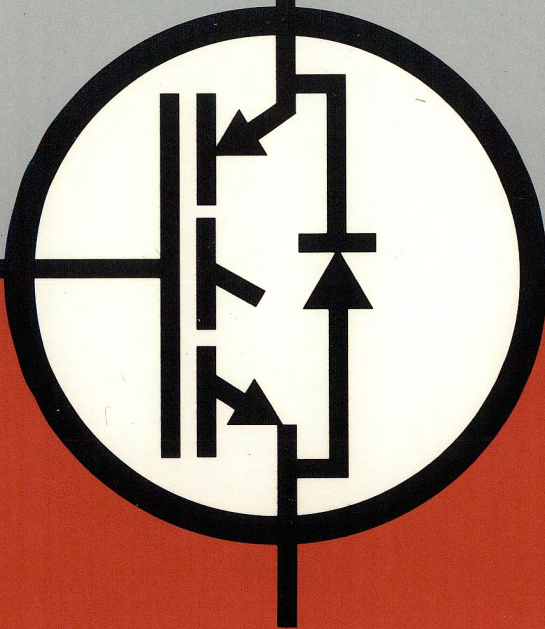


IGBT-3

IGBT Designer's Manual

Insulated Gate Bipolar Transistor



IR International Rectifier

International Rectifier

IGBT DESIGNER'S MANUAL

First Printing



Printed on recycled paper Weyerhaeuser
containing 10% total recovered fiber and
90% all post-consumer fiber.

PUBLISHED BY
INTERNATIONAL RECTIFIER, 233 KANSAS ST., EL SEGUNDO, CALIFORNIA 90245

IGBT Designer's Manual

International Rectifier does not recommend the use of its devices in life support applications wherein such use may directly threaten life or injury due to device failure or malfunction. Users of International Rectifier devices in life support applications assume all risks of such use and indemnify International Rectifier against all damages resulting from such use.

Copyright 1994, International Rectifier Corporation, El Segundo, CA. All rights reserved.
Reproduction or use of editorial or pictorial content without expressed permission in writing is prohibited.

IGBT

QUALITY STATEMENT

As an acknowledged leader in quality, International Rectifier is committed to a continuing process of improvement in our processes and products. As a visible demonstration of that commitment we recognize the value of an independent audit of our quality systems to recognized international standards, such as ISO9000. Our facility in England was one of the early registrants, achieving their certification in September of 1989. This was followed by our Italian factory in September of 1991. As the ISO standard began assuming a greater importance to customers in North America we undertook a campaign to register our facilities in California and Mexico. In September 1993, our El Segundo and Mexico manufacturing sites were certified to ISO9001, and our last remaining location in Temecula, California is scheduled for their certification audit during the first quarter of 1994.

International Rectifier believes that a product cannot be considered successful or of high quality if it is manufactured by processes that cause harm to the environment. It was based on this conviction that our newest manufacturing facility in Temecula California was built as a zero discharge facility exceeding even the tough environmental standards imposed by the state of California. Our facility in Tijuana Mexico is recognized by SEDESOL, the Mexican equivalent of the United States Environmental Protection Agency (EPA), as a model of environmental consciousness. Our water reclaim system was one of the first of its kind in Tijuana, and provides both water conservation and pollution control. The system satisfies the Mexican discharge standards and although not required, the even more stringent levels imposed in the United States by the EPA. We have reduced the VOC emissions in our El Segundo facility significantly every year since 1987, by both the installation of pollution control equipment and by

conversion to more environmentally friendly processes. Finally, our products themselves help in the drive toward a cleaner environment by allowing our customers to offer equipment that is more energy efficient, thereby requiring less power to be generated in the first place.

IGBT Quality Program

The quality programs of International Rectifier apply equally to all products. Our quality systems have been judged against the highest standards world wide, and as a result, have been certified to ISO9001 and other specific customer programs.

At International Rectifier we have been pursuing a policy of continuous improvement in the products we manufacture and the services we provide. This is a universal idea and crosses all international manufacturing boundaries. Each factory is responsible for their particular improvement programs but there is a universal theme throughout all locations. This is particularly important to the IGBT product line, because this is the first product that all factories of International Rectifier are involved with manufacturing.

The consistency and quality of our products is accomplished by the extensive use of Statistical Process Control. We abide by the axiom that a superior product is the result of "capable processes" tightly controlled, not extensive after the fact inspection to detect defects. The SPC program exists and is performed at the process operators level. They gather and plot the data and have initial responsibility for taking corrective action when an out of control condition occurs. Our process engineers are charged with developing processes that perform well within specification limits with a 6 sigma capability.

IGBT Reliability Programs

Maintaining and improving the reliability of all of our products is of prime importance to International Rectifier, and we have extended our existing reliability programs to include the IGBT product line. The objectives of that program are:

1. Define design weaknesses by stressing devices to failure under a variety of operating conditions. By establishing the cause of failure in the device, and applying techniques such as Pareto Analysis, we set the priorities for improvement.
2. Evaluate the consistency and predictability of production processes by monitoring device performance under varying conditions of stress.
3. Predict device lifetimes under realistic operating conditions by determining acceleration factors for known failure mechanisms.
4. Produce reports that can easily be used by customers to improve and predict the reliability of their products.
5. Appraise proposed process and design changes for their effect on reliability.
6. Conduct evaluations of competitive parts as a basis for benchmarking our products performance.

Additional information regarding this and the other elements of all our quality programs is contained in the booklet titled "Satisfying Our Customers" and can be obtained by contacting your local IR representative or writing for a copy to International Rectifier, 233 Kansas St., El Segundo, CA., 90245; ATTENTION: Advertising Department.

IGBT Designer's Manual

Table of Contents

Data Sheets	Alpha-Numeric Index	A	Alpha-Numeric Index	
	Selection Guide	B	Selection Guide	
	Low $V_{CE(on)}$ IGBTs For Low Frequency Power Applications Standard	Discretes	C	Low Frequency Standard Discrete
		Discretes Co-Packs Modules	C	Power Conversion Fast
	Medium Frequency IGBTs Fast	Discretes Co-Packs Modules	C	Motor Control Fast
		Discretes Co-Packs Modules	C	Power Conversion Ultra-Fast
	High Frequency IGBTs Ultra-Fast™	Discretes Co-Packs Modules	C	Motor Control Ultra-Fast
		Discretes Co-Packs Modules	C	Other Information
	Other Information	Appendix	D	Appendix
		Application Information	E	Application Information
Other Products		F	Other Information	

In the interest of product improvement, International Rectifier reserves the right to change specifications without notice.

IGBT Designer's Manual

Alpha-Numeric Index

IGBT Designer's Manual

INDEX



PART NUMBER	SECTION	DESCRIPTION
	Page Number	
AN-983A	E-3	Application Information
AN-988	E-33	Application Information
AN-990	E-15	Application Information
CPU165MF	C-133	Power Conversion
CPU165MK	C-961	Motor Control
CPU165MM	C-407	Motor Control
CPU165MU	C-733	Power Conversion
CPV362MF	C-141	Power Conversion
CPV362MK	C-963	Motor Control
CPV362MM	C-409	Motor Control
CPV362MU	C-741	Power Conversion
CPV363MF	C-149	Power Conversion
CPV363MK	C-971	Motor Control
CPV363MM	C-417	Motor Control
CPV363MU	C-749	Power Conversion
CPV364MF	C-157	Power Conversion
CPV364MK	C-979	Motor Control
CPV364MM	C-425	Motor Control
CPV364MU	C-757	Power Conversion
DT93-3	E-77	Application Information
DT93-6	E-81	Application Information
DT94-2	E-89	Application Information
DT94-4	E-95	Application Information
DT94-5	E-97	Application Information
DT94-6	E-99	Application Information
IRGB420U	C-575	Power Conversion
IRGB420UD2	C-617	Power Conversion
IRGB430U	C-581	Power Conversion
IRGB430UD2	C-625	Power Conversion
IRGB440U	C-587	Power Conversion
IRGBC20F	C-51	Power Conversion
IRGBC20FD2	C-93	Power Conversion
IRGBC20K	C-837	Motor Control
IRGBC20KD2	C-897	Motor Control
IRGBC20KD2-S	C-913	Motor Control
IRGBC20K-S	C-855	Motor Control
IRGBC20M	C-301	Motor Control
IRGBC20MD2	C-349	Motor Control
IRGBC20MD2-S	C-365	Motor Control
IRGBC20M-S	C-335	Motor Control
IRGBC20S	C-3	Low Frequency Power
IRGBC20U	C-651	Power Conversion
IRGBC20UD2	C-693	Power Conversion
IRGBC30F	C-57	Power Conversion
IRGBC30FD2	C-101	Power Conversion
IRGBC30K	C-843	Motor Control
IRGBC30KD2	C-905	Motor Control
IRGBC30KD2-S	C-921	Motor Control
IRGBC30K-S	C-861	Motor Control
IRGBC30M	C-307	Motor Control
IRGBC30MD2	C-357	Motor Control
IRGBC30MD2-S	C-373	Motor Control
IRGBC30M-S	C-341	Motor Control
IRGBC30S	C-9	Low Frequency Power
IRGBC30U	C-657	Power Conversion
IRGBC30UD2	C-701	Power Conversion
IRGBC40F	C-63	Power Conversion
IRGBC40K	C-849	Motor Control
IRGBC40K-S	C-867	Motor Control
IRGBC40M	C-313	Motor Control
IRGBC40M-S	C-347	Motor Control
IRGBC40S	C-15	Low Frequency Power
IRGBC40U	C-663	Power Conversion
IRGBF20F	C-237	Power Conversion
IRGBF30F	C-243	Power Conversion
IRGDDN200M12	C-549	Motor Control
IRGDDN300K06	C-1011	Motor Control
IRGDDN300M06	C-451	Motor Control
IRGDDN300M12	C-555	Motor Control

PART NUMBER	SECTION	DESCRIPTION
	Page Number	Application
IRGDDN400K06	C-1013	Motor Control
IRGDDN400M06	C-453	Motor Control
IRGDDN400M12	C-561	Motor Control
IRGDDN600K06	C-1015	Motor Control
IRGDDN600M06	C-455	Motor Control
IRGKI050U06	C-765	Power Conversion
IRGKI065F06	C-165	Power Conversion
IRGKI090U06	C-771	Power Conversion
IRGKI115U06	C-777	Power Conversion
IRGKI120F06	C-171	Power Conversion
IRGKI140U06	C-783	Power Conversion
IRGKI165F06	C-177	Power Conversion
IRGKI200F06	C-183	Power Conversion
IRGKIN025M12	C-489	Motor Control
IRGKIN050K06	C-987	Motor Control
IRGKIN050M06	C-427	Motor Control
IRGKIN050M12	C-495	Motor Control
IRGKIN075K06	C-989	Motor Control
IRGKIN075M06	C-429	Motor Control
IRGKIN075M12	C-501	Motor Control
IRGKIN100K06	C-991	Motor Control
IRGKIN100M06	C-431	Motor Control
IRGKIN100M12	C-507	Motor Control
IRGKIN150K06	C-993	Motor Control
IRGKIN150M06	C-433	Motor Control
IRGNI050U06	C-789	Power Conversion
IRGNI065F06	C-189	Power Conversion
IRGNI090U06	C-795	Power Conversion
IRGNI115U06	C-801	Power Conversion
IRGNI120F06	C-195	Power Conversion
IRGNI140U06	C-807	Power Conversion
IRGNI165F06	C-201	Power Conversion
IRGNI200F06	C-207	Power Conversion
IRGNIN025M12	C-509	Motor Control
IRGNIN050K06	C-995	Motor Control
IRGNIN050M06	C-435	Motor Control
IRGNIN050M12	C-515	Motor Control
IRGNIN075K06	C-997	Motor Control
IRGNIN075M06	C-437	Motor Control
IRGNIN075M12	C-521	Motor Control
IRGNIN100K06	C-999	Motor Control
IRGNIN100M06	C-439	Motor Control
IRGNIN100M12	C-527	Motor Control
IRGNIN150K06	C-1001	Motor Control
IRGNIN150M06	C-441	Motor Control
IRGP420U	C-593	Power Conversion
IRGP430U	C-599	Power Conversion
IRGP440U	C-605	Power Conversion
IRGP440UD2	C-641	Power Conversion
IRGP450U	C-611	Power Conversion
IRGP450UD2	C-649	Power Conversion
IRGPC20F	C-69	Power Conversion
IRGPC20K	C-873	Motor Control
IRGPC20KD2	C-929	Motor Control
IRGPC20M	C-315	Motor Control
IRGPC20MD2	C-381	Motor Control
IRGPC20U	C-669	Power Conversion
IRGPC30F	C-75	Power Conversion
IRGPC30FD2	C-109	Power Conversion
IRGPC30K	C-879	Motor Control
IRGPC30KD2	C-937	Motor Control
IRGPC30M	C-321	Motor Control
IRGPC30MD2	C-389	Motor Control
IRGPC30S	C-21	Low Frequency Power
IRGPC30U	C-675	Power Conversion
IRGPC30UD2	C-709	Power Conversion
IRGPC40F	C-81	Power Conversion
IRGPC40FD2	C-117	Power Conversion
IRGPC40K	C-885	Motor Control
IRGPC40KD2	C-945	Motor Control
IRGPC40M	C-327	Motor Control
IRGPC40MD2	C-397	Motor Control
IRGPC40S	C-27	Low Frequency Power
IRGPC40U	C-681	Power Conversion

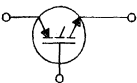
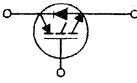
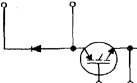
Alpha
Numeric
Index

PART NUMBER	SECTION Page Number	DESCRIPTION Application
IRGPC40UD2	C-717	Power Conversion
IRGPC50F	C-87	Power Conversion
IRGPC50FD2	C-125	Power Conversion
IRGPC50K	C-891	Motor Control
IRGPC50KD2	C-953	Motor Control
IRGPC50M	C-329	Motor Control
IRGPC50MD2	C-399	Motor Control
IRGPC50S	C-33	Low Frequency Power
IRGPC50U	C-687	Power Conversion
IRGPC50UD2	C-725	Power Conversion
IRGPF20F	C-249	Power Conversion
IRGPF30F	C-255	Power Conversion
IRGPF40F	C-261	Power Conversion
IRGPF50F	C-267	Power Conversion
IRGPH20M	C-463	Motor Control
IRGPH20S	C-39	Low Frequency Power
IRGPH30MD2	C-477	Motor Control
IRGPH30S	C-45	Low Frequency Power
IRGPH40F	C-273	Power Conversion
IRGPH40FD2	C-285	Power Conversion
IRGPH40M	C-469	Motor Control
IRGPH40MD2	C-479	Motor Control
IRGPH40S	C-47	Low Frequency Power
IRGPH50F	C-279	Power Conversion
IRGPH50FD2	C-293	Power Conversion
IRGPH50K	C-1023	Motor Control
IRGPH50KD2	C-1029	Motor Control
IRGPH50M	C-471	Motor Control
IRGPH50MD2	C-481	Motor Control
IRGPH50S	C-49	Low Frequency Power
IRGRDN200M12	C-549	Motor Control
IRGRDN300K06	C-1011	Motor Control
IRGRDN300M06	C-451	Motor Control
IRGRDN300M12	C-555	Motor Control
IRGRDN400K06	C-1013	Motor Control
IRGRDN400M06	C-453	Motor Control
IRGRDN400M12	C-561	Motor Control
IRGRDN600K06	C-1015	Motor Control
IRGRDN600M06	C-455	Motor Control
IRGTDN100M12	C-563	Motor Control
IRGTDN150K06	C-1017	Motor Control
IRGTDN150M06	C-457	Motor Control
IRGTDN150M12	C-569	Motor Control
IRGTDN200K06	C-1019	Motor Control
IRGTDN200M06	C-459	Motor Control
IRGTDN300K06	C-1021	Motor Control
IRGTDN300M06	C-461	Motor Control
IRGTI050U06	C-813	Power Conversion
IRGTI065F06	C-213	Power Conversion
IRGTI090U06	C-819	Power Conversion
IRGTI115U06	C-825	Power Conversion
IRGTI120F06	C-219	Power Conversion
IRGTI140U06	C-831	Power Conversion
IRGTI165F06	C-225	Power Conversion
IRGTI200F06	C-231	Power Conversion
IRGTIN025M12	C-529	Motor Control
IRGTIN050K06	C-1003	Motor Control
IRGTIN050M06	C-443	Motor Control
IRGTIN050M12	C-535	Motor Control
IRGTIN075K06	C-1005	Motor Control
IRGTIN075M06	C-445	Motor Control
IRGTIN075M12	C-541	Motor Control
IRGTIN100K06	C-1007	Motor Control
IRGTIN100M06	C-447	Motor Control
IRGTIN100M12	C-547	Motor Control
IRGTIN150K06	C-1009	Motor Control
IRGTIN150M06	C-449	Motor Control
OTHER CATALOGS	F-3	Other Designer's Manuals
TPAP-1	E-65	Application Information
TPAP-2	E-105	Application Information
TPAP-3	E-117	Application Information
TPAP-4	E-127	Application Information
TPAP-5	E-135	Application Information
TPAP-6	E-145	Application Information

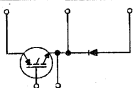
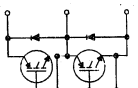
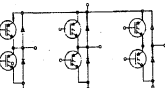
IGBT Designer's Manual

Selection Guide

Insulated Gate BiPolar Transistors — IGBTs and IGBT / UltraFast Diodes — CoPack Discrete and Module Types

Current Rating A	 Single Switch (without Diode)				 Single Switch (with Diode)				 Chopper Low Side Switch			
	Voltage Rating - V											
	500	600	900	1200	500	600	1200	600	1200			
5-10		IRGBC20K IRGPC20K IRGBC20K-S	IRGBF20F IRGPF20F	IRGPH20M IRGPH20S		IRGBC20KD2 IRGBC20KD2-S IRGPC20KD2						
11-15	IRGB420U IRGP420U	IRGBC20M IRGBC20M-S IRGPC20M IRGBC20U IRGPC20U			IRGB420UD2	IRGBC20MD2 IRGBC20MD2-S IRGPC20MD2 IRGBC20UD2	IRGPH30MD2					
16-20		IRGBC20F IRGPC20F IRGBC20S	IRGBF30F IRGPF30F			IRGBC20FD2						
21-25	IRGB430U IRGP430U	IRGBC30K IRGBC30K-S IRGPC30K IRGBC30U IRGPC30U		IRGPH30S	IRGB430UD2 IRGP430UD2	IRGBC30KD2 IRGBC30KD2-S IRGPC30KD2 IRGBC30UD2 IRGPC30UD2						
26-30		IRGBC30M IRGBC30M-S IRGPC30M		IRGPH40F		IRGBC30MD2 IRGBC30MD2-S IRGPC30MD2	IRGPH40FD2					
31-40	IRGB440U IRGP440U	IRGBC30F IRGPC30F IRGPC30S IRGBC40M IRGBC40M-S IRGPC40M IRGBC30S IRGBC40U IRGPC40U	IRGPF40F	IRGPH40M IRGPH40S IRGPH50K	IRGP440UD2	IRGBC30FD2 IRGPC30FD2 IRGPC40MD2 IRGPC40UD2	IRGPH40MD2 IRGPH50KD2					
41-50		IRGPC40K IRGBC40K IRGBC40F IRGPC40F IRGPC40K-S IRGPC40S IRGBC40S		IRGPH50F IRGPH50M		IRGPC40FD2 IRGPC40KD2	IRGPH50FD2 IRGPH50MD2	IRGKI050U06				
51-60	IRGP450U	IRGBC50K IRGPC50M IRGPC50U	IRGPF50F	IRGPH50S	IRGP450UD2	IRGPC50KD2 IRGPC50MD2 IRGPC50UD2		IRGKI050K06 IRGKI050M06		IRGKIN025M12		
61-70		IRGPC50F IRGPC50S				IRGPC50FD2		IRGKI065F06				
71-100								IRGKI090U06 IRGKI075K06 IRGKI120F06		IRGKIN050M12		
101-125								IRGKI120F06 IRGKI075M06				
126-150								IRGKI100K06 IRGKI100M06 IRGKI115U06		IRGKIN075M12		
151-175								IRGKI140U06 IRGKI165F06 IRGKI165F06 IRGKI150K06		IRGKIN100M12		
176-200								IRGKI200F06 IRGKI150M06				
201-300												
301-400						IRGDDN300K06 IRGRDN300K06 IRGDDN300M06 IRGRDN300M06	IRGDDN400M12 IRGDDN400M12					
401-600						IRGDDN400K06 IRGRDN400K06 IRGDDN400M06 IRGRDN400M06	IRGDDN200M12 IRGRDN200M12 IRGDDN300M12 IRGRDN300M12					
601-1000						IRGDDN600K06 IRGRDN600K06 IRGDDN600M06 IRGRDN600M06						

Part Numbers in Italics are Short Circuit Protected

Current Rating A					
	Chopper High Side Switch		Half Bridge		Three Phase Bridge
	Voltage Rating -V				
	600	1200	600	1200	600
5-10					CPV362MU CPV362MK CPV362MF
11-15					CPV363MK CPV363MU CPV363MM
16-20					CPV363MF CPV364MM CPV364MU CPV364MK
21-25					
26-30					CPV364MF
31-40			CPU165MU CPU165MK		
41-50	IRGN1050U06	IRGNIN025M12	CPU165MF CPU165MM IRGT1050U06	IRGTIN025M12	
51-60	IRGNIN050K06 IRGNIN050M06		IRGTIN050K06 IRGTIN050M06		
61-70	IRGN1065F06		IRGT1065F06		
71-100	IRGN1090U06 IRGNIN075K06	IRGNIN050M12	IRGT1090U06 IRGTIN075K06	IRGTIN050M12	
101-125	IRGN1120F06 IRGNIN075M06 IRGN1120F06		IRGTIN075M06 IRGT1120F06		
126-150	IRGNIN100K06 IRGNIN100M06 IRGN1115U06	IRGNIN075M12	IRGTIN100K06 IRGTIN100M06 IRGT1115U06	IRGTIN075M12	
151-175	IRGN1140U06 IRGNIN150K06 IRGN1165F06	IRGNIN100M12	IRGT1140U06 IRGT1165F06 IRGTIN150K06 IRGTDN150K06	IRGTIN100M12	
176-200	IRGNIN150M06 IRGN200F06 IRGTDN150M06		IRGTIN150M06 IRGT1200F06 IRGTDN150M06		
201-300			IRGTDN200K06 IRGTDN200M06	IRGTDN100M12 IRGTDN150M12	
301-400			IRGTDN300K06 IRGTDN300M06		
401-600					
601-1000					

IGBT Selection Guide

Low $V_{CE(on)}$ IGBTs for Low Frequency (DC~1kHz) Power Applications

STANDARD

Part Number	Page Number	V_{CES} Collector to Emitter Voltage (V)	Max $V_{CE(on)}$ Collector to Emitter Voltage (V)	I_C Continuous Collector Current		P_D Max. Power Dissipation (W)	Circuit	Case Outline Number
				$T_C = 25^\circ C$	$T_C = 100^\circ C$			
				(A)	(A)			
Discretes - (IGBT only)								
IRGBC20S	C-3	600	2.0	19	10	60	Circuit A	TO-220AB
IRGBC30S	C-9		2.2	34	18	100		
IRGBC40S	C-15		1.8	50	31	160		
IRGPC30S	C-21	1200	2.2	34	18	100	Circuit A	TO-247AC
IRGPC40S	C-27		1.8	50	31	160		
IRGPC50S	C-33		1.6	70	41	200		
IRGPH20S	C-39		3.3	10	6.6	60		
IRGPH30S	C-45		3.0	22	13	100		
IRGPH40S	C-47	3.0	33	20	160	Circuit A	TO-247AC	
IRGPH50S	C-49	2.0	57	33	200			
Fast IGBTs for Medium Frequency (3-10 kHz range) Power Applications High Efficiency — Optimized for Power Conversion								
FAST								
Discretes - (IGBT only)								
IRGBC20F	C-51	600	2.8	16	9.0	60	Circuit A	TO-220AB
IRGBC30F	C-57		2.1	31	17	100		
IRGBC40F	C-63		2.0	49	27	160		
IRGPC20F	C-69	1200	2.8	16	9.0	60	Circuit A	TO-247AC
IRGPC30F	C-75		2.1	31	17	100		
IRGPC40F	C-81		2.0	49	27	160		
IRGPC50F	C-87		1.7	70	39	200		
IRGBC20FD2	C-93		600	2.8	16	9.0		
IRGBC30FD2	C-101	2.1		31	17	100		
IRGPC30FD2	C-109	2.1		31	17	100		
IRGPC40FD2	C-117	1200	2.0	49	27	160	Circuit B	TO-247AC
IRGPC50FD2	C-125		1.7	70	39	200		
Co-Packs - (IGBT + HEXFRED™ Diode)								
IRGBC20FD2	C-93	600	2.8	16	9.0	60	Circuit B	TO-220AB
IRGBC30FD2	C-101		2.1	31	17	100		
IRGPC30FD2	C-109		2.1	31	17	100		
IRGPC40FD2	C-117	1200	2.0	49	27	160	Circuit B	TO-247AC
IRGPC50FD2	C-125		1.7	70	39	200		
Modules								
CPU165MF	C-133	600	1.5	42	23	83	Circuit E	IMS-1
CPV362MF	C-141		1.8	8.8	4.8	23	Circuit H	IMS-2
CPV363MF	C-149		1.6	16	8.7	36		
CPV364MF	C-157		1.6	27	15	63		
IRGKI065F06	C-165	1200	2.3	65	35	179	Circuit F	INT-A-Pak
IRGKI120F06	C-171		2.3	120	60	298		
IRGKI165F06	C-177		2.3	165	85	379		
IRGKI200F06	C-183		2.3	200	110	500		
IRGNI065F06	C-189	1200	2.3	65	35	179	Circuit G	INT-A-Pak
IRGNI120F06	C-195		2.3	120	60	298		
IRGNI165F06	C-201		2.3	165	85	379		
IRGNI200F06	C-207		2.3	200	110	500		
IRGTI065F06	C-213	1200	2.3	65	35	179	Circuit E	INT-A-Pak
IRGTI120F06	C-219		2.3	120	60	298		
IRGTI165F06	C-225		2.3	165	85	379		
IRGTI200F06	C-231		2.3	200	110	500		

IGBT Selection Guide

Fast IGBTs for Medium Frequency (3-10 kHz range) Power Applications
High Efficiency—Optimized for Power Conversion

FAST (cont.)

Part Number	Page Number	V _{CE} Collector to Emitter Voltage (V)	Max V _{CE(on)} Collector to Emitter Voltage (V)	I _C Continuous Collector Current		P _D Max. Power Dissipation (W)	Circuit	Case Outline Number	
				T _C = 25°C (A)	T _C = 100°C (A)				
Discretes - (IGBT only)									
IRGBF20F	C-237	900	4.3	9.0	5.3	60	Circuit A	TO-220AB	
IRGBF30F	C-243		3.7	20	11	100			
IRGPF20F	C-249		4.3	9.0	5.3	60			
IRGPF30F	C-255		3.7	20	11	100			
IRGPF40F	C-261		3.3	31	17	160			
IRGPF50F	C-267		2.7	51	28	200			
IRGPH40F	C-273	1200	3.3	29	17	160			
IRGPH50F	C-279		2.9	45	25	200			
Co-Packs - (IGBT + HEXFRED™ Diode)									
IRGPH40FD2	C-285	1200	3.3	29	17	160	Circuit B	TO-247AC	
IRGPH50FD2	C-293		2.9	45	25	200			
Short Circuit Rated—Optimized for Motor Control Applications									
Discretes - (IGBT only)									
IRGBC20M	C-301	600	2.5	13	8.0	60	Circuit A	TO-220AB	
IRGBC30M	C-307		2.9	26	16	100			
IRGBC40M	C-313		3.0	40	24	160			
IRGPC20M	C-315		2.3	13	8.0	60	Circuit B	TO-247AC	
IRGPC30M	C-321		2.9	26	16	100			
IRGPC40M	C-327		2.0	40	24	160			
IRGPC50M	C-329	2.2	60	35	200				
IRGBC20M-S	C-335		2.3	13	8.0	60		SMD-220	
IRGBC30M-S	C-341		2.9	26	16	100			
IRGBC40M-S	C-347		3.0	40	24	160			
Co-Packs - (IGBT + HEXFRED™ Diode)									
IRGBC20MD2	C-349	600	2.5	13	8.0	60	Circuit B	TO-220AB	
IRGBC30MD2	C-357		2.9	26	16	100			
IRGBC20MD2-S	C-365		2.5	13	8.0	60		SMD-220	
IRGBC30MD2-S	C-373		2.9	26	16	100			
IRGPC20MD2	C-381			2.5	13	8.0		60	TO-247AC
IRGPC30MD2	C-389			2.9	26	16		100	
IRGPC40MD2	C-397	3.0		40	24	160			
IRGPC50MD2	C-399	2.0		60	35	200			
Modules									
CPU165MM	C-407	600	2.0	42	23	83	Circuit E	IMS-1	
CPV362MM	C-409		3.3	7.9	4.6	23	Circuit H	IMS-2	
CPV363MM	C-417		2.4	13	7.0	36			
CPV364MM	C-425		1.7	22	12	62.5			
IRGKIN050M06	C-427		2.0	60	23	240	Circuit F	INT-A-Pak	
IRGKIN075M06	C-429		2.0	110	40	391			
IRGKIN100M06	C-431		2.0	150	60	500			
IRGKIN150M06	C-433		2.0	200	80	658			
IRGNIN050M06	C-435		2.0	60	23	240			Circuit G
IRGNIN075M06	C-437	2.0	110	40	391				
IRGNIN100M06	C-439	2.0	150	60	500				
IRGNIN150M06	C-441	2.0	200	80	658				



IGBT Selection Guide

Fast IGBTs for Medium Frequency (3-10 kHz range) Power Applications
Short Circuit Rated—Optimized for Motor Control Applications

FAST (cont.)

Part Number	Page Number	V _{CE(s)} Collector to Emitter Voltage (V)	Max V _{CE(on)} Collector to Emitter Voltage (V)	I _C Continuous Collector Current		P _D Max. Power Dissipation (W)	Circuit	Case Outline Number
				T _C = 25°C (A)	T _C = 100°C (A)			
Modules								
IRGTIN050M06	C-443	600	2.0	60	23	240	Circuit E	INT-A-Pak
IRGTIN075M06	C-445		2.0	110	40	391		
IRGTIN100M06	C-447		2.0	150	60	500		
IRGTIN150M06	C-449		2.0	200	80	658		
IRGDDN300M06	C-451	600	2.0	400	160	1563	Circuit C	Double INT-A-Pak
IRGDDN400M06	C-453		2.0	600	240	1984		
IRGDDN600M06	C-455		2.7	800	320	2604		
IRGRDN300M06	C-451	600	2.0	400	160	1563	Circuit D	
IRGRDN400M06	C-453		2.0	600	240	1984		
IRGRDN600M06	C-455		2.7	800	320	2604		
IRGTDN150M06	C-457	600	2.0	200	80	781	Circuit E	
IRGTDN200M06	C-459		2.0	300	120	1000		
IRGTDN300M06	C-461		2.0	400	160	1316		
Discretes - (IGBT only)								
IRGPH20M	C-463	1200	4.6	6.9	4.5	60	Circuit A	TO-247AC
IRGPH40M	C-469		3.4	31	18	160		
IRGPH50M	C-471		2.9	42	23	200		
Co-Packs - (IGBT + HEXFRED™ Diode)								
IRGPH30MD2	C-477	1200	3.5	15	9.0	100	Circuit B	TO-247AC
IRGPH40MD2	C-479		3.4	31	18	160		
IRGPH50MD2	C-481		2.9	42	23	200		
Modules								
IRGKIN025M12	C-489	1200	2.7	50	35	385	Circuit F	INT-A-Pak
IRGKIN050M12	C-495		2.7	100	45	455		
IRGKIN075M12	C-501		2.7	150	65	600		
IRGKIN100M12	C-507		2.7	175	75	665		
IRGNIN025M12	C-509		Circuit G	2.7	50	35	385	
IRGNIN050M12	C-515			2.7	100	45	455	
IRGNIN075M12	C-521			2.7	150	65	600	
IRGNIN100M12	C-527			2.7	175	75	665	
IRGTIN025M12	C-529		Circuit E	2.7	50	35	385	
IRGTIN050M12	C-535			2.7	100	45	455	
IRGTIN075M12	C-541			2.7	140	60	600	
IRGTIN100M12	C-547			2.7	175	75	665	
IRGDDN200M12	C-549		Circuit C	2.7	420	180	1800	
IRGDDN300M12	C-555			2.7	560	240	2400	
IRGDDN400M12	C-561			2.7	400	—	2770	
IRGRDN200M12	C-549		Circuit D	2.7	420	180	1800	
IRGRDN300M12	C-555	2.7		560	240	2400		
IRGRDN400M12	C-561	2.7		400	—	2770		
IRGTDN100M12	C-563	Circuit E	2.5	200	90	900		
IRGTDN150M12	C-569		2.5	280	120	1200		

IGBT Selection Guide

Ultra-Fast™ IGBTs for Higher Frequency (10-30 kHz range) Power Applications
High Efficiency—Optimized for Power Conversion

ULTRA-FAST

Part Number	Page Number	V _{CE(s)} Collector to Emitter Voltage (V)	Max V _{CE(on)} Collector to Emitter Voltage (V)	I _C Continuous Collector Current		P _D Max. Power Dissipation (W)	Circuit	Case Outline Number	
				T _C = 25°C (A)	T _C = 100°C (A)				
Discretes - (IGBT only)									
IRGB420U IRGB430U IRGB440U	C-575 C-581 C-587	500	3.0 3.0 3.0	14 25 40	7.5 15 22	60 100 160	Circuit A	TO-220AB TO247AC	
IRGP420U IRGP430U IRGP440U IRGP450U	C-593 C-599 C-605 C-611		3.0 3.0 3.0 3.2	14 25 40 59	7.5 15 22 33	60 100 160 200			
Co-Packs - (IGBT + HEXFRED™ Diode)									
IRGB420UD2 IRGB430UD2	C-617 C-625	500	2.9 3.0	14 25	7.5 15	60 100	Circuit B	TO-220AB TO-247AC	
IRGP430UD2 IRGP440UD2 IRGP450UD2	C-633 C-641 C-649		3.0 3.0 3.2	25 40 59	15 22 33	100 160 200			
Discretes - (IGBT only)									
IRGBC20U IRGBC30U IRGBC40U	C-651 C-657 C-663	600	3.0 3.0 3.0	13 23 40	6.5 12 20	60 100 160	Circuit A	TO-220-AB TO-247AC	
IRGPC20U IRGPC30U IRGPC40U IRGPC50U	C-669 C-675 C-681 C-687		3.0 3.0 3.0 3.0	13 23 40 55	6.5 12 20 27	60 100 160 200			
Co-Packs - (IGBT + HEXFRED™ Diode)									
IRGBC20UD2 IRGBC30UD2	C-693 C-701	600	3.0 3.0	13 23	6.5 12	60 100	Circuit B	TO-220AB TO-247AC	
IRGPC30UD2 IRGPC40UD2 IRGPC50UD2	C-709 C-717 C-725		3.0 3.0 3.0	23 40 55	12 20 27	100 160 200			
Modules									
CPU165MU	C-733	600	2.3	33	17	83	Circuit E	IMS-1	
CPV362MU	C-741		2.6	7.2	3.9	23	Circuit H	IMS-2	
CPV363MU	C-749		2.4	13	6.8	36			
CPV364MU	C-757		2.6	20	10	63			
IRGKI050U06 IRGKI090U06 IRGKI115U06 IRGKI140U06	C-765 C-771 C-777 C-783	600	3.1 3.0 2.8 2.7	50 90 130 170	30 50 70 95	179 298 379 500	Circuit F	INT-A-Pak	
IRGNI050U06 IRGNI090U06 IRGNI115U06 IRGNI140U06	C-789 C-795 C-801 C-807		3.1 3.0 2.8 2.7	50 90 130 170	30 50 70 95	179 298 379 500			Circuit G
IRGTI050U06 IRGTI090U06 IRGTI115U06 IRGTI140U06	C-813 C-819 C-825 C-831		3.1 3.0 2.8 2.7	50 90 130 170	30 50 70 95	179 298 379 500			Circuit E



IGBT Selection Guide

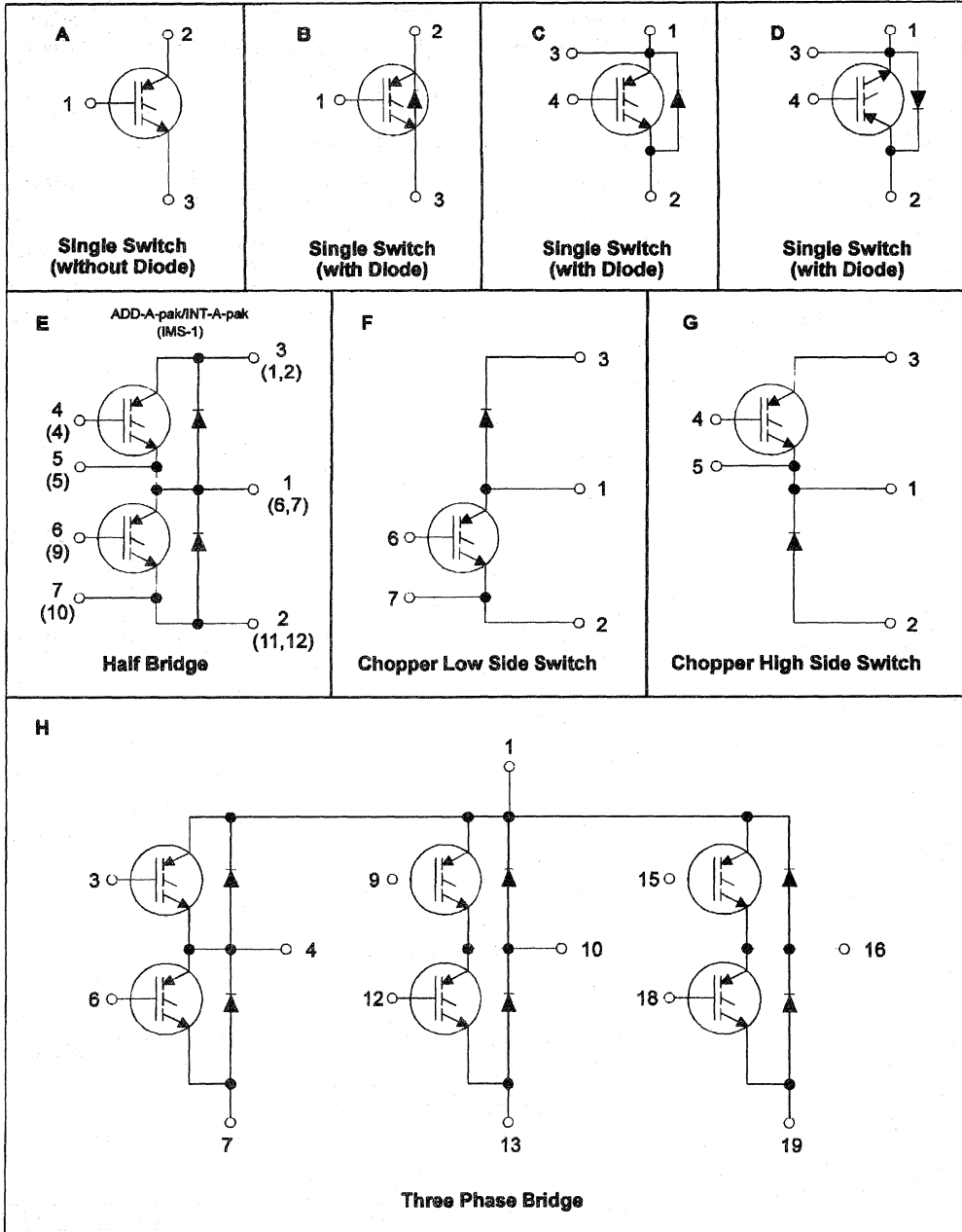
Ultra-Fast™ IGBTs for Higher Frequency (10-30 kHz range) Power Applications
Short Circuit Rated—Optimized for Motor Control Applications

ULTRA-FAST (cont.)

Part Number	Page Number	V _{CES} Collector to Emitter Voltage (V)	Max V _{CE(on)} Collector to Emitter Voltage (V)	I _C Continuous Collector Current		P _D Max. Power Dissipation (W)	Circuit	Case Outline Number
				T _C = 25°C (A)	T _C = 100°C (A)			
Discretes - (IGBT only)								
IRGBC20K	C-837	600	3.5	10	6.0	60	Circuit A	TO-220AB
IRGBC30K	C-843		3.8	23	14	100		
IRGBC40K	C-849		3.2	42	25	160		
IRGBC20K-S	C-855	3.5	10	6.0	60	SMD-220		
IRGBC30K-S	C-861	3.3	23	14	100			
IRGBC40K-S	C-867	3.2	42	25	160			
IRGPC20K	C-873	3.5	10	6.0	60	TO-247AC		
IRGPC30K	C-879	3.8	23	14	100			
IRGPC40K	C-885	3.2	42	25	160			
IRGPC50K	C-891	2.7	52	30	200			
Co-Packs - (IGBT + HEXFRED™ Diode)								
IRGBC20KD2	C-897	600	3.5	10	6.0	60	Circuit B	TO-220AB
IRGBC30KD2	C-905		3.8	23	14	100		
IRGBC20KD2-S	C-913		3.5	10	6.0	60		
IRGBC30KD2-S	C-921	3.8	23	14	100	SMD-220		
IRGPC20KD2	C-929	3.5	10	6.0	60			
IRGPC30KD2	C-937	3.8	23	14	100	TO-247AC		
IRGPC40KD2	C-945	3.2	42	25	160			
IRGPC50KD2	C-953	2.7	52	30	200			
Modules								
CPU165MK	C-961	600	2.7	33	17	83	Circuit E	IMS-1
CPV362MK	C-963		3.5	5.7	3.0	23	Circuit H	IMS-2
CPV363MK	C-971		3.0	11	6.0	36		
CPV364MK	C-979		3.1	24	13	63		
IRGKIN050K06	C-987	600	2.7	55	20	240	Circuit F	INT-A-Pak
IRGKIN075K06	C-989		2.7	95	40	391		
IRGKIN100K06	C-991		2.7	130	50	500		
IRGKIN150K06	C-993		2.7	170	70	658		
IRGNIN050K06	C-995	600	2.7	55	20	240	Circuit G	INT-A-Pak
IRGNIN075K06	C-997		2.7	95	40	391		
IRGNIN100K06	C-999		2.7	130	50	500		
IRGNIN150K06	C-1001		2.7	170	70	658		
IRGTIN050K06	C-1003	600	2.7	55	20	240	Circuit E	INT-A-Pak
IRGTIN075K06	C-1005		2.7	95	40	391		
IRGTIN100K06	C-1007		2.7	130	50	500		
IRGTIN150K06	C-1009		2.7	170	70	658		
IRGDDN300K06	C-1011	600	2.7	340	140	1563	Circuit C	Double INT-A-Pak
IRGDDN400K06	C-1013		2.7	520	200	1984		
IRGDDN600K06	C-1015		2.7	680	280	2604		
IRGRDN300K06	C-1011	600	2.7	340	140	1563	Circuit D	
IRGRDN400K06	C-1013		2.7	520	200	1984		
IRGRDN600K06	C-1015		2.7	680	280	2604		
IRGTDN150K06	C-1017	600	2.7	170	70	781	Circuit E	
IRGTDN200K06	C-1019		2.7	260	100	1000		
IRGTDN300K06	C-1021		2.7	340	140	1316		
Discretes - (IGBT only)								
IRGPH50K	C-1023	1200	3.5	36	20	200	Circuit A	TO-247AC
Co-Packs - (IGBT + HEXFRED™ Diode)								
IRGPH50KD2	C-1029	1200	3.5	36	20	200	Circuit B	TO-247AC

IGBT Selection Guide

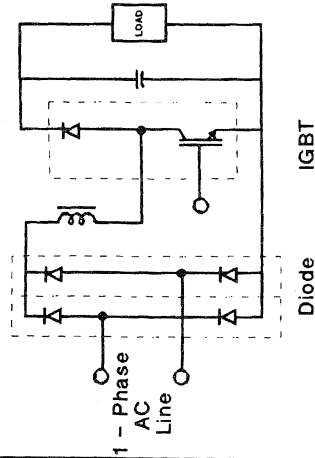
IGBT Circuit Configurations



Rectifier and IGBT Chopper Module Selection Guide for Boost-Converter (power factor correction)

Boost Converter Output Power kW	Minimum RMS Input Line Voltage V	Max RMS Input Line Voltage V	Max Continuous RMS Input Line Current A	Switching Frequency kHz	Suitable Rectifier Modules 1-phase Input	Suitable IGBT Chopper Modules
1	180	275	6	20 30 50	↕ 26MB60A 250JB6L	INT-A-PAK IRGK/NI050U06 IRGK/NI050U06 IRGK/NI050U06
	90	275	12	20 30 50	↕ 36MB60A 35MB60A	IRGK/NI090U06 IRGK/NI090U06 IRGK/NI115U06
	180	275	9	20 30 50	↕ 36MB60A 35MB60A	IRGK/NI050U06 IRGK/NI090U06 IRGK/NI090U06
1.5	90	275	18	20 30 50	↕ 2x B40D60	IRGK/NI090U06 IRGK/NI115U06 IRGK/NI140U06
	180	275	12	20 30 50	↕ 36MB60A 35MB60A	IRGK/NI090U06 IRGK/NI090U06 IRGK/NI115U06
	275	275	24	20 30	↕ 2x B40D60	IRGK/NI115U06 IRGK/NI140 U06
3	180	275	18	20 30	↕ 2x B40D60	IRGK/NI090U06 IRGK/NI115U06

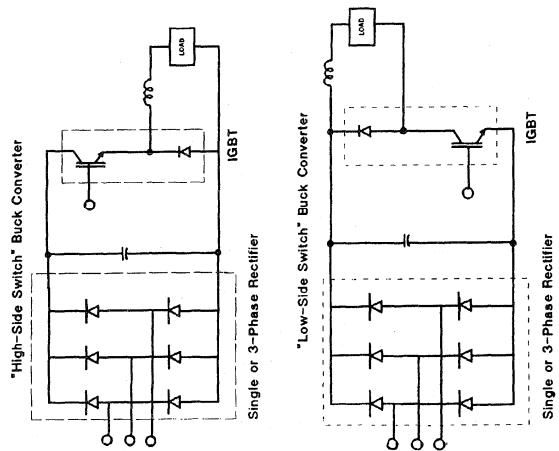
NOTE: DC output voltage of boost converter = 400V. T_{jc} @ continuous current is 20°-30°C.



Rectifier and IGBT Chopper Selection Guide for Buck Converter with 100% control range

Continuous Output Current A	Overload Current (1-minute) Typical A	Switching Frequency kHz	Suitable Rectifier Modules		Suitable IGBT Chopper Modules
			1-phase Input	3-phase Input	
10	15	2 5 10 15 20 30	36MB60A 35MB60A	36M160	INT-A-PAK IRGK/NI065F06 IRGK/NI065F06 IRGK/NI090F06 IRGK/NI090U06 IRGK/NI090U06 IRGK/NI090U06
15	22.5	2 5 10 15 20 30	2x B40D60	60M180K	IRGK/NI120F06 IRGK/NI120F06 IRGK/NI120F06 IRGK/NI090U06 IRGK/NI090U06 IRGK/NI115U06
20	30	2 5 10 15 20 30	—	60M180K	IRGK/NI120F06 IRGK/NI120F06 IRGK/NI115U06 IRGK/NI115U06 IRGK/NI140U06 IRGK/NI140U06
30	45	2 5 10	—	90M180K	IRGK/NI165F06 IRGK/NI165F06 IRGK/NI140F06
40	60	2 5	—	110M180K	IRGK/NI1200F06 IRGK/NI1200F06

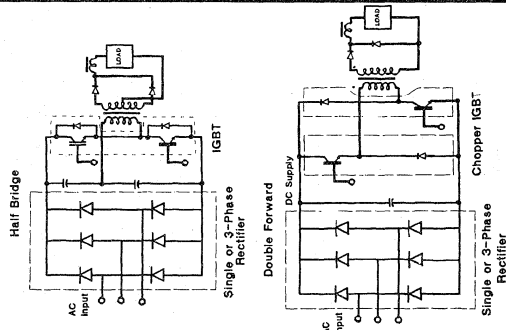
NOTE: DC output voltage = 360V. T_{jc} @ continuous current is 20°-30°C.



IGBT and Rectifier Module Selection Guide for Double-Forward and Half Bridge Converters

Cont. Output Power P ₀ W	Peak Rectangular IGBT Current at P ₀ A	Typical Max. Output Power P _{max} W	Typical Rectangular IGBT Current at P _{max} W	Switching Freq. kHz	Suitable Rectifier Modules - 230V Input		Suitable IGBT Modules	
					1-Phase Input	3-Phase Input	Double Forward Converter	Half Bridge
750	6	1125	9	20 30	100JB6L 26MT60	26MT60	IRGK1050U06+IRGN1050U06 IRGK1050U06+IRGN1050U06	IRGT1050U06 IRGT1050U06
1000	8	1500	12	20 30	26MB50A 250JB6L	26MT60	IRGK1050U06+IRGN1050U06 IRGK1050U06+IRGN1050U06	IRGT1050U06 IRGT1050U06
1500	12.2	2250	18.3	10 20	26MB60A 26MT60	26MT60	IRGK1050U06+IRGN1050U06 IRGK1050U06+IRGN1050U06	IRGT1050U06 IRGT1050U06
2000	16.3	3000	24.5	5 10 20 30	36MB60A 35MB60A	36MT60	IRGK1090U06+IRGN1090U06 IRGK115U06+IRGN115U06	IRGT1090U06 IRGT1090U06
3000	24.4	4500	36.6	2 5 10 20 30	2x B40D60 2x IRKD56-6	60MT80K	IRGK1065F06+IRGN1065F06 IRGK1050U06+IRGN1050U06 IRGK1090U06+IRGN1090U06 IRGK1090U06+IRGN1090U06 IRGK115U06+IRGN115U06	IRGT1065F06 IRGT1050U06 IRGT1090U06 IRGT1090U06 IRGT115U06
5000	40.7	7500	61	2 5 10 20	60MT80K	60MT80K	IRGK120F06+IRGN120F06 IRGK1090U06+IRGN1090U06 IRGK115U06+IRGN115U06 IRGK140U06+IRGN140U06	IRGT120F06 IRGT1090U06 IRGT115U06 IRGT140U06
7500	61	11250	91.5	2 5 10	90MT80K 3x B40D60	90MT80K 3x B40D60	IRGK120F06+IRGN120F06 IRGK140U06+IRGN140U06 IRGK140U06+IRGN140U06	IRGT130F06 IRGT140U06 IRGT140U06
10000	81.3	15000	122	2 5	110MT80K 3x B40D60	110MT80K 3x B40D60	IRGK165F06+IRGN165F06 IRGK200F06+IRGN200F06	IRGT165F06 IRGT200F06
15000	122	22500	183	2	160MT80K 3x IRKD56-6	160MT80K 3x IRKD56-6	IRGK200F06+IRGN200F06	IRGT200F06

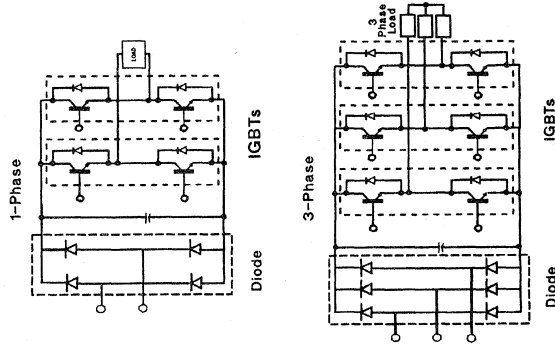
NOTE: DC voltage range approx: 265V to 400V. T_{jc} @ continuous P₀ is 20°-30°C.



IGBT and Rectifier Module Selection Guide for PWM Inverters

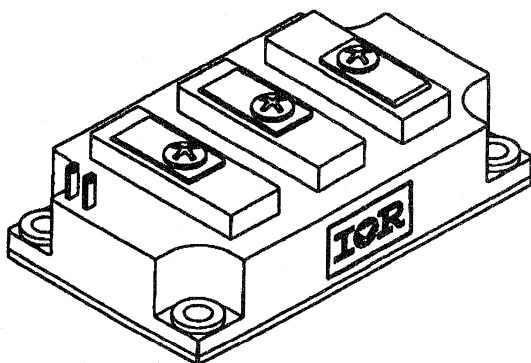
Cont. Output Current A	Overload Current (1-min.) Typical A	TYPICAL kVA		Switching Freq. kHz	Suitable rectifier modules		Suitable IGBT Module Type
		Three-Phase Bridge			3-Phase 230V line		
		Single-Phase Bridge Overload (1-minute) Typical Cont.	Three-Phase Bridge Overload (1-minute) Typical Cont.		For single-phase PWM IGBT Bridge	For three-phase PWM IGBT Bridge	
15	22.5	4	6	2	60MT80K	60MT80K	INT-A-PAK IRGT1065F06 IRGT1065F06 IRGT1050U06 IRGT1050U06 IRGT1050U06
20	30	5	7.5	5	60MT80K	60MT80K	IRGT1065F06 IRGT1065F06 IRGT1050U06 IRGT1050U06 IRGT1090U06
25	37.5	6.5	10	10	60MT80K	60MT80K	IRGT1065F06 IRGT1065F06 IRGT1090U06 IRGT1090U06 IRGT1090U06
30	45	8	12	15	60MT80K 3x B40D60	60MT80K 3x B40D60	IRGT1065F06 IRGT1065F06 IRGT1090U06 IRGT1090U06 IRGT1090U06
40	60.5	10	15	20	60MT80K 3x B40D60	60MT80K 3x B40D60	IRGT1065F06 IRGT1065F06 IRGT1090U06 IRGT1090U06 IRGT115U06
50	75	13	20	22.5	90MT80K 3x B40D60	90MT80K 3x B40D60	IRGT1120F06 IRGT1120F06 IRGT1090U06 IRGT115U06 IRGT1140U06
75	112.5	20	30	30	110MT80K 3x B40D60	110MT80K 3x B40D60	IRGT1120F06 IRGT1120F06 IRGT115U06 IRGT1140U06 IRGT1165F06
100	450	2.5	40	45	3x IRKD71-06	3x IRKD71-06	IRGT1200F06 IRGT1200F06 IRGT1200F06

NOTE: Nominal dc bus voltage = 360V. I_{Tc} @ continuous current is 20°-30°C.

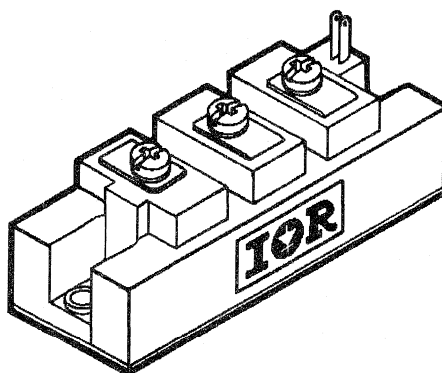


IGBT Selection Guide

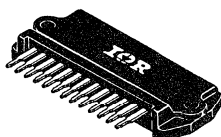
IGBT Case Styles



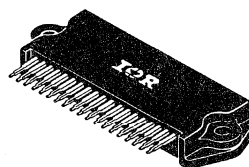
Double INT-A-PAK



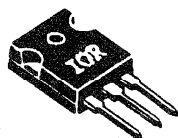
INT-A-PAK



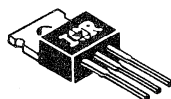
IMS-1



IMS-2



TO-247AC



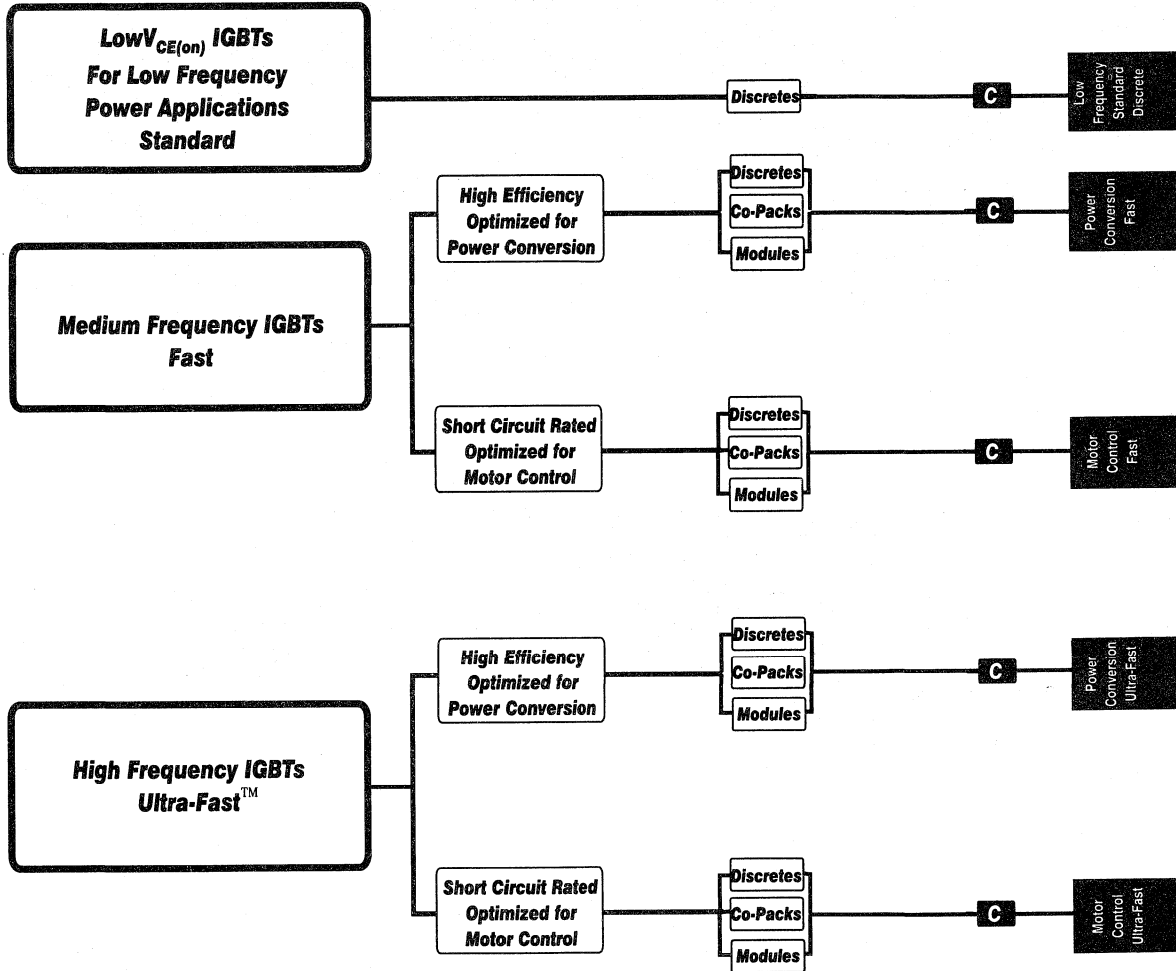
TO-220AB



SMD-220

IGBT Designer's Manual

Data Sheets



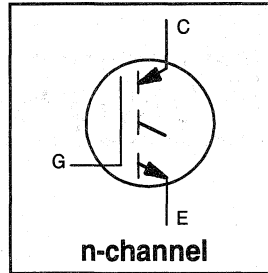
IGBT Designer's Manual

Data Sheets

The IGBT devices listed in this Designer's Manual represent International Rectifier's IGBT line as of August, 1994. The data presented in this manual supersedes all previous specifications.

Features

- Switching-loss rating includes all "tail" losses
- Optimized for line frequency operation (to 400 Hz)
See Fig. 1 for Current vs. Frequency curve



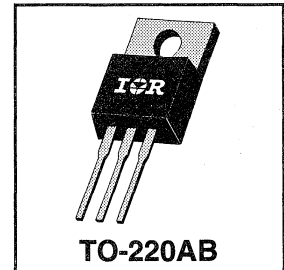
$$V_{CES} = 600V$$

$$V_{CE(sat)} \leq 2.4V$$

$$@V_{GE} = 15V, I_C = 10A$$

Description

Insulated Gate Bipolar Transistors (IGBTs) from International Rectifier have higher usable current densities than comparable bipolar transistors, while at the same time having simpler gate-drive requirements of the familiar power MOSFET. They provide substantial benefits to a host of high-voltage, high-current applications.



Absolute Maximum Ratings

	Parameter	Max.	Units
V_{CES}	Collector-to-Emitter Voltage	600	V
$I_C @ T_C = 25^\circ C$	Continuous Collector Current	19	A
$I_C @ T_C = 100^\circ C$	Continuous Collector Current	10	
I_{CM}	Pulsed Collector Current ①	76	
I_{LM}	Clamped Inductive Load Current ②	38	
V_{GE}	Gate-to-Emitter Voltage	± 20	V
E_{ARV}	Reverse Voltage Avalanche Energy ③	5.0	mJ
$P_D @ T_C = 25^\circ C$	Maximum Power Dissipation	60	W
$P_D @ T_C = 100^\circ C$	Maximum Power Dissipation	24	
T_J	Operating Junction and Storage Temperature Range	-55 to +150	°C
T_{STG}			
	Soldering Temperature, for 10 sec.	300 (0.063 in. (1.6mm) from case)	
	Mounting torque, 6-32 or M3 screw.	10 lbf•in (1.1N•m)	

Thermal Resistance

	Parameter	Min.	Typ.	Max.	Units
$R_{\theta JC}$	Junction-to-Case	—	—	2.1	°C/W
$R_{\theta CS}$	Case-to-Sink, flat, greased surface	—	0.50	—	
$R_{\theta JA}$	Junction-to-Ambient, typical socket mount	—	—	80	
Wt	Weight	—	2.0 (0.07)	—	g (oz)

Electrical Characteristics @ $T_J = 25^\circ\text{C}$ (unless otherwise specified)

	Parameter	Min.	Typ.	Max.	Units	Conditions
$V_{(BR)CES}$	Collector-to-Emitter Breakdown Voltage	600	—	—	V	$V_{GE} = 0V, I_C = 250\mu A$
$V_{(BR)ECS}$	Emitter-to-Collector Breakdown Voltage ④	20	—	—	V	$V_{GE} = 0V, I_C = 1.0A$
$\Delta V_{(BR)CES}/\Delta T_J$	Temperature Coeff. of Breakdown Voltage	—	0.75	—	$V/^\circ\text{C}$	$V_{GE} = 0V, I_C = 1.0mA$
$V_{CE(on)}$	Collector-to-Emitter Saturation Voltage	—	1.8	2.4	V	$I_C = 10A$ $I_C = 19A$ $I_C = 10A, T_J = 150^\circ\text{C}$ $V_{GE} = 15V$ See Fig. 2, 5
		—	2.4	—		
		—	1.9	—		
$V_{GE(th)}$	Gate Threshold Voltage	3.0	—	5.5		$V_{CE} = V_{GE}, I_C = 250\mu A$
$\Delta V_{GE(th)}/\Delta T_J$	Temperature Coeff. of Threshold Voltage	—	-11	—	$\text{mV}/^\circ\text{C}$	$V_{CE} = V_{GE}, I_C = 250\mu A$
g_{fe}	Forward Transconductance ⑤	2.0	5.8	—	S	$V_{CE} = 100V, I_C = 10A$
I_{CES}	Zero Gate Voltage Collector Current	—	—	250	μA	$V_{GE} = 0V, V_{CE} = 600V$ $V_{GE} = 0V, V_{CE} = 600V, T_J = 150^\circ\text{C}$
		—	—	1000		
I_{GES}	Gate-to-Emitter Leakage Current	—	—	± 100	nA	$V_{GE} = \pm 20V$

Switching Characteristics @ $T_J = 25^\circ\text{C}$ (unless otherwise specified)

	Parameter	Min.	Typ.	Max.	Units	Conditions
Q_g	Total Gate Charge (turn-on)	—	16	26	nC	$I_C = 10A$ $V_{CC} = 400V$ $V_{GE} = 15V$ See Fig. 8
Q_{ge}	Gate - Emitter Charge (turn-on)	—	2.3	4.0		
Q_{gc}	Gate - Collector Charge (turn-on)	—	7.0	12		
$t_{d(on)}$	Turn-On Delay Time	—	24	—	ns	$T_J = 25^\circ\text{C}$ $I_C = 10A, V_{CC} = 480V$ $V_{GE} = 15V, R_G = 50\Omega$ Energy losses include "tail"
t_r	Rise Time	—	23	—		
$t_{d(off)}$	Turn-Off Delay Time	—	820	1200		
t_f	Fall Time	—	910	1600		
E_{on}	Turn-On Switching Loss	—	0.24	—	mJ	See Fig. 9, 10, 11, 14
E_{off}	Turn-Off Switching Loss	—	3.9	—		
E_{ts}	Total Switching Loss	—	4.1	6.0		
$t_{d(on)}$	Turn-On Delay Time	—	26	—	ns	$T_J = 150^\circ\text{C}$, $I_C = 10A, V_{CC} = 480V$ $V_{GE} = 15V, R_G = 50\Omega$ Energy losses include "tail"
t_r	Rise Time	—	30	—		
$t_{d(off)}$	Turn-Off Delay Time	—	1100	—		
t_f	Fall Time	—	1800	—		
E_{ts}	Total Switching Loss	—	7.0	—	mJ	See Fig. 10, 14
L_E	Internal Emitter Inductance	—	7.5	—	nH	Measured 5mm from package
C_{ies}	Input Capacitance	—	360	—	pF	$V_{GE} = 0V$ $V_{CC} = 30V$ $f = 1.0\text{MHz}$ See Fig. 7
C_{oes}	Output Capacitance	—	36	—		
C_{res}	Reverse Transfer Capacitance	—	5.2	—		

Notes:

- ① Repetitive rating; $V_{GE}=20V$, pulse width limited by max. junction temperature. (See fig. 13b)
- ② $V_{CC}=80\%(V_{CES}), V_{GE}=20V, L=10\mu H, R_G=50\Omega$, (See fig. 13a)
- ③ Repetitive rating; pulse width limited by maximum junction temperature.
- ④ Pulse width $\leq 80\mu s$; duty factor $\leq 0.1\%$.
- ⑤ Pulse width $5.0\mu s$, single shot.

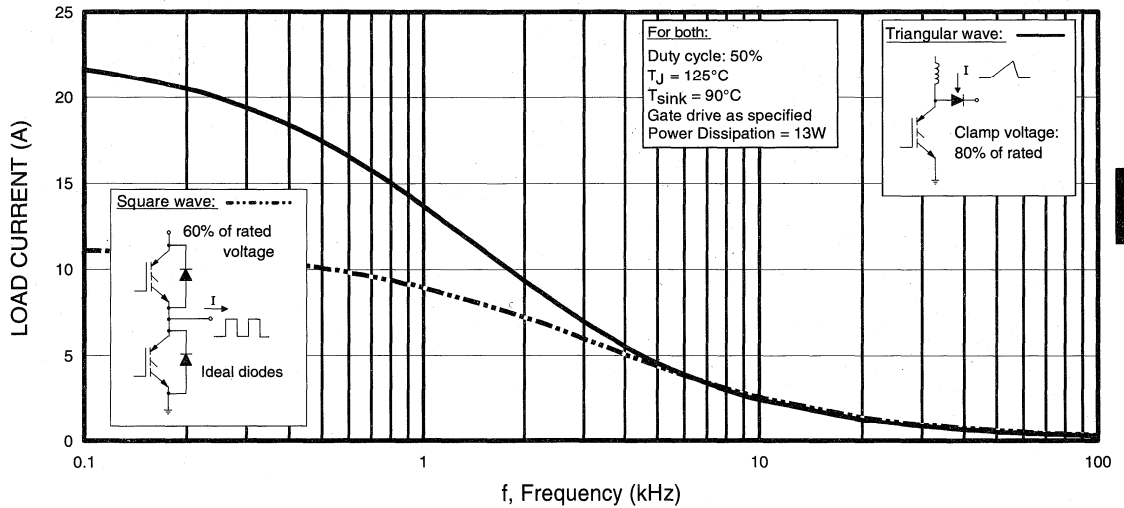


Fig. 1 - Typical Load Current vs. Frequency
 (For square wave, $I = I_{RMS}$ of fundamental; for triangular wave, $I = I_{PK}$)

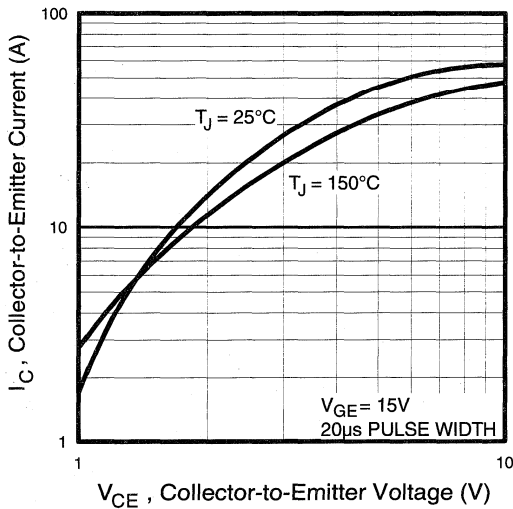


Fig. 2 - Typical Output Characteristics

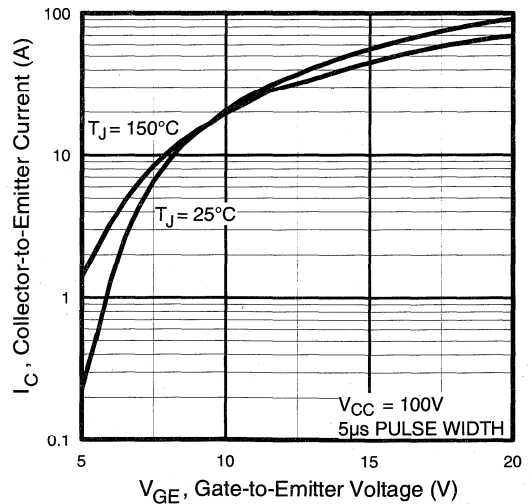


Fig. 3 - Typical Transfer Characteristics

Low
 Frequency
 Standard
 Discrete

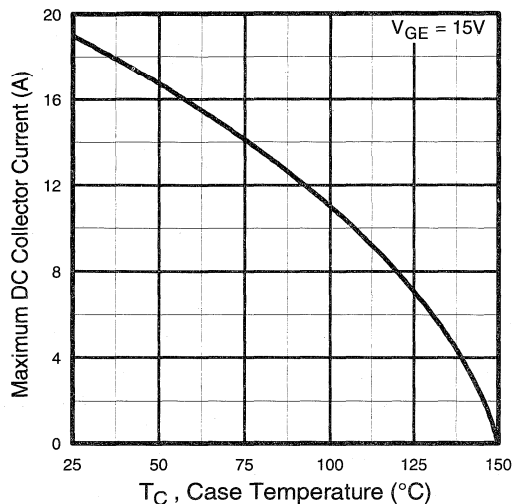


Fig. 4 - Maximum Collector Current vs. Case Temperature

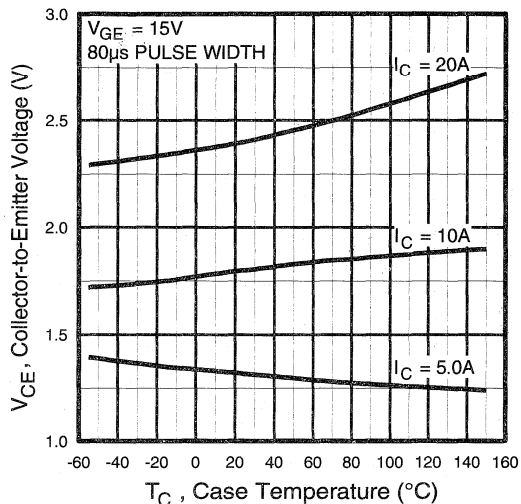


Fig. 5 - Collector-to-Emitter Voltage vs. Case Temperature

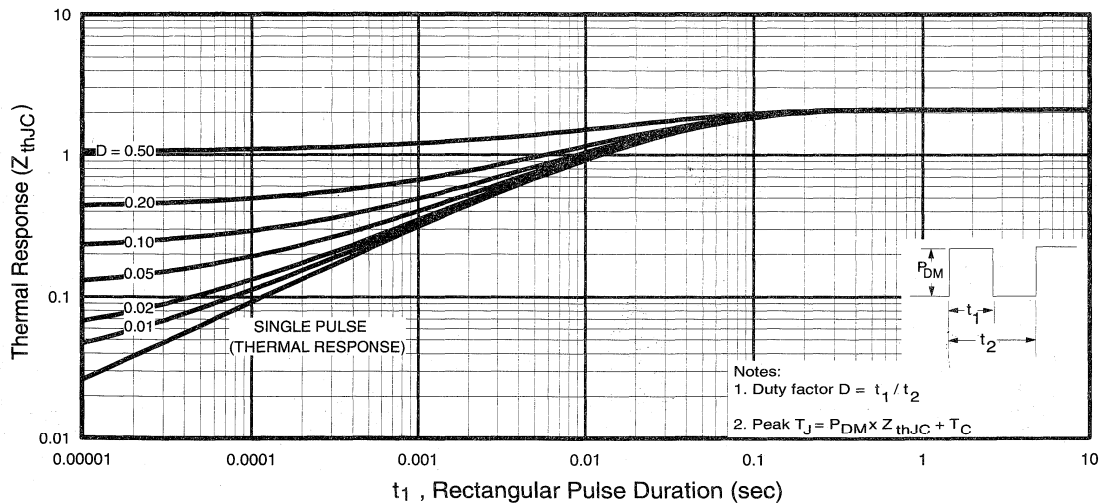


Fig. 6 - Maximum Effective Transient Thermal Impedance, Junction-to-Case

Low
Frequency
Standard
Device

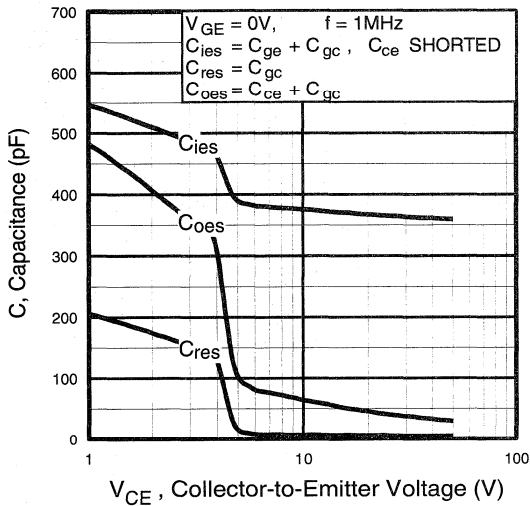


Fig. 7 - Typical Capacitance vs. Collector-to-Emitter Voltage

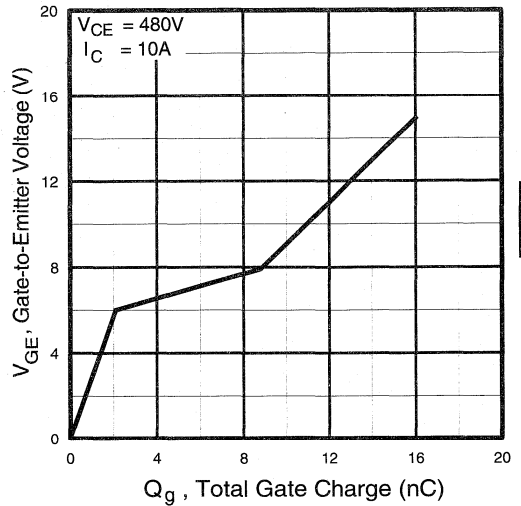


Fig. 8 - Typical Gate Charge vs. Gate-to-Emitter Voltage

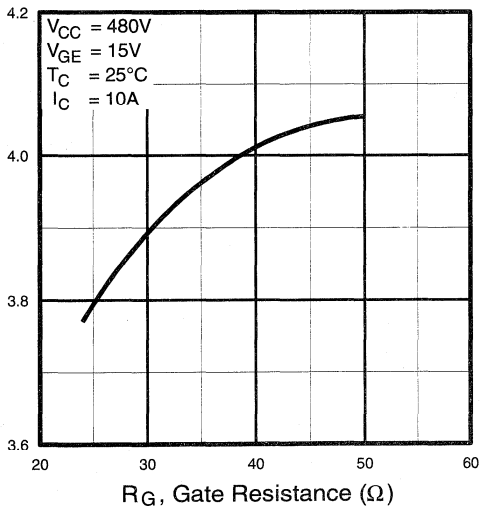


Fig. 9 - Typical Switching Losses vs. Gate Resistance

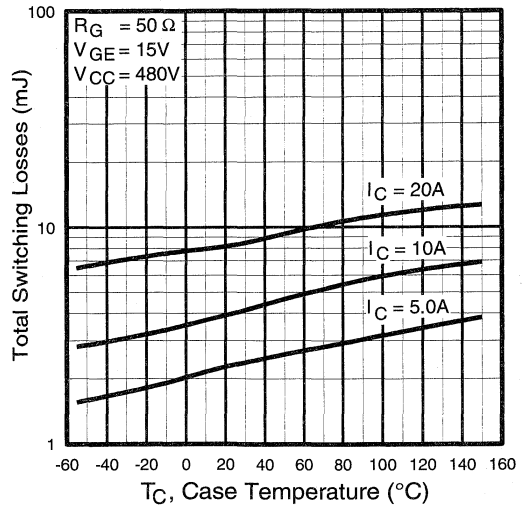


Fig. 10 - Typical Switching Losses vs. Case Temperature

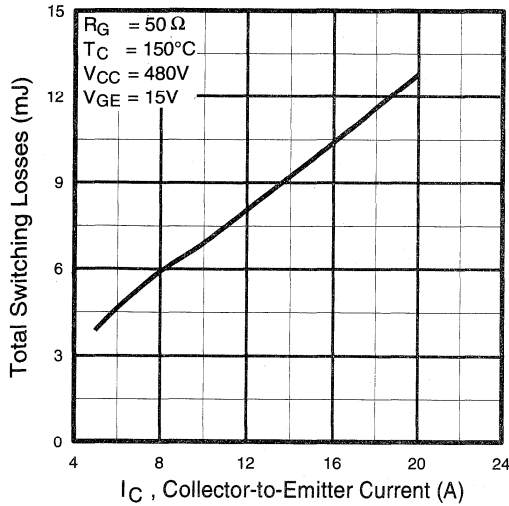


Fig. 11 - Typical Switching Losses vs. Collector-to-Emitter Current

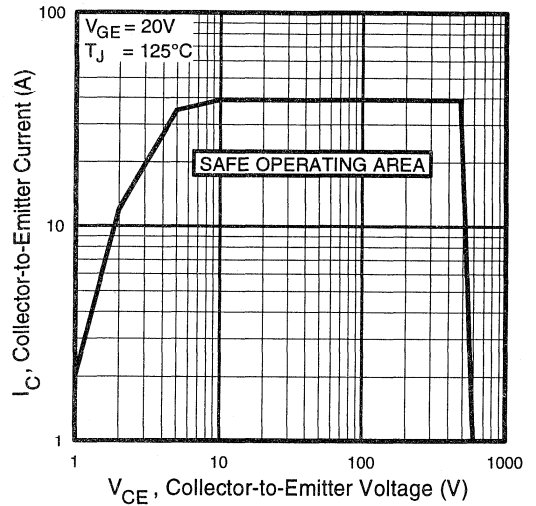


Fig. 12 - Turn-Off SOA

Refer to Section D for the following:

Appendix C: Section D - page D-5

Fig. 13a - Clamped Inductive Load Test Circuit

Fig. 13b - Pulsed Collector Current Test Circuit

Fig. 14a - Switching Loss Test Circuit

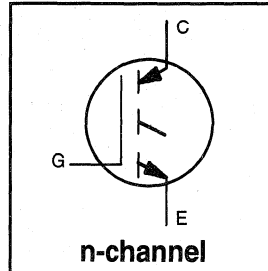
Fig. 14b - Switching Loss Waveform

Package Outline 1 - JEDEC Outline TO-220AB

Section D - page D-12

Features

- Switching-loss rating includes all "tail" losses
- Optimized for line frequency operation (to 400 Hz)
See Fig. 1 for Current vs. Frequency Curve



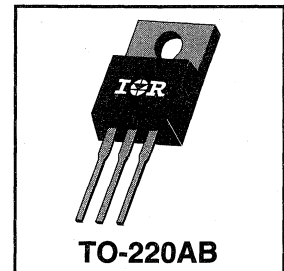
$$V_{CES} = 600V$$

$$V_{CE(sat)} \leq 2.2V$$

$$@ V_{GE} = 15V, I_C = 18A$$

Description

Insulated Gate Bipolar Transistors (IGBTs) from International Rectifier have higher usable current densities than comparable bipolar transistors, while at the same time having simpler gate-drive requirements of the familiar power MOSFET. They provide substantial benefits to a host of high-voltage, high-current applications.



Absolute Maximum Ratings

	Parameter	Max.	Units
V_{CES}	Collector-to-Emitter Voltage	600	V
$I_C @ T_C = 25^\circ C$	Continuous Collector Current	34	A
$I_C @ T_C = 100^\circ C$	Continuous Collector Current	18	
I_{CM}	Pulsed Collector Current ①	68	
I_{LM}	Clamped Inductive Load Current ②	68	
V_{GE}	Gate-to-Emitter Voltage	± 20	V
E_{ARV}	Reverse Voltage Avalanche Energy ③	10	mJ
$P_D @ T_C = 25^\circ C$	Maximum Power Dissipation	100	W
$P_D @ T_C = 100^\circ C$	Maximum Power Dissipation	42	
T_J	Operating Junction and	-55 to +150	°C
T_{STG}	Storage Temperature Range		
	Soldering Temperature, for 10 sec.		
	Mounting torque, 6-32 or M3 screw.	10 lbf•in (1.1N•m)	

Thermal Resistance

	Parameter	Min.	Typ.	Max.	Units
$R_{\theta JC}$	Junction-to-Case	—	—	1.2	°C/W
$R_{\theta CS}$	Case-to-Sink, flat, greased surface	—	0.50	—	
$R_{\theta JA}$	Junction-to-Ambient, typical socket mount	—	—	80	
Wt	Weight	—	2.0 (0.07)	—	g (oz)

Electrical Characteristics @ $T_J = 25^\circ\text{C}$ (unless otherwise specified)

	Parameter	Min.	Typ.	Max.	Units	Conditions
$V_{(BR)CES}$	Collector-to-Emitter Breakdown Voltage	600	—	—	V	$V_{GE} = 0V, I_C = 250\mu A$
$V_{(BR)ECS}$	Emitter-to-Collector Breakdown Voltage ④	20	—	—	V	$V_{GE} = 0V, I_C = 1.0A$
$\Delta V_{(BR)CES}/\Delta T_J$	Temperature Coeff. of Breakdown Voltage	—	0.75	—	V/ $^\circ\text{C}$	$V_{GE} = 0V, I_C = 1.0mA$
$V_{CE(on)}$	Collector-to-Emitter Saturation Voltage	—	1.7	2.2	V	$I_C = 18A$ $V_{GE} = 15V$ See Fig. 2, 5
		—	2.4	—		
		—	1.9	—		
$V_{GE(th)}$	Gate Threshold Voltage	3.0	—	5.5		$V_{CE} = V_{GE}, I_C = 250\mu A$
$\Delta V_{GE(th)}/\Delta T_J$	Temperature Coeff. of Threshold Voltage	—	-11	—	mV/ $^\circ\text{C}$	$V_{CE} = V_{GE}, I_C = 250\mu A$
g_{fe}	Forward Transconductance ⑤	6.0	11	—	S	$V_{CE} = 100V, I_C = 18A$
I_{CES}	Zero Gate Voltage Collector Current	—	—	250	μA	$V_{GE} = 0V, V_{CE} = 600V$
		—	—	1000		$V_{GE} = 0V, V_{CE} = 600V, T_J = 150^\circ\text{C}$
I_{GES}	Gate-to-Emitter Leakage Current	—	—	± 100	nA	$V_{GE} = \pm 20V$

Switching Characteristics @ $T_J = 25^\circ\text{C}$ (unless otherwise specified)

	Parameter	Min.	Typ.	Max.	Units	Conditions
Q_g	Total Gate Charge (turn-on)	—	28	40	nC	$I_C = 18A$ $V_{CC} = 400V$ See Fig. 8
Q_{ge}	Gate - Emitter Charge (turn-on)	—	5.0	8.0		
Q_{gc}	Gate - Collector Charge (turn-on)	—	12	20		
$t_{d(on)}$	Turn-On Delay Time	—	26	—	ns	$T_J = 25^\circ\text{C}$ $I_C = 18A, V_{CC} = 480V$ $V_{GE} = 15V, R_G = 23\Omega$ Energy losses include "tail"
t_r	Rise Time	—	32	—		
$t_{d(off)}$	Turn-Off Delay Time	—	820	1100		
t_f	Fall Time	—	720	1200		
E_{on}	Turn-On Switching Loss	—	0.51	—	mJ	See Fig. 9, 10, 11, 14
E_{off}	Turn-Off Switching Loss	—	6.6	—		
E_{ts}	Total Switching Loss	—	7.1	10		
$t_{d(on)}$	Turn-On Delay Time	—	26	—	ns	$T_J = 150^\circ\text{C}$, $I_C = 18A, V_{CC} = 480V$ $V_{GE} = 15V, R_G = 23\Omega$ Energy losses include "tail"
t_r	Rise Time	—	35	—		
$t_{d(off)}$	Turn-Off Delay Time	—	1200	—		
t_f	Fall Time	—	1500	—		
E_{ts}	Total Switching Loss	—	12	—	mJ	See Fig. 10, 14
L_E	Internal Emitter Inductance	—	7.5	—	nH	Measured 5mm from package
C_{ies}	Input Capacitance	—	700	—	pF	$V_{GE} = 0V$ $V_{CC} = 30V$ See Fig. 7
C_{oes}	Output Capacitance	—	70	—		
C_{res}	Reverse Transfer Capacitance	—	9.2	—		

Notes:

- ① Repetitive rating; $V_{GE}=20V$, pulse width limited by max. junction temperature. (See fig. 13b)
- ② $V_{CC}=80\%(V_{CES})$, $V_{GE}=20V$, $L=10\mu H$, $R_G=23\Omega$, (See fig. 13a)
- ③ Repetitive rating; pulse width limited by maximum junction temperature.
- ④ Pulse width $\leq 80\mu s$; duty factor $\leq 0.1\%$.
- ⑤ Pulse width $5.0\mu s$, single shot.

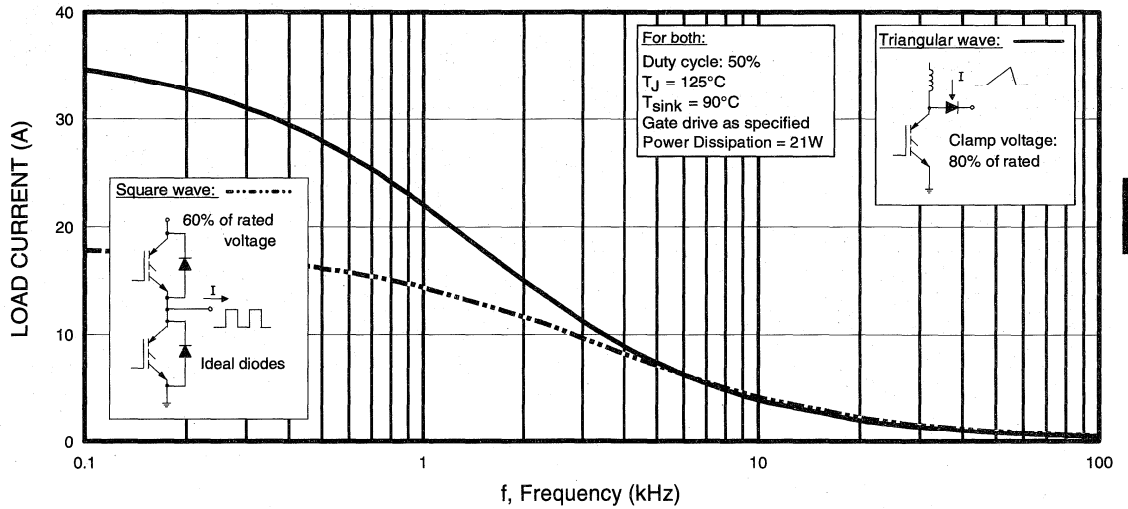


Fig. 1 - Typical Load Current vs. Frequency
 (For square wave, $I = I_{\text{RMS}}$ of fundamental; for triangular wave, $I = I_{\text{PK}}$)

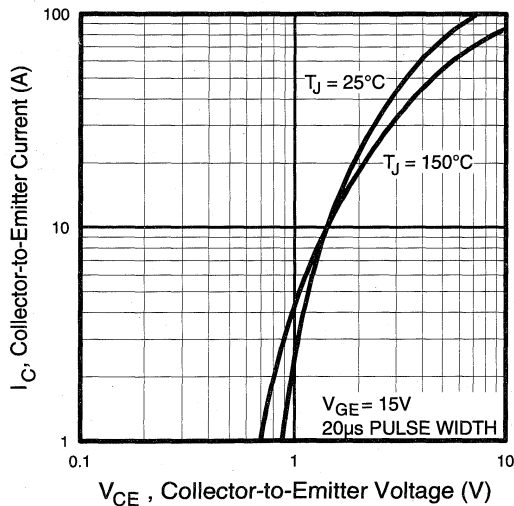


Fig. 2 - Typical Output Characteristics

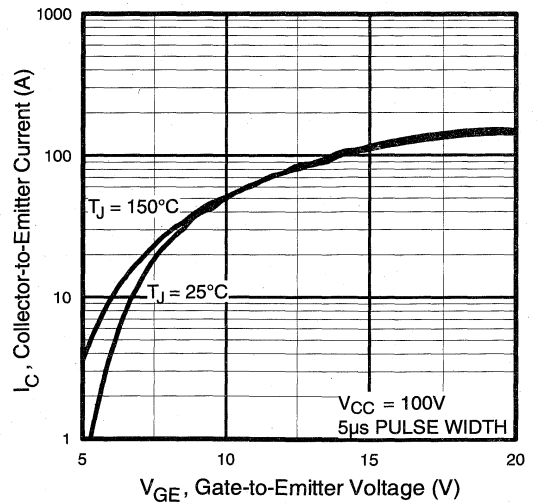


Fig. 3 - Typical Transfer Characteristics

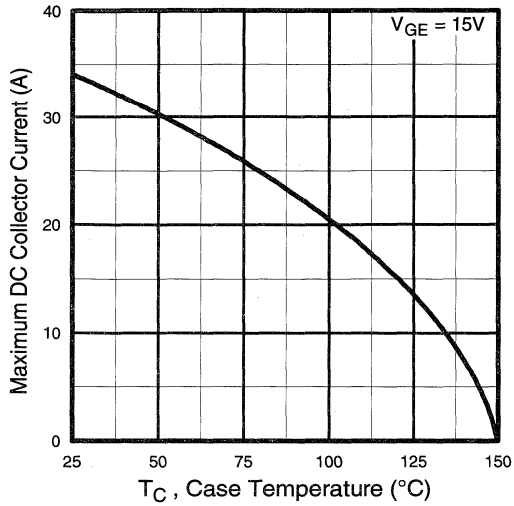


Fig. 4 - Maximum Collector Current vs. Case Temperature

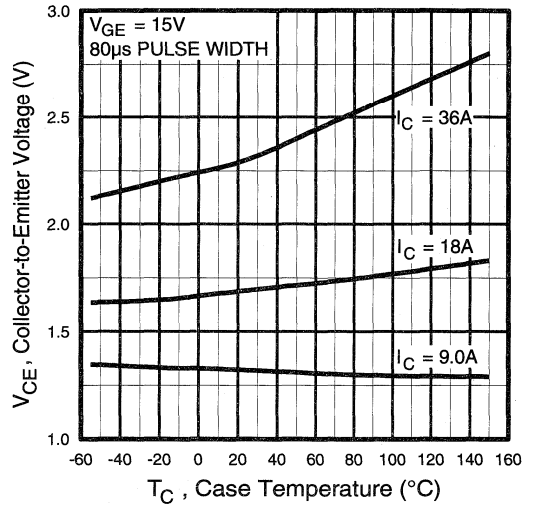


Fig. 5 - Collector-to-Emitter Voltage vs. Case Temperature

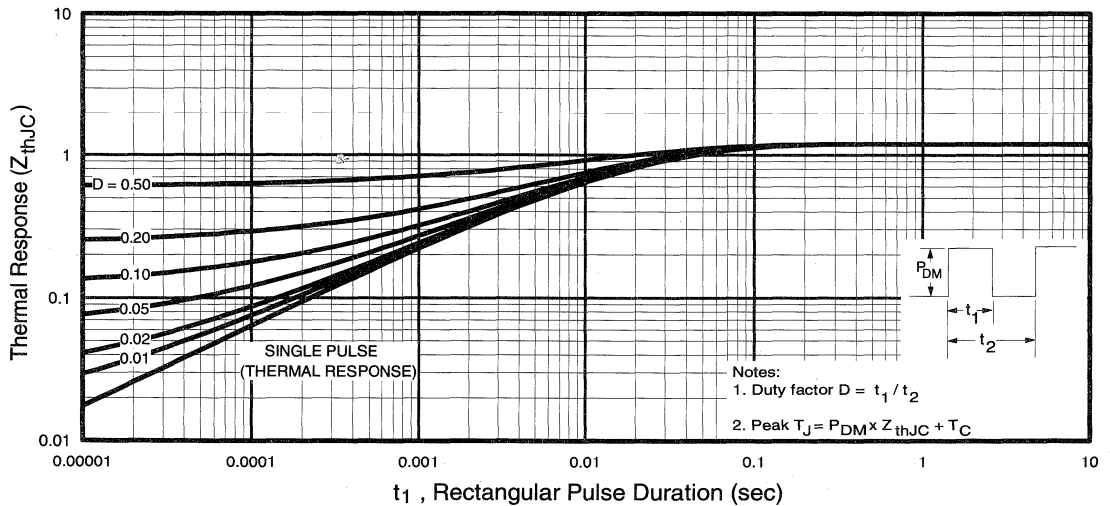


Fig. 6 - Maximum Effective Transient Thermal Impedance, Junction-to-Case

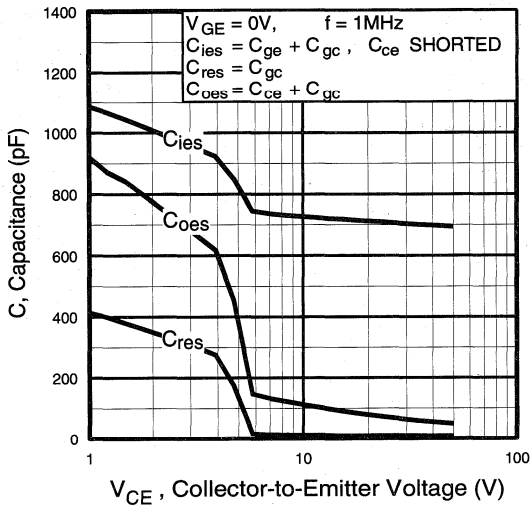


Fig. 7 - Typical Capacitance vs. Collector-to-Emitter Voltage

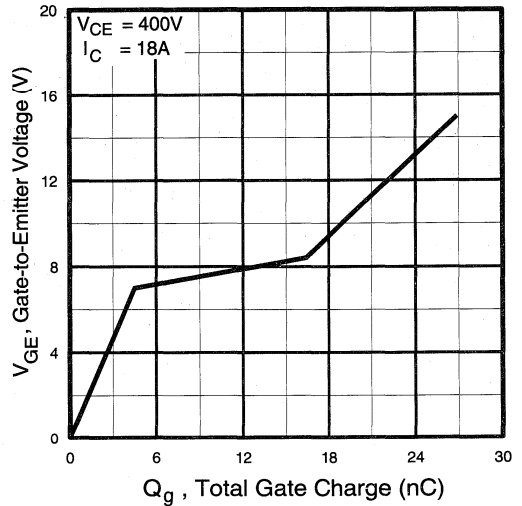


Fig. 8 - Typical Gate Charge vs. Gate-to-Emitter Voltage

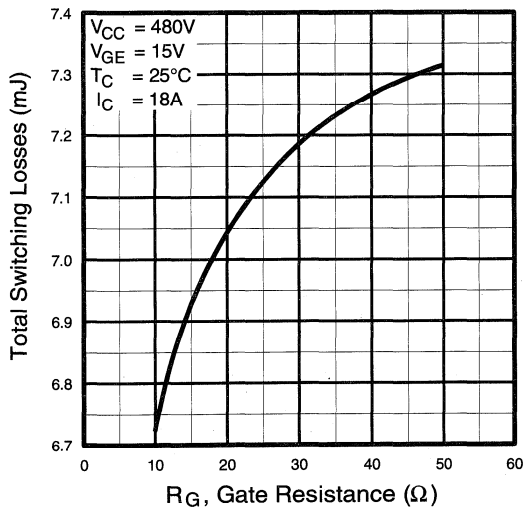


Fig. 9 - Typical Switching Losses vs. Gate Resistance

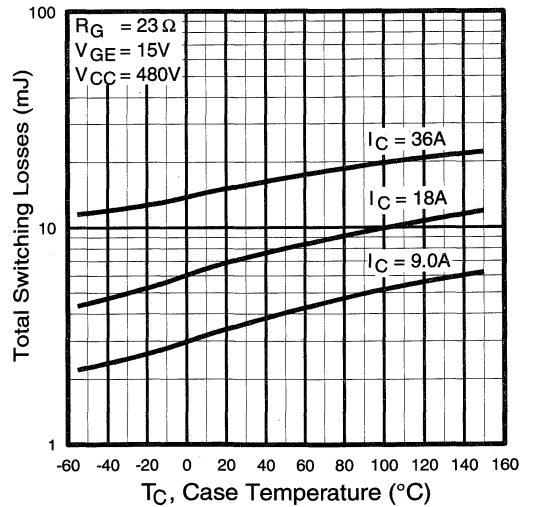


Fig. 10 - Typical Switching Losses vs. Case Temperature

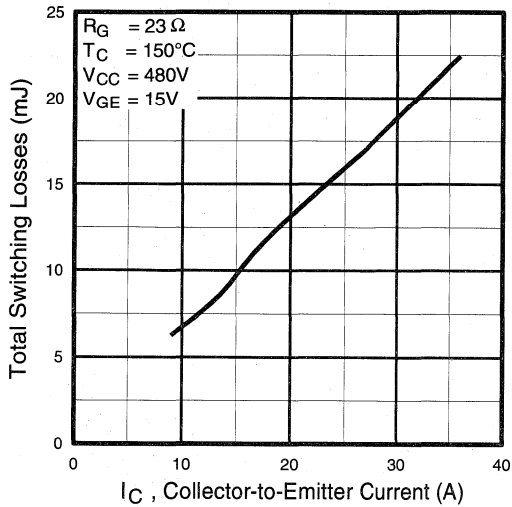


Fig. 11 - Typical Switching Losses vs. Collector-to-Emitter Current

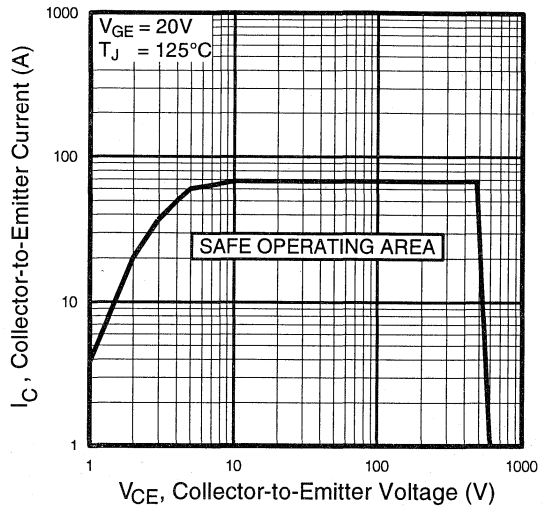


Fig. 12 - Turn-Off SOA

Refer to Section D for the following:

Appendix C: Section D - page D-5

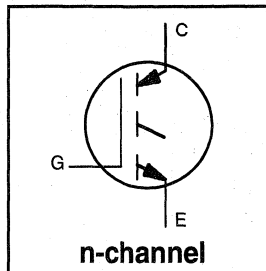
- Fig. 13a - Clamped Inductive Load Test Circuit
- Fig. 13b - Pulsed Collector Current Test Circuit
- Fig. 14a - Switching Loss Test Circuit
- Fig. 14b - Switching Loss Waveform

Package Outline 1 - JEDEC Outline TO-220AB

Section D - page D-12

Features

- Switching-loss rating includes all "tail" losses
- Optimized for line frequency operation (to 400 Hz)
See Fig. 1 for Current vs. Frequency curve



$$V_{CES} = 600V$$

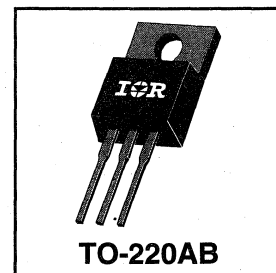
$$V_{CE(sat)} \leq 1.8V$$

$$@V_{GE} = 15V, I_C = 31A$$

 Low
Frequency
Standard
Discrete

Description

Insulated Gate Bipolar Transistors (IGBTs) from International Rectifier have higher usable current densities than comparable bipolar transistors, while at the same time having simpler gate-drive requirements of the familiar power MOSFET. They provide substantial benefits to a host of high-voltage, high-current applications.


TO-220AB

Absolute Maximum Ratings

	Parameter	Max.	Units
V_{CES}	Collector-to-Emitter Voltage	600	V
$I_C @ T_C = 25^\circ C$	Continuous Collector Current	50	A
$I_C @ T_C = 100^\circ C$	Continuous Collector Current	31	
I_{CM}	Pulsed Collector Current ①	240	
I_{LM}	Clamped Inductive Load Current ②	100	
V_{GE}	Gate-to-Emitter Voltage	± 20	V
E_{ARV}	Reverse Voltage Avalanche Energy ③	15	mJ
$P_D @ T_C = 25^\circ C$	Maximum Power Dissipation	160	W
$P_D @ T_C = 100^\circ C$	Maximum Power Dissipation	65	
T_J	Operating Junction and	-55 to +150	°C
T_{STG}	Storage Temperature Range		
	Soldering Temperature, for 10 sec.	300 (0.063 in. (1.6mm) from case)	
	Mounting torque, 6-32 or M3 screw.	10 lbf•in (1.1N•m)	

Thermal Resistance

	Parameter	Min.	Typ.	Max.	Units
$R_{\theta JC}$	Junction-to-Case	—	—	0.77	°C/W
$R_{\theta CS}$	Case-to-Sink, flat, greased surface	—	0.50	—	
$R_{\theta JA}$	Junction-to-Ambient, typical socket mount	—	—	80	
Wt	Weight	—	2.0 (0.07)	—	g (oz)

Electrical Characteristics @ $T_J = 25^\circ\text{C}$ (unless otherwise specified)

	Parameter	Min.	Typ.	Max.	Units	Conditions
$V_{(BR)CES}$	Collector-to-Emitter Breakdown Voltage	600	—	—	V	$V_{GE} = 0V, I_C = 250\mu A$
$V_{(BR)ECS}$	Emitter-to-Collector Breakdown Voltage ④	20	—	—	V	$V_{GE} = 0V, I_C = 1.0A$
$\Delta V_{(BR)CES}/\Delta T_J$	Temp. Coeff. of Breakdown Voltage	—	0.75	—	$V/^\circ\text{C}$	$V_{GE} = 0V, I_C = 1.0mA$
$V_{CE(on)}$	Collector-to-Emitter Saturation Voltage	—	1.6	1.8	V	$I_C = 31A$ $I_C = 60A$ $I_C = 31A, T_J = 150^\circ\text{C}$ $V_{GE} = 15V$ See Fig. 2, 5
		—	2.2	—		
		—	1.7	—		
$V_{GE(th)}$	Gate Threshold Voltage	3.0	—	5.5		$V_{CE} = V_{GE}, I_C = 250\mu A$
$\Delta V_{GE(th)}/\Delta T_J$	Temp. Coeff. of Threshold Voltage	—	-9.3	—	$mV/^\circ\text{C}$	$V_{CE} = V_{GE}, I_C = 250\mu A$
g_{fe}	Forward Transconductance ⑤	12	21	—	S	$V_{CE} = 100V, I_C = 31A$
I_{CES}	Zero Gate Voltage Collector Current	—	—	250	μA	$V_{GE} = 0V, V_{CE} = 600V$ $V_{GE} = 0V, V_{CE} = 600V, T_J = 150^\circ\text{C}$
		—	—	1000		
I_{GES}	Gate-to-Emitter Leakage Current	—	—	± 100	nA	$V_{GE} = \pm 20V$

Switching Characteristics @ $T_J = 25^\circ\text{C}$ (unless otherwise specified)

	Parameter	Min.	Typ.	Max.	Units	Conditions
Q_g	Total Gate Charge (turn-on)	—	62	90	nC	$I_C = 31A$ $V_{CC} = 400V$ $V_{GE} = 15V$ See Fig. 8
Q_{ge}	Gate - Emitter Charge (turn-on)	—	10	15		
Q_{gc}	Gate - Collector Charge (turn-on)	—	27	40		
$t_{d(on)}$	Turn-On Delay Time	—	28	—	ns	$T_J = 25^\circ\text{C}$ $I_C = 31A, V_{CC} = 480V$ $V_{GE} = 15V, R_G = 10\Omega$ Energy losses include "tail"
t_r	Rise Time	—	50	—		
$t_{d(off)}$	Turn-Off Delay Time	—	1100	1500		
t_f	Fall Time	—	620	1100		
E_{on}	Turn-On Switching Loss	—	1.0	—	mJ	See Fig. 9, 10, 11, 14
E_{off}	Turn-Off Switching Loss	—	12	—		
E_{ts}	Total Switching Loss	—	13	20		
$t_{d(on)}$	Turn-On Delay Time	—	29	—	ns	$T_J = 150^\circ\text{C}$, $I_C = 31A, V_{CC} = 480V$ $V_{GE} = 15V, R_G = 10\Omega$ Energy losses include "tail"
t_r	Rise Time	—	53	—		
$t_{d(off)}$	Turn-Off Delay Time	—	1600	—		
t_f	Fall Time	—	1200	—		
E_{ts}	Total Switching Loss	—	22	—	mJ	See Fig. 10, 14
L_E	Internal Emitter Inductance	—	7.5	—	nH	Measured 5mm from package
C_{ies}	Input Capacitance	—	1600	—	pF	$V_{GE} = 0V$ $V_{CC} = 30V$ $f = 1.0MHz$ See Fig. 7
C_{oes}	Output Capacitance	—	140	—		
C_{res}	Reverse Transfer Capacitance	—	20	—		

Notes:

- ① Repetitive rating; $V_{GE}=20V$, pulse width limited by max. junction temperature. (See fig. 13b)
- ② $V_{CC}=80\%(V_{CES}), V_{GE}=20V, L=10\mu H, R_G=10\Omega$, (See fig. 13a)
- ③ Repetitive rating; pulse width limited by maximum junction temperature.
- ④ Pulse width $\leq 80\mu s$; duty factor $\leq 0.1\%$.
- ⑤ Pulse width 5.0 μs , single shot.

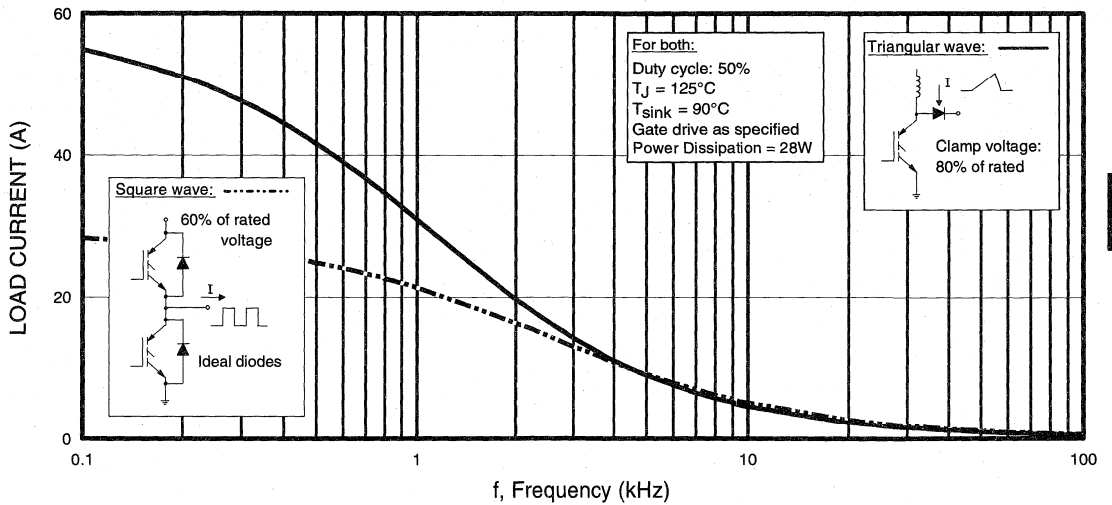


Fig. 1 - Typical Load Current vs. Frequency
 (For square wave, $I = I_{RMS}$ of fundamental; for triangular wave, $I = I_{PK}$)

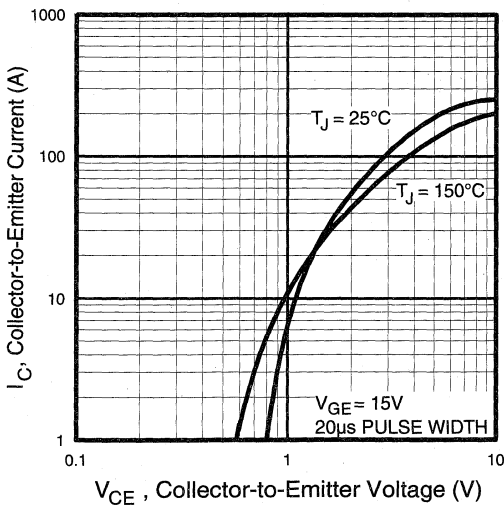


Fig. 2 - Typical Output Characteristics

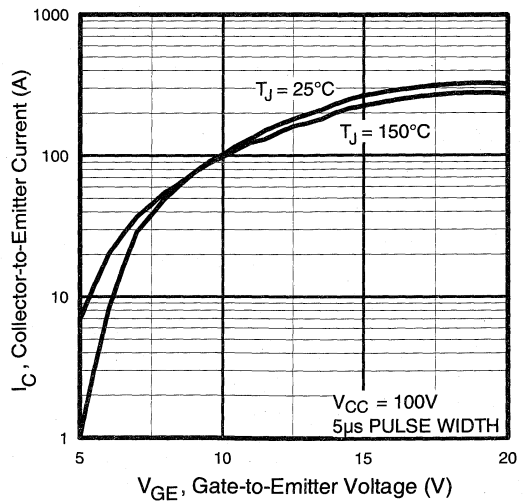


Fig. 3 - Typical Transfer Characteristics

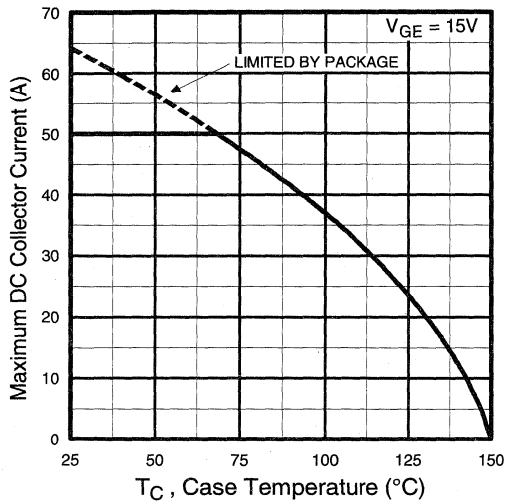


Fig. 4 - Maximum Collector Current vs. Case Temperature

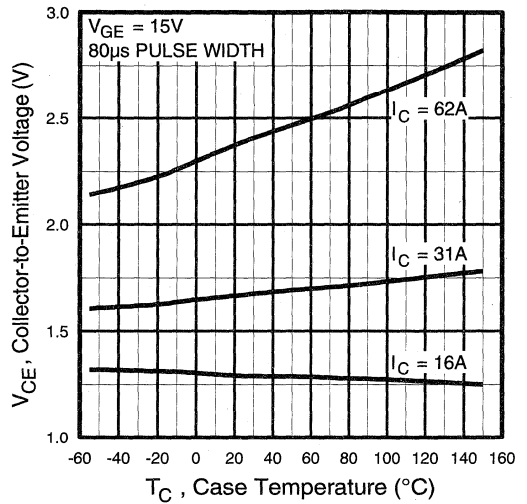


Fig. 5 - Collector-to-Emitter Voltage vs. Case Temperature

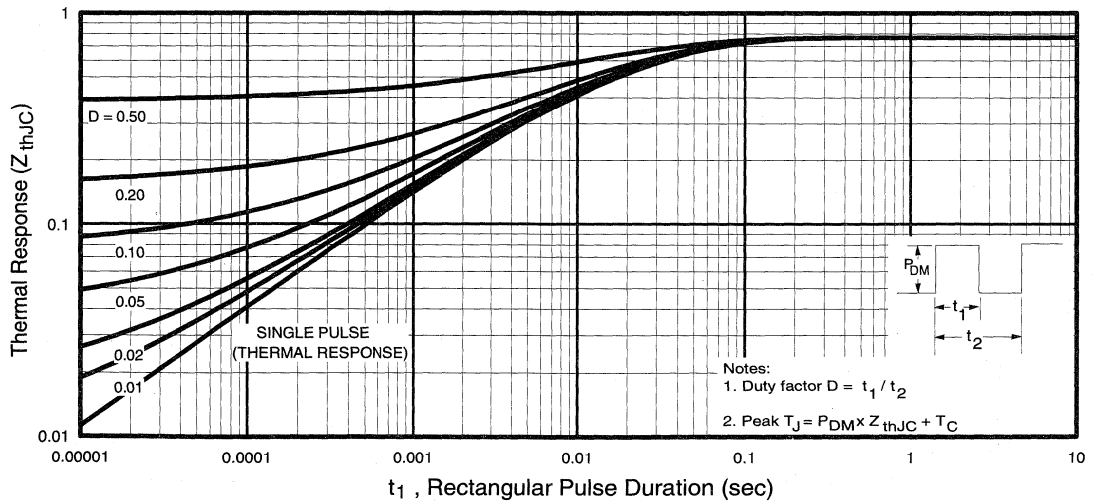


Fig. 6 - Maximum Effective Transient Thermal Impedance, Junction-to-Case

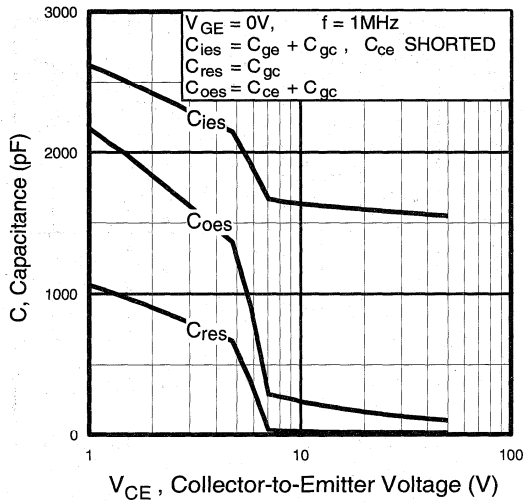


Fig. 7 - Typical Capacitance vs. Collector-to-Emitter Voltage

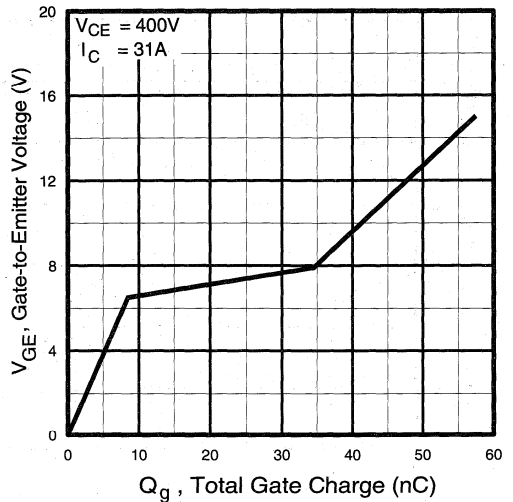


Fig. 8 - Typical Gate Charge vs. Gate-to-Emitter Voltage

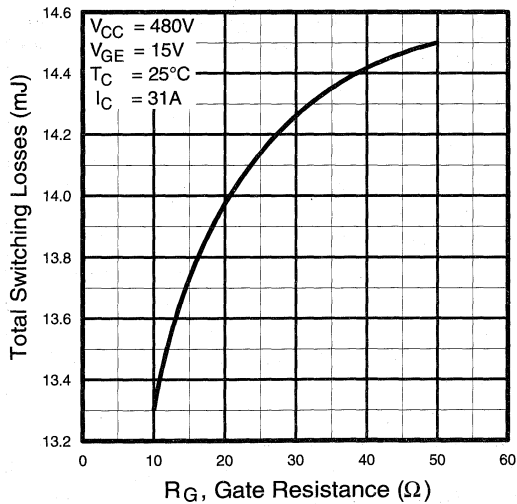


Fig. 9 - Typical Switching Losses vs. Gate Resistance

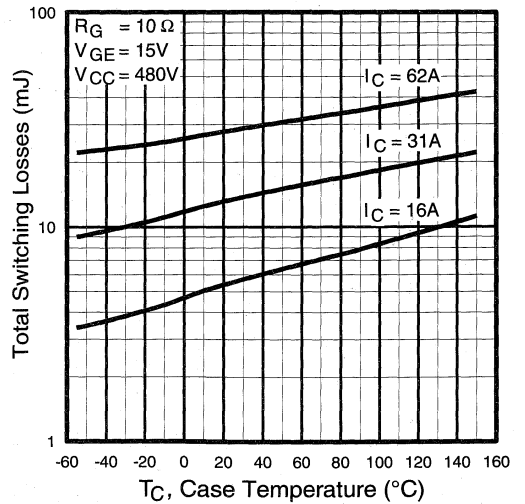


Fig. 10 - Typical Switching Losses vs. Case Temperature

IOR
 Frequency
 Standard
 Discrete

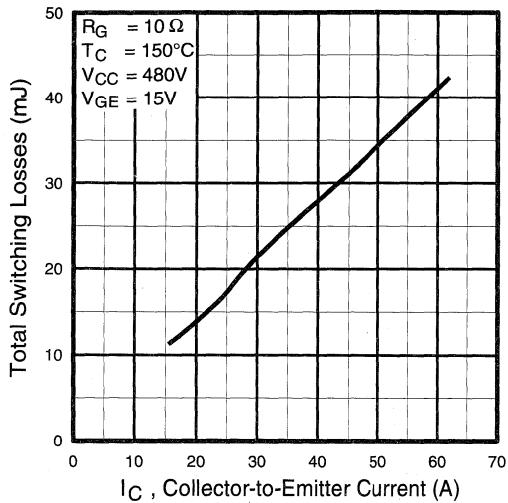


Fig. 11 - Typical Switching Losses vs. Collector-to-Emitter Current

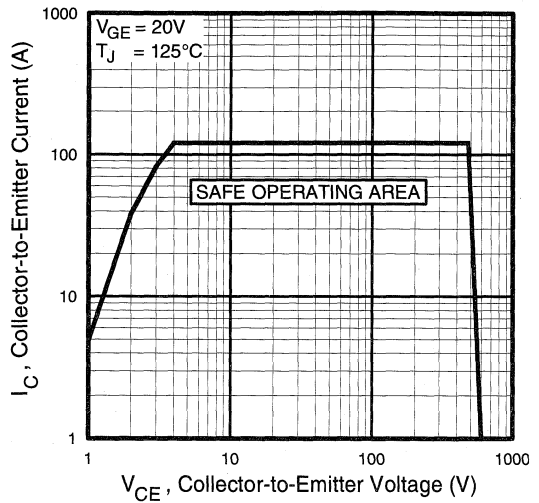


Fig. 12 - Turn-Off SOA

Refer to Section D for the following:

Appendix C: Section D - page D-5

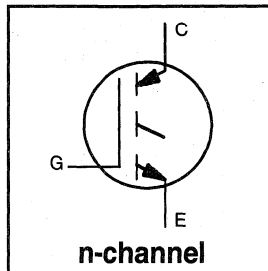
- Fig. 13a - Clamped Inductive Load Test Circuit
- Fig. 13b - Pulsed Collector Current Test Circuit
- Fig. 14a - Switching Loss Test Circuit
- Fig. 14b - Switching Loss Waveform

Package Outline 1 - JEDEC Outline TO-220AB

Section D - page D-12

Features

- Switching-loss rating includes all "tail" losses
- Optimized for line frequency operation (to 400Hz)
See Fig. 1 for Current vs. Frequency curve



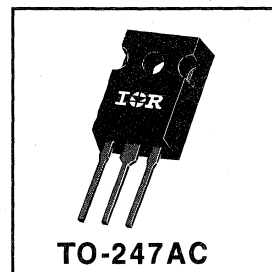
$$V_{CES} = 600V$$

$$V_{CE(sat)} \leq 2.2V$$

$$@V_{GE} = 15V, I_C = 18A$$

Description

Insulated Gate Bipolar Transistors (IGBTs) from International Rectifier have higher usable current densities than comparable bipolar transistors, while at the same time having simpler gate-drive requirements of the familiar power MOSFET. They provide substantial benefits to a host of high-voltage, high-current applications.



Absolute Maximum Ratings

	Parameter	Max.	Units
V_{CES}	Collector-to-Emitter Voltage	600	V
$I_C @ T_C = 25^\circ C$	Continuous Collector Current	34	A
$I_C @ T_C = 100^\circ C$	Continuous Collector Current	18	
I_{CM}	Pulsed Collector Current ①	68	
I_{LM}	Clamped Inductive Load Current ②	68	
V_{GE}	Gate-to-Emitter Voltage	± 20	V
E_{ARV}	Reverse Voltage Avalanche Energy ③	10	mJ
$P_D @ T_C = 25^\circ C$	Maximum Power Dissipation	100	W
$P_D @ T_C = 100^\circ C$	Maximum Power Dissipation	42	
T_J	Operating Junction and Storage Temperature Range	-55 to +150	°C
T_{STG}	Soldering Temperature, for 10 sec.	300 (0.063 in. (1.6mm) from case)	
	Mounting torque, 6-32 or M3 screw.	10 lbf•in (1.1N•m)	

Thermal Resistance

	Parameter	Min.	Typ.	Max.	Units
$R_{\theta JC}$	Junction-to-Case	—	—	1.2	°C/W
$R_{\theta CS}$	Case-to-Sink, flat, greased surface	—	0.24	—	
$R_{\theta JA}$	Junction-to-Ambient, typical socket mount	—	—	40	
Wt	Weight	—	6 (0.21)	—	g (oz)

Electrical Characteristics @ $T_J = 25^\circ\text{C}$ (unless otherwise specified)

	Parameter	Min.	Typ.	Max.	Units	Conditions
$V_{(BR)CES}$	Collector-to-Emitter Breakdown Voltage	600	—	—	V	$V_{GE} = 0V, I_C = 250\mu A$
$V_{(BR)ECS}$	Emitter-to-Collector Breakdown Voltage ④	20	—	—	V	$V_{GE} = 0V, I_C = 1.0A$
$\Delta V_{(BR)CES}/\Delta T_J$	Temperature Coeff. of Breakdown Voltage	—	0.75	—	V/ $^\circ\text{C}$	$V_{GE} = 0V, I_C = 1.0mA$
$V_{CE(on)}$	Collector-to-Emitter Saturation Voltage	—	1.7	2.2	V	$I_C = 18A, V_{GE} = 15V$ See Fig. 2, 5
		—	2.4	—		
		—	1.9	—		
$V_{GE(th)}$	Gate Threshold Voltage	3.0	—	5.5		$I_C = 18A, T_J = 150^\circ\text{C}$ $V_{CE} = V_{GE}, I_C = 250\mu A$
$\Delta V_{GE(th)}/\Delta T_J$	Temperature Coeff. of Threshold Voltage	—	-11	—	mV/ $^\circ\text{C}$	$V_{CE} = V_{GE}, I_C = 250\mu A$
g_{fe}	Forward Transconductance ⑤	6.0	11	—	S	$V_{CE} = 100V, I_C = 18A$
I_{CES}	Zero Gate Voltage Collector Current	—	—	250	μA	$V_{GE} = 0V, V_{CE} = 600V$ $V_{GE} = 0V, V_{CE} = 600V, T_J = 150^\circ\text{C}$
		—	—	1000		
I_{GES}	Gate-to-Emitter Leakage Current	—	—	± 100	nA	$V_{GE} = \pm 20V$

Switching Characteristics @ $T_J = 25^\circ\text{C}$ (unless otherwise specified)

	Parameter	Min.	Typ.	Max.	Units	Conditions
Q_g	Total Gate Charge (turn-on)	—	28	40	nC	$I_C = 18A, V_{CC} = 400V$ See Fig. 8
Q_{ge}	Gate - Emitter Charge (turn-on)	—	5.0	8.0		
Q_{gc}	Gate - Collector Charge (turn-on)	—	12	20		
$t_{d(on)}$	Turn-On Delay Time	—	26	—	ns	$T_J = 25^\circ\text{C}$ $I_C = 18A, V_{CC} = 480V$ $V_{GE} = 15V, R_G = 23\Omega$ Energy losses include "tail"
t_r	Rise Time	—	32	—		
$t_{d(off)}$	Turn-Off Delay Time	—	820	1100		
t_f	Fall Time	—	720	1200		
E_{on}	Turn-On Switching Loss	—	0.51	—	mJ	See Fig. 9, 10, 11, 14
E_{off}	Turn-Off Switching Loss	—	6.6	—		
E_{ts}	Total Switching Loss	—	7.1	10		
$t_{d(on)}$	Turn-On Delay Time	—	26	—	ns	$T_J = 150^\circ\text{C}$, $I_C = 18A, V_{CC} = 480V$ $V_{GE} = 15V, R_G = 23\Omega$ Energy losses include "tail"
t_r	Rise Time	—	35	—		
$t_{d(off)}$	Turn-Off Delay Time	—	1200	—		
t_f	Fall Time	—	1500	—		
E_{ts}	Total Switching Loss	—	12	—	mJ	See Fig. 10, 14
L_E	Internal Emitter Inductance	—	13	—	nH	Measured 5mm from package
C_{ies}	Input Capacitance	—	700	—	pF	$V_{GE} = 0V, V_{CC} = 30V$ See Fig. 7 $f = 1.0MHz$
C_{oes}	Output Capacitance	—	70	—		
C_{res}	Reverse Transfer Capacitance	—	9.2	—		

Notes:

- ① Repetitive rating; $V_{GE}=20V$, pulse width limited by max. junction temperature. (See fig. 13b)
- ② $V_{CC}=80\%(V_{CES}), V_{GE}=20V, L=10\mu H, R_G=23\Omega$, (See fig. 13a)
- ③ Repetitive rating; pulse width limited by maximum junction temperature.
- ④ Pulse width $\leq 80\mu s$; duty factor $\leq 0.1\%$.
- ⑤ Pulse width 5.0 μs , single shot.

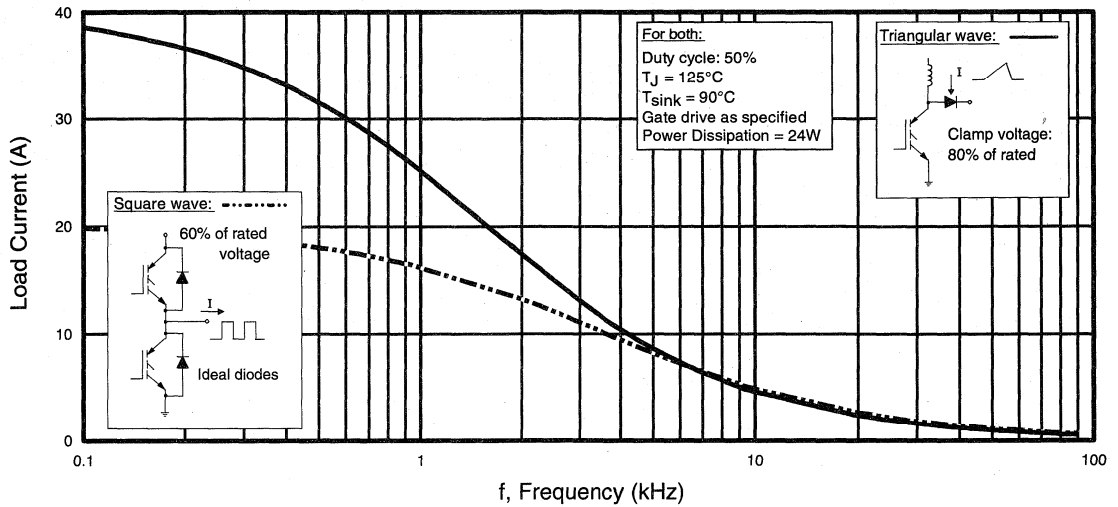


Fig. 1 - Typical Load Current vs. Frequency
 (For square wave, $I = I_{RMS}$ of fundamental; for triangular wave, $I = I_{PK}$)

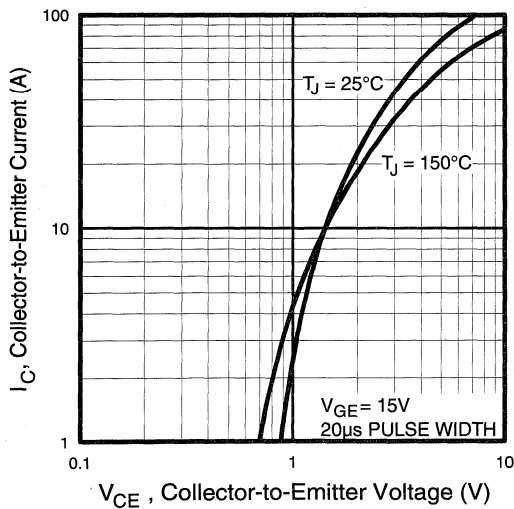


Fig. 2 - Typical Output Characteristics

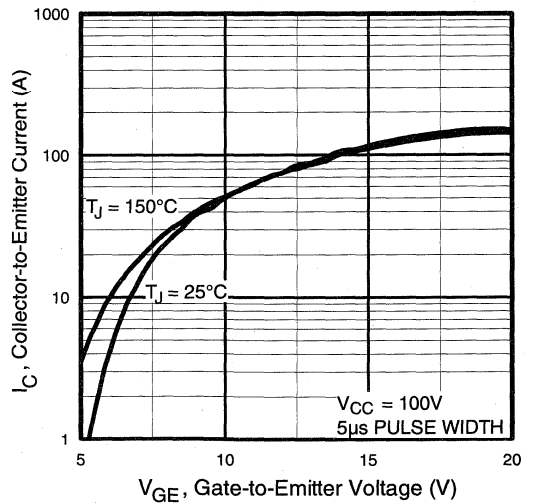


Fig. 3 - Typical Transfer Characteristics

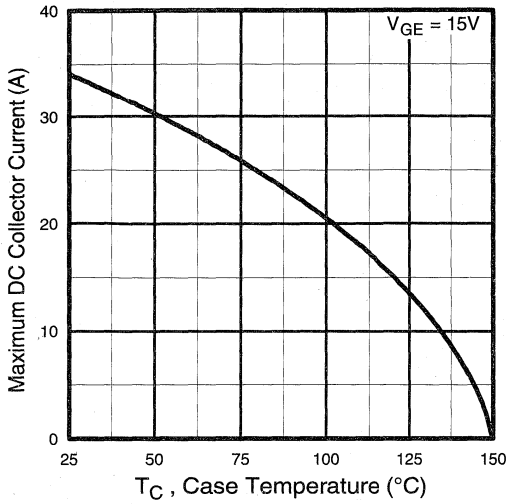


Fig. 4 - Maximum Collector Current vs. Case Temperature

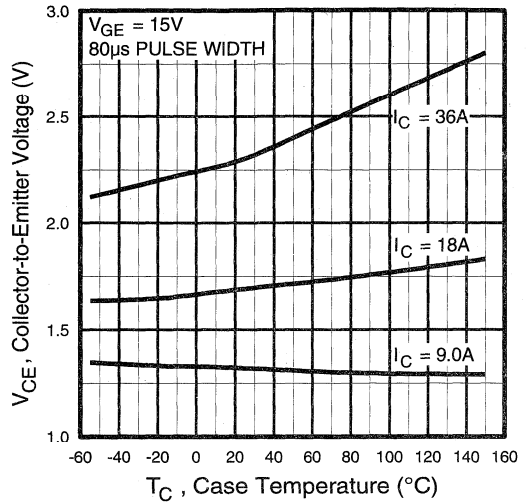


Fig. 5 - Collector-to-Emitter Voltage vs. Case Temperature

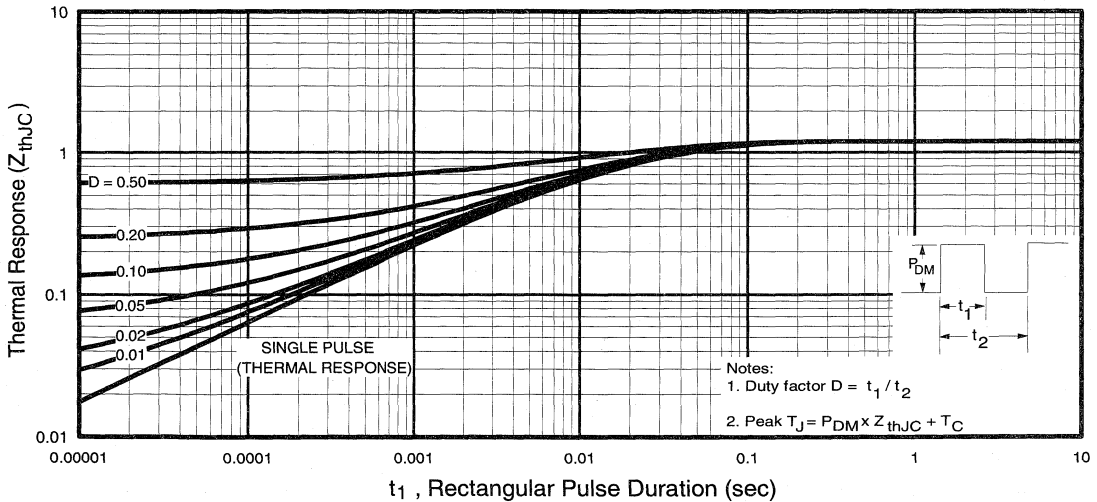


Fig. 6 - Maximum Effective Transient Thermal Impedance, Junction-to-Case

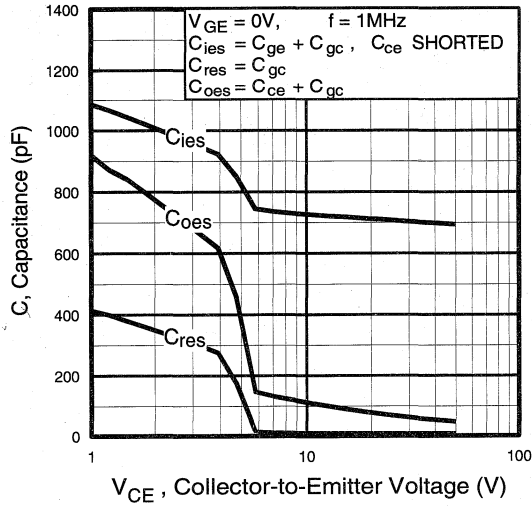


Fig. 7 - Typical Capacitance vs. Collector-to-Emitter Voltage

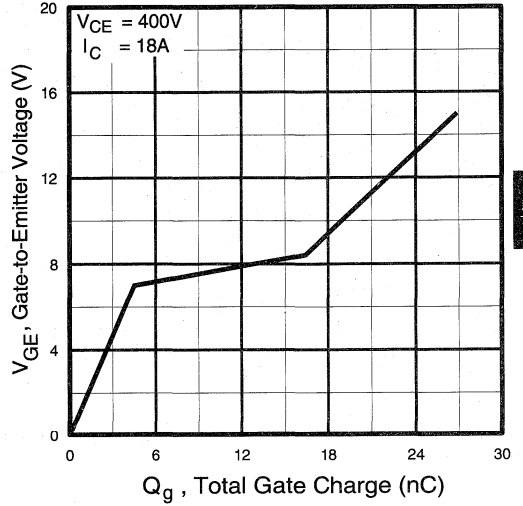


Fig. 8 - Typical Gate Charge vs. Gate-to-Emitter Voltage

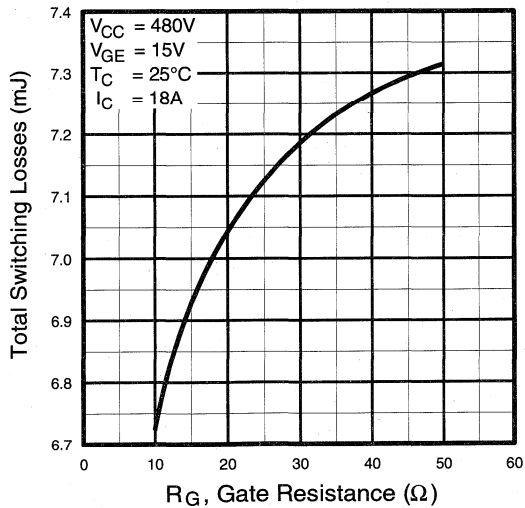


Fig. 9 - Typical Switching Losses vs. Gate Resistance

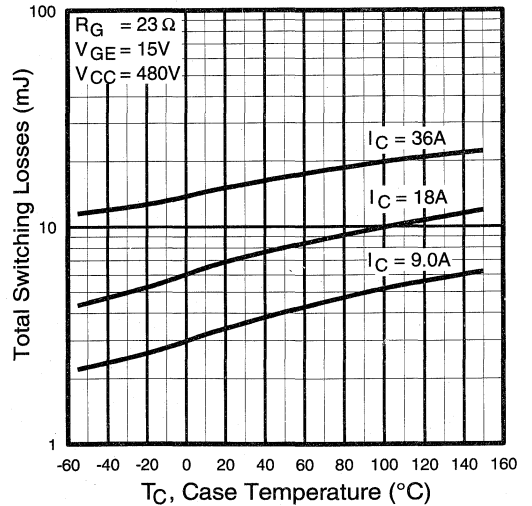


Fig. 10 - Typical Switching Losses vs. Case Temperature

Low
Frequency
Standard
Discrete

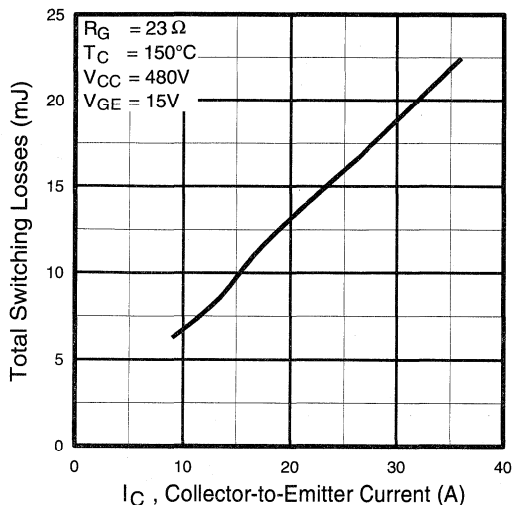


Fig. 11 - Typical Switching Losses vs. Collector-to-Emitter Current

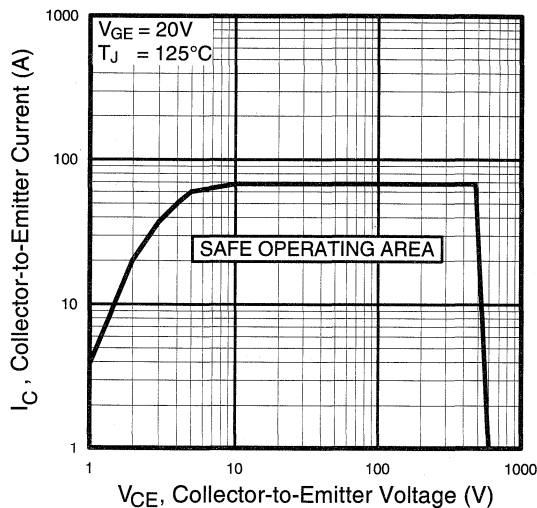


Fig. 12 - Turn-Off SOA

Refer to Section D for the following:

Appendix C: Section D - page D-5

Fig. 13a - Clamped Inductive Load Test Circuit

Fig. 13b - Pulsed Collector Current Test Circuit

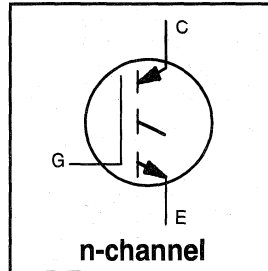
Fig. 14a - Switching Loss Test Circuit

Fig. 14b - Switching Loss Waveform

Package Outline 3 - JEDEC Outline TO-247AC (TO-3P) Section D - page D-13

Features

- Switching-loss rating includes all "tail" losses
- Optimized for line frequency operation (to 400Hz)
See Fig. 1 for Current vs. Frequency curve



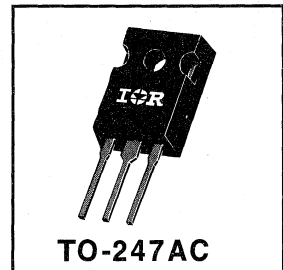
$$V_{CES} = 600V$$

$$V_{CE(sat)} \leq 1.8V$$

$$@V_{GE} = 15V, I_C = 31A$$

Description

Insulated Gate Bipolar Transistors (IGBTs) from International Rectifier have higher usable current densities than comparable bipolar transistors, while at the same time having simpler gate-drive requirements of the familiar power MOSFET. They provide substantial benefits to a host of high-voltage, high-current applications.



Absolute Maximum Ratings

	Parameter	Max.	Units
V_{CES}	Collector-to-Emitter Voltage	600	V
$I_C @ T_C = 25^\circ C$	Continuous Collector Current	50	A
$I_C @ T_C = 100^\circ C$	Continuous Collector Current	31	
I_{CM}	Pulsed Collector Current ①	240	
I_{LM}	Clamped Inductive Load Current ②	120	
V_{GE}	Gate-to-Emitter Voltage	± 20	V
E_{ARV}	Reverse Voltage Avalanche Energy ③	15	mJ
$P_D @ T_C = 25^\circ C$	Maximum Power Dissipation	160	W
$P_D @ T_C = 100^\circ C$	Maximum Power Dissipation	65	
T_J	Operating Junction and Storage Temperature Range	-55 to +150	$^\circ C$
	Soldering Temperature, for 10 sec.	300 (0.063 in. (1.6mm) from case)	
	Mounting torque, 6-32 or M3 screw.	10 lbf•in (1.1N•m)	

Thermal Resistance

	Parameter	Min.	Typ.	Max.	Units
$R_{\theta JC}$	Junction-to-Case	—	—	0.77	$^\circ C/W$
$R_{\theta CS}$	Case-to-Sink, flat, greased surface	—	0.24	—	
$R_{\theta JA}$	Junction-to-Ambient, typical socket mount	—	—	40	
Wt	Weight	—	6 (0.21)	—	g (oz)

Electrical Characteristics @ $T_J = 25^\circ\text{C}$ (unless otherwise specified)

	Parameter	Min.	Typ.	Max.	Units	Conditions
$V_{(BR)CES}$	Collector-to-Emitter Breakdown Voltage	600	—	—	V	$V_{GE} = 0V, I_C = 250\mu A$
$V_{(BR)ECS}$	Emitter-to-Collector Breakdown Voltage ④	20	—	—	V	$V_{GE} = 0V, I_C = 1.0A$
$\Delta V_{(BR)CES}/\Delta T_J$	Temp. Coeff. of Breakdown Voltage	—	0.75	—	$V/^\circ\text{C}$	$V_{GE} = 0V, I_C = 1.0mA$
$V_{CE(on)}$	Collector-to-Emitter Saturation Voltage	—	1.6	1.8	V	$I_C = 31A$ $V_{GE} = 15V$
		—	2.2	—		$I_C = 60A$ See Fig. 2, 5
		—	1.7	—		$I_C = 31A, T_J = 150^\circ\text{C}$
$V_{GE(th)}$	Gate Threshold Voltage	3.0	—	5.5		$V_{CE} = V_{GE}, I_C = 250\mu A$
$\Delta V_{GE(th)}/\Delta T_J$	Temp. Coeff. of Threshold Voltage	—	-9.3	—	$\text{mV}/^\circ\text{C}$	$V_{CE} = V_{GE}, I_C = 250\mu A$
g_{fe}	Forward Transconductance ⑤	12	21	—	S	$V_{CE} = 100V, I_C = 31A$
I_{CES}	Zero Gate Voltage Collector Current	—	—	250	μA	$V_{GE} = 0V, V_{CE} = 600V$
		—	—	1000		$V_{GE} = 0V, V_{CE} = 600V, T_J = 150^\circ\text{C}$
I_{GES}	Gate-to-Emitter Leakage Current	—	—	± 100	nA	$V_{GE} = \pm 20V$

Switching Characteristics @ $T_J = 25^\circ\text{C}$ (unless otherwise specified)

	Parameter	Min.	Typ.	Max.	Units	Conditions
Q_g	Total Gate Charge (turn-on)	—	62	90		$I_C = 31A$
Q_{ge}	Gate - Emitter Charge (turn-on)	—	10	15	nC	$V_{CC} = 400V$ See Fig. 8
Q_{gc}	Gate - Collector Charge (turn-on)	—	27	40		$V_{GE} = 15V$
$t_{d(on)}$	Turn-On Delay Time	—	28	—	ns	$T_J = 25^\circ\text{C}$
t_r	Rise Time	—	50	—		$I_C = 31A, V_{CC} = 480V$
$t_{d(off)}$	Turn-Off Delay Time	—	1100	1500		$V_{GE} = 15V, R_G = 10\Omega$
t_f	Fall Time	—	620	1100		Energy losses include "tail"
E_{on}	Turn-On Switching Loss	—	1.0	—	mJ	See Fig. 9, 10, 11, 14
E_{off}	Turn-Off Switching Loss	—	12	—		
E_{ts}	Total Switching Loss	—	13	20		
$t_{d(on)}$	Turn-On Delay Time	—	29	—	ns	$T_J = 150^\circ\text{C},$
t_r	Rise Time	—	53	—		$I_C = 31A, V_{CC} = 480V$
$t_{d(off)}$	Turn-Off Delay Time	—	1600	—		$V_{GE} = 15V, R_G = 10\Omega$
t_f	Fall Time	—	1200	—		Energy losses include "tail"
E_{ts}	Total Switching Loss	—	22	—	mJ	See Fig. 10, 14
L_E	Internal Emitter Inductance	—	7.5	—	nH	Measured 5mm from package
C_{ies}	Input Capacitance	—	1600	—	pF	$V_{GE} = 0V$
C_{oes}	Output Capacitance	—	140	—		$V_{CC} = 30V$ See Fig. 7
C_{res}	Reverse Transfer Capacitance	—	20	—		$f = 1.0\text{MHz}$

Notes:

- ① Repetitive rating; $V_{GE}=20V$, pulse width limited by max. junction temperature. (See fig. 13b)
- ② $V_{CC}=80\%(V_{CES}), V_{GE}=20V, L=10\mu H, R_G=10\Omega,$ (See fig. 13a)
- ③ Repetitive rating; pulse width limited by maximum junction temperature.
- ④ Pulse width $\leq 80\mu s$; duty factor $\leq 0.1\%$.
- ⑤ Pulse width $5.0\mu s$, single shot.

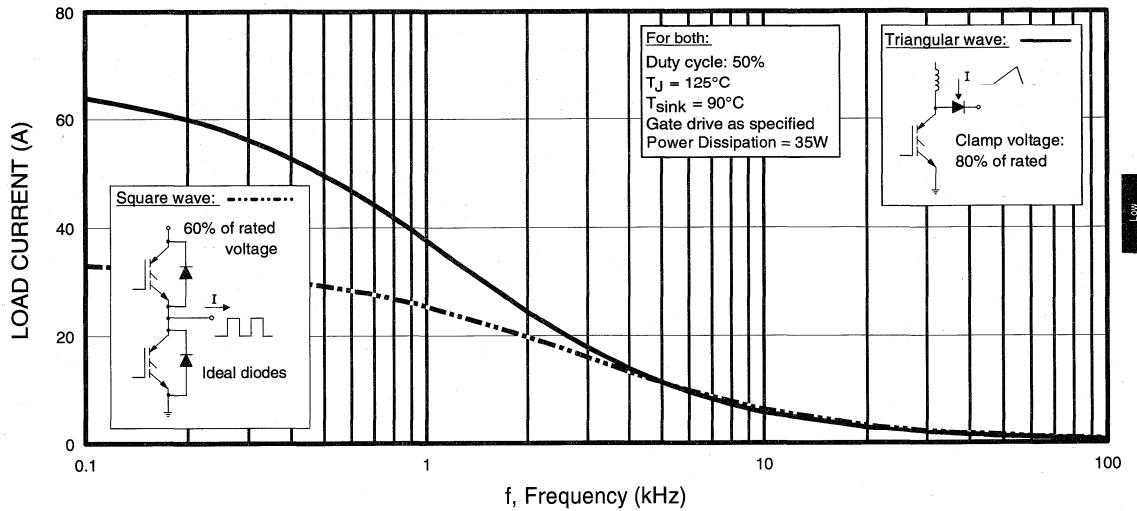


Fig. 1 - Typical Load Current vs. Frequency
 (For square wave, $I = I_{\text{RMS}}$ of fundamental; for triangular wave, $I = I_{\text{PK}}$)

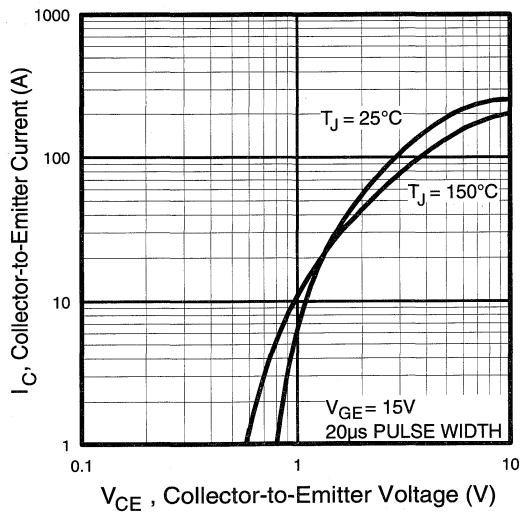


Fig. 2 - Typical Output Characteristics

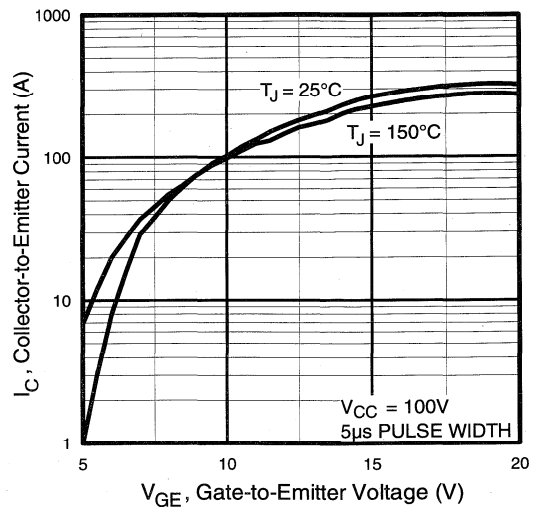


Fig. 3 - Typical Transfer Characteristics

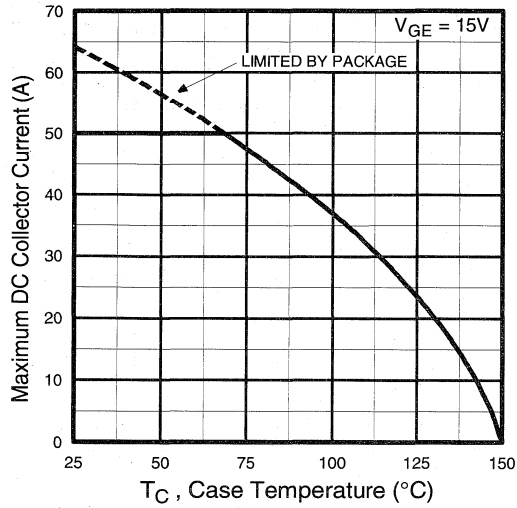


Fig. 4 - Maximum Collector Current vs. Case Temperature

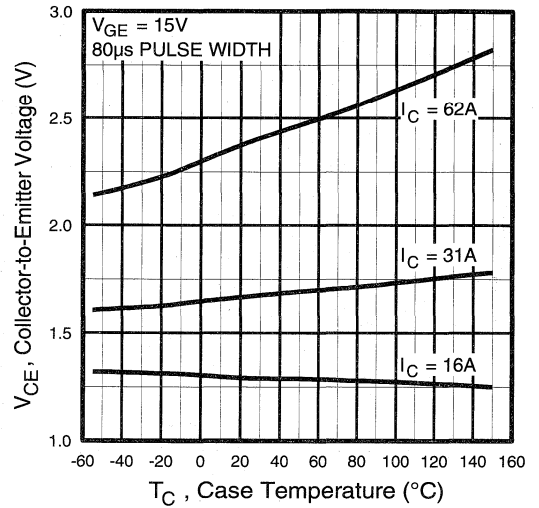


Fig. 5 - Collector-to-Emitter Voltage vs. Case Temperature

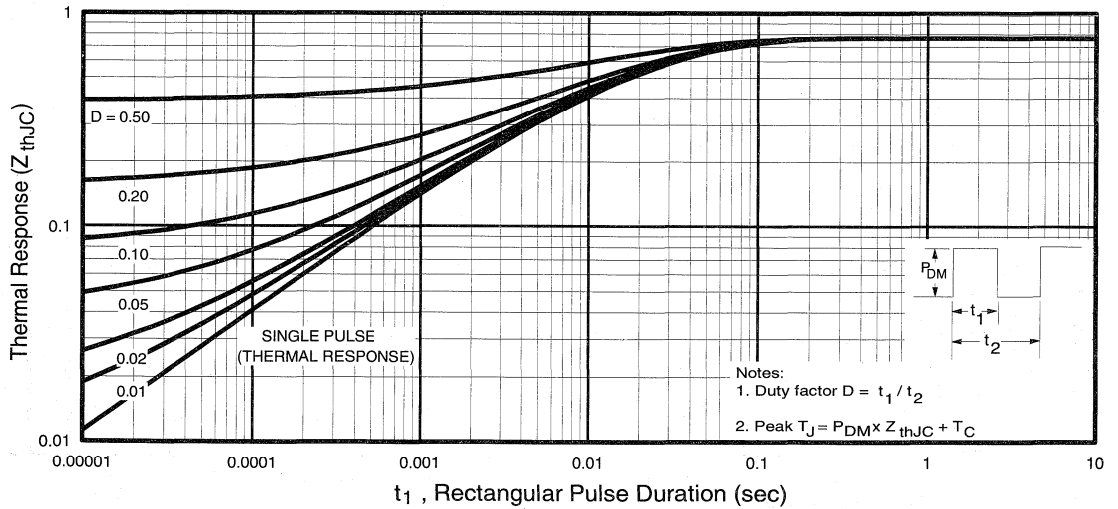


Fig. 6 - Maximum Effective Transient Thermal Impedance, Junction-to-Case

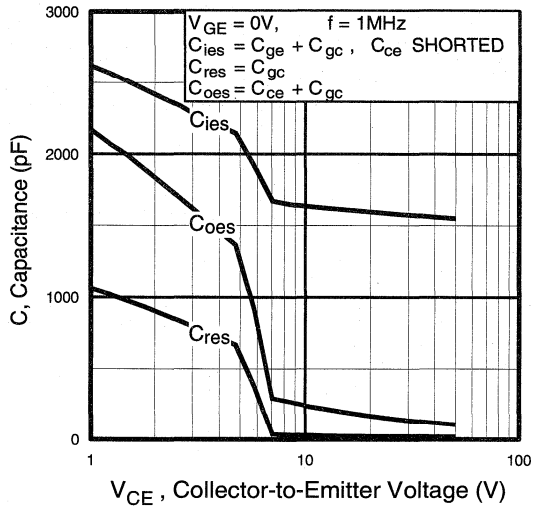


Fig. 7 - Typical Capacitance vs. Collector-to-Emitter Voltage

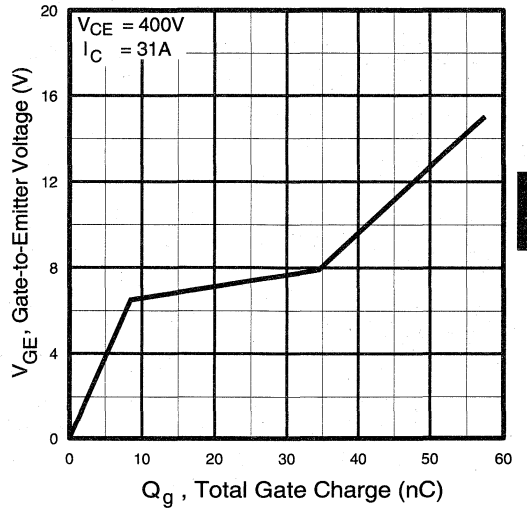


Fig. 8 - Typical Gate Charge vs. Gate-to-Emitter Voltage

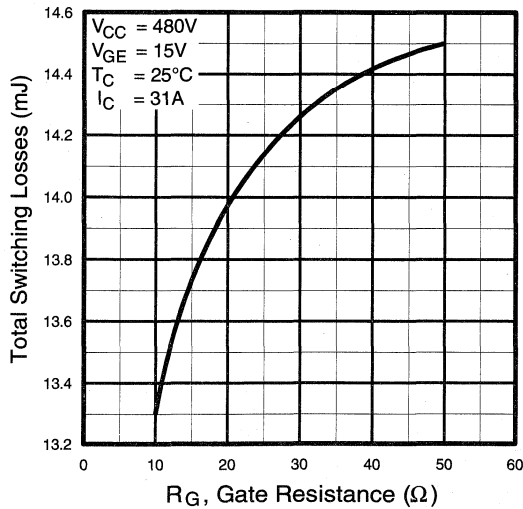


Fig. 9 - Typical Switching Losses vs. Gate Resistance

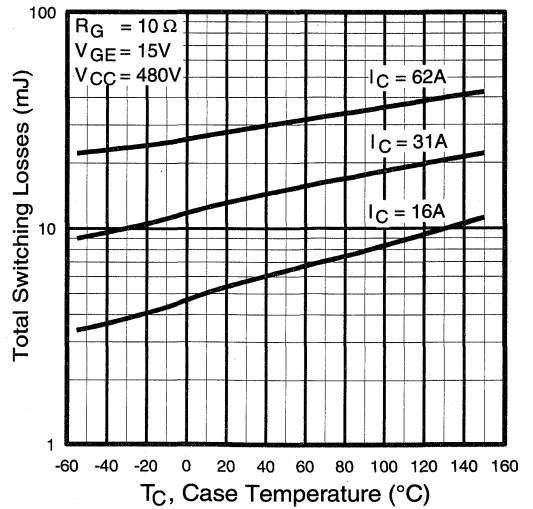


Fig. 10 - Typical Switching Losses vs. Case Temperature

Low Frequency Standard Discrete

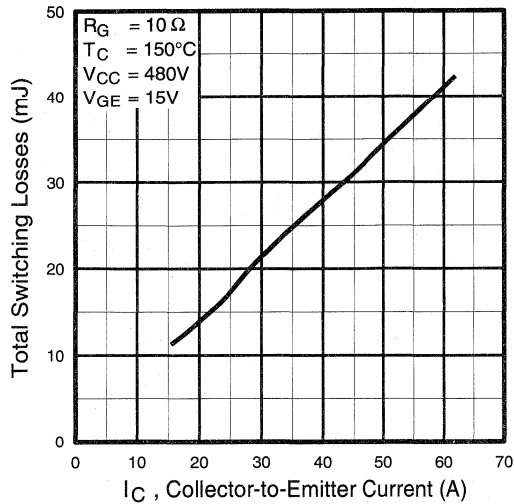


Fig. 11 - Typical Switching Losses vs. Collector-to-Emitter Current

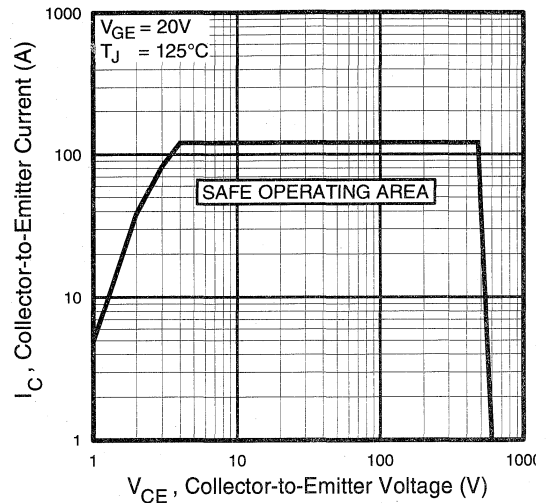


Fig. 12 - Turn-Off SOA

Refer to Section D for the following:

Appendix C: Section D - page D-5

Fig. 13a - Clamped Inductive Load Test Circuit

Fig. 13b - Pulsed Collector Current Test Circuit

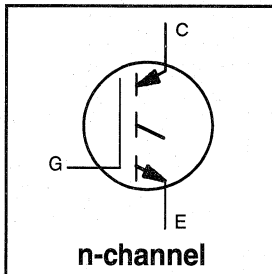
Fig. 14a - Switching Loss Test Circuit

Fig. 14b - Switching Loss Waveform

Package Outline 3 - JEDEC Outline TO-247AC (TO-3P) Section D - page D-13

Features

- Switching-loss rating includes all "tail" losses
- Optimized for line frequency operation (to 400Hz)
See Fig. 1 for Current vs. Frequency curve



$$V_{CES} = 600V$$

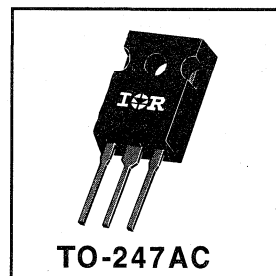
$$V_{CE(sat)} \leq 1.6V$$

$$@V_{GE} = 15V, I_C = 41A$$

Low
Frequency
Standard
Device

Description

Insulated Gate Bipolar Transistors (IGBTs) from International Rectifier have higher usable current densities than comparable bipolar transistors, while at the same time having simpler gate-drive requirements of the familiar power MOSFET. They provide substantial benefits to a host of high-voltage, high-current applications.



Absolute Maximum Ratings

	Parameter	Max.	Units
V_{CES}	Collector-to-Emitter Voltage	600	V
$I_C @ T_C = 25^\circ C$	Continuous Collector Current	70	A
$I_C @ T_C = 100^\circ C$	Continuous Collector Current	41	
I_{CM}	Pulsed Collector Current ①	320	
I_{LM}	Clamped Inductive Load Current ②	140	
V_{GE}	Gate-to-Emitter Voltage	± 20	V
E_{ARV}	Reverse Voltage Avalanche Energy ③	20	mJ
$P_D @ T_C = 25^\circ C$	Maximum Power Dissipation	200	W
$P_D @ T_C = 100^\circ C$	Maximum Power Dissipation	78	
T_J	Operating Junction and	-55 to +150	°C
T_{STG}	Storage Temperature Range		
	Soldering Temperature, for 10 sec.		
	Mounting torque, 6-32 or M3 screw.	10 lbf•in (1.1N•m)	

Thermal Resistance

	Parameter	Min.	Typ.	Max.	Units
$R_{\theta JC}$	Junction-to-Case	—	—	0.64	°C/W
$R_{\theta CS}$	Case-to-Sink, flat, greased surface	—	0.24	—	
$R_{\theta JA}$	Junction-to-Ambient, typical socket mount	—	—	40	
W_t	Weight	—	6 (0.21)	—	g (oz)

Electrical Characteristics @ $T_J = 25^\circ\text{C}$ (unless otherwise specified)

	Parameter	Min.	Typ.	Max.	Units	Conditions	
$V_{(BR)CES}$	Collector-to-Emitter Breakdown Voltage	600	—	—	V	$V_{GE} = 0V, I_C = 250\mu A$	
$V_{(BR)ECS}$	Emitter-to-Collector Breakdown Voltage ④	20	—	—	V	$V_{GE} = 0V, I_C = 1.0A$	
$\Delta V_{(BR)CES}/\Delta T_J$	Temp. Coeff. of Breakdown Voltage	—	0.75	—	V/ $^\circ\text{C}$	$V_{GE} = 0V, I_C = 1.0mA$	
$V_{CE(on)}$	Collector-to-Emitter Saturation Voltage	—	1.4	1.6	V	$V_{GE} = 15V$ See Fig. 2, 5	
		—	1.9	—			$I_C = 41A$
		—	1.5	—			$I_C = 80A, T_J = 150^\circ\text{C}$
$V_{GE(th)}$	Gate Threshold Voltage	3.0	—	5.5		$V_{CE} = V_{GE}, I_C = 250\mu A$	
$\Delta V_{GE(th)}/\Delta T_J$	Temp. Coeff. of Threshold Voltage	—	-9.3	—	mV/ $^\circ\text{C}$	$V_{CE} = V_{GE}, I_C = 250\mu A$	
g_{fe}	Forward Transconductance ⑤	17	34	—	S	$V_{CE} = 100V, I_C = 41A$	
I_{CES}	Zero Gate Voltage Collector Current	—	—	250	μA	$V_{GE} = 0V, V_{CE} = 600V$	
		—	—	1000		$V_{GE} = 0V, V_{CE} = 600V, T_J = 150^\circ\text{C}$	
I_{GES}	Gate-to-Emitter Leakage Current	—	—	± 100	nA	$V_{GE} = \pm 20V$	

Switching Characteristics @ $T_J = 25^\circ\text{C}$ (unless otherwise specified)

	Parameter	Min.	Typ.	Max.	Units	Conditions
Q_g	Total Gate Charge (turn-on)	—	120	150	nC	$I_C = 41A$ $V_{CC} = 400V$ See Fig. 8 $V_{GE} = 15V$
Q_{ge}	Gate - Emitter Charge (turn-on)	—	16	23		
Q_{gc}	Gate - Collector Charge (turn-on)	—	52	90		
$t_{d(on)}$	Turn-On Delay Time	—	52	—	ns	$T_J = 25^\circ\text{C}$ $I_C = 41A, V_{CC} = 480V$ $V_{GE} = 15V, R_G = 5.0\Omega$ Energy losses include "tail"
t_r	Rise Time	—	59	—		
$t_{d(off)}$	Turn-Off Delay Time	—	1200	1400		
t_f	Fall Time	—	500	700		
E_{on}	Turn-On Switching Loss	—	0.35	—	mJ	See Fig. 9, 10, 11, 14
E_{off}	Turn-Off Switching Loss	—	15	—		
E_{ts}	Total Switching Loss	—	16	22		
$t_{d(on)}$	Turn-On Delay Time	—	26	—	ns	$T_J = 150^\circ\text{C}$, $I_C = 41A, V_{CC} = 480V$ $V_{GE} = 15V, R_G = 5.0\Omega$ Energy losses include "tail"
t_r	Rise Time	—	58	—		
$t_{d(off)}$	Turn-Off Delay Time	—	2000	—		
t_f	Fall Time	—	1100	—		
E_{ts}	Total Switching Loss	—	28	—	mJ	See Fig. 10, 14
L_E	Internal Emitter Inductance	—	13	—	nH	Measured 5mm from package
C_{ies}	Input Capacitance	—	3100	—	pF	$V_{GE} = 0V$ $V_{CC} = 30V$ See Fig. 7 $f = 1.0MHz$
C_{oes}	Output Capacitance	—	240	—		
C_{res}	Reverse Transfer Capacitance	—	37	—		

Notes:

- ① Repetitive rating; $V_{GE}=20V$, pulse width limited by max. junction temperature. (See fig. 13b)
- ② $V_{CC}=80\%(V_{CES})$, $V_{GE}=20V$, $L=10\mu H$, $R_G=5.0\Omega$, (See fig. 13a)
- ③ Repetitive rating; pulse width limited by maximum junction temperature.
- ④ Pulse width $\leq 80\mu s$; duty factor $\leq 0.1\%$.
- ⑤ Pulse width $5.0\mu s$, single shot.

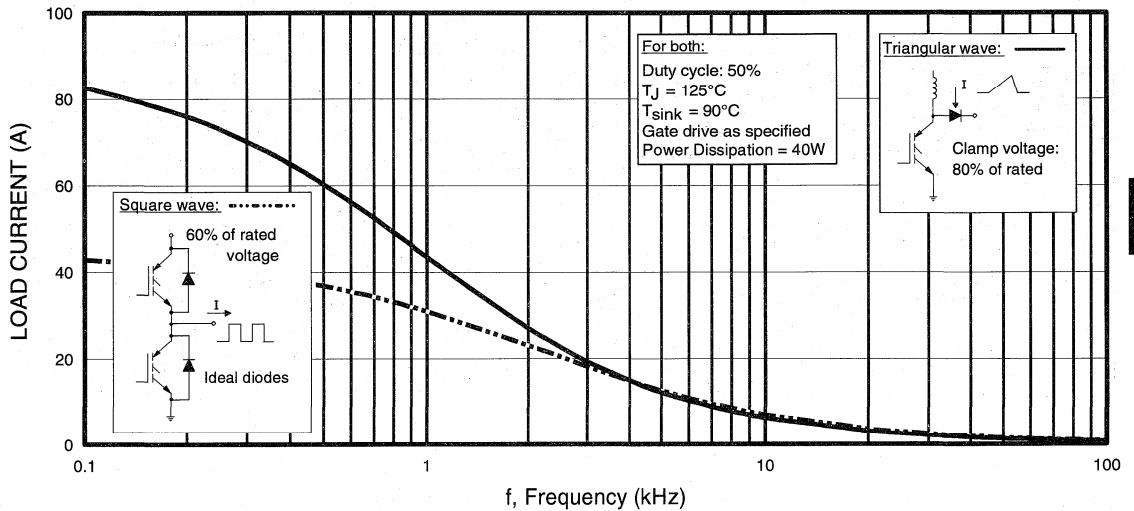


Fig. 1 - Typical Load Current vs. Frequency
 (For square wave, $I = I_{RMS}$ of fundamental; for triangular wave, $I = I_{PK}$)

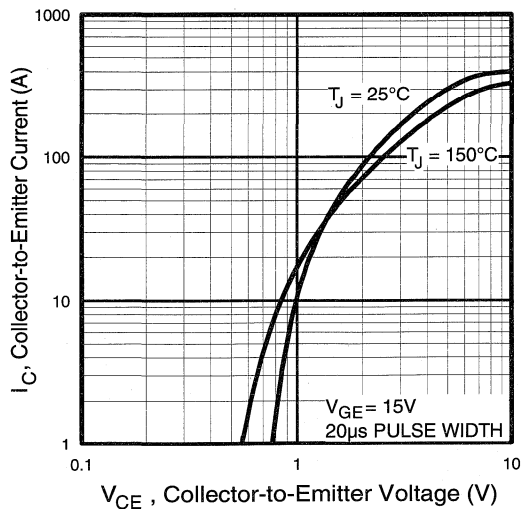


Fig. 2 - Typical Output Characteristics

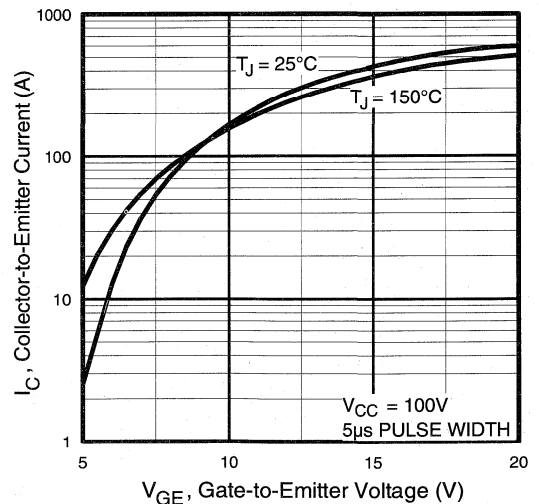


Fig. 3 - Typical Transfer Characteristics

Low
Frequency
Standard
Discrete

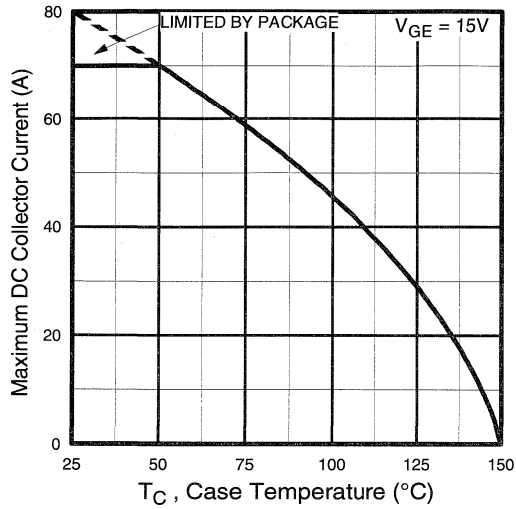


Fig. 4 - Maximum Collector Current vs. Case Temperature

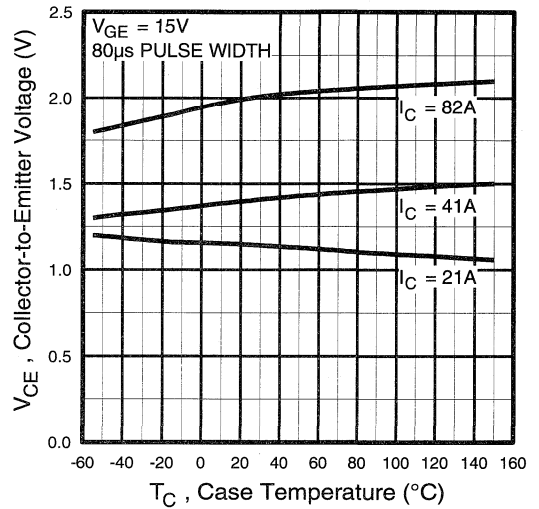


Fig. 5 - Collector-to-Emitter Voltage vs. Case Temperature

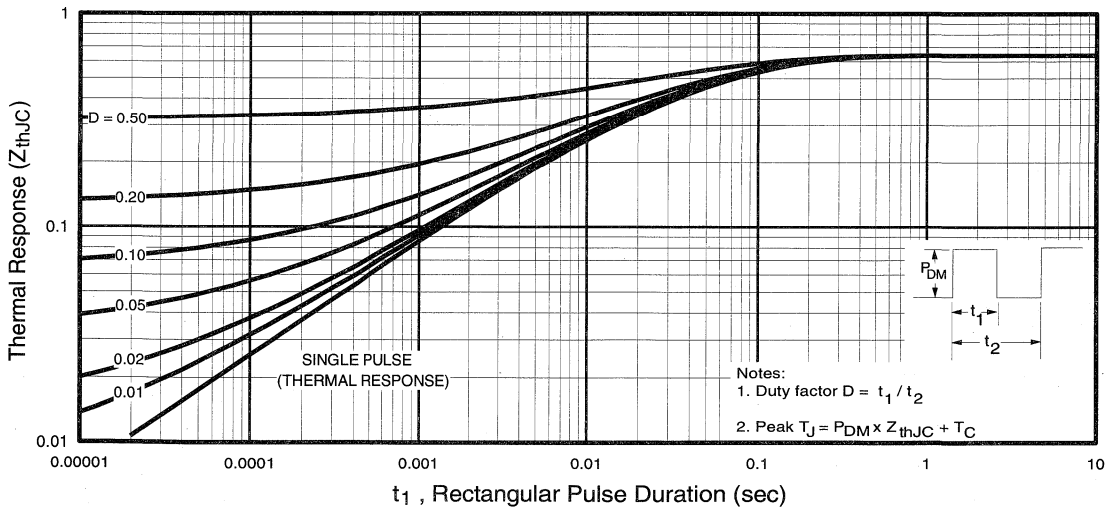


Fig. 6 - Maximum Effective Transient Thermal Impedance, Junction-to-Case

Low
Frequency
Standard
Discrete

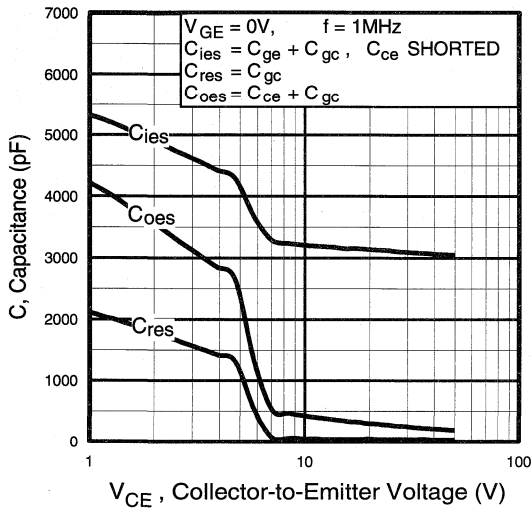


Fig. 7 - Typical Capacitance vs. Collector-to-Emitter Voltage

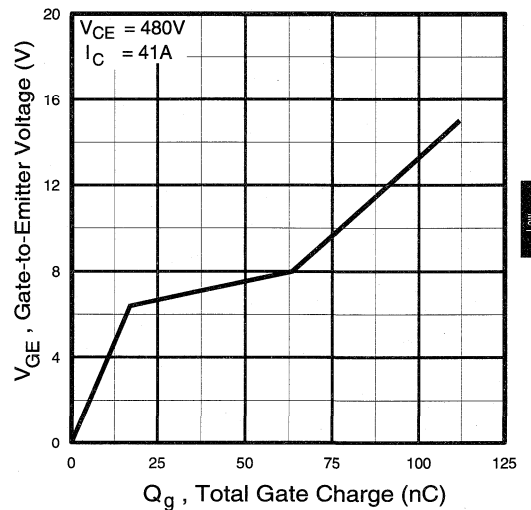


Fig. 8 - Typical Gate Charge vs. Gate-to-Emitter Voltage

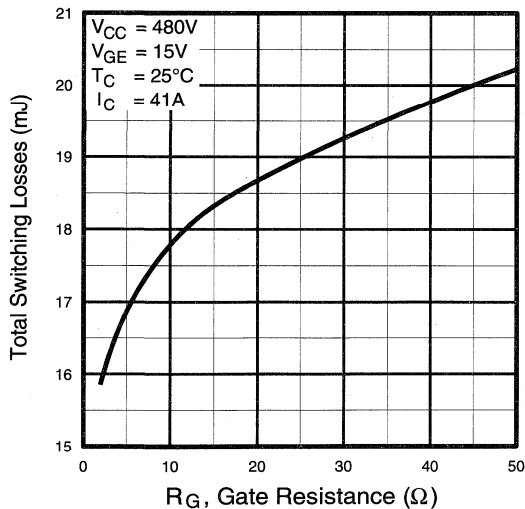


Fig. 9 - Typical Switching Losses vs. Gate Resistance

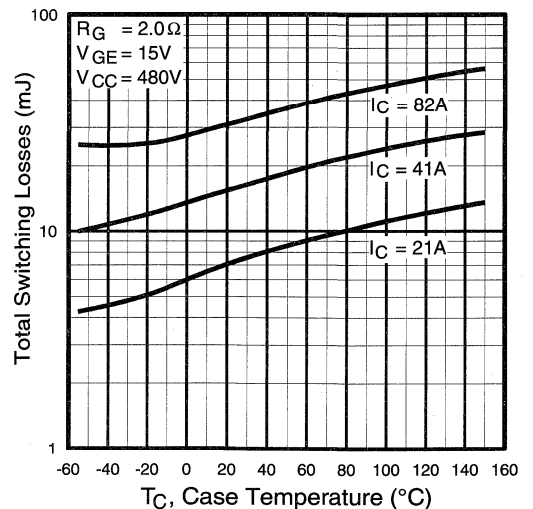


Fig. 10 - Typical Switching Losses vs. Case Temperature

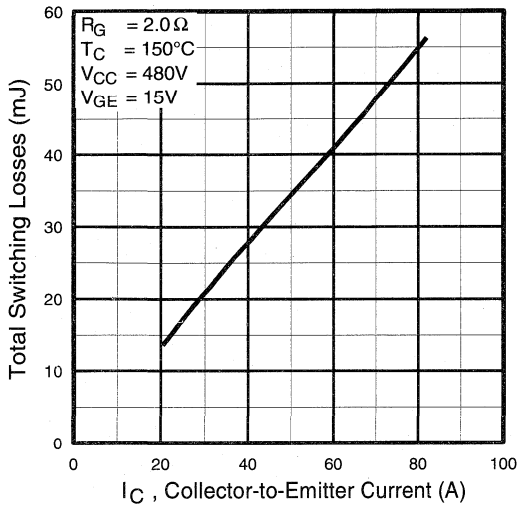


Fig. 11 - Typical Switching Losses vs. Collector-to-Emitter Current

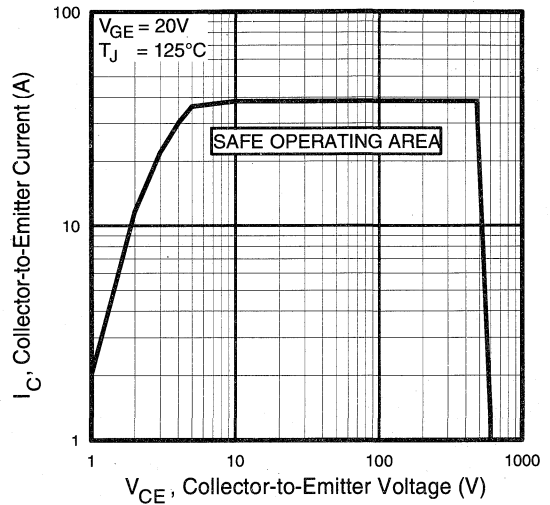


Fig. 12 - Turn-Off SOA

Refer to Section D for the following:

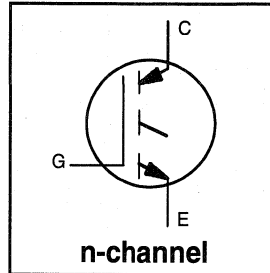
Appendix C: Section D - page D-5

- Fig. 13a - Clamped Inductive Load Test Circuit
- Fig. 13b - Pulsed Collector Current Test Circuit
- Fig. 14a - Switching Loss Test Circuit
- Fig. 14b - Switching Loss Waveform

Package Outline 3 - JEDEC Outline TO-247AC (TO-3P) Section D - page D-13

Features

- Switching-loss rating includes all "tail" losses
 - Optimized for line frequency operation (to 400Hz)
- See Fig. 1 for Current vs. Frequency curve



$$V_{CES} = 1200V$$

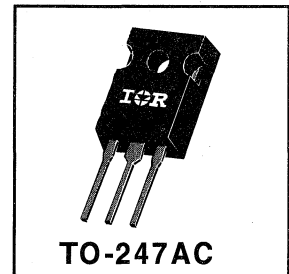
$$V_{CE(sat)} \leq 3.3V$$

$$@ V_{GE} = 15V, I_C = 6.6A$$

Low
Frequency
Standard
Diodes

Description

Insulated Gate Bipolar Transistors (IGBTs) from International Rectifier have higher usable current densities than comparable bipolar transistors, while at the same time having simpler gate-drive requirements of the familiar power MOSFET. They provide substantial benefits to a host of high-voltage, high-current applications.



Absolute Maximum Ratings

	Parameter	Max.	Units
V_{CES}	Collector-to-Emitter Voltage	1200	V
$I_C @ T_C = 25^\circ C$	Continuous Collector Current	10	A
$I_C @ T_C = 100^\circ C$	Continuous Collector Current	6.6	
I_{CM}	Pulsed Collector Current ①	20	
I_{LM}	Clamped Inductive Load Current ②	20	
V_{GE}	Gate-to-Emitter Voltage	± 20	V
E_{ARV}	Reverse Voltage Avalanche Energy ③	5.0	mJ
$P_D @ T_C = 25^\circ C$	Maximum Power Dissipation	60	W
$P_D @ T_C = 100^\circ C$	Maximum Power Dissipation	24	
T_J	Operating Junction and Storage Temperature Range	-55 to +150	°C
T_{STG}			
	Mounting torque, 6-32 or M3 screw.	10 lbf•in (1.1N•m)	

Thermal Resistance

	Parameter	Min.	Typ.	Max.	Units
$R_{\theta JC}$	Junction-to-Case	—	—	2.1	°C/W
$R_{\theta CS}$	Case-to-Sink, flat, greased surface	—	0.24	—	
$R_{\theta JA}$	Junction-to-Ambient, typical socket mount	—	—	40	
Wt	Weight	—	6 (0.21)	—	g (oz)

Electrical Characteristics @ $T_J = 25^\circ\text{C}$ (unless otherwise specified)

	Parameter	Min.	Typ.	Max.	Units	Conditions
$V_{(BR)CES}$	Collector-to-Emitter Breakdown Voltage	1200	—	—	V	$V_{GE} = 0V, I_C = 250\mu A$
$V_{(BR)ECS}$	Emitter-to-Collector Breakdown Voltage ④	20	—	—	V	$V_{GE} = 0V, I_C = 1.0A$
$\Delta V_{(BR)CES}/\Delta T_J$	Temperature Coeff. of Breakdown Voltage	—	1.3	—	V/ $^\circ\text{C}$	$V_{GE} = 0V, I_C = 1.0mA$
$V_{CE(on)}$	Collector-to-Emitter Saturation Voltage	—	2.2	3.3	V	$I_C = 6.6A$ $V_{GE} = 15V$ See Fig. 2, 5
		—	2.9	—		
		—	2.9	—		
$V_{GE(th)}$	Gate Threshold Voltage	3.0	—	5.5		$V_{CE} = V_{GE}, I_C = 250\mu A$
$\Delta V_{GE(th)}/\Delta T_J$	Temperature Coeff. of Threshold Voltage	—	-12	—	mV/ $^\circ\text{C}$	$V_{CE} = V_{GE}, I_C = 250\mu A$
g_{fe}	Forward Transconductance ⑤	1.5	3.0	—	S	$V_{CE} = 100V, I_C = 6.6A$
I_{CES}	Zero Gate Voltage Collector Current	—	—	250		$V_{GE} = 0V, V_{CE} = 1200V$
		—	—	1000		$V_{GE} = 0V, V_{CE} = 1200V, T_J = 150^\circ\text{C}$
I_{GES}	Gate-to-Emitter Leakage Current	—	—	± 100	nA	$V_{GE} = \pm 20V$

Switching Characteristics @ $T_J = 25^\circ\text{C}$ (unless otherwise specified)

	Parameter	Min.	Typ.	Max.	Units	Conditions
Q_g	Total Gate Charge (turn-on)	—	16	24	nC	$I_C = 6.6A$ $V_{CC} = 400V$ See Fig. 8
Q_{ge}	Gate - Emitter Charge (turn-on)	—	5.8	8.7		
Q_{gc}	Gate - Collector Charge (turn-on)	—	4.0	6.0		
$t_{d(on)}$	Turn-On Delay Time	—	28	—	ns	$T_J = 25^\circ\text{C}$ $I_C = 6.6A, V_{CC} = 960V$ $V_{GE} = 15V, R_G = 50\Omega$ Energy losses include "tail"
t_r	Rise Time	—	32	—		
$t_{d(off)}$	Turn-Off Delay Time	—	930	1400		
t_f	Fall Time	—	850	1550		
E_{on}	Turn-On Switching Loss	—	0.57	—	mJ	See Fig. 9, 10, 11, 14
E_{off}	Turn-Off Switching Loss	—	5.4	—		
E_{ts}	Total Switching Loss	—	6.0	9.0		
$t_{d(on)}$	Turn-On Delay Time	—	28	—	ns	$T_J = 150^\circ\text{C}$, $I_C = 6.6A, V_{CC} = 960V$ $V_{GE} = 15V, R_G = 50\Omega$ Energy losses include "tail"
t_r	Rise Time	—	45	—		
$t_{d(off)}$	Turn-Off Delay Time	—	1100	—		
t_f	Fall Time	—	1800	—		
E_{ts}	Total Switching Loss	—	10	—	mJ	See Fig. 10, 14
L_E	Internal Emitter Inductance	—	13	—	nH	Measured 5mm from package
C_{ies}	Input Capacitance	—	360	—	pF	$V_{GE} = 0V$ $V_{CC} = 30V$ See Fig. 7 $f = 1.0MHz$
C_{oes}	Output Capacitance	—	24	—		
C_{res}	Reverse Transfer Capacitance	—	4.8	—		

Notes:

- ① Repetitive rating; $V_{GE}=20V$, pulse width limited by max. junction temperature. (See fig. 13b)
- ② $V_{CC}=80\%(V_{CES}), V_{GE}=20V, L=10\mu H, R_G=50\Omega$, (See fig. 13a)
- ③ Repetitive rating; pulse width limited by maximum junction temperature.
- ④ Pulse width $\leq 80\mu s$; duty factor $\leq 0.1\%$.
- ⑤ Pulse width 5.0 μs , single shot.

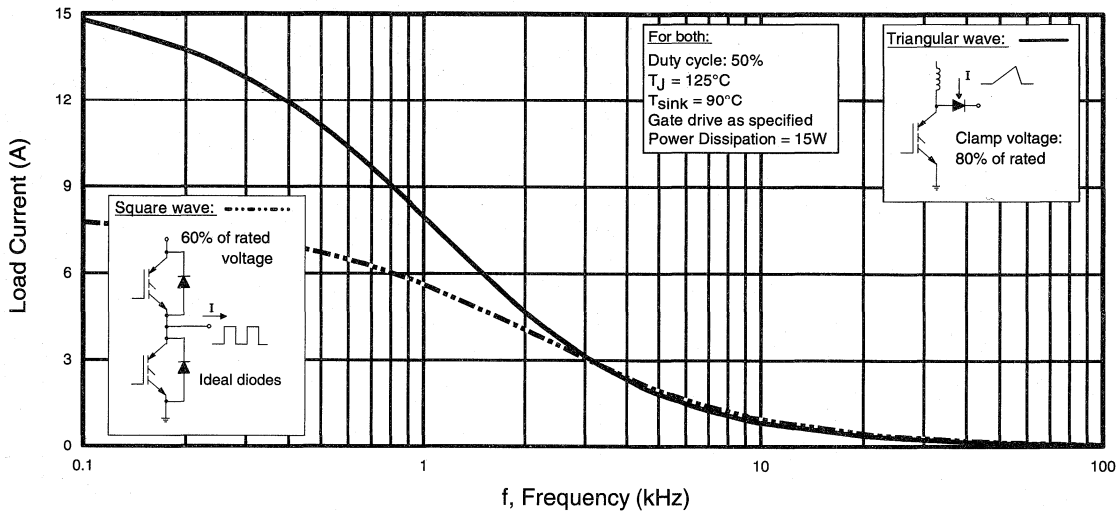


Fig. 1 - Typical Load Current vs. Frequency
 (For square wave, $I = I_{RMS}$ of fundamental; for triangular wave, $I = I_{PK}$)

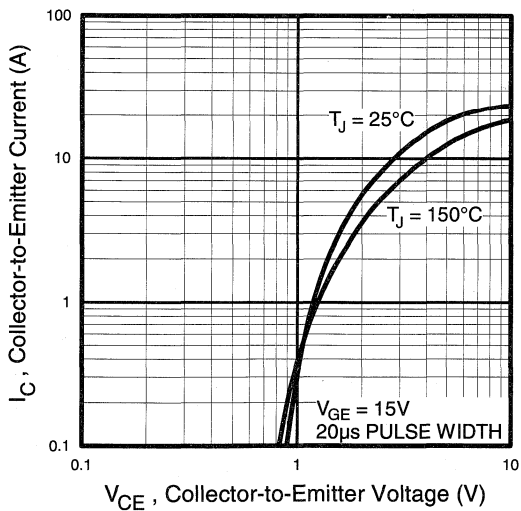


Fig. 2 - Typical Output Characteristics

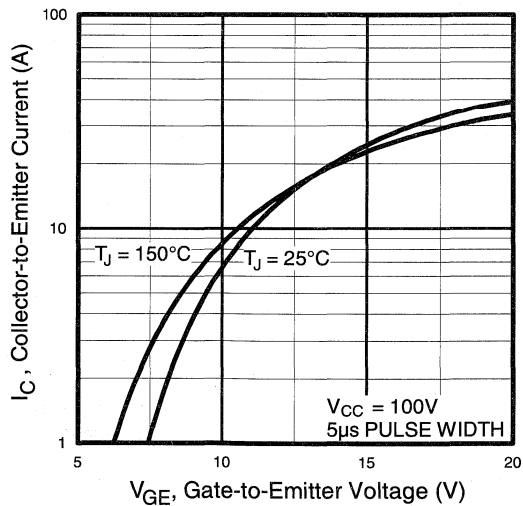


Fig. 3 - Typical Transfer Characteristics

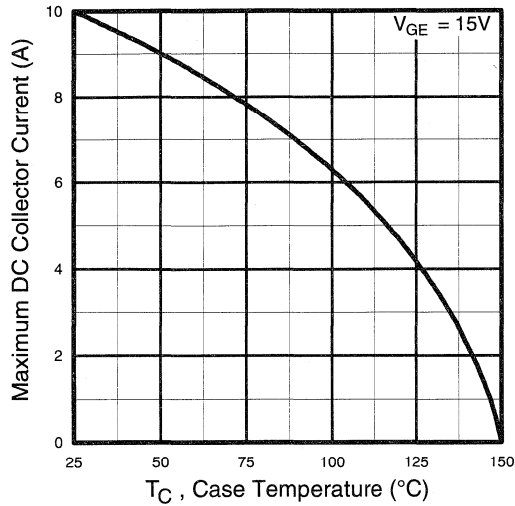


Fig. 4 - Maximum Collector Current vs. Case Temperature

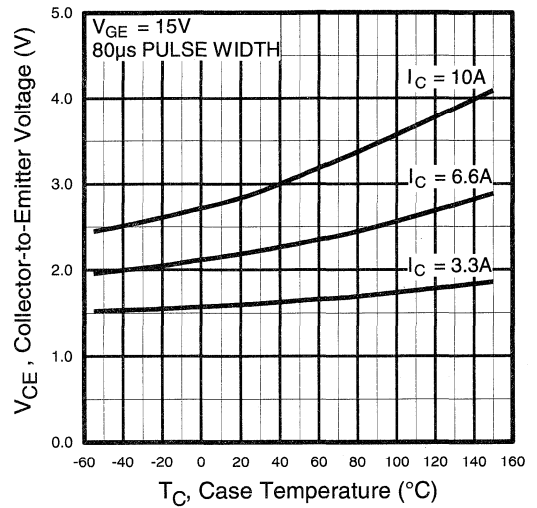


Fig. 5 - Collector-to-Emitter Voltage vs. Case Temperature

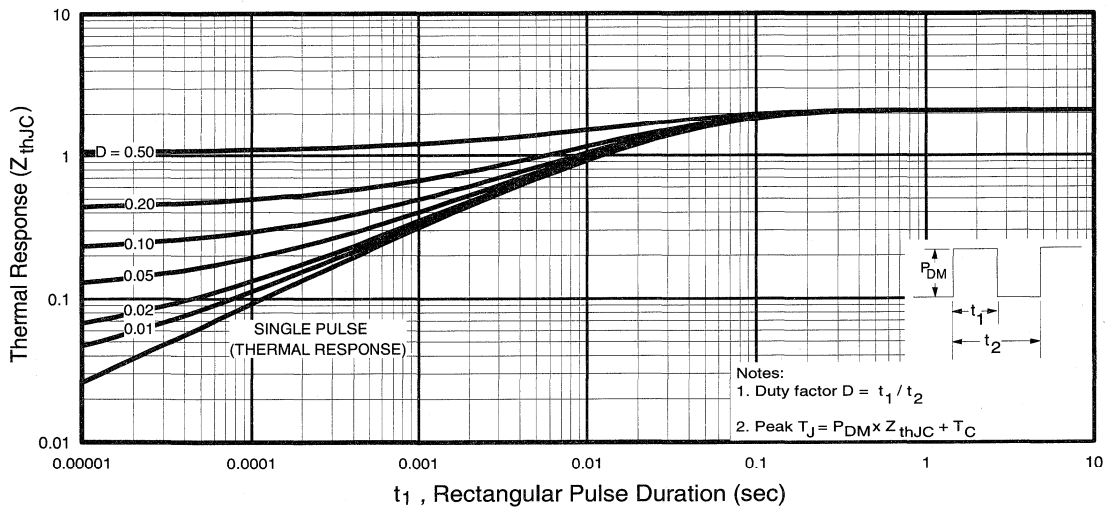


Fig. 6 - Maximum Effective Transient Thermal Impedance, Junction-to-Case

Low Frequency Standard Discrep.

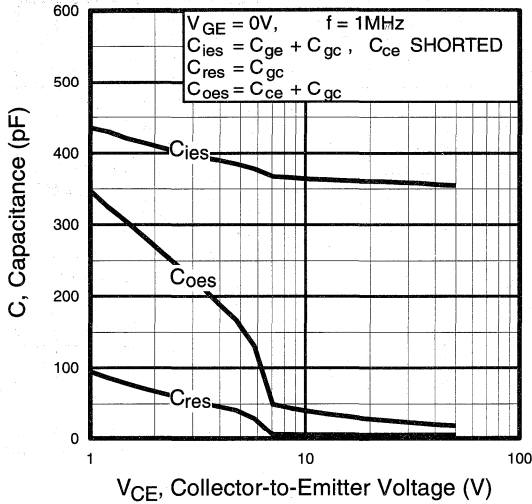


Fig. 7 - Typical Capacitance vs. Collector-to-Emitter Voltage

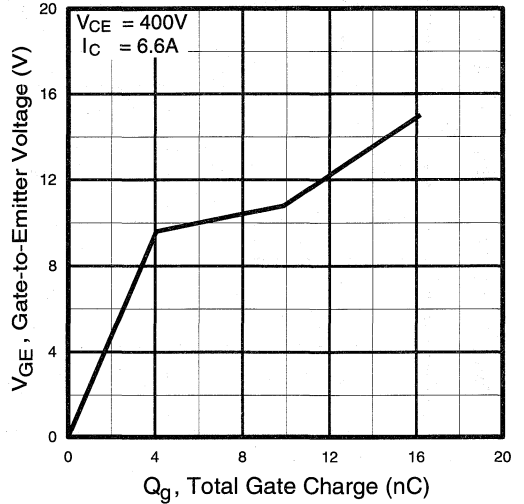


Fig. 8 - Typical Gate Charge vs. Gate-to-Emitter Voltage

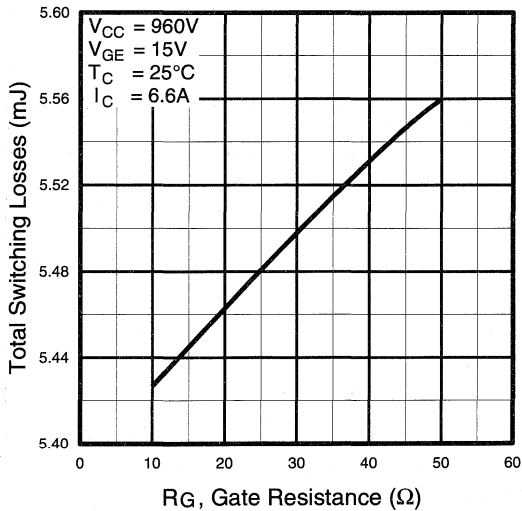


Fig. 9 - Typical Switching Losses vs. Gate Resistance

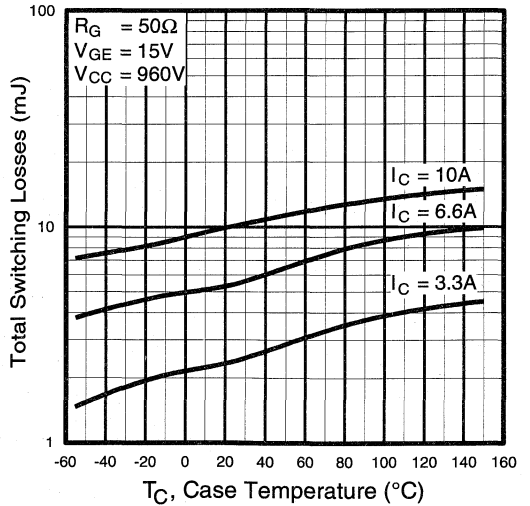


Fig. 10 - Typical Switching Losses vs. Case Temperature

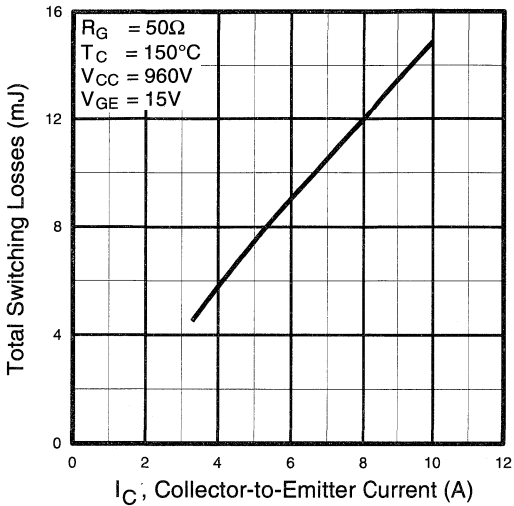


Fig. 11 - Typical Switching Losses vs. Collector-to-Emitter Current

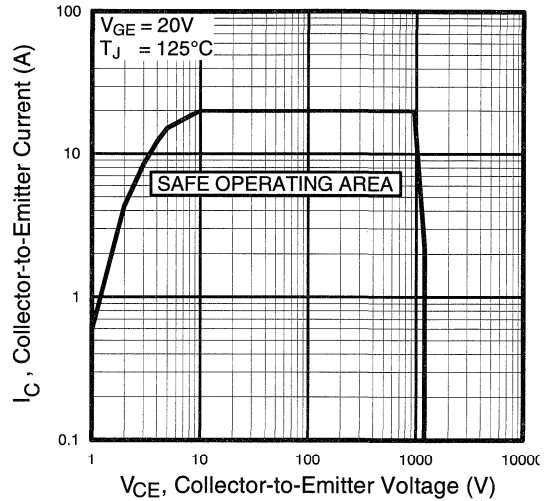


Fig. 12 - Turn-Off SOA

Refer to **Section D** for the following:

Appendix G: Section D - page D-9

Fig. 13a - Clamped Inductive Load Test Circuit

Fig. 13b - Pulsed Collector Current Test Circuit

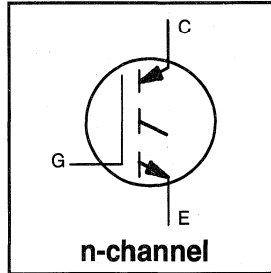
Fig. 14a - Switching Loss Test Circuit

Fig. 14b - Switching Loss Waveform

Package Outline 3 - JEDEC Outline TO-247AC (TO-3P) Section D - page D-13

Features

- Switching-loss rating includes all "tail" losses
- Optimized for line frequency operation (to 400Hz)



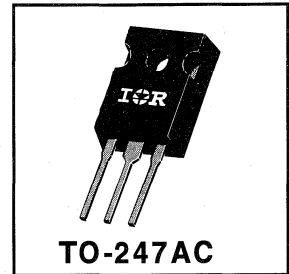
$$V_{CES} = 1200V$$

$$V_{CE(sat)} \leq 3.0V$$

$$@ V_{GE} = 15V, I_C = 13A$$

Description

Insulated Gate Bipolar Transistors (IGBTs) from International Rectifier have higher usable current densities than comparable bipolar transistors, while at the same time having simpler gate-drive requirements of the familiar power MOSFET. They provide substantial benefits to a host of high-voltage, high-current applications.



Absolute Maximum Ratings

	Parameter	Max.	Units
V_{CES}	Collector-to-Emitter Voltage	1200	V
$I_C @ T_C = 25^\circ C$	Continuous Collector Current	22	A
$I_C @ T_C = 100^\circ C$	Continuous Collector Current	13	
I_{CM}	Pulsed Collector Current ①	44	
I_{LM}	Clamped Inductive Load Current ②	44	
V_{GE}	Gate-to-Emitter Voltage	± 20	V
E_{ARV}	Reverse Voltage Avalanche Energy ③	10	mJ
$P_D @ T_C = 25^\circ C$	Maximum Power Dissipation	100	W
$P_D @ T_C = 100^\circ C$	Maximum Power Dissipation	13	
T_J	Operating Junction and	-55 to +150	°C
T_{STG}	Storage Temperature Range		
	Soldering Temperature, for 10 sec.		
	Mounting torque, 6-32 or M3 screw.	10 lbf•in (1.1N•m)	

Thermal Resistance

	Parameter	Min.	Typ.	Max.	Units
$R_{\theta JC}$	Junction-to-Case	—	—	1.2	°C/W
$R_{\theta CS}$	Case-to-Sink, flat, greased surface	—	0.24	—	
$R_{\theta JA}$	Junction-to-Ambient, typical socket mount	—	—	40	
Wt	Weight	—	6 (0.21)	—	g (oz)

Electrical Characteristics @ $T_J = 25^\circ\text{C}$ (unless otherwise specified)

	Parameter	Min.	Typ.	Max.	Units	Conditions
$V_{(BR)CES}$	Collector-to-Emitter Breakdown Voltage	1200	—	—	V	$V_{GE} = 0V, I_C = 250\mu A$
$V_{(BR)ECS}$	Emitter-to-Collector Breakdown Voltage ④	20	—	—	V	$V_{GE} = 0V, I_C = 1.0A$
$\Delta V_{(BR)CES}/\Delta T_J$	Temperature Coeff. of Breakdown Voltage	—	1.5	—	$V/^\circ\text{C}$	$V_{GE} = 0V, I_C = 1.0mA$
$V_{CE(on)}$	Collector-to-Emitter Saturation Voltage	—	2.0	3.0	V	$I_C = 13A$
		—	2.8	—		$I_C = 22A$
		—	2.6	—		$I_C = 13A, T_J = 150^\circ\text{C}$
$V_{GE(th)}$	Gate Threshold Voltage	3.0	—	5.5		$V_{CE} = V_{GE}, I_C = 250\mu A$
$\Delta V_{GE(th)}/\Delta T_J$	Temperature Coeff. of Threshold Voltage	—	-12	—	$mV/^\circ\text{C}$	$V_{CE} = V_{GE}, I_C = 250\mu A$
g_{fe}	Forward Transconductance ⑤	3.1	6.3	—	S	$V_{CE} = 100V, I_C = 13A$
I_{CES}	Zero Gate Voltage Collector Current	—	—	250	μA	$V_{GE} = 0V, V_{CE} = 1200V$
		—	—	1000		$V_{GE} = 0V, V_{CE} = 1200V, T_J = 150^\circ\text{C}$
I_{GES}	Gate-to-Emitter Leakage Current	—	—	± 100	nA	$V_{GE} = \pm 20V$

See Fig. 2, 5

Switching Characteristics @ $T_J = 25^\circ\text{C}$ (unless otherwise specified)

	Parameter	Min.	Typ.	Max.	Units	Conditions
Q_g	Total Gate Charge (turn-on)	—	28	42	nC	$I_C = 13A$ $V_{CC} = 400V$ $V_{GE} = 15V$
Q_{ge}	Gate - Emitter Charge (turn-on)	—	8.2	12		
Q_{gc}	Gate - Collector Charge (turn-on)	—	6.8	10		
$t_{d(on)}$	Turn-On Delay Time	—	28	—	ns	$T_J = 25^\circ\text{C}$ $I_C = 13A, V_{CC} = 960V$ $V_{GE} = 15V, R_G = 23\Omega$ Energy losses include "tail"
t_r	Rise Time	—	22	—		
$t_{d(off)}$	Turn-Off Delay Time	—	1200	1800		
t_f	Fall Time	—	680	1140		
E_{on}	Turn-On Switching Loss	—	0.90	—	mJ	
E_{off}	Turn-Off Switching Loss	—	12	—		
E_{ts}	Total Switching Loss	—	13	19		
$t_{d(on)}$	Turn-On Delay Time	—	26	—	ns	$T_J = 150^\circ\text{C}$, $I_C = 13A, V_{CC} = 960V$ $V_{GE} = 15V, R_G = 23\Omega$ Energy losses include "tail"
t_r	Rise Time	—	27	—		
$t_{d(off)}$	Turn-Off Delay Time	—	1280	—		
t_f	Fall Time	—	2000	—		
E_{ts}	Total Switching Loss	—	23	—	mJ	
L_E	Internal Emitter Inductance	—	13	—	nH	Measured 5mm from package
C_{ies}	Input Capacitance	—	685	—	pF	$V_{GE} = 0V$ $V_{CC} = 30V$ $f = 1.0MHz$
C_{oes}	Output Capacitance	—	43	—		
C_{res}	Reverse Transfer Capacitance	—	8.3	—		

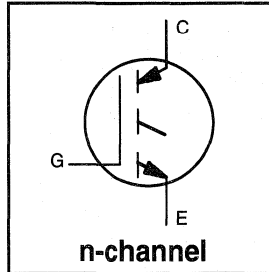
Notes:

- ① Repetitive rating; $V_{GE}=20V$, pulse width limited by max. junction temperature.
- ② $V_{CC}=80\%(V_{CES})$, $V_{GE}=20V$, $L=10\mu H$, $R_G=23\Omega$
- ③ Repetitive rating; pulse width limited by maximum junction temperature.
- ④ Pulse width $\leq 80\mu s$; duty factor $\leq 0.1\%$.
- ⑤ Pulse width $5.0\mu s$, single shot.

Refer to Section D - page D-13
Package Outline 3 - JEDEC Outline TO-247AC (TO-3P)

Features

- Switching-loss rating includes all "tail" losses
- Optimized for line frequency operation (to 400Hz)



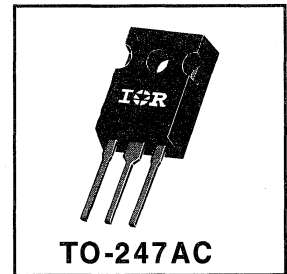
$$V_{CES} = 1200V$$

$$V_{CE(sat)} \leq 3.0V$$

$$@V_{GE} = 15V, I_C = 20A$$

Description

Insulated Gate Bipolar Transistors (IGBTs) from International Rectifier have higher usable current densities than comparable bipolar transistors, while at the same time having simpler gate-drive requirements of the familiar power MOSFET. They provide substantial benefits to a host of high-voltage, high-current applications.



Absolute Maximum Ratings

	Parameter	Max.	Units
V_{CES}	Collector-to-Emitter Voltage	1200	V
$I_C @ T_C = 25^\circ C$	Continuous Collector Current	33	A
$I_C @ T_C = 100^\circ C$	Continuous Collector Current	20	
I_{CM}	Pulsed Collector Current ①	66	
I_{LM}	Clamped Inductive Load Current ②	66	
V_{GE}	Gate-to-Emitter Voltage	± 20	
E_{ARV}	Reverse Voltage Avalanche Energy ③	15	mJ
$P_D @ T_C = 25^\circ C$	Maximum Power Dissipation	160	W
$P_D @ T_C = 100^\circ C$	Maximum Power Dissipation	65	
T_J	Operating Junction and	-55 to +150	°C
T_{STG}	Storage Temperature Range		
	Soldering Temperature, for 10 sec.		
	Mounting torque, 6-32 or M3 screw.	10 lb•in (1.1N•m)	

Thermal Resistance

	Parameter	Min.	Typ.	Max.	Units
$R_{\theta JC}$	Junction-to-Case	—	—	0.77	°C/W
$R_{\theta CS}$	Case-to-Sink, flat, greased surface	—	0.24	—	
$R_{\theta JA}$	Junction-to-Ambient, typical socket mount	—	—	40	
Wt	Weight	—	6 (0.21)	—	g (oz)

Electrical Characteristics @ $T_J = 25^\circ\text{C}$ (unless otherwise specified)

	Parameter	Min.	Typ.	Max.	Units	Conditions
$V_{(BR)CES}$	Collector-to-Emitter Breakdown Voltage	1200	—	—	V	$V_{GE} = 0V, I_C = 250\mu A$
$V_{(BR)ECS}$	Emitter-to-Collector Breakdown Voltage ①	20	—	—	V	$V_{GE} = 0V, I_C = 1.0A$
$\Delta V_{(BR)CES}/\Delta T_J$	Temperature Coeff. of Breakdown Voltage	—	1.3	—	V/ $^\circ\text{C}$	$V_{GE} = 0V, I_C = 1.0mA$
$V_{CE(on)}$	Collector-to-Emitter Saturation Voltage	—	2.5	3.0	V	$I_C = 20A$ $I_C = 33A$ $I_C = 20A, T_J = 150^\circ\text{C}$ $V_{GE} = 15V$
		—	2.9	—		
		—	2.8	—		
$V_{GE(th)}$	Gate Threshold Voltage	3.0	—	5.5		$V_{CE} = V_{GE}, I_C = 250\mu A$
$\Delta V_{GE(th)}/\Delta T_J$	Temperature Coeff. of Threshold Voltage	—	-12	—	mV/ $^\circ\text{C}$	$V_{CE} = V_{GE}, I_C = 250\mu A$
g_{fe}	Forward Transconductance ②	—	12	—	S	$V_{CE} = 100V, I_C = 20A$
I_{CES}	Zero Gate Voltage Collector Current	—	—	250	μA	$V_{GE} = 0V, V_{CE} = 1200V$ $V_{GE} = 0V, V_{CE} = 1200V, T_J = 150^\circ\text{C}$
		—	—	1000		
I_{GES}	Gate-to-Emitter Leakage Current	—	—	± 100	nA	$V_{GE} = \pm 20V$

Switching Characteristics @ $T_J = 25^\circ\text{C}$ (unless otherwise specified)

	Parameter	Min.	Typ.	Max.	Units	Conditions	
Q_g	Total Gate Charge (turn-on)	—	50	—	nC	$I_C = 20A$ $V_{CC} = 400V$ $V_{GE} = 15V$	
Q_{ge}	Gate - Emitter Charge (turn-on)	—	14	—			
Q_{gc}	Gate - Collector Charge (turn-on)	—	12	—			
$t_{d(on)}$	Turn-On Delay Time	—	30	—	ns	$T_J = 25^\circ\text{C}$ $I_C = 20A, V_{CC} = 960V$ $V_{GE} = 15V, R_G = 10\Omega$ Energy losses include "tail"	
t_r	Rise Time	—	22	—			
$t_{d(off)}$	Turn-Off Delay Time	—	1400	—			
t_f	Fall Time	—	680	—			
E_{on}	Turn-On Switching Loss	—	1.4	—			mJ
E_{off}	Turn-Off Switching Loss	—	20	—			
E_{ts}	Total Switching Loss	—	21.4	—			
$t_{d(on)}$	Turn-On Delay Time	—	28	—	ns	$T_J = 150^\circ\text{C}$, $I_C = 20A, V_{CC} = 960V$ $V_{GE} = 15V, R_G = 10\Omega$ Energy losses include "tail"	
t_r	Rise Time	—	27	—			
$t_{d(off)}$	Turn-Off Delay Time	—	1300	—			
t_f	Fall Time	—	2100	—			
E_{ts}	Total Switching Loss	—	50	—	mJ		
L_E	Internal Emitter Inductance	—	13	—	nH	Measured 5mm from package	
C_{ies}	Input Capacitance	—	1650	—	pF	$V_{GE} = 0V$ $V_{CC} = 30V$ $f = 1.0MHz$	
C_{oes}	Output Capacitance	—	73	—			
C_{res}	Reverse Transfer Capacitance	—	14	—			

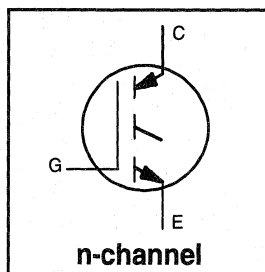
Notes:

- ① Repetitive rating; $V_{GE}=20V$, pulse width limited by max. junction temperature.
- ② $V_{CC}=80\%(V_{CES})$, $V_{GE}=20V$, $L=10\mu H$, $R_G=10\Omega$
- ③ Repetitive rating; pulse width limited by maximum junction temperature.
- ④ Pulse width $\leq 80\mu s$; duty factor $\leq 0.1\%$.
- ⑤ Pulse width 5.0 μs , single shot.

Refer to Section D - page D-13
Package Outline 3 - JEDEC Outline TO-247AC (TO-3P)

Features

- Switching-loss rating includes all "tail" losses
- Optimized for line frequency operation (to 400Hz)
See Fig. 1 for Current vs. Frequency curve

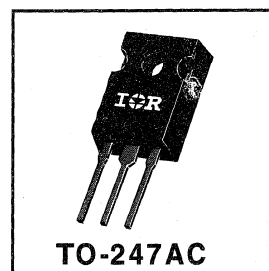


$V_{CES} = 1200V$
$V_{CE(sat)} \leq 2.0V$
@ $V_{GE} = 15V, I_C = 33A$

Low Frequency Standard Package

Description

Insulated Gate Bipolar Transistors (IGBTs) from International Rectifier have higher usable current densities than comparable bipolar transistors, while at the same time having simpler gate-drive requirements of the familiar power MOSFET. They provide substantial benefits to a host of high-voltage, high-current applications.



Absolute Maximum Ratings

	Parameter	Max.	Units
V_{CES}	Collector-to-Emitter Voltage	1200	V
$I_C @ T_C = 25^\circ C$	Continuous Collector Current	57	A
$I_C @ T_C = 100^\circ C$	Continuous Collector Current	33	
I_{CM}	Pulsed Collector Current ①	110	
I_{LM}	Clamped Inductive Load Current ②	110	
V_{GE}	Gate-to-Emitter Voltage	± 20	V
E_{ARV}	Reverse Voltage Avalanche Energy ③	20	mJ
$P_D @ T_C = 25^\circ C$	Maximum Power Dissipation	200	W
$P_D @ T_C = 100^\circ C$	Maximum Power Dissipation	78	
T_J	Operating Junction and Storage Temperature Range	-55 to +150	$^\circ C$
T_{STG}	Soldering Temperature, for 10 sec.	300 (0.063 in. (1.6mm) from case)	
	Mounting torque, 6-32 or M3 screw.	10 lbf•in (1.1N•m)	

Thermal Resistance

	Parameter	Min.	Typ.	Max.	Units
$R_{\theta JC}$	Junction-to-Case	—	—	0.64	$^\circ C/W$
$R_{\theta CS}$	Case-to-Sink, flat, greased surface	—	0.24	—	
$R_{\theta JA}$	Junction-to-Ambient, typical socket mount	—	—	40	
Wt	Weight	—	6 (0.21)	—	g (oz)

Electrical Characteristics @ $T_J = 25^\circ\text{C}$ (unless otherwise specified)

	Parameter	Min.	Typ.	Max.	Units	Conditions
$V_{(BR)CES}$	Collector-to-Emitter Breakdown Voltage	1200	—	—	V	$V_{GE} = 0V, I_C = 250\mu A$
$V_{(BR)ECS}$	Emitter-to-Collector Breakdown Voltage ④	20	—	—	V	$V_{GE} = 0V, I_C = 1.0A$
$\Delta V_{(BR)CES}/\Delta T_J$	Temperature Coeff. of Breakdown Voltage	—	1.3	—	V/°C	$V_{GE} = 0V, I_C = 1.0mA$
$V_{CE(on)}$	Collector-to-Emitter Saturation Voltage	—	1.7	2.0	V	$I_C = 33A$ $I_C = 57A$ $I_C = 33A, T_J = 150^\circ\text{C}$ $V_{GE} = 15V$ See Fig. 2, 5
		—	2.2	—		
		—	2.0	—		
$V_{GE(th)}$	Gate Threshold Voltage	3.0	—	5.5		$V_{CE} = V_{GE}, I_C = 250\mu A$
$\Delta V_{GE(th)}/\Delta T_J$	Temperature Coeff. of Threshold Voltage	—	-13	—	mV/°C	$V_{CE} = V_{GE}, I_C = 250\mu A$
g_{fe}	Forward Transconductance ⑤	—	19	—	S	$V_{CE} = 100V, I_C = 33A$
I_{CES}	Zero Gate Voltage Collector Current	—	—	250	μA	$V_{GE} = 0V, V_{CE} = 1200V$
		—	—	1000		$V_{GE} = 0V, V_{CE} = 1200V, T_J = 150^\circ\text{C}$
I_{GES}	Gate-to-Emitter Leakage Current	—	—	± 100	nA	$V_{GE} = \pm 20V$

Switching Characteristics @ $T_J = 25^\circ\text{C}$ (unless otherwise specified)

	Parameter	Min.	Typ.	Max.	Units	Conditions
Q_g	Total Gate Charge (turn-on)	—	72	108	nC	$I_C = 33A$ $V_{CC} = 400V$ $V_{GE} = 15V$ See Fig. 8
Q_{ge}	Gate - Emitter Charge (turn-on)	—	16	24		
Q_{gc}	Gate - Collector Charge (turn-on)	—	19	30		
$t_{d(on)}$	Turn-On Delay Time	—	62	—	ns	$T_J = 25^\circ\text{C}$ $I_C = 33A, V_{CC} = 960V$ $V_{GE} = 15V, R_G = 5.0\Omega$ Energy losses include "tail"
t_r	Rise Time	—	77	—		
$t_{d(off)}$	Turn-Off Delay Time	—	1200	1800		
t_f	Fall Time	—	780	1200		
E_{on}	Turn-On Switching Loss	—	3.0	—	mJ	See Fig. 9, 10, 11, 14
E_{off}	Turn-Off Switching Loss	—	26	—		
E_{ts}	Total Switching Loss	—	29	44		
$t_{d(on)}$	Turn-On Delay Time	—	52	—	ns	$T_J = 150^\circ\text{C}$, $I_C = 33A, V_{CC} = 960V$ $V_{GE} = 15V, R_G = 5.0\Omega$ Energy losses include "tail"
t_r	Rise Time	—	76	—		
$t_{d(off)}$	Turn-Off Delay Time	—	1300	—		
t_f	Fall Time	—	2100	—		
E_{ts}	Total Switching Loss	—	55	—	mJ	See Fig. 10, 14
L_E	Internal Emitter Inductance	—	13	—	nH	Measured 5mm from package
C_{ies}	Input Capacitance	—	1900	—	pF	$V_{GE} = 0V$ $V_{CC} = 30V$ $f = 1.0MHz$ See Fig. 7
C_{oes}	Output Capacitance	—	140	—		
C_{res}	Reverse Transfer Capacitance	—	24	—		

Notes:

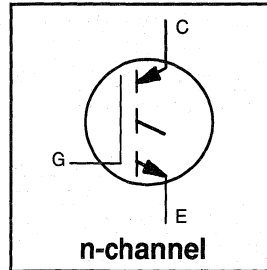
- ① Repetitive rating; $V_{GE}=20V$, pulse width limited by max. junction temperature. (See fig. 13b)
- ② $V_{CC}=80\%(V_{CES}), V_{GE}=20V, L=10\mu H, R_G=5.0\Omega$, (See fig. 13a)
- ③ Repetitive rating; pulse width limited by maximum junction temperature.
- ④ Pulse width $\leq 80\mu s$; duty factor $\leq 0.1\%$.
- ⑤ Pulse width $5.0\mu s$, single shot.

Refer to Section D - page D-13

Package Outline 3 - JEDEC Outline TO-247AC (TO-3P)

Features

- Switching-loss rating includes all "tail" losses
- Optimized for medium operating frequency (1 to 10kHz) See Fig. 1 for Current vs. Frequency curve



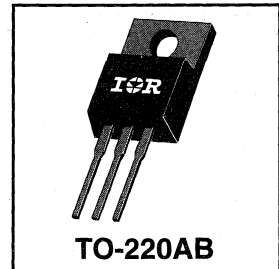
$$V_{CES} = 600V$$

$$V_{CE(sat)} \leq 2.8V$$

$$@V_{GE} = 15V, I_C = 9.0A$$

Description

Insulated Gate Bipolar Transistors (IGBTs) from International Rectifier have higher usable current densities than comparable bipolar transistors, while at the same time having simpler gate-drive requirements of the familiar power MOSFET. They provide substantial benefits to a host of high-voltage, high-current applications.



Absolute Maximum Ratings

	Parameter	Max.	Units
V_{CES}	Collector-to-Emitter Voltage	600	V
$I_C @ T_C = 25^\circ C$	Continuous Collector Current	16	A
$I_C @ T_C = 100^\circ C$	Continuous Collector Current	9.0	
I_{CM}	Pulsed Collector Current ①	64	
I_{LM}	Clamped Inductive Load Current ②	64	
V_{GE}	Gate-to-Emitter Voltage	± 20	V
E_{ARV}	Reverse Voltage Avalanche Energy ③	5.0	mJ
$P_D @ T_C = 25^\circ C$	Maximum Power Dissipation	60	W
$P_D @ T_C = 100^\circ C$	Maximum Power Dissipation	24	
T_J	Operating Junction and Storage Temperature Range	-55 to +150	$^\circ C$
T_{STG}	Soldering Temperature, for 10 sec.	300 (0.063 in. (1.6mm) from case)	
	Mounting torque, 6-32 or M3 screw.	10 lbf•in (1.1N•m)	

Thermal Resistance

	Parameter	Min.	Typ.	Max.	Units
$R_{\theta JC}$	Junction-to-Case	—	—	2.1	$^\circ C/W$
$R_{\theta CS}$	Case-to-Sink, flat, greased surface	—	0.50	—	
$R_{\theta JA}$	Junction-to-Ambient, typical socket mount	—	—	80	
Wt	Weight	—	2.0 (0.07)	—	g (oz)

Electrical Characteristics @ $T_J = 25^\circ\text{C}$ (unless otherwise specified)

	Parameter	Min.	Typ.	Max.	Units	Conditions
$V_{(BR)CES}$	Collector-to-Emitter Breakdown Voltage	600	—	—	V	$V_{GE} = 0V, I_C = 250\mu A$
$V_{(BR)ECS}$	Emitter-to-Collector Breakdown Voltage ④	20	—	—	V	$V_{GE} = 0V, I_C = 1.0A$
$\Delta V_{(BR)CES}/\Delta T_J$	Temp. Coeff. of Breakdown Voltage	—	0.72	—	V/°C	$V_{GE} = 0V, I_C = 1.0mA$
$V_{CE(on)}$	Collector-to-Emitter Saturation Voltage	—	2.0	2.8	V	$I_C = 9.0A, V_{GE} = 15V$
		—	2.6	—		$I_C = 16A$
		—	2.3	—		$I_C = 9.0A, T_J = 150^\circ\text{C}$
$V_{GE(th)}$	Gate Threshold Voltage	3.0	—	5.5		$V_{CE} = V_{GE}, I_C = 250\mu A$
$\Delta V_{GE(th)}/\Delta T_J$	Temp. Coeff. of Threshold Voltage	—	-11	—	mV/°C	$V_{CE} = V_{GE}, I_C = 250\mu A$
g_{fe}	Forward Transconductance ⑤	2.9	5.1	—	S	$V_{CE} = 100V, I_C = 9.0A$
I_{CES}	Zero Gate Voltage Collector Current	—	—	250	μA	$V_{GE} = 0V, V_{CE} = 600V$
		—	—	1000		$V_{GE} = 0V, V_{CE} = 600V, T_J = 150^\circ\text{C}$
I_{GES}	Gate-to-Emitter Leakage Current	—	—	± 100	nA	$V_{GE} = \pm 20V$

Switching Characteristics @ $T_J = 25^\circ\text{C}$ (unless otherwise specified)

	Parameter	Min.	Typ.	Max.	Units	Conditions	
Q_g	Total Gate Charge (turn-on)	—	16	21	nC	$I_C = 9.0A$	
Q_{ge}	Gate - Emitter Charge (turn-on)	—	2.4	3.4		$V_{CC} = 400V$	
Q_{gc}	Gate - Collector Charge (turn-on)	—	7.8	10		$V_{GE} = 15V$	
$t_{d(on)}$	Turn-On Delay Time	—	24	—	ns	$T_J = 25^\circ\text{C}$	
t_r	Rise Time	—	13	—		$I_C = 9.0A, V_{CC} = 480V$	
$t_{d(off)}$	Turn-Off Delay Time	—	160	270		$V_{GE} = 15V, R_G = 50\Omega$	
t_f	Fall Time	—	310	600		Energy losses include "tail"	
E_{on}	Turn-On Switching Loss	—	0.18	—		mJ	See Fig. 9, 10, 11, 14
E_{off}	Turn-Off Switching Loss	—	0.90	—			
E_{ts}	Total Switching Loss	—	1.08	2.0	ns	$T_J = 150^\circ\text{C},$ $I_C = 9.0A, V_{CC} = 480V$ $V_{GE} = 15V, R_G = 50\Omega$ Energy losses include "tail"	
$t_{d(on)}$	Turn-On Delay Time	—	25	—			
t_r	Rise Time	—	18	—			
$t_{d(off)}$	Turn-Off Delay Time	—	210	—			
t_f	Fall Time	—	600	—			
E_{ts}	Total Switching Loss	—	1.65	—	mJ	See Fig. 10, 14	
L_E	Internal Emitter Inductance	—	7.5	—	nH	Measured 5mm from package	
C_{ies}	Input Capacitance	—	340	—	pF	$V_{GE} = 0V$	
C_{oes}	Output Capacitance	—	63	—		$V_{CC} = 30V$	
C_{res}	Reverse Transfer Capacitance	—	5.9	—		$f = 1.0MHz$	

Notes:

- ① Repetitive rating; $V_{GE}=20V$, pulse width limited by max. junction temperature. (See fig. 13b)
- ② $V_{CC}=80\%(V_{CES}), V_{GE}=20V, L=10\mu H, R_G=50\Omega,$ (See fig. 13a)
- ③ Repetitive rating; pulse width limited by maximum junction temperature.
- ④ Pulse width $\leq 80\mu s$; duty factor $\leq 0.1\%$.
- ⑤ Pulse width $5.0\mu s$, single shot.

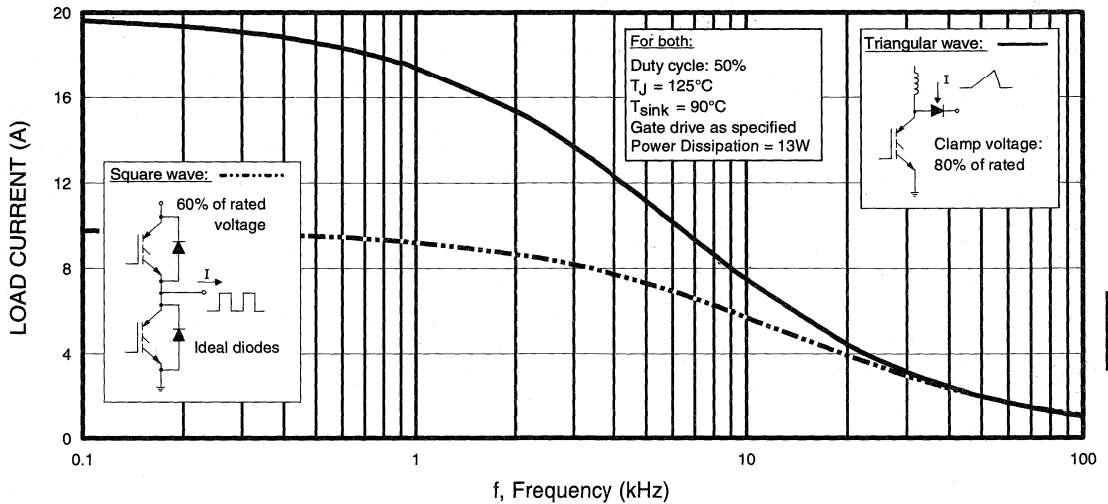


Fig. 1 - Typical Load Current vs. Frequency
 (For square wave, $I = I_{RMS}$ of fundamental; for triangular wave, $I = I_{PK}$)

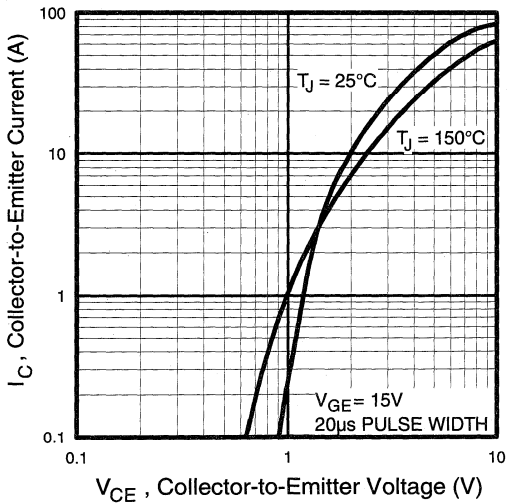


Fig. 2 - Typical Output Characteristics

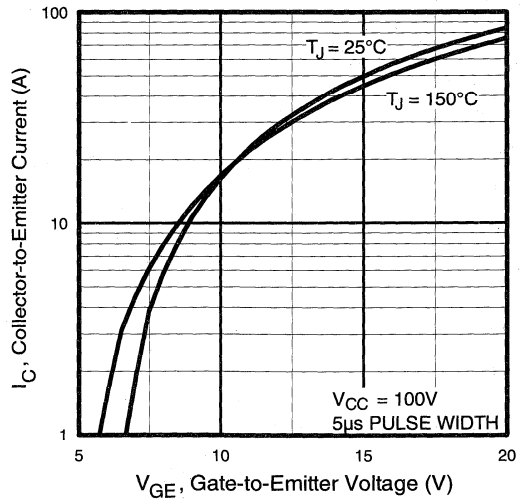


Fig. 3 - Typical Transfer Characteristics

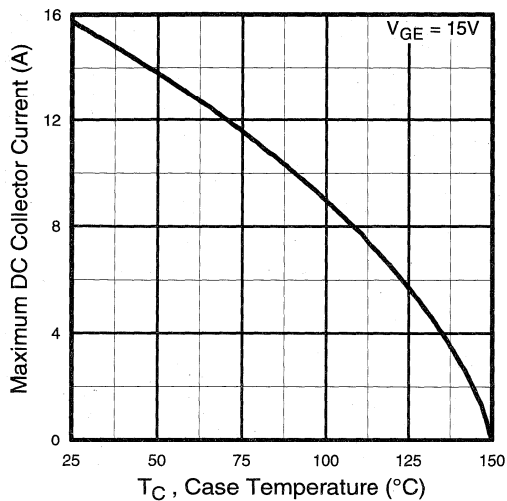


Fig. 4 - Maximum Collector Current vs. Case Temperature

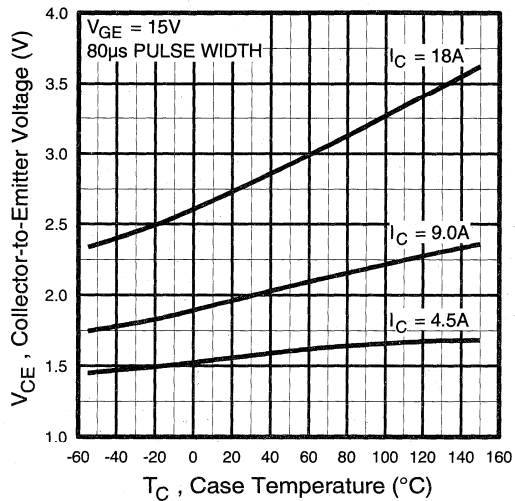


Fig. 5 - Collector-to-Emitter Voltage vs. Case Temperature

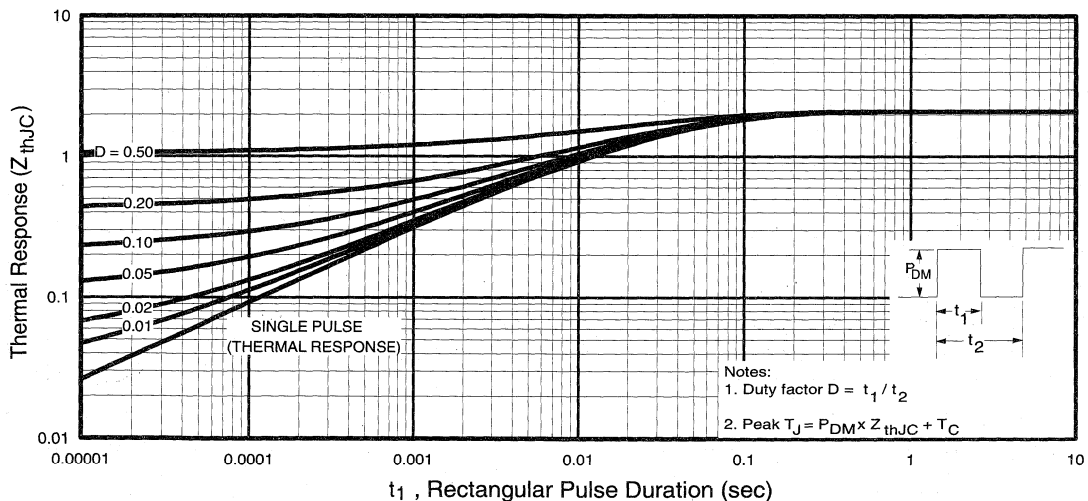


Fig. 6 - Maximum Effective Transient Thermal Impedance, Junction-to-Case

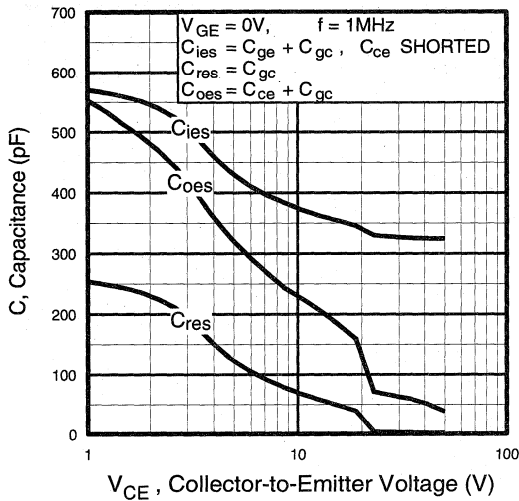


Fig. 7 - Typical Capacitance vs. Collector-to-Emitter Voltage

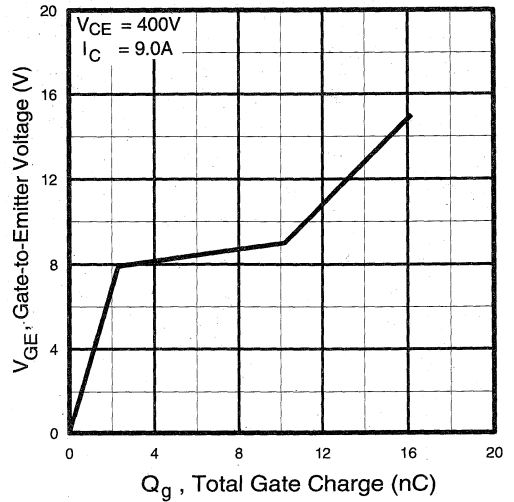


Fig. 8 - Typical Gate Charge vs. Gate-to-Emitter Voltage

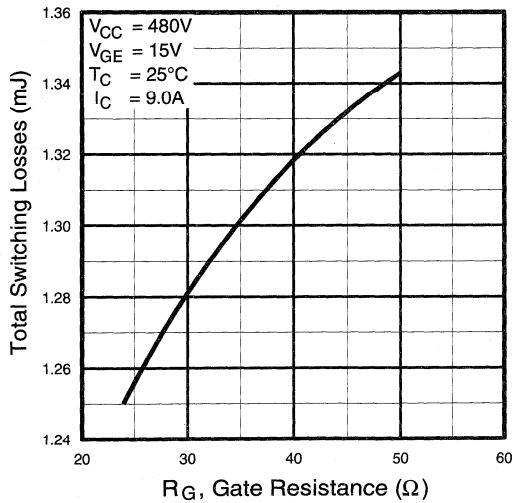


Fig. 9 - Typical Switching Losses vs. Gate Resistance

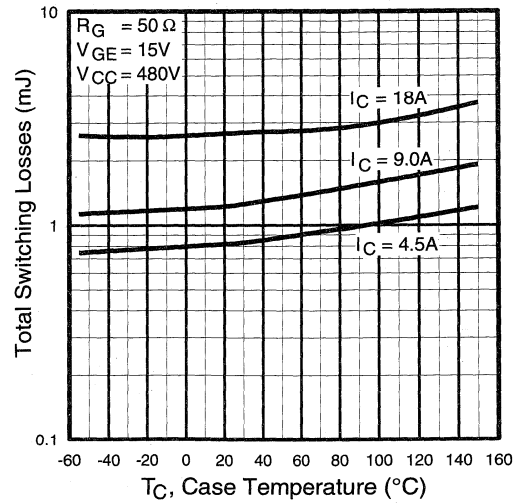


Fig. 10 - Typical Switching Losses vs. Case Temperature

Power Conversion First Devices

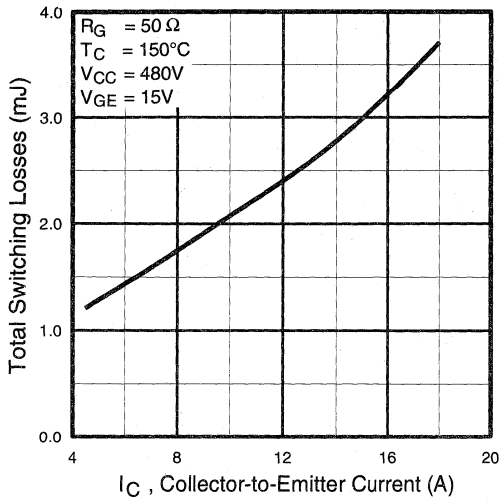


Fig. 11 - Typical Switching Losses vs. Collector-to-Emitter Current

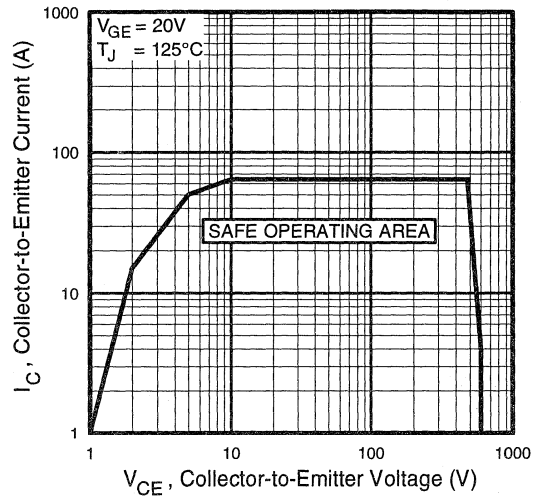


Fig. 12 - Turn-Off SOA

Refer to Section D for the following:

Appendix C: Section D - page D-5

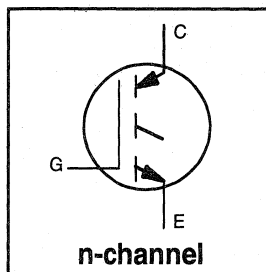
- Fig. 13a - Clamped Inductive Load Test Circuit
- Fig. 13b - Pulsed Collector Current Test Circuit
- Fig. 14a - Switching Loss Test Circuit
- Fig. 14b - Switching Loss Waveform

Package Outline 1 - JEDEC Outline TO-220AB

Section D - page D-12

Features

- Switching-loss rating includes all "tail" losses
- Optimized for medium operating frequency (1 to 10kHz) See Fig. 1 for Current vs. Frequency curve



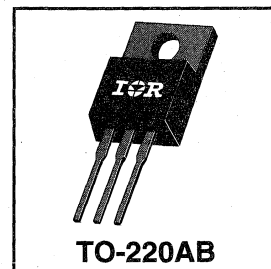
$$V_{CES} = 600V$$

$$V_{CE(sat)} \leq 2.1V$$

$$@ V_{GE} = 15V, I_C = 17A$$

Description

Insulated Gate Bipolar Transistors (IGBTs) from International Rectifier have higher usable current densities than comparable bipolar transistors, while at the same time having simpler gate-drive requirements of the familiar power MOSFET. They provide substantial benefits to a host of high-voltage, high-current applications.



Power Conversion Fast Discrete

Absolute Maximum Ratings

	Parameter	Max.	Units
V_{CES}	Collector-to-Emitter Voltage	600	V
$I_C @ T_C = 25^\circ C$	Continuous Collector Current	31	A
$I_C @ T_C = 100^\circ C$	Continuous Collector Current	17	
I_{CM}	Pulsed Collector Current ①	120	
I_{LM}	Clamped Inductive Load Current ②	120	
V_{GE}	Gate-to-Emitter Voltage	± 20	V
E_{ARV}	Reverse Voltage Avalanche Energy ③	10	mJ
$P_D @ T_C = 25^\circ C$	Maximum Power Dissipation	100	W
$P_D @ T_C = 100^\circ C$	Maximum Power Dissipation	42	
T_J	Operating Junction and	-55 to +150	°C
T_{STG}	Storage Temperature Range		
	Soldering Temperature, for 10 sec.	300 (0.063 in. (1.6mm) from case)	
	Mounting torque, 6-32 or M3 screw.	10 lbf•in (1.1N•m)	

Thermal Resistance

	Parameter	Min.	Typ.	Max.	Units
$R_{\theta JC}$	Junction-to-Case	—	—	1.2	°C/W
$R_{\theta CS}$	Case-to-Sink, flat, greased surface	—	0.50	—	
$R_{\theta JA}$	Junction-to-Ambient, typical socket mount	—	—	80	
Wt	Weight	—	2.0 (0.07)	—	g (oz)

Electrical Characteristics @ $T_J = 25^\circ\text{C}$ (unless otherwise specified)

	Parameter	Min.	Typ.	Max.	Units	Conditions
$V_{(BR)CES}$	Collector-to-Emitter Breakdown Voltage	600	—	—	V	$V_{GE} = 0V, I_C = 250\mu A$
$V_{(BR)ECS}$	Emitter-to-Collector Breakdown Voltage ④	20	—	—	V	$V_{GE} = 0V, I_C = 1.0A$
$\Delta V_{(BR)CES}/\Delta T_J$	Temperature Coeff. of Breakdown Voltage	—	0.69	—	V/ $^\circ\text{C}$	$V_{GE} = 0V, I_C = 1.0mA$
$V_{CE(on)}$	Collector-to-Emitter Saturation Voltage	—	1.8	2.1	V	$I_C = 17A, V_{GE} = 15V$ See Fig. 2, 5
		—	2.4	—		
		—	2.2	—		
$V_{GE(th)}$	Gate Threshold Voltage	3.0	—	5.5		$I_C = 17A, T_J = 150^\circ\text{C}$ $V_{CE} = V_{GE}, I_C = 250\mu A$
$\Delta V_{GE(th)}/\Delta T_J$	Temperature Coeff. of Threshold Voltage	—	-11	—	mV/ $^\circ\text{C}$	$V_{CE} = V_{GE}, I_C = 250\mu A$
g_{fe}	Forward Transconductance ⑤	6.1	10	—	S	$V_{CE} = 100V, I_C = 17A$
I_{CES}	Zero Gate Voltage Collector Current	—	—	250	μA	$V_{GE} = 0V, V_{CE} = 600V$
		—	—	1000		
I_{GES}	Gate-to-Emitter Leakage Current	—	—	± 100	nA	$V_{GE} = \pm 20V$

Switching Characteristics @ $T_J = 25^\circ\text{C}$ (unless otherwise specified)

	Parameter	Min.	Typ.	Max.	Units	Conditions
Q_g	Total Gate Charge (turn-on)	—	27	30	nC	$I_C = 17A$ $V_{CC} = 400V$ See Fig. 8 $V_{GE} = 15V$
Q_{ge}	Gate - Emitter Charge (turn-on)	—	4.1	5.9		
Q_{gc}	Gate - Collector Charge (turn-on)	—	12	15		
$t_{d(on)}$	Turn-On Delay Time	—	25	—	ns	$T_J = 25^\circ\text{C}$ $I_C = 17A, V_{CC} = 480V$ $V_{GE} = 15V, R_G = 23\Omega$ Energy losses include "tail"
t_r	Rise Time	—	21	—		
$t_{d(off)}$	Turn-Off Delay Time	—	210	320		
t_f	Fall Time	—	300	500		
E_{on}	Turn-On Switching Loss	—	0.30	—		
E_{off}	Turn-Off Switching Loss	—	2.1	—	mJ	See Fig. 9, 10, 11, 14
E_{ts}	Total Switching Loss	—	2.4	3.5		
$t_{d(on)}$	Turn-On Delay Time	—	25	—	ns	$T_J = 150^\circ\text{C}$, $I_C = 17A, V_{CC} = 480V$ $V_{GE} = 15V, R_G = 23\Omega$ Energy losses include "tail"
t_r	Rise Time	—	21	—		
$t_{d(off)}$	Turn-Off Delay Time	—	290	—		
t_f	Fall Time	—	590	—		
E_{ts}	Total Switching Loss	—	3.6	—		
L_E	Internal Emitter Inductance	—	7.5	—	nH	Measured 5mm from package
C_{ies}	Input Capacitance	—	670	—	pF	$V_{GE} = 0V$ $V_{CC} = 30V$ See Fig. 7 $f = 1.0MHz$
C_{oes}	Output Capacitance	—	100	—		
C_{res}	Reverse Transfer Capacitance	—	10	—		

Notes:

- ① Repetitive rating; $V_{GE}=20V$, pulse width limited by max. junction temperature. (See fig. 13b)
- ② $V_{CC}=80\%(V_{CES}), V_{GE}=20V, L=10\mu H, R_G=23\Omega$, (See fig. 13a)
- ③ Repetitive rating; pulse width limited by maximum junction temperature.
- ④ Pulse width $\leq 80\mu s$; duty factor $\leq 0.1\%$.
- ⑤ Pulse width $5.0\mu s$, single shot.

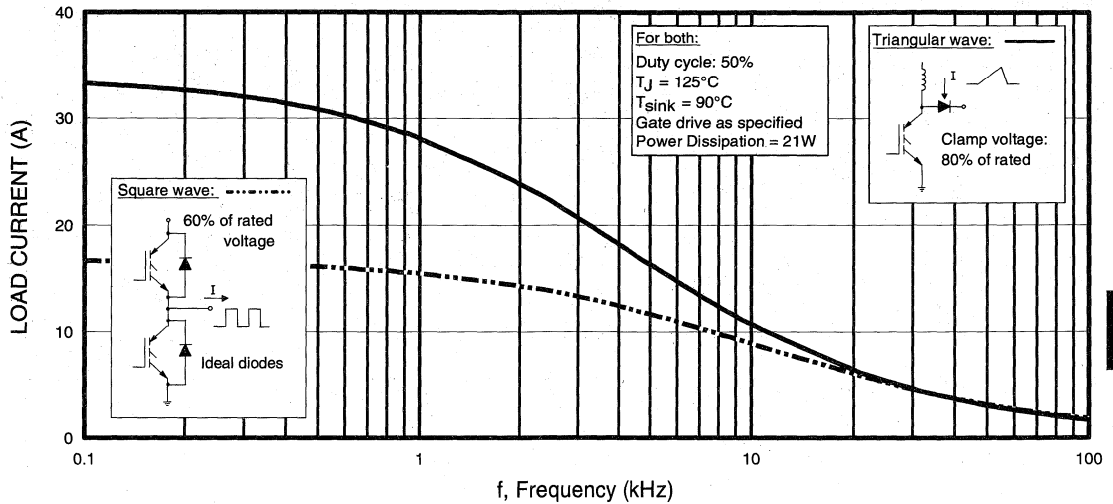


Fig. 1 - Typical Load Current vs. Frequency
 (For square wave, $I = I_{\text{RMS}}$ of fundamental; for triangular wave, $I = I_{\text{PK}}$)

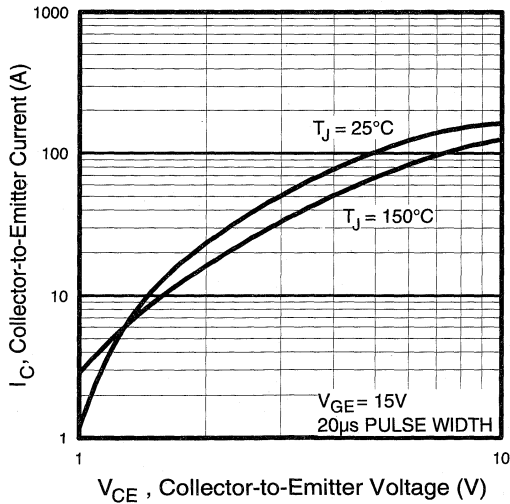


Fig. 2 - Typical Output Characteristics

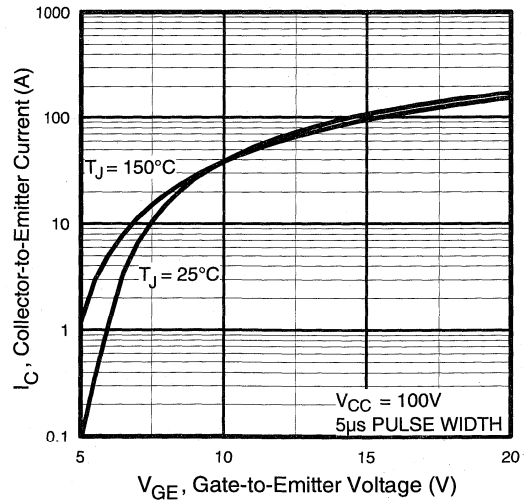


Fig. 3 - Typical Transfer Characteristics

Power
 Conversion,
 Fast
 Discretes

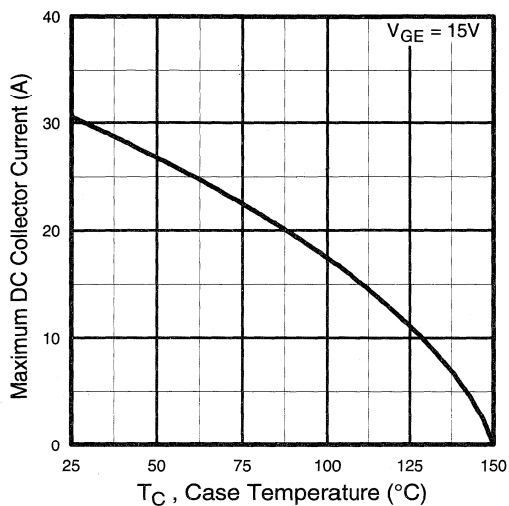


Fig. 4 - Maximum Collector Current vs. Case Temperature

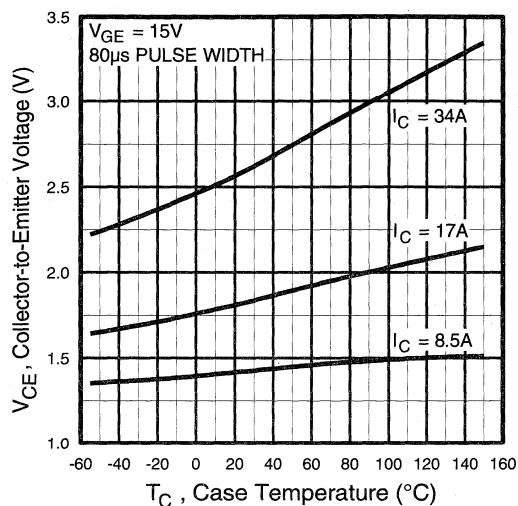


Fig. 5 - Collector-to-Emitter Voltage vs. Case Temperature

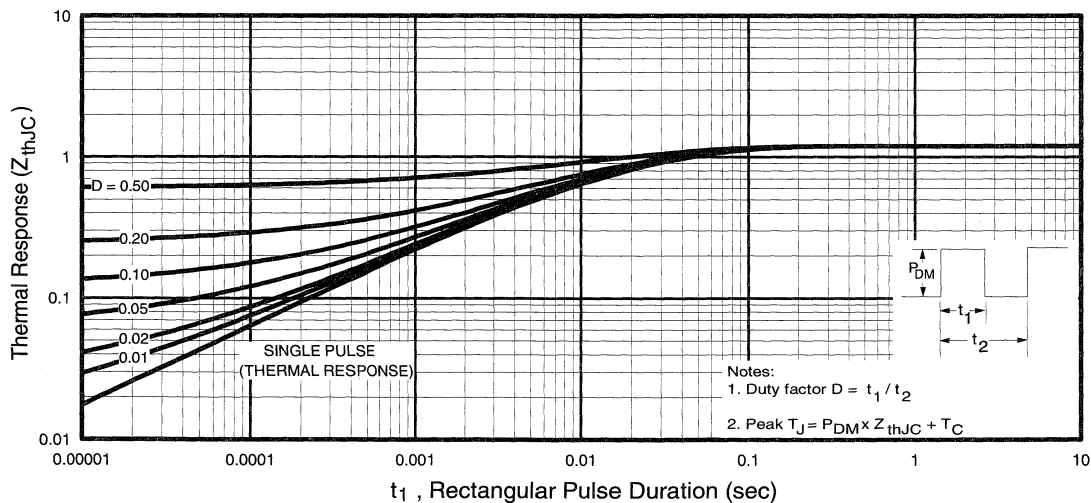


Fig. 6 - Maximum Effective Transient Thermal Impedance, Junction-to-Case

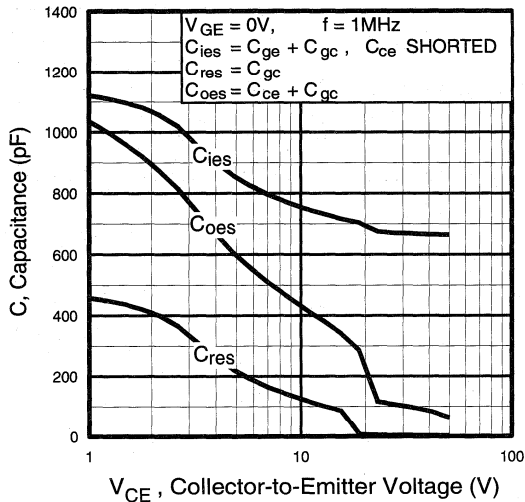


Fig. 7 - Typical Capacitance vs. Collector-to-Emitter Voltage

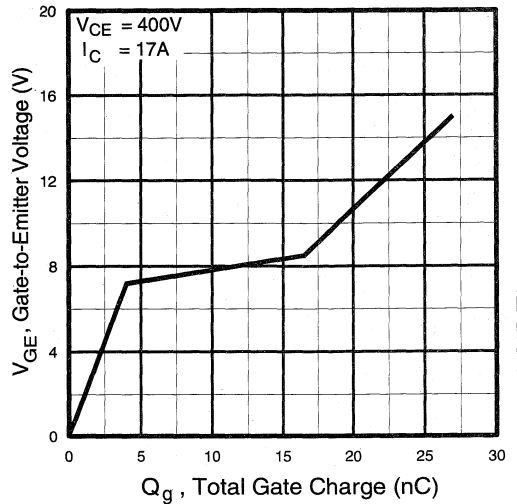


Fig. 8 - Typical Gate Charge vs. Gate-to-Emitter Voltage

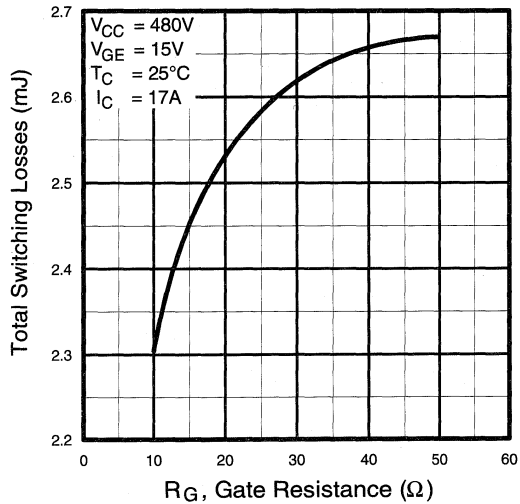


Fig. 9 - Typical Switching Losses vs. Gate Resistance

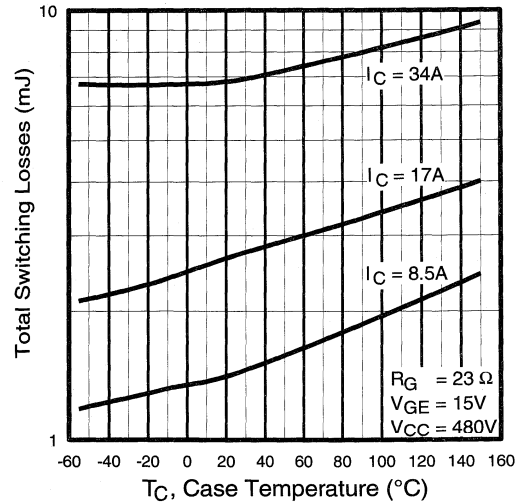


Fig. 10 - Typical Switching Losses vs. Case Temperature

Power
Conversion
Fast
Discrete

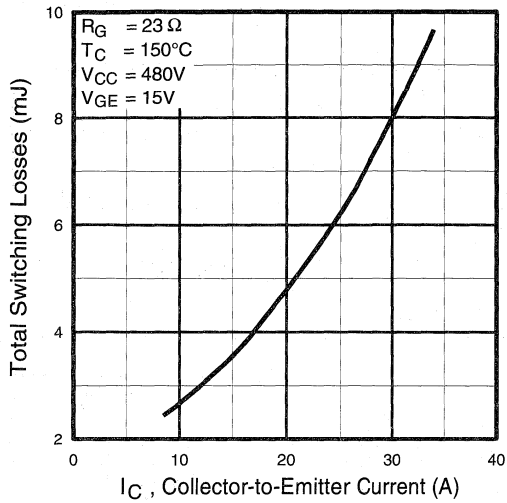


Fig. 11 - Typical Switching Losses vs. Collector-to-Emitter Current

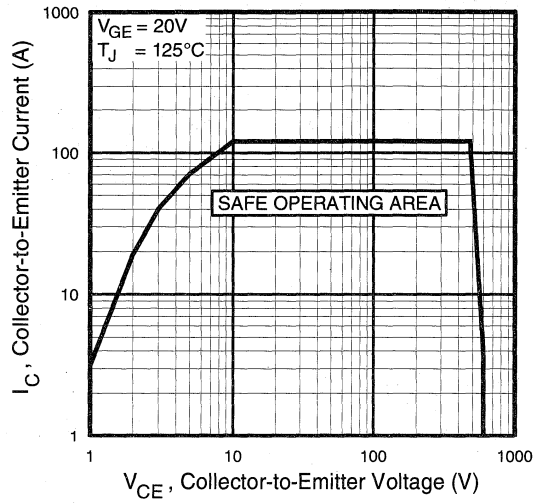


Fig. 12 - Turn-Off SOA

Refer to Section D for the following:

Appendix C: Section D - page D-5

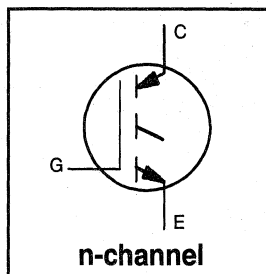
- Fig. 13a - Clamped Inductive Load Test Circuit
- Fig. 13b - Pulsed Collector Current Test Circuit
- Fig. 14a - Switching Loss Test Circuit
- Fig. 14b - Switching Loss Waveform

Package Outline 1 - JEDEC Outline TO-220AB

Section D - page D-12

Features

- Switching-loss rating includes all "tail" losses
- Optimized for medium operating frequency (1 to 10kHz) See Fig. 1 for Current vs. Frequency curve



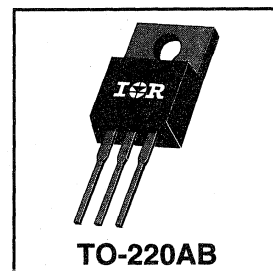
$$V_{CES} = 600V$$

$$V_{CE(sat)} \leq 2.0V$$

$$@ V_{GE} = 15V, I_C = 27A$$

Description

Insulated Gate Bipolar Transistors (IGBTs) from International Rectifier have higher usable current densities than comparable bipolar transistors, while at the same time having simpler gate-drive requirements of the familiar power MOSFET. They provide substantial benefits to a host of high-voltage, high-current applications.



Absolute Maximum Ratings

	Parameter	Max.	Units
V_{CES}	Collector-to-Emitter Voltage	600	V
$I_C @ T_C = 25^\circ C$	Continuous Collector Current	49	A
$I_C @ T_C = 100^\circ C$	Continuous Collector Current	27	
I_{CM}	Pulsed Collector Current ①	200	
I_{LM}	Clamped Inductive Load Current ②	200	
V_{GE}	Gate-to-Emitter Voltage	± 20	V
E_{ARV}	Reverse Voltage Avalanche Energy ③	15	mJ
$P_D @ T_C = 25^\circ C$	Maximum Power Dissipation	160	W
$P_D @ T_C = 100^\circ C$	Maximum Power Dissipation	65	
T_J	Operating Junction and	-55 to +150	$^\circ C$
T_{STG}	Storage Temperature Range		
	Soldering Temperature, for 10 sec.	300 (0.063 in. (1.6mm) from case)	
	Mounting torque, 6-32 or M3 screw.	10 lbf•in (1.1N•m)	

Thermal Resistance

	Parameter	Min.	Typ.	Max.	Units
$R_{\theta JC}$	Junction-to-Case	—	—	0.77	$^\circ C/W$
$R_{\theta CS}$	Case-to-Sink, flat, greased surface	—	0.50	—	
$R_{\theta JA}$	Junction-to-Ambient, typical socket mount	—	—	80	
Wt	Weight	—	2.0 (0.07)	—	g (oz)

Electrical Characteristics @ $T_J = 25^\circ\text{C}$ (unless otherwise specified)

	Parameter	Min.	Typ.	Max.	Units	Conditions
$V_{(BR)CES}$	Collector-to-Emitter Breakdown Voltage	600	—	—	V	$V_{GE} = 0V, I_C = 250\mu A$
$V_{(BR)ECS}$	Emitter-to-Collector Breakdown Voltage ②	20	—	—	V	$V_{GE} = 0V, I_C = 1.0A$
$\Delta V_{(BR)CES}/\Delta T_J$	Temp. Coeff. of Breakdown Voltage	—	0.70	—	V/ $^\circ\text{C}$	$V_{GE} = 0V, I_C = 1.0mA$
$V_{CE(on)}$	Collector-to-Emitter Saturation Voltage	—	1.7	2.0	V	$I_C = 27A$ $I_C = 49A$ $I_C = 27A, T_J = 150^\circ\text{C}$ $V_{GE} = 15V$ See Fig. 2, 5
		—	2.2	—		
		—	1.9	—		
$V_{GE(th)}$	Gate Threshold Voltage	3.0	—	5.5		$V_{CE} = V_{GE}, I_C = 250\mu A$
$\Delta V_{GE(th)}/\Delta T_J$	Temp. Coeff. of Threshold Voltage	—	-12	—	mV/ $^\circ\text{C}$	$V_{CE} = V_{GE}, I_C = 250\mu A$
g_{fe}	Forward Transconductance ③	9.2	12	—	S	$V_{CE} = 100V, I_C = 27A$
I_{CES}	Zero Gate Voltage Collector Current	—	—	250	μA	$V_{GE} = 0V, V_{CE} = 600V$ $V_{GE} = 0V, V_{CE} = 600V, T_J = 150^\circ\text{C}$
		—	—	1000		
I_{GES}	Gate-to-Emitter Leakage Current	—	—	± 100	nA	$V_{GE} = \pm 20V$

Switching Characteristics @ $T_J = 25^\circ\text{C}$ (unless otherwise specified)

	Parameter	Min.	Typ.	Max.	Units	Conditions
Q_g	Total Gate Charge (turn-on)	—	59	80	nC	$I_C = 27A$ $V_{CC} = 400V$ $V_{GE} = 15V$ See Fig. 8
Q_{ge}	Gate - Emitter Charge (turn-on)	—	8.6	10		
Q_{gc}	Gate - Collector Charge (turn-on)	—	25	42		
$t_{d(on)}$	Turn-On Delay Time	—	26	—	ns	$T_J = 25^\circ\text{C}$ $I_C = 27A, V_{CC} = 480V$ $V_{GE} = 15V, R_G = 10\Omega$ Energy losses include "tail"
t_r	Rise Time	—	37	—		
$t_{d(off)}$	Turn-Off Delay Time	—	240	410		
t_f	Fall Time	—	230	420		
E_{on}	Turn-On Switching Loss	—	0.65	—	mJ	See Fig. 9, 10, 11, 14
E_{off}	Turn-Off Switching Loss	—	3.0	—		
E_{ts}	Total Switching Loss	—	3.65	6.0		
$t_{d(on)}$	Turn-On Delay Time	—	28	—	ns	$T_J = 150^\circ\text{C}$, $I_C = 27A, V_{CC} = 480V$ $V_{GE} = 15V, R_G = 10\Omega$ Energy losses include "tail"
t_r	Rise Time	—	37	—		
$t_{d(off)}$	Turn-Off Delay Time	—	380	—		
t_f	Fall Time	—	460	—		
E_{ts}	Total Switching Loss	—	6.0	—	mJ	See Fig. 10, 14
L_E	Internal Emitter Inductance	—	7.5	—	nH	Measured 5mm from package
C_{ies}	Input Capacitance	—	1500	—	pF	$V_{GE} = 0V$ $V_{CC} = 30V$ $f = 1.0MHz$ See Fig. 7
C_{oes}	Output Capacitance	—	190	—		
C_{res}	Reverse Transfer Capacitance	—	20	—		

Notes:

- ① Repetitive rating; $V_{GE} = 20V$, pulse width limited by max. junction temperature. (See fig. 13b)
- ② $V_{CC} = 80\%(V_{CES}), V_{GE} = 20V, L = 10\mu H, R_G = 10\Omega$, (See fig. 13a)
- ③ Repetitive rating; pulse width limited by maximum junction temperature.
- ④ Pulse width $\leq 80\mu s$; duty factor $\leq 0.1\%$.
- ⑤ Pulse width $5.0\mu s$, single shot.

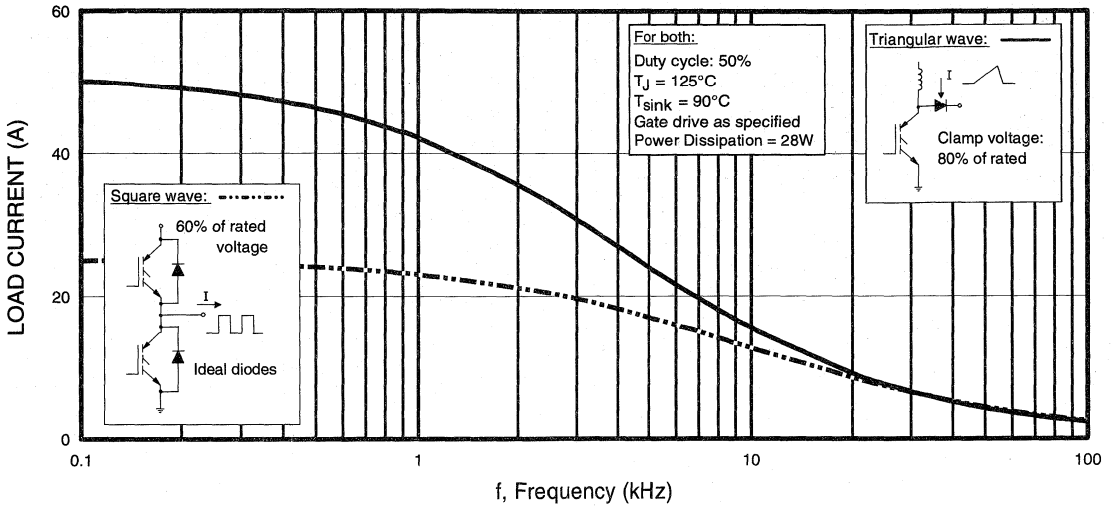


Fig. 1 - Typical Load Current vs. Frequency
 (For square wave, $I = I_{RMS}$ of fundamental; for triangular wave, $I = I_{PK}$)

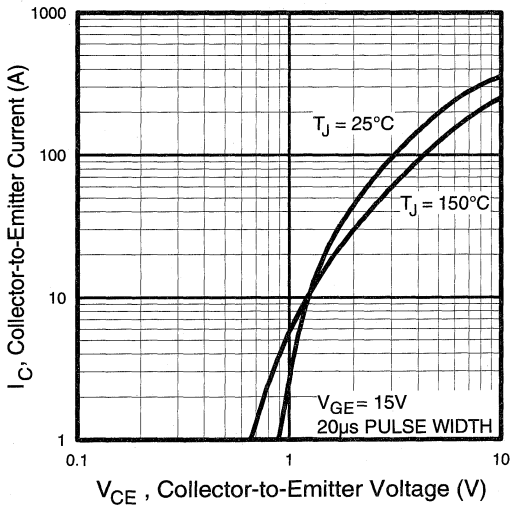


Fig. 2 - Typical Output Characteristics

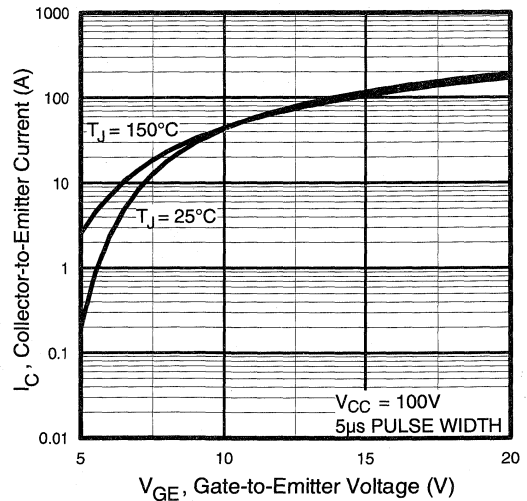


Fig. 3 - Typical Transfer Characteristics

Power
Conversion
Fast
Discrete

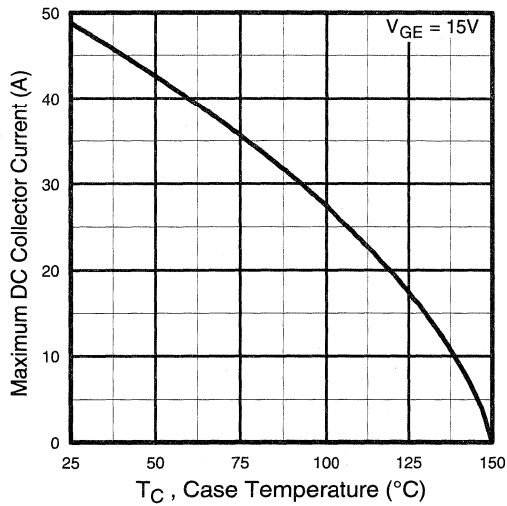


Fig. 4 - Maximum Collector Current vs. Case Temperature

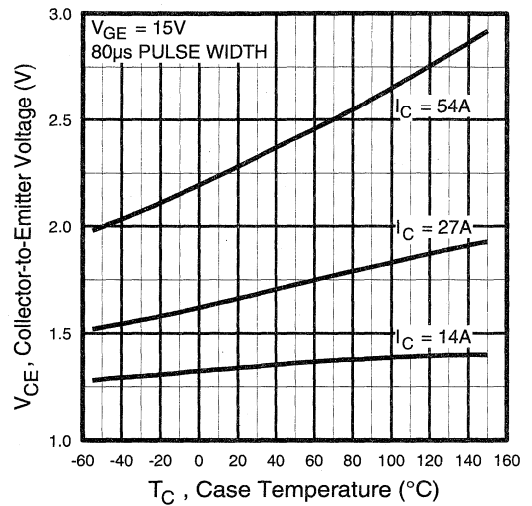


Fig. 5 - Collector-to-Emitter Voltage vs. Case Temperature

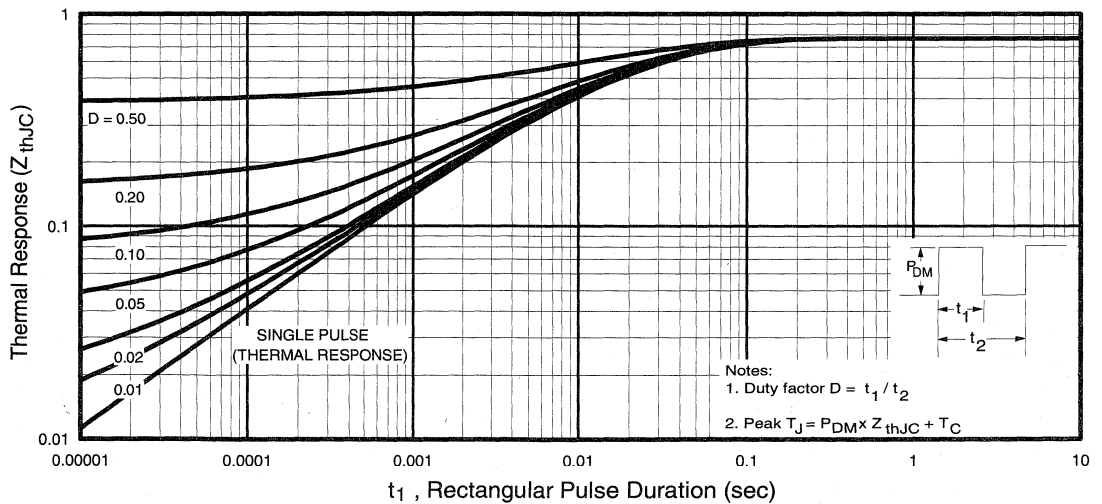


Fig. 6 - Maximum Effective Transient Thermal Impedance, Junction-to-Case

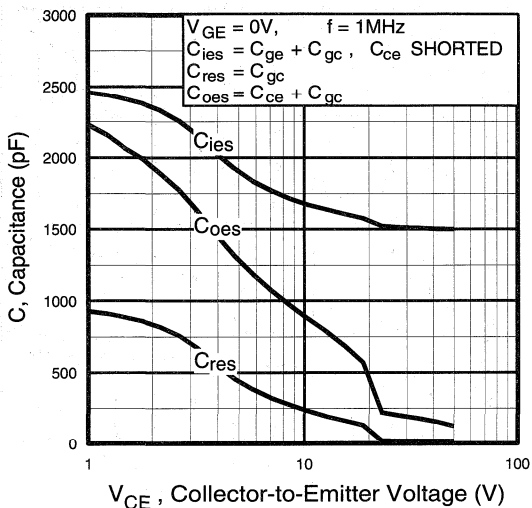


Fig. 7 - Typical Capacitance vs. Collector-to-Emitter Voltage

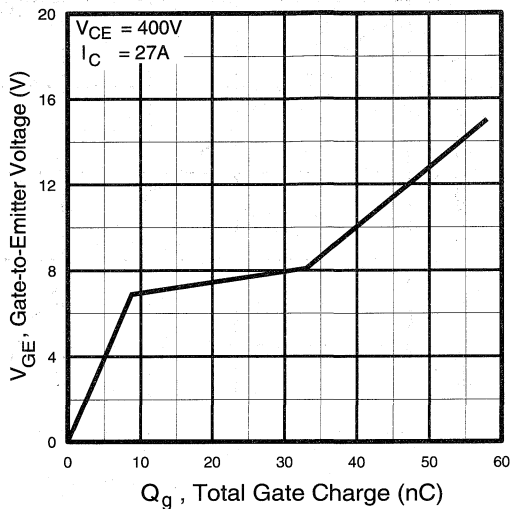


Fig. 8 - Typical Gate Charge vs. Gate-to-Emitter Voltage

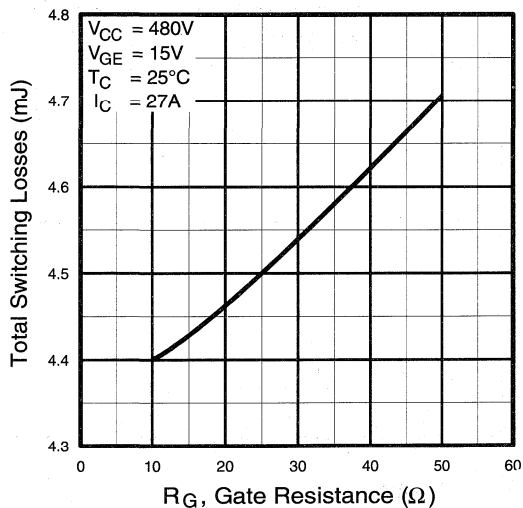


Fig. 9 - Typical Switching Losses vs. Gate Resistance

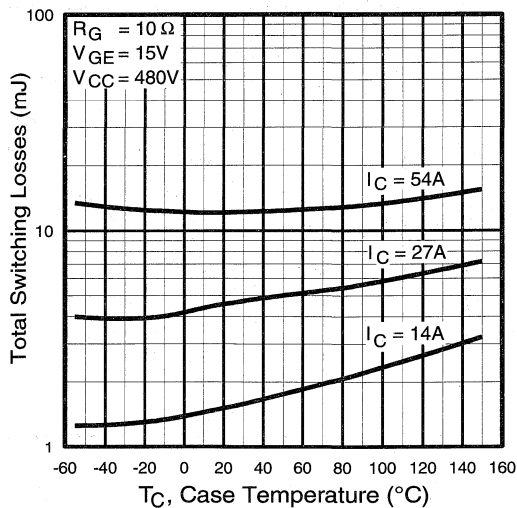


Fig. 10 - Typical Switching Losses vs. Case Temperature

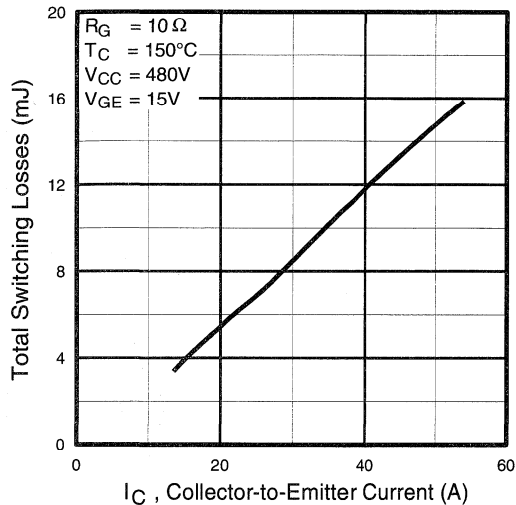


Fig. 11 - Typical Switching Losses vs. Collector-to-Emitter Current

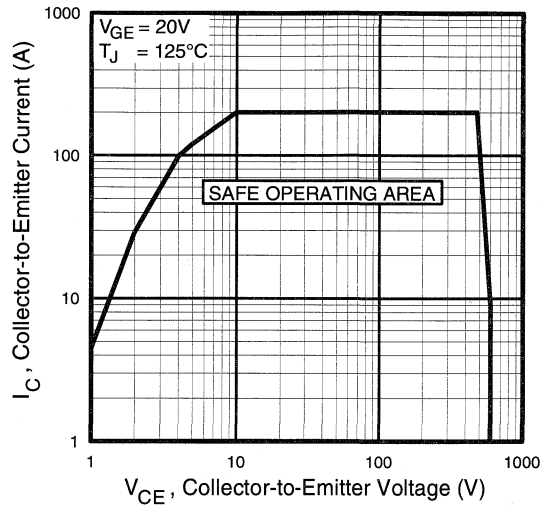


Fig. 12 - Turn-Off SOA

Refer to Section D for the following:

Appendix C: Section D - page D-5

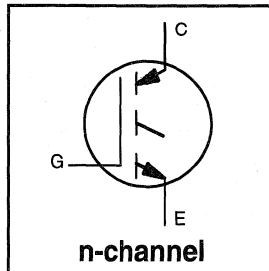
- Fig. 13a - Clamped Inductive Load Test Circuit
- Fig. 13b - Pulsed Collector Current Test Circuit
- Fig. 14a - Switching Loss Test Circuit
- Fig. 14b - Switching Loss Waveform

Package Outline 1 - JEDEC Outline TO-220AB

Section D - page D-12

Features

- Switching-loss rating includes all "tail" losses
- Optimized for medium operating frequency (1 to 10kHz) See Fig. 1 for Current vs. Frequency curve



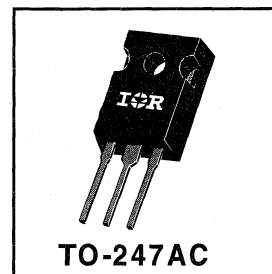
$$V_{CES} = 600V$$

$$V_{CE(sat)} \leq 2.8V$$

$$@V_{GE} = 15V, I_C = 9.0A$$

Description

Insulated Gate Bipolar Transistors (IGBTs) from International Rectifier have higher usable current densities than comparable bipolar transistors, while at the same time having simpler gate-drive requirements of the familiar power MOSFET. They provide substantial benefits to a host of high-voltage, high-current applications.



Absolute Maximum Ratings

	Parameter	Max.	Units
V_{CES}	Collector-to-Emitter Voltage	600	V
$I_C @ T_C = 25^\circ C$	Continuous Collector Current	16	A
$I_C @ T_C = 100^\circ C$	Continuous Collector Current	9.0	
I_{CM}	Pulsed Collector Current ①	64	
I_{LM}	Clamped Inductive Load Current ②	64	
V_{GE}	Gate-to-Emitter Voltage	± 20	V
E_{ARV}	Reverse Voltage Avalanche Energy ③	5.0	mJ
$P_D @ T_C = 25^\circ C$	Maximum Power Dissipation	60	W
$P_D @ T_C = 100^\circ C$	Maximum Power Dissipation	24	
T_J	Operating Junction and	-55 to +150	°C
T_{STG}	Storage Temperature Range		
	Soldering Temperature, for 10 sec.	300 (0.063 in. (1.6mm) from case)	
	Mounting torque, 6-32 or M3 screw.	10 lbf•in (1.1N•m)	

Thermal Resistance

	Parameter	Min.	Typ.	Max.	Units
$R_{\theta JC}$	Junction-to-Case	—	—	2.1	°C/W
$R_{\theta CS}$	Case-to-Sink, flat, greased surface	—	0.24	—	
$R_{\theta JA}$	Junction-to-Ambient, typical socket mount	—	—	40	
Wt	Weight	—	6 (0.21)	—	g (oz)

Electrical Characteristics @ $T_J = 25^\circ\text{C}$ (unless otherwise specified)

	Parameter	Min.	Typ.	Max.	Units	Conditions
$V_{(BR)CES}$	Collector-to-Emitter Breakdown Voltage	600	—	—	V	$V_{GE} = 0V, I_C = 250\mu A$
$V_{(BR)ECS}$	Emitter-to-Collector Breakdown Voltage ①	20	—	—	V	$V_{GE} = 0V, I_C = 1.0A$
$\Delta V_{(BR)CES}/\Delta T_J$	Temperature Coeff. of Breakdown Voltage	—	0.72	—	$V/^\circ\text{C}$	$V_{GE} = 0V, I_C = 1.0mA$
$V_{CE(on)}$	Collector-to-Emitter Saturation Voltage	—	2.0	2.8	V	$I_C = 9.0A$ $I_C = 16A$ $I_C = 9.0A, T_J = 150^\circ\text{C}$ $V_{CE} = V_{GE}, I_C = 250\mu A$
		—	2.6	—		
		—	2.3	—		
$V_{GE(th)}$	Gate Threshold Voltage	3.0	—	5.5		$V_{CE} = V_{GE}, I_C = 250\mu A$
$\Delta V_{GE(th)}/\Delta T_J$	Temperature Coeff. of Threshold Voltage	—	-11	—	$mV/^\circ\text{C}$	$V_{CE} = V_{GE}, I_C = 250\mu A$
g_{fe}	Forward Transconductance ②	2.9	5.1	—	S	$V_{CE} = 100V, I_C = 9.0A$
I_{CES}	Zero Gate Voltage Collector Current	—	—	250	μA	$V_{GE} = 0V, V_{CE} = 600V$
		—	—	1000		$V_{GE} = 0V, V_{CE} = 600V, T_J = 150^\circ\text{C}$
I_{GES}	Gate-to-Emitter Leakage Current	—	—	± 100	nA	$V_{GE} = \pm 20V$

Switching Characteristics @ $T_J = 25^\circ\text{C}$ (unless otherwise specified)

	Parameter	Min.	Typ.	Max.	Units	Conditions
Q_g	Total Gate Charge (turn-on)	—	16	21	nC	$I_C = 9.0A$ $V_{CC} = 400V$ $V_{GE} = 15V$ See Fig. 8
Q_{ge}	Gate - Emitter Charge (turn-on)	—	2.4	3.4		
Q_{gc}	Gate - Collector Charge (turn-on)	—	7.9	10		
$t_{d(on)}$	Turn-On Delay Time	—	24	—	ns	$T_J = 25^\circ\text{C}$ $I_C = 9.0A, V_{CC} = 480V$ $V_{GE} = 15V, R_G = 50\Omega$ Energy losses include "tail"
t_r	Rise Time	—	13	—		
$t_{d(off)}$	Turn-Off Delay Time	—	160	270		
t_f	Fall Time	—	310	600		
E_{on}	Turn-On Switching Loss	—	0.18	—	mJ	See Fig. 9, 10, 11, 14
E_{off}	Turn-Off Switching Loss	—	0.90	—		
E_{ts}	Total Switching Loss	—	1.08	2.0		
$t_{d(on)}$	Turn-On Delay Time	—	25	—	ns	$T_J = 150^\circ\text{C}$, $I_C = 9.0A, V_{CC} = 480V$ $V_{GE} = 15V, R_G = 50\Omega$ Energy losses include "tail"
t_r	Rise Time	—	18	—		
$t_{d(off)}$	Turn-Off Delay Time	—	210	—		
t_f	Fall Time	—	600	—		
E_{ts}	Total Switching Loss	—	1.65	—	mJ	See Fig. 10, 14
L_E	Internal Emitter Inductance	—	13	—	nH	Measured 5mm from package
C_{ies}	Input Capacitance	—	340	—	pF	$V_{GE} = 0V$ $V_{CC} = 30V$ $f = 1.0MHz$ See Fig. 7
C_{oes}	Output Capacitance	—	63	—		
C_{res}	Reverse Transfer Capacitance	—	5.9	—		

Notes:

- ① Repetitive rating; $V_{GE}=20V$, pulse width limited by max. junction temperature. (See fig. 13b)
- ② $V_{CC}=80\%(V_{CES}), V_{GE}=20V, L=10\mu H, R_G=50\Omega$, (See fig. 13a)
- ③ Repetitive rating; pulse width limited by maximum junction temperature.
- ④ Pulse width $\leq 80\mu s$; duty factor $\leq 0.1\%$.
- ⑤ Pulse width $5.0\mu s$, single shot.

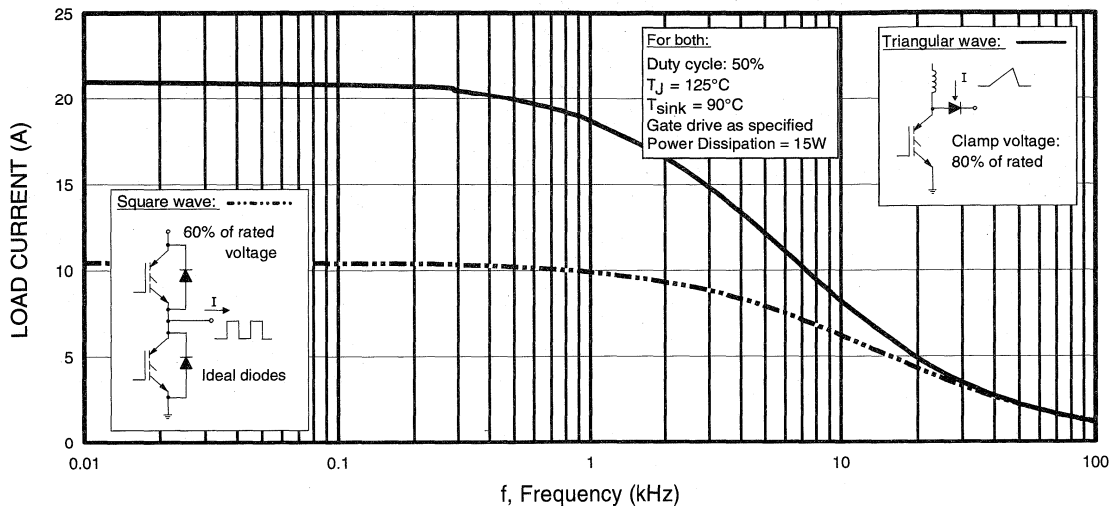


Fig. 1 - Typical Load Current vs. Frequency
 (For square wave, $I = I_{\text{RMS}}$ of fundamental; for triangular wave, $I = I_{\text{PK}}$)

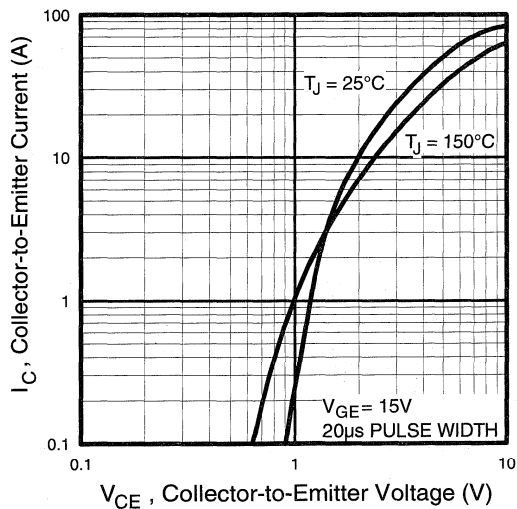


Fig. 2 - Typical Output Characteristics

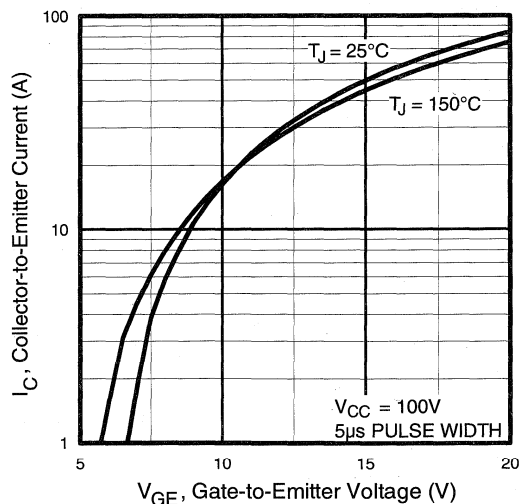


Fig. 3 - Typical Transfer Characteristics

Power
 Conversion
 Fast
 Discretes

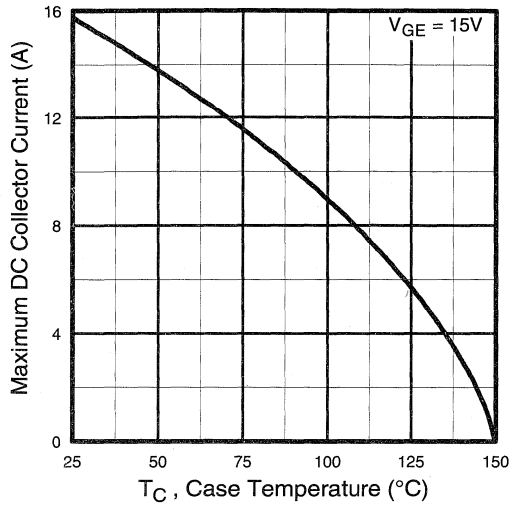


Fig. 4 - Maximum Collector Current vs. Case Temperature

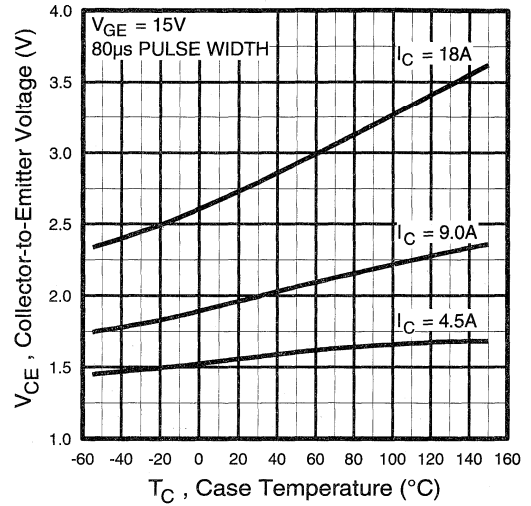


Fig. 5 - Collector-to-Emitter Voltage vs. Case Temperature

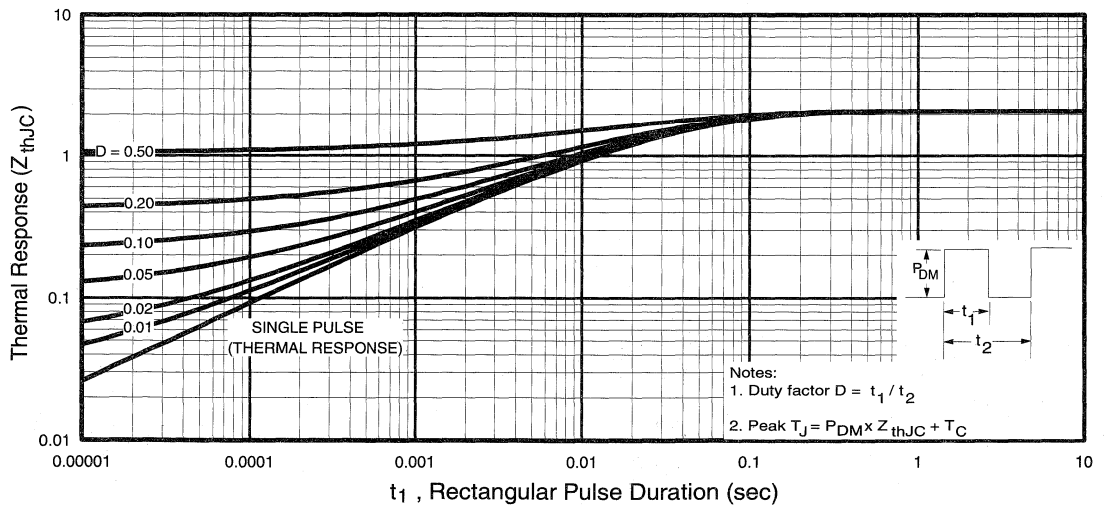


Fig. 6 - Maximum Effective Transient Thermal Impedance, Junction-to-Case

Power
Conversion
Fast
Discretes

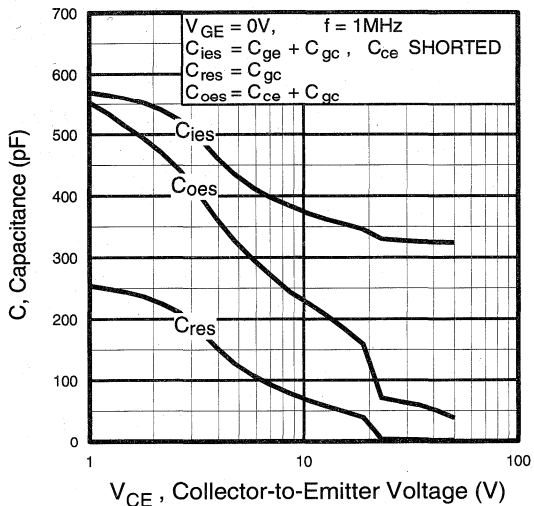


Fig. 7 - Typical Capacitance vs. Collector-to-Emitter Voltage

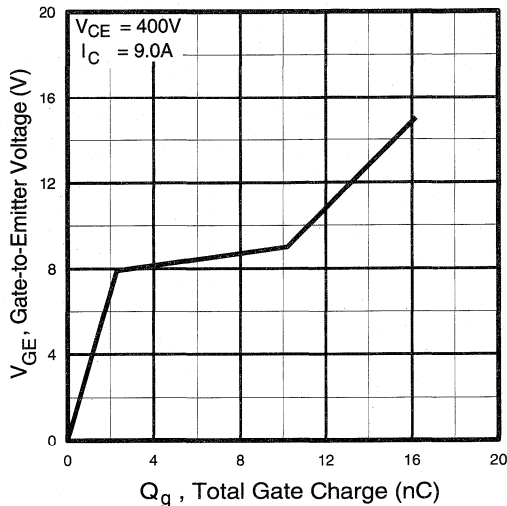


Fig. 8 - Typical Gate Charge vs. Gate-to-Emitter Voltage

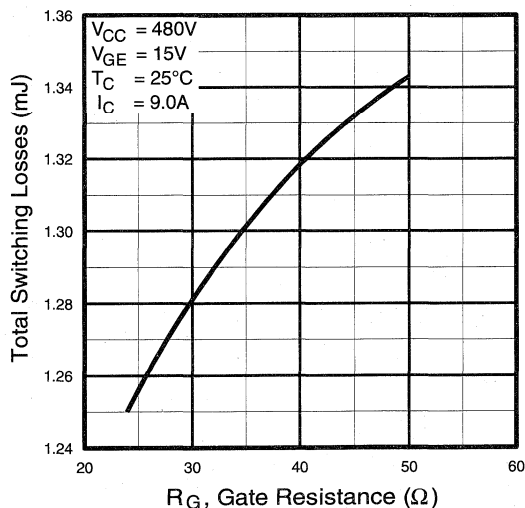


Fig. 9 - Typical Switching Losses vs. Gate Resistance

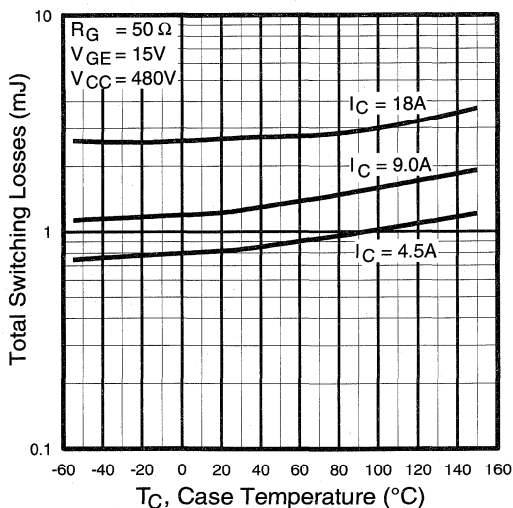


Fig. 10 - Typical Switching Losses vs. Case Temperature

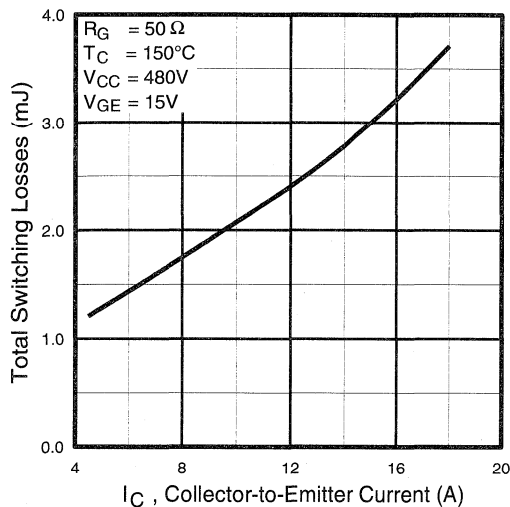


Fig. 11 - Typical Switching Losses vs. Collector-to-Emitter Current

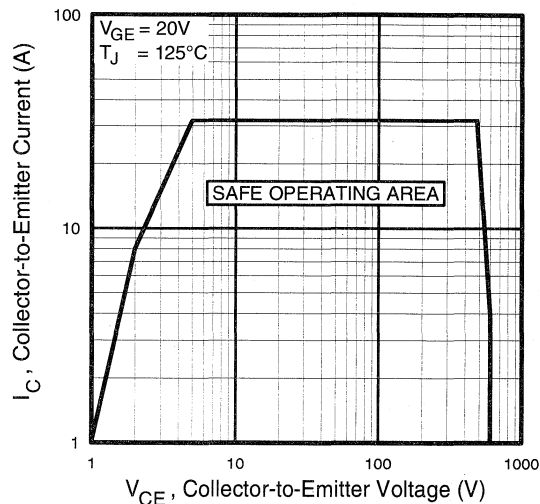


Fig. 12 - Turn-Off SOA

Refer to Section D for the following:

Appendix C: Section D - page D-5

Fig. 13a - Clamped Inductive Load Test Circuit

Fig. 13b - Pulsed Collector Current Test Circuit

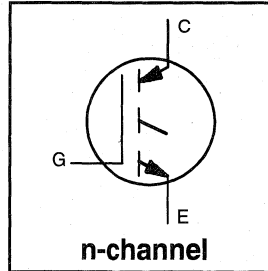
Fig. 14a - Switching Loss Test Circuit

Fig. 14b - Switching Loss Waveform

Package Outline 3 - JEDEC Outline TO-247AC (TO-3P) Section D - page D-13

Features

- Switching-loss rating includes all "tail" losses
- Optimized for medium operating frequency (1 to 10kHz) See Fig. 1 for Current vs. Frequency curve



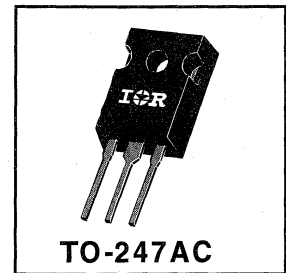
$$V_{CES} = 600V$$

$$V_{CE(sat)} \leq 2.1V$$

$$@V_{GE} = 15V, I_C = 17A$$

Description

Insulated Gate Bipolar Transistors (IGBTs) from International Rectifier have higher usable current densities than comparable bipolar transistors, while at the same time having simpler gate-drive requirements of the familiar power MOSFET. They provide substantial benefits to a host of high-voltage, high-current applications.



Absolute Maximum Ratings

	Parameter	Max.	Units
V_{CES}	Collector-to-Emitter Voltage	600	V
$I_C @ T_C = 25^\circ C$	Continuous Collector Current	31	A
$I_C @ T_C = 100^\circ C$	Continuous Collector Current	17	
I_{CM}	Pulsed Collector Current ①	120	
I_{LM}	Clamped Inductive Load Current ②	120	
V_{GE}	Gate-to-Emitter Voltage	± 20	V
E_{ARV}	Reverse Voltage Avalanche Energy ③	10	mJ
$P_D @ T_C = 25^\circ C$	Maximum Power Dissipation	100	W
$P_D @ T_C = 100^\circ C$	Maximum Power Dissipation	42	
T_J	Operating Junction and Storage Temperature Range	-55 to +150	°C
T_{STG}			
	Mounting torque, 6-32 or M3 screw.	10 lbf•in (1.1N•m)	

Thermal Resistance

	Parameter	Min.	Typ.	Max.	Units
$R_{\theta JC}$	Junction-to-Case	—	—	1.2	°C/W
$R_{\theta CS}$	Case-to-Sink, flat, greased surface	—	0.24	—	
$R_{\theta JA}$	Junction-to-Ambient, typical socket mount	—	—	40	
Wt	Weight	—	6 (0.21)	—	g (oz)

Electrical Characteristics @ $T_J = 25^\circ\text{C}$ (unless otherwise specified)

	Parameter	Min.	Typ.	Max.	Units	Conditions
$V_{(BR)CES}$	Collector-to-Emitter Breakdown Voltage	600	—	—	V	$V_{GE} = 0V, I_C = 250\mu A$
$V_{(BR)ECS}$	Emitter-to-Collector Breakdown Voltage ④	20	—	—	V	$V_{GE} = 0V, I_C = 1.0A$
$\Delta V_{(BR)CES}/\Delta T_J$	Temperature Coeff. of Breakdown Voltage	—	0.69	—	V/°C	$V_{GE} = 0V, I_C = 1.0mA$
$V_{CE(on)}$	Collector-to-Emitter Saturation Voltage	—	1.8	2.1	V	$I_C = 17A$ $I_C = 31A$ $I_C = 17A, T_J = 150^\circ\text{C}$ $V_{GE} = 15V$ See Fig. 2, 5
		—	2.4	—		
		—	2.2	—		
$V_{GE(th)}$	Gate Threshold Voltage	3.0	—	5.5		$V_{CE} = V_{GE}, I_C = 250\mu A$
$\Delta V_{GE(th)}/\Delta T_J$	Temperature Coeff. of Threshold Voltage	—	-11	—	mV/°C	$V_{CE} = V_{GE}, I_C = 250\mu A$
g_{fe}	Forward Transconductance ⑤	6.1	10	—	S	$V_{CE} = 100V, I_C = 17A$
I_{CES}	Zero Gate Voltage Collector Current	—	—	250	μA	$V_{GE} = 0V, V_{CE} = 600V$
		—	—	1000		$V_{GE} = 0V, V_{CE} = 600V, T_J = 150^\circ\text{C}$
I_{GES}	Gate-to-Emitter Leakage Current	—	—	± 100	nA	$V_{GE} = \pm 20V$

Switching Characteristics @ $T_J = 25^\circ\text{C}$ (unless otherwise specified)

	Parameter	Min.	Typ.	Max.	Units	Conditions
Q_g	Total Gate Charge (turn-on)	—	27	30	nC	$I_C = 17A$ $V_{CC} = 400V$ $V_{GE} = 15V$ See Fig. 8
Q_{ge}	Gate - Emitter Charge (turn-on)	—	4.1	5.9		
Q_{gc}	Gate - Collector Charge (turn-on)	—	12	15		
$t_{d(on)}$	Turn-On Delay Time	—	25	—	ns	$T_J = 25^\circ\text{C}$ $I_C = 17A, V_{CC} = 480V$ $V_{GE} = 15V, R_G = 23\Omega$ Energy losses include "tail"
t_r	Rise Time	—	21	—		
$t_{d(off)}$	Turn-Off Delay Time	—	210	320		
t_f	Fall Time	—	300	500		
E_{on}	Turn-On Switching Loss	—	0.30	—	mJ	See Fig. 9, 10, 11, 14
E_{off}	Turn-Off Switching Loss	—	2.1	—		
E_{ts}	Total Switching Loss	—	2.4	3.5		
$t_{d(on)}$	Turn-On Delay Time	—	25	—	ns	$T_J = 150^\circ\text{C}$, $I_C = 17A, V_{CC} = 480V$ $V_{GE} = 15V, R_G = 23\Omega$ Energy losses include "tail"
t_r	Rise Time	—	21	—		
$t_{d(off)}$	Turn-Off Delay Time	—	290	—		
t_f	Fall Time	—	590	—		
E_{ts}	Total Switching Loss	—	3.6	—	mJ	See Fig. 10, 14
L_E	Internal Emitter Inductance	—	7.5	—	nH	Measured 5mm from package
C_{ies}	Input Capacitance	—	670	—	pF	$V_{GE} = 0V$ $V_{CC} = 30V$ $f = 1.0MHz$ See Fig. 7
C_{oes}	Output Capacitance	—	100	—		
C_{res}	Reverse Transfer Capacitance	—	10	—		

Notes:

- ① Repetitive rating; $V_{GE}=20V$, pulse width limited by max. junction temperature. (See fig. 13b)
- ② $V_{CC}=80\%(V_{CES}), V_{GE}=20V, L=10\mu H, R_G=23\Omega$, (See fig. 13a)
- ③ Repetitive rating; pulse width limited by maximum junction temperature.
- ④ Pulse width $\leq 80\mu s$; duty factor $\leq 0.1\%$.
- ⑤ Pulse width $5.0\mu s$, single shot.

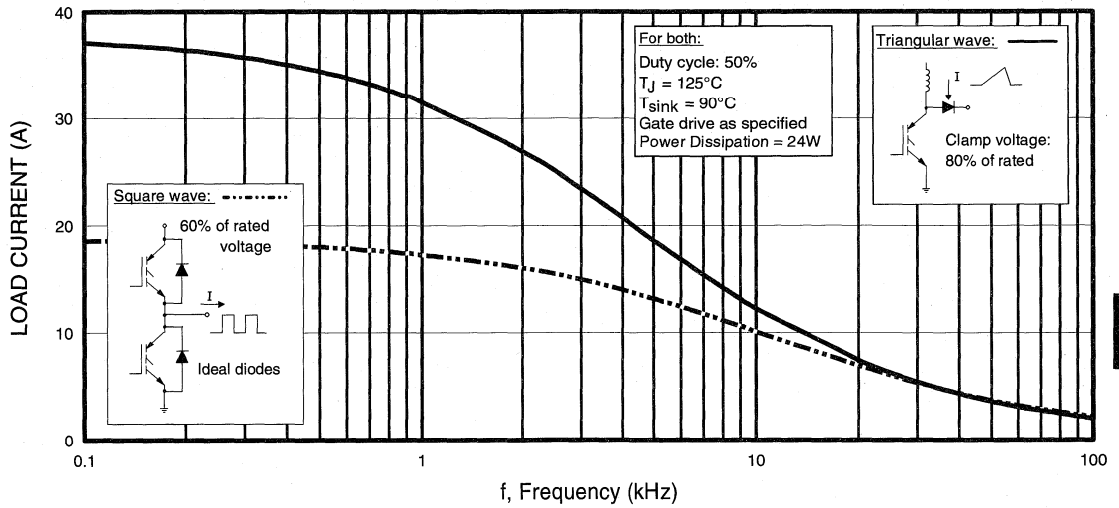


Fig. 1 - Typical Load Current vs. Frequency
 (For square wave, $I = I_{\text{RMS}}$ of fundamental; for triangular wave, $I = I_{\text{PK}}$)

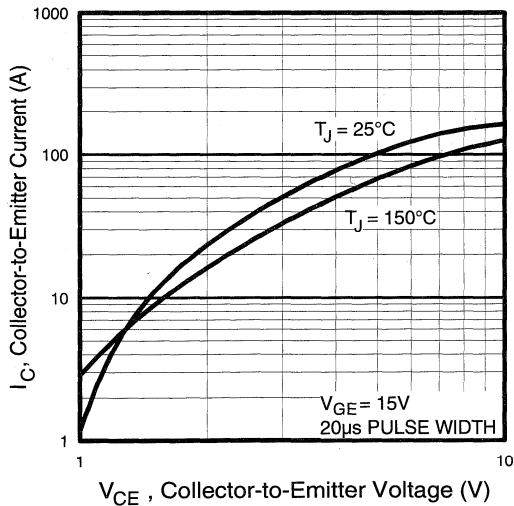


Fig. 2 - Typical Output Characteristics

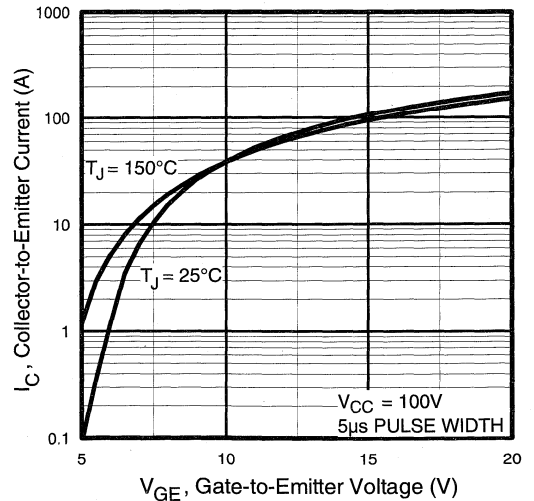


Fig. 3 - Typical Transfer Characteristics

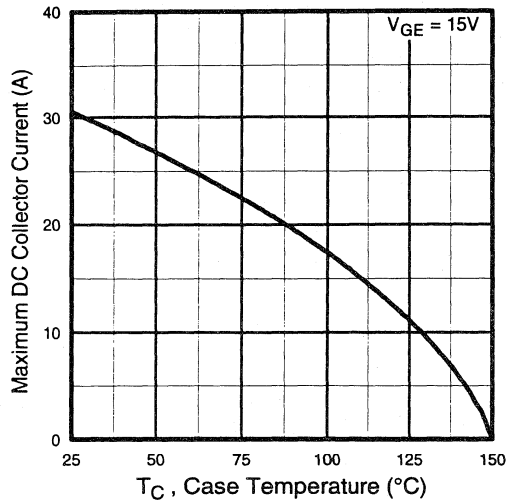


Fig. 4 - Maximum Collector Current vs. Case Temperature

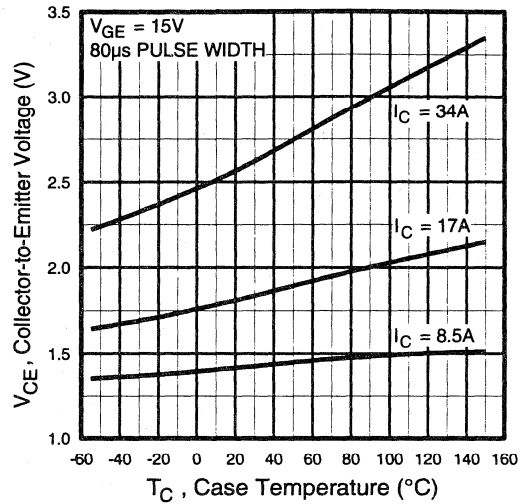


Fig. 5 - Collector-to-Emitter Voltage vs. Case Temperature

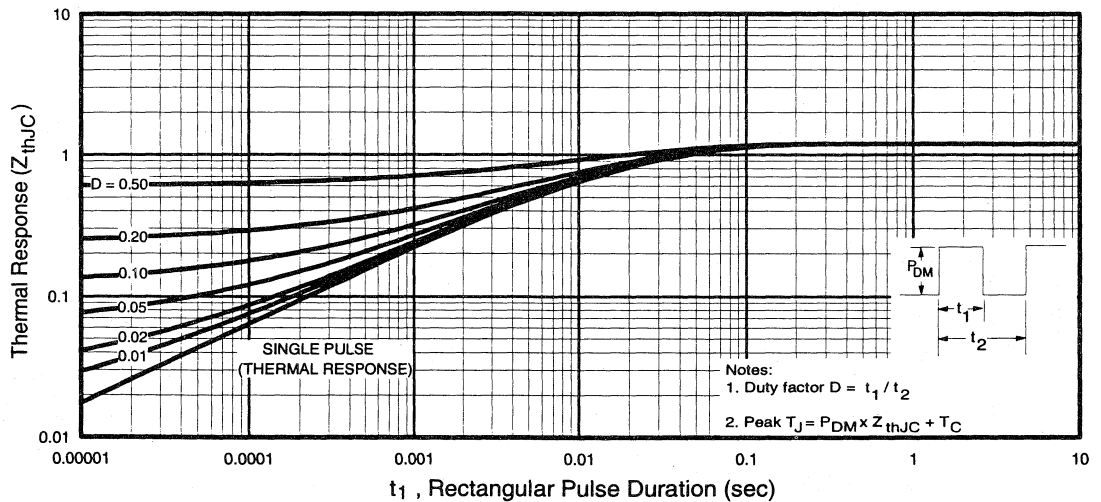


Fig. 6 - Maximum Effective Transient Thermal Impedance, Junction-to-Case

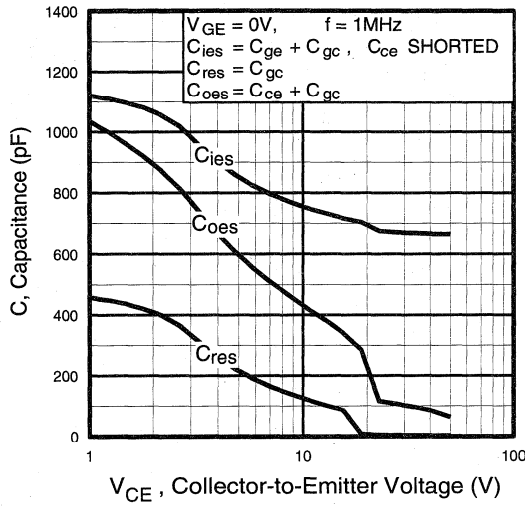


Fig. 7 - Typical Capacitance vs. Collector-to-Emitter Voltage

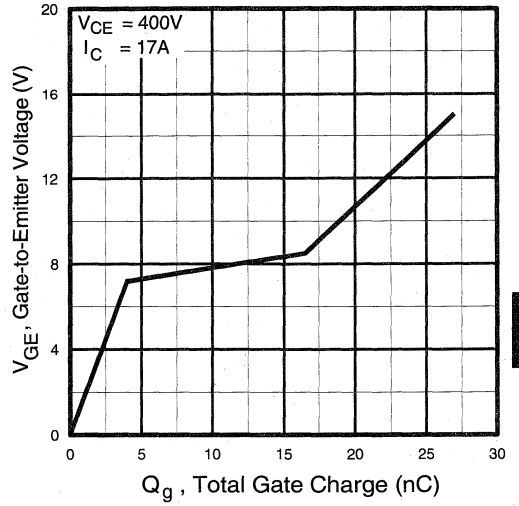


Fig. 8 - Typical Gate Charge vs. Gate-to-Emitter Voltage

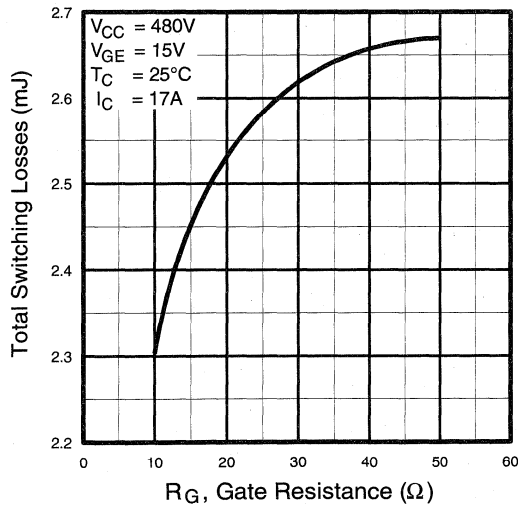


Fig. 9 - Typical Switching Losses vs. Gate Resistance

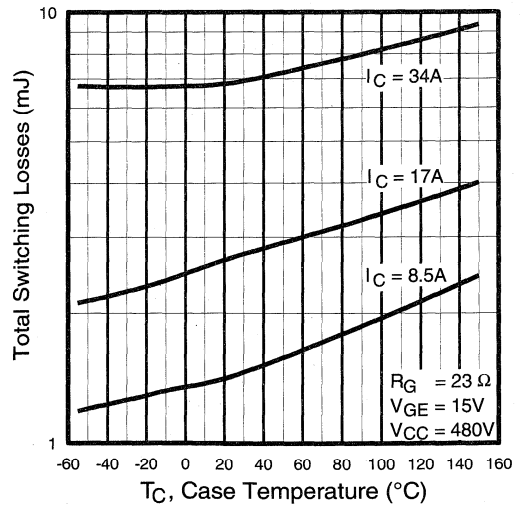


Fig. 10 - Typical Switching Losses vs. Case Temperature

Power
Conversion
Fast
Discretes

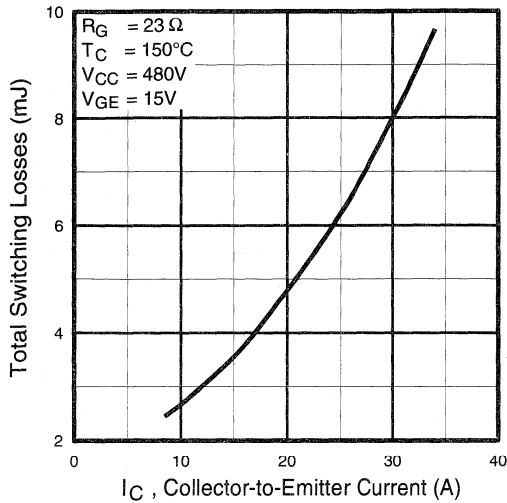


Fig. 11 - Typical Switching Losses vs. Collector-to-Emitter Current

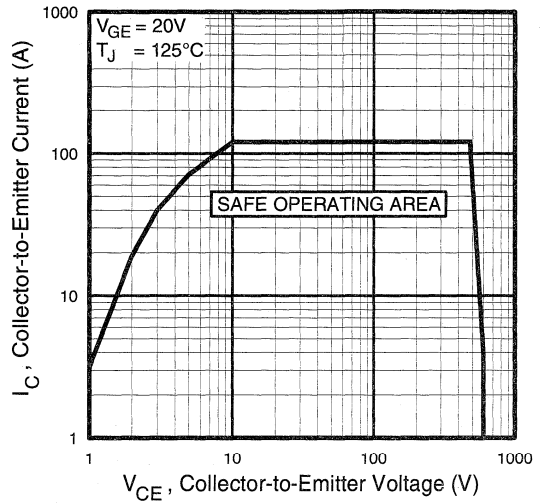


Fig. 12 - Turn-Off SOA

Refer to Section D for the following:

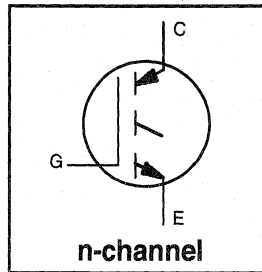
Appendix C: Section D - page D-5

- Fig. 13a - Clamped Inductive Load Test Circuit
- Fig. 13b - Pulsed Collector Current Test Circuit
- Fig. 14a - Switching Loss Test Circuit
- Fig. 14b - Switching Loss Waveform

Package Outline 3 - JEDEC Outline TO-247AC (TO-3P) Section D - page D-13

Features

- Switching-loss rating includes all "tail" losses
- Optimized for medium operating frequency (1 to 10kHz) See Fig. 1 for Current vs. Frequency curve



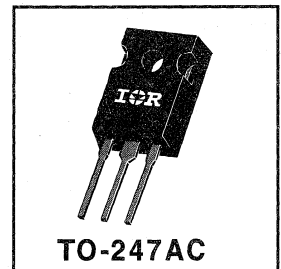
$$V_{CES} = 600V$$

$$V_{CE(sat)} \leq 2.0V$$

$$@ V_{GE} = 15V, I_C = 27A$$

Description

Insulated Gate Bipolar Transistors (IGBTs) from International Rectifier have higher usable current densities than comparable bipolar transistors, while at the same time having simpler gate-drive requirements of the familiar power MOSFET. They provide substantial benefits to a host of high-voltage, high-current applications.



TO-247AC

Absolute Maximum Ratings

	Parameter	Max.	Units
V_{CES}	Collector-to-Emitter Voltage	600	V
$I_C @ T_C = 25^\circ C$	Continuous Collector Current	49	A
$I_C @ T_C = 100^\circ C$	Continuous Collector Current	27	
I_{CM}	Pulsed Collector Current ①	200	
I_{LM}	Clamped Inductive Load Current ②	200	
V_{GE}	Gate-to-Emitter Voltage	± 20	V
E_{ARV}	Reverse Voltage Avalanche Energy ③	15	mJ
$P_D @ T_C = 25^\circ C$	Maximum Power Dissipation	160	W
$P_D @ T_C = 100^\circ C$	Maximum Power Dissipation	65	
T_J	Operating Junction and Storage Temperature Range	-55 to +150	°C
T_{STG}	Soldering Temperature, for 10 sec.	300 (0.063 in. (1.6mm) from case)	
	Mounting torque, 6-32 or M3 screw.	10 lbf•in (1.1N•m)	

Thermal Resistance

	Parameter	Min.	Typ.	Max.	Units
$R_{\theta JC}$	Junction-to-Case	—	—	0.77	°C/W
$R_{\theta CS}$	Case-to-Sink, flat, greased surface	—	0.24	—	
$R_{\theta JA}$	Junction-to-Ambient, typical socket mount	—	—	40	
Wt	Weight	—	6 (0.21)	—	g (oz)

Electrical Characteristics @ $T_J = 25^\circ\text{C}$ (unless otherwise specified)

	Parameter	Min.	Typ.	Max.	Units	Conditions	
$V_{(BR)CES}$	Collector-to-Emitter Breakdown Voltage	600	—	—	V	$V_{GE} = 0V, I_C = 250\mu A$	
$V_{(BR)ECS}$	Emitter-to-Collector Breakdown Voltage ④	20	—	—	V	$V_{GE} = 0V, I_C = 1.0A$	
$\Delta V_{(BR)CES}/\Delta T_J$	Temp. Coeff. of Breakdown Voltage	—	0.70	—	$V/^\circ\text{C}$	$V_{GE} = 0V, I_C = 1.0mA$	
$V_{CE(on)}$	Collector-to-Emitter Saturation Voltage	—	1.7	2.0	V	$I_C = 27A$ $I_C = 49A$ $I_C = 27A, T_J = 150^\circ\text{C}$ $V_{CE} = V_{GE}, I_C = 250\mu A$	
		—	2.2	—			$V_{GE} = 15V$ See Fig. 2, 5
		—	1.9	—			
$V_{GE(th)}$	Gate Threshold Voltage	3.0	—	5.5			
$\Delta V_{GE(th)}/\Delta T_J$	Temp. Coeff. of Threshold Voltage	—	-12	—	$mV/^\circ\text{C}$	$V_{CE} = V_{GE}, I_C = 250\mu A$	
g_{fe}	Forward Transconductance ⑤	9.2	12	—	S	$V_{CE} = 100V, I_C = 27A$	
I_{CES}	Zero Gate Voltage Collector Current	—	—	250	μA	$V_{GE} = 0V, V_{CE} = 600V$	
		—	—	1000		$V_{GE} = 0V, V_{CE} = 600V, T_J = 150^\circ\text{C}$	
I_{GES}	Gate-to-Emitter Leakage Current	—	—	± 100	nA	$V_{GE} = \pm 20V$	

Switching Characteristics @ $T_J = 25^\circ\text{C}$ (unless otherwise specified)

	Parameter	Min.	Typ.	Max.	Units	Conditions
Q_g	Total Gate Charge (turn-on)	—	59	80	nC	$I_C = 27A$ $V_{CC} = 400V$ $V_{GE} = 15V$ See Fig. 8
Q_{ge}	Gate - Emitter Charge (turn-on)	—	8.6	10		
Q_{gc}	Gate - Collector Charge (turn-on)	—	25	42		
$t_{d(on)}$	Turn-On Delay Time	—	25	—	ns	$T_J = 25^\circ\text{C}$ $I_C = 27A, V_{CC} = 480V$ $V_{GE} = 15V, R_G = 10\Omega$ Energy losses include "tail"
t_r	Rise Time	—	37	—		
$t_{d(off)}$	Turn-Off Delay Time	—	240	410		
t_f	Fall Time	—	230	420		
E_{on}	Turn-On Switching Loss	—	0.65	—	mJ	See Fig. 9, 10, 11, 14
E_{off}	Turn-Off Switching Loss	—	3.0	—		
E_{ts}	Total Switching Loss	—	3.65	6.0		
$t_{d(on)}$	Turn-On Delay Time	—	28	—	ns	$T_J = 150^\circ\text{C}$, $I_C = 27A, V_{CC} = 480V$ $V_{GE} = 15V, R_G = 10\Omega$ Energy losses include "tail"
t_r	Rise Time	—	37	—		
$t_{d(off)}$	Turn-Off Delay Time	—	380	—		
t_f	Fall Time	—	460	—		
E_{ts}	Total Switching Loss	—	6.0	—	mJ	See Fig. 10, 14
L_E	Internal Emitter Inductance	—	13	—	nH	Measured 5mm from package
C_{ies}	Input Capacitance	—	1500	—	pF	$V_{GE} = 0V$ $V_{CC} = 30V$ $f = 1.0MHz$ See Fig. 7
C_{oes}	Output Capacitance	—	190	—		
C_{res}	Reverse Transfer Capacitance	—	20	—		

Notes:

① Repetitive rating; $V_{GE}=20V$, pulse width limited by max. junction temperature. (See fig. 13b)

② $V_{CC}=80\%(V_{CES})$, $V_{GE}=20V$, $L=10\mu H$, $R_G=10\Omega$, (See fig. 13a)

③ Repetitive rating; pulse width limited by maximum junction temperature.

⑤ Pulse width 5.0 μs , single shot.

④ Pulse width $\leq 80\mu s$; duty factor $\leq 0.1\%$.

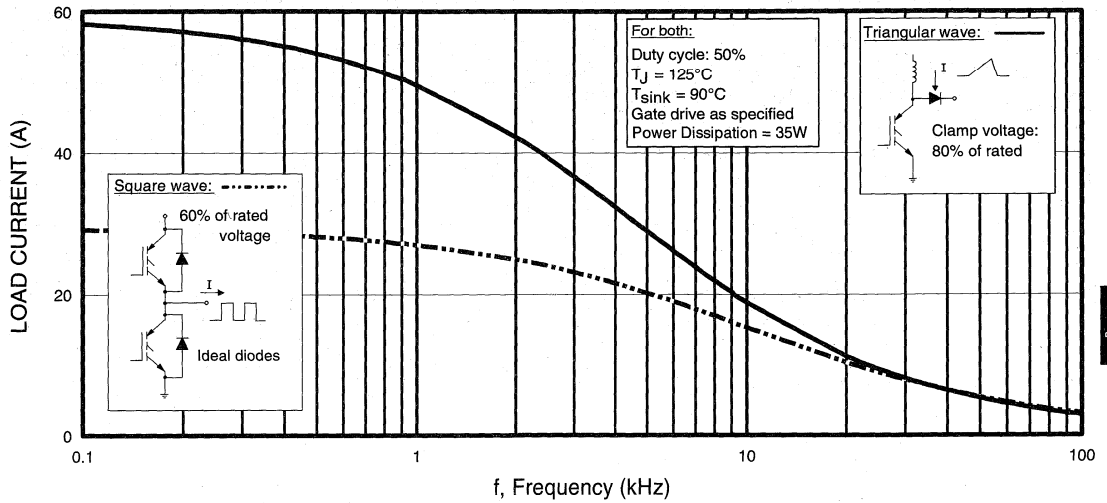


Fig. 1 - Typical Load Current vs. Frequency
 (For square wave, $I = I_{RMS}$ of fundamental; for triangular wave, $I = I_{PK}$)

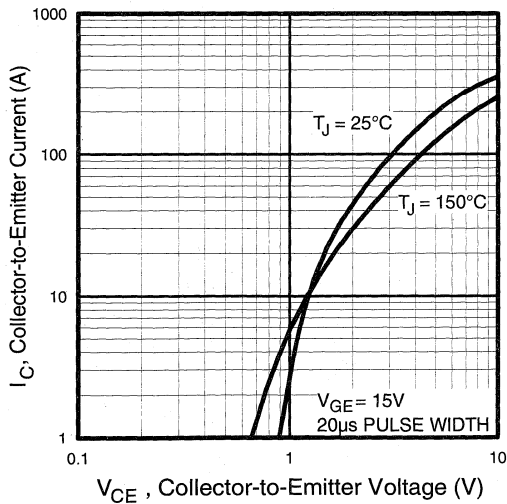


Fig. 2 - Typical Output Characteristics

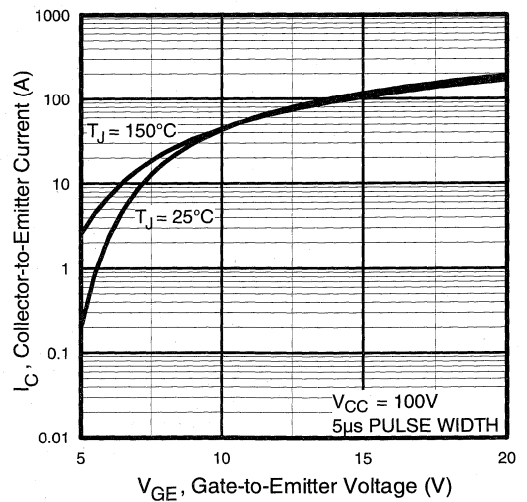


Fig. 3 - Typical Transfer Characteristics

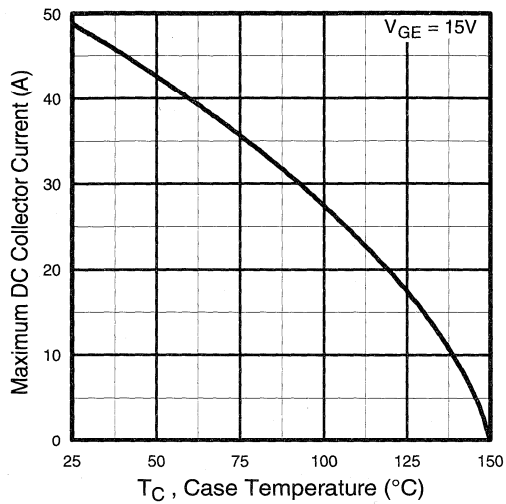


Fig. 4 - Maximum Collector Current vs. Case Temperature

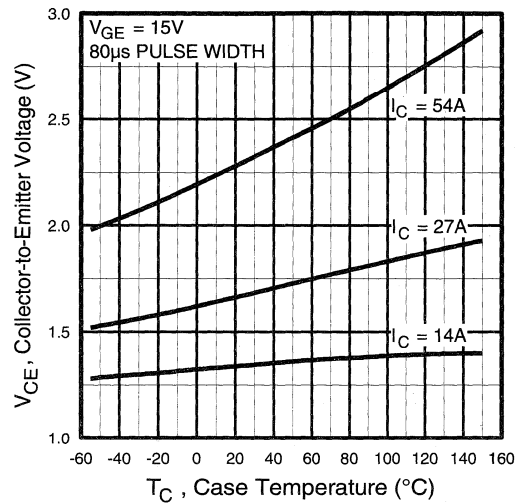


Fig. 5 - Collector-to-Emitter Voltage vs. Case Temperature

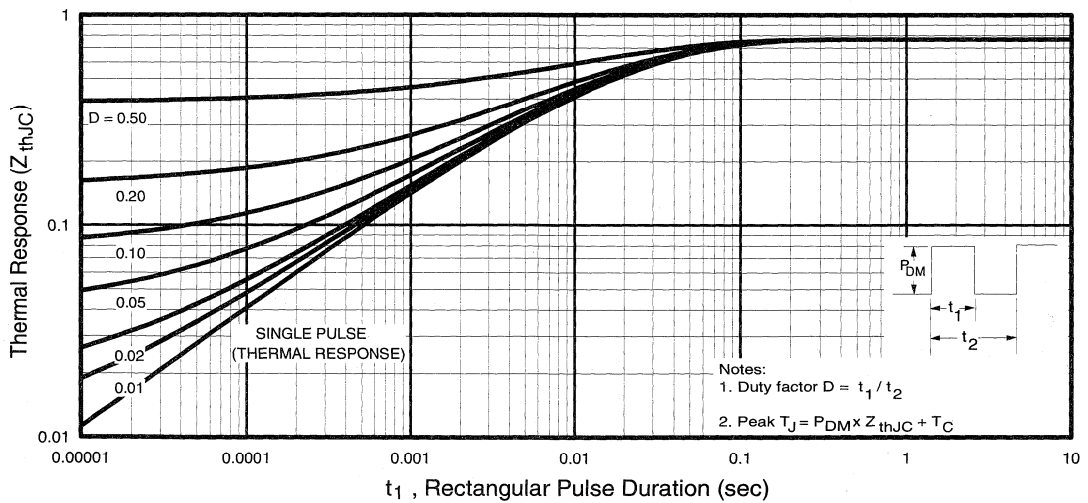


Fig. 6 - Maximum Effective Transient Thermal Impedance, Junction-to-Case

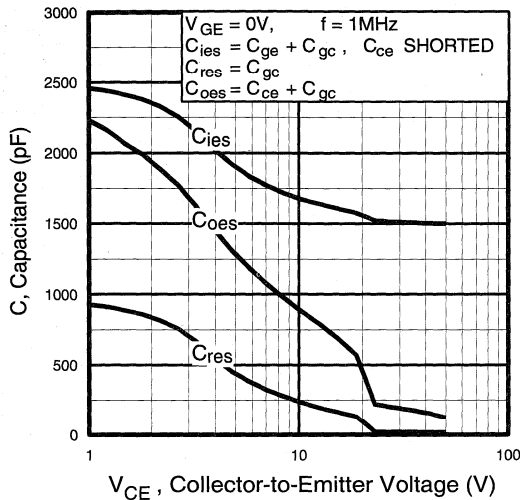


Fig. 7 - Typical Capacitance vs. Collector-to-Emitter Voltage

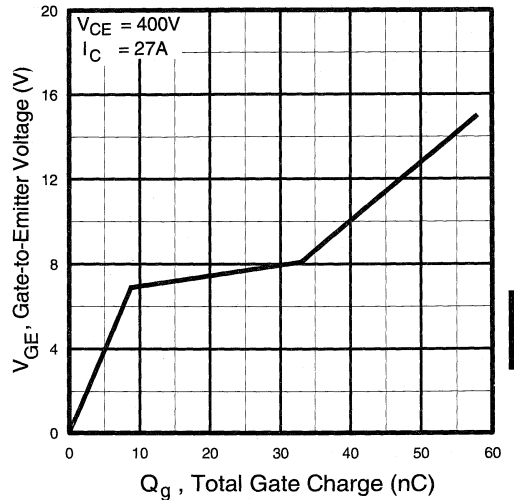


Fig. 8 - Typical Gate Charge vs. Gate-to-Emitter Voltage

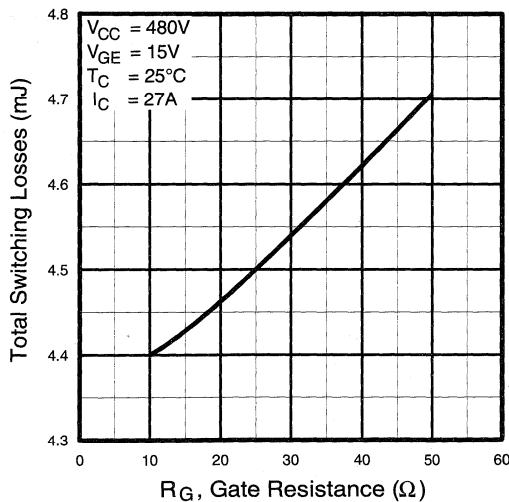


Fig. 9 - Typical Switching Losses vs. Gate Resistance

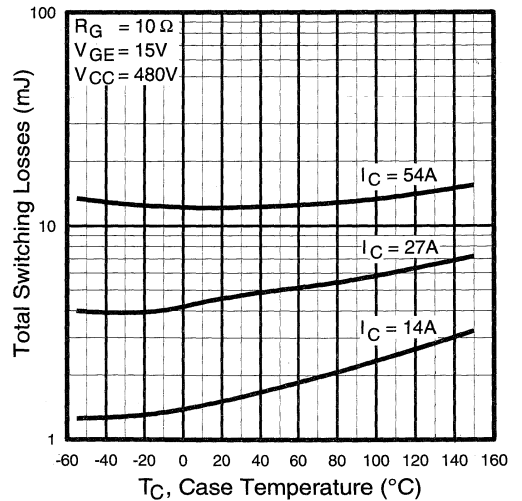


Fig. 10 - Typical Switching Losses vs. Case Temperature

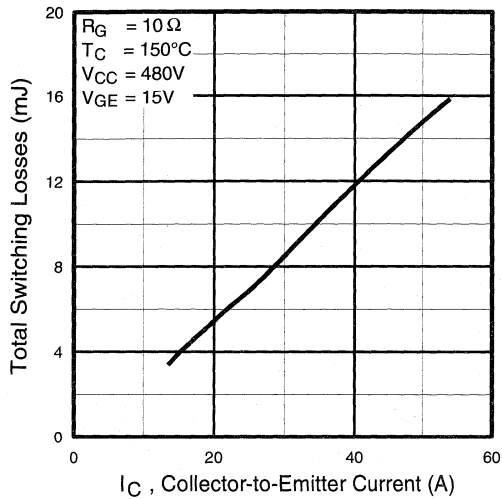


Fig. 11 - Typical Switching Losses vs. Collector-to-Emitter Current

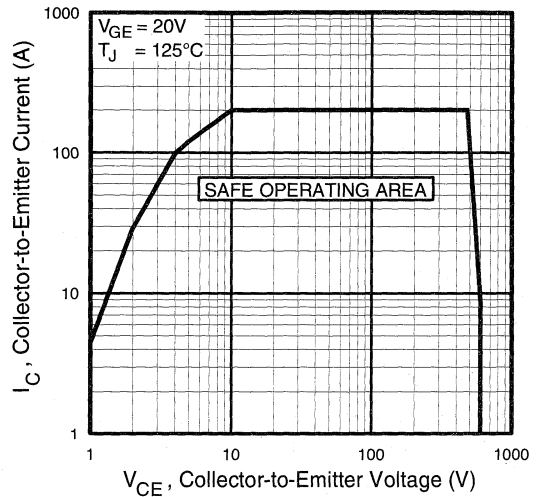


Fig. 12 - Turn-Off SOA

Refer to Section D for the following:

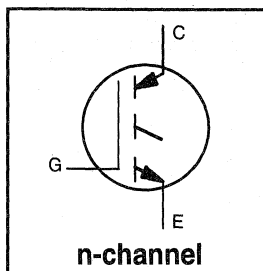
Appendix C: Section D - page D-5

- Fig. 13a - Clamped Inductive Load Test Circuit
- Fig. 13b - Pulsed Collector Current Test Circuit
- Fig. 14a - Switching Loss Test Circuit
- Fig. 14b - Switching Loss Waveform

Package Outline 3 - JEDEC Outline TO-247AC (TO-3P) Section D - page D-13

Features

- Switching-loss rating includes all "tail" losses
- Optimized for medium operating frequency (1 to 10kHz) See Fig. 1 for Current vs. Frequency curve



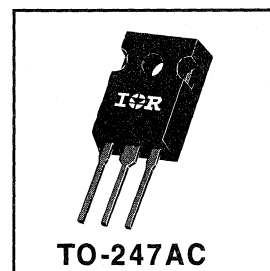
$$V_{CES} = 600V$$

$$V_{CE(sat)} \leq 1.7V$$

$$@V_{GE} = 15V, I_C = 39A$$

Description

Insulated Gate Bipolar Transistors (IGBTs) from International Rectifier have higher usable current densities than comparable bipolar transistors, while at the same time having simpler gate-drive requirements of the familiar power MOSFET. They provide substantial benefits to a host of high-voltage, high-current applications.



Absolute Maximum Ratings

	Parameter	Max.	Units
V_{CES}	Collector-to-Emitter Voltage	600	V
$I_C @ T_C = 25^\circ C$	Continuous Collector Current	70	A
$I_C @ T_C = 100^\circ C$	Continuous Collector Current	39	
I_{CM}	Pulsed Collector Current ①	280	
I_{LM}	Clamped Inductive Load Current ②	280	
V_{GE}	Gate-to-Emitter Voltage	± 20	V
E_{ARV}	Reverse Voltage Avalanche Energy ③	20	mJ
$P_D @ T_C = 25^\circ C$	Maximum Power Dissipation	200	W
$P_D @ T_C = 100^\circ C$	Maximum Power Dissipation	78	
T_J	Operating Junction and	-55 to +150	°C
T_{STG}	Storage Temperature Range		
	Soldering Temperature, for 10 sec.	300 (0.063 in. (1.6mm) from case)	
	Mounting torque, 6-32 or M3 screw.	10 lbf•in (1.1N•m)	

Thermal Resistance

	Parameter	Min.	Typ.	Max.	Units
$R_{\theta JC}$	Junction-to-Case	—	—	0.64	°C/W
$R_{\theta CS}$	Case-to-Sink, flat, greased surface	—	0.24	—	
$R_{\theta JA}$	Junction-to-Ambient, typical socket mount	—	—	40	
Wt	Weight	—	6 (0.21)	—	g (oz)

Electrical Characteristics @ $T_J = 25^\circ\text{C}$ (unless otherwise specified)

	Parameter	Min.	Typ.	Max.	Units	Conditions
$V_{(BR)CES}$	Collector-to-Emitter Breakdown Voltage	600	—	—	V	$V_{GE} = 0V, I_C = 250\mu A$
$V_{(BR)ECS}$	Emitter-to-Collector Breakdown Voltage ④	20	—	—	V	$V_{GE} = 0V, I_C = 1.0A$
$\Delta V_{(BR)CES}/\Delta T_J$	Temp. Coeff. of Breakdown Voltage	—	0.62	—	$V/^\circ\text{C}$	$V_{GE} = 0V, I_C = 1.0mA$
$V_{CE(on)}$	Collector-to-Emitter Saturation Voltage	—	1.4	1.7	V	$I_C = 39A$ $I_C = 70A$ $I_C = 39A, T_J = 150^\circ\text{C}$ $V_{GE} = 15V$ See Fig. 2, 5
		—	2.0	—		
		—	1.7	—		
$V_{GE(th)}$	Gate Threshold Voltage	3.0	—	5.5		$V_{CE} = V_{GE}, I_C = 250\mu A$
$\Delta V_{GE(th)}/\Delta T_J$	Temp. Coeff. of Threshold Voltage	—	-14	—	$mV/^\circ\text{C}$	$V_{CE} = V_{GE}, I_C = 250\mu A$
g_{fe}	Forward Transconductance ⑤	21	30	—	S	$V_{CE} = 100V, I_C = 39A$
I_{CES}	Zero Gate Voltage Collector Current	—	—	250	μA	$V_{GE} = 0V, V_{CE} = 600V$
		—	—	2000		$V_{GE} = 0V, V_{CE} = 600V, T_J = 150^\circ\text{C}$
I_{GES}	Gate-to-Emitter Leakage Current	—	—	± 100	nA	$V_{GE} = \pm 20V$

Switching Characteristics @ $T_J = 25^\circ\text{C}$ (unless otherwise specified)

	Parameter	Min.	Typ.	Max.	Units	Conditions
Q_g	Total Gate Charge (turn-on)	—	84	100	nC	$I_C = 39A$ $V_{CC} = 400V$ $V_{GE} = 15V$ See Fig. 8
Q_{ge}	Gate - Emitter Charge (turn-on)	—	20	25		
Q_{gc}	Gate - Collector Charge (turn-on)	—	51	67		
$t_{d(on)}$	Turn-On Delay Time	—	24	—	ns	$T_J = 25^\circ\text{C}$ $I_C = 39A, V_{CC} = 480V$ $V_{GE} = 15V, R_G = 5.0\Omega$ Energy losses include "tail"
t_r	Rise Time	—	50	—		
$t_{d(off)}$	Turn-Off Delay Time	—	270	540		
t_f	Fall Time	—	210	360		
E_{on}	Turn-On Switching Loss	—	1.7	—		
E_{off}	Turn-Off Switching Loss	—	4.3	—	mJ	See Fig. 9, 10, 11, 14
E_{ts}	Total Switching Loss	—	6.0	9.0		
$t_{d(on)}$	Turn-On Delay Time	—	25	—	ns	$T_J = 150^\circ\text{C}$, $I_C = 39A, V_{CC} = 480V$ $V_{GE} = 15V, R_G = 5.0\Omega$ Energy losses include "tail"
t_r	Rise Time	—	49	—		
$t_{d(off)}$	Turn-Off Delay Time	—	440	—		
t_f	Fall Time	—	410	—		
E_{ts}	Total Switching Loss	—	9.0	—		
L_E	Internal Emitter Inductance	—	13	—	nH	Measured 5mm from package
C_{ies}	Input Capacitance	—	3000	—	pF	$V_{GE} = 0V$ $V_{CC} = 30V$ $f = 1.0MHz$ See Fig. 7
C_{oes}	Output Capacitance	—	340	—		
C_{res}	Reverse Transfer Capacitance	—	40	—		

Notes:

- ① Repetitive rating; $V_{GE}=20V$, pulse width limited by max. junction temperature. (See fig. 13b)
- ② $V_{CC}=80\%(V_{CES}), V_{GE}=20V, L=10\mu H, R_G=5.0\Omega$, (See fig. 13a)
- ③ Repetitive rating; pulse width limited by maximum junction temperature.
- ④ Pulse width $\leq 80\mu s$; duty factor $\leq 0.1\%$.
- ⑤ Pulse width $5.0\mu s$, single shot.

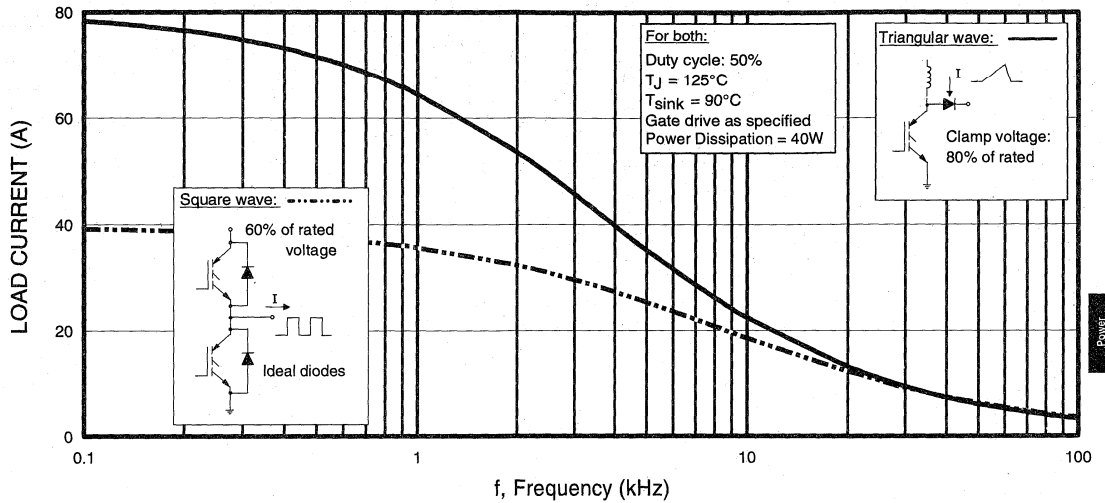


Fig. 1 - Typical Load Current vs. Frequency
 (For square wave, $I = I_{RMS}$ of fundamental; for triangular wave, $I = I_{PK}$)

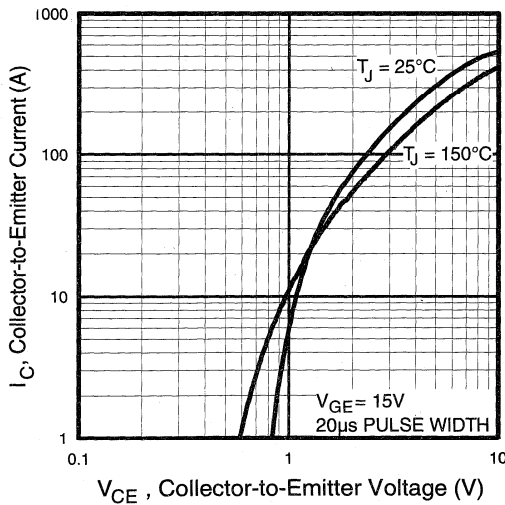


Fig. 2 - Typical Output Characteristics

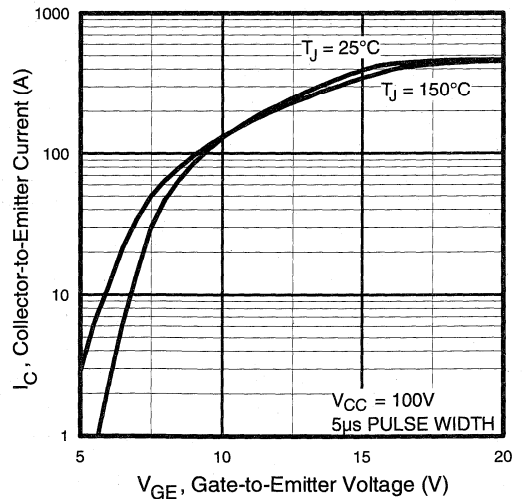


Fig. 3 - Typical Transfer Characteristics

Power
Conversion
Fast
Discretes

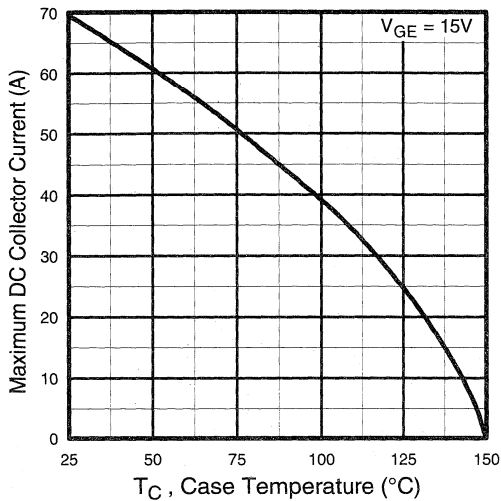


Fig. 4 - Maximum Collector Current vs. Case Temperature

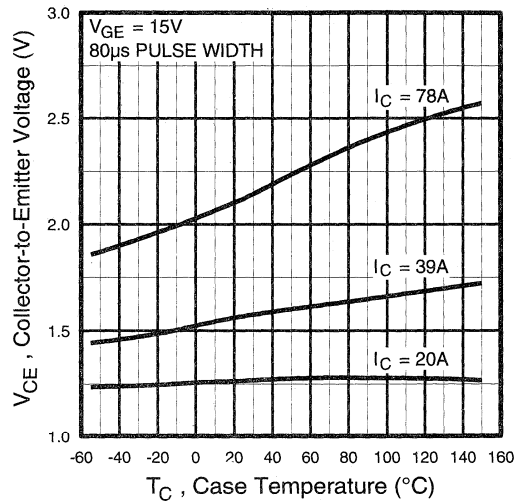


Fig. 5 - Collector-to-Emitter Voltage vs. Case Temperature

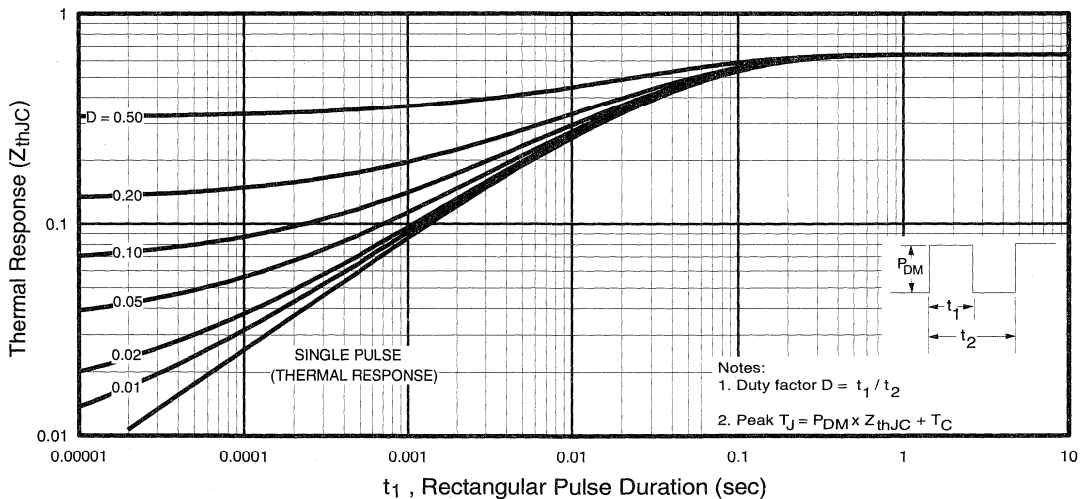


Fig. 6 - Maximum Effective Transient Thermal Impedance, Junction-to-Case

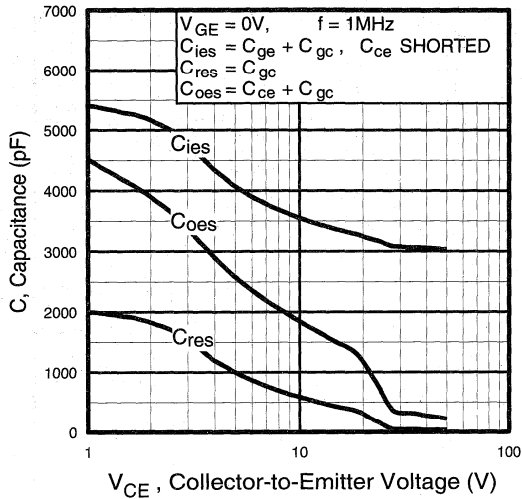


Fig. 7 - Typical Capacitance vs. Collector-to-Emitter Voltage

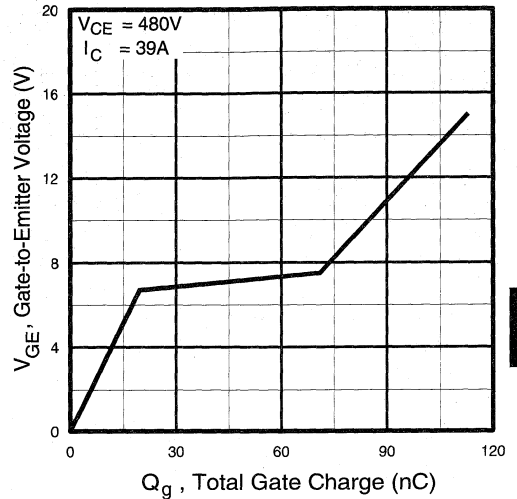


Fig. 8 - Typical Gate Charge vs. Gate-to-Emitter Voltage

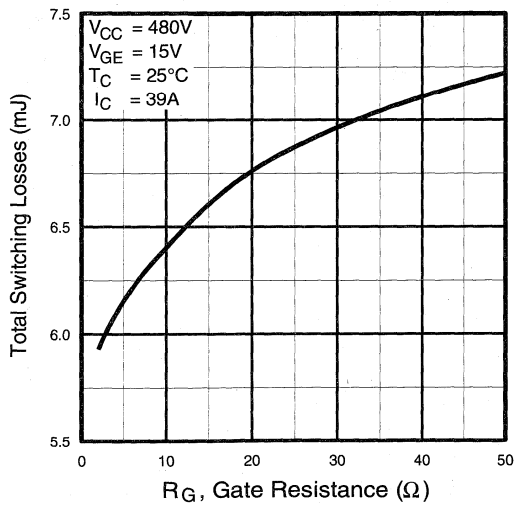


Fig. 9 - Typical Switching Losses vs. Gate Resistance

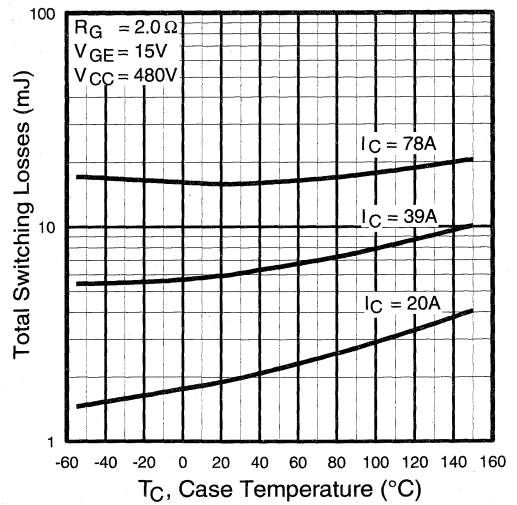


Fig. 10 - Typical Switching Losses vs. Case Temperature

Power
 Conversion
 Diodes

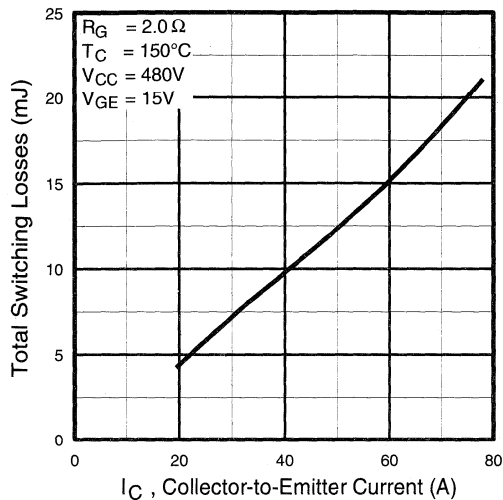


Fig. 11 - Typical Switching Losses vs. Collector-to-Emitter Current

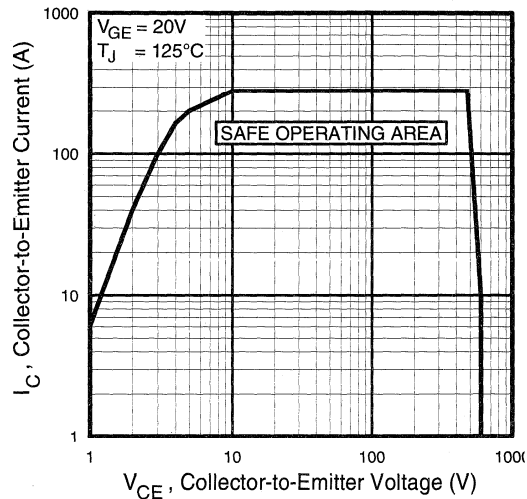


Fig. 12 - Turn-Off SOA

Refer to Section D for the following:

Appendix C: Section D- page D-5

- Fig. 13a - Clamped Inductive Load Test Circuit
- Fig. 13b - Pulsed Collector Current Test Circuit
- Fig. 14a - Switching Loss Test Circuit
- Fig. 14b - Switching Loss Waveform

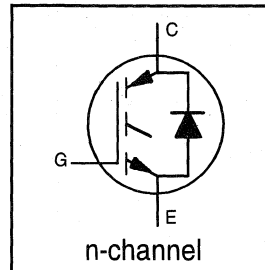
Package Outline 3 - JEDEC Outline TO-247AC (TO-3P) Section D - page D-13

INSULATED GATE BIPOLAR TRANSISTOR WITH ULTRAFAST SOFT RECOVERY DIODE

Fast CoPack IGBT

Features

- Switching-loss rating includes all "tail" losses
- HEXFRED™ soft ultrafast diodes
- Optimized for medium operating frequency (1 to 10kHz) See Fig. 1 for Current vs. Frequency curve



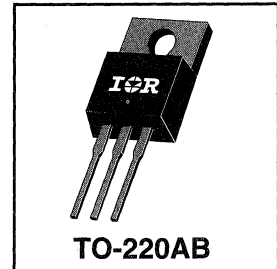
$$V_{CES} = 600V$$

$$V_{CE(sat)} \leq 2.8V$$

$$@ V_{GE} = 15V, I_C = 9.0A$$

Description

Co-packaged IGBTs are a natural extension of International Rectifier's well known IGBT line. They provide the convenience of an IGBT and an ultrafast recovery diode in one package, resulting in substantial benefits to a host of high-voltage, high-current, motor control, UPS and power supply applications.



Absolute Maximum Ratings

	Parameter	Max.	Units
V_{CES}	Collector-to-Emitter Voltage	600	V
$I_C @ T_C = 25^\circ C$	Continuous Collector Current	16	A
$I_C @ T_C = 100^\circ C$	Continuous Collector Current	9.0	
I_{CM}	Pulsed Collector Current $\text{\textcircled{D}}$	32	
I_{LM}	Clamped Inductive Load Current $\text{\textcircled{D}}$	32	
$I_F @ T_C = 100^\circ C$	Diode Continuous Forward Current	7.0	
I_{FM}	Diode Maximum Forward Current	32	
V_{GE}	Gate-to-Emitter Voltage	± 20	
$P_D @ T_C = 25^\circ C$	Maximum Power Dissipation	60	W
$P_D @ T_C = 100^\circ C$	Maximum Power Dissipation	24	
T_J	Operating Junction and	-55 to +150	$^\circ C$
T_{STG}	Storage Temperature Range		
	Soldering Temperature, for 10 sec.	300 (0.063 in. (1.6mm) from case)	
	Mounting Torque, 6-32 or M3 Screw.	10 lbf•in (1.1 N•m)	

Thermal Resistance

	Parameter	Min.	Typ.	Max.	Units
$R_{\theta JC}$	Junction-to-Case - IGBT	—	—	2.1	$^\circ C/W$
$R_{\theta JC}$	Junction-to-Case - Diode	—	—	3.5	
$R_{\theta CS}$	Case-to-Sink, flat, greased surface	—	0.50	—	
$R_{\theta JA}$	Junction-to-Ambient, typical socket mount	—	—	80	
Wt	Weight	—	2 (0.07)	—	g (oz)

Electrical Characteristics @ $T_J = 25^\circ\text{C}$ (unless otherwise specified)

	Parameter	Min.	Typ.	Max.	Units	Conditions
$V_{(BR)CES}$	Collector-to-Emitter Breakdown Voltage ^③	600	—	—	V	$V_{GE} = 0V, I_C = 250\mu A$
$\Delta V_{(BR)CES}/\Delta T_J$	Temp. Coeff. of Breakdown Voltage	—	0.72	—	V/ $^\circ\text{C}$	$V_{GE} = 0V, I_C = 1.0mA$
$V_{CE(on)}$	Collector-to-Emitter Saturation Voltage	—	2.0	2.8	V	$I_C = 9.0A$ $V_{GE} = 15V$ $I_C = 16A$ See Fig. 2, 5 $I_C = 9.0A, T_J = 150^\circ\text{C}$
		—	2.6	—		
		—	2.3	—		
$V_{GE(th)}$	Gate Threshold Voltage	3.0	—	5.5		$V_{CE} = V_{GE}, I_C = 250\mu A$
$\Delta V_{GE(th)}/\Delta T_J$	Temp. Coeff. of Threshold Voltage	—	-11	—	mV/ $^\circ\text{C}$	$V_{CE} = V_{GE}, I_C = 250\mu A$
g_{fe}	Forward Transconductance ^④	2.9	5.1	—	S	$V_{CE} = 100V, I_C = 600V$
	Zero Gate Voltage Collector Current	—	—	250	μA	$V_{GE} = 0V, V_{CE} = 600V$ $V_{GE} = 0V, V_{CE} = 600V, T_J = 150^\circ\text{C}$
		—	—	1700		
V_{FM}	Diode Forward Voltage Drop	—	1.4	1.7	V	$I_C = 8.0A$ See Fig. 13 $I_C = 8.0A, T_J = 150^\circ\text{C}$
		—	1.3	1.6		
I_{GES}	Gate-to-Emitter Leakage Current	—	—	± 100	nA	$V_{GE} = \pm 20V$

Switching Characteristics @ $T_J = 25^\circ\text{C}$ (unless otherwise specified)

	Parameter	Min.	Typ.	Max.	Units	Conditions
Q_g	Total Gate Charge (turn-on)	—	16	21	nC	$I_C = 9.0A$ $V_{CC} = 400V$ See Fig. 8
Q_{ge}	Gate - Emitter Charge (turn-on)	—	2.4	3.4		
Q_{gc}	Gate - Collector Charge (turn-on)	—	7.9	10		
$t_{d(on)}$	Turn-On Delay Time	—	62	—	ns	$T_J = 25^\circ\text{C}$ $I_C = 9.0A, V_{CC} = 480V$ $V_{GE} = 15V, R_G = 50\Omega$ Energy losses include "tail" and diode reverse recovery. See Fig. 9, 10, 11, 18
t_r	Rise Time	—	44	—		
$t_{d(off)}$	Turn-Off Delay Time	—	120	180		
t_f	Fall Time	—	58	93		
E_{on}	Turn-On Switching Loss	—	—	—		
E_{off}	Turn-Off Switching Loss	—	—	—	mJ	See Fig. 9, 10, 11, 18
E_{ts}	Total Switching Loss	—	—	0.83		
$t_{d(on)}$	Turn-On Delay Time	—	61	—	ns	$T_J = 150^\circ\text{C}$, See Fig. 9, 10, 11, 18 $I_C = 9.0A, V_{CC} = 480V$ $V_{GE} = 15V, R_G = 50\Omega$ Energy losses include "tail" and diode reverse recovery.
t_r	Rise Time	—	44	—		
$t_{d(off)}$	Turn-Off Delay Time	—	170	—		
t_f	Fall Time	—	160	—		
E_{ts}	Total Switching Loss	—	0.96	—		
L_E	Internal Emitter Inductance	—	7.5	—	nH	Measured 5mm from package
C_{ies}	Input Capacitance	—	340	—	pF	$V_{GE} = 0V$ $V_{CC} = 30V$ See Fig. 7 $f = 1.0MHz$
C_{oes}	Output Capacitance	—	63	—		
C_{res}	Reverse Transfer Capacitance	—	5.9	—		
t_{rr}	Diode Reverse Recovery Time	—	37	55	ns	$T_J = 25^\circ\text{C}$ See Fig. 14 $T_J = 125^\circ\text{C}$
		—	55	90		
I_{rr}	Diode Peak Reverse Recovery Current	—	3.5	5.0	A	$T_J = 25^\circ\text{C}$ See Fig. 15 $T_J = 125^\circ\text{C}$
		—	4.5	8.0		
Q_{rr}	Diode Reverse Recovery Charge	—	65	138	nC	$T_J = 25^\circ\text{C}$ See Fig. 16 $T_J = 125^\circ\text{C}$
		—	124	360		
$di_{(rec)M}/dt$	Diode Peak Rate of Fall of Recovery During t_b	—	240	—	A/ μs	$T_J = 25^\circ\text{C}$ See Fig. 17 $T_J = 125^\circ\text{C}$
		—	210	—		

Notes:

① Repetitive rating; $V_{GE}=20V$, pulse width limited by max. junction temperature. (See fig. 20)

② $V_{CC}=80\%(V_{CES})$, $V_{GE}=20V$, $L=10\mu H$, $R_G=50\Omega$, (See fig. 19)

③ Pulse width $\leq 80\mu s$; duty factor $\leq 0.1\%$.

④ Pulse width 5.0 μs , single shot.

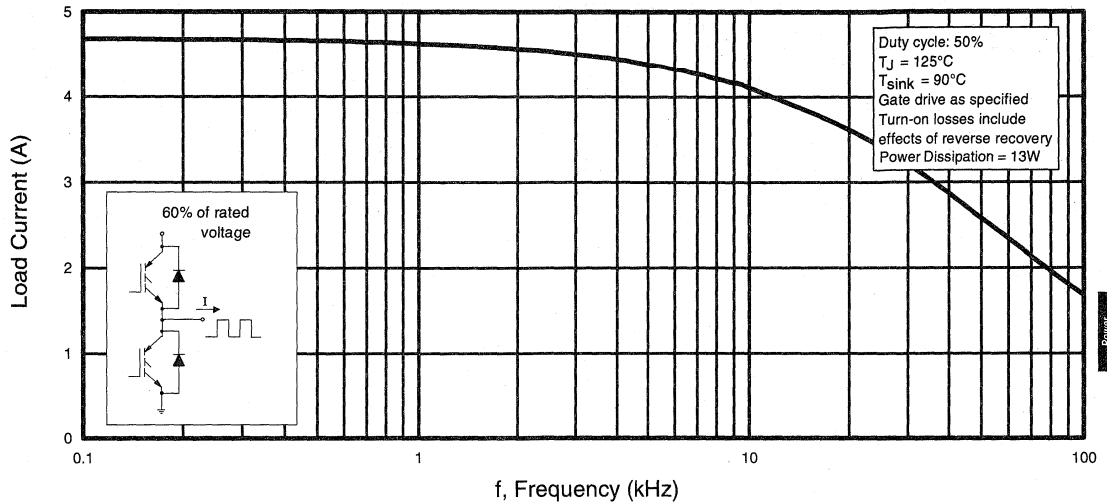


Fig. 1 - Typical Load Current vs. Frequency
(Load Current = I_{RMS} of fundamental)

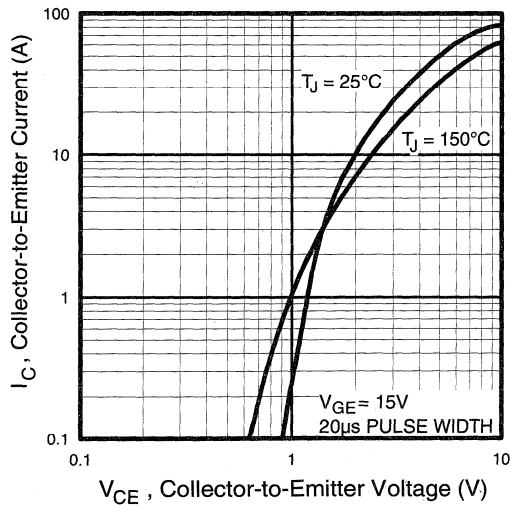


Fig. 2 - Typical Output Characteristics

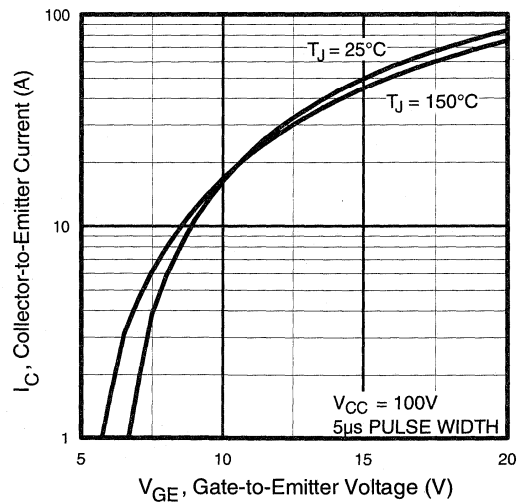


Fig. 3 - Typical Transfer Characteristics

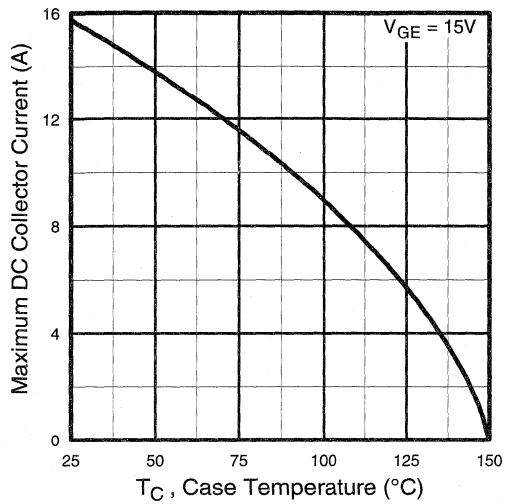


Fig. 4 - Maximum Collector Current vs. Case Temperature

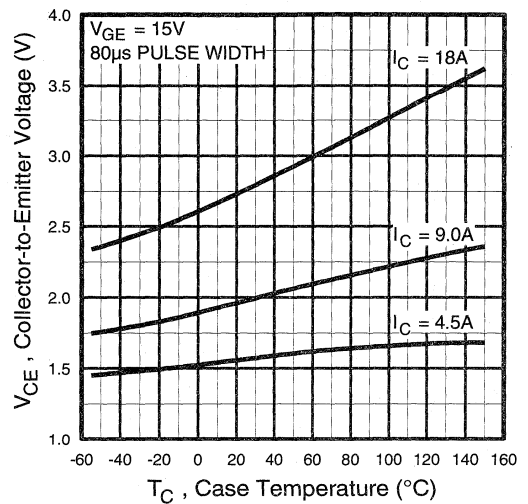


Fig. 5 - Collector-to-Emitter Voltage vs. Case Temperature

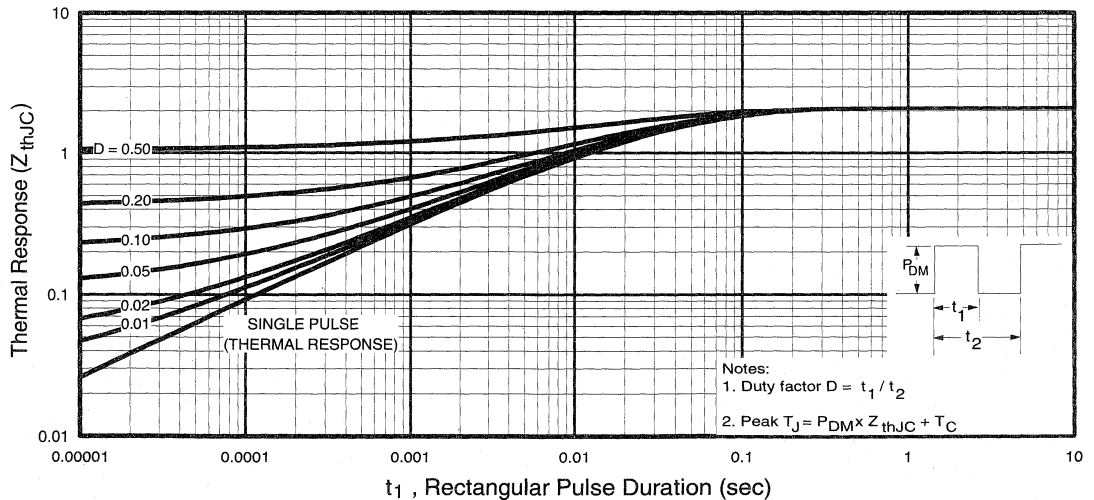


Fig. 6 - Maximum IGBT Effective Transient Thermal Impedance, Junction-to-Case

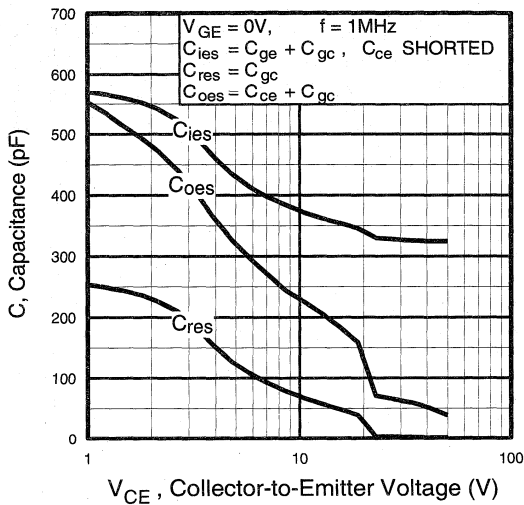


Fig. 7 - Typical Capacitance vs. Collector-to-Emitter Voltage

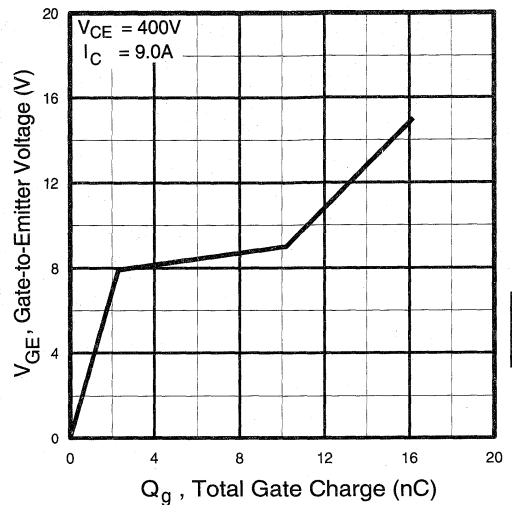


Fig. 8 - Typical Gate Charge vs. Gate-to-Emitter Voltage

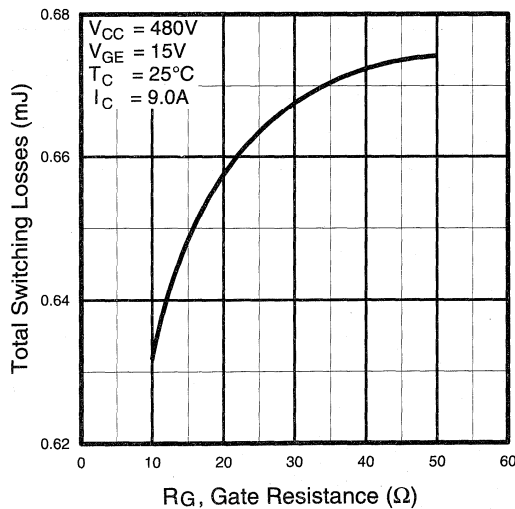


Fig. 9 - Typical Switching Losses vs. Gate Resistance

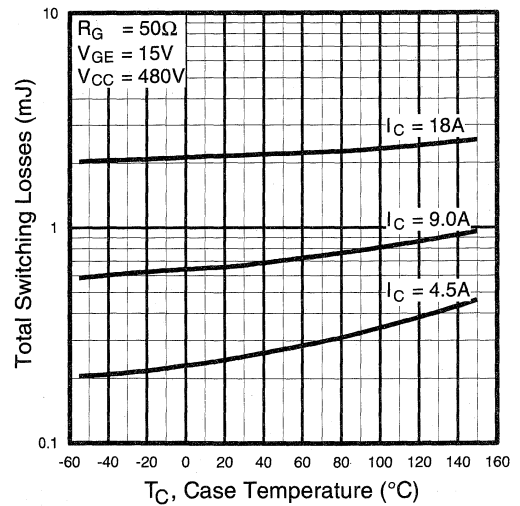


Fig. 10 - Typical Switching Losses vs. Case Temperature

Power
Conversion
Fast
Cu-Packs

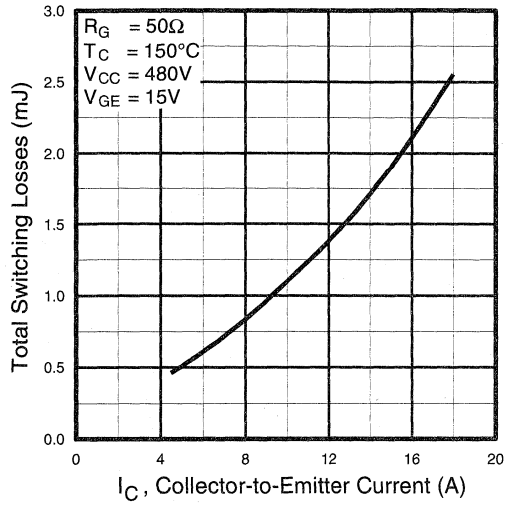


Fig. 11 - Typical Switching Losses vs. Collector-to-Emitter Current

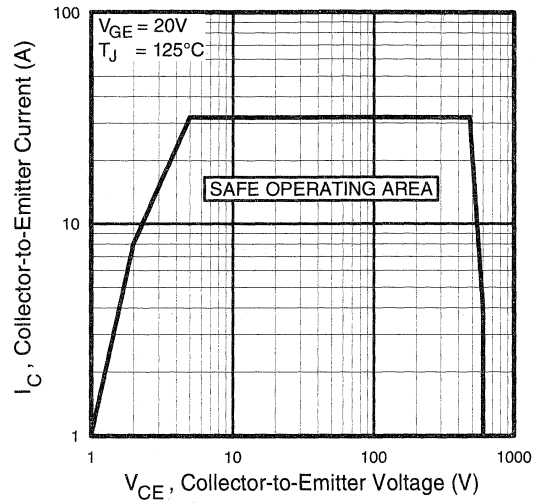


Fig. 12 - Turn-Off SOA

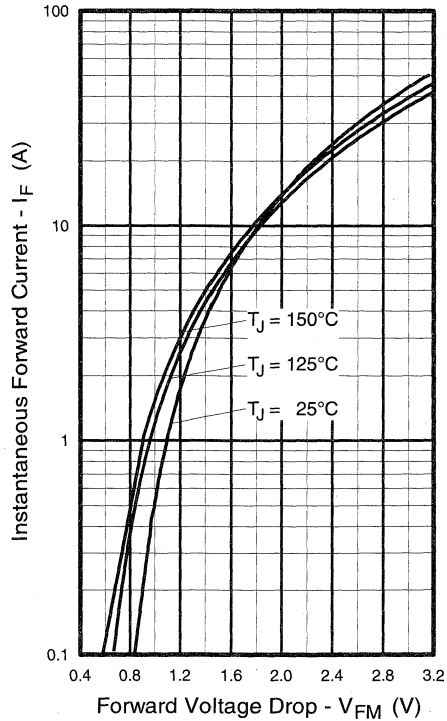


Fig. 13 - Maximum Forward Voltage Drop vs. Instantaneous Forward Current

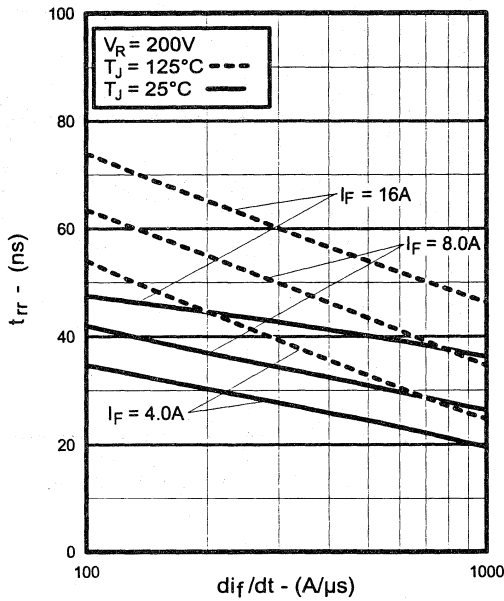


Fig. 14 - Typical Reverse Recovery vs. di_f/dt

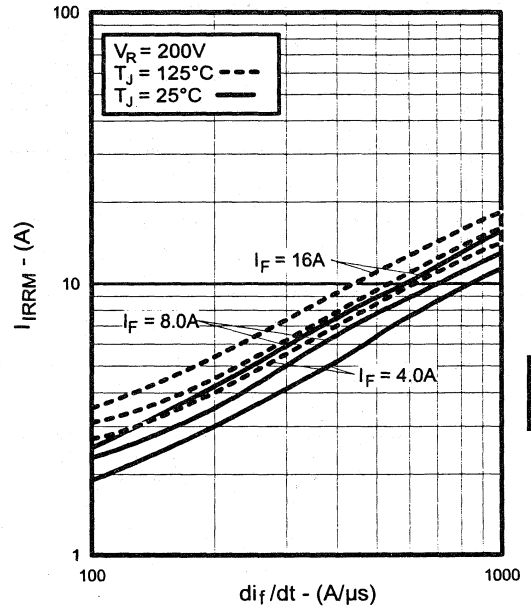


Fig. 15 - Typical Recovery Current vs. di_f/dt

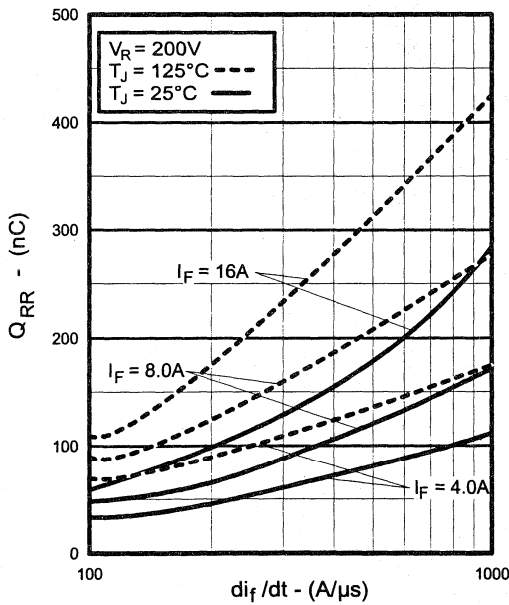


Fig. 16 - Typical Stored Charge vs. di_f/dt

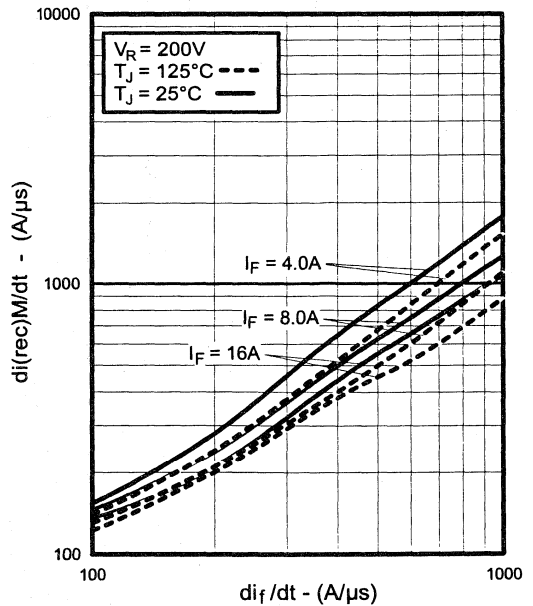


Fig. 17 - Typical $di_{(rec)}M/dt$ vs. di_f/dt

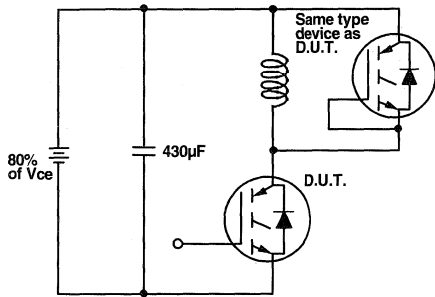


Fig. 18a - Test Circuit for Measurement of I_{LM} , E_{on} , $E_{off}(\text{diode})$, t_{rr} , Q_{rr} , I_{rr} , $t_{d(on)}$, t_r , $t_{d(off)}$, t_f

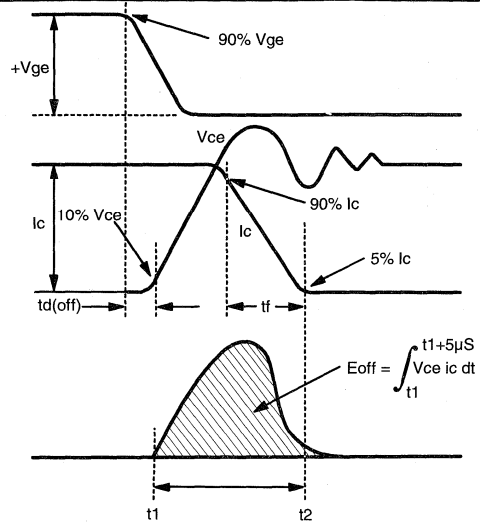


Fig. 18b - Test Waveforms for Circuit of Fig. 18a, Defining E_{off} , $t_{d(off)}$, t_f

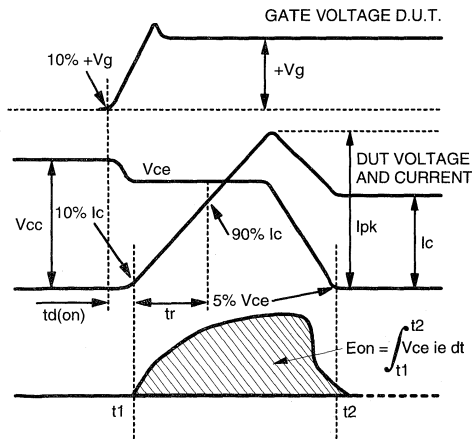


Fig. 18c - Test Waveforms for Circuit of Fig. 18a, Defining E_{on} , $t_{d(on)}$, t_r

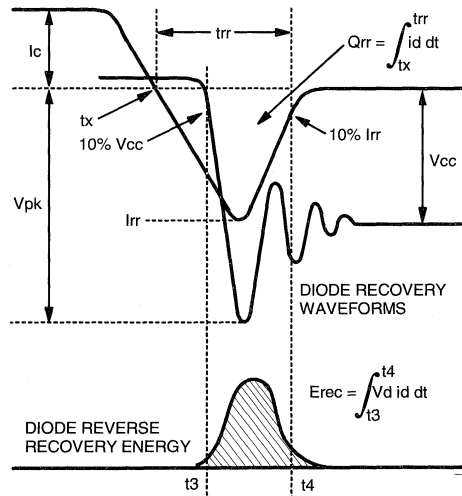


Fig. 18d - Test Waveforms for Circuit of Fig. 18a, Defining E_{rec} , t_{rr} , Q_{rr} , I_{rr}

**Refer to Section D for the following:
Appendix D: Section D - page D-6**

- Fig. 18e - Macro Waveforms for Test Circuit of Fig. 18a
- Fig. 19 - Clamped Inductive Load Test Circuit
- Fig. 20 - Pulsed Collector Current Test Circuit

IRGBC30FD2

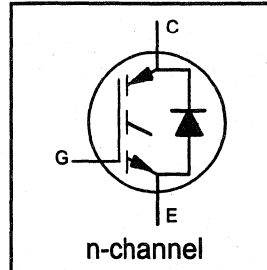
INSULATED GATE BIPOLAR TRANSISTOR
WITH ULTRAFAST SOFT RECOVERY

Fast CoPack IGBT

DIODE

Features

- Switching-loss rating includes all "tail" losses
- HEXFRED™ soft ultrafast diodes
- Optimized for medium operating frequency (1 to 10kHz) See Fig. 1 for Current vs. Frequency curve



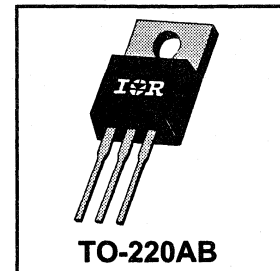
$$V_{CES} = 600V$$

$$V_{CE(sat)} \leq 2.1V$$

$$@V_{GE} = 15V, I_C = 31A$$

Description

Co-packaged IGBTs are a natural extension of International Rectifier's well known IGBT line. They provide the convenience of an IGBT and an ultrafast recovery diode in one package, resulting in substantial benefits to a host of high-voltage, high-current, motor control, UPS and power supply applications.



Absolute Maximum Ratings

	Parameter	Max.	Units
V_{CES}	Collector-to-Emitter Voltage	600	V
$I_C @ T_C = 25^\circ C$	Continuous Collector Current	31	A
$I_C @ T_C = 100^\circ C$	Continuous Collector Current	17	
I_{CM}	Pulsed Collector Current ①	120	
I_{LM}	Clamped Inductive Load Current ②	120	
$I_F @ T_C = 100^\circ C$	Diode Continuous Forward Current	12	
I_{FM}	Diode Maximum Forward Current	120	
V_{GE}	Gate-to-Emitter Voltage	± 20	
$P_D @ T_C = 25^\circ C$	Maximum Power Dissipation	100	W
$P_D @ T_C = 100^\circ C$	Maximum Power Dissipation	42	
T_J	Operating Junction and	-55 to +150	°C
T_{STG}	Storage Temperature Range		
	Soldering Temperature, for 10 sec.	300 (0.063 in. (1.6mm) from case)	
	Mounting Torque, 6-32 or M3 Screw.	10 lbf•in (1.1 N•m)	

Thermal Resistance

	Parameter	Min.	Typ.	Max.	Units
$R_{\theta JC}$	Junction-to-Case - IGBT	—	—	1.2	°C/W
$R_{\theta JC}$	Junction-to-Case - Diode	—	—	2.5	
$R_{\theta CS}$	Case-to-Sink, flat, greased surface	—	0.50	—	
$R_{\theta JA}$	Junction-to-Ambient, typical socket mount	—	—	80	
Wt	Weight	—	2 (0.07)	—	g (oz)

Electrical Characteristics @ T_J = 25°C (unless otherwise specified)

	Parameter	Min.	Typ.	Max.	Units	Conditions
V _{(BR)CES}	Collector-to-Emitter Breakdown Voltage ^①	600	—	—	V	V _{GE} = 0V, I _C = 250μA
ΔV _{(BR)CES} /ΔT _J	Temp. Coeff. of Breakdown Voltage	—	0.69	—	V/°C	V _{GE} = 0V, I _C = 1.0mA
V _{CE(on)}	Collector-to-Emitter Saturation Voltage	—	1.8	2.1	V	I _C = 17A, V _{GE} = 15V
		—	2.4	—		I _C = 31A
		—	2.2	—		I _C = 17A, T _J = 150°C
V _{GE(th)}	Gate Threshold Voltage	3.0	—	5.5		V _{CE} = V _{GE} , I _C = 250μA
ΔV _{GE(th)} /ΔT _J	Temp. Coeff. of Threshold Voltage	—	-11	—	mV/°C	V _{CE} = V _{GE} , I _C = 250μA
g _{fe}	Forward Transconductance ^②	6.1	10	—	S	V _{CE} = 100V, I _C = 17A
I _{CES}	Zero Gate Voltage Collector Current	—	—	250	μA	V _{GE} = 0V, V _{CE} = 600V
		—	—	2500		V _{GE} = 0V, V _{CE} = 600V, T _J = 150°C
V _{FM}	Diode Forward Voltage Drop	—	1.4	1.7	V	I _C = 12A
		—	1.3	1.6		I _C = 12A, T _J = 150°C
I _{GES}	Gate-to-Emitter Leakage Current	—	—	±100	nA	V _{GE} = ±20V

Switching Characteristics @ T_J = 25°C (unless otherwise specified)

	Parameter	Min.	Typ.	Max.	Units	Conditions
Q _g	Total Gate Charge (turn-on)	—	27	30		I _C = 17A
Q _{ge}	Gate - Emitter Charge (turn-on)	—	4.1	5.9	nC	V _{CC} = 400V
Q _{gc}	Gate - Collector Charge (turn-on)	—	12	15		See Fig. 8
t _{d(on)}	Turn-On Delay Time	—	72	—	ns	T _J = 25°C
t _r	Rise Time	—	75	—		I _C = 17A, V _{CC} = 480V
t _{d(off)}	Turn-Off Delay Time	—	300	450		V _{GE} = 15V, R _G = 23Ω
t _f	Fall Time	—	220	350	mJ	Energy losses include "tail" and diode reverse recovery.
E _{on}	Turn-On Switching Loss	—	0.9	—		See Fig. 9, 10, 11, 18
E _{off}	Turn-Off Switching Loss	—	2.1	—		
E _{is}	Total Switching Loss	—	3.0	4.6		
t _{d(on)}	Turn-On Delay Time	—	70	—	ns	T _J = 150°C, See Fig. 9, 10, 11, 18
t _r	Rise Time	—	75	—		I _C = 17A, V _{CC} = 480V
t _{d(off)}	Turn-Off Delay Time	—	420	—		V _{GE} = 15V, R _G = 23Ω
t _f	Fall Time	—	480	—	mJ	Energy losses include "tail" and diode reverse recovery.
E _{is}	Total Switching Loss	—	4.7	—		Measured 5mm from package
L _E	Internal Emitter Inductance	—	7.5	—		
C _{ies}	Input Capacitance	—	660	—	pF	
C _{oes}	Output Capacitance	—	100	—		V _{CC} = 30V
C _{res}	Reverse Transfer Capacitance	—	10	—		f = 1.0MHz
t _{rr}	Diode Reverse Recovery Time	—	42	60	ns	T _J = 25°C See Fig. 14
		—	80	120		T _J = 125°C
I _{rr}	Diode Peak Reverse Recovery Current	—	3.5	6.0	A	T _J = 25°C See Fig. 15
		—	5.6	10		T _J = 125°C
Q _{rr}	Diode Reverse Recovery Charge	—	80	180	nC	T _J = 25°C See Fig. 16
		—	220	600		T _J = 125°C
di _(rec) M/dt	Diode Peak Rate of Fall of Recovery During t _b	—	180	—	A/μs	T _J = 25°C See Fig. 17
		—	120	—		T _J = 125°C

Notes:

① Repetitive rating; V_{GE}=20V, pulse width limited by max. junction temperature. (See fig. 20)

② V_{CC}=80%(V_{CES}), V_{GE}=20V, L=10μH, R_G= 23Ω, (See fig. 19)

③ Pulse width ≤ 80μs; duty factor ≤ 0.1%.

④ Pulse width 5.0μs, single shot.

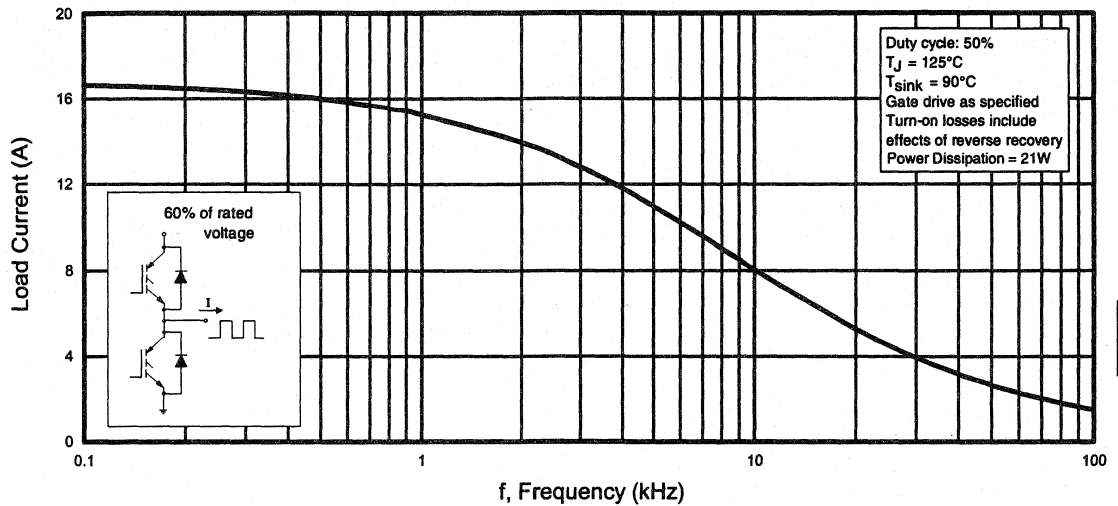


Fig. 1 - Typical Load Current vs. Frequency
 (Load Current = I_{RMS} of fundamental)

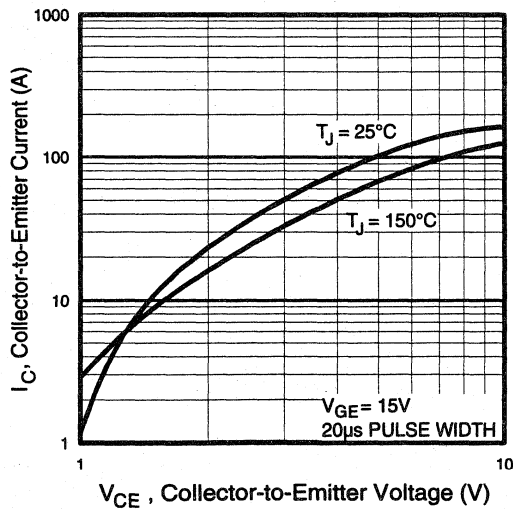


Fig. 2 - Typical Output Characteristics

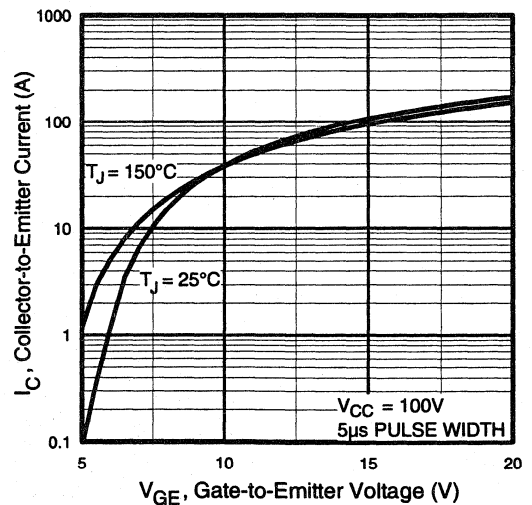


Fig. 3 - Typical Transfer Characteristics

Power
 Conversion
 Fast
 Co-Packs

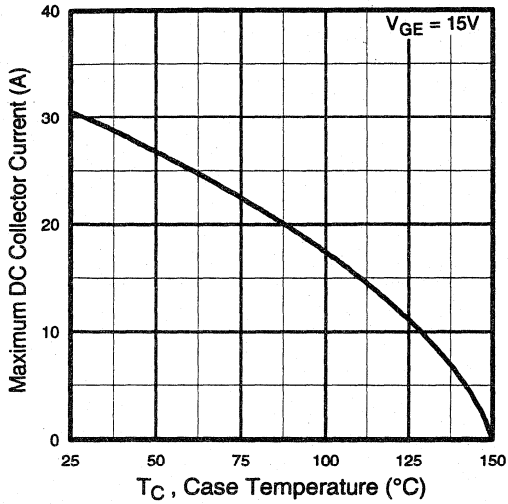


Fig. 4 - Maximum Collector Current vs. Case Temperature

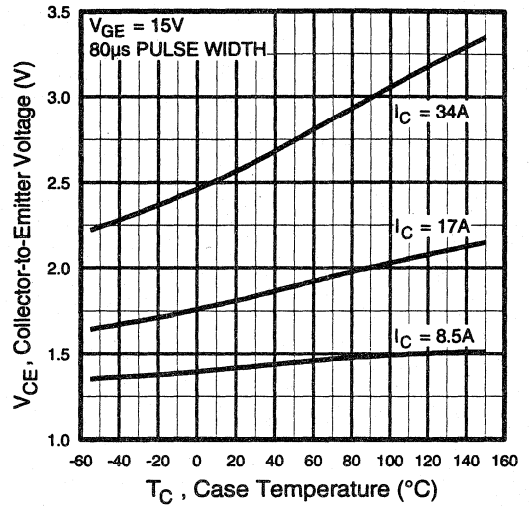


Fig. 5 - Collector-to-Emitter Voltage vs. Case Temperature

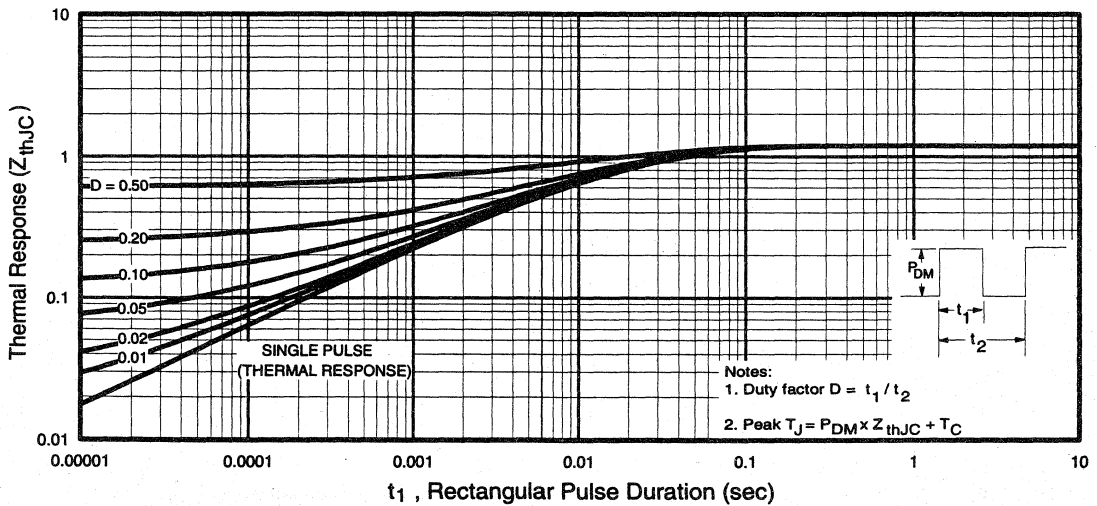


Fig. 6 - Maximum IGBT Effective Transient Thermal Impedance, Junction-to-Case

Power
Conversion
Fast
Co-Packs

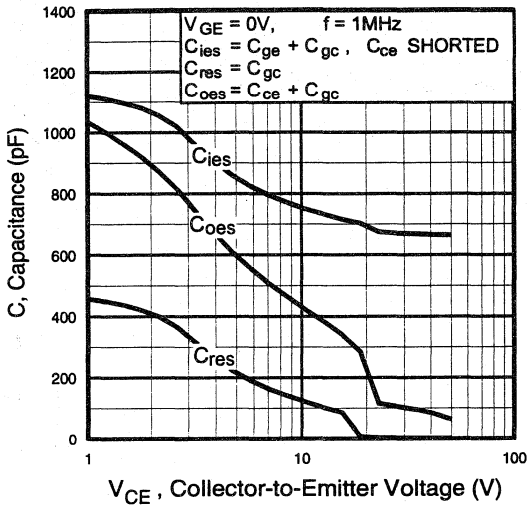


Fig. 7 - Typical Capacitance vs. Collector-to-Emitter Voltage

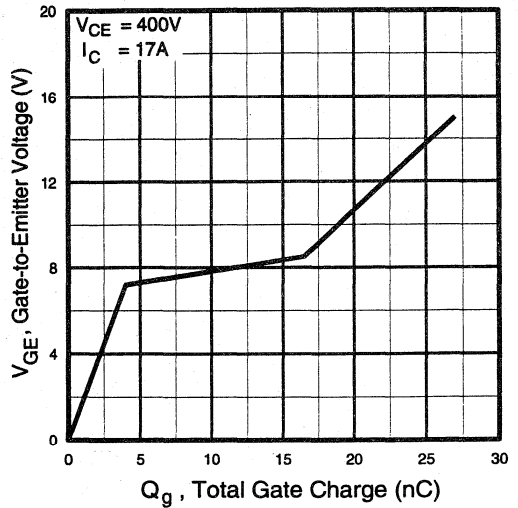


Fig. 8 - Typical Gate Charge vs. Gate-to-Emitter Voltage

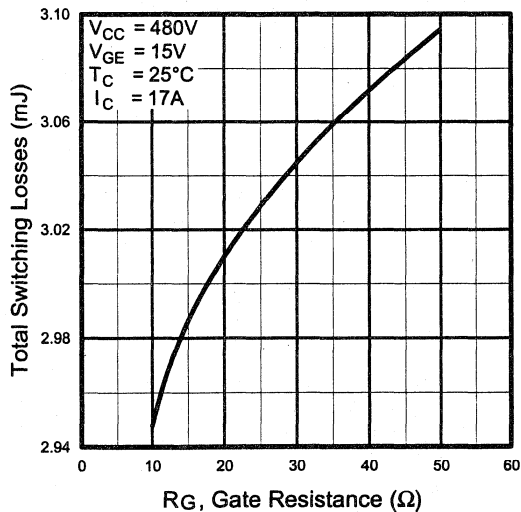


Fig. 9 - Typical Switching Losses vs. Gate Resistance

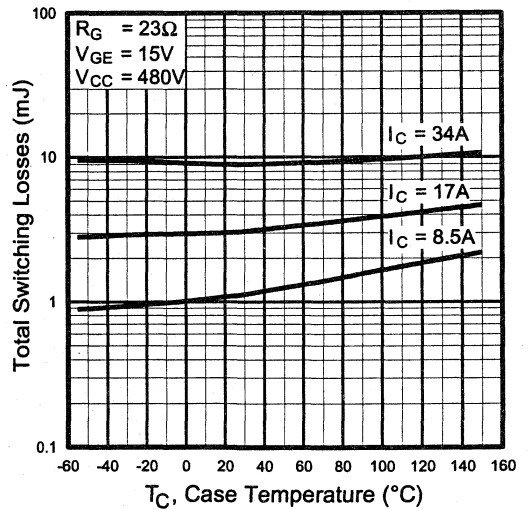


Fig. 10 - Typical Switching Losses vs. Case Temperature

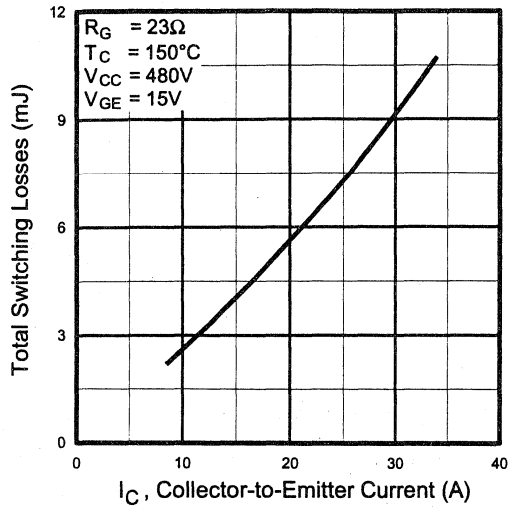


Fig. 11 - Typical Switching Losses vs. Collector-to-Emitter Current

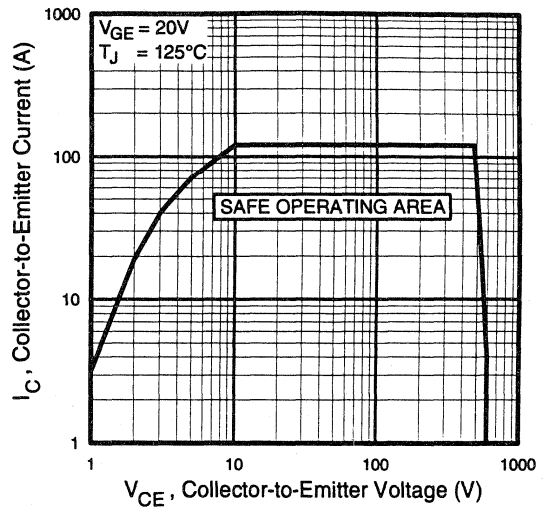


Fig. 12 - Turn-Off SOA

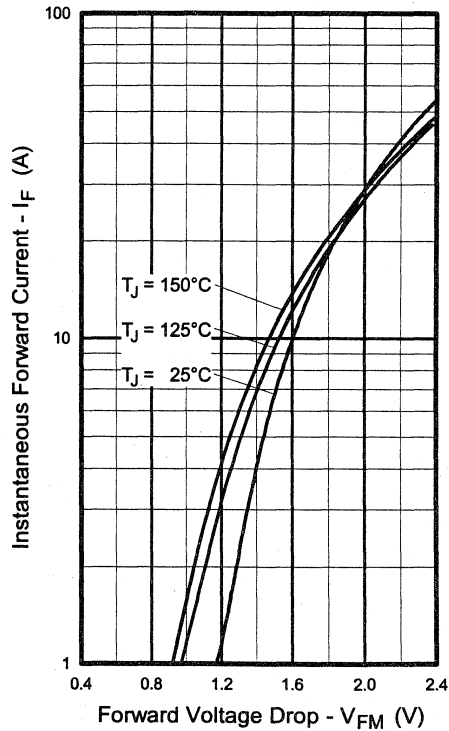


Fig. 13 - Maximum Forward Voltage Drop vs. Instantaneous Forward Current

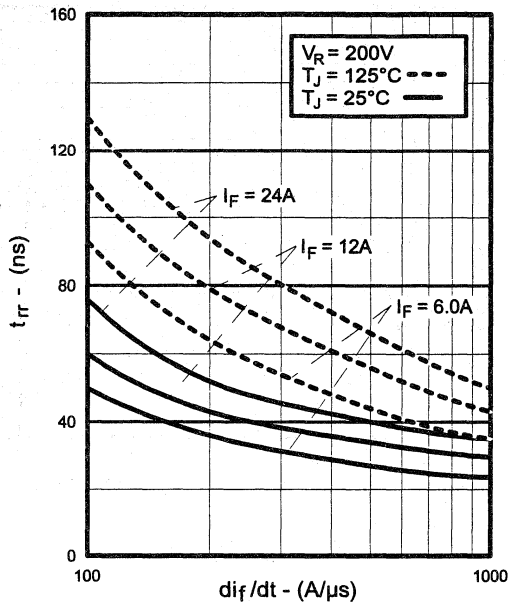


Fig. 14 - Typical Reverse Recovery vs. di_f/dt

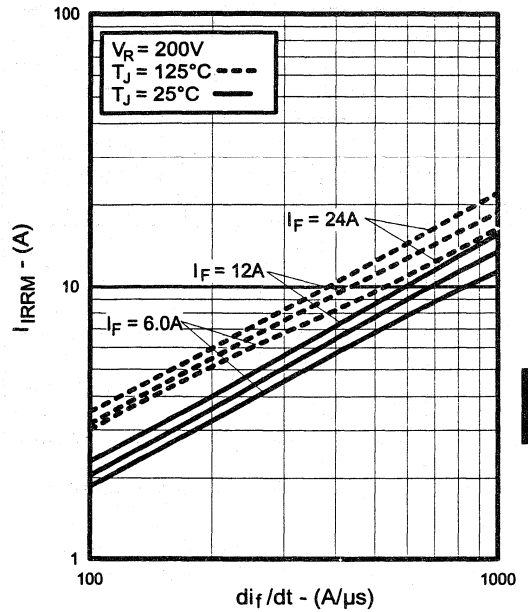


Fig. 15 - Typical Recovery Current vs. di_f/dt

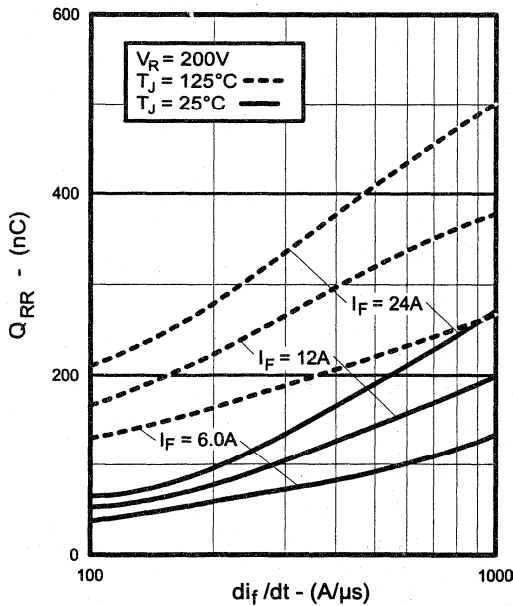


Fig. 16 - Typical Stored Charge vs. di_f/dt

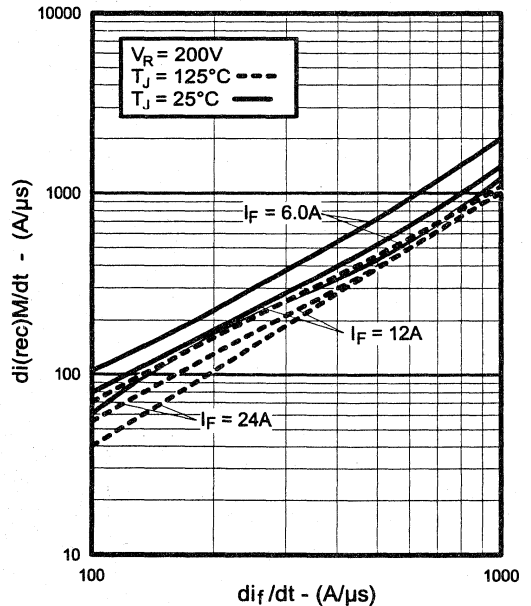


Fig. 17 - Typical $di_{(rec)M}/dt$ vs. di_f/dt

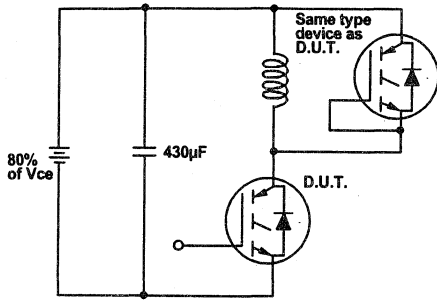


Fig. 18a - Test Circuit for Measurement of I_{LM} , E_{on} , $E_{off}(\text{diode})$, t_{rr} , Q_{rr} , I_{rr} , $t_{d(on)}$, t_r , $t_{d(off)}$, t_f

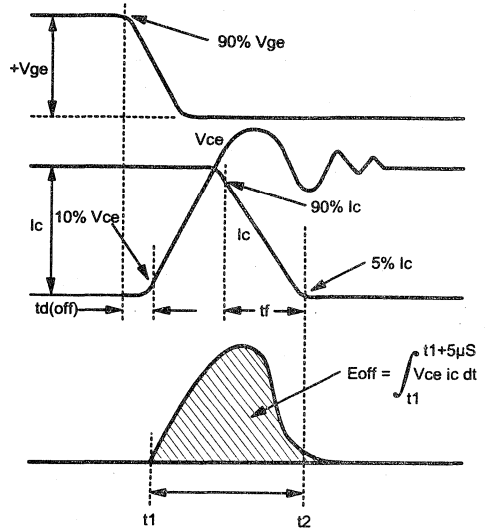


Fig. 18b - Test Waveforms for Circuit of Fig. 18a, Defining E_{off} , $t_{d(off)}$, t_f

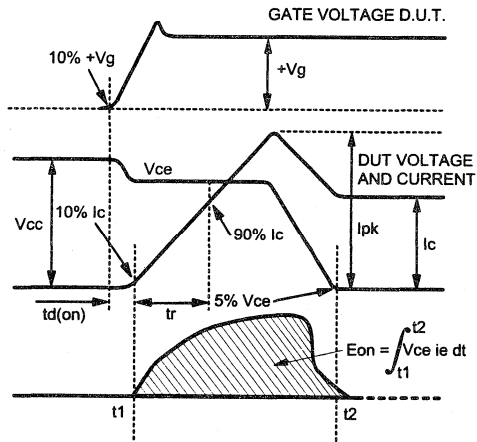


Fig. 18c - Test Waveforms for Circuit of Fig. 18a, Defining E_{on} , $t_{d(on)}$, t_r

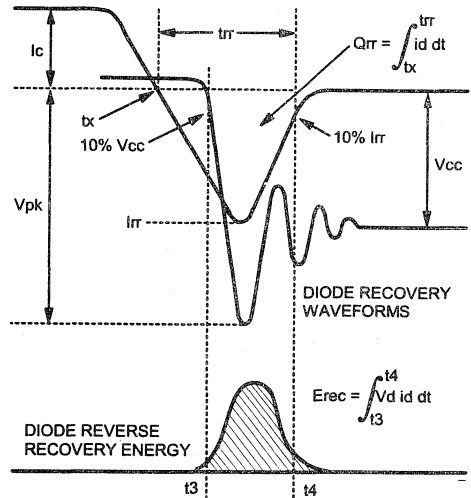


Fig. 18d - Test Waveforms for Circuit of Fig. 18a, Defining E_{rec} , t_{rr} , Q_{rr} , I_{rr}

Refer to Section D for the following:
Appendix D: Section D - page D-6

- Fig. 18e - Macro Waveforms for Test Circuit of Fig. 18a
- Fig. 19 - Clamped Inductive Load Test Circuit
- Fig. 20 - Pulsed Collector Current Test Circuit

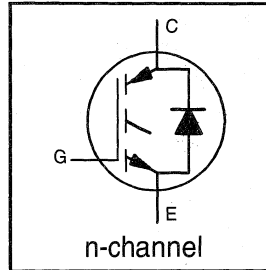
INSULATED GATE BIPOLAR TRANSISTOR
WITH ULTRAFAST SOFT RECOVERY

Fast CoPack IGBT

DIODE

Features

- Switching-loss rating includes all "tail" losses
- HEXFRED™ soft ultrafast diodes
- Optimized for medium operating frequency (1 to 10kHz) See Fig. 1 for Current vs. Frequency curve



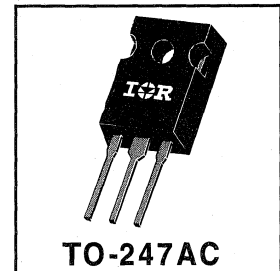
$$V_{CES} = 600V$$

$$V_{CE(sat)} \leq 2.1V$$

$$@V_{GE} = 15V, I_C = 17A$$

Description

Co-packaged IGBTs are a natural extension of International Rectifier's well known IGBT line. They provide the convenience of an IGBT and an ultrafast recovery diode in one package, resulting in substantial benefits to a host of high-voltage, high-current, motor control, UPS and power supply applications.



Absolute Maximum Ratings

	Parameter	Max.	Units
V_{CES}	Collector-to-Emitter Voltage	600	V
$I_C @ T_C = 25^\circ C$	Continuous Collector Current	31	A
$I_C @ T_C = 100^\circ C$	Continuous Collector Current	17	
I_{CM}	Pulsed Collector Current $\text{\textcircled{O}}$	120	
I_{LM}	Clamped Inductive Load Current $\text{\textcircled{O}}$	120	
$I_F @ T_C = 100^\circ C$	Diode Continuous Forward Current	12	
I_{FM}	Diode Maximum Forward Current	120	
V_{GE}	Gate-to-Emitter Voltage	± 20	V
$P_D @ T_C = 25^\circ C$	Maximum Power Dissipation	100	W
$P_D @ T_C = 100^\circ C$	Maximum Power Dissipation	42	
T_J	Operating Junction and	-55 to +150	°C
T_{STG}	Storage Temperature Range		
	Soldering Temperature, for 10 sec.	300 (0.063 in. (1.6mm) from case)	
	Mounting Torque, 6-32 or M3 Screw.	10 lbf•in (1.1 N•m)	

Thermal Resistance

	Parameter	Min.	Typ.	Max.	Units
$R_{\theta JC}$	Junction-to-Case - IGBT	—	—	1.2	°C/W
$R_{\theta JC}$	Junction-to-Case - Diode	—	—	2.5	
$R_{\theta CS}$	Case-to-Sink, flat, greased surface	—	0.24	—	
$R_{\theta JA}$	Junction-to-Ambient, typical socket mount	—	—	40	
Wt	Weight	—	6 (0.21)	—	g (oz)

Electrical Characteristics @ $T_J = 25^\circ\text{C}$ (unless otherwise specified)

	Parameter	Min.	Typ.	Max.	Units	Conditions
$V_{(BR)CES}$	Collector-to-Emitter Breakdown Voltage ^②	600	—	—	V	$V_{GE} = 0V, I_C = 250\mu A$
$\Delta V_{(BR)CES}/\Delta T_J$	Temp. Coeff. of Breakdown Voltage	—	0.69	—	V/ $^\circ\text{C}$	$V_{GE} = 0V, I_C = 1.0mA$
$V_{CE(on)}$	Collector-to-Emitter Saturation Voltage	—	1.8	2.1	V	$I_C = 17A$ $V_{GE} = 15V$
		—	2.4	—		$I_C = 31A$ See Fig. 2, 5
		—	2.2	—		$I_C = 17A, T_J = 150^\circ\text{C}$
$V_{GE(th)}$	Gate Threshold Voltage	3.0	—	5.5		$V_{CE} = V_{GE}, I_C = 250\mu A$
$\Delta V_{GE(th)}/\Delta T_J$	Temp. Coeff. of Threshold Voltage	—	-11	—	mV/ $^\circ\text{C}$	$V_{CE} = V_{GE}, I_C = 250\mu A$
g_{fe}	Forward Transconductance ^④	6.1	10	—	S	$V_{CE} = 100V, I_C = 17A$
I_{CES}	Zero Gate Voltage Collector Current	—	—	250	μA	$V_{GE} = 0V, V_{CE} = 600V$
		—	—	2500		$V_{GE} = 0V, V_{CE} = 600V, T_J = 150^\circ\text{C}$
V_{FM}	Diode Forward Voltage Drop	—	1.4	1.7	V	$I_C = 12A$ See Fig. 13
		—	1.3	1.6		$I_C = 12A, T_J = 150^\circ\text{C}$
I_{GES}	Gate-to-Emitter Leakage Current	—	—	± 100	nA	$V_{GE} = \pm 20V$

Switching Characteristics @ $T_J = 25^\circ\text{C}$ (unless otherwise specified)

	Parameter	Min.	Typ.	Max.	Units	Conditions
Q_g	Total Gate Charge (turn-on)	—	27	30	nC	$I_C = 17A$ $V_{CC} = 400V$ See Fig. 8
Q_{ge}	Gate - Emitter Charge (turn-on)	—	4.1	5.9		
Q_{gc}	Gate - Collector Charge (turn-on)	—	12	15		
$t_{d(on)}$	Turn-On Delay Time	—	72	—	ns	$T_J = 25^\circ\text{C}$ $I_C = 17A, V_{CC} = 480V$ $V_{GE} = 15V, R_G = 23\Omega$ Energy losses include "tail" and diode reverse recovery. See Fig. 9, 10, 11, 18
t_r	Rise Time	—	75	—		
$t_{d(off)}$	Turn-Off Delay Time	—	300	450		
t_f	Fall Time	—	220	350		
E_{on}	Turn-On Switching Loss	—	0.9	—		
E_{off}	Turn-Off Switching Loss	—	2.1	—		
E_{ts}	Total Switching Loss	—	3.0	4.6	mJ	$T_J = 150^\circ\text{C}$, See Fig. 9, 10, 11, 18 $I_C = 17A, V_{CC} = 480V$ $V_{GE} = 15V, R_G = 23\Omega$ Energy losses include "tail" and diode reverse recovery.
$t_{d(on)}$	Turn-On Delay Time	—	70	—		
t_r	Rise Time	—	75	—		
$t_{d(off)}$	Turn-Off Delay Time	—	420	—		
t_f	Fall Time	—	480	—		
E_{ts}	Total Switching Loss	—	4.7	—		
L_E	Internal Emitter Inductance	—	13	—	nH	Measured 5mm from package
C_{ies}	Input Capacitance	—	670	—	pF	$V_{GE} = 0V$ $V_{CC} = 30V$ See Fig. 7 $f = 1.0MHz$
C_{oes}	Output Capacitance	—	100	—		
C_{res}	Reverse Transfer Capacitance	—	10	—		
t_{rr}	Diode Reverse Recovery Time	—	42	60	ns	$T_J = 25^\circ\text{C}$ See Fig. 14 $T_J = 125^\circ\text{C}$ 14
		—	80	120		
I_{rr}	Diode Peak Reverse Recovery Current	—	3.5	6.0	A	$T_J = 25^\circ\text{C}$ See Fig. 15 $T_J = 125^\circ\text{C}$ 15
		—	5.6	10		
Q_{rr}	Diode Reverse Recovery Charge	—	80	180	nC	$T_J = 25^\circ\text{C}$ See Fig. 16 $T_J = 125^\circ\text{C}$ 16
		—	220	600		
$di_{(rec)M}/dt$	Diode Peak Rate of Fall of Recovery During t_b	—	180	—	A/ μs	$T_J = 25^\circ\text{C}$ See Fig. 17 $T_J = 125^\circ\text{C}$ 17
		—	120	—		

Notes:

- ① Repetitive rating; $V_{GE}=20V$, pulse width limited by max. junction temperature. (See fig. 20)
- ② $V_{CC}=80\%(V_{CES}), V_{GE}=20V, L=10\mu H, R_G=23\Omega$, (See fig. 19)
- ③ Pulse width $\leq 80\mu s$; duty factor $\leq 0.1\%$.
- ④ Pulse width 5.0 μs , single shot.

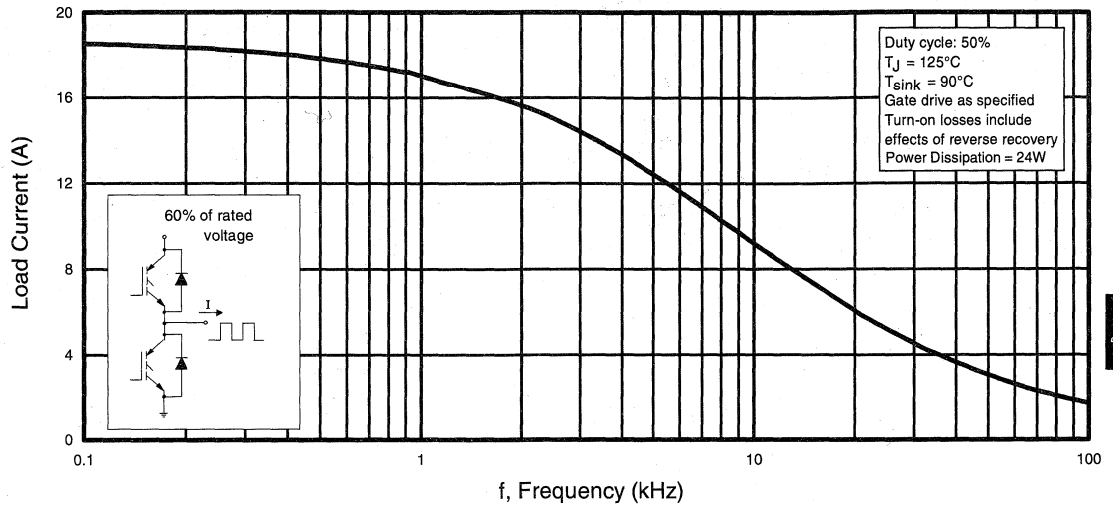


Fig. 1 - Typical Load Current vs. Frequency
(Load Current = I_{RMS} of fundamental)

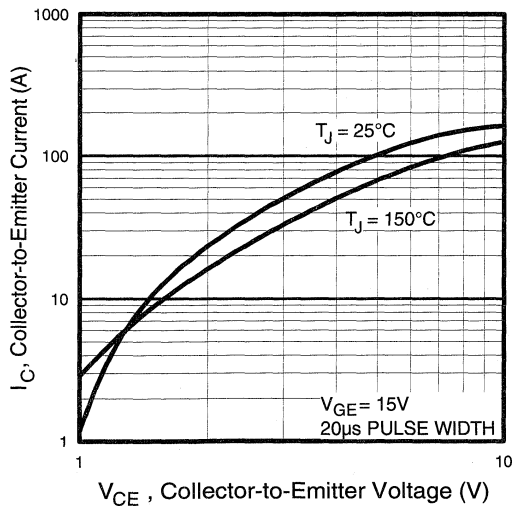


Fig. 2 - Typical Output Characteristics

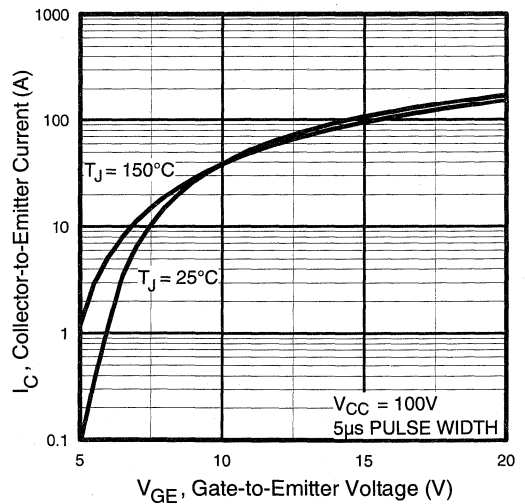


Fig. 3 - Typical Transfer Characteristics

Power
Conversion
Fast
Co-Packs

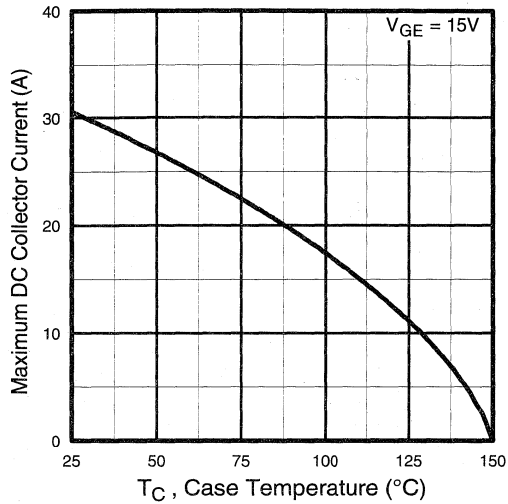


Fig. 4 - Maximum Collector Current vs. Case Temperature

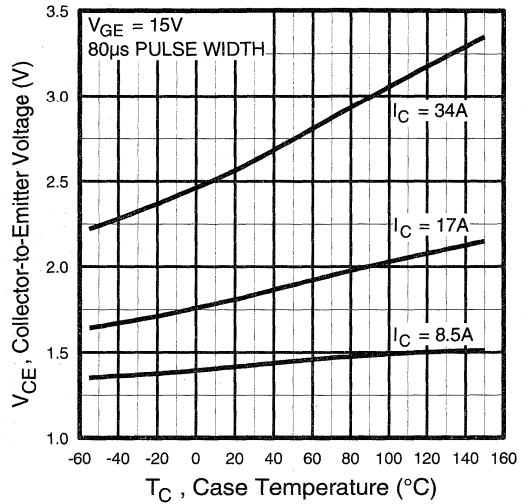


Fig. 5 - Collector-to-Emitter Voltage vs. Case Temperature

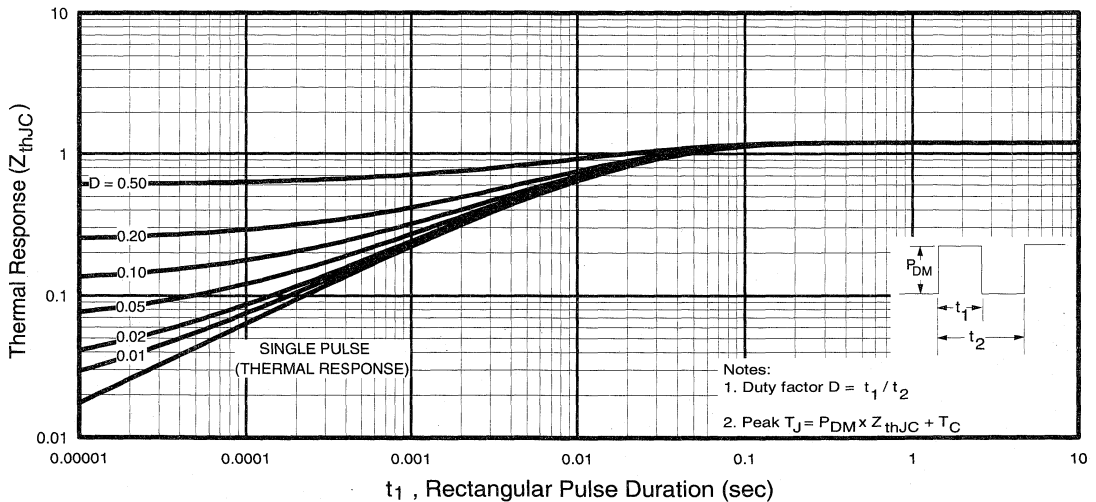


Fig. 6 - Maximum IGBT Effective Transient Thermal Impedance, Junction-to-Case

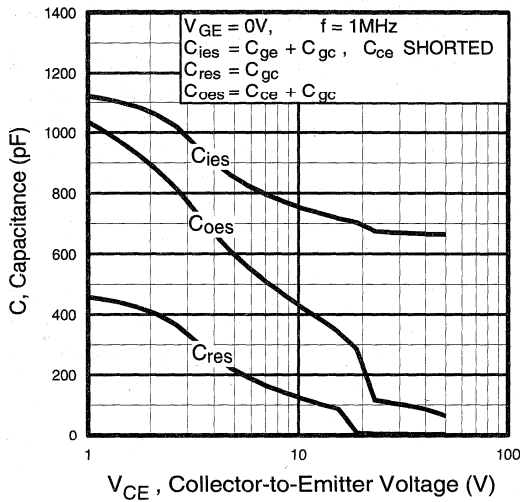


Fig. 7 - Typical Capacitance vs. Collector-to-Emitter Voltage

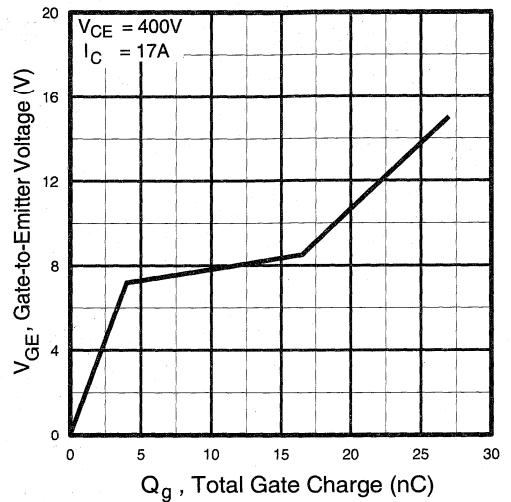


Fig. 8 - Typical Gate Charge vs. Gate-to-Emitter Voltage

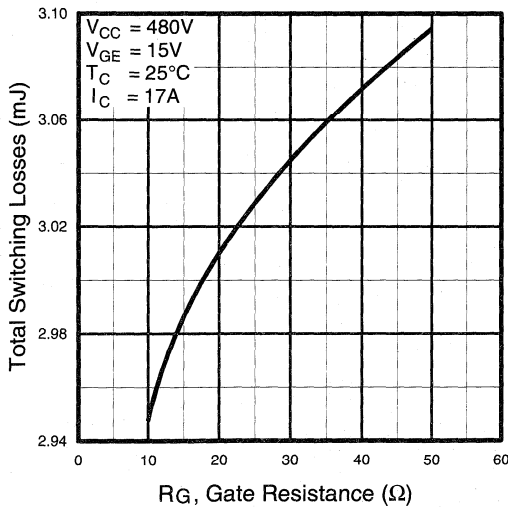


Fig. 9 - Typical Switching Losses vs. Gate Resistance

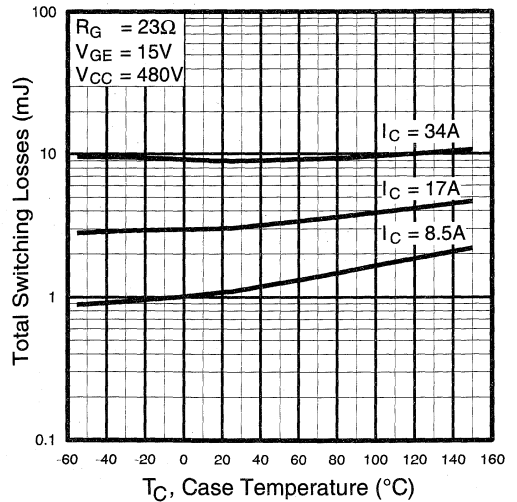


Fig. 10 - Typical Switching Losses vs. Case Temperature

Power
 Conversion
 Fast
 Co-Packs

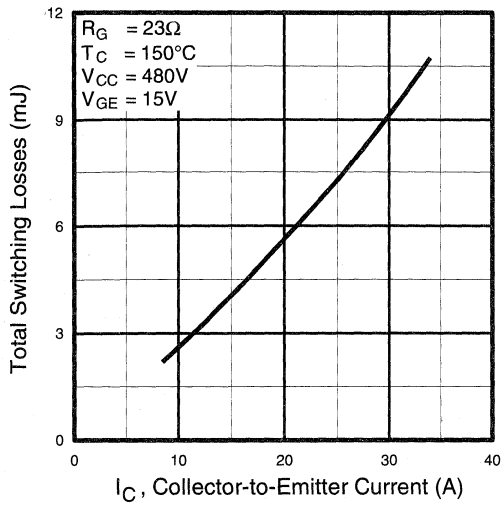


Fig. 11 - Typical Switching Losses vs. Collector-to-Emitter Current

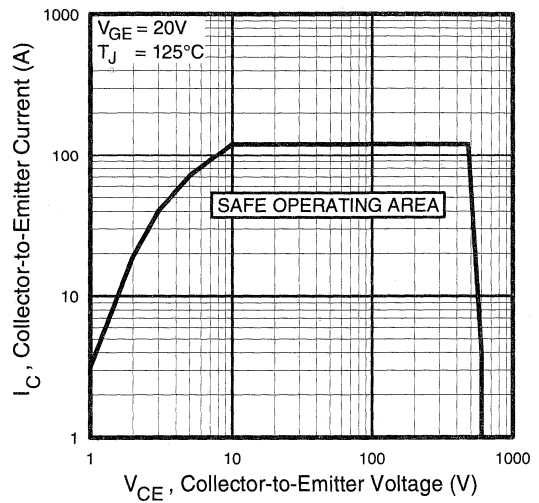


Fig. 12 - Turn-Off SOA

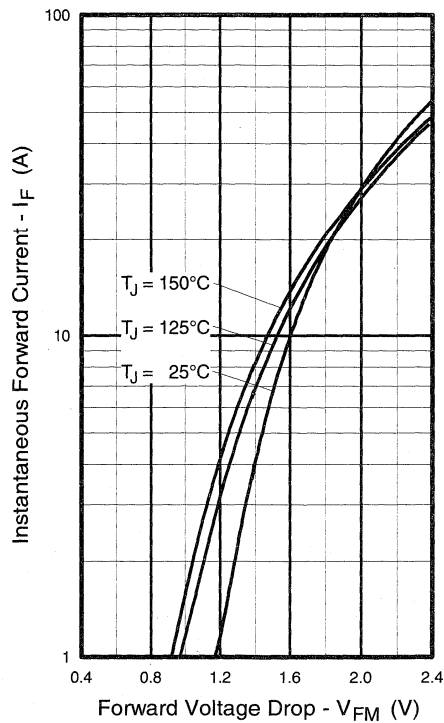


Fig. 13 - Maximum Forward Voltage Drop vs. Instantaneous Forward Current

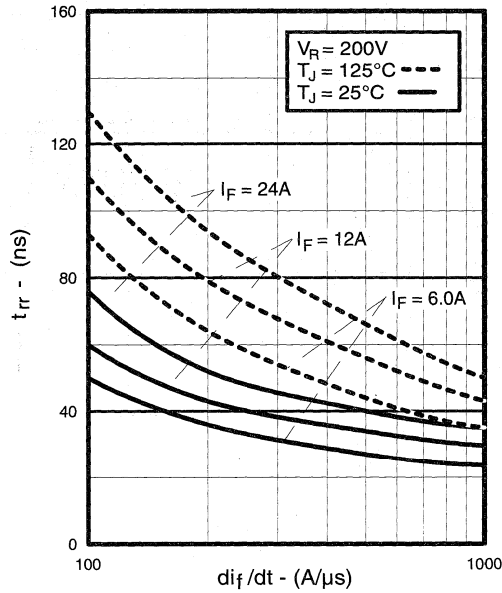


Fig. 14 - Typical Reverse Recovery vs. di_f/dt

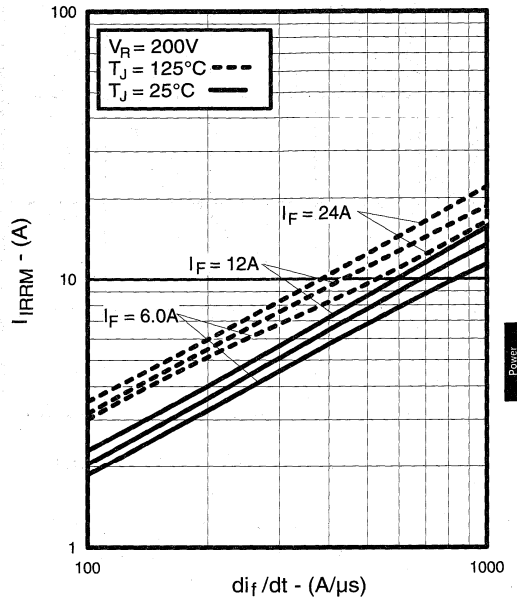


Fig. 15 - Typical Recovery Current vs. di_f/dt

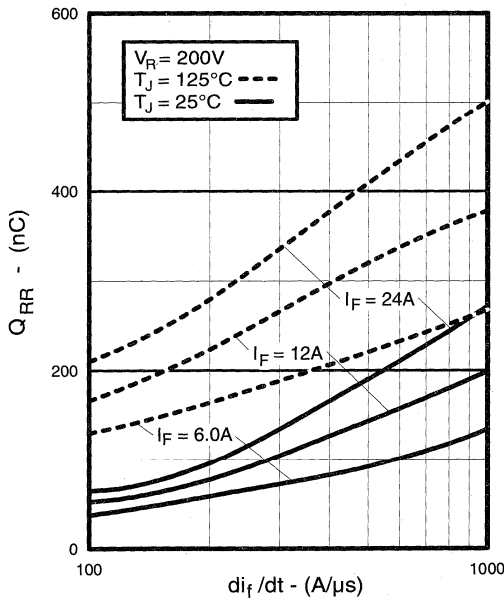


Fig. 16 - Typical Stored Charge vs. di_f/dt

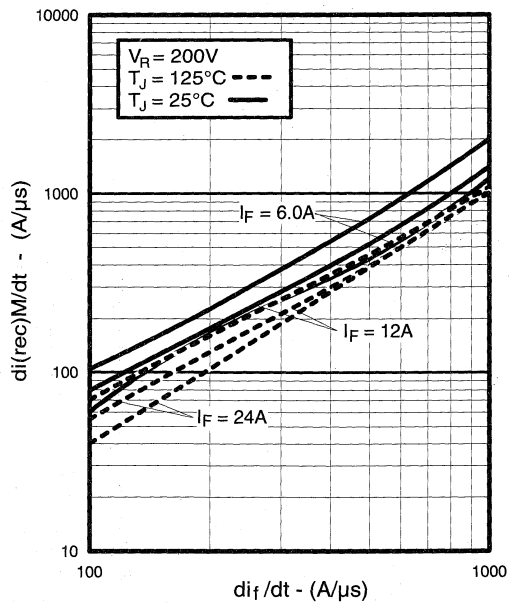


Fig. 17 - Typical $di_{(rec)}M/dt$ vs. di_f/dt

Power Conversion Fast Co-Packs

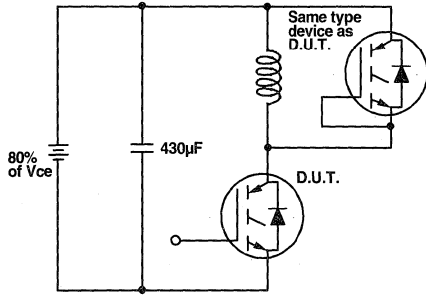


Fig. 18a - Test Circuit for Measurement of I_{LM} , E_{on} , $E_{off}(\text{diode})$, t_{rr} , Q_{rr} , I_{rr} , $t_{d(on)}$, t_r , $t_{d(off)}$, t_f

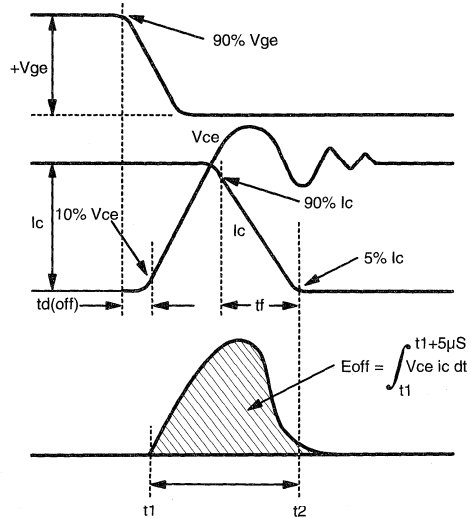


Fig. 18b - Test Waveforms for Circuit of Fig. 18a, Defining E_{off} , $t_{d(off)}$, t_f

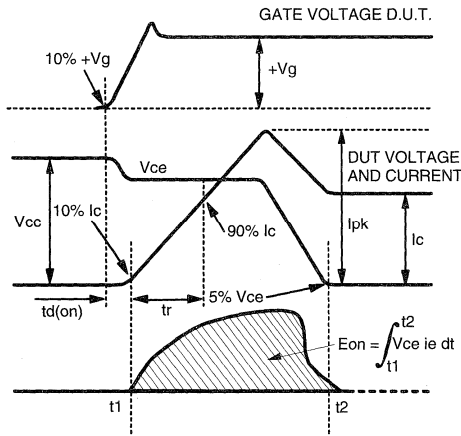


Fig. 18c - Test Waveforms for Circuit of Fig. 18a, Defining E_{on} , $t_{d(on)}$, t_r

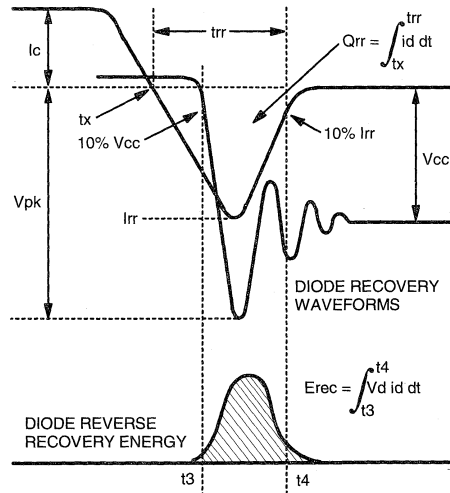


Fig. 18d - Test Waveforms for Circuit of Fig. 18a, Defining E_{rec} , t_{rr} , Q_{rr} , I_{rr}

Refer to Section D for the following Appendix D: Section D - page D-6

- Fig. 18e - Macro Waveforms for Test Circuit of Fig. 18a
- Fig. 19 - Clamped Inductive Load Test Circuit
- Fig. 20 - Pulsed Collector Current Test Circuit

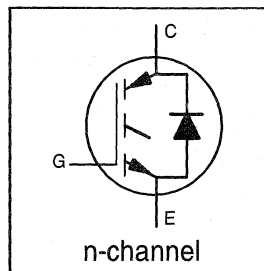
IRGPC40FD2

INSULATED GATE BIPOLAR TRANSISTOR
WITH ULTRAFAST SOFT RECOVERY

Fast CoPack IGBT

DIODE Features

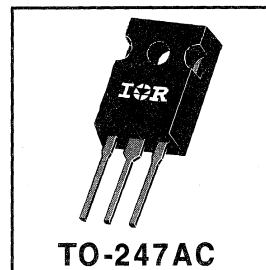
- Switching-loss rating includes all "tail" losses
- HEXFRED™ soft ultrafast diodes
- Optimized for medium operating frequency (1 to 10kHz) See Fig. 1 for Current vs. Frequency curve



$V_{CES} = 600V$
$V_{CE(sat)} \leq 2.0V$
@ $V_{GE} = 15V, I_C = 27A$

Description

Co-packaged IGBTs are a natural extension of International Rectifier's well known IGBT line. They provide the convenience of an IGBT and an ultrafast recovery diode in one package, resulting in substantial benefits to a host of high-voltage, high-current, motor control, UPS and power supply applications.



Absolute Maximum Ratings

	Parameter	Max.	Units
V_{CES}	Collector-to-Emitter Voltage	600	V
$I_C @ T_C = 25^\circ C$	Continuous Collector Current	49	A
$I_C @ T_C = 100^\circ C$	Continuous Collector Current	27	
I_{CM}	Pulsed Collector Current $\text{\textcircled{D}}$	200	
I_{LM}	Clamped Inductive Load Current $\text{\textcircled{D}}$	200	
$I_F @ T_C = 100^\circ C$	Diode Continuous Forward Current	15	
I_{FM}	Diode Maximum Forward Current	200	
V_{GE}	Gate-to-Emitter Voltage	± 20	V
$P_D @ T_C = 25^\circ C$	Maximum Power Dissipation	160	W
$P_D @ T_C = 100^\circ C$	Maximum Power Dissipation	65	
T_J	Operating Junction and	-55 to +150	$^\circ C$
T_{STG}	Storage Temperature Range		
	Soldering Temperature, for 10 sec.	300 (0.063 in. (1.6mm) from case)	
	Mounting Torque, 6-32 or M3 Screw.	10 lbf•in (1.1 N•m)	

Thermal Resistance

	Parameter	Min.	Typ.	Max.	Units
$R_{\theta JC}$	Junction-to-Case - IGBT	—	—	0.77	$^\circ C/W$
$R_{\theta JC}$	Junction-to-Case - Diode	—	—	1.7	
$R_{\theta CS}$	Case-to-Sink, flat, greased surface	—	0.24	—	
$R_{\theta JA}$	Junction-to-Ambient, typical socket mount	—	—	40	
W_t	Weight	—	6 (0.21)	—	g (oz)

Electrical Characteristics @ $T_J = 25^\circ\text{C}$ (unless otherwise specified)

	Parameter	Min.	Typ.	Max.	Units	Conditions
$V_{(BR)CES}$	Collector-to-Emitter Breakdown Voltage ^③	600	—	—	V	$V_{GE} = 0V, I_C = 250\mu A$
$\Delta V_{(BR)CES}/\Delta T_J$	Temp. Coeff. of Breakdown Voltage	—	0.70	—	V/°C	$V_{GE} = 0V, I_C = 1.0mA$
$V_{CE(on)}$	Collector-to-Emitter Saturation Voltage	—	1.7	2.0	V	$I_C = 27A$ $I_C = 49A$ $I_C = 27A, T_J = 150^\circ\text{C}$ $V_{GE} = 15V$ See Fig. 2, 5
		—	2.2	—		
		—	1.9	—		
$V_{GE(th)}$	Gate Threshold Voltage	3.0	—	5.5		$V_{CE} = V_{GE}, I_C = 250\mu A$
$\Delta V_{GE(th)}/\Delta T_J$	Temp. Coeff. of Threshold Voltage	—	-12	—	mV/°C	$V_{CE} = V_{GE}, I_C = 250\mu A$
g_{fe}	Forward Transconductance ^④	9.2	12	—	S	$V_{CE} = 100V, I_C = 27A$
I_{CES}	Zero Gate Voltage Collector Current	—	—	250	μA	$V_{GE} = 0V, V_{CE} = 600V$ $V_{GE} = 0V, V_{CE} = 600V, T_J = 150^\circ\text{C}$
		—	—	3500		
V_{FM}	Diode Forward Voltage Drop	—	1.3	1.7	V	$I_C = 15A$ $I_C = 15A, T_J = 150^\circ\text{C}$ See Fig. 13
		—	1.2	1.6		
I_{GES}	Gate-to-Emitter Leakage Current	—	—	± 100	nA	$V_{GE} = \pm 20V$

Switching Characteristics @ $T_J = 25^\circ\text{C}$ (unless otherwise specified)

	Parameter	Min.	Typ.	Max.	Units	Conditions
Q_g	Total Gate Charge (turn-on)	—	59	80	nC	$I_C = 27A$ $V_{CC} = 400V$ See Fig. 8
Q_{ge}	Gate - Emitter Charge (turn-on)	—	8.6	10		
Q_{gc}	Gate - Collector Charge (turn-on)	—	25	42		
$t_{d(on)}$	Turn-On Delay Time	—	71	—	ns	$T_J = 25^\circ\text{C}$ $I_C = 27A, V_{CC} = 480V$ $V_{GE} = 15V, R_G = 10\Omega$ Energy losses include "tail" and diode reverse recovery. See Fig. 9, 10, 11, 18
t_r	Rise Time	—	76	—		
$t_{d(off)}$	Turn-Off Delay Time	—	320	480		
t_f	Fall Time	—	210	320		
E_{on}	Turn-On Switching Loss	—	1.3	—		
E_{off}	Turn-Off Switching Loss	—	3.2	—		
E_{ts}	Total Switching Loss	—	4.5	6.8	mJ	
$t_{d(on)}$	Turn-On Delay Time	—	70	—	ns	$T_J = 150^\circ\text{C}$, See Fig. 9, 10, 11, 18 $I_C = 27A, V_{CC} = 480V$ $V_{GE} = 15V, R_G = 10\Omega$ Energy losses include "tail" and diode reverse recovery.
t_r	Rise Time	—	73	—		
$t_{d(off)}$	Turn-Off Delay Time	—	540	—		
t_f	Fall Time	—	480	—		
E_{ts}	Total Switching Loss	—	7.8	—	mJ	
L_E	Internal Emitter Inductance	—	13	—	nH	Measured 5mm from package
C_{ies}	Input Capacitance	—	1500	—	pF	$V_{GE} = 0V$ $V_{CC} = 30V$ $f = 1.0MHz$ See Fig. 7
C_{oes}	Output Capacitance	—	190	—		
C_{res}	Reverse Transfer Capacitance	—	20	—		
t_{rr}	Diode Reverse Recovery Time	—	42	60	ns	$T_J = 25^\circ\text{C}$ See Fig. 14 $T_J = 125^\circ\text{C}$ 14
		—	74	120		
I_{rr}	Diode Peak Reverse Recovery Current	—	4.0	6.0	A	$T_J = 25^\circ\text{C}$ See Fig. 15 $T_J = 125^\circ\text{C}$ 15
		—	6.5	10		
Q_{rr}	Diode Reverse Recovery Charge	—	80	180	nC	$T_J = 25^\circ\text{C}$ See Fig. 16 $T_J = 125^\circ\text{C}$ 16
		—	220	600		
$di_{(rec)}/dt$	Diode Peak Rate of Fall of Recovery During t_b	—	188	—	A/ μs	$T_J = 25^\circ\text{C}$ See Fig. 17 $T_J = 125^\circ\text{C}$ 17
		—	160	—		

Notes:

① Repetitive rating; $V_{GE}=20V$, pulse width limited by max. junction temperature. (See fig. 20)

② $V_{CC}=80\%(V_{CES}), V_{GE}=20V, L=10\mu H, R_G=10\Omega$, (See fig. 19)

③ Pulse width $\leq 80\mu s$; duty factor $\leq 0.1\%$.

④ Pulse width 5.0 μs , single shot.

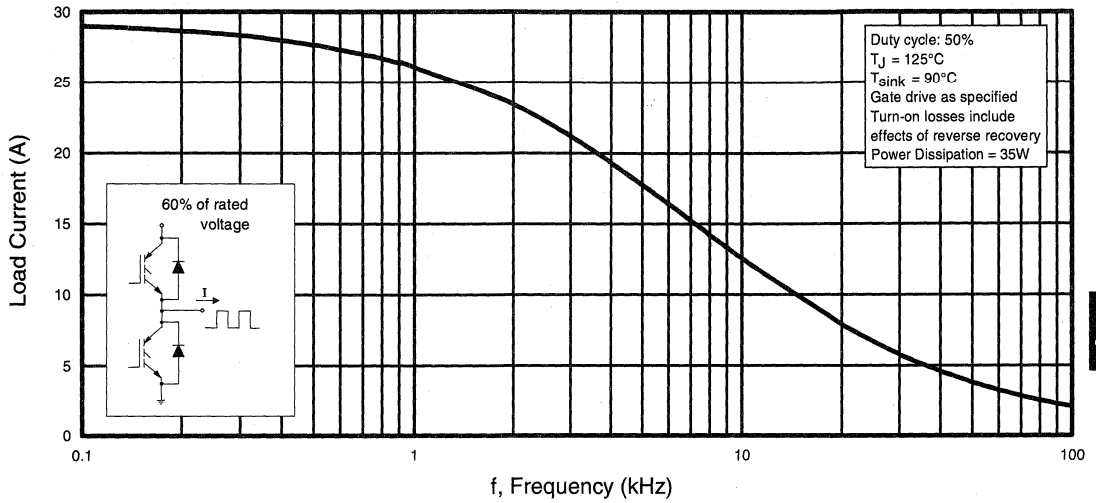


Fig. 1 - Typical Load Current vs. Frequency
(Load Current = I_{RMS} of fundamental)

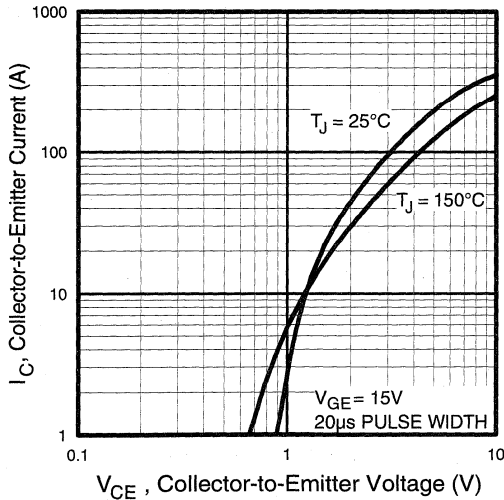


Fig. 2 - Typical Output Characteristics

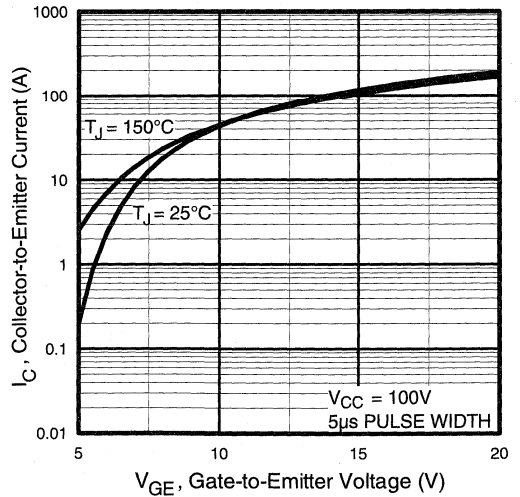


Fig. 3 - Typical Transfer Characteristics

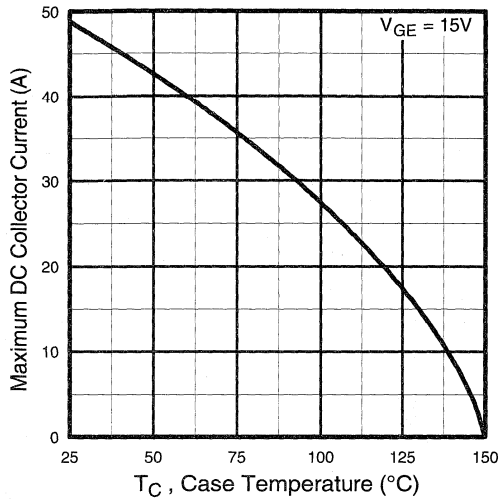


Fig. 4 - Maximum Collector Current vs. Case Temperature

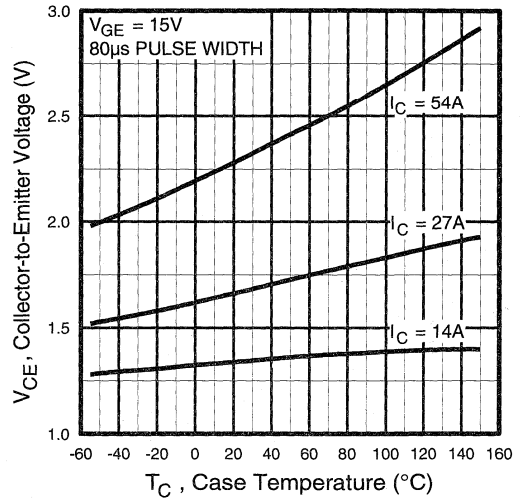


Fig. 5 - Collector-to-Emitter Voltage vs. Case Temperature

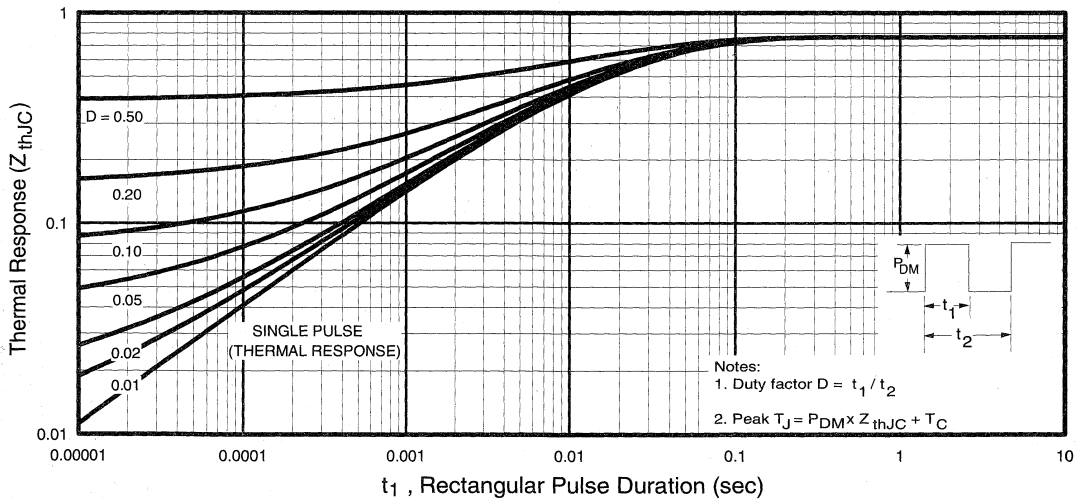


Fig. 6 - Maximum IGBT Effective Transient Thermal Impedance, Junction-to-Case

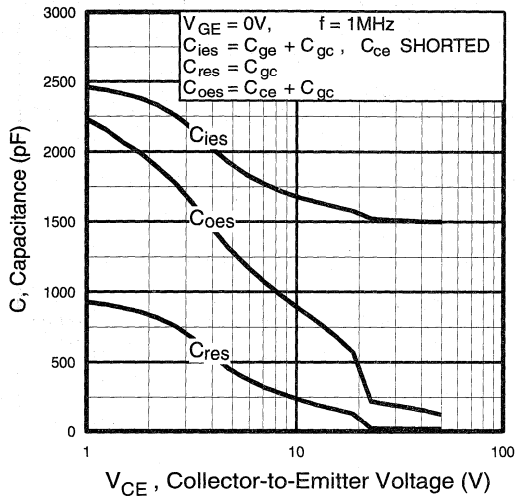


Fig. 7 - Typical Capacitance vs. Collector-to-Emitter Voltage

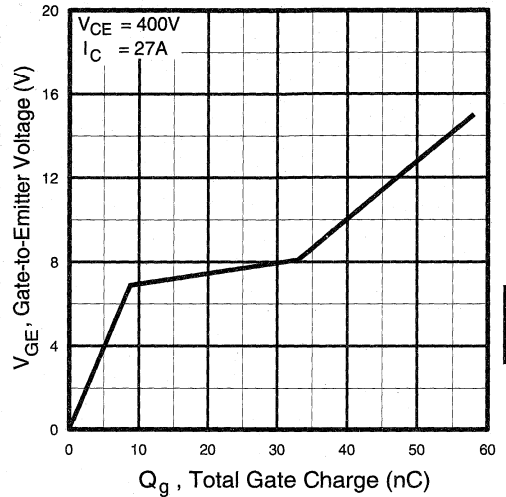


Fig. 8 - Typical Gate Charge vs. Gate-to-Emitter Voltage

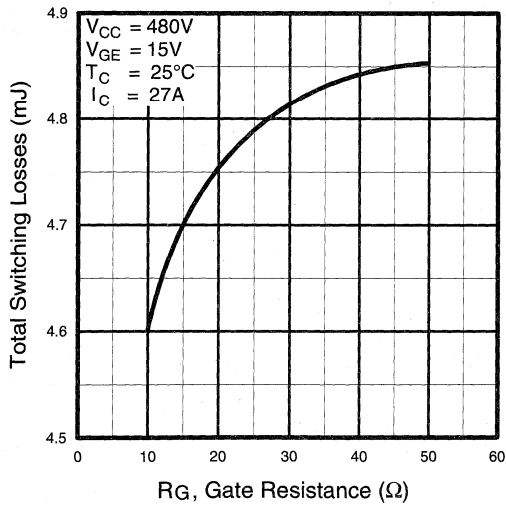


Fig. 9 - Typical Switching Losses vs. Gate Resistance

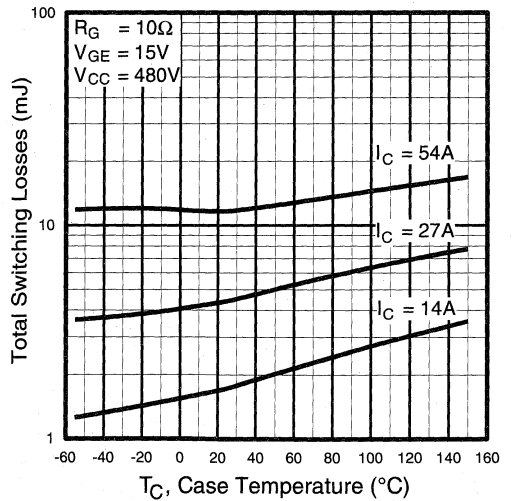


Fig. 10 - Typical Switching Losses vs. Case Temperature

Power Conversion Efficiency Co-Packs

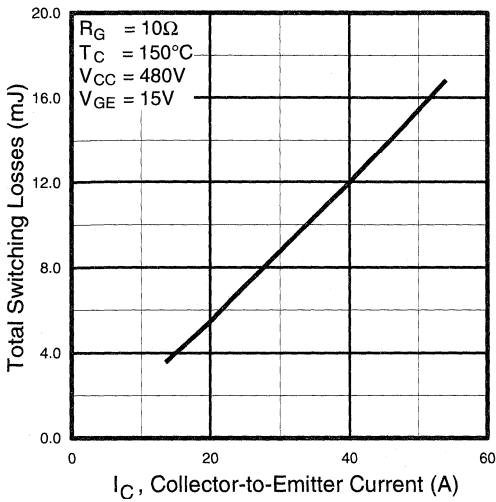


Fig. 11 - Typical Switching Losses vs. Collector-to-Emitter Current

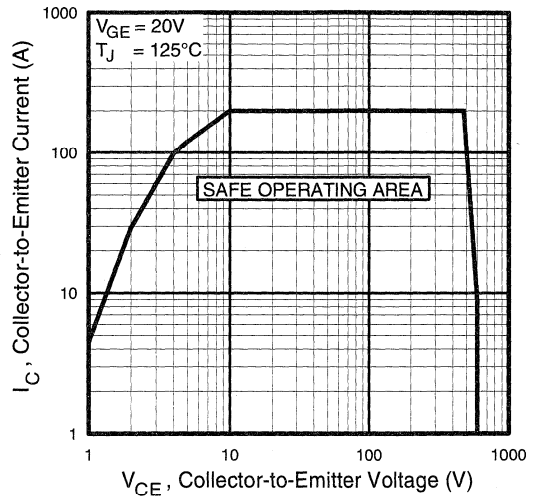


Fig. 12 - Turn-Off SOA

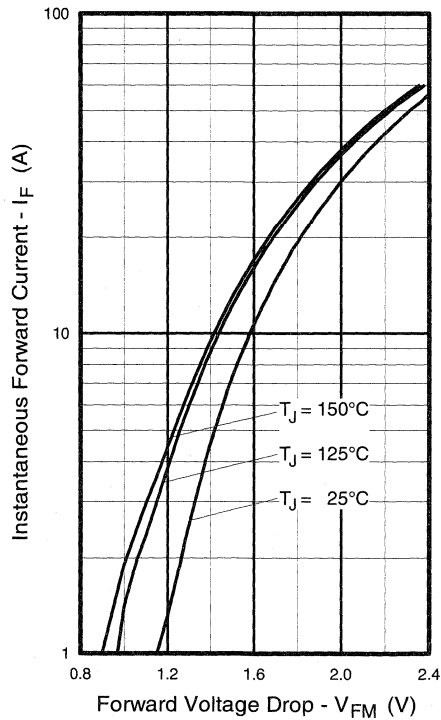


Fig. 13 - Maximum Forward Voltage Drop vs. Instantaneous Forward Current

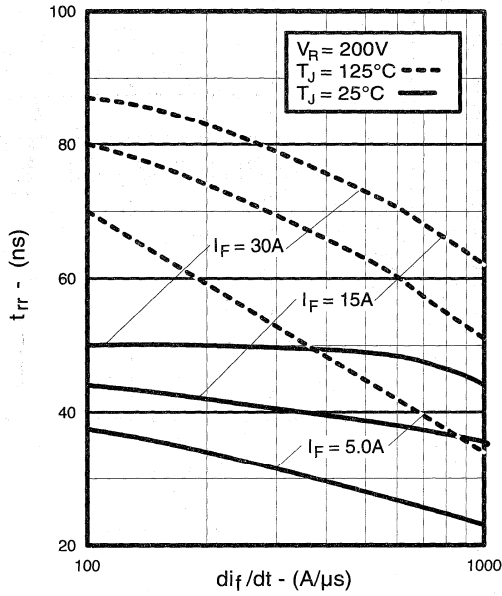


Fig. 14 - Typical Reverse Recovery vs. di_f/dt

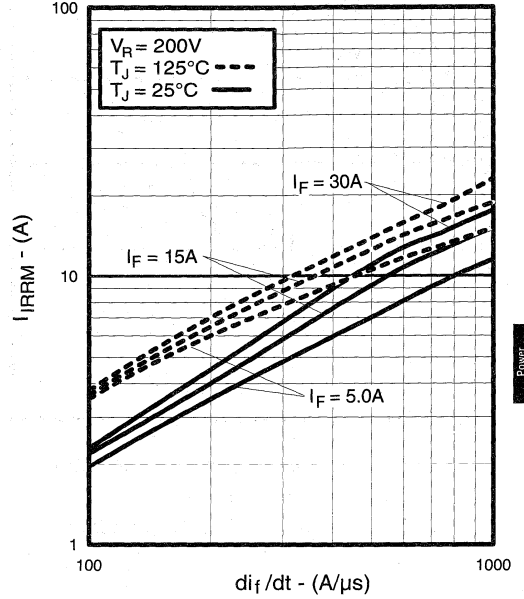


Fig. 15 - Typical Recovery Current vs. di_f/dt

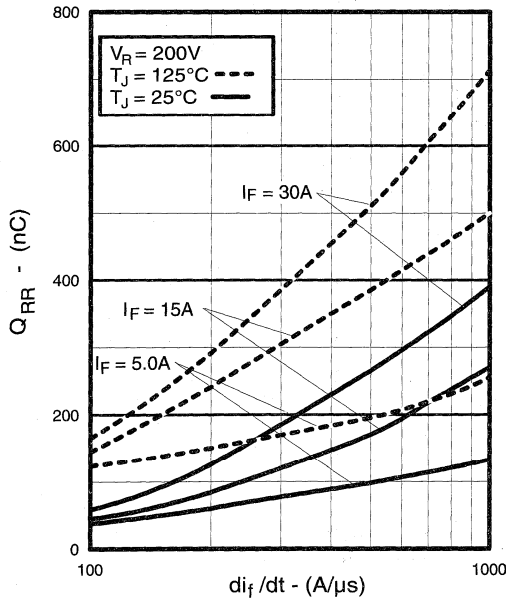


Fig. 16 - Typical Stored Charge vs. di_f/dt

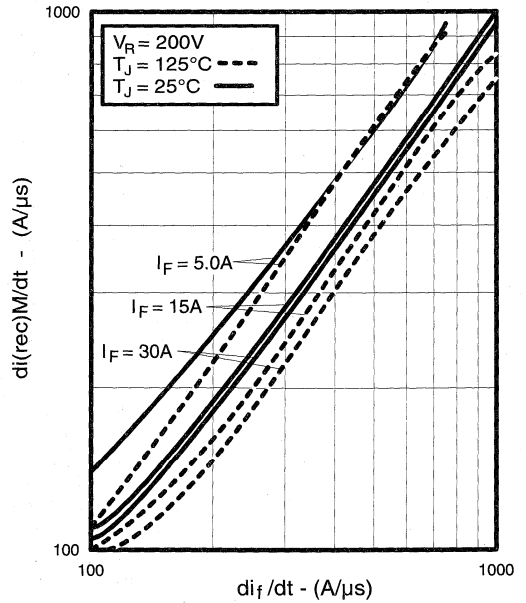


Fig. 17 - Typical $di_{(rec)M}/dt$ vs. di_f/dt

Power Conversion Fast Co-Packs

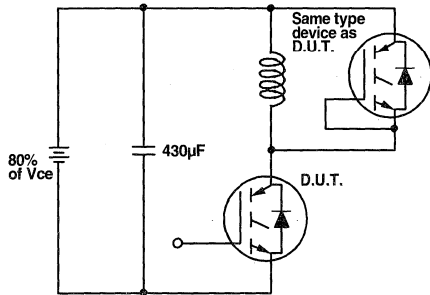


Fig. 18a - Test Circuit for Measurement of I_{LM} , E_{on} , $E_{off}(\text{diode})$, t_{rr} , Q_{rr} , I_{rr} , $t_{d(on)}$, t_r , $t_{d(off)}$, t_f

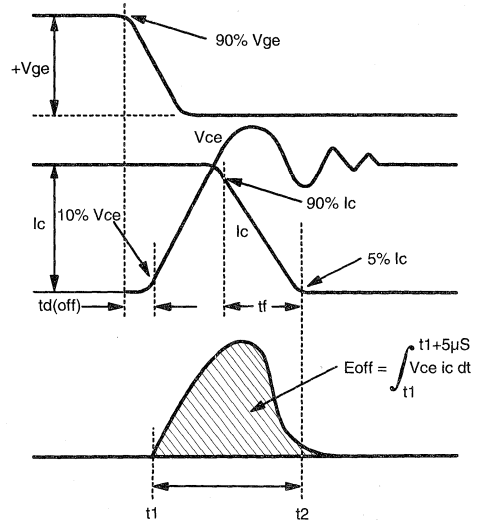


Fig. 18b - Test Waveforms for Circuit of Fig. 18a, Defining E_{off} , $t_{d(off)}$, t_f

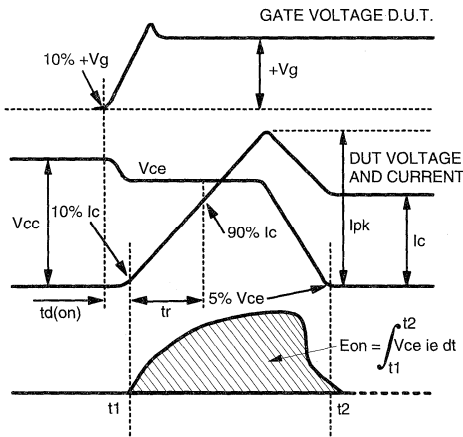


Fig. 18c - Test Waveforms for Circuit of Fig. 18a, Defining E_{on} , $t_{d(on)}$, t_r

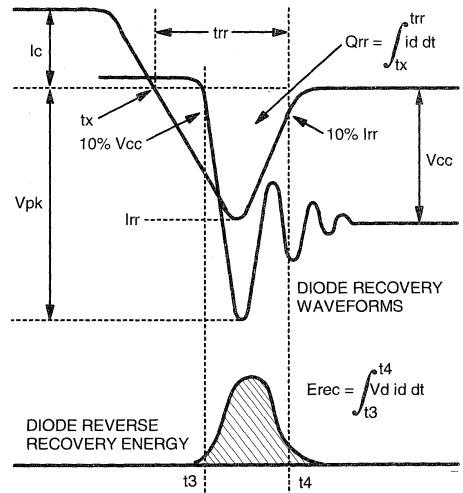


Fig. 18d - Test Waveforms for Circuit of Fig. 18a, Defining E_{rec} , t_{rr} , Q_{rr} , I_{rr}

**Refer to Section D for the following:
Appendix D: Section D - page D-6**

- Fig. 18e - Macro Waveforms for Test Circuit of Fig. 18a
- Fig. 19 - Clamped Inductive Load Test Circuit
- Fig. 20 - Pulsed Collector Current Test Circuit

IRGPC50FD2

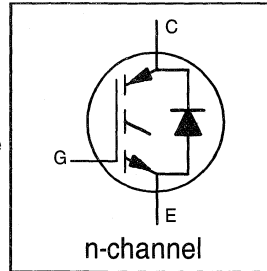
INSULATED GATE BIPOLAR TRANSISTOR
WITH ULTRAFAST SOFT RECOVERY

Fast CoPack IGBT

DIODE

Features

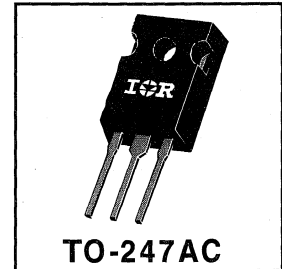
- Switching-loss rating includes all "tail" losses
- HEXFRED™ soft ultrafast diodes
- Optimized for medium operating frequency (1 to 10kHz) See Fig. 1 for Current vs. Frequency curve



$V_{CES} = 600V$
 $V_{CE(sat)} \leq 1.7V$
 @ $V_{GE} = 15V, I_C = 39A$

Description

Co-packaged IGBTs are a natural extension of International Rectifier's well known IGBT line. They provide the convenience of an IGBT and an ultrafast recovery diode in one package, resulting in substantial benefits to a host of high-voltage, high-current, motor control, UPS and power supply applications.



Absolute Maximum Ratings

	Parameter	Max.	Units
V_{CES}	Collector-to-Emitter Voltage	600	V
$I_C @ T_C = 25^\circ C$	Continuous Collector Current	70	A
$I_C @ T_C = 100^\circ C$	Continuous Collector Current	39	
I_{CM}	Pulsed Collector Current ^①	280	
I_{LM}	Clamped Inductive Load Current ^②	280	
$I_F @ T_C = 100^\circ C$	Diode Continuous Forward Current	25	
I_{FM}	Diode Maximum Forward Current	280	
V_{GE}	Gate-to-Emitter Voltage	± 20	V
$P_D @ T_C = 25^\circ C$	Maximum Power Dissipation	200	W
$P_D @ T_C = 100^\circ C$	Maximum Power Dissipation	78	
T_J	Operating Junction and	-55 to +150	°C
T_{STG}	Storage Temperature Range		
	Soldering Temperature, for 10 sec.	300 (0.063 in. (1.6mm) from case)	
	Mounting Torque, 6-32 or M3 Screw.	10 lbf•in (1.1 N•m)	

Thermal Resistance

	Parameter	Min.	Typ.	Max.	Units
$R_{\theta JC}$	Junction-to-Case - IGBT	—	—	0.64	°C/W
$R_{\theta JC}$	Junction-to-Case - Diode	—	—	0.83	
$R_{\theta CS}$	Case-to-Sink, flat, greased surface	—	0.24	—	
$R_{\theta JA}$	Junction-to-Ambient, typical socket mount	—	—	40	
Wt	Weight	—	6 (0.21)	—	

Electrical Characteristics @ $T_J = 25^\circ\text{C}$ (unless otherwise specified)

	Parameter	Min.	Typ.	Max.	Units	Conditions
$V_{(BR)CES}$	Collector-to-Emitter Breakdown Voltage ^③	600	—	—	V	$V_{GE} = 0V, I_C = 250\mu A$
$\Delta V_{(BR)CES}/\Delta T_J$	Temp. Coeff. of Breakdown Voltage	—	0.62	—	V/ $^\circ\text{C}$	$V_{GE} = 0V, I_C = 1.0mA$
$V_{CE(on)}$	Collector-to-Emitter Saturation Voltage	—	1.6	1.7	V	$I_C = 39A, V_{GE} = 15V$
		—	2.0	—		$I_C = 70A$ See Fig. 2, 5
		—	1.7	—		$I_C = 39A, T_J = 150^\circ\text{C}$
$V_{GE(th)}$	Gate Threshold Voltage	3.0	—	5.5		$V_{CE} = V_{GE}, I_C = 250\mu A$
$\Delta V_{GE(th)}/\Delta T_J$	Temperature Coeff. of Threshold Voltage	—	-14	—	mV/ $^\circ\text{C}$	$V_{CE} = V_{GE}, I_C = 250\mu A$
g_{fe}	Forward Transconductance ^④	21	24	—	S	$V_{CE} = 100V, I_C = 39A$
I_{CES}	Zero Gate Voltage Collector Current	—	—	250	μA	$V_{GE} = 0V, V_{CE} = 600V$
		—	—	6500		$V_{GE} = 0V, V_{CE} = 600V, T_J = 150^\circ\text{C}$
V_{FM}	Diode Forward Voltage Drop	—	1.3	1.7	V	$I_C = 25A$ See Fig. 13
		—	1.2	1.5		$I_C = 25A, T_J = 150^\circ\text{C}$
I_{GES}	Gate-to-Emitter Leakage Current	—	—	± 100	nA	$V_{GE} = \pm 20V$

Switching Characteristics @ $T_J = 25^\circ\text{C}$ (unless otherwise specified)

	Parameter	Min.	Typ.	Max.	Units	Conditions
Q_g	Total Gate Charge (turn-on)	—	110	170	nC	$I_C = 39A$
Q_{ge}	Gate - Emitter Charge (turn-on)	—	20	30		$V_{CC} = 400V$
Q_{gc}	Gate - Collector Charge (turn-on)	—	50	75		See Fig. 8
$t_{d(on)}$	Turn-On Delay Time	—	70	—	ns	$T_J = 25^\circ\text{C}$
t_r	Rise Time	—	110	—		$I_C = 39A, V_{CC} = 480V$
$t_{d(off)}$	Turn-Off Delay Time	—	400	600		$V_{GE} = 15V, R_G = 5.0\Omega$
t_f	Fall Time	—	290	400		Energy losses include "tail" and diode reverse recovery.
E_{on}	Turn-On Switching Loss	—	2.5	—		See Fig. 9, 10, 11, 18
E_{off}	Turn-Off Switching Loss	—	6.0	—	mJ	$T_J = 150^\circ\text{C}$, See Fig. 9, 10, 11, 18
E_{ts}	Total Switching Loss	—	8.5	13		
$t_{d(on)}$	Turn-On Delay Time	—	68	—		
t_r	Rise Time	—	100	—		
$t_{d(off)}$	Turn-Off Delay Time	—	760	—		
t_f	Fall Time	—	520	—	ns	$I_C = 39A, V_{CC} = 480V$ $V_{GE} = 15V, R_G = 5.0\Omega$
E_{ts}	Total Switching Loss	—	14	—		
L_E	Internal Emitter Inductance	—	13	—	nH	Measured 5mm from package
C_{ies}	Input Capacitance	—	3000	—	pF	$V_{GE} = 0V$
C_{oes}	Output Capacitance	—	340	—		$V_{CC} = 30V$ See Fig. 7
C_{res}	Reverse Transfer Capacitance	—	40	—		$f = 1.0MHz$
t_{rr}	Diode Reverse Recovery Time	—	50	75	ns	$T_J = 25^\circ\text{C}$ See Fig.
		—	105	160		$T_J = 125^\circ\text{C}$ 14
I_{rr}	Diode Peak Reverse Recovery Current	—	4.5	10	A	$T_J = 25^\circ\text{C}$ See Fig.
		—	8.0	15		$T_J = 125^\circ\text{C}$ 15
Q_{rr}	Diode Reverse Recovery Charge	—	112	375	nC	$T_J = 25^\circ\text{C}$ See Fig.
		—	420	1200		$T_J = 125^\circ\text{C}$ 16
$di_{(rec)M}/dt$	Diode Peak Rate of Fall of Recovery During t_b	—	250	—	A/ μs	$T_J = 25^\circ\text{C}$ See Fig.
		—	160	—		$T_J = 125^\circ\text{C}$ 17

Notes:

① Repetitive rating; $V_{GE}=20V$, pulse width limited by max. junction temperature. (See fig. 20)

② $V_{CC}=80\%(V_{CES}), V_{GE}=20V, L=10\mu H, R_G=5.0\Omega$, (See fig. 19)

④ Pulse width 5.0 μs , single shot.

③ Pulse width $\leq 80\mu s$; duty factor $\leq 0.1\%$.

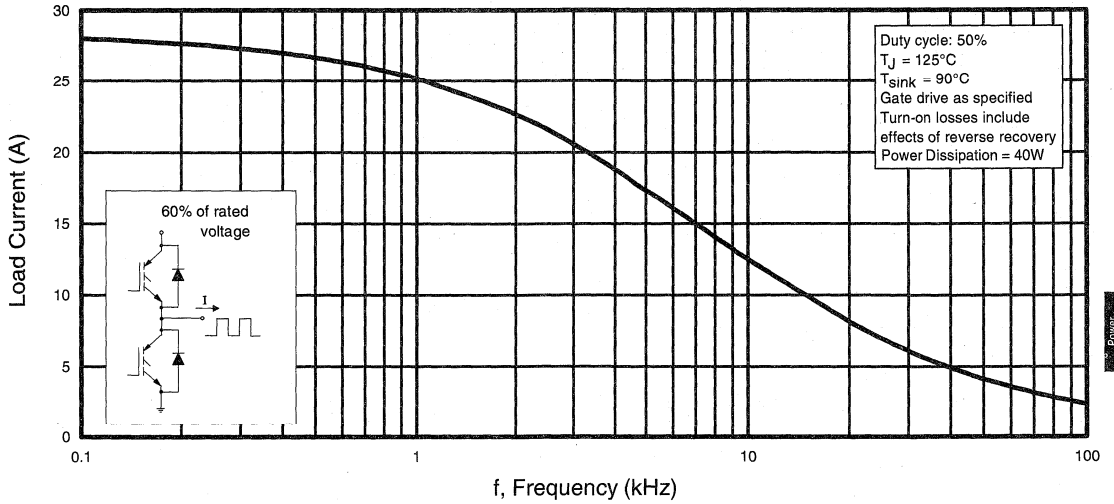


Fig. 1 - Typical Load Current vs. Frequency
 (Load Current = I_{RMS} of fundamental)

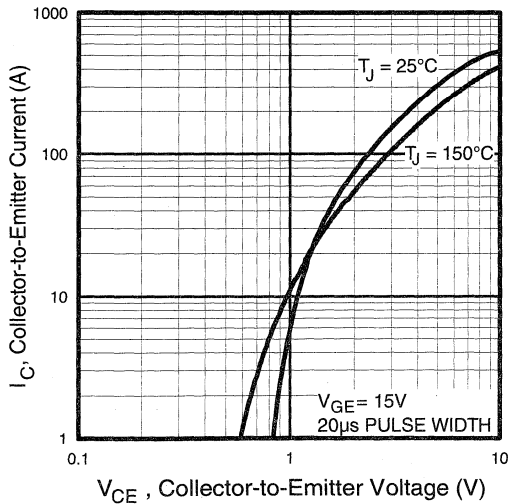


Fig. 2 - Typical Output Characteristics

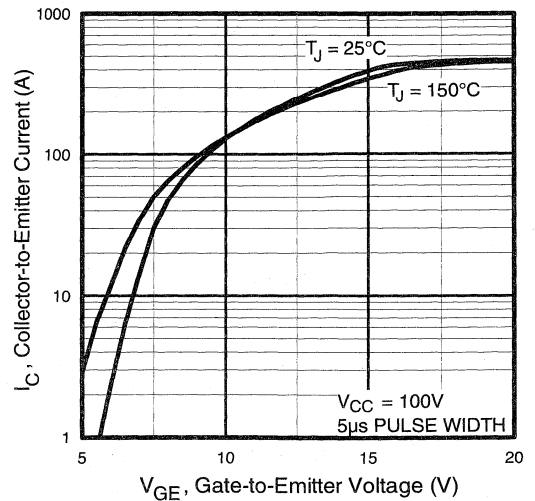


Fig. 3 - Typical Transfer Characteristics

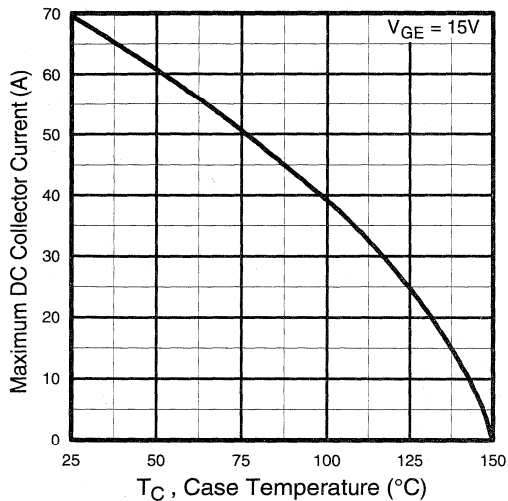


Fig. 4 - Maximum Collector Current vs. Case Temperature

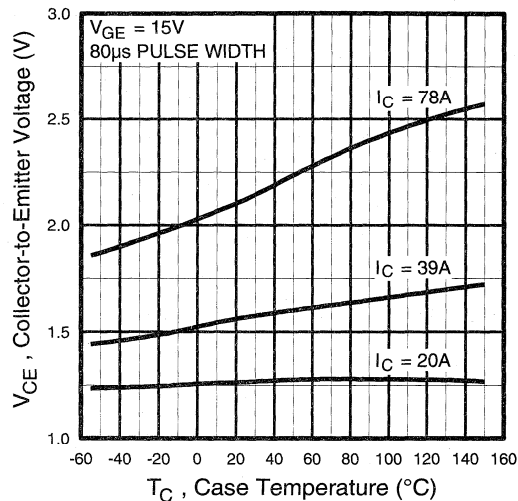


Fig. 5 - Collector-to-Emitter Voltage vs. Case Temperature

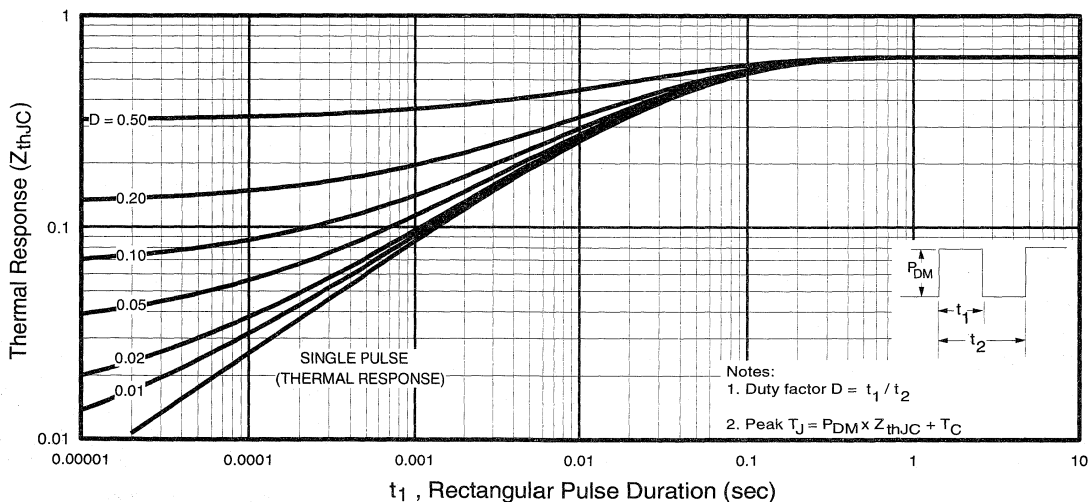


Fig. 6 - Maximum IGBT Effective Transient Thermal Impedance, Junction-to-Case

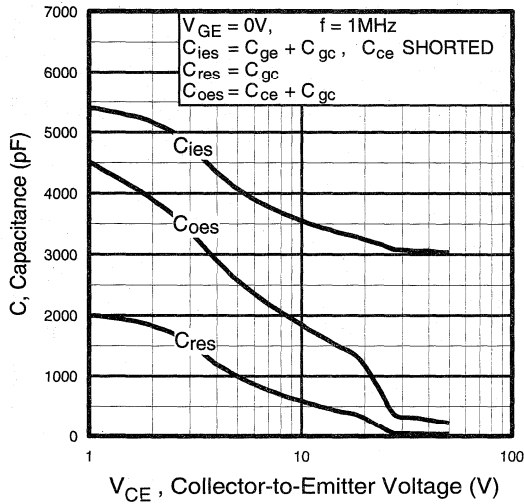


Fig. 7 - Typical Capacitance vs. Collector-to-Emitter Voltage

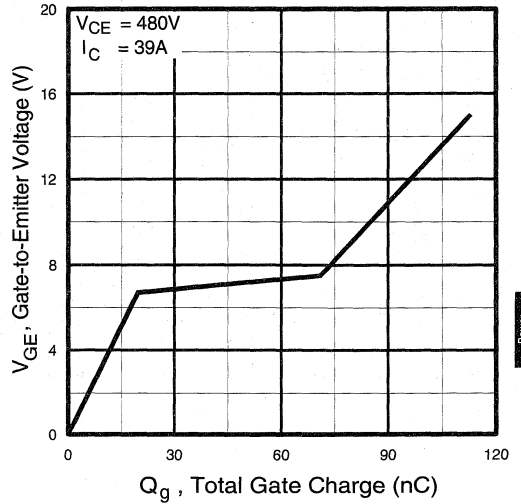


Fig. 8 - Typical Gate Charge vs. Gate-to-Emitter Voltage

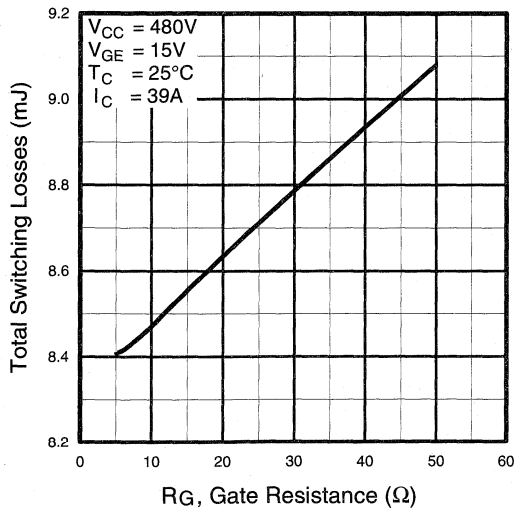


Fig. 9 - Typical Switching Losses vs. Gate Resistance

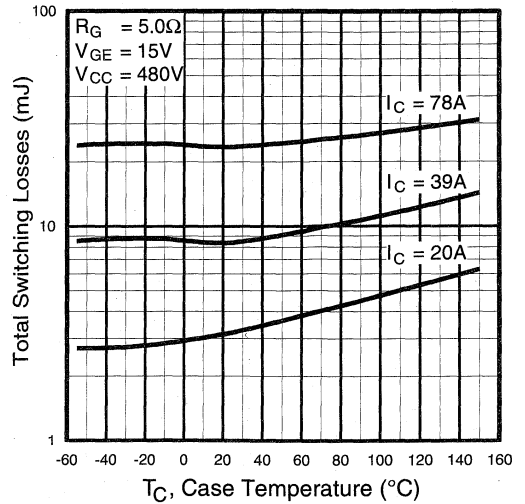


Fig. 10 - Typical Switching Losses vs. Case Temperature

Power
Conversion
Fast
Co-Packs

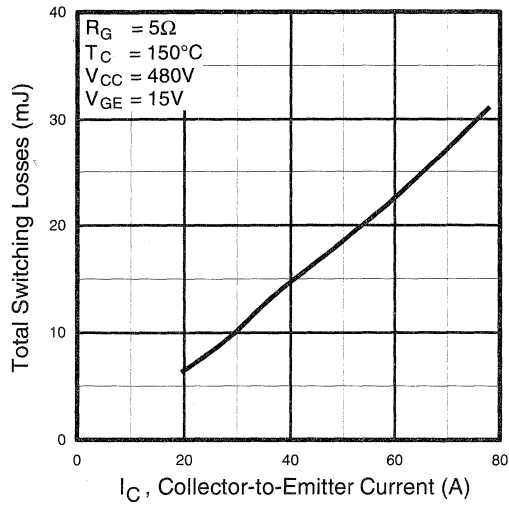


Fig. 11 - Typical Switching Losses vs. Collector-to-Emitter Current

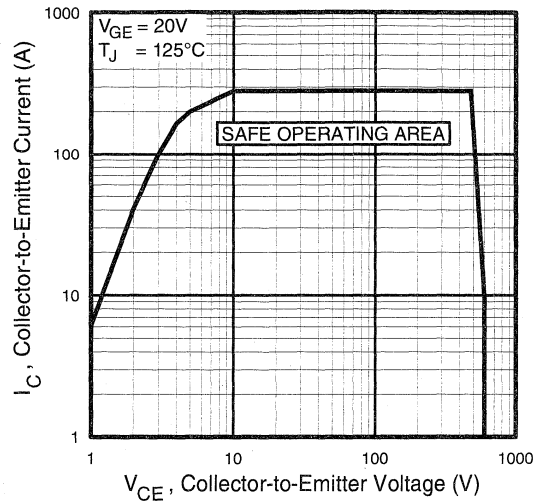


Fig. 12 - Turn-Off SOA

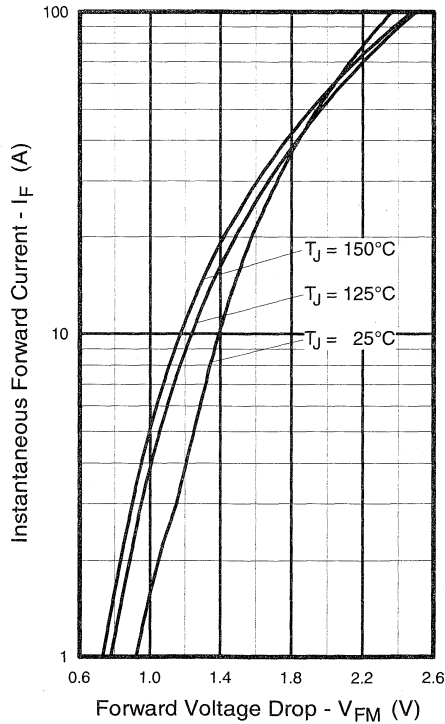


Fig. 13 - Maximum Forward Voltage Drop vs. Instantaneous Forward Current

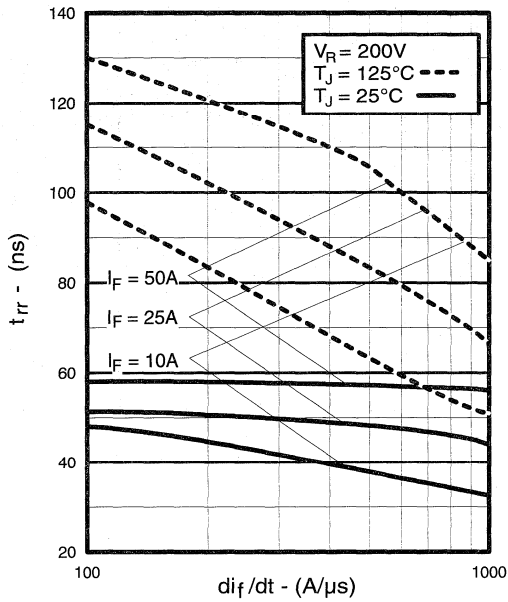


Fig. 14 - Typical Reverse Recovery vs. di_f/dt

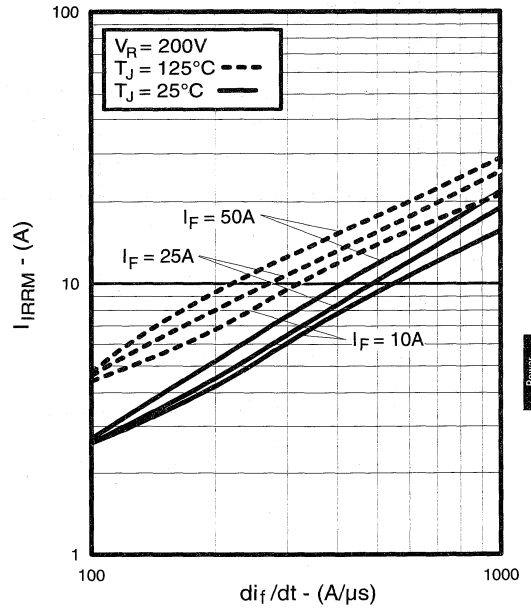


Fig. 15 - Typical Recovery Current vs. di_f/dt

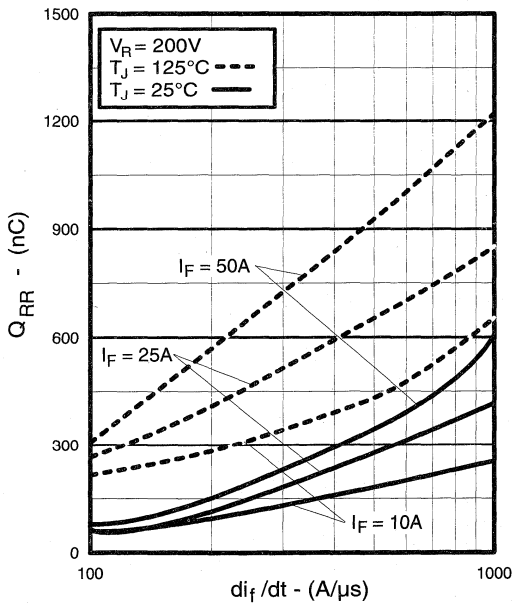


Fig. 16 - Typical Stored Charge vs. di_f/dt

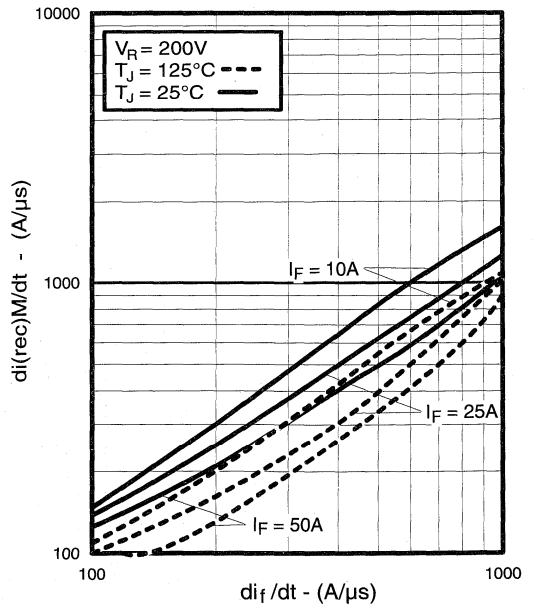


Fig. 17 - Typical $di_{(rec)M}/dt$ vs. di_f/dt

Power
 Conversion
 Fast
 Co-Packs

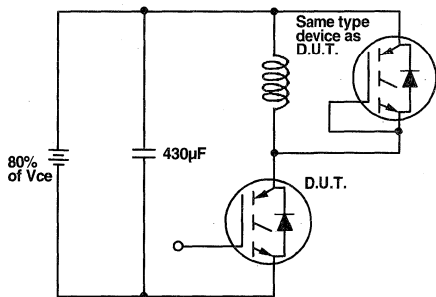


Fig. 18a - Test Circuit for Measurement of I_{LM} , E_{on} , $E_{off(diode)}$, t_{rr} , Q_{rr} , I_{rr} , $t_{d(on)}$, t_r , $t_{d(off)}$, t_f

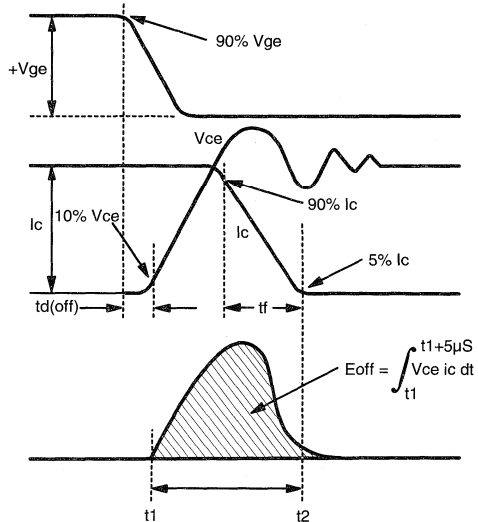


Fig. 18b - Test Waveforms for Circuit of Fig. 18a, Defining E_{off} , $t_{d(off)}$, t_f

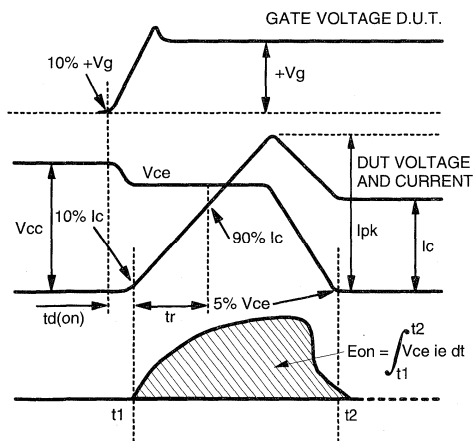


Fig. 18c - Test Waveforms for Circuit of Fig. 18a, Defining E_{on} , $t_{d(on)}$, t_r

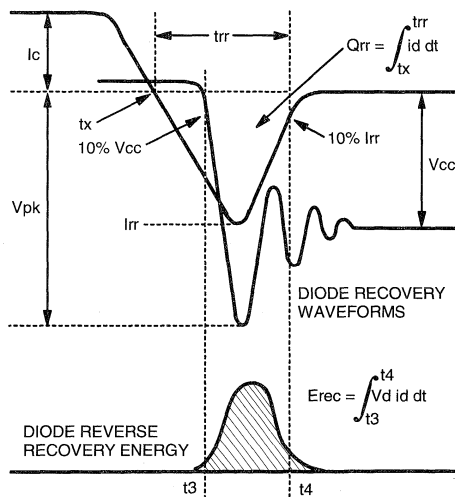


Fig. 18d - Test Waveforms for Circuit of Fig. 18a, Defining E_{rec} , t_{rr} , Q_{rr} , I_{rr}

**Refer to Section D for the following:
Appendix D: Section D - page D-6**

- Fig. 18e - Macro Waveforms for Test Circuit of Fig. 18a
- Fig. 19 - Clamped Inductive Load Test Circuit
- Fig. 20 - Pulsed Collector Current Test Circuit

IGBT SIP MODULE

Fast IGBT

Features

- Fully isolated printed circuit board mount package
- Switching-loss rating includes all "tail" losses
- HEXFRED™ soft ultrafast diodes
- Optimized for medium operating frequency (1 to 10kHz)
See Fig. 1 for Current vs. Frequency curve

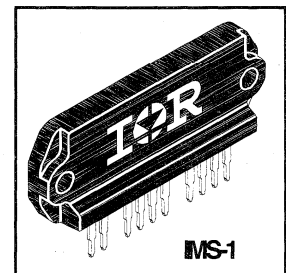
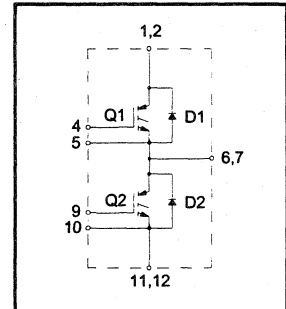
Product Summary

Output Current in a Typical 5.0 kHz Motor Drive

14 A_{RMS} with T_C = 90°C, T_J = 125°C, Supply Voltage 360Vdc,
Power Factor 0.8, Modulation Depth 80% (See Figure 1)

Description

The IGBT technology is the key to International Rectifier's advanced line of IMS (Insulated Metal Substrate) Power Modules. These modules are more efficient than comparable bipolar transistor modules, while at the same time having the simpler gate-drive requirements of the familiar power MOSFET. This superior technology has now been coupled to a state of the art materials system that maximizes power throughput with low thermal resistance. This package is highly suited to motor drive applications and where space is at a premium.



Power
Conversion
Fast
Modules

Absolute Maximum Ratings

	Parameter	Max.	Units
V _{CES}	Collector-to-Emitter Voltage	600	V
I _C @ T _C = 25°C	Continuous Collector Current, each IGBT	42	A
I _C @ T _C = 100°C	Continuous Collector Current, each IGBT	23	
I _{CM}	Pulsed Collector Current ①	120	
I _{LM}	Clamped Inductive Load Current ②	120	
I _F @ T _C = 100°C	Diode Continuous Forward Current	15	V
I _{FM}	Diode Maximum Forward Current	120	
V _{GE}	Gate-to-Emitter Voltage	±20	V
V _{ISOL}	Isolation Voltage, any terminal to case, 1 min.	2500	V _{RMS}
P _D @ T _C = 25°C	Maximum Power Dissipation, each IGBT	83	W
P _D @ T _C = 100°C	Maximum Power Dissipation, each IGBT	33	
T _J	Operating Junction and	-40 to +150	°C
T _{STG}	Storage Temperature Range		
	Soldering Temperature, for 10 sec.		
	Mounting torque, 6-32 or M3 screw.	5-7 lbf•in (0.55-0.8 N•m)	

Thermal Resistance

	Parameter	Typ.	Max.	Units
R _{θJC} (IGBT)	Junction-to-Case, each IGBT, one IGBT in conduction	—	1.5	°C/W
R _{θJC} (DIODE)	Junction-to-Case, each diode, one diode in conduction	—	2.0	
R _{θCS} (MODULE)	Case-to-Sink, flat, greased surface	0.1	—	
Wt	Weight of module	20 (0.7)	—	g (oz)

Electrical Characteristics @ T_J = 25°C (unless otherwise specified)

	Parameter	Min.	Typ.	Max.	Units	Conditions
V _{(BR)CES}	Collector-to-Emitter Breakdown Voltage ^③	600	—	—	V	V _{GE} = 0V, I _C = 250μA
ΔV _{(BR)CES/ΔT_J}	Temp. Coeff. of Breakdown Voltage	—	0.62	—	V/°C	V _{GE} = 0V, I _C = 1.0mA
V _{CE(on)}	Collector-to-Emitter Saturation Voltage	—	1.3	1.5	V	I _C = 23A V _{GE} = 15V
		—	1.7	—		I _C = 42A See Fig. 2, 5
		—	1.4	—		I _C = 23A, T _J = 150°C
V _{GE(th)}	Gate Threshold Voltage	3.0	—	5.5		V _{CE} = V _{GE} , I _C = 250μA
ΔV _{GE(th)/ΔT_J}	Temp. Coeff. of Threshold Voltage	—	-14	—	mV/°C	V _{CE} = V _{GE} , I _C = 250μA
g _{fe}	Forward Transconductance ^④	21	30	—	S	V _{CE} = 100V, I _C = 39A
I _{CES}	Zero Gate Voltage Collector Current	—	—	250	μA	V _{GE} = 0V, V _{CE} = 600V
		—	—	6500		V _{GE} = 0V, V _{CE} = 600V, T _J = 150°C
V _{FM}	Diode Forward Voltage Drop	—	1.3	1.7	V	I _C = 25A See Fig. 13
		—	1.2	1.5		I _C = 25A, T _J = 150°C
I _{GES}	Gate-to-Emitter Leakage Current	—	—	±500	nA	V _{GE} = ±20V

Switching Characteristics @ T_J = 25°C (unless otherwise specified)

	Parameter	Min.	Typ.	Max.	Units	Conditions	
Q _g	Total Gate Charge (turn-on)	—	84	100	nC	I _C = 39A	
Q _{ge}	Gate - Emitter Charge (turn-on)	—	20	25		V _{CC} = 400V	
Q _{gc}	Gate - Collector Charge (turn-on)	—	51	67		See Fig. 8	
t _{d(on)}	Turn-On Delay Time	—	24	—	ns	T _J = 25°C	
t _r	Rise Time	—	50	—		I _C = 39A, V _{CC} = 480V	
t _{d(off)}	Turn-Off Delay Time	—	270	540		V _{GE} = 15V, R _G = 5.0Ω	
t _f	Fall Time	—	210	360		Energy losses include "tail" and diode reverse recovery	
E _{on}	Turn-On Switching Loss	—	1.1	—		mJ	See Fig. 9, 10, 11, 18
E _{off}	Turn-Off Switching Loss	—	2.1	—			
E _{ts}	Total Switching Loss	—	3.2	5.4	mJ	T _J = 150°C, See Fig. 9, 10, 11, 18	
t _{d(on)}	Turn-On Delay Time	—	25	—			
t _r	Rise Time	—	49	—			
t _{d(off)}	Turn-Off Delay Time	—	440	—			
t _f	Fall Time	—	410	—			
E _{ts}	Total Switching Loss	—	5.8	—			
C _{ies}	Input Capacitance	—	3000	—	pF	V _{GE} = 0V	
C _{oes}	Output Capacitance	—	340	—		V _{CC} = 30V See Fig. 7	
C _{res}	Reverse Transfer Capacitance	—	40	—		f = 1.0MHz	
t _{rr}	Diode Reverse Recovery Time	—	50	75	ns	T _J = 25°C See Fig. 14	
		—	105	160		T _J = 125°C	
I _{rr}	Diode Peak Reverse Recovery Current	—	4.5	10	A	T _J = 25°C See Fig. 15	
		—	8.0	15		T _J = 125°C	
Q _{rr}	Diode Reverse Recovery Charge	—	112	375	nC	T _J = 25°C See Fig. 16	
		—	420	1200		T _J = 125°C	
di _{(rec)M/dt}	Diode Peak Rate of Fall of Recovery During t _b	—	250	—	A/μs	T _J = 25°C See Fig. 17	
		—	160	—		T _J = 125°C	

Notes:

① Repetitive rating; V_{GE}=20V, pulse width limited by max. junction temperature. (See fig. 20)

② V_{CC}=80%(V_{CES}), V_{GE}=20V, L=10μH, R_G=5.0Ω, (See fig. 19)

④ Pulse width 5.0μs, single shot.

③ Pulse width ≤ 80μs; duty factor ≤ 0.1%.

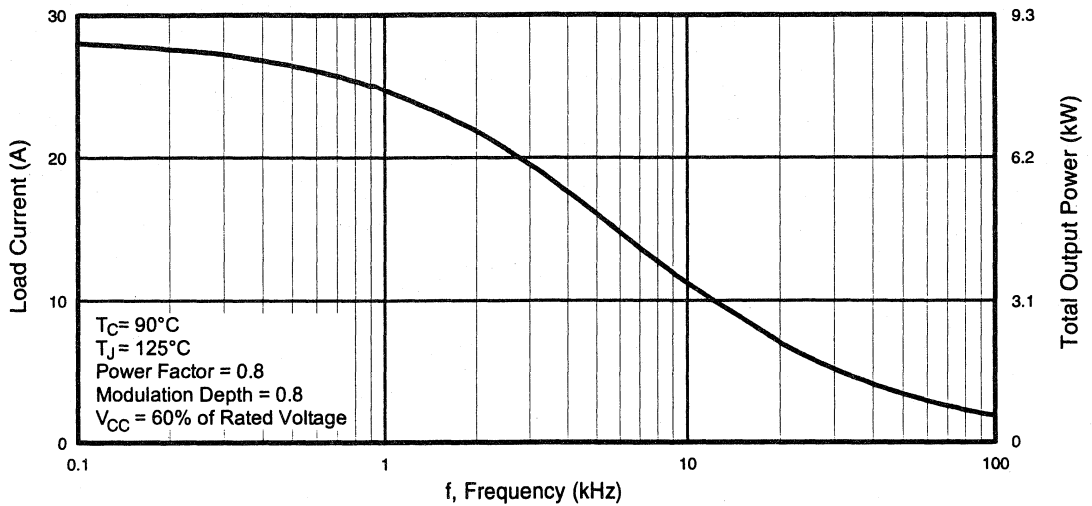


Fig. 1 - RMS Current and Output Power, Synthesized Sine Wave

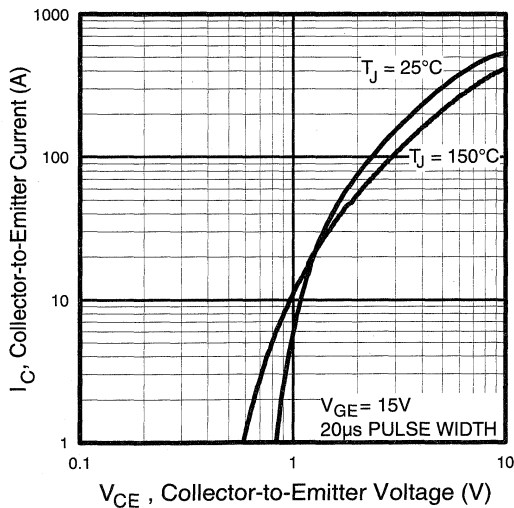


Fig. 2 - Typical Output Characteristics

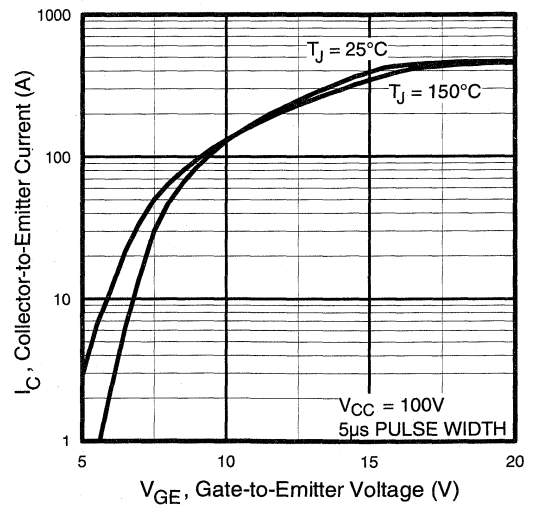


Fig. 3 - Typical Transfer Characteristics

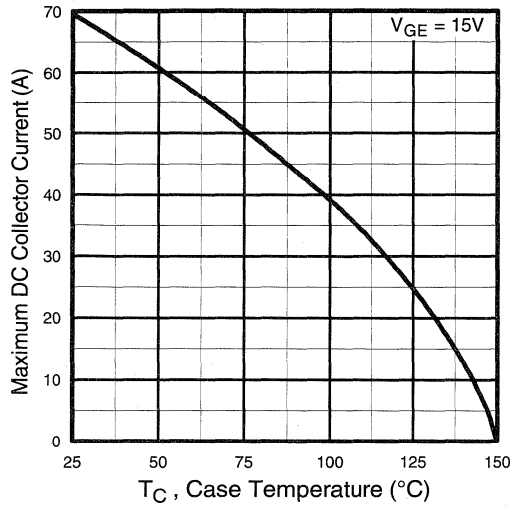


Fig. 4 - Maximum Collector Current vs. Case Temperature

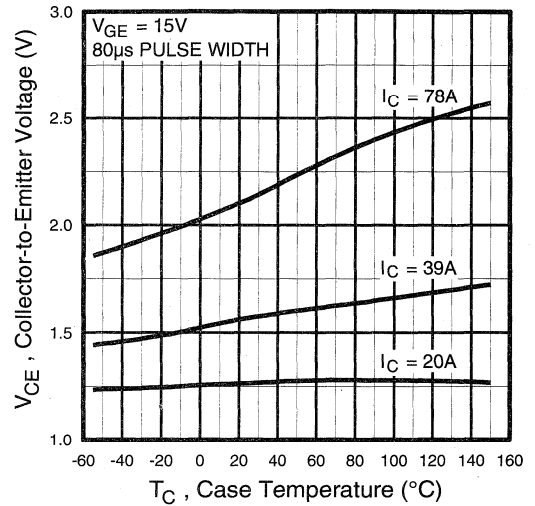


Fig. 5 - Collector-to-Emitter Voltage vs. Case Temperature

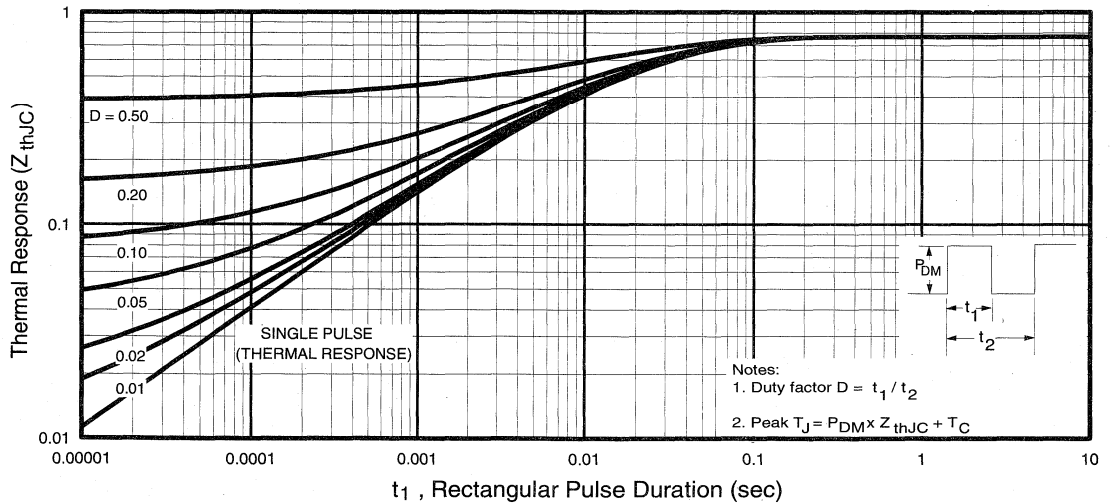


Fig. 6 - Maximum IGBT Effective Transient Thermal Impedance, Junction-to-Case

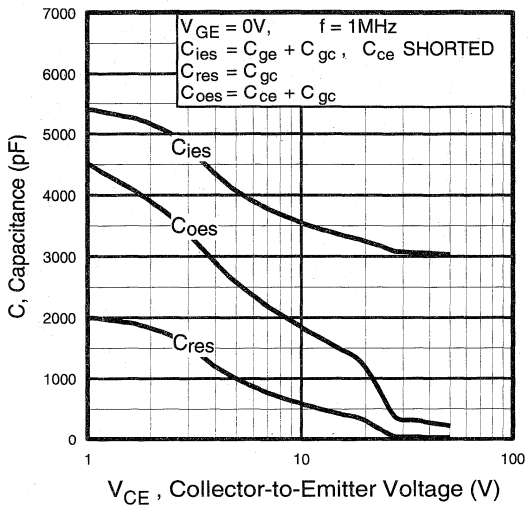


Fig. 7 - Typical Capacitance vs. Collector-to-Emitter Voltage

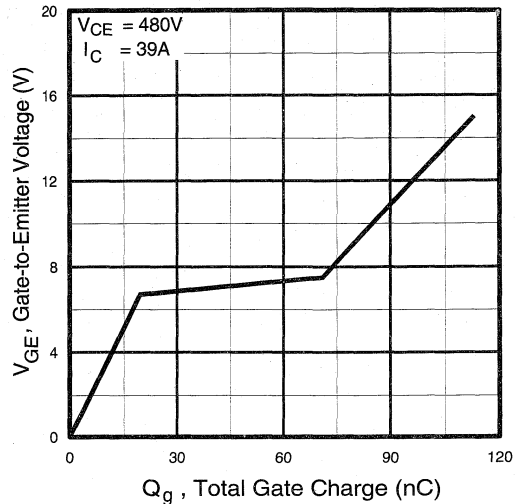


Fig. 8 - Typical Gate Charge vs. Gate-to-Emitter Voltage

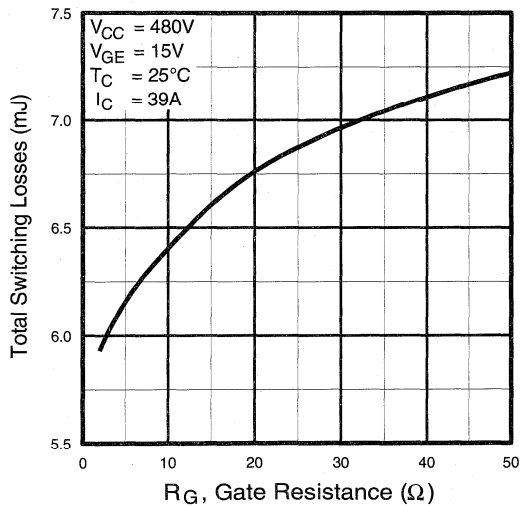


Fig. 9 - Typical Switching Losses vs. Gate Resistance

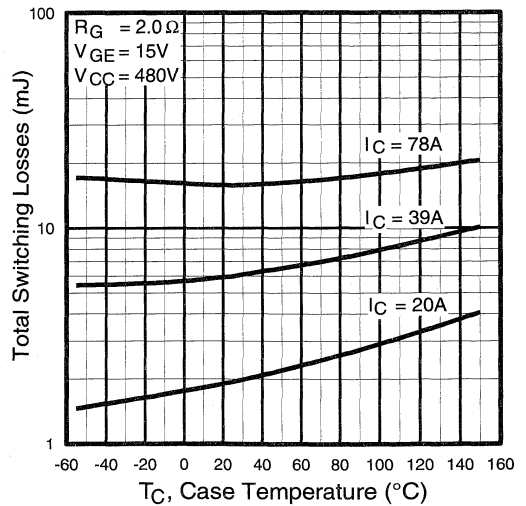


Fig. 10 - Typical Switching Losses vs. Case Temperature

Power
Conversion
Fast
Modules

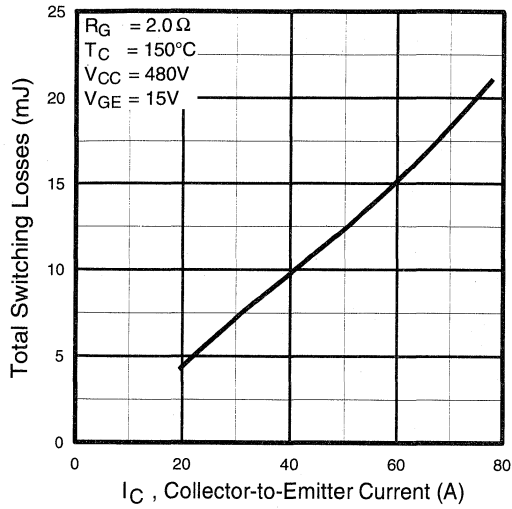


Fig. 11 - Typical Switching Losses vs. Collector-to-Emitter Current

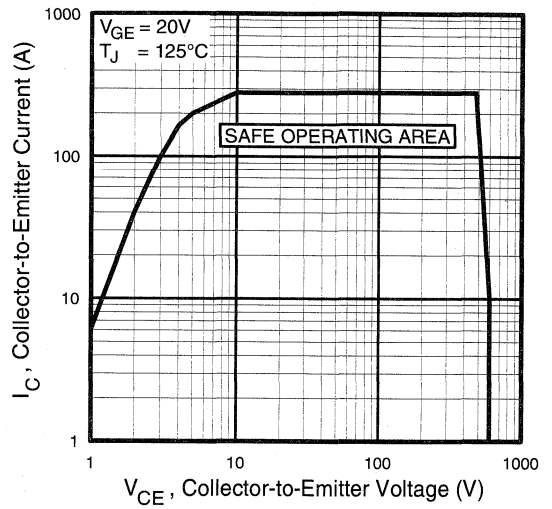


Fig. 12 - Turn-Off SOA

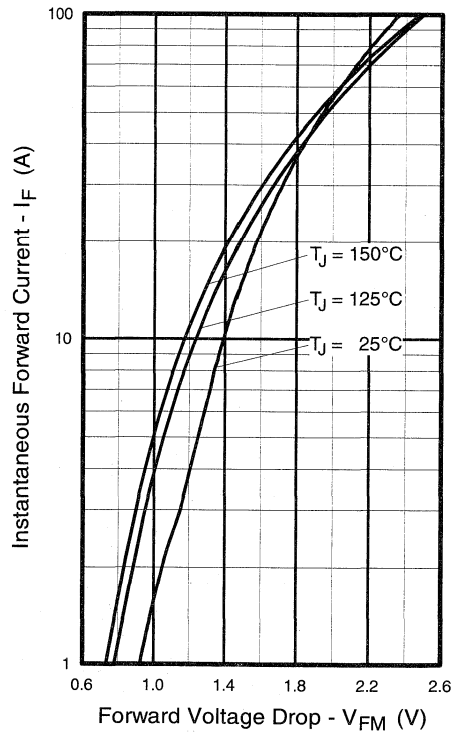


Fig. 13 - Maximum Forward Voltage Drop vs. Instantaneous Forward Current

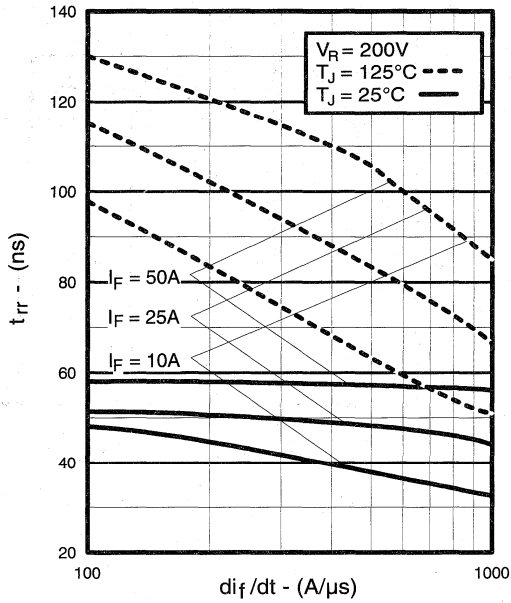


Fig. 14 - Typical Reverse Recovery vs. di_f/dt

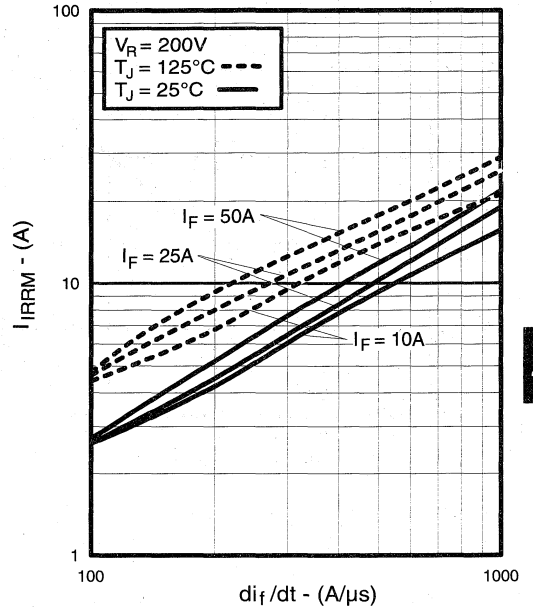


Fig. 15 - Typical Recovery Current vs. di_f/dt

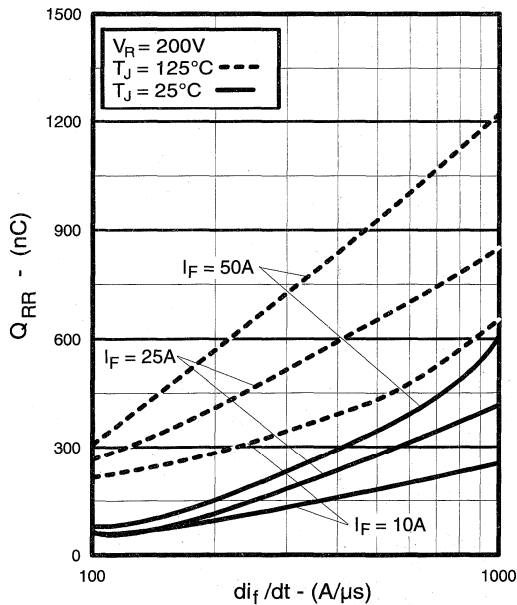


Fig. 16 - Typical Stored Charge vs. di_f/dt

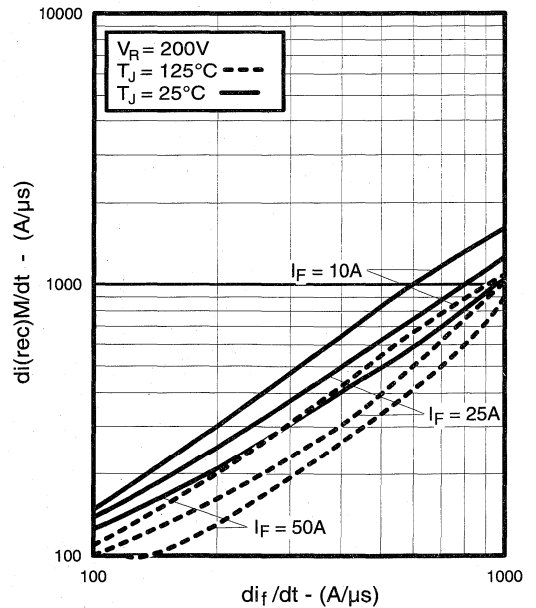


Fig. 17 - Typical $di_{(rec)M}/dt$ vs. di_f/dt

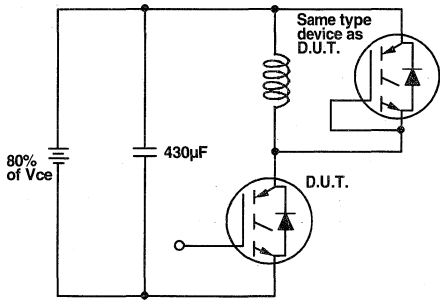


Fig. 18a - Test Circuit for Measurement of I_{LM} , E_{on} , $E_{off}(\text{diode})$, t_{rr} , Q_{rr} , I_{rr} , $t_{d(on)}$, t_r , $t_{d(off)}$, t_f

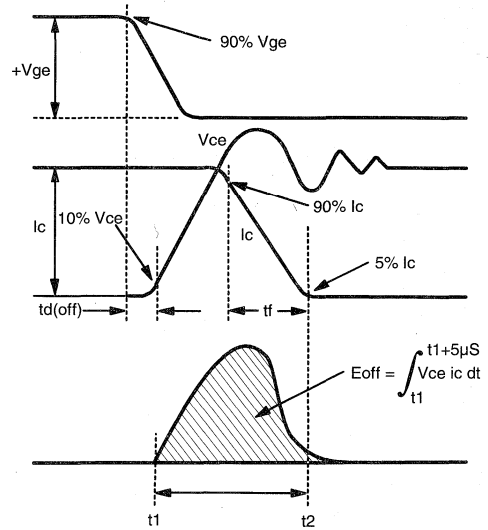


Fig. 18b - Test Waveforms for Circuit of Fig. 18a, Defining E_{off} , $t_{d(off)}$, t_f

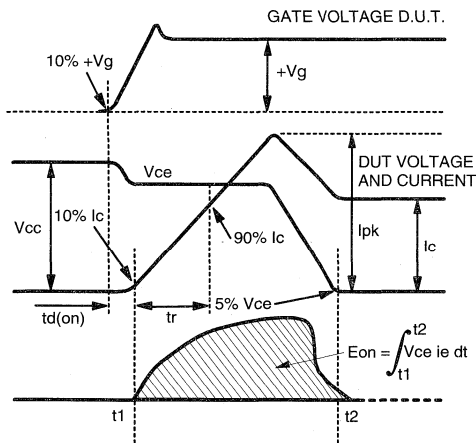


Fig. 18c - Test Waveforms for Circuit of Fig. 18a, Defining E_{on} , $t_{d(on)}$, t_r

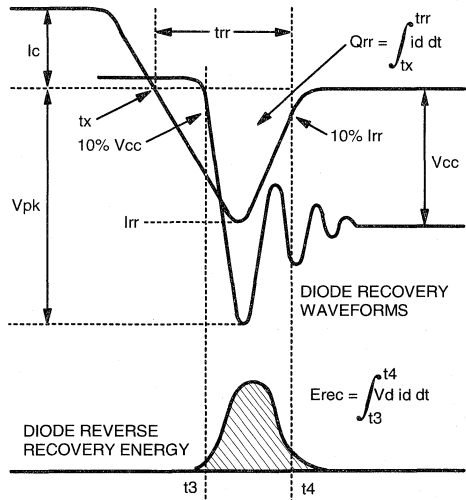


Fig. 18d - Test Waveforms for Circuit of Fig. 18a, Defining E_{rec} , t_{rr} , Q_{rr} , I_{rr}

Refer to **Section D** for the following:
Appendix D: Section D - page D-6

Fig. 18e - Macro Waveforms for Test Circuit Fig. 18a

Fig. 19 - Clamped Inductive Load Test Circuit

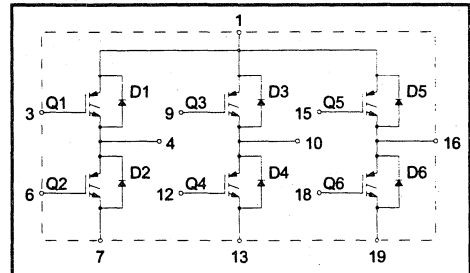
Fig. 20 - Pulsed Collector Current Test Circuit

IGBT SIP MODULE

Fast IGBT

Features

- Fully isolated printed circuit board mount package
- Switching-loss rating includes all "tail" losses
- HEXFRED™ soft ultrafast diodes
- Optimized for medium operating frequency (1 to 10kHz)
See Fig. 1 for Current vs. Frequency curve



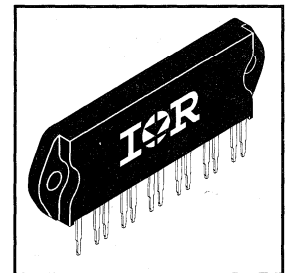
Product Summary

Output Current in a Typical 5.0 kHz Motor Drive

4.6 A_{RMS} per phase (1.4 kW total) with T_C = 90°C, T_J = 125°C, Supply Voltage 360Vdc, Power Factor 0.8, Modulation Depth 80% (See Figure 1)

Description

The IGBT technology is the key to International Rectifier's advanced line of IMS (Insulated Metal Substrate) Power Modules. These modules are more efficient than comparable bipolar transistor modules, while at the same time having the simpler gate-drive requirements of the familiar power MOSFET. This superior technology has now been coupled to a state of the art materials system that maximizes power throughput with low thermal resistance. This package is highly suited to motor drive applications and where space is at a premium.



Absolute Maximum Ratings

	Parameter	Max.	Units
V _{CES}	Collector-to-Emitter Voltage	600	V
I _C @ T _C = 25°C	Continuous Collector Current, each IGBT	8.8	A
I _C @ T _C = 100°C	Continuous Collector Current, each IGBT	4.8	
I _{CM}	Pulsed Collector Current ∅	26	
I _{LM}	Clamped Inductive Load Current ∅	26	
I _F @ T _C = 100°C	Diode Continuous Forward Current	3.4	
I _{FM}	Diode Maximum Forward Current	26	
V _{GE}	Gate-to-Emitter Voltage	±20	V
V _{ISOL}	Isolation Voltage, any terminal to case, 1 min.	2500	V _{RMS}
P _D @ T _C = 25°C	Maximum Power Dissipation, each IGBT	23	W
P _D @ T _C = 100°C	Maximum Power Dissipation, each IGBT	9.1	
T _J	Operating Junction and	-40 to +150	°C
T _{STG}	Storage Temperature Range		
	Soldering Temperature, for 10 sec.	300 (0.063 in. (1.6mm) from case)	
	Mounting torque, 6-32 or M3 screw.	5-7 lbf•in (0.55-0.8 N•m)	

Thermal Resistance

	Parameter	Typ.	Max.	Units
R _{θJC} (IGBT)	Junction-to-Case, each IGBT, one IGBT in conduction	—	5.5	°C/W
R _{θJC} (DIODE)	Junction-to-Case, each diode, one diode in conduction	—	9.0	
R _{θCS} (MODULE)	Case-to-Sink, flat, greased surface	0.1	—	
Wt	Weight of module	20 (0.7)	—	g (oz)

Electrical Characteristics @ T_J = 25°C (unless otherwise specified)

	Parameter	Min.	Typ.	Max.	Units	Conditions
V _{(BR)CES}	Collector-to-Emitter Breakdown Voltage ^③	600	—	—	V	V _{GE} = 0V, I _C = 250μA
ΔV _{(BR)CES} /ΔT _J	Temperature Coeff. of Breakdown Voltage	—	0.72	—	V/°C	V _{GE} = 0V, I _C = 1.0mA
V _{CE(on)}	Collector-to-Emitter Saturation Voltage	—	1.6	1.8	V	I _C = 4.8A V _{GE} = 15V See Fig. 2, 5
		—	2.0	—		
		—	1.7	—		
V _{GE(th)}	Gate Threshold Voltage	3.0	—	5.5		V _{CE} = V _{GE} , I _C = 250μA
ΔV _{GE(th)} /ΔT _J	Temperature Coeff. of Threshold Voltage	—	-11	—	mV/°C	V _{CE} = V _{GE} , I _C = 250μA
g _{fe}	Forward Transconductance ^④	2.9	5.0	—	S	V _{CE} = 100V, I _C = 9.0A
I _{CES}	Zero Gate Voltage Collector Current	—	—	250	μA	V _{GE} = 0V, V _{CE} = 600V V _{GE} = 0V, V _{CE} = 600V, T _J = 150°C
		—	—	1700		
V _{FM}	Diode Forward Voltage Drop	—	1.4	1.7	V	I _C = 8.0A See Fig. 13 I _C = 8.0A, T _J = 150°C
		—	1.3	1.6		
I _{GES}	Gate-to-Emitter Leakage Current	—	—	±500	nA	V _{GE} = ±20V

Switching Characteristics @ T_J = 25°C (unless otherwise specified)

	Parameter	Min.	Typ.	Max.	Units	Conditions
Q _g	Total Gate Charge (turn-on)	—	16	21	nC	I _C = 9.0A V _{CC} = 400V See Fig. 8
Q _{ge}	Gate - Emitter Charge (turn-on)	—	2.4	3.4		
Q _{gc}	Gate - Collector Charge (turn-on)	—	7.6	10		
t _{d(on)}	Turn-On Delay Time	—	24	—	ns	T _J = 25°C I _C = 9.0A, V _{CC} = 480V V _{GE} = 15V, R _G = 50Ω Energy losses include "tail" and diode reverse recovery
t _r	Rise Time	—	13	—		
t _{d(off)}	Turn-Off Delay Time	—	160	270		
t _f	Fall Time	—	310	600	mJ	See Fig. 9, 10, 11, 18
E _{on}	Turn-On Switching Loss	—	0.22	—		
E _{off}	Turn-Off Switching Loss	—	0.40	—		
E _{ts}	Total Switching Loss	—	0.62	1.04	ns	T _J = 150°C, See Fig. 9, 10, 11, 18 I _C = 9.0A, V _{CC} = 480V V _{GE} = 15V, R _G = 50Ω Energy losses include "tail" and diode reverse recovery
t _{d(on)}	Turn-On Delay Time	—	25	—		
t _r	Rise Time	—	18	—		
t _{d(off)}	Turn-Off Delay Time	—	210	—	mJ	See Fig. 7
t _f	Fall Time	—	600	—		
E _{ts}	Total Switching Loss	—	1.07	—		
C _{ies}	Input Capacitance	—	340	—	pF	V _{GE} = 0V V _{CC} = 30V f = 1.0MHz
C _{oes}	Output Capacitance	—	63	—		
C _{res}	Reverse Transfer Capacitance	—	5.9	—		
t _{rr}	Diode Reverse Recovery Time	—	37	55	ns	T _J = 25°C See Fig. 14 T _J = 125°C
		—	55	90		
I _{rr}	Diode Peak Reverse Recovery Current	—	3.5	50	A	T _J = 25°C See Fig. 15 T _J = 125°C
		—	4.5	8.0		
Q _{rr}	Diode Reverse Recovery Charge	—	65	138	nC	T _J = 25°C See Fig. 16 T _J = 125°C
		—	124	360		
di _{(rec)M} /dt	Diode Peak Rate of Fall of Recovery During t _b	—	240	—	A/μs	T _J = 25°C See Fig. 17 T _J = 125°C
		—	210	—		

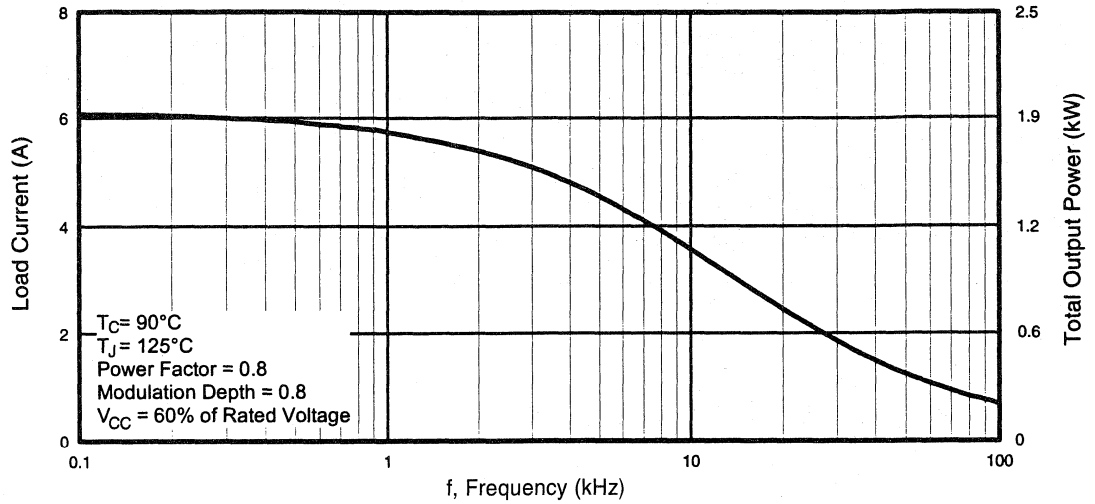
Notes:

① Repetitive rating; V_{GE}=20V, pulse width limited by max. junction temperature. (See fig. 20)

② V_{CC}=80%(V_{CES}), V_{GE}=20V, L=10μH, R_G = 50Ω, (See fig. 19)

③ Pulse width ≤ 80μs; duty factor ≤ 0.1%.

④ Pulse width 5.0μs, single shot.



Power Conversion Fast Modules

Fig. 1 - RMS Current and Output Power, Synthesized Sine Wave

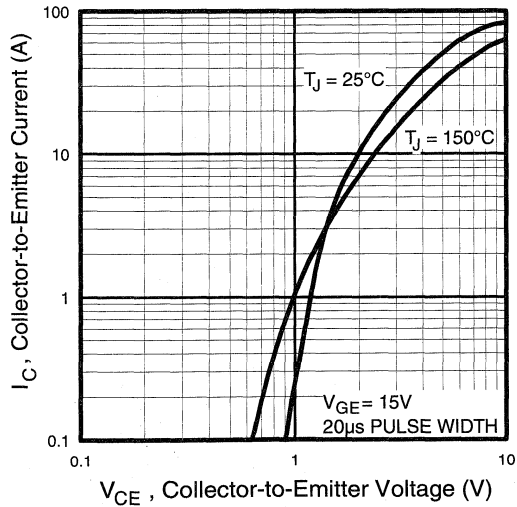


Fig. 2 - Typical Output Characteristics

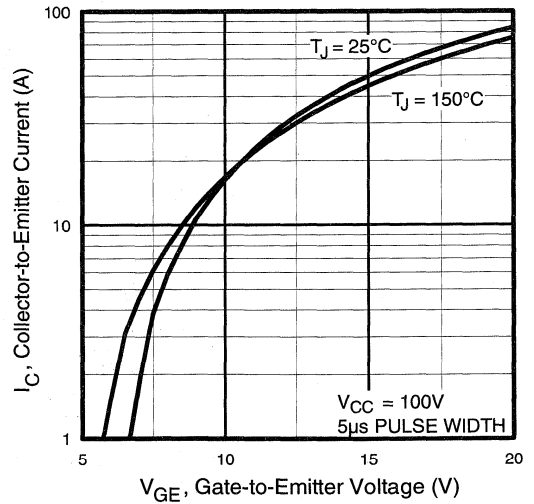


Fig. 3 - Typical Transfer Characteristics

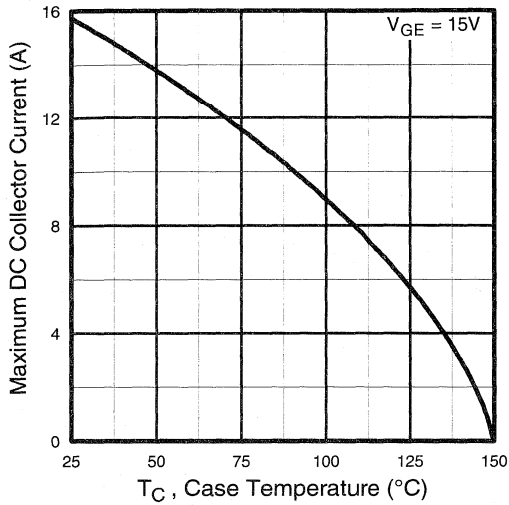


Fig. 4 - Maximum Collector Current vs. Case Temperature

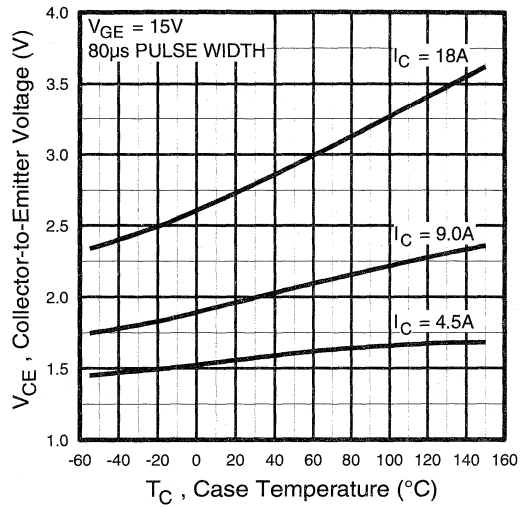


Fig. 5 - Collector-to-Emitter Voltage vs. Case Temperature

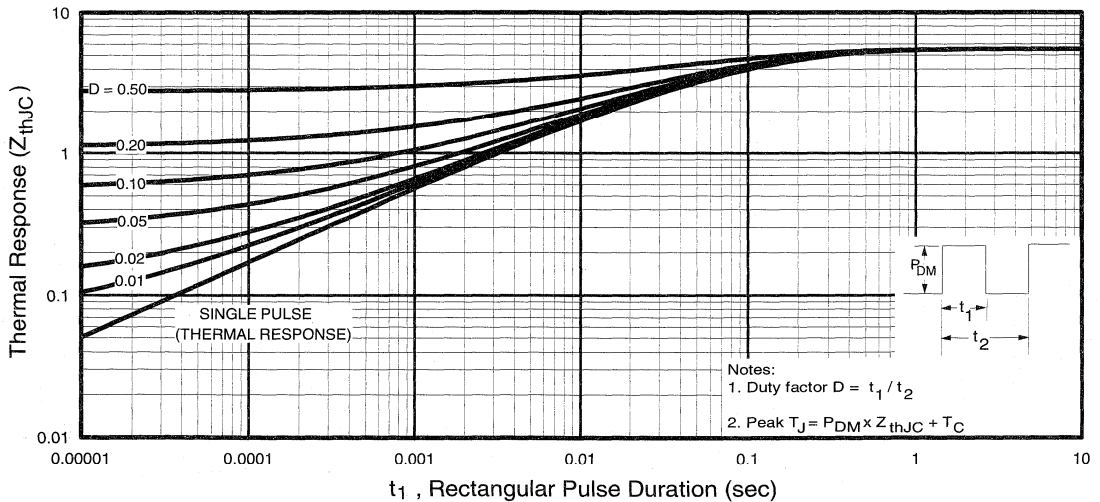


Fig. 6 - Maximum IGBT Effective Transient Thermal Impedance, Junction-to-Case

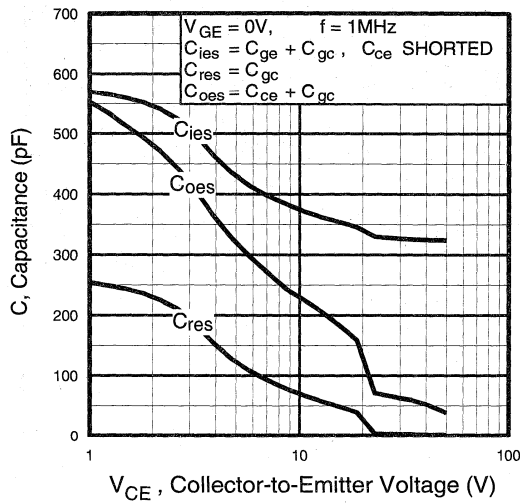


Fig. 7 - Typical Capacitance vs. Collector-to-Emitter Voltage

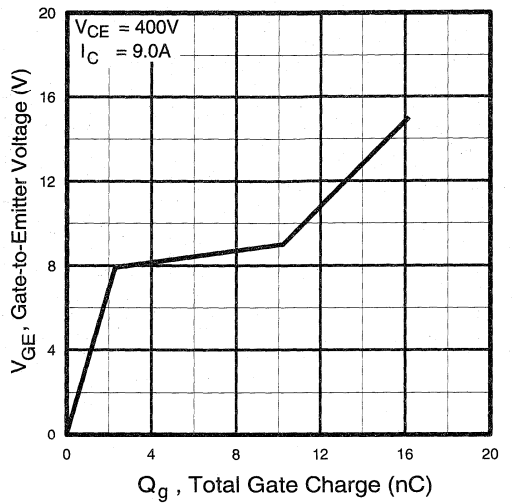


Fig. 8 - Typical Gate Charge vs. Gate-to-Emitter Voltage

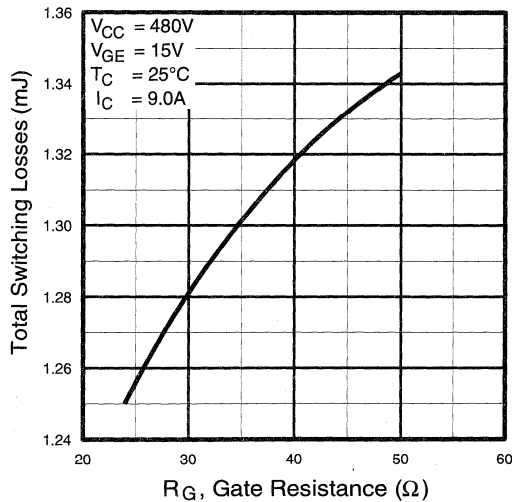


Fig. 9 - Typical Switching Losses vs. Gate Resistance

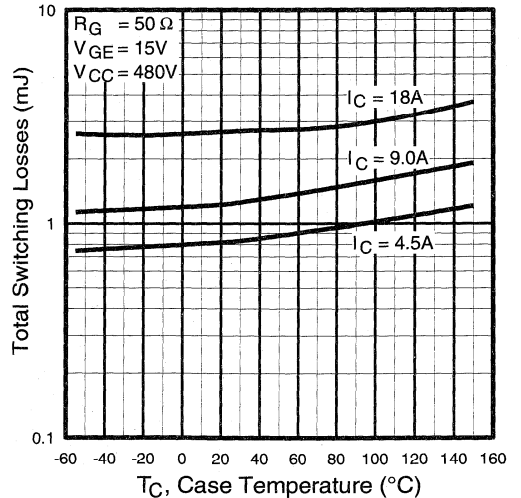


Fig. 10 - Typical Switching Losses vs. Case Temperature

Power
 Conversion
 Best
 Modules

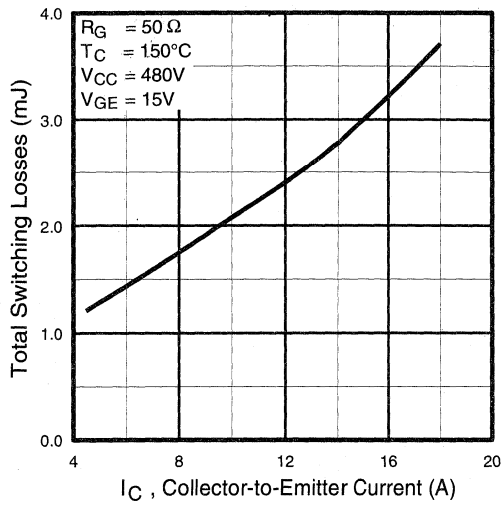


Fig. 11 - Typical Switching Losses vs. Collector-to-Emitter Current

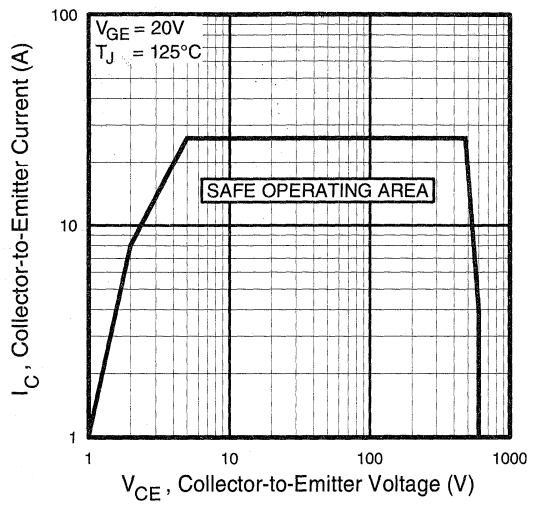


Fig. 12 - Turn-Off SOA

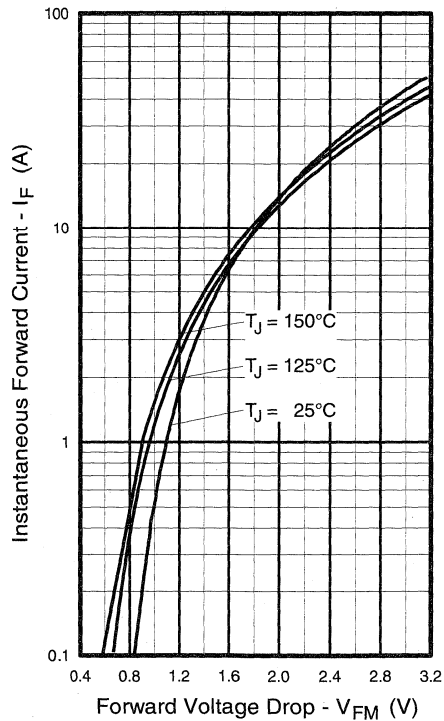


Fig. 13 - Maximum Forward Voltage Drop vs. Instantaneous Forward Current

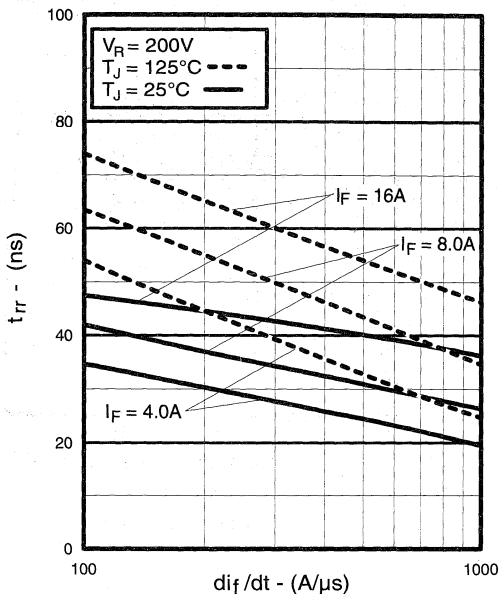


Fig. 14 - Typical Reverse Recovery vs. di_f/dt

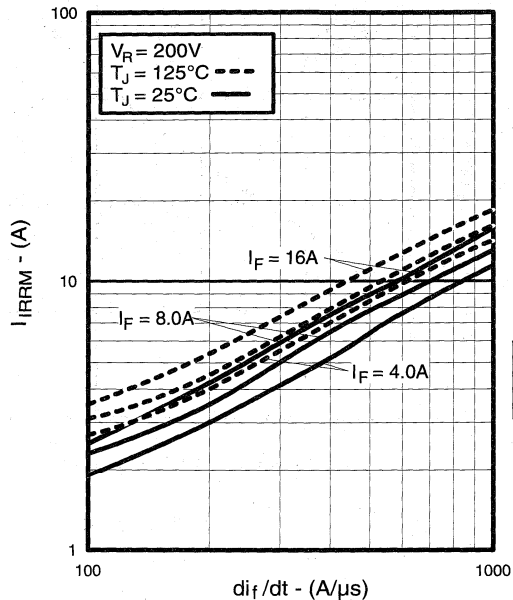


Fig. 15 - Typical Recovery Current vs. di_f/dt

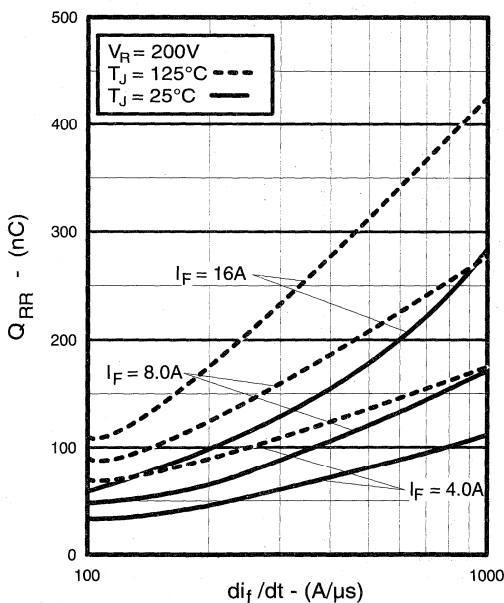


Fig. 16 - Typical Stored Charge vs. di_f/dt

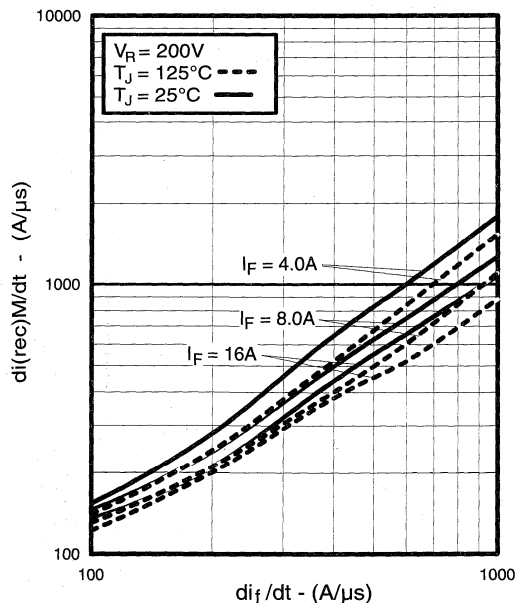


Fig. 17 - Typical $di_{(rec)M}/dt$ vs. di_f/dt

Power Conversion Fast Modules

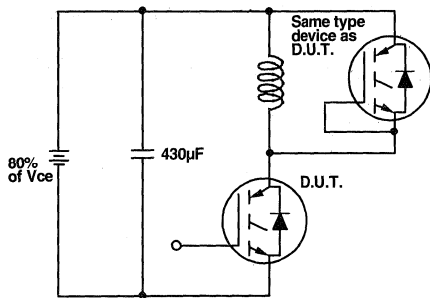


Fig. 18a - Test Circuit for Measurement of I_{LM} , E_{on} , $E_{off}(\text{diode})$, t_{rr} , Q_{rr} , I_{rr} , $t_{d(on)}$, t_r , $t_{d(off)}$, t_f

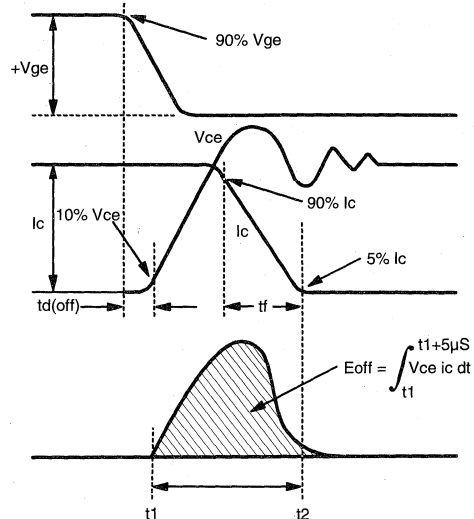


Fig. 18b - Test Waveforms for Circuit of Fig. 18a, Defining E_{off} , $t_{d(off)}$, t_f

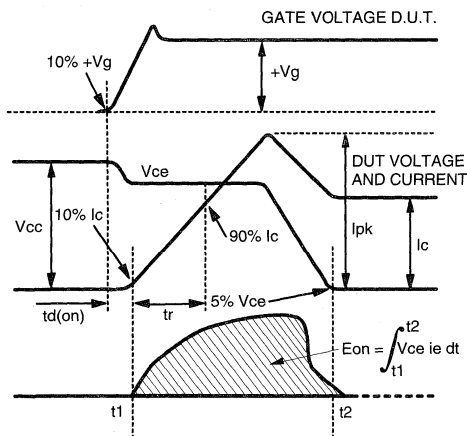


Fig. 18c - Test Waveforms for Circuit of Fig. 18a, Defining E_{on} , $t_{d(on)}$, t_r

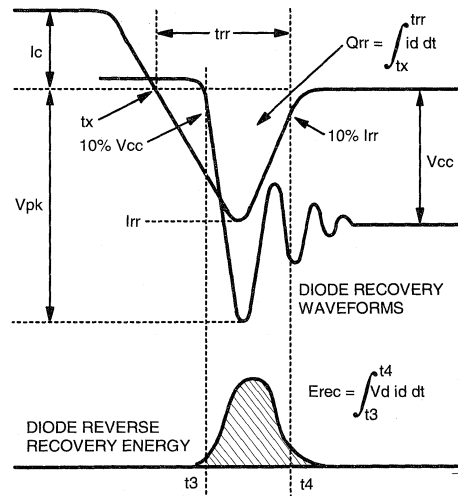


Fig. 18d - Test Waveforms for Circuit of Fig. 18a, Defining E_{rec} , t_{rr} , Q_{rr} , I_{rr}

Refer to Section D for the following:
Appendix D: Section D - page D-6

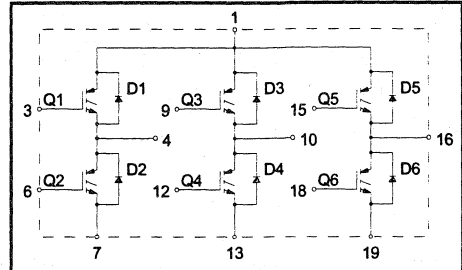
- Fig. 18e - Macro Waveforms for Test Circuit of Fig. 18a
- Fig. 19 - Clamped Inductive Load Test Circuit
- Fig. 20 - Pulsed Collector Current Test Circuit

IGBT SIP MODULE

Fast IGBT

Features

- Fully isolated printed circuit board mount package
- Switching-loss rating includes all "tail" losses
- HEXFRED™ soft ultrafast diodes
- Optimized for medium operating frequency (1 to 10kHz) See Fig. 1 for Current vs. Frequency curve



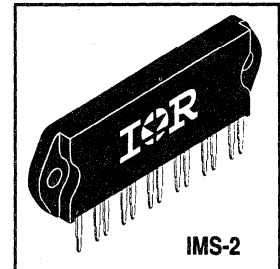
Product Summary

Output Current in a Typical 5.0 kHz Motor Drive

7.65 A_{RMS} per phase (2.4 kW total) with T_C = 90°C, T_J = 125°C, Supply Voltage 360Vdc, Power Factor 0.8, Modulation Depth 80% (See Figure 1)

Description

The IGBT technology is the key to International Rectifier's advanced line of IMS (Insulated Metal Substrate) Power Modules. These modules are more efficient than comparable bipolar transistor modules, while at the same time having the simpler gate-drive requirements of the familiar power MOSFET. This superior technology has now been coupled to a state of the art materials system that maximizes power throughput with low thermal resistance. This package is highly suited to motor drive applications and where space is at a premium.



Absolute Maximum Ratings

	Parameter	Max.	Units
V _{CES}	Collector-to-Emitter Voltage	600	V
I _C @ T _C = 25°C	Continuous Collector Current, each IGBT	16	A
I _C @ T _C = 100°C	Continuous Collector Current, each IGBT	8.7	
I _{CM}	Pulsed Collector Current ①	50	
I _{LM}	Clamped Inductive Load Current ②	50	
I _F @ T _C = 100°C	Diode Continuous Forward Current	6.1	
I _{FM}	Diode Maximum Forward Current	50	
V _{GE}	Gate-to-Emitter Voltage	±20	V
V _{ISOL}	Isolation Voltage, any terminal to case, 1 min.	2500	V _{RMS}
P _D @ T _C = 25°C	Maximum Power Dissipation, each IGBT	36	W
P _D @ T _C = 100°C	Maximum Power Dissipation, each IGBT	14	
T _J	Operating Junction and	-40 to +150	°C
T _{STG}	Storage Temperature Range		
	Soldering Temperature, for 10 sec.	300 (0.063 in. (1.6mm) from case)	
	Mounting torque, 6-32 or M3 screw.	5-7 lbf•in (0.55-0.8 N•m)	

Thermal Resistance

	Parameter	Typ.	Max.	Units
R _{θJC} (IGBT)	Junction-to-Case, each IGBT, one IGBT in conduction	—	3.5	°C/W
R _{θJC} (DIODE)	Junction-to-Case, each diode, one diode in conduction	—	5.5	
R _{θCS} (MODULE)	Case-to-Sink, flat, greased surface	0.1	—	
Wt	Weight of module	20 (0.7)	—	g (oz)

Electrical Characteristics @ $T_J = 25^\circ\text{C}$ (unless otherwise specified)

	Parameter	Min.	Typ.	Max.	Units	Conditions
$V_{(BR)CES}$	Collector-to-Emitter Breakdown Voltage ^②	600	—	—	V	$V_{GE} = 0V, I_C = 250\mu A$
$\Delta V_{(BR)CES}/\Delta T_J$	Temp. Coeff. of Breakdown Voltage	—	0.69	—	$V/^\circ\text{C}$	$V_{GE} = 0V, I_C = 1.0mA$
$V_{CE(on)}$	Collector-to-Emitter Saturation Voltage	—	1.5	1.6	V	$I_C = 8.7A$ $V_{GE} = 15V$
		—	1.9	—		$I_C = 16A$ See Fig. 2, 5
		—	1.6	—		$I_C = 8.7A, T_J = 150^\circ\text{C}$
$V_{GE(th)}$	Gate Threshold Voltage	3.0	—	5.5		$V_{CE} = V_{GE}, I_C = 250\mu A$
$\Delta V_{GE(th)}/\Delta T_J$	Temp. Coeff. of Threshold Voltage	—	-11	—	$mV/^\circ\text{C}$	$V_{CE} = V_{GE}, I_C = 250\mu A$
g_{fe}	Forward Transconductance ^④	6.0	8.0	—	S	$V_{CE} = 100V, I_C = 8.7A$
I_{CES}	Zero Gate Voltage Collector Current	—	—	250	μA	$V_{GE} = 0V, V_{CE} = 600V$
		—	—	2500		$V_{GE} = 0V, V_{CE} = 600V, T_J = 150^\circ\text{C}$
V_{FM}	Diode Forward Voltage Drop	—	1.4	1.7	V	$I_C = 12A$ See Fig. 13
		—	1.3	1.6		$I_C = 12A, T_J = 150^\circ\text{C}$
I_{GES}	Gate-to-Emitter Leakage Current	—	—	± 500	nA	$V_{GE} = \pm 20V$

Switching Characteristics @ $T_J = 25^\circ\text{C}$ (unless otherwise specified)

	Parameter	Min.	Typ.	Max.	Units	Conditions
Q_g	Total Gate Charge (turn-on)	—	23	30	nC	$I_C = 16A$
Q_{ge}	Gate - Emitter Charge (turn-on)	—	2.4	5.9		$V_{CC} = 400V$
Q_{gc}	Gate - Collector Charge (turn-on)	—	9.2	15		See Fig. 8
$t_{d(on)}$	Turn-On Delay Time	—	25	—	ns	$T_J = 25^\circ\text{C}$
t_r	Rise Time	—	21	—		$I_C = 8.7A, V_{CC} = 480V$
$t_{d(off)}$	Turn-Off Delay Time	—	210	300		$V_{GE} = 15V, R_G = 23\Omega$
t_f	Fall Time	—	300	450	mJ	Energy losses include "tail" and diode reverse recovery
E_{on}	Turn-On Switching Loss	—	0.44	—		See Fig. 9, 10, 11, 18
E_{off}	Turn-Off Switching Loss	—	2.0	—		
E_{ts}	Total Switching Loss	—	2.4	3.2	mJ	
$t_{d(on)}$	Turn-On Delay Time	—	25	—		$T_J = 150^\circ\text{C}$, See Fig. 9, 10, 11, 18
t_r	Rise Time	—	21	—		$I_C = 8.7A, V_{CC} = 480V$
$t_{d(off)}$	Turn-Off Delay Time	—	280	—	ns	$V_{GE} = 15V, R_G = 23\Omega$
t_f	Fall Time	—	550	—		Energy losses include "tail" and diode reverse recovery
E_{ts}	Total Switching Loss	—	3.4	—		
C_{ies}	Input Capacitance	—	670	—	pF	$V_{GE} = 0V$
C_{oes}	Output Capacitance	—	100	—		$V_{CC} = 30V$ See Fig. 7
C_{res}	Reverse Transfer Capacitance	—	10	—		$f = 1.0MHz$
t_{rr}	Diode Reverse Recovery Time	—	42	60	ns	$T_J = 25^\circ\text{C}$ See Fig.
		—	80	120		$T_J = 125^\circ\text{C}$ 14
I_{rr}	Diode Peak Reverse Recovery Current	—	3.5	6.0	A	$T_J = 25^\circ\text{C}$ See Fig.
		—	5.6	10		$T_J = 125^\circ\text{C}$ 15
Q_{rr}	Diode Reverse Recovery Charge	—	80	180	nC	$T_J = 25^\circ\text{C}$ See Fig.
		—	220	600		$T_J = 125^\circ\text{C}$ 16
$di_{(rec)M}/dt$	Diode Peak Rate of Fall of Recovery During t_b	—	180	—	A/ μs	$T_J = 25^\circ\text{C}$ See Fig.
		—	116	—		$T_J = 125^\circ\text{C}$ 17

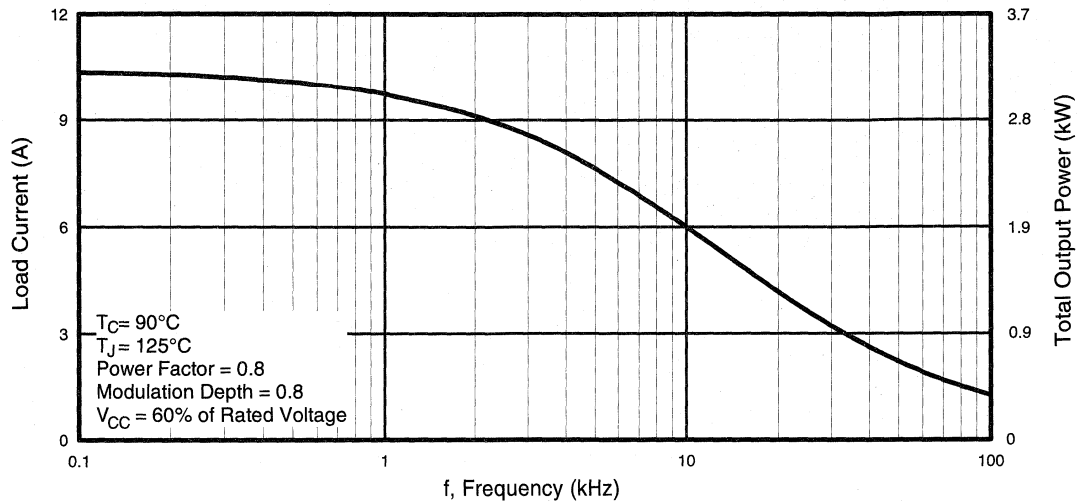
Notes:

① Repetitive rating; $V_{GE}=20V$, pulse width limited by max. junction temperature. (See fig. 20)

② $V_{CC}=80\%(V_{CES}), V_{GE}=20V, L=10\mu H, R_G=23\Omega$, (See fig. 19)

③ Pulse width $\leq 80\mu s$; duty factor $\leq 0.1\%$.

④ Pulse width 5.0 μs , single shot.



Power
 Conversion
 Fast
 Modules

Fig. 1 - RMS Current and Output Power, Synthesized Sine Wave

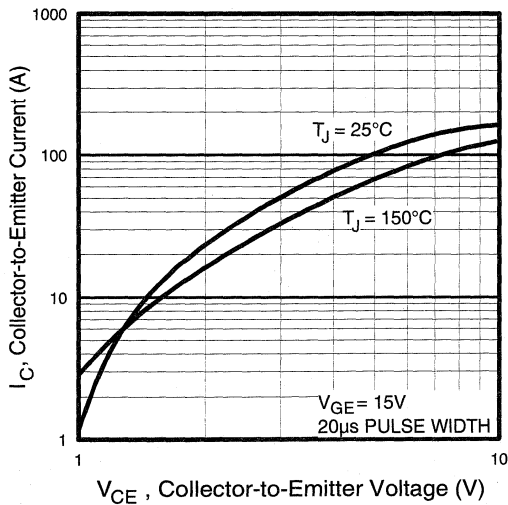


Fig. 2 - Typical Output Characteristics

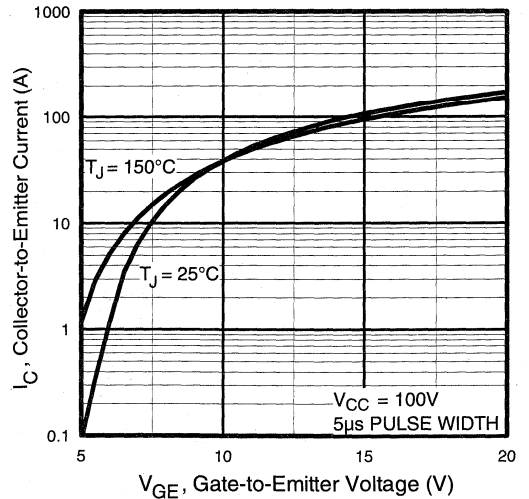


Fig. 3 - Typical Transfer Characteristics

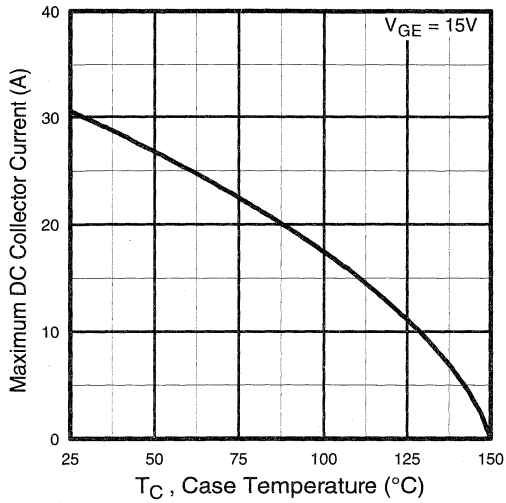


Fig. 4 - Maximum Collector Current vs. Case Temperature

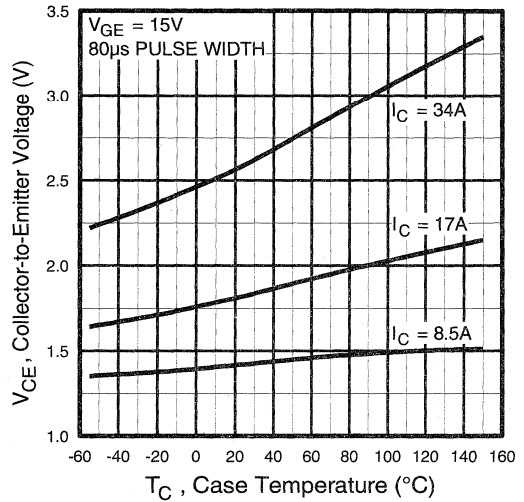


Fig. 5 - Collector-to-Emitter Voltage vs. Case Temperature

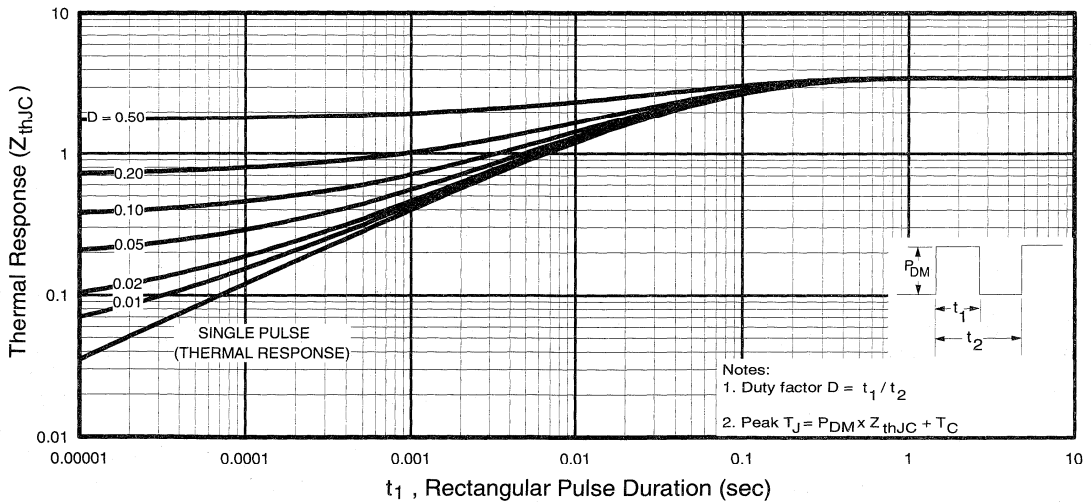


Fig. 6 - Maximum IGBT Effective Transient Thermal Impedance, Junction-to-Case

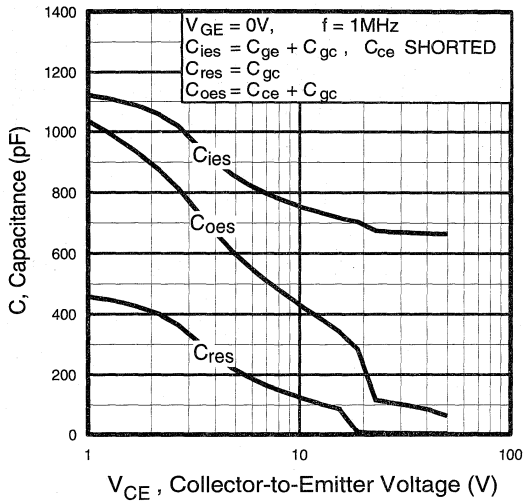


Fig. 7 - Typical Capacitance vs. Collector-to-Emitter Voltage

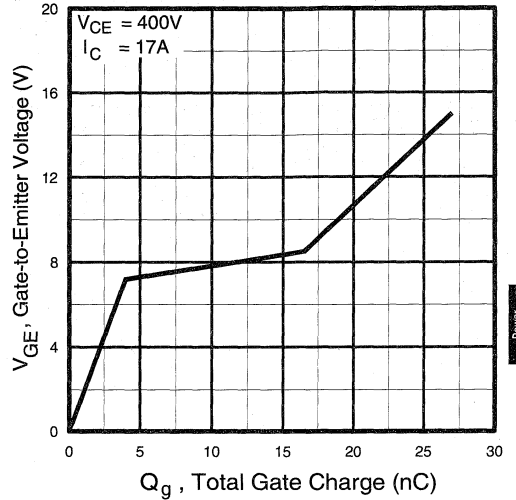


Fig. 8 - Typical Gate Charge vs. Gate-to-Emitter Voltage

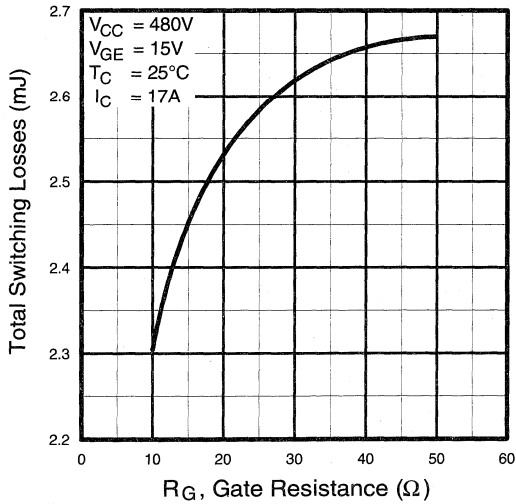


Fig. 9 - Typical Switching Losses vs. Gate Resistance

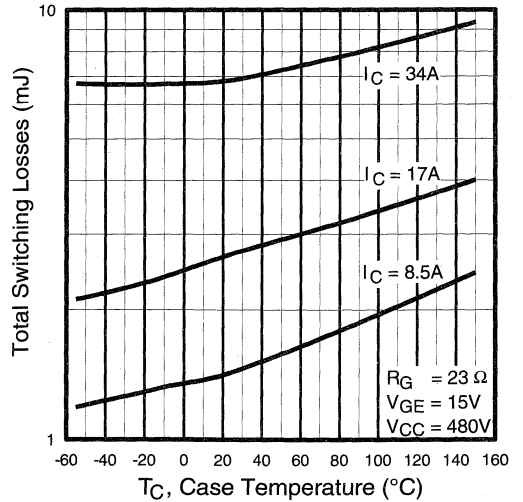


Fig. 10 - Typical Switching Losses vs. Case Temperature

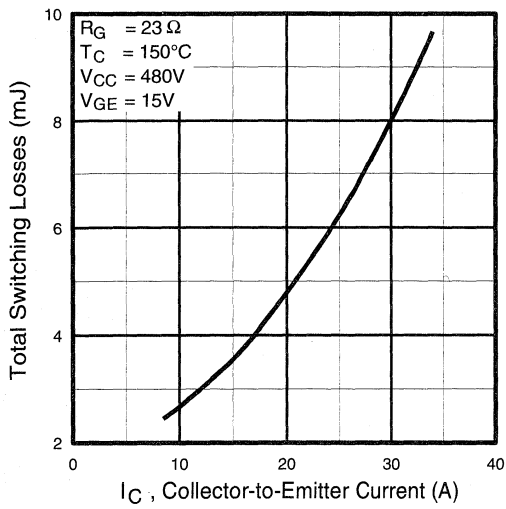


Fig. 11 - Typical Switching Losses vs. Collector-to-Emitter Current

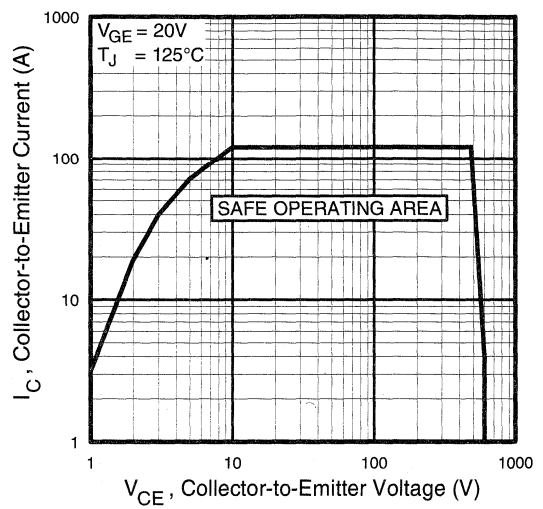


Fig. 12 - Turn-Off SOA

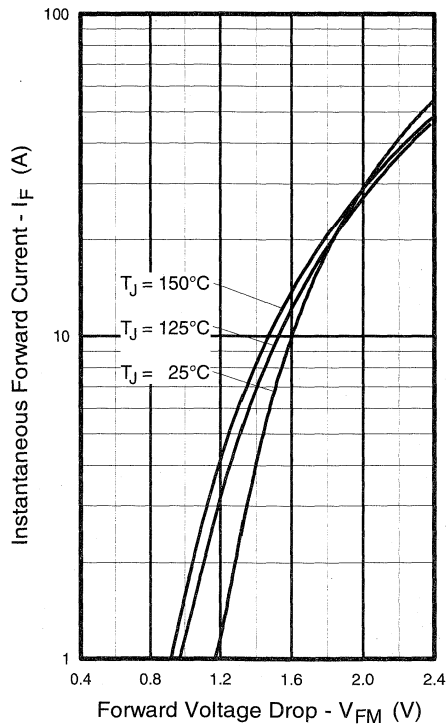


Fig. 13 - Maximum Forward Voltage Drop vs. Instantaneous Forward Current

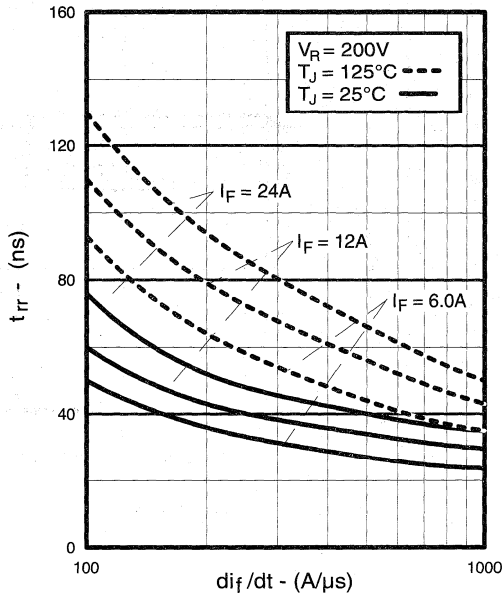


Fig. 14 - Typical Reverse Recovery vs. di/dt

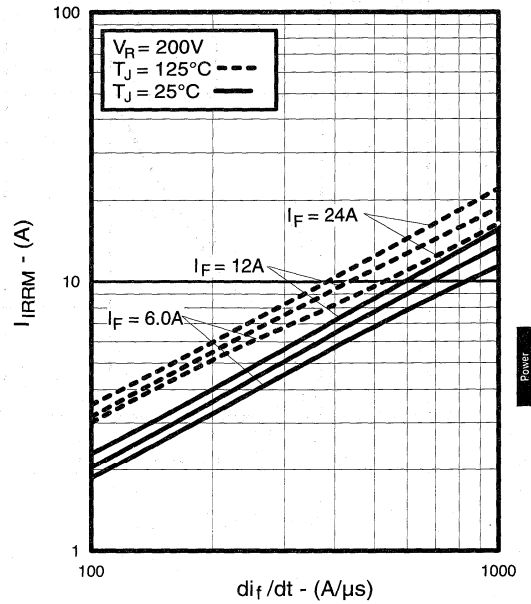


Fig. 15 - Typical Recovery Current vs. di/dt

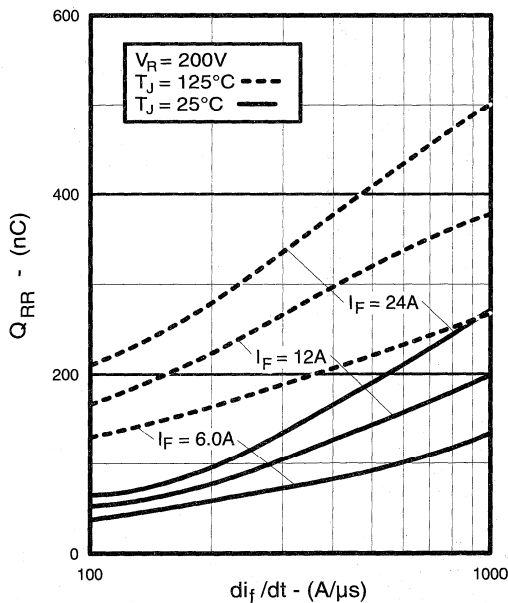


Fig. 16 - Typical Stored Charge vs. di/dt

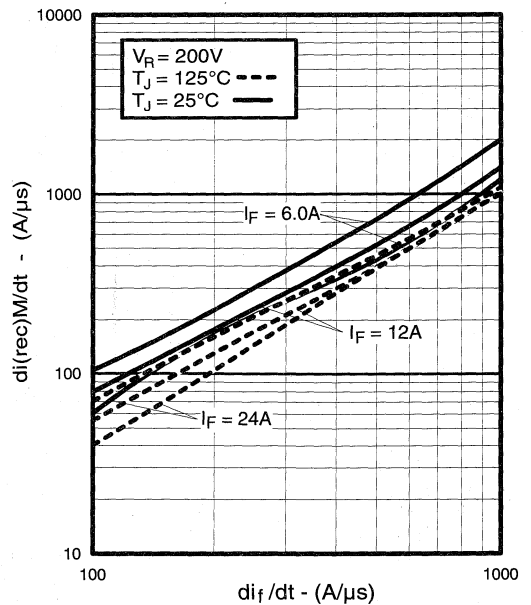


Fig. 17 - Typical $di_{(rec)M}/dt$ vs. di/dt

Power
Conversion
Fast
Modules

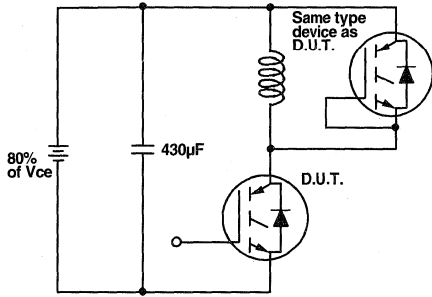


Fig. 18a - Test Circuit for Measurement of I_{LM} , E_{on} , $E_{off}(\text{diode})$, t_{rr} , Q_{rr} , I_{rr} , $t_{d(on)}$, t_r , $t_{d(off)}$, t_f

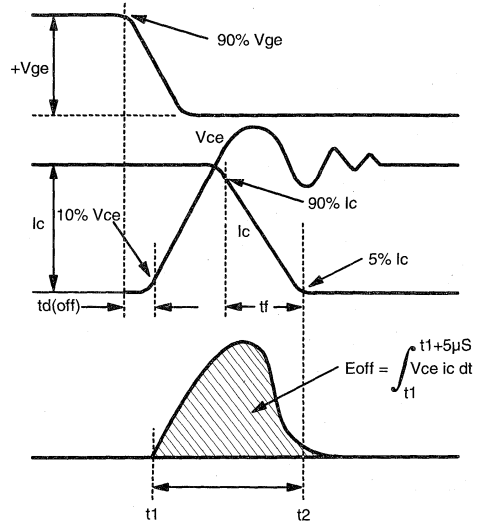


Fig. 18b - Test Waveforms for Circuit of Fig. 18a, Defining E_{off} , $t_{d(off)}$, t_f

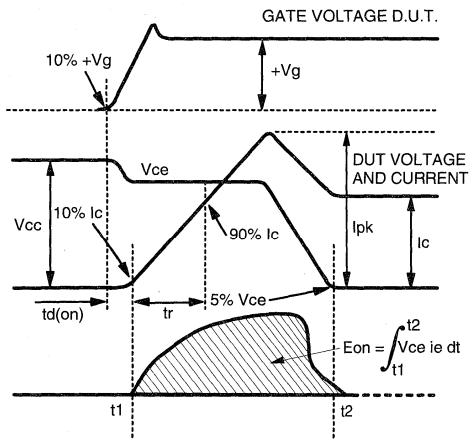


Fig. 18c - Test Waveforms for Circuit of Fig. 18a, Defining E_{on} , $t_{d(on)}$, t_r

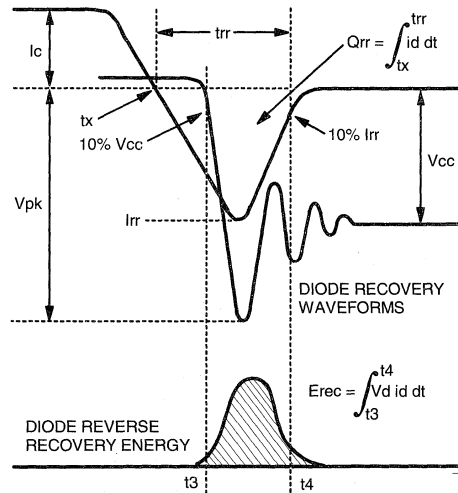


Fig. 18d - Test Waveforms for Circuit of Fig. 18a, Defining E_{rec} , t_{rr} , Q_{rr} , I_{rr}

Refer to Section D for the following:
Appendix D: Section D - page D-6

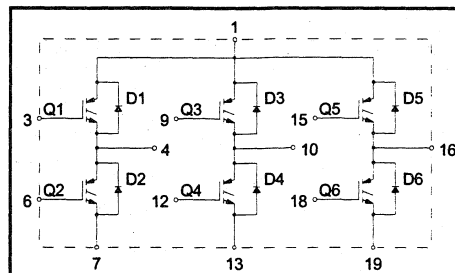
- Fig. 18e - Macro Waveforms for Test Circuit Fig. 18a
- Fig. 19 - Clamped Inductive Load Test Circuit
- Fig. 20 - Pulsed Collector Current Test Circuit

IGBT SIP MODULE

Fast IGBT

Features

- Fully isolated printed circuit board mount package
- Switching-loss rating includes all "tail" losses
- HEXFRED™ soft ultrafast diodes
- Optimized for medium operating frequency (1 to 10kHz) See Fig. 1 for Current vs. Frequency curve



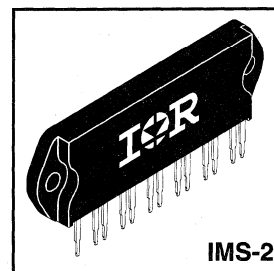
Product Summary

Output Current in a Typical 5.0 kHz Motor Drive

12 A_{RMS} per phase (3.8 kW total) with T_C = 90°C, T_J = 125°C, Supply Voltage 360Vdc, Power Factor 0.8, Modulation Depth 80% (See Figure 1)

Description

The IGBT technology is the key to International Rectifier's advanced line of IMS (Insulated Metal Substrate) Power Modules. These modules are more efficient than comparable bipolar transistor modules, while at the same time having the simpler gate-drive requirements of the familiar power MOSFET. This superior technology has now been coupled to a state of the art materials system that maximizes power throughput with low thermal resistance. This package is highly suited to motor drive applications and where space is at a premium.



Absolute Maximum Ratings

	Parameter	Max.	Units
V _{CES}	Collector-to-Emitter Voltage	600	V
I _C @ T _C = 25°C	Continuous Collector Current, each IGBT	27	A
I _C @ T _C = 100°C	Continuous Collector Current, each IGBT	15	
I _{CM}	Pulsed Collector Current ①	80	
I _{LM}	Clamped Inductive Load Current ②	80	
I _F @ T _C = 100°C	Diode Continuous Forward Current	9.3	
I _{FM}	Diode Maximum Forward Current	80	
V _{GE}	Gate-to-Emitter Voltage	±20	V
V _{ISOL}	Isolation Voltage, any terminal to case, 1 minute	2500	V _{RMS}
P _D @ T _C = 25°C	Maximum Power Dissipation, each IGBT	63	W
P _D @ T _C = 100°C	Maximum Power Dissipation, each IGBT	25	
T _J	Operating Junction and	-40 to +150	°C
T _{STG}	Storage Temperature Range		
	Soldering Temperature, for 10 sec.	300 (0.063 in. (1.6mm) from case)	
	Mounting torque, 6-32 or M3 screw.	5-7 lbf•in (0.55-0.8 N•m)	

Thermal Resistance

	Parameter	Typ.	Max.	Units
R _{θJC} (IGBT)	Junction-to-Case, each IGBT, one IGBT in conduction	—	2.0	°C/W
R _{θJC} (DIODE)	Junction-to-Case, each diode, one diode in conduction	—	3.0	
R _{θCS} (MODULE)	Case-to-Sink, flat, greased surface	0.1	—	
Wt	Weight of module	20 (0.7)	—	g (oz)

Electrical Characteristics @ $T_J = 25^\circ\text{C}$ (unless otherwise specified)

	Parameter	Min.	Typ.	Max.	Units	Conditions
$V_{(BR)CES}$	Collector-to-Emitter Breakdown Voltage ^③	600	—	—	V	$V_{GE} = 0V, I_C = 250\mu A$
$\Delta V_{(BR)CES}/\Delta T_J$	Temp. Coeff. of Breakdown Voltage	—	0.69	—	$V/^\circ\text{C}$	$V_{GE} = 0V, I_C = 1.0mA$
$V_{CE(on)}$	Collector-to-Emitter Saturation Voltage	—	1.4	1.6	V	$I_C = 15A$ $I_C = 27A$ $I_C = 15A, T_J = 150^\circ\text{C}$ $V_{GE} = 15V$ See Fig. 2, 5
		—	1.8	—		
		—	1.5	—		
$V_{GE(th)}$	Gate Threshold Voltage	3.0	—	5.5		$V_{CE} = V_{GE}, I_C = 250\mu A$
$\Delta V_{GE(th)}/\Delta T_J$	Temp. Coeff. of Threshold Voltage	—	-12	—	$mV/^\circ\text{C}$	$V_{CE} = V_{GE}, I_C = 250\mu A$
g_{fe}	Forward Transconductance ^④	9.2	12	—	S	$V_{CE} = 100V, I_C = 27A$
I_{CES}	Zero Gate Voltage Collector Current	—	—	250	μA	$V_{GE} = 0V, V_{CE} = 600V$ $V_{GE} = 0V, V_{CE} = 600V, T_J = 150^\circ\text{C}$
		—	—	3500		
V_{FM}	Diode Forward Voltage Drop	—	1.3	1.7	V	$I_C = 15A, T_J = 150^\circ\text{C}$ See Fig. 13
		—	1.2	1.6		
I_{GES}	Gate-to-Emitter Leakage Current	—	—	± 500	nA	$V_{GE} = \pm 20V$

Switching Characteristics @ $T_J = 25^\circ\text{C}$ (unless otherwise specified)

	Parameter	Min.	Typ.	Max.	Units	Conditions	
Q_g	Total Gate Charge (turn-on)	—	59	80	nC	$I_C = 27A$ $V_{CC} = 400V$ See Fig. 8	
Q_{ge}	Gate - Emitter Charge (turn-on)	—	8.6	10			
Q_{gc}	Gate - Collector Charge (turn-on)	—	25	42			
$t_{d(on)}$	Turn-On Delay Time	—	26	—	ns	$T_J = 25^\circ\text{C}$ $I_C = 27A, V_{CC} = 480V$ $V_{GE} = 15V, R_G = 10\Omega$ Energy losses include "tail" and diode reverse recovery	
t_r	Rise Time	—	37	—			
$t_{d(off)}$	Turn-Off Delay Time	—	240	410			
t_f	Fall Time	—	230	420	mJ	See Fig. 9, 10, 11, 18	
E_{on}	Turn-On Switching Loss	—	0.53	—			
E_{off}	Turn-Off Switching Loss	—	1.3	—			
E_{ts}	Total Switching Loss	—	1.8	2.8	mJ	$T_J = 150^\circ\text{C}$, See Fig. 9, 10, 11, 18 $I_C = 27A, V_{CC} = 480V$ $V_{GE} = 15V, R_G = 10\Omega$ Energy losses include "tail" and diode reverse recovery	
$t_{d(on)}$	Turn-On Delay Time	—	28	—			
t_r	Rise Time	—	37	—			
$t_{d(off)}$	Turn-Off Delay Time	—	380	—	ns	$T_J = 150^\circ\text{C}$, See Fig. 9, 10, 11, 18 $I_C = 27A, V_{CC} = 480V$ $V_{GE} = 15V, R_G = 10\Omega$ Energy losses include "tail" and diode reverse recovery	
t_f	Fall Time	—	460	—			
E_{ts}	Total Switching Loss	—	3.4	—			
C_{ies}	Input Capacitance	—	1500	—	pF	$V_{GE} = 0V$ $V_{CC} = 30V$ $f = 1.0MHz$ See Fig. 7	
C_{oes}	Output Capacitance	—	190	—			
C_{res}	Reverse Transfer Capacitance	—	20	—			
t_{rr}	Diode Reverse Recovery Time	—	42	60	ns	$T_J = 25^\circ\text{C}$ See Fig. 14 $T_J = 125^\circ\text{C}$ 14	$I_F = 15A$
		—	74	120			
I_{rr}	Diode Peak Reverse Recovery Current	—	4.0	6.0	A	$T_J = 25^\circ\text{C}$ See Fig. 15 $T_J = 125^\circ\text{C}$ 15	$V_R = 200V$
		—	6.5	10			
Q_{rr}	Diode Reverse Recovery Charge	—	80	180	nC	$T_J = 25^\circ\text{C}$ See Fig. 16 $T_J = 125^\circ\text{C}$ 16	$di/dt = 200A/\mu s$
		—	220	600			
$di_{(rec)M}/dt$	Diode Peak Rate of Fall of Recovery During t_b	—	188	—	A/ μs	$T_J = 25^\circ\text{C}$ See Fig. 17 $T_J = 125^\circ\text{C}$ 17	
		—	160	—			

Notes:

- ① Repetitive rating; $V_{GE}=20V$, pulse width limited by max. junction temperature. (See fig. 20)
- ② $V_{CC}=80\%(V_{CES}), V_{GE}=20V, L=10\mu H, R_G=10\Omega$, (See fig. 19)
- ③ Pulse width $\leq 80\mu s$; duty factor $\leq 0.1\%$.
- ④ Pulse width $5.0\mu s$, single shot.

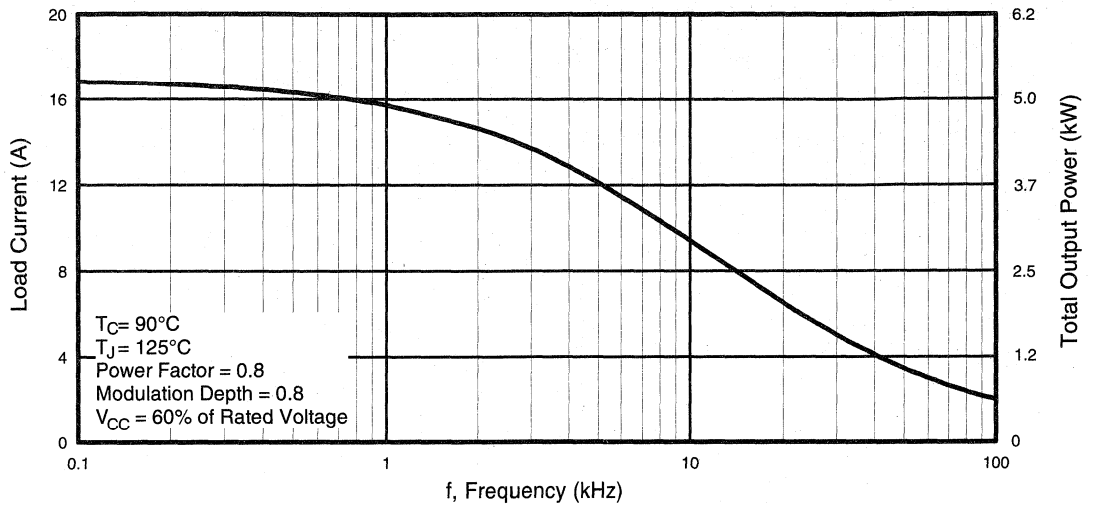


Fig. 1 - RMS Current and Output Power, Synthesized Sine Wave

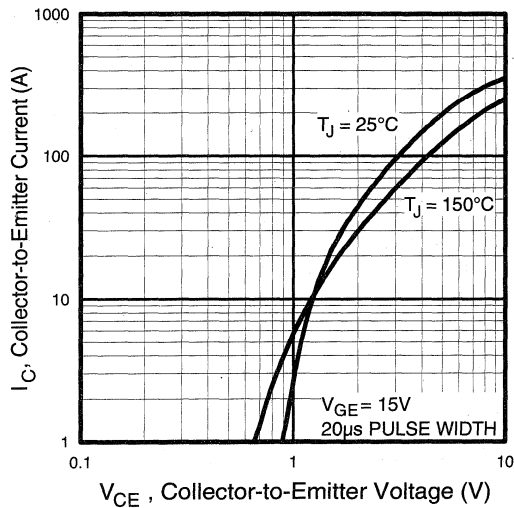


Fig. 2 - Typical Output Characteristics

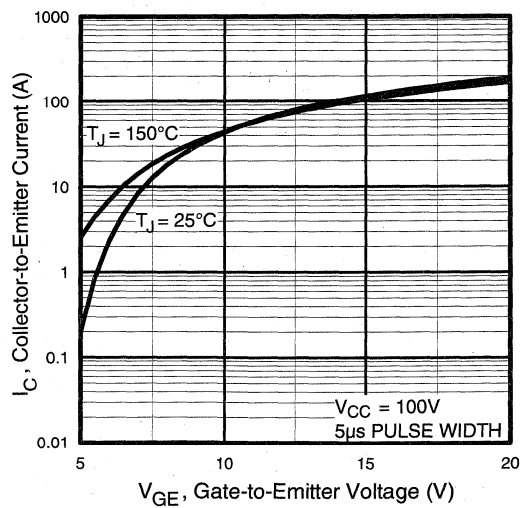


Fig. 3 - Typical Transfer Characteristics

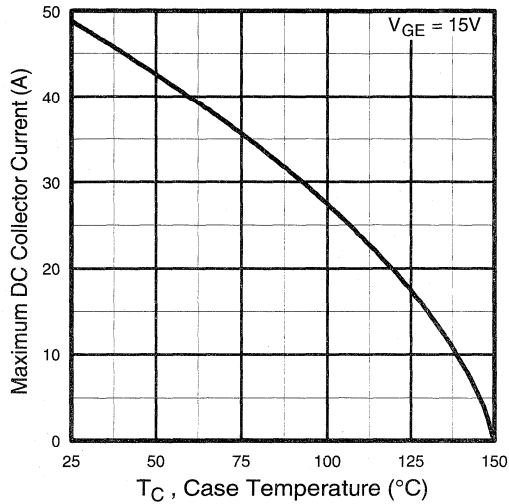


Fig. 4 - Maximum Collector Current vs. Case Temperature

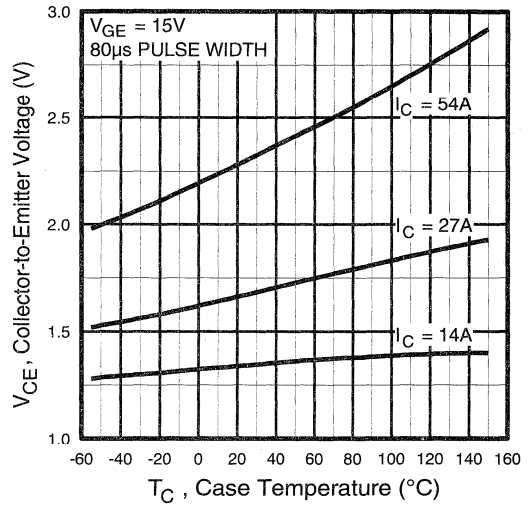


Fig. 5 - Collector-to-Emitter Voltage vs. Case Temperature

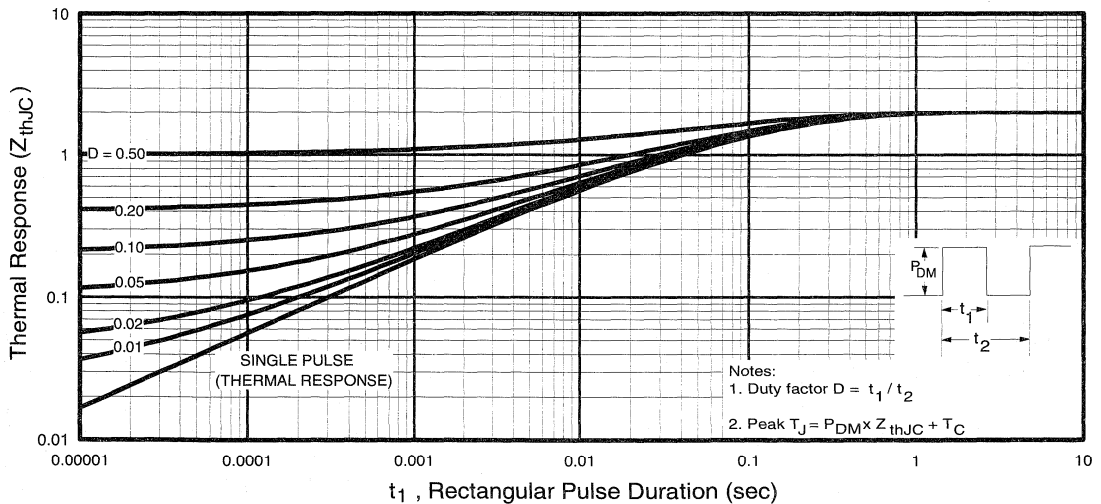


Fig. 6 - Maximum IGBT Effective Transient Thermal Impedance, Junction-to-Case

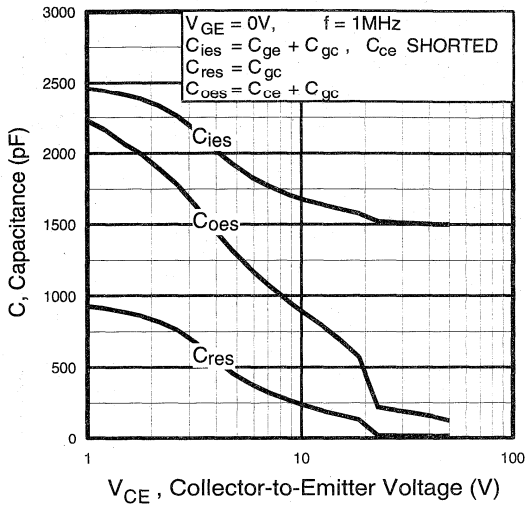


Fig. 7 - Typical Capacitance vs. Collector-to-Emitter Voltage

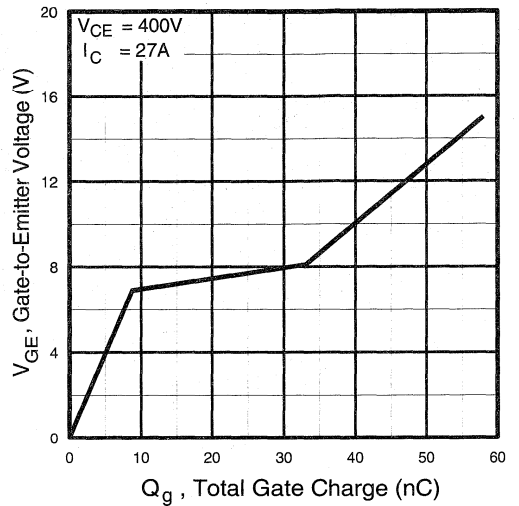


Fig. 8 - Typical Gate Charge vs. Gate-to-Emitter Voltage

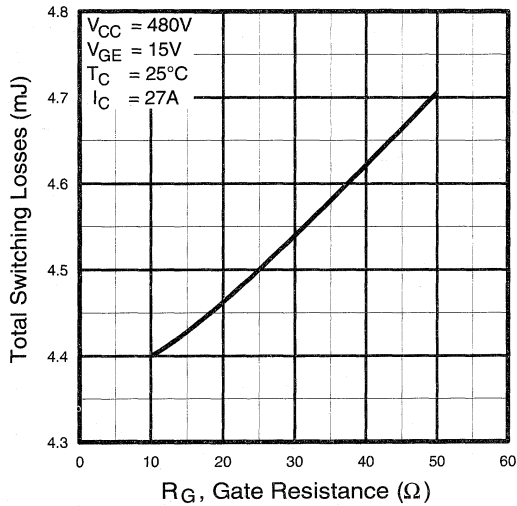


Fig. 9 - Typical Switching Losses vs. Gate Resistance

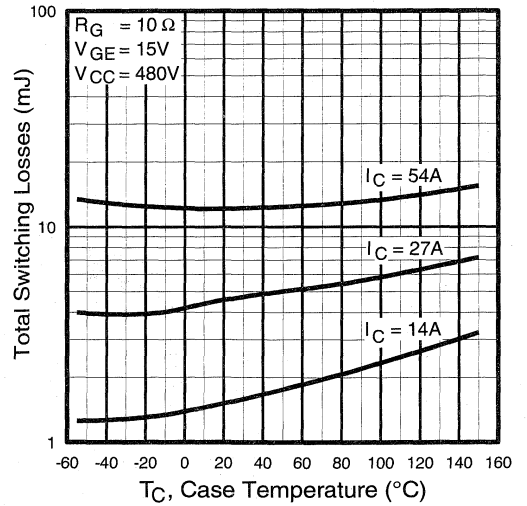


Fig. 10 - Typical Switching Losses vs. Case Temperature

Power Conversion Research Modules

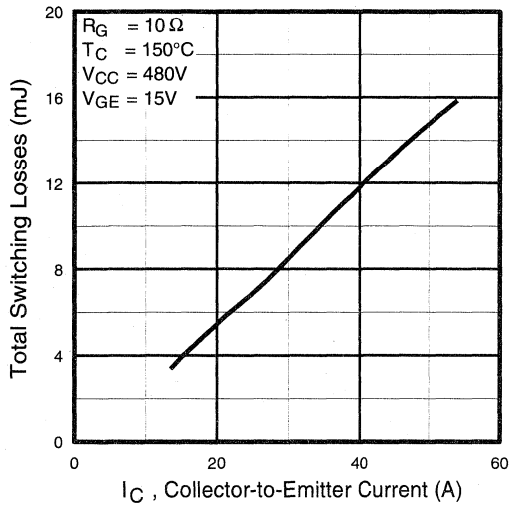


Fig. 11 - Typical Switching Losses vs. Collector-to-Emitter Current

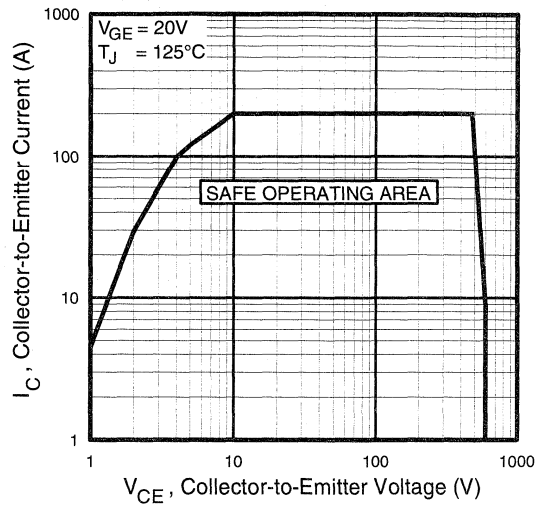


Fig. 12 - Turn-Off SOA

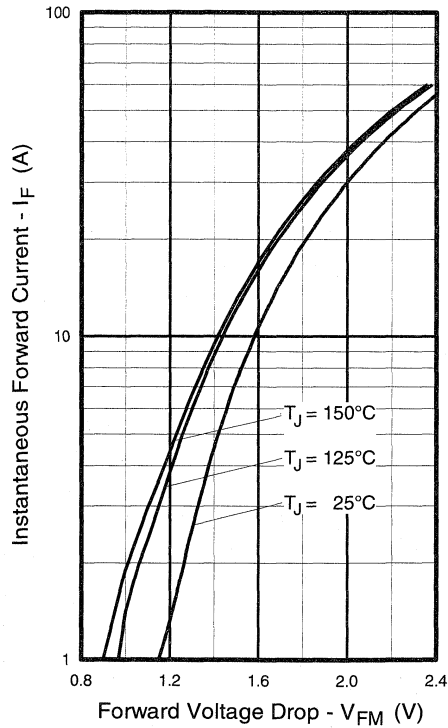


Fig. 13 - Maximum Forward Voltage Drop vs. Instantaneous Forward Current

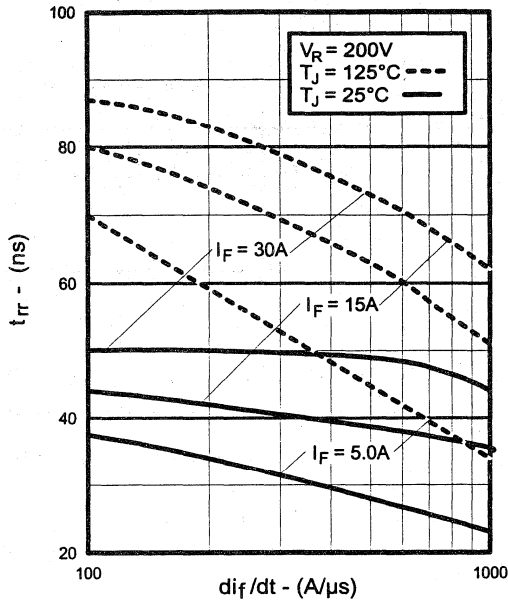


Fig. 14 - Typical Reverse Recovery vs. di_f/dt

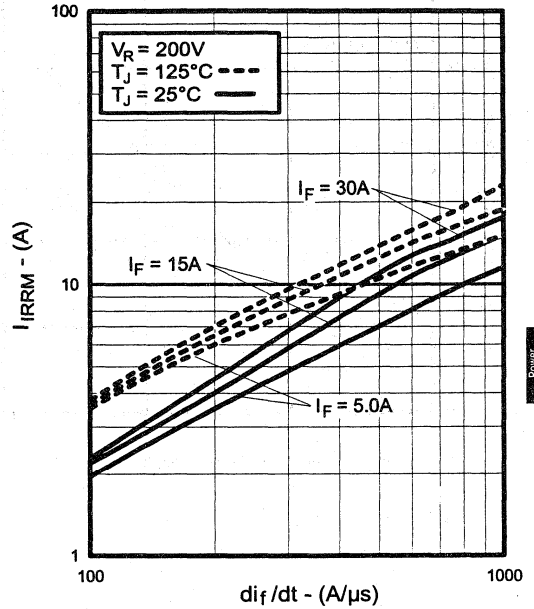


Fig. 15 - Typical Recovery Current vs. di_f/dt

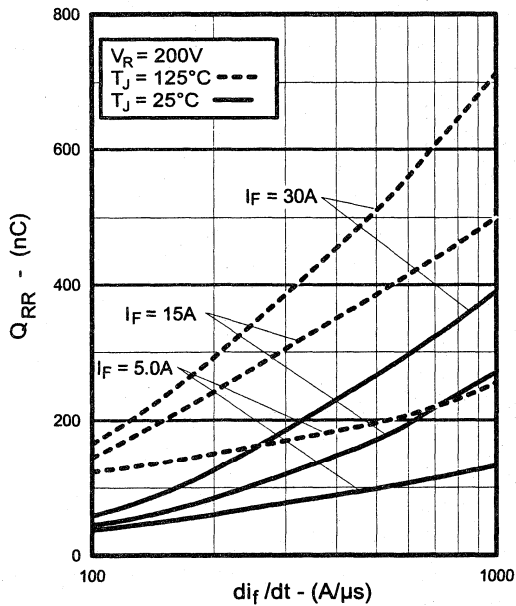


Fig. 16 - Typical Stored Charge vs. di_f/dt

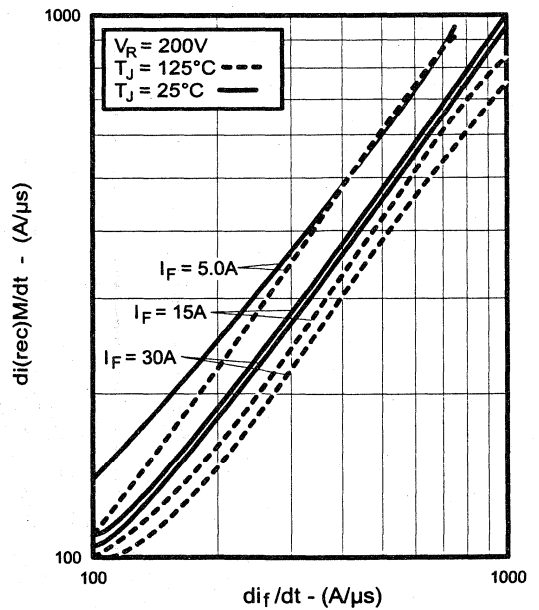


Fig. 17 - Typical $di_{(rec)M}/dt$ vs. di_f/dt

Power
Conversion
Fast
Modules

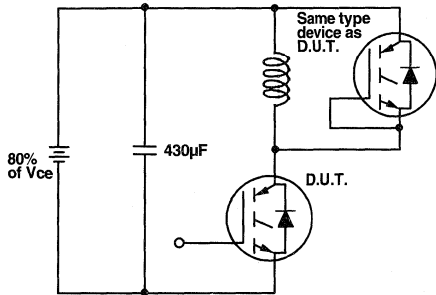


Fig. 18a - Test Circuit for Measurement of I_{LM} , E_{on} , $E_{off}(\text{diode})$, t_{rr} , Q_{rr} , I_{rr} , $t_{d(on)}$, t_r , $t_{d(off)}$, t_f

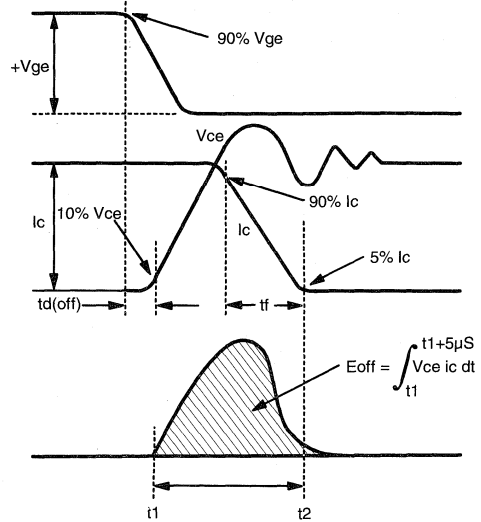


Fig. 18b - Test Waveforms for Circuit of Fig. 18a, Defining E_{off} , $t_{d(off)}$, t_f

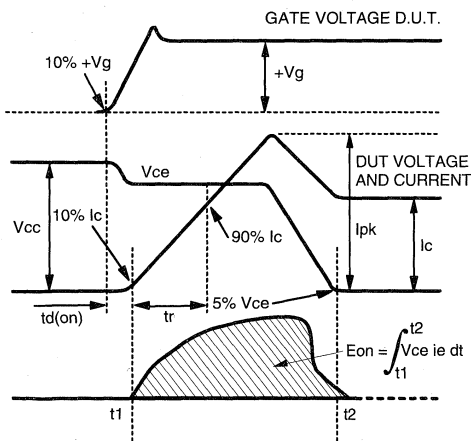


Fig. 18c - Test Waveforms for Circuit of Fig. 18a, Defining E_{on} , $t_{d(on)}$, t_r

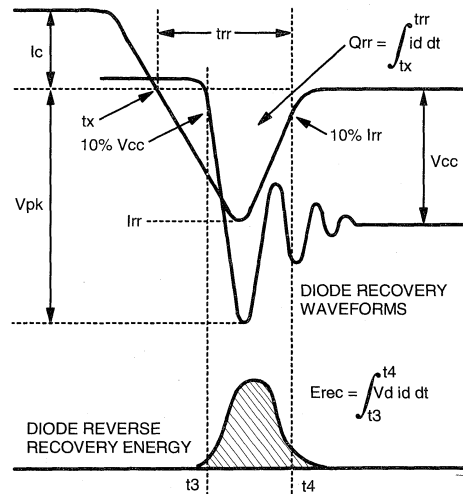


Fig. 18d - Test Waveforms for Circuit of Fig. 18a, Defining E_{rec} , t_{rr} , Q_{rr} , I_{rr}

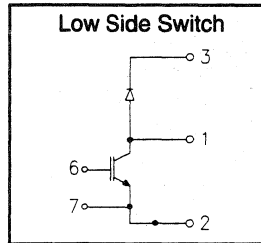
Refer to Section D for the following:
Appendix D: Section D - page D-6

- Fig. 18e - Macro Waveforms for Test Circuit Fig. 18a
- Fig. 19 - Clamped Inductive Load Test Circuit
- Fig. 20 - Pulsed Collector Current Test Circuit

"CHOPPER" IGBT INT-A-PAK

- Rugged Design
- Simple gate-drive
- Fast operation up to 10KHz hard switching, or 50KHz resonant
- Switching-Loss Rating includes all "tail" losses

Fast Speed IGBT



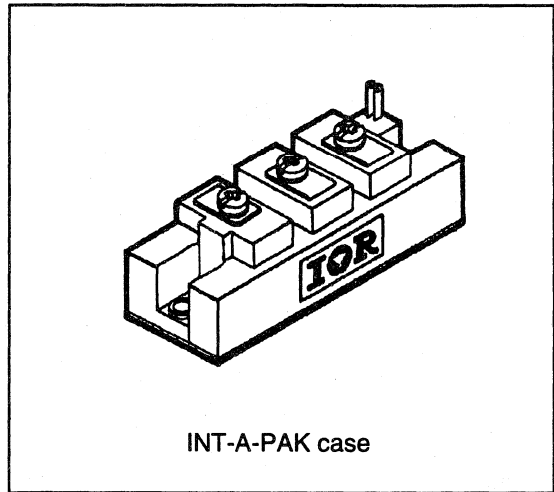
$$V_{CE} = 600V$$

$$I_C = 65A$$

$$V_{CE(ON)} < 2.3V$$

Description

IR's advanced IGBT technology is the key to this line of INT-A-pak Power Modules. The efficient geometry and unique processing of the IGBT allow higher current densities than comparable bipolar power module transistors, while at the same time requiring the simpler gate-drive of the familiar power MOSFET. This superior technology has now been coupled to state of the art assembly techniques to produce a higher current module that is highly suited to power applications such as motor drives, uninterruptible power supplies, welding, induction heating and ultrasonics.



Power
Conversion
Fast
Modules

Absolute Maximum Ratings

Parameter	Description	Value	Units
V_{CES}	Continuous collector to emitter voltage	600	V
$I_C @ T_C = 25^\circ C$	Continuous collector current	65	A
$I_C @ T_C = 85^\circ C$	Continuous collector current	40	
$I_C @ T_C = 100^\circ C$	Continuous collector current	35	
I_{LM}	Peak switching current	130	
I_{FM}	Peak diode forward current (1)	165	V
V_{GE}	Gate to emitter voltage	± 20	
V_{ISOL}	RMS isolation voltage, any terminal to case, $t = 1 \text{ min}$	2500	W
$P_D @ T_C = 25^\circ C$	Power dissipation	179	
T_J	Operating junction temperature range	-40 to 150	$^\circ C$
T_{STG}	Storage temperature range	-40 to 125	

(1) Duration limited by max junction temperature.

Electrical Characteristics - $T_J = 25^\circ\text{C}$, unless otherwise stated

Parameter	Description	Min	Typ	Max	Units	Test Conditions
BV_{CES}	Collector-to-emitter breakdown voltage	600	—	—	V	$V_{GE} = 0V, I_C = 500\mu A$
$V_{CE(ON)}$	Collector-to-emitter voltage	—	—	2.3		$V_{GE} = 15V, I_C = 65A$
		—	2.6	—		$V_{GE} = 15V, I_C = 65A, T_J = 150^\circ\text{C}$
V_{FM}	Diode forward voltage - maximum	—	—	2.3		$I_F = 65A, V_{GE} = 0V$
		—	2.3	—		$I_F = 65A, V_{GE} = 0V, T_J = 150^\circ\text{C}$
V_{GETh}	Gate threshold voltage	3.0	—	5.5	$I_C = 250\mu A$	
ΔV_{GETh}	Threshold voltage temp. coefficient	—	-11	—	mV/ $^\circ\text{C}$	$V_{CE} = V_{GE}, I_C = 250\mu A$
g_{fe}	Forward transconductance	26	—	36	S($\bar{\sigma}$)	$V_{CE} = 25V, I_C = 65A$
I_{CES}	Collector-to-emitter leakage current	—	—	500	μA	$V_{GE} = 0V, V_{CE} = 600V$
		—	—	5	mA	$V_{GE} = 0V, V_{CE} = 600V, T_J = 150^\circ\text{C}$
I_{GES}	Gate-to-emitter leakage current	—	—	± 500	nA	$V_{GE} = \pm 20V$

Dynamic Characteristics - $T_J = 150^\circ\text{C}$

Parameter	Description	Min	Typ	Max	Units	Test Conditions
E_{on}	Turn-on switching energy	—	0.05	—	mJ/A	$R_{G1} = 82\Omega, R_{G2} = 0\Omega$
E_{off} (1)	Turn-off switching energy	—	0.17	—		$I_C = 65A, L_S = 100nH$
E_{ts} (1)	Total switching energy	—	—	0.3		$V_{CC} = 360V, V_{GE} = \pm 15V$
$t_{d(on)}$	Turn-on delay time	—	80	—	ns	$R_{G1} = 82\Omega, R_{G2} = 0\Omega$
t_r	Rise time	—	150	—		$I_C = 65A$
$t_{d(off)}$	Turn-off delay time	—	450	—		$V_{CC} = 360V, V_{GE} = \pm 15V$
t_f	Fall time	—	900	—		$L_S = 100nH$
I_{rr}	Diode peak recovery current	—	30	—		$R_{G1} = 82\Omega, R_{G2} = 0\Omega$
t_{rr}	Diode recovery time	—	115	—	ns	$I_C = 65A$
Q_{rr}	Diode recovery charge	—	2.0	—	μC	$V_{CC} = 360V, V_{GE} = \pm 15V$
Q_{ge}	Gate-to-emitter charge (turn-on)	77	—	140	nC	$V_{CC} = 360V$
Q_{gc}	Gate-to-collector charge (turn-on)	35	—	70		$I_C = 65A$
Q_g	Total gate charge (turn-on)	13	—	21		$V_{GE} = 15V$
C_{ies}	Input capacitance	—	2900	—	pF	$V_{GE} = 0V$
C_{oes}	Output capacitance	—	330	—		$V_{CC} = 30V$
C_{res}	Reverse transfer capacitance	—	40	—		$f = 1MHz$

(1) Includes tail losses

Thermal and Mechanical Characteristics

Parameter	Description	Typ	Max	Units
R_{thJC} (IGBT)	Thermal resistance, junction to case, each IGBT	—	0.7	$^\circ\text{C/W}$
R_{thJC} (Diode)	Thermal resistance, junction to case, each diode	—	0.75	
R_{thCS} (Module)	Thermal resistance, case to sink	0.1	—	
Wt	Weight of module	140	—	g

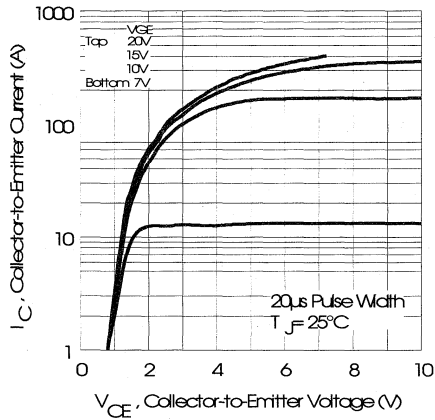


Fig. 1 - Typical Output Characteristics, $T_J = 25^\circ\text{C}$

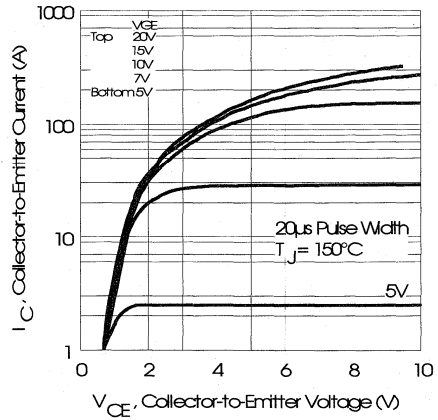


Fig. 2 - Typical Output Characteristics, $T_J = 150^\circ\text{C}$

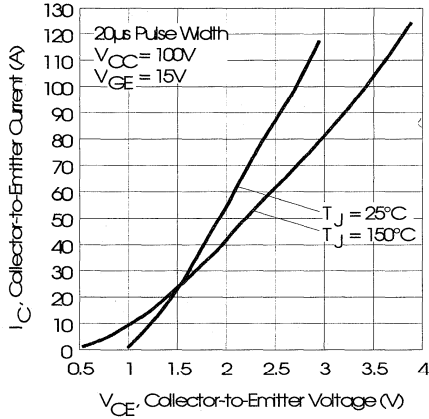


Fig. 3 - Typical Output Characteristics

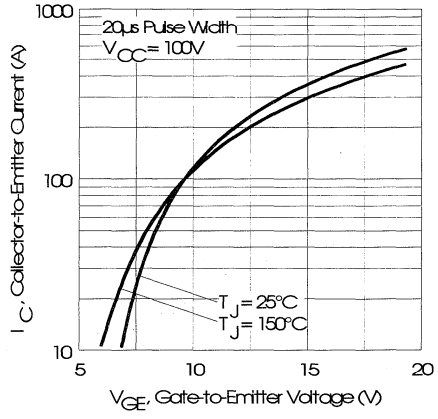


Fig. 4 - Typical Transfer Characteristics

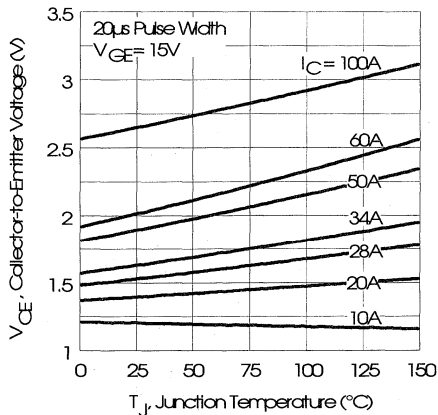


Fig. 5 - Collector-to-Emitter Saturation Typical Voltage vs. Junction Temperature

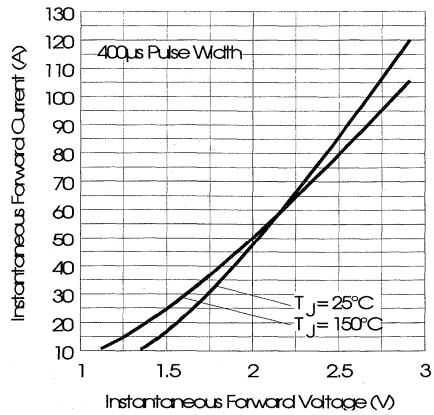


Fig. 6 - Forward Voltage Drop Characteristics

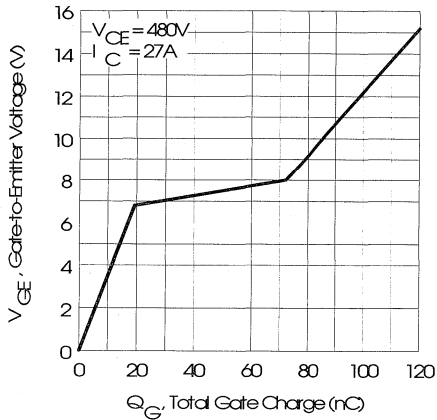


Fig. 7 - Typical Gate Charge vs. Gate-to-Emitter Voltage

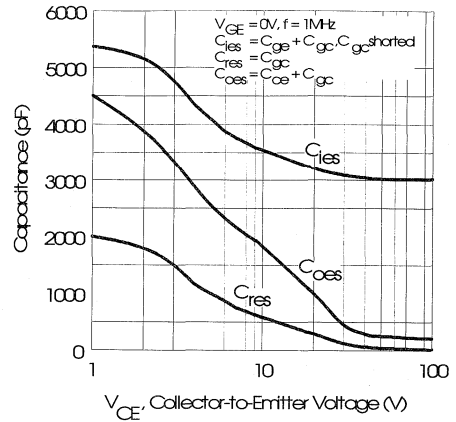


Fig. 8 - Typical Capacitance vs. Collector-to-Emitter Voltage

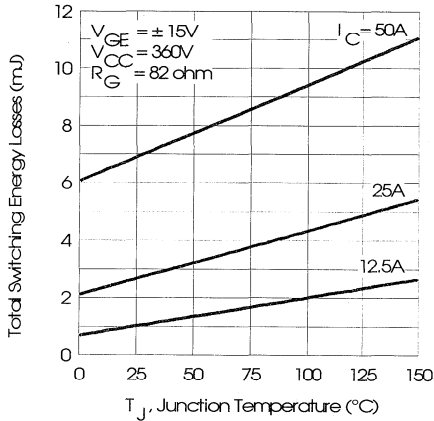


Fig. 9 - Typical Switching Losses vs. Junction Temperature

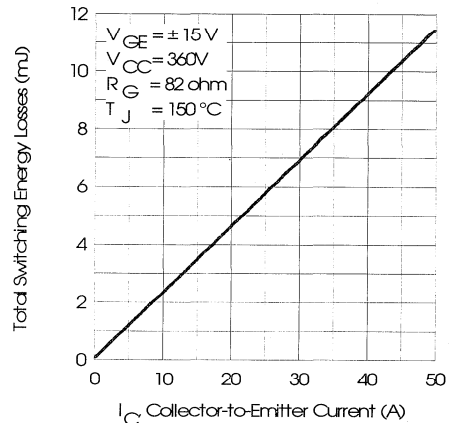


Fig. 10 - Typical Switching Losses vs. Collector-to-Emitter Current

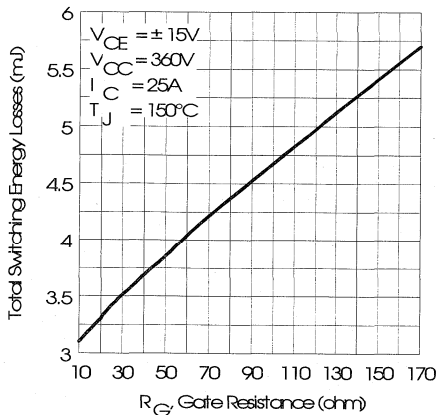


Fig. 11 - Typical Switching Losses vs. Gate Resistance

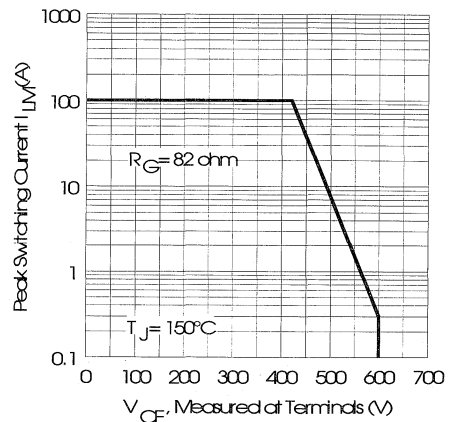


Fig. 12 - Reverse Bias Safe Operating Area

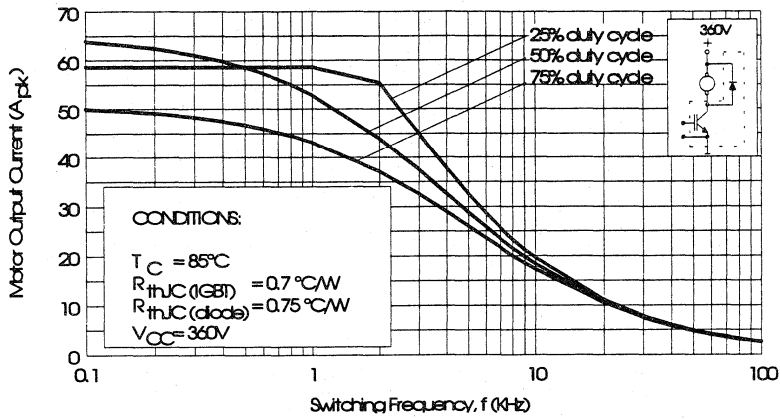


Fig. 13 - RMS Output Current vs. Frequency

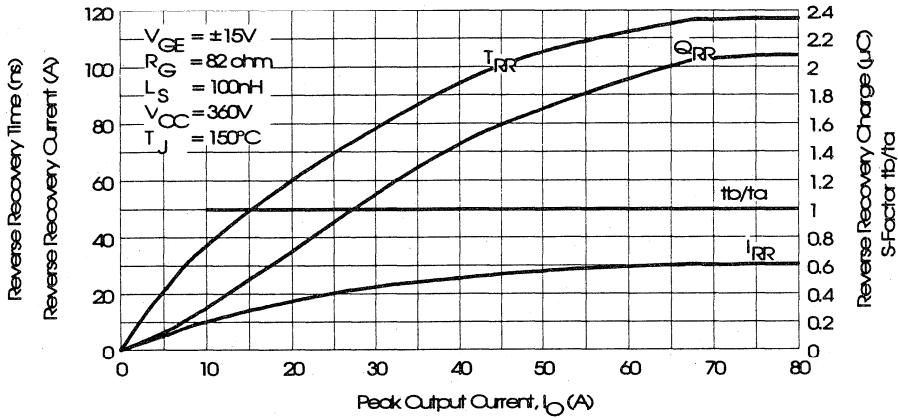


Fig. 14 - Typical Diode Recovery Characteristics as Function of Output Current I_O

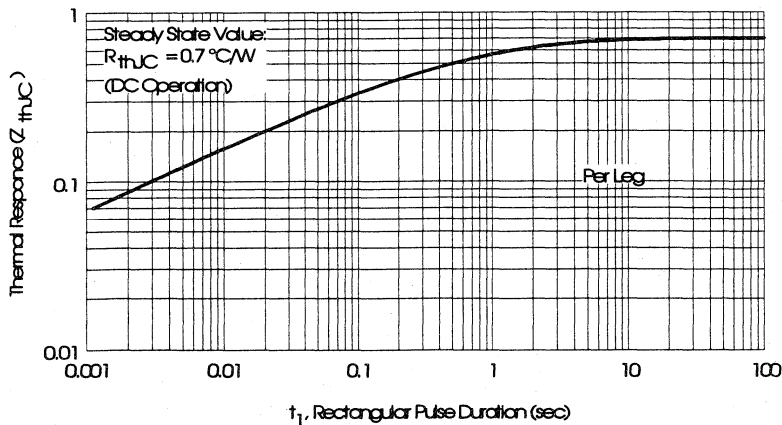


Fig. 15 - Maximum Effective Transient Thermal Impedance, Junction-to-Case

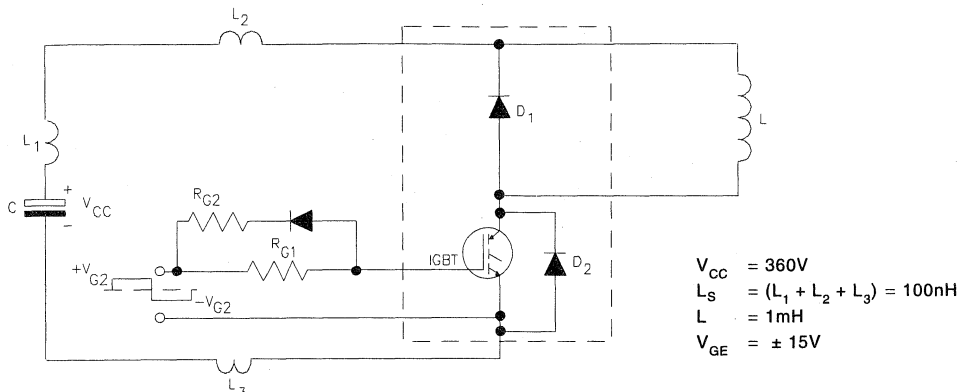


Fig. 16 - Test Circuit for Measurement of I_{LM} , E_{ON} , E_{OFF} , Q_{RR} , I_{RR} , $t_{D(ON)}$, t_r , $t_{D(OFF)}$, t_f

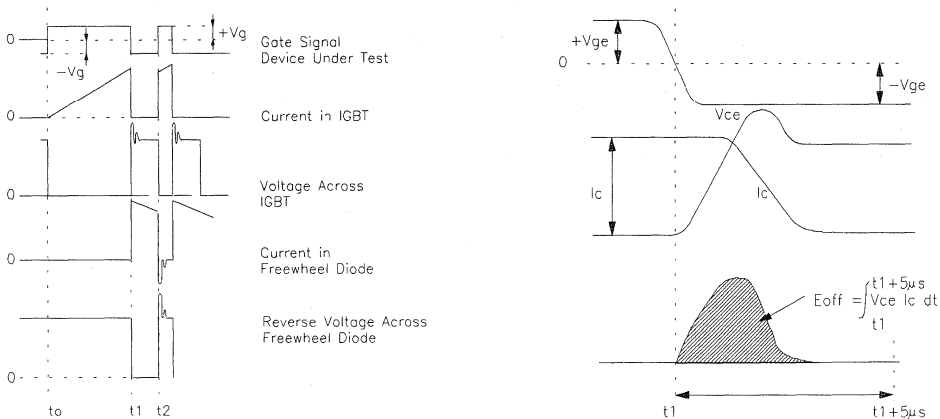


Fig. 17 - Test Waveforms for Circuit of Fig. 16

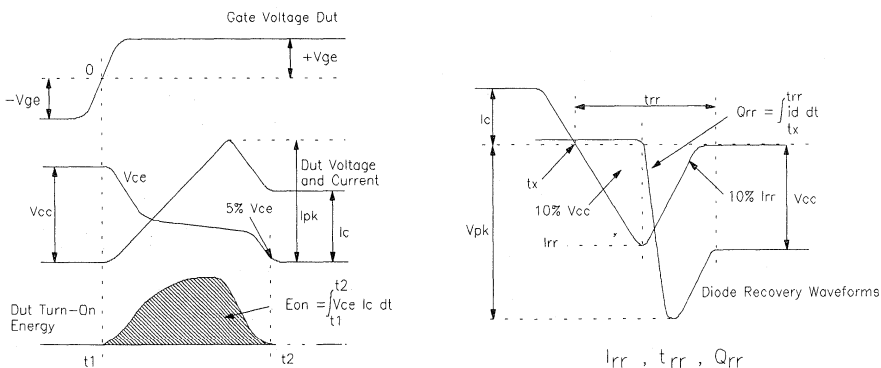


Fig. 18 - Test Waveforms for Circuit of Fig. 16, Defining E_{ON} , E_{REC} , $t_{D(ON)}$, t_r , I_{RR} , t_{RR} , Q_{RR}

Refer to Section D for the following:

Appendix E: Section D - page D-7

Figure 19 - Waveforms for switching time

Package Outline 6 - INT-A-PAK Low Side Switch

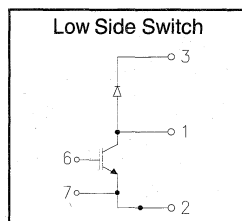
Section D - page D-14

IRGKI120F06

"CHOPPER" IGBT INT-A-PAK

Fast Speed IGBT

- Rugged Design
- Simple gate-drive
- Fast operation up to 10KHz hard switching, or 50KHz resonant
- Switching-Loss Rating includes all "tail" losses



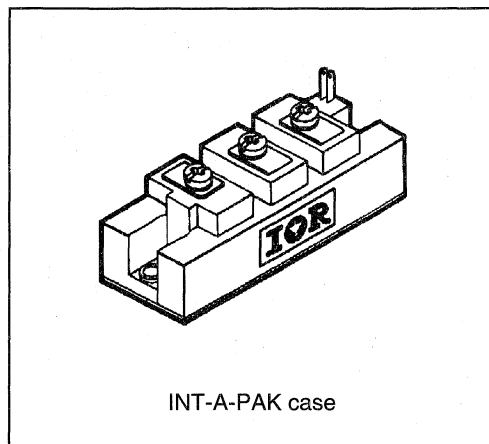
$$V_{CE} = 600V$$

$$I_C = 120A$$

$$V_{CE(ON)} < 2.3V$$

Description

IR's advanced IGBT technology is the key to this line of INT-A-pak Power Modules. The efficient geometry and unique processing of the IGBT allow higher current densities than comparable bipolar power module transistors, while at the same time requiring the simpler gate-drive of the familiar power MOSFET. This superior technology has now been coupled to state of the art assembly techniques to produce a higher current module that is highly suited to power applications such as motor drives, uninterruptible power supplies, welding, induction heating and ultrasonics.


 Power
Conversion
Fast
Modules

Absolute Maximum Ratings

Parameter	Description	Value	Units
V_{CES}	Continuous collector to emitter voltage	600	V
$I_C @ T_C = 25^\circ C$	Continuous collector current	120	A
$I_C @ T_C = 85^\circ C$	Continuous collector current	75	
$I_C @ T_C = 100^\circ C$	Continuous collector current	60	
I_{LM}	Peak switching current	240	
I_{FM}	Peak diode forward current (1)	300	
V_{GE}	Gate to emitter voltage	± 20	V
V_{ISOL}	RMS isolation voltage, any terminal to case, $t = 1 \text{ min}$	2500	
$P_D @ T_C = 25^\circ C$	Power dissipation	298	W
T_J	Operating junction temperature range	-40 to 150	$^\circ C$
T_{STG}	Storage temperature range	-40 to 125	

(1) Duration limited by max junction temperature.

Electrical Characteristics - $T_J = 25^\circ\text{C}$, unless otherwise stated

Parameter	Description	Min	Typ	Max	Units	Test Conditions
BV_{CES}	Collector-to-emitter breakdown voltage	600	—	—	V	$V_{GE} = 0V, I_C = 1mA$
$V_{CE(ON)}$	Collector-to-emitter voltage	—	—	2.3		$V_{GE} = 15V, I_C = 120A$
		—	2.4	—		$V_{GE} = 15V, I_C = 120A, T_J = 150^\circ\text{C}$
V_{FM}	Diode forward voltage - maximum	—	—	2.2		$I_F = 120A, V_{GE} = 0V$
		—	2.2	—		$I_F = 120A, V_{GE} = 0V, T_J = 150^\circ\text{C}$
V_{GEth}	Gate threshold voltage	3.0	—	5.5	$I_C = 500\mu A$	
ΔV_{GEth}	Threshold voltage temperature coefficient	—	-11	—	mV/°C	$V_{CE} = V_{GE}, I_C = 500\mu A$
g_{fe}	Forward transconductance	52	—	72	S(t)	$V_{CE} = 25V, I_C = 120A$
I_{CES}	Collector-to-emitter leakage current	—	—	1	mA	$V_{GE} = 0V, V_{CE} = 600V$
		—	—	10		$V_{GE} = 0V, V_{CE} = 600V, T_J = 150^\circ\text{C}$
I_{GES}	Gate-to-emitter leakage current	—	—	± 1	μA	$V_{GE} = \pm 20V$

Dynamic Characteristics - $T_J = 150^\circ\text{C}$

Parameter	Description	Min	Typ	Max	Units	Test Conditions
E_{on}	Turn-on switching energy	—	0.05	—	mJ/A	$R_{G1} = 47\Omega, R_{G2} = 0\Omega$
E_{off} (1)	Turn-off switching energy	—	0.17	—		$I_C = 120A, L_S = 100nH$
E_{ts} (1)	Total switching energy	—	—	0.3		$V_{CC} = 360V, V_{GE} = \pm 15V$
$t_{d(on)}$	Turn-on delay time	—	80	—	ns	$R_{G1} = 47\Omega, R_{G2} = 0\Omega$
t_r	Rise time	—	150	—		$I_C = 120A$
$t_{d(off)}$	Turn-off delay time	—	450	—		$V_{CC} = 360V, V_{GE} = \pm 15V$
t_f	Fall time	—	900	—		$L_S = 100nH$
I_{rr}	Diode peak recovery current	—	56	—	A	$R_{G1} = 47\Omega, R_{G2} = 0\Omega$
t_{rr}	Diode recovery time	—	115	—		$I_C = 120A$
Q_{rr}	Diode recovery charge	—	3.4	—	μC	$V_{CC} = 360V, V_{GE} = \pm 15V$
Q_{ge}	Gate-to-emitter charge (turn-on)	150	—	280	nC	$V_{CC} = 360V$
Q_{gc}	Gate-to-collector charge (turn-on)	70	—	140		$I_C = 54A$
Q_g	Total gate charge (turn-on)	26	—	42		$V_{GE} = 15V$
C_{ies}	Input capacitance	—	5800	—	pF	$V_{GE} = 0V$
C_{oes}	Output capacitance	—	660	—		$V_{CC} = 30V$
C_{res}	Reverse transfer capacitance	—	80	—		$f = 1MHz$

(1) Includes tail losses

Thermal and Mechanical Characteristics

Parameter	Description	Typ	Max	Units
R_{thJC} (IGBT)	Thermal resistance, junction to case, each IGBT	—	0.42	°C/W
R_{thJC} (Diode)	Thermal resistance, junction to case, each diode	—	0.45	
R_{thCS} (Module)	Thermal resistance, case to sink	0.1	—	
Wt	Weight of module	140	—	g

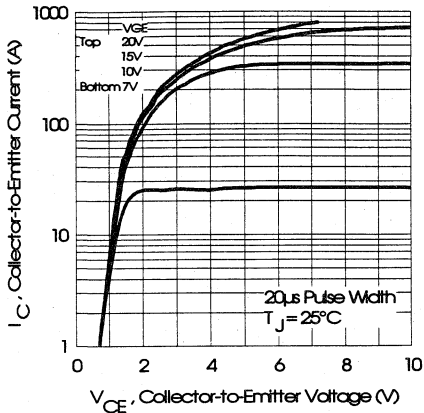


Fig. 1 - Typical Output Characteristics, $T_J = 25^\circ\text{C}$

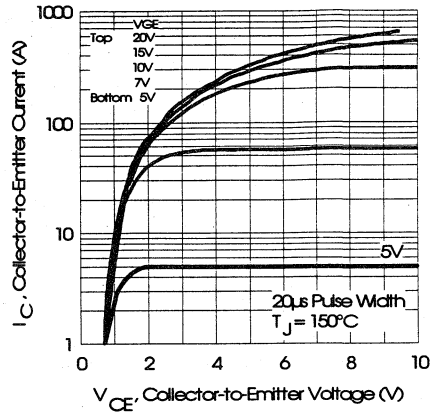


Fig. 2 - Typical Output Characteristics, $T_J = 150^\circ\text{C}$

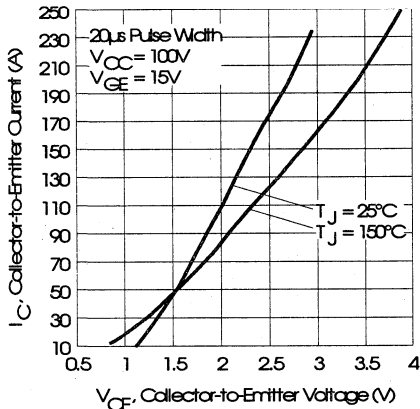


Fig. 3 - Typical Output Characteristics

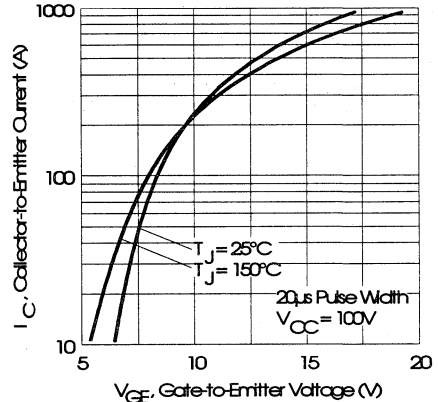


Fig. 4 - Typical Transfer Characteristics

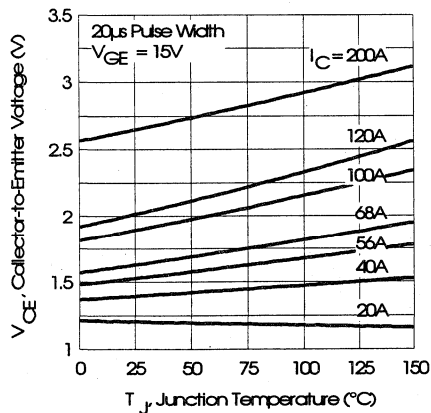


Fig. 5 - Collector-to-Emitter Saturation Typical Voltage vs. Junction Temperature

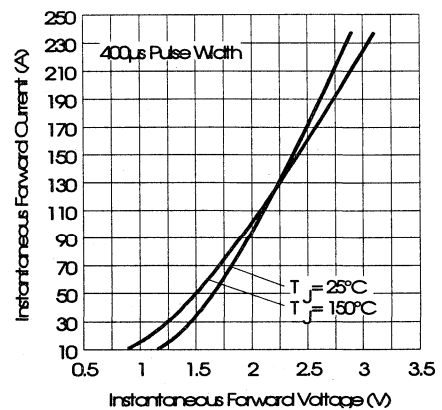


Fig. 6 - Forward Voltage Drop Characteristics

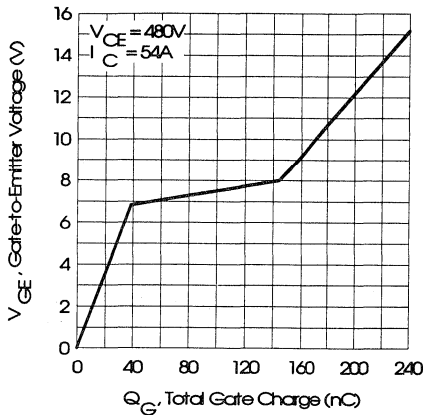


Fig. 7 - Typical Gate Charge vs. Gate-to-Emitter Voltage

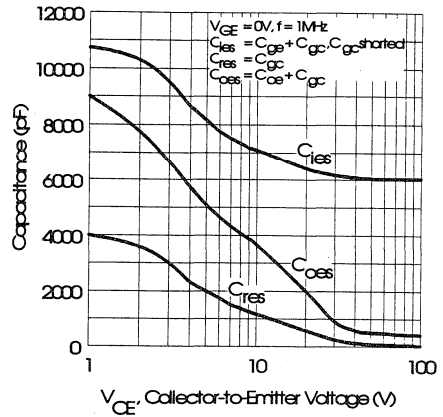


Fig. 8 - Typical Capacitance vs. Collector-to-Emitter Voltage

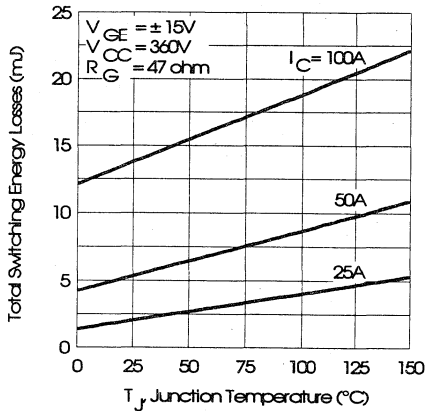


Fig. 9 - Typical Switching Losses vs. Junction Temperature

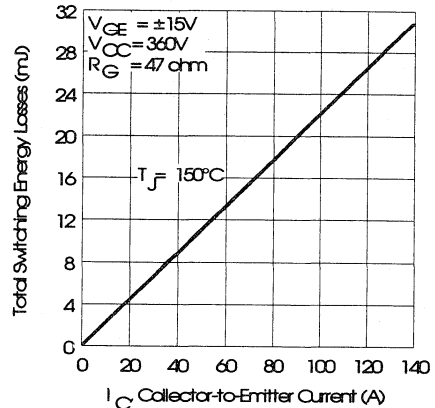


Fig. 10 - Typical Switching Losses vs. Collector-to-Emitter Current

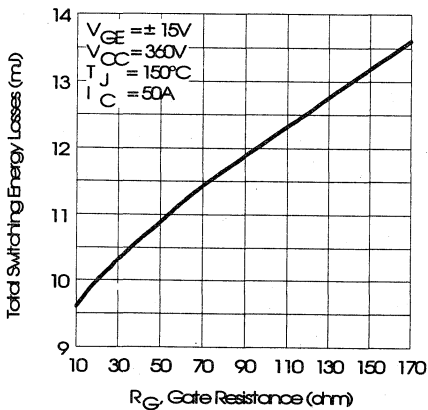


Fig. 11 - Typical Switching Losses vs. Gate Resistance

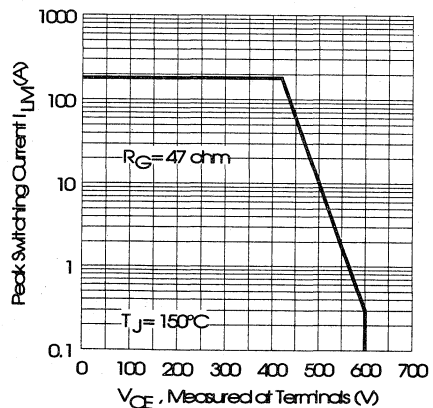


Fig. 12 - Reverse Bias Safe Operating Area

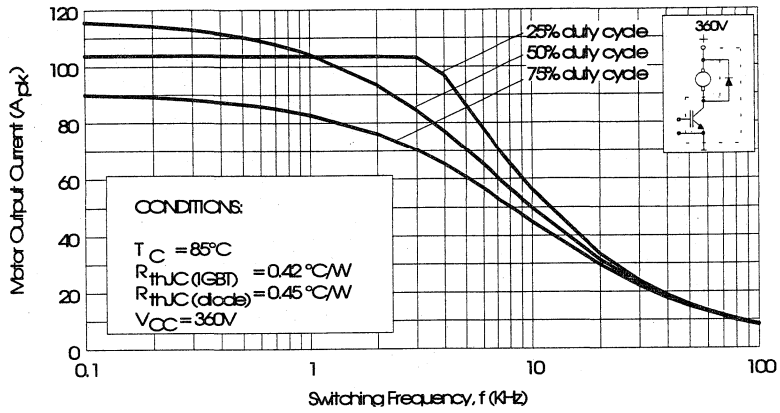


Fig. 13 - RMS Output Current vs. Frequency

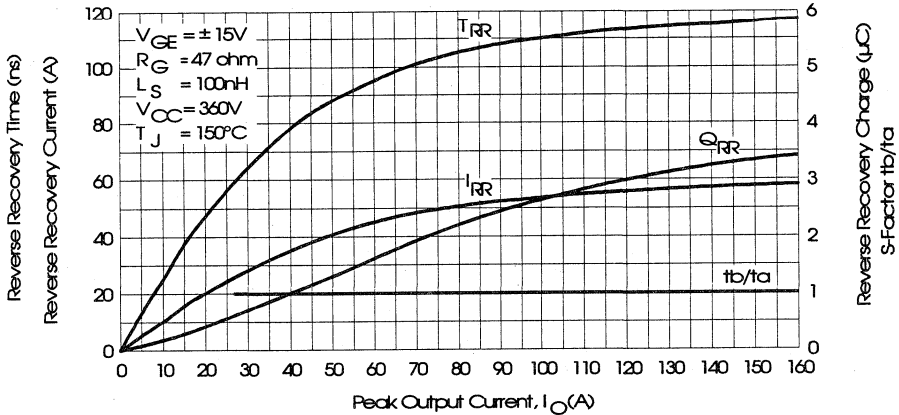


Fig. 14 - Typical Diode Recovery Characteristics as Function of Output Current I_o

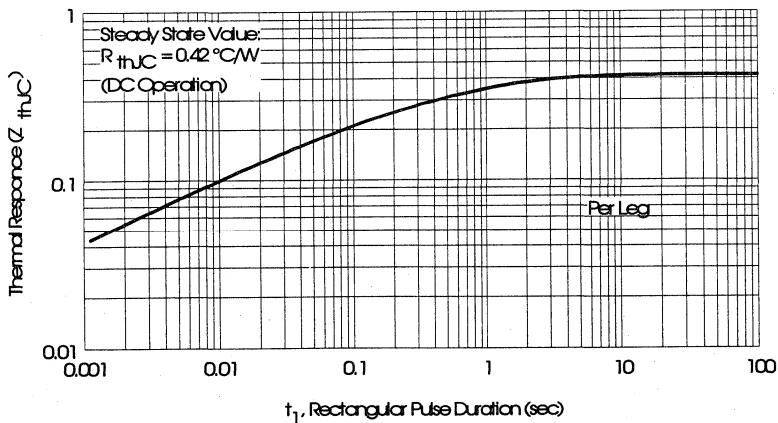


Fig. 15 - Maximum Effective Transient Thermal Impedance, Junction-to-Case

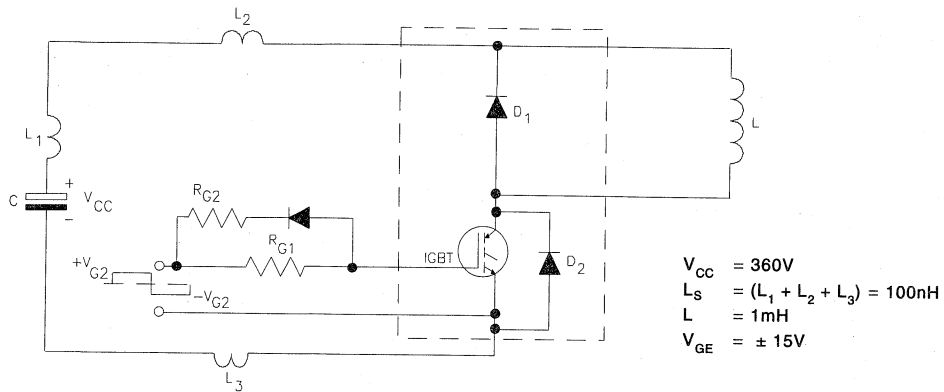


Fig. 16 - Test Circuit for Measurement of I_{LM} , E_{ON} , E_{OFF} , Q_{RR} , I_{RR} , $t_{D(ON)}$, t_r , $t_{D(OFF)}$, t_f

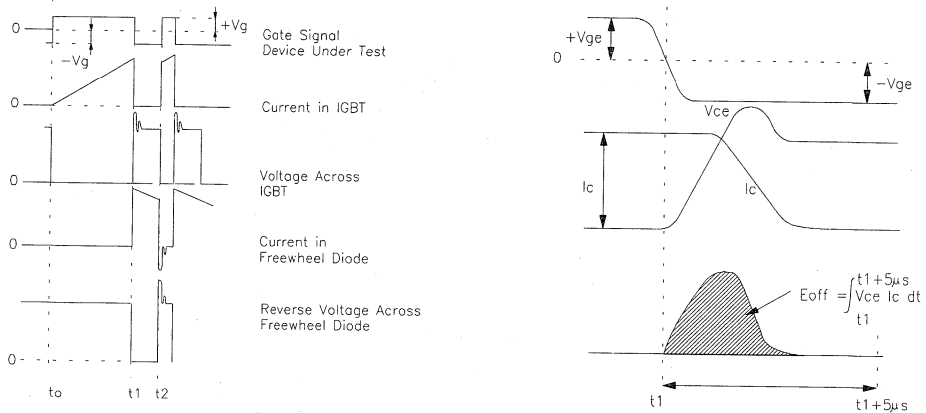


Fig. 17 - Test Waveforms for Circuit of Fig. 16

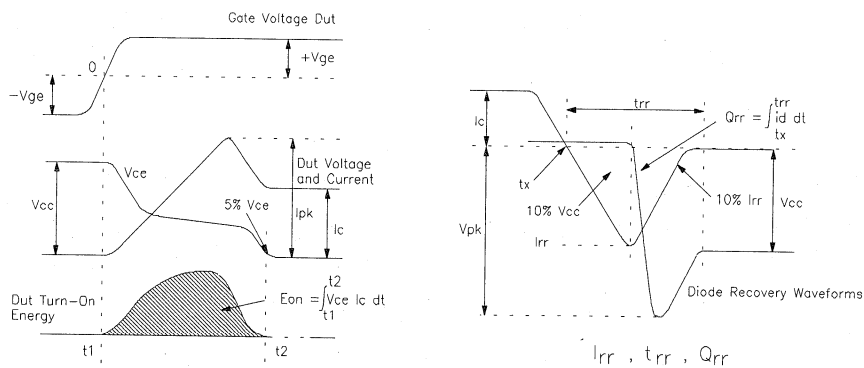


Fig. 18 - Test Waveforms for Circuit of Fig. 16, Defining E_{ON} , E_{REC} , $t_{D(ON)}$, t_r , I_{RR} , t_{RR} , Q_{RR}

Refer to Section D for the following:

Appendix E: Section D - page D-7

Fig. 19 - Waveforms for Switching Time

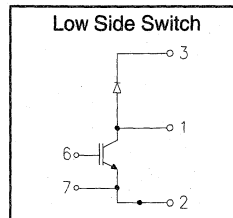
Package Outline 6 -INT-A-PAK Low Side Switch

Section D - page D-14

"CHOPPER" IGBT INT-A-PAK

Fast Speed IGBT

- Rugged Design
- Simple gate-drive
- Fast operation up to 10KHz hard switching, or 50KHz resonant
- Switching-Loss Rating includes all "tail" losses



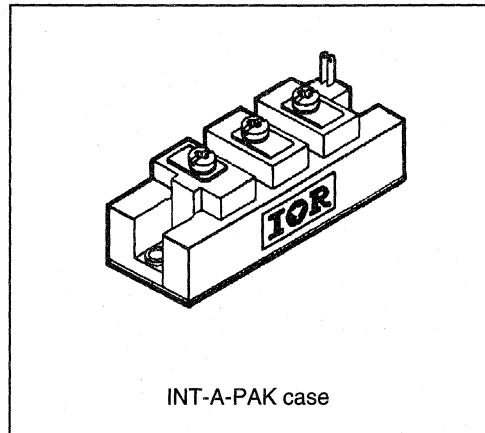
$$V_{CE} = 600V$$

$$I_C = 165A$$

$$V_{CE(ON)} < 2.3V$$

Description

IR's advanced IGBT technology is the key to this line of INT-A-pak Power Modules. The efficient geometry and unique processing of the IGBT allow higher current densities than comparable bipolar power module transistors, while at the same time requiring the simpler gate-drive of the familiar power MOSFET. This superior technology has now been coupled to state of the art assembly techniques to produce a higher current module that is highly suited to power applications such as motor drives, uninterruptible power supplies, welding, induction heating and ultrasonics.



Absolute Maximum Ratings

Parameter	Description	Value	Units
V _{CE}	Continuous collector to emitter voltage	600	V
I _C @ T _C = 25°C	Continuous collector current	165	A
I _C @ T _C = 85°C	Continuous collector current	100	
I _C @ T _C = 100°C	Continuous collector current	85	
I _{LM}	Peak switching current	330	
I _{FM}	Peak diode forward current (1)	400	
V _{GE}	Gate to emitter voltage	± 20	V
V _{ISOL}	RMS isolation voltage, any terminal to case, t = 1 min	2500	
P _D @ T _C = 25°C	Power dissipation	379	W
T _J	Operating junction temperature range	-40 to 150	°C
T _{STG}	Storage temperature range	-40 to 125	

(1) Duration limited by max junction temperature.

IRGKI165F06

Electrical Characteristics - $T_J = 25^\circ\text{C}$, unless otherwise stated

Parameter	Description	Min	Typ	Max	Units	Test Conditions
BV_{CES}	Collector-to-emitter breakdown voltage	600	—	—	V	$V_{GE} = 0V, I_C = 1.5mA$
$V_{CE(ON)}$	Collector-to-emitter voltage	—	—	2.3		$V_{GE} = 15V, I_C = 165A$
		—	2.3	—		$V_{GE} = 15V, I_C = 165A, T_J = 150^\circ\text{C}$
V_{FM}	Diode forward voltage - maximum	—	—	2.1		$I_F = 165A, V_{GE} = 0V$
		—	2.1	—		$I_F = 165A, V_{GE} = 0V, T_J = 150^\circ\text{C}$
V_{GEth}	Gate threshold voltage	3.0	—	5.5	$I_C = 750\mu A$	
ΔV_{GEth}	Threshold voltage temp. coefficient	—	-11	—	mV/ $^\circ\text{C}$	$V_{CE} = V_{GE}, I_C = 750\mu A$
g_{fe}	Forward transconductance	78	—	108	S(Ω)	$V_{CE} = 25V, I_C = 165A$
I_{CES}	Collector-to-emitter leakage current	—	—	1.5	mA	$V_{GE} = 0V, V_{CE} = 600V$
		—	—	15		$V_{GE} = 0V, V_{CE} = 600V, T_J = 150^\circ\text{C}$
I_{GES}	Gate-to-emitter leakage current	—	—	± 1.5	μA	$V_{GE} = \pm 20V$

Dynamic Characteristics - $T_J = 150^\circ\text{C}$

Parameter	Description	Min	Typ	Max	Units	Test Conditions
E_{on}	Turn-on switching energy	—	0.05	—	mJ/A	$R_{G1} = 33\Omega, R_{G2} = 0\Omega$
E_{off} (1)	Turn-off switching energy	—	0.17	—		$I_C = 165A, L_S = 100nH$
E_{ts} (1)	Total switching energy	—	—	0.3		$V_{CC} = 360V, V_{GE} = \pm 15V$
$t_{d(on)}$	Turn-on delay time	—	80	—	ns	$R_{G1} = 33\Omega, R_{G2} = 0\Omega$
t_r	Rise time	—	150	—		$I_C = 165A$
$t_{d(off)}$	Turn-off delay time	—	450	—		$V_{CC} = 360V, V_{GE} = \pm 15V$
t_f	Fall time	—	900	—		$L_S = 100nH$
I_{rr}	Diode peak recovery current	—	84	—		$R_{G1} = 33\Omega, R_{G2} = 0\Omega$
t_{rr}	Diode recovery time	—	115	—	ns	$I_C = 165A$
Q_{rr}	Diode recovery charge	—	5.0	—	μC	$V_{CC} = 360V, V_{GE} = \pm 15V$
Q_{ge}	Gate-to-emitter charge (turn-on)	225	—	420	nC	$V_{CC} = 360V$
Q_{gc}	Gate-to-collector charge (turn-on)	105	—	210		$I_C = 81A$
Q_g	Total gate charge (turn-on)	39	—	63		$V_{GE} = 15V$
C_{ies}	Input capacitance	—	8700	—	pF	$V_{GE} = 0V$
C_{oes}	Output capacitance	—	990	—		$V_{CC} = 30V$
C_{res}	Reverse transfer capacitance	—	120	—		$f = 1MHz$

(1) Includes tail losses

Thermal and Mechanical Characteristics

Parameter	Description	Typ	Max	Units
R_{thJC} (IGBT)	Thermal resistance, junction to case, each IGBT	—	0.33	$^\circ\text{C/W}$
R_{thJC} (Diode)	Thermal resistance, junction to case, each diode	—	0.35	
R_{thCS} (Module)	Thermal resistance, case to sink	0.1	—	
Wt	Weight of module	140	—	g

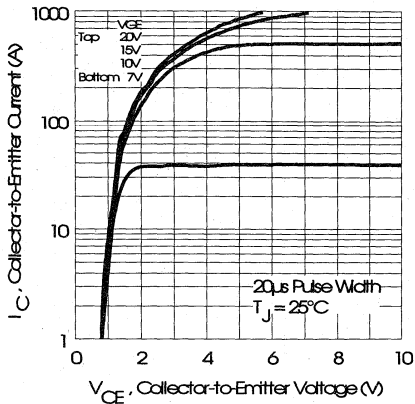


Fig. 1 - Typical Output Characteristics, $T_J = 25^\circ\text{C}$

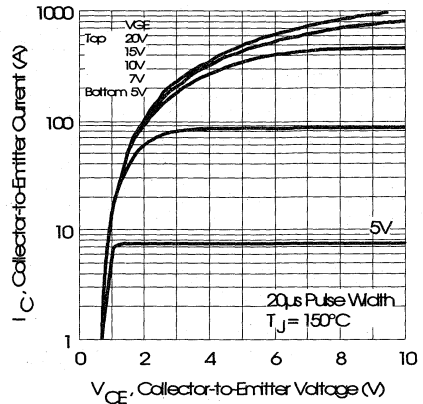


Fig. 2 - Typical Output Characteristics, $T_J = 150^\circ\text{C}$

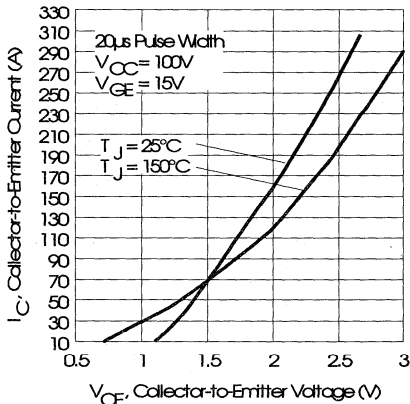


Fig. 3 - Typical Output Characteristics

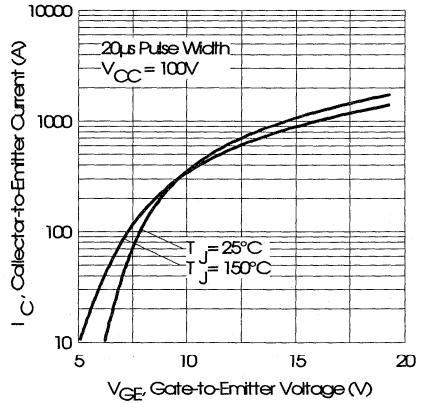


Fig. 4 - Typical Transfer Characteristics

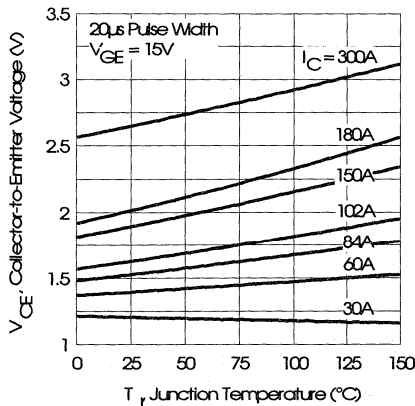


Fig. 5 - Collector-to-Emitter Saturation Typical Voltage vs. Junction Temperature

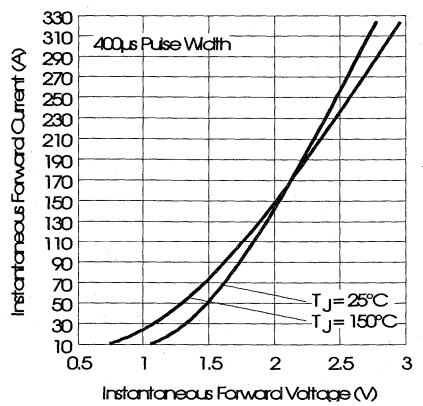


Fig. 6 - Forward Voltage Drop Characteristics



IRGKI165F06

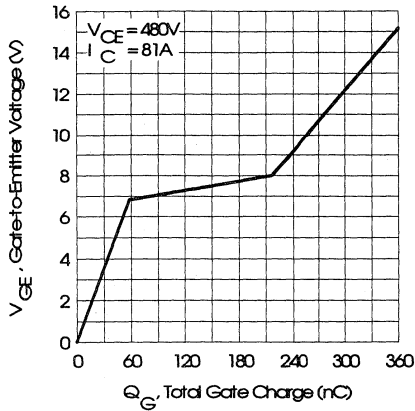


Fig. 7 - Typical Gate Charge vs. Gate-to-Emitter Voltage

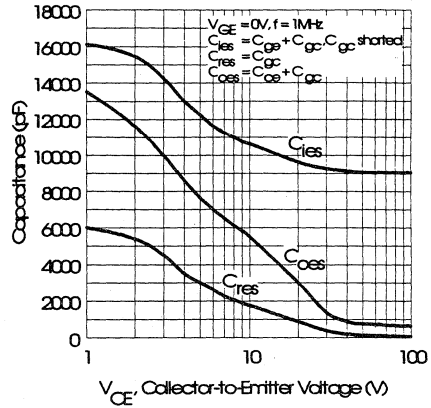


Fig. 8 - Typical Capacitance vs. Collector-to-Emitter Voltage

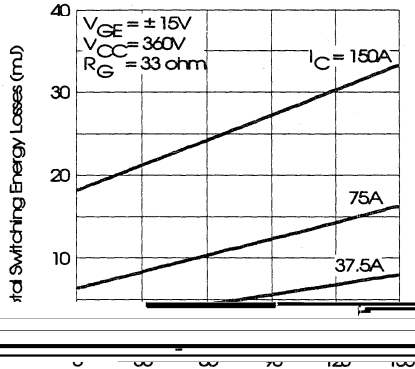


Fig. 9 - Typical Switching Losses vs. Junction Temperature

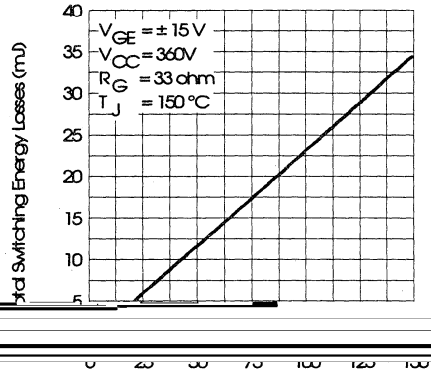


Fig. 10 - Typical Switching Losses vs. Collector-to-Emitter Current

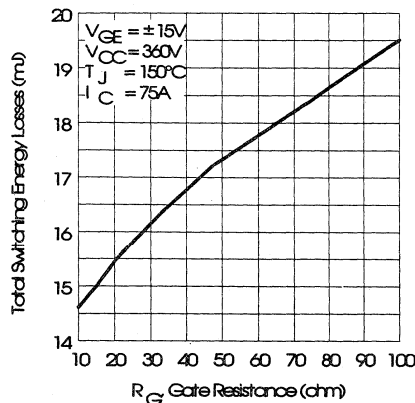


Fig. 11 - Typical Switching Losses vs. Gate Resistance

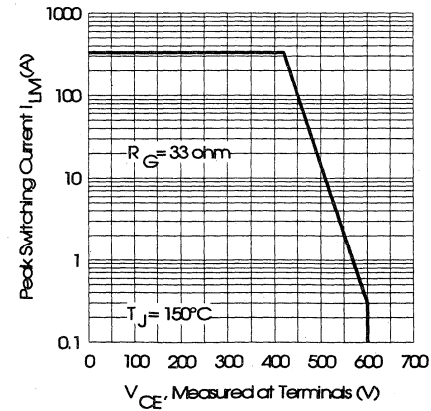


Fig. 12 - Reverse Bias Safe Operating Area

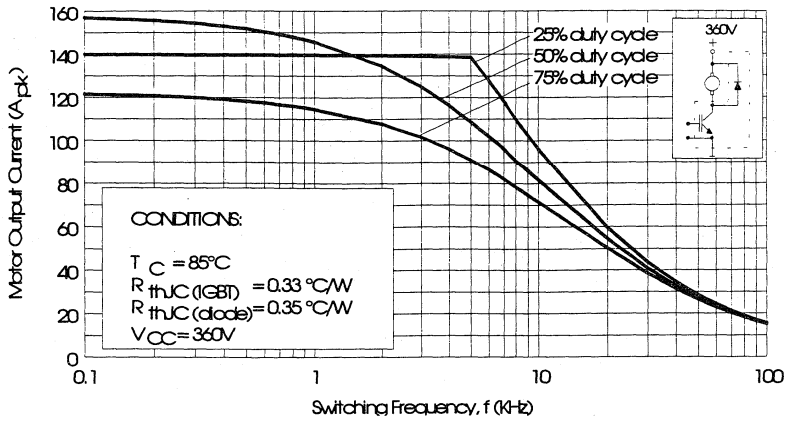


Fig. 13 - RMS Output Current vs. Frequency

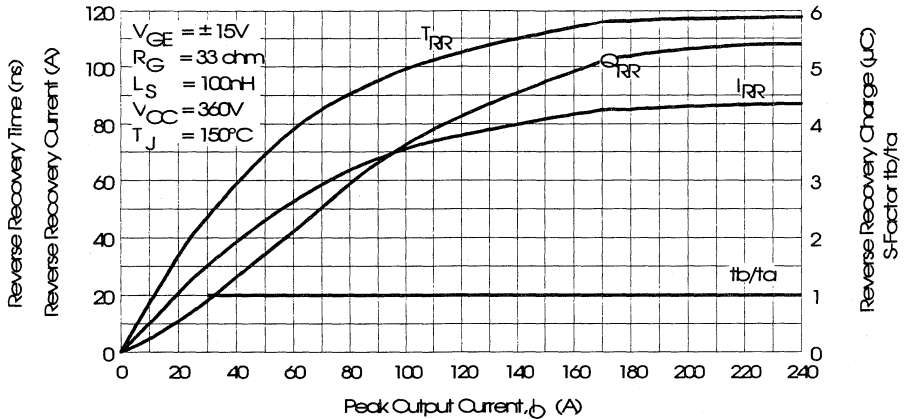


Fig. 14 - Typical Diode Recovery Characteristics as Function of Output Current I_o

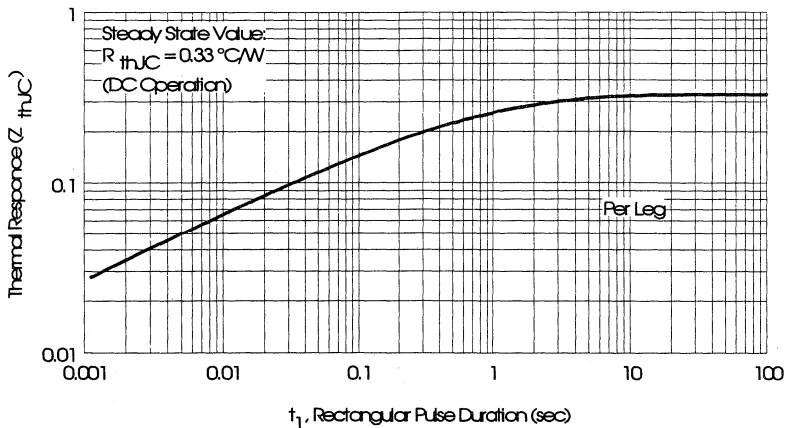


Fig. 15 - Maximum Effective Transient Thermal Impedance, Junction-to-Case

IRGKI165F06

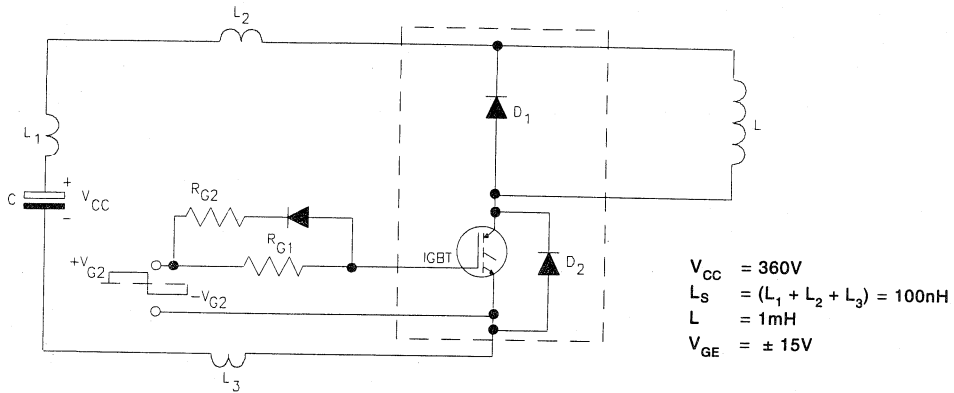


Fig. 16 - Test Circuit for Measurement of I_{LM} , E_{ON} , E_{OFF} , Q_{RR} , I_{RR} , $t_{D(ON)}$, t_r , $t_{D(OFF)}$, t_f

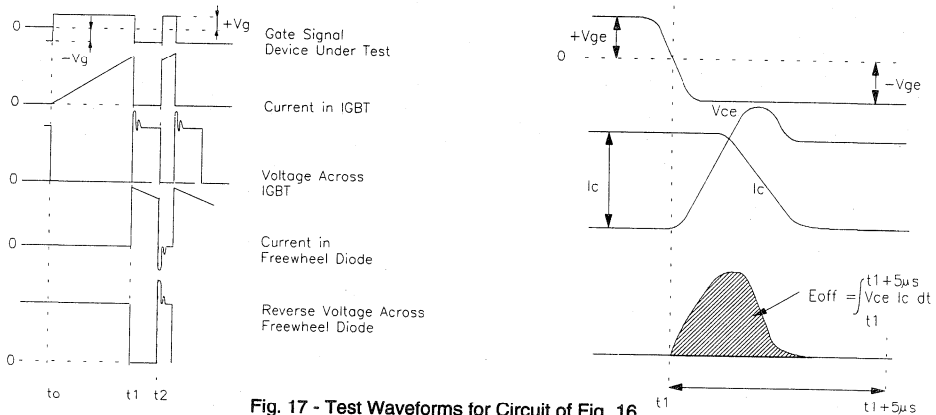


Fig. 17 - Test Waveforms for Circuit of Fig. 16

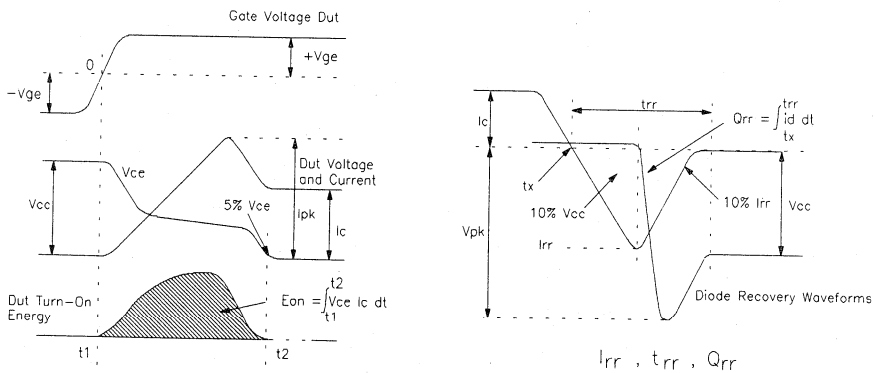


Fig. 18 - Test Waveforms for Circuit of Fig. 16, Defining E_{ON} , E_{REC} , $t_{D(ON)}$, t_r , I_{RR} , t_{RR} , Q_{RR}

Refer to Section D for the following:
 Appendix E: Section D - page D-7

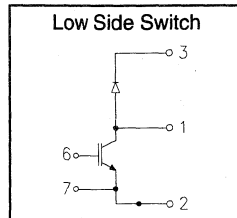
Fig. 19 - Waveforms for Switching Time

IRGKI200F06

"CHOPPER" IGBT INT-A-PAK

Fast Speed IGBT

- Rugged Design
- Simple gate-drive
- Fast operation up to 10KHz hard switching, or 50KHz resonant
- Switching-Loss Rating includes all "tail" losses



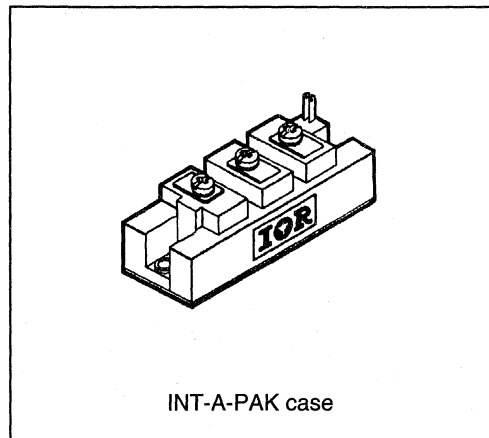
$$V_{CE} = 600V$$

$$I_C = 200A$$

$$V_{CE(ON)} < 2.3V$$

Description

IR's advanced IGBT technology is the key to this line of INT-A-pak Power Modules. The efficient geometry and unique processing of the IGBT allow higher current densities than comparable bipolar power module transistors, while at the same time requiring the simpler gate-drive of the familiar power MOSFET. This superior technology has now been coupled to state of the art assembly techniques to produce a higher current module that is highly suited to power applications such as motor drives, uninterruptible power supplies, welding, induction heating and ultrasonics.



Power
Conversion
Fast
Modules

Absolute Maximum Ratings

Parameter	Description	Value	Units
V_{CES}	Continuous collector to emitter voltage	600	V
$I_C @ T_C = 25^\circ C$	Continuous collector current	200	A
$I_C @ T_C = 85^\circ C$	Continuous collector current	130	
$I_C @ T_C = 100^\circ C$	Continuous collector current	110	
I_{LM}	Peak switching current	400	
I_{FM}	Peak diode forward current (1)	500	V
V_{GE}	Gate to emitter voltage	± 20	
V_{ISOL}	RMS isolation voltage, any terminal to case, $t = 1$ min	2500	W
$P_D @ T_C = 25^\circ C$	Power dissipation	500	
T_J	Operating junction temperature range	-40 to 150	$^\circ C$
T_{STG}	Storage temperature range	-40 to 125	

(1) Duration limited by max junction temperature.

Electrical Characteristics - $T_J = 25^\circ\text{C}$, unless otherwise stated

Parameter	Description	Min	Typ	Max	Units	Test Conditions
BV_{CES}	Collector-to-emitter breakdown voltage	600	—	—	V	$V_{GE} = 0V, I_C = 2mA$
$V_{CE(ON)}$	Collector-to-emitter voltage	—	—	2.3		$V_{GE} = 15V, I_C = 200A$
		—	2.2	—		$V_{GE} = 15V, I_C = 200A, T_J = 150^\circ\text{C}$
V_{FM}	Diode forward voltage - maximum	—	—	2.0		$I_F = 200A, V_{GE} = 0V$
		—	2.0	—		$I_F = 200A, V_{GE} = 0V, T_J = 150^\circ\text{C}$
V_{GEth}	Gate threshold voltage	3.0	—	5.5	$I_C = 1mA$	
ΔV_{GEth}	Threshold voltage temp. coefficient	—	-11	—	mV/°C	$V_{CE} = V_{GE}, I_C = 1mA$
g_{fe}	Forward transconductance	104	—	144	S(Ω)	$V_{CE} = 25V, I_C = 200A$
I_{CES}	Collector-to-emitter leakage current	—	—	2	mA	$V_{GE} = 0V, V_{CE} = 600V$
		—	—	20		$V_{GE} = 0V, V_{CE} = 600V, T_J = 150^\circ\text{C}$
I_{GES}	Gate-to-emitter leakage current	—	—	±2	µA	$V_{GE} = \pm 20V$

Dynamic Characteristics - $T_J = 150^\circ\text{C}$

Parameter	Description	Min	Typ	Max	Units	Test Conditions
E_{on}	Turn-on switching energy	—	0.05	—	mJ/A	$R_{G1} = 27\Omega, R_{G2} = 0\Omega$
E_{off} (1)	Turn-off switching energy	—	0.17	—		$I_C = 200A, L_S = 100nH$
E_{ts} (1)	Total switching energy	—	—	0.3		$V_{CC} = 360V, V_{GE} = \pm 15V$
$t_{d(on)}$	Turn-on delay time	—	80	—	ns	$R_{G1} = 27\Omega, R_{G2} = 0\Omega$
t_r	Rise time	—	150	—		$I_C = 200A$
$t_{d(off)}$	Turn-off delay time	—	450	—		$V_{CC} = 360V, V_{GE} = \pm 15V$
t_f	Fall time	—	900	—		$L_S = 100nH$
I_{rr}	Diode peak recovery current	—	108	—		$R_{G1} = 27\Omega, R_{G2} = 0\Omega$
t_{rr}	Diode recovery time	—	115	—	ns	$I_C = 200A$
Q_{rr}	Diode recovery charge	—	6.5	—	µC	$V_{CC} = 360V, V_{GE} = \pm 15V$
Q_{ge}	Gate-to-emitter charge (turn-on)	300	—	560	nC	$V_{CC} = 360V$
Q_{gc}	Gate-to-collector charge (turn-on)	140	—	280		$I_C = 108A$
Q_g	Total gate charge (turn-on)	52	—	84		$V_{GE} = 15V$
C_{ies}	Input capacitance	—	11600	—	pF	$V_{GE} = 0V$
C_{oes}	Output capacitance	—	1320	—		$V_{CC} = 30V$
C_{res}	Reverse transfer capacitance	—	160	—		$f = 1MHz$

(1) Includes tail losses

Thermal and Mechanical Characteristics

Parameter	Description	Typ	Max	Units
R_{thJC} (IGBT)	Thermal resistance, junction to case, each IGBT	—	0.25	°C/W
R_{thJC} (Diode)	Thermal resistance, junction to case, each diode	—	0.28	
R_{thCS} (Module)	Thermal resistance, case to sink	0.1	—	
Wt	Weight of module	140	—	g

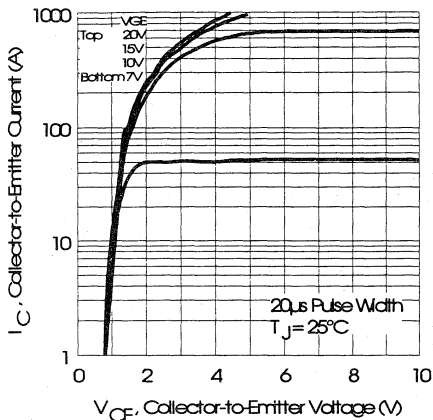


Fig. 1 - Typical Output Characteristics, $T_J = 25^\circ\text{C}$

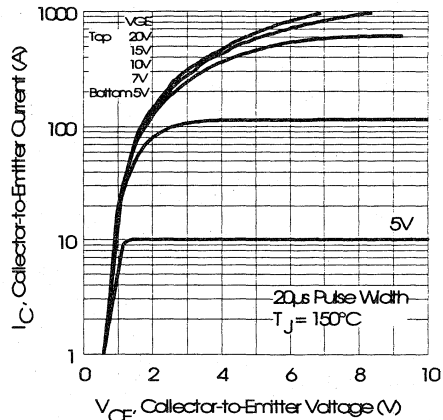


Fig. 2 - Typical Output Characteristics, $T_J = 150^\circ\text{C}$

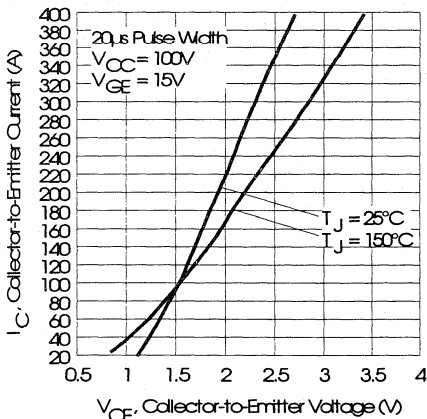


Fig. 3 - Typical Output Characteristics

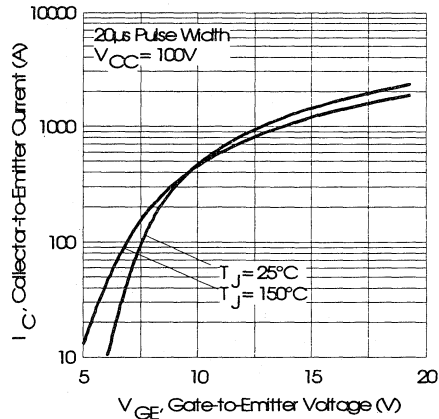


Fig. 4 - Typical Transfer Characteristics

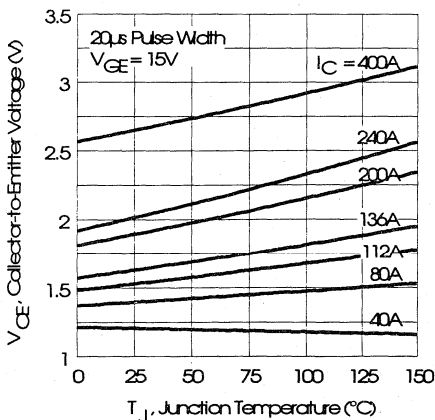


Fig. 5 - Collector-to-Emitter Saturation Typical Voltage vs. Junction Temperature

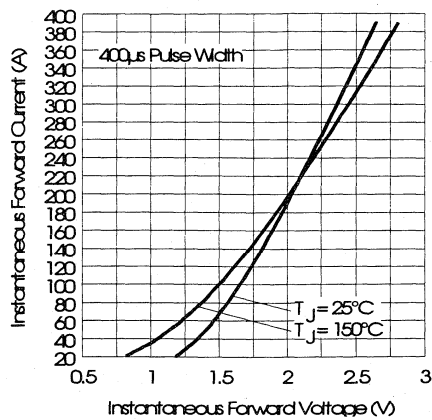


Fig. 6 - Forward Voltage Drop Characteristics

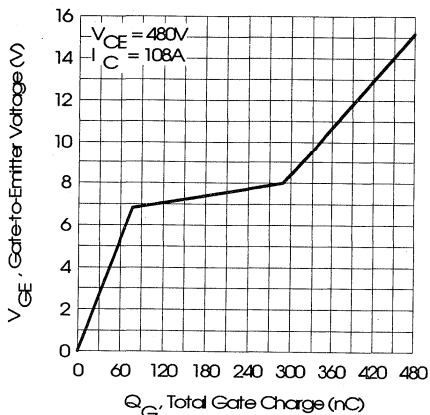


Fig. 7 - Typical Gate Charge vs. Gate-to-Emitter Voltage

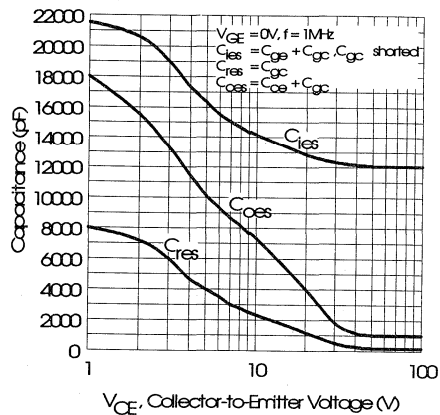


Fig. 8 - Typical Capacitance vs. Collector-to-Emitter Voltage

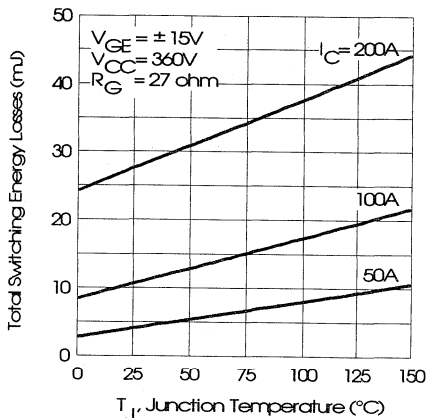


Fig. 9 - Typical Switching Losses vs. Junction Temperature

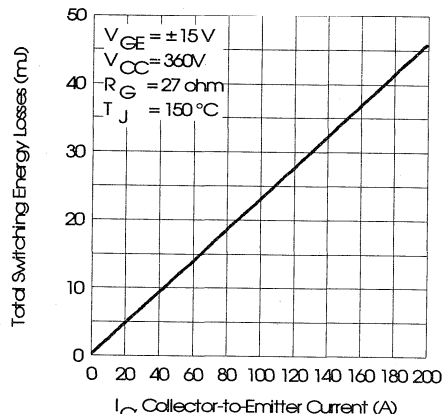


Fig. 10 - Typical Switching Losses vs. Collector-to-Emitter Current

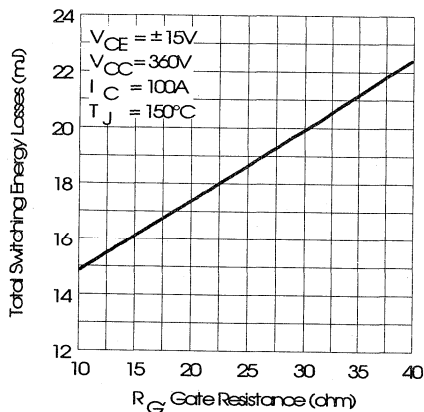


Fig. 11 - Typical Switching Losses vs. Gate Resistance

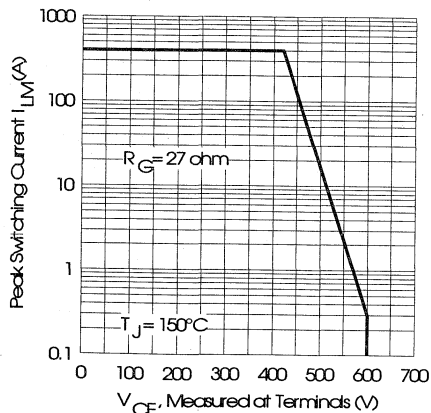


Fig. 12 - Reverse Bias Safe Operating Area

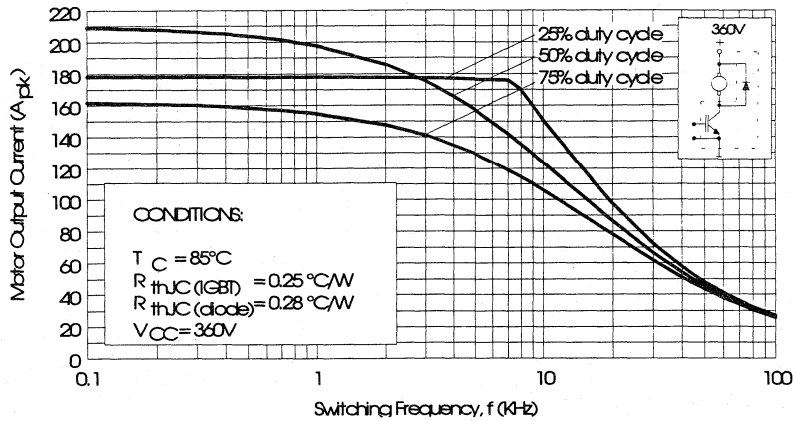


Fig. 13 - RMS Output Current vs. Frequency

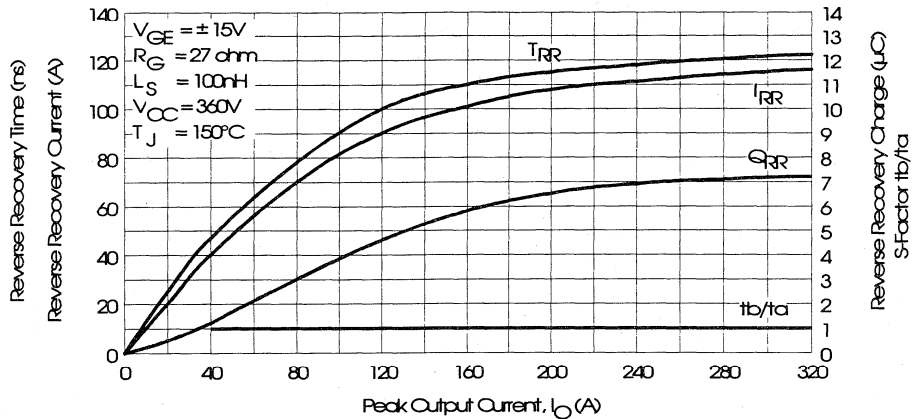


Fig. 14 - Typical Diode Recovery Characteristics as Function of Output Current I_o

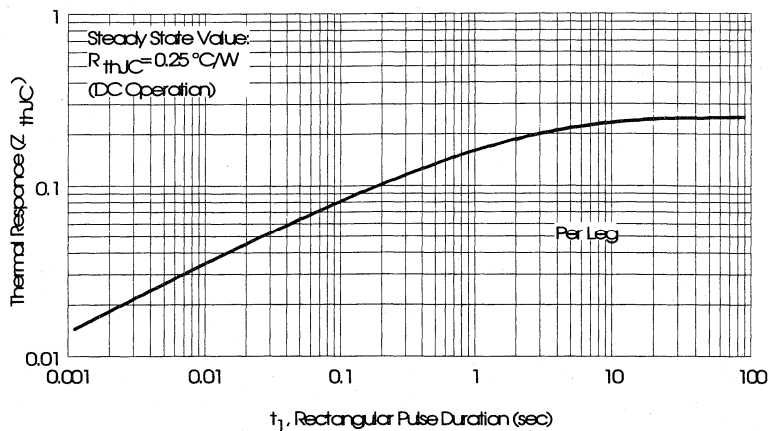


Fig. 15 - Maximum Effective Transient Thermal Impedance, Junction-to-Case

Power Conversion Fast Modules

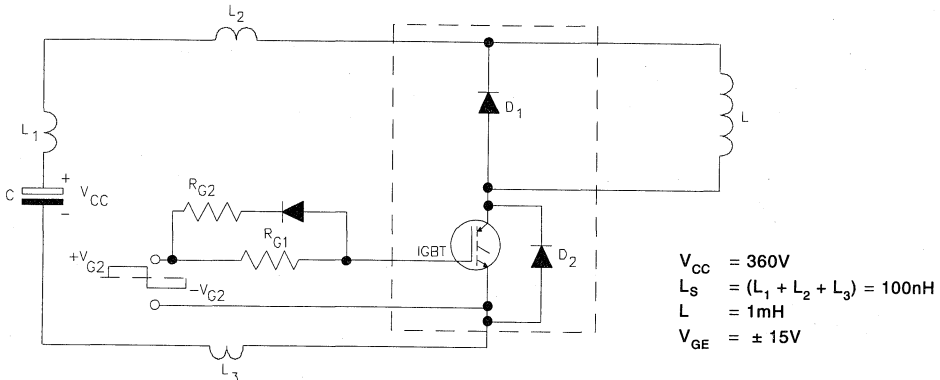


Fig. 16 - Test Circuit for Measurement of I_{LM} , E_{ON} , E_{OFF} , Q_{RR} , I_{RR} , $t_{D(ON)}$, t_r , $t_{D(OFF)}$, t_f

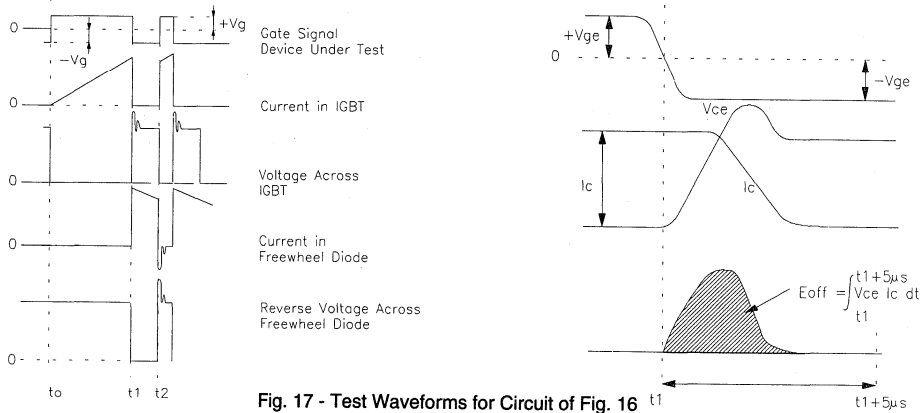


Fig. 17 - Test Waveforms for Circuit of Fig. 16

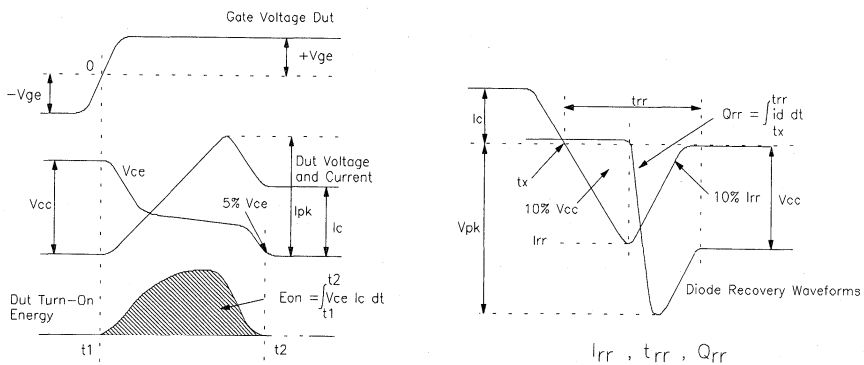


Fig. 18 - Test Waveforms for Circuit of Fig. 16, Defining E_{ON} , E_{REC} , $t_{D(ON)}$, t_r , I_{RR} , t_{RR} , Q_{RR}

Refer to Section D for the following:
 Appendix E: Section D - page D-7

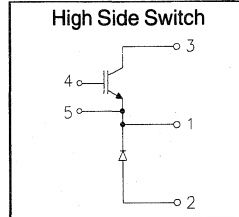
Fig. 19 - Waveforms for Switching Time

IRGNI065F06

"CHOPPER" IGBT INT-A-PAK

Fast Speed IGBT

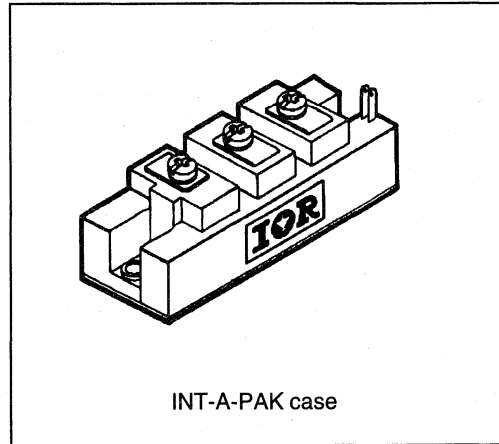
- Rugged Design
- Simple gate-drive
- Fast operation up to 10KHz hard switching, or 50KHz resonant
- Switching-Loss Rating includes all "tail" losses



$V_{CE} = 600V$
$I_C = 65A$
$V_{CE(ON)} < 2.3V$

Description

IR's advanced IGBT technology is the key to this line of INT-A-pak Power Modules. The efficient geometry and unique processing of the IGBT allow higher current densities than comparable bipolar power module transistors, while at the same time requiring the simpler gate-drive of the familiar power MOSFET. This superior technology has now been coupled to state of the art assembly techniques to produce a higher current module that is highly suited to power applications such as motor drives, uninterruptible power supplies, welding, induction heating and ultrasonics.



Power Conversion Fast Modules

Absolute Maximum Ratings

Parameter	Description	Value	Units
V_{CES}	Continuous collector to emitter voltage	600	V
$I_C @ T_C = 25^\circ C$	Continuous collector current	65	A
$I_C @ T_C = 85^\circ C$	Continuous collector current	40	
$I_C @ T_C = 100^\circ C$	Continuous collector current	35	
I_{LM}	Peak switching current	130	
I_{FM}	Peak diode forward current (1)	165	V
V_{GE}	Gate to emitter voltage	± 20	
V_{ISOL}	RMS isolation voltage, any terminal to case, $t = 1 \text{ min}$	2500	
$P_D @ T_C = 25^\circ C$	Power dissipation	179	W
T_J	Operating junction temperature range	-40 to 150	$^\circ C$
T_{STG}	Storage temperature range	-40 to 125	

(1) Duration limited by max junction temperature.

Electrical Characteristics - $T_J = 25^\circ\text{C}$, unless otherwise stated

Parameter	Description	Min	Typ	Max	Units	Test Conditions
BV_{CES}	Collector-to-emitter breakdown voltage	600	—	—	V	$V_{GE} = 0V, I_C = 500\mu A$
$V_{CE(ON)}$	Collector-to-emitter voltage	—	—	2.3		$V_{GE} = 15V, I_C = 65A$
		—	2.6	—		$V_{GE} = 15V, I_C = 65A, T_J = 150^\circ\text{C}$
V_{FM}	Diode forward voltage - maximum	—	—	2.3		$I_F = 65A, V_{GE} = 0V$
		—	2.3	—		$I_F = 65A, V_{GE} = 0V, T_J = 150^\circ\text{C}$
V_{GEth}	Gate threshold voltage	3.0	—	5.5	$I_C = 250\mu A$	
ΔV_{GEth}	Threshold voltage temp. coefficient	—	-11	—	mV/ $^\circ\text{C}$	$V_{CE} = V_{GE}, I_C = 250\mu A$
g_{fe}	Forward transconductance	26	—	36	S(τ)	$V_{CE} = 25V, I_C = 65A$
I_{CES}	Collector-to-emitter leakage current	—	—	500	μA	$V_{GE} = 0V, V_{CE} = 600V$
		—	—	5	mA	$V_{GE} = 0V, V_{CE} = 600V, T_J = 150^\circ\text{C}$
I_{GES}	Gate-to-emitter leakage current	—	—	± 500	nA	$V_{GE} = \pm 20V$

Dynamic Characteristics - $T_J = 150^\circ\text{C}$

Parameter	Description	Min	Typ	Max	Units	Test Conditions
E_{on}	Turn-on switching energy	—	0.05	—	mJ/A	$R_{G1} = 82\Omega, R_{G2} = 0\Omega$
E_{off} (1)	Turn-off switching energy	—	0.17	—		$I_C = 65A, L_S = 100nH$
E_{ts} (1)	Total switching energy	—	—	0.3		$V_{CC} = 360V, V_{GE} = \pm 15V$
$t_{d(on)}$	Turn-on delay time	—	80	—	ns	$R_{G1} = 82\Omega, R_{G2} = 0\Omega$
t_r	Rise time	—	150	—		$I_C = 65A$
$t_{d(off)}$	Turn-off delay time	—	450	—		$V_{CC} = 360V, V_{GE} = \pm 15V$
t_f	Fall time	—	900	—		$L_S = 100nH$
I_{rr}	Diode peak recovery current	—	30	—		$R_{G1} = 82\Omega, R_{G2} = 0\Omega$
t_{rr}	Diode recovery time	—	115	—	ns	$I_C = 65A$
Q_{rr}	Diode recovery charge	—	2.0	—	μC	$V_{CC} = 360V, V_{GE} = \pm 15V$
Q_{ge}	Gate-to-emitter charge (turn-on)	77	—	140	nC	$V_{CC} = 360V$
Q_{gc}	Gate-to-collector charge (turn-on)	35	—	70		$I_C = 65A$
Q_g	Total gate charge (turn-on)	13	—	21		$V_{GE} = 15V$
C_{ies}	Input capacitance	—	2900	—	pF	$V_{GE} = 0V$
C_{oes}	Output capacitance	—	330	—		$V_{CC} = 30V$
C_{res}	Reverse transfer capacitance	—	40	—		$f = 1MHz$

(1) Includes tail losses

Thermal and Mechanical Characteristics

Parameter	Description	Typ	Max	Units
R_{thJC} (IGBT)	Thermal resistance, junction to case, each IGBT	—	0.7	$^\circ\text{C/W}$
R_{thJC} (Diode)	Thermal resistance, junction to case, each diode	—	0.75	
R_{thCS} (Module)	Thermal resistance, case to sink	0.1	—	
Wt	Weight of module	140	—	g

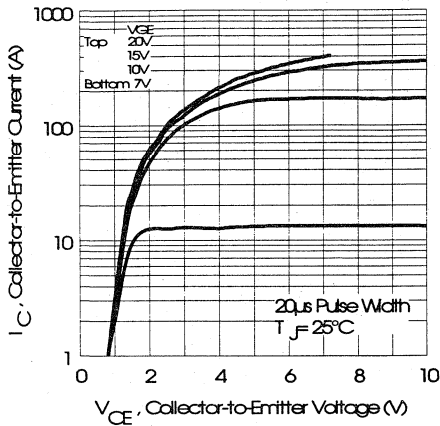


Fig. 1 - Typical Output Characteristics, $T_J = 25^\circ\text{C}$

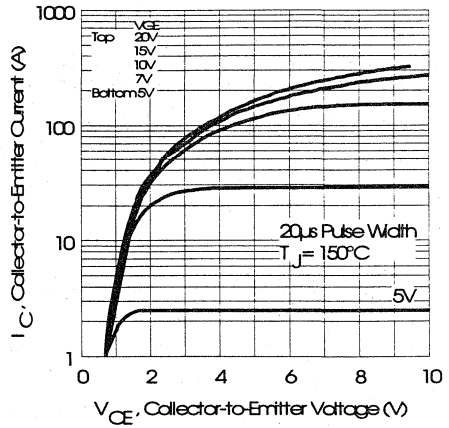


Fig. 2 - Typical Output Characteristics, $T_J = 150^\circ\text{C}$

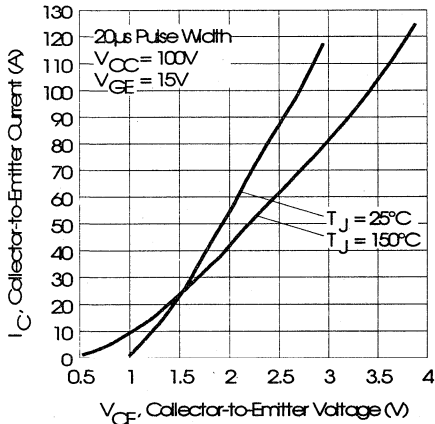


Fig. 3 - Typical Output Characteristics

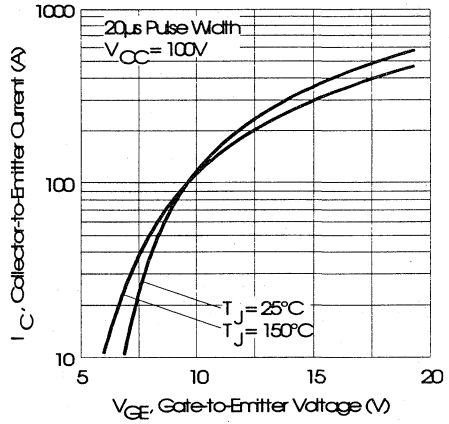


Fig. 4 - Typical Transfer Characteristics

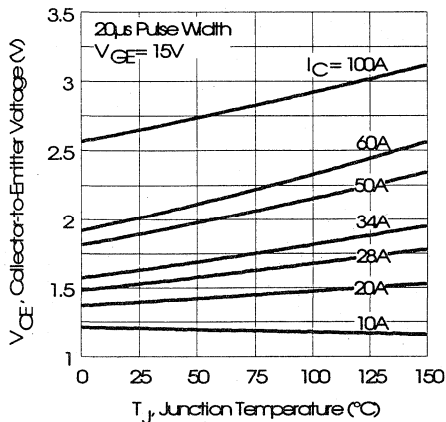


Fig. 5 - Collector-to-Emitter Saturation Typical Voltage vs. Junction Temperature

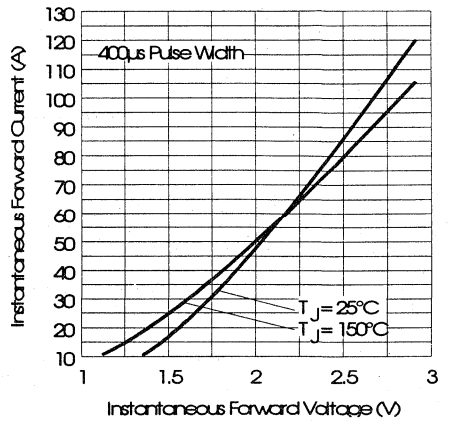


Fig. 6 - Forward Voltage Drop Characteristics



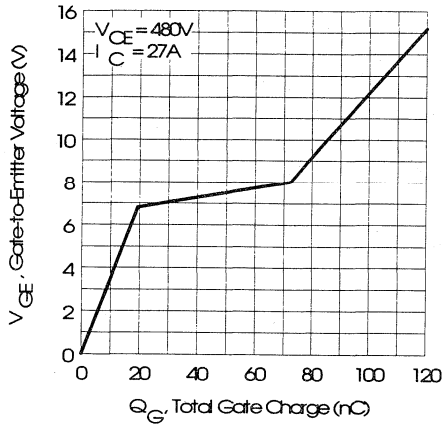


Fig. 7 - Typical Gate Charge vs. Gate-to-Emitter Voltage

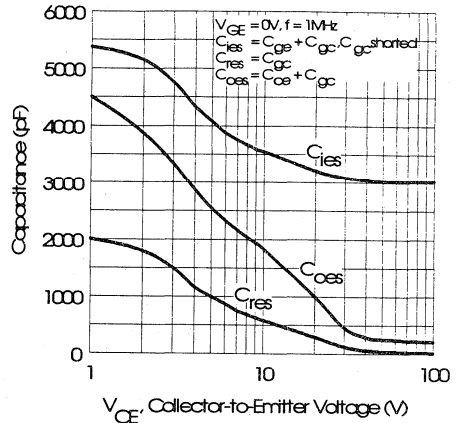


Fig. 8 - Typical Capacitance vs. Collector-to-Emitter Voltage

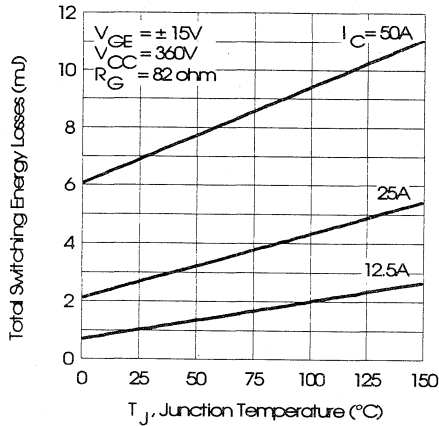


Fig. 9 - Typical Switching Losses vs. Junction Temperature

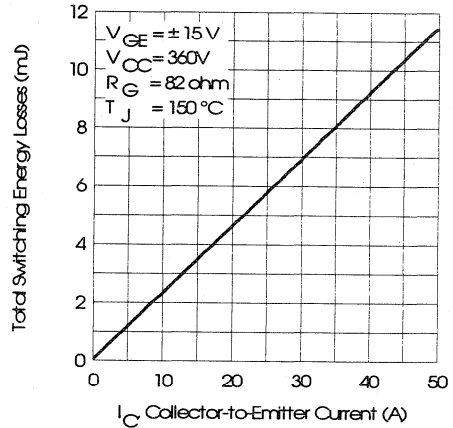


Fig. 10 - Typical Switching Losses vs. Collector-to-Emitter Current

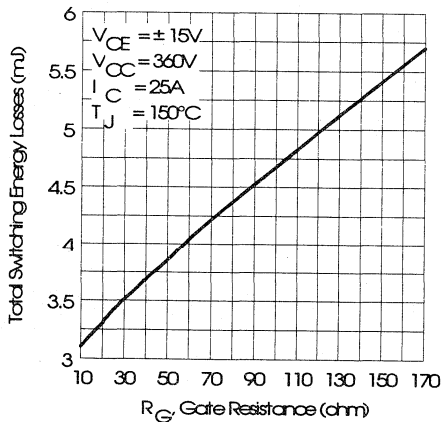


Fig. 11 - Typical Switching Losses vs. Gate Resistance

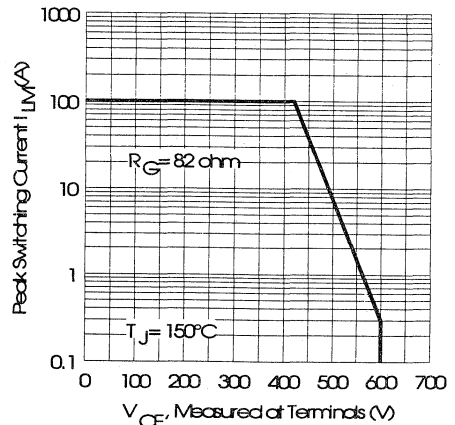


Fig. 12 - Reverse Bias Safe Operating Area

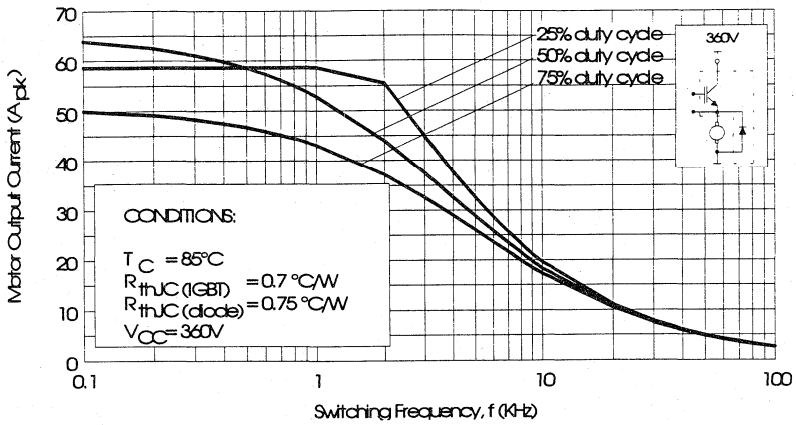


Fig. 13 - RMS Output Current vs. Frequency

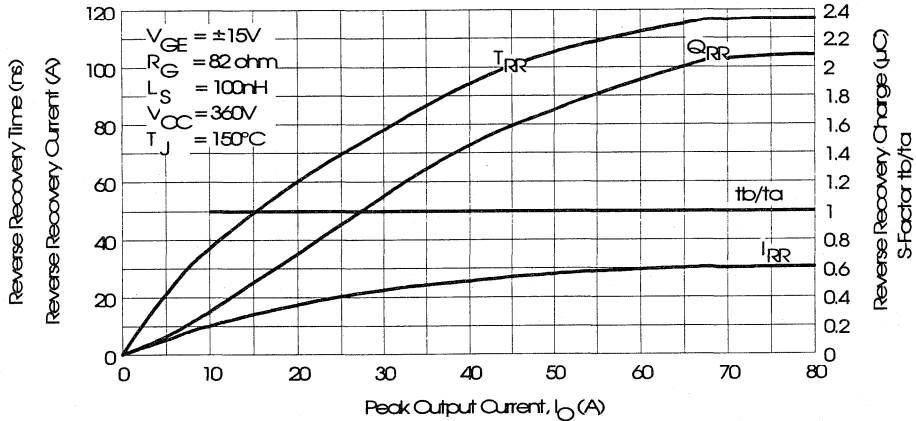


Fig. 14 - Typical Diode Recovery Characteristics as Function of Output Current I_O

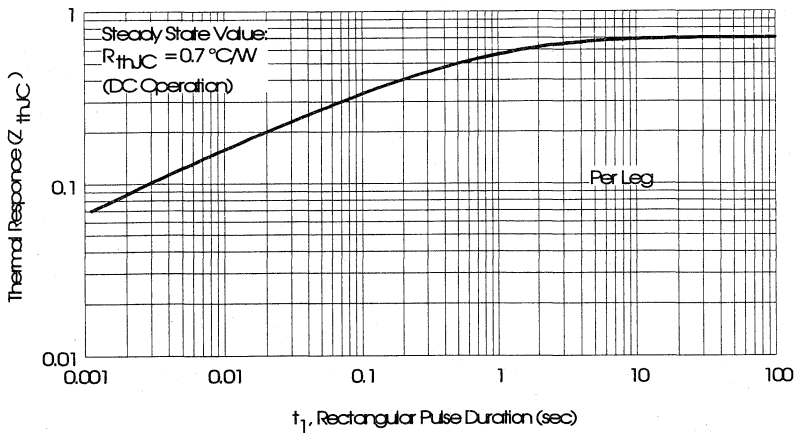


Fig. 15 - Maximum Effective Transient Thermal Impedance, Junction-to-Case

IRGNI065F06

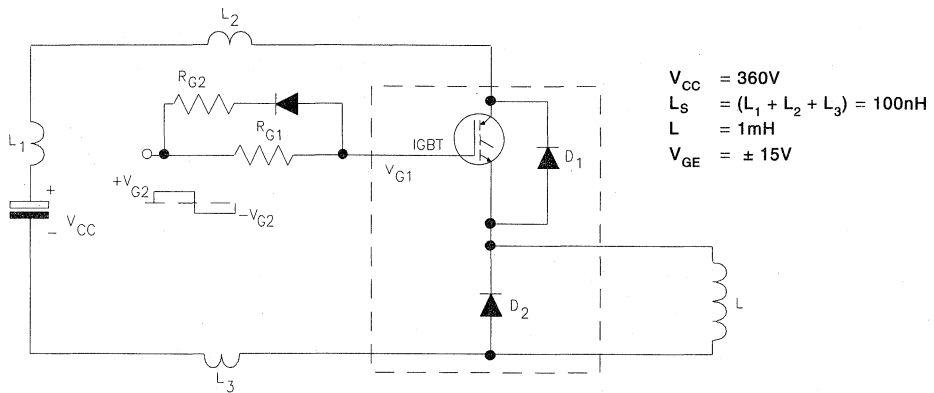


Fig. 16 - Test Circuit for Measurement of I_{LM} , E_{ON} , E_{OFF} , Q_{RR} , I_{RR} , $t_{D(ON)}$, t_r , $t_{D(OFF)}$, t_f

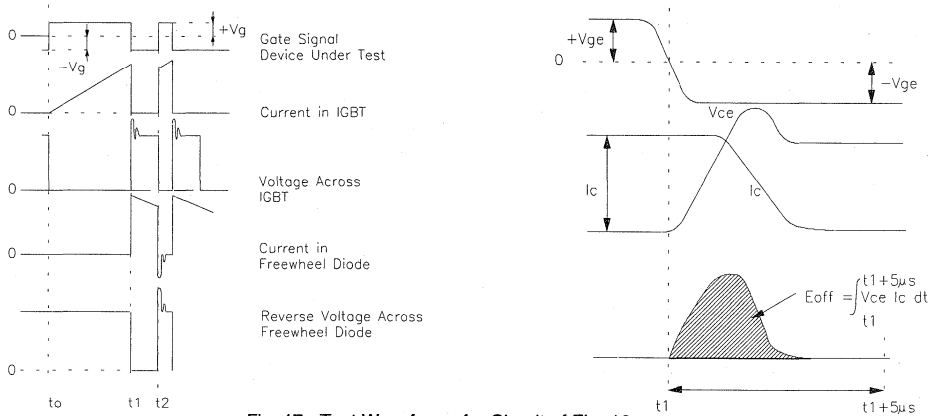


Fig. 17 - Test Waveforms for Circuit of Fig. 16

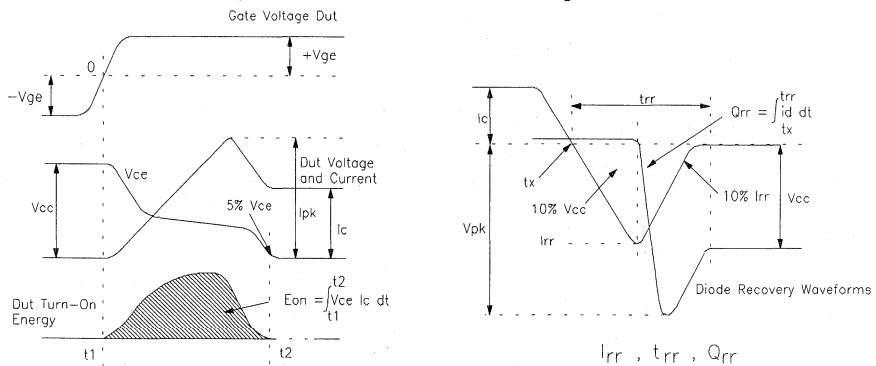


Fig. 18 - Test Waveforms for Circuit of Fig. 16, Defining E_{ON} , E_{REC} , $t_{D(ON)}$, t_r , I_{RR} , t_{RR} , Q_{RR}

Refer to Section D for the following:
Appendix E: Section D - page D-7

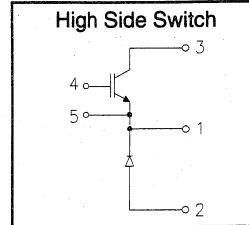
Fig. 19 - Waveforms for Switching Time

IRGNI120F06

"CHOPPER" IGBT INT-A-PAK

Fast Speed IGBT

- Rugged Design
- Simple gate-drive
- Fast operation up to 10KHz hard switching, or 50KHz resonant
- Switching-Loss Rating includes all "tail" losses



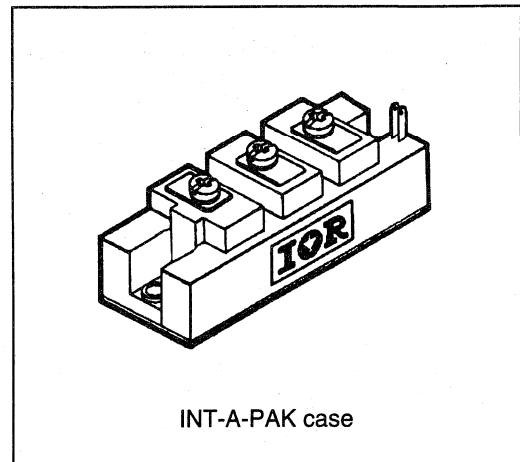
$$V_{CE} = 600V$$

$$I_C = 120A$$

$$V_{CE(ON)} < 2.3V$$

Description

IR's advanced IGBT technology is the key to this line of INT-A-pak Power Modules. The efficient geometry and unique processing of the IGBT allow higher current densities than comparable bipolar power module transistors, while at the same time requiring the simpler gate-drive of the familiar power MOSFET. This superior technology has now been coupled to state of the art assembly techniques to produce a higher current module that is highly suited to power applications such as motor drives, uninterruptible power supplies, welding, induction heating and ultrasonics.


 Power
Conversion
Fast
Modules

Absolute Maximum Ratings

Parameter	Description	Value	Units
V_{CES}	Continuous collector to emitter voltage	600	V
$I_C @ T_C = 25^\circ C$	Continuous collector current	120	A
$I_C @ T_C = 85^\circ C$	Continuous collector current	75	
$I_C @ T_C = 100^\circ C$	Continuous collector current	60	
I_{LM}	Peak switching current	240	
I_{FM}	Peak diode forward current (1)	300	V
V_{GE}	Gate to emitter voltage	± 20	
V_{ISOL}	RMS isolation voltage, any terminal to case, $t = 1$ min	2500	W
$P_D @ T_C = 25^\circ C$	Power dissipation	298	
T_J	Operating junction temperature range	-40 to 150	$^\circ C$
T_{STG}	Storage temperature range	-40 to 125	

(1) Duration limited by max junction temperature.

Electrical Characteristics - $T_J = 25^\circ\text{C}$, unless otherwise stated

Parameter	Description	Min	Typ	Max	Units	Test Conditions
BV_{CES}	Collector-to-emitter breakdown voltage	600	—	—	V	$V_{GE} = 0V, I_C = 1mA$
$V_{CE(ON)}$	Collector-to-emitter voltage	—	—	2.3		$V_{GE} = 15V, I_C = 120A$
		—	2.4	—		$V_{GE} = 15V, I_C = 120A, T_J = 150^\circ\text{C}$
V_{FM}	Diode forward voltage - maximum	—	—	2.2		$I_F = 120A, V_{GE} = 0V$
		—	2.2	—		$I_F = 120A, V_{GE} = 0V, T_J = 150^\circ\text{C}$
V_{GEth}	Gate threshold voltage	3.0	—	5.5	$I_C = 500\mu A$	
ΔV_{GEth}	Threshold voltage temp. coefficient	—	-11	—	mV/°C	$V_{CE} = V_{GE}, I_C = 500\mu A$
g_{fe}	Forward transconductance	52	—	72	S(τ)	$V_{CE} = 25V, I_C = 120A$
I_{CES}	Collector-to-emitter leakage current	—	—	1	mA	$V_{GE} = 0V, V_{CE} = 600V$
		—	—	10		$V_{GE} = 0V, V_{CE} = 600V, T_J = 150^\circ\text{C}$
I_{GES}	Gate-to-emitter leakage current	—	—	± 1	μA	$V_{GE} = \pm 20V$

Dynamic Characteristics - $T_J = 150^\circ\text{C}$

Parameter	Description	Min	Typ	Max	Units	Test Conditions
E_{on}	Turn-on switching energy	—	0.05	—	mJ/A	$R_{G1} = 47\Omega, R_{G2} = 0\Omega$
E_{off} (1)	Turn-off switching energy	—	0.17	—		$I_C = 120A, L_S = 100nH$
E_{ts} (1)	Total switching energy	—	—	0.3		$V_{CC} = 360V, V_{GE} = \pm 15V$
$t_{d(on)}$	Turn-on delay time	—	80	—	ns	$R_{G1} = 47\Omega, R_{G2} = 0\Omega$
t_r	Rise time	—	150	—		$I_C = 120A$
$t_{d(off)}$	Turn-off delay time	—	450	—		$V_{CC} = 360V, V_{GE} = \pm 15V$
t_f	Fall time	—	900	—		$L_S = 100nH$
I_{rr}	Diode peak recovery current	—	56	—		A
t_{rr}	Diode recovery time	—	115	—	ns	$I_C = 120A$
Q_{rr}	Diode recovery charge	—	3.4	—	μC	$V_{CC} = 360V, V_{GE} = \pm 15V$
Q_{ge}	Gate-to-emitter charge (turn-on)	150	—	280	nC	$V_{CC} = 360V$
Q_{gc}	Gate-to-collector charge (turn-on)	70	—	140		$I_C = 54A$
Q_g	Total gate charge (turn-on)	26	—	42		$V_{GE} = 15V$
C_{ies}	Input capacitance	—	5800	—	pF	$V_{GE} = 0V$
C_{oes}	Output capacitance	—	660	—		$V_{CC} = 30V$
C_{res}	Reverse transfer capacitance	—	80	—		$f = 1MHz$

(1) Includes tail losses

Thermal and Mechanical Characteristics

Parameter	Description	Typ	Max	Units
R_{thJC} (IGBT)	Thermal resistance, junction to case, each IGBT	—	0.42	°C/W
R_{thJC} (Diode)	Thermal resistance, junction to case, each diode	—	0.45	
R_{thCS} (Module)	Thermal resistance, case to sink	0.1	—	
Wt	Weight of module	140	—	g

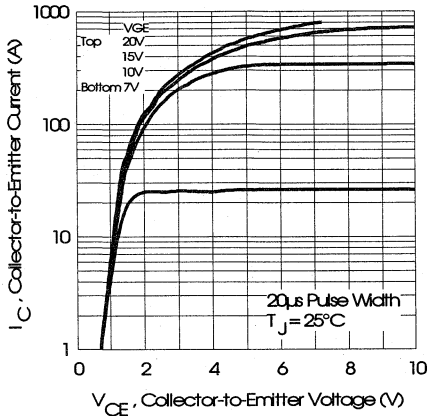


Fig. 1 - Typical Output Characteristics, $T_J = 25^\circ\text{C}$

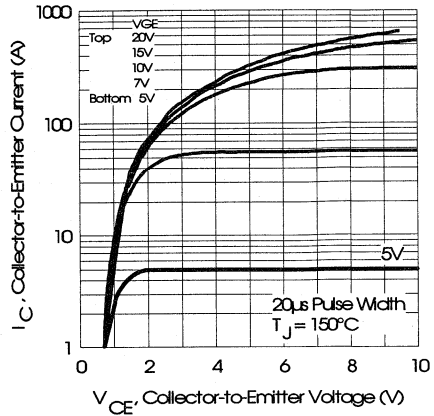


Fig. 2 - Typical Output Characteristics, $T_J = 150^\circ\text{C}$

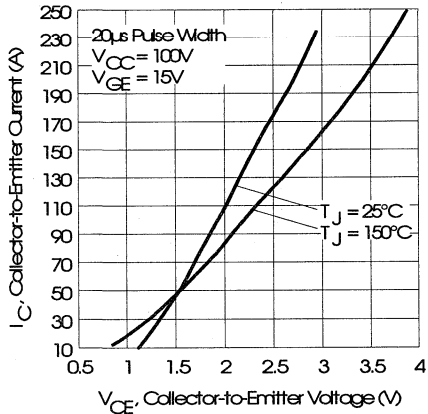


Fig. 3 - Typical Output Characteristics

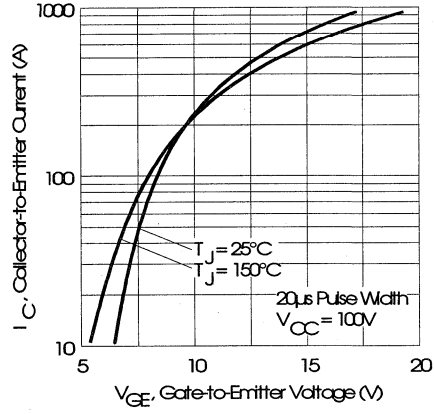


Fig. 4 - Typical Transfer Characteristics

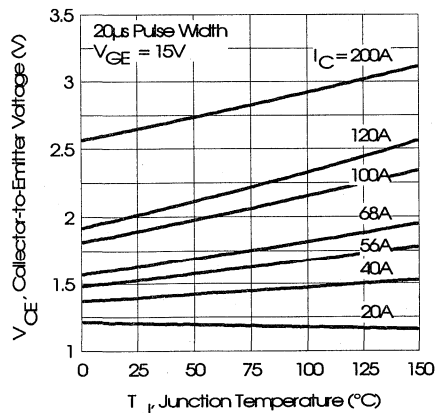


Fig. 5 - Collector-to-Emitter Saturation Typical Voltage vs. Junction Temperature

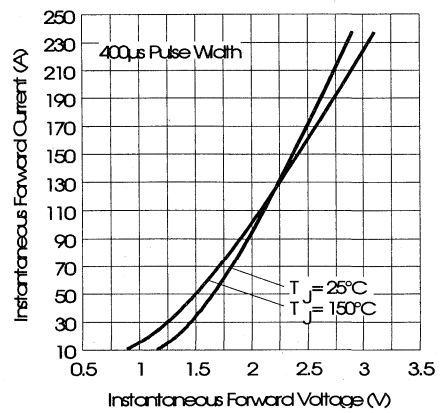


Fig. 6 - Forward Voltage Drop Characteristics

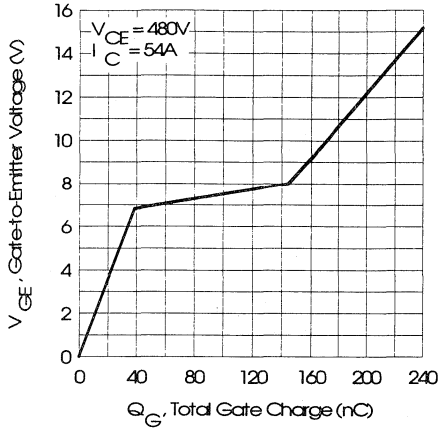


Fig. 7 - Typical Gate Charge vs. Gate-to-Emitter Voltage

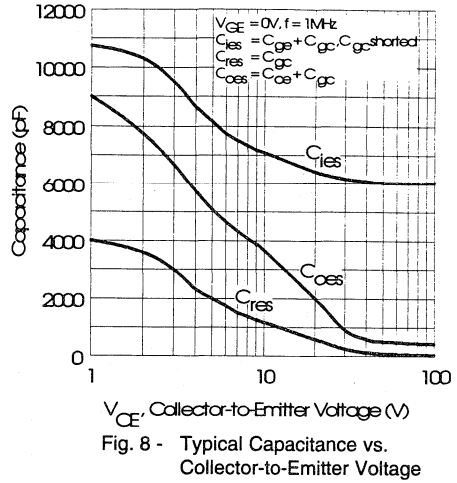


Fig. 8 - Typical Capacitance vs. Collector-to-Emitter Voltage

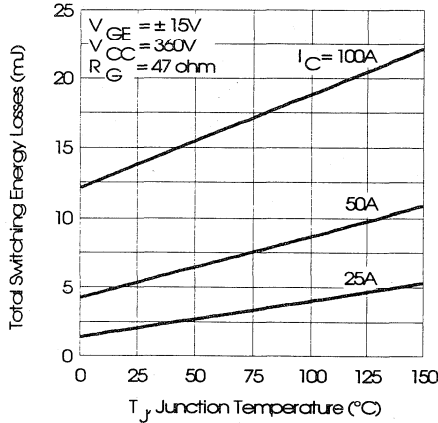


Fig. 9 - Typical Switching Losses vs. Junction Temperature

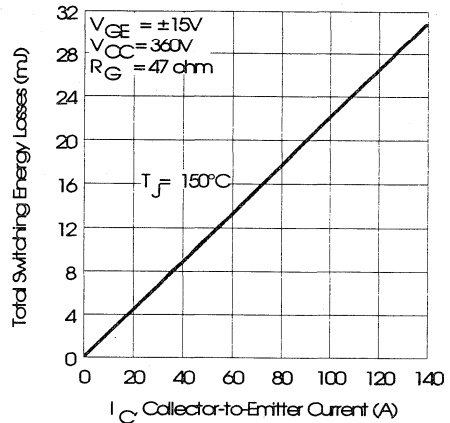


Fig. 10 - Typical Switching Losses vs. Collector-to-Emitter Current

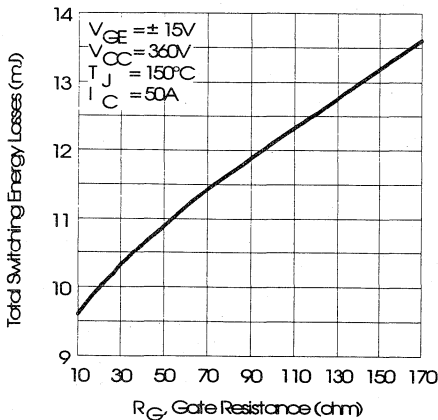


Fig. 11 - Typical Switching Losses vs. Gate Resistance

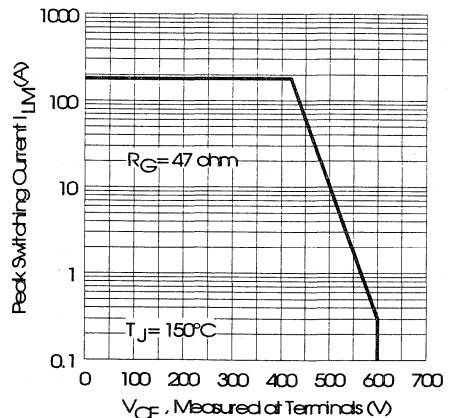


Fig. 12 - Reverse Bias Safe Operating Area

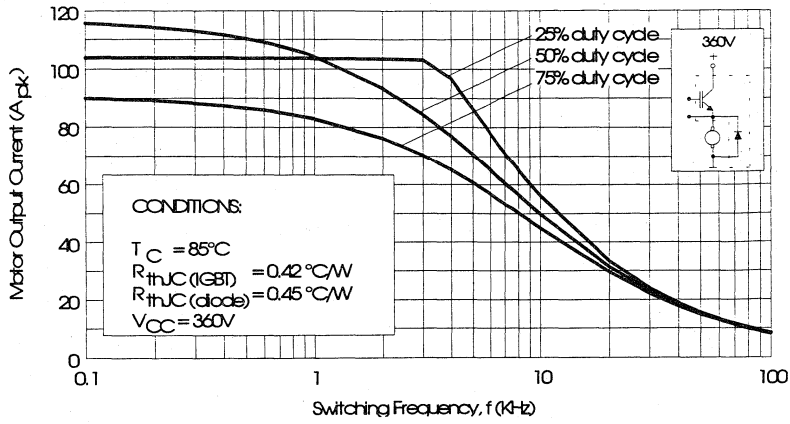


Fig. 13 - RMS Output Current vs. Frequency

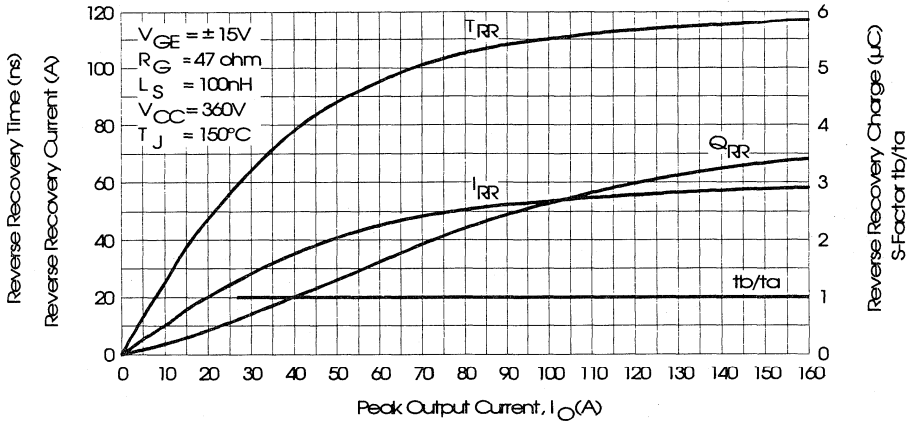


Fig. 14 - Typical Diode Recovery Characteristics as Function of Output Current I_O

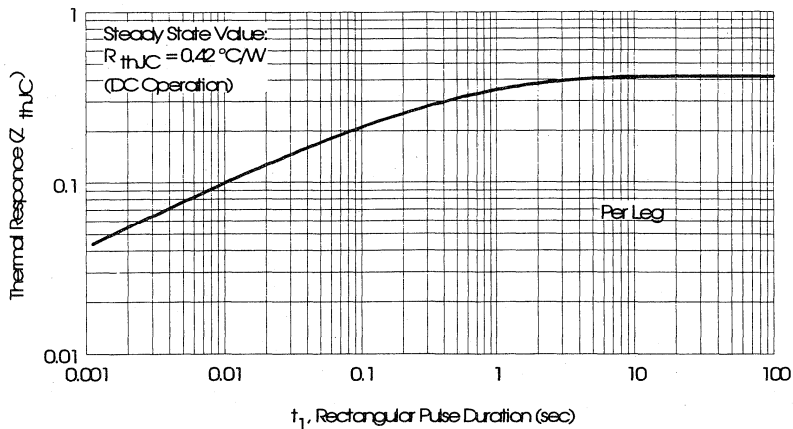


Fig. 15 - Maximum Effective Transient Thermal Impedance, Junction-to-Case

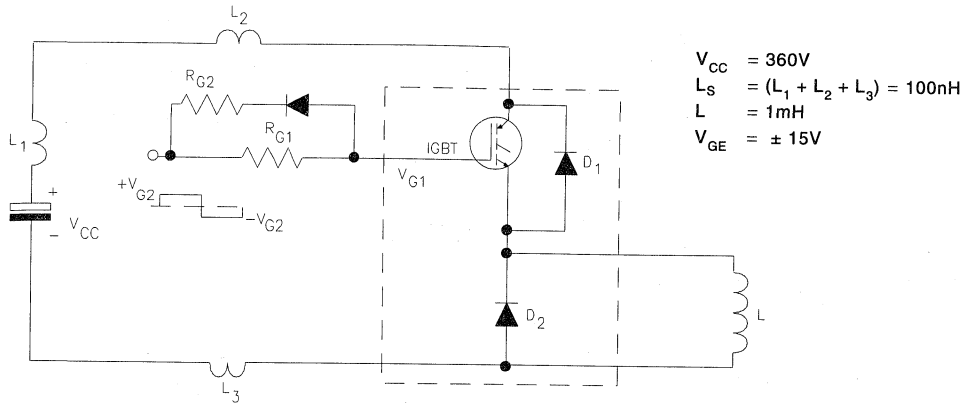


Fig. 16 - Test Circuit for Measurement of I_{LM} , E_{ON} , E_{OFF} , Q_{RR} , I_{RR} , $t_{D(ON)}$, t_r , $t_{D(OFF)}$, t_f

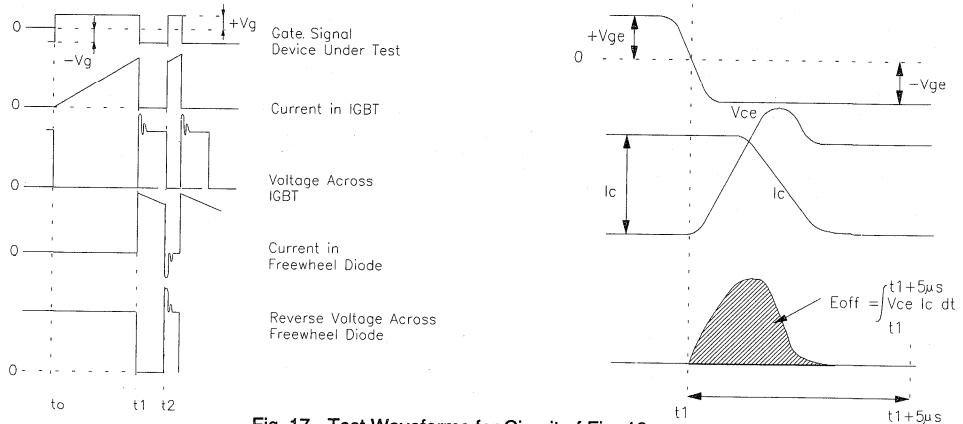


Fig. 17 - Test Waveforms for Circuit of Fig. 16

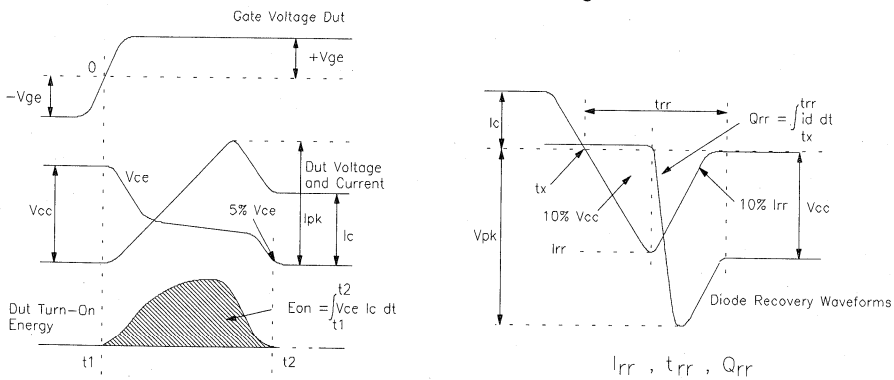


Fig. 18 - Test Waveforms for Circuit of Fig. 16, Defining E_{ON} , E_{REC} , $t_{D(ON)}$, t_r , I_{RR} , t_{RR} , Q_{RR}

Refer to Section D for the following:
Appendix E: Section D - page D-7

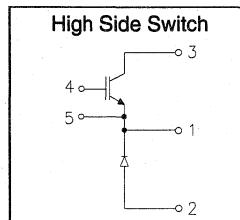
Fig. 19 - Waveforms for Switching Time

IRGNI165F06

"CHOPPER" IGBT INT-A-PAK

Fast Speed IGBT

- Rugged Design
- Simple gate-drive
- Fast operation up to 10KHz hard switching, or 50KHz resonant
- Switching-Loss Rating includes all "tail" losses



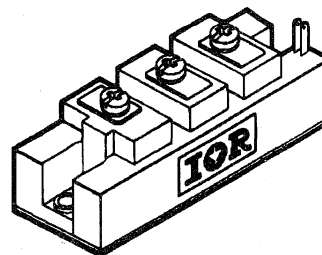
$$V_{CE} = 600V$$

$$I_C = 165A$$

$$V_{CE(ON)} < 2.3V$$

Description

IR's advanced IGBT technology is the key to this line of INT-A-pak Power Modules. The efficient geometry and unique processing of the IGBT allow higher current densities than comparable bipolar power module transistors, while at the same time requiring the simpler gate-drive of the familiar power MOSFET. This superior technology has now been coupled to state of the art assembly techniques to produce a higher current module that is highly suited to power applications such as motor drives, uninterruptible power supplies, welding, induction heating and ultrasonics.



INT-A-PAK case

Absolute Maximum Ratings

Parameter	Description	Value	Units
V_{CES}	Continuous collector to emitter voltage	600	V
$I_C @ T_C = 25^\circ C$	Continuous collector current	165	A
$I_C @ T_C = 85^\circ C$	Continuous collector current	100	
$I_C @ T_C = 100^\circ C$	Continuous collector current	85	
I_{LM}	Peak switching current	330	
I_{FM}	Peak diode forward current (1)	400	V
V_{GE}	Gate to emitter voltage	± 20	
V_{ISOL}	RMS isolation voltage, any terminal to case, $t = 1$ min	2500	W
$P_D @ T_C = 25^\circ C$	Power dissipation	379	
T_J	Operating junction temperature range	-40 to 150	
T_{STG}	Storage temperature range	-40 to 125	

(1) Duration limited by max junction temperature.

Electrical Characteristics - $T_J = 25^\circ\text{C}$, unless otherwise stated

Parameter	Description	Min	Typ	Max	Units	Test Conditions
BV_{CES}	Collector-to-emitter breakdown voltage	600	—	—	V	$V_{GE} = 0V, I_C = 1.5mA$
$V_{CE(ON)}$	Collector-to-emitter voltage	—	—	2.3		$V_{GE} = 15V, I_C = 165A$
		—	2.3	—		$V_{GE} = 15V, I_C = 165A, T_J = 150^\circ\text{C}$
V_{FM}	Diode forward voltage - maximum	—	—	2.1		$I_F = 165A, V_{GE} = 0V$
		—	2.1	—	$I_F = 165A, V_{GE} = 0V, T_J = 150^\circ\text{C}$	
V_{GEth}	Gate threshold voltage	3.0	—	5.5	mV/°C	$I_C = 750\mu A$
ΔV_{GEth}	Threshold voltage temperature coefficient	—	-11	—		$V_{CE} = V_{GE}, I_C = 750\mu A$
g_{fe}	Forward transconductance	78	—	108	S(τ)	$V_{CE} = 25V, I_C = 165A$
I_{CES}	Collector-to-emitter leakage current	—	—	1.5	mA	$V_{GE} = 0V, V_{CE} = 600V$
		—	—	15		$V_{GE} = 0V, V_{CE} = 600V, T_J = 150^\circ\text{C}$
I_{GES}	Gate-to-emitter leakage current	—	—	±1.5	μA	$V_{GE} = \pm 20V$

Dynamic Characteristics - $T_J = 150^\circ\text{C}$

Parameter	Description	Min	Typ	Max	Units	Test Conditions
E_{on}	Turn-on switching energy	—	0.05	—	mJ/A	$R_{G1} = 33\Omega, R_{G2} = 0\Omega$
$E_{off} (1)$	Turn-off switching energy	—	0.17	—		$I_C = 165A, L_S = 100nH$
$E_{ts} (1)$	Total switching energy	—	—	0.3		$V_{CC} = 360V, V_{GE} = \pm 15V$
$t_{d(on)}$	Turn-on delay time	—	80	—	ns	$R_{G1} = 33\Omega, R_{G2} = 0\Omega$
		—	150	—		$I_C = 165A$
t_r	Rise time	—	150	—		$V_{CC} = 360V, V_{GE} = \pm 15V$
$t_{d(off)}$	Turn-off delay time	—	450	—		$L_S = 100nH$
t_f	Fall time	—	900	—		
I_{rr}	Diode peak recovery current	—	84	—	A	$R_{G1} = 33\Omega, R_{G2} = 0\Omega$
t_{rr}	Diode recovery time	—	115	—	ns	$I_C = 165A$
Q_{rr}	Diode recovery charge	—	5.0	—	μC	$V_{CC} = 360V, V_{GE} = \pm 15V$
Q_{ge}	Gate-to-emitter charge (turn-on)	225	—	420	nC	$V_{CC} = 360V$
Q_{gc}	Gate-to-collector charge (turn-on)	105	—	210		$I_C = 81A$
Q_g	Total gate charge (turn-on)	39	—	63		$V_{GE} = 15V$
C_{ies}	Input capacitance	—	8700	—	pF	$V_{GE} = 0V$
C_{oes}	Output capacitance	—	990	—		$V_{CC} = 30V$
C_{res}	Reverse transfer capacitance	—	120	—		$f = 1MHz$

(1) Includes tail losses

Thermal and Mechanical Characteristics

Parameter	Description	Typ	Max	Units
R_{thJC} (IGBT)	Thermal resistance, junction to case, each IGBT	—	0.33	°C/W
R_{thJC} (Diode)	Thermal resistance, junction to case, each diode	—	0.35	
R_{thCS} (Module)	Thermal resistance, case to sink	0.1	—	
Wt	Weight of module	140	—	g

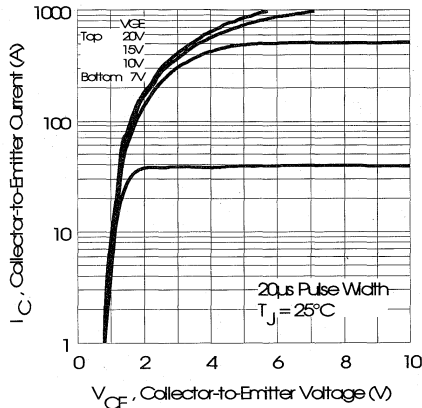


Fig. 1 - Typical Output Characteristics, $T_J = 25^\circ\text{C}$

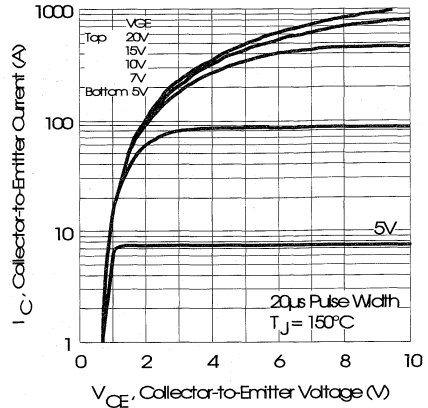


Fig. 2 - Typical Output Characteristics, $T_J = 150^\circ\text{C}$

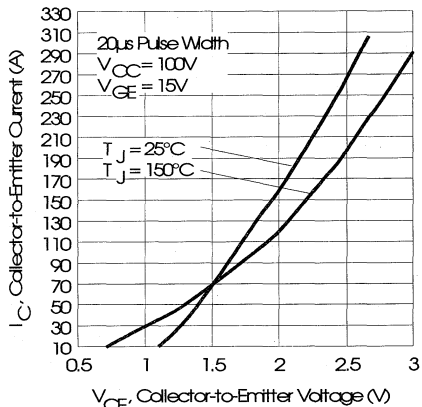


Fig. 3 - Typical Output Characteristics

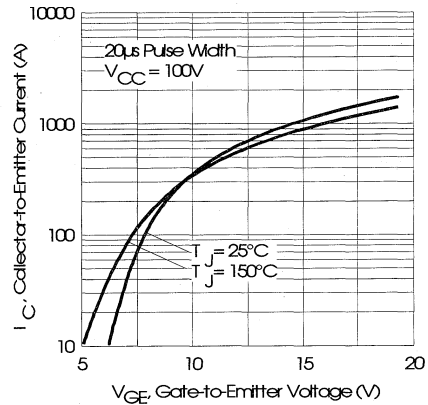


Fig. 4 - Typical Transfer Characteristics

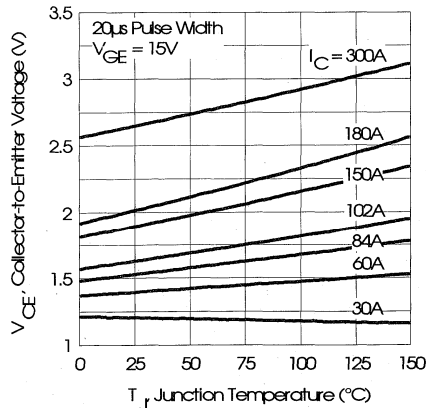


Fig. 5 - Collector-to-Emitter Saturation Typical Voltage vs. Junction Temperature

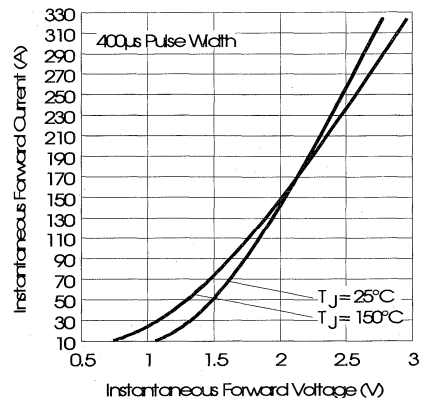


Fig. 6 - Forward Voltage Drop Characteristics

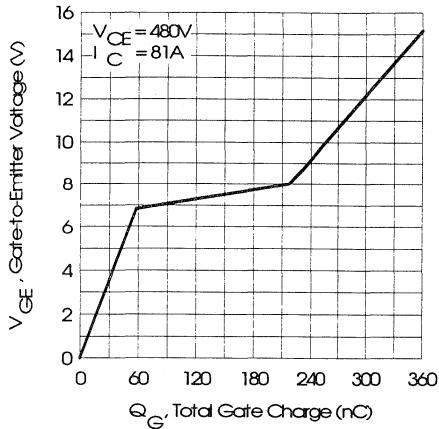


Fig. 7 - Typical Gate Charge vs. Gate-to-Emitter Voltage

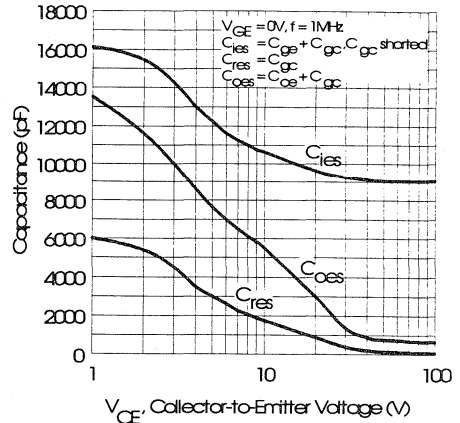


Fig. 8 - Typical Capacitance vs. Collector-to-Emitter Voltage

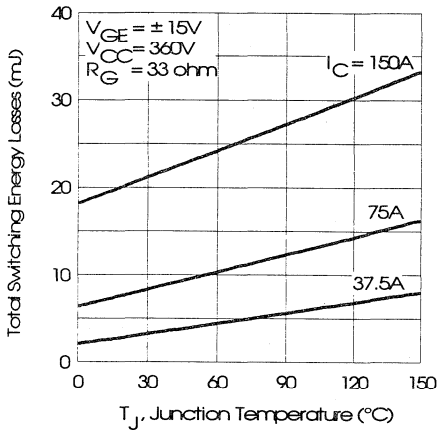


Fig. 9 - Typical Switching Losses vs. Junction Temperature

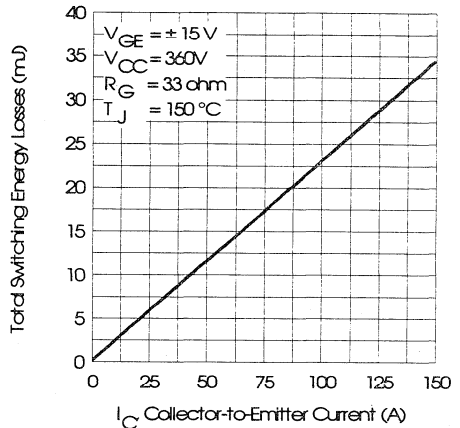


Fig. 10 - Typical Switching Losses vs. Collector-to-Emitter Current

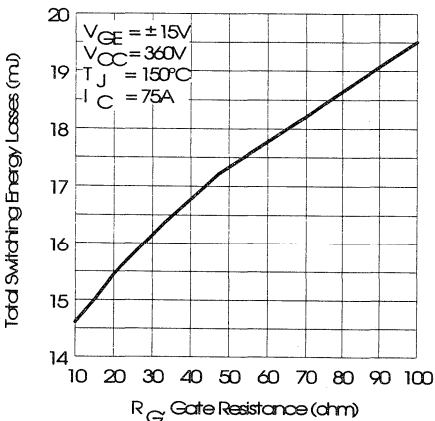


Fig. 11 - Typical Switching Losses vs. Gate Resistance

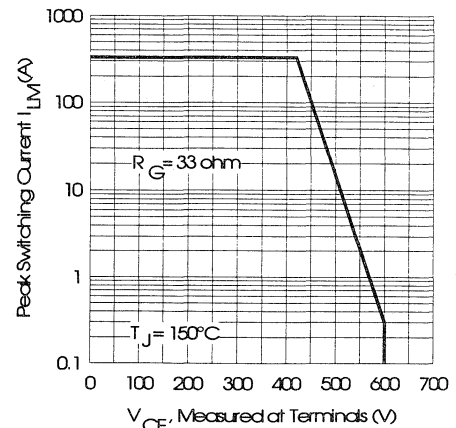


Fig. 12 - Reverse Bias Safe Operating Area

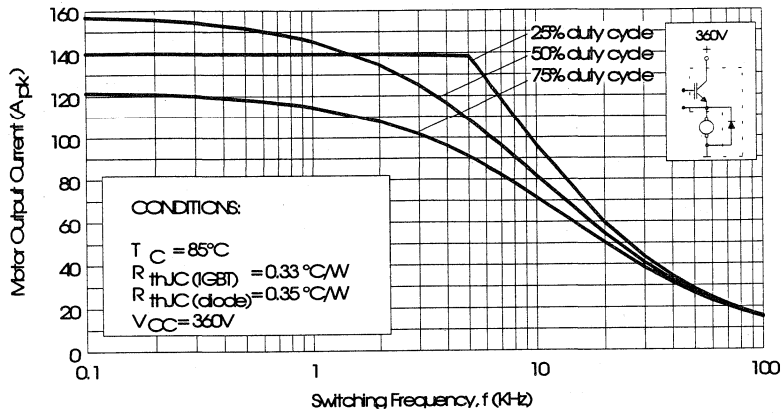


Fig. 13 - RMS Output Current vs. Frequency

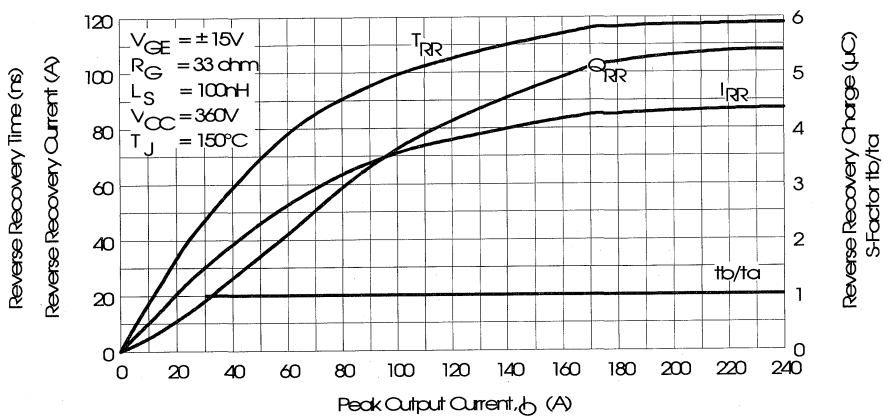


Fig. 14 - Typical Diode Recovery Characteristics as Function of Output Current I_o

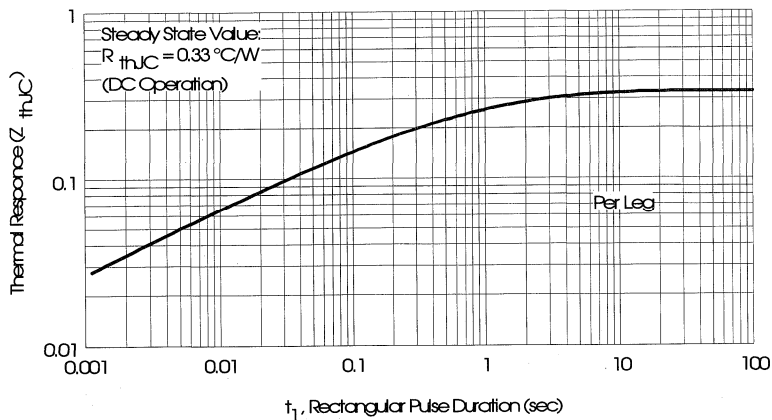


Fig. 15 - Maximum Effective Transient Thermal Impedance, Junction-to-Case

Power Conversion
 Fuses
 Modules

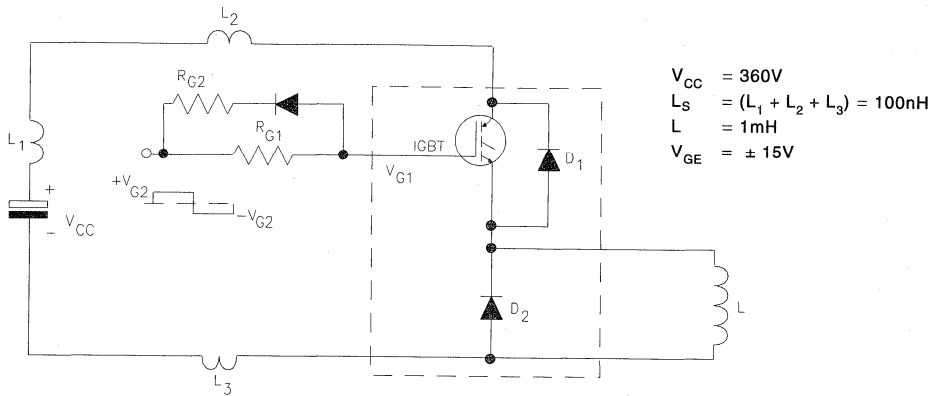


Fig. 16 - Test Circuit for Measurement of I_{LM} , E_{ON} , E_{OFF} , Q_{RR} , I_{RR} , $t_{D(ON)}$, t_r , $t_{D(OFF)}$, t_f

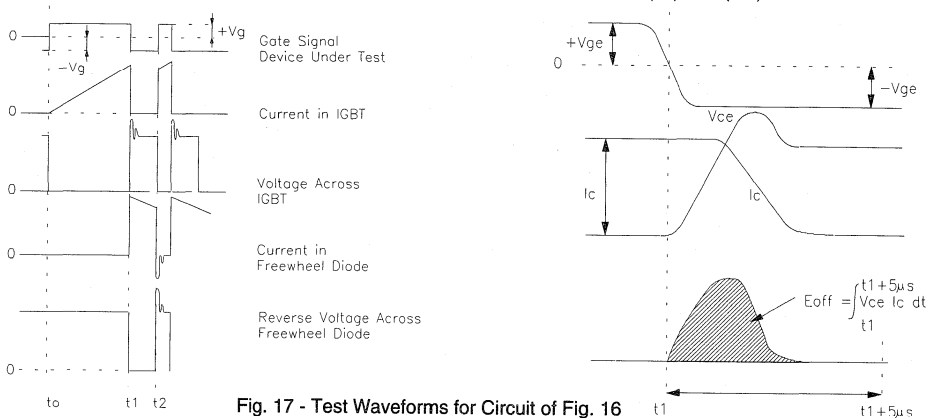


Fig. 17 - Test Waveforms for Circuit of Fig. 16

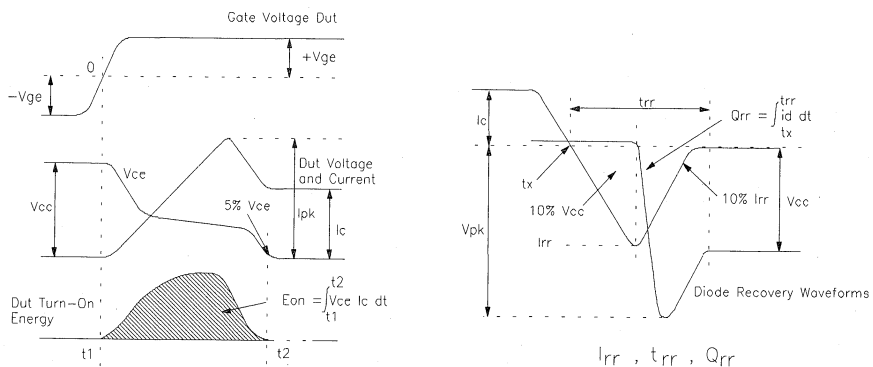


Fig. 18 - Test Waveforms for Circuit of Fig. 16, Defining E_{ON} , E_{REC} , $t_{D(ON)}$, t_r , I_{RR} , t_{RR} , Q_{RR}

**Refer to Section D for the following:
Appendix E: Sectio D - page D-7**

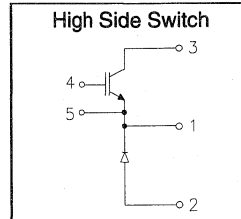
Fig. 19 - Waveforms for Switching Time

Package Outline 8 -INT-A-PAK High Side Switch Section D - page D-15

IRGNI200F06

"CHOPPER" IGBT INT-A-PAK

- Rugged Design
- Simple gate-drive
- Fast operation up to 10KHz hard switching, or 50KHz resonant
- Switching-Loss Rating includes all "tail" losses



Fast Speed IGBT

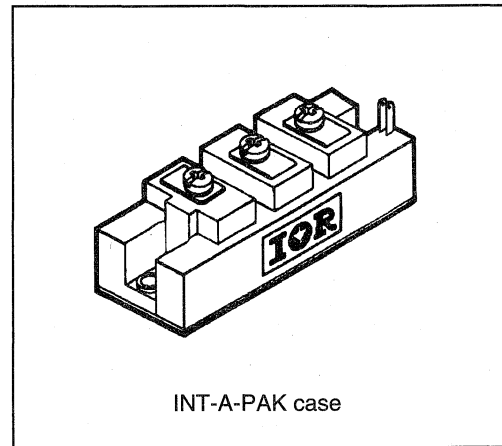
$$V_{CE} = 600V$$

$$I_C = 200A$$

$$V_{CE(ON)} < 2.3V$$

Description

IR's advanced IGBT technology is the key to this line of INT-A-pak Power Modules. The efficient geometry and unique processing of the IGBT allow higher current densities than comparable bipolar power module transistors, while at the same time requiring the simpler gate-drive of the familiar power MOSFET. This superior technology has now been coupled to state of the art assembly techniques to produce a higher current module that is highly suited to power applications such as motor drives, uninterruptible power supplies, welding, induction heating and ultrasonics.



Absolute Maximum Ratings

Parameter	Description	Value	Units	
V_{CES}	Continuous collector to emitter voltage	600	V	
$I_C @ T_C = 25^\circ C$	Continuous collector current	200	A	
$I_C @ T_C = 85^\circ C$	Continuous collector current	130		
$I_C @ T_C = 100^\circ C$	Continuous collector current	110		
I_{LM}	Peak switching current	400		
I_{FM}	Peak diode forward current (1)	500	V	
V_{GE}	Gate to emitter voltage	± 20		
V_{ISOL}	RMS isolation voltage, any terminal to case, $t = 1$ min	2500	W	
$P_D @ T_C = 25^\circ C$	Power dissipation	500		
T_J	Operating junction temperature range	-40 to 150		$^\circ C$
T_{STG}	Storage temperature range	-40 to 125		

(1) Duration limited by max junction temperature.

Electrical Characteristics - $T_J = 25^\circ\text{C}$, unless otherwise stated

Parameter	Description	Min	Typ	Max	Units	Test Conditions
BV_{CES}	Collector-to-emitter breakdown voltage	600	—	—	V	$V_{GE} = 0V, I_C = 2mA$
$V_{CE(ON)}$	Collector-to-emitter voltage	—	—	2.3		$V_{GE} = 15V, I_C = 200A$
		—	2.2	—		$V_{GE} = 15V, I_C = 200A, T_J = 150^\circ\text{C}$
V_{FM}	Diode forward voltage - maximum	—	—	2.0		$I_F = 200A, V_{GE} = 0V$
		—	2.0	—		$I_F = 200A, V_{GE} = 0V, T_J = 150^\circ\text{C}$
V_{GEth}	Gate threshold voltage	3.0	—	5.5	$I_C = 1mA$	
ΔV_{GEth}	Threshold voltage temp. coefficient	—	-11	—	mV/°C	$V_{CE} = V_{GE}, I_C = 1mA$
g_{fe}	Forward transconductance	104	—	144	S(Ω)	$V_{CE} = 25V, I_C = 200A$
I_{CES}	Collector-to-emitter leakage current	—	—	2	mA	$V_{GE} = 0V, V_{CE} = 600V$
		—	—	20		$V_{GE} = 0V, V_{CE} = 600V, T_J = 150^\circ\text{C}$
I_{GES}	Gate-to-emitter leakage current	—	—	± 2	μA	$V_{GE} = \pm 20V$

Dynamic Characteristics - $T_J = 150^\circ\text{C}$

Parameter	Description	Min	Typ	Max	Units	Test Conditions
E_{on}	Turn-on switching energy	—	0.05	—	mJ/A	$R_{G1} = 27\Omega, R_{G2} = 0\Omega$
E_{off} (1)	Turn-off switching energy	—	0.17	—		$I_C = 200A, L_S = 100nH$
E_{ts} (1)	Total switching energy	—	—	0.3		$V_{CC} = 360V, V_{GE} = \pm 15V$
$t_{d(on)}$	Turn-on delay time	—	80	—	ns	$R_{G1} = 27\Omega, R_{G2} = 0\Omega$
t_r	Rise time	—	150	—		$I_C = 200A$
$t_{d(off)}$	Turn-off delay time	—	450	—		$V_{CC} = 360V, V_{GE} = \pm 15V$
t_f	Fall time	—	900	—		$L_S = 100nH$
I_{rr}	Diode peak recovery current	—	108	—	A	$R_{G1} = 27\Omega, R_{G2} = 0\Omega$
t_{rr}	Diode recovery time	—	115	—		$I_C = 200A$
Q_{rr}	Diode recovery charge	—	6.5	—		$V_{CC} = 360V, V_{GE} = \pm 15V$
Q_{ge}	Gate-to-emitter charge (turn-on)	300	—	560	nC	$V_{CC} = 360V$
Q_{gc}	Gate-to-collector charge (turn-on)	140	—	280		$I_C = 108A$
Q_g	Total gate charge (turn-on)	52	—	84		$V_{GE} = 15V$
C_{ies}	Input capacitance	—	11600	—	pF	$V_{GE} = 0V$
C_{oes}	Output capacitance	—	1320	—		$V_{CC} = 30V$
C_{res}	Reverse transfer capacitance	—	160	—		$f = 1MHz$

(1) Includes tail losses

Thermal and Mechanical Characteristics

Parameter	Description	Typ	Max	Units
R_{thJC} (IGBT)	Thermal resistance, junction to case, each IGBT	—	0.25	°C/W
R_{thJC} (Diode)	Thermal resistance, junction to case, each diode	—	0.28	
R_{thCS} (Module)	Thermal resistance, case to sink	0.1	—	
Wt	Weight of module	140	—	g

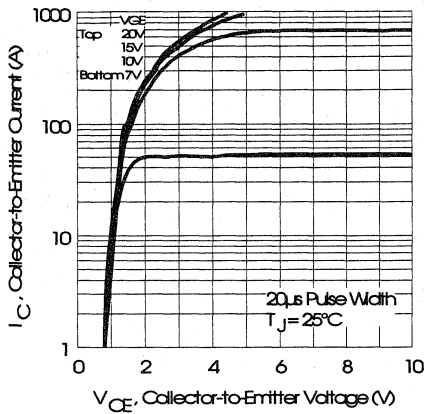


Fig. 1 - Typical Output Characteristics, $T_j = 25^\circ\text{C}$

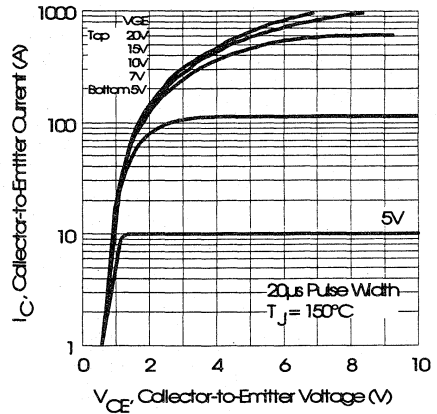


Fig. 2 - Typical Output Characteristics, $T_j = 150^\circ\text{C}$

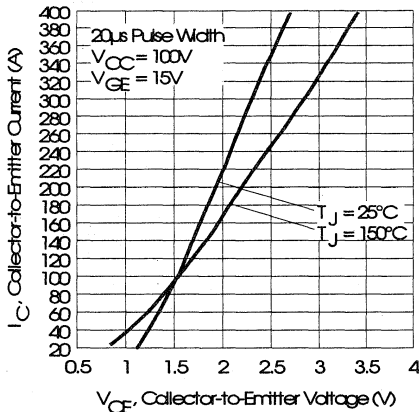


Fig. 3 - Typical Output Characteristics

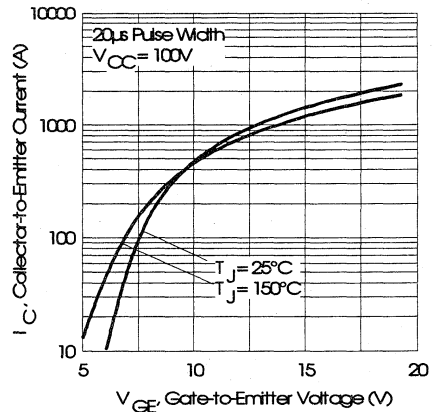


Fig. 4 - Typical Transfer Characteristics

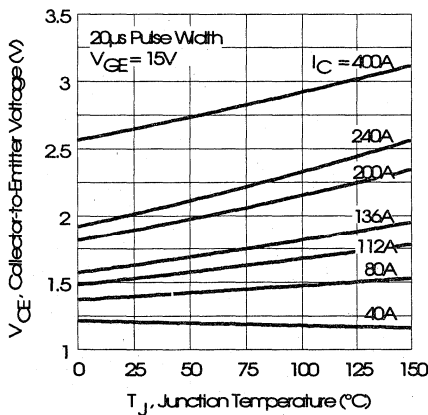


Fig. 5 - Collector-to-Emitter Saturation Typical Voltage vs. Junction Temperature

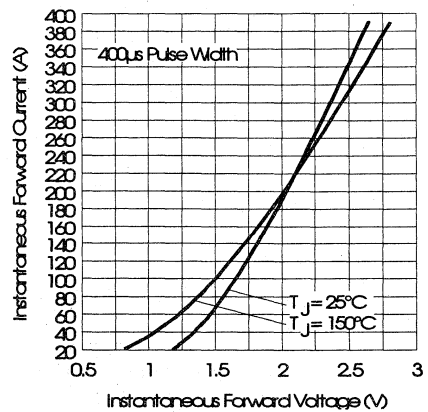


Fig. 6 - Forward Voltage Drop Characteristics

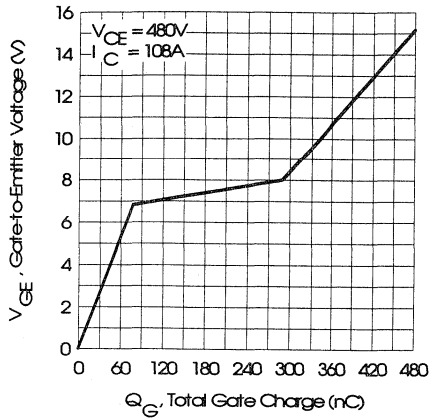


Fig. 7 - Typical Gate Charge vs. Gate-to-Emitter Voltage

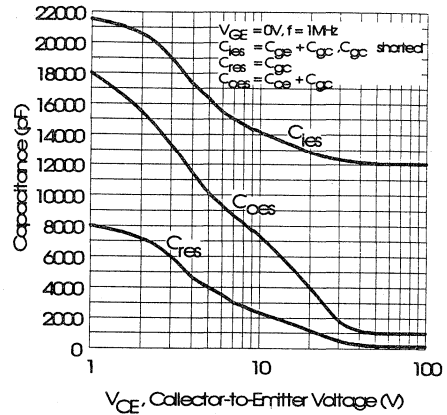


Fig. 8 - Typical Capacitance vs. Collector-to-Emitter Voltage

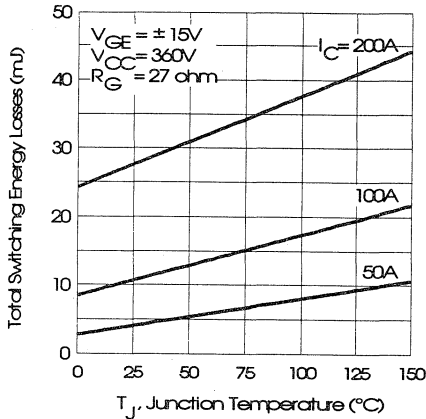


Fig. 9 - Typical Switching Losses vs. Junction Temperature

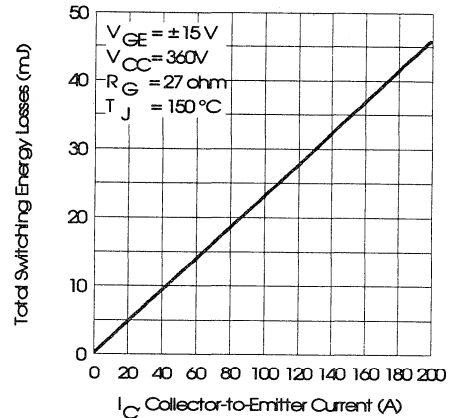


Fig. 10 - Typical Switching Losses vs. Collector-to-Emitter Current

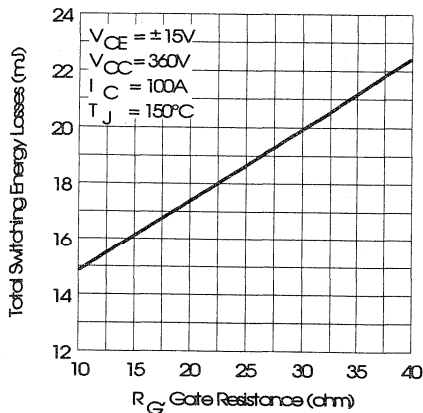


Fig. 11 - Typical Switching Losses vs. Gate Resistance

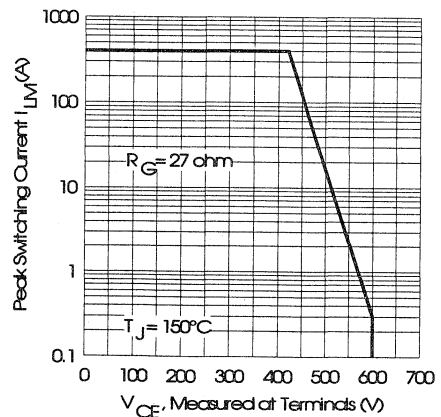


Fig. 12 - Reverse Bias Safe Operating Area

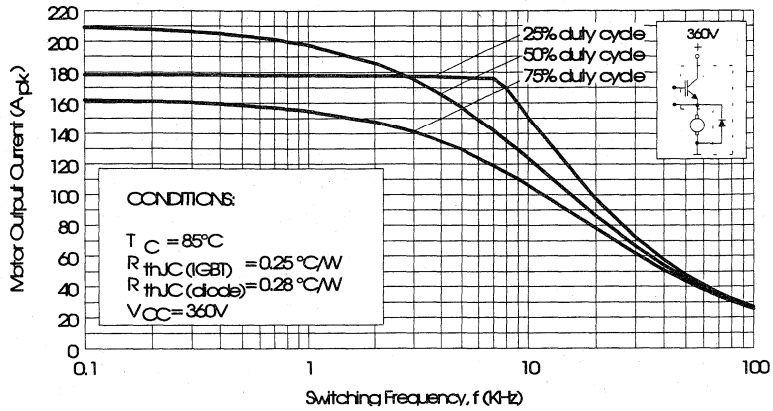


Fig. 13 - RMS Output Current vs. Frequency

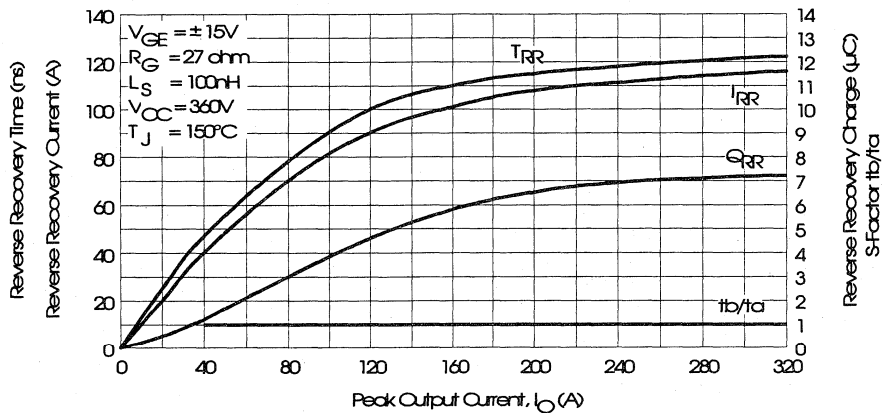


Fig. 14 - Typical Diode Recovery Characteristics as Function of Output Current I_O

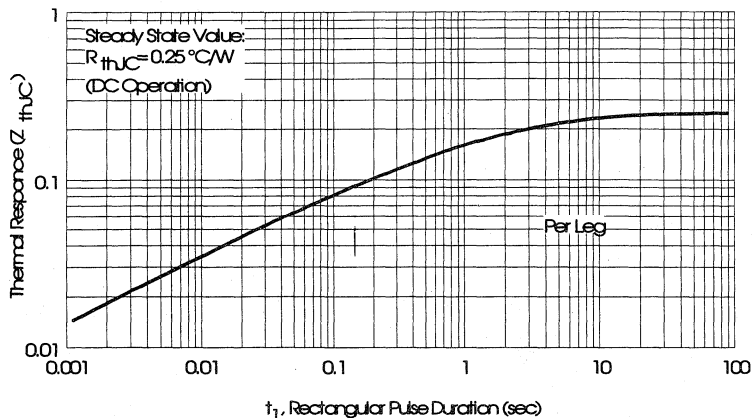


Fig. 15 - Maximum Effective Transient Thermal Impedance, Junction-to-Case

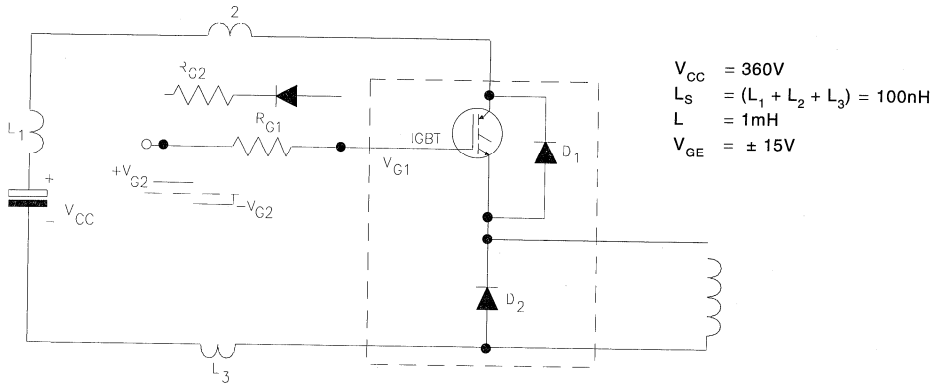


Fig. 16 - Test Circuit for Measurement of I_{LM} , E_{ON} , E_{OFF} , Q_{RR} , I_{RR} , $t_{D(ON)}$, t_r , $t_{D(OFF)}$, t_f

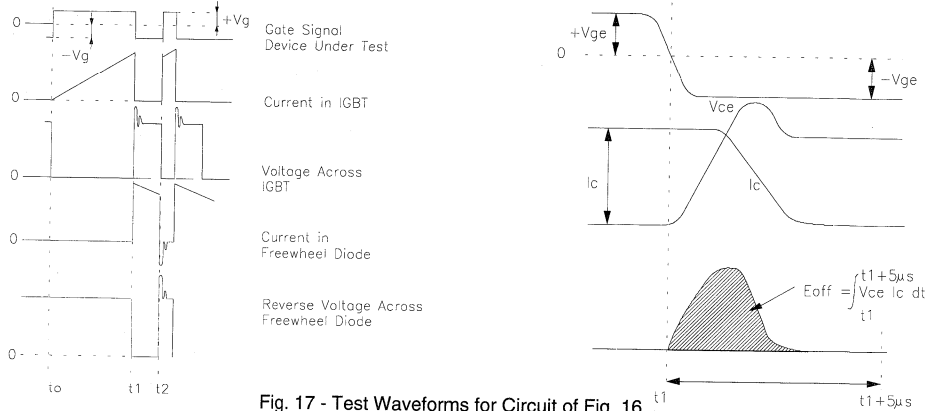


Fig. 17 - Test Waveforms for Circuit of Fig. 16

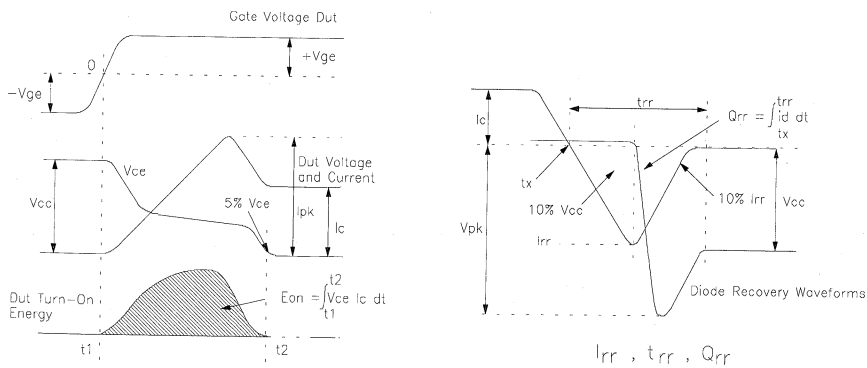


Fig. 18 - Test Waveforms for Circuit of Fig. 16, Defining E_{ON} , E_{REC} , $t_{D(ON)}$, t_r , I_{RR} , t_{RR} , Q_{RR}

Refer to Section D for the following:

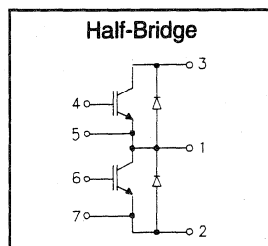
Appendix E: Section D - page D-7

Fig. 19 - Waveforms for Switching Time

"HALF-BRIDGE" IGBT INT-A-PAK

Fast Speed IGBT

- Rugged Design
- Simple gate-drive
- Fast operation up to 10KHz hard switching, or 50KHz resonant
- Switching-Loss Rating includes all "tail" losses



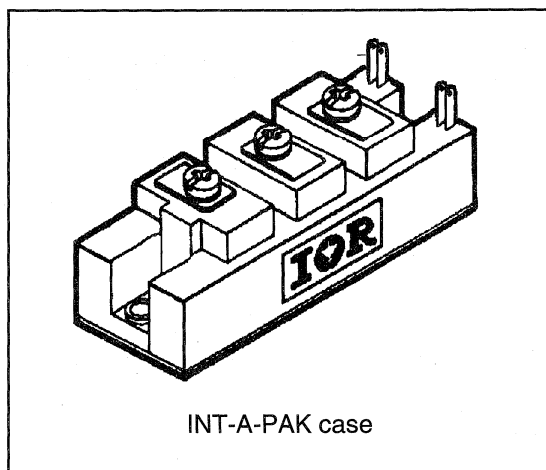
$$V_{CE} = 600V$$

$$I_C = 65A$$

$$V_{CE(ON)} < 2.3V$$

Description

IR's advanced IGBT technology is the key to this line of INT-A-pak Power Modules. The efficient geometry and unique processing of the IGBT allow higher current densities than comparable bipolar power module transistors, while at the same time requiring the simpler gate-drive of the familiar power MOSFET. This superior technology has now been coupled to state of the art assembly techniques to produce a higher current module that is highly suited to power applications such as motor drives, uninterruptible power supplies, welding, induction heating and ultrasonics.


 Power
Conversion
and
Energy
Modules

Absolute Maximum Ratings

Parameter	Description	Value	Units
V_{CES}	Continuous collector to emitter voltage	600	V
$I_C @ T_C = 25^\circ C$	Continuous collector current	65	A
$I_C @ T_C = 85^\circ C$	Continuous collector current	40	
$I_C @ T_C = 100^\circ C$	Continuous collector current	35	
I_{LM}	Peak switching current	130	
I_{FM}	Peak diode forward current (1)	165	
V_{GE}	Gate to emitter voltage	± 20	V
V_{ISOL}	RMS isolation voltage, any terminal to case, $t = 1$ min	2500	
$P_D @ T_C = 25^\circ C$	Power dissipation	179	W
T_J	Operating junction temperature range	-40 to 150	$^\circ C$
T_{STG}	Storage temperature range	-40 to 125	

(1) Duration limited by max junction temperature.

Electrical Characteristics - $T_J = 25^\circ\text{C}$, unless otherwise stated

Parameter	Description	Min	Typ	Max	Units	Test Conditions
BV_{CES}	Collector-to-emitter breakdown voltage	600	—	—	V	$V_{GE} = 0V, I_C = 500\mu A$
$V_{CE(ON)}$	Collector-to-emitter voltage	—	—	2.3		$V_{GE} = 15V, I_C = 65A$
		—	2.6	—		$V_{GE} = 15V, I_C = 65A, T_J = 150^\circ\text{C}$
V_{FM}	Diode forward voltage - maximum	—	—	3.2		$I_F = 65A, V_{GE} = 0V$
		—	3.2	—		$I_F = 65A, V_{GE} = 0V, T_J = 150^\circ\text{C}$
V_{GEth}	Gate threshold voltage	3.0	—	5.5	$I_C = 250\mu A$	
ΔV_{GEth}	Threshold voltage temp. coeff.	—	-11	—	mV/ $^\circ\text{C}$	$V_{CE} = V_{GE}, I_C = 250\mu A$
g_{fe}	Forward transconductance	26	—	36	S(τ)	$V_{CE} = 25V, I_C = 65A$
I_{CES}	Collector-to-emitter leakage current	—	—	500	μA	$V_{GE} = 0V, V_{CE} = 600V$
		—	—	5	mA	$V_{GE} = 0V, V_{CE} = 600V, T_J = 150^\circ\text{C}$
I_{GES}	Gate-to-emitter leakage current	—	—	± 500	nA	$V_{GE} = \pm 20V$

Dynamic Characteristics - $T_J = 150^\circ\text{C}$

Parameter	Description	Min	Typ	Max	Units	Test Conditions
E_{on}	Turn-on switching energy	—	0.05	—	mJ/A	$R_{G1} = 82\Omega, R_{G2} = 0\Omega$
E_{off} (1)	Turn-off switching energy	—	0.17	—		$I_C = 65A, L_S = 100nH$
E_{ts} (1)	Total switching energy	—	—	0.3		$V_{CC} = 360V, V_{GE} = \pm 15V$
$t_{d(on)}$	Turn-on delay time	—	80	—	ns	$R_{G1} = 82\Omega, R_{G2} = 0\Omega$
t_r	Rise time	—	150	—		$I_C = 65A$
$t_{d(off)}$	Turn-off delay time	—	450	—		$V_{CC} = 360V, V_{GE} = \pm 15V$
t_f	Fall time	—	900	—		$L_S = 100nH$
I_{rr}	Diode peak recovery current	—	30	—	A	$R_{G1} = 82\Omega, R_{G2} = 0\Omega$
t_{rr}	Diode recovery time	—	115	—	ns	$I_C = 65A$
Q_{rr}	Diode recovery charge	—	2.0	—	μC	$V_{CC} = 360V, V_{GE} = \pm 15V$
Q_{ge}	Gate-to-emitter charge (turn-on)	77	—	140	nC	$V_{CC} = 360V$
Q_{gc}	Gate-to-collector charge (turn-on)	35	—	70		$I_C = 65A$
Q_g	Total gate charge (turn-on)	13	—	21		$V_{GE} = 15V$
C_{ies}	Input capacitance	—	2900	—	pF	$V_{GE} = 0V$
C_{oes}	Output capacitance	—	330	—		$V_{CC} = 30V$
C_{res}	Reverse transfer capacitance	—	40	—		$f = 1MHz$

(1) Includes tail losses

Thermal and Mechanical Characteristics

Parameter	Description	Typ	Max	Units
R_{thJC} (IGBT)	Thermal resistance, junction to case, each IGBT	—	0.7	$^\circ\text{C/W}$
R_{thJC} (Diode)	Thermal resistance, junction to case, each diode	—	1.3	
R_{thCS} (Module)	Thermal resistance, case to sink	0.1	—	
Wt	Weight of module	140	—	g

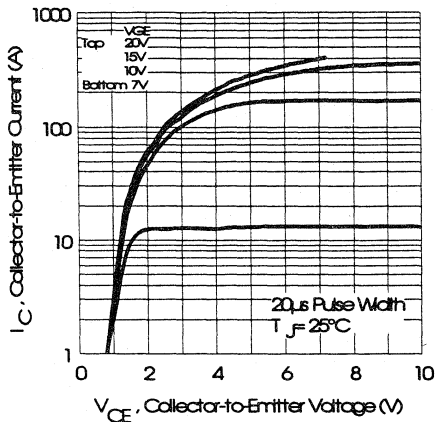


Fig. 1 - Typical Output Characteristics, $T_j = 25^\circ\text{C}$

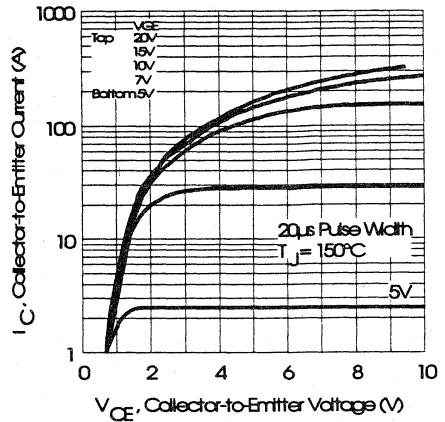


Fig. 2 - Typical Output Characteristics, $T_j = 150^\circ\text{C}$

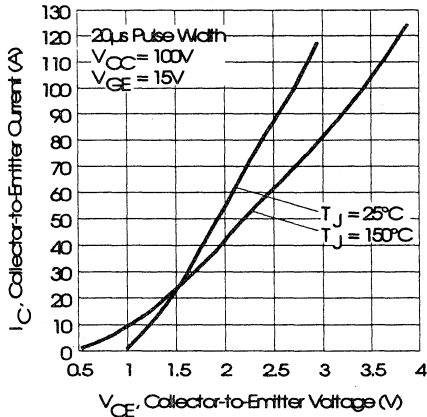


Fig. 3 - Typical Output Characteristics

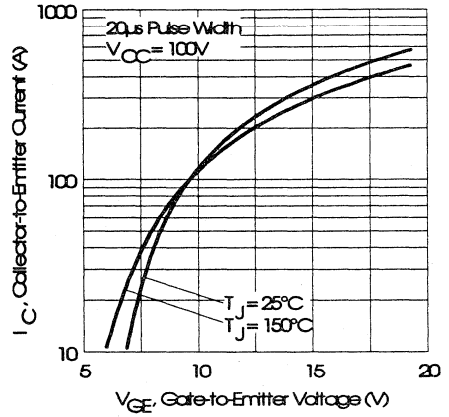


Fig. 4 - Typical Transfer Characteristics

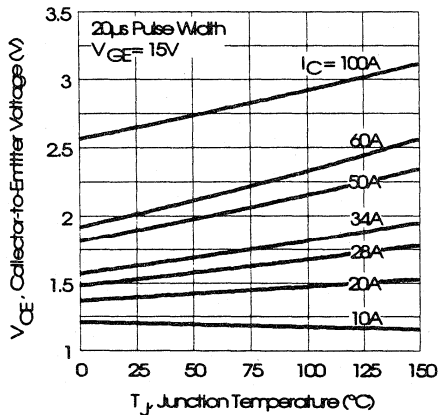


Fig. 5 - Collector-to-Emitter Saturation Typical Voltage vs. Junction Temperature

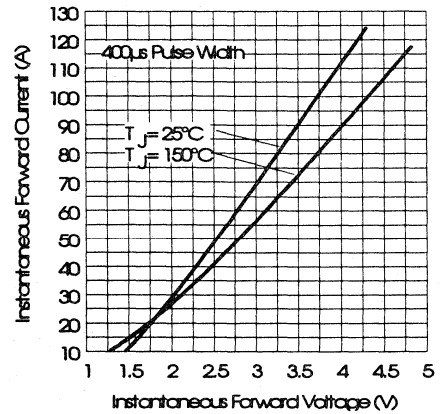


Fig. 6 - Forward Voltage Drop Characteristics

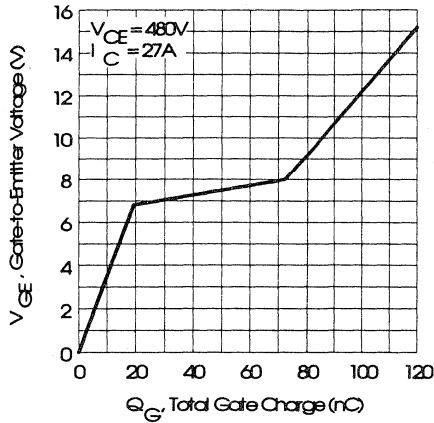


Fig. 7 - Typical Gate Charge vs. Gate-to-Emitter Voltage

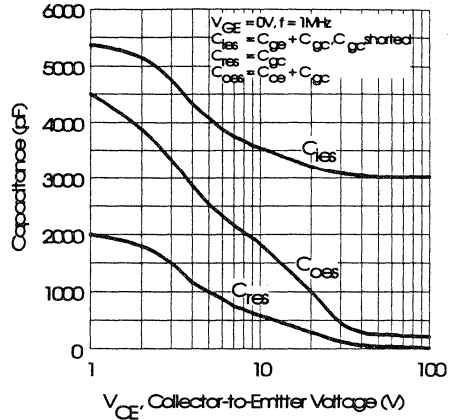


Fig. 8 - Typical Capacitance vs. Collector-to-Emitter Voltage

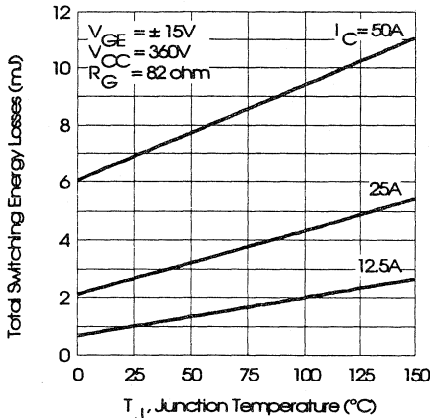


Fig. 9 - Typical Switching Losses vs. Junction Temperature

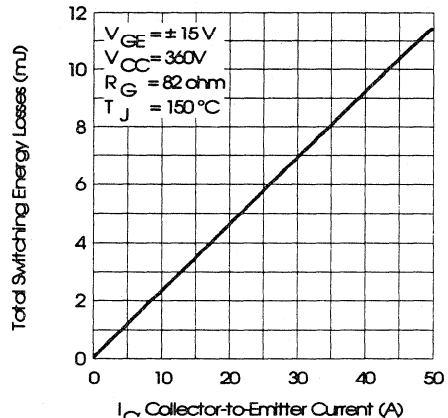


Fig. 10 - Typical Switching Losses vs. Collector-to-Emitter Current

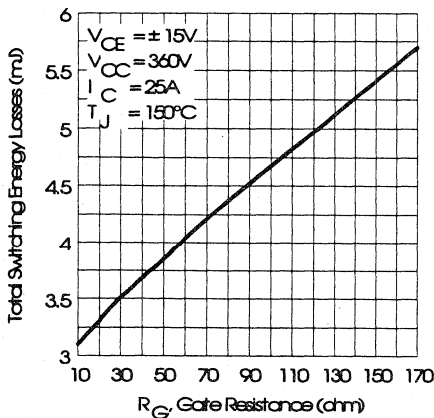


Fig. 11 - Typical Switching Losses vs. Gate Resistance

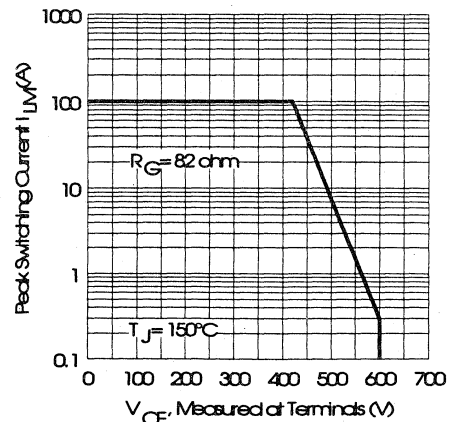


Fig. 12 - Reverse Bias Safe Operating Area

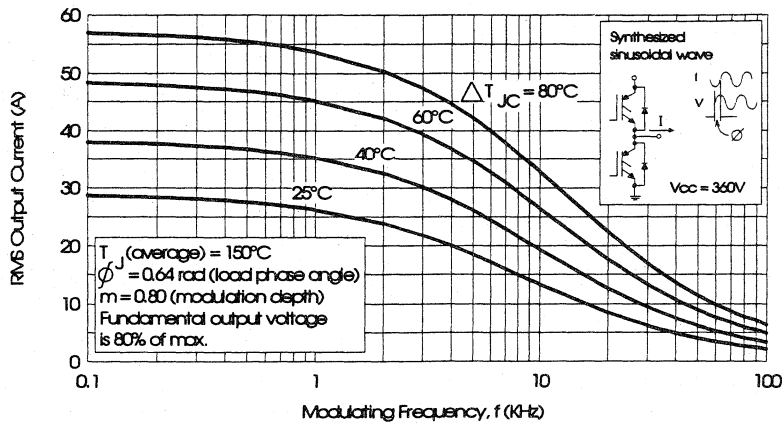


Fig. 13 - Typical RMS Output Current per phase vs. Frequency (Synthesized Sinusoidal Wave)

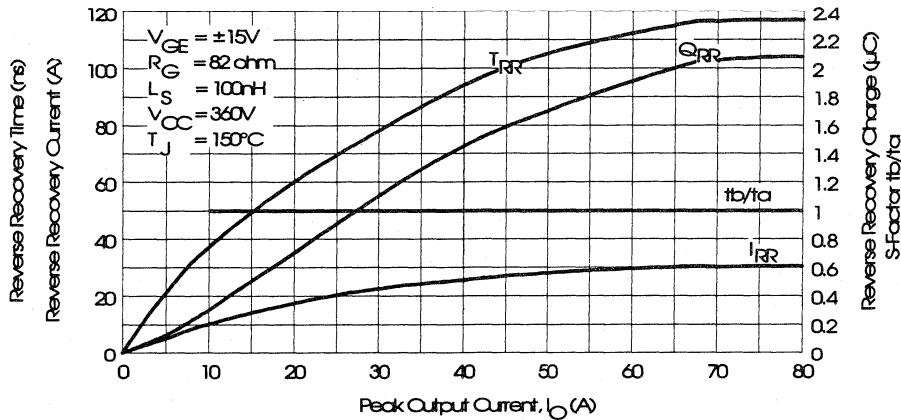


Fig. 14 - Typical Diode Recovery Characteristics as Function of Output Current I_o

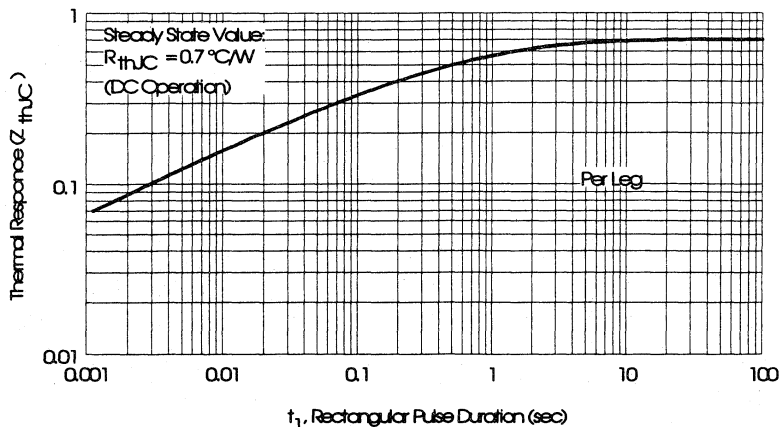


Fig. 15 - Maximum Effective Transient Thermal Impedance, Junction-to-Case

Power Conversion Fast Modules

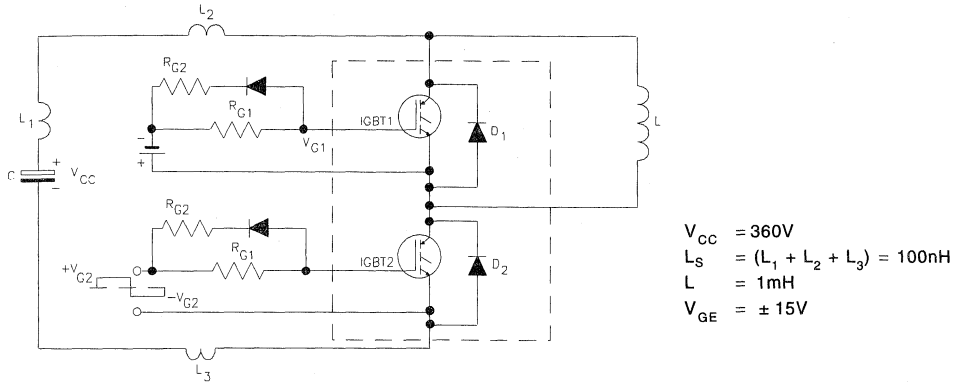


Fig. 16 - Test Circuit for Measurement of I_{LM} , E_{ON} , E_{OFF} , Q_{RR} , I_{RR} , $t_{D(ON)}$, t_r , $t_{D(OFF)}$, t_f

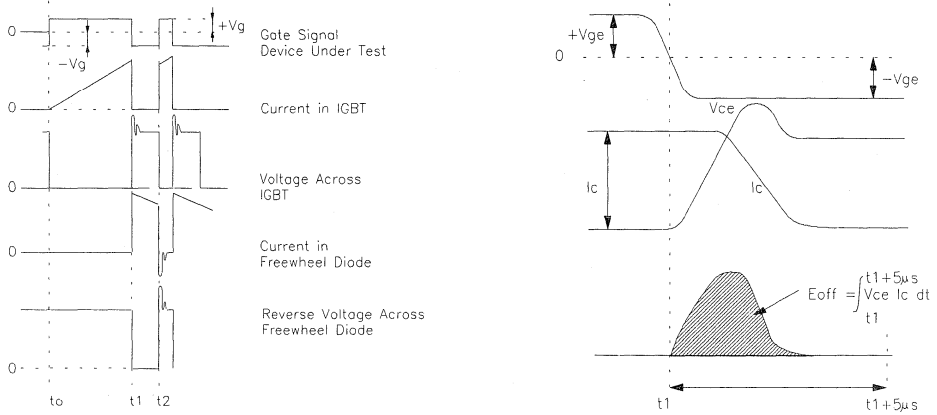


Fig. 17 - Test Waveforms for Circuit of Fig. 16

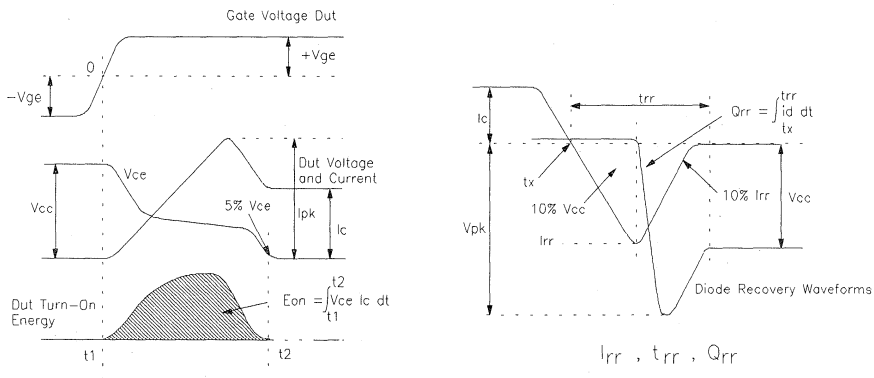


Fig. 18 - Test Waveforms for Circuit of Fig. 16, Defining E_{ON} , E_{REC} , $t_{D(ON)}$, t_r , I_{RR} , t_{RR} , Q_{RR}

Refer to Section D for the following:
Appendix E: Section D - page D-7

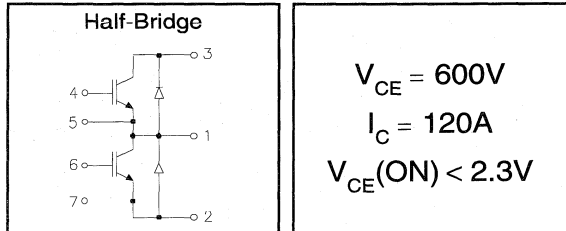
Fig. 19 - Waveforms for Switching Time

Package Outline 10 - INT-A-PAK Half Bridge Section D - page D-16

"HALF-BRIDGE" IGBT INT-A-PAK

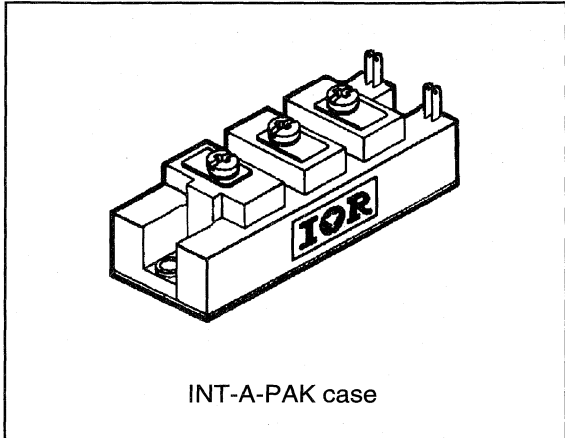
Fast Speed IGBT

- Rugged Design
- Simple gate-drive
- Fast operation up to 10KHz hard switching, or 50KHz resonant
- Switching-Loss Rating includes all "tail" losses



Description

IR's advanced IGBT technology is the key to this line of INT-A-pak Power Modules. The efficient geometry and unique processing of the IGBT allow higher current densities than comparable bipolar power module transistors, while at the same time requiring the simpler gate-drive of the familiar power MOSFET. This superior technology has now been coupled to state of the art assembly techniques to produce a higher current module that is highly suited to power applications such as motor drives, uninterruptible power supplies, welding, induction heating and ultrasonics.



Power Conversion Fast Modules

Absolute Maximum Ratings

Parameter	Description	Value	Units
V_{CES}	Continuous collector to emitter voltage	600	V
$I_C @ T_C = 25^\circ C$	Continuous collector current	120	A
$I_C @ T_C = 85^\circ C$	Continuous collector current	75	
$I_C @ T_C = 100^\circ C$	Continuous collector current	60	
I_{LM}	Peak switching current	240	
I_{FM}	Peak diode forward current (1)	300	
V_{GE}	Gate to emitter voltage	± 20	V
V_{ISOL}	RMS isolation voltage, any terminal to case, $t = 1$ min	2500	
$P_D @ T_C = 25^\circ C$	Power dissipation	298	W
T_J	Operating junction temperature range	-40 to 150	$^\circ C$
T_{STG}	Storage temperature range	-40 to 125	

(1) Duration limited by max junction temperature.

Electrical Characteristics - $T_J = 25^\circ\text{C}$, unless otherwise stated

Parameter	Description	Min	Typ	Max	Units	Test Conditions
BV_{CES}	Collector-to-emitter breakdown voltage	600	—	—	V	$V_{GE} = 0\text{V}, I_C = 1\text{mA}$
$V_{CE(ON)}$	Collector-to-emitter voltage	—	—	2.3		$V_{GE} = 15\text{V}, I_C = 120\text{A}$
V_{FM}	Diode forward voltage - maximum	—	2.4	—		$V_{GE} = 15\text{V}, I_C = 120\text{A}, T_J = 150^\circ\text{C}$
		—	—	3.1		$I_F = 120\text{A}, V_{GE} = 0\text{V}$
		—	3.1	—		$I_F = 120\text{A}, V_{GE} = 0\text{V}, T_J = 150^\circ\text{C}$
V_{Geth}	Gate threshold voltage	3.0	—	5.5	$I_C = 500\mu\text{A}$	
ΔV_{Geth}	Threshold voltage temp. coefficient	—	-11	—	$\text{mV}/^\circ\text{C}$	$V_{CE} = V_{GE}, I_C = 500\mu\text{A}$
g_{fe}	Forward transconductance	52	—	72	$\text{S}(\Omega)$	$V_{CE} = 25\text{V}, I_C = 120\text{A}$
I_{CES}	Collector-to-emitter leakage current	—	—	1	mA	$V_{GE} = 0\text{V}, V_{CE} = 600\text{V}$
		—	—	10		$V_{GE} = 0\text{V}, V_{CE} = 600\text{V}, T_J = 150^\circ\text{C}$
I_{GES}	Gate-to-emitter leakage current	—	—	± 1	μA	$V_{GE} = \pm 20\text{V}$

Dynamic Characteristics - $T_J = 150^\circ\text{C}$

Parameter	Description	Min	Typ	Max	Units	Test Conditions
E_{on}	Turn-on switching energy	—	0.05	—	mJ/A	$R_{G1} = 47\Omega, R_{G2} = 0\Omega$
E_{off} (1)	Turn-off switching energy	—	0.17	—		$I_C = 120\text{A}, L_S = 100\text{nH}$
E_{ts} (1)	Total switching energy	—	—	0.3		$V_{CC} = 360\text{V}, V_{GE} = \pm 15\text{V}$
$t_{d(on)}$	Turn-on delay time	—	80	—	ns	$R_{G1} = 47\Omega, R_{G2} = 0\Omega$
t_r	Rise time	—	150	—		$I_C = 120\text{A}$
$t_{d(off)}$	Turn-off delay time	—	450	—		$V_{GE} = \pm 15\text{V}$
t_f	Fall time	—	900	—		$L_S = 100\text{nH}$
I_{rr}	Diode peak recovery current	—	56	—		$R_{G1} = 47\Omega, R_{G2} = 0\Omega$
t_{rr}	Diode recovery time	—	115	—	ns	$I_C = 120\text{A}$
Q_{rr}	Diode recovery charge	—	3.4	—	μC	$V_{GE} = \pm 15\text{V}$
Q_{ge}	Gate-to-emitter charge (turn-on)	150	—	280	nC	$V_{CC} = 360\text{V}$
Q_{gc}	Gate-to-collector charge (turn-on)	70	—	140		$I_C = 54\text{A}$
Q_g	Total gate charge (turn-on)	26	—	42		$V_{GE} = 15\text{V}$
C_{ies}	Input capacitance	—	5800	—	pF	$V_{GE} = 0\text{V}$
C_{oes}	Output capacitance	—	660	—		$V_{CC} = 30\text{V}$
C_{res}	Reverse transfer capacitance	—	80	—		$f = 1\text{MHz}$

(1) Includes tail losses

Thermal and Mechanical Characteristics

Parameter	Description	Typ	Max	Units
R_{thJC} (IGBT)	Thermal resistance, junction to case, each IGBT	—	0.42	$^\circ\text{C}/\text{W}$
R_{thJC} (Diode)	Thermal resistance, junction to case, each diode	—	0.7	
R_{thCS} (Module)	Thermal resistance, case to sink	0.1	—	
Wt	Weight of module	140	—	g

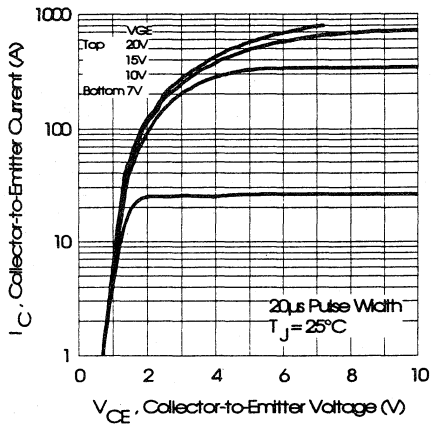


Fig. 1 - Typical Output Characteristics, $T_J = 25^\circ\text{C}$

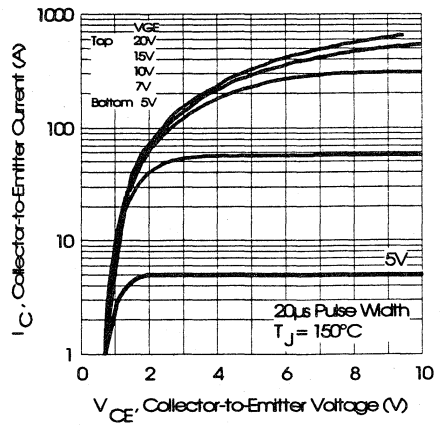


Fig. 2 - Typical Output Characteristics, $T_J = 150^\circ\text{C}$

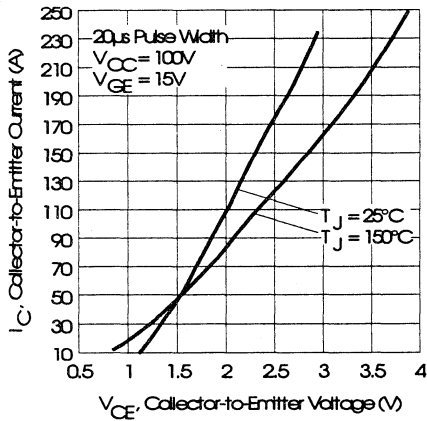


Fig. 3 - Typical Output Characteristics

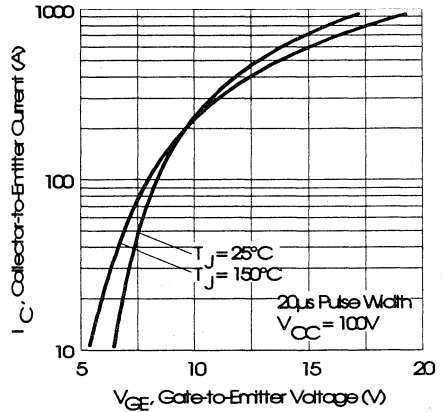


Fig. 4 - Typical Transfer Characteristics

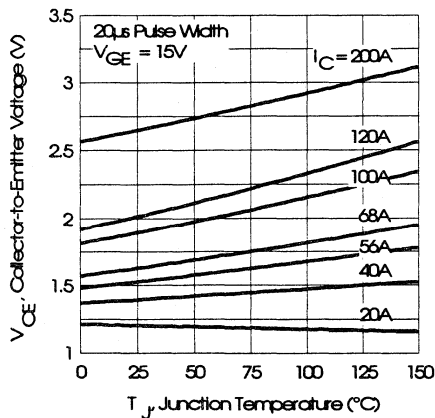


Fig. 5 - Collector-to-Emitter Saturation Typical Voltage vs. Junction Temperature

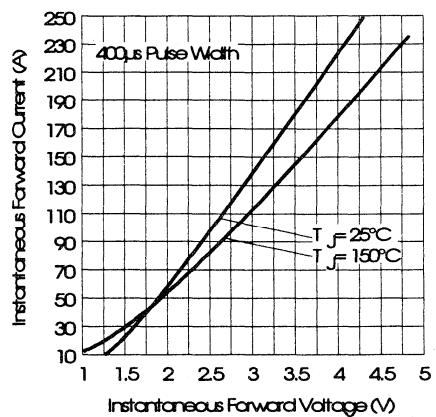


Fig. 6 - Forward Voltage Drop Characteristics

Power
Conversion
Fast
Modules

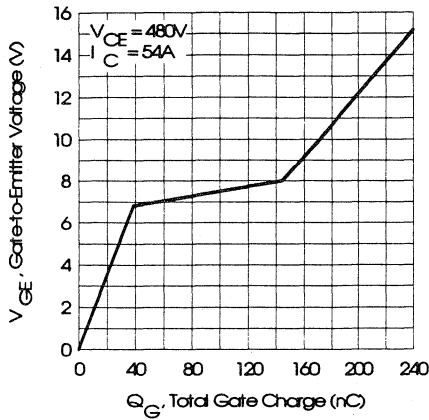


Fig. 7 - Typical Gate Charge vs. Gate-to-Emitter Voltage

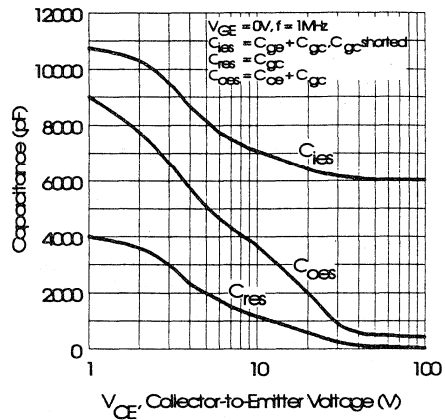


Fig. 8 - Typical Capacitance vs. Collector-to-Emitter Voltage

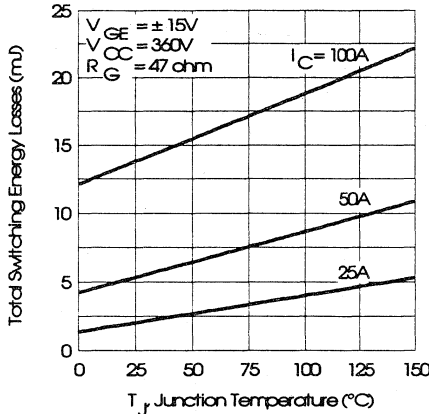


Fig. 9 - Typical Switching Losses vs. Junction Temperature

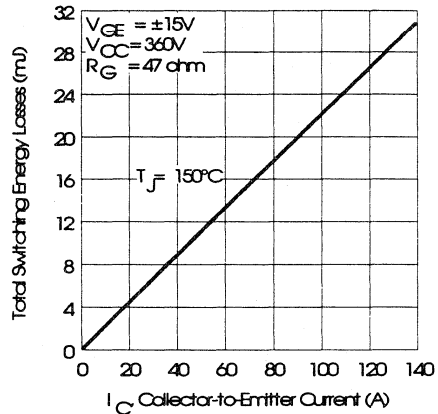


Fig. 10 - Typical Switching Losses vs. Collector-to-Emitter Current

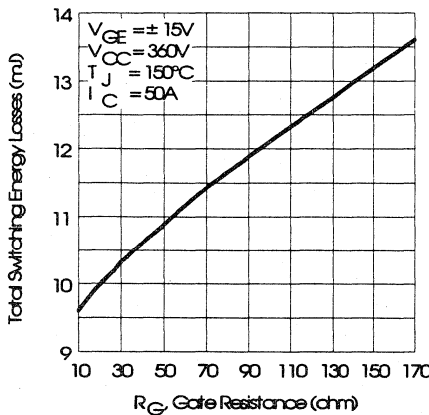


Fig. 11 - Typical Switching Losses vs. Gate Resistance

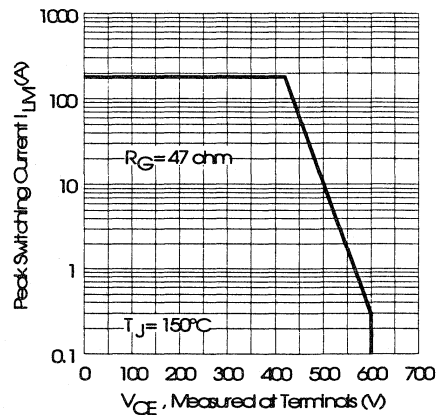


Fig. 12 - Reverse Bias Safe Operating Area

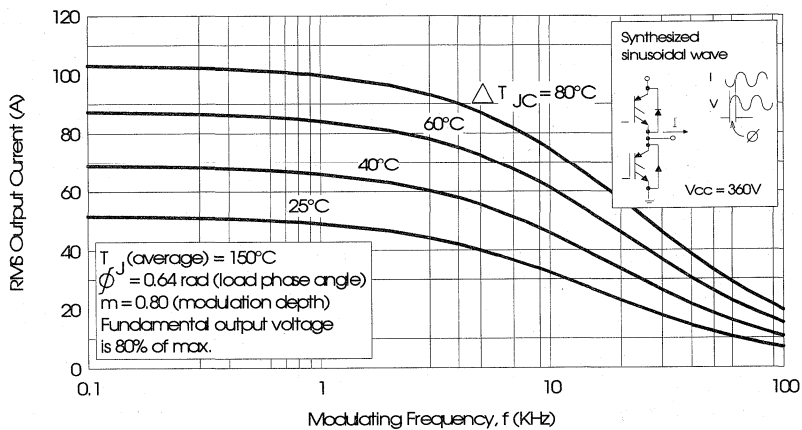


Fig. 13 - Typical RMS Output Current per phase vs. Frequency (Synthesized Sinusoidal Wave)

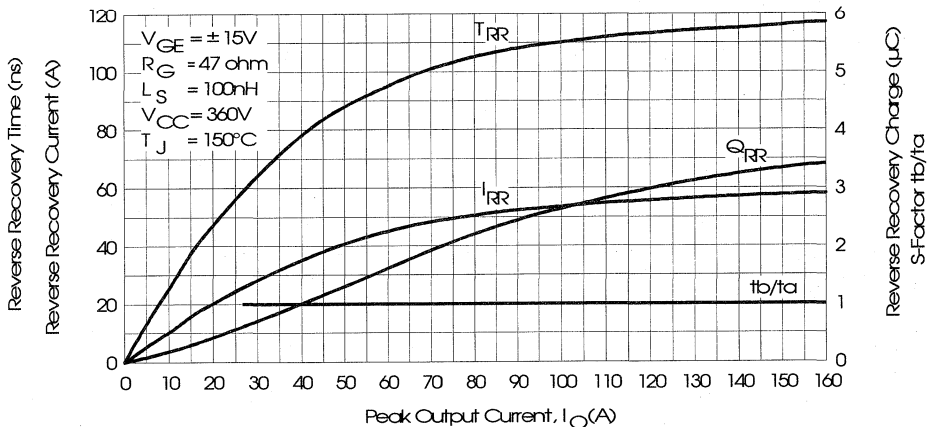


Fig. 14 - Typical Diode Recovery Characteristics as Function of Output Current I_o

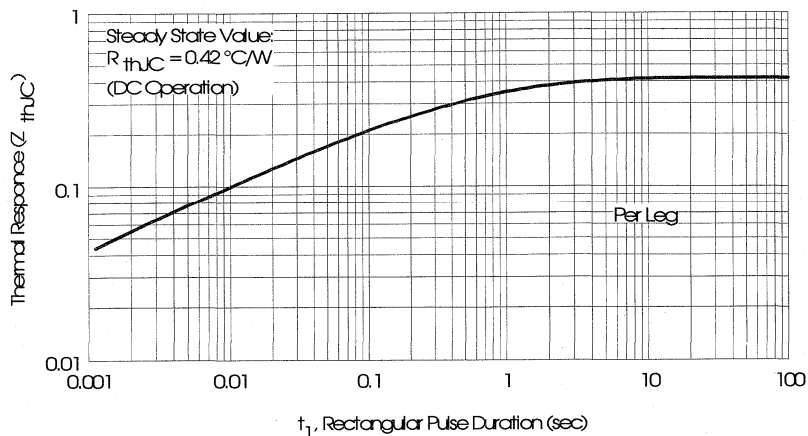


Fig. 15 - Maximum Effective Transient Thermal Impedance, Junction-to-Case

Power Conversion Fast Modules

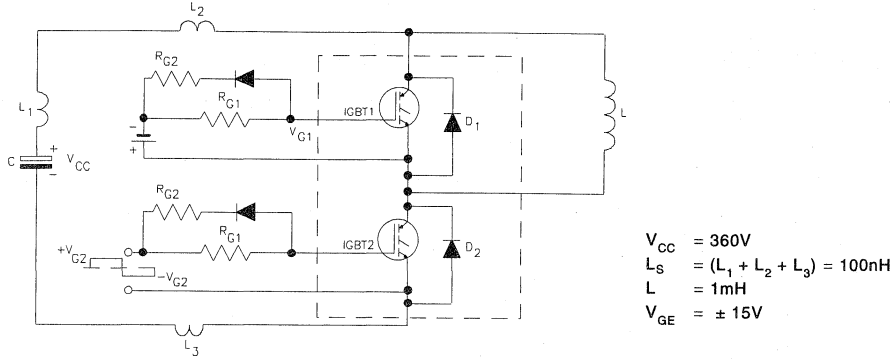


Fig. 16 - Test Circuit for Measurement of I_{LM} , E_{ON} , E_{OFF} , Q_{RR} , I_{RR} , $t_{D(ON)}$, t_r , $t_{D(OFF)}$, t_f

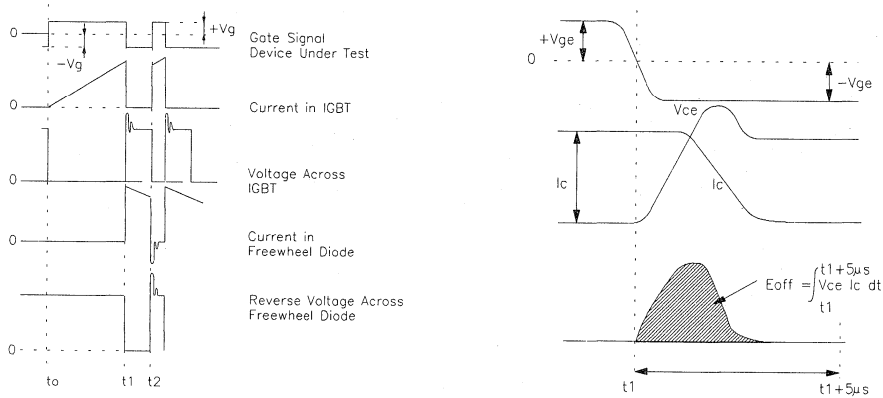


Fig. 17 - Test Waveforms for Circuit of Fig. 16

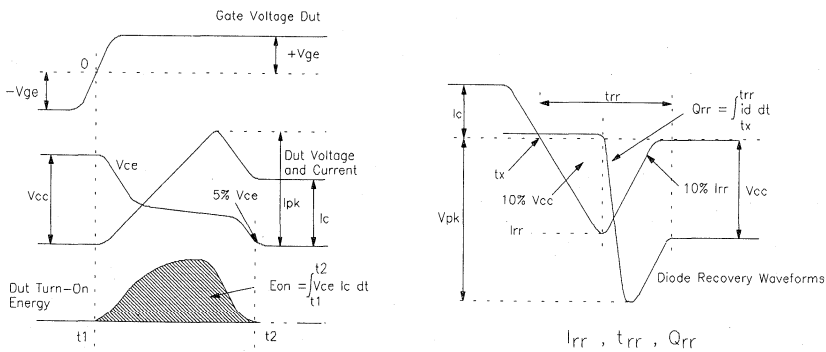


Fig. 18 - Test Waveforms for Circuit of Fig. 16, Defining E_{ON} , E_{REC} , $t_{D(ON)}$, t_r , I_{RR} , t_{RR} , Q_{RR}

Refer to Section D for the following:

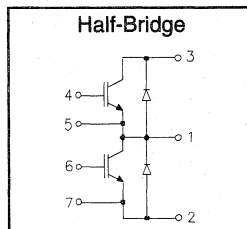
Appendix E: Section D - page D-7 Fig. 19 - Waveforms for Switching Time
 Package Outline 10 - INT-A-PAK Half Bridge Section D - Page D-16

IRGT1165F06

"HALF-BRIDGE" IGBT INT-A-PAK

Fast Speed IGBT

- Rugged Design
- Simple gate-drive
- Fast operation up to 10KHz hard switching, or 50KHz resonant
- Switching-Loss Rating includes all "tail" losses



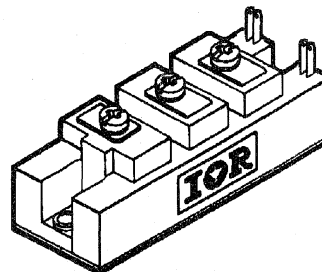
$$V_{CE} = 600V$$

$$I_C = 165A$$

$$V_{CE(ON)} < 2.3V$$

Description

IR's advanced IGBT technology is the key to this line of INT-A-pak Power Modules. The efficient geometry and unique processing of the IGBT allow higher current densities than comparable bipolar power module transistors, while at the same time requiring the simpler gate-drive of the familiar power MOSFET. This superior technology has now been coupled to state of the art assembly techniques to produce a higher current module that is highly suited to power applications such as motor drives, uninterruptible power supplies, welding, induction heating and ultrasonics.



INT-A-PAK case

Absolute Maximum Ratings

Parameter	Description	Value	Units
V_{CES}	Continuous collector to emitter voltage	600	V
$I_C @ T_C = 25^\circ C$	Continuous collector current	165	A
$I_C @ T_C = 85^\circ C$	Continuous collector current	100	
$I_C @ T_C = 100^\circ C$	Continuous collector current	85	
I_{LM}	Peak switching current	330	
I_{FM}	Peak diode forward current (1)	400	
V_{GE}	Gate to emitter voltage	± 20	V
V_{ISOL}	RMS isolation voltage, any terminal to case, $t = 1$ min	2500	
$P_D @ T_C = 25^\circ C$	Power dissipation	379	W
T_J	Operating junction temperature range	-40 to 150	$^\circ C$
T_{STG}	Storage temperature range	-40 to 125	

(1) Duration limited by max junction temperature.

Electrical Characteristics - $T_J = 25^\circ\text{C}$, unless otherwise stated

Parameter	Description	Min	Typ	Max	Units	Test Conditions
BV_{CES}	Collector-to-emitter breakdown voltage	600	—	—	V	$V_{GE} = 0\text{V}, I_C = 1.5\text{mA}$
$V_{CE(ON)}$	Collector-to-emitter voltage	—	—	2.3		$V_{GE} = 15\text{V}, I_C = 165\text{A}$
		—	2.3	—		$V_{GE} = 15\text{V}, I_C = 165\text{A}, T_J = 150^\circ\text{C}$
V_{FM}	Diode forward voltage - maximum	—	—	3.0		$I_F = 165\text{A}, V_{GE} = 0\text{V}$
		—	3.0	—		$I_F = 165\text{A}, V_{GE} = 0\text{V}, T_J = 150^\circ\text{C}$
V_{GEth}	Gate threshold voltage	3.0	—	5.5	$I_C = 750\mu\text{A}$	
ΔV_{GEth}	Threshold voltage temp. coefficient	—	-11	—	mV/ $^\circ\text{C}$	$V_{CE} = V_{GE}, I_C = 750\mu\text{A}$
g_{fe}	Forward transconductance	78	—	108	S(Ω)	$V_{CE} = 25\text{V}, I_C = 165\text{A}$
I_{CES}	Collector-to-emitter leakage current	—	—	1.5	mA	$V_{GE} = 0\text{V}, V_{CE} = 600\text{V}$
		—	—	15		$V_{GE} = 0\text{V}, V_{CE} = 600\text{V}, T_J = 150^\circ\text{C}$
I_{GES}	Gate-to-emitter leakage current	—	—	± 1.5	μA	$V_{GE} = \pm 20\text{V}$

Dynamic Characteristics - $T_J = 150^\circ\text{C}$

Parameter	Description	Min	Typ	Max	Units	Test Conditions
E_{on}	Turn-on switching energy	—	0.05	—	mJ/A	$R_{G1} = 33\Omega, R_{G2} = 0\Omega$
E_{off} (1)	Turn-off switching energy	—	0.17	—		$I_C = 165\text{A}, L_S = 100\text{nH}$
E_{ts} (1)	Total switching energy	—	—	0.3		$V_{CC} = 360\text{V}, V_{GE} = \pm 15\text{V}$
$t_{d(on)}$	Turn-on delay time	—	80	—	ns	$R_{G1} = 33\Omega, R_{G2} = 0\Omega$
t_r	Rise time	—	150	—		$I_C = 165\text{A}$
$t_{d(off)}$	Turn-off delay time	—	450	—		$V_{CC} = 360\text{V}, V_{GE} = \pm 15\text{V}$
t_f	Fall time	—	900	—		$L_S = 100\text{nH}$
I_{rr}	Diode peak recovery current	—	84	—	A	$R_{G1} = 33\Omega, R_{G2} = 0\Omega$
t_{rr}	Diode recovery time	—	115	—		$I_C = 165\text{A}$
Q_{rr}	Diode recovery charge	—	5.0	—		$V_{CC} = 360\text{V}, V_{GE} = \pm 15\text{V}$
Q_{ge}	Gate-to-emitter charge (turn-on)	225	—	420	nC	$V_{CC} = 360\text{V}$
Q_{gc}	Gate-to-collector charge (turn-on)	105	—	210		$I_C = 81\text{A}$
Q_g	Total gate charge (turn-on)	39	—	63		$V_{GE} = 15\text{V}$
C_{ies}	Input capacitance	—	8700	—	pF	$V_{GE} = 0\text{V}$
C_{oes}	Output capacitance	—	990	—		$V_{a_{CC}} = 30\text{V}$
C_{res}	Reverse transfer capacitance	—	120	—		$f = 1\text{MHz}$

(1) Includes tail losses

Thermal and Mechanical Characteristics

Parameter	Description	Typ	Max	Units
R_{thJC} (IGBT)	Thermal resistance, junction to case, each IGBT	—	0.33	$^\circ\text{C/W}$
R_{thJC} (Diode)	Thermal resistance, junction to case, each diode	—	0.55	
R_{thCS} (Module)	Thermal resistance, case to sink	0.1	—	
Wt	Weight of module	140	—	g

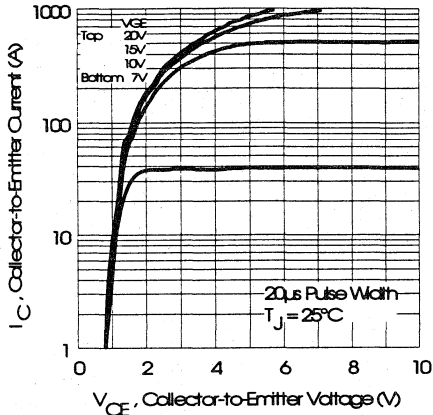


Fig. 1 - Typical Output Characteristics, $T_J = 25^\circ\text{C}$

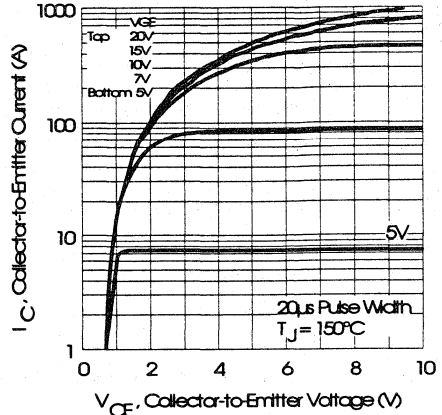


Fig. 2 - Typical Output Characteristics, $T_J = 150^\circ\text{C}$

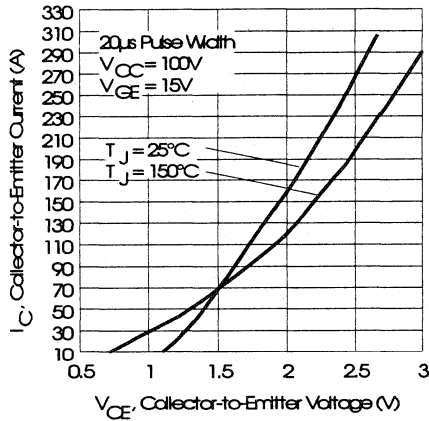


Fig. 3 - Typical Output Characteristics

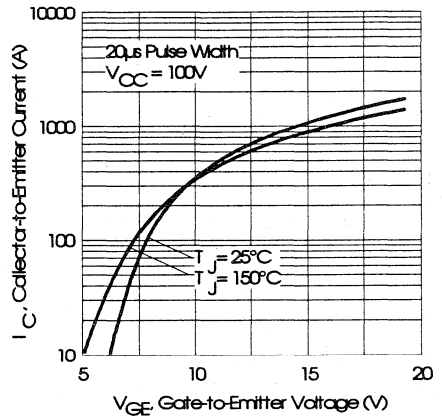


Fig. 4 - Typical Transfer Characteristics

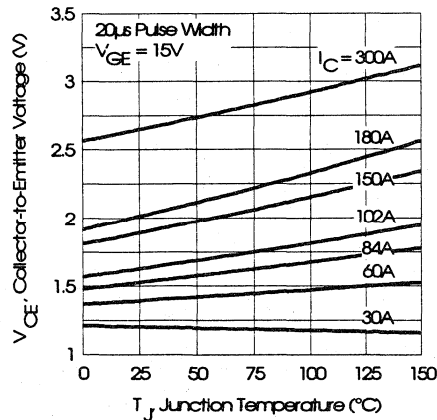


Fig. 5 - Collector-to-Emitter Saturation Typical Voltage vs. Junction Temperature

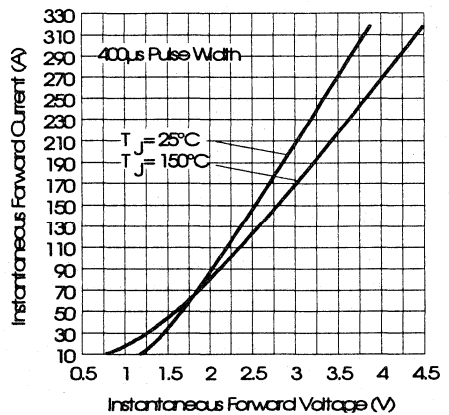


Fig. 6 - Forward Voltage Drop Characteristics

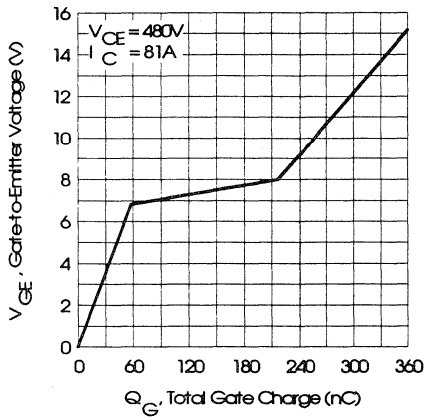


Fig. 7 - Typical Gate Charge vs. Gate-to-Emitter Voltage

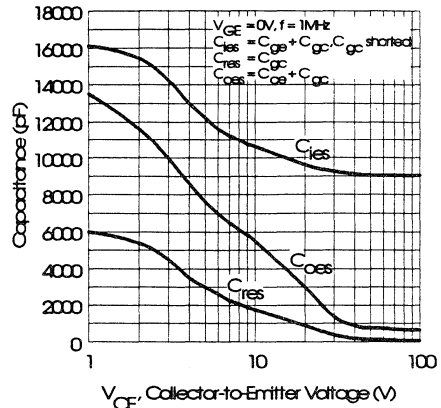


Fig. 8 - Typical Capacitance vs. Collector-to-Emitter Voltage

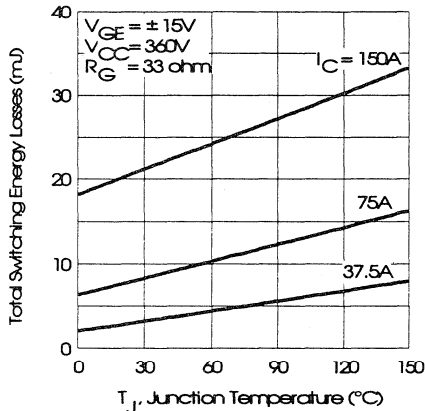


Fig. 9 - Typical Switching Losses vs. Junction Temperature

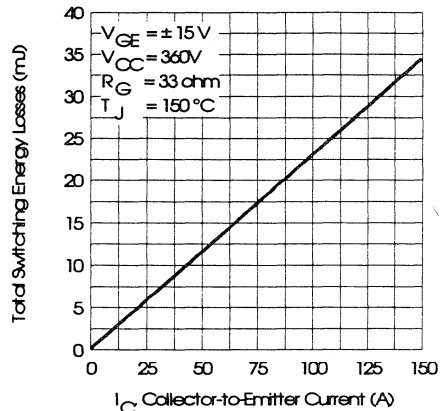


Fig. 10 - Typical Switching Losses vs. Collector-to-Emitter Current

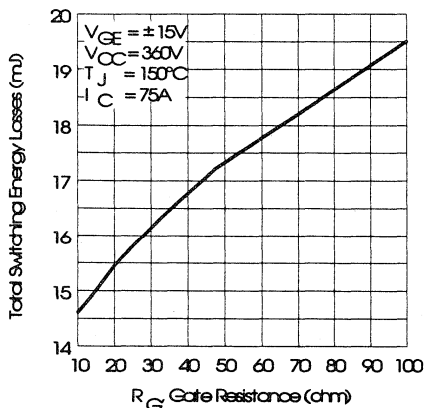


Fig. 11 - Typical Switching Losses vs. Gate Resistance

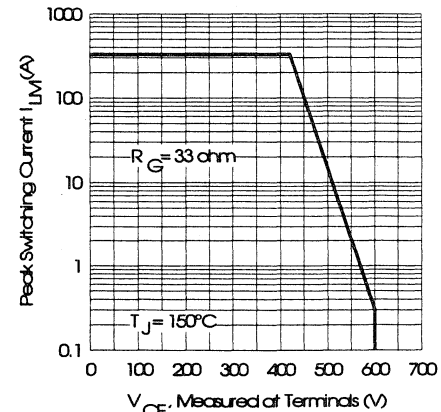


Fig. 12 - Reverse Bias Safe Operating Area

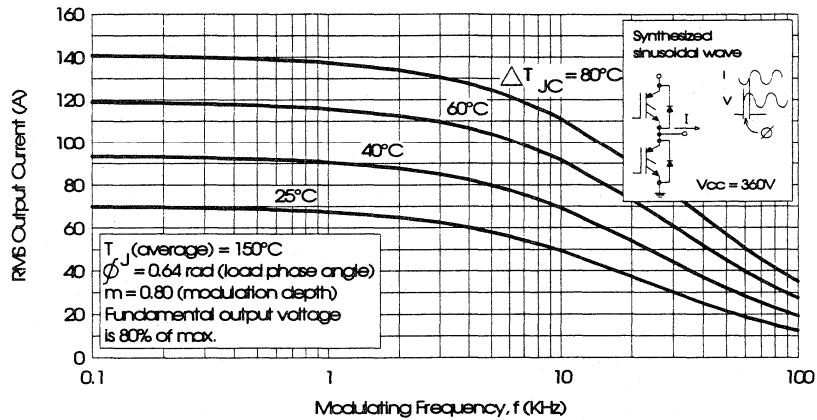


Fig. 13 - Typical RMS Output Current per phase vs. Frequency (Synthesized Sinusoidal Wave)

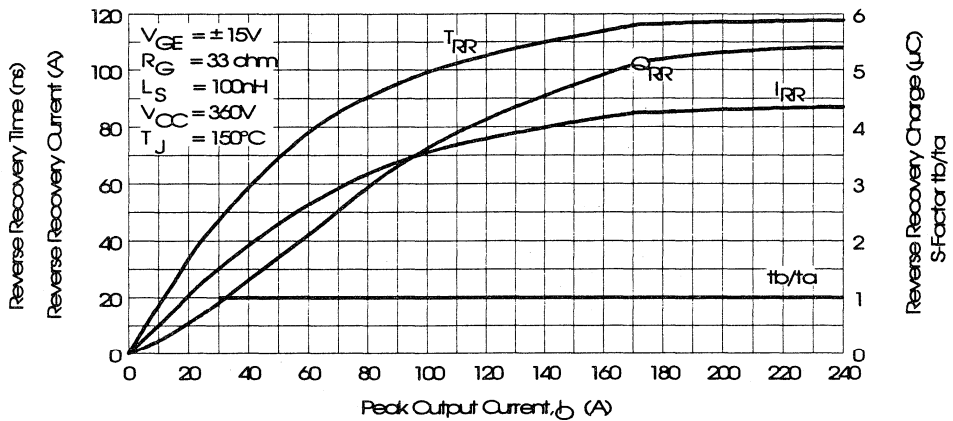


Fig. 14 - Typical Diode Recovery Characteristics as Function of Output Current I_o

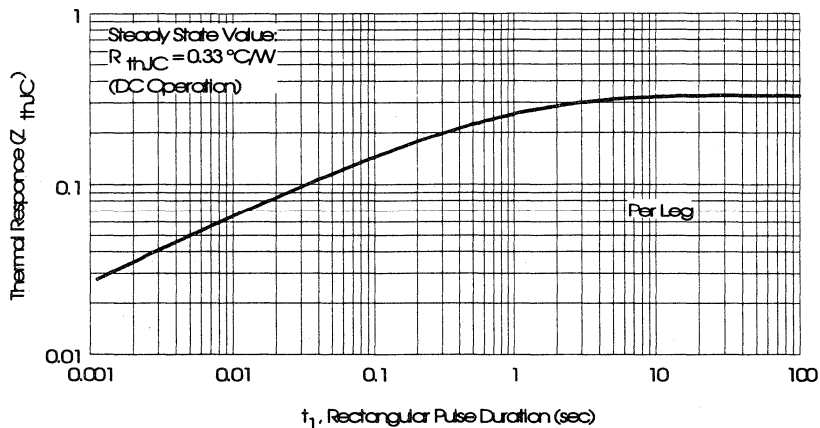


Fig. 15 - Maximum Effective Transient Thermal Impedance, Junction-to-Case

Power
Conversion
Fast
Modules

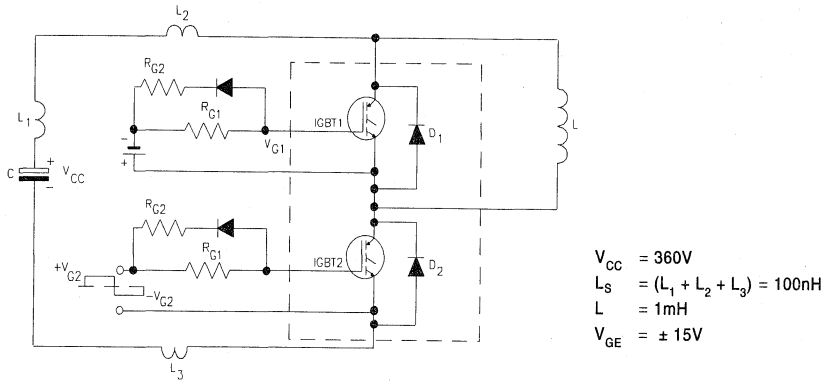


Fig. 16 - Test Circuit for Measurement of I_{LM} , E_{ON} , E_{OFF} , Q_{RR} , I_{RR} , $t_{D(ON)}$, t_r , $t_{D(OFF)}$, t_f

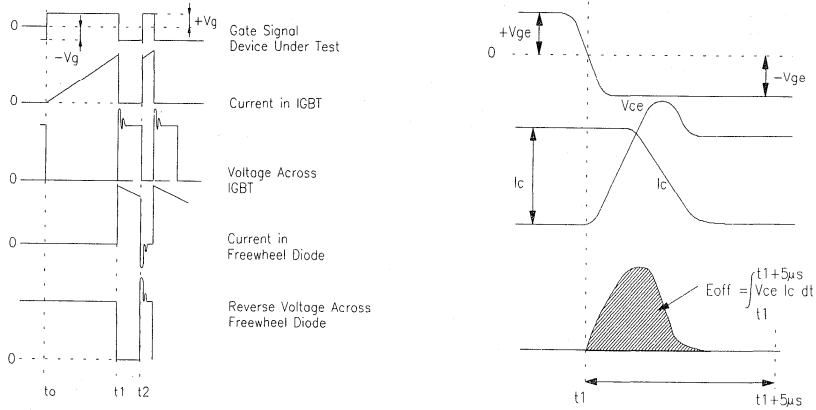


Fig. 17 - Test Waveforms for Circuit of Fig. 16

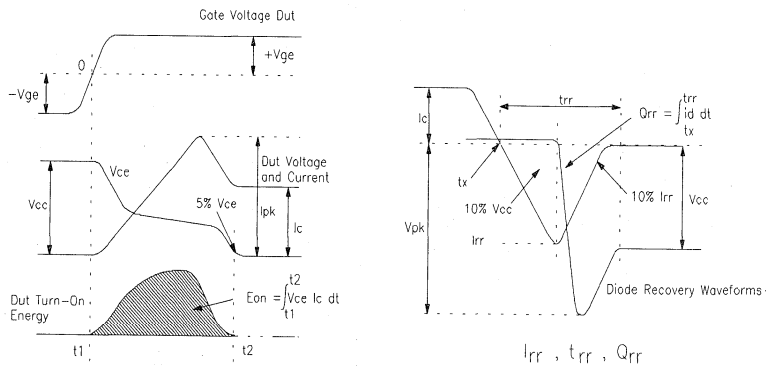


Fig. 18 - Test Waveforms for Circuit of Fig. 16, Defining E_{ON} , E_{REC} , $t_{D(ON)}$, t_r , I_{RR} , t_{RR} , Q_{RR}

Refer to Section D for the following:

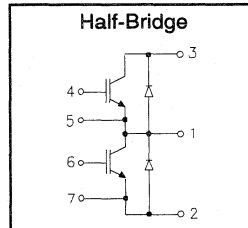
Appendix E: Section D - page D-7 Fig. 19 - Waveforms for Switching Time
 Package Outline 10 - INT-A-PAK Half Bridge Section D - Page D-16

IRGT1200F06

"HALF-BRIDGE" IGBT INT-A-PAK

Fast Speed IGBT

- Rugged Design
- Simple gate-drive
- Fast operation up to 10KHz hard switching, or 50KHz resonant
- Switching-Loss Rating includes all "tail" losses



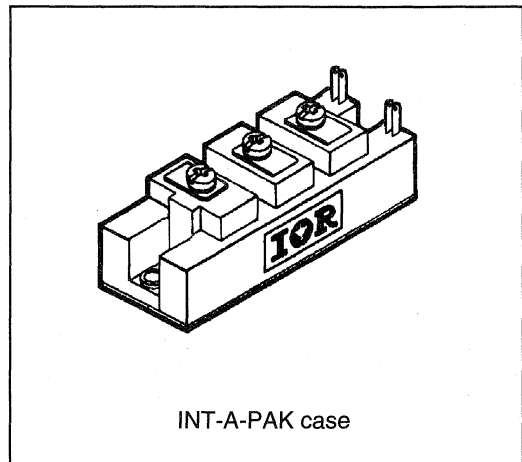
$$V_{CE} = 600V$$

$$I_C = 200A$$

$$V_{CE(ON)} < 2.3V$$

Description

IR's advanced IGBT technology is the key to this line of INT-A-pak Power Modules. The efficient geometry and unique processing of the IGBT allow higher current densities than comparable bipolar power module transistors, while at the same time requiring the simpler gate-drive of the familiar power MOSFET. This superior technology has now been coupled to state of the art assembly techniques to produce a higher current module that is highly suited to power applications such as motor drives, uninterruptible power supplies, welding, induction heating and ultrasonics.



Power
Conversion
Fast
Modules

Absolute Maximum Ratings

Parameter	Description	Value	Units
V_{CES}	Continuous collector to emitter voltage	600	V
$I_C @ T_C = 25^\circ C$	Continuous collector current	200	A
$I_C @ T_C = 85^\circ C$	Continuous collector current	130	
$I_C @ T_C = 100^\circ C$	Continuous collector current	110	
I_{LM}	Peak switching current	400	
I_{FM}	Peak diode forward current (1)	500	V
V_{GE}	Gate to emitter voltage	± 20	
V_{ISOL}	RMS isolation voltage, any terminal to case, $t = 1$ min	2500	W
$P_D @ T_C = 25^\circ C$	Power dissipation	500	
T_J	Operating junction temperature range	-40 to 150	
T_{STG}	Storage temperature range	-40 to 125	

(1) Duration limited by max junction temperature.

Electrical Characteristics - $T_J = 25^\circ\text{C}$, unless otherwise stated

Parameter	Description	Min	Typ	Max	Units	Test Conditions
BV_{CES}	Collector-to-emitter breakdown voltage	600	—	—	V	$V_{GE} = 0V, I_C = 2mA$
$V_{CE(ON)}$	Collector-to-emitter voltage	—	—	2.3		$V_{GE} = 15V, I_C = 200A$
		—	2.2	—		$V_{GE} = 15V, I_C = 200A, T_J = 150^\circ\text{C}$
		—	—	2.9		$I_F = 200A, V_{GE} = 0V$
V_{FM}	Diode forward voltage - maximum	—	—	2.9		$I_F = 200A, V_{GE} = 0V, T_J = 150^\circ\text{C}$
		—	2.8	—		$I_C = 1mA$
V_{GEth}	Gate threshold voltage	3.0	—	5.5	$V_{CE} = V_{GE}, I_C = 1mA$	
ΔV_{GEth}	Threshold voltage temp. coefficient	—	-11	—	mV/°C	$V_{CE} = 25V, I_C = 200A$
g_{fe}	Forward transconductance	104	—	144	S(Ω)	$V_{GE} = 0V, V_{CE} = 600V$
I_{CES}	Collector-to-emitter leakage current	—	—	2	mA	$V_{GE} = 0V, V_{CE} = 600V, T_J = 150^\circ\text{C}$
		—	—	20		$V_{GE} = 0V, V_{CE} = 600V, T_J = 150^\circ\text{C}$
I_{GES}	Gate-to-emitter leakage current	—	—	± 2	μA	$V_{GE} = \pm 20V$

Dynamic Characteristics - $T_J = 150^\circ\text{C}$

Parameter	Description	Min	Typ	Max	Units	Test Conditions
E_{on}	Turn-on switching energy	—	0.05	—	mJ/A	$R_{G1} = 27\Omega, R_{G2} = 0\Omega$
E_{off} (1)	Turn-off switching energy	—	0.17	—		$I_C = 200A, L_S = 100nH$
E_{ts} (1)	Total switching energy	—	—	0.3		$V_{CC} = 360V, V_{GE} = \pm 15V$
$t_{d(on)}$	Turn-on delay time	—	80	—	ns	$R_{G1} = 27\Omega, R_{G2} = 0\Omega$
t_r	Rise time	—	150	—		$I_C = 200A$
$t_{d(off)}$	Turn-off delay time	—	450	—		$V_{CC} = 360V, V_{GE} = \pm 15V$
t_f	Fall time	—	900	—		$L_S = 100nH$
I_{rr}	Diode peak recovery current	—	108	—	A	$R_{G1} = 27\Omega, R_{G2} = 0\Omega$
t_{rr}	Diode recovery time	—	115	—	ns	$I_C = 200A$
Q_{rr}	Diode recovery charge	—	6.5	—	μC	$V_{CC} = 360V, V_{GE} = \pm 15V$
Q_{ge}	Gate-to-emitter charge (turn-on)	300	—	560	nC	$V_{CC} = 360V$
Q_{gc}	Gate-to-collector charge (turn-on)	140	—	280		$I_C = 108A$
Q_g	Total gate charge (turn-on)	52	—	84		$V_{GE} = 15V$
C_{ies}	Input capacitance	—	11600	—	pF	$V_{GE} = 0V$
C_{oes}	Output capacitance	—	1320	—		$V_{CC} = 30V$
C_{res}	Reverse transfer capacitance	—	160	—		$f = 1MHz$

(1) Includes tail losses

Thermal and Mechanical Characteristics

Parameter	Description	Typ	Max	Units
R_{thJC} (IGBT)	Thermal resistance, junction to case, each IGBT	—	0.25	°C/W
R_{thJC} (Diode)	Thermal resistance, junction to case, each diode	—	0.4	
R_{thCS} (Module)	Thermal resistance, case to sink	0.1	—	
Wt	Weight of module	140	—	g

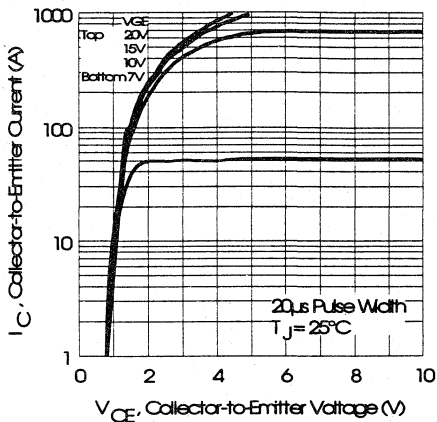


Fig. 1 - Typical Output Characteristics, $T_J = 25^\circ\text{C}$

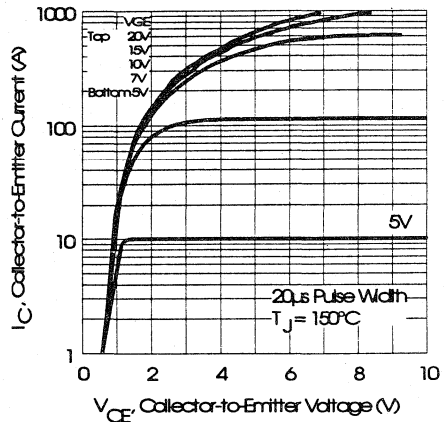


Fig. 2 - Typical Output Characteristics, $T_J = 150^\circ\text{C}$

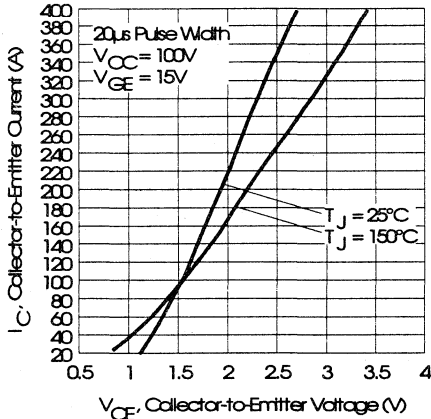


Fig. 3 - Typical Output Characteristics

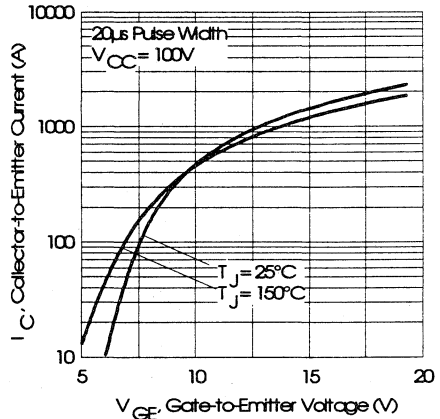


Fig. 4 - Typical Transfer Characteristics

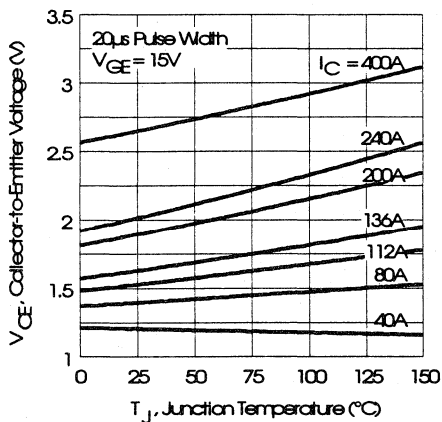


Fig. 5 - Collector-to-Emitter Saturation Typical Voltage vs. Junction Temperature

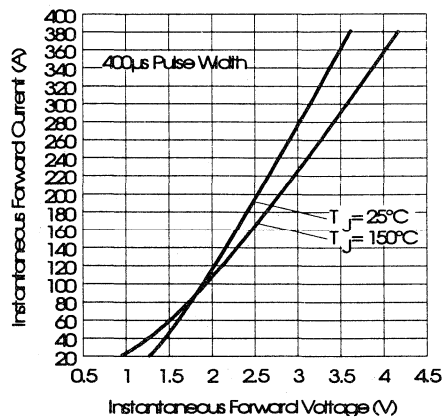


Fig. 6 - Forward Voltage Drop Characteristics

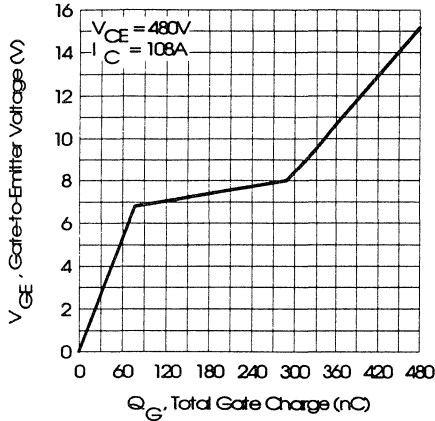


Fig. 7 - Typical Gate Charge vs. Gate-to-Emitter Voltage

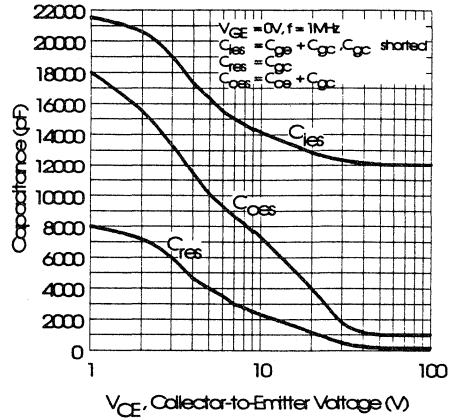


Fig. 8 - Typical Capacitance vs. Collector-to-Emitter Voltage

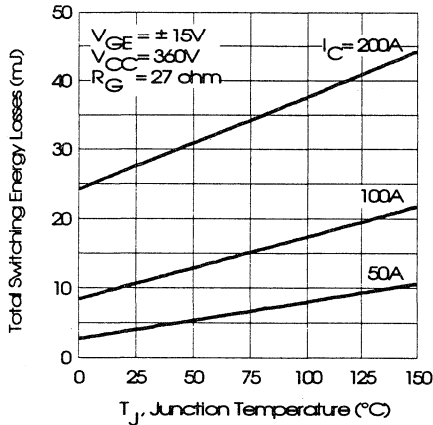


Fig. 9 - Typical Switching Losses vs. Junction Temperature

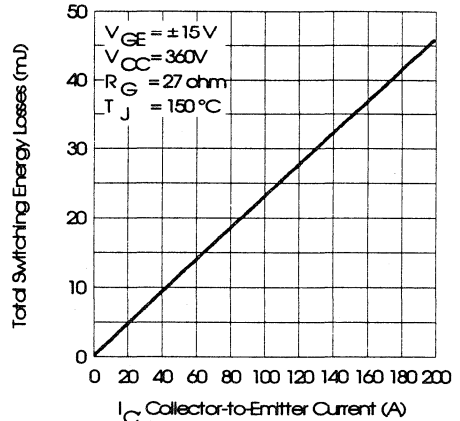


Fig. 10 - Typical Switching Losses vs. Collector-to-Emitter Current

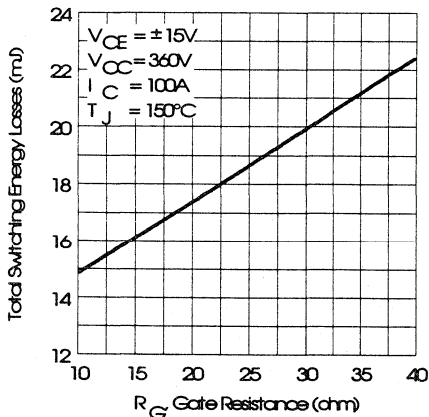


Fig. 11 - Typical Switching Losses vs. Gate Resistance

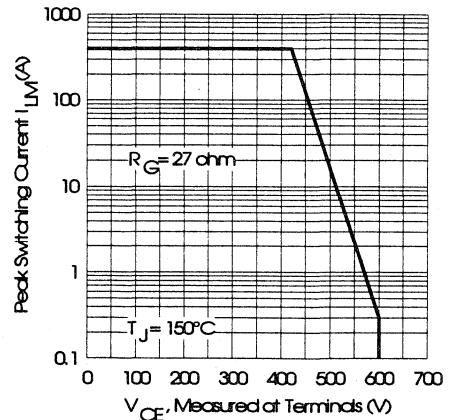


Fig. 12 - Reverse Bias Safe Operating Area

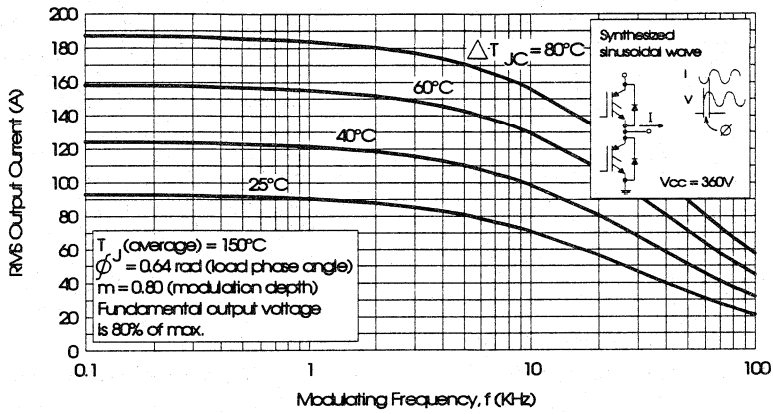


Fig. 13 - Typical RMS Output Current per phase vs. Frequency (Synthesized Sinusoidal Wave)

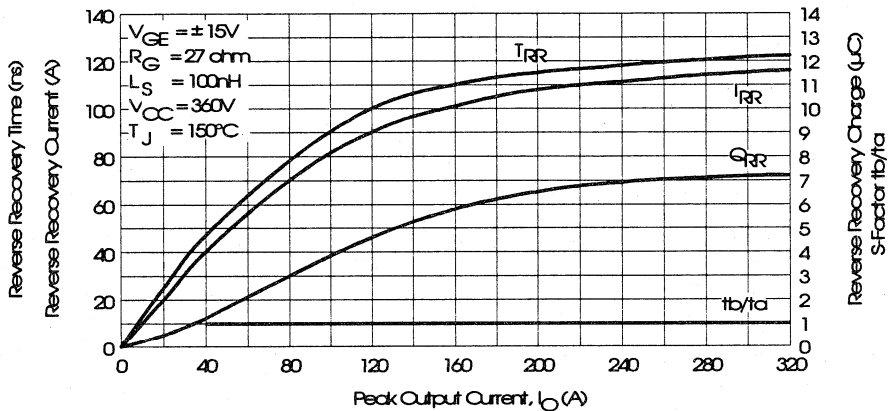


Fig. 14 - Typical Diode Recovery Characteristics as Function of Output Current I_o

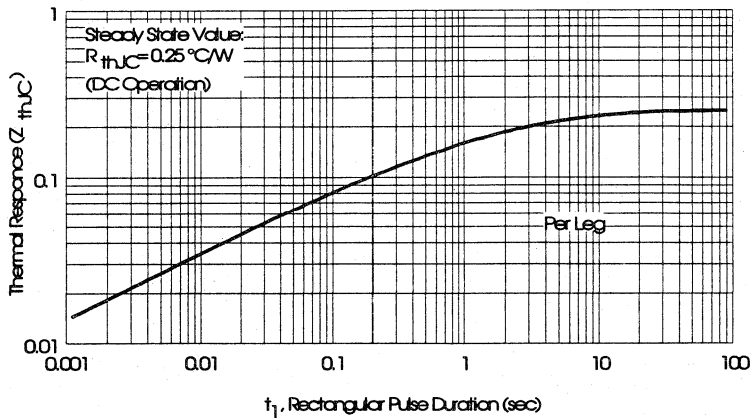


Fig. 15 - Maximum Effective Transient Thermal Impedance, Junction-to-Case

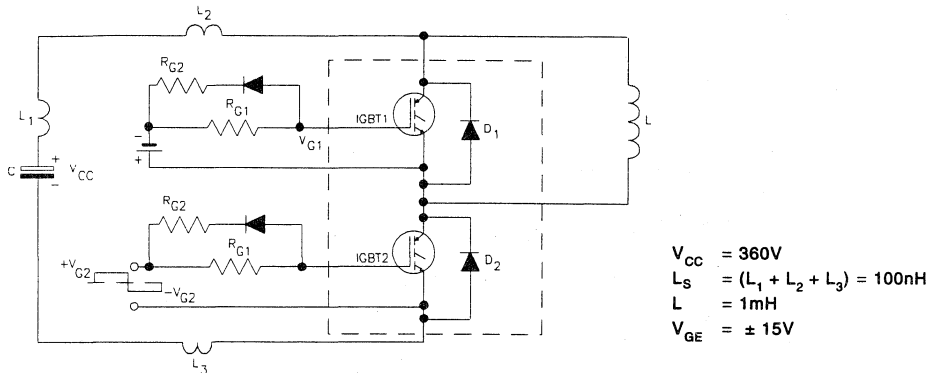


Fig. 16 - Test Circuit for Measurement of I_{LM} , E_{ON} , E_{OFF} , Q_{RR} , I_{RR} , $t_{D(ON)}$, t_r , $t_{D(OFF)}$, t_f

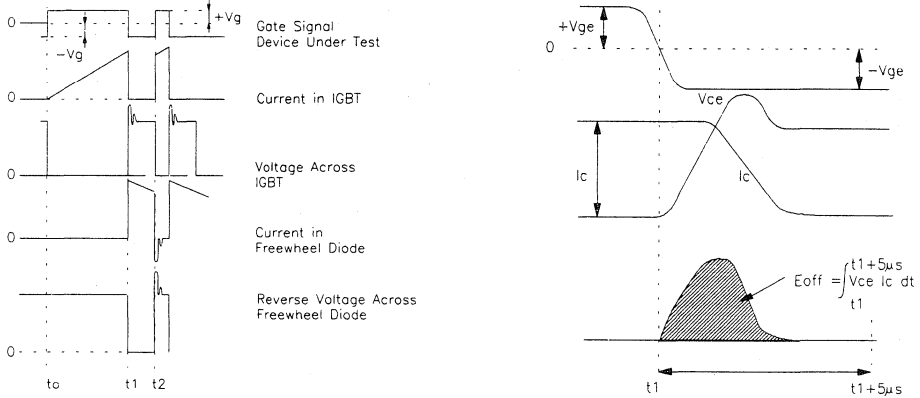


Fig. 17 - Test Waveforms for Circuit of Fig. 16

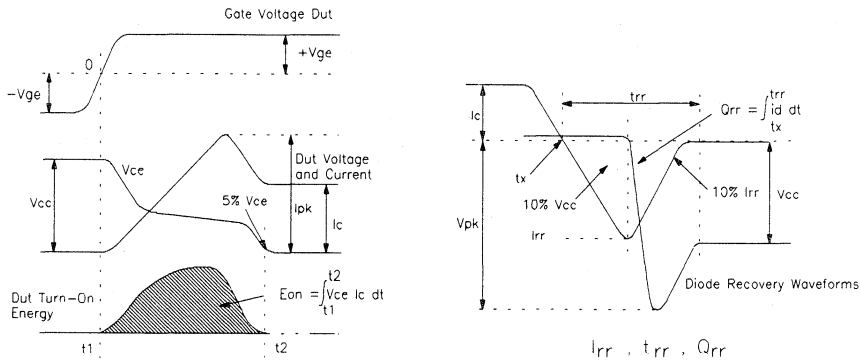


Fig. 18 - Test Waveforms for Circuit of Fig. 16, Defining E_{ON} , E_{REC} , $t_{D(ON)}$, t_r , I_{RR} , t_{RR} , Q_{RR}

Refer to Section D for the following:

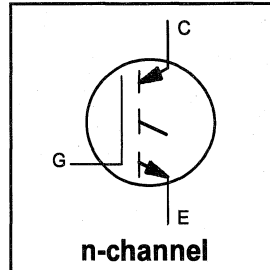
Appendix E: Section D - page D-7 Fig. 19 - Waveforms for Switching Time
 Package Outline 10 - INT-A-PAK Half Bridge Section D - Page D-16

INSULATED GATE BIPOLAR TRANSISTOR

Fast Speed IGBT

Features

- Switching-loss rating includes all "tail" losses
- Optimized for medium operating frequency (1 to 10kHz) See Fig. 1 for Current vs. Frequency curve



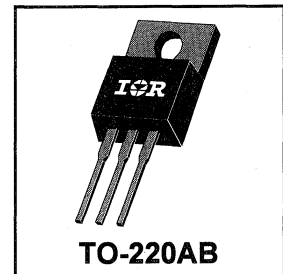
$$V_{CES} = 900V$$

$$V_{CE(sat)} \leq 4.3V$$

$$@V_{GE} = 15V, I_C = 5.3A$$

Description

Insulated Gate Bipolar Transistors (IGBTs) from International Rectifier have higher usable current densities than comparable bipolar transistors, while at the same time having simpler gate-drive requirements of the familiar power MOSFET. They provide substantial benefits to a host of high-voltage, high-current applications.



Absolute Maximum Ratings

	Parameter	Max.	Units
V_{CES}	Collector-to-Emitter Voltage	900	V
$I_C @ T_C = 25^\circ C$	Continuous Collector Current	9.0	A
$I_C @ T_C = 100^\circ C$	Continuous Collector Current	5.3	
I_{CM}	Pulsed Collector Current ①	18	
I_{LM}	Clamped Inductive Load Current ②	18	
V_{GE}	Gate-to-Emitter Voltage	± 20	V
E_{ARV}	Reverse Voltage Avalanche Energy ③	5.0	mJ
$P_D @ T_C = 25^\circ C$	Maximum Power Dissipation	60	W
$P_D @ T_C = 100^\circ C$	Maximum Power Dissipation	24	
T_J	Operating Junction and	-55 to +150	°C
T_{STG}	Storage Temperature Range		
	Soldering Temperature, for 10 sec.		
	Mounting torque, 6-32 or M3 screw.	10 lbf·in (1.1N·m)	

Thermal Resistance

	Parameter	Min.	Typ.	Max.	Units
$R_{\theta JC}$	Junction-to-Case	—	—	2.1	°C/W
$R_{\theta CS}$	Case-to-Sink, flat, greased surface	—	0.50	—	
$R_{\theta JA}$	Junction-to-Ambient, typical socket mount	—	—	80	
Wt	Weight	—	2.0 (0.07)	—	g (oz)

Electrical Characteristics @ $T_J = 25^\circ\text{C}$ (unless otherwise specified)

	Parameter	Min.	Typ.	Max.	Units	Conditions
$V_{(BR)CES}$	Collector-to-Emitter Breakdown Voltage	900	—	—	V	$V_{GE} = 0V, I_C = 250\mu A$
$V_{(BR)ECS}$	Emitter-to-Collector Breakdown Voltage ④	20	—	—	V	$V_{GE} = 0V, I_C = 1.0A$
$\Delta V_{(BR)CES}/\Delta T_J$	Temperature Coeff. of Breakdown Voltage	—	0.85	—	$V/^\circ\text{C}$	$V_{GE} = 0V, I_C = 1.0mA$
$V_{CE(on)}$	Collector-to-Emitter Saturation Voltage	—	2.9	4.3	V	$I_C = 5.3A$ $V_{GE} = 15V$ See Fig. 2, 5
		—	3.5	—		
		—	3.5	—		
$V_{GE(th)}$	Gate Threshold Voltage	3.0	—	5.5		$V_{CE} = V_{GE}, I_C = 250\mu A$
$\Delta V_{GE(th)}/\Delta T_J$	Temperature Coeff. of Threshold Voltage	—	-10	—	$mV/^\circ\text{C}$	$V_{CE} = V_{GE}, I_C = 250\mu A$
g_{fe}	Forward Transconductance ⑤	0.9	1.5	—	S	$V_{CE} = 100V, I_C = 5.3A$
I_{CES}	Zero Gate Voltage Collector Current	—	—	250	μA	$V_{GE} = 0V, V_{CE} = 900V$
		—	—	1000		$V_{GE} = 0V, V_{CE} = 900V, T_J = 150^\circ\text{C}$
I_{GES}	Gate-to-Emitter Leakage Current	—	—	± 100	nA	$V_{GE} = \pm 20V$

Switching Characteristics @ $T_J = 25^\circ\text{C}$ (unless otherwise specified)

	Parameter	Min.	Typ.	Max.	Units	Conditions
Q_g	Total Gate Charge (turn-on)	—	11	17	nC	$I_C = 5.3A$ See Fig. 8
Q_{ge}	Gate - Emitter Charge (turn-on)	—	2.6	3.9		$V_{CC} = 400V$
Q_{gc}	Gate - Collector Charge (turn-on)	—	4.6	6.9		$V_{GE} = 15V$
$t_{d(on)}$	Turn-On Delay Time	—	29	—	ns	$T_J = 25^\circ\text{C}$ $I_C = 5.3A, V_{CC} = 720V$ $V_{GE} = 15V, R_G = 50\Omega$ Energy losses include "tail"
t_r	Rise Time	—	12	—		
$t_{d(off)}$	Turn-Off Delay Time	—	170	300		
t_f	Fall Time	—	120	280		
E_{on}	Turn-On Switching Loss	—	0.25	—	mJ	See Fig. 9, 10, 11, 14
E_{off}	Turn-Off Switching Loss	—	0.36	—		
E_{ts}	Total Switching Loss	—	0.61	1.10		
$t_{d(on)}$	Turn-On Delay Time	—	27	—	ns	$T_J = 150^\circ\text{C}$, $I_C = 5.3A, V_{CC} = 720V$ $V_{GE} = 15V, R_G = 50\Omega$ Energy losses include "tail"
t_r	Rise Time	—	13	—		
$t_{d(off)}$	Turn-Off Delay Time	—	270	—		
t_f	Fall Time	—	240	—		
E_{ts}	Total Switching Loss	—	1.10	—	mJ	See Fig. 10, 14
L_E	Internal Emitter Inductance	—	7.5	—	nH	Measured 5mm from package
C_{ies}	Input Capacitance	—	220	—	pF	$V_{GE} = 0V$ $V_{CC} = 30V$ See Fig. 7 $f = 1.0MHz$
C_{oes}	Output Capacitance	—	25	—		
C_{res}	Reverse Transfer Capacitance	—	3.4	—		

Notes:

- ① Repetitive rating; $V_{GE} = 20V$, pulse width limited by max. junction temperature. (See fig. 13b)
- ② $V_{CC} = 80\%(V_{CES})$, $V_{GE} = 20V$, $L = 10\mu H$, $R_G = 50\Omega$, (See fig. 13a)
- ③ Repetitive rating; pulse width limited by maximum junction temperature.
- ④ Pulse width $\leq 80\mu s$; duty factor $\leq 0.1\%$.
- ⑤ Pulse width $5.0\mu s$, single shot.

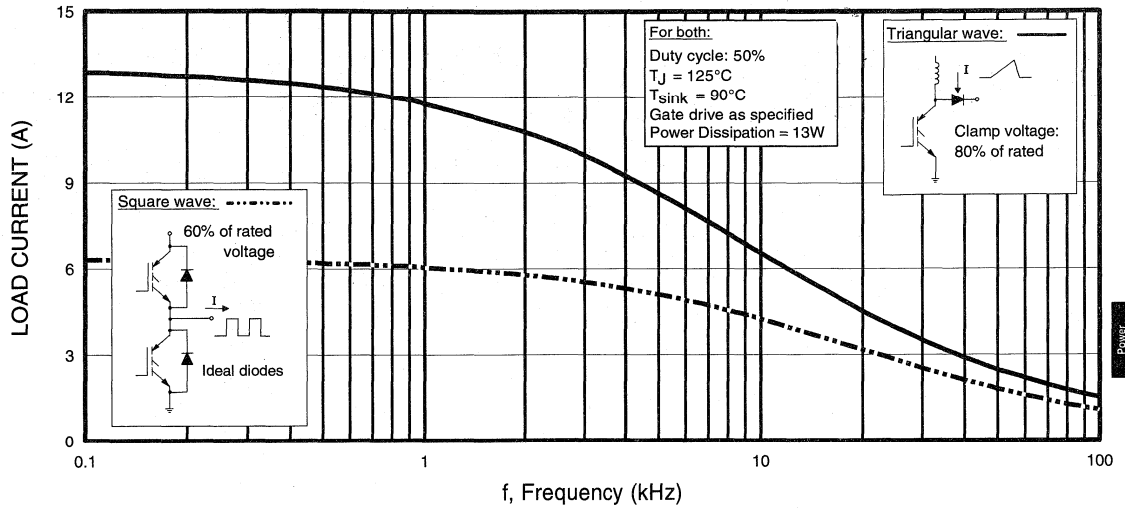


Fig. 1 - Typical Load Current vs. Frequency
 (For square wave, $I = I_{RMS}$ of fundamental; for triangular wave, $I = I_{PK}$)

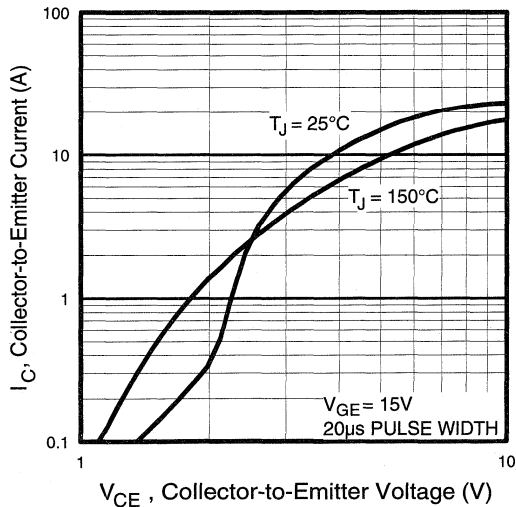


Fig. 2 - Typical Output Characteristics

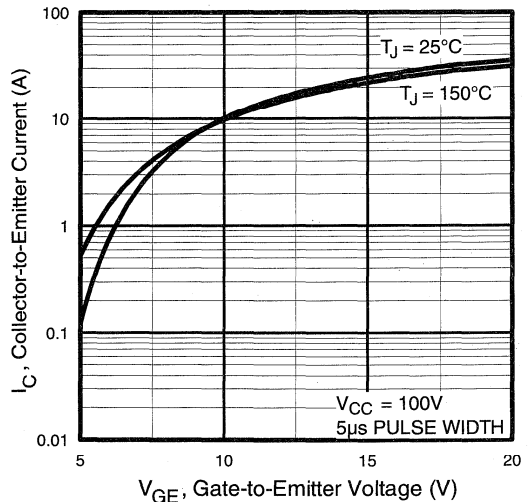


Fig. 3 - Typical Transfer Characteristics

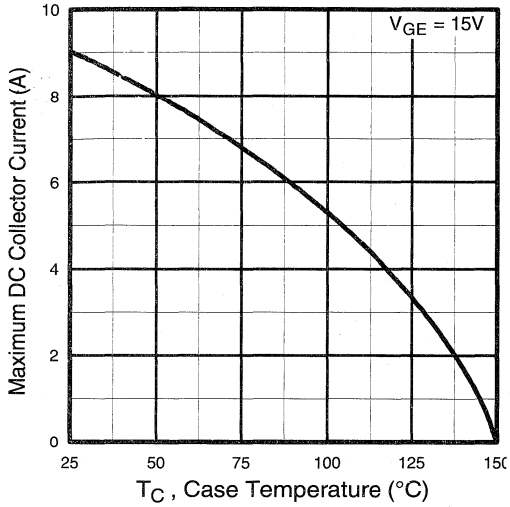


Fig. 4 - Maximum Collector Current vs. Case Temperature

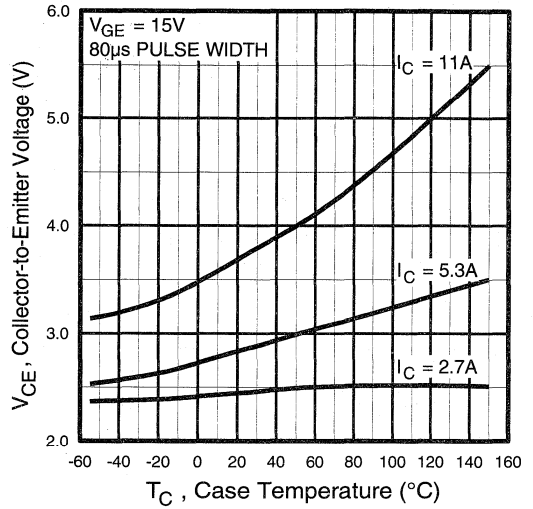


Fig. 5 - Collector-to-Emitter Voltage vs. Case Temperature

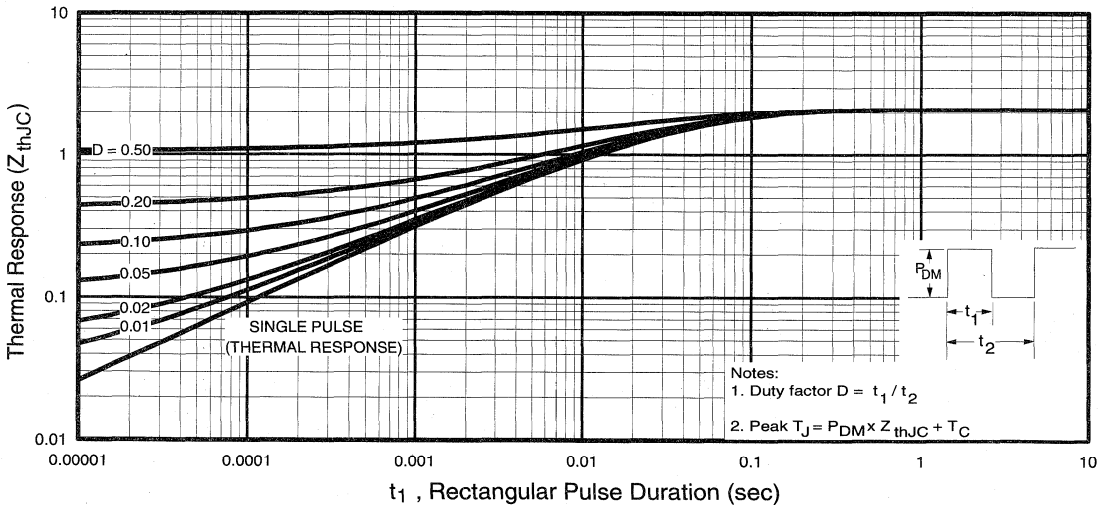


Fig. 6 - Maximum Effective Transient Thermal Impedance, Junction-to-Case

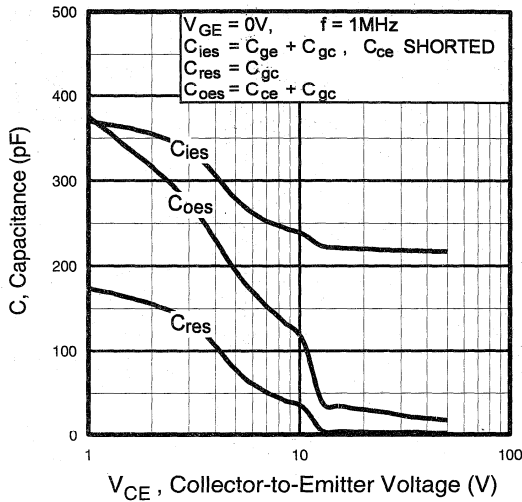


Fig. 7 - Typical Capacitance vs. Collector-to-Emitter Voltage

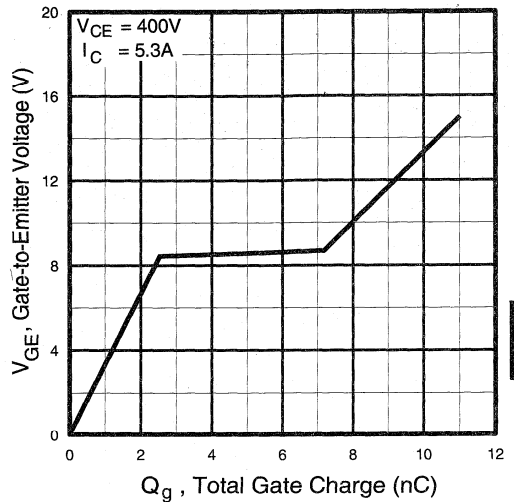


Fig. 8 - Typical Gate Charge vs. Gate-to-Emitter Voltage

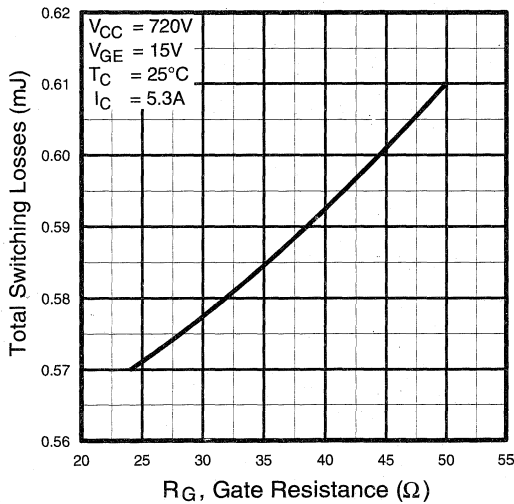


Fig. 9 - Typical Switching Losses vs. Gate Resistance

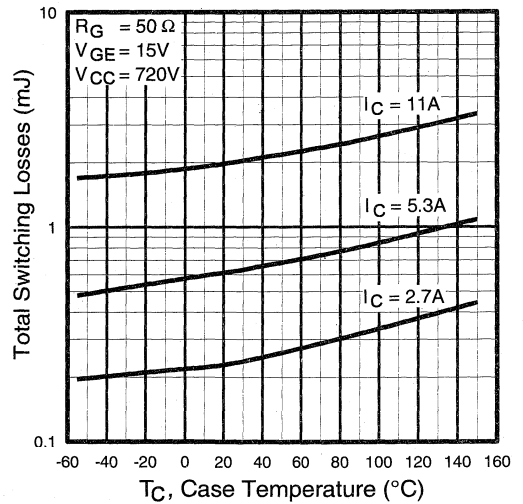


Fig. 10 - Typical Switching Losses vs. Case Temperature

Power Conversion Fast Discretes

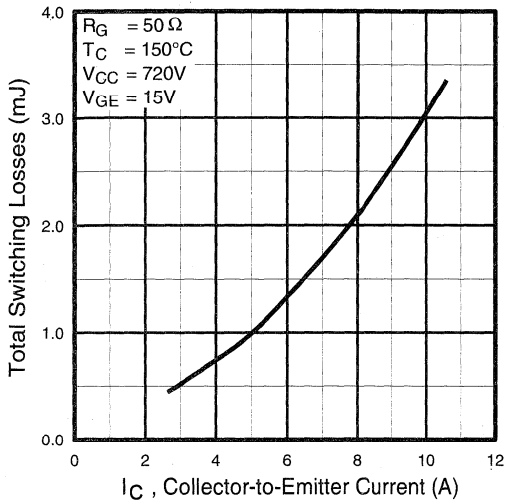


Fig. 11 - Typical Switching Losses vs. Collector-to-Emitter Current

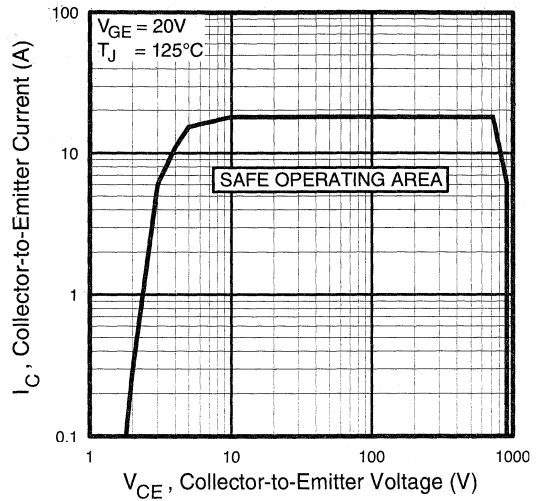


Fig. 12 - Turn-Off SOA

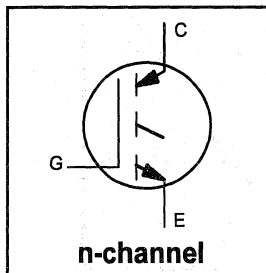
Refer to Section D for the following:

Appendix F: Section D - page D-8

- Fig. 13a - Clamped Inductive Load Test Circuit
- Fig. 13b - Pulsed Collector Current Test Circuit
- Fig. 14a - Switching Loss Test Circuit
- Fig. 14b - Switching Loss Waveform

Features

- Switching-loss rating includes all "tail" losses
- Optimized for medium operating frequency (1 to 10kHz) See Fig. 1 for Current vs. Frequency curve



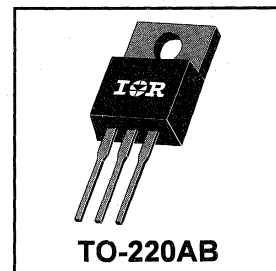
$$V_{CES} = 900V$$

$$V_{CE(sat)} \leq 3.7V$$

$$@V_{GE} = 15V, I_C = 11A$$

Description

Insulated Gate Bipolar Transistors (IGBTs) from International Rectifier have higher usable current densities than comparable bipolar transistors, while at the same time having simpler gate-drive requirements of the familiar power MOSFET. They provide substantial benefits to a host of high-voltage, high-current applications.


TO-220AB

Absolute Maximum Ratings

	Parameter	Max.	Units
V_{CES}	Collector-to-Emitter Voltage	900	V
$I_C @ T_C = 25^\circ C$	Continuous Collector Current	20	A
$I_C @ T_C = 100^\circ C$	Continuous Collector Current	11	
I_{CM}	Pulsed Collector Current ①	40	
I_{LM}	Clamped Inductive Load Current ②	40	
V_{GE}	Gate-to-Emitter Voltage	± 20	V
E_{ARV}	Reverse Voltage Avalanche Energy ③	10	mJ
$P_D @ T_C = 25^\circ C$	Maximum Power Dissipation	100	W
$P_D @ T_C = 100^\circ C$	Maximum Power Dissipation	42	
T_J	Operating Junction and Storage Temperature Range	-55 to +150	°C
T_{STG}	Soldering Temperature, for 10 sec.	300 (0.063 in. (1.6mm) from case)	
	Mounting torque, 6-32 or M3 screw.	10 lbf·in (1.1N·m)	

Thermal Resistance

	Parameter	Min.	Typ.	Max.	Units
$R_{\theta JC}$	Junction-to-Case	—	—	1.2	°C/W
$R_{\theta CS}$	Case-to-Sink, flat, greased surface	—	0.50	—	
$R_{\theta JA}$	Junction-to-Ambient, typical socket mount	—	—	80	
Wt	Weight	—	2.0 (0.07)	—	g (oz)

Electrical Characteristics @ $T_J = 25^\circ\text{C}$ (unless otherwise specified)

	Parameter	Min.	Typ.	Max.	Units	Conditions
$V_{(BR)CES}$	Collector-to-Emitter Breakdown Voltage	900	—	—	V	$V_{GE} = 0V, I_C = 250\mu A$
$V_{(BR)ECS}$	Emitter-to-Collector Breakdown Voltage ④	20	—	—	V	$V_{GE} = 0V, I_C = 1.0A$
$\Delta V_{(BR)CES}/\Delta T_J$	Temperature Coeff. of Breakdown Voltage	—	0.83	—	V/°C	$V_{GE} = 0V, I_C = 1.0mA$
$V_{CE(on)}$	Collector-to-Emitter Saturation Voltage	—	2.6	3.7	V	$I_C = 11A$
		—	3.3	—		$I_C = 20A$
		—	2.9	—		$I_C = 11A, T_J = 150^\circ\text{C}$
$V_{GE(th)}$	Gate Threshold Voltage	3.0	—	5.5		$V_{CE} = V_{GE}, I_C = 250\mu A$
$\Delta V_{GE(th)}/\Delta T_J$	Temperature Coeff. of Threshold Voltage	—	-11	—	mV/°C	$V_{CE} = V_{GE}, I_C = 250\mu A$
g_{fe}	Forward Transconductance ⑤	3.6	6.9	—	S	$V_{CE} = 100V, I_C = 11A$
I_{CES}	Zero Gate Voltage Collector Current	—	—	250	μA	$V_{GE} = 0V, V_{CE} = 900V$
		—	—	1000		$V_{GE} = 0V, V_{CE} = 900V, T_J = 150^\circ\text{C}$
I_{GES}	Gate-to-Emitter Leakage Current	—	—	± 100	nA	$V_{GE} = \pm 20V$

Switching Characteristics @ $T_J = 25^\circ\text{C}$ (unless otherwise specified)

	Parameter	Min.	Typ.	Max.	Units	Conditions
Q_g	Total Gate Charge (turn-on)	—	22	33	nC	$I_C = 11A$
Q_{ge}	Gate - Emitter Charge (turn-on)	—	5.1	7.7		$V_{CC} = 400V$
Q_{gc}	Gate - Collector Charge (turn-on)	—	8.0	12		$V_{GE} = 15V$
$t_{d(on)}$	Turn-On Delay Time	—	27	—	ns	$T_J = 25^\circ\text{C}$
t_r	Rise Time	—	9.7	—		$I_C = 11A, V_{CC} = 720V$
$t_{d(off)}$	Turn-Off Delay Time	—	160	280		$V_{GE} = 15V, R_G = 23\Omega$
t_f	Fall Time	—	140	240		Energy losses include "tail"
E_{on}	Turn-On Switching Loss	—	0.33	—	mJ	See Fig. 9, 10, 11, 14
E_{off}	Turn-Off Switching Loss	—	0.67	—		
E_{ts}	Total Switching Loss	—	1.0	1.9		
$t_{d(on)}$	Turn-On Delay Time	—	27	—	ns	$T_J = 150^\circ\text{C}$,
t_r	Rise Time	—	12	—		$I_C = 11A, V_{CC} = 720V$
$t_{d(off)}$	Turn-Off Delay Time	—	260	—		$V_{GE} = 15V, R_G = 23\Omega$
t_f	Fall Time	—	250	—		Energy losses include "tail"
E_{ts}	Total Switching Loss	—	2.0	—	mJ	See Fig. 10, 14
L_E	Internal Emitter Inductance	—	7.5	—	nH	Measured 5mm from package
C_{ies}	Input Capacitance	—	560	—	pF	$V_{GE} = 0V$
C_{oes}	Output Capacitance	—	50	—		$V_{CC} = 30V$
C_{res}	Reverse Transfer Capacitance	—	7.3	—		$f = 1.0MHz$

Notes:

- ① Repetitive rating; $V_{GE}=20V$, pulse width limited by max. junction temperature. (See fig. 13b)
- ② $V_{CC}=80\%(V_{CES}), V_{GE}=20V, L=10\mu H, R_G=23\Omega$, (See fig. 13a)
- ③ Repetitive rating; pulse width limited by maximum junction temperature.
- ④ Pulse width $\leq 80\mu s$; duty factor $\leq 0.1\%$.
- ⑤ Pulse width 5.0 μs , single shot.

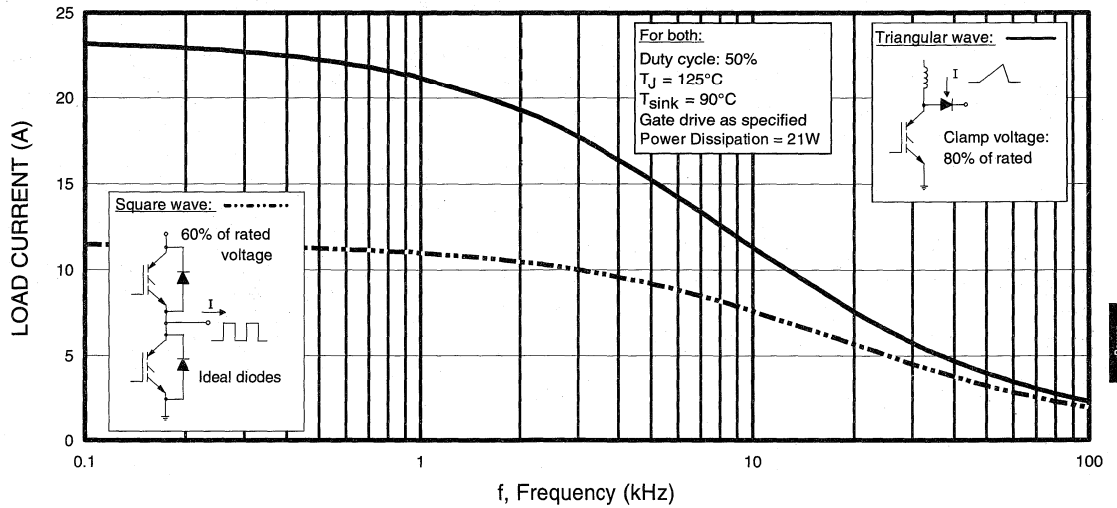


Fig. 1 - Typical Load Current vs. Frequency
 (For square wave, $I = I_{RMS}$ of fundamental; for triangular wave, $I = I_{PK}$)

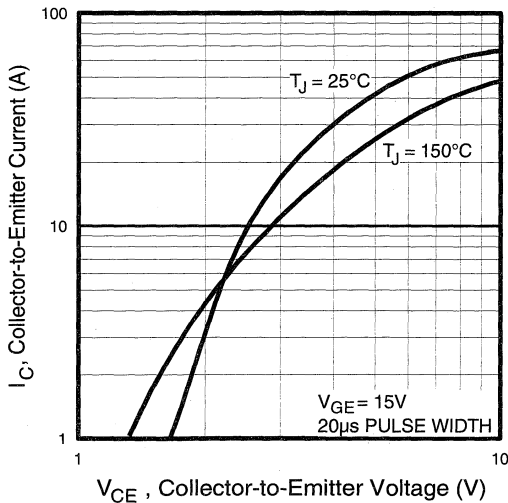


Fig. 2 - Typical Output Characteristics

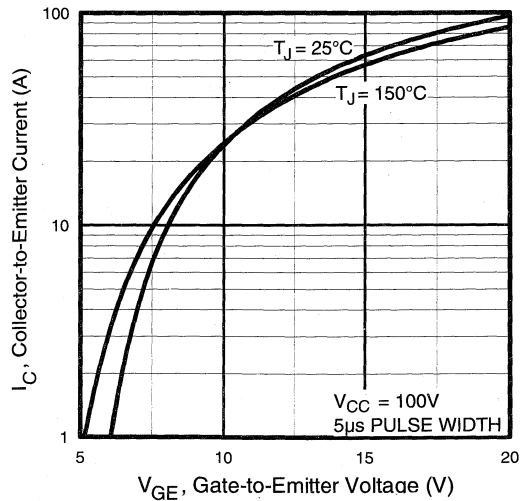


Fig. 3 - Typical Transfer Characteristics

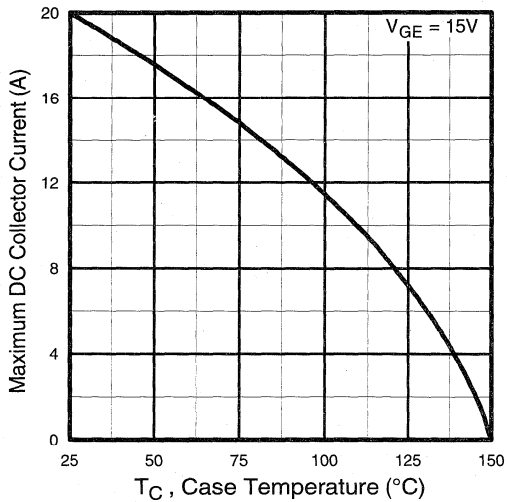


Fig. 4 - Maximum Collector Current vs. Case Temperature

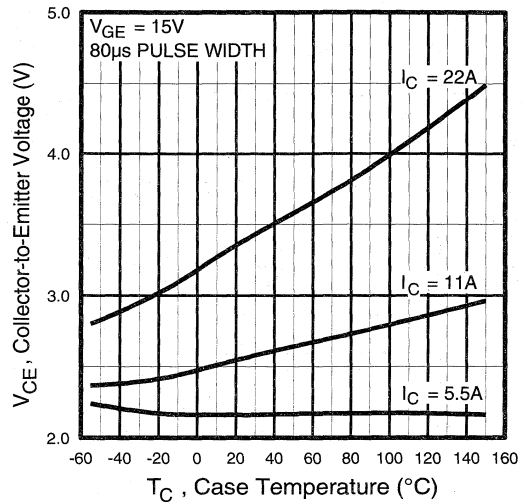


Fig. 5 - Collector-to-Emitter Voltage vs. Case Temperature

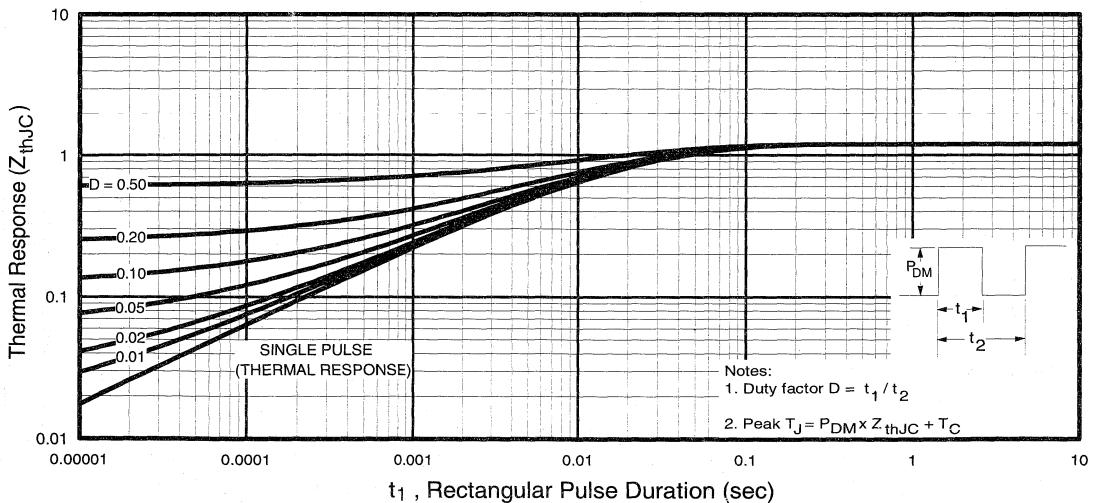


Fig. 6 - Maximum Effective Transient Thermal Impedance, Junction-to-Case

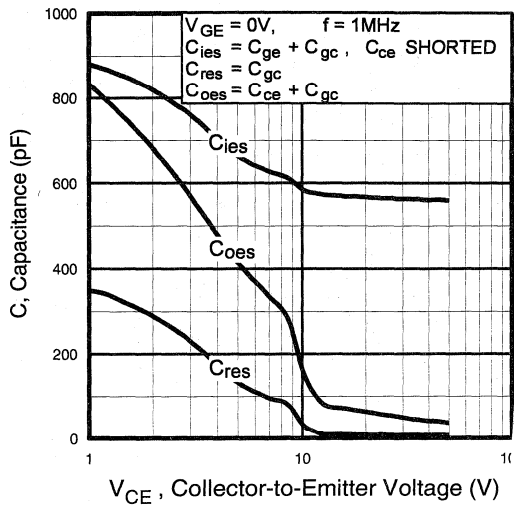


Fig. 7 - Typical Capacitance vs. Collector-to-Emitter Voltage

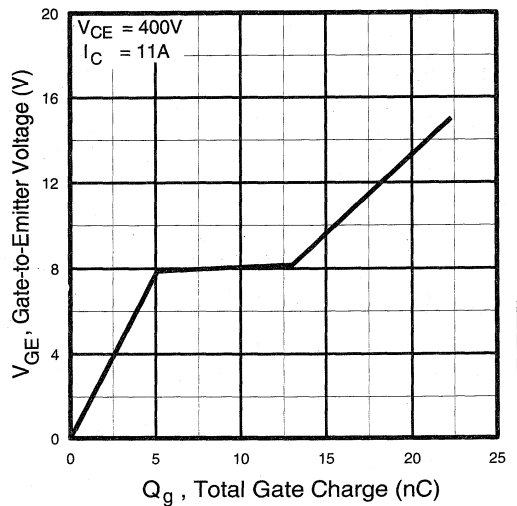


Fig. 8 - Typical Gate Charge vs. Gate-to-Emitter Voltage

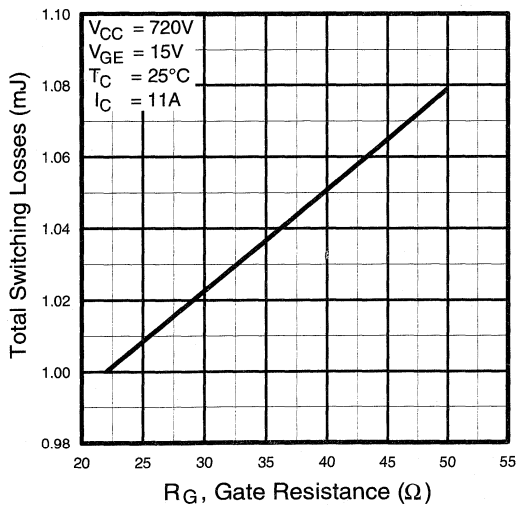


Fig. 9 - Typical Switching Losses vs. Gate Resistance

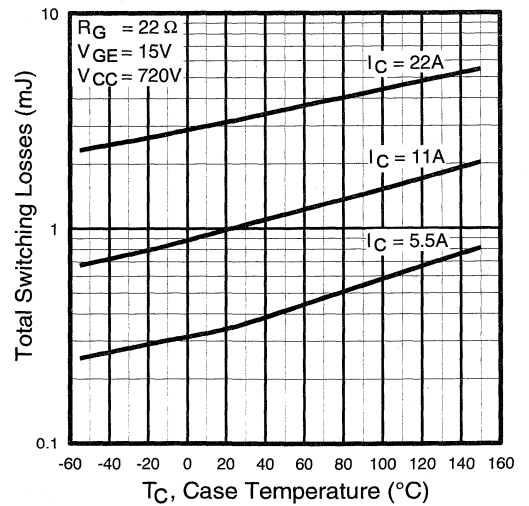


Fig. 10 - Typical Switching Losses vs. Case Temperature

Power Conversion Fast Discretes

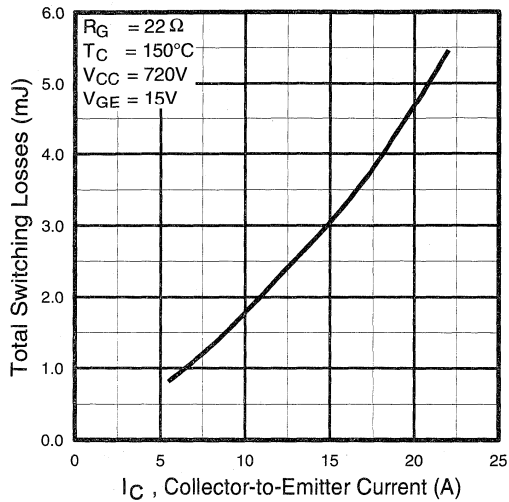


Fig. 11 - Typical Switching Losses vs. Collector-to-Emitter Current

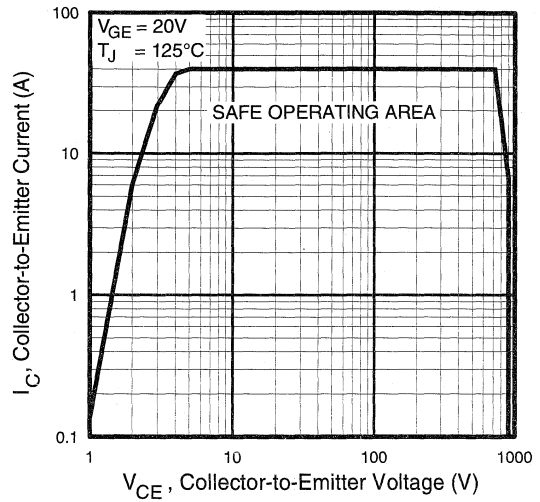


Fig. 12 - Turn-Off SOA

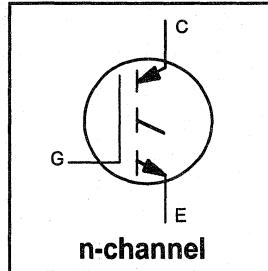
Refer to Section D for the following:

Appendix F: Section D - page D-8

- Fig. 13a - Clamped Inductive Load Test Circuit
- Fig. 13b - Pulsed Collector Current Test Circuit
- Fig. 14a - Switching Loss Test Circuit
- Fig. 14b - Switching Loss Waveform

Features

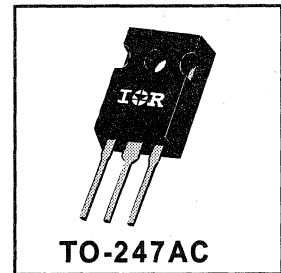
- Switching-loss rating includes all "tail" losses
- Optimized for medium operating frequency (1 to 10kHz) See Fig. 1 for Current vs. Frequency curve



$V_{CES} = 900V$
$V_{CE(sat)} \leq 4.3V$
@ $V_{GE} = 15V, I_C = 5.3A$

Description

Insulated Gate Bipolar Transistors (IGBTs) from International Rectifier have higher usable current densities than comparable bipolar transistors, while at the same time having simpler gate-drive requirements of the familiar power MOSFET. They provide substantial benefits to a host of high-voltage, high-current applications.



Power Conversion - Fast Discretes

Absolute Maximum Ratings

	Parameter	Max.	Units
V_{CES}	Collector-to-Emitter Voltage	900	V
$I_C @ T_C = 25^\circ C$	Continuous Collector Current	9.0	A
$I_C @ T_C = 100^\circ C$	Continuous Collector Current	5.3	
I_{CM}	Pulsed Collector Current ①	18	
I_{LM}	Clamped Inductive Load Current ②	18	
V_{GE}	Gate-to-Emitter Voltage	± 20	
E_{ARV}	Reverse Voltage Avalanche Energy ③	5.0	mJ
$P_D @ T_C = 25^\circ C$	Maximum Power Dissipation	60	W
$P_D @ T_C = 100^\circ C$	Maximum Power Dissipation	24	
T_J	Operating Junction and	-55 to +150	°C
T_{STG}	Storage Temperature Range		
	Soldering Temperature, for 10 sec.	300 (0.063 in. (1.6mm) from case)	
	Mounting torque, 6-32 or M3 screw.	10 lbf·in (1.1N·m)	

Thermal Resistance

	Parameter	Min.	Typ.	Max.	Units
$R_{\theta JC}$	Junction-to-Case	—	—	2.1	°C/W
$R_{\theta CS}$	Case-to-Sink, flat, greased surface	—	0.24	—	
$R_{\theta JA}$	Junction-to-Ambient, typical socket mount	—	—	40	
Wt	Weight	—	6 (0.21)	—	g (oz)

Electrical Characteristics @ $T_J = 25^\circ\text{C}$ (unless otherwise specified)

	Parameter	Min.	Typ.	Max.	Units	Conditions
$V_{(BR)CES}$	Collector-to-Emitter Breakdown Voltage	900	—	—	V	$V_{GE} = 0V, I_C = 250\mu A$
$V_{(BR)ECS}$	Emitter-to-Collector Breakdown Voltage ③	20	—	—	V	$V_{GE} = 0V, I_C = 1.0A$
$\Delta V_{(BR)CES}/\Delta T_J$	Temperature Coeff. of Breakdown Voltage	—	0.85	—	V/ $^\circ\text{C}$	$V_{GE} = 0V, I_C = 1.0mA$
$V_{CE(on)}$	Collector-to-Emitter Saturation Voltage	—	2.9	4.3	V	$I_C = 5.3A$ $V_{GE} = 15V$ $I_C = 9.0A$ See Fig. 2, 5 $I_C = 5.3A, T_J = 150^\circ\text{C}$
		—	3.5	—		
		—	3.5	—		
$V_{GE(th)}$	Gate Threshold Voltage	3.0	—	5.5		$V_{CE} = V_{GE}, I_C = 250\mu A$
$\Delta V_{GE(th)}/\Delta T_J$	Temperature Coeff. of Threshold Voltage	—	-10	—	mV/ $^\circ\text{C}$	$V_{CE} = V_{GE}, I_C = 250\mu A$
g_{fe}	Forward Transconductance ⑤	0.9	1.5	—	S	$V_{CE} = 100V, I_C = 5.3A$
I_{CES}	Zero Gate Voltage Collector Current	—	—	250	μA	$V_{GE} = 0V, V_{CE} = 900V$
		—	—	1000		$V_{GE} = 0V, V_{CE} = 900V, T_J = 150^\circ\text{C}$
I_{GES}	Gate-to-Emitter Leakage Current	—	—	± 100	nA	$V_{GE} = \pm 20V$

Switching Characteristics @ $T_J = 25^\circ\text{C}$ (unless otherwise specified)

	Parameter	Min.	Typ.	Max.	Units	Conditions
Q_g	Total Gate Charge (turn-on)	—	11	17	nC	$I_C = 5.3A$ $V_{CC} = 400V$ See Fig. 8 $V_{GE} = 15V$
Q_{ge}	Gate - Emitter Charge (turn-on)	—	2.6	3.9		
Q_{gc}	Gate - Collector Charge (turn-on)	—	4.6	6.9		
$t_{d(on)}$	Turn-On Delay Time	—	29	—	ns	$T_J = 25^\circ\text{C}$ $I_C = 5.3A, V_{CC} = 720V$ $V_{GE} = 15V, R_G = 50\Omega$ Energy losses include "tail"
t_r	Rise Time	—	12	—		
$t_{d(off)}$	Turn-Off Delay Time	—	170	300		
t_f	Fall Time	—	120	280		
E_{on}	Turn-On Switching Loss	—	0.25	—	mJ	See Fig. 9, 10, 11, 14
E_{off}	Turn-Off Switching Loss	—	0.36	—		
E_{ts}	Total Switching Loss	—	0.61	1.10		
$t_{d(on)}$	Turn-On Delay Time	—	27	—	ns	$T_J = 150^\circ\text{C}$, $I_C = 5.3A, V_{CC} = 720V$ $V_{GE} = 15V, R_G = 50\Omega$ Energy losses include "tail"
t_r	Rise Time	—	13	—		
$t_{d(off)}$	Turn-Off Delay Time	—	270	—		
t_f	Fall Time	—	240	—		
E_{ts}	Total Switching Loss	—	1.10	—	mJ	See Fig. 10, 14
L_E	Internal Emitter Inductance	—	13	—	nH	Measured 5mm from package
C_{ies}	Input Capacitance	—	220	—	pF	$V_{GE} = 0V$ $V_{CC} = 30V$ See Fig. 7 $f = 1.0MHz$
C_{oes}	Output Capacitance	—	25	—		
C_{res}	Reverse Transfer Capacitance	—	3.4	—		

Notes:

- ① Repetitive rating; $V_{GE}=20V$, pulse width limited by max. junction temperature. (See fig. 13b)
- ② $V_{CC}=80\%(V_{CES})$, $V_{GE}=20V$, $L=10\mu H$, $R_G=50\Omega$, (See fig. 13a)
- ③ Repetitive rating; pulse width limited by maximum junction temperature.
- ④ Pulse width $\leq 80\mu s$; duty factor $\leq 0.1\%$.
- ⑤ Pulse width 5.0 μs , single shot.

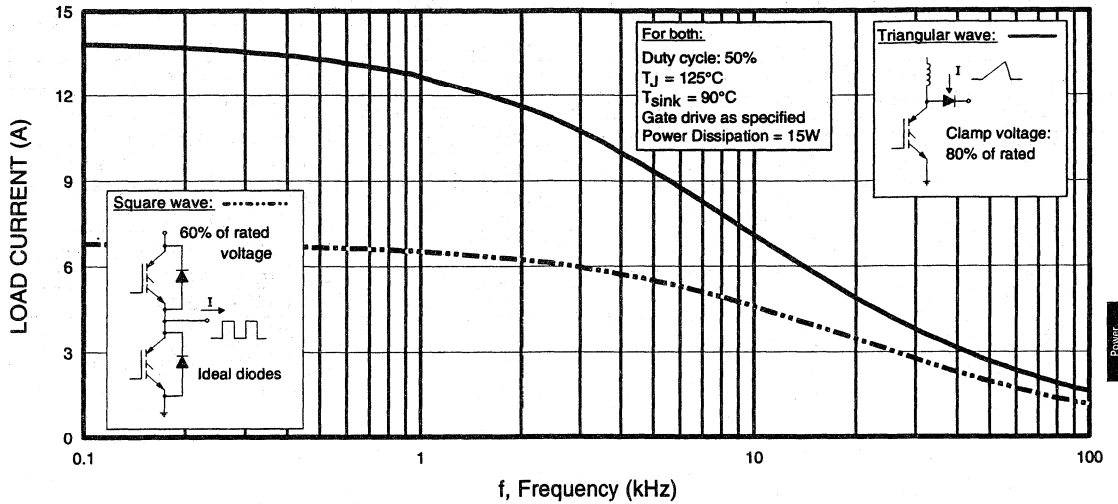


Fig. 1 - Typical Load Current vs. Frequency
 (For square wave, $I = I_{RMS}$ of fundamental; for triangular wave, $I = I_{PK}$)

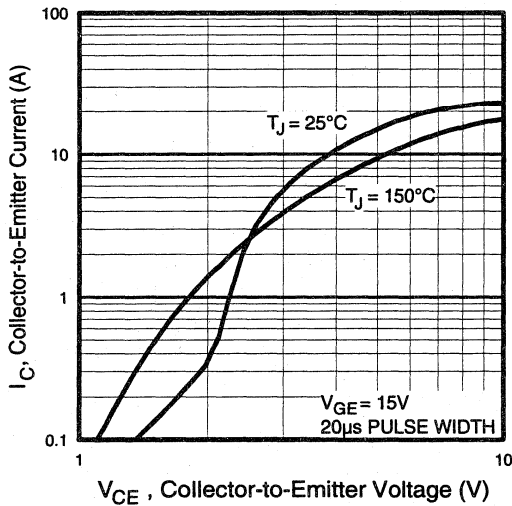


Fig. 2 - Typical Output Characteristics

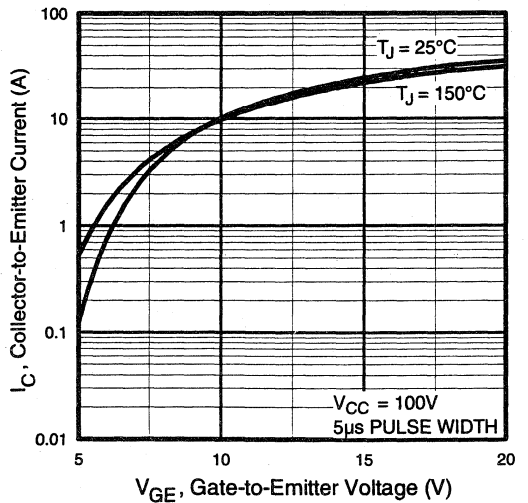


Fig. 3 - Typical Transfer Characteristics

Power
Conversion
Fast
Discretes

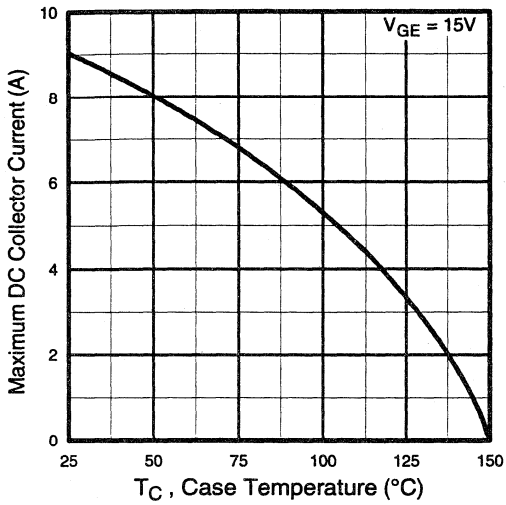


Fig. 4 - Maximum Collector Current vs. Case Temperature

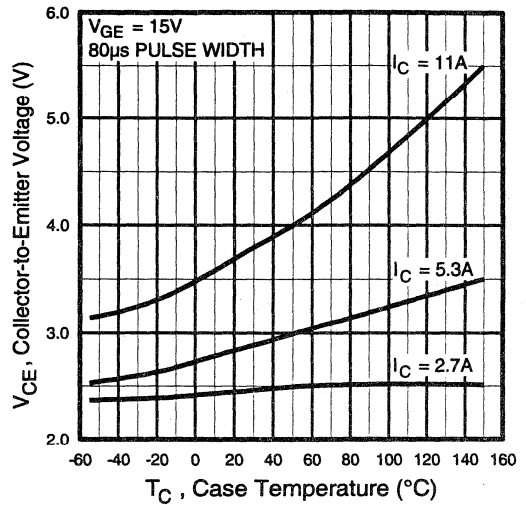


Fig. 5 - Collector-to-Emitter Voltage vs. Case Temperature

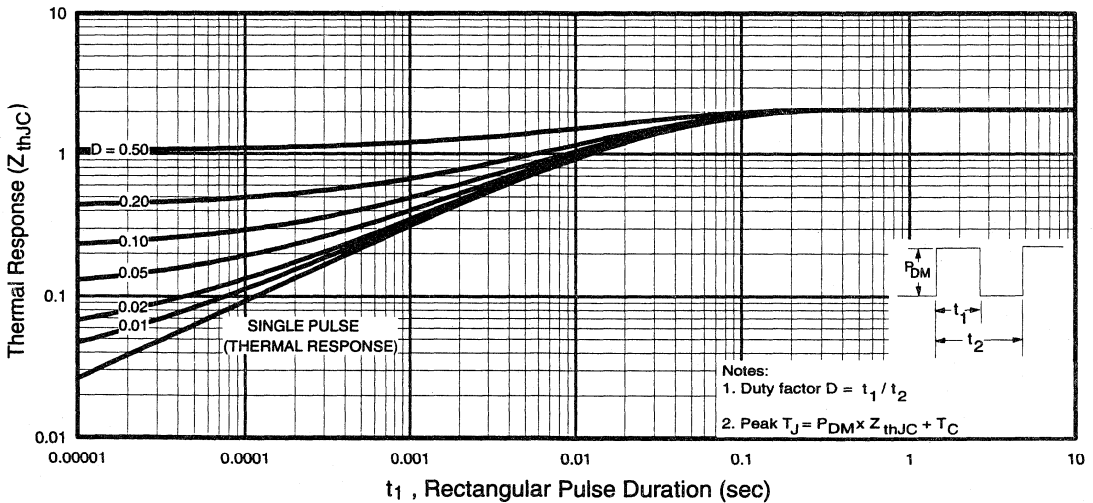


Fig. 6 - Maximum Effective Transient Thermal Impedance, Junction-to-Case

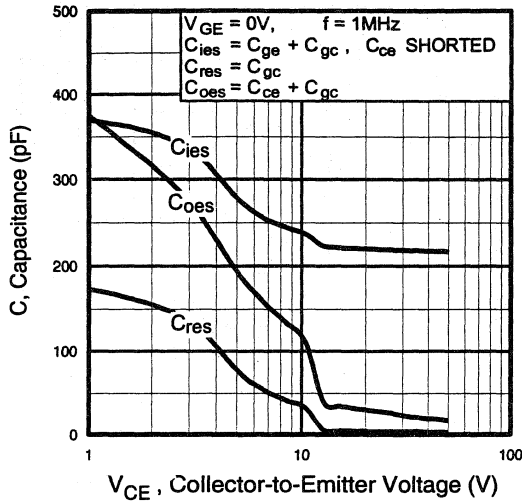


Fig. 7 - Typical Capacitance vs. Collector-to-Emitter Voltage

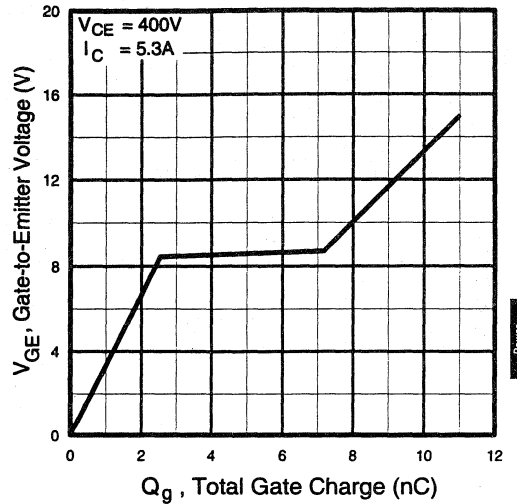


Fig. 8 - Typical Gate Charge vs. Gate-to-Emitter Voltage

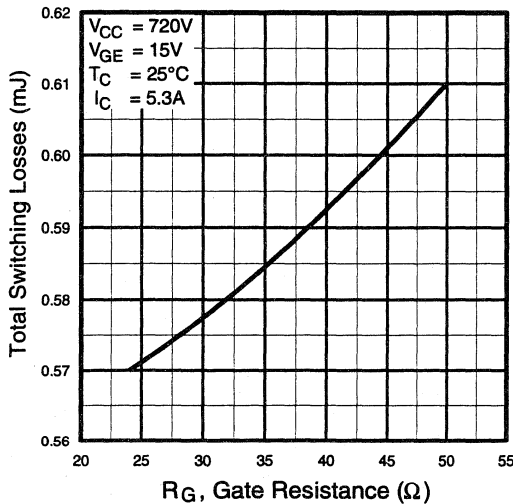


Fig. 9 - Typical Switching Losses vs. Gate Resistance

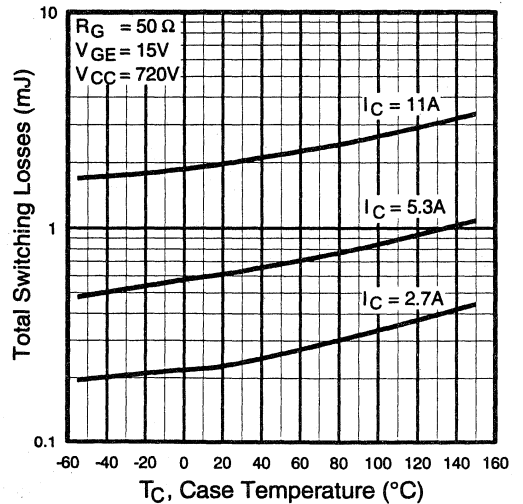


Fig. 10 - Typical Switching Losses vs. Case Temperature

Power
Conversion
Fast
Discretes

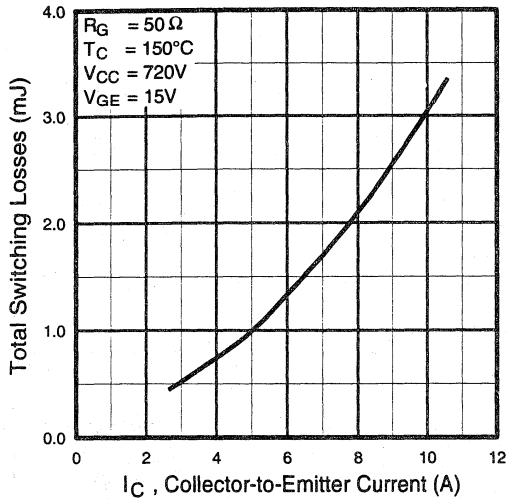


Fig. 11 - Typical Switching Losses vs. Collector-to-Emitter Current

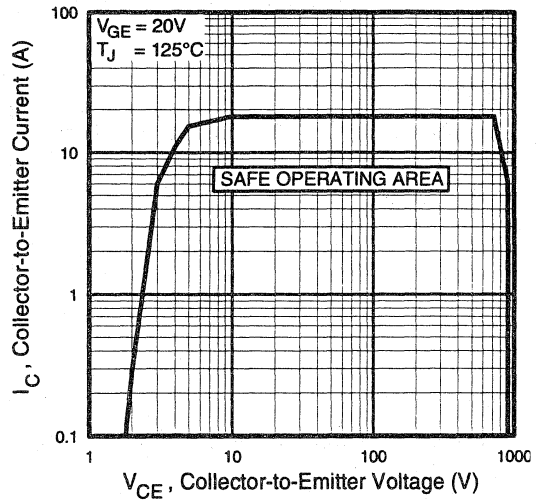


Fig. 12 - Turn-Off SOA

Refer to Section D for the following:

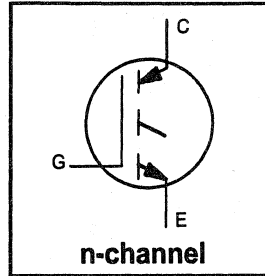
Appendix F: Section D - page D-8

- Fig. 13a - Clamped Inductive Load Test Circuit
- Fig. 13b - Pulsed Collector Current Test Circuit
- Fig. 14a - Switching Loss Test Circuit
- Fig. 14b - Switching Loss Waveform

Package Outline 3 - JEDEC Outline TO-247AC (TO-3P) Section D - page D-13

Features

- Switching-loss rating includes all "tail" losses
- Optimized for medium operating frequency (1 to 10kHz) See Fig. 1 for Current vs. Frequency curve



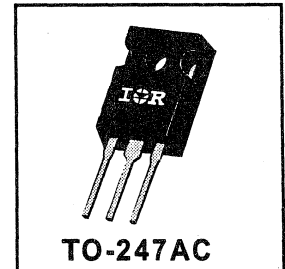
$$V_{CES} = 900V$$

$$V_{CE(sat)} \leq 3.7V$$

$$@V_{GE} = 15V, I_C = 11A$$

Description

Insulated Gate Bipolar Transistors (IGBTs) from International Rectifier have higher usable current densities than comparable bipolar transistors, while at the same time having simpler gate-drive requirements of the familiar power MOSFET. They provide substantial benefits to a host of high-voltage, high-current applications.



Absolute Maximum Ratings

	Parameter	Max.	Units
V_{CES}	Collector-to-Emitter Voltage	900	V
$I_C @ T_C = 25^\circ C$	Continuous Collector Current	20	A
$I_C @ T_C = 100^\circ C$	Continuous Collector Current	11	
I_{CM}	Pulsed Collector Current ①	40	
I_{LM}	Clamped Inductive Load Current ②	40	
V_{GE}	Gate-to-Emitter Voltage	± 20	V
E_{ARV}	Reverse Voltage Avalanche Energy ③	10	mJ
$P_D @ T_C = 25^\circ C$	Maximum Power Dissipation	100	W
$P_D @ T_C = 100^\circ C$	Maximum Power Dissipation	42	
T_J	Operating Junction and	-55 to +150	°C
T_{STG}	Storage Temperature Range		
	Soldering Temperature, for 10 sec.		
	Mounting torque, 6-32 or M3 screw.	10 lbf·in (1.1N·m)	

Thermal Resistance

	Parameter	Min.	Typ.	Max.	Units
$R_{\theta JC}$	Junction-to-Case	—	—	1.2	°C/W
$R_{\theta CS}$	Case-to-Sink, flat, greased surface	—	0.24	—	
$R_{\theta JA}$	Junction-to-Ambient, typical socket mount	—	—	40	
Wt	Weight	—	6 (0.21)	—	g (oz)

Electrical Characteristics @ $T_J = 25^\circ\text{C}$ (unless otherwise specified)

	Parameter	Min.	Typ.	Max.	Units	Conditions
$V_{(BR)CES}$	Collector-to-Emitter Breakdown Voltage	900	—	—	V	$V_{GE} = 0V, I_C = 250\mu A$
$V_{(BR)ECS}$	Emitter-to-Collector Breakdown Voltage ②	20	—	—	V	$V_{GE} = 0V, I_C = 1.0A$
$\Delta V_{(BR)CES}/\Delta T_J$	Temperature Coeff. of Breakdown Voltage	—	0.83	—	$V/^\circ\text{C}$	$V_{GE} = 0V, I_C = 1.0mA$
$V_{CE(on)}$	Collector-to-Emitter Saturation Voltage	—	2.6	3.7	V	$I_C = 11A, V_{GE} = 15V$
		—	3.3	—		$I_C = 20A$
		—	2.9	—		$I_C = 11A, T_J = 150^\circ\text{C}$
$V_{GE(th)}$	Gate Threshold Voltage	3.0	—	5.5		$V_{CE} = V_{GE}, I_C = 250\mu A$
$\Delta V_{GE(th)}/\Delta T_J$	Temperature Coeff. of Threshold Voltage	—	-11	—	$mV/^\circ\text{C}$	$V_{CE} = V_{GE}, I_C = 250\mu A$
g_{fe}	Forward Transconductance ③	3.6	6.9	—	S	$V_{CE} = 100V, I_C = 11A$
I_{CES}	Zero Gate Voltage Collector Current	—	—	250	μA	$V_{GE} = 0V, V_{CE} = 900V$
		—	—	1000		$V_{GE} = 0V, V_{CE} = 900V, T_J = 150^\circ\text{C}$
I_{GES}	Gate-to-Emitter Leakage Current	—	—	± 100	nA	$V_{GE} = \pm 20V$

Switching Characteristics @ $T_J = 25^\circ\text{C}$ (unless otherwise specified)

	Parameter	Min.	Typ.	Max.	Units	Conditions
Q_g	Total Gate Charge (turn-on)	—	22	33	nC	$I_C = 11A$
Q_{ge}	Gate - Emitter Charge (turn-on)	—	5.1	7.7		$V_{CC} = 400V$
Q_{gc}	Gate - Collector Charge (turn-on)	—	8.0	12		$V_{GE} = 15V$
$t_{d(on)}$	Turn-On Delay Time	—	27	—	ns	$T_J = 25^\circ\text{C}$
t_r	Rise Time	—	9.7	—		$I_C = 11A, V_{CC} = 720V$
$t_{d(off)}$	Turn-Off Delay Time	—	160	280		$V_{GE} = 15V, R_G = 23\Omega$
t_f	Fall Time	—	140	240		Energy losses include "tail"
E_{on}	Turn-On Switching Loss	—	0.33	—	mJ	See Fig. 9, 10, 11, 14
E_{off}	Turn-Off Switching Loss	—	0.67	—		
E_{ts}	Total Switching Loss	—	1.0	1.9		
$t_{d(on)}$	Turn-On Delay Time	—	27	—	ns	$T_J = 150^\circ\text{C}$,
t_r	Rise Time	—	12	—		$I_C = 11A, V_{CC} = 720V$
$t_{d(off)}$	Turn-Off Delay Time	—	260	—		$V_{GE} = 15V, R_G = 23\Omega$
t_f	Fall Time	—	250	—		Energy losses include "tail"
E_{ts}	Total Switching Loss	—	2.0	—	mJ	See Fig. 10, 14
L_E	Internal Emitter Inductance	—	13	—	nH	Measured 5mm from package
C_{ies}	Input Capacitance	—	560	—	pF	$V_{GE} = 0V$
C_{oes}	Output Capacitance	—	50	—		$V_{CC} = 30V$
C_{res}	Reverse Transfer Capacitance	—	7.3	—		$f = 1.0MHz$

Notes:

- ① Repetitive rating; $V_{GE}=20V$, pulse width limited by max. junction temperature. (See fig. 13b)
- ② $V_{CC}=80\%(V_{CES}), V_{GE}=20V, L=10\mu H, R_G=23\Omega$, (See fig. 13a)
- ③ Repetitive rating; pulse width limited by maximum junction temperature.
- ④ Pulse width $\leq 80\mu s$; duty factor $\leq 0.1\%$.
- ⑤ Pulse width 5.0 μs , single shot.

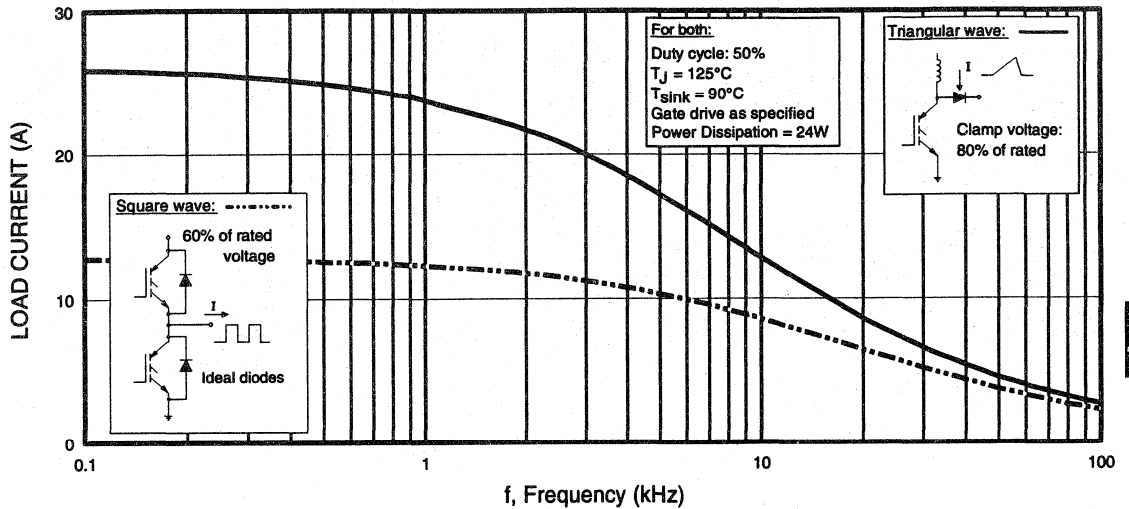


Fig. 1 - Typical Load Current vs. Frequency
 (For square wave, $I = I_{RMS}$ of fundamental; for triangular wave, $I = I_{PK}$)

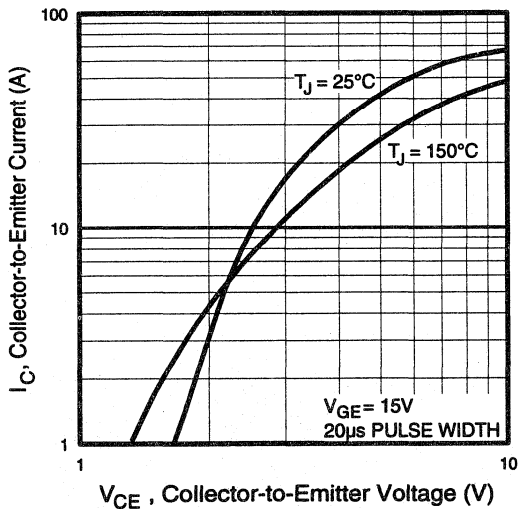


Fig. 2 - Typical Output Characteristics

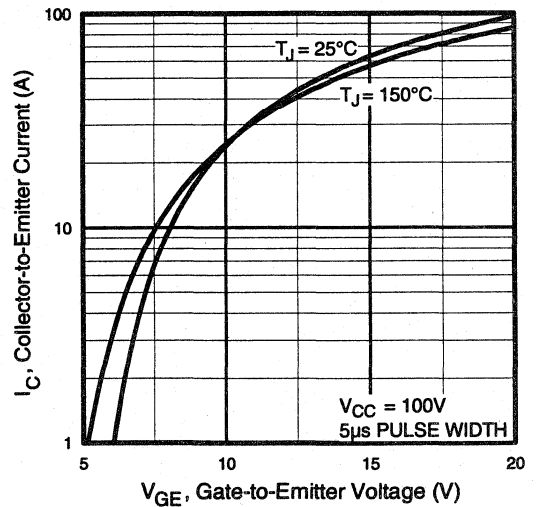


Fig. 3 - Typical Transfer Characteristics

Power
Conversion
Fast
Discretes

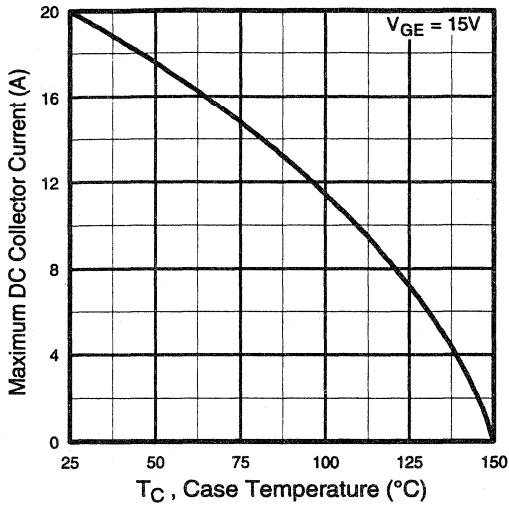


Fig. 4 - Maximum Collector Current vs. Case Temperature

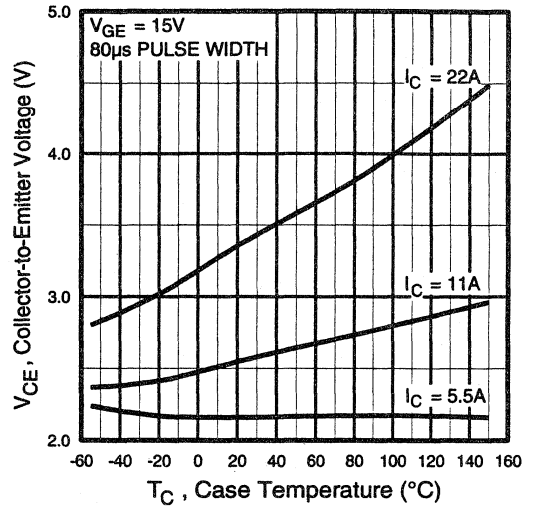


Fig. 5 - Collector-to-Emitter Voltage vs. Case Temperature

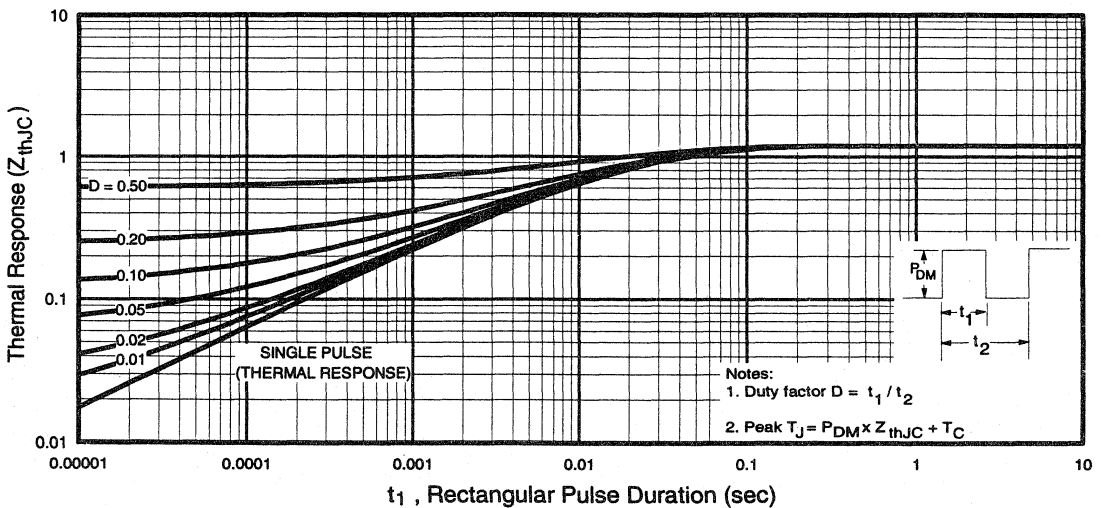


Fig. 6 - Maximum Effective Transient Thermal Impedance, Junction-to-Case

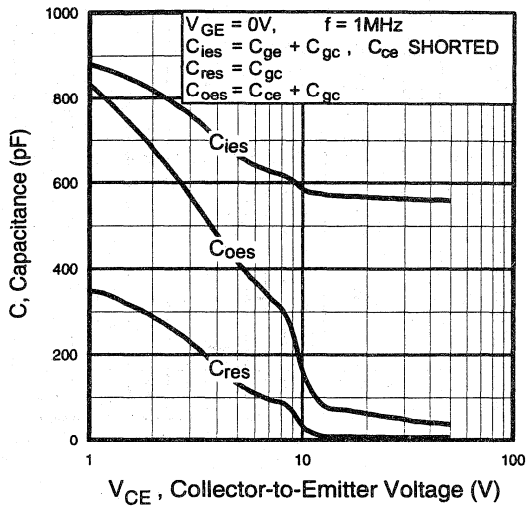


Fig. 7 - Typical Capacitance vs. Collector-to-Emitter Voltage

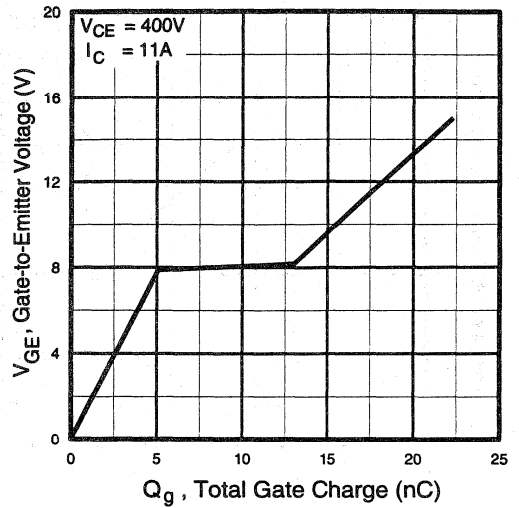


Fig. 8 - Typical Gate Charge vs. Gate-to-Emitter Voltage

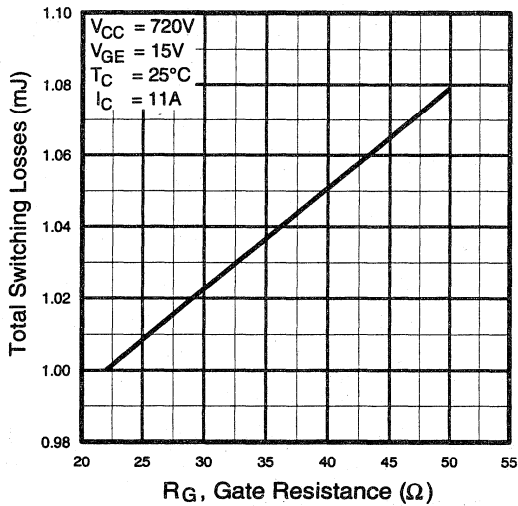


Fig. 9 - Typical Switching Losses vs. Gate Resistance

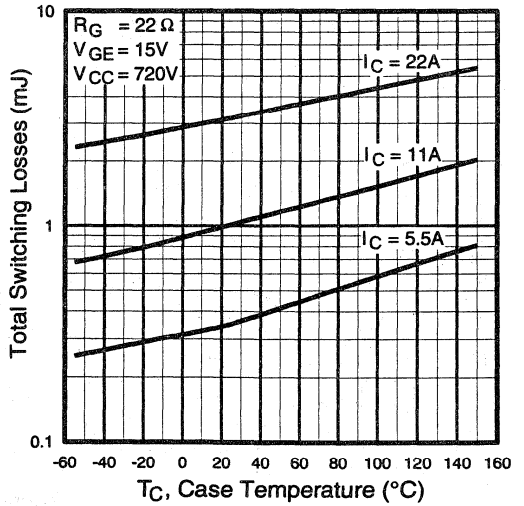


Fig. 10 - Typical Switching Losses vs. Case Temperature

Power
Conversion
Fast
Discretes

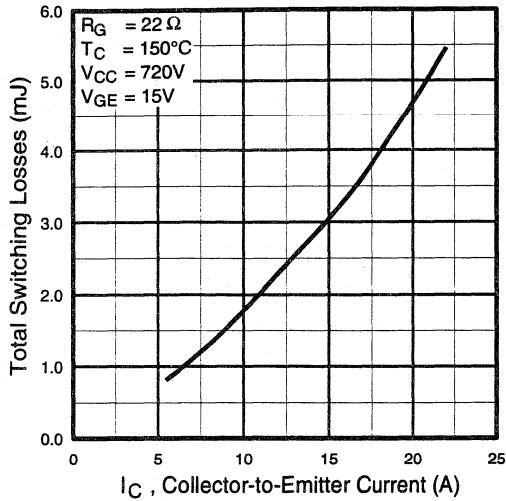


Fig. 11 - Typical Switching Losses vs. Collector-to-Emitter Current

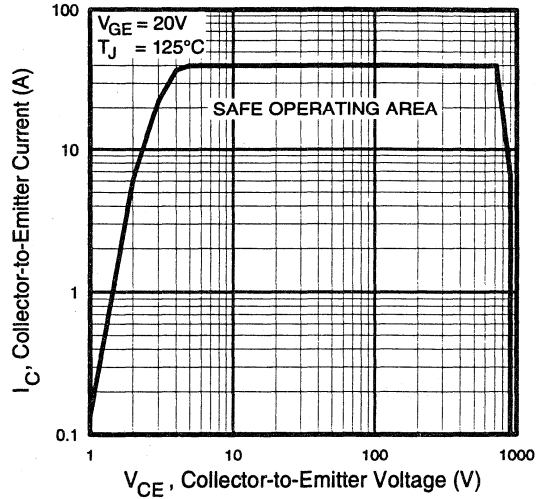


Fig. 12 - Turn-Off SOA

Refer to Section D for the following:

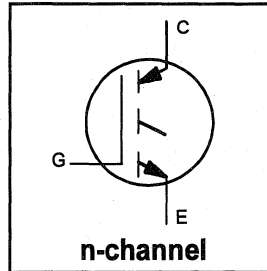
Appendix F: Section D - page D-8

- Fig. 13a - Clamped Inductive Load Test Circuit
- Fig. 13b - Pulsed Collector Current Test Circuit
- Fig. 14a - Switching Loss Test Circuit
- Fig. 14b - Switching Loss Waveform

Package Outline 3 - JEDEC Outline TO-247AC (TO-3P) Section D - page D-13

Features

- Switching-loss rating includes all "tail" losses
- Optimized for medium operating frequency (1 to 10kHz) See Fig. 1 for Current vs. Frequency curve



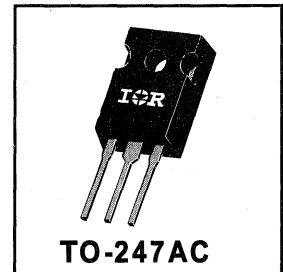
$$V_{CES} = 900V$$

$$V_{CE(sat)} \leq 3.3V$$

$$@V_{GE} = 15V, I_C = 17A$$

Description

Insulated Gate Bipolar Transistors (IGBTs) from International Rectifier have higher usable current densities than comparable bipolar transistors, while at the same time having simpler gate-drive requirements of the familiar power MOSFET. They provide substantial benefits to a host of high-voltage, high-current applications.



Absolute Maximum Ratings

	Parameter	Max.	Units
V_{CES}	Collector-to-Emitter Voltage	900	V
$I_C @ T_C = 25^\circ C$	Continuous Collector Current	31	A
$I_C @ T_C = 100^\circ C$	Continuous Collector Current	17	
I_{CM}	Pulsed Collector Current ①	62	
I_{LM}	Clamped Inductive Load Current ②	62	
V_{GE}	Gate-to-Emitter Voltage	± 20	V
E_{ARV}	Reverse Voltage Avalanche Energy ③	15	mJ
$P_D @ T_C = 25^\circ C$	Maximum Power Dissipation	160	W
$P_D @ T_C = 100^\circ C$	Maximum Power Dissipation	65	
T_J	Operating Junction and	-55 to +150	°C
T_{STG}	Storage Temperature Range		
	Soldering Temperature, for 10 sec.	300 (0.063 in. (1.6mm) from case)	
	Mounting torque, 6-32 or M3 screw.	10 lbf•in (1.1N•m)	

Thermal Resistance

	Parameter	Min.	Typ.	Max.	Units
$R_{\theta JC}$	Junction-to-Case	—	—	0.77	°C/W
$R_{\theta CS}$	Case-to-Sink, flat, greased surface	—	0.24	—	
$R_{\theta JA}$	Junction-to-Ambient, typical socket mount	—	—	40	
Wt	Weight	—	6 (0.21)	—	g (oz)

Electrical Characteristics @ $T_J = 25^\circ\text{C}$ (unless otherwise specified)

	Parameter	Min.	Typ.	Max.	Units	Conditions
$V_{(BR)CES}$	Collector-to-Emitter Breakdown Voltage	900	—	—	V	$V_{GE} = 0V, I_C = 250\mu\text{A}$
$V_{(BR)ECS}$	Emitter-to-Collector Breakdown Voltage ④	20	—	—	V	$V_{GE} = 0V, I_C = 1.0A$
$\Delta V_{(BR)CES}/\Delta T_J$	Temperature Coeff. of Breakdown Voltage	—	0.80	—	$V/^\circ\text{C}$	$V_{GE} = 0V, I_C = 1.0mA$
$V_{CE(on)}$	Collector-to-Emitter Saturation Voltage	—	2.5	3.3	V	$I_C = 17A$ $V_{GE} = 15V$ $I_C = 31A$ $V_{GE} = 15V$ $I_C = 17A, T_J = 150^\circ\text{C}$ See Fig. 2, 5
		—	3.2	—		
		—	2.9	—		
$V_{GE(th)}$	Gate Threshold Voltage	3.0	—	5.5		$V_{CE} = V_{GE}, I_C = 250\mu\text{A}$
$\Delta V_{GE(th)}/\Delta T_J$	Temperature Coeff. of Threshold Voltage	—	-12	—	$\text{mV}/^\circ\text{C}$	$V_{CE} = V_{GE}, I_C = 250\mu\text{A}$
g_{fe}	Forward Transconductance ⑤	5.2	13	—	S	$V_{CE} = 100V, I_C = 17A$
I_{CES}	Zero Gate Voltage Collector Current	—	—	250	μA	$V_{GE} = 0V, V_{CE} = 900V$
		—	—	1000		$V_{GE} = 0V, V_{CE} = 900V, T_J = 150^\circ\text{C}$
I_{GES}	Gate-to-Emitter Leakage Current	—	—	± 100	nA	$V_{GE} = \pm 20V$

Switching Characteristics @ $T_J = 25^\circ\text{C}$ (unless otherwise specified)

	Parameter	Min.	Typ.	Max.	Units	Conditions
Q_g	Total Gate Charge (turn-on)	—	45	68	nC	$I_C = 17A$ $V_{CC} = 400V$ See Fig. 8 $V_{GE} = 15V$
Q_{ge}	Gate - Emitter Charge (turn-on)	—	8.7	13		
Q_{gc}	Gate - Collector Charge (turn-on)	—	15	23		
$t_{d(on)}$	Turn-On Delay Time	—	28	—	ns	$T_J = 25^\circ\text{C}$ $I_C = 17A, V_{CC} = 720V$ $V_{GE} = 15V, R_G = 10\Omega$ Energy losses include "tail"
t_r	Rise Time	—	12	—		
$t_{d(off)}$	Turn-Off Delay Time	—	170	320		
t_f	Fall Time	—	110	300		
E_{on}	Turn-On Switching Loss	—	0.52	—	mJ	See Fig. 9, 10, 11, 14
E_{off}	Turn-Off Switching Loss	—	1.05	—		
E_{ts}	Total Switching Loss	—	1.57	3.1		
$t_{d(on)}$	Turn-On Delay Time	—	27	—	ns	$T_J = 150^\circ\text{C}$, $I_C = 17A, V_{CC} = 720V$ $V_{GE} = 15V, R_G = 10\Omega$ Energy losses include "tail"
t_r	Rise Time	—	14	—		
$t_{d(off)}$	Turn-Off Delay Time	—	250	—		
t_f	Fall Time	—	240	—		
E_{ts}	Total Switching Loss	—	3.0	—	mJ	See Fig. 10, 14
L_E	Internal Emitter Inductance	—	13	—	nH	Measured 5mm from package
C_{ies}	Input Capacitance	—	1200	—	pF	$V_{GE} = 0V$ $V_{CC} = 30V$ See Fig. 7 $f = 1.0\text{MHz}$
C_{oes}	Output Capacitance	—	91	—		
C_{res}	Reverse Transfer Capacitance	—	15	—		

Notes:

- ① Repetitive rating; $V_{GE}=20V$, pulse width limited by max. junction temperature. (See fig. 13b)
- ② $V_{CC}=80\%(V_{CES}), V_{GE}=20V, L=10\mu\text{H}, R_G=10\Omega$, (See fig. 13a)
- ③ Repetitive rating; pulse width limited by maximum junction temperature.
- ④ Pulse width $\leq 80\mu\text{s}$; duty factor $\leq 0.1\%$.
- ⑤ Pulse width $5.0\mu\text{s}$, single shot.

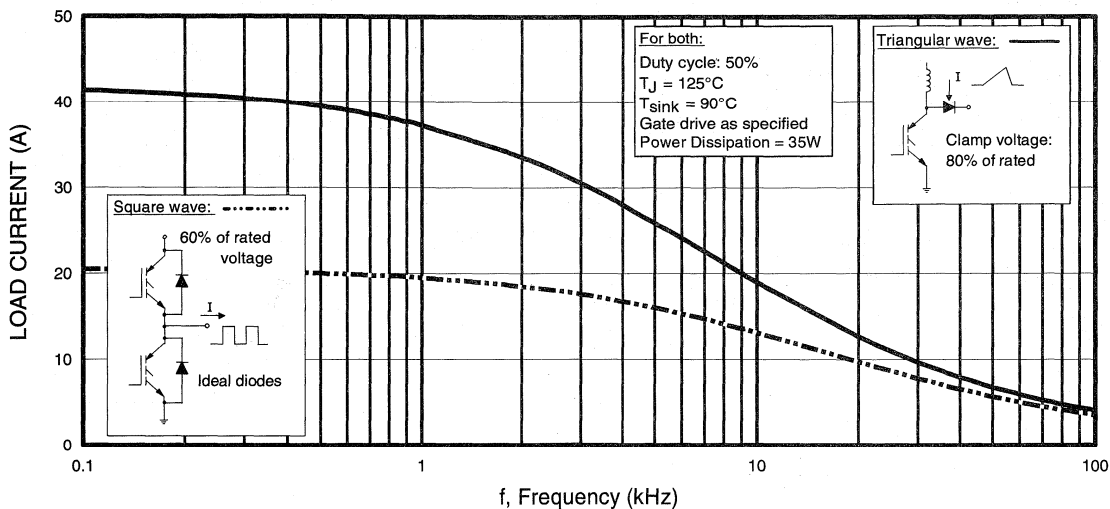


Fig. 1 - Typical Load Current vs. Frequency
 (For square wave, $I = I_{\text{RMS}}$ of fundamental; for triangular wave, $I = I_{\text{PK}}$)

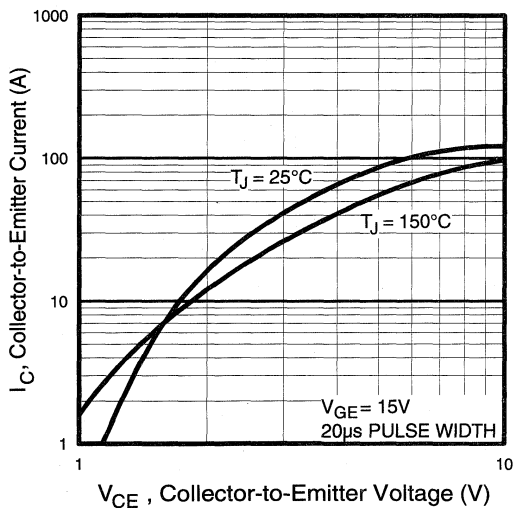


Fig. 2 - Typical Output Characteristics

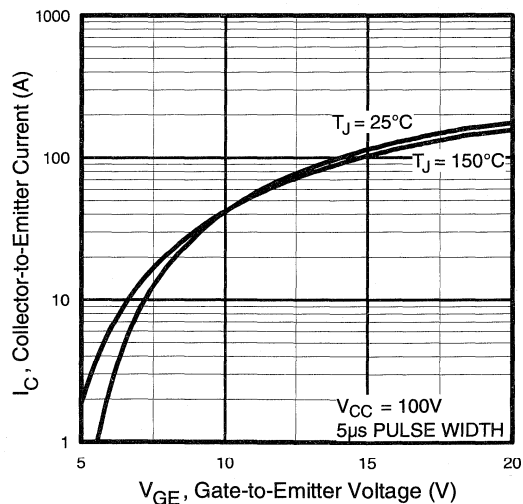


Fig. 3 - Typical Transfer Characteristics

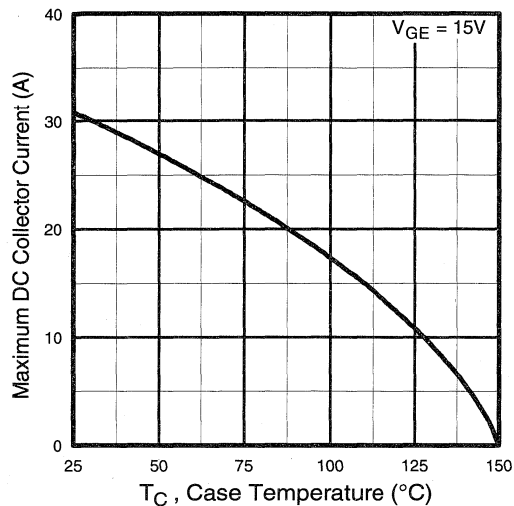


Fig. 4 - Maximum Collector Current vs. Case Temperature

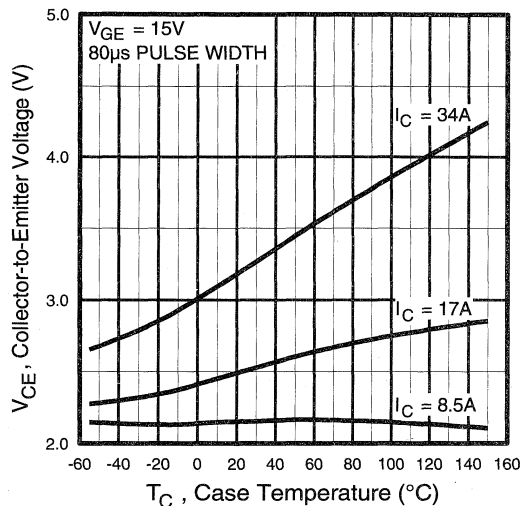


Fig. 5 - Collector-to-Emitter Voltage vs. Case Temperature

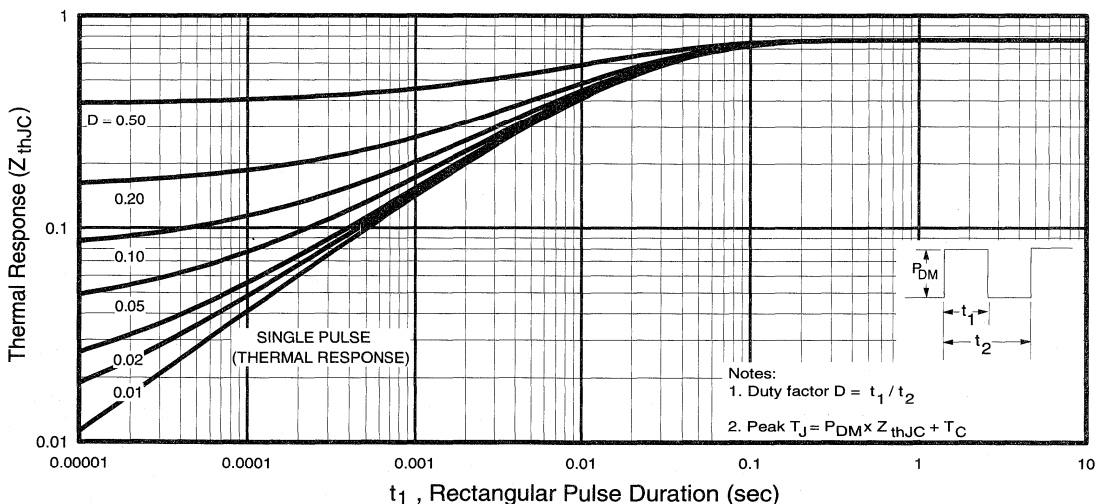


Fig. 6 - Maximum Effective Transient Thermal Impedance, Junction-to-Case

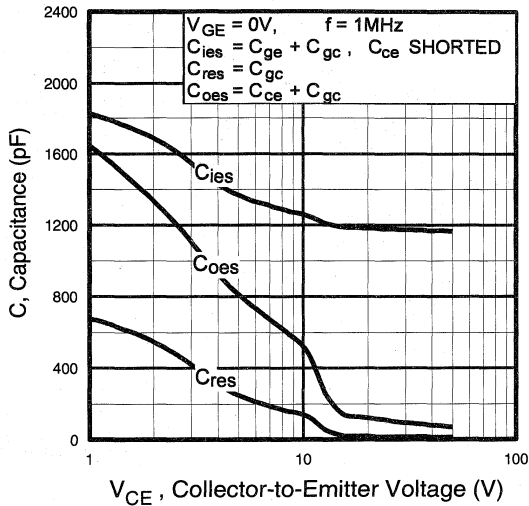


Fig. 7 - Typical Capacitance vs. Collector-to-Emitter Voltage

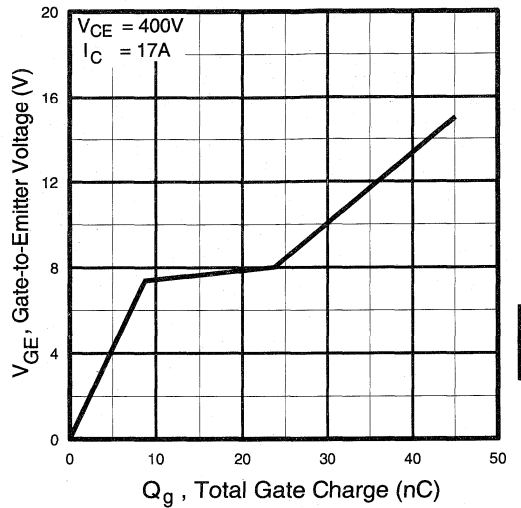


Fig. 8 - Typical Gate Charge vs. Gate-to-Emitter Voltage

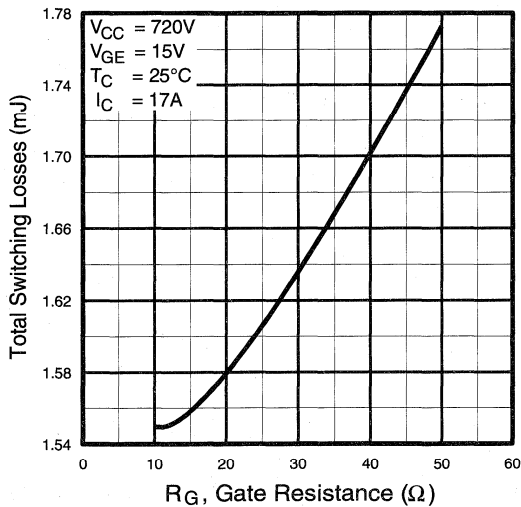


Fig. 9 - Typical Switching Losses vs. Gate Resistance

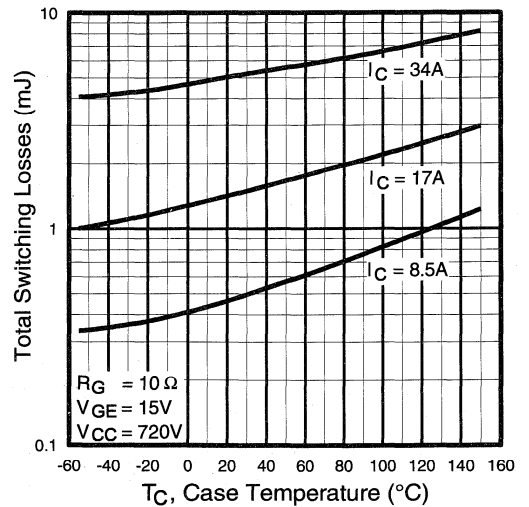


Fig. 10 - Typical Switching Losses vs. Case Temperature

Power Conversion
 IGBTs
 Discretes

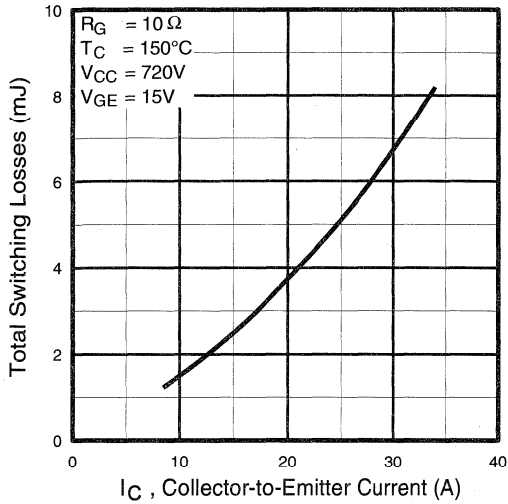


Fig. 11 - Typical Switching Losses vs. Collector-to-Emitter Current

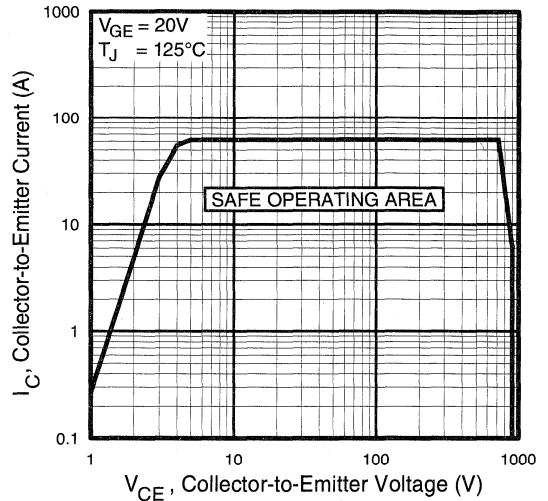


Fig. 12 - Turn-Off SOA

Refer to Section D for the following:

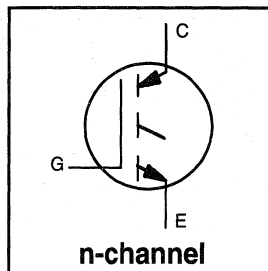
Appendix F: Section D - page D-8

- Fig. 13a - Clamped Inductive Load Test Circuit
- Fig. 13b - Pulsed Collector Current Test Circuit
- Fig. 14a - Switching Loss Test Circuit
- Fig. 14b - Switching Loss Waveform

Package Outline 3 - JEDEC Outline TO-247AC (TO-3P) Section D - page D-13

Features

- Switching-loss rating includes all "tail" losses
- Optimized for medium operating frequency (1 to 10kHz) See Fig. 1 for Current vs. Frequency curve



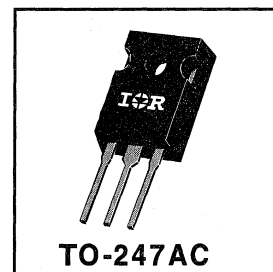
$$V_{CES} = 900V$$

$$V_{CE(sat)} \leq 2.7V$$

$$@V_{GE} = 15V, I_C = 28A$$

Description

Insulated Gate Bipolar Transistors (IGBTs) from International Rectifier have higher usable current densities than comparable bipolar transistors, while at the same time having simpler gate-drive requirements of the familiar power MOSFET. They provide substantial benefits to a host of high-voltage, high-current applications.



Absolute Maximum Ratings

	Parameter	Max.	Units
V_{CES}	Collector-to-Emitter Voltage	900	V
$I_C @ T_C = 25^\circ C$	Continuous Collector Current	51	A
$I_C @ T_C = 100^\circ C$	Continuous Collector Current	28	
I_{CM}	Pulsed Collector Current ①	100	
I_{LM}	Clamped Inductive Load Current ②	100	
V_{GE}	Gate-to-Emitter Voltage	± 20	V
E_{ARV}	Reverse Voltage Avalanche Energy ③	20	mJ
$P_D @ T_C = 25^\circ C$	Maximum Power Dissipation	200	W
$P_D @ T_C = 100^\circ C$	Maximum Power Dissipation	78	
T_J	Operating Junction and	-55 to +150	°C
T_{STG}	Storage Temperature Range		
	Soldering Temperature, for 10 sec.	300 (0.063 in. (1.6mm) from case)	
	Mounting torque, 6-32 or M3 screw.	10 lbf•in (1.1N•m)	

Thermal Resistance

	Parameter	Min.	Typ.	Max.	Units
$R_{\theta JC}$	Junction-to-Case	-----	-----	0.64	°C/W
$R_{\theta CS}$	Case-to-Sink, flat, greased surface	-----	0.24	-----	
$R_{\theta JA}$	Junction-to-Ambient, typical socket mount	-----	-----	40	
Wt	Weight	-----	6 (0.21)	-----	g (oz)

Electrical Characteristics @ $T_J = 25^\circ\text{C}$ (unless otherwise specified)

	Parameter	Min.	Typ.	Max.	Units	Conditions
$V_{(BR)CES}$	Collector-to-Emitter Breakdown Voltage	900	----	----	V	$V_{GE} = 0V, I_C = 250\mu A$
$V_{(BR)ECS}$	Emitter-to-Collector Breakdown Voltage ④	20	----	----	V	$V_{GE} = 0V, I_C = 1.0A$
$\Delta V_{(BR)CES}/\Delta T_J$	Temperature Coeff. of Breakdown Voltage	----	0.74	----	$V/^\circ\text{C}$	$V_{GE} = 0V, I_C = 1.0mA$
$V_{CE(on)}$	Collector-to-Emitter Saturation Voltage	----	2.1	2.7	V	$I_C = 28A$ $V_{GE} = 15V$
		----	2.7	----		$I_C = 51A$ See Fig. 2, 5
		----	2.4	----		$I_C = 28A, T_J = 150^\circ\text{C}$
$V_{GE(th)}$	Gate Threshold Voltage	3.0	----	5.5		$V_{CE} = V_{GE}, I_C = 250\mu A$
$\Delta V_{GE(th)}/\Delta T_J$	Temperature Coeff. of Threshold Voltage	----	-9.7	----	$mV/^\circ\text{C}$	$V_{CE} = V_{GE}, I_C = 250\mu A$
g_{fe}	Forward Transconductance ⑤	12	18	----	S	$V_{CE} = 100V, I_C = 28A$
I_{CES}	Zero Gate Voltage Collector Current	----	----	250	μA	$V_{GE} = 0V, V_{CE} = 900V$
		----	----	2000		$V_{GE} = 0V, V_{CE} = 900V, T_J = 150^\circ\text{C}$
I_{GES}	Gate-to-Emitter Leakage Current	----	----	± 100	nA	$V_{GE} = \pm 20V$

Switching Characteristics @ $T_J = 25^\circ\text{C}$ (unless otherwise specified)

	Parameter	Min.	Typ.	Max.	Units	Conditions
Q_g	Total Gate Charge (turn-on)	----	81	120	nC	$I_C = 28A$
Q_{ge}	Gate - Emitter Charge (turn-on)	----	16	24		$V_{CC} = 400V$ See Fig. 8
Q_{gc}	Gate - Collector Charge (turn-on)	----	29	44		$V_{GE} = 15V$
$t_{d(on)}$	Turn-On Delay Time	----	32	----	ns	$T_J = 25^\circ\text{C}$
t_r	Rise Time	----	22	----		$I_C = 28A, V_{CC} = 720V$
$t_{d(off)}$	Turn-Off Delay Time	----	200	280		$V_{GE} = 15V, R_G = 5.0\Omega$
t_f	Fall Time	----	130	180		Energy losses include "tail"
E_{on}	Turn-On Switching Loss	----	1.1	----	mJ	See Fig. 9, 10, 11, 14
E_{off}	Turn-Off Switching Loss	----	1.8	----		
E_{ts}	Total Switching Loss	----	2.9	4.1		
$t_{d(on)}$	Turn-On Delay Time	----	32	----	ns	$T_J = 150^\circ\text{C},$
t_r	Rise Time	----	20	----		$I_C = 28A, V_{CC} = 720V$
$t_{d(off)}$	Turn-Off Delay Time	----	480	----		$V_{GE} = 15V, R_G = 5.0\Omega$
t_f	Fall Time	----	450	----		Energy losses include "tail"
E_{ts}	Total Switching Loss	----	5.7	----	mJ	See Fig. 10, 14
L_E	Internal Emitter Inductance	----	13	----	nH	Measured 5mm from package
C_{ies}	Input Capacitance	----	2300	----	pF	$V_{GE} = 0V$
C_{oes}	Output Capacitance	----	180	----		$V_{CC} = 30V$ See Fig. 7
C_{res}	Reverse Transfer Capacitance	----	27	----		$f = 1.0MHz$

Notes:

- ① Repetitive rating; $V_{GE}=20V$, pulse width limited by max. junction temperature. (See fig. 13b)
- ② $V_{CC}=80\%(V_{CES}), V_{GE}=20V, L=10\mu H, R_G=5.0\Omega,$ (See fig. 13a)
- ③ Repetitive rating; pulse width limited by maximum junction temperature.
- ④ Pulse width $\leq 80\mu s$; duty factor $\leq 0.1\%$.
- ⑤ Pulse width 5.0 μs , single shot.

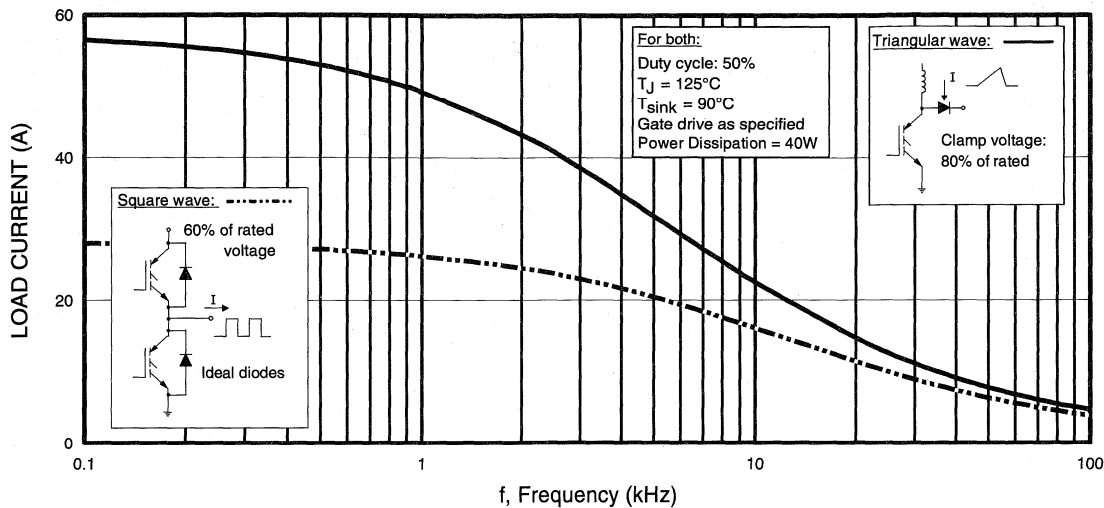


Fig. 1 - Typical Load Current vs. Frequency
 (For square wave, $I = I_{RMS}$ of fundamental; for triangular wave, $I = I_{PK}$)

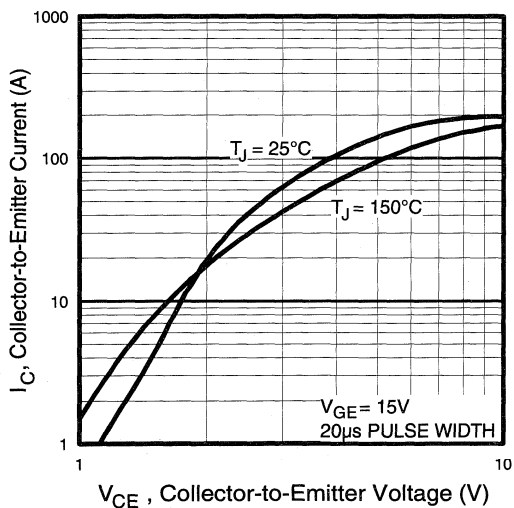


Fig. 2 - Typical Output Characteristics

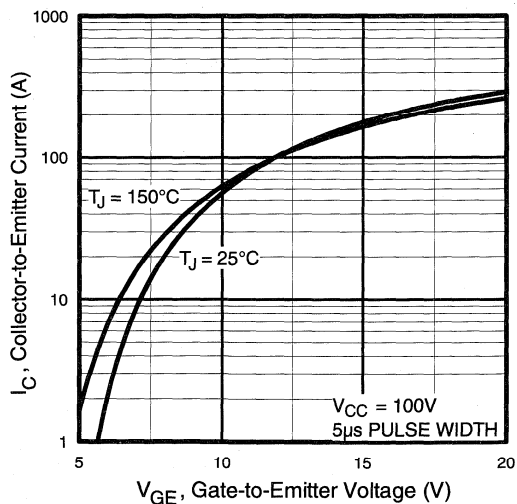


Fig. 3 - Typical Transfer Characteristics

Power
Conversion
Fast
Discretes

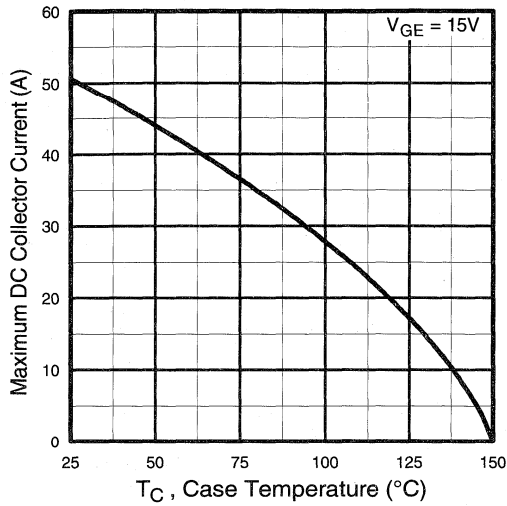


Fig. 4 - Maximum Collector Current vs. Case Temperature

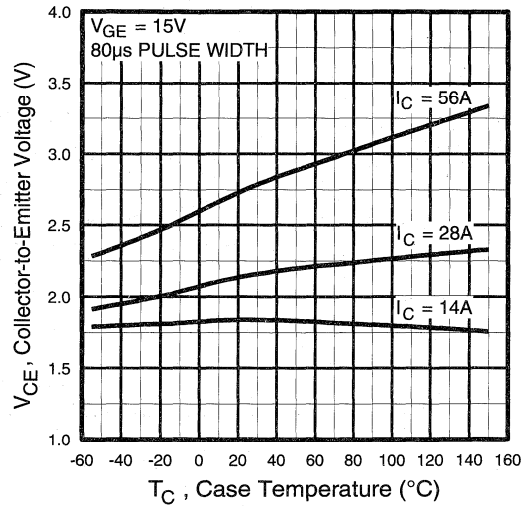


Fig. 5 - Collector-to-Emitter Voltage vs. Case Temperature

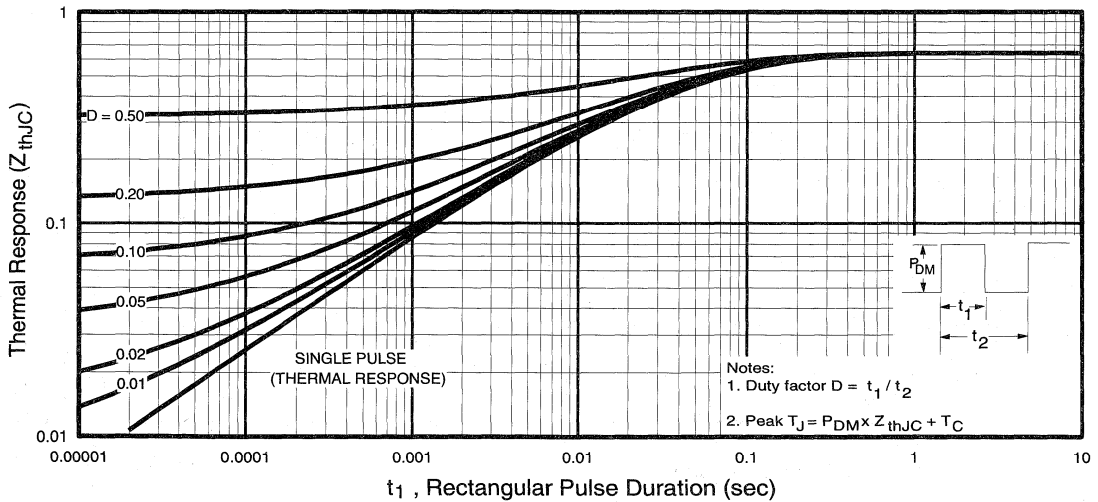


Fig. 6 - Maximum Effective Transient Thermal Impedance, Junction-to-Case

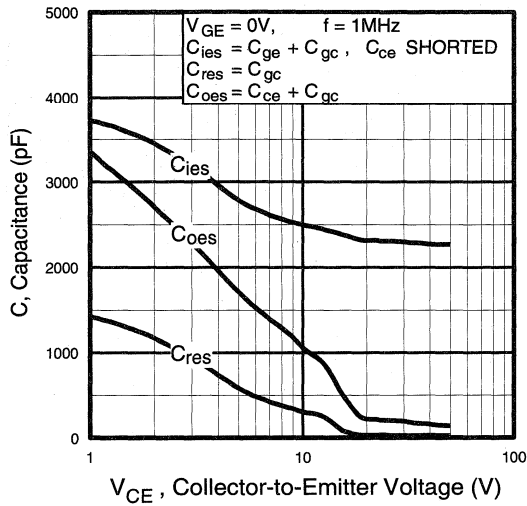


Fig. 7 - Typical Capacitance vs. Collector-to-Emitter Voltage

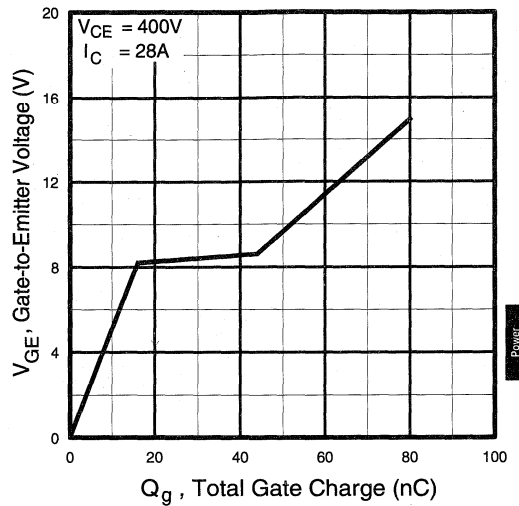


Fig. 8 - Typical Gate Charge vs. Gate-to-Emitter Voltage

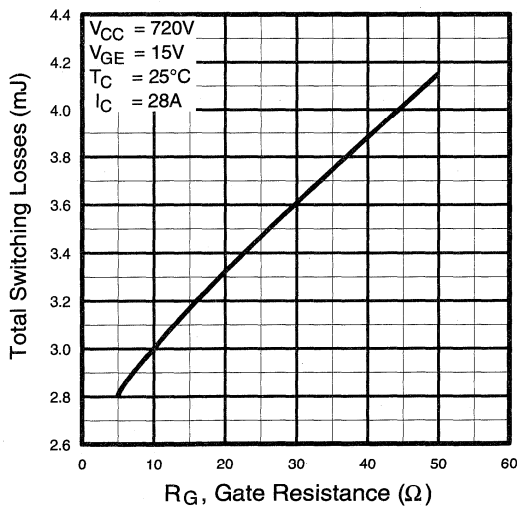


Fig. 9 - Typical Switching Losses vs. Gate Resistance

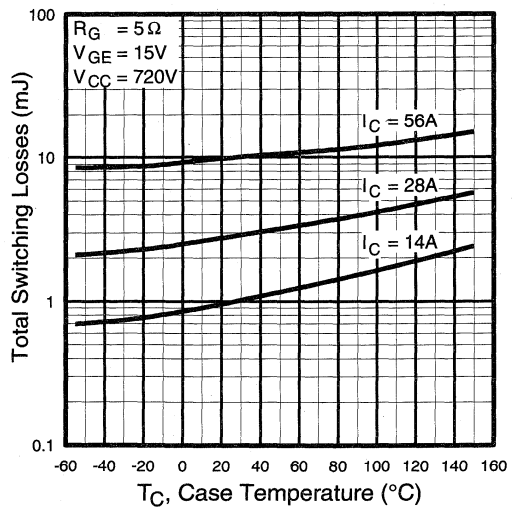


Fig. 10 - Typical Switching Losses vs. Case Temperature

Power Conversion Products Discretes

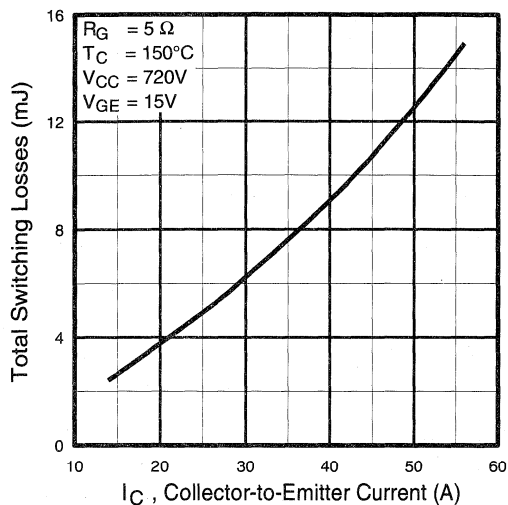


Fig. 11 - Typical Switching Losses vs. Collector-to-Emitter Current

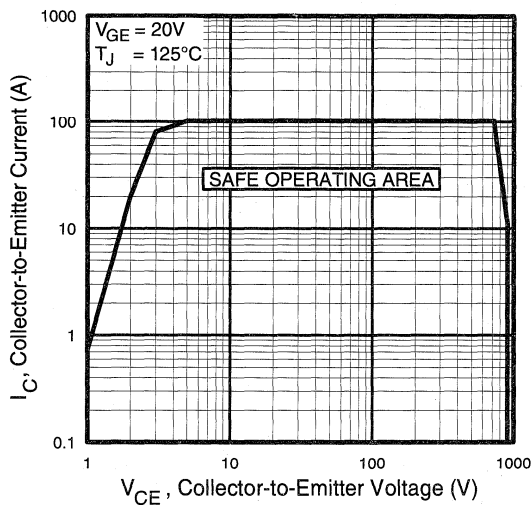


Fig. 12 - Turn-Off SOA

Refer to **Section D** for the following:

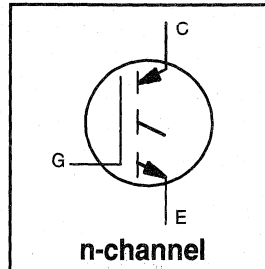
Appendix F: Section D - page D-8

- Fig. 13a - Clamped Inductive Load Test Circuit
- Fig. 13b - Pulsed Collector Current Test Circuit
- Fig. 14a - Switching Loss Test Circuit
- Fig. 14b - Switching Loss Waveform

Package Outline 3 - JEDEC Outline TO-247AC (TO-3P) Section D - page D-13

Features

- Switching-loss rating includes all "tail" losses
- Optimized for medium operating frequency (1 to 10kHz) See Fig. 1 for Current vs. Frequency curve



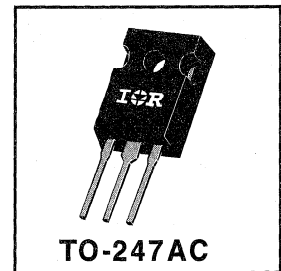
$$V_{CES} = 1200V$$

$$V_{CE(sat)} \leq 3.3V$$

$$@V_{GE} = 15V, I_C = 17A$$

Description

Insulated Gate Bipolar Transistors (IGBTs) from International Rectifier have higher usable current densities than comparable bipolar transistors, while at the same time having simpler gate-drive requirements of the familiar power MOSFET. They provide substantial benefits to a host of high-voltage, high-current applications.



Absolute Maximum Ratings

	Parameter	Max.	Units
V_{CES}	Collector-to-Emitter Voltage	1200	V
$I_C @ T_C = 25^\circ C$	Continuous Collector Current	29	A
$I_C @ T_C = 100^\circ C$	Continuous Collector Current	17	
I_{CM}	Pulsed Collector Current ①	58	
I_{LM}	Clamped Inductive Load Current ②	58	
V_{GE}	Gate-to-Emitter Voltage	± 20	V
E_{ARV}	Reverse Voltage Avalanche Energy ③	15	mJ
$P_D @ T_C = 25^\circ C$	Maximum Power Dissipation	160	W
$P_D @ T_C = 100^\circ C$	Maximum Power Dissipation	65	
T_J	Operating Junction and	-55 to +150	°C
T_{STG}	Storage Temperature Range		
	Soldering Temperature, for 10 sec.	300 (0.063 in. (1.6mm) from case)	
	Mounting torque, 6-32 or M3 screw.	10 lbf•in (1.1N•m)	

Thermal Resistance

	Parameter	Min.	Typ.	Max.	Units
$R_{\theta JC}$	Junction-to-Case	—	—	0.77	°C/W
$R_{\theta CS}$	Case-to-Sink, flat, greased surface	—	0.24	—	
$R_{\theta JA}$	Junction-to-Ambient, typical socket mount	—	—	40	
Wt	Weight	—	6 (0.21)	—	g (oz)

Electrical Characteristics @ $T_J = 25^\circ\text{C}$ (unless otherwise specified)

	Parameter	Min.	Typ.	Max.	Units	Conditions
$V_{(BR)CES}$	Collector-to-Emitter Breakdown Voltage	1200	—	—	V	$V_{GE} = 0V, I_C = 250\mu A$
$V_{(BR)ECS}$	Emitter-to-Collector Breakdown Voltage ④	20	—	—	V	$V_{GE} = 0V, I_C = 1.0A$
$\Delta V_{(BR)CES}/\Delta T_J$	Temperature Coeff. of Breakdown Voltage	—	1.3	—	$V/^\circ\text{C}$	$V_{GE} = 0V, I_C = 1.0mA$
$V_{CE(on)}$	Collector-to-Emitter Saturation Voltage	—	2.5	3.3	V	$I_C = 17A$ $I_C = 29A$ $I_C = 17A, T_J = 150^\circ\text{C}$ $V_{GE} = 15V$ See Fig. 2, 5
		—	3.2	—		
		—	3.0	—		
$V_{GE(th)}$	Gate Threshold Voltage	3.0	—	5.5		$V_{CE} = V_{GE}, I_C = 250\mu A$
$\Delta V_{GE(th)}/\Delta T_J$	Temperature Coeff. of Threshold Voltage	—	-13	—	$mV/^\circ\text{C}$	$V_{CE} = V_{GE}, I_C = 250\mu A$
g_{fe}	Forward Transconductance ⑤	5.0	11	—	S	$V_{CE} = 100V, I_C = 17A$
I_{CES}	Zero Gate Voltage Collector Current	—	—	250	μA	$V_{GE} = 0V, V_{CE} = 1200V$
		—	—	1000		$V_{GE} = 0V, V_{CE} = 1200V, T_J = 150^\circ\text{C}$
I_{GES}	Gate-to-Emitter Leakage Current	—	—	± 100	nA	$V_{GE} = \pm 20V$

Switching Characteristics @ $T_J = 25^\circ\text{C}$ (unless otherwise specified)

	Parameter	Min.	Typ.	Max.	Units	Conditions
Q_g	Total Gate Charge (turn-on)	—	45	67	nC	$I_C = 17A$ $V_{CC} = 400V$ $V_{GE} = 15V$ See Fig. 8
Q_{ge}	Gate - Emitter Charge (turn-on)	—	11	16		
Q_{gc}	Gate - Collector Charge (turn-on)	—	17	26		
$t_{d(on)}$	Turn-On Delay Time	—	33	—	ns	$T_J = 25^\circ\text{C}$ $I_C = 17A, V_{CC} = 960V$ $V_{GE} = 15V, R_G = 10\Omega$ Energy losses include "tail"
t_r	Rise Time	—	17	—		
$t_{d(off)}$	Turn-Off Delay Time	—	250	490		
t_f	Fall Time	—	210	390		
E_{on}	Turn-On Switching Loss	—	1.0	—	mJ	See Fig. 9, 10, 11, 14
E_{off}	Turn-Off Switching Loss	—	3.0	—		
E_{is}	Total Switching Loss	—	4.0	7.5		
$t_{d(on)}$	Turn-On Delay Time	—	32	—	ns	$T_J = 150^\circ\text{C}$, $I_C = 17A, V_{CC} = 960V$ $V_{GE} = 15V, R_G = 10\Omega$ Energy losses include "tail"
t_r	Rise Time	—	20	—		
$t_{d(off)}$	Turn-Off Delay Time	—	480	—		
t_f	Fall Time	—	450	—		
E_{is}	Total Switching Loss	—	8.3	—	mJ	See Fig. 10, 14
L_E	Internal Emitter Inductance	—	13	—	nH	Measured 5mm from package
C_{ies}	Input Capacitance	—	1200	—	pF	$V_{GE} = 0V$ $V_{CC} = 30V$ See Fig. 7 $f = 1.0MHz$
C_{oes}	Output Capacitance	—	75	—		
C_{res}	Reverse Transfer Capacitance	—	15	—		

Notes:

- ① Repetitive rating; $V_{GE}=20V$, pulse width limited by max. junction temperature. (See fig. 13b)
- ② $V_{CC}=80\%(V_{CES}), V_{GE}=20V, L=10\mu H, R_G=10\Omega$, (See fig. 13a)
- ③ Repetitive rating; pulse width limited by maximum junction temperature.
- ④ Pulse width $\leq 80\mu s$; duty factor $\leq 0.1\%$.
- ⑤ Pulse width 5.0 μs , single shot.

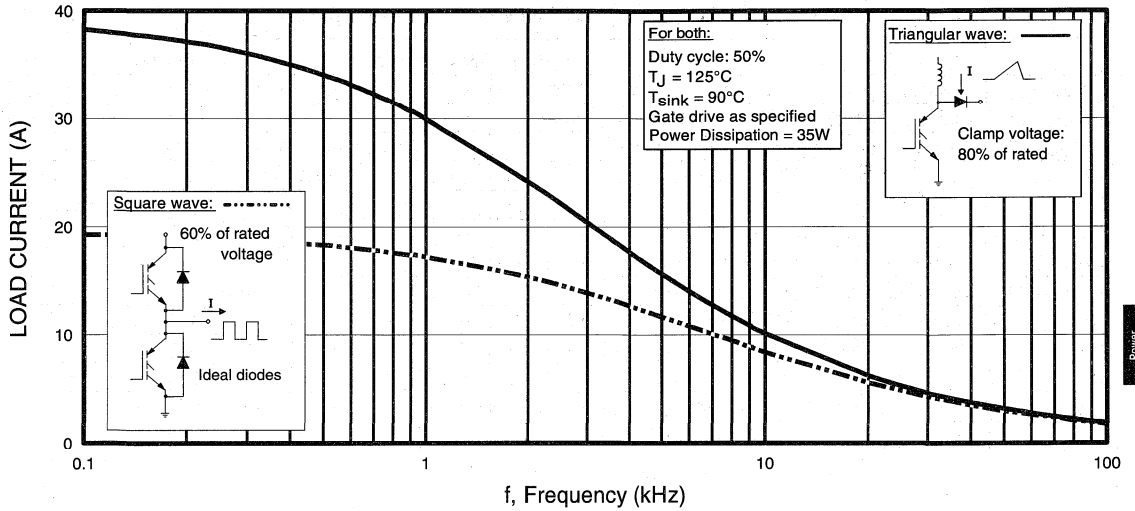


Fig. 1 - Typical Load Current vs. Frequency
 (For square wave, $I = I_{\text{RMS}}$ of fundamental; for triangular wave, $I = I_{\text{PK}}$)

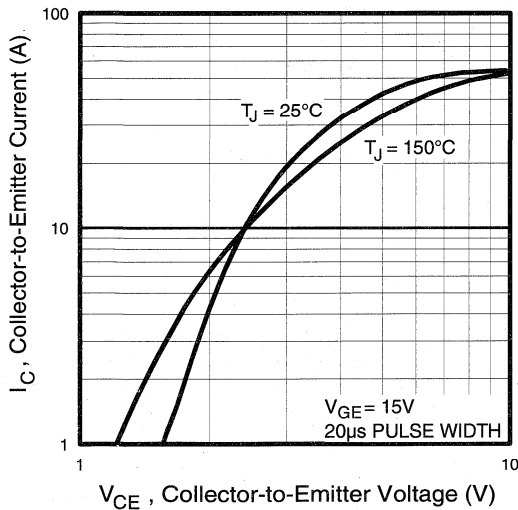


Fig. 2 - Typical Output Characteristics

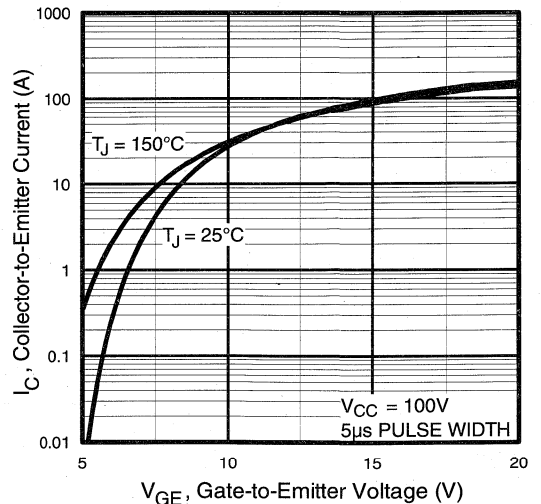


Fig. 3 - Typical Transfer Characteristics

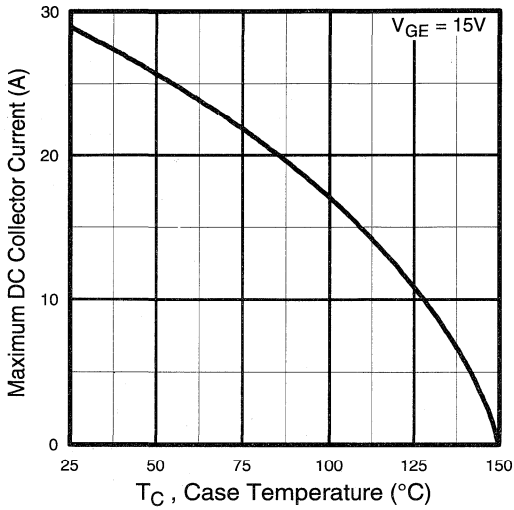


Fig. 4 - Maximum Collector Current vs. Case Temperature

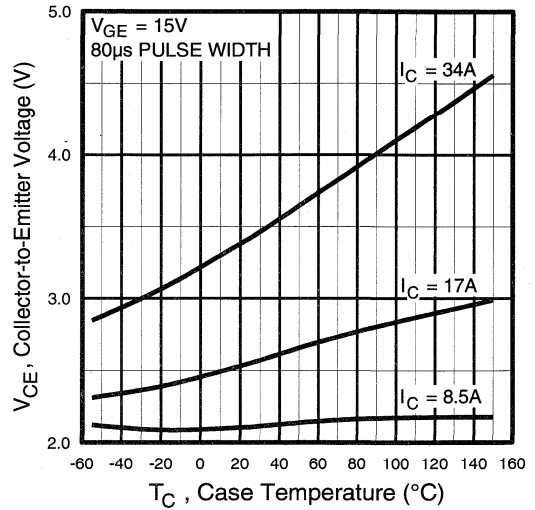


Fig. 5 - Collector-to-Emitter Voltage vs. Case Temperature

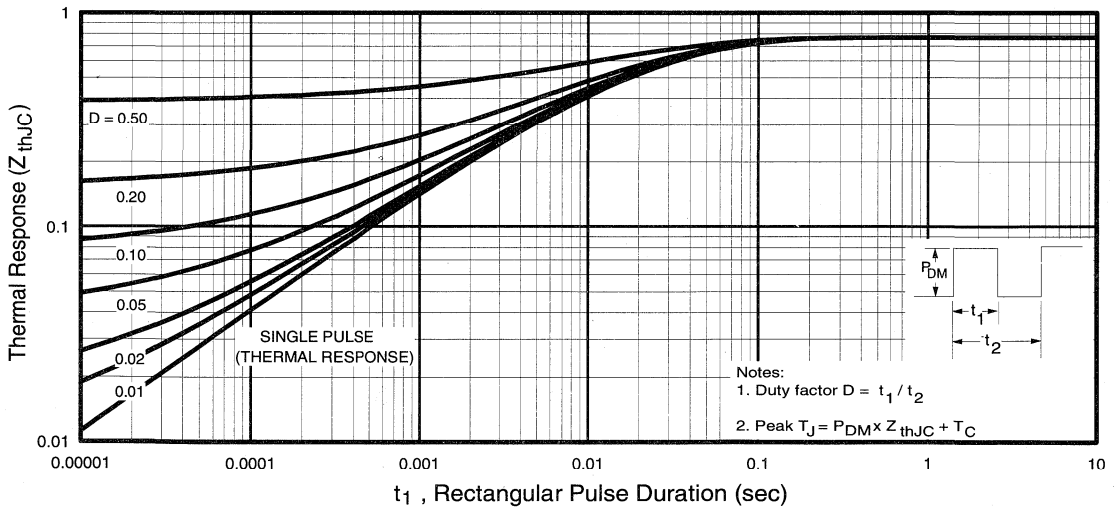


Fig. 6 - Maximum Effective Transient Thermal Impedance, Junction-to-Case

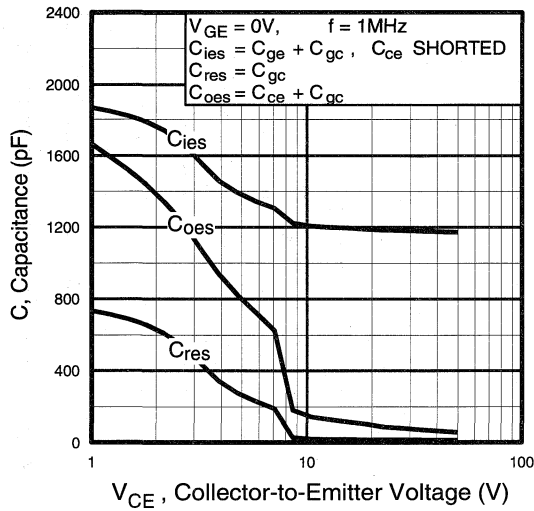


Fig. 7 - Typical Capacitance vs. Collector-to-Emitter Voltage

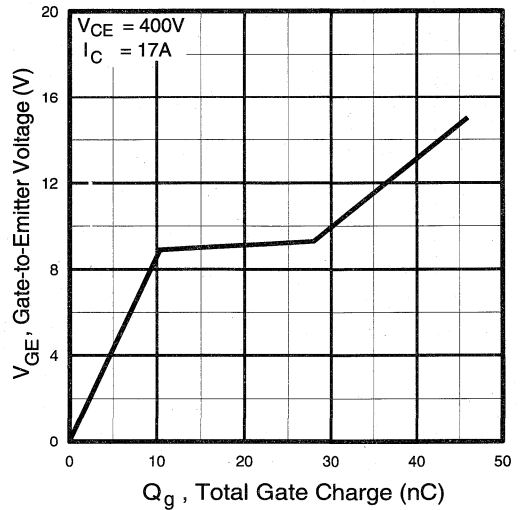


Fig. 8 - Typical Gate Charge vs. Gate-to-Emitter Voltage

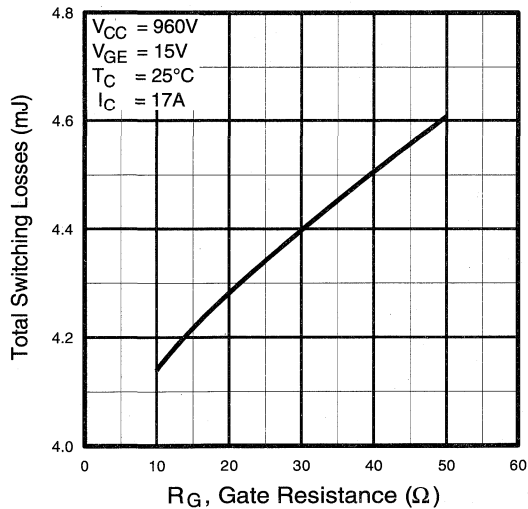


Fig. 9 - Typical Switching Losses vs. Gate Resistance

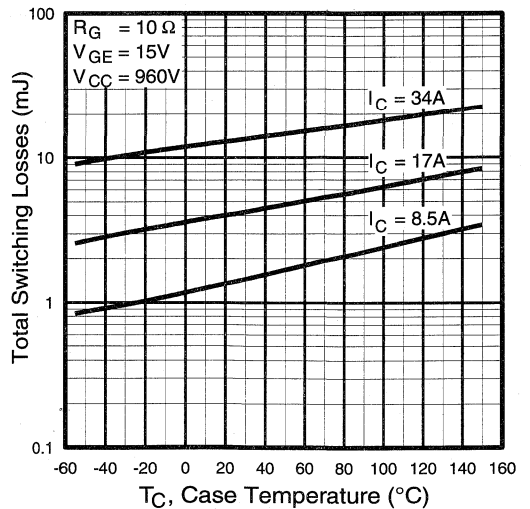


Fig. 10 - Typical Switching Losses vs. Case Temperature

Power
Conversion
Fast
Discretes

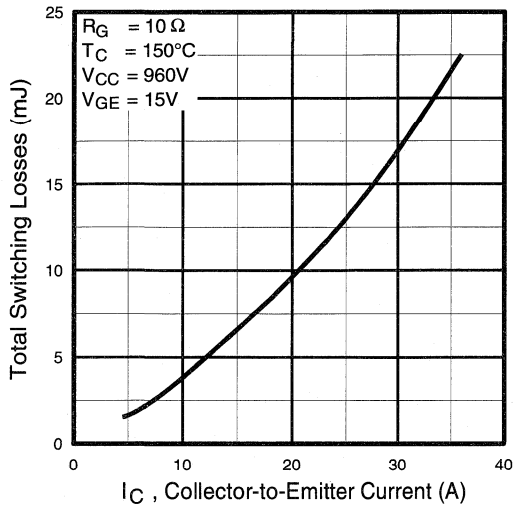


Fig. 11 - Typical Switching Losses vs. Collector-to-Emitter Current

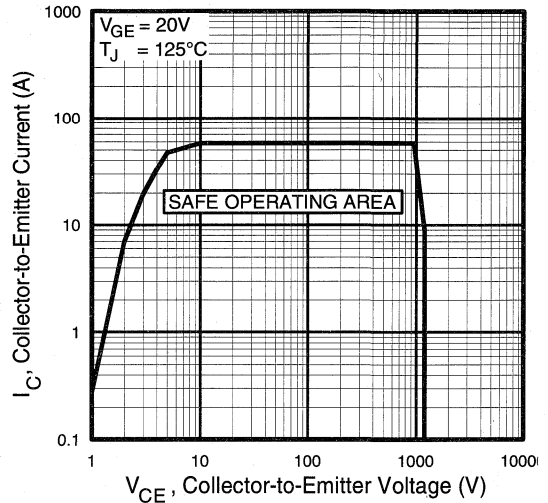


Fig. 12 - Turn-Off SOA

Refer to **Section D** for the following:

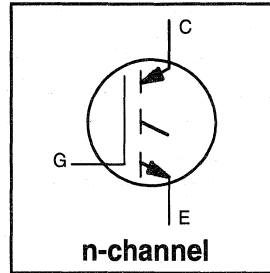
Appendix G: Section D - page D-9

- Fig. 13a - Clamped Inductive Load Test Circuit
- Fig. 13b - Pulsed Collector Current Test Circuit
- Fig. 14a - Switching Loss Test Circuit
- Fig. 14b - Switching Loss Waveform

Package Outline 3 - JEDEC Outline TO-247AC (TO-3P) Section D - page D-13

Features

- Switching-loss rating includes all "tail" losses
- Optimized for medium operating frequency (1 to 10kHz) See Fig. 1 for Current vs. Frequency curve



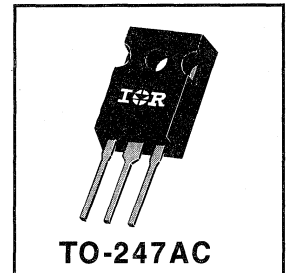
$$V_{CES} = 1200V$$

$$V_{CE(sat)} \leq 2.9V$$

$$@V_{GE} = 15V, I_C = 25A$$

Description

Insulated Gate Bipolar Transistors (IGBTs) from International Rectifier have higher usable current densities than comparable bipolar transistors, while at the same time having simpler gate-drive requirements of the familiar power MOSFET. They provide substantial benefits to a host of high-voltage, high-current applications.


TO-247AC

Absolute Maximum Ratings

	Parameter	Max.	Units
V_{CES}	Collector-to-Emitter Voltage	1200	V
$I_C @ T_C = 25^\circ C$	Continuous Collector Current	45	A
$I_C @ T_C = 100^\circ C$	Continuous Collector Current	25	
I_{CM}	Pulsed Collector Current ①	90	
I_{LM}	Clamped Inductive Load Current ②	90	
V_{GE}	Gate-to-Emitter Voltage	± 20	V
E_{ARV}	Reverse Voltage Avalanche Energy ③	20	mJ
$P_D @ T_C = 25^\circ C$	Maximum Power Dissipation	200	W
$P_D @ T_C = 100^\circ C$	Maximum Power Dissipation	78	
T_J	Operating Junction and	-55 to +150	°C
T_{STG}	Storage Temperature Range		
	Soldering Temperature, for 10 sec.	300 (0.063 in. (1.6mm) from case)	
	Mounting torque, 6-32 or M3 screw.	10 lbf•in (1.1N•m)	

Thermal Resistance

	Parameter	Min.	Typ.	Max.	Units
$R_{\theta JC}$	Junction-to-Case	—	—	0.64	°C/W
$R_{\theta CS}$	Case-to-Sink, flat, greased surface	—	0.24	—	
$R_{\theta JA}$	Junction-to-Ambient, typical socket mount	—	—	40	
Wt	Weight	—	6 (0.21)	—	g (oz)

Electrical Characteristics @ $T_J = 25^\circ\text{C}$ (unless otherwise specified)

	Parameter	Min.	Typ.	Max.	Units	Conditions
$V_{(BR)CES}$	Collector-to-Emitter Breakdown Voltage	1200	—	—	V	$V_{GE} = 0V, I_C = 250\mu A$
$V_{(BR)ECS}$	Emitter-to-Collector Breakdown Voltage ④	20	—	—	V	$V_{GE} = 0V, I_C = 1.0A$
$\Delta V_{(BR)CES}/\Delta T_J$	Temperature Coeff. of Breakdown Voltage	—	1.3	—	V/°C	$V_{GE} = 0V, I_C = 1.0mA$
$V_{CE(on)}$	Collector-to-Emitter Saturation Voltage	—	2.1	2.9	V	$I_C = 25A$ $I_C = 45A$ $I_C = 25A, T_J = 150^\circ\text{C}$ $V_{GE} = 15V$ See Fig. 2, 5
		—	2.5	—		
		—	2.4	—		
$V_{GE(th)}$	Gate Threshold Voltage	3.0	—	5.5		$V_{CE} = V_{GE}, I_C = 250\mu A$
$\Delta V_{GE(th)}/\Delta T_J$	Temperature Coeff. of Threshold Voltage	—	-14	—	mV/°C	$V_{CE} = V_{GE}, I_C = 250\mu A$
g_{fe}	Forward Transconductance ⑤	7.5	17	—	S	$V_{CE} = 100V, I_C = 25A$
I_{CES}	Zero Gate Voltage Collector Current	—	—	250	μA	$V_{GE} = 0V, V_{CE} = 1200V$
		—	—	1200		$V_{GE} = 0V, V_{CE} = 1200V, T_J = 150^\circ\text{C}$
I_{GES}	Gate-to-Emitter Leakage Current	—	—	± 100	nA	$V_{GE} = \pm 20V$

Switching Characteristics @ $T_J = 25^\circ\text{C}$ (unless otherwise specified)

	Parameter	Min.	Typ.	Max.	Units	Conditions
Q_g	Total Gate Charge (turn-on)	—	82	100	nC	$I_C = 25A$ $V_{CC} = 400V$ $V_{GE} = 15V$ See Fig. 8
Q_{ge}	Gate - Emitter Charge (turn-on)	—	16	21		
Q_{gc}	Gate - Collector Charge (turn-on)	—	30	43		
$t_{d(on)}$	Turn-On Delay Time	—	34	—	ns	$T_J = 25^\circ\text{C}$ $I_C = 25A, V_{CC} = 960V$ $V_{GE} = 15V, R_G = 5.0\Omega$ Energy losses include "tail"
t_r	Rise Time	—	13	—		
$t_{d(off)}$	Turn-Off Delay Time	—	320	480		
t_f	Fall Time	—	240	330		
E_{on}	Turn-On Switching Loss	—	1.4	—	mJ	See Fig. 9, 10, 11, 14
E_{off}	Turn-Off Switching Loss	—	4.5	—		
E_{ts}	Total Switching Loss	—	5.9	8.2		
$t_{d(on)}$	Turn-On Delay Time	—	33	—	ns	$T_J = 150^\circ\text{C}$, $I_C = 25A, V_{CC} = 960V$ $V_{GE} = 15V, R_G = 5.0\Omega$ Energy losses include "tail"
t_r	Rise Time	—	15	—		
$t_{d(off)}$	Turn-Off Delay Time	—	590	—		
t_f	Fall Time	—	500	—		
E_{ts}	Total Switching Loss	—	13	—	mJ	See Fig. 10, 14
L_E	Internal Emitter Inductance	—	13	—	nH	Measured 5mm from package
C_{ies}	Input Capacitance	—	2400	—	pF	$V_{GE} = 0V$ $V_{CC} = 30V$ $f = 1.0MHz$ See Fig. 7
C_{oes}	Output Capacitance	—	140	—		
C_{res}	Reverse Transfer Capacitance	—	28	—		

Notes:

- ① Repetitive rating; $V_{GE}=20V$, pulse width limited by max. junction temperature. (See fig. 13b)
- ② $V_{CC}=80\%(V_{CES})$, $V_{GE}=20V$, $L=10\mu H$, $R_G=5.0\Omega$, (See fig. 13a)
- ③ Repetitive rating; pulse width limited by maximum junction temperature.
- ④ Pulse width $\leq 80\mu s$; duty factor $\leq 0.1\%$.
- ⑤ Pulse width $5.0\mu s$, single shot.

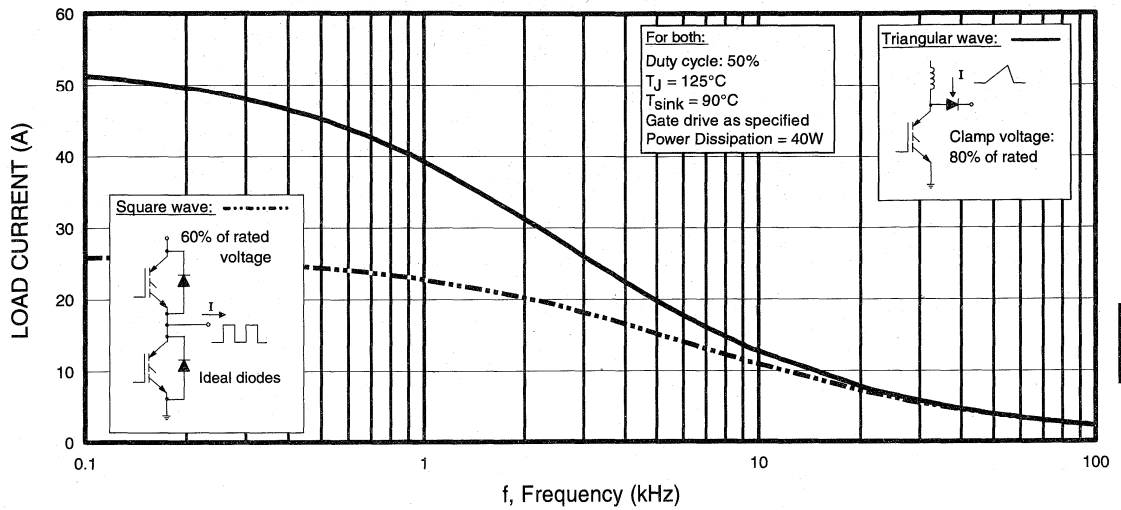


Fig. 1 - Typical Load Current vs. Frequency
 (For square wave, $I = I_{RMS}$ of fundamental; for triangular wave, $I = I_{PK}$)

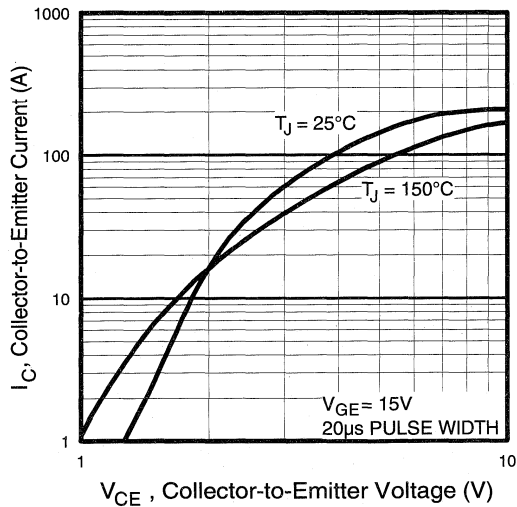


Fig. 2 - Typical Output Characteristics

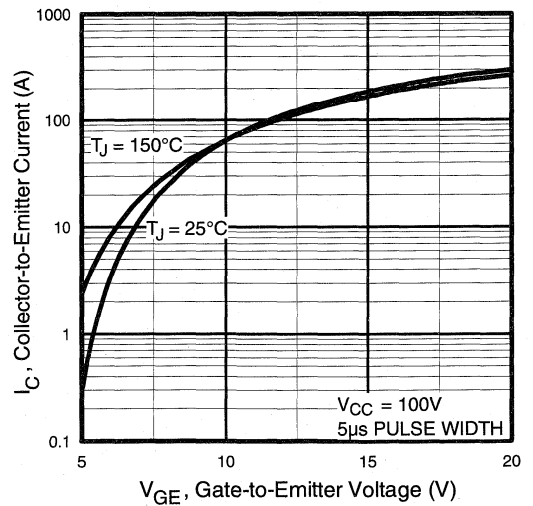


Fig. 3 - Typical Transfer Characteristics

Power
Conversion
Fast
Discretes

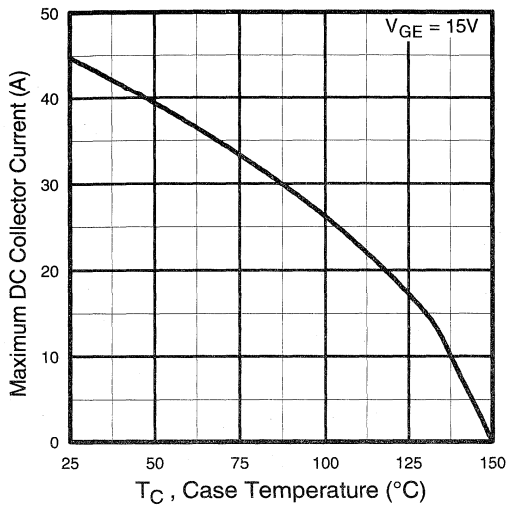


Fig. 4 - Maximum Collector Current vs. Case Temperature

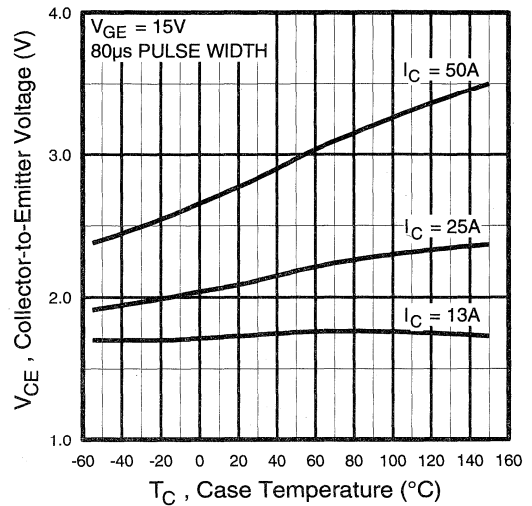


Fig. 5 - Collector-to-Emitter Voltage vs. Case Temperature

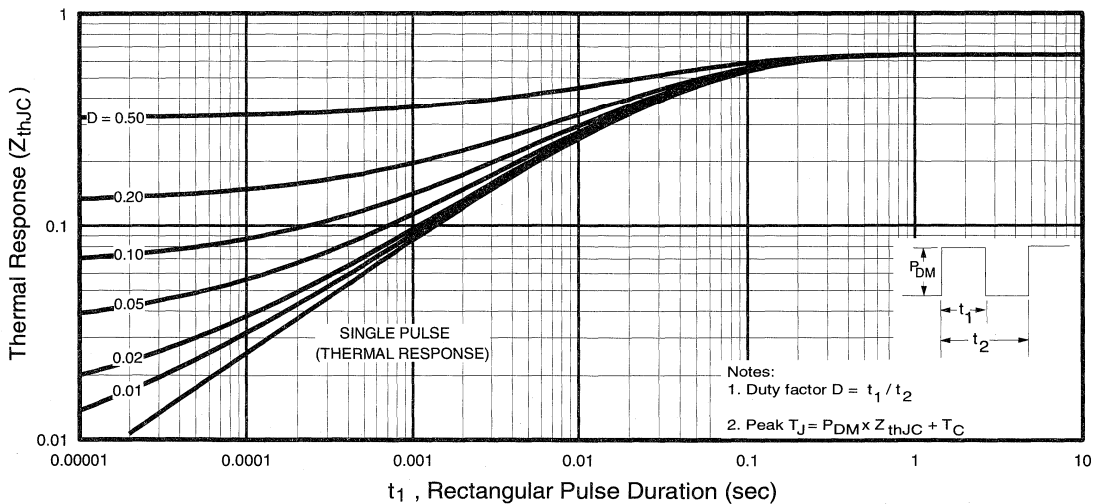


Fig. 6 - Maximum Effective Transient Thermal Impedance, Junction-to-Case

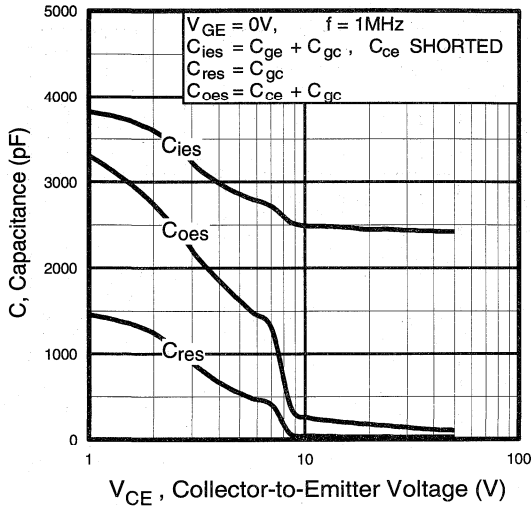


Fig. 7 - Typical Capacitance vs. Collector-to-Emitter Voltage

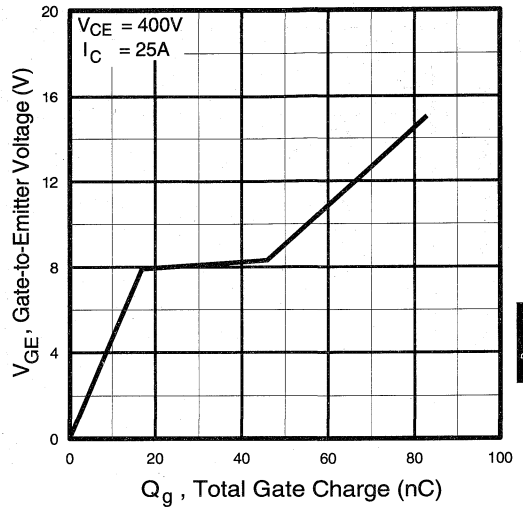


Fig. 8 - Typical Gate Charge vs. Gate-to-Emitter Voltage

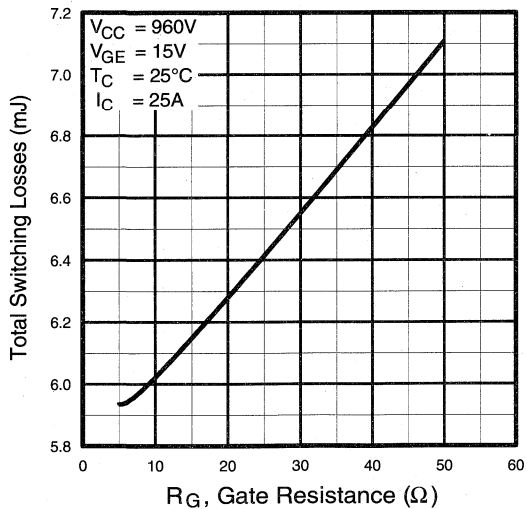


Fig. 9 - Typical Switching Losses vs. Gate Resistance

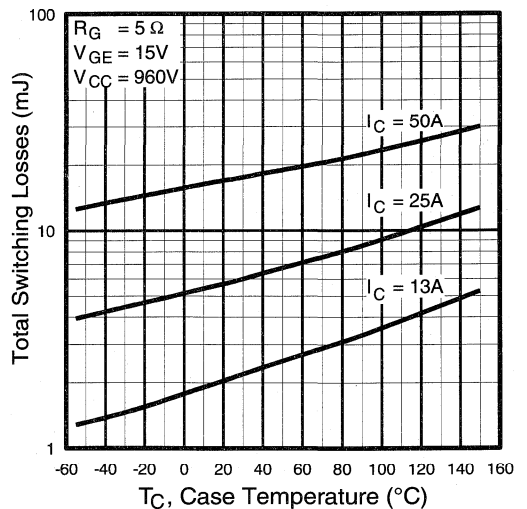


Fig. 10 - Typical Switching Losses vs. Case Temperature

Power
Conversion
Fast
Discretes

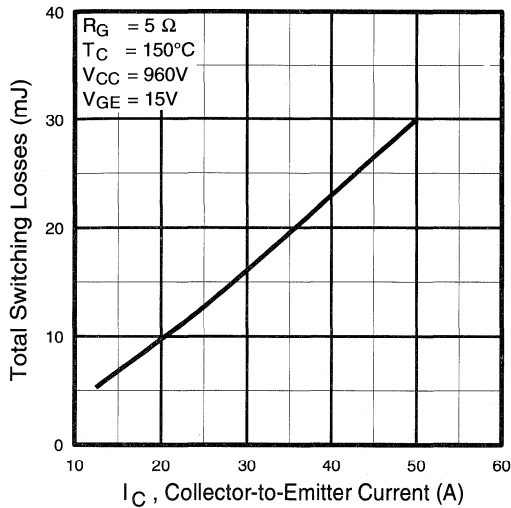


Fig. 11 - Typical Switching Losses vs. Collector-to-Emitter Current

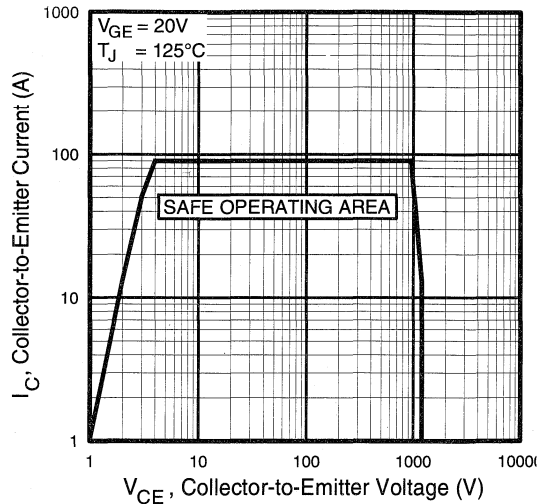


Fig. 12 - Turn-Off SOA

Refer to Section D for the following:

Appendix G: Section D - page D-9

- Fig. 13a - Clamped Inductive Load Test Circuit
- Fig. 13b - Pulsed Collector Current Test Circuit
- Fig. 14a - Switching Loss Test Circuit
- Fig. 14b - Switching Loss Waveform

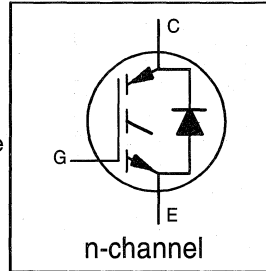
Package Outline 3 - JEDEC Outline TO-247AC (TO-3P) Section D - page D-13

INSULATED GATE BIPOLAR TRANSISTOR
WITH ULTRAFAST SOFT RECOVERY

Fast CoPack IGBT

DIODE Features

- Switching-loss rating includes all "tail" losses
- HEXFRED™ soft ultrafast diodes
- Optimized for medium operating frequency (1 to 10kHz) See Fig. 1 for Current vs. Frequency curve



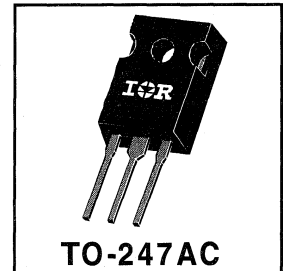
$$V_{CES} = 1200V$$

$$V_{CE(sat)} \leq 3.3V$$

$$@ V_{GE} = 15V, I_C = 17A$$

Description

Co-packaged IGBTs are a natural extension of International Rectifier's well known IGBT line. They provide the convenience of an IGBT and an ultrafast recovery diode in one package, resulting in substantial benefits to a host of high-voltage, high-current, motor control, UPS and power supply applications.



Absolute Maximum Ratings

	Parameter	Max.	Units
V_{CES}	Collector-to-Emitter Voltage	1200	V
$I_C @ T_C = 25^\circ C$	Continuous Collector Current	29	A
$I_C @ T_C = 100^\circ C$	Continuous Collector Current	17	
I_{CM}	Pulsed Collector Current ①	58	
I_{LM}	Clamped Inductive Load Current ②	58	
$I_F @ T_C = 100^\circ C$	Diode Continuous Forward Current	8.0	
I_{FM}	Diode Maximum Forward Current	130	
V_{GE}	Gate-to-Emitter Voltage	± 20	V
$P_D @ T_C = 25^\circ C$	Maximum Power Dissipation	160	W
$P_D @ T_C = 100^\circ C$	Maximum Power Dissipation	65	
T_J	Operating Junction and	-55 to +150	°C
T_{STG}	Storage Temperature Range		
	Soldering Temperature, for 10 sec.	300 (0.063 in. (1.6mm) from case)	
	Mounting Torque, 6-32 or M3 Screw.	10 lbf•in (1.1 N•m)	

Thermal Resistance

	Parameter	Min.	Typ.	Max.	Units
$R_{\theta JC}$	Junction-to-Case - IGBT	—	—	0.77	°C/W
$R_{\theta JC}$	Junction-to-Case - Diode	—	—	1.7	
$R_{\theta CS}$	Case-to-Sink, flat, greased surface	—	0.24	—	
$R_{\theta JA}$	Junction-to-Ambient, typical socket mount	—	—	40	
Wt	Weight	—	6 (0.21)	—	g (oz)

Electrical Characteristics @ $T_J = 25^\circ\text{C}$ (unless otherwise specified)

	Parameter	Min.	Typ.	Max.	Units	Conditions
$V_{(BR)CES}$	Collector-to-Emitter Breakdown Voltage ^②	1200	—	—	V	$V_{GE} = 0V, I_C = 250\mu A$
$\Delta V_{(BR)CES}/\Delta T_J$	Temperature Coeff. of Breakdown Voltage	—	1.3	—	V/ $^\circ\text{C}$	$V_{GE} = 0V, I_C = 1.0mA$
$V_{CE(on)}$	Collector-to-Emitter Saturation Voltage	—	2.5	3.3	V	$I_C = 17A, V_{GE} = 15V$
		—	3.2	—		$I_C = 29A$ See Fig. 2, 5
		—	3.0	—		$I_C = 17A, T_J = 150^\circ\text{C}$
$V_{GE(th)}$	Gate Threshold Voltage	3.0	—	5.5		$V_{CE} = V_{GE}, I_C = 250\mu A$
$\Delta V_{GE(th)}/\Delta T_J$	Temperature Coeff. of Threshold Voltage	—	-13	—	mV/ $^\circ\text{C}$	$V_{CE} = V_{GE}, I_C = 250\mu A$
g_{fe}	Forward Transconductance ^④	5.0	11	—	S	$V_{CE} = 100V, I_C = 17A$
I_{CES}	Zero Gate Voltage Collector Current	—	—	250	μA	$V_{GE} = 0V, V_{CE} = 1200V$
		—	—	1000		$V_{GE} = 0V, V_{CE} = 1200V, T_J = 150^\circ\text{C}$
V_{FM}	Diode Forward Voltage Drop	—	2.6	3.3	V	$I_C = 8.0A$ See Fig. 13
		—	2.3	3.0		$I_C = 8.0A, T_J = 150^\circ\text{C}$
		—	—	—		
I_{GES}	Gate-to-Emitter Leakage Current	—	—	± 100	nA	$V_{GE} = \pm 20V$

Switching Characteristics @ $T_J = 25^\circ\text{C}$ (unless otherwise specified)

	Parameter	Min.	Typ.	Max.	Units	Conditions
Q_g	Total Gate Charge (turn-on)	—	45	67	nC	$I_C = 17A$ $V_{CC} = 400V$ See Fig. 8
Q_{ge}	Gate - Emitter Charge (turn-on)	—	11	16		
Q_{gc}	Gate - Collector Charge (turn-on)	—	17	26		
$t_{d(on)}$	Turn-On Delay Time	—	70	—	ns	$T_J = 25^\circ\text{C}$ $I_C = 17A, V_{CC} = 800V$ $V_{GE} = 15V, R_G = 10\Omega$ Energy losses include "tail" and diode reverse recovery. See Fig. 9, 10, 11, 18
t_r	Rise Time	—	58	—		
$t_{d(off)}$	Turn-Off Delay Time	—	320	550		
t_f	Fall Time	—	370	630	mJ	$T_J = 150^\circ\text{C}$, See Fig. 9, 10, 11, 18 $I_C = 17A, V_{CC} = 800V$ $V_{GE} = 15V, R_G = 10\Omega$ Energy losses include "tail" and diode reverse recovery.
E_{on}	Turn-On Switching Loss	—	2.6	—		
E_{off}	Turn-Off Switching Loss	—	5.4	—		
E_{ts}	Total Switching Loss	—	8.0	15	mJ	$T_J = 150^\circ\text{C}$, See Fig. 9, 10, 11, 18 $I_C = 17A, V_{CC} = 800V$ $V_{GE} = 15V, R_G = 10\Omega$ Energy losses include "tail" and diode reverse recovery.
$t_{d(on)}$	Turn-On Delay Time	—	70	—		
t_r	Rise Time	—	54	—		
$t_{d(off)}$	Turn-Off Delay Time	—	670	—	ns	Measured 5mm from package
t_f	Fall Time	—	930	—		
E_{ts}	Total Switching Loss	—	15	—		
L_E	Internal Emitter Inductance	—	13	—	nH	Measured 5mm from package
C_{ies}	Input Capacitance	—	1200	—	pF	$V_{GE} = 0V$ $V_{CC} = 30V$ See Fig. 7 $f = 1.0MHz$
C_{oes}	Output Capacitance	—	75	—		
C_{res}	Reverse Transfer Capacitance	—	15	—		
t_{rr}	Diode Reverse Recovery Time	—	63	95	ns	$T_J = 25^\circ\text{C}$ See Fig.
		—	106	160		$T_J = 125^\circ\text{C}$ 14
I_{rr}	Diode Peak Reverse Recovery Current	—	4.5	8.0	A	$T_J = 25^\circ\text{C}$ See Fig.
		—	6.2	11		$T_J = 125^\circ\text{C}$ 15
Q_{rr}	Diode Reverse Recovery Charge	—	140	380	nC	$T_J = 25^\circ\text{C}$ See Fig.
		—	335	880		$T_J = 125^\circ\text{C}$ 16
$di_{(rec)M}/dt$	Diode Peak Rate of Fall of Recovery During t_b	—	133	—	A/ μs	$T_J = 25^\circ\text{C}$ See Fig.
		—	85	—		$T_J = 125^\circ\text{C}$ 17

Notes:

① Repetitive rating; $V_{GE}=20V$, pulse width limited by max. junction temperature.
(See fig. 20)

② $V_{CC}=80\%(V_{CES})$, $V_{GE}=20V$, $L=10\mu H$,
 $R_G = 10\Omega$, (See fig. 19)

③ Pulse width $\leq 80\mu s$; duty factor $\leq 0.1\%$.

④ Pulse width 5.0 μs ,
single shot.

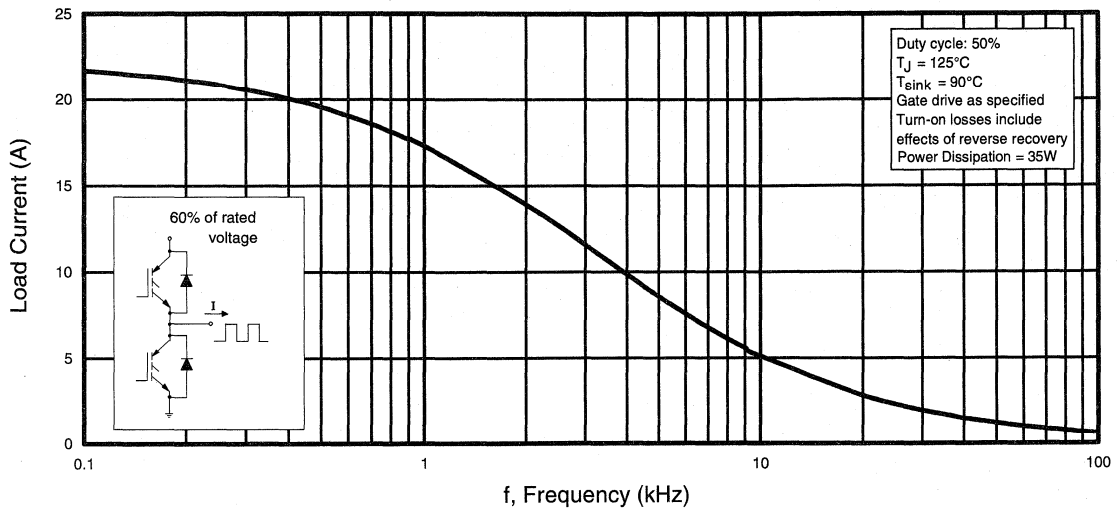


Fig. 1 - Typical Load Current vs. Frequency
 (Load Current = I_{RMS} of fundamental)

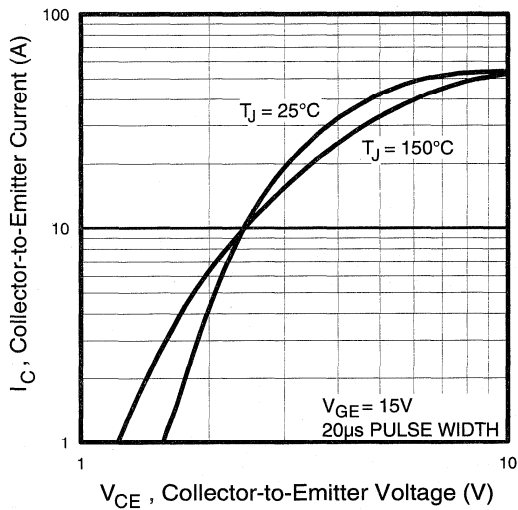


Fig. 2 - Typical Output Characteristics

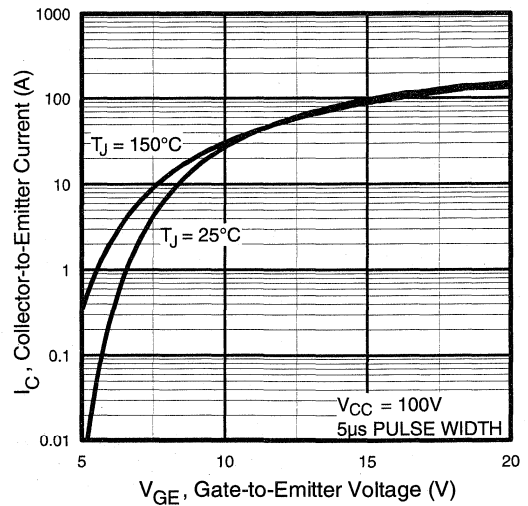


Fig. 3 - Typical Transfer Characteristics

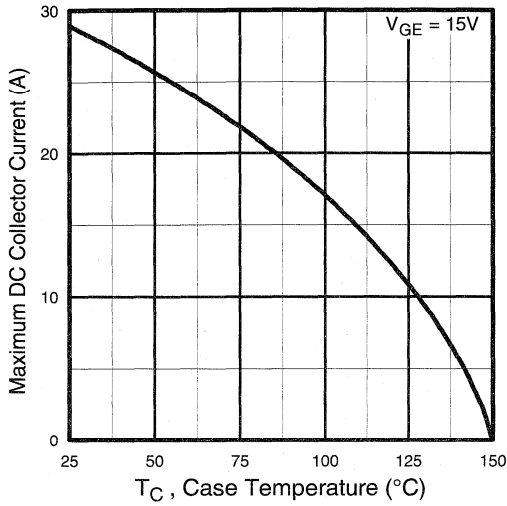


Fig. 4 - Maximum Collector Current vs. Case Temperature

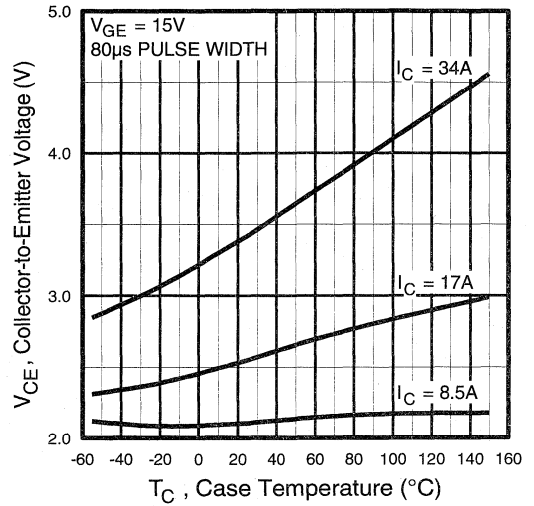


Fig. 5 - Collector-to-Emitter Voltage vs. Case Temperature

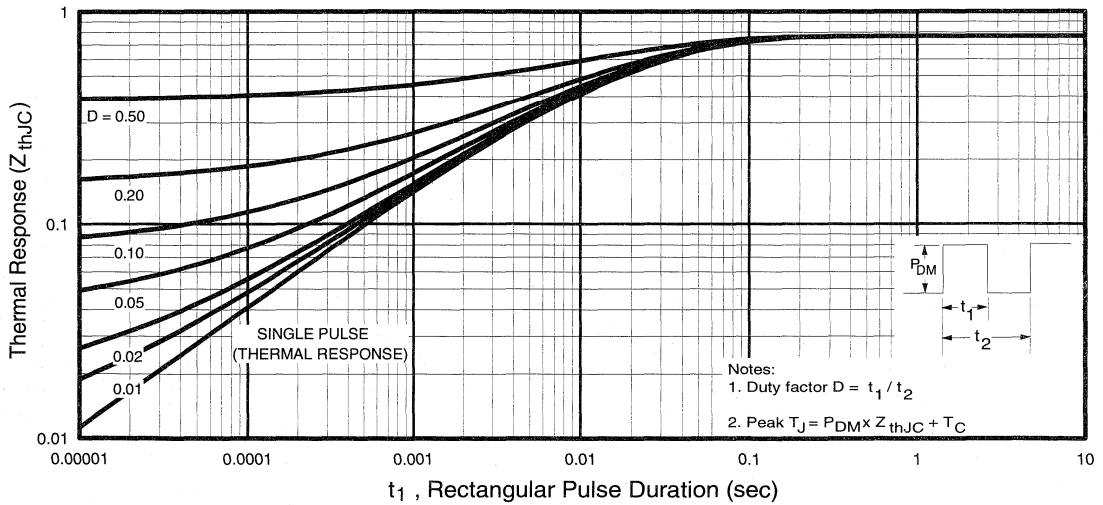


Fig. 6 - Maximum IGBT Effective Transient Thermal Impedance, Junction-to-Case

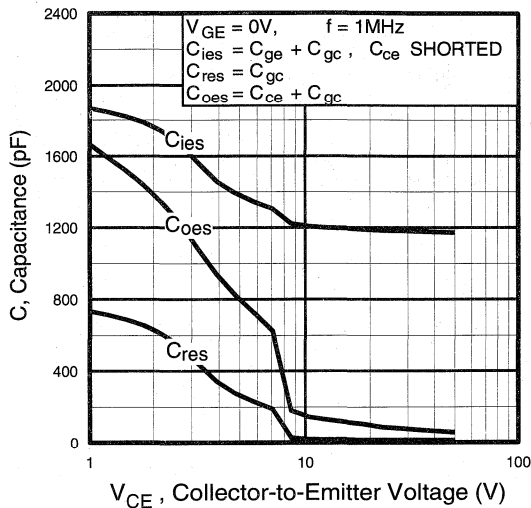


Fig. 7 - Typical Capacitance vs. Collector-to-Emitter Voltage

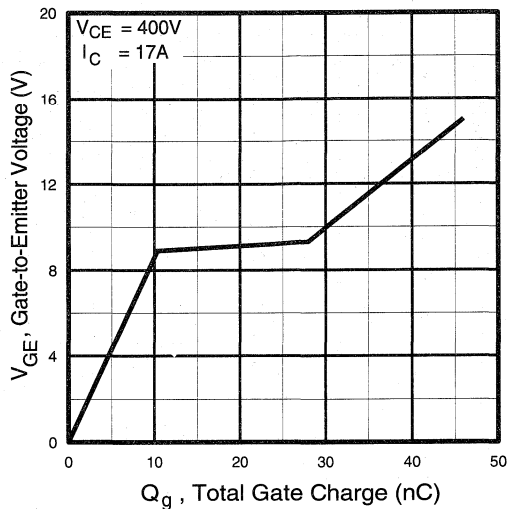


Fig. 8 - Typical Gate Charge vs. Gate-to-Emitter Voltage

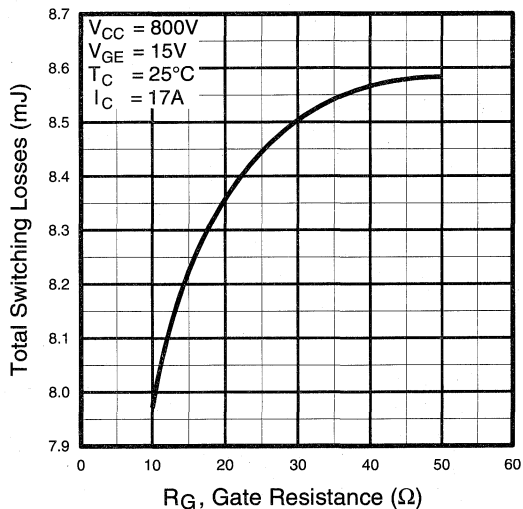


Fig. 9 - Typical Switching Losses vs. Gate Resistance

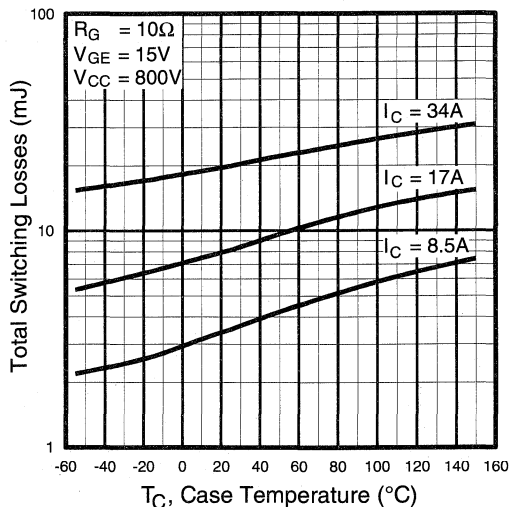


Fig. 10 - Typical Switching Losses vs. Case Temperature

Power Conversion
 Fast
 Co-Packs

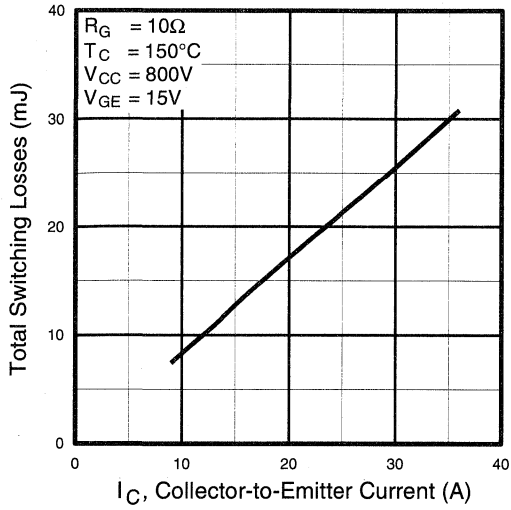


Fig. 11 - Typical Switching Losses vs. Collector-to-Emitter Current

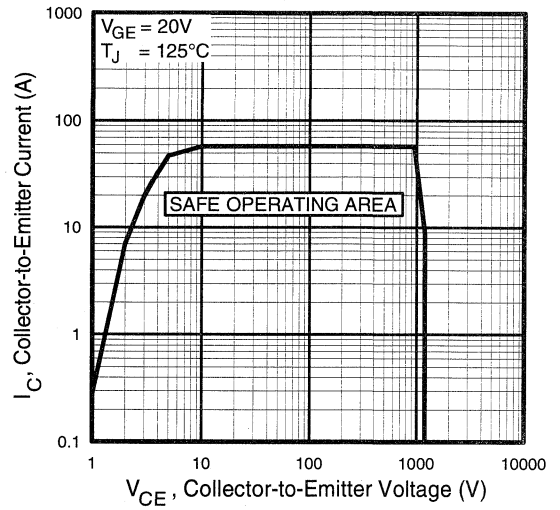


Fig. 12 - Turn-Off SOA

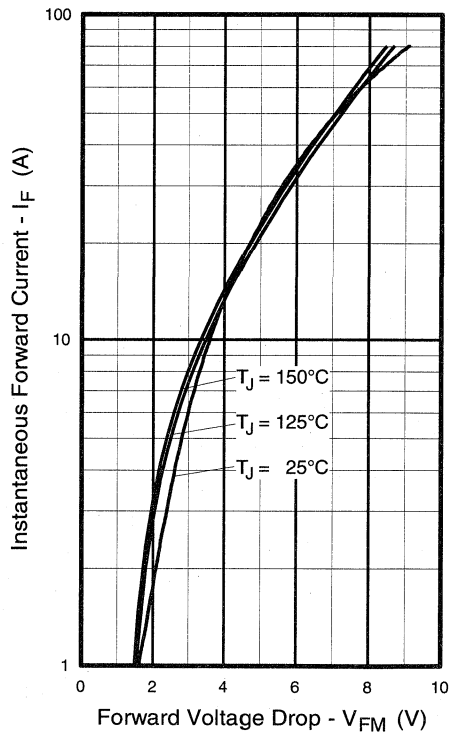


Fig. 13 - Maximum Forward Voltage Drop vs. Instantaneous Forward Current

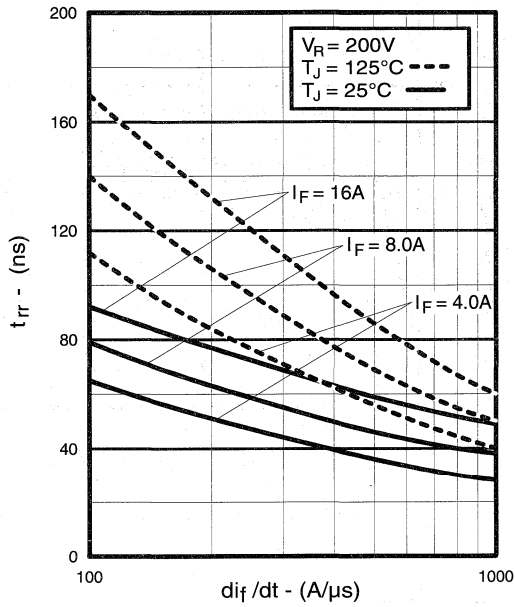


Fig. 14 - Typical Reverse Recovery vs. di_f/dt

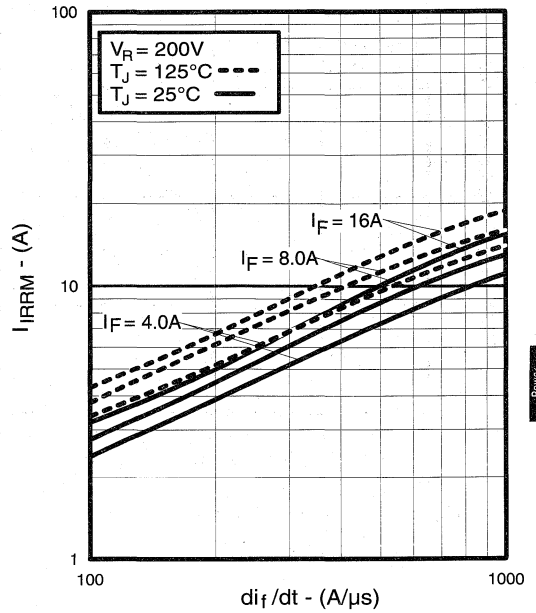


Fig. 15 - Typical Recovery Current vs. di_f/dt

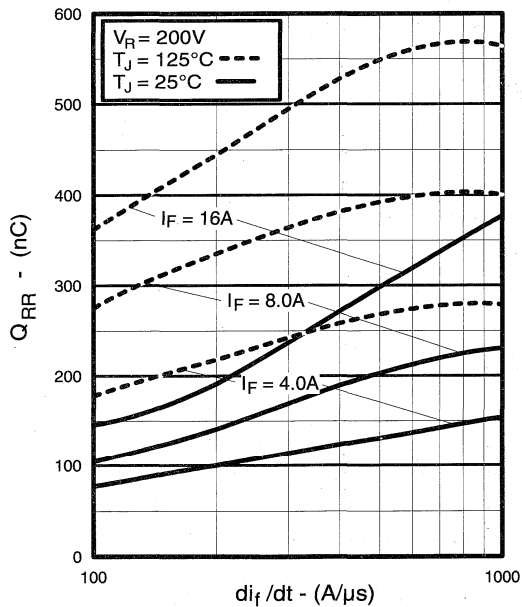


Fig. 16 - Typical Stored Charge vs. di_f/dt

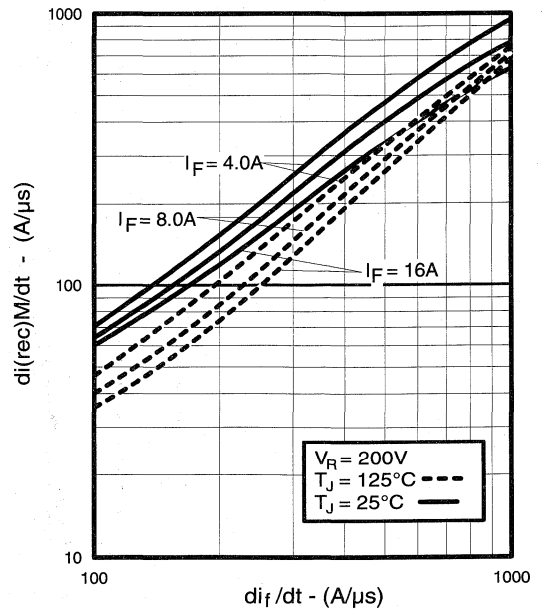


Fig. 17 - Typical $di_{(rec)M}/dt$ vs. di_f/dt

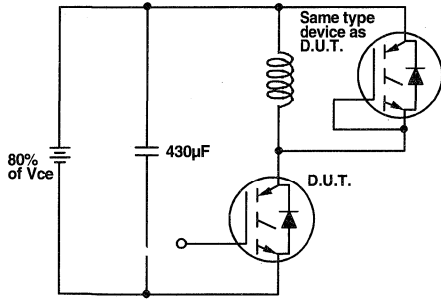


Fig. 18a - Test Circuit for Measurement of I_{LM} , E_{on} , $E_{off}(\text{diode})$, t_{rr} , Q_{rr} , I_{rr} , $t_{d(on)}$, t_r , $t_{d(off)}$, t_f

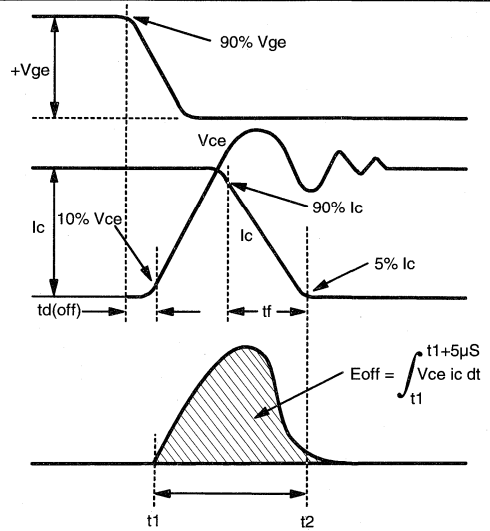


Fig. 18b - Test Waveforms for Circuit of Fig. 18a, Defining E_{off} , $t_{d(off)}$, t_f

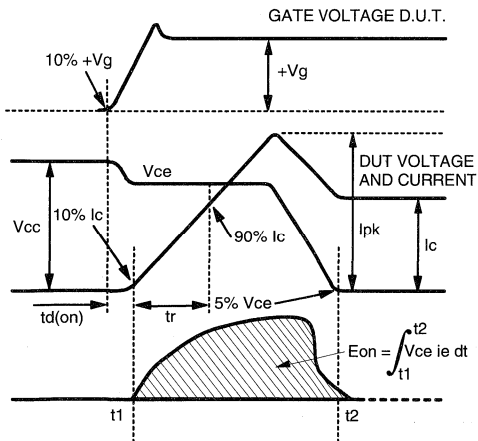


Fig. 18c - Test Waveforms for Circuit of Fig. 18a, Defining E_{on} , $t_{d(on)}$, t_r

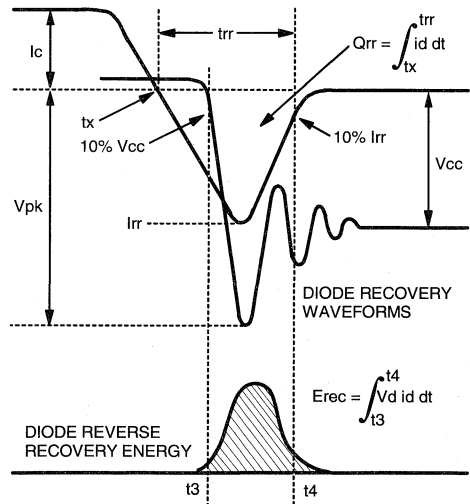


Fig. 18d - Test Waveforms for Circuit of Fig. 18a, Defining E_{rec} , t_{rr} , Q_{rr} , I_{rr}

**Refer to Section D for the following:
Appendix H: Section D - page D-10**

Fig. 18e - Macro Waveforms for Test Circuit Fig. 18a

Fig. 19 - Clamped Inductive Load Test Circuit

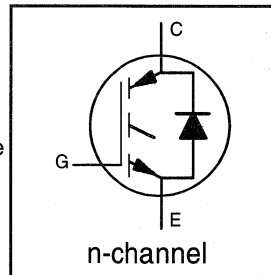
Fig. 20 - Pulsed Collector Current Test Circuit

INSULATED GATE BIPOLAR TRANSISTOR WITH ULTRAFAST SOFT RECOVERY DIODE

Fast CoPack IGBT

Features

- Switching-loss rating includes all "tail" losses
- HEXFRED™ soft ultrafast diodes
- Optimized for medium operating frequency (1 to 10kHz) See Fig. 1 for Current vs. Frequency curve



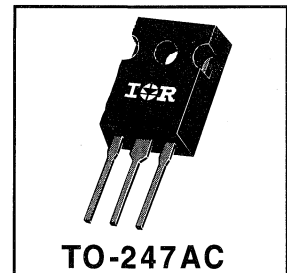
$$V_{CES} = 1200V$$

$$V_{CE(sat)} \leq 2.9V$$

$$@V_{GE} = 15V, I_C = 25A$$

Description

Co-packaged IGBTs are a natural extension of International Rectifier's well known IGBT line. They provide the convenience of an IGBT and an ultrafast recovery diode in one package, resulting in substantial benefits to a host of high-voltage, high-current, motor control, UPS and power supply applications.



Absolute Maximum Ratings

	Parameter	Max.	Units
V_{CES}	Collector-to-Emitter Voltage	1200	V
$I_C @ T_C = 25^\circ C$	Continuous Collector Current	45	A
$I_C @ T_C = 100^\circ C$	Continuous Collector Current	25	
I_{CM}	Pulsed Collector Current ①	90	
I_{LM}	Clamped Inductive Load Current ②	90	
$I_F @ T_C = 100^\circ C$	Diode Continuous Forward Current	16	
I_{FM}	Diode Maximum Forward Current	90	
V_{GE}	Gate-to-Emitter Voltage	± 20	V
$P_D @ T_C = 25^\circ C$	Maximum Power Dissipation	200	W
$P_D @ T_C = 100^\circ C$	Maximum Power Dissipation	78	
T_J	Operating Junction and	-55 to +150	°C
T_{STG}	Storage Temperature Range		
	Soldering Temperature, for 10 sec.	300 (0.063 in. (1.6mm) from case)	
	Mounting Torque, 6-32 or M3 Screw.	10 lbf•in (1.1 N•m)	

Thermal Resistance

	Parameter	Min.	Typ.	Max.	Units
$R_{\theta JC}$	Junction-to-Case - IGBT	—	—	0.64	°C/W
$R_{\theta JC}$	Junction-to-Case - Diode	—	—	0.83	
$R_{\theta CS}$	Case-to-Sink, flat, greased surface	—	0.24	—	
$R_{\theta JA}$	Junction-to-Ambient, typical socket mount	—	—	40	
Wt	Weight	—	6 (0.21)	—	g (oz)

Electrical Characteristics @ T_J = 25°C (unless otherwise specified)

	Parameter	Min.	Typ.	Max.	Units	Conditions
V _{(BR)CES}	Collector-to-Emitter Breakdown Voltage ^①	1200	—	—	V	V _{GE} = 0V, I _C = 250μA
ΔV _{(BR)CES} /ΔT _J	Temperature Coeff. of Breakdown Voltage	—	1.1	—	V/°C	V _{GE} = 0V, I _C = 1.0mA
V _{CE(on)}	Collector-to-Emitter Saturation Voltage	—	2.1	2.9	V	I _C = 25A V _{GE} = 15V
		—	2.5	—		I _C = 45A See Fig. 2, 5
		—	3.0	—		I _C = 25A, T _J = 150°C
V _{GE(th)}	Gate Threshold Voltage	3.0	—	5.5		V _{CE} = V _{GE} , I _C = 250μA
ΔV _{GE(th)} /ΔT _J	Temperature Coeff. of Threshold Voltage	—	-14	—	mV/°C	V _{CE} = V _{GE} , I _C = 250μA
g _{fe}	Forward Transconductance ^④	7.5	17	—	S	V _{CE} = 100V, I _C = 25A
I _{CES}	Zero Gate Voltage Collector Current	—	—	250	μA	V _{GE} = 0V, V _{CE} = 1200V
		—	—	6500		V _{GE} = 0V, V _{CE} = 1200V, T _J = 150°C
V _{FM}	Diode Forward Voltage Drop	—	2.5	3.0	V	I _C = 16A See Fig. 13
		—	2.1	2.5		I _C = 16A, T _J = 150°C
I _{GES}	Gate-to-Emitter Leakage Current	—	—	±100	nA	V _{GE} = ±20V

Switching Characteristics @ T_J = 25°C (unless otherwise specified)

	Parameter	Min.	Typ.	Max.	Units	Conditions
Q _g	Total Gate Charge (turn-on)	—	82	100	nC	I _C = 25A
Q _{ge}	Gate - Emitter Charge (turn-on)	—	16	21		V _{CC} = 400V
Q _{gc}	Gate - Collector Charge (turn-on)	—	30	43		See Fig. 8
t _{d(on)}	Turn-On Delay Time	—	77	—	ns	T _J = 25°C
t _r	Rise Time	—	75	—		I _C = 25A, V _{CC} = 800V
t _{d(off)}	Turn-Off Delay Time	—	360	540		V _{GE} = 15V, R _G = 5.0Ω
t _f	Fall Time	—	320	470		Energy losses include "tail" and diode reverse recovery.
E _{on}	Turn-On Switching Loss	—	3.2	—		See Fig. 9, 10, 11, 18
E _{off}	Turn-Off Switching Loss	—	5.8	—	mJ	
E _{ts}	Total Switching Loss	—	9.0	13.5		
t _{d(on)}	Turn-On Delay Time	—	70	—	ns	T _J = 150°C, See Fig. 9, 10, 11, 18
t _r	Rise Time	—	70	—		I _C = 25A, V _{CC} = 800V
t _{d(off)}	Turn-Off Delay Time	—	660	—		V _{GE} = 15V, R _G = 5.0Ω
t _f	Fall Time	—	640	—		Energy losses include "tail" and diode reverse recovery.
E _{ts}	Total Switching Loss	—	16.2	—		mJ
L _E	Internal Emitter Inductance	—	13	—	nH	Measured 5mm from package
C _{ies}	Input Capacitance	—	2400	—	pF	V _{GE} = 0V
C _{oes}	Output Capacitance	—	140	—		V _{CC} = 30V See Fig. 7
C _{res}	Reverse Transfer Capacitance	—	28	—		f = 1.0MHz
t _{rr}	Diode Reverse Recovery Time	—	90	135	ns	T _J = 25°C See Fig.
		—	164	245		T _J = 125°C 14
I _{rr}	Diode Peak Reverse Recovery Current	—	5.8	10	A	T _J = 25°C See Fig.
		—	8.3	15		T _J = 125°C 15
Q _{rr}	Diode Reverse Recovery Charge	—	260	675	nC	T _J = 25°C See Fig.
		—	680	1838		T _J = 125°C 16
di _{(rec)M} /dt	Diode Peak Rate of Fall of Recovery During t _b	—	120	—	A/μs	T _J = 25°C See Fig.
		—	76	—		T _J = 125°C 17

Notes:

① Repetitive rating; V_{GE}=20V, pulse width limited by max. junction temperature. (See fig. 20)

② V_{CC}=80%(V_{CES}). V_{GE}=20V, L=10μH, R_G= 5.0Ω, (See fig. 19)

③ Pulse width ≤ 80μs; duty factor ≤ 0.1%.

④ Pulse width 5.0μs, single shot.

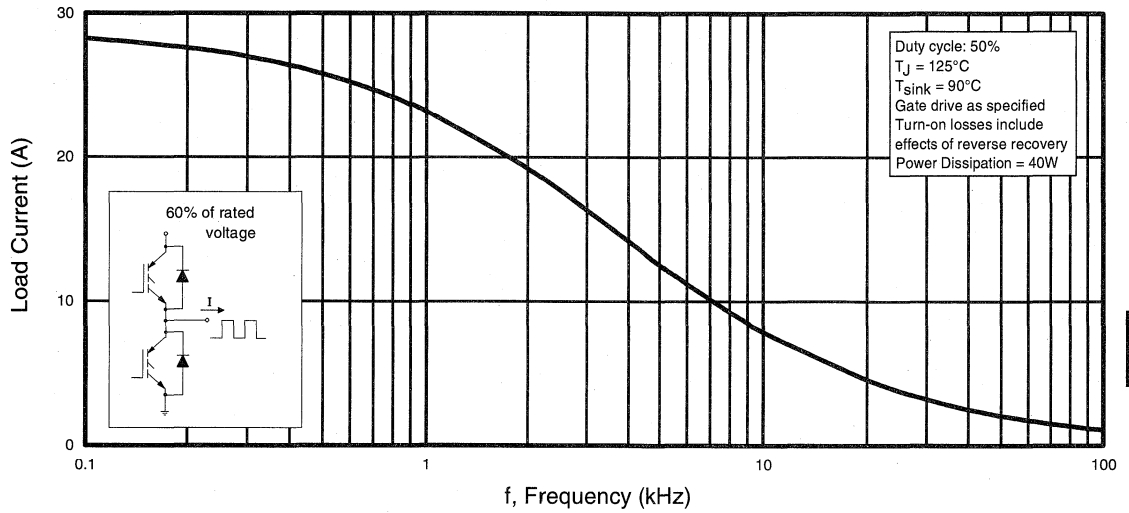


Fig. 1 - Typical Load Current vs. Frequency
 (Load Current = I_{RMS} of fundamental)

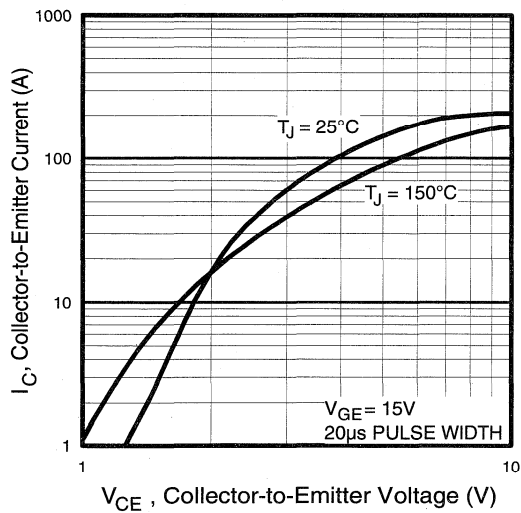


Fig. 2 - Typical Output Characteristics

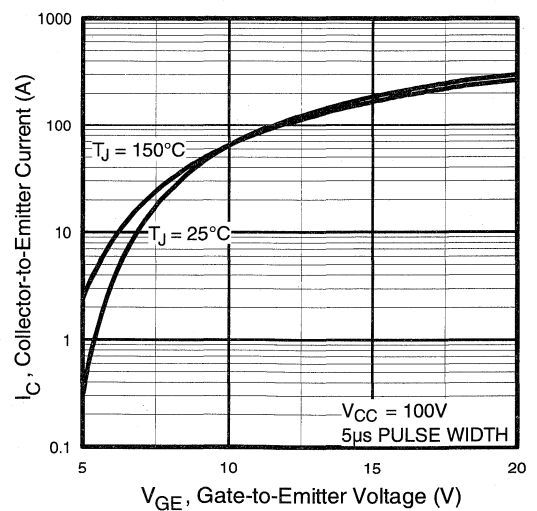


Fig. 3 - Typical Transfer Characteristics

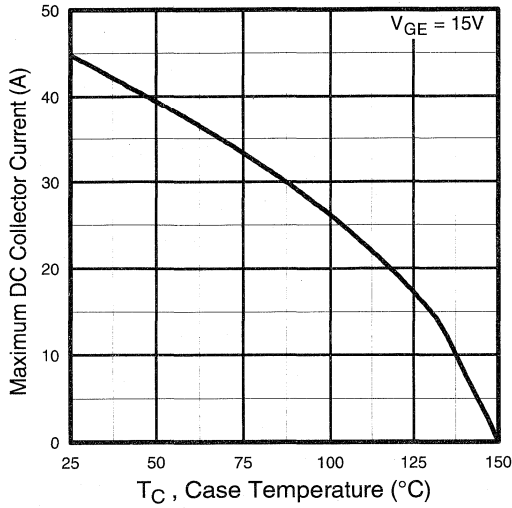


Fig. 4 - Maximum Collector Current vs. Case Temperature

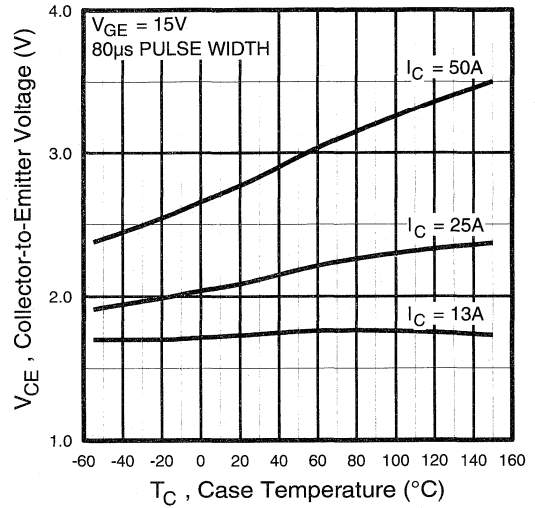


Fig. 5 - Collector-to-Emitter Voltage vs. Case Temperature

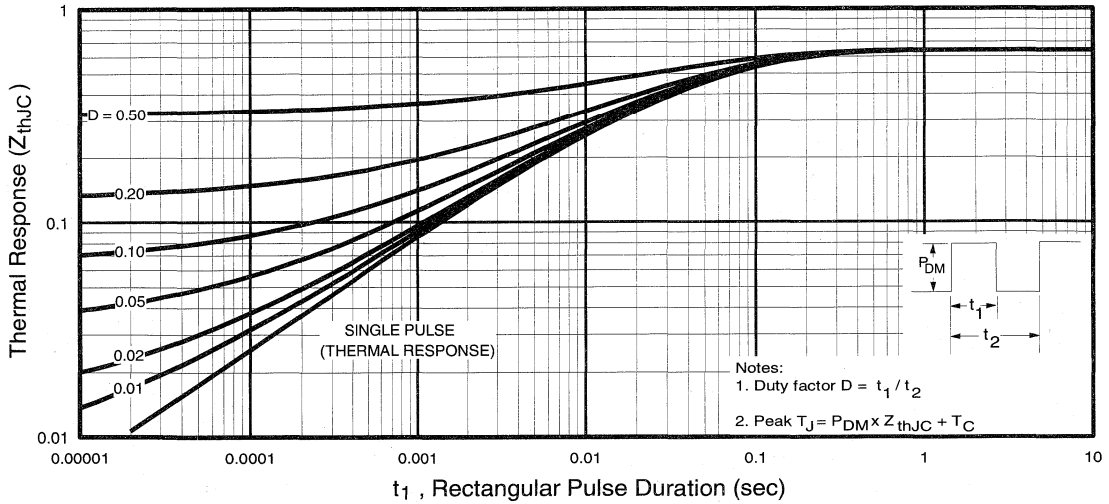


Fig. 6 - Maximum IGBT Effective Transient Thermal Impedance, Junction-to-Case

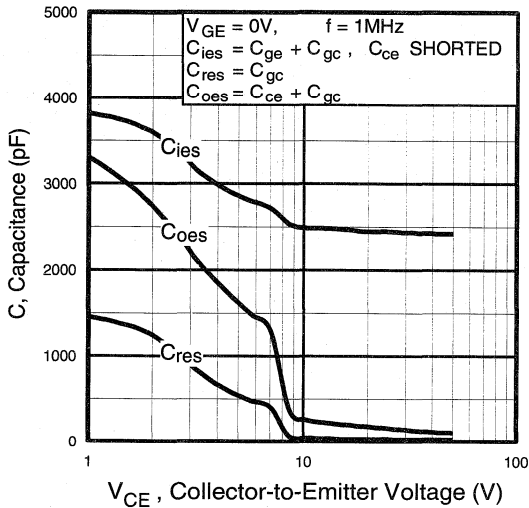


Fig. 7 - Typical Capacitance vs. Collector-to-Emitter Voltage

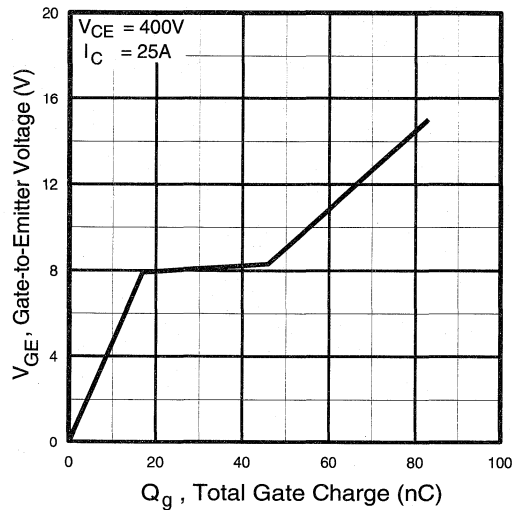


Fig. 8 - Typical Gate Charge vs. Gate-to-Emitter Voltage

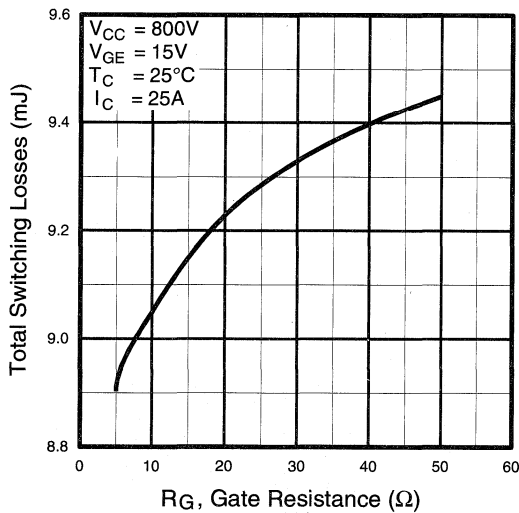


Fig. 9 - Typical Switching Losses vs. Gate Resistance

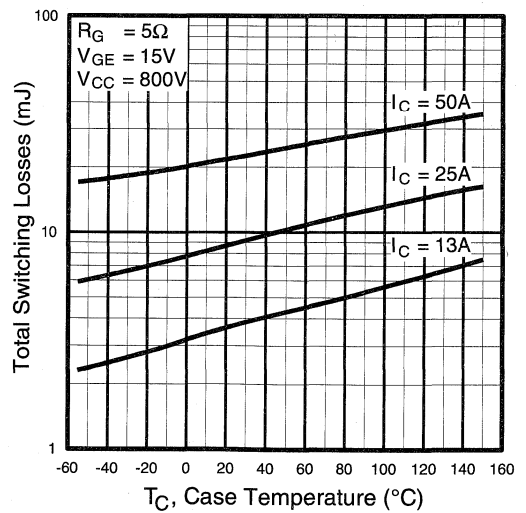


Fig. 10 - Typical Switching Losses vs. Case Temperature

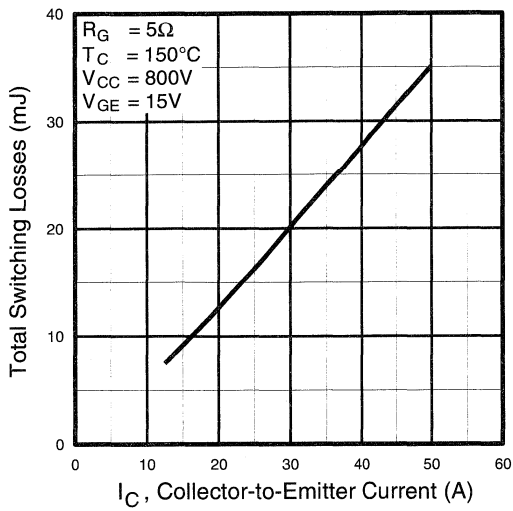


Fig. 11 - Typical Switching Losses vs. Collector-to-Emitter Current

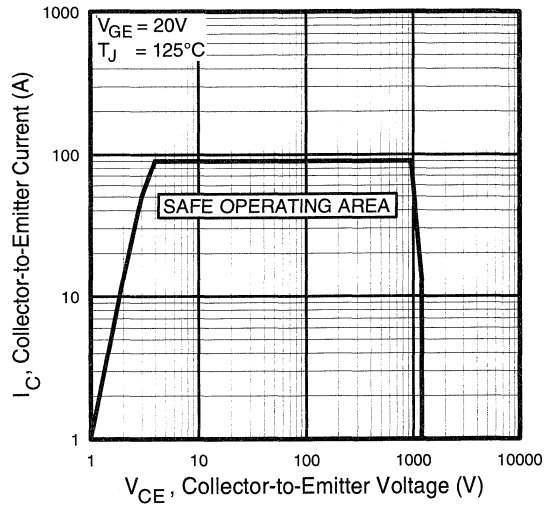


Fig. 12 - Turn-Off SOA

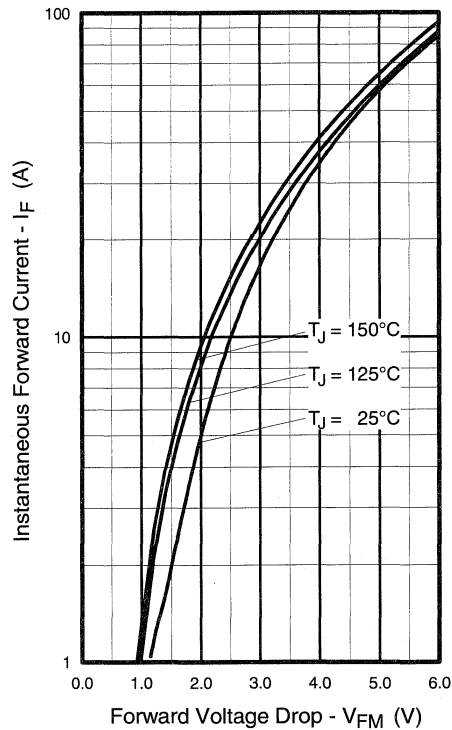


Fig. 13 - Maximum Forward Voltage Drop vs. Instantaneous Forward Current

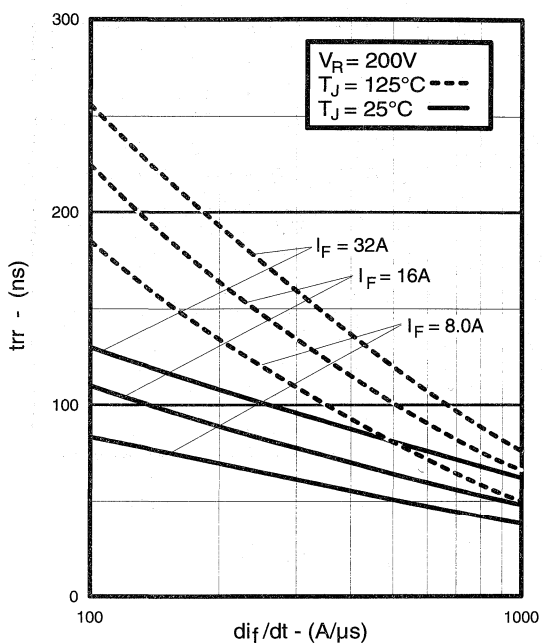


Fig. 14 - Typical Reverse Recovery vs. di_f/dt

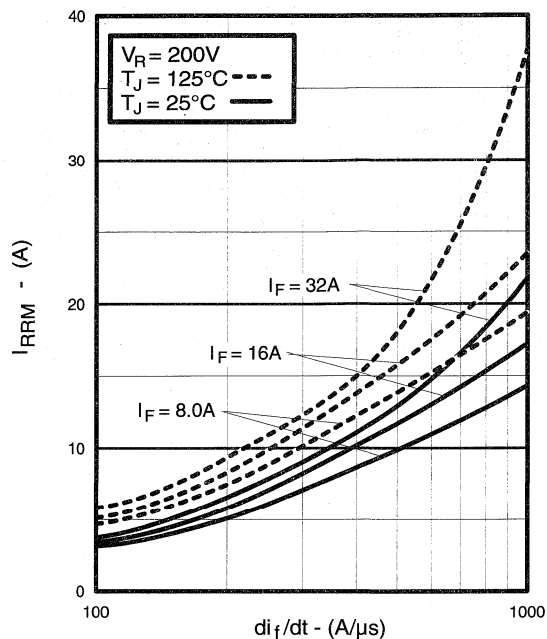


Fig. 15 - Typical Recovery Current vs. di_f/dt

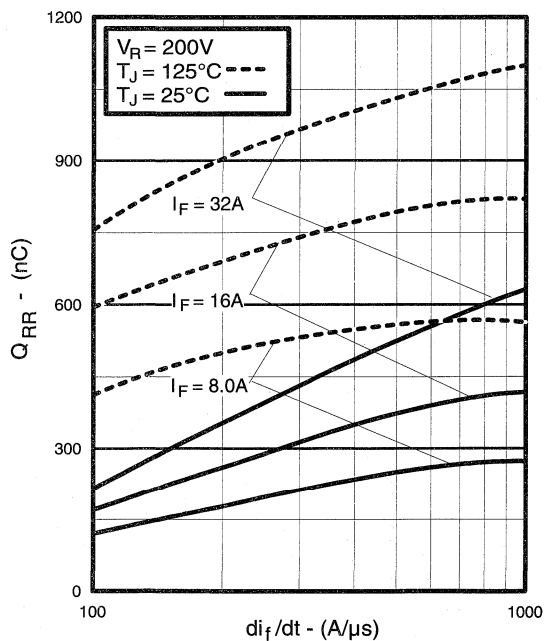


Fig. 16 - Typical Stored Charge vs. di_f/dt

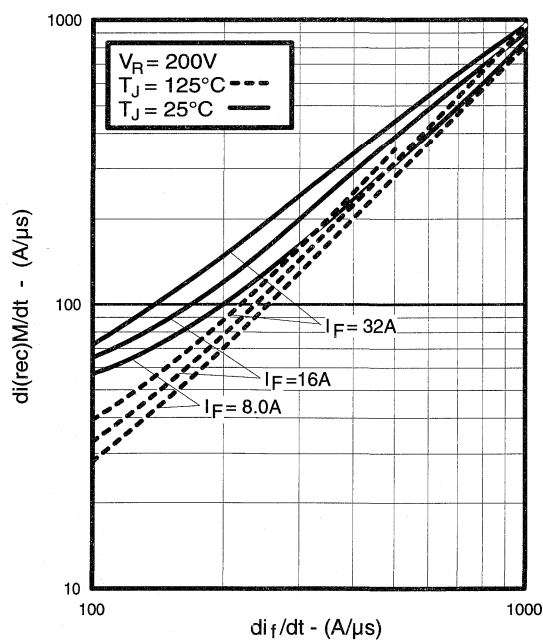


Fig. 17 - Typical $di_{(rec)}M/dt$ vs. di_f/dt

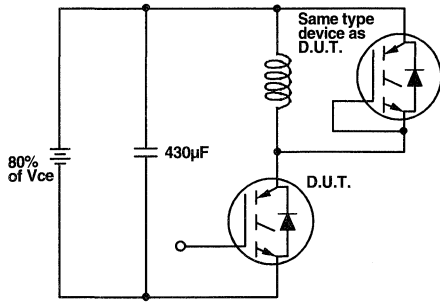


Fig. 18a - Test Circuit for Measurement of I_{LM} , E_{on} , $E_{off}(\text{diode})$, t_{rr} , Q_{rr} , I_{rr} , $t_{d(on)}$, t_r , $t_{d(off)}$, t_f

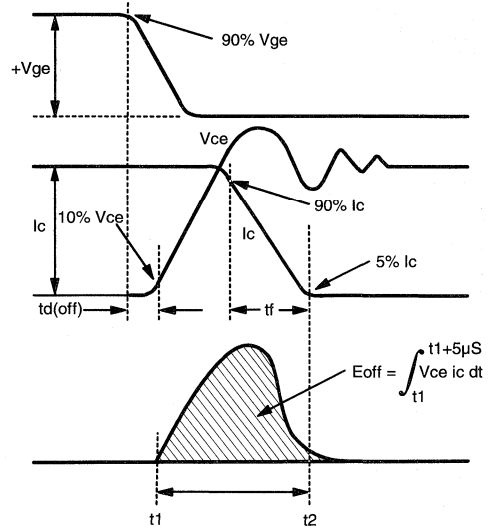


Fig. 18b - Test Waveforms for Circuit of Fig. 18a, Defining E_{off} , $t_{d(off)}$, t_f

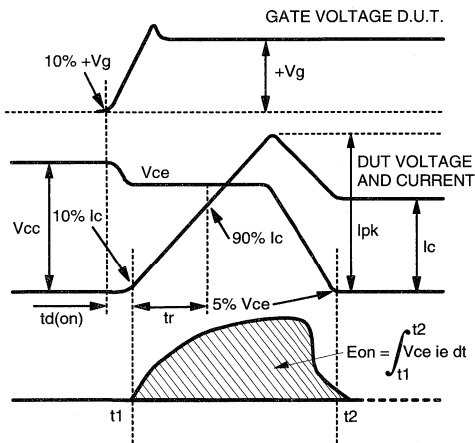


Fig. 18c - Test Waveforms for Circuit of Fig. 18a, Defining E_{on} , $t_{d(on)}$, t_r

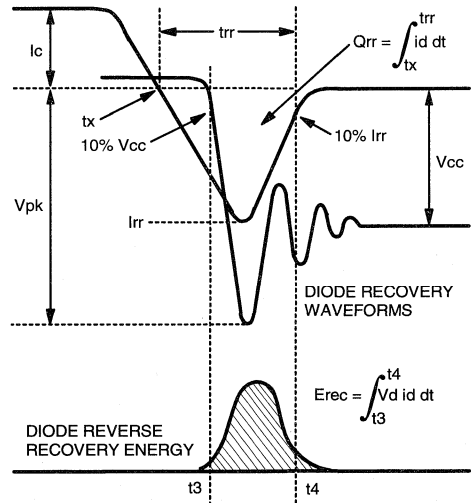


Fig. 18d - Test Waveforms for Circuit of Fig. 18a, Defining E_{rec} , t_{rr} , Q_{rr} , I_{rr}

**Refer to Section D for the following:
Appendix H: Section D - page D-10**

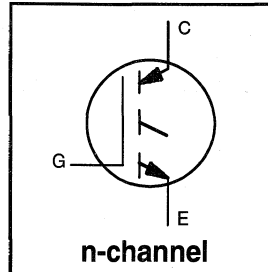
- Fig. 18e - Macro Waveforms for Test Circuit Fig. 18a
- Fig. 19 - Clamped Inductive Load Test Circuit
- Fig. 20 - Pulsed Collector Current Test Circuit

INSULATED GATE BIPOLAR TRANSISTOR

Short Circuit Rated
Fast IGBT

Features

- Short circuit rated - $10\mu\text{s}$ @ 125°C , $V_{\text{GE}} = 15\text{V}$
- Switching-loss rating includes all "tail" losses
- Optimized for medium operating frequency (1 to 10kHz) See Fig. 1 for Current vs. Frequency curve



$$V_{\text{CES}} = 600\text{V}$$

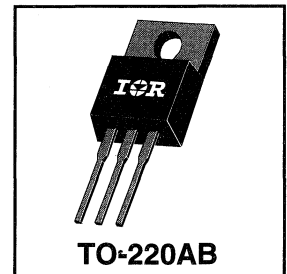
$$V_{\text{CE(sat)}} \leq 2.5\text{V}$$

$$\text{@ } V_{\text{GE}} = 15\text{V}, I_{\text{C}} = 8.0\text{A}$$

Description

Insulated Gate Bipolar Transistors (IGBTs) from International Rectifier have higher usable current densities than comparable bipolar transistors, while at the same time having simpler gate-drive requirements of the familiar power MOSFET. They provide substantial benefits to a host of high-voltage, high-current applications.

These new short circuit rated devices are especially suited for motor control and other applications requiring short circuit withstand capability.



Motor
Control
Fast
Discretes

Absolute Maximum Ratings

	Parameter	Max.	Units
V_{CES}	Collector-to-Emitter Voltage	600	V
$I_{\text{C}} @ T_{\text{C}} = 25^\circ\text{C}$	Continuous Collector Current	13	A
$I_{\text{C}} @ T_{\text{C}} = 100^\circ\text{C}$	Continuous Collector Current	8.0	
I_{CM}	Pulsed Collector Current ①	26	
I_{LM}	Clamped Inductive Load Current ②	26	
t_{sc}	Short Circuit Withstand Time	10	μs
V_{GE}	Gate-to-Emitter Voltage	± 20	V
E_{ARV}	Reverse Voltage Avalanche Energy ③	5.0	mJ
$P_{\text{D}} @ T_{\text{C}} = 25^\circ\text{C}$	Maximum Power Dissipation	60	W
$P_{\text{D}} @ T_{\text{C}} = 100^\circ\text{C}$	Maximum Power Dissipation	24	
T_{J}	Operating Junction and	-55 to +150	$^\circ\text{C}$
T_{STG}	Storage Temperature Range		
	Soldering Temperature, for 10 sec.	300 (0.063 in. (1.6mm) from case)	
	Mounting torque, 6-32 or M3 screw.	10 lbf•in (1.1N•m)	

Thermal Resistance

	Parameter	Min.	Typ.	Max.	Units
$R_{\theta\text{JC}}$	Junction-to-Case	—	—	2.1	$^\circ\text{C}/\text{W}$
$R_{\theta\text{CS}}$	Case-to-Sink, flat, greased surface	—	0.50	—	
$R_{\theta\text{JA}}$	Junction-to-Ambient, typical socket mount	—	—	80	
W_{t}	Weight	—	2 (0.07)	—	g (oz)

Electrical Characteristics @ $T_J = 25^\circ\text{C}$ (unless otherwise specified)

	Parameter	Min.	Typ.	Max.	Units	Conditions
$V_{(BR)CES}$	Collector-to-Emitter Breakdown Voltage	600	—	—	V	$V_{GE} = 0V, I_C = 250\mu A$
$V_{(BR)ECS}$	Emitter-to-Collector Breakdown Voltage ④	20	—	—	V	$V_{GE} = 0V, I_C = 1.0A$
$\Delta V_{(BR)CES}/\Delta T_J$	Temperature Coeff. of Breakdown Voltage	—	0.42	—	V/°C	$V_{GE} = 0V, I_C = 1.0mA$
$V_{CE(on)}$	Collector-to-Emitter Saturation Voltage	—	2.0	2.5	V	$I_C = 8.0A$ $I_C = 13A$ $I_C = 8.0A, T_J = 150^\circ\text{C}$ $V_{CE} = V_{GE}, I_C = 250\mu A$
		—	2.7	—		
		—	2.5	—		
$V_{GE(th)}$	Gate Threshold Voltage	3.0	—	5.5		
$\Delta V_{GE(th)}/\Delta T_J$	Temperature Coeff. of Threshold Voltage	—	-11	—	mV/°C	$V_{CE} = V_{GE}, I_C = 250\mu A$
g_{fe}	Forward Transconductance ⑤	2.7	3.8	—	S	$V_{CE} = 100V, I_C = 8.0A$
I_{CES}	Zero Gate Voltage Collector Current	—	—	250	μA	$V_{GE} = 0V, V_{CE} = 600V$
		—	—	1000		$V_{GE} = 0V, V_{CE} = 600V, T_J = 150^\circ\text{C}$
I_{GES}	Gate-to-Emitter Leakage Current	—	—	± 100	nA	$V_{GE} = \pm 20V$

Switching Characteristics @ $T_J = 25^\circ\text{C}$ (unless otherwise specified)

	Parameter	Min.	Typ.	Max.	Units	Conditions
Q_g	Total Gate Charge (turn-on)	—	7.9	16	nC	$I_C = 8.0A$ $V_{CC} = 400V$ $V_{GE} = 15V$ See Fig. 8
Q_{ge}	Gate - Emitter Charge (turn-on)	—	3.6	5.2		
Q_{gc}	Gate - Collector Charge (turn-on)	—	6.0	9.0		
$t_{d(on)}$	Turn-On Delay Time	—	29	—	ns	$T_J = 25^\circ\text{C}$ $I_C = 8.0A, V_{CC} = 480V$ $V_{GE} = 15V, R_G = 50\Omega$ Energy losses include "tail"
t_r	Rise Time	—	22	—		
$t_{d(off)}$	Turn-Off Delay Time	—	270	400		
t_f	Fall Time	—	280	510		
E_{on}	Turn-On Switching Loss	—	0.14	—		
E_{off}	Turn-Off Switching Loss	—	0.86	—		
E_{ts}	Total Switching Loss	—	1.0	2.0		
t_{sc}	Short Circuit Withstand Time	10	—	—	μs	$V_{CC} = 360V, T_J = 125^\circ\text{C}$ $V_{GE} = 15V, R_G = 50\Omega, V_{CPK} < 500V$
$t_{d(on)}$	Turn-On Delay Time	—	27	—	ns	$T_J = 150^\circ\text{C}$ $I_C = 8.0A, V_{CC} = 480V$ $V_{GE} = 15V, R_G = 50\Omega$ Energy losses include "tail"
t_r	Rise Time	—	21	—		
$t_{d(off)}$	Turn-Off Delay Time	—	370	—		
t_f	Fall Time	—	420	—		
E_{ts}	Total Switching Loss	—	1.4	—	mJ	See Fig. 10, 14
L_E	Internal Emitter Inductance	—	7.5	—	nH	Measured 5mm from package
C_{ies}	Input Capacitance	—	365	—	pF	$V_{GE} = 0V$ $V_{CC} = 30V$ $f = 1.0MHz$ See Fig. 7
C_{oes}	Output Capacitance	—	47	—		
C_{res}	Reverse Transfer Capacitance	—	4.8	—		

Notes:

- ① Repetitive rating; $V_{GE}=20V$, pulse width limited by max. junction temperature. (See fig. 13b)
- ② $V_{CC}=80\%(V_{CES}), V_{GE}=20V, L=10\mu H, R_G=50\Omega$, (See fig. 13a)
- ③ Repetitive rating; pulse width limited by maximum junction temperature.
- ④ Pulse width $\leq 80\mu s$; duty factor $\leq 0.1\%$.
- ⑤ Pulse width 5.0 μs , single shot.

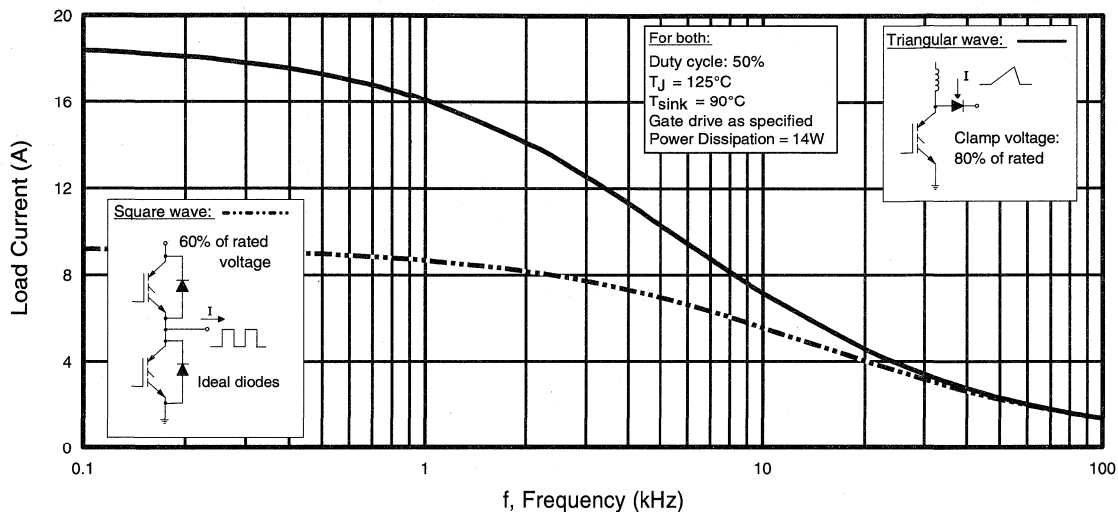


Fig. 1 - Typical Load Current vs. Frequency
 (For square wave, $I = I_{RMS}$ of fundamental; for triangular wave, $I = I_{PK}$)

Motor Control Fast Discretes

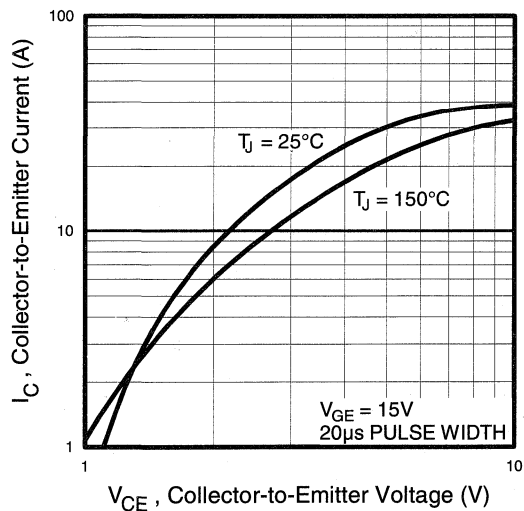


Fig. 2 - Typical Output Characteristics

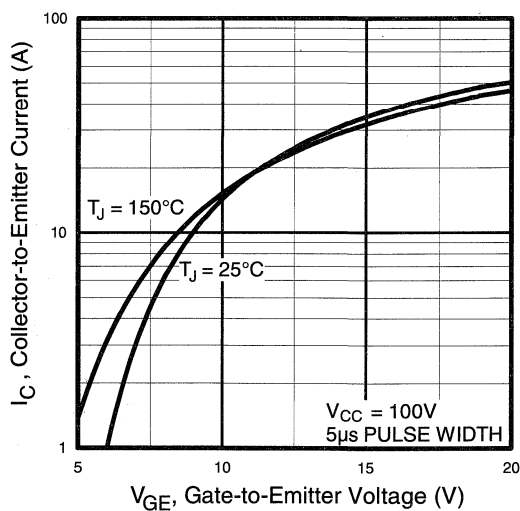


Fig. 3 - Typical Transfer Characteristics

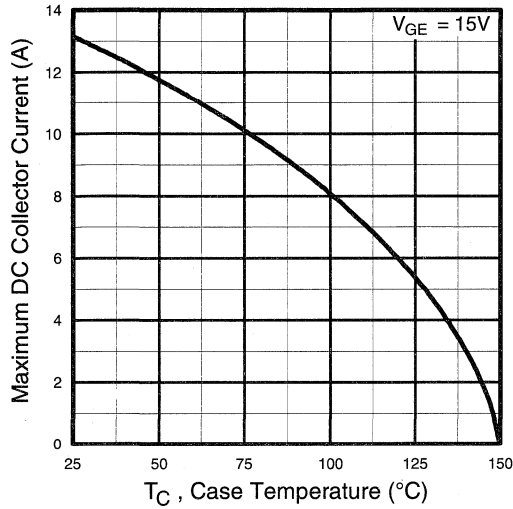


Fig. 4 - Maximum Collector Current vs. Case Temperature

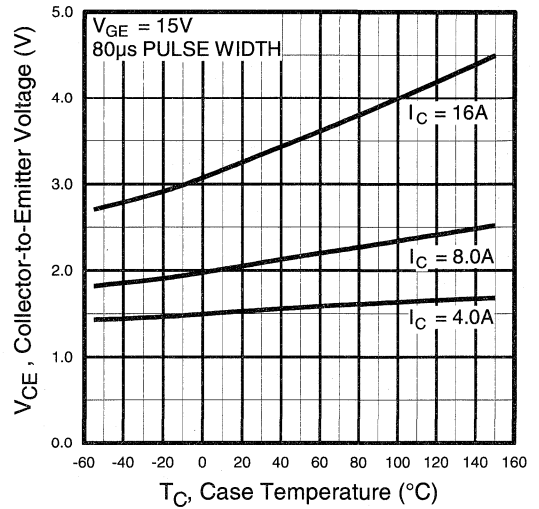


Fig. 5 - Collector-to-Emitter Voltage vs. Case Temperature

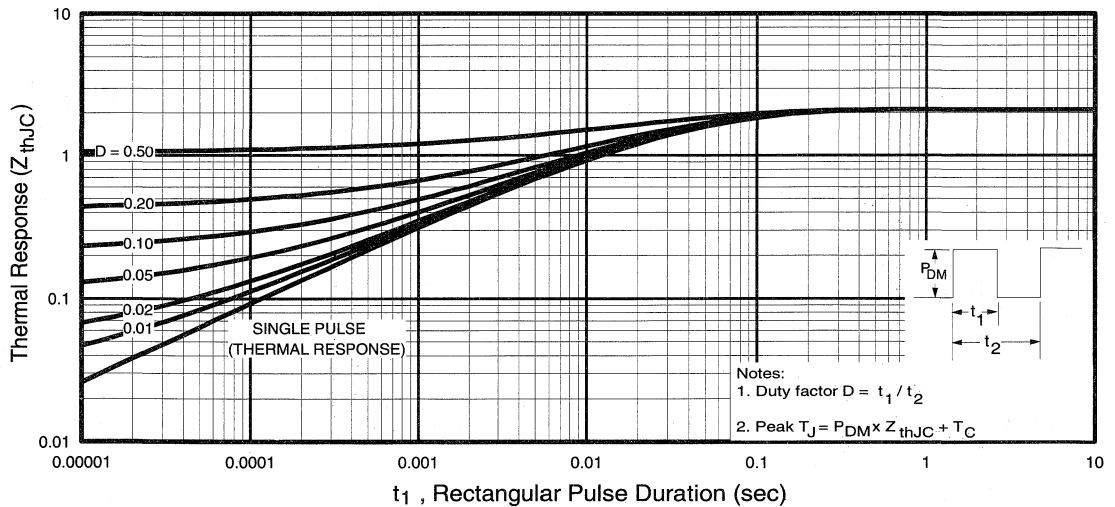


Fig. 6 - Maximum Effective Transient Thermal Impedance, Junction-to-Case

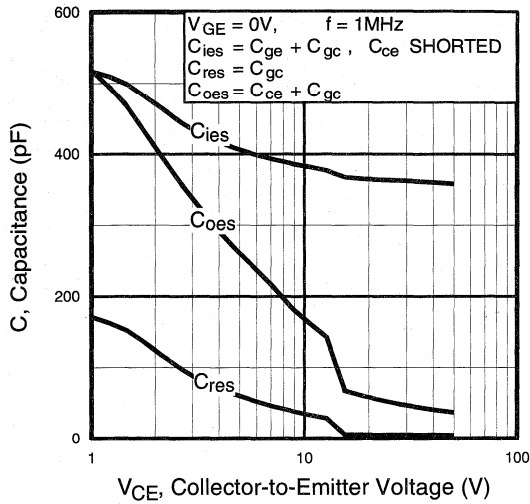


Fig. 7 - Typical Capacitance vs. Collector-to-Emitter Voltage

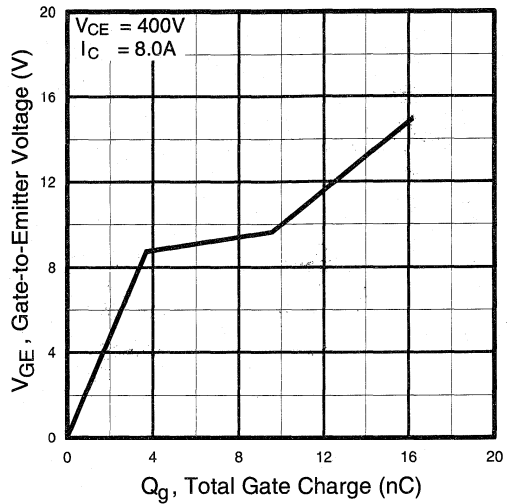


Fig. 8 - Typical Gate Charge vs. Gate-to-Emitter Voltage

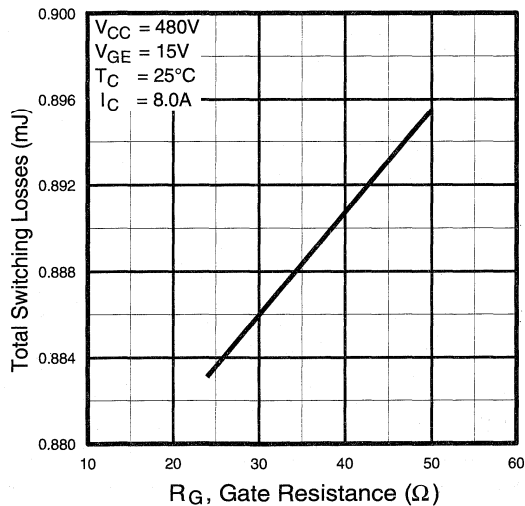


Fig. 9 - Typical Switching Losses vs. Gate Resistance

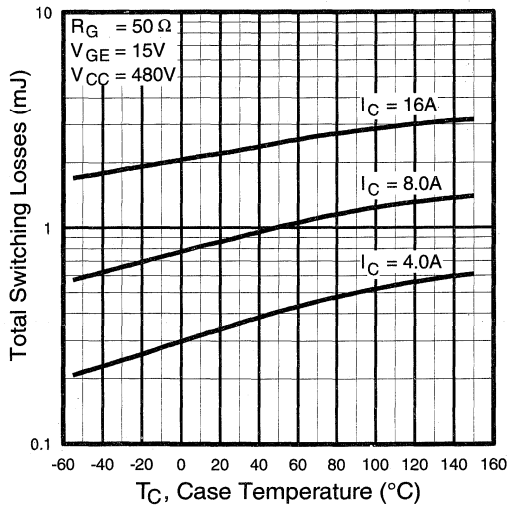


Fig. 10 - Typical Switching Losses vs. Case Temperature

Motor
Control
Fast
Discretes

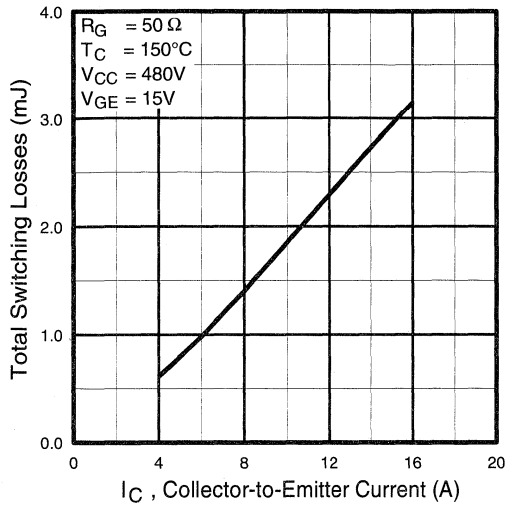


Fig. 11 - Typical Switching Losses vs. Collector-to-Emitter Current

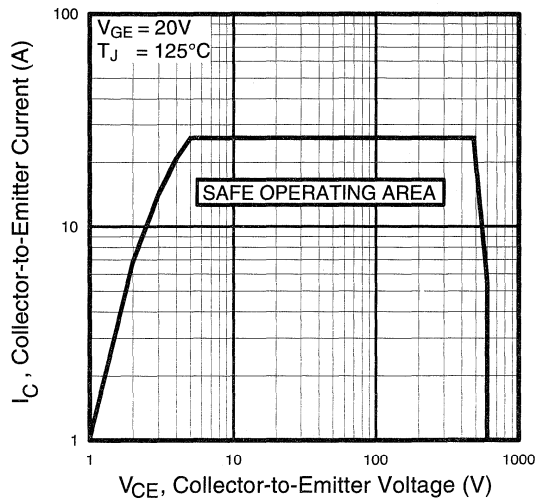


Fig. 12 - Turn-Off SOA

Refer to Section D for the following:

Appendix C: Section D - page D-5

Fig. 13a - Clamped Inductive Load Test Circuit

Fig. 13b - Pulsed Collector Current Test Circuit

Fig. 14a - Switching Loss Test Circuit

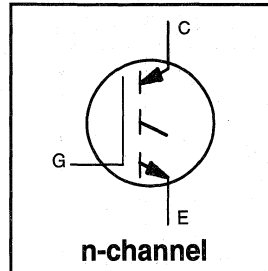
Fig. 14b - Switching Loss Waveform

Package Outline 1 - JEDEC Outline TO-220AB

Section D - page D-12

Features

- Short circuit rated - $10\mu\text{s}$ @ 125°C , $V_{\text{GE}} = 15\text{V}$
- Switching-loss rating includes all "tail" losses
- Optimized for medium operating frequency (1 to 10kHz) See Fig. 1 for Current vs. Frequency curve



$$V_{\text{CES}} = 600\text{V}$$

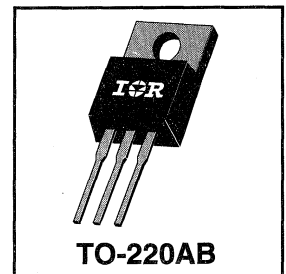
$$V_{\text{CE(sat)}} \leq 2.9\text{V}$$

$$\text{@ } V_{\text{GE}} = 15\text{V}, I_{\text{C}} = 16\text{A}$$

Description

Insulated Gate Bipolar Transistors (IGBTs) from International Rectifier have higher usable current densities than comparable bipolar transistors, while at the same time having simpler gate-drive requirements of the familiar power MOSFET. They provide substantial benefits to a host of high-voltage, high-current applications.

These new short circuit rated devices are especially suited for motor control and other applications requiring short circuit withstand capability.


 Motor
Control
Fast
Discretes

Absolute Maximum Ratings

	Parameter	Max.	Units
V_{CES}	Collector-to-Emitter Voltage	600	V
$I_{\text{C}} @ T_{\text{C}} = 25^\circ\text{C}$	Continuous Collector Current	26	A
$I_{\text{C}} @ T_{\text{C}} = 100^\circ\text{C}$	Continuous Collector Current	16	
I_{CM}	Pulsed Collector Current ①	52	
I_{LM}	Clamped Inductive Load Current ②	52	
t_{sc}	Short Circuit Withstand Time	10	μs
V_{GE}	Gate-to-Emitter Voltage	± 20	V
E_{ARV}	Reverse Voltage Avalanche Energy ③	10	mJ
$P_{\text{D}} @ T_{\text{C}} = 25^\circ\text{C}$	Maximum Power Dissipation	100	W
$P_{\text{D}} @ T_{\text{C}} = 100^\circ\text{C}$	Maximum Power Dissipation	42	
T_{J}	Operating Junction and	-55 to +150	$^\circ\text{C}$
T_{STG}	Storage Temperature Range		
	Soldering Temperature, for 10 sec.	300 (0.063 in. (1.6mm) from case)	
	Mounting torque, 6-32 or M3 screw.	10 lbf•in (1.1N•m)	

Thermal Resistance

	Parameter	Min.	Typ.	Max.	Units
$R_{\theta\text{JC}}$	Junction-to-Case	—	—	1.2	$^\circ\text{C/W}$
$R_{\theta\text{CS}}$	Case-to-Sink, flat, greased surface	—	0.50	—	
$R_{\theta\text{JA}}$	Junction-to-Ambient, typical socket mount	—	—	80	
W_t	Weight	—	2 (0.07)	—	g (oz)

Electrical Characteristics @ $T_J = 25^\circ\text{C}$ (unless otherwise specified)

	Parameter	Min.	Typ.	Max.	Units	Conditions
$V_{(BR)CES}$	Collector-to-Emitter Breakdown Voltage	600	—	—	V	$V_{GE} = 0V, I_C = 250\mu A$
$V_{(BR)ECS}$	Emitter-to-Collector Breakdown Voltage ④	20	—	—	V	$V_{GE} = 0V, I_C = 1.0A$
$\Delta V_{(BR)CES}/\Delta T_J$	Temp. Coeff. of Breakdown Voltage	—	0.65	—	V/°C	$V_{GE} = 0V, I_C = 1.0mA$
$V_{CE(on)}$	Collector-to-Emitter Saturation Voltage	—	1.9	2.9	V	$V_{GE} = 15V$ See Fig. 2, 5
		—	2.7	—		
		—	2.2	—		
$V_{GE(th)}$	Gate Threshold Voltage	3.0	—	5.5		$V_{CE} = V_{GE}, I_C = 250\mu A$
$\Delta V_{GE(th)}/\Delta T_J$	Temperature Coeff. of Threshold Voltage	—	-12	—	mV/°C	$V_{CE} = V_{GE}, I_C = 250\mu A$
g_{fe}	Forward Transconductance ⑤	3.3	6.5	—	S	$V_{CE} = 100V, I_C = 16A$
I_{CES}	Zero Gate Voltage Collector Current	—	—	250	μA	$V_{GE} = 0V, V_{CE} = 600V$
		—	—	1000		$V_{GE} = 0V, V_{CE} = 600V, T_J = 150^\circ C$
I_{GES}	Gate-to-Emitter Leakage Current	—	—	± 100	nA	$V_{GE} = \pm 20V$

Switching Characteristics @ $T_J = 25^\circ\text{C}$ (unless otherwise specified)

	Parameter	Min.	Typ.	Max.	Units	Conditions
Q_g	Total Gate Charge (turn-on)	—	35	53	nC	$I_C = 16A$ $V_{CC} = 400V$ See Fig. 8 $V_{GE} = 15V$
Q_{ge}	Gate - Emitter Charge (turn-on)	—	7.4	11		
Q_{gc}	Gate - Collector Charge (turn-on)	—	14	21		
$t_{d(on)}$	Turn-On Delay Time	—	31	—	ns	$T_J = 25^\circ C$ $I_C = 16A, V_{CC} = 480V$ $V_{GE} = 15V, R_G = 23\Omega$ Energy losses include "tail"
t_r	Rise Time	—	31	—		
$t_{d(off)}$	Turn-Off Delay Time	—	280	420		
t_f	Fall Time	—	310	470		
E_{on}	Turn-On Switching Loss	—	0.4	—		
E_{off}	Turn-Off Switching Loss	—	1.9	—	mJ	See Fig. 9, 10, 11, 14
E_{ts}	Total Switching Loss	—	2.3	3.5		
t_{sc}	Short Circuit Withstand Time	10	—	—	μs	$V_{CC} = 360V, T_J = 125^\circ C$ $V_{GE} = 15V, R_G = 23\Omega, V_{CPK} < 500V$
$t_{d(on)}$	Turn-On Delay Time	—	31	—	ns	$T_J = 150^\circ C,$ $I_C = 16A, V_{CC} = 480V$ $V_{GE} = 15V, R_G = 23\Omega$ Energy losses include "tail"
t_r	Rise Time	—	30	—		
$t_{d(off)}$	Turn-Off Delay Time	—	530	—		
t_f	Fall Time	—	660	—		
E_{ts}	Total Switching Loss	—	4.4	—		
L_E	Internal Emitter Inductance	—	7.5	—	nH	Measured 5mm from package
C_{ies}	Input Capacitance	—	750	—	pF	$V_{GE} = 0V$ $V_{CC} = 30V$ See Fig. 7 $f = 1.0MHz$
C_{oes}	Output Capacitance	—	110	—		
C_{res}	Reverse Transfer Capacitance	—	9.3	—		

Notes:

- ① Repetitive rating; $V_{GE} = 20V$, pulse width limited by max. junction temperature. (See fig. 13b)
- ② $V_{CC} = 80\%(V_{CES}), V_{GE} = 20V, L = 10\mu H, R_G = 23\Omega,$ (See fig. 13a)
- ③ Repetitive rating; pulse width limited by maximum junction temperature.
- ④ Pulse width $\leq 80\mu s$; duty factor $\leq 0.1\%$.
- ⑤ Pulse width $5.0\mu s$, single shot.

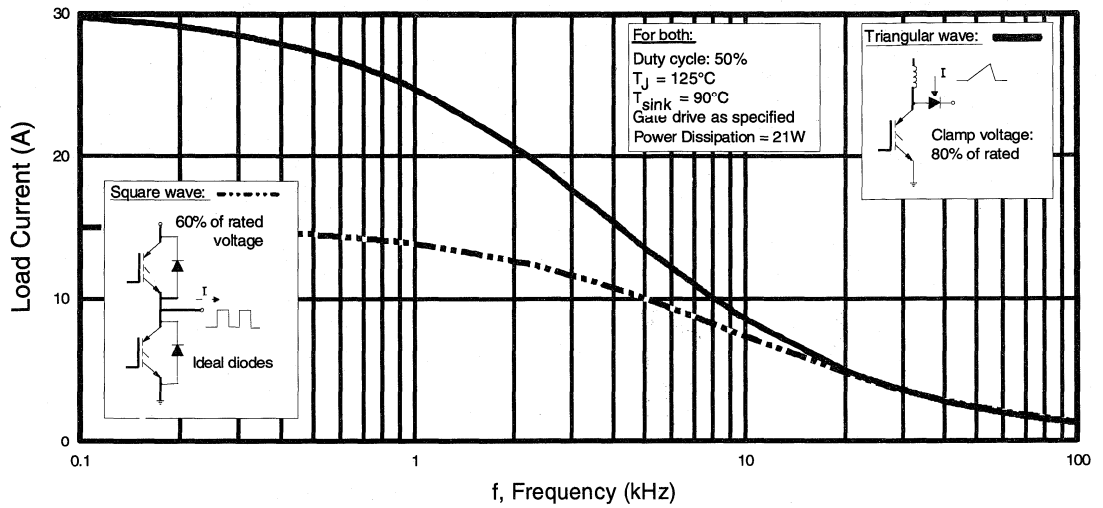


Fig. 1 - Typical Load Current vs. Frequency
 (For square wave, $I = I_{RMS}$ of fundamental; for triangular wave, $I = I_{PK}$)

Motor
Control
Fast
Discrete

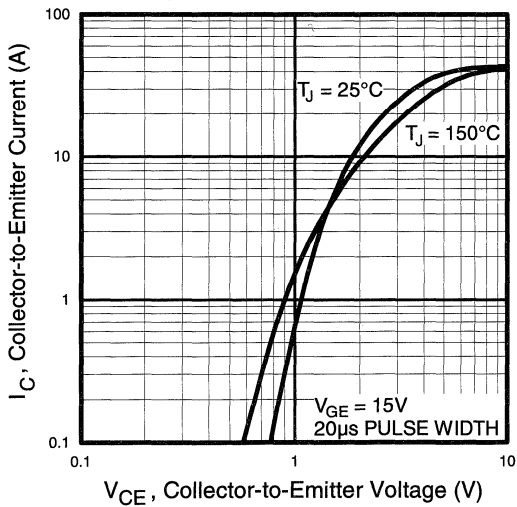


Fig. 2 - Typical Output Characteristics

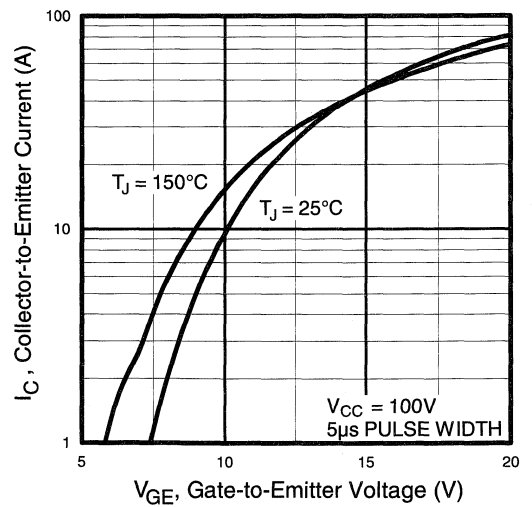


Fig. 3 - Typical Transfer Characteristics

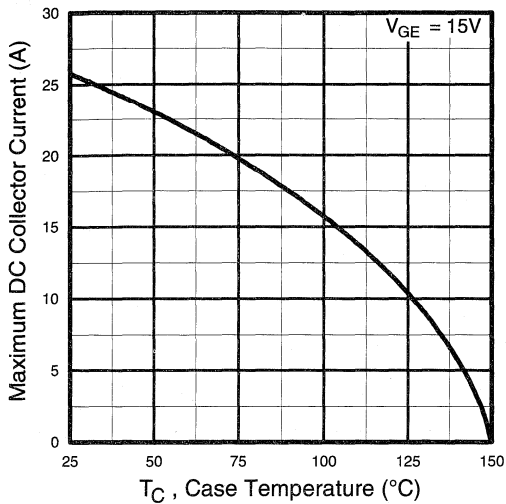


Fig. 4 - Maximum Collector Current vs. Case Temperature

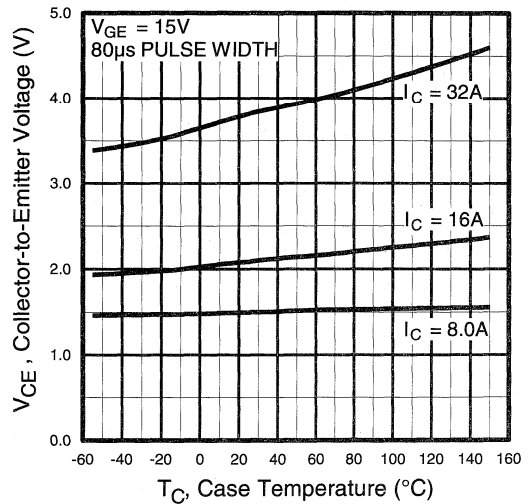


Fig. 5 - Collector-to-Emitter Voltage vs. Case Temperature

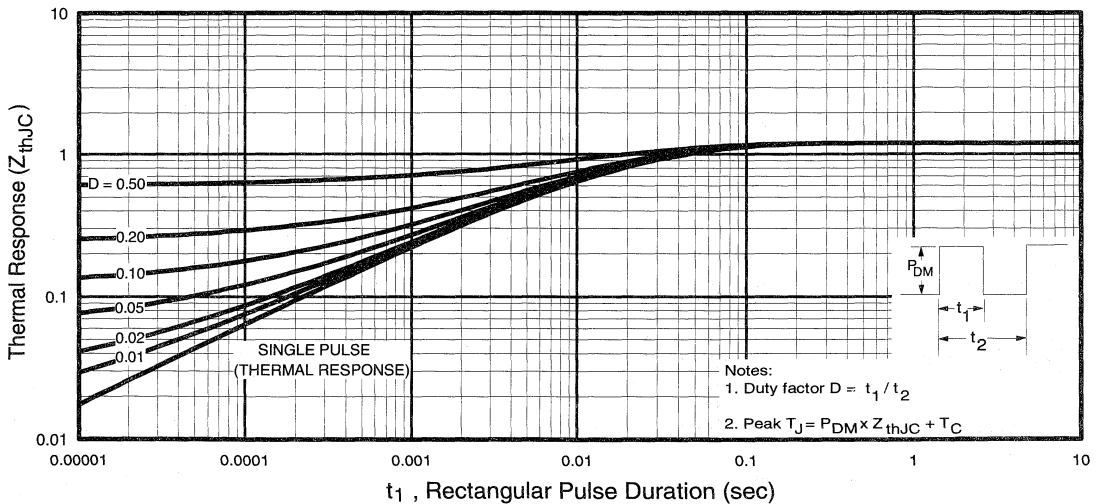


Fig. 6 - Maximum Effective Transient Thermal Impedance, Junction-to-Case

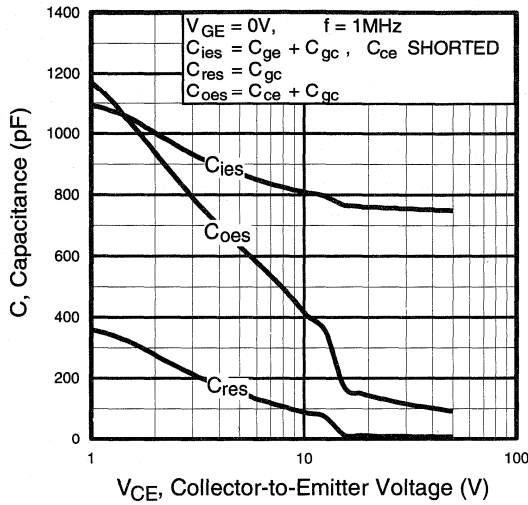


Fig. 7 - Typical Capacitance vs. Collector-to-Emitter Voltage

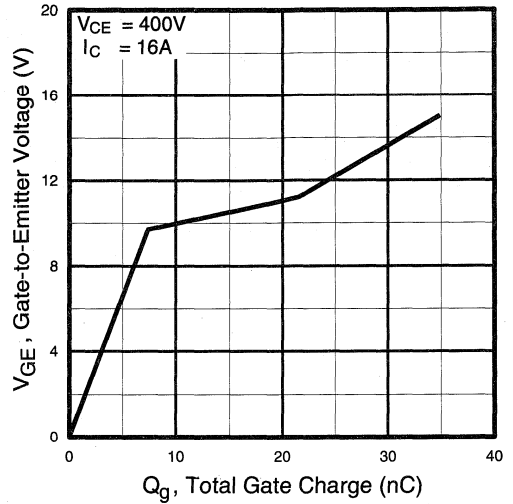


Fig. 8 - Typical Gate Charge vs. Gate-to-Emitter Voltage

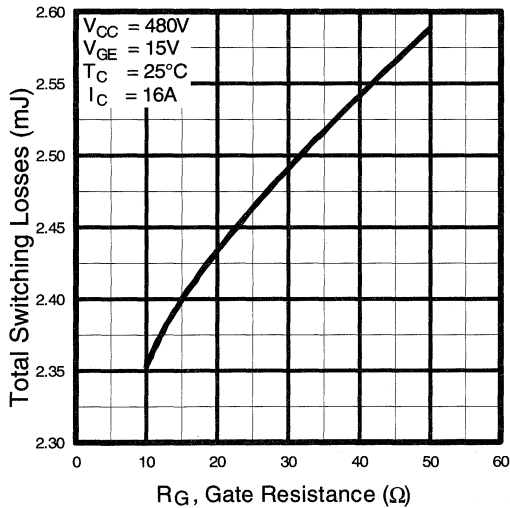


Fig. 9 - Typical Switching Losses vs. Gate Resistance

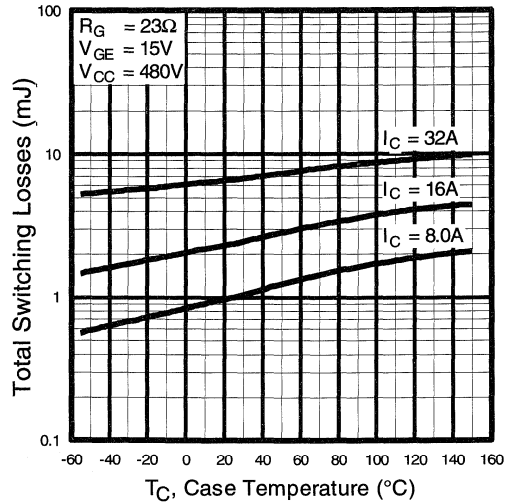


Fig. 10 - Typical Switching Losses vs. Case Temperature

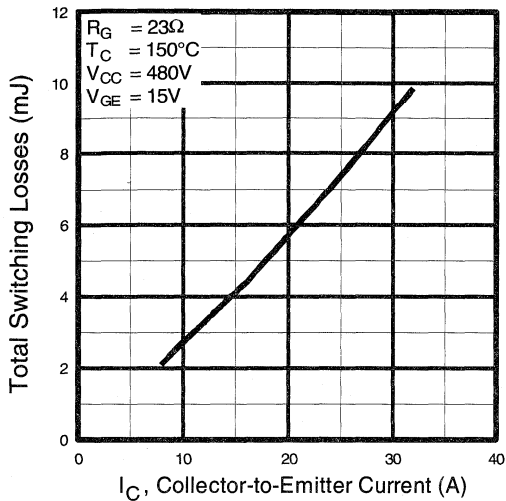


Fig. 11 - Typical Switching Losses vs. Collector-to-Emitter Current

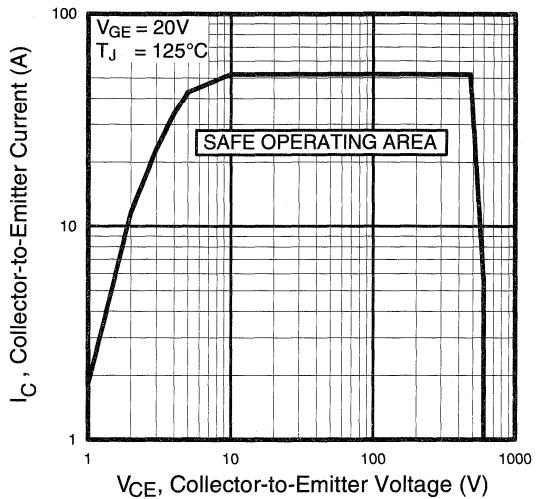


Fig. 12 - Turn-Off SOA

Refer to Section D for the following:

Appendix C: Section D - page D-5

- Fig. 13a - Clamped Inductive Load Test Circuit
- Fig. 13b - Pulsed Collector Current Test Circuit
- Fig. 14a - Switching Loss Test Circuit
- Fig. 14b - Switching Loss Waveform

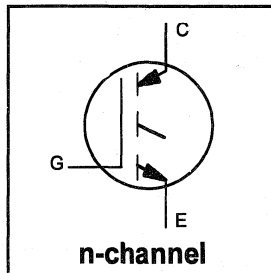
IRGBC40M

INSULATED GATE BIPOLAR TRANSISTOR

Short Circuit Rated
Fast IGBT

Features

- Short circuit rated - $10\mu\text{s}$ @ 125°C , $V_{GE} = 15\text{V}$
- Switching-loss rating includes all "tail" losses
- Optimized for medium operating frequency (1 to 10kHz)



$V_{CES} = 600\text{V}$

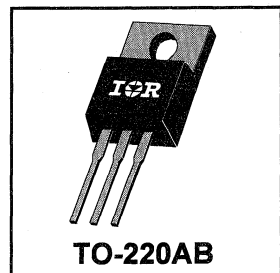
$V_{CE(sat)} \leq 3.0\text{V}$

@ $V_{GE} = 15\text{V}$, $I_C = 24\text{A}$

Description

Insulated Gate Bipolar Transistors (IGBTs) from International Rectifier have higher usable current densities than comparable bipolar transistors, while at the same time having simpler gate-drive requirements of the familiar power MOSFET. They provide substantial benefits to a host of high-voltage, high-current applications.

These new short circuit rated devices are especially suited for motor control and other applications requiring short circuit withstand capability.



Motor Control Fast Discretes

Absolute Maximum Ratings

	Parameter	Max.	Units
V_{CES}	Collector-to-Emitter Voltage	600	V
$I_C @ T_C = 25^\circ\text{C}$	Continuous Collector Current	40	A
$I_C @ T_C = 100^\circ\text{C}$	Continuous Collector Current	24	
I_{CM}	Pulsed Collector Current ①	80	
I_{LM}	Clamped Inductive Load Current ②	80	
t_{sc}	Short Circuit Withstand Time	10	μs
V_{GE}	Gate-to-Emitter Voltage	± 20	V
E_{ARV}	Reverse Voltage Avalanche Energy ③	15	mJ
$P_D @ T_C = 25^\circ\text{C}$	Maximum Power Dissipation	160	W
$P_D @ T_C = 100^\circ\text{C}$	Maximum Power Dissipation	65	
T_J	Operating Junction and Storage Temperature Range	-55 to +150	$^\circ\text{C}$
T_{STG}	Soldering Temperature, for 10 sec.	300 (0.063 in. (1.6mm) from case)	
	Mounting torque, 6-32 or M3 screw.	10 lbf·in (1.1N·m)	

Thermal Resistance

	Parameter	Min.	Typ.	Max.	Units
$R_{\theta JC}$	Junction-to-Case	—	—	0.77	$^\circ\text{C/W}$
$R_{\theta CS}$	Case-to-Sink, flat, greased surface	—	0.50	—	
$R_{\theta JA}$	Junction-to-Ambient, typical socket mount	—	—	80	
Wt	Weight	—	2 (0.07)	—	g (oz)

Electrical Characteristics @ $T_J = 25^\circ\text{C}$ (unless otherwise specified)

	Parameter	Min.	Typ.	Max.	Units	Conditions	
$V_{(BR)CES}$	Collector-to-Emitter Breakdown Voltage	600	—	—	V	$V_{GE} = 0V, I_C = 250\mu\text{A}$	
$V_{(BR)ECS}$	Emitter-to-Collector Breakdown Voltage ④	20	—	—	V	$V_{GE} = 0V, I_C = 1.0\text{A}$	
$\Delta V_{(BR)CES}/\Delta T_J$	Temp. Coeff. of Breakdown Voltage	—	0.70	—	$V/^\circ\text{C}$	$V_{GE} = 0V, I_C = 1.0\text{mA}$	
$V_{CE(on)}$	Collector-to-Emitter Saturation Voltage	—	2.0	3.0	V	$V_{GE} = 15V$ $I_C = 24\text{A}$	
		—	2.6	—			$I_C = 40\text{A}$
		—	2.4	—			$I_C = 24\text{A}, T_J = 150^\circ\text{C}$
$V_{GE(th)}$	Gate Threshold Voltage	3.0	—	5.5		$V_{CE} = V_{GE}, I_C = 250\mu\text{A}$	
$\Delta V_{GE(th)}/\Delta T_J$	Temperature Coeff. of Threshold Voltage	—	-12	—	$\text{mV}/^\circ\text{C}$	$V_{CE} = V_{GE}, I_C = 250\mu\text{A}$	
g_{fe}	Forward Transconductance ⑤	9.2	12	—	S	$V_{CE} = 100V, I_C = 24\text{A}$	
I_{CES}	Zero Gate Voltage Collector Current	—	—	250	μA	$V_{GE} = 0V, V_{CE} = 600V$	
		—	—	1000		$V_{GE} = 0V, V_{CE} = 600V, T_J = 150^\circ\text{C}$	
I_{GES}	Gate-to-Emitter Leakage Current	—	—	± 100	nA	$V_{GE} = \pm 20V$	

Switching Characteristics @ $T_J = 25^\circ\text{C}$ (unless otherwise specified)

	Parameter	Min.	Typ.	Max.	Units	Conditions
Q_g	Total Gate Charge (turn-on)	—	59	80	nC	$I_C = 24\text{A}$ $V_{CC} = 400V$ $V_{GE} = 15V$
Q_{ge}	Gate - Emitter Charge (turn-on)	—	8.6	10		
Q_{gc}	Gate - Collector Charge (turn-on)	—	25	42		
$t_{d(on)}$	Turn-On Delay Time	—	26	—	ns	$T_J = 25^\circ\text{C}$ $I_C = 24\text{A}, V_{CC} = 480V$ $V_{GE} = 15V, R_G = 10\Omega$ Energy losses include "tail"
t_r	Rise Time	—	37	—		
$t_{d(off)}$	Turn-Off Delay Time	—	240	410		
t_f	Fall Time	—	230	420	mJ	
E_{on}	Turn-On Switching Loss	—	0.75	—		
E_{off}	Turn-Off Switching Loss	—	1.65	—		
E_{ts}	Total Switching Loss	—	2.4	3.6	μs	$V_{CC} = 360V, T_J = 125^\circ\text{C}$ $V_{GE} = 15V, R_G = 10\Omega, V_{CPK} < 500V$
t_{sc}	Short Circuit Withstand Time	10	—	—		
$t_{d(on)}$	Turn-On Delay Time	—	28	—		
t_r	Rise Time	—	37	—	ns	$T_J = 150^\circ\text{C}$, $I_C = 24\text{A}, V_{CC} = 480V$ $V_{GE} = 15V, R_G = 10\Omega$ Energy losses include "tail"
$t_{d(off)}$	Turn-Off Delay Time	—	380	—		
t_f	Fall Time	—	460	—		
E_{ts}	Total Switching Loss	—	4.5	—	mJ	
L_E	Internal Emitter Inductance	—	7.5	—	nH	Measured 5mm from package
C_{ies}	Input Capacitance	—	1500	—	pF	$V_{GE} = 0V$ $V_{CC} = 30V$ $f = 1.0\text{MHz}$
C_{oes}	Output Capacitance	—	190	—		
C_{res}	Reverse Transfer Capacitance	—	20	—		

- Notes:**
- ① Repetitive rating; $V_{GE}=20V$, pulse width limited by max. junction temperature.
 - ② $V_{CC}=80\%(V_{CES}), V_{GE}=20V, L=10\mu\text{H}, R_G=10\Omega$
 - ③ Repetitive rating; pulse width limited by maximum junction temperature.
 - ④ Pulse width $\leq 80\mu\text{s}$; duty factor $\leq 0.1\%$.
 - ⑤ Pulse width $5.0\mu\text{s}$, single shot.

Refer to Section D for the following:

Package Outline 1 - JEDEC Outline TO-220AB

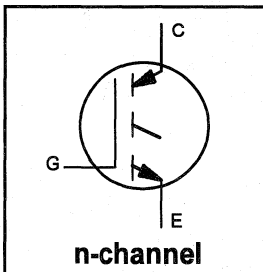
Section D - page D-12

INSULATED GATE BIPOLAR TRANSISTOR

Short Circuit Rated
Fast IGBT

Features

- Short circuit rated - $10\mu\text{s}$ @ 125°C , $V_{\text{GE}} = 15\text{V}$
- Switching-loss rating includes all "tail" losses
- Optimized for medium operating frequency (1 to 10kHz) See Fig. 1 for Current vs. Frequency curve

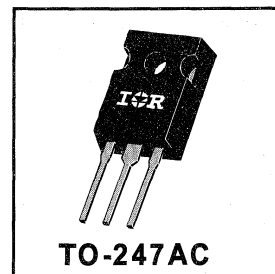


$V_{\text{CES}} = 600\text{V}$
$V_{\text{CE(sat)}} \leq 2.3\text{V}$
@ $V_{\text{GE}} = 15\text{V}$, $I_{\text{C}} = 8.0\text{A}$

Description

Insulated Gate Bipolar Transistors (IGBTs) from International Rectifier have higher usable current densities than comparable bipolar transistors, while at the same time having simpler gate-drive requirements of the familiar power MOSFET. They provide substantial benefits to a host of high-voltage, high-current applications.

These new short circuit rated devices are especially suited for motor control and other applications requiring short circuit withstand capability.



Motor
Control
Fast
Discretes

Absolute Maximum Ratings

	Parameter	Max.	Units
V_{CES}	Collector-to-Emitter Voltage	600	V
$I_{\text{C}} @ T_{\text{C}} = 25^\circ\text{C}$	Continuous Collector Current	13	A
$I_{\text{C}} @ T_{\text{C}} = 100^\circ\text{C}$	Continuous Collector Current	8.0	
I_{CM}	Pulsed Collector Current ①	26	
I_{LM}	Clamped Inductive Load Current ②	26	
t_{sc}	Short Circuit Withstand Time	10	μs
V_{GE}	Gate-to-Emitter Voltage	± 20	V
E_{ARV}	Reverse Voltage Avalanche Energy ③	5.0	mJ
$P_{\text{D}} @ T_{\text{C}} = 25^\circ\text{C}$	Maximum Power Dissipation	60	W
$P_{\text{D}} @ T_{\text{C}} = 100^\circ\text{C}$	Maximum Power Dissipation	24	
T_{J}	Operating Junction and	-55 to +150	$^\circ\text{C}$
T_{STG}	Storage Temperature Range		
	Soldering Temperature, for 10 sec.		
	Mounting torque, 6-32 or M3 screw.	10 lbf·in (1.1N·m)	

Thermal Resistance

	Parameter	Min.	Typ.	Max.	Units
$R_{\theta\text{JC}}$	Junction-to-Case	—	—	2.1	$^\circ\text{C}/\text{W}$
$R_{\theta\text{CS}}$	Case-to-Sink, flat, greased surface	—	0.24	—	
$R_{\theta\text{JA}}$	Junction-to-Ambient, typical socket mount	—	—	40	
Wt	Weight	—	6 (0.21)	—	g (oz)

Electrical Characteristics @ $T_J = 25^\circ\text{C}$ (unless otherwise specified)

	Parameter	Min.	Typ.	Max.	Units	Conditions
$V_{(BR)CES}$	Collector-to-Emitter Breakdown Voltage	600	—	—	V	$V_{GE} = 0V, I_C = 250\mu A$
$V_{(BR)ECS}$	Emitter-to-Collector Breakdown Voltage ④	20	—	—	V	$V_{GE} = 0V, I_C = 1.0A$
$\Delta V_{(BR)CES/\Delta T_J}$	Temperature Coeff. of Breakdown Voltage	—	0.42	—	V/ $^\circ\text{C}$	$V_{GE} = 0V, I_C = 1.0mA$
$V_{CE(on)}$	Collector-to-Emitter Saturation Voltage	—	2.0	2.3	V	$I_C = 8.0A$ $I_C = 13A$ $I_C = 8.0A, T_J = 150^\circ\text{C}$ $V_{CE} = V_{GE}, I_C = 250\mu A$
		—	2.7	—		
		—	2.5	—		
$V_{GE(th)}$	Gate Threshold Voltage	3.0	—	5.5		
$\Delta V_{GE(th)/\Delta T_J}$	Temperature Coeff. of Threshold Voltage	—	-11	—	mV/ $^\circ\text{C}$	$V_{CE} = V_{GE}, I_C = 250\mu A$
g_{fe}	Forward Transconductance ⑤	2.7	3.8	—	S	$V_{CE} = 100V, I_C = 8.0A$
I_{CES}	Zero Gate Voltage Collector Current	—	—	250	μA	$V_{GE} = 0V, V_{CE} = 600V$ $V_{GE} = 0V, V_{CE} = 600V, T_J = 150^\circ\text{C}$
		—	—	1000		
I_{GES}	Gate-to-Emitter Leakage Current	—	—	± 100	nA	$V_{GE} = \pm 20V$

Switching Characteristics @ $T_J = 25^\circ\text{C}$ (unless otherwise specified)

	Parameter	Min.	Typ.	Max.	Units	Conditions
Q_g	Total Gate Charge (turn-on)	—	16	24	nC	$I_C = 8.0A$ $V_{CC} = 400V$ $V_{GE} = 15V$ See Fig. 8
Q_{ge}	Gate - Emitter Charge (turn-on)	—	3.6	5.2		
Q_{gc}	Gate - Collector Charge (turn-on)	—	6.0	9.0		
$t_{d(on)}$	Turn-On Delay Time	—	29	—	ns	$T_J = 25^\circ\text{C}$ $I_C = 8.0A, V_{CC} = 480V$ $V_{GE} = 15V, R_G = 50\Omega$ Energy losses include "tail"
t_r	Rise Time	—	22	—		
$t_{d(off)}$	Turn-Off Delay Time	—	270	400		
t_f	Fall Time	—	280	510		
E_{on}	Turn-On Switching Loss	—	0.14	—		
E_{off}	Turn-Off Switching Loss	—	0.86	—		
E_{ts}	Total Switching Loss	—	1.0	2.0	mJ	See Fig. 9, 10, 11, 14
t_{sc}	Short Circuit Withstand Time	10	—	—	μs	$V_{CC} = 360V, T_J = 125^\circ\text{C}$ $V_{GE} = 15V, R_G = 50\Omega, V_{CPK} < 500V$
$t_{d(on)}$	Turn-On Delay Time	—	27	—	ns	$T_J = 150^\circ\text{C}$ $I_C = 8.0A, V_{CC} = 480V$ $V_{GE} = 15V, R_G = 50\Omega$ Energy losses include "tail"
t_r	Rise Time	—	21	—		
$t_{d(off)}$	Turn-Off Delay Time	—	370	—		
t_f	Fall Time	—	420	—		
E_{ts}	Total Switching Loss	—	1.4	—	mJ	See Fig. 10, 14
L_E	Internal Emitter Inductance	—	13	—	nH	Measured 5mm from package
C_{ies}	Input Capacitance	—	365	—	pF	$V_{GE} = 0V$ $V_{CC} = 30V$ $f = 1.0MHz$ See Fig. 7
C_{oes}	Output Capacitance	—	47	—		
C_{res}	Reverse Transfer Capacitance	—	4.8	—		

Notes:

- ① Repetitive rating; $V_{GE}=20V$, pulse width limited by max. junction temperature. (See fig. 13b)
- ② $V_{CC}=80\%(V_{CES}), V_{GE}=20V, L=10\mu H, R_G=50\Omega$, (See fig. 13a)
- ③ Repetitive rating; pulse width limited by maximum junction temperature.
- ④ Pulse width $\leq 80\mu s$; duty factor $\leq 0.1\%$.
- ⑤ Pulse width $5.0\mu s$, single shot.

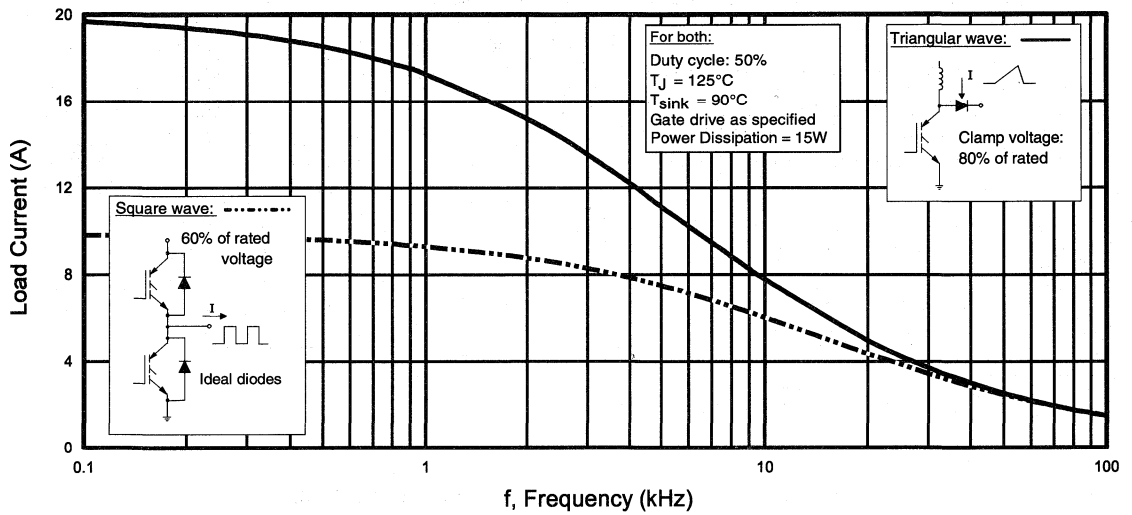


Fig. 1 - Typical Load Current vs. Frequency
 (For square wave, $I = I_{RMS}$ of fundamental; for triangular wave, $I = I_{PK}$)

Motor Control Fast Discretes

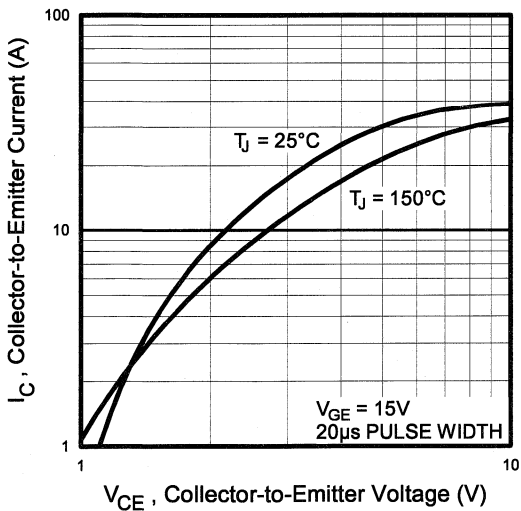


Fig. 2 - Typical Output Characteristics

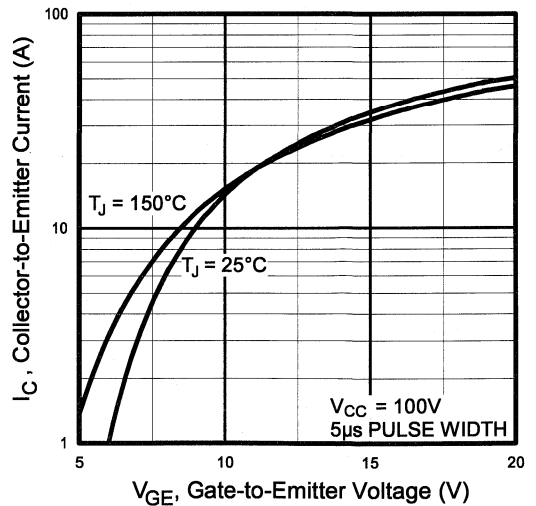


Fig. 3 - Typical Transfer Characteristics

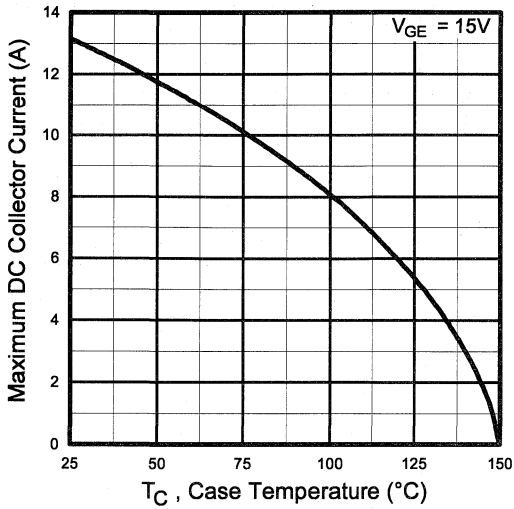


Fig. 4 - Maximum Collector Current vs. Case Temperature

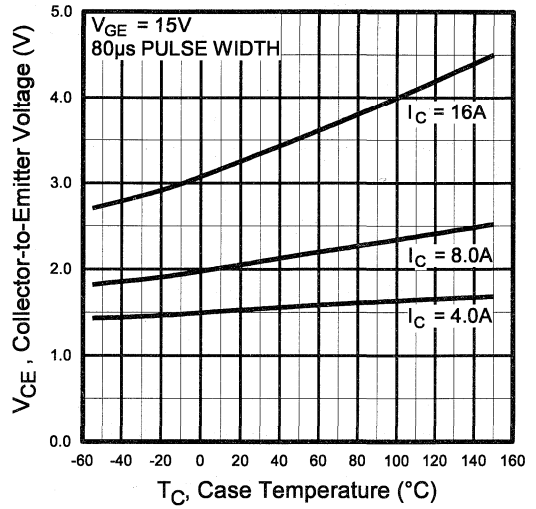


Fig. 5 - Collector-to-Emitter Voltage vs. Case Temperature

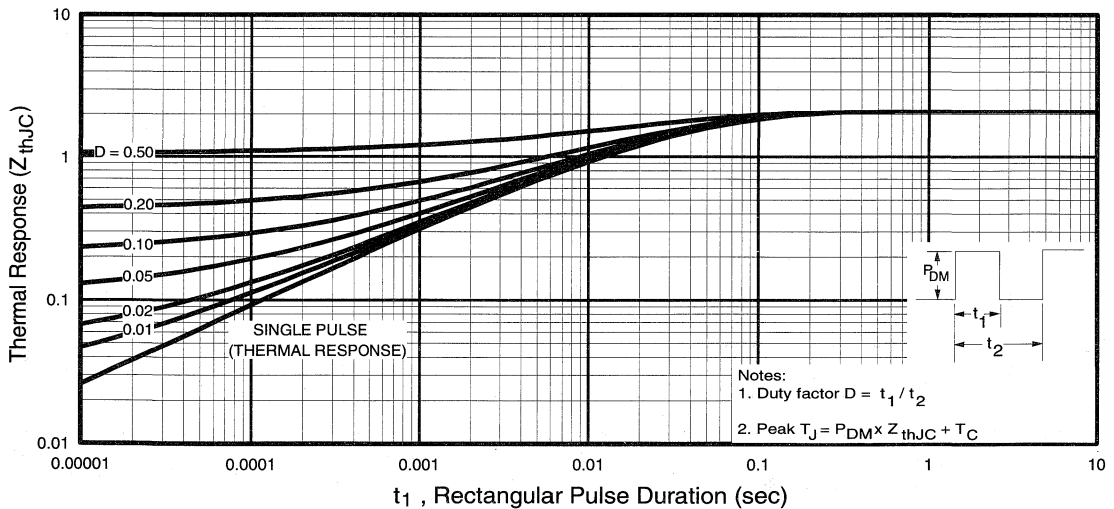


Fig. 6 - Maximum Effective Transient Thermal Impedance, Junction-to-Case

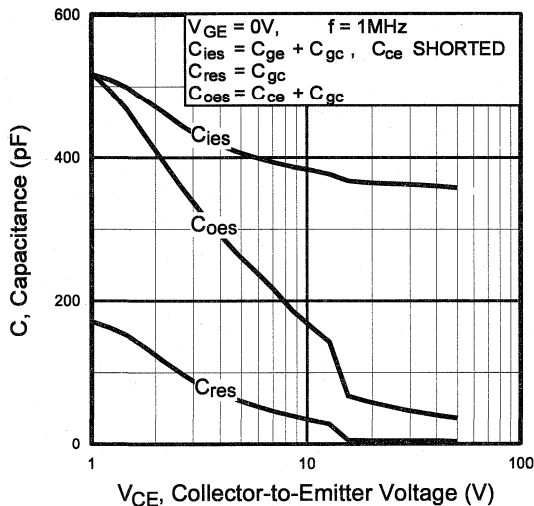


Fig. 7 - Typical Capacitance vs. Collector-to-Emitter Voltage

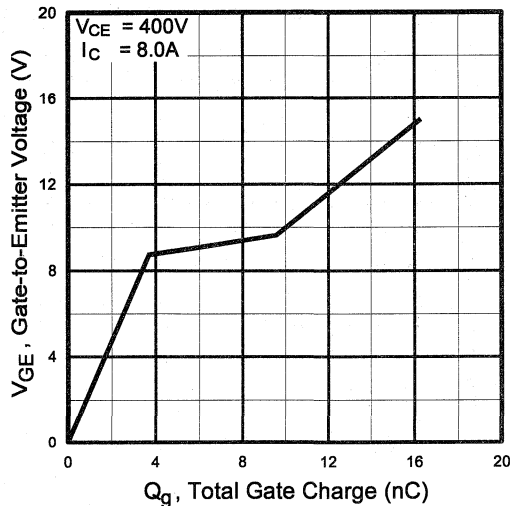


Fig. 8 - Typical Gate Charge vs. Gate-to-Emitter Voltage

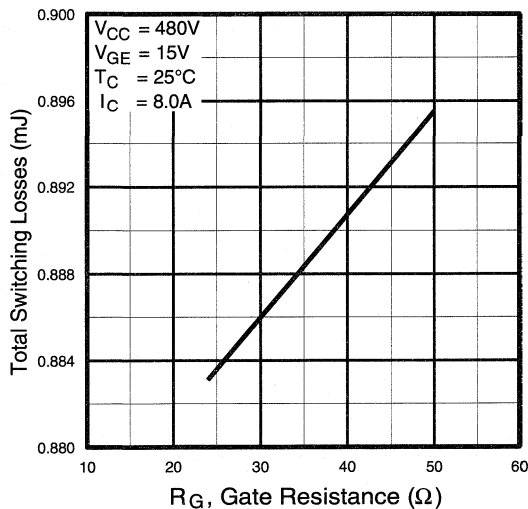


Fig. 9 - Typical Switching Losses vs. Gate Resistance

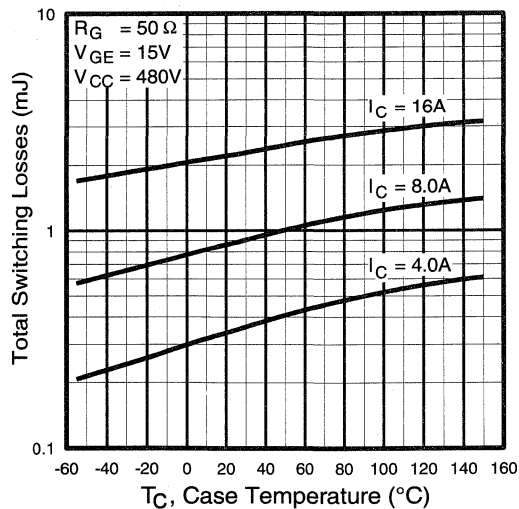


Fig. 10 - Typical Switching Losses vs. Case Temperature



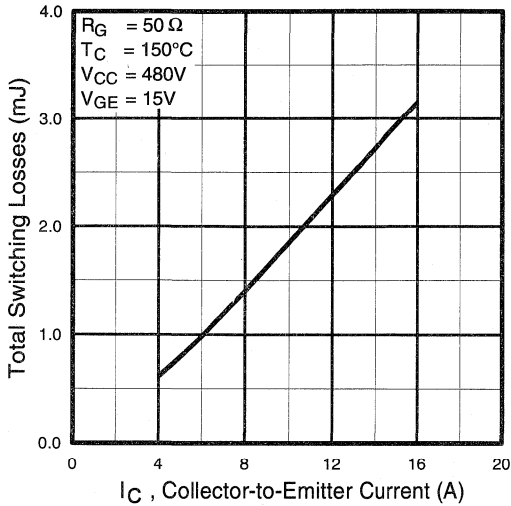


Fig. 11 - Typical Switching Losses vs. Collector-to-Emitter Current

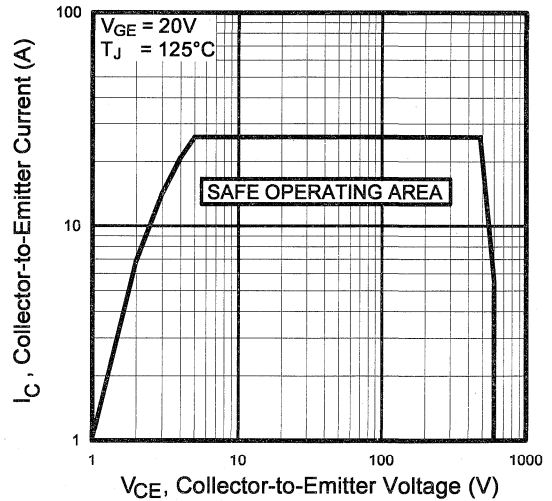


Fig. 12 - Turn-Off SOA

Refer to Section D for the following:

Appendix C: Section D - page D-5

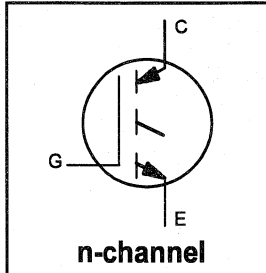
- Fig. 13a - Clamped Inductive Load Test Circuit
- Fig. 13b - Pulsed Collector Current Test Circuit
- Fig. 14a - Switching Loss Test Circuit
- Fig. 14b - Switching Loss Waveform

INSULATED GATE BIPOLAR TRANSISTOR

Short Circuit Rated
Fast IGBT

Features

- Short circuit rated - $10\mu\text{s}$ @ 125°C , $V_{GE} = 15\text{V}$
- Switching-loss rating includes all "tail" losses
- Optimized for medium operating frequency (1 to 10kHz) See Fig. 1 for Current vs. Frequency curve



$$V_{CES} = 600\text{V}$$

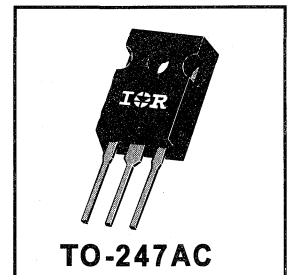
$$V_{CE(sat)} \leq 2.9\text{V}$$

$$\text{@}V_{GE} = 15\text{V}, I_C = 16\text{A}$$

Description

Insulated Gate Bipolar Transistors (IGBTs) from International Rectifier have higher usable current densities than comparable bipolar transistors, while at the same time having simpler gate-drive requirements of the familiar power MOSFET. They provide substantial benefits to a host of high-voltage, high-current applications.

These new short circuit rated devices are especially suited for motor control and other applications requiring short circuit withstand capability.



Motor Control Fast Discretes

Absolute Maximum Ratings

	Parameter	Max.	Units
V_{CES}	Collector-to-Emitter Voltage	600	V
$I_C @ T_C = 25^\circ\text{C}$	Continuous Collector Current	26	A
$I_C @ T_C = 100^\circ\text{C}$	Continuous Collector Current	16	
I_{CM}	Pulsed Collector Current ①	52	
I_{LM}	Clamped Inductive Load Current ②	52	
t_{sc}	Short Circuit Withstand Time	10	μs
V_{GE}	Gate-to-Emitter Voltage	± 20	V
E_{ARV}	Reverse Voltage Avalanche Energy ③	10	mJ
$P_D @ T_C = 25^\circ\text{C}$	Maximum Power Dissipation	100	W
$P_D @ T_C = 100^\circ\text{C}$	Maximum Power Dissipation	42	
T_J	Operating Junction and	-55 to +150	$^\circ\text{C}$
T_{STG}	Storage Temperature Range		
	Soldering Temperature, for 10 sec.		
	Mounting torque, 6-32 or M3 screw.	10 lbf•in (1.1N•m)	

Thermal Resistance

	Parameter	Min.	Typ.	Max.	Units
$R_{\theta JC}$	Junction-to-Case	—	—	1.2	$^\circ\text{C}/\text{W}$
$R_{\theta CS}$	Case-to-Sink, flat, greased surface	—	0.24	—	
$R_{\theta JA}$	Junction-to-Ambient, typical socket mount	—	—	40	
Wt	Weight	—	6 (0.21)	—	g (oz)

Electrical Characteristics @ $T_J = 25^\circ\text{C}$ (unless otherwise specified)

	Parameter	Min.	Typ.	Max.	Units	Conditions
$V_{(BR)CES}$	Collector-to-Emitter Breakdown Voltage	600	—	—	V	$V_{GE} = 0V, I_C = 250\mu A$
$V_{(BR)ECS}$	Emitter-to-Collector Breakdown Voltage ④	20	—	—	V	$V_{GE} = 0V, I_C = 1.0A$
$\Delta V_{(BR)CES}/\Delta T_J$	Temperature Coeff. of Breakdown Voltage	—	0.65	—	V/°C	$V_{GE} = 0V, I_C = 1.0mA$
$V_{CE(on)}$	Collector-to-Emitter Saturation Voltage	—	1.9	2.9	V	$I_C = 16A, V_{GE} = 15V$ See Fig. 2, 5
		—	2.7	—		
		—	2.2	—		
$V_{GE(th)}$	Gate Threshold Voltage	3.0	—	5.5		$V_{CE} = V_{GE}, I_C = 250\mu A$
$\Delta V_{GE(th)}/\Delta T_J$	Temperature Coeff. of Threshold Voltage	—	-12	—	mV/°C	$V_{CE} = V_{GE}, I_C = 250\mu A$
g_{fe}	Forward Transconductance ⑤	3.3	6.5	—	S	$V_{CE} = 100V, I_C = 16A$
I_{CES}	Zero Gate Voltage Collector Current	—	—	250	μA	$V_{GE} = 0V, V_{CE} = 600V$
		—	—	1000		$V_{GE} = 0V, V_{CE} = 600V, T_J = 150^\circ\text{C}$
I_{GES}	Gate-to-Emitter Leakage Current	—	—	± 100	nA	$V_{GE} = \pm 20V$

Switching Characteristics @ $T_J = 25^\circ\text{C}$ (unless otherwise specified)

	Parameter	Min.	Typ.	Max.	Units	Conditions
Q_g	Total Gate Charge (turn-on)	—	35	53	nC	$I_C = 16A, V_{CC} = 400V$ See Fig. 8
Q_{ge}	Gate - Emitter Charge (turn-on)	—	7.4	11		
Q_{gc}	Gate - Collector Charge (turn-on)	—	14	21		
$t_{d(on)}$	Turn-On Delay Time	—	31	—	ns	$T_J = 25^\circ\text{C}$ $I_C = 16A, V_{CC} = 480V$ $V_{GE} = 15V, R_G = 23\Omega$ Energy losses include "tail"
t_r	Rise Time	—	31	—		
$t_{d(off)}$	Turn-Off Delay Time	—	280	420		
t_f	Fall Time	—	310	470		
E_{on}	Turn-On Switching Loss	—	0.4	—	mJ	See Fig. 9, 10, 11, 14
E_{off}	Turn-Off Switching Loss	—	1.9	—		
E_{ts}	Total Switching Loss	—	2.3	3.5		
t_{sc}	Short Circuit Withstand Time	10	—	—	μs	$V_{CC} = 360V, T_J = 125^\circ\text{C}$ $V_{GE} = 15V, R_G = 23\Omega, V_{CPK} < 500V$
$t_{d(on)}$	Turn-On Delay Time	—	31	—	ns	$T_J = 150^\circ\text{C}$ $I_C = 14A, V_{CC} = 480V$ $V_{GE} = 15V, R_G = 23\Omega$ Energy losses include "tail"
t_r	Rise Time	—	30	—		
$t_{d(off)}$	Turn-Off Delay Time	—	530	—		
t_f	Fall Time	—	660	—		
E_{ts}	Total Switching Loss	—	4.4	—	mJ	See Fig. 10, 14
L_E	Internal Emitter Inductance	—	13	—	nH	Measured 5mm from package
C_{ies}	Input Capacitance	—	750	—	pF	$V_{GE} = 0V, V_{CC} = 30V$ See Fig. 7 $f = 1.0MHz$
C_{oes}	Output Capacitance	—	110	—		
C_{res}	Reverse Transfer Capacitance	—	9.3	—		

Notes:

- ① Repetitive rating; $V_{GE}=20V$, pulse width limited by max. junction temperature. (See fig. 13b)
- ② $V_{CC}=80\%(V_{CES}), V_{GE}=20V, L=10\mu H, R_G=23\Omega$, (See fig. 13a)
- ③ Repetitive rating; pulse width limited by maximum junction temperature.
- ④ Pulse width $\leq 80\mu s$; duty factor $\leq 0.1\%$.
- ⑤ Pulse width 5.0 μs , single shot.

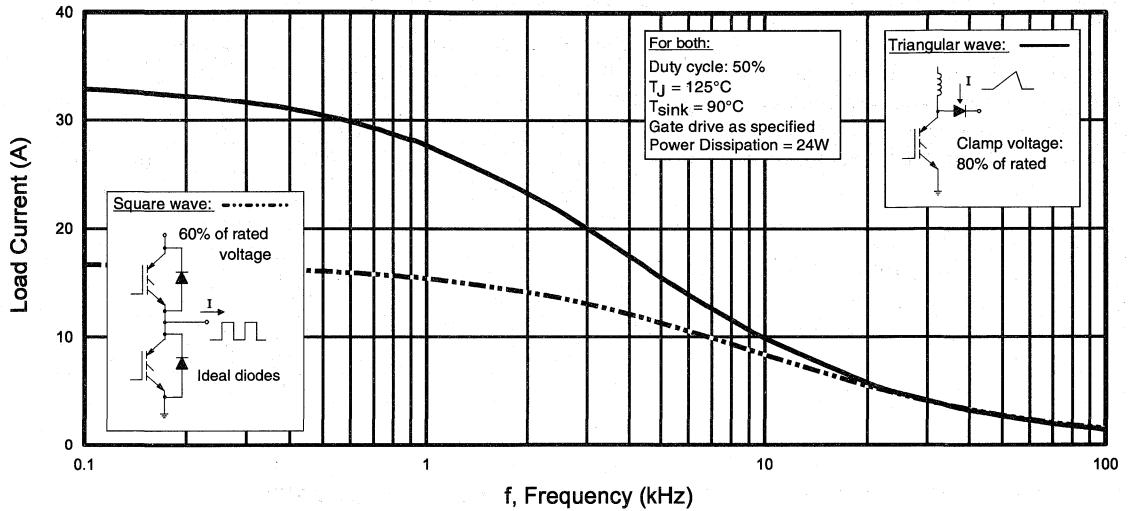


Fig. 1 - Typical Load Current vs. Frequency
 (For square wave, $I = I_{RMS}$ of fundamental; for triangular wave, $I = I_{PK}$)

Major
Control
Fast
Discretes

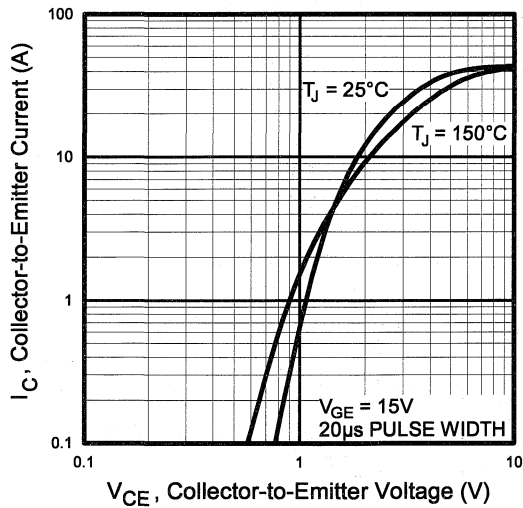


Fig. 2 - Typical Output Characteristics

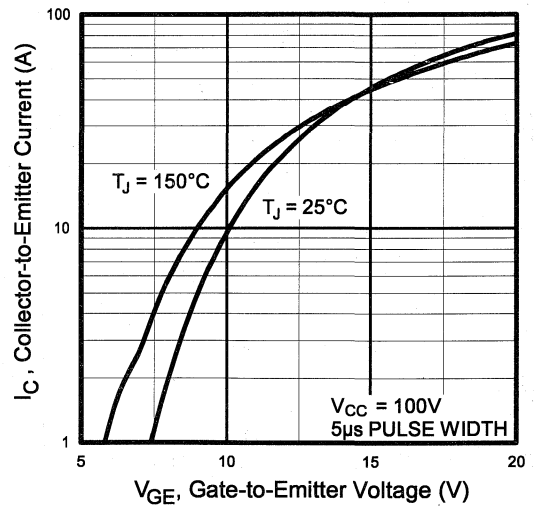


Fig. 3 - Typical Transfer Characteristics

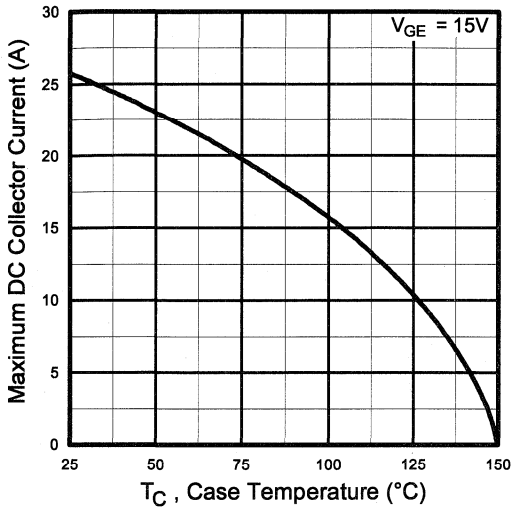


Fig. 4 - Maximum Collector Current vs. Case Temperature

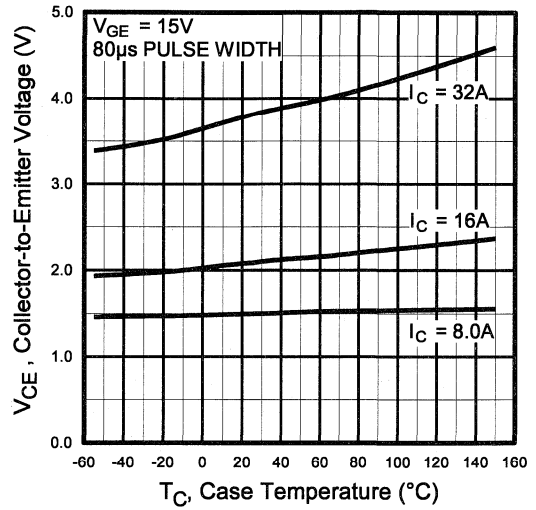


Fig. 5 - Collector-to-Emitter Voltage vs. Case Temperature

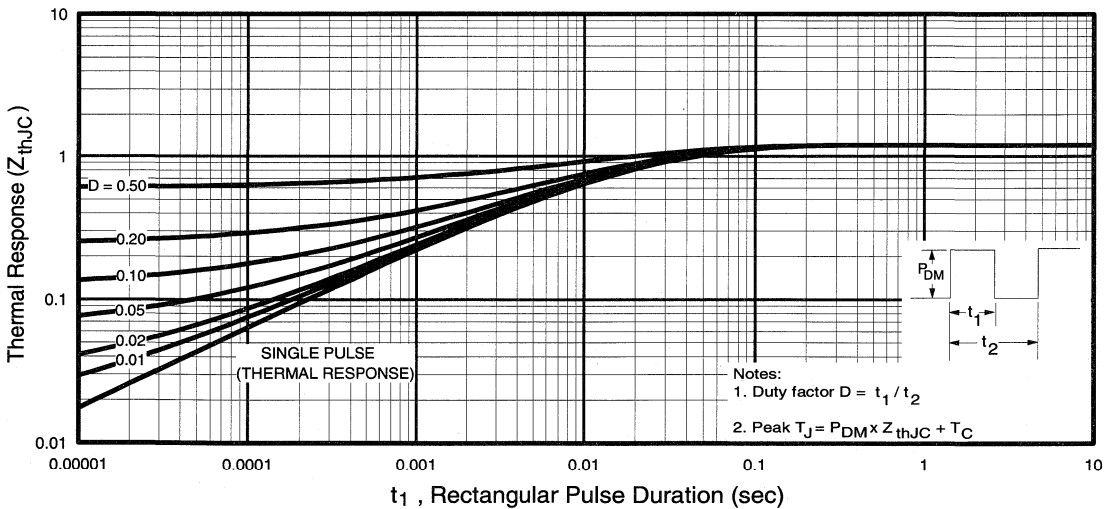


Fig. 6 - Maximum Effective Transient Thermal Impedance, Junction-to-Case

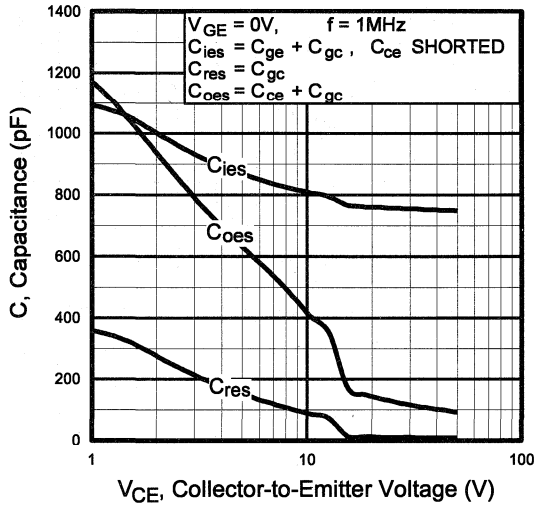


Fig. 7 - Typical Capacitance vs. Collector-to-Emitter Voltage

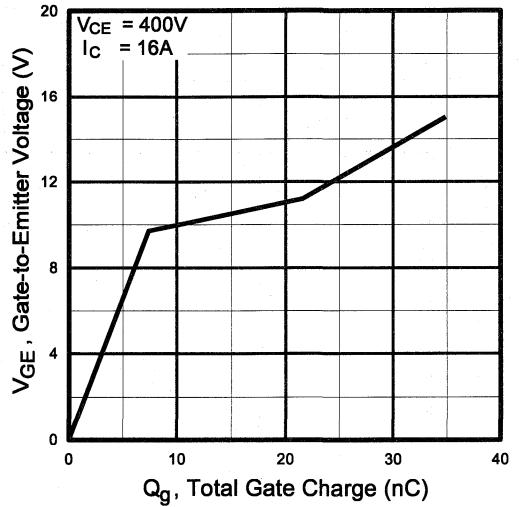


Fig. 8 - Typical Gate Charge vs. Gate-to-Emitter Voltage

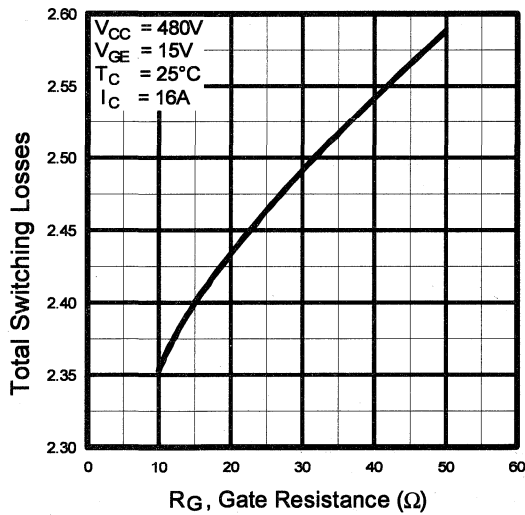


Fig. 9 - Typical Switching Losses vs. Gate Resistance

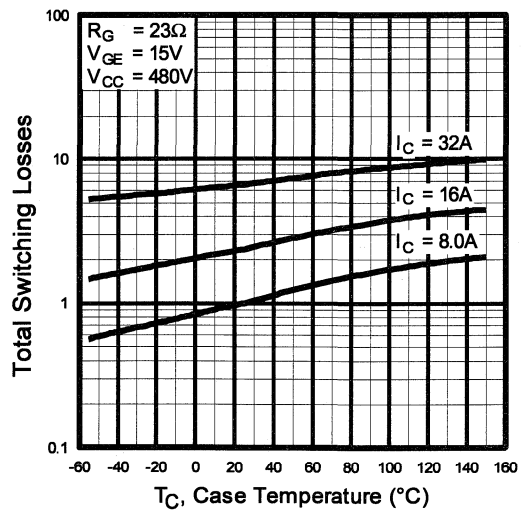


Fig. 10 - Typical Switching Losses vs. Case Temperature

Motor
Control
Fast
Discretics

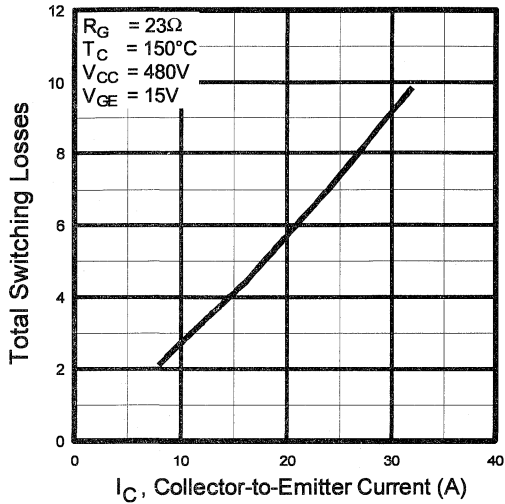


Fig. 11 - Typical Switching Losses vs. Collector-to-Emitter Current

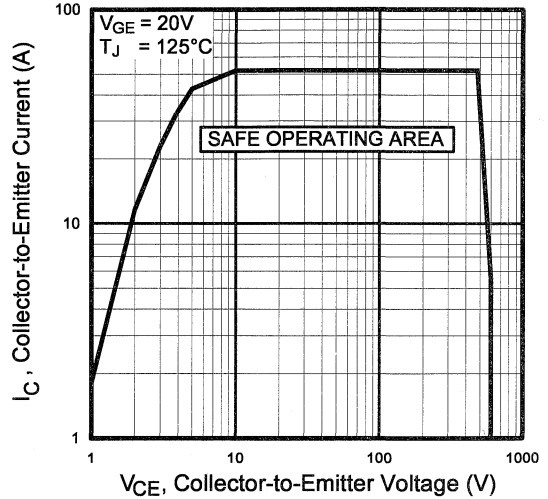


Fig. 12 - Turn-Off SOA

Refer to Section D for the following:

Appendix C: Section D - page D-5

- Fig. 13a - Clamped Inductive Load Test Circuit
- Fig. 13b - Pulsed Collector Current Test Circuit
- Fig. 14a - Switching Loss Test Circuit
- Fig. 14b - Switching Loss Waveform

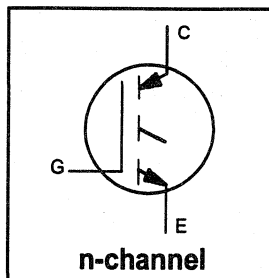
IRGPC40M

INSULATED GATE BIPOLAR TRANSISTOR

Short Circuit Rated
Fast IGBT

Features

- Short circuit rated - $10\mu\text{s}$ @ 125°C , $V_{\text{GE}} = 15\text{V}$
- Switching-loss rating includes all "tail" losses
- Optimized for medium operating frequency (1 to 10kHz)



$$V_{\text{CES}} = 600\text{V}$$

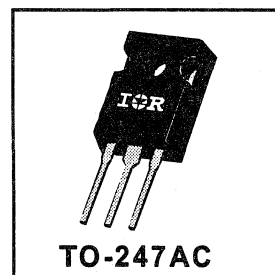
$$V_{\text{CE}(\text{typ})} \leq 2.0\text{V}$$

$$\text{@}V_{\text{GE}} = 15\text{V}, I_{\text{C}} = 24\text{A}$$

Description

Insulated Gate Bipolar Transistors (IGBTs) from International Rectifier have higher usable current densities than comparable bipolar transistors, while at the same time having simpler gate-drive requirements of the familiar power MOSFET. They provide substantial benefits to a host of high-voltage, high-current applications.

These new short circuit rated devices are especially suited for motor control and other applications requiring short circuit withstand capability.



Motor
Control
Fast
Discretes

Absolute Maximum Ratings

	Parameter	Max.	Units
V_{CES}	Collector-to-Emitter Voltage	600	V
$I_{\text{C}} @ T_{\text{C}} = 25^\circ\text{C}$	Continuous Collector Current	40	A
$I_{\text{C}} @ T_{\text{C}} = 100^\circ\text{C}$	Continuous Collector Current	24	
I_{CM}	Pulsed Collector Current ①	80	
I_{LM}	Clamped Inductive Load Current ②	80	
t_{sc}	Short Circuit Withstand Time	10	μs
V_{GE}	Gate-to-Emitter Voltage	± 20	V
E_{ARV}	Reverse Voltage Avalanche Energy ③	15	mJ
$P_{\text{D}} @ T_{\text{C}} = 25^\circ\text{C}$	Maximum Power Dissipation	160	W
$P_{\text{D}} @ T_{\text{C}} = 100^\circ\text{C}$	Maximum Power Dissipation	65	
T_{J}	Operating Junction and	-55 to +150	$^\circ\text{C}$
T_{STG}	Storage Temperature Range		
	Soldering Temperature, for 10 sec.	300 (0.063 in. (1.6mm) from case)	
	Mounting torque, 6-32 or M3 screw.	10 lbf•in (1.1N•m)	

Thermal Resistance

	Parameter	Min.	Typ.	Max.	Units
$R_{\theta\text{JC}}$	Junction-to-Case	—	—	0.77	$^\circ\text{C}/\text{W}$
$R_{\theta\text{CS}}$	Case-to-Sink, flat, greased surface	—	0.24	—	
$R_{\theta\text{JA}}$	Junction-to-Ambient, typical socket mount	—	—	40	
W_{t}	Weight	—	6 (0.21)	—	g (oz)

Electrical Characteristics @ $T_J = 25^\circ\text{C}$ (unless otherwise specified)

	Parameter	Min.	Typ.	Max.	Units	Conditions
$V_{(BR)CES}$	Collector-to-Emitter Breakdown Voltage	600	—	—	V	$V_{GE} = 0V, I_C = 250\mu A$
$V_{(BR)ECS}$	Emitter-to-Collector Breakdown Voltage ④	20	—	—	V	$V_{GE} = 0V, I_C = 1.0A$
$\Delta V_{(BR)CES}/\Delta T_J$	Temp. Coeff. of Breakdown Voltage	—	0.70	—	$V/^\circ\text{C}$	$V_{GE} = 0V, I_C = 1.0mA$
$V_{CE(on)}$	Collector-to-Emitter Saturation Voltage	—	2.0	—	V	$I_C = 24A$ $I_C = 40A$ $I_C = 24A, T_J = 150^\circ\text{C}$ $V_{GE} = 15V$
		—	2.6	—		
		—	2.4	—		
$V_{GE(th)}$	Gate Threshold Voltage	3.0	—	5.5		$V_{CE} = V_{GE}, I_C = 250\mu A$
$\Delta V_{GE(th)}/\Delta T_J$	Temperature Coeff. of Threshold Voltage	—	-12	—	$mV/^\circ\text{C}$	$V_{CE} = V_{GE}, I_C = 250\mu A$
g_{fe}	Forward Transconductance ⑤	9.2	12	—	S	$V_{CE} = 100V, I_C = 24A$
I_{CES}	Zero Gate Voltage Collector Current	—	—	250	μA	$V_{GE} = 0V, V_{CE} = 600V$
		—	—	1000		$V_{GE} = 0V, V_{CE} = 600V, T_J = 150^\circ\text{C}$
I_{GES}	Gate-to-Emitter Leakage Current	—	—	± 100	nA	$V_{GE} = \pm 20V$

Switching Characteristics @ $T_J = 25^\circ\text{C}$ (unless otherwise specified)

	Parameter	Min.	Typ.	Max.	Units	Conditions
Q_g	Total Gate Charge (turn-on)	—	59	80	nC	$I_C = 24A$ $V_{CC} = 400V$ $V_{GE} = 15V$
Q_{ge}	Gate - Emitter Charge (turn-on)	—	8.6	10		
Q_{gc}	Gate - Collector Charge (turn-on)	—	25	42		
$t_{d(on)}$	Turn-On Delay Time	—	26	—	ns	$T_J = 25^\circ\text{C}$ $I_C = 24A, V_{CC} = 480V$ $V_{GE} = 15V, R_G = 10\Omega$ Energy losses include "tail"
t_r	Rise Time	—	37	—		
$t_{d(off)}$	Turn-Off Delay Time	—	240	410		
t_f	Fall Time	—	230	420		
E_{on}	Turn-On Switching Loss	—	0.75	—	mJ	
E_{off}	Turn-Off Switching Loss	—	1.65	—		
E_{ts}	Total Switching Loss	—	2.4	3.6		
t_{sc}	Short Circuit Withstand Time	10	—	—	μs	$V_{CC} = 360V, T_J = 125^\circ\text{C}$ $V_{GE} = 15V, R_G = 10\Omega, V_{CPK} < 500V$
$t_{d(on)}$	Turn-On Delay Time	—	28	—	ns	$T_J = 150^\circ\text{C}$ $I_C = 24A, V_{CC} = 480V$ $V_{GE} = 15V, R_G = 10\Omega$ Energy losses include "tail"
t_r	Rise Time	—	37	—		
$t_{d(off)}$	Turn-Off Delay Time	—	380	—		
t_f	Fall Time	—	460	—		
E_{ts}	Total Switching Loss	—	4.5	—	mJ	
L_E	Internal Emitter Inductance	—	13	—	nH	Measured 5mm from package
C_{ies}	Input Capacitance	—	1500	—	pF	$V_{GE} = 0V$ $V_{CC} = 30V$ $f = 1.0MHz$
C_{oes}	Output Capacitance	—	190	—		
C_{res}	Reverse Transfer Capacitance	—	20	—		

Notes: ① Repetitive rating; $V_{GE}=20V$, pulse width limited by max. junction temperature.

③ Repetitive rating; pulse width limited by maximum junction temperature.

⑤ Pulse width 5.0 μs , single shot.

② $V_{CC}=80\%(V_{CES}), V_{GE}=20V, L=10\mu H, R_G=10\Omega$

④ Pulse width $\leq 80\mu s$; duty factor $\leq 0.1\%$.

Refer to Section D for the following:

Package Outline 3 - JEDEC Outline TO-247AC

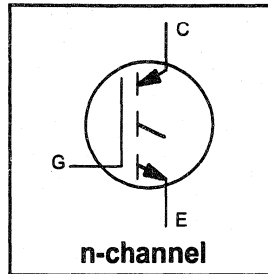
Section D - page D-13

INSULATED GATE BIPOLAR TRANSISTOR

Short Circuit Rated
Fast IGBT

Features

- Short circuit rated - 10 μ s @ 125°C, $V_{GE} = 15V$
- Switching-loss rating includes all "tail" losses
- Optimized for medium operating frequency (1 to 10kHz) See Fig. 1 for Current vs. Frequency curve



$$V_{CES} = 600V$$

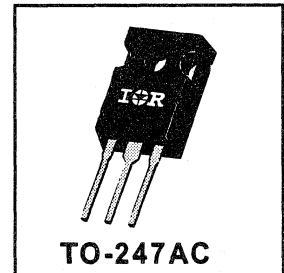
$$V_{CE(sat)} \leq 2.2V$$

$$@V_{GE} = 15V, I_C = 35A$$

Description

Insulated Gate Bipolar Transistors (IGBTs) from International Rectifier have higher usable current densities than comparable bipolar transistors, while at the same time having simpler gate-drive requirements of the familiar power MOSFET. They provide substantial benefits to a host of high-voltage, high-current applications.

These new short circuit rated devices are especially suited for motor control and other applications requiring short circuit withstand capability.



Motor
Control
Fast
Discretes

Absolute Maximum Ratings

	Parameter	Max.	Units
V_{CES}	Collector-to-Emitter Voltage	600	V
$I_C @ T_C = 25^\circ C$	Continuous Collector Current	60	A
$I_C @ T_C = 100^\circ C$	Continuous Collector Current	35	
I_{CM}	Pulsed Collector Current ①	120	
I_{LM}	Clamped Inductive Load Current ②	120	
t_{sc}	Short Circuit Withstand Time	10	μ s
V_{GE}	Gate-to-Emitter Voltage	± 20	V
E_{ARV}	Reverse Voltage Avalanche Energy ③	20	mJ
$P_D @ T_C = 25^\circ C$	Maximum Power Dissipation	200	W
$P_D @ T_C = 100^\circ C$	Maximum Power Dissipation	78	
T_J	Operating Junction and	-55 to +150	$^\circ C$
T_{STG}	Storage Temperature Range		
	Soldering Temperature, for 10 sec.	300 (0.063 in. (1.6mm) from case)	
	Mounting torque, 6-32 or M3 screw.	10 lbf·in (1.1N·m)	

Thermal Resistance

	Parameter	Min.	Typ.	Max.	Units
$R_{\theta JC}$	Junction-to-Case	—	—	0.64	$^\circ C/W$
$R_{\theta CS}$	Case-to-Sink, flat, greased surface	—	0.24	—	
$R_{\theta JA}$	Junction-to-Ambient, typical socket mount	—	—	40	
Wt	Weight	—	6 (0.21)	—	g (oz)

Electrical Characteristics @ $T_J = 25^\circ\text{C}$ (unless otherwise specified)

	Parameter	Min.	Typ.	Max.	Units	Conditions
$V_{(BR)CES}$	Collector-to-Emitter Breakdown Voltage	600	—	—	V	$V_{GE} = 0V, I_C = 250\mu A$
$V_{(BR)ECS}$	Emitter-to-Collector Breakdown Voltage ④	20	—	—	V	$V_{GE} = 0V, I_C = 1.0A$
$\Delta V_{(BR)CES}/\Delta T_J$	Temp. Coeff. of Breakdown Voltage	—	0.62	—	V/ $^\circ\text{C}$	$V_{GE} = 0V, I_C = 1.0mA$
$V_{CE(on)}$	Collector-to-Emitter Saturation Voltage	—	1.8	2.2	V	$I_C = 35A$ $I_C = 60A$ $I_C = 35A, T_J = 150^\circ\text{C}$ $V_{CE} = V_{GE}, I_C = 250\mu A$
		—	2.3	—		
		—	2.0	—		
$V_{GE(th)}$	Gate Threshold Voltage	3.0	—	5.5		$V_{CE} = V_{GE}, I_C = 250\mu A$
$\Delta V_{GE(th)}/\Delta T_J$	Temperature Coeff. of Threshold Voltage	—	-14	—	mV/ $^\circ\text{C}$	$V_{CE} = V_{GE}, I_C = 250\mu A$
g_{fe}	Forward Transconductance ⑤	11	20	—	S	$V_{CE} = 100V, I_C = 35A$
I_{CES}	Zero Gate Voltage Collector Current	—	—	250	μA	$V_{GE} = 0V, V_{CE} = 600V$
		—	—	2000		$V_{GE} = 0V, V_{CE} = 600V, T_J = 150^\circ\text{C}$
I_{GES}	Gate-to-Emitter Leakage Current	—	—	± 100	nA	$V_{GE} = \pm 20V$

Switching Characteristics @ $T_J = 25^\circ\text{C}$ (unless otherwise specified)

	Parameter	Min.	Typ.	Max.	Units	Conditions
Q_g	Total Gate Charge (turn-on)	—	120	180	nC	$I_C = 35A$ $V_{CC} = 400V$ $V_{GE} = 15V$ See Fig. 8
Q_{ge}	Gate - Emitter Charge (turn-on)	—	25	38		
Q_{gc}	Gate - Collector Charge (turn-on)	—	40	60		
$t_{d(on)}$	Turn-On Delay Time	—	35	—	ns	$T_J = 25^\circ\text{C}$ $I_C = 35A, V_{CC} = 480V$ $V_{GE} = 15V, R_G = 5.0\Omega$ Energy losses include "tail"
t_r	Rise Time	—	33	—		
$t_{d(off)}$	Turn-Off Delay Time	—	260	400		
t_f	Fall Time	—	170	260		
E_{on}	Turn-On Switching Loss	—	1.1	—	mJ	See Fig. 9, 10, 11, 14
E_{off}	Turn-Off Switching Loss	—	2.4	—		
E_{ts}	Total Switching Loss	—	3.5	5.3		
t_{sc}	Short Circuit Withstand Time	10	—	—	μs	$V_{CC} = 360V, T_J = 125^\circ\text{C}$ $V_{GE} = 15V, R_G = 5.0\Omega, V_{CPK} < 500V$
$t_{d(on)}$	Turn-On Delay Time	—	35	—	ns	$T_J = 150^\circ\text{C}$, $I_C = 35A, V_{CC} = 480V$ $V_{GE} = 15V, R_G = 5.0\Omega$ Energy losses include "tail"
t_r	Rise Time	—	32	—		
$t_{d(off)}$	Turn-Off Delay Time	—	460	—		
t_f	Fall Time	—	320	—		
E_{ts}	Total Switching Loss	—	6.5	—	mJ	See Fig. 10, 14
L_E	Internal Emitter Inductance	—	13	—	nH	Measured 5mm from package
C_{ies}	Input Capacitance	—	2900	—	pF	$V_{GE} = 0V$ $V_{CC} = 30V$ $f = 1.0MHz$ See Fig. 7
C_{oes}	Output Capacitance	—	230	—		
C_{res}	Reverse Transfer Capacitance	—	30	—		

Notes:

- ① Repetitive rating; $V_{GE}=20V$, pulse width limited by max. junction temperature. (See fig. 13b)
- ② $V_{CC}=80\%(V_{CES})$, $V_{GE}=20V$, $L=10\mu H$, $R_G = 5.0\Omega$, (See fig. 13a)
- ③ Repetitive rating; pulse width limited by maximum junction temperature.
- ④ Pulse width $\leq 80\mu s$; duty factor $\leq 0.1\%$.
- ⑤ Pulse width $5.0\mu s$, single shot.

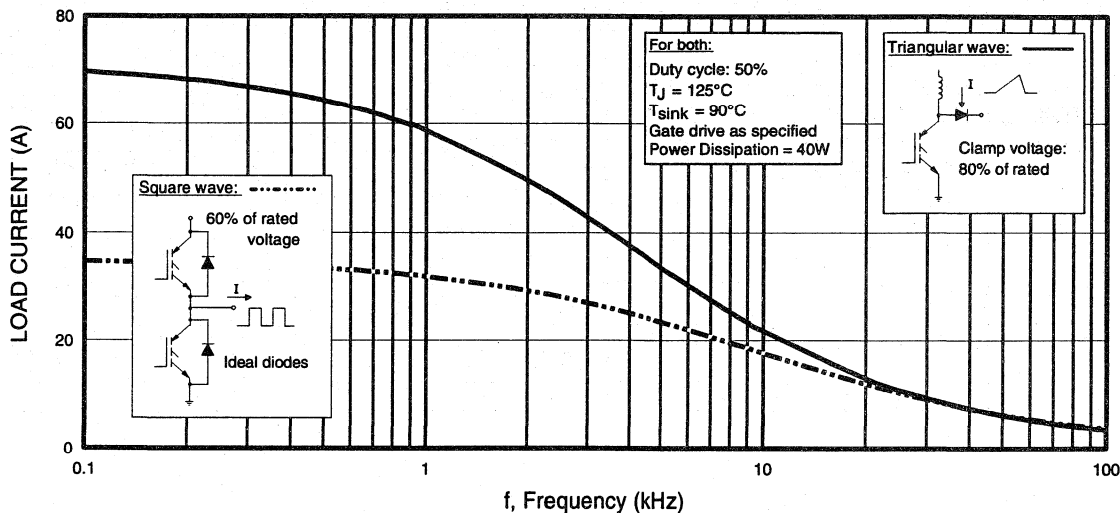


Fig. 1 - Typical Load Current vs. Frequency
 (For square wave, $I = I_{RMS}$ of fundamental; for triangular wave, $I = I_{PK}$)

Major
 Control
 Fast
 Discretes

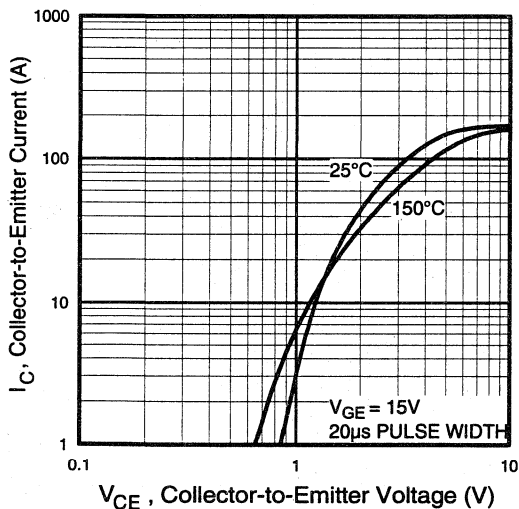


Fig. 2 - Typical Output Characteristics

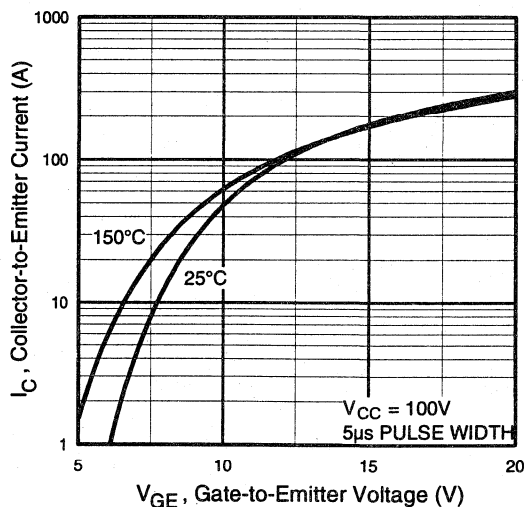


Fig. 3 - Typical Transfer Characteristics

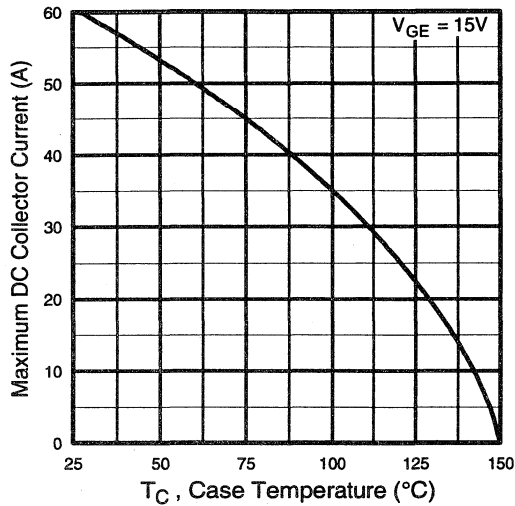


Fig. 4 - Maximum Collector Current vs. Case Temperature

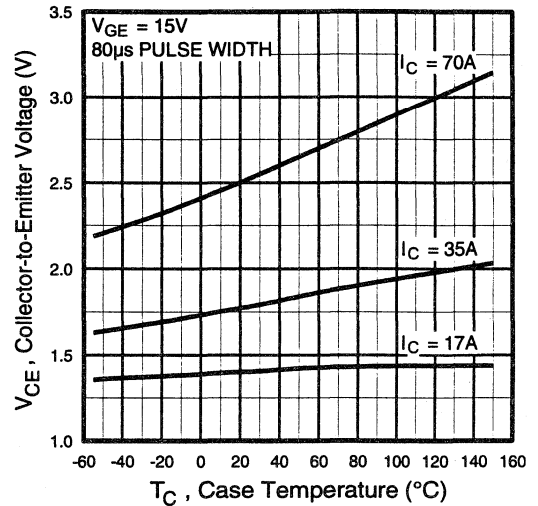


Fig. 5 - Collector-to-Emitter Voltage vs. Case Temperature

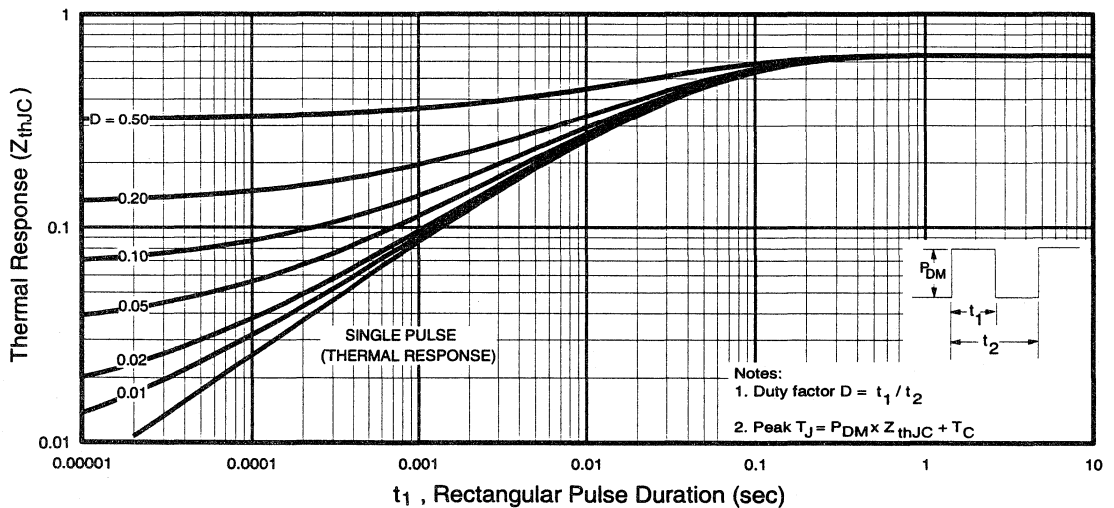


Fig. 6 - Maximum Effective Transient Thermal Impedance, Junction-to-Case

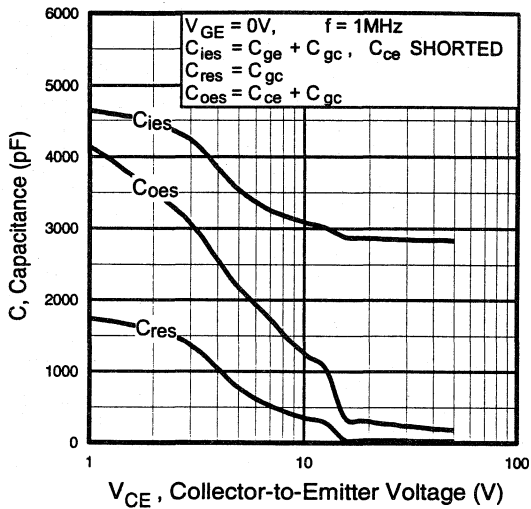


Fig. 7 - Typical Capacitance vs. Collector-to-Emitter Voltage

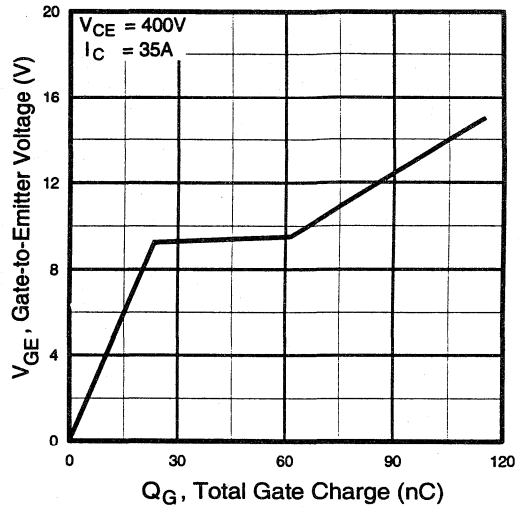


Fig. 8 - Typical Gate Charge vs. Gate-to-Emitter Voltage

Motor
 Control
 Fan
 Discretes

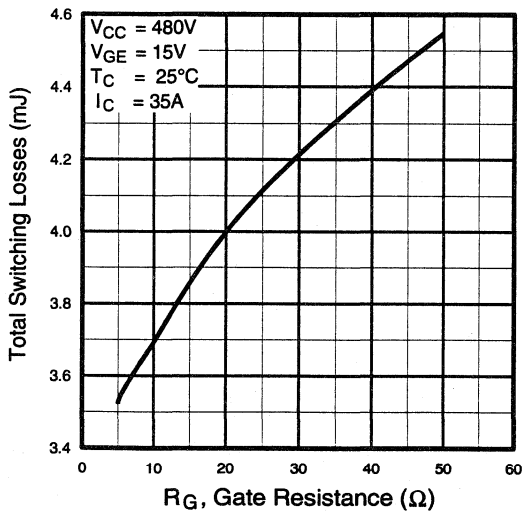


Fig. 9 - Typical Switching Losses vs. Gate Resistance

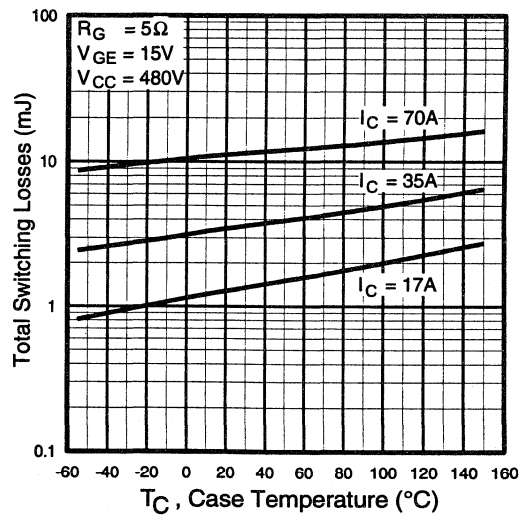


Fig. 10 - Typical Switching Losses vs. Case Temperature

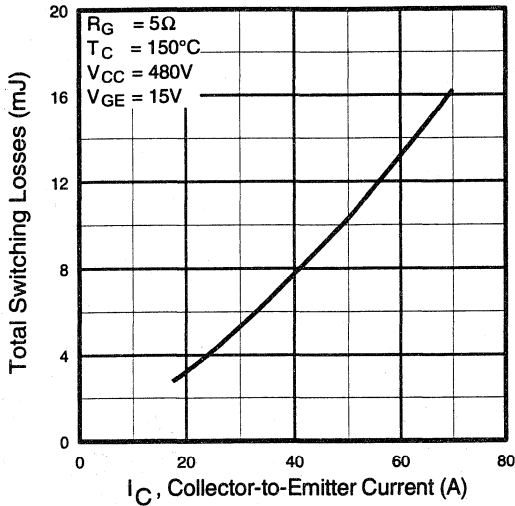


Fig. 11 - Typical Switching Losses vs. Collector-to-Emitter Current

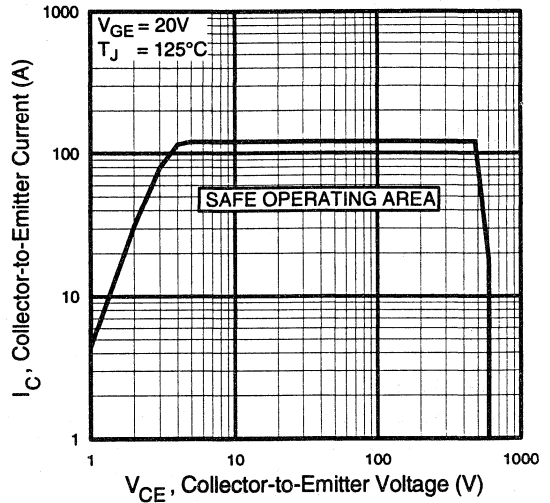


Fig. 12 - Turn-Off SOA

Refer to Section D for the following:

Appendix C: Section D - page D-5

Fig. 13a - Clamped Inductive Load Test Circuit

Fig. 13b - Pulsed Collector Current Test Circuit

Fig. 14a - Switching Loss Test Circuit

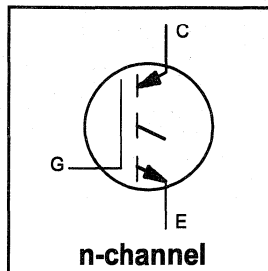
Fig. 14b - Switching Loss Waveform

INSULATED GATE BIPOLAR TRANSISTOR

Short Circuit Rated
Fast IGBT

Features

- Short circuit rated - $10\mu\text{s}$ @ 125°C , $V_{GE} = 15\text{V}$
- Switching-loss rating includes all "tail" losses
- Optimized for medium operating frequency (1 to 10kHz) See Fig. 1 for Current vs. Frequency curve



$$V_{CES} = 600\text{V}$$

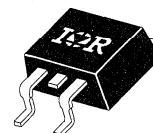
$$V_{CE(sat)} \leq 2.3\text{V}$$

$$@V_{GE} = 15\text{V}, I_C = 8.0\text{A}$$

Description

Insulated Gate Bipolar Transistors (IGBTs) from International Rectifier have higher usable current densities than comparable bipolar transistors, while at the same time having simpler gate-drive requirements of the familiar power MOSFET. They provide substantial benefits to a host of high-voltage, high-current applications.

These new short circuit rated devices are especially suited for motor control and other applications requiring short circuit withstand capability.



SMD-220

Motor
Control
Fast
Discretes

Absolute Maximum Ratings

	Parameter	Max.	Units
V_{CES}	Collector-to-Emitter Voltage	600	V
$I_C @ T_C = 25^\circ\text{C}$	Continuous Collector Current	13	A
$I_C @ T_C = 100^\circ\text{C}$	Continuous Collector Current	8.0	
I_{CM}	Pulsed Collector Current ①	26	
I_{LM}	Clamped Inductive Load Current ②	26	
t_{sc}	Short Circuit Withstand Time	10	μs
V_{GE}	Gate-to-Emitter Voltage	± 20	V
E_{ARV}	Reverse Voltage Avalanche Energy ③	5.0	mJ
$P_D @ T_C = 25^\circ\text{C}$	Maximum Power Dissipation	60	W
$P_D @ T_C = 100^\circ\text{C}$	Maximum Power Dissipation	24	
T_J	Operating Junction and	-55 to +150	$^\circ\text{C}$
T_{STG}	Storage Temperature Range		
	Soldering Temperature, for 10 sec.		
	Mounting torque, 6-32 or M3 screw.	10 lbf·in (1.1N·m)	

Thermal Resistance

	Parameter	Min.	Typ.	Max.	Units
$R_{\theta JC}$	Junction-to-Case	—	—	2.1	$^\circ\text{C/W}$
$R_{\theta JA}$	Junction-to-Ambient, (PCB mount)**	—	—	40	
$R_{\theta JA}$	Junction-to-Ambient, typical socket mount	—	—	80	
Wt	Weight	—	2 (0.07)	—	g (oz)

** When mounted on 1" square PCB (FR-4 or G-10 Material)

For recommended footprint and soldering techniques refer to application note #AN-994.

Electrical Characteristics @ $T_J = 25^\circ\text{C}$ (unless otherwise specified)

	Parameter	Min.	Typ.	Max.	Units	Conditions
$V_{(BR)CES}$	Collector-to-Emitter Breakdown Voltage	600	—	—	V	$V_{GE} = 0V, I_C = 250\mu A$
$V_{(BR)ECS}$	Emitter-to-Collector Breakdown Voltage ④	20	—	—	V	$V_{GE} = 0V, I_C = 1.0A$
$\Delta V_{(BR)CES}/\Delta T_J$	Temperature Coeff. of Breakdown Voltage	—	0.42	—	V/°C	$V_{GE} = 0V, I_C = 1.0mA$
$V_{CE(on)}$	Collector-to-Emitter Saturation Voltage	—	2.0	2.3	V	$V_{GE} = 15V$ See Fig. 2, 5
		—	2.7	—		
		—	2.5	—		
$V_{GE(th)}$	Gate Threshold Voltage	3.0	—	5.5		$I_C = 8.0A, T_J = 150^\circ\text{C}$ $V_{CE} = V_{GE}, I_C = 250\mu A$
$\Delta V_{GE(th)}/\Delta T_J$	Temperature Coeff. of Threshold Voltage	—	-11	—	mV/°C	$V_{CE} = V_{GE}, I_C = 250\mu A$
g_{fe}	Forward Transconductance ⑤	2.7	3.8	—	S	$V_{CE} = 100V, I_C = 8.0A$
I_{CES}	Zero Gate Voltage Collector Current	—	—	250	μA	$V_{GE} = 0V, V_{CE} = 600V$ $V_{GE} = 0V, V_{CE} = 600V, T_J = 150^\circ\text{C}$
		—	—	1000		
I_{GES}	Gate-to-Emitter Leakage Current	—	—	± 100	nA	$V_{GE} = \pm 20V$

Switching Characteristics @ $T_J = 25^\circ\text{C}$ (unless otherwise specified)

	Parameter	Min.	Typ.	Max.	Units	Conditions
Q_g	Total Gate Charge (turn-on)	—	7.9	16	nC	$I_C = 8.0A$ $V_{CE} = 400V$ $V_{GE} = 15V$ See Fig. 8
Q_{ge}	Gate - Emitter Charge (turn-on)	—	3.6	5.2		
Q_{gc}	Gate - Collector Charge (turn-on)	—	6.0	9.0		
$t_{d(on)}$	Turn-On Delay Time	—	29	—	ns	$T_J = 25^\circ\text{C}$ $I_C = 8.0A, V_{CC} = 480V$ $V_{GE} = 15V, R_G = 50\Omega$ Energy losses include "tail"
t_r	Rise Time	—	22	—		
$t_{d(off)}$	Turn-Off Delay Time	—	270	400		
t_f	Fall Time	—	280	510		
E_{on}	Turn-On Switching Loss	—	0.14	—		
E_{off}	Turn-Off Switching Loss	—	0.86	—		
E_{ts}	Total Switching Loss	—	1.0	2.0		
t_{sc}	Short Circuit Withstand Time	10	—	—	μs	$V_{CC} = 360V, T_J = 125^\circ\text{C}$ $V_{GE} = 15V, R_G = 50\Omega, V_{CPK} < 500V$
$t_{d(on)}$	Turn-On Delay Time	—	27	—	ns	$T_J = 150^\circ\text{C}$, $I_C = 8.0A, V_{CC} = 480V$ $V_{GE} = 15V, R_G = 50\Omega$ Energy losses include "tail"
t_r	Rise Time	—	21	—		
$t_{d(off)}$	Turn-Off Delay Time	—	370	—		
t_f	Fall Time	—	420	—		
E_{ts}	Total Switching Loss	—	1.4	—		
L_E	Internal Emitter Inductance	—	7.5	—	nH	Measured 5mm from package
C_{ies}	Input Capacitance	—	365	—	pF	$V_{GE} = 0V$ $V_{CC} = 30V$ $f = 1.0MHz$ See Fig. 7
C_{oes}	Output Capacitance	—	47	—		
C_{res}	Reverse Transfer Capacitance	—	4.8	—		

Notes:

- ① Repetitive rating; $V_{GE}=20V$, pulse width limited by max. junction temperature. (See fig. 13b)
- ② $V_{CC}=80\%(V_{CES}), V_{GE}=20V, L=10\mu H, R_G=50\Omega$, (See fig. 13a)
- ③ Repetitive rating; pulse width limited by maximum junction temperature.
- ④ Pulse width $\leq 80\mu s$; duty factor $\leq 0.1\%$.
- ⑤ Pulse width $5.0\mu s$, single shot.

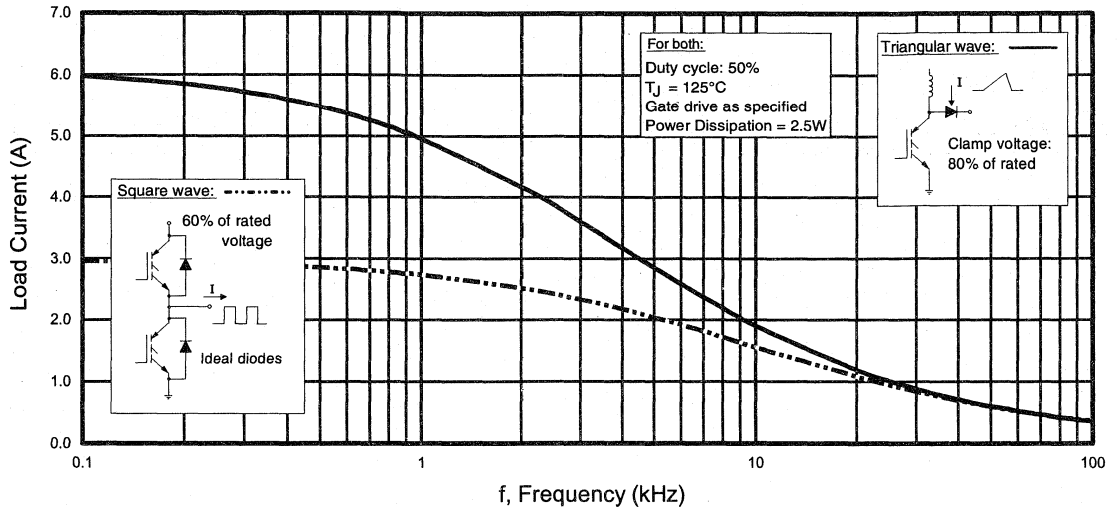


Fig. 1 - Typical Load Current vs. Frequency
 (For square wave, $I = I_{RMS}$ of fundamental; for triangular wave, $I = I_{PK}$)

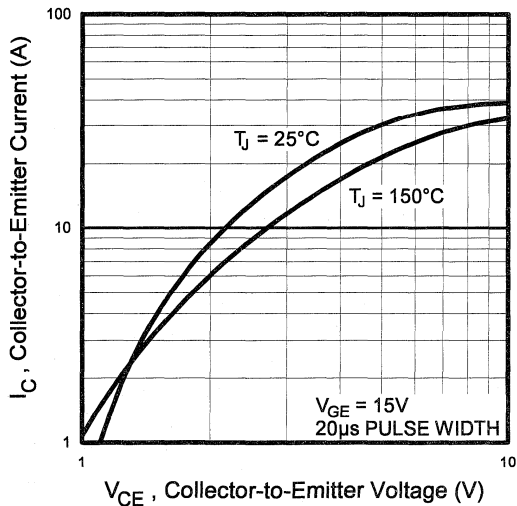


Fig. 2 - Typical Output Characteristics

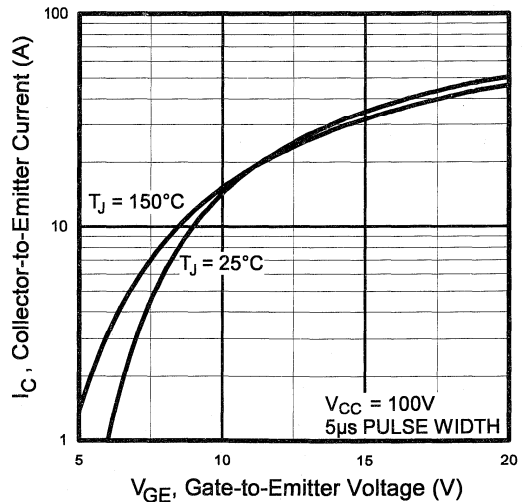


Fig. 3 - Typical Transfer Characteristics

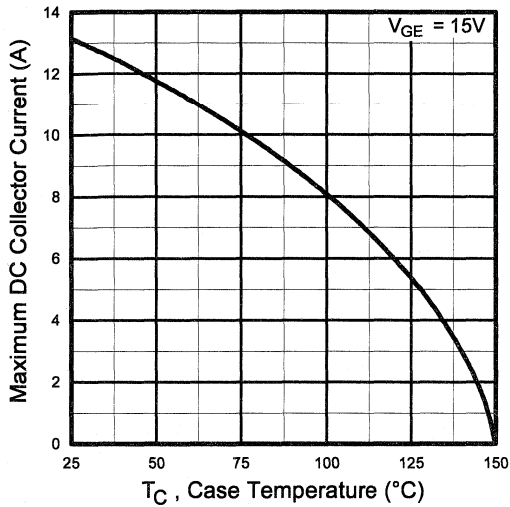


Fig. 4 - Maximum Collector Current vs. Case Temperature

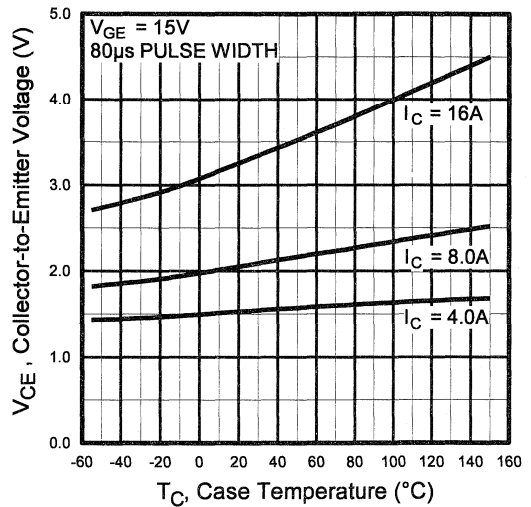


Fig. 5 - Collector-to-Emitter Voltage vs. Case Temperature

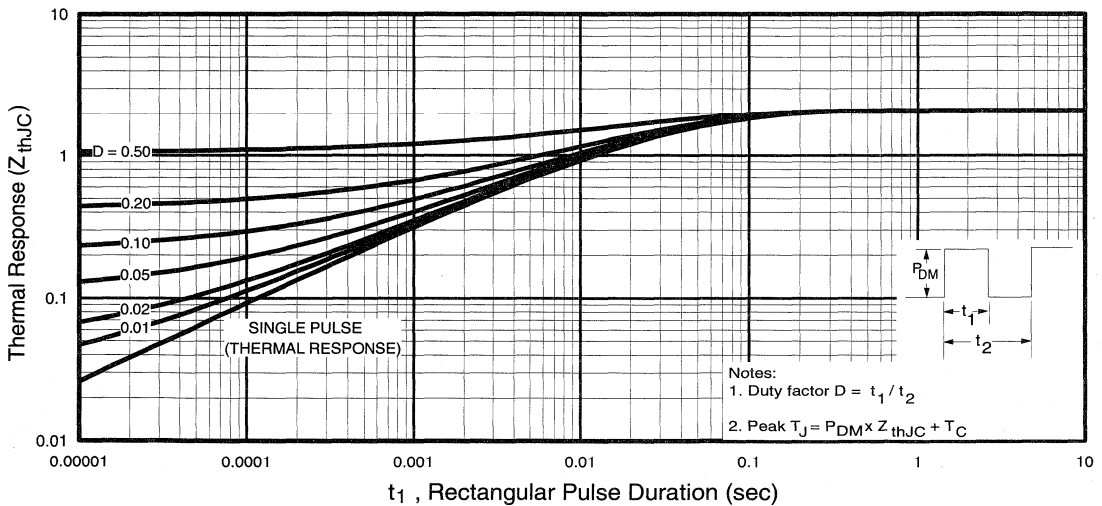


Fig. 6 - Maximum Effective Transient Thermal Impedance, Junction-to-Case

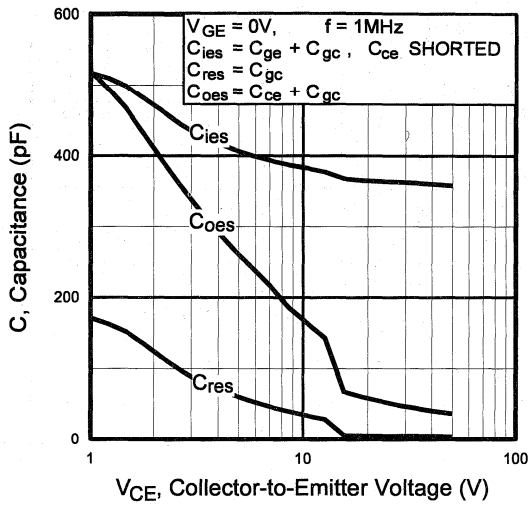


Fig. 7 - Typical Capacitance vs. Collector-to-Emitter Voltage

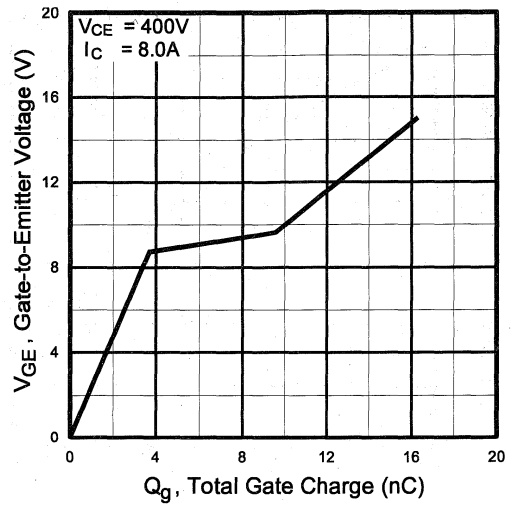


Fig. 8 - Typical Gate Charge vs. Gate-to-Emitter Voltage

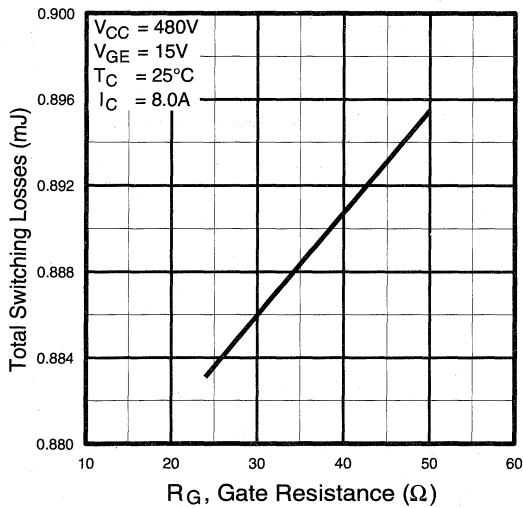


Fig. 9 - Typical Switching Losses vs. Gate Resistance

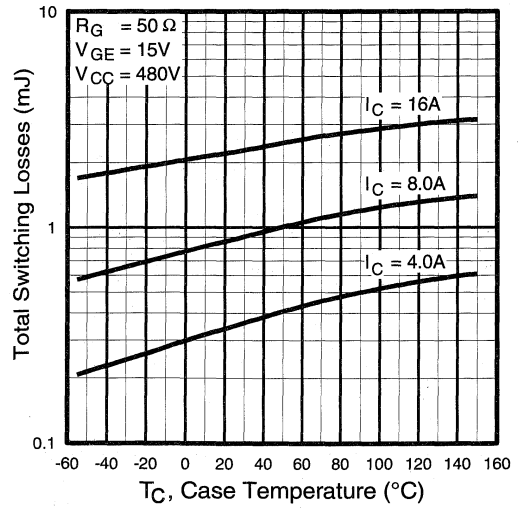


Fig. 10 - Typical Switching Losses vs. Case Temperature

Motor
 Control
 Fast
 Discretes

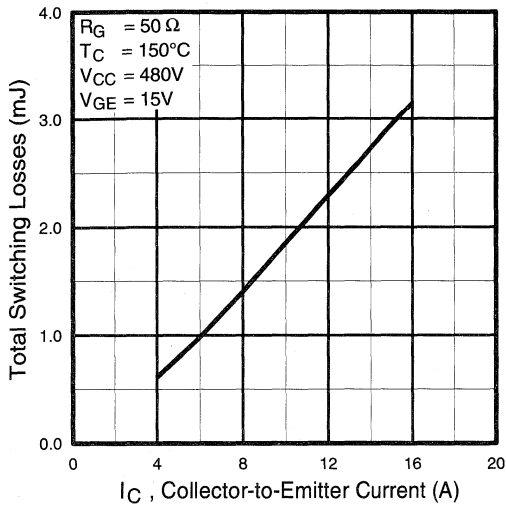


Fig. 11 - Typical Switching Losses vs. Collector-to-Emitter Current

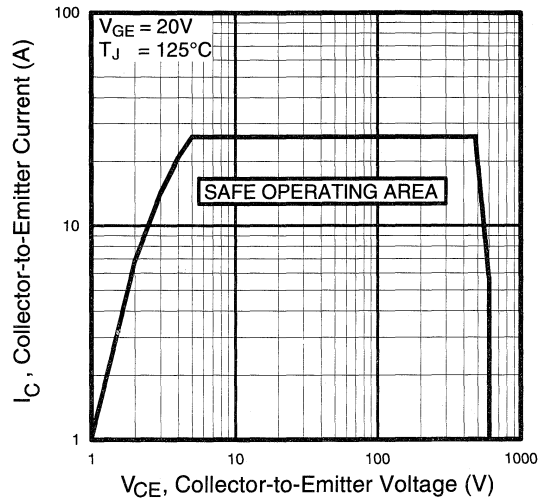


Fig. 12 - Turn-Off SOA

Refer to Section D for the following:

Appendix C: Section D - page D-5

Fig. 13a - Clamped Inductive Load Test Circuit

Fig. 13b - Pulsed Collector Current Test Circuit

Fig. 14a - Switching Loss Test Circuit

Fig. 14b - Switching Loss Waveform

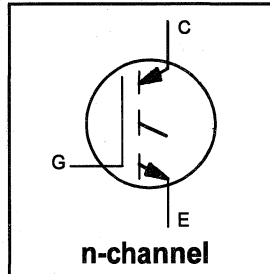
Package Outline 2 - SMD-220 Section D - page D-12

INSULATED GATE BIPOLAR TRANSISTOR

**Short Circuit Rated
Fast IGBT**

Features

- Short circuit rated - 10 μ s @ 125°C, V_{GE} = 15V
- Switching-loss rating includes all "tail" losses
- Optimized for medium operating frequency (1 to 10kHz) See Fig. 1 for Current vs. Frequency curve



V_{CES} = 600V

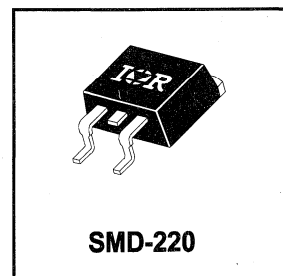
V_{CE(sat)} ≤ 2.9V

@V_{GE} = 15V, I_C = 16A

Description

Insulated Gate Bipolar Transistors (IGBTs) from International Rectifier have higher usable current densities than comparable bipolar transistors, while at the same time having simpler gate-drive requirements of the familiar power MOSFET. They provide substantial benefits to a host of high-voltage, high-current applications.

These new short circuit rated devices are especially suited for motor control and other applications requiring short circuit withstand capability.



Motor Control Fast Discretes

Absolute Maximum Ratings

	Parameter	Max.	Units
V _{CES}	Collector-to-Emitter Voltage	600	V
I _C @ T _C = 25°C	Continuous Collector Current	26	A
I _C @ T _C = 100°C	Continuous Collector Current	16	
I _{CM}	Pulsed Collector Current ①	52	
I _{LM}	Clamped Inductive Load Current ②	52	
t _{sc}	Short Circuit Withstand Time	10	μ s
V _{GE}	Gate-to-Emitter Voltage	±20	V
E _{ARV}	Reverse Voltage Avalanche Energy ③	10	mJ
P _D @ T _C = 25°C	Maximum Power Dissipation	100	W
P _D @ T _C = 100°C	Maximum Power Dissipation	42	
T _J	Operating Junction and	-55 to +150	°C
T _{STG}	Storage Temperature Range		
	Soldering Temperature, for 10 sec.	300 (0.063 in. (1.6mm) from case)	
	Mounting torque, 6-32 or M3 screw.	10 lbf•in (1.1N•m)	

Thermal Resistance

	Parameter	Min.	Typ.	Max.	Units
R _{θJC}	Junction-to-Case	—	—	1.2	°C/W
R _{θJA}	Junction-to-Ambient, (PCB mount)**	—	—	40	
R _{θJA}	Junction-to-Ambient, typical socket mount	—	—	80	
Wt	Weight	—	2 (0.07)	—	g (oz)

** When mounted on 1" square PCB (FR-4 or G-10 Material)

For recommended footprint and soldering techniques refer to application note #AN-994.

Electrical Characteristics @ $T_J = 25^\circ\text{C}$ (unless otherwise specified)

	Parameter	Min.	Typ.	Max.	Units	Conditions
$V_{(BR)CES}$	Collector-to-Emitter Breakdown Voltage	600	—	—	V	$V_{GE} = 0V, I_C = 250\mu A$
$V_{(BR)ECS}$	Emitter-to-Collector Breakdown Voltage ④	20	—	—	V	$V_{GE} = 0V, I_C = 1.0A$
$\Delta V_{(BR)CES}/\Delta T_J$	Temperature Coeff. of Breakdown Voltage	—	0.65	—	V/°C	$V_{GE} = 0V, I_C = 1.0mA$
$V_{CE(on)}$	Collector-to-Emitter Saturation Voltage	—	1.9	2.9	V	$I_C = 14A, T_J = 150^\circ\text{C}$ See Fig. 2, 5
		—	2.7	—		
		—	2.2	—		
$V_{GE(th)}$	Gate Threshold Voltage	3.0	—	5.5		$V_{CE} = V_{GE}, I_C = 250\mu A$
$\Delta V_{GE(th)}/\Delta T_J$	Temperature Coeff. of Threshold Voltage	—	-12	—	mV/°C	$V_{CE} = V_{GE}, I_C = 250\mu A$
g_{fe}	Forward Transconductance ⑤	3.3	6.5	—	S	$V_{CE} = 100V, I_C = 14A$
I_{CES}	Zero Gate Voltage Collector Current	—	—	250	μA	$V_{GE} = 0V, V_{CE} = 600V$
		—	—	1000		$V_{GE} = 0V, V_{CE} = 600V, T_J = 150^\circ\text{C}$
I_{GES}	Gate-to-Emitter Leakage Current	—	—	± 100	nA	$V_{GE} = \pm 20V$

Switching Characteristics @ $T_J = 25^\circ\text{C}$ (unless otherwise specified)

	Parameter	Min.	Typ.	Max.	Units	Conditions
Q_g	Total Gate Charge (turn-on)	—	35	53	nC	$I_C = 16A$ $V_{CC} = 400V$ $V_{GE} = 15V$ See Fig. 8
Q_{ge}	Gate - Emitter Charge (turn-on)	—	7.4	11		
Q_{gc}	Gate - Collector Charge (turn-on)	—	14	21		
$t_{d(on)}$	Turn-On Delay Time	—	31	—	ns	$T_J = 25^\circ\text{C}$ $I_C = 16A, V_{CC} = 480V$ $V_{GE} = 15V, R_G = 23\Omega$ Energy losses include "tail"
t_r	Rise Time	—	31	—		
$t_{d(off)}$	Turn-Off Delay Time	—	280	420		
t_f	Fall Time	—	310	470	mJ	See Fig. 9, 10, 11, 14
E_{on}	Turn-On Switching Loss	—	0.4	—		
E_{off}	Turn-Off Switching Loss	—	1.9	—		
E_{ts}	Total Switching Loss	—	2.3	3.5	μs	$V_{CC} = 360V, T_J = 125^\circ\text{C}$ $V_{GE} = 15V, R_G = 23\Omega, V_{CPK} < 500V$
t_{sc}	Short Circuit Withstand Time	10	—	—		
$t_{d(on)}$	Turn-On Delay Time	—	31	—		
t_r	Rise Time	—	30	—	ns	$T_J = 150^\circ\text{C}$, $I_C = 16A, V_{CC} = 480V$ $V_{GE} = 15V, R_G = 23\Omega$ Energy losses include "tail"
$t_{d(off)}$	Turn-Off Delay Time	—	530	—		
t_f	Fall Time	—	660	—		
E_{ts}	Total Switching Loss	—	4.4	—	mJ	See Fig. 10, 14
L_E	Internal Emitter Inductance	—	7.5	—	nH	Measured 5mm from package
C_{ies}	Input Capacitance	—	750	—	pF	$V_{GE} = 0V$ $V_{CC} = 30V$ See Fig. 7
C_{oes}	Output Capacitance	—	110	—		
C_{res}	Reverse Transfer Capacitance	—	9.3	—		

Notes:

- ① Repetitive rating; $V_{GE}=20V$, pulse width limited by max. junction temperature. (See fig. 13b)
- ② $V_{CC}=80\%(V_{CES}), V_{GE}=20V, L=10\mu H, R_G=23\Omega$, (See fig. 13a)
- ③ Repetitive rating; pulse width limited by maximum junction temperature.
- ④ Pulse width $\leq 80\mu s$; duty factor $\leq 0.1\%$.
- ⑤ Pulse width 5.0 μs , single shot.

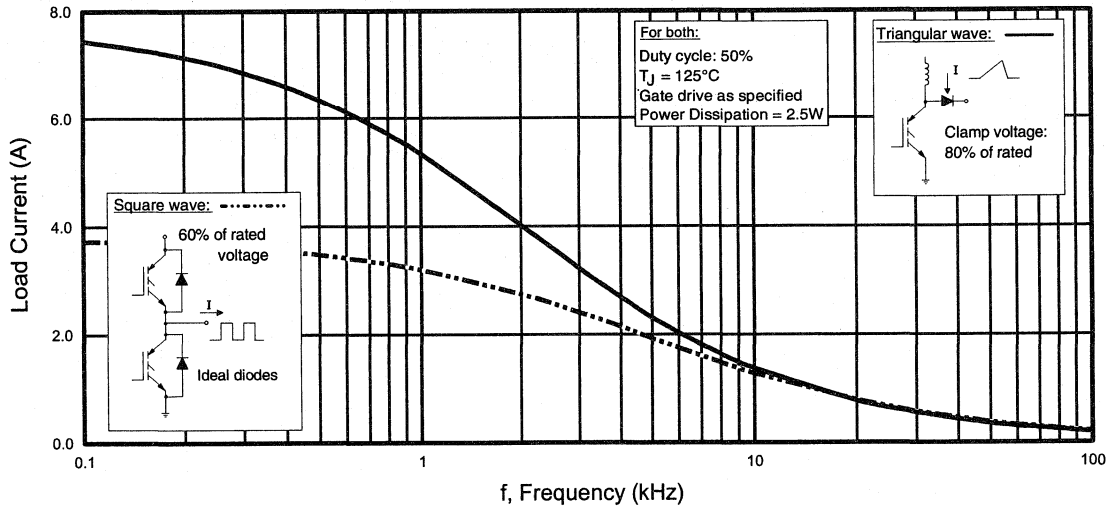


Fig. 1 - Typical Load Current vs. Frequency
 (For square wave, $I = I_{RMS}$ of fundamental; for triangular wave, $I = I_{PK}$)

Motor
 Control
 Fast
 Discretes

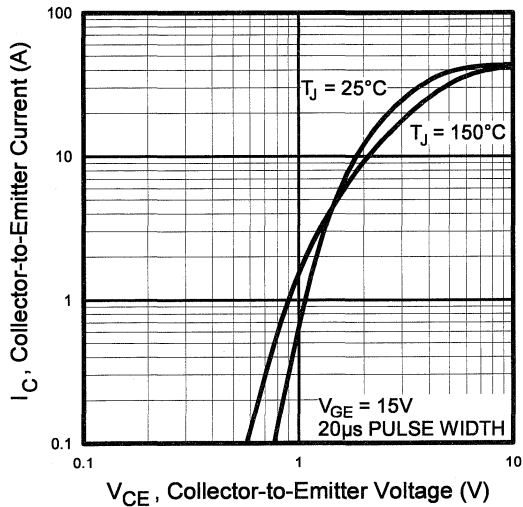


Fig. 2 - Typical Output Characteristics

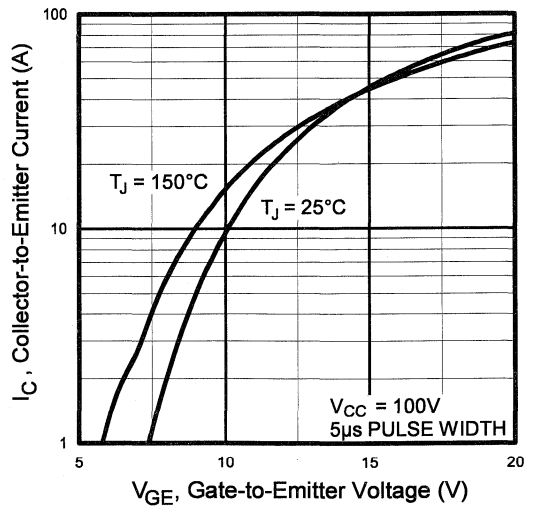


Fig. 3 - Typical Transfer Characteristics

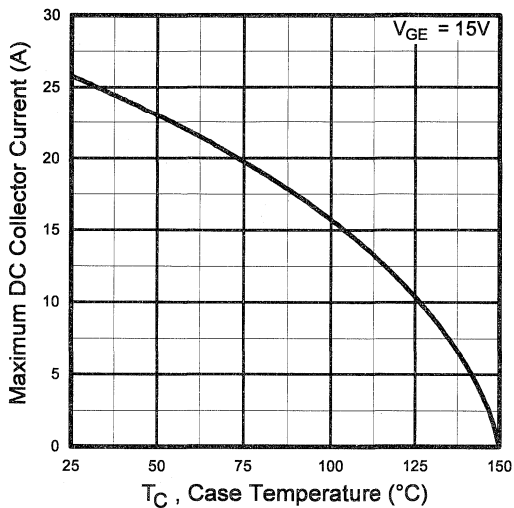


Fig. 4 - Maximum Collector Current vs. Case Temperature

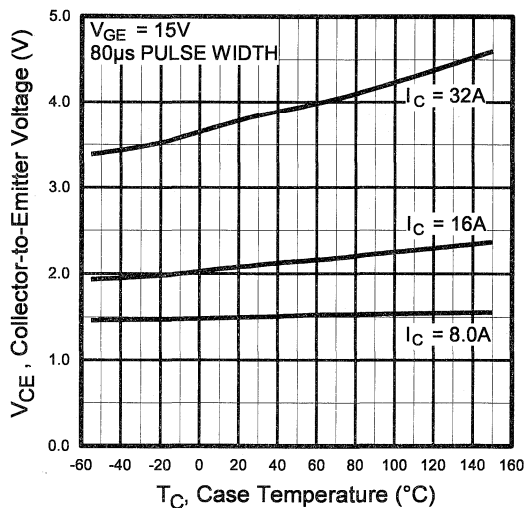


Fig. 5 - Collector-to-Emitter Voltage vs. Case Temperature

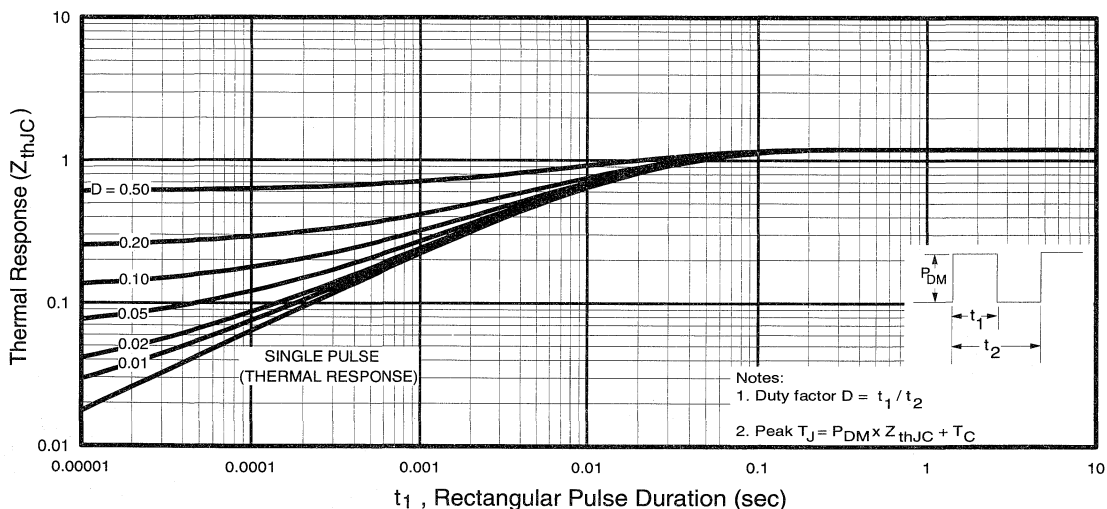


Fig. 6 - Maximum Effective Transient Thermal Impedance, Junction-to-Case

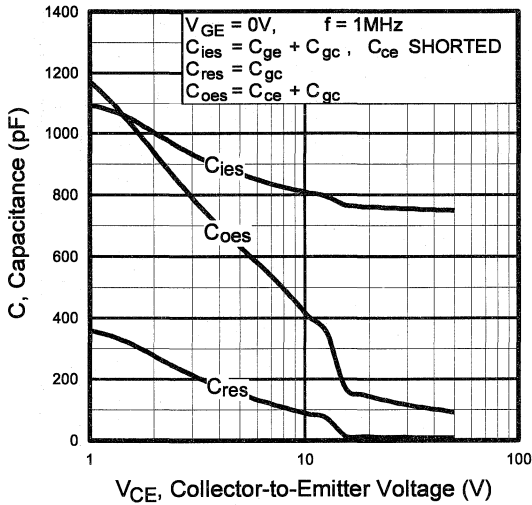


Fig. 7 - Typical Capacitance vs. Collector-to-Emitter Voltage

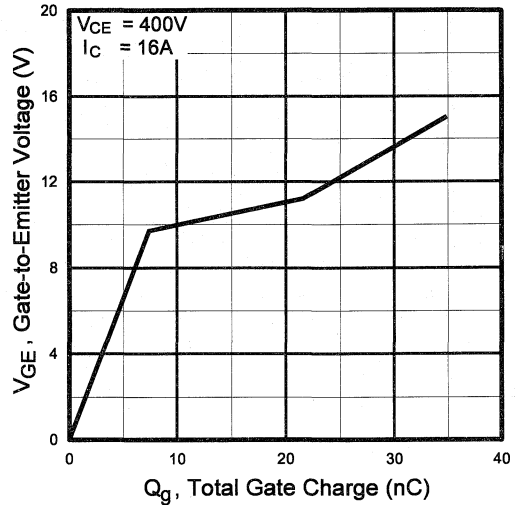


Fig. 8 - Typical Gate Charge vs. Gate-to-Emitter Voltage

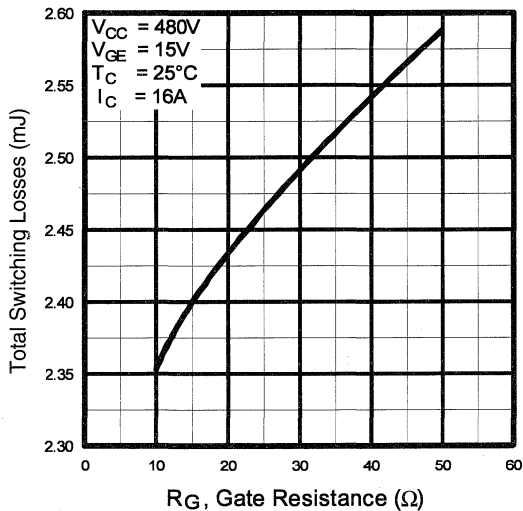


Fig. 9 - Typical Switching Losses vs. Gate Resistance

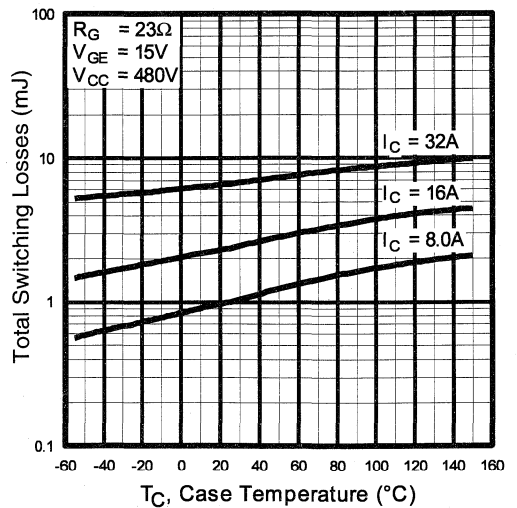


Fig. 10 - Typical Switching Losses vs. Case Temperature



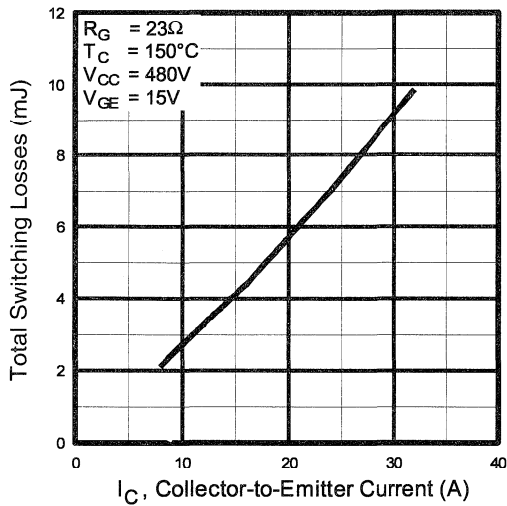


Fig. 11 - Typical Switching Losses vs. Collector-to-Emitter Current

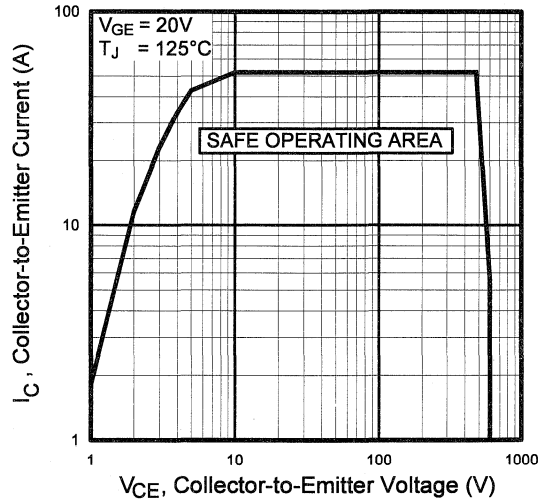


Fig. 12 - Turn-Off SOA

Refer to Section D for the following:

Appendix C: Section D - page D-5

- Fig. 13a - Clamped Inductive Load Test Circuit
- Fig. 13b - Pulsed Collector Current Test Circuit
- Fig. 14a - Switching Loss Test Circuit
- Fig. 14b - Switching Loss Waveform

Package Outline 2 - SMD-220 Section D - page D-12

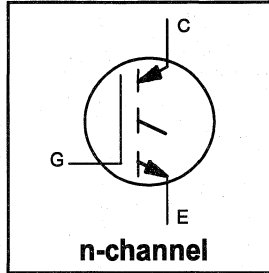
IRGBC40M-S

INSULATED GATE BIPOLAR TRANSISTOR

Short Circuit Rated
Fast IGBT

Features

- Short circuit rated - 10 μ s @ 125°C, $V_{GE} = 15V$
- Switching-loss rating includes all "tail" losses
- Optimized for medium operating frequency (1 to 10kHz)



$$V_{CES} = 600V$$

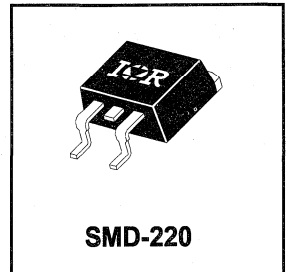
$$V_{CE(sat)} \leq 3.0V$$

$$@V_{GE} = 15V, I_C = 24A$$

Description

Insulated Gate Bipolar Transistors (IGBTs) from International Rectifier have higher usable current densities than comparable bipolar transistors, while at the same time having simpler gate-drive requirements of the familiar power MOSFET. They provide substantial benefits to a host of high-voltage, high-current applications.

These new short circuit rated devices are especially suited for motor control and other applications requiring short circuit withstand capability.



SMD-220

Motor
Control
Fast
Discretes

Absolute Maximum Ratings

	Parameter	Max.	Units
V_{CES}	Collector-to-Emitter Voltage	600	V
$I_C @ T_C = 25^\circ C$	Continuous Collector Current	40	A
$I_C @ T_C = 100^\circ C$	Continuous Collector Current	24	
I_{CM}	Pulsed Collector Current ①	80	
I_{LM}	Clamped Inductive Load Current ②	80	
t_{sc}	Short Circuit Withstand Time	10	μ s
V_{GE}	Gate-to-Emitter Voltage	± 20	V
E_{ARV}	Reverse Voltage Avalanche Energy ③	15	mJ
$P_D @ T_C = 25^\circ C$	Maximum Power Dissipation	160	W
$P_D @ T_C = 100^\circ C$	Maximum Power Dissipation	65	
T_J	Operating Junction and	-55 to +150	°C
T_{STG}	Storage Temperature Range		
	Soldering Temperature, for 10 sec.	300 (0.063 in. (1.6mm) from case)	
	Mounting torque, 6-32 or M3 screw.	10 lbf•in (1.1N•m)	

Thermal Resistance

	Parameter	Min.	Typ.	Max.	Units
$R_{\theta JC}$	Junction-to-Case	—	—	0.77	°C/W
$R_{\theta JA}$	Junction-to-Ambient, (PCB mount)**	—	—	40	
$R_{\theta JA}$	Junction-to-Ambient, typical socket mount	—	—	80	
Wt	Weight	—	2 (0.07)	—	g (oz)

** When mounted on 1" square PCB (FR-4 or G-10 Material)

For recommended footprint and soldering techniques refer to application note #AN-994.

Electrical Characteristics @ $T_J = 25^\circ\text{C}$ (unless otherwise specified)

	Parameter	Min.	Typ.	Max.	Units	Conditions	
$V_{(BR)CES}$	Collector-to-Emitter Breakdown Voltage	600	—	—	V	$V_{GE} = 0V, I_C = 250\mu A$	
$V_{(BR)ECS}$	Emitter-to-Collector Breakdown Voltage ④	20	—	—	V	$V_{GE} = 0V, I_C = 1.0A$	
$\Delta V_{(BR)CES}/\Delta T_J$	Temp. Coeff. of Breakdown Voltage	—	0.70	—	V/ $^\circ\text{C}$	$V_{GE} = 0V, I_C = 1.0mA$	
$V_{CE(on)}$	Collector-to-Emitter Saturation Voltage	—	2.0	3.0	V	$V_{GE} = 15V$ $I_C = 24A$	
		—	2.6	—			$I_C = 40A$
		—	2.4	—			$I_C = 24A, T_J = 150^\circ\text{C}$
$V_{GE(th)}$	Gate Threshold Voltage	3.0	—	5.5		$V_{CE} = V_{GE}, I_C = 250\mu A$	
$\Delta V_{GE(th)}/\Delta T_J$	Temperature Coeff. of Threshold Voltage	—	-12	—	mV/ $^\circ\text{C}$	$V_{CE} = V_{GE}, I_C = 250\mu A$	
g_{fe}	Forward Transconductance ⑤	9.2	12	—	S	$V_{CE} = 100V, I_C = 24A$	
I_{CES}	Zero Gate Voltage Collector Current	—	—	250	μA	$V_{GE} = 0V, V_{CE} = 600V$	
		—	—	1000		$V_{GE} = 0V, V_{CE} = 600V, T_J = 150^\circ\text{C}$	
I_{GES}	Gate-to-Emitter Leakage Current	—	—	± 100	nA	$V_{GE} = \pm 20V$	

Switching Characteristics @ $T_J = 25^\circ\text{C}$ (unless otherwise specified)

	Parameter	Min.	Typ.	Max.	Units	Conditions
Q_g	Total Gate Charge (turn-on)	—	59	80	nC	$I_C = 24A$ $V_{CC} = 400V$ $V_{GE} = 15V$
Q_{ge}	Gate - Emitter Charge (turn-on)	—	8.6	10		
Q_{gc}	Gate - Collector Charge (turn-on)	—	25	42		
$t_{d(on)}$	Turn-On Delay Time	—	26	—	ns	$T_J = 25^\circ\text{C}$ $I_C = 24A, V_{CC} = 480V$ $V_{GE} = 15V, R_G = 10\Omega$ Energy losses include "tail"
t_r	Rise Time	—	37	—		
$t_{d(off)}$	Turn-Off Delay Time	—	240	410		
t_f	Fall Time	—	230	420		
E_{on}	Turn-On Switching Loss	—	0.75	—	mJ	
E_{off}	Turn-Off Switching Loss	—	1.65	—		
E_{ts}	Total Switching Loss	—	2.4	3.6		
t_{sc}	Short Circuit Withstand Time	10	—	—	μs	$V_{CC} = 360V, T_J = 125^\circ\text{C}$ $V_{GE} = 15V, R_G = 10\Omega, V_{CPK} < 500V$
$t_{d(on)}$	Turn-On Delay Time	—	28	—	ns	$T_J = 150^\circ\text{C}$, $I_C = 24A, V_{CC} = 480V$ $V_{GE} = 15V, R_G = 10\Omega$ Energy losses include "tail"
t_r	Rise Time	—	37	—		
$t_{d(off)}$	Turn-Off Delay Time	—	380	—		
t_f	Fall Time	—	460	—		
E_{ts}	Total Switching Loss	—	4.5	—		
L_E	Internal Emitter Inductance	—	7.5	—	nH	Measured 5mm from package
C_{ies}	Input Capacitance	—	1500	—	pF	$V_{GE} = 0V$ $V_{CC} = 30V$ $f = 1.0MHz$
C_{oes}	Output Capacitance	—	190	—		
C_{res}	Reverse Transfer Capacitance	—	20	—		

Notes:

- ① Repetitive rating; $V_{GE}=20V$, pulse width limited by max. junction temperature.
- ② $V_{CC}=80\%(V_{CES})$, $V_{GE}=20V$, $L=10\mu H$, $R_G=10\Omega$
- ③ Repetitive rating; pulse width limited by maximum junction temperature.
- ④ Pulse width $\leq 80\mu s$; duty factor $\leq 0.1\%$.
- ⑤ Pulse width 5.0 μs , single shot.

Refer to Section D for the following:

Package Outline 2 - SMD-220 Section D - page D-12

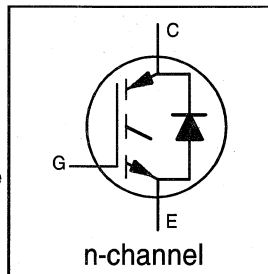
IRGBC20MD2

INSULATED GATE BIPOLAR TRANSISTOR
WITH ULTRAFAST SOFT RECOVERY

Short Circuit Rated
Fast Copack IGBT

DIODE Features

- Short circuit rated -10 μ s @125°C, $V_{GE} = 15V$
- Switching-loss rating includes all "tail" losses
- HEXFRED™ soft ultrafast diodes
- Optimized for medium operating frequency (1 to 10kHz) See Fig. 1 for Current vs. Frequency curve



$$V_{CES} = 600V$$

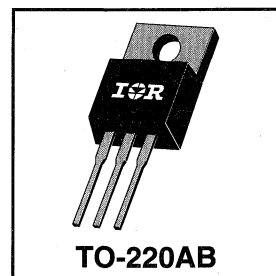
$$V_{CE(sat)} \leq 2.5V$$

$$@V_{GE} = 15V, I_C = 8.0A$$

Description

Co-packaged IGBTs are a natural extension of International Rectifier's well known IGBT line. They provide the convenience of an IGBT and an ultrafast recovery diode in one package, resulting in substantial benefits to a host of high-voltage, high-current, applications.

These new short circuit rated devices are especially suited for motor control and other applications requiring short circuit withstand capability.



Motor
Control
Fast
Co-Packs

Absolute Maximum Ratings

	Parameter	Max.	Units
V_{CES}	Collector-to-Emitter Voltage	600	V
$I_C @ T_C = 25^\circ C$	Continuous Collector Current	13	A
$I_C @ T_C = 100^\circ C$	Continuous Collector Current	8.0	
I_{CM}	Pulsed Collector Current $\text{\textcircled{D}}$	26	
I_{LM}	Clamped Inductive Load Current $\text{\textcircled{D}}$	26	
$I_F @ T_C = 100^\circ C$	Diode Continuous Forward Current	7.0	
I_{FM}	Diode Maximum Forward Current	60	
t_{sc}	Short Circuit Withstand Time	10	
V_{GE}	Gate-to-Emitter Voltage	± 20	V
$P_D @ T_C = 25^\circ C$	Maximum Power Dissipation	60	W
$P_D @ T_C = 100^\circ C$	Maximum Power Dissipation	24	
T_J	Operating Junction and	-55 to +150	$^\circ C$
T_{STG}	Storage Temperature Range		
	Soldering Temperature, for 10 sec.	300 (0.063 in. (1.6mm) from case)	
	Mounting Torque, 6-32 or M3 Screw.	10 lbf•in (1.1 N•m)	

Thermal Resistance

	Parameter	Min.	Typ.	Max.	Units
$R_{\theta JC}$	Junction-to-Case - IGBT	—	—	2.1	$^\circ C/W$
$R_{\theta JC}$	Junction-to-Case - Diode	—	—	3.5	
$R_{\theta CS}$	Case-to-Sink, flat, greased surface	—	0.50	—	
$R_{\theta JA}$	Junction-to-Ambient, typical socket mount	—	—	80	
Wt	Weight	—	2 (0.07)	—	g (oz)

Electrical Characteristics @ $T_J = 25^\circ\text{C}$ (unless otherwise specified)

	Parameter	Min.	Typ.	Max.	Units	Conditions
$V_{(BR)CES}$	Collector-to-Emitter Breakdown Voltage ^①	600	—	—	V	$V_{GE} = 0V, I_C = 250\mu A$
$\Delta V_{(BR)CES}/\Delta T_J$	Temperature Coeff. of Breakdown Voltage	—	0.42	—	V/ $^\circ\text{C}$	$V_{GE} = 0V, I_C = 1.0mA$
$V_{CE(on)}$	Collector-to-Emitter Saturation Voltage	—	2.0	2.5	V	$I_C = 8.0A, V_{GE} = 15V$
		—	2.7	—		$I_C = 13A$
		—	2.5	—		$I_C = 8.0A, T_J = 150^\circ\text{C}$
$V_{GE(th)}$	Gate Threshold Voltage	3.0	—	5.5		$V_{CE} = V_{GE}, I_C = 250\mu A$
$\Delta V_{GE(th)}/\Delta T_J$	Temperature Coeff. of Threshold Voltage	—	-11	—	mV/ $^\circ\text{C}$	$V_{CE} = V_{GE}, I_C = 250\mu A$
g_{fe}	Forward Transconductance ^②	2.7	3.8	—	S	$V_{CE} = 100V, I_C = 8.0A$
I_{CES}	Zero Gate Voltage Collector Current	—	—	250	μA	$V_{GE} = 0V, V_{CE} = 600V$
		—	—	1700		$V_{GE} = 0V, V_{CE} = 600V, T_J = 150^\circ\text{C}$
V_{FM}	Diode Forward Voltage Drop	—	1.4	1.7	V	$I_C = 8.0A$
		—	1.4	1.7		$I_C = 8.0A, T_J = 150^\circ\text{C}$
I_{GES}	Gate-to-Emitter Leakage Current	—	—	± 100	nA	$V_{GE} = \pm 20V$

Switching Characteristics @ $T_J = 25^\circ\text{C}$ (unless otherwise specified)

	Parameter	Min.	Typ.	Max.	Units	Conditions
Q_g	Total Gate Charge (turn-on)	—	16	24	nC	$I_C = 8.0A$
Q_{ge}	Gate - Emitter Charge (turn-on)	—	3.6	5.2		$V_{CC} = 400V$
Q_{gc}	Gate - Collector Charge (turn-on)	—	6.0	9.0		See Fig. 8
$t_{d(on)}$	Turn-On Delay Time	—	66	—	ns	$T_J = 25^\circ\text{C}$
t_r	Rise Time	—	40	—		$I_C = 8.0A, V_{CC} = 480V$
$t_{d(off)}$	Turn-Off Delay Time	—	330	540		$V_{GE} = 15V, R_G = 50\Omega$
t_f	Fall Time	—	260	480		Energy losses include "tail" and diode reverse recovery.
E_{on}	Turn-On Switching Loss	—	0.5	—		See Fig. 9, 10, 11, 18
E_{off}	Turn-Off Switching Loss	—	1.0	—	mJ	
E_{ts}	Total Switching Loss	—	1.5	2.5		
t_{sc}	Short Circuit Withstand Time	10	—	—	μs	$V_{CC} = 360V, T_J = 125^\circ\text{C}$ $V_{GE} = 15V, R_G = 50\Omega, V_{CPK} < 500V$
$t_{d(on)}$	Turn-On Delay Time	—	65	—	ns	$T_J = 150^\circ\text{C}$, See Fig. 9, 10, 11, 18
t_r	Rise Time	—	46	—		$I_C = 8.0A, V_{CC} = 480V$
$t_{d(off)}$	Turn-Off Delay Time	—	520	—		$V_{GE} = 15V, R_G = 50\Omega$
t_f	Fall Time	—	560	—		Energy losses include "tail" and diode reverse recovery.
E_{ts}	Total Switching Loss	—	2.3	—	mJ	diode reverse recovery.
L_E	Internal Emitter Inductance	—	7.5	—	nH	Measured 5mm from package
C_{ies}	Input Capacitance	—	365	—	pF	$V_{GE} = 0V$
C_{oes}	Output Capacitance	—	47	—		$V_{CC} = 30V$
C_{res}	Reverse Transfer Capacitance	—	4.8	—		$f = 1.0MHz$
t_{rr}	Diode Reverse Recovery Time	—	37	55	ns	$T_J = 25^\circ\text{C}$ See Fig.
		—	55	90		$T_J = 125^\circ\text{C}$ 14
I_{rr}	Diode Peak Reverse Recovery Current	—	3.5	5.0	A	$T_J = 25^\circ\text{C}$ See Fig.
		—	4.5	8.0		$T_J = 125^\circ\text{C}$ 15
Q_{rr}	Diode Reverse Recovery Charge	—	65	138	nC	$T_J = 25^\circ\text{C}$ See Fig.
		—	124	360		$T_J = 125^\circ\text{C}$ 16
$di_{(rec)M}/dt$	Diode Peak Rate of Fall of Recovery During t_b	—	240	—	A/ μs	$T_J = 25^\circ\text{C}$ See Fig.
		—	210	—		$T_J = 125^\circ\text{C}$ 17

Notes:

① Repetitive rating; $V_{GE}=20V$, pulse width limited by max. junction temperature. (See fig. 20)

② $V_{CC}=80\%(V_{CES}), V_{GE}=20V, L=10\mu H, R_G=50\Omega$, (See fig. 19)

③ Pulse width $\leq 80\mu s$; duty factor $\leq 0.1\%$.

④ Pulse width 5.0 μs , single shot.

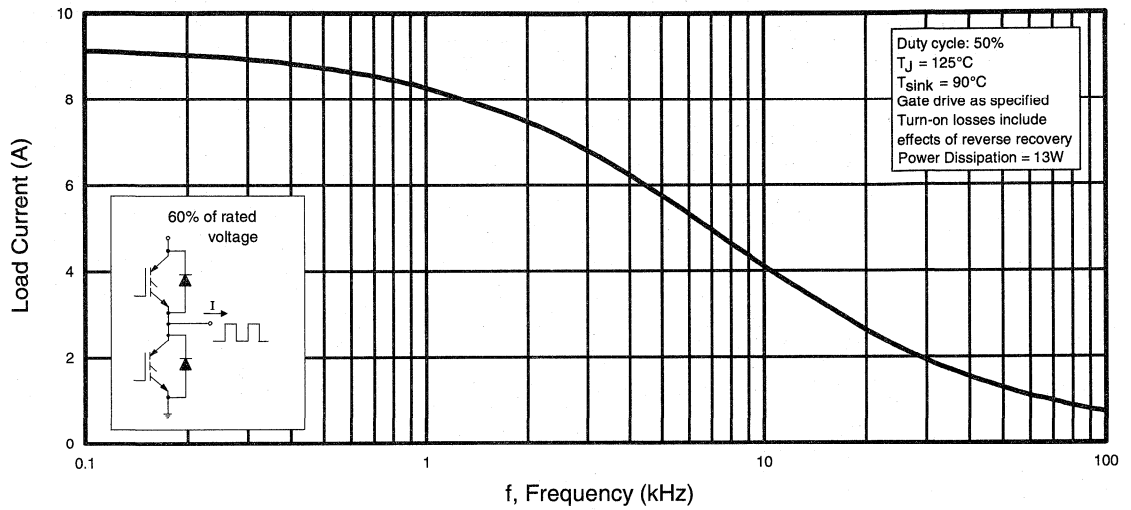


Fig. 1 - Typical Load Current vs. Frequency
(Load Current = I_{RMS} of fundamental)

Motor Control Fast Co-Packs

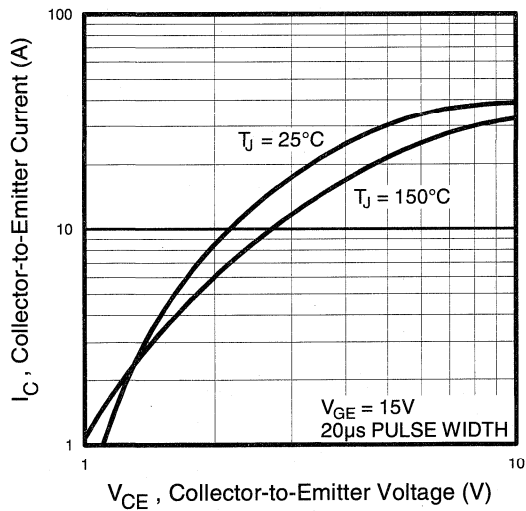


Fig. 2 - Typical Output Characteristics

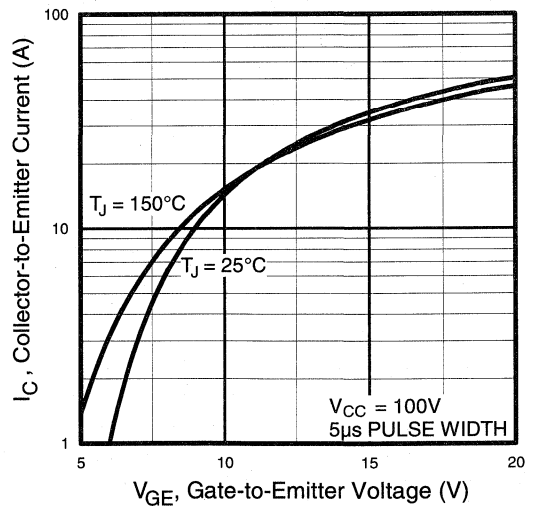


Fig. 3 - Typical Transfer Characteristics

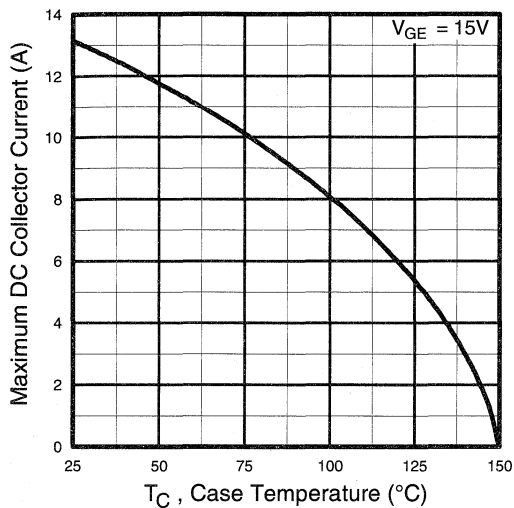


Fig. 4 - Maximum Collector Current vs. Case Temperature

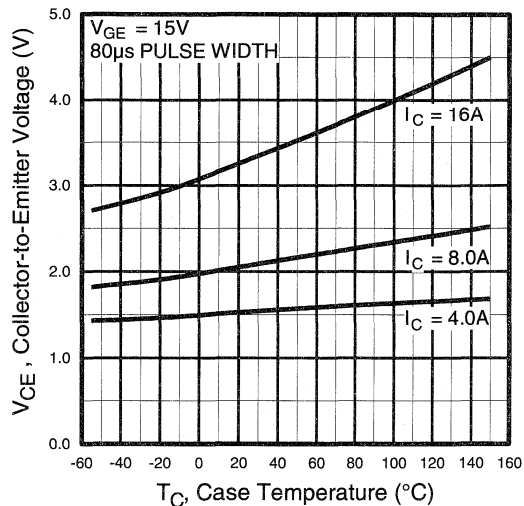


Fig. 5 - Collector-to-Emitter Voltage vs. Case Temperature

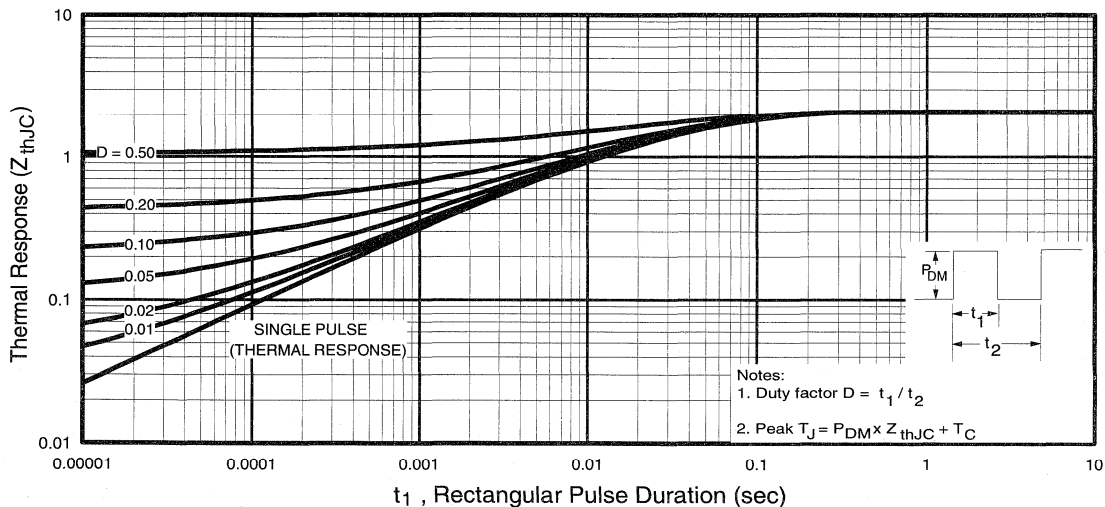


Fig. 6 - Maximum IGBT Effective Transient Thermal Impedance, Junction-to-Case

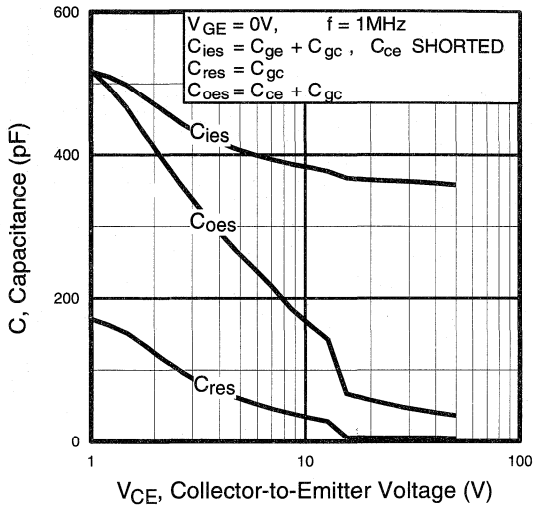


Fig. 7 - Typical Capacitance vs. Collector-to-Emitter Voltage

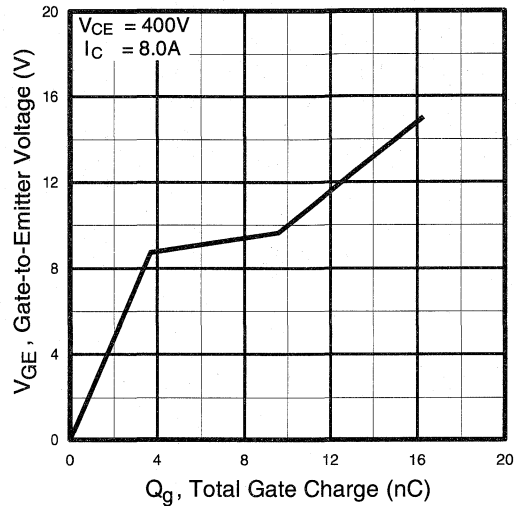


Fig. 8 - Typical Gate Charge vs. Gate-to-Emitter Voltage

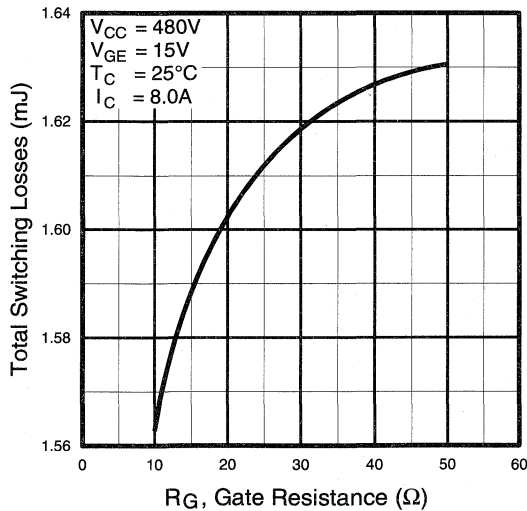


Fig. 9 - Typical Switching Losses vs. Gate Resistance

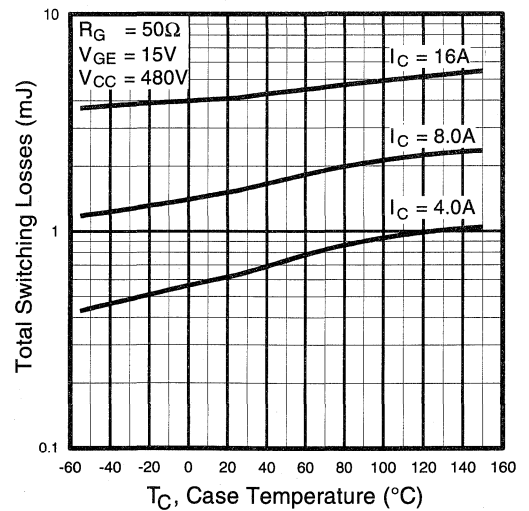


Fig. 10 - Typical Switching Losses vs. Case Temperature



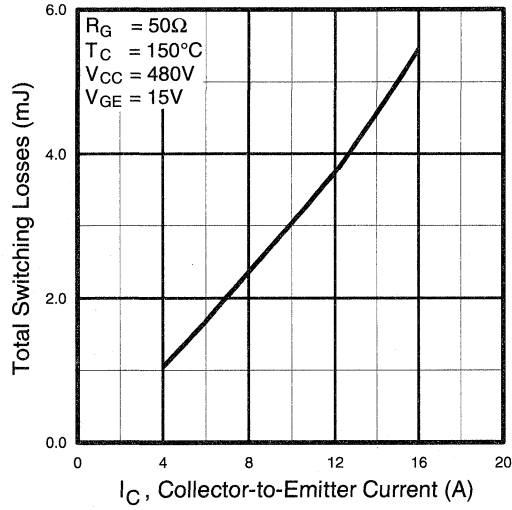


Fig. 11 - Typical Switching Losses vs. Collector-to-Emitter Current

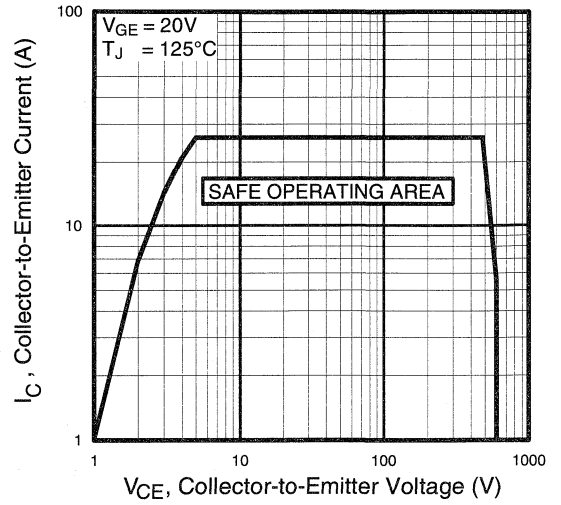


Fig. 12 - Turn-Off SOA

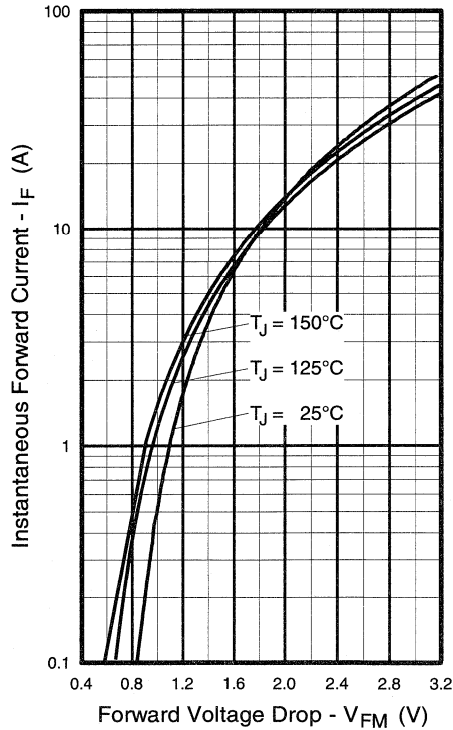


Fig. 13 - Maximum Forward Voltage Drop vs. Instantaneous Forward Current

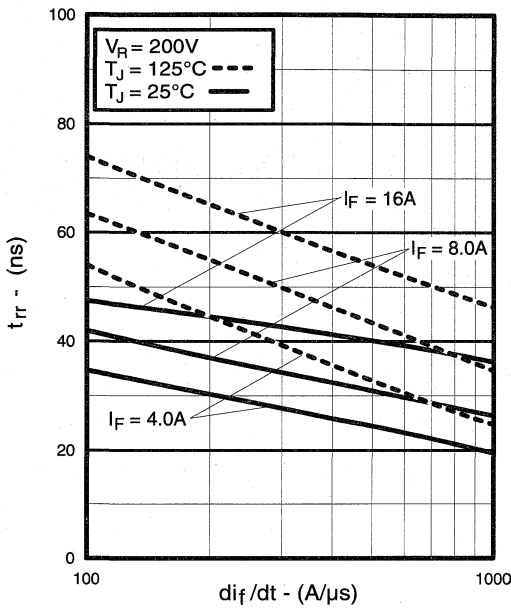


Fig. 14 - Typical Reverse Recovery vs. di_f/dt

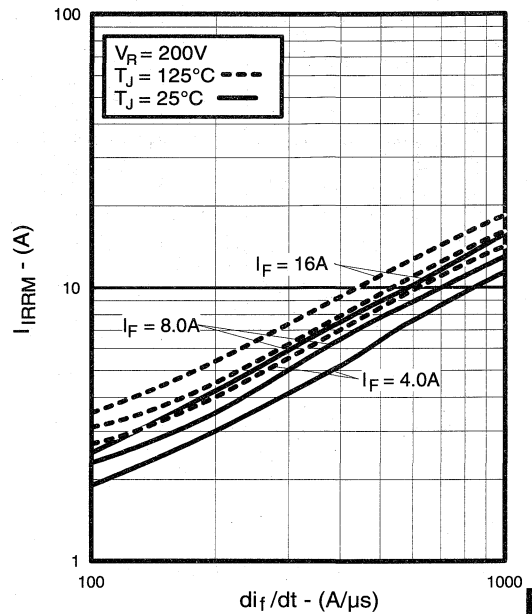


Fig. 15 - Typical Recovery Current vs. di_f/dt

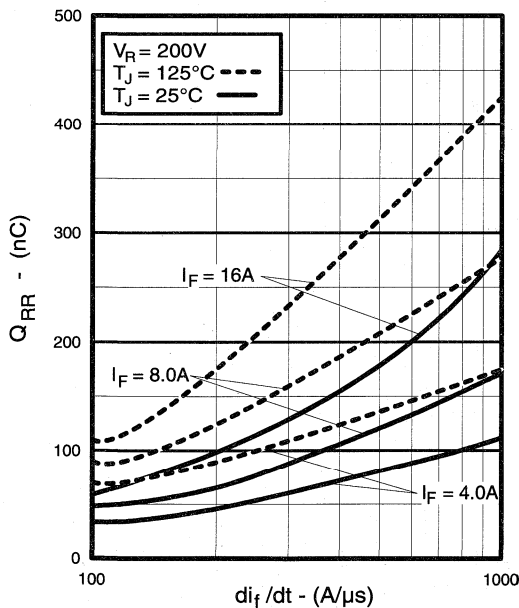


Fig. 16 - Typical Stored Charge vs. di_f/dt

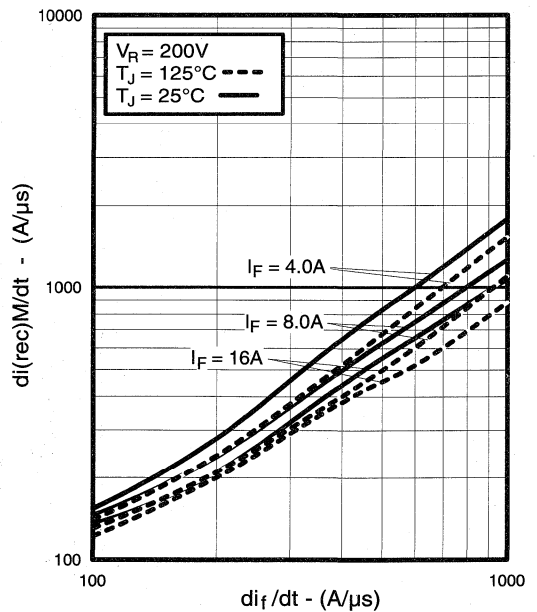


Fig. 17 - Typical $di_{(rec)M}/dt$ vs. di_f/dt

Motor
Control
Fast
Co-Packs

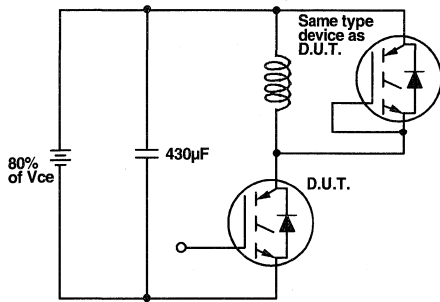


Fig. 18a - Test Circuit for Measurement of I_{LM} , E_{on} , $E_{off}(\text{diode})$, t_{rr} , Q_{rr} , I_{rr} , $t_{d(on)}$, t_r , $t_{d(off)}$, t_f

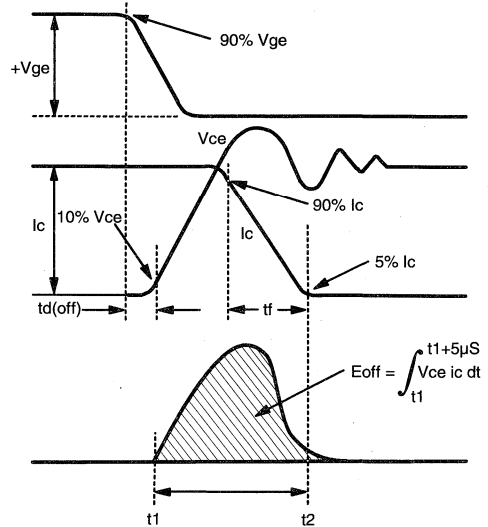


Fig. 18b - Test Waveforms for Circuit of Fig. 18a, Defining E_{off} , $t_{d(off)}$, t_f

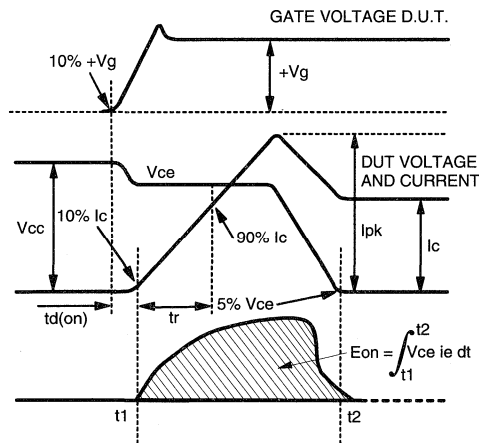


Fig. 18c - Test Waveforms for Circuit of Fig. 18a, Defining E_{on} , $t_{d(on)}$, t_r

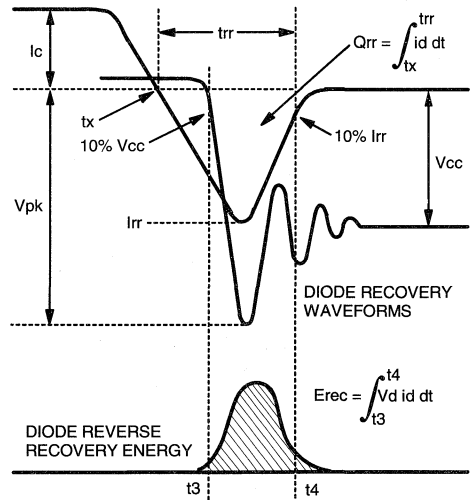


Fig. 18d - Test Waveforms for Circuit of Fig. 18a, Defining E_{rec} , t_{rr} , Q_{rr} , I_{rr}

Refer to Section D for the following:

Appendix D: Section D - page D-6

Fig. 18e - Macro Waveforms for Test Circuit Fig. 18a

Fig. 19 - Clamped Inductive Load Test Circuit

Fig. 20 - Pulsed Collector Current Test Circuit

IRGBC30MD2

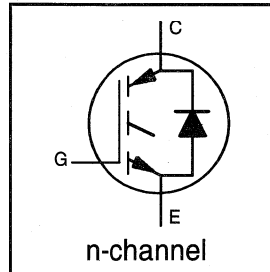
INSULATED GATE BIPOLAR TRANSISTOR
WITH ULTRAFAST SOFT RECOVERY

Short Circuit Rated
Fast Copack IGBT

DIODE

Features

- Short circuit rated -10 μ s @ 125°C, $V_{GE} = 15V$
- Switching-loss rating includes all "tail" losses
- HEXFRED™ soft ultrafast diodes
- Optimized for medium operating frequency (1 to 10kHz) See Fig. 1 for Current vs. Frequency curve



$$V_{CES} = 600V$$

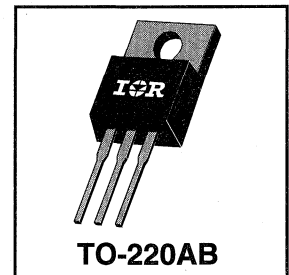
$$V_{CE(sat)} \leq 2.9V$$

$$@ V_{GE} = 15V, I_C = 16A$$

Description

Co-packaged IGBTs are a natural extension of International Rectifier's well known IGBT line. They provide the convenience of an IGBT and an ultrafast recovery diode in one package, resulting in substantial benefits to a host of high-voltage, high-current, applications.

These new short circuit rated devices are especially suited for motor control and other applications requiring short circuit withstand capability.



Absolute Maximum Ratings

	Parameter	Max.	Units
V_{CES}	Collector-to-Emitter Voltage	600	V
$I_C @ T_C = 25^\circ C$	Continuous Collector Current	26	A
$I_C @ T_C = 100^\circ C$	Continuous Collector Current	16	
I_{CM}	Pulsed Collector Current ①	52	
I_{LM}	Clamped Inductive Load Current ②	52	
$I_F @ T_C = 100^\circ C$	Diode Continuous Forward Current	12	
I_{FM}	Diode Maximum Forward Current	52	
t_{sc}	Short Circuit Withstand Time	10	μ s
V_{GE}	Gate-to-Emitter Voltage	± 20	V
$P_D @ T_C = 25^\circ C$	Maximum Power Dissipation	100	W
$P_D @ T_C = 100^\circ C$	Maximum Power Dissipation	42	
T_J	Operating Junction and	-55 to +150	$^\circ C$
T_{STG}	Storage Temperature Range		
	Soldering Temperature, for 10 sec.		
	Mounting Torque, 6-32 or M3 Screw.	10 lbf•in (1.1 N•m)	

Thermal Resistance

	Parameter	Min.	Typ.	Max.	Units
$R_{\theta JC}$	Junction-to-Case - IGBT	—	—	1.2	$^\circ C/W$
$R_{\theta JC}$	Junction-to-Case - Diode	—	—	2.5	
$R_{\theta CS}$	Case-to-Sink, flat, greased surface	—	0.50	—	
$R_{\theta JA}$	Junction-to-Ambient, typical socket mount	—	—	80	
Wt	Weight	—	2 (0.07)	—	g (oz)

Electrical Characteristics @ $T_J = 25^\circ\text{C}$ (unless otherwise specified)

	Parameter	Min.	Typ.	Max.	Units	Conditions
$V_{(BR)CES}$	Collector-to-Emitter Breakdown Voltage ^③	600	—	—	V	$V_{GE} = 0V, I_C = 250\mu A$
$\Delta V_{(BR)CES}/\Delta T_J$	Temp. Coeff. of Breakdown Voltage	—	0.65	—	V/ $^\circ\text{C}$	$V_{GE} = 0V, I_C = 1.0mA$
$V_{CE(on)}$	Collector-to-Emitter Saturation Voltage	—	1.9	2.9	V	$I_C = 16A$ $V_{GE} = 15V$
		—	2.7	—		$I_C = 26A$ See Fig. 2, 5
		—	2.2	—		$I_C = 16A, T_J = 150^\circ\text{C}$
$V_{GE(th)}$	Gate Threshold Voltage	3.0	—	5.5		$V_{CE} = V_{GE}, I_C = 250\mu A$
$\Delta V_{GE(th)}/\Delta T_J$	Temperature Coeff. of Threshold Voltage	—	-12	—	mV/ $^\circ\text{C}$	$V_{CE} = V_{GE}, I_C = 250\mu A$
g_{fe}	Forward Transconductance ^④	3.3	6.5	—	S	$V_{CE} = 100V, I_C = 16A$
I_{CES}	Zero Gate Voltage Collector Current	—	—	250	μA	$V_{GE} = 0V, V_{CE} = 600V$
		—	—	2500		$V_{GE} = 0V, V_{CE} = 600V, T_J = 150^\circ\text{C}$
V_{FM}	Diode Forward Voltage Drop	—	1.4	1.7	V	$I_C = 12A$ See Fig. 13
		—	1.3	1.6		$I_C = 12A, T_J = 150^\circ\text{C}$
I_{GES}	Gate-to-Emitter Leakage Current	—	—	± 100	nA	$V_{GE} = \pm 20V$

Switching Characteristics @ $T_J = 25^\circ\text{C}$ (unless otherwise specified)

	Parameter	Min.	Typ.	Max.	Units	Conditions
Q_g	Total Gate Charge (turn-on)	—	35	53	nC	$I_C = 16A$ $V_{CC} = 400V$ See Fig. 8
Q_{ge}	Gate - Emitter Charge (turn-on)	—	7.4	11		
Q_{gc}	Gate - Collector Charge (turn-on)	—	14	21		
$t_{d(on)}$	Turn-On Delay Time	—	68	—	ns	$T_J = 25^\circ\text{C}$ $I_C = 16A, V_{CC} = 480V$ $V_{GE} = 15V, R_G = 23\Omega$ Energy losses include "tail" and diode reverse recovery. See Fig. 9, 10, 11, 18
t_r	Rise Time	—	130	—		
$t_{d(off)}$	Turn-Off Delay Time	—	330	500		
t_f	Fall Time	—	310	470		
E_{on}	Turn-On Switching Loss	—	1.5	—		
E_{off}	Turn-Off Switching Loss	—	2.1	—	mJ	See Fig. 9, 10, 11, 18
E_{ts}	Total Switching Loss	—	3.6	5.4		
t_{sc}	Short Circuit Withstand Time	10	—	—	μs	$V_{CC} = 360V, T_J = 125^\circ\text{C}$ $V_{GE} = 15V, R_G = 23\Omega, V_{CPK} < 500V$
$t_{d(on)}$	Turn-On Delay Time	—	66	—	ns	$T_J = 150^\circ\text{C}$, See Fig. 9, 10, 11, 18 $I_C = 16A, V_{CC} = 480V$ $V_{GE} = 15V, R_G = 23\Omega$ Energy losses include "tail" and diode reverse recovery.
t_r	Rise Time	—	120	—		
$t_{d(off)}$	Turn-Off Delay Time	—	580	—		
t_f	Fall Time	—	630	—		
E_{ts}	Total Switching Loss	—	5.7	—	mJ	diode reverse recovery.
L_E	Internal Emitter Inductance	—	7.5	—	nH	Measured 5mm from package
C_{ies}	Input Capacitance	—	750	—	pF	$V_{GE} = 0V$ $V_{CC} = 30V$ See Fig. 7 $f = 1.0MHz$
C_{oes}	Output Capacitance	—	110	—		
C_{res}	Reverse Transfer Capacitance	—	9.3	—		
t_{rr}	Diode Reverse Recovery Time	—	42	60	ns	$T_J = 25^\circ\text{C}$ See Fig. 14
		—	80	120		$T_J = 125^\circ\text{C}$
I_{rr}	Diode Peak Reverse Recovery Current	—	3.5	6.0	A	$T_J = 25^\circ\text{C}$ See Fig. 15
		—	5.6	10		$T_J = 125^\circ\text{C}$
Q_{rr}	Diode Reverse Recovery Charge	—	80	180	nC	$T_J = 25^\circ\text{C}$ See Fig. 16
		—	220	600		$T_J = 125^\circ\text{C}$
$di_{(rec)M}/dt$	Diode Peak Rate of Fall of Recovery During t_b	—	180	—	A/ μs	$T_J = 25^\circ\text{C}$ See Fig. 17
		—	120	—		$T_J = 125^\circ\text{C}$

Notes:

① Repetitive rating; $V_{GE}=20V$, pulse width limited by max. junction temperature. (See fig. 20)

② $V_{CC}=80\%(V_{CES}), V_{GE}=20V, L=10\mu H, R_G = 23\Omega$, (See fig. 19)
③ Pulse width $\leq 80\mu s$; duty factor $\leq 0.1\%$.

④ Pulse width 5.0 μs , single shot.

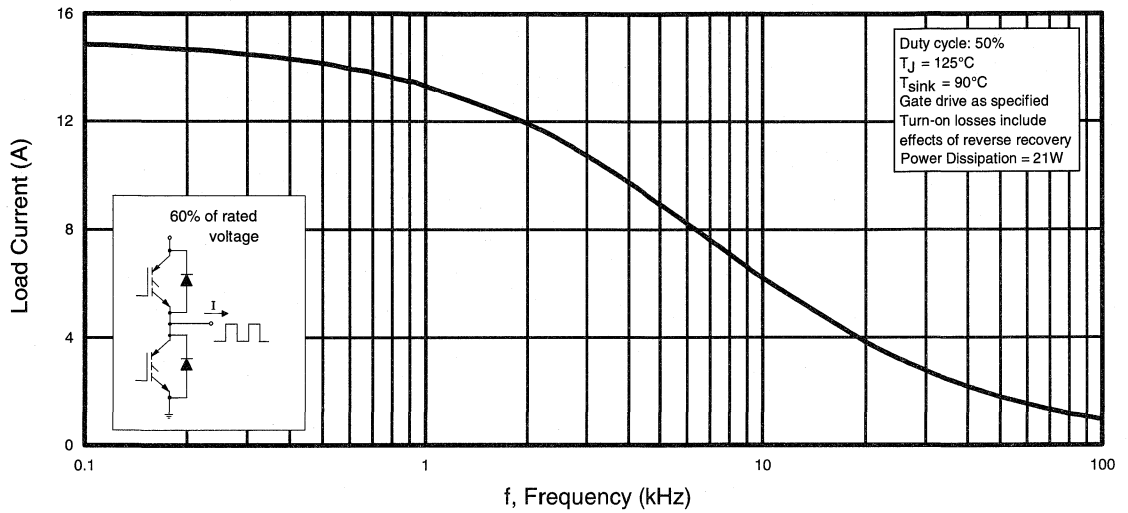


Fig. 1 - Typical Load Current vs. Frequency
 (Load Current = I_{RMS} of fundamental)

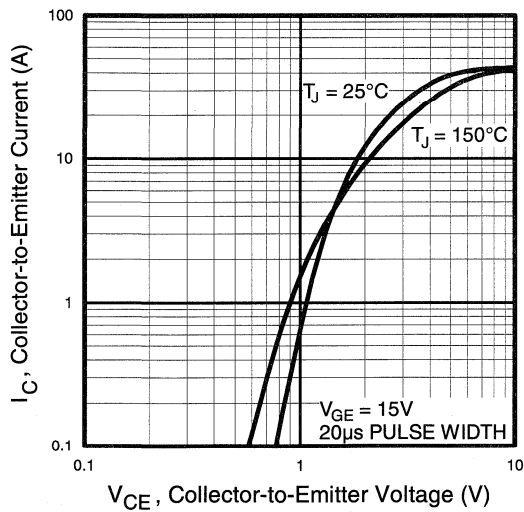


Fig. 2 - Typical Output Characteristics

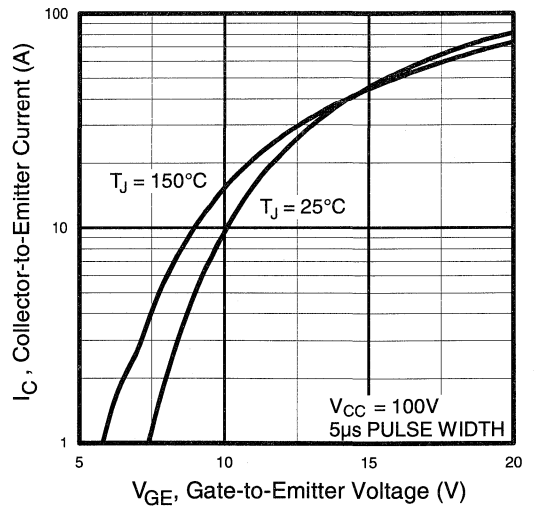


Fig. 3 - Typical Transfer Characteristics

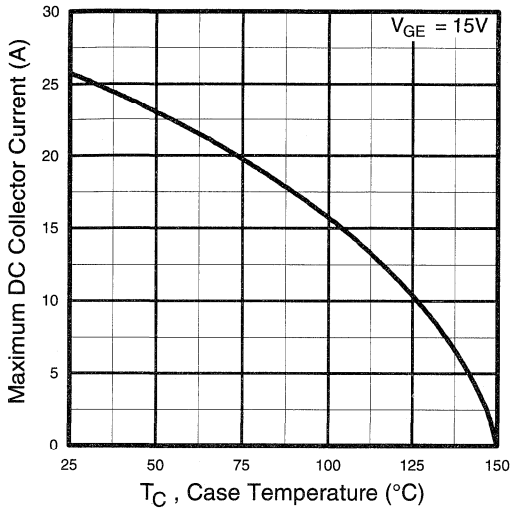


Fig. 4 - Maximum Collector Current vs. Case Temperature

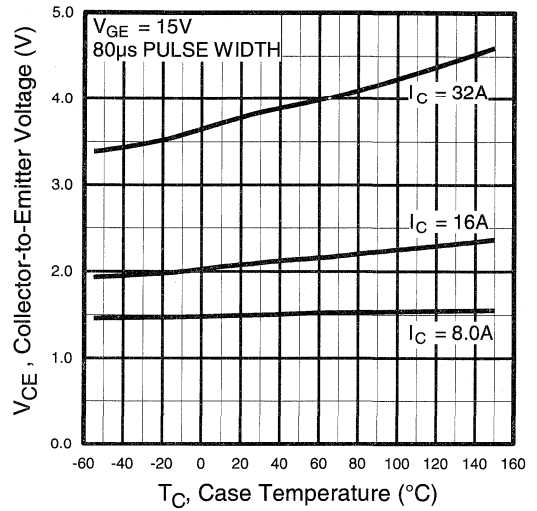


Fig. 5 - Collector-to-Emitter Voltage vs. Case Temperature

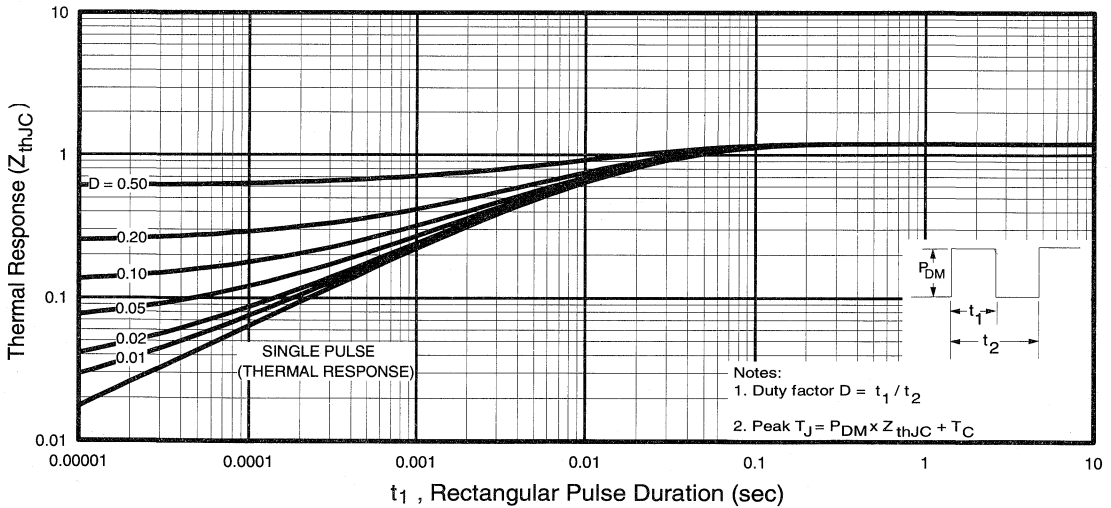


Fig. 6 - Maximum IGBT Effective Transient Thermal Impedance, Junction-to-Case

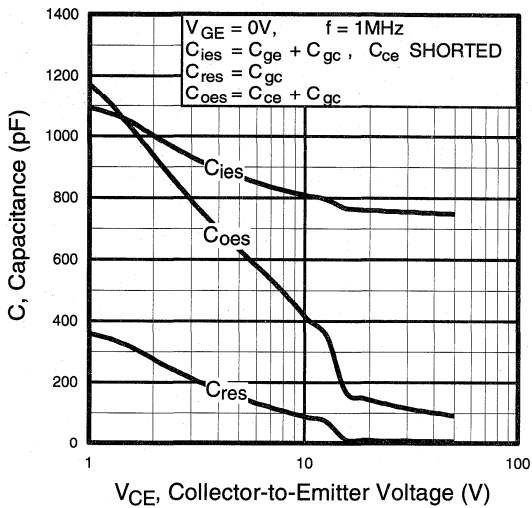


Fig. 7 - Typical Capacitance vs. Collector-to-Emitter Voltage

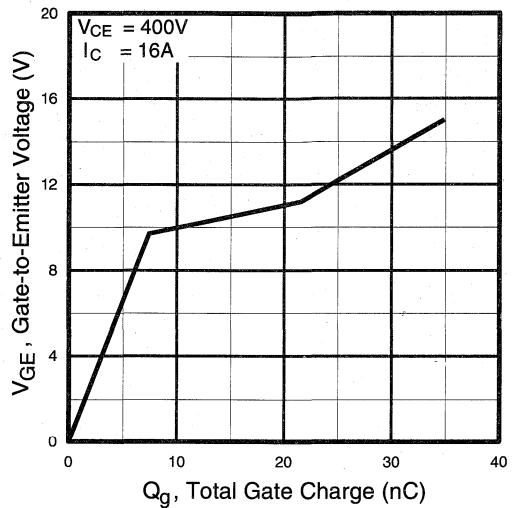


Fig. 8 - Typical Gate Charge vs. Gate-to-Emitter Voltage

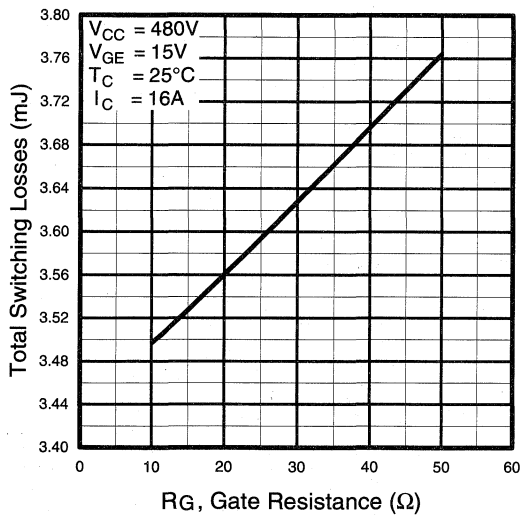


Fig. 9 - Typical Switching Losses vs. Gate Resistance

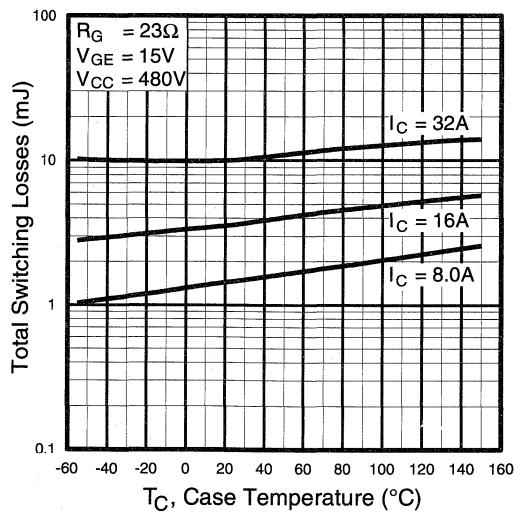


Fig. 10 - Typical Switching Losses vs. Case Temperature



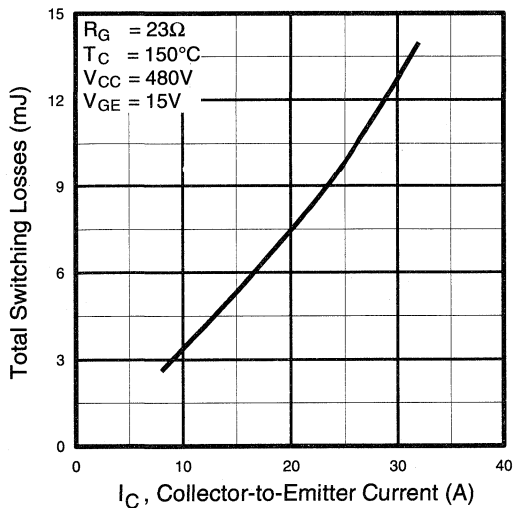


Fig. 11 - Typical Switching Losses vs. Collector-to-Emitter Current

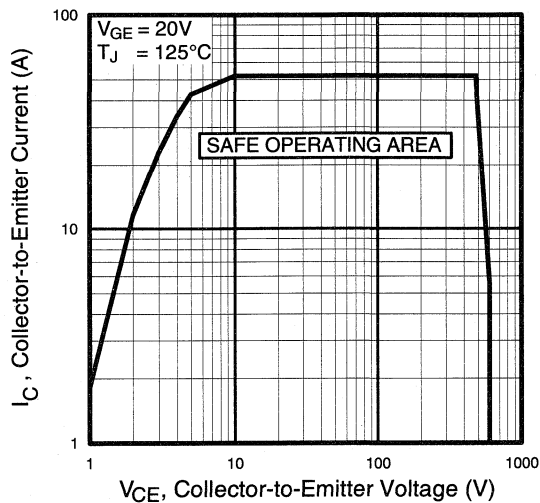


Fig. 12 - Turn-Off SOA

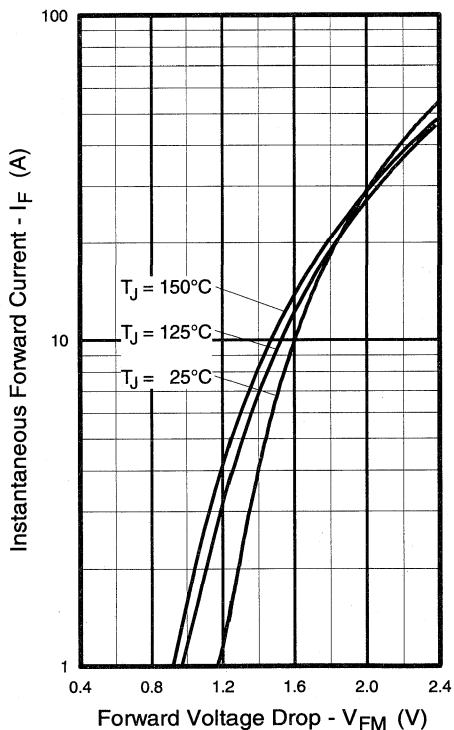


Fig. 13 - Maximum Forward Voltage Drop vs. Instantaneous Forward Current

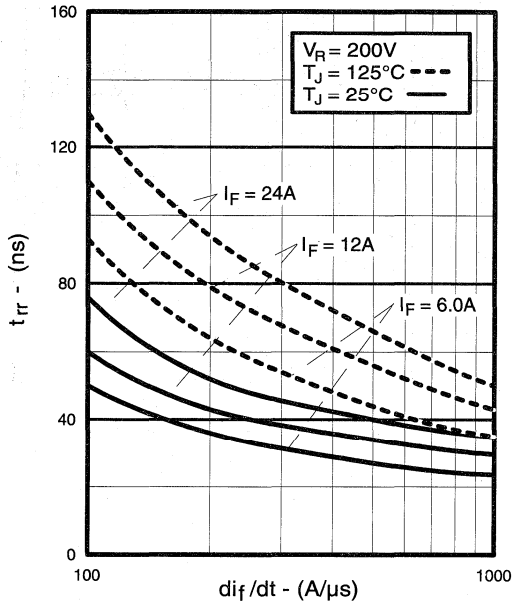


Fig. 14 - Typical Reverse Recovery vs. di_f/dt

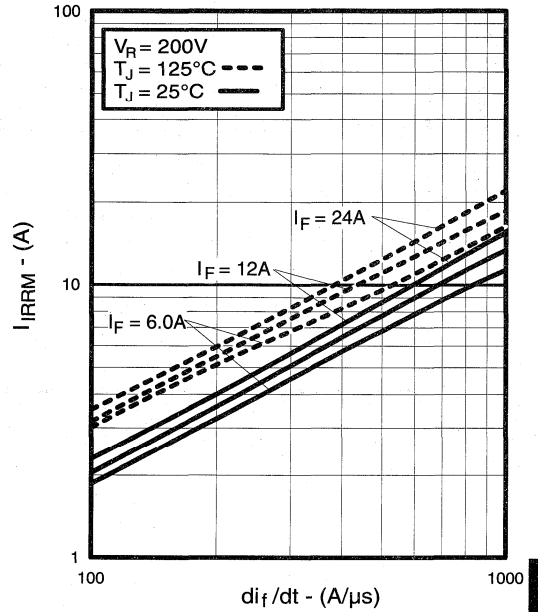


Fig. 15 - Typical Recovery Current vs. di_f/dt

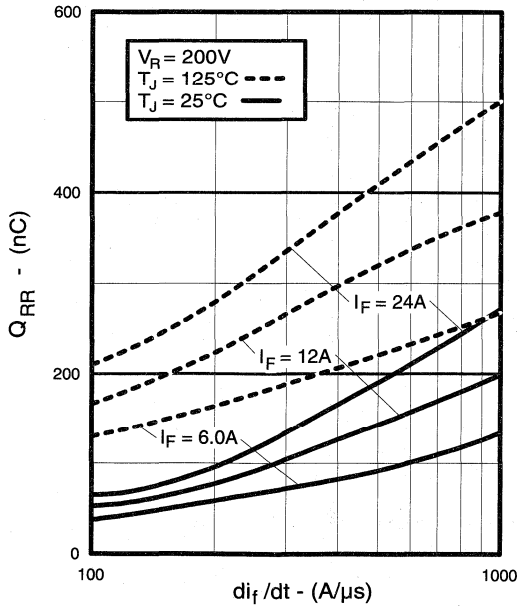


Fig. 16 - Typical Stored Charge vs. di_f/dt

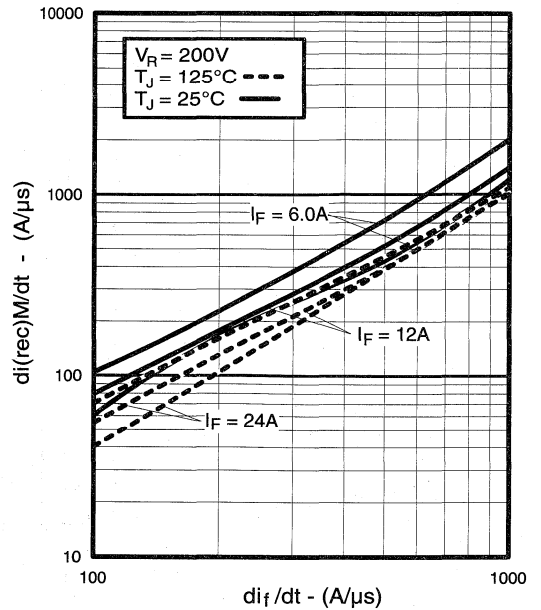


Fig. 17 - Typical $di_{(rec)}M/dt$ vs. di_f/dt

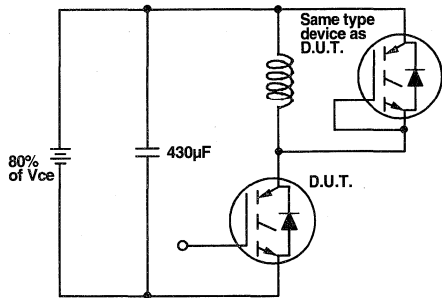


Fig. 18a - Test Circuit for Measurement of I_{LM} , E_{on} , $E_{off}(\text{diode})$, t_{rr} , Q_{rr} , I_{rr} , $t_{d(on)}$, t_r , $t_{d(off)}$, t_f

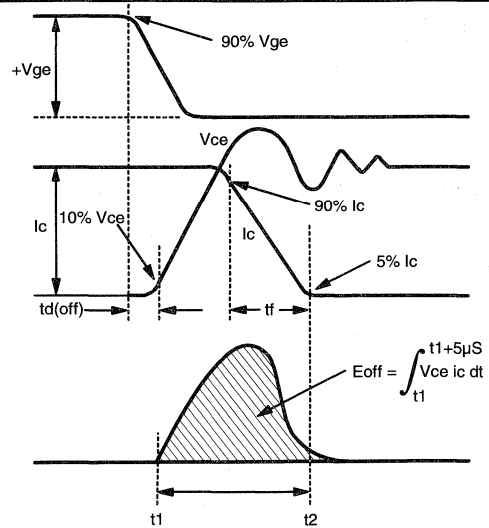


Fig. 18b - Test Waveforms for Circuit of Fig. 18a, Defining E_{off} , $t_{d(off)}$, t_f

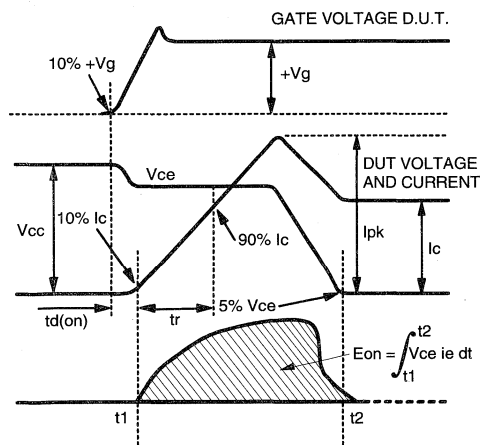


Fig. 18c - Test Waveforms for Circuit of Fig. 18a, Defining E_{on} , $t_{d(on)}$, t_r

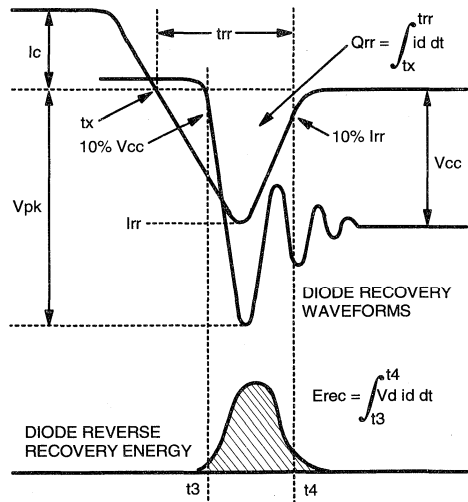


Fig. 18d - Test Waveforms for Circuit of Fig. 18a, Defining E_{rec} , t_{rr} , Q_{rr} , I_{rr}

Refer to Section D for the following:

Appendix D: Section D - page D-6

Fig. 18e - Macro Waveforms for Test Circuit Fig. 18a

Fig. 19 - Clamped Inductive Load Test Circuit

Fig. 20 - Pulsed Collector Current Test Circuit

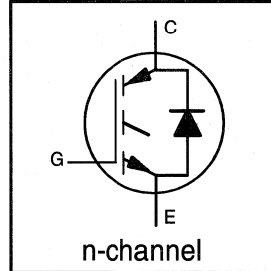
IRGBC20MD2-S

INSULATED GATE BIPOLAR TRANSISTOR
WITH ULTRAFAST SOFT RECOVERY DIODE

Short Circuit Rated
Fast CoPack IGBT

Features

- Short circuit rated -10 μ s @ 125°C, $V_{GE} = 15V$
- Switching-loss rating includes all "tail" losses
- HEXFRED™ soft ultrafast diodes
- Optimized for medium operating frequency (1 to 10kHz) See Fig. 1 for Current vs. Frequency curve



$$V_{CES} = 600V$$

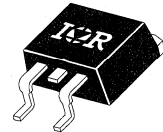
$$V_{CE(sat)} \leq 2.5V$$

@ $V_{GE} = 15V, I_C = 8.0A$

Description

Co-packaged IGBTs are a natural extension of International Rectifier's well known IGBT line. They provide the convenience of an IGBT and an ultrafast recovery diode in one package, resulting in substantial benefits to a host of high-voltage, high-current, applications.

These new short circuit rated devices are especially suited for motor control and other applications requiring short circuit withstand capability.



SMD-220

Absolute Maximum Ratings

	Parameter	Max.	Units
V_{CES}	Collector-to-Emitter Voltage	600	V
$I_C @ T_C = 25^\circ C$	Continuous Collector Current	13	A
$I_C @ T_C = 100^\circ C$	Continuous Collector Current	8.0	
I_{CM}	Pulsed Collector Current $\text{\textcircled{D}}$	26	
I_{LM}	Clamped Inductive Load Current $\text{\textcircled{D}}$	26	
$I_F @ T_C = 100^\circ C$	Diode Continuous Forward Current	7.0	
I_{FM}	Diode Maximum Forward Current	26	μs
t_{sc}	Short Circuit Withstand Time	10	
V_{GE}	Gate-to-Emitter Voltage	± 20	V
$P_D @ T_C = 25^\circ C$	Maximum Power Dissipation	60	W
$P_D @ T_C = 100^\circ C$	Maximum Power Dissipation	24	
T_J	Operating Junction and	-55 to +150	$^\circ C$
T_{STG}	Storage Temperature Range		
	Soldering Temperature, for 10 sec.	300 (0.063 in. (1.6mm) from case)	
	Mounting Torque, 6-32 or M3 Screw.	10 lbf•in (1.1 N•m)	

Thermal Resistance

	Parameter	Min.	Typ.	Max.	Units
$R_{\theta JC}$	Junction-to-Case - IGBT	—	—	2.1	$^\circ C/W$
$R_{\theta JC}$	Junction-to-Case - Diode	—	—	3.5	
$R_{\theta JA}$	Junction-to-Ambient, (PCB Mount)**	—	—	40	
$R_{\theta JA}$	Junction-to-Ambient, typical socket mount	—	—	80	
Wt	Weight	—	2 (0.07)	—	g (oz)

** When mounted on 1" square PCB (FR-4 or G-10 Material)

For recommended footprint and soldering techniques refer to application note #AN-994.

Electrical Characteristics @ $T_J = 25^\circ\text{C}$ (unless otherwise specified)

	Parameter	Min.	Typ.	Max.	Units	Conditions
$V_{(BR)CES}$	Collector-to-Emitter Breakdown Voltage ^②	600	—	—	V	$V_{GE} = 0V, I_C = 250\mu A$
$\Delta V_{(BR)CES}/\Delta T_J$	Temperature Coeff. of Breakdown Voltage	—	0.42	—	V/ $^\circ\text{C}$	$V_{GE} = 0V, I_C = 1.0mA$
$V_{CE(on)}$	Collector-to-Emitter Saturation Voltage	—	2.0	2.5	V	$I_C = 8.0A, V_{GE} = 15V$ See Fig. 2, 5
		—	2.7	—		
		—	2.5	—		
$V_{GE(th)}$	Gate Threshold Voltage	3.0	—	5.5		$V_{CE} = V_{GE}, I_C = 250\mu A$
$\Delta V_{GE(th)}/\Delta T_J$	Temperature Coeff. of Threshold Voltage	—	-11	—	mV/ $^\circ\text{C}$	$V_{CE} = V_{GE}, I_C = 250\mu A$
g_{fe}	Forward Transconductance ^④	2.7	3.8	—	S	$V_{CE} = 100V, I_C = 8.0A$
I_{CES}	Zero Gate Voltage Collector Current	—	—	250	μA	$V_{GE} = 0V, V_{CE} = 600V$
		—	—	1700		$V_{GE} = 0V, V_{CE} = 600V, T_J = 150^\circ\text{C}$
V_{FM}	Diode Forward Voltage Drop	—	1.4	1.7	V	$I_C = 8.0A$ See Fig. 13
		—	1.3	1.6		
I_{GES}	Gate-to-Emitter Leakage Current	—	—	± 100	nA	$V_{GE} = \pm 20V$

Switching Characteristics @ $T_J = 25^\circ\text{C}$ (unless otherwise specified)

	Parameter	Min.	Typ.	Max.	Units	Conditions
Q_g	Total Gate Charge (turn-on)	—	16	24	nC	$I_C = 8.0A$ $V_{CC} = 400V$ See Fig. 8
Q_{ge}	Gate - Emitter Charge (turn-on)	—	3.6	5.2		
Q_{gc}	Gate - Collector Charge (turn-on)	—	6.0	9.0		
$t_{d(on)}$	Turn-On Delay Time	—	66	—	ns	$T_J = 25^\circ\text{C}$ $I_C = 8.0A, V_{CC} = 480V$ $V_{GE} = 15V, R_G = 50\Omega$ Energy losses include "tail" and diode reverse recovery. See Fig. 9, 10, 11, 18
t_r	Rise Time	—	40	—		
$t_{d(off)}$	Turn-Off Delay Time	—	330	540		
t_f	Fall Time	—	260	480		
E_{on}	Turn-On Switching Loss	—	0.50	—		
E_{off}	Turn-Off Switching Loss	—	1.0	—	mJ	See Fig. 9, 10, 11, 18
E_{ts}	Total Switching Loss	—	1.5	2.5		
t_{sc}	Short Circuit Withstand Time	10	—	—	μs	$V_{CC} = 360V, T_J = 125^\circ\text{C}$ $V_{GE} = 15V, R_G = 50\Omega, V_{CPK} < 500V$
$t_{d(on)}$	Turn-On Delay Time	—	65	—	ns	$T_J = 150^\circ\text{C}$, See Fig. 9, 10, 11, 18 $I_C = 8.0A, V_{CC} = 480V$ $V_{GE} = 15V, R_G = 50\Omega$ Energy losses include "tail" and diode reverse recovery.
t_r	Rise Time	—	46	—		
$t_{d(off)}$	Turn-Off Delay Time	—	520	—		
t_f	Fall Time	—	560	—		
E_{ts}	Total Switching Loss	—	2.3	—		
L_E	Internal Emitter Inductance	—	7.5	—	nH	Measured 5mm from package
C_{ies}	Input Capacitance	—	365	—	pF	$V_{GE} = 0V$ $V_{CC} = 30V$ $f = 1.0MHz$ See Fig. 7
C_{oes}	Output Capacitance	—	47	—		
C_{res}	Reverse Transfer Capacitance	—	4.8	—		
t_{rr}	Diode Reverse Recovery Time	—	37	55	ns	$T_J = 25^\circ\text{C}$ See Fig. 14 $T_J = 125^\circ\text{C}$ 14
		—	55	90		
I_{rr}	Diode Peak Reverse Recovery Current	—	3.5	5.0	A	$T_J = 25^\circ\text{C}$ See Fig. 15 $T_J = 125^\circ\text{C}$ 15
		—	4.5	8.0		
Q_{rr}	Diode Reverse Recovery Charge	—	65	138	nC	$T_J = 25^\circ\text{C}$ See Fig. 16 $T_J = 125^\circ\text{C}$ 16
		—	124	360		
$di_{(rec)M}/dt$	Diode Peak Rate of Fall of Recovery During t_b	—	240	—	A/ μs	$T_J = 25^\circ\text{C}$ See Fig. 17 $T_J = 125^\circ\text{C}$ 17
		—	210	—		

Notes:

① Repetitive rating; $V_{GE}=20V$, pulse width limited by max. junction temperature. (See fig. 20)

② $V_{CC}=80\%(V_{CES}), V_{GE}=20V, L=10\mu H, R_G=50\Omega$, (See fig. 19)
③ Pulse width $\leq 80\mu s$; duty factor $\leq 0.1\%$.

④ Pulse width 5.0 μs , single shot.

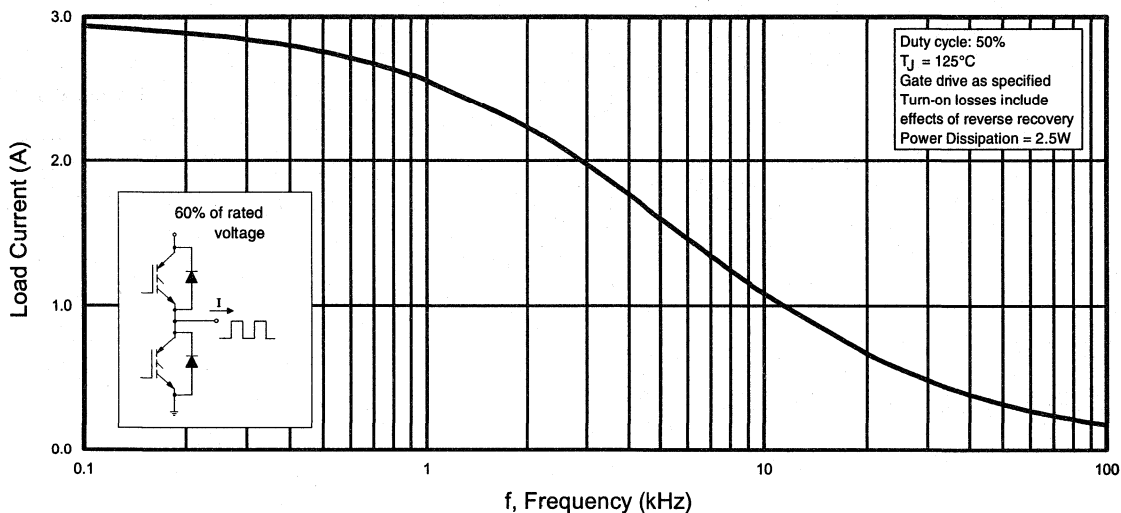


Fig. 1 - Typical Load Current vs. Frequency
(Load Current = I_{RMS} of fundamental)

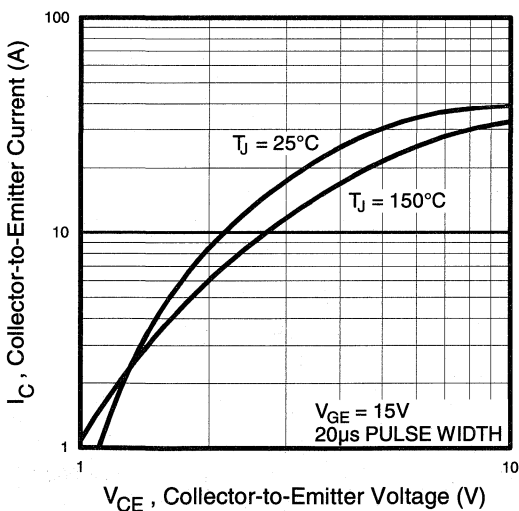


Fig. 2 - Typical Output Characteristics

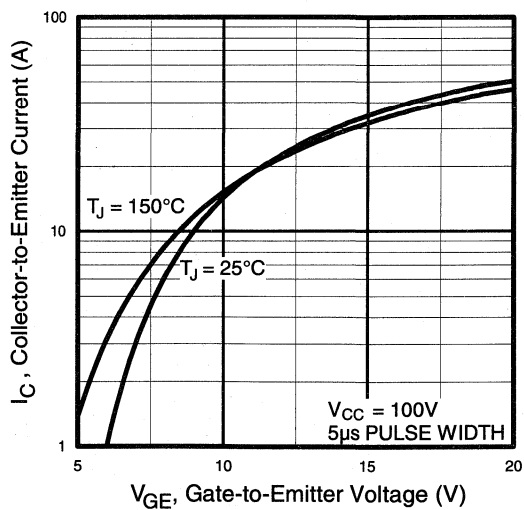


Fig. 3 - Typical Transfer Characteristics

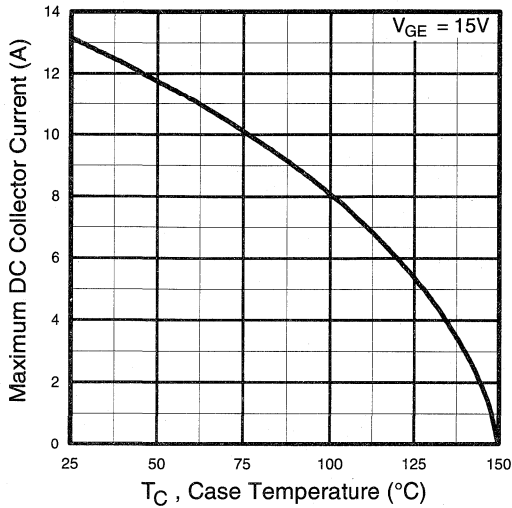


Fig. 4 - Maximum Collector Current vs. Case Temperature

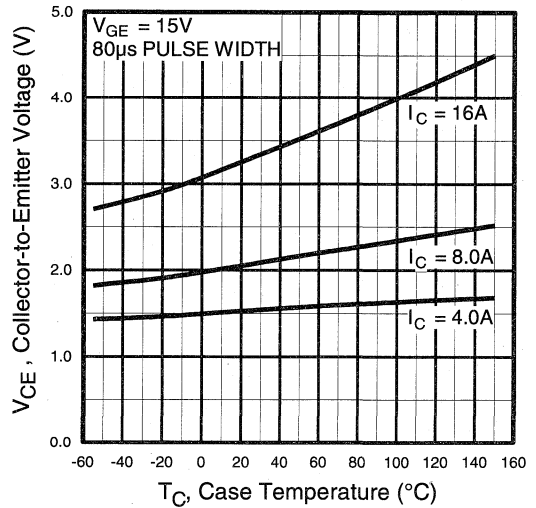


Fig. 5 - Collector-to-Emitter Voltage vs. Case Temperature

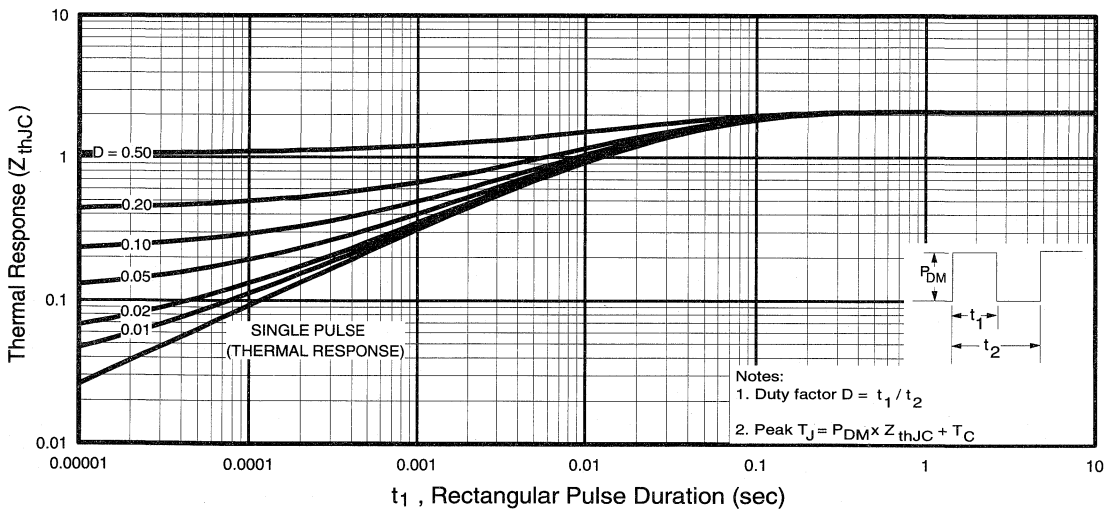


Fig. 6 - Maximum IGBT Effective Transient Thermal Impedance, Junction-to-Case

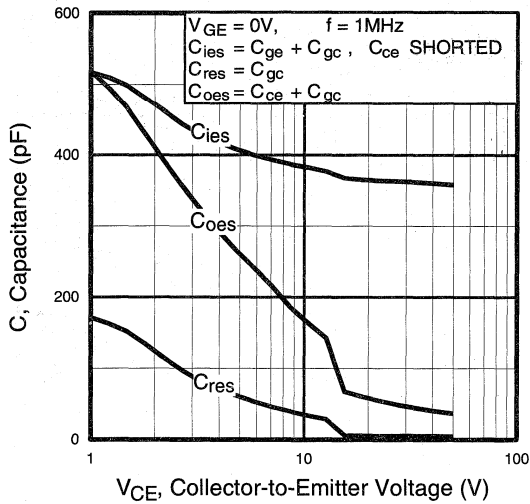


Fig. 7 - Typical Capacitance vs. Collector-to-Emitter Voltage

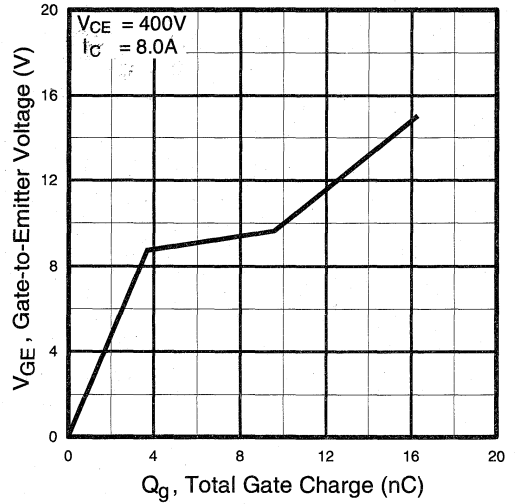


Fig. 8 - Typical Gate Charge vs. Gate-to-Emitter Voltage

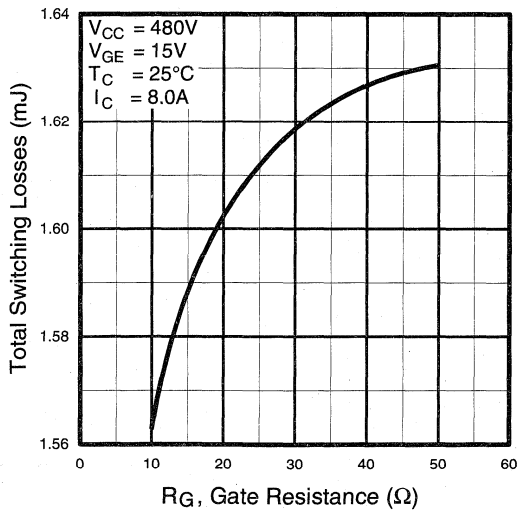


Fig. 9 - Typical Switching Losses vs. Gate Resistance

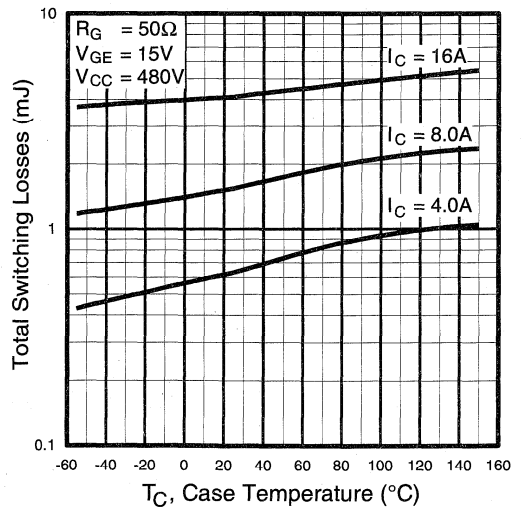


Fig. 10 - Typical Switching Losses vs. Case Temperature



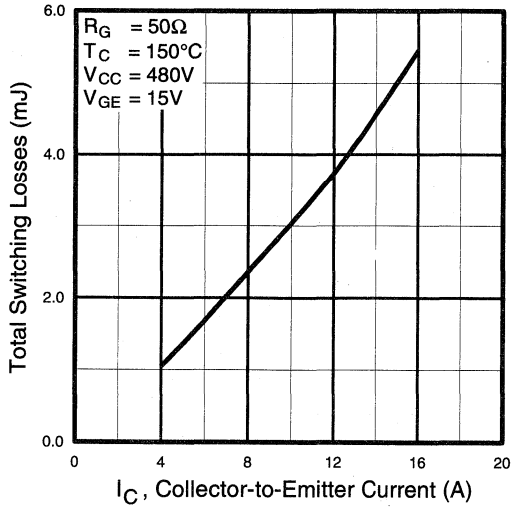


Fig. 11 - Typical Switching Losses vs. Collector-to-Emitter Current

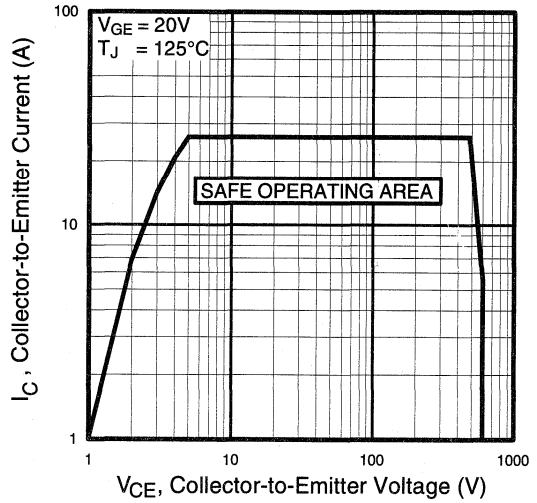


Fig. 12 - Turn-Off SOA

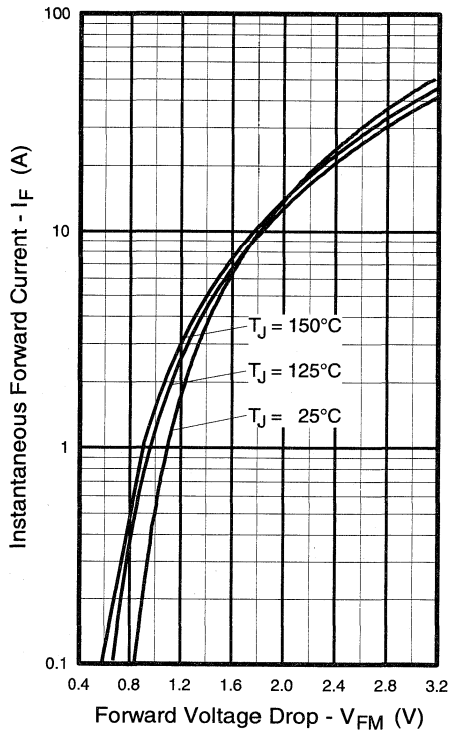


Fig. 13 - Maximum Forward Voltage Drop vs. Instantaneous Forward Current

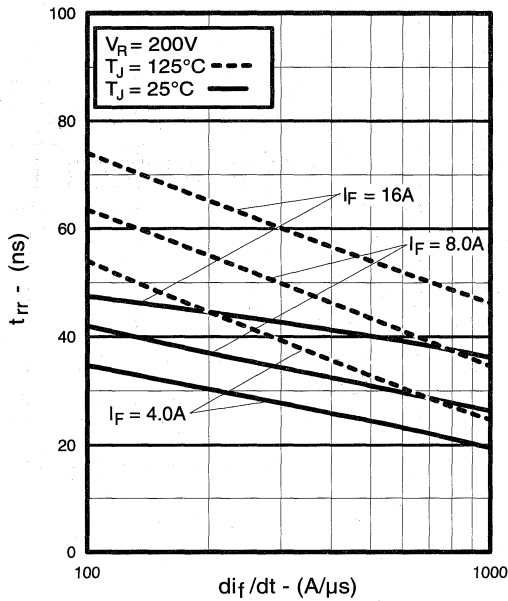


Fig. 14 - Typical Reverse Recovery vs. di_f/dt

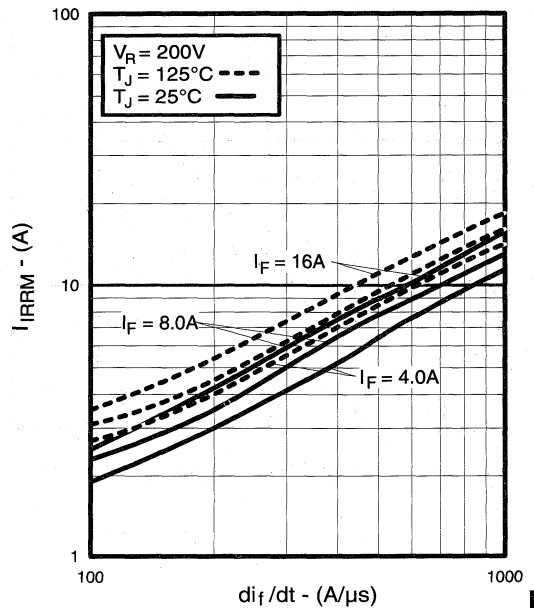


Fig. 15 - Typical Recovery Current vs. di_f/dt

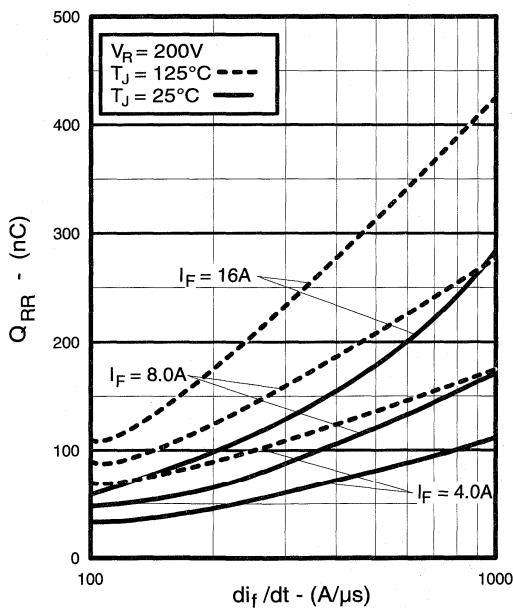


Fig. 16 - Typical Stored Charge vs. di_f/dt

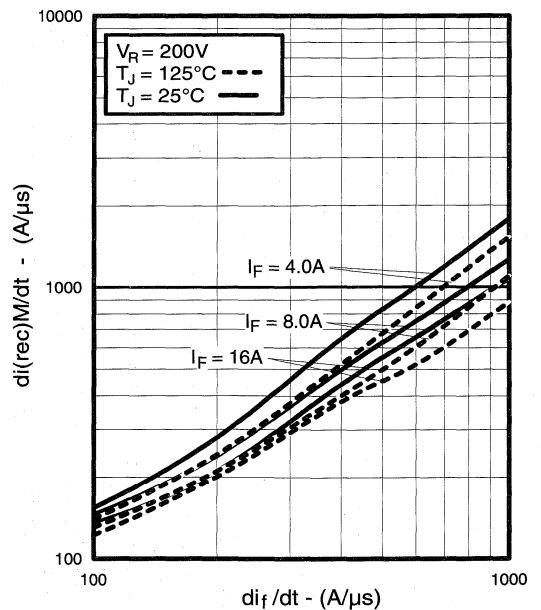


Fig. 17 - Typical $di_{(rec)M}/dt$ vs. di_f/dt

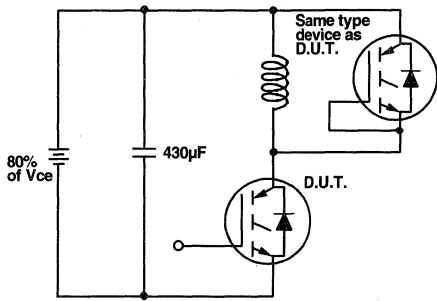


Fig. 18a - Test Circuit for Measurement of I_{LM} , E_{on} , $E_{off}(\text{diode})$, t_{rr} , Q_{rr} , I_{rr} , $t_{d(on)}$, t_r , $t_{d(off)}$, t_f

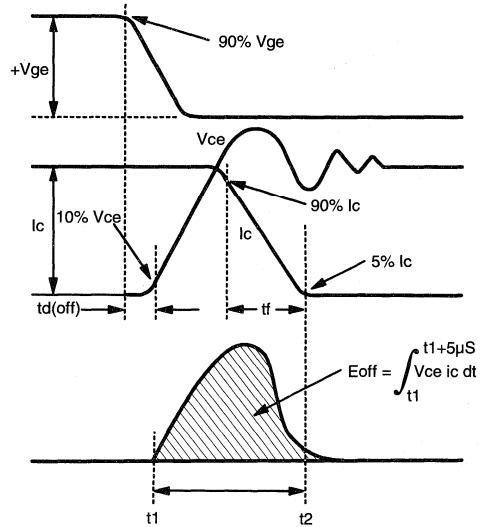


Fig. 18b - Test Waveforms for Circuit of Fig. 18a, Defining E_{off} , $t_{d(off)}$, t_f

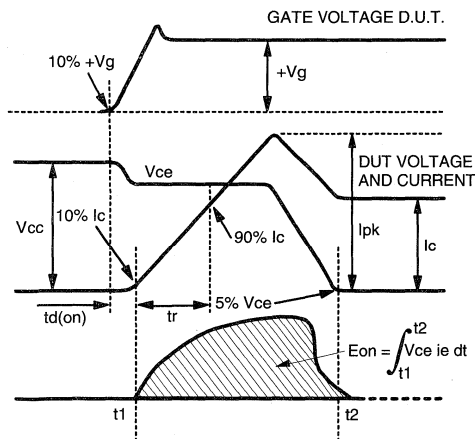


Fig. 18c - Test Waveforms for Circuit of Fig. 18a, Defining E_{on} , $t_{d(on)}$, t_r

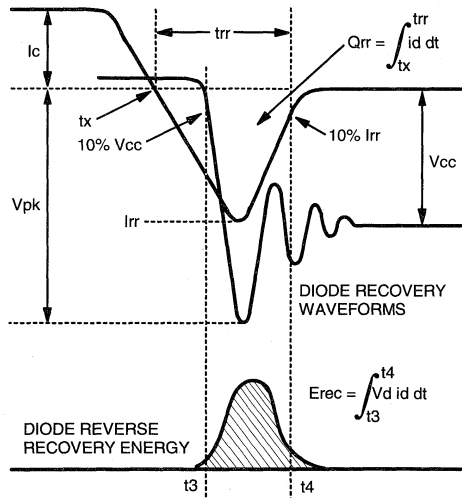


Fig. 18d - Test Waveforms for Circuit of Fig. 18a, Defining E_{rec} , t_{rr} , Q_{rr} , I_{rr}

Refer to Section D for the following:

Appendix D: Section D - page D-6

- Fig. 18e - Macro Waveforms for Test Circuit Fig. 18a
- Fig. 19 - Clamped Inductive Load Test Circuit
- Fig. 20 - Pulsed Collector Current Test Circuit

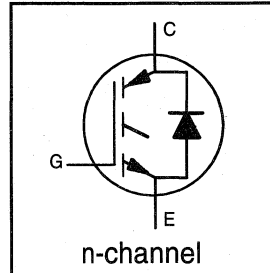
IRGBC30MD2-S

**INSULATED GATE BIPOLAR TRANSISTOR
WITH ULTRAFAST SOFT RECOVERY DIODE**

**Short Circuit Rated
Fast CoPack IGBT**

Features

- Short circuit rated -10µs @ 125°C, V_{GE} = 15V
- Switching-loss rating includes all "tail" losses
- HEXFRED™ soft ultrafast diodes
- Optimized for medium operating frequency (1 to 10kHz) See Fig. 1 for Current vs. Frequency curve

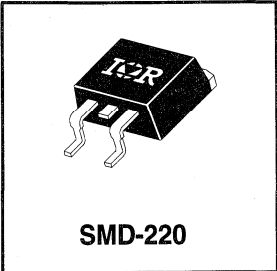


V_{CES} = 600V
V_{CE(sat)} ≤ 2.9V
@ V_{GE} = 15V, I_C = 16A

Description

Co-packaged IGBTs are a natural extension of International Rectifier's well known IGBT line. They provide the convenience of an IGBT and an ultrafast recovery diode in one package, resulting in substantial benefits to a host of high-voltage, high-current, applications.

These new short circuit rated devices are especially suited for motor control and other applications requiring short circuit withstand capability.



Absolute Maximum Ratings

	Parameter	Max.	Units
V _{CES}	Collector-to-Emitter Voltage	600	V
I _C @ T _C = 25°C	Continuous Collector Current	26	A
I _C @ T _C = 100°C	Continuous Collector Current	16	
I _{CM}	Pulsed Collector Current Ⓞ	52	
I _{LM}	Clamped Inductive Load Current Ⓞ	52	
I _F @ T _C = 100°C	Diode Continuous Forward Current	12	
I _{FM}	Diode Maximum Forward Current	52	
t _{sc}	Short Circuit Withstand Time	10	µs
V _{GE}	Gate-to-Emitter Voltage	± 20	V
P _D @ T _C = 25°C	Maximum Power Dissipation	100	W
P _D @ T _C = 100°C	Maximum Power Dissipation	42	
T _J	Operating Junction and Storage Temperature Range	-55 to +150	°C
T _{STG}	Soldering Temperature, for 10 sec.	300 (0.063 in. (1.6mm) from case)	
	Mounting Torque, 6-32 or M3 Screw.	10 lbf•in (1.1 N•m)	

Thermal Resistance

	Parameter	Min.	Typ.	Max.	Units
R _{θJC}	Junction-to-Case - IGBT	—	—	1.2	°C/W
R _{θJC}	Junction-to-Case - Diode	—	—	2.5	
R _{θJA}	Junction-to-Ambient, (PCB Mount)**	—	—	40	
R _{θJA}	Junction-to-Ambient, typical socket mount	—	—	80	
Wt	Weight	—	2 (0.07)	—	g (oz)

** When mounted on 1" square PCB (FR-4 or G-10 Material)
For recommended footprint and soldering techniques refer to application note #AN-994.

Electrical Characteristics @ $T_J = 25^\circ\text{C}$ (unless otherwise specified)

	Parameter	Min.	Typ.	Max.	Units	Conditions
$V_{(BR)CES}$	Collector-to-Emitter Breakdown Voltage ^③	600	—	—	V	$V_{GE} = 0V, I_C = 250\mu A$
$\Delta V_{(BR)CES}/\Delta T_J$	Temperature Coeff. of Breakdown Voltage	—	0.65	—	V/ $^\circ\text{C}$	$V_{GE} = 0V, I_C = 1.0mA$
$V_{CE(on)}$	Collector-to-Emitter Saturation Voltage	—	1.9	2.9	V	$I_C = 16A$ $V_{GE} = 15V$
		—	2.7	—		$I_C = 26A$ See Fig. 2, 5
		—	2.2	—		$I_C = 16A, T_J = 150^\circ\text{C}$
$V_{GE(th)}$	Gate Threshold Voltage	3.0	—	5.5		$V_{CE} = V_{GE}, I_C = 250\mu A$
$\Delta V_{GE(th)}/\Delta T_J$	Temperature Coeff. of Threshold Voltage	—	-12	—	mV/ $^\circ\text{C}$	$V_{CE} = V_{GE}, I_C = 250\mu A$
g_{fe}	Forward Transconductance ^④	3.3	6.5	—	S	$V_{CE} = 100V, I_C = 16A$
I_{CES}	Zero Gate Voltage Collector Current	—	—	250	μA	$V_{GE} = 0V, V_{CE} = 600V$
		—	—	2500		$V_{GE} = 0V, V_{CE} = 600V, T_J = 150^\circ\text{C}$
V_{FM}	Diode Forward Voltage Drop	—	1.4	1.7	V	$I_C = 12A$ See Fig. 13
		—	1.3	1.6		$I_C = 12A, T_J = 150^\circ\text{C}$
I_{GES}	Gate-to-Emitter Leakage Current	—	—	± 100	nA	$V_{GE} = \pm 20V$

Switching Characteristics @ $T_J = 25^\circ\text{C}$ (unless otherwise specified)

	Parameter	Min.	Typ.	Max.	Units	Conditions	
Q_g	Total Gate Charge (turn-on)	—	35	53	nC	$I_C = 16A$	
Q_{ge}	Gate - Emitter Charge (turn-on)	—	7.4	11		$V_{CC} = 400V$	
Q_{gc}	Gate - Collector Charge (turn-on)	—	14	21		See Fig. 8	
$t_{d(on)}$	Turn-On Delay Time	—	68	—	ns	$T_J = 25^\circ\text{C}$	
t_r	Rise Time	—	130	—		$I_C = 16A, V_{CC} = 480V$	
$t_{d(off)}$	Turn-Off Delay Time	—	330	500		$V_{GE} = 15V, R_G = 23\Omega$	
t_f	Fall Time	—	310	470		Energy losses include "tail" and diode reverse recovery.	
E_{on}	Turn-On Switching Loss	—	1.5	—		mJ	See Fig. 9, 10, 11, 18
E_{off}	Turn-Off Switching Loss	—	2.1	—			
E_{ts}	Total Switching Loss	—	3.6	5.4			
t_{sc}	Short Circuit Withstand Time	10	—	—	μs	$V_{CC} = 360V, T_J = 125^\circ\text{C}$ $V_{GE} = 15V, R_G = 23\Omega, V_{CPK} < 500V$	
$t_{d(on)}$	Turn-On Delay Time	—	66	—	ns	$T_J = 150^\circ\text{C}$, See Fig. 9, 10, 11, 18	
t_r	Rise Time	—	120	—		$I_C = 16A, V_{CC} = 480V$	
$t_{d(off)}$	Turn-Off Delay Time	—	580	—		$V_{GE} = 15V, R_G = 23\Omega$	
t_f	Fall Time	—	630	—		Energy losses include "tail" and diode reverse recovery.	
E_{ts}	Total Switching Loss	—	5.7	—	mJ		
L_E	Internal Emitter Inductance	—	7.5	—	nH	Measured 5mm from package	
C_{ies}	Input Capacitance	—	750	—	pF	$V_{GE} = 0V$	
C_{oes}	Output Capacitance	—	110	—		$V_{CC} = 30V$ See Fig. 7	
C_{res}	Reverse Transfer Capacitance	—	9.3	—		$f = 1.0MHz$	
t_{rr}	Diode Reverse Recovery Time	—	42	60	ns	$T_J = 25^\circ\text{C}$ See Fig. 14	
		—	80	120		$T_J = 125^\circ\text{C}$	
I_{rr}	Diode Peak Reverse Recovery Current	—	3.5	6.0	A	$T_J = 25^\circ\text{C}$ See Fig. 15	
		—	5.6	10		$T_J = 125^\circ\text{C}$	
Q_{rr}	Diode Reverse Recovery Charge	—	80	180	nC	$T_J = 25^\circ\text{C}$ See Fig. 16	
		—	220	600		$T_J = 125^\circ\text{C}$	
$di_{(rec)M}/dt$	Diode Peak Rate of Fall of Recovery During t_b	—	180	—	A/ μs	$T_J = 25^\circ\text{C}$ See Fig. 17	
		—	120	—		$T_J = 125^\circ\text{C}$	

Notes:

① Repetitive rating; $V_{GE}=20V$, pulse width limited by max. junction temperature. (See fig. 20)

② $V_{CC}=80\%(V_{CES}), V_{GE}=20V, L=10\mu H, R_G=23\Omega,$ (See fig. 19)

③ Pulse width $\leq 80\mu s$; duty factor $\leq 0.1\%$.

④ Pulse width 5.0 μs , single shot.

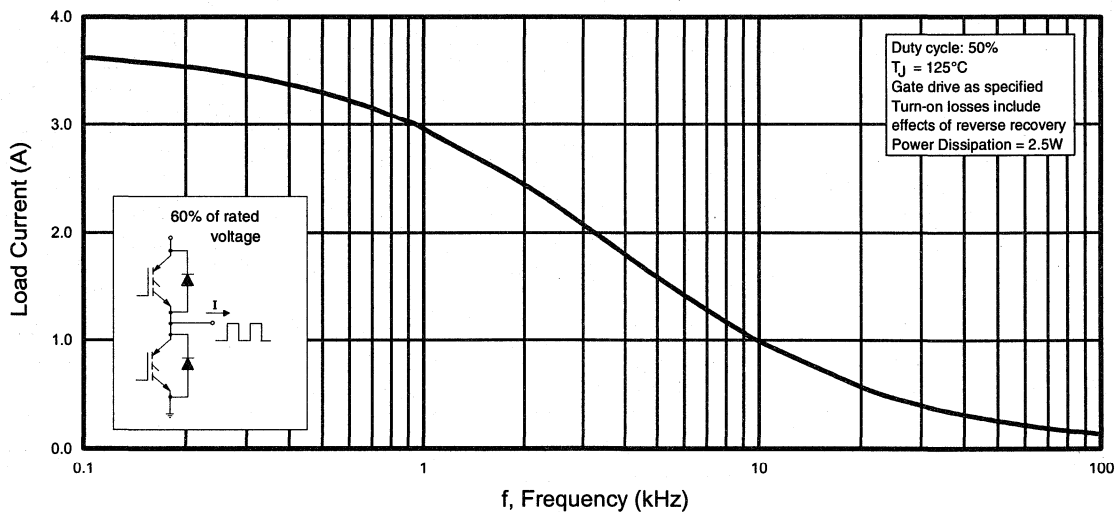


Fig. 1 - Typical Load Current vs. Frequency
(Load Current = I_{RMS} of fundamental)

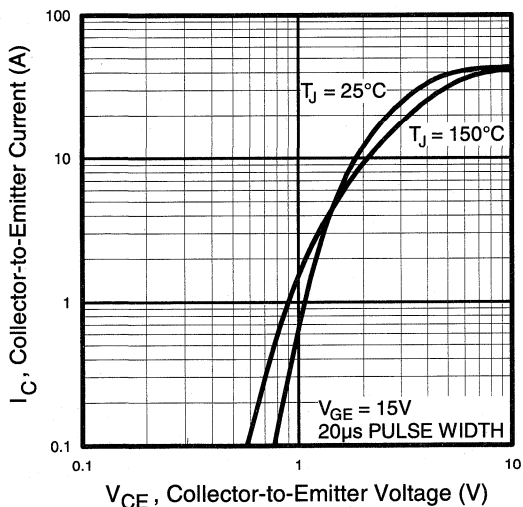


Fig. 2 - Typical Output Characteristics

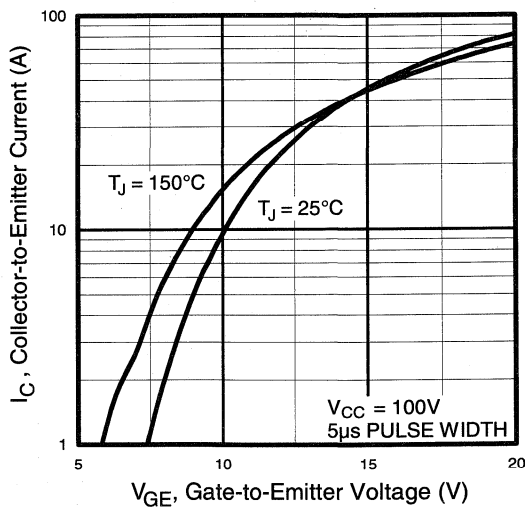


Fig. 3 - Typical Transfer Characteristics

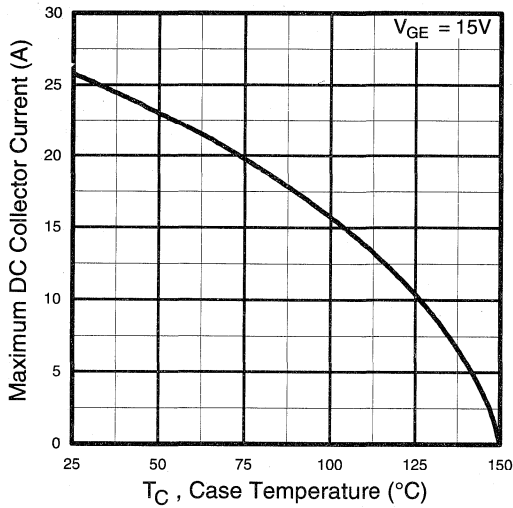


Fig. 4 - Maximum Collector Current vs. Case Temperature

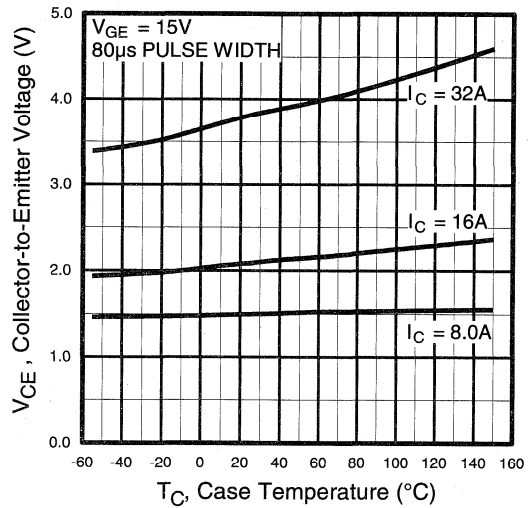


Fig. 5 - Collector-to-Emitter Voltage vs. Case Temperature

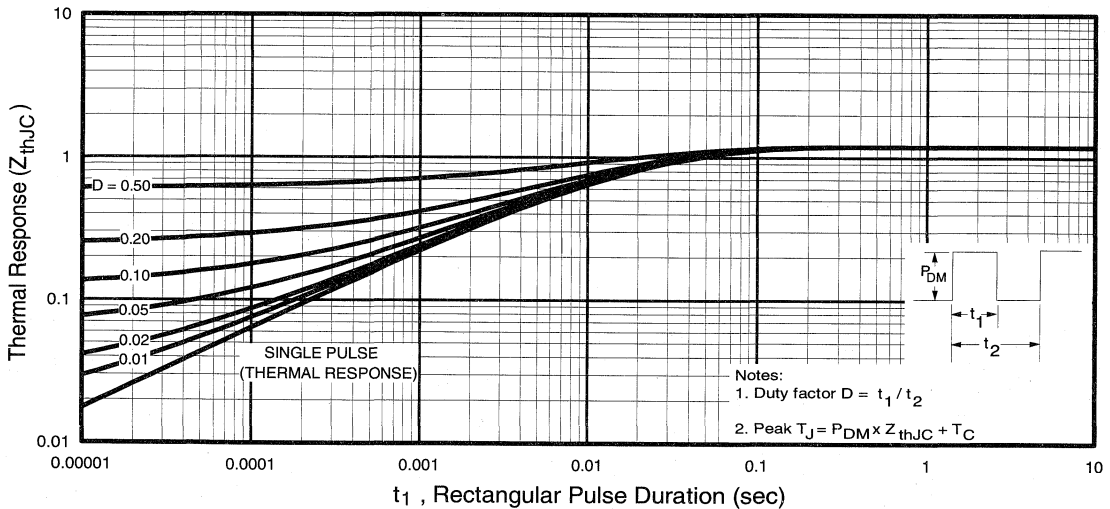


Fig. 6 - Maximum IGBT Effective Transient Thermal Impedance, Junction-to-Case

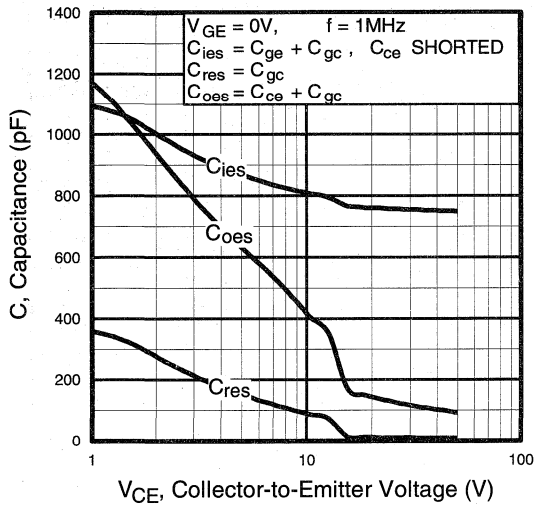


Fig. 7 - Typical Capacitance vs. Collector-to-Emitter Voltage

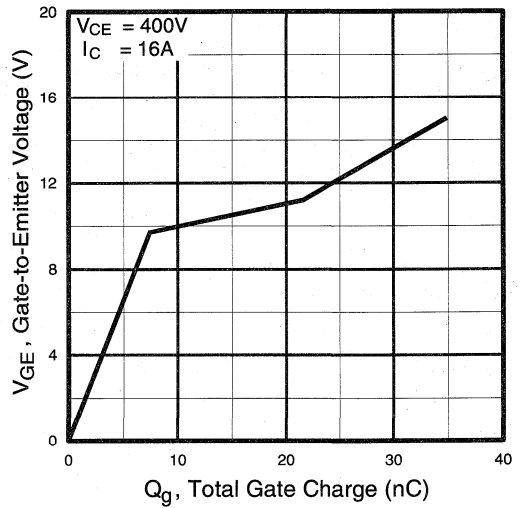


Fig. 8 - Typical Gate Charge vs. Gate-to-Emitter Voltage

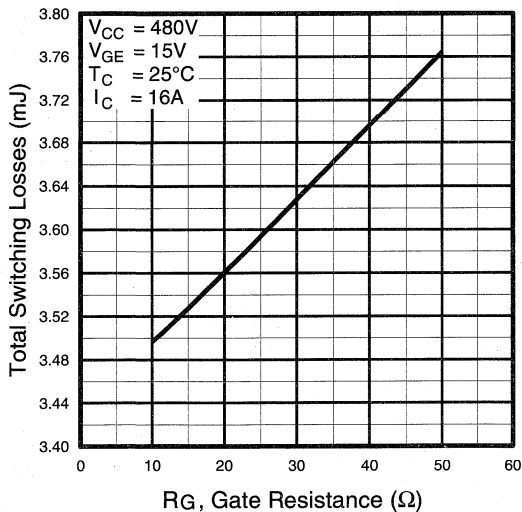


Fig. 9 - Typical Switching Losses vs. Gate Resistance

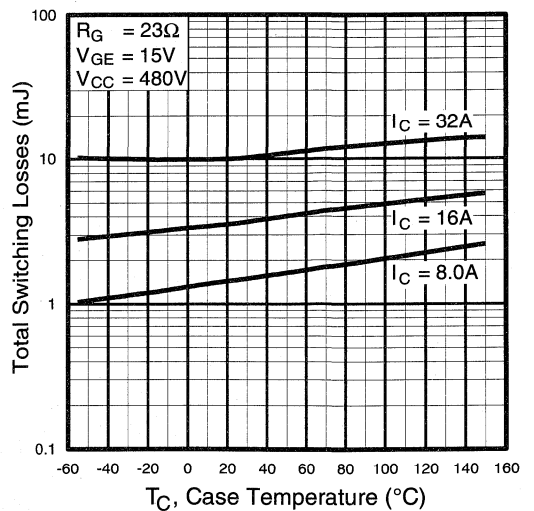


Fig. 10 - Typical Switching Losses vs. Case Temperature

Motor
Control
Fast
Capacitors

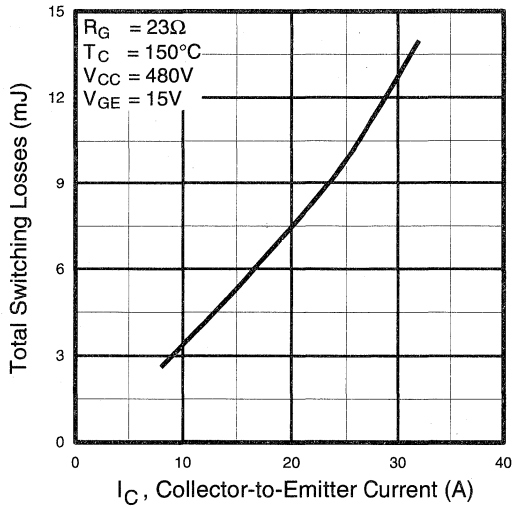


Fig. 11 - Typical Switching Losses vs. Collector-to-Emitter Current

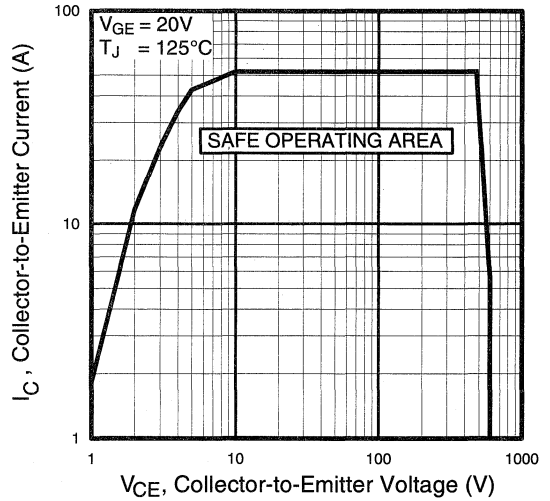


Fig. 12 - Turn-Off SOA

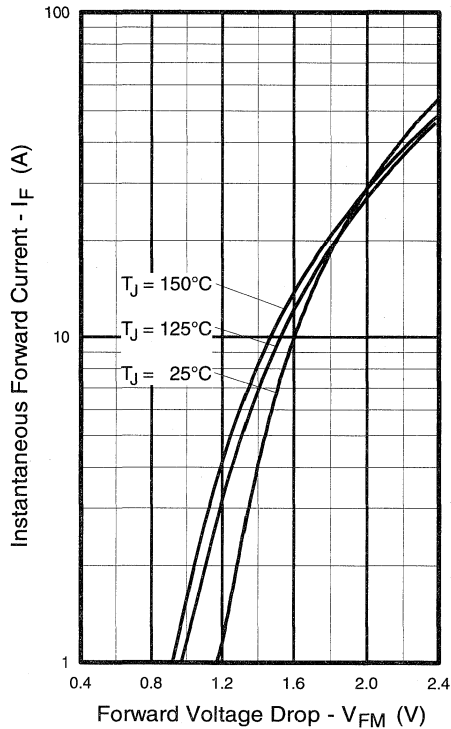


Fig. 13 - Maximum Forward Voltage Drop vs. Instantaneous Forward Current

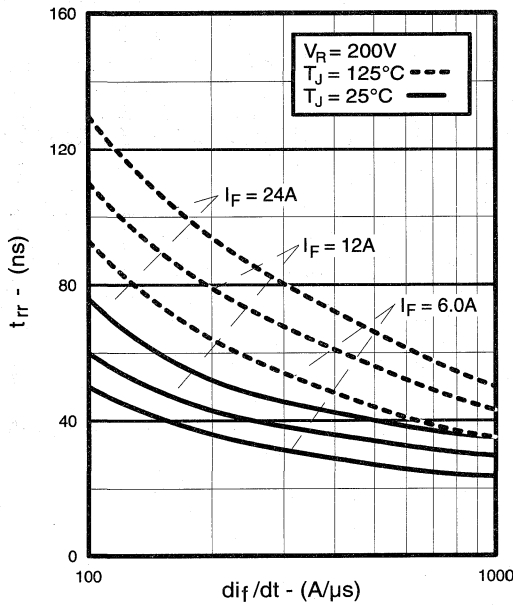


Fig. 14 - Typical Reverse Recovery vs. di_f/dt

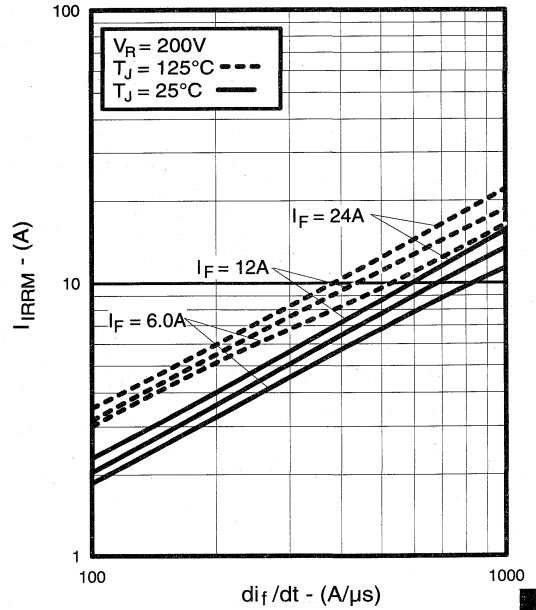


Fig. 15 - Typical Recovery Current vs. di_f/dt

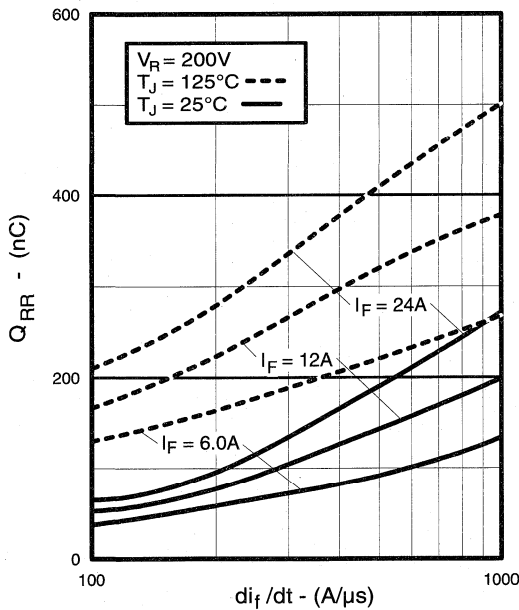


Fig. 16 - Typical Stored Charge vs. di_f/dt

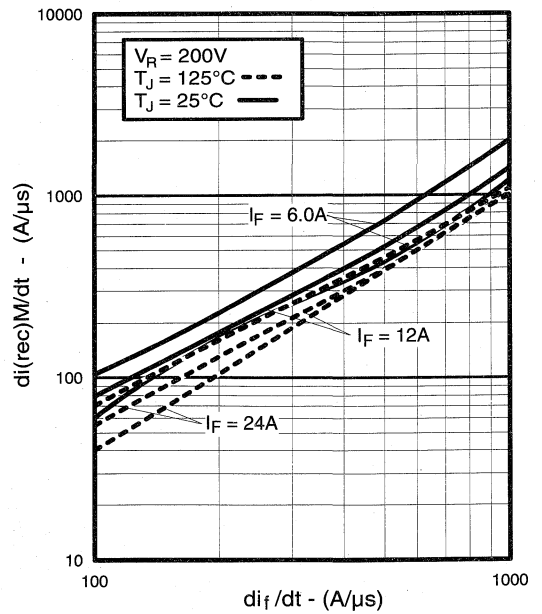


Fig. 17 - Typical $di_{(rec)M}/dt$ vs. di_f/dt

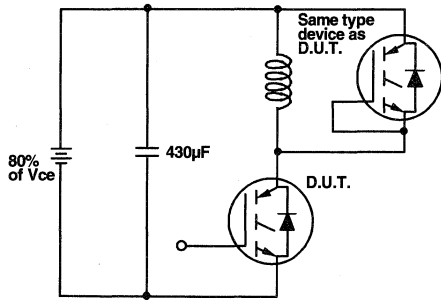


Fig. 18a - Test Circuit for Measurement of I_{LM} , E_{on} , $E_{off}(\text{diode})$, t_{rr} , Q_{rr} , I_{rr} , $t_{d(on)}$, t_r , $t_{d(off)}$, t_f

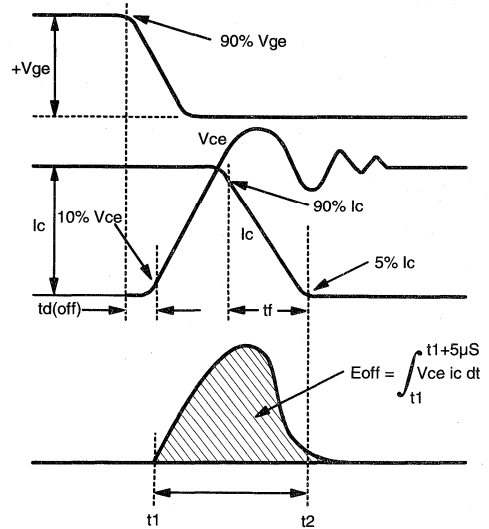


Fig. 18b - Test Waveforms for Circuit of Fig. 18a, Defining E_{off} , $t_{d(off)}$, t_f

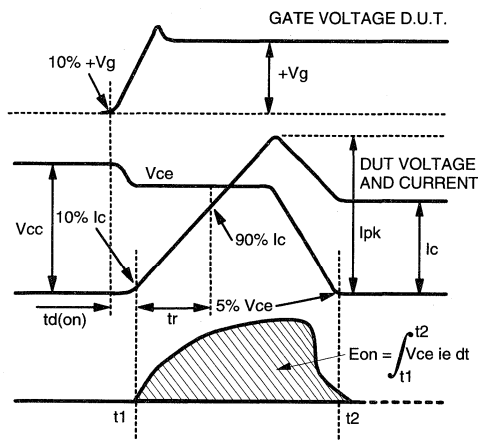


Fig. 18c - Test Waveforms for Circuit of Fig. 18a, Defining E_{on} , $t_{d(on)}$, t_r

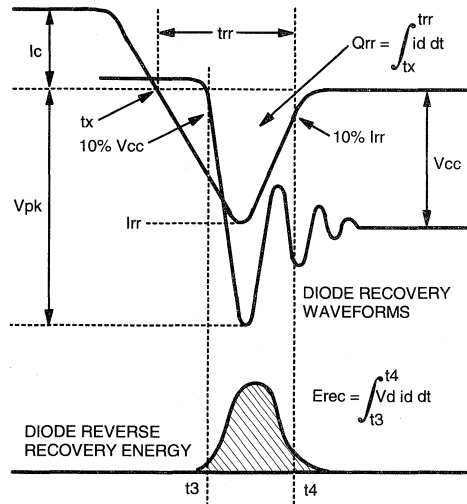


Fig. 18d - Test Waveforms for Circuit of Fig. 18a, Defining E_{rec} , t_{rr} , Q_{rr} , I_{rr}

Refer to Section D for the following:

Appendix D: Section D - page D-6

- Fig. 18e - Macro Waveforms for Test Circuit Fig. 18a
- Fig. 19 - Clamped Inductive Load Test Circuit
- Fig. 20 - Pulsed Collector Current Test Circuit

IRGPC20MD2

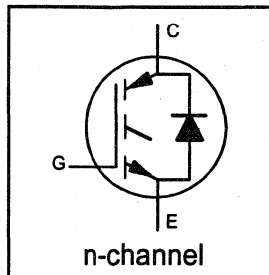
INSULATED GATE BIPOLAR TRANSISTOR
WITH ULTRAFAST SOFT RECOVERY

Short Circuit Rated
Fast CoPack IGBT

DIODE

Features

- Short circuit rated $-10\mu\text{s}$ @ 125°C , $V_{\text{GE}} = 15\text{V}$
- Switching-loss rating includes all "tail" losses
- HEXFRED™ soft ultrafast diodes
- Optimized for medium operating frequency (1 to 10kHz) See Fig. 1 for Current vs. Frequency curve



$$V_{\text{CES}} = 600\text{V}$$

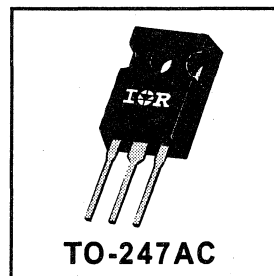
$$V_{\text{CE(sat)}} \leq 2.5\text{V}$$

$$\text{@}V_{\text{GE}} = 15\text{V}, I_{\text{C}} = 8.0\text{A}$$

Description

Co-packaged IGBTs are a natural extension of International Rectifier's well known IGBT line. They provide the convenience of an IGBT and an ultrafast recovery diode in one package, resulting in substantial benefits to a host of high-voltage, high-current, applications.

These new short circuit rated devices are especially suited for motor control and other applications requiring short circuit withstand capability.



TO-247AC

Absolute Maximum Ratings

	Parameter	Max.	Units
V_{CES}	Collector-to-Emitter Voltage	600	V
$I_{\text{C}} @ T_{\text{C}} = 25^\circ\text{C}$	Continuous Collector Current	13	A
$I_{\text{C}} @ T_{\text{C}} = 100^\circ\text{C}$	Continuous Collector Current	8.0	
I_{CM}	Pulsed Collector Current ①	26	
I_{LM}	Clamped Inductive Load Current ②	26	
$I_{\text{F}} @ T_{\text{C}} = 100^\circ\text{C}$	Diode Continuous Forward Current	7.0	
I_{FM}	Diode Maximum Forward Current	60	μs
t_{sc}	Short Circuit Withstand Time	10	
V_{GE}	Gate-to-Emitter Voltage	± 20	V
$P_{\text{D}} @ T_{\text{C}} = 25^\circ\text{C}$	Maximum Power Dissipation	60	W
$P_{\text{D}} @ T_{\text{C}} = 100^\circ\text{C}$	Maximum Power Dissipation	24	
T_{J}	Operating Junction and	-55 to +150	$^\circ\text{C}$
T_{STG}	Storage Temperature Range		
	Soldering Temperature, for 10 sec.	300 (0.063 in. (1.6mm) from case)	
	Mounting Torque, 6-32 or M3 Screw.	10 lbf·in (1.1 N·m)	

Thermal Resistance

	Parameter	Min.	Typ.	Max.	Units
$R_{\theta\text{JC}}$	Junction-to-Case - IGBT	—	—	2.1	$^\circ\text{C/W}$
$R_{\theta\text{JC}}$	Junction-to-Case - Diode	—	—	3.5	
$R_{\theta\text{CS}}$	Case-to-Sink, flat, greased surface	—	0.24	—	
$R_{\theta\text{JA}}$	Junction-to-Ambient, typical socket mount	—	—	40	
Wt	Weight	—	6 (0.21)	—	g (oz)

Electrical Characteristics @ T_J = 25°C (unless otherwise specified)

	Parameter	Min.	Typ.	Max.	Units	Conditions
V _{(BR)CES}	Collector-to-Emitter Breakdown Voltage ^③	600	—	—	V	V _{GE} = 0V, I _C = 250μA
ΔV _{(BR)CES} /ΔT _J	Temp. Coeff. of Breakdown Voltage	—	0.42	—	V/°C	V _{GE} = 0V, I _C = 1.0mA
V _{CE(on)}	Collector-to-Emitter Saturation Voltage	—	2.0	2.5	V	I _C = 8.0A V _{GE} = 15V I _C = 13A See Fig. 2, 5 I _C = 8.0A, T _J = 150°C
V _{GE(th)}	Gate Threshold Voltage	3.0	—	5.5		V _{CE} = V _{GE} , I _C = 250μA
ΔV _{GE(th)} /ΔT _J	Temperature Coeff. of Threshold Voltage	—	-11	—		mV/°C
g _{fe}	Forward Transconductance ^④	2.7	3.8	—	S	V _{CE} = 100V, I _C = 8.0A
I _{CES}	Zero Gate Voltage Collector Current	—	—	250	μA	V _{GE} = 0V, V _{CE} = 600V
		—	—	1700		V _{GE} = 0V, V _{CE} = 600V, T _J = 150°C
V _{FM}	Diode Forward Voltage Drop	—	1.4	1.7	V	I _C = 8.0A See Fig. 13 I _C = 8.0A, T _J = 150°C
I _{GES}	Gate-to-Emitter Leakage Current	—	—	±100		nA

Switching Characteristics @ T_J = 25°C (unless otherwise specified)

	Parameter	Min.	Typ.	Max.	Units	Conditions	
Q _g	Total Gate Charge (turn-on)	—	16	24	nC	I _C = 8.0A V _{CC} = 400V See Fig. 8	
Q _{ge}	Gate - Emitter Charge (turn-on)	—	3.6	5.2			
Q _{gc}	Gate - Collector Charge (turn-on)	—	6.0	9.0			
t _{d(on)}	Turn-On Delay Time	—	66	—	ns	T _J = 25°C I _C = 8.0A, V _{CC} = 480V	
t _r	Rise Time	—	40	—		V _{GE} = 15V, R _G = 50Ω Energy losses include "tail" and diode reverse recovery.	
t _{d(off)}	Turn-Off Delay Time	—	330	540	mJ	See Fig. 9, 10, 11, 18	
t _f	Fall Time	—	260	480			
E _{on}	Turn-On Switching Loss	—	0.5	—	μs	V _{CC} = 360V, T _J = 125°C V _{GE} = 15V, R _G = 50Ω, V _{CPK} < 500V	
E _{off}	Turn-Off Switching Loss	—	1.0	—			
E _{ts}	Total Switching Loss	—	1.5	2.5			
t _{sc}	Short Circuit Withstand Time	10	—	—	ns	T _J = 150°C, See Fig. 9, 10, 11, 18 I _C = 8.0A, V _{CC} = 480V V _{GE} = 15V, R _G = 50Ω Energy losses include "tail" and diode reverse recovery.	
t _{d(on)}	Turn-On Delay Time	—	65	—			
t _r	Rise Time	—	46	—	mJ	Measured 5mm from package	
t _{d(off)}	Turn-Off Delay Time	—	520	—			
t _f	Fall Time	—	560	—	pF	V _{GE} = 0V V _{CC} = 30V See Fig. 7 f = 1.0MHz	
E _{ts}	Total Switching Loss	—	2.3	—			
L _E	Internal Emitter Inductance	—	13	—			
C _{ies}	Input Capacitance	—	365	—	ns	T _J = 25°C See Fig. 14 T _J = 125°C	
C _{oes}	Output Capacitance	—	47	—		A	T _J = 25°C See Fig. 15 T _J = 125°C
C _{res}	Reverse Transfer Capacitance	—	4.8	—			nC
t _{rr}	Diode Reverse Recovery Time	—	37	55	A/μs	T _J = 25°C See Fig. 17 T _J = 125°C	
I _{rr}	Diode Peak Reverse Recovery Current	—	3.5	5.0		—	—
Q _{rr}	Diode Reverse Recovery Charge	—	65	138	—		—
di _{(rec)M} /dt	Diode Peak Rate of Fall of Recovery During t _b	—	240	—		—	—
		—	210	—			

Notes:

① Repetitive rating; V_{GE}=20V, pulse width limited by max. junction temperature. (See fig. 20)

② V_{CC}=80%(V_{CES}), V_{GE}=20V, L=10μH, R_G= 50Ω, (See fig. 19)

④ Pulse width 5.0μs, single shot.

③ Pulse width ≤ 80μs; duty factor ≤ 0.1%.

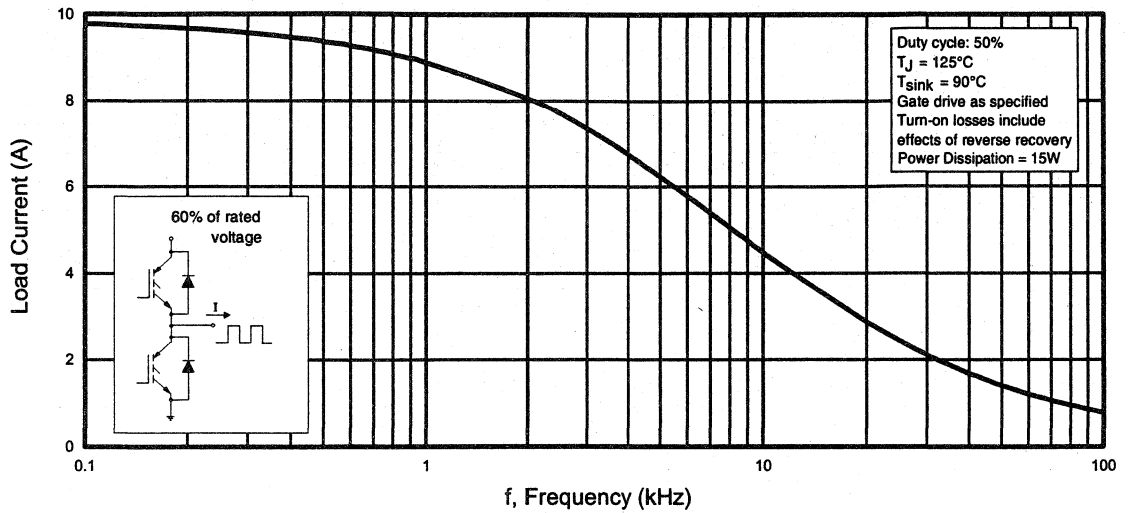


Fig. 1 - Typical Load Current vs. Frequency
(Load Current = I_{RMS} of fundamental)

Motor
Control
Fast
Co-Packs

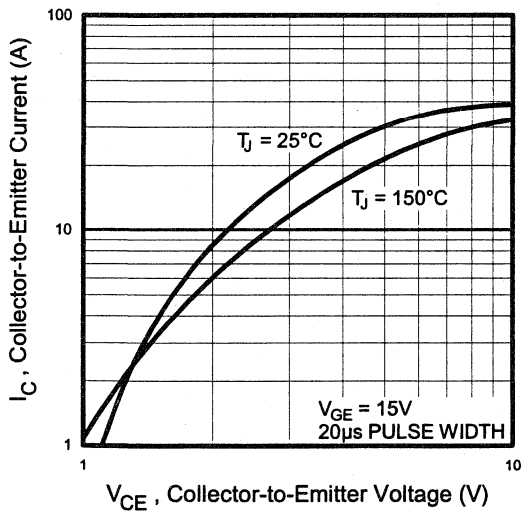


Fig. 2 - Typical Output Characteristics

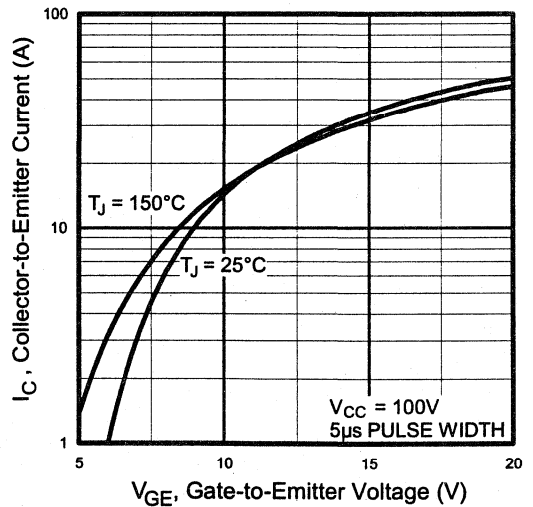


Fig. 3 - Typical Transfer Characteristics

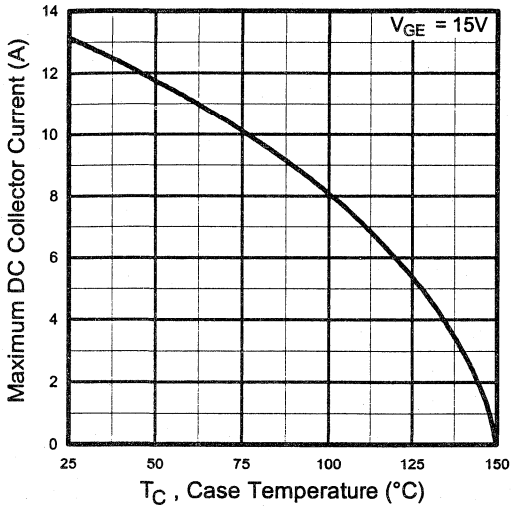


Fig. 4 - Maximum Collector Current vs. Case Temperature

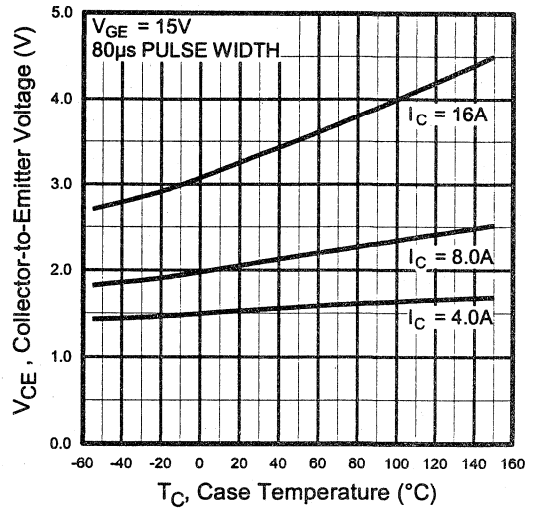


Fig. 5 - Collector-to-Emitter Voltage vs. Case Temperature

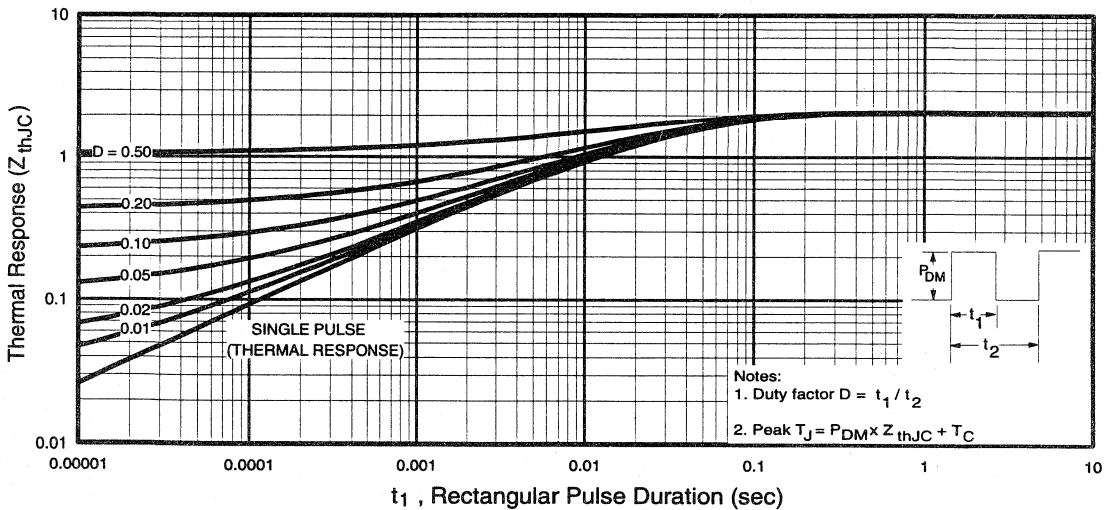


Fig. 6 - Maximum IGBT Effective Transient Thermal Impedance, Junction-to-Case

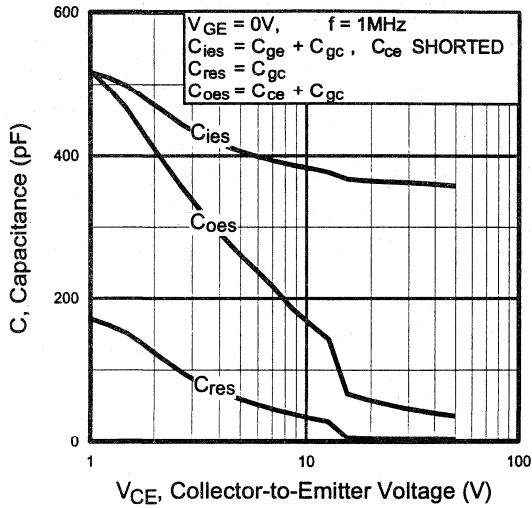


Fig. 7 - Typical Capacitance vs. Collector-to-Emitter Voltage

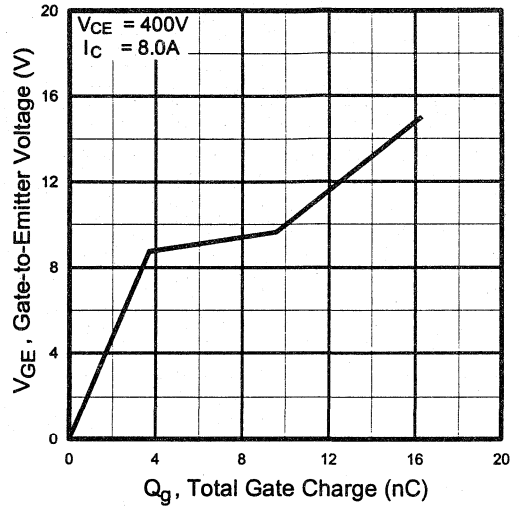


Fig. 8 - Typical Gate Charge vs. Gate-to-Emitter Voltage

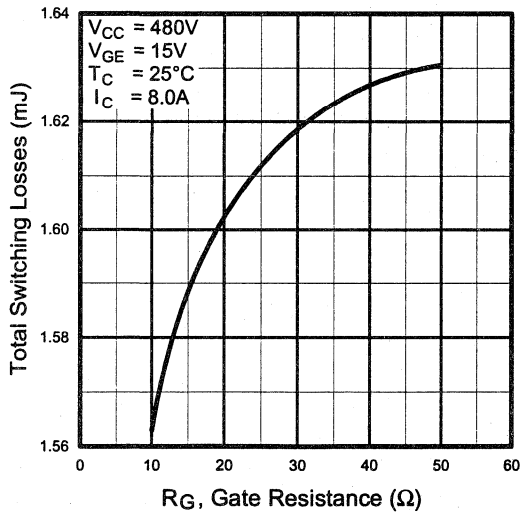


Fig. 9 - Typical Switching Losses vs. Gate Resistance

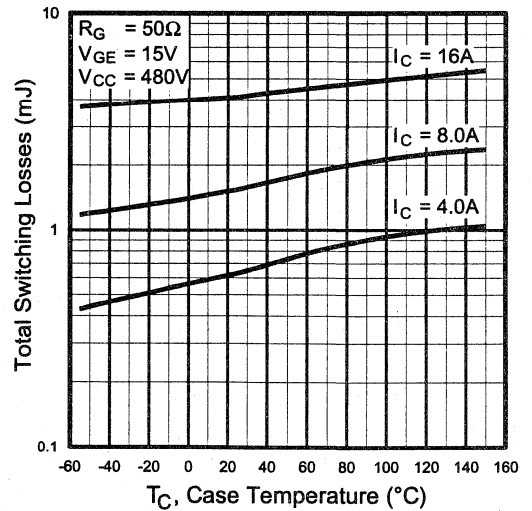


Fig. 10 - Typical Switching Losses vs. Case Temperature



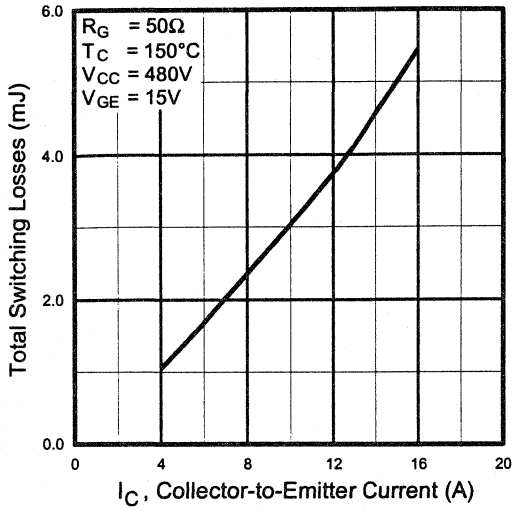


Fig. 11 - Typical Switching Losses vs. Collector-to-Emitter Current

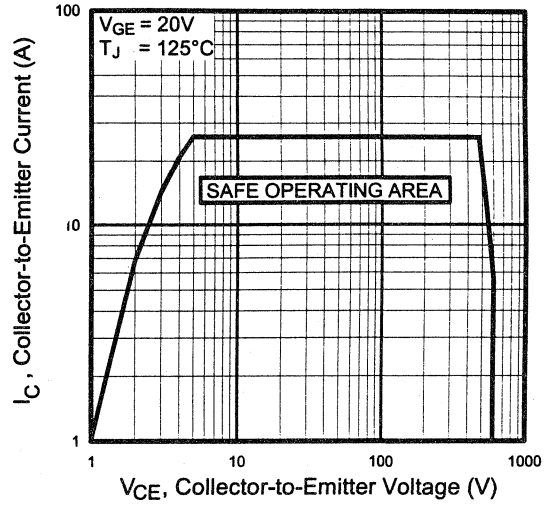


Fig. 12 - Turn-Off SOA

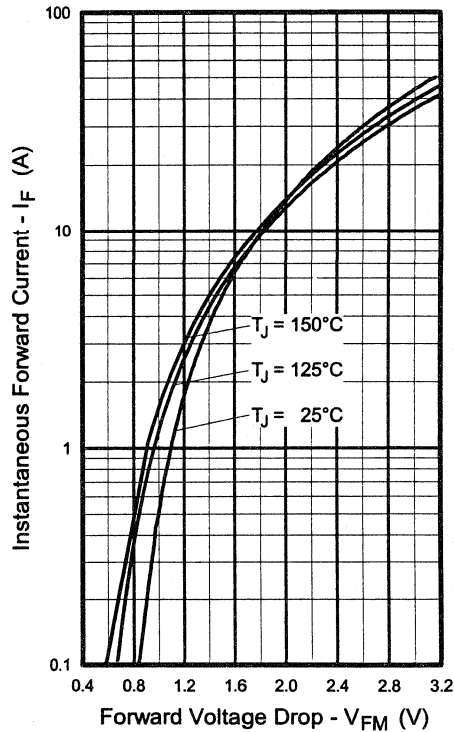


Fig. 13 - Maximum Forward Voltage Drop vs. Instantaneous Forward Current

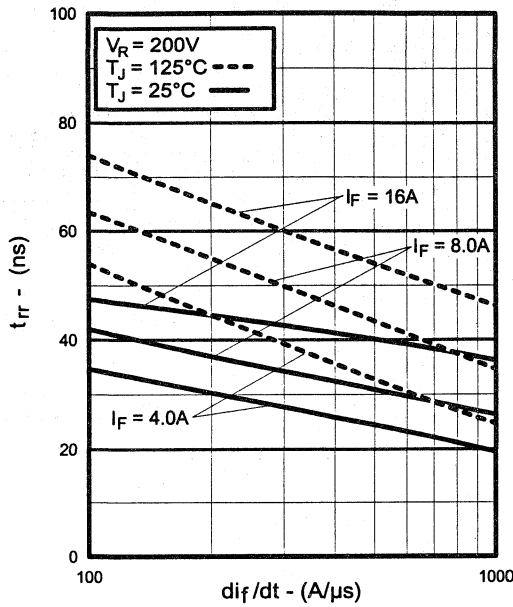


Fig. 14 - Typical Reverse Recovery vs. di_f/dt

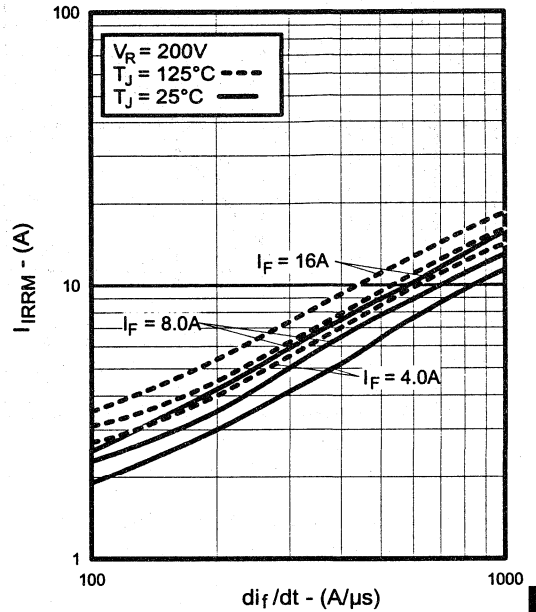


Fig. 15 - Typical Recovery Current vs. di_f/dt

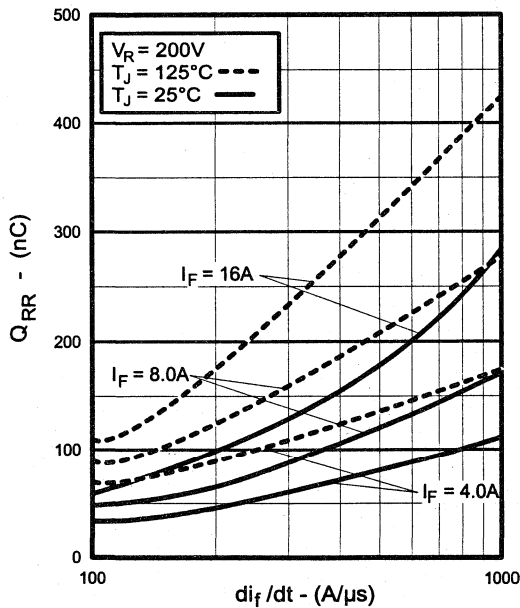


Fig. 16 - Typical Stored Charge vs. di_f/dt

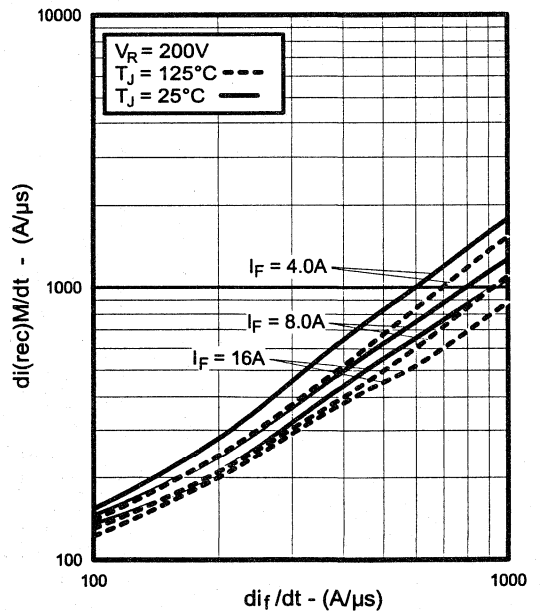


Fig. 17 - Typical $di_{(rec)M}/dt$ vs. di_f/dt

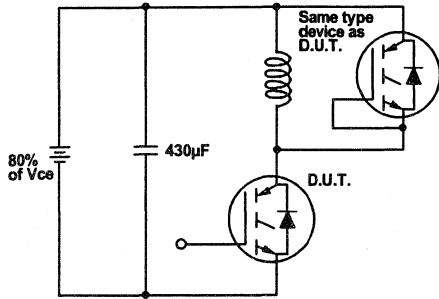


Fig. 18a - Test Circuit for Measurement of I_{LM} , V_{ce} , $E_{off}(\text{diode})$, t_{rr} , Q_{rr} , I_{rr} , $t_{d(on)}$, t_r , $t_{d(off)}$, t_f

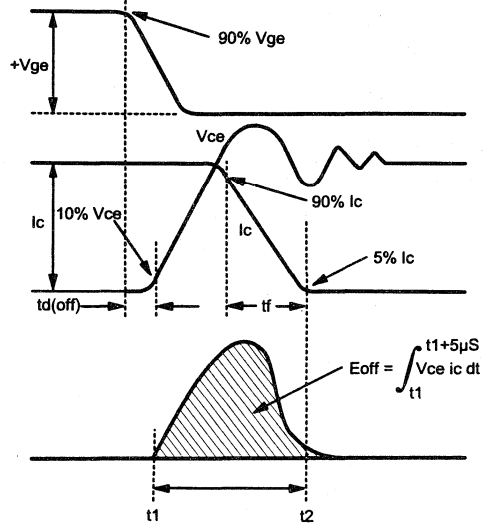


Fig. 18b - Test Waveforms for Circuit of Fig. 18a, Defining E_{off} , $t_{d(off)}$, t_f

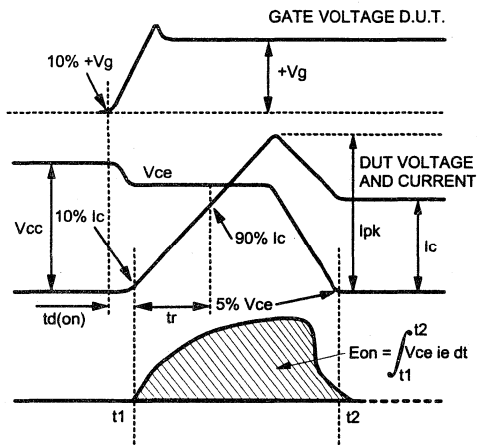


Fig. 18c - Test Waveforms for Circuit of Fig. 18a, Defining E_{on} , $t_{d(on)}$, t_r

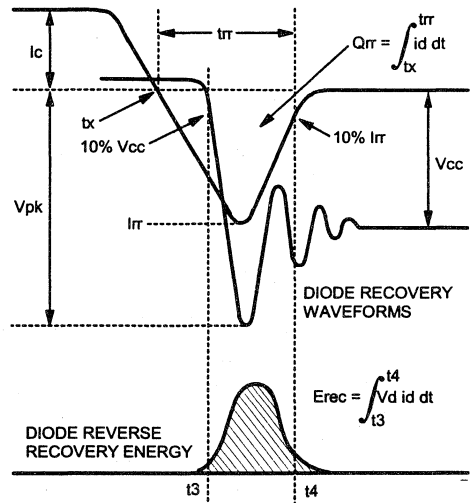


Fig. 18d - Test Waveforms for Circuit of Fig. 18a, Defining E_{rec} , t_{rr} , Q_{rr} , I_{rr}

Refer to Section D for the following:

Appendix D: Section D - page D-6

Fig. 18e - Macro Waveforms for Test Circuit of Fig. 18a

Fig. 19 - Clamped Inductive Load Test Circuit

Fig. 20 - Pulsed Collector Current Test Circuit

IRGPC30MD2

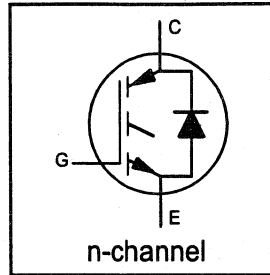
INSULATED GATE BIPOLAR TRANSISTOR
WITH ULTRAFAST SOFT RECOVERY

Short Circuit Rated
Fast CoPack IGBT

DIODE

Features

- Short circuit rated $-10\mu\text{s}$ @ 125°C , $V_{GE} = 15\text{V}$
- Switching-loss rating includes all "tail" losses
- HEXFRED™ soft ultrafast diodes
- Optimized for medium operating frequency (1 to 10kHz) See Fig. 1 for Current vs. Frequency curve



$$V_{CES} = 600\text{V}$$

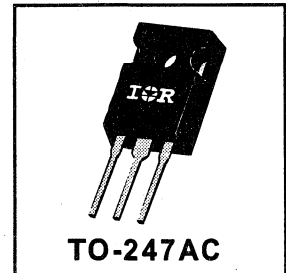
$$V_{CE(sat)} \leq 2.9\text{V}$$

$$\text{@ } V_{GE} = 15\text{V}, I_C = 16\text{A}$$

Description

Co-packaged IGBTs are a natural extension of International Rectifier's well known IGBT line. They provide the convenience of an IGBT and an ultrafast recovery diode in one package, resulting in substantial benefits to a host of high-voltage, high-current, applications.

These new short circuit rated devices are especially suited for motor control and other applications requiring short circuit withstand capability.



Motor
Control
Fast
Co-Packs

Absolute Maximum Ratings

	Parameter	Max.	Units
V_{CES}	Collector-to-Emitter Voltage	600	V
$I_C @ T_C = 25^\circ\text{C}$	Continuous Collector Current	26	A
$I_C @ T_C = 100^\circ\text{C}$	Continuous Collector Current	16	
I_{CM}	Pulsed Collector Current ①	52	
I_{LM}	Clamped Inductive Load Current ②	52	
$I_F @ T_C = 100^\circ\text{C}$	Diode Continuous Forward Current	12	
I_{FM}	Diode Maximum Forward Current	52	
t_{sc}	Short Circuit Withstand Time	10	μs
V_{GE}	Gate-to-Emitter Voltage	± 20	V
$P_D @ T_C = 25^\circ\text{C}$	Maximum Power Dissipation	100	W
$P_D @ T_C = 100^\circ\text{C}$	Maximum Power Dissipation	42	
T_J	Operating Junction and	-55 to +150	$^\circ\text{C}$
T_{STG}	Storage Temperature Range		
	Soldering Temperature, for 10 sec.	300 (0.063 in. (1.6mm) from case)	
	Mounting Torque, 6-32 or M3 Screw.	10 lbf·in (1.1 N·m)	

Thermal Resistance

	Parameter	Min.	Typ.	Max.	Units
$R_{\theta JC}$	Junction-to-Case - IGBT	—	—	1.2	$^\circ\text{C/W}$
$R_{\theta JC}$	Junction-to-Case - Diode	—	—	2.5	
$R_{\theta CS}$	Case-to-Sink, flat, greased surface	—	0.24	—	
$R_{\theta JA}$	Junction-to-Ambient, typical socket mount	—	—	40	
Wt	Weight	—	6 (0.21)	—	g (oz)

Electrical Characteristics @ $T_J = 25^\circ\text{C}$ (unless otherwise specified)

	Parameter	Min.	Typ.	Max.	Units	Conditions
$V_{(BR)CES}$	Collector-to-Emitter Breakdown Voltage ^③	600	—	—	V	$V_{GE} = 0V, I_C = 250\mu A$
$\Delta V_{(BR)CES}/\Delta T_J$	Temp. Coeff. of Breakdown Voltage	—	0.65	—	V/°C	$V_{GE} = 0V, I_C = 1.0mA$
$V_{CE(on)}$	Collector-to-Emitter Saturation Voltage	—	1.9	2.9	V	$I_C = 16A, V_{GE} = 15V$
		—	2.7	—		$I_C = 26A$
		—	2.2	—		$I_C = 16A, T_J = 150^\circ\text{C}$
$V_{GE(th)}$	Gate Threshold Voltage	3.0	—	5.5		$V_{CE} = V_{GE}, I_C = 250\mu A$
$\Delta V_{GE(th)}/\Delta T_J$	Temperature Coeff. of Threshold Voltage	—	-12	—	mV/°C	$V_{CE} = V_{GE}, I_C = 250\mu A$
g_{fe}	Forward Transconductance ^④	3.3	6.5	—	S	$V_{CE} = 100V, I_C = 16A$
I_{CES}	Zero Gate Voltage Collector Current	—	—	250	μA	$V_{GE} = 0V, V_{CE} = 600V$
		—	—	2500		$V_{GE} = 0V, V_{CE} = 600V, T_J = 150^\circ\text{C}$
V_{FM}	Diode Forward Voltage Drop	—	1.4	1.7	V	$I_C = 12A$
		—	1.3	1.6		$I_C = 12A, T_J = 150^\circ\text{C}$
I_{GES}	Gate-to-Emitter Leakage Current	—	—	± 100	nA	$V_{GE} = \pm 20V$

Switching Characteristics @ $T_J = 25^\circ\text{C}$ (unless otherwise specified)

	Parameter	Min.	Typ.	Max.	Units	Conditions	
Q_g	Total Gate Charge (turn-on)	—	35	53	nC	$I_C = 16A$	
Q_{ge}	Gate - Emitter Charge (turn-on)	—	7.4	11		$V_{CC} = 400V$	
Q_{gc}	Gate - Collector Charge (turn-on)	—	14	21		See Fig. 8	
$t_{d(on)}$	Turn-On Delay Time	—	68	—	ns	$T_J = 25^\circ\text{C}$	
t_r	Rise Time	—	130	—		$I_C = 16A, V_{CC} = 480V$	
$t_{d(off)}$	Turn-Off Delay Time	—	330	500		$V_{GE} = 15V, R_G = 23\Omega$	
t_f	Fall Time	—	310	470		Energy losses include "tail" and diode reverse recovery.	
E_{on}	Turn-On Switching Loss	—	1.5	—		mJ	See Fig. 9, 10, 11, 18
E_{off}	Turn-Off Switching Loss	—	2.1	—			
E_{ts}	Total Switching Loss	—	3.6	5.4			
t_{sc}	Short Circuit Withstand Time	10	—	—	μs	$V_{CC} = 360V, T_J = 125^\circ\text{C}$ $V_{GE} = 15V, R_G = 23\Omega, V_{CPK} < 500V$	
$t_{d(on)}$	Turn-On Delay Time	—	66	—	ns	$T_J = 150^\circ\text{C}$, See Fig. 9, 10, 11, 18	
t_r	Rise Time	—	120	—		$I_C = 14A, V_{CC} = 480V$	
$t_{d(off)}$	Turn-Off Delay Time	—	580	—		$V_{GE} = 15V, R_G = 23\Omega$	
t_f	Fall Time	—	630	—		Energy losses include "tail" and diode reverse recovery.	
E_{ts}	Total Switching Loss	—	5.7	—		mJ	
L_E	Internal Emitter Inductance	—	13	—		nH	Measured 5mm from package
C_{ies}	Input Capacitance	—	750	—	pF	$V_{GE} = 0V$	
C_{oes}	Output Capacitance	—	110	—		$V_{CC} = 30V$	
C_{res}	Reverse Transfer Capacitance	—	9.3	—		$f = 1.0MHz$	
t_{rr}	Diode Reverse Recovery Time	—	42	60	ns	$T_J = 25^\circ\text{C}$ See Fig. 14	
		—	80	120		$T_J = 125^\circ\text{C}$	
I_{rr}	Diode Peak Reverse Recovery Current	—	3.5	6.0	A	$T_J = 25^\circ\text{C}$ See Fig. 15	
		—	5.6	10		$T_J = 125^\circ\text{C}$	
Q_{rr}	Diode Reverse Recovery Charge	—	80	180	nC	$T_J = 25^\circ\text{C}$ See Fig. 16	
		—	220	600		$T_J = 125^\circ\text{C}$	
$di_{(rec)M}/dt$	Diode Peak Rate of Fall of Recovery During t_b	—	180	—	A/ μs	$T_J = 25^\circ\text{C}$ See Fig. 17	
		—	120	—		$T_J = 125^\circ\text{C}$	

Notes:

① Repetitive rating; $V_{GE}=20V$, pulse width limited by max. junction temperature. (See fig. 20)

② $V_{CC}=80\%(V_{CES}), V_{GE}=20V, L=10\mu H, R_G = 23\Omega$, (See fig. 19)
③ Pulse width $\leq 80\mu s$; duty factor $\leq 0.1\%$.

④ Pulse width 5.0 μs , single shot.

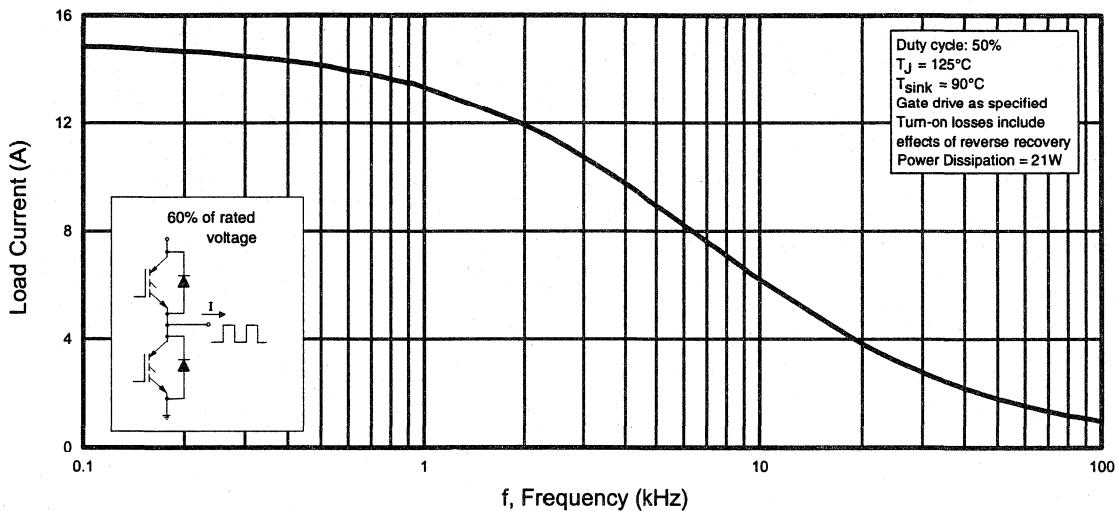


Fig. 1 - Typical Load Current vs. Frequency
(Load Current = I_{RMS} of fundamental)

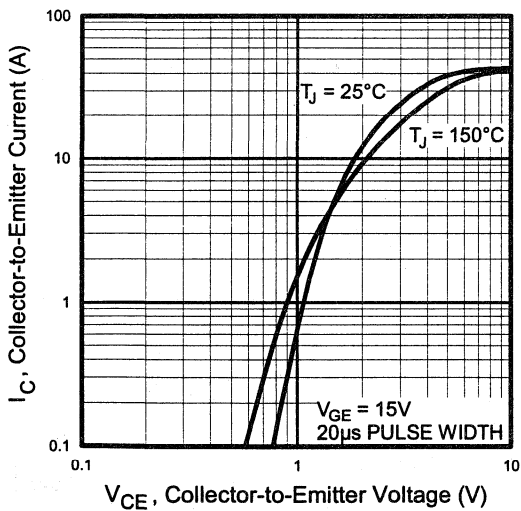


Fig. 2 - Typical Output Characteristics

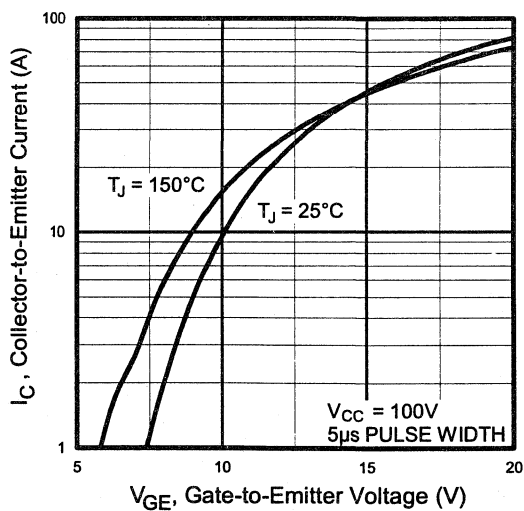


Fig. 3 - Typical Transfer Characteristics

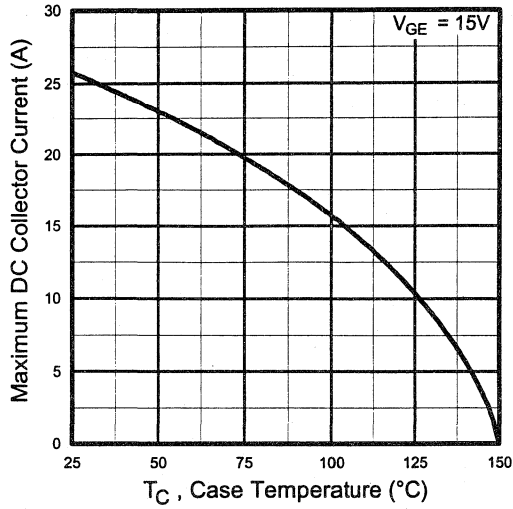


Fig. 4 - Maximum Collector Current vs. Case Temperature

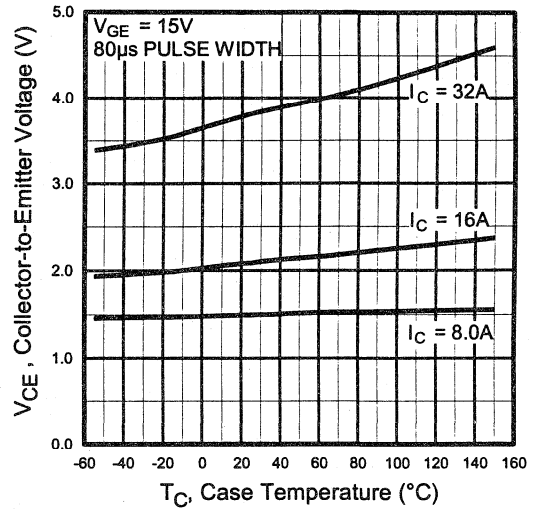


Fig. 5 - Collector-to-Emitter Voltage vs. Case Temperature

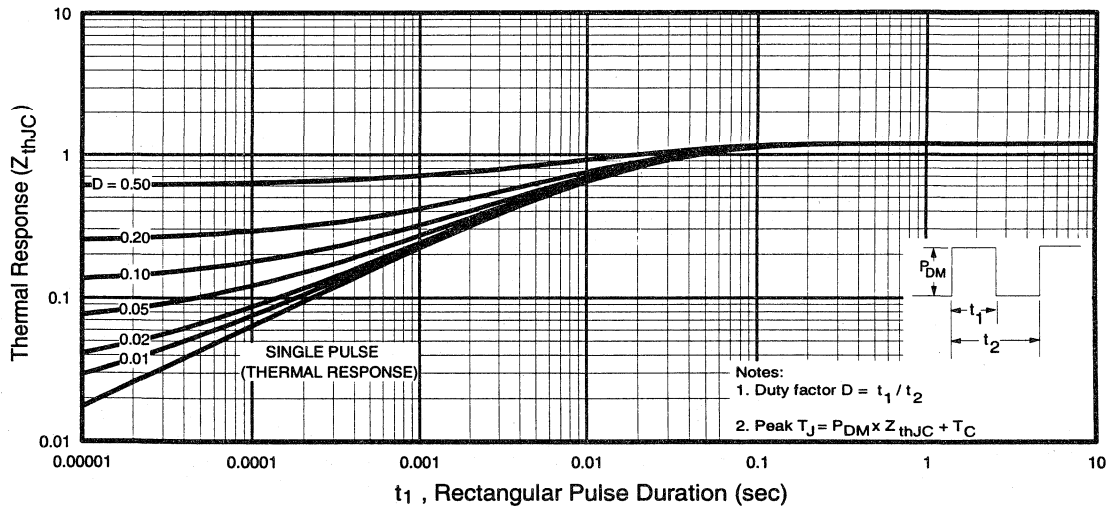


Fig. 6 - Maximum Effective Transient Thermal Impedance, Junction-to-Case

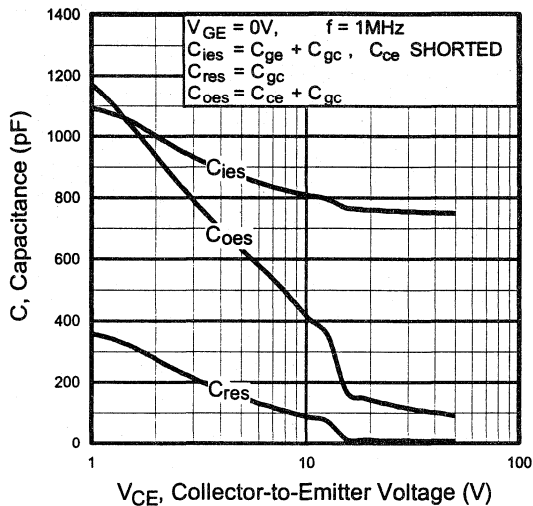


Fig. 7 - Typical Capacitance vs. Collector-to-Emitter Voltage

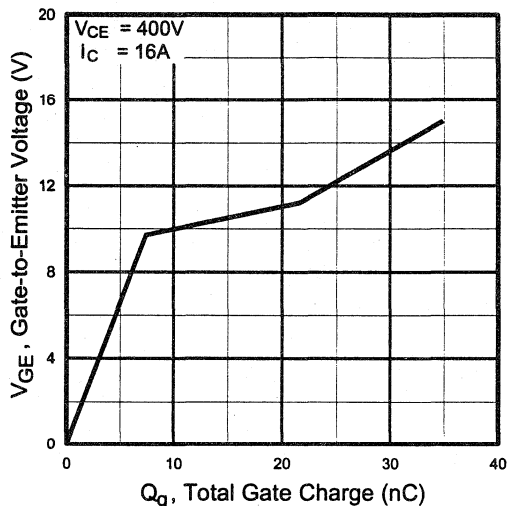


Fig. 8 - Typical Gate Charge vs. Gate-to-Emitter Voltage

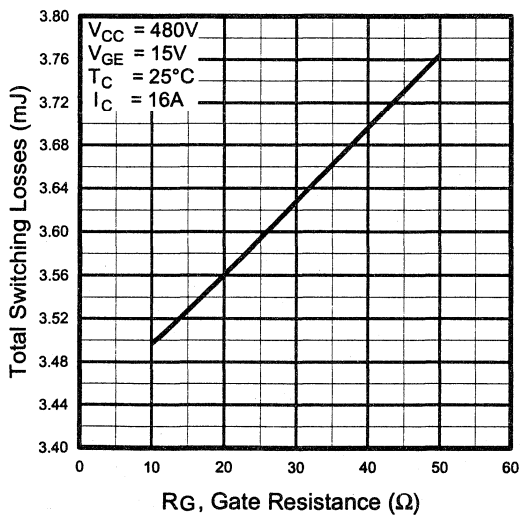


Fig. 9 - Typical Switching Losses vs. Gate Resistance

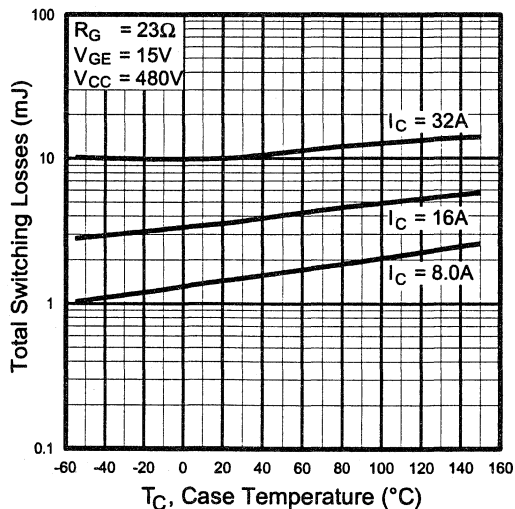


Fig. 10 - Typical Switching Losses vs. Case Temperature

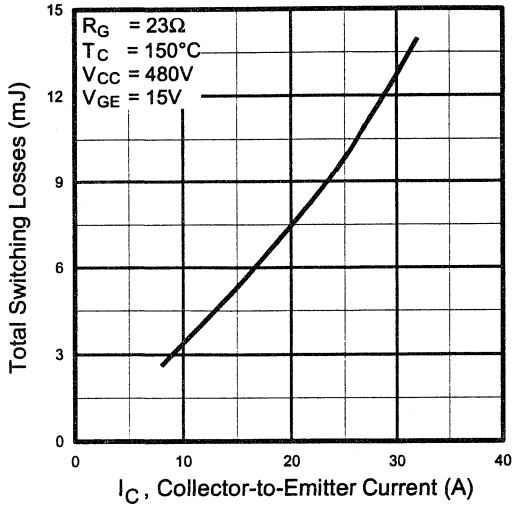


Fig. 11 - Typical Switching Losses vs. Collector-to-Emitter Current

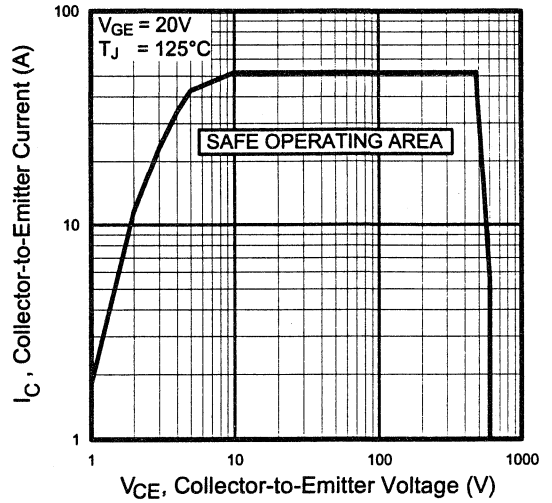


Fig. 12 - Turn-Off SOA

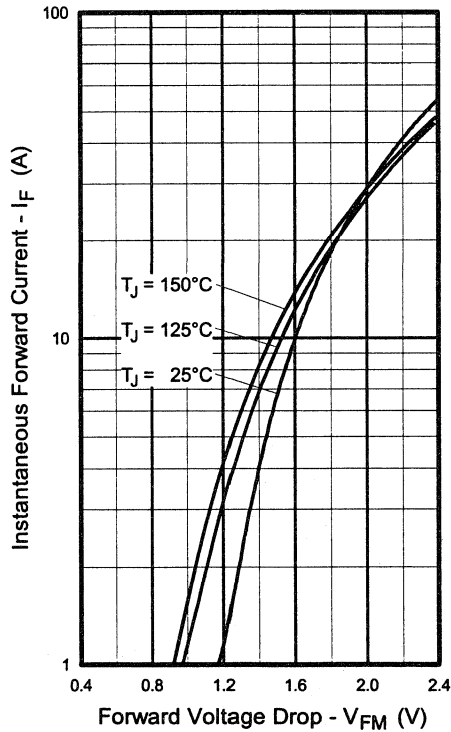


Fig. 13 - Maximum Forward Voltage Drop vs. Instantaneous Forward Current

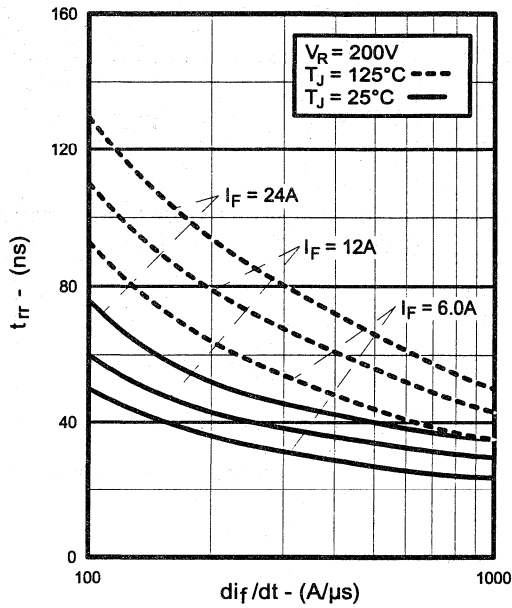


Fig. 14 - Typical Reverse Recovery vs. di_F/dt

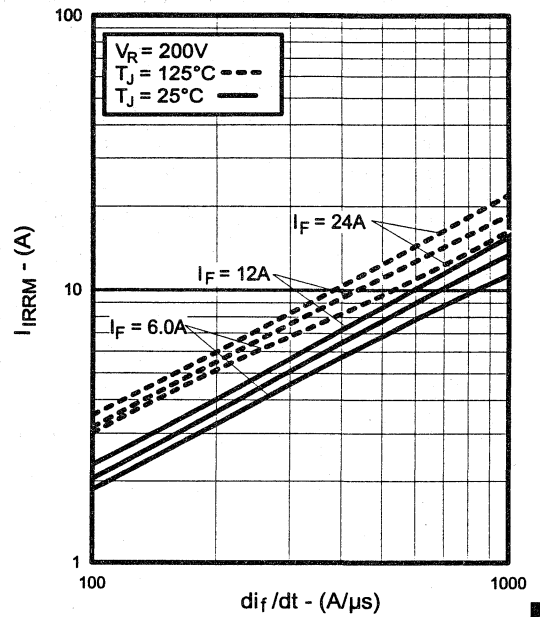


Fig. 15 - Typical Recovery Current vs. di_F/dt

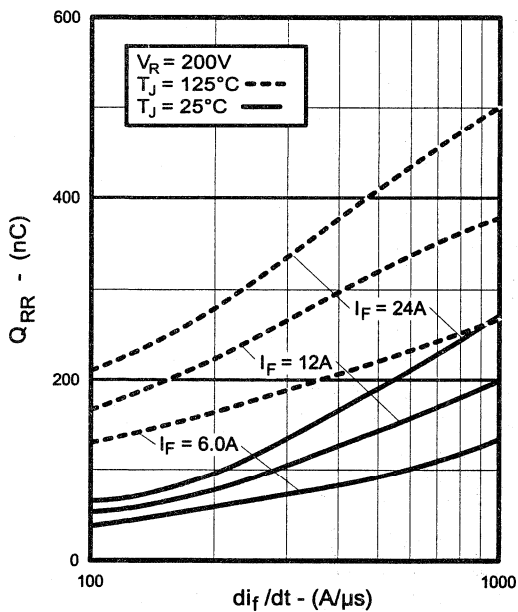


Fig. 16 - Typical Stored Charge vs. di_F/dt

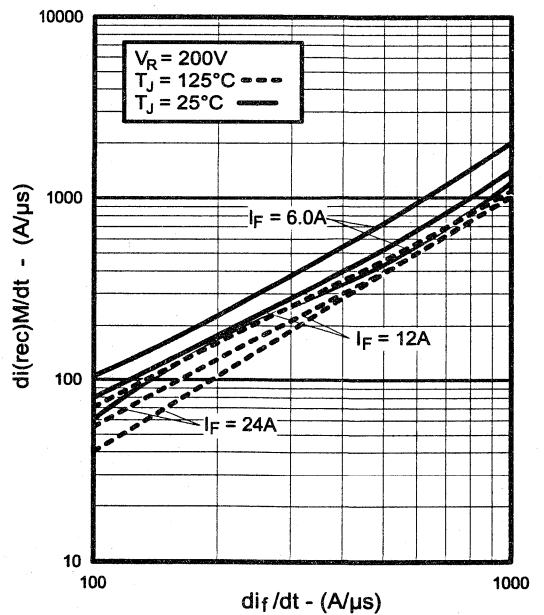


Fig. 17 - Typical $di_{(rec)M}/dt$ vs. di_F/dt

Motor
Control
Fast
Co-Packs

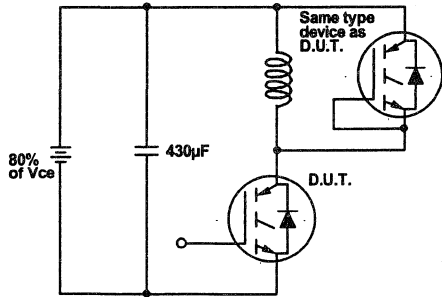


Fig. 18a - Test Circuit for Measurement of I_{LM} , E_{on} , $E_{off}(\text{diode})$, t_{rr} , Q_{rr} , I_{rr} , $t_{d(on)}$, t_r , $t_{d(off)}$, t_f

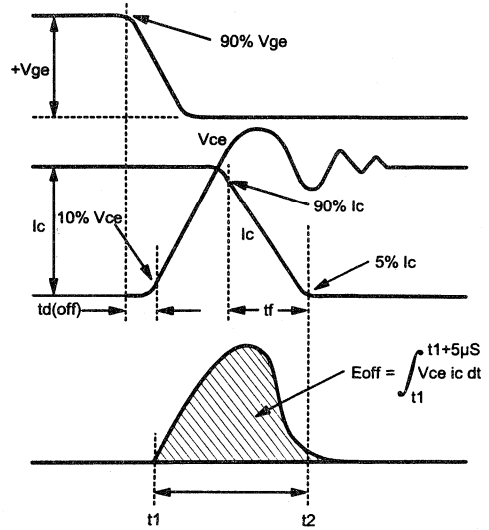


Fig. 18b - Test Waveforms for Circuit of Fig. 18a, Defining E_{off} , $t_{d(off)}$, t_f

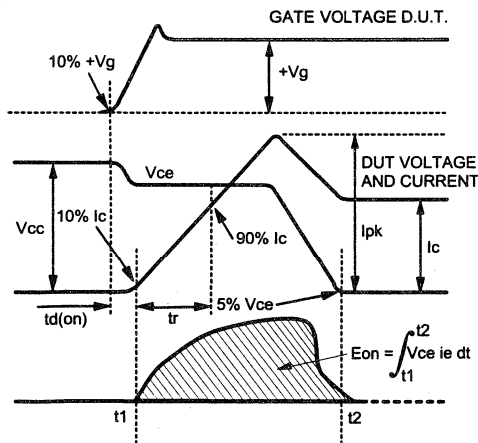


Fig. 18c - Test Waveforms for Circuit of Fig. 18a, Defining E_{on} , $t_{d(on)}$, t_r

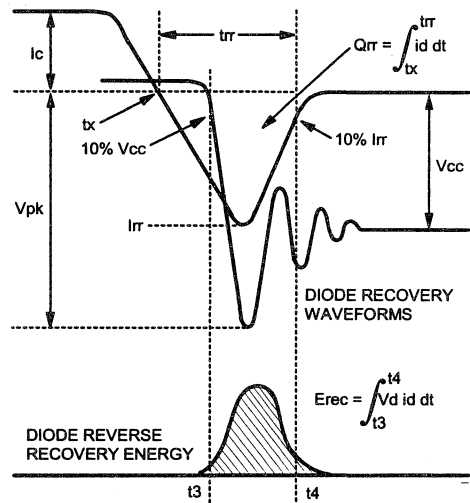


Fig. 18d - Test Waveforms for Circuit of Fig. 18a, Defining E_{rec} , t_{rr} , Q_{rr} , I_{rr}

Refer to Section D for the following:

Appendix D: Section D - page D-6

Fig. 18e - Macro Waveforms for Test Circuit of Fig. 18a

Fig. 19 - Clamped Inductive Load Test Circuit

Fig. 20 - Pulsed Collector Current Test Circuit

IRGPC40MD2

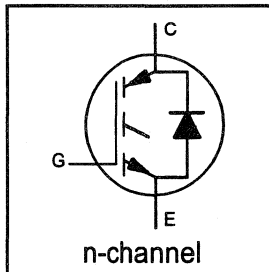
INSULATED GATE BIPOLAR TRANSISTOR
WITH ULTRAFAST SOFT RECOVERY

Short Circuit Rated
Fast CoPack IGBT

DIODE

Features

- Short circuit rated -10 μ s @125°C, $V_{GE} = 15V$
- Switching-loss rating includes all "tail" losses
- HEXFRED™ soft ultrafast diodes
- Optimized for medium operating frequency (1 to 10kHz)



$$V_{CES} = 600V$$

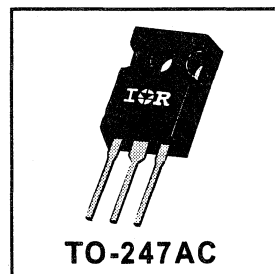
$$V_{CE(sat)} \leq 3.0V$$

$$@V_{GE} = 15V, I_C = 24A$$

Description

Co-packaged IGBTs are a natural extension of International Rectifier's well known IGBT line. They provide the convenience of an IGBT and an ultrafast recovery diode in one package, resulting in substantial benefits to a host of high-voltage, high-current, applications.

These new short circuit rated devices are especially suited for motor control and other applications requiring short circuit withstand capability.



Motor
Control
Fast
Co-Packs

Absolute Maximum Ratings

	Parameter	Max.	Units
V_{CES}	Collector-to-Emitter Voltage	600	V
$I_C @ T_C = 25^\circ C$	Continuous Collector Current	40	A
$I_C @ T_C = 100^\circ C$	Continuous Collector Current	24	
I_{CM}	Pulsed Collector Current ①	80	
I_{LM}	Clamped Inductive Load Current ②	80	
$I_F @ T_C = 100^\circ C$	Diode Continuous Forward Current	15	
I_{FM}	Diode Maximum Forward Current	80	
t_{sc}	Short Circuit Withstand Time	10	μ s
V_{GE}	Gate-to-Emitter Voltage	± 20	V
$P_D @ T_C = 25^\circ C$	Maximum Power Dissipation	160	W
$P_D @ T_C = 100^\circ C$	Maximum Power Dissipation	65	
T_J	Operating Junction and	-55 to +150	°C
T_{STG}	Storage Temperature Range		
	Soldering Temperature, for 10 sec.		
	Mounting Torque, 6-32 or M3 Screw.	10 lbf·in (1.1 N·m)	

Thermal Resistance

	Parameter	Min.	Typ.	Max.	Units
$R_{\theta JC}$	Junction-to-Case - IGBT	—	—	0.77	°C/W
$R_{\theta JC}$	Junction-to-Case - Diode	—	—	1.7	
$R_{\theta CS}$	Case-to-Sink, flat, greased surface	—	0.24	—	
$R_{\theta JA}$	Junction-to-Ambient, typical socket mount	—	—	40	
Wt	Weight	—	6 (0.21)	—	g (oz)

Electrical Characteristics @ T_J = 25°C (unless otherwise specified)

	Parameter	Min.	Typ.	Max.	Units	Conditions
V _{(BR)CES}	Collector-to-Emitter Breakdown Voltage ^①	600	—	—	V	V _{GE} = 0V, I _C = 250μA
ΔV _{(BR)CES} /ΔT _J	Temperature Coeff. of Breakdown Voltage	—	0.70	—	V/°C	V _{GE} = 0V, I _C = 1.0mA
V _{CE(on)}	Collector-to-Emitter Saturation Voltage	—	2.0	3.0	V	I _C = 24A, V _{GE} = 15V
		—	2.6	—		I _C = 40A
		—	2.4	—		I _C = 24A, T _J = 150°C
V _{GE(th)}	Gate Threshold Voltage	3.0	—	5.5		V _{CE} = V _{GE} , I _C = 250μA
ΔV _{GE(th)} /ΔT _J	Temperature Coeff. of Threshold Voltage	—	-12	—	mV/°C	V _{CE} = V _{GE} , I _C = 250μA
g _{fe}	Forward Transconductance ^②	9.2	12	—	S	V _{CE} = 100V, I _C = 24A
I _{CES}	Zero Gate Voltage Collector Current	—	—	250	μA	V _{GE} = 0V, V _{CE} = 600V
		—	—	3500		V _{GE} = 0V, V _{CE} = 600V, T _J = 150°C
V _{FM}	Diode Forward Voltage Drop	—	1.3	1.7	V	I _C = 15A
		—	1.2	1.6		I _C = 15A, T _J = 150°C
I _{GES}	Gate-to-Emitter Leakage Current	—	—	±100	nA	V _{GE} = ±20V

Switching Characteristics @ T_J = 25°C (unless otherwise specified)

	Parameter	Min.	Typ.	Max.	Units	Conditions	
Q _g	Total Gate Charge (turn-on)	—	59	80	nC	I _C = 24A V _{CC} = 400V	
Q _{ge}	Gate - Emitter Charge (turn-on)	—	8.6	10			
Q _{gc}	Gate - Collector Charge (turn-on)	—	25	42			
t _{d(on)}	Turn-On Delay Time	—	26	—	ns	T _J = 25°C I _C = 24A, V _{CC} = 480V V _{GE} = 15V, R _G = 10Ω Energy losses include "tail" and diode reverse recovery.	
t _r	Rise Time	—	37	—			
t _{d(off)}	Turn-Off Delay Time	—	240	410			
t _f	Fall Time	—	230	420			
E _{on}	Turn-On Switching Loss	—	0.75	—	mJ		
E _{off}	Turn-Off Switching Loss	—	1.65	—			
E _{ts}	Total Switching Loss	—	2.4	3.6			
t _{sc}	Short Circuit Withstand Time	10	—	—	μs	V _{CC} = 360V, T _J = 125°C V _{GE} = 15V, R _G = 10Ω, V _{CPK} < 500V	
t _{d(on)}	Turn-On Delay Time	—	28	—	ns	T _J = 150°C, I _C = 24A, V _{CC} = 480V V _{GE} = 15V, R _G = 10Ω Energy losses include "tail" and diode reverse recovery.	
t _r	Rise Time	—	37	—			
t _{d(off)}	Turn-Off Delay Time	—	380	—			
t _f	Fall Time	—	460	—			
E _{ts}	Total Switching Loss	—	4.5	—	mJ		
L _E	Internal Emitter Inductance	—	13	—	nH	Measured 5mm from package	
C _{ies}	Input Capacitance	—	1500	—	pF	V _{GE} = 0V V _{CC} = 30V f = 1.0MHz	
C _{oes}	Output Capacitance	—	190	—			
C _{res}	Reverse Transfer Capacitance	—	20	—			
t _{rr}	Diode Reverse Recovery Time	—	42	60	ns	T _J = 25°C	I _F = 15A V _R = 200V di/dt = 200A/μs
		—	74	120		T _J = 125°C	
I _{rr}	Diode Peak Reverse Recovery Current	—	4.0	6.0	A	T _J = 25°C	
		—	6.5	10		T _J = 125°C	
Q _{rr}	Diode Reverse Recovery Charge	—	80	180	nC	T _J = 25°C	
		—	220	600		T _J = 125°C	
di _(rec) M/dt	Diode Peak Rate of Fall of Recovery During t _b	—	188	—	A/μs	T _J = 25°C	
		—	160	—		T _J = 125°C	

Notes: ① Repetitive rating; V_{GE}=20V, pulse width limited by max. junction temperature. ② V_{CC}=80%(V_{CES}), V_{GE}=20V, L=10μH, R_G= 10Ω. ③ Pulse width ≤ 80μs; duty factor ≤ 0.1%, single shot.

Refer to Section D for the following:

Package Outline 3 - JEDEC Outline TO-247AC

Section D - page D-13

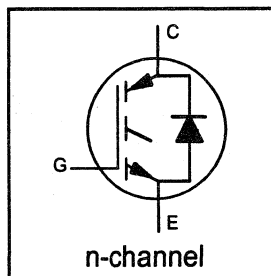
IRGPC50MD2

INSULATED GATE BIPOLAR TRANSISTOR
WITH ULTRAFAST SOFT RECOVERY

Short Circuit Rated
Fast CoPack IGBT

DIODE Features

- Short circuit rated -10 μ s @125°C, $V_{GE} = 15V$
- Switching-loss rating includes all "tail" losses
- HEXFRED™ soft ultrafast diodes
- Optimized for medium operating frequency (1 to 10kHz) See Fig. 1 for Current vs. Frequency curve

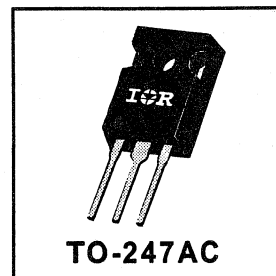


$V_{CES} = 600V$
$V_{CE(sat)} \leq 2.0V$
@ $V_{GE} = 15V, I_C = 35A$

Description

Co-packaged IGBTs are a natural extension of International Rectifier's well known IGBT line. They provide the convenience of an IGBT and an ultrafast recovery diode in one package, resulting in substantial benefits to a host of high-voltage, high-current, applications.

These new short circuit rated devices are especially suited for motor control and other applications requiring short circuit withstand capability.



Motor
Control
Fast
CoPacks

Absolute Maximum Ratings

	Parameter	Max.	Units
V_{CES}	Collector-to-Emitter Voltage	600	V
$I_C @ T_C = 25^\circ C$	Continuous Collector Current	60	A
$I_C @ T_C = 100^\circ C$	Continuous Collector Current	35	
I_{CM}	Pulsed Collector Current ①	120	
I_{LM}	Clamped Inductive Load Current ②	120	
$I_F @ T_C = 100^\circ C$	Diode Continuous Forward Current	25	
I_{FM}	Diode Maximum Forward Current	120	
t_{sc}	Short Circuit Withstand Time	10	μ s
V_{GE}	Gate-to-Emitter Voltage	± 20	V
$P_D @ T_C = 25^\circ C$	Maximum Power Dissipation	200	W
$P_D @ T_C = 100^\circ C$	Maximum Power Dissipation	78	
T_J	Operating Junction and	-55 to +150	$^\circ C$
T_{STG}	Storage Temperature Range		
	Soldering Temperature, for 10 sec.	300 (0.063 in. (1.6mm) from case)	
	Mounting Torque, 6-32 or M3 Screw.	10 lbf·in (1.1 N·m)	

Thermal Resistance

	Parameter	Min.	Typ.	Max.	Units
$R_{\theta JC}$	Junction-to-Case - IGBT	—	—	0.64	$^\circ C/W$
$R_{\theta JC}$	Junction-to-Case - Diode	—	—	0.83	
$R_{\theta CS}$	Case-to-Sink, flat, greased surface	—	0.24	—	
$R_{\theta JA}$	Junction-to-Ambient, typical socket mount	—	—	40	
Wt	Weight	—	6 (0.21)	—	g (oz)

Electrical Characteristics @ $T_J = 25^\circ\text{C}$ (unless otherwise specified)

	Parameter	Min.	Typ.	Max.	Units	Conditions
$V_{(BR)CES}$	Collector-to-Emitter Breakdown Voltage ^②	600	—	—	V	$V_{GE} = 0V, I_C = 250\mu A$
$\Delta V_{(BR)CES}/\Delta T_J$	Temp. Coeff. of Breakdown Voltage	—	0.62	—	V/ $^\circ\text{C}$	$V_{GE} = 0V, I_C = 1.0mA$
$V_{CE(on)}$	Collector-to-Emitter Saturation Voltage	—	1.8	2.0	V	$I_C = 35A$
		—	2.3	—		$I_C = 60A$
		—	2.0	—		$I_C = 35A, T_J = 150^\circ\text{C}$
$V_{GE(th)}$	Gate Threshold Voltage	3.0	—	5.5		$V_{CE} = V_{GE}, I_C = 250\mu A$
$\Delta V_{GE(th)}/\Delta T_J$	Temperature Coeff. of Threshold Voltage	—	-14	—	mV/ $^\circ\text{C}$	$V_{CE} = V_{GE}, I_C = 250\mu A$
g_{fe}	Forward Transconductance ^④	11	20	—	S	$V_{CE} = 100V, I_C = 35A$
I_{CES}	Zero Gate Voltage Collector Current	—	—	250	μA	$V_{GE} = 0V, V_{CE} = 600V$
		—	—	6500		$V_{GE} = 0V, V_{CE} = 600V, T_J = 150^\circ\text{C}$
V_{FM}	Diode Forward Voltage Drop	—	1.3	1.7	V	$I_C = 25A$
		—	1.2	1.5		$I_C = 25A, T_J = 150^\circ\text{C}$
I_{GES}	Gate-to-Emitter Leakage Current	—	—	± 100	nA	$V_{GE} = \pm 20V$

Switching Characteristics @ $T_J = 25^\circ\text{C}$ (unless otherwise specified)

	Parameter	Min.	Typ.	Max.	Units	Conditions
Q_g	Total Gate Charge (turn-on)	—	120	180	nC	$I_C = 35A$
Q_{ge}	Gate - Emitter Charge (turn-on)	—	25	38		$V_{CC} = 400V$
Q_{gc}	Gate - Collector Charge (turn-on)	—	40	60		See Fig. 8
$t_{d(on)}$	Turn-On Delay Time	—	78	—	ns	$T_J = 25^\circ\text{C}$
t_r	Rise Time	—	110	—		$I_C = 35A, V_{CC} = 480V$
$t_{d(off)}$	Turn-Off Delay Time	—	340	510		$V_{GE} = 15V, R_G = 5.0\Omega$
t_f	Fall Time	—	265	400		Energy losses include "tail" and diode reverse recovery.
E_{on}	Turn-On Switching Loss	—	2.1	—		See Fig. 9, 10, 11, 18
E_{off}	Turn-Off Switching Loss	—	4.0	—	mJ	
E_{ts}	Total Switching Loss	—	6.1	9.5		
t_{sc}	Short Circuit Withstand Time	10	—	—	μs	$V_{CC} = 360V, T_J = 125^\circ\text{C}$ $V_{GE} = 15V, R_G = 5.0\Omega, V_{CPK} < 500V$
$t_{d(on)}$	Turn-On Delay Time	—	80	—	ns	$T_J = 150^\circ\text{C}$, See Fig. 9, 10, 11, 18
t_r	Rise Time	—	110	—		$I_C = 35A, V_{CC} = 480V$
$t_{d(off)}$	Turn-Off Delay Time	—	610	—		$V_{GE} = 15V, R_G = 5.0\Omega$
t_f	Fall Time	—	440	—		Energy losses include "tail" and diode reverse recovery.
E_{ts}	Total Switching Loss	—	9.4	—		mJ
L_E	Internal Emitter Inductance	—	13	—	nH	Measured 5mm from package
C_{ies}	Input Capacitance	—	2900	—	pF	$V_{GE} = 0V$
C_{oes}	Output Capacitance	—	230	—		$V_{CC} = 30V$
C_{res}	Reverse Transfer Capacitance	—	30	—		$f = 1.0MHz$
t_{rr}	Diode Reverse Recovery Time	—	50	75	ns	$T_J = 25^\circ\text{C}$ See Fig.
		—	105	160		$T_J = 125^\circ\text{C}$ 14
I_{rr}	Diode Peak Reverse Recovery Current	—	4.5	10	A	$T_J = 25^\circ\text{C}$ See Fig.
		—	8.0	15		$T_J = 125^\circ\text{C}$ 15
Q_{rr}	Diode Reverse Recovery Charge	—	112	375	nC	$T_J = 25^\circ\text{C}$ See Fig.
		—	420	1200		$T_J = 125^\circ\text{C}$ 16
$di_{(rec)M}/dt$	Diode Peak Rate of Fall of Recovery During t_b	—	250	—	A/ μs	$T_J = 25^\circ\text{C}$ See Fig.
		—	160	—		$T_J = 125^\circ\text{C}$ 17

Notes:

① Repetitive rating; $V_{GE}=20V$, pulse width limited by max. junction temperature. (See fig. 20)

② $V_{CE}=80\%(V_{CES}), V_{GE}=20V, L=10\mu H, R_G=5.0\Omega, (\text{ See fig. 19 })$

③ Pulse width $\leq 80\mu s$; duty factor $\leq 0.1\%$.

④ Pulse width 5.0 μs , single shot.

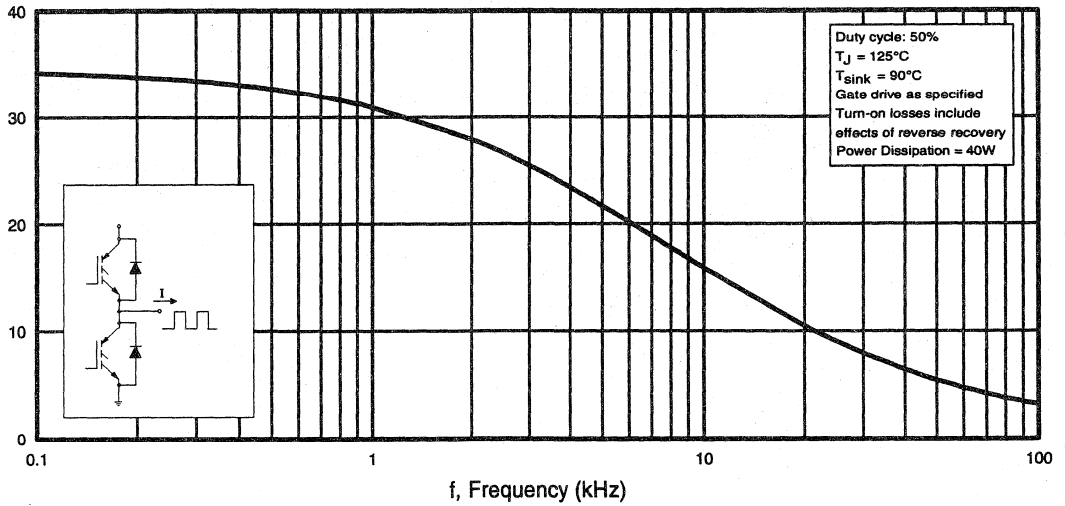


Fig. 1 - Typical Load Current vs. Frequency
 (Load Current = I_{RMS} of fundamental)

Motor Control Fast Car-Brakes

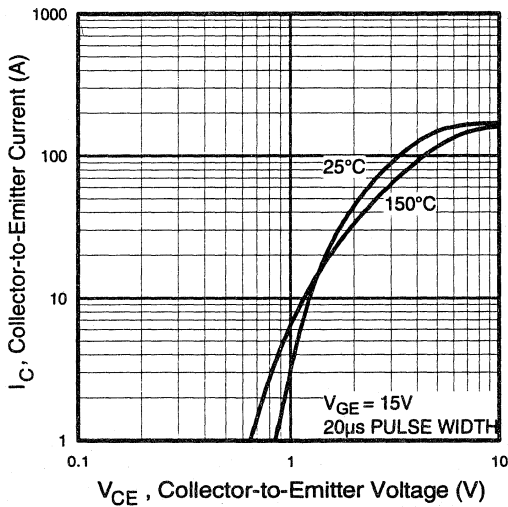


Fig. 2 - Typical Output Characteristics

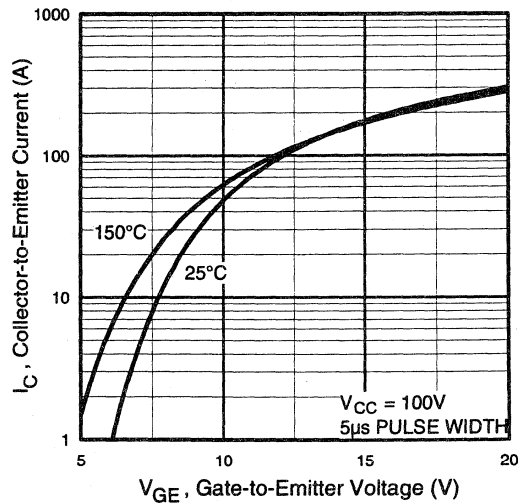


Fig. 3 - Typical Transfer Characteristics

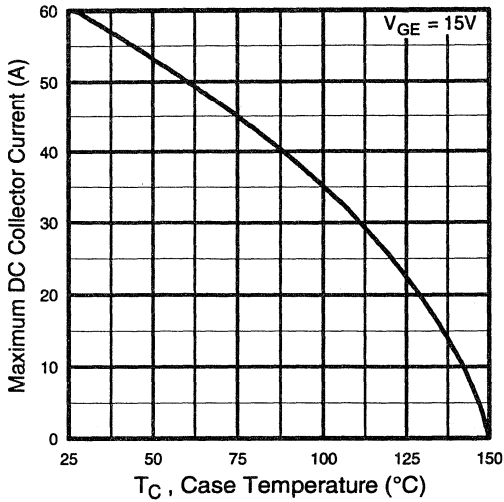


Fig. 4 - Maximum Collector Current vs. Case Temperature

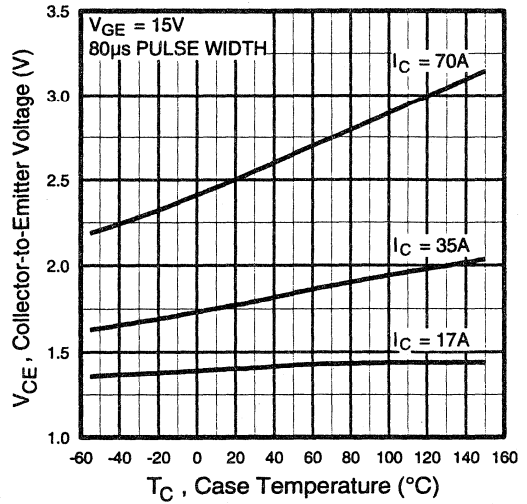


Fig. 5 - Collector-to-Emitter Voltage vs. Case Temperature

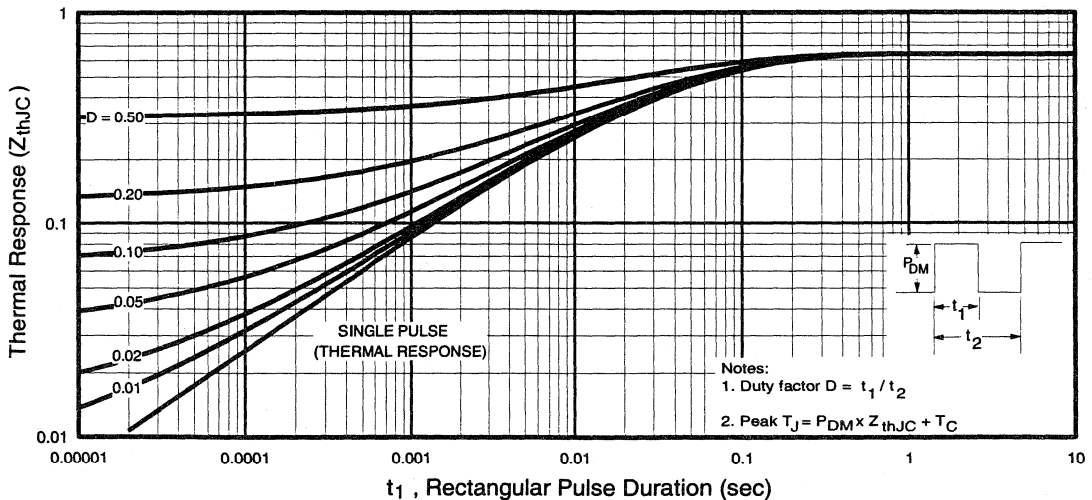


Fig. 6 - Maximum IGBT Effective Transient Thermal Impedance, Junction-to-Case

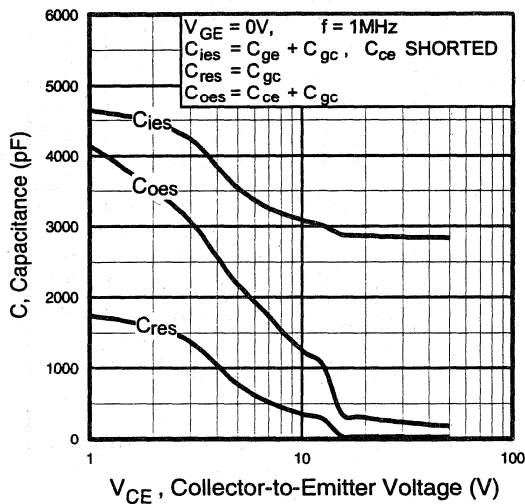


Fig. 7 - Typical Capacitance vs. Collector-to-Emitter Voltage

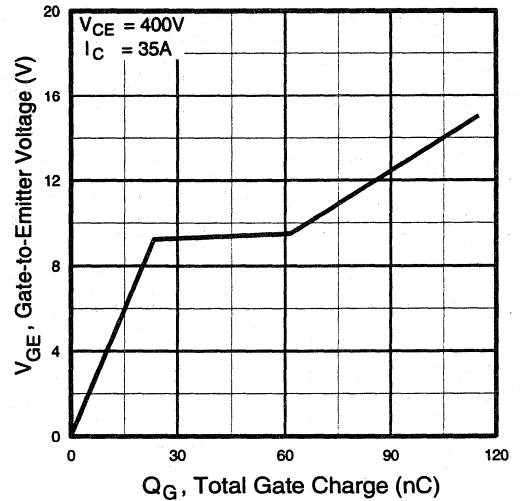


Fig. 8 - Typical Gate Charge vs. Gate-to-Emitter Voltage

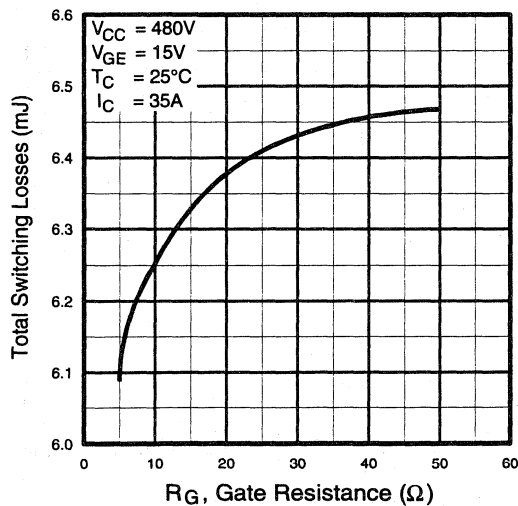


Fig. 9 - Typical Switching Losses vs. Gate Resistance

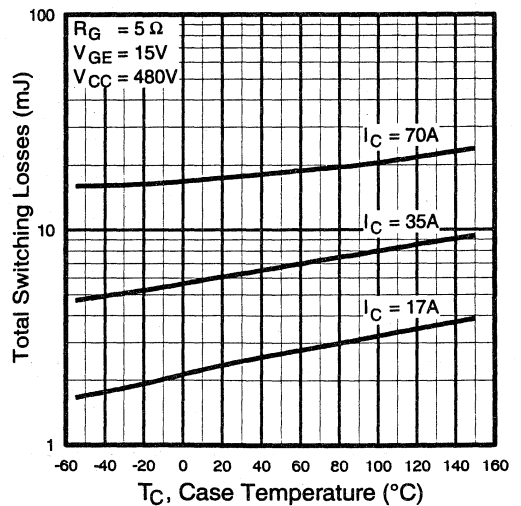


Fig. 10 - Typical Switching Losses vs. Case Temperature

Motor Control Fast Co-Packs

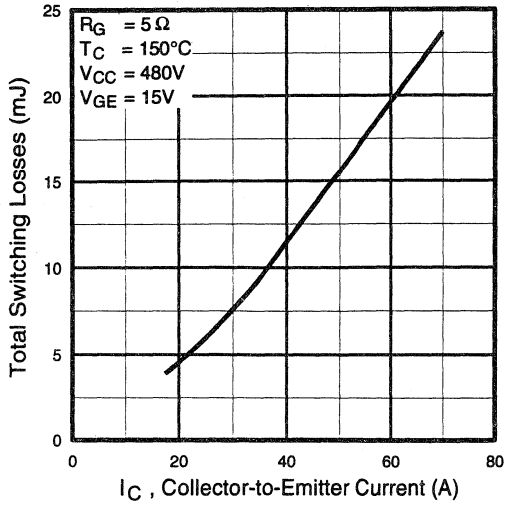


Fig. 11 - Typical Switching Losses vs. Collector-to-Emitter Current

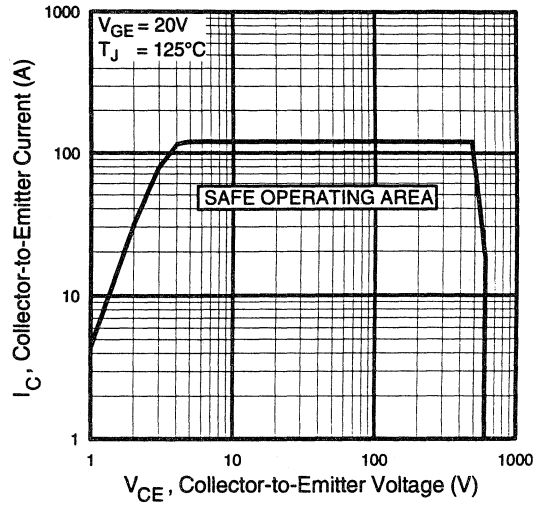


Fig. 12 - Turn-Off SOA

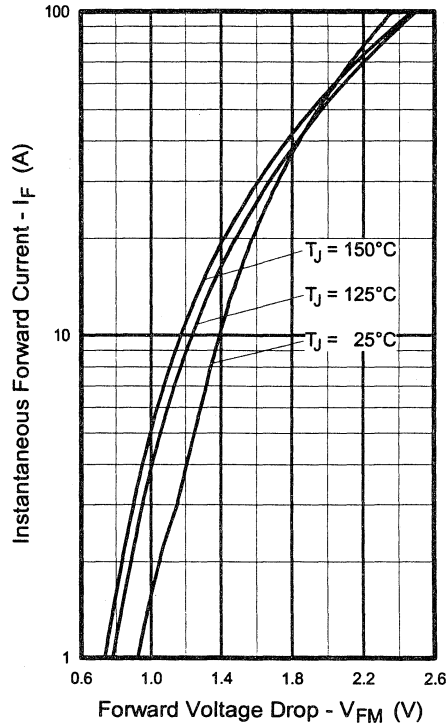


Fig. 13 - Maximum Forward Voltage Drop vs. Instantaneous Forward Current

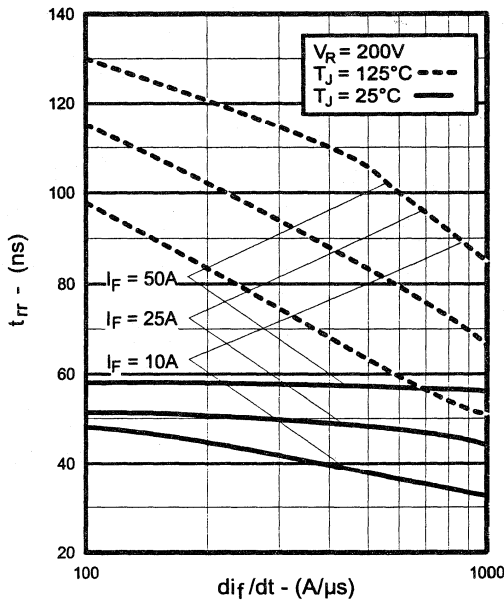


Fig. 14 - Typical Reverse Recovery vs. di_f/dt

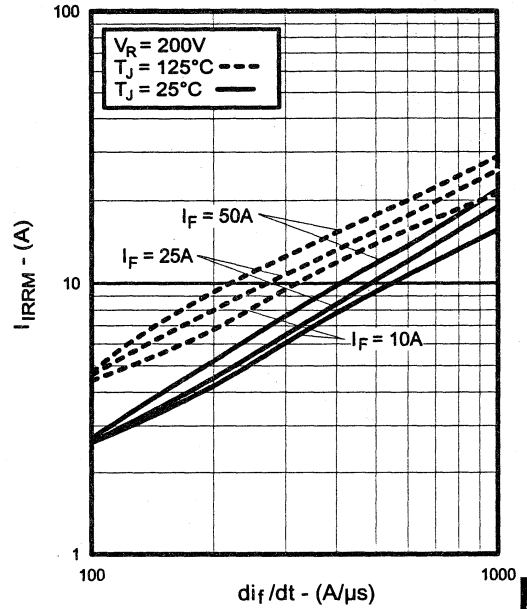


Fig. 15 - Typical Recovery Current vs. di_f/dt

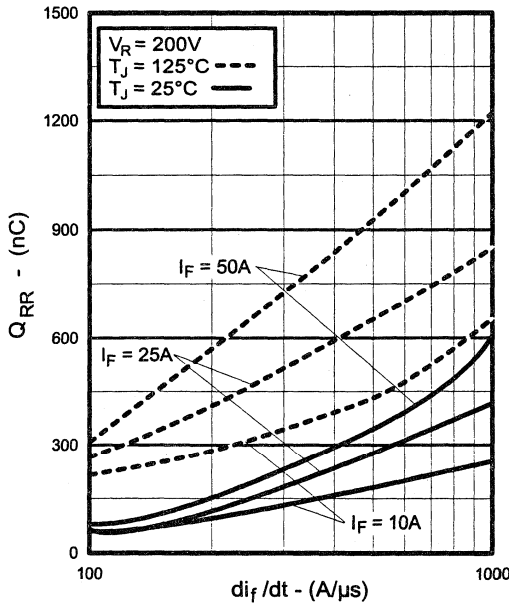


Fig. 16 - Typical Stored Charge vs. di_f/dt

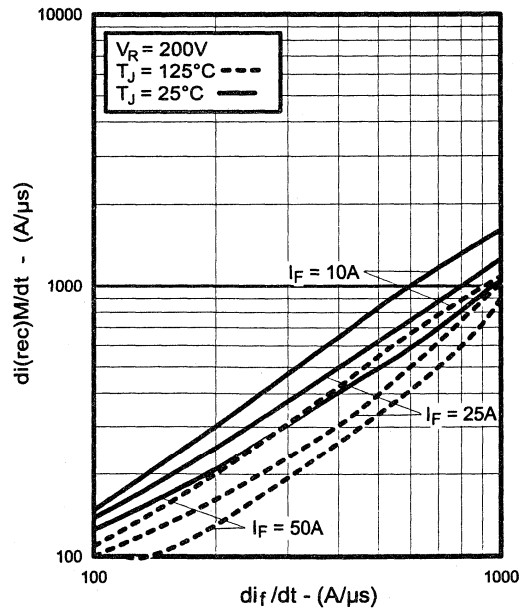


Fig. 17 - Typical $di_{(rec)M}/dt$ vs. di_f/dt

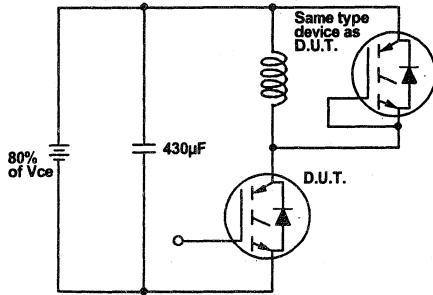


Fig. 18a - Test Circuit for Measurement of I_{LM} , E_{on} , $E_{off}(\text{diode})$, t_{rr} , Q_{rr} , I_{rr} , $t_{d(on)}$, t_r , $t_{d(off)}$, t_f

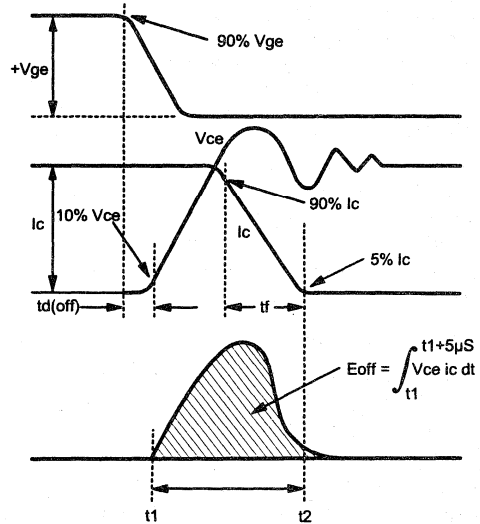


Fig. 18b - Test Waveforms for Circuit of Fig. 18a, Defining E_{off} , $t_{d(off)}$, t_f

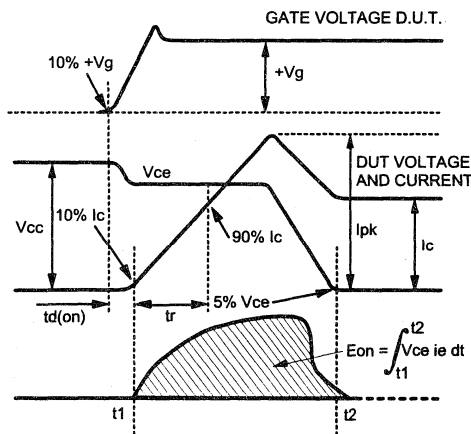


Fig. 18c - Test Waveforms for Circuit of Fig. 18a, Defining E_{on} , $t_{d(on)}$, t_r

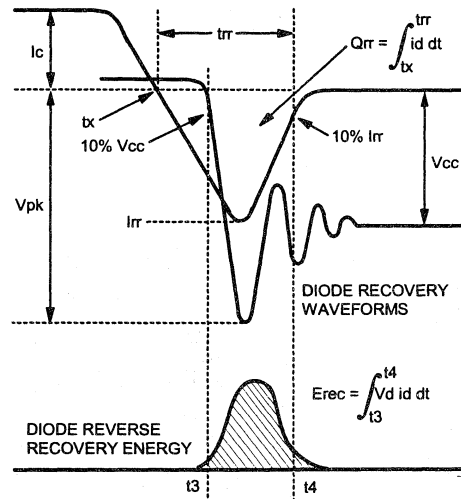


Fig. 18d - Test Waveforms for Circuit of Fig. 18a, Defining E_{rec} , t_{rr} , Q_{rr} , I_{rr}

Refer to Section D for the following:

Appendix D: Section D - page D-6

Fig. 18e - Macro Waveforms for Test Circuit of Fig. 18a

Fig. 19 - Clamped Inductive Load Test Circuit

Fig. 20 - Pulsed Collector Current Test Circuit

IGBT SIP MODULE

Short Circuit Rated Fast IGBT

Features

- Short Circuit Rated - 10 μ s @ 125°C, V_{GE} = 15V Fully isolated printed circuit board mount package
- Switching-loss rating includes all "tail" losses
- HEXFRED™ soft ultrafast diodes
- Optimized for medium operating frequency (1 to 10kHz).

Product Summary

Output Current in a Typical 5.0 kHz Motor Drive

14 A_{RMS} with T_C = 90°C, T_J = 125°C, Supply Voltage 360Vdc, Power Factor 0.8, Modulation Depth 80%.

Description

The IGBT technology is the key to International Rectifier's advanced line of IMS (Insulated Metal Substrate) Power Modules. These modules are more efficient than comparable bipolar transistor modules, while at the same time having the simpler gate-drive requirements of the familiar power MOSFET. This superior technology has now been coupled to a state of the art materials system that maximizes power throughput with low thermal resistance. This package is highly suited to power applications and where space is at a premium.

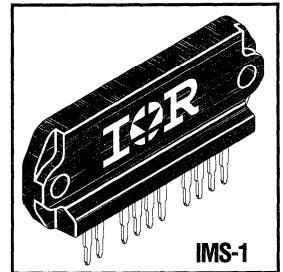
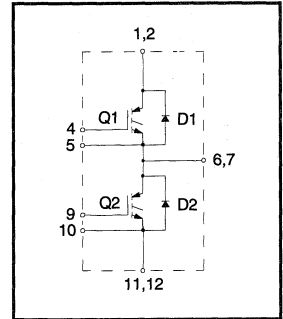
These new short circuit rated devices are especially suited for motor control and other totem-pole applications requiring short circuit withstand capability.

Absolute Maximum Ratings

	Parameter	Max.	Units
V _{CES}	Collector-to-Emitter Voltage	600	V
I _C @ T _C = 25°C	Continuous Collector Current, each IGBT	42	A
I _C @ T _C = 100°C	Continuous Collector Current, each IGBT	23	
I _{CM}	Pulsed Collector Current Ⓞ	120	
I _{LM}	Clamped Inductive Load Current Ⓞ	120	
I _F @ T _C = 100°C	Diode Continuous Forward Current	15	
I _{FM}	Diode Maximum Forward Current	120	
t _{sc}	Short Circuit Withstand Time	10	μ s
V _{GE}	Gate-to-Emitter Voltage	\pm 20	V
V _{ISOL}	Isolation Voltage, any terminal to case, 1 minute	2500	V _{RMS}
P _D @ T _C = 25°C	Maximum Power Dissipation, each IGBT	83	W
P _D @ T _C = 100°C	Maximum Power Dissipation, each IGBT	33	
T _J	Operating Junction and	-40 to +150	°C
T _{STG}	Storage Temperature Range		
	Soldering Temperature, for 10 sec.	300 (0.063 in. (1.6mm) from case)	
	Mounting torque, 6-32 or M3 screw.	5-7 lbf•in (0.55 - 0.8 N•m)	

Thermal Resistance

	Parameter	Typ.	Max.	Units
R _{θJC} (IGBT)	Junction-to-Case, each IGBT, one IGBT in conduction	—	1.5	°C/W
R _{θJC} (DIODE)	Junction-to-Case, each diode, one diode in conduction	—	2.0	
R _{θCS} (MODULE)	Case-to-Sink, flat, greased surface	0.1	—	
Wt	Weight of module	20 (0.7)	—	g (oz)



Motor
Control
Modules

Electrical Characteristics @ $T_J = 25^\circ\text{C}$ (unless otherwise specified)

	Parameter	Min.	Typ.	Max.	Units	Conditions
$V_{(BR)CES}$	Collector-to-Emitter Breakdown Voltage ^③	600	—	—	V	$V_{GE} = 0V, I_C = 250\mu A$
$\Delta V_{(BR)CES}/\Delta T_J$	Temp.Coeff. of Breakdown Voltage	—	0.62	—	V/°C	$V_{GE} = 0V, I_C = 1.0mA$
$V_{CE(on)}$	Collector-to-Emitter Saturation Voltage	—	1.8	2.0	V	$I_C = 35A, V_{GE} = 15V$
		—	2.3	—		$I_C = 60A$
		—	2.0	—		$I_C = 35A, T_J = 150^\circ\text{C}$
$V_{GE(th)}$	Gate Threshold Voltage	3.0	—	5.5		$V_{CE} = V_{GE}, I_C = 250\mu A$
$\Delta V_{GE(th)}/\Delta T_J$	Temp. Coeff. of Threshold Voltage	—	-14	—	mV/°C	$V_{CE} = V_{GE}, I_C = 250\mu A$
g_{fe}	Forward Transconductance ^④	11	20	—	S	$V_{CE} = 100V, I_C = 35A$
I_{CES}	Zero Gate Voltage Collector Current	—	—	250	μA	$V_{GE} = 0V, V_{CE} = 600V$
		—	—	6500		$V_{GE} = 0V, V_{CE} = 600V, T_J = 150^\circ\text{C}$
V_{FM}	Diode Forward Voltage Drop	—	1.3	1.7	V	$I_C = 25A$
		—	1.2	1.5		$I_C = 25A, T_J = 150^\circ\text{C}$
I_{GES}	Gate-to-Emitter Leakage Current	—	—	± 500	nA	$V_{GE} = \pm 20V$

Switching Characteristics @ $T_J = 25^\circ\text{C}$ (unless otherwise specified)

	Parameter	Min.	Typ.	Max.	Units	Conditions	
Q_g	Total Gate Charge (turn-on)	—	120	180	nC	$I_C = 35A$	
Q_{ge}	Gate - Emitter Charge (turn-on)	—	25	38		$V_{CC} = 400V$	
Q_{gc}	Gate - Collector Charge (turn-on)	—	40	60			
$t_{d(on)}$	Turn-On Delay Time	—	78	—	ns	$T_J = 25^\circ\text{C}$	
t_r	Rise Time	—	110	—		$I_C = 35A, V_{CC} = 480V$	
$t_{d(off)}$	Turn-Off Delay Time	—	340	510		$V_{GE} = 15V, R_G = 5.0\Omega$	
t_f	Fall Time	—	265	400		Energy losses include "tail" and diode reverse recovery.	
E_{on}	Turn-On Switching Loss	—	2.1	—		mJ	
E_{off}	Turn-Off Switching Loss	—	4.0	—			
E_{ts}	Total Switching Loss	—	6.1	9.5			
t_{sc}	Short Circuit Withstand Time	10	—	—		μs	$V_{CC} = 360V, T_J = 125^\circ\text{C}$ $V_{GE} = 15V, R_G = 5.0\Omega, V_{CPK} < 500V$
$t_{d(on)}$	Turn-On Delay Time	—	80	—		ns	$T_J = 150^\circ\text{C}$,
t_r	Rise Time	—	110	—			$I_C = 35A, V_{CC} = 480V$
$t_{d(off)}$	Turn-Off Delay Time	—	610	—	$V_{GE} = 15V, R_G = 5.0\Omega$		
t_f	Fall Time	—	440	—	Energy losses include "tail" and diode reverse recovery.		
E_{ts}	Total Switching Loss	—	9.4	—	mJ		
C_{ies}	Input Capacitance	—	2900	—	pF	$V_{GE} = 0V$	
C_{oes}	Output Capacitance	—	230	—		$V_{CC} = 30V$	
C_{res}	Reverse Transfer Capacitance	—	30	—		$f = 1.0MHz$	
t_{rr}	Diode Reverse Recovery Time	—	50	75	ns	$T_J = 25^\circ\text{C}$	
		—	105	160		$T_J = 125^\circ\text{C}$	
I_{rr}	Diode Peak Reverse Recovery Current	—	4.5	10	A	$T_J = 25^\circ\text{C}$	
		—	8.0	15		$T_J = 125^\circ\text{C}$	
Q_{rr}	Diode Reverse Recovery Charge	—	112	375	nC	$T_J = 25^\circ\text{C}$	
		—	420	1200		$T_J = 125^\circ\text{C}$	
$di_{(rec)M}/dt$	Diode Peak Rate of Fall of Recovery During t_b	—	250	—	A/ μs	$T_J = 25^\circ\text{C}$	
		—	160	—		$T_J = 125^\circ\text{C}$	

Notes: ① Repetitive rating; $V_{GE}=20V$, pulse width limited by max. junction temperature.

② $V_{CC}=80\%(V_{CES}), V_{GE}=20V, L=10\mu H, R_G=5.0\Omega$.

④ Pulse width 5.0 μs , single shot.

Refer to Section D for the following: ③ Pulse width $\leq 80\mu s$; duty factor $\leq 0.1\%$.

Package Outline 4 - IMS-1 Package (10 pins) Section D - page D-13

CPV362MM

IGBT SIP MODULE

Short Circuit Rated Fast IGBT

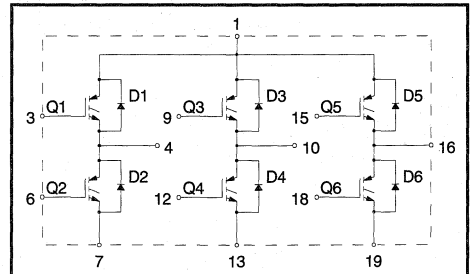
Features

- Short Circuit Rated - $10\mu\text{s}$ @ 125°C , $V_{\text{GE}} = 15\text{V}$
- Fully isolated printed circuit board mount package
- Switching-loss rating includes all "tail" losses
- HEXFRED™ soft ultrafast diodes
- Optimized for medium operating frequency (1 to 10kHz) See Fig. 1 for Current vs. Frequency curve

Product Summary

Output Current in a Typical 5.0 kHz Motor Drive

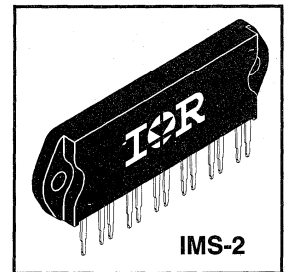
4.6 A_{RMS} per phase (1.4 kW total) with $T_{\text{C}} = 90^\circ\text{C}$, $T_{\text{J}} = 125^\circ\text{C}$, Supply Voltage 360Vdc, Power Factor 0.8, Modulation Depth 80% (See Figure 1)



Description

The IGBT technology is the key to International Rectifier's advanced line of IMS (Insulated Metal Substrate) Power Modules. These modules are more efficient than comparable bipolar transistor modules, while at the same time having the simpler gate-drive requirements of the familiar power MOSFET. This superior technology has now been coupled to a state of the art materials system that maximizes power throughput with low thermal resistance. This package is highly suited to power applications and where space is at a premium.

These new short circuit rated devices are especially suited for motor control and other totem-pole applications requiring short circuit withstand capability.



Motor Control Fast Modules

Absolute Maximum Ratings

	Parameter	Max.	Units
V_{CES}	Collector-to-Emitter Voltage	600	V
$I_{\text{C}} @ T_{\text{C}} = 25^\circ\text{C}$	Continuous Collector Current, each IGBT	7.9	A
$I_{\text{C}} @ T_{\text{C}} = 100^\circ\text{C}$	Continuous Collector Current, each IGBT	4.6	
I_{CM}	Pulsed Collector Current $\text{\textcircled{D}}$	16	
I_{LM}	Clamped Inductive Load Current $\text{\textcircled{D}}$	16	
$I_{\text{F}} @ T_{\text{C}} = 100^\circ\text{C}$	Diode Continuous Forward Current	3.4	
I_{FM}	Diode Maximum Forward Current	16	
t_{sc}	Short Circuit Withstand Time	10	μs
V_{GE}	Gate-to-Emitter Voltage	± 20	V
V_{ISOL}	Isolation Voltage, any terminal to case, 1 minute	2500	V_{RMS}
$P_{\text{D}} @ T_{\text{C}} = 25^\circ\text{C}$	Maximum Power Dissipation, each IGBT	23	W
$P_{\text{D}} @ T_{\text{C}} = 100^\circ\text{C}$	Maximum Power Dissipation, each IGBT	9.1	
T_{J}	Operating Junction and	-40 to +150	$^\circ\text{C}$
T_{STG}	Storage Temperature Range		
	Soldering Temperature, for 10 sec.	300 (0.063 in. (1.6mm) from case)	
	Mounting torque, 6-32 or M3 screw.	5-7 lbf•in (0.55 - 0.8 N•m)	

Thermal Resistance

	Parameter	Typ.	Max.	Units
$R_{\theta\text{JC}}$ (IGBT)	Junction-to-Case, each IGBT, one IGBT in conduction	—	5.5	$^\circ\text{C}/\text{W}$
$R_{\theta\text{JC}}$ (DIODE)	Junction-to-Case, each diode, one diode in conduction	—	9.0	
$R_{\theta\text{CS}}$ (MODULE)	Case-to-Sink, flat, greased surface	0.1	—	g (oz)
Wt	Weight of module	20 (0.7)	—	

Electrical Characteristics @ $T_J = 25^\circ\text{C}$ (unless otherwise specified)

	Parameter	Min.	Typ.	Max.	Units	Conditions
$V_{(BR)CES}$	Collector-to-Emitter Breakdown Voltage ^③	600	—	—	V	$V_{GE} = 0V, I_C = 250\mu A$
$\Delta V_{(BR)CES}/\Delta T_J$	Temperature Coeff. of Breakdown Voltage	—	0.42	—	V/ $^\circ\text{C}$	$V_{GE} = 0V, I_C = 1.0mA$
$V_{CE(on)}$	Collector-to-Emitter Saturation Voltage	—	2.2	3.3	V	$I_C = 4.6A, V_{GE} = 15V$
		—	2.8	—		$I_C = 7.9A$
		—	2.5	—		$I_C = 4.6A, T_J = 150^\circ\text{C}$
$V_{GE(th)}$	Gate Threshold Voltage	3.0	—	5.5		$V_{CE} = V_{GE}, I_C = 250\mu A$
$\Delta V_{GE(th)}/\Delta T_J$	Temperature Coeff. of Threshold Voltage	—	-11	—	mV/ $^\circ\text{C}$	$V_{CE} = V_{GE}, I_C = 250\mu A$
g_{fe}	Forward Transconductance ^④	2.7	3.8	—	S	$V_{CE} = 100V, I_C = 8.0A$
I_{CES}	Zero Gate Voltage Collector Current	—	—	250	μA	$V_{GE} = 0V, V_{CE} = 600V$
		—	—	1700		$V_{GE} = 0V, V_{CE} = 600V, T_J = 150^\circ\text{C}$
V_{FM}	Diode Forward Voltage Drop	—	1.4	1.7	V	$I_C = 8.0A$
		—	1.3	1.6		$I_C = 8.0A, T_J = 150^\circ\text{C}$
I_{GES}	Gate-to-Emitter Leakage Current	—	—	± 500	nA	$V_{GE} = \pm 20V$

Switching Characteristics @ $T_J = 25^\circ\text{C}$ (unless otherwise specified)

	Parameter	Min.	Typ.	Max.	Units	Conditions
Q_g	Total Gate Charge (turn-on)	—	16	24	nC	$I_C = 8.0A$
Q_{ge}	Gate - Emitter Charge (turn-on)	—	3.6	5.2		$V_{CC} = 400V$
Q_{gc}	Gate - Collector Charge (turn-on)	—	6.0	9.0		See Fig. 8
$t_{d(on)}$	Turn-On Delay Time	—	66	—	ns	$T_J = 25^\circ\text{C}$
t_r	Rise Time	—	28	—		$I_C = 4.6A, V_{CC} = 480V$
$t_{d(off)}$	Turn-Off Delay Time	—	140	210		$V_{GE} = 15V, R_G = 50\Omega$
t_f	Fall Time	—	53	100		Energy losses include "tail" and diode reverse recovery.
E_{on}	Turn-On Switching Loss	—	0.18	—		mJ
E_{off}	Turn-Off Switching Loss	—	0.14	—		
E_{ts}	Total Switching Loss	—	0.32	0.48		
t_{sc}	Short Circuit Withstand Time	10	—	—	μs	$V_{CC} = 360V, T_J = 125^\circ\text{C}$ $V_{GE} = 15V, R_G = 50\Omega, V_{CPK} < 500V$
$t_{d(on)}$	Turn-On Delay Time	—	64	—	ns	$T_J = 150^\circ\text{C}$, See Fig. 9, 10, 11, 18
t_r	Rise Time	—	25	—		$I_C = 4.6A, V_{CC} = 480V$
$t_{d(off)}$	Turn-Off Delay Time	—	240	—		$V_{GE} = 15V, R_G = 50\Omega$
t_f	Fall Time	—	160	—		Energy losses include "tail" and diode reverse recovery.
E_{ts}	Total Switching Loss	—	0.56	—		mJ
C_{ies}	Input Capacitance	—	365	—	pF	$V_{GE} = 0V$
C_{oes}	Output Capacitance	—	47	—		$V_{CC} = 30V$
C_{res}	Reverse Transfer Capacitance	—	4.8	—		$f = 1.0MHz$
t_{rr}	Diode Reverse Recovery Time	—	37	55	ns	$T_J = 25^\circ\text{C}$ See Fig. 14
		—	55	90		$T_J = 125^\circ\text{C}$
I_{rr}	Diode Peak Reverse Recovery Current	—	3.5	5.0	A	$T_J = 25^\circ\text{C}$ See Fig. 15
		—	4.5	8.0		$T_J = 125^\circ\text{C}$
Q_{rr}	Diode Reverse Recovery Charge	—	65	138	nC	$T_J = 25^\circ\text{C}$ See Fig. 16
		—	124	360		$T_J = 125^\circ\text{C}$
$di_{(rec)M}/dt$	Diode Peak Rate of Fall of Recovery During t_b	—	240	—	A/ μs	$T_J = 25^\circ\text{C}$ See Fig. 17
		—	210	—		$T_J = 125^\circ\text{C}$

Notes:

① Repetitive rating; $V_{GE}=20V$, pulse width limited by max. junction temperature. (See fig. 20)

② $V_{CC}=80\%(V_{CES}), V_{GE}=20V, L=10\mu H, R_G=50\Omega$, (See fig. 19)

③ Pulse width $\leq 80\mu s$; duty factor $\leq 0.1\%$.

④ Pulse width 5.0 μs , single shot.

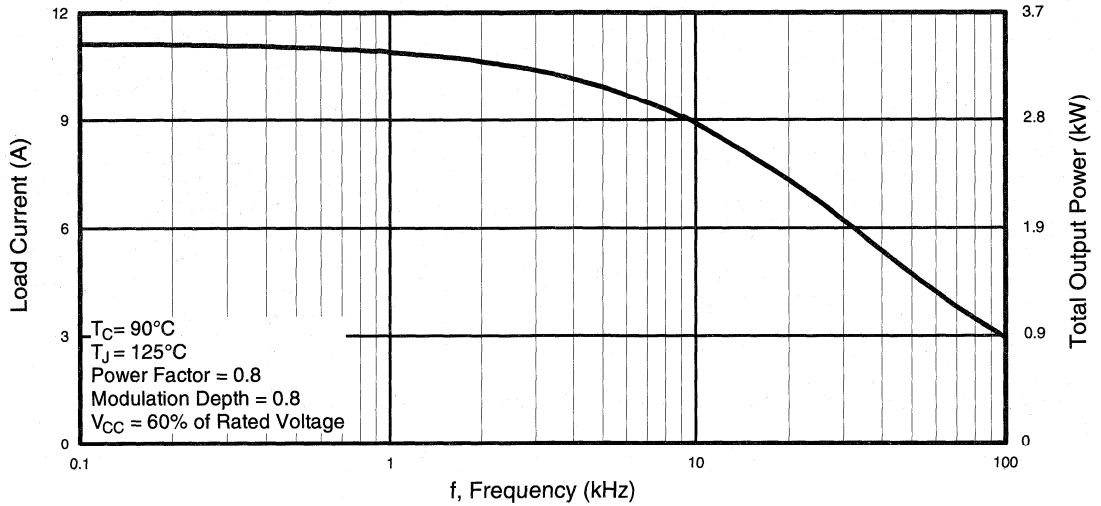


Fig. 1 - RMS Current and Output Power, Synthesized Sine Wave

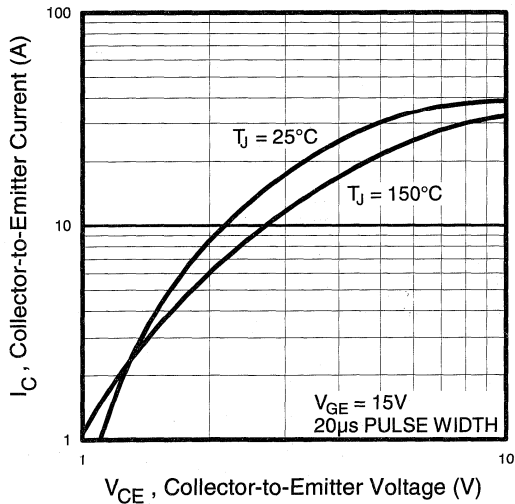


Fig. 2 - Typical Output Characteristics

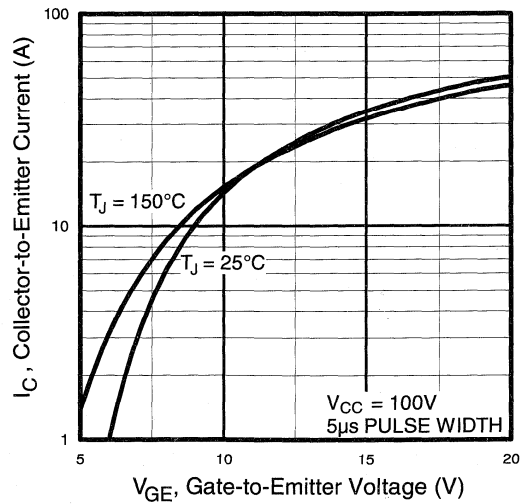


Fig. 3 - Typical Transfer Characteristics

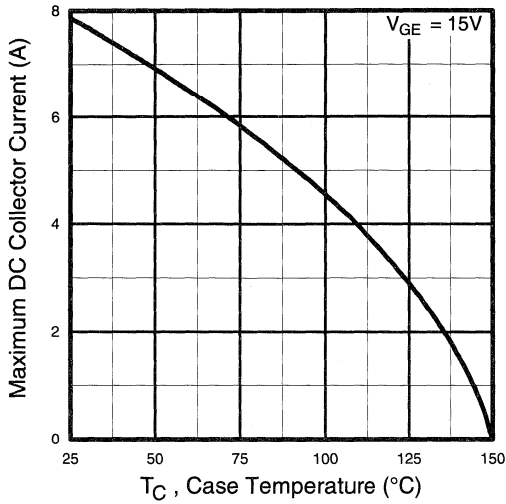


Fig. 4 - Maximum Collector Current vs. Case Temperature

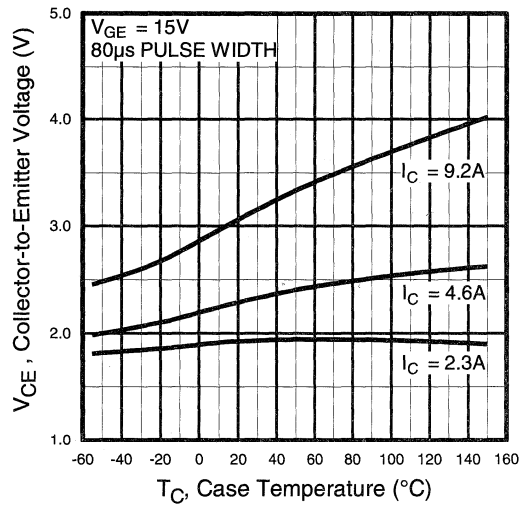


Fig. 5 - Collector-to-Emitter Voltage vs. Case Temperature

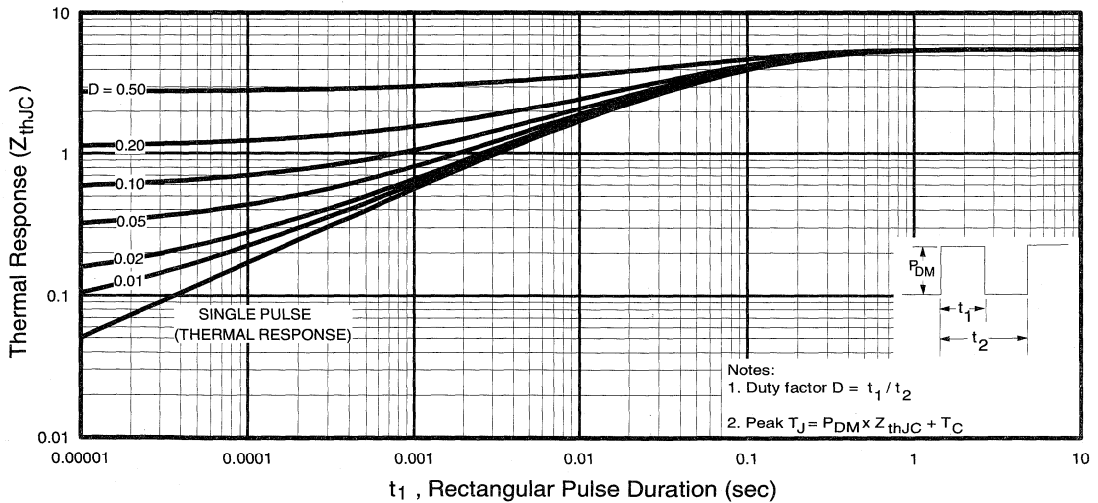


Fig. 6 - Maximum IGBT Effective Transient Thermal Impedance, Junction-to-Case

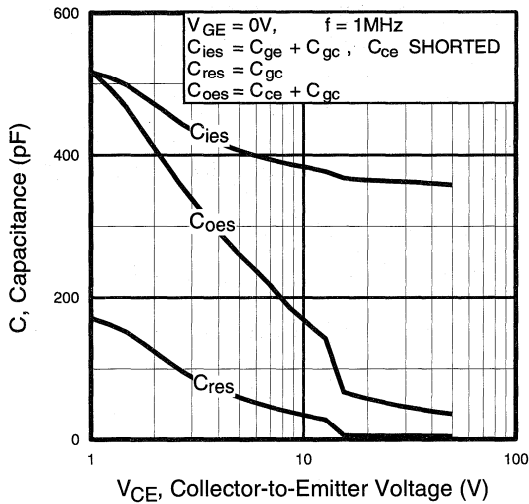


Fig. 7 - Typical Capacitance vs. Collector-to-Emitter Voltage

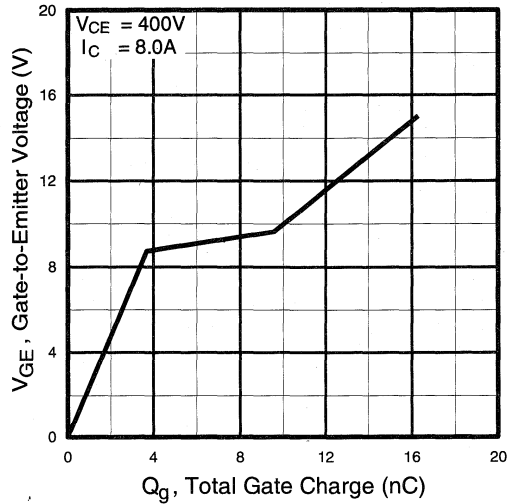


Fig. 8 - Typical Gate Charge vs. Gate-to-Emitter Voltage

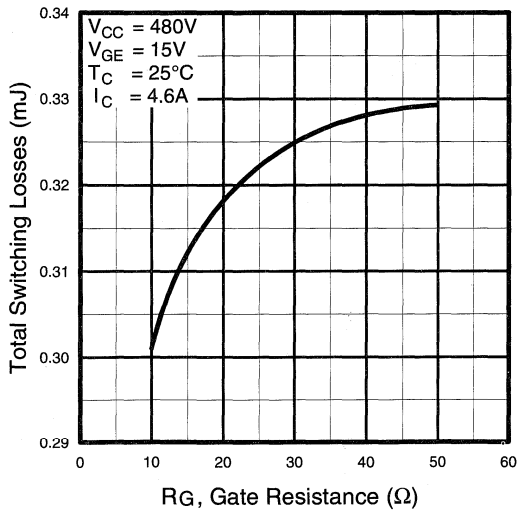


Fig. 9 - Typical Switching Losses vs. Gate Resistance

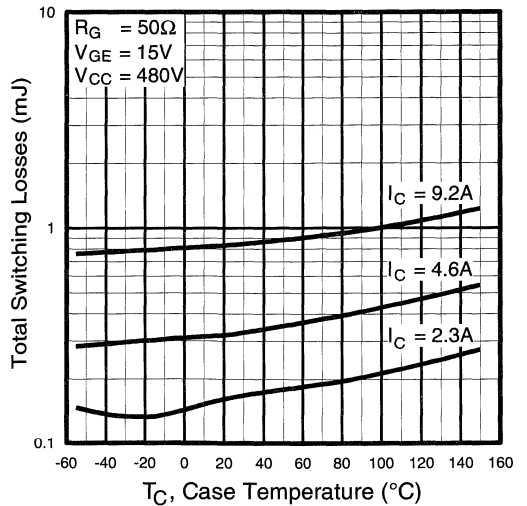


Fig. 10 - Typical Switching Losses vs. Case Temperature

Motor
Control
Fast
Modules

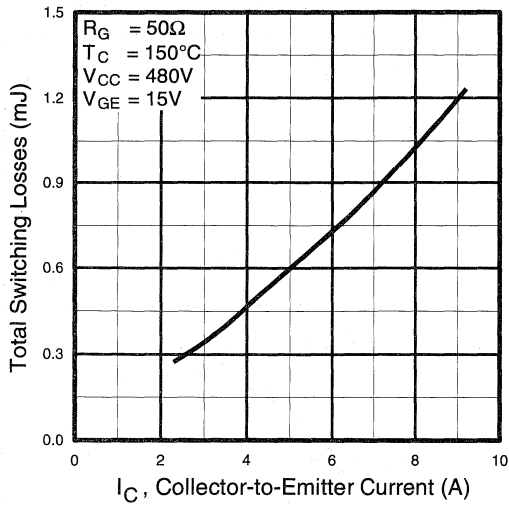


Fig. 11 - Typical Switching Losses vs. Collector-to-Emitter Current

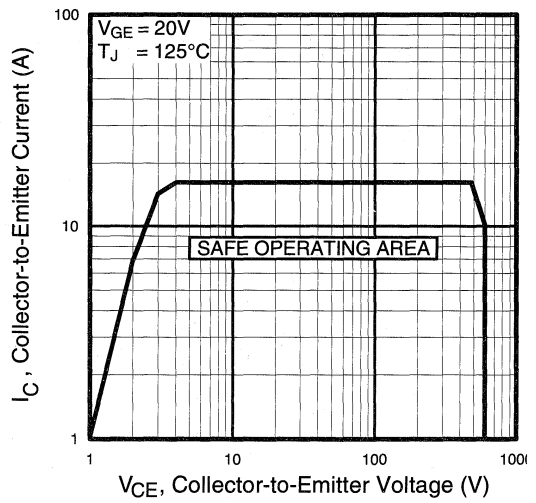


Fig. 12 - Turn-Off SOA

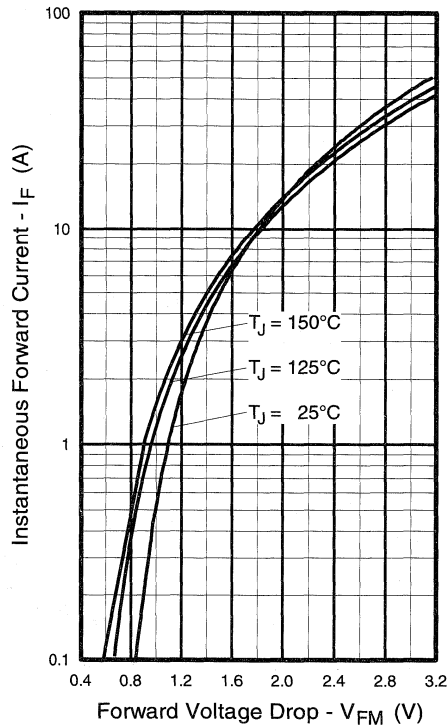


Fig. 13 - Maximum Forward Voltage Drop vs. Instantaneous Forward Current

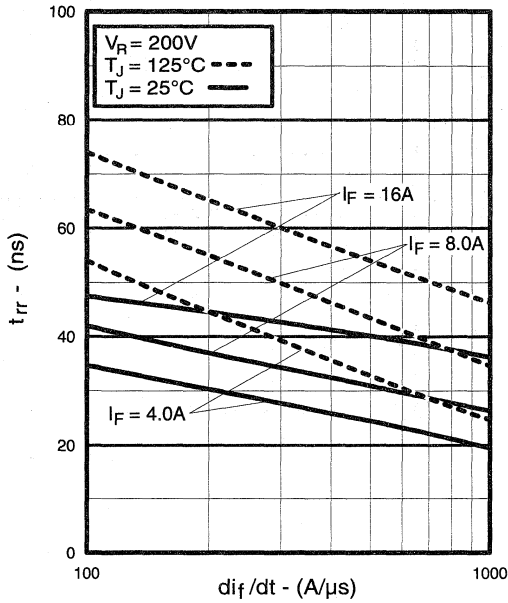


Fig. 14 - Typical Reverse Recovery vs. di_f/dt

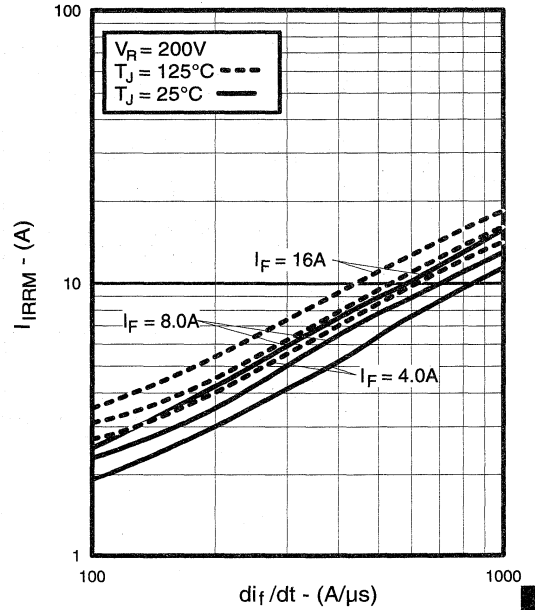


Fig. 15 - Typical Recovery Current vs. di_f/dt

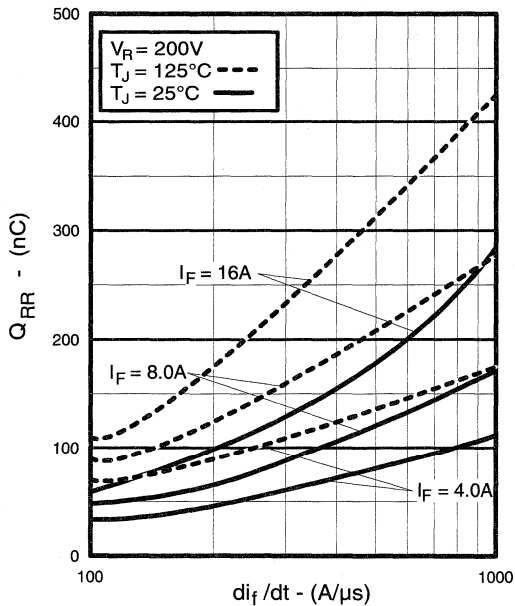


Fig. 16 - Typical Stored Charge vs. di_f/dt

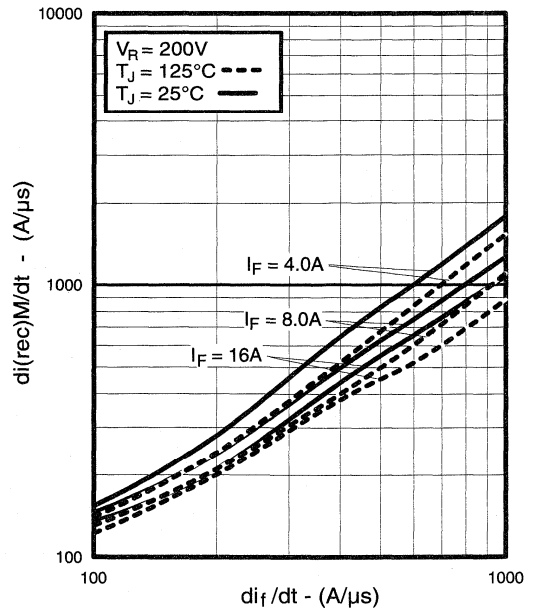


Fig. 17 - Typical $di_{(rec)M}/dt$ vs. di_f/dt

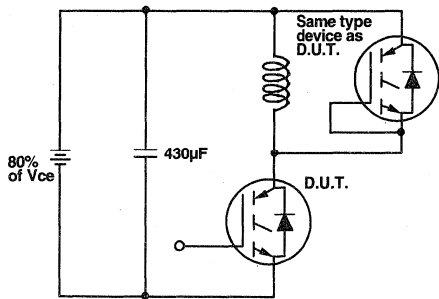


Fig. 18a - Test Circuit for Measurement of I_{LM} , V_{on} , $E_{off}(\text{diode})$, t_{rr} , Q_{rr} , I_{rr} , $t_{d(on)}$, t_r , $t_{d(off)}$, t_f

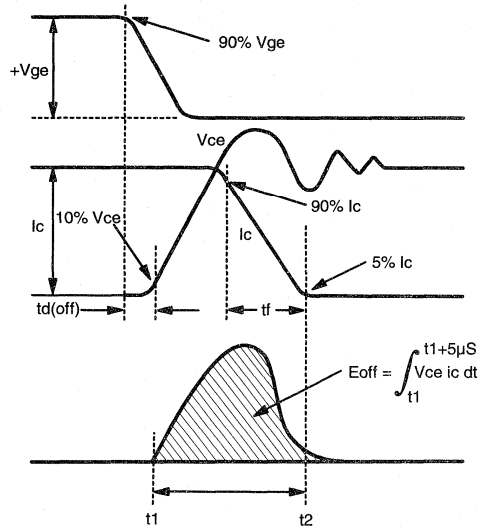


Fig. 18b - Test Waveforms for Circuit of Fig. 18a, Defining E_{off} , $t_{d(off)}$, t_f

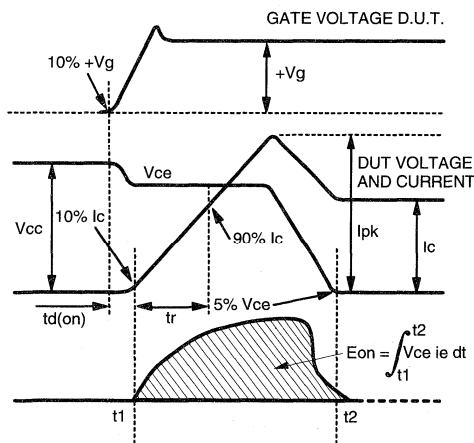


Fig. 18c - Test Waveforms for Circuit of Fig. 18a, Defining E_{on} , $t_{d(on)}$, t_r

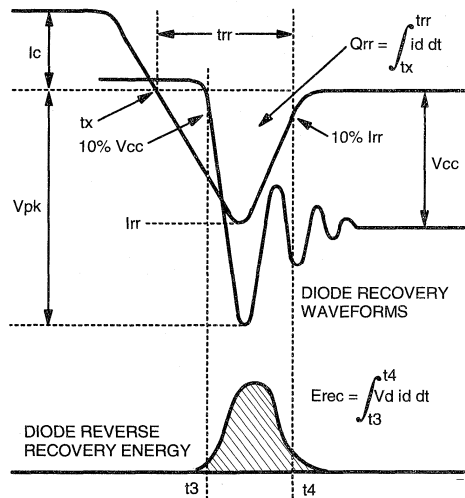


Fig. 18d - Test Waveforms for Circuit of Fig. 18a, Defining E_{rec} , t_{rr} , Q_{rr} , I_{rr}

Refer to Section D for the following:

Appendix D: Section D - page D-6

Fig. 18e - Macro Waveforms for Test Circuit of Fig. 18a

Fig. 19 - Clamped Inductive Load Test Circuit

Fig. 20 - Pulsed Collector Current Test Circuit

IGBT SIP MODULE

Short Circuit Rated Fast IGBT

Features

- Short Circuit Rated - $10\mu\text{s}$ @ 125°C , $V_{\text{GE}} = 15\text{V}$
- Fully isolated printed circuit board mount package
- Switching-loss rating includes all "tail" losses
- HEXFRED™ soft ultrafast diodes
- Optimized for medium operating frequency (1 to 10kHz) See Fig. 1 for Current vs. Frequency curve

Product Summary

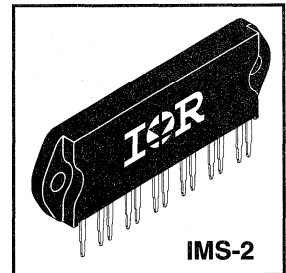
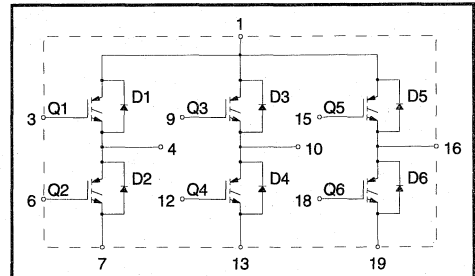
Output Current in a Typical 5.0 kHz Motor Drive

7.65 A_{RMS} per phase (2.4 kW total) with $T_{\text{C}} = 90^\circ\text{C}$, $T_{\text{J}} = 125^\circ\text{C}$, Supply Voltage 360Vdc, Power Factor 0.8, Modulation Depth 80% (See Figure 1)

Description

The IGBT technology is the key to International Rectifier's advanced line of IMS (Insulated Metal Substrate) Power Modules. These modules are more efficient than comparable bipolar transistor modules, while at the same time having the simpler gate-drive requirements of the familiar power MOSFET. This superior technology has now been coupled to a state of the art materials system that maximizes power throughput with low thermal resistance. This package is highly suited to power applications and where space is at a premium.

These new short circuit rated devices are especially suited for motor control and other totem-pole applications requiring short circuit withstand capability.



Motor
Control
Fast
Modules

Absolute Maximum Ratings

	Parameter	Max.	Units
V_{CES}	Collector-to-Emitter Voltage	600	V
$I_{\text{C}} @ T_{\text{C}} = 25^\circ\text{C}$	Continuous Collector Current, each IGBT	13	A
$I_{\text{C}} @ T_{\text{C}} = 100^\circ\text{C}$	Continuous Collector Current, each IGBT	7.0	
I_{CM}	Pulsed Collector Current ①	26	
I_{LM}	Clamped Inductive Load Current ②	26	
$I_{\text{F}} @ T_{\text{C}} = 100^\circ\text{C}$	Diode Continuous Forward Current	6.1	
I_{FM}	Diode Maximum Forward Current	26	
t_{sc}	Short Circuit Withstand Time	10	μs
V_{GE}	Gate-to-Emitter Voltage	± 20	V
V_{ISOL}	Isolation Voltage, any terminal to case, 1 min.	2500	V_{RMS}
$P_{\text{D}} @ T_{\text{C}} = 25^\circ\text{C}$	Maximum Power Dissipation, each IGBT	36	W
$P_{\text{D}} @ T_{\text{C}} = 100^\circ\text{C}$	Maximum Power Dissipation, each IGBT	14	
T_{J}	Operating Junction and	-40 to +150	$^\circ\text{C}$
T_{STG}	Storage Temperature Range		
	Soldering Temperature, for 10 sec.		
	Mounting torque, 6-32 or M3 screw.	5-7 lbf•in (0.55 - 0.8 N•m)	

Thermal Resistance

	Parameter	Typ.	Max.	Units
$R_{\theta\text{JC}}$ (IGBT)	Junction-to-Case, each IGBT, one IGBT in conduction	—	3.5	$^\circ\text{C/W}$
$R_{\theta\text{JC}}$ (DIODE)	Junction-to-Case, each diode, one diode in conduction	—	5.5	
$R_{\theta\text{CS}}$ (MODULE)	Case-to-Sink, flat, greased surface	0.1	—	
Wt	Weight of module	20 (0.7)	—	g (oz)

Electrical Characteristics @ $T_J = 25^\circ\text{C}$ (unless otherwise specified)

	Parameter	Min.	Typ.	Max.	Units	Conditions
$V_{(BR)CES}$	Collector-to-Emitter Breakdown Voltage ^③	600	—	—	V	$V_{GE} = 0V, I_C = 250\mu A$
$\Delta V_{(BR)CES}/\Delta T_J$	Temperature Coeff. of Breakdown Voltage	—	0.68	—	V/ $^\circ\text{C}$	$V_{GE} = 0V, I_C = 1.0mA$
$V_{CE(on)}$	Collector-to-Emitter Saturation Voltage	—	1.6	2.4	V	$I_C = 7.0A$ $V_{GE} = 15V$ See Fig. 2, 5
		—	2.0	—		
		—	1.7	—		
$V_{GE(th)}$	Gate Threshold Voltage	3.0	—	5.5		$V_{CE} = V_{GE}, I_C = 250\mu A$
$\Delta V_{GE(th)}/\Delta T_J$	Temperature Coeff. of Threshold Voltage	—	-13	—	mV/ $^\circ\text{C}$	$V_{CE} = V_{GE}, I_C = 250\mu A$
g_{fe}	Forward Transconductance ^④	3.2	6.3	—	S	$V_{CE} = 100V, I_C = 14A$
I_{CES}	Zero Gate Voltage Collector Current	—	—	250	μA	$V_{GE} = 0V, V_{CE} = 600V$
		—	—	2500		$V_{GE} = 0V, V_{CE} = 600V, T_J = 150^\circ\text{C}$
V_{FM}	Diode Forward Voltage Drop	—	1.4	1.7	V	$I_C = 12A$ See Fig. 13
		—	1.3	1.6		$I_C = 12A, T_J = 150^\circ\text{C}$
I_{GES}	Gate-to-Emitter Leakage Current	—	—	± 500	nA	$V_{GE} = \pm 20V$

Switching Characteristics @ $T_J = 25^\circ\text{C}$ (unless otherwise specified)

	Parameter	Min.	Typ.	Max.	Units	Conditions
Q_g	Total Gate Charge (turn-on)	—	32	49	nC	$I_C = 14A$ $V_{CC} = 400V$ See Fig. 8
Q_{ge}	Gate - Emitter Charge (turn-on)	—	6.7	10		
Q_{gc}	Gate - Collector Charge (turn-on)	—	13	21		
$t_{d(on)}$	Turn-On Delay Time	—	64	—	ns	$T_J = 25^\circ\text{C}$ $I_C = 7.0A, V_{CC} = 480V$ $V_{GE} = 15V, R_G = 23\Omega$ Energy losses include "tail" and diode reverse recovery.
t_r	Rise Time	—	29	—		
$t_{d(off)}$	Turn-Off Delay Time	—	340	500		
t_f	Fall Time	—	240	350		
E_{on}	Turn-On Switching Loss	—	0.28	—		
E_{off}	Turn-Off Switching Loss	—	0.70	—	mJ	See Fig. 9, 10, 11, 18
E_{ts}	Total Switching Loss	—	0.98	1.5		
t_{sc}	Short Circuit Withstand Time	10	—	—	μs	$V_{CC} = 360V, T_J = 125^\circ\text{C}$ $V_{GE} = 15V, R_G = 23\Omega, V_{CPK} < 500V$
$t_{d(on)}$	Turn-On Delay Time	—	62	—	ns	$T_J = 150^\circ\text{C}$, See Fig. 9, 10, 11, 18 $I_C = 7.0A, V_{CC} = 480V$ $V_{GE} = 15V, R_G = 23\Omega$ Energy losses include "tail" and diode reverse recovery.
t_r	Rise Time	—	28	—		
$t_{d(off)}$	Turn-Off Delay Time	—	620	—		
t_f	Fall Time	—	420	—		
E_{ts}	Total Switching Loss	—	1.8	—		
C_{ies}	Input Capacitance	—	750	—	pF	$V_{GE} = 0V$ $V_{CC} = 30V$ $f = 1.0MHz$ See Fig. 7
C_{oes}	Output Capacitance	—	100	—		
C_{res}	Reverse Transfer Capacitance	—	9.3	—		
t_{rr}	Diode Reverse Recovery Time	—	42	60	ns	$T_J = 25^\circ\text{C}$ See Fig. 14 $T_J = 125^\circ\text{C}$
		—	80	120		
I_{rr}	Diode Peak Reverse Recovery Current	—	3.5	6.0	A	$T_J = 25^\circ\text{C}$ See Fig. 15 $T_J = 125^\circ\text{C}$
		—	5.6	10		
Q_{rr}	Diode Reverse Recovery Charge	—	80	180	nC	$T_J = 25^\circ\text{C}$ See Fig. 16 $T_J = 125^\circ\text{C}$
		—	220	600		
$di_{(rec)M}/dt$	Diode Peak Rate of Fall of Recovery During t_b	—	180	—	A/ μs	$T_J = 25^\circ\text{C}$ See Fig. 17 $T_J = 125^\circ\text{C}$
		—	120	—		

Notes:

① Repetitive rating; $V_{GE} = 20V$, pulse width limited by max. junction temperature. (See fig. 20)

② $V_{CC} = 80\%(V_{CES}), V_{GE} = 20V, L = 10\mu H, R_G = 23\Omega$, (See fig. 19)

③ Pulse width $\leq 80\mu s$; duty factor $\leq 0.1\%$.

④ Pulse width 5.0 μs , single shot.

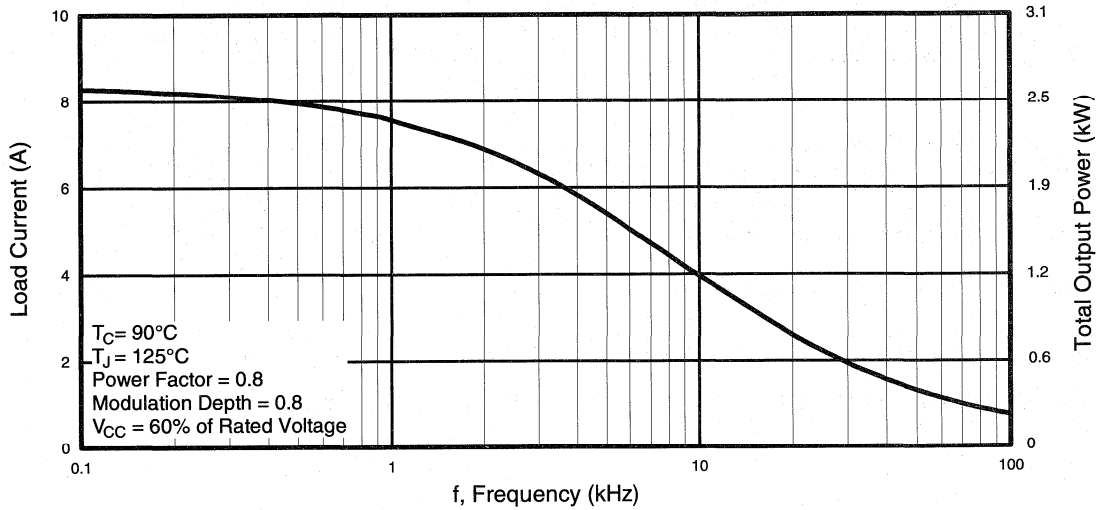


Fig. 1 - RMS Current and Output Power, Synthesized Sine Wave

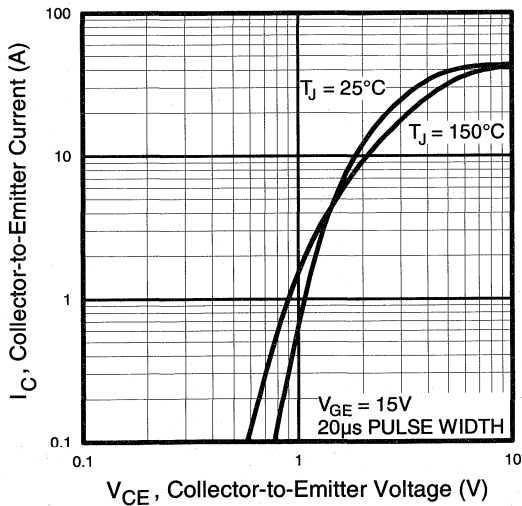


Fig. 2 - Typical Output Characteristics

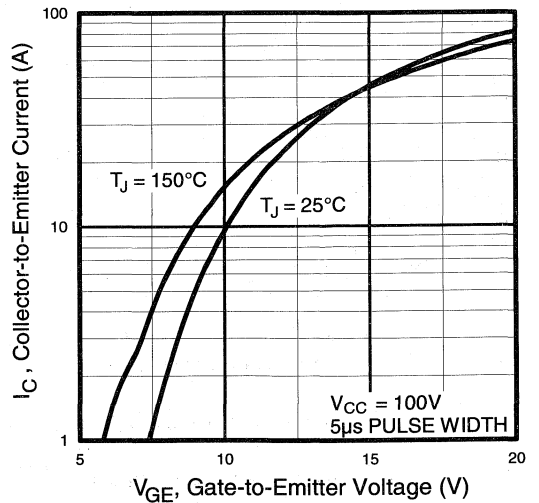


Fig. 3 - Typical Transfer Characteristics

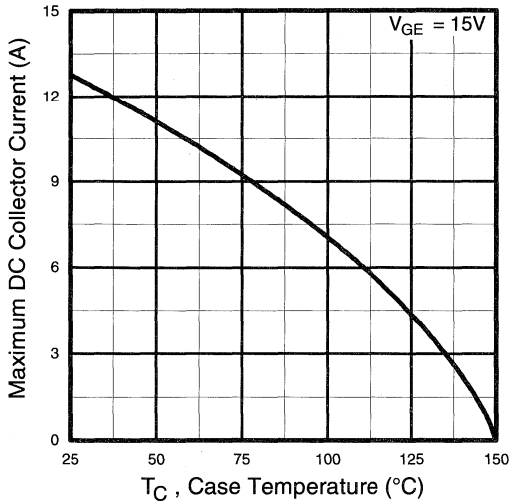


Fig. 4 - Maximum Collector Current vs. Case Temperature

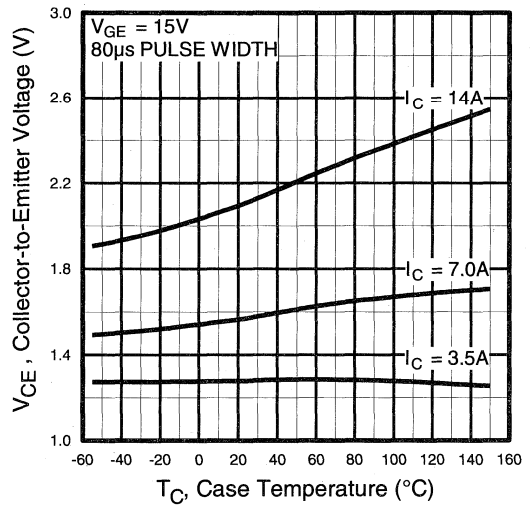


Fig. 5 - Collector-to-Emitter Voltage vs. Case Temperature

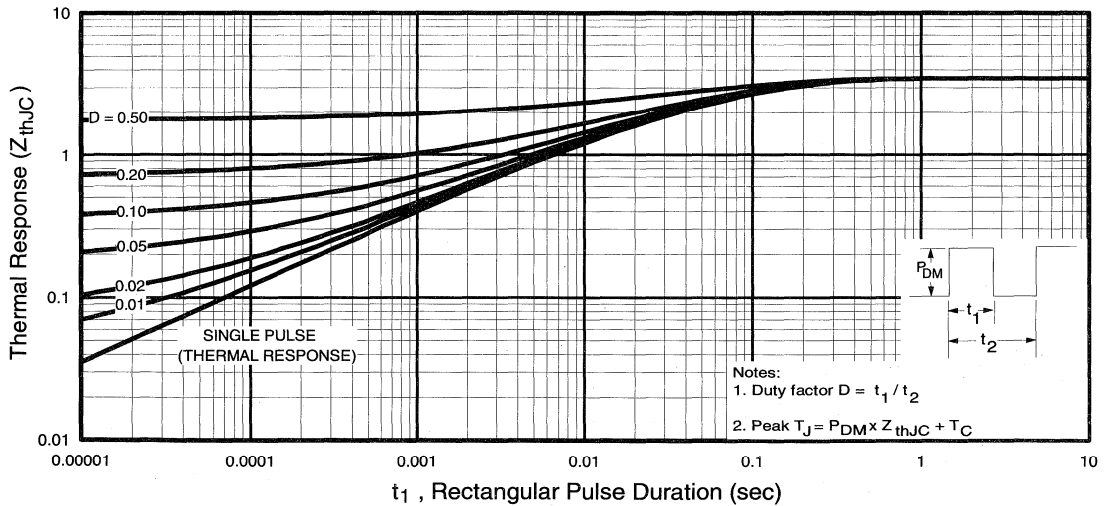


Fig. 6 - Maximum IGBT Effective Transient Thermal Impedance, Junction-to-Case

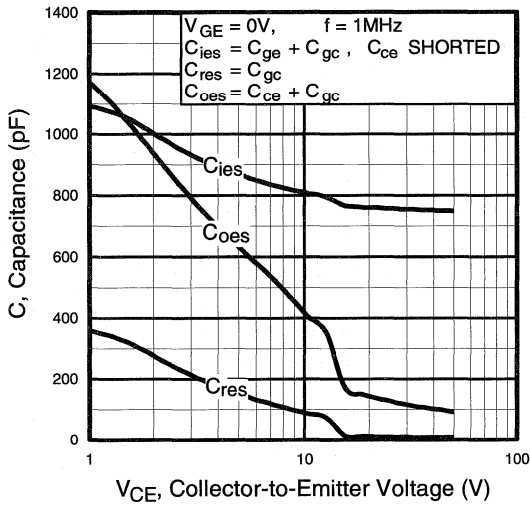


Fig. 7 - Typical Capacitance vs. Collector-to-Emitter Voltage

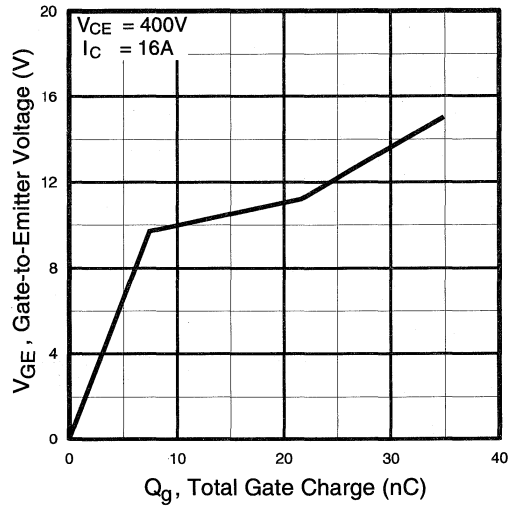


Fig. 8 - Typical Gate Charge vs. Gate-to-Emitter Voltage

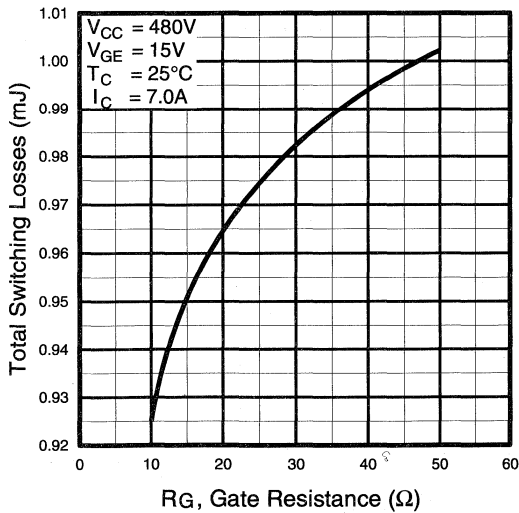


Fig. 9 - Typical Switching Losses vs. Gate Resistance

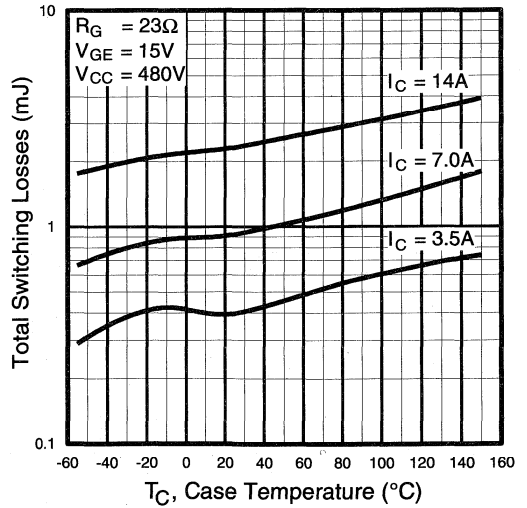


Fig. 10 - Typical Switching Losses vs. Case Temperature

Motor Control Modules

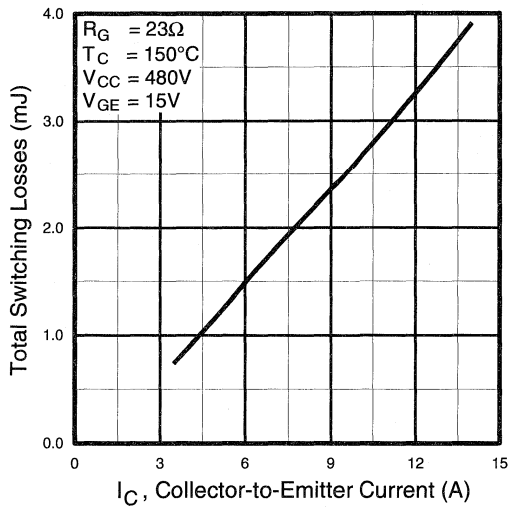


Fig. 11 - Typical Switching Losses vs. Collector-to-Emitter Current

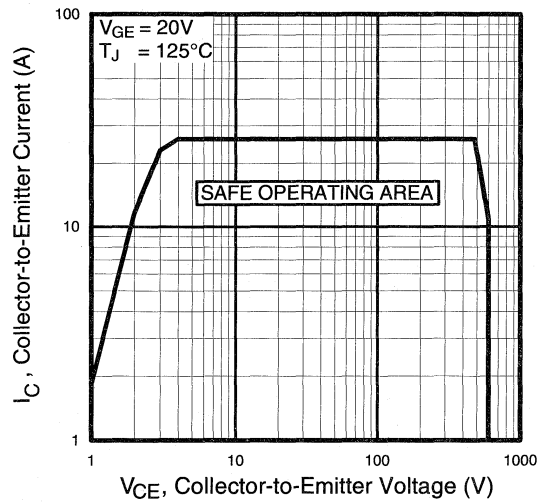


Fig. 12 - Turn-Off SOA

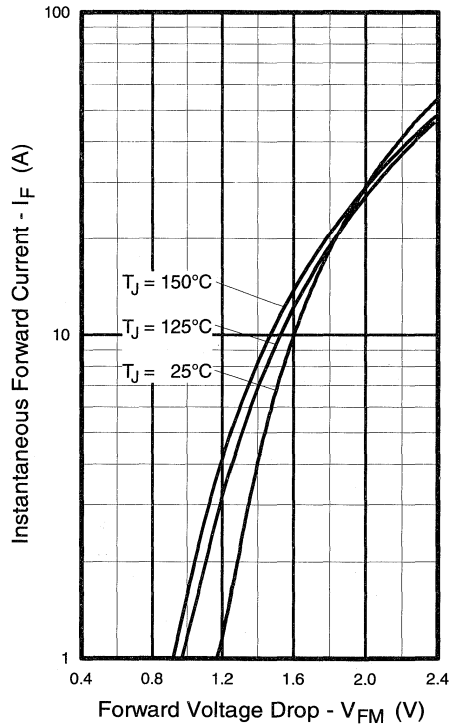


Fig. 13 - Maximum Forward Voltage Drop vs. Instantaneous Forward Current

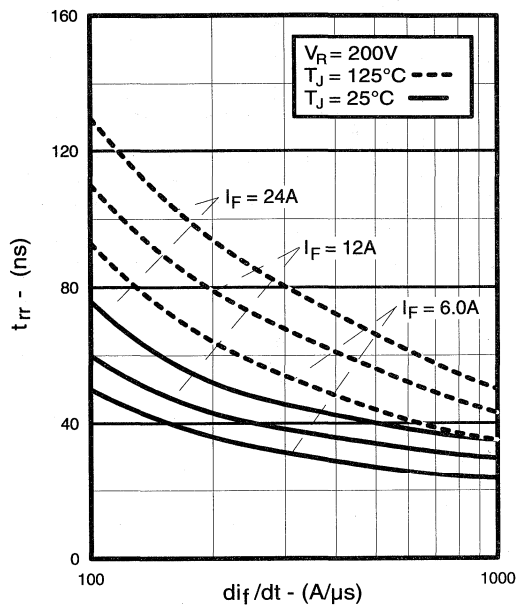


Fig. 14 - Typical Reverse Recovery vs. di_f/dt

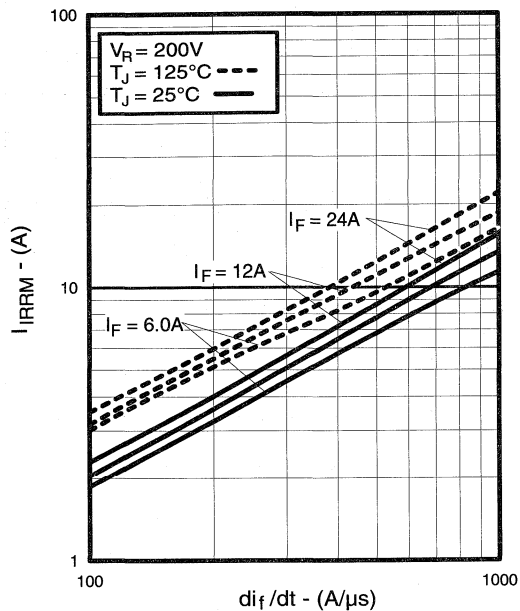


Fig. 15 - Typical Recovery Current vs. di_f/dt

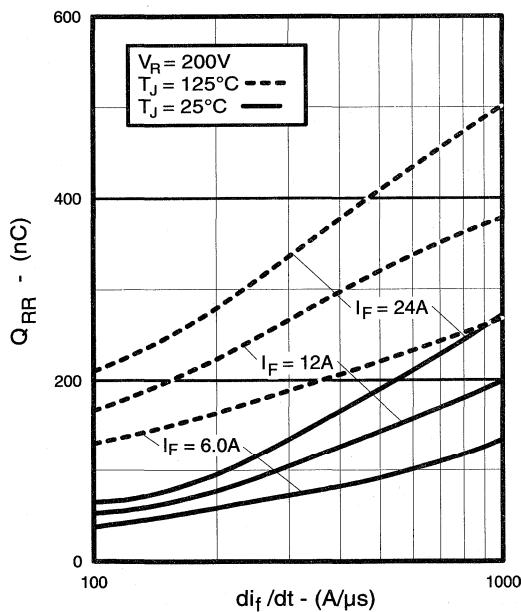


Fig. 16 - Typical Stored Charge vs. di_f/dt

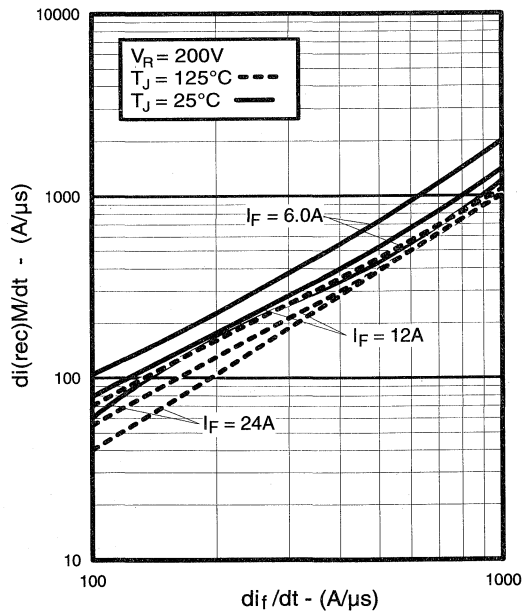


Fig. 17 - Typical $di_{(rec)M}/dt$ vs. di_f/dt

Motor Control Fast Modules

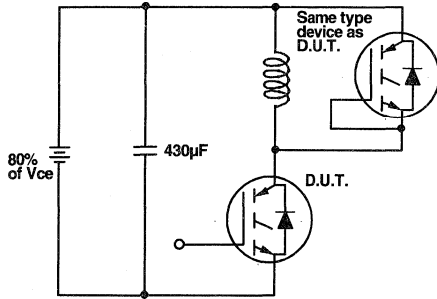


Fig. 18a - Test Circuit for Measurement of I_{LM} , E_{on} , $E_{off}(\text{diode})$, t_{rr} , Q_{rr} , I_{rr} , $t_{d(on)}$, t_r , $t_{d(off)}$, t_f

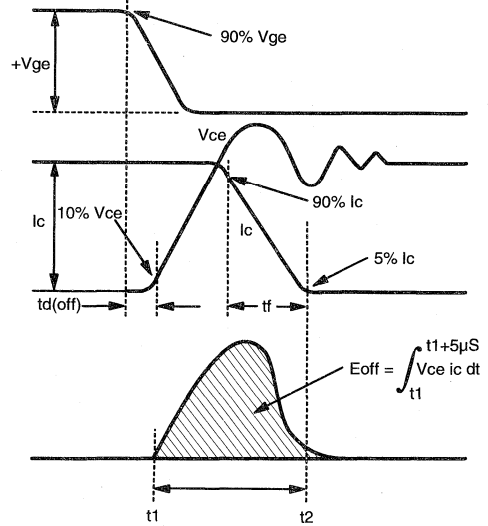


Fig. 18b - Test Waveforms for Circuit of Fig. 18a, Defining E_{off} , $t_{d(off)}$, t_f

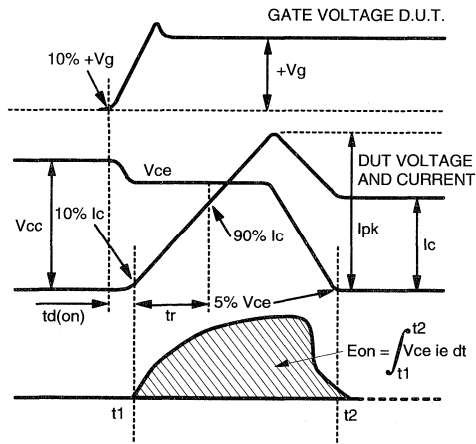


Fig. 18c - Test Waveforms for Circuit of Fig. 18a, Defining E_{on} , $t_{d(on)}$, t_r

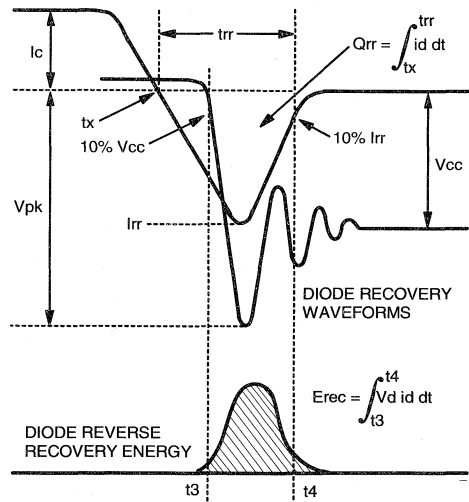


Fig. 18d - Test Waveforms for Circuit of Fig. 18a, Defining E_{rec} , t_{rr} , Q_{rr} , I_{rr}

**Refer to Section D for the following:
Appendix D: Section D - page D-6**

Fig. 18e - Macro Waveforms for Test Circuit of Fig. 18a

Fig. 19 - Clamped Inductive Load Test Circuit

Fig. 20 - Pulsed Collector Current Test Circuit

IGBT SIP MODULE

Short Circuit Rated Fast IGBT

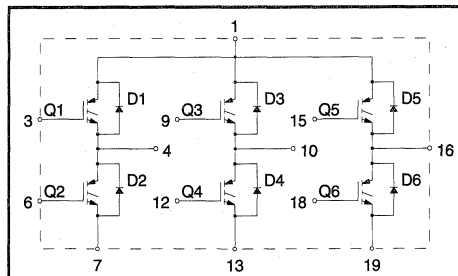
Features

- Short Circuit Rated - $10\mu\text{s}$ @ 125°C , $V_{\text{GE}} = 15\text{V}$
- Fully isolated printed circuit board mount package
- Switching-loss rating includes all "tail" losses
- HEXFRED™ soft ultrafast diodes
- Optimized for medium operating frequency (1 to 10kHz)

Product Summary

Output Current in a Typical 5.0 kHz Motor Drive

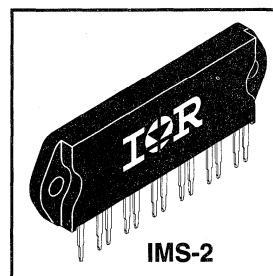
13 A_{RMS} per phase (4.1 kW total) with $T_{\text{C}} = 90^\circ\text{C}$, $T_{\text{J}} = 125^\circ\text{C}$, Supply Voltage 360Vdc,
Power Factor 0.8, Modulation Depth 80%



Description

The IGBT technology is the key to International Rectifier's advanced line of IMS (Insulated Metal Substrate) Power Modules. These modules are more efficient than comparable bipolar transistor modules, while at the same time having the simpler gate-drive requirements of the familiar power MOSFET. This superior technology has now been coupled to a state of the art materials system that maximizes power throughput with low thermal resistance. This package is highly suited to power applications and where space is at a premium.

These new short circuit rated devices are especially suited for motor control and other totem-pole applications requiring short circuit withstand capability.



Motor
Control
Fast
Modules

Absolute Maximum Ratings

	Parameter	Max.	Units
V_{CES}	Collector-to-Emitter Voltage	600	V
$I_{\text{C}} @ T_{\text{C}} = 25^\circ\text{C}$	Continuous Collector Current, each IGBT	22	A
$I_{\text{C}} @ T_{\text{C}} = 100^\circ\text{C}$	Continuous Collector Current, each IGBT	12	
I_{CM}	Pulsed Collector Current $\text{\textcircled{D}}$	44	
I_{LM}	Clamped Inductive Load Current $\text{\textcircled{D}}$	44	
$I_{\text{F}} @ T_{\text{C}} = 100^\circ\text{C}$	Diode Continuous Forward Current	9.3	
I_{FM}	Diode Maximum Forward Current	44	
t_{sc}	Short Circuit Withstand Time	10	μs
V_{GE}	Gate-to-Emitter Voltage	± 20	V
V_{ISOL}	Isolation Voltage, any terminal to case, 1 minute	2500	V_{RMS}
$P_{\text{D}} @ T_{\text{C}} = 25^\circ\text{C}$	Maximum Power Dissipation, each IGBT	62.5	W
$P_{\text{D}} @ T_{\text{C}} = 100^\circ\text{C}$	Maximum Power Dissipation, each IGBT	25	
T_{J}	Operating Junction and	-40 to +150	$^\circ\text{C}$
T_{STG}	Storage Temperature Range		
	Soldering Temperature, for 10 sec.		
	Mounting torque, 6-32 or M3 screw.	5-7 lbf•in (0.55 - 0.8 N•m)	

Thermal Resistance

	Parameter	Typ.	Max.	Units
$R_{\theta\text{JC}}$ (IGBT)	Junction-to-Case, each IGBT, one IGBT in conduction	—	2.0	$^\circ\text{C}/\text{W}$
$R_{\theta\text{JC}}$ (DIODE)	Junction-to-Case, each diode, one diode in conduction	—	3.0	
$R_{\theta\text{CS}}$ (MODULE)	Case-to-Sink, flat, greased surface	0.1	—	
Wt	Weight of module	20 (0.7)	—	g (oz)

Electrical Characteristics @ $T_J = 25^\circ\text{C}$ (unless otherwise specified)

	Parameter	Min.	Typ.	Max.	Units	Conditions
$V_{(BR)CES}$	Collector-to-Emitter Breakdown Voltage ^①	600	—	—	V	$V_{GE} = 0V, I_C = 250\mu A$
$\Delta V_{(BR)CES}/\Delta T_J$	Temp. Coeff. of Breakdown Voltage	—	0.69	—	V/ $^\circ\text{C}$	$V_{GE} = 0V, I_C = 1.0mA$
$V_{CE(on)}$	Collector-to-Emitter Saturation Voltage	—	1.7	—	V	$I_C = 12A, V_{GE} = 15V$
		—	2.0	—		
		—	1.9	—		
$V_{GE(th)}$	Gate Threshold Voltage	3.0	—	5.5		$V_{CE} = V_{GE}, I_C = 250\mu A$
$\Delta V_{GE(th)}/\Delta T_J$	Temp. Coeff. of Threshold Voltage	—	-12	—	mV/ $^\circ\text{C}$	$V_{CE} = V_{GE}, I_C = 250\mu A$
g_{fe}	Forward Transconductance ^④	9.2	12	—	S	$V_{CE} = 100V, I_C = 24A$
I_{CES}	Zero Gate Voltage Collector Current	—	—	250	μA	$V_{GE} = 0V, V_{CE} = 600V$
		—	—	3500		$V_{GE} = 0V, V_{CE} = 600V, T_J = 150^\circ\text{C}$
V_{FM}	Diode Forward Voltage Drop	—	1.3	1.7	V	$I_C = 15A$
		—	1.2	1.6		$I_C = 15A, T_J = 150^\circ\text{C}$
I_{GES}	Gate-to-Emitter Leakage Current	—	—	± 500	nA	$V_{GE} = \pm 20V$

Switching Characteristics @ $T_J = 25^\circ\text{C}$ (unless otherwise specified)

	Parameter	Min.	Typ.	Max.	Units	Conditions
Q_g	Total Gate Charge (turn-on)	—	59	80	nC	$I_C = 24A, V_{CC} = 400V$
Q_{ge}	Gate - Emitter Charge (turn-on)	—	8.6	10		
Q_{gc}	Gate - Collector Charge (turn-on)	—	25	42		
$t_{d(on)}$	Turn-On Delay Time	—	26	—	ns	$T_J = 25^\circ\text{C}$ $I_C = 24A, V_{CC} = 480V$ $V_{GE} = 15V, R_G = 10\Omega$ Energy losses include "tail" and diode reverse recovery.
t_r	Rise Time	—	37	—		
$t_{d(off)}$	Turn-Off Delay Time	—	240	410		
t_f	Fall Time	—	230	420		
E_{on}	Turn-On Switching Loss	—	0.75	—	mJ	
E_{off}	Turn-Off Switching Loss	—	1.65	—		
E_{ts}	Total Switching Loss	—	2.4	3.6		
t_{sc}	Short Circuit Withstand Time	10	—	—	μs	$V_{CC} = 360V, T_J = 125^\circ\text{C}$ $V_{GE} = 15V, R_G = 10\Omega, V_{CPK} < 500V$
$t_{d(on)}$	Turn-On Delay Time	—	28	—	ns	$T_J = 150^\circ\text{C}$, $I_C = 24A, V_{CC} = 480V$ $V_{GE} = 15V, R_G = 10\Omega$ Energy losses include "tail" and diode reverse recovery.
t_r	Rise Time	—	37	—		
$t_{d(off)}$	Turn-Off Delay Time	—	380	—		
t_f	Fall Time	—	460	—		
E_{ts}	Total Switching Loss	—	4.5	—	mJ	
C_{ies}	Input Capacitance	—	1500	—	pF	$V_{GE} = 0V$ $V_{CC} = 30V$ $f = 1.0MHz$
C_{oes}	Output Capacitance	—	190	—		
C_{res}	Reverse Transfer Capacitance	—	20	—		
t_{rr}	Diode Reverse Recovery Time	—	42	60	ns	$T_J = 25^\circ\text{C}$ $T_J = 125^\circ\text{C}$
		—	74	120		
I_{rr}	Diode Peak Reverse Recovery Current	—	4.0	6.0	A	$T_J = 25^\circ\text{C}$ $T_J = 125^\circ\text{C}$
		—	6.5	10		
Q_{rr}	Diode Reverse Recovery Charge	—	80	180	nC	$T_J = 25^\circ\text{C}$ $T_J = 125^\circ\text{C}$
		—	220	600		
$di_{(rec)M}/dt$	Diode Peak Rate of Fall of Recovery During t_b	—	188	—	A/ μs	$T_J = 25^\circ\text{C}$ $T_J = 125^\circ\text{C}$
		—	160	—		

Notes: ① Repetitive rating; $V_{GE}=20V$, pulse width limited by maximum junction temperature.

② $V_{CC}=80\%(V_{CES}), V_{GE}=20V, L=10\mu H, R_G=10\Omega$

④ Pulse width 5.0 μs , single shot.

③ Pulse width $\leq 80\mu s$; duty factor $\leq 0.1\%$.

Refer to Section D for the following:

Package Outline 5 - IMS-2

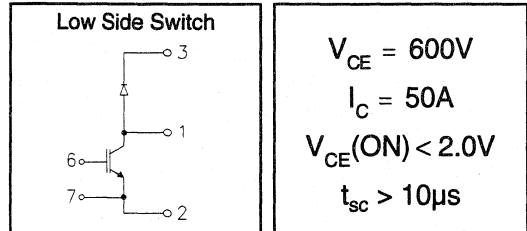
Section D - page D-14

IRGKIN050M06

"CHOPPER" IGBT INT-A-PAK

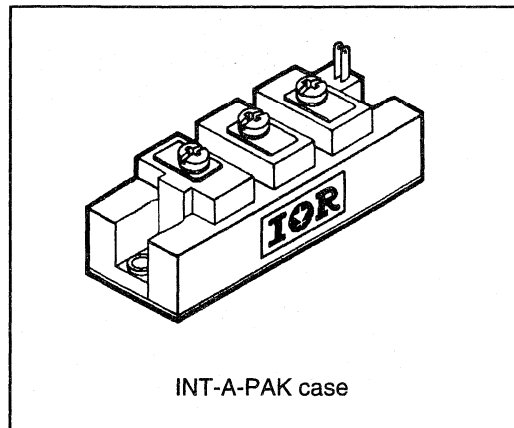
Low conduction loss IGBT

- Rugged Design
- Simple gate-drive
- Switching-Loss Rating includes all "tail" losses
- Short circuit rated



Description

IR's advanced IGBT technology is the key to this line of INT-A-PAK Power Modules. The efficient geometry and unique processing of the IGBT allow higher current densities than comparable bipolar power module transistors, while at the same time requiring the simpler gate-drive of the familiar power MOSFET. These modules are short circuit rated for applications such as motor control requiring this important feature.



Absolute Maximum Ratings

Parameter	Description	Value	Units
V_{CES}	Continuous collector to emitter voltage	600	V
$I_C @ T_C = 25^\circ C$	Continuous collector current	60	A
$I_C @ T_C = 85^\circ C$	Continuous collector current	35	
$I_C @ T_C = 100^\circ C$	Continuous collector current	23	
I_{LM}	Peak switching current	100	
I_{FM}	Peak diode forward current (1)	100	V
V_{GE}	Gate to emitter voltage	± 20	
V_{ISOL}	RMS isolation voltage, any terminal to case, $t = 1$ min	2500	W
$P_D @ T_C = 25^\circ C$	Power dissipation	240	
T_J	Operating junction temperature range	-40 to 150	
T_{STG}	Storage temperature range	-40 to 125	

(1) Duration limited by max junction temperature.

Electrical Characteristics - $T_J = 25^\circ\text{C}$, unless otherwise stated

Parameter	Description	Min	Typ	Max	Units	Test Conditions
V_{CES}	Collector-to-emitter breakdown voltage	600	—	—	v	$V_{GE} = 0V, I_C = 500\mu A$
$V_{CE(ON)}$	Collector-to-emitter voltage	—	—	2.0		$V_{GE} = 15V, I_C = 50A$
		—	2.2	—		$V_{GE} = 15V, I_C = 50A, T_J = 125^\circ\text{C}$
V_{FM}	Diode forward voltage - maximum	—	1.8	2.0		$I_F = 50A, V_{GE} = 0V$
		—	1.75	—		$I_F = 50A, V_{GE} = 0V, T_J = 125^\circ\text{C}$
V_{GEth}	Gate threshold voltage	3.0	—	5.5	$I_C = 250\mu A$	
ΔV_{GEth}	Threshold voltage temp. coefficient	—	-11	—	mV/ $^\circ\text{C}$	$V_{CE} = V_{GE}, I_C = 250\mu A$
g_{fe}	Forward transconductance	26	—	36	S(τ)	$V_{CE} = 25V, I_C = 50A$
I_{CES}	Collector-to-emitter leakage current	—	—	500	μA	$V_{GE} = 0V, V_{CE} = 600V$
		—	—	5	mA	$V_{GE} = 0V, V_{CE} = 600V, T_J = 125^\circ\text{C}$
I_{GES}	Gate-to-emitter leakage current	—	—	± 500	nA	$V_{GE} = \pm 20V$

Dynamic Characteristics - $T_J = 125^\circ\text{C}$, unless otherwise stated

Parameter	Description	Min	Typ	Max	Units	Test Conditions
E_{on}	Turn-on switching energy	—	0.03	—	mJ/A	$R_G = 18\Omega, V_{CC} = 300V$
$E_{off} (1)$	Turn-off switching energy	—	0.11	—		$I_C = 50A, L_S = 100nH$
$E_{ts} (1)$	Total switching energy	—	—	0.18		$V_{GE} = \pm 15V$
$t_{d(on)}$	Turn-on delay time	—	200	—	ns	$R_G = 18\Omega, V_{CC} = 300V$
t_r	Rise time	—	400	—		$I_C = 50A$
$t_{d(off)}$	Turn-off delay time	—	250	—		$V_{GE} = \pm 15V$
t_f	Fall time	—	350	—		Resistive load, $T_J = 25^\circ\text{C}$
I_{rr}	Diode peak recovery current	—	20	—		A
t_{rr}	Diode recovery time	—	110	—	ns	$I_C = 50A$
Q_{rr}	Diode recovery charge	—	1.2	—	μC	$V_{GE} = \pm 15V$
Q_{ge}	Gate-to-emitter charge (turn-on)	13	—	21	nC	$V_{CC} = 480V$
Q_{gc}	Gate-to-collector charge (turn-on)	35	—	70		$I_C = 27A$
Q_g	Total gate charge (turn-on)	77	—	140		$V_{GE} = 15V$
C_{ies}	Input capacitance	—	2900	—	pF	$V_{GE} = 0V$
C_{oes}	Output capacitance	—	330	—		$V_{CC} = 30V$
C_{res}	Reverse transfer capacitance	—	40	—		$f = 1MHz$
t_{sc}	Short circuit withstand time	10	—	—	μs	$V_{CC} = 360V, V_{GE} = \pm 15V$ Min. $R_G = 18\Omega, V_{CEP} = 500V$

(1) Includes tail losses

Thermal and Mechanical Characteristics

Parameter	Description	Typ	Max	Units
R_{thJC} (IGBT)	Thermal resistance, junction to case, each IGBT	—	0.52	$^\circ\text{C/W}$
R_{thJC} (Diode)	Thermal resistance, junction to case, each diode	—	0.90	
R_{thCS} (Module)	Thermal resistance, case to sink	0.041	0.100	
Wt	Weight of module	150	—	g

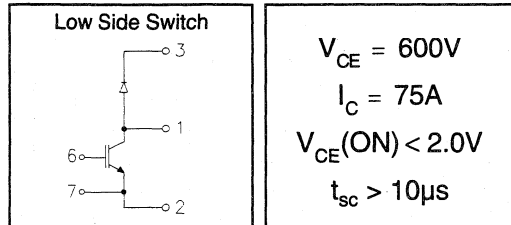
Refer to Section D - page D-15 for Package Outline 7 -INT-A-PAK, New - Low Side Switch

IRGKIN075M06

"CHOPPER" IGBT INT-A-PAK

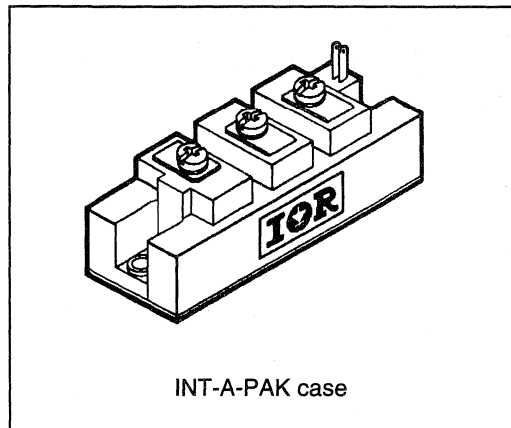
Low conduction loss IGBT

- Rugged Design
- Simple gate-drive
- Switching-Loss Rating includes all "tail" losses
- Short circuit rated



Description

IR's advanced IGBT technology is the key to this line of INT-A-PAK Power Modules. The efficient geometry and unique processing of the IGBT allow higher current densities than comparable bipolar power module transistors, while at the same time requiring the simpler gate-drive of the familiar power MOSFET. These modules are short circuit rated for applications such as motor control requiring this important feature.



Absolute Maximum Ratings

Parameter	Description	Value	Units
V_{CES}	Continuous collector to emitter voltage	600	V
$I_C @ T_C = 25^\circ C$	Continuous collector current	110	A
$I_C @ T_C = 85^\circ C$	Continuous collector current	60	
$I_C @ T_C = 100^\circ C$	Continuous collector current	40	
I_{LM}	Peak switching current	150	
I_{FM}	Peak diode forward current (1)	150	V
V_{GE}	Gate to emitter voltage	± 20	
V_{ISOL}	RMS isolation voltage, any terminal to case, $t = 1 \text{ min}$	2500	W
$P_D @ T_C = 25^\circ C$	Power dissipation	391	
T_J	Operating junction temperature range	-40 to 150	$^\circ C$
T_{STG}	Storage temperature range	-40 to 125	

(1) Duration limited by max junction temperature.

Electrical Characteristics - $T_J = 25^\circ\text{C}$, unless otherwise stated

Parameter	Description	Min	Typ	Max	Units	Test Conditions
BV_{CES}	Collector-to-emitter breakdown voltage	600	—	—	V	$V_{GE} = 0\text{V}, I_C = 1\text{mA}$
$V_{CE(ON)}$	Collector-to-emitter voltage	—	—	2.0		$V_{GE} = 15\text{V}, I_C = 75\text{A}$
		—	2.2	—		$V_{GE} = 15\text{V}, I_C = 75\text{A}, T_J = 125^\circ\text{C}$
V_{FM}	Diode forward voltage - maximum	—	1.8	2.0		$I_F = 75\text{A}, V_{GE} = 0\text{V}$
		—	1.75	—	$I_F = 75\text{A}, V_{GE} = 0\text{V}, T_J = 125^\circ\text{C}$	
V_{GEth}	Gate threshold voltage	3.0	—	5.5	$I_C = 500\mu\text{A}$	
ΔV_{GEth}	Threshold voltage temp. coefficient	—	-11	—	mV/°C	$V_{CE} = V_{GE}, I_C = 500\mu\text{A}$
g_{fe}	Forward transconductance	52	—	72	S(t)	$V_{CE} = 25\text{V}, I_C = 75\text{A}$
I_{CES}	Collector-to-emitter leakage current	—	—	1	mA	$V_{GE} = 0\text{V}, V_{CE} = 600\text{V}$
		—	—	10		$V_{GE} = 0\text{V}, V_{CE} = 600\text{V}, T_J = 125^\circ\text{C}$
I_{GES}	Gate-to-emitter leakage current	—	—	± 1	μA	$V_{GE} = \pm 20\text{V}$

Dynamic Characteristics - $T_J = 125^\circ\text{C}$, unless otherwise stated

Parameter	Description	Min	Typ	Max	Units	Test Conditions
E_{on}	Turn-on switching energy	—	0.03	—	mJ/A	$R_G = 18\Omega, V_{CC} = 300\text{V}$
E_{off} (1)	Turn-off switching energy	—	0.11	—		$I_C = 75\text{A}, L_S = 100\text{nH}$
E_{ts} (1)	Total switching energy	—	—	0.18		$V_{GE} = \pm 15\text{V}$
$t_{d(on)}$	Turn-on delay time	—	200	—	ns	$R_G = 18\Omega, V_{CC} = 300\text{V}$
t_r	Rise time	—	400	—		$I_C = 75\text{A}$
$t_{d(off)}$	Turn-off delay time	—	250	—		$V_{GE} = \pm 15\text{V}$
t_f	Fall time	—	350	—		Resistive load, $T_J = 25^\circ\text{C}$
I_{rr}	Diode peak recovery current	—	27	—		$R_G = 18\Omega, V_{CC} = 300\text{V}$
t_{rr}	Diode recovery time	—	110	—	$I_C = 75\text{A}$	
Q_{rr}	Diode recovery charge	—	1.7	—	μC	$V_{GE} = \pm 15\text{V}$
Q_{ge}	Gate-to-emitter charge (turn-on)	26	—	42	nC	$V_{CC} = 480\text{V}$
Q_{gc}	Gate-to-collector charge (turn-on)	70	—	140		$I_C = 54\text{A}$
Q_g	Total gate charge (turn-on)	150	—	280		$V_{GE} = 15\text{V}$
C_{ies}	Input capacitance	—	5800	—	pF	$V_{GE} = 0\text{V}$
C_{oes}	Output capacitance	—	660	—		$V_{CC} = 30\text{V}$
C_{res}	Reverse transfer capacitance	—	80	—		$f = 1\text{MHz}$
t_{sc}	Short circuit withstand time	10	—	—	μs	$V_{CC} = 360\text{V}, V_{GE} = \pm 15\text{V}$ Min. $R_G = 18\Omega, V_{CEP} = 500\text{V}$

(1) Includes tail losses

Thermal and Mechanical Characteristics

Parameter	Description	Typ	Max	Units
R_{thJC} (IGBT)	Thermal resistance, junction to case, each IGBT	—	0.32	°C/W
R_{thJC} (Diode)	Thermal resistance, junction to case, each diode	—	0.48	
R_{thCS} (Module)	Thermal resistance, case to sink	0.041	0.100	
Wt	Weight of module	150	—	g

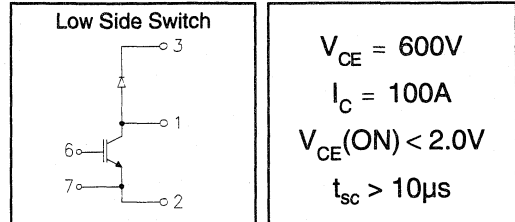
Refer to Section D - page D-15 for Package Outline 7 -INT-A-PAK, New - Low Side Switch

IRGKIN100M06

"CHOPPER" IGBT INT-A-PAK

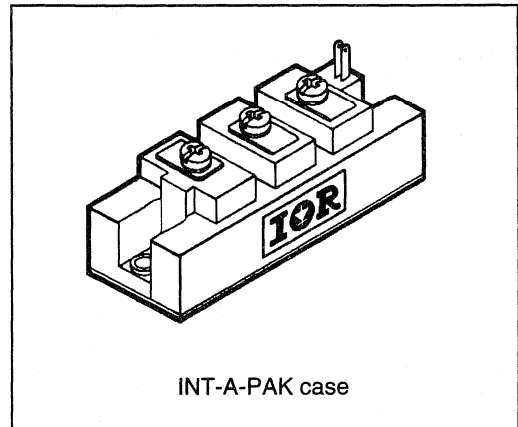
Low conduction loss IGBT

- Rugged Design
- Simple gate-drive
- Switching-Loss Rating includes all "tail" losses
- Short circuit rated



Description

IR's advanced IGBT technology is the key to this line of INT-A-PAK Power Modules. The efficient geometry and unique processing of the IGBT allow higher current densities than comparable bipolar power module transistors, while at the same time requiring the simpler gate-drive of the familiar power MOSFET. These modules are short circuit rated for applications such as motor control requiring this important feature.


 Motor
Control
Power
Modules

Absolute Maximum Ratings

Parameter	Description	Value	Units
V_{CES}	Continuous collector to emitter voltage	600	V
$I_C @ T_C = 25^\circ C$	Continuous collector current	150	A
$I_C @ T_C = 85^\circ C$	Continuous collector current	80	
$I_C @ T_C = 100^\circ C$	Continuous collector current	60	
I_{LM}	Peak switching current	200	
I_{FM}	Peak diode forward current (1)	200	V
V_{GE}	Gate to emitter voltage	± 20	
V_{ISOL}	RMS isolation voltage, any terminal to case, $t = 1$ min	2500	
$P_D @ T_C = 25^\circ C$	Power dissipation	500	W
T_J	Operating junction temperature range	-40 to 150	$^\circ C$
T_{STG}	Storage temperature range	-40 to 125	

(1) Duration limited by max junction temperature.



Electrical Characteristics - $T_J = 25^\circ\text{C}$, unless otherwise stated

Parameter	Description	Min	Typ	Max	Units	Test Conditions
BV_{CES}	Collector-to-emitter breakdown voltage	600	—	—	V	$V_{GE} = 0V, I_C = 1.5mA$
$V_{CE(ON)}$	Collector-to-emitter voltage	—	—	2.0		$V_{GE} = 15V, I_C = 100A$
		—	2.2	—		$V_{GE} = 15V, I_C = 100A, T_J = 125^\circ\text{C}$
V_{FM}	Diode forward voltage - maximum	—	1.8	2.0		$I_F = 100A, V_{GE} = 0V$
		—	1.75	—	$I_F = 100A, V_{GE} = 0V, T_J = 125^\circ\text{C}$	
V_{GEth}	Gate threshold voltage	3.0	—	5.5	mV/°C	$I_C = 750\mu A$
ΔV_{GEth}	Threshold voltage temp. coefficient	—	-11	—		$V_{CE} = V_{GE}, I_C = 750\mu A$
g_{fe}	Forward transconductance	78	—	108	S(t)	$V_{CE} = 25V, I_C = 100A$
I_{CES}	Collector-to-emitter leakage current	—	—	1.5	mA	$V_{GE} = 0V, V_{CE} = 600V$
		—	—	15		$V_{GE} = 0V, V_{CE} = 600V, T_J = 125^\circ\text{C}$
I_{GES}	Gate-to-emitter leakage current	—	—	± 1.5	μA	$V_{GE} = \pm 20V$

Dynamic Characteristics - $T_J = 125^\circ\text{C}$, unless otherwise stated

Parameter	Description	Min	Typ	Max	Units	Test Conditions
E_{on}	Turn-on switching energy	—	0.03	—	mJ/A	$R_G = 18\Omega, V_{CC} = 300V$
$E_{off} (1)$	Turn-off switching energy	—	0.11	—		$I_C = 100A, L_S = 100nH$
$E_{ts} (1)$	Total switching energy	—	—	0.18		$V_{GE} = \pm 15V$
$t_{d(on)}$	Turn-on delay time	—	200	—	ns	$R_G = 18\Omega, V_{CC} = 300V$
t_r	Rise time	—	400	—		$I_C = 100A$
$t_{d(off)}$	Turn-off delay time	—	250	—		$V_{GE} = \pm 15V$
t_f	Fall time	—	350	—		Resistive load, $T_J = 25^\circ\text{C}$
I_{rr}	Diode peak recovery current	—	40	—	A	$R_G = 18\Omega, V_{CC} = 300V$
t_{rr}	Diode recovery time	—	110	—	ns	$I_C = 100A$
Q_{rr}	Diode recovery charge	—	2.2	—	μC	$V_{GE} = \pm 15V$
Q_{ge}	Gate-to-emitter charge (turn-on)	39	—	63	nC	$V_{CC} = 480V$
Q_{gc}	Gate-to-collector charge (turn-on)	105	—	210		$I_C = 81A$
Q_g	Total gate charge (turn-on)	225	—	420		$V_{GE} = 15V$
C_{ies}	Input capacitance	—	8700	—	pF	$V_{GE} = 0V$
C_{oes}	Output capacitance	—	990	—		$V_{CC} = 30V$
C_{res}	Reverse transfer capacitance	—	120	—		$f = 1MHz$
t_{sc}	Short circuit withstand time	10	—	—	μs	$V_{CC} = 360V, V_{GE} = \pm 15V$ Min. $R_G = 18\Omega, V_{CEP} = 500V$

(1) Includes tail losses

Thermal and Mechanical Characteristics

Parameter	Description	Typ	Max	Units
R_{thJC} (IGBT)	Thermal resistance, junction to case, each IGBT	—	0.25	°C/W
R_{thJC} (Diode)	Thermal resistance, junction to case, each diode	—	0.38	
R_{thCS} (Module)	Thermal resistance, case to sink	0.041	0.100	
Wt	Weight of module	150	—	g

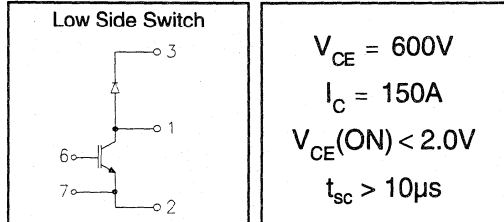
Refer to Section D - page D-15 for Package Outline 7 -INT-A-PAK, New - Low Side Switch

IRGKIN150M06

"CHOPPER" IGBT INT-A-PAK

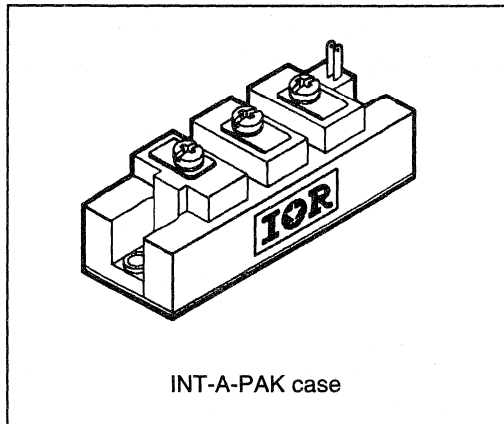
Low conduction loss IGBT

- Rugged Design
- Simple gate-drive
- Switching-Loss Rating includes all "tail" losses
- Short circuit rated



Description

IR's advanced IGBT technology is the key to this line of INT-A-PAK Power Modules. The efficient geometry and unique processing of the IGBT allow higher current densities than comparable bipolar power module transistors, while at the same time requiring the simpler gate-drive of the familiar power MOSFET. These modules are short circuit rated for applications such as motor control requiring this important feature.



Absolute Maximum Ratings

Parameter	Description	Value	Units
V_{CES}	Continuous collector to emitter voltage	600	V
$I_C @ T_C = 25^\circ C$	Continuous collector current	200	A
$I_C @ T_C = 85^\circ C$	Continuous collector current	110	
$I_C @ T_C = 100^\circ C$	Continuous collector current	80	
I_{LM}	Peak switching current	300	
I_{FM}	Peak diode forward current (1)	300	V
V_{GE}	Gate to emitter voltage	± 20	
V_{ISOL}	RMS isolation voltage, any terminal to case, $t = 1$ min	2500	W
$P_D @ T_C = 25^\circ C$	Power dissipation	658	
T_J	Operating junction temperature range	-40 to 150	
T_{STG}	Storage temperature range	-40 to 125	

(1) Duration limited by max junction temperature.



Electrical Characteristics - $T_J = 25^\circ\text{C}$, unless otherwise stated

Parameter	Description	Min	Typ	Max	Units	Test Conditions
BV_{CES}	Collector-to-emitter breakdown voltage	600	—	—	V	$V_{GE} = 0V, I_C = 2mA$
$V_{CE(ON)}$	Collector-to-emitter voltage	—	—	2.0		$V_{GE} = 15V, I_C = 150A$
		—	2.2	—		$V_{GE}=15V, I_C=150A, T_J=125^\circ\text{C}$
V_{FM}	Diode forward voltage - maximum	—	1.8	2.0		$I_F = 150A, V_{GE} = 0V$
		—	1.75	—		$I_F=150A, V_{GE}=0V, T_J= 125^\circ\text{C}$
V_{GEth}	Gate threshold voltage	3.0	—	5.5	$I_C = 1mA$	
ΔV_{GEth}	Threshold voltage temperature coefficient	—	- 11	—	mV/ $^\circ\text{C}$	$V_{CE} = V_{GE}, I_C = 1mA$
g_{fe}	Forward transconductance	104	—	144	S(Ω)	$V_{CE} = 25V, I_C = 150A$
I_{CES}	Collector-to-emitter leakage current	—	—	2	mA	$V_{GE} = 0V, V_{CE} = 600V$
		—	—	20		$V_{GE}=0V, V_{CE}=600V, T_J=125^\circ\text{C}$
I_{GES}	Gate-to-emitter leakage current	—	—	± 2	μA	$V_{GE} = \pm 20V$

Dynamic Characteristics - $T_J = 125^\circ\text{C}$, unless otherwise stated

Parameter	Description	Min	Typ	Max	Units	Test Conditions
E_{on}	Turn-on switching energy	—	0.03	—	mJ/A	$R_G = 18\Omega, V_{CC} = 300V$
E_{off} (1)	Turn-off switching energy	—	0.11	—		$I_C = 150A, L_S = 100nH$
E_{ts} (1)	Total switching energy	—	—	0.18		$V_{GE} = \pm 15V$
$t_{d(on)}$	Turn-on delay time	—	200	—	ns	$R_G = 18\Omega, V_{CC} = 300V$
t_r	Rise time	—	400	—		$I_C = 150A$
$t_{d(off)}$	Turn-off delay time	—	250	—		$V_{GE} = \pm 15V$
t_f	Fall time	—	350	—		Resistive load, $T_J = 25^\circ\text{C}$
I_{rr}	Diode peak recovery current	—	50	—	A	$R_G = 18\Omega, V_{CC} = 300V$
t_{rr}	Diode recovery time	—	110	—	ns	$I_C = 150A$
Q_{rr}	Diode recovery charge	—	3	—	μC	$V_{GE} = \pm 15V$
Q_{ge}	Gate-to-emitter charge (turn-on)	52	—	84	nC	$V_{CC} = 480V$
Q_{gc}	Gate-to-collector charge (turn-on)	140	—	280		$I_C = 108A$
Q_g	Total gate charge (turn-on)	300	—	560		$V_{GE} = 15V$
C_{ies}	Input capacitance	—	11600	—	pF	$V_{GE} = 0V$
C_{oes}	Output capacitance	—	1320	—		$V_{CC} = 30V$
C_{res}	Reverse transfer capacitance	—	160	—		$f = 1MHz$
t_{sc}	Short circuit withstand time	10	—	—	μs	$V_{CC} = 360V, V_{GE} = \pm 15V$ Min. $R_G = 18\Omega, V_{CEP} = 500V$

(1) Includes tail losses

Thermal and Mechanical Characteristics

Parameter	Description	Typ	Max	Units
R_{thJC} (IGBT)	Thermal resistance, junction to case, each IGBT	—	0.19	$^\circ\text{C/W}$
R_{thJC} (Diode)	Thermal resistance, junction to case, each diode	—	0.28	
R_{thCS} (Module)	Thermal resistance, case to sink	0.041	0.100	
Wt	Weight of module	150	—	g

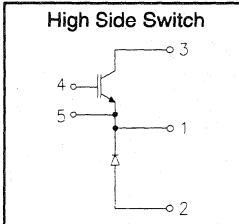
Refer to Section D - page D-15 for Package Outline 7 -INT-A-PAK, New - Low Side Switch

IRGNIN050M06

"CHOPPER" IGBT INT-A-PAK

Low conduction loss IGBT

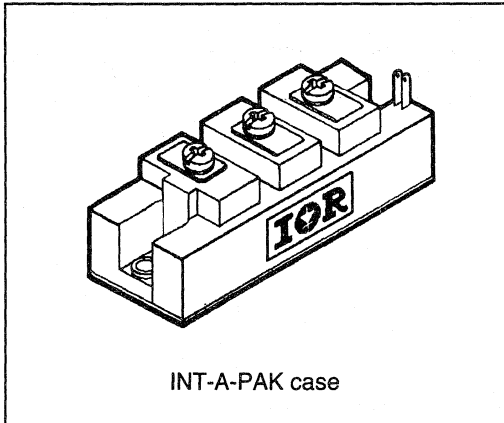
- Rugged Design
- Simple gate-drive
- Switching-Loss Rating includes all "tail" losses
- Short circuit rated



$V_{CE} = 600V$
$I_C = 50A$
$V_{CE(ON)} < 2.0V$
$t_{sc} > 10\mu s$

Description

IR's advanced IGBT technology is the key to this line of INT-A-PAK Power Modules. The efficient geometry and unique processing of the IGBT allow higher current densities than comparable bipolar power module transistors, while at the same time requiring the simpler gate-drive of the familiar power MOSFET. These modules are short circuit rated for applications such as motor control requiring this important feature.



Absolute Maximum Ratings

Parameter	Description	Value	Units
V_{CES}	Continuous collector to emitter voltage	600	V
$I_C @ T_C = 25^\circ C$	Continuous collector current	60	A
$I_C @ T_C = 85^\circ C$	Continuous collector current	35	
$I_C @ T_C = 100^\circ C$	Continuous collector current	23	
I_{LM}	Peak switching current	100	
I_{FM}	Peak diode forward current (1)	100	V
V_{GE}	Gate to emitter voltage	± 20	
V_{ISOL}	RMS isolation voltage, any terminal to case, $t = 1$ min	2500	
$P_D @ T_C = 25^\circ C$	Power dissipation	240	W
T_J	Operating junction temperature range	-40 to 150	$^\circ C$
T_{STG}	Storage temperature range	-40 to 125	

(1) Duration limited by max junction temperature.

Electrical Characteristics - $T_J = 25^\circ\text{C}$, unless otherwise stated

Parameter	Description	Min	Typ	Max	Units	Test Conditions
BV_{CES}	Collector-to-emitter breakdown voltage	600	—	—	V	$V_{GE} = 0V, I_C = 500\mu A$
$V_{CE(ON)}$	Collector-to-emitter voltage	—	—	2.0		$V_{GE} = 15V, I_C = 50A$
		—	2.2	—		$V_{GE} = 15V, I_C = 50A, T_J = 125^\circ\text{C}$
V_{FM}	Diode forward voltage - maximum	—	1.8	2.0		$I_F = 50A, V_{GE} = 0V$
		—	1.75	—		$I_F = 50A, V_{GE} = 0V, T_J = 125^\circ\text{C}$
V_{GEth}	Gate threshold voltage	3.0	—	5.5	$I_C = 250\mu A$	
ΔV_{GEth}	Threshold voltage temp. coefficient	—	-11	—	mV/ $^\circ\text{C}$	$V_{CE} = V_{GE}, I_C = 250\mu A$
g_{fe}	Forward transconductance	26	—	36	S(τ)	$V_{CE} = 25V, I_C = 50A$
I_{CES}	Collector-to-emitter leakage current	—	—	500	μA	$V_{GE} = 0V, V_{CE} = 600V$
		—	—	5	mA	$V_{GE} = 0V, V_{CE} = 600V, T_J = 125^\circ\text{C}$
I_{GES}	Gate-to-emitter leakage current	—	—	± 500	nA	$V_{GE} = \pm 20V$

Dynamic Characteristics - $T_J = 125^\circ\text{C}$, unless otherwise stated

Parameter	Description	Min	Typ	Max	Units	Test Conditions
E_{on}	Turn-on switching energy	—	0.03	—	mJ/A	$R_G = 18\Omega, V_{CC} = 300V$
E_{off} (1)	Turn-off switching energy	—	0.11	—		$I_C = 50A, L_S = 100nH$
E_{ts} (1)	Total switching energy	—	—	0.18		$V_{GE} = \pm 15V$
$t_{d(on)}$	Turn-on delay time	—	200	—	ns	$R_G = 18\Omega, V_{CC} = 300V$
t_r	Rise time	—	400	—		$I_C = 50A$
$t_{d(off)}$	Turn-off delay time	—	250	—		$V_{GE} = \pm 15V$
t_f	Fall time	—	350	—		Resistive load, $T_J = 25^\circ\text{C}$
I_{rr}	Diode peak recovery current	—	20	—		$R_G = 18\Omega, V_{CC} = 300V$
t_{rr}	Diode recovery time	—	110	—	ns	$I_C = 50A$
Q_{rr}	Diode recovery charge	—	1.2	—	μC	$V_{GE} = \pm 15V$
Q_{ge}	Gate-to-emitter charge (turn-on)	13	—	21	nC	$V_{CC} = 480V$
Q_{gc}	Gate-to-collector charge (turn-on)	35	—	70		$I_C = 27A$
Q_g	Total gate charge (turn-on)	77	—	140		$V_{GE} = 15V$
C_{ies}	Input capacitance	—	2900	—	pF	$V_{GE} = 0V$
C_{oes}	Output capacitance	—	330	—		$V_{CC} = 30V$
C_{res}	Reverse transfer capacitance	—	40	—		$f = 1MHz$
t_{sc}	Short circuit withstand time	10	—	—	μs	$V_{CC} = 360V, V_{GE} = \pm 15V$ Min. $R_G = 18\Omega, V_{CEP} = 500V$

(1) Includes tail losses

Thermal and Mechanical Characteristics

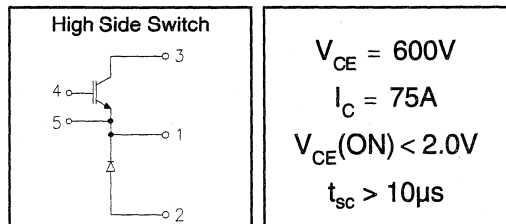
Parameter	Description	Typ	Max	Units
R_{thJC} (IGBT)	Thermal resistance, junction to case, each IGBT	—	0.52	$^\circ\text{C/W}$
R_{thJC} (Diode)	Thermal resistance, junction to case, each diode	—	0.90	
R_{thCS} (Module)	Thermal resistance, case to sink	0.041	0.100	
Wt	Weight of module	150	—	g

Refer to Section D - page D-16 for Package Outline 9 -INT-A-PAK, New - High Side Switch

"CHOPPER" IGBT INT-A-PAK

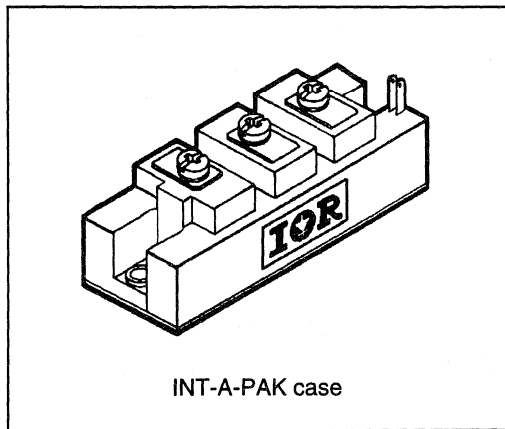
Low conduction loss IGBT

- Rugged Design
- Simple gate-drive
- Switching-Loss Rating includes all "tail" losses
- Short circuit rated



Description

IR's advanced IGBT technology is the key to this line of INT-A-PAK Power Modules. The efficient geometry and unique processing of the IGBT allow higher current densities than comparable bipolar power module transistors, while at the same time requiring the simpler gate-drive of the familiar power MOSFET. These modules are short circuit rated for applications such as motor control requiring this important feature.



Absolute Maximum Ratings

Parameter	Description	Value	Units
V_{CES}	Continuous collector to emitter voltage	600	V
$I_C @ T_C = 25^\circ C$	Continuous collector current	110	A
$I_C @ T_C = 85^\circ C$	Continuous collector current	60	
$I_C @ T_C = 100^\circ C$	Continuous collector current	40	
I_{LM}	Peak switching current	150	
I_{FM}	Peak diode forward current (1)	150	
V_{GE}	Gate to emitter voltage	± 20	V
V_{ISOL}	RMS isolation voltage, any terminal to case, $t = 1 \text{ min}$	2500	
$P_D @ T_C = 25^\circ C$	Power dissipation	391	W
T_J	Operating junction temperature range	-40 to 150	$^\circ C$
T_{STG}	Storage temperature range	-40 to 125	

(1) Duration limited by max junction temperature.

Electrical Characteristics - $T_J = 25^\circ\text{C}$, unless otherwise stated

Parameter	Description	Min	Typ	Max	Units	Test Conditions
BV_{CES}	Collector-to-emitter breakdown voltage	600	—	—	V	$V_{GE} = 0V, I_C = 1mA$
$V_{CE(ON)}$	Collector-to-emitter voltage	—	—	2.0		$V_{GE} = 15V, I_C = 75A$
		—	2.2	—		$V_{GE} = 15V, I_C = 75A, T_J = 125^\circ\text{C}$
V_{FM}	Diode forward voltage - maximum	—	1.8	2.0		$I_F = 75A, V_{GE} = 0V$
		—	1.75	—		$I_F = 75A, V_{GE} = 0V, T_J = 125^\circ\text{C}$
V_{GEth}	Gate threshold voltage	3.0	—	5.5	$I_C = 500\mu A$	
ΔV_{GEth}	Threshold voltage temp. coefficient	—	-11	—	mV/°C	$V_{CE} = V_{GE}, I_C = 500\mu A$
g_{fe}	Forward transconductance	52	—	72	S(Ω)	$V_{CE} = 25V, I_C = 75A$
I_{CES}	Collector-to-emitter leakage current	—	—	1	mA	$V_{GE} = 0V, V_{CE} = 600V$
		—	—	10		$V_{GE} = 0V, V_{CE} = 600V, T_J = 125^\circ\text{C}$
I_{GES}	Gate-to-emitter leakage current	—	—	±1	μA	$V_{GE} = \pm 20V$

Dynamic Characteristics - $T_J = 125^\circ\text{C}$, unless otherwise stated

Parameter	Description	Min	Typ	Max	Units	Test Conditions
E_{on}	Turn-on switching energy	—	0.03	—	mJ/A	$R_G = 18\Omega, V_{CC} = 300V$
E_{off} (1)	Turn-off switching energy	—	0.11	—		$I_C = 75A, L_S = 100nH$
E_{ts} (1)	Total switching energy	—	—	0.18		$V_{GE} = \pm 15V$
$t_{d(on)}$	Turn-on delay time	—	200	—	ns	$R_G = 18\Omega, V_{CC} = 300V$
t_r	Rise time	—	400	—		$I_C = 75A$
$t_{d(off)}$	Turn-off delay time	—	250	—		$V_{GE} = \pm 15V$
t_f	Fall time	—	350	—		Resistive load, $T_J = 25^\circ\text{C}$
I_{rr}	Diode peak recovery current	—	27	—	A	$R_G = 18\Omega, V_{CC} = 300V$
t_{rr}	Diode recovery time	—	110	—	ns	$I_C = 75A$
Q_{rr}	Diode recovery charge	—	1.7	—	μC	$V_{GE} = \pm 15V$
Q_{ge}	Gate-to-emitter charge (turn-on)	26	—	42	nC	$V_{CC} = 480V$
Q_{gc}	Gate-to-collector charge (turn-on)	70	—	140		$I_C = 54A$
Q_g	Total gate charge (turn-on)	150	—	280		$V_{GE} = 15V$
C_{ies}	Input capacitance	—	5800	—	pF	$V_{GE} = 0V$
C_{oes}	Output capacitance	—	660	—		$V_{CC} = 30V$
C_{res}	Reverse transfer capacitance	—	80	—		$f = 1MHz$
t_{sc}	Short circuit withstand time	10	—	—	μs	$V_{CC} = 360V, V_{GE} = \pm 15V$ Min. $R_G = 18\Omega, V_{CEP} = 500V$

(1) Includes tail losses

Thermal and Mechanical Characteristics

Parameter	Description	Typ	Max	Units
R_{thJC} (IGBT)	Thermal resistance, junction to case, each IGBT	—	0.32	°C/W
R_{thJC} (Diode)	Thermal resistance, junction to case, each diode	—	0.48	
R_{thCS} (Module)	Thermal resistance, case to sink	0.041	0.100	
Wt	Weight of module	150	—	g

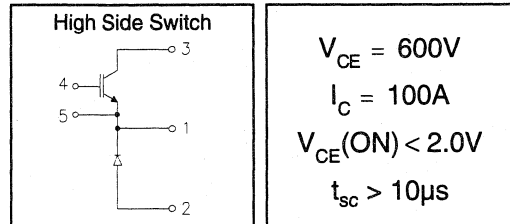
Refer to Section D - page D-16 for Package Outline 9 -INT-A-PAK, New - High Side Switch

IRGNIN100M06

"CHOPPER" IGBT INT-A-PAK

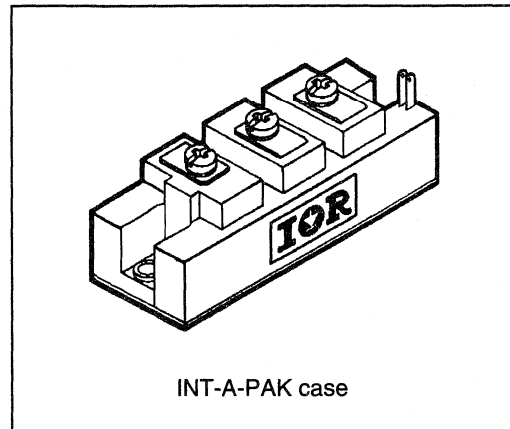
Low conduction loss IGBT

- Rugged Design
- Simple gate-drive
- Switching-Loss Rating includes all "tail" losses
- Short circuit rated



Description

IR's advanced IGBT technology is the key to this line of INT-A-PAK Power Modules. The efficient geometry and unique processing of the IGBT allow higher current densities than comparable bipolar power module transistors, while at the same time requiring the simpler gate-drive of the familiar power MOSFET. These modules are short circuit rated for applications such as motor control requiring this important feature.


 Motor
Control
Power
Modules

Absolute Maximum Ratings

Parameter	Description	Value	Units
V_{CES}	Continuous collector to emitter voltage	600	V
$I_C @ T_C = 25^\circ C$	Continuous collector current	150	A
$I_C @ T_C = 85^\circ C$	Continuous collector current	80	
$I_C @ T_C = 100^\circ C$	Continuous collector current	60	
I_{LM}	Peak switching current	200	
I_{FM}	Peak diode forward current (1)	200	V
V_{GE}	Gate to emitter voltage	± 20	
V_{ISOL}	RMS isolation voltage, any terminal to case, $t = 1 \text{ min}$	2500	
$P_D @ T_C = 25^\circ C$	Power dissipation	500	W
T_J	Operating junction temperature range	-40 to 150	$^\circ C$
T_{STG}	Storage temperature range	-40 to 125	

(1) Duration limited by max junction temperature.

Electrical Characteristics - $T_J = 25^\circ\text{C}$, unless otherwise stated

Parameter	Description	Min	Typ	Max	Units	Test Conditions
BV_{CES}	Collector-to-emitter breakdown voltage	600	—	—	V	$V_{GE} = 0\text{V}, I_C = 1.5\text{mA}$
$V_{CE(ON)}$	Collector-to-emitter voltage	—	—	2.0		$V_{GE} = 15\text{V}, I_C = 100\text{A}$
		—	2.2	—		$V_{GE} = 15\text{V}, I_C = 100\text{A}, T_J = 125^\circ\text{C}$
V_{FM}	Diode forward voltage - maximum	—	1.8	2.0		$I_F = 100\text{A}, V_{GE} = 0\text{V}$
		—	1.75	—		$I_F = 100\text{A}, V_{GE} = 0\text{V}, T_J = 125^\circ\text{C}$
V_{Geth}	Gate threshold voltage	3.0	—	5.5	$I_C = 750\mu\text{A}$	
ΔV_{Geth}	Threshold voltage temp. coefficient	—	-11	—	mV/°C	$V_{CE} = V_{GE}, I_C = 750\mu\text{A}$
g_{fe}	Forward transconductance	78	—	108	S(τ)	$V_{CE} = 25\text{V}, I_C = 100\text{A}$
I_{CES}	Collector-to-emitter leakage current	—	—	1.5	mA	$V_{GE} = 0\text{V}, V_{CE} = 600\text{V}$
		—	—	15		$V_{GE} = 0\text{V}, V_{CE} = 600\text{V}, T_J = 125^\circ\text{C}$
I_{GES}	Gate-to-emitter leakage current	—	—	± 1.5	μA	$V_{GE} = \pm 20\text{V}$

Dynamic Characteristics - $T_J = 125^\circ\text{C}$, unless otherwise stated

Parameter	Description	Min	Typ	Max	Units	Test Conditions
E_{on}	Turn-on switching energy	—	0.03	—	mJ/A	$R_G = 18\Omega, V_{CC} = 300\text{V}$
E_{off} (1)	Turn-off switching energy	—	0.11	—		$I_C = 100\text{A}, L_S = 100\text{nH}$
E_{ts} (1)	Total switching energy	—	—	0.18		$V_{GE} = \pm 15\text{V}$
$t_{d(on)}$	Turn-on delay time	—	200	—	ns	$R_G = 18\Omega, V_{CC} = 300\text{V}$
t_r	Rise time	—	400	—		$I_C = 100\text{A}$
$t_{d(off)}$	Turn-off delay time	—	250	—		$V_{GE} = \pm 15\text{V}$
t_f	Fall time	—	350	—		Resistive load, $T_J = 25^\circ\text{C}$
I_{rr}	Diode peak recovery current	—	40	—	A	$R_G = 18\Omega, V_{CC} = 300\text{V}$
t_{rr}	Diode recovery time	—	110	—	ns	$I_C = 100\text{A}$
Q_{rr}	Diode recovery charge	—	2.2	—	μC	$V_{GE} = \pm 15\text{V}$
Q_{ge}	Gate-to-emitter charge (turn-on)	39	—	63	nC	$V_{CC} = 480\text{V}$
Q_{gc}	Gate-to-collector charge (turn-on)	105	—	210	nC	$I_C = 81\text{A}$
Q_g	Total gate charge (turn-on)	225	—	420		$V_{GE} = 15\text{V}$
C_{ies}	Input capacitance	—	8700	—		pF
C_{oes}	Output capacitance	—	990	—	$V_{CC} = 30\text{V}$	
C_{res}	Reverse transfer capacitance	—	120	—	$f = 1\text{MHz}$	
t_{sc}	Short circuit withstand time	10	—	—	μs	$V_{CC} = 360\text{V}, V_{GE} = \pm 15\text{V}$ Min. $R_G = 18\Omega, V_{CEP} = 500\text{V}$

(1) Includes tail losses

Thermal and Mechanical Characteristics

Parameter	Description	Typ	Max	Units
R_{thJC} (IGBT)	Thermal resistance, junction to case, each IGBT	—	0.25	°C/W
R_{thJC} (Diode)	Thermal resistance, junction to case, each diode	—	0.38	
R_{thCS} (Module)	Thermal resistance, case to sink	0.041	0.100	
Wt	Weight of module	150	—	g

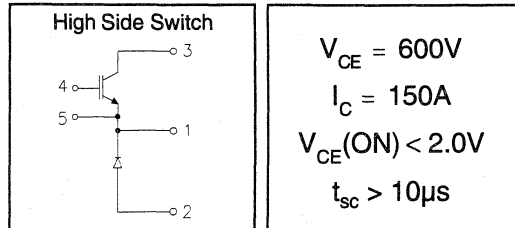
Refer to Section D - page D-16 for Package Outline 9 -INT-A-PAK, New - High Side Switch

IRGNIN150M06

"CHOPPER" IGBT INT-A-PAK

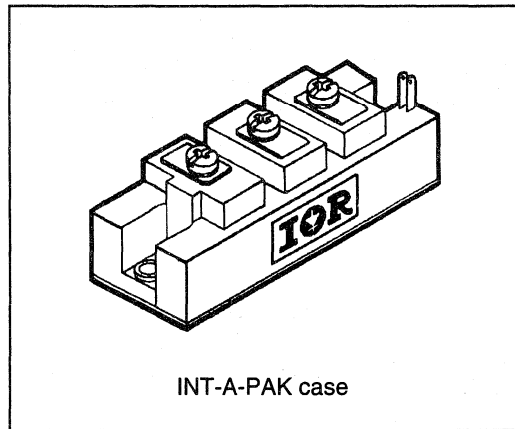
Low conduction loss IGBT

- Rugged Design
- Simple gate-drive
- Switching-Loss Rating includes all "tail" losses
- Short circuit rated



Description

IR's advanced IGBT technology is the key to this line of INT-A-PAK Power Modules. The efficient geometry and unique processing of the IGBT allow higher current densities than comparable bipolar power module transistors, while at the same time requiring the simpler gate-drive of the familiar power MOSFET. These modules are short circuit rated for applications such as motor control requiring this important feature.



Absolute Maximum Ratings

Parameter	Description	Value	Units
V_{CES}	Continuous collector to emitter voltage	600	V
$I_C @ T_C = 25^\circ C$	Continuous collector current	200	A
$I_C @ T_C = 85^\circ C$	Continuous collector current	110	
$I_C @ T_C = 100^\circ C$	Continuous collector current	80	
I_{LM}	Peak switching current	300	
I_{FM}	Peak diode forward current (1)	300	
V_{GE}	Gate to emitter voltage	± 20	V
V_{ISOL}	RMS isolation voltage, any terminal to case, $t = 1$ min	2500	W
$P_D @ T_C = 25^\circ C$	Power dissipation	658	
T_J	Operating junction temperature range	-40 to 150	
T_{STG}	Storage temperature range	-40 to 125	

(1) Duration limited by max junction temperature.

Target Data

Electrical Characteristics - $T_J = 25^\circ\text{C}$, unless otherwise stated

Parameter	Description	Min	Typ	Max	Units	Test Conditions
BV_{CES}	Collector-to-emitter breakdown voltage	600	—	—	V	$V_{GE} = 0V, I_C = 2mA$
$V_{CE(ON)}$	Collector-to-emitter voltage	—	—	2.0		$V_{GE} = 15V, I_C = 150A$
		—	2.2	—		$V_{GE} = 15V, I_C = 150A, T_J = 125^\circ\text{C}$
V_{FM}	Diode forward voltage - maximum	—	1.8	2.0		$I_F = 150A, V_{GE} = 0V$
		—	1.75	—		$I_F = 150A, V_{GE} = 0V, T_J = 125^\circ\text{C}$
V_{Geth}	Gate threshold voltage	3.0	—	5.5	$I_C = 1mA$	
ΔV_{Geth}	Threshold voltage temperature coefficient	—	-11	—	$mV/^\circ\text{C}$	$V_{CE} = V_{GE}, I_C = 1mA$
g_{fe}	Forward transconductance	104	—	144	S($\bar{\omega}$)	$V_{CE} = 25V, I_C = 150A$
I_{CES}	Collector-to-emitter leakage current	—	—	2	mA	$V_{GE} = 0V, V_{CE} = 600V$
		—	—	20		$V_{GE} = 0V, V_{CE} = 600V, T_J = 125^\circ\text{C}$
I_{GES}	Gate-to-emitter leakage current	—	—	± 2	μA	$V_{GE} = \pm 20V$

Dynamic Characteristics - $T_J = 125^\circ\text{C}$, unless otherwise stated

Parameter	Description	Min	Typ	Max	Units	Test Conditions
E_{on}	Turn-on switching energy	—	0.03	—	mJ/A	$R_G = 18\Omega, V_{CC} = 300V$
E_{off} (1)	Turn-off switching energy	—	0.11	—		$I_C = 150A, L_S = 100nH$
E_{ts} (1)	Total switching energy	—	—	0.18		$V_{GE} = \pm 15V$
$t_{d(on)}$	Turn-on delay time	—	200	—	ns	$R_G = 18\Omega, V_{CC} = 300V$
t_r	Rise time	—	400	—		$I_C = 150A$
$t_{d(off)}$	Turn-off delay time	—	250	—		$V_{GE} = \pm 15V$
t_f	Fall time	—	350	—		Resistive load, $T_J = 25^\circ\text{C}$
I_{rr}	Diode peak recovery current	—	50	—		A
t_{rr}	Diode recovery time	—	110	—	ns	$I_C = 150A$
Q_{rr}	Diode recovery charge	—	3	—	μC	$V_{GE} = \pm 15V$
Q_{ge}	Gate-to-emitter charge (turn-on)	52	—	84	nC	$V_{CC} = 480V$
Q_{gc}	Gate-to-collector charge (turn-on)	140	—	280		$I_C = 108A$
Q_g	Total gate charge (turn-on)	300	—	560		$V_{GE} = 15V$
C_{ies}	Input capacitance	—	11600	—	pF	$V_{GE} = 0V$
C_{oes}	Output capacitance	—	1320	—		$V_{CC} = 30V$
C_{res}	Reverse transfer capacitance	—	160	—		$f = 1MHz$
t_{sc}	Short circuit withstand time	10	—	—	μs	$V_{CC} = 360V, V_{GE} = \pm 15V$ Min. $R_G = 18\Omega, V_{CEP} = 500V$

(1) Includes tail losses

Thermal and Mechanical Characteristics

Parameter	Description	Typ	Max	Units
R_{thJC} (IGBT)	Thermal resistance, junction to case, each IGBT	—	0.19	$^\circ\text{C/W}$
R_{thJC} (Diode)	Thermal resistance, junction to case, each diode	—	0.28	
R_{thCS} (Module)	Thermal resistance, case to sink	0.041	0.100	
Wt	Weight of module	150	—	g

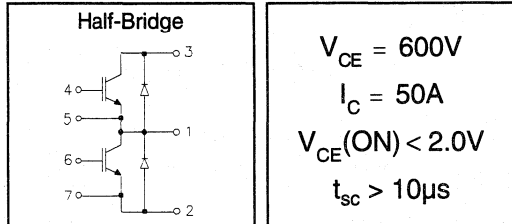
Refer to Section D - page D-16 for Package Outline 9 -INT-A-PAK, New - High Side Switch

IRGTIN050M06

"HALF-BRIDGE" IGBT INT-A-PAK

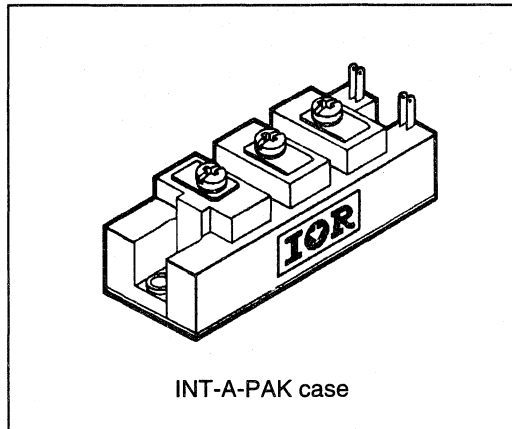
Low conduction loss IGBT

- Rugged Design
- Simple gate-drive
- Switching-Loss Rating includes all "tail" losses
- Short circuit rated



Description

IR's advanced IGBT technology is the key to this line of INT-A-PAK Power Modules. The efficient geometry and unique processing of the IGBT allow higher current densities than comparable bipolar power module transistors, while at the same time requiring the simpler gate-drive of the familiar power MOSFET. These modules are short circuit rated for applications such as motor control requiring this important feature.



Motor
Control
Pak
Modules

Absolute Maximum Ratings

Parameter	Description	Value	Units
V_{CES}	Continuous collector to emitter voltage	600	V
$I_C @ T_C = 25^\circ C$	Continuous collector current	60	A
$I_C @ T_C = 85^\circ C$	Continuous collector current	35	
$I_C @ T_C = 100^\circ C$	Continuous collector current	23	
I_{LM}	Peak switching current	100	
I_{FM}	Peak diode forward current (1)	100	V
V_{GE}	Gate to emitter voltage	± 20	
V_{ISOL}	RMS isolation voltage, any terminal to case, $t = 1$ min	2500	W
$P_D @ T_C = 25^\circ C$	Power dissipation	240	
T_J	Operating junction temperature range	-40 to 150	$^\circ C$
T_{STG}	Storage temperature range	-40 to 125	

(1) Duration limited by max junction temperature.

Electrical Characteristics - $T_J = 25^\circ\text{C}$, unless otherwise stated

Parameter	Description	Min	Typ	Max	Units	Test Conditions
BV_{CES}	Collector-to-emitter breakdown voltage	600	—	—	V	$V_{GE} = 0V, I_C = 500\mu A$
$V_{CE(ON)}$	Collector-to-emitter voltage	—	—	2.0		$V_{GE} = 15V, I_C = 50A$
		—	2.2	—		$V_{GE} = 15V, I_C = 50A, T_J = 125^\circ\text{C}$
V_{FM}	Diode forward voltage - maximum	—	1.8	2.0		$I_F = 50A, V_{GE} = 0V$
		—	1.75	—		$I_F = 50A, V_{GE} = 0V, T_J = 125^\circ\text{C}$
V_{GEth}	Gate threshold voltage	3.0	—	5.5	$I_C = 250\mu A$	
ΔV_{GEth}	Threshold voltage temperature coefficient	—	-11	—	mV/ $^\circ\text{C}$	$V_{CE} = V_{GE}, I_C = 250\mu A$
g_{fe}	Forward transconductance	26	—	36	S(\bar{v})	$V_{CE} = 25V, I_C = 50A$
I_{CES}	Collector-to-emitter leakage current	—	—	500	μA	$V_{GE} = 0V, V_{CE} = 600V$
		—	—	5	mA	$V_{GE} = 0V, V_{CE} = 600V, T_J = 125^\circ\text{C}$
I_{GES}	Gate-to-emitter leakage current	—	—	± 500	nA	$V_{GE} = \pm 20V$

Dynamic Characteristics - $T_J = 125^\circ\text{C}$, unless otherwise stated

Parameter	Description	Min	Typ	Max	Units	Test Conditions
E_{on}	Turn-on switching energy	—	0.03	—	mJ/A	$R_G = 18\Omega, V_{CC} = 300V$
E_{off} (1)	Turn-off switching energy	—	0.11	—		$I_C = 50A, L_S = 100nH$
E_{ts} (1)	Total switching energy	—	—	0.18		$V_{GE} = \pm 15V$
$t_{d(on)}$	Turn-on delay time	—	200	—	ns	$R_G = 18\Omega, V_{CC} = 300V$
t_r	Rise time	—	400	—		$I_C = 50A$
$t_{d(off)}$	Turn-off delay time	—	250	—		$V_{GE} = \pm 15V$
t_f	Fall time	—	350	—		Resistive load, $T_J = 25^\circ\text{C}$
I_{rr}	Diode peak recovery current	—	20	—	A	$R_G = 18\Omega, V_{CC} = 300V$
t_{rr}	Diode recovery time	—	110	—	ns	$I_C = 50A$
Q_{rr}	Diode recovery charge	—	1.2	—	μC	$V_{GE} = \pm 15V$
Q_{ge}	Gate-to-emitter charge (turn-on)	13	—	21	nC	$V_{CC} = 480V$
Q_{gc}	Gate-to-collector charge (turn-on)	35	—	70		$I_C = 27A$
Q_g	Total gate charge (turn-on)	77	—	140		$V_{GE} = 15V$
C_{ies}	Input capacitance	—	2900	—	pF	$V_{GE} = 0V$
C_{oes}	Output capacitance	—	330	—		$V_{CC} = 30V$
C_{res}	Reverse transfer capacitance	—	40	—		$f = 1MHz$
t_{sc}	Short circuit withstand time	10	—	—	μs	$V_{CC} = 360V, V_{GE} = \pm 15V$ Min. $R_G = 18\Omega, V_{CEP} = 500V$

(1) Includes tail losses

Thermal and Mechanical Characteristics

Parameter	Description	Typ	Max	Units
R_{thJC} (IGBT)	Thermal resistance, junction to case, each IGBT	—	0.52	$^\circ\text{C/W}$
R_{thJC} (Diode)	Thermal resistance, junction to case, each diode	—	0.90	
R_{thCS} (Module)	Thermal resistance, case to sink	0.041	0.100	
Wt	Weight of module	150	—	g

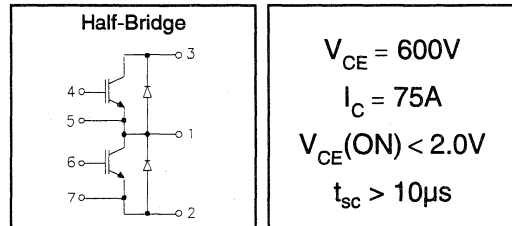
Refer to Section D - page D-17 for Package Outline11 -INT-A-PAK, New -Half Bridge

IRGTIN075M06

"HALF-BRIDGE" IGBT INT-A-PAK

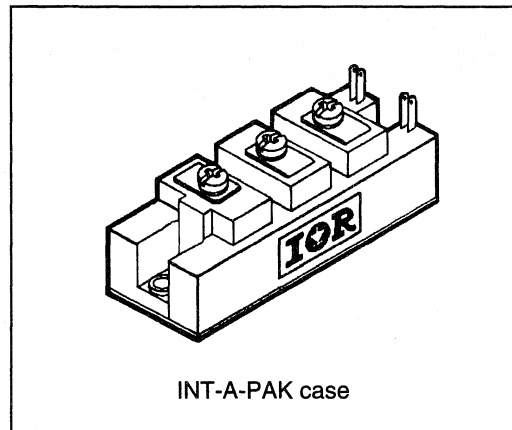
Low conduction loss IGBT

- Rugged Design
- Simple gate-drive
- Switching-Loss Rating includes all "tail" losses
- Short circuit rated



Description

IR's advanced IGBT technology is the key to this line of INT-A-PAK Power Modules. The efficient geometry and unique processing of the IGBT allow higher current densities than comparable bipolar power module transistors, while at the same time requiring the simpler gate-drive of the familiar power MOSFET. These modules are short circuit rated for applications such as motor control requiring this important feature.



Absolute Maximum Ratings

Parameter	Description	Value	Units
V_{CES}	Continuous collector to emitter voltage	600	V
$I_C @ T_C = 25^\circ C$	Continuous collector current	110	A
$I_C @ T_C = 85^\circ C$	Continuous collector current	60	
$I_C @ T_C = 100^\circ C$	Continuous collector current	40	
I_{LM}	Peak switching current	150	
I_{FM}	Peak diode forward current (1)	150	
V_{GE}	Gate to emitter voltage	± 20	V
V_{ISOL}	RMS isolation voltage, any terminal to case, $t = 1$ min	2500	
$P_D @ T_C = 25^\circ C$	Power dissipation	391	W
T_J	Operating junction temperature range	-40 to 150	$^\circ C$
T_{STG}	Storage temperature range	-40 to 125	

(1) Duration limited by max junction temperature.

Electrical Characteristics - $T_J = 25^\circ\text{C}$, unless otherwise stated

Parameter	Description	Min	Typ	Max	Units	Test Conditions
BV_{CES}	Collector-to-emitter breakdown voltage	600	—	—	V	$V_{GE} = 0V, I_C = 1mA$
$V_{CE(ON)}$	Collector-to-emitter voltage	—	—	2.0		$V_{GE} = 15V, I_C = 75A$
		—	2.2	—		$V_{GE} = 15V, I_C = 75A, T_J = 125^\circ\text{C}$
V_{FM}	Diode forward voltage - maximum	—	1.8	2.0		$I_F = 75A, V_{GE} = 0V$
		—	1.75	—		$I_F = 75A, V_{GE} = 0V, T_J = 125^\circ\text{C}$
V_{GEth}	Gate threshold voltage	3.0	—	5.5	$I_C = 500\mu A$	
ΔV_{GEth}	Threshold voltage temp. coefficient	—	-11	—	mV/ $^\circ\text{C}$	$V_{CE} = V_{GE}, I_C = 500\mu A$
g_{fe}	Forward transconductance	52	—	72	S(τ)	$V_{CE} = 25V, I_C = 75A$
I_{CES}	Collector-to-emitter leakage current	—	—	1	mA	$V_{GE} = 0V, V_{CE} = 600V$
		—	—	10		$V_{GE} = 0V, V_{CE} = 600V, T_J = 125^\circ\text{C}$
I_{GES}	Gate-to-emitter leakage current	—	—	± 1	μA	$V_{GE} = \pm 20V$

Dynamic Characteristics - $T_J = 125^\circ\text{C}$, unless otherwise stated

Parameter	Description	Min	Typ	Max	Units	Test Conditions
E_{on}	Turn-on switching energy	—	0.03	—	mJ/A	$R_G = 18\Omega, V_{CC} = 300V$
E_{off} (1)	Turn-off switching energy	—	0.11	—		$I_C = 75A, L_S = 100nH$
E_{ts} (1)	Total switching energy	—	—	0.18		$V_{GE} = \pm 15V$
$t_{d(on)}$	Turn-on delay time	—	200	—	ns	$R_G = 18\Omega, V_{CC} = 300V$
t_r	Rise time	—	400	—		$I_C = 75A$
$t_{d(off)}$	Turn-off delay time	—	250	—		$V_{GE} = \pm 15V$
t_f	Fall time	—	350	—		Resistive load, $T_J = 25^\circ\text{C}$
I_{rr}	Diode peak recovery current	—	27	—	A	$R_G = 18\Omega, V_{CC} = 300V$
t_{rr}	Diode recovery time	—	110	—	ns	$I_C = 75A$
Q_{rr}	Diode recovery charge	—	1.7	—	μC	$V_{GE} = \pm 15V$
Q_{ge}	Gate-to-emitter charge (turn-on)	26	—	42	nC	$V_{CC} = 480V$
Q_{gc}	Gate-to-collector charge (turn-on)	70	—	140		$I_C = 54A$
Q_g	Total gate charge (turn-on)	150	—	280		$V_{GE} = 15V$
C_{ies}	Input capacitance	—	5800	—	pF	$V_{GE} = 0V$
C_{oes}	Output capacitance	—	660	—		$V_{CC} = 30V$
C_{res}	Reverse transfer capacitance	—	80	—		$f = 1MHz$
t_{sc}	Short circuit withstand time	10	—	—	μs	$V_{CC} = 360V, V_{GE} = \pm 15V$ Min. $R_G = 18\Omega, V_{CEP} = 500V$

(1) Includes tail losses

Thermal and Mechanical Characteristics

Parameter	Description	Typ	Max	Units
R_{thJC} (IGBT)	Thermal resistance, junction to case, each IGBT	—	0.32	$^\circ\text{C/W}$
R_{thJC} (Diode)	Thermal resistance, junction to case, each diode	—	0.48	
R_{thCS} (Module)	Thermal resistance, case to sink	0.041	0.100	
Wt	Weight of module	150	—	g

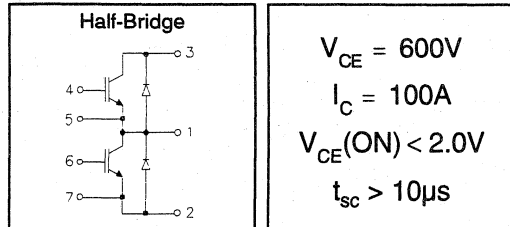
Refer to Section D - page D-17 for Package Outline11 -INT-A-PAK, New -Half Bridge

IRGTIN100M06

"HALF-BRIDGE" IGBT INT-A-PAK

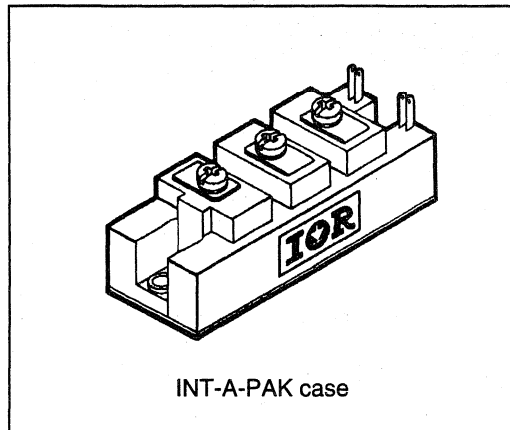
Low conduction loss IGBT

- Rugged Design
- Simple gate-drive
- Switching-Loss Rating includes all "tail" losses
- Short circuit rated



Description

IR's advanced IGBT technology is the key to this line of INT-A-PAK Power Modules. The efficient geometry and unique processing of the IGBT allow higher current densities than comparable bipolar power module transistors, while at the same time requiring the simpler gate-drive of the familiar power MOSFET. These modules are short circuit rated for applications such as motor control requiring this important feature.



Absolute Maximum Ratings

Parameter	Description	Value	Units
V_{CES}	Continuous collector to emitter voltage	600	V
$I_C @ T_C = 25^\circ C$	Continuous collector current	150	A
$I_C @ T_C = 85^\circ C$	Continuous collector current	80	
$I_C @ T_C = 100^\circ C$	Continuous collector current	60	
I_{LM}	Peak switching current	200	
I_{FM}	Peak diode forward current (1)	200	
V_{GE}	Gate to emitter voltage	± 20	V
V_{ISOL}	RMS isolation voltage, any terminal to case, $t = 1$ min	2500	
$P_D @ T_C = 25^\circ C$	Power dissipation	500	W
T_J	Operating junction temperature range	-40 to 150	$^\circ C$
T_{STG}	Storage temperature range	-40 to 125	

(1) Duration limited by max junction temperature.

Electrical Characteristics - $T_J = 25^\circ\text{C}$, unless otherwise stated

Parameter	Description	Min	Typ	Max	Units	Test Conditions
BV_{CES}	Collector-to-emitter breakdown voltage	600	—	—	V	$V_{GE} = 0V, I_C = 1.5mA$
$V_{CE(ON)}$	Collector-to-emitter voltage	—	—	2.0		$V_{GE} = 15V, I_C = 100A$
		—	2.2	—		$V_{GE} = 15V, I_C = 100A, T_J = 125^\circ\text{C}$
V_{FM}	Diode forward voltage - maximum	—	1.8	2.0		$I_F = 100A, V_{GE} = 0V$
		—	1.75	—		$I_F = 100A, V_{GE} = 0V, T_J = 125^\circ\text{C}$
V_{GEth}	Gate threshold voltage	3.0	—	5.5	$I_C = 750\mu A$	
ΔV_{GEth}	Threshold voltage temp. coefficient	—	-11	—	mV/°C	$V_{CE} = V_{GE}, I_C = 750\mu A$
g_{fe}	Forward transconductance	78	—	108	S(τ)	$V_{CE} = 25V, I_C = 100A$
I_{CES}	Collector-to-emitter leakage current	—	—	1.5	mA	$V_{GE} = 0V, V_{CE} = 600V$
		—	—	15		$V_{GE} = 0V, V_{CE} = 600V, T_J = 125^\circ\text{C}$
I_{GES}	Gate-to-emitter leakage current	—	—	± 1.5	μA	$V_{GE} = \pm 20V$

Dynamic Characteristics - $T_J = 125^\circ\text{C}$, unless otherwise stated

Parameter	Description	Min	Typ	Max	Units	Test Conditions
E_{on}	Turn-on switching energy	—	0.03	—	mJ/A	$R_G = 18\Omega, V_{CC} = 300V$
E_{off} (1)	Turn-off switching energy	—	0.11	—		$I_C = 100A, L_S = 100nH$
E_{ts} (1)	Total switching energy	—	—	0.18		$V_{GE} = \pm 15V$
$t_{d(on)}$	Turn-on delay time	—	200	—	ns	$R_G = 18\Omega, V_{CC} = 300V$
t_r	Rise time	—	400	—		$I_C = 100A$
$t_{d(off)}$	Turn-off delay time	—	250	—		$V_{GE} = \pm 15V$
t_f	Fall time	—	350	—		Resistive load, $T_J = 25^\circ\text{C}$
I_{rr}	Diode peak recovery current	—	40	—	A	$R_G = 18\Omega, V_{CC} = 300V$
t_{rr}	Diode recovery time	—	110	—		$I_C = 100A$
Q_{rr}	Diode recovery charge	—	2.2	—		$V_{GE} = \pm 15V$
Q_{ge}	Gate-to-emitter charge (turn-on)	39	—	63	nC	$V_{CC} = 480V$
Q_{gc}	Gate-to-collector charge (turn-on)	105	—	210		$I_C = 81A$
Q_g	Total gate charge (turn-on)	225	—	420		$V_{GE} = 15V$
C_{ies}	Input capacitance	—	8700	—	pF	$V_{GE} = 0V$
C_{oes}	Output capacitance	—	990	—		$V_{CC} = 30V$
C_{res}	Reverse transfer capacitance	—	120	—		$f = 1MHz$
t_{sc}	Short circuit withstand time	10	—	—	μs	$V_{CC} = 360V, V_{GE} = \pm 15V$ Min. $R_G = 18\Omega, V_{CEP} = 500V$

(1) Includes tail losses

Thermal and Mechanical Characteristics

Parameter	Description	Typ	Max	Units
R_{thJC} (IGBT)	Thermal resistance, junction to case, each IGBT	—	0.25	°C/W
R_{thJC} (Diode)	Thermal resistance, junction to case, each diode	—	0.38	
R_{thCS} (Module)	Thermal resistance, case to sink	0.041	0.100	
Wt	Weight of module	150	—	g

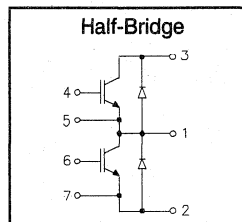
Refer to Section D - page D-17 for Package Outline11 -INT-A-PAK, New -Half Bridge

IRGTIN150M06

"HALF-BRIDGE" IGBT INT-A-PAK

Low conduction loss IGBT

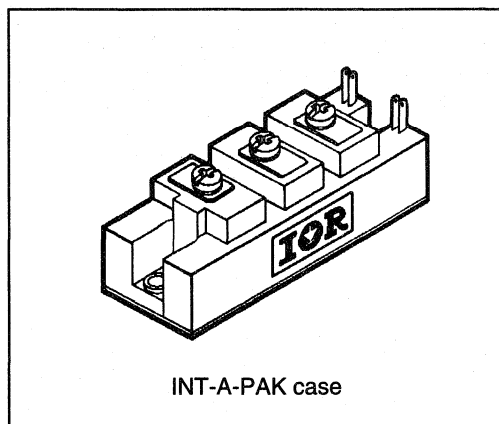
- Rugged Design
- Simple gate-drive
- Switching-Loss Rating includes all "tail" losses
- Short circuit rated



$V_{CE} = 600V$
$I_C = 150A$
$V_{CE(ON)} < 2.0V$
$t_{sc} > 10\mu s$

Description

IR's advanced IGBT technology is the key to this line of INT-A-PAK Power Modules. The efficient geometry and unique processing of the IGBT allow higher current densities than comparable bipolar power module transistors, while at the same time requiring the simpler gate-drive of the familiar power MOSFET. These modules are short circuit rated for applications such as motor control requiring this important feature.



Motor Control Fast Modules

Absolute Maximum Ratings

Parameter	Description	Value	Units
V_{CES}	Continuous collector to emitter voltage	600	V
$I_C @ T_C = 25^\circ C$	Continuous collector current	200	A
$I_C @ T_C = 85^\circ C$	Continuous collector current	110	
$I_C @ T_C = 100^\circ C$	Continuous collector current	80	
I_{LM}	Peak switching current	300	
I_{FM}	Peak diode forward current (1)	300	V
V_{GE}	Gate to emitter voltage	± 20	
V_{ISOL}	RMS isolation voltage, any terminal to case, $t = 1$ min	2500	°C
$P_D @ T_C = 25^\circ C$	Power dissipation	658	
T_J	Operating junction temperature range	-40 to 150	
T_{STG}	Storage temperature range	-40 to 125	

(1) Duration limited by max junction temperature.

Target Data

Electrical Characteristics - $T_J = 25^\circ\text{C}$, unless otherwise stated

Parameter	Description	Min	Typ	Max	Units	Test Conditions
BV_{CES}	Collector-to-emitter breakdown voltage	600	—	—	V	$V_{GE} = 0V, I_C = 2mA$
$V_{CE(ON)}$	Collector-to-emitter voltage	—	—	2.0		$V_{GE} = 15V, I_C = 150A$
		—	2.2	—		$V_{GE} = 15V, I_C = 150A, T_J = 125^\circ\text{C}$
V_{FM}	Diode forward voltage - maximum	—	1.8	2.0		$I_F = 150A, V_{GE} = 0V$
		—	1.75	—	$I_F = 150A, V_{GE} = 0V, T_J = 125^\circ\text{C}$	
V_{GEth}	Gate threshold voltage	3.0	—	5.5	mV/°C	$I_C = 1mA$
ΔV_{GEth}	Threshold voltage temp. coefficient	—	-11	—		$V_{CE} = V_{GE}, I_C = 1mA$
g_{fe}	Forward transconductance	104	—	144	S(Ω)	$V_{CE} = 25V, I_C = 150A$
I_{CES}	Collector-to-emitter leakage current	—	—	2	mA	$V_{GE} = 0V, V_{CE} = 600V$
		—	—	20		$V_{GE} = 0V, V_{CE} = 600V, T_J = 125^\circ\text{C}$
I_{GES}	Gate-to-emitter leakage current	—	—	±2	μA	$V_{GE} = \pm 20V$

Dynamic Characteristics - $T_J = 125^\circ\text{C}$, unless otherwise stated

Parameter	Description	Min	Typ	Max	Units	Test Conditions
E_{on}	Turn-on switching energy	—	0.03	—	mJ/A	$R_G = 18\Omega, V_{CC} = 300V$
E_{off} (1)	Turn-off switching energy	—	0.11	—		$I_C = 150A, L_S = 100nH$
E_{ts} (1)	Total switching energy	—	—	0.18		$V_{GE} = \pm 15V$
$t_{d(on)}$	Turn-on delay time	—	200	—	ns	$R_G = 18\Omega, V_{CC} = 300V$
t_r	Rise time	—	400	—		$I_C = 150A$
$t_{d(off)}$	Turn-off delay time	—	250	—		$V_{GE} = \pm 15V$
t_f	Fall time	—	350	—		Resistive load, $T_J = 25^\circ\text{C}$
I_{rr}	Diode peak recovery current	—	50	—		$R_G = 18\Omega, V_{CC} = 300V$
t_{rr}	Diode recovery time	—	110	—	ns	$I_C = 150A$
Q_{rr}	Diode recovery charge	—	3	—		$V_{GE} = \pm 15V$
Q_{ge}	Gate-to-emitter charge (turn-on)	52	—	84	nC	$V_{CC} = 480V$
Q_{gc}	Gate-to-collector charge (turn-on)	140	—	280		$I_C = 108A$
Q_g	Total gate charge (turn-on)	300	—	560		$V_{GE} = 15V$
C_{ies}	Input capacitance	—	11600	—	pF	$V_{GE} = 0V$
C_{oes}	Output capacitance	—	1320	—		$V_{CC} = 30V$
C_{res}	Reverse transfer capacitance	—	160	—		$f = 1MHz$
t_{sc}	Short circuit withstand time	10	—	—	μs	$V_{CC} = 360V, V_{GE} = \pm 15V$ Min. $R_G = 18\Omega, V_{CEP} = 500V$

(1) Includes tail losses

Thermal and Mechanical Characteristics

Parameter	Description	Typ	Max	Units
R_{thJC} (IGBT)	Thermal resistance, junction to case, each IGBT	—	0.19	°C/W
R_{thJC} (Diode)	Thermal resistance, junction to case, each diode	—	0.28	
R_{thCS} (Module)	Thermal resistance, case to sink	0.041	0.100	
Wt	Weight of module	150	—	g

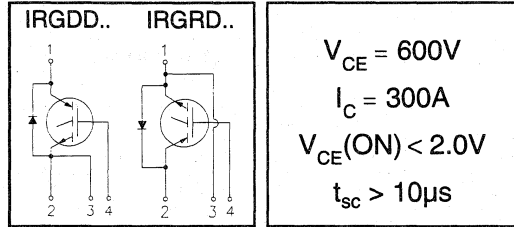
Refer to Section D - page D-17 for Package Outline11 -INT-A-PAK, New -Half Bridge

IRGDDN300M06 IRGRDN300M06

"SINGLE SWITCH" IGBT DOUBLE INT-A-PAK

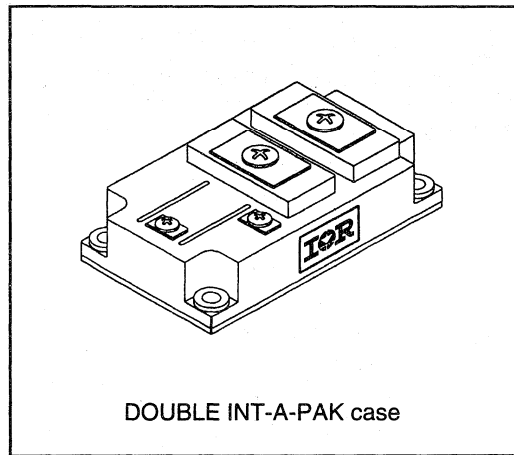
Low conduction loss IGBT

- Rugged Design
- Simple gate-drive
- Switching-Loss Rating includes all "tail" losses
- Short circuit rated



Description

IR's advanced IGBT technology is the key to this line of DOUBLE INT-A-PAK Power Modules. The efficient geometry and unique processing of the IGBT allow higher current densities than comparable bipolar power module transistors, while at the same time requiring the simpler gate-drive of the familiar power MOSFET. This superior technology has now been coupled to state of the art assembly techniques to produce a higher current module that is highly suited to power applications such as motor drives, uninterruptible power supplies, welding and power factor correction.


 Motor
Control
Fast
Modules

Absolute Maximum Ratings

Parameter	Description	Value	Units
V_{CES}	Continuous collector to emitter voltage	600	V
$I_C @ T_c = 25^\circ\text{C}$	Maximum Continuous collector current	400	A
$I_C @ T_c = 85^\circ\text{C}$	Maximum Continuous collector current	220	
$I_C @ T_c = 100^\circ\text{C}$	Maximum Continuous collector current	160	
I_{LM}	Peak switching current	600	
I_{FM}	Peak diode forward current (1)	600	V
V_{GE}	Gate to emitter voltage	± 20	
V_{ISOL}	RMS isolation voltage, any terminal to case, $t = 1 \text{ min}$	2500	
$P_D @ T_c = 25^\circ\text{C}$	Power dissipation	1563	$^\circ\text{C}$
T_J	Operating junction temperature range	-40 to 150	
T_{STG}	Storage temperature range	-40 to 125	

(1) Duration limited by max junction temperature.

IRGDDN300M06 IRGRDN300M06

Target Data



Electrical Characteristics - $T_J = 25^\circ\text{C}$, unless otherwise stated

Parameter	Description	Min	Typ	Max	Units	Test Conditions
BV_{CES}	Collector-to-emitter breakdown voltage	600	—	—	V	$V_{GE} = 0V, I_C = 4mA$
$V_{CE(ON)}$	Collector-to-emitter voltage	—	—	2.0		$V_{GE} = 15V, I_C = 300A$
		—	2.2	—		$V_{GE} = 15V, I_C = 300A, T_J = 125^\circ\text{C}$
V_{FM}	Diode forward voltage - maximum	—	1.8	2.0		$I_F = 300A, V_{GE} = 0V$
		—	1.8	—		$I_F = 300A, V_{GE} = 0V, T_J = 125^\circ\text{C}$
V_{GEth}	Gate threshold voltage	3.0	—	5.5	$I_C = 2mA$	
ΔV_{GEth}	Threshold voltage temperature coefficient	—	- 11	—	mV/ $^\circ\text{C}$	$V_{CE} = V_{GE}, I_C = 2mA$
g_{fe}	Forward transconductance	208	—	296	S(τ)	$V_{CE} = 25V, I_C = 300A$
I_{CES}	Collector-to-emitter leakage current	—	—	4	mA	$V_{GE} = 0V, V_{CE} = 600V$
		—	—	40		$V_{GE} = 0V, V_{CE} = 600V, T_J = 125^\circ\text{C}$
I_{GES}	Gate-to-emitter leakage current	—	—	± 4	μA	$V_{GE} = \pm 20V$

Dynamic Characteristics - $T_J = 125^\circ\text{C}$

Parameter	Description	Min	Typ	Max	Units	Test Conditions
E_{on}	Turn-on switching energy	—	0.03	—	mJ/A	$R_G = 15\Omega, V_{CC} = 300V$
E_{off} (1)	Turn-off switching energy	—	0.11	—		$I_C = 300A, L_S = 100nH$
E_{ts} (1)	Total switching energy	—	—	0.2		$V_{GE} = \pm 15V$
$t_{d(on)}$	Turn-on delay time	—	300	—	ns	$R_G = 15\Omega, V_{CC} = 300V$
t_r	Rise time	—	900	—		$I_C = 300A$
$t_{d(off)}$	Turn-off delay time	—	700	—		$V_{GE} = \pm 15V$
t_f	Fall time	—	350	—		Resistive Load, $T_J = 25^\circ\text{C}$
I_{rr}	Diode peak recovery current	—	110	—		A
t_{rr}	Diode recovery time	—	110	—	ns	$I_C = 300A$
Q_{rr}	Diode recovery charge	—	6	—	μC	$V_{GE} = \pm 15V$
Q_{ge}	Gate-to-emitter charge (turn-on)	104	—	168	nC	$V_{CC} = 480V$
Q_{gc}	Gate-to-collector charge (turn-on)	280	—	560		$I_C = 216A$
Q_g	Total gate charge (turn-on)	600	—	1120		$V_{GE} = 15V$
C_{ies}	Input capacitance	—	23200	—	pF	$V_{GE} = 0V$
C_{oes}	Output capacitance	—	2640	—		$V_{CC} = 30V$
C_{res}	Reverse transfer capacitance	—	320	—		$f = 1MHz$
t_{sc}	Short circuit withstand time	10	—	—	μs	$V_{CC} = 360V, V_{GE} = \pm 15V$ Min. $R_G = 15\Omega, V_{CEP} = 500V$

(1) Includes tail losses

Thermal and Mechanical Characteristics

Parameter	Description	Typ	Max	Units
R_{thJC} (IGBT)	Thermal resistance, junction to case, each IGBT	—	0.08	$^\circ\text{C/W}$
R_{thJC} (Diode)	Thermal resistance, junction to case, each diode	—	0.12	
R_{thCS} (Module)	Thermal resistance, case to sink	0.023	0.050	
Wt	Weight of module	242	—	g

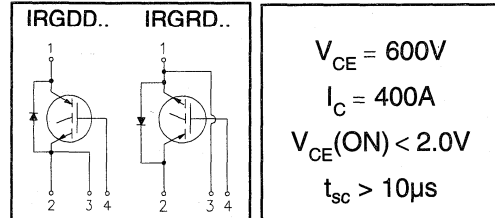
**Refer to Section D - page D-18 for the following:
Package Outline13 -Double INT-A-PAK Single Switch**

IRGDDN400M06 IRGRDN400M06

"SINGLE SWITCH" IGBT DOUBLE INT-A-PAK

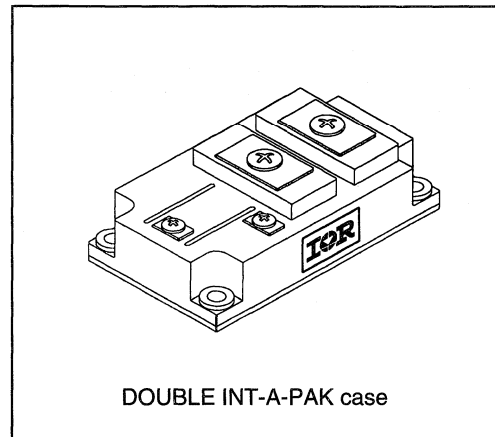
Low conduction loss IGBT

- Rugged Design
- Simple gate-drive
- Switching-Loss Rating includes all "tail" losses
- Short circuit rated



Description

IR's advanced IGBT technology is the key to this line of DOUBLE INT-A-PAK Power Modules. The efficient geometry and unique processing of the IGBT allow higher current densities than comparable bipolar power module transistors, while at the same time requiring the simpler gate-drive of the familiar power MOSFET. This superior technology has now been coupled to state of the art assembly techniques to produce a higher current module that is highly suited to power applications such as motor drives, uninterruptible power supplies, welding and power factor correction.



Absolute Maximum Ratings

Parameter	Description	Value	Units
V_{CES}	Continuous collector to emitter voltage	600	V
$I_C @ T_c = 25^\circ\text{C}$	Maximum Continuous collector current	600	A
$I_C @ T_c = 85^\circ\text{C}$	Maximum Continuous collector current	320	
$I_C @ T_c = 100^\circ\text{C}$	Maximum Continuous collector current	240	
I_{LM}	Peak switching current	800	
I_{FM}	Peak diode forward current (1)	800	V
V_{GE}	Gate to emitter voltage	± 20	
V_{ISOL}	RMS isolation voltage, any terminal to case, $t = 1 \text{ min}$	2500	
$P_D @ T_c = 25^\circ\text{C}$	Power dissipation	1984	$^\circ\text{C}$
T_J	Operating junction temperature range	-40 to 150	
T_{STG}	Storage temperature range	-40 to 125	

(1) Duration limited by max junction temperature.

Target Data

IRGDDN400M06

IRGRDN400M06

Target Data



Electrical Characteristics - $T_J = 25^\circ\text{C}$, unless otherwise stated

Parameter	Description	Min	Typ	Max	Units	Test Conditions
BV_{CES}	Collector-to-emitter breakdown voltage	600	—	—	V	$V_{GE} = 0V, I_C = 6mA$
$V_{CE(ON)}$	Collector-to-emitter voltage	—	—	2.0		$V_{GE} = 15V, I_C = 400A$
		—	2.2	—		$V_{GE} = 15V, I_C = 400A, T_J = 125^\circ\text{C}$
V_{FM}	Diode forward voltage - maximum	—	1.8	2.0		$I_F = 400A, V_{GE} = 0V$
		—	1.8	—		$I_F = 400A, V_{GE} = 0V, T_J = 125^\circ\text{C}$
V_{GEth}	Gate threshold voltage	3.0	—	5.5	$I_C = 3mA$	
ΔV_{GEth}	Threshold voltage temperature coefficient	—	- 11	—	mV/ $^\circ\text{C}$	$V_{CE} = V_{GE}, I_C = 3mA$
g_{fe}	Forward transconductance	312	—	432	S(τ)	$V_{CE} = 25V, I_C = 300A$
I_{CES}	Collector-to-emitter leakage current	—	—	6	mA	$V_{GE} = 0V, V_{CE} = 600V$
		—	—	60		$V_{GE} = 0V, V_{CE} = 600V, T_J = 125^\circ\text{C}$
I_{GES}	Gate-to-emitter leakage current	—	—	± 6	μA	$V_{GE} = \pm 20V$

Dynamic Characteristics - $T_J = 125^\circ\text{C}$

Parameter	Description	Min	Typ	Max	Units	Test Conditions
E_{on}	Turn-on switching energy	—	0.03	—	mJ/A	$R_G = 15\Omega, V_{CC} = 300V$
E_{off} (1)	Turn-off switching energy	—	0.11	—		$I_C = 400A, L_S = 100nH$
E_{ts} (1)	Total switching energy	—	—	0.2		$V_{GE} = \pm 15V$
$t_{d(on)}$	Turn-on delay time	—	300	—	ns	$R_G = 15\Omega, V_{CC} = 300V$
t_r	Rise time	—	900	—		$I_C = 400A$
$t_{d(off)}$	Turn-off delay time	—	700	—		$V_{GE} = \pm 15V$
t_f	Fall time	—	350	—		Resistive Load, $T_J = 25^\circ\text{C}$
i_{rr}	Diode peak recovery current	—	90	—		A
t_{rr}	Diode recovery time	—	110	—	ns	$I_C = 400A$
Q_{rr}	Diode recovery charge	—	4.5	—	μC	$V_{GE} = \pm 15V$
Q_{ge}	Gate-to-emitter charge (turn-on)	156	—	252	nC	$V_{CC} = 480V$
Q_{gc}	Gate-to-collector charge (turn-on)	420	—	840		$I_C = 324A$
Q_g	Total gate charge (turn-on)	900	—	1680		$V_{GE} = 15V$
C_{ies}	Input capacitance	—	34800	—	pF	$V_{GE} = 0V$
C_{oes}	Output capacitance	—	3960	—		$V_{CC} = 30V$
C_{res}	Reverse transfer capacitance	—	480	—		$f = 1MHz$
t_{sc}	Short circuit withstand time	10	—	—	μs	$V_{CC} = 360V, V_{GE} = \pm 15V$ Min. $R_G = 15\Omega, V_{CEP} = 500V$

(1) Includes tail losses

Thermal and Mechanical Characteristics

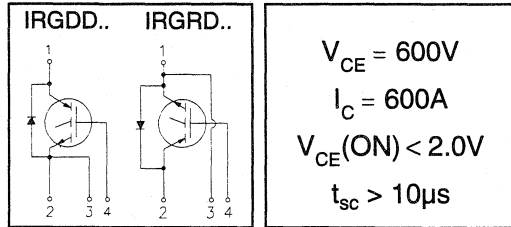
Parameter	Description	Typ	Max	Units
R_{thJC} (IGBT)	Thermal resistance, junction to case, each IGBT	—	0.063	$^\circ\text{C/W}$
R_{thJC} (Diode)	Thermal resistance, junction to case, each diode	—	0.095	
R_{thCS} (Module)	Thermal resistance, case to sink	0.023	0.050	
Wt	Weight of module	242	—	g

Refer to Section D - page D-18 for the following:
Package Outline13 -Double INT-A-PAK Single Switch

"SINGLE SWITCH" IGBT DOUBLE INT-A-PAK

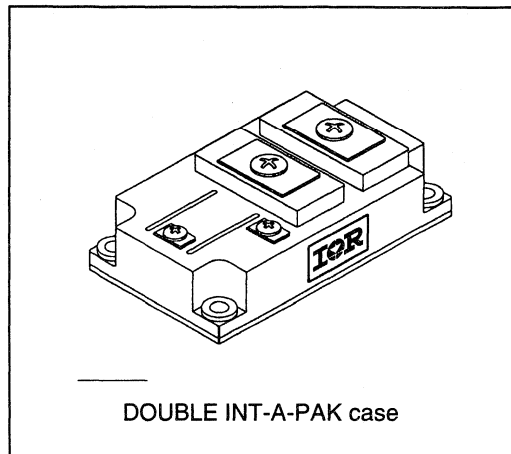
Low conduction loss IGBT

- Rugged Design
- Simple gate-drive
- Switching-Loss Rating includes all "tail" losses
- Short circuit rated



Description

IR's advanced IGBT technology is the key to this line of DOUBLE INT-A-PAK Power Modules. The efficient geometry and unique processing of the IGBT allow higher current densities than comparable bipolar power module transistors, while at the same time requiring the simpler gate-drive of the familiar power MOSFET. This superior technology has now been coupled to state of the art assembly techniques to produce a higher current module that is highly suited to power applications such as motor drives, uninterruptible power supplies, welding and power factor correction.


 Motor
Control
Fast
Modules

Absolute Maximum Ratings

Parameter	Description	Value	Units
V_{CES}	Continuous collector to emitter voltage	600	V
$I_C @ T_C = 25^\circ C$	Maximum Continuous collector current	800	A
$I_C @ T_C = 85^\circ C$	Maximum Continuous collector current	440	
$I_C @ T_C = 100^\circ C$	Maximum Continuous collector current	320	
I_{LM}	Peak switching current	1200	
I_{FM}	Peak diode forward current (1)	1200	
V_{GE}	Gate to emitter voltage	± 20	V
V_{ISOL}	RMS isolation voltage, any terminal to case, $t = 1$ min	2500	
$P_D @ T_C = 25^\circ C$	Power dissipation	2604	
T_J	Operating junction temperature range	-40 to 150	$^\circ C$
T_{STG}	Storage temperature range	-40 to 125	

(1) Duration limited by max junction temperature.

IRGDDN600M06 IRGRDN600M06

Target Data



Electrical Characteristics - $T_J = 25^\circ\text{C}$, unless otherwise stated

Parameter	Description	Min	Typ	Max	Units	Test Conditions
BV_{CES}	Collector-to-emitter breakdown voltage	600	—	—	V	$V_{GE} = 0V, I_C = 8mA$
$V_{CE(ON)}$	Collector-to-emitter voltage	—	—	2.7		$V_{GE} = 15V, I_C = 600A$
		—	2.7	—		$V_{GE} = 15V, I_C = 600A, T_J = 125^\circ\text{C}$
V_{FM}	Diode forward voltage - maximum	—	1.8	2.0		$I_F = 600A, V_{GE} = 0V$
		—	1.8	—	$I_F = 600A, V_{GE} = 0V, T_J = 125^\circ\text{C}$	
V_{Geth}	Gate threshold voltage	3.0	—	5.5	mV/°C	$I_C = 4mA$
ΔV_{Geth}	Threshold voltage temperature coefficient	—	- 11	—		$V_{CE} = V_{GE}, I_C = 4mA$
g_{fe}	Forward transconductance	416	—	596	S(Ω)	$V_{CE} = 25V, I_C = 600A$
I_{CES}	Collector-to-emitter leakage current	—	—	8	mA	$V_{GE} = 0V, V_{CE} = 600V$
		—	—	80		$V_{GE} = 0V, V_{CE} = 600V, T_J = 125^\circ\text{C}$
I_{GES}	Gate-to-emitter leakage current	—	—	± 8	μA	$V_{GE} = \pm 20V$

Dynamic Characteristics - $T_J = 125^\circ\text{C}$

Parameter	Description	Min	Typ	Max	Units	Test Conditions
E_{on}	Turn-on switching energy	—	0.03	—	mJ/A	$R_G = 15\Omega, V_{CC} = 300V$
$E_{off} (1)$	Turn-off switching energy	—	0.11	—		$I_C = 600A, L_S = 100nH$
$E_{ts} (1)$	Total switching energy	—	—	0.2		$V_{GE} = \pm 15V$
$t_{d(on)}$	Turn-on delay time	—	300	—	ns	$R_G = 15\Omega, V_{CC} = 300V$
t_r	Rise time	—	900	—		$I_C = 600A$
$t_{d(off)}$	Turn-off delay time	—	700	—		$V_{GE} = \pm 15V$
t_f	Fall time	—	350	—		Resistive Load, $T_J = 25^\circ\text{C}$
I_{rr}	Diode peak recovery current	—	110	—	A	$R_G = 15\Omega, V_{CC} = 300V$
t_{rr}	Diode recovery time	—	110	—	ns	$I_C = 600A$
Q_{rr}	Diode recovery charge	—	6	—	μC	$V_{GE} = \pm 15V$
Q_{ge}	Gate-to-emitter charge (turn-on)	208	—	336	nC	$V_{CC} = 480V$
Q_{gc}	Gate-to-collector charge (turn-on)	560	—	1120		$I_C = 432A$
Q_g	Total gate charge (turn-on)	1200	—	2240		$V_{GE} = 15V$
C_{ies}	Input capacitance	—	46400	—	pF	$V_{GE} = 0V$
C_{oes}	Output capacitance	—	5280	—		$V_{CC} = 30V$
C_{res}	Reverse transfer capacitance	—	640	—		$f = 1MHz$
t_{sc}	Short circuit withstand time	10	---	---	μs	$V_{CC} = 360V, V_{GE} = \pm 15V$ Min. $R_G = 15\Omega, V_{CEP} = 500V$

(1) Includes tail losses

Thermal and Mechanical Characteristics

Parameter	Description	Typ	Max	Units
R_{thJC} (IGBT)	Thermal resistance, junction to case, each IGBT	—	0.048	°C/W
R_{thJC} (Diode)	Thermal resistance, junction to case, each diode	—	0.07	
R_{thCS} (Module)	Thermal resistance, case to sink	0.023	0.050	
Wt	Weight of module	242	—	g

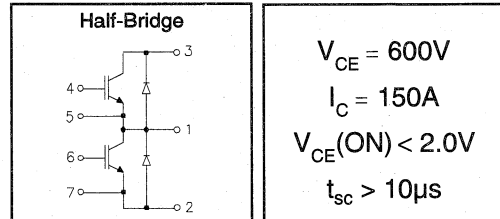
Refer to Section D - page D-18 for the following:
Package Outline13 -Double INT-A-PAK Single Switch

IRGTDN150M06

"HALF-BRIDGE" IGBT DOUBLE INT-A-PAK

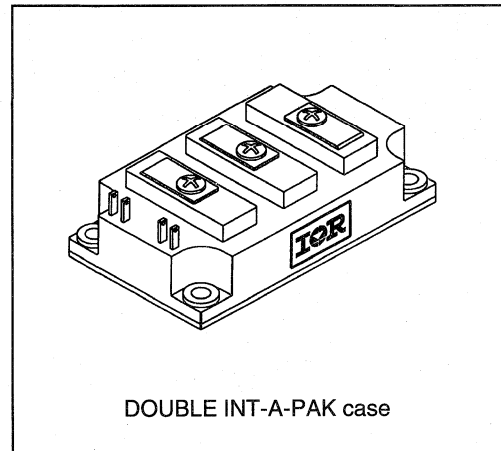
Low conduction loss IGBT

- Rugged Design
- Simple gate-drive
- Switching-Loss Rating includes all "tail" losses
- Short circuit rated



Description

IR's advanced IGBT technology is the key to this line of DOUBLE INT-A-PAK Power Modules. The efficient geometry and unique processing of the IGBT allow higher current densities than comparable bipolar power module transistors, while at the same time requiring the simpler gate-drive of the familiar power MOSFET. This superior technology has now been coupled to state of the art assembly techniques to produce a higher current module that is highly suited to power applications such as motor drives, uninterruptible power supplies, welding and power factor correction.



Absolute Maximum Ratings

Parameter	Description	Value	Units
V_{CES}	Continuous collector to emitter voltage	600	V
$I_C @ T_C = 25^\circ C$	Maximum Continuous collector current	200	A
$I_C @ T_C = 85^\circ C$	Maximum Continuous collector current	110	
$I_C @ T_C = 100^\circ C$	Maximum Continuous collector current	80	
I_{LM}	Peak IGBT switching current	300	
I_{FM}	Peak diode forward switching current (1)	300	
V_{GE}	Gate to emitter voltage	± 20	V
V_{ISOL}	RMS isolation voltage, any terminal to case, $t = 1$ min	2500	
$P_D @ T_C = 25^\circ C$	Power dissipation	781	W
T_J	Operating junction temperature range	-40 to 150	°C
T_{STG}	Storage temperature range	-40 to 125	

(1) Duration limited by max junction temperature.

Target Data

Electrical Characteristics - $T_J = 25^\circ\text{C}$, unless otherwise stated

Parameter	Description	Min	Typ	Max	Units	Test Conditions
BV_{CES}	Collector-to-emitter breakdown voltage	600	—	—	V	$V_{GE} = 0V, I_C = 2mA$
$V_{CE(ON)}$	Collector-to-emitter voltage	—	—	2.0		$V_{GE} = 15V, I_C = 150A$
		—	2.2	—		$V_{GE} = 15V, I_C = 150A, T_J = 125^\circ\text{C}$
V_{FM}	Diode forward voltage - maximum	—	1.8	2.0		$I_F = 150A, V_{GE} = 0V$
		—	1.75	—		$I_F = 150A, V_{GE} = 0V, T_J = 125^\circ\text{C}$
V_{GEth}	Gate threshold voltage	3.0	—	5.5	$I_C = 1mA$	
ΔV_{GEth}	Threshold voltage temp. coefficient	—	-11	—	mV/ $^\circ\text{C}$	$V_{CE} = V_{GE}, I_C = 1mA$
g_{fe}	Forward transconductance	104	—	144	S(τ)	$V_{CE} = 25V, I_C = 150A$
I_{CES}	Collector-to-emitter leakage current	—	—	2	mA	$V_{GE} = 0V, V_{CE} = 600V$
		—	—	20		$V_{GE} = 0V, V_{CE} = 600V, T_J = 125^\circ\text{C}$
I_{GES}	Gate-to-emitter leakage current	—	—	± 2	μA	$V_{GE} = \pm 20V$

Dynamic Characteristics - $T_J = 125^\circ\text{C}$

Parameter	Description	Min	Typ	Max	Units	Test Conditions
E_{on}	Turn-on switching energy	—	0.03	—	mJ/A	$R_G = 15\Omega, V_{CC} = 300V$
E_{off} (1)	Turn-off switching energy	—	0.11	—		$I_C = 150A, L_S = 100nH$
E_{ts} (1)	Total switching energy	—	—	0.18		$V_{GE} = \pm 15V$
$t_{d(on)}$	Turn-on delay time	—	300	—	ns	$R_G = 15\Omega, V_{CC} = 300V$
t_r	Rise time	—	600	—		$I_C = 150A$
$t_{d(off)}$	Turn-off delay time	—	350	—		$V_{GE} = \pm 15V$
t_f	Fall time	—	350	—		Resistive Load, $T_J = 25^\circ\text{C}$
I_{rr}	Diode peak recovery current	—	60	—	A	$R_G = 15\Omega, V_{CC} = 300V$
t_{rr}	Diode recovery time	—	110	—	ns	$I_C = 150A$
Q_{rr}	Diode recovery charge	—	3	—	μC	$V_{GE} = \pm 15V$
Q_{ge}	Gate-to-emitter charge (turn-on)	52	—	84	nC	$V_{CC} = 480V$
Q_{gc}	Gate-to-collector charge (turn-on)	140	—	280		$I_C = 108A$
Q_g	Total gate charge (turn-on)	300	—	560		$V_{GE} = 15V$
C_{ies}	Input capacitance	—	11600	—	pF	$V_{GE} = 0V$
C_{oes}	Output capacitance	—	1320	—		$V_{CC} = 30V$
C_{res}	Reverse transfer capacitance	—	160	—		$f = 1MHz$
t_{sc}	Short circuit withstand time	10	—	—	μs	$V_{CC} = 360V, V_{GE} = \pm 15V$ Min. $R_G = 15\Omega, V_{CEP} = 500V$

(1) Includes tail losses

Thermal and Mechanical Characteristics

Parameter	Description	Typ	Max	Units
R_{thJC} (IGBT)	Thermal resistance, junction to case, each IGBT	—	0.16	$^\circ\text{C/W}$
R_{thJC} (Diode)	Thermal resistance, junction to case, each diode	—	0.24	
R_{thCS} (Module)	Thermal resistance, case to sink	0.032	0.075	
Wt	Weight of module	242	—	g

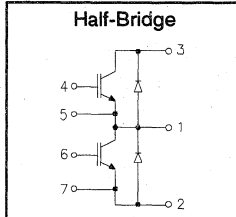
Refer to Section D -page D-17 for Package Outline 12 -Double INT-A-PAK Half Bridge

IRGTDN200K06

"HALF-BRIDGE" IGBT DOUBLE INT-A-PAK

Low conduction loss IGBT

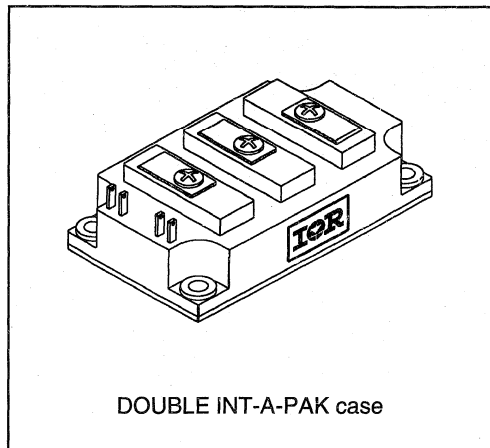
- Rugged Design
- Simple gate-drive
- Switching-Loss Rating includes all "tail" losses
- Short circuit rated



$V_{CE} = 600V$
$I_C = 200A$
$V_{CE(ON)} < 2.7V$
$t_{sc} > 10\mu s$

Description

IR's advanced IGBT technology is the key to this line of DOUBLE INT-A-PAK Power Modules. The efficient geometry and unique processing of the IGBT allow higher current densities than comparable bipolar power module transistors, while at the same time requiring the simpler gate-drive of the familiar power MOSFET. This superior technology has now been coupled to state of the art assembly techniques to produce a higher current module that is highly suited to power applications such as motor drives, uninterruptible power supplies, welding and power factor correction.


 Motor
Control
Fast
Modules

Absolute Maximum Ratings

Parameter	Description	Value	Units
V_{CES}	Continuous collector to emitter voltage	600	V
$I_C @ T_C = 25^\circ C$	Maximum Continuous collector current	260	A
$I_C @ T_C = 85^\circ C$	Maximum Continuous collector current	140	
$I_C @ T_C = 100^\circ C$	Maximum Continuous collector current	100	
I_{LM}	Peak IGBT switching current	400	
I_{FM}	Peak diode forward switching current (1)	400	
V_{GE}	Gate to emitter voltage	± 20	V
V_{ISOL}	RMS isolation voltage, any terminal to case, $t = 1$ min	2500	
$P_D @ T_C = 25^\circ C$	Power dissipation	1000	W
T_J	Operating junction temperature range	-40 to 150	$^\circ C$
T_{STG}	Storage temperature range	-40 to 125	

(1) Duration limited by max junction temperature.

Target Data

Electrical Characteristics - $T_J = 25^\circ\text{C}$, unless otherwise stated

Parameter	Description	Min	Typ	Max	Units	Test Conditions
BV_{CES}	Collector-to-emitter breakdown voltage	600	—	—	V	$V_{GE} = 0V, I_C = 3mA$
$V_{CE(ON)}$	Collector-to-emitter voltage	—	—	2.7		$V_{GE} = 15V, I_C = 200A$
		—	2.7	—		$V_{GE} = 15V, I_C = 200A, T_J = 125^\circ\text{C}$
V_{FM}	Diode forward voltage - maximum	—	1.8	2.0		$I_F = 200A, V_{GE} = 0V$
		—	1.75	—	$I_F = 200A, V_{GE} = 0V, T_J = 125^\circ\text{C}$	
V_{GETh}	Gate threshold voltage	3.0	—	5.5	mV/°C	$I_C = 1.5mA$
ΔV_{GETh}	Threshold voltage temp. coefficient	—	-11	—		$V_{CE} = V_{GE}, I_C = 1.5mA$
g_{fe}	Forward transconductance	102	—	174	S(Ω)	$V_{CE} = 25V, I_C = 200A$
I_{CES}	Collector-to-emitter leakage current	—	—	3	mA	$V_{GE} = 0V, V_{CE} = 600V$
		—	—	30		$V_{GE} = 0V, V_{CE} = 600V, T_J = 125^\circ\text{C}$
I_{GES}	Gate-to-emitter leakage current	—	—	±3	μA	$V_{GE} = \pm 20V$

Dynamic Characteristics - $T_J = 125^\circ\text{C}$

Parameter	Description	Min	Typ	Max	Units	Test Conditions
E_{on}	Turn-on switching energy	—	0.04	—	mJ/A	$R_G = 15\Omega, V_{CC} = 300V$
E_{off} (1)	Turn-off switching energy	—	0.06	—		$I_C = 200A, L_S = 100nH$
E_{ts} (1)	Total switching energy	—	—	0.13		$V_{GE} = \pm 15V$
$t_{d(on)}$	Turn-on delay time	—	300	—	ns	$R_G = 15\Omega, V_{CC} = 300V$
t_r	Rise time	—	500	—		$I_C = 200A$
$t_{d(off)}$	Turn-off delay time	—	350	—		$V_{GE} = \pm 15V$
t_f	Fall time	—	120	—		Resistive Load, $T_J = 25^\circ\text{C}$
I_{rr}	Diode peak recovery current	—	90	—	A	$R_G = 15\Omega, V_{CC} = 300V$
t_{rr}	Diode recovery time	—	110	—		$I_C = 200A$
Q_{rr}	Diode recovery charge	—	4.5	—		$V_{GE} = \pm 15V$
Q_{ge}	Gate-to-emitter charge (turn-on)	78	—	126	nC	$V_{CC} = 480V$
Q_{gc}	Gate-to-collector charge (turn-on)	210	—	420		$I_C = 162A$
Q_g	Total gate charge (turn-on)	450	—	840		$V_{GE} = 15V$
C_{ies}	Input capacitance	—	17400	—	pF	$V_{GE} = 0V$
C_{oes}	Output capacitance	—	1980	—		$V_{CC} = 30V$
C_{res}	Reverse transfer capacitance	—	240	—		$f = 1MHz$
t_{sc}	Short circuit withstand time	10	---	---	μs	$V_{CC} = 360V, V_{GE} = \pm 15V$ Min. $R_G = 15\Omega, V_{CEP} = 500V$

(1) Includes tail losses

Thermal and Mechanical Characteristics

Parameter	Description	Typ	Max	Units
R_{thJC} (IGBT)	Thermal resistance, junction to case, each IGBT	—	0.125	°C/W
R_{thJC} (Diode)	Thermal resistance, junction to case, each diode	—	0.190	
R_{thCS} (Module)	Thermal resistance, case to sink	0.032	0.075	
Wt	Weight of module	242	—	g

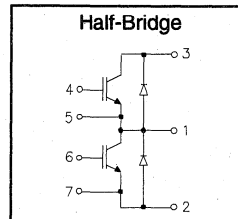
Refer to Section D - page D-17 for Package Outline 12 -Double INT-A-PAK Half Bridge

IRGTDN300M06

"HALF-BRIDGE" IGBT DOUBLE INT-A-PAK

Low conduction loss IGBT

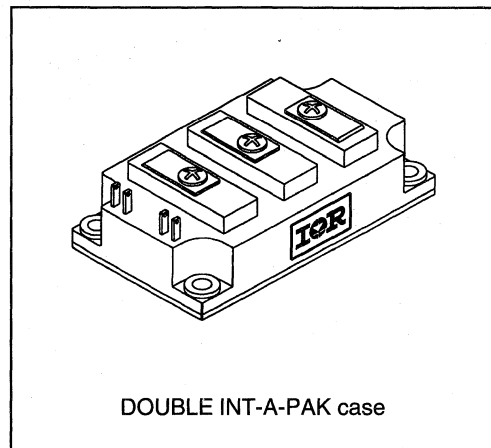
- Rugged Design
- Simple gate-drive
- Switching-Loss Rating includes all "tail" losses
- Short circuit rated



$V_{CE} = 600V$
$I_C = 300A$
$V_{CE(ON)} < 2.0V$
$t_{sc} > 10\mu s$

Description

IR's advanced IGBT technology is the key to this line of DOUBLE INT-A-PAK Power Modules. The efficient geometry and unique processing of the IGBT allow higher current densities than comparable bipolar power module transistors, while at the same time requiring the simpler gate-drive of the familiar power MOSFET. This superior technology has now been coupled to state of the art assembly techniques to produce a higher current module that is highly suited to power applications such as motor drives, uninterruptible power supplies, welding and power factor correction.



Motor Control Fast Modules

Absolute Maximum Ratings

Parameter	Description	Value	Units
V_{CES}	Continuous collector to emitter voltage	600	V
$I_C @ T_C = 25^\circ C$	Maximum Continuous collector current	400	A
$I_C @ T_C = 85^\circ C$	Maximum Continuous collector current	220	
$I_C @ T_C = 100^\circ C$	Maximum Continuous collector current	160	
I_{LM}	Peak IGBT switching current	600	
I_{FM}	Peak diode forward switching current (1)	600	V
V_{GE}	Gate to emitter voltage	± 20	
V_{ISOL}	RMS isolation voltage, any terminal to case, $t = 1 \text{ min}$	2500	W
$P_D @ T_C = 25^\circ C$	Power dissipation	1316	
T_J	Operating junction temperature range	-40 to 150	$^\circ C$
T_{STG}	Storage temperature range	-40 to 125	

(1) Duration limited by max junction temperature.

Target Data

Electrical Characteristics - $T_J = 25^\circ\text{C}$, unless otherwise stated

Parameter	Description	Min	Typ	Max	Units	Test Conditions
BV_{CES}	Collector-to-emitter breakdown voltage	600	—	—	v	$V_{GE} = 0V, I_C = 4mA$
$V_{CE(ON)}$	Collector-to-emitter voltage	—	—	2.0		$V_{GE} = 15V, I_C = 300A$
		—	2.2	—		$V_{GE} = 15V, I_C = 300A, T_J = 125^\circ\text{C}$
V_{FM}	Diode forward voltage - maximum	—	1.8	2.0		$I_F = 300A, V_{GE} = 0V$
		—	1.75	—	$I_F = 300A, V_{GE} = 0V, T_J = 125^\circ\text{C}$	
V_{GEth}	Gate threshold voltage	3.0	—	5.5	$I_C = 2mA$	
ΔV_{GEth}	Threshold voltage temperature coefficient	—	-11	—	mV/ $^\circ\text{C}$	$V_{CE} = V_{GE}, I_C = 2mA$
g_{fe}	Forward transconductance	208	—	296	S(τ)	$V_{CE} = 25V, I_C = 300A$
I_{CES}	Collector-to-emitter leakage current	—	—	4	mA	$V_{GE} = 0V, V_{CE} = 600V$
		—	—	40		$V_{GE} = 0V, V_{CE} = 600V, T_J = 125^\circ\text{C}$
I_{GES}	Gate-to-emitter leakage current	—	—	± 4	μA	$V_{GE} = \pm 20V$

Dynamic Characteristics - $T_J = 125^\circ\text{C}$

Parameter	Description	Min	Typ	Max	Units	Test Conditions
E_{on}	Turn-on switching energy	—	0.03	—	mJ/A	$R_G = 15\Omega, V_{CC} = 300V$
E_{off} (1)	Turn-off switching energy	—	0.11	—		$I_C = 300A, L_S = 100nH$
E_{ts} (1)	Total switching energy	—	—	0.18		$V_{GE} = \pm 15V$
$t_{d(on)}$	Turn-on delay time	—	300	—	ns	$R_G = 15\Omega, V_{CC} = 300V$
t_r	Rise time	—	400	—		$I_C = 300A$
$t_{d(off)}$	Turn-off delay time	—	350	—		$V_{GE} = \pm 15V$
t_f	Fall time	—	350	—		Resistive Load, $T_J = 25^\circ\text{C}$
I_{rr}	Diode peak recovery current	—	110	—	A	$R_G = 15\Omega, V_{CC} = 300V$
t_{rr}	Diode recovery time	—	110	—	ns	$I_C = 300A$
Q_{rr}	Diode recovery charge	—	6	—	μC	$V_{GE} = \pm 15V$
Q_{ge}	Gate-to-emitter charge (turn-on)	104	—	168	nC	$V_{CC} = 480V$
Q_{gc}	Gate-to-collector charge (turn-on)	280	—	560		$I_C = 216A$
Q_g	Total gate charge (turn-on)	600	—	1120		$V_{GE} = 15V$
C_{ies}	Input capacitance	—	23200	—	pF	$V_{GE} = 0V$
C_{oes}	Output capacitance	—	2640	—		$V_{CC} = 30V$
C_{res}	Reverse transfer capacitance	—	320	—		$f = 1\text{MHz}$
t_{sc}	Short circuit withstand time	10	—	—	μs	$V_{CC} = 360V, V_{GE} = \pm 15V$ Min. $R_G = 15\Omega, V_{CEP} = 500V$

(1) Includes tail losses

Thermal and Mechanical Characteristics

Parameter	Description	Typ	Max	Units
R_{thJC} (IGBT)	Thermal resistance, junction to case, each IGBT	—	0.095	$^\circ\text{C/W}$
R_{thJC} (Diode)	Thermal resistance, junction to case, each diode	—	0.140	
R_{thCS} (Module)	Thermal resistance, case to sink	0.032	0.075	
Wt	Weight of module	242	—	g

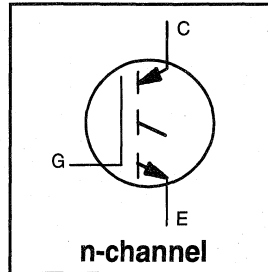
Refer to Section D - page D-17 for Package Outline 12 - Double INT-A-PAK Half Bridge

INSULATED GATE BIPOLAR TRANSISTOR

Short Circuit Rated
Fast IGBT

Features

- Short circuit rated - $10\mu\text{s}$ @ 125°C , $V_{\text{GE}} = 15\text{V}$
- Switching-loss rating includes all "tail" losses
- Optimized for medium operating frequency (1 to 10kHz) See Fig. 1 for Current vs. Frequency curve



$$V_{\text{CES}} = 1200\text{V}$$

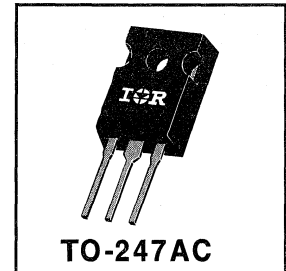
$$V_{\text{CE(sat)}} \leq 4.6\text{V}$$

$$\text{@ } V_{\text{GE}} = 15\text{V}, I_{\text{C}} = 4.5\text{A}$$

Description

Insulated Gate Bipolar Transistors (IGBTs) from International Rectifier have higher usable current densities than comparable bipolar transistors, while at the same time having simpler gate-drive requirements of the familiar power MOSFET. They provide substantial benefits to a host of high-voltage, high-current applications.

These new short circuit rated devices are especially suited for motor control and other applications requiring short circuit withstand capability.



Motor
Control
Fast
Discretes

Absolute Maximum Ratings

	Parameter	Max.	Units
V_{CES}	Collector-to-Emitter Voltage	1200	V
$I_{\text{C}} @ T_{\text{C}} = 25^\circ\text{C}$	Continuous Collector Current	6.9	A
$I_{\text{C}} @ T_{\text{C}} = 100^\circ\text{C}$	Continuous Collector Current	4.5	
I_{CM}	Pulsed Collector Current ①	14	
I_{LM}	Clamped Inductive Load Current ②	14	
t_{sc}	Short Circuit Withstand Time	10	μs
V_{GE}	Gate-to-Emitter Voltage	± 20	V
E_{ARV}	Reverse Voltage Avalanche Energy ③	5.0	mJ
$P_{\text{D}} @ T_{\text{C}} = 25^\circ\text{C}$	Maximum Power Dissipation	60	W
$P_{\text{D}} @ T_{\text{C}} = 100^\circ\text{C}$	Maximum Power Dissipation	24	
T_{J}	Operating Junction and	-55 to +150	$^\circ\text{C}$
T_{STG}	Storage Temperature Range		
	Soldering Temperature, for 10 sec.	300 (0.063 in. (1.6mm) from case)	
	Mounting torque, 6-32 or M3 screw.	10 lb•in (1.1N•m)	

Thermal Resistance

	Parameter	Min.	Typ.	Max.	Units
$R_{\theta\text{JC}}$	Junction-to-Case	—	—	2.1	$^\circ\text{C}/\text{W}$
$R_{\theta\text{CS}}$	Case-to-Sink, flat, greased surface	—	0.24	—	
$R_{\theta\text{JA}}$	Junction-to-Ambient, typical socket mount	—	—	40	
Wt	Weight	—	6 (0.21)	—	g (oz)

Electrical Characteristics @ $T_J = 25^\circ\text{C}$ (unless otherwise specified)

	Parameter	Min.	Typ.	Max.	Units	Conditions
$V_{(BR)CES}$	Collector-to-Emitter Breakdown Voltage	1200	—	—	V	$V_{GE} = 0V, I_C = 250\mu A$
$V_{(BR)ECS}$	Emitter-to-Collector Breakdown Voltage ①	20	—	—	V	$V_{GE} = 0V, I_C = 1.0A$
$\Delta V_{(BR)CES}/\Delta T_J$	Temperature Coeff. of Breakdown Voltage	—	1.3	—	V/°C	$V_{GE} = 0V, I_C = 1.0mA$
$V_{CE(on)}$	Collector-to-Emitter Saturation Voltage	—	3.1	4.6	V	$I_C = 4.5A, V_{GE} = 15V$
		—	3.9	—		$I_C = 6.9A$
		—	4.0	—		$I_C = 4.5A, T_J = 150^\circ\text{C}$
						See Fig. 2, 5
$V_{GE(th)}$	Gate Threshold Voltage	3.0	—	5.5		$V_{CE} = V_{GE}, I_C = 250\mu A$
$\Delta V_{GE(th)}/\Delta T_J$	Temperature Coeff. of Threshold Voltage	—	-11	—	mV/°C	$V_{CE} = V_{GE}, I_C = 250\mu A$
g_{fe}	Forward Transconductance ②	1.3	2.6	—	S	$V_{CE} = 100V, I_C = 4.5A$
I_{CES}	Zero Gate Voltage Collector Current	—	—	250	μA	$V_{GE} = 0V, V_{CE} = 1200V$
		—	—	1000		$V_{GE} = 0V, V_{CE} = 1200V, T_J = 150^\circ\text{C}$
I_{GES}	Gate-to-Emitter Leakage Current	—	—	± 100	nA	$V_{GE} = \pm 20V$

Switching Characteristics @ $T_J = 25^\circ\text{C}$ (unless otherwise specified)

	Parameter	Min.	Typ.	Max.	Units	Conditions
Q_g	Total Gate Charge (turn-on)	—	16	24	nC	$I_C = 4.5A$ $V_{CC} = 400V$ See Fig. 8 $V_{GE} = 15V$
Q_{ge}	Gate - Emitter Charge (turn-on)	—	4.4	7.0		
Q_{gc}	Gate - Collector Charge (turn-on)	—	5.5	8.3		
$t_{d(on)}$	Turn-On Delay Time	—	26	—	ns	$T_J = 25^\circ\text{C}$ $I_C = 4.5A, V_{CC} = 960V$ $V_{GE} = 15V, R_G = 50\Omega$ Energy losses include "tail"
t_r	Rise Time	—	13	—		
$t_{d(off)}$	Turn-Off Delay Time	—	43	65		
t_f	Fall Time	—	430	640		
E_{on}	Turn-On Switching Loss	—	0.33	—	mJ	See Fig. 9, 10, 11, 14
E_{off}	Turn-Off Switching Loss	—	0.78	—		
E_{ts}	Total Switching Loss	—	1.1	1.7		
t_{sc}	Short Circuit Withstand Time	10	—	—	μs	$V_{CC} = 720V, T_J = 125^\circ\text{C}$ $V_{GE} = 15V, R_G = 50\Omega, V_{CPK} < 1000V$
$t_{d(on)}$	Turn-On Delay Time	—	32	—	ns	$T_J = 150^\circ\text{C},$ $I_C = 4.5A, V_{CC} = 960V$ $V_{GE} = 15V, R_G = 50\Omega$ Energy losses include "tail"
t_r	Rise Time	—	20	—		
$t_{d(off)}$	Turn-Off Delay Time	—	480	—		
t_f	Fall Time	—	450	—		
E_{ts}	Total Switching Loss	—	2.4	—	mJ	See Fig. 10, 14
L_E	Internal Emitter Inductance	—	13	—	nH	Measured 5mm from package
C_{ies}	Input Capacitance	—	340	—	μF	$V_{GE} = 0V$ $V_{CC} = 30V$ See Fig. 7 $f = 1.0MHz$
C_{oes}	Output Capacitance	—	25	—		
C_{res}	Reverse Transfer Capacitance	—	4.7	—		

Notes:

- ① Repetitive rating; $V_{GE}=20V$, pulse width limited by max. junction temperature. (See fig. 13b)
- ② $V_{CC}=80\%(V_{CES}), V_{GE}=20V, L=10\mu H, R_G=50\Omega$, (See fig. 13a)
- ③ Repetitive rating; pulse width limited by maximum junction temperature.
- ④ Pulse width $\leq 80\mu s$; duty factor $\leq 0.1\%$.
- ⑤ Pulse width 5.0 μs , single shot.

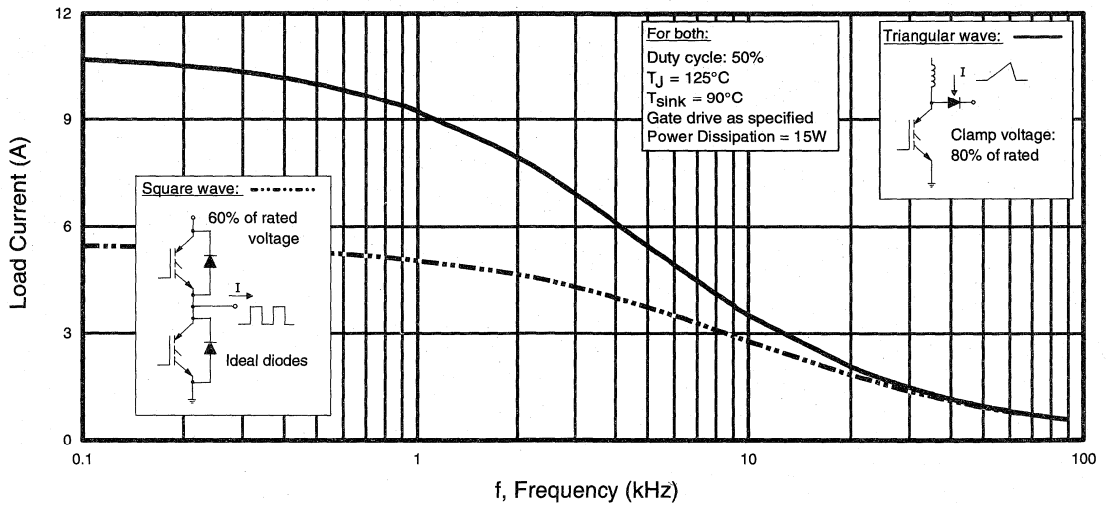


Fig. 1 - Typical Load Current vs. Frequency
 (For square wave, $I = I_{\text{RMS}}$ of fundamental; for triangular wave, $I = I_{\text{PK}}$)

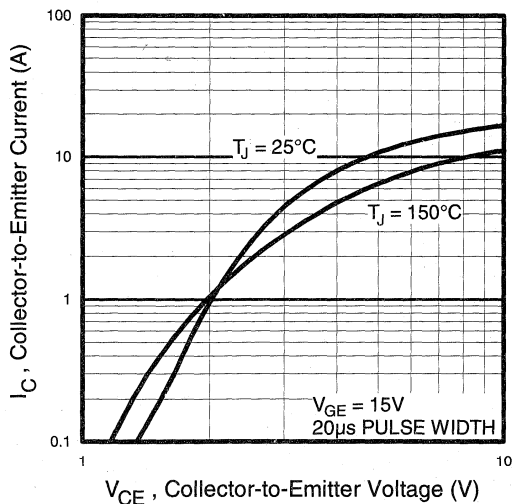


Fig. 2 - Typical Output Characteristics

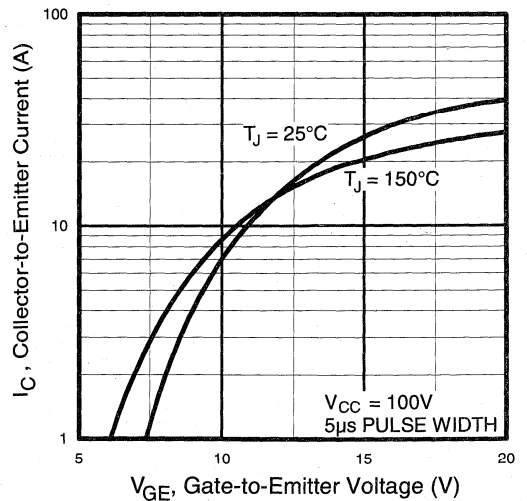


Fig. 3 - Typical Transfer Characteristics

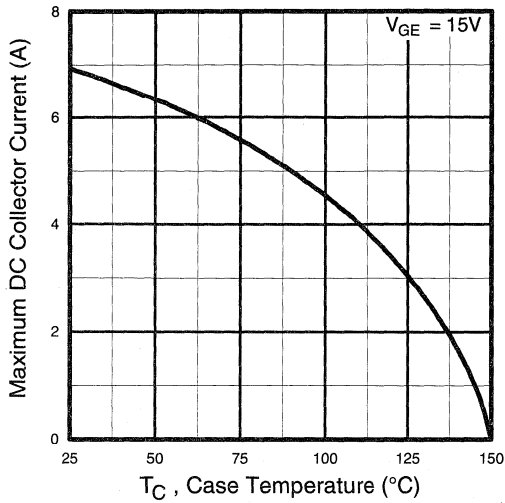


Fig. 4 - Maximum Collector Current vs. Case Temperature

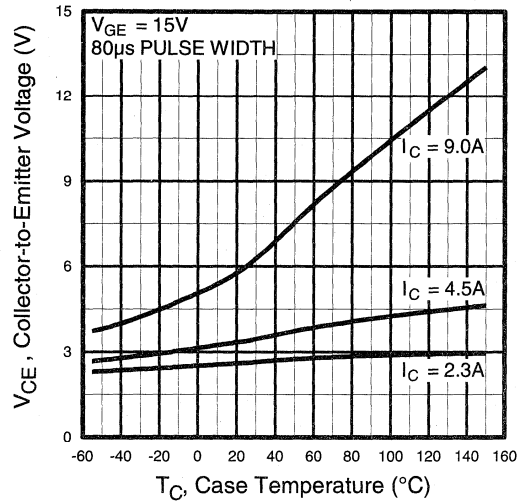


Fig. 5 - Collector-to-Emitter Voltage vs. Case Temperature

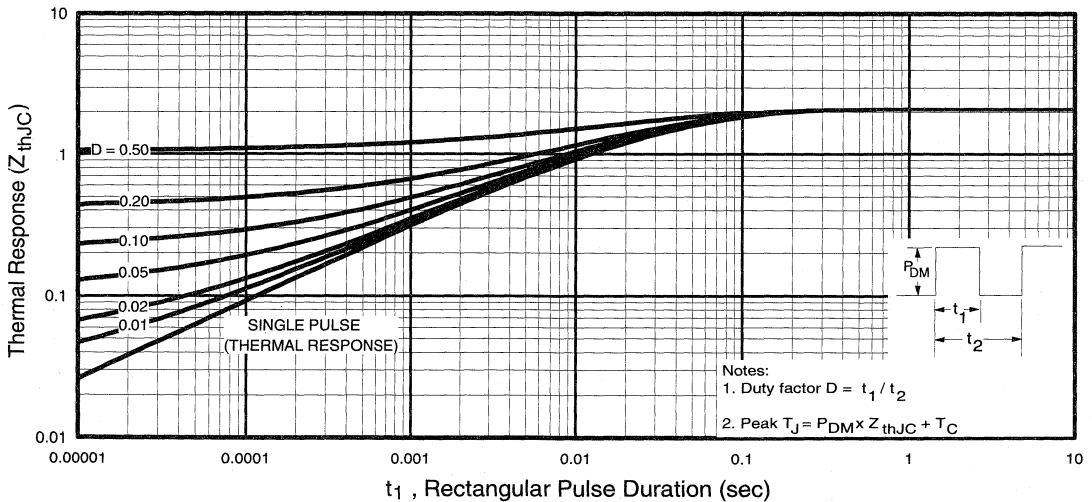


Fig. 6 - Maximum Effective Transient Thermal Impedance, Junction-to-Case

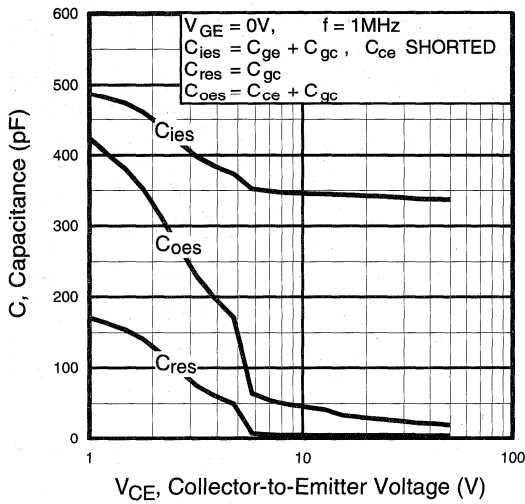


Fig. 7 - Typical Capacitance vs. Collector-to-Emitter Voltage

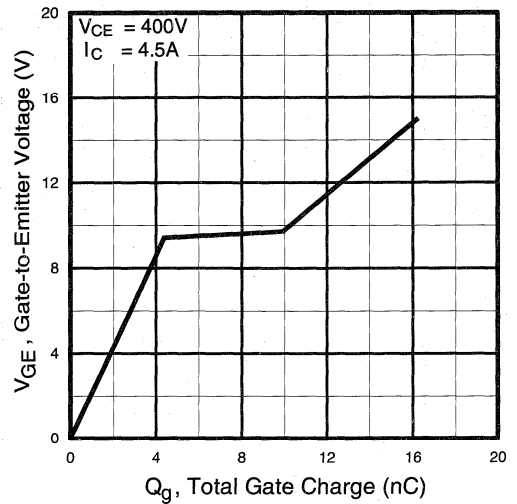


Fig. 8 - Typical Gate Charge vs. Gate-to-Emitter Voltage

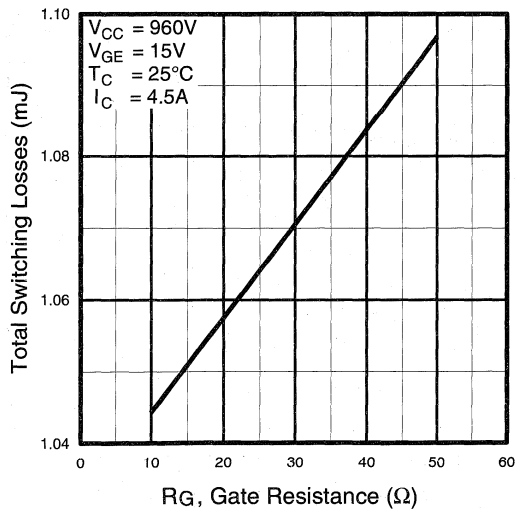


Fig. 9 - Typical Switching Losses vs. Gate Resistance

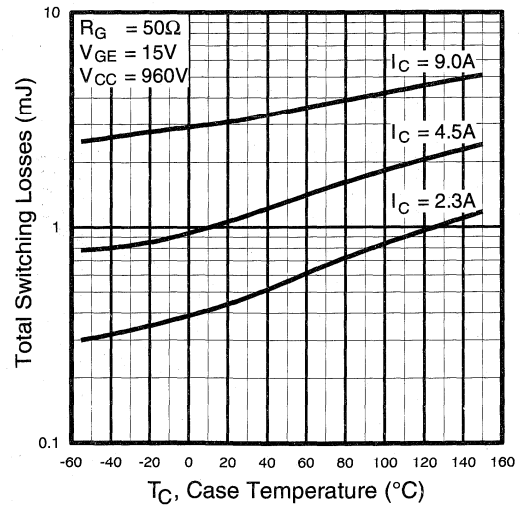


Fig. 10 - Typical Switching Losses vs. Case Temperature

Motor Control Fast Discretes

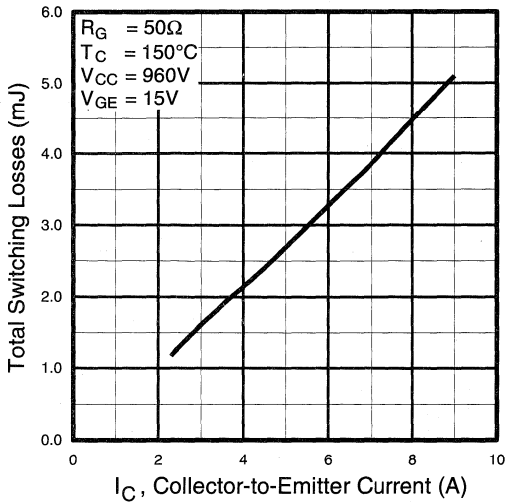


Fig. 11 - Typical Switching Losses vs. Collector-to-Emitter Current

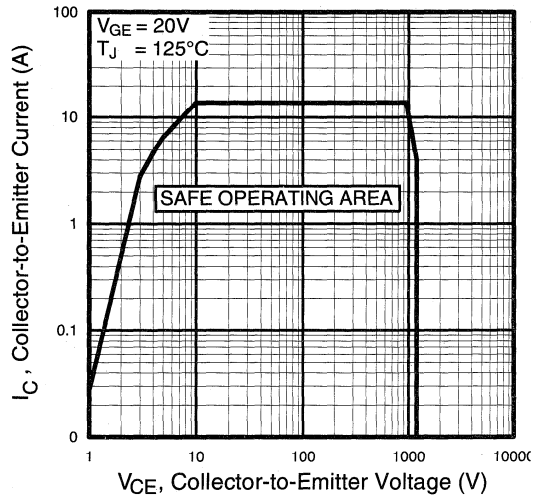


Fig. 12 - Turn-Off SOA

Refer to Section D for the following:

Appendix G: Section D - page D-9

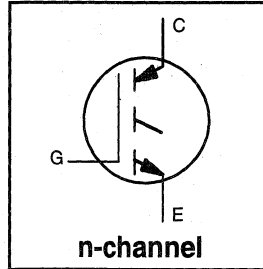
- Fig. 13a - Clamped Inductive Load Test Circuit
- Fig. 13b - Pulsed Collector Current Test Circuit
- Fig. 14a - Switching Loss Test Circuit
- Fig. 14b - Switching Loss Waveform

INSULATED GATE BIPOLAR TRANSISTOR

Short Circuit Rated
Fast IGBT

Features

- Short circuit rated - $10\mu\text{s}$ @ 125°C , $V_{\text{GE}} = 15\text{V}$
- Switching-loss rating includes all "tail" losses
- Optimized for medium operating frequency (1 to 10kHz)



$$V_{\text{CES}} = 1200\text{V}$$

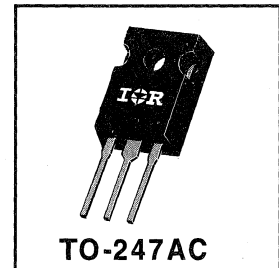
$$V_{\text{CE(sat)}} \leq 3.4\text{V}$$

$$\text{@ } V_{\text{GE}} = 15\text{V}, I_{\text{C}} = 18\text{A}$$

Description

Insulated Gate Bipolar Transistors (IGBTs) from International Rectifier have higher usable current densities than comparable bipolar transistors, while at the same time having simpler gate-drive requirements of the familiar power MOSFET. They provide substantial benefits to a host of high-voltage, high-current applications.

These new short circuit rated devices are especially suited for motor control and other applications requiring short circuit withstand capability.



Absolute Maximum Ratings

	Parameter	Max.	Units
V_{CES}	Collector-to-Emitter Voltage	1200	V
$I_{\text{C}} @ T_{\text{C}} = 25^\circ\text{C}$	Continuous Collector Current	31	A
$I_{\text{C}} @ T_{\text{C}} = 100^\circ\text{C}$	Continuous Collector Current	18	
I_{CM}	Pulsed Collector Current ①	62	
I_{LM}	Clamped Inductive Load Current ②	62	
t_{sc}	Short Circuit Withstand Time	10	μs
V_{GE}	Gate-to-Emitter Voltage	± 20	V
E_{ARV}	Reverse Voltage Avalanche Energy ③	15	mJ
$P_{\text{D}} @ T_{\text{C}} = 25^\circ\text{C}$	Maximum Power Dissipation	160	W
$P_{\text{D}} @ T_{\text{C}} = 100^\circ\text{C}$	Maximum Power Dissipation	65	
T_{J}	Operating Junction and	-55 to +150	°C
T_{STG}	Storage Temperature Range		
	Soldering Temperature, for 10 sec.	300 (0.063 in. (1.6mm) from case)	
	Mounting torque, 6-32 or M3 screw.	10 lbf•in (1.1N•m)	

Thermal Resistance

	Parameter	Min.	Typ.	Max.	Units
$R_{\theta\text{JC}}$	Junction-to-Case	—	—	0.77	°C/W
$R_{\theta\text{CS}}$	Case-to-Sink, flat, greased surface	—	0.24	—	
$R_{\theta\text{JA}}$	Junction-to-Ambient, typical socket mount	—	—	40	
Wt	Weight	—	6 (0.21)	—	g (oz)

Electrical Characteristics @ $T_J = 25^\circ\text{C}$ (unless otherwise specified)

	Parameter	Min.	Typ.	Max.	Units	Conditions	
$V_{(BR)CES}$	Collector-to-Emitter Breakdown Voltage	1200	—	—	V	$V_{GE} = 0V, I_C = 250\mu A$	
$V_{(BR)ECS}$	Emitter-to-Collector Breakdown Voltage ④	20	—	—	V	$V_{GE} = 0V, I_C = 1.0A$	
$\Delta V_{(BR)CES}/\Delta T_J$	Temperature Coeff. of Breakdown Voltage	—	1.1	—	$V/^\circ\text{C}$	$V_{GE} = 0V, I_C = 1.0mA$	
$V_{CE(on)}$	Collector-to-Emitter Saturation Voltage	—	2.3	3.4	V	$V_{GE} = 15V$ $I_C = 18A$	
		—	3.0	—			$I_C = 31A$
		—	2.8	—			$I_C = 18A, T_J = 150^\circ\text{C}$
$V_{GE(th)}$	Gate Threshold Voltage	3.0	—	5.5		$V_{CE} = V_{GE}, I_C = 250\mu A$	
$\Delta V_{GE(th)}/\Delta T_J$	Temperature Coeff. of Threshold Voltage	—	-14	—	$mV/^\circ\text{C}$	$V_{CE} = V_{GE}, I_C = 250\mu A$	
g_{fe}	Forward Transconductance ⑤	4.0	10	—	S	$V_{CE} = 100V, I_C = 18A$	
I_{CES}	Zero Gate Voltage Collector Current	—	—	250	μA	$V_{GE} = 0V, V_{CE} = 1200V$	
		—	—	3500		$V_{GE} = 0V, V_{CE} = 1200V, T_J = 150^\circ\text{C}$	
I_{GES}	Gate-to-Emitter Leakage Current	—	—	± 100	nA	$V_{GE} = \pm 20V$	

Switching Characteristics @ $T_J = 25^\circ\text{C}$ (unless otherwise specified)

	Parameter	Min.	Typ.	Max.	Units	Conditions		
Q_g	Total Gate Charge (turn-on)	—	50	75	nC	$I_C = 18A$ $V_{CC} = 400V$ $V_{GE} = 15V$		
Q_{ge}	Gate - Emitter Charge (turn-on)	—	11	21				
Q_{gc}	Gate - Collector Charge (turn-on)	—	15	30				
$t_{d(on)}$	Turn-On Delay Time	—	30	—	ns	$T_J = 25^\circ\text{C}$ $I_C = 18A, V_{CC} = 960V$ $V_{GE} = 15V, R_G = 10\Omega$ Energy losses include "tail"		
t_r	Rise Time	—	21	—				
$t_{d(off)}$	Turn-Off Delay Time	—	400	890				
t_f	Fall Time	—	390	740				
E_{on}	Turn-On Switching Loss	—	1.1	—				
E_{off}	Turn-Off Switching Loss	—	6.3	—				
E_{ts}	Total Switching Loss	—	7.4	14				
t_{sc}	Short Circuit Withstand Time	10	—	—			μs	$V_{CC} = 720V, T_J = 125^\circ\text{C}$ $V_{GE} = 15V, R_G = 10\Omega, V_{CPK} < 1000V$
$t_{d(on)}$	Turn-On Delay Time	—	28	—			ns	$T_J = 150^\circ\text{C}$, $I_C = 18A, V_{CC} = 960V$ $V_{GE} = 15V, R_G = 10\Omega$ Energy losses include "tail"
t_r	Rise Time	—	24	—				
$t_{d(off)}$	Turn-Off Delay Time	—	600	—				
t_f	Fall Time	—	870	—				
E_{ts}	Total Switching Loss	—	15	—	mJ			
L_E	Internal Emitter Inductance	—	13	—	nH	Measured 5mm from package		
C_{ies}	Input Capacitance	—	1360	—	pF	$V_{GE} = 0V$ $V_{CC} = 30V$ $f = 1.0MHz$		
C_{oes}	Output Capacitance	—	100	—				
C_{res}	Reverse Transfer Capacitance	—	15	—				

Notes:

- ① Repetitive rating; $V_{GE}=20V$, pulse width limited by max. junction temperature.
- ② $V_{CC}=80\%(V_{CES}), V_{GE}=20V, L=10\mu H, R_G=10\Omega$
- ③ Repetitive rating; pulse width limited by maximum junction temperature.
- ④ Pulse width $\leq 80\mu s$; duty factor $\leq 0.1\%$.
- ⑤ Pulse width $5.0\mu s$, single shot.

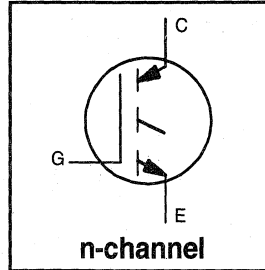
Refer to Section D - page D-13 for Package Outline 3 - JEDEC Outline TO-247AC

INSULATED GATE BIPOLAR TRANSISTOR

Short Circuit Rated
Fast IGBT

Features

- Short circuit rated - $10\mu\text{s}$ @ 125°C , $V_{GE} = 15\text{V}$
- Switching-loss rating includes all "tail" losses
- Optimized for medium operating frequency (1 to 10kHz) See Fig. 1 for Current vs. Frequency curve



$$V_{CES} = 1200\text{V}$$

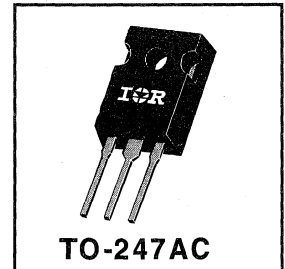
$$V_{CE(sat)} \leq 2.9\text{V}$$

$$\text{@ } V_{GE} = 15\text{V}, I_C = 23\text{A}$$

Description

Insulated Gate Bipolar Transistors (IGBTs) from International Rectifier have higher usable current densities than comparable bipolar transistors, while at the same time having simpler gate-drive requirements of the familiar power MOSFET. They provide substantial benefits to a host of high-voltage, high-current applications.

These new short circuit rated devices are especially suited for motor control and other applications requiring short circuit withstand capability.



Motor Control Fast Discretes

Absolute Maximum Ratings

	Parameter	Max.	Units
V_{CES}	Collector-to-Emitter Voltage	1200	V
$I_C @ T_C = 25^\circ\text{C}$	Continuous Collector Current	42	A
$I_C @ T_C = 100^\circ\text{C}$	Continuous Collector Current	23	
I_{CM}	Pulsed Collector Current $\text{\textcircled{D}}$	84	
I_{LM}	Clamped Inductive Load Current $\text{\textcircled{D}}$	84	
t_{sc}	Short Circuit Withstand Time	10	μs
V_{GE}	Gate-to-Emitter Voltage	± 20	V
E_{ARV}	Reverse Voltage Avalanche Energy $\text{\textcircled{D}}$	20	mJ
$P_D @ T_C = 25^\circ\text{C}$	Maximum Power Dissipation	200	W
$P_D @ T_C = 100^\circ\text{C}$	Maximum Power Dissipation	78	
T_J	Operating Junction and	-55 to +150	$^\circ\text{C}$
T_{STG}	Storage Temperature Range		
	Soldering Temperature, for 10 sec.		
	Mounting torque, 6-32 or M3 screw.	10 lbf•in (1.1N•m)	

Thermal Resistance

	Parameter	Min.	Typ.	Max.	Units
$R_{\theta JC}$	Junction-to-Case	—	—	0.64	$^\circ\text{C/W}$
$R_{\theta CS}$	Case-to-Sink, flat, greased surface	—	0.24	—	
$R_{\theta JA}$	Junction-to-Ambient, typical socket mount	—	—	40	
W_t	Weight	—	6 (0.21)	—	g (oz)

Electrical Characteristics @ $T_J = 25^\circ\text{C}$ (unless otherwise specified)

	Parameter	Min.	Typ.	Max.	Units	Conditions
$V_{(BR)CES}$	Collector-to-Emitter Breakdown Voltage	1200	—	—	V	$V_{GE} = 0V, I_C = 250\mu A$
$V_{(BR)ECS}$	Emitter-to-Collector Breakdown Voltage ④	20	—	—	V	$V_{GF} = 0V, I_C = 1.0A$
$\Delta V_{(BR)CES}/\Delta T_J$	Temp. Coeff. of Breakdown Voltage	—	1.1	—	$V/^\circ\text{C}$	$V_{GE} = 0V, I_C = 1.0mA$
$V_{CE(on)}$	Collector-to-Emitter Saturation Voltage	—	2.3	2.9	V	$I_C = 23A$ $I_C = 42A$ $I_C = 23A, T_J = 150^\circ\text{C}$ $V_{CE} = V_{GE}, I_C = 250\mu A$
		—	3.0	—		
		—	2.8	—		
$V_{GE(th)}$	Gate Threshold Voltage	3.0	—	5.5		$V_{CE} = V_{GE}, I_C = 250\mu A$
$\Delta V_{GE(th)}/\Delta T_J$	Temp. Coeff. of Threshold Voltage	—	-13	—	$mV/^\circ\text{C}$	$V_{CE} = V_{GE}, I_C = 250\mu A$
g_{fe}	Forward Transconductance ⑤	11	15	—	S	$V_{CE} = 100V, I_C = 23A$
I_{CES}	Zero Gate Voltage Collector Current	—	—	250	μA	$V_{GE} = 0V, V_{CE} = 1200V$
		—	—	2000		$V_{GE} = 0V, V_{CE} = 1200V, T_J = 150^\circ\text{C}$
I_{GES}	Gate-to-Emitter Leakage Current	—	—	± 100	nA	$V_{GE} = \pm 20V$

Switching Characteristics @ $T_J = 25^\circ\text{C}$ (unless otherwise specified)

	Parameter	Min.	Typ.	Max.	Units	Conditions
Q_g	Total Gate Charge (turn-on)	—	89	130	nC	$I_C = 23A$ $V_{CC} = 400V$ $V_{GE} = 15V$ See Fig. 8
Q_{ge}	Gate - Emitter Charge (turn-on)	—	22	33		
Q_{gc}	Gate - Collector Charge (turn-on)	—	26	39		
$t_{d(on)}$	Turn-On Delay Time	—	42	—	ns	$T_J = 25^\circ\text{C}$ $I_C = 23A, V_{CC} = 960V$ $V_{GE} = 15V, R_G = 5.0\Omega$ Energy losses include "tail"
t_r	Rise Time	—	32	—		
$t_{d(off)}$	Turn-Off Delay Time	—	280	820		
t_f	Fall Time	—	190	410	mJ	See Fig. 9, 10, 11, 14
E_{on}	Turn-On Switching Loss	—	1.6	—		
E_{off}	Turn-Off Switching Loss	—	3.3	—		
E_{ts}	Total Switching Loss	—	4.9	11	μs	$V_{CC} = 720V, T_J = 125^\circ\text{C}$ $V_{GE} = 15V, R_G = 5.0\Omega, V_{CPK} < 1000V$
t_{sc}	Short Circuit Withstand Time	10	—	—		
$t_{d(on)}$	Turn-On Delay Time	—	32	—		
t_r	Rise Time	—	21	—	ns	$T_J = 150^\circ\text{C}$ $I_C = 23A, V_{CC} = 960V$ $V_{GE} = 15V, R_G = 5.0\Omega$ Energy losses include "tail"
$t_{d(off)}$	Turn-Off Delay Time	—	490	—		
t_f	Fall Time	—	440	—		
E_{ts}	Total Switching Loss	—	10	—	mJ	See Fig. 10, 14
L_E	Internal Emitter Inductance	—	13	—	nH	Measured 5mm from package
C_{ies}	Input Capacitance	—	1900	—	pF	$V_{GE} = 0V$ $V_{CC} = 30V$ $f = 1.0MHz$ See Fig. 7
C_{oes}	Output Capacitance	—	140	—		
C_{res}	Reverse Transfer Capacitance	—	24	—		

Notes:

- ① Repetitive rating; $V_{GE}=20V$, pulse width limited by max. junction temperature. (See fig. 13b)
- ② $V_{CC}=80\%(V_{CES})$, $V_{GE}=20V$, $L=10\mu H$, $R_G=5.0\Omega$, (See fig. 13a)
- ③ Repetitive rating; pulse width limited by maximum junction temperature.
- ④ Pulse width $\leq 80\mu s$; duty factor $\leq 0.1\%$.
- ⑤ Pulse width $5.0\mu s$, single shot.

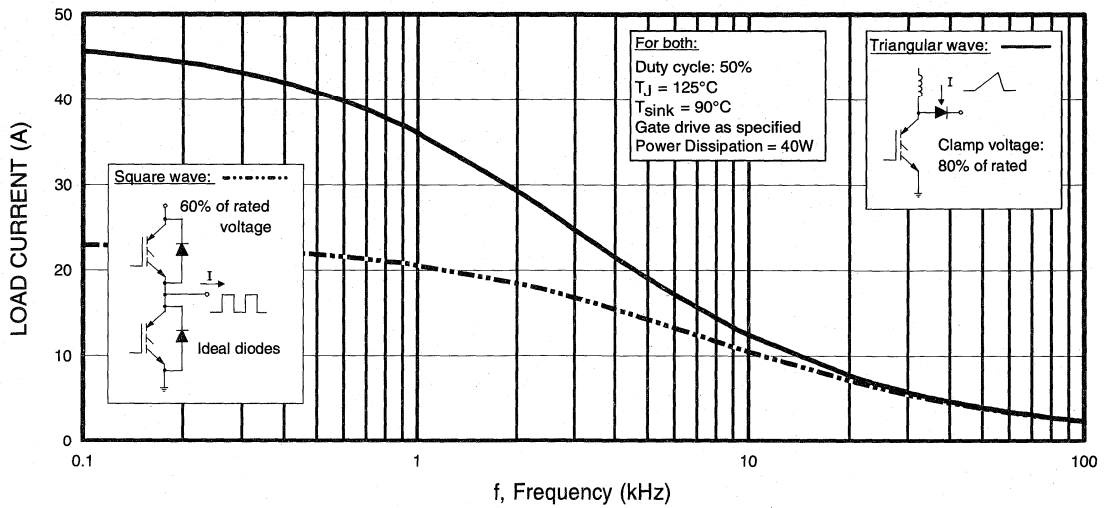


Fig. 1 - Typical Load Current vs. Frequency
 (For square wave, $I = I_{RMS}$ of fundamental; for triangular wave, $I = I_{PK}$)

Motor
Control
Fast
Discretels

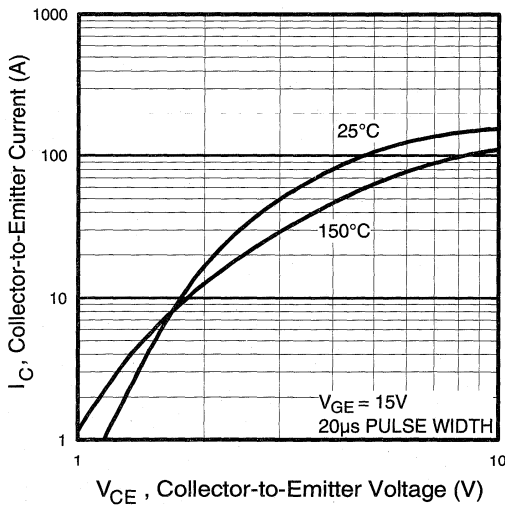


Fig. 2 - Typical Output Characteristics

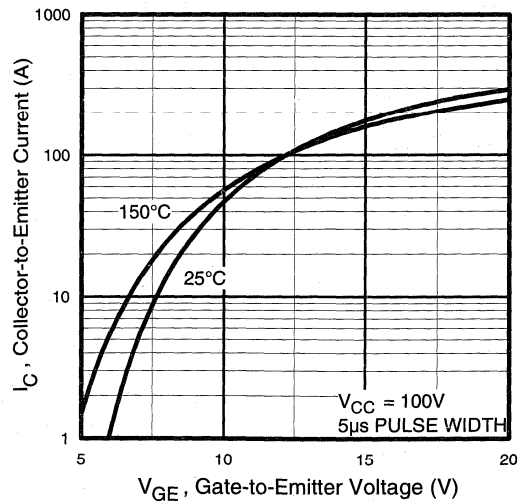


Fig. 3 - Typical Transfer Characteristics

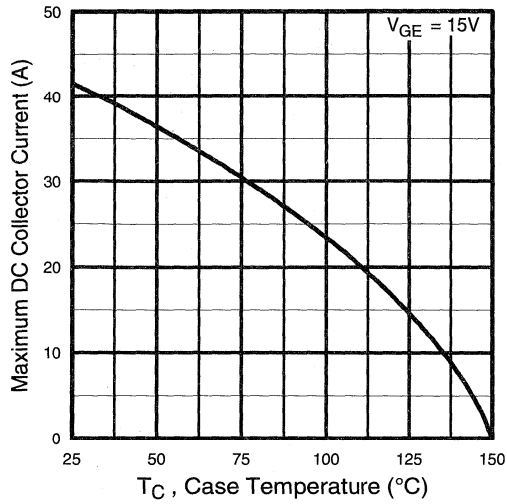


Fig. 4 - Maximum Collector Current vs. Case Temperature

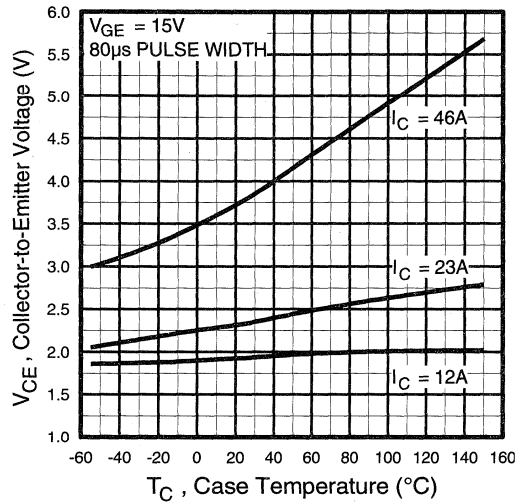


Fig. 5 - Collector-to-Emitter Voltage vs. Case Temperature

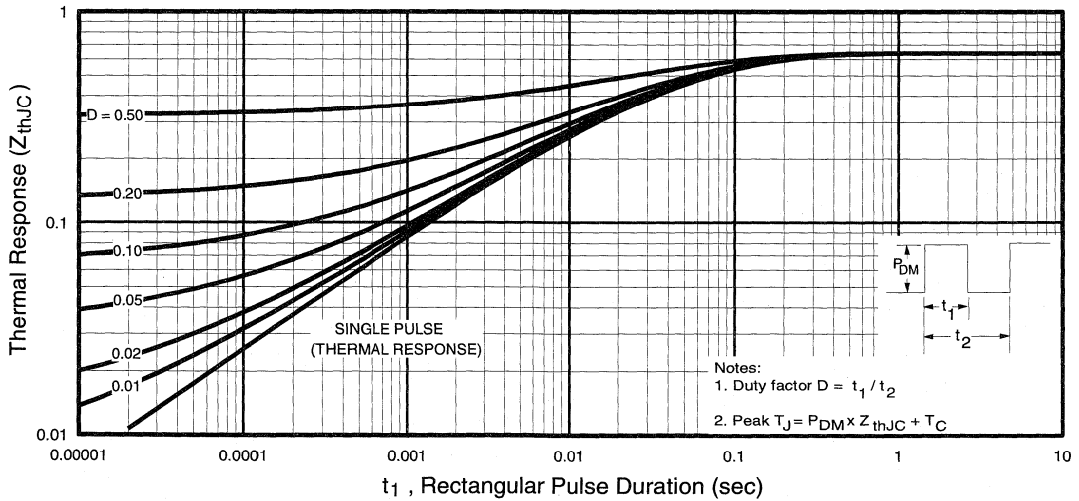


Fig. 6 - Maximum Effective Transient Thermal Impedance, Junction-to-Case

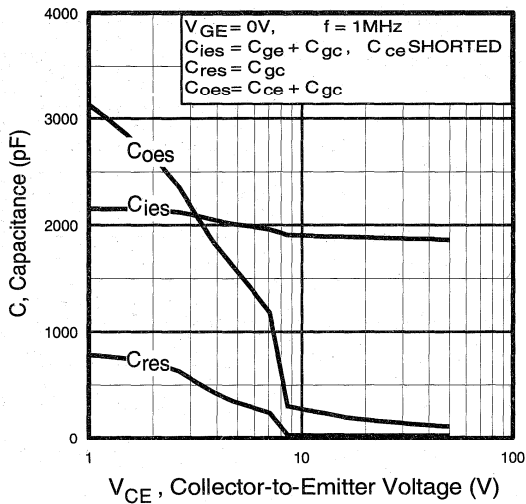


Fig. 7 - Typical Capacitance vs. Collector-to-Emitter Voltage

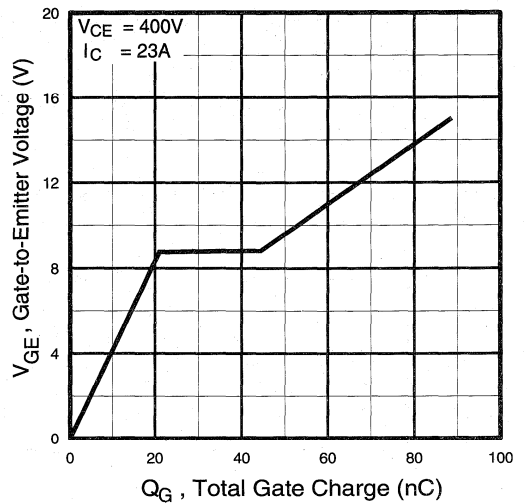


Fig. 8 - Typical Gate Charge vs. Gate-to-Emitter Voltage

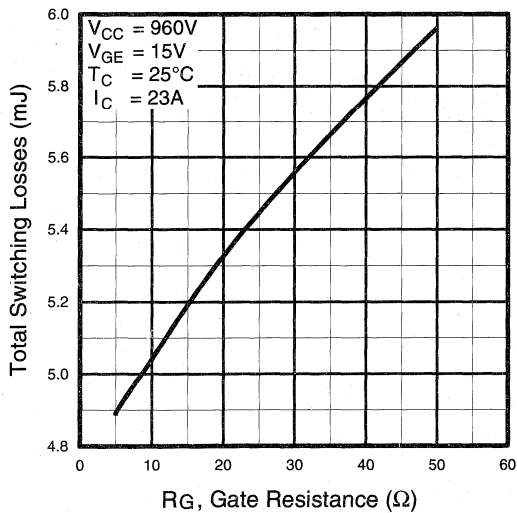


Fig. 9 - Typical Switching Losses vs. Gate Resistance

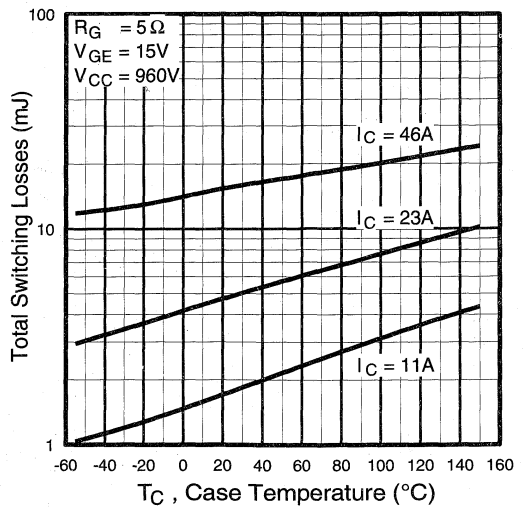


Fig. 10 - Typical Switching Losses vs. Case Temperature

Motor Control Fast Discretes

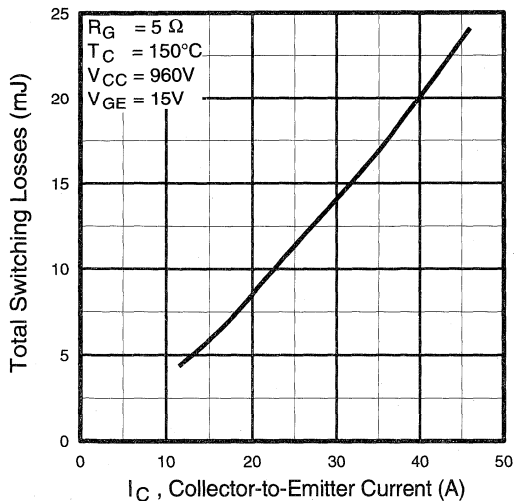


Fig. 11 - Typical Switching Losses vs. Collector-to-Emitter Current

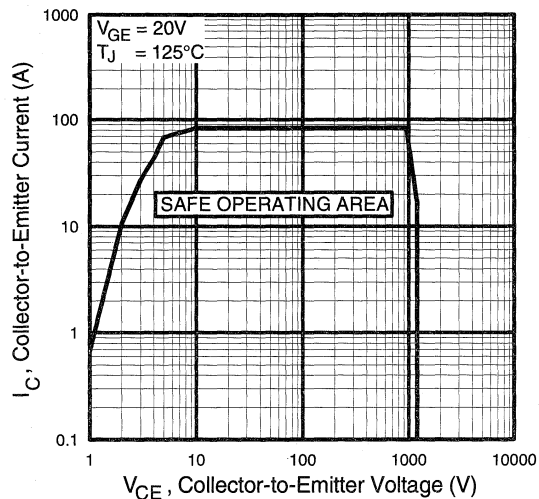


Fig. 12 - Turn-Off SOA

Refer to Section D for the following:

Appendix G: Section D - page D-9

Fig. 13a - Clamped Inductive Load Test Circuit

Fig. 13b - Pulsed Collector Current Test Circuit

Fig. 14a - Switching Loss Test Circuit

Fig. 14b - Switching Loss Waveform

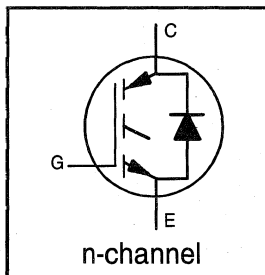
IRGPH30MD2

INSULATED GATE BIPOLAR TRANSISTOR
WITH ULTRAFAST SOFT RECOVERY

Short Circuit Rated
Fast CoPack IGBT

DIODE Features

- Short circuit rated -10 μ s @ 125°C, $V_{GE} = 15V$
- Switching-loss rating includes all "tail" losses
- HEXFRED™ soft ultrafast diodes
- Optimized for medium operating frequency (1 to 10kHz)

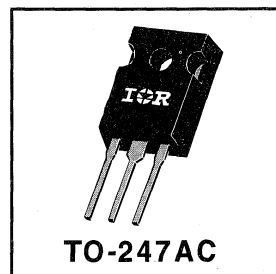


$V_{CES} = 1200V$
$V_{CE(sat)} \leq 3.5V$
@ $V_{GE} = 15V, I_C = 9.0A$

Description

Co-packaged IGBTs are a natural extension of International Rectifier's well known IGBT line. They provide the convenience of an IGBT and an ultrafast recovery diode in one package, resulting in substantial benefits to a host of high-voltage, high-current, applications.

These new short circuit rated devices are especially suited for motor control and other applications requiring short circuit withstand capability.



Absolute Maximum Ratings

	Parameter	Max.	Units
V_{CES}	Collector-to-Emitter Voltage	1200	V
$I_C @ T_C = 25^\circ C$	Continuous Collector Current	15	A
$I_C @ T_C = 100^\circ C$	Continuous Collector Current	9.0	
I_{CM}	Pulsed Collector Current $\text{\textcircled{D}}$	30	
I_{LM}	Clamped Inductive Load Current $\text{\textcircled{2}}$	30	
$I_F @ T_C = 100^\circ C$	Diode Continuous Forward Current	6.0	
I_{FM}	Diode Maximum Forward Current	30	
t_{sc}	Short Circuit Withstand Time	10	μ s
V_{GE}	Gate-to-Emitter Voltage	± 20	V
$P_D @ T_C = 25^\circ C$	Maximum Power Dissipation	100	W
$P_D @ T_C = 100^\circ C$	Maximum Power Dissipation	42	
T_J	Operating Junction and	-55 to +150	$^\circ C$
T_{STG}	Storage Temperature Range		
	Soldering Temperature, for 10 sec.		
	Mounting Torque, 6-32 or M3 Screw.	10 lbf*in (1.1 N*m)	

Thermal Resistance

	Parameter	Min.	Typ.	Max.	Units
$R_{\theta JC}$	Junction-to-Case - IGBT	—	—	1.2	$^\circ C/W$
$R_{\theta JC}$	Junction-to-Case - Diode	—	—	2.5	
$R_{\theta CS}$	Case-to-Sink, flat, greased surface	—	0.24	—	
$R_{\theta JA}$	Junction-to-Ambient, typical socket mount	—	—	40	
Wt	Weight	—	6 (0.21)	—	g (oz)

Electrical Characteristics @ $T_J = 25^\circ\text{C}$ (unless otherwise specified)

	Parameter	Min.	Typ.	Max.	Units	Conditions
$V_{(BR)CES}$	Collector-to-Emitter Breakdown Voltage ^①	1200	—	—	V	$V_{GE} = 0V, I_C = 250\mu A$
$\Delta V_{(BR)CES}/\Delta T_J$	Temperature Coeff. of Breakdown Voltage	—	—	—	V/ $^\circ\text{C}$	$V_{GE} = 0V, I_C = 1.0mA$
$V_{CE(on)}$	Collector-to-Emitter Saturation Voltage	—	3.1	3.5	V	$I_C = 9.0A, V_{GE} = 15V$
		—	4.9	—		$I_C = 15A$
		—	3.6	—		$I_C = 9.0A, T_J = 150^\circ\text{C}$
$V_{GE(th)}$	Gate Threshold Voltage	3.0	—	5.5		$V_{CE} = V_{GE}, I_C = 250\mu A$
$\Delta V_{GE(th)}/\Delta T_J$	Temperature Coeff. of Threshold Voltage	—	-14	—	mV/ $^\circ\text{C}$	$V_{CE} = V_{GE}, I_C = 250\mu A$
g_{fe}	Forward Transconductance ^④	2.5	—	—	S	$V_{CE} = 100V, I_C = 9.0A$
I_{CES}	Zero Gate Voltage Collector Current	—	—	250	μA	$V_{GE} = 0V, V_{CE} = 1200V$
		—	—	2500		$V_{GE} = 0V, V_{CE} = 1200V, T_J = 150^\circ\text{C}$
V_{FM}	Diode Forward Voltage Drop	—	2.7	3.0	V	$I_C = 6.0A$
		—	2.4	2.7		$I_C = 6.0A, T_J = 150^\circ\text{C}$
I_{GES}	Gate-to-Emitter Leakage Current	—	—	± 100	nA	$V_{GE} = \pm 20V$

Switching Characteristics @ $T_J = 25^\circ\text{C}$ (unless otherwise specified)

	Parameter	Min.	Typ.	Max.	Units	Conditions	
Q_g	Total Gate Charge (turn-on)	—	25	30	nC	$I_C = 9.0A, V_{CC} = 960V$	
Q_{ge}	Gate - Emitter Charge (turn-on)	—	—	6.0			
Q_{gc}	Gate - Collector Charge (turn-on)	—	—	15			
$t_{d(on)}$	Turn-On Delay Time	—	2.3	—	ns	$T_J = 25^\circ\text{C}, I_C = 9.0A, V_{CC} = 960V, V_{GE} = 15V, R_G = 23\Omega$ Energy losses include "tail" and diode reverse recovery.	
t_r	Rise Time	—	10	—			
$t_{d(off)}$	Turn-Off Delay Time	—	200	450			
t_f	Fall Time	—	210	390			
E_{on}	Turn-On Switching Loss	—	—	—			
E_{off}	Turn-Off Switching Loss	—	—	—	mJ		
E_{ts}	Total Switching Loss	—	4.0	7.0			
t_{sc}	Short Circuit Withstand Time	10	—	—	μs	$V_{CC} = 720V, T_J = 125^\circ\text{C}, V_{GE} = 15V, R_G = 23\Omega, V_{CPK} < 1000V$	
$t_{d(on)}$	Turn-On Delay Time	—	33	—	ns	$T_J = 150^\circ\text{C}, I_C = 9.0A, V_{CC} = 960V, V_{GE} = 15V, R_G = 23\Omega$ Energy losses include "tail" and diode reverse recovery.	
t_r	Rise Time	—	20	—			
$t_{d(off)}$	Turn-Off Delay Time	—	480	—			
t_f	Fall Time	—	450	—			
E_{ts}	Total Switching Loss	—	8.0	—			
L_E	Internal Emitter Inductance	—	13	—	nH	Measured 5mm from package	
C_{ies}	Input Capacitance	—	670	—	pF	$V_{GE} = 0V, V_{CC} = 30V, f = 1.0MHz$	
C_{oes}	Output Capacitance	—	50	—			
C_{res}	Reverse Transfer Capacitance	—	10	—			
t_{rr}	Diode Reverse Recovery Time	—	53	80	ns	$T_J = 25^\circ\text{C}$	$I_F = 6.0A, V_R = 200V, di/dt = 200A/\mu s$
		—	87	130			
I_{rr}	Diode Peak Reverse Recovery Current	—	4.4	8.0	A	$T_J = 25^\circ\text{C}$	
		—	5.0	9.0		$T_J = 125^\circ\text{C}$	
Q_{rr}	Diode Reverse Recovery Charge	—	116	320	nC	$T_J = 25^\circ\text{C}$	
		—	233	585		$T_J = 125^\circ\text{C}$	
$di_{(rec)M}/dt$	Diode Peak Rate of Fall of Recovery During t_b	—	180	—	A/ μs	$T_J = 25^\circ\text{C}$	
		—	100	—		$T_J = 125^\circ\text{C}$	

Notes: ① Repetitive rating; $V_{GE}=20V$, pulse width limited by max. junction temperature.

② $V_{CC}=80\%(V_{CES}), V_{GE}=20V, L=10\mu H, R_G=23\Omega$

④ Pulse width 5.0 μs , single shot.

③ Pulse width $\leq 80\mu s$; duty factor $\leq 0.1\%$.

Refer to Section D - page D-13 for Package Outline 3 - JEDEC Outline TO-247AC

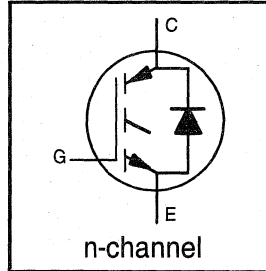
IRGPH40MD2

INSULATED GATE BIPOLAR TRANSISTOR
WITH ULTRAFAST SOFT RECOVERY

Short Circuit Rated
Fast CoPack IGBT

DIODE Features

- Short circuit rated -10 μ s @ 125°C, $V_{GE} = 15V$
- Switching-loss rating includes all "tail" losses
- HEXFRED™ soft ultrafast diodes
- Optimized for medium operating frequency (1 to 10kHz)

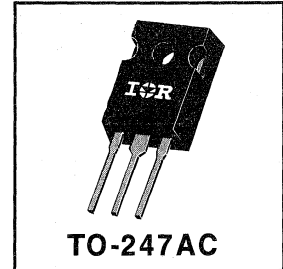


$V_{CES} = 1200V$
 $V_{CE(sat)} \leq 3.4V$
@ $V_{GE} = 15V, I_C = 18A$

Description

Co-packaged IGBTs are a natural extension of International Rectifier's well known IGBT line. They provide the convenience of an IGBT and an ultrafast recovery diode in one package, resulting in substantial benefits to a host of high-voltage, high-current, applications.

These new short circuit rated devices are especially suited for motor control and other applications requiring short circuit withstand capability.



Motor
Control
Fast
CoPacks

Absolute Maximum Ratings

	Parameter	Max.	Units
V_{CES}	Collector-to-Emitter Voltage	1200	V
$I_C @ T_C = 25^\circ C$	Continuous Collector Current	31	A
$I_C @ T_C = 100^\circ C$	Continuous Collector Current	18	
I_{CM}	Pulsed Collector Current ①	62	
I_{LM}	Clamped Inductive Load Current ②	62	
$I_F @ T_C = 100^\circ C$	Diode Continuous Forward Current	8.0	
I_{FM}	Diode Maximum Forward Current	62	μ s
t_{sc}	Short Circuit Withstand Time	10	
V_{GE}	Gate-to-Emitter Voltage	± 20	V
$P_D @ T_C = 25^\circ C$	Maximum Power Dissipation	160	W
$P_D @ T_C = 100^\circ C$	Maximum Power Dissipation	65	
T_J	Operating Junction and	-55 to +150	$^\circ C$
T_{STG}	Storage Temperature Range		
	Soldering Temperature, for 10 sec.	300 (0.063 in. (1.6mm) from case)	
	Mounting Torque, 6-32 or M3 Screw.	10 lbf•in (1.1 N•m)	

Thermal Resistance

	Parameter	Min.	Typ.	Max.	Units
$R_{\theta JC}$	Junction-to-Case - IGBT	—	—	0.77	$^\circ C/W$
$R_{\theta JC}$	Junction-to-Case - Diode	—	—	1.7	
$R_{\theta CS}$	Case-to-Sink, flat, greased surface	—	0.24	—	
$R_{\theta JA}$	Junction-to-Ambient, typical socket mount	—	—	40	
Wt	Weight	—	6 (0.21)	—	g (oz)

Electrical Characteristics @ $T_J = 25^\circ\text{C}$ (unless otherwise specified)

	Parameter	Min.	Typ.	Max.	Units	Conditions
$V_{(BR)CES}$	Collector-to-Emitter Breakdown Voltage ^③	1200	—	—	V	$V_{GE} = 0V, I_C = 250\mu A$
$\Delta V_{(BR)CES}/\Delta T_J$	Temp. Coeff. of Breakdown Voltage	—	1.1	—	V/ $^\circ\text{C}$	$V_{GE} = 0V, I_C = 1.0mA$
$V_{CE(on)}$	Collector-to-Emitter Saturation Voltage	—	2.3	3.4	V	$I_C = 18A$ $V_{GE} = 15V$
		—	3.0	—		$I_C = 31A$
		—	2.8	—		$I_C = 18A, T_J = 150^\circ\text{C}$
$V_{GE(th)}$	Gate Threshold Voltage	3.0	—	5.5		$V_{CE} = V_{GE}, I_C = 250\mu A$
$\Delta V_{GE(th)}/\Delta T_J$	Temp. Coeff. of Threshold Voltage	—	-14	—	mV/ $^\circ\text{C}$	$V_{CE} = V_{GE}, I_C = 250\mu A$
g_{fe}	Forward Transconductance ^④	4.0	10	—	S	$V_{CE} = 100V, I_C = 18A$
I_{CES}	Zero Gate Voltage Collector Current	—	—	250	μA	$V_{GE} = 0V, V_{CE} = 1200V$
		—	—	3500		$V_{GE} = 0V, V_{CE} = 1200V, T_J = 150^\circ\text{C}$
V_{FM}	Diode Forward Voltage Drop	—	2.6	3.3	V	$I_C = 8A$
		—	2.3	3.0		$I_C = 8A, T_J = 150^\circ\text{C}$
I_{GES}	Gate-to-Emitter Leakage Current	—	—	± 100	nA	$V_{GE} = \pm 20V$

Switching Characteristics @ $T_J = 25^\circ\text{C}$ (unless otherwise specified)

	Parameter	Min.	Typ.	Max.	Units	Conditions	
Q_g	Total Gate Charge (turn-on)	—	50	75	nC	$I_C = 18A$ $V_{CC} = 400V$	
Q_{ge}	Gate - Emitter Charge (turn-on)	—	11	21			
Q_{gc}	Gate - Collector Charge (turn-on)	—	15	30			
$t_{d(on)}$	Turn-On Delay Time	—	67	—	ns	$T_J = 25^\circ\text{C}$ $I_C = 18A, V_{CC} = 800V$ $V_{GE} = 15V, R_G = 10\Omega$ Energy losses include "tail" and diode reverse recovery.	
t_r	Rise Time	—	89	—			
$t_{d(off)}$	Turn-Off Delay Time	—	340	930			
t_f	Fall Time	—	510	930			
E_{on}	Turn-On Switching Loss	—	2.1	—			
E_{off}	Turn-Off Switching Loss	—	5.9	—	mJ		
E_{ts}	Total Switching Loss	—	8.0	13			
t_{sc}	Short Circuit Withstand Time	10	—	—	μs	$V_{CC} = 720V, T_J = 125^\circ\text{C}$ $V_{GE} = 15V, R_G = 10\Omega, V_{CPK} < 1000V$	
$t_{d(on)}$	Turn-On Delay Time	—	64	—	ns	$T_J = 150^\circ\text{C}$, $I_C = 18A, V_{CC} = 800V$ $V_{GE} = 15V, R_G = 10\Omega$ Energy losses include "tail" and diode reverse recovery.	
t_r	Rise Time	—	74	—			
$t_{d(off)}$	Turn-Off Delay Time	—	550	—			
t_f	Fall Time	—	1200	—			
E_{ts}	Total Switching Loss	—	16	—			
L_E	Internal Emitter Inductance	—	13	—	nH	Measured 5mm from package	
C_{ies}	Input Capacitance	—	1400	—	pF	$V_{GE} = 0V$ $V_{CC} = 30V$ $f = 1.0MHz$	
C_{oes}	Output Capacitance	—	100	—			
C_{res}	Reverse Transfer Capacitance	—	15	—			
t_{rr}	Diode Reverse Recovery Time	—	63	95	ns	$T_J = 25^\circ\text{C}$ $T_J = 125^\circ\text{C}$	$I_F = 8A$ $V_R = 200V$ $di/dt = 200A/\mu s$
		—	106	160			
I_{rr}	Diode Peak Reverse Recovery Current	—	4.5	8.0	A	$T_J = 25^\circ\text{C}$	
		—	6.2	11		$T_J = 125^\circ\text{C}$	
Q_{rr}	Diode Reverse Recovery Charge	—	140	380	nC	$T_J = 25^\circ\text{C}$	
		—	335	880		$T_J = 125^\circ\text{C}$	
$di_{(rec)M}/dt$	Diode Peak Rate of Fall of Recovery During t_b	—	133	—	A/ μs	$T_J = 25^\circ\text{C}$	
		—	85	—		$T_J = 125^\circ\text{C}$	

Notes: ① Repetitive rating; $V_{GE}=20V$, pulse width limited by max. junction temperature.

② $V_{CC}=80\%(V_{CES})$, $V_{GE}=20V$, $L=10\mu H$, $R_G=10\Omega$

④ Pulse width 5.0 μs , single shot.

③ Pulse width $\leq 80\mu s$; duty factor $\leq 0.1\%$.

Refer to Section D - page D-13 for Package Outline 3 - JEDEC Outline TO-247AC

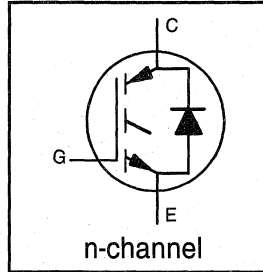
IRGPH50MD2

**INSULATED GATE BIPOLAR TRANSISTOR
WITH ULTRAFAST SOFT RECOVERY**

**Short Circuit Rated
Fast CoPack IGBT**

**DIODE
Features**

- Short circuit rated -10 μ s @ 125°C, V_{GE} = 15V
- Switching-loss rating includes all "tail" losses
- HEXFRED™ soft ultrafast diodes
- Optimized for medium operating frequency (1 to 10kHz) See Fig. 1 for Current vs. Frequency curve

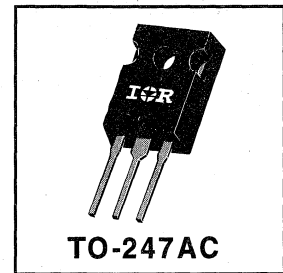


V_{CES} = 1200V
V_{CE(sat)} ≤ 2.9V
@ V_{GE} = 15V, I_C = 23A

Description

Co-packaged IGBTs are a natural extension of International Rectifier's well known IGBT line. They provide the convenience of an IGBT and an ultrafast recovery diode in one package, resulting in substantial benefits to a host of high-voltage, high-current, applications.

These new short circuit rated devices are especially suited for motor control and other applications requiring short circuit withstand capability.



Motor
Control
Fast
CoPacks

Absolute Maximum Ratings

	Parameter	Max.	Units
V _{CES}	Collector-to-Emitter Voltage	1200	V
I _C @ T _C = 25°C	Continuous Collector Current	42	A
I _C @ T _C = 100°C	Continuous Collector Current	23	
I _{CM}	Pulsed Collector Current ①	84	
I _{LM}	Clamped Inductive Load Current ②	84	
I _F @ T _C = 100°C	Diode Continuous Forward Current	16	
I _{FM}	Diode Maximum Forward Current	84	μs
t _{sc}	Short Circuit Withstand Time	10	
V _{GE}	Gate-to-Emitter Voltage	± 20	V
P _D @ T _C = 25°C	Maximum Power Dissipation	200	W
P _D @ T _C = 100°C	Maximum Power Dissipation	78	
T _J	Operating Junction and	-55 to +150	°C
T _{STG}	Storage Temperature Range		
	Soldering Temperature, for 10 sec.	300 (0.063 in. (1.6mm) from case)	
	Mounting torque, 6-32 or M3 screw.	10 lbf•in (1.1 N•m)	

Thermal Resistance

	Parameter	Min.	Typ.	Max.	Units
R _{θJC}	Junction-to-Case - IGBT	—	—	0.64	°C/W
R _{θJC}	Junction-to-Case - Diode	—	—	0.83	
R _{θCS}	Case-to-Sink, flat, greased surface	—	0.24	—	
R _{θJA}	Junction-to-Ambient, typical socket mount	—	—	40	
Wt	Weight	—	6 (0.21)	—	g (oz)

Electrical Characteristics @ $T_J = 25^\circ\text{C}$ (unless otherwise specified)

	Parameter	Min.	Typ.	Max.	Units	Conditions
$V_{(BR)CES}$	Collector-to-Emitter Breakdown Voltage ^③	1200	—	—	V	$V_{GE} = 0\text{V}$, $I_C = 250\mu\text{A}$
$\Delta V_{(BR)CES}/\Delta T_J$	Temperature Coeff. of Breakdown Voltage	—	1.1	—	V/ $^\circ\text{C}$	$V_{GE} = 0\text{V}$, $I_C = 1.0\text{mA}$
$V_{CE(on)}$	Collector-to-Emitter Saturation Voltage	—	2.3	2.9	V	$I_C = 23\text{A}$ $V_{GE} = 15\text{V}$ $I_C = 42\text{A}$ See Fig. 2, 5 $I_C = 23\text{A}$, $T_J = 150^\circ\text{C}$
		—	3.0	—		
		—	2.8	—		
$V_{GE(th)}$	Gate Threshold Voltage	3.0	—	5.5		$V_{CE} = V_{GE}$, $I_C = 250\mu\text{A}$
$\Delta V_{GE(th)}/\Delta T_J$	Temperature Coeff. of Threshold Voltage	—	-13	—	mV/ $^\circ\text{C}$	$V_{CE} = V_{GE}$, $I_C = 250\mu\text{A}$
g_{fe}	Forward Transconductance ^④	11	15	—	S	$V_{CE} = 100\text{V}$, $I_C = 23\text{A}$
I_{CES}	Zero Gate Voltage Collector Current	—	—	250	μA	$V_{GE} = 0\text{V}$, $V_{CE} = 1200\text{V}$
		—	—	6500		$V_{GE} = 0\text{V}$, $V_{CE} = 1200\text{V}$, $T_J = 150^\circ\text{C}$
V_{FM}	Diode Forward Voltage Drop	—	2.5	3.0	V	$I_C = 16\text{A}$ See Fig. 13 $I_C = 16\text{A}$, $T_J = 150^\circ\text{C}$
		—	2.1	2.5		
I_{GES}	Gate-to-Emitter Leakage Current	—	—	± 100	nA	$V_{GE} = \pm 20\text{V}$

Switching Characteristics @ $T_J = 25^\circ\text{C}$ (unless otherwise specified)

	Parameter	Min.	Typ.	Max.	Units	Conditions
Q_g	Total Gate Charge (turn-on)	—	89	130	nC	$I_C = 23\text{A}$ $V_{CC} = 400\text{V}$ See Fig. 8
Q_{ge}	Gate - Emitter Charge (turn-on)	—	22	33		
Q_{gc}	Gate - Collector Charge (turn-on)	—	26	39		
$t_{d(on)}$	Turn-On Delay Time	—	100	—	ns	$T_J = 25^\circ\text{C}$ $I_C = 23\text{A}$, $V_{CC} = 960\text{V}$ $V_{GE} = 15\text{V}$, $R_G = 5.0\Omega$ Energy losses include "tail" and diode reverse recovery. See Fig. 9, 10, 11, 18
t_r	Rise Time	—	140	—		
$t_{d(off)}$	Turn-Off Delay Time	—	510	770		
t_f	Fall Time	—	470	730		
E_{on}	Turn-On Switching Loss	—	3.0	—		
E_{off}	Turn-Off Switching Loss	—	8.0	—		
E_{ts}	Total Switching Loss	—	11	17	mJ	
t_{sc}	Short Circuit Withstand Time	10	—	—	μs	$V_{CC} = 720\text{V}$, $T_J = 125^\circ\text{C}$ $V_{GE} = 15\text{V}$, $R_G = 5.0\Omega$
$t_{d(on)}$	Turn-On Delay Time	—	86	—	ns	$T_J = 150^\circ\text{C}$, See Fig. 9, 10, 11, 18 $I_C = 23\text{A}$, $V_{CC} = 960\text{V}$ $V_{GE} = 15\text{V}$, $R_G = 5.0\Omega$ Energy losses include "tail" and diode reverse recovery
t_r	Rise Time	—	130	—		
$t_{d(off)}$	Turn-Off Delay Time	—	800	—		
t_f	Fall Time	—	920	—		
E_{ts}	Total Switching Loss	—	20	—		
L_E	Internal Emitter Inductance	—	13	—	nH	Measured 5mm from package
C_{ies}	Input Capacitance	—	1900	—	pF	$V_{GE} = 0\text{V}$ $V_{CC} = 30\text{V}$ See Fig. 7 $f = 1.0\text{MHz}$
C_{oes}	Output Capacitance	—	140	—		
C_{res}	Reverse Transfer Capacitance	—	24	—		
t_{rr}	Diode Reverse Recovery Time	—	90	135	ns	$T_J = 25^\circ\text{C}$ See Fig. 14 $T_J = 125^\circ\text{C}$ 14
		—	164	245		
I_{rr}	Diode Peak Reverse Recovery Charge	—	5.8	10	A	$T_J = 25^\circ\text{C}$ See Fig. 15 $T_J = 125^\circ\text{C}$ 15
		—	8.3	15		
Q_{rr}	Diode Reverse Recovery Charge	—	260	675	nC	$T_J = 25^\circ\text{C}$ See Fig. 16 $T_J = 125^\circ\text{C}$ 16
		—	680	1838		
$di_{(rec)M}/dt$	Diode Peak Rate of Fall of Recovery During t_b	—	120	—	A/ μs	$T_J = 25^\circ\text{C}$ See Fig. 17 $T_J = 125^\circ\text{C}$ 17
		—	76	—		

Notes:

① Repetitive rating; $V_{GE} = 20\text{V}$, pulse width limited by max. junction temperature. (See fig. 20)

② $V_{CC} = 80\%(V_{CES})$, $V_{GE} = 20\text{V}$, $L = 10\mu\text{H}$, $R_G = 5.0\Omega$, (See fig. 19)

③ Pulse width $\leq 80\mu\text{s}$; duty factor $\leq 0.1\%$.

④ Pulse width $5.0\mu\text{s}$, single shot.

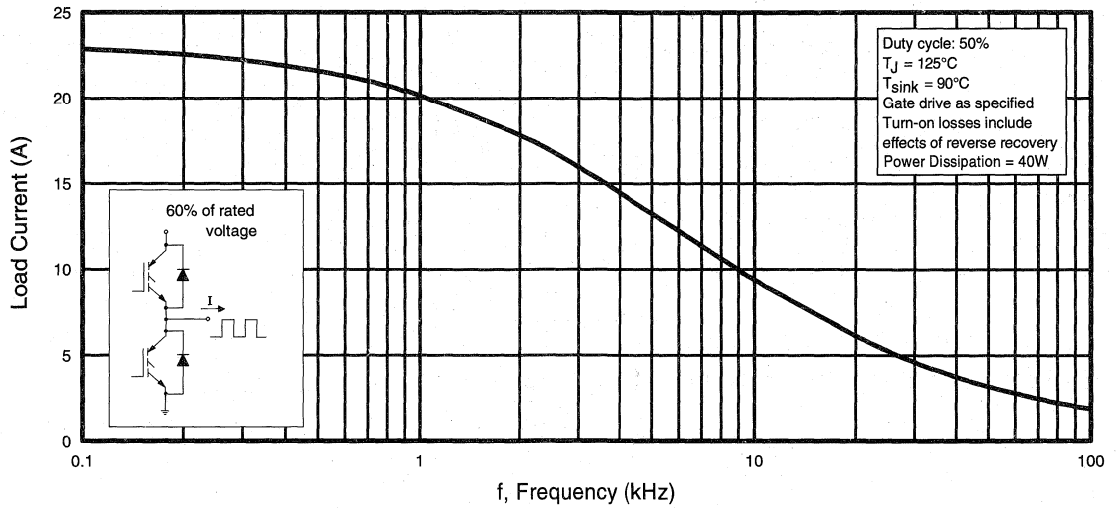


Fig. 1 - Typical Load Current vs. Frequency
(Load Current = I_{RMS} of fundamental)

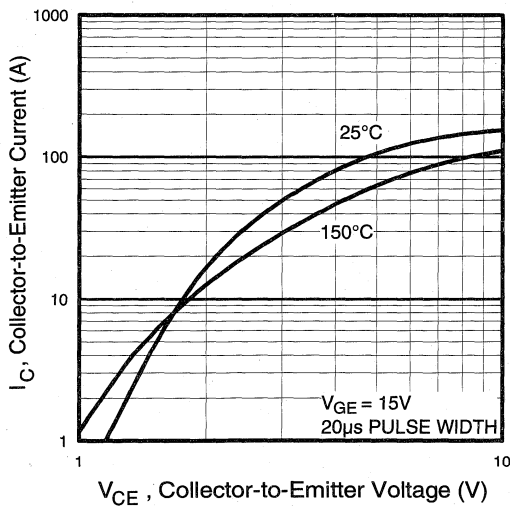


Fig. 2 - Typical Output Characteristics

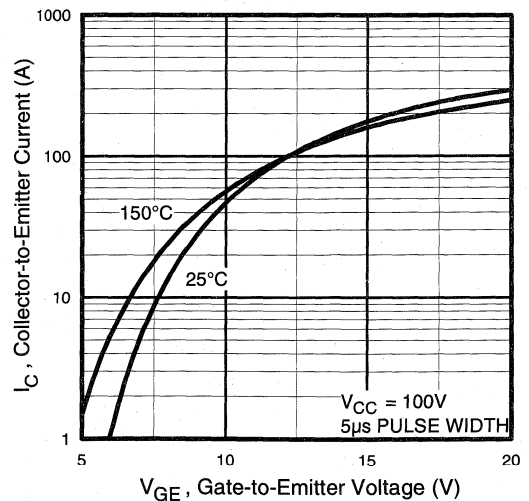


Fig. 3 - Typical Transfer Characteristics

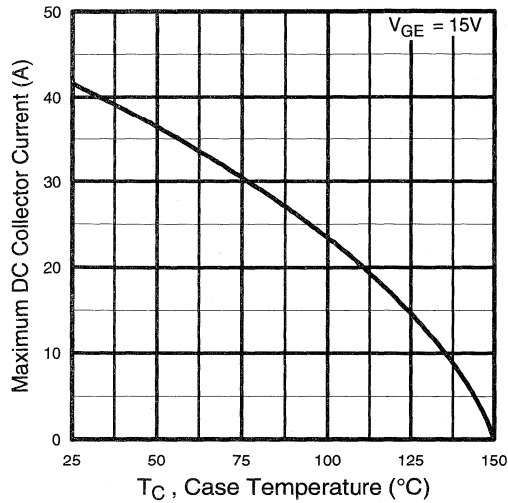


Fig. 4 - Maximum Collector Current vs. Case Temperature

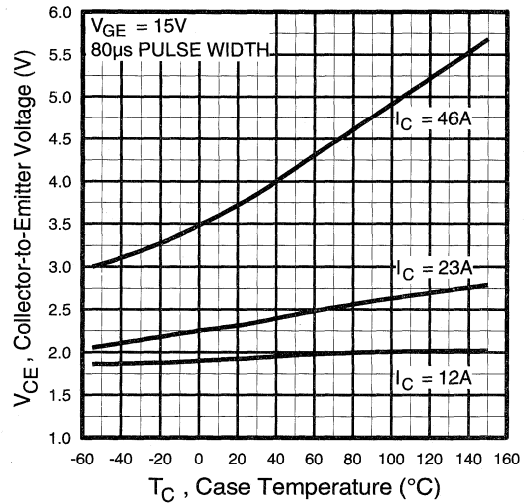


Fig. 5 - Collector-to-Emitter Voltage vs. Case Temperature

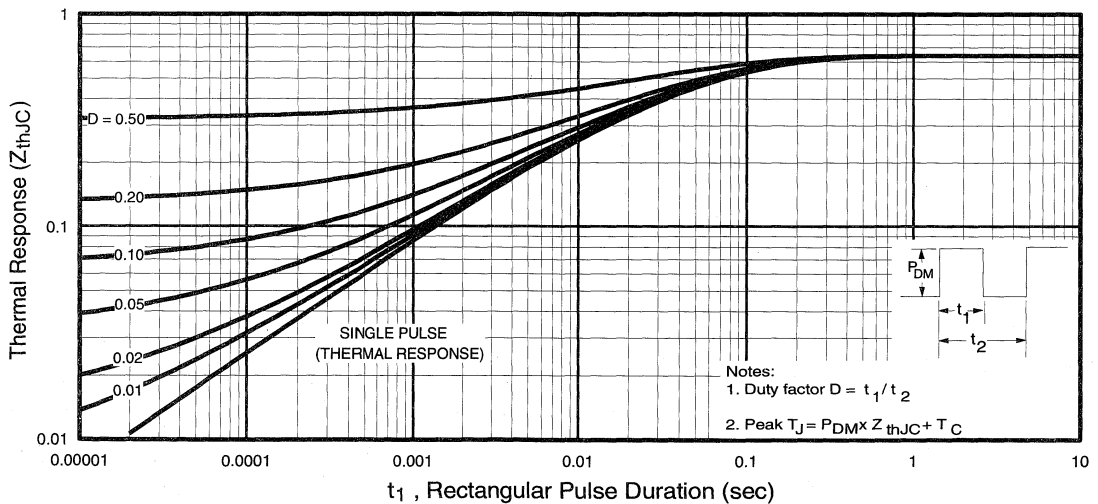


Fig. 6 - Maximum IGBT Effective Transient Thermal Impedance, Junction-to-Case

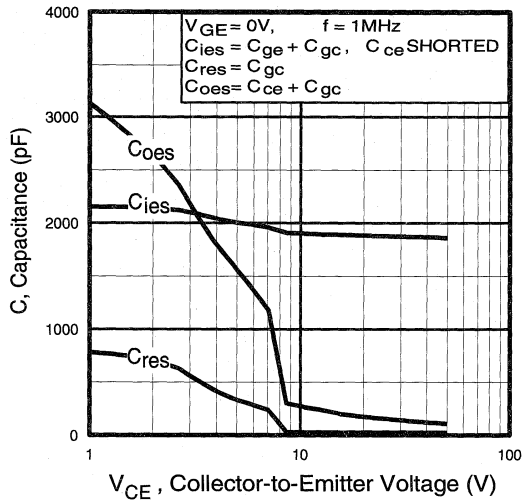


Fig. 7 - Typical Capacitance vs. Collector-to-Emitter Voltage

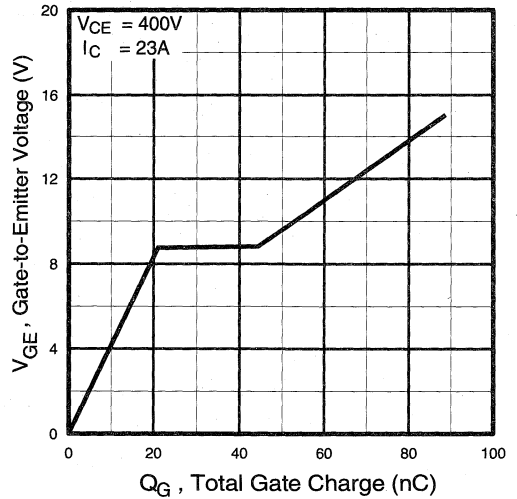


Fig. 8 - Typical Gate Charge vs. Gate-to-Emitter Voltage

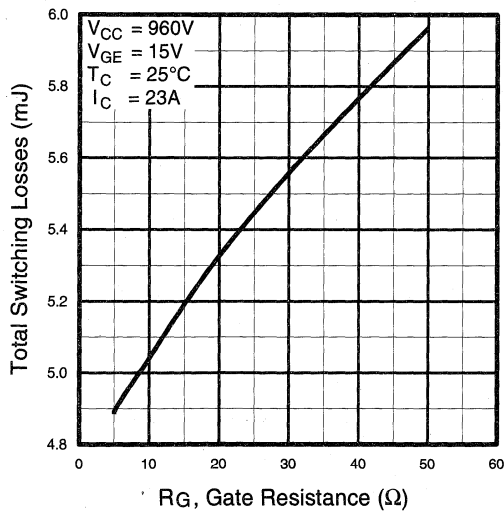


Fig. 9 - Typical Switching Losses vs. Gate Resistance

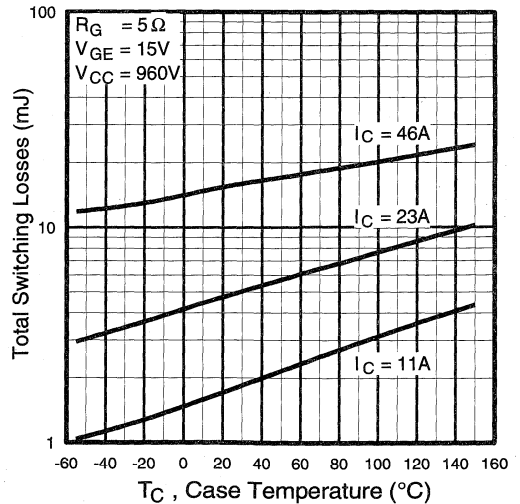


Fig. 10 - Typical Switching Losses vs. Case Temperature



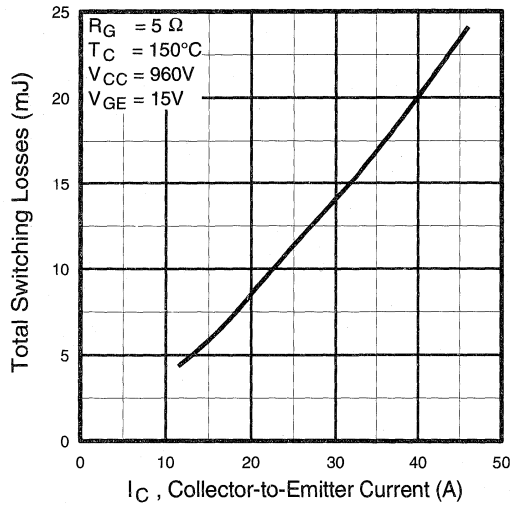


Fig. 11 - Typical Switching Losses vs. Collector-to-Emitter Current

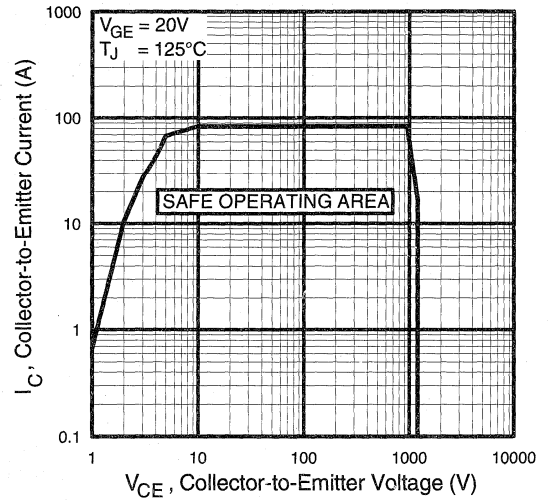


Fig. 12 - Turn-Off SOA

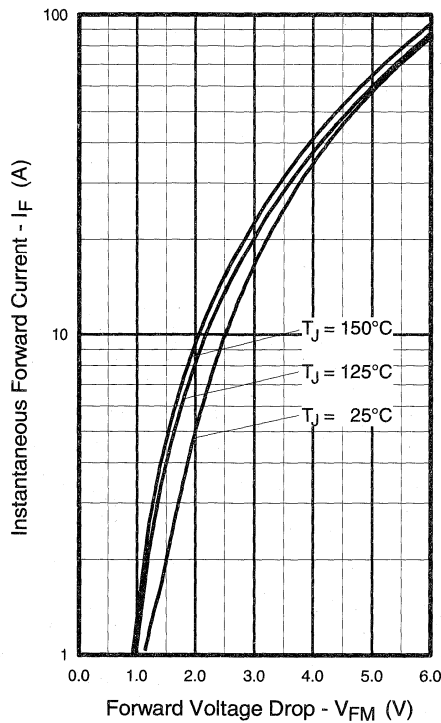


Fig. 13 - Maximum Forward Voltage Drop vs. Instantaneous Forward Current

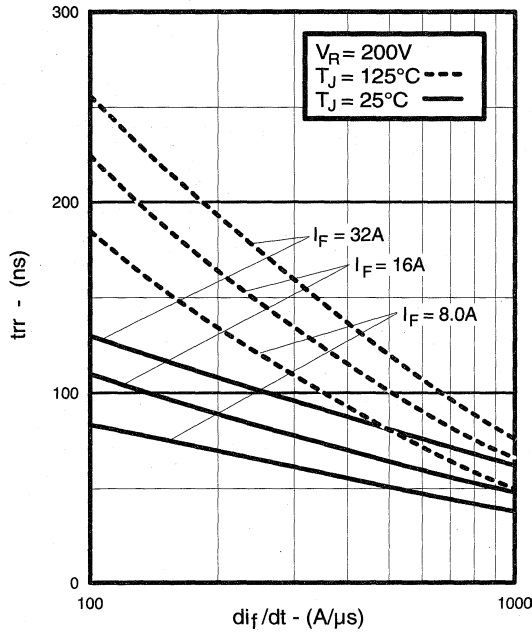


Fig. 14 - Typical Reverse Recovery vs. di_f/dt

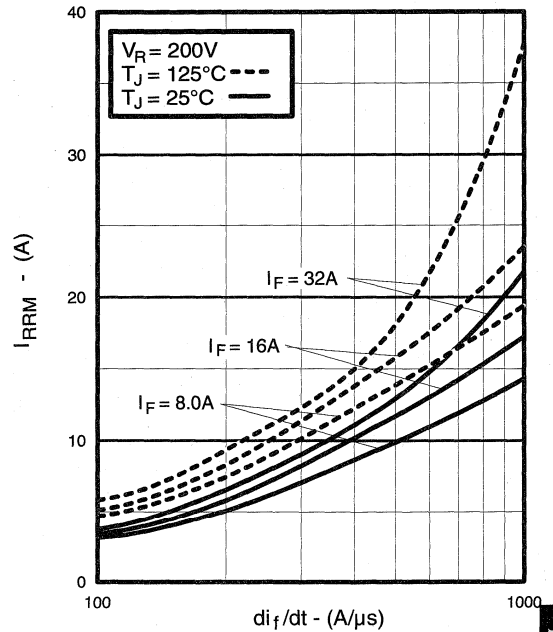


Fig. 15 - Typical Recovery Current vs. di_f/dt

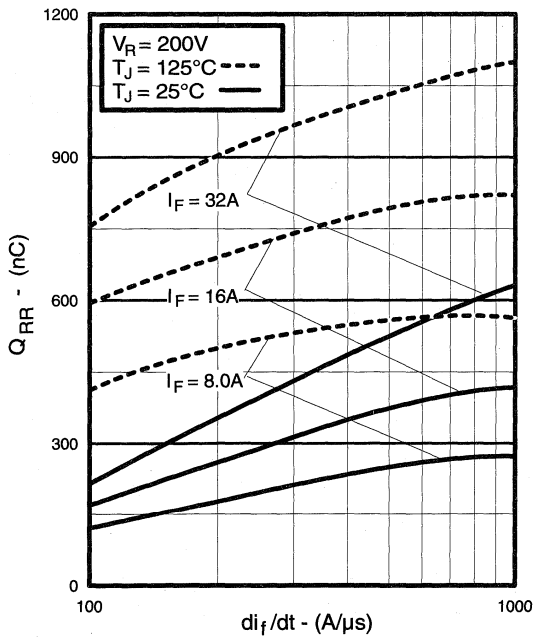


Fig. 16 - Typical Stored Charge vs. di_f/dt

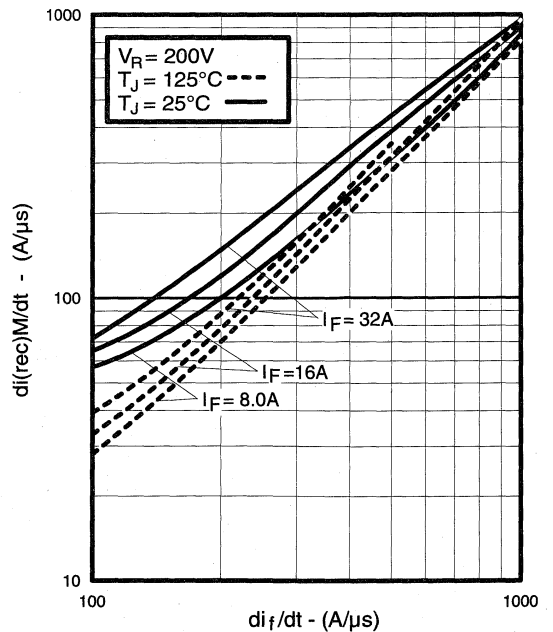


Fig. 17 - Typical $di_{(rec)M}/dt$ vs. di_f/dt

Motor Control Fast Co-Packs

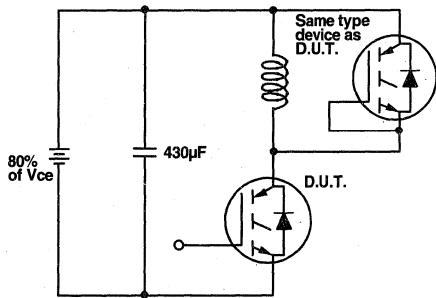


Fig. 18a - Test Circuit for Measurement of I_{LM} , E_{on} , $E_{off(diode)}$, t_{rr} , Q_{rr} , I_{rr} , $t_{d(on)}$, t_r , $t_{d(off)}$, t_f

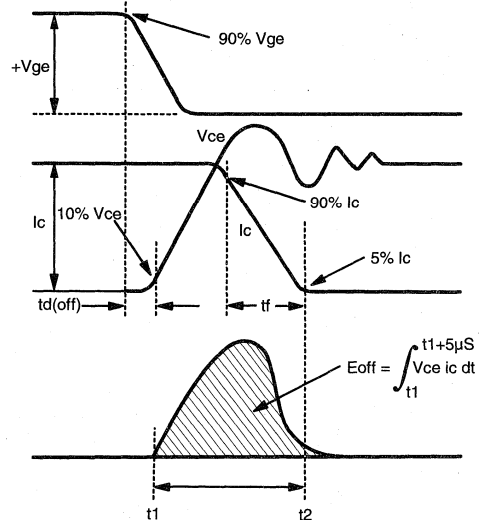


Fig. 18b - Test Waveforms for Circuit of Fig. 18a, Defining E_{off} , $t_{d(off)}$, t_f

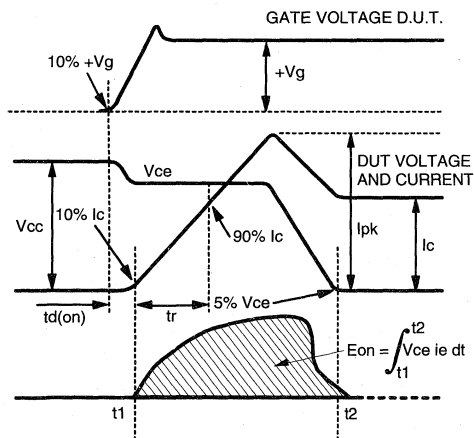


Fig. 18c - Test Waveforms for Circuit of Fig. 18a, Defining E_{on} , $t_{d(on)}$, t_r

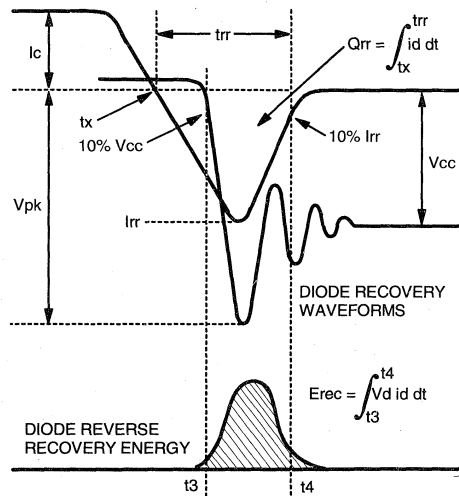


Fig. 18d - Test Waveforms for Circuit of Fig. 18a, Defining E_{rec} , t_{rr} , Q_{rr} , I_{rr}

Refer to Section D for the following:

Appendix H: Section D - page D-10

Fig. 18e - Macro Waveforms for Test Circuit Fig. 18a

Fig. 19 - Clamped Inductive Load Test Circuit

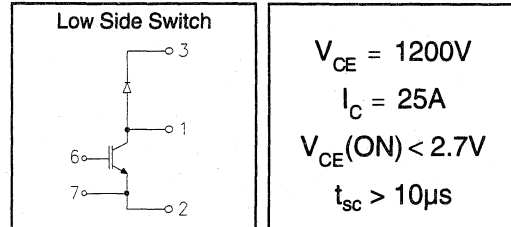
Fig. 20 - Pulsed Collector Current Test Circuit

IRGKIN025M12

"CHOPPER LOW SIDE SWITCH" IGBT INT-A-PAK

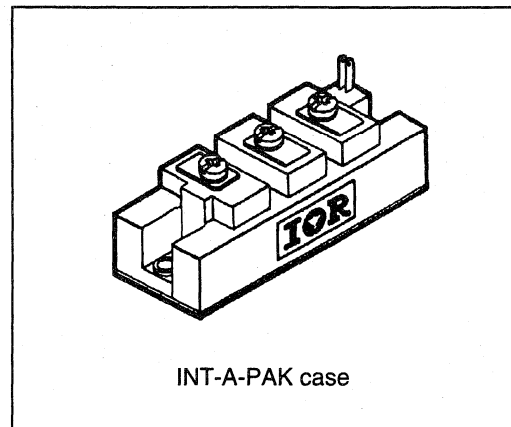
Low conduction loss IGBT

- Rugged Design
- Simple gate-drive
- Switching-Loss Rating includes all "tail" losses
- Short circuit rated



Description

IR's advanced IGBT technology is the key to this line of INT-A-PAK Power Modules. The efficient geometry and unique processing of the IGBT allow higher current densities than comparable bipolar power module transistors, while at the same time requiring the simpler gate-drive of the familiar power MOSFET. These modules are short circuit rated for applications such as motor control requiring this important feature.



Motor Control Fast Modules

Absolute Maximum Ratings

Parameter	Description	Value	Units
V_{CES}	Continuous collector to emitter voltage	1200	V
$I_C @ T_C = 25^\circ C$	Maximum Continuous collector current	50	A
$I_C @ T_C = 85^\circ C$	Maximum Continuous collector current	45	
$I_C @ T_C = 100^\circ C$	Maximum Continuous collector current	35	
I_{LM}	Peak switching current	50	
I_{FM}	Peak diode forward current (1)	50	V
V_{GE}	Gate to emitter voltage	± 20	
V_{ISOL}	RMS isolation voltage, any terminal to case, $t = 1$ min	2500	
$P_D @ T_C = 25^\circ C$	Power dissipation	385	W
T_J	Operating junction temperature range	-40 to 150	$^\circ C$
T_{STG}	Storage temperature range	-40 to 125	

(1) Duration limited by max junction temperature.

Electrical Characteristics - $T_J = 25^\circ\text{C}$, unless otherwise stated

Parameter	Description	Min	Typ	Max	Units	Test Conditions
BV_{CES}	Collector-to-emitter breakdown voltage	1200	—	—	V	$V_{GE} = 0V, I_C = 1mA$
$V_{CE(ON)}$	Collector-to-emitter voltage	—	2.2	2.7		$V_{GE} = 15V, I_C = 25A$
		—	1.85	—		$V_{GE} = 15V, I_C = 15A, T_J = 150^\circ\text{C}$
V_{FM}	Diode forward voltage - maximum	—	3.2	3.4		$I_F = 25A, V_{GE} = 0V$
		—	2.6	—		$I_F = 25A, V_{GE} = 0V, T_J = 150^\circ\text{C}$
V_{GEth}	Gate threshold voltage	3.0	—	5.5	$I_C = 500\mu A$	
ΔV_{GEth}	Threshold voltage temp. coefficient	—	-11	—	mV/ $^\circ\text{C}$	$V_{CE} = V_{GE}, I_C = 500\mu A$
g_{fe}	Forward transconductance	18	—	35	S(τ)	$V_{CE} = 25V, I_C = 25A$
I_{CES}	Collector-to-emitter leakage current	—	—	1	mA	$V_{GE} = 0V, V_{CE} = 1200V$
		—	—	10		$V_{GE} = 0V, V_{CE} = 1200V, T_J = 150^\circ\text{C}$
I_{GES}	Gate-to-emitter leakage current	—	—	± 1	μA	$V_{GE} = \pm 20V$

Dynamic Characteristics - $T_J = 125^\circ\text{C}$, unless otherwise stated

Parameter	Description	Min	Typ	Max	Units	Test Conditions
E_{on}	Turn-on switching energy	—	0.19	—	mJ/A	$R_G = 15\Omega, V_{CC} = 600V$
E_{off} (1)	Turn-off switching energy	—	0.36	—		$I_C = 25A, L_S = 100nH$
E_{ts} (1)	Total switching energy	—	—	0.60		$V_{GE} = \pm 15V$
$t_{d(on)}$	Turn-on delay time	—	200	250	ns	$R_G = 15\Omega, V_{CC} = 600V$
t_r	Rise time	—	200	250		$I_C = 25A$
$t_{d(off)}$	Turn-off delay time	—	125	200		$V_{GE} = \pm 15V$
t_f	Fall time	—	650	—		Resistive load, $T_J = 25^\circ\text{C}$
I_{rr}	Diode peak recovery current	—	25	—		A
t_{rr}	Diode recovery time	—	215	—	ns	$I_C = 25A$
Q_{rr}	Diode recovery charge	—	3	—	μC	$V_{GE} = \pm 15V$
Q_{ge}	Gate-to-emitter charge (turn-on)	23	—	88	nC	$V_{CC} = 600V$
Q_{gc}	Gate-to-collector charge (turn-on)	80	—	170		$I_C = 25A$
Q_g	Total gate charge (turn-on)	250	—	450		$V_{GE} = 15V$
C_{ies}	Input capacitance	5250	—	5500	pF	$V_{GE} = 0V$
C_{oes}	Output capacitance	330	—	550		$V_{CC} = 30V$
C_{res}	Reverse transfer capacitance	330	—	500		$f = 1MHz$
t_{sc}	Short circuit withstand time	10	—	—	μs	$V_{CC} = 720V, V_{GE} = \pm 15V$ Min. $R_G = 15\Omega, V_{CEP} = 1000V$

(1) Includes tail losses

Thermal and Mechanical Characteristics

Parameter	Description	Typ	Max	Units
R_{thJC} (IGBT)	Thermal resistance, junction to case, each IGBT	—	0.352	$^\circ\text{C/W}$
R_{thJC} (Diode)	Thermal resistance, junction to case, each diode	—	0.480	
R_{thCS} (Module)	Thermal resistance, case to sink	0.041	0.100	
Wt	Weight of module	150	—	g

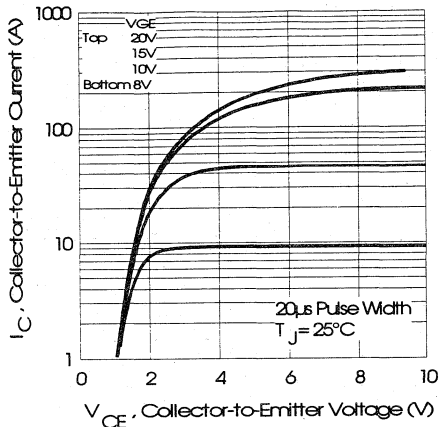


Fig. 1 - Typical Output Characteristics, $T_J = 25^\circ\text{C}$

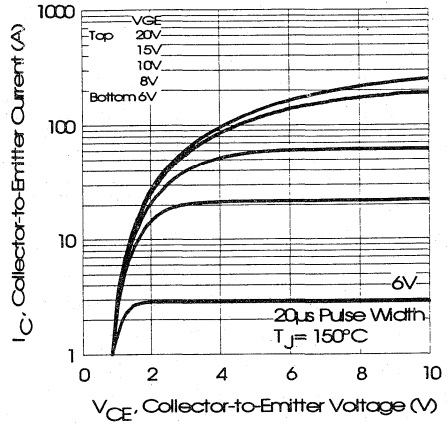


Fig. 2 - Typical Output Characteristics, $T_J = 150^\circ\text{C}$

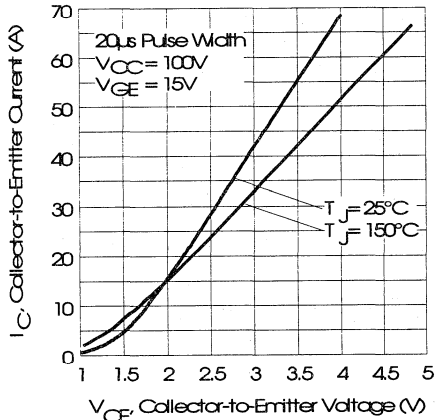


Fig. 3 - Typical Output Characteristics

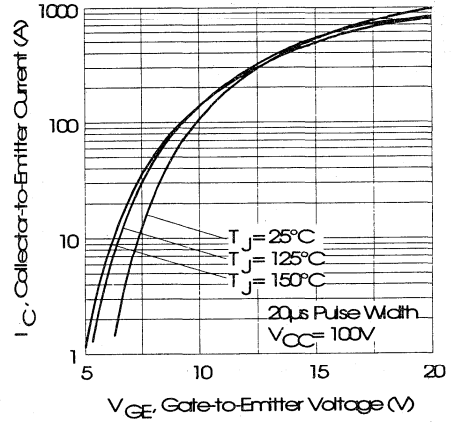


Fig. 4 - Typical Transfer Characteristics

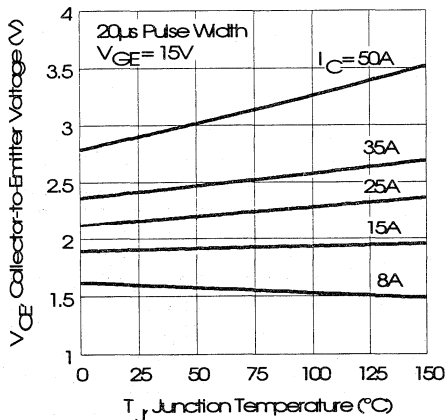


Fig. 5 - Collector-to-Emitter Saturation Typical Voltage vs. Junction Temperature

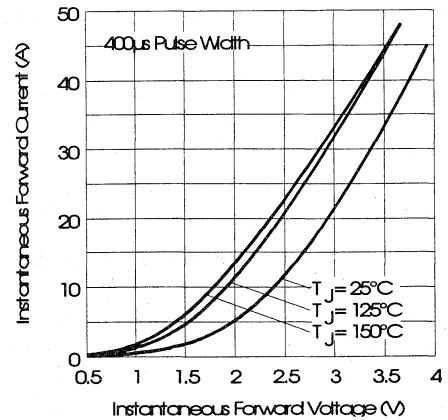


Fig. 6 - Forward Voltage Drop Characteristics

Motor
Control
First
Modules

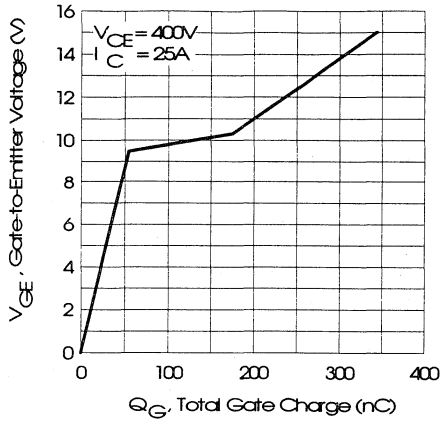


Fig. 7 - Typical Gate Charge vs. Gate-to-Emitter Voltage

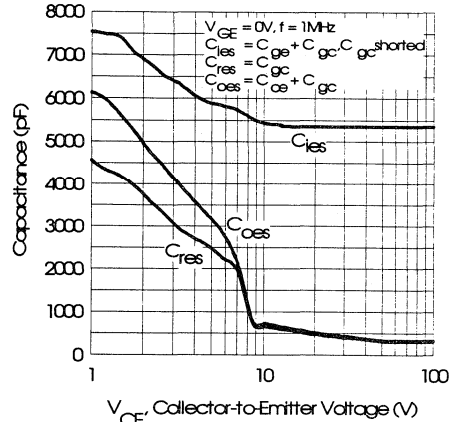


Fig. 8 - Typical Capacitance vs. Collector-to-Emitter Voltage

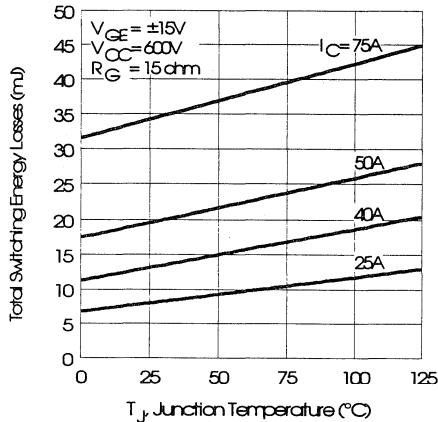


Fig. 9 - Typical Switching Losses vs. Junction Temperature

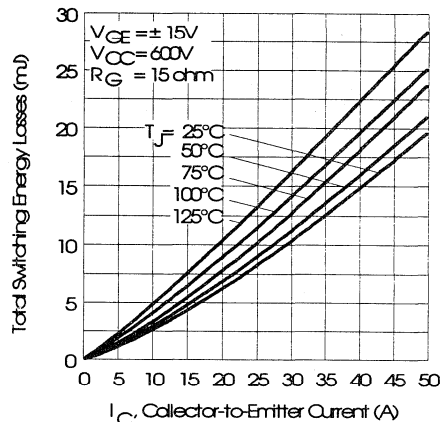


Fig. 10 - Typical Switching Losses vs. Collector-to-Emitter Current

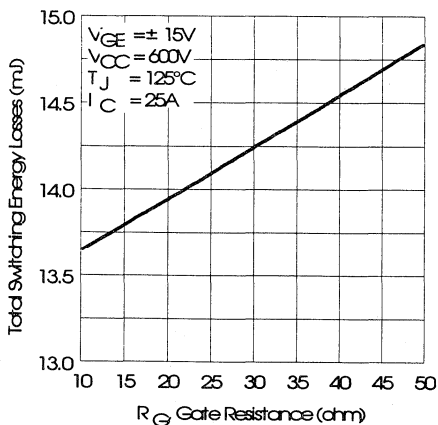


Fig. 11 - Typical Switching Losses vs. Gate Resistance

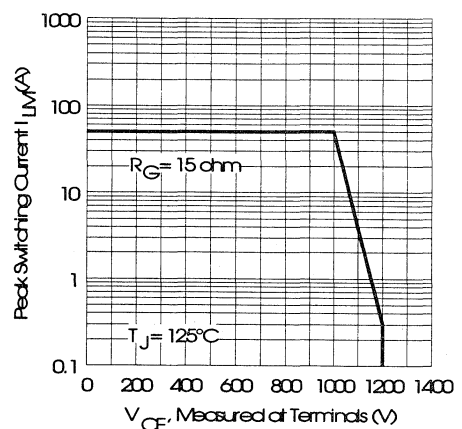


Fig. 12 - Reverse Bias Safe Operating Area

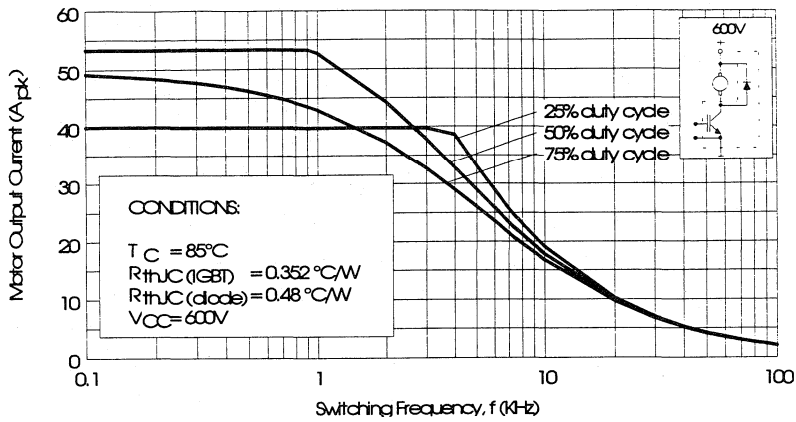


Fig. 13 - RMS Output Current vs. Frequency

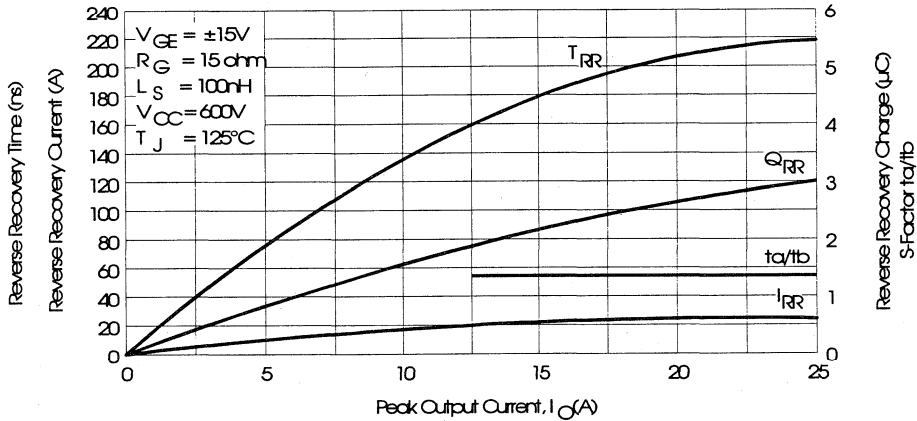


Fig. 14 - Typical Diode Recovery Characteristics as Function of Output Current I_o

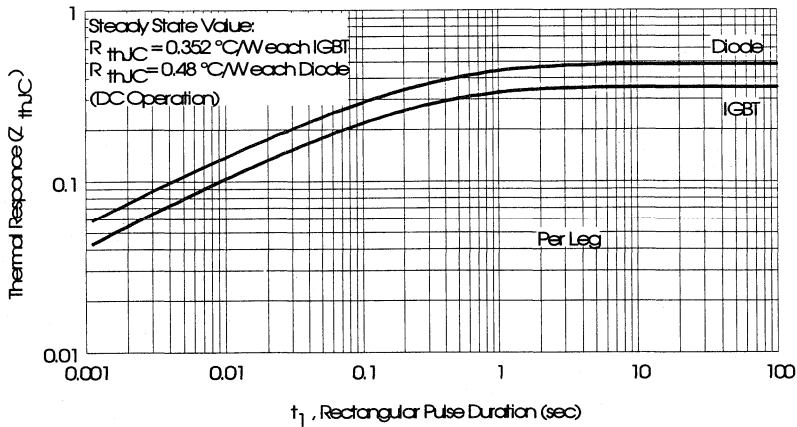


Fig. 15 - Maximum Effective Transient Thermal Impedance, Junction-to-Case

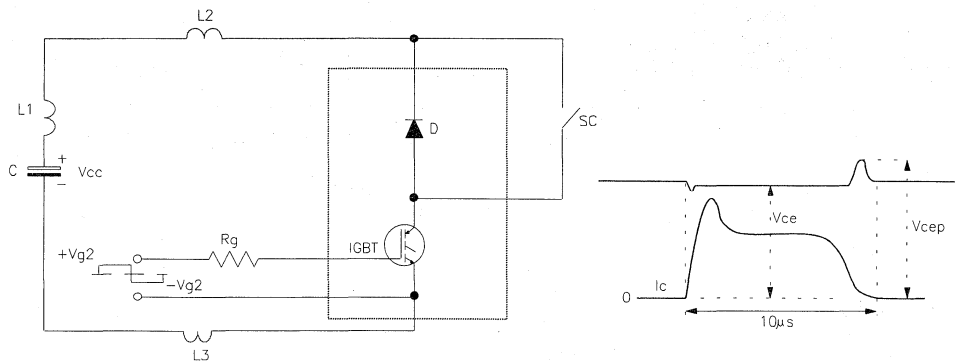


Fig. 16 - Test Circuit for Short Circuit

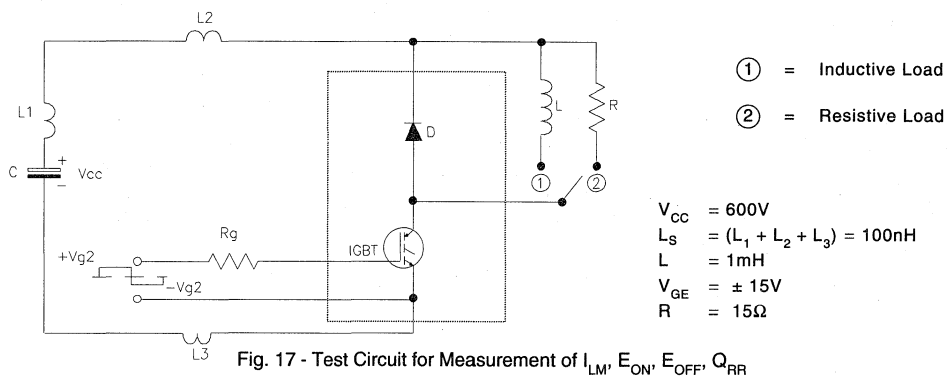


Fig. 17 - Test Circuit for Measurement of I_{LM} , E_{ON} , E_{OFF} , Q_{RR}

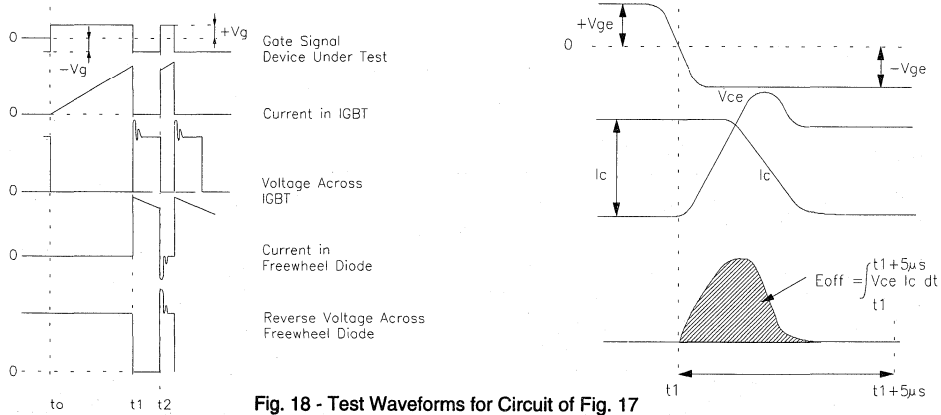


Fig. 18 - Test Waveforms for Circuit of Fig. 17

Refer to Section D for the following:

Appendix I: Section D - page D-11

Fig. 19 - Test Waveforms for Circuit of Fig. 17,

Defining E_{ON} , E_{REC} , Q_{RR}

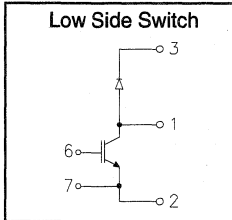
Fig. 20 - Waveforms for Switching Time

IRGKIN050M12

"CHOPPER LOW SIDE SWITCH" IGBT INT-A-PAK

Low conduction loss IGBT

- Rugged Design
- Simple gate-drive
- Switching-Loss Rating includes all "tail" losses
- Short circuit rated



$$V_{CE} = 1200V$$

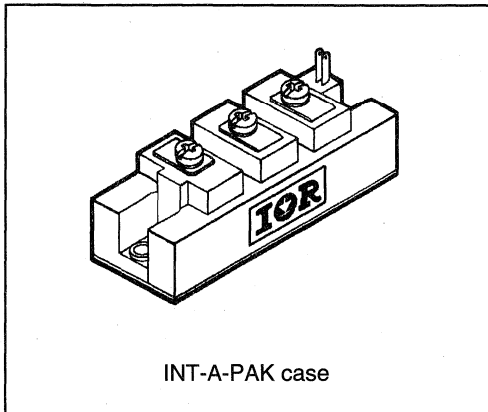
$$I_C = 50A$$

$$V_{CE(ON)} < 2.7V$$

$$t_{sc} > 10\mu s$$

Description

IR's advanced IGBT technology is the key to this line of INT-A-PAK Power Modules. The efficient geometry and unique processing of the IGBT allow higher current densities than comparable bipolar power module transistors, while at the same time requiring the simpler gate-drive of the familiar power MOSFET. These modules are short circuit rated for applications such as motor control requiring this important feature.



Motor
Control
Fast
Modules

Absolute Maximum Ratings

Parameter	Description	Value	Units
V_{CES}	Continuous collector to emitter voltage	1200	V
$I_C @ T_C = 25^\circ C$	Maximum Continuous collector current	100	A
$I_C @ T_C = 85^\circ C$	Maximum Continuous collector current	65	
$I_C @ T_C = 100^\circ C$	Maximum Continuous collector current	45	
I_{LM}	Peak switching current	100	
I_{FM}	Peak diode forward current (1)	100	V
V_{GE}	Gate to emitter voltage	± 20	
V_{ISOL}	RMS isolation voltage, any terminal to case, $t = 1 \text{ min}$	2500	W
$P_D @ T_C = 25^\circ C$	Power dissipation	455	
T_J	Operating junction temperature range	-40 to 150	$^\circ C$
T_{STG}	Storage temperature range	-40 to 125	

(1) Duration limited by max junction temperature.

Electrical Characteristics - $T_J = 25^\circ\text{C}$, unless otherwise stated

Parameter	Description	Min	Typ	Max	Units	Test Conditions
BV_{CES}	Collector-to-emitter breakdown voltage	1200	—	—	V	$V_{GE} = 0V, I_C = 1.5mA$
$V_{CE(ON)}$	Collector-to-emitter voltage	—	2.2	2.7		$V_{GE} = 15V, I_C = 50A$
		—	1.8	—		$V_{GE} = 15V, I_C = 25A, T_J = 150^\circ\text{C}$
V_{FM}	Diode forward voltage - maximum	—	3.2	3.4		$I_F = 50A, V_{GE} = 0V$
		—	2.6	—		$I_F = 50A, V_{GE} = 0V, T_J = 150^\circ\text{C}$
V_{GEth}	Gate threshold voltage	3.0	—	5.5	$I_C = 750\mu A$	
ΔV_{GEth}	Threshold voltage temp. coefficient	—	-11	—	$mV/^\circ\text{C}$	$V_{CE} = V_{GE}, I_C = 750\mu A$
g_{fe}	Forward transconductance	27	—	53	S($\bar{\omega}$)	$V_{CE} = 25V, I_C = 50A$
I_{CES}	Collector-to-emitter leakage current	—	—	1.5	mA	$V_{GE} = 0V, V_{CE} = 1200V$
		—	—	15		$V_{GE} = 0V, V_{CE} = 1200V, T_J = 150^\circ\text{C}$
I_{GES}	Gate-to-emitter leakage current	—	—	± 1.5	μA	$V_{GE} = \pm 20V$

Dynamic Characteristics - $T_J = 125^\circ\text{C}$, unless otherwise stated

Parameter	Description	Min	Typ	Max	Units	Test Conditions
E_{on}	Turn-on switching energy	—	0.19	—	mJ/A	$R_G = 10\Omega, V_{CC} = 600V$
E_{off} (1)	Turn-off switching energy	—	0.36	—		$I_C = 50A, L_S = 100nH$
E_{ts} (1)	Total switching energy	—	—	0.60		$V_{GE} = \pm 15V$
$t_{d(on)}$	Turn-on delay time	—	200	250	ns	$R_G = 10\Omega, V_{CC} = 600V$
t_r	Rise time	—	200	250		$I_C = 50A$
$t_{d(off)}$	Turn-off delay time	—	125	200		$V_{GE} = \pm 15V$
t_f	Fall time	—	650	—		Resistive load, $T_J = 25^\circ\text{C}$
I_{rr}	Diode peak recovery current	—	35	—	A	$R_G = 10\Omega, V_{CC} = 600V$
t_{rr}	Diode recovery time	—	215	—	ns	$I_C = 50A$
Q_{rr}	Diode recovery charge	—	4.5	—	μC	$V_{GE} = \pm 15V$
Q_{ge}	Gate-to-emitter charge (turn-on)	35	—	130	nC	$V_{CC} = 600V$
Q_{gc}	Gate-to-collector charge (turn-on)	120	—	250		$I_C = 50A$
Q_g	Total gate charge (turn-on)	380	—	680		$V_{GE} = 15V$
C_{ies}	Input capacitance	8000	—	8300	pF	$V_{GE} = 0V$
C_{oes}	Output capacitance	490	—	820		$V_{CC} = 30V$
C_{res}	Reverse transfer capacitance	490	—	750		$f = 1MHz$
t_{sc}	Short circuit withstand time	10	—	—	μs	$V_{CC} = 720V, V_{GE} = \pm 15V$ Min. $R_G = 10\Omega, V_{CEP} = 1000V$

(1) Includes tail losses

Thermal and Mechanical Characteristics

Parameter	Description	Typ	Max	Units
R_{thJC} (IGBT)	Thermal resistance, junction to case, each IGBT	—	0.275	$^\circ\text{C/W}$
R_{thJC} (Diode)	Thermal resistance, junction to case, each diode	—	0.380	
R_{thCS} (Module)	Thermal resistance, case to sink	0.041	0.100	
Wt	Weight of module	150	—	g

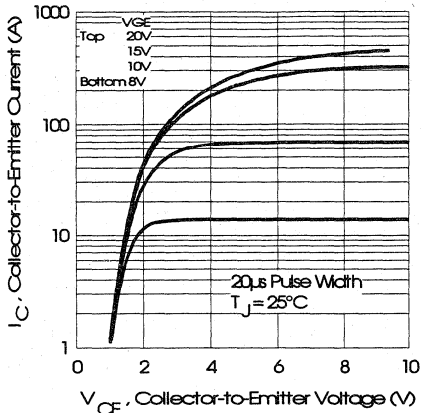


Fig. 1 - Typical Output Characteristics, $T_J = 25^\circ\text{C}$

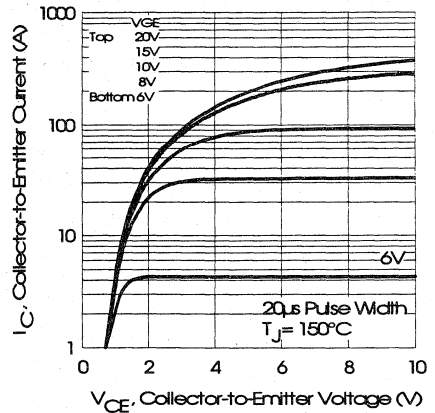


Fig. 2 - Typical Output Characteristics, $T_J = 150^\circ\text{C}$

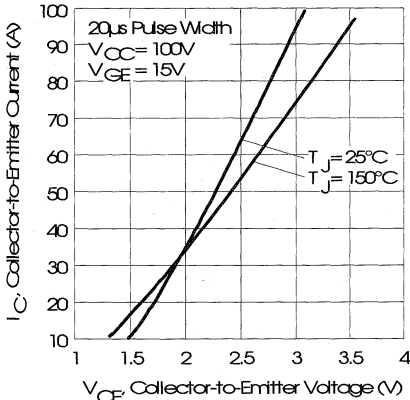


Fig. 3 - Typical Output Characteristics

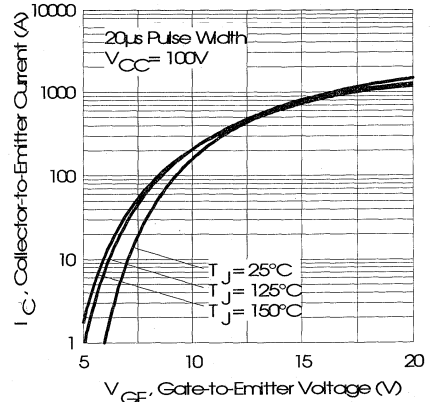


Fig. 4 - Typical Transfer Characteristics

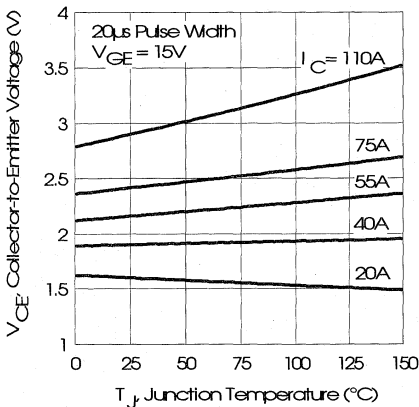


Fig. 5 - Collector-to-Emitter Saturation Typical Voltage vs. Junction Temperature

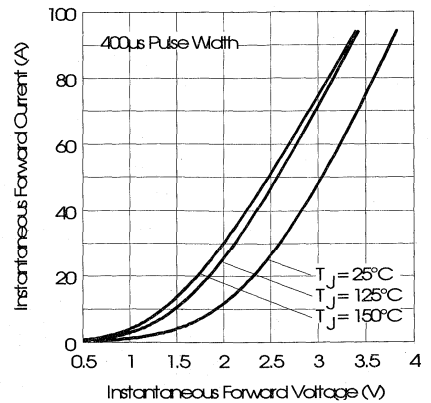


Fig. 6 - Forward Voltage Drop Characteristics

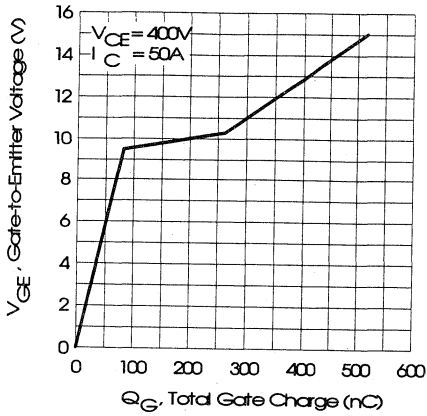


Fig. 7 - Typical Gate Charge vs. Gate-to-Emitter Voltage

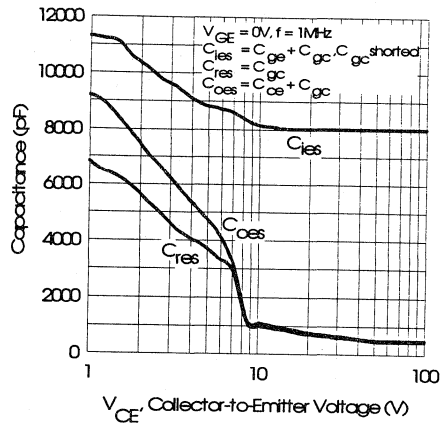


Fig. 8 - Typical Capacitance vs. Collector-to-Emitter Voltage

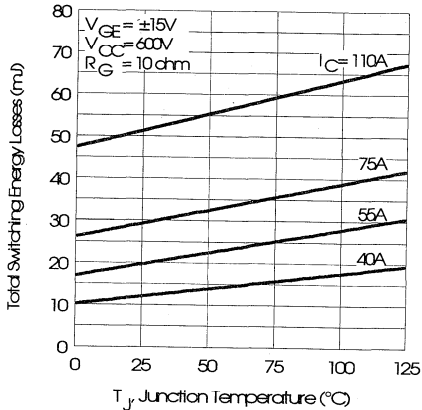


Fig. 9 - Typical Switching Losses vs. Junction Temperature

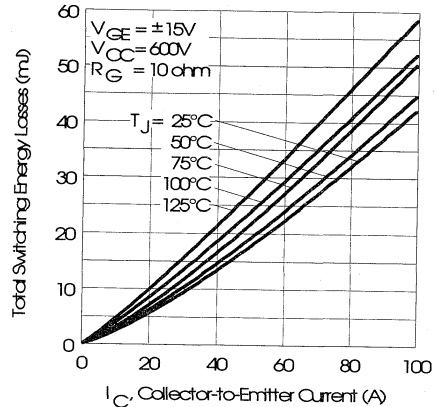


Fig. 10 - Typical Switching Losses vs. Collector-to-Emitter Current

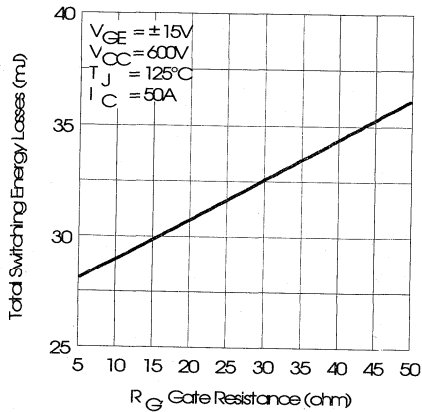


Fig. 11 - Typical Switching Losses vs. Gate Resistance

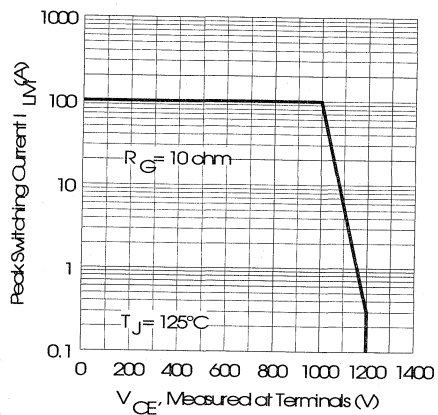


Fig. 12 - Reverse Bias Safe Operating Area

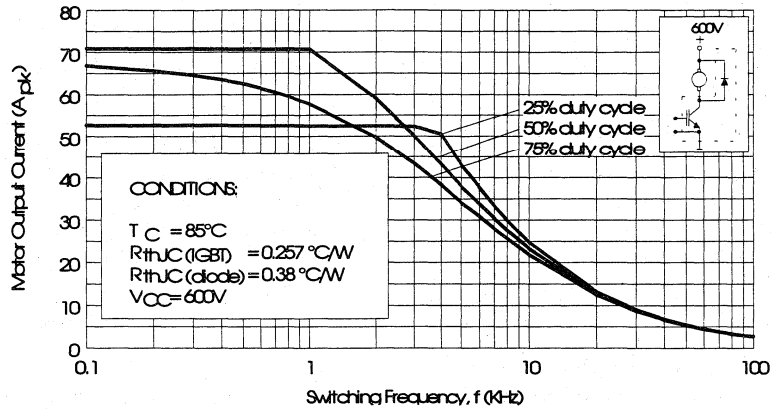


Fig. 13 - RMS Output Current vs. Frequency

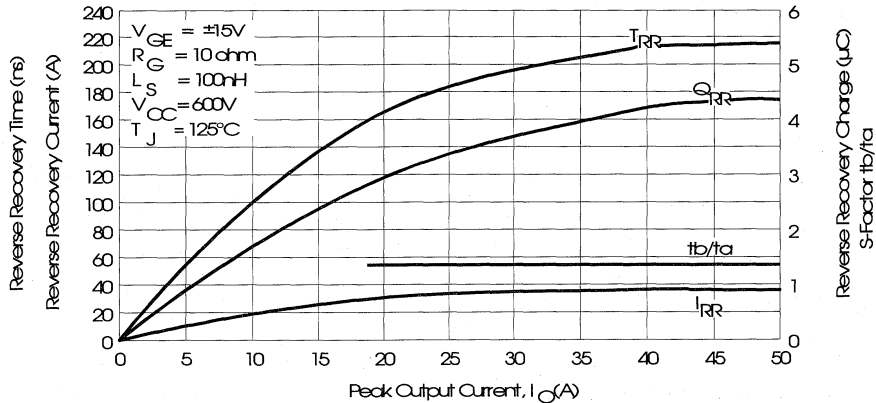


Fig. 14 - Typical Diode Recovery Characteristics as Function of Output Current I_o

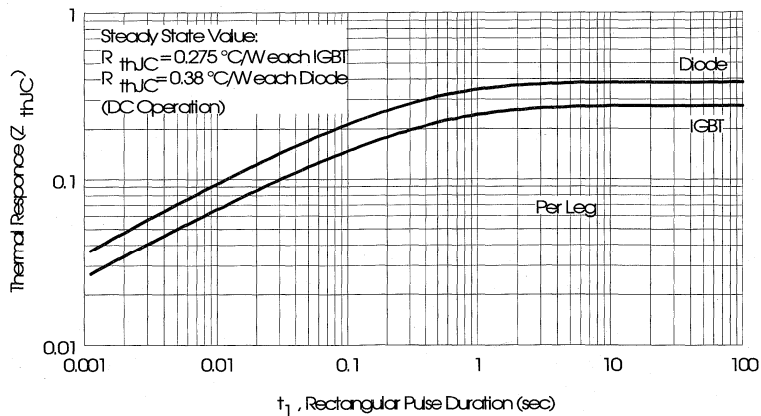


Fig. 15 - Maximum Effective Transient Thermal Impedance, Junction-to-Case

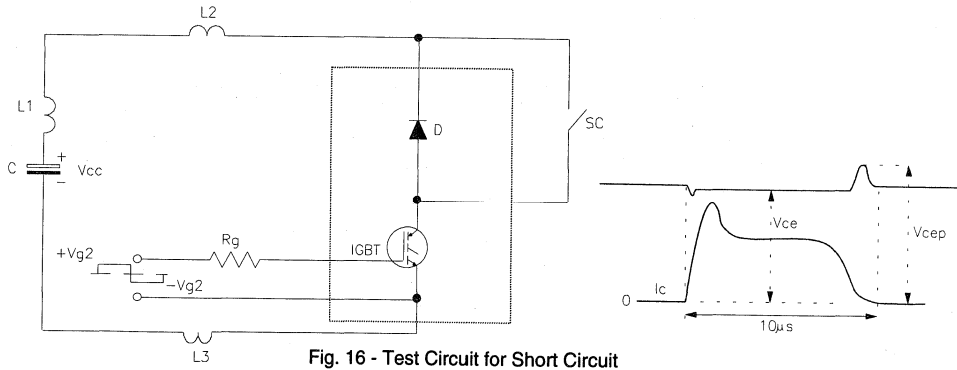


Fig. 16 - Test Circuit for Short Circuit

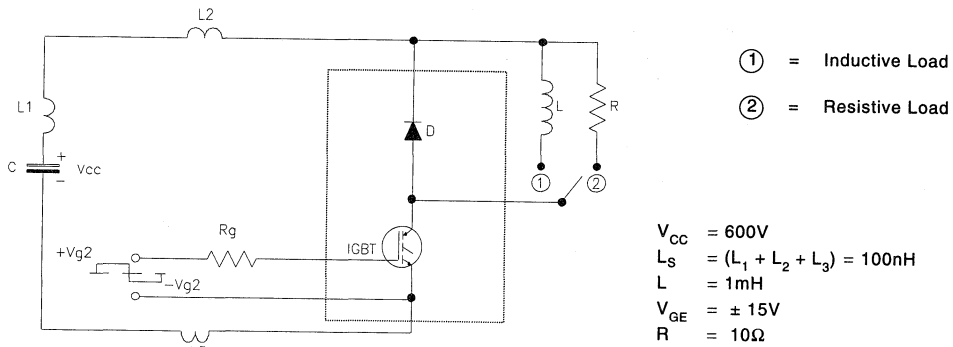


Fig. 17 - Test Circuit for Measurement of I_{LM} , E_{ON} , E_{OFF} , Q_{RR}

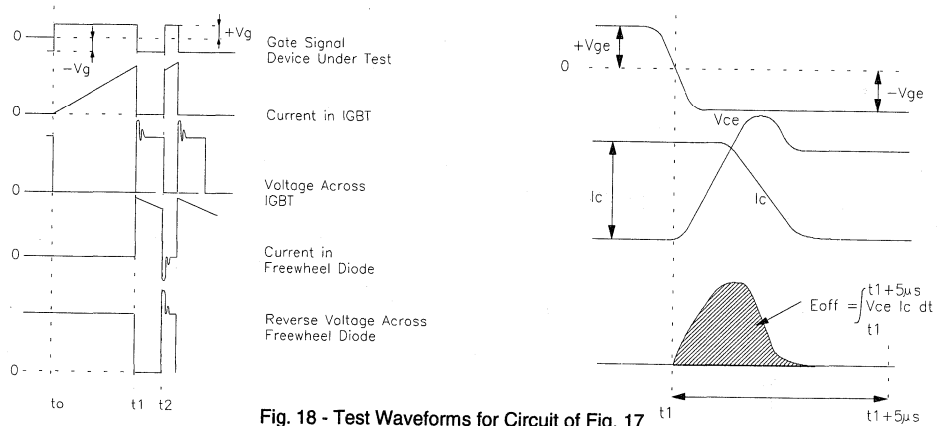


Fig. 18 - Test Waveforms for Circuit of Fig. 17

Refer to Section D for the following:

Appendix I: Section D - page D-11

Fig. 19 - Test Waveforms for Circuit of Fig. 17,

Defining E_{ON} , E_{REC} , Q_{RR}

Fig. 20 - Waveforms for Switching Time

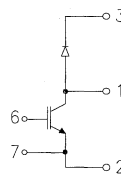
IRGKIN075M12

"CHOPPER LOW SIDE SWITCH" IGBT INT-A-PAK

Low conduction loss IGBT

- Rugged Design
- Simple gate-drive
- Switching-Loss Rating includes all "tail" losses
- Short circuit rated

Low Side Switch



$$V_{CE} = 1200V$$

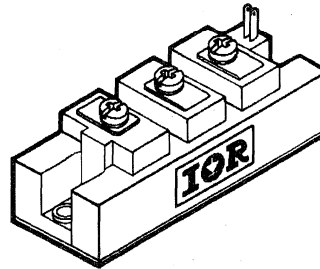
$$I_C = 75A$$

$$V_{CE(ON)} < 2.7V$$

$$t_{sc} > 10\mu s$$

Description

IR's advanced IGBT technology is the key to this line of INT-A-PAK Power Modules. The efficient geometry and unique processing of the IGBT allow higher current densities than comparable bipolar power module transistors, while at the same time requiring the simpler gate-drive of the familiar power MOSFET. These modules are short circuit rated for applications such as motor control requiring this important feature.



INT-A-PAK case

 Motor
Control
Fast
Modules

Absolute Maximum Ratings

Parameter	Description	Value	Units
V_{CES}	Continuous collector to emitter voltage	1200	V
$I_C @ T_C = 25^\circ C$	Maximum Continuous collector current	150	A
$I_C @ T_C = 85^\circ C$	Maximum Continuous collector current	85	
$I_C @ T_C = 100^\circ C$	Maximum Continuous collector current	65	
I_{LM}	Peak IGBT switching current	150	
I_{FM}	Peak diode forward switching current (1)	150	V
V_{GE}	Gate to emitter voltage	± 20	
V_{ISOL}	RMS isolation voltage, any terminal to case, $t = 1$ min	2500	W
$P_D @ T_C = 25^\circ C$	Power dissipation	600	
T_J	Operating junction temperature range	-40 to 150	$^\circ C$
T_{STG}	Storage temperature range	-40 to 125	

(1) Duration limited by max junction temperature.

Electrical Characteristics - $T_J = 25^\circ\text{C}$, unless otherwise stated

Parameter	Description	Min	Typ	Max	Units	Test Conditions
BV_{CES}	Collector-to-emitter breakdown voltage	1200	—	—	V	$V_{GE} = 0V, I_C = 2mA$
$V_{CE(ON)}$	Collector-to-emitter voltage	—	2.2	2.7		$V_{GE} = 15V, I_C = 75A$
		—	1.8	—		$V_{GE} = 15V, I_C = 40A, T_J = 150^\circ\text{C}$
V_{FM}	Diode forward voltage - maximum	—	3.2	3.4		$I_F = 75A, V_{GE} = 0V$
		—	2.6	—		$I_F = 75A, V_{GE} = 0V, T_J = 150^\circ\text{C}$
V_{GEth}	Gate threshold voltage	3.0	—	5.5	$I_C = 1mA$	
ΔV_{GEth}	Threshold voltage temp. coefficient	—	-11	—	$mV/^\circ\text{C}$	$V_{CE} = V_{GE}, I_C = 1mA$
g_{fe}	Forward transconductance	35	—	70	S(τ)	$V_{CE} = 25V, I_C = 75A$
I_{CES}	Collector-to-emitter leakage current	—	—	2	mA	$V_{GE} = 0V, V_{CE} = 1200V$
		—	—	20		$V_{GE} = 0V, V_{CE} = 1200V, T_J = 150^\circ\text{C}$
I_{GES}	Gate-to-emitter leakage current	—	—	± 2	μA	$V_{GE} = \pm 20V$

Dynamic Characteristics - $T_J = 125^\circ\text{C}$, unless otherwise stated

Parameter	Description	Min	Typ	Max	Units	Test Conditions
E_{on}	Turn-on switching energy	—	0.19	—	mJ/A	$R_G = 6.8\Omega, V_{CC} = 600V$
E_{off} (1)	Turn-off switching energy	—	0.36	—		$I_C = 75A, L_S = 100nH$
E_{ts} (1)	Total switching energy	—	—	0.60		$V_{GE} = \pm 15V$
$t_{d(on)}$	Turn-on delay time	—	200	250	ns	$R_G = 6.8\Omega, V_{CC} = 600V$
t_r	Rise time	—	200	250		$I_C = 75A$
$t_{d(off)}$	Turn-off delay time	—	125	200		$V_{GE} = \pm 15V$
t_f	Fall time	—	650	—		Resistive load, $T_J = 25^\circ\text{C}$
I_{rr}	Diode peak recovery current	—	45	—		$R_G = 6.8\Omega, V_{CC} = 600V$
t_{rr}	Diode recovery time	—	215	—	$I_C = 75A$	
Q_{rr}	Diode recovery charge	—	6	—	μC	$V_{GE} = \pm 15V$
Q_{ge}	Gate-to-emitter charge (turn-on)	45	—	175	nC	$V_{CC} = 600V$
Q_{gc}	Gate-to-collector charge (turn-on)	160	—	330		$I_C = 75A$
Q_g	Total gate charge (turn-on)	500	—	900		$V_{GE} = 15V$
C_{ies}	Input capacitance	10500	—	11000	pF	$V_{GE} = 0V$
C_{oes}	Output capacitance	650	—	1100		$V_{CC} = 30V$
C_{res}	Reverse transfer capacitance	650	—	1000		$f = 1MHz$
t_{sc}	Short circuit withstand time	10	—	—	μs	$V_{CC} = 720V, V_{GE} = \pm 15V$ Min. $R_G = 6.8\Omega, V_{CEP} = 1000V$

(1) Includes tail losses

Thermal and Mechanical Characteristics

Parameter	Description	Typ	Max	Units
R_{thJC} (IGBT)	Thermal resistance, junction to case, each IGBT	—	0.209	$^\circ\text{C/W}$
R_{thJC} (Diode)	Thermal resistance, junction to case, each diode	—	0.280	
R_{thCS} (Module)	Thermal resistance, case to sink	0.041	0.100	
Wt	Weight of module	150	—	g

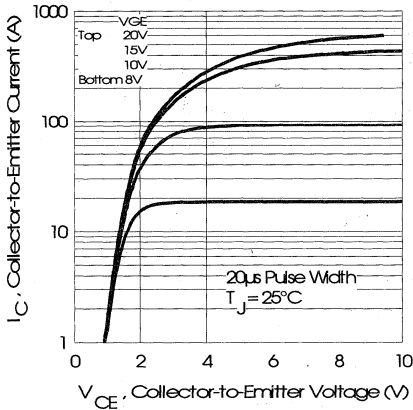


Fig. 1 - Typical Output Characteristics, $T_J = 25^\circ\text{C}$

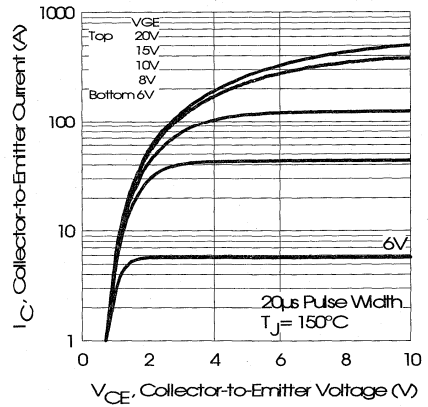


Fig. 2 - Typical Output Characteristics, $T_J = 150^\circ\text{C}$

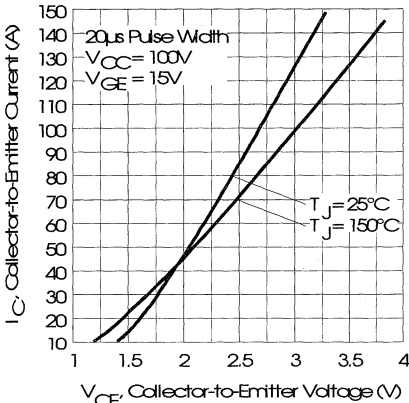


Fig. 3 - Typical Output Characteristics

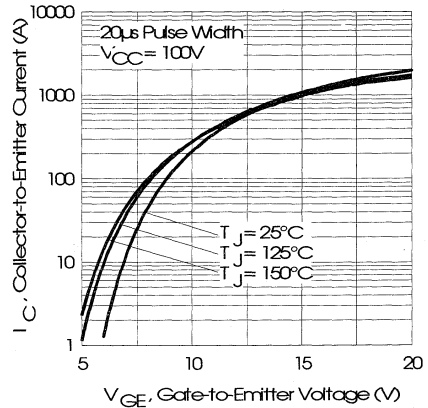


Fig. 4 - Typical Transfer Characteristics

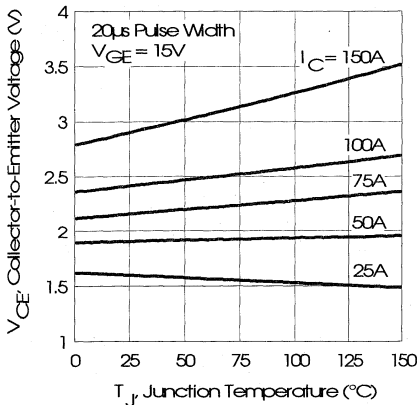


Fig. 5 - Collector-to-Emitter Saturation Typical Voltage vs. Junction Temperature

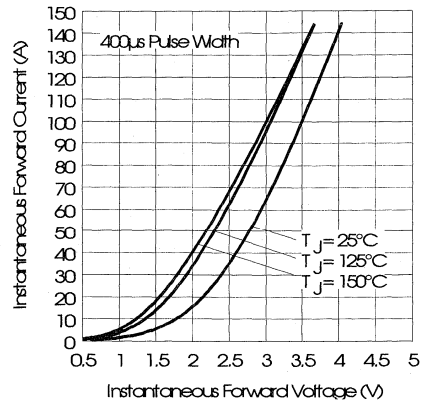


Fig. 6 - Forward Voltage Drop Characteristics

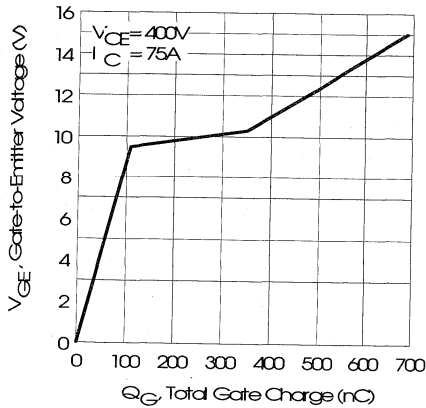


Fig. 7 - Typical Gate Charge vs. Gate-to-Emitter Voltage

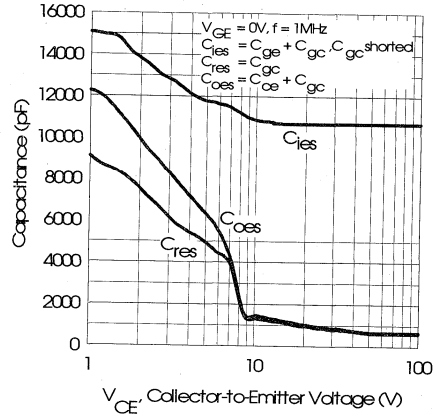


Fig. 8 - Typical Capacitance vs. Collector-to-Emitter Voltage

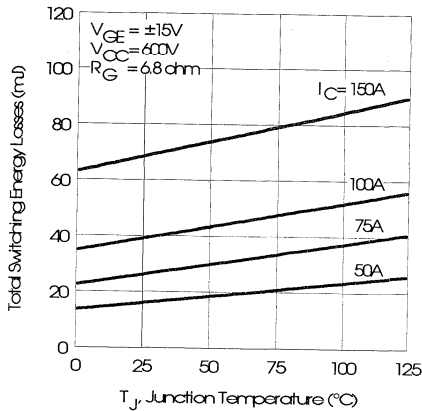


Fig. 9 - Typical Switching Losses vs. Junction Temperature

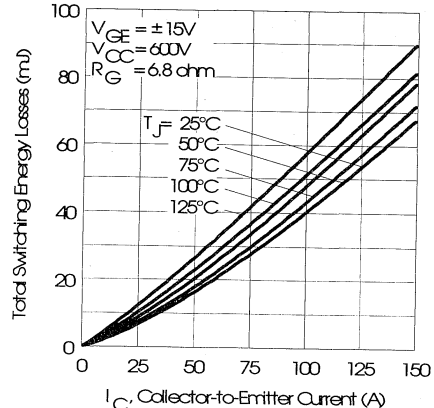


Fig. 10 - Typical Switching Losses vs. Collector-to-Emitter Current

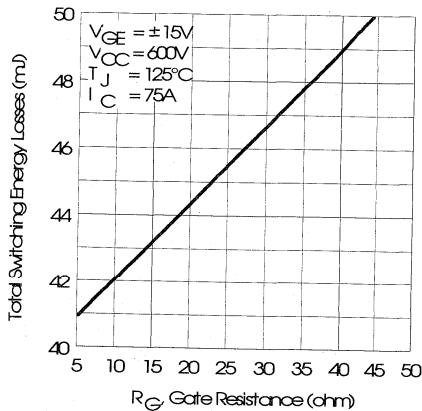


Fig. 11 - Typical Switching Losses vs. Gate Resistance

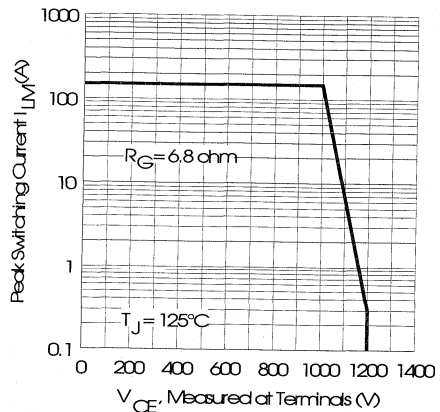


Fig. 12 - Reverse Bias Safe Operating Area

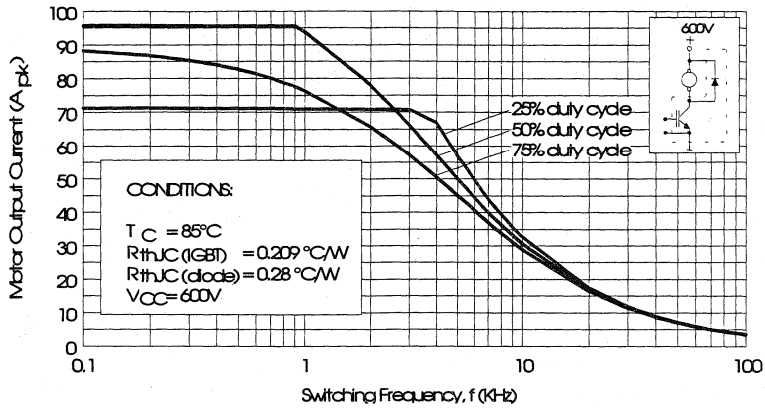


Fig. 13 - RMS Output Current vs. Frequency

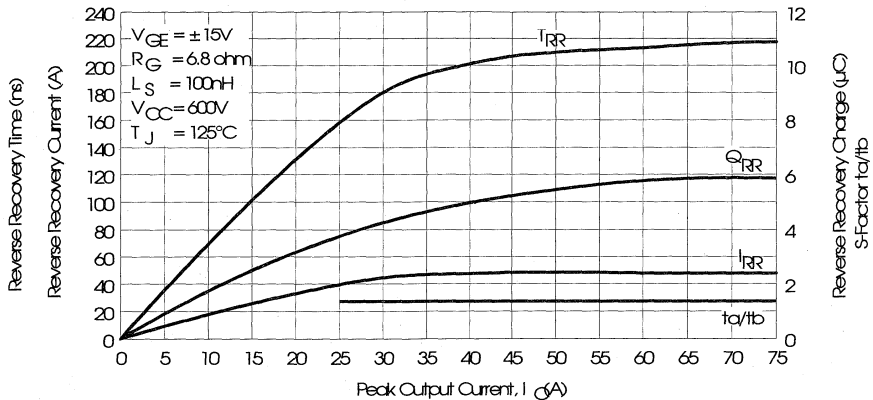


Fig. 14 - Typical Diode Recovery Characteristics as Function of Output Current I_o

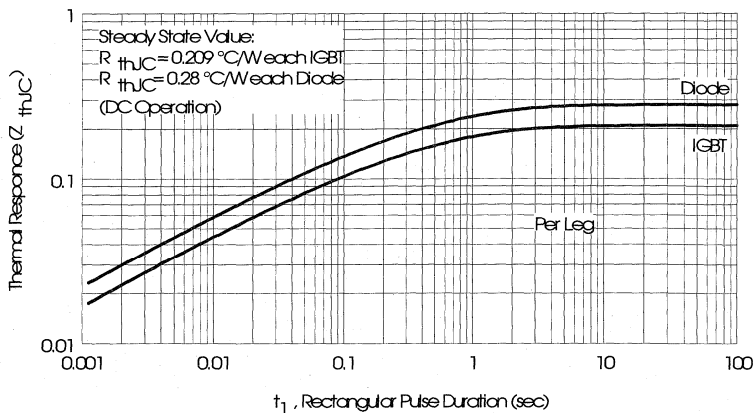


Fig. 15 - Maximum Effective Transient Thermal Impedance, Junction-to-Case

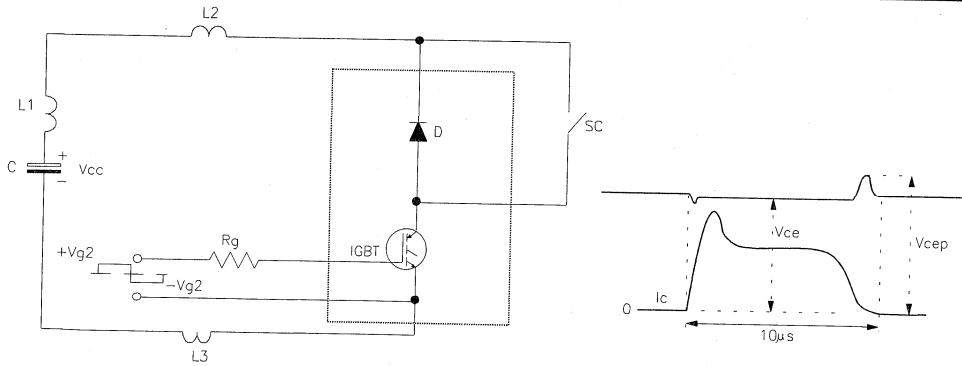


Fig. 16 - Test Circuit for Short Circuit

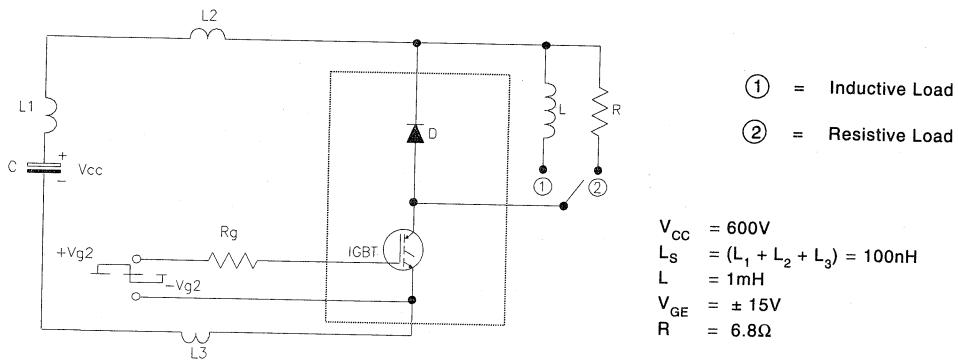


Fig. 17 - Test Circuit for Measurement of I_{LM} , E_{ON} , E_{OFF} , Q_{RR}

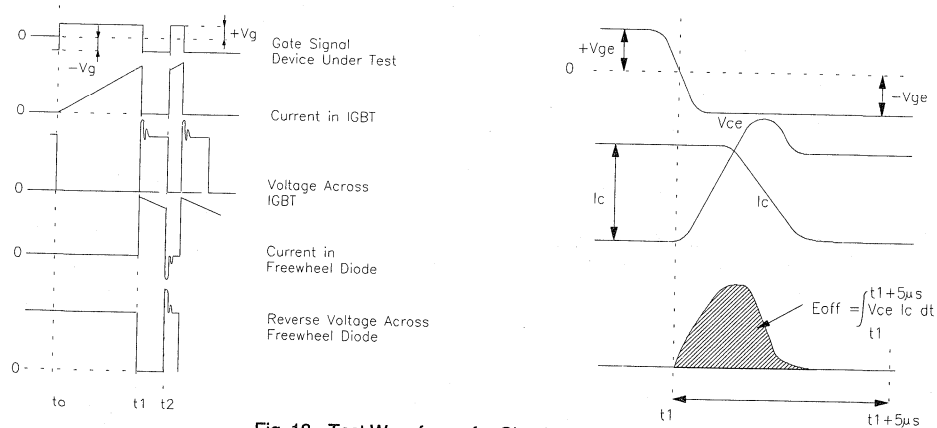


Fig. 18 - Test Waveforms for Circuit of Fig. 17

Refer to Section D for the following:

Appendix I: Section D - page D-11

Fig. 19 - Test Waveforms for Circuit of Fig. 17,

Defining E_{ON} , E_{REC} , Q_{RR}

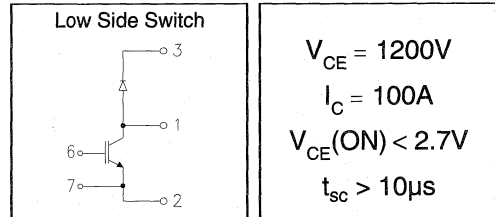
Fig. 20 - Waveforms for Switching Time

IRGKIN100M12

"CHOPPER LOW SIDE SWITCH" IGBT INT-A-PAK

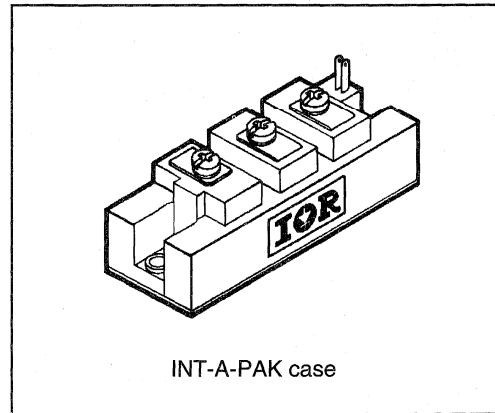
Low conduction loss IGBT

- Rugged Design
- Simple gate-drive
- Switching-Loss Rating includes all "tail" losses
- Short circuit rated



Description

IR's advanced IGBT technology is the key to this line of INT-A-PAK Power Modules. The efficient geometry and unique processing of the IGBT allow higher current densities than comparable bipolar power module transistors, while at the same time requiring the simpler gate-drive of the familiar power MOSFET. These modules are short circuit rated for applications such as motor control requiring this important feature.



Micro
Control
Fast
Modules

Absolute Maximum Ratings

Parameter	Description	Value	Units
V_{CES}	Continuous collector to emitter voltage	1200	V
$I_C @ T_C = 25^\circ C$	Maximum Continuous collector current	175	A
$I_C @ T_C = 85^\circ C$	Maximum Continuous collector current	100	
$I_C @ T_C = 100^\circ C$	Maximum Continuous collector current	75	
I_{LM}	Peak IGBT switching current	200	
I_{FM}	Peak diode forward switching current (1)	200	V
V_{GE}	Gate to emitter voltage	± 20	
V_{ISOL}	RMS isolation voltage, any terminal to case, $t = 1$ min	2500	
$P_D @ T_C = 25^\circ C$	Power dissipation	665	W
T_J	Operating junction temperature range	-40 to 150	$^\circ C$
T_{STG}	Storage temperature range	-40 to 125	

(1) Duration limited by max junction temperature.

IRGKIN100M12



Electrical Characteristics - $T_J = 25^\circ\text{C}$, unless otherwise stated

Parameter	Description	Min	Typ	Max	Units	Test Conditions
BV_{CES}	Collector-to-emitter breakdown voltage	1200	—	—	V	$V_{GE} = 0V, I_C = 3mA$
$V_{CE(ON)}$	Collector-to-emitter voltage	—	2.2	2.7		$V_{GE} = 15V, I_C = 100A$
		—	1.8	—		$V_{GE} = 15V, I_C = 80A, T_J = 150^\circ\text{C}$
V_{FM}	Diode forward voltage - maximum	—	3.2	3.4		$I_F = 100A, V_{GE} = 0V$
		—	2.6	—		$I_F = 100A, V_{GE} = 0V, T_J = 150^\circ\text{C}$
V_{GEth}	Gate threshold voltage	3.0	—	5.5	$I_C = 1mA$	
ΔV_{GEth}	Threshold voltage temp. coefficient	—	-11	—	mV/ $^\circ\text{C}$	$V_{CE} = V_{GE}, I_C = 1mA$
g_{fe}	Forward transconductance	35	—	70	S(τ)	$V_{CE} = 25V, I_C = 100A$
I_{CES}	Collector-to-emitter leakage current	—	—	3	mA	$V_{GE} = 0V, V_{CE} = 1200V$
		—	—	30		$V_{GE} = 0V, V_{CE} = 1200V, T_J = 150^\circ\text{C}$
I_{GES}	Gate-to-emitter leakage current	—	—	± 3	μA	$V_{GE} = \pm 20V$

Dynamic Characteristics - $T_J = 125^\circ\text{C}$, unless otherwise stated

Parameter	Description	Min	Typ	Max	Units	Test Conditions
E_{on}	Turn-on switching energy	—	0.19	—	mJ/A	$R_G = 6.8\Omega, V_{CC} = 600V$
E_{off} (1)	Turn-off switching energy	—	0.36	—		$I_C = 100A, L_S = 100nH$
E_{ts} (1)	Total switching energy	—	—	0.60		$V_{GE} = \pm 15V$
$t_{d(on)}$	Turn-on delay time	—	200	250	ns	$R_G = 6.8\Omega, V_{CC} = 600V$
t_r	Rise time	—	200	250		$I_C = 100A$
$t_{d(off)}$	Turn-off delay time	—	125	200		$V_{GE} = \pm 15V$
t_f	Fall time	—	650	—		Resistive load, $T_J = 25^\circ\text{C}$
I_{rr}	Diode peak recovery current	—	50	—	A	$R_G = 6.8\Omega, V_{CC} = 600V$
t_{rr}	Diode recovery time	—	215	—	ns	$I_C = 100A$
Q_{rr}	Diode recovery charge	—	8	—	μC	$V_{GE} = \pm 15V$
Q_{ge}	Gate-to-emitter charge (turn-on)	65	—	260	nC	$V_{CC} = 600V$
Q_{gc}	Gate-to-collector charge (turn-on)	240	—	500		$I_C = 100A$
Q_g	Total gate charge (turn-on)	750	—	1350		$V_{GE} = 15V$
C_{ies}	Input capacitance	15500	—	16500	pF	$V_{GE} = 0V$
C_{oes}	Output capacitance	950	—	1650		$V_{CC} = 30V$
C_{res}	Reverse transfer capacitance	950	—	1650		$f = 1MHz$
t_{sc}	Short circuit withstand time	10	—	—	μs	$V_{CC} = 720V, V_{GE} = \pm 15V$ Min. $R_G = 6.8\Omega, V_{CEP} = 1000V$

(1) Includes tail losses

Thermal and Mechanical Characteristics

Parameter	Description	Typ	Max	Units
R_{thJC} (IGBT)	Thermal resistance, junction to case, each IGBT	—	0.188	$^\circ\text{C/W}$
R_{thJC} (Diode)	Thermal resistance, junction to case, each diode	—	0.209	
R_{thCS} (Module)	Thermal resistance, case to sink	0.041	0.100	
Wt	Weight of module	150	—	g

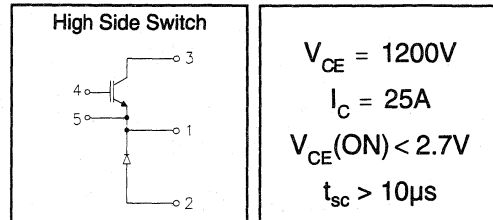
Refer to Section D - page D-15 for Package Outline 7 -INT-A-PAK, New - Low Side Switch

IRGNIN025M12

"CHOPPER HIGH SIDE SWITCH" IGBT INT-A-PAK

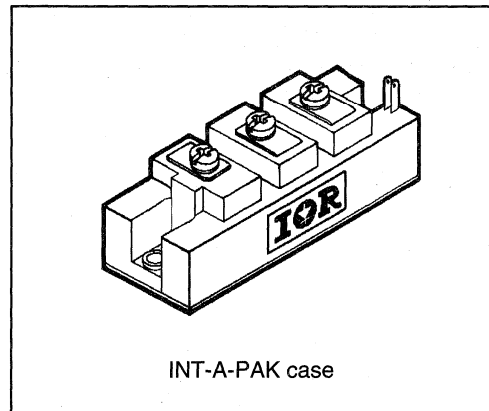
Low conduction loss IGBT

- Rugged Design
- Simple gate-drive
- Switching-Loss Rating includes all "tail" losses
- Short circuit rated



Description

IR's advanced IGBT technology is the key to this line of INT-A-PAK Power Modules. The efficient geometry and unique processing of the IGBT allow higher current densities than comparable bipolar power module transistors, while at the same time requiring the simpler gate-drive of the familiar power MOSFET. These modules are short circuit rated for applications such as motor control requiring this important feature.



Absolute Maximum Ratings

Parameter	Description	Value	Units
V_{CES}	Continuous collector to emitter voltage	1200	V
$I_C @ T_C = 25^\circ C$	Maximum Continuous collector current	50	A
$I_C @ T_C = 85^\circ C$	Maximum Continuous collector current	45	
$I_C @ T_C = 100^\circ C$	Maximum Continuous collector current	35	
I_{LM}	Peak switching current	50	
I_{FM}	Peak diode forward current (1)	50	
V_{GE}	Gate to emitter voltage	± 20	V
V_{ISOL}	RMS isolation voltage, any terminal to case, $t = 1$ min	2500	
$P_D @ T_C = 25^\circ C$	Power dissipation	385	W
T_J	Operating junction temperature range	-40 to 150	$^\circ C$
T_{STG}	Storage temperature range	-40 to 125	

(1) Duration limited by max junction temperature.

Electrical Characteristics - $T_J = 25^\circ\text{C}$, unless otherwise stated

Parameter	Description	Min	Typ	Max	Units	Test Conditions
BV_{CES}	Collector-to-emitter breakdown voltage	1200	—	—	V	$V_{GE} = 0V, I_C = 1mA$
$V_{CE(ON)}$	Collector-to-emitter voltage	—	2.2	2.7		$V_{GE} = 15V, I_C = 25A$
		—	1.85	—		$V_{GE} = 15V, I_C = 15A, T_J = 150^\circ\text{C}$
V_{FM}	Diode forward voltage - maximum	—	3.2	3.4		$I_F = 25A, V_{GE} = 0V$
		—	2.6	—		$I_F = 25A, V_{GE} = 0V, T_J = 150^\circ\text{C}$
V_{GEth}	Gate threshold voltage	3.0	—	5.5	$I_C = 500\mu A$	
ΔV_{GEth}	Threshold voltage temp. coefficient	—	-11	—	mV/ $^\circ\text{C}$	$V_{CE} = V_{GE}, I_C = 500\mu A$
g_{fe}	Forward transconductance	18	—	35	S(τ)	$V_{CE} = 25V, I_C = 25A$
I_{CES}	Collector-to-emitter leakage current	—	—	1	mA	$V_{GE} = 0V, V_{CE} = 1200V$
		—	—	10		$V_{GE} = 0V, V_{CE} = 1200V, T_J = 150^\circ\text{C}$
I_{GES}	Gate-to-emitter leakage current	—	—	± 1	μA	$V_{GE} = \pm 20V$

Dynamic Characteristics - $T_J = 125^\circ\text{C}$, unless otherwise stated

Parameter	Description	Min	Typ	Max	Units	Test Conditions
E_{on}	Turn-on switching energy	—	0.19	—	mJ/A	$R_G = 15\Omega, V_{CC} = 600V$
E_{off} (1)	Turn-off switching energy	—	0.36	—		$I_C = 25A, L_S = 100nH$
E_{ts} (1)	Total switching energy	—	—	0.60		$V_{GE} = \pm 15V$
$t_{d(on)}$	Turn-on delay time	—	200	250	ns	$R_G = 15\Omega, V_{CC} = 600V$
t_r	Rise time	—	200	250		$I_C = 25A$
$t_{d(off)}$	Turn-off delay time	—	125	200		$V_{GE} = \pm 15V$
t_f	Fall time	—	650	—		Resistive load, $T_J = 25^\circ\text{C}$
I_{rr}	Diode peak recovery current	—	25	—	A	$R_G = 15\Omega, V_{CC} = 600V$
t_{rr}	Diode recovery time	—	215	—	ns	$I_C = 25A$
Q_{rr}	Diode recovery charge	—	3	—	μC	$V_{GE} = \pm 15V$
Q_{ge}	Gate-to-emitter charge (turn-on)	23	—	88	nC	$V_{CC} = 600V$
Q_{gc}	Gate-to-collector charge (turn-on)	80	—	170		$I_C = 25A$
Q_g	Total gate charge (turn-on)	250	—	450		$V_{GE} = 15V$
C_{ies}	Input capacitance	5250	—	5500	pF	$V_{GE} = 0V$
C_{oes}	Output capacitance	330	—	550		$V_{CC} = 30V$
C_{res}	Reverse transfer capacitance	330	—	500		$f = 1MHz$
t_{sc}	Short circuit withstand time	10	—	—	μs	$V_{CC} = 720V, V_{GE} = \pm 15V$ Min. $R_G = 15\Omega, V_{CEP} = 1000V$

(1) Includes tail losses

Thermal and Mechanical Characteristics

Parameter	Description	Typ	Max	Units
R_{thJC} (IGBT)	Thermal resistance, junction to case, each IGBT	—	0.352	$^\circ\text{C/W}$
R_{thJC} (Diode)	Thermal resistance, junction to case, each diode	—	0.480	
R_{thCS} (Module)	Thermal resistance, case to sink	0.041	0.100	
Wt	Weight of module	150	—	g

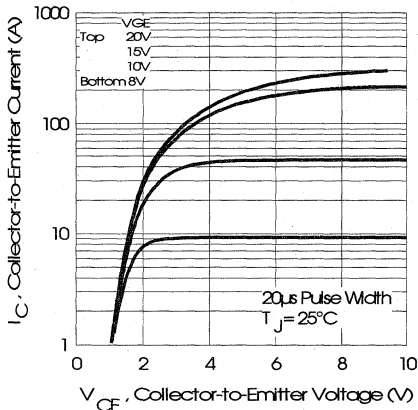


Fig. 1 - Typical Output Characteristics, $T_J = 25^\circ\text{C}$

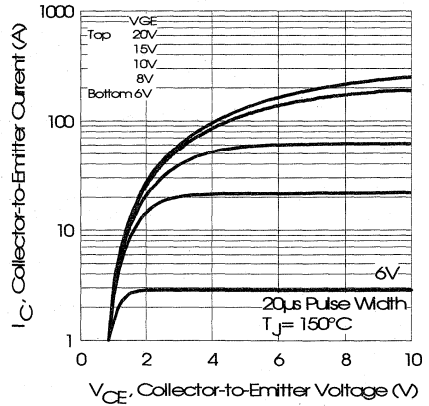


Fig. 2 - Typical Output Characteristics, $T_J = 150^\circ\text{C}$

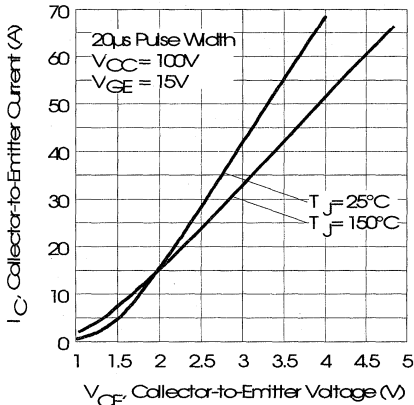


Fig. 3 - Typical Output Characteristics

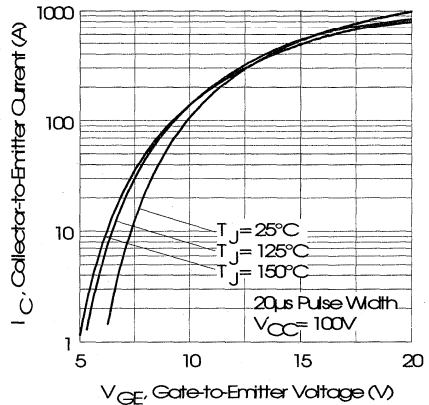


Fig. 4 - Typical Transfer Characteristics

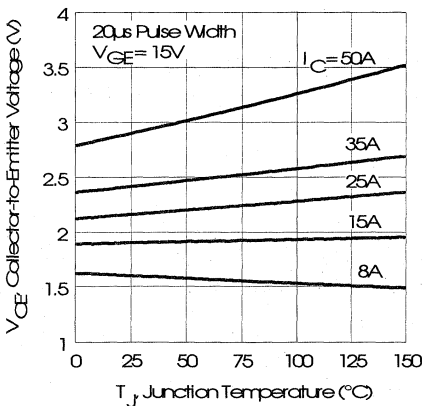


Fig. 5 - Collector-to-Emitter Saturation Typical Voltage vs. Junction Temperature

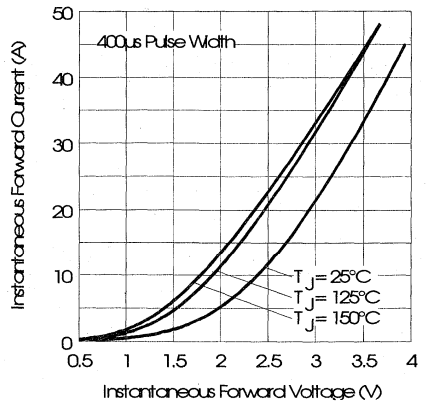


Fig. 6 - Forward Voltage Drop Characteristics



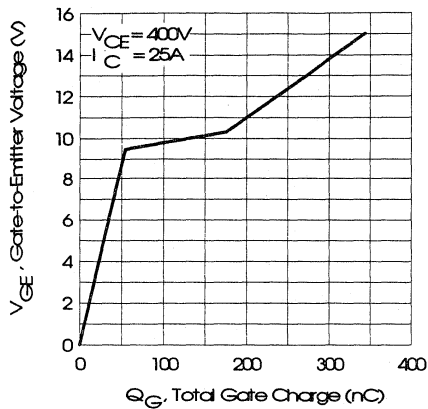


Fig. 7 - Typical Gate Charge vs. Gate-to-Emitter Voltage

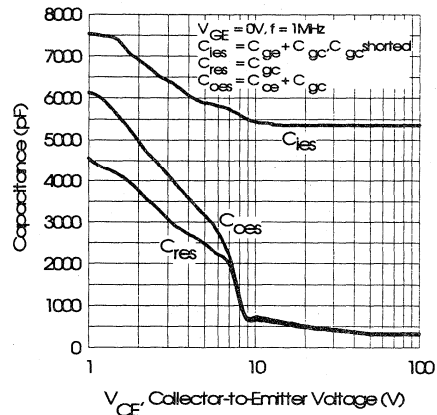


Fig. 8 - Typical Capacitance vs. Collector-to-Emitter Voltage

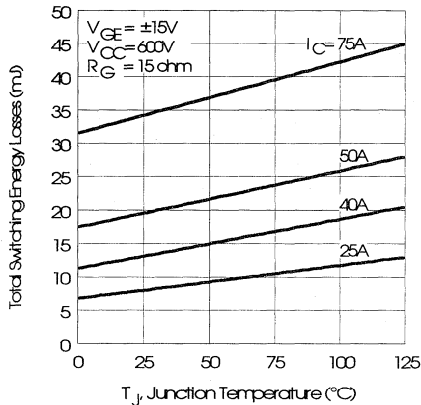


Fig. 9 - Typical Switching Losses vs. Junction Temperature

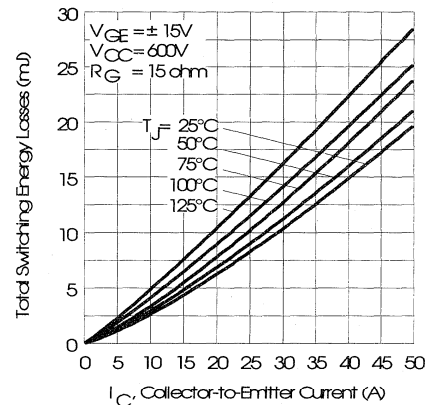


Fig. 10 - Typical Switching Losses vs. Collector-to-Emitter Current

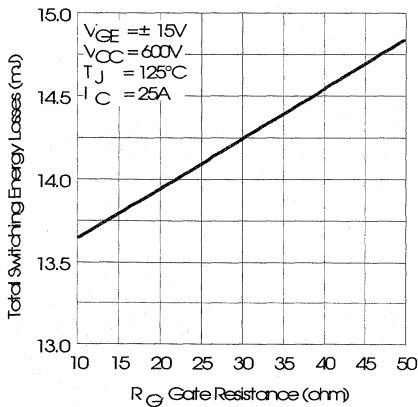


Fig. 11 - Typical Switching Losses vs. Gate Resistance

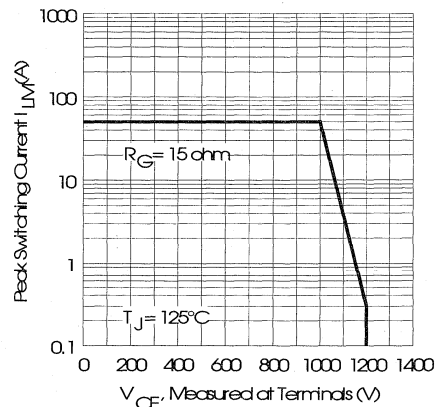


Fig. 12 - Reverse Bias Safe Operating Area

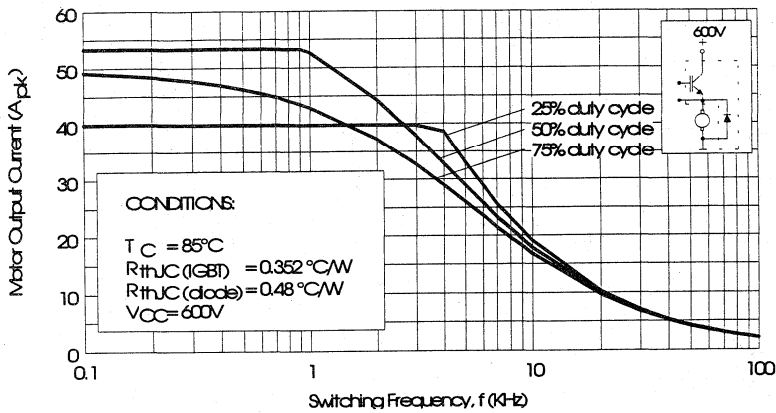


Fig. 13 - RMS Output Current vs. Frequency

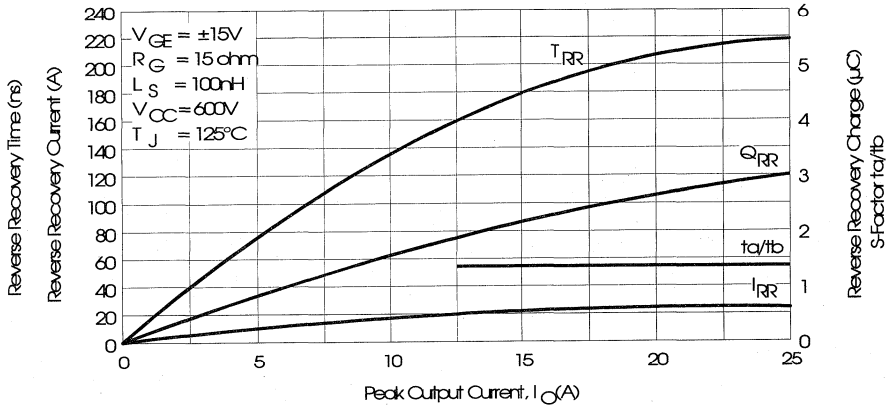


Fig. 14 - Typical Diode Recovery Characteristics as Function of Output Current I_O

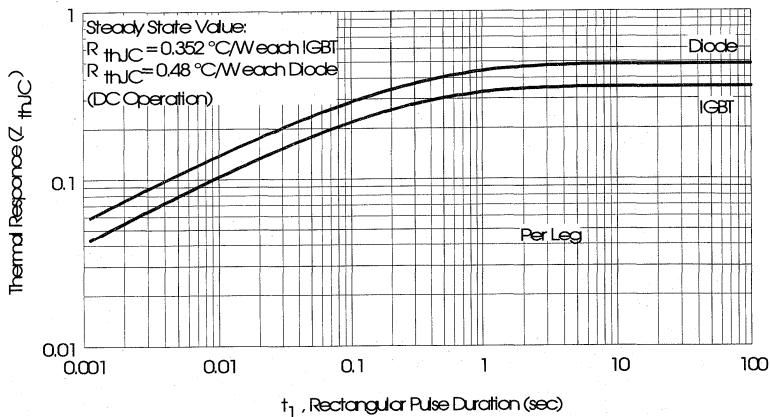


Fig. 15 - Maximum Effective Transient Thermal Impedance, Junction-to-Case

Motor
Control
Fast
Modules

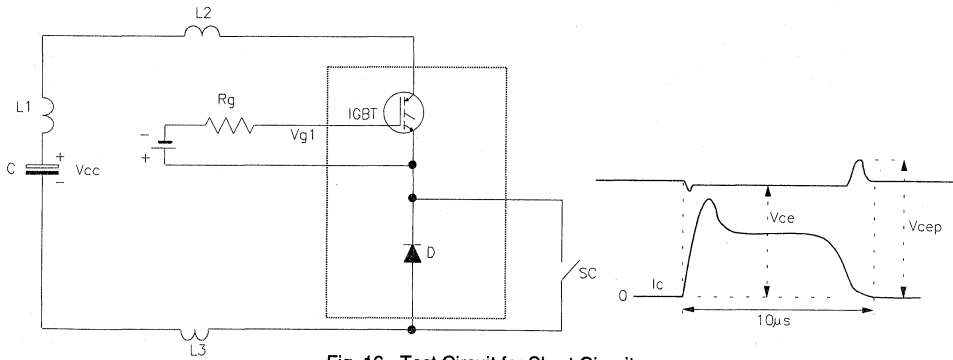


Fig. 16 - Test Circuit for Short Circuit

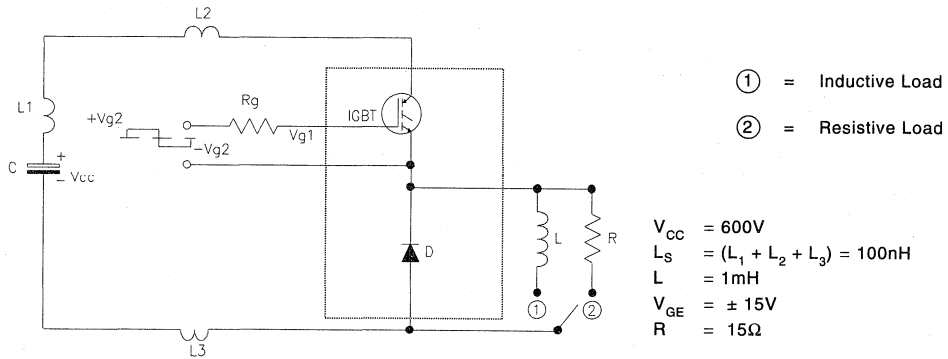


Fig. 17 - Test Circuit for Measurement of I_{LM} , E_{ON} , E_{OFF} , Q_{RR}

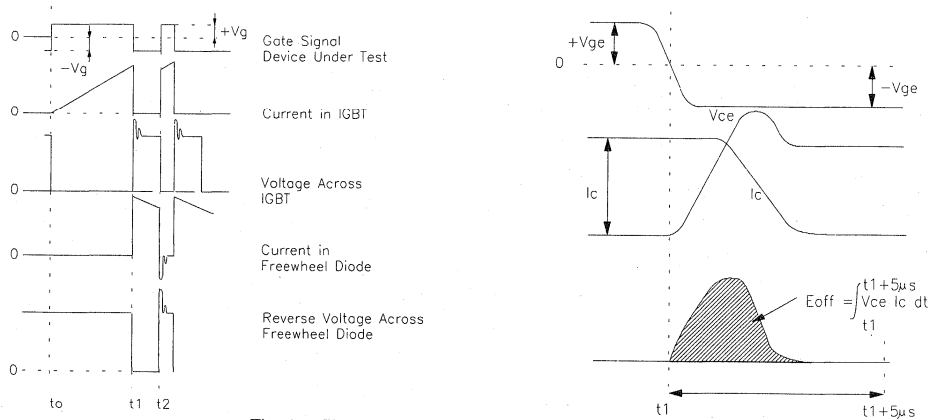


Fig. 18 - Test Waveforms for Circuit of Fig. 17

Refer to Section D for the following:
 Appendix I: Section D - page D-11

Fig. 19 - Test Waveforms for Circuit of Fig. 17,

Defining E_{ON} , E_{REC} , Q_{RR}

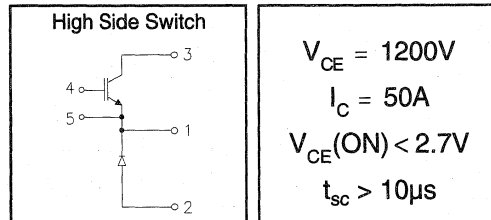
Fig. 20 - Waveforms for Switching Time

IRGNIN050M12

"CHOPPER HIGH SIDE SWITCH" IGBT INT-A-PAK

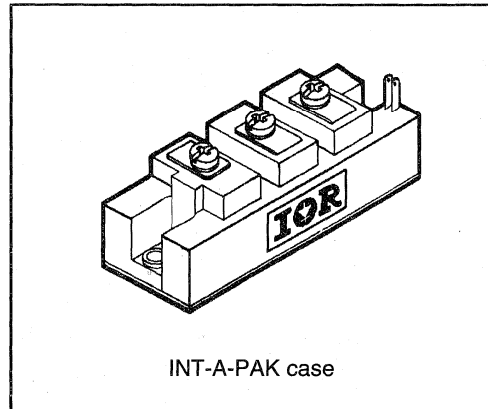
Low conduction loss IGBT

- Rugged Design
- Simple gate-drive
- Switching-Loss Rating includes all "tail" losses
- Short circuit rated



Description

IR's advanced IGBT technology is the key to this line of INT-A-PAK Power Modules. The efficient geometry and unique processing of the IGBT allow higher current densities than comparable bipolar power module transistors, while at the same time requiring the simpler gate-drive of the familiar power MOSFET. These modules are short circuit rated for applications such as motor control requiring this important feature.



Motor
Control
Fast
Modules

Absolute Maximum Ratings

Parameter	Description	Value	Units
V_{CES}	Continuous collector to emitter voltage	1200	V
$I_C @ T_C = 25^\circ C$	Maximum Continuous collector current	100	A
$I_C @ T_C = 85^\circ C$	Maximum Continuous collector current	65	
$I_C @ T_C = 100^\circ C$	Maximum Continuous collector current	45	
I_{LM}	Peak switching current	100	
I_{FM}	Peak diode forward current (1)	100	
V_{GE}	Gate to emitter voltage	± 20	V
V_{ISOL}	RMS isolation voltage, any terminal to case, $t = 1 \text{ min}$	2500	
$P_D @ T_C = 25^\circ C$	Power dissipation	455	W
T_J	Operating junction temperature range	-40 to 150	$^\circ C$
T_{STG}	Storage temperature range	-40 to 125	

(1) Duration limited by max junction temperature.

Electrical Characteristics - $T_J = 25^\circ\text{C}$, unless otherwise stated

Parameter	Description	Min	Typ	Max	Units	Test Conditions
BV_{CES}	Collector-to-emitter breakdown voltage	1200	—	—	V	$V_{GE} = 0V, I_C = 1.5mA$
$V_{CE(ON)}$	Collector-to-emitter voltage	—	2.2	2.7		$V_{GE} = 15V, I_C = 50A$
		—	1.8	—		$V_{GE} = 15V, I_C = 25A, T_J = 150^\circ\text{C}$
V_{FM}	Diode forward voltage - maximum	—	3.2	3.4		$I_F = 50A, V_{GE} = 0V$
		—	2.6	—		$I_F = 50A, V_{GE} = 0V, T_J = 150^\circ\text{C}$
V_{GEth}	Gate threshold voltage	3.0	—	5.5	$I_C = 750\mu A$	
ΔV_{GEth}	Threshold voltage temp. coefficient	—	-11	—	mV/ $^\circ\text{C}$	$V_{CE} = V_{GE}, I_C = 750\mu A$
g_{fe}	Forward transconductance	27	—	53	S(τ)	$V_{CE} = 25V, I_C = 50A$
I_{CES}	Collector-to-emitter leakage current	—	—	1.5	mA	$V_{GE} = 0V, V_{CE} = 1200V$
		—	—	15		$V_{GE} = 0V, V_{CE} = 1200V, T_J = 150^\circ\text{C}$
I_{GES}	Gate-to-emitter leakage current	—	—	± 1.5	μA	$V_{GE} = \pm 20V$

Dynamic Characteristics - $T_J = 125^\circ\text{C}$, unless otherwise stated

Parameter	Description	Min	Typ	Max	Units	Test Conditions
E_{on}	Turn-on switching energy	—	0.19	—	mJ/A	$R_G = 10\Omega, V_{CC} = 600V$
E_{off} (1)	Turn-off switching energy	—	0.36	—		$I_C = 50A, L_S = 100nH$
E_{ts} (1)	Total switching energy	—	—	0.60		$V_{GE} = \pm 15V$
$t_{d(on)}$	Turn-on delay time	—	200	250	ns	$R_G = 10\Omega, V_{CC} = 600V$
t_r	Rise time	—	200	250		$I_C = 50A$
$t_{d(off)}$	Turn-off delay time	—	125	200		$V_{GE} = \pm 15V$
t_f	Fall time	—	650	—		Resistive load, $T_J = 25^\circ\text{C}$
I_{rr}	Diode peak recovery current	—	35	—		A
t_{rr}	Diode recovery time	—	215	—	ns	$I_C = 50A$
Q_{rr}	Diode recovery charge	—	4.5	—	μC	$V_{GE} = \pm 15V$
Q_{ge}	Gate-to-emitter charge (turn-on)	35	—	130	nC	$V_{CC} = 600V$
Q_{gc}	Gate-to-collector charge (turn-on)	120	—	250		$I_C = 50A$
Q_g	Total gate charge (turn-on)	380	—	680		$V_{GE} = 15V$
C_{ies}	Input capacitance	8000	—	8300	pF	$V_{GE} = 0V$
C_{oes}	Output capacitance	490	—	820		$V_{CC} = 30V$
C_{res}	Reverse transfer capacitance	490	—	750		$f = 1MHz$
t_{sc}	Short circuit withstand time	10	—	—	μs	$V_{CC} = 720V, V_{GE} = \pm 15V$ Min. $R_G = 10\Omega, V_{CEP} = 1000V$

(1) Includes tail losses

Thermal and Mechanical Characteristics

Parameter	Description	Typ	Max	Units
R_{thJC} (IGBT)	Thermal resistance, junction to case, each IGBT	—	0.275	$^\circ\text{C/W}$
R_{thJC} (Diode)	Thermal resistance, junction to case, each diode	—	0.380	
R_{thCS} (Module)	Thermal resistance, case to sink	0.041	0.100	
Wt	Weight of module	150	—	g



IRGNIN050M12

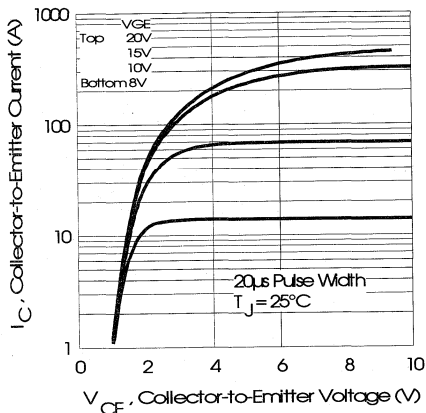


Fig. 1 - Typical Output Characteristics, $T_J = 25^\circ\text{C}$

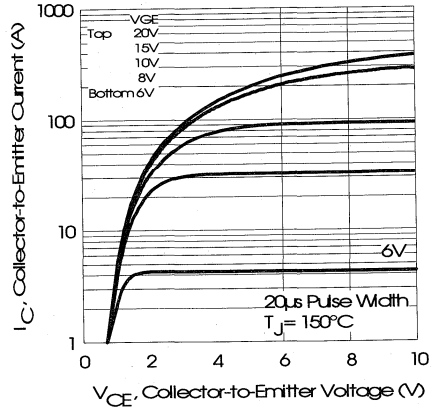


Fig. 2 - Typical Output Characteristics, $T_J = 150^\circ\text{C}$

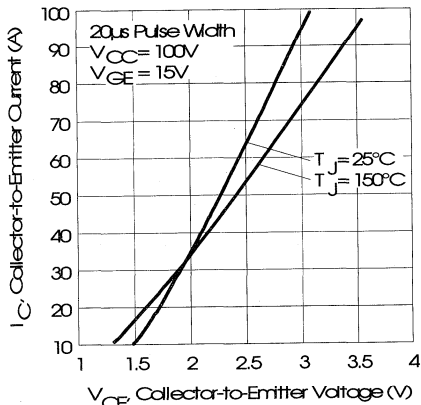


Fig. 3 - Typical Output Characteristics

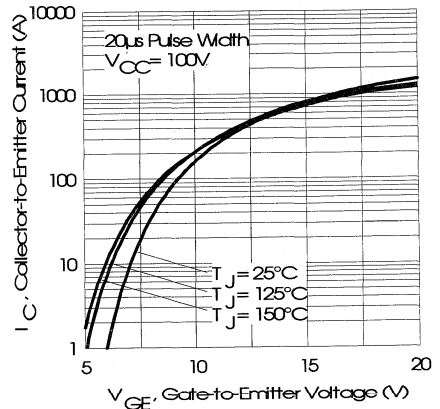


Fig. 4 - Typical Transfer Characteristics

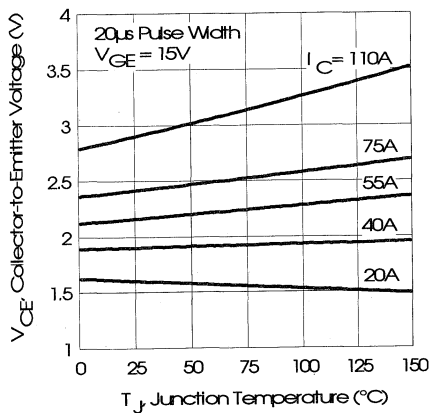


Fig. 5 - Collector-to-Emitter Saturation Typical Voltage vs. Junction Temperature

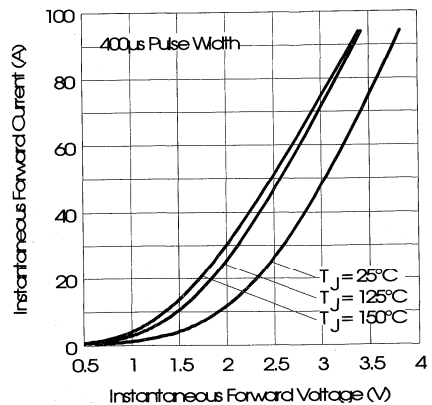


Fig. 6 - Forward Voltage Drop Characteristics

Motor
Control
Fast
Modules.

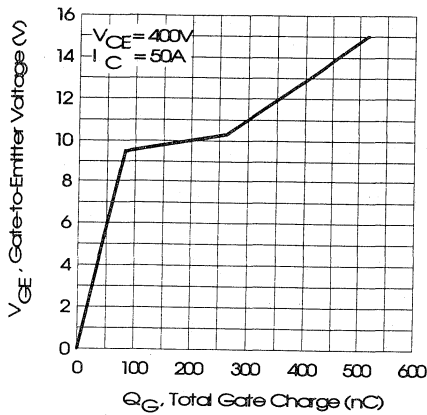


Fig. 7 - Typical Gate Charge vs. Gate-to-Emitter Voltage

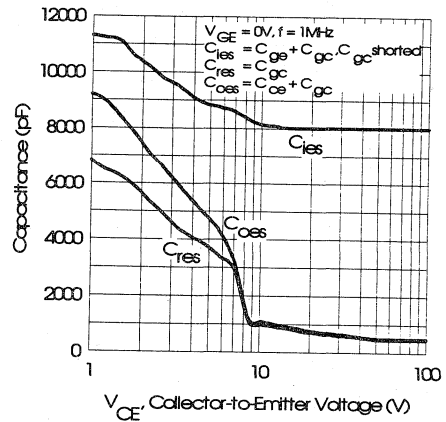


Fig. 8 - Typical Capacitance vs. Collector-to-Emitter Voltage

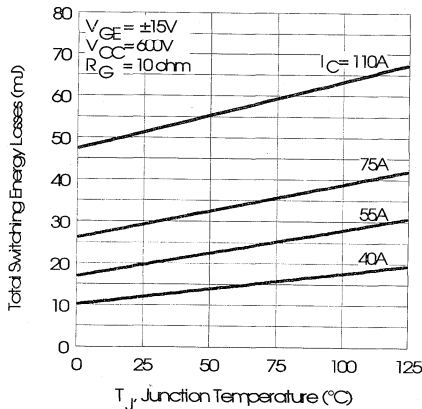


Fig. 9 - Typical Switching Losses vs. Junction Temperature

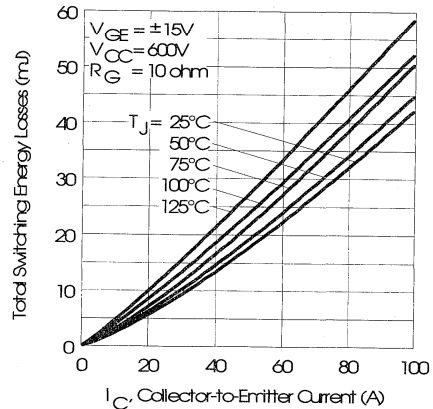


Fig. 10 - Typical Switching Losses vs. Collector-to-Emitter Current

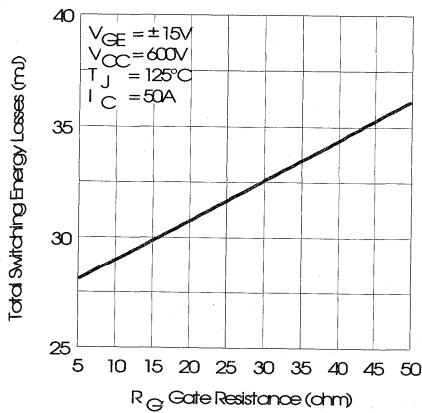


Fig. 11 - Typical Switching Losses vs. Gate Resistance

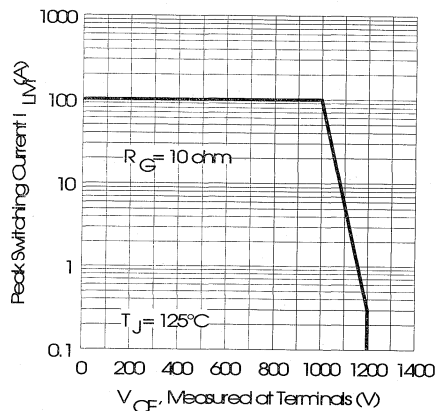


Fig. 12 - Reverse Bias Safe Operating Area

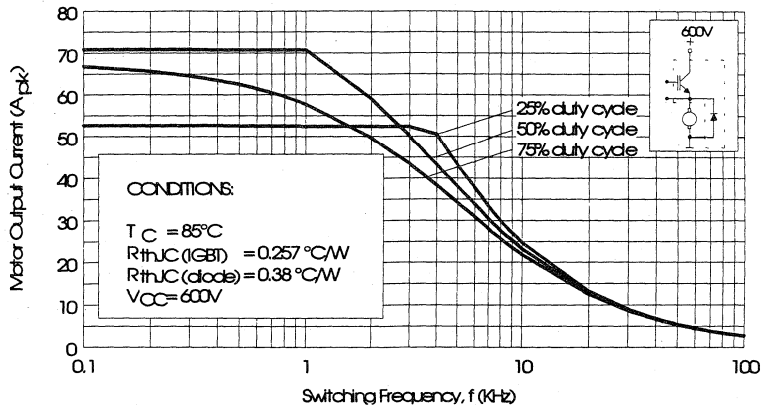


Fig. 13 - RMS Output Current vs. Frequency

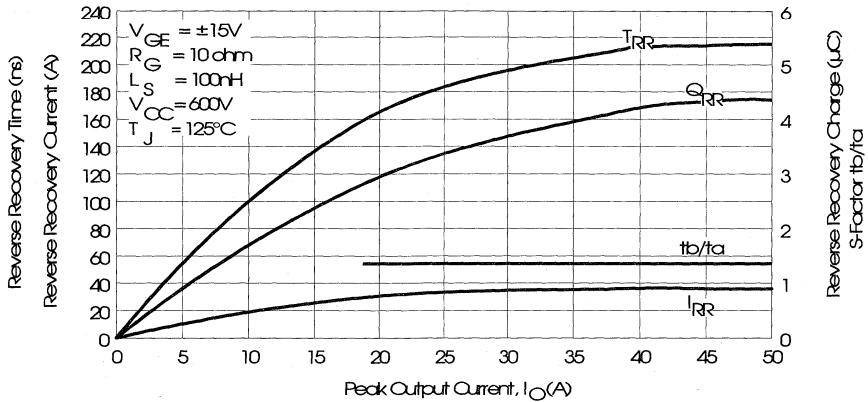


Fig. 14 - Typical Diode Recovery Characteristics as Function of Output Current I_O

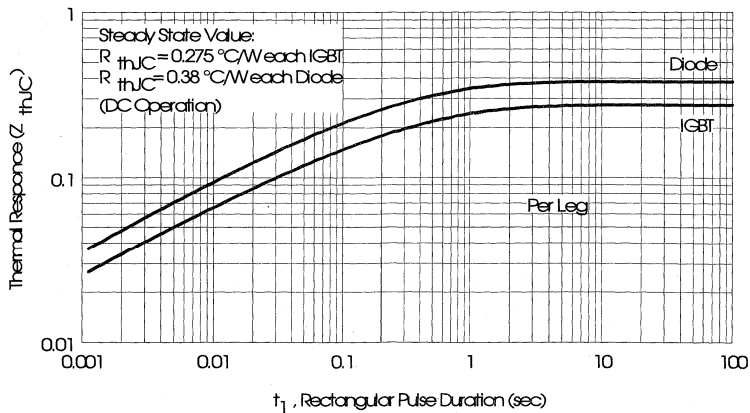


Fig. 15 - Maximum Effective Transient Thermal Impedance, Junction-to-Case

Motor Control Fast Modules

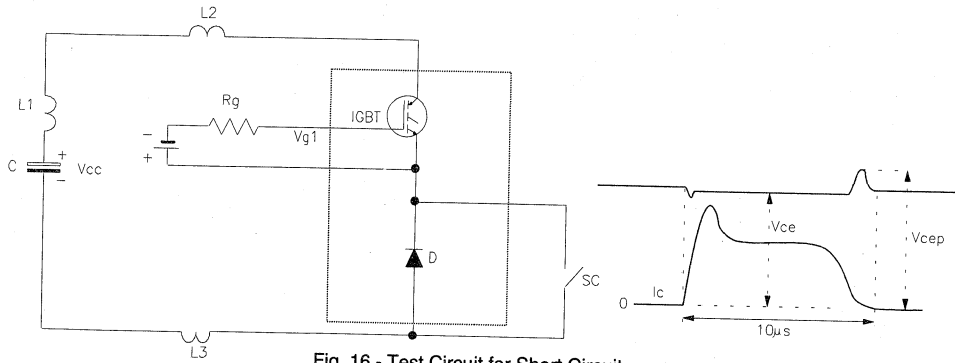


Fig. 16 - Test Circuit for Short Circuit

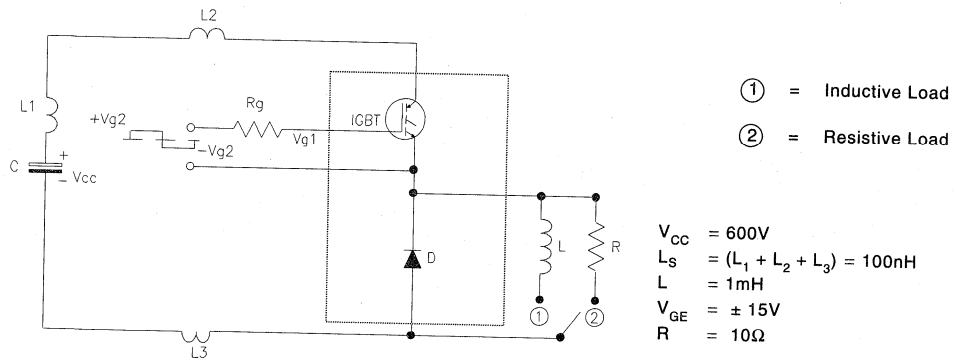


Fig. 17 - Test Circuit for Measurement of I_{LM} , E_{ON} , E_{OFF} , Q_{RR}

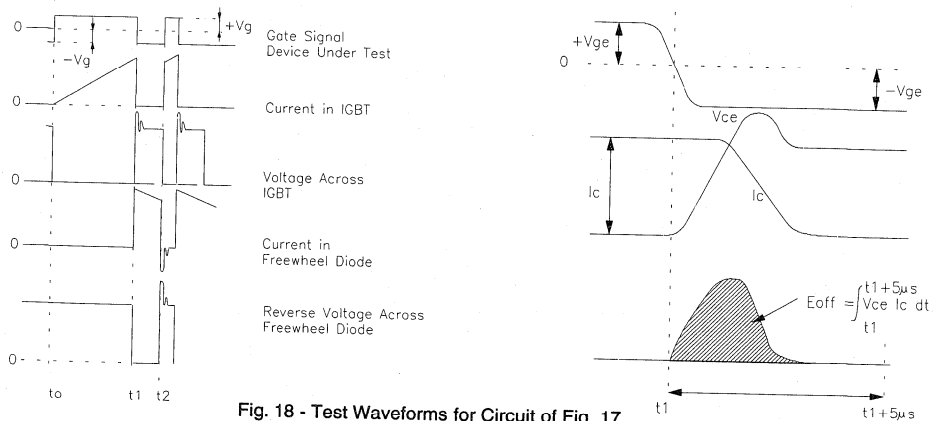


Fig. 18 - Test Waveforms for Circuit of Fig. 17

Refer to Section D for the following:
 Appendix I: Section D - page D-11

Fig. 19 - Test Waveforms for Circuit of Fig. 17,
 Defining E_{ON} , E_{REC} , Q_{RR}

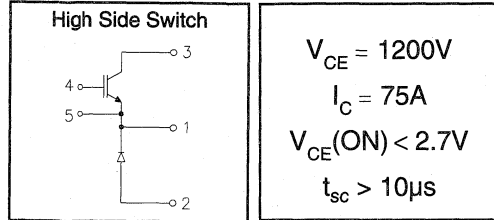
Fig. 20 - Waveforms for Switching Time

IRGNIN075M12

"CHOPPER HIGH SIDE SWITCH" IGBT INT-A-PAK

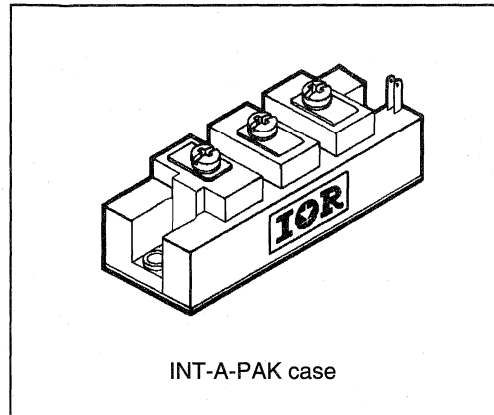
Low conduction loss IGBT

- Rugged Design
- Simple gate-drive
- Switching-Loss Rating includes all "tail" losses
- Short circuit rated



Description

IR's advanced IGBT technology is the key to this line of INT-A-PAK Power Modules. The efficient geometry and unique processing of the IGBT allow higher current densities than comparable bipolar power module transistors, while at the same time requiring the simpler gate-drive of the familiar power MOSFET. These modules are short circuit rated for applications such as motor control requiring this important feature.



Absolute Maximum Ratings

Parameter	Description	Value	Units
V_{CES}	Continuous collector to emitter voltage	1200	V
$I_C @ T_C = 25^\circ C$	Maximum Continuous collector current	150	A
$I_C @ T_C = 85^\circ C$	Maximum Continuous collector current	85	
$I_C @ T_C = 100^\circ C$	Maximum Continuous collector current	65	
I_{LM}	Peak switching current	150	
I_{FM}	Peak diode forward current (1)	150	
V_{GE}	Gate to emitter voltage	± 20	V
V_{ISOL}	RMS isolation voltage, any terminal to case, $t = 1 \text{ min}$	2500	
$P_D @ T_C = 25^\circ C$	Power dissipation	600	W
T_J	Operating junction temperature range	-40 to 150	$^\circ C$
T_{STG}	Storage temperature range	-40 to 125	

(1) Duration limited by max junction temperature.

Electrical Characteristics - $T_J = 25^\circ\text{C}$, unless otherwise stated

Parameter	Description	Min	Typ	Max	Units	Test Conditions
BV_{CES}	Collector-to-emitter breakdown voltage	1200	—	—	v	$V_{GE} = 0V, I_C = 2mA$
$V_{CE(ON)}$	Collector-to-emitter voltage	—	2.2	2.7		$V_{GE} = 15V, I_C = 75A$
V_{FM}	Diode forward voltage - maximum	—	1.8	—		$V_{GE} = 15V, I_C = 40A, T_J = 150^\circ\text{C}$
		—	3.2	3.4		$I_F = 75A, V_{GE} = 0V$
V_{GEth}	Gate threshold voltage	3.0	—	5.5		$I_C = 1mA$
ΔV_{GEth}	Threshold voltage temp. coefficient	—	-11	—	$mV/^\circ\text{C}$	$V_{CE} = V_{GE}, I_C = 1mA$
g_{fe}	Forward transconductance	35	—	70	$S(\tau)$	$V_{CE} = 25V, I_C = 75A$
I_{CES}	Collector-to-emitter leakage current	—	—	2	mA	$V_{GE} = 0V, V_{CE} = 1200V$
		—	—	20		$V_{GE} = 0V, V_{CE} = 1200V, T_J = 150^\circ\text{C}$
I_{GES}	Gate-to-emitter leakage current	—	—	± 2	μA	$V_{GE} = \pm 20V$

Dynamic Characteristics - $T_J = 125^\circ\text{C}$, unless otherwise stated

Parameter	Description	Min	Typ	Max	Units	Test Conditions
E_{on}	Turn-on switching energy	—	0.19	—	mJ/A	$R_G = 6.8\Omega, V_{CC} = 600V$
$E_{off} (1)$	Turn-off switching energy	—	0.36	—		$I_C = 75A, L_S = 100nH$
$E_{ts} (1)$	Total switching energy	—	—	0.60		$V_{GE} = \pm 15V$
$t_{d(on)}$	Turn-on delay time	—	200	250	ns	$R_G = 6.8\Omega, V_{CC} = 600V$
t_r	Rise time	—	200	250		$I_C = 75A$
$t_{d(off)}$	Turn-off delay time	—	125	200		$V_{GE} = \pm 15V$
t_f	Fall time	—	650	—		Resistive load, $T_J = 25^\circ\text{C}$
I_{rr}	Diode peak recovery current	—	45	—	A	$R_G = 6.8\Omega, V_{CC} = 600V$
t_{rr}	Diode recovery time	—	215	—	ns	$I_C = 75A$
Q_{rr}	Diode recovery charge	—	6	—	μC	$V_{GE} = \pm 15V$
Q_{ge}	Gate-to-emitter charge (turn-on)	45	—	175	nC	$V_{CC} = 600V$
Q_{gc}	Gate-to-collector charge (turn-on)	160	—	330		$I_C = 75A$
Q_g	Total gate charge (turn-on)	500	—	900		$V_{GE} = 15V$
C_{ies}	Input capacitance	10500	—	11000	pF	$V_{GE} = 0V$
C_{oes}	Output capacitance	650	—	1100		$V_{CC} = 30V$
C_{res}	Reverse transfer capacitance	650	—	1000		$f = 1MHz$
t_{sc}	Short circuit withstand time	10	—	—	μs	$V_{CC} = 720V, V_{GE} = \pm 15V$ Min. $R_G = 6.8\Omega, V_{CEP} = 1000V$

(1) Includes tail losses

Thermal and Mechanical Characteristics

Parameter	Description	Typ	Max	Units
R_{thJC} (IGBT)	Thermal resistance, junction to case, each IGBT	—	0.209	$^\circ\text{C/W}$
R_{thJC} (Diode)	Thermal resistance, junction to case, each diode	—	0.280	
R_{thCS} (Module)	Thermal resistance, case to sink	0.041	0.100	
Wt	Weight of module	150	—	g

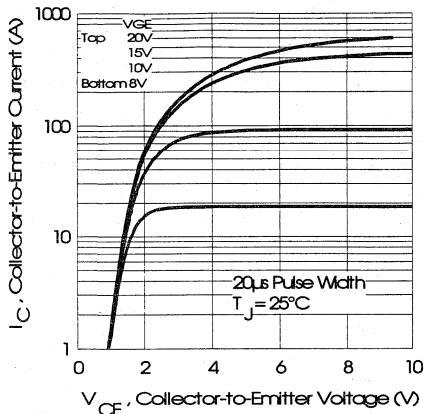


Fig. 1 - Typical Output Characteristics, $T_J = 25^\circ\text{C}$

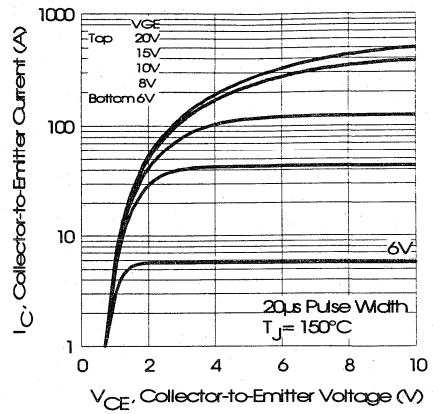


Fig. 2 - Typical Output Characteristics, $T_J = 150^\circ\text{C}$

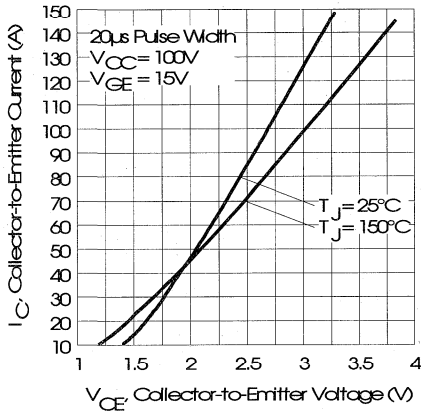


Fig. 3 - Typical Output Characteristics

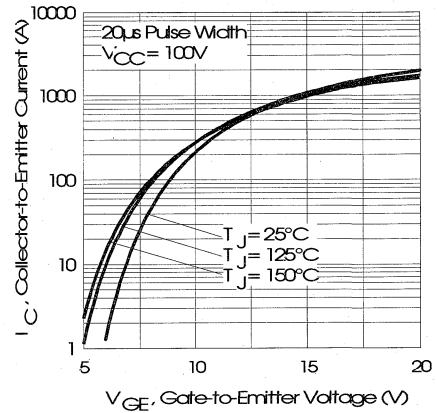


Fig. 4 - Typical Transfer Characteristics

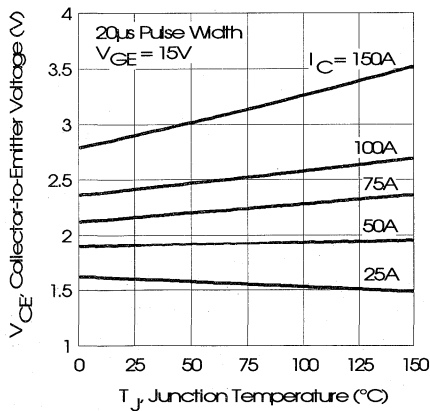


Fig. 5 - Collector-to-Emitter Saturation Typical Voltage vs. Junction Temperature

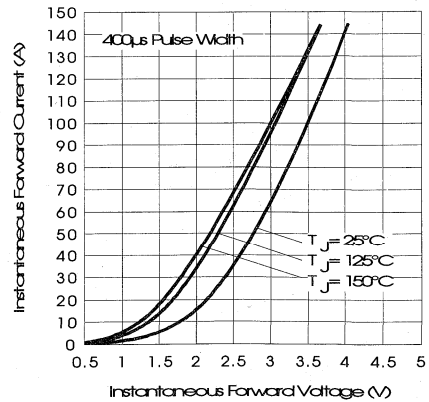


Fig. 6 - Forward Voltage Drop Characteristics

Motor
Control
Fast
Modules

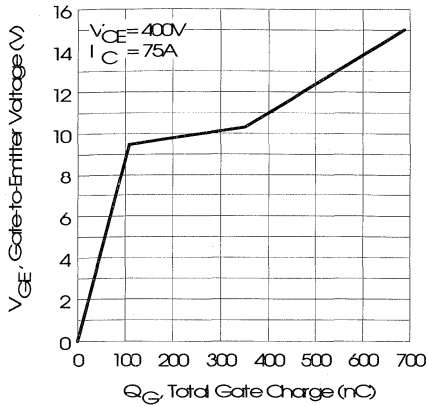


Fig. 7 - Typical Gate Charge vs. Gate-to-Emitter Voltage

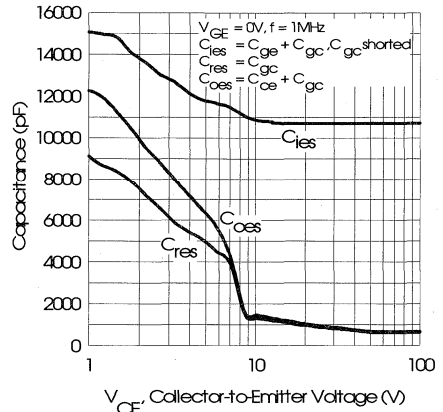


Fig. 8 - Typical Capacitance vs. Collector-to-Emitter Voltage

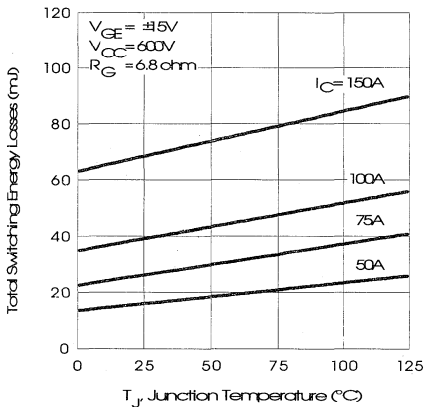


Fig. 9 - Typical Switching Losses vs. Junction Temperature

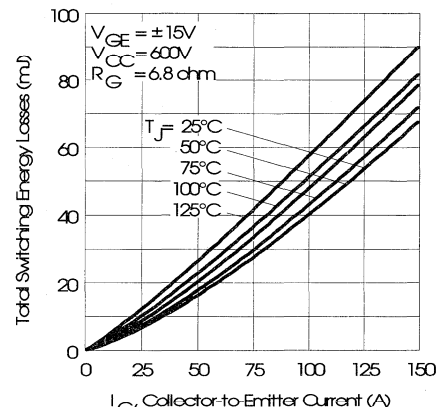


Fig. 10 - Typical Switching Losses vs. Collector-to-Emitter Current

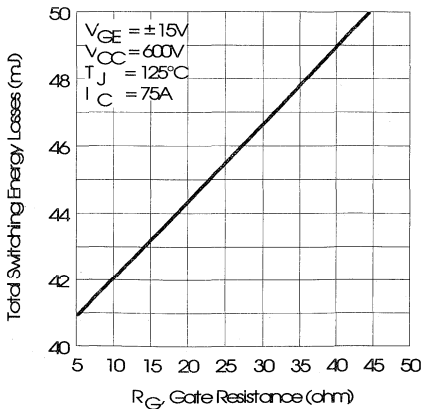


Fig. 11 - Typical Switching Losses vs. Gate Resistance

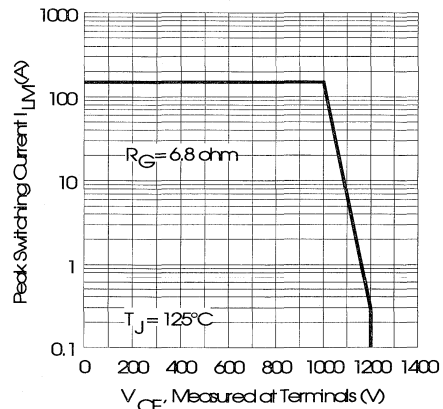


Fig. 12 - Reverse Bias Safe Operating Area

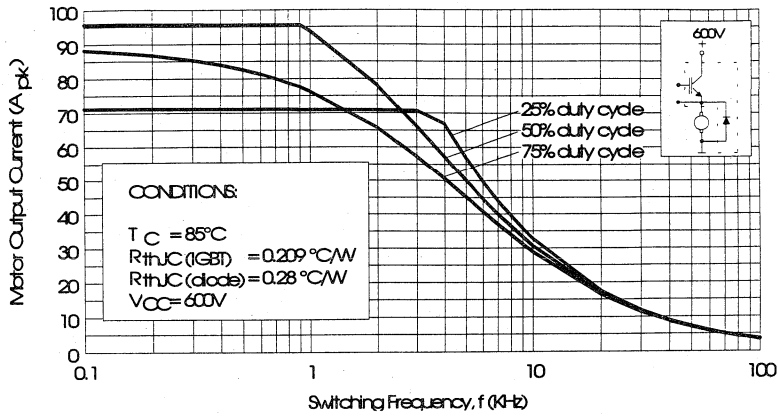


Fig. 13 - RMS Output Current vs. Frequency

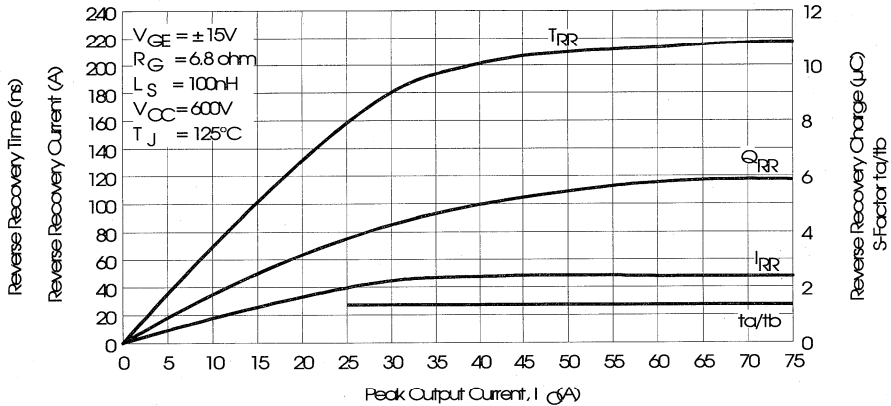


Fig. 14 - Typical Diode Recovery Characteristics as Function of Output Current I_o

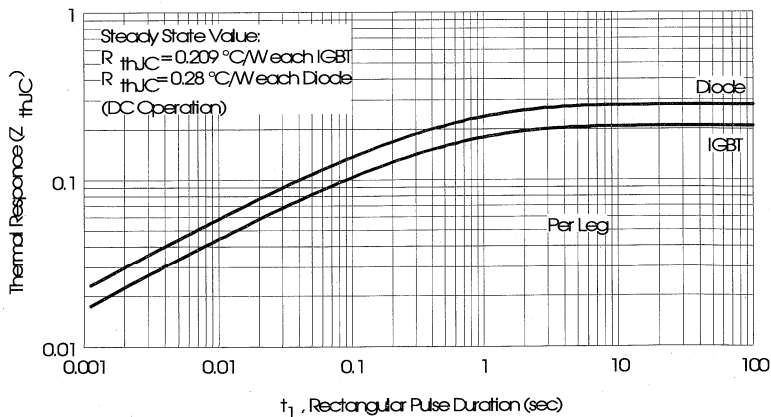


Fig. 15 - Maximum Effective Transient Thermal Impedance, Junction-to-Case

Motor
Control
Fast
Modules

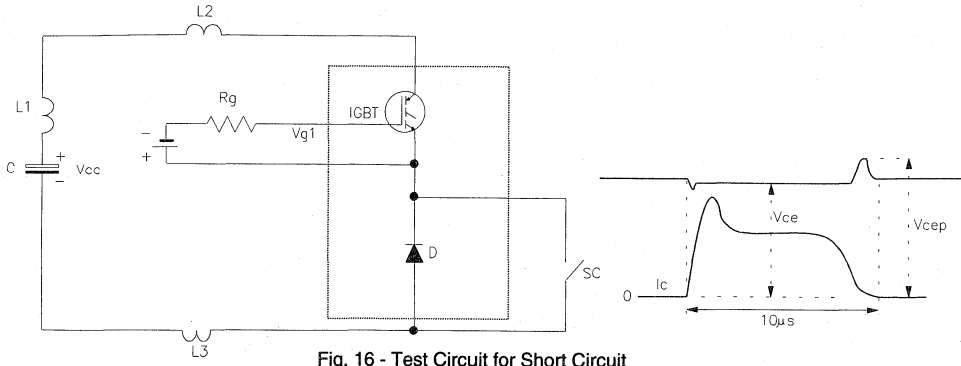


Fig. 16 - Test Circuit for Short Circuit

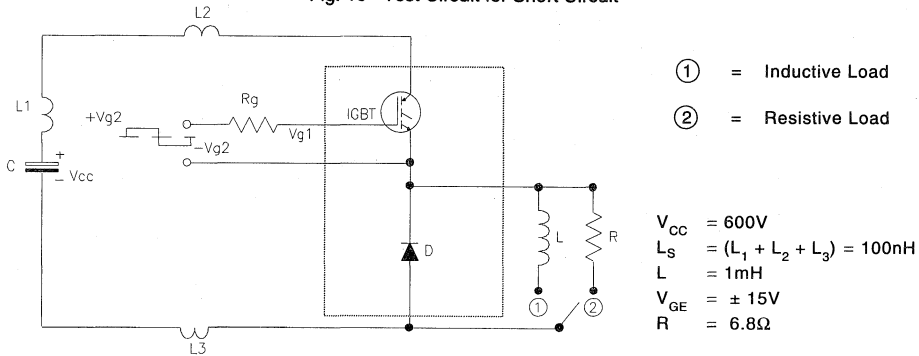


Fig. 17 - Test Circuit for Measurement of I_{LM} , E_{ON} , E_{OFF} , Q_{RR}

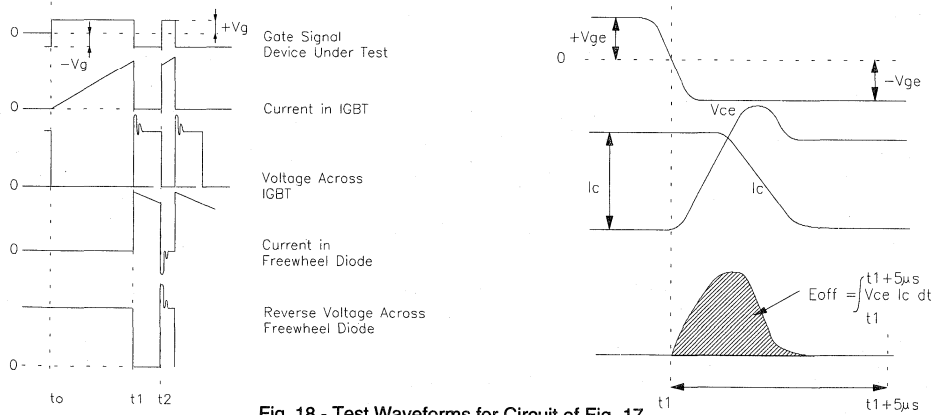


Fig. 18 - Test Waveforms for Circuit of Fig. 17

Refer to Section D for the following:
Appendix I: Section D - page D-11

Fig. 19 - Test Waveforms for Circuit of Fig. 17,

Defining E_{ON} , E_{REC} , Q_{RR}

Fig. 20 - Waveforms for Switching Time

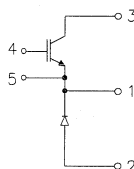
IRGNIN100M12

"CHOPPER HIGH SIDE SWITCH" IGBT INT-A-PAK

Low conduction loss IGBT

- Rugged Design
- Simple gate-drive
- Switching-Loss Rating includes all "tail" losses
- Short circuit rated

High Side Switch



$$V_{CE} = 1200V$$

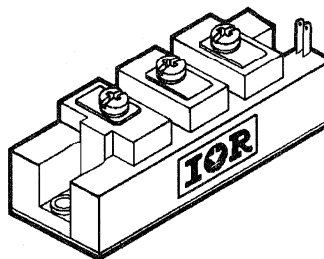
$$I_C = 100A$$

$$V_{CE(ON)} < 2.7V$$

$$t_{sc} > 10\mu s$$

Description

IR's advanced IGBT technology is the key to this line of INT-A-PAK Power Modules. The efficient geometry and unique processing of the IGBT allow higher current densities than comparable bipolar power module transistors, while at the same time requiring the simpler gate-drive of the familiar power MOSFET. These modules are short circuit rated for applications such as motor control requiring this important feature.



INT-A-PAK case

 Motor
Control
Fast
Modules

Absolute Maximum Ratings

Parameter	Description	Value	Units
V_{CES}	Continuous collector to emitter voltage	1200	V
$I_C @ T_c = 25^\circ C$	Maximum Continuous collector current	175	A
$I_C @ T_c = 85^\circ C$	Maximum Continuous collector current	100	
$I_C @ T_c = 100^\circ C$	Maximum Continuous collector current	75	
I_{LM}	Peak switching current	200	
I_{FM}	Peak diode forward current (1)	200	V
V_{GE}	Gate to emitter voltage	± 20	
V_{ISOL}	RMS isolation voltage, any terminal to case, $t = 1$ min	2500	
$P_D @ T_c = 25^\circ C$	Power dissipation	665	W
T_J	Operating junction temperature range	-40 to 150	$^\circ C$
T_{STG}	Storage temperature range	-40 to 125	

(1) Duration limited by max junction temperature.

IRGNIN100M12



Electrical Characteristics - $T_J = 25^\circ\text{C}$, unless otherwise stated

Parameter	Description	Min	Typ	Max	Units	Test Conditions
BV_{CES}	Collector-to-emitter breakdown voltage	1200	—	—	V	$V_{GE} = 0V, I_C = 3mA$
$V_{CE(ON)}$	Collector-to-emitter voltage	—	2.2	2.7		$V_{GE} = 15V, I_C = 100A$
		—	1.8	—		$V_{GE} = 15V, I_C = 80A, T_J = 150^\circ\text{C}$
V_{FM}	Diode forward voltage - maximum	—	3.2	3.4		$I_F = 100A, V_{GE} = 0V$
		—	2.6	—		$I_F = 100A, V_{GE} = 0V, T_J = 150^\circ\text{C}$
V_{Geth}	Gate threshold voltage	3.0	—	5.5	$I_C = 1mA$	
ΔV_{Geth}	Threshold voltage temp. coefficient	—	-11	—	mV/ $^\circ\text{C}$	$V_{CE} = V_{GE}, I_C = 1mA$
g_{fe}	Forward transconductance	35	—	70	S(t)	$V_{CE} = 25V, I_C = 100A$
I_{CES}	Collector-to-emitter leakage current	—	—	3	mA	$V_{GE} = 0V, V_{CE} = 1200V$
		—	—	30		$V_{GE} = 0V, V_{CE} = 1200V, T_J = 150^\circ\text{C}$
I_{GES}	Gate-to-emitter leakage current	—	—	± 3	μA	$V_{GE} = \pm 20V$

Dynamic Characteristics - $T_J = 125^\circ\text{C}$, unless otherwise stated

Parameter	Description	Min	Typ	Max	Units	Test Conditions
E_{on}	Turn-on switching energy	—	0.19	—	mJ/A	$R_G = 6.8\Omega, V_{CC} = 600V$
$E_{off(1)}$	Turn-off switching energy	—	0.36	—		$I_C = 100A, L_S = 100nH$
$E_{ts(1)}$	Total switching energy	—	—	0.60		$V_{GE} = \pm 15V$
$t_{d(on)}$	Turn-on delay time	—	200	250	ns	$R_G = 6.8\Omega, V_{CC} = 600V$
t_r	Rise time	—	200	250		$I_C = 100A$
$t_{d(off)}$	Turn-off delay time	—	125	200		$V_{GE} = \pm 15V$
t_f	Fall time	—	650	—		Resistive load, $T_J = 25^\circ\text{C}$
I_{rr}	Diode peak recovery current	—	50	—	A	$R_G = 6.8\Omega, V_{CC} = 600V$
t_{rr}	Diode recovery time	—	215	—	ns	$I_C = 100A$
Q_{rr}	Diode recovery charge	—	8	—	μC	$V_{GE} = \pm 15V$
Q_{ge}	Gate-to-emitter charge (turn-on)	65	—	260	nC	$V_{CC} = 600V$
Q_{gc}	Gate-to-collector charge (turn-on)	240	—	500		$I_C = 100A$
Q_g	Total gate charge (turn-on)	750	—	1350		$V_{GE} = 15V$
C_{ies}	Input capacitance	15500	—	16500	pF	$V_{GE} = 0V$
C_{oes}	Output capacitance	950	—	1650		$V_{CC} = 30V$
C_{res}	Reverse transfer capacitance	950	—	1650		$f = 1MHz$
t_{sc}	Short circuit withstand time	10	—	—	μs	$V_{CC} = 720V, V_{GE} = \pm 15V$ Min. $R_G = 6.8\Omega, V_{CEP} = 1000V$

(1) Includes tail losses

Thermal and Mechanical Characteristics

Parameter	Description	Typ	Max	Units
R_{thJC} (IGBT)	Thermal resistance, junction to case, each IGBT	—	0.188	$^\circ\text{C/W}$
R_{thJC} (Diode)	Thermal resistance, junction to case, each diode	—	0.209	
R_{thCS} (Module)	Thermal resistance, case to sink	0.041	0.100	
Wt	Weight of module	150	—	g

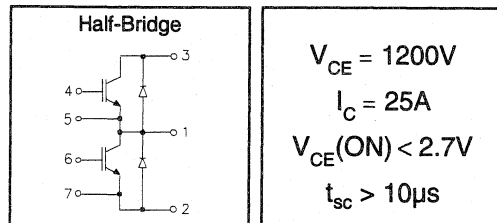
Refer to Section D - page D-16 for Package Outline 9 -INT-A-PAK, New - High Side Switch

IRGTIN025M12

"HALF-BRIDGE" IGBT INT-A-PAK

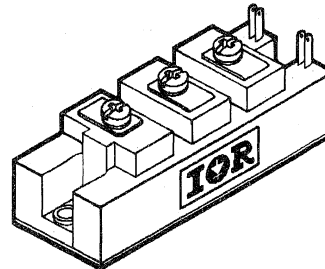
Low conduction loss IGBT

- Rugged Design
- Simple gate-drive
- Switching-Loss Rating includes all "tail" losses
- Short circuit rated



Description

IR's advanced IGBT technology is the key to this line of INT-A-PAK Power Modules. The efficient geometry and unique processing of the IGBT allow higher current densities than comparable bipolar power module transistors, while at the same time requiring the simpler gate-drive of the familiar power MOSFET. These modules are short circuit rated for applications such as motor control requiring this important feature.



INT-A-PAK case

Absolute Maximum Ratings

Parameter	Description	Value	Units
V_{CES}	Continuous collector to emitter voltage	1200	V
$I_C @ T_C = 25^\circ C$	Maximum Continuous collector current	50	A
$I_C @ T_C = 85^\circ C$	Maximum Continuous collector current	45	
$I_C @ T_C = 100^\circ C$	Maximum Continuous collector current	35	
I_{LM}	Peak IGBT switching current	50	
I_{FM}	Peak diode forward switching current (1)	50	
V_{GE}	Gate to emitter voltage	± 20	V
V_{ISOL}	RMS isolation voltage, any terminal to case, $t = 1$ min	2500	
$P_D @ T_C = 25^\circ C$	Power dissipation	385	W
T_J	Operating junction temperature range	-40 to 150	$^\circ C$
T_{STG}	Storage temperature range	-40 to 125	

(1) Duration limited by max junction temperature.

Electrical Characteristics - $T_J = 25^\circ\text{C}$, unless otherwise stated

Parameter	Description	Min	Typ	Max	Units	Test Conditions
BV_{CES}	Collector-to-emitter breakdown voltage	1200	—	—	V	$V_{GE} = 0V, I_C = 1mA$
$V_{CE(ON)}$	Collector-to-emitter voltage	—	2.2	2.7		$V_{GE} = 15V, I_C = 25A$
		—	1.85	—		$V_{GE} = 15V, I_C = 15A, T_J = 150^\circ\text{C}$
V_{FM}	Diode forward voltage - maximum	—	3.2	3.4		$I_F = 25A, V_{GE} = 0V$
		—	2.6	—		$I_F = 25A, V_{GE} = 0V, T_J = 150^\circ\text{C}$
V_{GEth}	Gate threshold voltage	3.0	—	5.5	$I_C = 500\mu A$	
ΔV_{GEth}	Threshold voltage temp. coefficient	—	-11	—	mV/ $^\circ\text{C}$	$V_{CE} = V_{GE}, I_C = 500\mu A$
g_{fe}	Forward transconductance	18	—	35	S(τ)	$V_{CE} = 25V, I_C = 25A$
I_{CES}	Collector-to-emitter leakage current	—	—	1	mA	$V_{GE} = 0V, V_{CE} = 1200V$
		—	—	10		$V_{GE} = 0V, V_{CE} = 1200V, T_J = 150^\circ\text{C}$
I_{GES}	Gate-to-emitter leakage current	—	—	± 1	μA	$V_{GE} = \pm 20V$

Dynamic Characteristics - $T_J = 125^\circ\text{C}$, unless otherwise stated

Parameter	Description	Min	Typ	Max	Units	Test Conditions
E_{on}	Turn-on switching energy	—	0.19	—	mJ/A	$R_G = 15\Omega, V_{CC} = 600V$
E_{off} (1)	Turn-off switching energy	—	0.36	—		$I_C = 25A, L_S = 100nH$
E_{ts} (1)	Total switching energy	—	—	0.60		$V_{GE} = \pm 15V$
$t_{d(on)}$	Turn-on delay time	—	200	250	ns	$R_G = 15\Omega, V_{CC} = 600V$
t_r	Rise time	—	200	250		$I_C = 25A$
$t_{d(off)}$	Turn-off delay time	—	125	200		$V_{GE} = \pm 15V$
t_f	Fall time	—	650	—		Resistive load, $T_J = 25^\circ\text{C}$
I_{rr}	Diode peak recovery current	—	25	—	A	$R_G = 15\Omega, V_{CC} = 600V$
t_{rr}	Diode recovery time	—	215	—	ns	$I_C = 25A$
Q_{rr}	Diode recovery charge	—	3	—	μC	$V_{GE} = \pm 15V$
Q_{ge}	Gate-to-emitter charge (turn-on)	23	—	88	nC	$V_{CC} = 600V$
Q_{gc}	Gate-to-collector charge (turn-on)	80	—	170		$I_C = 25A$
Q_g	Total gate charge (turn-on)	250	—	450		$V_{GE} = 15V$
C_{ies}	Input capacitance	5250	—	5500	pF	$V_{GE} = 0V$
C_{oes}	Output capacitance	330	—	550		$V_{CC} = 30V$
C_{res}	Reverse transfer capacitance	330	—	500		$f = 1MHz$
t_{sc}	Short circuit withstand time	10	---	---	μs	$V_{CC} = 720V, V_{GE} = \pm 15V$ Min. $R_G = 15\Omega, V_{CEP} = 1000V$

(1) Includes tail losses

Thermal and Mechanical Characteristics

Parameter	Description	Typ	Max	Units
R_{thJC} (IGBT)	Thermal resistance, junction to case, each IGBT	—	0.352	$^\circ\text{C/W}$
R_{thJC} (Diode)	Thermal resistance, junction to case, each diode	—	0.480	
R_{thCS} (Module)	Thermal resistance, case to sink	0.041	0.100	
Wt	Weight of module	150	—	g

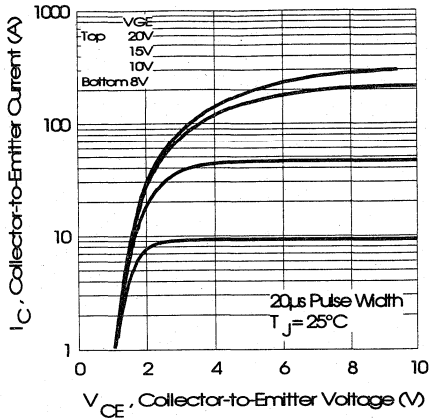


Fig. 1 - Typical Output Characteristics, $T_j = 25^\circ\text{C}$

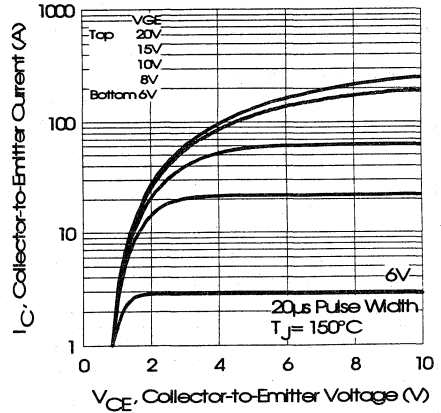


Fig. 2 - Typical Output Characteristics, $T_j = 150^\circ\text{C}$

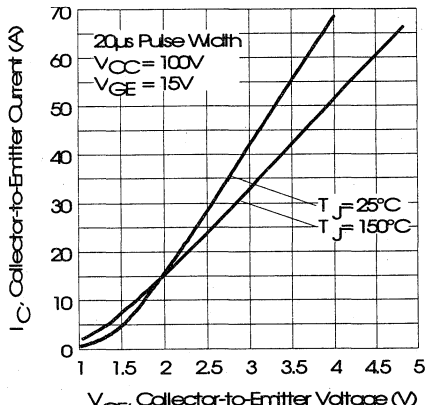


Fig. 3 - Typical Output Characteristics

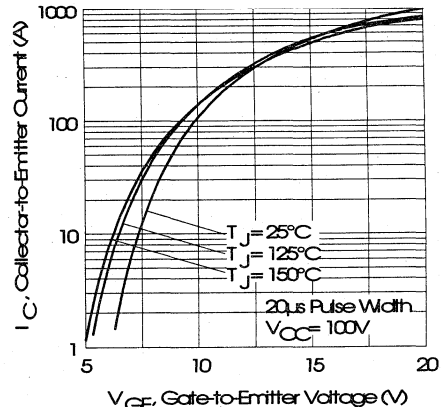


Fig. 4 - Typical Transfer Characteristics

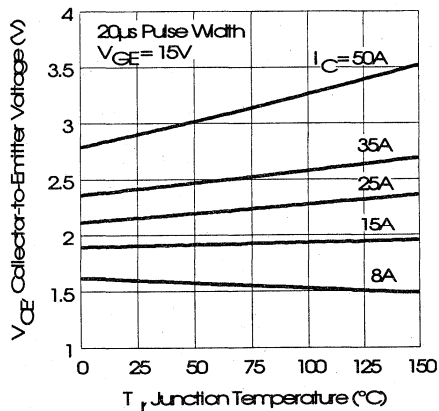


Fig. 5 - Collector-to-Emitter Saturation Typical Voltage vs. Junction Temperature

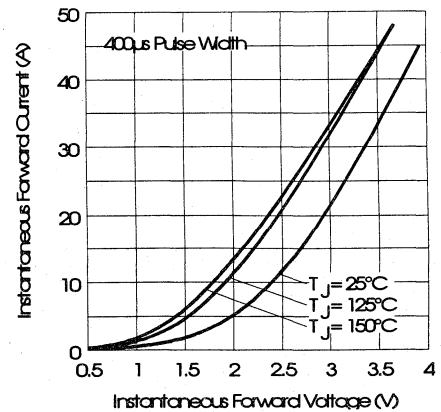


Fig. 6 - Forward Voltage Drop Characteristics

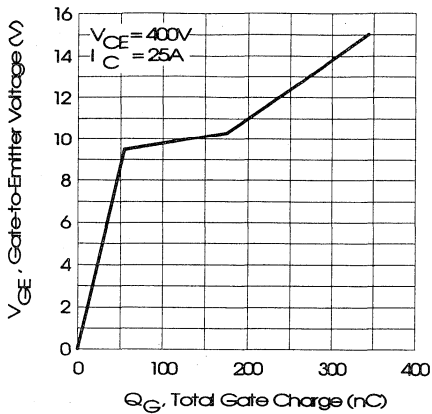


Fig. 7 - Typical Gate Charge vs. Gate-to-Emitter Voltage

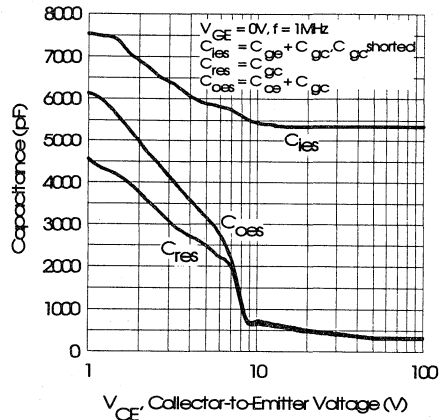


Fig. 8 - Typical Capacitance vs. Collector-to-Emitter Voltage

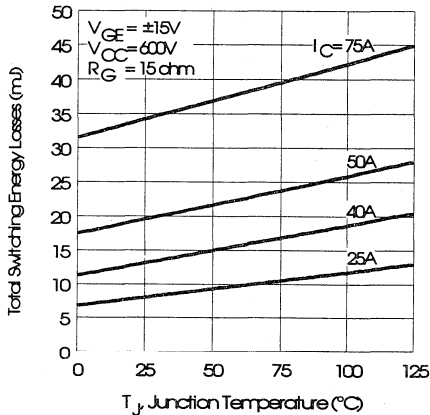


Fig. 9 - Typical Switching Losses vs. Junction Temperature

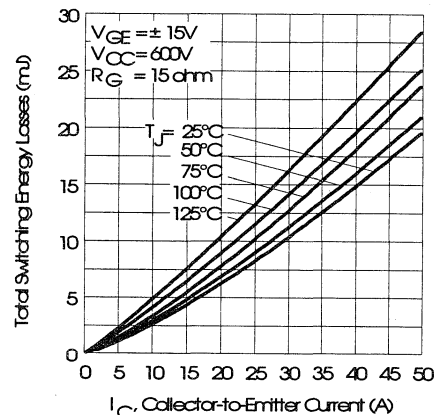


Fig. 10 - Typical Switching Losses vs. Collector-to-Emitter Current

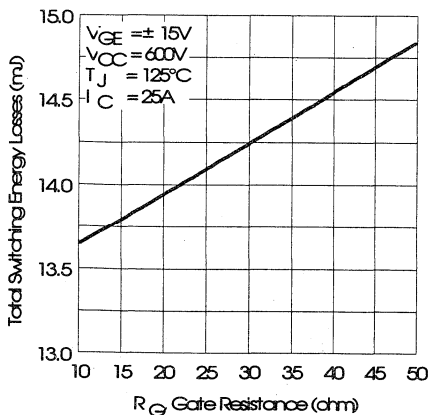


Fig. 11 - Typical Switching Losses vs. Gate Resistance

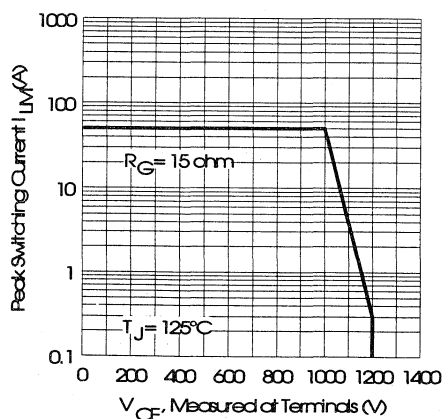


Fig. 12 - Reverse Bias Safe Operating Area

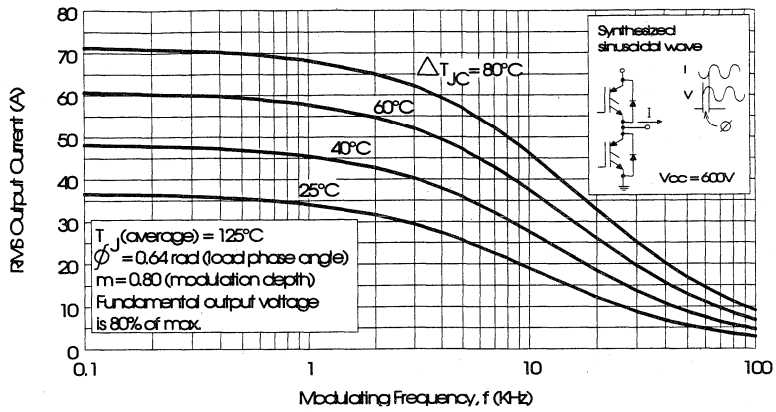


Fig. 13 - Typical RMS Output Current per phase vs. Frequency (Synthesized Sinusoidal Wave)

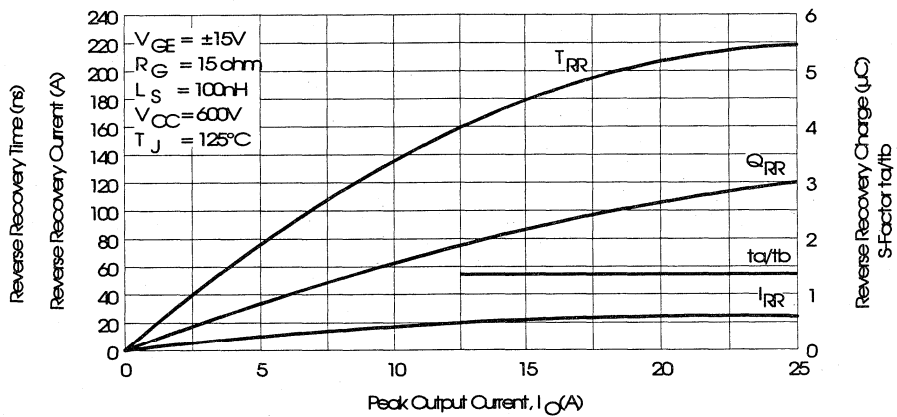


Fig. 14 - Typical Diode Recovery Characteristics as Function of Output Current I_o

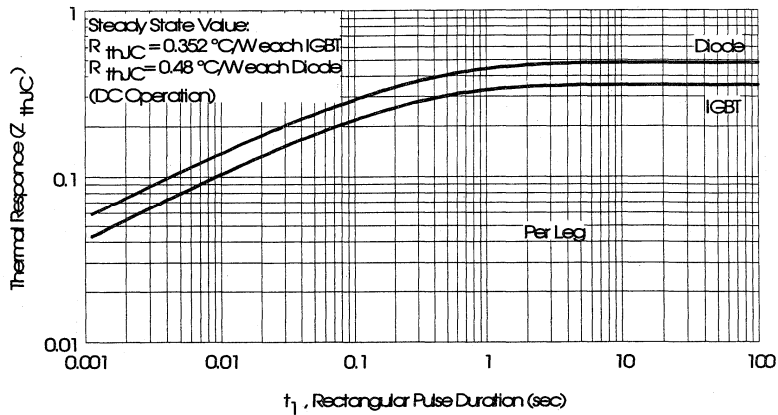


Fig. 15 - Maximum Effective Transient Thermal Impedance, Junction-to-Case

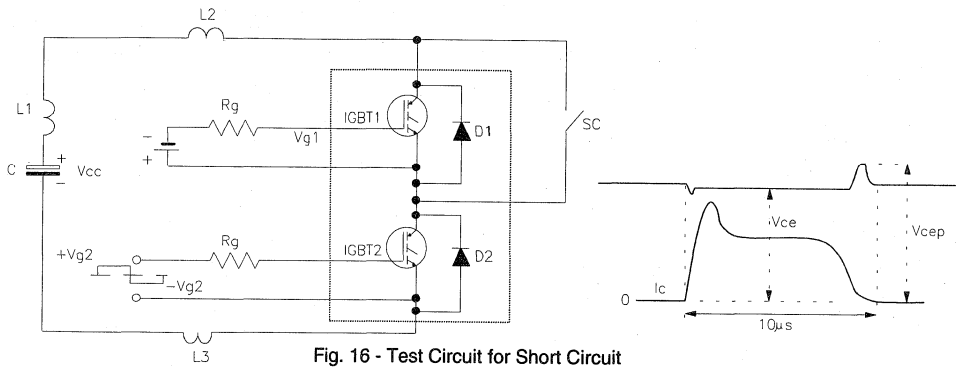


Fig. 16 - Test Circuit for Short Circuit

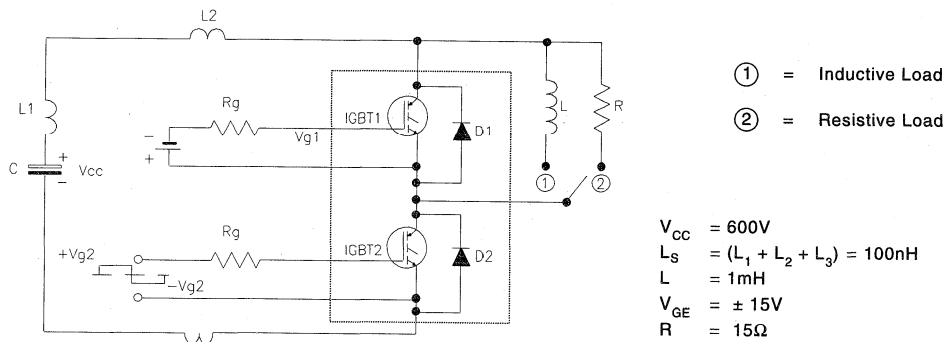


Fig. 17 - Test Circuit for Measurement of I_{LM} , E_{ON} , E_{OFF} , Q_{RR}

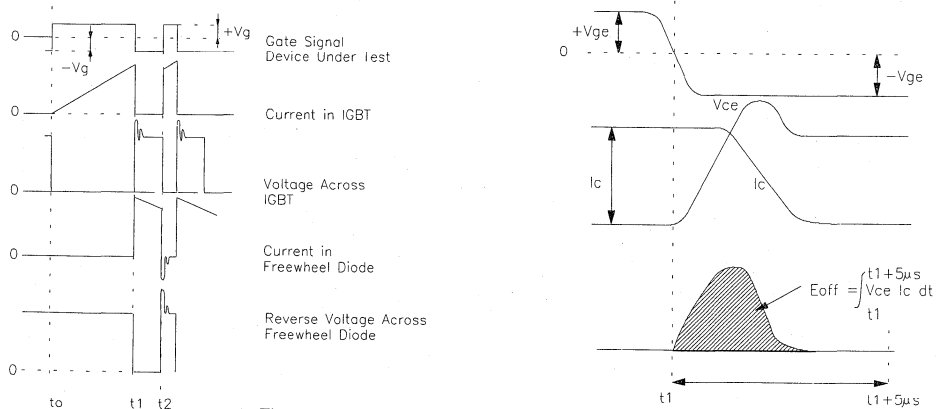


Fig. 18 - Test Waveforms for Circuit of Fig. 17

Refer to Section D for the following:

Appendix I: Section D - page D-11

Fig. 19 - Test Waveforms for Circuit of Fig. 17,
Defining E_{ON} , E_{REC} , Q_{RR}

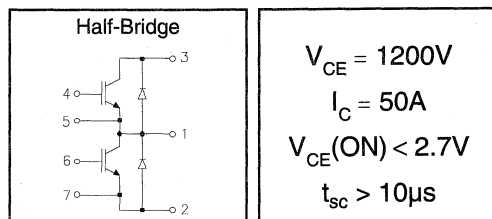
Fig. 20 - Waveforms for Switching Time

IRGTIN050M12

"HALF-BRIDGE" IGBT INT-A-PAK

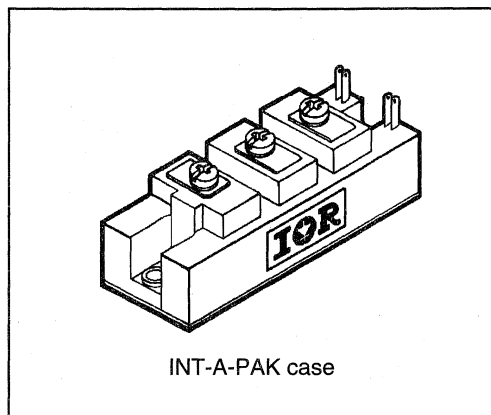
Low conduction loss IGBT

- Rugged Design
- Simple gate-drive
- Switching-Loss Rating includes all "tail" losses
- Short circuit rated



Description

IR's advanced IGBT technology is the key to this line of INT-A-PAK Power Modules. The efficient geometry and unique processing of the IGBT allow higher current densities than comparable bipolar power module transistors, while at the same time requiring the simpler gate-drive of the familiar power MOSFET. These modules are short circuit rated for applications such as motor control requiring this important feature.



Absolute Maximum Ratings

Parameter	Description	Value	Units
V_{CES}	Continuous collector to emitter voltage	1200	V
$I_C @ T_C = 25^\circ C$	Maximum Continuous collector current	100	A
$I_C @ T_C = 85^\circ C$	Maximum Continuous collector current	65	
$I_C @ T_C = 100^\circ C$	Maximum Continuous collector current	45	
I_{LM}	Peak IGBT switching current	100	
I_{FM}	Peak diode forward switching current (1)	100	
V_{GE}	Gate to emitter voltage	± 20	V
V_{ISOL}	RMS isolation voltage, any terminal to case, $t = 1 \text{ min}$	2500	
$P_D @ T_C = 25^\circ C$	Power dissipation	455	W
T_J	Operating junction temperature range	-40 to 150	$^\circ C$
T_{STG}	Storage temperature range	-40 to 125	

(1) Duration limited by max junction temperature.

Electrical Characteristics - $T_J = 25^\circ\text{C}$, unless otherwise stated

Parameter	Description	Min	Typ	Max	Units	Test Conditions
BV_{CES}	Collector-to-emitter breakdown voltage	1200	—	—	V	$V_{GE} = 0V, I_C = 1.5mA$
$V_{CE(ON)}$	Collector-to-emitter voltage	—	2.2	2.7		$V_{GE} = 15V, I_C = 50A$
		—	1.8	—		$V_{GE} = 15V, I_C = 25A, T_J = 150^\circ\text{C}$
V_{FM}	Diode forward voltage - maximum	—	3.2	3.4		$I_F = 50A, V_{GE} = 0V$
		—	2.6	—		$I_F = 50A, V_{GE} = 0V, T_J = 150^\circ\text{C}$
V_{GEth}	Gate threshold voltage	3.0	—	5.5	$I_C = 750\mu A$	
ΔV_{GEth}	Threshold voltage temp. coefficient	—	-11	—	mV/°C	$V_{CE} = V_{GE}, I_C = 750\mu A$
g_{fe}	Forward transconductance	27	—	53	S(Ω)	$V_{CE} = 25V, I_C = 50A$
I_{CES}	Collector-to-emitter leakage current	—	—	1.5	mA	$V_{GE} = 0V, V_{CE} = 1200V$
		—	—	15		$V_{GE} = 0V, V_{CE} = 1200V, T_J = 150^\circ\text{C}$
I_{GES}	Gate-to-emitter leakage current	—	—	± 1.5	μA	$V_{GE} = \pm 20V$

Dynamic Characteristics - $T_J = 125^\circ\text{C}$, unless otherwise stated

Parameter	Description	Min	Typ	Max	Units	Test Conditions
E_{on}	Turn-on switching energy	—	0.19	—	mJ/A	$R_G = 10\Omega, V_{CC} = 600V$
E_{off} (1)	Turn-off switching energy	—	0.36	—		$I_C = 50A, L_S = 100nH$
E_{ts} (1)	Total switching energy	—	—	0.60		$V_{GE} = \pm 15V$
$t_{d(on)}$	Turn-on delay time	—	200	250	ns	$R_G = 10\Omega, V_{CC} = 600V$
t_r	Rise time	—	200	250		$I_C = 50A$
$t_{d(off)}$	Turn-off delay time	—	125	200		$V_{GE} = \pm 15V$
t_f	Fall time	—	650	—		Resistive load, $T_J = 25^\circ\text{C}$
I_{rr}	Diode peak recovery current	—	35	—	A	$R_G = 10\Omega, V_{CC} = 600V$
t_{rr}	Diode recovery time	—	215	—	ns	$I_C = 50A$
Q_{rr}	Diode recovery charge	—	4.5	—	μC	$V_{GE} = \pm 15V$
Q_{ge}	Gate-to-emitter charge (turn-on)	35	—	130	nC	$V_{CC} = 600V$
Q_{gc}	Gate-to-collector charge (turn-on)	120	—	250		$I_C = 50A$
Q_g	Total gate charge (turn-on)	380	—	680		$V_{GE} = 15V$
C_{ies}	Input capacitance	8000	—	8300	pF	$V_{GE} = 0V$
C_{oes}	Output capacitance	490	—	820		$V_{CC} = 30V$
C_{res}	Reverse transfer capacitance	490	—	750		$f = 1MHz$
t_{sc}	Short circuit withstand time	10	—	—	μs	$V_{CC} = 720V, V_{GE} = \pm 15V$ Min. $R_G = 10\Omega, V_{CEP} = 1000V$

(1) Includes tail losses

Thermal and Mechanical Characteristics

Parameter	Description	Typ	Max	Units
R_{thJC} (IGBT)	Thermal resistance, junction to case, each IGBT	—	0.275	°C/W
R_{thJC} (Diode)	Thermal resistance, junction to case, each diode	—	0.380	
R_{thCS} (Module)	Thermal resistance, case to sink	0.041	0.100	
Wt	Weight of module	150	—	g

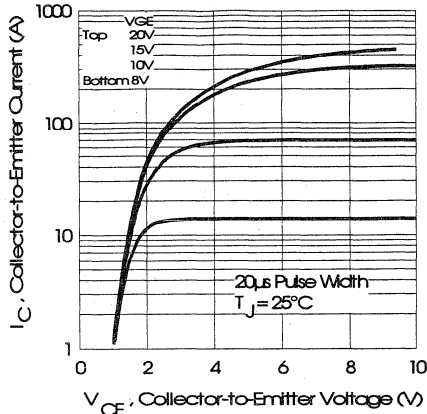


Fig. 1 - Typical Output Characteristics, $T_j = 25^\circ\text{C}$

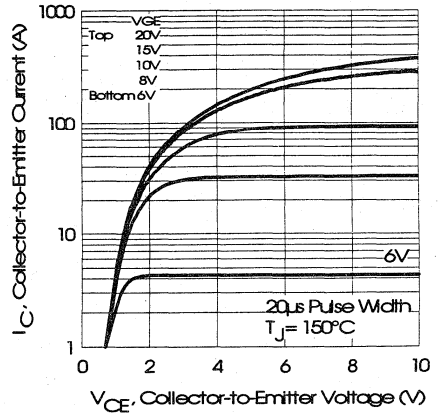


Fig. 2 - Typical Output Characteristics, $T_j = 150^\circ\text{C}$

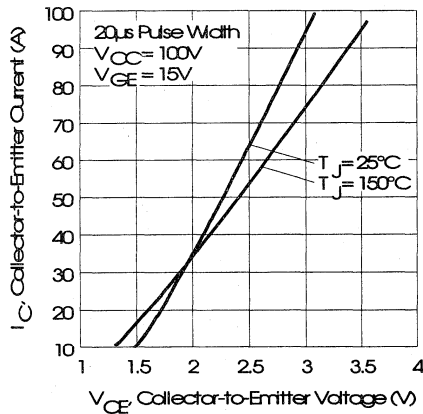


Fig. 3 - Typical Output Characteristics

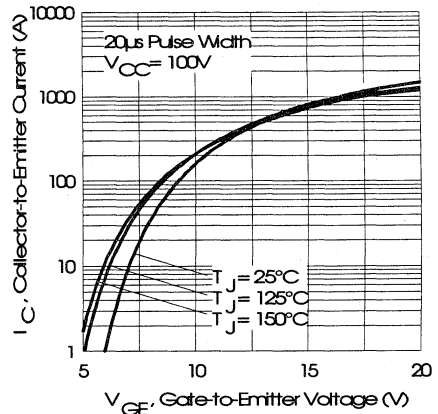


Fig. 4 - Typical Transfer Characteristics

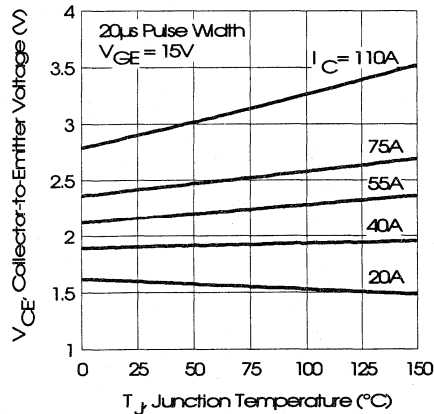


Fig. 5 - Collector-to-Emitter Saturation Typical Voltage vs. Junction Temperature

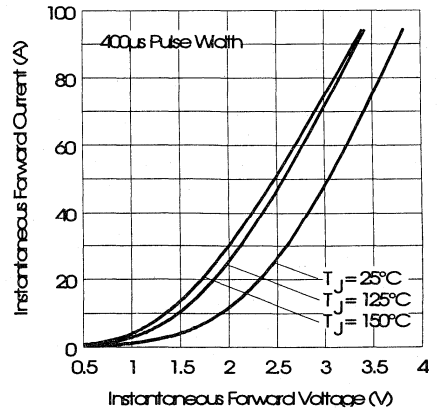


Fig. 6 - Forward Voltage Drop Characteristics

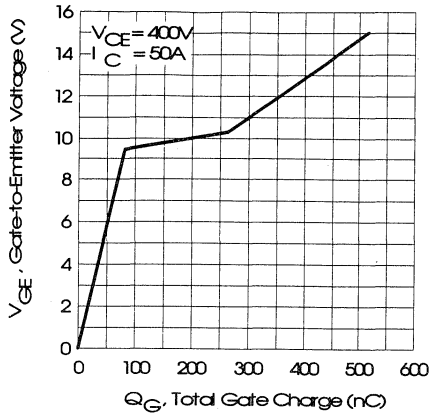


Fig. 7 - Typical Gate Charge vs. Gate-to-Emitter Voltage

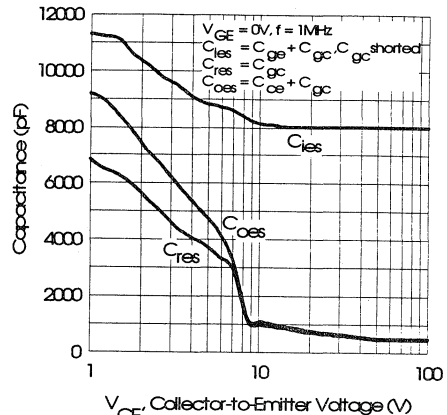


Fig. 8 - Typical Capacitance vs. Collector-to-Emitter Voltage

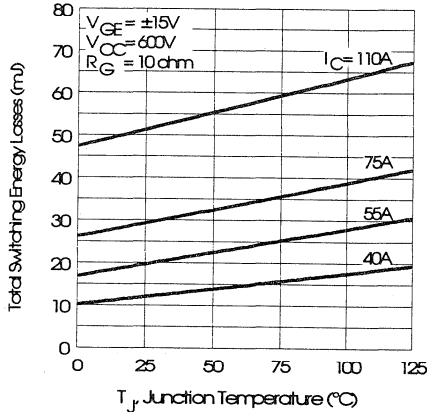


Fig. 9 - Typical Switching Losses vs. Junction Temperature

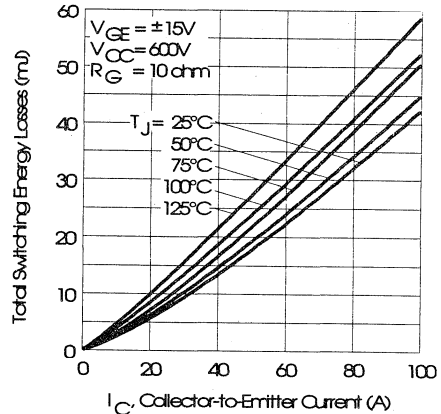


Fig. 10 - Typical Switching Losses vs. Collector-to-Emitter Current

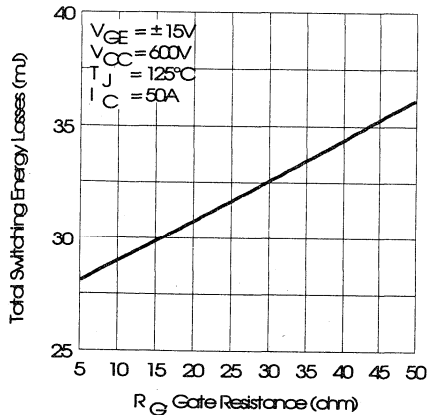


Fig. 11 - Typical Switching Losses vs. Gate Resistance

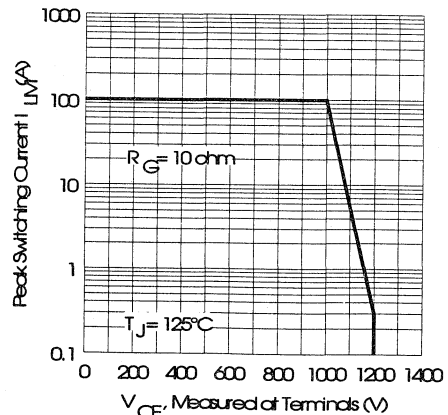


Fig. 12 - Reverse Bias Safe Operating Area

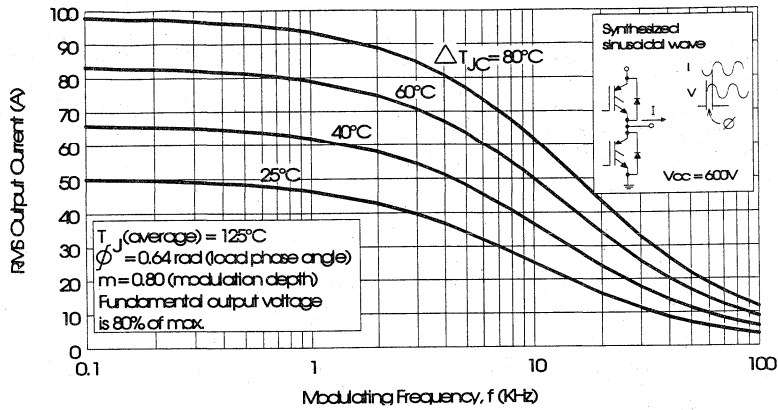


Fig. 13 - Typical RMS Output Current per phase vs. Frequency (Synthesized Sinusoidal Wave)

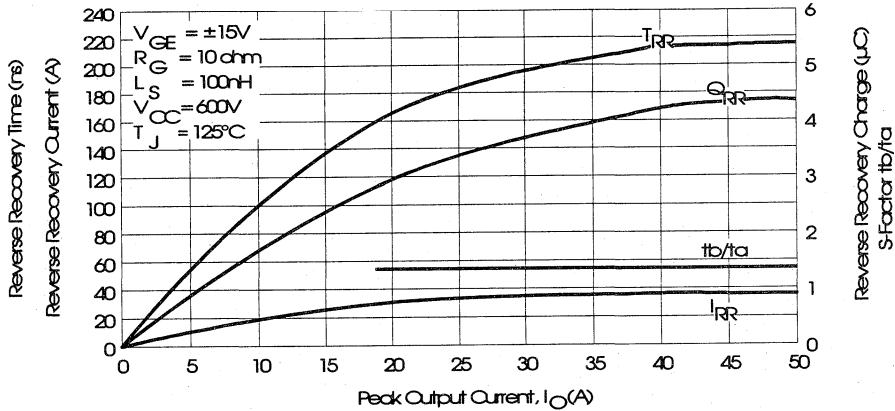


Fig. 14 - Typical Diode Recovery Characteristics as Function of Output Current I_o

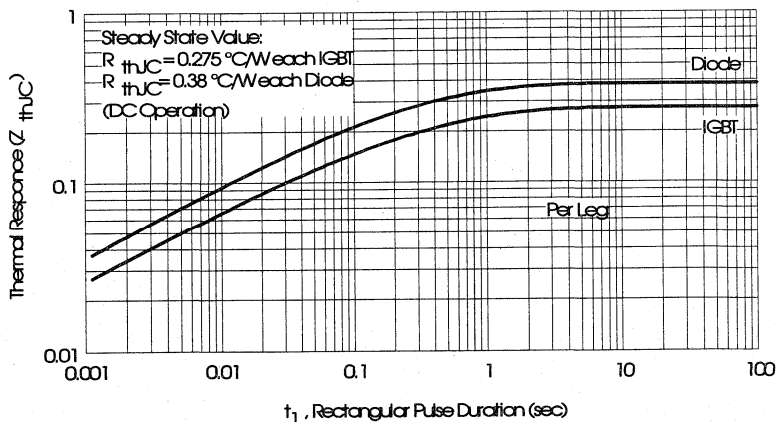


Fig. 15 - Maximum Effective Transient Thermal Impedance, Junction-to-Case

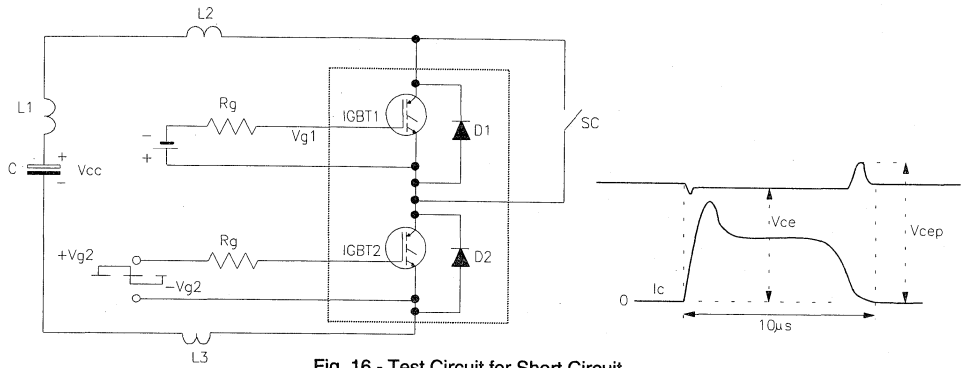


Fig. 16 - Test Circuit for Short Circuit

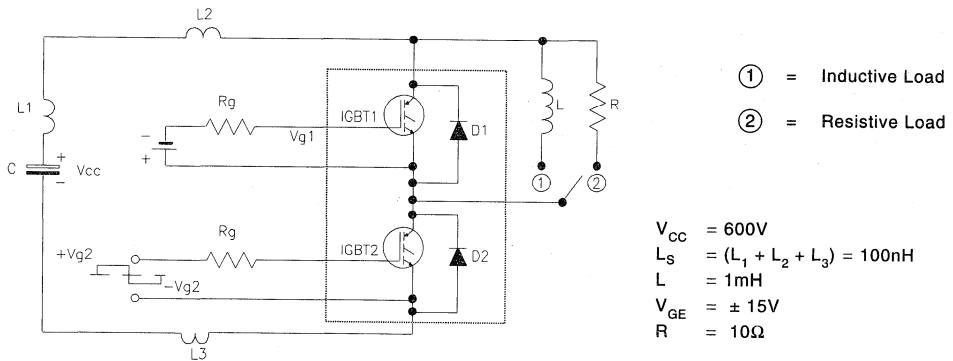


Fig. 17 - Test Circuit for Measurement of I_{LM} , E_{ON} , E_{OFF} , Q_{RR}

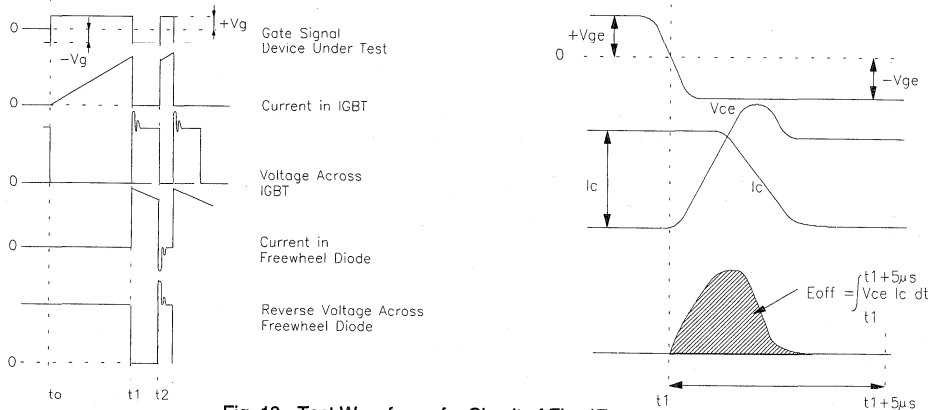


Fig. 18 - Test Waveforms for Circuit of Fig. 17

Refer to Section D for the following:

Appendix I: Section D - page D-11

Fig. 19 - Test Waveforms for Circuit of Fig. 17,

Defining E_{ON} , E_{REC} , Q_{RR}

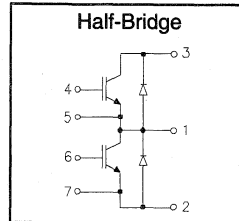
Fig. 20 - Waveforms for Switching Time

IRGTIN075M12

"HALF-BRIDGE" IGBT INT-A-PAK

Low conduction loss IGBT

- Rugged Design
- Simple gate-drive
- Switching-Loss Rating includes all "tail" losses
- Short circuit rated



$$V_{CE} = 1200V$$

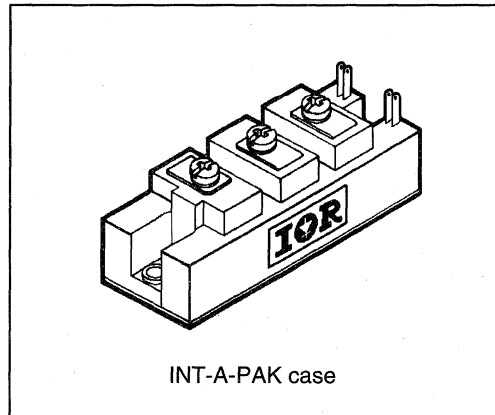
$$I_C = 75A$$

$$V_{CE(ON)} < 2.7V$$

$$t_{sc} > 10\mu s$$

Description

IR's advanced IGBT technology is the key to this line of INT-A-PAK Power Modules. The efficient geometry and unique processing of the IGBT allow higher current densities than comparable bipolar power module transistors, while at the same time requiring the simpler gate-drive of the familiar power MOSFET. These modules are short circuit rated for applications such as motor control requiring this important feature.



Absolute Maximum Ratings

Parameter	Description	Value	Units
V_{CES}	Continuous collector to emitter voltage	1200	V
$I_C @ T_C = 25^\circ C$	Maximum Continuous collector current	140	A
$I_C @ T_C = 85^\circ C$	Maximum Continuous collector current	80	
$I_C @ T_C = 100^\circ C$	Maximum Continuous collector current	60	
I_{LM}	Peak IGBT switching current	150	
I_{FM}	Peak diode forward switching current (1)	150	
V_{GE}	Gate to emitter voltage	± 20	V
V_{ISOL}	RMS isolation voltage, any terminal to case, $t = 1 \text{ min}$	2500	
$P_D @ T_C = 25^\circ C$	Power dissipation	600	W
T_J	Operating junction temperature range	-40 to 150	$^\circ C$
T_{STG}	Storage temperature range	-40 to 125	

(1) Duration limited by max junction temperature.

Electrical Characteristics - $T_J = 25^\circ\text{C}$, unless otherwise stated

Parameter	Description	Min	Typ	Max	Units	Test Conditions
BV_{CES}	Collector-to-emitter breakdown voltage	1200	—	—	V	$V_{GE} = 0V, I_C = 2mA$
$V_{CE(ON)}$	Collector-to-emitter voltage	—	2.2	2.7		$V_{GE} = 15V, I_C = 75A$
		—	1.8	—		$V_{GE} = 15V, I_C = 40A, T_J = 150^\circ\text{C}$
V_{FM}	Diode forward voltage - maximum	—	3.2	3.4		$I_F = 75A, V_{GE} = 0V$
		—	2.6	—		$I_F = 75A, V_{GE} = 0V, T_J = 150^\circ\text{C}$
V_{GEth}	Gate threshold voltage	3.0	—	5.5	$I_C = 1mA$	
ΔV_{GEth}	Threshold voltage temp. coefficient	—	-11	—	mV/°C	$V_{CE} = V_{GE}, I_C = 1mA$
g_{fe}	Forward transconductance	35	—	70	S(Ω)	$V_{CE} = 25V, I_C = 75A$
I_{CES}	Collector-to-emitter leakage current	—	—	2	mA	$V_{GE} = 0V, V_{CE} = 1200V$
		—	—	20		$V_{GE} = 0V, V_{CE} = 1200V, T_J = 150^\circ\text{C}$
I_{GES}	Gate-to-emitter leakage current	—	—	±2	μA	$V_{GE} = \pm 20V$

Dynamic Characteristics - $T_J = 125^\circ\text{C}$, unless otherwise stated

Parameter	Description	Min	Typ	Max	Units	Test Conditions
E_{on}	Turn-on switching energy	—	0.19	—	mJ/A	$R_G = 6.8\Omega, V_{CC} = 600V$
E_{off} (1)	Turn-off switching energy	—	0.36	—		$I_C = 75A, L_S = 100nH$
E_{ts} (1)	Total switching energy	—	—	0.60		$V_{GE} = \pm 15V$
$t_{d(on)}$	Turn-on delay time	—	200	250	ns	$R_G = 6.8\Omega, V_{CC} = 600V$
t_r	Rise time	—	200	250		$I_C = 75A$
$t_{d(off)}$	Turn-off delay time	—	125	200		$V_{GE} = \pm 15V$
t_f	Fall time	—	650	—		Resistive load, $T_J = 25^\circ\text{C}$
I_{rr}	Diode peak recovery current	—	45	—		$R_G = 6.8\Omega, V_{CC} = 600V$
t_{rr}	Diode recovery time	—	215	—	ns	$I_C = 75A$
Q_{rr}	Diode recovery charge	—	6	—	μC	$V_{GE} = \pm 15V$
Q_{ge}	Gate-to-emitter charge (turn-on)	45	—	175	nC	$V_{CC} = 600V$
Q_{gc}	Gate-to-collector charge (turn-on)	160	—	330		$I_C = 75A$
Q_g	Total gate charge (turn-on)	500	—	900		$V_{GE} = 15V$
C_{ies}	Input capacitance	10500	—	11000	pF	$V_{GE} = 0V$
C_{oes}	Output capacitance	650	—	1100		$V_{CC} = 30V$
C_{res}	Reverse transfer capacitance	650	—	1000		$f = 1MHz$
t_{sc}	Short circuit withstand time	10	—	—	μs	$V_{CC} = 720V, V_{GE} = \pm 15V$ Min. $R_G = 6.8\Omega, V_{CEP} = 1000V$

(1) Includes tail losses

Thermal and Mechanical Characteristics

Parameter	Description	Typ	Max	Units
R_{thJC} (IGBT)	Thermal resistance, junction to case, each IGBT	—	0.209	°C/W
R_{thJC} (Diode)	Thermal resistance, junction to case, each diode	—	0.280	
R_{thCS} (Module)	Thermal resistance, case to sink	0.041	0.100	
Wt	Weight of module	150	—	g

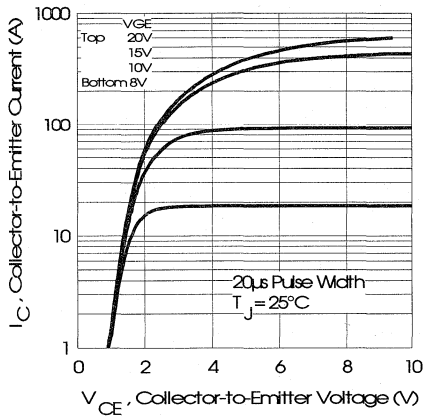


Fig. 1 - Typical Output Characteristics, $T_J = 25^\circ\text{C}$

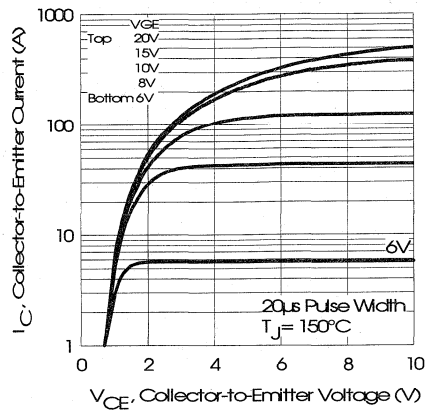


Fig. 2 - Typical Output Characteristics, $T_J = 150^\circ\text{C}$

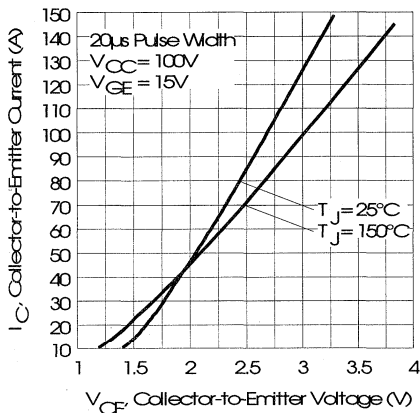


Fig. 3 - Typical Output Characteristics

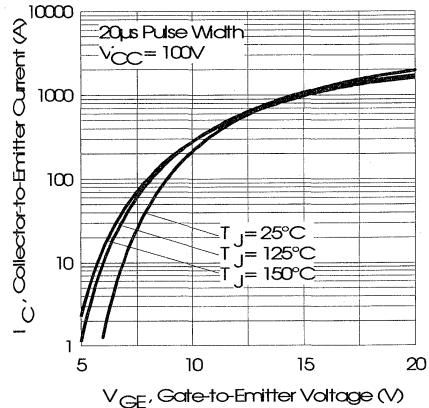


Fig. 4 - Typical Transfer Characteristics

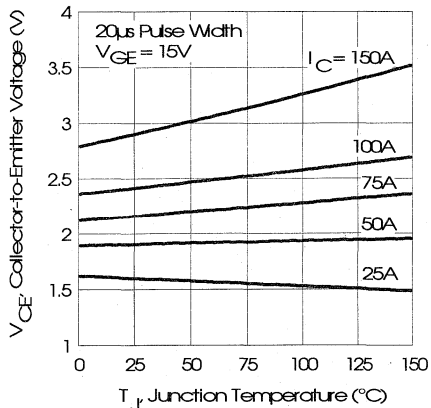


Fig. 5 - Collector-to-Emitter Saturation Typical Voltage vs. Junction Temperature

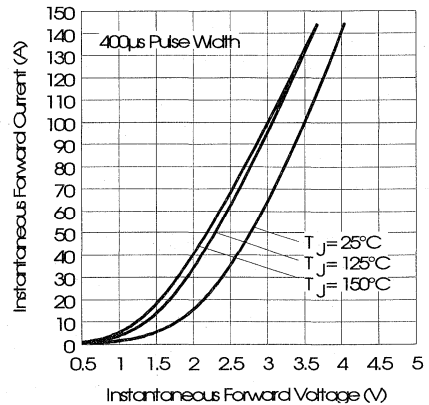


Fig. 6 - Forward Voltage Drop Characteristics



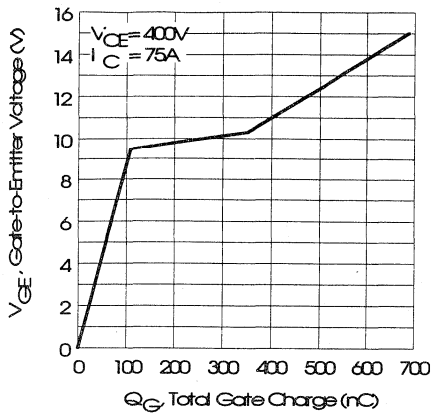


Fig. 7 - Typical Gate Charge vs. Gate-to-Emitter Voltage

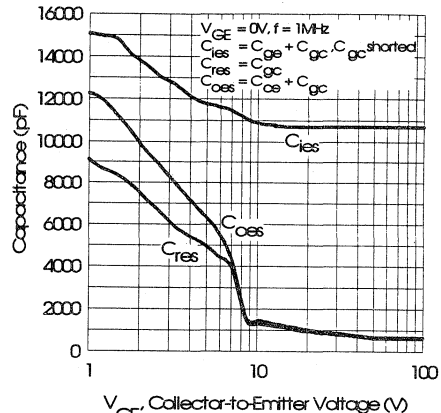


Fig. 8 - Typical Capacitance vs. Collector-to-Emitter Voltage

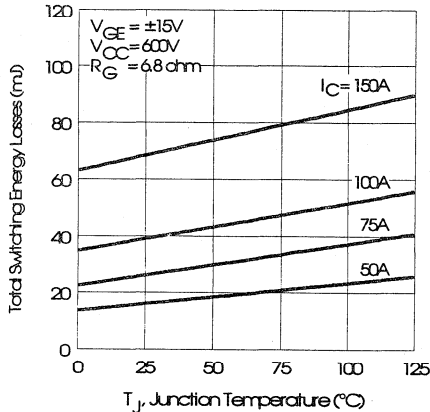


Fig. 9 - Typical Switching Losses vs. Junction Temperature

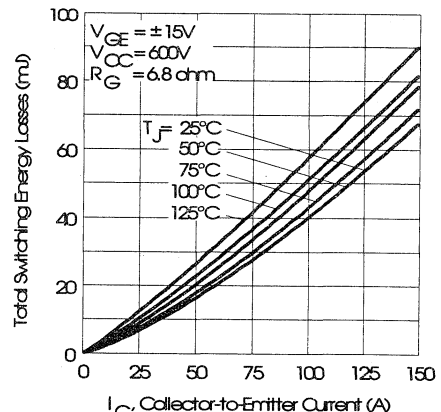


Fig. 10 - Typical Switching Losses vs. Collector-to-Emitter Current

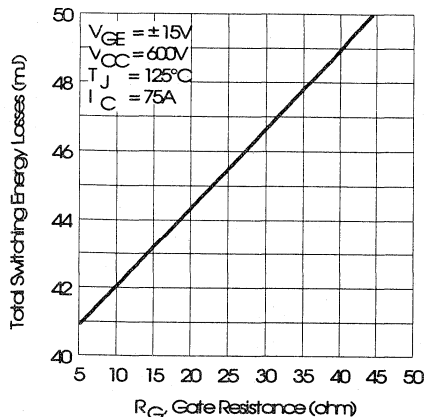


Fig. 11 - Typical Switching Losses vs. Gate Resistance

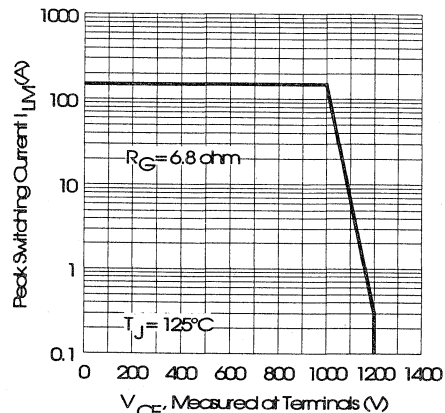


Fig. 12 - Reverse Bias Safe Operating Area

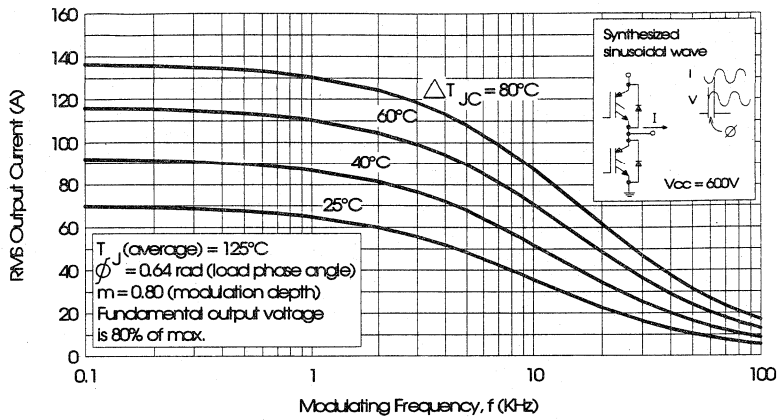


Fig. 13 - Typical RMS Output Current per phase vs. Frequency (Synthesized Sinusoidal Wave)

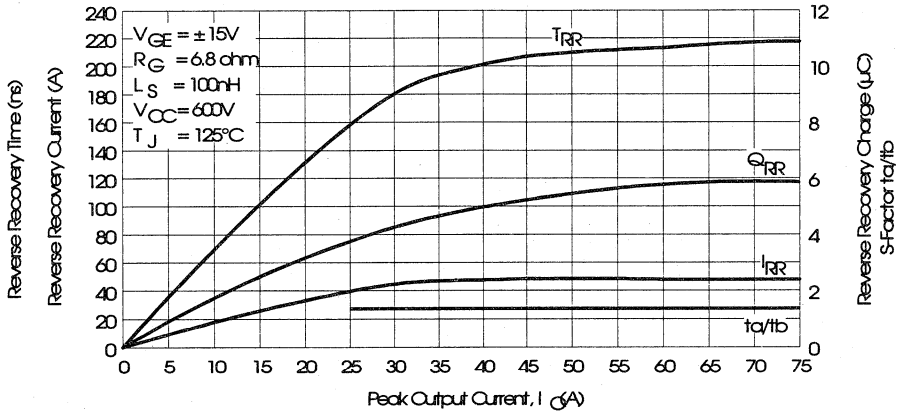


Fig. 14 - Typical Diode Recovery Characteristics as Function of Output Current I_o

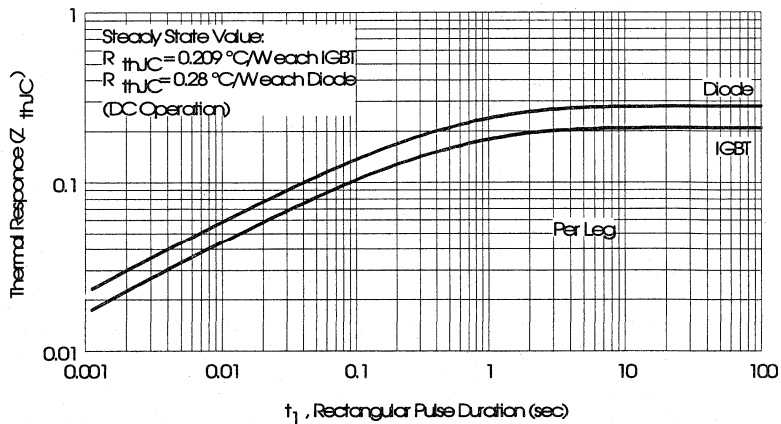


Fig. 15 - Maximum Effective Transient Thermal Impedance, Junction-to-Case

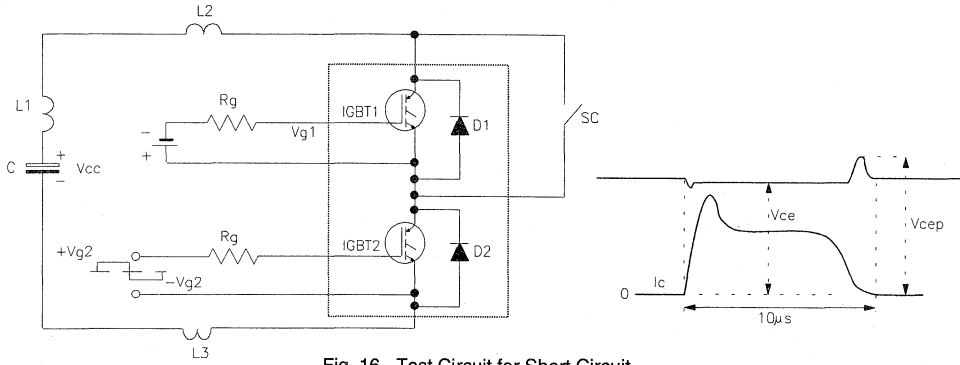


Fig. 16 - Test Circuit for Short Circuit

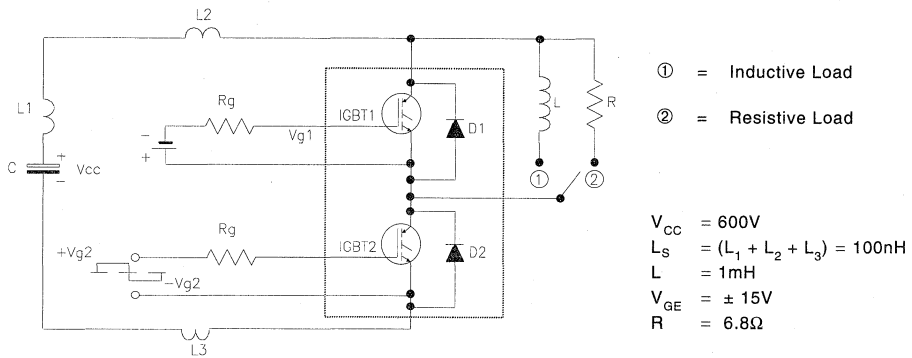


Fig. 17 - Test Circuit for Measurement of I_{LM} , E_{ON} , E_{OFF} , Q_{RR}

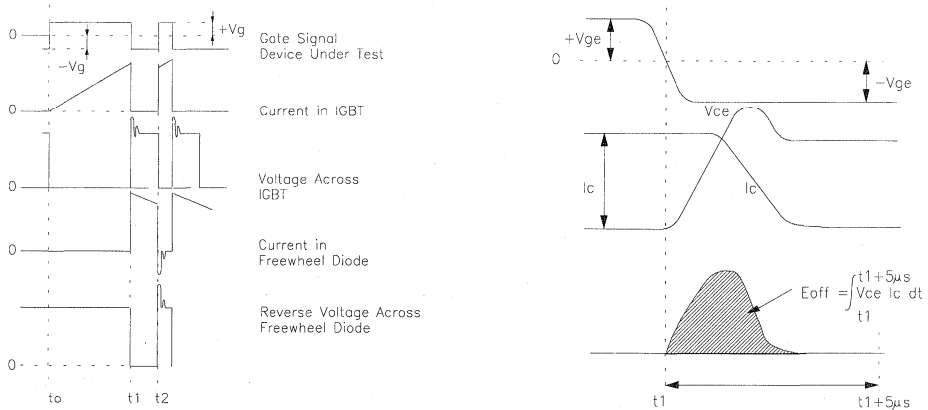


Fig. 18 - Test Waveforms for Circuit of Fig. 17

Refer to Section D for the following:
Appendix I: Section D - page D-11

Fig. 19 - Test Waveforms for Circuit of Fig. 17,

Defining E_{ON} , E_{REC} , Q_{RR}

Fig. 20 - Waveforms for Switching Time

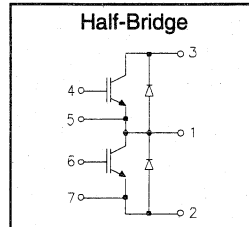
Package Outline 11- INT-A-PAK, New -Half Bridge Section D - page D-17

IRGTIN100M12

"HALF-BRIDGE" IGBT INT-A-PAK

Low conduction loss IGBT

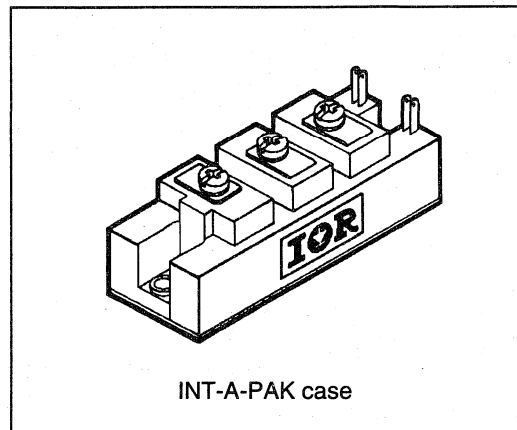
- Rugged Design
- Simple gate-drive
- Switching-Loss Rating includes all "tail" losses
- Short circuit rated



$V_{CE} = 1200V$
$I_C = 100A$
$V_{CE(ON)} < 2.7V$
$t_{SC} > 10\mu s$

Description

IR's advanced IGBT technology is the key to this line of INT-A-PAK Power Modules. The efficient geometry and unique processing of the IGBT allow higher current densities than comparable bipolar power module transistors, while at the same time requiring the simpler gate-drive of the familiar power MOSFET. These modules are short circuit rated for applications such as motor control requiring this important feature.



Absolute Maximum Ratings

Parameter	Description	Value	Units
V_{CES}	Continuous collector to emitter voltage	1200	V
$I_C @ T_C = 25^\circ C$	Maximum Continuous collector current	175	A
$I_C @ T_C = 85^\circ C$	Maximum Continuous collector current	100	
$I_C @ T_C = 100^\circ C$	Maximum Continuous collector current	75	
I_{LM}	Peak IGBT switching current	200	
I_{FM}	Peak diode forward switching current (1)	200	V
V_{GE}	Gate to emitter voltage	± 20	
V_{ISOL}	RMS isolation voltage, any terminal to case, $t = 1 \text{ min}$	2500	
$P_D @ T_C = 25^\circ C$	Power dissipation	665	W
T_J	Operating junction temperature range	-40 to 150	$^\circ C$
T_{STG}	Storage temperature range	-40 to 125	

(1) Duration limited by max junction temperature.

Electrical Characteristics - $T_J = 25^\circ\text{C}$, unless otherwise stated

Parameter	Description	Min	Typ	Max	Units	Test Conditions
BV_{CES}	Collector-to-emitter breakdown voltage	1200	—	—	V	$V_{GE} = 0V, I_C = 3mA$
$V_{CE(ON)}$	Collector-to-emitter voltage	—	2.2	2.7		$V_{GE} = 15V, I_C = 100A$
		—	1.8	—		$V_{GE} = 15V, I_C = 80A, T_J = 150^\circ\text{C}$
V_{FM}	Diode forward voltage - maximum	—	3.2	3.4		$I_F = 100A, V_{GE} = 0V$
		—	2.6	—		$I_F = 100A, V_{GE} = 0V, T_J = 150^\circ\text{C}$
V_{GEth}	Gate threshold voltage	3.0	—	5.5	$I_C = 1mA$	
ΔV_{GEth}	Threshold voltage temp. coefficient	—	-11	—	mV/ $^\circ\text{C}$	$V_{CE} = V_{GE}, I_C = 1mA$
g_{fe}	Forward transconductance	35	—	70	S(t)	$V_{CE} = 25V, I_C = 100A$
I_{CES}	Collector-to-emitter leakage current	—	—	3	mA	$V_{GE} = 0V, V_{CE} = 1200V$
		—	—	30		$V_{GE} = 0V, V_{CE} = 1200V, T_J = 150^\circ\text{C}$
I_{GES}	Gate-to-emitter leakage current	—	—	± 3	μA	$V_{GE} = \pm 20V$

Dynamic Characteristics - $T_J = 125^\circ\text{C}$, unless otherwise stated

Parameter	Description	Min	Typ	Max	Units	Test Conditions
E_{on}	Turn-on switching energy	—	0.19	—	mJ/A	$R_G = 6.8\Omega, V_{CC} = 600V$
E_{off} (1)	Turn-off switching energy	—	0.36	—		$I_C = 100A, L_S = 100nH$
E_{ts} (1)	Total switching energy	—	—	0.60		$V_{GE} = \pm 15V$
$t_{d(on)}$	Turn-on delay time	—	200	250	ns	$R_G = 6.8\Omega, V_{CC} = 600V$
t_r	Rise time	—	200	250		$I_C = 100A$
$t_{d(off)}$	Turn-off delay time	—	125	200		$V_{GE} = \pm 15V$
t_f	Fall time	—	650	—		Resistive load, $T_J = 25^\circ\text{C}$
I_{rr}	Diode peak recovery current	—	50	—		A
t_{rr}	Diode recovery time	—	215	—	ns	$I_C = 100A$
Q_{rr}	Diode recovery charge	—	8	—	μC	$V_{GE} = \pm 15V$
Q_{ge}	Gate-to-emitter charge (turn-on)	65	—	260	nC	$V_{CC} = 600V$
Q_{gc}	Gate-to-collector charge (turn-on)	240	—	500		$I_C = 100A$
Q_g	Total gate charge (turn-on)	750	—	1350		$V_{GE} = 15V$
C_{ies}	Input capacitance	15500	—	16500	pF	$V_{GE} = 0V$
C_{oes}	Output capacitance	950	—	1650		$V_{CC} = 30V$
C_{res}	Reverse transfer capacitance	950	—	1650		$f = 1MHz$
t_{sc}	Short circuit withstand time	10	—	—	μs	$V_{CC} = 720V, V_{GE} = \pm 15V$ Min. $R_G = 6.8\Omega, V_{CEP} = 1000V$

(1) Includes tail losses

Thermal and Mechanical Characteristics

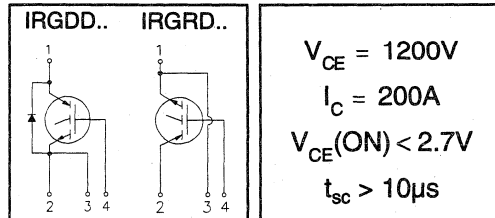
Parameter	Description	Typ	Max	Units
R_{thJC} (IGBT)	Thermal resistance, junction to case, each IGBT	—	0.188	$^\circ\text{C/W}$
R_{thJC} (Diode)	Thermal resistance, junction to case, each diode	—	0.209	
R_{thCS} (Module)	Thermal resistance, case to sink	0.041	0.100	
Wt	Weight of module	150	—	g

Refer to Section D - page D-17 for Package Outline11 -INT-A-PAK, New -Half Bridge

"SINGLE SWITCH" IGBT DOUBLE INT-A-PAK

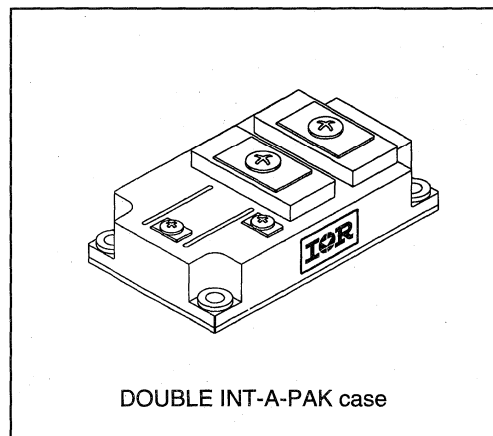
Low conduction loss IGBT

- Rugged Design
- Simple gate-drive
- Switching-Loss Rating includes all "tail" losses
- Short circuit rated



Description

IR's advanced IGBT technology is the key to this line of DOUBLE INT-A-PAK Power Modules. The efficient geometry and unique processing of the IGBT allow higher current densities than comparable bipolar power module transistors, while at the same time requiring the simpler gate-drive of the familiar power MOSFET. This superior technology has now been coupled to state of the art assembly techniques to produce a higher current module that is highly suited to power applications such as motor drives, uninterruptible power supplies, welding and power factor correction.


 Motor
Control
Fresh
Modules

Absolute Maximum Ratings

Parameter	Description	Value	Units
V_{CES}	Continuous collector to emitter voltage	1200	V
$I_C @ T_C = 25^\circ\text{C}$	Maximum Continuous collector current	420	A
$I_C @ T_C = 85^\circ\text{C}$	Maximum Continuous collector current	240	
$I_C @ T_C = 100^\circ\text{C}$	Maximum Continuous collector current	180	
I_{LM}	Peak switching current	400	
I_{FM}	Peak diode forward current (1)	400	
V_{GE}	Gate to emitter voltage	± 20	V
V_{ISOL}	RMS isolation voltage, any terminal to case, $t = 1 \text{ min}$	2500	
$P_D @ T_C = 25^\circ\text{C}$	Power dissipation	1800	W
T_J	Operating junction temperature range	-40 to 150	$^\circ\text{C}$
T_{STG}	Storage temperature range	-40 to 125	

(1) Duration limited by max junction temperature.

IRGDDN200M12

IRGRDN200M12



Electrical Characteristics - $T_J = 25^\circ\text{C}$, unless otherwise stated

Parameter	Description	Min	Typ	Max	Units	Test Conditions
BV_{CES}	Collector-to-emitter breakdown voltage	1200	—	—	V	$V_{GE} = 0V, I_C = 6mA$
$V_{CE(ON)}$	Collector-to-emitter voltage	—	2.3	2.7		$V_{GE} = 15V, I_C = 200A$
		—	1.8	—		$V_{GE} = 15V, I_C = 100A, T_J = 150^\circ\text{C}$
V_{FM}	Diode forward voltage - maximum	—	3.2	3.4		$I_F = 200A, V_{GE} = 0V$
		—	2.6	—		$I_F = 200A, V_{GE} = 0V, T_J = 150^\circ\text{C}$
V_{GEth}	Gate threshold voltage	3.0	—	5.5	$I_C = 3mA$	
ΔV_{GEth}	Threshold voltage temp. coefficient	—	-11	—	mV/°C	$V_{CE} = V_{GE}, I_C = 3mA$
g_{fe}	Forward transconductance	105	—	210	S(±)	$V_{CE} = 25V, I_C = 200A$
I_{CES}	Collector-to-emitter leakage current	—	—	6	mA	$V_{GE} = 0V, V_{CE} = 1200V$
		—	—	60		$V_{GE} = -0V, V_{CE} = 1200V, T_J = 150^\circ\text{C}$
I_{GES}	Gate-to-emitter leakage current	—	—	±6	µA	$V_{GE} = \pm 20V$

Dynamic Characteristics - $T_J = 125^\circ\text{C}$

Parameter	Description	Min	Typ	Max	Units	Test Conditions
E_{on}	Turn-on switching energy	—	0.19	—	mJ/A	$R_G = 15\Omega, V_{CC} = 600V$
E_{off} (1)	Turn-off switching energy	—	0.34	—		$I_C = 200A, L_S = 100nH$
E_{ts} (1)	Total switching energy	—	—	0.6		$V_{GE} = \pm 15V$
$t_{d(on)}$	Turn-on delay time	—	400	550	ns	$R_G = 15\Omega, V_{CC} = 600V$
t_r	Rise time	—	600	800		$I_C = 200A$
$t_{d(off)}$	Turn-off delay time	—	550	650		$V_{GE} = \pm 15V$
t_f	Fall time	—	650	—		Resistive Load, $T_J = 25^\circ\text{C}$
I_{rr}	Diode peak recovery current	—	83	—	A	$R_G = 15\Omega, V_{CC} = 600V$
t_{rr}	Diode recovery time	—	240	—	ns	$I_C = 200A$
Q_{rr}	Diode recovery charge	—	13	—	µC	$V_{GE} = \pm 15V$
Q_{ge}	Gate-to-emitter charge (turn-on)	225	—	495	nC	$V_{CC} = 600V$
Q_{gc}	Gate-to-collector charge (turn-on)	315	—	975		$I_C = 200A$
Q_g	Total gate charge (turn-on)	190	—	2250		$V_{GE} = 15V$
C_{ies}	Input capacitance	31500	—	33000	pF	$V_{GE} = 0V$
C_{oes}	Output capacitance	1950	—	3300		$V_{CC} = 30V$
C_{res}	Reverse transfer capacitance	1950	—	3000		$f = 1MHz$
t_{sc}	Short circuit withstand time	10	—	—	µs	$V_{CC} = 720V, V_{GE} = \pm 15V$ Min. $R_G = 15\Omega, V_{CEP} = 1000V$

(1) Includes tail losses

Thermal and Mechanical Characteristics

Parameter	Description	Typ	Max	Units
R_{thJC} (IGBT)	Thermal resistance, junction to case, each IGBT	—	0.069	°C/W
R_{thJC} (Diode)	Thermal resistance, junction to case, each diode	—	0.095	
R_{thCS} (Module)	Thermal resistance, case to sink	0.023	0.050	
Wt	Weight of module	242	—	g



IRGDDN200M12

IRGRDN200M12

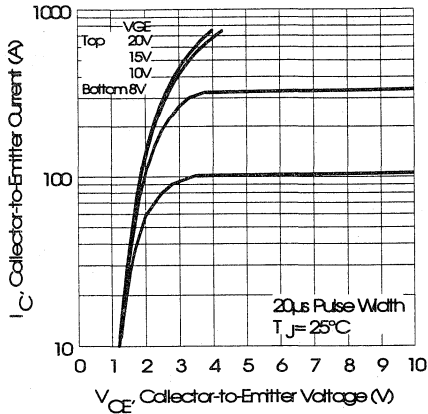


Fig. 1 - Typical Output Characteristics, $T_J = 25^\circ\text{C}$

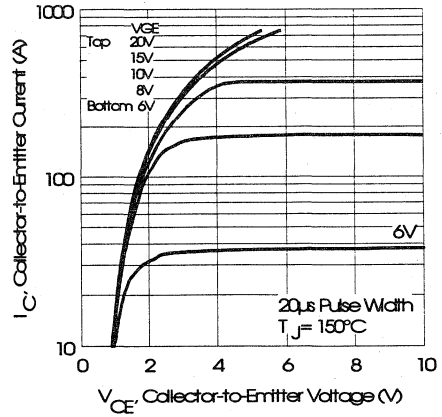


Fig. 2 - Typical Output Characteristics, $T_J = 150^\circ\text{C}$

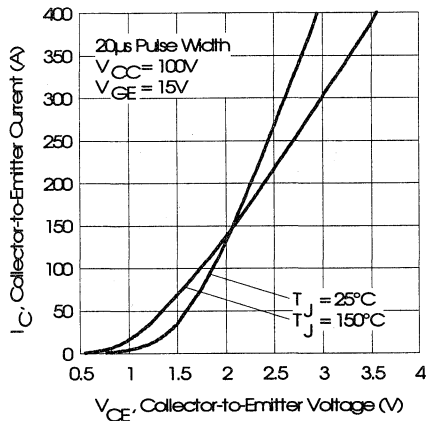


Fig. 3 - Typical Output Characteristics

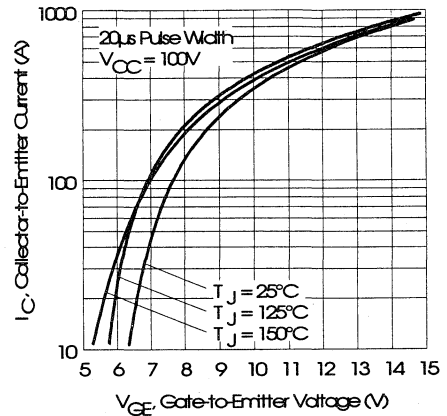


Fig. 4 - Typical Transfer Characteristics

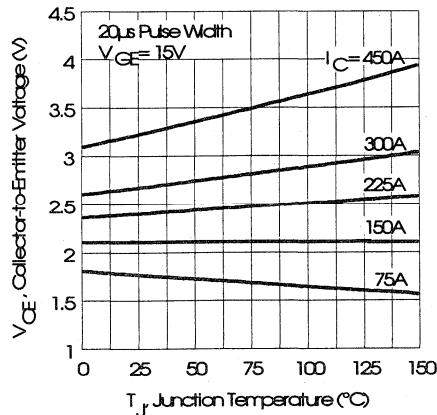


Fig. 5 - Collector-to-Emitter Saturation Typical Voltage vs. Junction Temperature

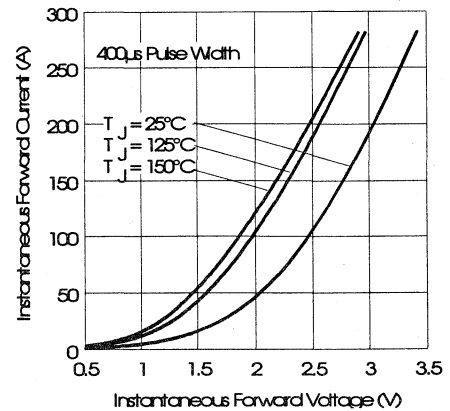


Fig. 6 - Forward Voltage Drop Characteristics



IRGDDN200M12

IRGRDN200M12

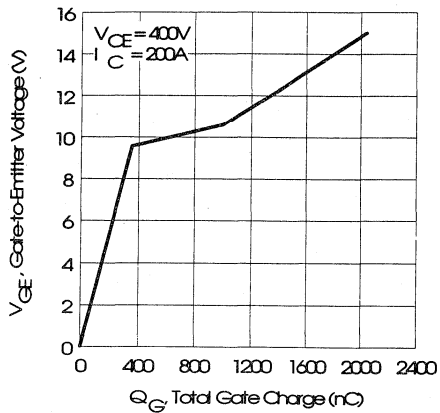


Fig. 7 - Typical Gate Charge vs. Gate-to-Emitter Voltage

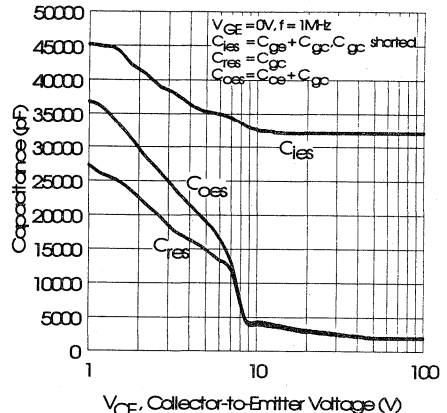


Fig. 8 - Typical Capacitance vs. Collector-to-Emitter Voltage

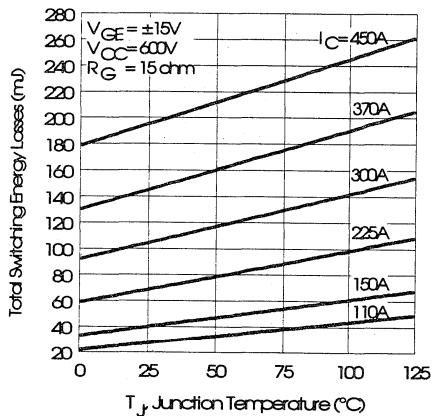


Fig. 9 - Typical Switching Losses vs. Junction Temperature

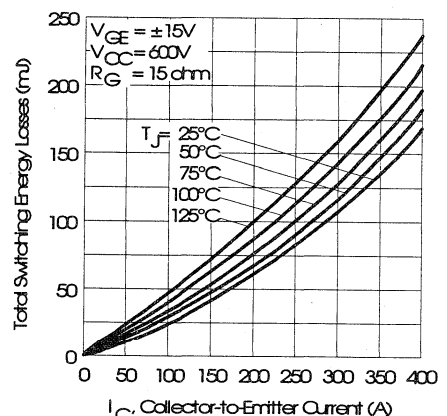


Fig. 10 - Typical Switching Losses vs. Collector-to-Emitter Current

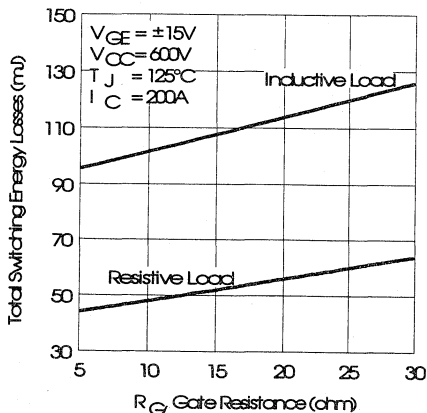


Fig. 11 - Typical Switching Losses vs. Gate Resistance

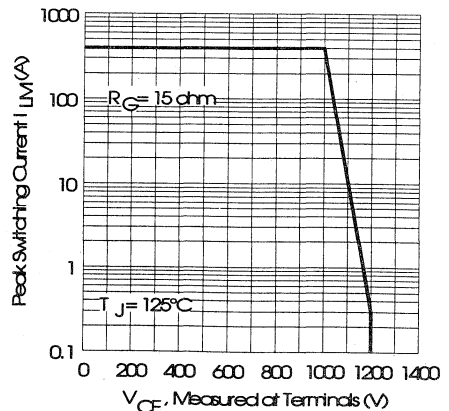


Fig. 12 - Reverse Bias Safe Operating Area



IRGDDN200M12

IRGRDN200M12

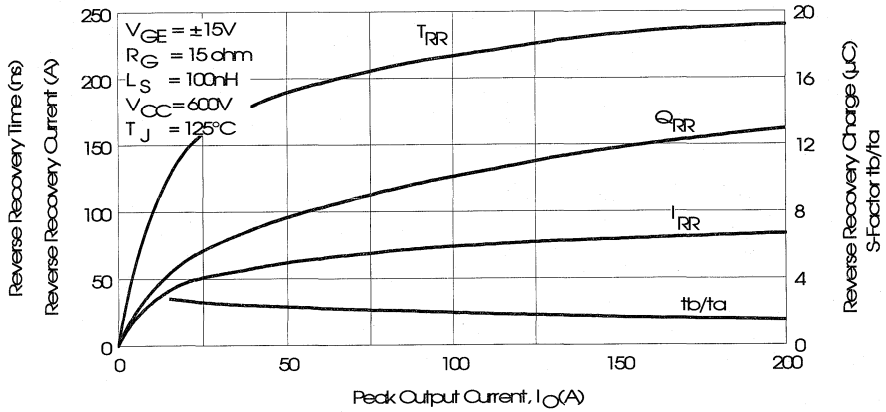


Fig. 13 - Typical Diode Recovery Characteristics as Function of Output Current I_O

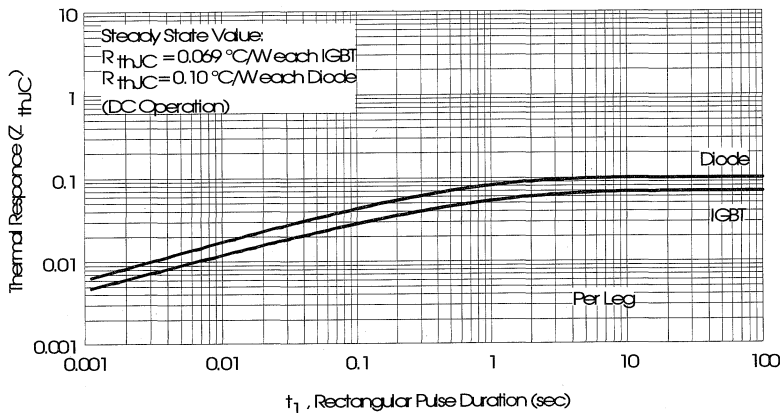


Fig. 14 - Maximum Effective Transient Thermal Impedance, Junction-to-Case

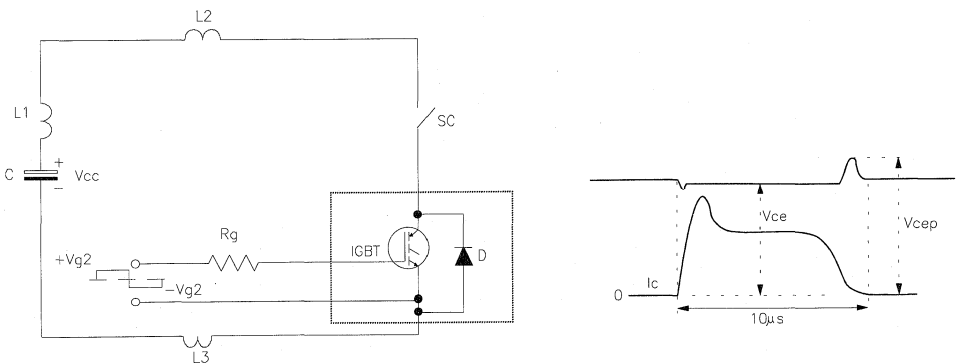


Fig. 15 - Test Circuit for Short Circuit

Motor Control Fast Modules

IRGDDN200M12

IRGRDN200M12

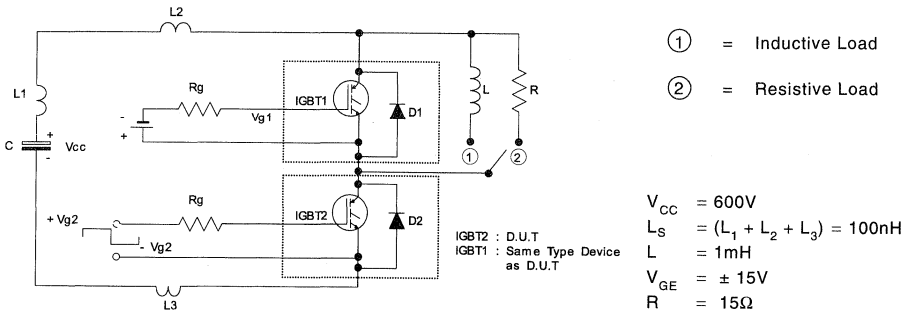


Fig. 16 - Test Circuit for Measurement of I_{LM} , E_{ON} , E_{OFF} , Q_{RR}

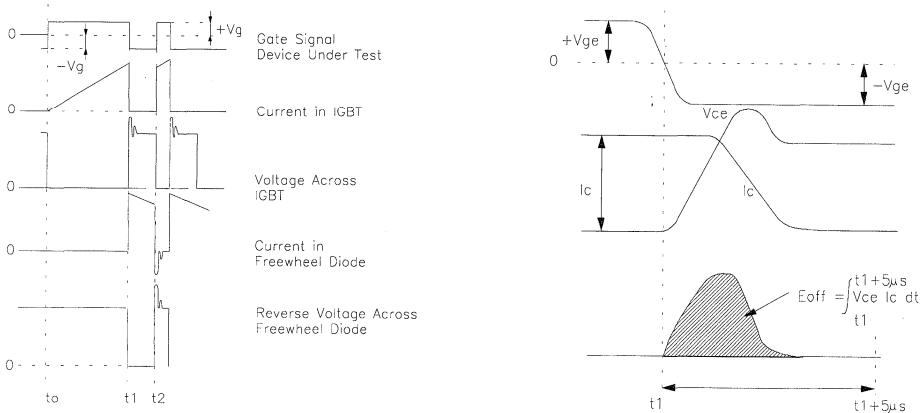


Fig. 17 - Test Waveforms for Circuit of Fig. 16

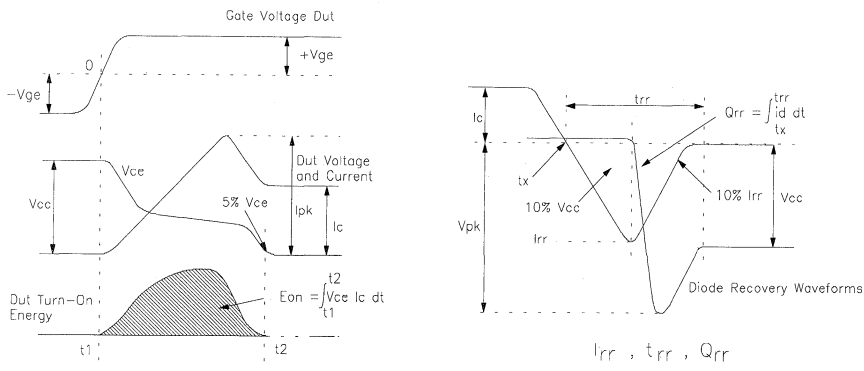


Fig. 18 - Test Waveforms for Circuit of Fig. 16, Defining E_{ON} , E_{REC} , Q_{RR}

Refer to Section D for the following:
 Appendix I: Section D - page D-11

Fig. 19 - Test Waveforms for Circuit of Fig. 17, Defining E_{ON} , E_{REC} , Q_{RR}

Fig. 20 - Waveforms for Switching Time

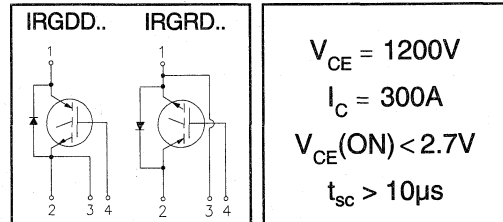
Package Outline 13 - Double INT-A-PAK Single Switch

Section D - page D-18

"SINGLE SWITCH" IGBT DOUBLE INT-A-PAK

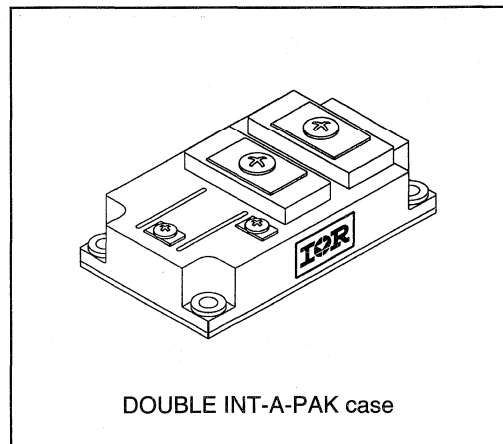
Low conduction loss IGBT

- Rugged Design
- Simple gate-drive
- Switching-Loss Rating includes all "tail" losses
- Short circuit rated



Description

IR's advanced IGBT technology is the key to this line of DOUBLE INT-A-PAK Power Modules. The efficient geometry and unique processing of the IGBT allow higher current densities than comparable bipolar power module transistors, while at the same time requiring the simpler gate-drive of the familiar power MOSFET. This superior technology has now been coupled to state of the art assembly techniques to produce a higher current module that is highly suited to power applications such as motor drives, uninterruptible power supplies, welding and power factor correction.



Absolute Maximum Ratings

Parameter	Description	Value	Units
V_{CES}	Continuous collector to emitter voltage	1200	V
$I_C @ T_C = 25^\circ C$	Maximum Continuous collector current	560	A
$I_C @ T_C = 85^\circ C$	Maximum Continuous collector current	320	
$I_C @ T_C = 100^\circ C$	Maximum Continuous collector current	240	
I_{LM}	Peak switching current	600	
I_{FM}	Peak diode forward current (1)	600	V
V_{GE}	Gate to emitter voltage	± 20	
V_{ISOL}	RMS isolation voltage, any terminal to case, $t = 1$ min	2500	W
$P_D @ T_C = 25^\circ C$	Power dissipation	2400	
T_J	Operating junction temperature range	-40 to 150	$^\circ C$
T_{STG}	Storage temperature range	-40 to 125	

(1) Duration limited by max junction temperature.

IRGDDN300M12

IRGRDN300M12



Electrical Characteristics - $T_J = 25^\circ\text{C}$, unless otherwise stated

Parameter	Description	Min	Typ	Max	Units	Test Conditions
BV_{CES}	Collector-to-emitter breakdown voltage	1200	—	—	V	$V_{GE} = 0V, I_C = 8mA$
$V_{CE(ON)}$	Collector-to-emitter voltage	—	2.3	2.7		$V_{GE} = 15V, I_C = 300A$
		—	1.8	—		$V_{GE} = 15V, I_C = 150A, T_J = 150^\circ\text{C}$
V_{FM}	Diode forward voltage - maximum	—	3.2	3.4		$I_F = 300A, V_{GE} = 0V$
		—	2.6	—	$I_F = 300A, V_{GE} = 0V, T_J = 150^\circ\text{C}$	
V_{GEth}	Gate threshold voltage	3.0	—	5.5	mV/°C	$I_C = 4mA$
ΔV_{GEth}	Threshold voltage temp. coefficient	—	-11	—		$V_{CE} = V_{GE}, I_C = 4mA$
g_{fe}	Forward transconductance	140	—	280	S(Ω)	$V_{CE} = 25V, I_C = 300A$
I_{CES}	Collector-to-emitter leakage current	—	—	8	mA	$V_{GE} = 0V, V_{CE} = 1200V$
		—	—	80		$V_{GE} = 0V, V_{CE} = 1200V, T_J = 150^\circ\text{C}$
I_{GES}	Gate-to-emitter leakage current	—	—	±8	μA	$V_{GE} = \pm 20V$

Dynamic Characteristics - $T_J = 125^\circ\text{C}$

Parameter	Description	Min	Typ	Max	Units	Test Conditions
E_{on}	Turn-on switching energy	—	0.19	—	mJ/A	$R_G = 15\Omega, V_{CC} = 600V$
$E_{off} (1)$	Turn-off switching energy	—	0.34	—		$I_C = 300A, L_S = 100nH$
$E_{ts} (1)$	Total switching energy	—	—	0.60		$V_{GE} = \pm 15V$
$t_{d(on)}$	Turn-on delay time	—	400	550	ns	$R_G = 15\Omega, V_{CC} = 600V$
t_r	Rise time	—	600	800		$I_C = 300A$
$t_{d(off)}$	Turn-off delay time	—	550	650		$V_{GE} = \pm 15V$
t_f	Fall time	—	650	—		Resistive Load, $T_J = 25^\circ\text{C}$
I_{rr}	Diode peak recovery current	—	111	—	A	$R_G = 15\Omega, V_{CC} = 600V$
t_{rr}	Diode recovery time	—	240	—	ns	$I_C = 300A$
Q_{rr}	Diode recovery charge	—	17	—	μC	$V_{GE} = \pm 15V$
Q_{ge}	Gate-to-emitter charge (turn-on)	300	—	660	nC	$V_{CC} = 600V$
Q_{gc}	Gate-to-collector charge (turn-on)	420	—	1300		$I_C = 300A$
Q_g	Total gate charge (turn-on)	250	—	3000		$V_{GE} = 15V$
C_{ies}	Input capacitance	42000	—	44000	pF	$V_{GE} = 0V$
C_{oes}	Output capacitance	2600	—	4400		$V_{CC} = 30V$
C_{res}	Reverse transfer capacitance	2600	—	4000		$f = 1MHz$
t_{sc}	Short circuit withstand time	10	—	—	μs	$V_{CC} = 720V, V_{GE} = \pm 15V$ Min. $R_G = 15\Omega, V_{CEP} = 1000V$

(1) Includes tail losses

Thermal and Mechanical Characteristics

Parameter	Description	Typ	Max	Units
R_{thJC} (IGBT)	Thermal resistance, junction to case, each IGBT	—	0.052	°C/W
R_{thJC} (Diode)	Thermal resistance, junction to case, each diode	—	0.070	
R_{thCS} (Module)	Thermal resistance, case to sink	0.023	0.050	
Wt	Weight of module	242	—	g



IRGDDN300M12

IRGRDN300M12

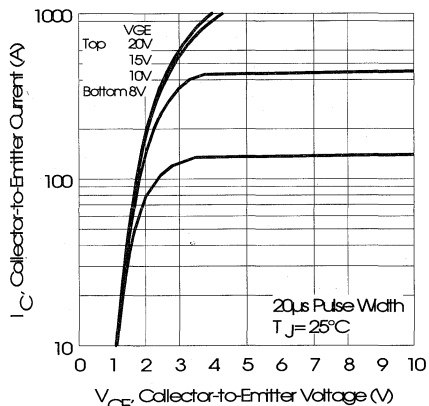


Fig. 1 - Typical Output Characteristics, $T_J = 25^\circ\text{C}$

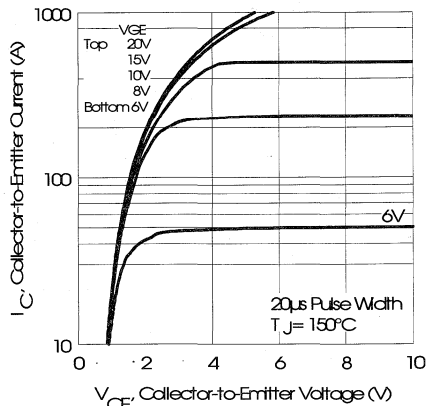


Fig. 2 - Typical Output Characteristics, $T_J = 150^\circ\text{C}$

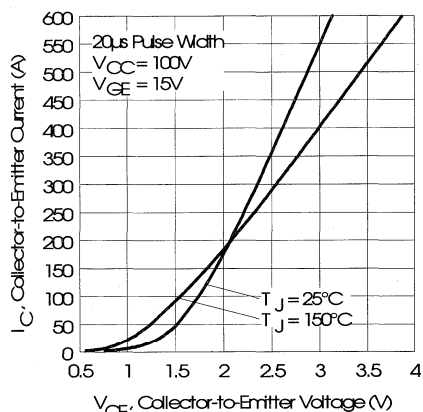


Fig. 3 - Typical Output Characteristics

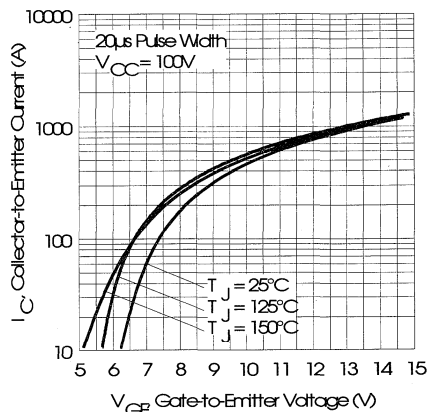


Fig. 4 - Typical Transfer Characteristics

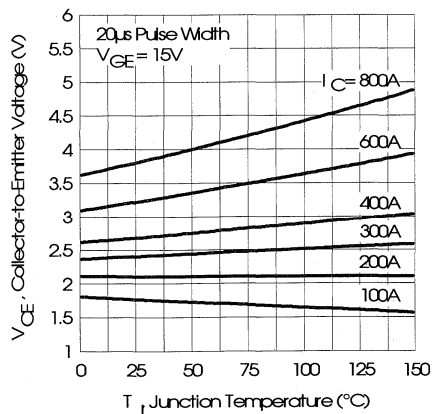


Fig. 5 - Collector-to-Emitter Saturation Typical Voltage vs. Junction Temperature

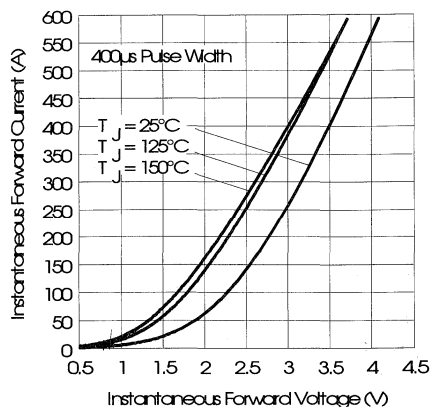


Fig. 6 - Forward Voltage Drop Characteristics



IRGDDN300M12

IRGRDN300M12

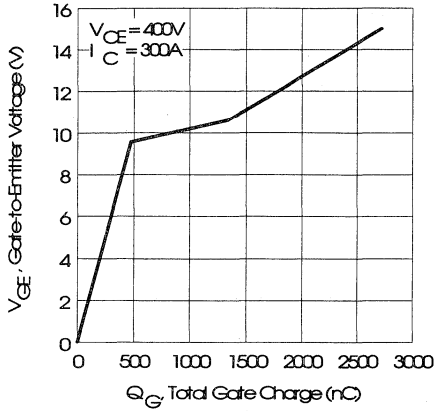


Fig. 7 - Typical Gate Charge vs. Gate-to-Emitter Voltage

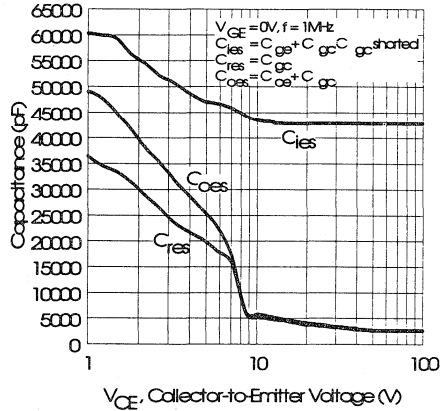


Fig. 8 - Typical Capacitance vs. Collector-to-Emitter Voltage

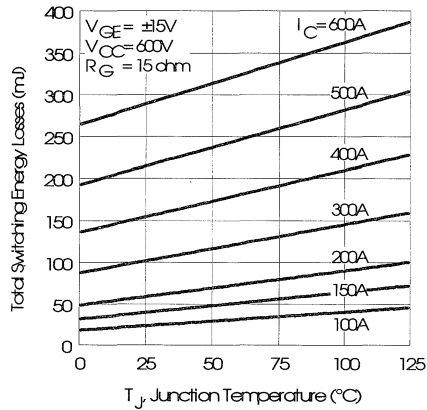


Fig. 9 - Typical Switching Losses vs. Junction Temperature

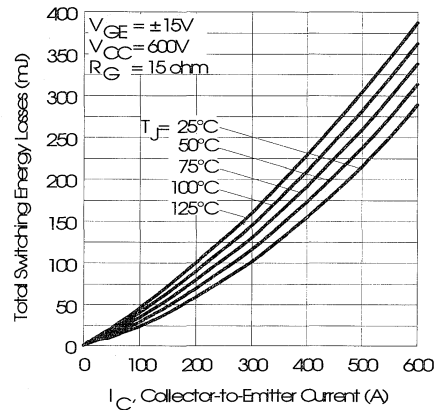


Fig. 10 - Typical Switching Losses vs. Collector-to-Emitter Current

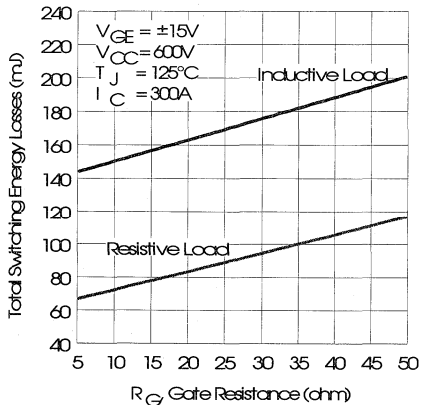


Fig. 11 - Typical Switching Losses vs. Gate Resistance

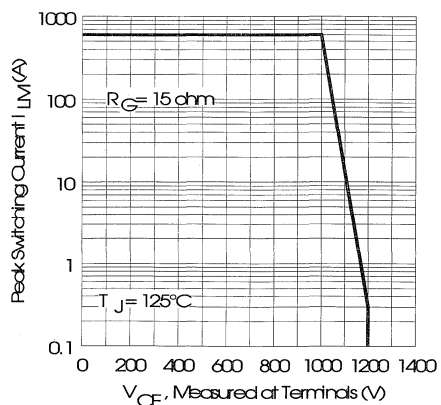


Fig. 12 - Reverse Bias Safe Operating Area



IRGDDN300M12

IRGRDN300M12

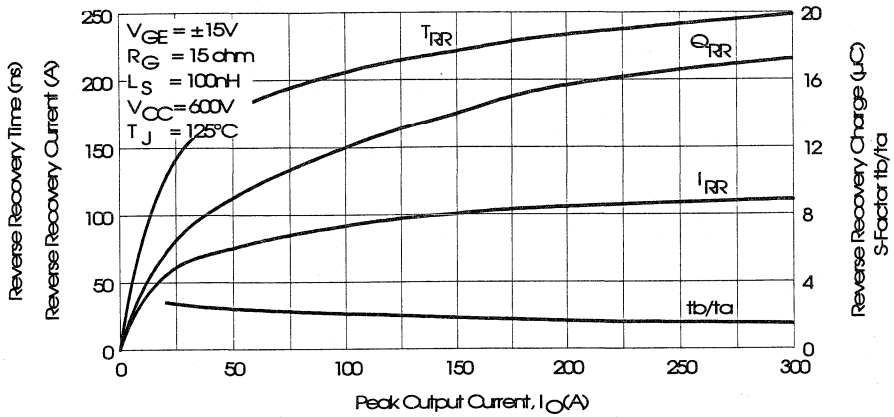


Fig. 13 - Typical Diode Recovery Characteristics as Function of Output Current I_o

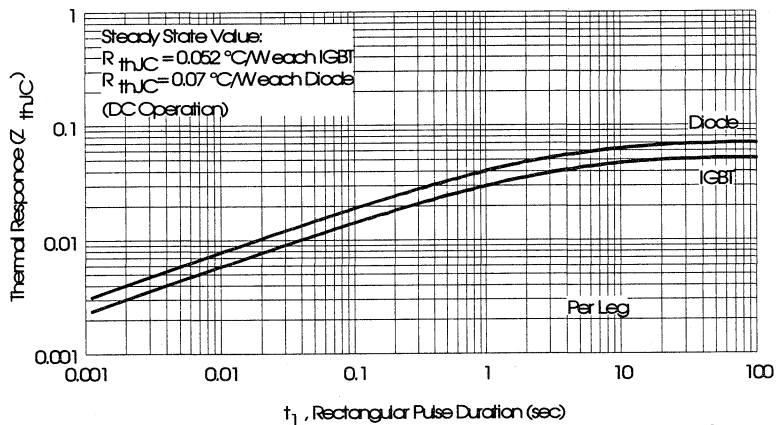


Fig. 14 - Maximum Effective Transient Thermal Impedance, Junction-to-Case

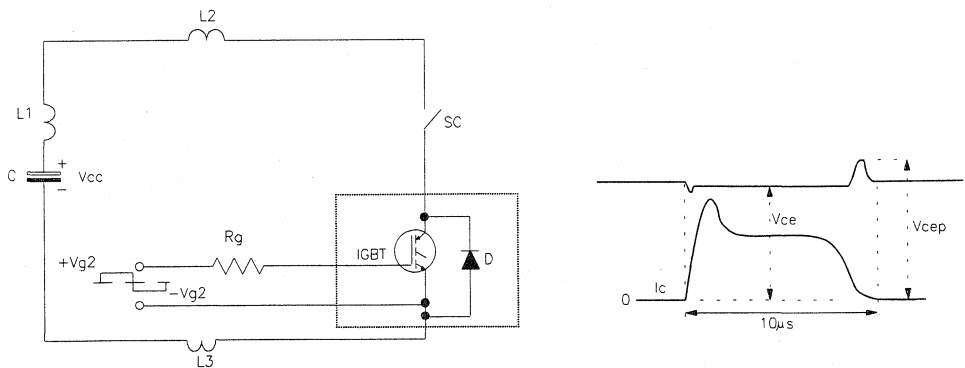


Fig. 15 - Test Circuit for Short Circuit



IRGDDN300M12

IRGRDN300M12

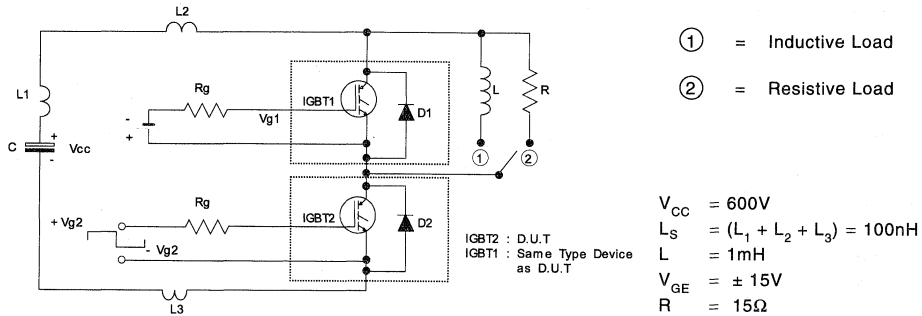


Fig. 16 - Test Circuit for Measurement of I_{LM} , E_{ON} , E_{OFF} , Q_{RR}

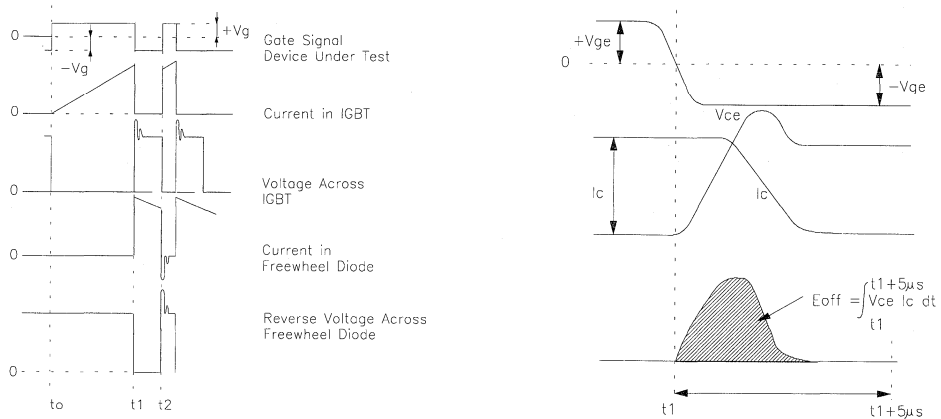


Fig. 17 - Test Waveforms for Circuit of Fig. 16

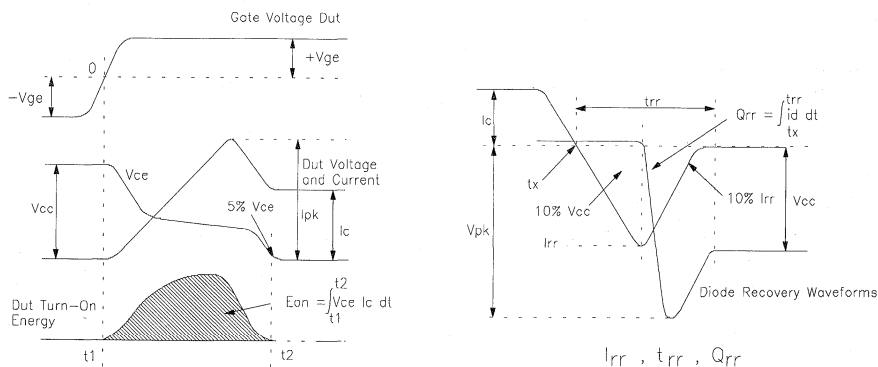


Fig. 18 - Test Waveforms for Circuit of Fig. 16, Defining E_{ON} , E_{REC} , Q_{RR}

Refer to Section D for the following:
 Appendix I: Section D - page D-11

Fig. 19 - Test Waveforms for Circuit of Fig. 17, Defining E_{ON} , E_{REC} , Q_{RR}

Fig. 20 - Waveforms for Switching Time

Package Outline 13 - Double INT-A-PAK Single Switch

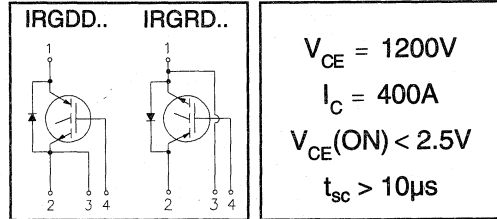
Section D - page D-18

IRGDDN400M12 IRGRDN400M12

"SINGLE SWITCH" IGBT DOUBLE INT-A-PAK

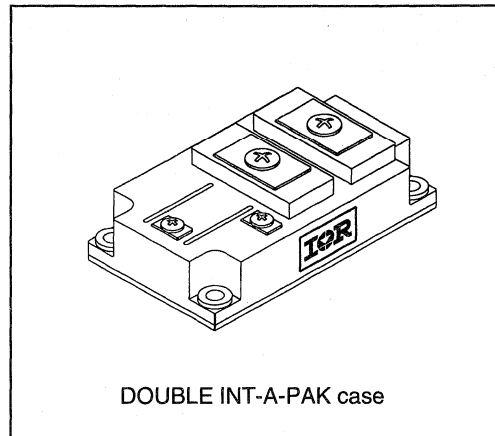
Low conduction loss IGBT

- Rugged Design
- Simple gate-drive
- Switching-Loss Rating includes all "tail" losses
- Short circuit rated



Description

IR's advanced IGBT technology is the key to this line of DOUBLE INT-A-PAK Power Modules. The efficient geometry and unique processing of the IGBT allow higher current densities than comparable bipolar power module transistors, while at the same time requiring the simpler gate-drive of the familiar power MOSFET. This superior technology has now been coupled to state of the art assembly techniques to produce a higher current module that is highly suited to power applications such as motor drives, uninterruptible power supplies, welding and power factor correction.



Motor
Control
Fast
Modules

Absolute Maximum Ratings

Parameter	Description	Value	Units
V_{CES}	Continuous collector to emitter voltage	1200	V
$I_C @ T_C = 25^\circ C$	Maximum continuous collector current	400	A
R_{thJC}	Thermal resistance junction to case	0.045	$^\circ C/W$
$E_{ts} @ T_J = 125^\circ C$	Total switching energy, $R_G = 4.7\Omega$, $V_{CC} = 600V$, $I_C = 400A$	0.55	mJ/A
I_{LM}	Peak switching current	800	A
I_{FM}	Peak diode forward current (1)	800	
V_{GE}	Gate to emitter voltage	± 20	V
V_{ISOL}	RMS isolation voltage, any terminal to case, $t = 1 \text{ min}$	2500	
$P_D @ T_C = 25^\circ C$	Power dissipation	2770	W
T_J	Operating junction temperature range	-40 to 150	$^\circ C$
T_{STG}	Storage temperature range	-40 to 125	

(1) Duration limited by max junction temperature.

Target Data

IRGDDN400M12

IRGRDN400M12



Electrical Characteristics - $T_J = 25^\circ\text{C}$, unless otherwise stated

Parameter	Description	Min	Typ	Max	Units	Test Conditions
BV_{CES}	Collector-to-emitter breakdown voltage	1200	—	—	V	$V_{GE} = 0V, I_C = 12mA$
$V_{CE(ON)}$	Collector-to-emitter voltage	—	2.3	2.7		$V_{GE} = 15V, I_C = 400A$
		—	1.8	—		$V_{GE} = 15V, I_C = 300A, T_J = 150^\circ\text{C}$
V_{FM}	Diode forward voltage - maximum	—	3.2	3.4		$I_F = 400A, V_{GE} = 0V$
		—	2.6	—		$I_F = 400A, V_{GE} = 0V, T_J = 150^\circ\text{C}$
V_{GEth}	Gate threshold voltage	3.0	—	5.5		$I_C = 4mA$
ΔV_{GEth}	Threshold voltage temperature coefficient	—	-11	—	mV/ $^\circ\text{C}$	$V_{CE} = V_{GE}, I_C = 4mA$
g_{fe}	Forward transconductance	140	—	280	S(τ)	$V_{CE} = 25V, I_C = 400A$
I_{CES}	Collector-to-emitter leakage current	—	—	12	mA	$V_{GE} = 0V, V_{CE} = 1200V$
		—	—	120		$V_{GE} = 0V, V_{CE} = 1200V, T_J = 150^\circ\text{C}$
I_{GES}	Gate-to-emitter leakage current	—	—	± 12	μA	$V_{GE} = \pm 20V$

Dynamic Characteristics - $T_J = 125^\circ\text{C}$

Parameter	Description	Min	Typ	Max	Units	Test Conditions
E_{on}	Turn-on switching energy	—	0.19	—	mJ/A	$R_G = 15\Omega, V_{CC} = 600V$
$E_{off} (1)$	Turn-off switching energy	—	0.34	—		$I_C = 400A, L_S = 100nH$
$E_{is} (1)$	Total switching energy	—	—	0.60		$V_{GE} = \pm 15V$
$t_{d(on)}$	Turn-on delay time	—	400	550	ns	$R_G = 15\Omega, V_{CC} = 600V$
t_r	Rise time	—	600	800		$I_C = 400A$
$t_{d(off)}$	Turn-off delay time	—	550	650		$V_{GE} = \pm 15V$
t_f	Fall time	—	650	—		Resistive Load, $T_J = 25^\circ\text{C}$
I_{rr}	Diode peak recovery current	—	130	—		$R_G = 15\Omega, V_{CC} = 600V$
t_{rr}	Diode recovery time	—	220	—	ns	$I_C = 400A$
Q_{rr}	Diode recovery charge	—	16.5	—	μC	$V_{GE} = \pm 15V$
Q_{ge}	Gate-to-emitter charge (turn-on)	440	—	1000	nC	$V_{CC} = 600V$
Q_{gc}	Gate-to-collector charge (turn-on)	600	—	1900	nC	$I_C = 400A$
Q_g	Total gate charge (turn-on)	3700	—	4500	nC	$V_{GE} = 15V$
C_{ies}	Input capacitance	63000	—	66000	pF	$V_{GE} = 0V$
C_{oes}	Output capacitance	3900	—	6600		$V_{CC} = 30V$
C_{res}	Reverse transfer capacitance	3900	—	6600		$f = 1MHz$
t_{sc}	Short circuit withstand time	10	—	—	μS	$V_{CC} = 720V, V_{GE} = \pm 15V$ Min. $R_G = 15\Omega, V_{CEP} = 1000V$

(1) Includes tail losses

Thermal and Mechanical Characteristics

Parameter	Description	Typ	Max	Units
R_{thJC} (IGBT)	Thermal resistance, junction to case, each IGBT	—	0.047	$^\circ\text{C/W}$
R_{thJC} (Diode)	Thermal resistance, junction to case, each diode	—	0.052	
R_{thCS} (Module)	Thermal resistance, case to sink	0.023	0.050	
Wt	Weight of module	242	—	g

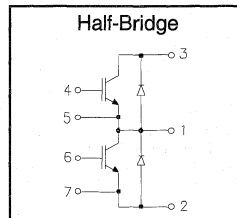
Refer to Section D - page D-18 for Package Outline 13 - Double INT-A-PAK Single Switch

IRGTDN100M12

"HALF-BRIDGE" IGBT DOUBLE INT-A-PAK

Low conduction loss IGBT

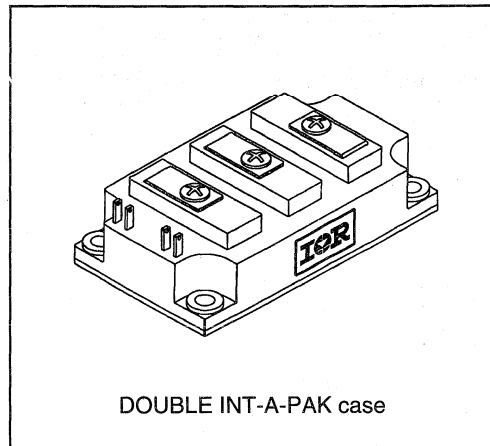
- Rugged Design
- Simple gate-drive
- Switching-Loss Rating includes all "tail" losses
- Short circuit rated



$V_{CE} = 1200V$
$I_C = 100A$
$V_{CE(ON)} < 2.5V$
$t_{sc} > 10\mu s$

Description

IR's advanced IGBT technology is the key to this line of DOUBLE INT-A-PAK Power Modules. The efficient geometry and unique processing of the IGBT allow higher current densities than comparable bipolar power module transistors, while at the same time requiring the simpler gate-drive of the familiar power MOSFET. This superior technology has now been coupled to state of the art assembly techniques to produce a higher current module that is highly suited to power applications such as motor drives, uninterruptible power supplies, welding and power factor correction.



Absolute Maximum Ratings

Parameter	Description	Value	Units
V_{CES}	Continuous collector to emitter voltage	1200	V
$I_C @ T_C = 25^\circ C$	Maximum Continuous collector current	200	A
$I_C @ T_C = 85^\circ C$	Maximum Continuous collector current	120	
$I_C @ T_C = 100^\circ C$	Maximum Continuous collector current	90	
I_{LM}	Peak IGBT switching current	200	
I_{FM}	Peak diode forward switching current (1)	200	
V_{GE}	Gate to emitter voltage	± 20	V
V_{ISOL}	RMS isolation voltage, any terminal to case, $t = 1$ min	2500	
$P_D @ T_C = 25^\circ C$	Power dissipation	900	W
T_J	Operating junction temperature range	-40 to 150	$^\circ C$
T_{STG}	Storage temperature range	-40 to 125	

(1) Duration limited by max junction temperature.

Electrical Characteristics - $T_J = 25^\circ\text{C}$, unless otherwise stated

Parameter	Description	Min	Typ	Max	Units	Test Conditions
BV_{CES}	Collector-to-emitter breakdown voltage	1200	—	—	V	$V_{GE} = 0V, I_C = 3mA$
$V_{CE(ON)}$	Collector-to-emitter voltage	—	2.3	2.5		$V_{GE} = 15V, I_C = 100A$
		—	1.8	—		$V_{GE} = 15V, I_C = 50A, T_J = 150^\circ\text{C}$
V_{FM}	Diode forward voltage - maximum	—	3.2	3.4		$I_F = 100A, V_{GE} = 0V$
		—	2.6	—		$I_F = 100A, V_{GE} = 0V, T_J = 150^\circ\text{C}$
V_{GEth}	Gate threshold voltage	3.0	—	5.5	$I_C = 1.5mA$	
ΔV_{GEth}	Threshold voltage temperature coefficient	—	-11	—	mV/ $^\circ\text{C}$	$V_{CE} = V_{GE}, I_C = 1.5mA$
g_{fe}	Forward transconductance	53	—	105	S(τ)	$V_{CE} = 25V, I_C = 100A$
I_{CES}	Collector-to-emitter leakage current	—	—	3	mA	$V_{GE} = 0V, V_{CE} = 1200V$
		—	—	30		$V_{GE} = 0V, V_{CE} = 1200V, T_J = 150^\circ\text{C}$
I_{GES}	Gate-to-emitter leakage current	—	—	± 3	μA	$V_{GE} = \pm 20V$

Dynamic Characteristics - $T_J = 125^\circ\text{C}$

Parameter	Description	Min	Typ	Max	Units	Test Conditions
E_{on}	Turn-on switching energy	—	0.14	—	mJ/A	$R_G = 10\Omega, V_{CC} = 600V$
E_{off} (1)	Turn-off switching energy	—	0.36	—		$I_C = 100A, L_S = 100nH$
E_{ts} (1)	Total switching energy	—	—	0.60		$V_{GE} = \pm 15V$
$t_{d(on)}$	Turn-on delay time	—	100	150	ns	$R_G = 10\Omega, V_{CC} = 600V$
t_r	Rise time	—	450	600		$I_C = 100A$
$t_{d(off)}$	Turn-off delay time	—	350	500		$V_{GE} = \pm 15V$
t_f	Fall time	—	1500	1800		Resistive Load, $T_J = 25^\circ\text{C}$
I_{rr}	Diode peak recovery current	—	70	—		A
t_{rr}	Diode recovery time	—	220	—	ns	$I_C = 100A$
Q_{rr}	Diode recovery charge	—	8.0	—	μC	$V_{GE} = \pm 15V$
Q_{ge}	Gate-to-emitter charge (turn-on)	115	—	250	nC	$V_{CC} = 600V$
Q_{gc}	Gate-to-collector charge (turn-on)	160	—	485		$I_C = 100A$
Q_g	Total gate charge (turn-on)	950	—	1120		$V_{GE} = 15V$
C_{ies}	Input capacitance	15700	—	16500	pF	$V_{GE} = 0V$
C_{oes}	Output capacitance	980	—	1650		$V_{CC} = 30V$
C_{res}	Reverse transfer capacitance	980	—	1500		$f = 1MHz$
t_{sc}	Short circuit withstand time	10	—	—	μs	$V_{CC} = 720V, V_{GE} = \pm 15V$ Min. $R_G = 10\Omega, V_{CEP} = 1000V$

(1) Includes tail losses

Thermal and Mechanical Characteristics

Parameter	Description	Typ	Max	Units
R_{thJC} (IGBT)	Thermal resistance, junction to case, each IGBT	—	0.138	$^\circ\text{C/W}$
R_{thJC} (Diode)	Thermal resistance, junction to case, each diode	—	0.190	
R_{thCS} (Module)	Thermal resistance, case to sink	0.032	0.075	
Wt	Weight of module	242	—	g

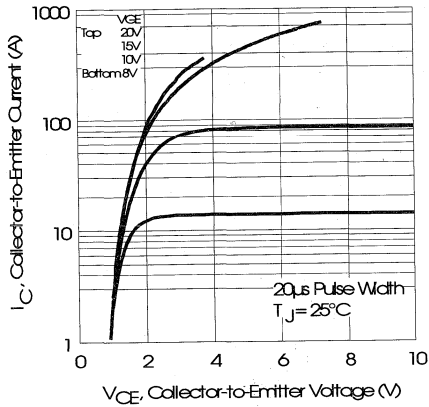


Fig. 1 - Typical Output Characteristics, $T_J = 25^\circ\text{C}$

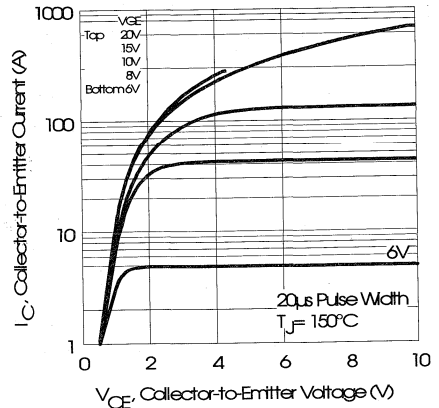


Fig. 2 - Typical Output Characteristics, $T_J = 150^\circ\text{C}$

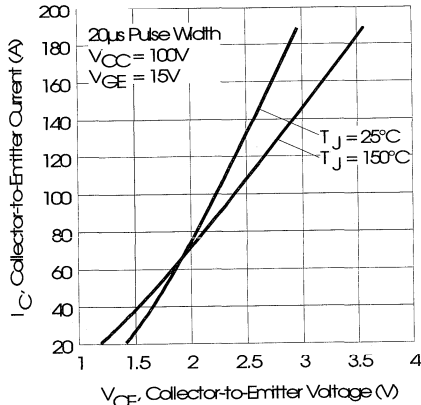


Fig. 3 - Typical Output Characteristics

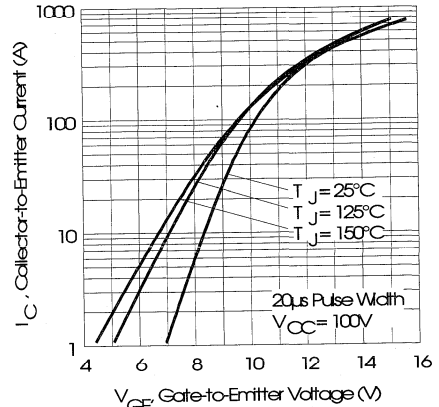


Fig. 4 - Typical Transfer Characteristics

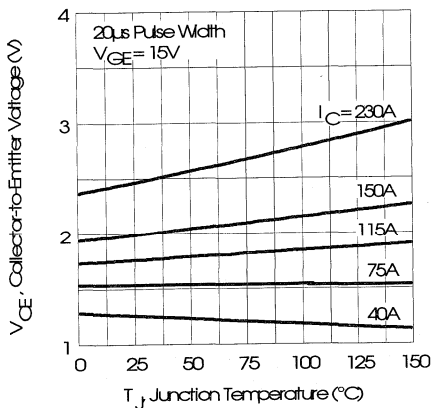


Fig. 5 - Collector-to-Emitter Saturation Typical Voltage vs. Junction Temperature

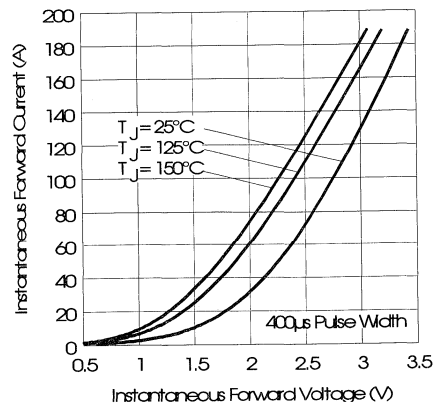


Fig. 6 - Forward Voltage Drop Characteristics

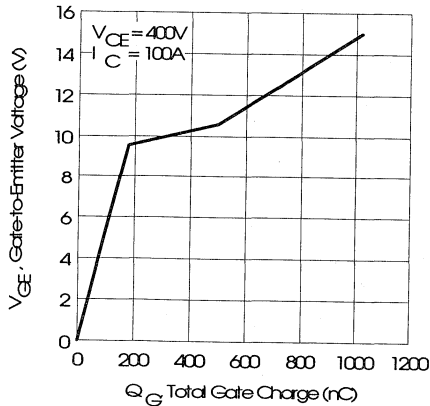


Fig. 7 - Typical Gate Charge vs. Gate-to-Emitter Voltage

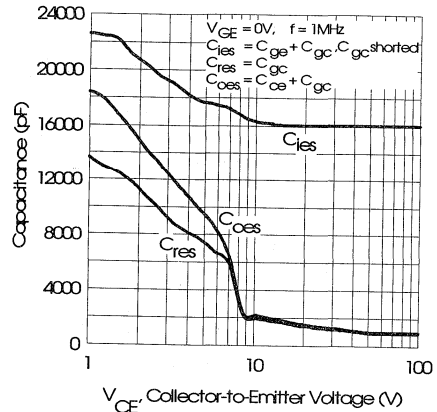


Fig. 8 - Typical Capacitance vs. Collector-to-Emitter Voltage

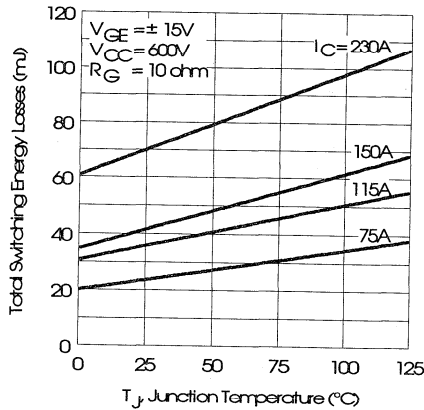


Fig. 9 - Typical Switching Losses vs. Junction Temperature

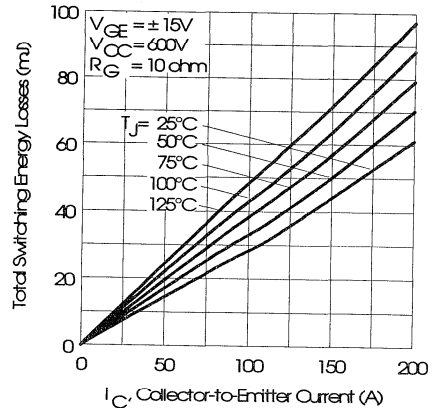


Fig. 10 - Typical Switching Losses vs. Collector-to-Emitter Current

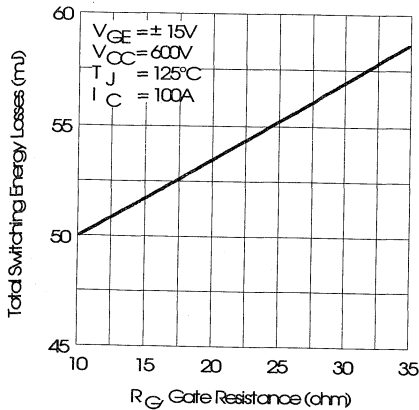


Fig. 11 - Typical Switching Losses vs. Gate Resistance

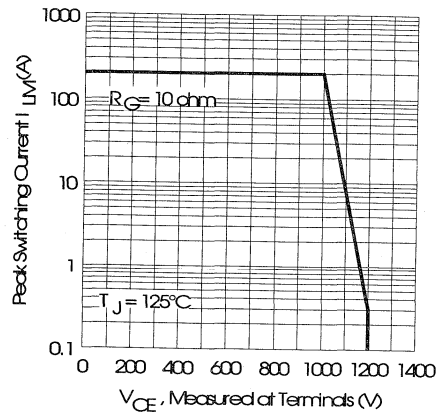


Fig. 12 - Reverse Bias Safe Operating Area

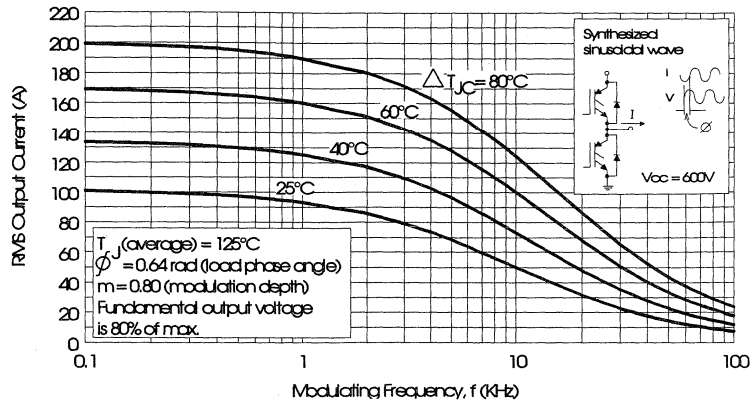


Fig. 13 - Typical RMS Output Current per phase vs. Frequency (Synthesized Sinusoidal Wave)

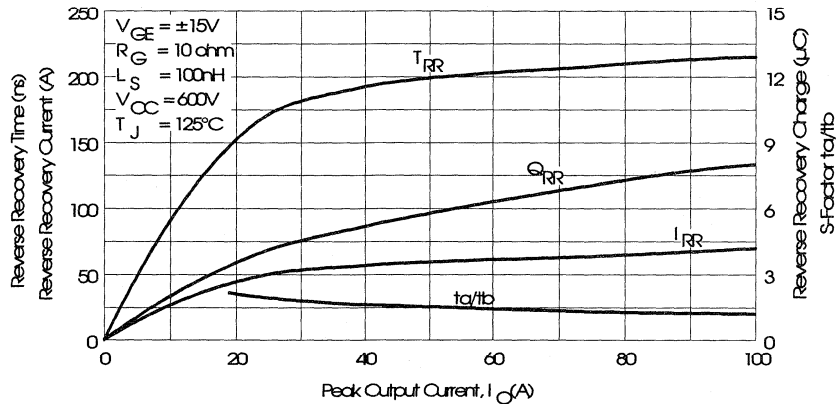


Fig. 14 - Typical Diode Recovery Characteristics as Function of Output Current I_o

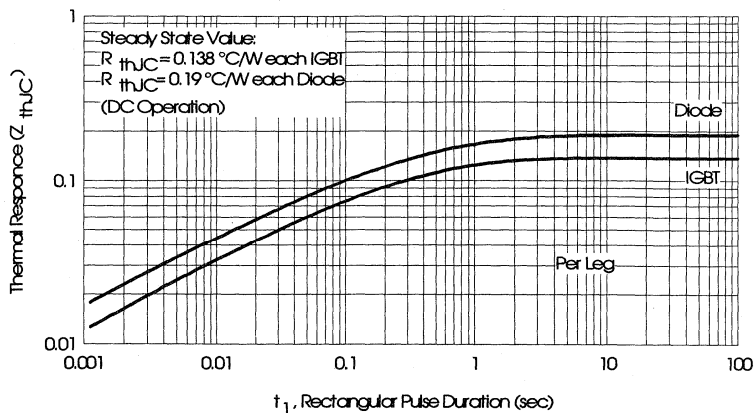


Fig. 15 - Maximum Effective Transient Thermal Impedance, Junction-to-Case

Motor Control Fast Modules

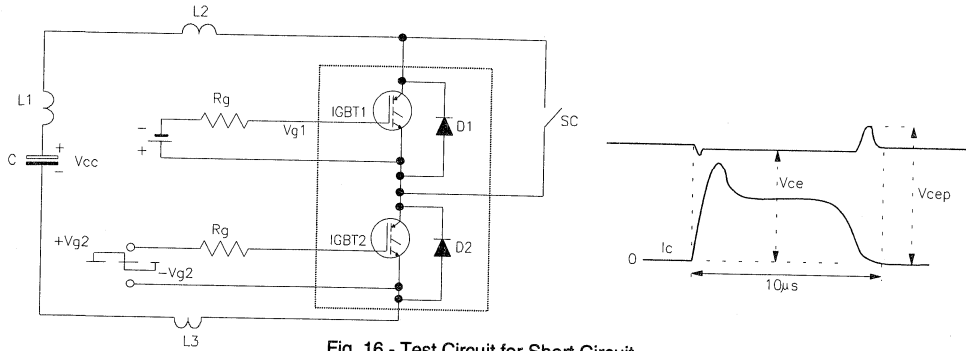


Fig. 16 - Test Circuit for Short Circuit

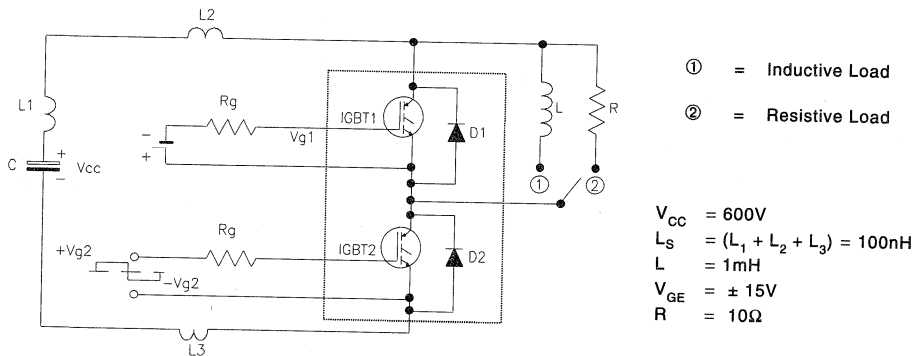


Fig. 17 - Test Circuit for Measurement of I_{LM} , E_{ON} , E_{OFF} , Q_{RR}

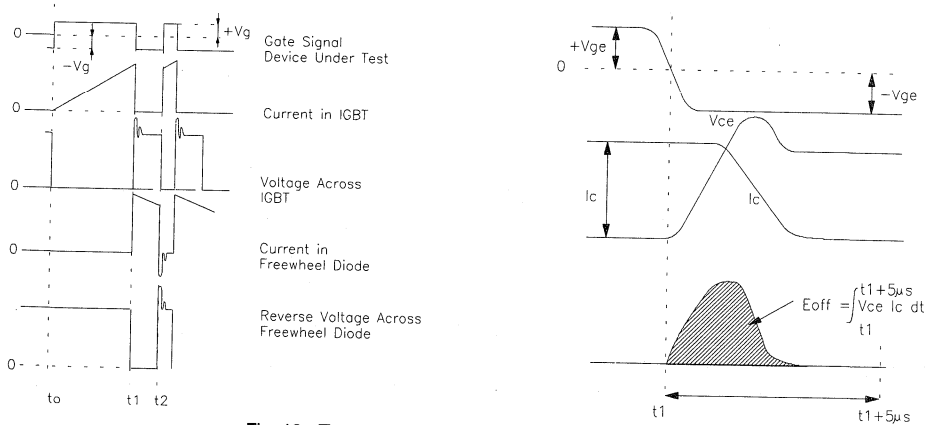


Fig. 18 - Test Waveforms for Circuit of Fig. 17

Refer to Section D for the following:
 Appendix I: Section D - page D-11

Fig. 19 - Test Waveforms for Circuit of Fig. 17,
 Defining E_{ON} , E_{REC} , Q_{RR}

Fig. 20 - Waveforms for Switching Time

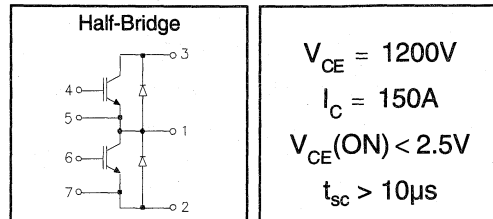
Package Outline 12- Double INT-A-PAK, New Half Bridge Section D - page D-17

IRGTDN150M12

"HALF-BRIDGE" IGBT DOUBLE INT-A-PAK

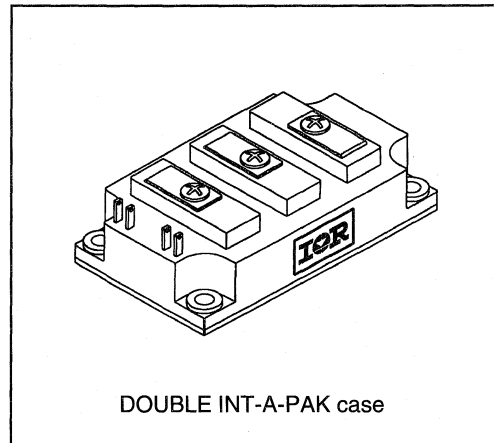
Low conduction loss IGBT

- Rugged Design
- Simple gate-drive
- Switching-Loss Rating includes all "tail" losses
- Short circuit rated



Description

IR's advanced IGBT technology is the key to this line of DOUBLE INT-A-PAK Power Modules. The efficient geometry and unique processing of the IGBT allow higher current densities than comparable bipolar power module transistors, while at the same time requiring the simpler gate-drive of the familiar power MOSFET. This superior technology has now been coupled to state of the art assembly techniques to produce a higher current module that is highly suited to power applications such as motor drives, uninterruptible power supplies, welding and power factor correction.


 Motor
Control
Fast
Modules

Absolute Maximum Ratings

Parameter	Description	Value	Units
V_{CES}	Continuous collector to emitter voltage	1200	V
$I_C @ T_C = 25^\circ C$	Maximum Continuous collector current	280	A
$I_C @ T_C = 85^\circ C$	Maximum Continuous collector current	160	
$I_C @ T_C = 100^\circ C$	Maximum Continuous collector current	120	
I_{LM}	Peak IGBT switching current	300	
I_{FM}	Peak diode forward switching current (1)	300	
V_{GE}	Gate to emitter voltage	± 20	V
V_{ISOL}	RMS isolation voltage, any terminal to case, $t = 1$ min	2500	
$P_D @ T_C = 25^\circ C$	Power dissipation	1200	W
T_J	Operating junction temperature range	-40 to 150	$^\circ C$
T_{STG}	Storage temperature range	-40 to 125	

(1) Duration limited by max junction temperature.

Electrical Characteristics - $T_J = 25^\circ\text{C}$, unless otherwise stated

Parameter	Description	Min	Typ	Max	Units	Test Conditions
BV_{CES}	Collector-to-emitter breakdown voltage	1200	—	—	V	$V_{GE} = 0V, I_C = 4mA$
$V_{CE(ON)}$	Collector-to-emitter voltage	—	2.3	2.5		$V_{GE} = 15V, I_C = 150A$
		—	1.8	—		$V_{GE} = 15V, I_C = 75A, T_J = 150^\circ\text{C}$
V_{FM}	Diode forward voltage - maximum	—	3.2	3.4		$I_F = 150A, V_{GE} = 0V$
		—	2.6	—		$I_F = 150A, V_{GE} = 0V, T_J = 150^\circ\text{C}$
V_{GEth}	Gate threshold voltage	3.0	—	5.5	$I_C = 2mA$	
ΔV_{GEth}	Threshold voltage temp. coefficient	—	-11	—	mV/ $^\circ\text{C}$	$V_{CE} = V_{GE}, I_C = 2mA$
g_{fe}	Forward transconductance	70	—	140	S(τ)	$V_{CE} = 25V, I_C = 150A$
I_{CES}	Collector-to-emitter leakage current	—	—	4	mA	$V_{GE} = 0V, V_{CE} = 1200V$
		—	—	40		$V_{GE} = 0V, V_{CE} = 1200V, T_J = 150^\circ\text{C}$
I_{GES}	Gate-to-emitter leakage current	—	—	± 4	μA	$V_{GE} = \pm 20V$

Dynamic Characteristics - $T_J = 125^\circ\text{C}$

Parameter	Description	Min	Typ	Max	Units	Test Conditions
E_{on}	Turn-on switching energy	—	0.14	—	mJ/A	$R_G = 10\Omega, V_{CC} = 600V$
E_{off} (1)	Turn-off switching energy	—	0.36	—		$I_C = 150A, L_S = 100nH$
E_{ts} (1)	Total switching energy	—	—	0.60		$V_{GE} = \pm 15V$
$t_{d(on)}$	Turn-on delay time	—	100	150	ns	$R_G = 10\Omega, V_{CC} = 600V$
t_r	Rise time	—	450	600		$I_C = 150A$
$t_{d(off)}$	Turn-off delay time	—	350	500		$V_{GE} = \pm 15V$
t_f	Fall time	—	1500	1800		Resistive Load, $T_J = 25^\circ\text{C}$
I_{rr}	Diode peak recovery current	—	90	—	A	$R_G = 10\Omega, V_{CC} = 600V$
t_{rr}	Diode recovery time	—	220	—	ns	$I_C = 150A$
Q_{rr}	Diode recovery charge	—	11.0	—	μC	$V_{GE} = \pm 15V$
Q_{ge}	Gate-to-emitter charge (turn-on)	150	—	330	nC	$V_{CC} = 600V$
Q_{gc}	Gate-to-collector charge (turn-on)	210	—	650		$I_C = 150A$
Q_g	Total gate charge (turn-on)	1250	—	1500		$V_{GE} = 15V$
C_{ies}	Input capacitance	21000	—	22000	pF	$V_{GE} = 0V$
C_{oes}	Output capacitance	1300	—	2200		$V_{CC} = 30V$
C_{res}	Reverse transfer capacitance	1300	—	2000		$f = 1MHz$
t_{sc}	Short circuit withstand time	10	—	—	μs	$V_{CC} = 720V, V_{GE} = \pm 15V$ Min. $R_G = 10\Omega, V_{CEP} = 1000V$

(1) Includes tail losses

Thermal and Mechanical Characteristics

Parameter	Description	Typ	Max	Units
R_{thJC} (IGBT)	Thermal resistance, junction to case, each IGBT	—	0.105	$^\circ\text{C/W}$
R_{thJC} (Diode)	Thermal resistance, junction to case, each diode	—	0.140	
R_{thCS} (Module)	Thermal resistance, case to sink	0.032	0.075	
Wt	Weight of module	242	—	g



IRGTDN150M12

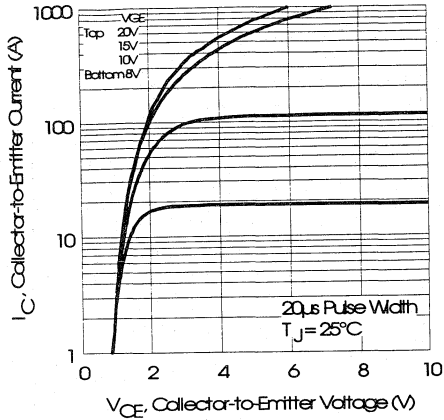


Fig. 1 - Typical Output Characteristics, $T_J = 25^\circ\text{C}$

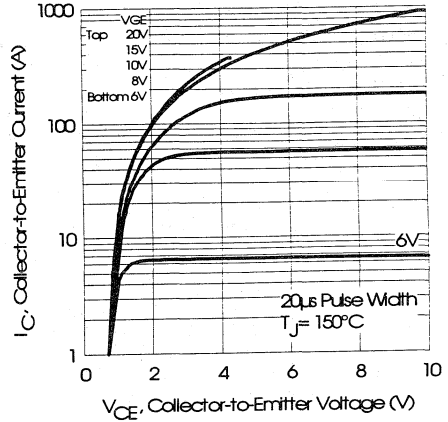


Fig. 2 - Typical Output Characteristics, $T_J = 150^\circ\text{C}$

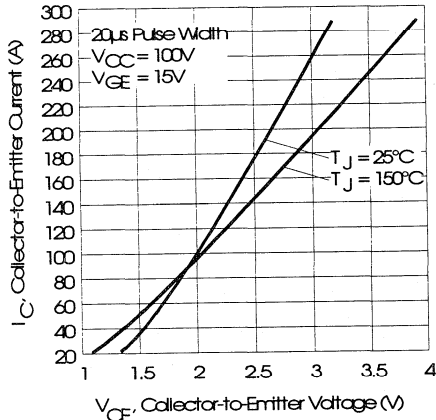


Fig. 3 - Typical Output Characteristics

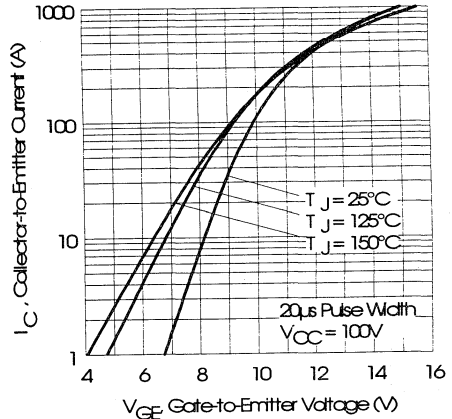


Fig. 4 - Typical Transfer Characteristics

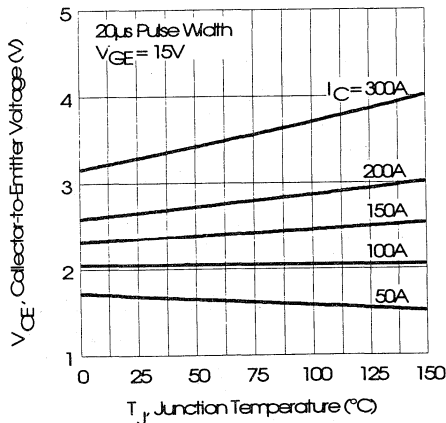


Fig. 5 - Collector-to-Emitter Saturation Typical Voltage vs. Junction Temperature

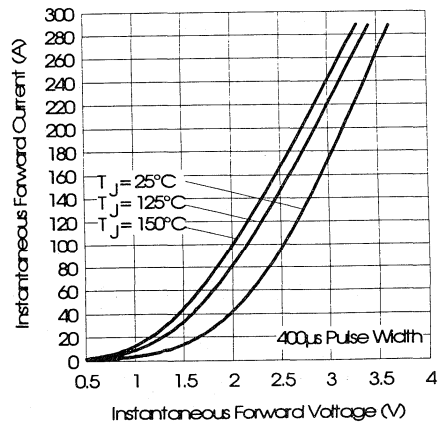


Fig. 6 - Forward Voltage Drop Characteristics



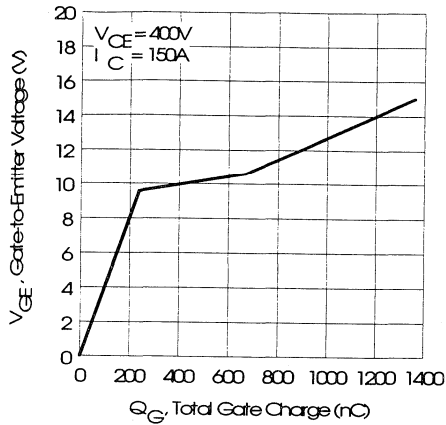


Fig. 7 - Typical Gate Charge vs. Gate-to-Emitter Voltage

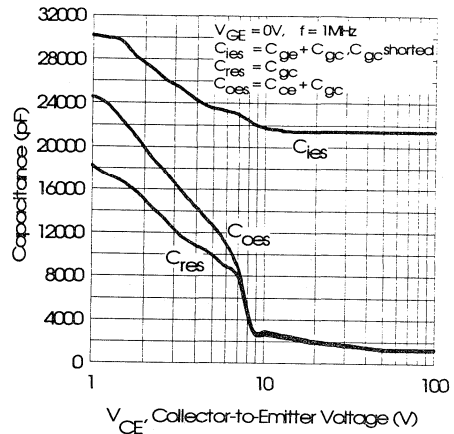


Fig. 8 - Typical Capacitance vs. Collector-to-Emitter Voltage

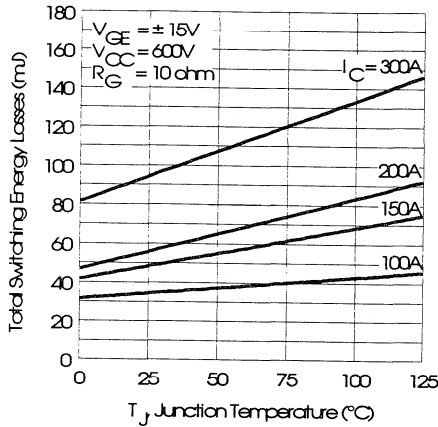


Fig. 9 - Typical Switching Losses vs. Junction Temperature

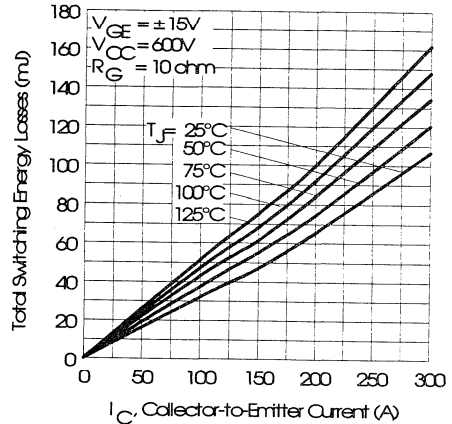


Fig. 10 - Typical Switching Losses vs. Collector-to-Emitter Current

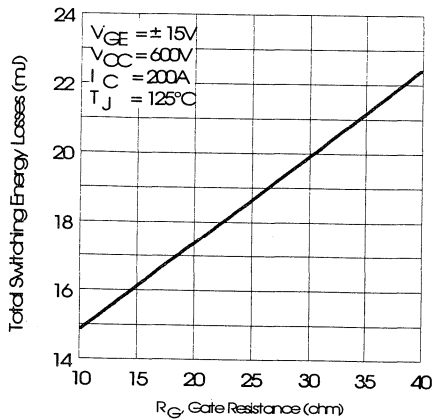


Fig. 11 - Typical Switching Losses vs. Gate Resistance

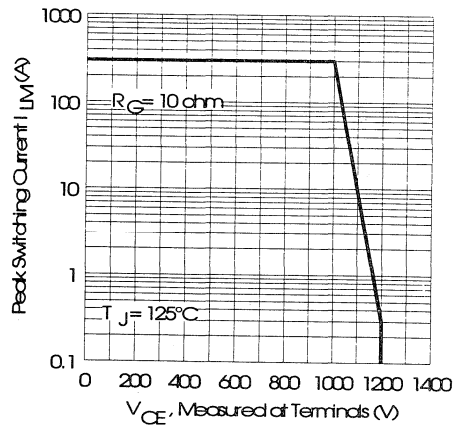


Fig. 12 - Reverse Bias Safe Operating Area

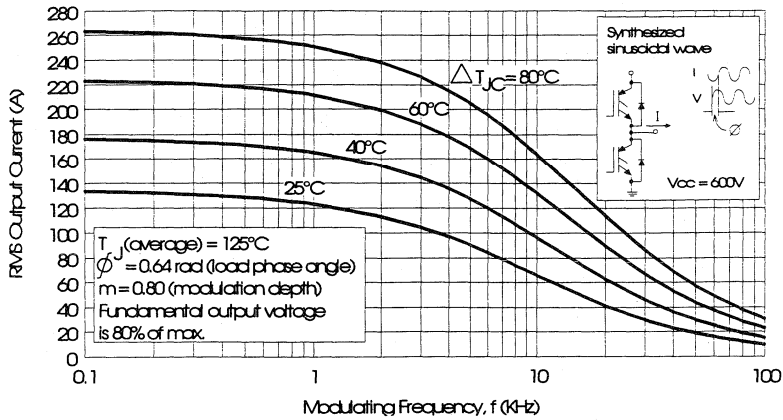


Fig. 13 - Typical RMS Output Current per phase vs. Frequency (Synthesized Sinusoidal Wave)

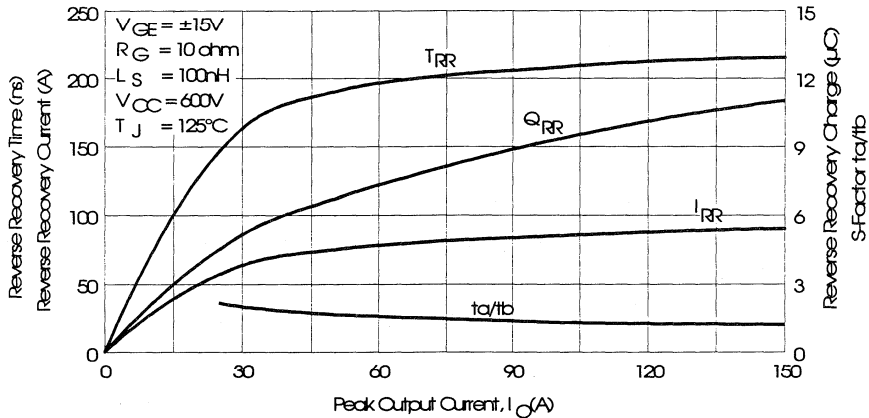


Fig. 14 - Typical Diode Recovery Characteristics as Function of Output Current I_0

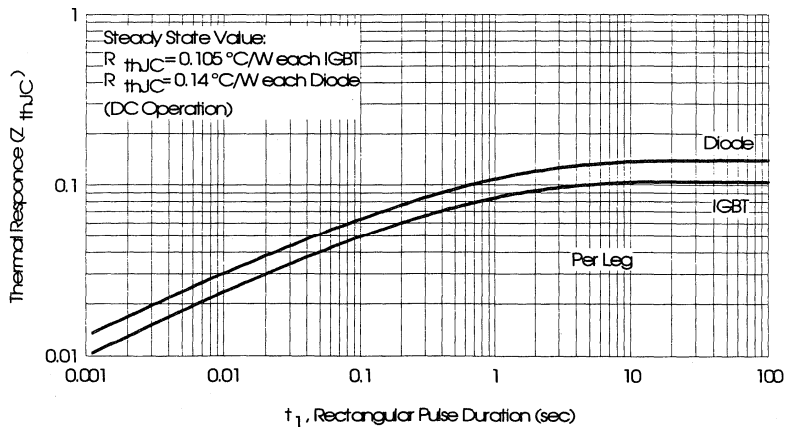


Fig. 15 - Maximum Effective Transient Thermal Impedance, Junction-to-Case

Motor
Control
Fast
Modules

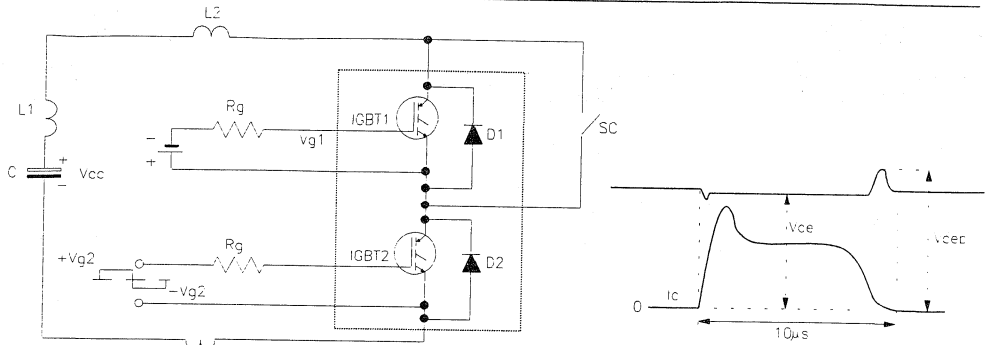


Fig. 16 - Test Circuit for Short Circuit

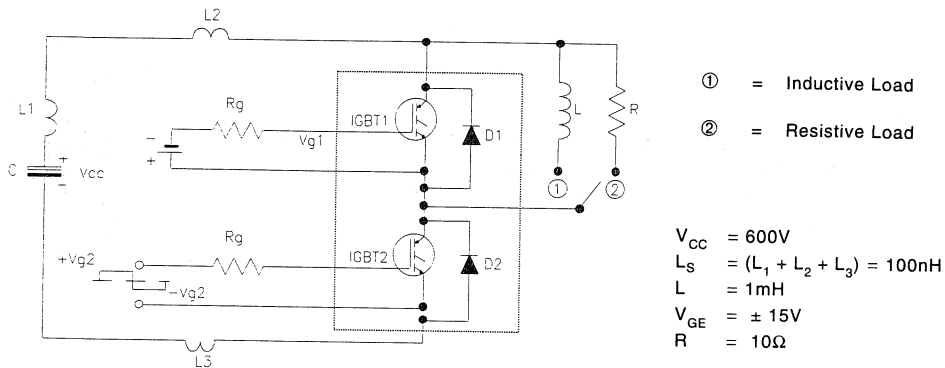


Fig. 17 - Test Circuit for Measurement of I_{LM} , E_{ON} , E_{OFF} , Q_{RR}

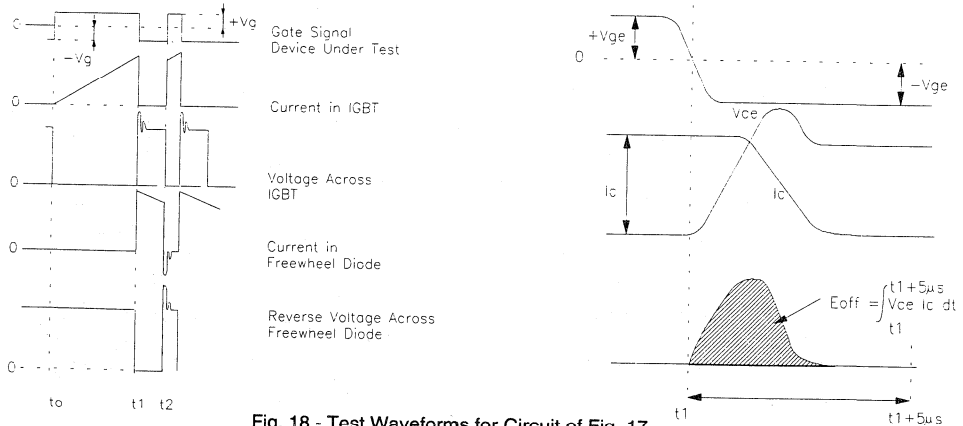


Fig. 18 - Test Waveforms for Circuit of Fig. 17

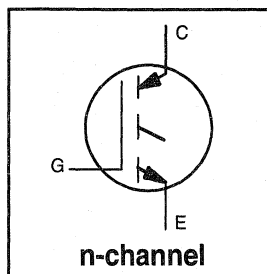
Refer to Section D for the following:
Appendix I: Section D - page D-11

Fig. 19 - Test Waveforms for Circuit of Fig. 17,
 Defining E_{ON} , E_{REC} , Q_{RR}

Fig. 20 - Waveforms for Switching Time

Features

- Switching-loss rating includes all "tail" losses
- Optimized for high operating frequency (over 5kHz)
See Fig. 1 for Current vs. Frequency curve



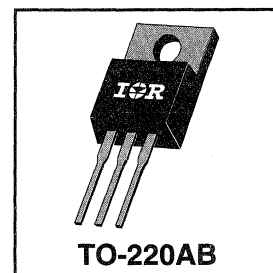
$$V_{CES} = 500V$$

$$V_{CE(sat)} \leq 3.0V$$

$$@ V_{GE} = 15V, I_C = 7.5A$$

Description

Insulated Gate Bipolar Transistors (IGBTs) from International Rectifier have higher usable current densities than comparable bipolar transistors, while at the same time having simpler gate-drive requirements of the familiar power MOSFET. They provide substantial benefits to a host of high-voltage, high-current applications.



Absolute Maximum Ratings

	Parameter	Max.	Units
V_{CES}	Collector-to-Emitter Voltage	500	V
$I_C @ T_C = 25^\circ C$	Continuous Collector Current	14	A
$I_C @ T_C = 100^\circ C$	Continuous Collector Current	7.5	
I_{CM}	Pulsed Collector Current ①	28	A
I_{LM}	Clamped Inductive Load Current ②	28	
V_{GE}	Gate-to-Emitter Voltage	± 20	V
E_{ARV}	Reverse Voltage Avalanche Energy ③	5.0	mJ
$P_D @ T_C = 25^\circ C$	Maximum Power Dissipation	60	W
$P_D @ T_C = 100^\circ C$	Maximum Power Dissipation	24	
T_J	Operating Junction and	-55 to +150	°C
T_{STG}	Storage Temperature Range		
	Soldering Temperature, for 10 sec.	300 (0.063 in. (1.6mm) from case)	
	Mounting torque, 6-32 or M3 screw.	10 lbf•in (1.1N•m)	

Thermal Resistance

	Parameter	Min.	Typ.	Max.	Units
$R_{\theta JC}$	Junction-to-Case	—	—	2.1	°C/W
$R_{\theta CS}$	Case-to-Sink, flat, greased surface	—	0.50	—	
$R_{\theta JA}$	Junction-to-Ambient, typical socket mount	—	—	80	
Wt	Weight	—	2.0 (0.07)	—	g (oz)

Electrical Characteristics @ $T_J = 25^\circ\text{C}$ (unless otherwise specified)

	Parameter	Min.	Typ.	Max.	Units	Conditions
$V_{(BR)CES}$	Collector-to-Emitter Breakdown Voltage	500	—	—	V	$V_{GE} = 0V, I_C = 250\mu A$
$V_{(BR)ECS}$	Emitter-to-Collector Breakdown Voltage ④	20	—	—	V	$V_{GE} = 0V, I_C = 1.0A$
$\Delta V_{(BR)CES}/\Delta T_J$	Temp. Coeff. of Breakdown Voltage	—	0.47	—	V/ $^\circ\text{C}$	$V_{GE} = 0V, I_C = 1.0mA$
$V_{CE(on)}$	Collector-to-Emitter Saturation Voltage	—	2.4	3.0	V	$I_C = 7.5A$ $I_C = 14A$ $I_C = 7.5A, T_J = 150^\circ\text{C}$ $V_{GE} = 15V$ See Fig. 2, 5
		—	3.1	—		
		—	2.7	—		
$V_{GE(th)}$	Gate Threshold Voltage	3.0	—	5.5		$V_{CE} = V_{GE}, I_C = 250\mu A$
$\Delta V_{GE(th)}/\Delta T_J$	Temperature Coeff. of Threshold Voltage	—	-10	—	mV/ $^\circ\text{C}$	$V_{CE} = V_{GE}, I_C = 250\mu A$
g_{fe}	Forward Transconductance ⑤	1.2	2.0	—	S	$V_{CE} = 100V, I_C = 7.5A$
I_{CES}	Zero Gate Voltage Collector Current	—	—	250	μA	$V_{GE} = 0V, V_{CE} = 500V$
		—	—	1000		$V_{GE} = 0V, V_{CE} = 500V, T_J = 150^\circ\text{C}$
I_{GES}	Gate-to-Emitter Leakage Current	—	—	± 100	nA	$V_{GE} = \pm 20V$

Switching Characteristics @ $T_J = 25^\circ\text{C}$ (unless otherwise specified)

	Parameter	Min.	Typ.	Max.	Units	Conditions
Q_g	Total Gate Charge (turn-on)	—	15	23	nC	$I_C = 7.5A$ $V_{CC} = 400V$ $V_{GE} = 15V$ See Fig. 8
Q_{ge}	Gate - Emitter Charge (turn-on)	—	3.7	5.6		
Q_{gc}	Gate - Collector Charge (turn-on)	—	6.5	9.8		
$t_{d(on)}$	Turn-On Delay Time	—	28	—	ns	$T_J = 25^\circ\text{C}$ $I_C = 7.5A, V_{CC} = 400V$ $V_{GE} = 15V, R_G = 50\Omega$ Energy losses include "tail"
t_r	Rise Time	—	11	—		
$t_{d(off)}$	Turn-Off Delay Time	—	72	110		
t_f	Fall Time	—	96	140		
E_{on}	Turn-On Switching Loss	—	0.13	—	mJ	See Fig. 9, 10, 11, 14
E_{off}	Turn-Off Switching Loss	—	0.08	—		
E_{ts}	Total Switching Loss	—	0.21	0.28		
$t_{d(on)}$	Turn-On Delay Time	—	26	—	ns	$T_J = 150^\circ\text{C}$, $I_C = 7.5A, V_{CC} = 400V$ $V_{GE} = 15V, R_G = 50\Omega$ Energy losses include "tail"
t_r	Rise Time	—	12	—		
$t_{d(off)}$	Turn-Off Delay Time	—	120	—		
t_f	Fall Time	—	140	—		
E_{ts}	Total Switching Loss	—	0.35	—	mJ	See Fig. 10, 14
L_E	Internal Emitter Inductance	—	7.5	—	nH	Measured 5mm from package
C_{ies}	Input Capacitance	—	330	—	pF	$V_{GE} = 0V$ $V_{CC} = 30V$ $f = 1.0MHz$ See Fig. 7
C_{oes}	Output Capacitance	—	47	—		
C_{res}	Reverse Transfer Capacitance	—	5.9	—		

Notes:

- ① Repetitive rating; $V_{GE}=20V$, pulse width limited by max. junction temperature. (See fig. 13b)
- ② $V_{CC}=80\%(V_{CES})$, $V_{GE}=20V$, $L=10\mu H$, $R_G=50\Omega$, (See fig. 13a)
- ③ Repetitive rating; pulse width limited by maximum junction temperature.
- ④ Pulse width $\leq 80\mu s$; duty factor $\leq 0.1\%$.
- ⑤ Pulse width 5.0 μs , single shot.

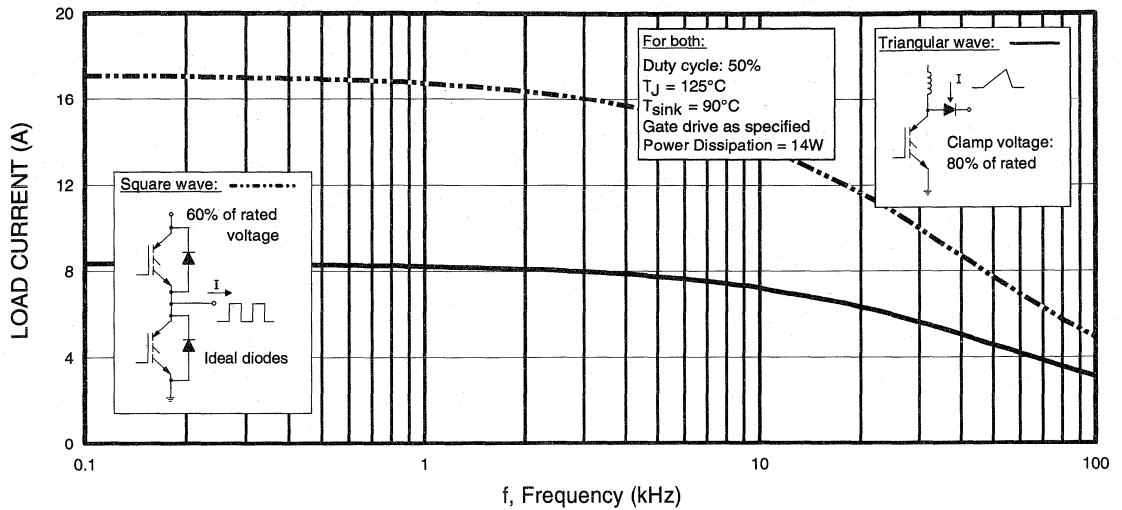


Fig. 1 - Typical Load Current vs. Frequency
 (For square wave, $I = I_{RMS}$ of fundamental; for triangular wave, $I = I_{PK}$)

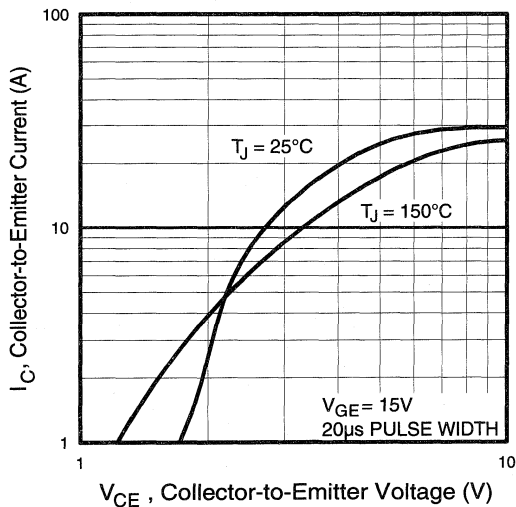


Fig. 2 - Typical Output Characteristics

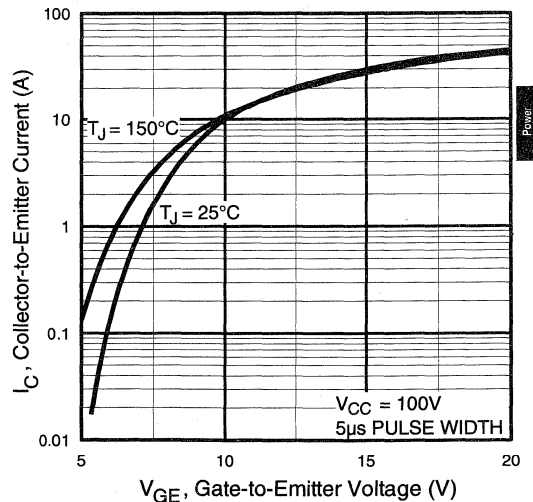


Fig. 3 - Typical Transfer Characteristics

Power Conversion Ultra-Fast Discrets

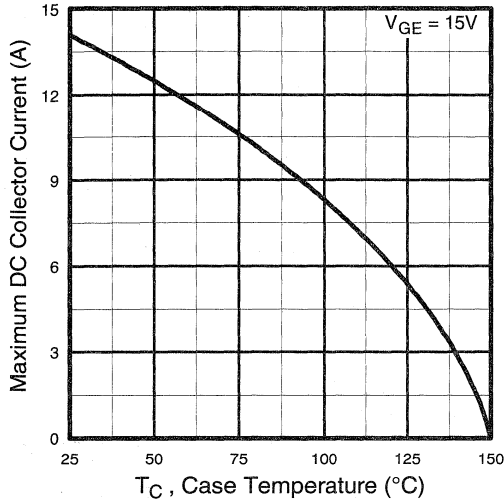


Fig. 4 - Maximum Collector Current vs. Case Temperature

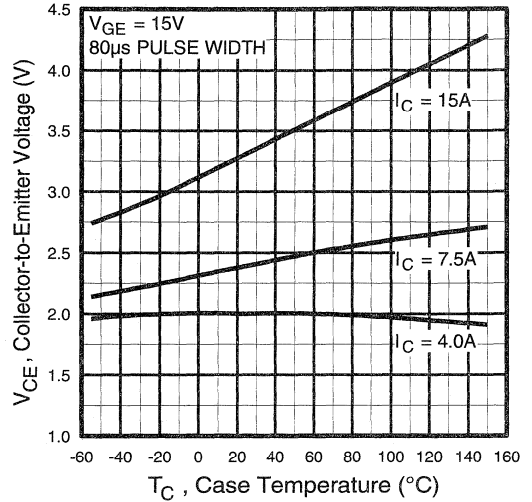


Fig. 5 - Collector-to-Emitter Voltage vs. Case Temperature

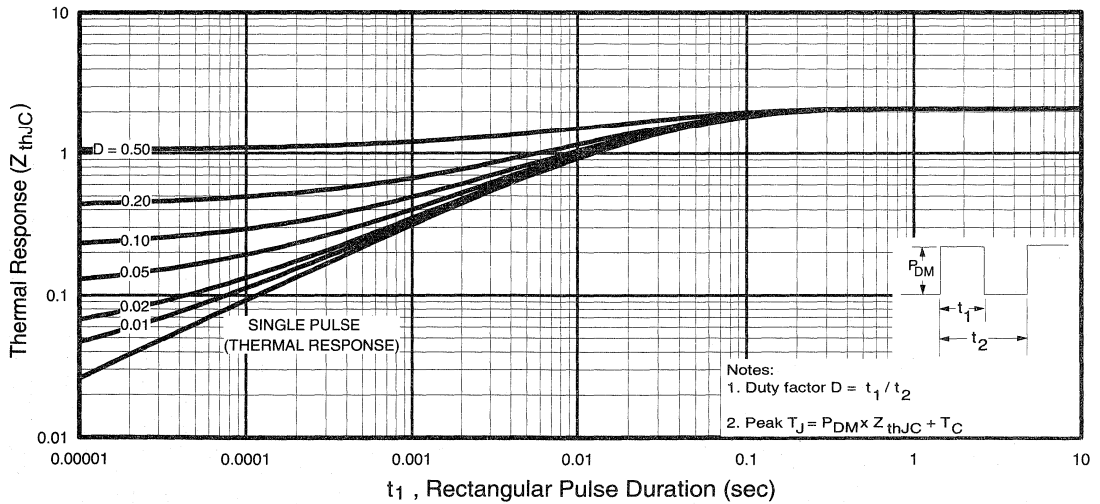


Fig. 6 - Maximum Effective Transient Thermal Impedance, Junction-to-Case

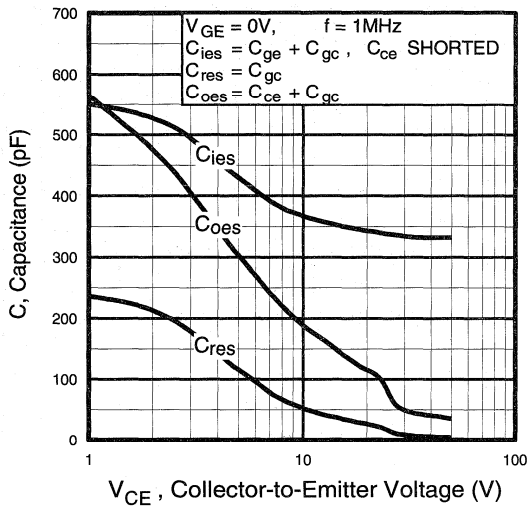


Fig. 7 - Typical Capacitance vs. Collector-to-Emitter Voltage

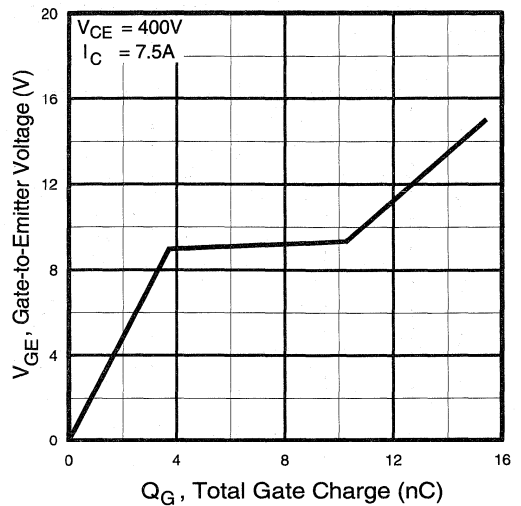


Fig. 8 - Typical Gate Charge vs. Gate-to-Emitter Voltage

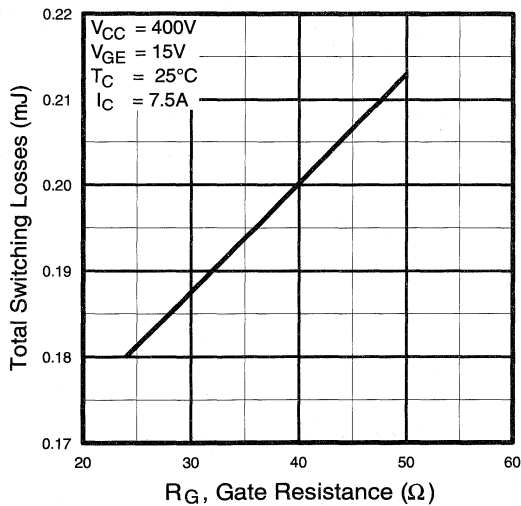


Fig. 9 - Typical Switching Losses vs. Gate Resistance

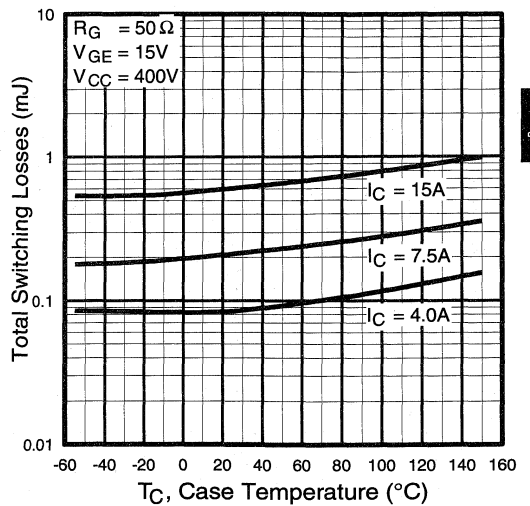


Fig. 10 - Typical Switching Losses vs. Case Temperature

Power Conversion Ultra-Fast Discrets

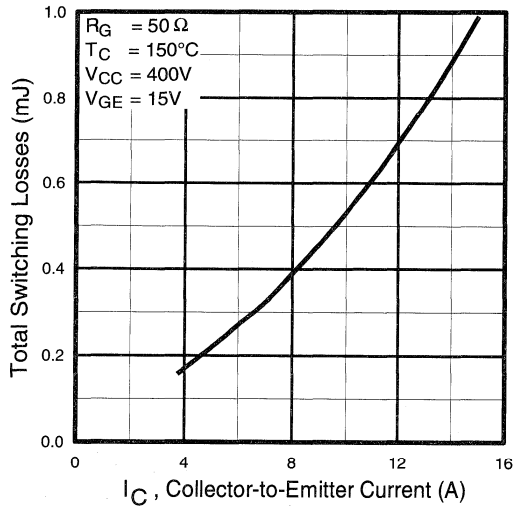


Fig. 11 - Typical Switching Losses vs. Collector-to-Emitter Current

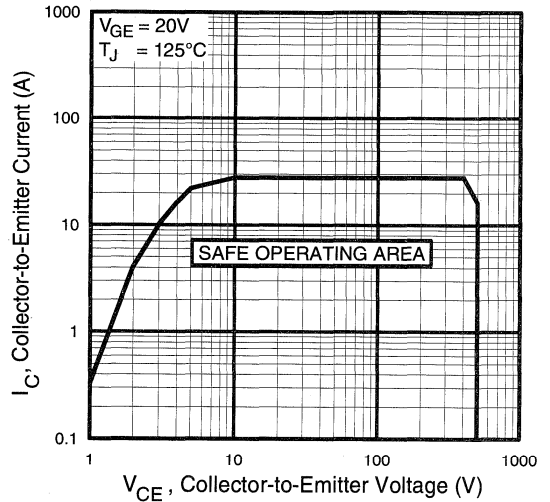


Fig. 12 - Turn-Off SOA

Refer to Section D for the following:

Appendix A: Section D - page D-3

Fig. 13a - Clamped Inductive Load Test Circuit

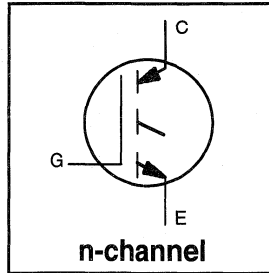
Fig. 13b - Pulsed Collector Current Test Circuit

Fig. 14a - Switching Loss Test Circuit

Fig. 14b - Switching Loss Waveform

Features

- Switching-loss rating includes all "tail" losses
- Optimized for high operating frequency (over 5kHz) See Fig. 1 for Current vs. Frequency curve



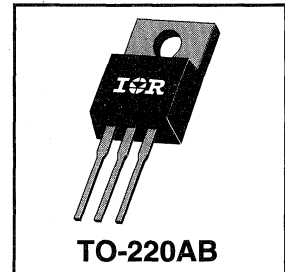
$$V_{CES} = 500V$$

$$V_{CE(sat)} \leq 3.0V$$

$$@V_{GE} = 15V, I_C = 15A$$

Description

Insulated Gate Bipolar Transistors (IGBTs) from International Rectifier have higher usable current densities than comparable bipolar transistors, while at the same time having simpler gate-drive requirements of the familiar power MOSFET. They provide substantial benefits to a host of high-voltage, high-current applications.



Absolute Maximum Ratings

	Parameter	Max.	Units
V_{CES}	Collector-to-Emitter Voltage	500	V
$I_C @ T_C = 25^\circ C$	Continuous Collector Current	25	A
$I_C @ T_C = 100^\circ C$	Continuous Collector Current	15	
I_{CM}	Pulsed Collector Current ①	50	
I_{LM}	Clamped Inductive Load Current ②	50	
V_{GE}	Gate-to-Emitter Voltage	± 20	V
E_{ARV}	Reverse Voltage Avalanche Energy ③	10	mJ
$P_D @ T_C = 25^\circ C$	Maximum Power Dissipation	100	W
$P_D @ T_C = 100^\circ C$	Maximum Power Dissipation	42	
T_J	Operating Junction and	-55 to +150	°C
T_{STG}	Storage Temperature Range		
	Soldering Temperature, for 10 sec.	300 (0.063 in. (1.6mm) from case)	
	Mounting torque, 6-32 or M3 screw.	10 lbf•in (1.1N•m)	

 Power
Conversion
Fast
Modules

Thermal Resistance

	Parameter	Min.	Typ.	Max.	Units
$R_{\theta JC}$	Junction-to-Case	—	—	1.2	°C/W
$R_{\theta CS}$	Case-to-Sink, flat, greased surface	—	0.50	—	
$R_{\theta JA}$	Junction-to-Ambient, typical socket mount	—	—	80	
W_t	Weight	—	2.0 (0.07)	—	g (oz)

Electrical Characteristics @ $T_J = 25^\circ\text{C}$ (unless otherwise specified)

	Parameter	Min.	Typ.	Max.	Units	Conditions
$V_{(BR)CES}$	Collector-to-Emitter Breakdown Voltage	500	—	—	V	$V_{GE} = 0V, I_C = 250\mu A$
$V_{(BR)ECS}$	Emitter-to-Collector Breakdown Voltage ④	20	—	—	V	$V_{GE} = 0V, I_C = 1.0A$
$\Delta V_{(BR)CES}/\Delta T_J$	Temperature Coeff. of Breakdown Voltage	—	0.46	—	V/°C	$V_{GE} = 0V, I_C = 1.0mA$
$V_{CE(on)}$	Collector-to-Emitter Saturation Voltage	—	2.3	3.0	V	$I_C = 15A$ $V_{GE} = 15V$ See Fig. 2, 5
		—	2.8	—		
		—	2.6	—		
$V_{GE(th)}$	Gate Threshold Voltage	3.0	—	5.5		$V_{CE} = V_{GE}, I_C = 250\mu A$
$\Delta V_{GE(th)}/\Delta T_J$	Temperature Coeff. of Threshold Voltage	—	-11	—	mV/°C	$V_{CE} = V_{GE}, I_C = 250\mu A$
g_{fe}	Forward Transconductance ⑤	2.3	8.1	—	S	$V_{CE} = 100V, I_C = 15A$
I_{CES}	Zero Gate Voltage Collector Current	—	—	250	μA	$V_{GE} = 0V, V_{CE} = 500V$
		—	—	1000		$V_{GE} = 0V, V_{CE} = 500V, T_J = 150^\circ\text{C}$
I_{GES}	Gate-to-Emitter Leakage Current	—	—	± 100	nA	$V_{GE} = \pm 20V$

Switching Characteristics @ $T_J = 25^\circ\text{C}$ (unless otherwise specified)

	Parameter	Min.	Typ.	Max.	Units	Conditions
Q_g	Total Gate Charge (turn-on)	—	31	47	nC	$I_C = 15A$ $V_{CC} = 400V$ See Fig. 8
Q_{ge}	Gate - Emitter Charge (turn-on)	—	6.2	9.3		
Q_{gc}	Gate - Collector Charge (turn-on)	—	12	19		
$t_{d(on)}$	Turn-On Delay Time	—	29	—	ns	$T_J = 25^\circ\text{C}$ $I_C = 15A, V_{CC} = 400V$ $V_{GE} = 15V, R_G = 23\Omega$ Energy losses include "tail"
t_r	Rise Time	—	11	—		
$t_{d(off)}$	Turn-Off Delay Time	—	91	160		
t_f	Fall Time	—	66	120		
E_{on}	Turn-On Switching Loss	—	0.24	—	mJ	See Fig. 9, 10, 11, 14
E_{off}	Turn-Off Switching Loss	—	0.17	—		
E_{ts}	Total Switching Loss	—	0.41	0.61		
$t_{d(on)}$	Turn-On Delay Time	—	13	—	ns	$T_J = 150^\circ\text{C}$, $I_C = 15A, V_{CC} = 400V$ $V_{GE} = 15V, R_G = 23\Omega$ Energy losses include "tail"
t_r	Rise Time	—	27	—		
$t_{d(off)}$	Turn-Off Delay Time	—	130	—		
t_f	Fall Time	—	130	—		
E_{ts}	Total Switching Loss	—	0.76	—	mJ	See Fig. 10, 14
L_E	Internal Emitter Inductance	—	7.5	—	nH	Measured 5mm from package
C_{ies}	Input Capacitance	—	660	—	pF	$V_{GE} = 0V$ $V_{CC} = 30V$ See Fig. 7
C_{oes}	Output Capacitance	—	110	—		
C_{res}	Reverse Transfer Capacitance	—	12	—		

Notes:

- ① Repetitive rating; $V_{GE}=20V$, pulse width limited by max. junction temperature. (See fig. 13b)
- ② $V_{CC}=80\%(V_{CES}), V_{GE}=20V, L=10\mu H, R_G=23\Omega$, (See fig. 13a)
- ③ Repetitive rating; pulse width limited by maximum junction temperature.
- ④ Pulse width $\leq 80\mu s$; duty factor $\leq 0.1\%$.
- ⑤ Pulse width 5.0 μs , single shot.

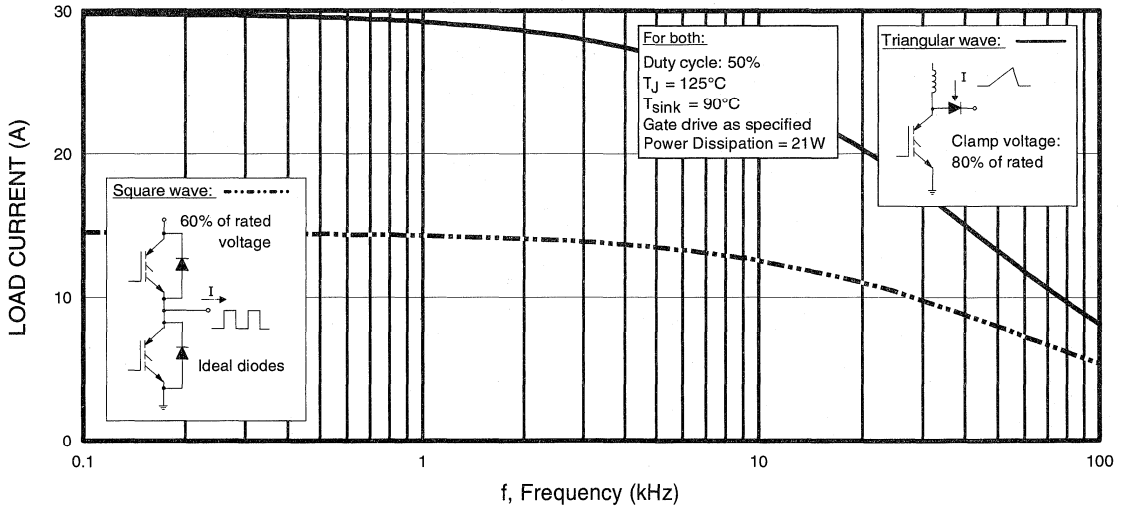


Fig. 1 - Typical Load Current vs. Frequency
 (For square wave, $I = I_{RMS}$ of fundamental; for triangular wave, $I = I_{PK}$)

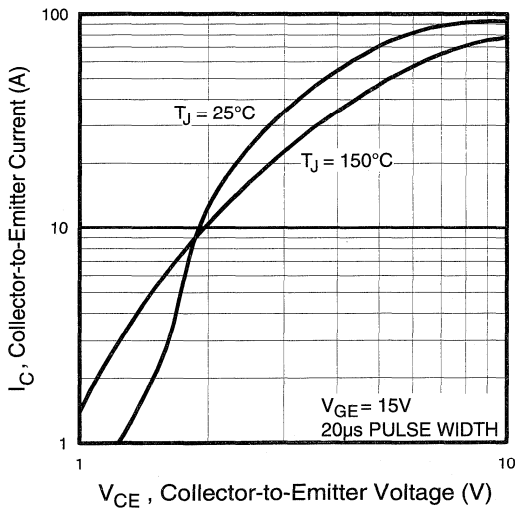


Fig. 2 - Typical Output Characteristics

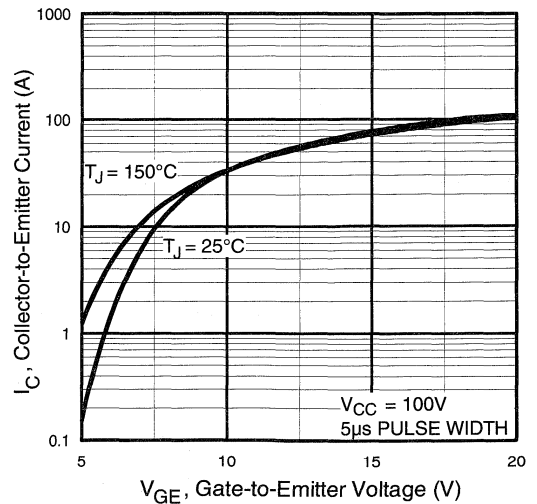


Fig. 3 - Typical Transfer Characteristics

Power Conversion Ultra-Fast Discreets

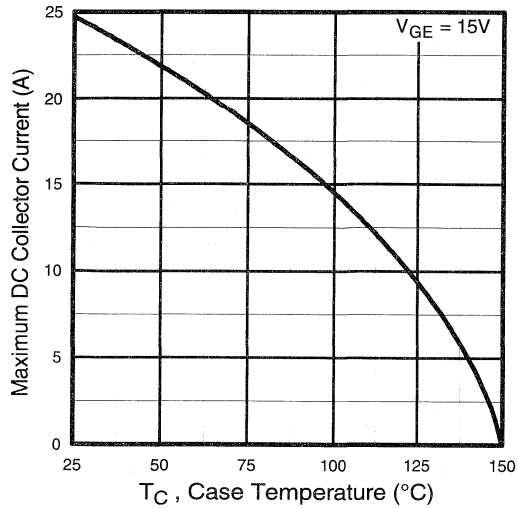


Fig. 4 - Maximum Collector Current vs. Case Temperature

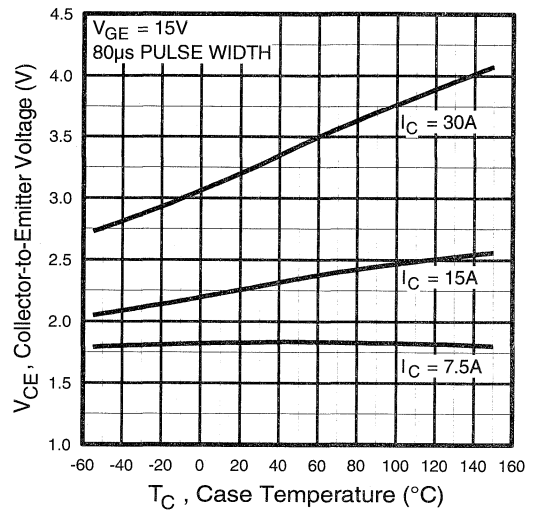


Fig. 5 - Collector-to-Emitter Voltage vs. Case Temperature

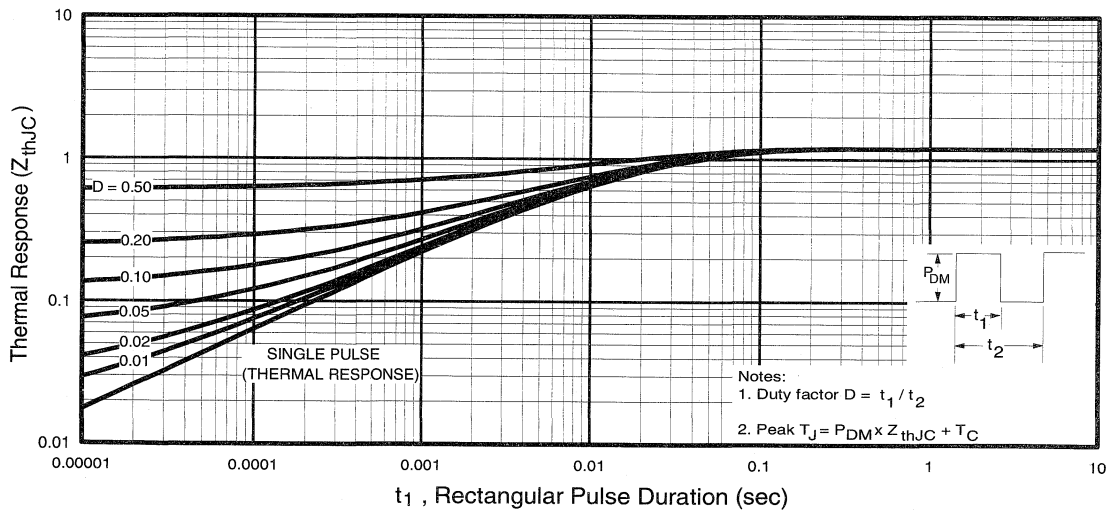


Fig. 6 - Maximum Effective Transient Thermal Impedance, Junction-to-Case

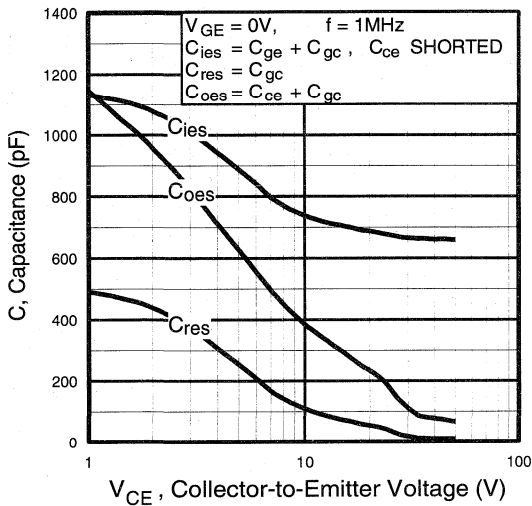


Fig. 7 - Typical Capacitance vs. Collector-to-Emitter Voltage

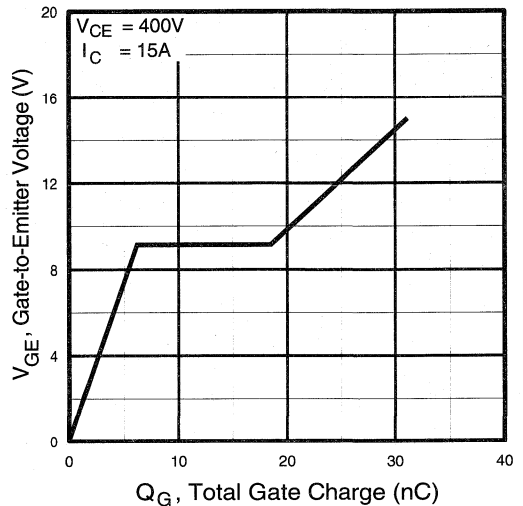


Fig. 8 - Typical Gate Charge vs. Gate-to-Emitter Voltage

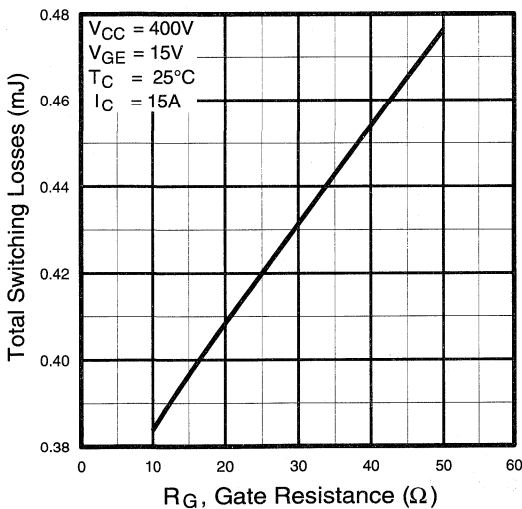


Fig. 9 - Typical Switching Losses vs. Gate Resistance

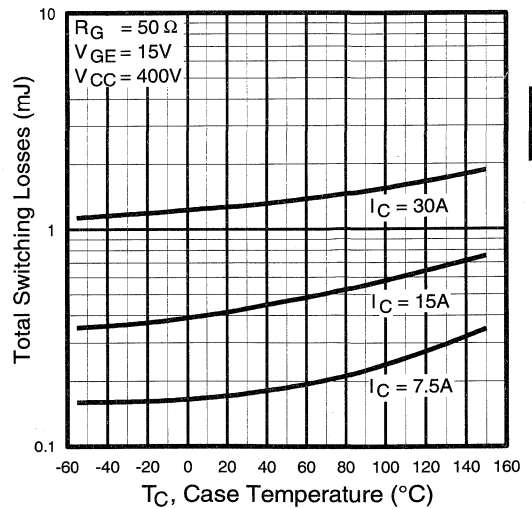


Fig. 10 - Typical Switching Losses vs. Case Temperature

Power
Conversion
Ultra-Fast
Discretes

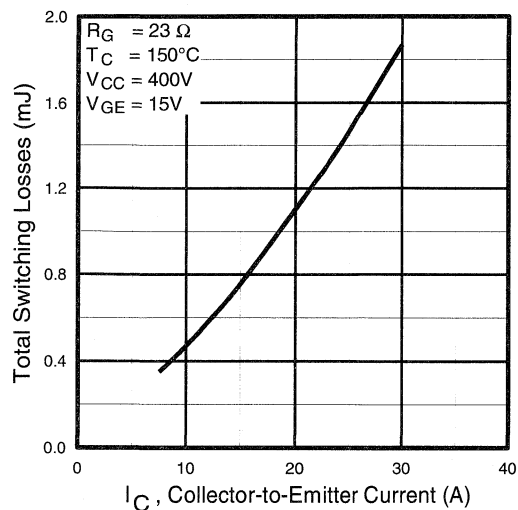


Fig. 11 - Typical Switching Losses vs. Collector-to-Emitter Current

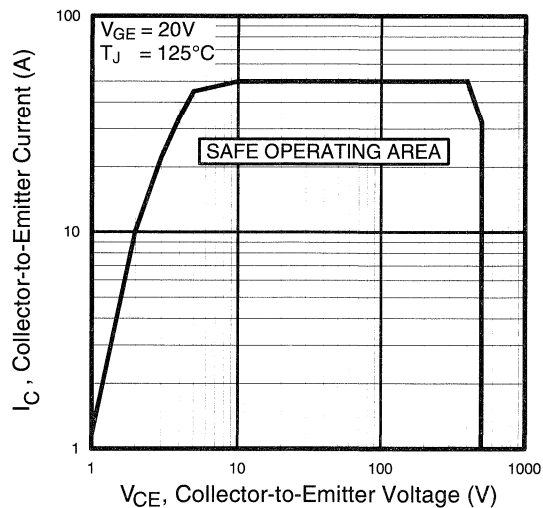


Fig. 12 - Turn-Off SOA

Refer to Section D for the following:

Appendix A: Section D - page D-3

Fig. 13a - Clamped Inductive Load Test Circuit

Fig. 13b - Pulsed Collector Current Test Circuit

Fig. 14a - Switching Loss Test Circuit

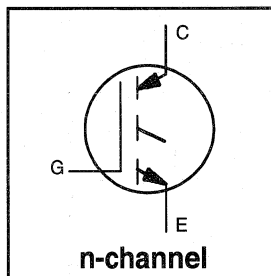
Fig. 14b - Switching Loss Waveform

Package Outline 1 - JEDEC Outline TO-220AB

Section D - page D-12

Features

- Switching-loss rating includes all "tail" losses
 - Optimized for high operating frequency (over 5kHz)
- See Fig. 1 for Current vs. Frequency curve



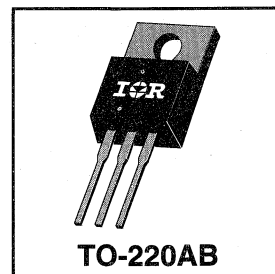
$$V_{CES} = 500V$$

$$V_{CE(sat)} \leq 3.0V$$

$$@V_{GE} = 15V, I_C = 22A$$

Description

Insulated Gate Bipolar Transistors (IGBTs) from International Rectifier have higher usable current densities than comparable bipolar transistors, while at the same time having simpler gate-drive requirements of the familiar power MOSFET. They provide substantial benefits to a host of high-voltage, high-current applications.



Absolute Maximum Ratings

	Parameter	Max.	Units
V_{CES}	Collector-to-Emitter Voltage	500	V
$I_C @ T_C = 25^\circ C$	Continuous Collector Current	40	A
$I_C @ T_C = 100^\circ C$	Continuous Collector Current	22	
I_{CM}	Pulsed Collector Current ①	80	
I_{LM}	Clamped Inductive Load Current ②	80	
V_{GE}	Gate-to-Emitter Voltage	± 20	V
E_{ARV}	Reverse Voltage Avalanche Energy ③	15	mJ
$P_D @ T_C = 25^\circ C$	Maximum Power Dissipation	160	W
$P_D @ T_C = 100^\circ C$	Maximum Power Dissipation	65	
T_J	Operating Junction and	-55 to +150	°C
T_{STG}	Storage Temperature Range		
	Soldering Temperature, for 10 sec.	300 (0.063 in. (1.6mm) from case)	
	Mounting torque, 6-32 or M3 screw.	10 lbf•in (1.1N•m)	

Thermal Resistance

	Parameter	Min.	Typ.	Max.	Units
$R_{\theta JC}$	Junction-to-Case	—	—	0.77	°C/W
$R_{\theta CS}$	Case-to-Sink, flat, greased surface	—	0.50	—	
$R_{\theta JA}$	Junction-to-Ambient, typical socket mount	—	—	80	
Wt	Weight	—	2.0 (0.07)	—	g (oz)

Electrical Characteristics @ $T_J = 25^\circ\text{C}$ (unless otherwise specified)

	Parameter	Min.	Typ.	Max.	Units	Conditions
$V_{(BR)CES}$	Collector-to-Emitter Breakdown Voltage	500	—	—	V	$V_{GE} = 0V, I_C = 250\mu A$
$V_{(BR)ECS}$	Emitter-to-Collector Breakdown Voltage ④	20	—	—	V	$V_{GE} = 0V, I_C = 1.0A$
$\Delta V_{(BR)CES}/\Delta T_J$	Temperature Coeff. of Breakdown Voltage	—	0.35	—	V/°C	$V_{GE} = 0V, I_C = 1.0mA$
$V_{CE(on)}$	Collector-to-Emitter Saturation Voltage	—	2.4	3.0	V	$I_C = 22A$ $V_{GE} = 15V$ See Fig. 2, 5
		—	2.8	—		
		—	2.4	—		
$V_{GE(th)}$	Gate Threshold Voltage	3.0	—	5.5		$V_{CE} = V_{GE}, I_C = 250\mu A$
$\Delta V_{GE(th)}/\Delta T_J$	Temperature Coeff. of Threshold Voltage	—	-11	—	mV/°C	$V_{CE} = V_{GE}, I_C = 250\mu A$
g_{fe}	Forward Transconductance ⑤	6.6	13	—	S	$V_{CE} = 100V, I_C = 22A$
I_{CES}	Zero Gate Voltage Collector Current	—	—	250	μA	$V_{GE} = 0V, V_{CE} = 500V$ $V_{GE} = 0V, V_{CE} = 500V, T_J = 150^\circ\text{C}$
		—	—	1000		
I_{GES}	Gate-to-Emitter Leakage Current	—	—	± 100	nA	$V_{GE} = \pm 20V$

Switching Characteristics @ $T_J = 25^\circ\text{C}$ (unless otherwise specified)

	Parameter	Min.	Typ.	Max.	Units	Conditions
Q_g	Total Gate Charge (turn-on)	—	55	83	nC	$I_C = 22A$ $V_{CC} = 400V$ $V_{GE} = 15V$ See Fig. 8
Q_{ge}	Gate - Emitter Charge (turn-on)	—	11	17		
Q_{gc}	Gate - Collector Charge (turn-on)	—	19	29		
$t_{d(on)}$	Turn-On Delay Time	—	27	—	ns	$T_J = 25^\circ\text{C}$ $I_C = 22A, V_{CC} = 400V$ $V_{GE} = 15V, R_G = 10\Omega$ Energy losses include "tail"
t_r	Rise Time	—	13	—		
$t_{d(off)}$	Turn-Off Delay Time	—	100	150		
t_f	Fall Time	—	56	100		
E_{on}	Turn-On Switching Loss	—	0.37	—	mJ	See Fig. 9, 10, 11, 14
E_{off}	Turn-Off Switching Loss	—	0.18	—		
E_{ts}	Total Switching Loss	—	0.55	0.70		
$t_{d(on)}$	Turn-On Delay Time	—	27	—	ns	$T_J = 150^\circ\text{C}$, $I_C = 22A, V_{CC} = 400V$ $V_{GE} = 15V, R_G = 10\Omega$ Energy losses include "tail"
t_r	Rise Time	—	15	—		
$t_{d(off)}$	Turn-Off Delay Time	—	137	—		
t_f	Fall Time	—	100	—		
E_{ts}	Total Switching Loss	—	0.96	—	mJ	See Fig. 10, 14
L_E	Internal Emitter Inductance	—	7.5	—	nH	Measured 5mm from package
C_{ies}	Input Capacitance	—	1400	—	pF	$V_{GE} = 0V$ $V_{CC} = 30V$ See Fig. 7 $f = 1.0\text{MHz}$
C_{oes}	Output Capacitance	—	250	—		
C_{res}	Reverse Transfer Capacitance	—	42	—		

Notes:

- ① Repetitive rating; $V_{GE}=20V$, pulse width limited by max. junction temperature. (See fig. 13b)
- ② $V_{CC}=80\%(V_{CES})$, $V_{GE}=20V$, $L=10\mu H$, $R_G=10\Omega$, (See fig. 13a)
- ③ Repetitive rating; pulse width limited by maximum junction temperature.
- ④ Pulse width $\leq 80\mu s$; duty factor $\leq 0.1\%$.
- ⑤ Pulse width 5.0 μs , single shot.

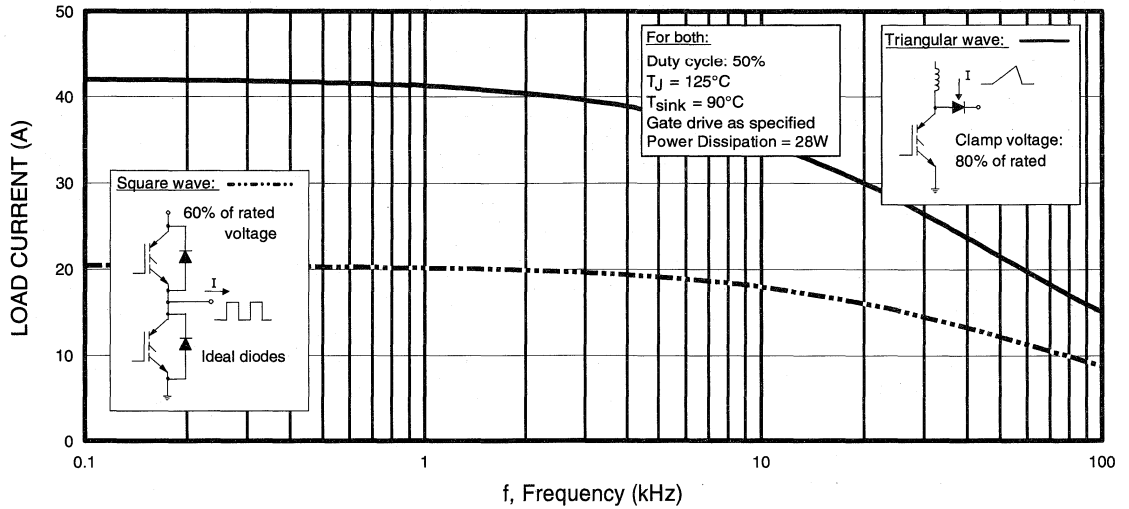


Fig. 1 - Typical Load Current vs. Frequency
 (For square wave, $I = I_{RMS}$ of fundamental; for triangular wave, $I = I_{PK}$)

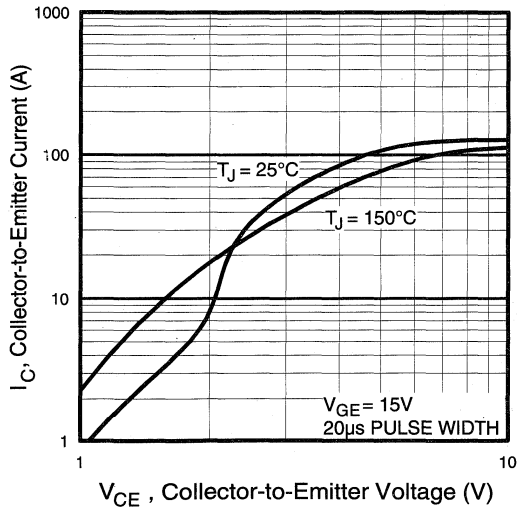


Fig. 2 - Typical Output Characteristics

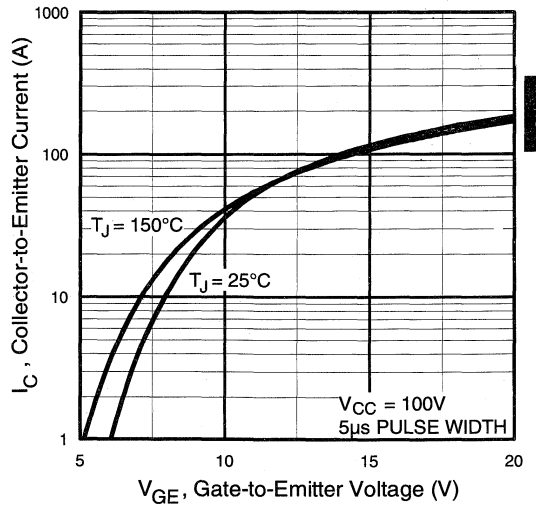


Fig. 3 - Typical Transfer Characteristics

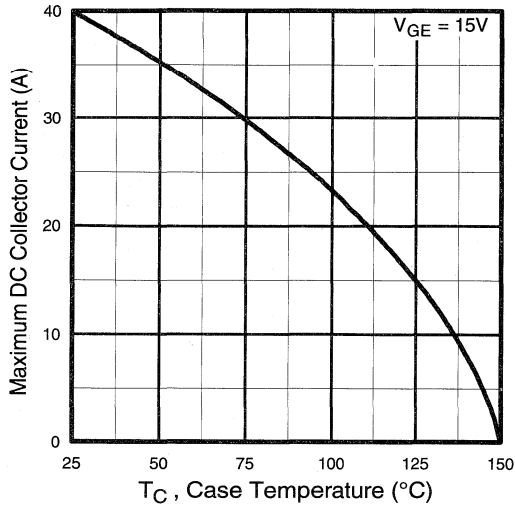


Fig. 4 - Maximum Collector Current vs. Case Temperature

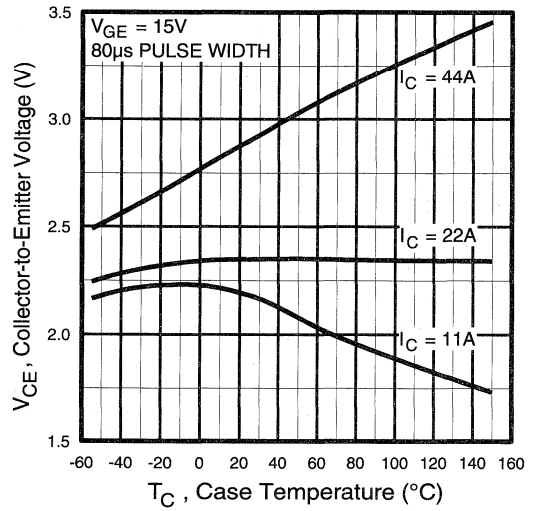


Fig. 5 - Collector-to-Emitter Voltage vs. Case Temperature

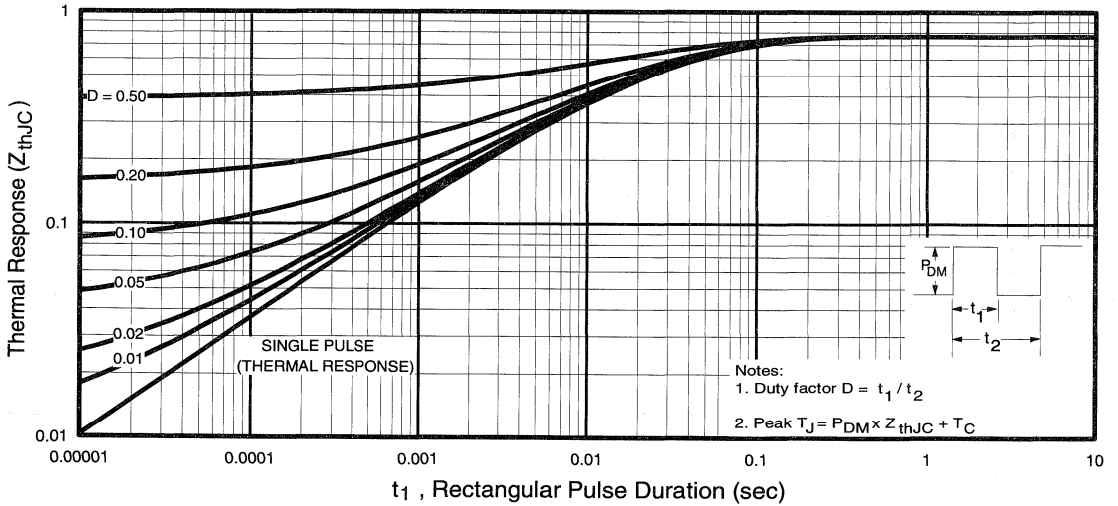


Fig. 6 - Maximum Effective Transient Thermal Impedance, Junction-to-Case

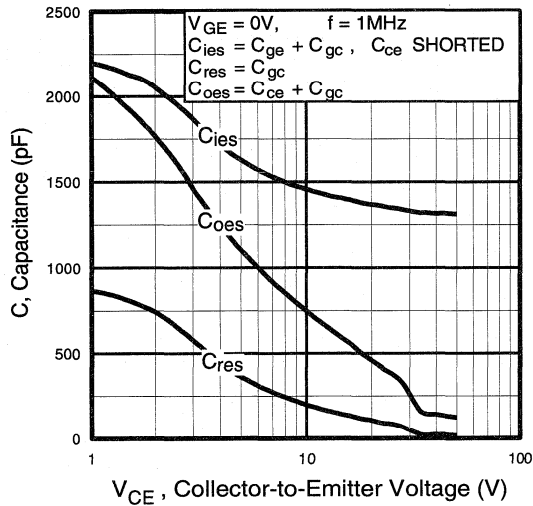


Fig. 7 - Typical Capacitance vs. Collector-to-Emitter Voltage

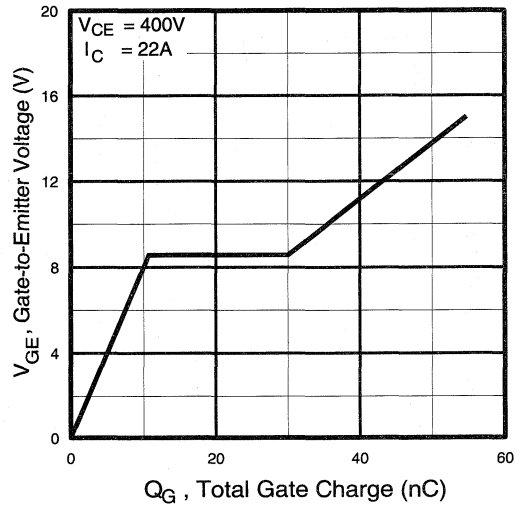


Fig. 8 - Typical Gate Charge vs. Gate-to-Emitter Voltage

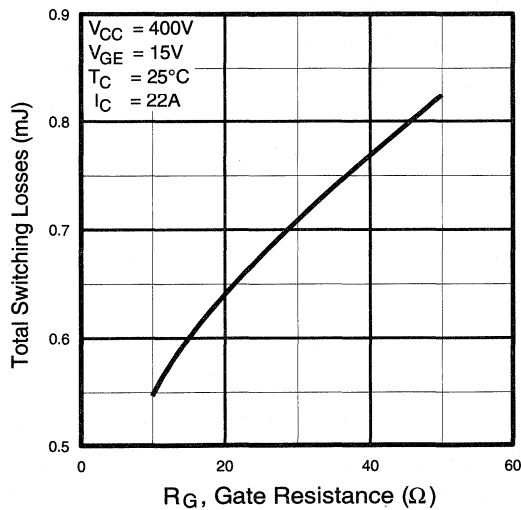


Fig. 9 - Typical Switching Losses vs. Gate Resistance

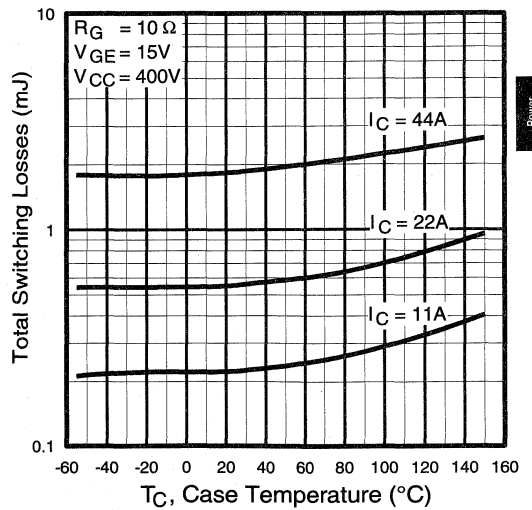


Fig. 10 - Typical Switching Losses vs. Case Temperature

Power Conversion
Ultra-Fast
Discretes

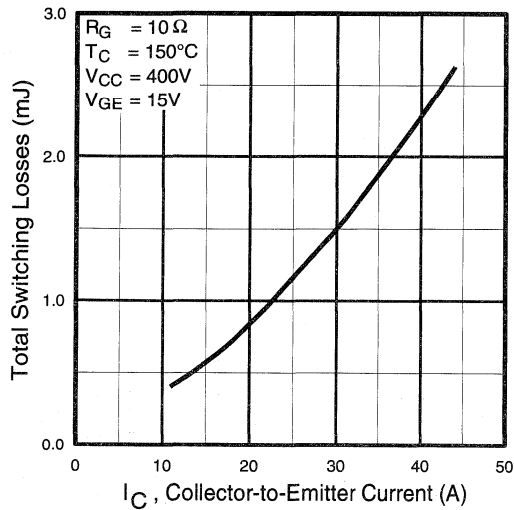


Fig. 11 - Typical Switching Losses vs. Collector-to-Emitter Current

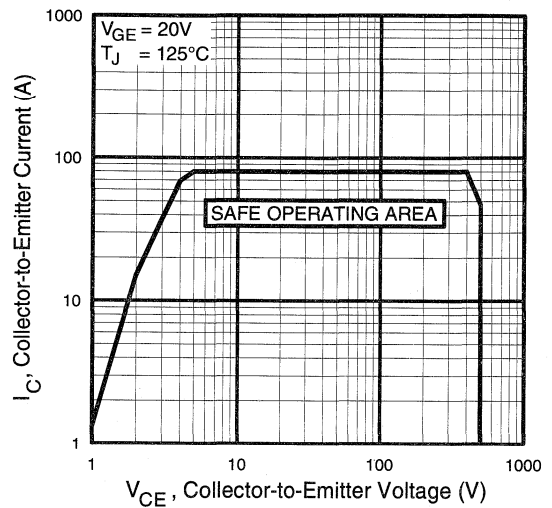


Fig. 12 - Turn-Off SOA

Refer to Section D for the following:

Appendix A: Section D - page D-3

Fig. 13a - Clamped Inductive Load Test Circuit

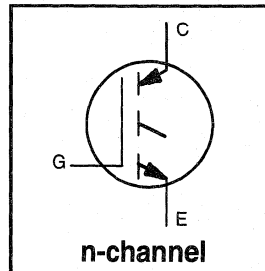
Fig. 13b - Pulsed Collector Current Test Circuit

Fig. 14a - Switching Loss Test Circuit

Fig. 14b - Switching Loss Waveform

Features

- Switching-loss rating includes all "tail" losses
- Optimized for high operating frequency (over 5kHz)
See Fig. 1 for Current vs. Frequency curve



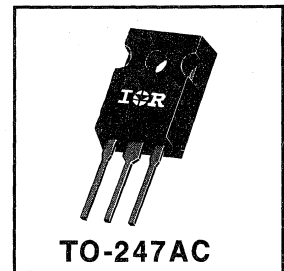
$$V_{CES} = 500V$$

$$V_{CE(sat)} \leq 3.0V$$

$$@V_{GE} = 15V, I_C = 7.5A$$

Description

Insulated Gate Bipolar Transistors (IGBTs) from International Rectifier have higher usable current densities than comparable bipolar transistors, while at the same time having simpler gate-drive requirements of the familiar power MOSFET. They provide substantial benefits to a host of high-voltage, high-current applications.


TO-247AC

Absolute Maximum Ratings

	Parameter	Max.	Units
V_{CES}	Collector-to-Emitter Voltage	500	V
$I_C @ T_C = 25^\circ C$	Continuous Collector Current	14	A
$I_C @ T_C = 100^\circ C$	Continuous Collector Current	7.5	
I_{CM}	Pulsed Collector Current ①	28	
I_{LM}	Clamped Inductive Load Current ②	28	
V_{GE}	Gate-to-Emitter Voltage	± 20	V
E_{ARV}	Reverse Voltage Avalanche Energy ③	5.0	mJ
$P_D @ T_C = 25^\circ C$	Maximum Power Dissipation	60	W
$P_D @ T_C = 100^\circ C$	Maximum Power Dissipation	24	
T_J	Operating Junction and	-55 to +150	°C
T_{STG}	Storage Temperature Range		
	Soldering Temperature, for 10 sec.	300 (0.063 in. (1.6mm) from case)	
	Mounting torque, 6-32 or M3 screw.	10 lbf•in (1.1N•m)	

Thermal Resistance

	Parameter	Min.	Typ.	Max.	Units
$R_{\theta JC}$	Junction-to-Case	—	—	2.1	°C/W
$R_{\theta CS}$	Case-to-Sink, flat, greased surface	—	0.24	—	
$R_{\theta JA}$	Junction-to-Ambient, typical socket mount	—	—	40	
Wt	Weight	—	6 (0.21)	—	g (oz)

Electrical Characteristics @ $T_J = 25^\circ\text{C}$ (unless otherwise specified)

	Parameter	Min.	Typ.	Max.	Units	Conditions
$V_{(BR)CES}$	Collector-to-Emitter Breakdown Voltage	500	—	—	V	$V_{GE} = 0V, I_C = 250\mu A$
$V_{(BR)ECS}$	Emitter-to-Collector Breakdown Voltage ④	20	—	—	V	$V_{GE} = 0V, I_C = 1.0A$
$\Delta V_{(BR)CES}/\Delta T_J$	Temperature Coeff. of Breakdown Voltage	—	0.47	—	$V/^\circ\text{C}$	$V_{GE} = 0V, I_C = 1.0mA$
$V_{CE(on)}$	Collector-to-Emitter Saturation Voltage	—	2.4	3.0	V	$I_C = 7.5A$ $V_{GE} = 15V$ See Fig. 2, 5
		—	3.1	—		
		—	2.7	—		
$V_{GE(th)}$	Gate Threshold Voltage	3.0	—	5.5		$V_{CE} = V_{GE}, I_C = 250\mu A$
$\Delta V_{GE(th)}/\Delta T_J$	Temperature Coeff. of Threshold Voltage	—	-1.0	—	$mV/^\circ\text{C}$	$V_{CE} = V_{GE}, I_C = 250\mu A$
g_{fe}	Forward Transconductance ⑤	1.2	2.0	—	S	$V_{CE} = 100V, I_C = 7.5A$
I_{CES}	Zero Gate Voltage Collector Current	—	—	250	μA	$V_{GE} = 0V, V_{CE} = 500V$
		—	—	1000		$V_{GE} = 0V, V_{CE} = 500V, T_J = 150^\circ\text{C}$
I_{GES}	Gate-to-Emitter Leakage Current	—	—	± 100	nA	$V_{GE} = \pm 20V$

Switching Characteristics @ $T_J = 25^\circ\text{C}$ (unless otherwise specified)

	Parameter	Min.	Typ.	Max.	Units	Conditions
Q_g	Total Gate Charge (turn-on)	—	15	23	nC	$I_C = 7.5A$ $V_{CC} = 400V$ $V_{GE} = 15V$ See Fig. 8
Q_{ge}	Gate - Emitter Charge (turn-on)	—	3.7	5.6		
Q_{gc}	Gate - Collector Charge (turn-on)	—	6.5	9.8		
$t_{d(on)}$	Turn-On Delay Time	—	28	—	ns	$T_J = 25^\circ\text{C}$ $I_C = 7.5A, V_{CC} = 400V$ $V_{GE} = 15V, R_G = 50\Omega$ Energy losses include "tail"
t_r	Rise Time	—	11	—		
$t_{d(off)}$	Turn-Off Delay Time	—	72	110		
t_f	Fall Time	—	96	140		
E_{on}	Turn-On Switching Loss	—	0.13	—	mJ	See Fig. 9, 10, 11, 14
E_{off}	Turn-Off Switching Loss	—	0.08	—		
E_{ts}	Total Switching Loss	—	0.21	0.28		
$t_{d(on)}$	Turn-On Delay Time	—	26	—	ns	$T_J = 150^\circ\text{C}$, $I_C = 7.5A, V_{CC} = 400V$ $V_{GE} = 15V, R_G = 50\Omega$ Energy losses include "tail"
t_r	Rise Time	—	12	—		
$t_{d(off)}$	Turn-Off Delay Time	—	120	—		
t_f	Fall Time	—	140	—		
E_{ts}	Total Switching Loss	—	0.35	—	mJ	See Fig. 10, 14
L_E	Internal Emitter Inductance	—	13	—	nH	Measured 5mm from package
C_{ies}	Input Capacitance	—	330	—	pF	$V_{GE} = 0V$ $V_{CC} = 30V$ See Fig. 7 $f = 1.0MHz$
C_{oes}	Output Capacitance	—	47	—		
C_{res}	Reverse Transfer Capacitance	—	5.9	—		

Notes:

- ① Repetitive rating; $V_{GE}=20V$, pulse width limited by max. junction temperature. (See fig. 13b)
- ② $V_{CC}=80\%(V_{CES}), V_{GE}=20V, L=10\mu H, R_G=50\Omega$, (See fig. 13a)
- ③ Repetitive rating; pulse width limited by maximum junction temperature.
- ④ Pulse width $\leq 80\mu s$; duty factor $\leq 0.1\%$.
- ⑤ Pulse width $5.0\mu s$, single shot.

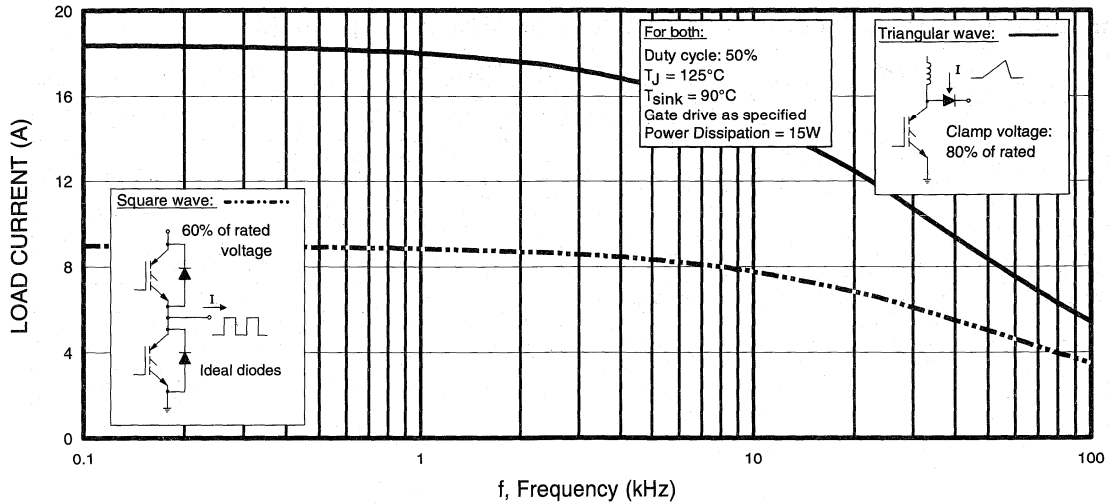


Fig. 1 - Typical Load Current vs. Frequency
 (For square wave, $I = I_{\text{RMS}}$ of fundamental; for triangular wave, $I = I_{\text{PK}}$)

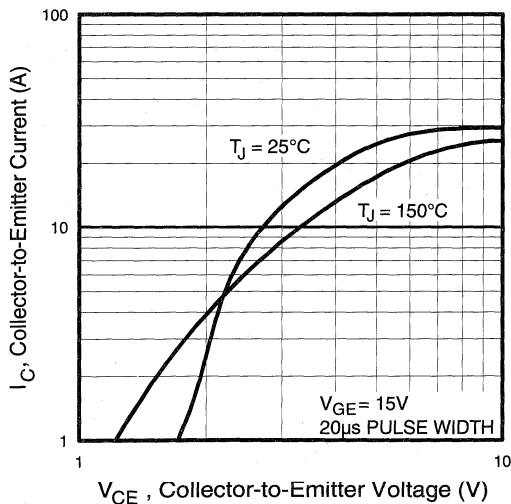


Fig. 2 - Typical Output Characteristics

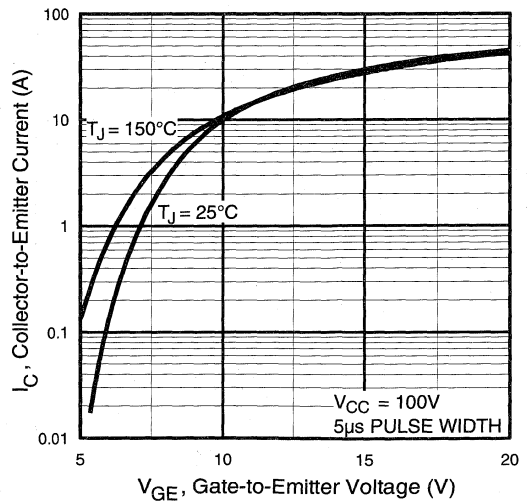


Fig. 3 - Typical Transfer Characteristics

Power
 Conversion
 Ultrafast
 Discrete

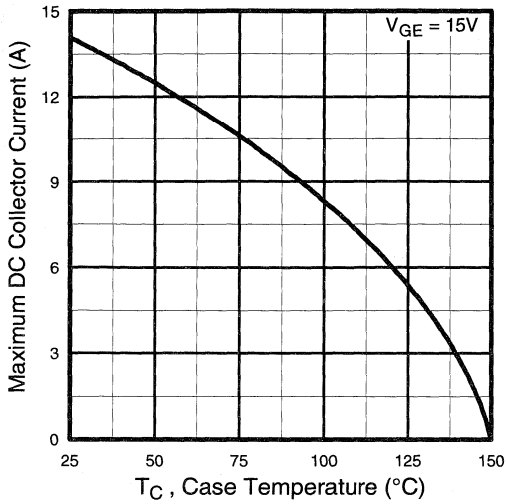


Fig. 4 - Maximum Collector Current vs. Case Temperature

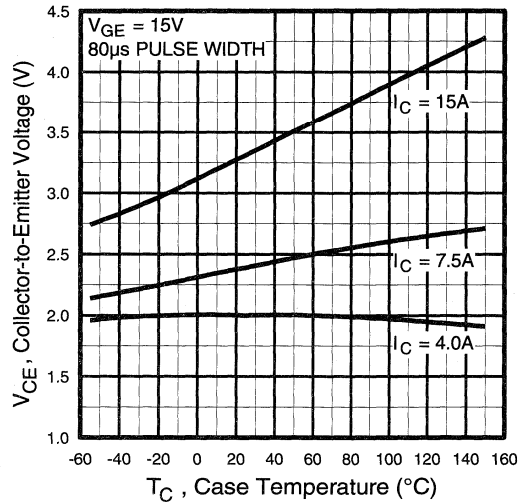


Fig. 5 - Collector-to-Emitter Voltage vs. Case Temperature

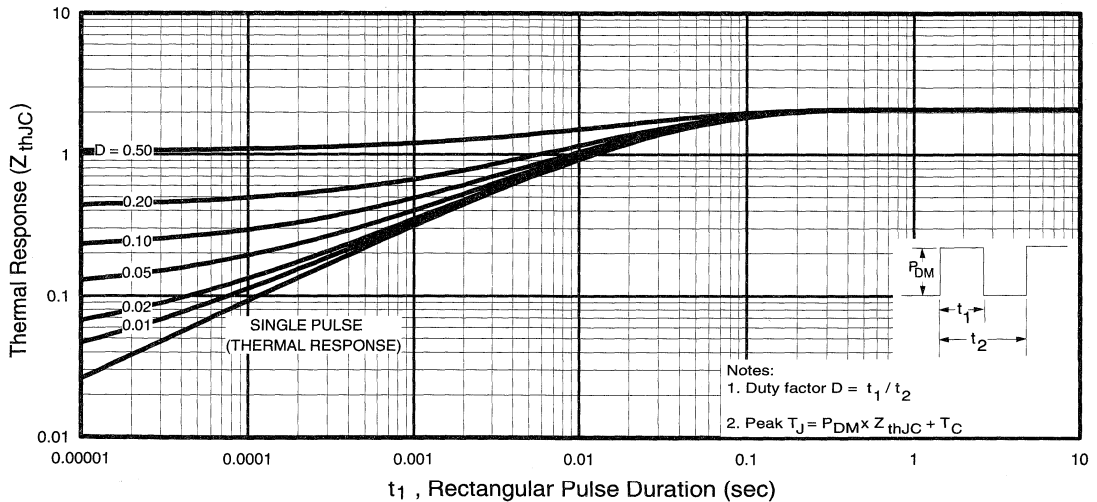


Fig. 6 - Maximum Effective Transient Thermal Impedance, Junction-to-Case

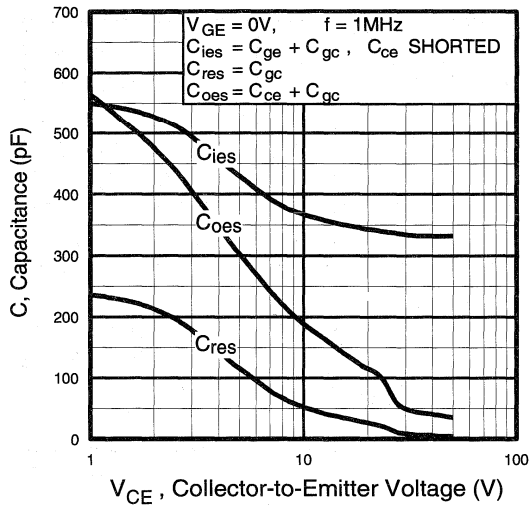


Fig. 7 - Typical Capacitance vs. Collector-to-Emitter Voltage

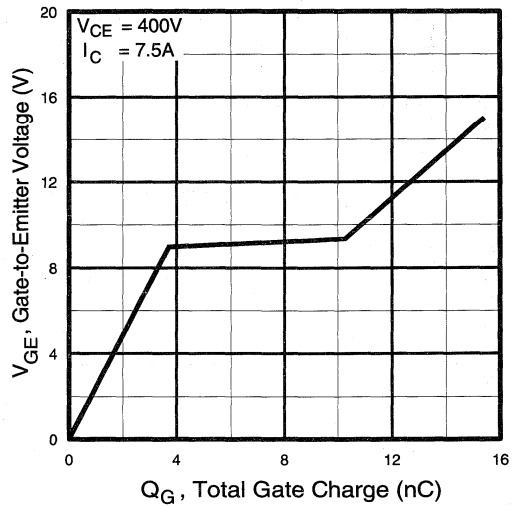


Fig. 8 - Typical Gate Charge vs. Gate-to-Emitter Voltage

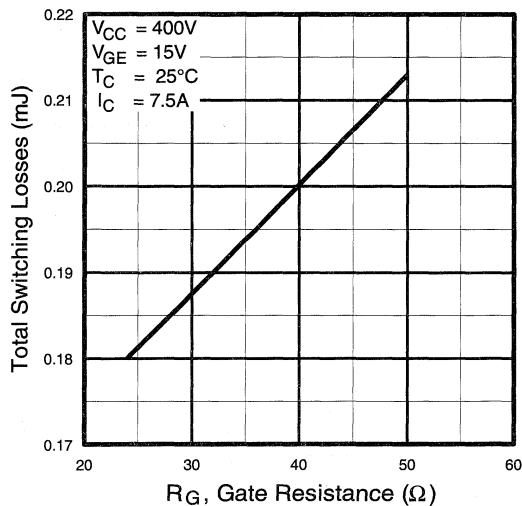


Fig. 9 - Typical Switching Losses vs. Gate Resistance

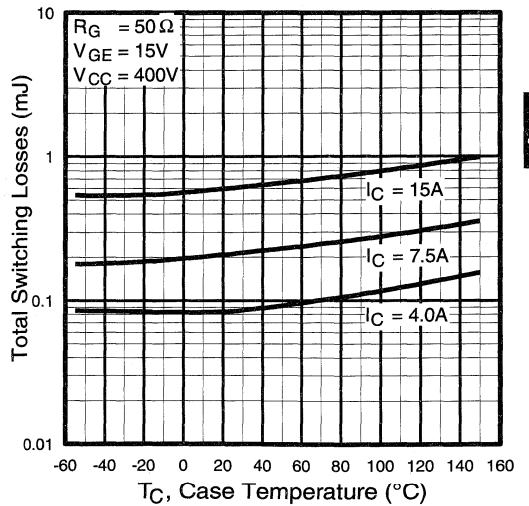


Fig. 10 - Typical Switching Losses vs. Case Temperature

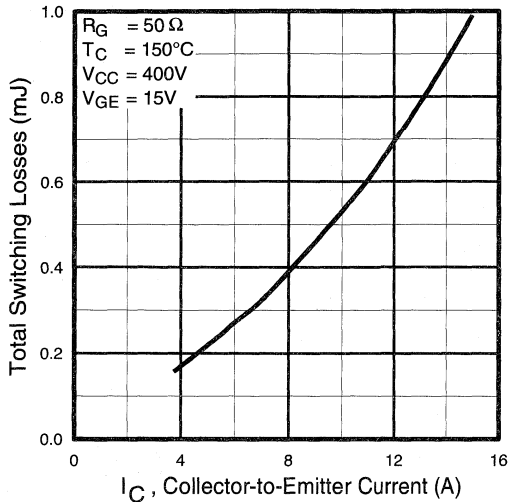


Fig. 11 - Typical Switching Losses vs. Collector-to-Emitter Current

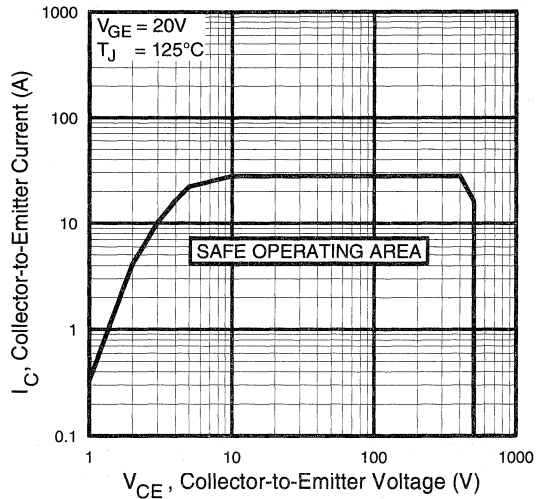


Fig. 12 - Turn-Off SOA

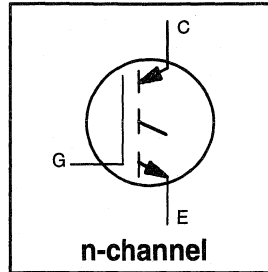
Refer to Section D for the following:

Appendix A: Section D - page D-3

- Fig. 13a - Clamped Inductive Load Test Circuit
- Fig. 13b - Pulsed Collector Current Test Circuit
- Fig. 14a - Switching Loss Test Circuit
- Fig. 14b - Switching Loss Waveform

Features

- Switching-loss rating includes all "tail" losses
- Optimized for high operating frequency (over 5kHz)
See Fig. 1 for Current vs. Frequency curve



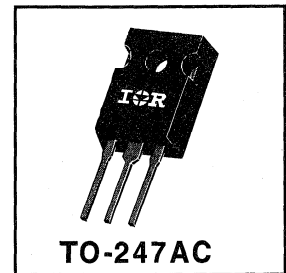
$$V_{CES} = 500V$$

$$V_{CE(sat)} \leq 3.0V$$

$$@ V_{GE} = 15V, I_C = 15A$$

Description

Insulated Gate Bipolar Transistors (IGBTs) from International Rectifier have higher usable current densities than comparable bipolar transistors, while at the same time having simpler gate-drive requirements of the familiar power MOSFET. They provide substantial benefits to a host of high-voltage, high-current applications.



Absolute Maximum Ratings

	Parameter	Max.	Units
V_{CES}	Collector-to-Emitter Voltage	500	V
$I_C @ T_C = 25^\circ C$	Continuous Collector Current	25	A
$I_C @ T_C = 100^\circ C$	Continuous Collector Current	15	
I_{CM}	Pulsed Collector Current ①	50	
I_{LM}	Clamped Inductive Load Current ②	50	
V_{GE}	Gate-to-Emitter Voltage	± 20	
E_{ARV}	Reverse Voltage Avalanche Energy ③	10	mJ
$P_D @ T_C = 25^\circ C$	Maximum Power Dissipation	100	W
$P_D @ T_C = 100^\circ C$	Maximum Power Dissipation	42	
T_J	Operating Junction and	-55 to +150	°C
T_{STG}	Storage Temperature Range		
	Soldering Temperature, for 10 sec.	300 (0.063 in. (1.6mm) from case)	
	Mounting torque, 6-32 or M3 screw.	10 lbf•in (1.1N•m)	

Thermal Resistance

	Parameter	Min.	Typ.	Max.	Units
$R_{\theta JC}$	Junction-to-Case	—	—	1.2	°C/W
$R_{\theta CS}$	Case-to-Sink, flat, greased surface	—	0.24	—	
$R_{\theta JA}$	Junction-to-Ambient, typical socket mount	—	—	40	
Wt	Weight	—	6 (0.21)	—	g (oz)

Electrical Characteristics @ $T_J = 25^\circ\text{C}$ (unless otherwise specified)

	Parameter	Min.	Typ.	Max.	Units	Conditions
$V_{(BR)CES}$	Collector-to-Emitter Breakdown Voltage	500	—	—	V	$V_{GE} = 0V, I_C = 250\mu A$
$V_{(BR)ECS}$	Emitter-to-Collector Breakdown Voltage ④	20	—	—	V	$V_{GE} = 0V, I_C = 1.0A$
$\Delta V_{(BR)CES}/\Delta T_J$	Temperature Coeff. of Breakdown Voltage	—	0.46	—	V/°C	$V_{GE} = 0V, I_C = 1.0mA$
$V_{CE(on)}$	Collector-to-Emitter Saturation Voltage	—	2.3	3.0	V	$V_{GE} = 15V$ See Fig. 2, 5
		—	2.8	—		
		—	2.6	—		
$V_{GE(th)}$	Gate Threshold Voltage	3.0	—	5.5		$I_C = 15A, T_J = 150^\circ\text{C}$
$\Delta V_{GE(th)}/\Delta T_J$	Temperature Coeff. of Threshold Voltage	—	-11	—	mV/°C	$V_{CE} = V_{GE}, I_C = 250\mu A$
g_{fe}	Forward Transconductance ⑤	2.3	8.1	—	S	$V_{CE} = 100V, I_C = 15A$
I_{CES}	Zero Gate Voltage Collector Current	—	—	250	μA	$V_{GE} = 0V, V_{CE} = 500V$
		—	—	1000		$V_{GE} = 0V, V_{CE} = 500V, T_J = 150^\circ\text{C}$
I_{GES}	Gate-to-Emitter Leakage Current	—	—	± 100	nA	$V_{GE} = \pm 20V$

Switching Characteristics @ $T_J = 25^\circ\text{C}$ (unless otherwise specified)

	Parameter	Min.	Typ.	Max.	Units	Conditions
Q_g	Total Gate Charge (turn-on)	—	31	47	nC	$I_C = 15A$ $V_{CC} = 400V$ $V_{GE} = 15V$ See Fig. 8
Q_{ge}	Gate - Emitter Charge (turn-on)	—	6.2	9.3		
Q_{gc}	Gate - Collector Charge (turn-on)	—	12	19		
$t_{d(on)}$	Turn-On Delay Time	—	29	—	ns	$T_J = 25^\circ\text{C}$ $I_C = 15A, V_{CC} = 400V$ $V_{GE} = 15V, R_G = 23\Omega$ Energy losses include "tail"
t_r	Rise Time	—	11	—		
$t_{d(off)}$	Turn-Off Delay Time	—	91	160		
t_f	Fall Time	—	66	120		
E_{on}	Turn-On Switching Loss	—	0.24	—	mJ	See Fig. 9, 10, 11, 14
E_{off}	Turn-Off Switching Loss	—	0.17	—		
E_{ts}	Total Switching Loss	—	0.41	0.61		
$t_{d(on)}$	Turn-On Delay Time	—	13	—	ns	$T_J = 150^\circ\text{C}$, $I_C = 15A, V_{CC} = 400V$ $V_{GE} = 15V, R_G = 23\Omega$ Energy losses include "tail"
t_r	Rise Time	—	27	—		
$t_{d(off)}$	Turn-Off Delay Time	—	130	—		
t_f	Fall Time	—	130	—		
E_{ts}	Total Switching Loss	—	0.76	—	mJ	See Fig. 10, 14
L_E	Internal Emitter Inductance	—	13	—	nH	Measured 5mm from package
C_{ies}	Input Capacitance	—	660	—	pF	$V_{GE} = 0V$ $V_{CC} = 30V$ $f = 1.0MHz$ See Fig. 7
C_{oes}	Output Capacitance	—	110	—		
C_{res}	Reverse Transfer Capacitance	—	12	—		

Notes:

- ① Repetitive rating; $V_{GE}=20V$, pulse width limited by max. junction temperature. (See fig. 13b)
- ② $V_{CC}=80\%(V_{CES}), V_{GE}=20V, L=10\mu H, R_G=23\Omega$, (See fig. 13a)
- ③ Repetitive rating; pulse width limited by maximum junction temperature.
- ④ Pulse width $\leq 80\mu s$; duty factor $\leq 0.1\%$.
- ⑤ Pulse width 5.0 μs , single shot.

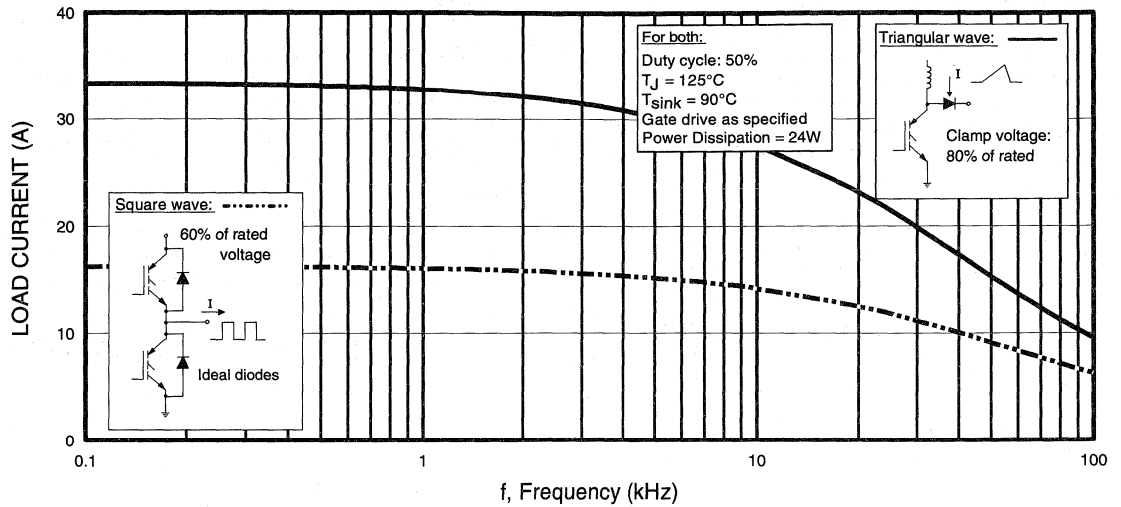


Fig. 1 - Typical Load Current vs. Frequency
 (For square wave, $I = I_{RMS}$ of fundamental; for triangular wave, $I = I_{PK}$)

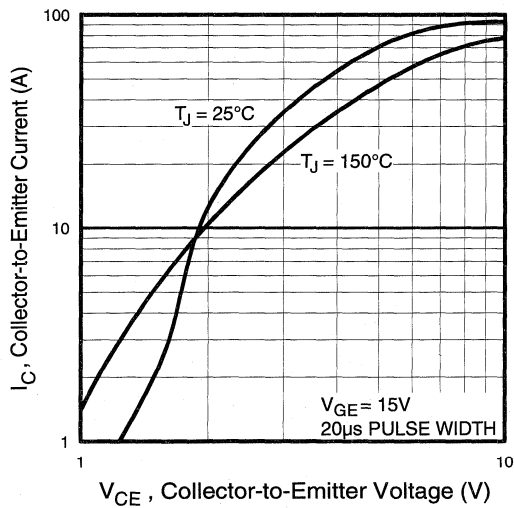


Fig. 2 - Typical Output Characteristics

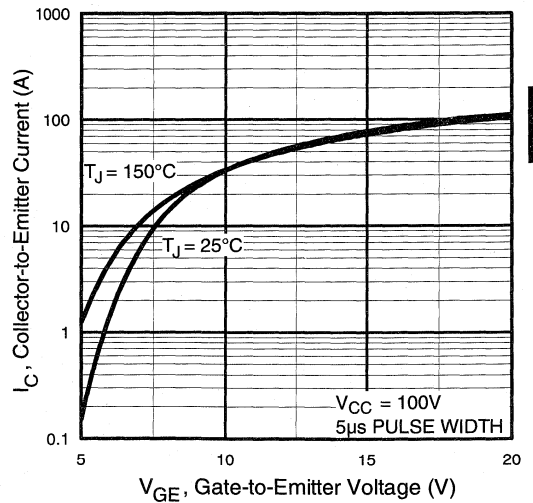


Fig. 3 - Typical Transfer Characteristics

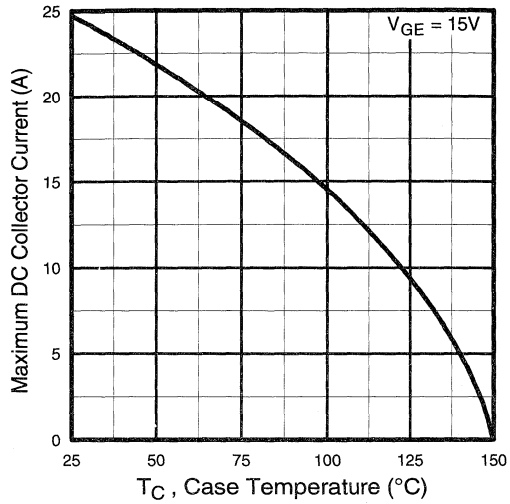


Fig. 4 - Maximum Collector Current vs. Case Temperature

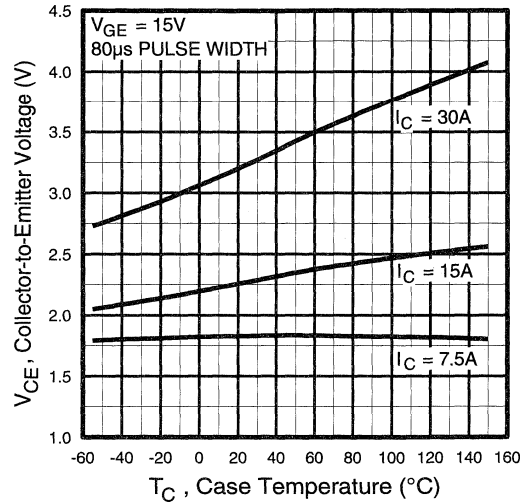


Fig. 5 - Collector-to-Emitter Voltage vs. Case Temperature

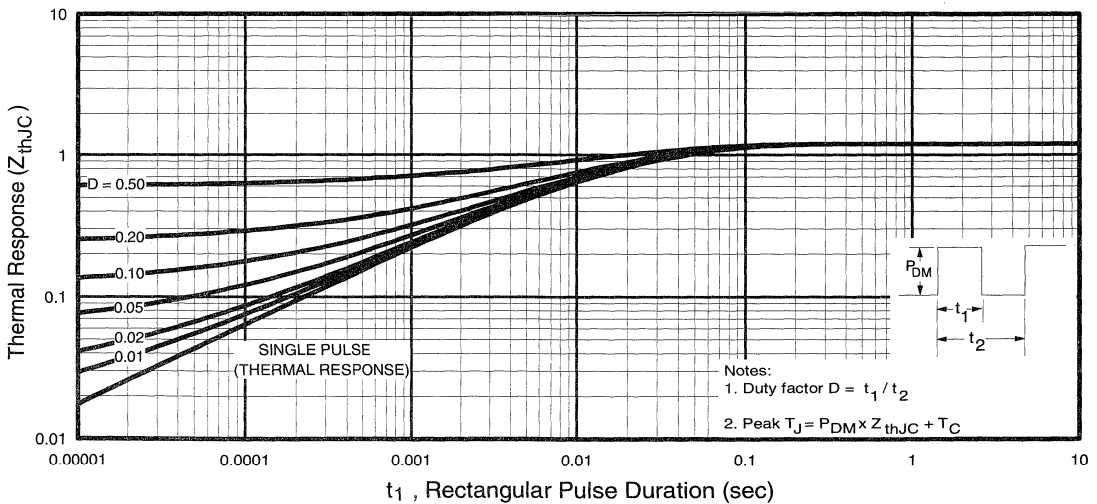


Fig. 6 - Maximum Effective Transient Thermal Impedance, Junction-to-Case

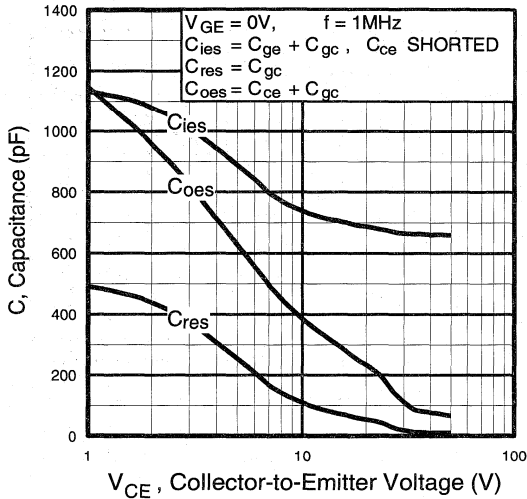


Fig. 7 - Typical Capacitance vs. Collector-to-Emitter Voltage

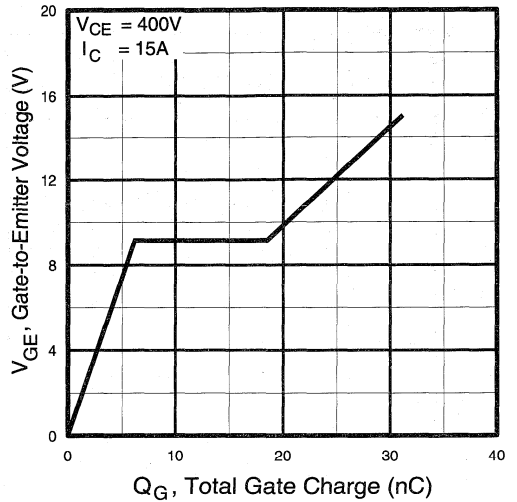


Fig. 8 - Typical Gate Charge vs. Gate-to-Emitter Voltage

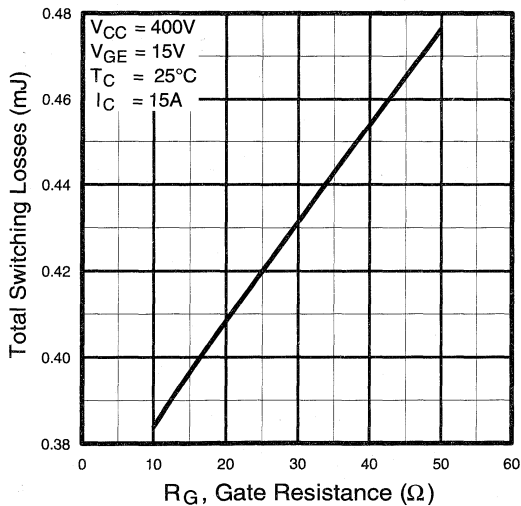


Fig. 9 - Typical Switching Losses vs. Gate Resistance

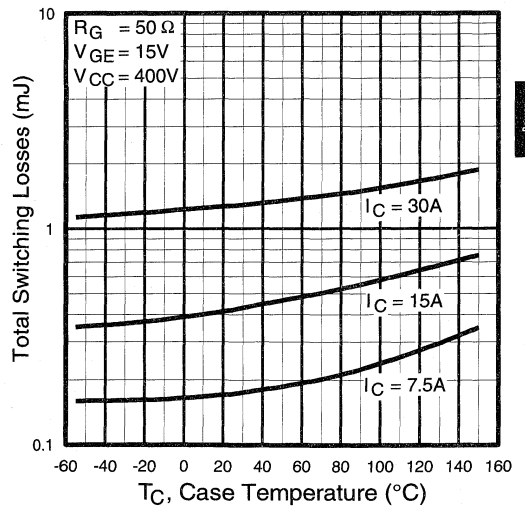


Fig. 10 - Typical Switching Losses vs. Case Temperature

Power
Conversion
Ultra-Fast
Discretes

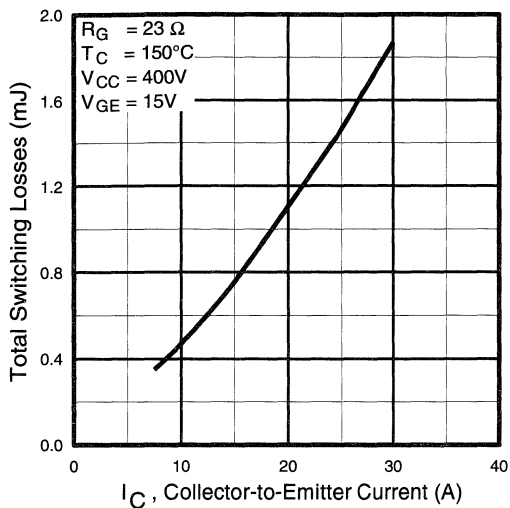


Fig. 11 - Typical Switching Losses vs. Collector-to-Emitter Current

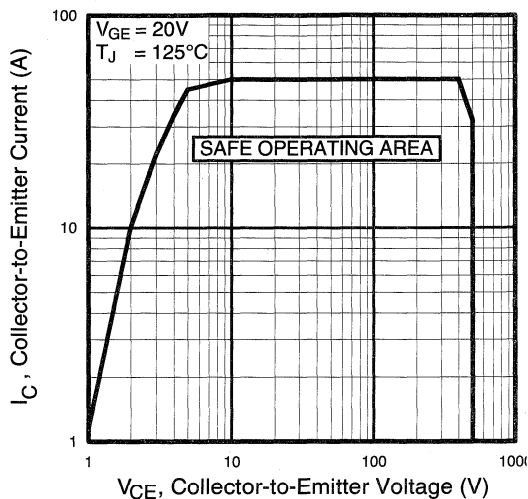


Fig. 12 - Turn-Off SOA

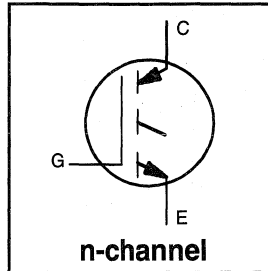
Refer to Section D for the following:

Appendix A: Section D - page D-3

- Fig. 13a - Clamped Inductive Load Test Circuit
- Fig. 13b - Pulsed Collector Current Test Circuit
- Fig. 14a - Switching Loss Test Circuit
- Fig. 14b - Switching Loss Waveform

Features

- Switching-loss rating includes all "tail" losses
- Optimized for high operating frequency (over 5kHz)
See Fig. 1 for Current vs. Frequency curve



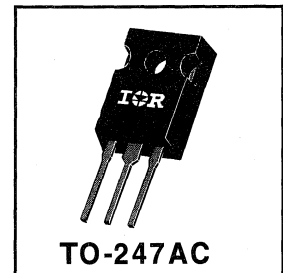
$$V_{CES} = 500V$$

$$V_{CE(sat)} \leq 3.0V$$

$$@V_{GE} = 15V, I_C = 22A$$

Description

Insulated Gate Bipolar Transistors (IGBTs) from International Rectifier have higher usable current densities than comparable bipolar transistors, while at the same time having simpler gate-drive requirements of the familiar power MOSFET. They provide substantial benefits to a host of high-voltage, high-current applications.



Absolute Maximum Ratings

	Parameter	Max.	Units
V_{CES}	Collector-to-Emitter Voltage	500	V
$I_C @ T_C = 25^\circ C$	Continuous Collector Current	40	A
$I_C @ T_C = 100^\circ C$	Continuous Collector Current	22	
I_{CM}	Pulsed Collector Current ①	80	
I_{LM}	Clamped Inductive Load Current ②	80	
V_{GE}	Gate-to-Emitter Voltage	± 20	V
E_{ARV}	Reverse Voltage Avalanche Energy ③	15	mJ
$P_D @ T_C = 25^\circ C$	Maximum Power Dissipation	160	W
$P_D @ T_C = 100^\circ C$	Maximum Power Dissipation	65	
T_J	Operating Junction and Storage Temperature Range	-55 to +150	$^\circ C$
T_{STG}			
	Mounting torque, 6-32 or M3 screw.	10 lbf•in (1.1N•m)	

Thermal Resistance

	Parameter	Min.	Typ.	Max.	Units
$R_{\theta JC}$	Junction-to-Case	—	—	0.77	$^\circ C/W$
$R_{\theta CS}$	Case-to-Sink, flat, greased surface	—	0.24	—	
$R_{\theta JA}$	Junction-to-Ambient, typical socket mount	—	—	40	
Wt	Weight	—	6 (0.21)	—	g (oz)

 Power
Conversion
Ultra-Fast
Discretes

Electrical Characteristics @ $T_J = 25^\circ\text{C}$ (unless otherwise specified)

	Parameter	Min.	Typ.	Max.	Units	Conditions
$V_{(BR)CES}$	Collector-to-Emitter Breakdown Voltage	500	—	—	V	$V_{GE} = 0V, I_C = 250\mu A$
$V_{(BR)ECS}$	Emitter-to-Collector Breakdown Voltage ④	20	—	—	V	$V_{GE} = 0V, I_C = 1.0A$
$\Delta V_{(BR)CES}/\Delta T_J$	Temp. Coeff. of Breakdown Voltage	—	0.35	—	V/°C	$V_{GE} = 0V, I_C = 1.0mA$
$V_{CE(on)}$	Collector-to-Emitter Saturation Voltage	—	2.4	3.0	V	$I_C = 22A$ $I_C = 40A$ $I_C = 22A, T_J = 150^\circ\text{C}$ See Fig. 2, 5
		—	2.8	—		
		—	2.4	—		
$V_{GE(th)}$	Gate Threshold Voltage	3.0	—	5.5		$V_{CE} = V_{GE}, I_C = 250\mu A$
$\Delta V_{GE(th)}/\Delta T_J$	Temperature Coeff. of Threshold Voltage	—	-11	—	mV/°C	$V_{CE} = V_{GE}, I_C = 250\mu A$
g_{fe}	Forward Transconductance ⑤	6.6	13	—	S	$V_{CE} = 100V, I_C = 22A$
I_{CES}	Zero Gate Voltage Collector Current	—	—	250	μA	$V_{GE} = 0V, V_{CE} = 500V$ $V_{GE} = 0V, V_{CE} = 500V, T_J = 150^\circ\text{C}$
		—	—	1000		
I_{GES}	Gate-to-Emitter Leakage Current	—	—	± 100	nA	$V_{GE} = \pm 20V$

Switching Characteristics @ $T_J = 25^\circ\text{C}$ (unless otherwise specified)

	Parameter	Min.	Typ.	Max.	Units	Conditions
Q_g	Total Gate Charge (turn-on)	—	55	83	nC	$I_C = 22A$ $V_{CC} = 400V$ $V_{GE} = 15V$ See Fig. 8
Q_{ge}	Gate - Emitter Charge (turn-on)	—	11	17		
Q_{gc}	Gate - Collector Charge (turn-on)	—	19	29		
$t_{d(on)}$	Turn-On Delay Time	—	27	—	ns	$T_J = 25^\circ\text{C}$ $I_C = 22A, V_{CC} = 400V$ $V_{GE} = 15V, R_G = 10\Omega$ Energy losses include "tail"
t_r	Rise Time	—	13	—		
$t_{d(off)}$	Turn-Off Delay Time	—	100	150		
t_f	Fall Time	—	56	100		
E_{on}	Turn-On Switching Loss	—	0.37	—	mJ	See Fig. 9, 10, 11, 14
E_{off}	Turn-Off Switching Loss	—	0.18	—		
E_{ts}	Total Switching Loss	—	0.55	0.70		
$t_{d(on)}$	Turn-On Delay Time	—	27	—	ns	$T_J = 150^\circ\text{C}$, $I_C = 22A, V_{CC} = 400V$ $V_{GE} = 15V, R_G = 10\Omega$ Energy losses include "tail"
t_r	Rise Time	—	15	—		
$t_{d(off)}$	Turn-Off Delay Time	—	137	—		
t_f	Fall Time	—	100	—		
E_{ts}	Total Switching Loss	—	0.96	—	mJ	See Fig. 10, 14
L_E	Internal Emitter Inductance	—	13	—	nH	Measured 5mm from package
C_{ies}	Input Capacitance	—	1400	—	pF	$V_{GE} = 0V$ $V_{CC} = 30V$ $f = 1.0MHz$ See Fig. 7
C_{oes}	Output Capacitance	—	250	—		
C_{res}	Reverse Transfer Capacitance	—	42	—		

Notes:

- ① Repetitive rating; $V_{GE}=20V$, pulse width limited by max. junction temperature. (See fig. 13b)
- ② $V_{CC}=80\%(V_{CES})$, $V_{GE}=20V$, $L=10\mu H$, $R_G=10\Omega$, (See fig. 13a)
- ③ Repetitive rating; pulse width limited by maximum junction temperature.
- ④ Pulse width $\leq 80\mu s$; duty factor $\leq 0.1\%$.
- ⑤ Pulse width $5.0\mu s$, single shot.

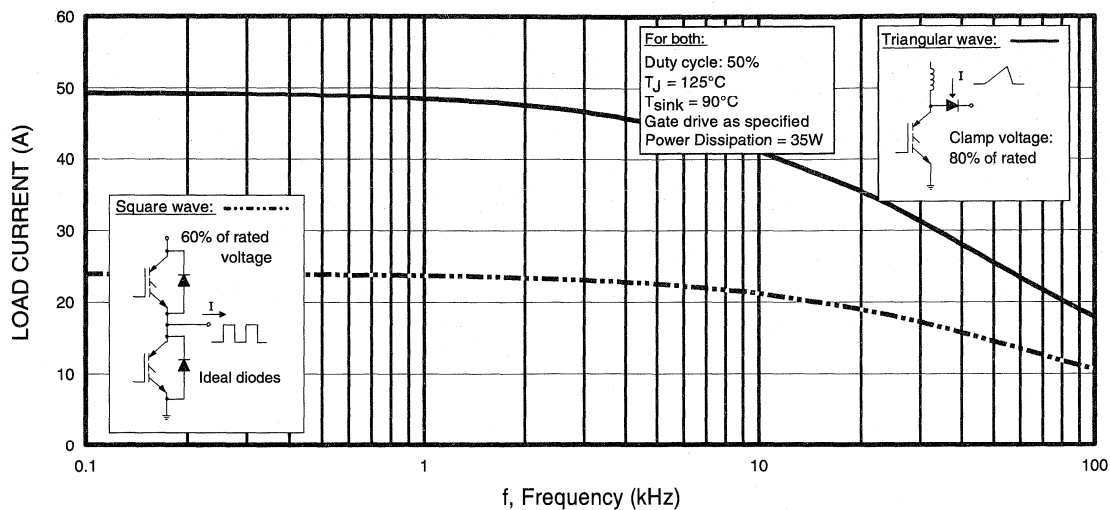


Fig. 1 - Typical Load Current vs. Frequency
 (For square wave, $I = I_{RMS}$ of fundamental; for triangular wave, $I = I_{PK}$)

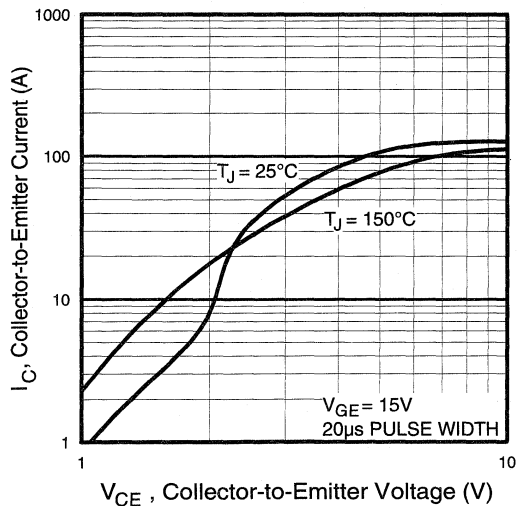


Fig. 2 - Typical Output Characteristics

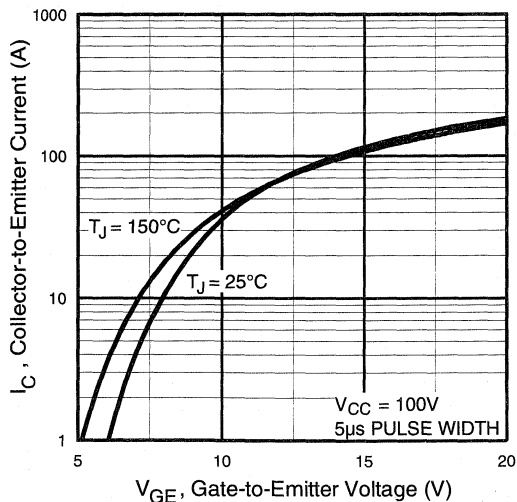


Fig. 3 - Typical Transfer Characteristics

Power
Conversion
Ultra-Fast
Discretes

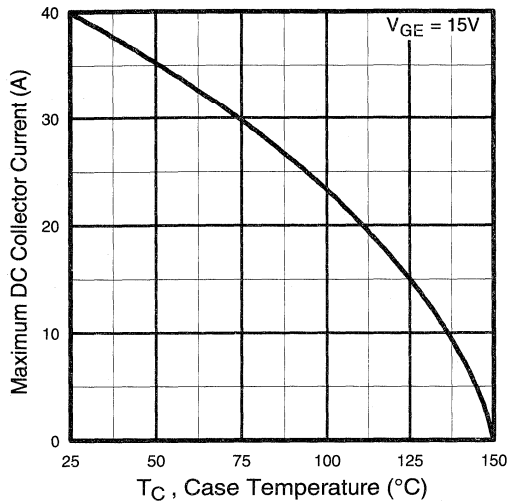


Fig. 4 - Maximum Collector Current vs. Case Temperature

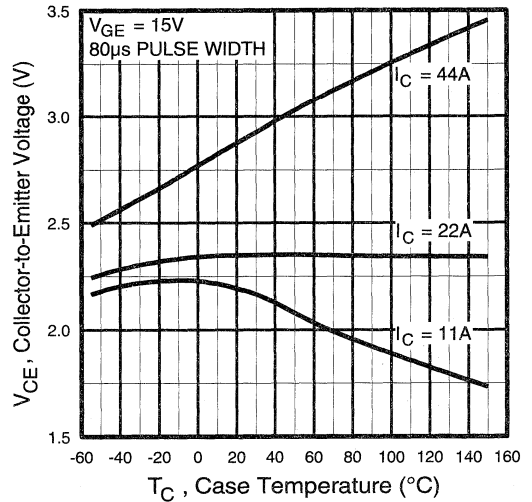


Fig. 5 - Collector-to-Emitter Voltage vs. Case Temperature

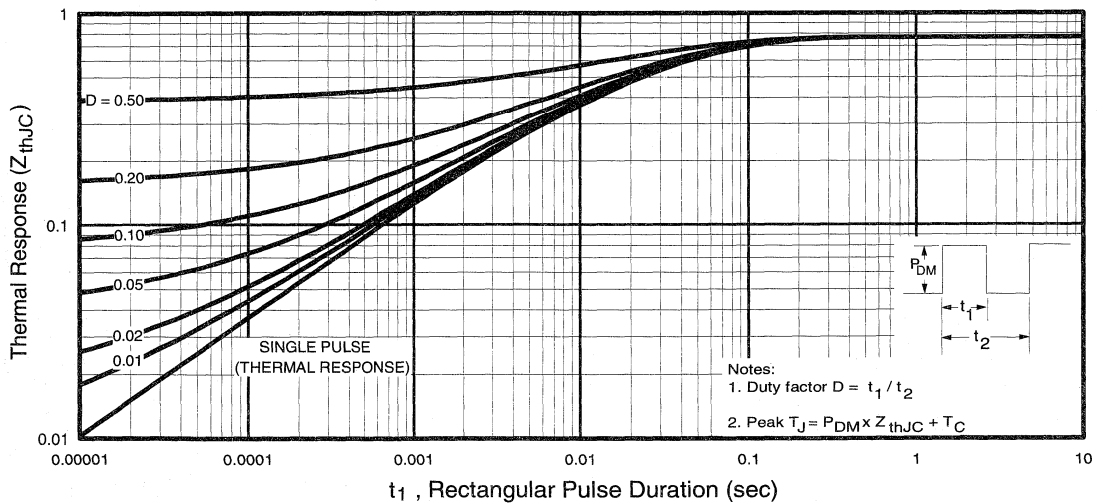


Fig. 6 - Maximum Effective Transient Thermal Impedance, Junction-to-Case

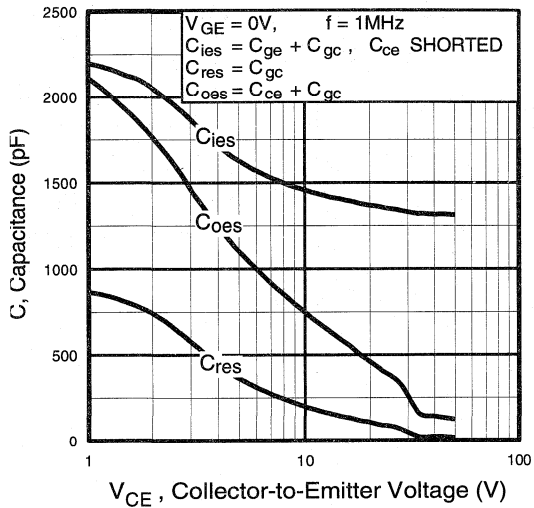


Fig. 7 - Typical Capacitance vs. Collector-to-Emitter Voltage

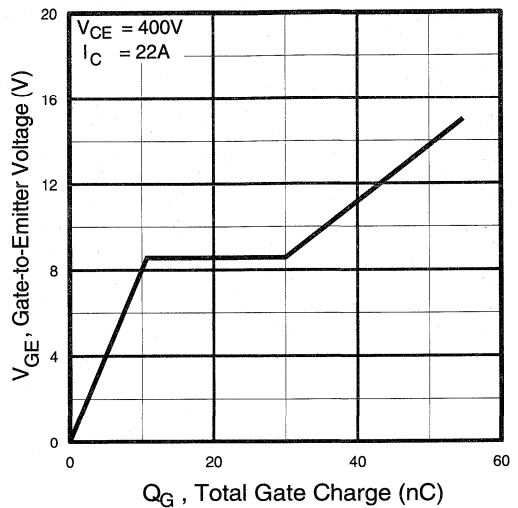


Fig. 8 - Typical Gate Charge vs. Gate-to-Emitter Voltage

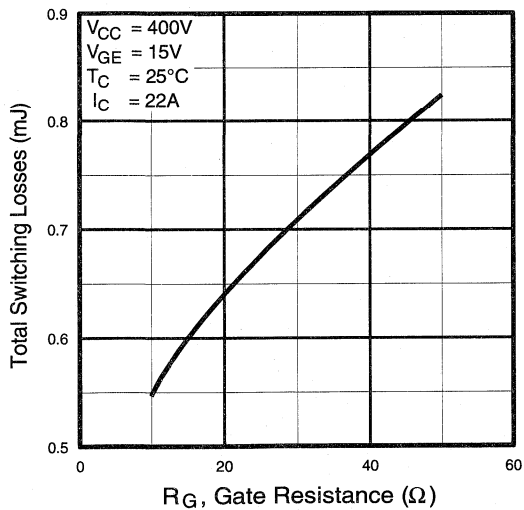


Fig. 9 - Typical Switching Losses vs. Gate Resistance

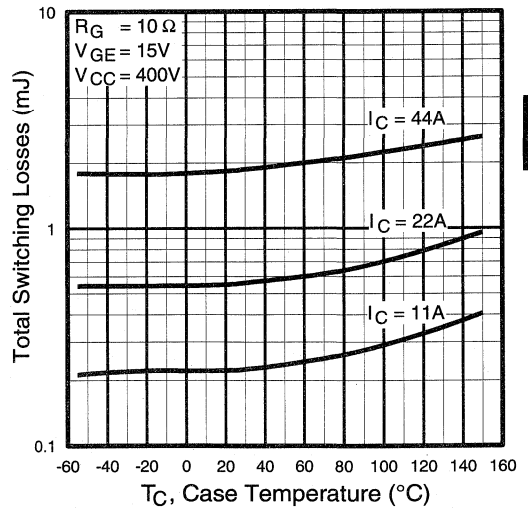


Fig. 10 - Typical Switching Losses vs. Case Temperature

Power Conversion
Ultra-Fast
Discretes

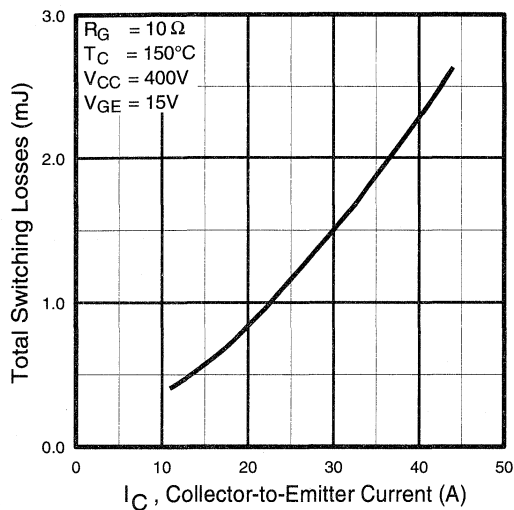


Fig. 11 - Typical Switching Losses vs. Collector-to-Emitter Current

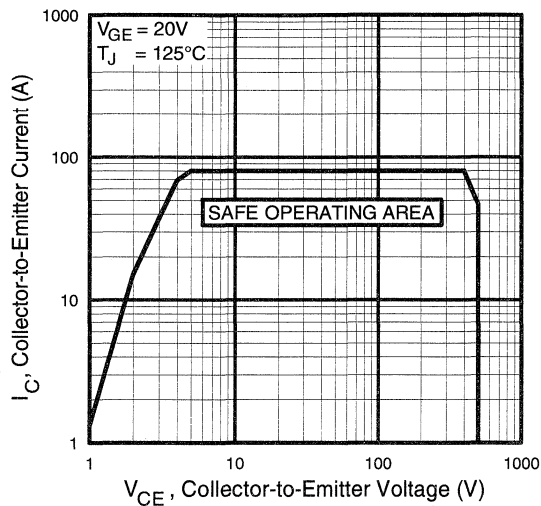


Fig. 12 - Turn-Off SOA

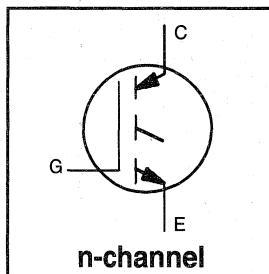
Refer to **Section D** for the following:

Appendix A: Section D - page D-3

- Fig. 13a - Clamped Inductive Load Test Circuit
- Fig. 13b - Pulsed Collector Current Test Circuit
- Fig. 14a - Switching Loss Test Circuit
- Fig. 14b - Switching Loss Waveform

Features

- Switching-loss rating includes all "tail" losses
- Optimized for high operating frequency (over 5kHz)
See Fig. 1 for Current vs. Frequency curve



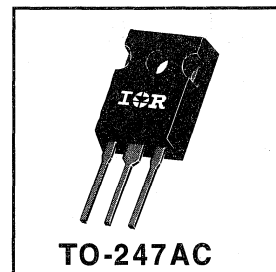
$$V_{CES} = 500V$$

$$V_{CE(sat)} \leq 3.2V$$

$$@V_{GE} = 15V, I_C = 33A$$

Description

Insulated Gate Bipolar Transistors (IGBTs) from International Rectifier have higher usable current densities than comparable bipolar transistors, while at the same time having simpler gate-drive requirements of the familiar power MOSFET. They provide substantial benefits to a host of high-voltage, high-current applications.



Absolute Maximum Ratings

	Parameter	Max.	Units
V_{CES}	Collector-to-Emitter Voltage	500	V
$I_C @ T_C = 25^\circ C$	Continuous Collector Current	59	A
$I_C @ T_C = 100^\circ C$	Continuous Collector Current	33	
I_{CM}	Pulsed Collector Current ①	120	
I_{LM}	Clamped Inductive Load Current ②	120	
V_{GE}	Gate-to-Emitter Voltage	± 20	V
E_{ARV}	Reverse Voltage Avalanche Energy ③	20	mJ
$P_D @ T_C = 25^\circ C$	Maximum Power Dissipation	200	W
$P_D @ T_C = 100^\circ C$	Maximum Power Dissipation	78	
T_J	Operating Junction and	-55 to +150	$^\circ C$
T_{STG}	Storage Temperature Range		
	Soldering Temperature, for 10 sec.		
	Mounting torque, 6-32 or M3 screw.	10 lbf•in (1.1N•m)	

Thermal Resistance

	Parameter	Min.	Typ.	Max.	Units
$R_{\theta JC}$	Junction-to-Case	—	—	0.64	$^\circ C/W$
$R_{\theta CS}$	Case-to-Sink, flat, greased surface	—	0.24	—	
$R_{\theta JA}$	Junction-to-Ambient, typical socket mount	—	—	40	
Wt	Weight	—	6 (0.21)	—	g (oz)

Electrical Characteristics @ $T_J = 25^\circ\text{C}$ (unless otherwise specified)

	Parameter	Min.	Typ.	Max.	Units	Conditions
$V_{(BR)CES}$	Collector-to-Emitter Breakdown Voltage	500	—	—	V	$V_{GE} = 0V, I_C = 250\mu A$
$V_{(BR)ECS}$	Emitter-to-Collector Breakdown Voltage ④	20	—	—	V	$V_{GE} = 0V, I_C = 1.0A$
$\Delta V_{(BR)CES}/\Delta T_J$	Temperature Coeff. of Breakdown Voltage	—	0.41	—	$V/^\circ\text{C}$	$V_{GE} = 0V, I_C = 1.0mA$
$V_{CE(on)}$	Collector-to-Emitter Saturation Voltage	—	2.1	3.2	V	$I_C = 33A$ $V_{GE} = 15V$ See Fig. 2, 5
		—	2.6	—		
		—	2.1	—		
$V_{GE(th)}$	Gate Threshold Voltage	3.0	—	5.5		$V_{CE} = V_{GE}, I_C = 250\mu A$
$\Delta V_{GE(th)}/\Delta T_J$	Temperature Coeff. of Threshold Voltage	—	-11	—	$mV/^\circ\text{C}$	$V_{CE} = V_{GE}, I_C = 250\mu A$
g_{fe}	Forward Transconductance ⑤	7.2	2.1	—	S	$V_{CE} = 100V, I_C = 33A$
I_{CES}	Zero Gate Voltage Collector Current	—	—	250	μA	$V_{GE} = 0V, V_{CE} = 500V$
		—	—	2000		$V_{GE} = 0V, V_{CE} = 500V, T_J = 150^\circ\text{C}$
I_{GES}	Gate-to-Emitter Leakage Current	—	—	± 100	nA	$V_{GE} = \pm 20V$

Switching Characteristics @ $T_J = 25^\circ\text{C}$ (unless otherwise specified)

	Parameter	Min.	Typ.	Max.	Units	Conditions
Q_g	Total Gate Charge (turn-on)	—	120	180	nC	$I_C = 33A$ $V_{CC} = 400V$ See Fig. 8
Q_{ge}	Gate - Emitter Charge (turn-on)	—	22	33		
Q_{gc}	Gate - Collector Charge (turn-on)	—	41	62		
$t_{d(on)}$	Turn-On Delay Time	—	33	—	ns	$T_J = 25^\circ\text{C}$ $I_C = 33A, V_{CC} = 400V$ $V_{GE} = 15V, R_G = 5.0\Omega$ Energy losses include "tail"
t_r	Rise Time	—	26	—		
$t_{d(off)}$	Turn-Off Delay Time	—	110	170		
t_f	Fall Time	—	91	140		
E_{on}	Turn-On Switching Loss	—	0.73	—	mJ	See Fig. 9, 10, 11, 14
E_{off}	Turn-Off Switching Loss	—	0.25	—		
E_{ts}	Total Switching Loss	—	0.98	1.5		
$t_{d(on)}$	Turn-On Delay Time	—	31	—	ns	$T_J = 150^\circ\text{C}$, $I_C = 33A, V_{CC} = 400V$ $V_{GE} = 15V, R_G = 5.0\Omega$ Energy losses include "tail"
t_r	Rise Time	—	29	—		
$t_{d(off)}$	Turn-Off Delay Time	—	160	—		
t_f	Fall Time	—	110	—		
E_{ts}	Total Switching Loss	—	1.4	—	mJ	See Fig. 10, 14
L_E	Internal Emitter Inductance	—	13	—	nH	Measured 5mm from package
C_{ies}	Input Capacitance	—	2700	—	pF	$V_{GE} = 0V$ $V_{CC} = 30V$ See Fig. 7
C_{oes}	Output Capacitance	—	280	—		
C_{res}	Reverse Transfer Capacitance	—	34	—		

Notes:

- ① Repetitive rating; $V_{GE} = 20V$, pulse width limited by max. junction temperature. (See fig. 13b)
- ② $V_{CC} = 80\%(V_{CES}), V_{GE} = 20V, L = 10\mu H, R_G = 5.0\Omega$, (See fig. 13a)
- ③ Repetitive rating; pulse width limited by maximum junction temperature.
- ④ Pulse width $\leq 80\mu s$; duty factor $\leq 0.1\%$.
- ⑤ Pulse width $5.0\mu s$, single shot.

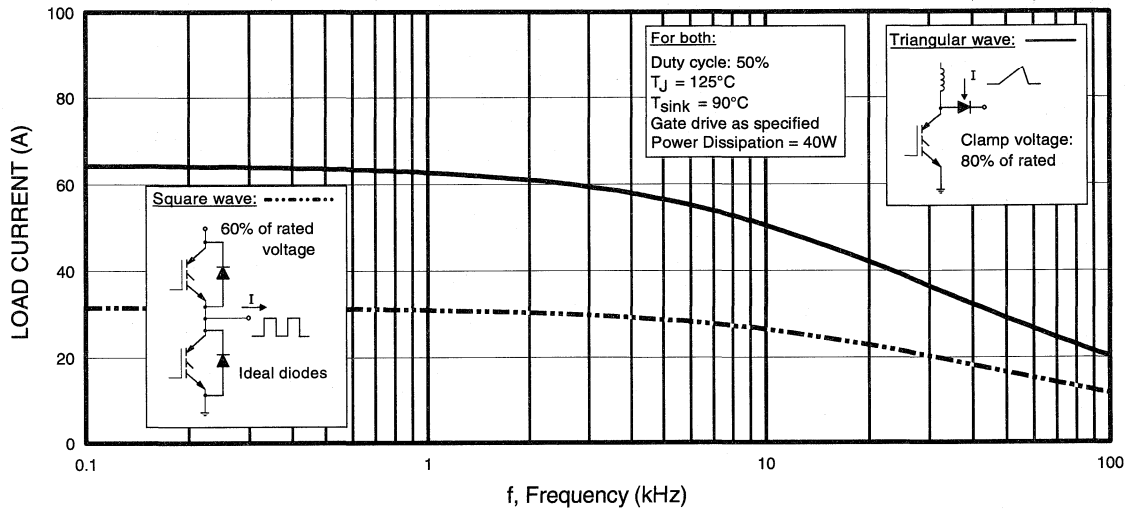


Fig. 1 - Typical Load Current vs. Frequency
 (For square wave, $I = I_{RMS}$ of fundamental; for triangular wave, $I = I_{PK}$)

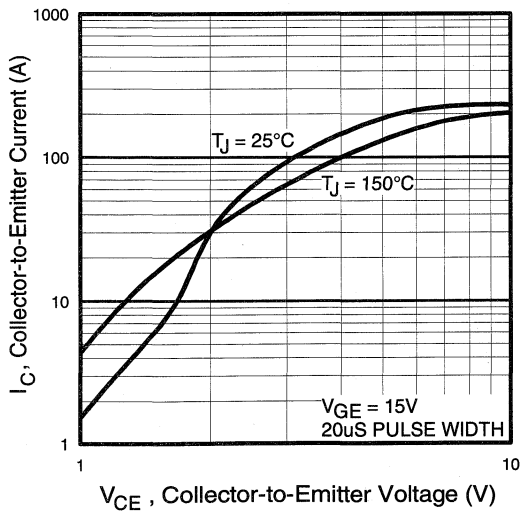


Fig. 2 - Typical Output Characteristics

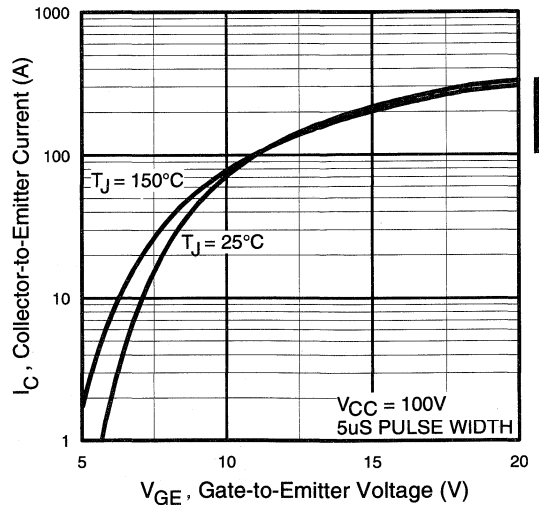


Fig. 3 - Typical Transfer Characteristics

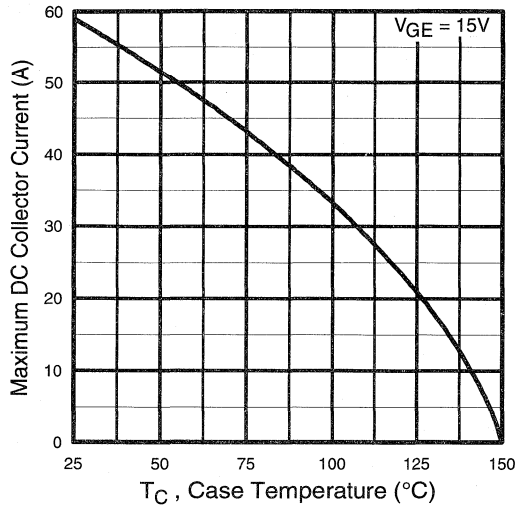


Fig. 4 - Maximum Collector Current vs. Case Temperature

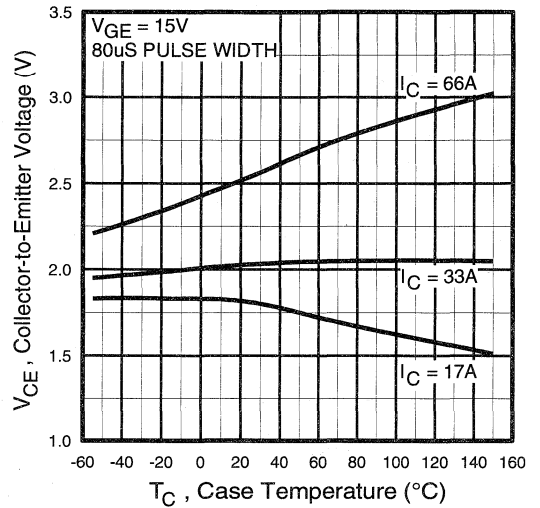


Fig. 5 - Collector-to-Emitter Voltage vs. Case Temperature

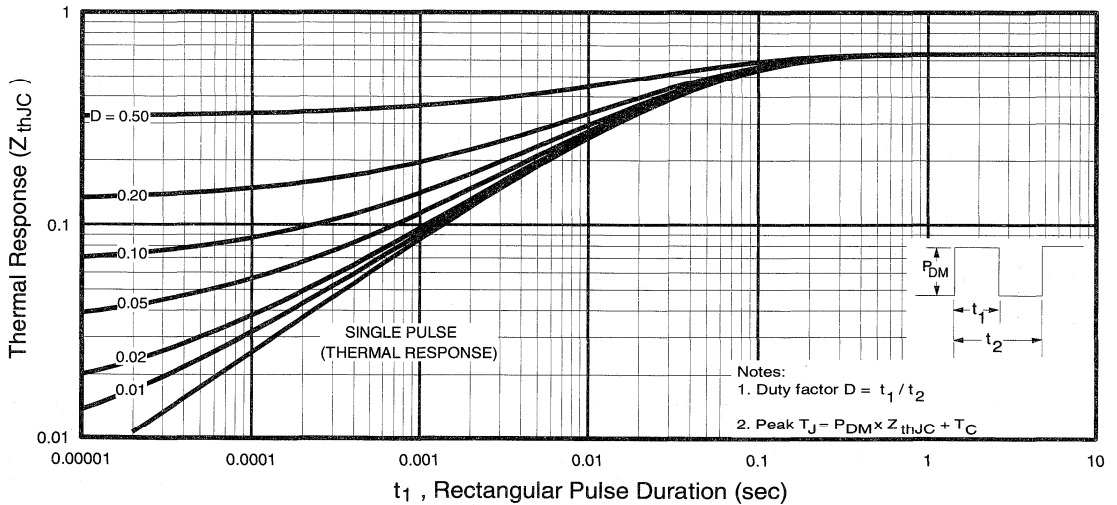


Fig. 6 - Maximum Effective Transient Thermal Impedance, Junction-to-Case

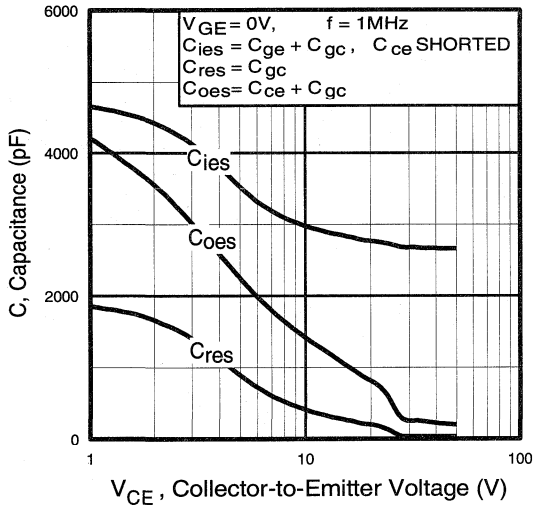


Fig. 7 - Typical Capacitance vs. Collector-to-Emitter Voltage

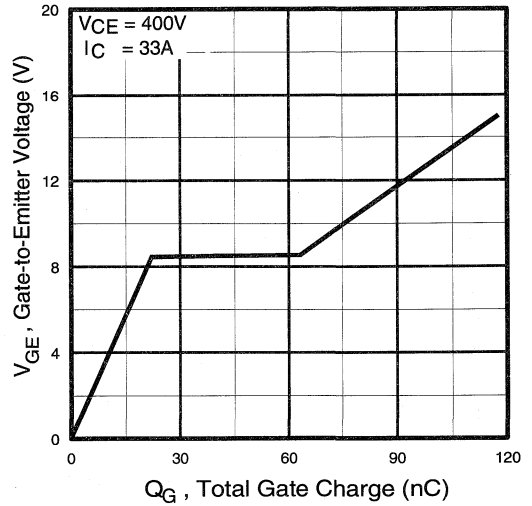


Fig. 8 - Typical Gate Charge vs. Gate-to-Emitter Voltage

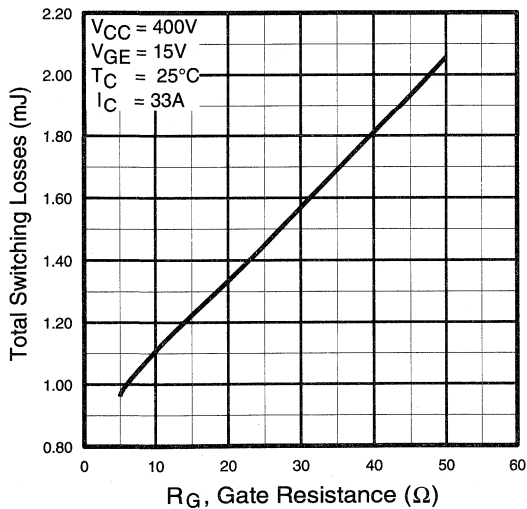


Fig. 9 - Typical Switching Losses vs. Gate Resistance

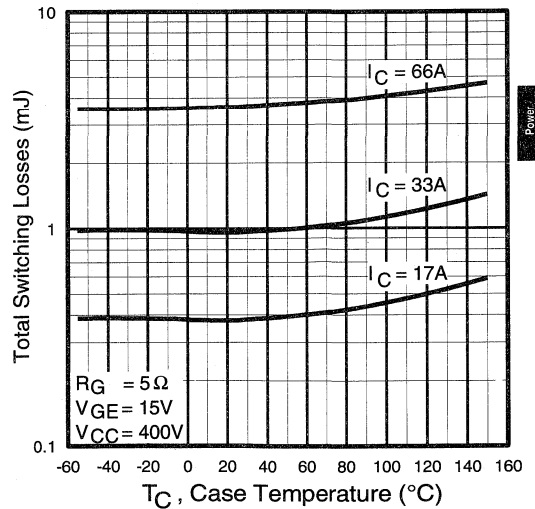


Fig. 10 - Typical Switching Losses vs. Case Temperature

Power Conversion Ultra-Fast Diodes

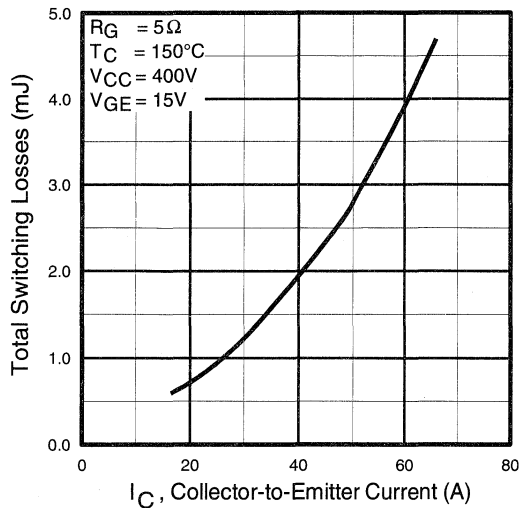


Fig. 11 - Typical Switching Losses vs. Collector-to-Emitter Current

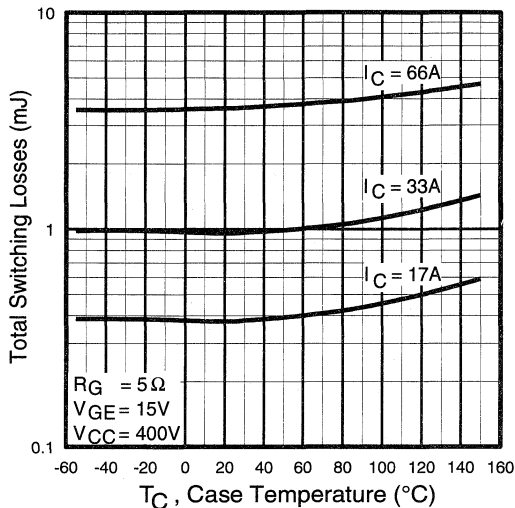


Fig. 12 - Turn-Off SOA

Refer to Section D for the following:

Appendix A: Section D - page D-3

Fig. 13a - Clamped Inductive Load Test Circuit

Fig. 13b - Pulsed Collector Current Test Circuit

Fig. 14a - Switching Loss Test Circuit

Fig. 14b - Switching Loss Waveform

Package Outline 3 - JEDEC Outline TO-247AC

Section D - page D-13

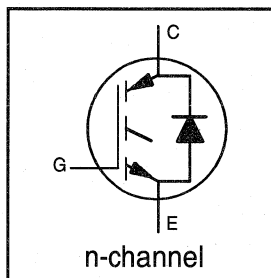
INSULATED GATE BIPOLAR TRANSISTOR
WITH ULTRAFAST SOFT RECOVERY

UltraFast CoPack IGBT

DIODE

Features

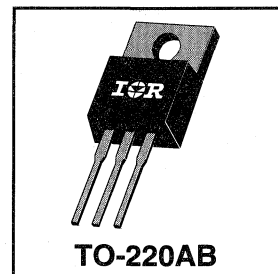
- Switching-loss rating includes all "tail" losses
- HEXFRED™ soft ultrafast diodes
- Optimized for high operating frequency (over 5kHz)
See Fig. 1 for Current vs. Frequency curve



$V_{CES} = 500V$
$V_{CE(sat)} \leq 2.9V$
@ $V_{GE} = 15V, I_C = 7.5A$

Description

Co-packaged IGBTs are a natural extension of International Rectifier's well known IGBT line. They provide the convenience of an IGBT and an ultrafast recovery diode in one package, resulting in substantial benefits to a host of high-voltage, high-current, motor control, UPS and power supply applications.



Absolute Maximum Ratings

	Parameter	Max.	Units
V_{CES}	Collector-to-Emitter Voltage	500	V
$I_C @ T_C = 25^\circ C$	Continuous Collector Current	14	A
$I_C @ T_C = 100^\circ C$	Continuous Collector Current	7.5	
I_{CM}	Pulsed Collector Current ①	28	
I_{LM}	Clamped Inductive Load Current ②	28	
$I_F @ T_C = 100^\circ C$	Diode Continuous Forward Current	7.0	
I_{FM}	Diode Maximum Forward Current	28	
V_{GE}	Gate-to-Emitter Voltage	± 20	V
$P_D @ T_C = 25^\circ C$	Maximum Power Dissipation	60	W
$P_D @ T_C = 100^\circ C$	Maximum Power Dissipation	24	
T_J	Operating Junction and Storage Temperature Range	-55 to +150	°C
T_{STG}			
	Mounting Torque, 6-32 or M3 Screw.	10 lbf•in (1.1 N•m)	

Power
Conversion
Ultra-Fast
Co-Packs

Thermal Resistance

	Parameter	Min.	Typ.	Max.	Units
$R_{\theta JC}$	Junction-to-Case - IGBT	—	—	2.1	°C/W
$R_{\theta JC}$	Junction-to-Case - Diode	—	—	3.5	
$R_{\theta CS}$	Case-to-Sink, flat, greased surface	—	0.50	—	
$R_{\theta JA}$	Junction-to-Ambient, typical socket mount	—	—	80	
Wt	Weight	—	2 (0.07)	—	g (oz)

Electrical Characteristics @ $T_J = 25^\circ\text{C}$ (unless otherwise specified)

	Parameter	Min.	Typ.	Max.	Units	Conditions
$V_{(BR)CES}$	Collector-to-Emitter Breakdown Voltage ^③	500	—	—	V	$V_{GE} = 0V, I_C = 250\mu A$
$\Delta V_{(BR)CES}/\Delta T_J$	Temp. Coeff. of Breakdown Voltage	—	0.47	—	V/°C	$V_{GE} = 0V, I_C = 1.0mA$
$V_{CE(on)}$	Collector-to-Emitter Saturation Voltage	—	2.4	2.9	V	$I_C = 7.5A, V_{GE} = 15V$
		—	3.1	—		$I_C = 14A$
		—	2.7	—		$I_C = 7.5A, T_J = 150^\circ\text{C}$
$V_{GE(th)}$	Gate Threshold Voltage	3.0	—	5.5		$V_{CE} = V_{GE}, I_C = 250\mu A$
$\Delta V_{GE(th)}/\Delta T_J$	Temp. Coeff. of Threshold Voltage	—	-10	—	mV/°C	$V_{CE} = V_{GE}, I_C = 250\mu A$
g_{fe}	Forward Transconductance ^④	1.2	2.0	—	S	$V_{CE} = 100V, I_C = 7.5A$
I_{CES}	Zero Gate Voltage Collector Current	—	—	250	μA	$V_{GE} = 0V, V_{CE} = 500V$
		—	—	1700		$V_{GE} = 0V, V_{CE} = 500V, T_J = 150^\circ\text{C}$
V_{FM}	Diode Forward Voltage Drop	—	1.4	1.7	V	$I_C = 8.0A$
		—	1.3	1.6		$I_C = 8.0A, T_J = 150^\circ\text{C}$
I_{GES}	Gate-to-Emitter Leakage Current	—	—	± 100	nA	$V_{GE} = \pm 20V$

Switching Characteristics @ $T_J = 25^\circ\text{C}$ (unless otherwise specified)

	Parameter	Min.	Typ.	Max.	Units	Conditions
Q_g	Total Gate Charge (turn-on)	—	15	23	nC	$I_C = 7.5A$
Q_{ge}	Gate - Emitter Charge (turn-on)	—	3.7	5.6		$V_{CC} = 400V$
Q_{gc}	Gate - Collector Charge (turn-on)	—	6.5	9.8		See Fig. 8
$t_{d(on)}$	Turn-On Delay Time	—	65	—	ns	$T_J = 25^\circ\text{C}$
t_r	Rise Time	—	44	—		$I_C = 7.5A, V_{CC} = 400V$
$t_{d(off)}$	Turn-Off Delay Time	—	140	210	ns	$V_{GE} = 15V, R_G = 50\Omega$
t_f	Fall Time	—	110	160		Energy losses include "tail" and diode reverse recovery.
E_{on}	Turn-On Switching Loss	—	0.25	—	mJ	See Fig. 9, 10, 11, 18
E_{off}	Turn-Off Switching Loss	—	0.25	—		
E_{ts}	Total Switching Loss	—	0.50	0.80	mJ	
$t_{d(on)}$	Turn-On Delay Time	—	60	—		ns
t_r	Rise Time	—	44	—	$I_C = 7.5A, V_{CC} = 480V$	
$t_{d(off)}$	Turn-Off Delay Time	—	230	—	ns	$V_{GE} = 15V, R_G = 50\Omega$
t_f	Fall Time	—	220	—		Energy losses include "tail" and diode reverse recovery.
E_{ts}	Total Switching Loss	—	0.8	—	mJ	
L_E	Internal Emitter Inductance	—	7.5	—	nH	Measured 5mm from package
C_{ies}	Input Capacitance	—	330	—	pF	$V_{GE} = 0V$
C_{oes}	Output Capacitance	—	47	—		$V_{CC} = 30V$
C_{res}	Reverse Transfer Capacitance	—	5.9	—		$f = 1.0MHz$
t_{rr}	Diode Reverse Recovery Time	—	37	55	ns	$T_J = 25^\circ\text{C}$ See Fig.
		—	55	90		$T_J = 125^\circ\text{C}$ 14
I_{rr}	Diode Peak Reverse Recovery Current	—	3.5	5.0	A	$T_J = 25^\circ\text{C}$ See Fig.
		—	4.5	8.0		$T_J = 125^\circ\text{C}$ 15
Q_{rr}	Diode Reverse Recovery Charge	—	65	138	nC	$T_J = 25^\circ\text{C}$ See Fig.
		—	124	360		$T_J = 125^\circ\text{C}$ 16
$di_{(rec)M}/dt$	Diode Peak Rate of Fall of Recovery During t_b	—	240	—	A/ μs	$T_J = 25^\circ\text{C}$ See Fig.
		—	210	—		$T_J = 125^\circ\text{C}$ 17

Notes:

① Repetitive rating; $V_{GE}=20V$, pulse width limited by max. junction temperature.
(See fig. 20)

② $V_{CC}=80\%(V_{CES}), V_{GE}=20V, L=10\mu H,$
 $R_G = 50\Omega,$ (See fig. 19)

③ Pulse width $\leq 80\mu s$; duty factor $\leq 0.1\%$.

④ Pulse width 5.0 μs ,
single shot.

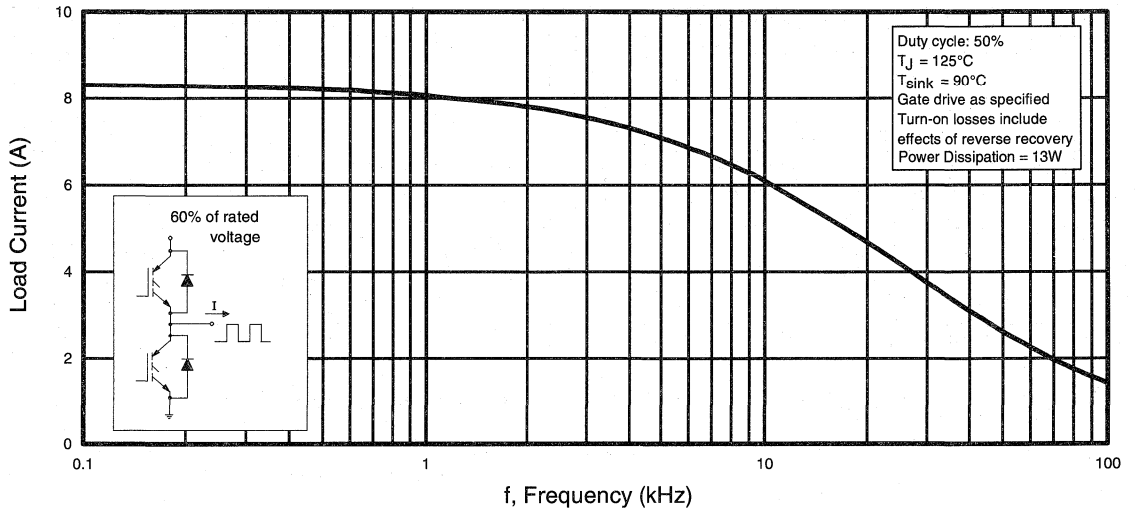


Fig. 1 - Typical Load Current vs. Frequency
(Load Current = I_{RMS} of fundamental)

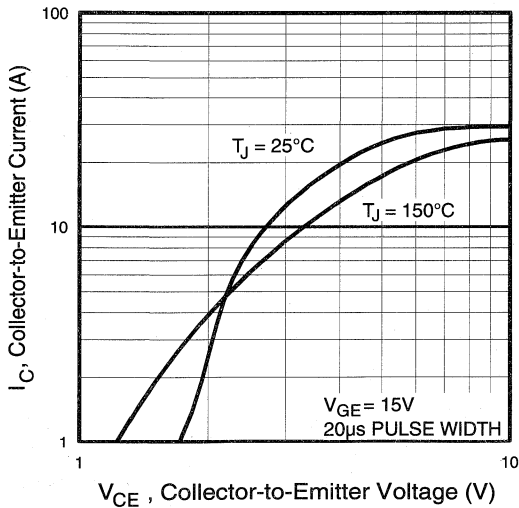


Fig. 2 - Typical Output Characteristics

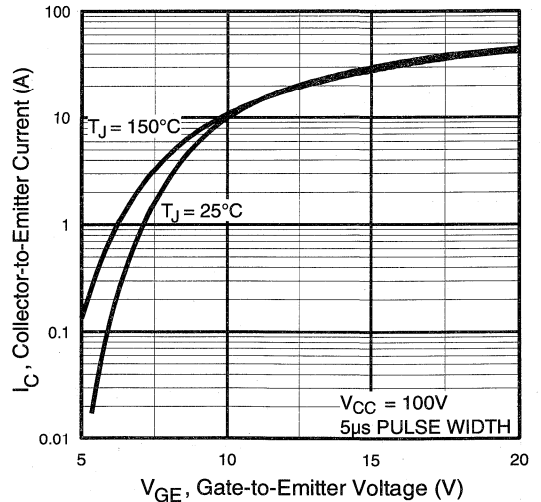


Fig. 3 - Typical Transfer Characteristics

Power
Conversion
Ultra-Fast
IGBTs

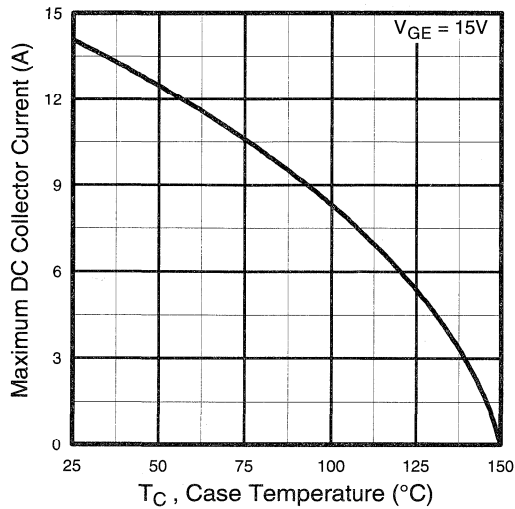


Fig. 4 - Maximum Collector Current vs. Case Temperature

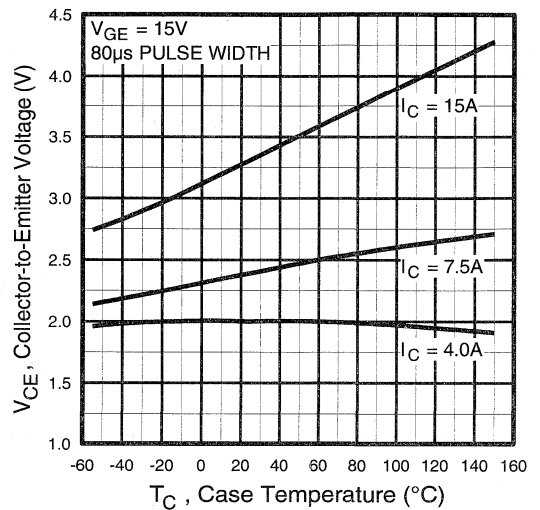


Fig. 5 - Collector-to-Emitter Voltage vs. Case Temperature

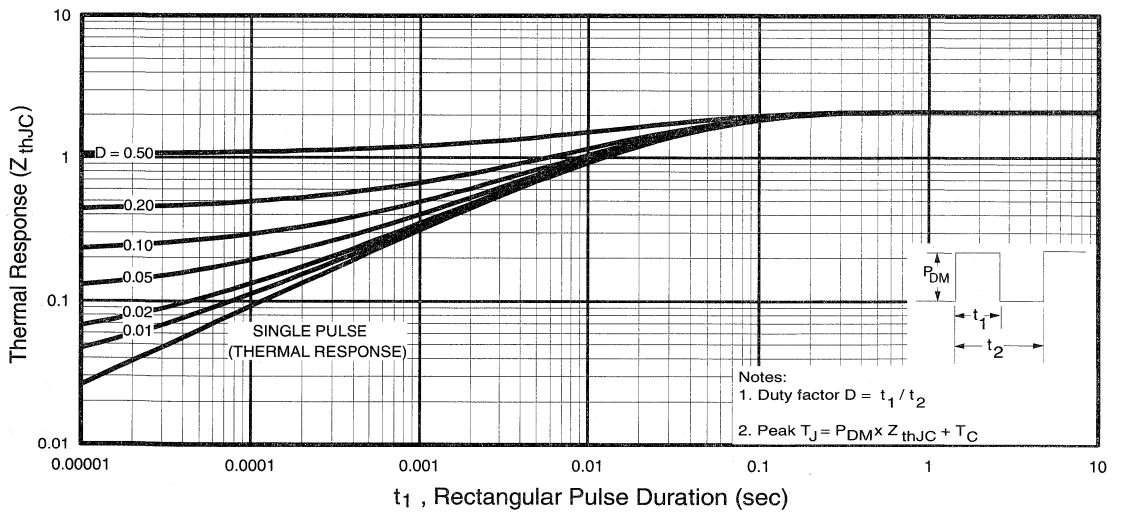


Fig. 6 - Maximum IGBT Effective Transient Thermal Impedance, Junction-to-Case

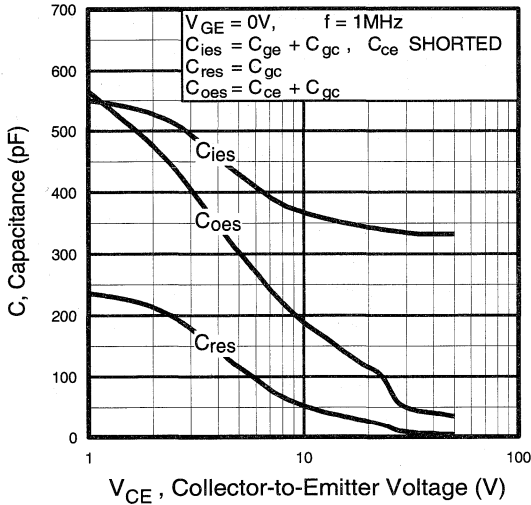


Fig. 7 - Typical Capacitance vs. Collector-to-Emitter Voltage

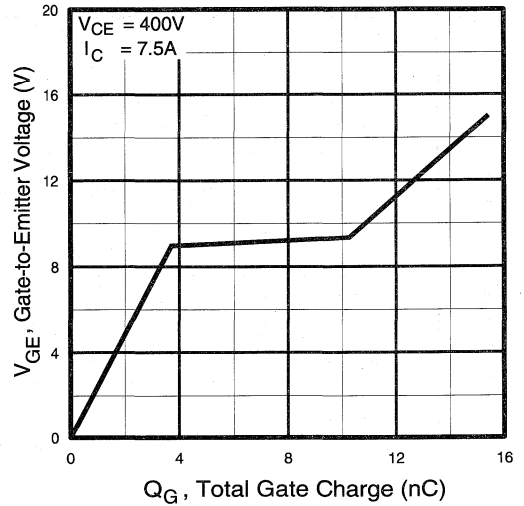


Fig. 8 - Typical Gate Charge vs. Gate-to-Emitter Voltage

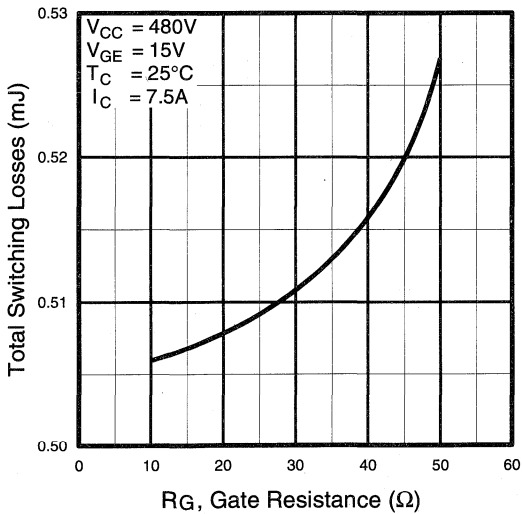


Fig. 9 - Typical Switching Losses vs. Gate Resistance

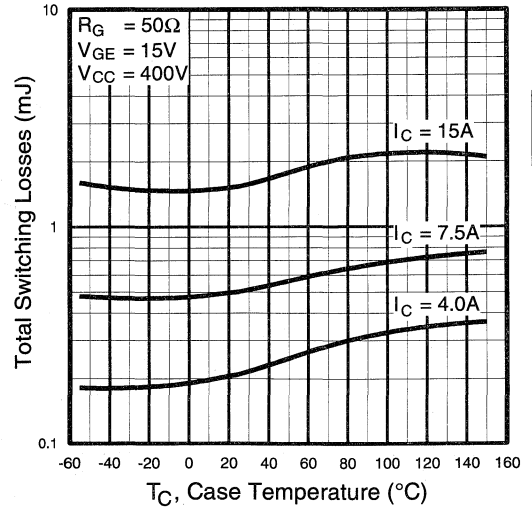


Fig. 10 - Typical Switching Losses vs. Case Temperature

Power Conversion
 Ultra-Fast
 Co-Packs

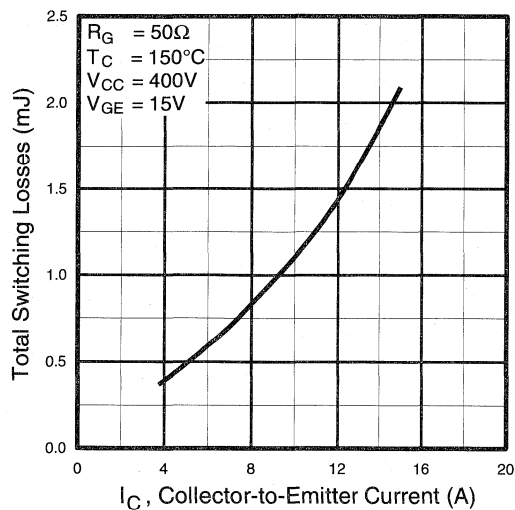


Fig. 11 - Typical Switching Losses vs. Collector-to-Emitter Current

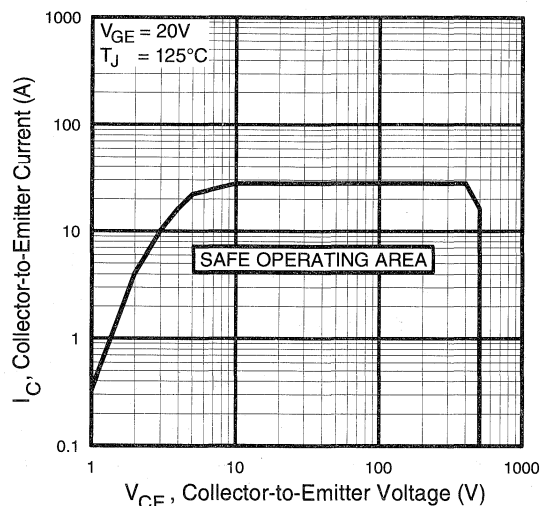


Fig. 12 - Turn-Off SOA

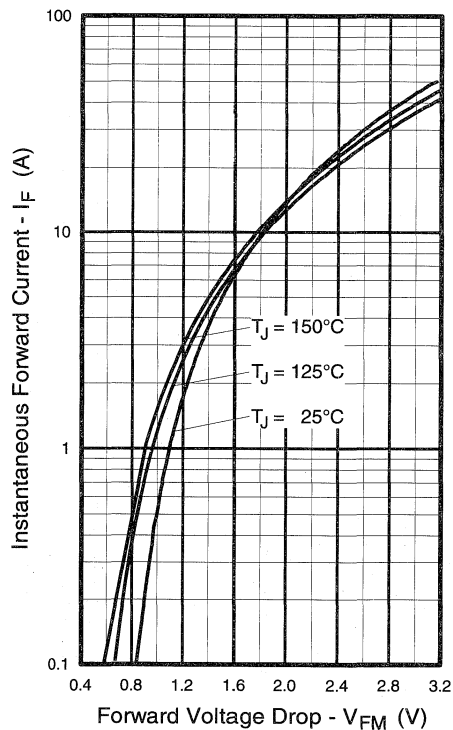


Fig. 13 - Maximum Forward Voltage Drop vs. Instantaneous Forward Current

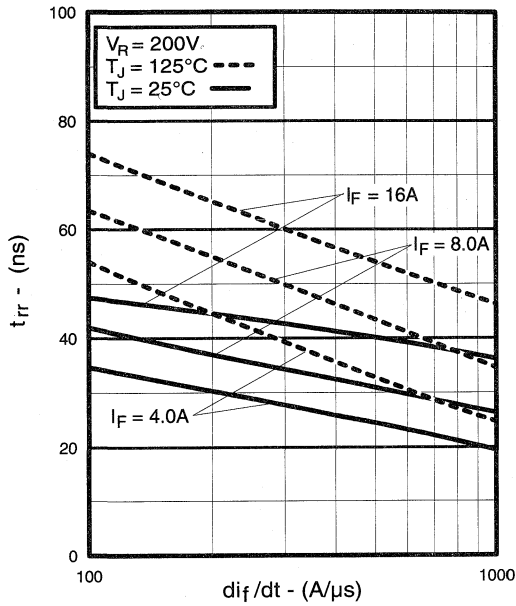


Fig. 14 - Typical Reverse Recovery vs. di_f/dt

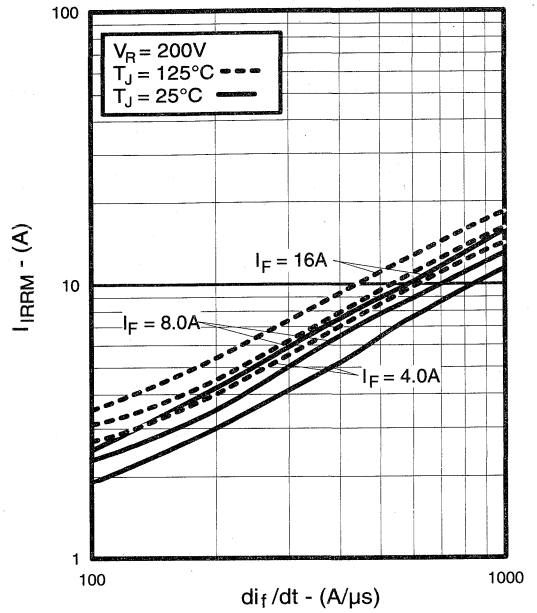


Fig. 15 - Typical Recovery Current vs. di_f/dt

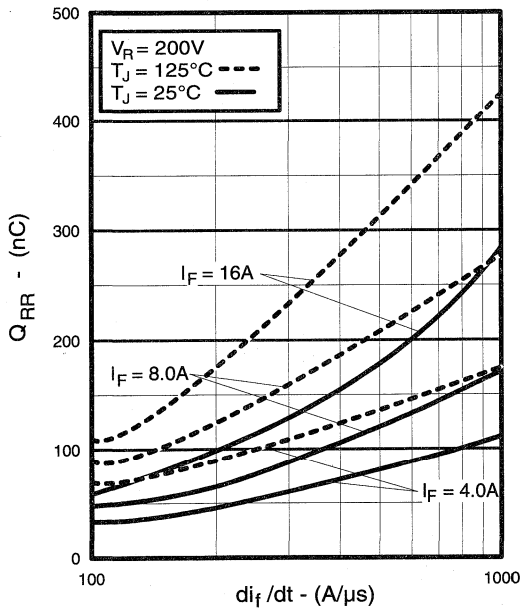


Fig. 16 - Typical Stored Charge vs. di_f/dt

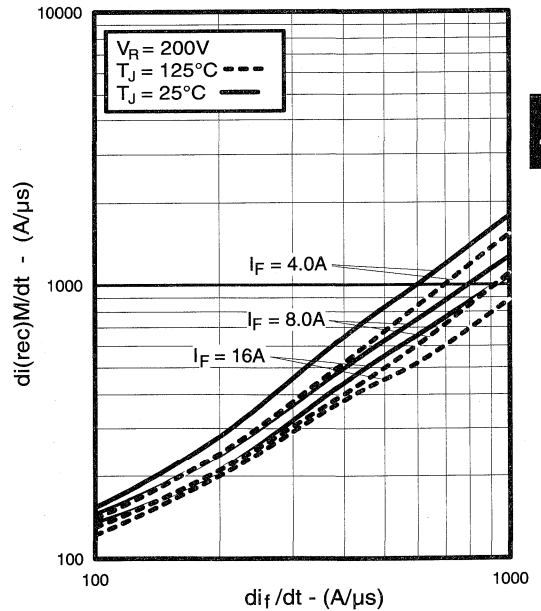


Fig. 17 - Typical $di_{(rec)M}/dt$ vs. di_f/dt

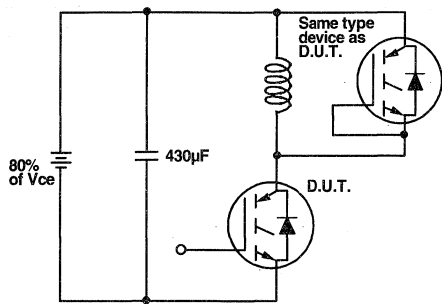


Fig. 18a - Test Circuit for Measurement of I_{LM} , E_{on} , $E_{off(diode)}$, t_{rr} , Q_{rr} , I_{rr} , $t_{d(on)}$, t_r , $t_{d(off)}$, t_f

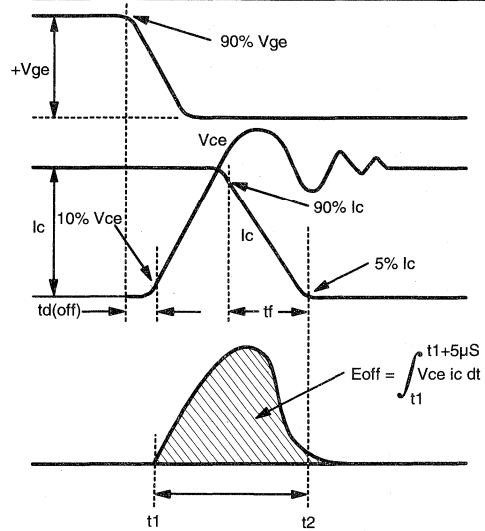


Fig. 18b - Test Waveforms for Circuit of Fig. 18a, Defining E_{off} , $t_{d(off)}$, t_f

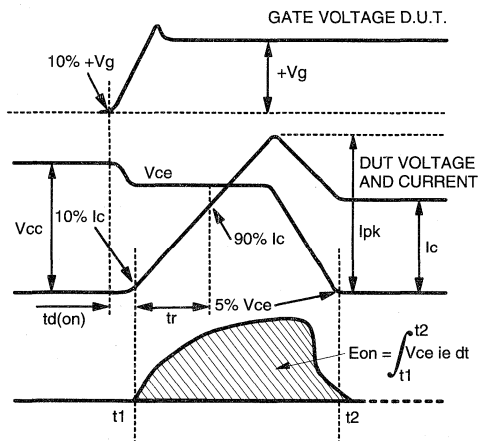


Fig. 18c - Test Waveforms for Circuit of Fig. 18a, Defining E_{on} , $t_{d(on)}$, t_r

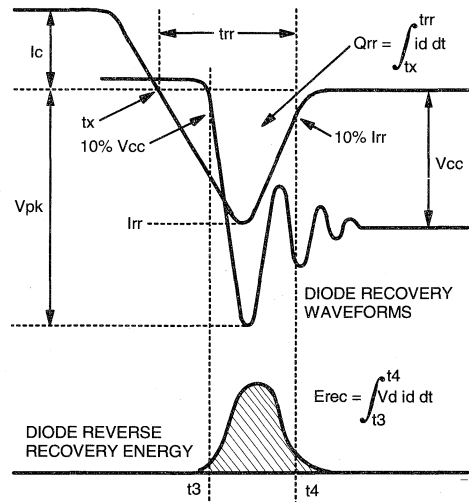


Fig. 18d - Test Waveforms for Circuit of Fig. 18a, Defining E_{rec} , t_{rr} , Q_{rr} , I_{rr}

Refer to Section D for the following:

Appendix B: Section D - page D-4

Fig. 18e - Macro Waveforms for Test Circuit of Fig. 18a

Fig. 19 - Clamped Inductive Load Test Circuit

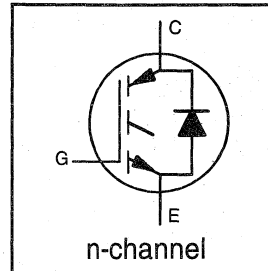
Fig. 20 - Pulsed Collector Current Test Circuit

INSULATED GATE BIPOLAR TRANSISTOR WITH ULTRAFAST SOFT RECOVERY DIODE

UltraFast CoPack IGBT

Features

- Switching-loss rating includes all "tail" losses
- HEXFRED™ soft ultrafast diodes
- Optimized for high operating frequency (over 5kHz)
See Fig. 1 for Current vs. Frequency curve



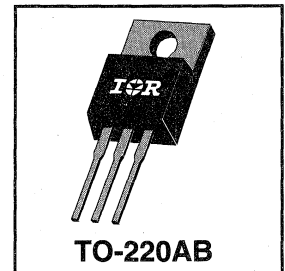
$$V_{CES} = 500V$$

$$V_{CE(sat)} \leq 3.0V$$

$$@ V_{GE} = 15V, I_C = 15A$$

Description

Co-packaged IGBTs are a natural extension of International Rectifier's well known IGBT line. They provide the convenience of an IGBT and an ultrafast recovery diode in one package, resulting in substantial benefits to a host of high-voltage, high-current, motor control, UPS and power supply applications.



Absolute Maximum Ratings

	Parameter	Max.	Units
V_{CES}	Collector-to-Emitter Voltage	500	V
$I_C @ T_C = 25^\circ C$	Continuous Collector Current	25	A
$I_C @ T_C = 100^\circ C$	Continuous Collector Current	15	
I_{CM}	Pulsed Collector Current ①	50	
I_{LM}	Clamped Inductive Load Current ②	50	
$I_F @ T_C = 100^\circ C$	Diode Continuous Forward Current	12	
I_{FM}	Diode Maximum Forward Current	50	
V_{GE}	Gate-to-Emitter Voltage	± 20	
$P_D @ T_C = 25^\circ C$	Maximum Power Dissipation	100	W
$P_D @ T_C = 100^\circ C$	Maximum Power Dissipation	42	
T_J	Operating Junction and	-55 to +150	°C
T_{STG}	Storage Temperature Range		
	Soldering Temperature, for 10 sec.		
	Mounting Torque, 6-32 or M3 Screw.	10 lbf•in (1.1 N•m)	

Thermal Resistance

	Parameter	Min.	Typ.	Max.	Units
$R_{\theta JC}$	Junction-to-Case - IGBT	—	—	1.2	°C/W
$R_{\theta JC}$	Junction-to-Case - Diode	—	—	2.5	
$R_{\theta CS}$	Case-to-Sink, flat, greased surface	—	0.50	—	
$R_{\theta JA}$	Junction-to-Ambient, typical socket mount	—	—	80	
Wt	Weight	—	2 (0.07)	—	g (oz)

Electrical Characteristics @ $T_J = 25^\circ\text{C}$ (unless otherwise specified)

	Parameter	Min.	Typ.	Max.	Units	Conditions
$V_{(BR)CES}$	Collector-to-Emitter Breakdown Voltage ^③	500	—	—	V	$V_{GE} = 0V, I_C = 250\mu A$
$\Delta V_{(BR)CES}/\Delta T_J$	Temp. Coeff. of Breakdown Voltage	—	0.46	—	V/°C	$V_{GE} = 0V, I_C = 1.0mA$
$V_{CE(on)}$	Collector-to-Emitter Saturation Voltage	—	2.3	3.0	V	$I_C = 15A$ $V_{GE} = 15V$
		—	2.8	—		$I_C = 25A$ See Fig. 2, 5
		—	2.6	—		$I_C = 15A, T_J = 150^\circ\text{C}$
$V_{GE(th)}$	Gate Threshold Voltage	3.0	—	5.5		$V_{CE} = V_{GE}, I_C = 250\mu A$
$\Delta V_{GE(th)}/\Delta T_J$	Temp. Coeff. of Threshold Voltage	—	-11	—	mV/°C	$V_{CE} = V_{GE}, I_C = 250\mu A$
g_{fe}	Forward Transconductance ^④	2.3	8.1	—	S	$V_{CE} = 100V, I_C = 15A$
I_{CES}	Zero Gate Voltage Collector Current	—	—	250	μA	$V_{GE} = 0V, V_{CE} = 500V$
		—	—	2500		$V_{GE} = 0V, V_{CE} = 500V, T_J = 150^\circ\text{C}$
V_{FM}	Diode Forward Voltage Drop	—	1.4	1.7	V	$I_C = 12A$ See Fig. 13
		—	1.3	1.6		$I_C = 12A, T_J = 150^\circ\text{C}$
I_{GES}	Gate-to-Emitter Leakage Current	—	—	± 100	nA	$V_{GE} = \pm 20V$

Switching Characteristics @ $T_J = 25^\circ\text{C}$ (unless otherwise specified)

	Parameter	Min.	Typ.	Max.	Units	Conditions	
Q_g	Total Gate Charge (turn-on)	—	31	47	nC	$I_C = 15A$ $V_{CC} = 400V$ See Fig. 8	
Q_{ge}	Gate - Emitter Charge (turn-on)	—	6.2	9.2			
Q_{gc}	Gate - Collector Charge (turn-on)	—	12	19			
$t_{d(on)}$	Turn-On Delay Time	—	73	—	ns	$T_J = 25^\circ\text{C}$ $I_C = 15A, V_{CC} = 400V$ $V_{GE} = 15V, R_G = 23\Omega$ Energy losses include "tail" and diode reverse recovery. See Fig. 9, 10, 11, 18	
t_r	Rise Time	—	72	—			
$t_{d(off)}$	Turn-Off Delay Time	—	120	180			
t_f	Fall Time	—	100	150			
E_{on}	Turn-On Switching Loss	—	0.7	—			
E_{off}	Turn-Off Switching Loss	—	0.4	—	mJ		
E_{ts}	Total Switching Loss	—	1.1	1.7			
$t_{d(on)}$	Turn-On Delay Time	—	77	—	ns	$T_J = 150^\circ\text{C}$, See Fig. 9, 10, 11, 18 $I_C = 15A, V_{CC} = 400V$ $V_{GE} = 15V, R_G = 23\Omega$ Energy losses include "tail" and diode reverse recovery.	
t_r	Rise Time	—	75	—			
$t_{d(off)}$	Turn-Off Delay Time	—	200	—			
t_f	Fall Time	—	190	—			
E_{ts}	Total Switching Loss	—	1.5	—	mJ		
L_E	Internal Emitter Inductance	—	7.5	—	nH	Measured 5mm from package	
C_{ies}	Input Capacitance	—	660	—	pF	$V_{GE} = 0V$ $V_{CC} = 30V$ See Fig. 7 $f = 1.0MHz$	
C_{oes}	Output Capacitance	—	110	—			
C_{res}	Reverse Transfer Capacitance	—	12	—			
t_{rr}	Diode Reverse Recovery Time	—	42	60	ns	$T_J = 25^\circ\text{C}$ See Fig.	$I_F = 12A$ $V_R = 200V$ $di/dt = 200A/\mu s$
		—	80	120		$T_J = 125^\circ\text{C}$ 14	
I_{rr}	Diode Peak Reverse Recovery Current	—	3.5	6.0	A	$T_J = 25^\circ\text{C}$ See Fig.	
		—	5.6	10		$T_J = 125^\circ\text{C}$ 15	
Q_{rr}	Diode Reverse Recovery Charge	—	80	180	nC	$T_J = 25^\circ\text{C}$ See Fig.	
		—	220	600		$T_J = 125^\circ\text{C}$ 16	
$di_{(rec)M}/dt$	Diode Peak Rate of Fall of Recovery During t_b	—	180	—	A/ μs	$T_J = 25^\circ\text{C}$ See Fig.	
		—	120	—		$T_J = 125^\circ\text{C}$ 17	

Notes:

① Repetitive rating; $V_{GE}=20V$, pulse width limited by max. junction temperature. (See fig. 20)

② $V_{CC}=80\%(V_{CES})$, $V_{GE}=20V$, $L=10\mu H$, $R_G = 23\Omega$, (See fig. 19)

④ Pulse width 5.0 μs , single shot.

③ Pulse width $\leq 80\mu s$; duty factor $\leq 0.1\%$.

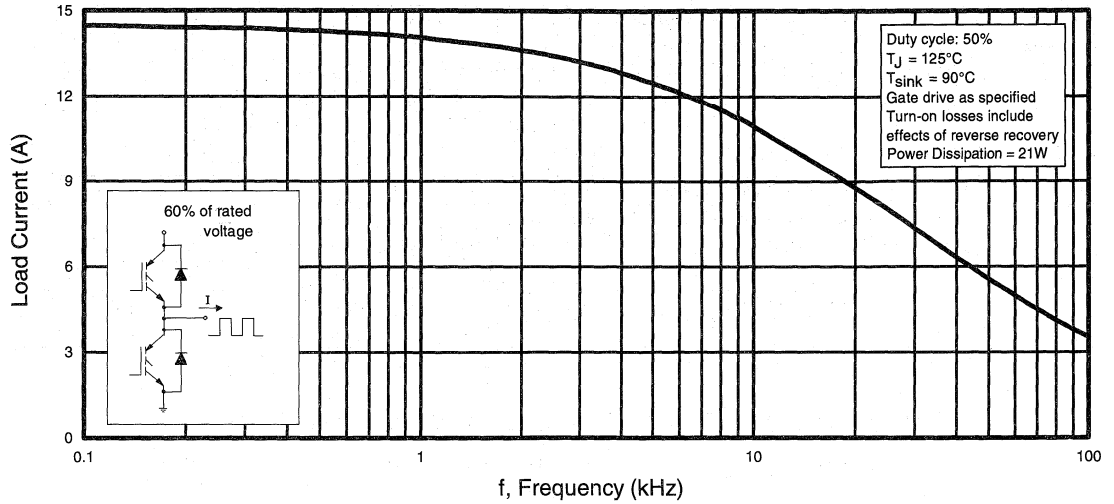


Fig. 1 - Typical Load Current vs. Frequency
(Load Current = I_{RMS} of fundamental)

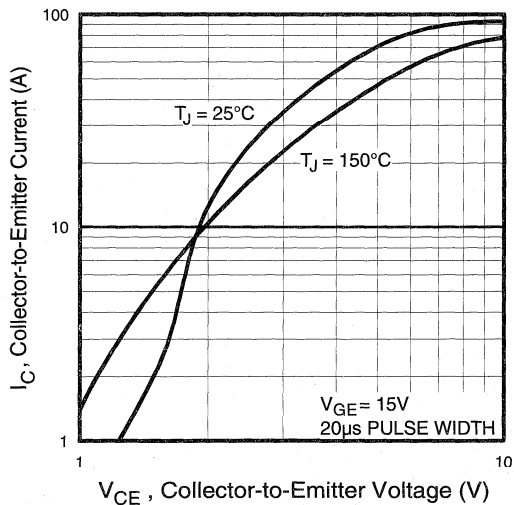


Fig. 2 - Typical Output Characteristics

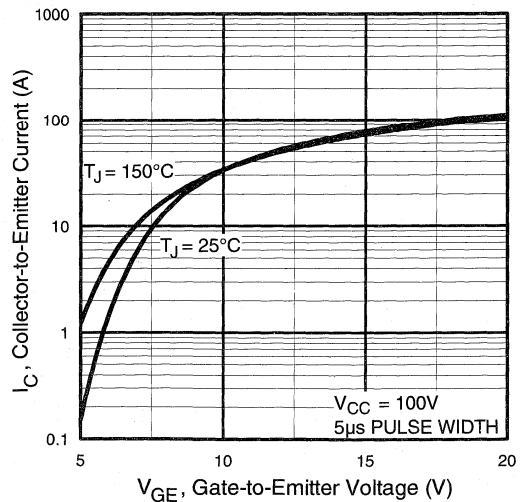


Fig. 3 - Typical Transfer Characteristics

Power
Conversion
Ultra-Fast
Co-Packs

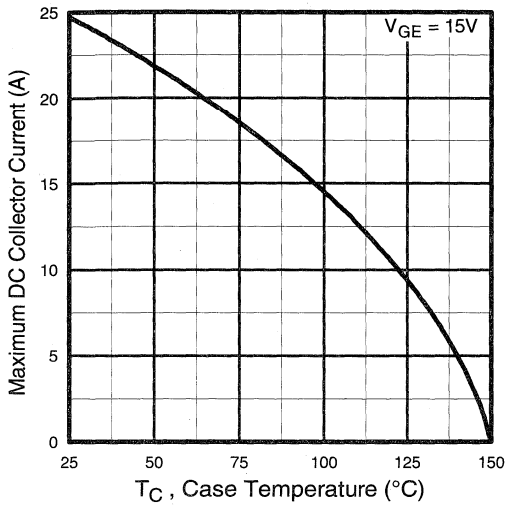


Fig. 4 - Maximum Collector Current vs. Case Temperature

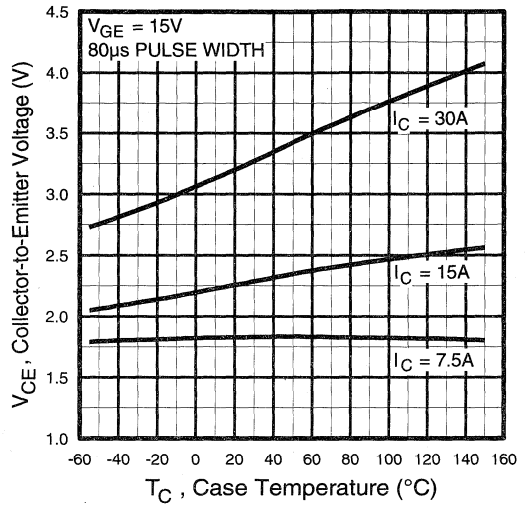


Fig. 5 - Collector-to-Emitter Voltage vs. Case Temperature

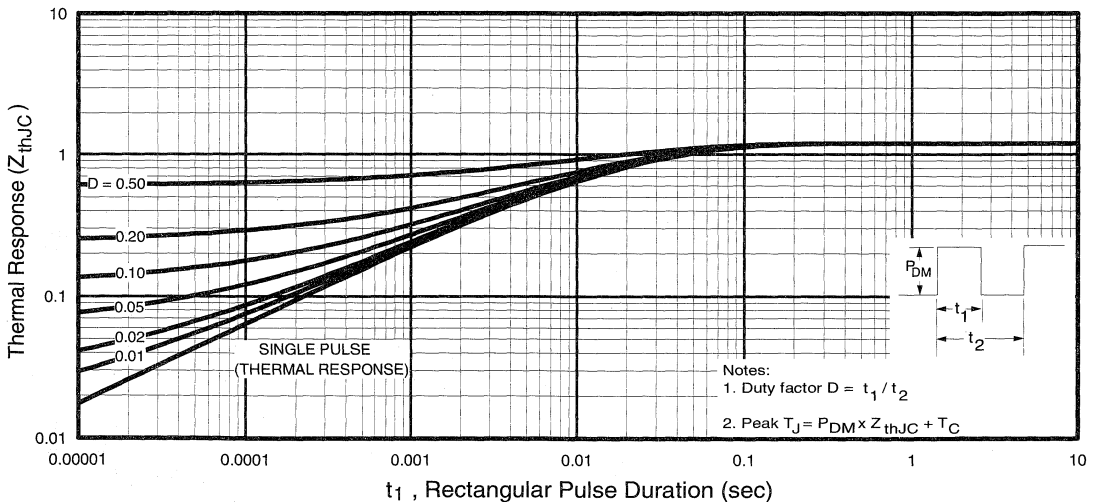


Fig. 6 - Maximum IGBT Effective Transient Thermal Impedance, Junction-to-Case

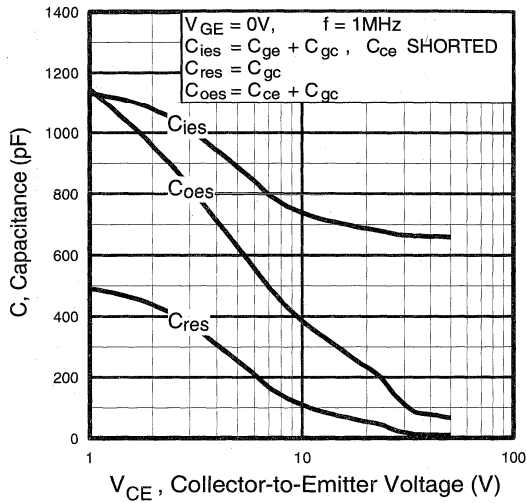


Fig. 7 - Typical Capacitance vs. Collector-to-Emitter Voltage

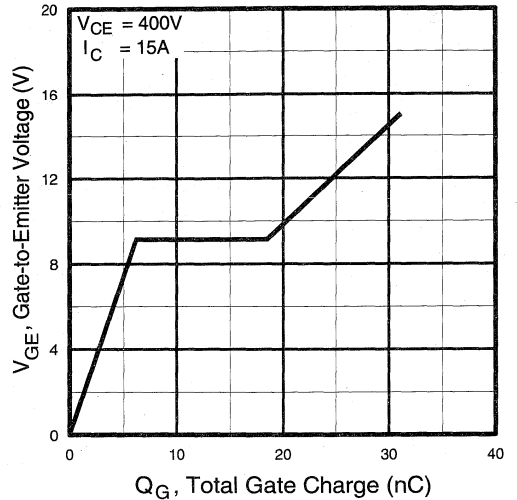


Fig. 8 - Typical Gate Charge vs. Gate-to-Emitter Voltage

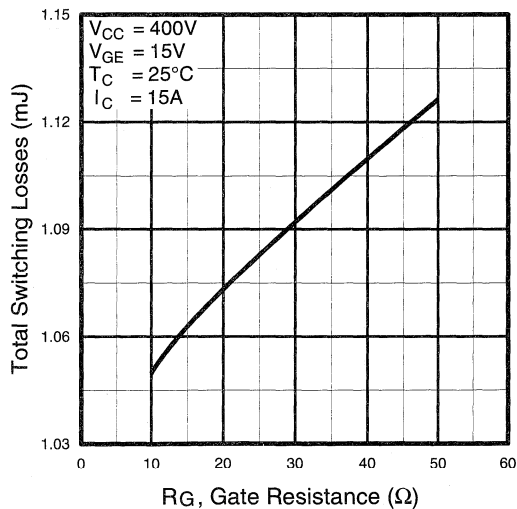


Fig. 9 - Typical Switching Losses vs. Gate Resistance

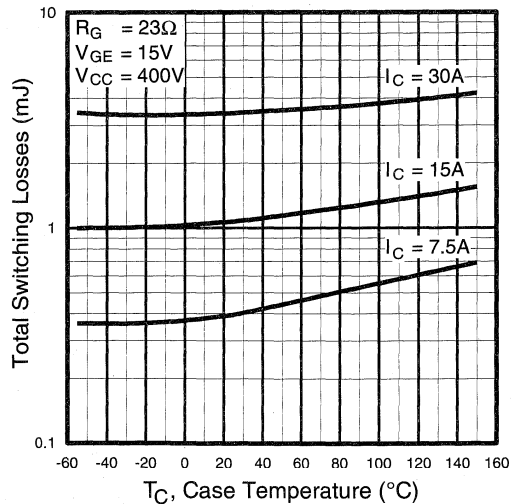


Fig. 10 - Typical Switching Losses vs. Case Temperature

Power Conversion
 Ultra-Fast
 Co-Packs

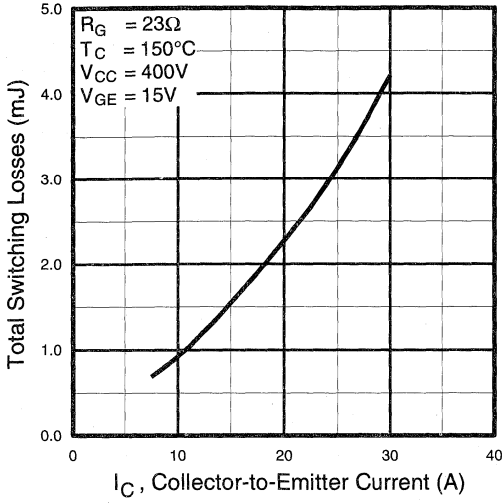


Fig. 11 - Typical Switching Losses vs. Collector-to-Emitter Current

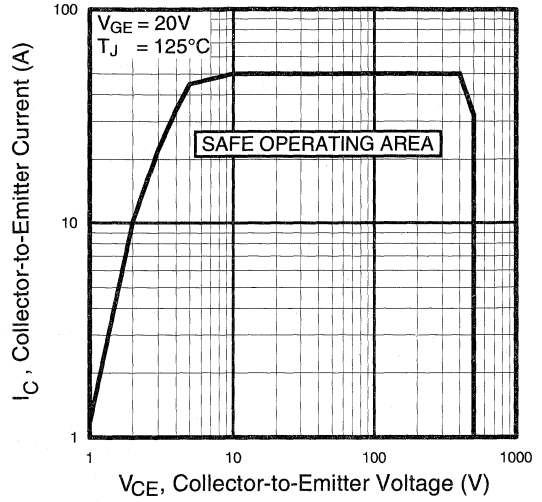


Fig. 12 - Turn-Off SOA

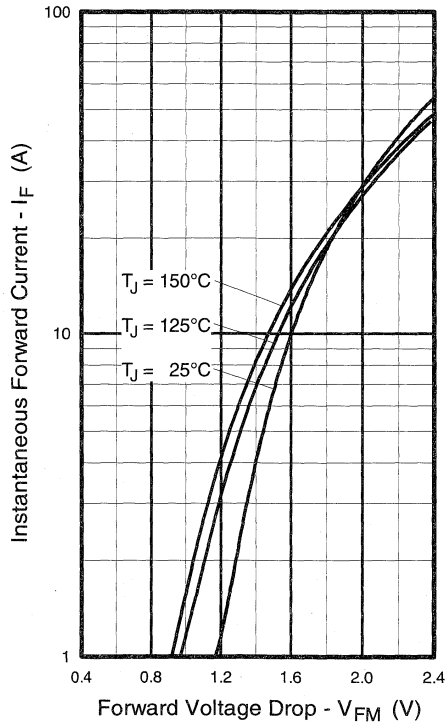


Fig. 13 - Maximum Forward Voltage Drop vs. Instantaneous Forward Current

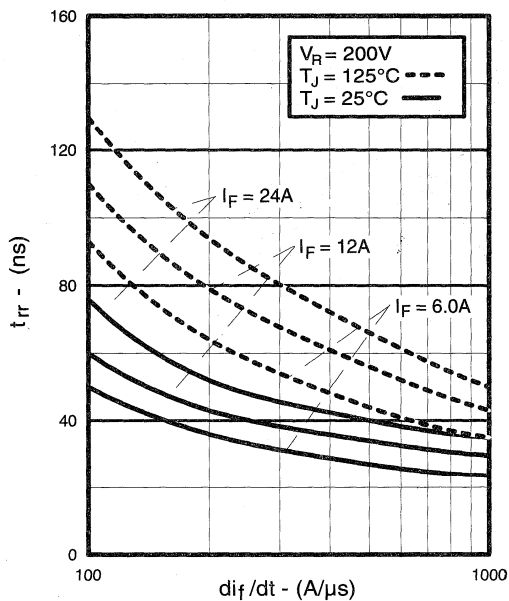


Fig. 14 - Typical Reverse Recovery vs. di_f/dt

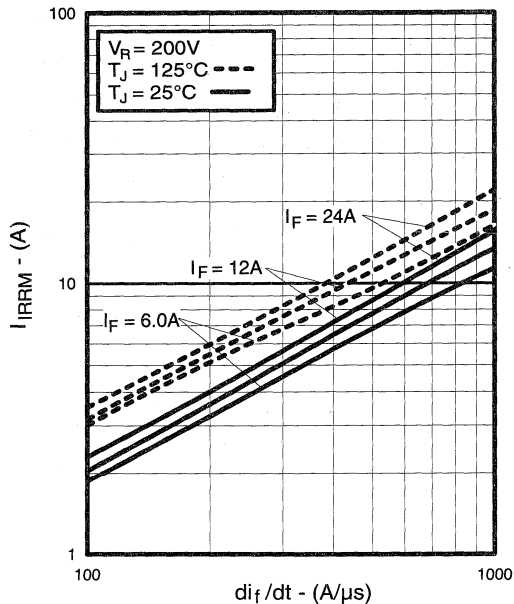


Fig. 15 - Typical Recovery Current vs. di_f/dt

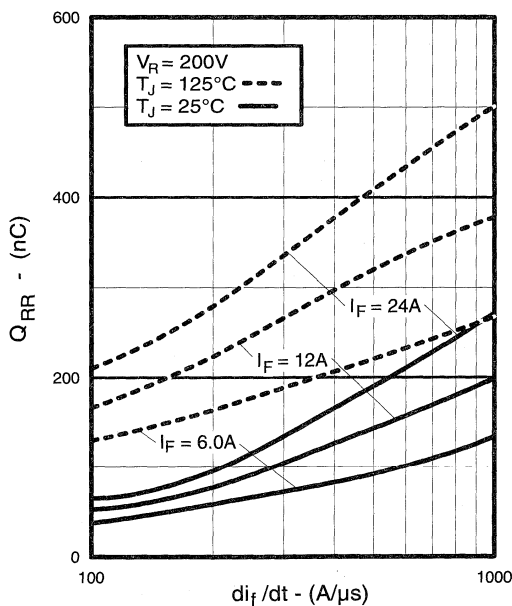


Fig. 16 - Typical Stored Charge vs. di_f/dt

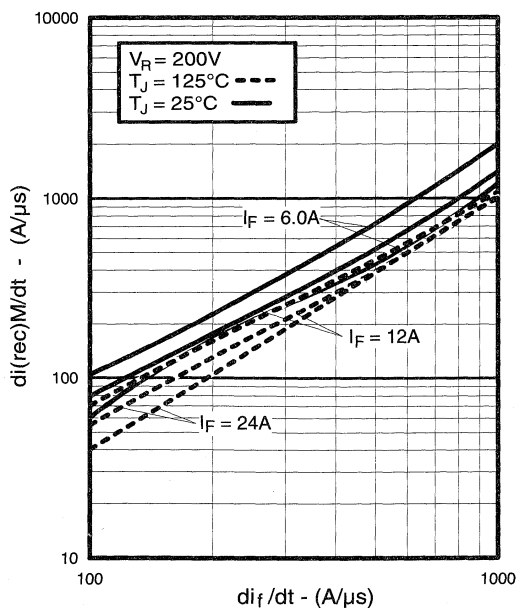


Fig. 17 - Typical $di_{(rec)M}/dt$ vs. di_f/dt

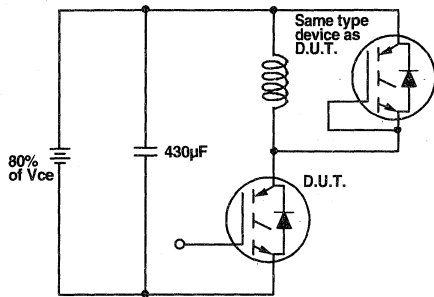


Fig. 18a - Test Circuit for Measurement of I_{LM} , E_{on} , $E_{off}(\text{diode})$, t_{rr} , Q_{rr} , I_{rr} , $t_{d(on)}$, t_r , $t_{d(off)}$, t_f

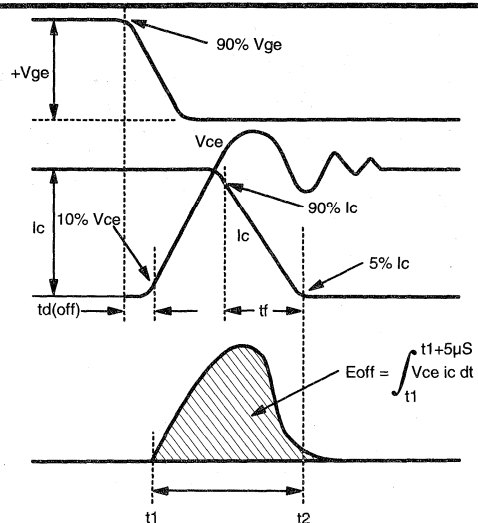


Fig. 18b - Test Waveforms for Circuit of Fig. 18a, Defining E_{off} , $t_{d(off)}$, t_f

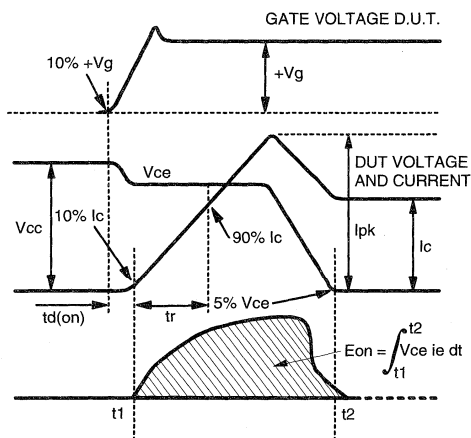


Fig. 18c - Test Waveforms for Circuit of Fig. 18a, Defining E_{on} , $t_{d(on)}$, t_r

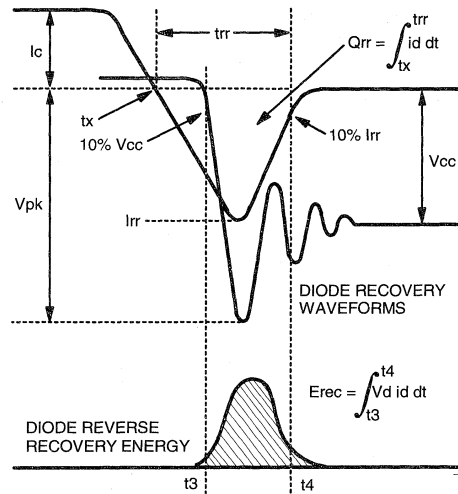


Fig. 18d - Test Waveforms for Circuit of Fig. 18a, Defining E_{rec} , t_{rr} , Q_{rr} , I_{rr}

Refer to Section D for the following:

Appendix B: Section D - page D-4

Fig. 18e - Macro Waveforms for Test Circuit Fig. 18a

Fig. 19 - Clamped Inductive Load Test Circuit

Fig. 20 - Pulsed Collector Current Test Circuit

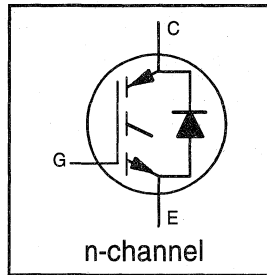
IRGP430UD2

**INSULATED GATE BIPOLAR TRANSISTOR
WITH ULTRAFAST SOFT RECOVERY DIODE**

UltraFast CoPack IGBT

Features

- Switching-loss rating includes all "tail" losses
- HEXFRED™ soft ultrafast diodes
- Optimized for high operating frequency (over 5kHz)
See Fig. 1 for Current vs. Frequency curve



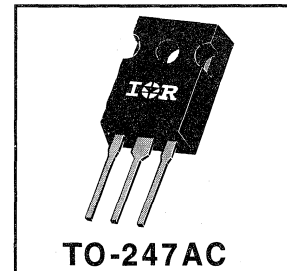
$V_{CES} = 500V$

$V_{CE(sat)} \leq 3.0V$

@ $V_{GE} = 15V, I_C = 15A$

Description

Co-packaged IGBTs are a natural extension of International Rectifier's well known IGBT line. They provide the convenience of an IGBT and an ultrafast recovery diode in one package, resulting in substantial benefits to a host of high-voltage, high-current, motor control, UPS and power supply applications.



Absolute Maximum Ratings

	Parameter	Max.	Units
V_{CES}	Collector-to-Emitter Voltage	500	V
$I_C @ T_C = 25^\circ C$	Continuous Collector Current	25	A
$I_C @ T_C = 100^\circ C$	Continuous Collector Current	15	
I_{CM}	Pulsed Collector Current ①	50	
I_{LM}	Clamped Inductive Load Current ②	50	
$I_F @ T_C = 100^\circ C$	Diode Continuous Forward Current	12	
I_{FM}	Diode Maximum Forward Current	50	
V_{GE}	Gate-to-Emitter Voltage	± 20	V
$P_D @ T_C = 25^\circ C$	Maximum Power Dissipation	100	W
$P_D @ T_C = 100^\circ C$	Maximum Power Dissipation	42	
T_J	Operating Junction and	-55 to +150	°C
T_{STG}	Storage Temperature Range		
	Soldering Temperature, for 10 sec.	300 (0.063 in. (1.6mm) from case)	
	Mounting Torque, 6-32 or M3 Screw.	10 lbf•in (1.1 N•m)	

Thermal Resistance

	Parameter	Min.	Typ.	Max.	Units
$R_{\theta JC}$	Junction-to-Case - IGBT	—	—	1.2	°C/W
$R_{\theta JC}$	Junction-to-Case - Diode	—	—	2.5	
$R_{\theta CS}$	Case-to-Sink, flat, greased surface	—	0.24	—	
$R_{\theta JA}$	Junction-to-Ambient, typical socket mount	—	—	40	
Wt	Weight	—	6 (0.21)	—	g (oz)

Power Conversion Ultra-Fast Co-Packs

Electrical Characteristics @ $T_J = 25^\circ\text{C}$ (unless otherwise specified)

	Parameter	Min.	Typ.	Max.	Units	Conditions
$V_{(BR)CES}$	Collector-to-Emitter Breakdown Voltage ^③	500	—	—	V	$V_{GE} = 0V, I_C = 250\mu A$
$\Delta V_{(BR)CES}/\Delta T_J$	Temp. Coeff. of Breakdown Voltage	—	0.46	—	$V/^\circ\text{C}$	$V_{GE} = 0V, I_C = 1.0mA$
$V_{CE(on)}$	Collector-to-Emitter Saturation Voltage	—	2.3	3.0	V	$I_C = 15A$ $V_{GE} = 15V$
		—	2.8	—		$I_C = 25A$ See Fig. 2, 5
		—	2.6	—		$I_C = 15A, T_J = 150^\circ\text{C}$
$V_{GE(th)}$	Gate Threshold Voltage	3.0	—	5.5		$V_{CE} = V_{GE}, I_C = 250\mu A$
$\Delta V_{GE(th)}/\Delta T_J$	Temp. Coeff. of Threshold Voltage	—	-11	—	$mV/^\circ\text{C}$	$V_{CE} = V_{GE}, I_C = 250\mu A$
g_{fe}	Forward Transconductance ^④	2.3	8.1	—	S	$V_{CE} = 100V, I_C = 15A$
I_{CES}	Zero Gate Voltage Collector Current	—	—	250	μA	$V_{GE} = 0V, V_{CE} = 500V$
		—	—	2500		$V_{GE} = 0V, V_{CE} = 500V, T_J = 150^\circ\text{C}$
V_{FM}	Diode Forward Voltage Drop	—	1.4	1.7	V	$I_C = 12A$ See Fig. 13
		—	1.3	1.6		$I_C = 12A, T_J = 150^\circ\text{C}$
I_{GES}	Gate-to-Emitter Leakage Current	—	—	± 100	nA	$V_{GE} = \pm 20V$

Switching Characteristics @ $T_J = 25^\circ\text{C}$ (unless otherwise specified)

	Parameter	Min.	Typ.	Max.	Units	Conditions
Q_g	Total Gate Charge (turn-on)	—	31	47	nC	$I_C = 15A$ $V_{CC} = 400V$ See Fig. 8
Q_{ge}	Gate - Emitter Charge (turn-on)	—	6.2	9.2		
Q_{gc}	Gate - Collector Charge (turn-on)	—	12	19		
$t_{d(on)}$	Turn-On Delay Time	—	73	—	ns	$T_J = 25^\circ\text{C}$ $I_C = 15A, V_{CC} = 400V$ $V_{GE} = 15V, R_G = 23\Omega$ Energy losses include "tail" and diode reverse recovery.
t_r	Rise Time	—	72	—		
$t_{d(off)}$	Turn-Off Delay Time	—	120	180	mJ	See Fig. 9, 10, 11, 18
t_f	Fall Time	—	100	150		
E_{on}	Turn-On Switching Loss	—	0.7	—	mJ	See Fig. 9, 10, 11, 18
E_{off}	Turn-Off Switching Loss	—	0.4	—		
E_{ts}	Total Switching Loss	—	1.1	1.7		
$t_{d(on)}$	Turn-On Delay Time	—	77	—	ns	$T_J = 150^\circ\text{C}$, See Fig. 9, 10, 11, 18 $I_C = 15A, V_{CC} = 400V$ $V_{GE} = 15V, R_G = 23\Omega$ Energy losses include "tail" and diode reverse recovery.
t_r	Rise Time	—	75	—		
$t_{d(off)}$	Turn-Off Delay Time	—	200	—	mJ	Measured 5mm from package
t_f	Fall Time	—	190	—		
E_{ts}	Total Switching Loss	—	1.5	—	pF	$V_{GE} = 0V$ $V_{CC} = 30V$ See Fig. 7 $f = 1.0MHz$
L_E	Internal Emitter Inductance	—	13	—		
C_{ies}	Input Capacitance	—	660	—		
C_{oes}	Output Capacitance	—	110	—	ns	$T_J = 25^\circ\text{C}$ See Fig. 14 $T_J = 125^\circ\text{C}$ 14
C_{res}	Reverse Transfer Capacitance	—	12	—		
t_{rr}	Diode Reverse Recovery Time	—	42	60	A	$T_J = 25^\circ\text{C}$ See Fig. 15 $T_J = 125^\circ\text{C}$ 15
		—	80	120		
I_{rr}	Diode Peak Reverse Recovery Current	—	3.5	6.0	nC	$T_J = 25^\circ\text{C}$ See Fig. 16 $T_J = 125^\circ\text{C}$ 16
		—	5.6	10		
Q_{rr}	Diode Reverse Recovery Charge	—	80	180	A/ μs	$T_J = 25^\circ\text{C}$ See Fig. 17 $T_J = 125^\circ\text{C}$ 17
		—	220	600		
$di_{(rec)M}/dt$	Diode Peak Rate of Fall of Recovery During t_b	—	180	—		$I_F = 12A$ $V_R = 200V$ $di/dt = 200A/\mu s$
		—	116	—		

Notes:

① Repetitive rating; $V_{GE}=20V$, pulse width limited by max. junction temperature. (See fig. 20)

② $V_{CC}=80\%(V_{CES})$, $V_{GE}=20V$, $L=10\mu H$, $R_G = 23\Omega$, (See fig. 19)

④ Pulse width 5.0 μs , single shot.

③ Pulse width $\leq 80\mu s$; duty factor $\leq 0.1\%$.

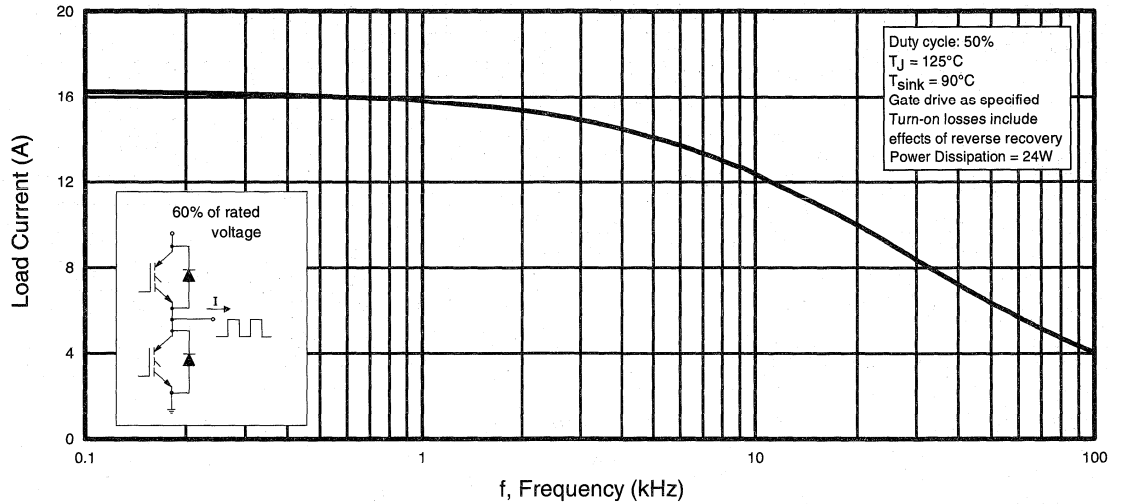


Fig. 1 - Typical Load Current vs. Frequency
(Load Current = I_{RMS} of fundamental)

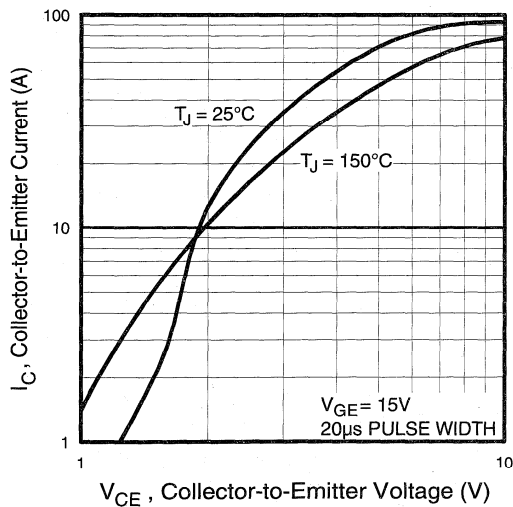


Fig. 2 - Typical Output Characteristics

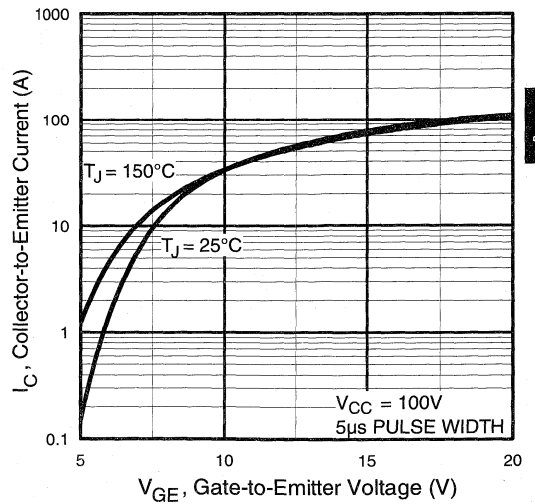


Fig. 3 - Typical Transfer Characteristics

Power Conversion
Ultra-Fast
Co-Packs

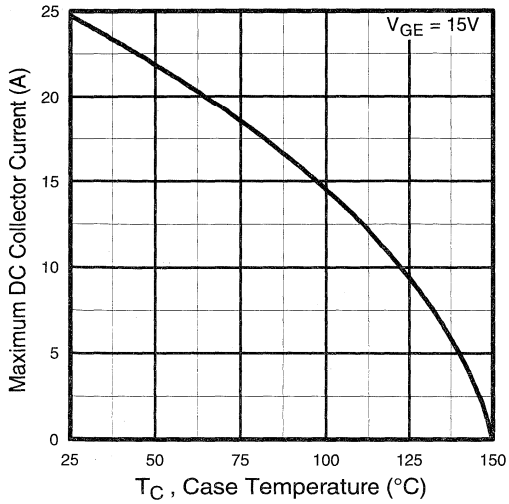


Fig. 4 - Maximum Collector Current vs. Case Temperature

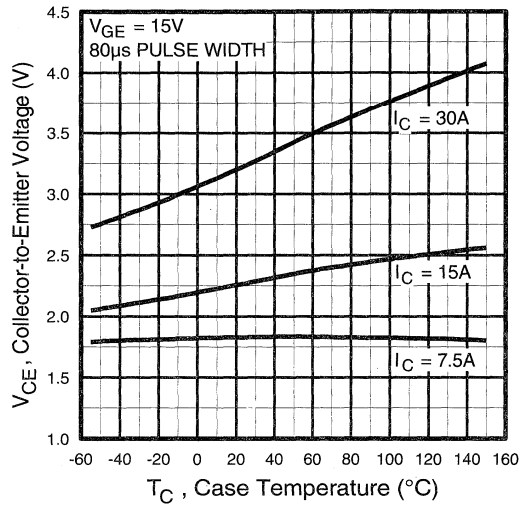


Fig. 5 - Collector-to-Emitter Voltage vs. Case Temperature

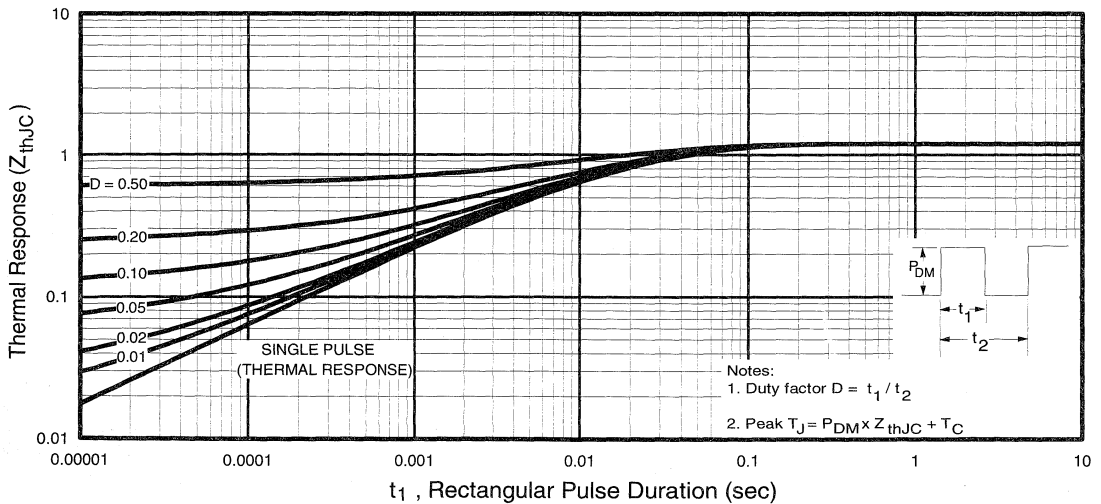


Fig. 6 - Maximum IGBT Effective Transient Thermal Impedance, Junction-to-Case

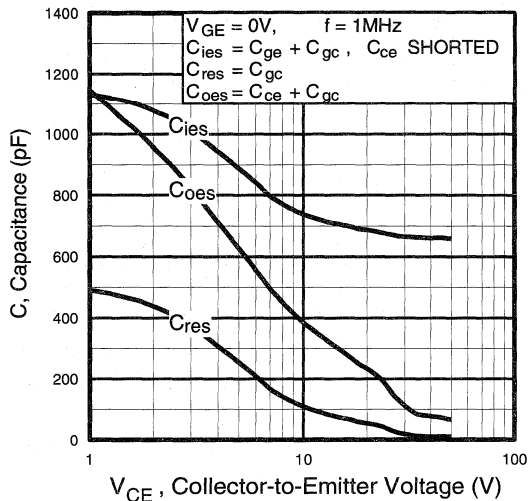


Fig. 7 - Typical Capacitance vs. Collector-to-Emitter Voltage

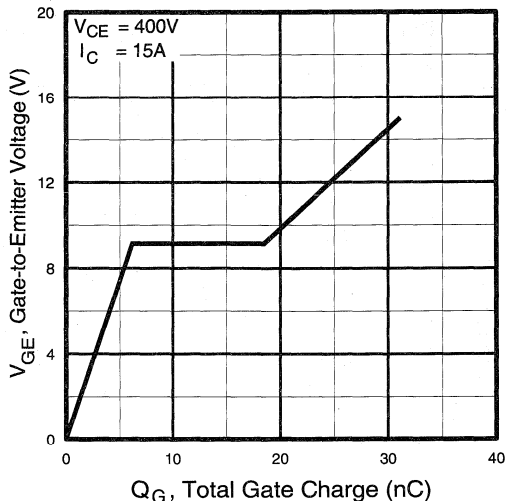


Fig. 8 - Typical Gate Charge vs. Gate-to-Emitter Voltage

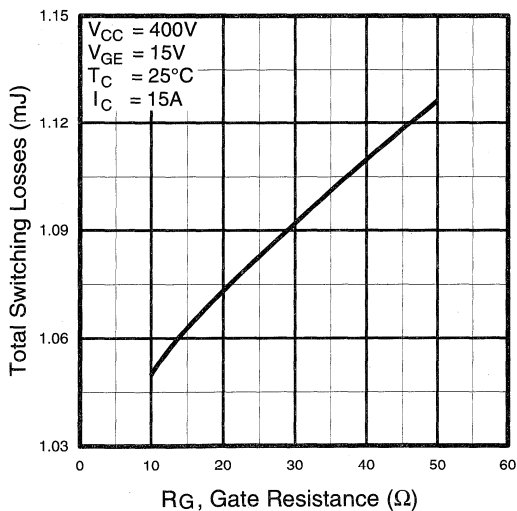


Fig. 9 - Typical Switching Losses vs. Gate Resistance

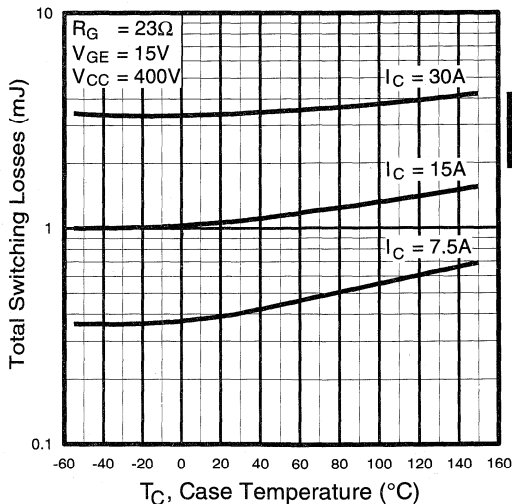


Fig. 10 - Typical Switching Losses vs. Case Temperature

Power Conversion
 Ultra-Fast
 Co-Packs

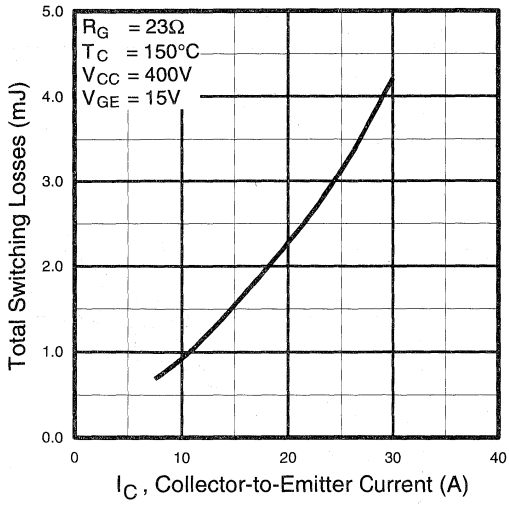


Fig. 11 - Typical Switching Losses vs. Collector-to-Emitter Current

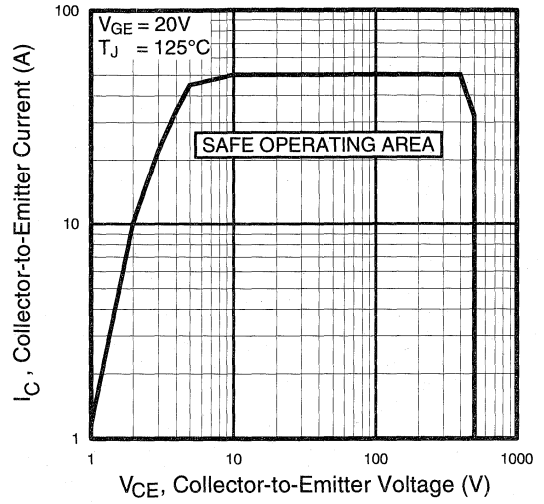


Fig. 12 - Turn-Off SOA

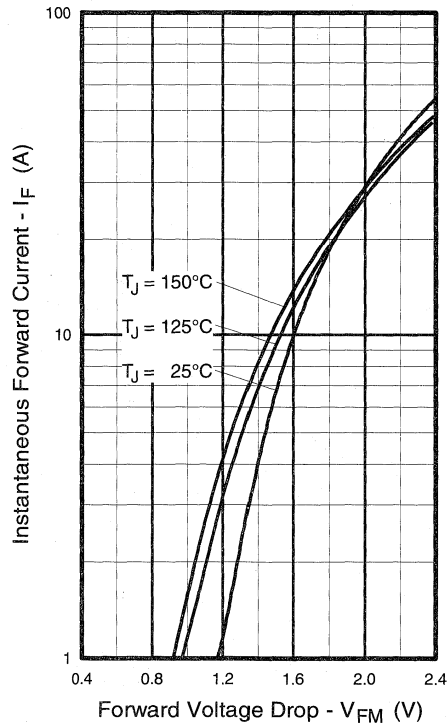


Fig. 13 - Maximum Forward Voltage Drop vs. Instantaneous Forward Current

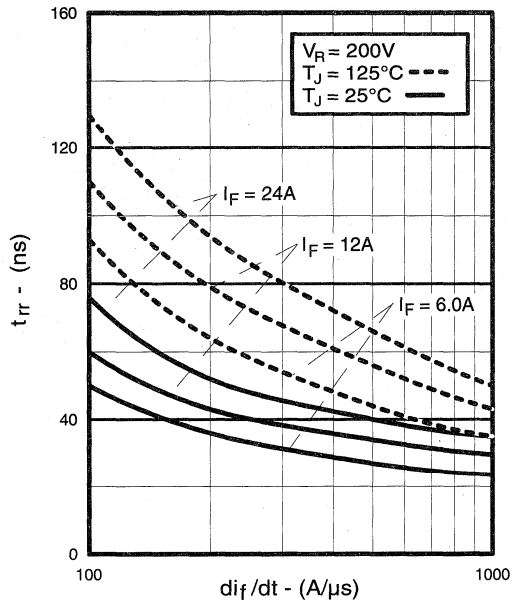


Fig. 14 - Typical Reverse Recovery vs. di_f/dt

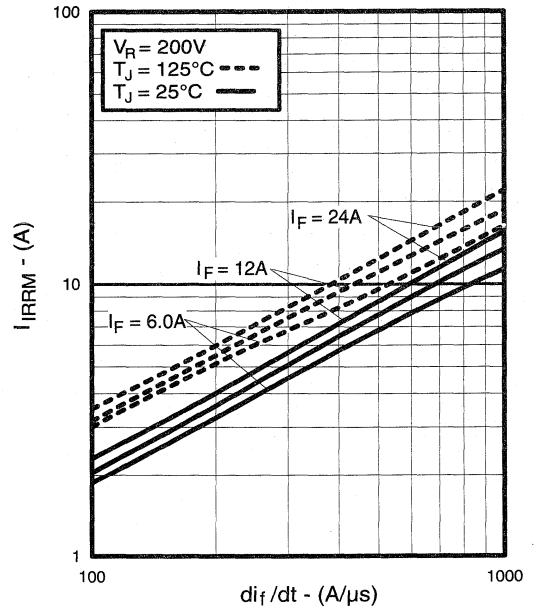


Fig. 15 - Typical Recovery Current vs. di_f/dt

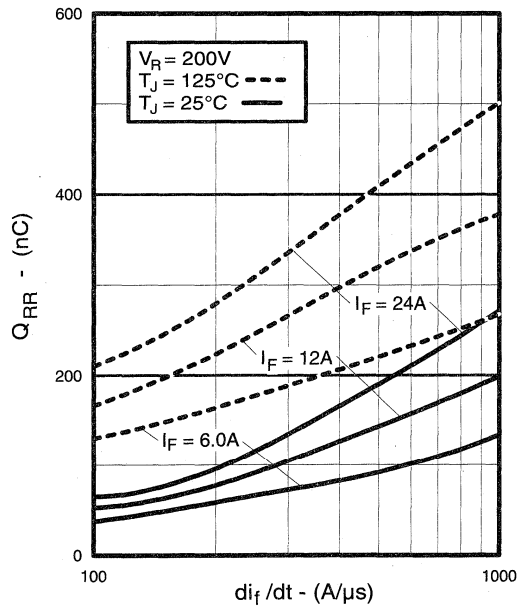


Fig. 16 - Typical Stored Charge vs. di_f/dt

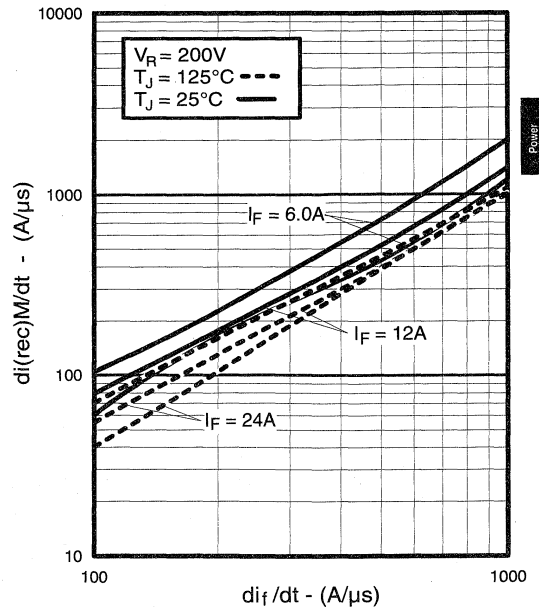


Fig. 17 - Typical $di_{(rec)}M/dt$ vs. di_f/dt

Power
 Conversion
 Ultra-Fast
 Capacitors

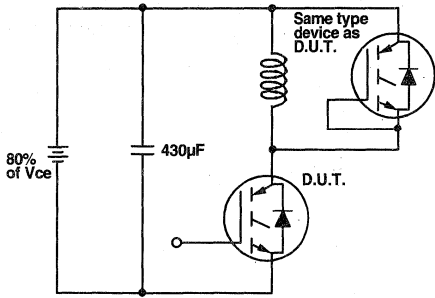


Fig. 18a - Test Circuit for Measurement of I_{LM} , E_{on} , $E_{off}(\text{diode})$, t_{rr} , Q_{rr} , I_{rr} , $t_{d(on)}$, t_r , $t_{d(off)}$, t_f

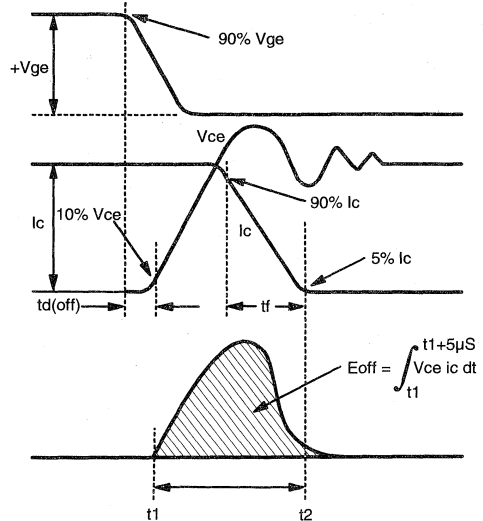


Fig. 18b - Test Waveforms for Circuit of Fig. 18a, Defining E_{off} , $t_{d(off)}$, t_f

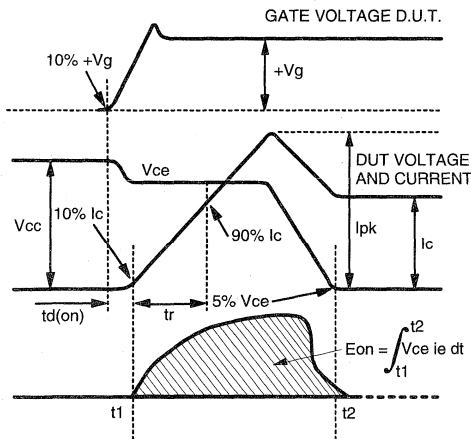


Fig. 18c - Test Waveforms for Circuit of Fig. 18a, Defining E_{on} , $t_{d(on)}$, t_r

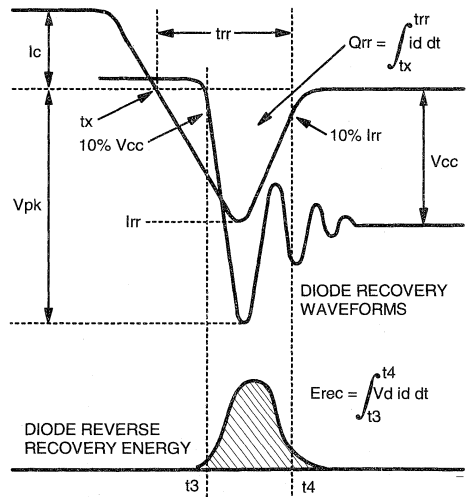


Fig. 18d - Test Waveforms for Circuit of Fig. 18a, Defining E_{rec} , t_{rr} , Q_{rr} , I_{rr}

**Refer to Section D for the following:
Appendix B: Section D - page D-4**

Fig. 18e - Macro Waveforms for Test Circuit Fig. 18a

Fig. 19 - Clamped Inductive Load Test Circuit

Fig. 20 - Pulsed Collector Current Test Circuit

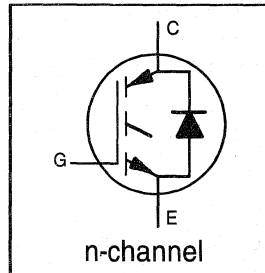
IRGP440UD2

INSULATED GATE BIPOLAR TRANSISTOR
WITH ULTRAFAST SOFT RECOVERY DIODE

UltraFast CoPack IGBT

Features

- Switching-loss rating includes all "tail" losses
- HEXFRED™ soft ultrafast diodes
- Optimized for high operating frequency (over 5kHz)
See Fig. 1 for Current vs. Frequency curve



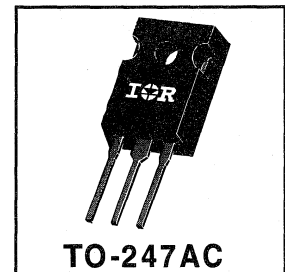
$$V_{CES} = 500V$$

$$V_{CE(sat)} \leq 3.0V$$

$$@ V_{GE} = 15V, I_C = 22A$$

Description

Co-packaged IGBTs are a natural extension of International Rectifier's well known IGBT line. They provide the convenience of an IGBT and an ultrafast recovery diode in one package, resulting in substantial benefits to a host of high-voltage, high-current, motor control, UPS and power supply applications.



Absolute Maximum Ratings

	Parameter	Max.	Units
V_{CES}	Collector-to-Emitter Voltage	500	V
$I_C @ T_C = 25^\circ C$	Continuous Collector Current	40	A
$I_C @ T_C = 100^\circ C$	Continuous Collector Current	22	
I_{CM}	Pulsed Collector Current ①	80	
I_{LM}	Clamped Inductive Load Current ②	80	
$I_F @ T_C = 100^\circ C$	Diode Continuous Forward Current	15	
I_{FM}	Diode Maximum Forward Current	80	
V_{GE}	Gate-to-Emitter Voltage	± 20	V
$P_D @ T_C = 25^\circ C$	Maximum Power Dissipation	160	W
$P_D @ T_C = 100^\circ C$	Maximum Power Dissipation	65	
T_J T_{STG}	Operating Junction and Storage Temperature Range	-55 to +150	°C
	Soldering Temperature, for 10 sec.	300 (0.063 in. (1.6mm) from case)	
	Mounting Torque, 6-32 or M3 Screw.	10 lbf•in (1.1 N•m)	

Thermal Resistance

	Parameter	Min.	Typ.	Max.	Units
$R_{\theta JC}$	Junction-to-Case - IGBT	—	—	0.77	°C/W
$R_{\theta JC}$	Junction-to-Case - Diode	—	—	1.7	
$R_{\theta CS}$	Case-to-Sink, flat, greased surface	—	0.24	—	
$R_{\theta JA}$	Junction-to-Ambient, typical socket mount	—	—	40	
Wt	Weight	—	6 (0.21)	—	g (oz)

Electrical Characteristics @ $T_J = 25^\circ\text{C}$ (unless otherwise specified)

	Parameter	Min.	Typ.	Max.	Units	Conditions
$V_{(BR)CES}$	Collector-to-Emitter Breakdown Voltage ^③	500	—	—	V	$V_{GE} = 0V, I_C = 250\mu A$
$\Delta V_{(BR)CES}/\Delta T_J$	Temp. Coeff. of Breakdown Voltage	—	0.35	—	V/°C	$V_{GE} = 0V, I_C = 1.0mA$
$V_{CE(on)}$	Collector-to-Emitter Saturation Voltage	—	2.4	3.0	V	$I_C = 22A, V_{GE} = 15V$
		—	2.8	—		$I_C = 40A$
		—	2.4	—		$I_C = 22A, T_J = 150^\circ\text{C}$
$V_{GE(th)}$	Gate Threshold Voltage	3.0	—	5.5		$V_{CE} = V_{GE}, I_C = 250\mu A$
$\Delta V_{GE(th)}/\Delta T_J$	Temp. Coeff. of Threshold Voltage	—	-11	—	mV/°C	$V_{CE} = V_{GE}, I_C = 250\mu A$
g_{fe}	Forward Transconductance ^④	6.6	13	—	S	$V_{CE} = 100V, I_C = 22A$
I_{CES}	Zero Gate Voltage Collector Current	—	—	250	μA	$V_{GE} = 0V, V_{CE} = 500V$
		—	—	3500		$V_{GE} = 0V, V_{CE} = 500V, T_J = 150^\circ\text{C}$
V_{FM}	Diode Forward Voltage Drop	—	1.3	1.7	V	$I_C = 15A$
		—	1.2	1.6		$I_C = 15A, T_J = 150^\circ\text{C}$
I_{GES}	Gate-to-Emitter Leakage Current	—	—	± 100	nA	$V_{GE} = \pm 20V$

Switching Characteristics @ $T_J = 25^\circ\text{C}$ (unless otherwise specified)

	Parameter	Min.	Typ.	Max.	Units	Conditions
Q_g	Total Gate Charge (turn-on)	—	55	83	nC	$I_C = 22A$
Q_{ge}	Gate - Emitter Charge (turn-on)	—	11	17		$V_{CC} = 400V$
Q_{gc}	Gate - Collector Charge (turn-on)	—	19	29		See Fig. 8
$t_{d(on)}$	Turn-On Delay Time	—	80	—	ns	$T_J = 25^\circ\text{C}$
t_r	Rise Time	—	68	—		$I_C = 22A, V_{CC} = 400V$
$t_{d(off)}$	Turn-Off Delay Time	—	160	240		$V_{GE} = 15V, R_G = 10\Omega$
t_f	Fall Time	—	130	220		Energy losses include "tail" and diode reverse recovery.
E_{on}	Turn-On Switching Loss	—	0.81	—	mJ	See Fig. 9, 10, 11, 18
E_{off}	Turn-Off Switching Loss	—	0.82	—		
E_{ts}	Total Switching Loss	—	1.6	2.4	mJ	$T_J = 150^\circ\text{C}$, See Fig. 9, 10, 11, 18
$t_{d(on)}$	Turn-On Delay Time	—	78	—		$I_C = 22A, V_{CC} = 400V$
t_r	Rise Time	—	64	—		$V_{GE} = 15V, R_G = 10\Omega$
$t_{d(off)}$	Turn-Off Delay Time	—	290	—		Energy losses include "tail" and diode reverse recovery.
t_f	Fall Time	—	250	—	mJ	
E_{ts}	Total Switching Loss	—	2.6	—		
L_E	Internal Emitter Inductance	—	13	—	nH	Measured 5mm from package
C_{ies}	Input Capacitance	—	1400	—	pF	$V_{GE} = 0V$
C_{oes}	Output Capacitance	—	250	—		$V_{CC} = 30V$
C_{res}	Reverse Transfer Capacitance	—	42	—		$f = 1.0MHz$
t_{rr}	Diode Reverse Recovery Time	—	42	60	ns	$T_J = 25^\circ\text{C}$ See Fig.
		—	74	120		$T_J = 125^\circ\text{C}$ 14
I_{rr}	Diode Peak Reverse Recovery Current	—	4.0	6.0	A	$T_J = 25^\circ\text{C}$ See Fig.
		—	6.5	10		$T_J = 125^\circ\text{C}$ 15
Q_{rr}	Diode Reverse Recovery Charge	—	80	180	nC	$T_J = 25^\circ\text{C}$ See Fig.
		—	220	600		$T_J = 125^\circ\text{C}$ 16
$di_{(rec)M}/dt$	Diode Peak Rate of Fall of Recovery During t_b	—	188	—	A/ μs	$T_J = 25^\circ\text{C}$ See Fig.
		—	160	—		$T_J = 125^\circ\text{C}$ 17

Notes:

① Repetitive rating; $V_{GE}=20V$, pulse width limited by max. junction temperature. (See fig. 20)

② $V_{CC}=80\%(V_{CES})$, $V_{GE}=20V$, $L=10\mu H$, $R_G=10\Omega$, (See fig. 19)

③ Pulse width $\leq 80\mu s$; duty factor $\leq 0.1\%$.

④ Pulse width 5.0 μs , single shot.

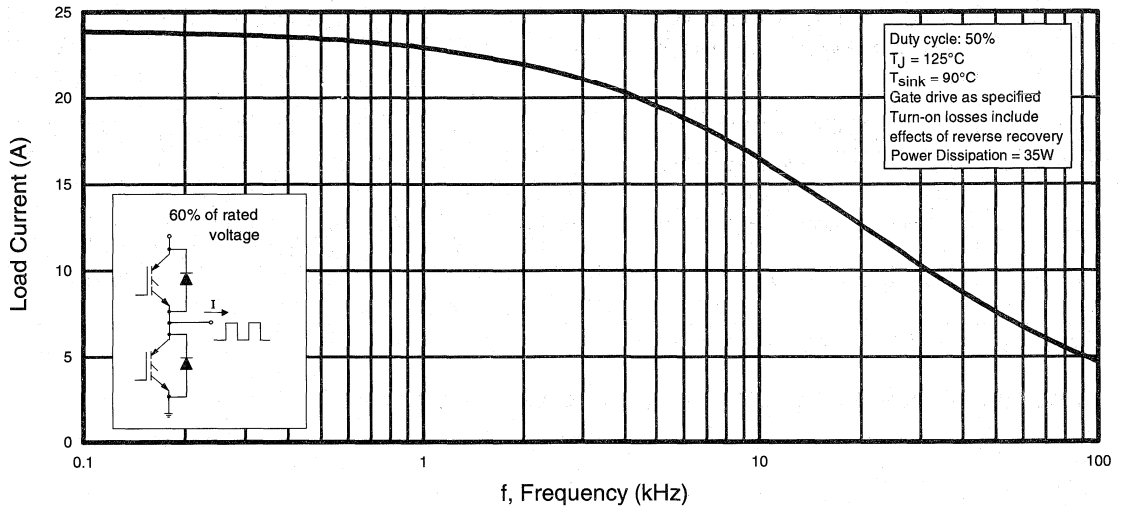


Fig. 1 - Typical Load Current vs. Frequency
(Load Current = I_{RMS} of fundamental)

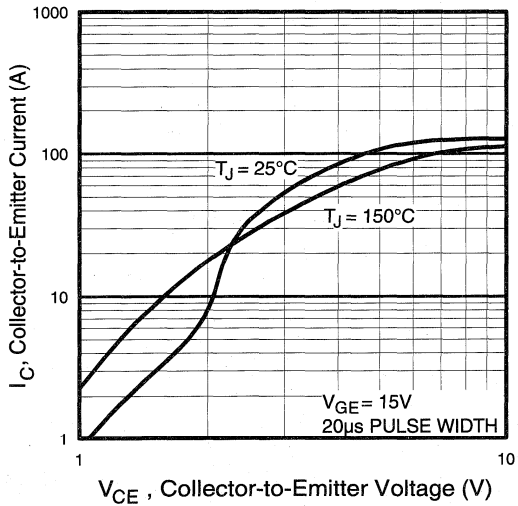


Fig. 2 - Typical Output Characteristics

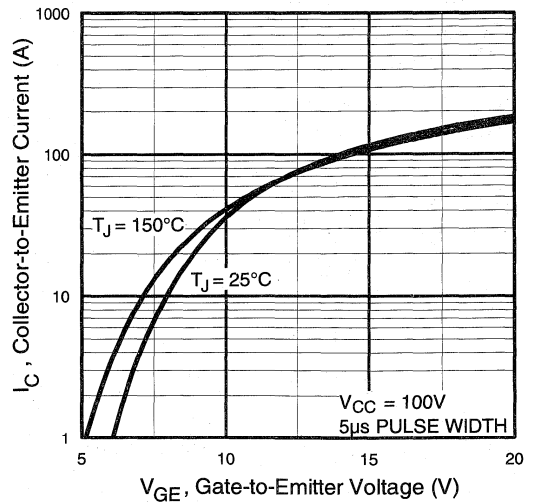


Fig. 3 - Typical Transfer Characteristics

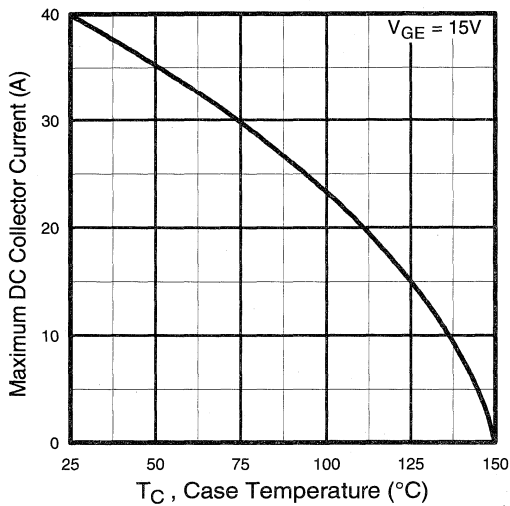


Fig. 4 - Maximum Collector Current vs. Case Temperature

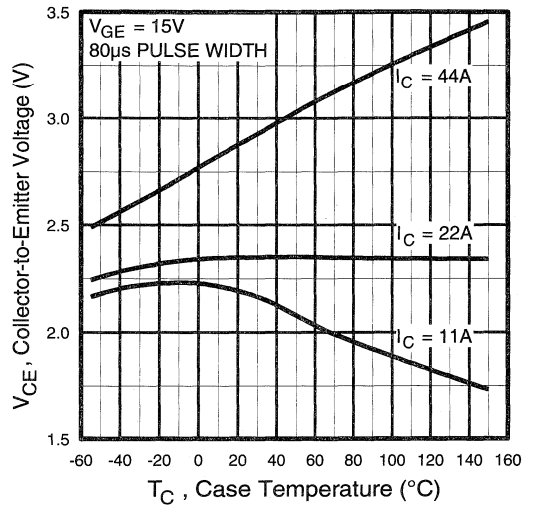


Fig. 5 - Collector-to-Emitter Voltage vs. Case Temperature

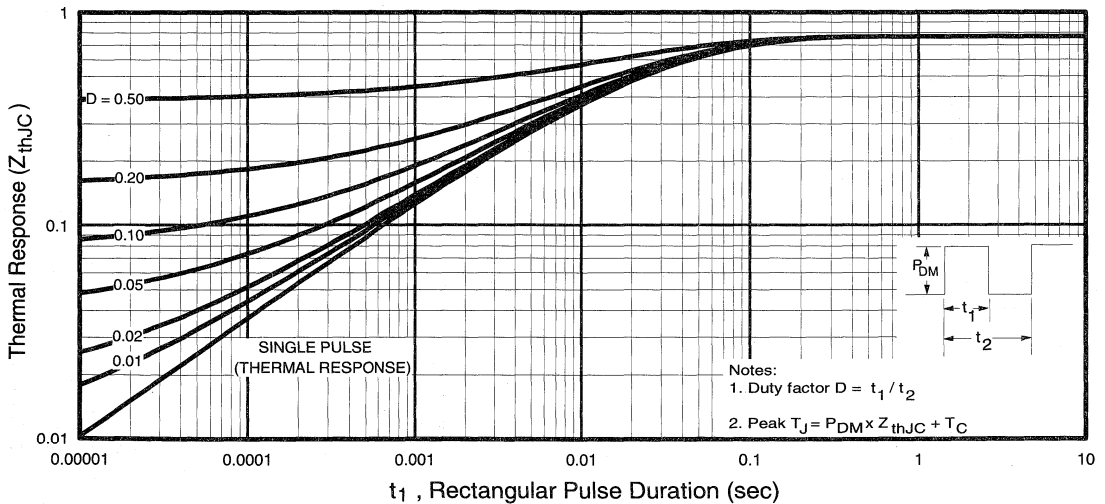


Fig. 6 - Maximum IGBT Effective Transient Thermal Impedance, Junction-to-Case

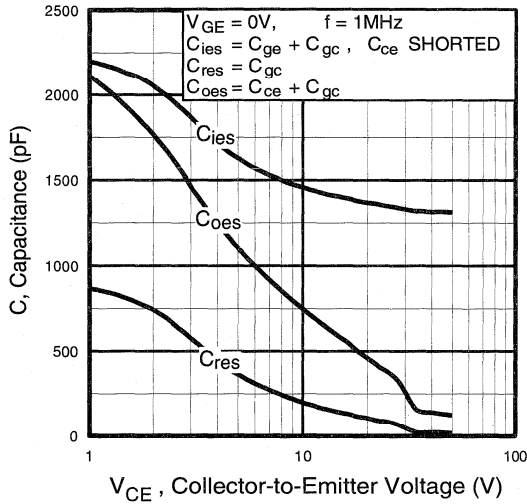


Fig. 7 - Typical Capacitance vs. Collector-to-Emitter Voltage

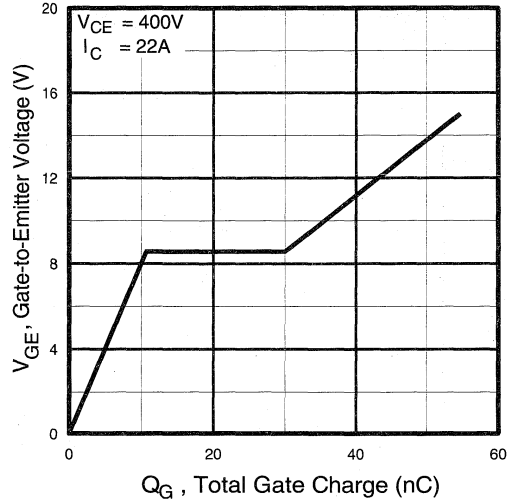


Fig. 8 - Typical Gate Charge vs. Gate-to-Emitter Voltage

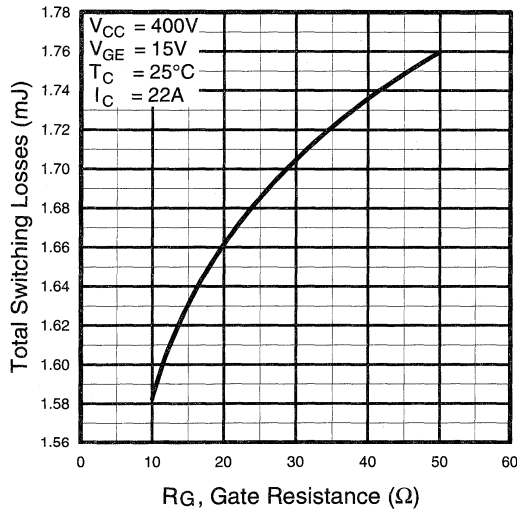


Fig. 9 - Typical Switching Losses vs. Gate Resistance

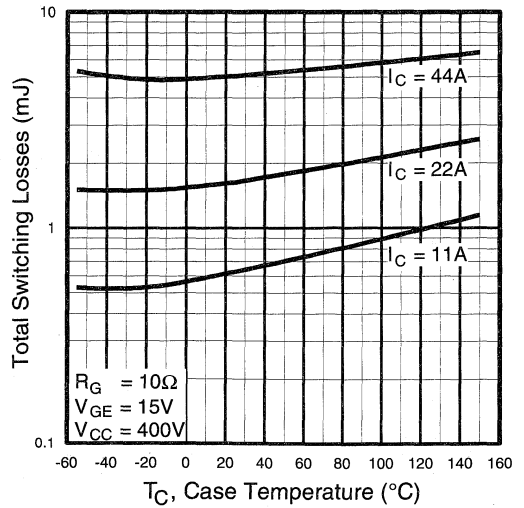


Fig. 10 - Typical Switching Losses vs. Case Temperature

Power Conversion
Ultra-Fast
Co-Packs

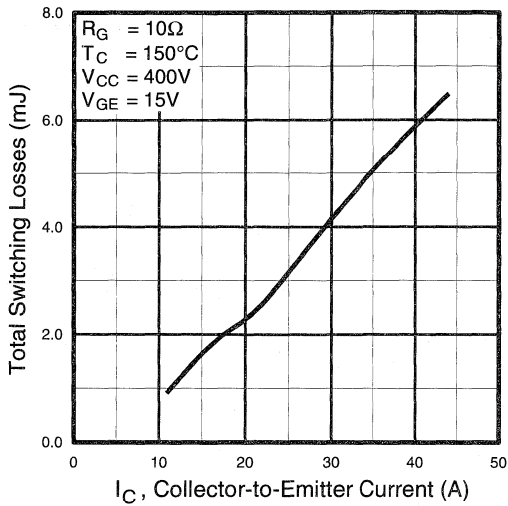


Fig. 11 - Typical Switching Losses vs. Collector-to-Emitter Current

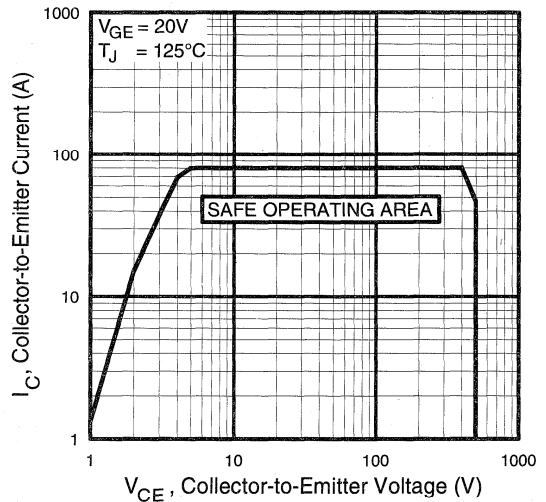


Fig. 12 - Turn-Off SOA

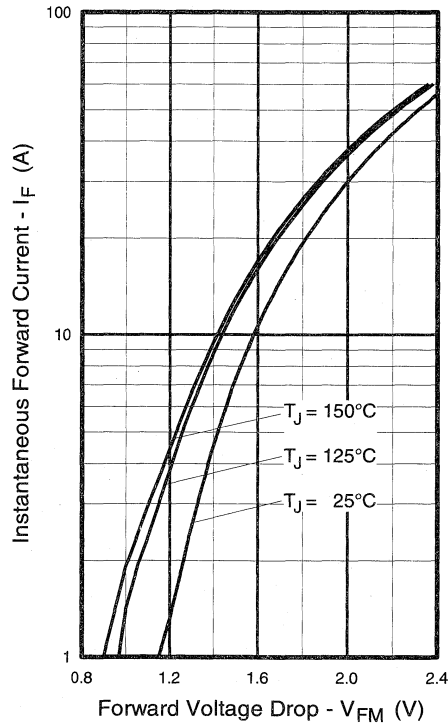


Fig. 13 - Maximum Forward Voltage Drop vs. Instantaneous Forward Current

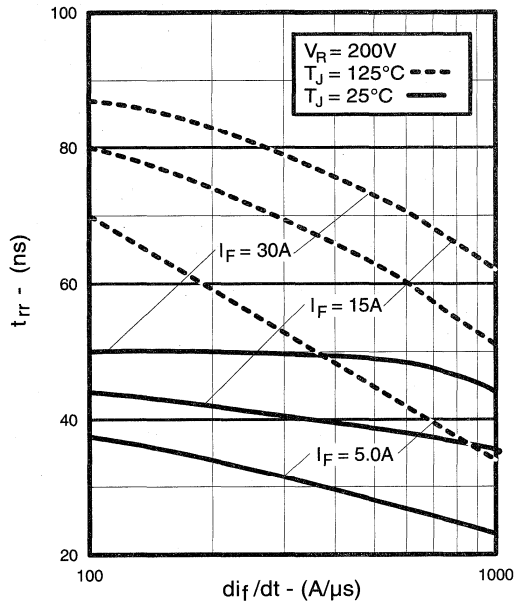


Fig. 14 - Typical Reverse Recovery vs. di_f/dt

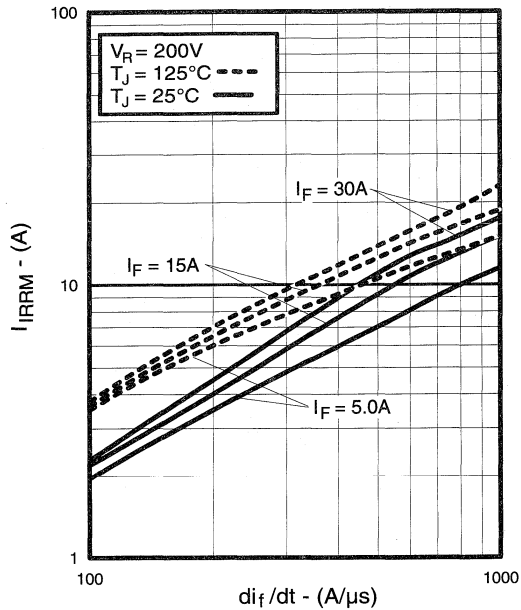


Fig. 15 - Typical Recovery Current vs. di_f/dt

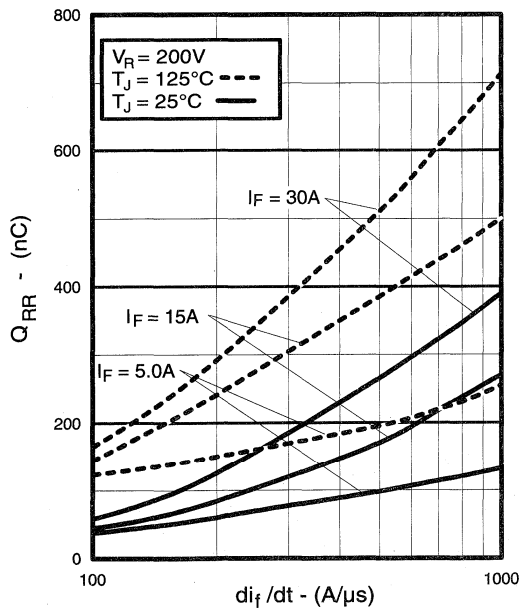


Fig. 16 - Typical Stored Charge vs. di_f/dt

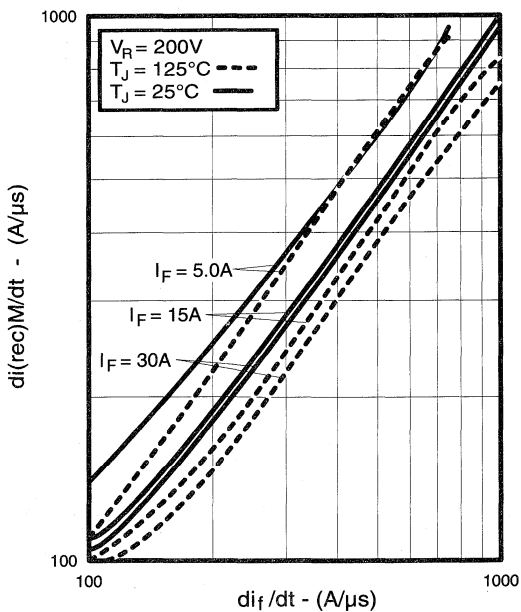


Fig. 17 - Typical $di_{(rec)M}/dt$ vs. di_f/dt

Power
Conversion
Ultra-Fast
Co-Pack

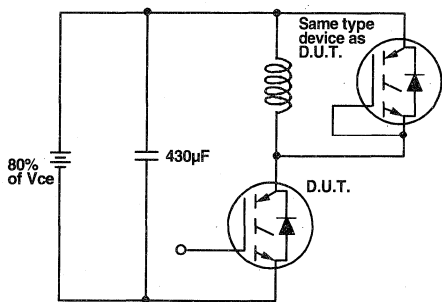


Fig. 18a - Test Circuit for Measurement of I_{LM} , E_{on} , $E_{off}(\text{diode})$, t_{rr} , Q_{rr} , I_{rr} , $t_{d(on)}$, t_r , $t_{d(off)}$, t_f

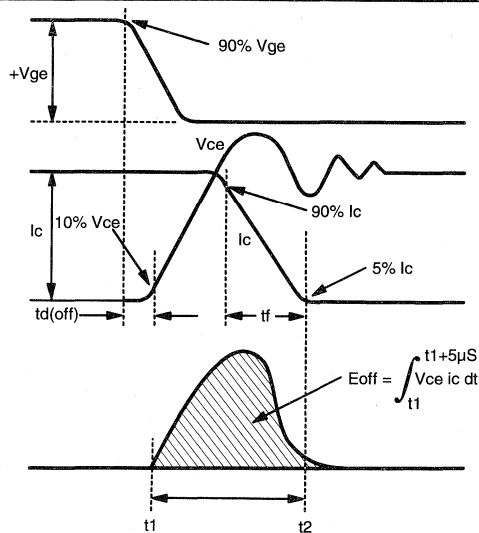


Fig. 18b - Test Waveforms for Circuit of Fig. 18a, Defining E_{off} , $t_{d(off)}$, t_f

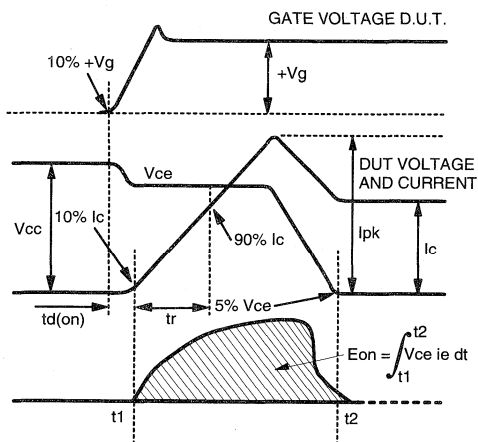


Fig. 18c - Test Waveforms for Circuit of Fig. 18a, Defining E_{on} , $t_{d(on)}$, t_r

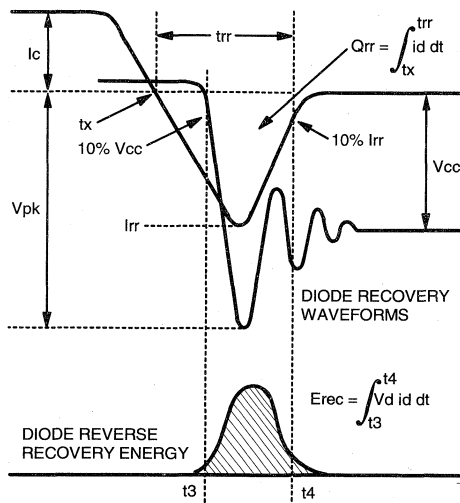


Fig. 18d - Test Waveforms for Circuit of Fig. 18a, Defining E_{rec} , t_{rr} , Q_{rr} , I_{rr}

**Refer to Section D for the following:
Appendix B: Section D - page D-4**

- Fig. 18e - Clamped Inductive Load Test Circuit
- Fig. 19 - Pulsed Collector Current Test Circuit
- Fig. 20 - Switching Loss Test Circuit

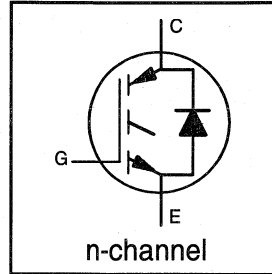
IRGP450UD2

**INSULATED GATE BIPOLAR TRANSISTOR
WITH ULTRAFAST SOFT RECOVERY**

UltraFast CoPack IGBT

**DIODE
Features**

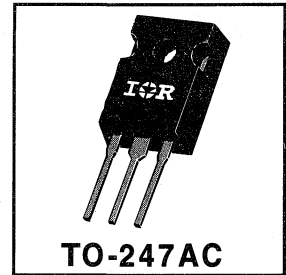
- Switching-loss rating includes all "tail" losses
- HEXFRED™ soft ultrafast diodes
- Optimized for high operating frequency (over 5kHz)



$V_{CES} = 500V$
 $V_{CE(sat)} \leq 3.2V$
@ $V_{GE} = 15V, I_C = 33A$

Description

Co-packaged IGBTs are a natural extension of International Rectifier's well known IGBT line. They provide the convenience of an IGBT and an ultrafast recovery diode in one package, resulting in substantial benefits to a host of high-voltage, high-current, motor control, UPS and power supply applications.



Absolute Maximum Ratings

	Parameter	Max.	Units
V_{CES}	Collector-to-Emitter Voltage	500	V
$I_C @ T_C = 25^\circ C$	Continuous Collector Current	59	A
$I_C @ T_C = 100^\circ C$	Continuous Collector Current	33	
I_{CM}	Pulsed Collector Current ①	120	
I_{LM}	Clamped Inductive Load Current ②	120	
$I_F @ T_C = 100^\circ C$	Diode Continuous Forward Current	29	
I_{FM}	Diode Maximum Forward Current	120	
V_{GE}	Gate-to-Emitter Voltage	± 20	V
$P_D @ T_C = 25^\circ C$	Maximum Power Dissipation	200	W
$P_D @ T_C = 100^\circ C$	Maximum Power Dissipation	78	
T_J	Operating Junction and Storage Temperature Range	-55 to +150	°C
T_{STG}	Soldering Temperature, for 10 sec.	300 (0.063 in. (1.6mm) from case)	
	Mounting Torque, 6-32 or M3 Screw.	10 lbf•in (1.1 N•m)	

Thermal Resistance

	Parameter	Min.	Typ.	Max.	Units
$R_{\theta JC}$	Junction-to-Case - IGBT	—	—	0.64	°C/W
$R_{\theta JC}$	Junction-to-Case - Diode	—	—	0.83	
$R_{\theta CS}$	Case-to-Sink, flat, greased surface	—	0.24	—	
$R_{\theta JA}$	Junction-to-Ambient, typical socket mount	—	—	40	
Wt	Weight	—	6 (0.21)	—	g (oz)

Power
Conversion
Ultra-Fast
Co-Packs

Electrical Characteristics @ $T_J = 25^\circ\text{C}$ (unless otherwise specified)

	Parameter	Min.	Typ.	Max.	Units	Conditions
$V_{(BR)CES}$	Collector-to-Emitter Breakdown Voltage ^③	500	—	—	V	$V_{GE} = 0V, I_C = 250\mu A$
$\Delta V_{(BR)CES}/\Delta T_J$	Temperature Coeff. of Breakdown Voltage	—	0.41	—	$V/^\circ\text{C}$	$V_{GE} = 0V, I_C = 1.0mA$
$V_{CE(on)}$	Collector-to-Emitter Saturation Voltage	—	2.1	3.2	V	$I_C = 33A$ $V_{GE} = 15V$
		—	2.6	—		
		—	2.1	—		
$V_{GE(th)}$	Gate Threshold Voltage	3.0	—	5.5		$V_{CE} = V_{GE}, I_C = 250\mu A$
$\Delta V_{GE(th)}/\Delta T_J$	Temperature Coeff. of Threshold Voltage	—	-10	—	$mV/^\circ\text{C}$	$V_{CE} = V_{GE}, I_C = 250\mu A$
g_{fe}	Forward Transconductance ^④	7.0	22	—	S	$V_{CE} = 100V, I_C = 33A$
I_{CES}	Zero Gate Voltage Collector Current	—	—	250	μA	$V_{GE} = 0V, V_{CE} = 500V$
		—	—	6500		$V_{GE} = 0V, V_{CE} = 500V, T_J = 150^\circ\text{C}$
V_{FM}	Diode Forward Voltage Drop	—	1.3	1.7	V	$I_C = 25A$
		—	1.2	1.5		$I_C = 25A, T_J = 150^\circ\text{C}$
I_{GES}	Gate-to-Emitter Leakage Current	—	—	± 100	nA	$V_{GE} = \pm 20V$

Switching Characteristics @ $T_J = 25^\circ\text{C}$ (unless otherwise specified)

	Parameter	Min.	Typ.	Max.	Units	Conditions	
Q_g	Total Gate Charge (turn-on)	—	120	180	nC	$I_C = 33A$ $V_{CC} = 400V$	
Q_{ge}	Gate - Emitter Charge (turn-on)	—	22	33			
Q_{gc}	Gate - Collector Charge (turn-on)	—	41	62			
$t_{d(on)}$	Turn-On Delay Time	—	33	—	ns	$T_J = 25^\circ\text{C}$ $I_C = 33A, V_{CC} = 400V$ $V_{GE} = 15V, R_G = 5.0\Omega$ Energy losses include "tail" and diode reverse recovery.	
t_r	Rise Time	—	26	—			
$t_{d(off)}$	Turn-Off Delay Time	—	110	170			
t_f	Fall Time	—	91	140			
E_{on}	Turn-On Switching Loss	—	0.91	—	mJ		
E_{off}	Turn-Off Switching Loss	—	0.25	—			
E_{ts}	Total Switching Loss	—	1.2	1.7	mJ	$T_J = 150^\circ\text{C}$, $I_C = 33A, V_{CC} = 400V$ $V_{GE} = 15V, R_G = 5.0\Omega$ Energy losses include "tail" and diode reverse recovery.	
$t_{d(on)}$	Turn-On Delay Time	—	37	—			
t_r	Rise Time	—	29	—			
$t_{d(off)}$	Turn-Off Delay Time	—	160	—			
t_f	Fall Time	—	110	—	ns		
E_{ts}	Total Switching Loss	—	1.8	—			
L_E	Internal Emitter Inductance	—	13	—	nH	Measured 5mm from package	
C_{ies}	Input Capacitance	—	2700	—	pF	$V_{GE} = 0V$ $V_{CC} = 30V$ $f = 1.0MHz$	
C_{oes}	Output Capacitance	—	280	—			
C_{res}	Reverse Transfer Capacitance	—	34	—			
t_{rr}	Diode Reverse Recovery Time	—	50	75	ns	$T_J = 25^\circ\text{C}$	$I_F = 25A$ $V_R = 200V$ $di/dt = 200A/\mu s$
		—	105	160			
I_{rr}	Diode Peak Reverse Recovery Current	—	4.5	10	A	$T_J = 25^\circ\text{C}$	
		—	8.0	15		$T_J = 125^\circ\text{C}$	
Q_{rr}	Diode Reverse Recovery Charge	—	112	375	nC	$T_J = 25^\circ\text{C}$	
		—	420	1200		$T_J = 125^\circ\text{C}$	
$di_{(rec)M}/dt$	Diode Peak Rate of Fall of Recovery During t_b	—	250	—	$A/\mu s$	$T_J = 25^\circ\text{C}$	
		—	160	—		$T_J = 125^\circ\text{C}$	

Notes: ① Repetitive rating; $V_{GE}=20V$, pulse width limited by max. junction temperature. (See fig. 20)

② $V_{CC}=80\%(V_{CES}), V_{GE}=20V, L=10\mu H, R_G=5.0\Omega,$ (See fig. 19)

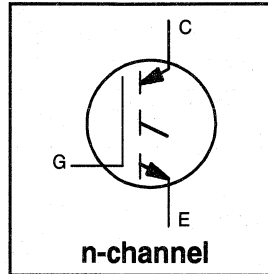
④ Pulse width $5.0\mu s$, single shot.

③ Pulse width $\leq 80\mu s$; duty factor $\leq 0.1\%$.

Refer to Section D - page D-13 for Package Outline 3 - JEDEC Outline TO-247AC

Features

- Switching-loss rating includes all "tail" losses
- Optimized for high operating frequency (over 5kHz)
See Fig. 1 for Current vs. Frequency curve



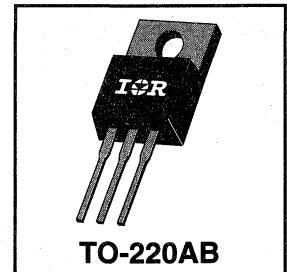
$$V_{CES} = 600V$$

$$V_{CE(sat)} \leq 3.0V$$

$$@ V_{GE} = 15V, I_C = 6.5A$$

Description

Insulated Gate Bipolar Transistors (IGBTs) from International Rectifier have higher usable current densities than comparable bipolar transistors, while at the same time having simpler gate-drive requirements of the familiar power MOSFET. They provide substantial benefits to a host of high-voltage, high-current applications.



Absolute Maximum Ratings

	Parameter	Max.	Units
V_{CES}	Collector-to-Emitter Voltage	600	V
$I_C @ T_C = 25^\circ C$	Continuous Collector Current	13	A
$I_C @ T_C = 100^\circ C$	Continuous Collector Current	6.5	
I_{CM}	Pulsed Collector Current ①	52	
I_{LM}	Clamped Inductive Load Current ②	52	
V_{GE}	Gate-to-Emitter Voltage	± 20	V
E_{ARV}	Reverse Voltage Avalanche Energy ③	5	mJ
$P_D @ T_C = 25^\circ C$	Maximum Power Dissipation	60	W
$P_D @ T_C = 100^\circ C$	Maximum Power Dissipation	24	
T_J	Operating Junction and	-55 to +150	°C
T_{STG}	Storage Temperature Range		
	Soldering Temperature, for 10 sec.	300 (0.063 in. (1.6mm) from case)	
	Mounting torque, 6-32 or M3 screw.	10 lbf•in (1.1N•m)	

Thermal Resistance

	Parameter	Min.	Typ.	Max.	Units
$R_{\theta JC}$	Junction-to-Case	—	—	2.1	°C/W
$R_{\theta CS}$	Case-to-Sink, flat, greased surface	—	0.50	—	
$R_{\theta JA}$	Junction-to-Ambient, typical socket mount	—	—	80	
Wt	Weight	—	2.0 (0.07)	—	g (oz)

Electrical Characteristics @ $T_J = 25^\circ\text{C}$ (unless otherwise specified)

	Parameter	Min.	Typ.	Max.	Units	Conditions
$V_{(BR)CES}$	Collector-to-Emitter Breakdown Voltage	600	—	—	V	$V_{GE} = 0V, I_C = 250\mu A$
$V_{(BR)ECS}$	Emitter-to-Collector Breakdown Voltage ④	20	—	—	V	$V_{GE} = 0V, I_C = 1.0A$
$\Delta V_{(BR)CES}/\Delta T_J$	Temperature Coeff. of Breakdown Voltage	—	0.69	—	V/ $^\circ\text{C}$	$V_{GE} = 0V, I_C = 1.0mA$
$V_{CE(on)}$	Collector-to-Emitter Saturation Voltage	—	2.2	3.0	V	$I_C = 6.5A$ $V_{GE} = 15V$
		—	2.8	—		$I_C = 13A$ See Fig. 2, 5
		—	2.5	—		$I_C = 6.5A, T_J = 150^\circ\text{C}$
$V_{GE(th)}$	Gate Threshold Voltage	3.0	—	5.5		$V_{CE} = V_{GE}, I_C = 250\mu A$
$\Delta V_{GE(th)}/\Delta T_J$	Temperature Coeff. of Threshold Voltage	—	-11	—	mV/ $^\circ\text{C}$	$V_{CE} = V_{GE}, I_C = 250\mu A$
g_{fe}	Forward Transconductance ⑤	1.4	4.3	—	S	$V_{CE} = 100V, I_C = 6.5A$
I_{CES}	Zero Gate Voltage Collector Current	—	—	250	μA	$V_{GE} = 0V, V_{CE} = 600V$
		—	—	1000		$V_{GE} = 0V, V_{CE} = 600V, T_J = 150^\circ\text{C}$
I_{GES}	Gate-to-Emitter Leakage Current	—	—	± 100	nA	$V_{GE} = \pm 20V$

Switching Characteristics @ $T_J = 25^\circ\text{C}$ (unless otherwise specified)

	Parameter	Min.	Typ.	Max.	Units	Conditions
Q_g	Total Gate Charge (turn-on)	—	16	22	nC	$I_C = 6.5A$ $V_{CC} = 400V$ See Fig. 8 $V_{GE} = 15V$
Q_{ge}	Gate - Emitter Charge (turn-on)	—	2.5	3.8		
Q_{gc}	Gate - Collector Charge (turn-on)	—	7.8	13		
$t_{d(on)}$	Turn-On Delay Time	—	22	—	ns	$T_J = 25^\circ\text{C}$ $I_C = 6.5A, V_{CC} = 480V$ $V_{GE} = 15V, R_G = 50\Omega$ Energy losses include "tail"
t_r	Rise Time	—	12	—		
$t_{d(off)}$	Turn-Off Delay Time	—	71	95		
t_f	Fall Time	—	91	280		
E_{on}	Turn-On Switching Loss	—	0.11	—	mJ	See Fig. 9, 10, 11, 14
E_{off}	Turn-Off Switching Loss	—	0.14	—		
E_{ts}	Total Switching Loss	—	0.25	0.50		
$t_{d(on)}$	Turn-On Delay Time	—	23	—	ns	$T_J = 150^\circ\text{C}$, $I_C = 6.5A, V_{CC} = 480V$ $V_{GE} = 15V, R_G = 50\Omega$ Energy losses include "tail"
t_r	Rise Time	—	13	—		
$t_{d(off)}$	Turn-Off Delay Time	—	140	—		
t_f	Fall Time	—	200	—		
E_{ts}	Total Switching Loss	—	0.45	—	mJ	See Fig. 10, 14
L_E	Internal Emitter Inductance	—	7.5	—	nH	Measured 5mm from package
C_{ies}	Input Capacitance	—	330	—	pF	$V_{GE} = 0V$ $V_{CC} = 30V$ See Fig. 7 $f = 1.0MHz$
C_{oes}	Output Capacitance	—	65	—		
C_{res}	Reverse Transfer Capacitance	—	6.0	—		

Notes:

- ① Repetitive rating; $V_{GE}=20V$, pulse width limited by max. junction temperature. (See fig. 13b)
- ② $V_{CC}=80\%(V_{CES}), V_{GE}=20V, L=10\mu H, R_G=50\Omega$, (See fig. 13a)
- ③ Repetitive rating; pulse width limited by maximum junction temperature.
- ④ Pulse width $\leq 80\mu s$; duty factor $\leq 0.1\%$.
- ⑤ Pulse width 5.0 μs , single shot.

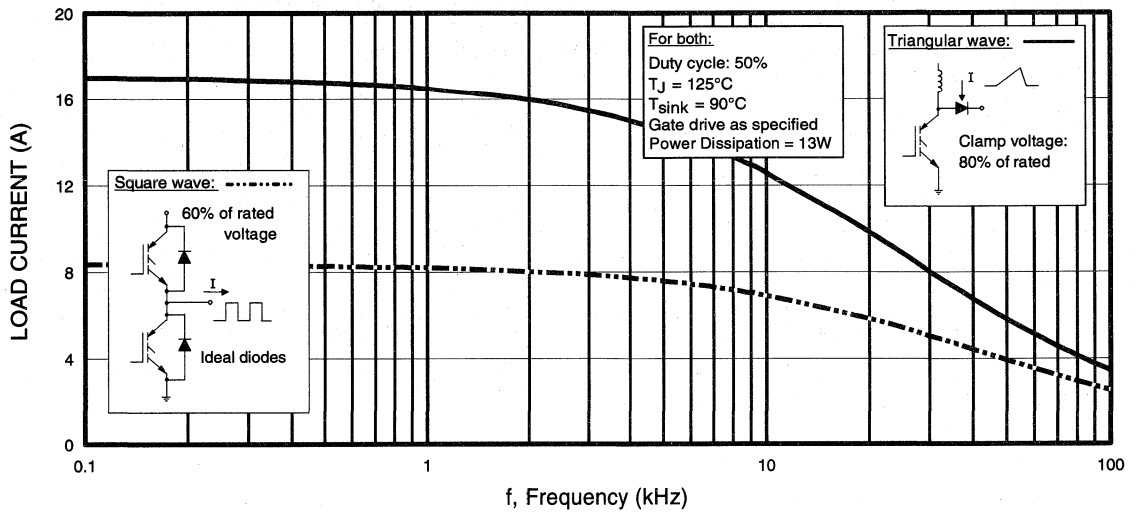


Fig. 1 - Typical Load Current vs. Frequency
 (For square wave, $I = I_{RMS}$ of fundamental; for triangular wave, $I = I_{PK}$)

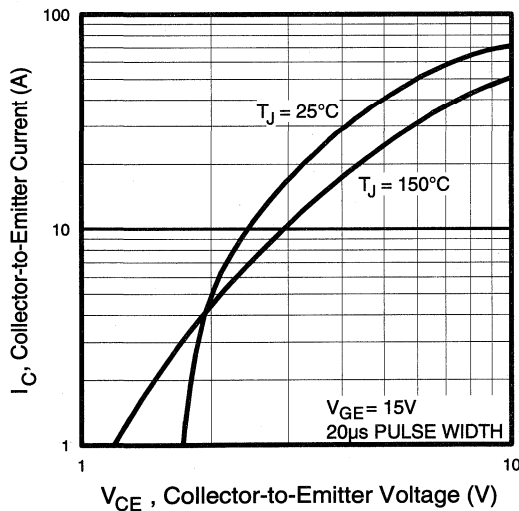


Fig. 2 - Typical Output Characteristics

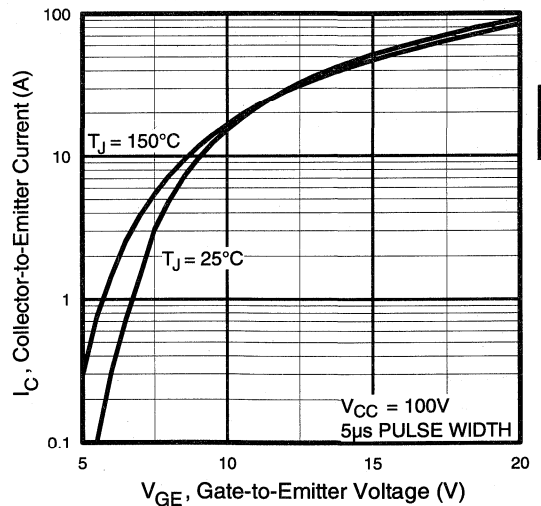


Fig. 3 - Typical Transfer Characteristics

Power
Conversion
Ultra-Fast
Discretes

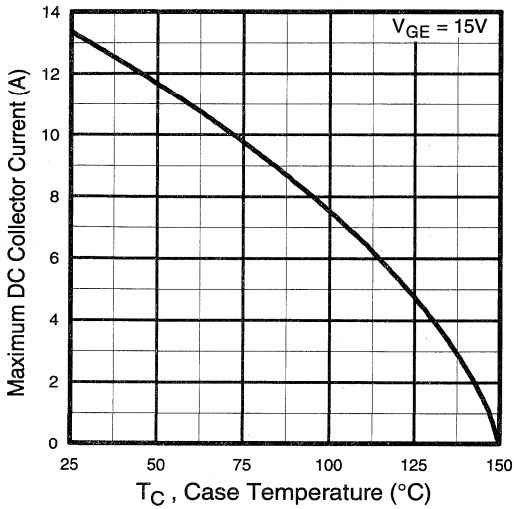


Fig. 4 - Maximum Collector Current vs. Case Temperature

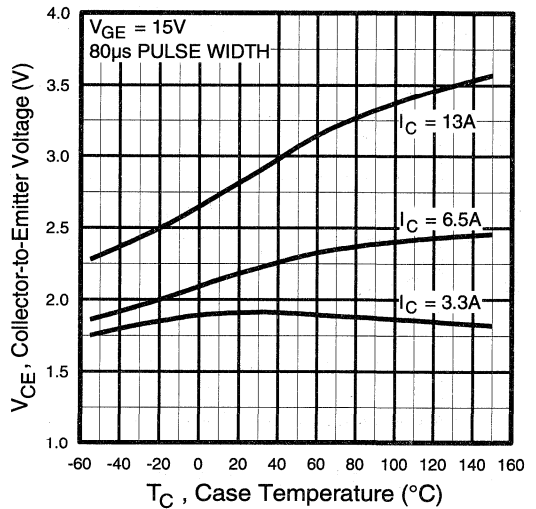


Fig. 5 - Collector-to-Emitter Voltage vs. Case Temperature

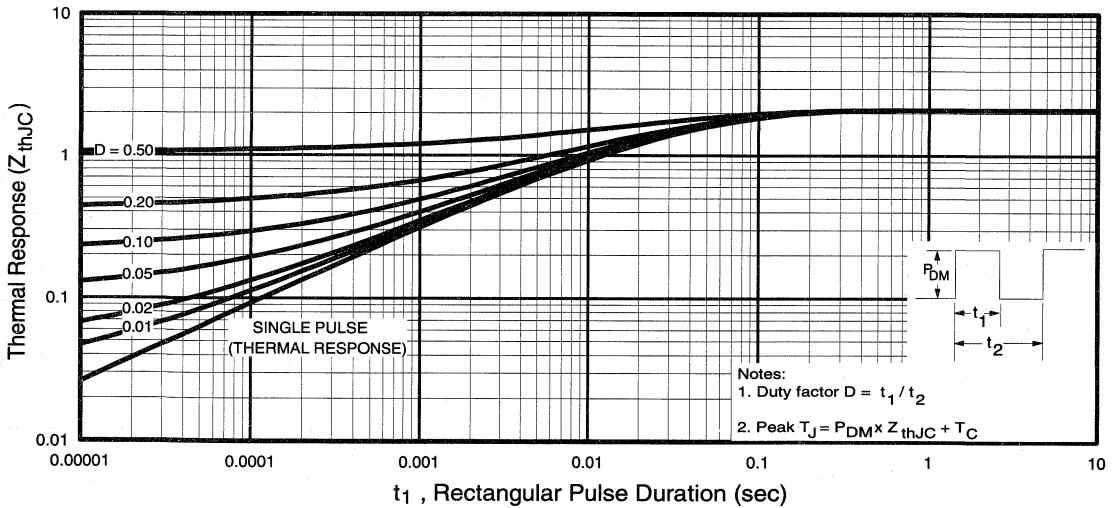


Fig. 6 - Maximum Effective Transient Thermal Impedance, Junction-to-Case

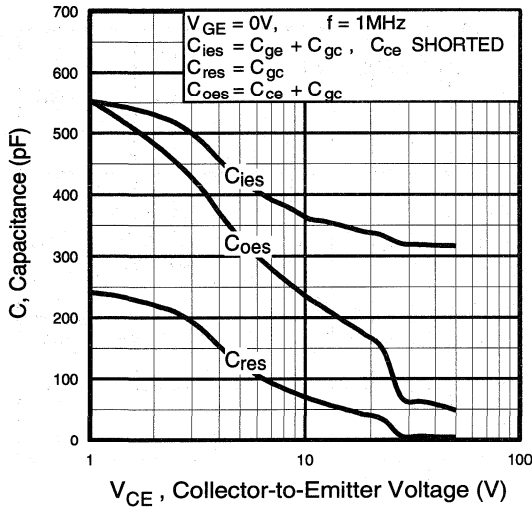


Fig. 7 - Typical Capacitance vs. Collector-to-Emitter Voltage

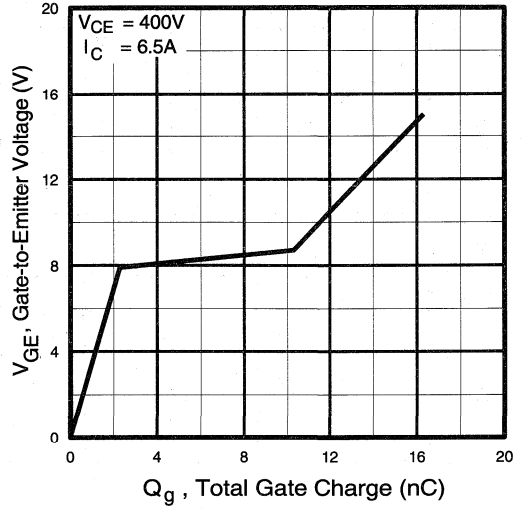


Fig. 8 - Typical Gate Charge vs. Gate-to-Emitter Voltage

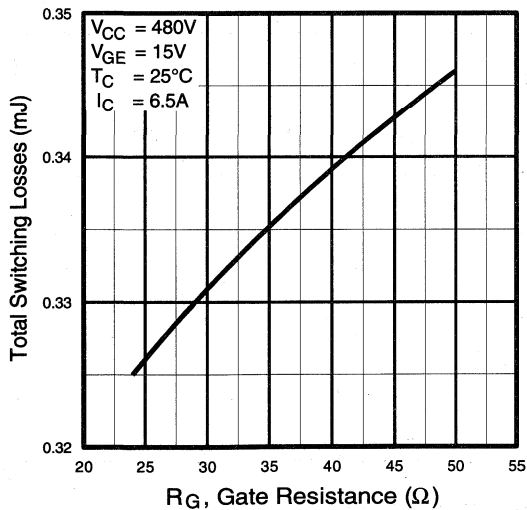


Fig. 9 - Typical Switching Losses vs. Gate Resistance

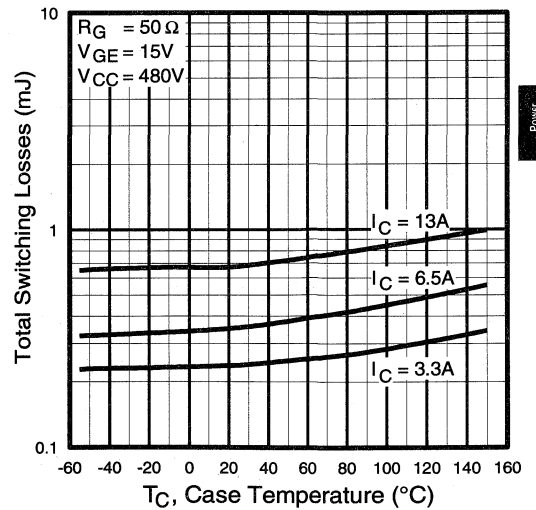


Fig. 10 - Typical Switching Losses vs. Case Temperature

Power Conversion
Ultra-Fast
Diodes

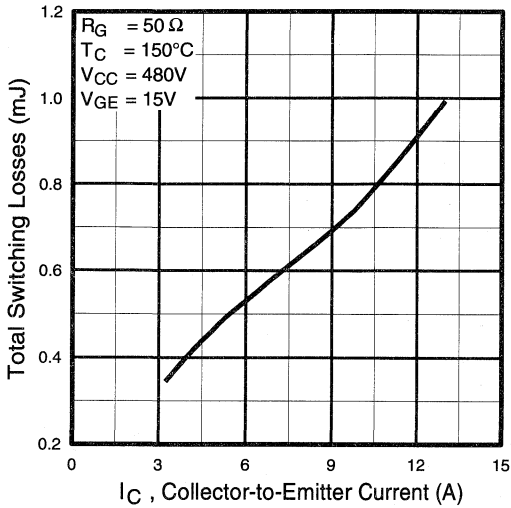


Fig. 11 - Typical Switching Losses vs. Collector-to-Emitter Current

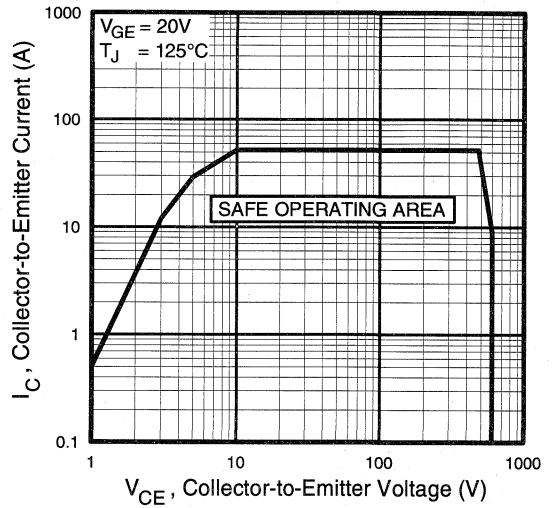


Fig. 12 - Turn-Off SOA

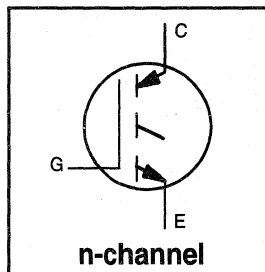
Refer to Section D for the following:

Appendix C: Section D - page D-5

- Fig. 13a - Clamped Inductive Load Test Circuit
- Fig. 13b - Pulsed Collector Current Test Circuit
- Fig. 14a - Switching Loss Test Circuit
- Fig. 14b - Switching Loss Waveform

Features

- Switching-loss rating includes all "tail" losses
- Optimized for high operating frequency (over 5kHz)
See Fig. 1 for Current vs. Frequency curve



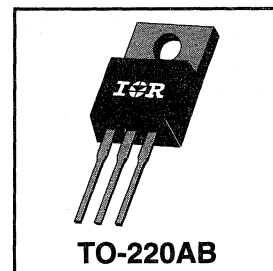
$$V_{CES} = 600V$$

$$V_{CE(sat)} \leq 3.0V$$

$$@V_{GE} = 15V, I_C = 12A$$

Description

Insulated Gate Bipolar Transistors (IGBTs) from International Rectifier have higher usable current densities than comparable bipolar transistors, while at the same time having simpler gate-drive requirements of the familiar power MOSFET. They provide substantial benefits to a host of high-voltage, high-current applications.



Absolute Maximum Ratings

	Parameter	Max.	Units
V_{CES}	Collector-to-Emitter Voltage	600	V
$I_C @ T_C = 25^\circ C$	Continuous Collector Current	23	A
$I_C @ T_C = 100^\circ C$	Continuous Collector Current	12	
I_{CM}	Pulsed Collector Current ①	92	
I_{LM}	Clamped Inductive Load Current ②	92	
V_{GE}	Gate-to-Emitter Voltage	± 20	V
E_{ARV}	Reverse Voltage Avalanche Energy ③	10	mJ
$P_D @ T_C = 25^\circ C$	Maximum Power Dissipation	100	W
$P_D @ T_C = 100^\circ C$	Maximum Power Dissipation	42	
T_J	Operating Junction and	-55 to +150	°C
T_{STG}	Storage Temperature Range		
	Soldering Temperature, for 10 sec.	300 (0.063 in. (1.6mm) from case)	
	Mounting torque, 6-32 or M3 screw.	10 lbf•in (1.1N•m)	

Thermal Resistance

	Parameter	Min.	Typ.	Max.	Units
$R_{\theta JC}$	Junction-to-Case	—	—	1.2	°C/W
$R_{\theta CS}$	Case-to-Sink, flat, greased surface	—	0.50	—	
$R_{\theta JA}$	Junction-to-Ambient, typical socket mount	—	—	80	
Wt	Weight	—	2.0 (0.07)	—	g (oz)

Electrical Characteristics @ $T_J = 25^\circ\text{C}$ (unless otherwise specified)

	Parameter	Min.	Typ.	Max.	Units	Conditions
$V_{(BR)CES}$	Collector-to-Emitter Breakdown Voltage	600	—	—	V	$V_{GE} = 0V, I_C = 250\mu A$
$V_{(BR)ECS}$	Emitter-to-Collector Breakdown Voltage ④	20	—	—	V	$V_{GE} = 0V, I_C = 1.0A$
$\Delta V_{(BR)CES}/\Delta T_J$	Temperature Coeff. of Breakdown Voltage	—	0.63	—	V/°C	$V_{GE} = 0V, I_C = 1.0mA$
$V_{CE(on)}$	Collector-to-Emitter Saturation Voltage	—	2.2	3.0	V	$I_C = 12A$ $V_{GE} = 15V$ See Fig. 2, 5
		—	2.7	—		
		—	2.4	—		
$V_{GE(th)}$	Gate Threshold Voltage	3.0	—	5.5		$I_C = 12A, T_J = 150^\circ\text{C}$ $V_{CE} = V_{GE}, I_C = 250\mu A$
$\Delta V_{GE(th)}/\Delta T_J$	Temperature Coeff. of Threshold Voltage	—	-11	—	mV/°C	$V_{CE} = V_{GE}, I_C = 250\mu A$
g_{fe}	Forward Transconductance ⑤	3.1	8.6	—	S	$V_{CE} = 100V, I_C = 12A$
I_{CES}	Zero Gate Voltage Collector Current	—	—	250	μA	$V_{GE} = 0V, V_{CE} = 600V$ $V_{GE} = 0V, V_{CE} = 600V, T_J = 150^\circ\text{C}$
		—	—	1000		
I_{GES}	Gate-to-Emitter Leakage Current	—	—	± 100	nA	$V_{GE} = \pm 20V$

Switching Characteristics @ $T_J = 25^\circ\text{C}$ (unless otherwise specified)

	Parameter	Min.	Typ.	Max.	Units	Conditions
Q_g	Total Gate Charge (turn-on)	—	29	36	nC	$I_C = 12A$ $V_{CC} = 400V$ $V_{GE} = 15V$ See Fig. 8
Q_{ge}	Gate - Emitter Charge (turn-on)	—	4.8	6.8		
Q_{gc}	Gate - Collector Charge (turn-on)	—	12	17		
$t_{d(on)}$	Turn-On Delay Time	—	24	—	ns	$T_J = 25^\circ\text{C}$ $I_C = 12A, V_{CC} = 480V$ $V_{GE} = 15V, R_G = 23\Omega$ Energy losses include "tail"
t_r	Rise Time	—	15	—		
$t_{d(off)}$	Turn-Off Delay Time	—	92	200		
t_f	Fall Time	—	93	190		
E_{on}	Turn-On Switching Loss	—	0.18	—	mJ	See Fig. 9, 10, 11, 14
E_{off}	Turn-Off Switching Loss	—	0.35	—		
E_{ts}	Total Switching Loss	—	0.53	1.0		
$t_{d(on)}$	Turn-On Delay Time	—	24	—	ns	$T_J = 150^\circ\text{C}$, $I_C = 12A, V_{CC} = 480V$ $V_{GE} = 15V, R_G = 23\Omega$ Energy losses include "tail"
t_r	Rise Time	—	15	—		
$t_{d(off)}$	Turn-Off Delay Time	—	160	—		
t_f	Fall Time	—	200	—		
E_{ts}	Total Switching Loss	—	0.9	—	mJ	See Fig. 10, 14
L_E	Internal Emitter Inductance	—	7.5	—	nH	Measured 5mm from package
C_{ies}	Input Capacitance	—	660	—	pF	$V_{GE} = 0V$ $V_{CC} = 30V$ See Fig. 7 $f = 1.0MHz$
C_{oes}	Output Capacitance	—	100	—		
C_{res}	Reverse Transfer Capacitance	—	11	—		

Notes:

- ① Repetitive rating; $V_{GE}=20V$, pulse width limited by max. junction temperature. (See fig. 13b)
- ② $V_{CC}=80\%(V_{CES}), V_{GE}=20V, L=10\mu H, R_G=23\Omega$, (See fig. 13a)
- ③ Repetitive rating; pulse width limited by maximum junction temperature.
- ④ Pulse width $\leq 80\mu s$; duty factor $\leq 0.1\%$.
- ⑤ Pulse width 5.0 μs , single shot.

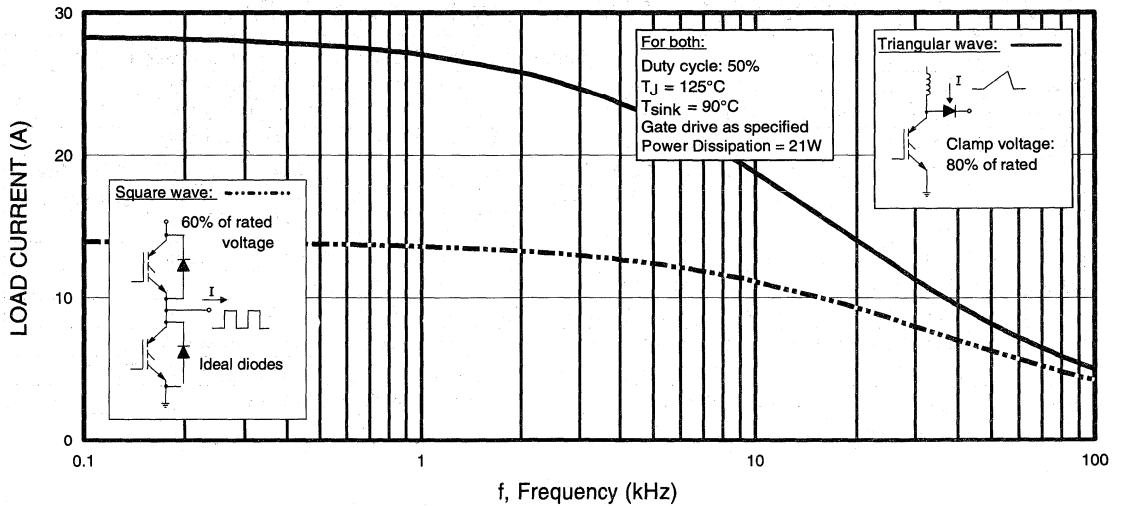


Fig. 1 - Typical Load Current vs. Frequency
 (For square wave, $I = I_{RMS}$ of fundamental; for triangular wave, $I = I_{PK}$)

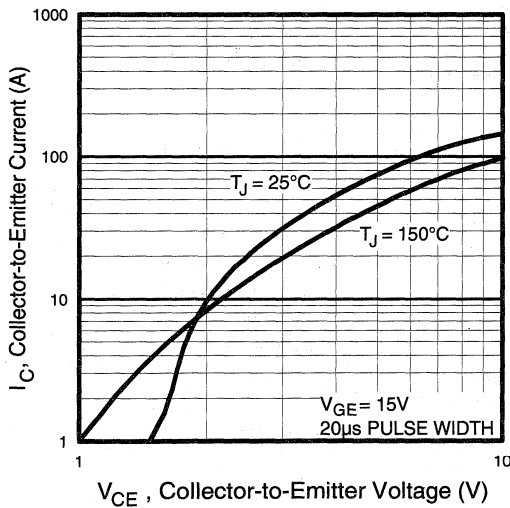


Fig. 2 - Typical Output Characteristics

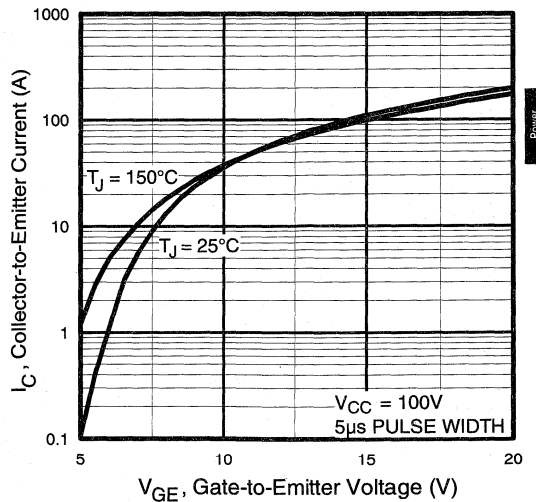


Fig. 3 - Typical Transfer Characteristics

Power Conversion Ultra-Fast Discretes

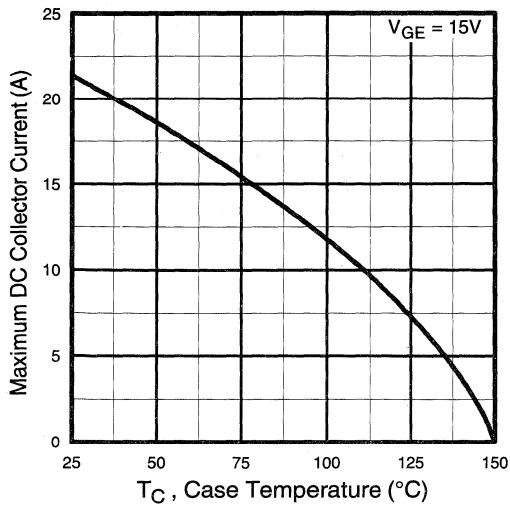


Fig. 4 - Maximum Collector Current vs. Case Temperature

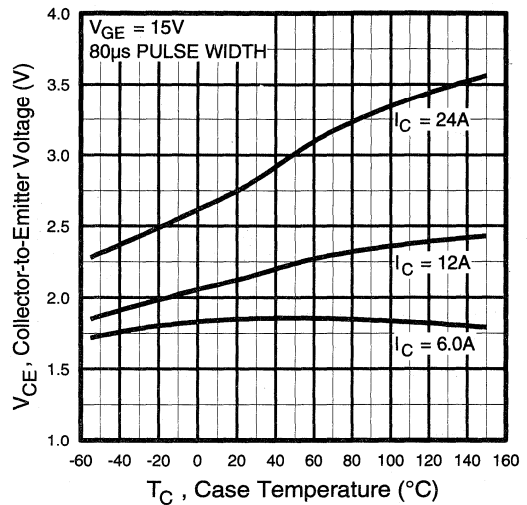


Fig. 5 - Collector-to-Emitter Voltage vs. Case Temperature

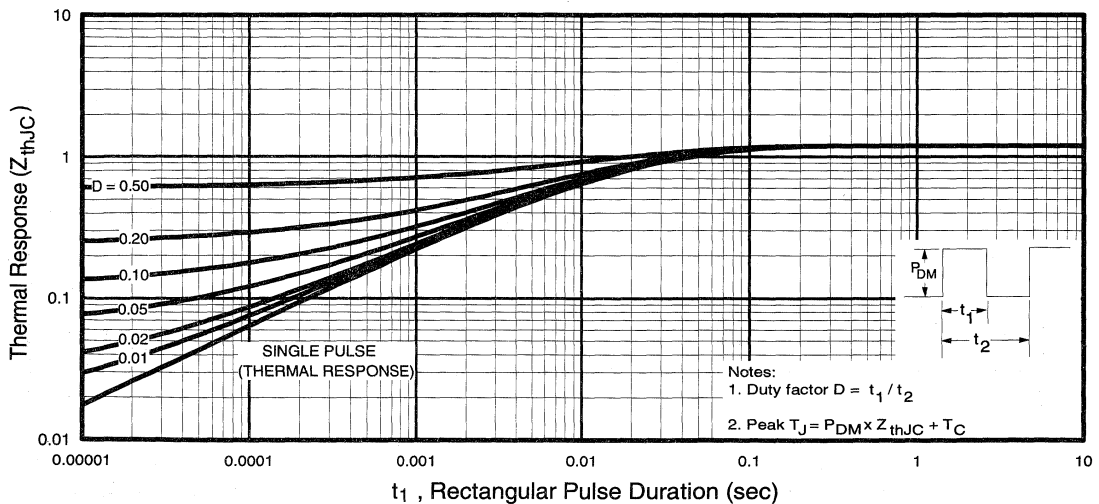


Fig. 6 - Maximum Effective Transient Thermal Impedance, Junction-to-Case

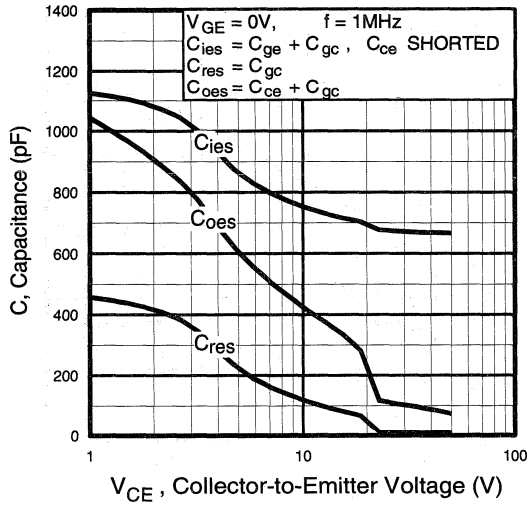


Fig. 7 - Typical Capacitance vs. Collector-to-Emitter Voltage

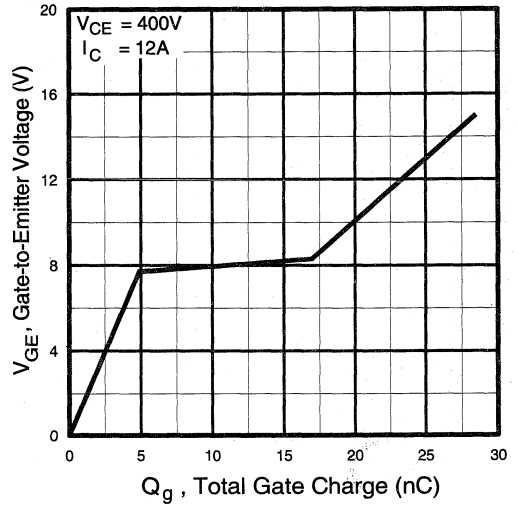


Fig. 8 - Typical Gate Charge vs. Gate-to-Emitter Voltage

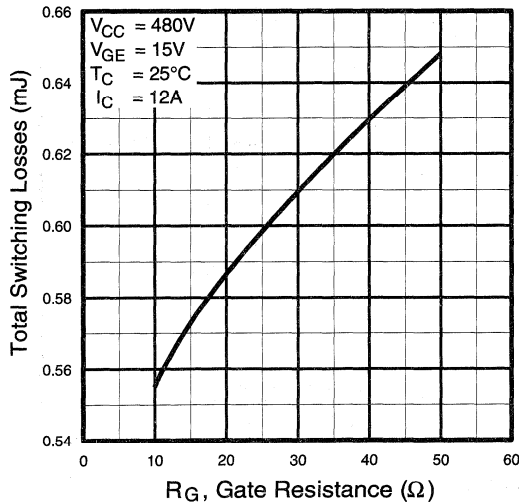


Fig. 9 - Typical Switching Losses vs. Gate Resistance

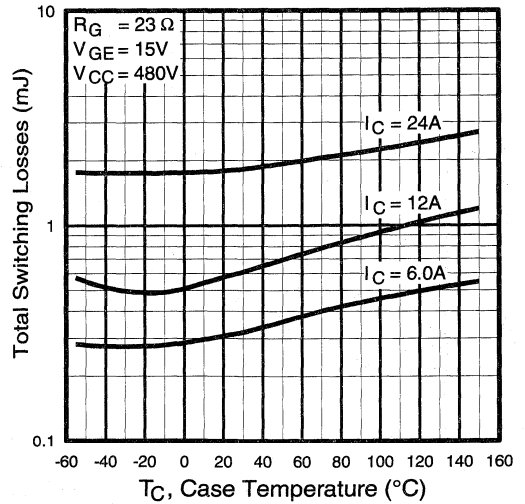


Fig. 10 - Typical Switching Losses vs. Case Temperature

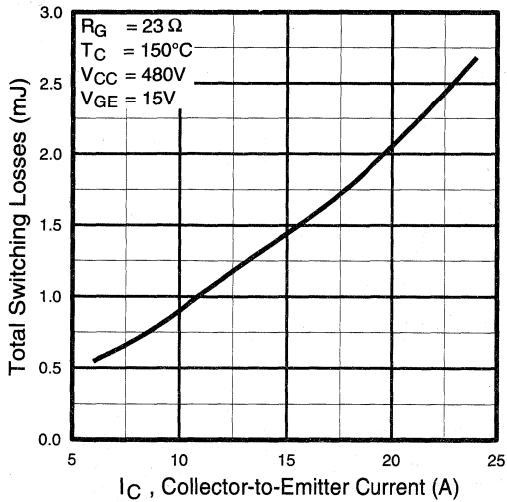


Fig. 11 - Typical Switching Losses vs. Collector-to-Emitter Current

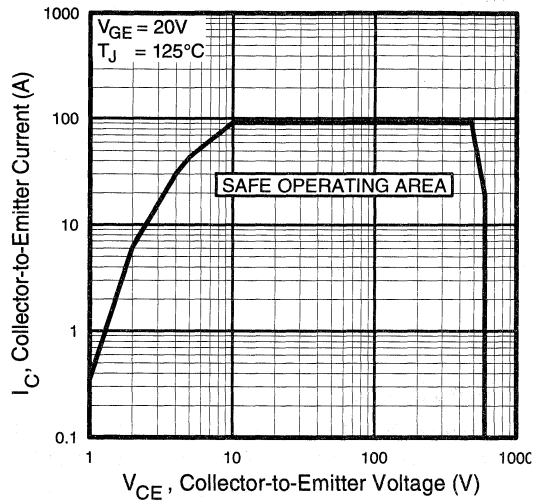


Fig. 12 - Turn-Off SOA

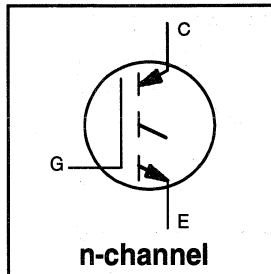
Refer to Section D for the following:

Appendix C: Section D - page D-5

- Fig. 13a - Clamped Inductive Load Test Circuit
- Fig. 13b - Pulsed Collector Current Test Circuit
- Fig. 14a - Switching Loss Test Circuit
- Fig. 14b - Switching Loss Waveform

Features

- Switching-loss rating includes all "tail" losses
- Optimized for high operating frequency (over 5kHz)
See Fig. 1 for Current vs. Frequency curve



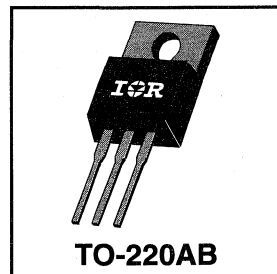
$$V_{CES} = 600V$$

$$V_{CE(sat)} \leq 3.0V$$

$$@V_{GE} = 15V, I_C = 20A$$

Description

Insulated Gate Bipolar Transistors (IGBTs) from International Rectifier have higher usable current densities than comparable bipolar transistors, while at the same time having simpler gate-drive requirements of the familiar power MOSFET. They provide substantial benefits to a host of high-voltage, high-current applications.



Absolute Maximum Ratings

	Parameter	Max.	Units
V_{CES}	Collector-to-Emitter Voltage	600	V
$I_C @ T_C = 25^\circ C$	Continuous Collector Current	40	A
$I_C @ T_C = 100^\circ C$	Continuous Collector Current	20	
I_{CM}	Pulsed Collector Current ①	160	
I_{LM}	Clamped Inductive Load Current ②	160	
V_{GE}	Gate-to-Emitter Voltage	± 20	V
E_{ARV}	Reverse Voltage Avalanche Energy ③	15	mJ
$P_D @ T_C = 25^\circ C$	Maximum Power Dissipation	160	W
$P_D @ T_C = 100^\circ C$	Maximum Power Dissipation	65	
T_J	Operating Junction and	-55 to +150	°C
T_{STG}	Storage Temperature Range		
	Soldering Temperature, for 10 sec.	300 (0.063 in. (1.6mm) from case)	
	Mounting torque, 6-32 or M3 screw.	10 lbf•in (1.1N•m)	

Thermal Resistance

	Parameter	Min.	Typ.	Max.	Units
$R_{\theta JC}$	Junction-to-Case	—	—	0.77	°C/W
$R_{\theta CS}$	Case-to-Sink, flat, greased surface	—	0.50	—	
$R_{\theta JA}$	Junction-to-Ambient, typical socket mount	—	—	80	
Wt	Weight	—	2.0 (0.07)	—	g (oz)

Electrical Characteristics @ $T_J = 25^\circ\text{C}$ (unless otherwise specified)

	Parameter	Min.	Typ.	Max.	Units	Conditions
$V_{(BR)CES}$	Collector-to-Emitter Breakdown Voltage	600	—	—	V	$V_{GE} = 0V, I_C = 250\mu A$
$V_{(BR)ECS}$	Emitter-to-Collector Breakdown Voltage ④	20	—	—	V	$V_{GE} = 0V, I_C = 1.0A$
$\Delta V_{(BR)CES}/\Delta T_J$	Temp. Coeff. of Breakdown Voltage	—	0.63	—	V/°C	$V_{GE} = 0V, I_C = 1.0mA$
$V_{CE(on)}$	Collector-to-Emitter Saturation Voltage	—	2.2	3.0	V	$I_C = 20A$ $I_C = 40A$ $I_C = 20A, T_J = 150^\circ\text{C}$ $V_{CE} = V_{GE}, I_C = 250\mu A$
		—	2.7	—		
		—	2.3	—		
$V_{GE(th)}$	Gate Threshold Voltage	3.0	—	5.5		$V_{CE} = V_{GE}, I_C = 250\mu A$
$\Delta V_{GE(th)}/\Delta T_J$	Temperature Coeff. of Threshold Voltage	—	-13	—	mV/°C	$V_{CE} = V_{GE}, I_C = 250\mu A$
g_{fe}	Forward Transconductance ⑤	11	18	—	S	$V_{CE} = 100V, I_C = 20A$
I_{CES}	Zero Gate Voltage Collector Current	—	—	250	μA	$V_{GE} = 0V, V_{CE} = 600V$
		—	—	1000		$V_{GE} = 0V, V_{CE} = 600V, T_J = 150^\circ\text{C}$
I_{GES}	Gate-to-Emitter Leakage Current	—	—	± 100	nA	$V_{GE} = \pm 20V$

Switching Characteristics @ $T_J = 25^\circ\text{C}$ (unless otherwise specified)

	Parameter	Min.	Typ.	Max.	Units	Conditions
Q_g	Total Gate Charge (turn-on)	—	51	67	nC	$I_C = 20A$ $V_{CC} = 400V$ $V_{GE} = 15V$ See Fig. 8
Q_{ge}	Gate - Emitter Charge (turn-on)	—	8.9	11		
Q_{gc}	Gate - Collector Charge (turn-on)	—	20	33		
$t_{d(on)}$	Turn-On Delay Time	—	25	—	ns	$T_J = 25^\circ\text{C}$ $I_C = 20A, V_{CC} = 480V$ $V_{GE} = 15V, R_G = 10\Omega$ Energy losses include "tail"
t_r	Rise Time	—	21	—		
$t_{d(off)}$	Turn-Off Delay Time	—	96	190		
t_f	Fall Time	—	43	120		
E_{on}	Turn-On Switching Loss	—	0.34	—	mJ	See Fig. 9, 10, 11, 14
E_{off}	Turn-Off Switching Loss	—	0.41	—		
E_{ts}	Total Switching Loss	—	0.75	1.6		
$t_{d(on)}$	Turn-On Delay Time	—	25	—	ns	$T_J = 150^\circ\text{C}$, $I_C = 20A, V_{CC} = 480V$ $V_{GE} = 15V, R_G = 10\Omega$ Energy losses include "tail"
t_r	Rise Time	—	23	—		
$t_{d(off)}$	Turn-Off Delay Time	—	174	—		
t_f	Fall Time	—	140	—		
E_{ts}	Total Switching Loss	—	1.4	—	mJ	See Fig. 10, 14
L_E	Internal Emitter Inductance	—	7.5	—	nH	Measured 5mm from package
C_{ies}	Input Capacitance	—	1500	—	pF	$V_{GE} = 0V$ $V_{CC} = 30V$ $f = 1.0MHz$ See Fig. 7
C_{oes}	Output Capacitance	—	190	—		
C_{res}	Reverse Transfer Capacitance	—	17	—		

Notes:

- ① Repetitive rating; $V_{GE}=20V$, pulse width limited by max. junction temperature. (See fig. 13b)
- ② $V_{CC}=80\%(V_{CES}), V_{GE}=20V, L=10\mu H, R_G=10\Omega$, (See fig. 13a)
- ③ Repetitive rating; pulse width limited by maximum junction temperature.
- ④ Pulse width $\leq 80\mu s$; duty factor $\leq 0.1\%$.
- ⑤ Pulse width $5.0\mu s$, single shot.

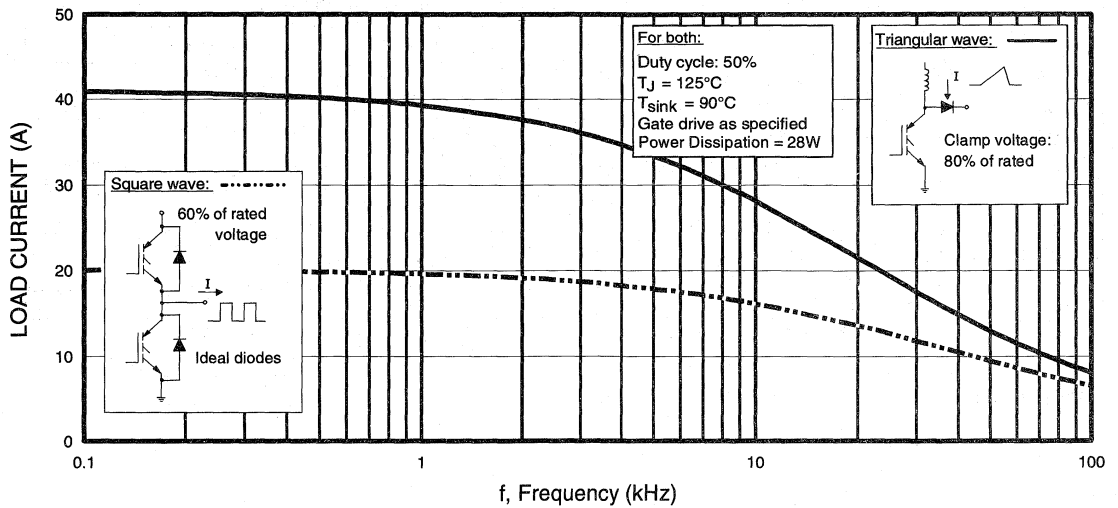


Fig. 1 - Typical Load Current vs. Frequency
 (For square wave, $I = I_{RMS}$ of fundamental; for triangular wave, $I = I_{PK}$)

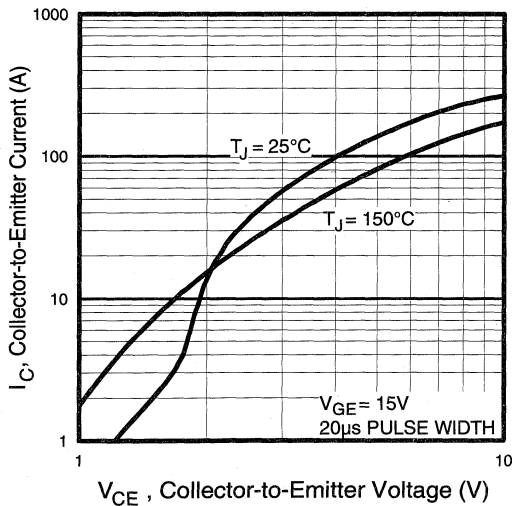


Fig. 2 - Typical Output Characteristics

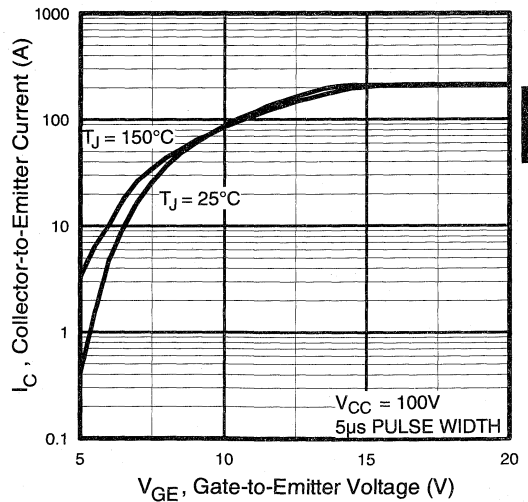


Fig. 3 - Typical Transfer Characteristics

Power
Conversion
UltraFast
Discretes

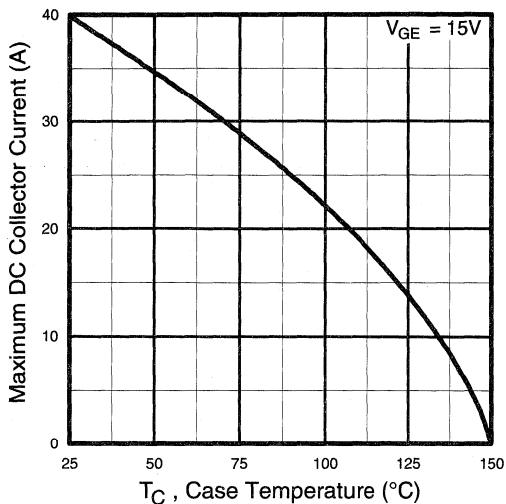


Fig. 4 - Maximum Collector Current vs. Case Temperature

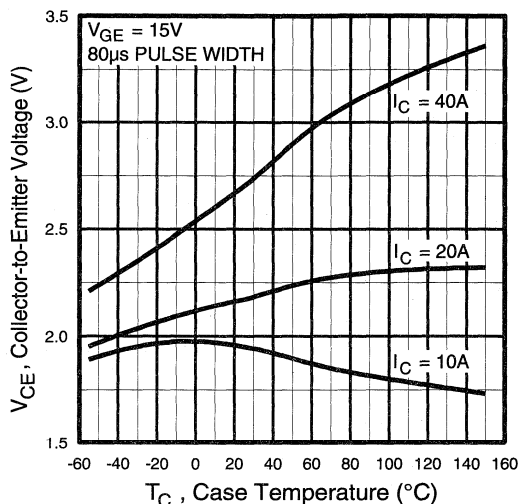


Fig. 5 - Collector-to-Emitter Voltage vs. Case Temperature

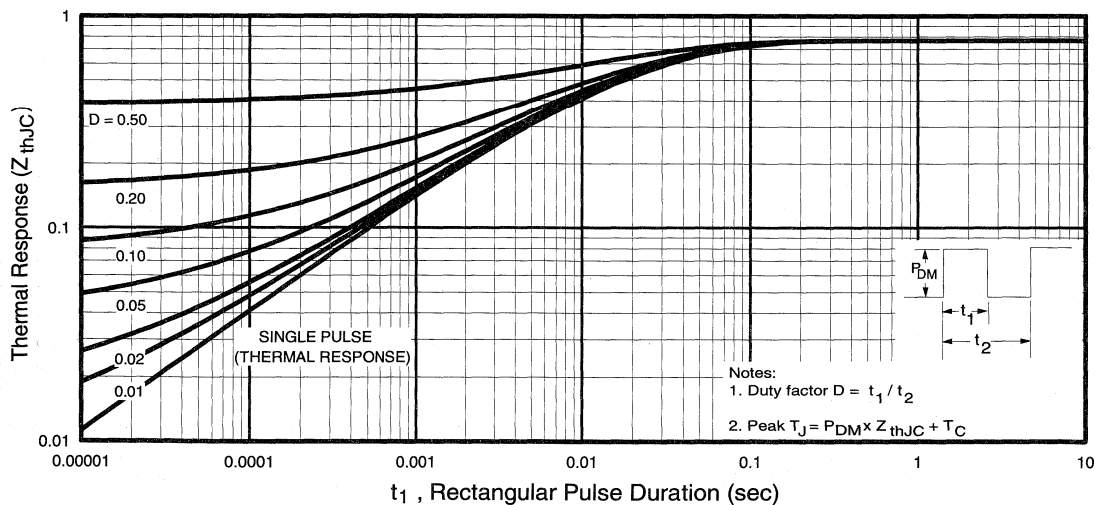


Fig. 6 - Maximum Effective Transient Thermal Impedance, Junction-to-Case

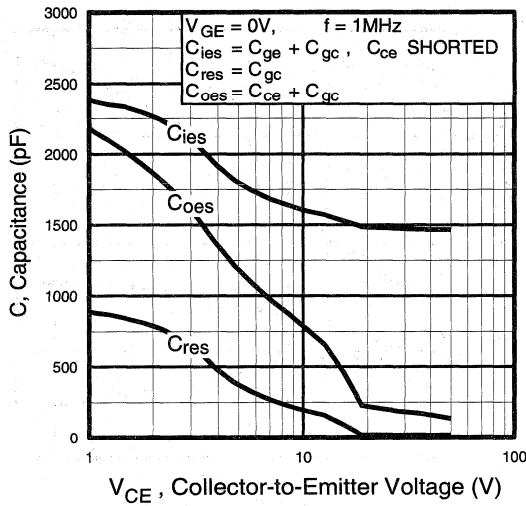


Fig. 7 - Typical Capacitance vs. Collector-to-Emitter Voltage

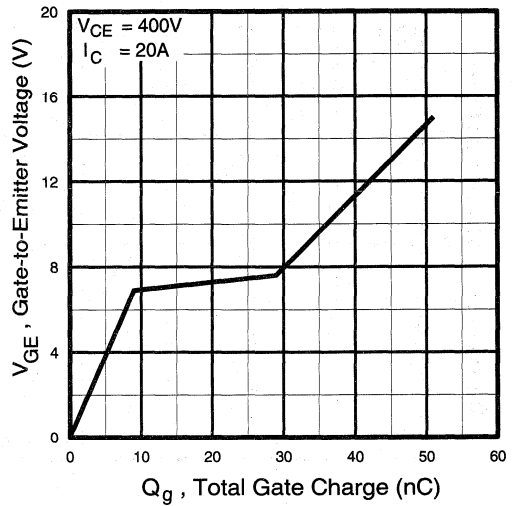


Fig. 8 - Typical Gate Charge vs. Gate-to-Emitter Voltage

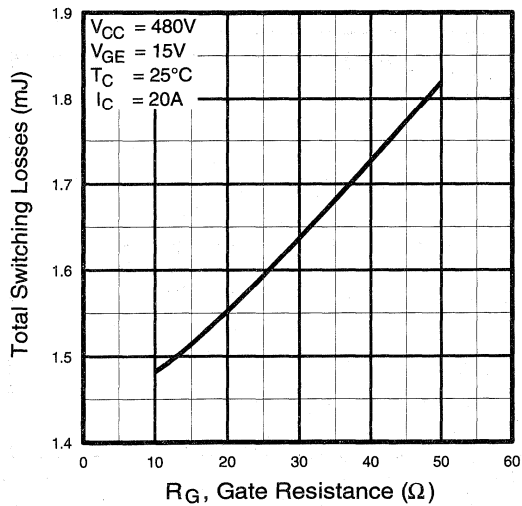


Fig. 9 - Typical Switching Losses vs. Gate Resistance

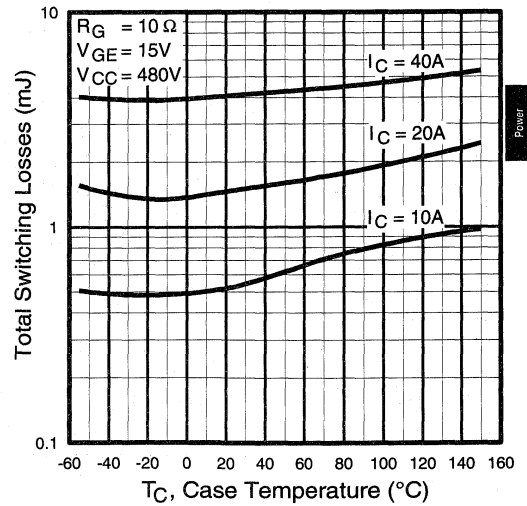


Fig. 10 - Typical Switching Losses vs. Case Temperature

Power Conversion
Ultra-Fast
Discreets

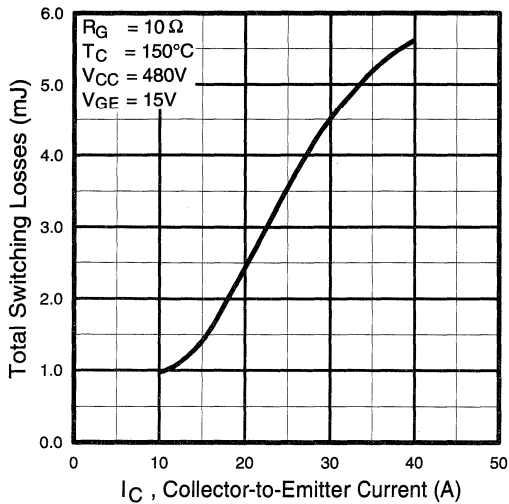


Fig. 11 - Typical Switching Losses vs. Collector-to-Emitter Current

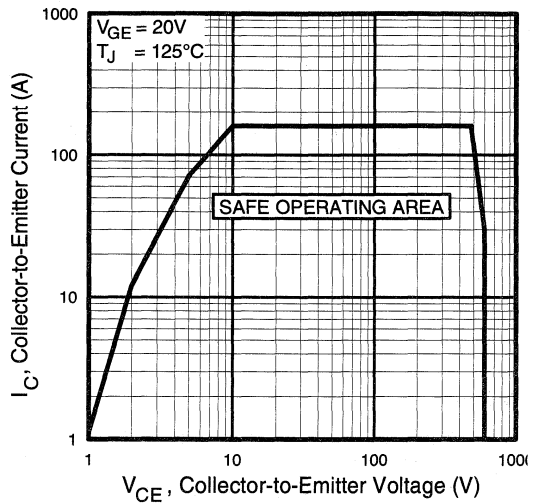


Fig. 12 - Turn-Off SOA

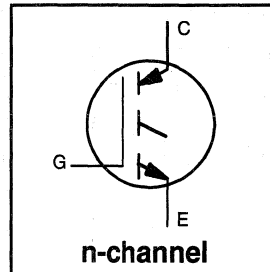
Refer to Section D for the following:

Appendix C: Section D - page D-5

- Fig. 13a - Clamped Inductive Load Test Circuit
- Fig. 13b - Pulsed Collector Current Test Circuit
- Fig. 14a - Switching Loss Test Circuit
- Fig. 14b - Switching Loss Waveform

Features

- Switching-loss rating includes all "tail" losses
- Optimized for high operating frequency (over 5kHz)
See Fig. 1 for Current vs. Frequency curve



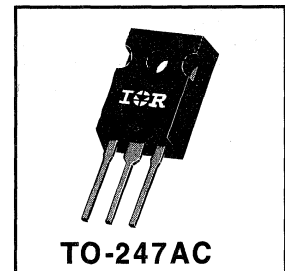
$$V_{CES} = 600V$$

$$V_{CE(sat)} \leq 3.0V$$

$$@V_{GE} = 15V, I_C = 6.5A$$

Description

Insulated Gate Bipolar Transistors (IGBTs) from International Rectifier have higher usable current densities than comparable bipolar transistors, while at the same time having simpler gate-drive requirements of the familiar power MOSFET. They provide substantial benefits to a host of high-voltage, high-current applications.



Absolute Maximum Ratings

	Parameter	Max.	Units
V_{CES}	Collector-to-Emitter Voltage	600	V
$I_C @ T_C = 25^\circ C$	Continuous Collector Current	13	A
$I_C @ T_C = 100^\circ C$	Continuous Collector Current	6.5	
I_{CM}	Pulsed Collector Current ①	52	
I_{LM}	Clamped Inductive Load Current ②	52	
V_{GE}	Gate-to-Emitter Voltage	± 20	V
E_{ARV}	Reverse Voltage Avalanche Energy ③	5	mJ
$P_D @ T_C = 25^\circ C$	Maximum Power Dissipation	60	W
$P_D @ T_C = 100^\circ C$	Maximum Power Dissipation	24	
T_J	Operating Junction and	-55 to +150	°C
T_{STG}	Storage Temperature Range		
	Soldering Temperature, for 10 sec.	300 (0.063 in. (1.6mm) from case)	
	Mounting torque, 6-32 or M3 screw.	10 lbf•in (1.1N•m)	

Thermal Resistance

	Parameter	Min.	Typ.	Max.	Units
$R_{\theta JC}$	Junction-to-Case	—	—	2.1	°C/W
$R_{\theta CS}$	Case-to-Sink, flat, greased surface	—	0.24	—	
$R_{\theta JA}$	Junction-to-Ambient, typical socket mount	—	—	40	
Wt	Weight	—	6 (0.21)	—	g (oz)

Electrical Characteristics @ $T_J = 25^\circ\text{C}$ (unless otherwise specified)

	Parameter	Min.	Typ.	Max.	Units	Conditions
$V_{(BR)CES}$	Collector-to-Emitter Breakdown Voltage	600	—	—	V	$V_{GE} = 0V, I_C = 250\mu A$
$V_{(BR)ECS}$	Emitter-to-Collector Breakdown Voltage ④	20	—	—	V	$V_{GE} = 0V, I_C = 1.0A$
$\Delta V_{(BR)CES}/\Delta T_J$	Temp. Coeff. of Breakdown Voltage	—	0.69	—	V/°C	$V_{GE} = 0V, I_C = 1.0mA$
$V_{CE(on)}$	Collector-to-Emitter Saturation Voltage	—	2.2	3.0	V	$I_C = 6.5A, V_{GE} = 15V$ See Fig. 2, 5
		—	2.8	—		
		—	2.5	—		
$V_{GE(th)}$	Gate Threshold Voltage	3.0	—	5.5		$V_{CE} = V_{GE}, I_C = 250\mu A$
$\Delta V_{GE(th)}/\Delta T_J$	Temperature Coeff. of Threshold Voltage	—	-11	—	mV/°C	$V_{CE} = V_{GE}, I_C = 250\mu A$
g_{fe}	Forward Transconductance ⑤	1.4	4.3	—	S	$V_{CE} = 100V, I_C = 6.5A$
I_{CES}	Zero Gate Voltage Collector Current	—	—	250	μA	$V_{GE} = 0V, V_{CE} = 600V$ $V_{GE} = 0V, V_{CE} = 600V, T_J = 150^\circ\text{C}$
		—	—	1000		
I_{GES}	Gate-to-Emitter Leakage Current	—	—	± 100	nA	$V_{GE} = \pm 20V$

Switching Characteristics @ $T_J = 25^\circ\text{C}$ (unless otherwise specified)

	Parameter	Min.	Typ.	Max.	Units	Conditions
Q_g	Total Gate Charge (turn-on)	—	16	22	nC	$I_C = 6.5A$ $V_{CC} = 400V$ See Fig. 8 $V_{GE} = 15V$
Q_{ge}	Gate - Emitter Charge (turn-on)	—	2.5	3.8		
Q_{gc}	Gate - Collector Charge (turn-on)	—	7.8	13		
$t_{d(on)}$	Turn-On Delay Time	—	22	—	ns	$T_J = 25^\circ\text{C}$ $I_C = 6.5A, V_{CC} = 480V$ $V_{GE} = 15V, R_G = 50\Omega$ Energy losses include "tail"
t_r	Rise Time	—	12	—		
$t_{d(off)}$	Turn-Off Delay Time	—	71	95		
t_f	Fall Time	—	91	280		
E_{on}	Turn-On Switching Loss	—	0.11	—	mJ	See Fig. 9, 10, 11, 14
E_{off}	Turn-Off Switching Loss	—	0.14	—		
E_{ts}	Total Switching Loss	—	0.25	0.50		
$t_{d(on)}$	Turn-On Delay Time	—	23	—	ns	$T_J = 150^\circ\text{C}$, $I_C = 6.5A, V_{CC} = 480V$ $V_{GE} = 15V, R_G = 50\Omega$ Energy losses include "tail"
t_r	Rise Time	—	13	—		
$t_{d(off)}$	Turn-Off Delay Time	—	140	—		
t_f	Fall Time	—	200	—		
E_{ts}	Total Switching Loss	—	0.45	—	mJ	See Fig. 10, 14
L_E	Internal Emitter Inductance	—	13	—	nH	Measured 5mm from package
C_{ies}	Input Capacitance	—	330	—	pF	$V_{GE} = 0V$ $V_{CC} = 30V$ See Fig. 7 $f = 1.0MHz$
C_{oes}	Output Capacitance	—	65	—		
C_{res}	Reverse Transfer Capacitance	—	6.0	—		

Notes:

- ① Repetitive rating; $V_{GE}=20V$, pulse width limited by max. junction temperature. (See fig. 13b)
- ② $V_{CC}=80\%(V_{CES}), V_{GE}=20V, L=10\mu H, R_G=50\Omega$, (See fig. 13a)
- ③ Repetitive rating; pulse width limited by maximum junction temperature.
- ④ Pulse width $\leq 80\mu s$; duty factor $\leq 0.1\%$.
- ⑤ Pulse width 5.0 μs , single shot.

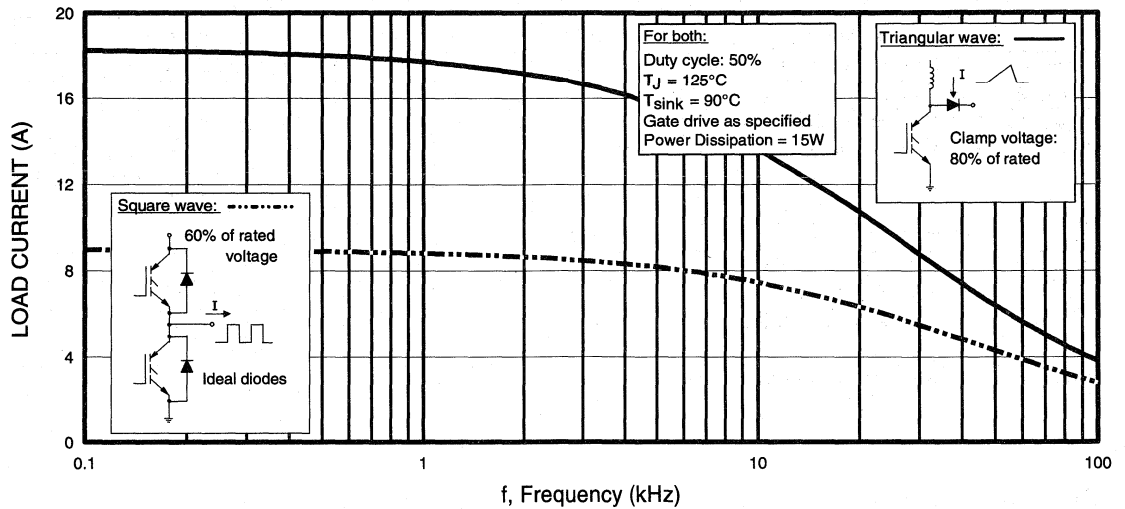


Fig. 1 - Typical Load Current vs. Frequency
 (For square wave, $I = I_{RMS}$ of fundamental; for triangular wave, $I = I_{PK}$)

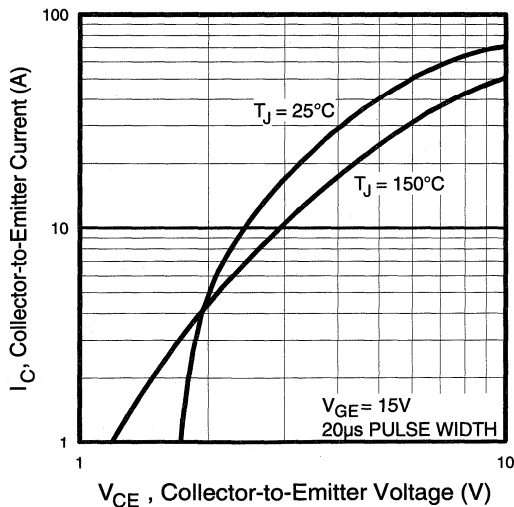


Fig. 2 - Typical Output Characteristics

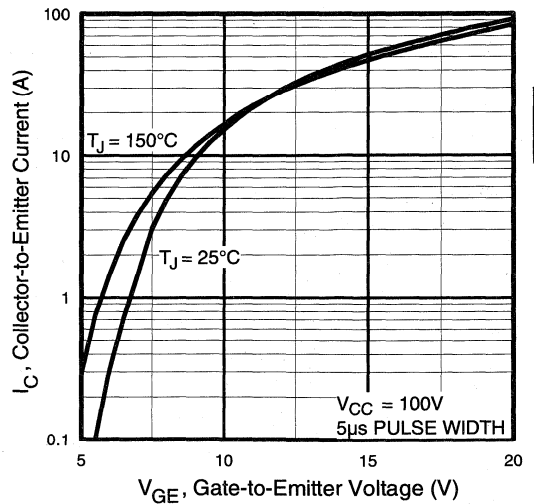


Fig. 3 - Typical Transfer Characteristics

Power
Conversion
Ultra-Fast
Discretes

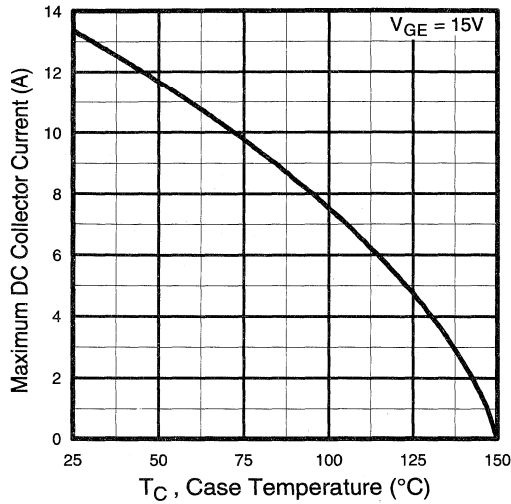


Fig. 4 - Maximum Collector Current vs. Case Temperature

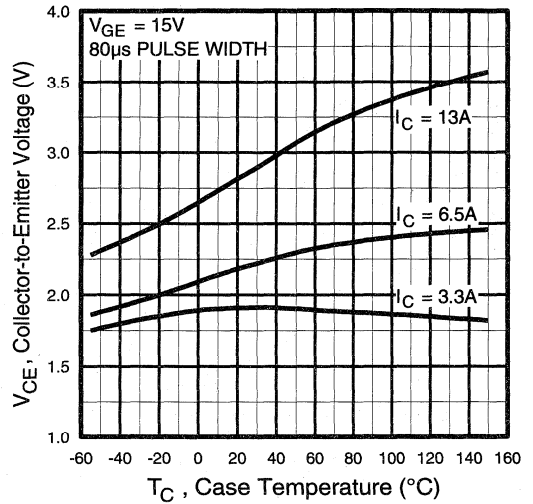


Fig. 5 - Collector-to-Emitter Voltage vs. Case Temperature

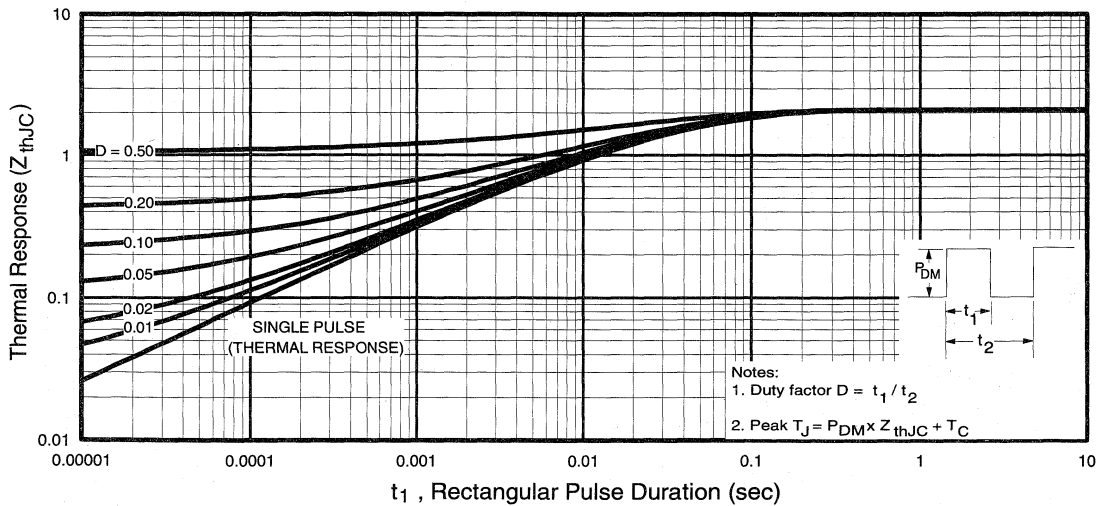


Fig. 6 - Maximum Effective Transient Thermal Impedance, Junction-to-Case

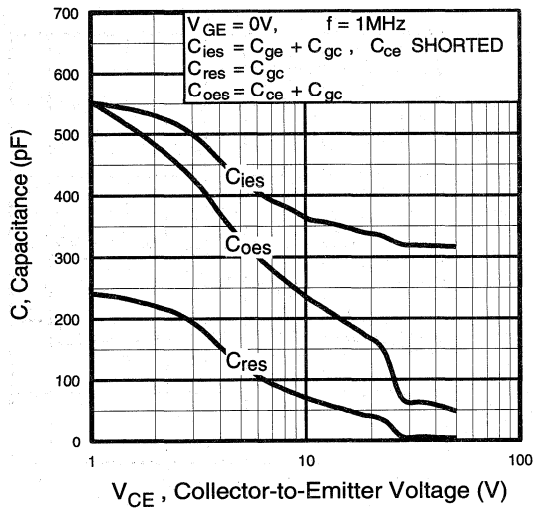


Fig. 7 - Typical Capacitance vs. Collector-to-Emitter Voltage

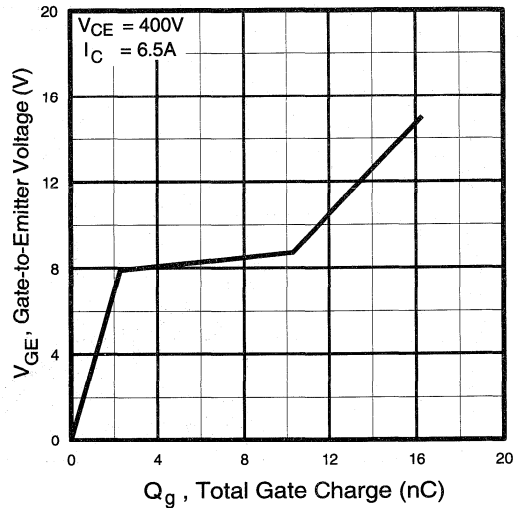


Fig. 8 - Typical Gate Charge vs. Gate-to-Emitter Voltage

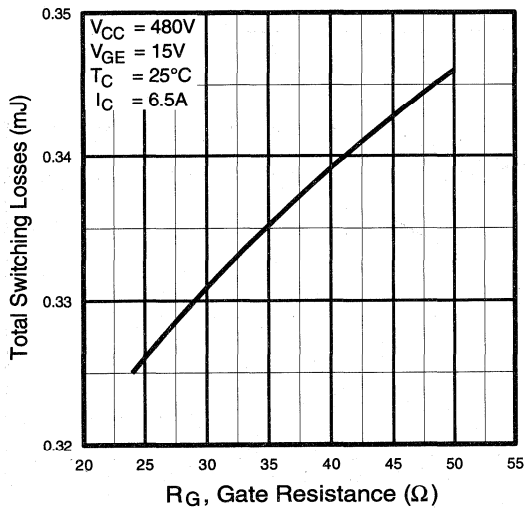


Fig. 9 - Typical Switching Losses vs. Gate Resistance

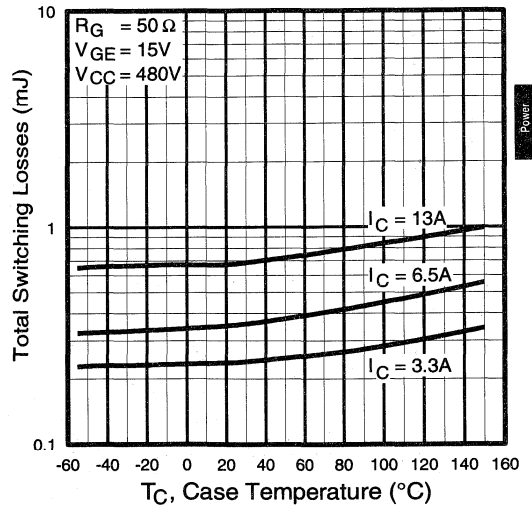


Fig. 10 - Typical Switching Losses vs. Case Temperature

Power Conversion
 Ultra-Fast
 Discretes

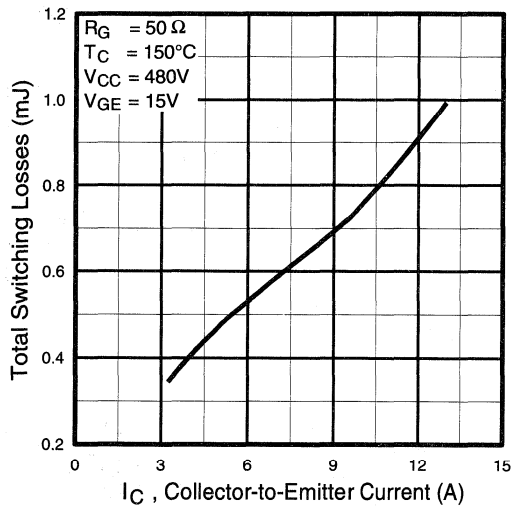


Fig. 11 - Typical Switching Losses vs. Collector-to-Emitter Current

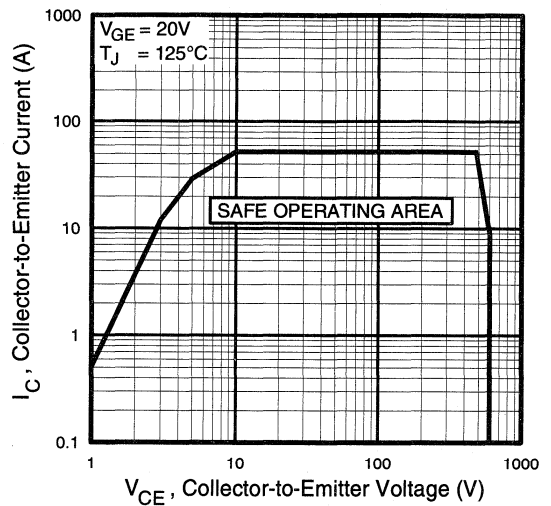


Fig. 12 - Turn-Off SOA

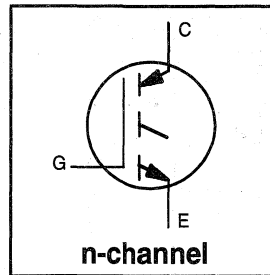
Refer to Section D for the following:

Appendix C: Section D - page D-5

- Fig. 13a - Clamped Inductive Load Test Circuit
- Fig. 13b - Pulsed Collector Current Test Circuit
- Fig. 14a - Switching Loss Test Circuit
- Fig. 14b - Switching Loss Waveform

Features

- Switching-loss rating includes all "tail" losses
- Optimized for high operating frequency (over 5kHz)
See Fig. 1 for Current vs. Frequency curve



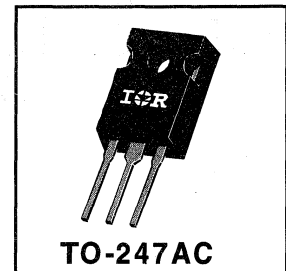
$$V_{CES} = 600V$$

$$V_{CE(sat)} \leq 3.0V$$

$$@V_{GE} = 15V, I_C = 12A$$

Description

Insulated Gate Bipolar Transistors (IGBTs) from International Rectifier have higher usable current densities than comparable bipolar transistors, while at the same time having simpler gate-drive requirements of the familiar power MOSFET. They provide substantial benefits to a host of high-voltage, high-current applications.



Absolute Maximum Ratings

	Parameter	Max.	Units
V_{CES}	Collector-to-Emitter Voltage	600	V
$I_C @ T_C = 25^\circ C$	Continuous Collector Current	23	A
$I_C @ T_C = 100^\circ C$	Continuous Collector Current	12	
I_{CM}	Pulsed Collector Current ①	92	
I_{LM}	Clamped Inductive Load Current ②	92	
V_{GE}	Gate-to-Emitter Voltage	± 20	V
E_{ARV}	Reverse Voltage Avalanche Energy ③	10	mJ
$P_D @ T_C = 25^\circ C$	Maximum Power Dissipation	100	W
$P_D @ T_C = 100^\circ C$	Maximum Power Dissipation	42	
T_J	Operating Junction and	-55 to +150	°C
T_{STG}	Storage Temperature Range		
	Soldering Temperature, for 10 sec.	300 (0.063 in. (1.6mm) from case)	
	Mounting torque, 6-32 or M3 screw.	10 lbf•in (1.1N•m)	

Thermal Resistance

	Parameter	Min.	Typ.	Max.	Units
$R_{\theta JC}$	Junction-to-Case	—	—	1.2	°C/W
$R_{\theta CS}$	Case-to-Sink, flat, greased surface	—	0.24	—	
$R_{\theta JA}$	Junction-to-Ambient, typical socket mount	—	—	40	
Wt	Weight	—	6 (0.21)	—	g (oz)

Electrical Characteristics @ $T_J = 25^\circ\text{C}$ (unless otherwise specified)

	Parameter	Min.	Typ.	Max.	Units	Conditions
$V_{(BR)CES}$	Collector-to-Emitter Breakdown Voltage	600	—	—	V	$V_{GE} = 0V, I_C = 250\mu A$
$V_{(BR)ECS}$	Emitter-to-Collector Breakdown Voltage ②	20	—	—	V	$V_{GE} = 0V, I_C = 1.0A$
$\Delta V_{(BR)CES}/\Delta T_J$	Temp. Coeff. of Breakdown Voltage	—	0.63	—	$V/^\circ\text{C}$	$V_{GE} = 0V, I_C = 1.0mA$
$V_{CE(on)}$	Collector-to-Emitter Saturation Voltage	—	2.2	3.0	V	$I_C = 12A$ $V_{GE} = 15V$
		—	2.7	—		$I_C = 23A$ See Fig. 2, 5
		—	2.4	—		$I_C = 12A, T_J = 150^\circ\text{C}$
$V_{GE(th)}$	Gate Threshold Voltage	3.0	—	5.5		$V_{CE} = V_{GE}, I_C = 250\mu A$
$\Delta V_{GE(th)}/\Delta T_J$	Temperature Coeff. of Threshold Voltage	—	-11	—	$mV/^\circ\text{C}$	$V_{CE} = V_{GE}, I_C = 250\mu A$
g_{fe}	Forward Transconductance ③	3.1	8.6	—	S	$V_{CE} = 100V, I_C = 12A$
I_{CES}	Zero Gate Voltage Collector Current	—	—	250	μA	$V_{GE} = 0V, V_{CE} = 600V$
		—	—	1000		$V_{GE} = 0V, V_{CE} = 600V, T_J = 150^\circ\text{C}$
I_{GES}	Gate-to-Emitter Leakage Current	—	—	± 100	nA	$V_{GE} = \pm 20V$

Switching Characteristics @ $T_J = 25^\circ\text{C}$ (unless otherwise specified)

	Parameter	Min.	Typ.	Max.	Units	Conditions
Q_g	Total Gate Charge (turn-on)	—	29	36	nC	$I_C = 12A$
Q_{ge}	Gate - Emitter Charge (turn-on)	—	4.8	6.8		$V_{CC} = 400V$ See Fig. 8
Q_{gc}	Gate - Collector Charge (turn-on)	—	12	17		$V_{GE} = 15V$
$t_{d(on)}$	Turn-On Delay Time	—	24	—	ns	$T_J = 25^\circ\text{C}$
t_r	Rise Time	—	15	—		$I_C = 12A, V_{CC} = 480V$
$t_{d(off)}$	Turn-Off Delay Time	—	92	200		$V_{GE} = 15V, R_G = 23\Omega$
t_f	Fall Time	—	93	190		Energy losses include "tail"
E_{on}	Turn-On Switching Loss	—	0.18	—	mJ	See Fig. 9, 10, 11, 14
E_{off}	Turn-Off Switching Loss	—	0.35	—		
E_{ts}	Total Switching Loss	—	0.53	1.0		
$t_{d(on)}$	Turn-On Delay Time	—	24	—	ns	$T_J = 150^\circ\text{C},$
t_r	Rise Time	—	15	—		$I_C = 12A, V_{CC} = 480V$
$t_{d(off)}$	Turn-Off Delay Time	—	160	—		$V_{GE} = 15V, R_G = 23\Omega$
t_f	Fall Time	—	200	—		Energy losses include "tail"
E_{ts}	Total Switching Loss	—	0.90	—	mJ	See Fig. 10, 14
L_E	Internal Emitter Inductance	—	13	—	nH	Measured 5mm from package
C_{ies}	Input Capacitance	—	660	—	pF	$V_{GE} = 0V$
C_{oes}	Output Capacitance	—	100	—		$V_{CC} = 30V$ See Fig. 7
C_{res}	Reverse Transfer Capacitance	—	11	—		$f = 1.0MHz$

Notes:

- ① Repetitive rating; $V_{GE}=20V$, pulse width limited by max. junction temperature. (See fig. 13b)
- ② $V_{CC}=80\%(V_{CES}), V_{GE}=20V, L=10\mu H, R_G=23\Omega,$ (See fig. 13a)
- ③ Repetitive rating; pulse width limited by maximum junction temperature.
- ④ Pulse width $\leq 80\mu s$; duty factor $\leq 0.1\%$.
- ⑤ Pulse width 5.0 μs , single shot.

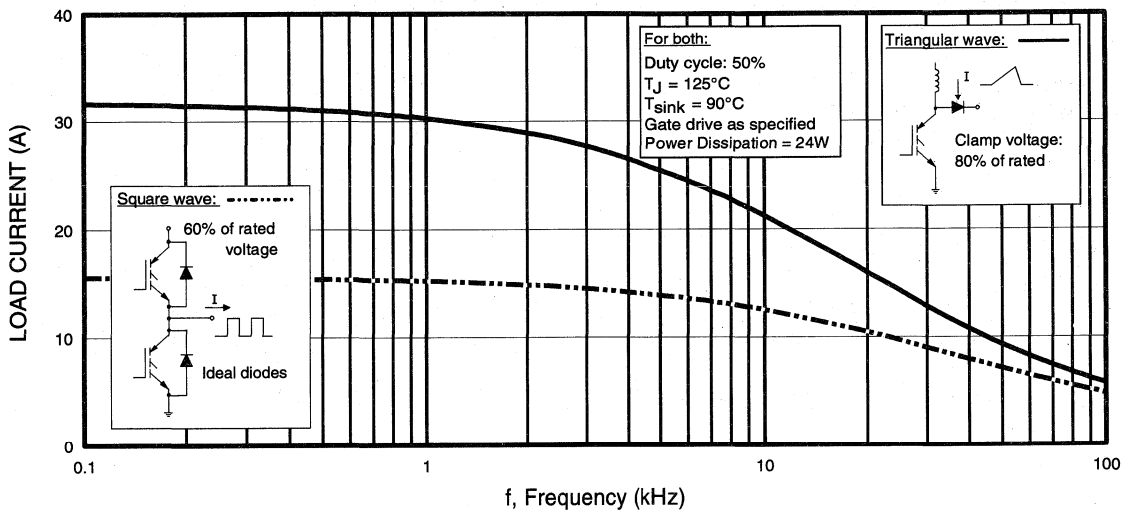


Fig. 1 - Typical Load Current vs. Frequency
 (For square wave, $I = I_{RMS}$ of fundamental; for triangular wave, $I = I_{PK}$)

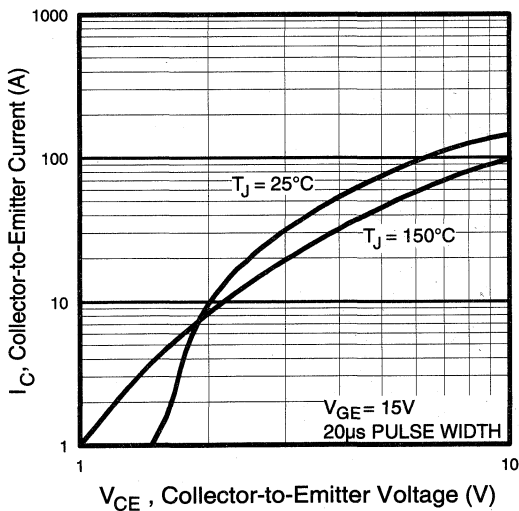


Fig. 2 - Typical Output Characteristics

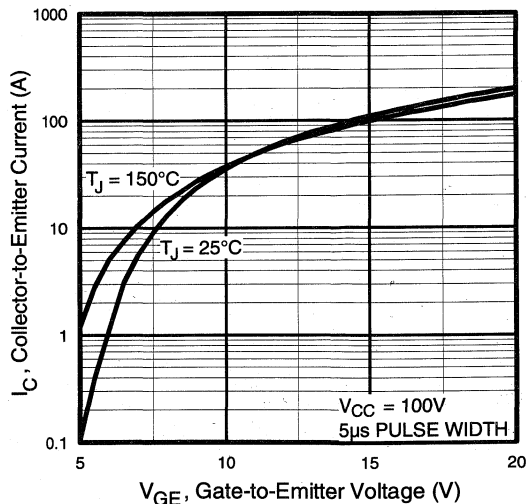


Fig. 3 - Typical Transfer Characteristics

Power
Conversion
Ultra-Fast
Discretes

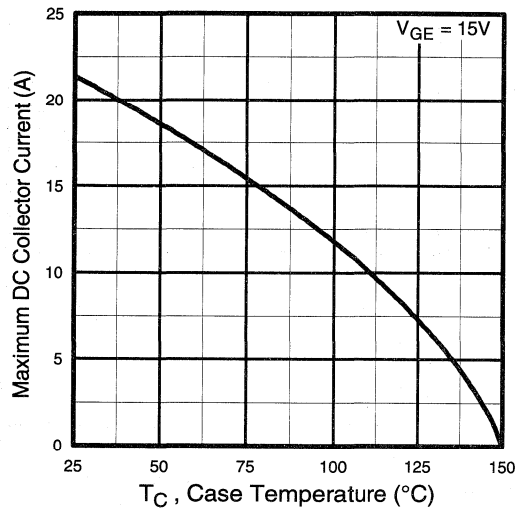


Fig. 4 - Maximum Collector Current vs. Case Temperature

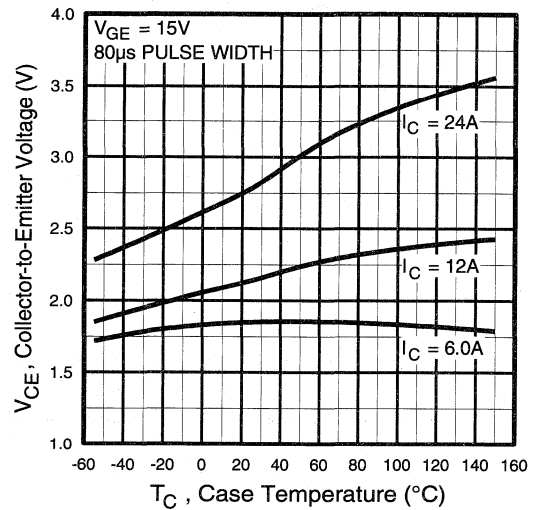


Fig. 5 - Collector-to-Emitter Voltage vs. Case Temperature

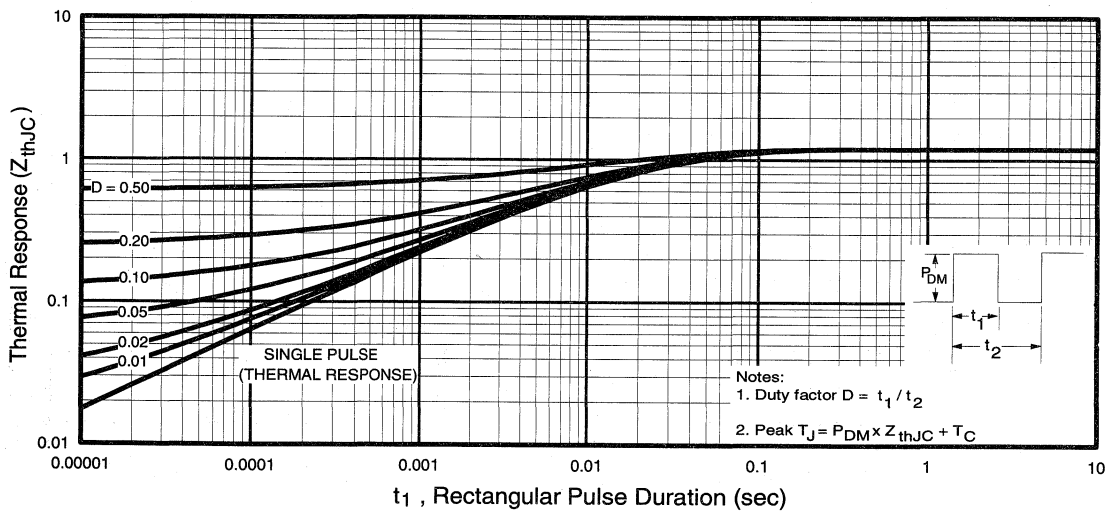


Fig. 6 - Maximum Effective Transient Thermal Impedance, Junction-to-Case

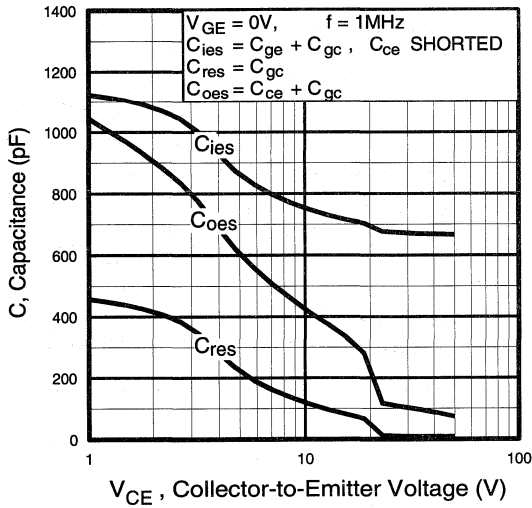


Fig. 7 - Typical Capacitance vs. Collector-to-Emitter Voltage

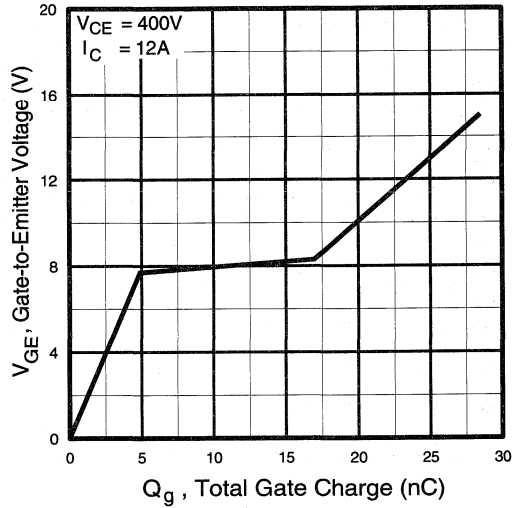


Fig. 8 - Typical Gate Charge vs. Gate-to-Emitter Voltage

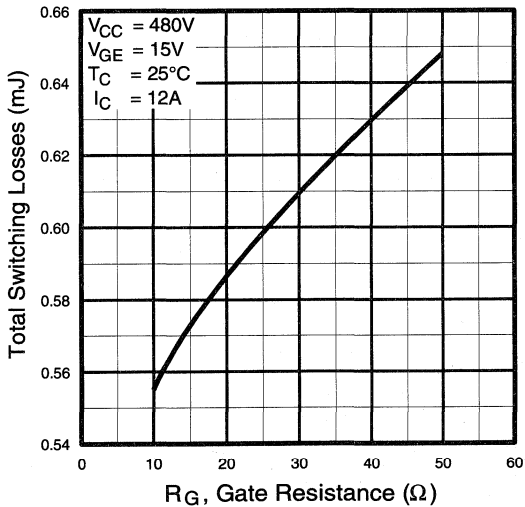


Fig. 9 - Typical Switching Losses vs. Gate Resistance

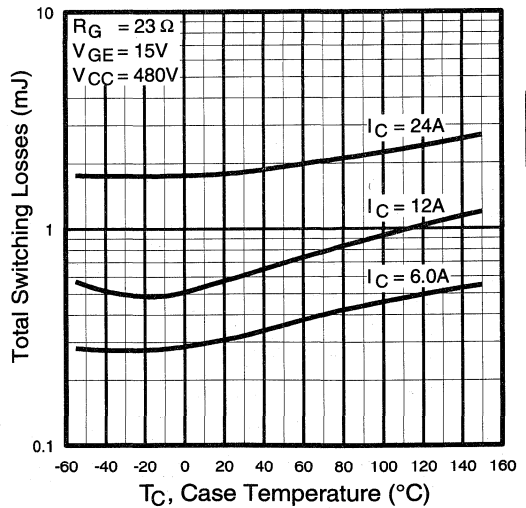


Fig. 10 - Typical Switching Losses vs. Case Temperature

Power Conversion
Ultra-Fast
Discrete

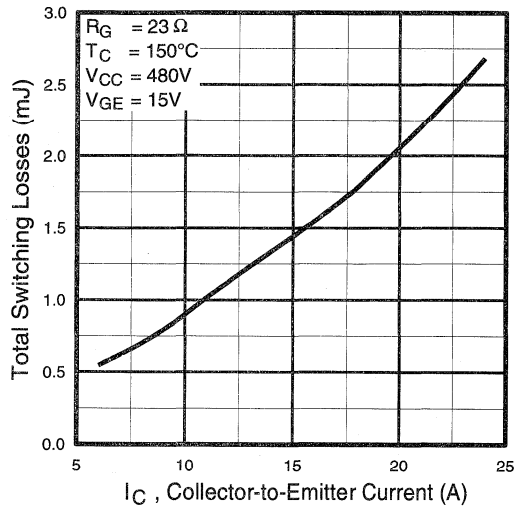


Fig. 11 - Typical Switching Losses vs. Collector-to-Emitter Current

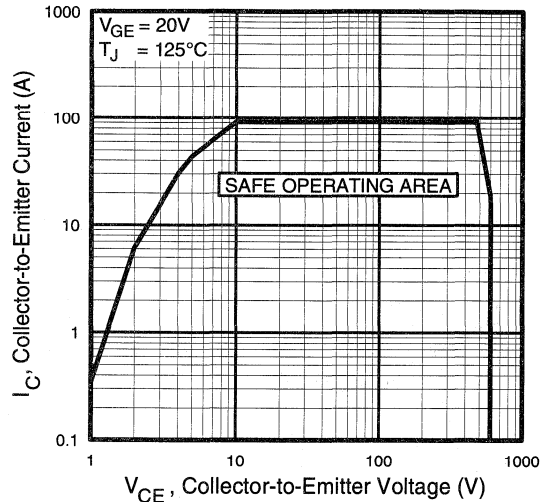


Fig. 12 - Turn-Off SOA

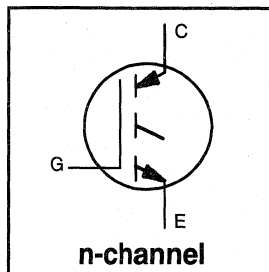
Refer to Section D for the following:

Appendix C: Section D - page D-5

- Fig. 13a - Clamped Inductive Load Test Circuit
- Fig. 13b - Pulsed Collector Current Test Circuit
- Fig. 14a - Switching Loss Test Circuit
- Fig. 14b - Switching Loss Waveform

Features

- Switching-loss rating includes all "tail" losses
- Optimized for high operating frequency (over 5kHz)
See Fig. 1 for Current vs. Frequency curve



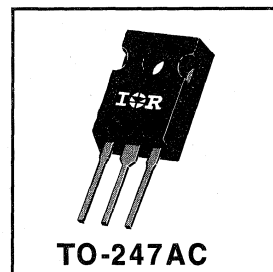
$$V_{CES} = 600V$$

$$V_{CE(sat)} \leq 3.0V$$

$$@V_{GE} = 15V, I_C = 20A$$

Description

Insulated Gate Bipolar Transistors (IGBTs) from International Rectifier have higher usable current densities than comparable bipolar transistors, while at the same time having simpler gate-drive requirements of the familiar power MOSFET. They provide substantial benefits to a host of high-voltage, high-current applications.



Absolute Maximum Ratings

	Parameter	Max.	Units
V_{CES}	Collector-to-Emitter Voltage	600	V
$I_C @ T_C = 25^\circ C$	Continuous Collector Current	40	A
$I_C @ T_C = 100^\circ C$	Continuous Collector Current	20	
I_{CM}	Pulsed Collector Current ①	160	
I_{LM}	Clamped Inductive Load Current ②	160	
V_{GE}	Gate-to-Emitter Voltage	± 20	V
E_{ARV}	Reverse Voltage Avalanche Energy ③	15	mJ
$P_D @ T_C = 25^\circ C$	Maximum Power Dissipation	160	W
$P_D @ T_C = 100^\circ C$	Maximum Power Dissipation	65	
T_J	Operating Junction and	-55 to +150	$^\circ C$
T_{STG}	Storage Temperature Range		
	Soldering Temperature, for 10 sec.	300 (0.063 in. (1.6mm) from case)	
	Mounting torque, 6-32 or M3 screw.	10 lbf•in (1.1N•m)	

Thermal Resistance

	Parameter	Min.	Typ.	Max.	Units
$R_{\theta JC}$	Junction-to-Case	—	—	0.77	$^\circ C/W$
$R_{\theta CS}$	Case-to-Sink, flat, greased surface	—	0.24	—	
$R_{\theta JA}$	Junction-to-Ambient, typical socket mount	—	—	40	
Wt	Weight	—	6 (0.21)	—	g (oz)

Electrical Characteristics @ $T_J = 25^\circ\text{C}$ (unless otherwise specified)

	Parameter	Min.	Typ.	Max.	Units	Conditions
$V_{(BR)CES}$	Collector-to-Emitter Breakdown Voltage	600	—	—	V	$V_{GE} = 0V, I_C = 250\mu A$
$V_{(BR)ECS}$	Emitter-to-Collector Breakdown Voltage ④	20	—	—	V	$V_{GE} = 0V, I_C = 1.0A$
$\Delta V_{(BR)CES}/\Delta T_J$	Temperature Coeff. of Breakdown Voltage	—	0.63	—	$V/^\circ\text{C}$	$V_{GE} = 0V, I_C = 1.0mA$
$V_{CE(on)}$	Collector-to-Emitter Saturation Voltage	—	2.2	3.0	V	$I_C = 20A$ $V_{GE} = 15V$
		—	2.7	—		$I_C = 40A$ See Fig. 2, 5
		—	2.3	—		$I_C = 20A, T_J = 150^\circ\text{C}$
$V_{GE(th)}$	Gate Threshold Voltage	3.0	—	5.5		$V_{CE} = V_{GE}, I_C = 250\mu A$
$\Delta V_{GE(th)}/\Delta T_J$	Temperature Coeff. of Threshold Voltage	—	-13	—	$\text{mV}/^\circ\text{C}$	$V_{CE} = V_{GE}, I_C = 250\mu A$
g_{fe}	Forward Transconductance ⑤	11	18	—	S	$V_{CE} = 100V, I_C = 20A$
I_{CES}	Zero Gate Voltage Collector Current	—	—	250	μA	$V_{GE} = 0V, V_{CE} = 600V$
		—	—	2500		$V_{GE} = 0V, V_{CE} = 600V, T_J = 150^\circ\text{C}$
I_{GES}	Gate-to-Emitter Leakage Current	—	—	± 100	nA	$V_{GE} = \pm 20V$

Switching Characteristics @ $T_J = 25^\circ\text{C}$ (unless otherwise specified)

	Parameter	Min.	Typ.	Max.	Units	Conditions
Q_g	Total Gate Charge (turn-on)	—	51	67	nC	$I_C = 20A$ $V_{CC} = 400V$ See Fig. 8 $V_{GE} = 15V$
Q_{ge}	Gate - Emitter Charge (turn-on)	—	8.9	11		
Q_{gc}	Gate - Collector Charge (turn-on)	—	20	33		
$t_{d(on)}$	Turn-On Delay Time	—	25	—	ns	$T_J = 25^\circ\text{C}$ $I_C = 20A, V_{CC} = 480V$ $V_{GE} = 15V, R_G = 10\Omega$ Energy losses include "tail"
t_r	Rise Time	—	21	—		
$t_{d(off)}$	Turn-Off Delay Time	—	96	190		
t_f	Fall Time	—	43	120		
E_{on}	Turn-On Switching Loss	—	0.34	—	mJ	See Fig. 9, 10, 11, 14
E_{off}	Turn-Off Switching Loss	—	0.41	—		
E_{ts}	Total Switching Loss	—	0.75	1.6		
$t_{d(on)}$	Turn-On Delay Time	—	25	—	ns	$T_J = 150^\circ\text{C}$, $I_C = 20A, V_{CC} = 480V$ $V_{GE} = 15V, R_G = 10\Omega$ Energy losses include "tail"
t_r	Rise Time	—	23	—		
$t_{d(off)}$	Turn-Off Delay Time	—	174	—		
t_f	Fall Time	—	140	—		
E_{ts}	Total Switching Loss	—	1.4	—	mJ	See Fig. 10, 14
L_E	Internal Emitter Inductance	—	13	—	nH	Measured 5mm from package
C_{ies}	Input Capacitance	—	1500	—	pF	$V_{GE} = 0V$ $V_{CC} = 30V$ See Fig. 7 $f = 1.0\text{MHz}$
C_{oes}	Output Capacitance	—	190	—		
C_{res}	Reverse Transfer Capacitance	—	17	—		

Notes:

- ① Repetitive rating; $V_{GE}=20V$, pulse width limited by max. junction temperature. (See fig. 13b)
- ② $V_{CC}=80\%(V_{CES}), V_{GE}=20V, L=10\mu H, R_G=10\Omega$, (See fig. 13a)
- ③ Repetitive rating; pulse width limited by maximum junction temperature.
- ④ Pulse width $\leq 80\mu s$; duty factor $\leq 0.1\%$.
- ⑤ Pulse width $5.0\mu s$, single shot.

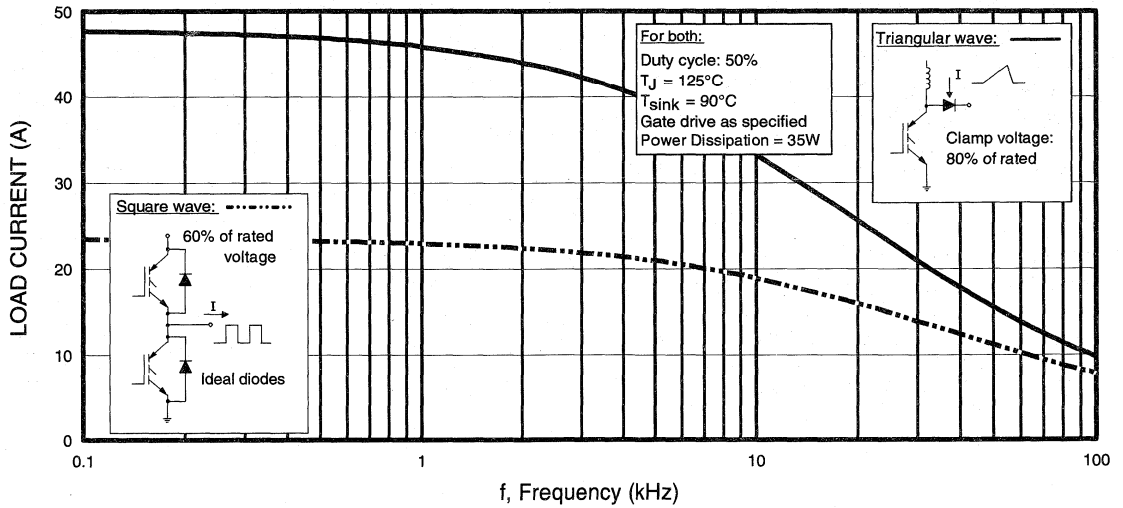


Fig. 1 - Typical Load Current vs. Frequency
 (For square wave, $I = I_{RMS}$ of fundamental; for triangular wave, $I = I_{PK}$)

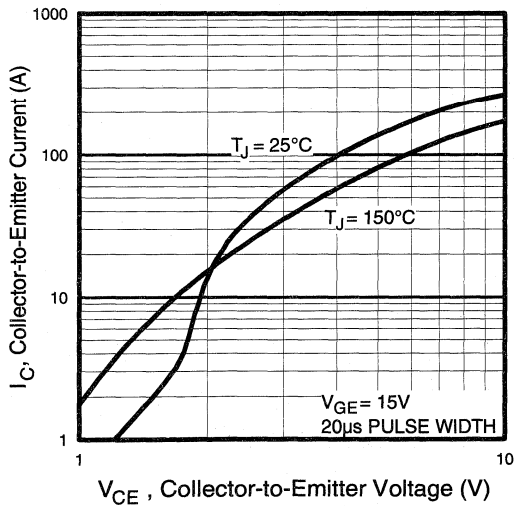


Fig. 2 - Typical Output Characteristics

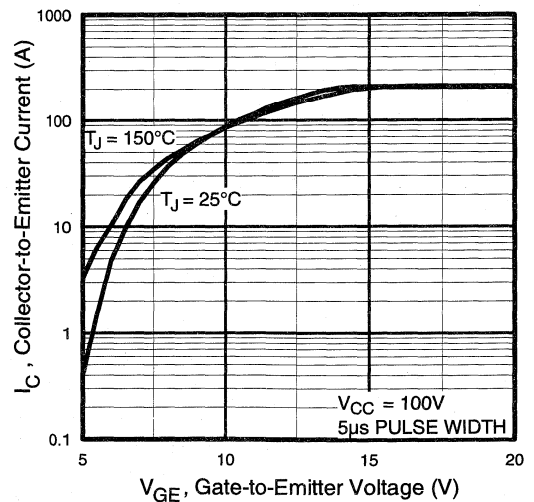


Fig. 3 - Typical Transfer Characteristics

Power Conversion Ultra-Fast Discretes

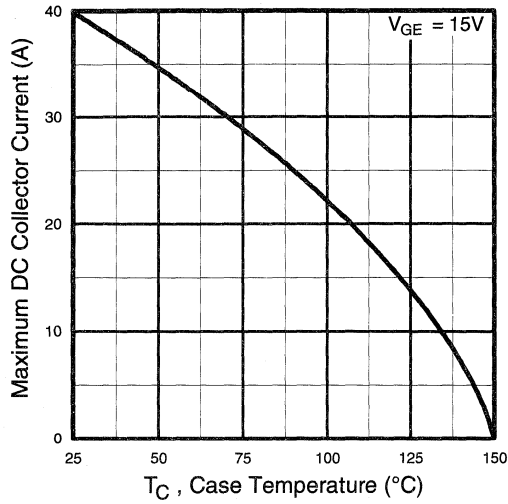


Fig. 4 - Maximum Collector Current vs. Case Temperature

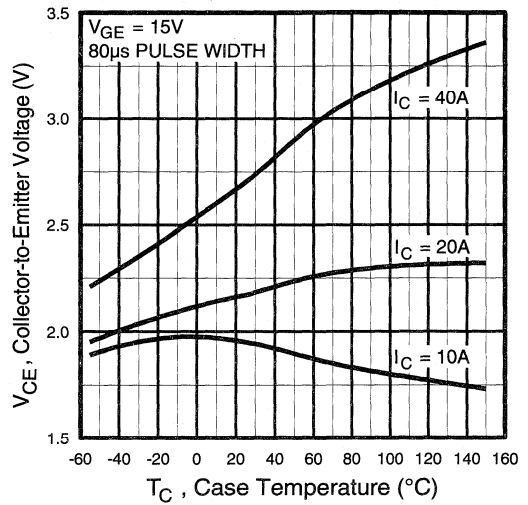


Fig. 5 - Collector-to-Emitter Voltage vs. Case Temperature

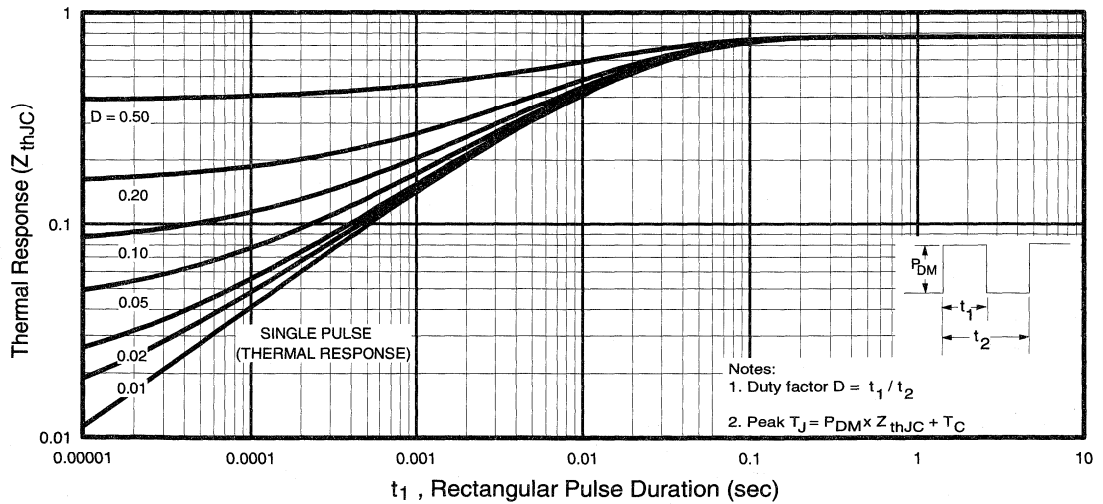


Fig. 6 - Maximum Effective Transient Thermal Impedance, Junction-to-Case

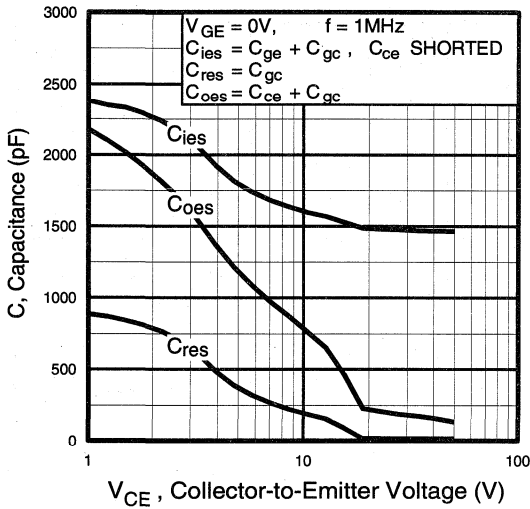


Fig. 7 - Typical Capacitance vs. Collector-to-Emitter Voltage

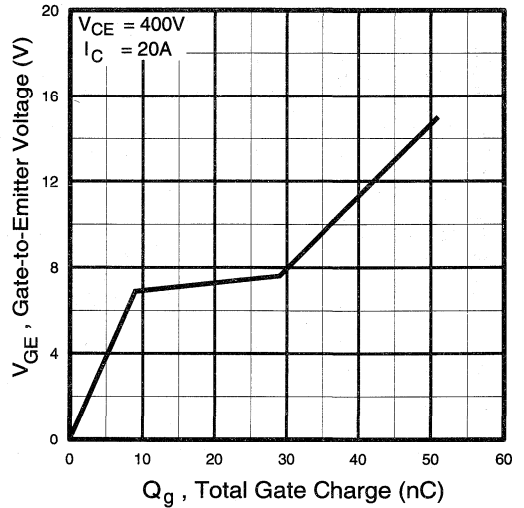


Fig. 8 - Typical Gate Charge vs. Gate-to-Emitter Voltage

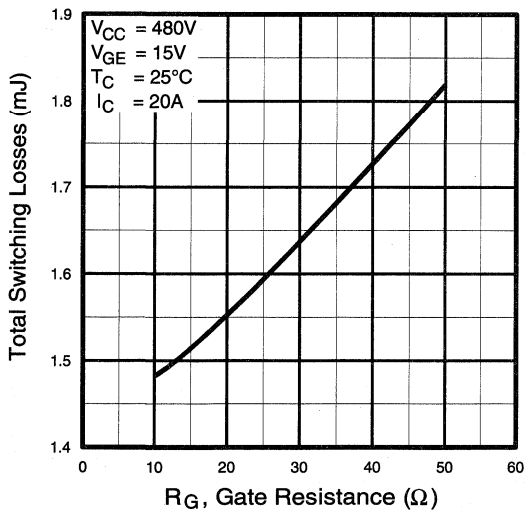


Fig. 9 - Typical Switching Losses vs. Gate Resistance

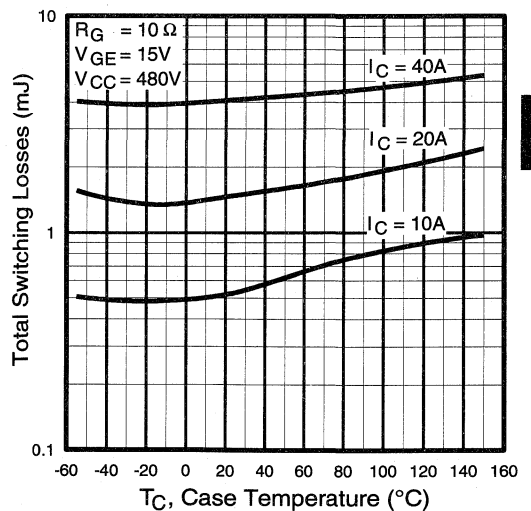


Fig. 10 - Typical Switching Losses vs. Case Temperature

Power Conversion
Ultra-Fast
IGBTs

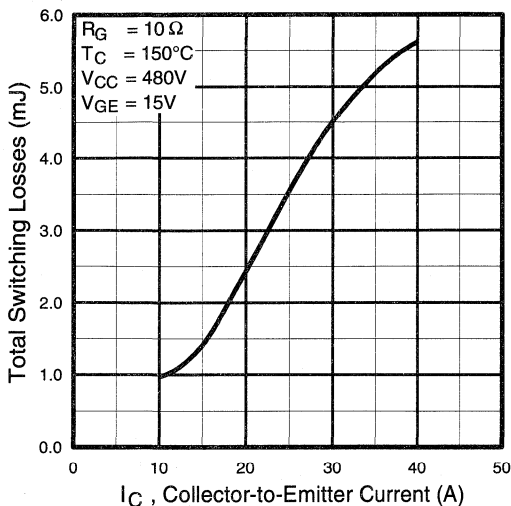


Fig. 11 - Typical Switching Losses vs. Collector-to-Emitter Current

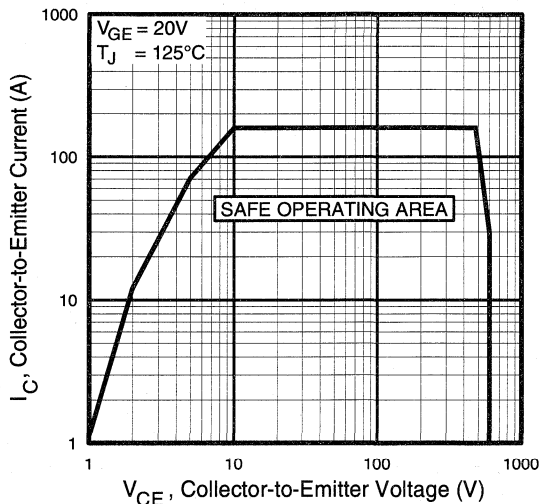


Fig. 12 - Turn-Off SOA

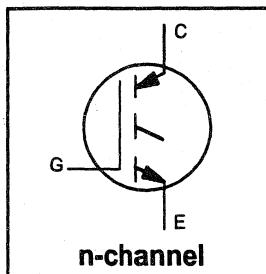
Refer to Section D for the following:

Appendix C: Section D - page D-5

- Fig. 13a - Clamped Inductive Load Test Circuit
- Fig. 13b - Pulsed Collector Current Test Circuit
- Fig. 14a - Switching Loss Test Circuit
- Fig. 14b - Switching Loss Waveform

Features

- Switching-loss rating includes all "tail" losses
- Optimized for high operating frequency (over 5kHz)
See Fig. 1 for Current vs. Frequency curve



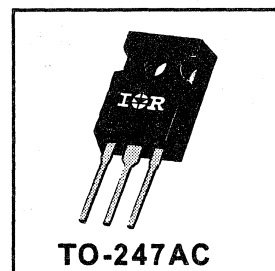
$$V_{CES} = 600V$$

$$V_{CE(sat)} \leq 3.0V$$

$$@V_{GE} = 15V, I_C = 27A$$

Description

Insulated Gate Bipolar Transistors (IGBTs) from International Rectifier have higher usable current densities than comparable bipolar transistors, while at the same time having simpler gate-drive requirements of the familiar power MOSFET. They provide substantial benefits to a host of high-voltage, high-current applications.



Absolute Maximum Ratings

	Parameter	Max.	Units
V_{CES}	Collector-to-Emitter Voltage	600	V
$I_C @ T_C = 25^\circ C$	Continuous Collector Current	55	A
$I_C @ T_C = 100^\circ C$	Continuous Collector Current	27	
I_{CM}	Pulsed Collector Current ①	220	
I_{LM}	Clamped Inductive Load Current ②	220	
V_{GE}	Gate-to-Emitter Voltage	± 20	V
E_{ARV}	Reverse Voltage Avalanche Energy ③	20	mJ
$P_D @ T_C = 25^\circ C$	Maximum Power Dissipation	200	W
$P_D @ T_C = 100^\circ C$	Maximum Power Dissipation	78	
T_J	Operating Junction and	-55 to +150	°C
T_{STG}	Storage Temperature Range		
	Soldering Temperature, for 10 sec.		
	Mounting torque, 6-32 or M3 screw.	10 lbf·in (1.1N·m)	

Thermal Resistance

	Parameter	Min.	Typ.	Max.	Units
$R_{\theta JC}$	Junction-to-Case	—	—	0.64	°C/W
$R_{\theta CS}$	Case-to-Sink, flat, greased surface	—	0.24	—	
$R_{\theta JA}$	Junction-to-Ambient, typical socket mount	—	—	40	
Wt	Weight	—	6 (0.21)	—	g (oz)

Electrical Characteristics @ $T_J = 25^\circ\text{C}$ (unless otherwise specified)

	Parameter	Min.	Typ.	Max.	Units	Conditions
$V_{(BR)CES}$	Collector-to-Emitter Breakdown Voltage	600	—	—	V	$V_{GE} = 0V, I_C = 250\mu\text{A}$
$V_{(BR)ECS}$	Emitter-to-Collector Breakdown Voltage ③	20	—	—	V	$V_{GE} = 0V, I_C = 1.0A$
$\Delta V_{(BR)CES}/\Delta T_J$	Temp. Coeff. of Breakdown Voltage	—	0.60	—	V/°C	$V_{GE} = 0V, I_C = 1.0mA$
$V_{CE(on)}$	Collector-to-Emitter Saturation Voltage	—	2.0	3.0	V	$I_C = 27A$ $I_C = 55A$ $I_C = 27A, T_J = 150^\circ\text{C}$ $V_{GE} = 15V$ See Fig. 2, 5
		—	2.4	—		
		—	1.9	—		
$V_{GE(th)}$	Gate Threshold Voltage	3.0	—	5.5		$V_{CE} = V_{GE}, I_C = 250\mu\text{A}$
$\Delta V_{GE(th)}/\Delta T_J$	Temperature Coeff. of Threshold Voltage	—	-13	—	mV/°C	$V_{CE} = V_{GE}, I_C = 250\mu\text{A}$
g_{fe}	Forward Transconductance ⑤	16	24	—	S	$V_{CE} = 100V, I_C = 27A$
I_{CES}	Zero Gate Voltage Collector Current	—	—	250	μA	$V_{GE} = 0V, V_{CE} = 600V$
		—	—	5000		$V_{GE} = 0V, V_{CE} = 600V, T_J = 150^\circ\text{C}$
I_{GES}	Gate-to-Emitter Leakage Current	—	—	± 100	nA	$V_{GE} = \pm 20V$

Switching Characteristics @ $T_J = 25^\circ\text{C}$ (unless otherwise specified)

	Parameter	Min.	Typ.	Max.	Units	Conditions
Q_g	Total Gate Charge (turn-on)	—	110	140	nC	$I_C = 27A$ $V_{CC} = 400V$ $V_{GE} = 15V$ See Fig. 8
Q_{ge}	Gate - Emitter Charge (turn-on)	—	17	21		
Q_{gc}	Gate - Collector Charge (turn-on)	—	53	70		
$t_{d(on)}$	Turn-On Delay Time	—	23	—	ns	$T_J = 25^\circ\text{C}$ $I_C = 27A, V_{CC} = 480V$ $V_{GE} = 15V, R_G = 5.0\Omega$ Energy losses include "tail"
t_r	Rise Time	—	28	—		
$t_{d(off)}$	Turn-Off Delay Time	—	100	200		
t_f	Fall Time	—	45	140		
E_{on}	Turn-On Switching Loss	—	0.80	—	mJ	See Fig. 9, 10, 11, 14
E_{off}	Turn-Off Switching Loss	—	0.6	—		
E_{ts}	Total Switching Loss	—	1.4	2.4		
$t_{d(on)}$	Turn-On Delay Time	—	24	—	ns	$T_J = 150^\circ\text{C}$, $I_C = 27A, V_{CC} = 480V$ $V_{GE} = 15V, R_G = 5.0\Omega$ Energy losses include "tail"
t_r	Rise Time	—	27	—		
$t_{d(off)}$	Turn-Off Delay Time	—	180	—		
t_f	Fall Time	—	130	—		
E_{ts}	Total Switching Loss	—	2.5	—	mJ	See Fig. 10, 14
L_E	Internal Emitter Inductance	—	13	—	nH	Measured 5mm from package
C_{ies}	Input Capacitance	—	2900	—	pF	$V_{GE} = 0V$ $V_{CC} = 30V$ $f = 1.0\text{MHz}$ See Fig. 7
C_{oes}	Output Capacitance	—	330	—		
C_{res}	Reverse Transfer Capacitance	—	41	—		

Notes:

- ① Repetitive rating; $V_{GE} = 20V$, pulse width limited by max. junction temperature. (See fig. 13b)
- ② $V_{CC} = 80\%(V_{CES}), V_{GE} = 20V, L = 10\mu\text{H}, R_G = 5.0\Omega$, (See fig. 13a)
- ③ Repetitive rating; pulse width limited by maximum junction temperature.
- ④ Pulse width $\leq 80\mu\text{s}$; duty factor $\leq 0.1\%$.
- ⑤ Pulse width 5.0 μs , single shot.

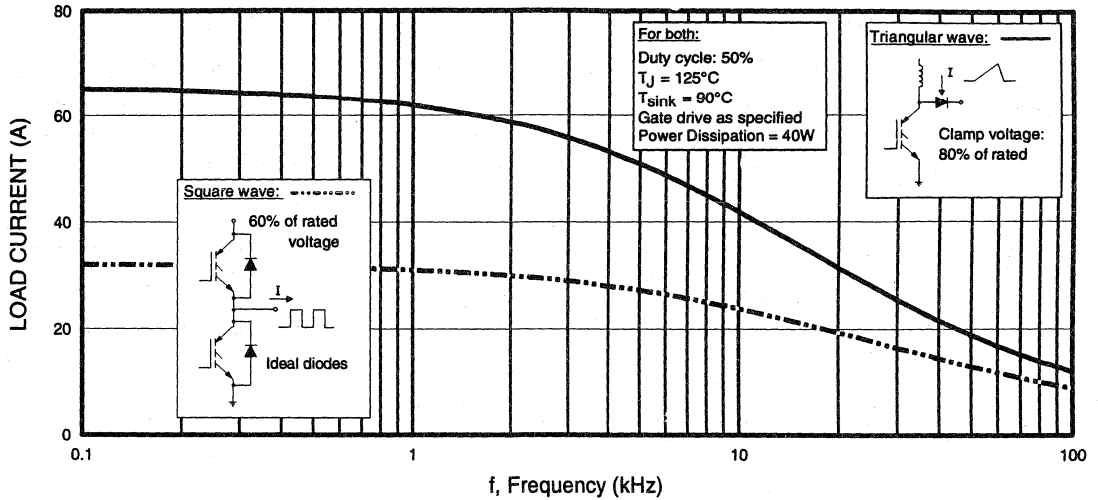


Fig. 1 - Typical Load Current vs. Frequency
 (For square wave, $I = I_{RMS}$ of fundamental; for triangular wave, $I = I_{PK}$)

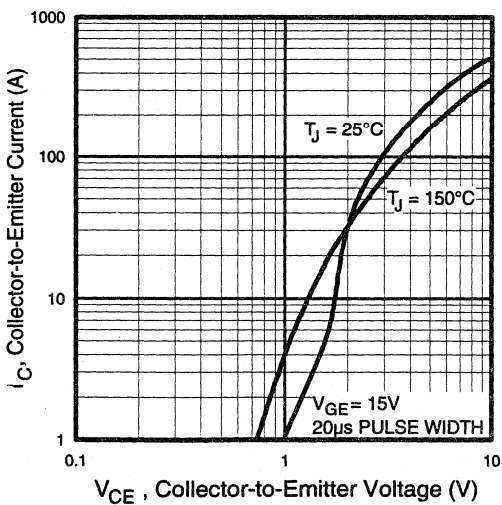


Fig. 2 - Typical Output Characteristics

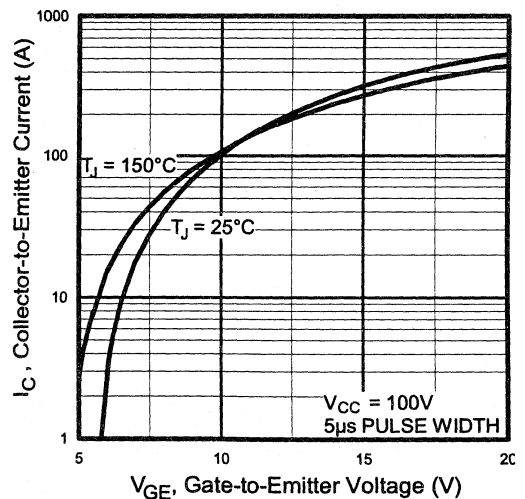


Fig. 3 - Typical Transfer Characteristics

Power
Conversion
UltraFast
Discrete

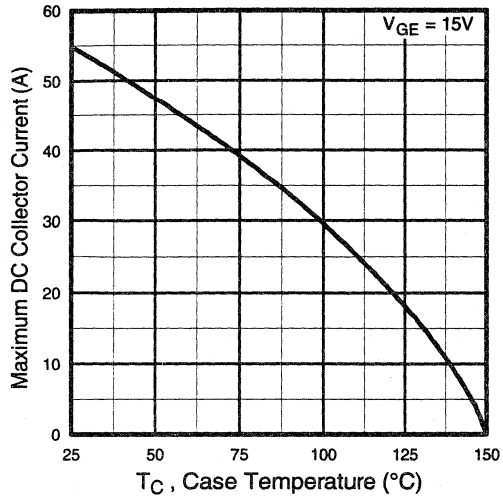


Fig. 4 - Maximum Collector Current vs. Case Temperature

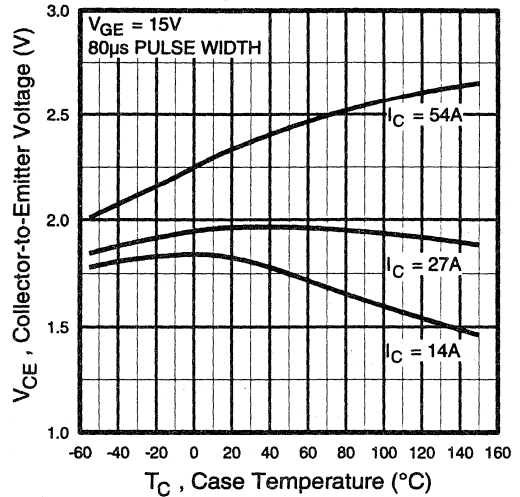


Fig. 5 - Collector-to-Emitter Voltage vs. Case Temperature

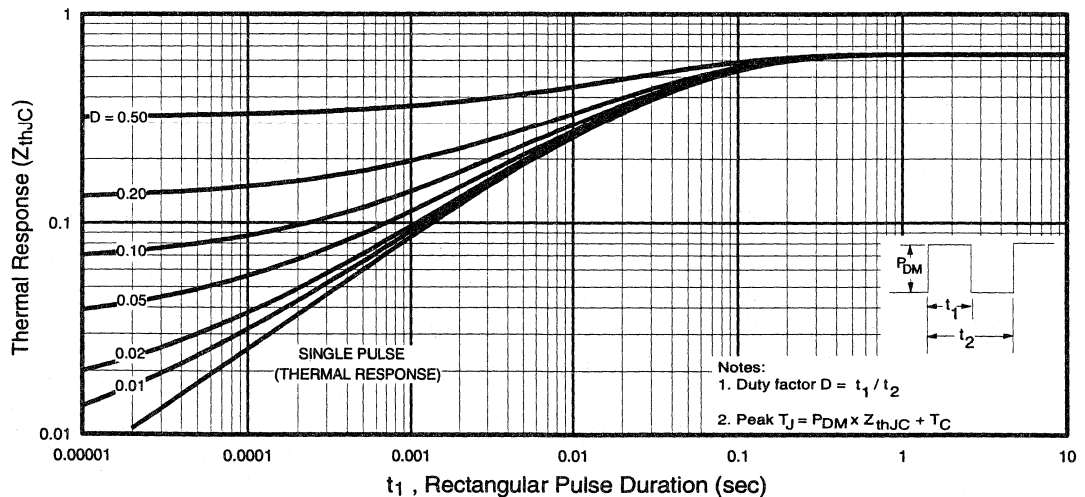


Fig. 6 - Maximum Effective Transient Thermal Impedance, Junction-to-Case

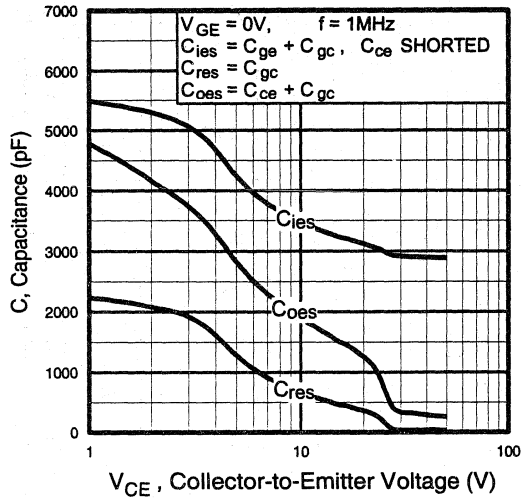


Fig. 7 - Typical Capacitance vs. Collector-to-Emitter Voltage

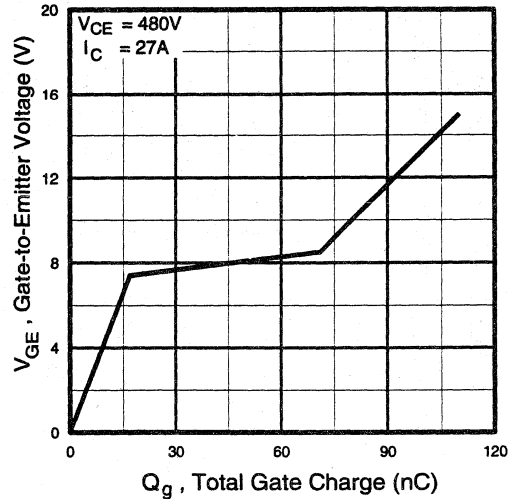


Fig. 8 - Typical Gate Charge vs. Gate-to-Emitter Voltage

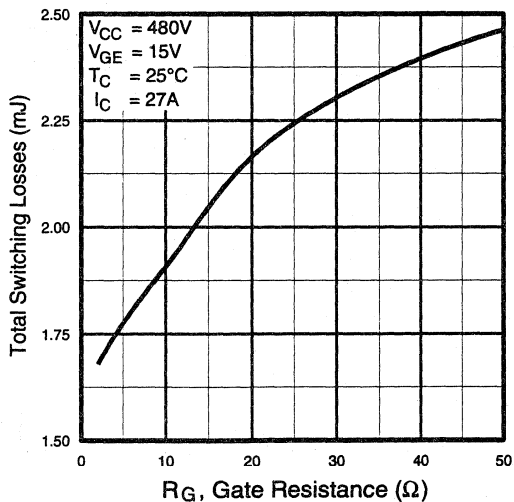


Fig. 9 - Typical Switching Losses vs. Gate Resistance

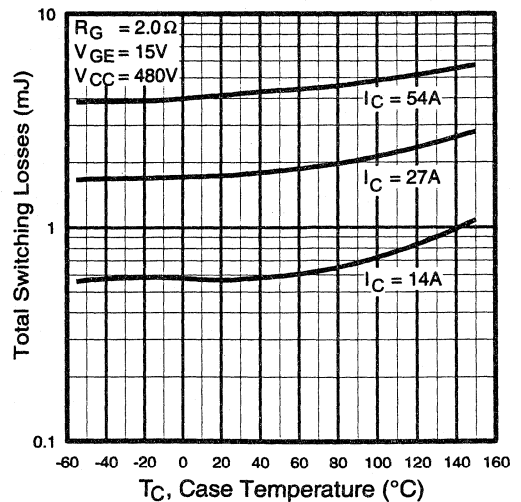


Fig. 10 - Typical Switching Losses vs. Case Temperature

Power Conversion
Ultra-Fast
Discretes

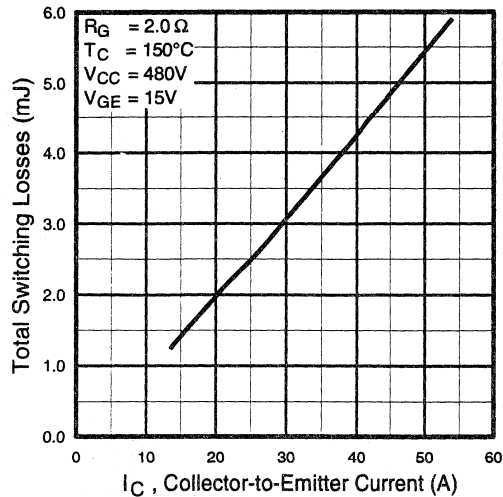


Fig. 11 - Typical Switching Losses vs. Collector-to-Emitter Current

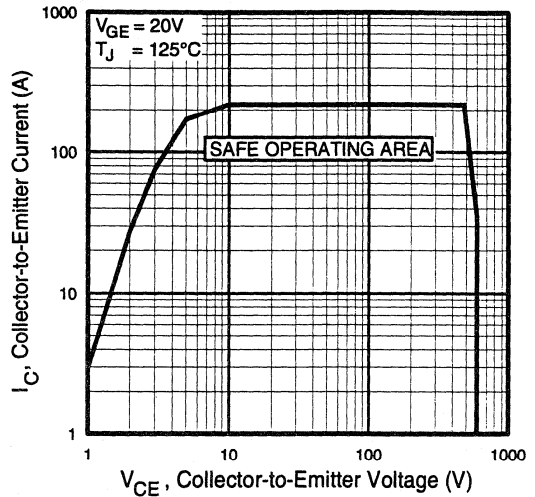


Fig. 12 - Turn-Off SOA

Refer to Section D for the following:

Appendix C: Section D - page D-5

Fig. 13a - Clamped Inductive Load Test Circuit

Fig. 13b - Pulsed Collector Current Test Circuit

Fig. 14a - Switching Loss Test Circuit

Fig. 14b - Switching Loss Waveform

Package Outline 3 - JEDEC Outline TO-247AC

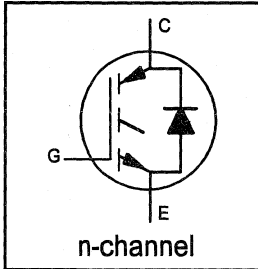
Section D - page D-13

INSULATED GATE BIPOLAR TRANSISTOR
WITH ULTRAFAST SOFT RECOVERY DIODE

UltraFast CoPack IGBT

Features

- Switching-loss rating includes all "tail" losses
- HEXFRED™ soft ultrafast diodes
- Optimized for high operating frequency (over 5kHz)
See Fig. 1 for Current vs. Frequency curve



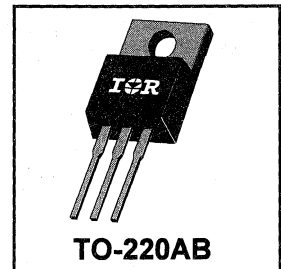
$$V_{CES} = 600V$$

$$V_{CE(sat)} \leq 3.0V$$

$$@V_{GE} = 15V, I_C = 6.5A$$

Description

Co-packaged IGBTs are a natural extension of International Rectifier's well known IGBT line. They provide the convenience of an IGBT and an ultrafast recovery diode in one package, resulting in substantial benefits to a host of high-voltage, high-current, motor control, UPS and power supply applications.



Absolute Maximum Ratings

	Parameter	Max.	Units
V_{CES}	Collector-to-Emitter Voltage	600	V
$I_C @ T_C = 25^\circ C$	Continuous Collector Current	13	A
$I_C @ T_C = 100^\circ C$	Continuous Collector Current	6.5	
I_{CM}	Pulsed Collector Current ①	52	
I_{LM}	Clamped Inductive Load Current ②	52	
$I_F @ T_C = 100^\circ C$	Diode Continuous Forward Current	7.0	
I_{FM}	Diode Maximum Forward Current	52	
V_{GE}	Gate-to-Emitter Voltage	± 20	V
$P_D @ T_C = 25^\circ C$	Maximum Power Dissipation	60	W
$P_D @ T_C = 100^\circ C$	Maximum Power Dissipation	24	
T_J	Operating Junction and	-55 to +150	°C
T_{STG}	Storage Temperature Range		
	Soldering Temperature, for 10 sec.	300 (0.063 in. (1.6mm) from case)	
	Mounting Torque, 6-32 or M3 Screw.	10 lbf•in (1.1 N•m)	

Thermal Resistance

	Parameter	Min.	Typ.	Max.	Units
$R_{\theta JC}$	Junction-to-Case - IGBT	—	—	2.1	°C/W
$R_{\theta JC}$	Junction-to-Case - Diode	—	—	3.5	
$R_{\theta CS}$	Case-to-Sink, flat, greased surface	—	0.50	—	
$R_{\theta JA}$	Junction-to-Ambient, typical socket mount	—	—	80	
Wt	Weight	—	2 (0.07)	—	g (oz)

Power
Conversion
Ultra-Fast
Co-Packs

Electrical Characteristics @ $T_J = 25^\circ\text{C}$ (unless otherwise specified)

	Parameter	Min.	Typ.	Max.	Units	Conditions
$V_{(BR)CES}$	Collector-to-Emitter Breakdown Voltage ^③	600	—	—	V	$V_{GE} = 0V, I_C = 250\mu A$
$\Delta V_{(BR)CES}/\Delta T_J$	Temp. Coeff. of Breakdown Voltage	—	0.69	—	V/°C	$V_{GE} = 0V, I_C = 1.0mA$
$V_{CE(on)}$	Collector-to-Emitter Saturation Voltage	—	2.2	3.0	V	$I_C = 6.5A, V_{GE} = 15V$ See Fig. 2, 5
		—	2.8	—		
		—	2.5	—		
$V_{GE(th)}$	Gate Threshold Voltage	3.0	—	5.5		$V_{CE} = V_{GE}, I_C = 250\mu A$
$\Delta V_{GE(th)}/\Delta T_J$	Temp. Coeff. of Threshold Voltage	—	-11	—	mV/°C	$V_{CE} = V_{GE}, I_C = 250\mu A$
g_{fe}	Forward Transconductance ^④	1.4	4.3	—	S	$V_{CE} = 100V, I_C = 6.5A$
I_{CES}	Zero Gate Voltage Collector Current	—	—	250	μA	$V_{GE} = 0V, V_{CE} = 600V$ $V_{GE} = 0V, V_{CE} = 600V, T_J = 150^\circ C$
		—	—	1700		
V_{FM}	Diode Forward Voltage Drop	—	1.4	1.7	V	$I_C = 8.0A$ See Fig. 13
		—	1.3	1.6		
I_{GES}	Gate-to-Emitter Leakage Current	—	—	± 100	nA	$V_{GE} = \pm 20V$

Switching Characteristics @ $T_J = 25^\circ\text{C}$ (unless otherwise specified)

	Parameter	Min.	Typ.	Max.	Units	Conditions	
Q_g	Total Gate Charge (turn-on)	—	16	22	nC	$I_C = 6.5A$ $V_{CC} = 400V$ See Fig. 8	
Q_{ge}	Gate - Emitter Charge (turn-on)	—	2.5	3.8			
Q_{gc}	Gate - Collector Charge (turn-on)	—	7.8	13			
$t_{d(on)}$	Turn-On Delay Time	—	60	—	ns	$T_J = 25^\circ C$ $I_C = 6.5A, V_{CC} = 480V$ $V_{GE} = 15V, R_G = 50\Omega$ Energy losses include "tail" and diode reverse recovery. See Fig. 9, 10, 11, 18	
t_r	Rise Time	—	29	—			
$t_{d(off)}$	Turn-Off Delay Time	—	130	200			
t_f	Fall Time	—	65	120			
E_{on}	Turn-On Switching Loss	—	0.21	—			
E_{off}	Turn-Off Switching Loss	—	0.22	—	mJ	See Fig. 9, 10, 11, 18	
E_{ts}	Total Switching Loss	—	0.43	0.65			
$t_{d(on)}$	Turn-On Delay Time	—	60	—	ns	$T_J = 150^\circ C$, See Fig. 9, 10, 11, 18 $I_C = 6.5A, V_{CC} = 480V$ $V_{GE} = 15V, R_G = 50\Omega$ Energy losses include "tail" and diode reverse recovery.	
t_r	Rise Time	—	30	—			
$t_{d(off)}$	Turn-Off Delay Time	—	210	—			
t_f	Fall Time	—	180	—			
E_{ts}	Total Switching Loss	—	0.71	—	mJ		
L_E	Internal Emitter Inductance	—	7.5	—	nH	Measured 5mm from package	
C_{ies}	Input Capacitance	—	330	—	pF	$V_{GE} = 0V$ $V_{CC} = 30V$ See Fig. 7 $f = 1.0MHz$	
C_{oes}	Output Capacitance	—	65	—			
C_{res}	Reverse Transfer Capacitance	—	6.0	—			
t_{rr}	Diode Reverse Recovery Time	—	37	55	ns	$T_J = 25^\circ C$ See Fig. 14 $T_J = 125^\circ C$ 14	$I_F = 8.0A$ $V_R = 200V$ $di/dt = 200A/\mu s$
		—	55	90			
I_{rr}	Diode Peak Reverse Recovery Current	—	3.5	5.0	A	$T_J = 25^\circ C$ See Fig. 15 $T_J = 125^\circ C$ 15	
		—	4.5	8.0			
Q_{rr}	Diode Reverse Recovery Charge	—	65	138	nC	$T_J = 25^\circ C$ See Fig. 16 $T_J = 125^\circ C$ 16	
		—	124	360			
$di_{(rec)M}/dt$	Diode Peak Rate of Fall of Recovery During t_b	—	240	—	A/ μs	$T_J = 25^\circ C$ See Fig. 17 $T_J = 125^\circ C$ 17	
		—	210	—			

Notes:

① Repetitive rating; $V_{GE}=20V$, pulse width limited by max. junction temperature. (See fig. 20)

② $V_{CC}=80\%(V_{CES}), V_{GE}=20V, L=10\mu H, R_G=50\Omega,$ (See fig. 19)

③ Pulse width $\leq 80\mu s$; duty factor $\leq 0.1\%$.

④ Pulse width $5.0\mu s$, single shot.

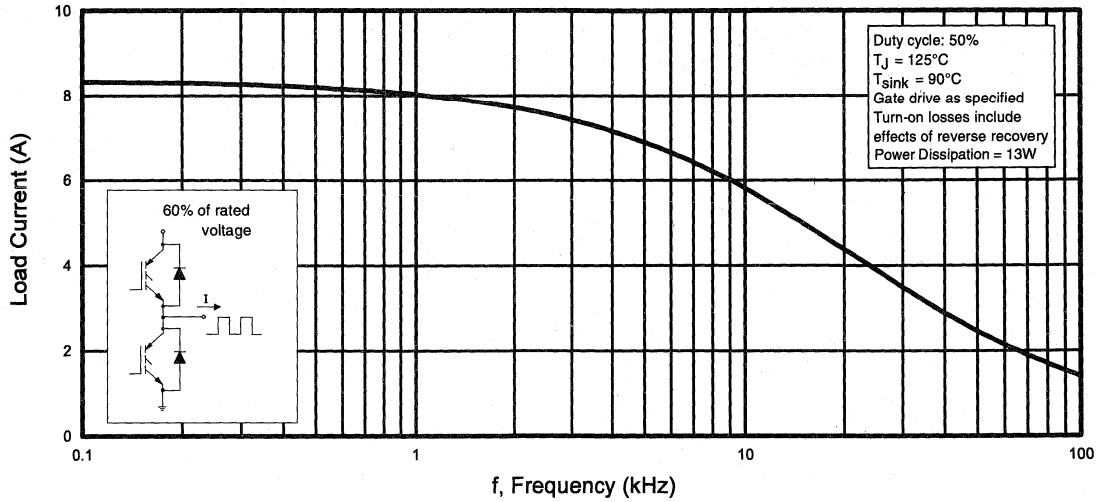


Fig. 1 - Typical Load Current vs. Frequency
(Load Current = I_{RMS} of fundamental)

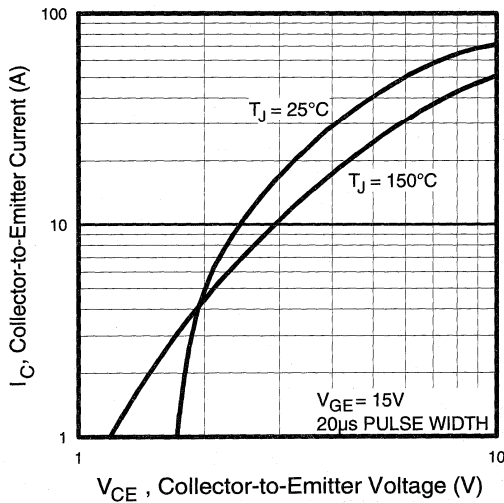


Fig. 2 - Typical Output Characteristics

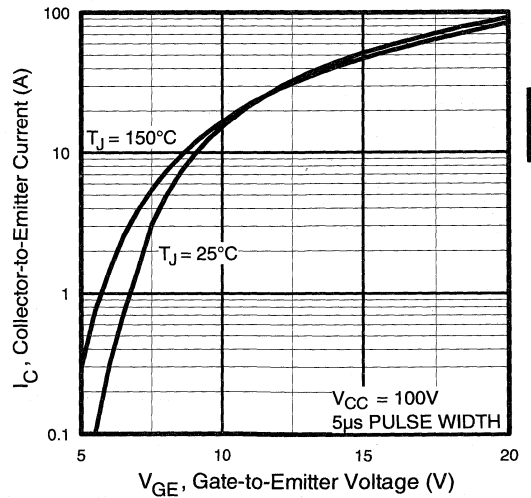


Fig. 3 - Typical Transfer Characteristics

Power Conversion
Ultra-Fast
Ce-Packs

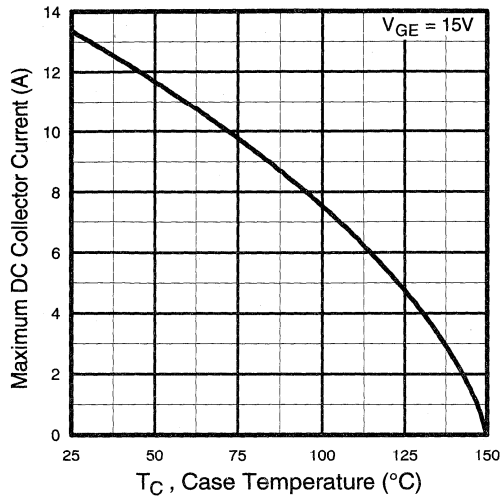


Fig. 4 - Maximum Collector Current vs. Case Temperature

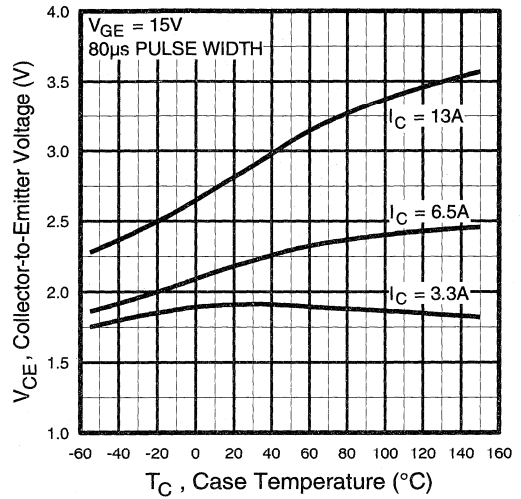


Fig. 5 - Collector-to-Emitter Voltage vs. Case Temperature

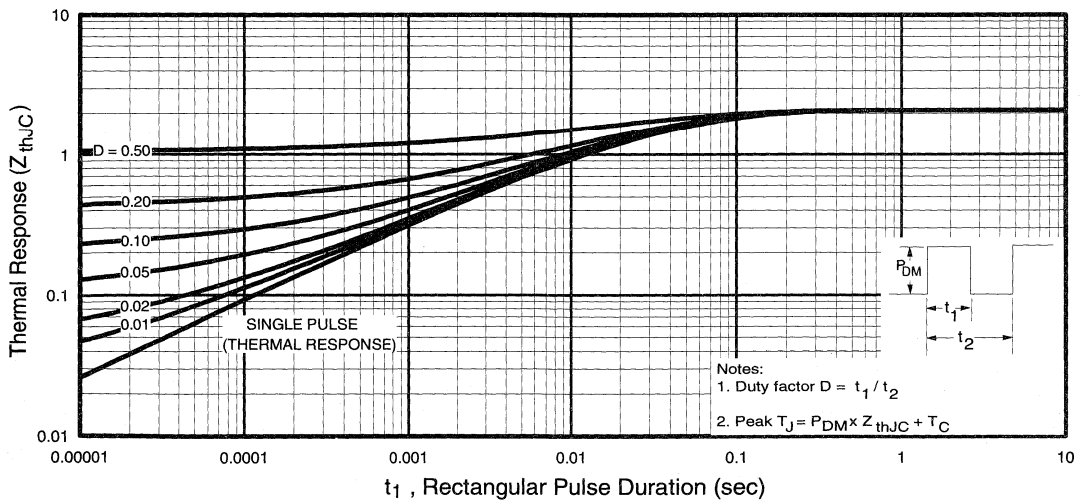


Fig. 6 - Maximum IGBT Effective Transient Thermal Impedance, Junction-to-Case

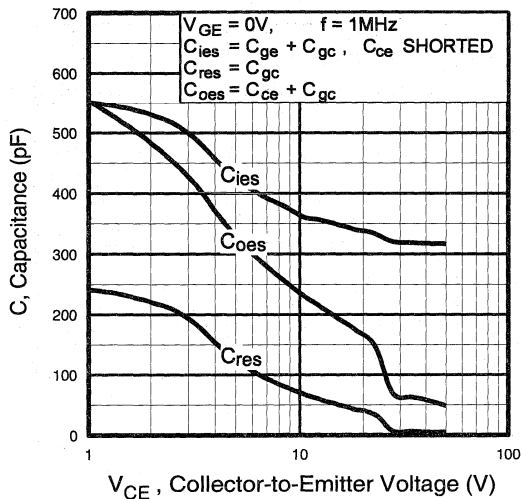


Fig. 7 - Typical Capacitance vs. Collector-to-Emitter Voltage

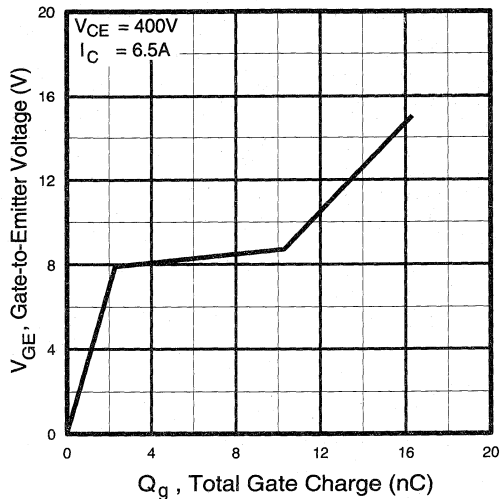


Fig. 8 - Typical Gate Charge vs. Gate-to-Emitter Voltage

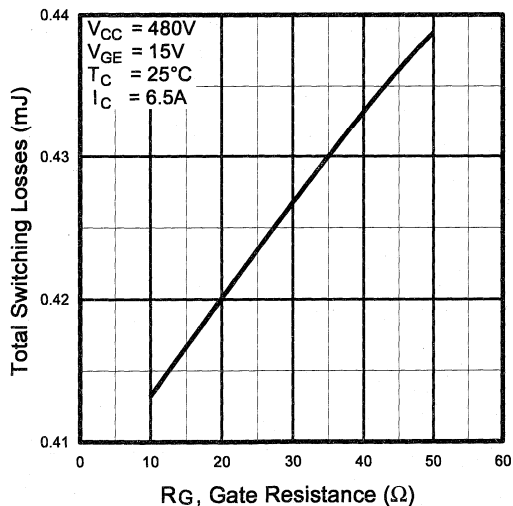


Fig. 9 - Typical Switching Losses vs. Gate Resistance

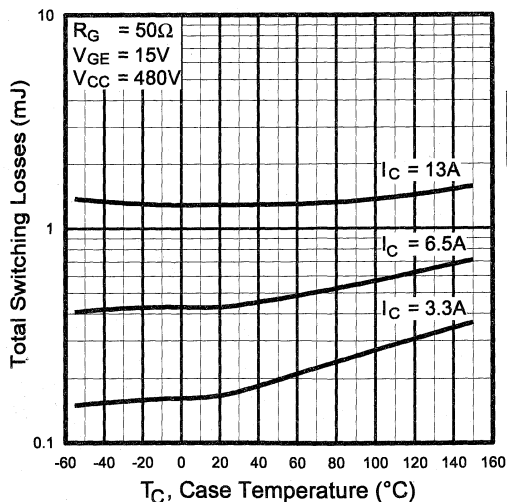


Fig. 10 - Typical Switching Losses vs. Case Temperature

Power Conversion
Ultra-Fast
Co-Packs

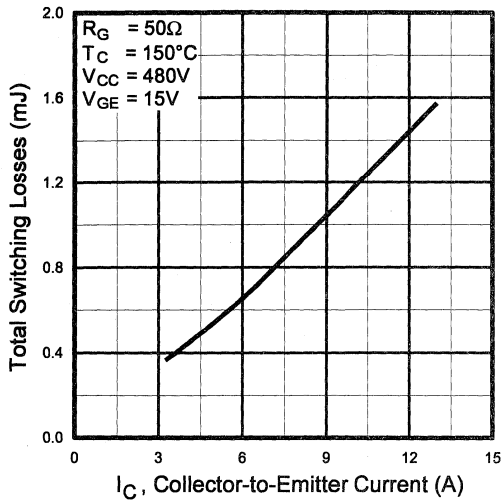


Fig. 11 - Typical Switching Losses vs. Collector-to-Emitter Current

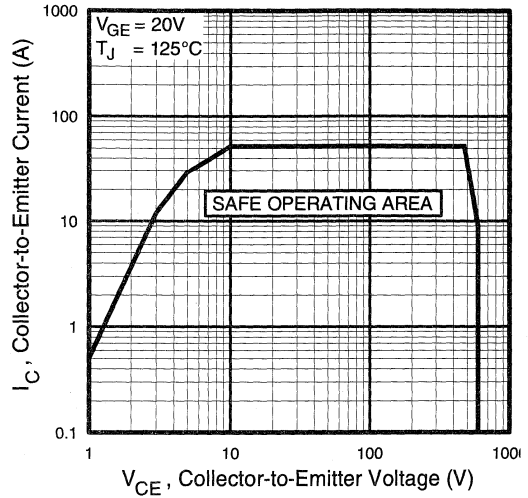


Fig. 12 - Turn-Off SOA

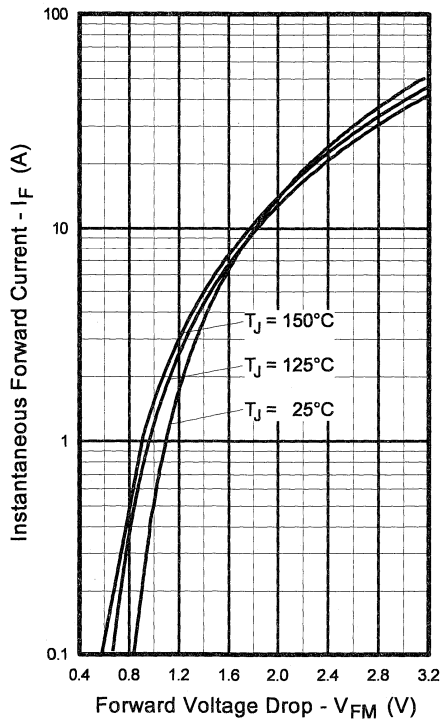


Fig. 13 - Maximum Forward Voltage Drop vs. Instantaneous Forward Current

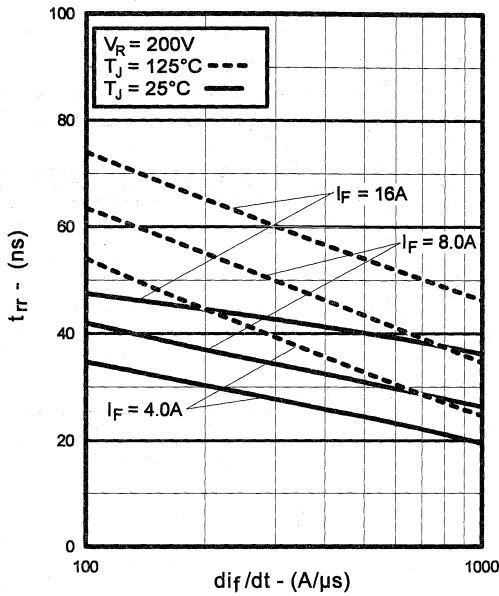


Fig. 14 - Typical Reverse Recovery vs. di_f/dt

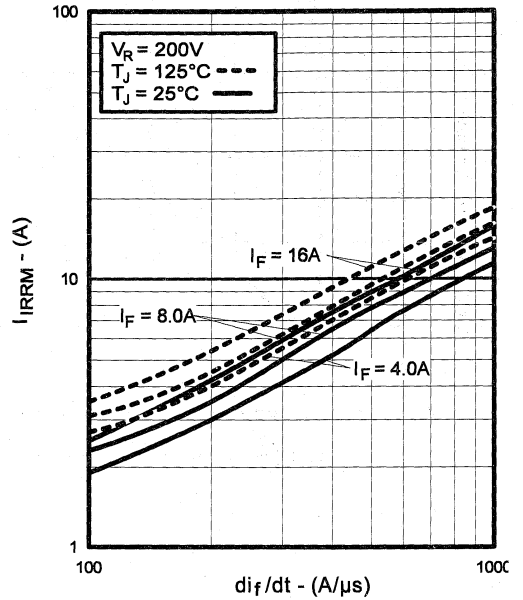


Fig. 15 - Typical Recovery Current vs. di_f/dt

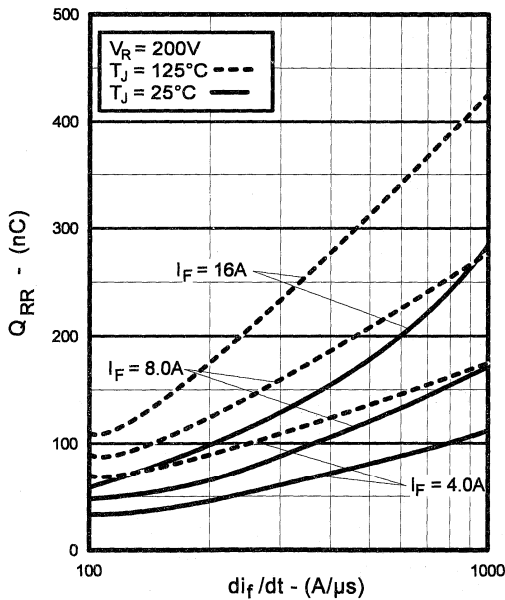


Fig. 16 - Typical Stored Charge vs. di_f/dt

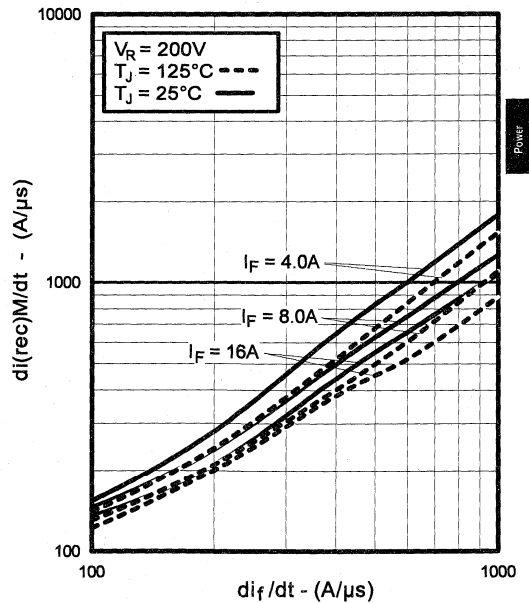


Fig. 17 - Typical $di_{(rec)M}/dt$ vs. di_f/dt

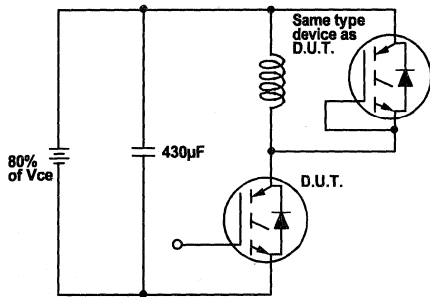


Fig. 18a - Test Circuit for Measurement of I_{LM} , E_{on} , $E_{off(diode)}$, t_{rr} , Q_{rr} , I_{rr} , $t_{d(on)}$, t_r , $t_{d(off)}$, t_f

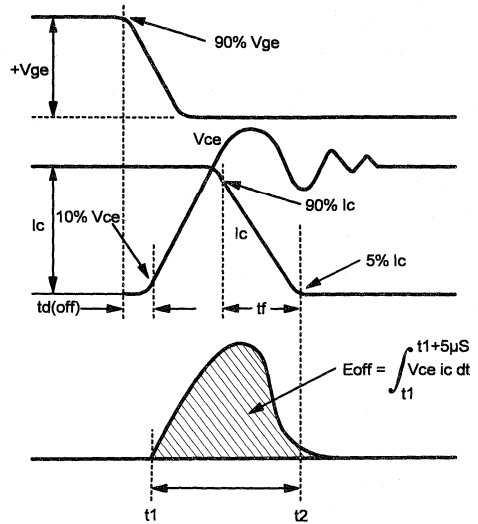


Fig. 18b - Test Waveforms for Circuit of Fig. 18a, Defining E_{off} , $t_{d(off)}$, t_f

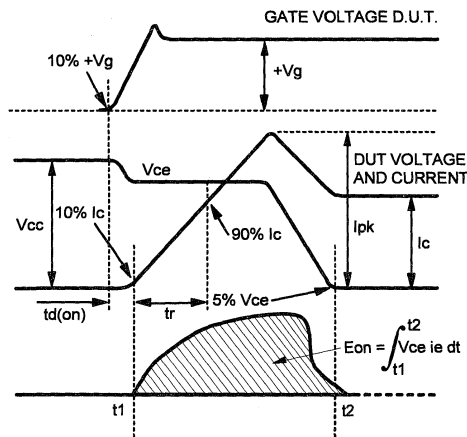


Fig. 18c - Test Waveforms for Circuit of Fig. 18a, Defining E_{on} , $t_{d(on)}$, t_r

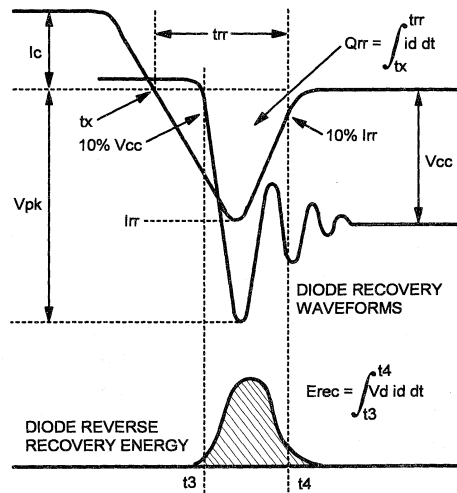


Fig. 18d - Test Waveforms for Circuit of Fig. 18a, Defining E_{rec} , t_{rr} , Q_{rr} , I_{rr}

Refer to Section D for the following:
Appendix D: Section D - page D-6

- Fig. 18e - Macro Waveforms for Test Circuit Fig. 18a
- Fig. 19 - Clamped Inductive Load Test Circuit
- Fig. 20 - Pulsed Collector Current Test Circuit

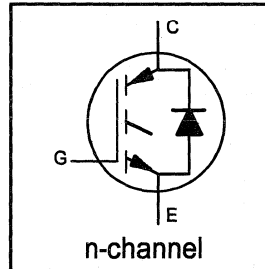
IRGBC30UD2

INSULATED GATE BIPOLAR TRANSISTOR
WITH ULTRAFAST SOFT RECOVERY DIODE

UltraFast CoPack IGBT

Features

- Switching-loss rating includes all "tail" losses
- HEXFRED™ soft ultrafast diodes
- Optimized for high operating frequency (over 5kHz)
See Fig. 1 for Current vs. Frequency curve



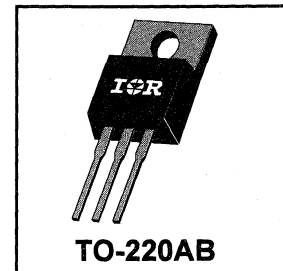
$$V_{CES} = 600V$$

$$V_{CE(sat)} \leq 3.0V$$

$$@V_{GE} = 15V, I_C = 12A$$

Description

Co-packaged IGBTs are a natural extension of International Rectifier's well known IGBT line. They provide the convenience of an IGBT and an ultrafast recovery diode in one package, resulting in substantial benefits to a host of high-voltage, high-current, motor control, UPS and power supply applications.



Absolute Maximum Ratings

	Parameter	Max.	Units
V_{CES}	Collector-to-Emitter Voltage	600	V
$I_C @ T_C = 25^\circ C$	Continuous Collector Current	23	A
$I_C @ T_C = 100^\circ C$	Continuous Collector Current	12	
I_{CM}	Pulsed Collector Current ①	92	
I_{LM}	Clamped Inductive Load Current ②	92	
$I_F @ T_C = 100^\circ C$	Diode Continuous Forward Current	12	
I_{FM}	Diode Maximum Forward Current	92	
V_{GE}	Gate-to-Emitter Voltage	± 20	V
$P_D @ T_C = 25^\circ C$	Maximum Power Dissipation	100	W
$P_D @ T_C = 100^\circ C$	Maximum Power Dissipation	42	
T_J	Operating Junction and	-55 to +150	$^\circ C$
T_{STG}	Storage Temperature Range		
	Soldering Temperature, for 10 sec.	300 (0.063 in. (1.6mm) from case)	
	Mounting Torque, 6-32 or M3 Screw.	10 lbf·in (1.1 N·m)	

Thermal Resistance

	Parameter	Min.	Typ.	Max.	Units
$R_{\theta JC}$	Junction-to-Case - IGBT	—	—	1.2	$^\circ C/W$
$R_{\theta JC}$	Junction-to-Case - Diode	—	—	2.5	
$R_{\theta CS}$	Case-to-Sink, flat, greased surface	—	0.50	—	
$R_{\theta JA}$	Junction-to-Ambient, typical socket mount	—	—	80	
Wt	Weight	—	2 (0.07)	—	g (oz)

Electrical Characteristics @ $T_J = 25^\circ\text{C}$ (unless otherwise specified)

	Parameter	Min.	Typ.	Max.	Units	Conditions
$V_{(BR)CES}$	Collector-to-Emitter Breakdown Voltage ^①	600	—	—	V	$V_{GE} = 0V, I_C = 250\mu A$
$\Delta V_{(BR)CES}/\Delta T_J$	Temperature Coeff. of Breakdown Voltage	—	0.63	—	$V/^\circ\text{C}$	$V_{GE} = 0V, I_C = 1.0mA$
$V_{CE(on)}$	Collector-to-Emitter Saturation Voltage	—	2.2	3.0	V	$I_C = 12A$ $V_{GE} = 15V$
		—	2.7	—		$I_C = 23A$ See Fig. 2, 5
		—	2.4	—		$I_C = 12A, T_J = 150^\circ\text{C}$
$V_{GE(th)}$	Gate Threshold Voltage	3.0	—	5.5		$V_{CE} = V_{GE}, I_C = 250\mu A$
$\Delta V_{GE(th)}/\Delta T_J$	Temperature Coeff. of Threshold Voltage	—	-11	—	$mV/^\circ\text{C}$	$V_{CE} = V_{GE}, I_C = 250\mu A$
g_{fe}	Forward Transconductance ^②	3.1	8.6	—	S	$V_{CE} = 100V, I_C = 12A$
I_{CES}	Zero Gate Voltage Collector Current	—	—	250	μA	$V_{GE} = 0V, V_{CE} = 600V$
		—	—	2500		$V_{GE} = 0V, V_{CE} = 600V, T_J = 150^\circ\text{C}$
V_{FM}	Diode Forward Voltage Drop	—	1.4	1.7	V	$I_C = 12A$ See Fig. 13
		—	1.3	1.6		$I_C = 12A, T_J = 150^\circ\text{C}$
I_{GES}	Gate-to-Emitter Leakage Current	—	—	± 100	nA	$V_{GE} = \pm 20V$

Switching Characteristics @ $T_J = 25^\circ\text{C}$ (unless otherwise specified)

	Parameter	Min.	Typ.	Max.	Units	Conditions
Q_g	Total Gate Charge (turn-on)	—	29	36	nC	$I_C = 12A$
Q_{ge}	Gate - Emitter Charge (turn-on)	—	4.8	6.8		$V_{CC} = 400V$
Q_{gc}	Gate - Collector Charge (turn-on)	—	12	17		See Fig. 8
$t_{d(on)}$	Turn-On Delay Time	—	67	—	ns	$T_J = 25^\circ\text{C}$
t_r	Rise Time	—	56	—		$I_C = 12A, V_{CC} = 480V$
$t_{d(off)}$	Turn-Off Delay Time	—	170	250		$V_{GE} = 15V, R_G = 23\Omega$
t_f	Fall Time	—	140	270		Energy losses include "tail" and diode reverse recovery.
E_{on}	Turn-On Switching Loss	—	0.70	—		See Fig. 9, 10, 11, 18
E_{off}	Turn-Off Switching Loss	—	0.80	—	mJ	
E_{ts}	Total Switching Loss	—	1.5	2.5		
$t_{d(on)}$	Turn-On Delay Time	—	61	—	ns	$T_J = 150^\circ\text{C}$, See Fig. 9, 10, 11, 18
t_r	Rise Time	—	51	—		$I_C = 12A, V_{CC} = 480V$
$t_{d(off)}$	Turn-Off Delay Time	—	190	—		$V_{GE} = 15V, R_G = 23\Omega$
t_f	Fall Time	—	190	—		Energy losses include "tail" and diode reverse recovery.
E_{ts}	Total Switching Loss	—	1.9	—	mJ	
L_E	Internal Emitter Inductance	—	7.5	—	nH	Measured 5mm from package
C_{ies}	Input Capacitance	—	680	—	pF	$V_{GE} = 0V$
C_{oes}	Output Capacitance	—	100	—		$V_{CC} = 30V$ See Fig. 7
C_{res}	Reverse Transfer Capacitance	—	11	—		$f = 1.0MHz$
t_{rr}	Diode Reverse Recovery Time	—	42	60	ns	$T_J = 25^\circ\text{C}$ See Fig. 14
		—	80	120		$T_J = 125^\circ\text{C}$ 14
I_{rr}	Diode Peak Reverse Recovery Current	—	3.5	6.0	A	$T_J = 25^\circ\text{C}$ See Fig. 15
		—	5.6	10		$T_J = 125^\circ\text{C}$ 15
Q_{rr}	Diode Reverse Recovery Charge	—	80	180	nC	$T_J = 25^\circ\text{C}$ See Fig. 16
		—	220	600		$T_J = 125^\circ\text{C}$ 16
$di_{(rec)M}/dt$	Diode Peak Rate of Fall of Recovery During t_b	—	180	—	$A/\mu s$	$T_J = 25^\circ\text{C}$ See Fig. 17
		—	120	—		$T_J = 125^\circ\text{C}$ 17

Notes:

① Repetitive rating; $V_{GE}=20V$, pulse width limited by max. junction temperature. (See fig. 20)

② $V_{CC}=80\%(V_{CES}), V_{GE}=20V, L=10\mu H, R_G=23\Omega,$ (See fig. 19)

③ Pulse width $\leq 80\mu s$; duty factor $\leq 0.1\%$.

④ Pulse width $5.0\mu s$, single shot.

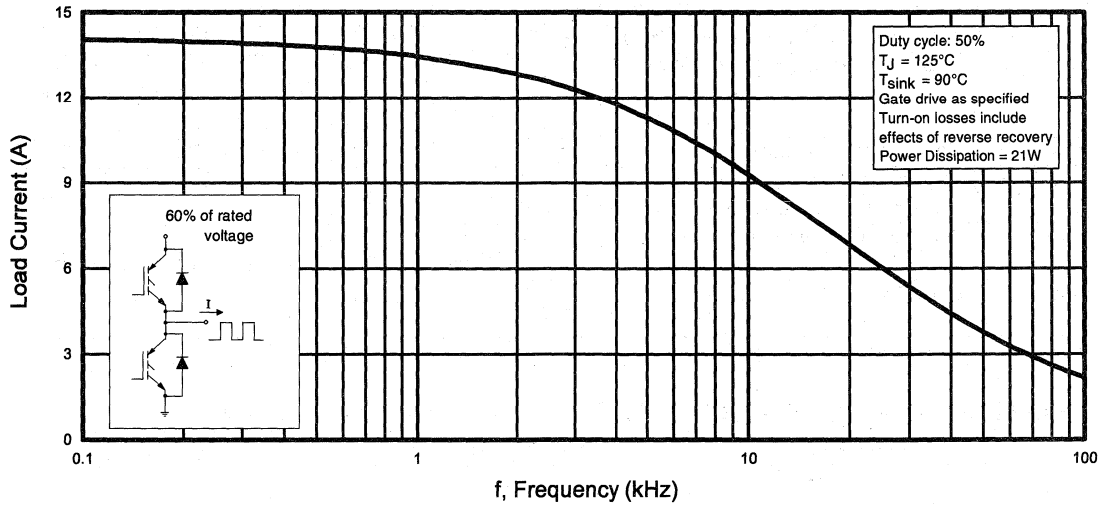


Fig. 1 - Typical Load Current vs. Frequency
(Load Current = I_{RMS} of fundamental)

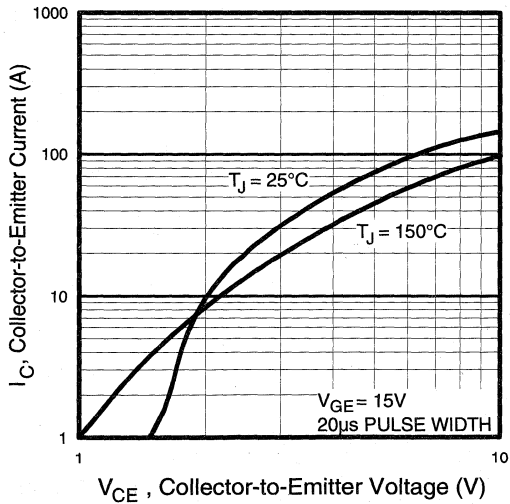


Fig. 2 - Typical Output Characteristics

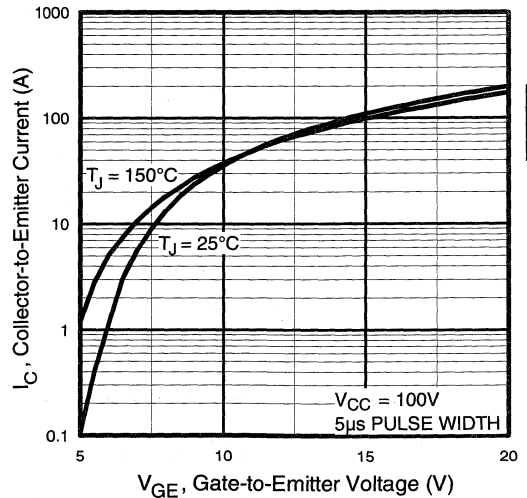


Fig. 3 - Typical Transfer Characteristics

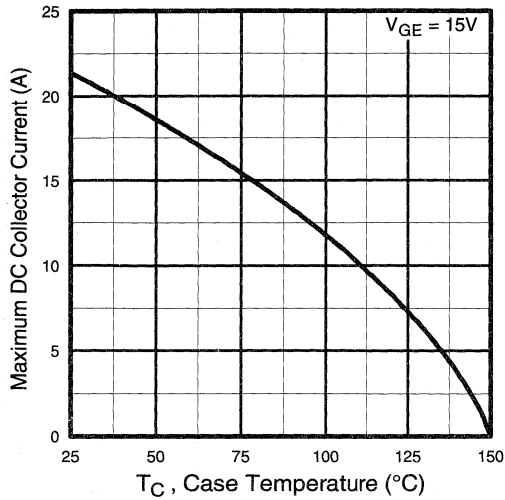


Fig. 4 - Maximum Collector Current vs. Case Temperature

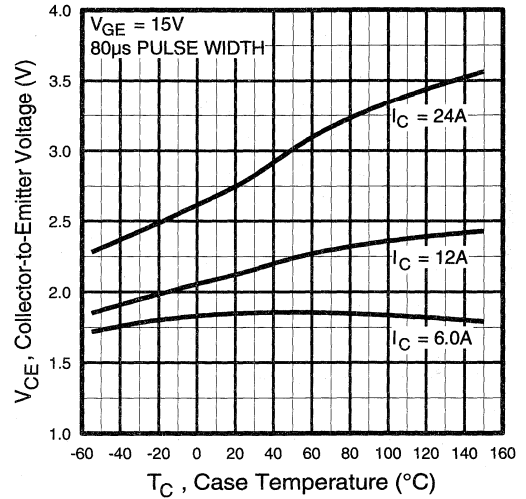


Fig. 5 - Collector-to-Emitter Voltage vs. Case Temperature

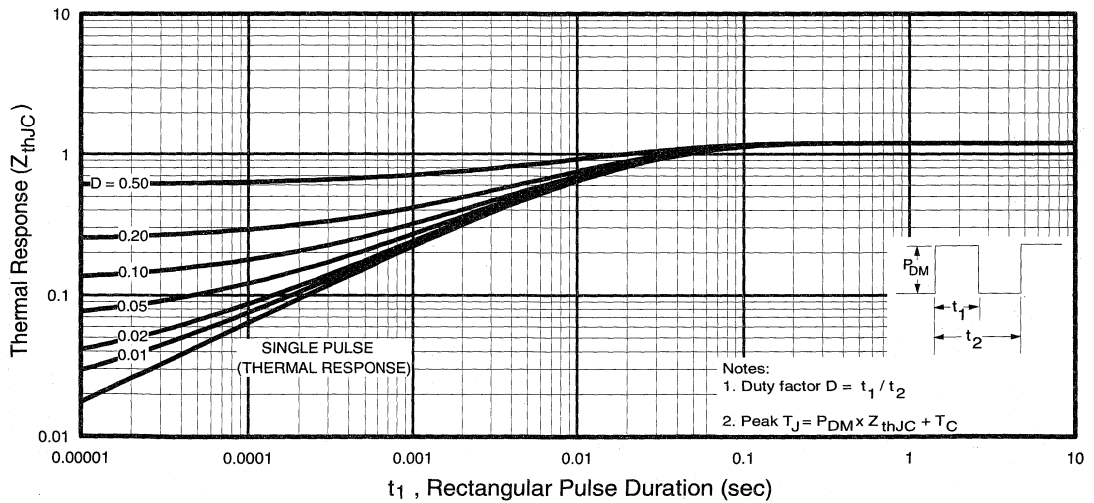


Fig. 6 - Maximum IGBT Effective Transient Thermal Impedance, Junction-to-Case

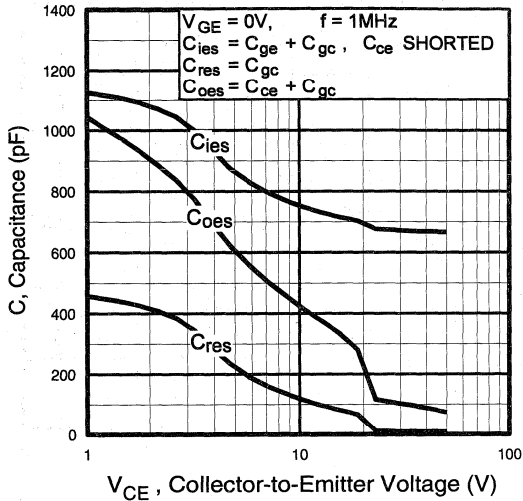


Fig. 7 - Typical Capacitance vs. Collector-to-Emitter Voltage

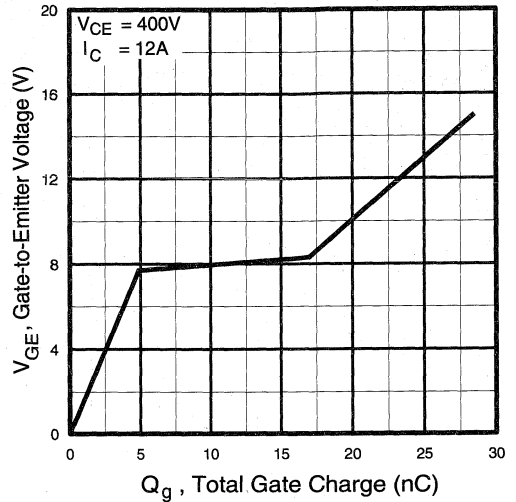


Fig. 8 - Typical Gate Charge vs. Gate-to-Emitter Voltage

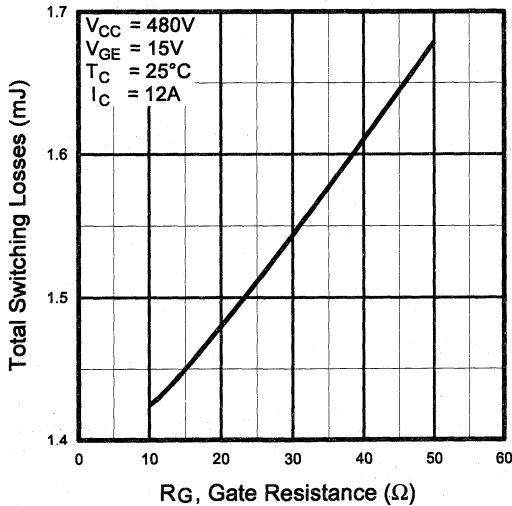


Fig. 9 - Typical Switching Losses vs. Gate Resistance

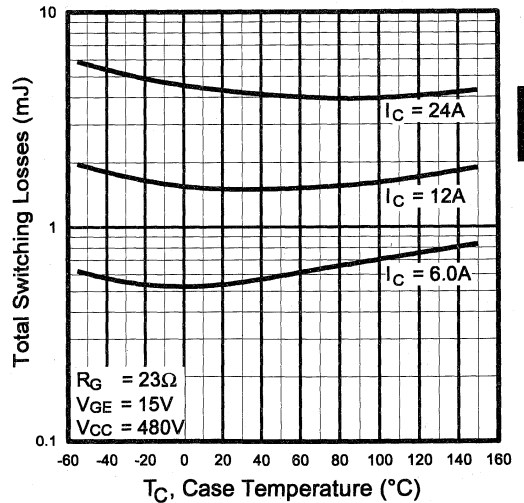


Fig. 10 - Typical Switching Losses vs. Case Temperature

Power
Conversion
Ultra-Fast
Co-Packs

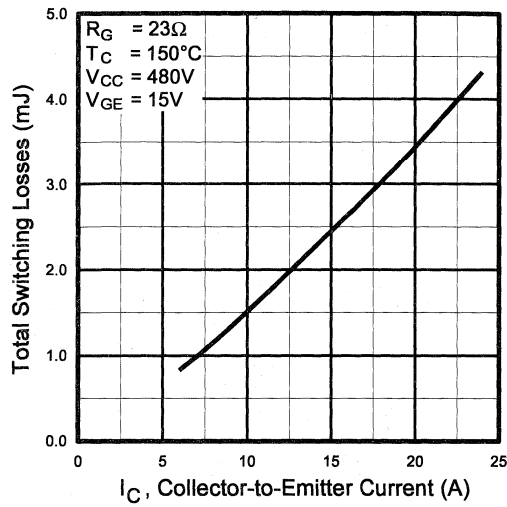


Fig. 11 - Typical Switching Losses vs. Collector-to-Emitter Current

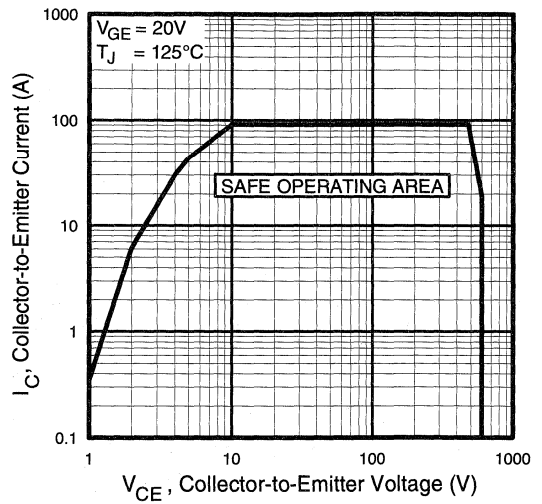


Fig. 12 - Turn-Off SOA

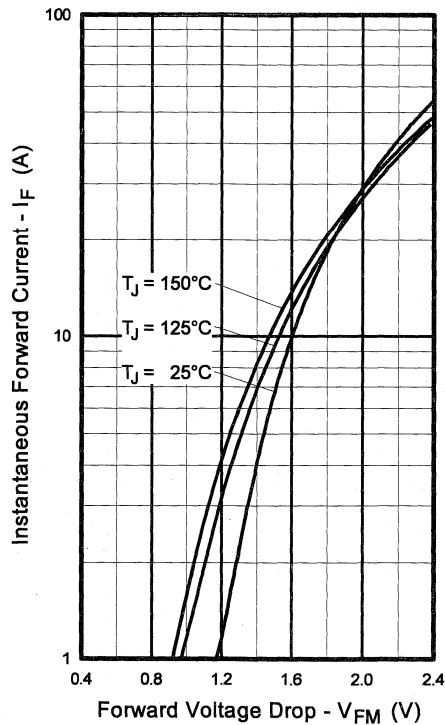


Fig. 13 - Maximum Forward Voltage Drop vs. Instantaneous Forward Current

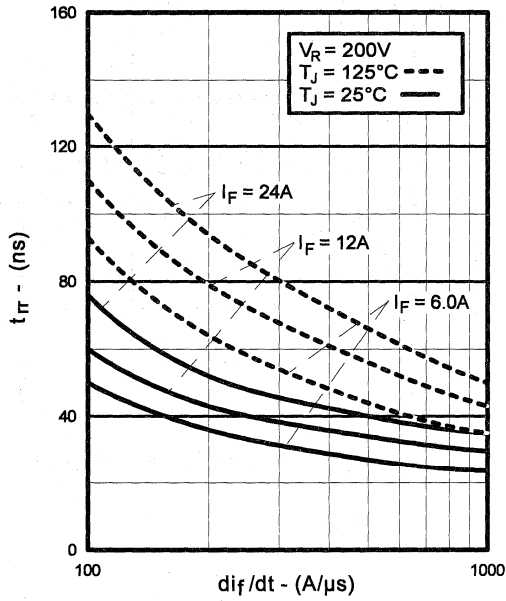


Fig. 14 - Typical Reverse Recovery vs. di_f/dt

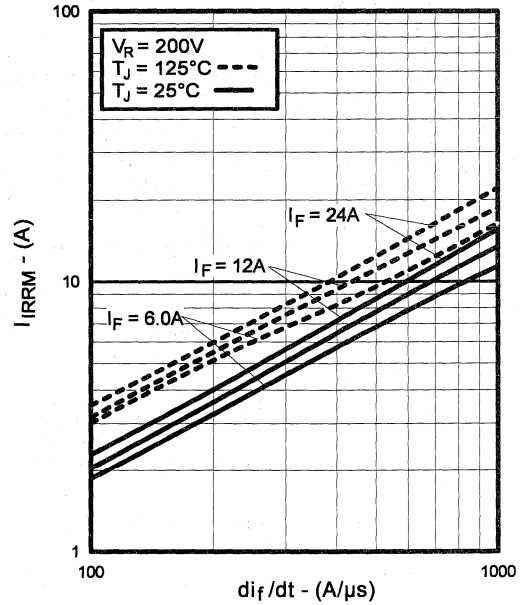


Fig. 15 - Typical Recovery Current vs. di_f/dt

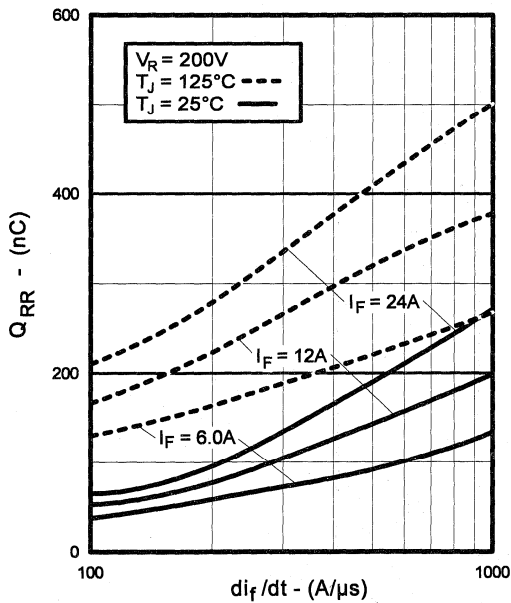


Fig. 16 - Typical Stored Charge vs. di_f/dt

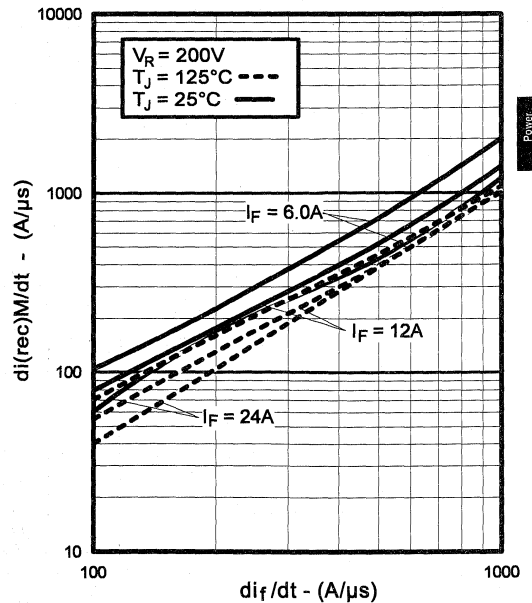


Fig. 17 - Typical $di_{(rec)}M/dt$ vs. di_f/dt

Power
Conversion
Ultra-Fast
Co-Packs

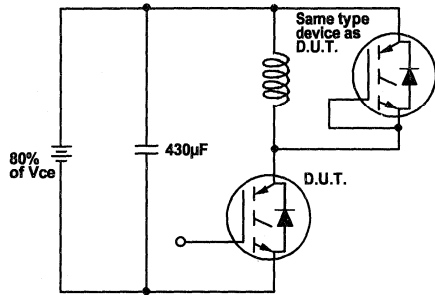


Fig. 18a - Test Circuit for Measurement of I_{LM} , E_{on} , $E_{off}(\text{diode})$, t_{rr} , Q_{rr} , I_{rr} , $t_{d(on)}$, t_r , $t_{d(off)}$, t_f

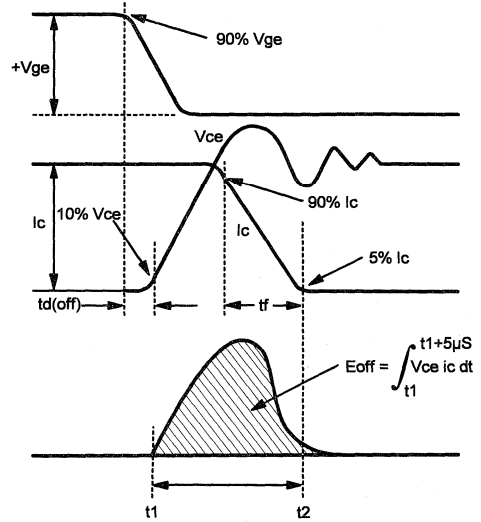


Fig. 18b - Test Waveforms for Circuit of Fig. 18a, Defining E_{off} , $t_{d(off)}$, t_f

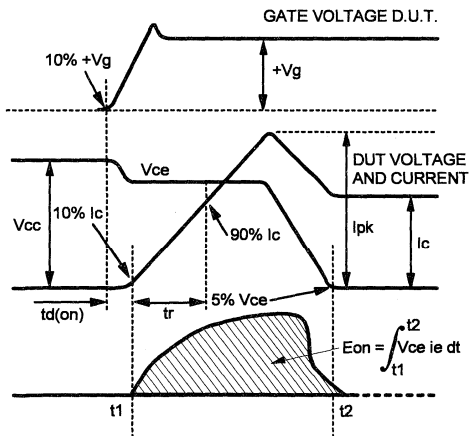


Fig. 18c - Test Waveforms for Circuit of Fig. 18a, Defining E_{on} , $t_{d(on)}$, t_r

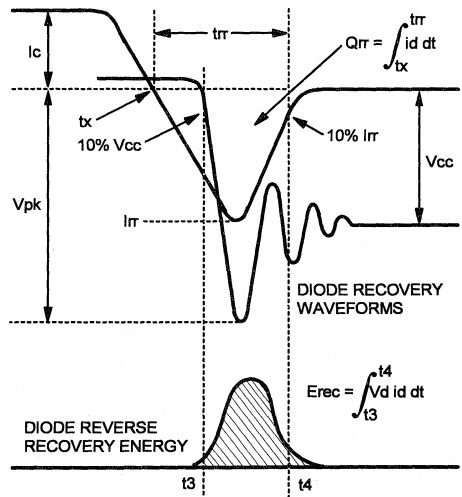


Fig. 18d - Test Waveforms for Circuit of Fig. 18a, Defining E_{rec} , t_{rr} , Q_{rr} , I_{rr}

Refer to Section D for the following:
Appendix D: Section D - page D-6

Fig. 18e - Macro Waveforms for Test Circuit Fig. 18a

Fig. 19 - Clamped Inductive Load Test Circuit

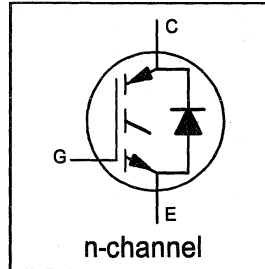
Fig. 20 - Pulsed Collector Current Test Circuit

INSULATED GATE BIPOLAR TRANSISTOR
WITH ULTRAFAST SOFT RECOVERY DIODE

UltraFast CoPack IGBT

Features

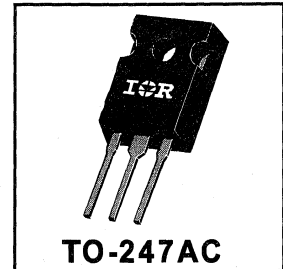
- Switching-loss rating includes all "tail" losses
- HEXFRED™ soft ultrafast diodes
- Optimized for high operating frequency (over 5kHz)
See Fig. 1 for Current vs. Frequency curve



$V_{CES} = 600V$
 $V_{CE(sat)} \leq 3.0V$
@ $V_{GE} = 15V, I_C = 12A$

Description

Co-packaged IGBTs are a natural extension of International Rectifier's well known IGBT line. They provide the convenience of an IGBT and an ultrafast recovery diode in one package, resulting in substantial benefits to a host of high-voltage, high-current, motor control, UPS and power supply applications.



Absolute Maximum Ratings

	Parameter	Max.	Units
V_{CES}	Collector-to-Emitter Voltage	600	V
$I_C @ T_C = 25^\circ C$	Continuous Collector Current	23	A
$I_C @ T_C = 100^\circ C$	Continuous Collector Current	12	
I_{CM}	Pulsed Collector Current $\text{\textcircled{1}}$	92	
I_{LM}	Clamped Inductive Load Current $\text{\textcircled{2}}$	92	
$I_F @ T_C = 100^\circ C$	Diode Continuous Forward Current	12	
I_{FM}	Diode Maximum Forward Current	92	
V_{GE}	Gate-to-Emitter Voltage	± 20	V
$P_D @ T_C = 25^\circ C$	Maximum Power Dissipation	100	W
$P_D @ T_C = 100^\circ C$	Maximum Power Dissipation	42	
T_J	Operating Junction and	-55 to +150	$^\circ C$
T_{STG}	Storage Temperature Range		
	Soldering Temperature, for 10 sec.		
	Mounting Torque, 6-32 or M3 Screw.	10 lbf·in (1.1 N·m)	

Thermal Resistance

	Parameter	Min.	Typ.	Max.	Units
$R_{\theta JC}$	Junction-to-Case - IGBT	—	—	1.2	$^\circ C/W$
$R_{\theta JC}$	Junction-to-Case - Diode	—	—	2.5	
$R_{\theta CS}$	Case-to-Sink, flat, greased surface	—	0.24	—	
$R_{\theta JA}$	Junction-to-Ambient, typical socket mount	—	—	40	
Wt	Weight	—	6 (0.21)	—	g (oz)

Electrical Characteristics @ $T_J = 25^\circ\text{C}$ (unless otherwise specified)

	Parameter	Min.	Typ.	Max.	Units	Conditions
$V_{(BR)CES}$	Collector-to-Emitter Breakdown Voltage ^①	600	—	—	V	$V_{GE} = 0V, I_C = 250\mu A$
$\Delta V_{(BR)CES}/\Delta T_J$	Temp. Coeff. of Breakdown Voltage	—	0.63	—	V/ $^\circ\text{C}$	$V_{GE} = 0V, I_C = 1.0mA$
$V_{CE(on)}$	Collector-to-Emitter Saturation Voltage	—	2.2	3.0	V	$I_C = 12A$ $V_{GE} = 15V$
		—	2.7	—		$I_C = 23A$ See Fig. 2, 5
		—	2.4	—		$I_C = 12A, T_J = 150^\circ\text{C}$
$V_{GE(th)}$	Gate Threshold Voltage	3.0	—	5.5		$V_{CE} = V_{GE}, I_C = 250\mu A$
$\Delta V_{GE(th)}/\Delta T_J$	Temp. Coeff. of Threshold Voltage	—	-11	—	mV/ $^\circ\text{C}$	$V_{CE} = V_{GE}, I_C = 250\mu A$
g_{fe}	Forward Transconductance ^②	3.1	8.6	—	S	$V_{CE} = 100V, I_C = 12A$
I_{CES}	Zero Gate Voltage Collector Current	—	—	250	μA	$V_{GE} = 0V, V_{CE} = 600V$
		—	—	2500		$V_{GE} = 0V, V_{CE} = 600V, T_J = 150^\circ\text{C}$
V_{FM}	Diode Forward Voltage Drop	—	1.4	1.7	V	$I_C = 12A$ See Fig. 13
		—	1.3	1.6		$I_C = 12A, T_J = 150^\circ\text{C}$
I_{GES}	Gate-to-Emitter Leakage Current	—	—	± 100	nA	$V_{GE} = \pm 20V$

Switching Characteristics @ $T_J = 25^\circ\text{C}$ (unless otherwise specified)

	Parameter	Min.	Typ.	Max.	Units	Conditions
Q_g	Total Gate Charge (turn-on)	—	29	36	nC	$I_C = 12A$
Q_{ge}	Gate - Emitter Charge (turn-on)	—	4.8	6.8		$V_{CC} = 400V$
Q_{gc}	Gate - Collector Charge (turn-on)	—	12	17		See Fig. 8
$t_{d(on)}$	Turn-On Delay Time	—	67	—	ns	$T_J = 25^\circ\text{C}$
t_r	Rise Time	—	56	—		$I_C = 12A, V_{CC} = 480V$
$t_{d(off)}$	Turn-Off Delay Time	—	170	250		$V_{GE} = 15V, R_G = 23\Omega$
t_f	Fall Time	—	140	270		Energy losses include "tail" and diode reverse recovery.
E_{on}	Turn-On Switching Loss	—	0.70	—		See Fig. 9, 10, 11, 18
E_{off}	Turn-Off Switching Loss	—	0.80	—	mJ	
E_{ts}	Total Switching Loss	—	1.5	2.5		
$t_{d(on)}$	Turn-On Delay Time	—	61	—	ns	$T_J = 150^\circ\text{C}$, See Fig. 9, 10, 11, 18
t_r	Rise Time	—	51	—		$I_C = 12A, V_{CC} = 480V$
$t_{d(off)}$	Turn-Off Delay Time	—	190	—		$V_{GE} = 15V, R_G = 23\Omega$
t_f	Fall Time	—	190	—		Energy losses include "tail" and diode reverse recovery.
E_{ts}	Total Switching Loss	—	1.9	—		mJ
L_E	Internal Emitter Inductance	—	13	—	nH	Measured 5mm from package
C_{ies}	Input Capacitance	—	680	—	pF	$V_{GE} = 0V$
C_{oes}	Output Capacitance	—	110	—		$V_{CC} = 30V$ See Fig. 7
C_{res}	Reverse Transfer Capacitance	—	11	—		$f = 1.0MHz$
t_{rr}	Diode Reverse Recovery Time	—	42	60	ns	$T_J = 25^\circ\text{C}$ See Fig.
		—	80	120		$T_J = 125^\circ\text{C}$ 14
I_{rr}	Diode Peak Reverse Recovery Current	—	3.5	6.0	A	$T_J = 25^\circ\text{C}$ See Fig.
		—	5.6	10		$T_J = 125^\circ\text{C}$ 15
Q_{rr}	Diode Reverse Recovery Charge	—	80	180	nC	$T_J = 25^\circ\text{C}$ See Fig.
		—	220	600		$T_J = 125^\circ\text{C}$ 16
$di_{(rec)M}/dt$	Diode Peak Rate of Fall of Recovery During t_b	—	180	—	A/ μs	$T_J = 25^\circ\text{C}$ See Fig.
		—	120	—		$T_J = 125^\circ\text{C}$ 17

Notes:

① Repetitive rating; $V_{GE}=20V$, pulse width limited by max. junction temperature. (See fig. 20)

② $V_{CC}=80\%(V_{CES}), V_{GE}=20V, L=10\mu H, R_G=23\Omega$, (See fig. 19)

③ Pulse width 5.0 μs , single shot.

④ Pulse width $\leq 80\mu s$; duty factor $\leq 0.1\%$.

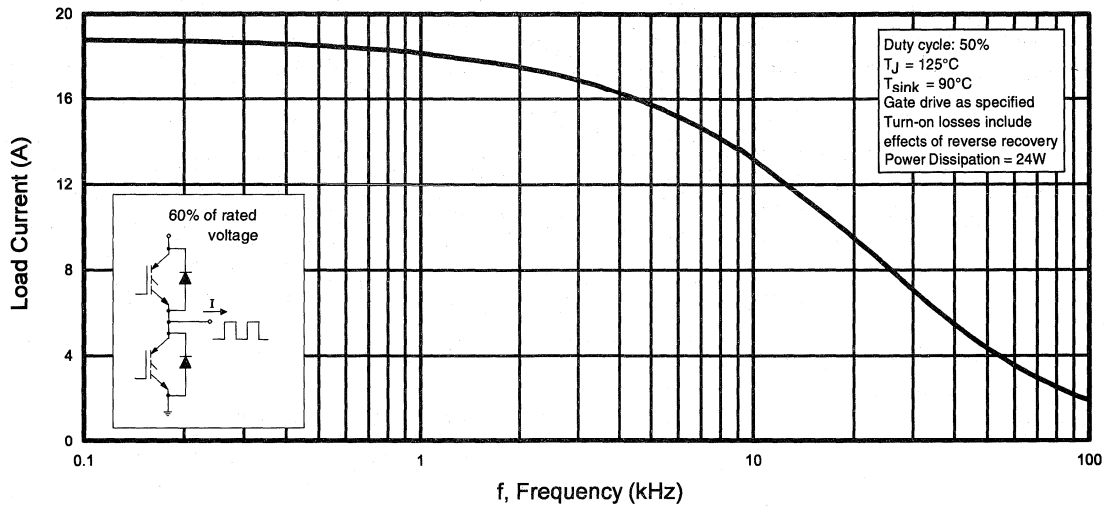


Fig. 1 - Typical Load Current vs. Frequency
(Load Current = I_{RMS} of fundamental)

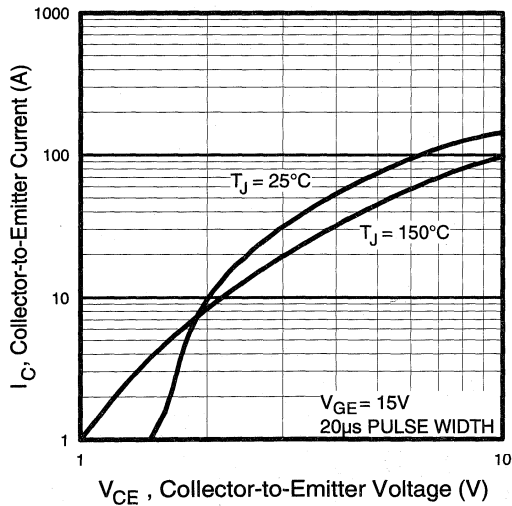


Fig. 2 - Typical Output Characteristics

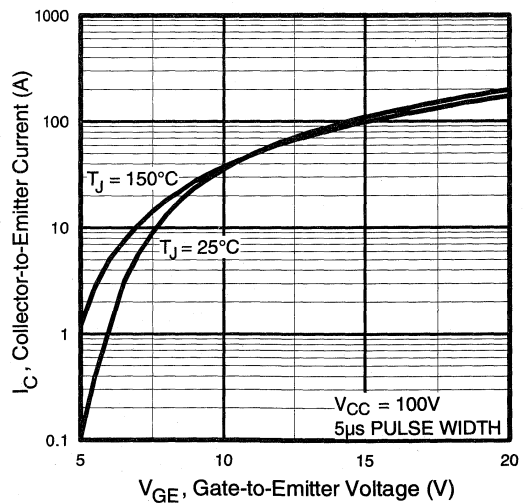


Fig. 3 - Typical Transfer Characteristics

Power
Conversion
Ultra-Fast
Co-Packs

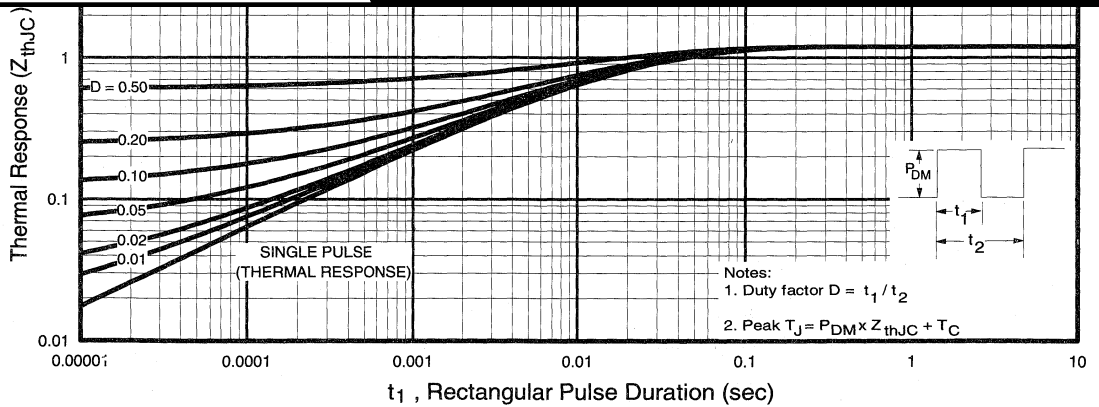
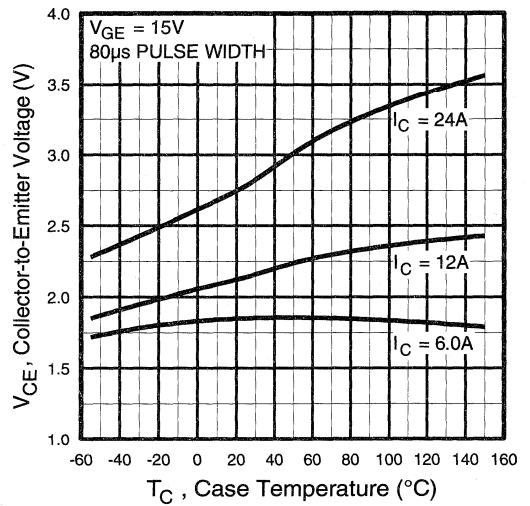
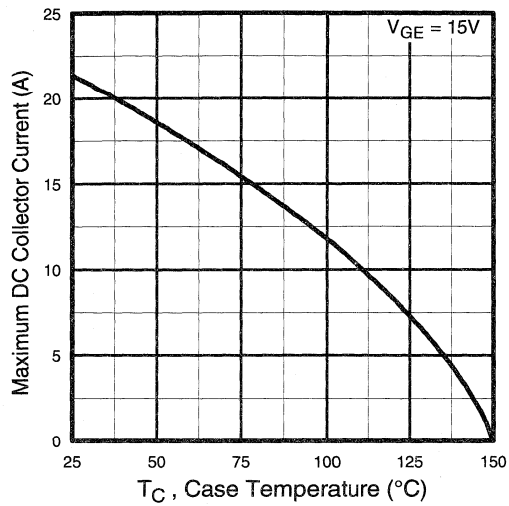


Fig. 6 - Maximum IGBT Effective Transient Thermal Impedance, Junction-to-Case

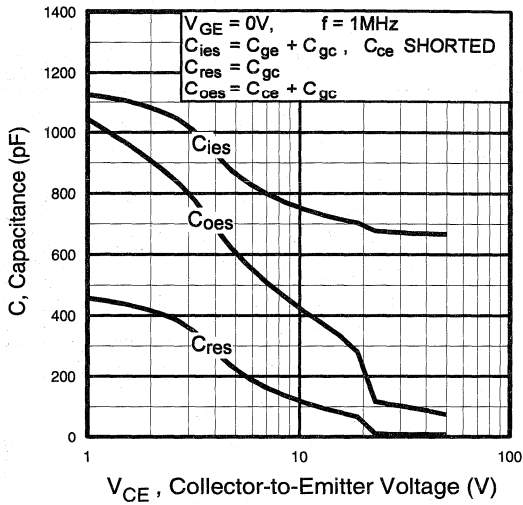


Fig. 7 - Typical Capacitance vs. Collector-to-Emitter Voltage

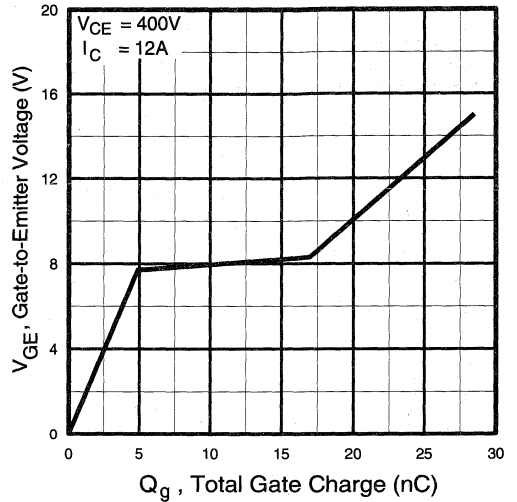


Fig. 8 - Typical Gate Charge vs. Gate-to-Emitter Voltage

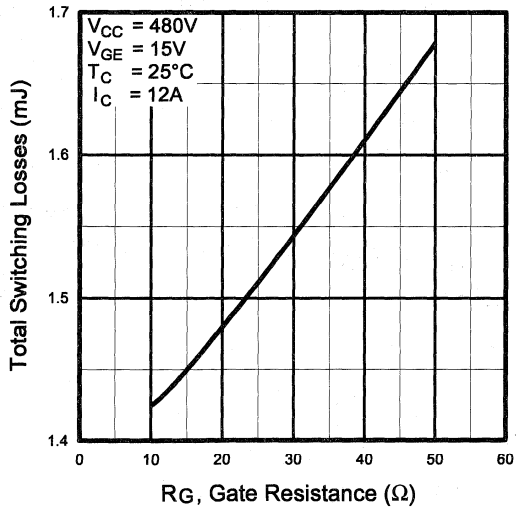


Fig. 9 - Typical Switching Losses vs. Gate Resistance

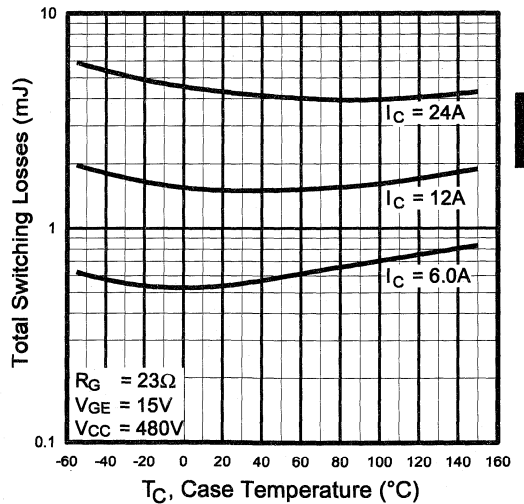


Fig. 10 - Typical Switching Losses vs. Case Temperature

Power Conversion
Ultra-Fast
Co-Packs

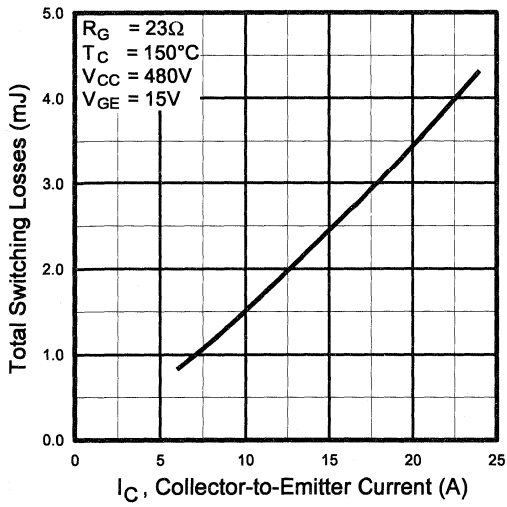


Fig. 11 - Typical Switching Losses vs. Collector-to-Emitter Current

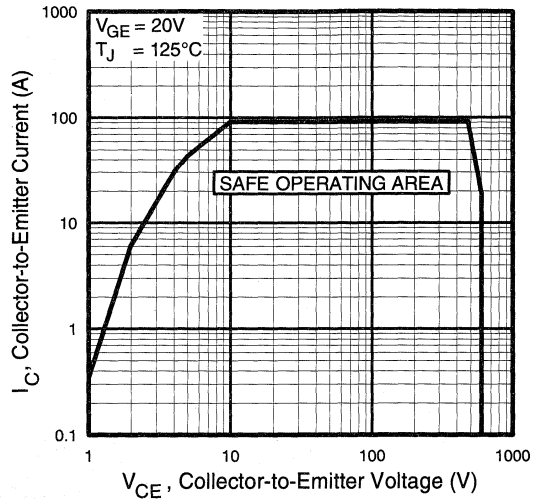


Fig. 12 - Turn-Off SOA

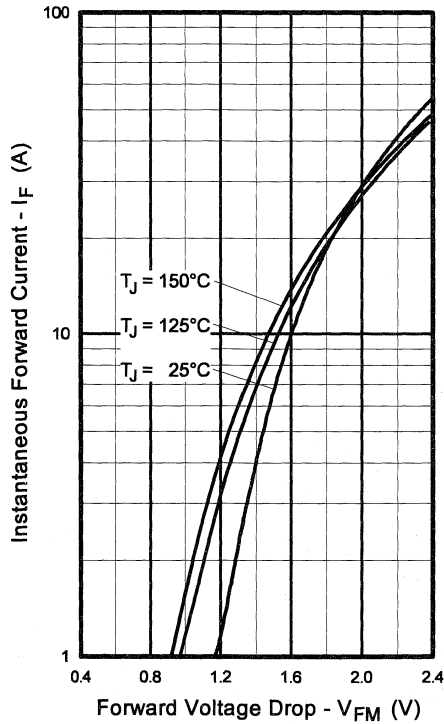


Fig. 13 - Maximum Forward Voltage Drop vs. Instantaneous Forward Current

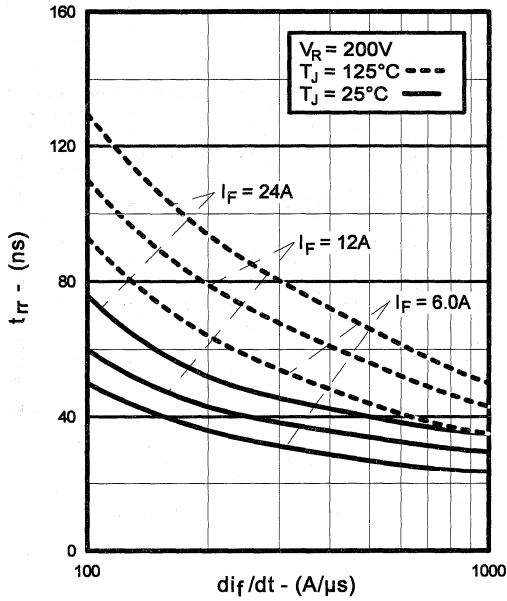


Fig. 14 - Typical Reverse Recovery vs. di_f/dt

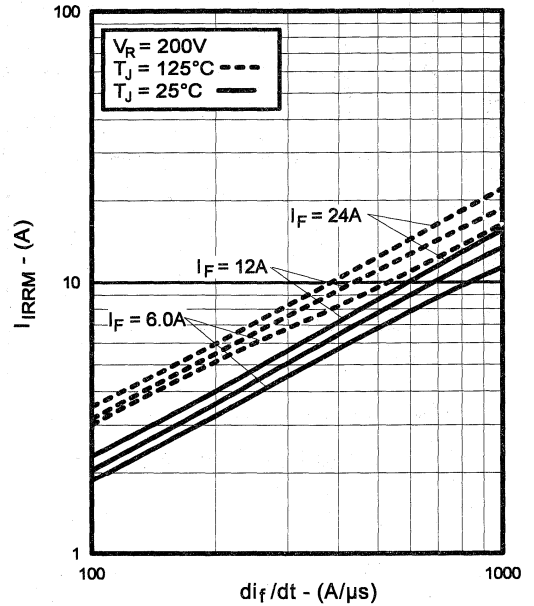


Fig. 15 - Typical Recovery Current vs. di_f/dt

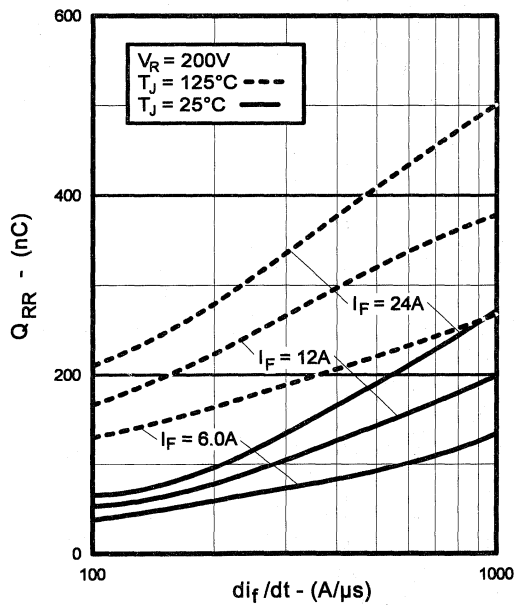


Fig. 16 - Typical Stored Charge vs. di_f/dt

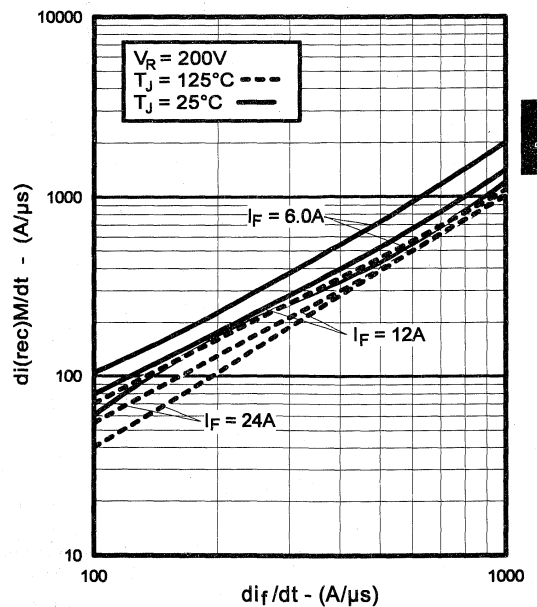


Fig. 17 - Typical $di_{(rec)}M/dt$ vs. di_f/dt

Power
 Conversion
 Ultra-Fast
 Co-Packs

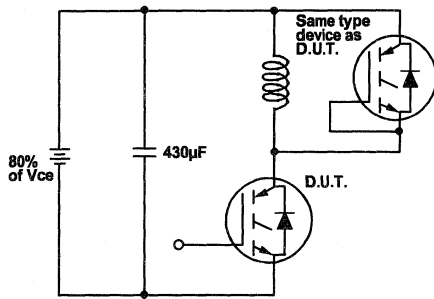


Fig. 18a - Test Circuit for Measurement of I_{LM} , E_{on} , $E_{off}(\text{diode})$, t_{rr} , Q_{rr} , I_{rr} , $t_{d(on)}$, t_r , $t_{d(off)}$, t_f

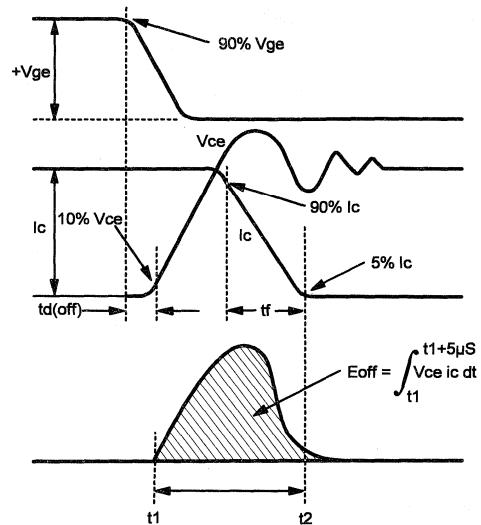


Fig. 18b - Test Waveforms for Circuit of Fig. 18a, Defining E_{off} , $t_{d(off)}$, t_f

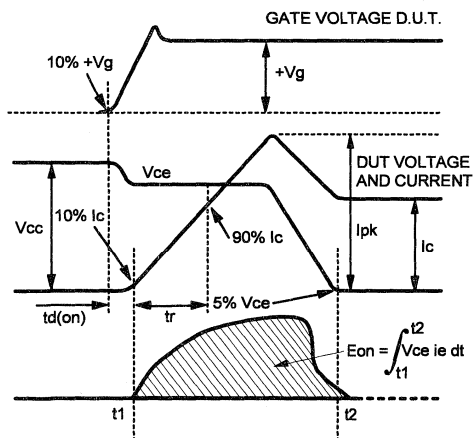


Fig. 18c - Test Waveforms for Circuit of Fig. 18a, Defining E_{on} , $t_{d(on)}$, t_r

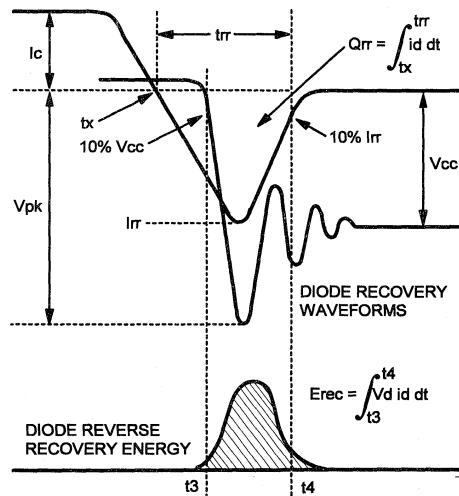


Fig. 18d - Test Waveforms for Circuit of Fig. 18a, Defining E_{rec} , t_{rr} , Q_{rr} , I_{rr}

Refer to Section D for the following:
Appendix D: Section D - page D-6

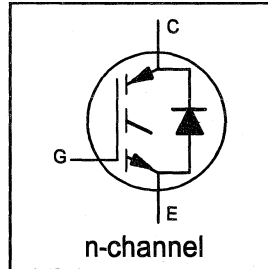
- Fig. 18e - Macro Waveforms for Test Circuit of Fig. 18a
- Fig. 19 - Clamped Inductive Load Test Circuit
- Fig. 20 - Pulsed Collector Current Test Circuit

INSULATED GATE BIPOLAR TRANSISTOR
WITH ULTRAFAST SOFT RECOVERY DIODE

UltraFast CoPack IGBT

Features

- Switching-loss rating includes all "tail" losses
- HEXFRED™ soft ultrafast diodes
- Optimized for high operating frequency (over 5kHz)
See Fig. 1 for Current vs. Frequency curve



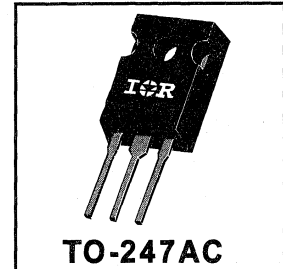
$$V_{CES} = 600V$$

$$V_{CE(sat)} \leq 3.0V$$

$$@V_{GE} = 15V, I_C = 20A$$

Description

Co-packaged IGBTs are a natural extension of International Rectifier's well known IGBT line. They provide the convenience of an IGBT and an ultrafast recovery diode in one package, resulting in substantial benefits to a host of high-voltage, high-current, motor control, UPS and power supply applications.



Absolute Maximum Ratings

	Parameter	Max.	Units
V_{CES}	Collector-to-Emitter Voltage	600	V
$I_C @ T_C = 25^\circ C$	Continuous Collector Current	40	A
$I_C @ T_C = 100^\circ C$	Continuous Collector Current	20	
I_{CM}	Pulsed Collector Current $\text{\textcircled{D}}$	160	
I_{LM}	Clamped Inductive Load Current $\text{\textcircled{D}}$	160	
$I_F @ T_C = 100^\circ C$	Diode Continuous Forward Current	15	
I_{FM}	Diode Maximum Forward Current	160	
V_{GE}	Gate-to-Emitter Voltage	± 20	V
$P_D @ T_C = 25^\circ C$	Maximum Power Dissipation	160	W
$P_D @ T_C = 100^\circ C$	Maximum Power Dissipation	65	
T_J	Operating Junction and	-55 to +150	$^\circ C$
T_{STG}	Storage Temperature Range		
	Soldering Temperature, for 10 sec.		
	Mounting Torque, 6-32 or M3 Screw.	10 lbf·in (1.1 N·m)	

Thermal Resistance

	Parameter	Min.	Typ.	Max.	Units
$R_{\theta JC}$	Junction-to-Case - IGBT	—	—	0.77	$^\circ C/W$
$R_{\theta JC}$	Junction-to-Case - Diode	—	—	1.7	
$R_{\theta CS}$	Case-to-Sink, flat, greased surface	—	0.24	—	
$R_{\theta JA}$	Junction-to-Ambient, typical socket mount	—	—	40	
Wt	Weight	—	6 (0.21)	—	g (oz)

Electrical Characteristics @ $T_J = 25^\circ\text{C}$ (unless otherwise specified)

	Parameter	Min.	Typ.	Max.	Units	Conditions
$V_{(BR)CES}$	Collector-to-Emitter Breakdown Voltage ^③	600	—	—	V	$V_{GE} = 0V, I_C = 250\mu A$
$\Delta V_{(BR)CES}/\Delta T_J$	Temp. Coeff. of Breakdown Voltage	—	0.63	—	V/ $^\circ\text{C}$	$V_{GE} = 0V, I_C = 1.0mA$
$V_{CE(on)}$	Collector-to-Emitter Saturation Voltage	—	2.2	3.0	V	$I_C = 20A$ $V_{GE} = 15V$ See Fig. 2, 5 $I_C = 40A$ $I_C = 20A, T_J = 150^\circ\text{C}$
		—	2.7	—		
		—	2.3	—		
$V_{GE(th)}$	Gate Threshold Voltage	3.0	—	5.5		$V_{CE} = V_{GE}, I_C = 250\mu A$
$\Delta V_{GE(th)}/\Delta T_J$	Temp. Coeff. of Threshold Voltage	—	-13	—	mV/ $^\circ\text{C}$	$V_{CE} = V_{GE}, I_C = 250\mu A$
g_{fe}	Forward Transconductance ^④	11	18	—	S	$V_{CE} = 100V, I_C = 20A$
I_{CES}	Zero Gate Voltage Collector Current	—	—	250	μA	$V_{GE} = 0V, V_{CE} = 600V$ $V_{GE} = 0V, V_{CE} = 600V, T_J = 150^\circ\text{C}$
		—	—	3500		
V_{FM}	Diode Forward Voltage Drop	—	1.3	1.7	V	$I_C = 15A$ See Fig. 13 $I_C = 15A, T_J = 150^\circ\text{C}$
		—	1.2	1.6		
I_{GES}	Gate-to-Emitter Leakage Current	—	—	± 100	nA	$V_{GE} = \pm 20V$

Switching Characteristics @ $T_J = 25^\circ\text{C}$ (unless otherwise specified)

	Parameter	Min.	Typ.	Max.	Units	Conditions
Q_g	Total Gate Charge (turn-on)	—	51	67	nC	$I_C = 20A$ $V_{CC} = 400V$ See Fig. 8
Q_{ge}	Gate - Emitter Charge (turn-on)	—	8.9	11		
Q_{gc}	Gate - Collector Charge (turn-on)	—	20	33		
$t_{d(on)}$	Turn-On Delay Time	—	63	—	ns	$T_J = 25^\circ\text{C}$ $I_C = 20A, V_{CC} = 480V$ $V_{GE} = 15V, R_G = 10\Omega$ Energy losses include "tail" and diode reverse recovery. See Fig. 9, 10, 11, 18
t_r	Rise Time	—	54	—		
$t_{d(off)}$	Turn-Off Delay Time	—	160	240		
t_f	Fall Time	—	120	200	mJ	$T_J = 150^\circ\text{C}$, See Fig. 9, 10, 11, 18 $I_C = 20A, V_{CC} = 480V$ $V_{GE} = 15V, R_G = 10\Omega$ Energy losses include "tail" and diode reverse recovery.
E_{on}	Turn-On Switching Loss	—	0.65	—		
E_{off}	Turn-Off Switching Loss	—	1.25	—		
E_{ts}	Total Switching Loss	—	1.90	3.0	mJ	$T_J = 150^\circ\text{C}$, See Fig. 9, 10, 11, 18 $I_C = 20A, V_{CC} = 480V$ $V_{GE} = 15V, R_G = 10\Omega$ Energy losses include "tail" and diode reverse recovery.
$t_{d(on)}$	Turn-On Delay Time	—	65	—		
t_r	Rise Time	—	53	—		
$t_{d(off)}$	Turn-Off Delay Time	—	280	—	ns	$T_J = 150^\circ\text{C}$, See Fig. 9, 10, 11, 18 $I_C = 20A, V_{CC} = 480V$ $V_{GE} = 15V, R_G = 10\Omega$ Energy losses include "tail" and diode reverse recovery.
t_f	Fall Time	—	210	—		
E_{ts}	Total Switching Loss	—	3.0	—		
L_E	Internal Emitter Inductance	—	13	—	nH	Measured 5mm from package
C_{ies}	Input Capacitance	—	1500	—	pF	$V_{GE} = 0V$ $V_{CC} = 30V$ See Fig. 7 $f = 1.0MHz$
C_{oes}	Output Capacitance	—	190	—		
C_{res}	Reverse Transfer Capacitance	—	17	—		
t_{rr}	Diode Reverse Recovery Time	—	42	60	ns	$T_J = 25^\circ\text{C}$ See Fig. 14 $T_J = 125^\circ\text{C}$ 14
		—	74	120		
I_{rr}	Diode Peak Reverse Recovery Current	—	4.0	6.0	A	$T_J = 25^\circ\text{C}$ See Fig. 15 $T_J = 125^\circ\text{C}$ 15
		—	6.5	10		
Q_{rr}	Diode Reverse Recovery Charge	—	80	180	nC	$T_J = 25^\circ\text{C}$ See Fig. 16 $T_J = 125^\circ\text{C}$ 16
		—	220	600		
$di_{(rec)M}/dt$	Diode Peak Rate of Fall of Recovery During t_b	—	188	—	A/ μs	$T_J = 25^\circ\text{C}$ See Fig. 17 $T_J = 125^\circ\text{C}$ 17
		—	160	—		

Notes:

- ① Repetitive rating; $V_{GE}=20V$, pulse width limited by max. junction temperature. (See fig. 20)
- ② $V_{CC}=80\%(V_{CES}), V_{GE}=20V, L=10\mu H, R_G=10\Omega$, (See fig. 19)
- ③ Pulse width $\leq 80\mu s$; duty factor $\leq 0.1\%$.
- ④ Pulse width 5.0 μs , single shot.

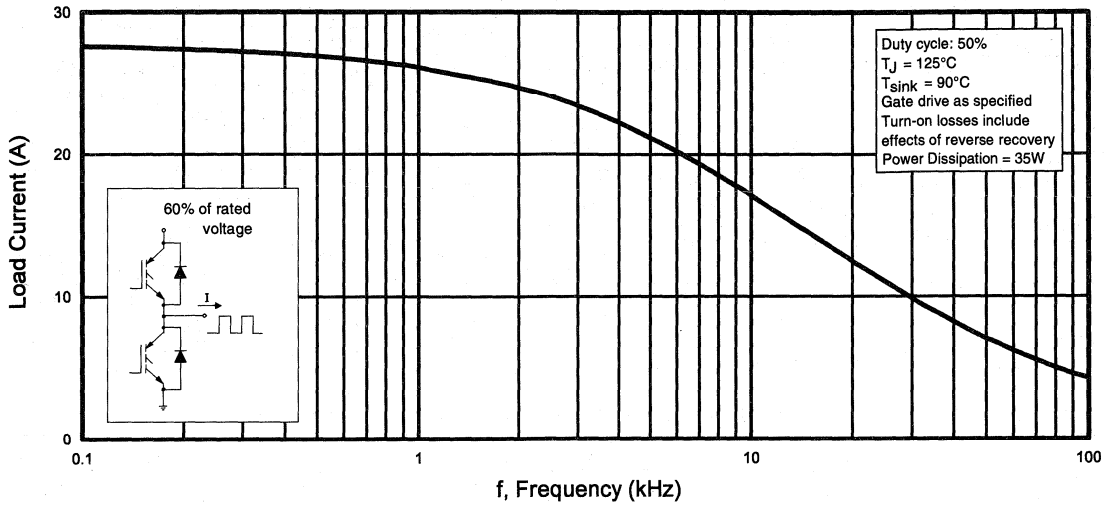


Fig. 1 - Typical Load Current vs. Frequency
(Load Current = I_{RMS} of fundamental)

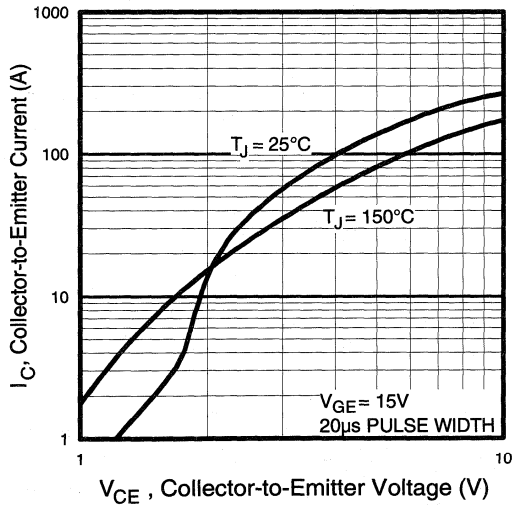


Fig. 2 - Typical Output Characteristics

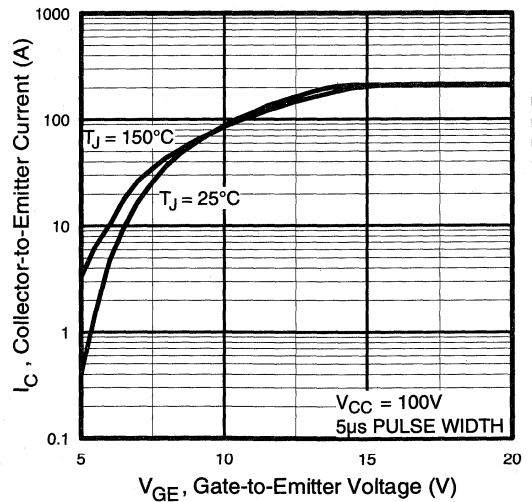


Fig. 3 - Typical Transfer Characteristics

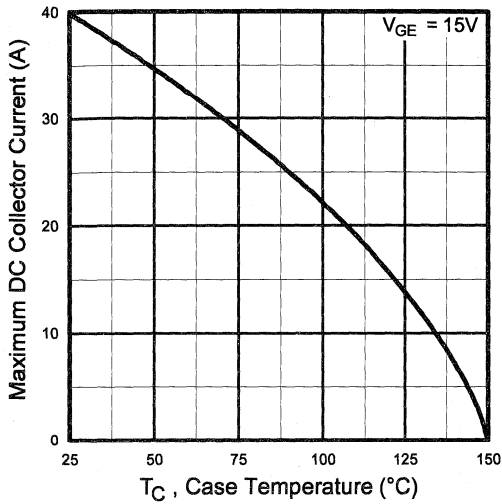


Fig. 4 - Maximum Collector Current vs. Case Temperature

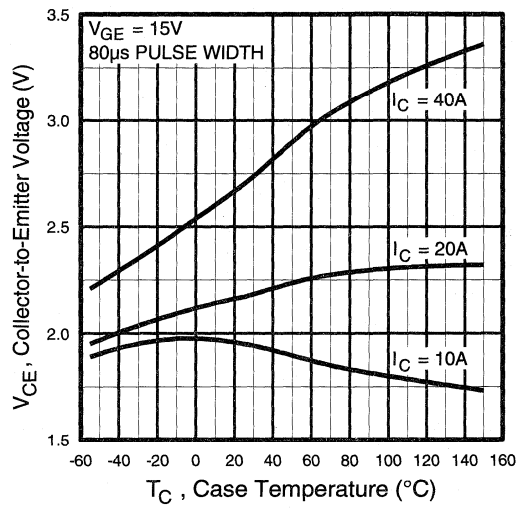


Fig. 5 - Collector-to-Emitter Voltage vs. Case Temperature

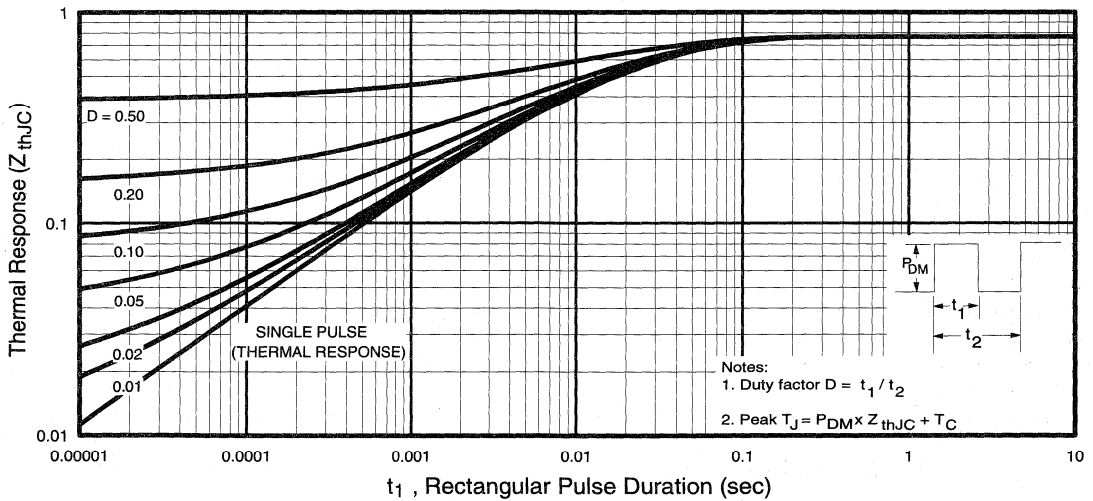


Fig. 6 - Maximum IGBT Effective Transient Thermal Impedance, Junction-to-Case

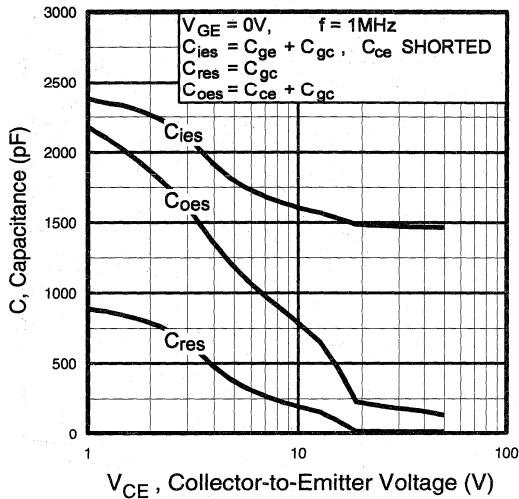


Fig. 7 - Typical Capacitance vs. Collector-to-Emitter Voltage

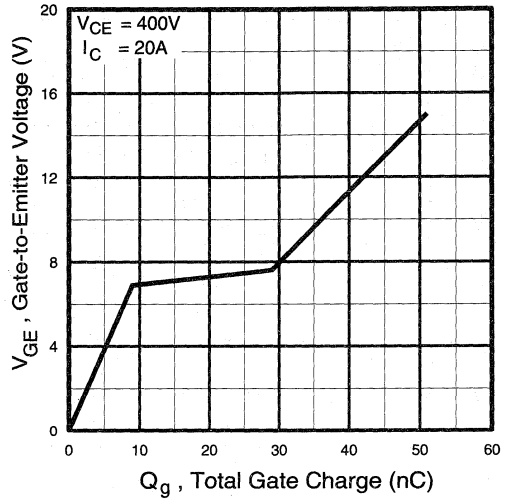


Fig. 8 - Typical Gate Charge vs. Gate-to-Emitter Voltage

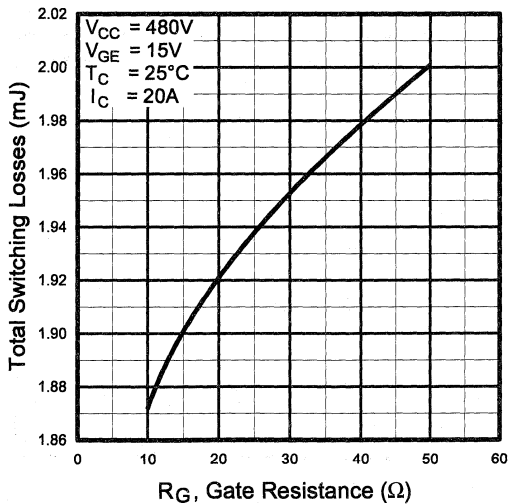


Fig. 9 - Typical Switching Losses vs. Gate Resistance

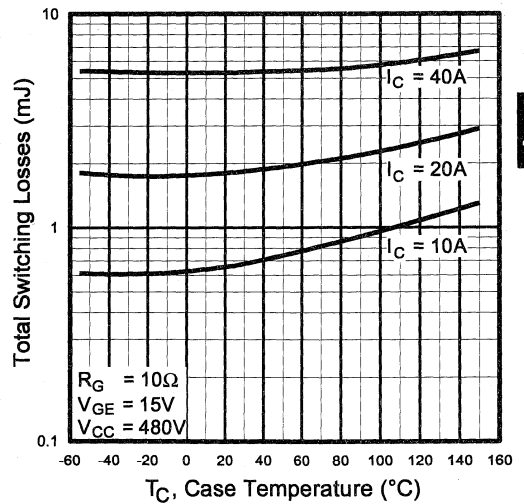


Fig. 10 - Typical Switching Losses vs. Case Temperature

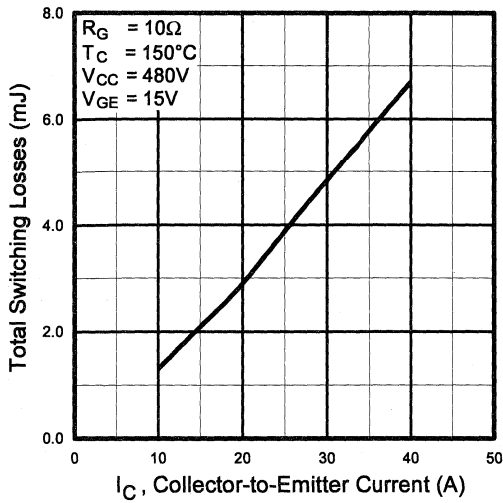


Fig. 11 - Typical Switching Losses vs. Collector-to-Emitter Current

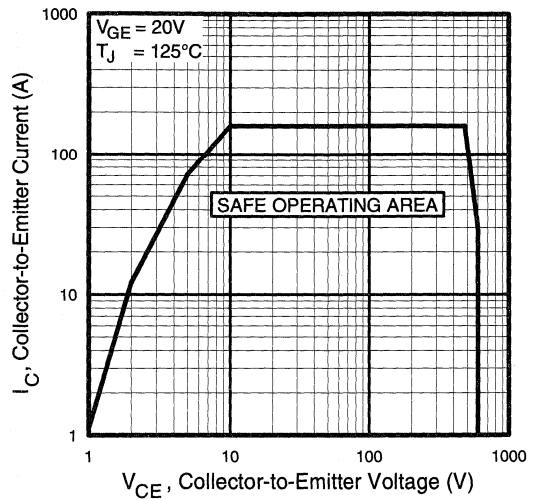


Fig. 12 - Turn-Off SOA

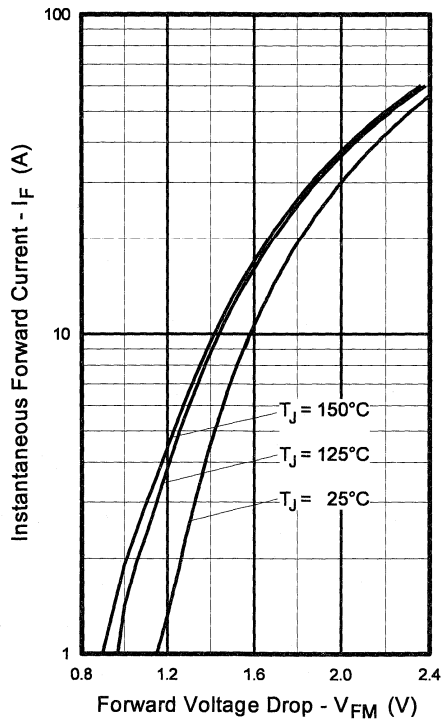


Fig. 13 - Maximum Forward Voltage Drop vs. Instantaneous Forward Current

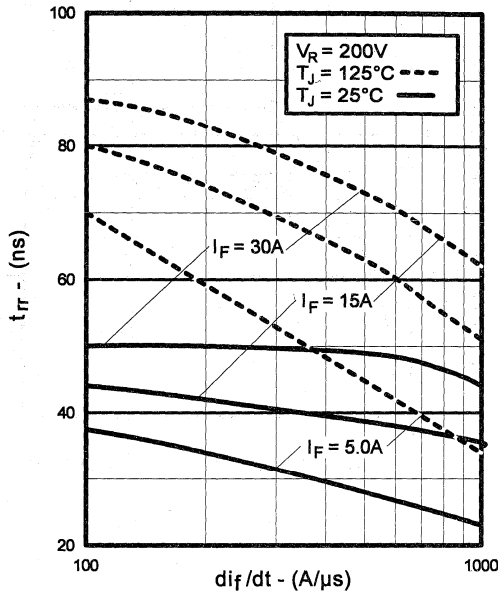


Fig. 14 - Typical Reverse Recovery vs. di_f/dt

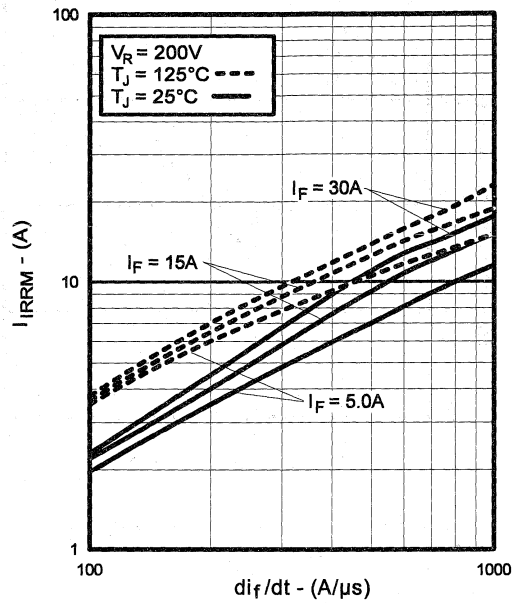


Fig. 15 - Typical Recovery Current vs. di_f/dt

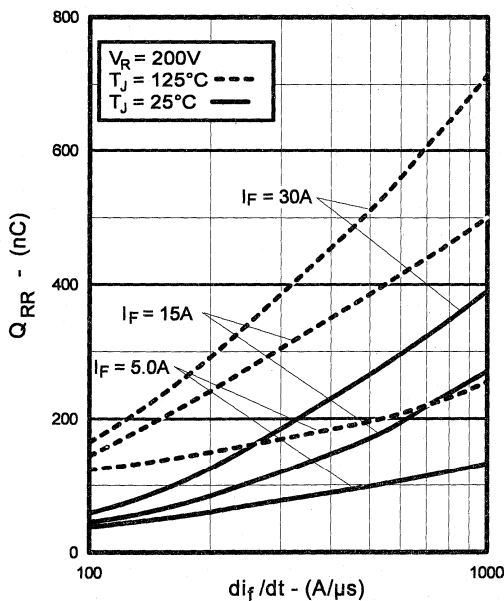


Fig. 16 - Typical Stored Charge vs. di_f/dt

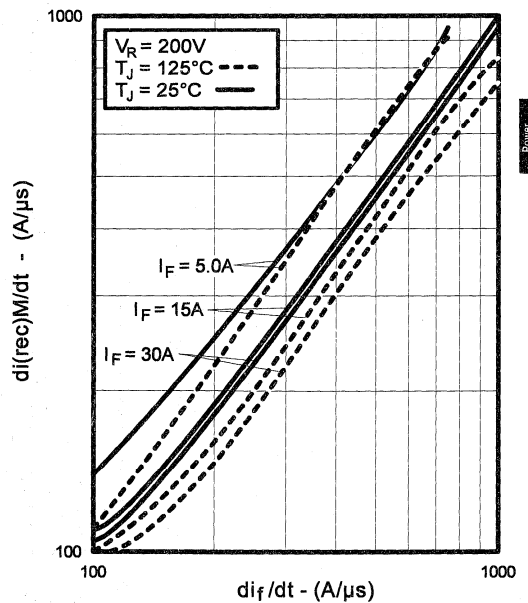


Fig. 17 - Typical $di_{(rec)M}/dt$ vs. di_f/dt

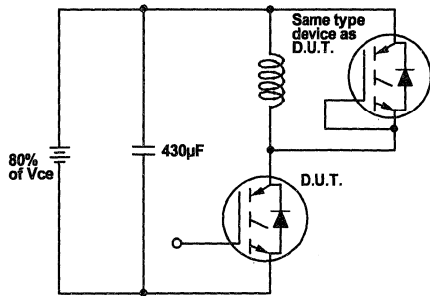


Fig. 18a - Test Circuit for Measurement of I_{LM} , E_{on} , $E_{off}(\text{diode})$, t_{rr} , Q_{rr} , I_{rr} , $t_{d(on)}$, t_r , $t_{d(off)}$, t_f

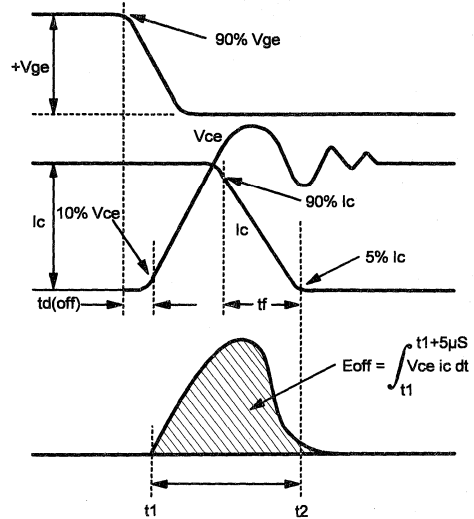


Fig. 18b - Test Waveforms for Circuit of Fig. 18a, Defining E_{off} , $t_{d(off)}$, t_f

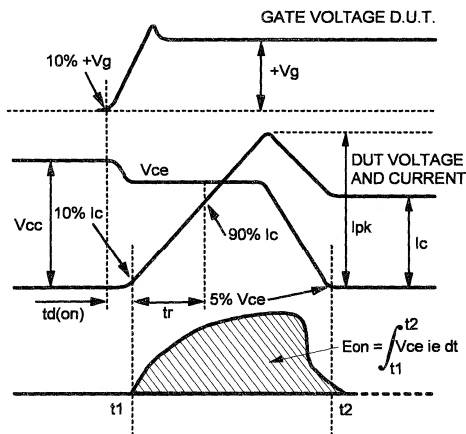


Fig. 18c - Test Waveforms for Circuit of Fig. 18a, Defining E_{on} , $t_{d(on)}$, t_r

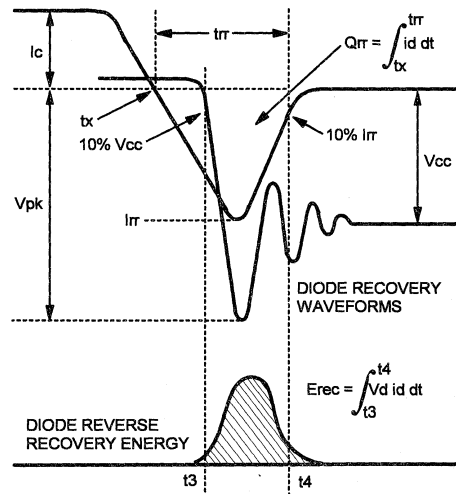


Fig. 18d - Test Waveforms for Circuit of Fig. 18a, Defining E_{rec} , t_{rr} , Q_{rr} , I_{rr}

Refer to Section D for the following:
Appendix D: Section D - page D-6

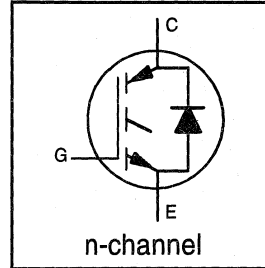
- Fig. 18e - Macro Waveforms for Test Circuit of Fig. 18a
- Fig. 19 - Clamped Inductive Load Test Circuit
- Fig. 20 - Pulsed Collector Current Test Circuit

INSULATED GATE BIPOLAR TRANSISTOR WITH ULTRAFAST SOFT RECOVERY

UltraFast CoPack IGBT

DIODE Features

- Switching-loss rating includes all "tail" losses
- HEXFRED™ soft ultrafast diodes
- Optimized for high operating frequency (over 5kHz)
See Fig. 1 for Current vs. Frequency curve



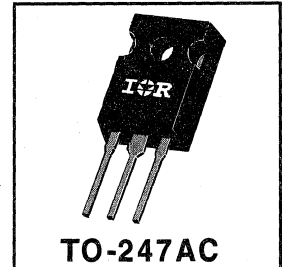
$$V_{CES} = 600V$$

$$V_{CE(sat)} \leq 3.0V$$

$$@ V_{GE} = 15V, I_C = 27A$$

Description

Co-packaged IGBTs are a natural extension of International Rectifier's well known IGBT line. They provide the convenience of an IGBT and an ultrafast recovery diode in one package, resulting in substantial benefits to a host of high-voltage, high-current, motor control, UPS and power supply applications.



Absolute Maximum Ratings

	Parameter	Max.	Units
V_{CES}	Collector-to-Emitter Voltage	600	V
$I_C @ T_C = 25^\circ C$	Continuous Collector Current	55	A
$I_C @ T_C = 100^\circ C$	Continuous Collector Current	27	
I_{CM}	Pulsed Collector Current \ominus	220	
I_{LM}	Clamped Inductive Load Current \ominus	220	
$I_F @ T_C = 100^\circ C$	Diode Continuous Forward Current	25	
I_{FM}	Diode Maximum Forward Current	220	
V_{GE}	Gate-to-Emitter Voltage	± 20	V
$P_D @ T_C = 25^\circ C$	Maximum Power Dissipation	200	W
$P_D @ T_C = 100^\circ C$	Maximum Power Dissipation	78	
T_J	Operating Junction and Storage Temperature Range	-55 to +150	$^\circ C$
T_{STG}	Soldering Temperature, for 10 sec.	300 (0.063 in. (1.6mm) from case)	
	Mounting Torque, 6-32 or M3 Screw.	10 lbf•in (1.1 N•m)	

Thermal Resistance

	Parameter	Min.	Typ.	Max.	Units
$R_{\theta JC}$	Junction-to-Case - IGBT	—	—	0.64	$^\circ C/W$
$R_{\theta JC}$	Junction-to-Case - Diode	—	—	0.83	
$R_{\theta CS}$	Case-to-Sink, flat, greased surface	—	0.24	—	
$R_{\theta JA}$	Junction-to-Ambient, typical socket mount	—	—	40	
Wt	Weight	—	6 (0.21)	—	g (oz)

Electrical Characteristics @ $T_J = 25^\circ\text{C}$ (unless otherwise specified)

	Parameter	Min.	Typ.	Max.	Units	Conditions
$V_{(BR)CES}$	Collector-to-Emitter Breakdown Voltage ^③	600	—	—	V	$V_{GE} = 0V, I_C = 250\mu A$
$\Delta V_{(BR)CES}/\Delta T_J$	Temp. Coeff. of Breakdown Voltage	—	0.60	—	V/ $^\circ\text{C}$	$V_{GE} = 0V, I_C = 1.0mA$
$V_{CE(on)}$	Collector-to-Emitter Saturation Voltage	—	1.9	3.0	V	$I_C = 27A$ $V_{GE} = 15V$
		—	2.4	—		$I_C = 55A$ See Fig. 2, 5
		—	1.9	—		$I_C = 27A, T_J = 150^\circ\text{C}$
$V_{GE(th)}$	Gate Threshold Voltage	3.0	—	5.5		$V_{CE} = V_{GE}, I_C = 250\mu A$
$\Delta V_{GE(th)}/\Delta T_J$	Temp. Coeff. of Threshold Voltage	—	-13	—	mV/ $^\circ\text{C}$	$V_{CE} = V_{GE}, I_C = 250\mu A$
g_{fe}	Forward Transconductance ^④	16	24	—	S	$V_{CE} = 100V, I_C = 27A$
I_{CES}	Zero Gate Voltage Collector Current	—	—	250	μA	$V_{GE} = 0V, V_{CE} = 600V$
		—	—	6500		$V_{GE} = 0V, V_{CE} = 600V, T_J = 150^\circ\text{C}$
V_{FM}	Diode Forward Voltage Drop	—	1.3	1.7	V	$I_C = 25A$ See Fig. 13
		—	1.2	1.5		$I_C = 25A, T_J = 150^\circ\text{C}$
I_{GES}	Gate-to-Emitter Leakage Current	—	—	± 100	nA	$V_{GE} = \pm 20V$

Switching Characteristics @ $T_J = 25^\circ\text{C}$ (unless otherwise specified)

	Parameter	Min.	Typ.	Max.	Units	Conditions
Q_g	Total Gate Charge (turn-on)	—	110	140	nC	$I_C = 27A$ $V_{CC} = 400V$ See Fig. 8
Q_{ge}	Gate - Emitter Charge (turn-on)	—	17	21		
Q_{gc}	Gate - Collector Charge (turn-on)	—	53	70		
$t_{d(on)}$	Turn-On Delay Time	—	73	—	ns	$T_J = 25^\circ\text{C}$ $I_C = 27A, V_{CC} = 480V$ $V_{GE} = 15V, R_G = 5.0\Omega$ Energy losses include "tail" and diode reverse recovery.
t_r	Rise Time	—	71	—		
$t_{d(off)}$	Turn-Off Delay Time	—	210	320		
t_f	Fall Time	—	150	280		
E_{on}	Turn-On Switching Loss	—	1.4	—	mJ	See Fig. 9, 10, 11, 18
E_{off}	Turn-Off Switching Loss	—	1.6	—		
E_{ts}	Total Switching Loss	—	3.0	4.5		
$t_{d(on)}$	Turn-On Delay Time	—	73	—	ns	$T_J = 150^\circ\text{C}$, See Fig. 9, 10, 11, 18 $I_C = 27A, V_{CC} = 480V$ $V_{GE} = 15V, R_G = 5.0\Omega$ Energy losses include "tail" and diode reverse recovery.
t_r	Rise Time	—	67	—		
$t_{d(off)}$	Turn-Off Delay Time	—	360	—		
t_f	Fall Time	—	230	—		
E_{ts}	Total Switching Loss	—	4.5	—	mJ	
L_E	Internal Emitter Inductance	—	13	—	nH	Measured 5mm from package
C_{ies}	Input Capacitance	—	2900	—	pF	$V_{GE} = 0V$ $V_{CC} = 30V$ See Fig. 7 $f = 1.0MHz$
C_{oes}	Output Capacitance	—	330	—		
C_{res}	Reverse Transfer Capacitance	—	40	—		
t_{rr}	Diode Reverse Recovery Time	—	50	75	ns	$T_J = 25^\circ\text{C}$ See Fig. 14 $T_J = 125^\circ\text{C}$ 14
		—	105	160		
I_{rr}	Diode Peak Reverse Recovery Current	—	4.5	10	A	$T_J = 25^\circ\text{C}$ See Fig. 15 $T_J = 125^\circ\text{C}$ 15
		—	8.0	15		
Q_{rr}	Diode Reverse Recovery Charge	—	112	375	nC	$T_J = 25^\circ\text{C}$ See Fig. 16 $T_J = 125^\circ\text{C}$ 16
		—	420	1200		
$di_{(rec)M}/dt$	Diode Peak Rate of Fall of Recovery During t_b	—	250	—	A/ μs	$T_J = 25^\circ\text{C}$ See Fig. 17 $T_J = 125^\circ\text{C}$ 17
		—	160	—		

Notes:

① Repetitive rating; $V_{GE}=20V$, pulse width limited by max. junction temperature. (See fig. 20)

② $V_{CC}=80\%(V_{CES}), V_{GE}=20V, L=10\mu H, R_G = 5.0\Omega,$ (See fig. 19)

③ Pulse width $\leq 80\mu s$; duty factor $\leq 0.1\%$.

④ Pulse width 5.0 μs , single shot.

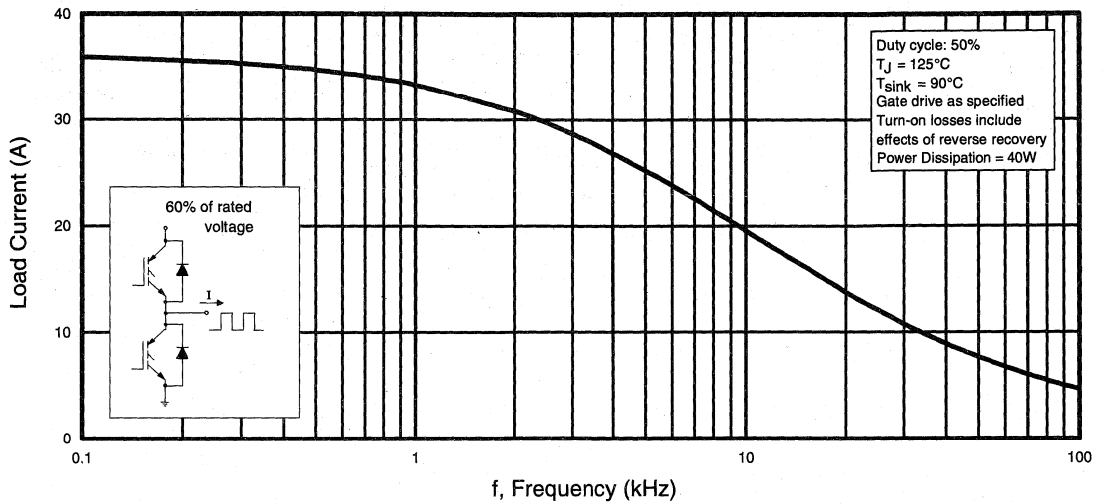


Fig. 1 - Typical Load Current vs. Frequency
(Load Current = I_{RMS} of fundamental)

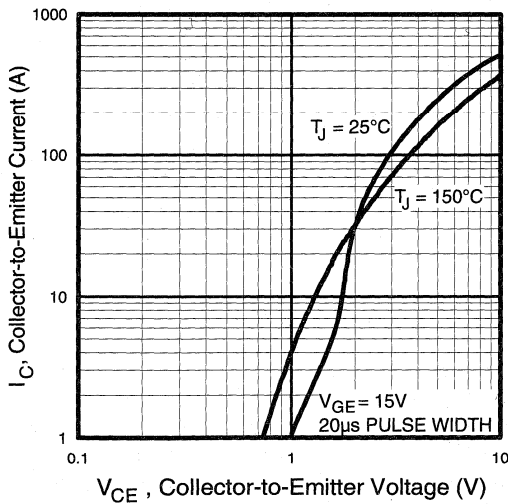


Fig. 2 - Typical Output Characteristics

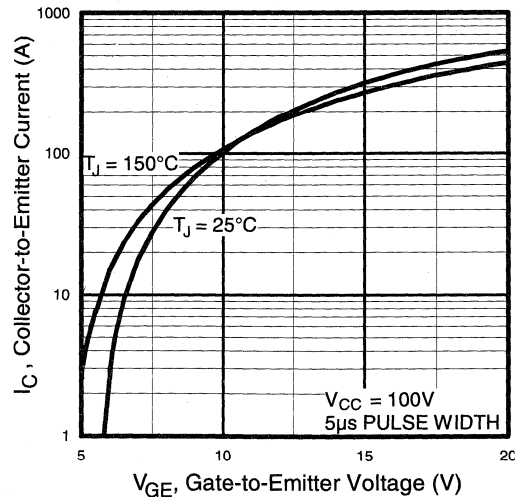


Fig. 3 - Typical Transfer Characteristics

Power Conversion Ultra-Fast Cool-Plots

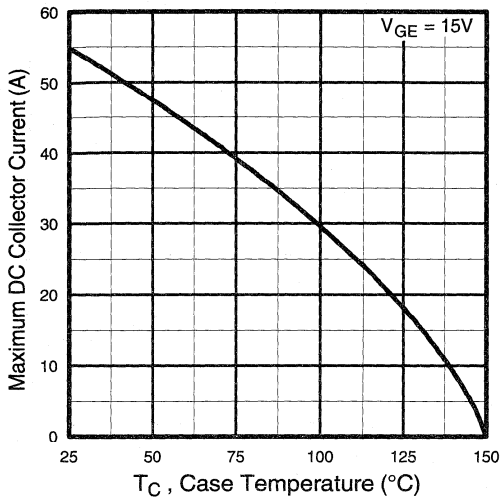


Fig. 4 - Maximum Collector Current vs. Case Temperature

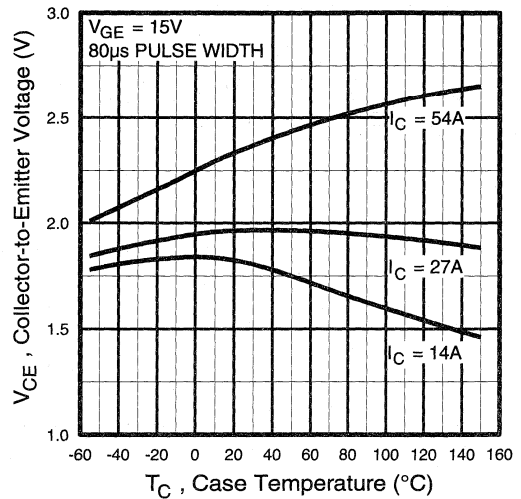


Fig. 5 - Collector-to-Emitter Voltage vs. Case Temperature

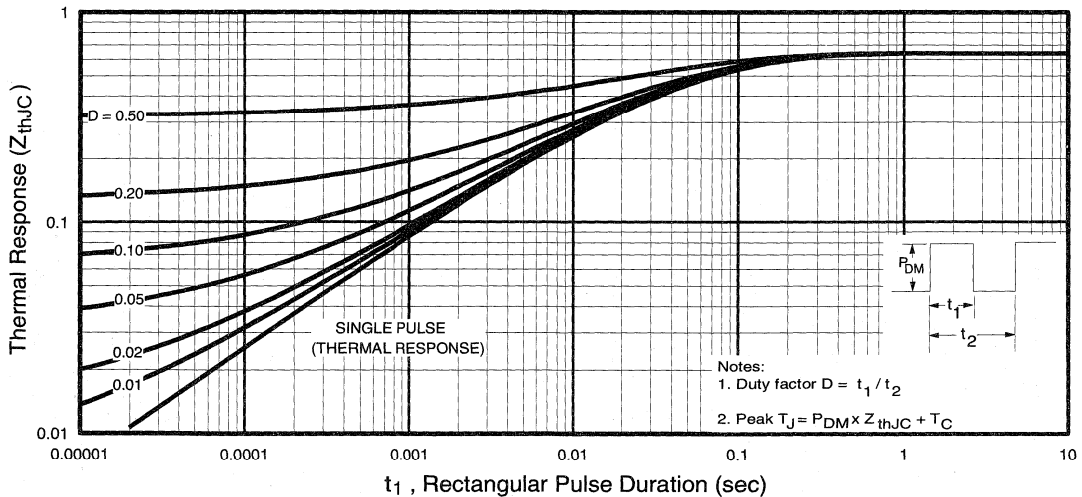


Fig. 6 - Maximum IGBT Effective Transient Thermal Impedance, Junction-to-Case

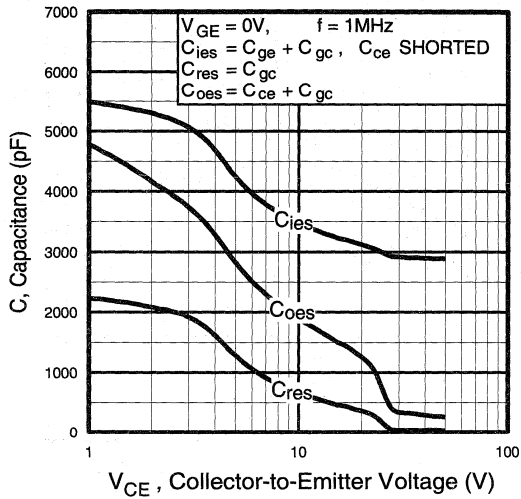


Fig. 7 - Typical Capacitance vs. Collector-to-Emitter Voltage

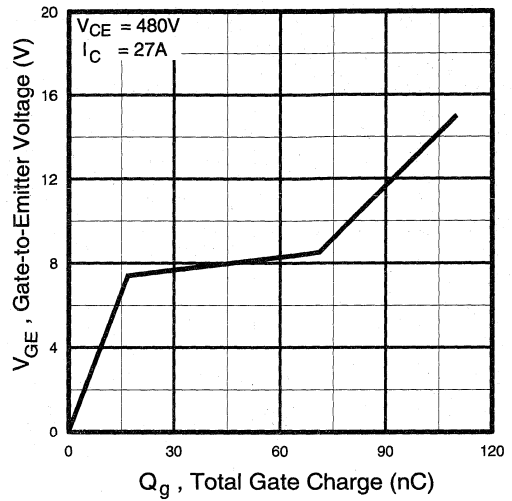


Fig. 8 - Typical Gate Charge vs. Gate-to-Emitter Voltage

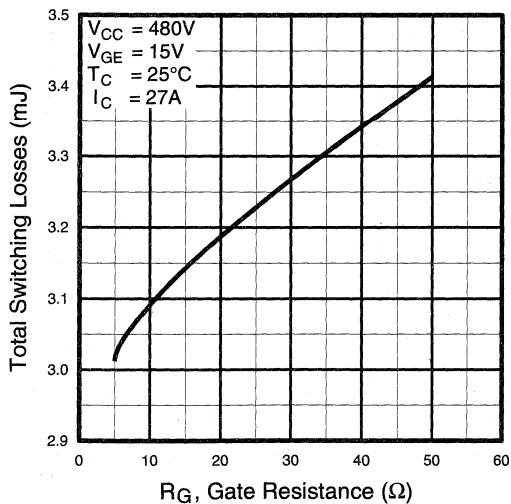


Fig. 9 - Typical Switching Losses vs. Gate Resistance

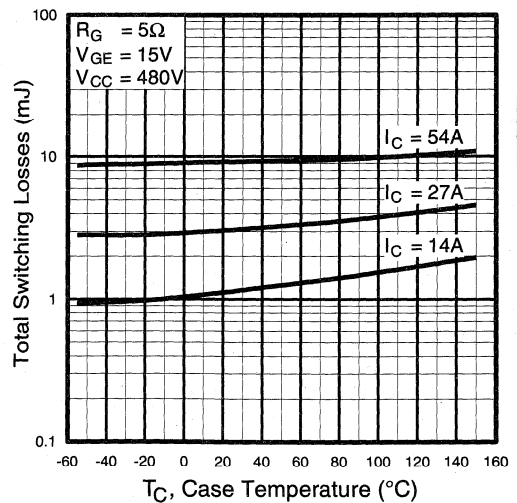


Fig. 10 - Typical Switching Losses vs. Case Temperature

Power Conversion
Ultra-Fast
Co-Packs

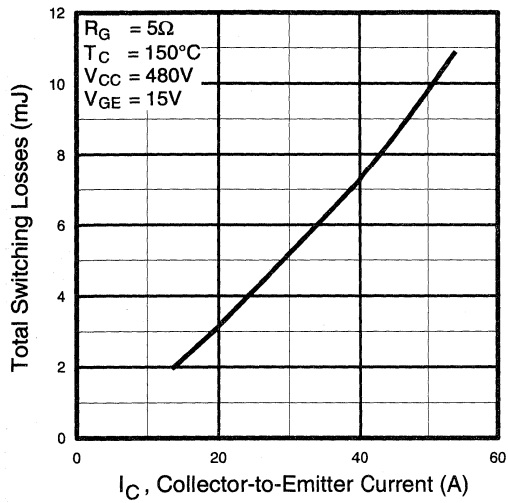


Fig. 11 - Typical Switching Losses vs. Collector-to-Emitter Current

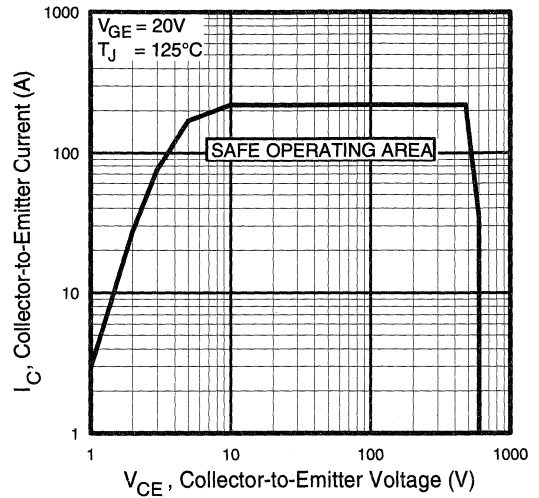


Fig. 12 - Turn-Off SOA

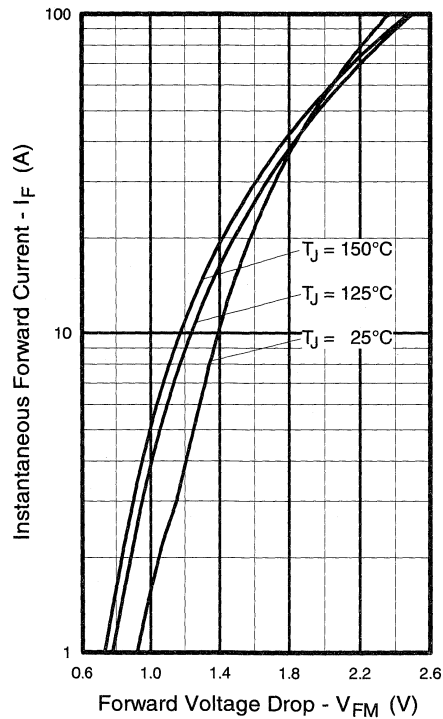


Fig. 13 - Maximum Forward Voltage Drop vs. Instantaneous Forward Current

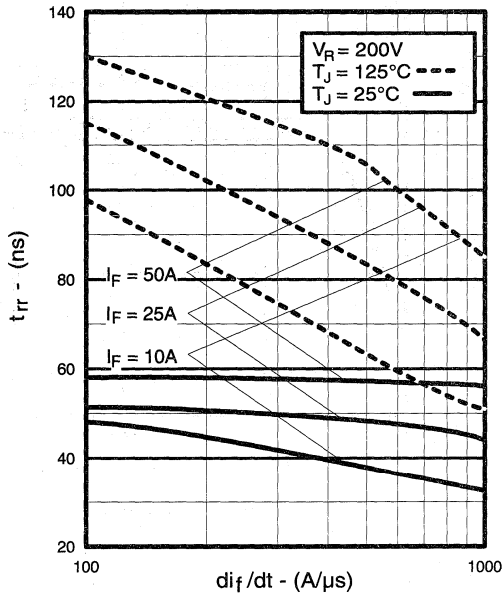


Fig. 14 - Typical Reverse Recovery vs. di_f/dt

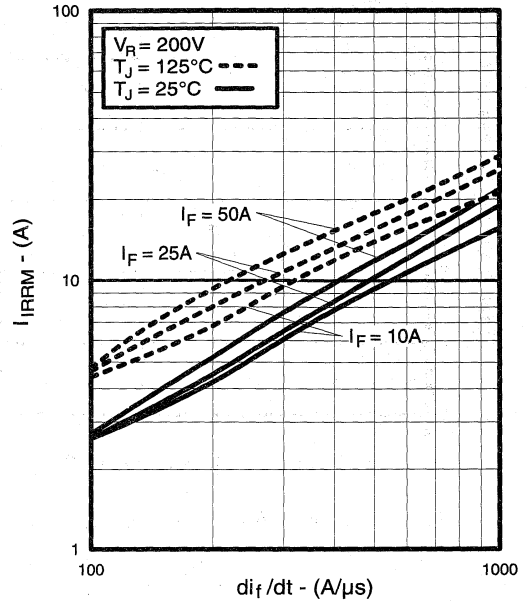


Fig. 15 - Typical Recovery Current vs. di_f/dt

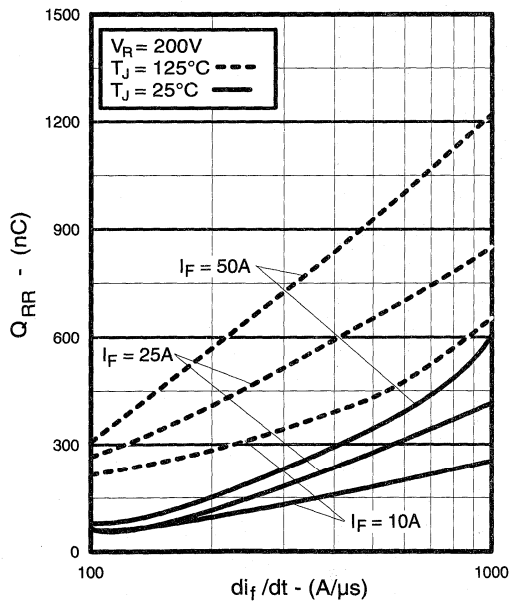


Fig. 16 - Typical Stored Charge vs. di_f/dt

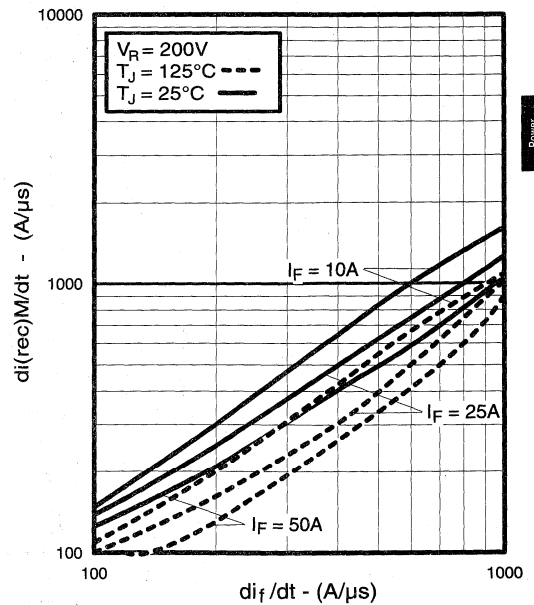


Fig. 17 - Typical $di_{(rec)M}/dt$ vs. di_f/dt

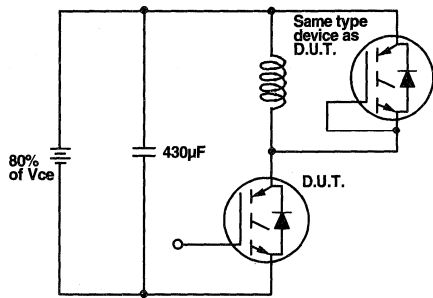


Fig. 18a - Test Circuit for Measurement of I_{LM} , E_{on} , $E_{off}(\text{diode})$, t_{rr} , Q_{rr} , I_{rr} , $t_{d(on)}$, t_r , $t_{d(off)}$, t_f

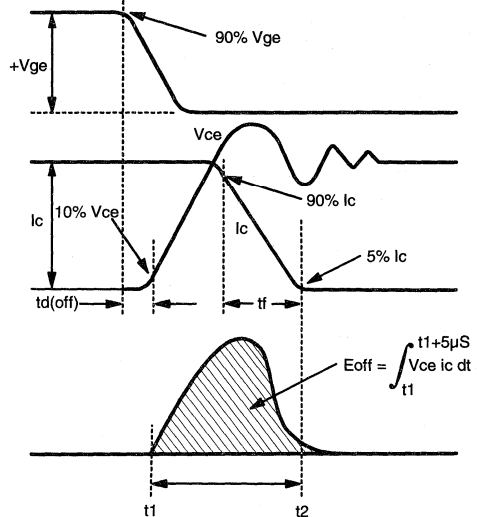


Fig. 18b - Test Waveforms for Circuit of Fig. 18a, Defining E_{off} , $t_{d(off)}$, t_f

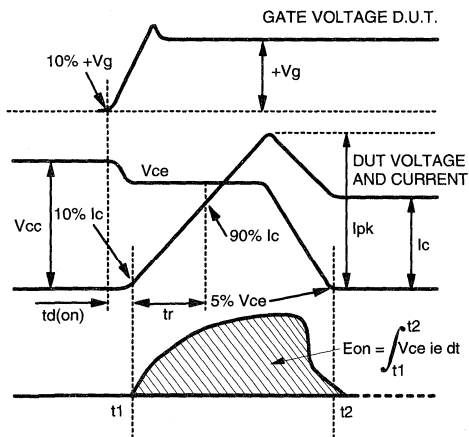


Fig. 18c - Test Waveforms for Circuit of Fig. 18a, Defining E_{on} , $t_{d(on)}$, t_r

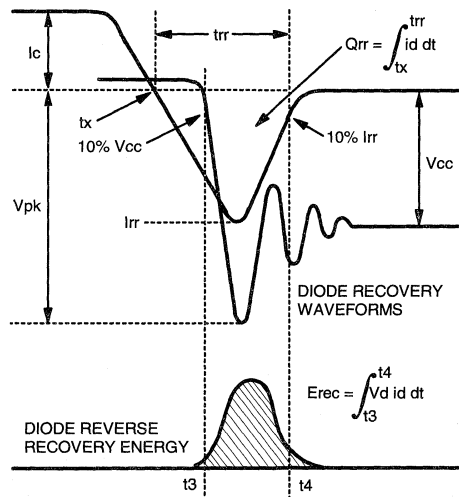


Fig. 18d - Test Waveforms for Circuit of Fig. 18a, Defining E_{rec} , t_{rr} , Q_{rr} , I_{rr}

**Refer to Section D for the following:
Appendix D: Section D - page D-6**

Fig. 18e - Macro Waveforms for Test Circuit of Fig. 18a

Fig. 19 - Clamped Inductive Load Test Circuit

Fig. 20 - Pulsed Collector Current Test Circuit

IGBT SIP MODULE

Ultra-Fast IGBT

Features

- Fully isolated printed circuit board mount package
 - Switching-loss rating includes all "tail" losses
 - HEXFRED™ soft ultrafast diodes
 - Optimized for high operating frequency (over 5kHz)
- See Fig. 1 for Current vs. Frequency curve

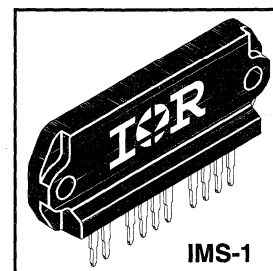
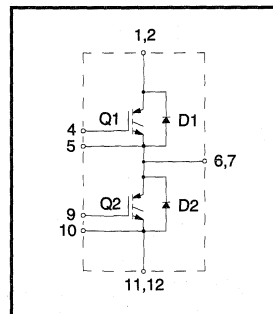
Product Summary

Output Current in a Typical 20 kHz Motor Drive

10 A_{RMS} with T_C = 90°C, T_J = 125°C, Supply Voltage 360Vdc,
Power Factor 0.8, Modulation Depth 80% (See Figure 1)

Description

The IGBT technology is the key to International Rectifier's advanced line of IMS (Insulated Metal Substrate) Power Modules. These modules are more efficient than comparable bipolar transistor modules, while at the same time having the simpler gate-drive requirements of the familiar power MOSFET. This superior technology has now been coupled to a state of the art materials system that maximizes power throughput with low thermal resistance. This package is highly suited to motor drive applications and where space is at a premium.



Absolute Maximum Ratings

	Parameter	Max.	Units
V _{CES}	Collector-to-Emitter Voltage	600	V
I _C @ T _C = 25°C	Continuous Collector Current, each IGBT	33	A
I _C @ T _C = 100°C	Continuous Collector Current, each IGBT	17	
I _{CM}	Pulsed Collector Current Ⓞ	100	
I _{LM}	Clamped Inductive Load Current Ⓞ	100	
I _F @ T _C = 100°C	Diode Continuous Forward Current	15	
I _{FM}	Diode Maximum Forward Current	100	
V _{GE}	Gate-to-Emitter Voltage	±20	V
V _{ISOL}	Isolation Voltage, any terminal to case, 1 minute	2500	V _{RMS}
P _D @ T _C = 25°C	Maximum Power Dissipation, each IGBT	83	W
P _D @ T _C = 100°C	Maximum Power Dissipation, each IGBT	33	
T _J	Operating Junction and Storage Temperature Range	-40 to +150	°C
T _{STG}	Soldering Temperature, for 10 sec.	300 (0.063 in. (1.6mm) from case)	
	Mounting torque, 6-32 or M3 screw.	5-7 lbf•in (0.55-0.8 N•m)	

Thermal Resistance

	Parameter	Typ.	Max.	Units
R _{θJC} (IGBT)	Junction-to-Case, each IGBT, one IGBT in conduction	—	1.5	°C/W
R _{θJC} (DIODE)	Junction-to-Case, each diode, one diode in conduction	—	2.0	
R _{θCS} (MODULE)	Case-to-Sink, flat, greased surface	0.1	—	
Wt	Weight of module	20 (0.7)	—	g (oz)

Electrical Characteristics @ T_J = 25°C (unless otherwise specified)

	Parameter	Min.	Typ.	Max.	Units	Conditions
V _{(BR)CES}	Collector-to-Emitter Breakdown Voltage ^③	600	—	—	V	V _{GE} = 0V, I _C = 250μA
ΔV _{(BR)CES} /ΔT _J	Temperature Coeff. of Breakdown Voltage	—	0.60	—	V/°C	V _{GE} = 0V, I _C = 1.0mA
V _{CE(on)}	Collector-to-Emitter Saturation Voltage	—	1.8	2.3	V	I _C = 17A V _{GE} = 15V
		—	2.2	—		I _C = 33A See Fig. 2, 5
		—	1.6	—		I _C = 17A, T _J = 150°C
V _{GE(th)}	Gate Threshold Voltage	3.0	—	5.5		V _{CE} = V _{GE} , I _C = 250μA
ΔV _{GE(th)} /ΔT _J	Temperature Coeff. of Threshold Voltage	—	-13	—	mV/°C	V _{CE} = V _{GE} , I _C = 250μA
g _{fe}	Forward Transconductance ^④	16	24	—	S	V _{CE} = 100V, I _C = 27A
I _{CES}	Zero Gate Voltage Collector Current	—	—	250	μA	V _{GE} = 0V, V _{CE} = 600V
		—	—	6500		V _{GE} = 0V, V _{CE} = 600V, T _J = 150°C
V _{FM}	Diode Forward Voltage Drop	—	1.3	1.7	V	I _C = 25A See Fig. 13
		—	1.2	1.5		I _C = 25A, T _J = 150°C
I _{GES}	Gate-to-Emitter Leakage Current	—	—	±500	nA	V _{GE} = ±20V

Switching Characteristics @ T_J = 25°C (unless otherwise specified)

	Parameter	Min.	Typ.	Max.	Units	Conditions
Q _g	Total Gate Charge (turn-on)	—	108	140	nC	I _C = 27A
Q _{ge}	Gate - Emitter Charge (turn-on)	—	17	21		V _{CC} = 400V
Q _{gc}	Gate - Collector Charge (turn-on)	—	52	70		See Fig. 8
t _{d(on)}	Turn-On Delay Time	—	23	—	ns	T _J = 25°C
t _r	Rise Time	—	28	—		I _C = 27A, V _{CC} = 480V
t _{d(off)}	Turn-Off Delay Time	—	100	200		V _{GE} = 15V, R _G = 5.0Ω
t _f	Fall Time	—	45	140		Energy losses include "tail" and diode reverse recovery.
E _{on}	Turn-On Switching Loss	—	0.76	—	mJ	See Fig. 9, 10, 11, 18
E _{off}	Turn-Off Switching Loss	—	0.26	—		
E _{ts}	Total Switching Loss	—	1.0	2.0		
t _{d(on)}	Turn-On Delay Time	—	24	—	ns	T _J = 150°C, See Fig. 9, 10, 11, 18
t _r	Rise Time	—	27	—		I _C = 27A, V _{CC} = 480V
t _{d(off)}	Turn-Off Delay Time	—	180	—		V _{GE} = 15V, R _G = 5.0Ω
t _f	Fall Time	—	130	—		Energy losses include "tail" and diode reverse recovery.
E _{ts}	Total Switching Loss	—	3.7	—	mJ	
C _{ies}	Input Capacitance	—	2900	—	pF	V _{GE} = 0V
C _{oes}	Output Capacitance	—	330	—		V _{CC} = 30V See Fig. 7
C _{res}	Reverse Transfer Capacitance	—	41	—		f = 1.0MHz
t _{rr}	Diode Reverse Recovery Time	—	50	75	ns	T _J = 25°C See Fig. 14
		—	105	160		T _J = 125°C
I _{rr}	Diode Peak Reverse Recovery Current	—	4.5	10	A	T _J = 25°C See Fig. 15
		—	8.0	15		T _J = 125°C
Q _{rr}	Diode Reverse Recovery Charge	—	112	375	nC	T _J = 25°C See Fig. 16
		—	420	1200		T _J = 125°C
di _{(rec)M} /dt	Diode Peak Rate of Fall of Recovery During t _b	—	250	—	A/μs	T _J = 25°C See Fig. 17
		—	160	—		T _J = 125°C

Notes:

① Repetitive rating; V_{GE}=20V, pulse width limited by max. junction temperature. (See fig. 20)

② V_{CC}=80%(V_{CES}), V_{GE}=20V, L=10μH, R_G= 5.0Ω, (See fig. 19)

④ Pulse width 5.0μs, single shot.

③ Pulse width ≤ 80μs; duty factor ≤ 0.1%.

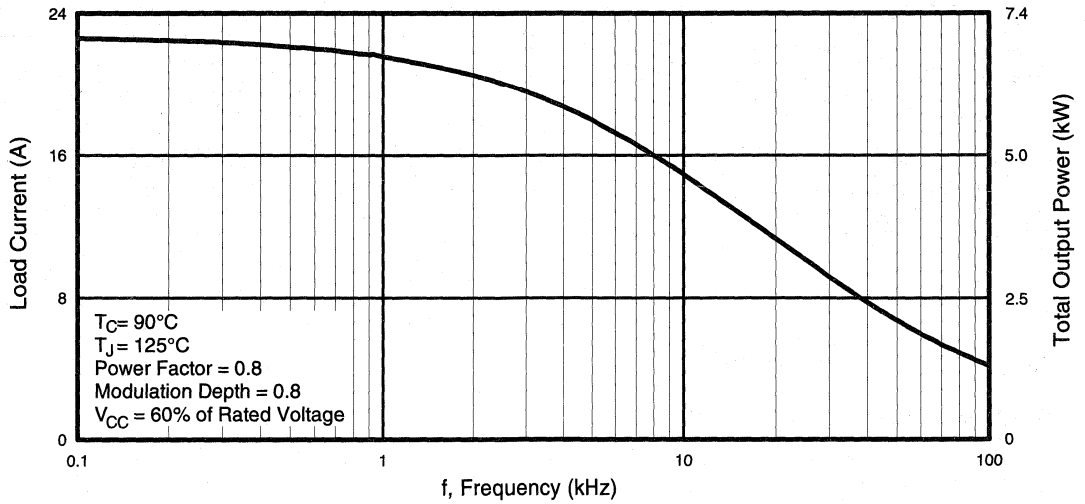


Fig. 1 - RMS Current and Output Power, Synthesized Sine Wave

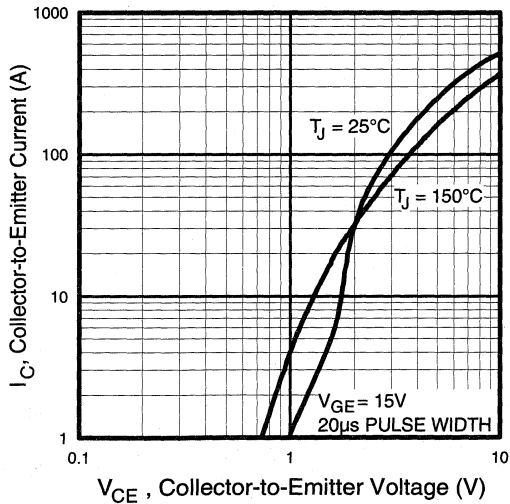


Fig. 2 - Typical Output Characteristics

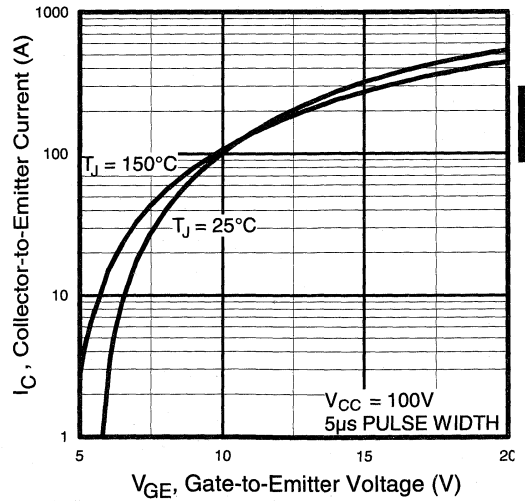


Fig. 3 - Typical Transfer Characteristics

Power Conversion Ultra-Fast Modules

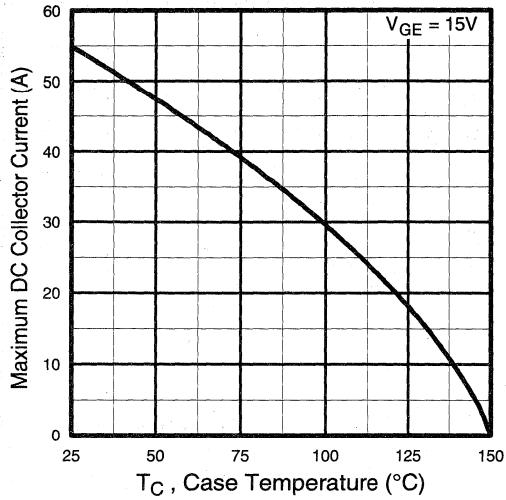


Fig. 4 - Maximum Collector Current vs. Case Temperature

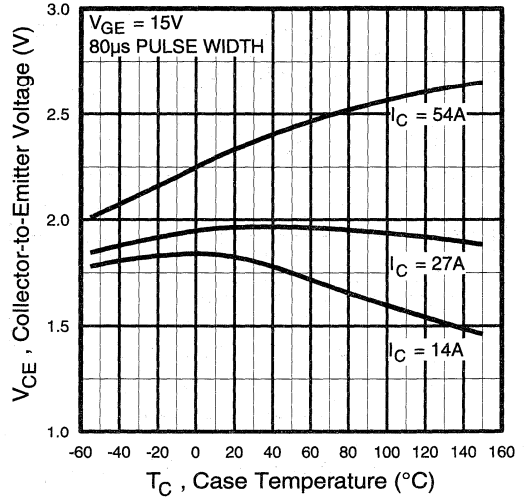


Fig. 5 - Collector-to-Emitter Voltage vs. Case Temperature

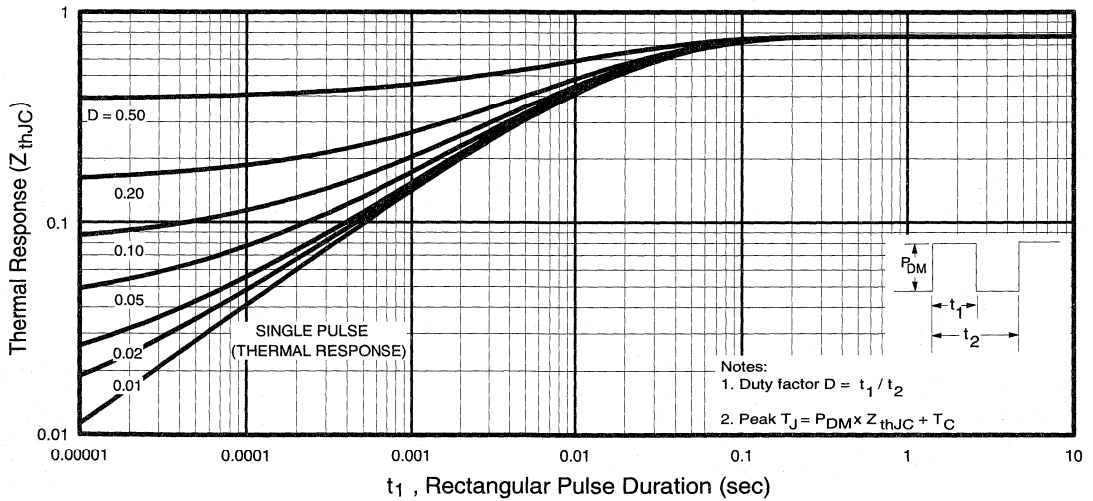


Fig. 6 - Maximum IGBT Effective Transient Thermal Impedance, Junction-to-Case

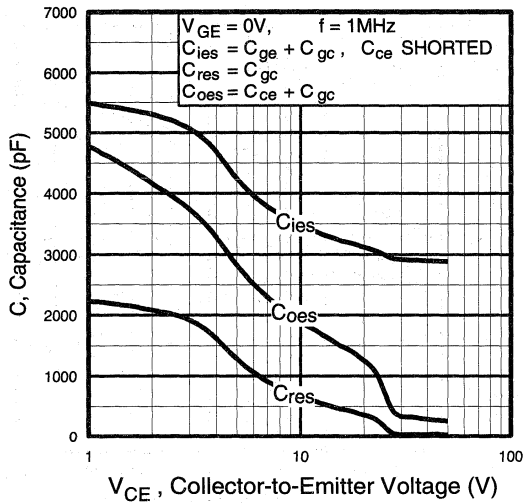


Fig. 7 - Typical Capacitance vs. Collector-to-Emitter Voltage

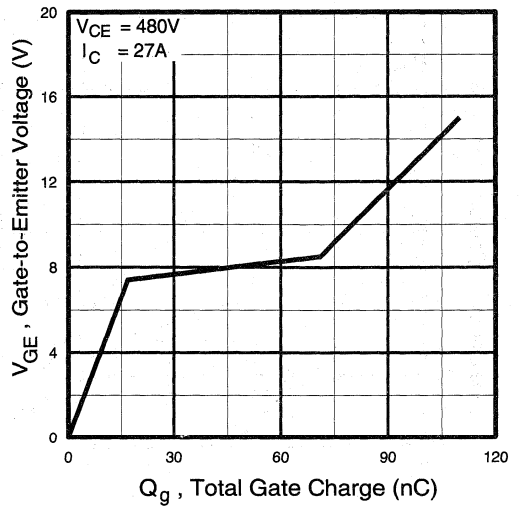


Fig. 8 - Typical Gate Charge vs. Gate-to-Emitter Voltage

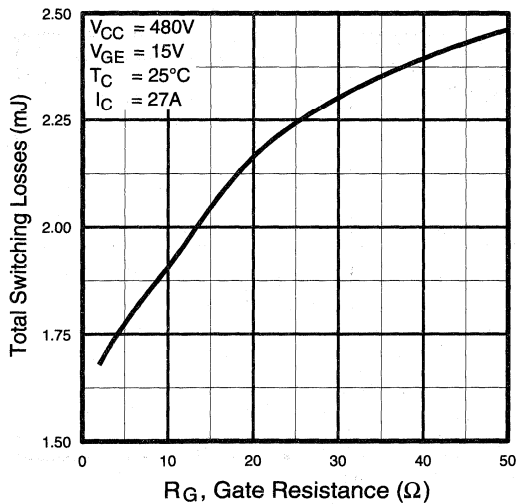


Fig. 9 - Typical Switching Losses vs. Gate Resistance

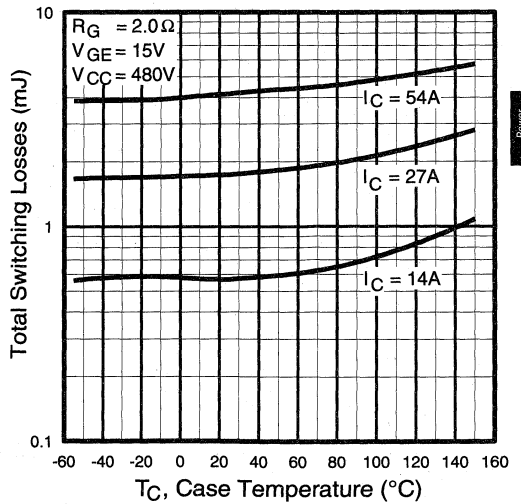


Fig. 10 - Typical Switching Losses vs. Case Temperature

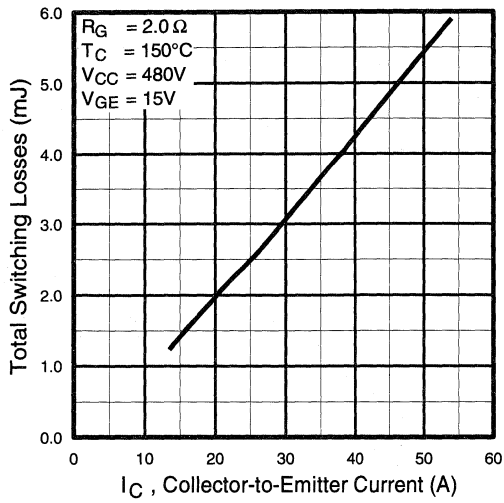


Fig. 11 - Typical Switching Losses vs. Collector-to-Emitter Current

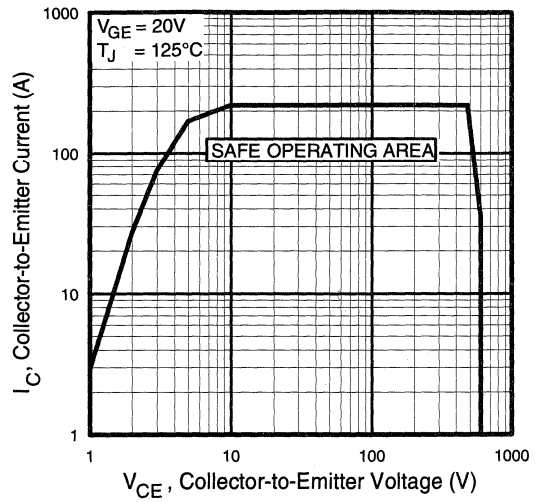


Fig. 12 - Turn-Off SOA

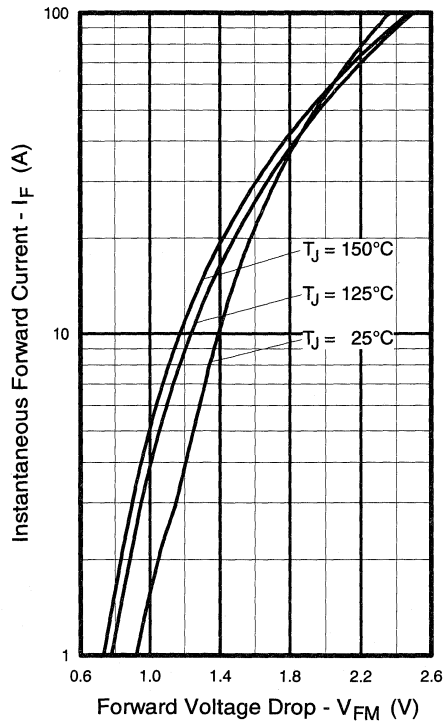


Fig. 13 - Maximum Forward Voltage Drop vs. Instantaneous Forward Current

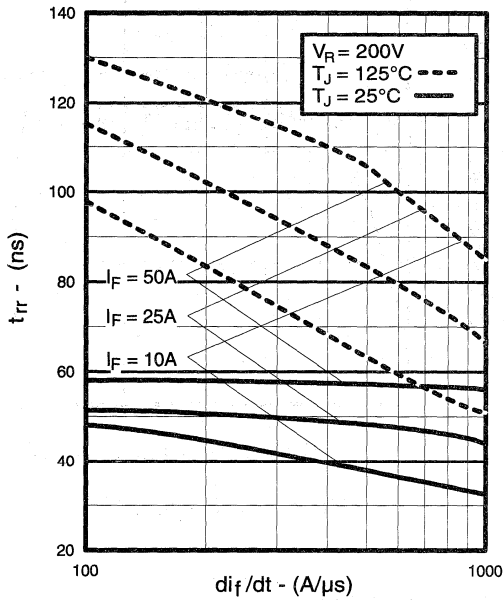


Fig. 14 - Typical Reverse Recovery vs. di_f/dt

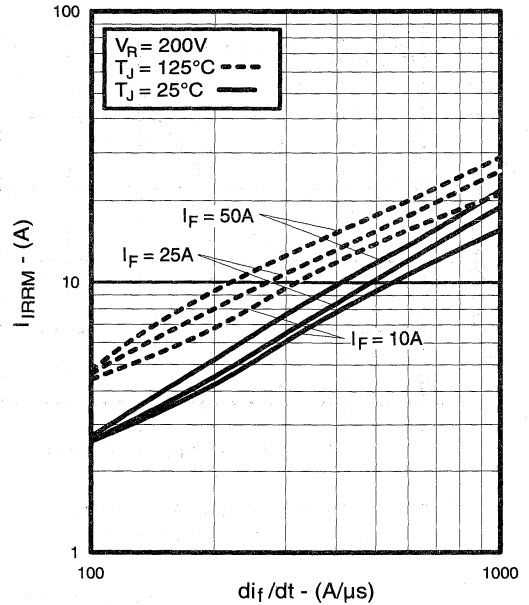


Fig. 15 - Typical Recovery Current vs. di_f/dt

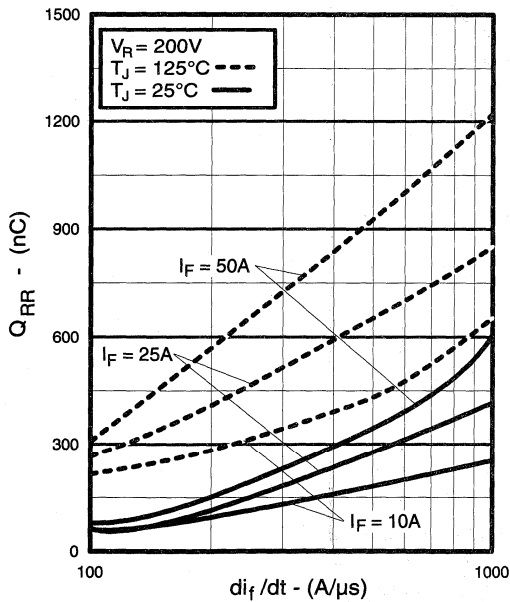


Fig. 16 - Typical Stored Charge vs. di_f/dt

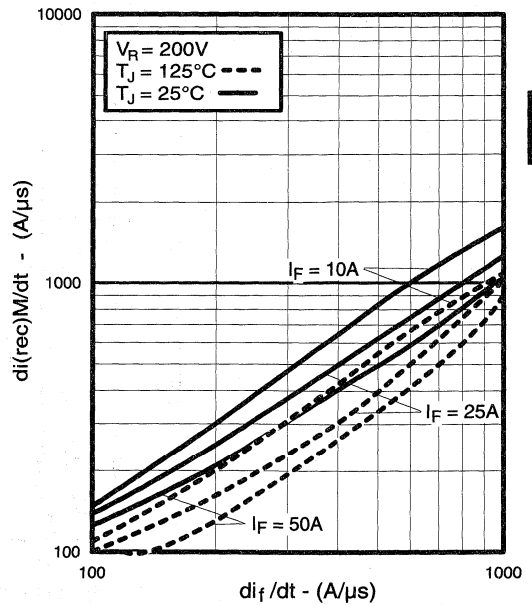


Fig. 17 - Typical $di_{(rec)M}/dt$ vs. di_f/dt

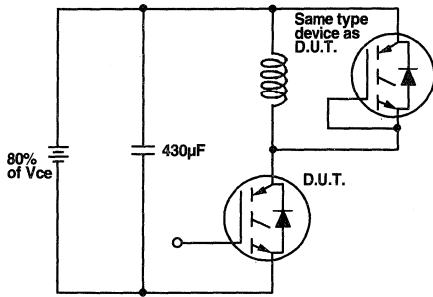


Fig. 18a - Test Circuit for Measurement of I_{LM} , E_{on} , $E_{off}(\text{diode})$, t_{rr} , Q_{rr} , I_{rr} , $t_{d(on)}$, t_r , $t_{d(off)}$, t_f

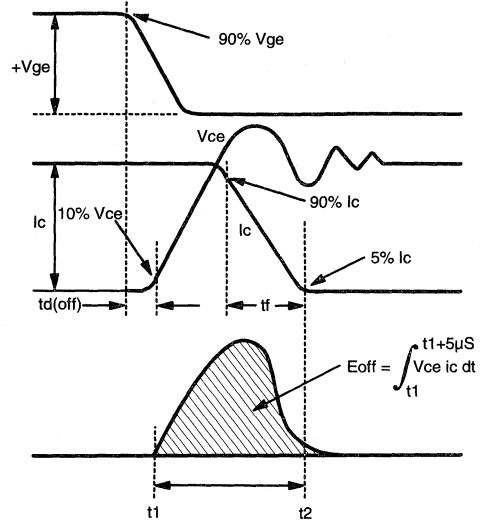


Fig. 18b - Test Waveforms for Circuit of Fig. 18a, Defining E_{off} , $t_{d(off)}$, t_f

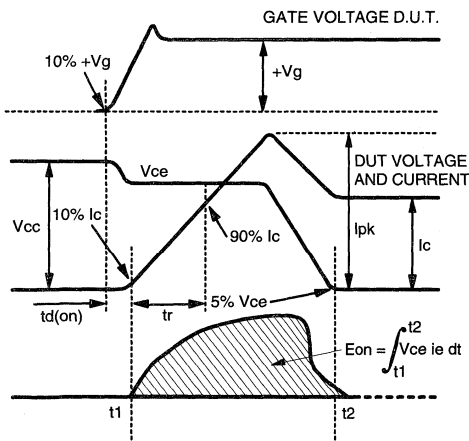


Fig. 18c - Test Waveforms for Circuit of Fig. 18a, Defining E_{on} , $t_{d(on)}$, t_r

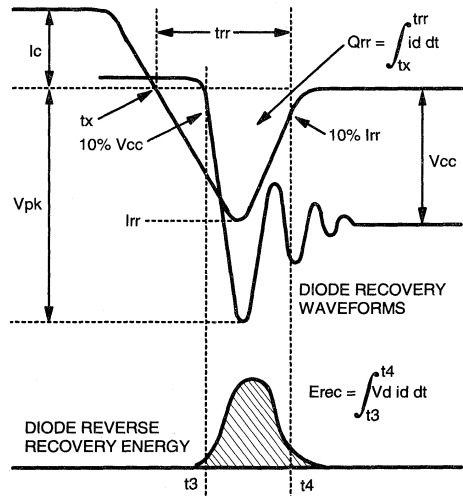


Fig. 18d - Test Waveforms for Circuit of Fig. 18a, Defining E_{rec} , t_{rr} , Q_{rr} , I_{rr}

Refer to Section D for the following:
Appendix D: Section D - page D-6

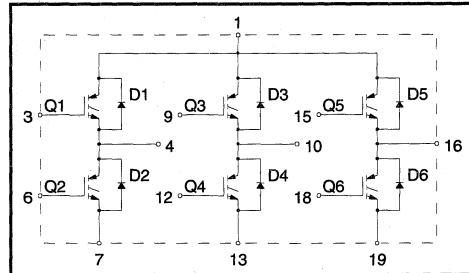
- Fig. 18e - Macro Waveforms for Test Circuit of Fig. 18a
- Fig. 19 - Clamped Inductive Load Test Circuit
- Fig. 20 - Pulsed Collector Current Test Circuit

IGBT SIP MODULE

Ultra-Fast IGBT

Features

- Fully isolated printed circuit board mount package
- Switching-loss rating includes all "tail" losses
- HEXFRED™ soft ultrafast diodes
- Optimized for high operating frequency (over 5kHz)
See Fig. 1 for Current vs. Frequency curve



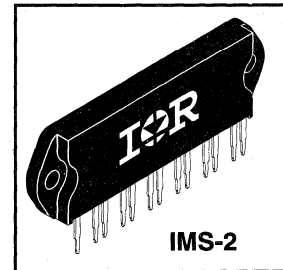
Product Summary

Output Current in a Typical 20 kHz Motor Drive

3.5 A_{RMS} per phase (1.1 kW total) with T_C = 90°C, T_J = 125°C, Supply Voltage 360Vdc, Power Factor 0.8, Modulation Depth 80% (See Figure 1)

Description

The IGBT technology is the key to International Rectifier's advanced line of IMS (Insulated Metal Substrate) Power Modules. These modules are more efficient than comparable bipolar transistor modules, while at the same time having the simpler gate-drive requirements of the familiar power MOSFET. This superior technology has now been coupled to a state of the art materials system that maximizes power throughput with low thermal resistance. This package is highly suited to motor drive applications and where space is at a premium.



Absolute Maximum Ratings

	Parameter	Max.	Units
V _{CES}	Collector-to-Emitter Voltage	600	V
I _C @ T _C = 25°C	Continuous Collector Current, each IGBT	7.2	A
I _C @ T _C = 100°C	Continuous Collector Current, each IGBT	3.9	
I _{CM}	Pulsed Collector Current ①	22	
I _{LM}	Clamped Inductive Load Current ②	22	
I _F @ T _C = 100°C	Diode Continuous Forward Current	3.4	
I _{FM}	Diode Maximum Forward Current	22	
V _{GE}	Gate-to-Emitter Voltage	±20	V
V _{ISOL}	Isolation Voltage, any terminal to case, 1 min.	2500	V _{RMS}
P _D @ T _C = 25°C	Maximum Power Dissipation, each IGBT	23	W
P _D @ T _C = 100°C	Maximum Power Dissipation, each IGBT	9.1	
T _J	Operating Junction and	-40 to +150	°C
T _{STG}	Storage Temperature Range		
	Soldering Temperature, for 10 sec.		
	Mounting torque, 6-32 or M3 screw.	5-7 lbf•in (0.55-0.8 N•m)	

Thermal Resistance

	Parameter	Typ.	Max.	Units
R _{θJC} (IGBT)	Junction-to-Case, each IGBT, one IGBT in conduction	—	5.5	°C/W
R _{θJC} (DIODE)	Junction-to-Case, each diode, one diode in conduction	—	9.0	
R _{θCS} (MODULE)	Case-to-Sink, flat, greased surface	0.1	—	
Wt	Weight of module	20 (0.7)	—	g (oz)

Power Conversion Ultra-Fast Modules

Electrical Characteristics @ $T_J = 25^\circ\text{C}$ (unless otherwise specified)

	Parameter	Min.	Typ.	Max.	Units	Conditions
$V_{(BR)CES}$	Collector-to-Emitter Breakdown Voltage ^③	600	—	—	V	$V_{GE} = 0V, I_C = 250\mu\text{A}$
$\Delta V_{(BR)CES}/\Delta T_J$	Temperature Coeff. of Breakdown Voltage	—	0.69	—	V/ $^\circ\text{C}$	$V_{GE} = 0V, I_C = 1.0\text{mA}$
$V_{CE(on)}$	Collector-to-Emitter Saturation Voltage	—	2.1	2.6	V	$I_C = 3.9A, V_{GE} = 15V$
		—	2.5	—		$I_C = 7.2A$
		—	2.0	—		$I_C = 3.9A, T_J = 150^\circ\text{C}$
$V_{GE(th)}$	Gate Threshold Voltage	3.0	—	5.5		$V_{CE} = V_{GE}, I_C = 250\mu\text{A}$
$\Delta V_{GE(th)}/\Delta T_J$	Temperature Coeff. of Threshold Voltage	—	-11	—	mV/ $^\circ\text{C}$	$V_{CE} = V_{GE}, I_C = 250\mu\text{A}$
g_{fe}	Forward Transconductance ^④	1.4	4.3	—	S	$V_{CE} = 100V, I_C = 6.5A$
I_{CES}	Zero Gate Voltage Collector Current	—	—	250	μA	$V_{GE} = 0V, V_{CE} = 600V$
		—	—	1700		$V_{GE} = 0V, V_{CE} = 600V, T_J = 150^\circ\text{C}$
V_{FM}	Diode Forward Voltage Drop	—	1.4	1.7	V	$I_C = 8.0A$
		—	1.3	1.6		$I_C = 8.0A, T_J = 150^\circ\text{C}$
I_{GES}	Gate-to-Emitter Leakage Current	—	—	± 500	nA	$V_{GE} = \pm 20V$

Switching Characteristics @ $T_J = 25^\circ\text{C}$ (unless otherwise specified)

	Parameter	Min.	Typ.	Max.	Units	Conditions
Q_g	Total Gate Charge (turn-on)	—	16	22	nC	$I_C = 6.5A$ $V_{CC} = 400V$ See Fig. 8
Q_{ge}	Gate - Emitter Charge (turn-on)	—	2.4	3.8		
Q_{gc}	Gate - Collector Charge (turn-on)	—	7.8	13		
$t_{d(on)}$	Turn-On Delay Time	—	22	—	ns	$T_J = 25^\circ\text{C}$ $I_C = 6.5A, V_{CC} = 480V$ $V_{GE} = 15V, R_G = 50\Omega$ Energy losses include "tail" and diode reverse recovery.
t_r	Rise Time	—	12	—		
$t_{d(off)}$	Turn-Off Delay Time	—	71	95		
t_f	Fall Time	—	91	280		
E_{on}	Turn-On Switching Loss	—	0.19	—		
E_{off}	Turn-Off Switching Loss	—	0.07	—	mJ	See Fig. 9, 10, 11, 18
E_{ts}	Total Switching Loss	—	0.26	0.42		
$t_{d(on)}$	Turn-On Delay Time	—	23	—	ns	$T_J = 150^\circ\text{C}$, See Fig. 9, 10, 11, 18 $I_C = 6.5A, V_{CC} = 480V$ $V_{GE} = 15V, R_G = 50\Omega$ Energy losses include "tail" and diode reverse recovery.
t_r	Rise Time	—	13	—		
$t_{d(off)}$	Turn-Off Delay Time	—	140	—		
t_f	Fall Time	—	200	—		
E_{ts}	Total Switching Loss	—	0.83	—	mJ	
C_{ies}	Input Capacitance	—	330	—	pF	$V_{GE} = 0V$ $V_{CC} = 30V$ $f = 1.0\text{MHz}$ See Fig. 7
C_{oes}	Output Capacitance	—	65	—		
C_{res}	Reverse Transfer Capacitance	—	6.0	—		
t_{rr}	Diode Reverse Recovery Time	—	37	55	ns	$T_J = 25^\circ\text{C}$ See Fig.
		—	55	90		$T_J = 125^\circ\text{C}$ 14
I_{rr}	Diode Peak Reverse Recovery Current	—	3.5	5.0	A	$T_J = 25^\circ\text{C}$ See Fig.
		—	4.5	8.0		$T_J = 125^\circ\text{C}$ 15
Q_{rr}	Diode Reverse Recovery Charge	—	65	138	nC	$T_J = 25^\circ\text{C}$ See Fig.
		—	124	360		$T_J = 125^\circ\text{C}$ 16
$di_{(rec)}/dt$	Diode Peak Rate of Fall of Recovery During t_b	—	240	—	A/ μs	$T_J = 25^\circ\text{C}$ See Fig.
		—	210	—		$T_J = 125^\circ\text{C}$ 17

Notes:

① Repetitive rating; $V_{GE}=20V$, pulse width limited by max. junction temperature. (See fig. 20)

② $V_{CC}=80\%(V_{CES}), V_{GE}=20V, L=10\mu\text{H}, R_G=50\Omega$, (See fig. 19)

③ Pulse width $\leq 80\mu\text{s}$; duty factor $\leq 0.1\%$.

④ Pulse width $5.0\mu\text{s}$, single shot.

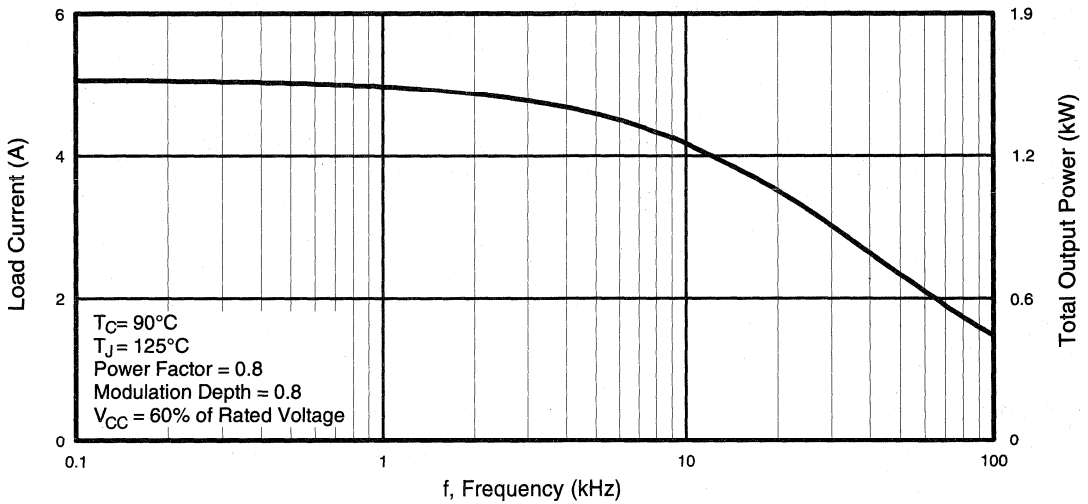


Fig. 1 - RMS Current and Output Power, Synthesized Sine Wave

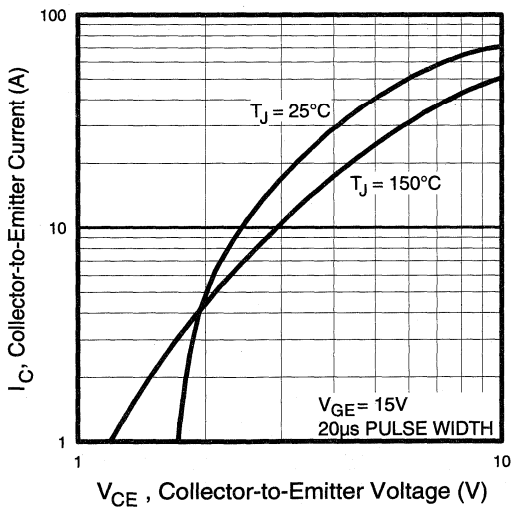


Fig. 2 - Typical Output Characteristics

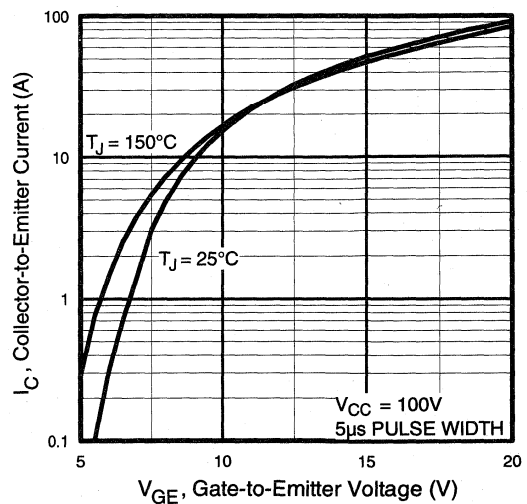


Fig. 3 - Typical Transfer Characteristics

Power Conversion
 Universal
 Modules

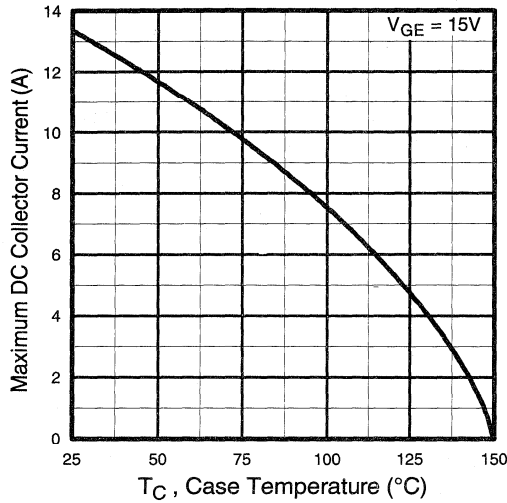


Fig. 4 - Maximum Collector Current vs. Case Temperature

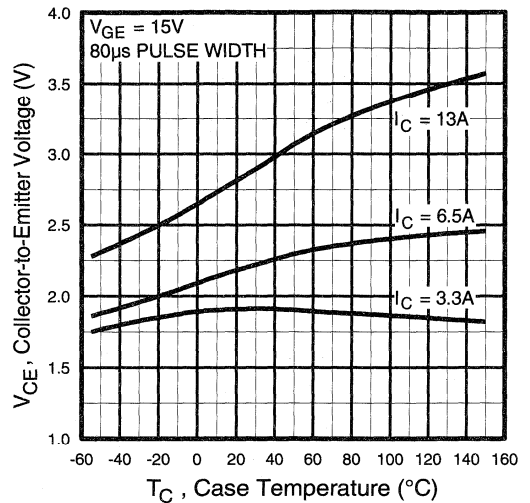


Fig. 5 - Collector-to-Emitter Voltage vs. Case Temperature

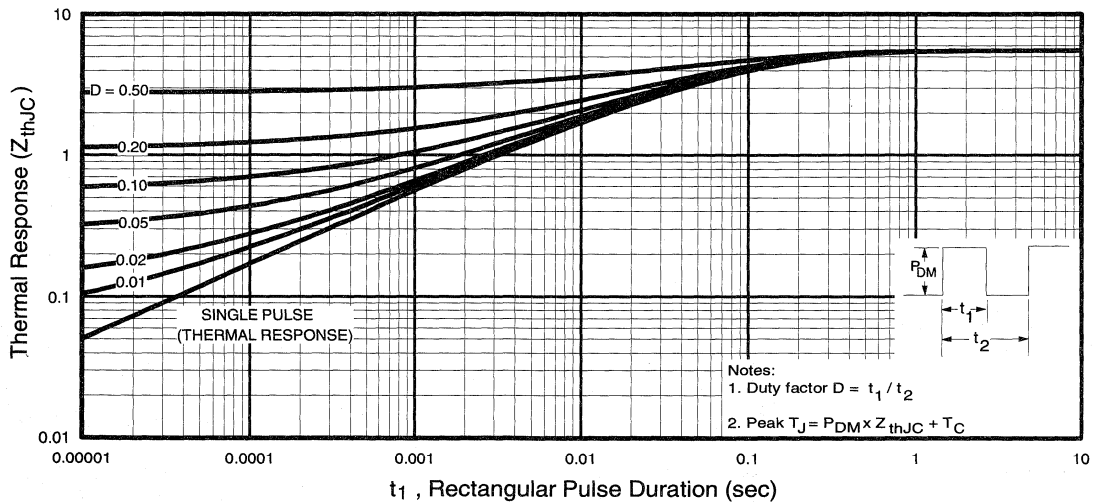


Fig. 6 - Maximum IGBT Effective Transient Thermal Impedance, Junction-to-Case

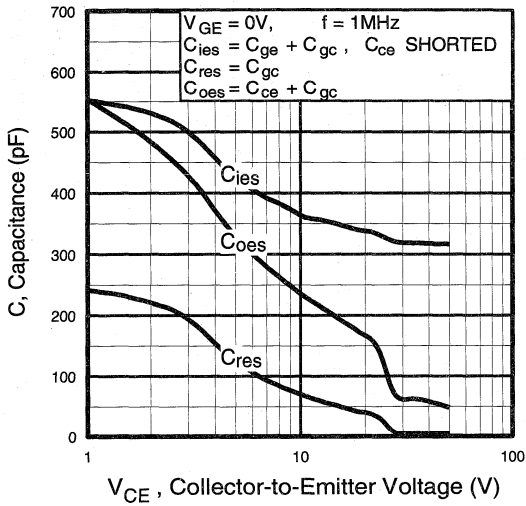


Fig. 7 - Typical Capacitance vs. Collector-to-Emitter Voltage

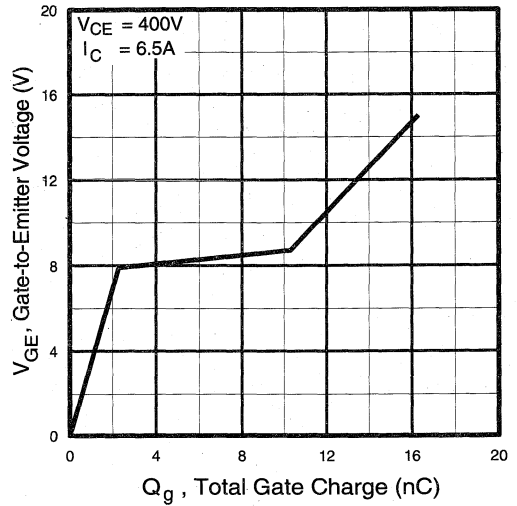


Fig. 8 - Typical Gate Charge vs. Gate-to-Emitter Voltage

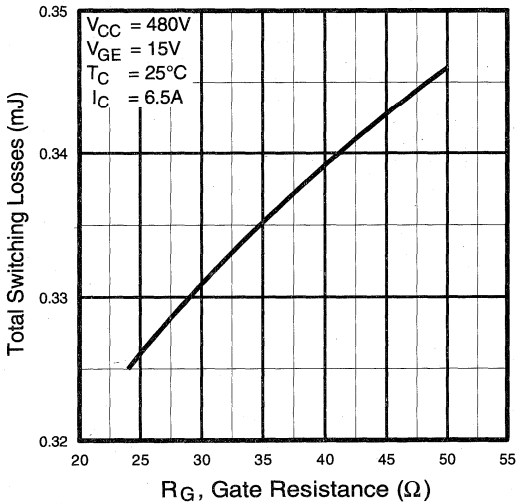


Fig. 9 - Typical Switching Losses vs. Gate Resistance

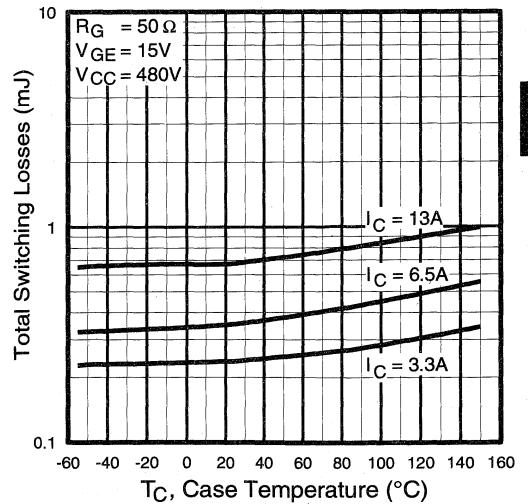


Fig. 10 - Typical Switching Losses vs. Case Temperature

Power Conversion Ultra-Fast Modules

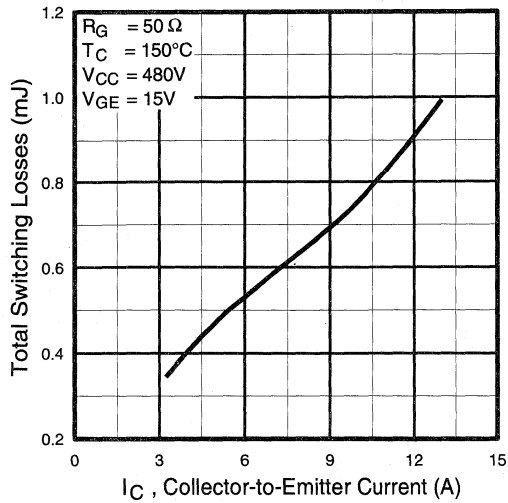


Fig. 11 - Typical Switching Losses vs. Collector-to-Emitter Current

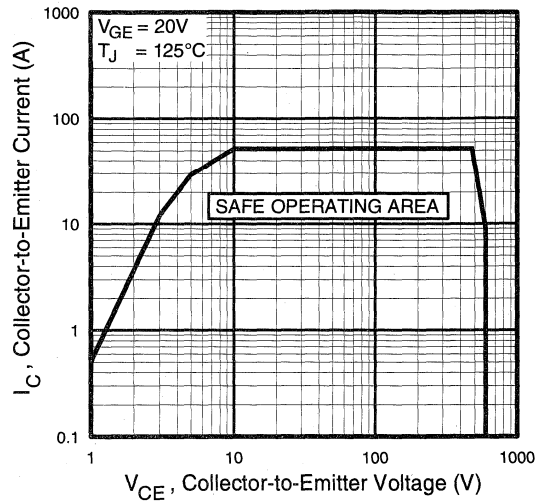


Fig. 12 - Turn-Off SOA

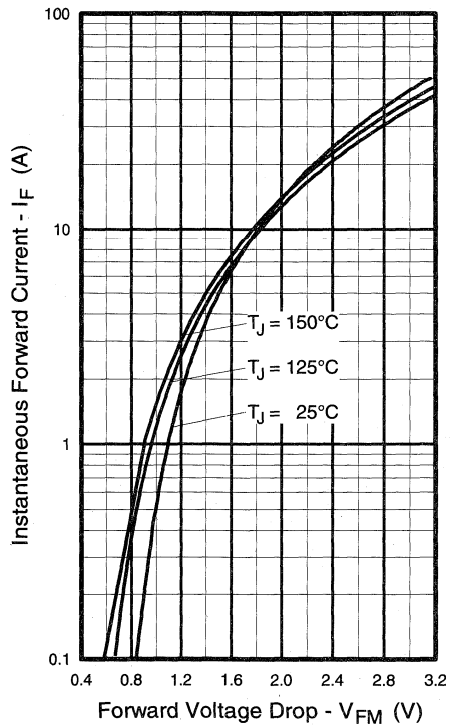


Fig. 13 - Maximum Forward Voltage Drop vs. Instantaneous Forward Current

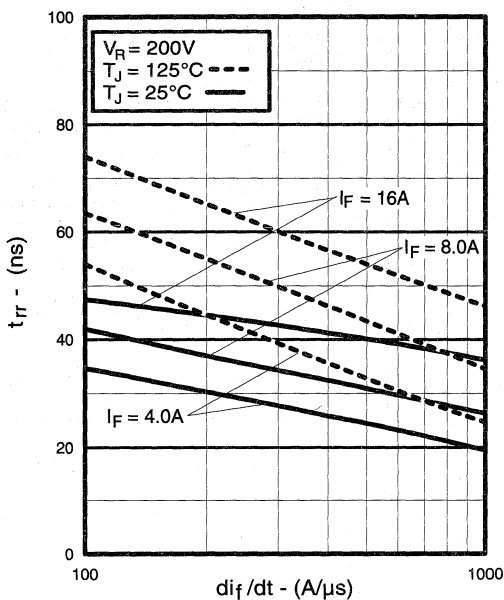


Fig. 14 - Typical Reverse Recovery vs. di_f/dt

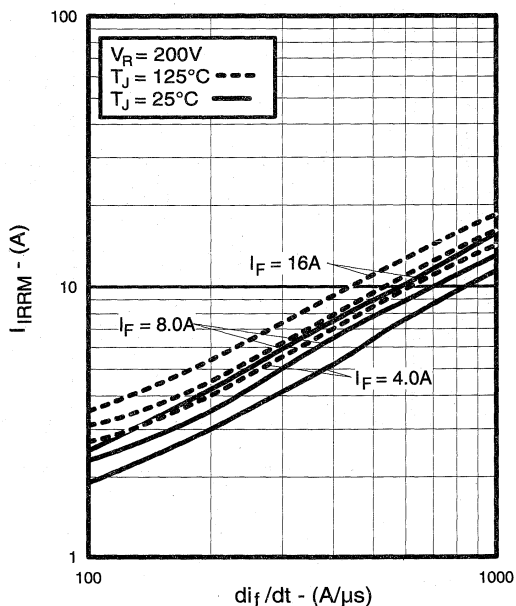


Fig. 15 - Typical Recovery Current vs. di_f/dt

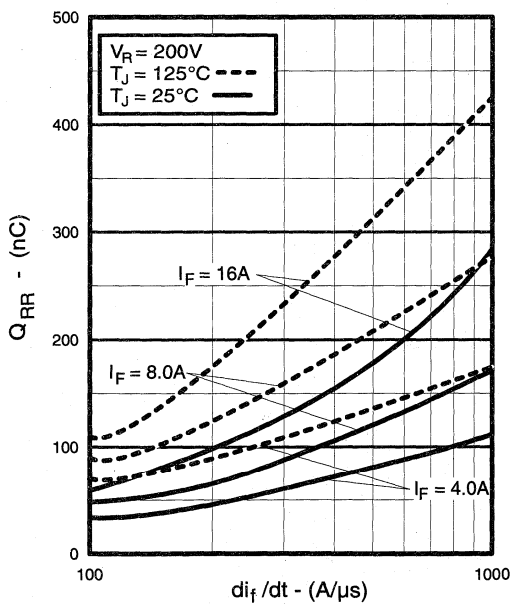


Fig. 16 - Typical Stored Charge vs. di_f/dt

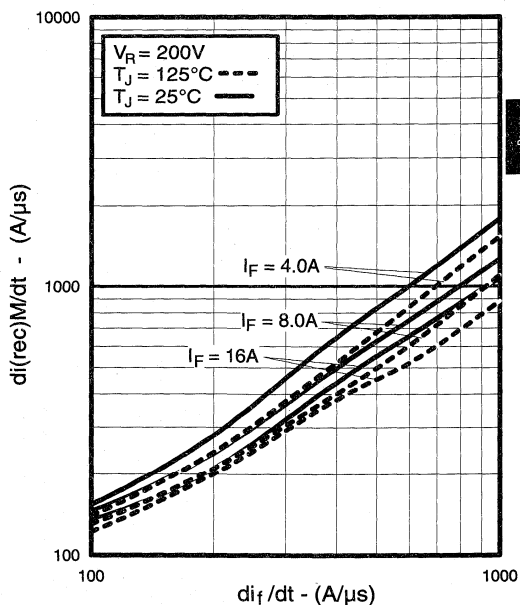


Fig. 17 - Typical $di_{(rec)M}/dt$ vs. di_f/dt

Power Conversion Ultra-Fast Modules

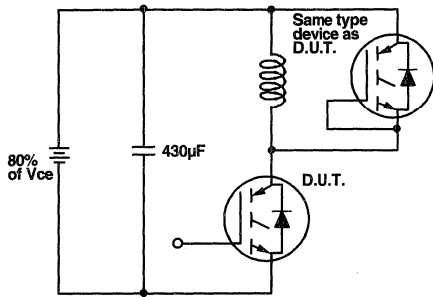


Fig. 18a - Test Circuit for Measurement of I_{LM} , E_{on} , $E_{off}(\text{diode})$, t_{rr} , Q_{rr} , I_{rr} , $t_{d(on)}$, t_r , $t_{d(off)}$, t_f

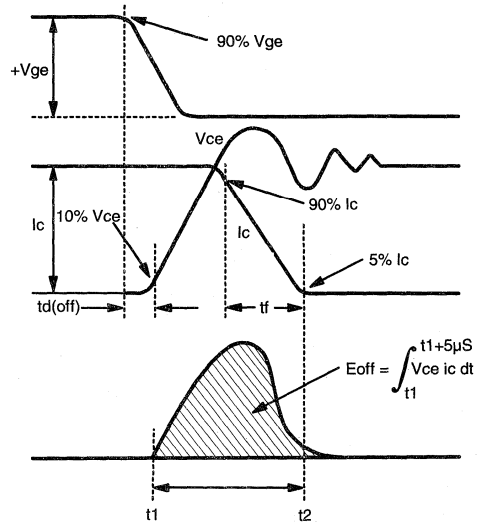


Fig. 18b - Test Waveforms for Circuit of Fig. 18a, Defining E_{off} , $t_{d(off)}$, t_f

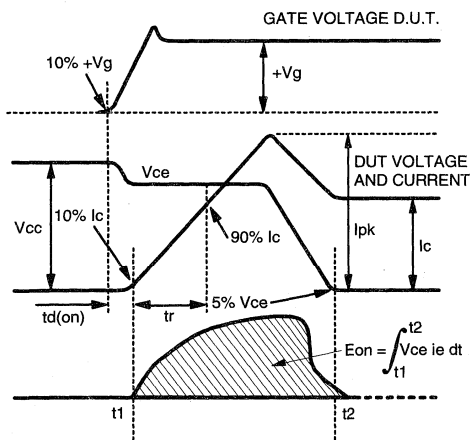


Fig. 18c - Test Waveforms for Circuit of Fig. 18a, Defining E_{on} , $t_{d(on)}$, t_r

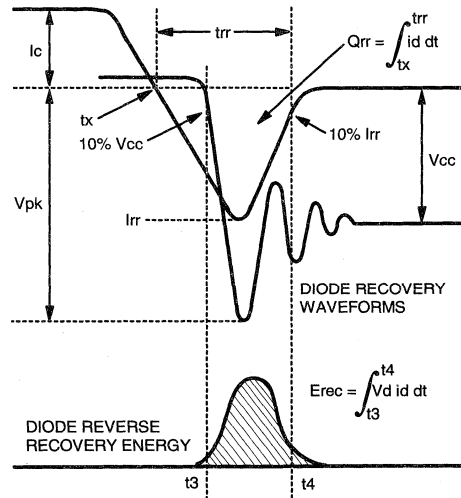


Fig. 18d - Test Waveforms for Circuit of Fig. 18a, Defining E_{rec} , t_{rr} , Q_{rr} , I_{rr}

**Refer to Section D for the following:
Appendix D: Section D - page D-6**

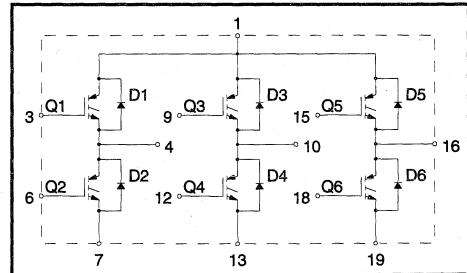
- Fig. 18e - Macro Waveforms for Test Circuit of Fig. 18a
- Fig. 19 - Clamped Inductive Load Test Circuit
- Fig. 20 - Pulsed Collector Current Test Circuit

IGBT SIP MODULE

Ultra-Fast IGBT

Features

- Fully isolated printed circuit board mount package
 - Switching-loss rating includes all "tail" losses
 - HEXFRED™ soft ultrafast diodes
 - Optimized for high operating frequency (over 5kHz)
- See Fig. 1 for Current vs. Frequency curve



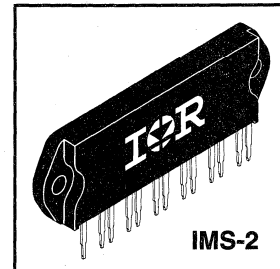
Product Summary

Output Current in a Typical 20 kHz Motor Drive

5.4 A_{RMS} per phase (1.7 kW total) with T_C = 90°C, T_J = 125°C, Supply Voltage 360Vdc, Power Factor 0.8, Modulation Depth 80% (See Figure 1)

Description

The IGBT technology is the key to International Rectifier's advanced line of IMS (Insulated Metal Substrate) Power Modules. These modules are more efficient than comparable bipolar transistor modules, while at the same time having the simpler gate-drive requirements of the familiar power MOSFET. This superior technology has now been coupled to a state of the art materials system that maximizes power throughput with low thermal resistance. This package is highly suited to motor drive applications and where space is at a premium.



Absolute Maximum Ratings

	Parameter	Max.	Units
V _{CES}	Collector-to-Emitter Voltage	600	V
I _C @ T _C = 25°C	Continuous Collector Current, each IGBT	13	A
I _C @ T _C = 100°C	Continuous Collector Current, each IGBT	6.8	
I _{CM}	Pulsed Collector Current ①	40	
I _{LM}	Clamped Inductive Load Current ②	40	
I _F @ T _C = 100°C	Diode Continuous Forward Current	6.1	
I _{FM}	Diode Maximum Forward Current	40	
V _{GE}	Gate-to-Emitter Voltage	±20	V
V _{ISOL}	Isolation Voltage, any terminal to case, 1 min.	2500	V _{RMS}
P _D @ T _C = 25°C	Maximum Power Dissipation, each IGBT	36	W
P _D @ T _C = 100°C	Maximum Power Dissipation, each IGBT	14	
T _J	Operating Junction and	-40 to +150	°C
T _{STG}	Storage Temperature Range		
	Soldering Temperature, for 10 sec.	300 (0.063 in. (1.6mm) from case)	
	Mounting torque, 6-32 or M3 screw.	5-7 lb•in (0.55-0.8 N•m)	

Thermal Resistance

	Parameter	Typ.	Max.	Units
R _{θJC} (IGBT)	Junction-to-Case, each IGBT, one IGBT in conduction	—	3.5	°C/W
R _{θJC} (DIODE)	Junction-to-Case, each diode, one diode in conduction	—	5.5	
R _{θCS} (MODULE)	Case-to-Sink, flat, greased surface	0.1	—	
Wt	Weight of module	20 (0.7)	—	g (oz)

Electrical Characteristics @ $T_J = 25^\circ\text{C}$ (unless otherwise specified)

	Parameter	Min.	Typ.	Max.	Units	Conditions
$V_{(BR)CES}$	Collector-to-Emitter Breakdown Voltage ^③	600	—	—	V	$V_{GE} = 0V, I_C = 250\mu A$
$\Delta V_{(BR)CES}/\Delta T_J$	Temperature Coeff. of Breakdown Voltage	—	0.63	—	$V/^\circ\text{C}$	$V_{GE} = 0V, I_C = 1.0mA$
$V_{CE(on)}$	Collector-to-Emitter Saturation Voltage	—	1.9	2.4	V	$I_C = 6.8A$ $I_C = 13A$ $I_C = 6.8A, T_J = 150^\circ\text{C}$ $V_{GE} = 15V$ See Fig. 2, 5
		—	2.3	—		
		—	1.8	—		
$V_{GE(th)}$	Gate Threshold Voltage	3.0	—	5.5		$V_{CE} = V_{GE}, I_C = 250\mu A$
$\Delta V_{GE(th)}/\Delta T_J$	Temperature Coeff. of Threshold Voltage	—	-11	—	$mV/^\circ\text{C}$	$V_{CE} = V_{GE}, I_C = 250\mu A$
g_{fe}	Forward Transconductance ^④	4.0	6.0	—	S	$V_{CE} = 100V, I_C = 6.8A$
I_{CES}	Zero Gate Voltage Collector Current	—	—	250	μA	$V_{GE} = 0V, V_{CE} = 600V$
		—	—	2500		$V_{GE} = 0V, V_{CE} = 600V, T_J = 150^\circ\text{C}$
V_{FM}	Diode Forward Voltage Drop	—	1.4	1.7	V	$I_C = 12A$ $I_C = 12A, T_J = 150^\circ\text{C}$ See Fig. 13
		—	1.3	1.6		
I_{GES}	Gate-to-Emitter Leakage Current	—	—	± 500	nA	$V_{GE} = \pm 20V$

Switching Characteristics @ $T_J = 25^\circ\text{C}$ (unless otherwise specified)

	Parameter	Min.	Typ.	Max.	Units	Conditions
Q_g	Total Gate Charge (turn-on)	—	29	36	nC	$I_C = 6.8A$ $V_{CC} = 400V$ See Fig. 8
Q_{ge}	Gate - Emitter Charge (turn-on)	—	4.8	6.8		
Q_{gc}	Gate - Collector Charge (turn-on)	—	12	17		
$t_{d(on)}$	Turn-On Delay Time	—	25	—	ns	$T_J = 25^\circ\text{C}$ $I_C = 6.8A, V_{CC} = 480V$ $V_{GE} = 15V, R_G = 23\Omega$ Energy losses include "tail" and diode reverse recovery. See Fig. 9, 10, 11, 18
t_r	Rise Time	—	15	—		
$t_{d(off)}$	Turn-Off Delay Time	—	92	200		
t_f	Fall Time	—	93	190		
E_{on}	Turn-On Switching Loss	—	0.23	—	mJ	See Fig. 9, 10, 11, 18
E_{off}	Turn-Off Switching Loss	—	0.13	—		
E_{ts}	Total Switching Loss	—	0.36	0.62		
$t_{d(on)}$	Turn-On Delay Time	—	25	—	ns	$T_J = 150^\circ\text{C}$, See Fig. 9, 10, 11, 18 $I_C = 6.8A, V_{CC} = 480V$ $V_{GE} = 15V, R_G = 23\Omega$ Energy losses include "tail" and diode reverse recovery.
t_r	Rise Time	—	15	—		
$t_{d(off)}$	Turn-Off Delay Time	—	160	—		
t_f	Fall Time	—	200	—		
E_{ts}	Total Switching Loss	—	0.71	—	mJ	
C_{ies}	Input Capacitance	—	660	—	pF	$V_{GE} = 0V$ $V_{CC} = 30V$ $f = 1.0MHz$ See Fig. 7
C_{oes}	Output Capacitance	—	100	—		
C_{res}	Reverse Transfer Capacitance	—	11	—		
t_{rr}	Diode Reverse Recovery Time	—	42	60	ns	$T_J = 25^\circ\text{C}$ See Fig. 14 $T_J = 125^\circ\text{C}$ 14
		—	80	120		
I_{rr}	Diode Peak Reverse Recovery Current	—	3.5	6.0	A	$T_J = 25^\circ\text{C}$ See Fig. 15 $T_J = 125^\circ\text{C}$ 15
		—	5.6	10		
Q_{rr}	Diode Reverse Recovery Charge	—	80	180	nC	$T_J = 25^\circ\text{C}$ See Fig. 16 $T_J = 125^\circ\text{C}$ 16
		—	220	600		
$di_{(rec)M}/dt$	Diode Peak Rate of Fall of Recovery During t_b	—	180	—	$A/\mu s$	$T_J = 25^\circ\text{C}$ See Fig. 17 $T_J = 125^\circ\text{C}$ 17
		—	116	—		

Notes:

① Repetitive rating; $V_{GE}=20V$, pulse width limited by max. junction temperature. (See fig. 20)

② $V_{CC}=80\%(V_{CES}), V_{GE}=20V, L=10\mu H, R_G=23\Omega$, (See fig. 19)

③ Pulse width $\leq 80\mu s$; duty factor $\leq 0.1\%$.

④ Pulse width $5.0\mu s$, single shot.

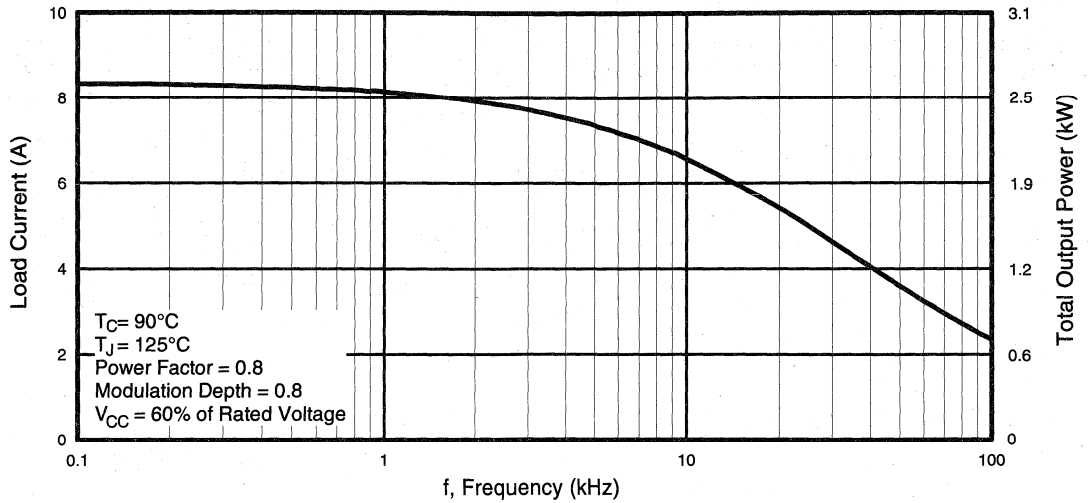


Fig. 1 - RMS Current and Output Power, Synthesized Sine Wave

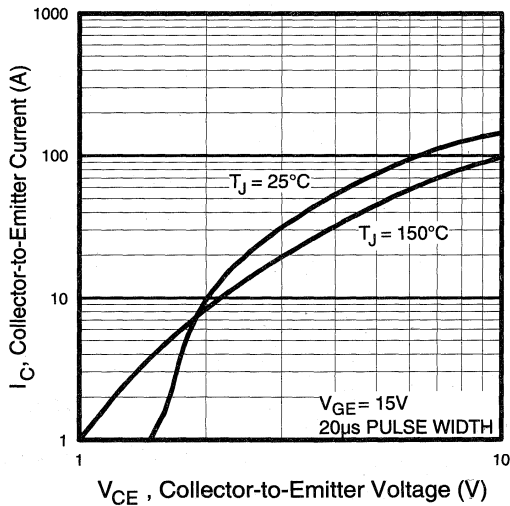


Fig. 2 - Typical Output Characteristics

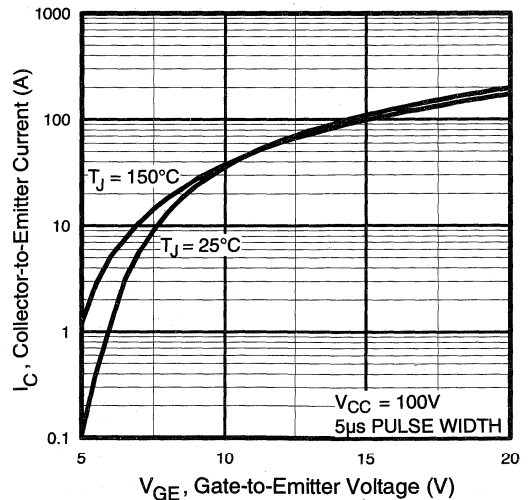


Fig. 3 - Typical Transfer Characteristics

Power
 Conversion
 Ultra-Fast
 Modules

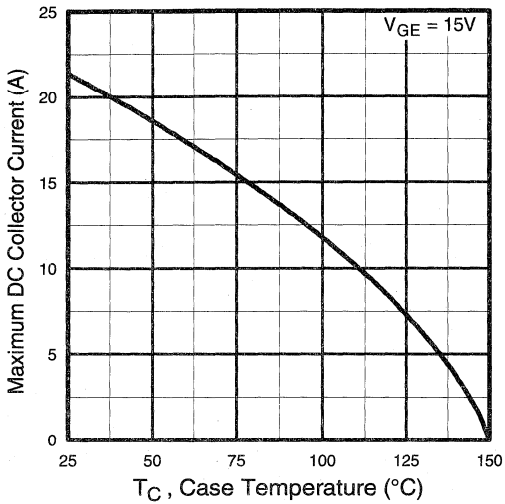


Fig. 4 - Maximum Collector Current vs. Case Temperature

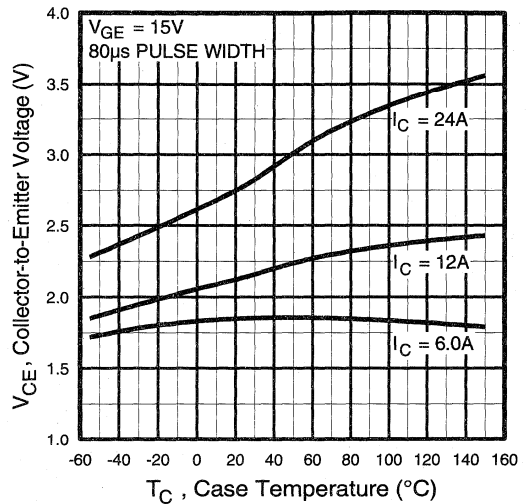


Fig. 5 - Collector-to-Emitter Voltage vs. Case Temperature

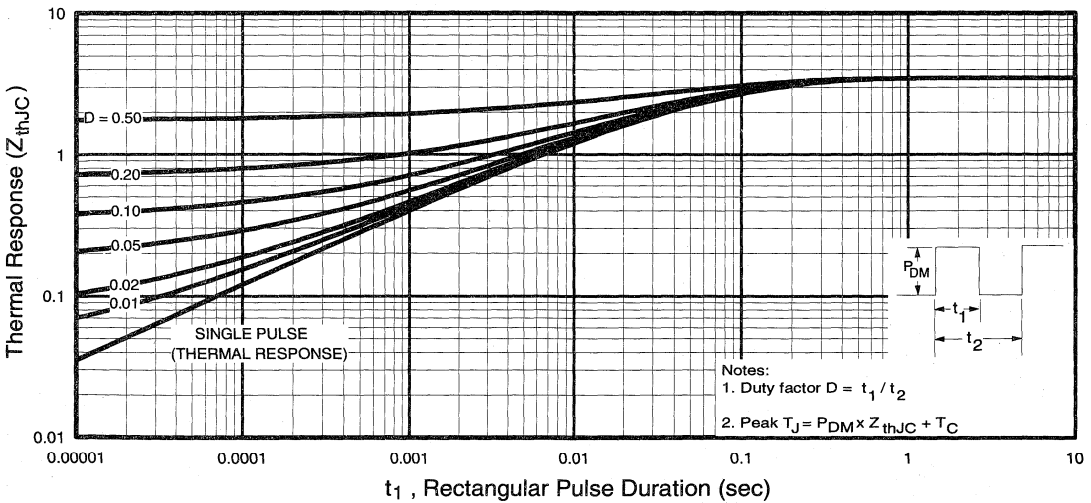


Fig. 6 - Maximum IGBT Effective Transient Thermal Impedance, Junction-to-Case

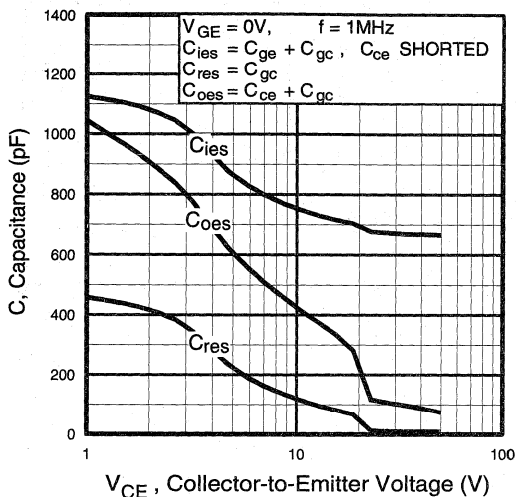


Fig. 7 - Typical Capacitance vs. Collector-to-Emitter Voltage

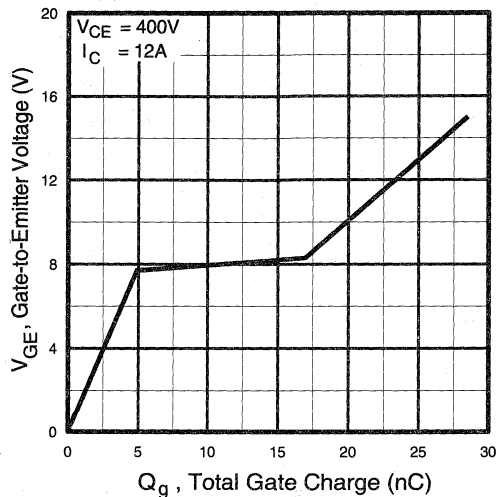


Fig. 8 - Typical Gate Charge vs. Gate-to-Emitter Voltage

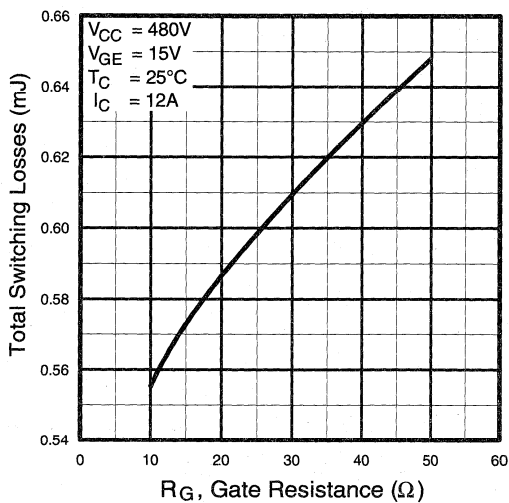


Fig. 9 - Typical Switching Losses vs. Gate Resistance

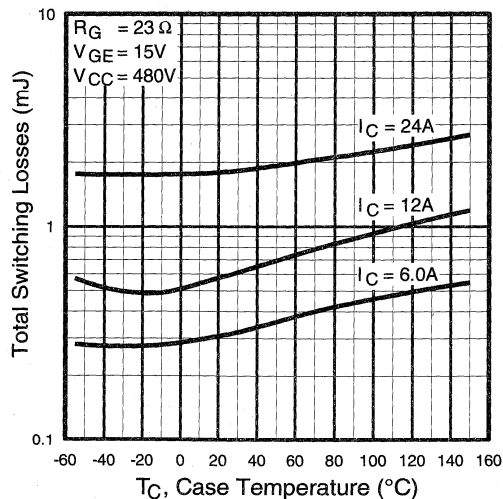


Fig. 10 - Typical Switching Losses vs. Case Temperature

Power Conversion
 Ultra-Fast
 Modules

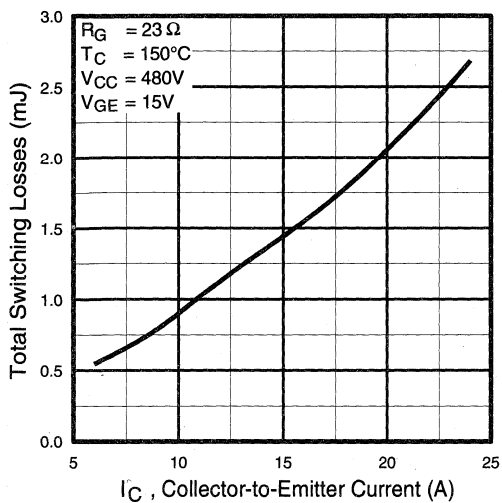


Fig. 11 - Typical Switching Losses vs. Collector-to-Emitter Current

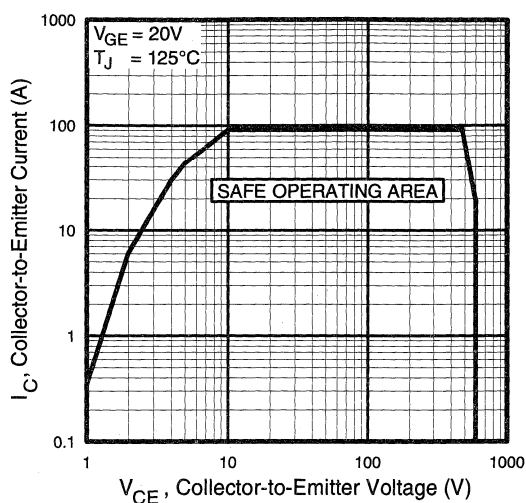


Fig. 12 - Turn-Off SOA

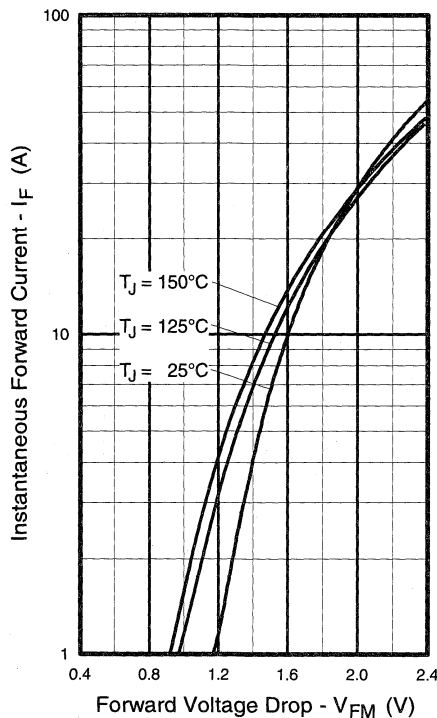


Fig. 13 - Maximum Forward Voltage Drop vs. Instantaneous Forward Current

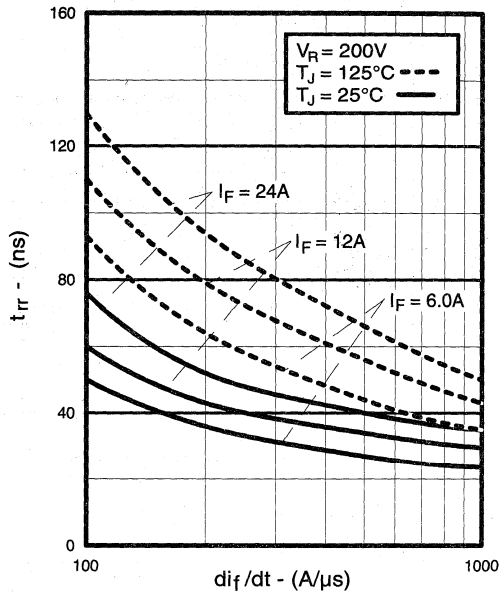


Fig. 14 - Typical Reverse Recovery vs. di_f/dt

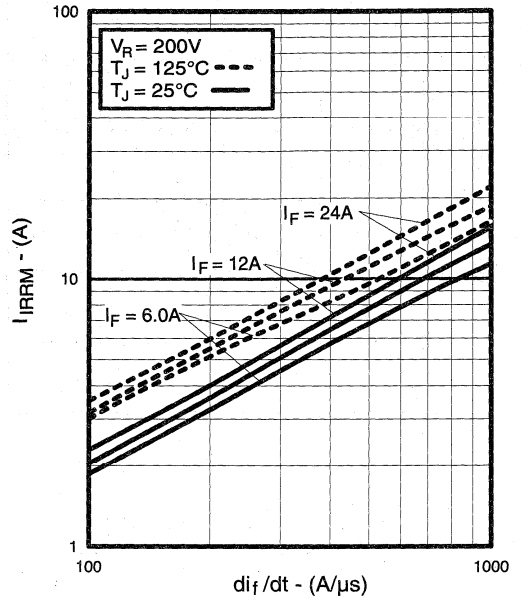


Fig. 15 - Typical Recovery Current vs. di_f/dt

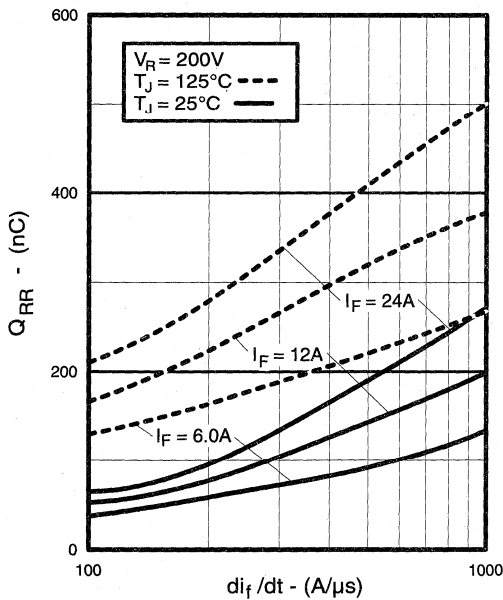


Fig. 16 - Typical Stored Charge vs. di_f/dt

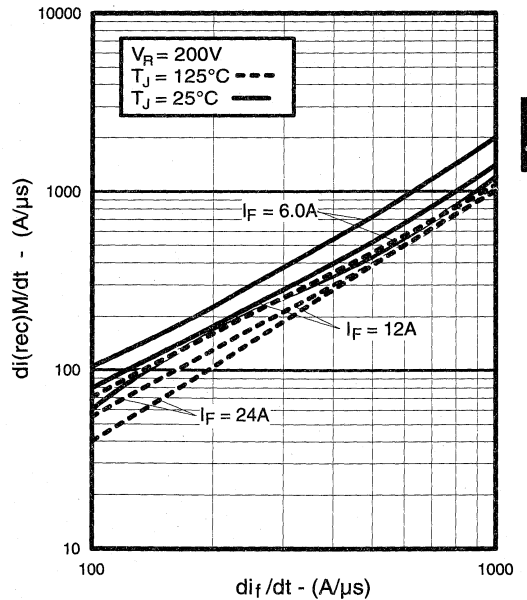


Fig. 17 - Typical $di_{(rec)M}/dt$ vs. di_f/dt

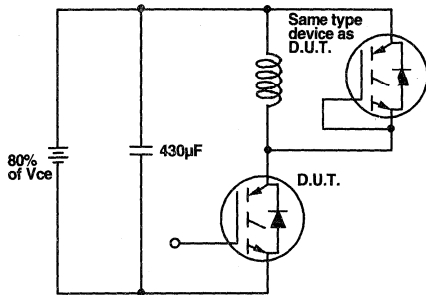


Fig.18a - Test Circuit for Measurement of I_{LM} , E_{on} , $E_{off}(\text{diode})$, t_{rr} , Q_{rr} , I_{rr} , $t_{d(on)}$, t_r , $t_{d(off)}$, t_f

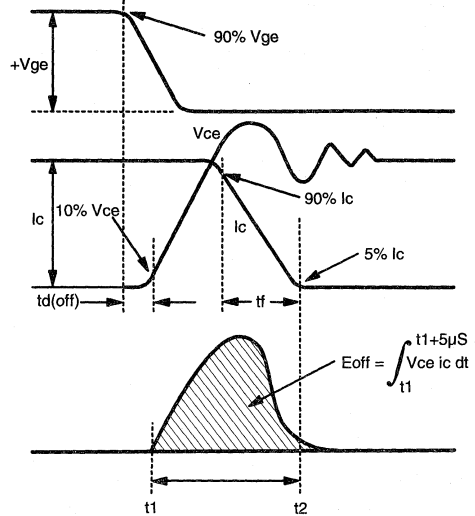


Fig. 18b - Test Waveforms for Circuit of Fig. 18a, Defining E_{off} , $t_{d(off)}$, t_f

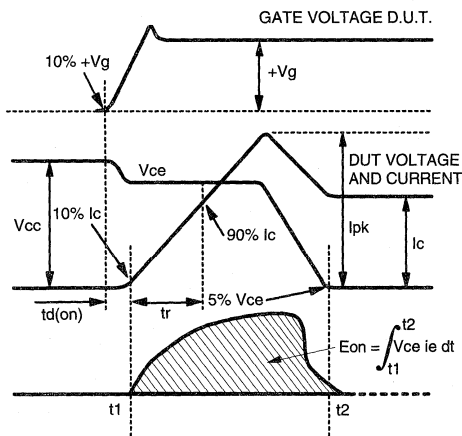


Fig. 18c - Test Waveforms for Circuit of Fig. 18a, Defining E_{on} , $t_{d(on)}$, t_r

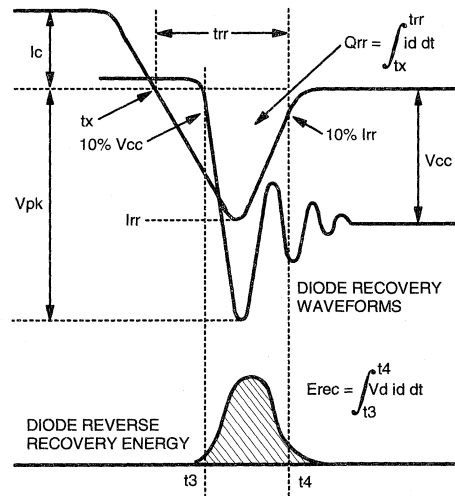


Fig. 18d - Test Waveforms for Circuit of Fig. 18a, Defining E_{rec} , t_{rr} , Q_{rr} , I_{rr}

Refer to Section D for the following:
Appendix D: Section D - page D-6

Fig. 18e - Macro Waveforms for Test Circuit of Fig. 18a

Fig. 19 - Clamped Inductive Load Test Circuit

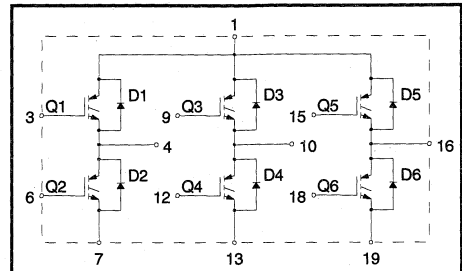
Fig. 20 - Pulsed Collector Current Test Circuit

IGBT SIP MODULE

Ultra-Fast IGBT

Features

- Fully isolated printed circuit board mount package
 - Switching-loss rating includes all "tail" losses
 - HEXFRED™ soft ultrafast diodes
 - Optimized for high operating frequency (over 5kHz)
- See Fig. 1 for Current vs. Frequency curve



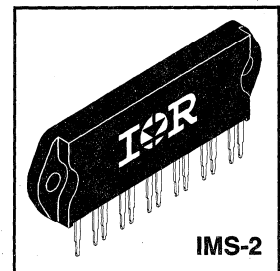
Product Summary

Output Current in a Typical 20 kHz Motor Drive

5.4 A_{RMS} per phase (1.7 kW total) with T_C = 90°C, T_J = 125°C, Supply Voltage 360Vdc, Power Factor 0.8, Modulation Depth 80% (See Figure 1)

Description

The IGBT technology is the key to International Rectifier's advanced line of IMS (Insulated Metal Substrate) Power Modules. These modules are more efficient than comparable bipolar transistor modules, while at the same time having the simpler gate-drive requirements of the familiar power MOSFET. This superior technology has now been coupled to a state of the art materials system that maximizes power throughput with low thermal resistance. This package is highly suited to motor drive applications and where space is at a premium.



Absolute Maximum Ratings

	Parameter	Max.	Units
V _{CES}	Collector-to-Emitter Voltage	600	V
I _C @ T _C = 25°C	Continuous Collector Current, each IGBT	20	A
I _C @ T _C = 100°C	Continuous Collector Current, each IGBT	10	
I _{CM}	Pulsed Collector Current ①	60	
I _{LM}	Clamped Inductive Load Current ②	60	
I _F @ T _C = 100°C	Diode Continuous Forward Current	9.3	
I _{FM}	Diode Maximum Forward Current	60	
V _{GE}	Gate-to-Emitter Voltage	±20	V
V _{ISOL}	Isolation Voltage, any terminal to case, 1 min.	2500	V _{RMS}
P _D @ T _C = 25°C	Maximum Power Dissipation, each IGBT	63	W
P _D @ T _C = 100°C	Maximum Power Dissipation, each IGBT	25	
T _J	Operating Junction and	-40 to +150	°C
T _{STG}	Storage Temperature Range		
	Soldering Temperature, for 10 sec.	300 (0.063 in. (1.6mm) from case)	
	Mounting torque, 6-32 or M3 screw.	5-7 lbf•in (0.55-0.8 N•m)	

Thermal Resistance

	Parameter	Typ.	Max.	Units
R _{θJC} (IGBT)	Junction-to-Case, each IGBT, one IGBT in conduction	—	2.0	°C/W
R _{θJC} (DIODE)	Junction-to-Case, each diode, one diode in conduction	—	3.0	
R _{θCS} (MODULE)	Case-to-Sink, flat, greased surface	0.1	—	
Wt	Weight of module	20 (0.7)	—	g (oz)

Electrical Characteristics @ $T_J = 25^\circ\text{C}$ (unless otherwise specified)

	Parameter	Min.	Typ.	Max.	Units	Conditions
$V_{(BR)CES}$	Collector-to-Emitter Breakdown Voltage ^②	600	—	—	V	$V_{GE} = 0V, I_C = 250\mu\text{A}$
$\Delta V_{(BR)CES}/\Delta T_J$	Temp. Coeff. of Breakdown Voltage	—	0.63	—	$V/^\circ\text{C}$	$V_{GE} = 0V, I_C = 1.0\text{mA}$
$V_{CE(on)}$	Collector-to-Emitter Saturation Voltage	—	2.0	2.6	V	$I_C = 10A$ $V_{GE} = 15V$ See Fig. 2, 5
		—	2.3	—		
		—	1.7	—		
$V_{GE(th)}$	Gate Threshold Voltage	3.0	—	5.5		$V_{CE} = V_{GE}, I_C = 250\mu\text{A}$
$\Delta V_{GE(th)}/\Delta T_J$	Temp. Coeff. of Threshold Voltage	—	-13	—	$\text{mV}/^\circ\text{C}$	$V_{CE} = V_{GE}, I_C = 250\mu\text{A}$
g_{fe}	Forward Transconductance ^④	11	18	—	S	$V_{CE} = 100V, I_C = 20A$
I_{CES}	Zero Gate Voltage Collector Current	—	—	250	μA	$V_{GE} = 0V, V_{CE} = 600V$ $V_{GE} = 0V, V_{CE} = 600V, T_J = 150^\circ\text{C}$
		—	—	3500		
V_{FM}	Diode Forward Voltage Drop	—	1.3	1.7	V	$I_C = 15A$ See Fig. 13 $I_C = 15A, T_J = 150^\circ\text{C}$
		—	1.2	1.6		
I_{GES}	Gate-to-Emitter Leakage Current	—	—	± 500	nA	$V_{GE} = \pm 20V$

Switching Characteristics @ $T_J = 25^\circ\text{C}$ (unless otherwise specified)

	Parameter	Min.	Typ.	Max.	Units	Conditions
Q_g	Total Gate Charge (turn-on)	—	51	67	nC	$I_C = 20A$ $V_{CC} = 400V$ See Fig. 8
Q_{ge}	Gate - Emitter Charge (turn-on)	—	8.8	11		
Q_{gc}	Gate - Collector Charge (turn-on)	—	19	33		
$t_{d(on)}$	Turn-On Delay Time	—	25	—	ns	$T_J = 25^\circ\text{C}$ $I_C = 20A, V_{CC} = 480V$ $V_{GE} = 15V; R_G = 10\Omega$ Energy losses include "tail" and diode reverse recovery. See Fig. 9, 10, 11, 18
t_r	Rise Time	—	21	—		
$t_{d(off)}$	Turn-Off Delay Time	—	96	190		
t_f	Fall Time	—	43	120		
E_{on}	Turn-On Switching Loss	—	0.32	—	mJ	See Fig. 9, 10, 11, 18
E_{off}	Turn-Off Switching Loss	—	0.13	—		
E_{ts}	Total Switching Loss	—	0.45	0.8		
$t_{d(on)}$	Turn-On Delay Time	—	25	—	ns	$T_J = 150^\circ\text{C}$, See Fig. 9, 10, 11, 18 $I_C = 20A, V_{CC} = 480V$ $V_{GE} = 15V, R_G = 10\Omega$ Energy losses include "tail" and diode reverse recovery.
t_r	Rise Time	—	23	—		
$t_{d(off)}$	Turn-Off Delay Time	—	175	—		
t_f	Fall Time	—	140	—		
E_{ts}	Total Switching Loss	—	1.6	—	mJ	
C_{ies}	Input Capacitance	—	1500	—	pF	$V_{GE} = 0V$ $V_{CC} = 30V$ See Fig. 7 $f = 1.0\text{MHz}$
C_{oes}	Output Capacitance	—	190	—		
C_{res}	Reverse Transfer Capacitance	—	17	—		
t_{rr}	Diode Reverse Recovery Time	—	42	60	ns	$T_J = 25^\circ\text{C}$ See Fig. 14 $T_J = 125^\circ\text{C}$ 14
		—	74	120		
I_{rr}	Diode Peak Reverse Recovery Current	—	4.0	6.0	A	$T_J = 25^\circ\text{C}$ See Fig. 15 $T_J = 125^\circ\text{C}$ 15
		—	6.5	10		
Q_{rr}	Diode Reverse Recovery Charge	—	80	180	nC	$T_J = 25^\circ\text{C}$ See Fig. 16 $T_J = 125^\circ\text{C}$ 16
		—	220	600		
$di_{(rec)M}/dt$	Diode Peak Rate of Fall of Recovery During t_b	—	188	—	$\text{A}/\mu\text{s}$	$T_J = 25^\circ\text{C}$ See Fig. 17 $T_J = 125^\circ\text{C}$ 17
		—	160	—		

Notes:

① Repetitive rating; $V_{GE}=20V$, pulse width limited by max. junction temperature. (See fig. 20)

② $V_{CC}=80\%(V_{CES})$, $V_{GE}=20V$, $L=10\mu\text{H}$, $R_G=10\Omega$, (See fig. 19)

③ Pulse width $\leq 80\mu\text{s}$; duty factor $\leq 0.1\%$.

④ Pulse width 5.0 μs , single shot.

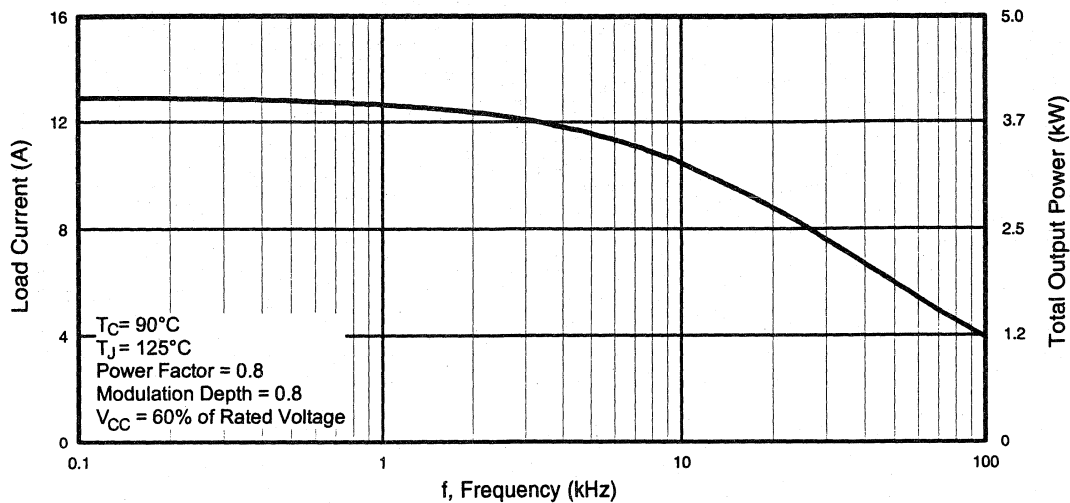


Fig. 1 - RMS Current and Output Power, Synthesized Sine Wave

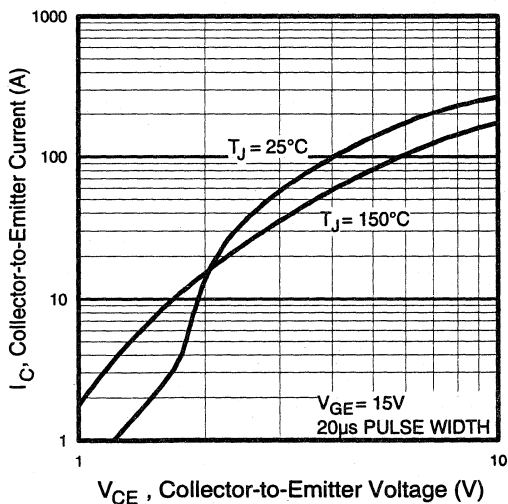


Fig. 2 - Typical Output Characteristics

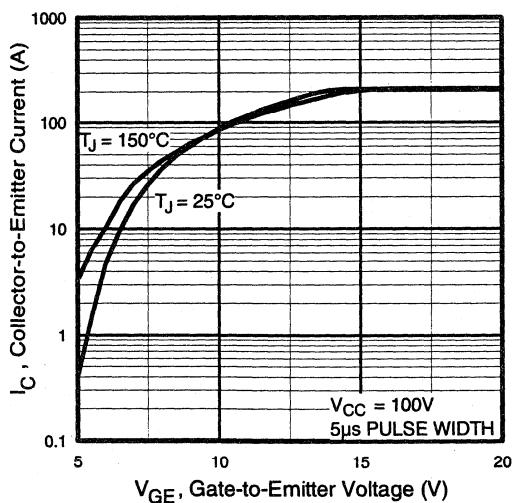


Fig. 3 - Typical Transfer Characteristics

Power Conversion
 Ultra-Fast Modules

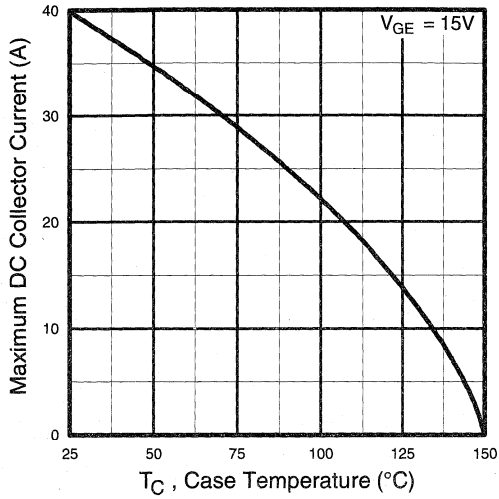


Fig. 4 - Maximum Collector Current vs. Case Temperature

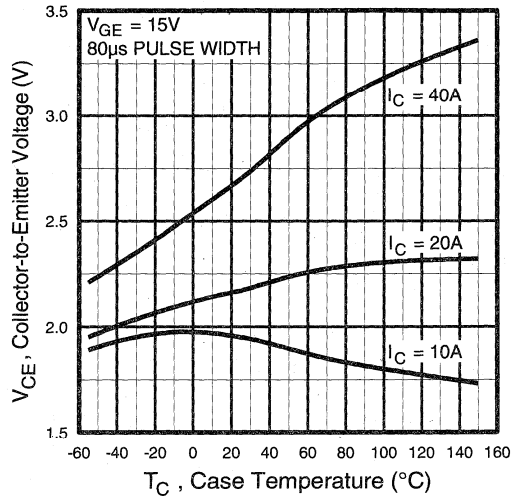


Fig. 5 - Collector-to-Emitter Voltage vs. Case Temperature

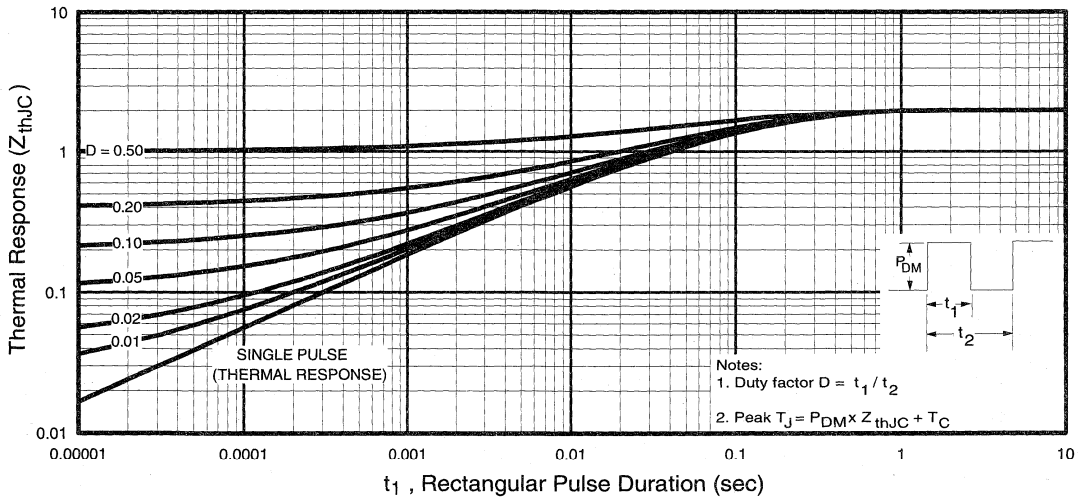


Fig. 6 - Maximum IGBT Effective Transient Thermal Impedance, Junction-to-Case

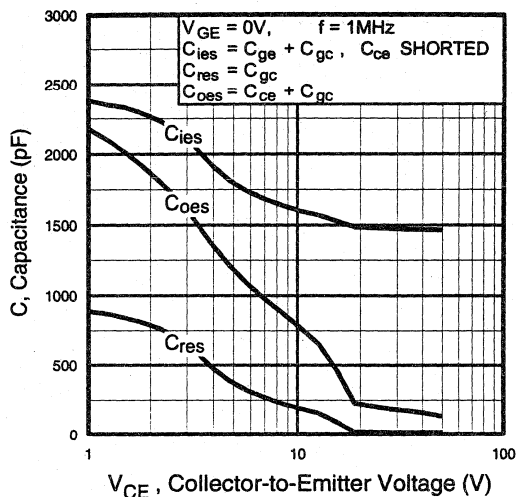


Fig. 7 - Typical Capacitance vs. Collector-to-Emitter Voltage

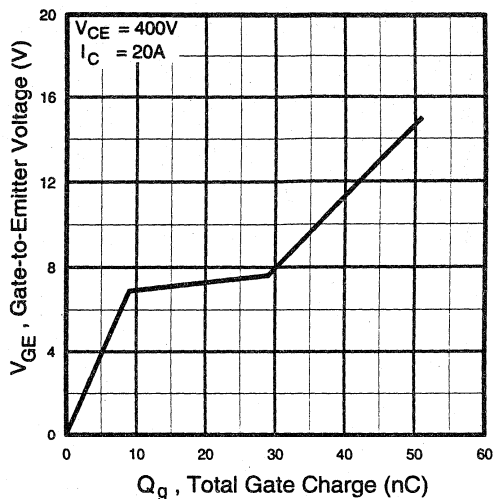


Fig. 8 - Typical Gate Charge vs. Gate-to-Emitter Voltage

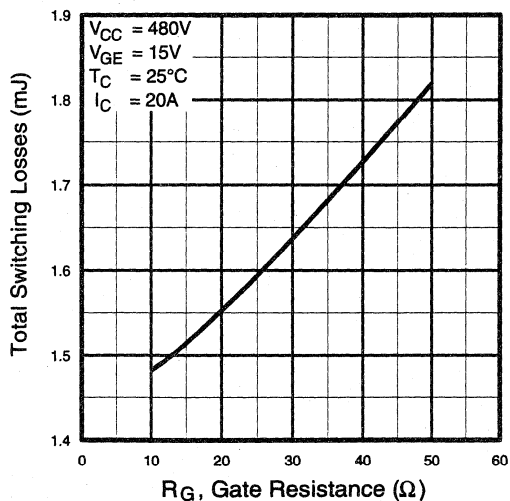


Fig. 9 - Typical Switching Losses vs. Gate Resistance

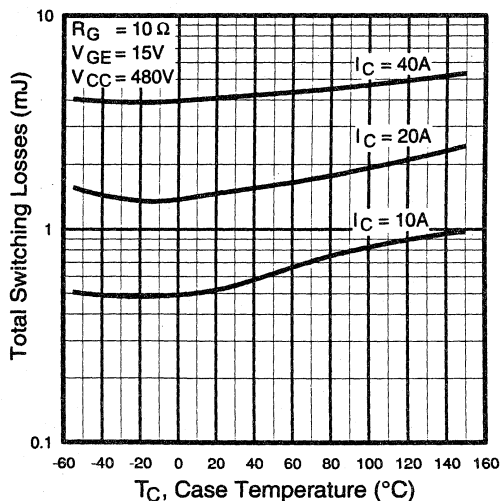


Fig. 10 - Typical Switching Losses vs. Case Temperature

Power
Conversion
Ultra-Fast
Modules

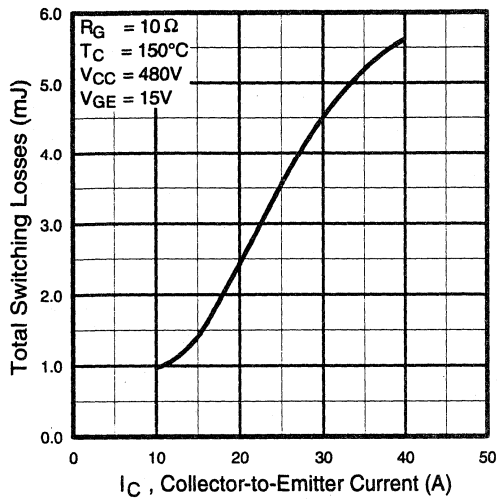


Fig. 11 - Typical Switching Losses vs. Collector-to-Emitter Current

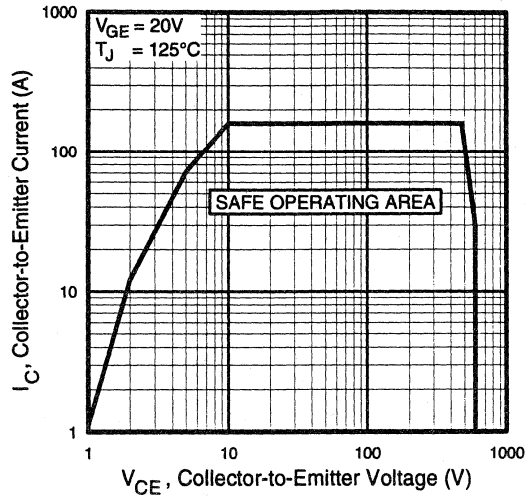


Fig. 12 - Turn-Off SOA

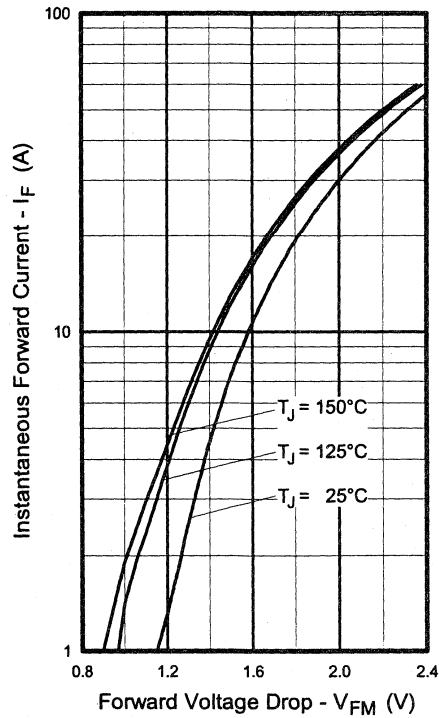


Fig. 13 - Maximum Forward Voltage Drop vs. Instantaneous Forward Current

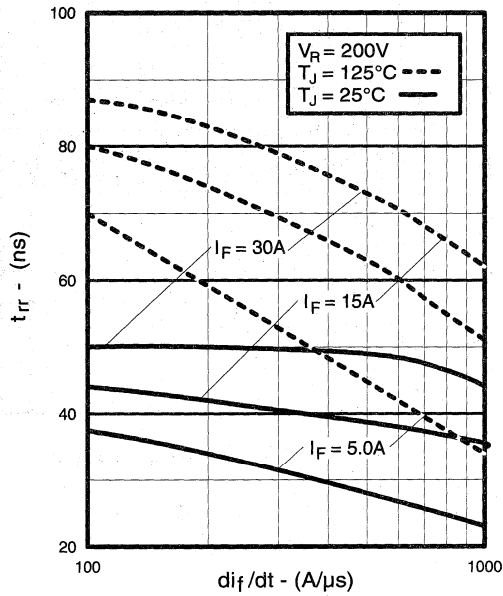


Fig. 14 - Typical Reverse Recovery vs. di_f/dt

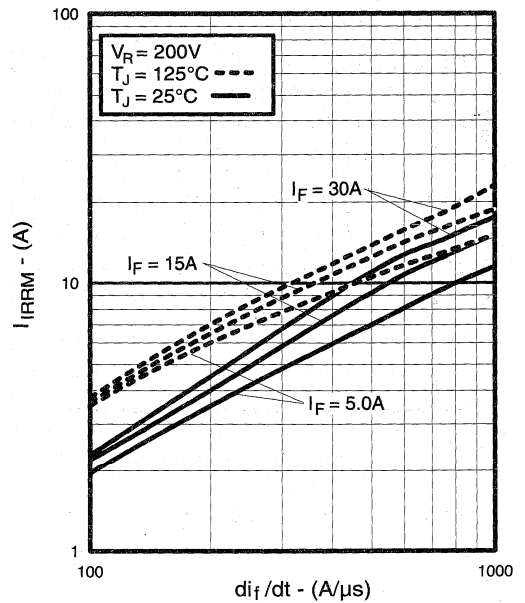


Fig. 15 - Typical Recovery Current vs. di_f/dt

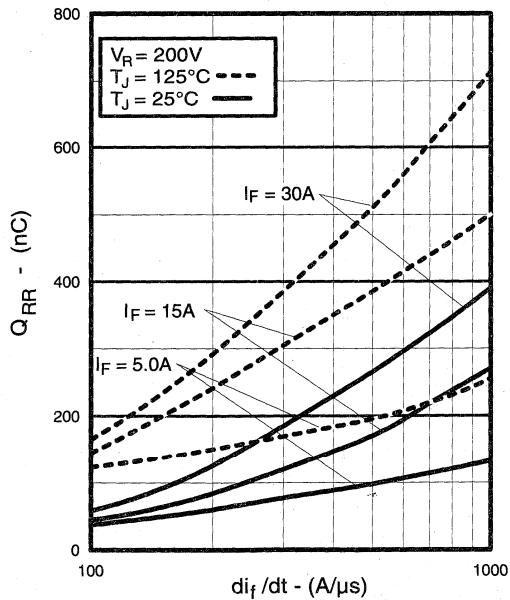


Fig. 16 - Typical Stored Charge vs. di_f/dt

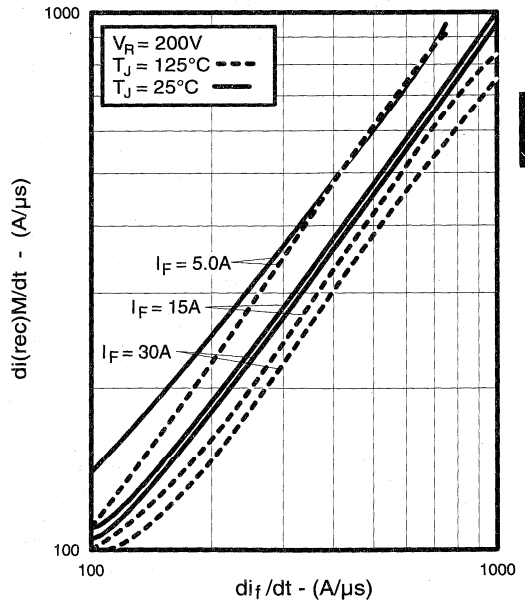


Fig. 17 - Typical $di_{(rec)M}/dt$ vs. di_f/dt

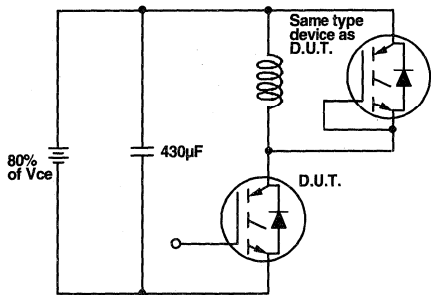


Fig. 18a - Test Circuit for Measurement of I_{LM} , E_{on} , $E_{off}(\text{diode})$, t_{rr} , Q_{rr} , I_{rr} , $t_{d(on)}$, t_r , $t_{d(off)}$, t_f

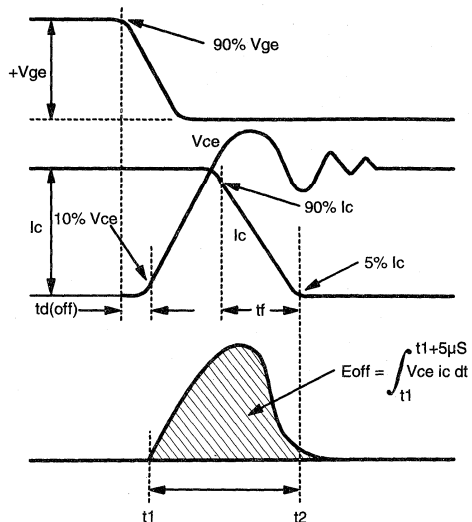


Fig. 18b - Test Waveforms for Circuit of Fig. 18a, Defining E_{off} , $t_{d(off)}$, t_f

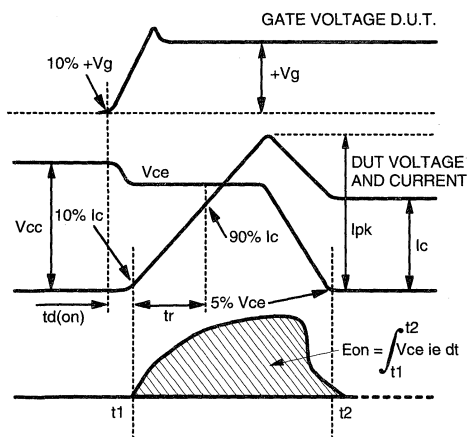


Fig. 18c - Test Waveforms for Circuit of Fig. 18a, Defining E_{on} , $t_{d(on)}$, t_r

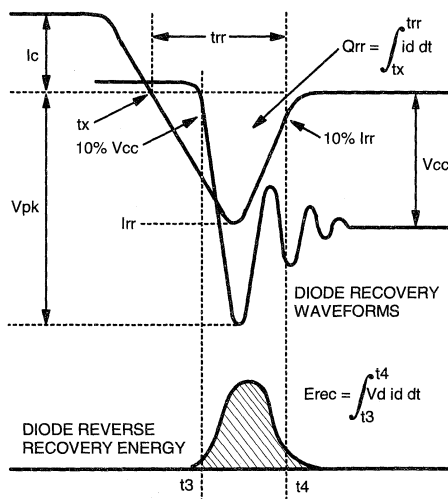


Fig. 18d - Test Waveforms for Circuit of Fig. 18a, Defining E_{rec} , t_{rr} , Q_{rr} , I_{rr}

Refer to Section D for the following:
Appendix D: Section D - page D-6

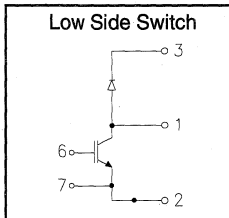
- Fig. 18e - Macro Waveforms for Test Circuit of Fig. 18a
- Fig. 19 - Clamped Inductive Load Test Circuit
- Fig. 20 - Pulsed Collector Current Test Circuit

IRGKI050U06

"CHOPPER" IGBT INT-A-PAK

Ultra-fast™ Speed IGBT

- Rugged Design
- Simple gate-drive
- Ultra-fast operation up to 25KHz hard switching, or 100KHz resonant
- Switching-Loss Rating includes all "tail" losses



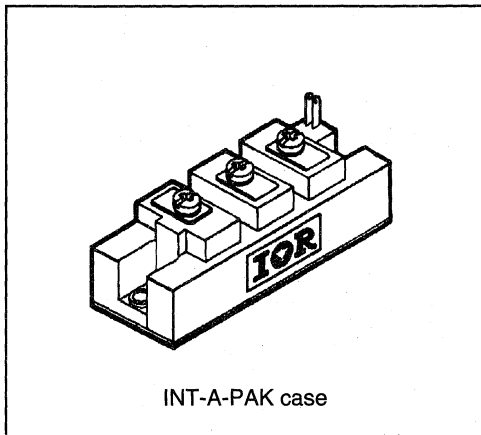
$$V_{CE} = 600V$$

$$I_C = 50A$$

$$V_{CE(ON)} < 3.1V$$

Description

IR's advanced IGBT technology is the key to this line of INT-A-pak Power Modules. The efficient geometry and unique processing of the IGBT allow higher current densities than comparable bipolar power module transistors, while at the same time requiring the simpler gate-drive of the familiar power MOSFET. This superior technology has now been coupled to state of the art assembly techniques to produce a higher current module that is highly suited to power applications such as motor drives, uninterruptible power supplies, welding, induction heating and ultrasonics.



Absolute Maximum Ratings

Parameter	Description	Value	Units
V_{CES}	Continuous collector to emitter voltage	600	V
$I_C @ T_C = 25^\circ C$	Continuous collector current	50	A
$I_C @ T_C = 85^\circ C$	Continuous collector current	35	
$I_C @ T_C = 100^\circ C$	Continuous collector current	30	
I_{LM}	Peak switching current	100	
I_{FM}	Peak diode forward current (1)	125	
V_{GE}	Gate to emitter voltage	± 20	V
V_{ISOL}	RMS isolation voltage, any terminal to case, $t = 1$ min	2500	
$P_D @ T_C = 25^\circ C$	Power dissipation	179	W
T_J	Operating junction temperature range	-40 to 150	$^\circ C$
T_{STG}	Storage temperature range	-40 to 125	

(1) Duration limited by max junction temperature.

Electrical Characteristics - $T_J = 25^\circ\text{C}$, unless otherwise stated

Parameter	Description	Min	Typ	Max	Units	Test Conditions
BV_{CES}	Collector-to-emitter breakdown voltage	600	—	—	V	$V_{GE} = 0V, I_C = 500\mu A$
$V_{CE(ON)}$	Collector-to-emitter voltage	—	—	3.1		$V_{GE} = 15V, I_C = 50A$
		—	3.3	—		$V_{GE} = 15V, I_C = 50A, T_J = 150^\circ\text{C}$
V_{FM}	Diode forward voltage - maximum	—	—	2.9		$I_F = 50A, V_{GE} = 0V$
		—	2.8	—		$I_F = 50A, V_{GE} = 0V, T_J = 150^\circ\text{C}$
V_{Geth}	Gate threshold voltage	3.0	—	5.5	$I_C = 250\mu A$	
ΔV_{Geth}	Threshold voltage temp. coefficient	—	-11	—	mV/°C	$V_{CE} = V_{GE}, I_C = 250\mu A$
g_{fe}	Forward transconductance	17.3	—	29.6	S(Ω)	$V_{CE} = 25V, I_C = 50A$
I_{CES}	Collector-to-emitter leakage current	—	—	500	μA	$V_{GE} = 0V, V_{CE} = 600V$
		—	—	5	mA	$V_{GE} = 0V, V_{CE} = 600V, T_J = 150^\circ\text{C}$
I_{GES}	Gate-to-emitter leakage current	—	—	±500	nA	$V_{GE} = \pm 20V$

Dynamic Characteristics - $T_J = 150^\circ\text{C}$

Parameter	Description	Min	Typ	Max	Units	Test Conditions
E_{on}	Turn-on switching energy	—	0.05	—	mJ/A	$R_{G1} = 82\Omega, R_{G2} = 0\Omega$
E_{off} (1)	Turn-off switching energy	—	0.05	—		$I_C = 50A, L_S = 100nH$
E_{ts} (1)	Total switching energy	—	—	0.12		$V_{CC} = 360V, V_{GE} = \pm 15V$
$t_{d(on)}$	Turn-on delay time	—	70	—	ns	$R_{G1} = 82\Omega, R_{G2} = 0\Omega$
t_r	Rise time	—	90	—		$I_C = 50A$
$t_{d(off)}$	Turn-off delay time	—	180	—		$V_{CC} = 360V, V_{GE} = \pm 15V$
t_f	Fall time	—	250	—		$L_S = 100nH$
I_{rr}	Diode peak recovery current	—	27	—		A
t_{rr}	Diode recovery time	—	110	—	ns	$I_C = 50A$
Q_{rr}	Diode recovery charge	—	1.6	—	μC	$V_{CC} = 360V, V_{GE} = \pm 15V$
Q_{ge}	Gate-to-emitter charge (turn-on)	77	—	140	nC	$V_{CC} = 360V$
Q_{gc}	Gate-to-collector charge (turn-on)	35	—	70		$I_C = 50A$
Q_g	Total gate charge (turn-on)	13	—	21		$V_{GE} = 15V$
C_{ies}	Input capacitance	—	2900	—	pF	$V_{GE} = 0V$
C_{oes}	Output capacitance	—	330	—		$V_{CC} = 30V$
C_{res}	Reverse transfer capacitance	—	40	—		$f = 1MHz$

(1) Includes tail losses

Thermal and Mechanical Characteristics

Parameter	Description	Typ	Max	Units
R_{thJC} (IGBT)	Thermal resistance, junction to case, each IGBT	—	0.7	°C/W
R_{thJC} (Diode)	Thermal resistance, junction to case, each diode	—	1.3	
R_{thCS} (Module)	Thermal resistance, case to sink	0.1	—	
Wt	Weight of module	140	—	g

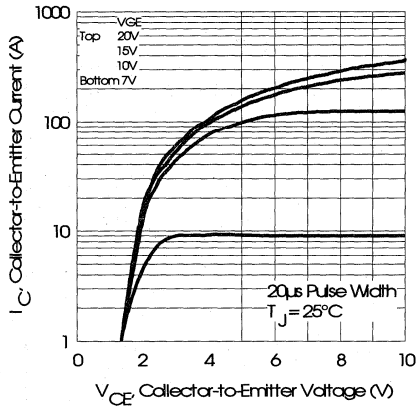


Fig. 1 - Typical Output Characteristics, $T_J = 25^\circ\text{C}$

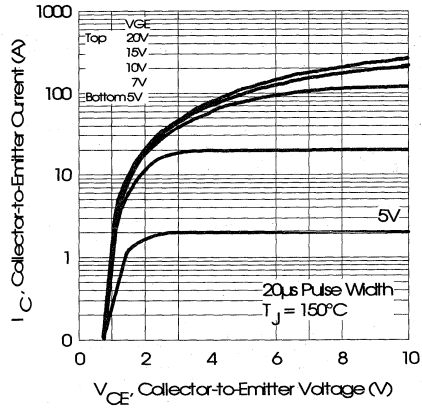


Fig. 2 - Typical Output Characteristics, $T_J = 150^\circ\text{C}$

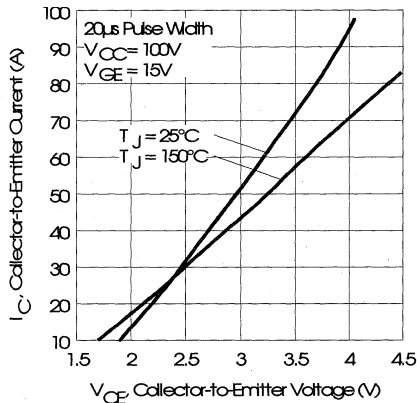


Fig. 3 - Typical Output Characteristics

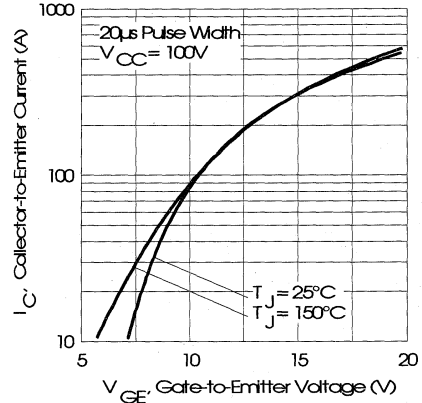


Fig. 4 - Typical Transfer Characteristics

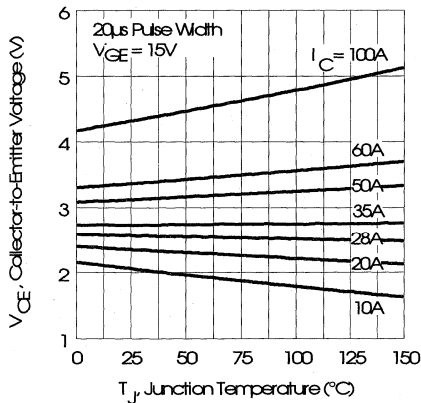


Fig. 5 - Collector-to-Emitter Saturation Typical Voltage vs. Junction Temperature

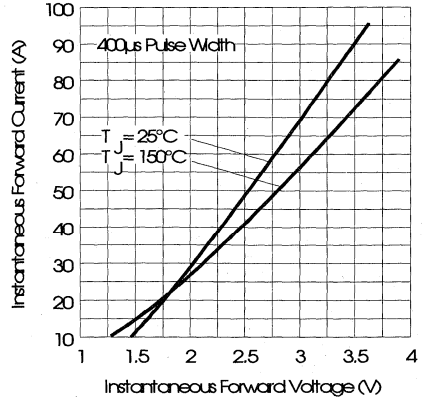


Fig. 6 - Forward Voltage Drop Characteristics

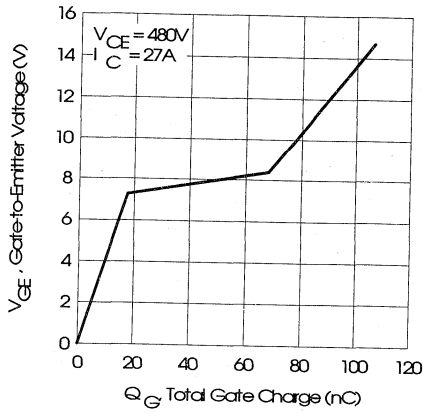


Fig. 7 - Typical Gate Charge vs. Gate-to-Emitter Voltage

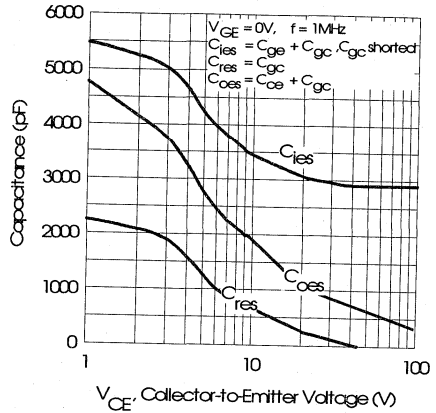


Fig. 8 - Typical Capacitance vs. Collector-to-Emitter Voltage

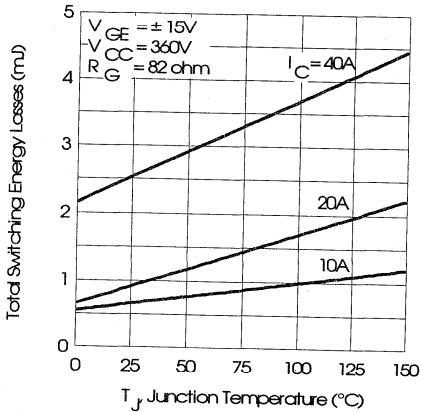


Fig. 9 - Typical Switching Losses vs. Junction Temperature

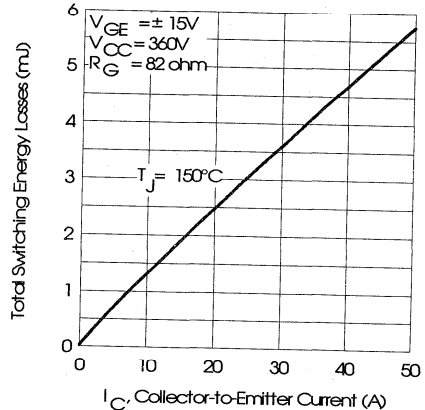


Fig. 10 - Typical Switching Losses vs. Collector-to-Emitter Current

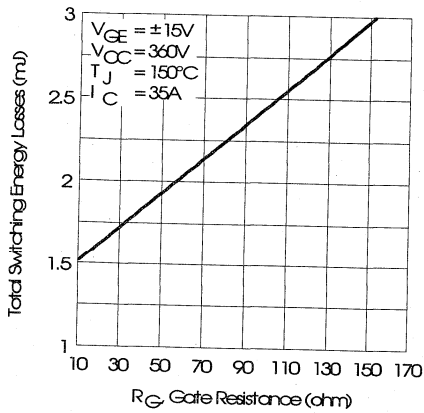


Fig. 11 - Typical Switching Losses vs. Gate Resistance

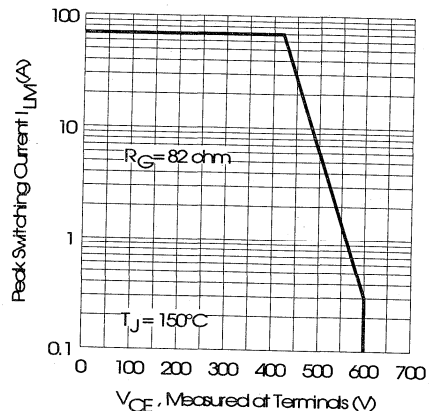


Fig. 12 - Reverse Bias Safe Operating Area

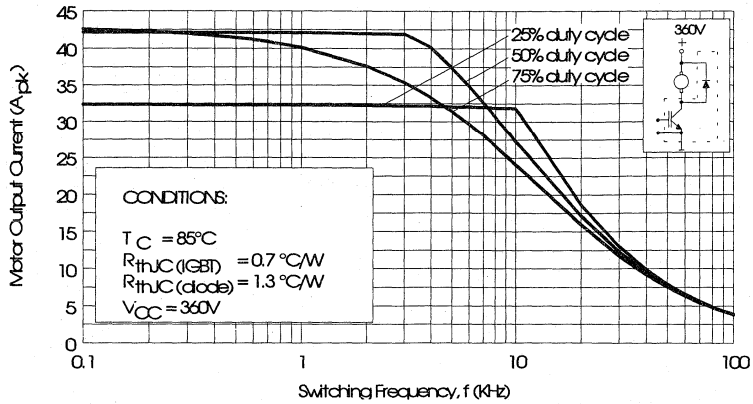


Fig. 13 - RMS Output Current vs. Frequency

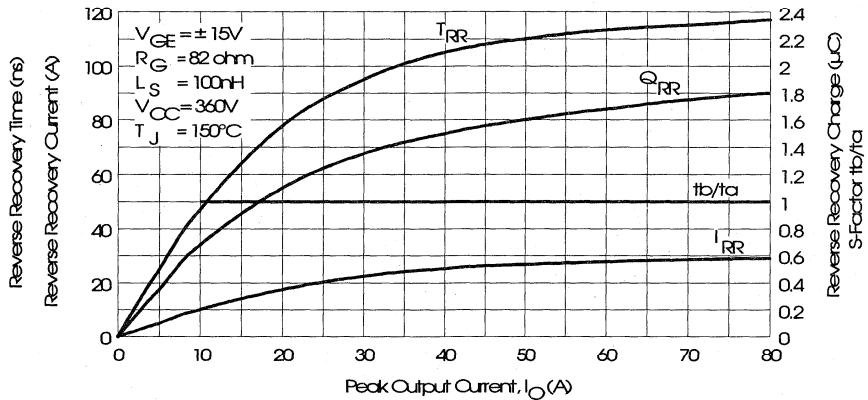


Fig. 14 - Typical Diode Recovery Characteristics as Function of Output Current I_o

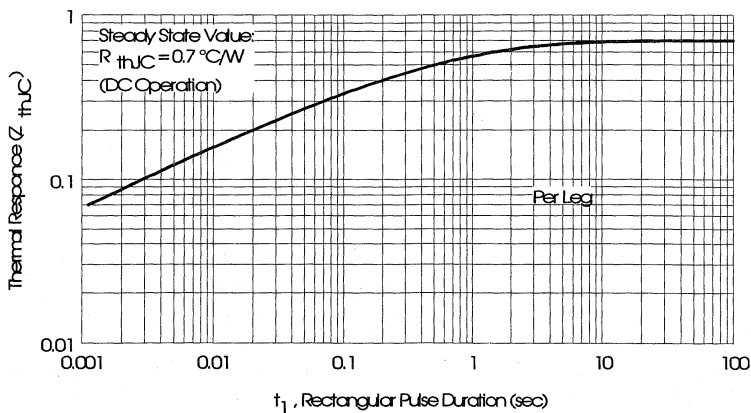


Fig. 15 - Maximum Effective Transient Thermal Impedance, Junction-to-Case

Power Conversion
Ultra-Fast
Modules

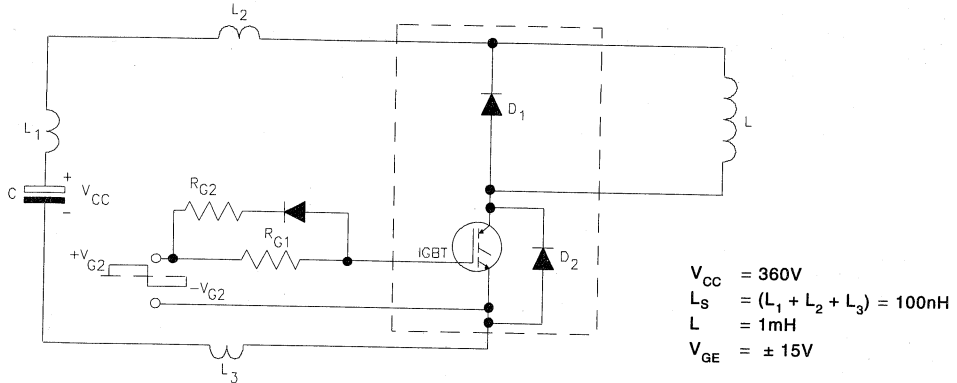


Fig. 16 - Test Circuit for Measurement of I_{LM} , E_{ON} , E_{OFF} , Q_{RR} , I_{RR} , $t_{D(ON)}$, t_r , $t_{D(OFF)}$, t_f

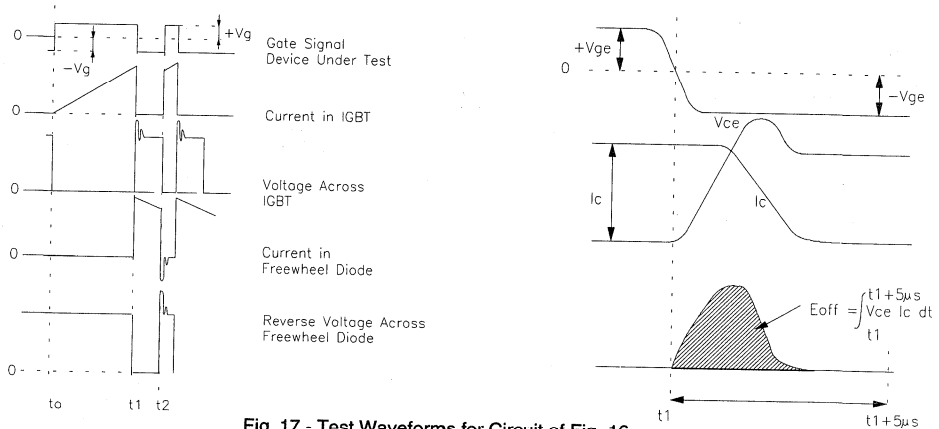


Fig. 17 - Test Waveforms for Circuit of Fig. 16

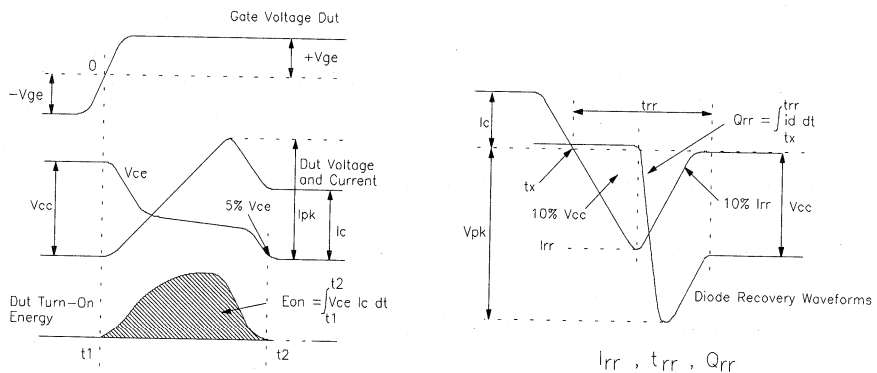


Fig. 18 - Test Waveforms for Circuit of Fig. 16, Defining E_{ON} , E_{REC} , $t_{D(ON)}$, t_r , I_{RR} , t_{RR} , Q_{RR}

Refer to Section D for the following:
 Appendix E: Section D - page D-7

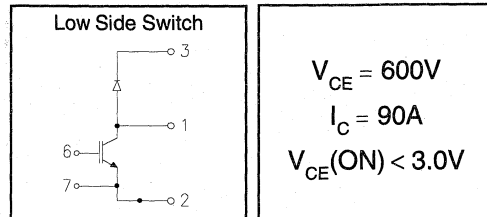
Fig. 19 - Waveforms for Switching Time

IRGKI090U06

"CHOPPER" IGBT INT-A-PAK

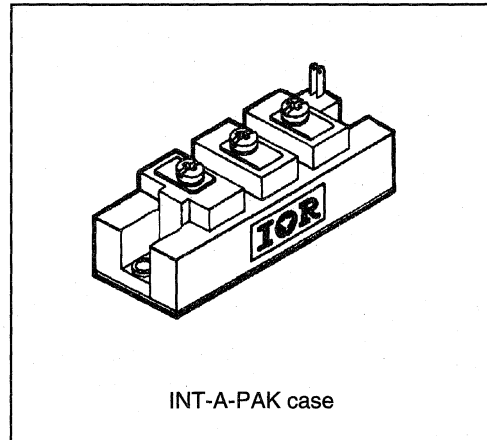
Ultra-fast™ Speed IGBT

- Rugged Design
- Simple gate-drive
- Ultra-fast operation up to 25KHz hard switching, or 100KHz resonant
- Switching-Loss Rating includes all "tail" losses



Description

IR's advanced IGBT technology is the key to this line of INT-A-pak Power Modules. The efficient geometry and unique processing of the IGBT allow higher current densities than comparable bipolar power module transistors, while at the same time requiring the simpler gate-drive of the familiar power MOSFET. This superior technology has now been coupled to state of the art assembly techniques to produce a higher current module that is highly suited to power applications such as motor drives, uninterruptible power supplies, welding, induction heating and ultrasonics.



Absolute Maximum Ratings

Parameter	Description	Value	Units
V_{CES}	Continuous collector to emitter voltage	600	V
$I_C @ T_C = 25^\circ C$	Continuous collector current	90	A
$I_C @ T_C = 85^\circ C$	Continuous collector current	60	
$I_C @ T_C = 100^\circ C$	Continuous collector current	50	
I_{LM}	Peak switching current	180	
I_{FM}	Peak diode forward current (1)	225	V
V_{GE}	Gate to emitter voltage	± 20	
V_{ISOL}	RMS isolation voltage, any terminal to case, $t = 1 \text{ min}$	2500	
$P_D @ T_C = 25^\circ C$	Power dissipation	298	W
T_J	Operating junction temperature range	-40 to 150	$^\circ C$
T_{STG}	Storage temperature range	-40 to 125	

(1) Duration limited by max junction temperature.

Electrical Characteristics - $T_J = 25^\circ\text{C}$, unless otherwise stated

Parameter	Description	Min	Typ	Max	Units	Test Conditions
BV_{CES}	Collector-to-emitter breakdown voltage	600	—	—	V	$V_{GE} = 0V, I_C = 1mA$
$V_{CE(ON)}$	Collector-to-emitter voltage	—	—	3.0		$V_{GE} = 15V, I_C = 90A$
		—	3.1	—		$V_{GE} = 15V, I_C = 90A, T_J = 150^\circ\text{C}$
V_{FM}	Diode forward voltage - maximum	—	—	2.8		$I_F = 90A, V_{GE} = 0V$
		—	2.6	—		$I_F = 90A, V_{GE} = 0V, T_J = 150^\circ\text{C}$
V_{GEth}	Gate threshold voltage	3.0	—	5.5	$I_C = 500\mu A$	
ΔV_{GEth}	Threshold voltage temp. coefficient	—	-11	—	mV/°C	$V_{CE} = V_{GE}, I_C = 500\mu A$
g_{fe}	Forward transconductance	34	—	58	S(Ω)	$V_{CE} = 25V, I_C = 90A$
I_{CES}	Collector-to-emitter leakage current	—	—	1	mA	$V_{GE} = 0V, V_{CE} = 600V$
		—	—	10		$V_{GE} = 0V, V_{CE} = 600V, T_J = 150^\circ\text{C}$
I_{GES}	Gate-to-emitter leakage current	—	—	±1	μA	$V_{GE} = \pm 20V$

Dynamic Characteristics - $T_J = 150^\circ\text{C}$

Parameter	Description	Min	Typ	Max	Units	Test Conditions
E_{on}	Turn-on switching energy	—	0.05	—	mJ/A	$R_{G1} = 47\Omega, R_{G2} = 0\Omega$
E_{off} (1)	Turn-off switching energy	—	0.05	—		$I_C = 90A, L_S = 100nH$
E_{ts} (1)	Total switching energy	—	—	0.12		$V_{CC} = 360V, V_{GE} = \pm 15V$
$t_{d(on)}$	Turn-on delay time	—	70	—	ns	$R_{G1} = 47\Omega, R_{G2} = 0\Omega$
t_r	Rise time	—	90	—		$I_C = 90A$
$t_{d(off)}$	Turn-off delay time	—	180	—		$V_{CC} = 360V, V_{GE} = \pm 15V$
t_f	Fall time	—	250	—		$L_S = 100nH$
I_{rr}	Diode peak recovery current	—	52	—		A
t_{rr}	Diode recovery time	—	110	—	ns	$I_C = 90A$
Q_{rr}	Diode recovery charge	—	3.0	—	μC	$V_{CC} = 360V, V_{GE} = \pm 15V$
Q_{ge}	Gate-to-emitter charge (turn-on)	150	—	280	nC	$V_{CC} = 360V$
Q_{gc}	Gate-to-collector charge (turn-on)	70	—	140		$I_C = 90A$
Q_g	Total gate charge (turn-on)	26	—	42		$V_{GE} = 15V$
C_{ies}	Input capacitance	—	5800	—	pF	$V_{GE} = 0V$
C_{oes}	Output capacitance	—	660	—		$V_{CC} = 30V$
C_{res}	Reverse transfer capacitance	—	80	—		$f = 1MHz$

(1) Includes tail losses

Thermal and Mechanical Characteristics

Parameter	Description	Typ	Max	Units
R_{thJC} (IGBT)	Thermal resistance, junction to case, each IGBT	—	0.42	°C/W
R_{thJC} (Diode)	Thermal resistance, junction to case, each diode	—	0.7	
R_{thCS} (Module)	Thermal resistance, case to sink	0.1	—	
Wt	Weight of module	140	—	g

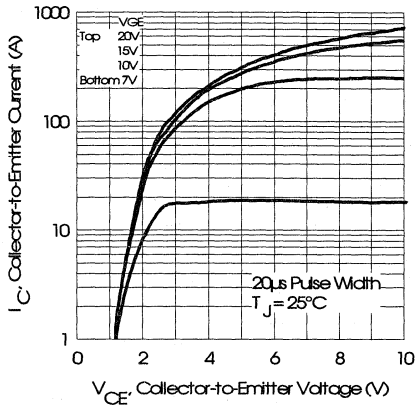


Fig. 1 - Typical Output Characteristics, $T_J = 25^\circ\text{C}$

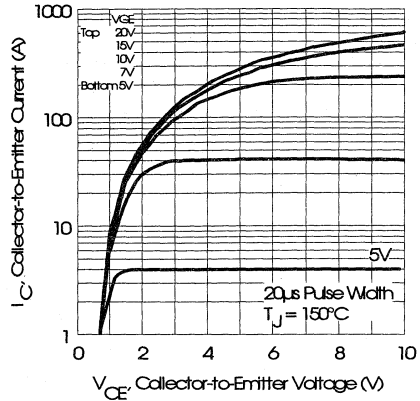


Fig. 2 - Typical Output Characteristics, $T_J = 150^\circ\text{C}$

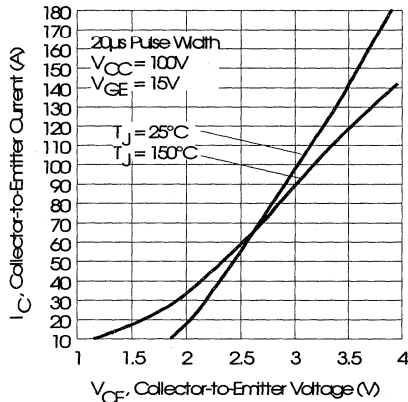


Fig. 3 - Typical Output Characteristics

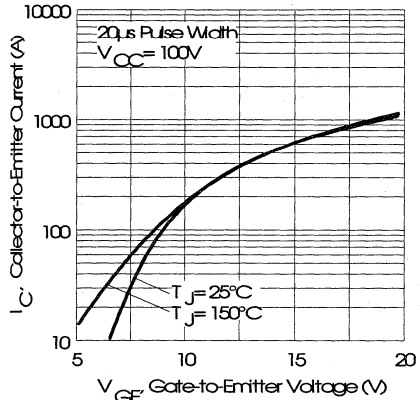


Fig. 4 - Typical Transfer Characteristics

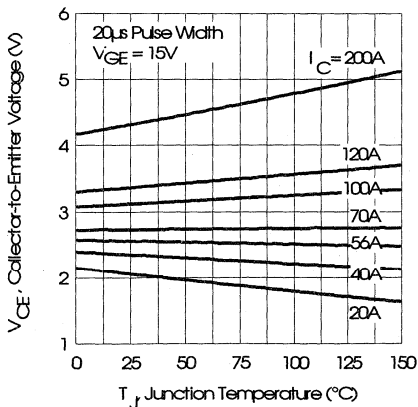


Fig. 5 - Collector-to-Emitter Saturation Typical Voltage vs. Junction Temperature

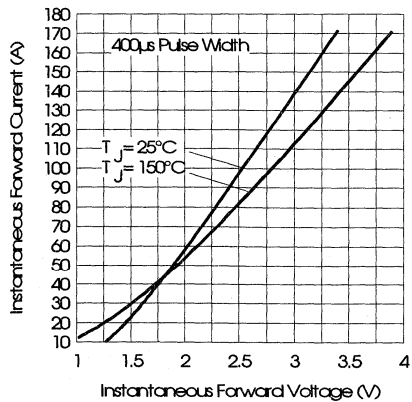


Fig. 6 - Forward Voltage Drop Characteristics

Power
Conversion
Ultra-Fast
Modules

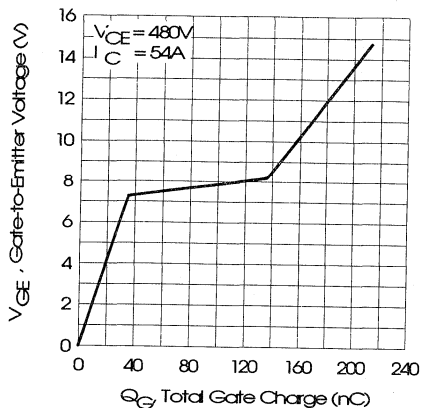


Fig. 7 - Typical Gate Charge vs. Gate-to-Emitter Voltage

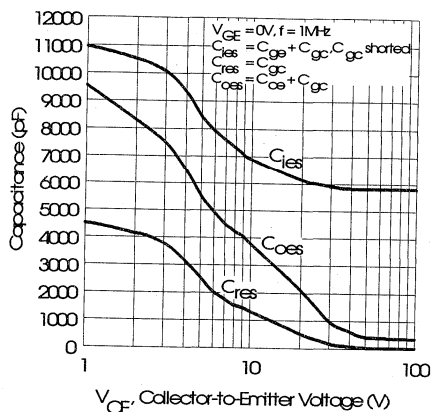


Fig. 8 - Typical Capacitance vs. Collector-to-Emitter Voltage

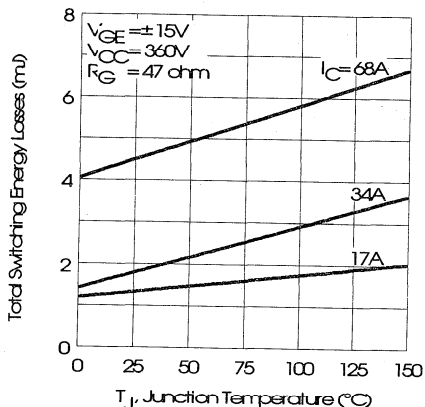


Fig. 9 - Typical Switching Losses vs. Junction Temperature

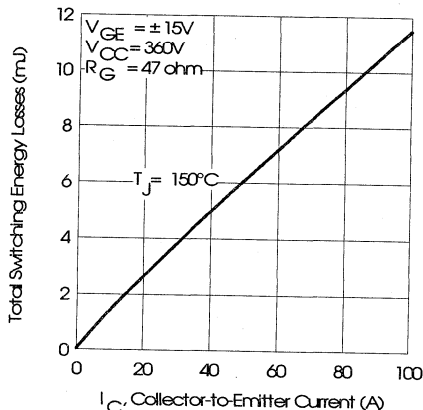


Fig. 10 - Typical Switching Losses vs. Collector-to-Emitter Current

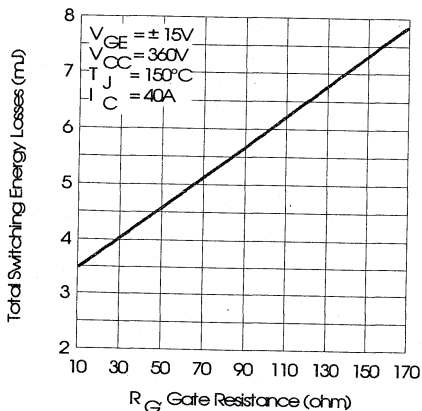


Fig. 11 - Typical Switching Losses vs. Gate Resistance

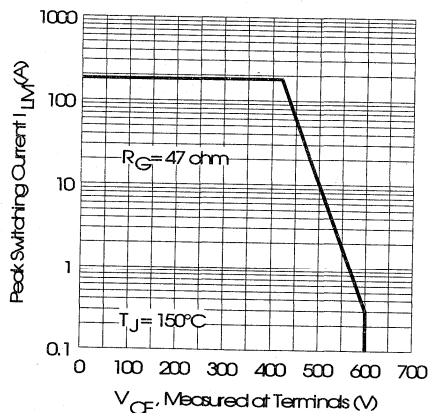


Fig. 12 - Reverse Bias Safe Operating Area

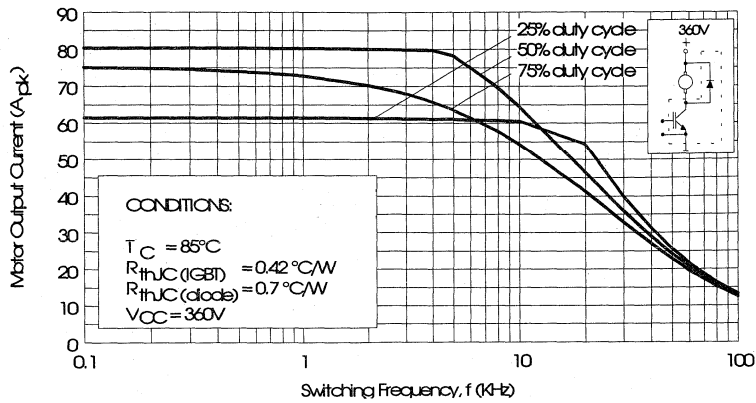


Fig. 13 - RMS Output Current vs. Frequency

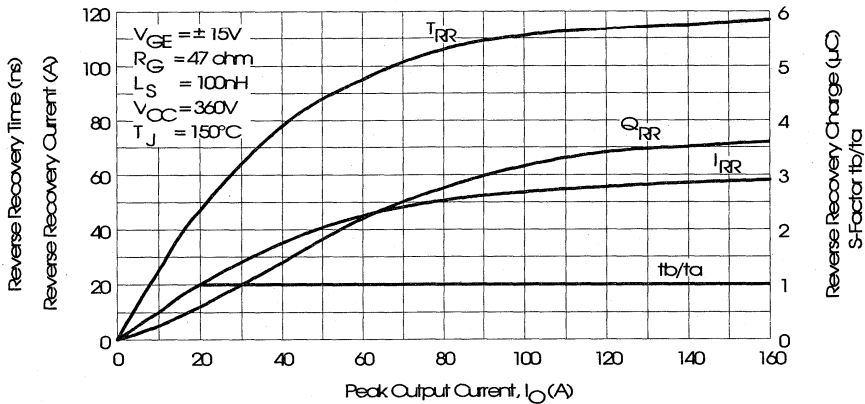


Fig. 14 - Typical Diode Recovery Characteristics as Function of Output Current I_O

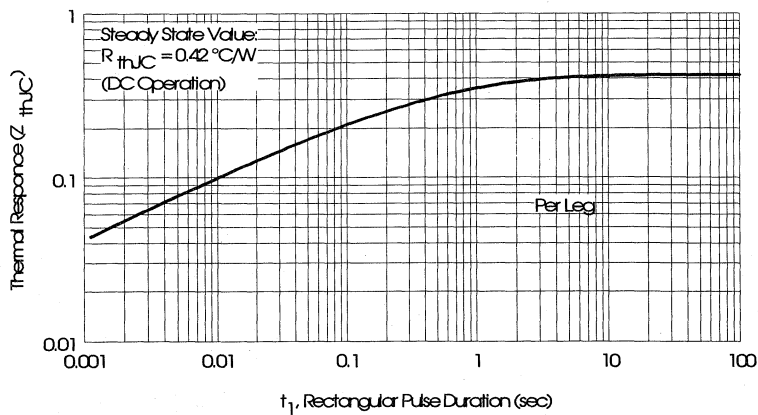


Fig. 15 - Maximum Effective Transient Thermal Impedance, Junction-to-Case

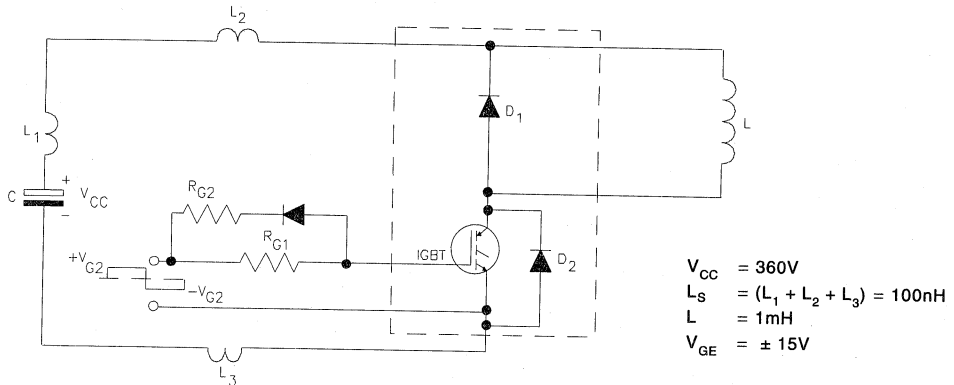


Fig. 16 - Test Circuit for Measurement of I_{LM} , E_{ON} , E_{OFF} , Q_{RR} , I_{RR} , $t_{D(ON)}$, t_r , $t_{D(OFF)}$, t_f

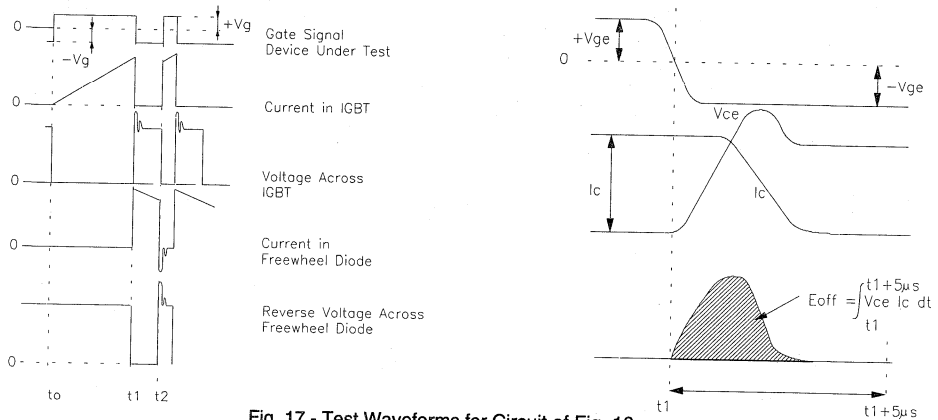


Fig. 17 - Test Waveforms for Circuit of Fig. 16

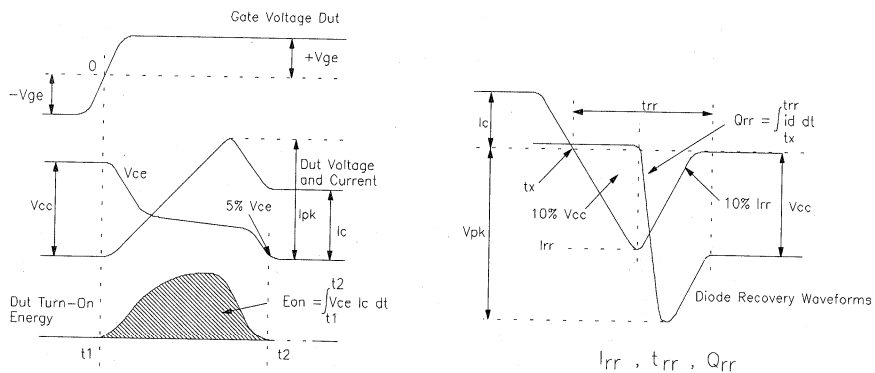


Fig. 18 - Test Waveforms for Circuit of Fig. 16, Defining E_{ON} , E_{REC} , $t_{D(ON)}$, t_r , I_{RR} , t_{RR} , Q_{RR}

Refer to Section D for the following:

Appendix E: Section D - page D-7

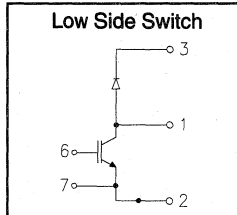
Fig. 19 - Waveforms for Switching Time

IRGKI115U06

"CHOPPER" IGBT INT-A-PAK

Ultra-fast™ Speed IGBT

- Rugged Design
- Simple gate-drive
- Ultra-fast operation up to 25KHz hard switching, or 100KHz resonant
- Switching-Loss Rating includes all "tail" losses



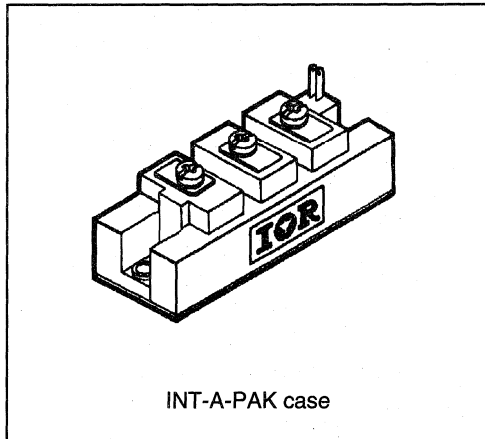
$$V_{CE} = 600V$$

$$I_C = 115A$$

$$V_{CE(ON)} < 2.8V$$

Description

IR's advanced IGBT technology is the key to this line of INT-A-pak Power Modules. The efficient geometry and unique processing of the IGBT allow higher current densities than comparable bipolar power module transistors, while at the same time requiring the simpler gate-drive of the familiar power MOSFET. This superior technology has now been coupled to state of the art assembly techniques to produce a higher current module that is highly suited to power applications such as motor drives, uninterruptible power supplies, welding, induction heating and ultrasonics.



Absolute Maximum Ratings

Parameter	Description	Value	Units
V_{CES}	Continuous collector to emitter voltage	600	V
$I_C @ T_C = 25^\circ C$	Continuous collector current	130	A
$I_C @ T_C = 85^\circ C$	Continuous collector current	85	
$I_C @ T_C = 100^\circ C$	Continuous collector current	70	
I_{LM}	Peak switching current	230	
I_{FM}	Peak diode forward current (1)	290	V
V_{GE}	Gate to emitter voltage	± 20	
V_{ISOL}	RMS isolation voltage, any terminal to case, $t = 1$ min	2500	W
$P_D @ T_C = 25^\circ C$	Power dissipation	379	
T_J	Operating junction temperature range	-40 to 150	$^\circ C$
T_{STG}	Storage temperature range	-40 to 125	

(1) Duration limited by max junction temperature.

Power
Conversion
Ultra-fast
Modules

Electrical Characteristics - $T_J = 25^\circ\text{C}$, unless otherwise stated

Parameter	Description	Min	Typ	Max	Units	Test Conditions
BV_{CES}	Collector-to-emitter breakdown voltage	600	—	—	V	$V_{GE} = 0V, I_C = 1.5mA$
$V_{CE(ON)}$	Collector-to-emitter voltage	—	—	2.8		$V_{GE} = 15V, I_C = 115A$
		—	2.9	—		$V_{GE} = 15V, I_C = 115A, T_J = 150^\circ\text{C}$
V_{FM}	Diode forward voltage - maximum	—	—	2.7		$I_F = 115A, V_{GE} = 0V$
		—	2.4	—		$I_F = 115A, V_{GE} = 0V, T_J = 150^\circ\text{C}$
V_{GEth}	Gate threshold voltage	3.0	—	5.5	$I_C = 750\mu A$	
ΔV_{GEth}	Threshold voltage temperature coefficient	—	-11	—	mV/°C	$V_{CE} = V_{GE}, I_C = 750\mu A$
g_{fe}	Forward transconductance	51	—	87	S(Ω)	$V_{CE} = 25V, I_C = 115A$
I_{CES}	Collector-to-emitter leakage current	—	—	1.5	mA	$V_{GE} = 0V, V_{CE} = 600V$
		—	—	15		$V_{GE} = 0V, V_{CE} = 600V, T_J = 150^\circ\text{C}$
I_{GES}	Gate-to-emitter leakage current	—	—	± 1.5	μA	$V_{GE} = \pm 20V$

Dynamic Characteristics - $T_J = 150^\circ\text{C}$

Parameter	Description	Min	Typ	Max	Units	Test Conditions
E_{on}	Turn-on switching energy	—	0.05	—	mJ/A	$R_{G1} = 33\Omega, R_{G2} = 0\Omega$
E_{off} (1)	Turn-off switching energy	—	0.05	—		$I_C = 115A, L_S = 100nH$
E_{ts} (1)	Total switching energy	—	—	0.12		$V_{CC} = 360V, V_{GE} = \pm 15V$
$t_{d(on)}$	Turn-on delay time	—	70	—	ns	$R_{G1} = 33\Omega, R_{G2} = 0\Omega$
t_r	Rise time	—	90	—		$I_C = 115A$
$t_{d(off)}$	Turn-off delay time	—	180	—		$V_{CC} = 360V, V_{GE} = \pm 15V$
t_f	Fall time	—	250	—		$L_S = 100nH$
I_{rr}	Diode peak recovery current	—	72	—		$R_{G1} = 33\Omega, R_{G2} = 0\Omega$
t_{rr}	Diode recovery time	—	110	—	ns	$I_C = 115A$
Q_{rr}	Diode recovery charge	—	4.0	—	μC	$V_{CC} = 360V, V_{GE} = \pm 15V$
Q_{ge}	Gate-to-emitter charge (turn-on)	225	—	420	nC	$V_{CC} = 360V$
Q_{gc}	Gate-to-collector charge (turn-on)	105	—	210		$I_C = 115A$
Q_g	Total gate charge (turn-on)	39	—	63		$V_{GE} = 15V$
C_{ies}	Input capacitance	—	8700	—	pF	$V_{GE} = 0V$
C_{oes}	Output capacitance	—	990	—		$V_{CC} = 30V$
C_{res}	Reverse transfer capacitance	—	120	—		$f = 1MHz$

(1) Includes tail losses

Thermal and Mechanical Characteristics

Parameter	Description	Typ	Max	Units
R_{thJC} (IGBT)	Thermal resistance, junction to case, each IGBT	—	0.33	°C/W
R_{thJC} (Diode)	Thermal resistance, junction to case, each diode	—	0.55	
R_{thCS} (Module)	Thermal resistance, case to sink	0.1	—	
Wt	Weight of module	140	—	g

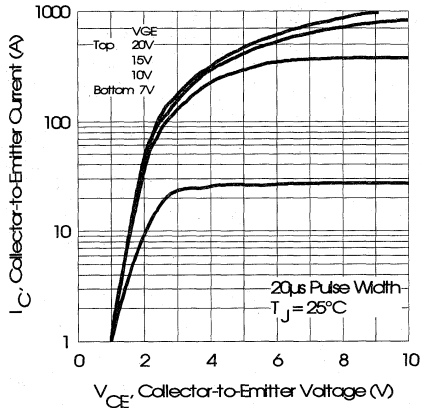


Fig. 1 - Typical Output Characteristics, $T_J = 25^\circ\text{C}$

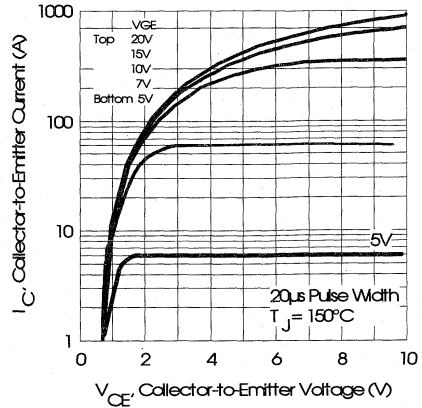


Fig. 2 - Typical Output Characteristics, $T_J = 150^\circ\text{C}$

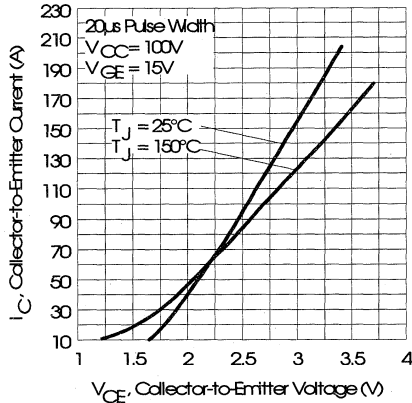


Fig. 3 - Typical Output Characteristics

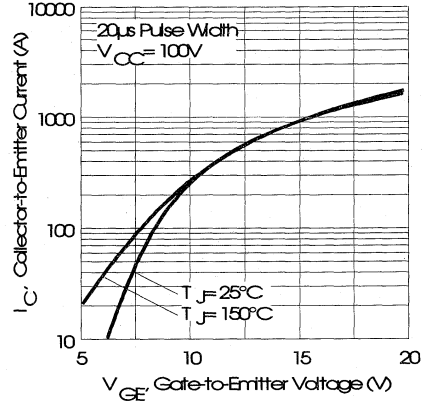


Fig. 4 - Typical Transfer Characteristics

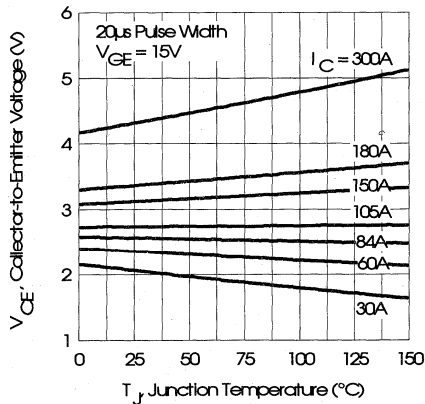


Fig. 5 - Collector-to-Emitter Saturation Typical Voltage vs. Junction Temperature

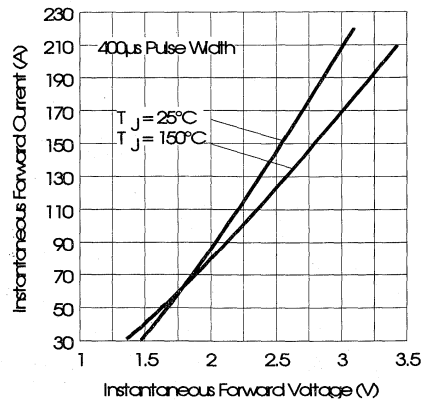


Fig. 6 - Forward Voltage Drop Characteristics

Power
Conversion
Ultra-Fast
Modules

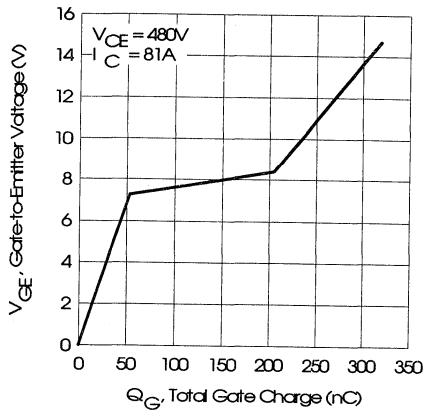


Fig. 7 - Typical Gate Charge vs. Gate-to-Emitter Voltage

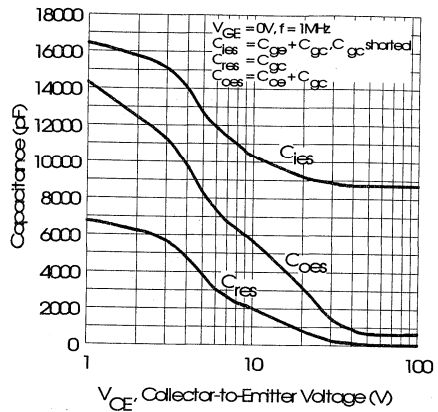


Fig. 8 - Typical Capacitance vs. Collector-to-Emitter Voltage

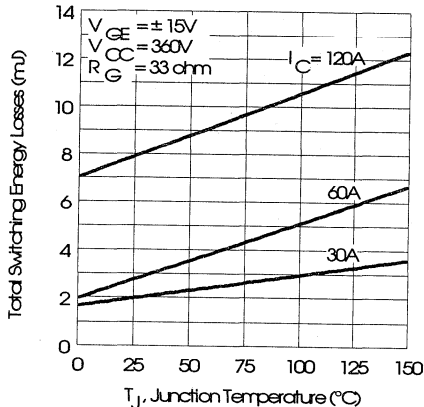


Fig. 9 - Typical Switching Losses vs. Junction Temperature

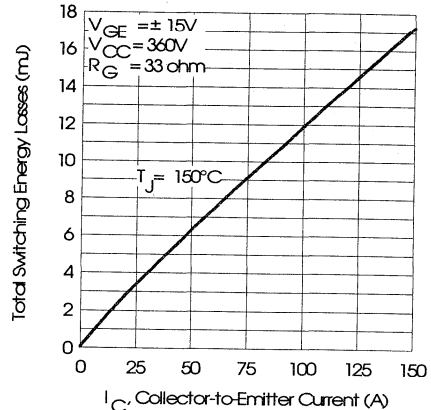


Fig. 10 - Typical Switching Losses vs. Collector-to-Emitter Current

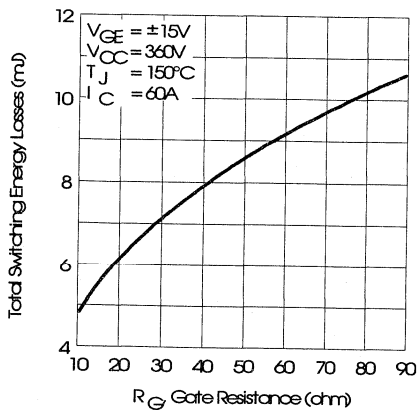


Fig. 11 - Typical Switching Losses vs. Gate Resistance

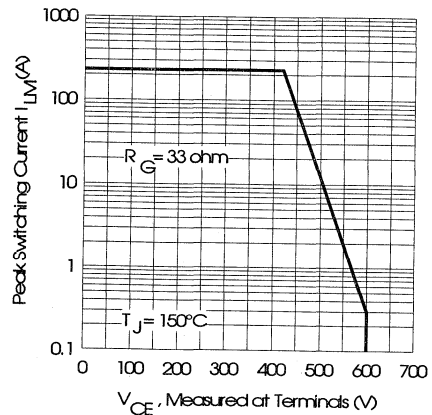


Fig. 12 - Reverse Bias Safe Operating Area

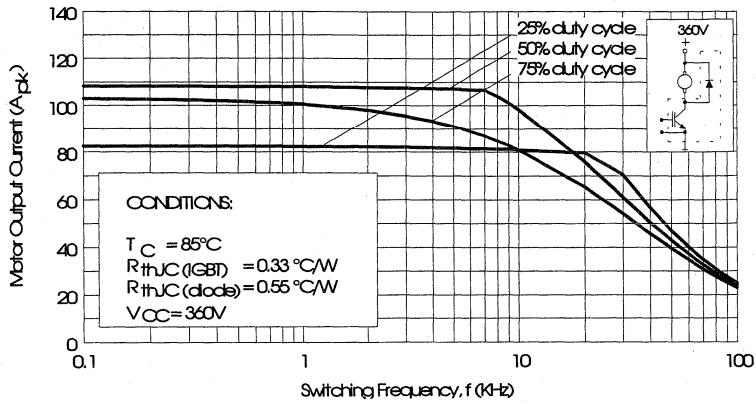


Fig. 13 - RMS Output Current vs. Frequency

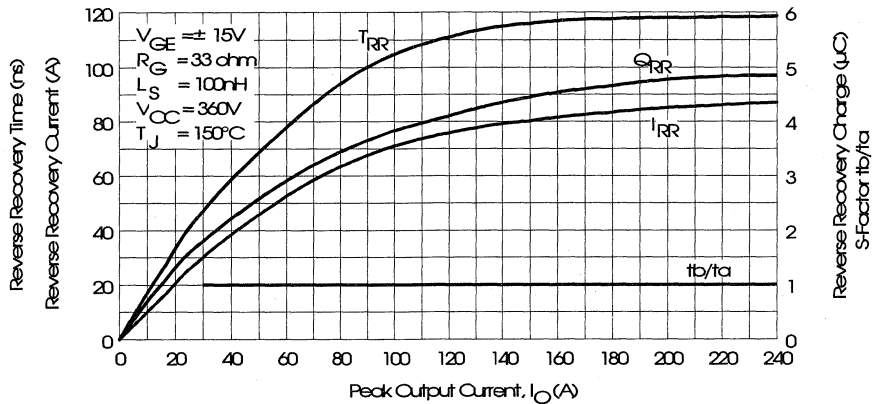


Fig. 14 - Typical Diode Recovery Characteristics as Function of Output Current I_o

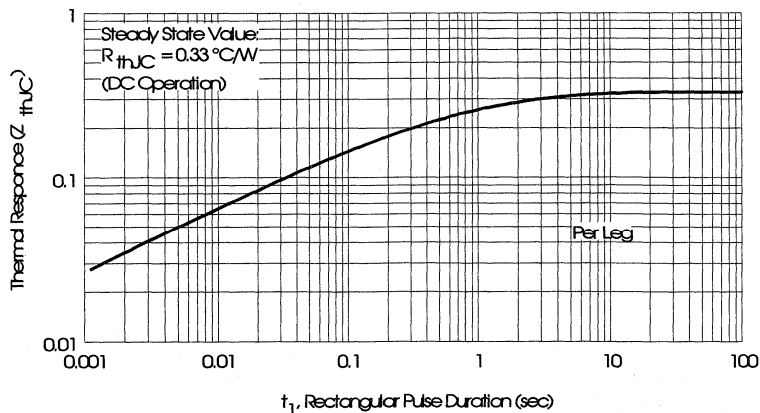


Fig. 15 - Maximum Effective Transient Thermal Impedance, Junction-to-Case

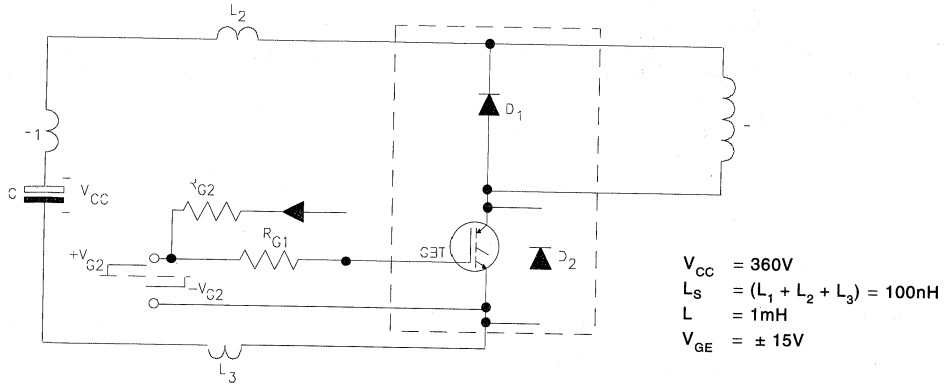


Fig. 16 - Test Circuit for Measurement of I_{LM} , E_{ON} , E_{OFF} , Q_{RR} , I_{RR} , $t_{D(ON)}$, t_r , $t_{D(OFF)}$, t_f

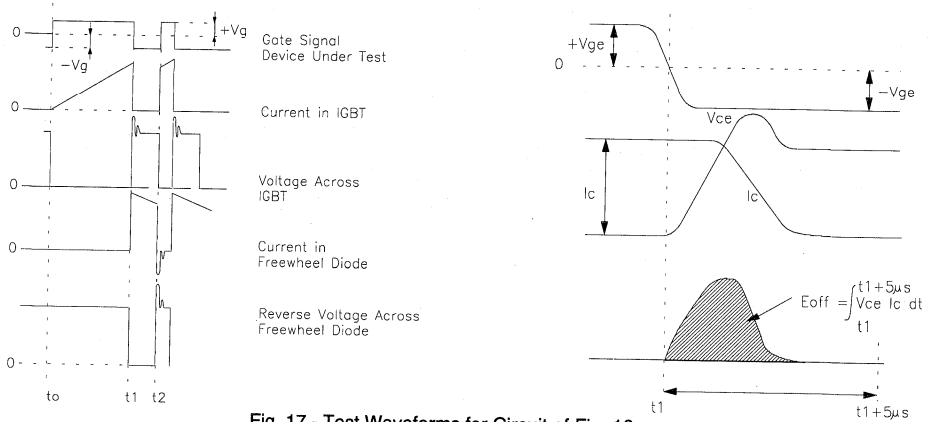


Fig. 17 - Test Waveforms for Circuit of Fig. 16

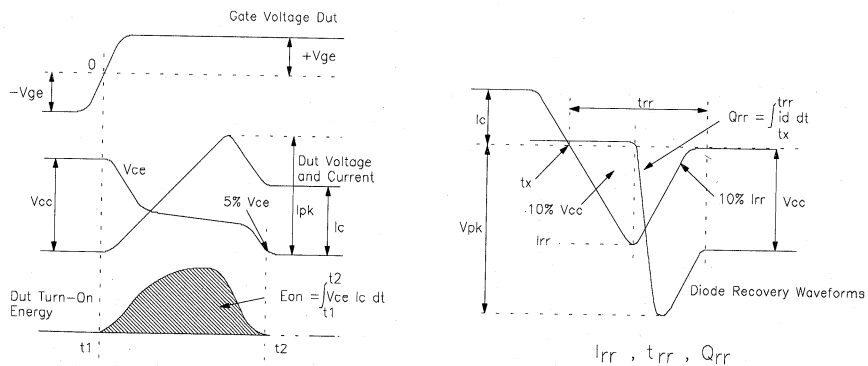


Fig. 18 - Test Waveforms for Circuit of Fig. 16, Defining E_{ON} , E_{REC} , $t_{D(ON)}$, t_r , I_{RR} , t_{RR} , Q_{RR}

Refer to Section D for the following:
Appendix E: Section D - page D-7

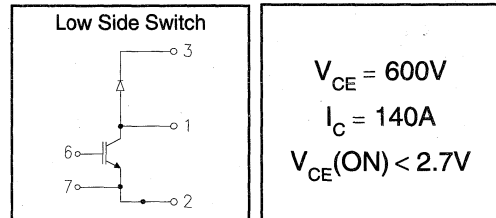
Fig. 19 - Waveforms for Switching Time

IRGKI140U06

"CHOPPER" IGBT INT-A-PAK

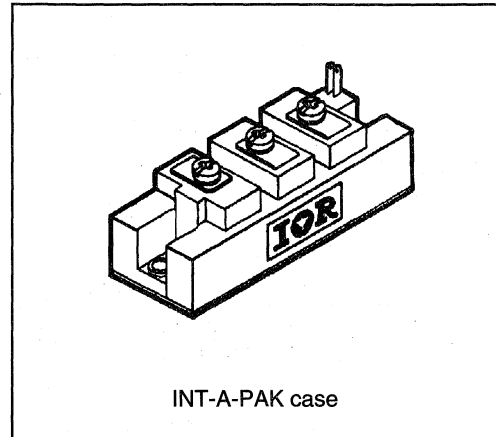
Ultra-fast™ Speed IGBT

- Rugged Design
- Simple gate-drive
- Ultra-fast operation up to 25KHz hard switching, or 100KHz resonant
- Switching-Loss Rating includes all "tail" losses



Description

IR's advanced IGBT technology is the key to this line of INT-A-pak Power Modules. The efficient geometry and unique processing of the IGBT allow higher current densities than comparable bipolar power module transistors, while at the same time requiring the simpler gate-drive of the familiar power MOSFET. This superior technology has now been coupled to state of the art assembly techniques to produce a higher current module that is highly suited to power applications such as motor drives, uninterruptible power supplies, welding, induction heating and ultrasonics.



Absolute Maximum Ratings

Parameter	Description	Value	Units
V_{CES}	Continuous collector to emitter voltage	600	V
$I_C @ T_C = 25^\circ C$	Continuous collector current	170	A
$I_C @ T_C = 85^\circ C$	Continuous collector current	110	
$I_C @ T_C = 100^\circ C$	Continuous collector current	95	
I_{LM}	Peak switching current	280	
I_{FM}	Peak diode forward current (1)	315	V
V_{GE}	Gate to emitter voltage	± 20	
V_{ISOL}	RMS isolation voltage, any terminal to case, $t = 1$ min	2500	W
$P_D @ T_C = 25^\circ C$	Power dissipation	500	
T_J	Operating junction temperature range	-40 to 150	$^\circ C$
T_{STG}	Storage temperature range	-40 to 125	

(1) Duration limited by max junction temperature.

Electrical Characteristics - $T_J = 25^\circ\text{C}$, unless otherwise stated

Parameter	Description	Min	Typ	Max	Units	Test Conditions
BV_{CES}	Collector-to-emitter breakdown voltage	600	—	—	V	$V_{GE} = 0V, I_C = 2mA$
$V_{CE(ON)}$	Collector-to-emitter voltage	—	—	2.7		$V_{GE} = 15V, I_C = 140A$
		—	2.7	—		$V_{GE} = 15V, I_C = 140A, T_J = 150^\circ\text{C}$
V_{FM}	Diode forward voltage - maximum	—	—	2.6		$I_F = 140A, V_{GE} = 0V$
		—	2.3	—		$I_F = 140A, V_{GE} = 0V, T_J = 150^\circ\text{C}$
V_{GEth}	Gate threshold voltage	3.0	—	5.5	$I_C = 1mA$	
ΔV_{GEth}	Threshold voltage temp. coefficient	—	-11	—	mV/°C	$V_{CE} = V_{GE}, I_C = 1mA$
g_{fe}	Forward transconductance	68	—	120	S(Ω)	$V_{CE} = 25V, I_C = 140A$
I_{CES}	Collector-to-emitter leakage current	—	—	2	mA	$V_{GE} = 0V, V_{CE} = 600V$
		—	—	20		$V_{GE} = 0V, V_{CE} = 600V, T_J = 150^\circ\text{C}$
I_{GES}	Gate-to-emitter leakage current	—	—	± 2	μA	$V_{GE} = \pm 20V$

Dynamic Characteristics - $T_J = 150^\circ\text{C}$

Parameter	Description	Min	Typ	Max	Units	Test Conditions
E_{on}	Turn-on switching energy	—	0.05	—	mJ/A	$R_{G1} = 27\Omega, R_{G2} = 0\Omega$
E_{off} (1)	Turn-off switching energy	—	0.05	—		$I_C = 140A, L_S = 100nH$
E_{ts} (1)	Total switching energy	—	—	0.12		$V_{CC} = 360V, V_{GE} = \pm 15V$
$t_{d(on)}$	Turn-on delay time	—	70	—	ns	$R_{G1} = 27\Omega, R_{G2} = 0\Omega$
t_r	Rise time	—	90	—		$I_C = 140A$
$t_{d(off)}$	Turn-off delay time	—	180	—		$V_{CC} = 360V, V_{GE} = \pm 15V$
t_f	Fall time	—	250	—		$L_S = 100nH$
I_{rr}	Diode peak recovery current	—	80	—	A	$R_{G1} = 27\Omega, R_{G2} = 0\Omega$
t_{rr}	Diode recovery time	—	110	—	ns	$I_C = 140A$
Q_{rr}	Diode recovery charge	—	5.0	—	μC	$V_{CC} = 360V, V_{GE} = \pm 15V$
Q_{ge}	Gate-to-emitter charge (turn-on)	310	—	560	nC	$V_{CC} = 360V$
Q_{gc}	Gate-to-collector charge (turn-on)	140	—	280		$I_C = 108A$
Q_g	Total gate charge (turn-on)	52	—	84		$V_{GE} = 15V$
C_{ies}	Input capacitance	—	11600	—	pF	$V_{GE} = 0V$
C_{oes}	Output capacitance	—	1320	—		$V_{CC} = 30V$
C_{res}	Reverse transfer capacitance	—	160	—		$f = 1MHz$

(1) Includes tail losses

Thermal and Mechanical Characteristics

Parameter	Description	Typ	Max	Units
R_{thJC} (IGBT)	Thermal resistance, junction to case, each IGBT	—	0.25	°C/W
R_{thJC} (Diode)	Thermal resistance, junction to case, each diode	—	0.4	
R_{thCS} (Module)	Thermal resistance, case to sink	0.1	—	
Wt	Weight of module	140	—	g

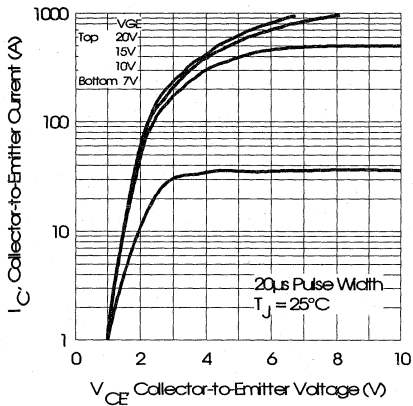


Fig. 1 - Typical Output Characteristics, $T_J = 25^\circ\text{C}$

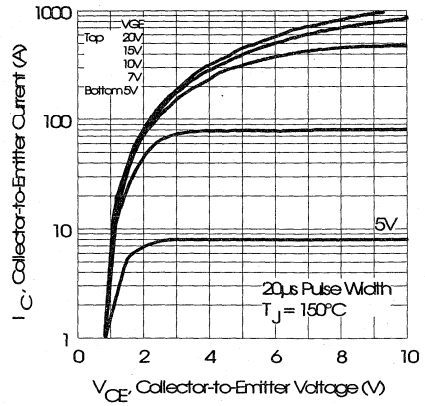


Fig. 2 - Typical Output Characteristics, $T_J = 150^\circ\text{C}$

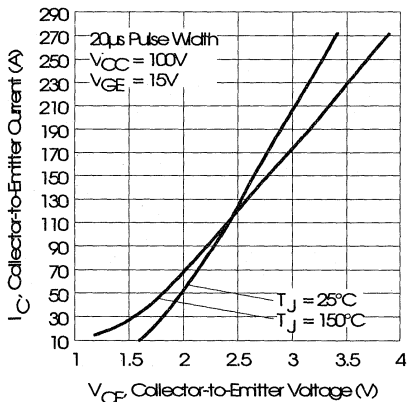


Fig. 3 - Typical Output Characteristics

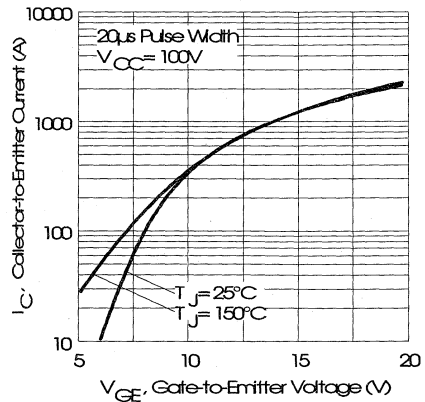


Fig. 4 - Typical Transfer Characteristics

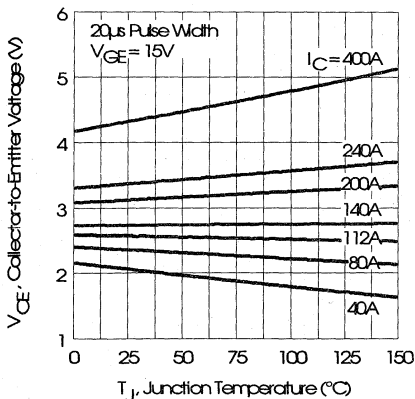


Fig. 5 - Collector-to-Emitter Saturation Typical Voltage vs. Junction Temperature

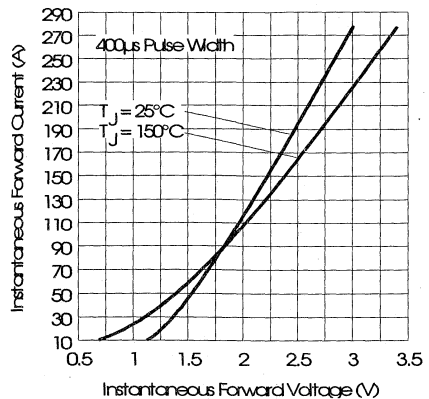


Fig. 6 - Forward Voltage Drop Characteristics

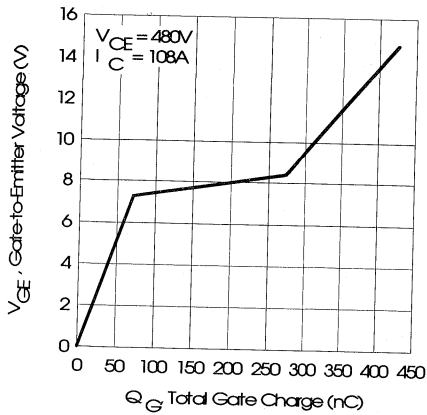


Fig. 7 - Typical Gate Charge vs. Gate-to-Emitter Voltage

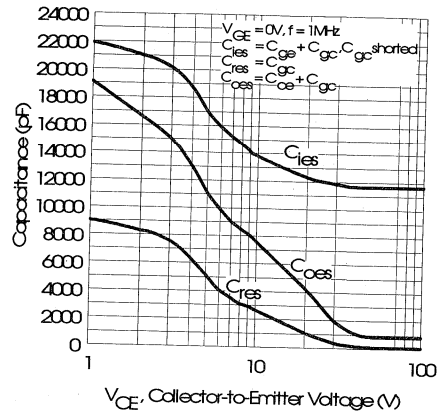


Fig. 8 - Typical Capacitance vs. Collector-to-Emitter Voltage

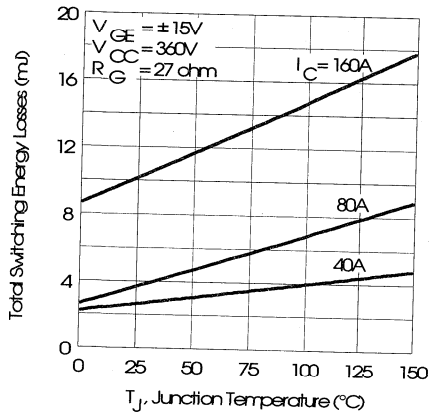


Fig. 9 - Typical Switching Losses vs. Junction Temperature

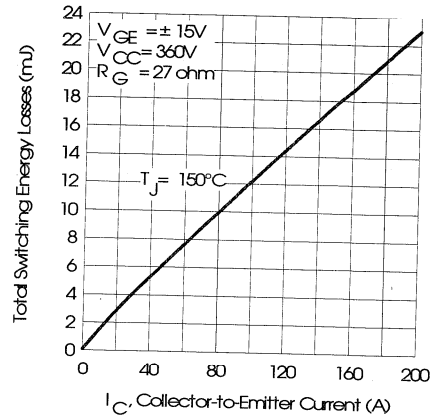


Fig. 10 - Typical Switching Losses vs. Collector-to-Emitter Current

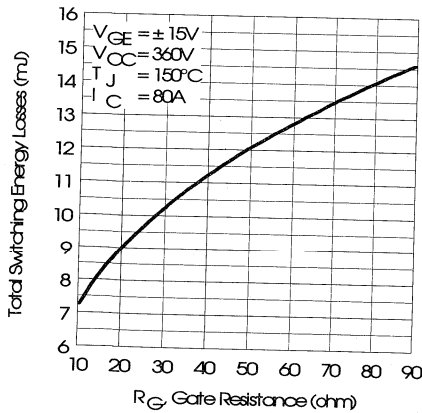


Fig. 11 - Typical Switching Losses vs. Gate Resistance

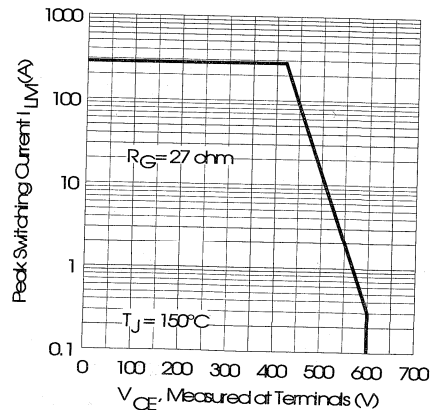


Fig. 12 - Reverse Bias Safe Operating Area

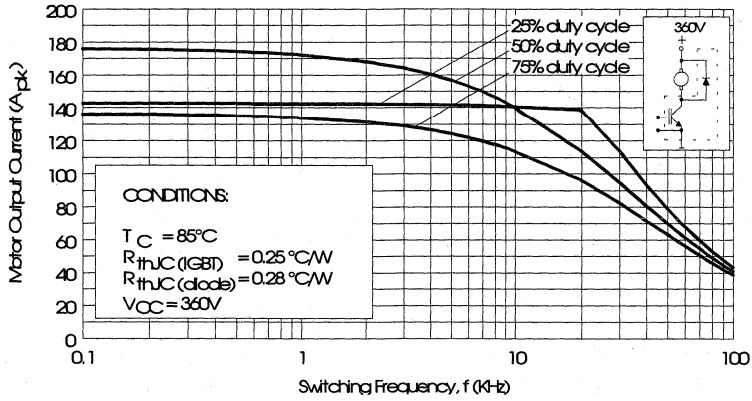


Fig. 13 - RMS Output Current vs. Frequency

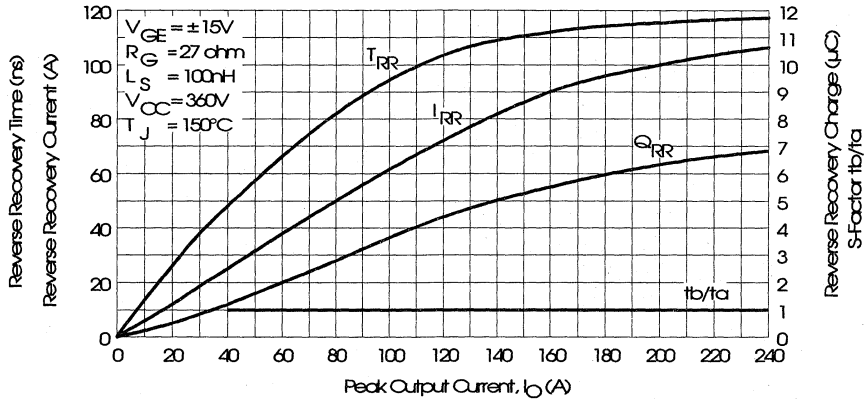


Fig. 14 - Typical Diode Recovery Characteristics as Function of Output Current I_o

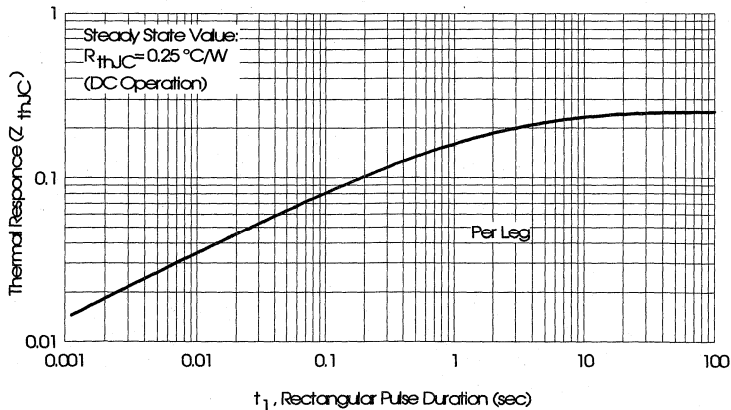


Fig. 15 - Maximum Effective Transient Thermal Impedance, Junction-to-Case

Power
 Conversion
 Ultra-Fast
 Modules

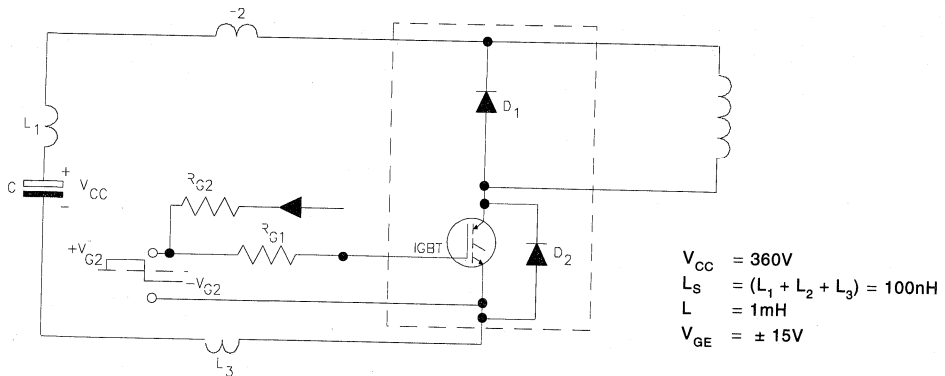


Fig. 16 - Test Circuit for Measurement of I_{LM} , E_{ON} , E_{OFF} , Q_{RR} , I_{RR} , $t_{D(ON)}$, t_r , $t_{D(OFF)}$, t_f

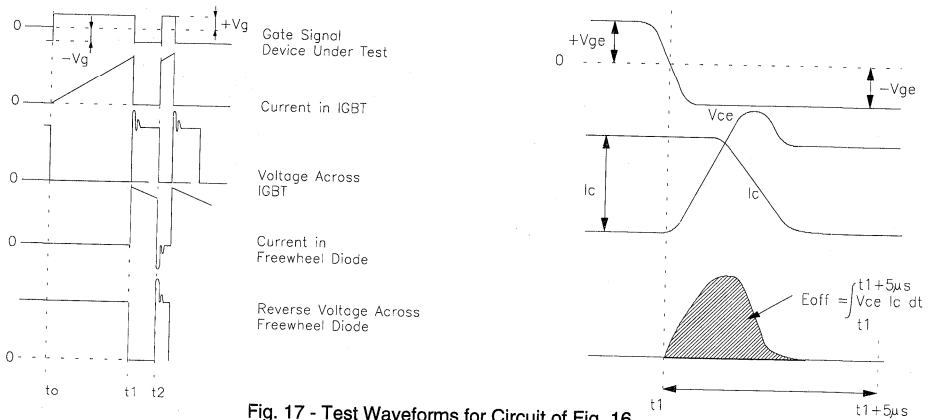


Fig. 17 - Test Waveforms for Circuit of Fig. 16

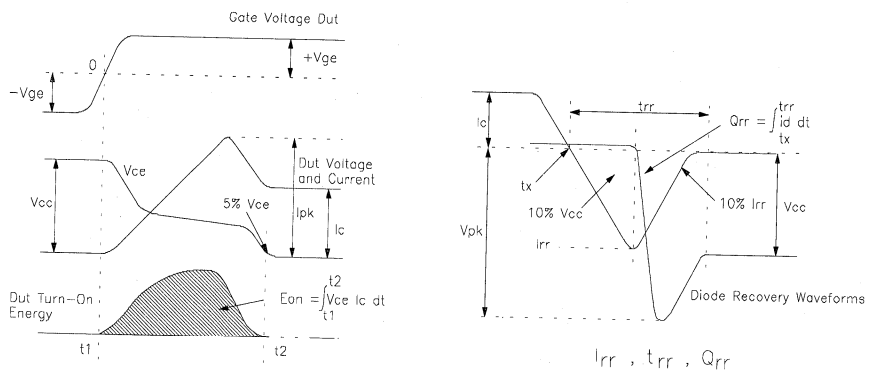


Fig. 18 - Test Waveforms for Circuit of Fig. 16, Defining E_{ON} , E_{REC} , $t_{D(ON)}$, t_r , I_{RR} , t_{RR} , Q_{RR}

Refer to Section D for the following:

Appendix E: Section D - page D-7

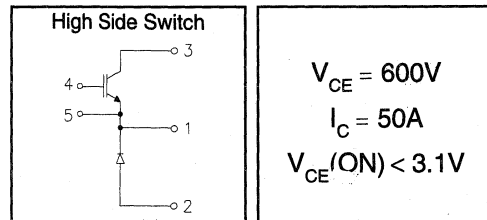
Fig. 19 - Waveforms for Switching Time

IRGNI050U06

"CHOPPER" IGBT INT-A-PAK

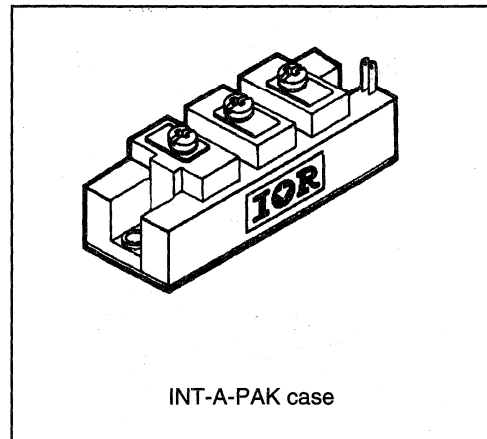
Ultra-fast™ Speed IGBT

- Rugged Design
- Simple gate-drive
- Ultra-fast operation up to 25KHz hard switching, or 100KHz resonant
- Switching-Loss Rating includes all "tail" losses



Description

IR's advanced IGBT technology is the key to this line of INT-A-pak Power Modules. The efficient geometry and unique processing of the IGBT allow higher current densities than comparable bipolar power module transistors, while at the same time requiring the simpler gate-drive of the familiar power MOSFET. This superior technology has now been coupled to state of the art assembly techniques to produce a higher current module that is highly suited to power applications such as motor drives, uninterruptible power supplies, welding, induction heating and ultrasonics.



Absolute Maximum Ratings

Parameter	Description	Value	Units
V_{CES}	Continuous collector to emitter voltage	600	V
$I_C @ T_C = 25^\circ C$	Continuous collector current	50	A
$I_C @ T_C = 85^\circ C$	Continuous collector current	35	
$I_C @ T_C = 100^\circ C$	Continuous collector current	30	
I_{LM}	Peak switching current	100	
I_{FM}	Peak diode forward current (1)	125	V
V_{GE}	Gate to emitter voltage	± 20	
V_{ISOL}	RMS isolation voltage, any terminal to case, $t = 1 \text{ min}$	2500	
$P_D @ T_C = 25^\circ C$	Power dissipation	179	W
T_J	Operating junction temperature range	-40 to 150	$^\circ C$
T_{STG}	Storage temperature range	-40 to 125	

(1) Duration limited by max junction temperature.

Electrical Characteristics - $T_J = 25^\circ\text{C}$, unless otherwise stated

Parameter	Description	Min	Typ	Max	Units	Test Conditions
BV_{CES}	Collector-to-emitter breakdown voltage	600	—	—	V	$V_{GE} = 0V, I_C = 500\mu A$
$V_{CE(ON)}$	Collector-to-emitter voltage	—	—	3.1		$V_{GE} = 15V, I_C = 50A$
		—	3.3	—		$V_{GE} = 15V, I_C = 50A, T_J = 150^\circ\text{C}$
V_{FM}	Diode forward voltage - maximum	—	—	2.9		$I_F = 50A, V_{GE} = 0V$
		—	2.8	—		$I_F = 50A, V_{GE} = 0V, T_J = 150^\circ\text{C}$
V_{GEth}	Gate threshold voltage	3.0	—	5.5		$I_C = 250\mu A$
ΔV_{GEth}	Threshold voltage temperature coeff.	—	-11	—	$mV/^\circ\text{C}$	$V_{CE} = V_{GE}, I_C = 250\mu A$
g_{fe}	Forward transconductance	17.3	—	29.6	$S(\text{V})$	$V_{CE} = 25V, I_C = 50A$
I_{CES}	Collector-to-emitter leakage current	—	—	500	μA	$V_{GE} = 0V, V_{CE} = 600V$
		—	—	5	mA	$V_{GE} = 0V, V_{CE} = 600V, T_J = 150^\circ\text{C}$
I_{GES}	Gate-to-emitter leakage current	—	—	± 500	nA	$V_{GE} = \pm 20V$

Dynamic Characteristics - $T_J = 150^\circ\text{C}$

Parameter	Description	Min	Typ	Max	Units	Test Conditions
E_{on}	Turn-on switching energy	—	0.05	—	mJ/A	$R_{G1} = 82\Omega, R_{G2} = 0\Omega$
$E_{off} (1)$	Turn-off switching energy	—	0.05	—		$I_C = 50A, L_S = 100nH$
$E_{ts} (1)$	Total switching energy	—	—	0.12		$V_{CC} = 360V, V_{GE} = \pm 15V$
$t_{d(on)}$	Turn-on delay time	—	70	—	ns	$R_{G1} = 82\Omega, R_{G2} = 0\Omega$
t_r	Rise time	—	90	—		$I_C = 50A$
$t_{d(off)}$	Turn-off delay time	—	180	—		$V_{CC} = 360V, V_{GE} = \pm 15V$
t_f	Fall time	—	250	—		$L_S = 100nH$
I_{rr}	Diode peak recovery current	—	27	—	A	$R_{G1} = 82\Omega, R_{G2} = 0\Omega$
t_{rr}	Diode recovery time	—	110	—	ns	$I_C = 50A$
Q_{rr}	Diode recovery charge	—	1.6	—	μC	$V_{CC} = 360V, V_{GE} = \pm 15V$
Q_{ge}	Gate-to-emitter charge (turn-on)	77	—	140	nC	$V_{CC} = 360V$
Q_{gc}	Gate-to-collector charge (turn-on)	35	—	70	nC	$I_C = 50A$
Q_g	Total gate charge (turn-on)	13	—	21	nC	$V_{GE} = 15V$
C_{ies}	Input capacitance	—	2900	—	pF	$V_{GE} = 0V$
C_{oes}	Output capacitance	—	330	—	pF	$V_{CC} = 30V$
C_{res}	Reverse transfer capacitance	—	40	—	pF	$f = 1MHz$

(1) Includes tail losses

Thermal and Mechanical Characteristics

Parameter	Description	Typ	Max	Units
R_{thJC} (IGBT)	Thermal resistance, junction to case, each IGBT	—	0.7	$^\circ\text{C/W}$
R_{thJC} (Diode)	Thermal resistance, junction to case, each diode	—	1.3	
R_{thCS} (Module)	Thermal resistance, case to sink	0.1	—	
Wt	Weight of module	140	—	g

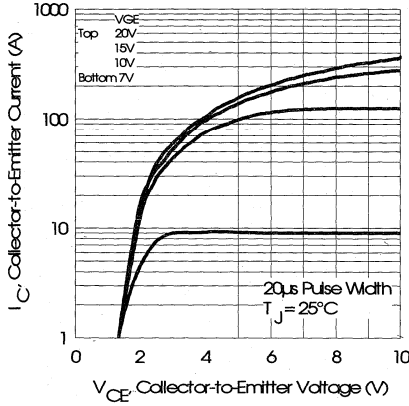


Fig. 1 - Typical Output Characteristics, $T_J = 25^\circ\text{C}$

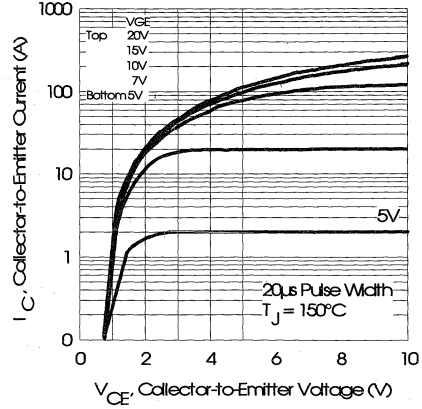


Fig. 2 - Typical Output Characteristics, $T_J = 150^\circ\text{C}$

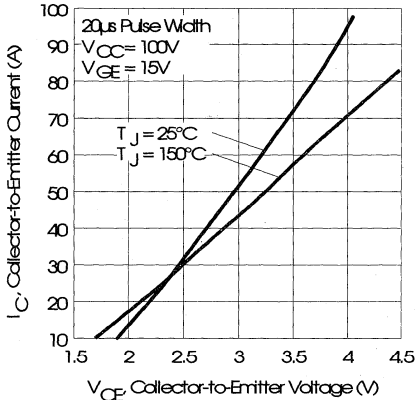


Fig. 3 - Typical Output Characteristics

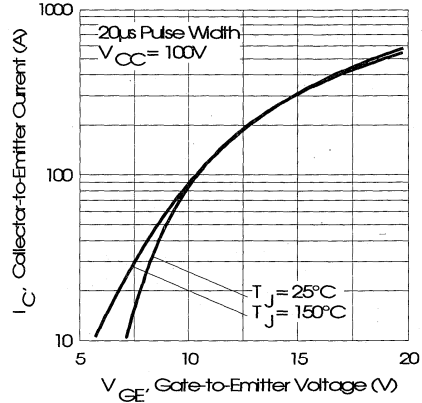


Fig. 4 - Typical Transfer Characteristics

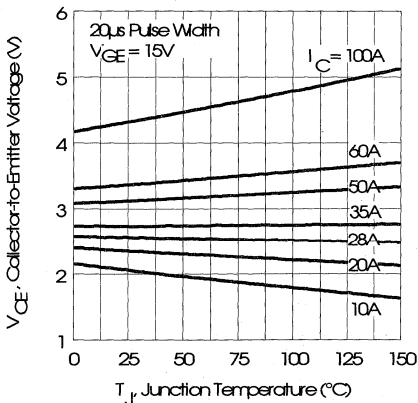


Fig. 5 - Collector-to-Emitter Saturation Typical Voltage vs. Junction Temperature

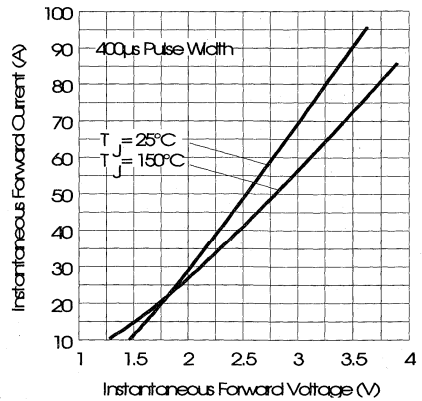


Fig. 6 - Forward Voltage Drop Characteristics

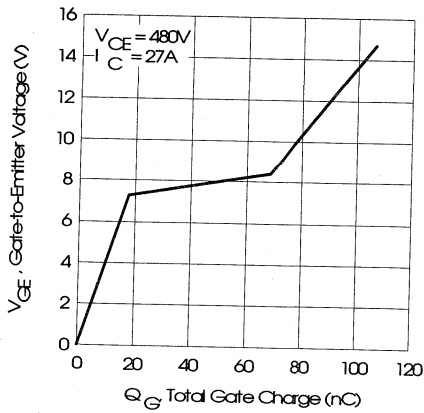


Fig. 7 - Typical Gate Charge vs. Gate-to-Emitter Voltage

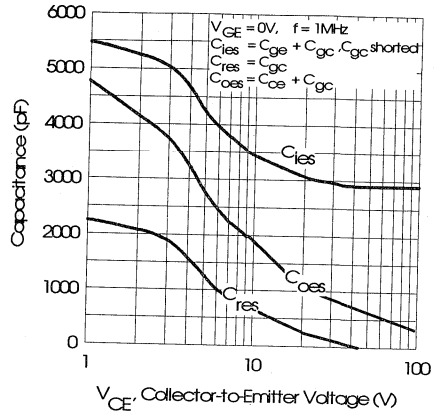


Fig. 8 - Typical Capacitance vs. Collector-to-Emitter Voltage

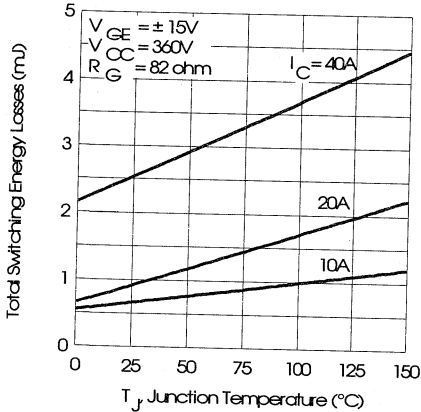


Fig. 9 - Typical Switching Losses vs. Junction Temperature

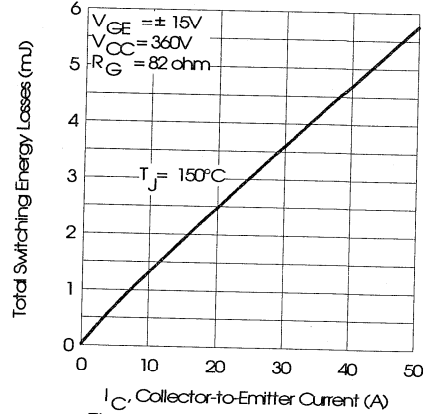


Fig. 10 - Typical Switching Losses vs. Collector-to-Emitter Current

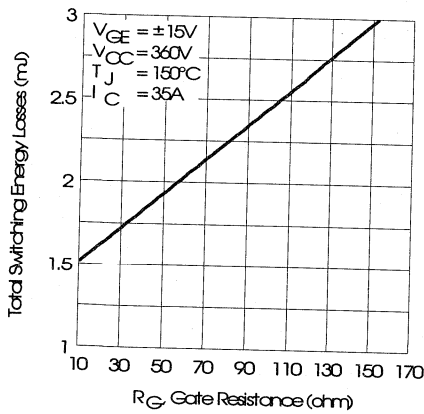


Fig. 11 - Typical Switching Losses vs. Gate Resistance

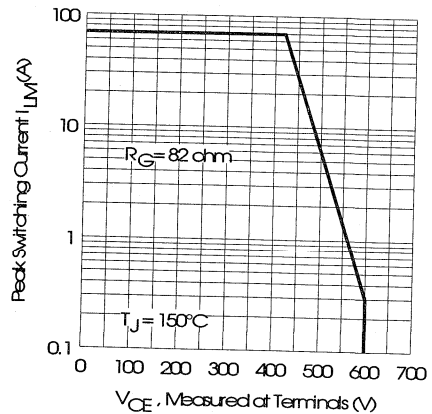


Fig. 12 - Reverse Bias Safe Operating Area

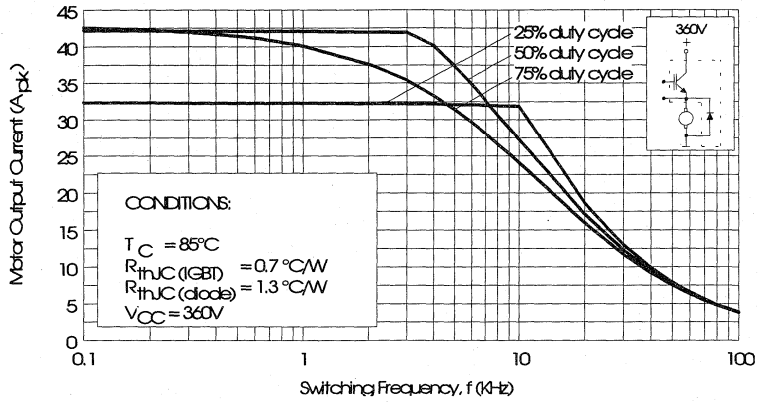


Fig. 13 - RMS Output Current vs. Frequency

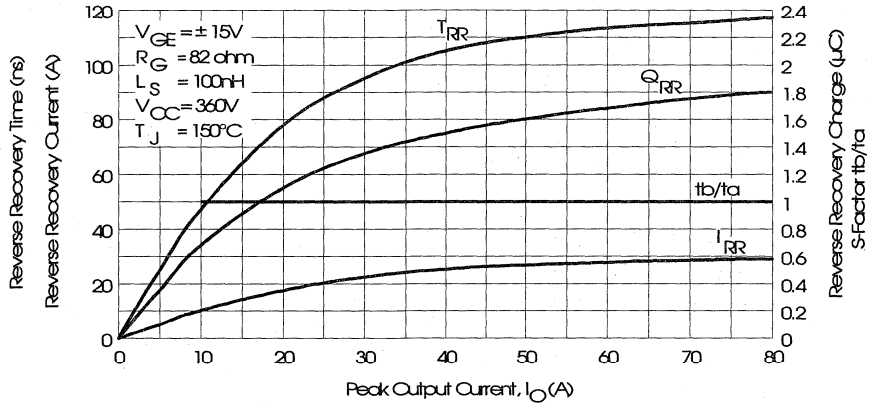


Fig. 14 - Typical Diode Recovery Characteristics as Function of Output Current I_o

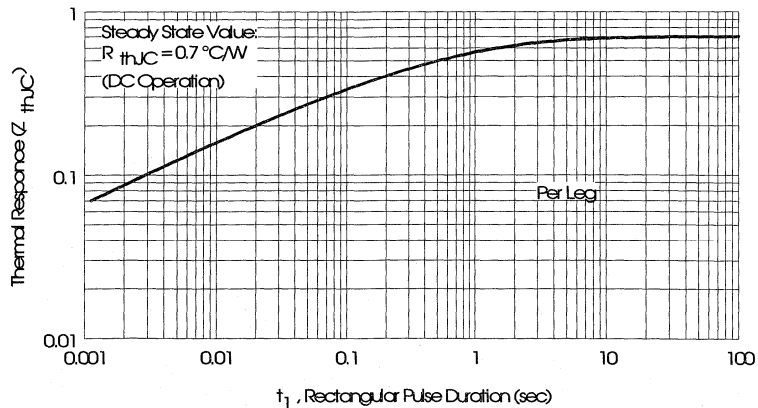


Fig. 15 - Maximum Effective Transient Thermal Impedance, Junction-to-Case

Power Conversion Ultra-Pass Modules

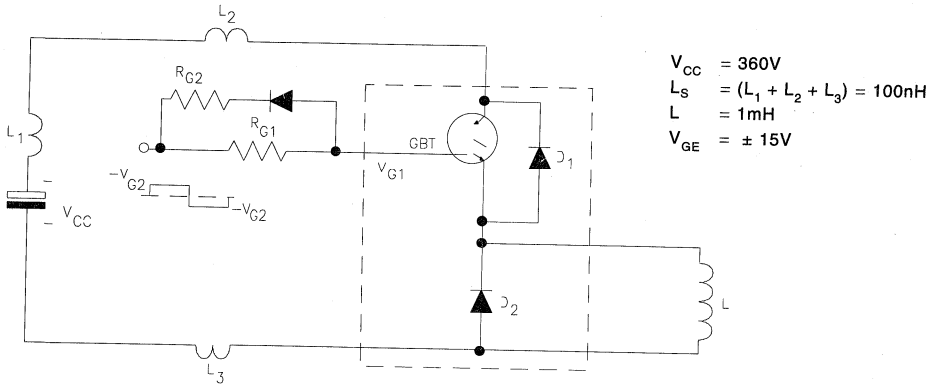


Fig. 16 - Test Circuit for Measurement of I_{LM} , E_{ON} , E_{OFF} , Q_{RR} , I_{RR} , $t_{D(ON)}$, t_r , $t_{D(OFF)}$, t_f

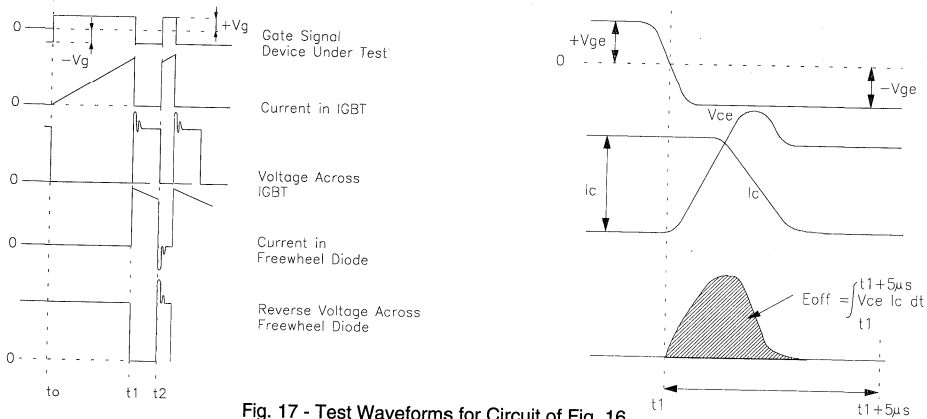


Fig. 17 - Test Waveforms for Circuit of Fig. 16

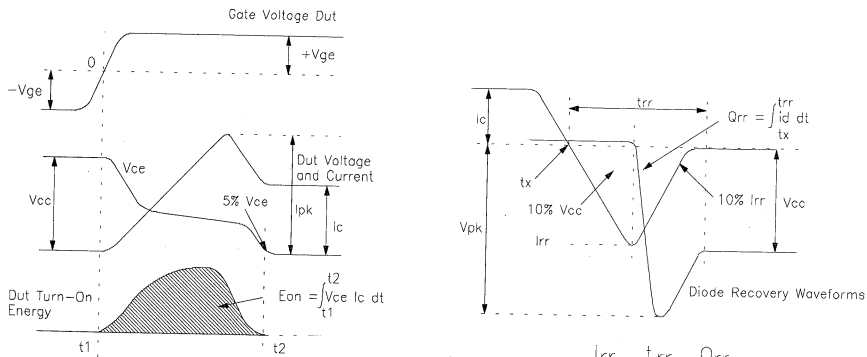


Fig. 18 - Test Waveforms for Circuit of Fig. 16, Defining E_{ON} , E_{REC} , $t_{D(ON)}$, t_r , I_{RR} , t_{RR} , Q_{RR}

Refer to Section D for the following:
 Appendix E: Section D - page D-7

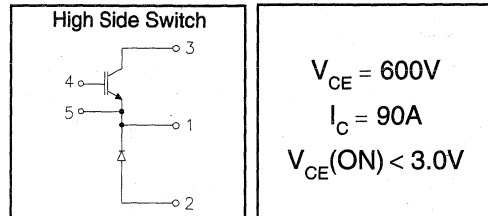
Fig. 19 - Waveforms for Switching Time

IRGNI090U06

"CHOPPER" IGBT INT-A-PAK

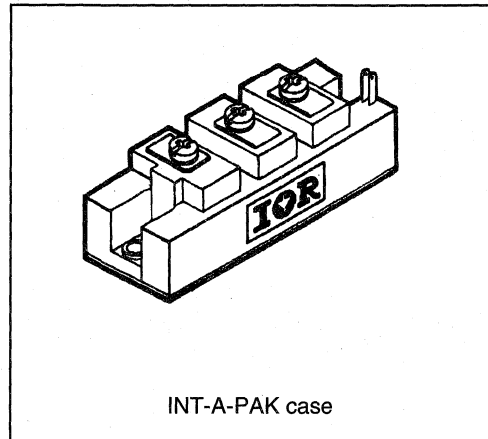
Ultra-fast™ Speed IGBT

- Rugged Design
- Simple gate-drive
- Ultra-fast operation up to 25KHz hard switching, or 100KHz resonant
- Switching-Loss Rating includes all "tail" losses



Description

IR's advanced IGBT technology is the key to this line of INT-A-pak Power Modules. The efficient geometry and unique processing of the IGBT allow higher current densities than comparable bipolar power module transistors, while at the same time requiring the simpler gate-drive of the familiar power MOSFET. This superior technology has now been coupled to state of the art assembly techniques to produce a higher current module that is highly suited to power applications such as motor drives, uninterruptible power supplies, welding, induction heating and ultrasonics.



Absolute Maximum Ratings

Parameter	Description	Value	Units
V_{CES}	Continuous collector to emitter voltage	600	V
$I_C @ T_C = 25^\circ C$	Continuous collector current	90	A
$I_C @ T_C = 85^\circ C$	Continuous collector current	60	
$I_C @ T_C = 100^\circ C$	Continuous collector current	50	
I_{LM}	Peak switching current	180	
I_{FM}	Peak diode forward current (1)	225	V
V_{GE}	Gate to emitter voltage	± 20	
V_{ISOL}	RMS isolation voltage, any terminal to case, $t = 1$ min	2500	W
$P_D @ T_C = 25^\circ C$	Power dissipation	298	
T_J	Operating junction temperature range	-40 to 150	$^\circ C$
T_{STG}	Storage temperature range	-40 to 125	

(1) Duration limited by max junction temperature.

Electrical Characteristics - $T_J = 25^\circ\text{C}$, unless otherwise stated

Parameter	Description	Min	Typ	Max	Units	Test Conditions
BV_{CES}	Collector-to-emitter breakdown voltage	600	—	—	V	$V_{GE} = 0V, I_C = 1mA$
$V_{CE(ON)}$	Collector-to-emitter voltage	—	—	3.0		$V_{GE} = 15V, I_C = 90A$
		—	3.1	—		$V_{GE} = 15V, I_C = 90A, T_J = 150^\circ\text{C}$
V_{FM}	Diode forward voltage - maximum	—	—	2.8		$I_F = 90A, V_{GE} = 0V$
		—	2.6	—		$I_F = 90A, V_{GE} = 0V, T_J = 150^\circ\text{C}$
V_{GEth}	Gate threshold voltage	3.0	—	5.5	$I_C = 500\mu A$	
ΔV_{GEth}	Threshold voltage temperature coeff.	—	-11	—	mV/°C	$V_{CE} = V_{GE}, I_C = 500\mu A$
g_{fe}	Forward transconductance	34	—	58	S(τ)	$V_{CE} = 25V, I_C = 90A$
I_{CES}	Collector-to-emitter leakage current	—	—	1	mA	$V_{GE} = 0V, V_{CE} = 600V$
		—	—	10		$V_{GE} = 0V, V_{CE} = 600V, T_J = 150^\circ\text{C}$
I_{GES}	Gate-to-emitter leakage current	—	—	± 1	μA	$V_{GE} = \pm 20V$

Dynamic Characteristics - $T_J = 150^\circ\text{C}$

Parameter	Description	Min	Typ	Max	Units	Test Conditions
E_{on}	Turn-on switching energy	—	0.05	—	mJ/A	$R_{G1} = 47\Omega, R_{G2} = 0\Omega$
E_{off} (1)	Turn-off switching energy	—	0.05	—		$I_C = 90A, L_S = 100nH$
E_{ts} (1)	Total switching energy	—	—	0.12		$V_{CC} = 360V, V_{GE} = \pm 15V$
$t_{d(on)}$	Turn-on delay time	—	70	—	ns	$R_{G1} = 47\Omega, R_{G2} = 0\Omega$
t_r	Rise time	—	90	—		$I_C = 90A$
$t_{d(off)}$	Turn-off delay time	—	180	—		$V_{CC} = 360V, V_{GE} = \pm 15V$
t_f	Fall time	—	250	—		$L_S = 100nH$
I_{rr}	Diode peak recovery current	—	52	—		A
t_{rr}	Diode recovery time	—	110	—	ns	$I_C = 90A$
Q_{rr}	Diode recovery charge	—	3.0	—	μC	$V_{CC} = 360V, V_{GE} = \pm 15V$
Q_{ge}	Gate-to-emitter charge (turn-on)	150	—	280	nC	$V_{CC} = 360V$
Q_{gc}	Gate-to-collector charge (turn-on)	70	—	140		$I_C = 90A$
Q_g	Total gate charge (turn-on)	26	—	42		$V_{GE} = 15V$
C_{ies}	Input capacitance	—	5800	—	pF	$V_{GE} = 0V$
C_{oes}	Output capacitance	—	660	—		$V_{CC} = 30V$
C_{res}	Reverse transfer capacitance	—	80	—		$f = 1MHz$

(1) Includes tail losses

Thermal and Mechanical Characteristics

Parameter	Description	Typ	Max	Units
R_{thJC} (IGBT)	Thermal resistance, junction to case, each IGBT	—	0.42	°C/W
R_{thJC} (Diode)	Thermal resistance, junction to case, each diode	—	0.7	
R_{thCS} (Module)	Thermal resistance, case to sink	0.1	—	
Wt	Weight of module	140	—	g

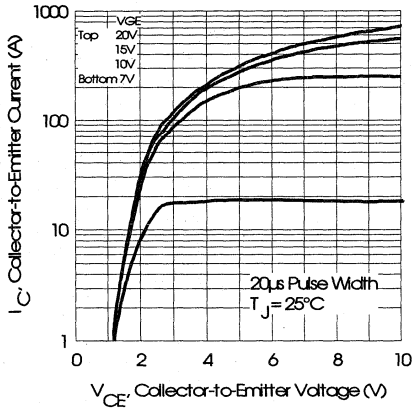


Fig. 1 - Typical Output Characteristics, $T_j = 25^\circ\text{C}$

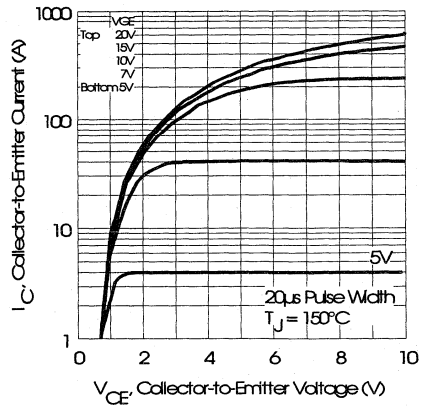


Fig. 2 - Typical Output Characteristics, $T_j = 150^\circ\text{C}$

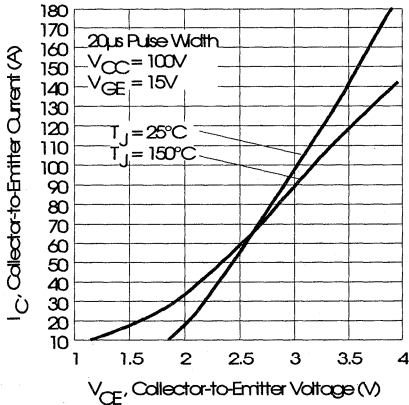


Fig. 3 - Typical Output Characteristics

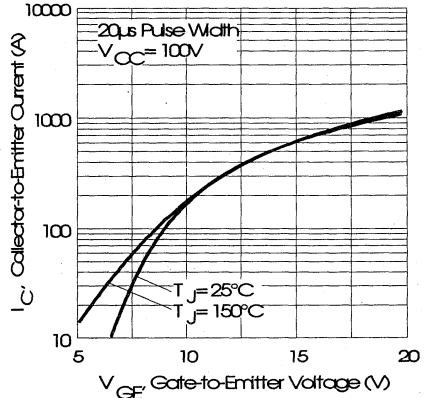


Fig. 4 - Typical Transfer Characteristics

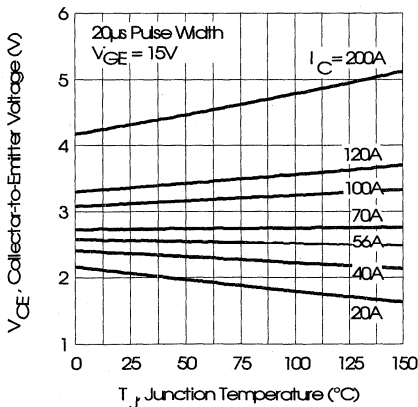


Fig. 5 - Collector-to-Emitter Saturation Typical Voltage vs. Junction Temperature

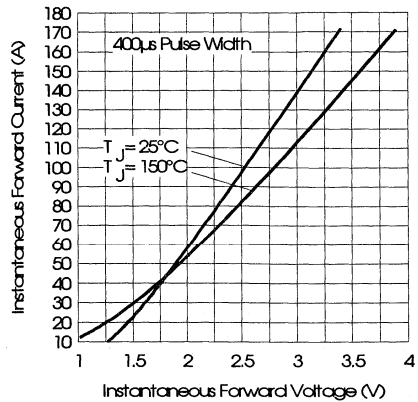


Fig. 6 - Forward Voltage Drop Characteristics

Power Conversion Ultra-Fast Modules

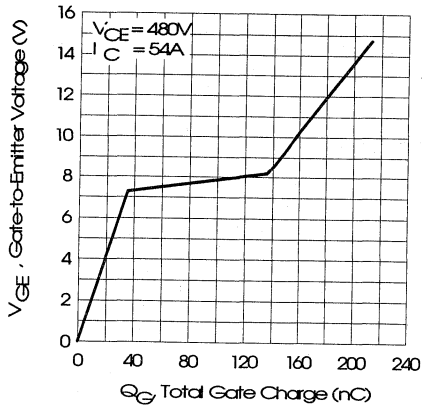


Fig. 7 - Typical Gate Charge vs. Gate-to-Emitter Voltage

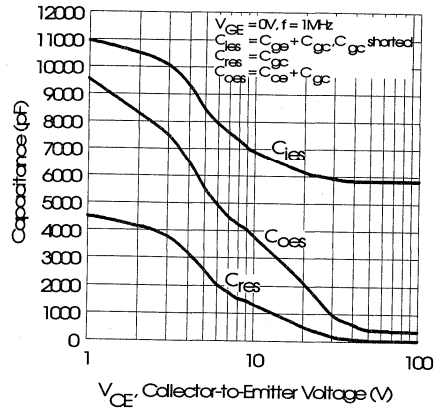


Fig. 8 - Typical Capacitance vs. Collector-to-Emitter Voltage

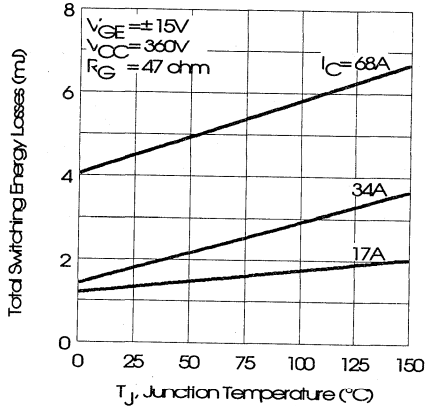


Fig. 9 - Typical Switching Losses vs. Junction Temperature

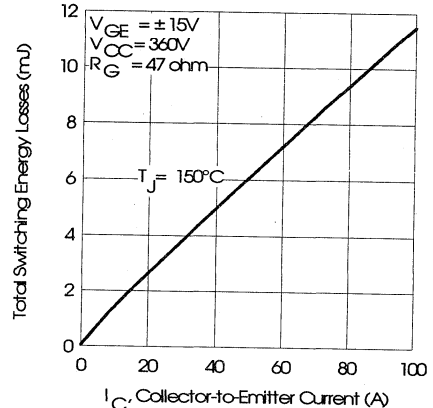


Fig. 10 - Typical Switching Losses vs. Collector-to-Emitter Current

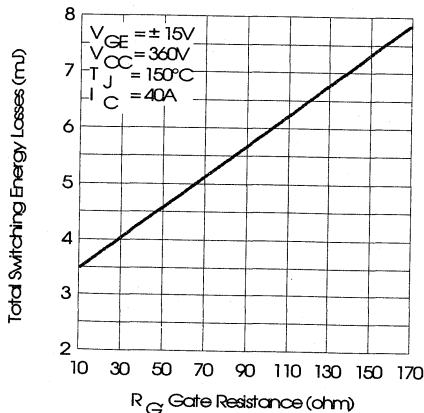


Fig. 11 - Typical Switching Losses vs. Gate Resistance

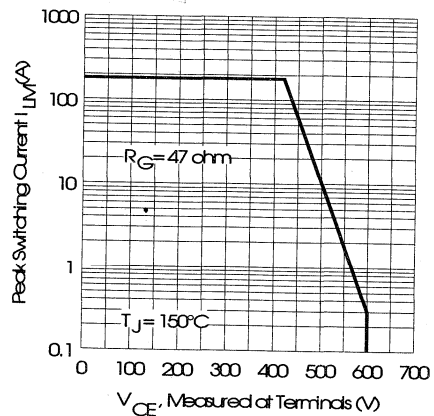


Fig. 12 - Reverse Bias Safe Operating Area

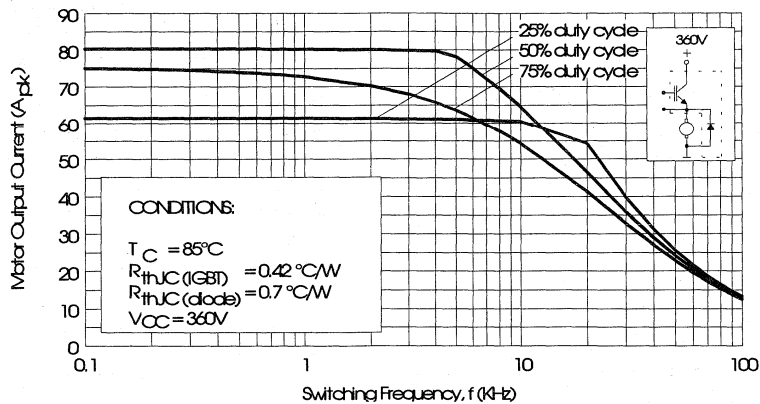


Fig. 13 - RMS Output Current vs. Frequency

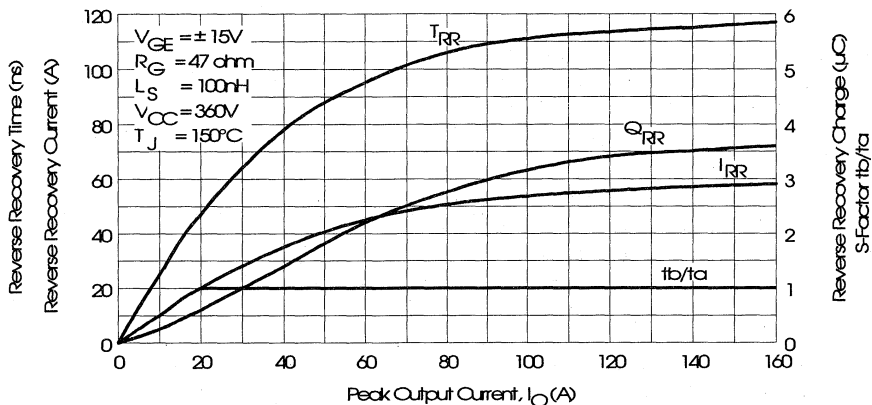


Fig. 14 - Typical Diode Recovery Characteristics as Function of Output Current I_O

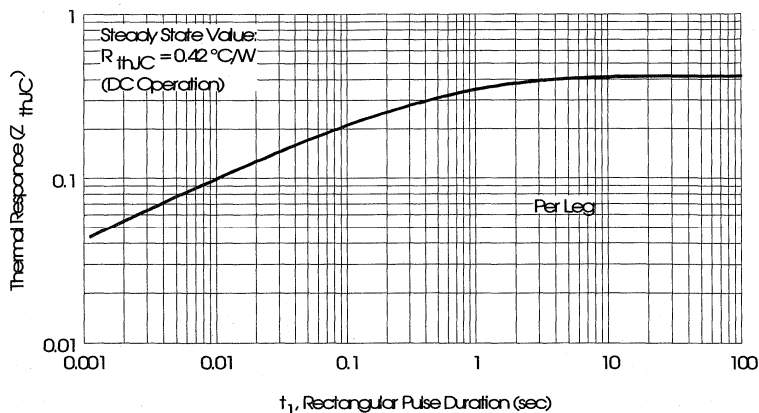


Fig. 15 - Maximum Effective Transient Thermal Impedance, Junction-to-Case

Power Conversion
Ultra-Fast
Modules

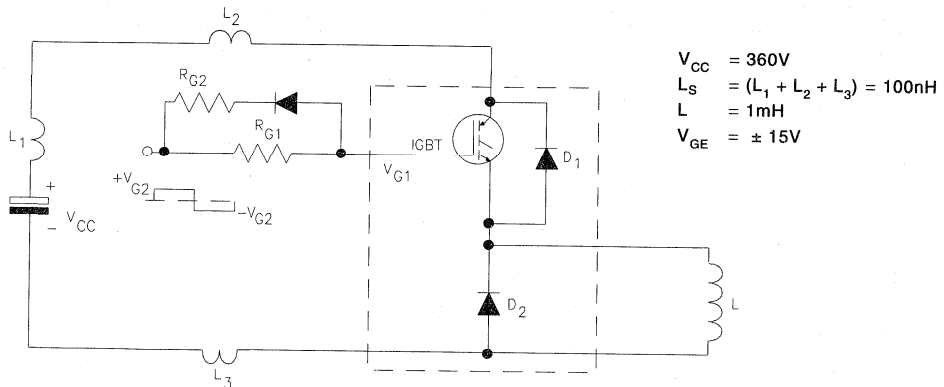


Fig. 16 - Test Circuit for Measurement of I_{LM} , E_{ON} , E_{OFF} , Q_{RR} , I_{RR} , $t_{D(ON)}$, t_r , $t_{D(OFF)}$, t_f

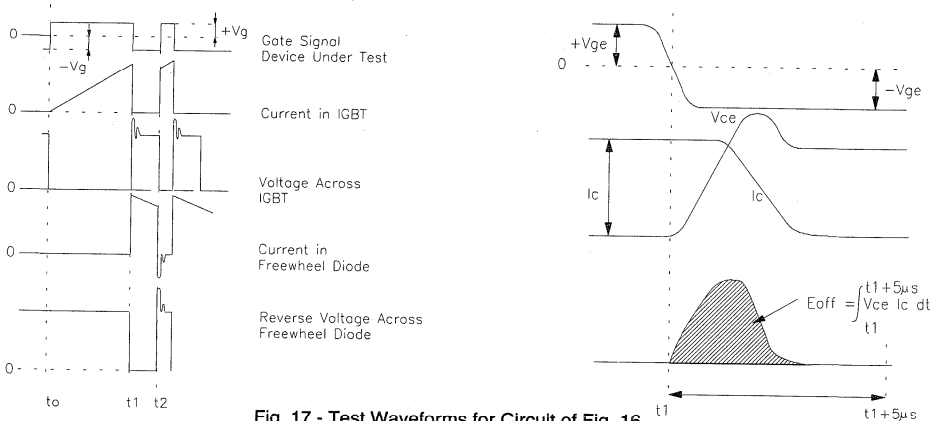


Fig. 17 - Test Waveforms for Circuit of Fig. 16

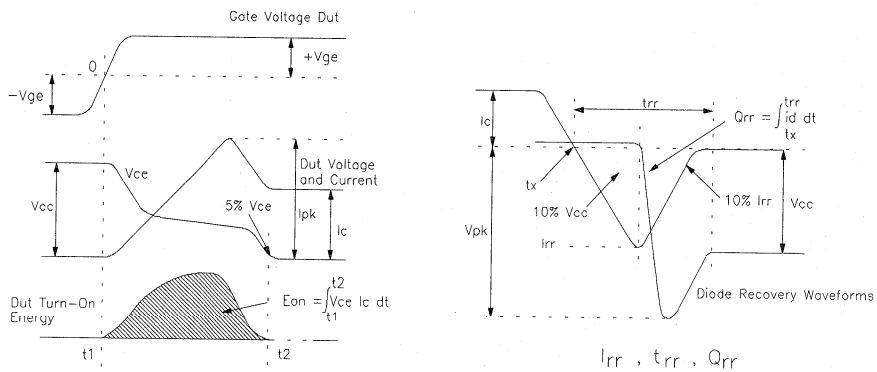


Fig. 18 - Test Waveforms for Circuit of Fig. 16, Defining E_{ON} , E_{REC} , $t_{D(ON)}$, t_r , I_{RR} , t_{RR} , Q_{RR}

Refer to Section D for the following:

Appendix E: Section D - page D-7

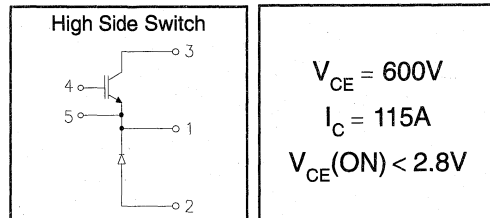
Fig. 19 - Waveforms for Switching Time

IRGNI115U06

"CHOPPER" IGBT INT-A-PAK

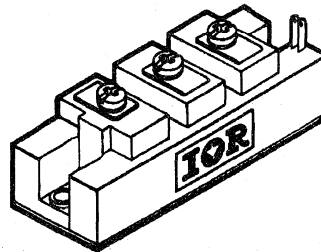
Ultra-fast™ Speed IGBT

- Rugged Design
- Simple gate-drive
- Ultra-fast operation up to 25KHz hard switching, or 100KHz resonant
- Switching-Loss Rating includes all "tail" losses



Description

IR's advanced IGBT technology is the key to this line of INT-A-pak Power Modules. The efficient geometry and unique processing of the IGBT allow higher current densities than comparable bipolar power module transistors, while at the same time requiring the simpler gate-drive of the familiar power MOSFET. This superior technology has now been coupled to state of the art assembly techniques to produce a higher current module that is highly suited to power applications such as motor drives, uninterruptible power supplies, welding, induction heating and ultrasonics.



INT-A-PAK case

Absolute Maximum Ratings

Parameter	Description	Value	Units
V_{CES}	Continuous collector to emitter voltage	600	V
$I_C @ T_C = 25^\circ C$	Continuous collector current	130	A
$I_C @ T_C = 85^\circ C$	Continuous collector current	85	
$I_C @ T_C = 100^\circ C$	Continuous collector current	70	
I_{LM}	Peak switching current	230	
I_{FM}	Peak diode forward current (1)	290	V
V_{GE}	Gate to emitter voltage	± 20	
V_{ISOL}	RMS isolation voltage, any terminal to case, $t = 1$ min	2500	W
$P_D @ T_C = 25^\circ C$	Power dissipation	379	
T_J	Operating junction temperature range	-40 to 150	
T_{STG}	Storage temperature range	-40 to 125	

(1) Duration limited by max junction temperature.

Electrical Characteristics - $T_J = 25^\circ\text{C}$, unless otherwise stated

Parameter	Description	Min	Typ	Max	Units	Test Conditions
BV_{CES}	Collector-to-emitter breakdown voltage	600	—	—	V	$V_{GE} = 0V, I_C = 1.5mA$
$V_{CE(ON)}$	Collector-to-emitter voltage	—	—	2.8		$V_{GE} = 15V, I_C = 115A$
		—	2.9	—		$V_{GE} = 15V, I_C = 115A, T_J = 150^\circ\text{C}$
V_{FM}	Diode forward voltage - maximum	—	—	2.7		$I_F = 115A, V_{GE} = 0V$
		—	2.4	—	$I_F = 115A, V_{GE} = 0V, T_J = 150^\circ\text{C}$	
V_{GEth}	Gate threshold voltage	3.0	—	5.5	$I_C = 750\mu A$	
ΔV_{GEth}	Threshold voltage temperature coeff.	—	-11	—	mV/°C	$V_{CE} = V_{GE}, I_C = 750\mu A$
g_{fe}	Forward transconductance	51	—	87	S(Ω)	$V_{CE} = 25V, I_C = 115A$
I_{CES}	Collector-to-emitter leakage current	—	—	1.5	mA	$V_{GE} = 0V, V_{CE} = 600V$
		—	—	15		$V_{GE} = 0V, V_{CE} = 600V, T_J = 150^\circ\text{C}$
I_{GES}	Gate-to-emitter leakage current	—	—	± 1.5	μA	$V_{GE} = \pm 20V$

Dynamic Characteristics - $T_J = 150^\circ\text{C}$

Parameter	Description	Min	Typ	Max	Units	Test Conditions
E_{on}	Turn-on switching energy	—	0.05	—	mJ/A	$R_{G1} = 33\Omega, R_{G2} = 0\Omega$
$E_{off} (1)$	Turn-off switching energy	—	0.05	—		$I_C = 115A, L_S = 100nH$
$E_{ts} (1)$	Total switching energy	—	—	0.12		$V_{CC} = 360V, V_{GE} = \pm 15V$
$t_{d(on)}$	Turn-on delay time	—	70	—	ns	$R_{G1} = 33\Omega, R_{G2} = 0\Omega$
t_r	Rise time	—	90	—		$I_C = 115A$
$t_{d(off)}$	Turn-off delay time	—	180	—		$V_{CC} = 360V, V_{GE} = \pm 15V$
t_f	Fall time	—	250	—		$L_S = 100nH$
I_{rr}	Diode peak recovery current	—	72	—		$R_{G1} = 33\Omega, R_{G2} = 0\Omega$
t_{rr}	Diode recovery time	—	110	—	$I_C = 115A$	
Q_{rr}	Diode recovery charge	—	4.0	—	μC	$V_{CC} = 360V, V_{GE} = \pm 15V$
Q_{ge}	Gate-to-emitter charge (turn-on)	225	—	420	nC	$V_{CC} = 360V$
Q_{gc}	Gate-to-collector charge (turn-on)	105	—	210		$I_C = 115A$
Q_g	Total gate charge (turn-on)	39	—	63		$V_{GE} = 15V$
C_{ies}	Input capacitance	—	8700	—	pF	$V_{GE} = 0V$
C_{oes}	Output capacitance	—	990	—		$V_{CC} = 30V$
C_{res}	Reverse transfer capacitance	—	120	—		$f = 1MHz$

(1) Includes tail losses

Thermal and Mechanical Characteristics

Parameter	Description	Typ	Max	Units
R_{thJC} (IGBT)	Thermal resistance, junction to case, each IGBT	—	0.33	°C/W
R_{thJC} (Diode)	Thermal resistance, junction to case, each diode	—	0.55	
R_{thCS} (Module)	Thermal resistance, case to sink	0.1	—	
Wt	Weight of module	140	—	g

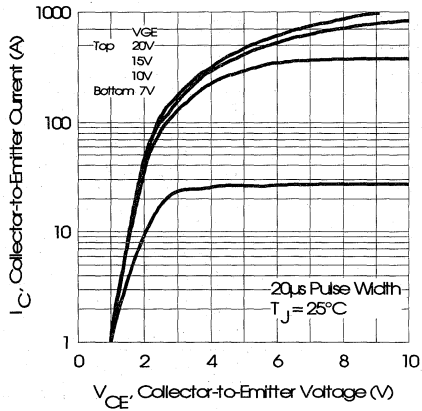


Fig. 1 - Typical Output Characteristics, $T_J = 25^\circ\text{C}$

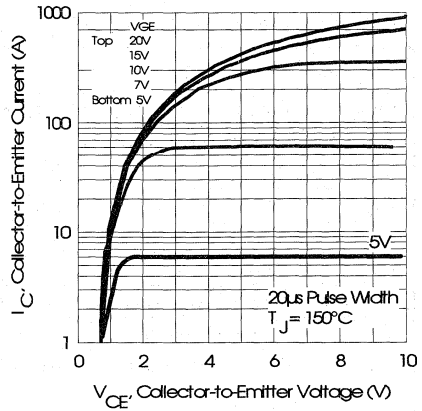


Fig. 2 - Typical Output Characteristics, $T_J = 150^\circ\text{C}$

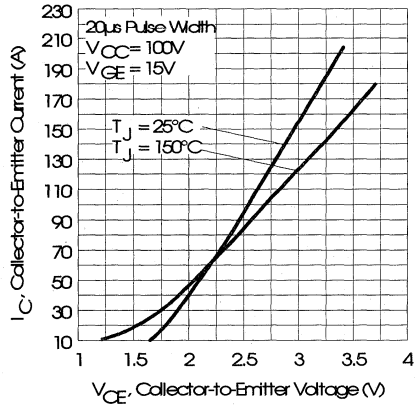


Fig. 3 - Typical Output Characteristics

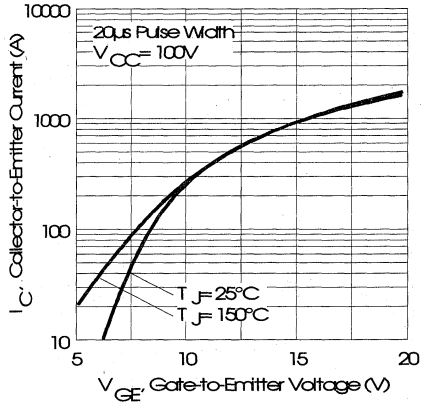


Fig. 4 - Typical Transfer Characteristics

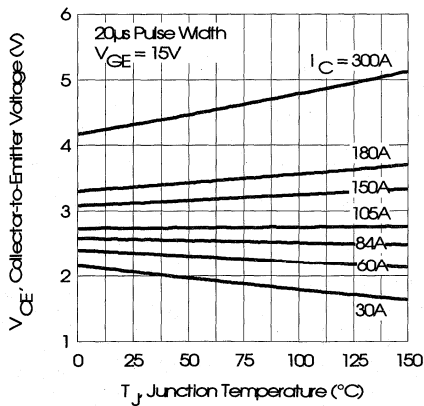


Fig. 5 - Collector-to-Emitter Saturation Typical Voltage vs. Junction Temperature

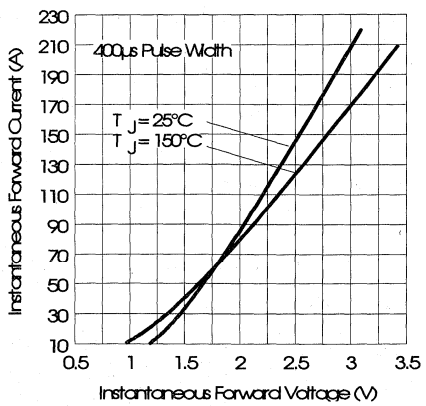


Fig. 6 - Forward Voltage Drop Characteristics

Power
Conversion
Ultra-Fast
Modules

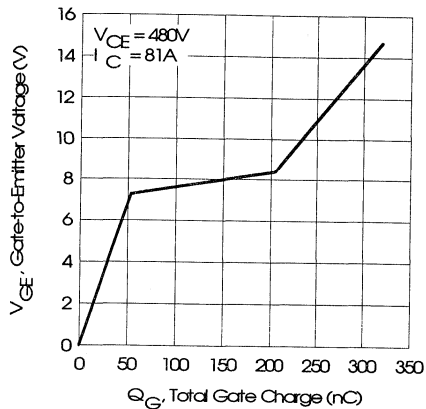


Fig. 7 - Typical Gate Charge vs. Gate-to-Emitter Voltage

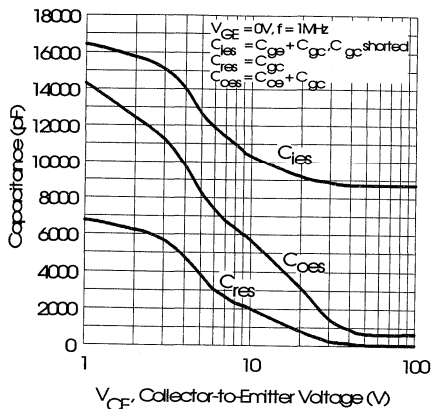


Fig. 8 - Typical Capacitance vs. Collector-to-Emitter Voltage

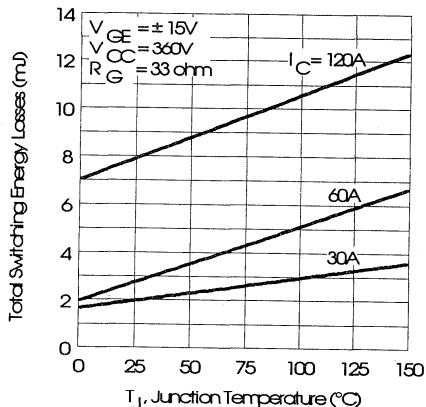


Fig. 9 - Typical Switching Losses vs. Junction Temperature

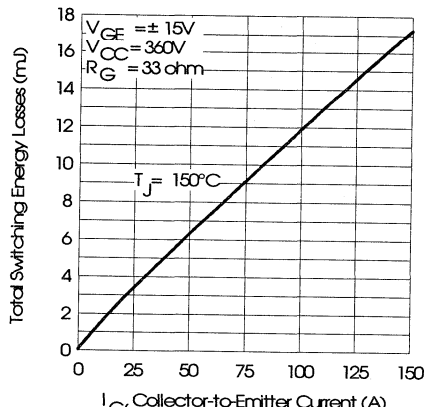


Fig. 10 - Typical Switching Losses vs. Collector-to-Emitter Current

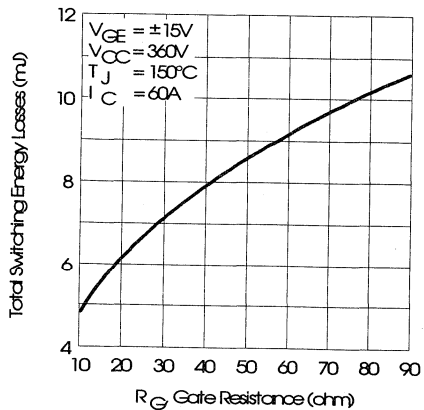


Fig. 11 - Typical Switching Losses vs. Gate Resistance

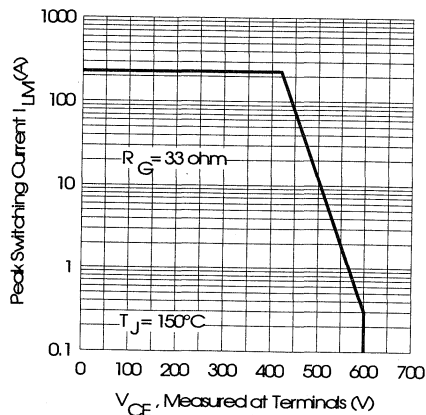


Fig. 12 - Reverse Bias Safe Operating Area

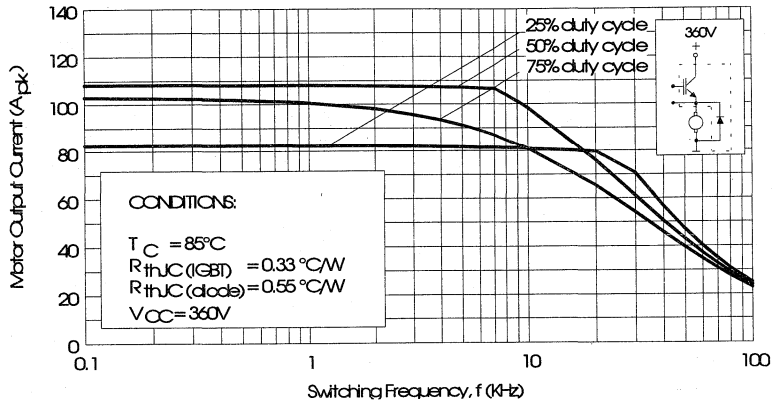


Fig. 13 - RMS Output Current vs. Frequency

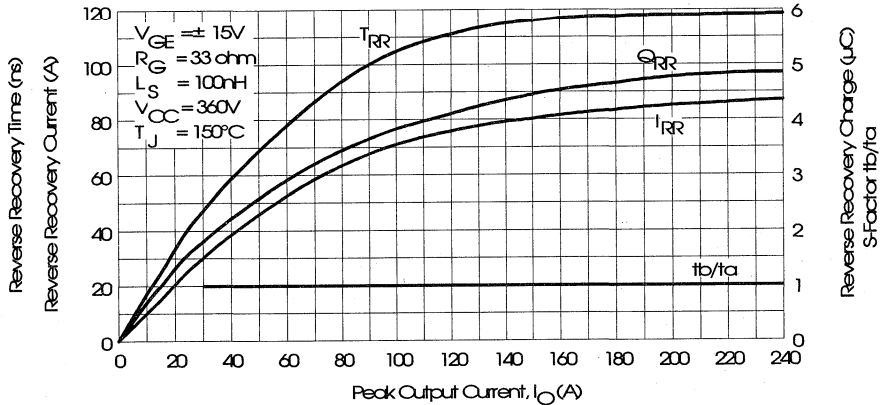


Fig. 14 - Typical Diode Recovery Characteristics as Function of Output Current I_O

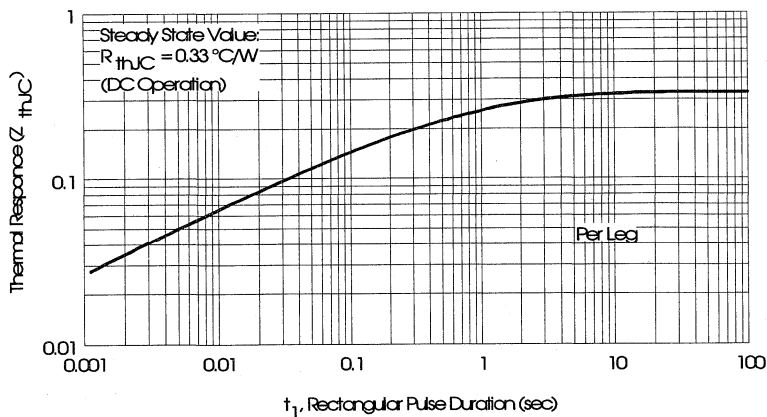


Fig. 15 - Maximum Effective Transient Thermal Impedance, Junction-to-Case

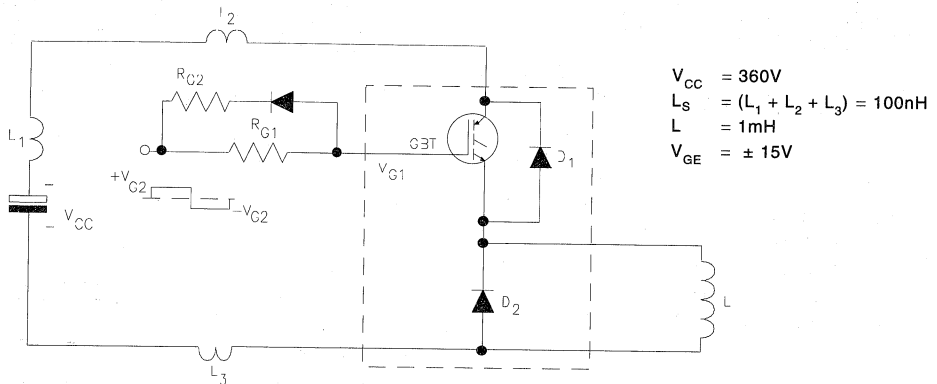


Fig. 16 - Test Circuit for Measurement of I_{LM} , E_{ON} , E_{OFF} , Q_{RR} , I_{RR} , $t_{D(ON)}$, t_r , $t_{D(OFF)}$, t_f

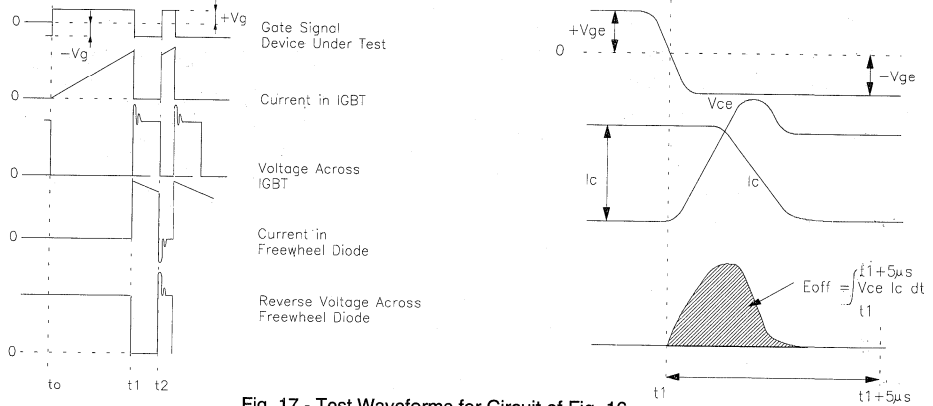


Fig. 17 - Test Waveforms for Circuit of Fig. 16

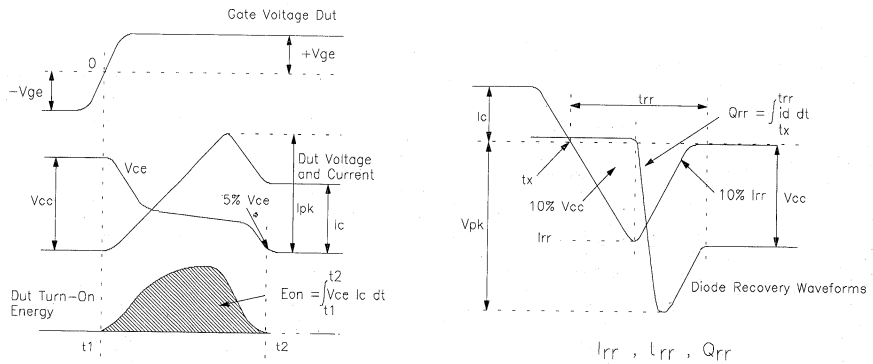


Fig. 18 - Test Waveforms for Circuit of Fig. 16, Defining E_{ON} , E_{REC} , $t_{D(ON)}$, t_r , I_{RR} , t_{RR} , Q_{RR}

Refer to Section D for the following:

Appendix E: Section D - page D-7

Fig. 19 - Waveforms for Switching Time

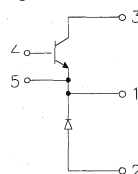
IRGNI140U06

"CHOPPER" IGBT INT-A-PAK

Ultra-fast™ Speed IGBT

- Rugged Design
- Simple gate-drive
- Ultra-fast operation up to 25KHz hard switching, or 100KHz resonant
- Switching-Loss Rating includes all "tail" losses

High Side Switch



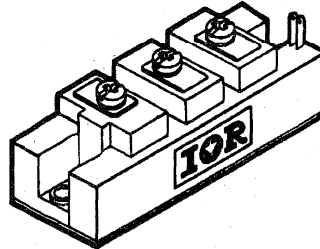
$$V_{CE} = 600V$$

$$I_C = 140A$$

$$V_{CE(ON)} < 2.7V$$

Description

IR's advanced IGBT technology is the key to this line of INT-A-pak Power Modules. The efficient geometry and unique processing of the IGBT allow higher current densities than comparable bipolar power module transistors, while at the same time requiring the simpler gate-drive of the familiar power MOSFET. This superior technology has now been coupled to state of the art assembly techniques to produce a higher current module that is highly suited to power applications such as motor drives, uninterruptible power supplies, welding, induction heating and ultrasonics.



INT-A-PAK case

Absolute Maximum Ratings

Parameter	Description	Value	Units
V_{CES}	Continuous collector to emitter voltage	600	V
$I_C @ T_C = 25^\circ C$	Continuous collector current	170	A
$I_C @ T_C = 85^\circ C$	Continuous collector current	110	
$I_C @ T_C = 100^\circ C$	Continuous collector current	95	
I_{LM}	Peak switching current	280	
I_{FM}	Peak diode forward current (1)	315	
V_{GE}	Gate to emitter voltage	± 20	V
V_{ISOL}	RMS isolation voltage, any terminal to case, $t = 1 \text{ min}$	2500	
$P_D @ T_C = 25^\circ C$	Power dissipation	500	W
T_J	Operating junction temperature range	-40 to 150	$^\circ C$
T_{STG}	Storage temperature range	-40 to 125	

(1) Duration limited by max junction temperature.

Electrical Characteristics - $T_J = 25^\circ\text{C}$, unless otherwise stated

Parameter	Description	Min	Typ	Max	Units	Test Conditions
BV_{CES}	Collector-to-emitter breakdown voltage	600	—	—	v	$V_{GE} = 0V, I_C = 2mA$
$V_{CE(ON)}$	Collector-to-emitter voltage	—	—	2.7		$V_{GE} = 15V, I_C = 140A$
		—	2.7	—		$V_{GE} = 15V, I_C = 140A, T_J = 150^\circ\text{C}$
V_{FM}	Diode forward voltage - maximum	—	—	2.6		$I_F = 140A, V_{GE} = 0V$
		—	2.3	—	$I_F = 140A, V_{GE} = 0V, T_J = 150^\circ\text{C}$	
V_{GEth}	Gate threshold voltage	3.0	—	5.5	$I_C = 1mA$	
ΔV_{GEth}	Threshold voltage temperature coeff.	—	-11	—	mV/ $^\circ\text{C}$	$V_{CE} = V_{GE}, I_C = 1mA$
g_{fe}	Forward transconductance	68	—	120	S(τ)	$V_{CE} = 25V, I_C = 140A$
I_{CES}	Collector-to-emitter leakage current	—	—	2	mA	$V_{GE} = 0V, V_{CE} = 600V$
		—	—	20		$V_{GE} = 0V, V_{CE} = 600V, T_J = 150^\circ\text{C}$
I_{GES}	Gate-to-emitter leakage current	—	—	± 2	μA	$V_{GE} = \pm 20V$

Dynamic Characteristics - $T_J = 150^\circ\text{C}$

Parameter	Description	Min	Typ	Max	Units	Test Conditions
E_{on}	Turn-on switching energy	—	0.05	—	mJ/A	$R_{G1} = 27\Omega, R_{G2} = 0\Omega$
E_{off} (1)	Turn-off switching energy	—	0.05	—		$I_C = 140A, L_S = 100nH$
E_{is} (1)	Total switching energy	—	—	0.12		$V_{CC} = 360V, V_{GE} = \pm 15V$
$t_{d(on)}$	Turn-on delay time	—	70	—	ns	$R_{G1} = 27\Omega, R_{G2} = 0\Omega$
t_r	Rise time	—	90	—		$I_C = 140A$
$t_{d(off)}$	Turn-off delay time	—	180	—		$V_{CC} = 360V, V_{GE} = \pm 15V$
t_f	Fall time	—	250	—		$L_S = 100nH$
I_{rr}	Diode peak recovery current	—	80	—	A	$R_{G1} = 27\Omega, R_{G2} = 0\Omega$
t_{rr}	Diode recovery time	—	110	—	ns	$I_C = 140A$
Q_{rr}	Diode recovery charge	—	5.0	—	μC	$V_{CC} = 360V, V_{GE} = \pm 15V$
Q_{ge}	Gate-to-emitter charge (turn-on)	310	—	560	nC	$V_{CC} = 360V$
Q_{gc}	Gate-to-collector charge (turn-on)	140	—	280		$I_C = 108A$
Q_g	Total gate charge (turn-on)	52	—	84		$V_{GE} = 15V$
C_{ies}	Input capacitance	—	11600	—	pF	$V_{GE} = 0V$
C_{oes}	Output capacitance	—	1320	—		$V_{CC} = 30V$
C_{res}	Reverse transfer capacitance	—	160	—		$f = 1MHz$

(1) Includes tail losses

Thermal and Mechanical Characteristics

Parameter	Description	Typ	Max	Units
R_{thJC} (IGBT)	Thermal resistance, junction to case, each IGBT	—	0.25	$^\circ\text{C/W}$
R_{thJC} (Diode)	Thermal resistance, junction to case, each diode	—	0.4	
R_{thCS} (Module)	Thermal resistance, case to sink	0.1	—	
Wt	Weight of module	140	—	g

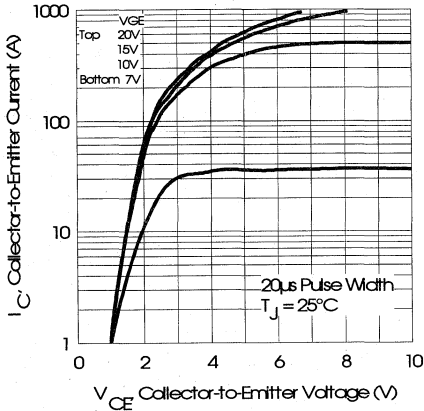


Fig. 1 - Typical Output Characteristics, $T_J = 25^\circ\text{C}$

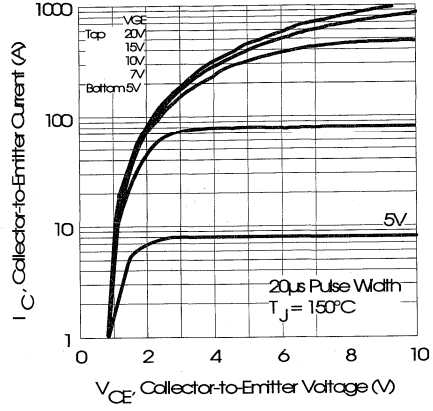


Fig. 2 - Typical Output Characteristics, $T_J = 150^\circ\text{C}$

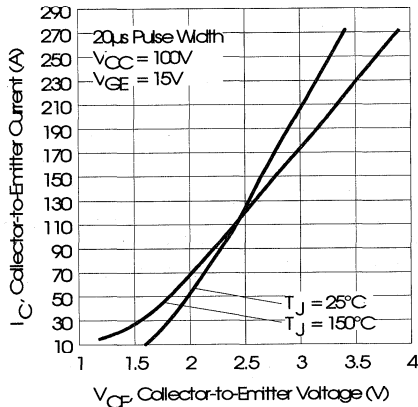


Fig. 3 - Typical Output Characteristics

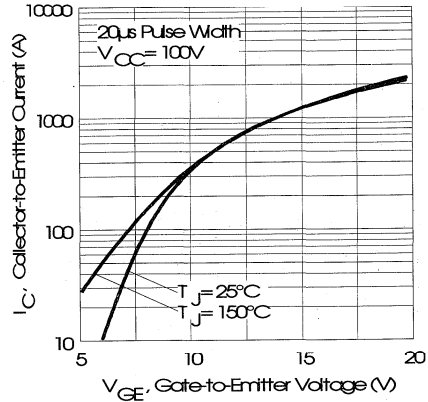


Fig. 4 - Typical Transfer Characteristics

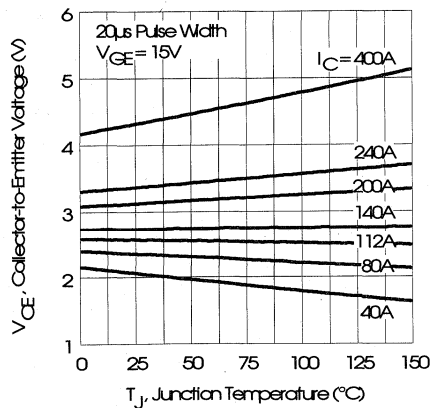


Fig. 5 - Collector-to-Emitter Saturation Typical Voltage vs. Junction Temperature

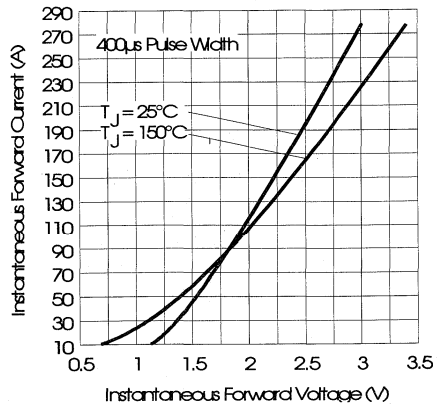


Fig. 6 - Forward Voltage Drop Characteristics

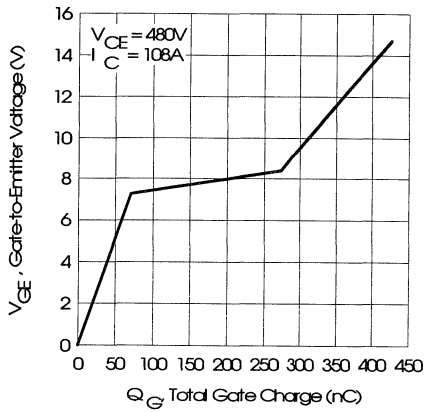


Fig. 7 - Typical Gate Charge vs. Gate-to-Emitter Voltage

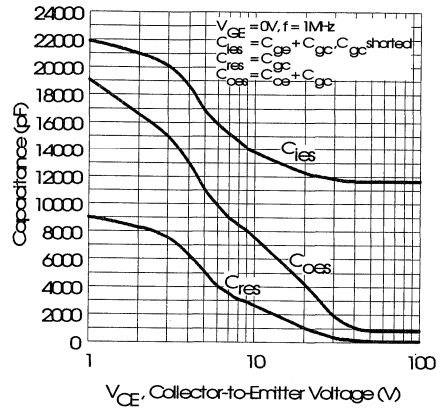


Fig. 8 - Typical Capacitance vs. Collector-to-Emitter Voltage

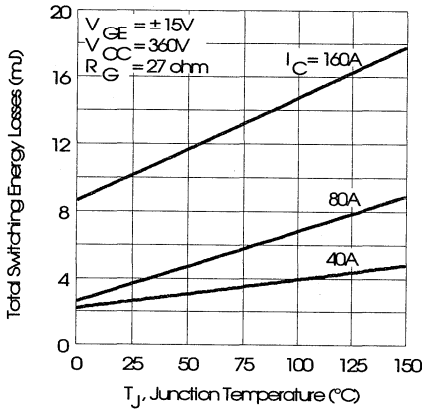


Fig. 9 - Typical Switching Losses vs. Junction Temperature

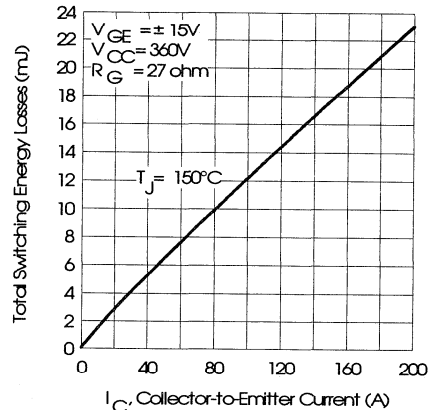


Fig. 10 - Typical Switching Losses vs. Collector-to-Emitter Current

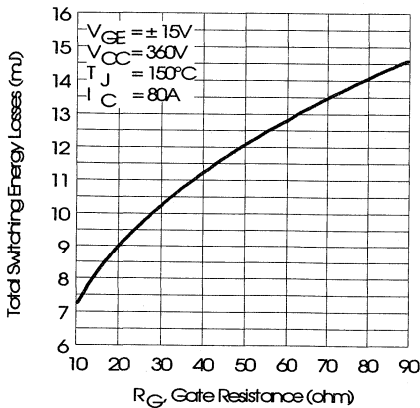


Fig. 11 - Typical Switching Losses vs. Gate Resistance

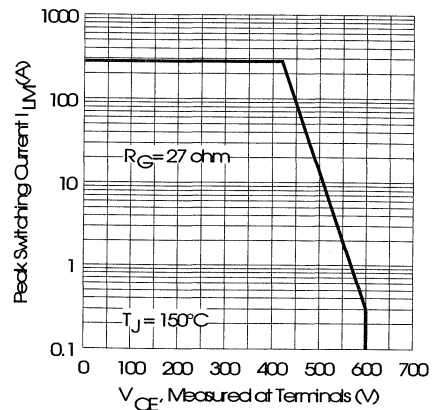


Fig. 12 - Reverse Bias Safe Operating Area

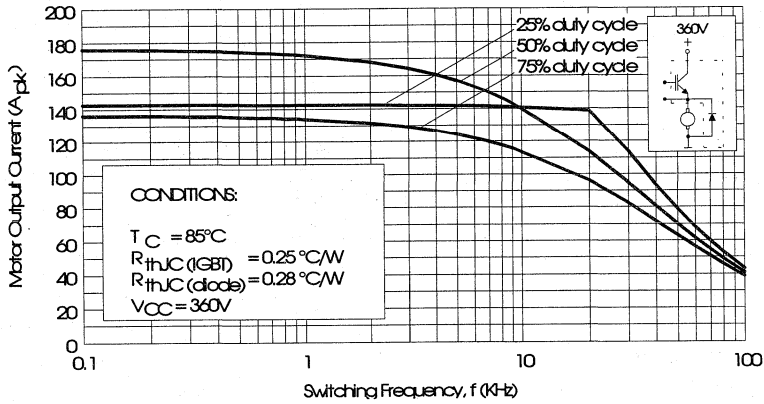


Fig. 13 - RMS Output Current vs. Frequency

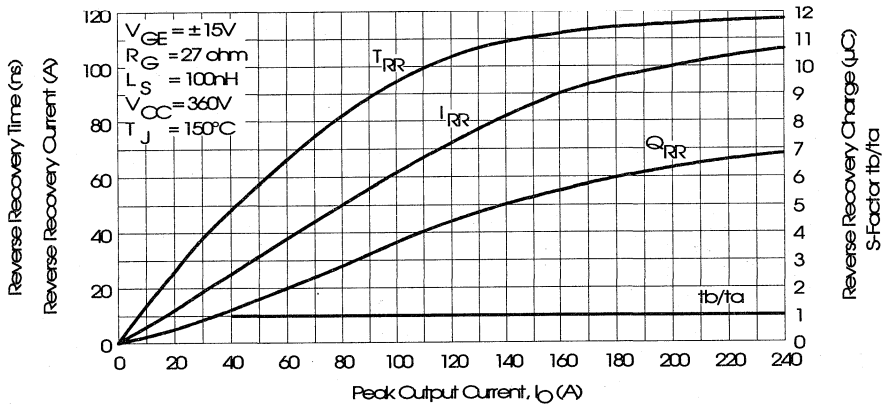


Fig. 14 - Typical Diode Recovery Characteristics as Function of Output Current I_o

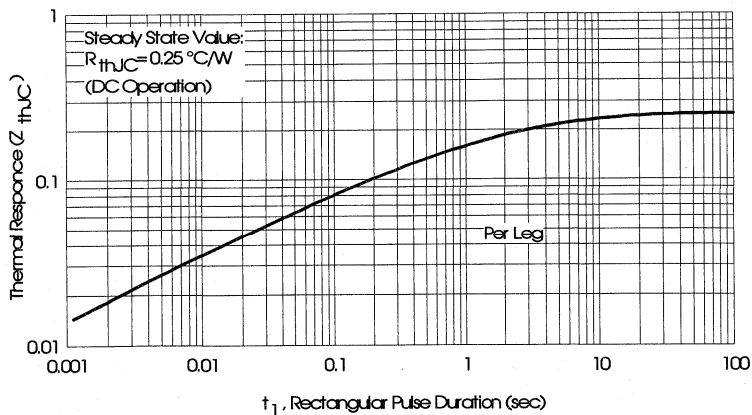


Fig. 15 - Maximum Effective Transient Thermal Impedance, Junction-to-Case

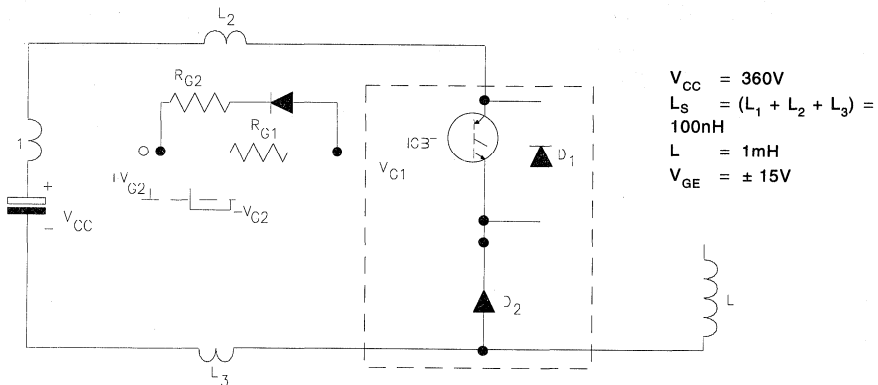


Fig. 16 - Test Circuit for Measurement of I_{LM} , E_{ON} , E_{OFF} , Q_{RR} , I_{RR} , $t_{D(ON)}$, t_r , $t_{D(OFF)}$, t_f

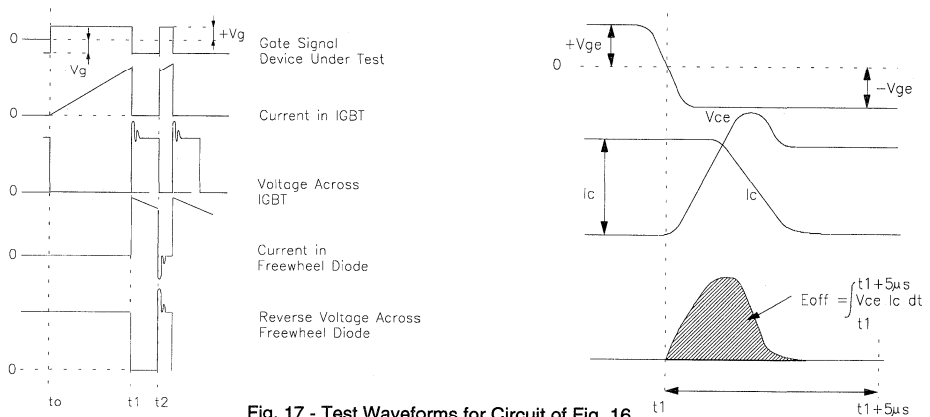


Fig. 17 - Test Waveforms for Circuit of Fig. 16

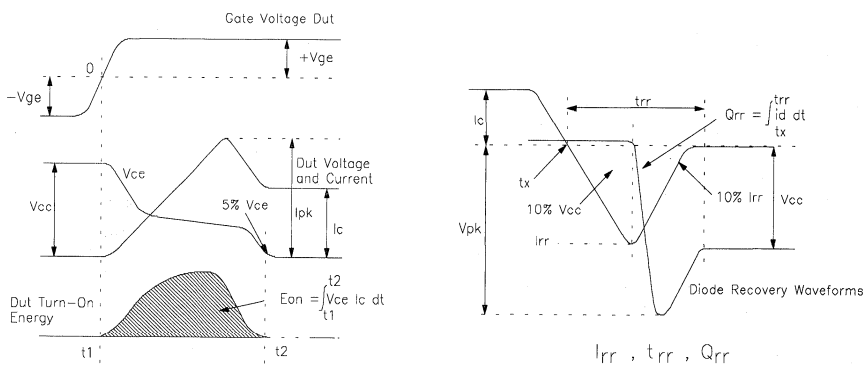


Fig. 18 - Test Waveforms for Circuit of Fig. 16, Defining E_{ON} , E_{REC} , $t_{D(ON)}$, t_r , I_{RR} , t_{RR} , Q_{RR}

Refer to Section D for the following:
 Appendix E: Section D - page D-7

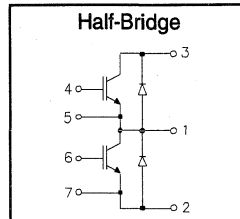
Fig. 19 - Waveforms for Switching Time

IRGT1050U06

"HALF-BRIDGE" IGBT INT-A-PAK

Ultra-fast™ Speed IGBT

- Rugged Design
- Simple gate-drive
- Ultra-fast operation up to 25KHz hard switching, or 100KHz resonant
- Switching-Loss Rating includes all "tail" losses



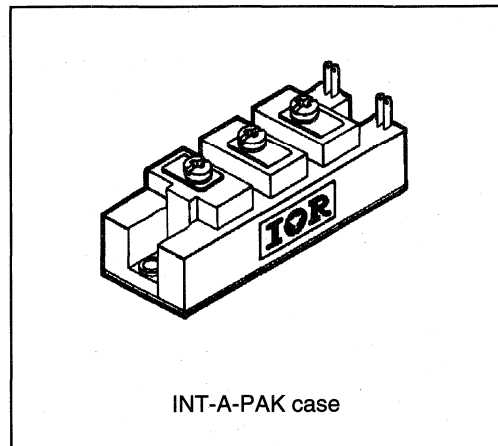
$$V_{CE} = 600V$$

$$I_C = 50A$$

$$V_{CE(ON)} < 3.1V$$

Description

IR's advanced IGBT technology is the key to this line of INT-A-pak Power Modules. The efficient geometry and unique processing of the IGBT allow higher current densities than comparable bipolar power module transistors, while at the same time requiring the simpler gate-drive of the familiar power MOSFET. This superior technology has now been coupled to state of the art assembly techniques to produce a higher current module that is highly suited to power applications such as motor drives, uninterruptible power supplies, welding, induction heating and ultrasonics.



Absolute Maximum Ratings

Parameter	Description	Value	Units
V_{CES}	Continuous collector to emitter voltage	600	V
$I_C @ T_C = 25^\circ C$	Continuous collector current	50	A
$I_C @ T_C = 85^\circ C$	Continuous collector current	35	
$I_C @ T_C = 100^\circ C$	Continuous collector current	30	
I_{LM}	Peak switching current	100	
I_{FM}	Peak diode forward current (1)	125	V
V_{GE}	Gate to emitter voltage	± 20	
V_{ISOL}	RMS isolation voltage, any terminal to case, $t = 1$ min	2500	W
$P_D @ T_C = 25^\circ C$	Power dissipation	179	
T_J	Operating junction temperature range	-40 to 150	$^\circ C$
T_{STG}	Storage temperature range	-40 to 125	

(1) Duration limited by max junction temperature.

Power Conversion Ultra-fast Modules

Electrical Characteristics - $T_J = 25^\circ\text{C}$, unless otherwise stated

Parameter	Description	Min	Typ	Max	Units	Test Conditions
BV_{CES}	Collector-to-emitter breakdown voltage	600	—	—		$V_{GE} = 0V, I_C = 500\mu A$
$V_{CE(ON)}$	Collector-to-emitter voltage	—	—	3.1	V	$V_{GE} = 15V, I_C = 50A$
		—	3.3	—		$V_{GE} = 15V, I_C = 50A, T_J = 150^\circ\text{C}$
V_{FM}	Diode forward voltage - maximum	—	—	2.9		$I_F = 50A, V_{GE} = 0V$
		—	2.8	—		$I_F = 50A, V_{GE} = 0V, T_J = 150^\circ\text{C}$
V_{GEth}	Gate threshold voltage	3.0	—	5.5		$I_C = 250\mu A$
ΔV_{GEth}	Threshold voltage temperature coeff.	—	-11	—	mV/°C	$V_{CE} = V_{GE}, I_C = 250\mu A$
g_{fe}	Forward transconductance	17.3	—	29.6	S(r)	$V_{CE} = 25V, I_C = 50A$
I_{CES}	Collector-to-emitter leakage current	—	—	500	μA	$V_{GE} = 0V, V_{CE} = 600V$
		—	—	5	mA	$V_{GE} = 0V, V_{CE} = 600V, T_J = 150^\circ\text{C}$
I_{GES}	Gate-to-emitter leakage current	—	—	± 500	nA	$V_{GE} = \pm 20V$

Dynamic Characteristics - $T_J = 150^\circ\text{C}$

Parameter	Description	Min	Typ	Max	Units	Test Conditions
E_{on}	Turn-on switching energy	—	0.05	—		$R_{G1} = 82\Omega, R_{G2} = 0\Omega$
E_{off} (1)	Turn-off switching energy	—	0.05	—	mJ/A	$I_C = 50A, L_S = 100nH$
E_{ts} (1)	Total switching energy	—	—	0.12		$V_{CC} = 360V, V_{GE} = \pm 15V$
$t_{d(on)}$	Turn-on delay time	—	70	—	ns	$R_{G1} = 82\Omega, R_{G2} = 0\Omega$
t_r	Rise time	—	90	—		$I_C = 50A$
$t_{d(off)}$	Turn-off delay time	—	180	—		$V_{CC} = 360V, V_{GE} = \pm 15V$
t_f	Fall time	—	250	—		$L_S = 100nH$
I_{rr}	Diode peak recovery current	—	27	—	A	$R_{G1} = 82\Omega, R_{G2} = 0\Omega$
t_{rr}	Diode recovery time	—	110	—	ns	$I_C = 50A$
Q_{rr}	Diode recovery charge	—	1.6	—	μC	$V_{CC} = 360V, V_{GE} = \pm 15V$
Q_{ge}	Gate-to-emitter charge (turn-on)	77	—	140	nC	$V_{CC} = 360V$
Q_{gc}	Gate-to-collector charge (turn-on)	35	—	70		$I_C = 50A$
Q_g	Total gate charge (turn-on)	13	—	21		$V_{GE} = 15V$
C_{ies}	Input capacitance	—	2900	—	pF	$V_{GE} = 0V$
C_{oes}	Output capacitance	—	330	—		$V_{CC} = 30V$
C_{res}	Reverse transfer capacitance	—	40	—		$f = 1MHz$

(1) Includes tail losses

Thermal and Mechanical Characteristics

Parameter	Description	Typ	Max	Units
R_{thJC} (IGBT)	Thermal resistance, junction to case, each IGBT	—	0.7	°C/W
R_{thJC} (Diode)	Thermal resistance, junction to case, each diode	—	1.3	
R_{thCS} (Module)	Thermal resistance, case to sink	0.1	—	
Wt	Weight of module	140	—	g

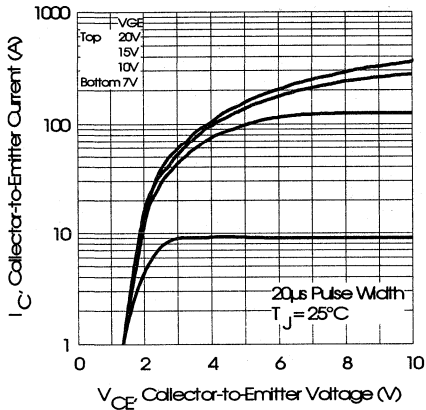


Fig. 1 - Typical Output Characteristics, $T_J = 25^\circ\text{C}$

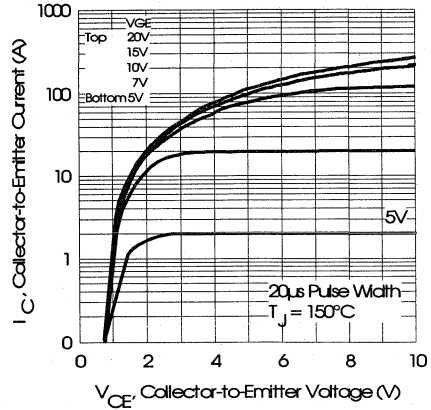


Fig. 2 - Typical Output Characteristics, $T_J = 150^\circ\text{C}$

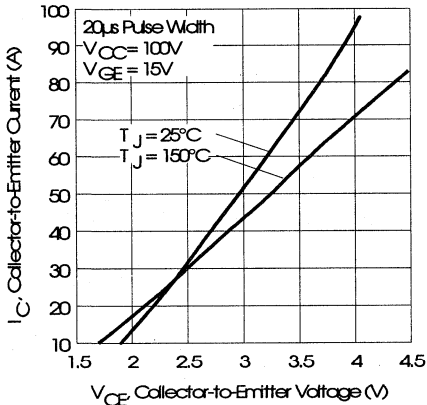


Fig. 3 - Typical Output Characteristics

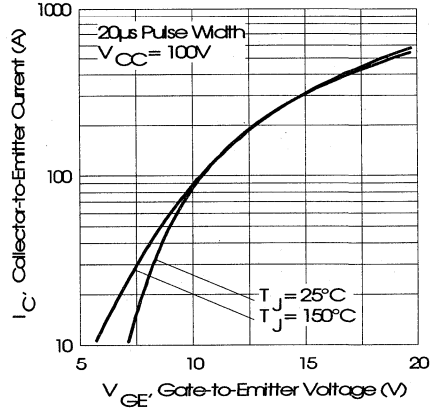


Fig. 4 - Typical Transfer Characteristics

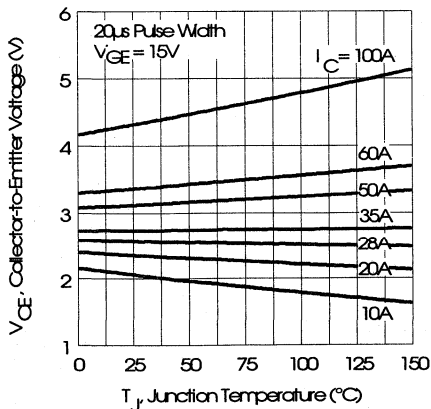


Fig. 5 - Collector-to-Emitter Saturation Typical Voltage vs. Junction Temperature

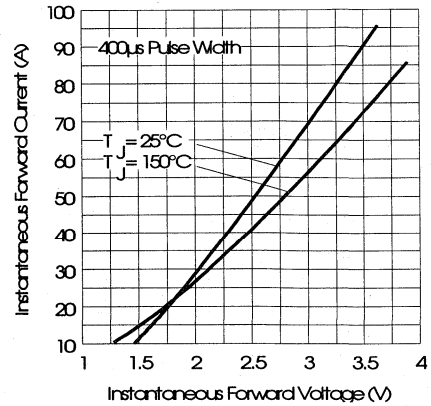


Fig. 6 - Forward Voltage Drop Characteristics

Power Conversion
Ultra-Fast
Modules

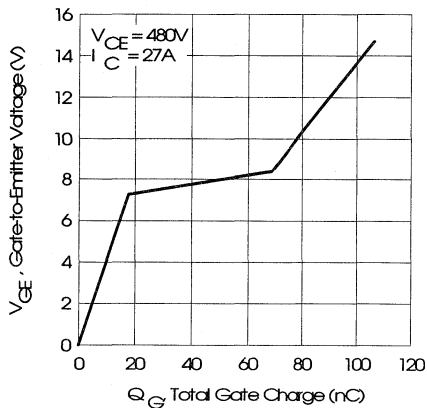


Fig. 7 - Typical Gate Charge vs. Gate-to-Emitter Voltage

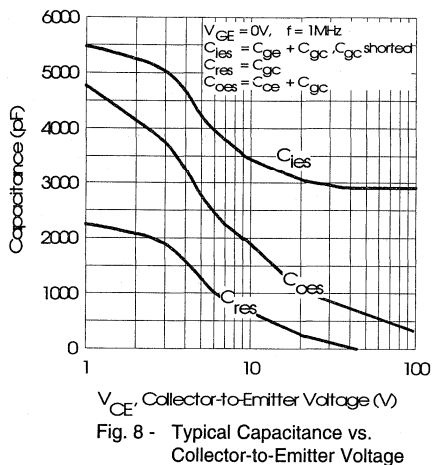


Fig. 8 - Typical Capacitance vs. Collector-to-Emitter Voltage

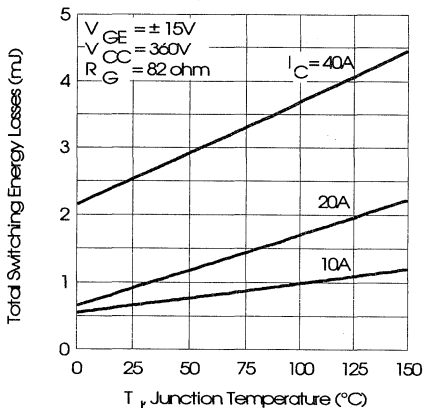


Fig. 9 - Typical Switching Losses vs. Junction Temperature

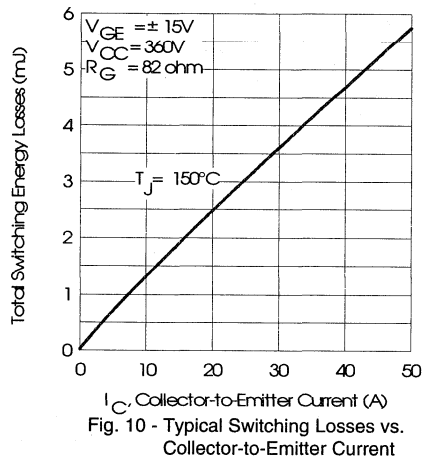


Fig. 10 - Typical Switching Losses vs. Collector-to-Emitter Current

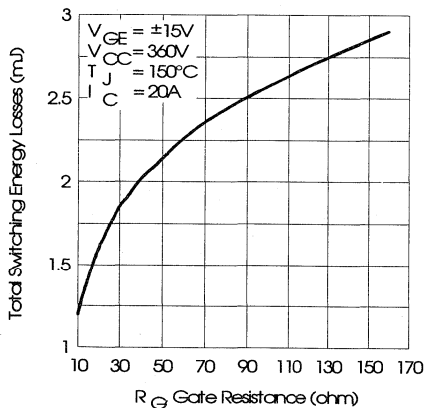


Fig. 11 - Typical Switching Losses vs. Gate Resistance

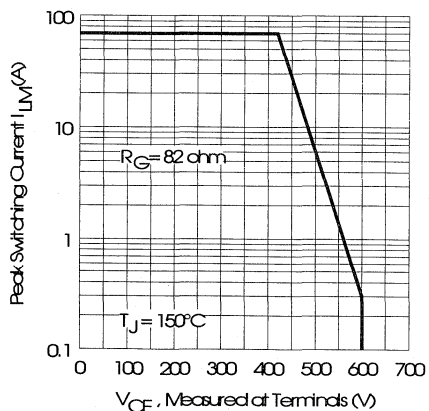


Fig. 12 - Reverse Bias Safe Operating Area

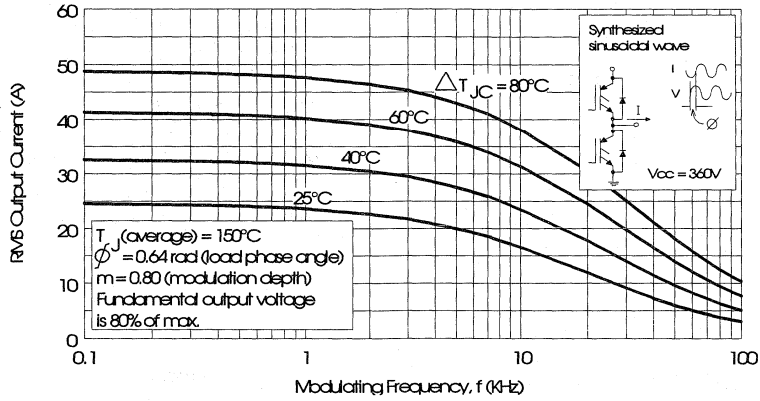


Fig. 13 - Typical RMS Output Current per phase vs. Frequency (Synthesized Sinusoidal Wave)

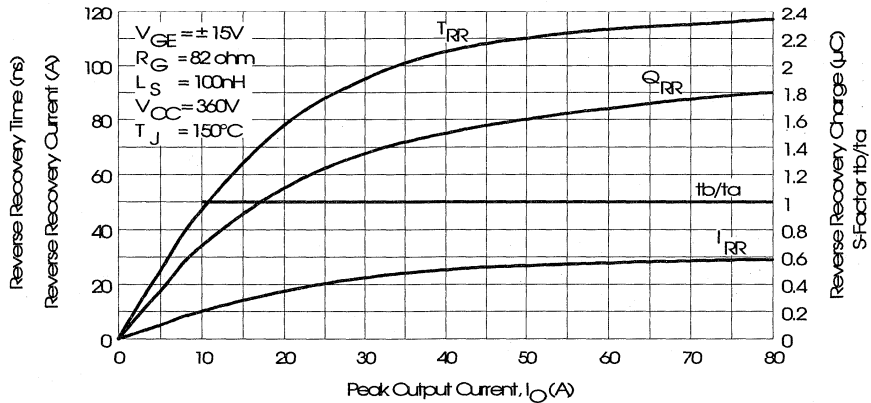


Fig. 14 - Typical Diode Recovery Characteristics as Function of Output Current I_o

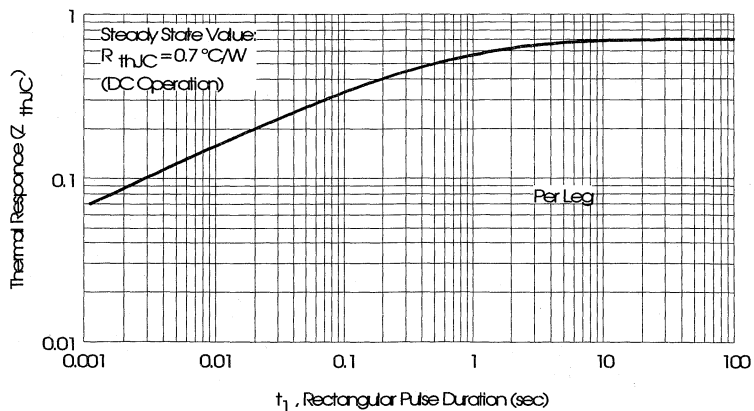


Fig. 15 - Maximum Effective Transient Thermal Impedance, Junction-to-Case

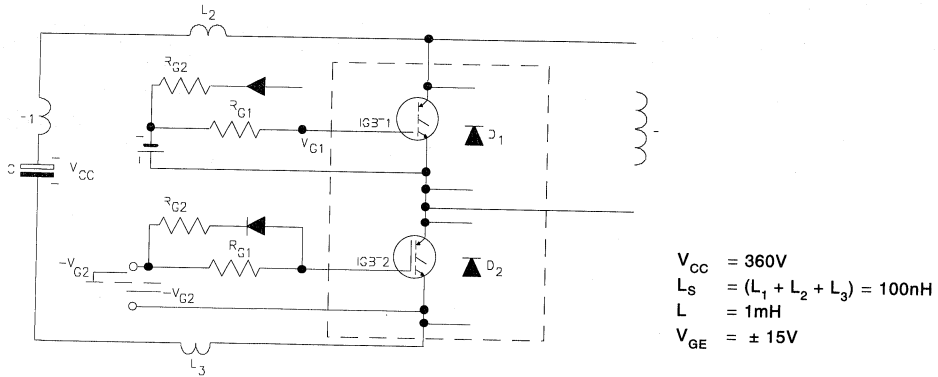


Fig. 16 - Test Circuit for Measurement of I_{LM} , E_{ON} , E_{OFF} , Q_{RR} , I_{RR} , $t_{D(ON)}$, t_r , $t_{D(OFF)}$, t_f

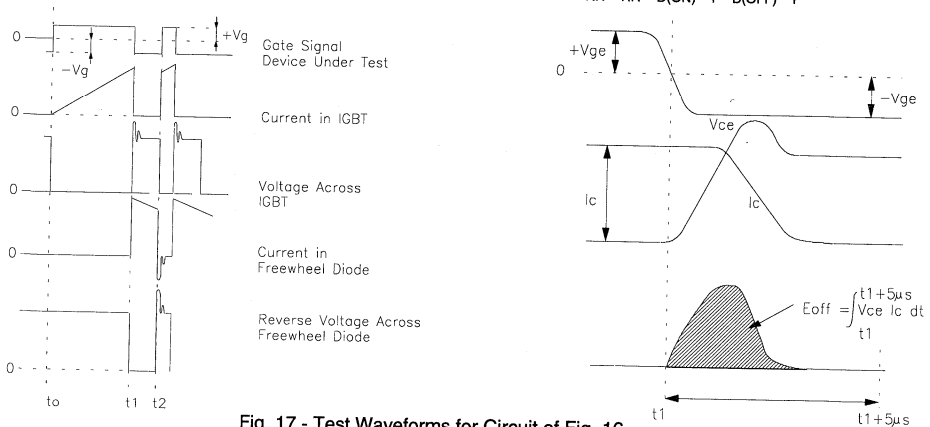


Fig. 17 - Test Waveforms for Circuit of Fig. 16

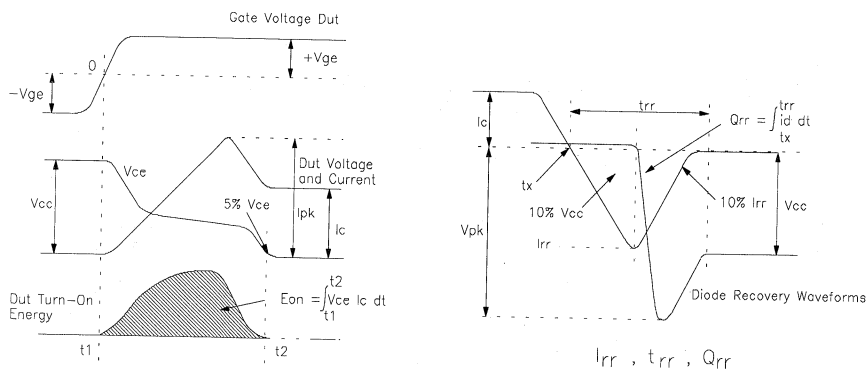


Fig. 18 - Test Waveforms for Circuit of Fig. 16, Defining E_{ON} , E_{REC} , $t_{D(ON)}$, t_r , I_{RR} , t_{RR} , Q_{RR}

Refer to Section D for the following:
Appendix E: Section D - page D-7

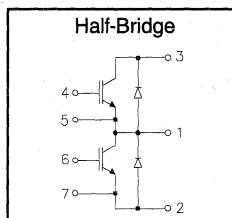
Fig. 19 - Waveforms for Switching Time

IRGT1090U06

"HALF-BRIDGE" IGBT INT-A-PAK

Ultra-fast™ Speed IGBT

- Rugged Design
- Simple gate-drive
- Ultra-fast operation up to 25KHz hard switching, or 100KHz resonant
- Switching-Loss Rating includes all "tail" losses



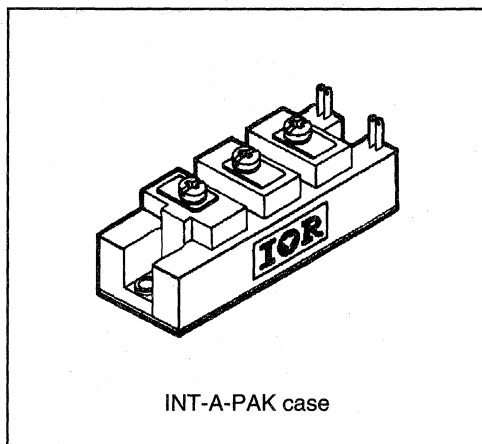
$$V_{CE} = 600V$$

$$I_C = 90A$$

$$V_{CE(ON)} < 3.0V$$

Description

IR's advanced IGBT technology is the key to this line of INT-A-pak Power Modules. The efficient geometry and unique processing of the IGBT allow higher current densities than comparable bipolar power module transistors, while at the same time requiring the simpler gate-drive of the familiar power MOSFET. This superior technology has now been coupled to state of the art assembly techniques to produce a higher current module that is highly suited to power applications such as motor drives, uninterruptible power supplies, welding, induction heating and ultrasonics.



Absolute Maximum Ratings

Parameter	Description	Value	Units
V_{CES}	Continuous collector to emitter voltage	600	V
$I_C @ T_C = 25^\circ C$	Continuous collector current	90	A
$I_C @ T_C = 85^\circ C$	Continuous collector current	60	
$I_C @ T_C = 100^\circ C$	Continuous collector current	50	
I_{LM}	Peak switching current	180	
I_{FM}	Peak diode forward current (1)	225	
V_{GE}	Gate to emitter voltage	± 20	V
V_{ISOL}	RMS isolation voltage, any terminal to case, $t = 1$ min	2500	
$P_D @ T_C = 25^\circ C$	Power dissipation	298	W
T_J	Operating junction temperature range	-40 to 150	$^\circ C$
T_{STG}	Storage temperature range	-40 to 125	

(1) Duration limited by max junction temperature.

Electrical Characteristics - $T_J = 25^\circ\text{C}$, unless otherwise stated

Parameter	Description	Min	Typ	Max	Units	Test Conditions
BV_{CES}	Collector-to-emitter breakdown voltage	600	—	—	V	$V_{GE} = 0V, I_C = 1mA$
$V_{CE(ON)}$	Collector-to-emitter voltage	—	—	3.0		$V_{GE} = 15V, I_C = 90A$
		—	3.1	—		$V_{GE} = 15V, I_C = 90A, T_J = 150^\circ\text{C}$
V_{FM}	Diode forward voltage - maximum	—	—	2.8		$I_F = 90A, V_{GE} = 0V$
		—	2.6	—		$I_F = 90A, V_{GE} = 0V, T_J = 150^\circ\text{C}$
V_{Geth}	Gate threshold voltage	3.0	—	5.5	$I_C = 500\mu A$	
ΔV_{Geth}	Threshold voltage temperature coeff.	—	-11	—	mV/°C	$V_{CE} = V_{GE}, I_C = 500\mu A$
g_{fe}	Forward transconductance	34	—	58	S(Ω)	$V_{CE} = 25V, I_C = 90A$
I_{CES}	Collector-to-emitter leakage current	—	—	1	mA	$V_{GE} = 0V, V_{CE} = 600V$
		—	—	10		$V_{GE} = 0V, V_{CE} = 600V, T_J = 150^\circ\text{C}$
I_{GES}	Gate-to-emitter leakage current	—	—	± 1	μA	$V_{GE} = \pm 20V$

Dynamic Characteristics - $T_J = 150^\circ\text{C}$

Parameter	Description	Min	Typ	Max	Units	Test Conditions
E_{on}	Turn-on switching energy	—	0.05	—	mJ/A	$R_{G1} = 47\Omega, R_{G2} = 0\Omega$
E_{off} (1)	Turn-off switching energy	—	0.05	—		$I_C = 90A, L_S = 100nH$
E_{IS} (1)	Total switching energy	—	—	0.12		$V_{CC} = 360V, V_{GE} = \pm 15V$
$t_{d(on)}$	Turn-on delay time	—	70	—	ns	$R_{G1} = 47\Omega, R_{G2} = 0\Omega$
t_r	Rise time	—	90	—		$I_C = 90A$
$t_{d(off)}$	Turn-off delay time	—	180	—		$V_{CC} = 360V, V_{GE} = \pm 15V$
t_f	Fall time	—	250	—		$L_S = 100nH$
I_{rr}	Diode peak recovery current	—	52	—	A	$R_{G1} = 47\Omega, R_{G2} = 0\Omega$
t_{rr}	Diode recovery time	—	110	—	ns	$I_C = 90A$
Q_{rr}	Diode recovery charge	—	3.0	—	μC	$V_{CC} = 360V, V_{GE} = \pm 15V$
Q_{ge}	Gate-to-emitter charge (turn-on)	150	—	280	nC	$V_{CC} = 360V$
Q_{gc}	Gate-to-collector charge (turn-on)	70	—	140		$I_C = 90A$
Q_g	Total gate charge (turn-on)	26	—	42		$V_{GE} = 15V$
C_{ies}	Input capacitance	—	5800	—	pF	$V_{GE} = 0V$
C_{oes}	Output capacitance	—	660	—		$V_{CC} = 30V$
C_{res}	Reverse transfer capacitance	—	80	—		$f = 1MHz$

(1) Includes tail losses

Thermal and Mechanical Characteristics

Parameter	Description	Typ	Max	Units
R_{thJC} (IGBT)	Thermal resistance, junction to case, each IGBT	—	0.42	°C/W
R_{thJC} (Diode)	Thermal resistance, junction to case, each diode	—	0.7	
R_{thCS} (Module)	Thermal resistance, case to sink	0.1	—	
Wt	Weight of module	140	—	g

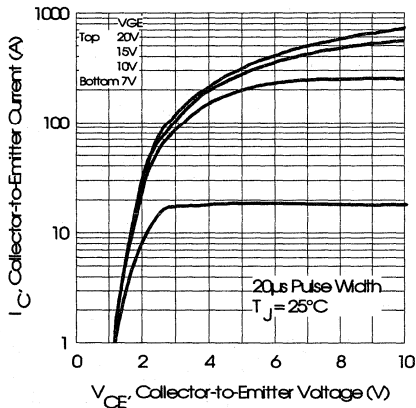


Fig. 1 - Typical Output Characteristics, $T_J = 25^\circ\text{C}$

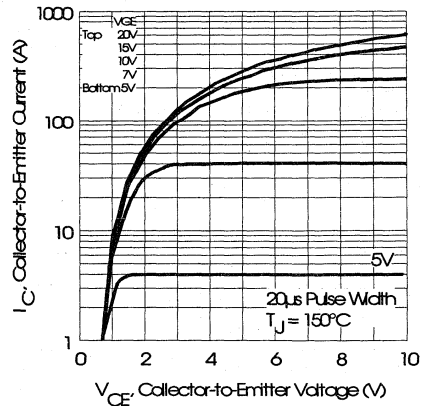


Fig. 2 - Typical Output Characteristics, $T_J = 150^\circ\text{C}$

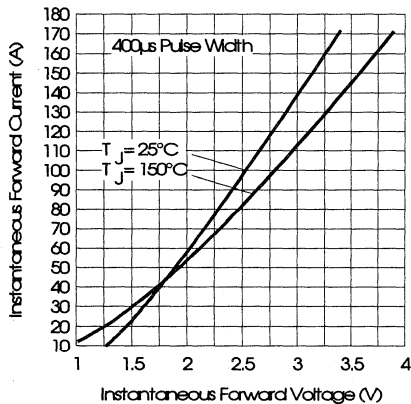


Fig. 3 - Typical Output Characteristics

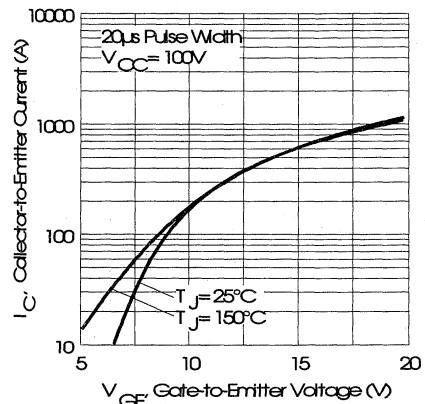


Fig. 4 - Typical Transfer Characteristics

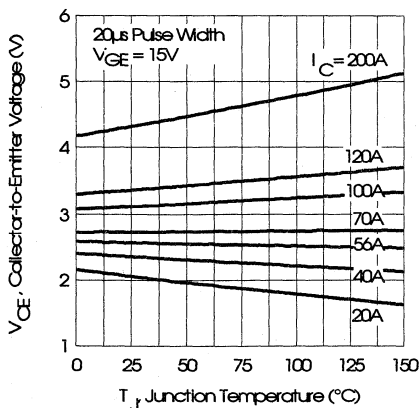


Fig. 5 - Collector-to-Emitter Saturation Typical Voltage vs. Junction Temperature

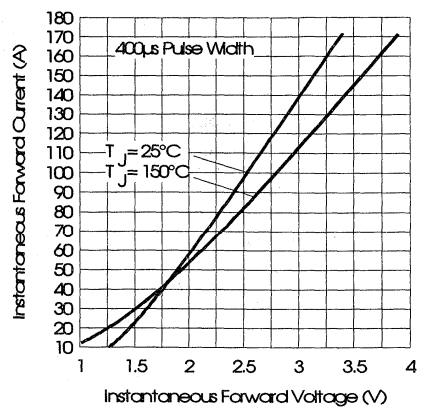


Fig. 6 - Forward Voltage Drop Characteristics

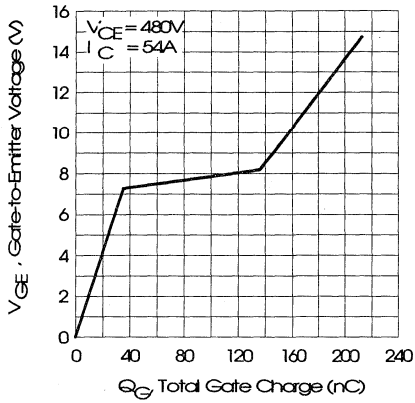


Fig. 7 - Typical Gate Charge vs. Gate-to-Emitter Voltage

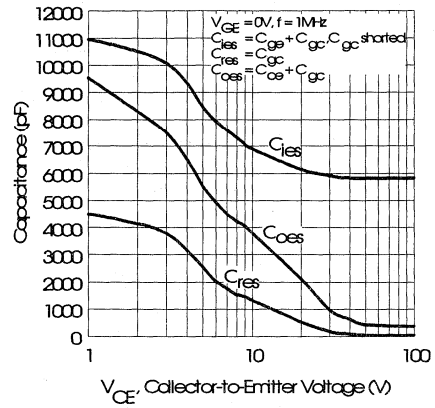


Fig. 8 - Typical Capacitance vs. Collector-to-Emitter Voltage

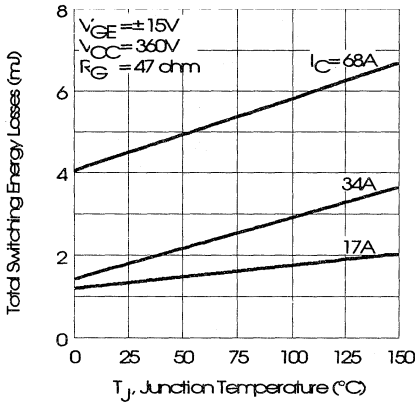


Fig. 9 - Typical Switching Losses vs. Junction Temperature

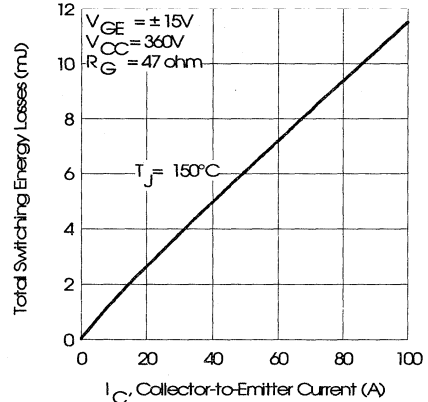


Fig. 10 - Typical Switching Losses vs. Collector-to-Emitter Current

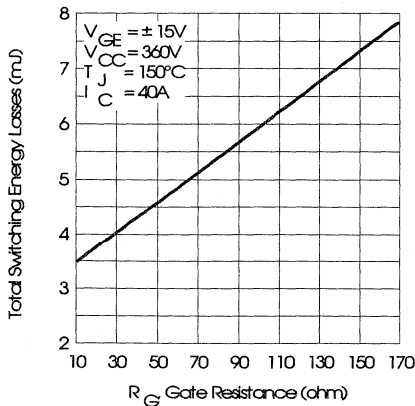


Fig. 11 - Typical Switching Losses vs. Gate Resistance

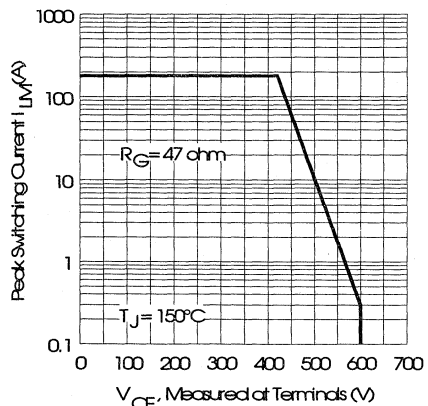


Fig. 12 - Reverse Bias Safe Operating Area

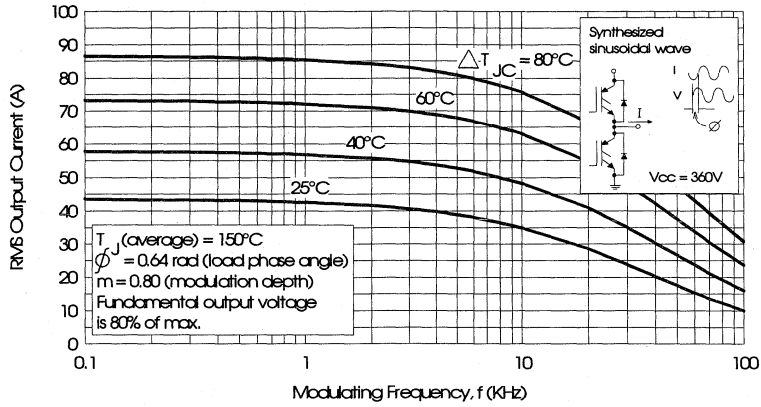


Fig. 13 - Typical RMS Output Current per phase vs. Frequency (Synthesized Sinusoidal Wave)

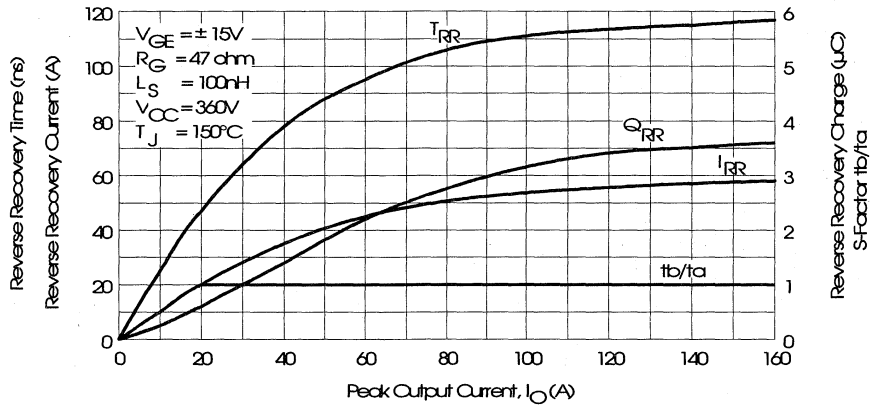


Fig. 14 - Typical Diode Recovery Characteristics as Function of Output Current I_o

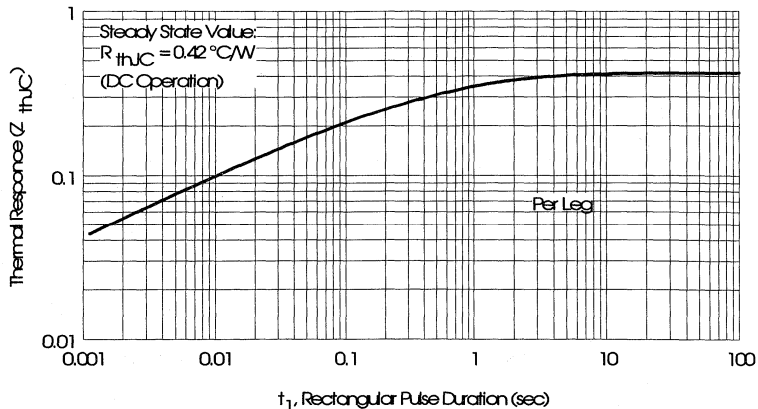


Fig. 15 - Maximum Effective Transient Thermal Impedance, Junction-to-Case

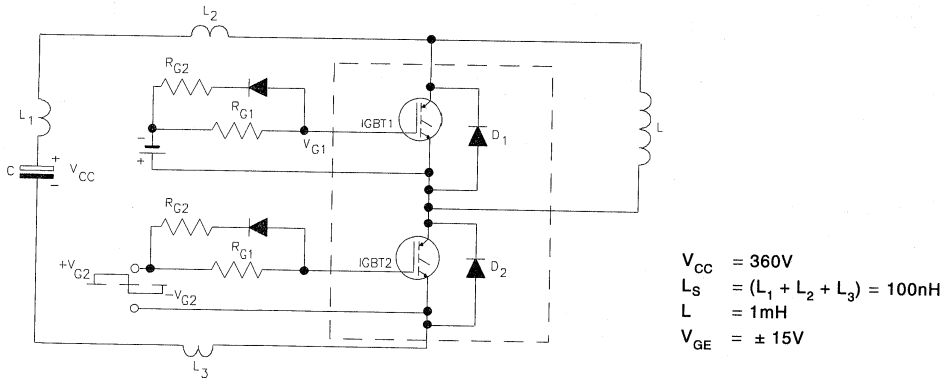


Fig. 16 - Test Circuit for Measurement of I_{LM} , E_{ON} , E_{OFF} , Q_{RR} , I_{RR} , $t_{D(ON)}$, t_r , $t_{D(OFF)}$, t_f

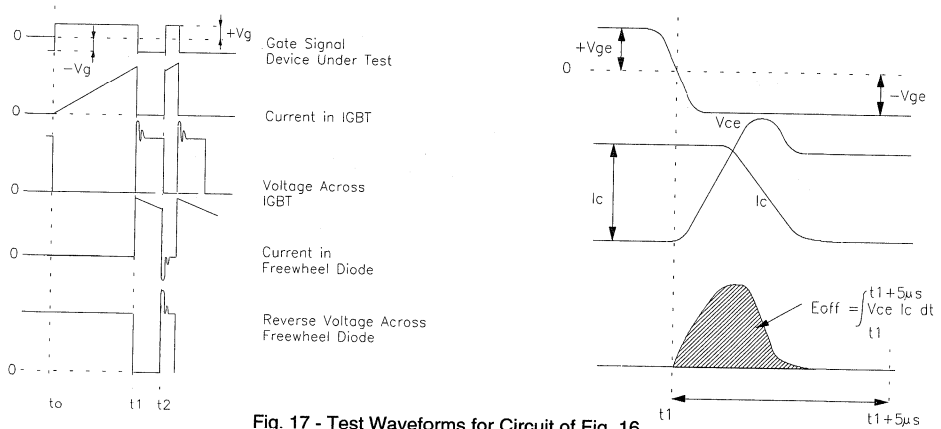


Fig. 17 - Test Waveforms for Circuit of Fig. 16

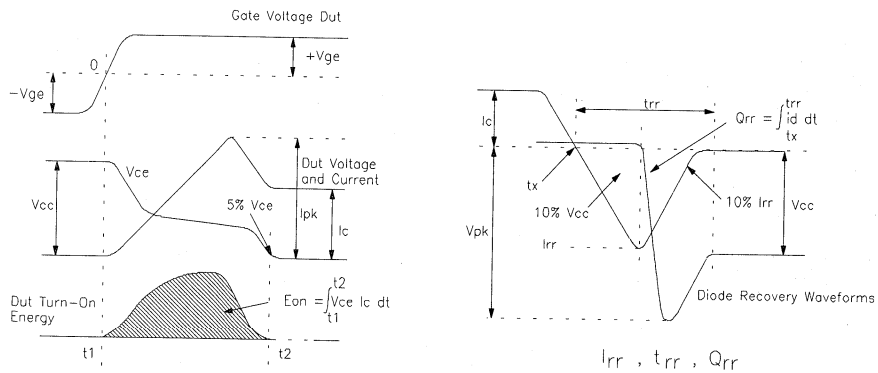


Fig. 18 - Test Waveforms for Circuit of Fig. 16, Defining E_{ON} , E_{REC} , $t_{D(ON)}$, t_r , I_{RR} , t_{RR} , Q_{RR}

Refer to Section D for the following:
 Appendix E: Section D - page D-7

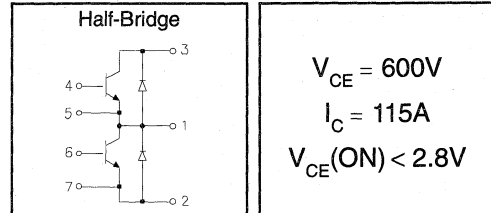
Fig. 19 - Waveforms for Switching Time

IRGT115U06

"HALF-BRIDGE" IGBT INT-A-PAK

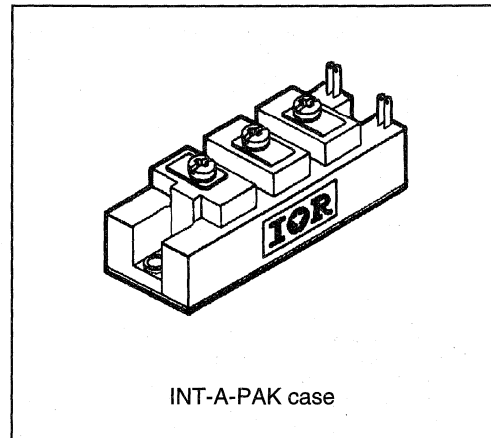
Ultra-fast™ Speed IGBT

- Rugged Design
- Simple gate-drive
- Ultra-fast operation up to 25KHz hard switching, or 100KHz resonant
- Switching-Loss Rating includes all "tail" losses



Description

IR's advanced IGBT technology is the key to this line of INT-A-pak Power Modules. The efficient geometry and unique processing of the IGBT allow higher current densities than comparable bipolar power module transistors, while at the same time requiring the simpler gate-drive of the familiar power MOSFET. This superior technology has now been coupled to state of the art assembly techniques to produce a higher current module that is highly suited to power applications such as motor drives, uninterruptible power supplies, welding, induction heating and ultrasonics.



Absolute Maximum Ratings

Parameter	Description	Value	Units
V_{CES}	Continuous collector to emitter voltage	600	V
$I_C @ T_C = 25^\circ C$	Continuous collector current	130	A
$I_C @ T_C = 85^\circ C$	Continuous collector current	85	
$I_C @ T_C = 100^\circ C$	Continuous collector current	70	
I_{LM}	Peak switching current	230	
I_{FM}	Peak diode forward current (1)	290	
V_{GE}	Gate to emitter voltage	± 20	V
V_{ISOL}	RMS isolation voltage, any terminal to case, $t = 1$ min	2500	
$P_D @ T_C = 25^\circ C$	Power dissipation	379	W
T_J	Operating junction temperature range	-40 to 150	$^\circ C$
T_{STG}	Storage temperature range	-40 to 125	

(1) Duration limited by max junction temperature.

Electrical Characteristics - $T_J = 25^\circ\text{C}$, unless otherwise stated

Parameter	Description	Min	Typ	Max	Units	Test Conditions
BV_{CES}	Collector-to-emitter breakdown voltage	600	—	—	v	$V_{GE} = 0V, I_C = 1.5mA$
$V_{CE(ON)}$	Collector-to-emitter voltage	—	—	2.8		$V_{GE} = 15V, I_C = 115A$
		—	2.9	—		$V_{GE} = 15V, I_C = 115A, T_J = 150^\circ\text{C}$
V_{FM}	Diode forward voltage - maximum	—	—	2.7		$I_F = 115A, V_{GE} = 0V$
		—	2.4	—		$I_F = 115A, V_{GE} = 0V, T_J = 150^\circ\text{C}$
V_{GEth}	Gate threshold voltage	3.0	—	5.5	$I_C = 750\mu A$	
ΔV_{GEth}	Threshold voltage temperature coeff.	—	-11	—	mV/ $^\circ\text{C}$	$V_{CE} = V_{GE}, I_C = 750\mu A$
g_{fe}	Forward transconductance	51	—	87	S(ω)	$V_{CE} = 25V, I_C = 115A$
I_{CES}	Collector-to-emitter leakage current	—	—	1.5	mA	$V_{GE} = 0V, V_{CE} = 600V$
		—	—	15		$V_{GE} = 0V, V_{CE} = 600V, T_J = 150^\circ\text{C}$
I_{GES}	Gate-to-emitter leakage current	—	—	± 1.5	μA	$V_{GE} = \pm 20V$

Dynamic Characteristics - $T_J = 150^\circ\text{C}$

Parameter	Description	Min	Typ	Max	Units	Test Conditions
E_{on}	Turn-on switching energy	—	0.05	—	mJ/A	$R_{G1} = 33\Omega, R_{G2} = 0\Omega$
E_{off} (1)	Turn-off switching energy	—	0.05	—		$I_C = 115A, L_S = 100nH$
E_{ts} (1)	Total switching energy	—	—	0.12		$V_{CC} = 360V, V_{GE} = \pm 15V$
$t_{d(on)}$	Turn-on delay time	—	70	—	ns	$R_{G1} = 33\Omega, R_{G2} = 0\Omega$
t_r	Rise time	—	90	—		$I_C = 115A$
$t_{d(off)}$	Turn-off delay time	—	180	—		$V_{CC} = 360V, V_{GE} = \pm 15V$
t_f	Fall time	—	250	—		$L_S = 100nH$
I_{rr}	Diode peak recovery current	—	72	—		A
t_{rr}	Diode recovery time	—	110	—	ns	$I_C = 115A$
Q_{rr}	Diode recovery charge	—	4.0	—	μC	$V_{CC} = 360V, V_{GE} = \pm 15V$
Q_{ge}	Gate-to-emitter charge (turn-on)	225	—	420	nC	$V_{CC} = 360V$
Q_{gc}	Gate-to-collector charge (turn-on)	105	—	210	nC	$I_C = 115A$
Q_g	Total gate charge (turn-on)	39	—	63	nC	$V_{GE} = 15V$
C_{ies}	Input capacitance	—	8700	—	pF	$V_{GE} = 0V$
C_{oes}	Output capacitance	—	990	—		$V_{CC} = 30V$
C_{res}	Reverse transfer capacitance	—	120	—		$f = 1MHz$

(1) Includes tail losses

Thermal and Mechanical Characteristics

Parameter	Description	Typ	Max	Units
R_{thJC} (IGBT)	Thermal resistance, junction to case, each IGBT	—	0.33	$^\circ\text{C/W}$
R_{thJC} (Diode)	Thermal resistance, junction to case, each diode	—	0.55	
R_{thCS} (Module)	Thermal resistance, case to sink	0.1	—	
Wt	Weight of module	140	—	g

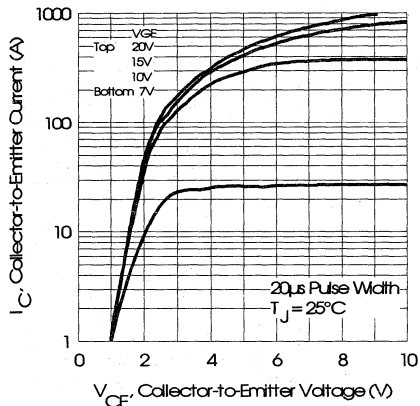


Fig. 1 - Typical Output Characteristics, $T_J = 25^\circ\text{C}$

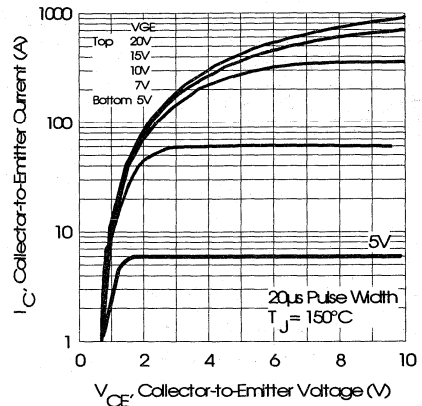


Fig. 2 - Typical Output Characteristics, $T_J = 150^\circ\text{C}$

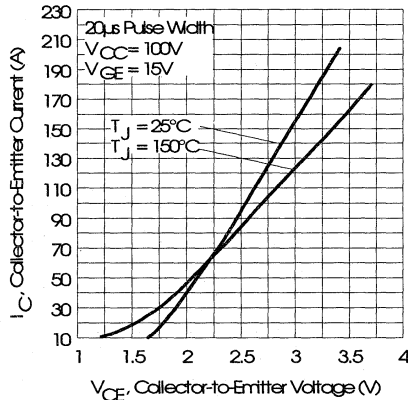


Fig. 3 - Typical Output Characteristics

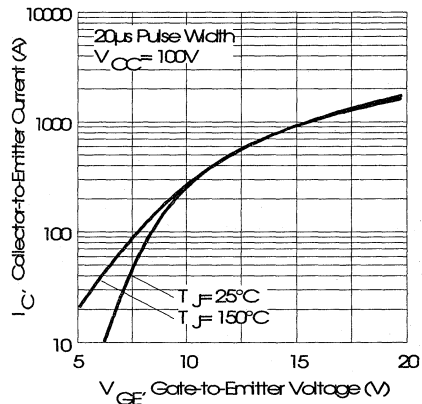


Fig. 4 - Typical Transfer Characteristics

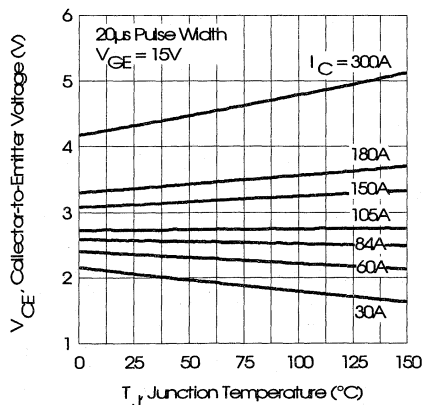


Fig. 5 - Collector-to-Emitter Saturation Typical Voltage vs. Junction Temperature

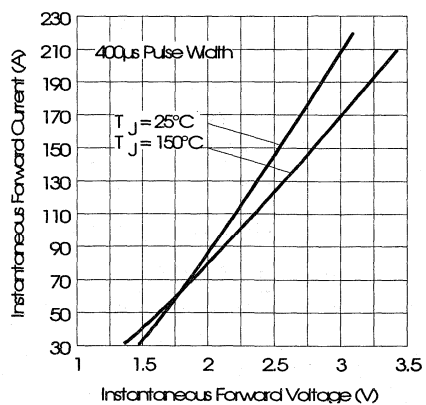


Fig. 6 - Forward Voltage Drop Characteristics

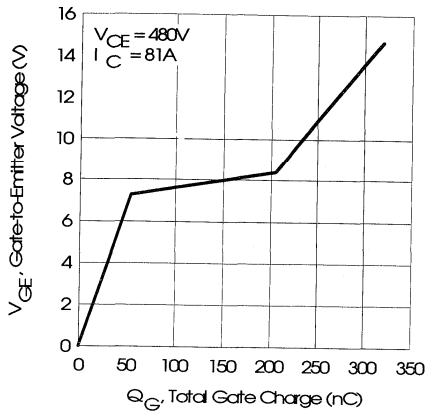


Fig. 7 - Typical Gate Charge vs. Gate-to-Emitter Voltage

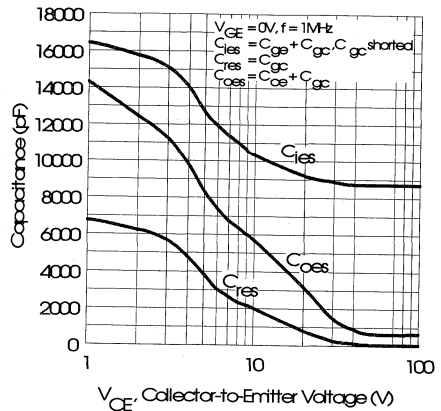


Fig. 8 - Typical Capacitance vs. Collector-to-Emitter Voltage

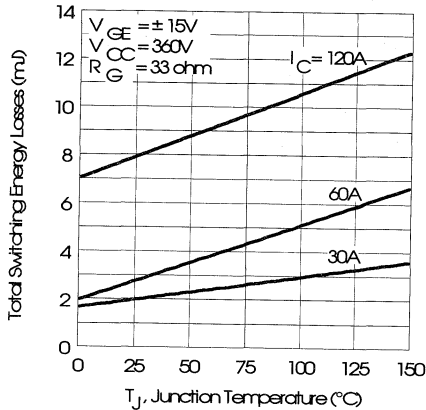


Fig. 9 - Typical Switching Losses vs. Junction Temperature

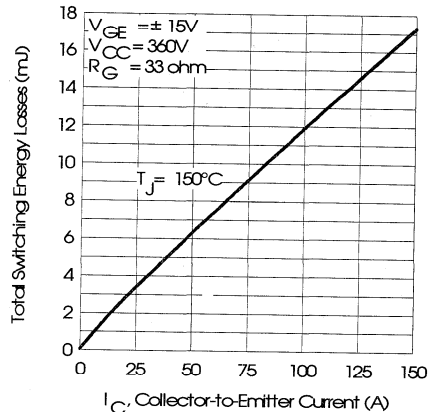


Fig. 10 - Typical Switching Losses vs. Collector-to-Emitter Current

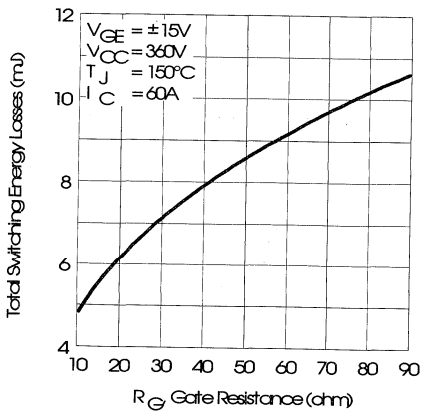


Fig. 11 - Typical Switching Losses vs. Gate Resistance

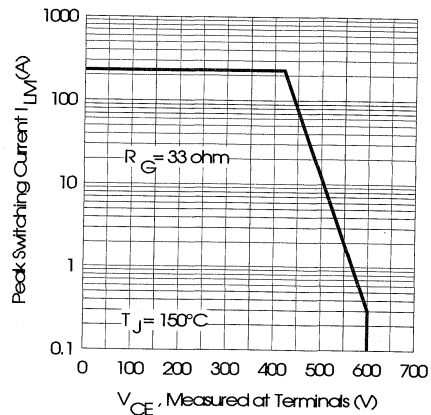


Fig. 12 - Reverse Bias Safe Operating Area

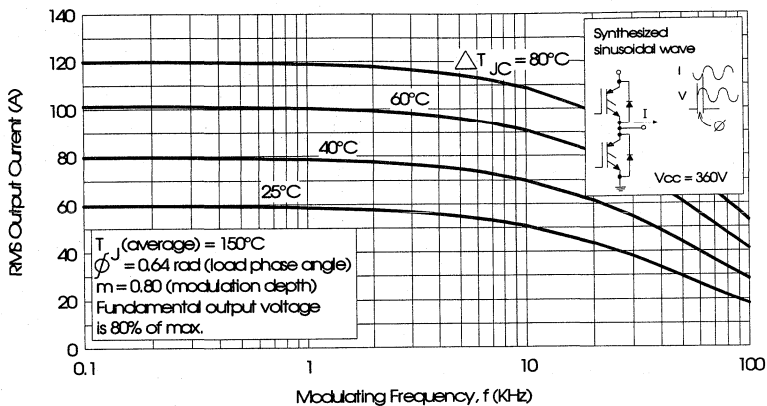


Fig. 13 - Typical RMS Output Current per phase vs. Frequency (Synthesized Sinusoidal Wave)

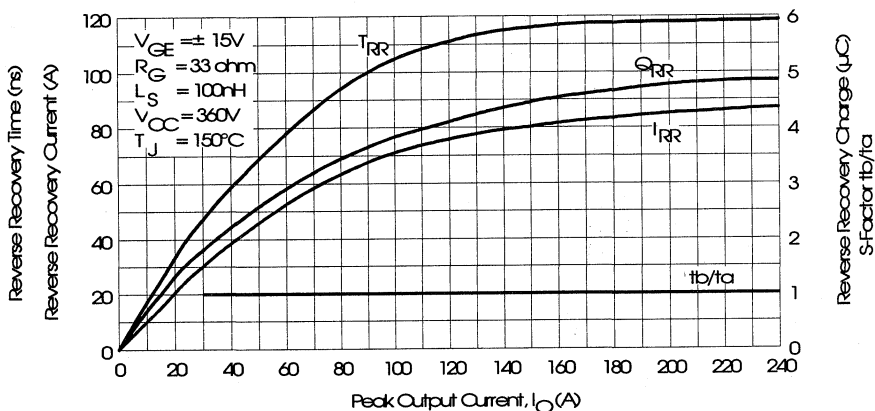


Fig. 14 - Typical Diode Recovery Characteristics as Function of Output Current I_o

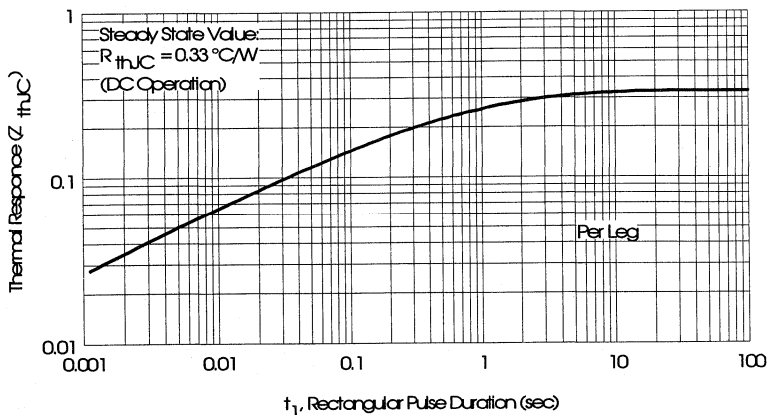


Fig. 15 - Maximum Effective Transient Thermal Impedance, Junction-to-Case

Power Conversion Ultra-Fast Modules

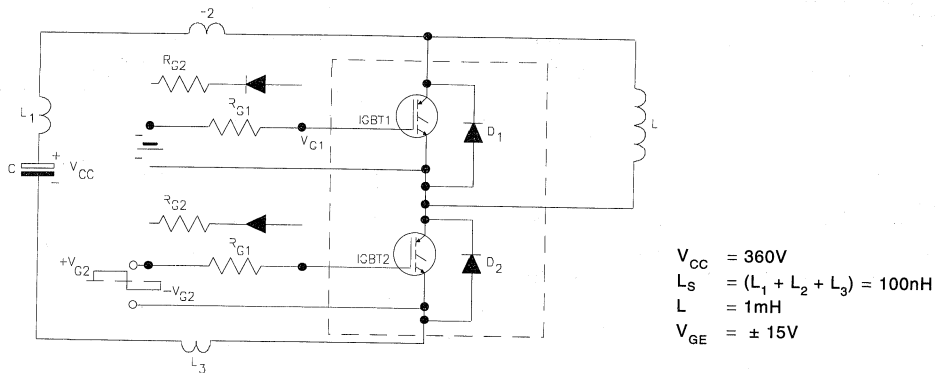


Fig. 16 - Test Circuit for Measurement of I_{LM} , E_{ON} , E_{OFF} , Q_{RR} , I_{RR} , $t_{D(ON)}$, t_r , $t_{D(OFF)}$, t_f

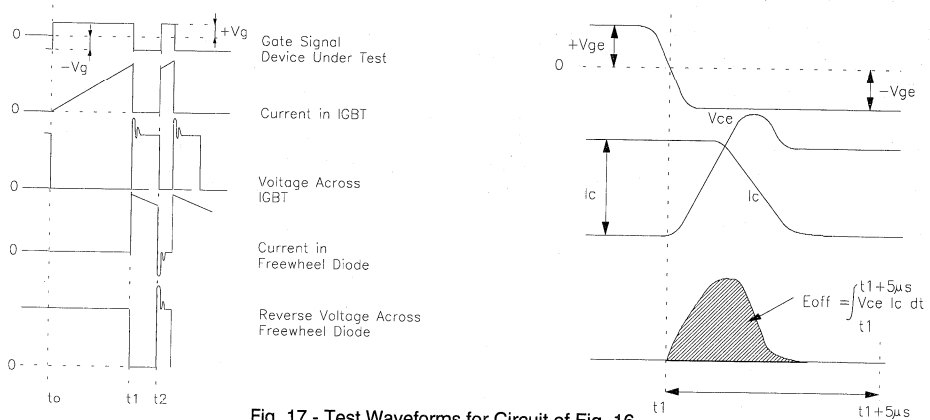


Fig. 17 - Test Waveforms for Circuit of Fig. 16

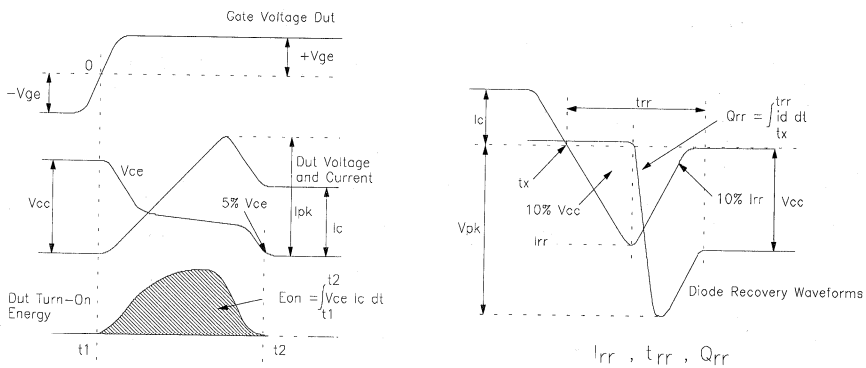


Fig. 18 - Test Waveforms for Circuit of Fig. 16, Defining E_{ON} , E_{REC} , $t_{D(ON)}$, t_r , I_{RR} , t_{RR} , Q_{RR}

Refer to Section D for the following:
Appendix E: Section D - page D-7

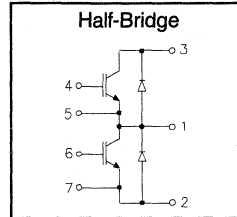
Fig. 19 - Waveforms for Switching Time

IRGT1140U06

"HALF-BRIDGE" IGBT INT-A-PAK

Ultra-fast™ Speed IGBT

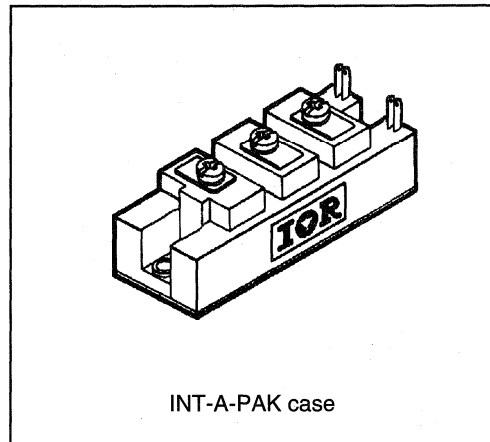
- Rugged Design
- Simple gate-drive
- Ultra-fast operation up to 25KHz hard switching, or 100KHz resonant
- Switching-Loss Rating includes all "tail" losses



$V_{CE} = 600V$
$I_C = 140A$
$V_{CE(ON)} < 2.7V$

Description

IR's advanced IGBT technology is the key to this line of INT-A-pak Power Modules. The efficient geometry and unique processing of the IGBT allow higher current densities than comparable bipolar power module transistors, while at the same time requiring the simpler gate-drive of the familiar power MOSFET. This superior technology has now been coupled to state of the art assembly techniques to produce a higher current module that is highly suited to power applications such as motor drives, uninterruptible power supplies, welding, induction heating and ultrasonics.



Absolute Maximum Ratings

Parameter	Description	Value	Units
V_{CES}	Continuous collector to emitter voltage	600	V
$I_C @ T_C = 25^\circ C$	Continuous collector current	170	A
$I_C @ T_C = 85^\circ C$	Continuous collector current	110	
$I_C @ T_C = 100^\circ C$	Continuous collector current	95	
I_{LM}	Peak switching current	280	
I_{FM}	Peak diode forward current (1)	315	V
V_{GE}	Gate to emitter voltage	± 20	
V_{ISOL}	RMS isolation voltage, any terminal to case, $t = 1$ min	2500	
$P_D @ T_C = 25^\circ C$	Power dissipation	500	W
T_J	Operating junction temperature range	-40 to 150	$^\circ C$
T_{STG}	Storage temperature range	-40 to 125	

(1) Duration limited by max junction temperature.

Power Conversion Ultra-Fast Modules

Electrical Characteristics - $T_J = 25^\circ\text{C}$, unless otherwise stated

Parameter	Description	Min	Typ	Max	Units	Test Conditions
BV_{CES}	Collector-to-emitter breakdown voltage	600	—	—	V	$V_{GE} = 0V, I_C = 2mA$
$V_{CE(ON)}$	Collector-to-emitter voltage	—	—	2.7		$V_{GE} = 15V, I_C = 140A$
		—	2.7	—		$V_{GE} = 15V, I_C = 140A, T_J = 150^\circ\text{C}$
V_{FM}	Diode forward voltage - maximum	—	—	2.6		$I_F = 140A, V_{GE} = 0V$
		—	2.3	—		$I_F = 140A, V_{GE} = 0V, T_J = 150^\circ\text{C}$
V_{GEth}	Gate threshold voltage	3.0	—	5.5	$I_C = 1mA$	
ΔV_{GEth}	Threshold voltage temperature coeff.	—	-11	—	mV/ $^\circ\text{C}$	$V_{CE} = V_{GE}, I_C = 1mA$
g_{fe}	Forward transconductance	68	—	120	S(τ)	$V_{CE} = 25V, I_C = 140A$
I_{CES}	Collector-to-emitter leakage current	—	—	2	mA	$V_{GE} = 0V, V_{CE} = 600V$
		—	—	20		$V_{GE} = 0V, V_{CE} = 600V, T_J = 150^\circ\text{C}$
I_{GES}	Gate-to-emitter leakage current	—	—	± 2	μA	$V_{GE} = \pm 20V$

Dynamic Characteristics - $T_J = 150^\circ\text{C}$

Parameter	Description	Min	Typ	Max	Units	Test Conditions
E_{on}	Turn-on switching energy	—	0.05	—	mJ/A	$R_{G1} = 27\Omega, R_{G2} = 0\Omega$
$E_{off} (1)$	Turn-off switching energy	—	0.05	—		$I_C = 140A, L_S = 100nH$
$E_{ts} (1)$	Total switching energy	—	—	0.12		$V_{CC} = 360V, V_{GE} = \pm 15V$
$t_{d(on)}$	Turn-on delay time	—	70	—	ns	$R_{G1} = 27\Omega, R_{G2} = 0\Omega$
t_r	Rise time	—	90	—		$I_C = 140A$
$t_{d(off)}$	Turn-off delay time	—	180	—		$V_{CC} = 360V, V_{GE} = \pm 15V$
t_f	Fall time	—	250	—		$L_S = 100nH$
I_{rr}	Diode peak recovery current	—	80	—		$R_{G1} = 27\Omega, R_{G2} = 0\Omega$
t_{rr}	Diode recovery time	—	110	—	ns	$I_C = 140A$
Q_{rr}	Diode recovery charge	—	5.0	—	μC	$V_{CC} = 360V, V_{GE} = \pm 15V$
Q_{ge}	Gate-to-emitter charge (turn-on)	310	—	560	nC	$V_{CC} = 360V$
Q_{gc}	Gate-to-collector charge (turn-on)	140	—	280		$I_C = 108A$
Q_g	Total gate charge (turn-on)	52	—	84		$V_{GE} = 15V$
C_{ies}	Input capacitance	—	11600	—	pF	$V_{GE} = 0V$
C_{oes}	Output capacitance	—	1320	—		$V_{CC} = 30V$
C_{res}	Reverse transfer capacitance	—	160	—		$f = 1MHz$

(1) Includes tail losses

Thermal and Mechanical Characteristics

Parameter	Description	Typ	Max	Units
R_{thJC} (IGBT)	Thermal resistance, junction to case, each IGBT	—	0.25	$^\circ\text{C/W}$
R_{thJC} (Diode)	Thermal resistance, junction to case, each diode	—	0.4	
R_{thCS} (Module)	Thermal resistance, case to sink	0.1	—	
Wt	Weight of module	140	—	g

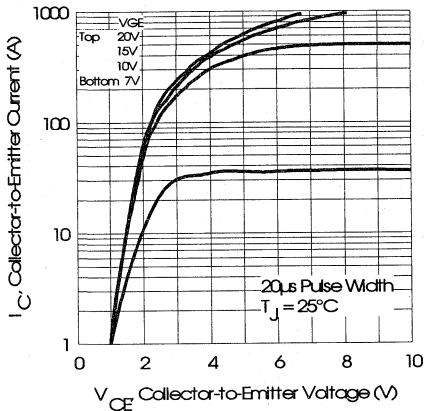


Fig. 1 - Typical Output Characteristics, $T_J = 25^\circ\text{C}$

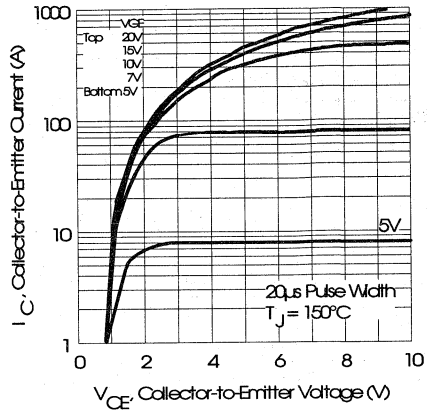


Fig. 2 - Typical Output Characteristics, $T_J = 150^\circ\text{C}$

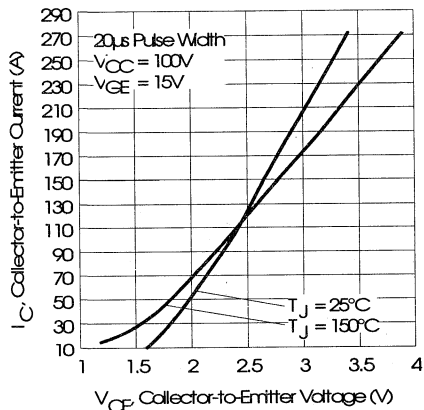


Fig. 3 - Typical Output Characteristics

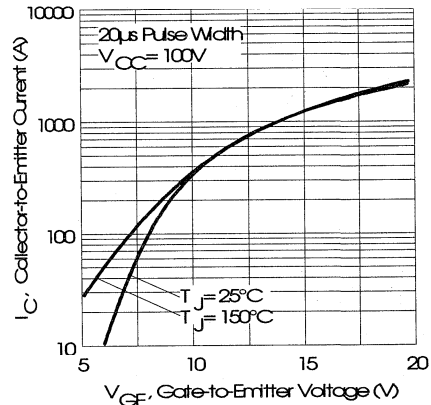


Fig. 4 - Typical Transfer Characteristics

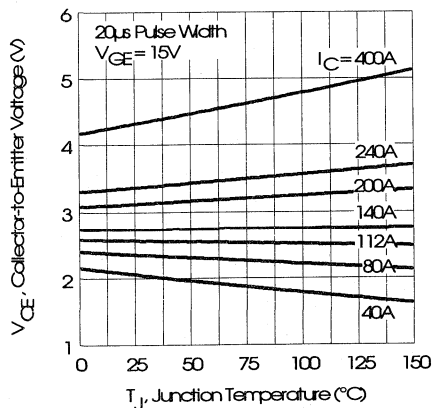


Fig. 5 - Collector-to-Emitter Saturation Typical Voltage vs. Junction Temperature

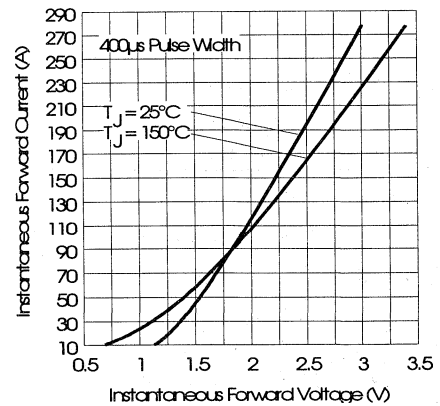


Fig. 6 - Forward Voltage Drop Characteristics

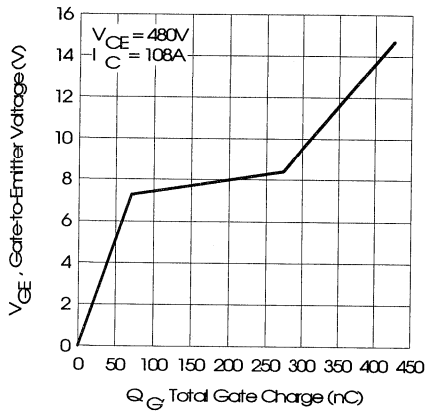


Fig. 7 - Typical Gate Charge vs. Gate-to-Emitter Voltage

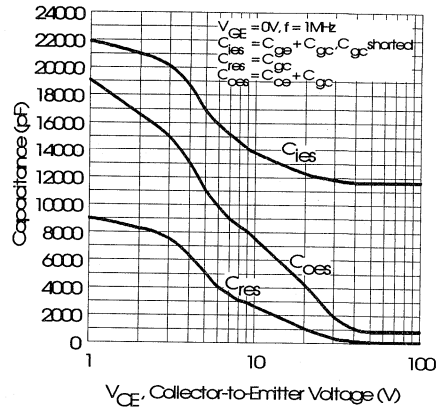


Fig. 8 - Typical Capacitance vs. Collector-to-Emitter Voltage

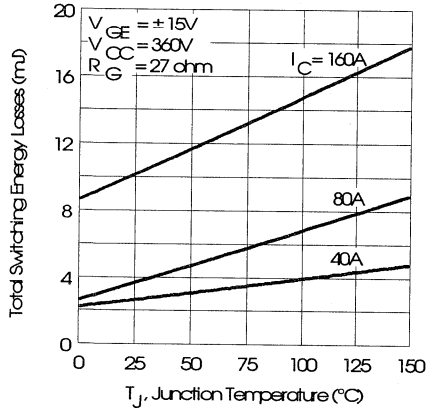


Fig. 9 - Typical Switching Losses vs. Junction Temperature

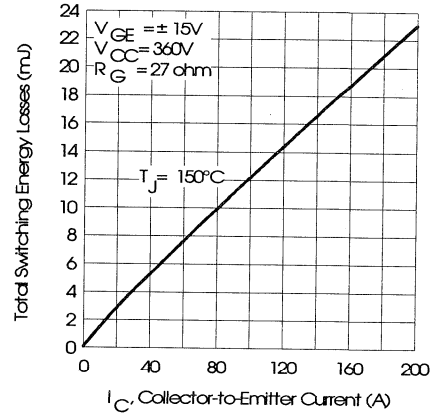


Fig. 10 - Typical Switching Losses vs. Collector-to-Emitter Current

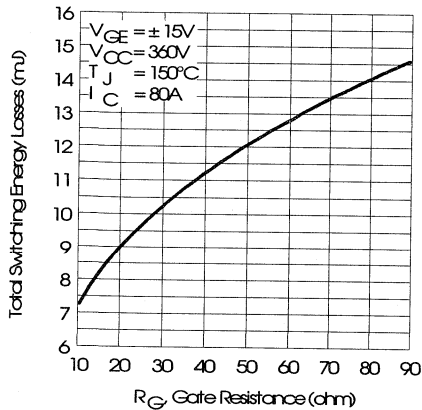


Fig. 11 - Typical Switching Losses vs. Gate Resistance

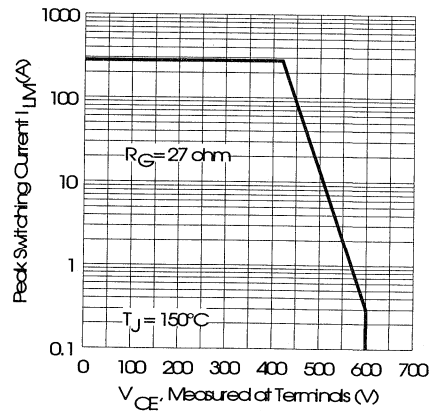


Fig. 12 - Reverse Bias Safe Operating Area

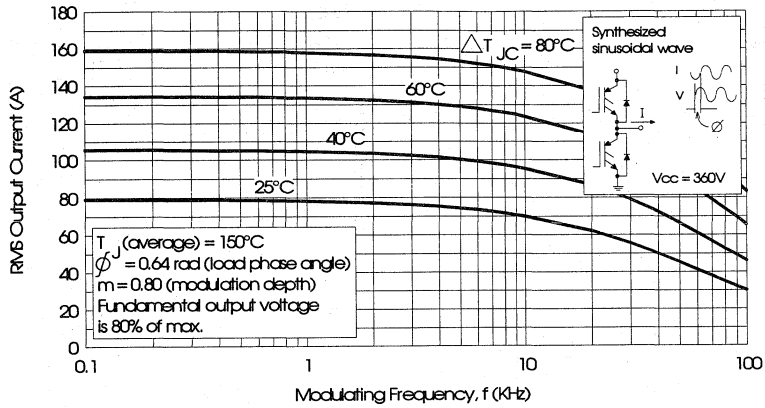


Fig. 13 - Typical RMS Output Current per phase vs. Frequency (Synthesized Sinusoidal Wave)

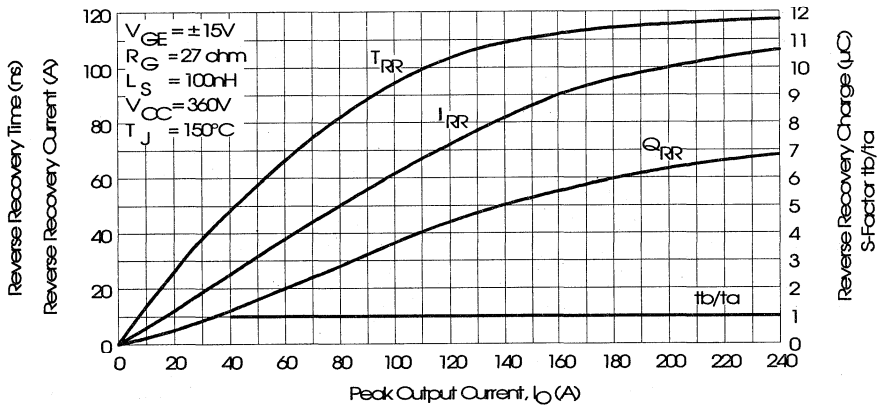


Fig. 14 - Typical Diode Recovery Characteristics as Function of Output Current I_o

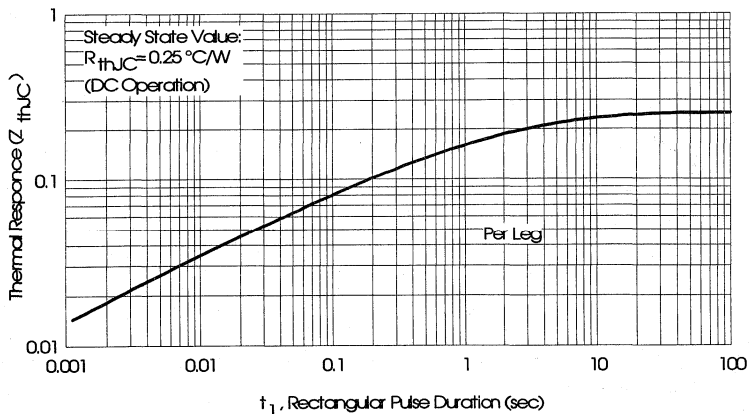


Fig. 15 - Maximum Effective Transient Thermal Impedance, Junction-to-Case

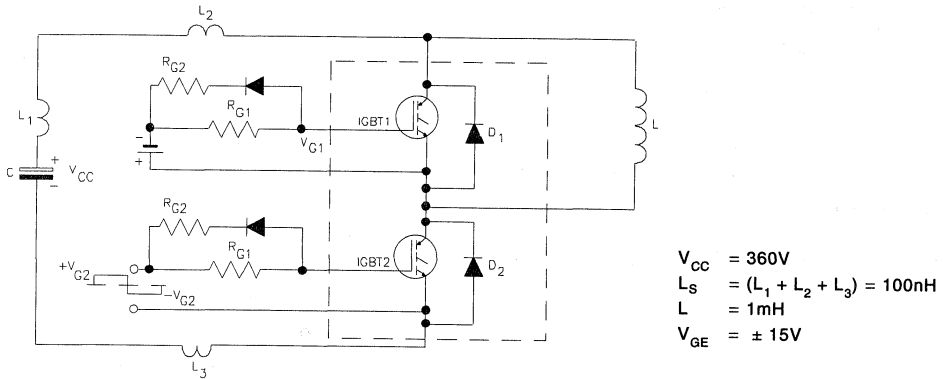


Fig. 16 - Test Circuit for Measurement of I_{LM} , E_{ON} , E_{OFF} , Q_{RR} , I_{RR} , $t_{D(ON)}$, t_r , $t_{D(OFF)}$, t_f

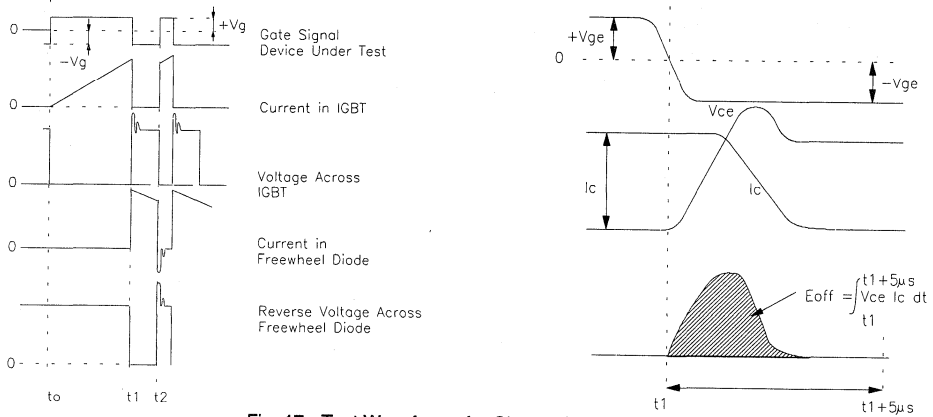


Fig. 17 - Test Waveforms for Circuit of Fig. 16

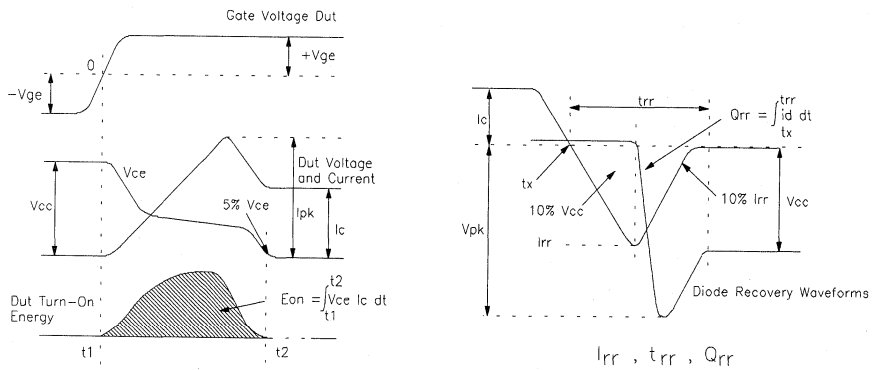


Fig. 18 - Test Waveforms for Circuit of Fig. 16, Defining E_{ON} , E_{REC} , $t_{D(ON)}$, t_r , I_{RR} , t_{RR} , Q_{RR}

Refer to Section D for the following:
Appendix E: Section D - page D-7

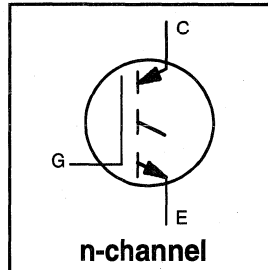
Fig. 19 - Waveforms for Switching Time

INSULATED GATE BIPOLAR TRANSISTOR

Short Circuit Rated
UltraFast IGBT

Features

- Short circuit rated - $10\mu\text{s}$ @ 125°C , $V_{\text{GE}} = 15\text{V}$
- Switching-loss rating includes all "tail" losses
- Optimized for high operating frequency (over 5kHz)
See Fig. 1 for Current vs. Frequency curve



$$V_{\text{CES}} = 600\text{V}$$

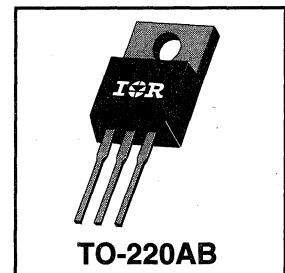
$$V_{\text{CE(sat)}} \leq 3.5\text{V}$$

$$\text{@ } V_{\text{GE}} = 15\text{V}, I_{\text{C}} = 6.0\text{A}$$

Description

Insulated Gate Bipolar Transistors (IGBTs) from International Rectifier have higher usable current densities than comparable bipolar transistors, while at the same time having simpler gate-drive requirements of the familiar power MOSFET. They provide substantial benefits to a host of high-voltage, high-current applications.

These new short circuit rated devices are especially suited for motor control and other applications requiring short circuit withstand capability.



Absolute Maximum Ratings

	Parameter	Max.	Units
V_{CES}	Collector-to-Emitter Voltage	600	V
$I_{\text{C}} @ T_{\text{C}} = 25^\circ\text{C}$	Continuous Collector Current	10	A
$I_{\text{C}} @ T_{\text{C}} = 100^\circ\text{C}$	Continuous Collector Current	6.0	
I_{CM}	Pulsed Collector Current ①	20	
I_{LM}	Clamped Inductive Load Current ②	20	
t_{sc}	Short Circuit Withstand Time	10	μs
V_{GE}	Gate-to-Emitter Voltage	± 20	V
E_{ARV}	Reverse Voltage Avalanche Energy ③	5.0	mJ
$P_{\text{D}} @ T_{\text{C}} = 25^\circ\text{C}$	Maximum Power Dissipation	60	W
$P_{\text{D}} @ T_{\text{C}} = 100^\circ\text{C}$	Maximum Power Dissipation	24	
T_{J}	Operating Junction and Storage Temperature Range	-55 to +150	$^\circ\text{C}$
T_{STG}	Soldering Temperature, for 10 sec.	300 (0.063 in. (1.6mm) from case)	
	Mounting torque, 6-32 or M3 screw.	10 lbf•in (1.1N•m)	

Thermal Resistance

	Parameter	Min.	Typ.	Max.	Units
$R_{\theta\text{JC}}$	Junction-to-Case	—	—	2.1	$^\circ\text{C}/\text{W}$
$R_{\theta\text{CS}}$	Case-to-Sink, flat, greased surface	—	0.50	—	
$R_{\theta\text{JA}}$	Junction-to-Ambient, typical socket mount	—	—	80	
Wt	Weight	—	2 (0.07)	—	g (oz)

Electrical Characteristics @ $T_J = 25^\circ\text{C}$ (unless otherwise specified)

	Parameter	Min.	Typ.	Max.	Units	Conditions
$V_{(BR)CES}$	Collector-to-Emitter Breakdown Voltage	600	—	—	V	$V_{GE} = 0V, I_C = 250\mu A$
$V_{(BR)ECS}$	Emitter-to-Collector Breakdown Voltage ④	20	—	—	V	$V_{GE} = 0V, I_C = 1.0A$
$\Delta V_{(BR)CES}/\Delta T_J$	Temp. Coeff. of Breakdown Voltage	—	0.37	—	V/ $^\circ\text{C}$	$V_{GE} = 0V, I_C = 1.0mA$
$V_{CE(on)}$	Collector-to-Emitter Saturation Voltage	—	2.4	3.5	V	$I_C = 6.0A$ $V_{GE} = 15V$ See Fig. 2, 5
		—	3.6	—		
		—	2.9	—		
$V_{GE(th)}$	Gate Threshold Voltage	3.0	—	5.5		$V_{CE} = V_{GE}, I_C = 250\mu A$
$\Delta V_{GE(th)}/\Delta T_J$	Temperature Coeff. of Threshold Voltage	—	-11	—	mV/ $^\circ\text{C}$	$V_{CE} = V_{GE}, I_C = 250\mu A$
g_{fe}	Forward Transconductance ⑤	1.9	3.3	—	S	$V_{CE} = 100V, I_C = 6.0A$
I_{CES}	Zero Gate Voltage Collector Current	—	—	250	μA	$V_{GE} = 0V, V_{CE} = 600V$
		—	—	1000		$V_{GE} = 0V, V_{CE} = 600V, T_J = 150^\circ\text{C}$
I_{GES}	Gate-to-Emitter Leakage Current	—	—	± 100	nA	$V_{GE} = \pm 20V$

Switching Characteristics @ $T_J = 25^\circ\text{C}$ (unless otherwise specified)

	Parameter	Min.	Typ.	Max.	Units	Conditions
Q_g	Total Gate Charge (turn-on)	—	17	26	nC	$I_C = 6.0A$ $V_{CC} = 400V$ $V_{GE} = 15V$ See Fig. 8
Q_{ge}	Gate - Emitter Charge (turn-on)	—	4.3	6.8		
Q_{gc}	Gate - Collector Charge (turn-on)	—	6.4	11		
$t_{d(on)}$	Turn-On Delay Time	—	29	—	ns	$T_J = 25^\circ\text{C}$ $I_C = 6.0A, V_{CC} = 480V$ $V_{GE} = 15V, R_G = 50\Omega$ Energy losses include "tail"
t_r	Rise Time	—	18	—		
$t_{d(off)}$	Turn-Off Delay Time	—	58	90		
t_f	Fall Time	—	120	200		
E_{on}	Turn-On Switching Loss	—	0.11	—	mJ	See Fig. 9, 10, 11, 14
E_{off}	Turn-Off Switching Loss	—	0.13	—		
E_{is}	Total Switching Loss	—	0.24	0.31		
t_{sc}	Short Circuit Withstand Time	10	—	—	μs	$V_{CC} = 360V, T_J = 125^\circ\text{C}$ $V_{GE} = 15V, R_G = 50\Omega, V_{CPK} < 500V$
$t_{d(on)}$	Turn-On Delay Time	—	28	—	ns	$T_J = 150^\circ\text{C}$, $I_C = 6.0A, V_{CC} = 480V$ $V_{GE} = 15V, R_G = 50\Omega$ Energy losses include "tail"
t_r	Rise Time	—	22	—		
$t_{d(off)}$	Turn-Off Delay Time	—	200	—		
t_f	Fall Time	—	145	—		
E_{is}	Total Switching Loss	—	0.50	—	mJ	See Fig. 10, 14
L_E	Internal Emitter Inductance	—	7.5	—	nH	Measured 5mm from package
C_{ies}	Input Capacitance	—	360	—	pF	$V_{GE} = 0V$ $V_{CC} = 30V$ See Fig. 7 $f = 1.0MHz$
C_{oes}	Output Capacitance	—	45	—		
C_{res}	Reverse Transfer Capacitance	—	4.7	—		

Notes:

- ① Repetitive rating; $V_{GE}=20V$, pulse width limited by max. junction temperature. (See fig. 13b)
- ② $V_{CC}=80\%(V_{CES}), V_{GE}=20V, L=10\mu H, R_G=50\Omega$, (See fig. 13a)
- ③ Repetitive rating; pulse width limited by maximum junction temperature.
- ④ Pulse width $\leq 80\mu s$; duty factor $\leq 0.1\%$.
- ⑤ Pulse width $5.0\mu s$, single shot.

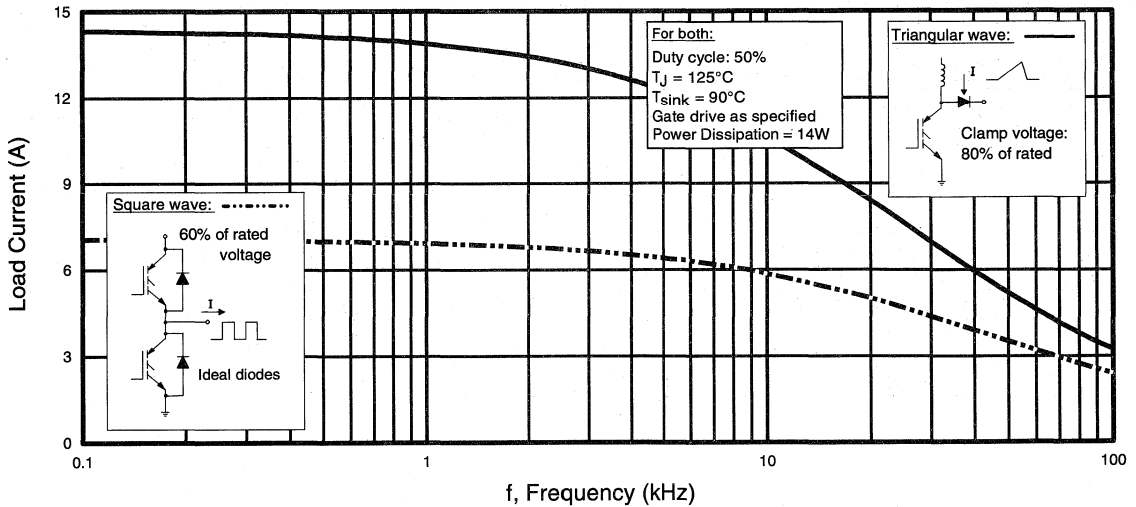


Fig. 1 - Typical Load Current vs. Frequency
 (For square wave, $I = I_{RMS}$ of fundamental; for triangular wave, $I = I_{PK}$)

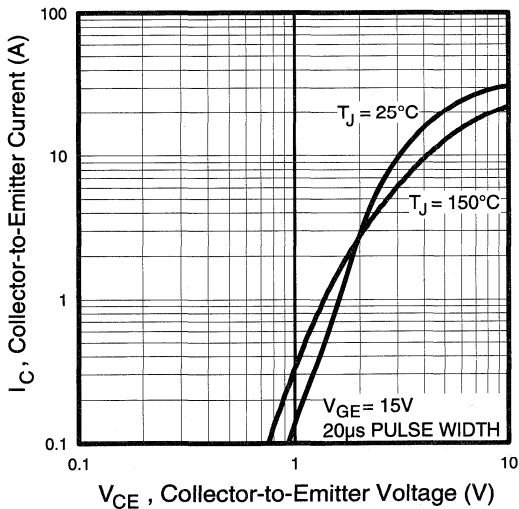


Fig. 2 - Typical Output Characteristics

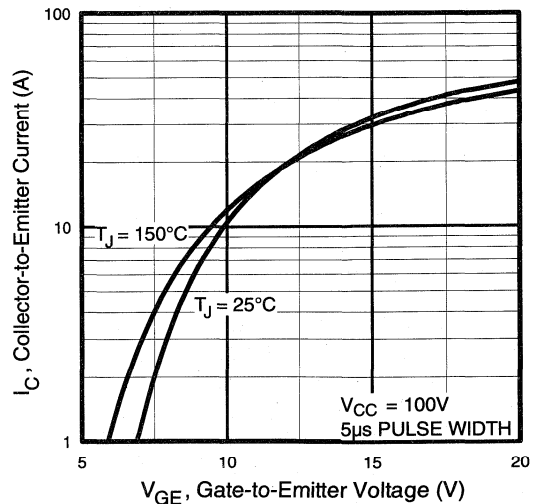


Fig. 3 - Typical Transfer Characteristics

Motor
 Control
 UnderPass
 Discreets

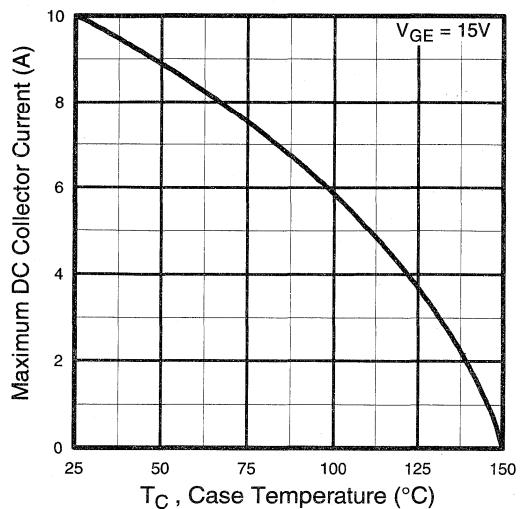


Fig. 4 - Maximum Collector Current vs. Case Temperature

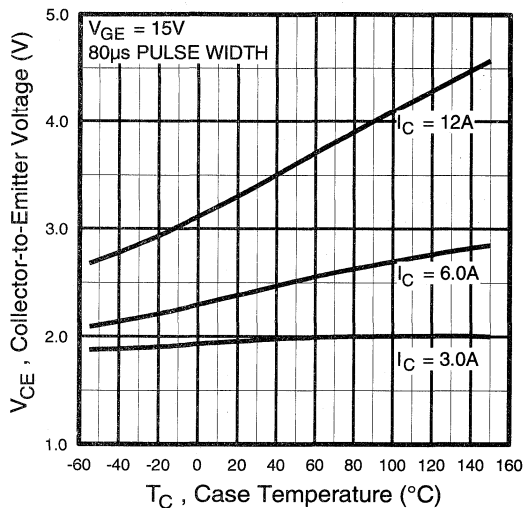


Fig. 5 - Collector-to-Emitter Voltage vs. Case Temperature

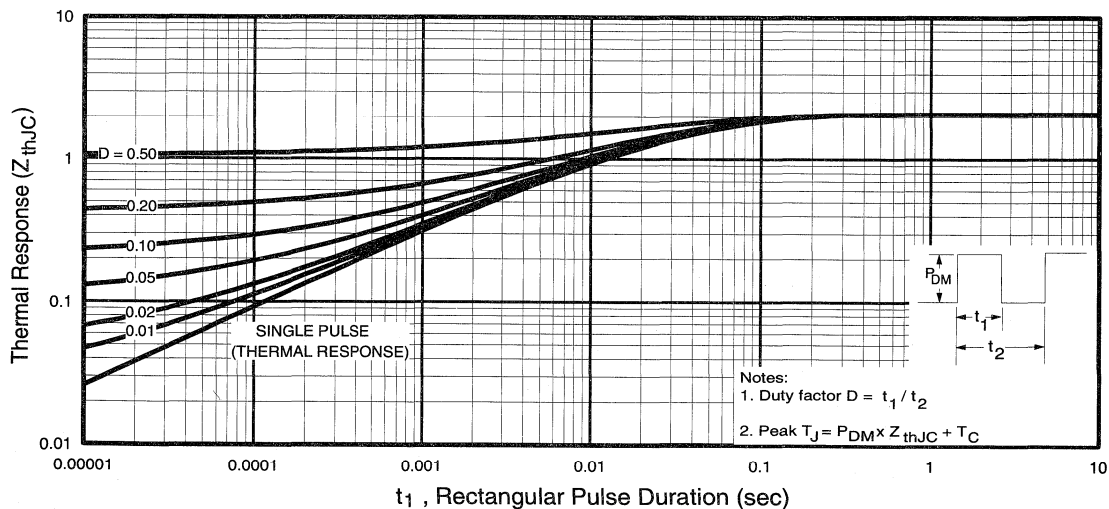


Fig. 6 - Maximum Effective Transient Thermal Impedance, Junction-to-Case

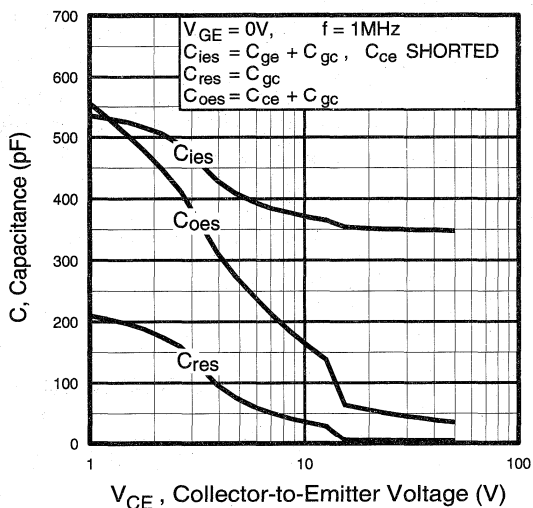


Fig. 7 - Typical Capacitance vs. Collector-to-Emitter Voltage

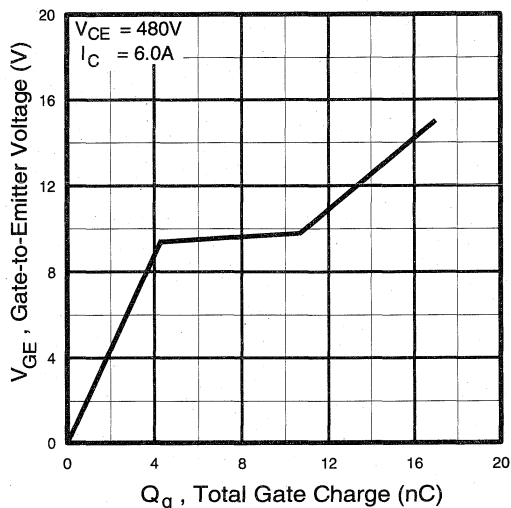


Fig. 8 - Typical Gate Charge vs. Gate-to-Emitter Voltage

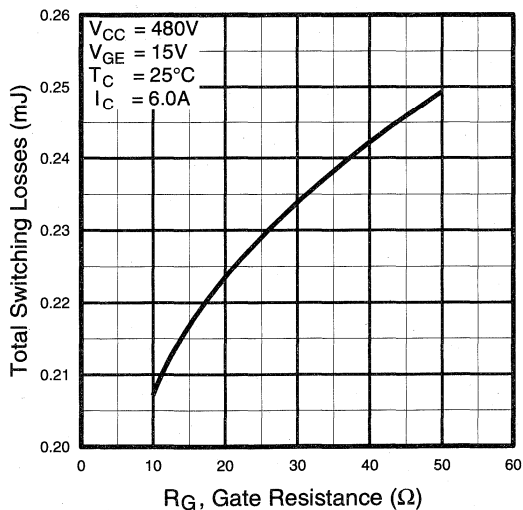


Fig. 9 - Typical Switching Losses vs. Gate Resistance

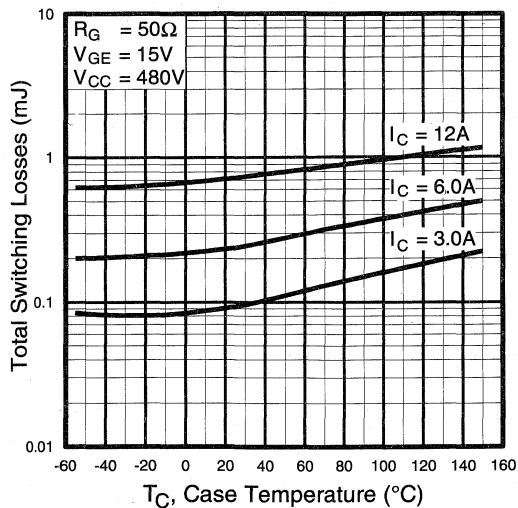


Fig. 10 - Typical Switching Losses vs. Case Temperature

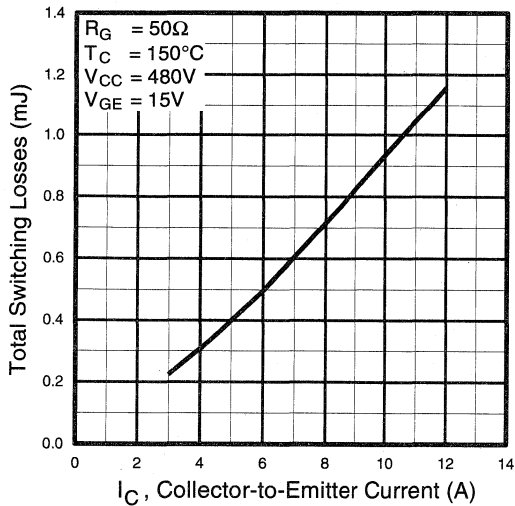


Fig. 11 - Typical Switching Losses vs. Collector-to-Emitter Current

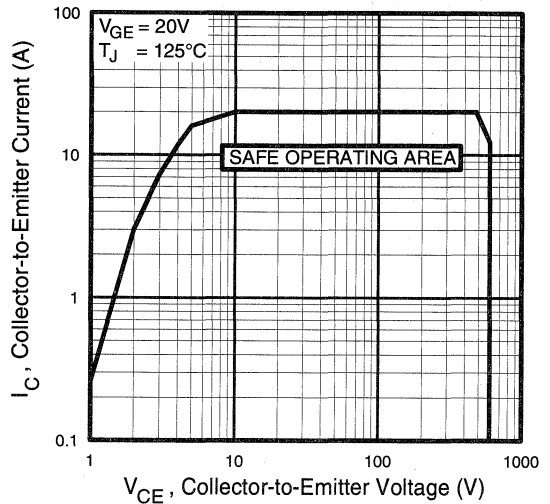


Fig. 12 - Turn-Off SOA

Refer to Section D for the following:

Appendix C: Section D - page D-5

Fig. 13a - Clamped Inductive Load Test Circuit

Fig. 13b - Pulsed Collector Current Test Circuit

Fig. 14a - Switching Loss Test Circuit

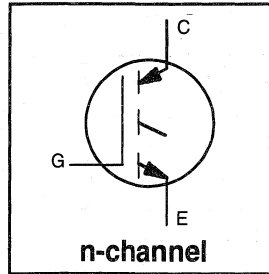
Fig. 14b - Switching Loss Waveform

INSULATED GATE BIPOLAR TRANSISTOR

Short Circuit Rated
UltraFast IGBT

Features

- Short circuit rated - $10\mu\text{s}$ @ 125°C , $V_{\text{GE}} = 15\text{V}$
- Switching-loss rating includes all "tail" losses
- Optimized for high operating frequency (over 5kHz)
See Fig. 1 for Current vs. Frequency curve



$$V_{\text{CES}} = 600\text{V}$$

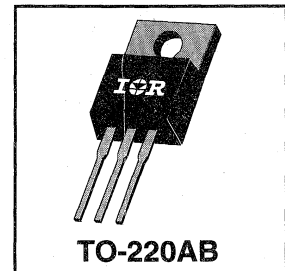
$$V_{\text{CE(sat)}} \leq 3.8\text{V}$$

$$\text{@ } V_{\text{GE}} = 15\text{V}, I_{\text{C}} = 14\text{A}$$

Description

Insulated Gate Bipolar Transistors (IGBTs) from International Rectifier have higher usable current densities than comparable bipolar transistors, while at the same time having simpler gate-drive requirements of the familiar power MOSFET. They provide substantial benefits to a host of high-voltage, high-current applications.

These new short circuit rated devices are especially suited for motor control and other applications requiring short circuit withstand capability.



Absolute Maximum Ratings

	Parameter	Max.	Units
V_{CES}	Collector-to-Emitter Voltage	600	V
$I_{\text{C}} @ T_{\text{C}} = 25^\circ\text{C}$	Continuous Collector Current	23	A
$I_{\text{C}} @ T_{\text{C}} = 100^\circ\text{C}$	Continuous Collector Current	14	
I_{CM}	Pulsed Collector Current ①	46	
I_{LM}	Clamped Inductive Load Current ②	46	
t_{sc}	Short Circuit Withstand Time	10	μs
V_{GE}	Gate-to-Emitter Voltage	± 20	V
E_{ARV}	Reverse Voltage Avalanche Energy ③	10	mJ
$P_{\text{D}} @ T_{\text{C}} = 25^\circ\text{C}$	Maximum Power Dissipation	100	W
$P_{\text{D}} @ T_{\text{C}} = 100^\circ\text{C}$	Maximum Power Dissipation	42	
T_{J}	Operating Junction and	-55 to +150	$^\circ\text{C}$
T_{STG}	Storage Temperature Range		
	Soldering Temperature, for 10 sec.		
	Mounting torque, 6-32 or M3 screw.	10 lbf•in (1.1N•m)	

Thermal Resistance

	Parameter	Min.	Typ.	Max.	Units
$R_{\theta\text{JC}}$	Junction-to-Case	—	—	1.2	$^\circ\text{C/W}$
$R_{\theta\text{CS}}$	Case-to-Sink, flat, greased surface	—	0.50	—	
$R_{\theta\text{JA}}$	Junction-to-Ambient, typical socket mount	—	—	80	
Wt	Weight	—	2 (0.07)	—	g (oz)

Electrical Characteristics @ $T_J = 25^\circ\text{C}$ (unless otherwise specified)

	Parameter	Min.	Typ.	Max.	Units	Conditions
$V_{(BR)CES}$	Collector-to-Emitter Breakdown Voltage	600	—	—	V	$V_{GE} = 0V, I_C = 250\mu A$
$V_{(BR)ECS}$	Emitter-to-Collector Breakdown Voltage ④	20	—	—	V	$V_{GE} = 0V, I_C = 1.0A$
$\Delta V_{(BR)CES}/\Delta T_J$	Temperature Coeff. of Breakdown Voltage	—	0.30	—	V/ $^\circ\text{C}$	$V_{GE} = 0V, I_C = 1.0mA$
$V_{CE(on)}$	Collector-to-Emitter Saturation Voltage	—	2.5	3.8	V	$I_C = 14A$ $V_{GE} = 15V$
		—	3.3	—		$I_C = 23A$ See Fig. 2, 5
		—	2.5	—		$I_C = 14A, T_J = 150^\circ\text{C}$
$V_{GE(th)}$	Gate Threshold Voltage	3.0	—	5.5		$V_{CE} = V_{GE}, I_C = 250\mu A$
$\Delta V_{GE(th)}/\Delta T_J$	Temperature Coeff. of Threshold Voltage	—	-13	—	mV/ $^\circ\text{C}$	$V_{CE} = V_{GE}, I_C = 250\mu A$
g_{fe}	Forward Transconductance ⑤	3.3	6.5	—	S	$V_{CE} = 100V, I_C = 14A$
I_{CES}	Zero Gate Voltage Collector Current	—	—	600	μA	$V_{GE} = 0V, V_{CE} = 600V$
		—	—	1100		$V_{GE} = 0V, V_{CE} = 600V, T_J = 150^\circ\text{C}$
I_{GES}	Gate-to-Emitter Leakage Current	—	—	± 100	nA	$V_{GE} = \pm 20V$

Switching Characteristics @ $T_J = 25^\circ\text{C}$ (unless otherwise specified)

	Parameter	Min.	Typ.	Max.	Units	Conditions	
Q_g	Total Gate Charge (turn-on)	—	39	58	nC	$I_C = 14A$	
Q_{ge}	Gate - Emitter Charge (turn-on)	—	8.7	13		$V_{CC} = 400V$ See Fig. 8	
Q_{gc}	Gate - Collector Charge (turn-on)	—	15	23		$V_{GE} = 15V$	
$t_{d(on)}$	Turn-On Delay Time	—	31	—	ns	$T_J = 25^\circ\text{C}$	
t_r	Rise Time	—	23	—		$I_C = 14A, V_{CC} = 480V$	
$t_{d(off)}$	Turn-Off Delay Time	—	100	150		$V_{GE} = 15V, R_G = 23\Omega$	
t_f	Fall Time	—	84	130		Energy losses include "tail"	
E_{on}	Turn-On Switching Loss	—	0.3	—		mJ	See Fig. 9, 10, 11, 14
E_{off}	Turn-Off Switching Loss	—	0.3	—			
E_{ts}	Total Switching Loss	—	0.6	0.9			
t_{sc}	Short Circuit Withstand Time	10	—	—	μs	$V_{CC} = 360V, T_J = 125^\circ\text{C}$ $V_{GE} = 15V, R_G = 23\Omega, V_{CPK} < 500V$	
$t_{d(on)}$	Turn-On Delay Time	—	30	—	ns	$T_J = 150^\circ\text{C}$,	
t_r	Rise Time	—	23	—		$I_C = 14A, V_{CC} = 480V$	
$t_{d(off)}$	Turn-Off Delay Time	—	170	—		$V_{GE} = 15V, R_G = 23\Omega$	
t_f	Fall Time	—	170	—		Energy losses include "tail"	
E_{ts}	Total Switching Loss	—	1.2	—		mJ	See Fig. 10, 14
L_E	Internal Emitter Inductance	—	7.5	—		nH	Measured 5mm from package
C_{ies}	Input Capacitance	—	740	—		pF	$V_{GE} = 0V$
C_{oes}	Output Capacitance	—	92	—	$V_{CC} = 30V$ See Fig. 7		
C_{res}	Reverse Transfer Capacitance	—	9.4	—	$f = 1.0MHz$		

Notes:

- ① Repetitive rating; $V_{GE}=20V$, pulse width limited by max. junction temperature. (See fig. 13b)
- ② $V_{CC}=80\%(V_{CES}), V_{GE}=20V, L=10\mu H, R_G=23\Omega$, (See fig. 13a)
- ③ Repetitive rating; pulse width limited by maximum junction temperature.
- ④ Pulse width $\leq 80\mu s$; duty factor $\leq 0.1\%$.
- ⑤ Pulse width 5.0 μs , single shot.

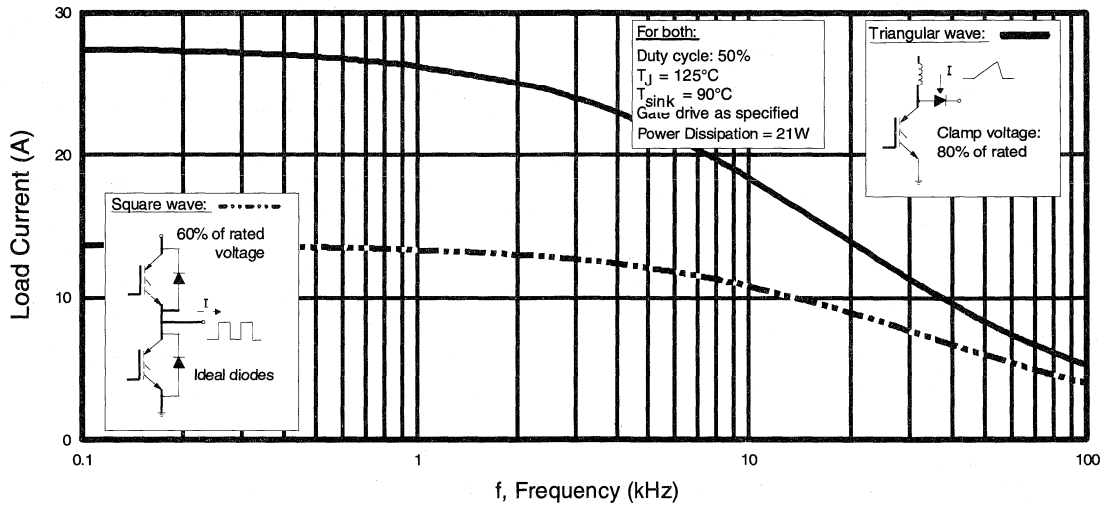


Fig. 1 - Typical Load Current vs. Frequency
 (For square wave, $I = I_{RMS}$ of fundamental; for triangular wave, $I = I_{PK}$)

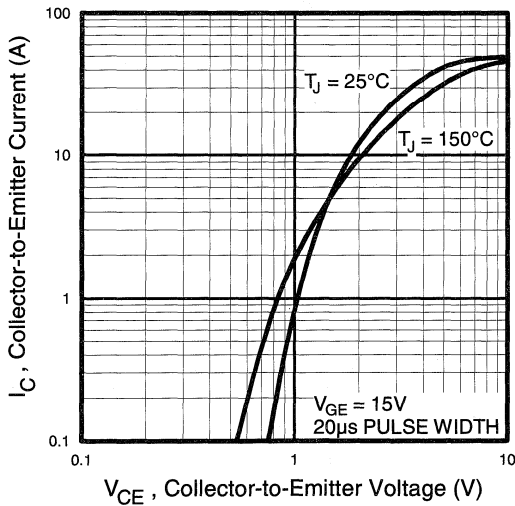


Fig. 2 - Typical Output Characteristics

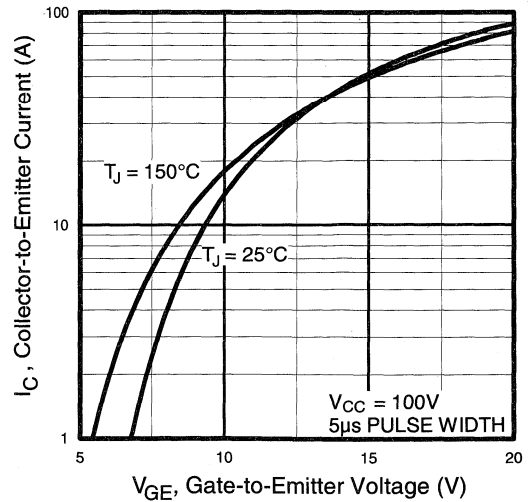


Fig. 3 - Typical Transfer Characteristics

Motor
Control
Ultra-Fast
Discretes

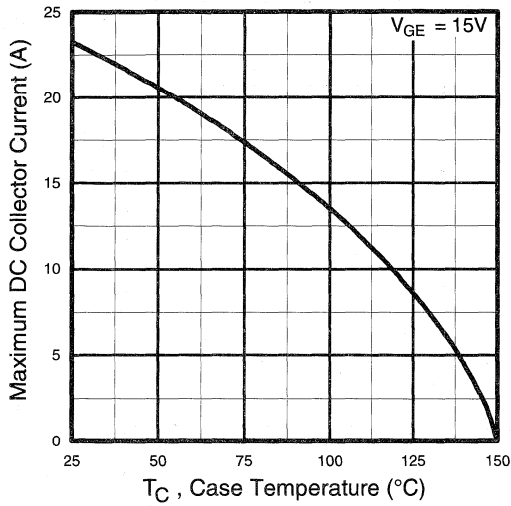


Fig. 4 - Maximum Collector Current vs. Case Temperature

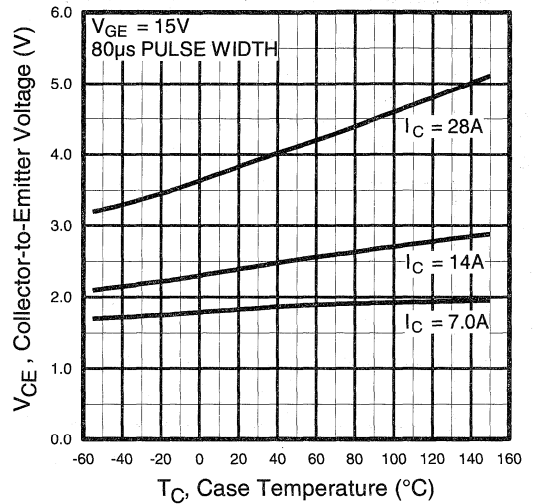


Fig. 5 - Collector-to-Emitter Voltage vs. Case Temperature

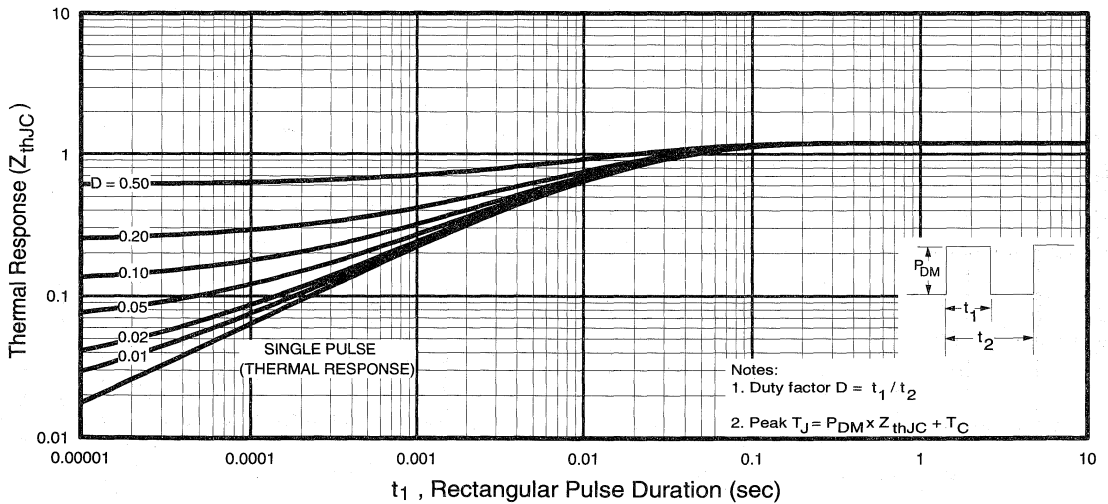


Fig. 6 - Maximum Effective Transient Thermal Impedance, Junction-to-Case

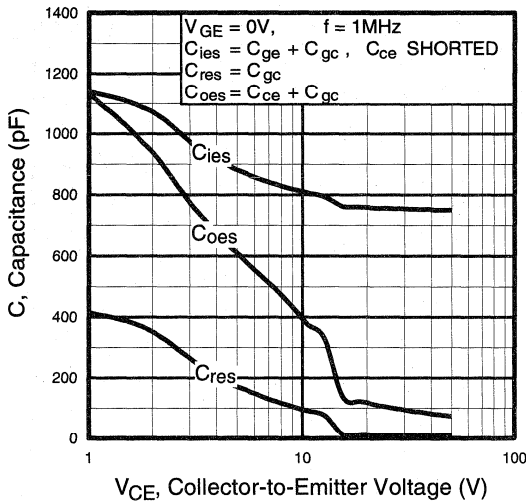


Fig. 7 - Typical Capacitance vs. Collector-to-Emitter Voltage

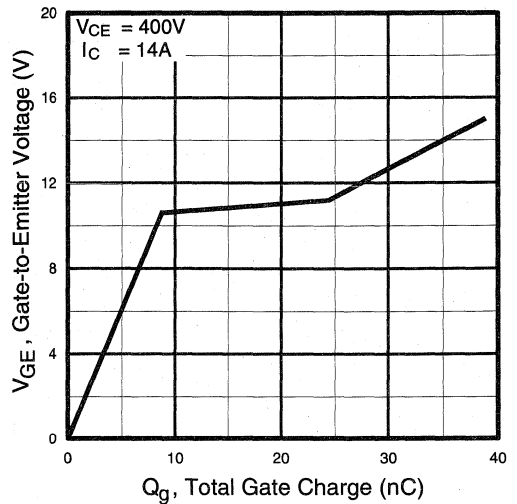


Fig. 8 - Typical Gate Charge vs. Gate-to-Emitter Voltage

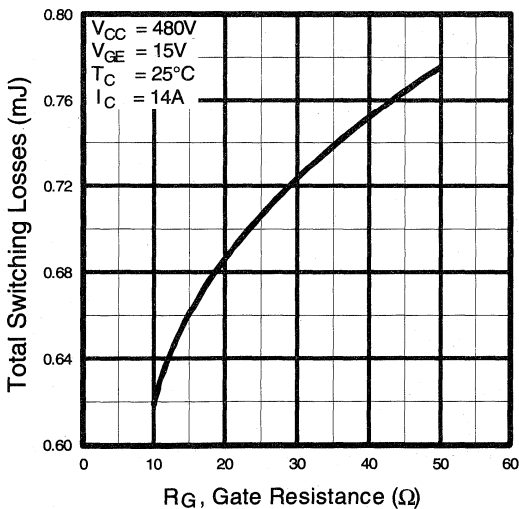


Fig. 9 - Typical Switching Losses vs. Gate Resistance

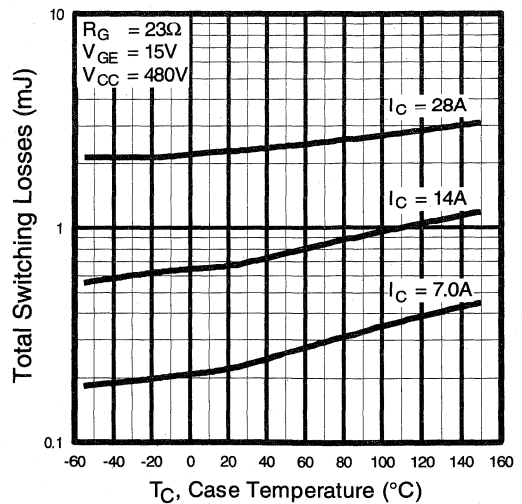


Fig. 10 - Typical Switching Losses vs. Case Temperature

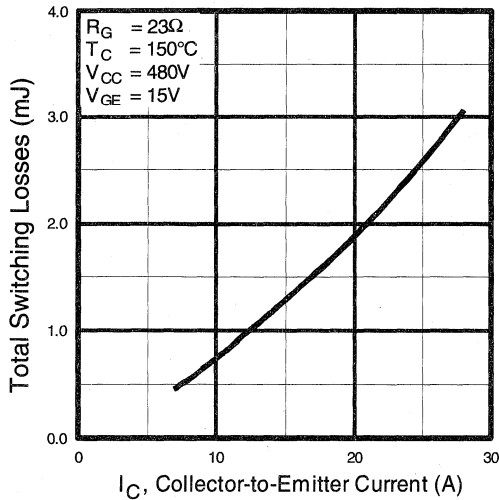


Fig. 11 - Typical Switching Losses vs. Collector-to-Emitter Current

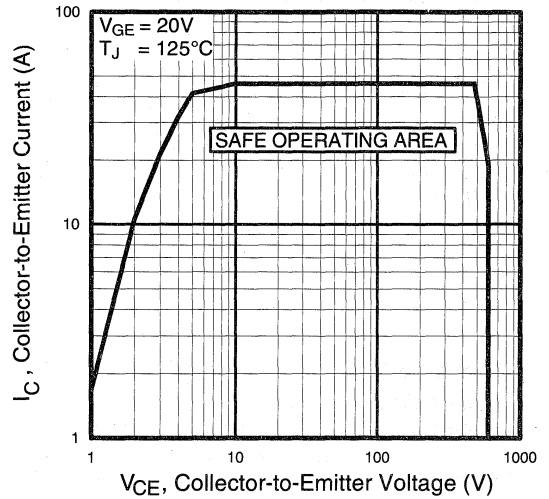


Fig. 12 - Turn-Off SOA

Refer to Section D for the following:

Appendix C: Section D - page D-5

- Fig. 13a - Clamped Inductive Load Test Circuit
- Fig. 13b - Pulsed Collector Current Test Circuit
- Fig. 14a - Switching Loss Test Circuit
- Fig. 14b - Switching Loss Waveform

Package Outline 1 - JEDEC Outline TO-220AB

Section D - page D-12

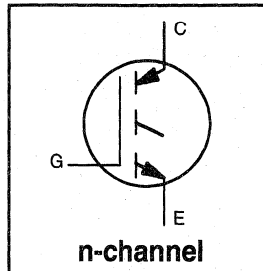
IRGBC40K

INSULATED GATE BIPOLAR TRANSISTOR

Short Circuit Rated
UltraFast IGBT

Features

- Short circuit rated - 10 μ s @ 125°C, V_{GE} = 15V
- Switching-loss rating includes all "tail" losses
- Optimized for high operating frequency (over 5kHz)
See Fig. 1 for Current vs. Frequency curve



$$V_{CES} = 600V$$

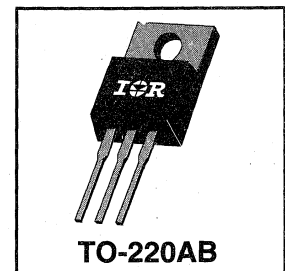
$$V_{CE(sat)} \leq 3.2V$$

$$@ V_{GE} = 15V, I_C = 25A$$

Description

Insulated Gate Bipolar Transistors (IGBTs) from International Rectifier have higher usable current densities than comparable bipolar transistors, while at the same time having simpler gate-drive requirements of the familiar power MOSFET. They provide substantial benefits to a host of high-voltage, high-current applications.

These new short circuit rated devices are especially suited for motor control and other applications requiring short circuit withstand capability.



Absolute Maximum Ratings

	Parameter	Max.	Units
V _{CES}	Collector-to-Emitter Voltage	600	V
I _C @ T _C = 25°C	Continuous Collector Current	42	A
I _C @ T _C = 100°C	Continuous Collector Current	25	
I _{CM}	Pulsed Collector Current ①	84	
I _{LM}	Clamped Inductive Load Current ②	84	
t _{sc}	Short Circuit Withstand Time	10	μ s
V _{GE}	Gate-to-Emitter Voltage	± 20	V
E _{ARV}	Reverse Voltage Avalanche Energy ③	15	mJ
P _D @ T _C = 25°C	Maximum Power Dissipation	160	W
P _D @ T _C = 100°C	Maximum Power Dissipation	65	
T _J	Operating Junction and Storage Temperature Range	-55 to +150	°C
T _{STG}	Soldering Temperature, for 10 sec.	300 (0.063 in. (1.6mm) from case)	
	Mounting torque, 6-32 or M3 screw.	10 lbf•in (1.1N•m)	

Thermal Resistance

	Parameter	Min.	Typ.	Max.	Units
R _{θJC}	Junction-to-Case	—	—	0.77	°C/W
R _{θCS}	Case-to-Sink, flat, greased surface	—	0.50	—	
R _{θJA}	Junction-to-Ambient, typical socket mount	—	—	80	
Wt	Weight	—	2 (0.07)	—	g (oz)

Motor Control UltraFast Discretes

Electrical Characteristics @ $T_J = 25^\circ\text{C}$ (unless otherwise specified)

	Parameter	Min.	Typ.	Max.	Units	Conditions
$V_{(BR)CES}$	Collector-to-Emitter Breakdown Voltage	600	—	—	V	$V_{GE} = 0V, I_C = 250\mu A$
$V_{(BR)ECS}$	Emitter-to-Collector Breakdown Voltage ①	20	—	—	V	$V_{GE} = 0V, I_C = 1.0A$
$\Delta V_{(BR)CES}/\Delta T_J$	Temperature Coeff. of Breakdown Voltage	—	0.46	—	V/ $^\circ\text{C}$	$V_{GE} = 0V, I_C = 1.0mA$
$V_{CE(on)}$	Collector-to-Emitter Saturation Voltage	—	2.1	3.2	V	$I_C = 25A$ $I_C = 42A$ $I_C = 25A, T_J = 150^\circ\text{C}$ $V_{GE} = 15V$ See Fig. 2, 5
		—	2.8	—		
		—	2.5	—		
$V_{GE(th)}$	Gate Threshold Voltage	3.0	—	5.5		$V_{CE} = V_{GE}, I_C = 250\mu A$
$\Delta V_{GE(th)}/\Delta T_J$	Temperature Coeff. of Threshold Voltage	—	-13	—	mV/ $^\circ\text{C}$	$V_{CE} = V_{GE}, I_C = 250\mu A$
g_{fe}	Forward Transconductance ⑤	7.0	14	—	S	$V_{CE} = 100V, I_C = 25A$
I_{CES}	Zero Gate Voltage Collector Current	—	—	250	μA	$V_{GE} = 0V, V_{CE} = 600V$ $V_{GE} = 0V, V_{CE} = 600V, T_J = 150^\circ\text{C}$
		—	—	1000		
I_{GES}	Gate-to-Emitter Leakage Current	—	—	± 100	nA	$V_{GE} = \pm 20V$

Switching Characteristics @ $T_J = 25^\circ\text{C}$ (unless otherwise specified)

	Parameter	Min.	Typ.	Max.	Units	Conditions
Q_g	Total Gate Charge (turn-on)	—	61	92	nC	$I_C = 25A$ $V_{CC} = 400V$ $V_{GE} = 15V$ See Fig. 8
Q_{ge}	Gate - Emitter Charge (turn-on)	—	13	19		
Q_{gc}	Gate - Collector Charge (turn-on)	—	22	33		
$t_{d(on)}$	Turn-On Delay Time	—	35	—	ns	$T_J = 25^\circ\text{C}$ $I_C = 25A, V_{CC} = 480V$ $V_{GE} = 15V, R_G = 10\Omega$ Energy losses include "tail"
t_r	Rise Time	—	27	—		
$t_{d(off)}$	Turn-Off Delay Time	—	160	240		
t_f	Fall Time	—	130	200		
E_{on}	Turn-On Switching Loss	—	0.52	—		
E_{off}	Turn-Off Switching Loss	—	1.2	—		
E_{ts}	Total Switching Loss	—	1.7	2.6		
t_{sc}	Short Circuit Withstand Time	10	—	—	μs	$V_{CC} = 360V, T_J = 125^\circ\text{C}$ $V_{GE} = 15V, R_G = 10\Omega, V_{CPK} < 500V$
$t_{d(on)}$	Turn-On Delay Time	—	34	—	ns	$T_J = 150^\circ\text{C}$ $I_C = 25A, V_{CC} = 480V$ $V_{GE} = 15V, R_G = 10\Omega$ Energy losses include "tail"
t_r	Rise Time	—	28	—		
$t_{d(off)}$	Turn-Off Delay Time	—	300	—		
t_f	Fall Time	—	310	—		
E_{ts}	Total Switching Loss	—	3.6	—		
L_E	Internal Emitter Inductance	—	7.5	—	nH	Measured 5mm from package
C_{ies}	Input Capacitance	—	1500	—	pF	$V_{GE} = 0V$ $V_{CC} = 30V$ See Fig. 7 $f = 1.0MHz$
C_{oes}	Output Capacitance	—	190	—		
C_{res}	Reverse Transfer Capacitance	—	17	—		

Notes:

- ① Repetitive rating; $V_{GE} = 20V$, pulse width limited by max. junction temperature. (See fig. 13b)
- ② $V_{CC} = 80\%(V_{CES}), V_{GE} = 20V, L = 10\mu H, R_G = 10\Omega$, (See fig. 13a)
- ③ Repetitive rating; pulse width limited by maximum junction temperature.
- ④ Pulse width $\leq 80\mu s$; duty factor $\leq 0.1\%$.
- ⑤ Pulse width 5.0 μs , single shot.

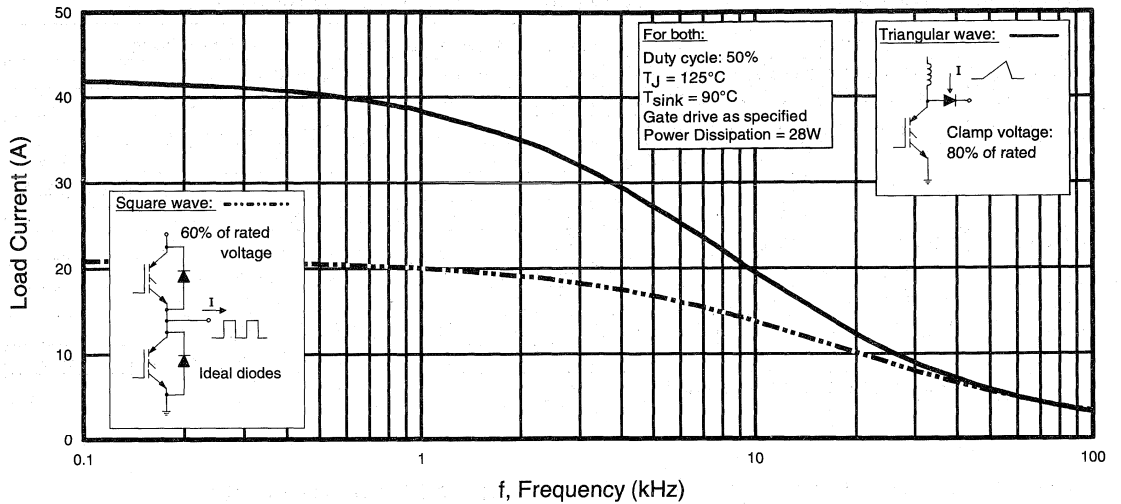


Fig. 1 - Typical Load Current vs. Frequency
 (For square wave, $I = I_{RMS}$ of fundamental; for triangular wave, $I = I_{PK}$)

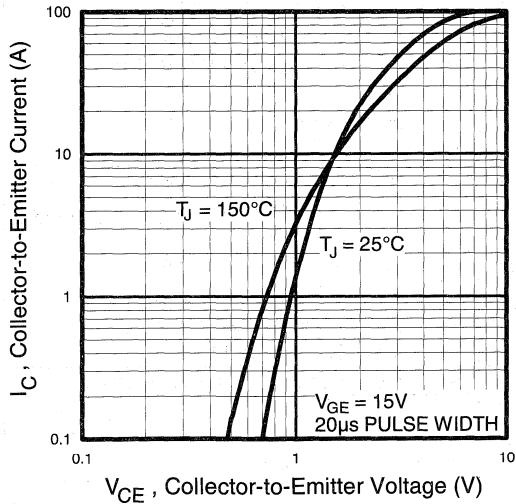


Fig. 2 - Typical Output Characteristics

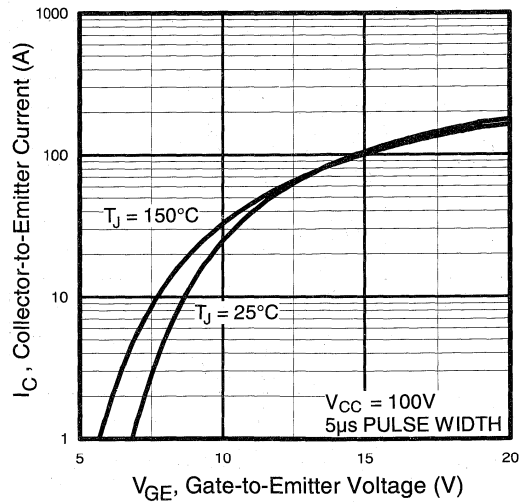


Fig. 3 - Typical Transfer Characteristics

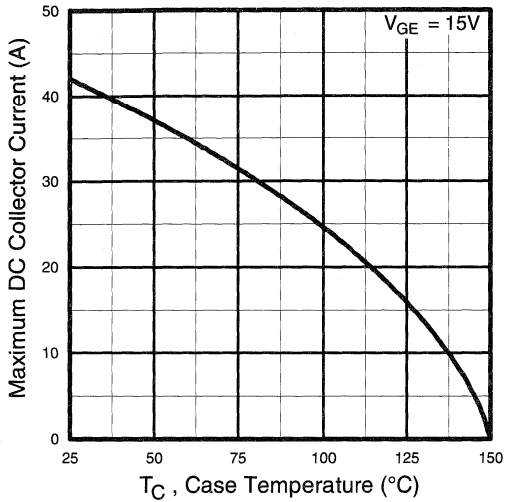


Fig. 4 - Maximum Collector Current vs. Case Temperature

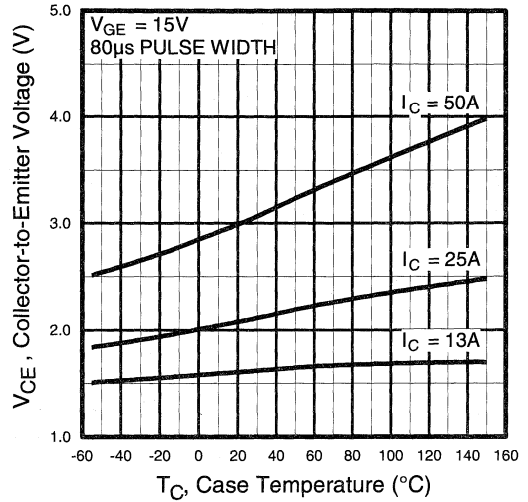


Fig. 5 - Collector-to-Emitter Voltage vs. Case Temperature

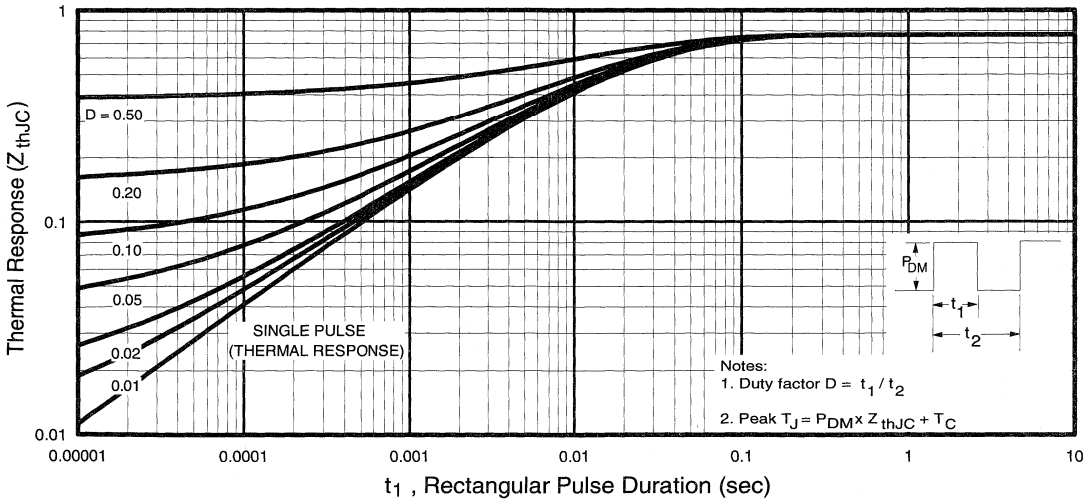


Fig. 6 - Maximum Effective Transient Thermal Impedance, Junction-to-Case

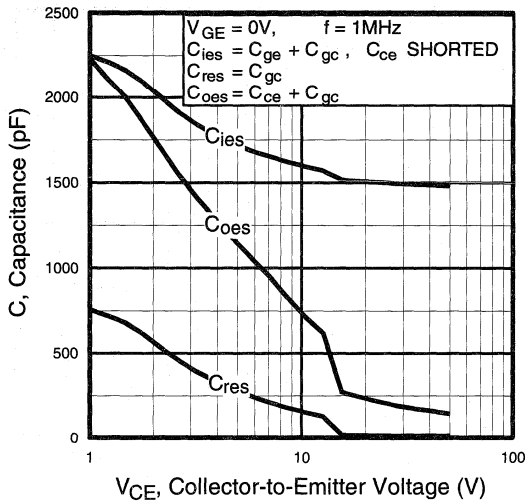


Fig. 7 - Typical Capacitance vs. Collector-to-Emitter Voltage

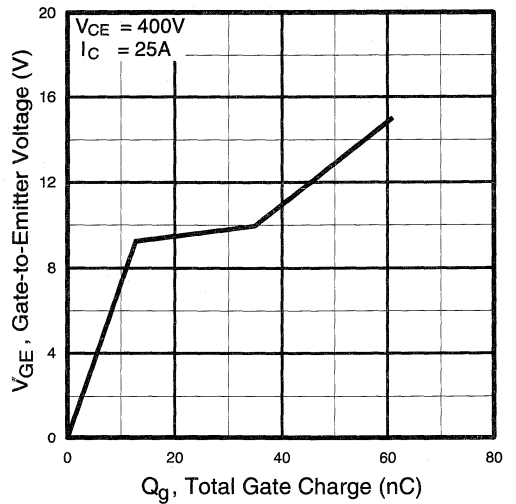


Fig. 8 - Typical Gate Charge vs. Gate-to-Emitter Voltage

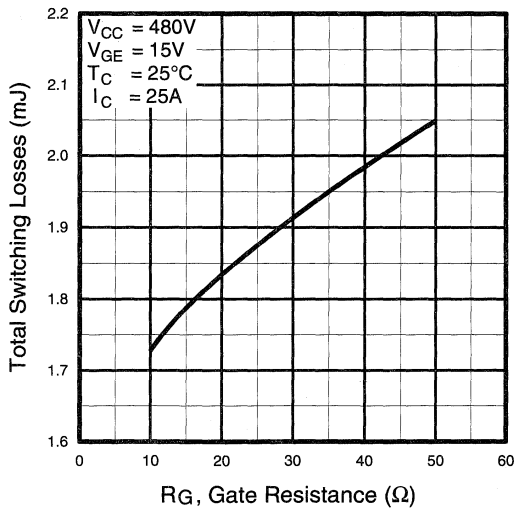


Fig. 9 - Typical Switching Losses vs. Gate Resistance

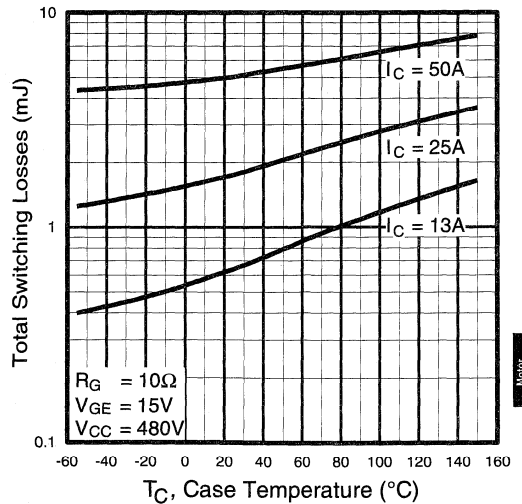


Fig. 10 - Typical Switching Losses vs. Case Temperature

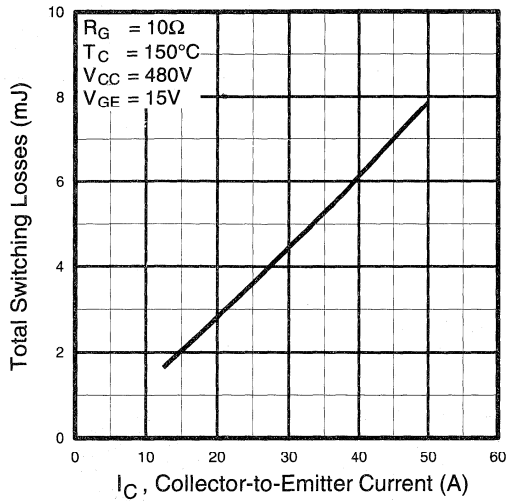


Fig. 11 - Typical Switching Losses vs. Collector-to-Emitter Current

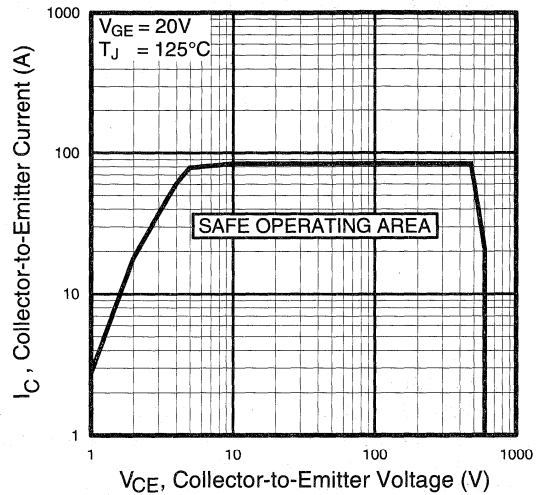


Fig. 12 - Turn-Off SOA

Refer to Section D for the following:

Appendix C: Section D - page D-5

- Fig. 13a - Clamped Inductive Load Test Circuit
- Fig. 13b - Pulsed Collector Current Test Circuit
- Fig. 14a - Switching Loss Test Circuit
- Fig. 14b - Switching Loss Waveform

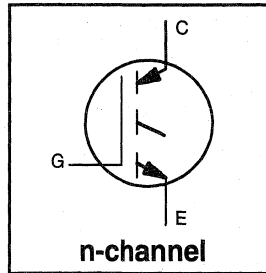
IRGBC20K-S

INSULATED GATE BIPOLAR TRANSISTOR

Short Circuit Rated
UltraFast Fast IGBT

Features

- Short circuit rated - $10\mu\text{s}$ @ 125°C , $V_{GE} = 15\text{V}$
- Switching-loss rating includes all "tail" losses
- Optimized for high operating frequency (over 5kHz)
See Fig. 1 for Current vs. Frequency curve



$$V_{CES} = 600\text{V}$$

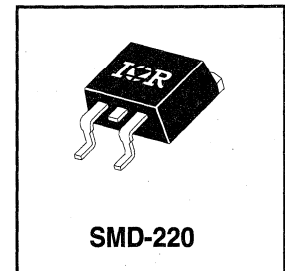
$$V_{CE(sat)} \leq 3.5\text{V}$$

$$\text{@ } V_{GE} = 15\text{V}, I_C = 6.0\text{A}$$

Description

Insulated Gate Bipolar Transistors (IGBTs) from International Rectifier have higher usable current densities than comparable bipolar transistors, while at the same time having simpler gate-drive requirements of the familiar power MOSFET. They provide substantial benefits to a host of high-voltage, high-current applications.

These new short circuit rated devices are especially suited for motor control and other applications requiring short circuit withstand capability.



Absolute Maximum Ratings

	Parameter	Max.	Units
V_{CES}	Collector-to-Emitter Voltage	600	V
$I_C @ T_C = 25^\circ\text{C}$	Continuous Collector Current	10	A
$I_C @ T_C = 100^\circ\text{C}$	Continuous Collector Current	6.0	
I_{CM}	Pulsed Collector Current ①	20	
I_{LM}	Clamped Inductive Load Current ②	20	
t_{sc}	Short Circuit Withstand Time	10	μs
V_{GE}	Gate-to-Emitter Voltage	± 20	V
E_{ARV}	Reverse Voltage Avalanche Energy ③	5.0	mJ
$P_D @ T_C = 25^\circ\text{C}$	Maximum Power Dissipation	60	W
$P_D @ T_C = 100^\circ\text{C}$	Maximum Power Dissipation	24	
T_J	Operating Junction and	-55 to +150	$^\circ\text{C}$
T_{STG}	Storage Temperature Range		
	Soldering Temperature, for 10 sec.	300 (0.063 in. (1.6mm) from case)	
	Mounting torque, 6-32 or M3 screw.	10 lbf*in (1.1N*m)	

Thermal Resistance

	Parameter	Min.	Typ.	Max.	Units
$R_{\theta JC}$	Junction-to-Case	—	—	2.1	$^\circ\text{C/W}$
$R_{\theta JA}$	Junction-to-Ambient (PCB mount)**	—	—	40	
$R_{\theta JA}$	Junction-to-Ambient, typical socket mount	—	—	80	
Wt	Weight	—	2 (0.07)	—	g (oz)

** When mounted on 1" square PCB (FR-4 or G-10 Material)

For recommended footprint and soldering techniques refer to application note #AN-994.

Electrical Characteristics @ $T_J = 25^\circ\text{C}$ (unless otherwise specified)

	Parameter	Min.	Typ.	Max.	Units	Conditions	
$V_{(BR)CES}$	Collector-to-Emitter Breakdown Voltage	600	—	—	V	$V_{GE} = 0V, I_C = 250\mu A$	
$V_{(BR)ECS}$	Emitter-to-Collector Breakdown Voltage ④	20	—	—	V	$V_{GE} = 0V, I_C = 1.0A$	
$\Delta V_{(BR)CES}/\Delta T_J$	Temp. Coeff. of Breakdown Voltage	—	0.37	—	V/°C	$V_{GE} = 0V, I_C = 1.0mA$	
$V_{CE(on)}$	Collector-to-Emitter Saturation Voltage	—	2.4	3.5	V	$V_{GE} = 15V$ See Fig. 2, 5	
		—	3.6	—			$I_C = 6.0A$
		—	2.9	—			$I_C = 10A, T_J = 150^\circ\text{C}$
$V_{GE(th)}$	Gate Threshold Voltage	3.0	—	5.5		$V_{CE} = V_{GE}, I_C = 250\mu A$	
$\Delta V_{GE(th)}/\Delta T_J$	Temperature Coeff. of Threshold Voltage	—	-11	—	mV/°C	$V_{CE} = V_{GE}, I_C = 250\mu A$	
g_{fe}	Forward Transconductance ⑤	1.9	3.3	—	S	$V_{CE} = 100V, I_C = 6.0A$	
I_{CES}	Zero Gate Voltage Collector Current	—	—	250	μA	$V_{GE} = 0V, V_{CE} = 600V$	
		—	—	1000		$V_{GE} = 0V, V_{CE} = 600V, T_J = 150^\circ\text{C}$	
I_{GES}	Gate-to-Emitter Leakage Current	—	—	± 100	nA	$V_{GE} = \pm 20V$	

Switching Characteristics @ $T_J = 25^\circ\text{C}$ (unless otherwise specified)

	Parameter	Min.	Typ.	Max.	Units	Conditions
Q_g	Total Gate Charge (turn-on)	—	17	26	nC	$I_C = 6.0A$ $V_{CC} = 400V$ $V_{GE} = 15V$ See Fig. 8
Q_{ge}	Gate - Emitter Charge (turn-on)	—	4.3	6.8		
Q_{gc}	Gate - Collector Charge (turn-on)	—	6.4	11		
$t_{d(on)}$	Turn-On Delay Time	—	29	—	ns	$T_J = 25^\circ\text{C}$ $I_C = 6.0A, V_{CC} = 480V$ $V_{GE} = 15V, R_G = 50\Omega$ Energy losses include "tail"
t_r	Rise Time	—	18	—		
$t_{d(off)}$	Turn-Off Delay Time	—	58	90		
t_f	Fall Time	—	120	195		
E_{on}	Turn-On Switching Loss	—	0.11	—		
E_{off}	Turn-Off Switching Loss	—	0.13	—	mJ	See Fig. 9, 10, 11, 14
E_{ts}	Total Switching Loss	—	0.24	0.31		
t_{sc}	Short Circuit Withstand Time	10	—	—	μs	$V_{CC} = 360V, T_J = 125^\circ\text{C}$ $V_{GE} = 15V, R_G = 50\Omega, V_{CPK} < 500V$
$t_{d(on)}$	Turn-On Delay Time	—	28	—	ns	$T_J = 150^\circ\text{C}$, $I_C = 6.0A, V_{CC} = 480V$ $V_{GE} = 15V, R_G = 50\Omega$ Energy losses include "tail"
t_r	Rise Time	—	22	—		
$t_{d(off)}$	Turn-Off Delay Time	—	200	—		
t_f	Fall Time	—	145	—		
E_{ts}	Total Switching Loss	—	0.50	—		
L_E	Internal Emitter Inductance	—	7.5	—	nH	Measured 5mm from package
C_{ies}	Input Capacitance	—	360	—	pF	$V_{GE} = 0V$ $V_{CC} = 30V$ See Fig. 7
C_{oes}	Output Capacitance	—	45	—		
C_{res}	Reverse Transfer Capacitance	—	4.7	—		

Notes:

- ① Repetitive rating; $V_{GE}=20V$, pulse width limited by max. junction temperature. (See fig. 13b)
- ② $V_{CC}=80\%(V_{CES}), V_{GE}=20V, L=10\mu H, R_G=50\Omega$, (See fig. 13a)
- ③ Repetitive rating; pulse width limited by maximum junction temperature.
- ④ Pulse width $\leq 80\mu s$; duty factor $\leq 0.1\%$.
- ⑤ Pulse width $5.0\mu s$, single shot.

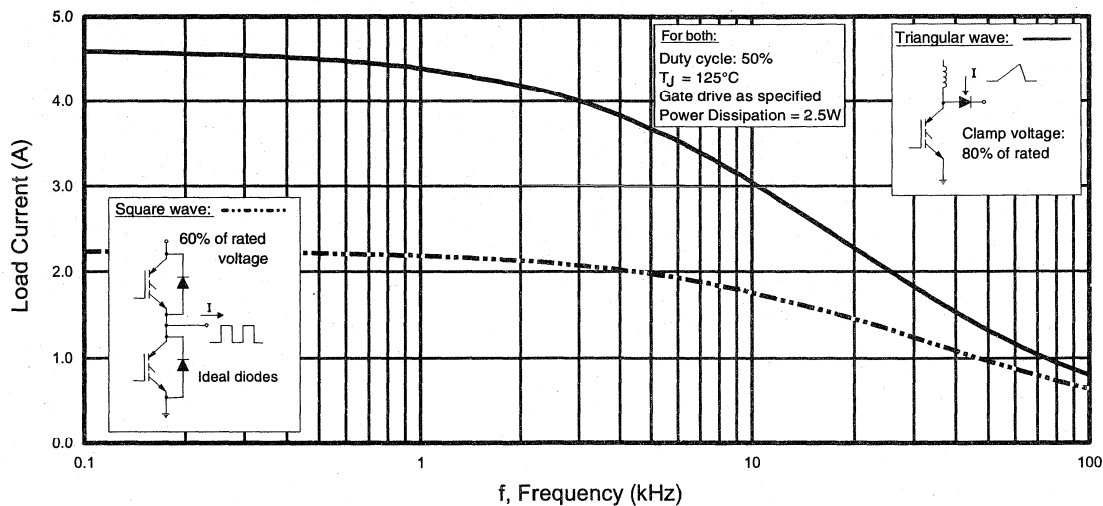


Fig. 1 - Typical Load Current vs. Frequency
 (For square wave, $I = I_{RMS}$ of fundamental; for triangular wave, $I = I_{PK}$)

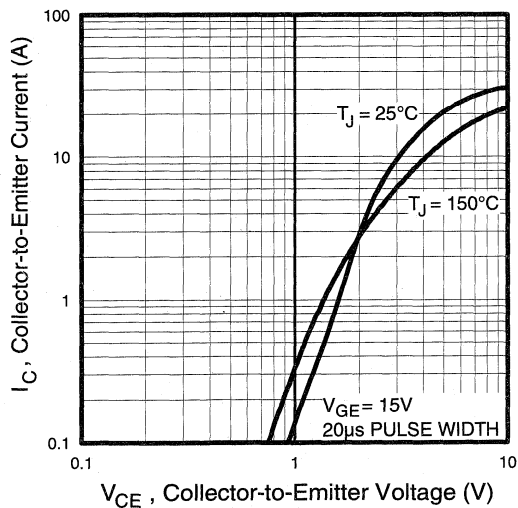


Fig. 2 - Typical Output Characteristics

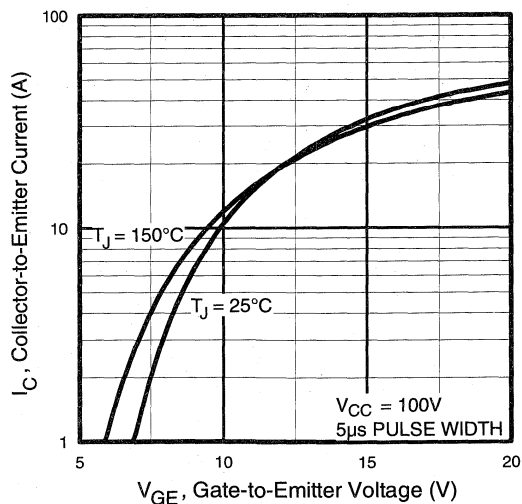


Fig. 3 - Typical Transfer Characteristics

Motor
 Control
 Ultra-Fast
 Discretes

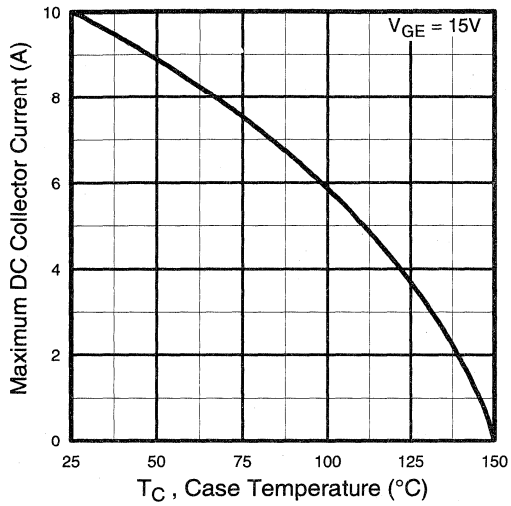


Fig. 4 - Maximum Collector Current vs. Case Temperature

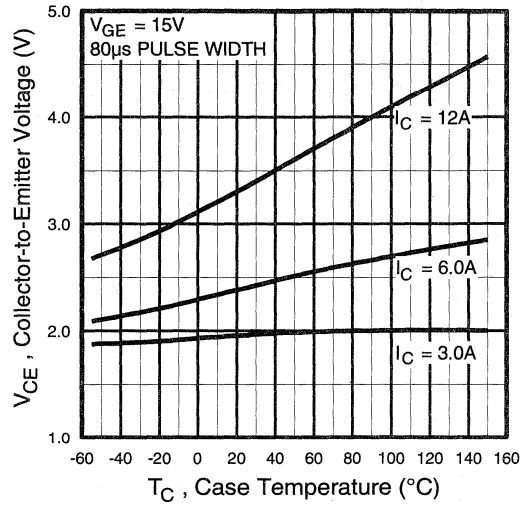


Fig. 5 - Collector-to-Emitter Voltage vs. Case Temperature

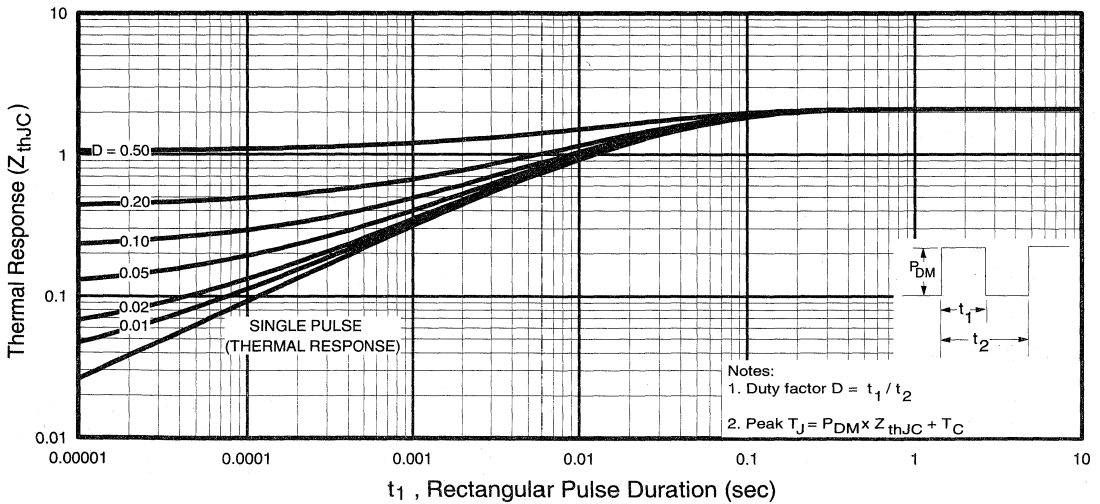


Fig. 6 - Maximum Effective Transient Thermal Impedance, Junction-to-Case

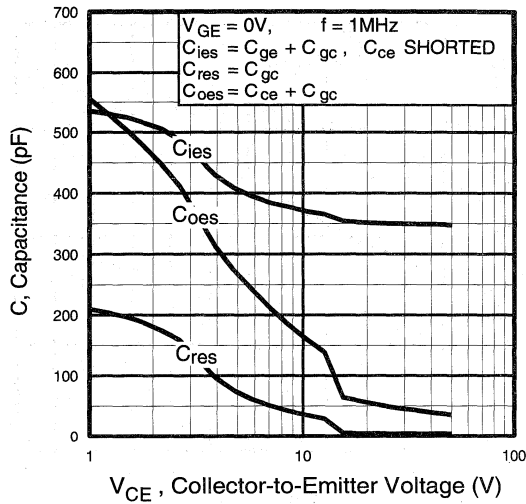


Fig. 7 - Typical Capacitance vs. Collector-to-Emitter Voltage

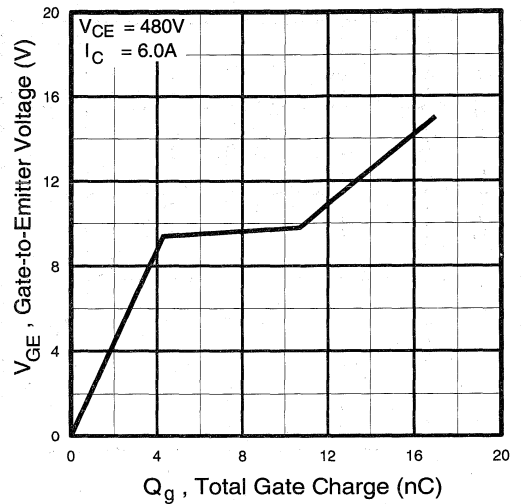


Fig. 8 - Typical Gate Charge vs. Gate-to-Emitter Voltage

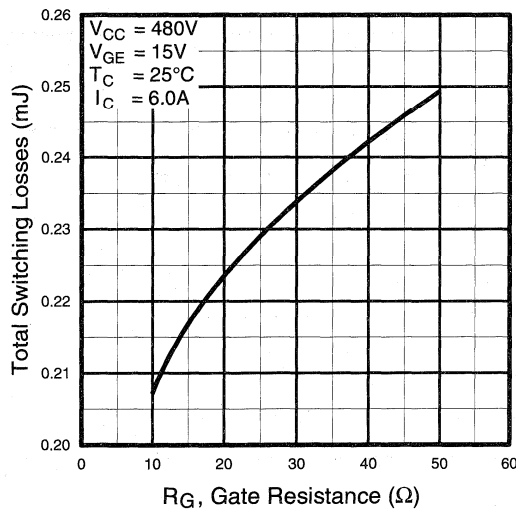


Fig. 9 - Typical Switching Losses vs. Gate Resistance

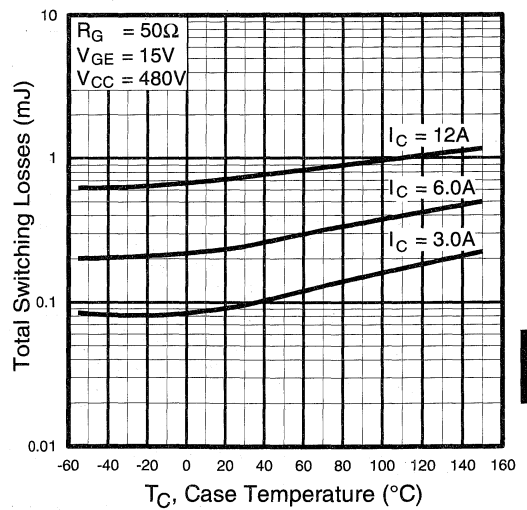


Fig. 10 - Typical Switching Losses vs. Case Temperature

Moser
 Control
 Ultra-Fast
 Discretes

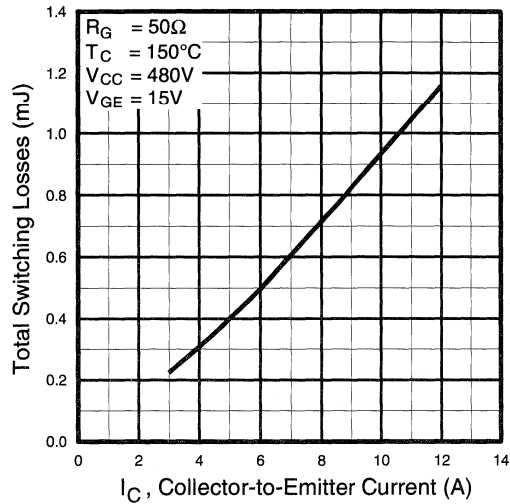


Fig. 11 - Typical Switching Losses vs. Collector-to-Emitter Current

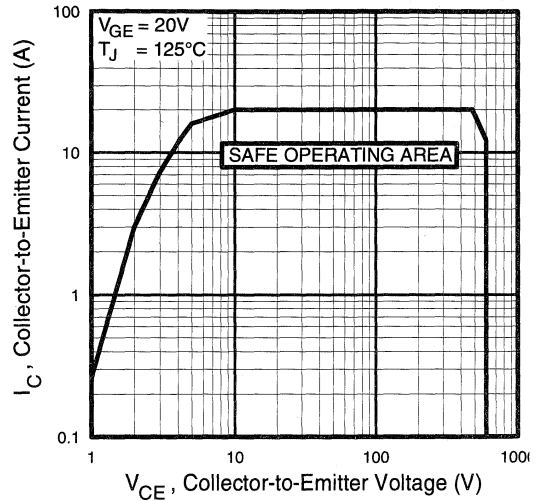


Fig. 12 - Turn-Off SOA

Refer to Section D for the following:

Appendix C: Section D - page D-5

- Fig. 13a - Clamped Inductive Load Test Circuit
- Fig. 13b - Pulsed Collector Current Test Circuit
- Fig. 14a - Switching Loss Test Circuit
- Fig. 14b - Switching Loss Waveform

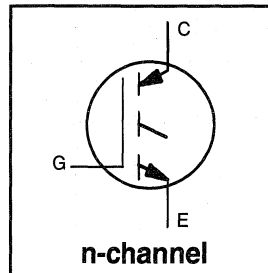
IRGBC30K-S

INSULATED GATE BIPOLAR TRANSISTOR

Short Circuit Rated
UltraFast Fast IGBT

Features

- Short circuit rated - 10 μ s @ 125°C, $V_{GE} = 15V$
 - Switching-loss rating includes all "tail" losses
 - Optimized for high operating frequency (over 5kHz)
- See Fig. 1 for Current vs. Frequency curve



$$V_{CES} = 600V$$

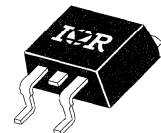
$$V_{CE(sat)} \leq 3.8V$$

$$@V_{GE} = 15V, I_C = 14A$$

Description

Insulated Gate Bipolar Transistors (IGBTs) from International Rectifier have higher usable current densities than comparable bipolar transistors, while at the same time having simpler gate-drive requirements of the familiar power MOSFET. They provide substantial benefits to a host of high-voltage, high-current applications.

These new short circuit rated devices are especially suited for motor control and other applications requiring short circuit withstand capability.



SMD-220

Absolute Maximum Ratings

	Parameter	Max.	Units
V_{CES}	Collector-to-Emitter Voltage	600	V
$I_C @ T_C = 25^\circ C$	Continuous Collector Current	23	A
$I_C @ T_C = 100^\circ C$	Continuous Collector Current	14	
I_{CM}	Pulsed Collector Current ①	46	
I_{LM}	Clamped Inductive Load Current ②	46	
t_{sc}	Short Circuit Withstand Time	10	μ s
V_{GE}	Gate-to-Emitter Voltage	± 20	V
E_{ARV}	Reverse Voltage Avalanche Energy ③	10	mJ
$P_D @ T_C = 25^\circ C$	Maximum Power Dissipation	100	W
$P_D @ T_C = 100^\circ C$	Maximum Power Dissipation	42	
T_J	Operating Junction and	-55 to +150	$^\circ C$
T_{STG}	Storage Temperature Range		
	Soldering Temperature, for 10 sec.	300 (0.063 in. (1.6mm) from case)	
	Mounting torque, 6-32 or M3 screw.	10 lbf•in (1.1N•m)	

Thermal Resistance

	Parameter	Min.	Typ.	Max.	Units
$R_{\theta JC}$	Junction-to-Case	—	—	1.2	$^\circ C/W$
$R_{\theta JA}$	Junction-to-Ambient, (PCB mount)**	—	—	40	
$R_{\theta JA}$	Junction-to-Ambient, typical socket mount	—	—	80	
Wt	Weight	—	2 (0.07)	—	g (oz)

** When mounted on 1" square PCB (FR-4 or G-10 Material)

For recommended footprint and soldering techniques refer to application note #AN-994.

Electrical Characteristics @ $T_J = 25^\circ\text{C}$ (unless otherwise specified)

	Parameter	Min.	Typ.	Max.	Units	Conditions
$V_{(BR)CES}$	Collector-to-Emitter Breakdown Voltage	600	—	—	V	$V_{GE} = 0V, I_C = 250\mu A$
$V_{(BR)ECS}$	Emitter-to-Collector Breakdown Voltage ④	20	—	—	V	$V_{GE} = 0V, I_C = 1.0A$
$\Delta V_{(BR)CES}/\Delta T_J$	Temperature Coeff. of Breakdown Voltage	—	0.30	—	V/°C	$V_{GE} = 0V, I_C = 1.0mA$
$V_{CE(on)}$	Collector-to-Emitter Saturation Voltage	—	2.5	3.8	V	$I_C = 14A$ $V_{GE} = 15V$ See Fig. 2, 5
		—	3.3	—		
		—	2.5	—		
$V_{GE(th)}$	Gate Threshold Voltage	3.0	—	5.5		$V_{CE} = V_{GE}, I_C = 250\mu A$
$\Delta V_{GE(th)}/\Delta T_J$	Temperature Coeff. of Threshold Voltage	—	-13	—	mV/°C	$V_{CE} = V_{GE}, I_C = 250\mu A$
g_{fe}	Forward Transconductance ⑤	3.3	6.5	—	S	$V_{CE} = 100V, I_C = 14A$
I_{CES}	Zero Gate Voltage Collector Current	—	—	600	μA	$V_{GE} = 0V, V_{CE} = 600V$
		—	—	1100		$V_{GE} = 0V, V_{CE} = 600V, T_J = 150^\circ\text{C}$
I_{GES}	Gate-to-Emitter Leakage Current	—	—	± 100	nA	$V_{GE} = \pm 20V$

Switching Characteristics @ $T_J = 25^\circ\text{C}$ (unless otherwise specified)

	Parameter	Min.	Typ.	Max.	Units	Conditions
Q_g	Total Gate Charge (turn-on)	—	39	58	nC	$I_C = 14A$ $V_{CC} = 400V$ $V_{GE} = 15V$ See Fig. 8
Q_{ge}	Gate - Emitter Charge (turn-on)	—	8.7	13		
Q_{gc}	Gate - Collector Charge (turn-on)	—	15	23		
$t_{d(on)}$	Turn-On Delay Time	—	31	—	ns	$T_J = 25^\circ\text{C}$ $I_C = 14A, V_{CC} = 480V$ $V_{GE} = 15V, R_G = 23\Omega$ Energy losses include "tail"
t_r	Rise Time	—	23	—		
$t_{d(off)}$	Turn-Off Delay Time	—	100	150		
t_f	Fall Time	—	84	130		
E_{on}	Turn-On Switching Loss	—	0.3	—		
E_{off}	Turn-Off Switching Loss	—	0.3	—	mJ	See Fig. 9, 10, 11, 14
E_{ts}	Total Switching Loss	—	0.6	0.9		
t_{sc}	Short Circuit Withstand Time	10	—	—	μs	$V_{CC} = 360V, T_J = 125^\circ\text{C}$ $V_{GE} = 15V, R_G = 23\Omega, V_{CPK} < 500V$
$t_{d(on)}$	Turn-On Delay Time	—	30	—	ns	$T_J = 150^\circ\text{C}$, $I_C = 14A, V_{CC} = 480V$ $V_{GE} = 15V, R_G = 23\Omega$ Energy losses include "tail"
t_r	Rise Time	—	23	—		
$t_{d(off)}$	Turn-Off Delay Time	—	170	—		
t_f	Fall Time	—	170	—		
E_{ts}	Total Switching Loss	—	1.2	—		
L_E	Internal Emitter Inductance	—	7.5	—	nH	Measured 5mm from package
C_{ies}	Input Capacitance	—	740	—	pF	$V_{GE} = 0V$ $V_{CC} = 30V$ See Fig. 7
C_{oes}	Output Capacitance	—	92	—		
C_{res}	Reverse Transfer Capacitance	—	9.4	—		

Notes:

- ① Repetitive rating; $V_{GE}=20V$, pulse width limited by max. junction temperature. (See fig. 13b)
- ② $V_{CC}=80\%(V_{CES}), V_{GE}=20V, L=10\mu H, R_G=23\Omega$, (See fig. 13a)
- ③ Repetitive rating; pulse width limited by maximum junction temperature.
- ④ Pulse width $\leq 80\mu s$; duty factor $\leq 0.1\%$.
- ⑤ Pulse width $5.0\mu s$, single shot.

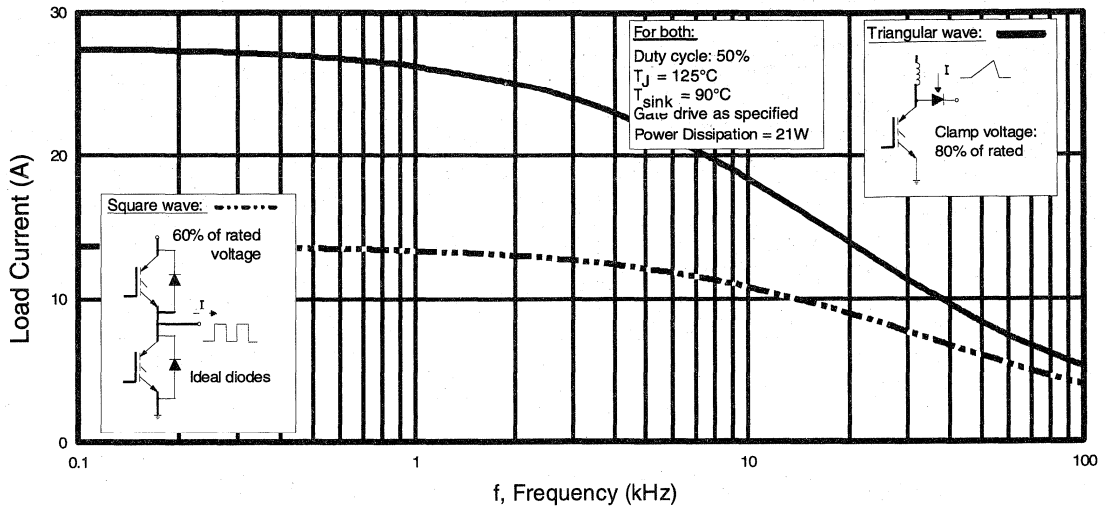


Fig. 1 - Typical Load Current vs. Frequency
 (For square wave, $I = I_{RMS}$ of fundamental; for triangular wave, $I = I_{PK}$)

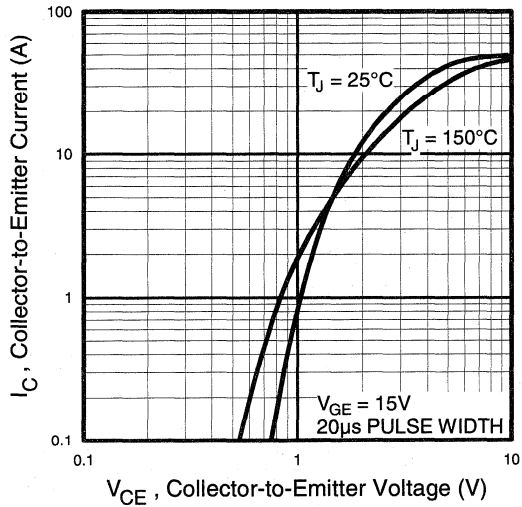


Fig. 2 - Typical Output Characteristics

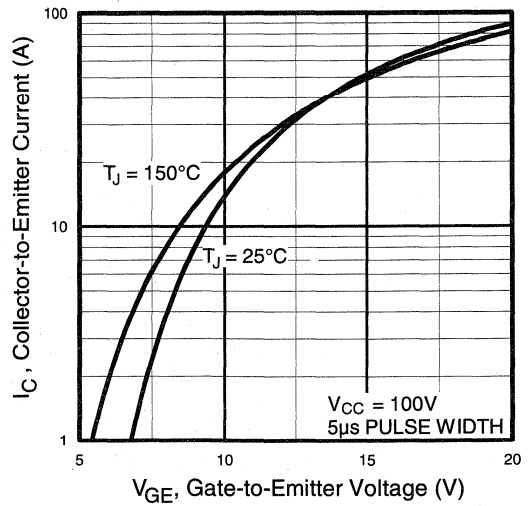


Fig. 3 - Typical Transfer Characteristics

Motor
Control
Ultra-Fast
Discretes

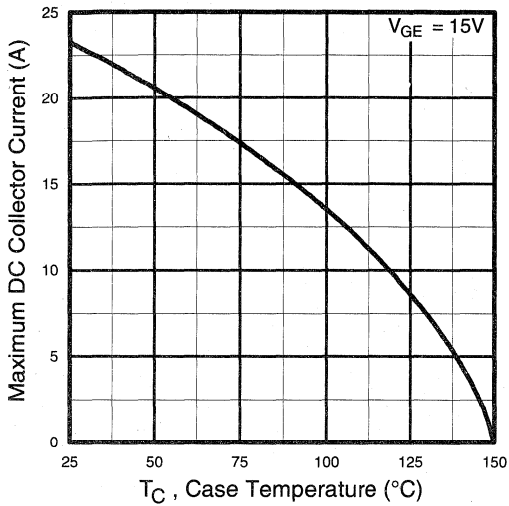


Fig. 4 - Maximum Collector Current vs. Case Temperature

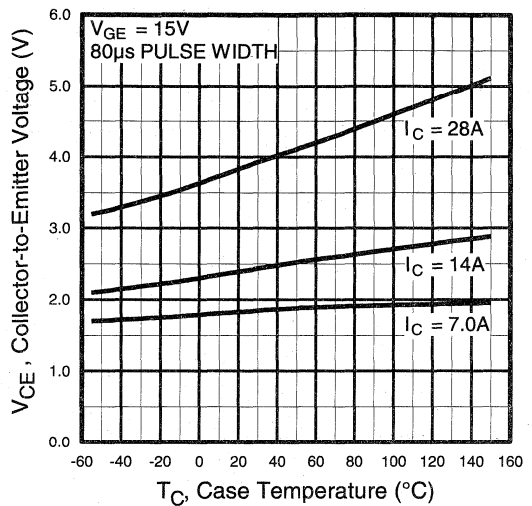


Fig. 5 - Collector-to-Emitter Voltage vs. Case Temperature

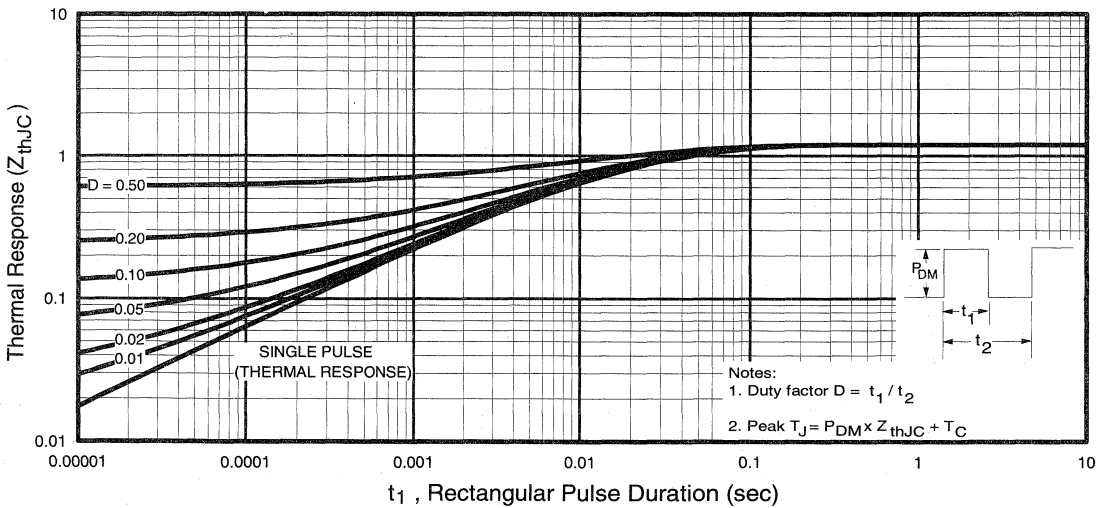


Fig. 6 - Maximum Effective Transient Thermal Impedance, Junction-to-Case

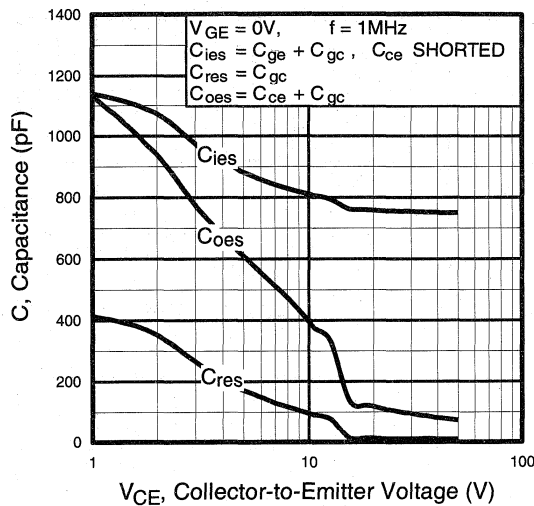


Fig. 7 - Typical Capacitance vs. Collector-to-Emitter Voltage

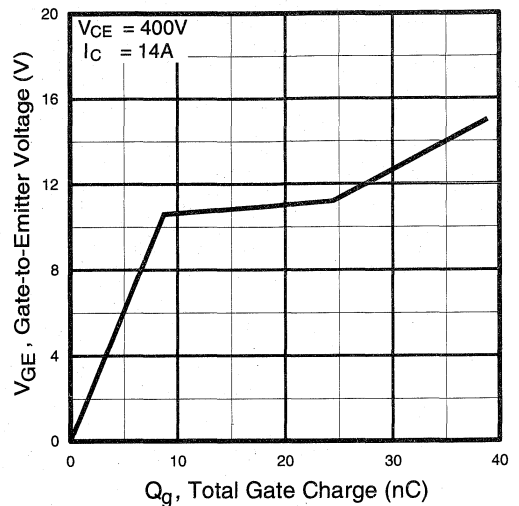


Fig. 8 - Typical Gate Charge vs. Gate-to-Emitter Voltage

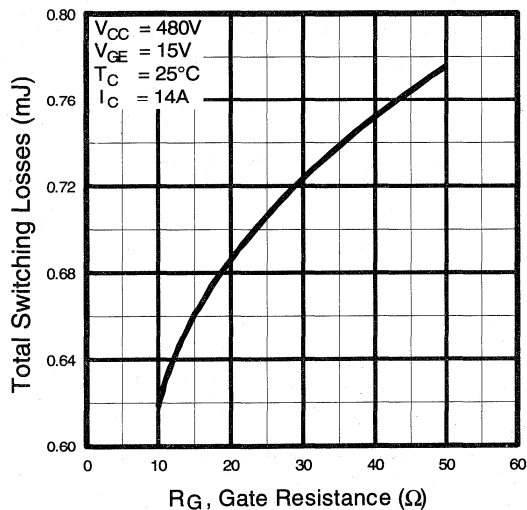


Fig. 9 - Typical Switching Losses vs. Gate Resistance

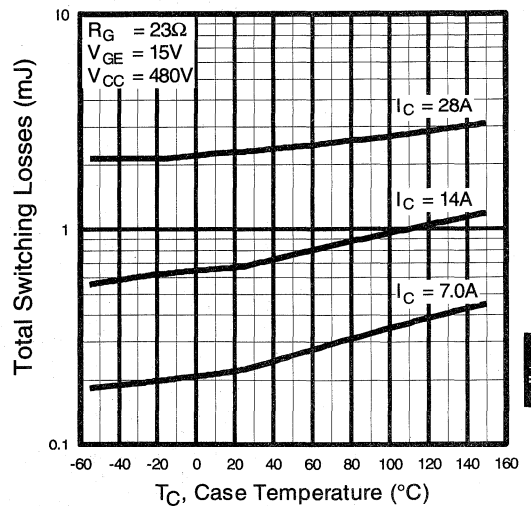


Fig. 10 - Typical Switching Losses vs. Case Temperature

Motor Control
Ultra-Fast
Discretes

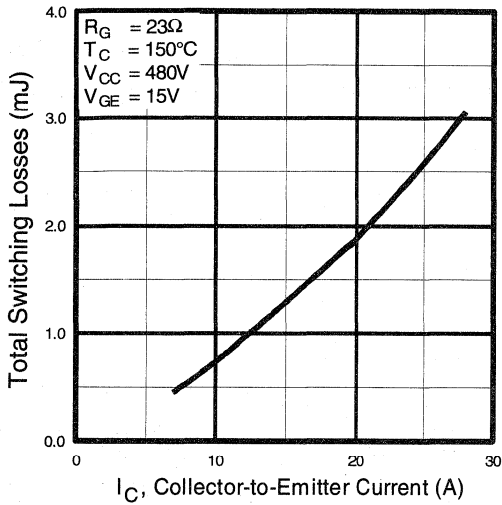


Fig. 11 - Typical Switching Losses vs. Collector-to-Emitter Current

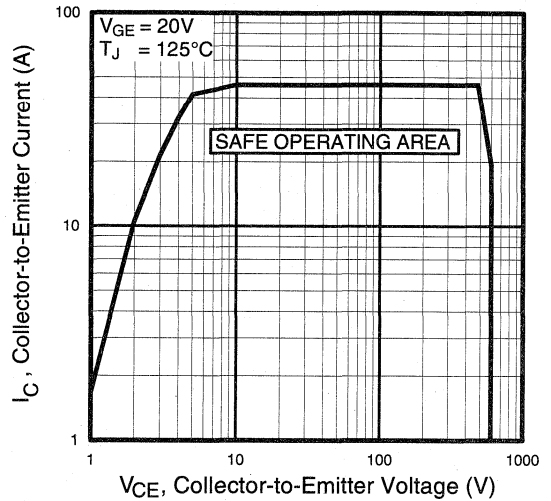


Fig. 12 - Turn-Off SOA

Refer to Section D for the following:

Appendix C: Section D - page D-5

- Fig. 13a - Clamped Inductive Load Test Circuit
- Fig. 13b - Pulsed Collector Current Test Circuit
- Fig. 14a - Switching Loss Test Circuit
- Fig. 14b - Switching Loss Waveform

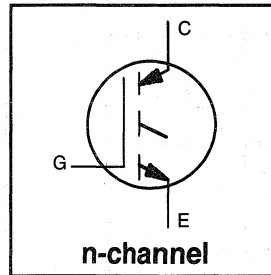
IRGBC40K-S

INSULATED GATE BIPOLAR TRANSISTOR

Short Circuit Rated
UltraFast Fast IGBT

Features

- Short circuit rated - $10\mu\text{s}$ @ 125°C , $V_{\text{GE}} = 15\text{V}$
- Switching-loss rating includes all "tail" losses
- Optimized for high operating frequency (over 5kHz)
See Fig. 1 for Current vs. Frequency curve



$$V_{\text{CES}} = 600\text{V}$$

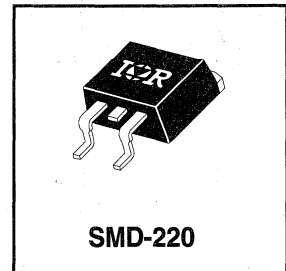
$$V_{\text{CE(sat)}} \leq 3.2\text{V}$$

$$\text{@ } V_{\text{GE}} = 15\text{V}, I_{\text{C}} = 25\text{A}$$

Description

Insulated Gate Bipolar Transistors (IGBTs) from International Rectifier have higher usable current densities than comparable bipolar transistors, while at the same time having simpler gate-drive requirements of the familiar power MOSFET. They provide substantial benefits to a host of high-voltage, high-current applications.

These new short circuit rated devices are especially suited for motor control and other applications requiring short circuit withstand capability.



SMD-220

Absolute Maximum Ratings

	Parameter	Max.	Units
V_{CES}	Collector-to-Emitter Voltage	600	V
$I_{\text{C}} @ T_{\text{C}} = 25^\circ\text{C}$	Continuous Collector Current	42	A
$I_{\text{C}} @ T_{\text{C}} = 100^\circ\text{C}$	Continuous Collector Current	25	
I_{CM}	Pulsed Collector Current ①	84	
I_{LM}	Clamped Inductive Load Current ②	84	
t_{sc}	Short Circuit Withstand Time	10	μs
V_{GE}	Gate-to-Emitter Voltage	± 20	V
E_{ARV}	Reverse Voltage Avalanche Energy ③	15	mJ
$P_{\text{D}} @ T_{\text{C}} = 25^\circ\text{C}$	Maximum Power Dissipation	160	W
$P_{\text{D}} @ T_{\text{C}} = 100^\circ\text{C}$	Maximum Power Dissipation	65	
T_{J}	Operating Junction and	-55 to +150	$^\circ\text{C}$
T_{STG}	Storage Temperature Range		
	Soldering Temperature, for 10 sec.	300 (0.063 in. (1.6mm) from case)	
	Mounting torque, 6-32 or M3 screw.	10 lbf•in (1.1N•m)	

Thermal Resistance

	Parameter	Min.	Typ.	Max.	Units
$R_{\theta\text{JC}}$	Junction-to-Case	—	—	0.77	$^\circ\text{C}/\text{W}$
$R_{\theta\text{JA}}$	Junction-to-Ambient, (PCB mount)**	—	—	40	
$R_{\theta\text{JA}}$	Junction-to-Ambient, typical socket mount	—	—	80	
Wt	Weight	—	2 (0.07)	—	g (oz)

** When mounted on 1" square PCB (FR-4 or G-10 Material)

For recommended footprint and soldering techniques refer to application note #AN-994.

Electrical Characteristics @ $T_J = 25^\circ\text{C}$ (unless otherwise specified)

	Parameter	Min.	Typ.	Max.	Units	Conditions
$V_{(BR)CES}$	Collector-to-Emitter Breakdown Voltage	600	—	—	V	$V_{GE} = 0V, I_C = 250\mu A$
$V_{(BR)ECS}$	Emitter-to-Collector Breakdown Voltage ④	20	—	—	V	$V_{GE} = 0V, I_C = 1.0A$
$\Delta V_{(BR)CES}/\Delta T_J$	Temp. Coeff. of Breakdown Voltage	—	0.46	—	V/ $^\circ\text{C}$	$V_{GE} = 0V, I_C = 1.0mA$
$V_{CE(on)}$	Collector-to-Emitter Saturation Voltage	—	2.1	3.2	V	$I_C = 25A$ $I_C = 42A$ $I_C = 25A, T_J = 150^\circ\text{C}$ $V_{GE} = 15V$ See Fig. 2, 5
		—	2.8	—		
		—	2.5	—		
$V_{GE(th)}$	Gate Threshold Voltage	3.0	—	5.5		$V_{CE} = V_{GE}, I_C = 250\mu A$
$\Delta V_{GE(th)}/\Delta T_J$	Temperature Coeff. of Threshold Voltage	—	-13	—	mV/ $^\circ\text{C}$	$V_{CE} = V_{GE}, I_C = 250\mu A$
g_{fe}	Forward Transconductance ⑤	7.0	14	—	S	$V_{CE} = 100V, I_C = 25A$
I_{CES}	Zero Gate Voltage Collector Current	—	—	250	μA	$V_{GE} = 0V, V_{CE} = 600V$ $V_{GE} = 0V, V_{CE} = 600V, T_J = 150^\circ\text{C}$
		—	—	1000		
I_{GES}	Gate-to-Emitter Leakage Current	—	—	± 100	nA	$V_{GE} = \pm 20V$

Switching Characteristics @ $T_J = 25^\circ\text{C}$ (unless otherwise specified)

	Parameter	Min.	Typ.	Max.	Units	Conditions
Q_g	Total Gate Charge (turn-on)	—	61	92	nC	$I_C = 25A$ $V_{CC} = 400V$ $V_{GE} = 15V$ See Fig. 8
Q_{ge}	Gate - Emitter Charge (turn-on)	—	13	19		
Q_{gc}	Gate - Collector Charge (turn-on)	—	22	33		
$t_{d(on)}$	Turn-On Delay Time	—	35	—	ns	$T_J = 25^\circ\text{C}$ $I_C = 25A, V_{CC} = 480V$ $V_{GE} = 15V, R_G = 10\Omega$ Energy losses include "tail"
t_r	Rise Time	—	27	—		
$t_{d(off)}$	Turn-Off Delay Time	—	160	240		
t_f	Fall Time	—	130	200		
E_{on}	Turn-On Switching Loss	—	0.52	—	mJ	See Fig. 9, 10, 11, 14
E_{off}	Turn-Off Switching Loss	—	1.2	—		
E_{ts}	Total Switching Loss	—	1.7	2.6		
t_{sc}	Short Circuit Withstand Time	10	—	—	μs	$V_{CC} = 360V, T_J = 125^\circ\text{C}$ $V_{GE} = 15V, R_G = 10\Omega, V_{CPK} < 500V$
$t_{d(on)}$	Turn-On Delay Time	—	34	—	ns	$T_J = 150^\circ\text{C}$, $I_C = 25A, V_{CC} = 480V$ $V_{GE} = 15V, R_G = 10\Omega$ Energy losses include "tail"
t_r	Rise Time	—	28	—		
$t_{d(off)}$	Turn-Off Delay Time	—	300	—		
t_f	Fall Time	—	310	—		
E_{ts}	Total Switching Loss	—	3.6	—	mJ	See Fig. 10, 14
L_E	Internal Emitter Inductance	—	7.5	—	nH	Measured 5mm from package
C_{ies}	Input Capacitance	—	1500	—	pF	$V_{GE} = 0V$ $V_{CC} = 30V$ $f = 1.0MHz$ See Fig. 7
C_{oes}	Output Capacitance	—	190	—		
C_{res}	Reverse Transfer Capacitance	—	17	—		

Notes:

- ① Repetitive rating; $V_{GE}=20V$, pulse width limited by max. junction temperature. (See fig. 13b)
- ② $V_{CC}=80\%(V_{CES}), V_{GE}=20V, L=10\mu H, R_G=10\Omega$, (See fig. 13a)
- ③ Repetitive rating; pulse width limited by maximum junction temperature.
- ④ Pulse width $\leq 80\mu s$; duty factor $\leq 0.1\%$.
- ⑤ Pulse width 5.0 μs , single shot.

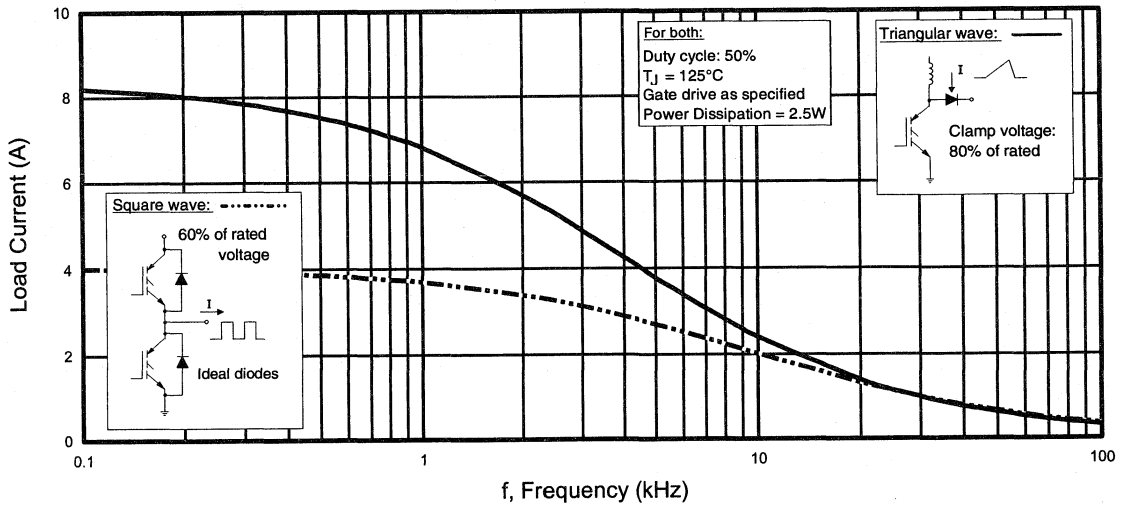


Fig. 1 - Typical Load Current vs. Frequency
 (For square wave, $I = I_{RMS}$ of fundamental; for triangular wave, $I = I_{PK}$)

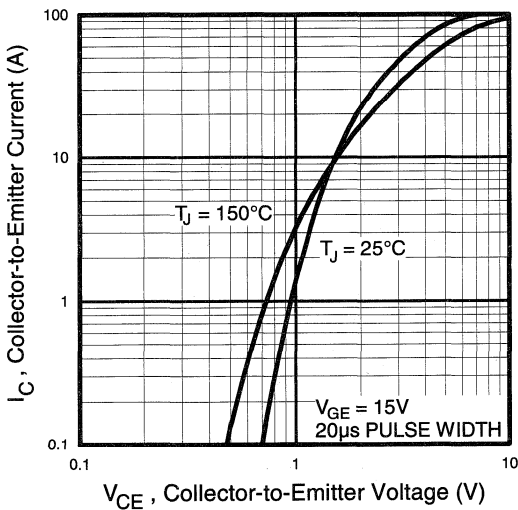


Fig. 2 - Typical Output Characteristics

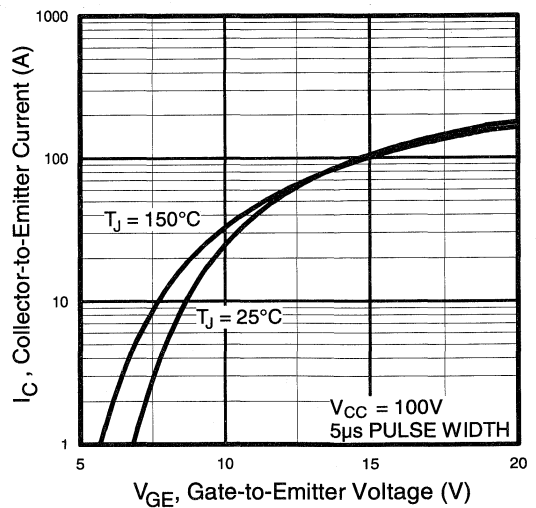


Fig. 3 - Typical Transfer Characteristics

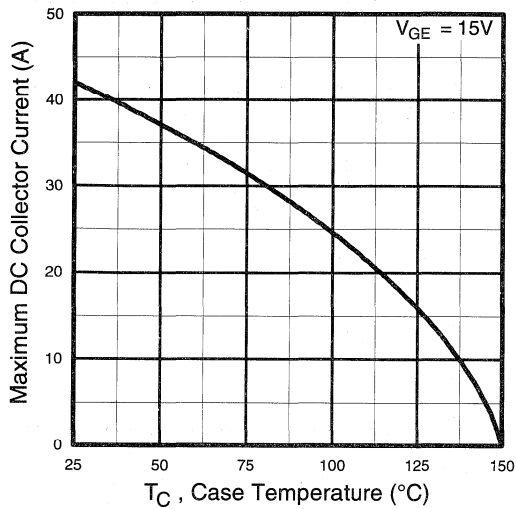


Fig. 4 - Maximum Collector Current vs. Case Temperature

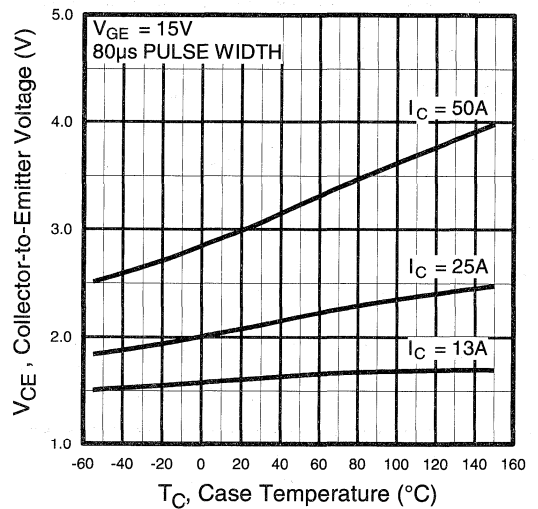


Fig. 5 - Collector-to-Emitter Voltage vs. Case Temperature

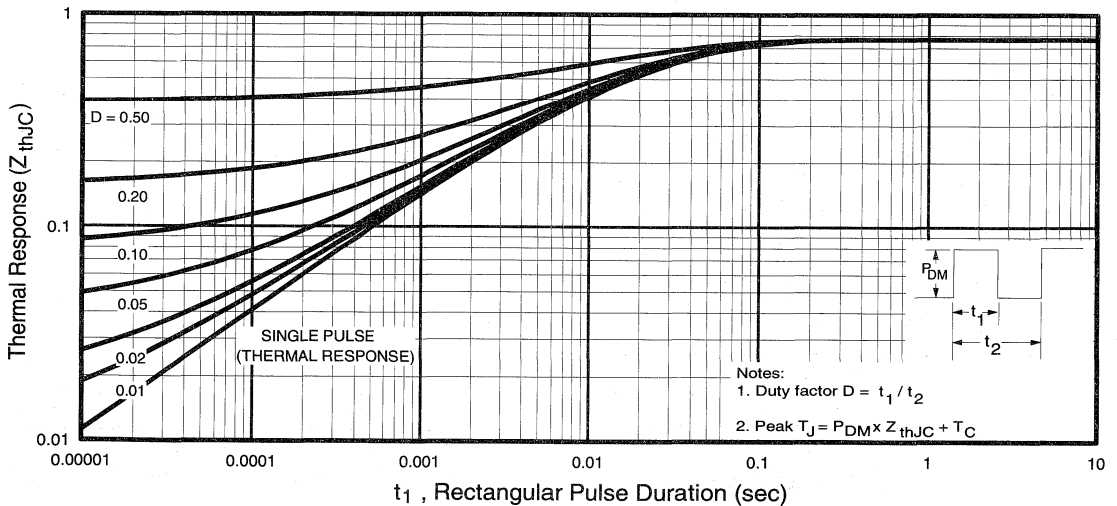


Fig. 6 - Maximum Effective Transient Thermal Impedance, Junction-to-Case

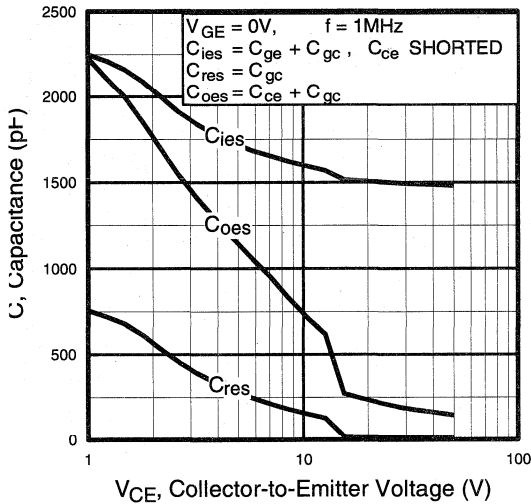


Fig. 7 - Typical Capacitance vs. Collector-to-Emitter Voltage

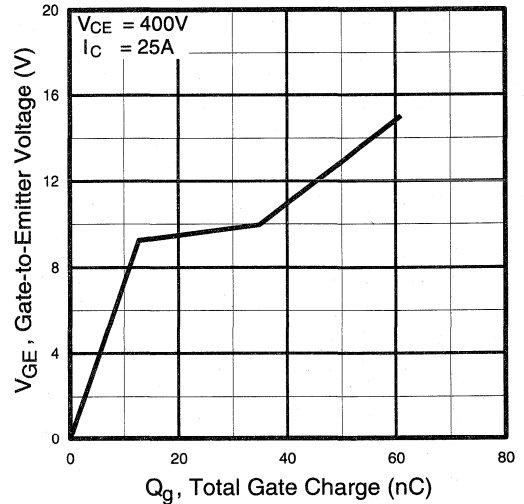


Fig. 8 - Typical Gate Charge vs. Gate-to-Emitter Voltage

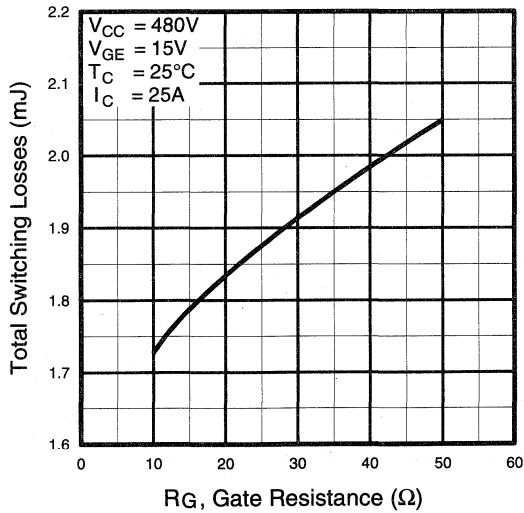


Fig. 9 - Typical Switching Losses vs. Gate Resistance

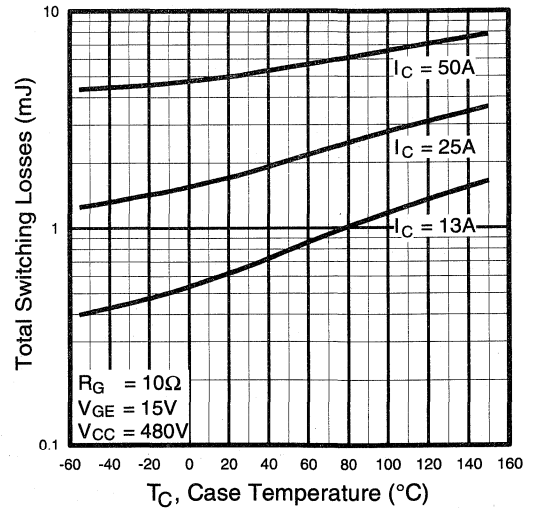


Fig. 10 - Typical Switching Losses vs. Case Temperature

Motor
 Control
 Ultra Fast
 Discretes

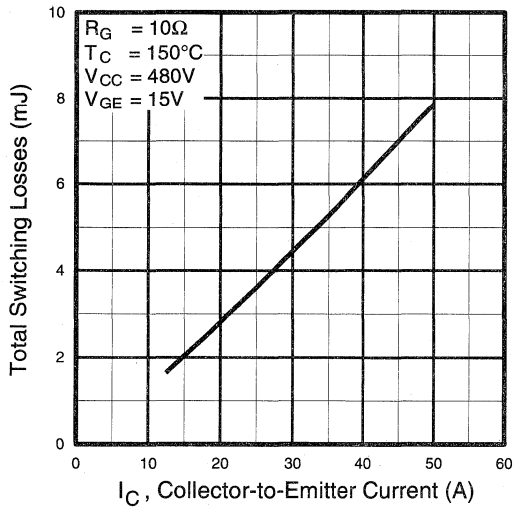


Fig. 11 - Typical Switching Losses vs. Collector-to-Emitter Current

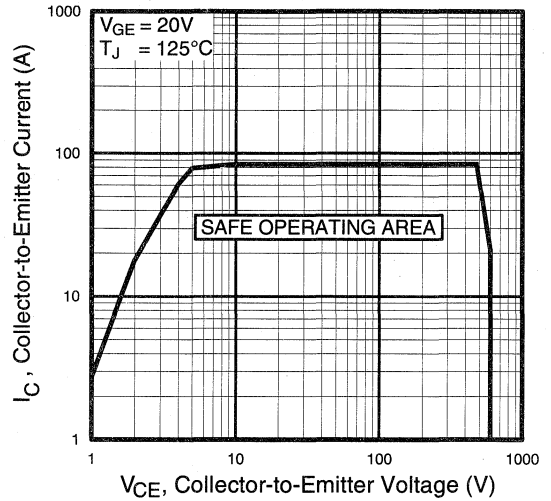


Fig. 12 - Turn-Off SOA

Refer to Section D for the following:

Appendix C: Section D - page D-5

Fig. 13a - Clamped Inductive Load Test Circuit

Fig. 13b - Pulsed Collector Current Test Circuit

Fig. 14a - Switching Loss Test Circuit

Fig. 14b - Switching Loss Waveform

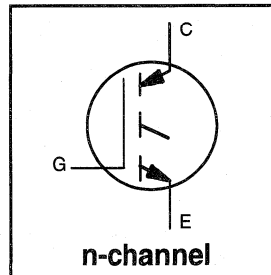
INSULATED GATE BIPOLAR TRANSISTOR

Short Circuit Rated
UltraFast IGBT

Features

- Short circuit rated - $10\mu\text{s}$ @ 125°C , $V_{GE} = 15\text{V}$
- Switching-loss rating includes all "tail" losses
- Optimized for high operating frequency (over 5kHz)

See Fig. 1 for Current vs. Frequency curve



$$V_{CES} = 600\text{V}$$

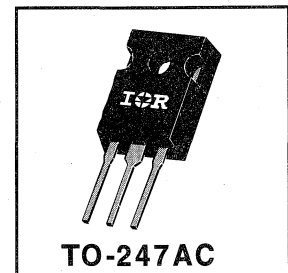
$$V_{CE(sat)} \leq 3.5\text{V}$$

$$\text{@ } V_{GE} = 15\text{V}, I_C = 6.0\text{A}$$

Description

Insulated Gate Bipolar Transistors (IGBTs) from International Rectifier have higher usable current densities than comparable bipolar transistors, while at the same time having simpler gate-drive requirements of the familiar power MOSFET. They provide substantial benefits to a host of high-voltage, high-current applications.

These new short circuit rated devices are especially suited for motor control and other applications requiring short circuit withstand capability.



Absolute Maximum Ratings

	Parameter	Max.	Units
V_{CES}	Collector-to-Emitter Voltage	600	V
I_C @ $T_C = 25^\circ\text{C}$	Continuous Collector Current	10	A
I_C @ $T_C = 100^\circ\text{C}$	Continuous Collector Current	6.0	
I_{CM}	Pulsed Collector Current ①	20	
I_{LM}	Clamped Inductive Load Current ②	20	
t_{sc}	Short Circuit Withstand Time	10	μs
V_{GE}	Gate-to-Emitter Voltage	± 20	V
E_{ARV}	Reverse Voltage Avalanche Energy ③	5.0	mJ
P_D @ $T_C = 25^\circ\text{C}$	Maximum Power Dissipation	60	W
P_D @ $T_C = 100^\circ\text{C}$	Maximum Power Dissipation	24	
T_J	Operating Junction and	-55 to +150	$^\circ\text{C}$
T_{STG}	Storage Temperature Range		
	Soldering Temperature, for 10 sec.	300 (0.063 in. (1.6mm) from case)	
	Mounting torque, 6-32 or M3 screw.	10 lbf•in (1.1N•m)	

Thermal Resistance

	Parameter	Min.	Typ.	Max.	Units
$R_{\theta JC}$	Junction-to-Case	—	—	2.1	$^\circ\text{C/W}$
$R_{\theta CS}$	Case-to-Sink, flat, greased surface	—	0.24	—	
$R_{\theta JA}$	Junction-to-Ambient, typical socket mount	—	—	40	
Wt	Weight	—	6 (0.21)	—	g (oz)

Electrical Characteristics @ $T_J = 25^\circ\text{C}$ (unless otherwise specified)

	Parameter	Min.	Typ.	Max.	Units	Conditions
$V_{(BR)CES}$	Collector-to-Emitter Breakdown Voltage	600	—	—	V	$V_{GE} = 0V, I_C = 250\mu A$
$V_{(BR)ECS}$	Emitter-to-Collector Breakdown Voltage ④	20	—	—	V	$V_{GE} = 0V, I_C = 1.0A$
$\Delta V_{(BR)CES}/\Delta T_J$	Temperature Coeff. of Breakdown Voltage	—	0.37	—	V/ $^\circ\text{C}$	$V_{GE} = 0V, I_C = 1.0mA$
$V_{CE(on)}$	Collector-to-Emitter Saturation Voltage	—	2.4	3.5	V	$I_C = 6.0A$ $V_{GE} = 15V$ See Fig. 2, 5
		—	3.6	—		
		—	2.9	—		
$V_{GE(th)}$	Gate Threshold Voltage	3.0	—	5.5		$V_{CE} = V_{GE}, I_C = 250\mu A$
$\Delta V_{GE(th)}/\Delta T_J$	Temperature Coeff. of Threshold Voltage	—	-11	—	mV/ $^\circ\text{C}$	$V_{CE} = V_{GE}, I_C = 250\mu A$
g_{fe}	Forward Transconductance ⑤	1.9	3.3	—	S	$V_{CE} = 100V, I_C = 6.0A$
I_{CES}	Zero Gate Voltage Collector Current	—	—	250	μA	$V_{GE} = 0V, V_{CE} = 600V$
		—	—	1000		
I_{GES}	Gate-to-Emitter Leakage Current	—	—	± 100	nA	$V_{GE} = \pm 20V$

Switching Characteristics @ $T_J = 25^\circ\text{C}$ (unless otherwise specified)

	Parameter	Min.	Typ.	Max.	Units	Conditions
Q_g	Total Gate Charge (turn-on)	—	17	26	nC	$I_C = 6.0A$ $V_{CC} = 400V$ $V_{GE} = 15V$ See Fig. 8
Q_{ge}	Gate - Emitter Charge (turn-on)	—	4.3	6.8		
Q_{gc}	Gate - Collector Charge (turn-on)	—	6.4	11		
$t_{d(on)}$	Turn-On Delay Time	—	29	—	ns	$T_J = 25^\circ\text{C}$ $I_C = 6.0A, V_{CC} = 480V$ $V_{GE} = 15V, R_G = 50\Omega$ Energy losses include "tail"
t_r	Rise Time	—	18	—		
$t_{d(off)}$	Turn-Off Delay Time	—	58	90		
t_f	Fall Time	—	120	200		
E_{on}	Turn-On Switching Loss	—	0.11	—	mJ	See Fig. 9, 10, 11, 14
E_{off}	Turn-Off Switching Loss	—	0.13	—		
E_{ts}	Total Switching Loss	—	0.24	0.31		
t_{sc}	Short Circuit Withstand Time	10	—	—	μs	$V_{CC} = 400V, T_J = 125^\circ\text{C}$ $V_{GE} = 15V, R_G = 50\Omega, V_{CPK} < 500V$
$t_{d(on)}$	Turn-On Delay Time	—	28	—	ns	$T_J = 150^\circ\text{C}$, $I_C = 6.0A, V_{CC} = 480V$ $V_{GE} = 15V, R_G = 50\Omega$ Energy losses include "tail"
t_r	Rise Time	—	22	—		
$t_{d(off)}$	Turn-Off Delay Time	—	200	—		
t_f	Fall Time	—	145	—		
E_{ts}	Total Switching Loss	—	0.50	—	mJ	See Fig. 10, 14
L_E	Internal Emitter Inductance	—	13	—	nH	Measured 5mm from package
C_{ies}	Input Capacitance	—	360	—	pF	$V_{GE} = 0V$ $V_{CC} = 30V$ See Fig. 7 $f = 1.0MHz$
C_{oes}	Output Capacitance	—	45	—		
C_{res}	Reverse Transfer Capacitance	—	4.7	—		

Notes:

- ① Repetitive rating; $V_{GE}=20V$, pulse width limited by max. junction temperature. (See fig. 13b)
- ② $V_{CC}=80\%(V_{CES}), V_{GE}=20V, L=10\mu H, R_G=50\Omega$, (See fig. 13a)
- ③ Repetitive rating; pulse width limited by maximum junction temperature.
- ④ Pulse width $\leq 80\mu s$; duty factor $\leq 0.1\%$.
- ⑤ Pulse width $5.0\mu s$, single shot.

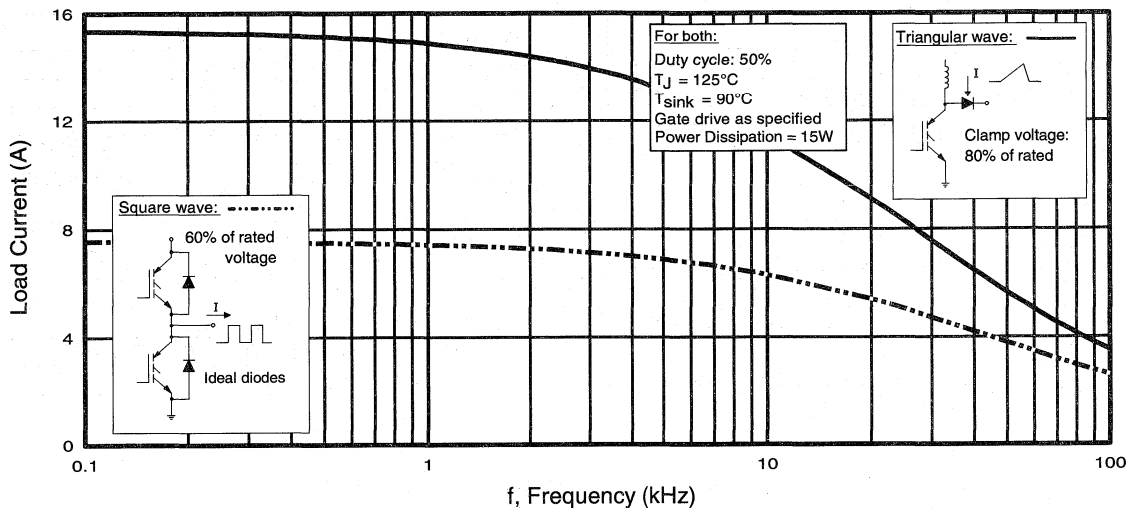


Fig. 1 - Typical Load Current vs. Frequency
 (For square wave, $I = I_{RMS}$ of fundamental; for triangular wave, $I = I_{PK}$)

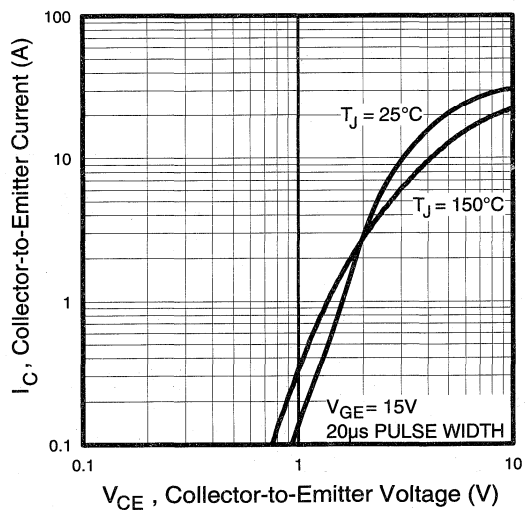


Fig. 2 - Typical Output Characteristics

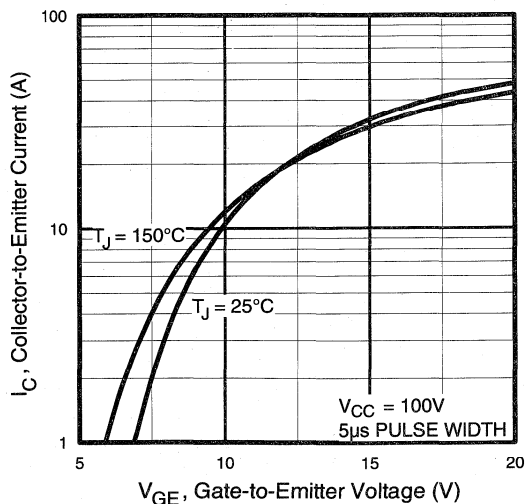


Fig. 3 - Typical Transfer Characteristics

Motor Control
 Ultra-Fast
 Discretes

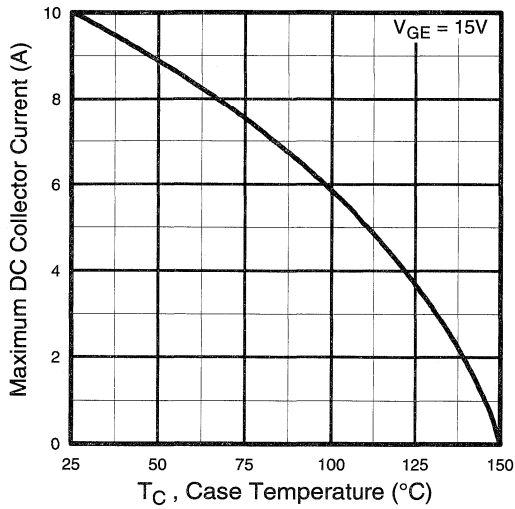


Fig. 4 - Maximum Collector Current vs. Case Temperature

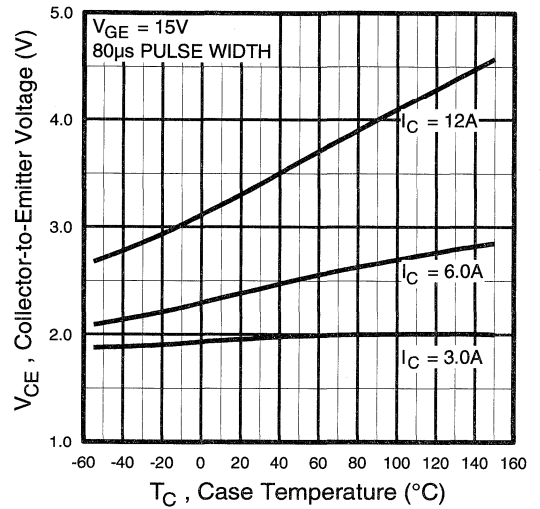


Fig. 5 - Collector-to-Emitter Voltage vs. Case Temperature

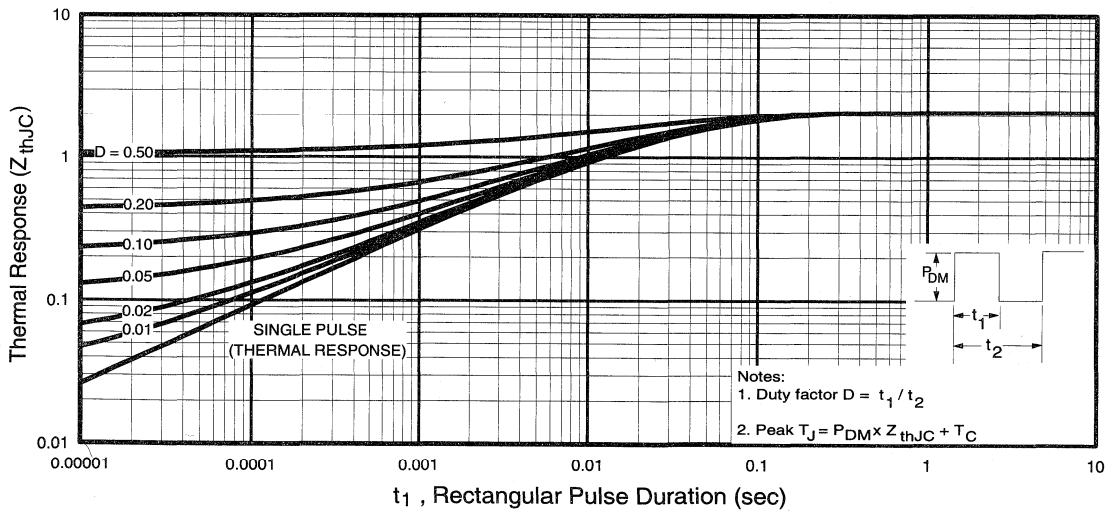


Fig. 6 - Maximum Effective Transient Thermal Impedance, Junction-to-Case

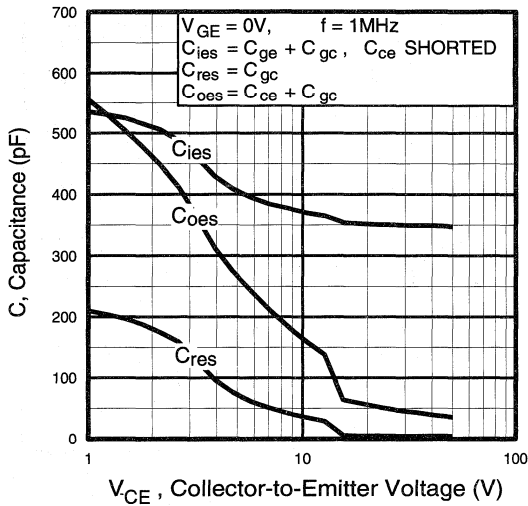


Fig. 7 - Typical Capacitance vs. Collector-to-Emitter Voltage

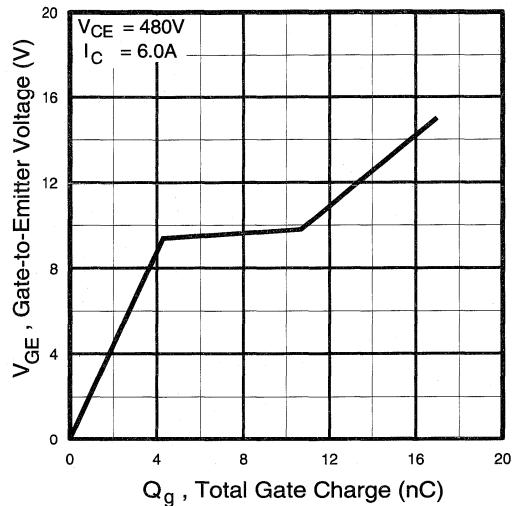


Fig. 8 - Typical Gate Charge vs. Gate-to-Emitter Voltage

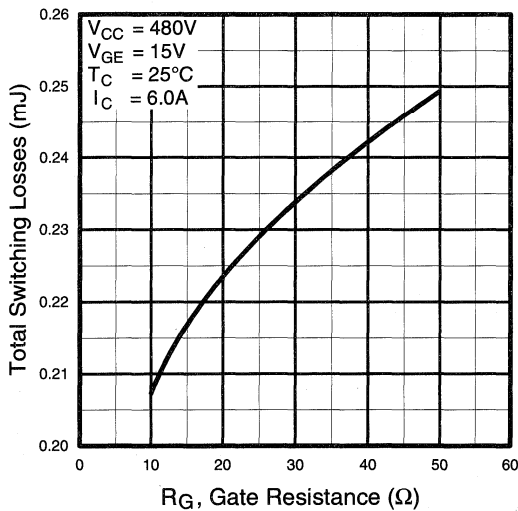


Fig. 9 - Typical Switching Losses vs. Gate Resistance

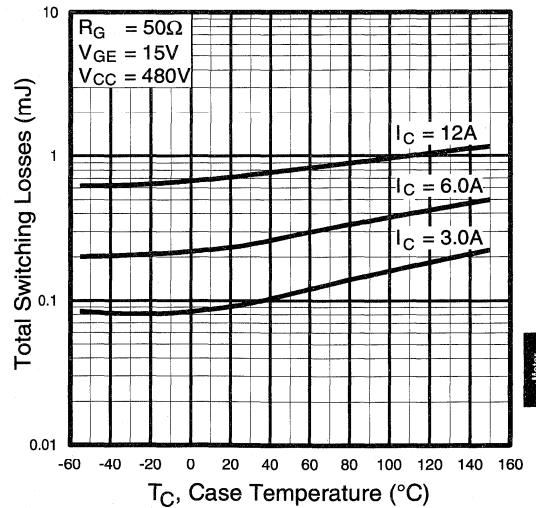


Fig. 10 - Typical Switching Losses vs. Case Temperature

Motor
Control
Ultra-Fast
Discretes

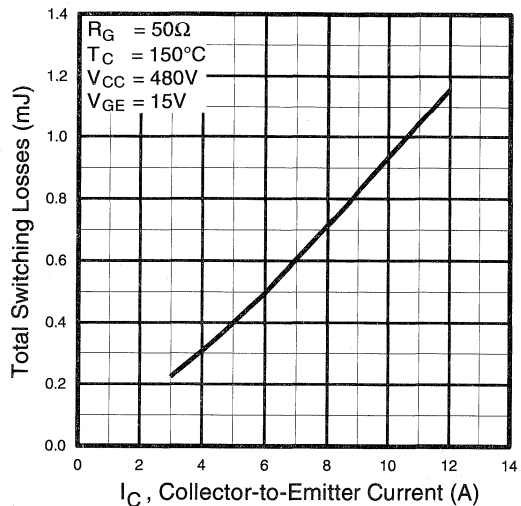


Fig. 11 - Typical Switching Losses vs. Collector-to-Emitter Current

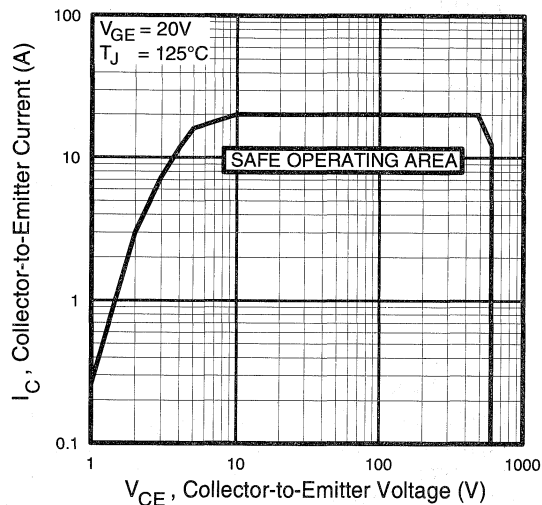


Fig. 12 - Turn-Off SOA

Refer to Section D for the following:

Appendix C: Section D - page D-5

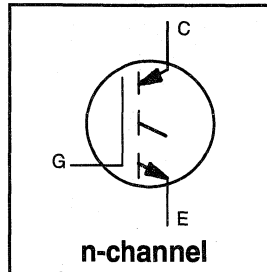
- Fig. 13a - Clamped Inductive Load Test Circuit
- Fig. 13b - Pulsed Collector Current Test Circuit
- Fig. 14a - Switching Loss Test Circuit
- Fig. 14b - Switching Loss Waveform

INSULATED GATE BIPOLAR TRANSISTOR

Short Circuit Rated
UltraFast IGBT

Features

- Short circuit rated - $10\mu\text{s}$ @ 125°C , $V_{GE} = 15\text{V}$
- Switching-loss rating includes all "tail" losses
- Optimized for high operating frequency (over 5kHz)
See Fig. 1 for Current vs. Frequency curve



$$V_{CES} = 600\text{V}$$

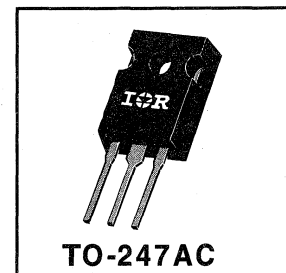
$$V_{CE(sat)} \leq 3.8\text{V}$$

$$\text{@ } V_{GE} = 15\text{V}, I_C = 14\text{A}$$

Description

Insulated Gate Bipolar Transistors (IGBTs) from International Rectifier have higher usable current densities than comparable bipolar transistors, while at the same time having simpler gate-drive requirements of the familiar power MOSFET. They provide substantial benefits to a host of high-voltage, high-current applications.

These new short circuit rated devices are especially suited for motor control and other applications requiring short circuit withstand capability.



Absolute Maximum Ratings

	Parameter	Max.	Units
V_{CES}	Collector-to-Emitter Voltage	600	V
$I_C @ T_C = 25^\circ\text{C}$	Continuous Collector Current	23	A
$I_C @ T_C = 100^\circ\text{C}$	Continuous Collector Current	14	
I_{CM}	Pulsed Collector Current ①	46	
I_{LM}	Clamped Inductive Load Current ②	46	
t_{sc}	Short Circuit Withstand Time	10	μs
V_{GE}	Gate-to-Emitter Voltage	± 20	V
E_{ARV}	Reverse Voltage Avalanche Energy ③	10	mJ
$P_D @ T_C = 25^\circ\text{C}$	Maximum Power Dissipation	100	W
$P_D @ T_C = 100^\circ\text{C}$	Maximum Power Dissipation	42	
T_J	Operating Junction and	-55 to +150	$^\circ\text{C}$
T_{STG}	Storage Temperature Range		
	Soldering Temperature, for 10 sec.	300 (0.063 in. (1.6mm) from case)	
	Mounting torque, 6-32 or M3 screw.	10 lbf•in (1.1N•m)	

Thermal Resistance

	Parameter	Min.	Typ.	Max.	Units
$R_{\theta JC}$	Junction-to-Case	—	—	1.2	$^\circ\text{C/W}$
$R_{\theta CS}$	Case-to-Sink, flat, greased surface	—	0.24	—	
$R_{\theta JA}$	Junction-to-Ambient, typical socket mount	—	—	40	
Wt	Weight	—	6 (0.21)	—	g (oz)

Electrical Characteristics @ $T_J = 25^\circ\text{C}$ (unless otherwise specified)

	Parameter	Min.	Typ.	Max.	Units	Conditions
$V_{(BR)CES}$	Collector-to-Emitter Breakdown Voltage	600	—	—	V	$V_{GE} = 0V, I_C = 250\mu A$
$V_{(BR)ECS}$	Emitter-to-Collector Breakdown Voltage ④	20	—	—	V	$V_{GE} = 0V, I_C = 1.0A$
$\Delta V_{(BR)CES}/\Delta T_J$	Temperature Coeff. of Breakdown Voltage	—	0.30	—	V/°C	$V_{GE} = 0V, I_C = 1.0mA$
$V_{CE(on)}$	Collector-to-Emitter Saturation Voltage	—	2.5	3.8	V	$I_C = 14A, V_{GE} = 15V$ See Fig. 2, 5
		—	3.3	—		
		—	2.5	—		
$V_{GE(th)}$	Gate Threshold Voltage	3.0	—	5.5		$V_{CE} = V_{GE}, I_C = 250\mu A$
$\Delta V_{GE(th)}/\Delta T_J$	Temperature Coeff. of Threshold Voltage	—	-13	—	mV/°C	$V_{CE} = V_{GE}, I_C = 250\mu A$
g_{fe}	Forward Transconductance ⑤	3.3	6.5	—	S	$V_{CE} = 100V, I_C = 14A$
I_{CES}	Zero Gate Voltage Collector Current	—	—	600	μA	$V_{GE} = 0V, V_{CE} = 600V$
		—	—	1100		$V_{GE} = 0V, V_{CE} = 600V, T_J = 150^\circ C$
I_{GES}	Gate-to-Emitter Leakage Current	—	—	± 100	nA	$V_{GE} = \pm 20V$

Switching Characteristics @ $T_J = 25^\circ\text{C}$ (unless otherwise specified)

	Parameter	Min.	Typ.	Max.	Units	Conditions
Q_g	Total Gate Charge (turn-on)	—	39	58	nC	$I_C = 14A, V_{CC} = 400V$ See Fig. 8
Q_{ge}	Gate - Emitter Charge (turn-on)	—	8.7	13		
Q_{gc}	Gate - Collector Charge (turn-on)	—	15	23		
$t_{d(on)}$	Turn-On Delay Time	—	31	—	ns	$T_J = 25^\circ C, I_C = 14A, V_{CC} = 480V, V_{GE} = 15V, R_G = 23\Omega$ Energy losses include "tail"
t_r	Rise Time	—	23	—		
$t_{d(off)}$	Turn-Off Delay Time	—	100	150		
t_f	Fall Time	—	84	130		
E_{on}	Turn-On Switching Loss	—	0.3	—	mJ	See Fig. 9, 10, 11, 14
E_{off}	Turn-Off Switching Loss	—	0.3	—		
E_{is}	Total Switching Loss	—	0.6	0.9		
t_{sc}	Short Circuit Withstand Time	10	—	—	μs	$V_{CC} = 360V, T_J = 125^\circ C, V_{GE} = 15V, R_G = 23\Omega, V_{CPK} < 500V$
$t_{d(on)}$	Turn-On Delay Time	—	30	—	ns	$T_J = 150^\circ C, I_C = 14A, V_{CC} = 480V, V_{GE} = 15V, R_G = 23\Omega$ Energy losses include "tail"
t_r	Rise Time	—	23	—		
$t_{d(off)}$	Turn-Off Delay Time	—	170	—		
t_f	Fall Time	—	170	—		
E_{is}	Total Switching Loss	—	1.4	—	mJ	See Fig. 10, 14
L_E	Internal Emitter Inductance	—	13	—	nH	Measured 5mm from package
C_{ies}	Input Capacitance	—	740	—	pF	$V_{GE} = 0V, V_{CC} = 30V$ See Fig. 7
C_{oes}	Output Capacitance	—	92	—		
C_{ros}	Reverse Transfer Capacitance	—	9.4	—		

Notes:

- ① Repetitive rating; $V_{GE}=20V$, pulse width limited by max. junction temperature. (See fig. 13b)
- ② $V_{CC}=80\%(V_{CES}), V_{GE}=20V, L=10\mu H, R_G=23\Omega$, (See fig. 13a)
- ③ Repetitive rating; pulse width limited by maximum junction temperature.
- ④ Pulse width $\leq 80\mu s$; duty factor $\leq 0.1\%$.
- ⑤ Pulse width 5.0 μs , single shot.

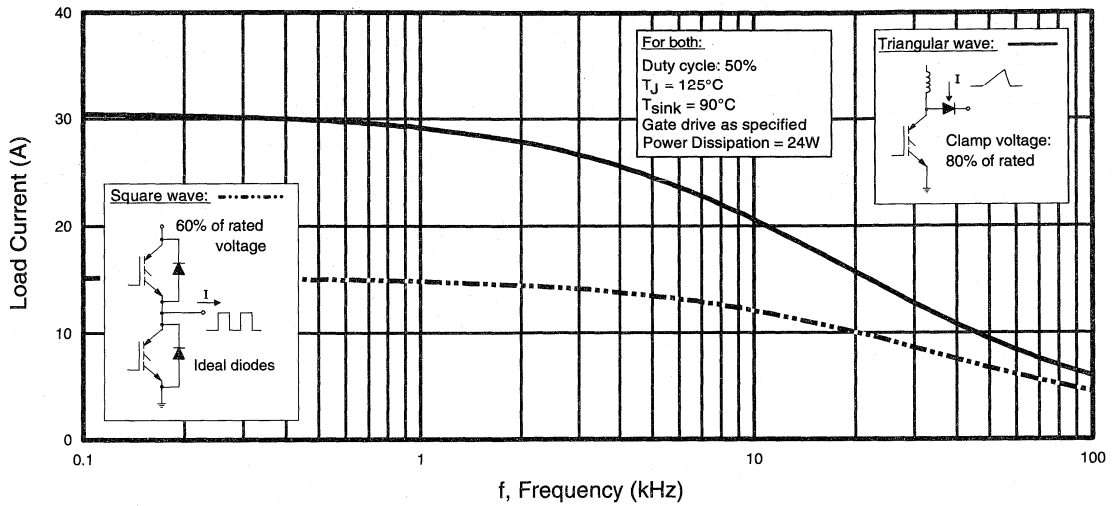


Fig. 1 - Typical Load Current vs. Frequency
 (For square wave, $I = I_{RMS}$ of fundamental; for triangular wave, $I = I_{PK}$)

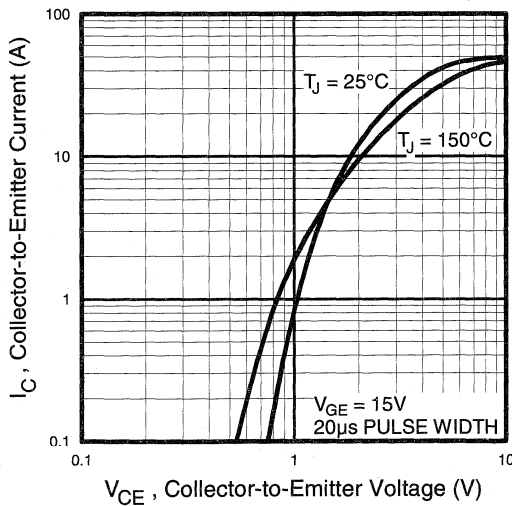


Fig. 2 - Typical Output Characteristics

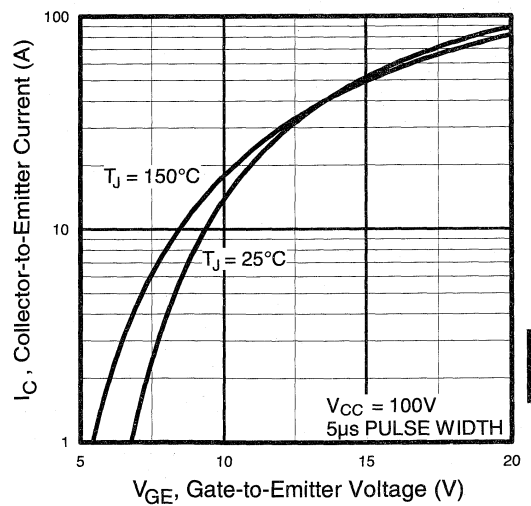


Fig. 3 - Typical Transfer Characteristics

Motor Control Ultra-Fast Discretes

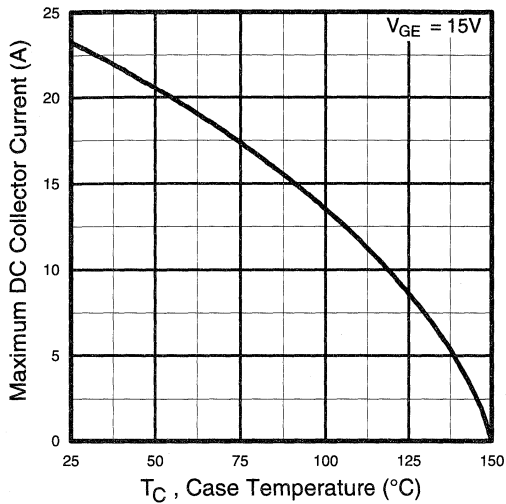


Fig. 4 - Maximum Collector Current vs. Case Temperature

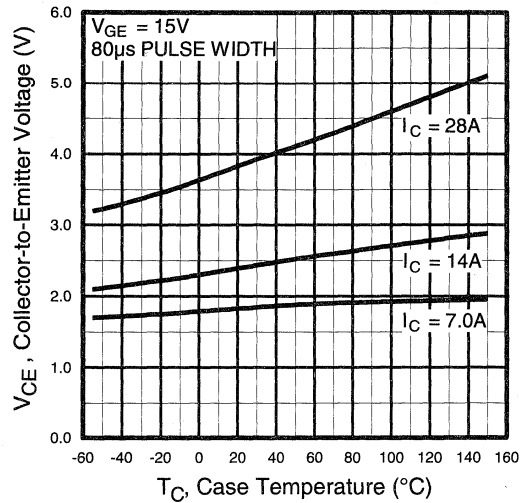


Fig. 5 - Collector-to-Emitter Voltage vs. Case Temperature

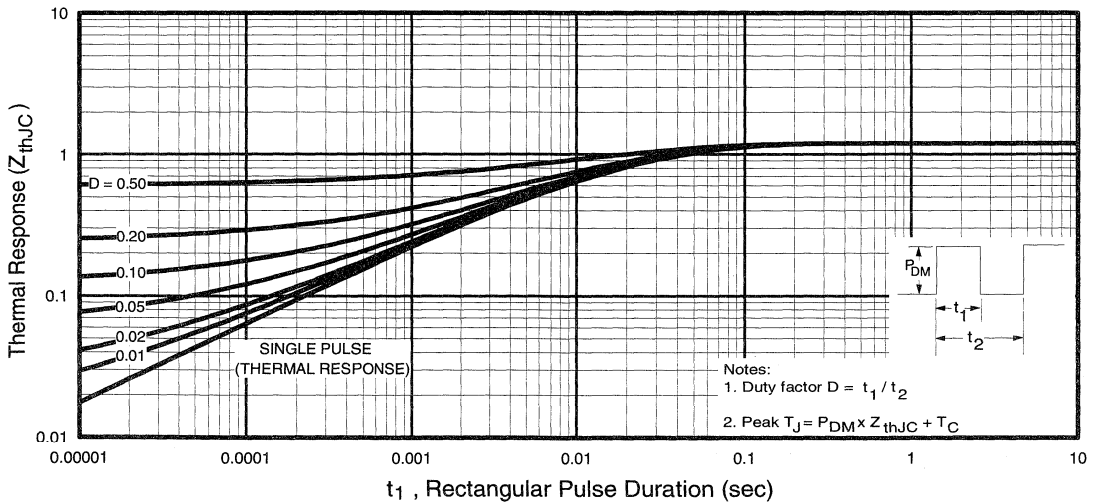


Fig. 6 - Maximum Effective Transient Thermal Impedance, Junction-to-Case

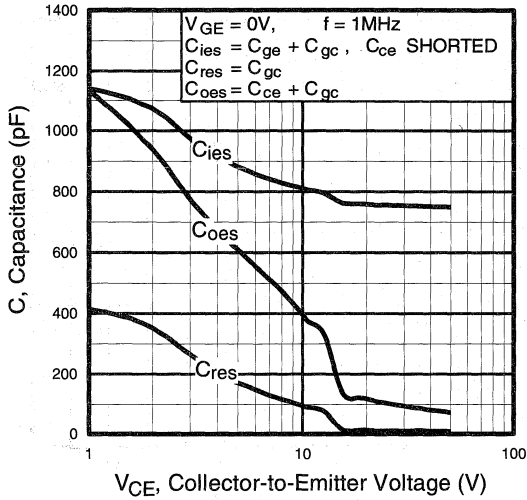


Fig. 7 - Typical Capacitance vs. Collector-to-Emitter Voltage

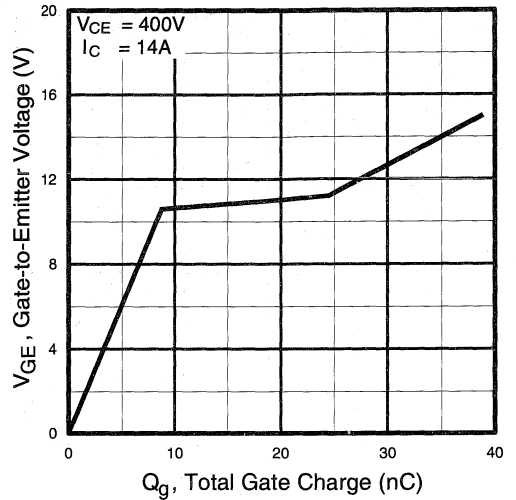


Fig. 8 - Typical Gate Charge vs. Gate-to-Emitter Voltage

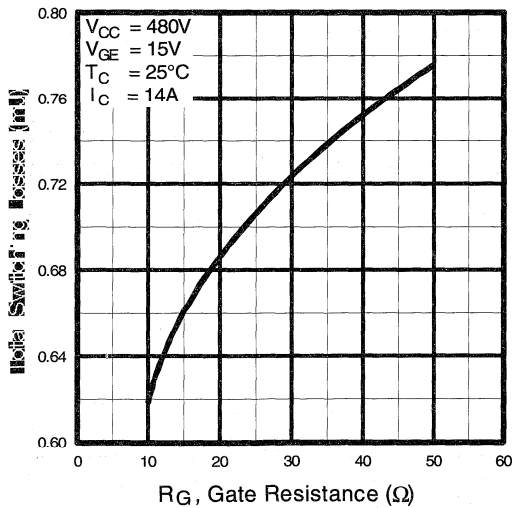


Fig. 9 - Typical Switching Losses vs. Gate Resistance

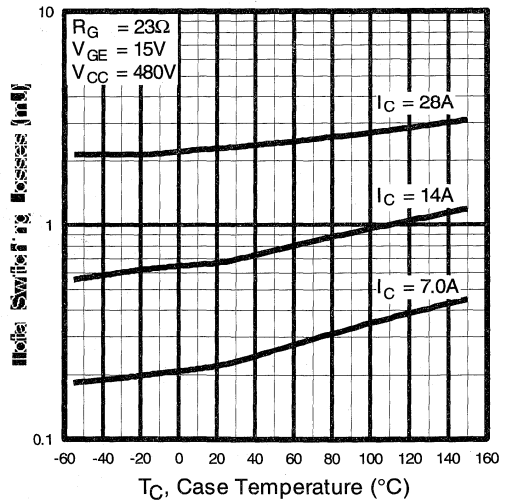


Fig. 10 - Typical Switching Losses vs. Case Temperature

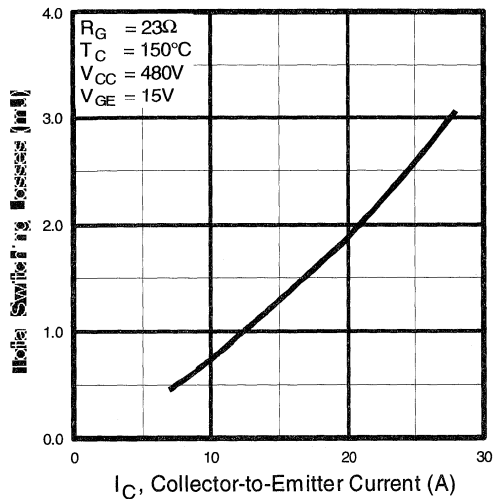


Fig. 11 - Typical Switching Losses vs. Collector-to-Emitter Current

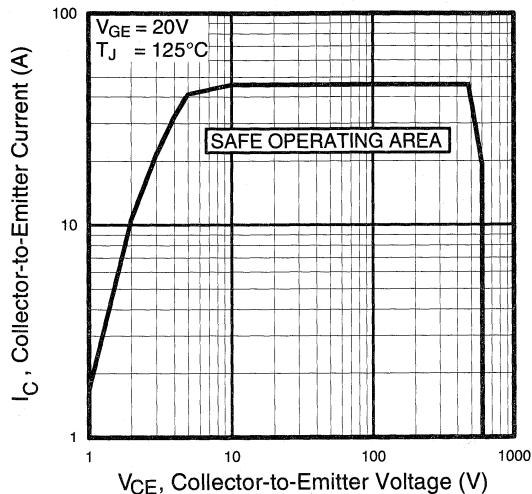


Fig. 12 - Turn-Off SOA

Refer to Section D for the following:

Appendix C: Section D - page D-5

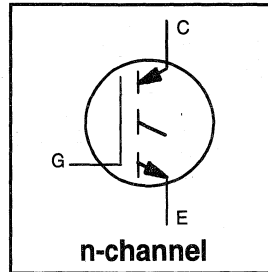
- Fig. 13a - Clamped Inductive Load Test Circuit
- Fig. 13b - Pulsed Collector Current Test Circuit
- Fig. 14a - Switching Loss Test Circuit
- Fig. 14b - Switching Loss Waveform

INSULATED GATE BIPOLAR TRANSISTOR

Short Circuit Rated
UltraFast IGBT

Features

- Short circuit rated - $10\mu\text{s}$ @ 125°C , $V_{\text{GE}} = 15\text{V}$
- Switching-loss rating includes all "tail" losses
- Optimized for high operating frequency (over 5kHz)
See Fig. 1 for Current vs. Frequency curve



$$V_{\text{CES}} = 600\text{V}$$

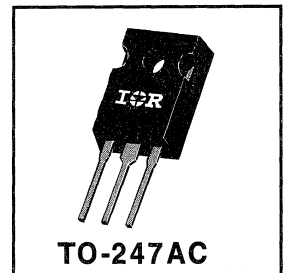
$$V_{\text{CE(sat)}} \leq 3.2\text{V}$$

$$\text{@ } V_{\text{GE}} = 15\text{V}, I_{\text{C}} = 25\text{A}$$

Description

Insulated Gate Bipolar Transistors (IGBTs) from International Rectifier have higher usable current densities than comparable bipolar transistors, while at the same time having simpler gate-drive requirements of the familiar power MOSFET. They provide substantial benefits to a host of high-voltage, high-current applications.

These new short circuit rated devices are especially suited for motor control and other applications requiring short circuit withstand capability.



Absolute Maximum Ratings

	Parameter	Max.	Units		
V_{CES}	Collector-to-Emitter Voltage	600	V		
$I_{\text{C}} @ T_{\text{C}} = 25^\circ\text{C}$	Continuous Collector Current	42	A		
$I_{\text{C}} @ T_{\text{C}} = 100^\circ\text{C}$	Continuous Collector Current	25			
I_{CM}	Pulsed Collector Current ①	84			
I_{LM}	Clamped Inductive Load Current ②	84			
t_{sc}	Short Circuit Withstand Time	10	μs		
V_{GE}	Gate-to-Emitter Voltage	± 20	V		
E_{ARV}	Reverse Voltage Avalanche Energy ③	15	mJ		
$P_{\text{D}} @ T_{\text{C}} = 25^\circ\text{C}$	Maximum Power Dissipation	160	W		
$P_{\text{D}} @ T_{\text{C}} = 100^\circ\text{C}$	Maximum Power Dissipation	65			
T_{J}	Operating Junction and Storage Temperature Range	-55 to +150	$^\circ\text{C}$		
				Soldering Temperature, for 10 sec.	300 (0.063 in. (1.6mm) from case)
				Mounting torque, 6-32 or M3 screw.	10 lbf•in (1.1N•m)

Thermal Resistance

	Parameter	Min.	Typ.	Max.	Units
$R_{\theta\text{JC}}$	Junction-to-Case	—	—	0.77	$^\circ\text{C/W}$
$R_{\theta\text{CS}}$	Case-to-Sink, flat, greased surface	—	0.24	—	
$R_{\theta\text{JA}}$	Junction-to-Ambient, typical socket mount	—	—	40	
Wt	Weight	—	6 (0.21)	—	g (oz)

Electrical Characteristics @ $T_J = 25^\circ\text{C}$ (unless otherwise specified)

	Parameter	Min.	Typ.	Max.	Units	Conditions
$V_{(BR)CES}$	Collector-to-Emitter Breakdown Voltage	600	—	—	V	$V_{GE} = 0V, I_C = 250\mu A$
$V_{(BR)ECS}$	Emitter-to-Collector Breakdown Voltage ①	20	—	—	V	$V_{GE} = 0V, I_C = 1.0A$
$\Delta V_{(BR)CES}/\Delta T_J$	Temp. Coeff. of Breakdown Voltage	—	0.46	—	V/°C	$V_{GE} = 0V, I_C = 1.0mA$
$V_{CE(on)}$	Collector-to-Emitter Saturation Voltage	—	2.1	3.2	V	$I_C = 25A$ $I_C = 42A$ $I_C = 25A, T_J = 150^\circ\text{C}$ $V_{GE} = 15V$ See Fig. 2, 5
		—	2.8	—		
		—	2.5	—		
$V_{GE(th)}$	Gate Threshold Voltage	3.0	—	5.5		$V_{CE} = V_{GE}, I_C = 250\mu A$
$\Delta V_{GE(th)}/\Delta T_J$	Temperature Coeff. of Threshold Voltage	—	-13	—	mV/°C	$V_{CE} = V_{GE}, I_C = 250\mu A$
g_{fe}	Forward Transconductance ②	7.0	14	—	S	$V_{CE} = 100V, I_C = 25A$
I_{CES}	Zero Gate Voltage Collector Current	—	—	250	μA	$V_{GE} = 0V, V_{CE} = 600V$ $V_{GE} = 0V, V_{CE} = 600V, T_J = 150^\circ\text{C}$
		—	—	1000		
I_{GES}	Gate-to-Emitter Leakage Current	—	—	± 100	nA	$V_{GE} = \pm 20V$

Switching Characteristics @ $T_J = 25^\circ\text{C}$ (unless otherwise specified)

	Parameter	Min.	Typ.	Max.	Units	Conditions		
Q_g	Total Gate Charge (turn-on)	—	61	92	nC	$I_C = 25A$ $V_{CC} = 400V$ $V_{GE} = 15V$ See Fig. 8		
Q_{ge}	Gate - Emitter Charge (turn-on)	—	13	19				
Q_{gc}	Gate - Collector Charge (turn-on)	—	22	33				
$t_{d(on)}$	Turn-On Delay Time	—	35	—	ns	$T_J = 25^\circ\text{C}$ $I_C = 25A, V_{CC} = 480V$ $V_{GE} = 15V, R_G = 10\Omega$ Energy losses include "tail"		
t_r	Rise Time	—	27	—				
$t_{d(off)}$	Turn-Off Delay Time	—	160	240				
t_f	Fall Time	—	130	200				
E_{on}	Turn-On Switching Loss	—	0.52	—			mJ	See Fig. 9, 10, 11, 14
E_{off}	Turn-Off Switching Loss	—	1.2	—				
E_{ts}	Total Switching Loss	—	1.7	2.6				
t_{sc}	Short Circuit Withstand Time	10	—	—	μs	$V_{CC} = 360V, T_J = 125^\circ\text{C}$ $V_{GE} = 15V, R_G = 10\Omega, V_{CPK} < 500V$		
$t_{d(on)}$	Turn-On Delay Time	—	34	—	ns	$T_J = 150^\circ\text{C}$ $I_C = 25A, V_{CC} = 480V$ $V_{GE} = 15V, R_G = 10\Omega$ Energy losses include "tail"		
t_r	Rise Time	—	28	—				
$t_{d(off)}$	Turn-Off Delay Time	—	300	—				
t_f	Fall Time	—	310	—				
E_{ts}	Total Switching Loss	—	3.6	—			mJ	See Fig. 10, 14
L_E	Internal Emitter Inductance	—	7.5	—				
C_{ies}	Input Capacitance	—	1500	—			pF	$V_{GE} = 0V$ $V_{CC} = 30V$ $f = 1.0MHz$ See Fig. 7
C_{oes}	Output Capacitance	—	190	—				
C_{res}	Reverse Transfer Capacitance	—	17	—				

Notes:

- ① Repetitive rating; $V_{GE}=20V$, pulse width limited by max. junction temperature. (See fig. 13b)
- ② $V_{CC}=80\%(V_{CES}), V_{GE}=20V, L=10\mu H, R_G=10\Omega$, (See fig. 13a)
- ③ Repetitive rating; pulse width limited by maximum junction temperature.
- ④ Pulse width $\leq 80\mu s$; duty factor $\leq 0.1\%$.
- ⑤ Pulse width 5.0 μs , single shot.

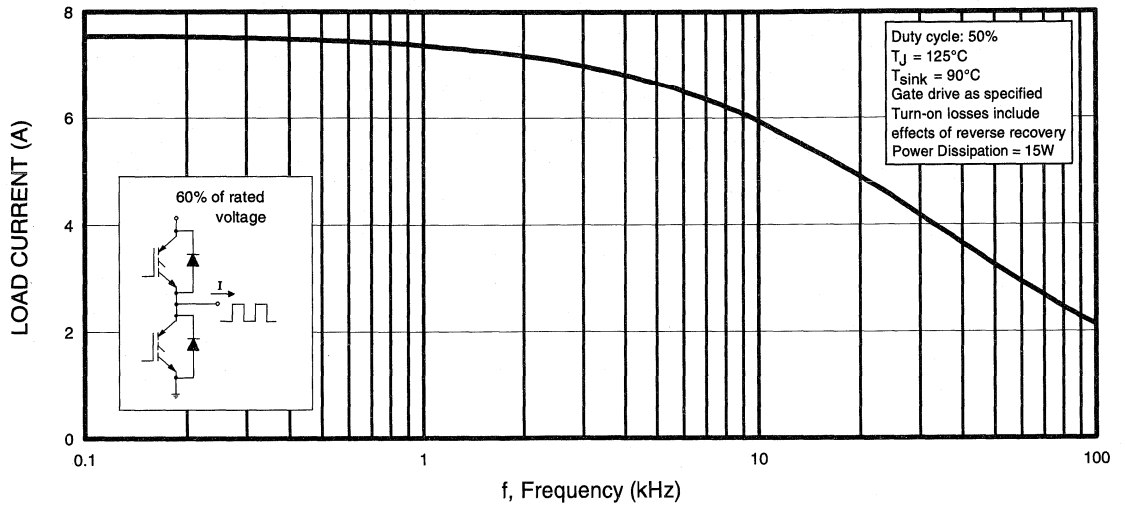


Fig. 1 - Typical Load Current vs. Frequency
 (For square wave, $I = I_{RMS}$ of fundamental; for triangular wave, $I = I_{PK}$)

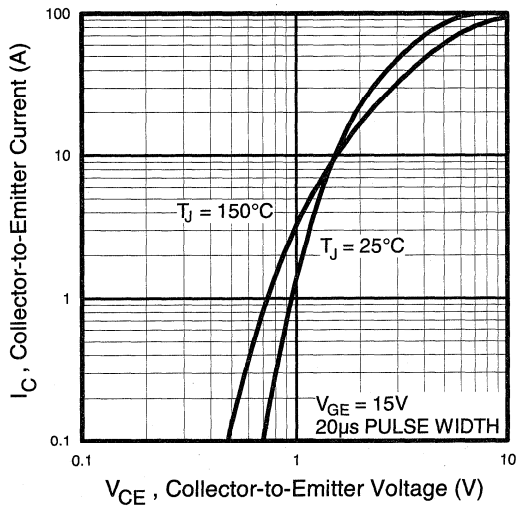


Fig. 2 - Typical Output Characteristics

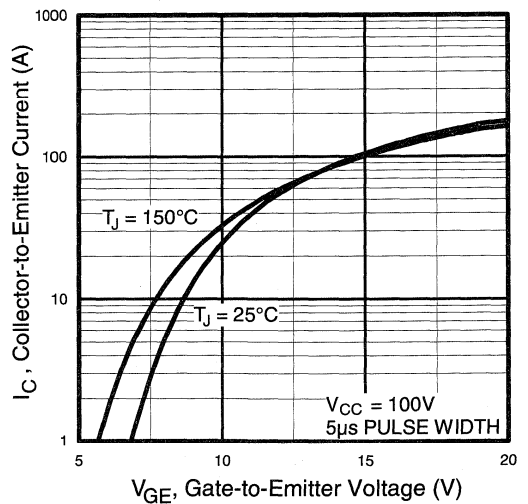


Fig. 3 - Typical Transfer Characteristics

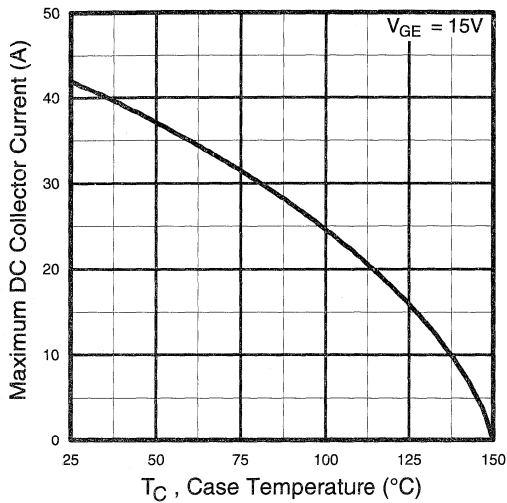


Fig. 4 - Maximum Collector Current vs. Case Temperature

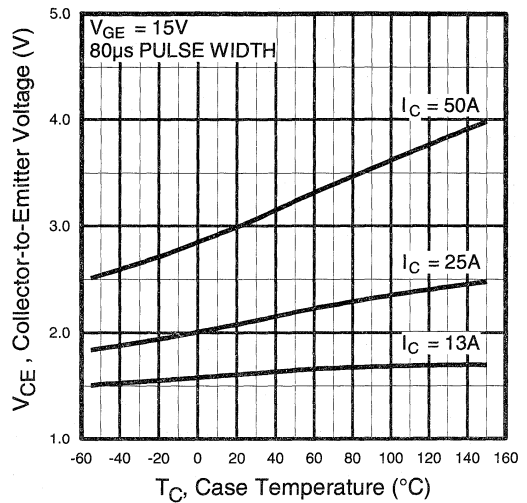


Fig. 5 - Collector-to-Emitter Voltage vs. Case Temperature

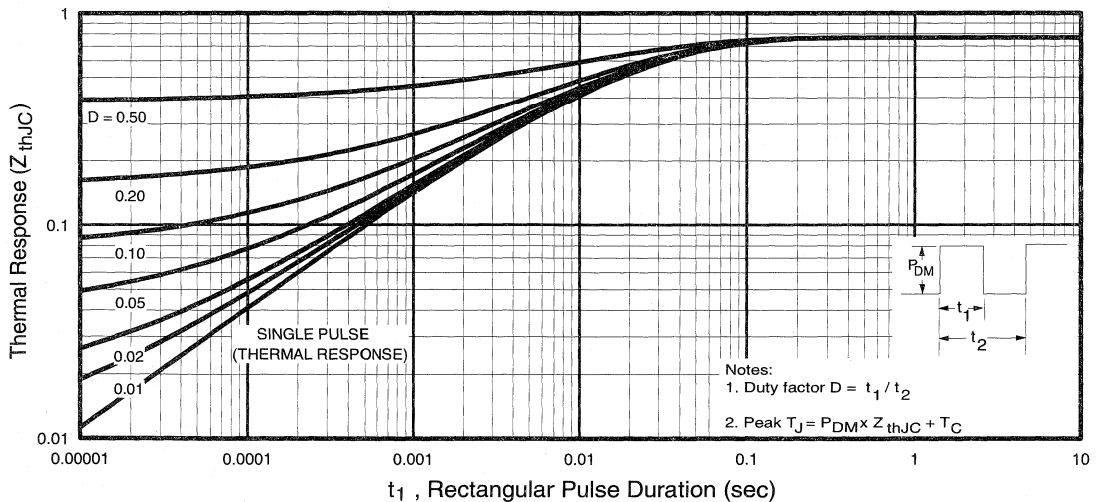


Fig. 6 - Maximum Effective Transient Thermal Impedance, Junction-to-Case

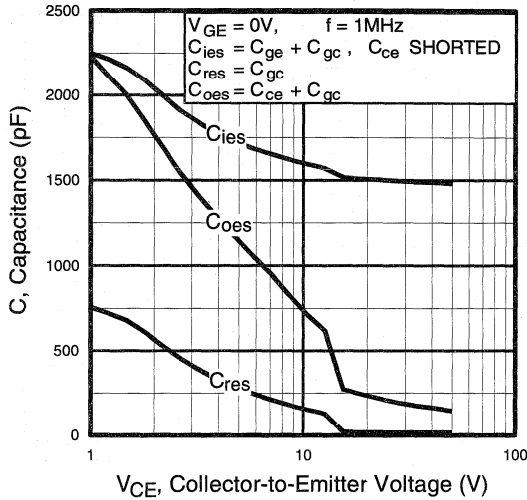


Fig. 7 - Typical Capacitance vs. Collector-to-Emitter Voltage

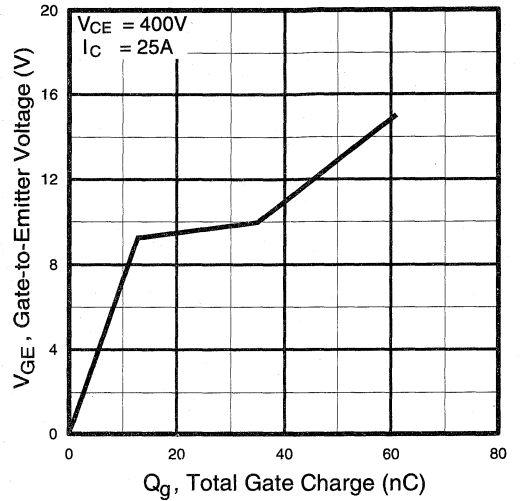


Fig. 8 - Typical Gate Charge vs. Gate-to-Emitter Voltage

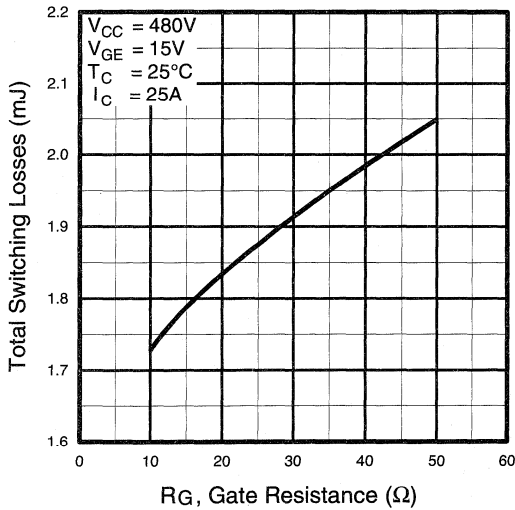


Fig. 9 - Typical Switching Losses vs. Gate Resistance

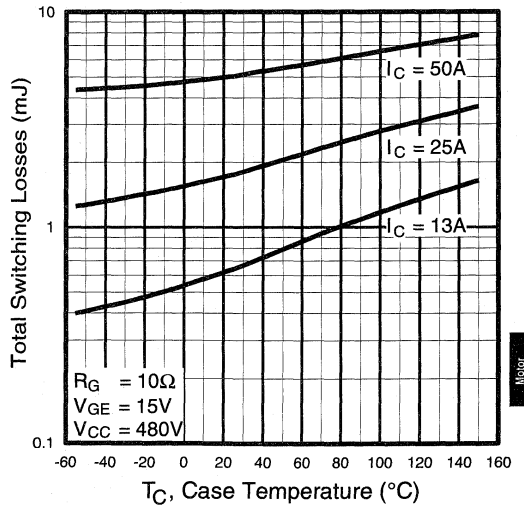


Fig. 10 - Typical Switching Losses vs. Case Temperature

Motor Control
 Ultra-Fast
 Discrets

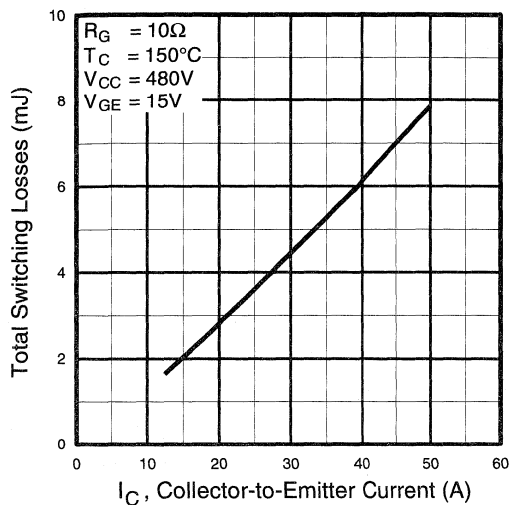


Fig. 11 - Typical Switching Losses vs. Collector-to-Emitter Current

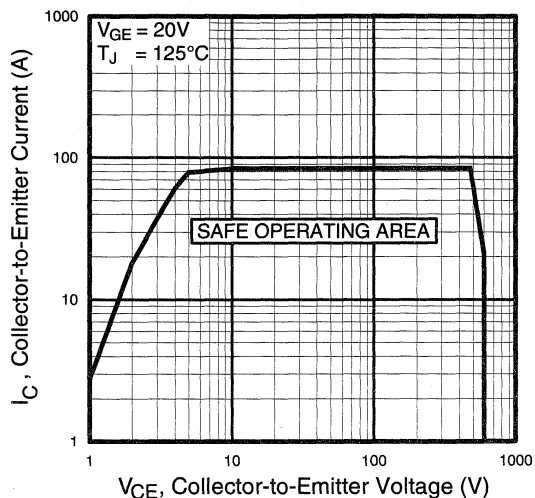


Fig. 12 - Turn-Off SOA

Refer to Section D for the following:

Appendix C: Section D - page D-5

- Fig. 13a - Clamped Inductive Load Test Circuit
- Fig. 13b - Pulsed Collector Current Test Circuit
- Fig. 14a - Switching Loss Test Circuit
- Fig. 14b - Switching Loss Waveform

Package Outline 3 - JEDEC Outline TO-247AC

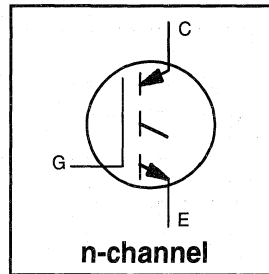
Section D - page D-13

INSULATED GATE BIPOLAR TRANSISTOR

Short Circuit Rated
UltraFast IGBT

Features

- Short circuit rated - $10\mu\text{s}$ @ 125°C , $V_{\text{GE}} = 15\text{V}$
- Switching-loss rating includes all "tail" losses
- Optimized for high operating frequency (over 5kHz)
See Fig. 1 for Current vs. Frequency Curve



$$V_{\text{CES}} = 600\text{V}$$

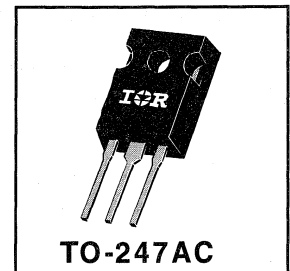
$$V_{\text{CE(sat)}} \leq 2.7\text{V}$$

$$\text{@ } V_{\text{GE}} = 15\text{V}, I_{\text{C}} = 30\text{A}$$

Description

Insulated Gate Bipolar Transistors (IGBTs) from International Rectifier have higher usable current densities than comparable bipolar transistors, while at the same time having simpler gate-drive requirements of the familiar power MOSFET. They provide substantial benefits to a host of high-voltage, high-current applications.

These new short circuit rated devices are especially suited for motor control and other applications requiring short circuit withstand capability.



Absolute Maximum Ratings

	Parameter	Max.	Units
V_{CES}	Collector-to-Emitter Voltage	600	V
$I_{\text{C}} @ T_{\text{C}} = 25^\circ\text{C}$	Continuous Collector Current	52	A
$I_{\text{C}} @ T_{\text{C}} = 100^\circ\text{C}$	Continuous Collector Current	30	
I_{CM}	Pulsed Collector Current ①	100	
I_{LM}	Clamped Inductive Load Current ②	100	
t_{sc}	Short Circuit Withstand Time	10	μs
V_{GE}	Gate-to-Emitter Voltage	± 20	V
E_{ARV}	Reverse Voltage Avalanche Energy ③	20	mJ
$P_{\text{D}} @ T_{\text{C}} = 25^\circ\text{C}$	Maximum Power Dissipation	200	W
$P_{\text{D}} @ T_{\text{C}} = 100^\circ\text{C}$	Maximum Power Dissipation	52	
T_{J}	Operating Junction and Storage Temperature Range	-55 to +150	$^\circ\text{C}$
T_{STG}			
	Soldering Temperature, for 10 sec.	300 (0.063 in. (1.6mm) from case)	
	Mounting torque, 6-32 or M3 screw.	10 lbf•in (1.1N•m)	

Thermal Resistance

	Parameter	Min.	Typ.	Max.	Units
$R_{\theta\text{JC}}$	Junction-to-Case	—	—	0.64	$^\circ\text{C/W}$
$R_{\theta\text{CS}}$	Case-to-Sink, flat, greased surface	—	0.24	—	
$R_{\theta\text{JA}}$	Junction-to-Ambient, typical socket mount	—	—	40	
Wt	Weight	—	6 (0.21)	—	g (oz)

Electrical Characteristics @ $T_J = 25^\circ\text{C}$ (unless otherwise specified)

	Parameter	Min.	Typ.	Max.	Units	Conditions
$V_{(BR)CES}$	Collector-to-Emitter Breakdown Voltage	600	—	—	V	$V_{GE} = 0V, I_C = 250\mu A$
$V_{(BR)ECS}$	Emitter-to-Collector Breakdown Voltage ④	20	—	—	V	$V_{GE} = 0V, I_C = 1.0A$
$\Delta V_{(BR)CES}/\Delta T_J$	Temp. Coeff. of Breakdown Voltage	—	0.60	—	V/ $^\circ\text{C}$	$V_{GE} = 0V, I_C = 1.0mA$
$V_{CE(on)}$	Collector-to-Emitter Saturation Voltage	—	2.1	2.7	V	$I_C = 30A$ $I_C = 52A$ $I_C = 30A, T_J = 150^\circ\text{C}$ $V_{CE} = V_{GE}, I_C = 250\mu A$
		—	2.6	—		
		—	2.3	—		
$V_{GE(th)}$	Gate Threshold Voltage	3.0	—	5.5		$V_{CE} = V_{GE}, I_C = 250\mu A$
$\Delta V_{GE(th)}/\Delta T_J$	Temperature Coeff. of Threshold Voltage	—	-14	—	mV/ $^\circ\text{C}$	$V_{CE} = V_{GE}, I_C = 250\mu A$
g_{fe}	Forward Transconductance ⑤	9.8	17	—	S	$V_{CE} = 100V, I_C = 30A$
I_{CES}	Zero Gate Voltage Collector Current	—	—	250	μA	$V_{GE} = 0V, V_{CE} = 600V$ $V_{GE} = 0V, V_{CE} = 600V, T_J = 150^\circ\text{C}$
		—	—	5000		
I_{GES}	Gate-to-Emitter Leakage Current	—	—	± 100	nA	$V_{GE} = \pm 20V$

Switching Characteristics @ $T_J = 25^\circ\text{C}$ (unless otherwise specified)

	Parameter	Min.	Typ.	Max.	Units	Conditions
Q_g	Total Gate Charge (turn-on)	—	120	200	nC	$I_C = 30A$ $V_{CC} = 400V$ $V_{GE} = 15V$ See Fig. 8
Q_{ge}	Gate - Emitter Charge (turn-on)	—	27	42		
Q_{gc}	Gate - Collector Charge (turn-on)	—	44	73		
$t_{d(on)}$	Turn-On Delay Time	—	35	—	ns	$T_J = 25^\circ\text{C}$ $I_C = 30A, V_{CC} = 480V$ $V_{GE} = 15V, R_G = 5.0\Omega$ Energy losses include "tail"
t_r	Rise Time	—	27	—		
$t_{d(off)}$	Turn-Off Delay Time	—	130	200		
t_f	Fall Time	—	76	110		
E_{on}	Turn-On Switching Loss	—	0.9	—		
E_{off}	Turn-Off Switching Loss	—	0.5	—	mJ	See Fig. 9, 10, 11, 14
E_{ts}	Total Switching Loss	—	1.4	2.1		
t_{sc}	Short Circuit Withstand Time	10	—	—	μs	$V_{CC} = 360V, T_J = 125^\circ\text{C}$ $V_{GE} = 15V, R_G = 5.0\Omega$
$t_{d(on)}$	Turn-On Delay Time	—	32	—	ns	$T_J = 150^\circ\text{C}$, $I_C = 30A, V_{CC} = 480V$ $V_{GE} = 15V, R_G = 5.0\Omega$ Energy losses include "tail"
t_r	Rise Time	—	27	—		
$t_{d(off)}$	Turn-Off Delay Time	—	480	—		
t_f	Fall Time	—	450	—		
E_{ts}	Total Switching Loss	—	2.8	—		
L_E	Internal Emitter Inductance	—	13	—	nH	Measured 5mm from package
C_{ies}	Input Capacitance	—	2900	—	pF	$V_{GE} = 0V$ $V_{CC} = 30V$ $f = 1.0MHz$ See Fig. 7
C_{oes}	Output Capacitance	—	220	—		
C_{res}	Reverse Transfer Capacitance	—	30	—		

Notes:

- ① Repetitive rating; $V_{GE}=20V$, pulse width limited by max. junction temperature. (See fig. 13b)
- ② $V_{CC}=80\%(V_{CES})$, $V_{GE}=20V$, $L=10\mu H$, $R_G=5.0\Omega$, (See fig. 13a)
- ③ Repetitive rating; pulse width limited by maximum junction temperature.
- ④ Pulse width $\leq 80\mu s$; duty factor $\leq 0.1\%$.
- ⑤ Pulse width $5.0\mu s$, single shot.

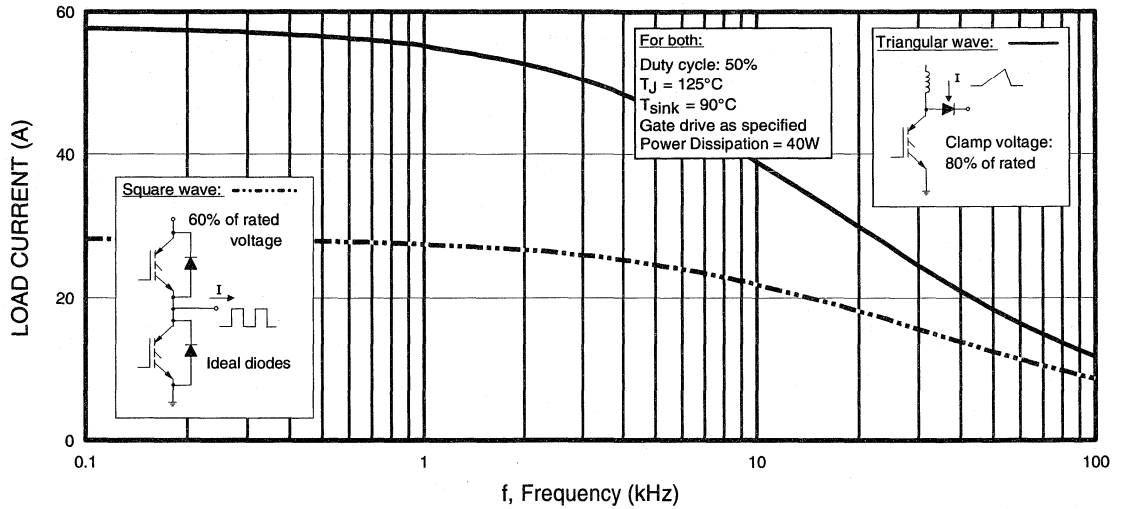


Fig. 1 - Typical Load Current vs. Frequency
 (For square wave, $I = I_{RMS}$ of fundamental; for triangular wave, $I = I_{PK}$)

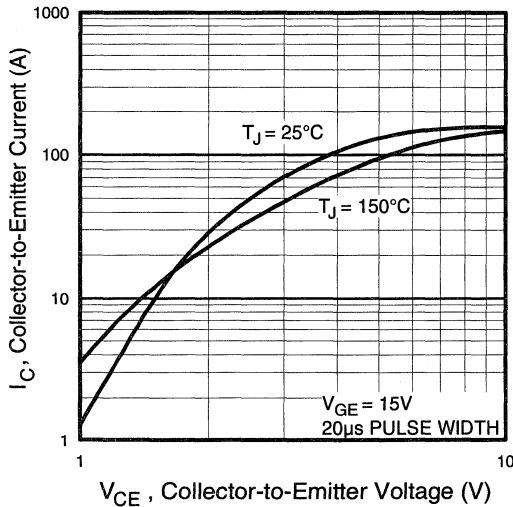


Fig. 2 - Typical Output Characteristics

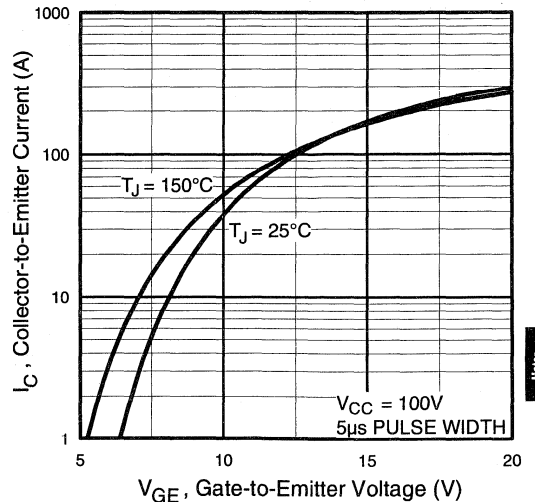


Fig. 3 - Typical Transfer Characteristics

Motor Control
 Ultra-Fast
 Discretes

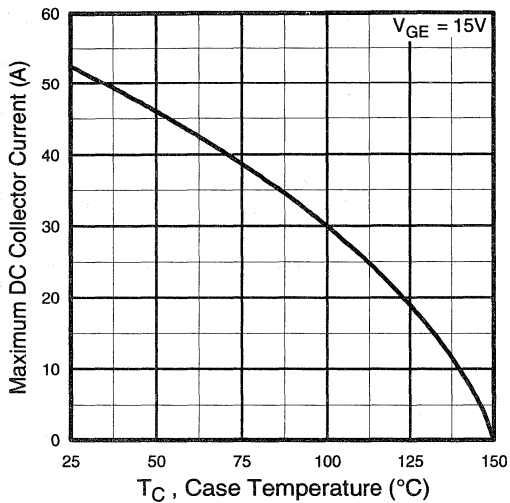


Fig. 4 - Maximum Collector Current vs. Case Temperature

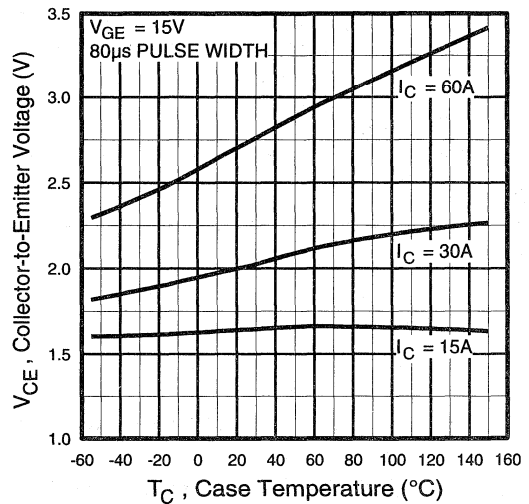


Fig. 5 - Collector-to-Emitter Voltage vs. Case Temperature

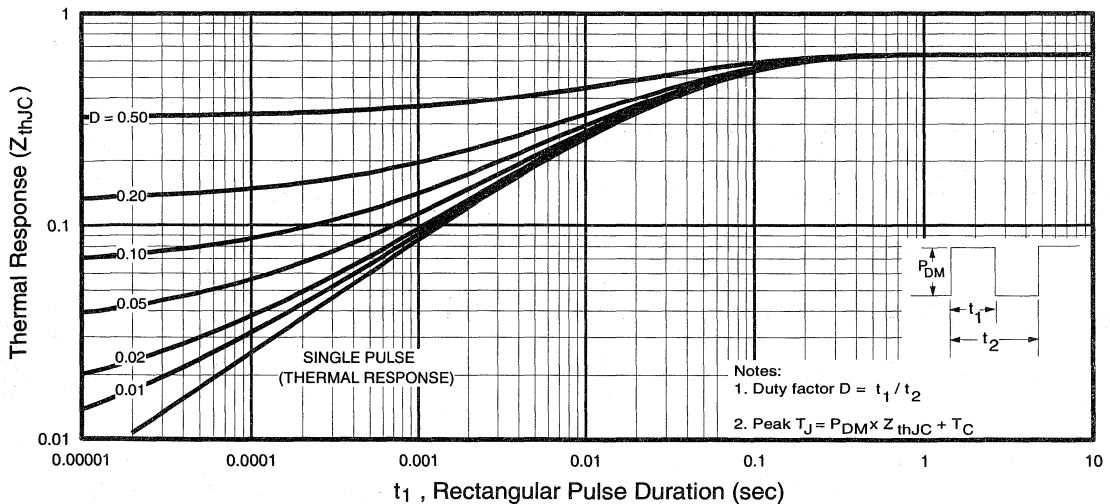


Fig. 6 - Maximum Effective Transient Thermal Impedance, Junction-to-Case

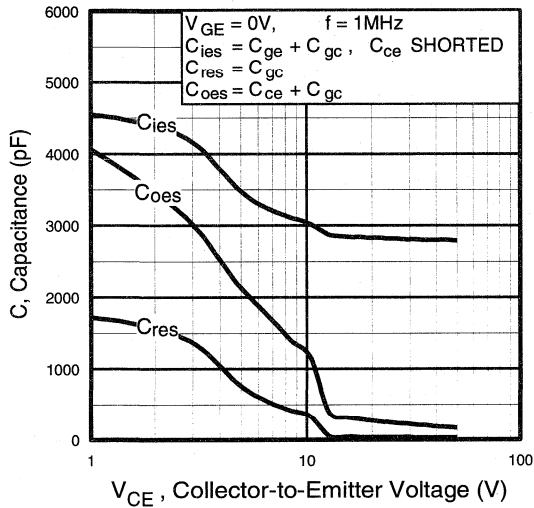


Fig. 7 - Typical Capacitance vs. Collector-to-Emitter Voltage

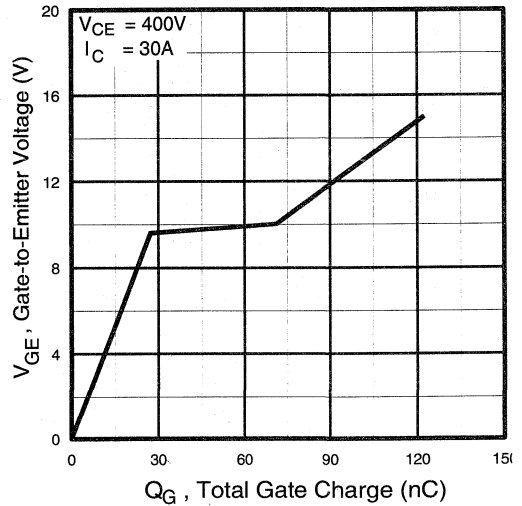


Fig. 8 - Typical Gate Charge vs. Gate-to-Emitter Voltage

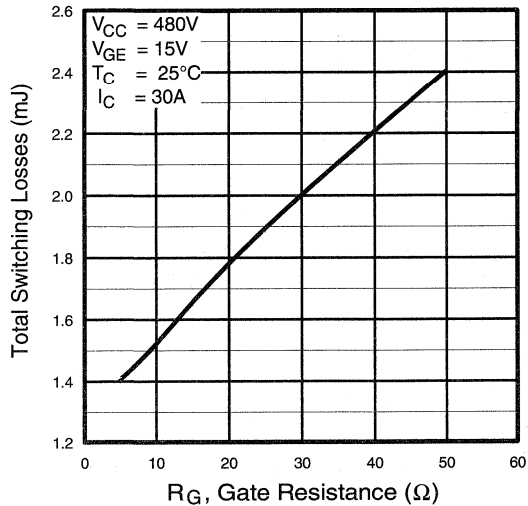


Fig. 9 - Typical Switching Losses vs. Gate Resistance

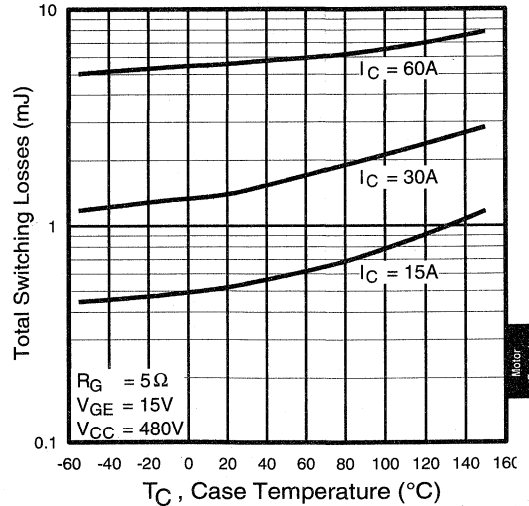


Fig. 10 - Typical Switching Losses vs. Case Temperature

Motor Control
 Ultra-Fast
 Discretes

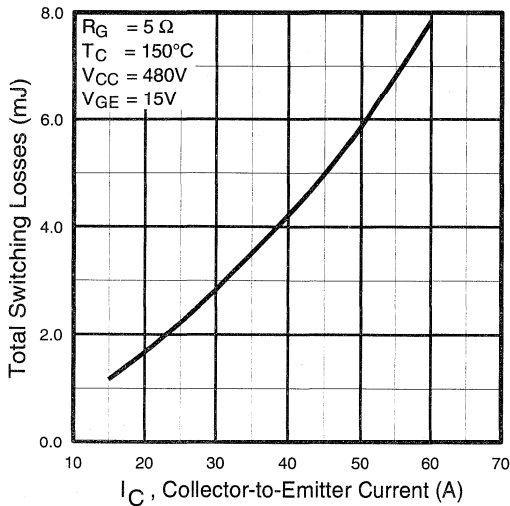


Fig. 11 - Typical Switching Losses vs. Collector-to-Emitter Current

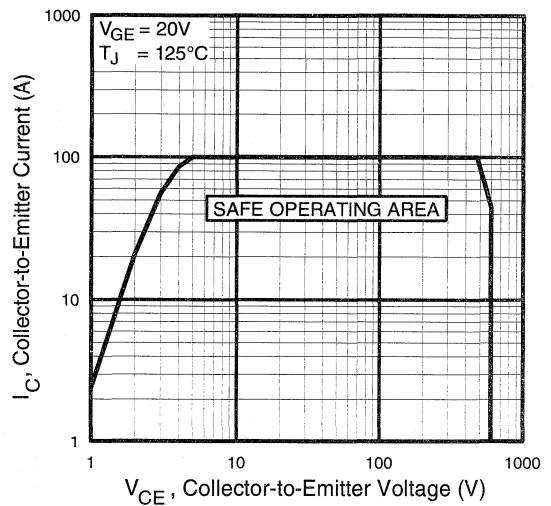


Fig. 12 - Turn-Off SOA

Refer to Section D for the following:

Appendix C: Section D - page D-5

- Fig. 13a - Clamped Inductive Load Test Circuit
- Fig. 13b - Pulsed Collector Current Test Circuit
- Fig. 14a - Switching Loss Test Circuit
- Fig. 14b - Switching Loss Waveform

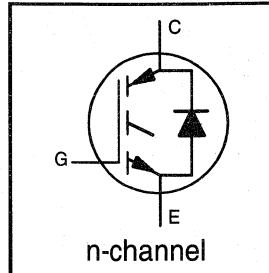
IRGBC20KD2

INSULATED GATE BIPOLAR TRANSISTOR
WITH ULTRAFAST SOFT RECOVERY DIODE

Short Circuit Rated
UltraFast CoPack IGBT

Features

- Short circuit rated -10 μ s @ 125°C, $V_{GE} = 15V$
- Switching-loss rating includes all "tail" losses
- HEXFRED™ soft ultrafast diodes
- Optimized for high operating frequency (over 5kHz)
See Fig. 1 for Current vs. Frequency curve

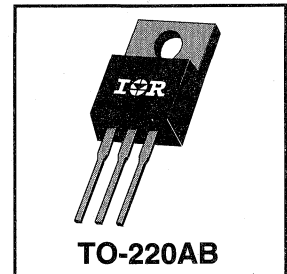


$V_{CES} = 600V$
$V_{CE(sat)} \leq 3.5V$
@ $V_{GE} = 15V, I_C = 6.0A$

Description

Co-packaged IGBTs are a natural extension of International Rectifier's well known IGBT line. They provide the convenience of an IGBT and an ultrafast recovery diode in one package, resulting in substantial benefits to a host of high-voltage, high-current, applications.

These new short circuit rated devices are especially suited for motor control and other applications requiring short circuit withstand capability.



Absolute Maximum Ratings

	Parameter	Max.	Units
V_{CES}	Collector-to-Emitter Voltage	600	V
$I_C @ T_C = 25^\circ C$	Continuous Collector Current	10	A
$I_C @ T_C = 100^\circ C$	Continuous Collector Current	6.0	
I_{CM}	Pulsed Collector Current ①	20	
I_{LM}	Clamped Inductive Load Current ②	20	
$I_F @ T_C = 100^\circ C$	Diode Continuous Forward Current	7.0	
I_{FM}	Diode Maximum Forward Current	20	
t_{sc}	Short Circuit Withstand Time	10	μ s
V_{GE}	Gate-to-Emitter Voltage	± 20	V
$P_D @ T_C = 25^\circ C$	Maximum Power Dissipation	60	W
$P_D @ T_C = 100^\circ C$	Maximum Power Dissipation	24	
T_J	Operating Junction and Storage Temperature Range	-55 to +150	$^\circ C$
T_{STG}			
	Mounting Torque, 6-32 or M3 Screw.	10 lbf•in (1.1 N•m)	

Thermal Resistance

	Parameter	Min.	Typ.	Max.	Units
$R_{\theta JC}$	Junction-to-Case - IGBT	—	—	2.1	$^\circ C/W$
$R_{\theta JC}$	Junction-to-Case - Diode	—	—	3.5	
$R_{\theta CS}$	Case-to-Sink, flat, greased surface	—	0.50	—	
$R_{\theta JA}$	Junction-to-Ambient, typical socket mount	—	—	80	
Wt	Weight	—	2 (0.07)	—	g (oz)

Electrical Characteristics @ T_J = 25°C (unless otherwise specified)

	Parameter	Min.	Typ.	Max.	Units	Conditions
V _{(BR)CES}	Collector-to-Emitter Breakdown Voltage ^①	600	—	—	V	V _{GE} = 0V, I _C = 250μA
ΔV _{(BR)CES} /ΔT _J	Temp. Coeff. of Breakdown Voltage	—	0.37	—	V/°C	V _{GE} = 0V, I _C = 1.0mA
V _{CE(on)}	Collector-to-Emitter Saturation Voltage	—	2.4	3.5	V	I _C = 6.0A V _{GE} = 15V
		—	3.6	—		I _C = 10A See Fig. 2, 5
		—	2.8	—		I _C = 6.0A, T _J = 150°C
V _{GE(th)}	Gate Threshold Voltage	3.0	—	5.5		V _{CE} = V _{GE} , I _C = 250μA
ΔV _{GE(th)} /ΔT _J	Temperature Coeff. of Threshold Voltage	—	-11	—	mV/°C	V _{CE} = V _{GE} , I _C = 250μA
g _{fe}	Forward Transconductance ^②	1.9	3.3	—	S	V _{CE} = 100V, I _C = 6.0A
I _{CES}	Zero Gate Voltage Collector Current	—	—	250	μA	V _{GE} = 0V, V _{CE} = 600V
		—	—	1700		V _{GE} = 0V, V _{CE} = 600V, T _J = 150°C
V _{FM}	Diode Forward Voltage Drop	—	1.4	1.7	V	I _C = 8.0A See Fig. 13
		—	1.4	1.7		I _C = 8.0A, T _J = 150°C
I _{GES}	Gate-to-Emitter Leakage Current	—	—	±100	nA	V _{GE} = ±20V

Switching Characteristics @ T_J = 25°C (unless otherwise specified)

	Parameter	Min.	Typ.	Max.	Units	Conditions
Q _g	Total Gate Charge (turn-on)	—	17	26		I _C = 6.0A
Q _{ge}	Gate - Emitter Charge (turn-on)	—	4.3	6.8	nC	V _{CC} = 480V
Q _{gc}	Gate - Collector Charge (turn-on)	—	6.4	11		See Fig. 8
t _{d(on)}	Turn-On Delay Time	—	59	—	ns	T _J = 25°C
t _r	Rise Time	—	38	—		I _C = 6.0A, V _{CC} = 480V
t _{d(off)}	Turn-Off Delay Time	—	110	210		V _{GE} = 15V, R _G = 50Ω
t _f	Fall Time	—	80	120		Energy losses include "tail" and diode reverse recovery.
E _{on}	Turn-On Switching Loss	—	0.28	—	mJ	See Fig. 9, 10, 11, 18
E _{off}	Turn-Off Switching Loss	—	0.15	—		
E _{ts}	Total Switching Loss	—	0.43	0.90		
t _{sc}	Short Circuit Withstand Time	10	—	—	μs	V _{CC} = 360V, T _J = 125°C V _{GE} = 15V, R _G = 50Ω, V _{CPK} < 500V
t _{d(on)}	Turn-On Delay Time	—	52	—	ns	T _J = 150°C, See Fig. 9, 10, 11, 18
t _r	Rise Time	—	35	—		I _C = 6.0A, V _{CC} = 480V
t _{d(off)}	Turn-Off Delay Time	—	170	—		V _{GE} = 15V, R _G = 50Ω
t _f	Fall Time	—	170	—		Energy losses include "tail" and diode reverse recovery.
E _{ts}	Total Switching Loss	—	0.7	—	mJ	
L _E	Internal Emitter Inductance	—	7.5	—	nH	Measured 5mm from package
C _{ies}	Input Capacitance	—	350	—	pF	V _{GE} = 0V
C _{oes}	Output Capacitance	—	50	—		V _{CC} = 30V See Fig. 7
C _{res}	Reverse Transfer Capacitance	—	4.7	—		f = 1.0MHz
t _{rr}	Diode Reverse Recovery Time	—	37	55	ns	T _J = 25°C See Fig.
		—	55	90		T _J = 125°C 14
I _{rr}	Diode Peak Reverse Recovery Current	—	3.5	5.0	A	T _J = 25°C See Fig.
		—	4.5	8.0		T _J = 125°C 15
Q _{rr}	Diode Reverse Recovery Charge	—	65	138	nC	T _J = 25°C See Fig.
		—	124	360		T _J = 125°C 16
di _(rec) M/dt	Diode Peak Rate of Fall of Recovery During t _b	—	240	—	A/μs	T _J = 25°C See Fig.
		—	210	—		T _J = 125°C 17

Notes:

① Repetitive rating; V_{GE}=20V, pulse width limited by max. junction temperature. (See fig. 20)

② V_{CC}=80%(V_{CES}), V_{GE}=20V, L=10μH, R_G= 50Ω, (See fig. 19)

③ Pulse width 5.0μs, single shot.

④ Pulse width ≤ 80μs; duty factor ≤ 0.1%.

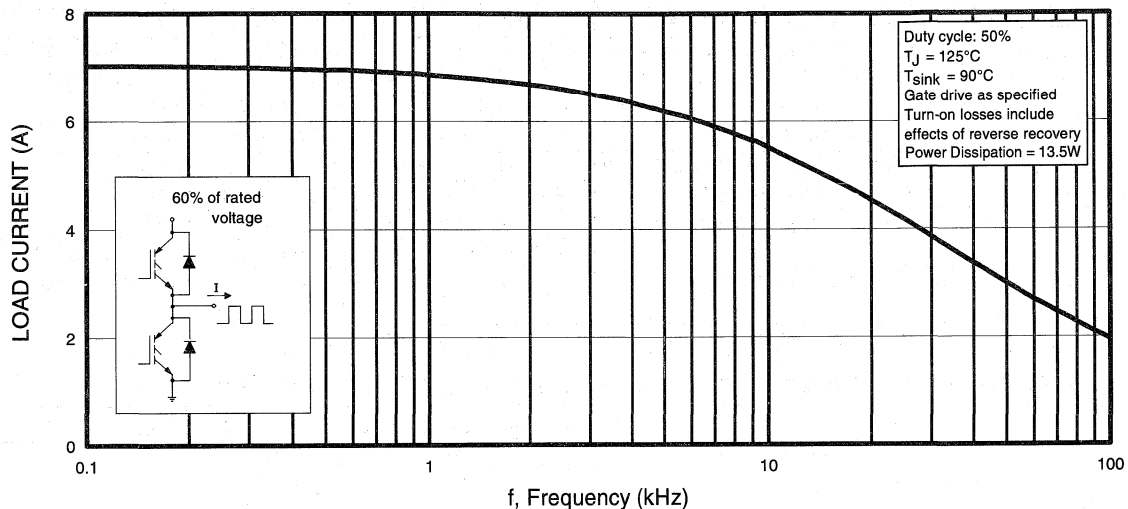


Fig. 1 - Typical Load Current vs. Frequency
(Load Current = I_{RMS} of fundamental)

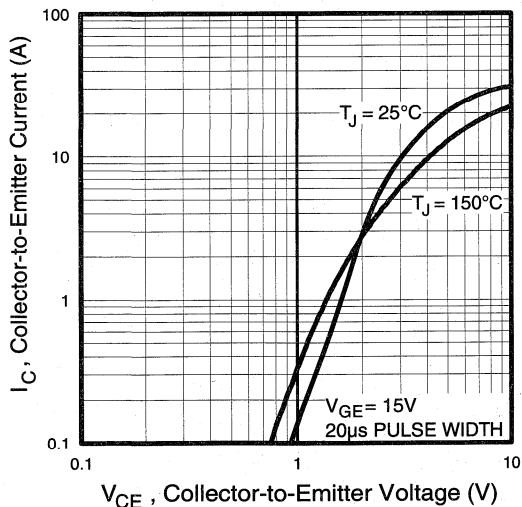


Fig. 2 - Typical Output Characteristics

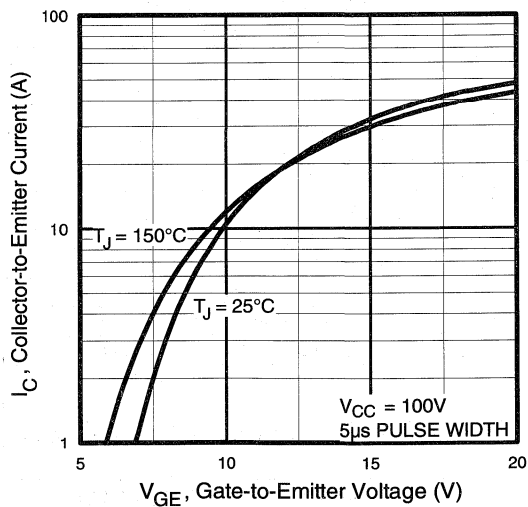


Fig. 3 - Typical Transfer Characteristics

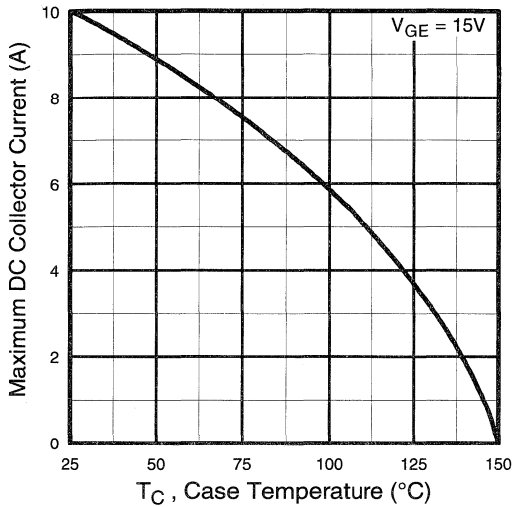


Fig. 4 - Maximum Collector Current vs. Case Temperature

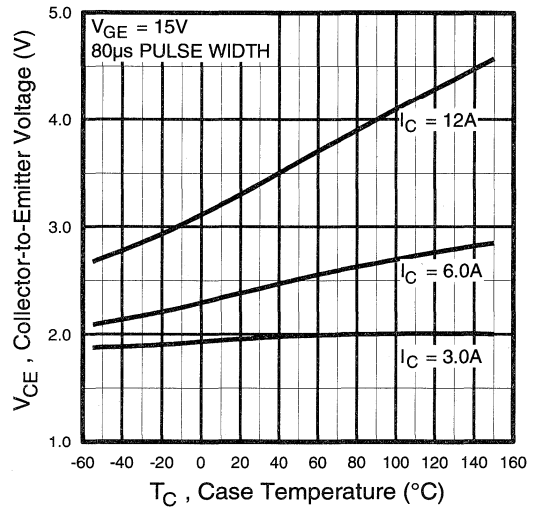


Fig. 5 - Collector-to-Emitter Voltage vs. Case Temperature

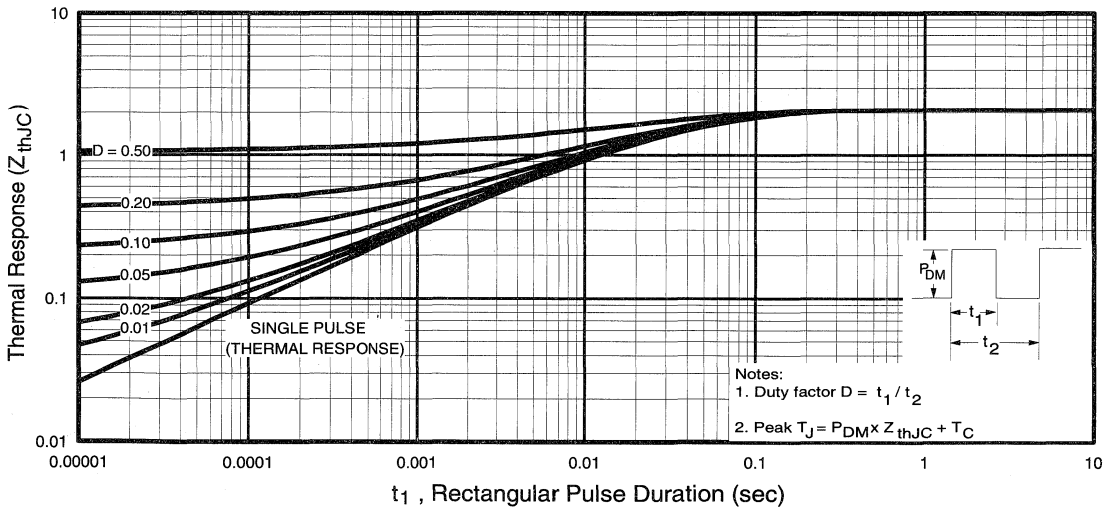


Fig. 6 - Maximum IGBT Effective Transient Thermal Impedance, Junction-to-Case

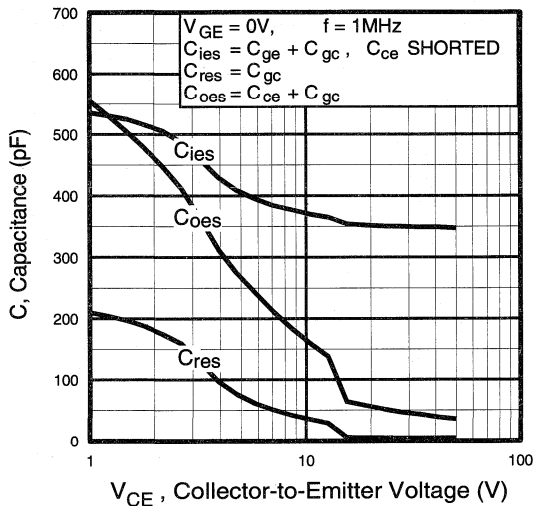


Fig. 7 - Typical Capacitance vs. Collector-to-Emitter Voltage

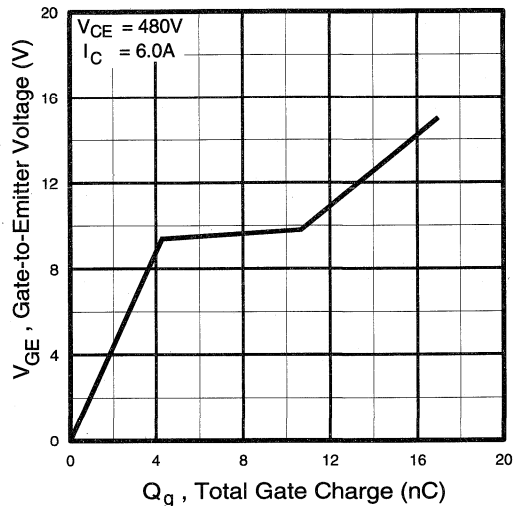


Fig. 8 - Typical Gate Charge vs. Gate-to-Emitter Voltage

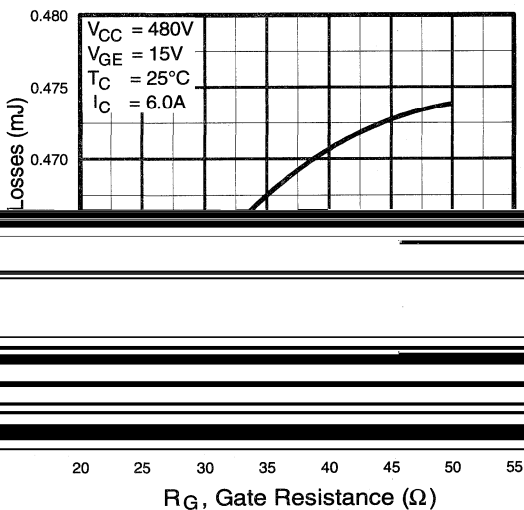


Fig. 9 - Typical Switching Losses vs. Gate Resistance

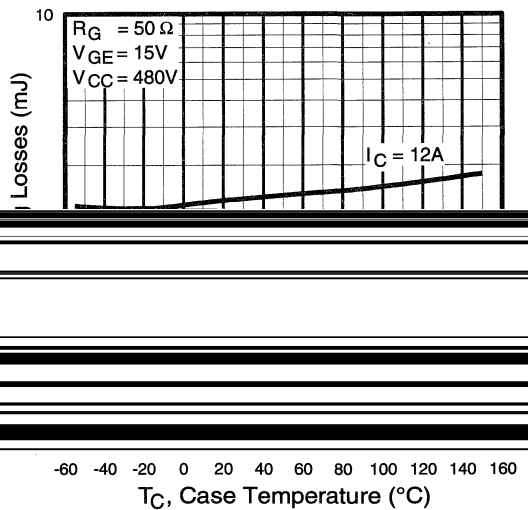


Fig. 10 - Typical Switching Losses vs. Case Temperature

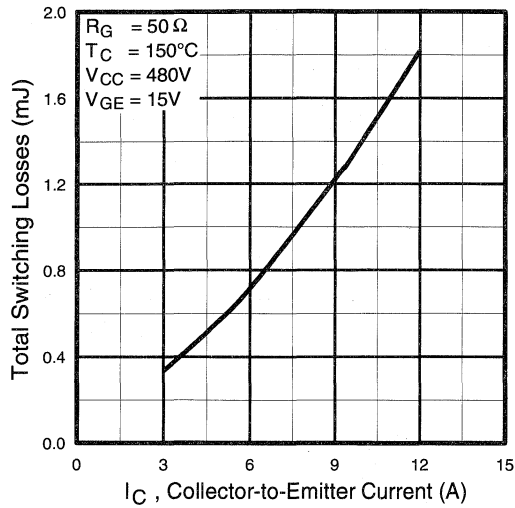


Fig. 11 - Typical Switching Losses vs. Collector-to-Emitter Current

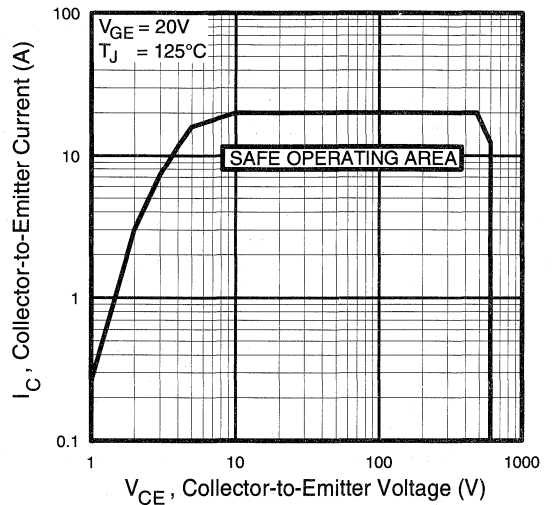


Fig. 12 - Turn-Off SOA

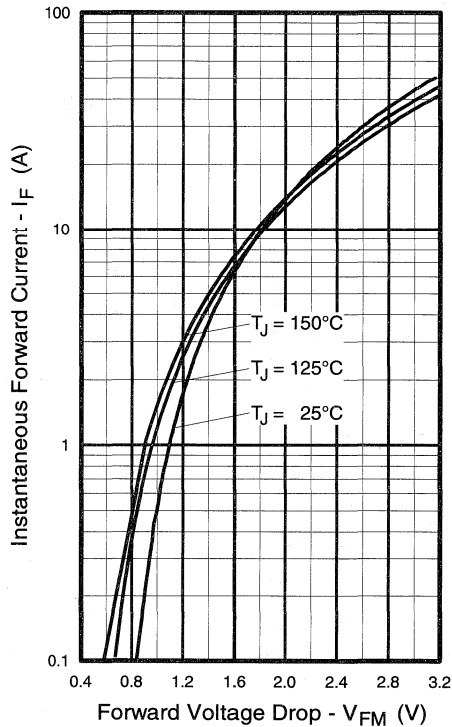


Fig. 13 - Maximum Forward Voltage Drop vs. Instantaneous Forward Current

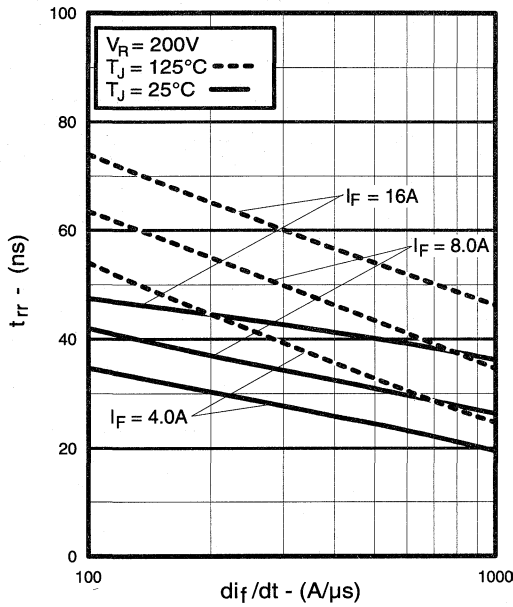


Fig. 14 - Typical Reverse Recovery vs. di_f/dt

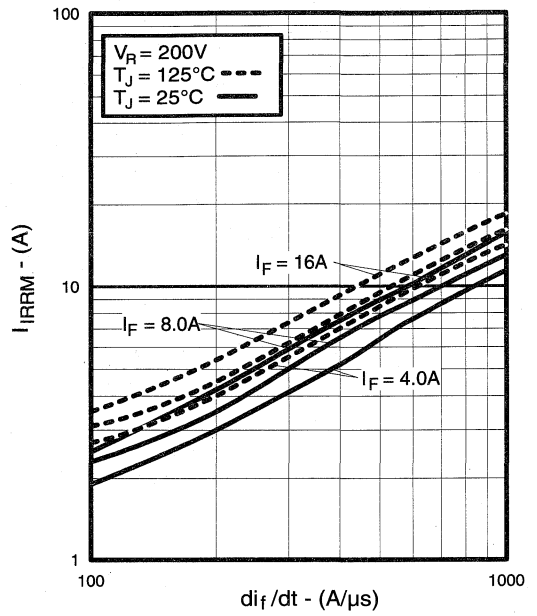


Fig. 15 - Typical Recovery Current vs. di_f/dt

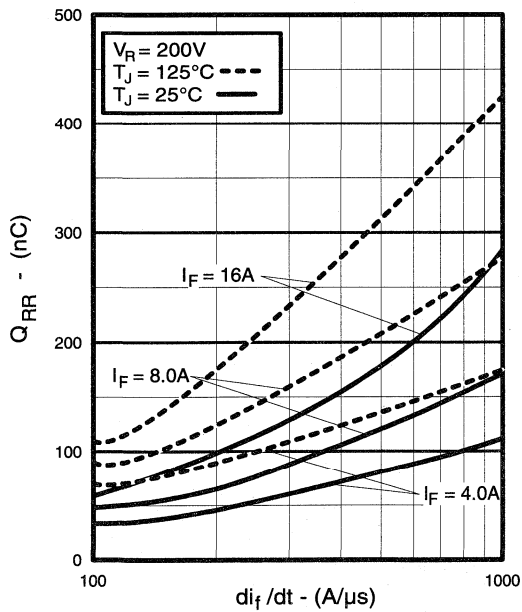


Fig. 16 - Typical Stored Charge vs. di_f/dt

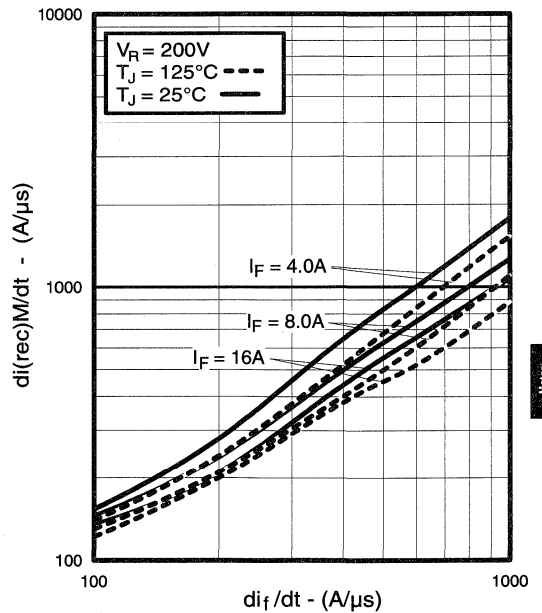


Fig. 17 - Typical $di_{(rec)M}/dt$ vs. di_f/dt

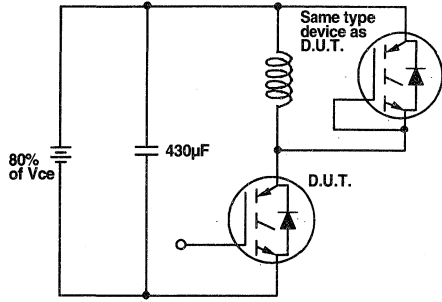


Fig. 18a - Test Circuit for Measurement of I_{LM} , E_{on} , $E_{off(diode)}$, t_{rr} , Q_{rr} , I_{rr} , $t_{d(on)}$, t_r , $t_{d(off)}$, t_f

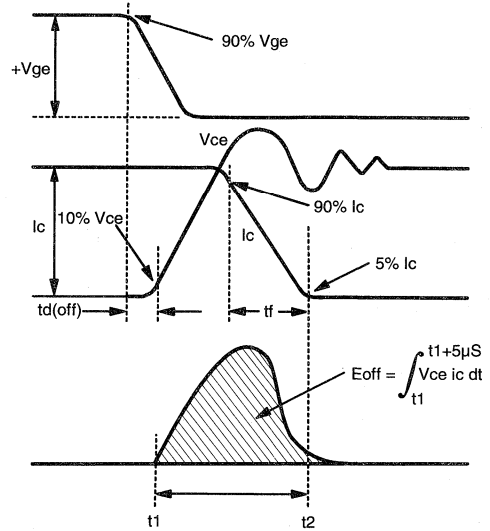


Fig. 18b - Test Waveforms for Circuit of Fig. 18a, Defining E_{off} , $t_{d(off)}$, t_f

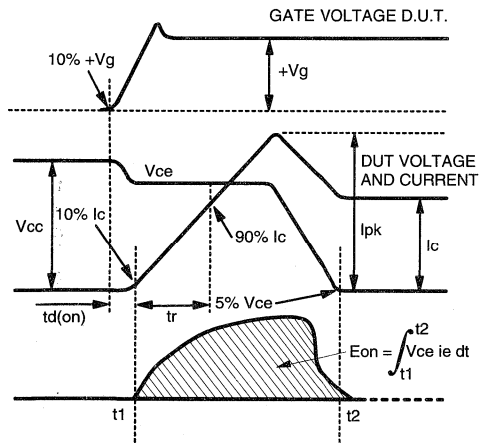


Fig. 18c - Test Waveforms for Circuit of Fig. 18a, Defining E_{on} , $t_{d(on)}$, t_r

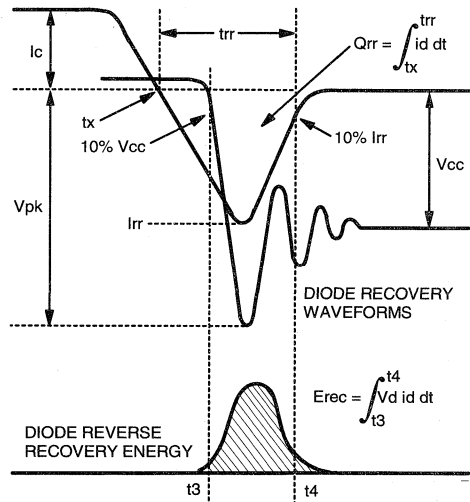


Fig. 18d - Test Waveforms for Circuit of Fig. 18a, Defining E_{rec} , t_{rr} , Q_{rr} , I_{rr}

Refer to Section D for the following:
Appendix D: Section D - page D-6

Fig. 18e - Macro Waveforms for Test Circuit of Fig. 18a

Fig. 19 - Clamped Inductive Load Test Circuit

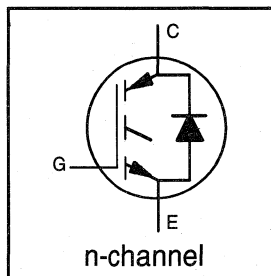
Fig. 20 - Pulsed Collector Current Test Circuit

INSULATED GATE BIPOLAR TRANSISTOR
WITH ULTRAFAST SOFT RECOVERY DIODE

Short Circuit Rated
UltraFast CoPack IGBT

Features

- Short circuit rated - $10\mu\text{s}$ @ 125°C , $V_{GE} = 15\text{V}$
- Switching-loss rating includes all "tail" losses
- HEXFRED™ soft ultrafast diodes
- Optimized for high operating frequency (over 5kHz)
See Fig. 1 for Current vs. Frequency curve



$$V_{CES} = 600\text{V}$$

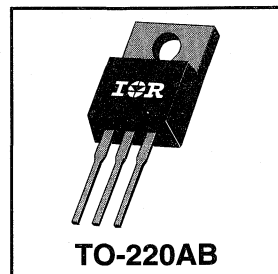
$$V_{CE(sat)} \leq 3.8\text{V}$$

$$\text{@ } V_{GE} = 15\text{V}, I_C = 14\text{A}$$

Description

Co-packaged IGBTs are a natural extension of International Rectifier's well known IGBT line. They provide the convenience of an IGBT and an ultrafast recovery diode in one package, resulting in substantial benefits to a host of high-voltage, high-current, applications.

These new short circuit rated devices are especially suited for motor control and other applications requiring short circuit withstand capability.



Absolute Maximum Ratings

	Parameter	Max.	Units
V_{CES}	Collector-to-Emitter Voltage	600	V
$I_C @ T_C = 25^\circ\text{C}$	Continuous Collector Current	23	A
$I_C @ T_C = 100^\circ\text{C}$	Continuous Collector Current	14	
I_{CM}	Pulsed Collector Current ①	46	
I_{LM}	Clamped Inductive Load Current ②	46	
$I_F @ T_C = 100^\circ\text{C}$	Diode Continuous Forward Current	12	
I_{FM}	Diode Maximum Forward Current	46	
t_{sc}	Short Circuit Withstand Time	10	μs
V_{GE}	Gate-to-Emitter Voltage	± 20	V
$P_D @ T_C = 25^\circ\text{C}$	Maximum Power Dissipation	100	W
$P_D @ T_C = 100^\circ\text{C}$	Maximum Power Dissipation	42	
T_J	Operating Junction and	-55 to +150	$^\circ\text{C}$
T_{STG}	Storage Temperature Range		
	Soldering Temperature, for 10 sec.	300 (0.063 in. (1.6mm) from case)	
	Mounting Torque, 6-32 or M3 Screw.	10 lbf•in (1.1 N•m)	

Thermal Resistance

	Parameter	Min.	Typ.	Max.	Units
$R_{\theta JC}$	Junction-to-Case - IGBT	—	—	1.2	$^\circ\text{C}/\text{W}$
$R_{\theta JC}$	Junction-to-Case - Diode	—	—	2.5	
$R_{\theta CS}$	Case-to-Sink, flat, greased surface	—	0.50	—	
$R_{\theta JA}$	Junction-to-Ambient, typical socket mount	—	—	80	
Wt	Weight	—	2 (0.07)	—	g (oz)

Electrical Characteristics @ T_J = 25°C (unless otherwise specified)

	Parameter	Min.	Typ.	Max.	Units	Conditions
V _{(BR)CES}	Collector-to-Emitter Breakdown Voltage ^③	600	—	—	V	V _{GE} = 0V, I _C = 250μA
ΔV _{(BR)CES/ΔT_J}	Temp. Coeff. of Breakdown Voltage	—	0.30	—	V/°C	V _{GE} = 0V, I _C = 1.0mA
V _{CE(on)}	Collector-to-Emitter Saturation Voltage	—	2.5	3.8	V	I _C = 14A
		—	3.3	—		I _C = 23A
		—	2.5	—		I _C = 14A, T _J = 150°C
		V _{GE} = 15V		See Fig. 2, 5		
V _{GE(th)}	Gate Threshold Voltage	3.0	—	5.5		V _{CE} = V _{GE} , I _C = 250μA
ΔV _{GE(th)/ΔT_J}	Temperature Coeff. of Threshold Voltage	—	-13	—	mV/°C	V _{CE} = V _{GE} , I _C = 250μA
g _{fe}	Forward Transconductance ^④	3.3	6.5	—	S	V _{CE} = 100V, I _C = 14A
I _{CES}	Zero Gate Voltage Collector Current	—	—	250	μA	V _{GE} = 0V, V _{CE} = 600V
		—	—	2500		V _{GE} = 0V, V _{CE} = 600V, T _J = 150°C
V _{FM}	Diode Forward Voltage Drop	—	1.4	1.7	V	I _C = 12A
		—	1.3	1.6		I _C = 12A, T _J = 150°C
I _{GES}	Gate-to-Emitter Leakage Current	—	—	±100	nA	V _{GE} = ±20V

Switching Characteristics @ T_J = 25°C (unless otherwise specified)

	Parameter	Min.	Typ.	Max.	Units	Conditions
Q _g	Total Gate Charge (turn-on)	—	39	58		I _C = 14A
Q _{ge}	Gate - Emitter Charge (turn-on)	—	8.7	13	nC	V _{CC} = 400V
Q _{gc}	Gate - Collector Charge (turn-on)	—	15	23		See Fig. 8
t _{d(on)}	Turn-On Delay Time	—	67	—	ns	T _J = 25°C
t _r	Rise Time	—	120	—		I _C = 14A, V _{CC} = 480V
t _{d(off)}	Turn-Off Delay Time	—	110	170		V _{GE} = 15V, R _G = 23Ω
t _f	Fall Time	—	94	140		Energy losses include "tail" and diode reverse recovery.
E _{on}	Turn-On Switching Loss	—	1.1	—	mJ	See Fig. 9, 10, 11, 18
E _{off}	Turn-Off Switching Loss	—	0.5	—		
E _{ts}	Total Switching Loss	—	1.6	2.4		
t _{sc}	Short Circuit Withstand Time	10	—	—	μs	V _{CC} = 360V, T _J = 125°C V _{GE} = 15V, R _G = 23Ω, V _{C_{PK}} < 500V
t _{d(on)}	Turn-On Delay Time	—	64	—	ns	T _J = 150°C, See Fig. 9, 10, 11, 18
t _r	Rise Time	—	100	—		I _C = 14A, V _{CC} = 480V
t _{d(off)}	Turn-Off Delay Time	—	190	—		V _{GE} = 15V, R _G = 23Ω
t _f	Fall Time	—	180	—		Energy losses include "tail" and diode reverse recovery.
E _{ts}	Total Switching Loss	—	2.2	—	mJ	
L _E	Internal Emitter Inductance	—	7.5	—	nH	Measured 5mm from package
C _{ies}	Input Capacitance	—	740	—	pF	V _{GE} = 0V
C _{oes}	Output Capacitance	—	92	—		V _{CC} = 30V
C _{res}	Reverse Transfer Capacitance	—	9.4	—		f = 1.0MHz
t _{rr}	Diode Reverse Recovery Time	—	42	60	ns	T _J = 25°C
		—	80	120		T _J = 125°C
I _{rr}	Diode Peak Reverse Recovery Current	—	3.5	6.0	A	T _J = 25°C
		—	5.6	10		T _J = 125°C
Q _{rr}	Diode Reverse Recovery Charge	—	80	180	nC	T _J = 25°C
		—	220	600		T _J = 125°C
di _(rec) /dt	Diode Peak Rate of Fall of Recovery During t _b	—	180	—	A/μs	T _J = 25°C
		—	120	—		T _J = 125°C

Notes:

① Repetitive rating; V_{GE}=20V, pulse width limited by max. junction temperature. (See fig. 20)

② V_{CC}=80%(V_{CES}), V_{GE}=20V, L=10μH, R_G= 23Ω, (See fig. 19)

③ Pulse width ≤ 80μs; duty factor ≤ 0.1%.

④ Pulse width 5.0μs, single shot.

I_F = 12A
V_R = 200V
di/dt = 200A/μs

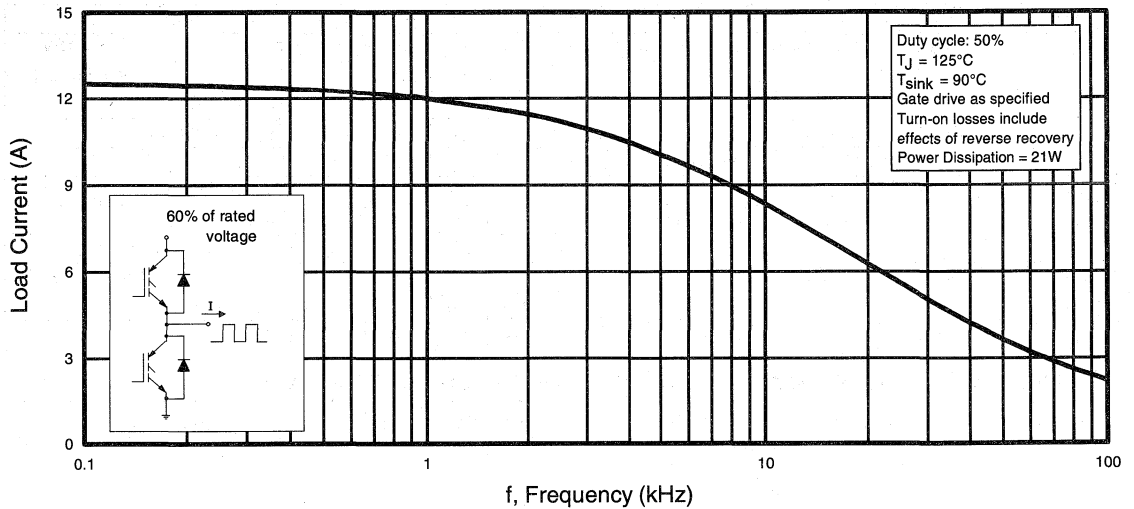


Fig. 1 - Typical Load Current vs. Frequency
(Load Current = I_{RMS} of fundamental)

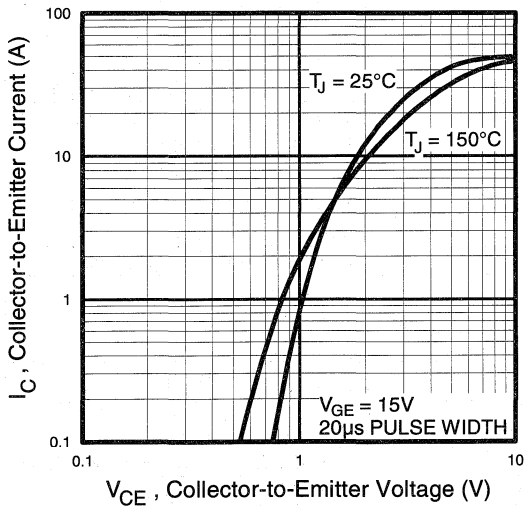


Fig. 2 - Typical Output Characteristics

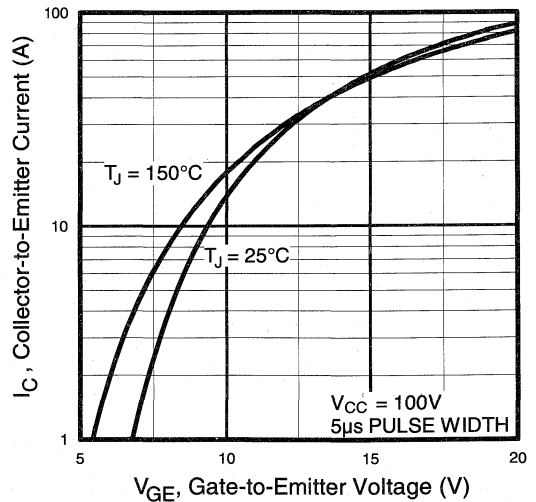


Fig. 3 - Typical Transfer Characteristics

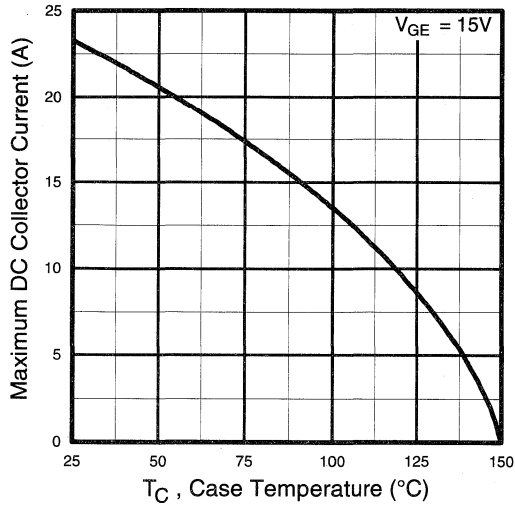


Fig. 4 - Maximum Collector Current vs. Case Temperature

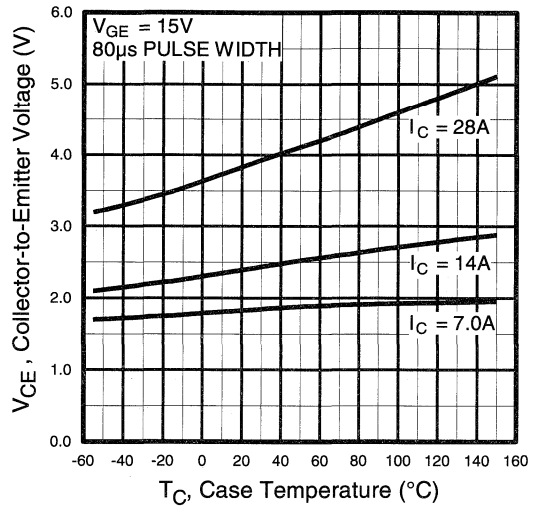


Fig. 5 - Collector-to-Emitter Voltage vs. Case Temperature

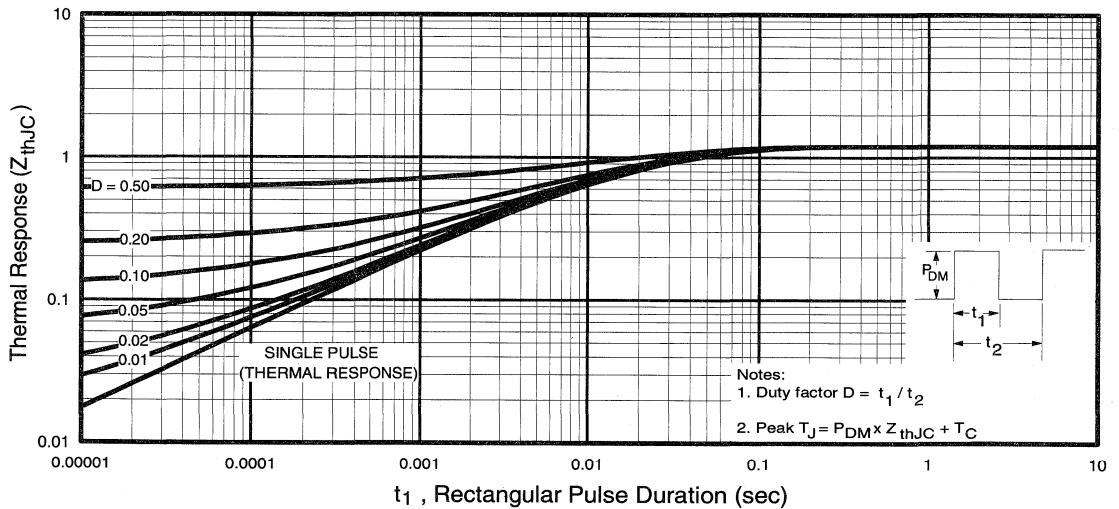


Fig. 6 - Maximum IGBT Effective Transient Thermal Impedance, Junction-to-Case

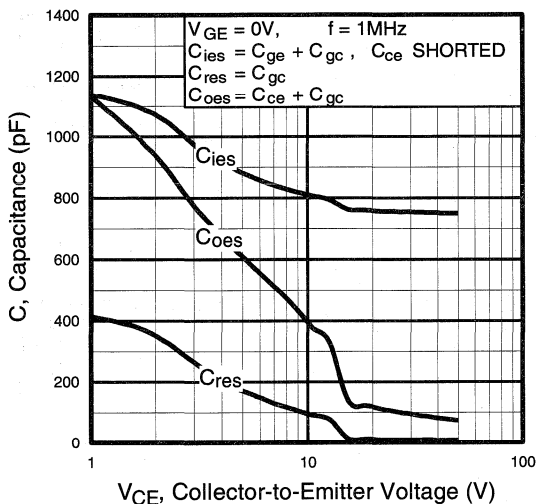


Fig. 7 - Typical Capacitance vs. Collector-to-Emitter Voltage

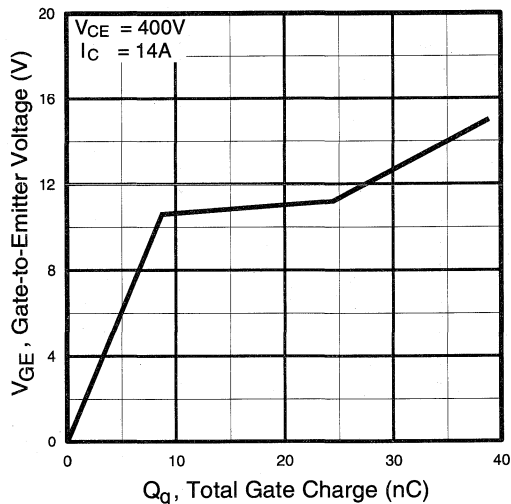


Fig. 8 - Typical Gate Charge vs. Gate-to-Emitter Voltage

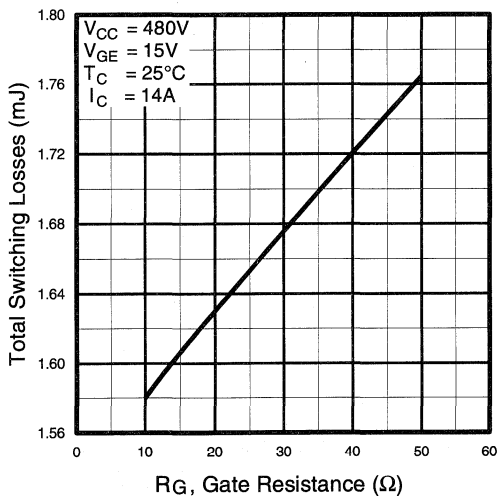


Fig. 9 - Typical Switching Losses vs. Gate Resistance

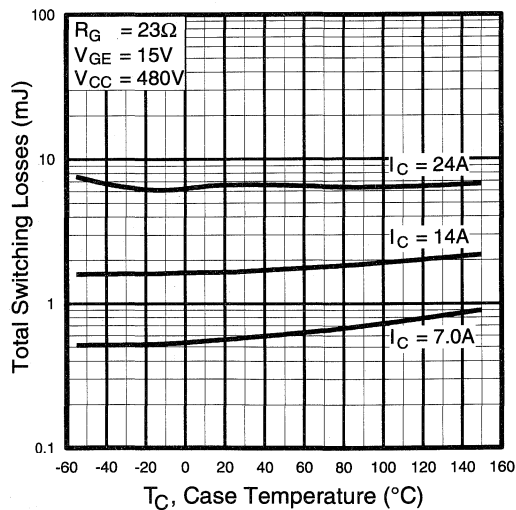


Fig. 10 - Typical Switching Losses vs. Case Temperature

Motor
Control
Ultra-Fast
Co-Packs

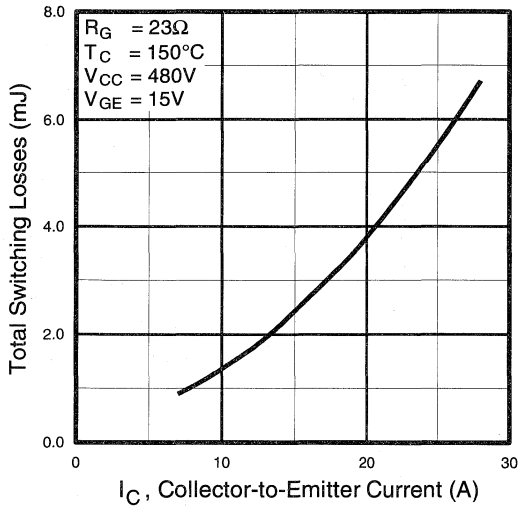


Fig. 11 - Typical Switching Losses vs. Collector-to-Emitter Current

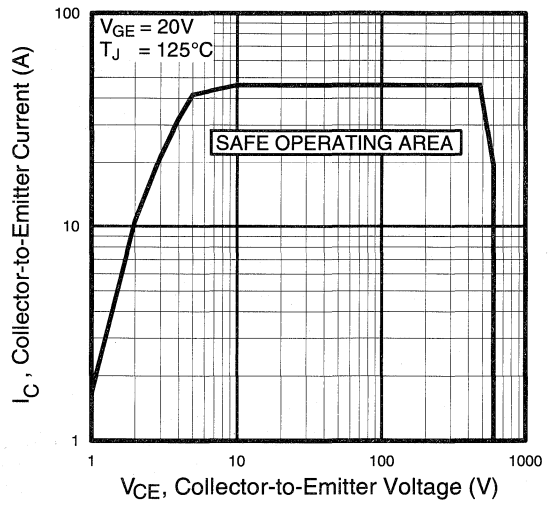


Fig. 12 - Turn-Off SOA

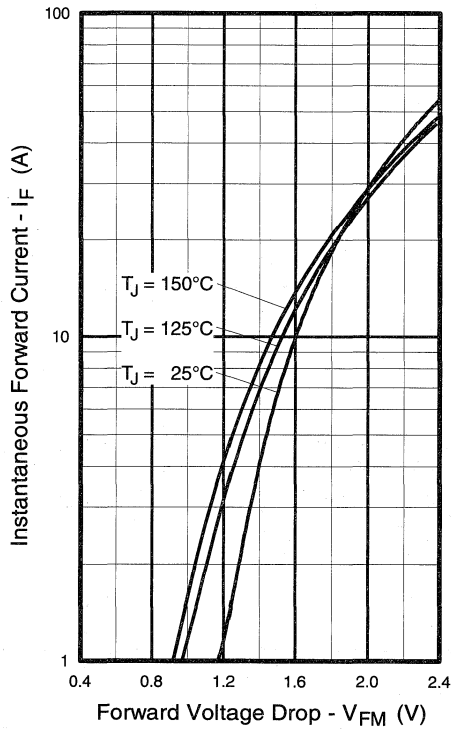


Fig. 13 - Maximum Forward Voltage Drop vs. Instantaneous Forward Current

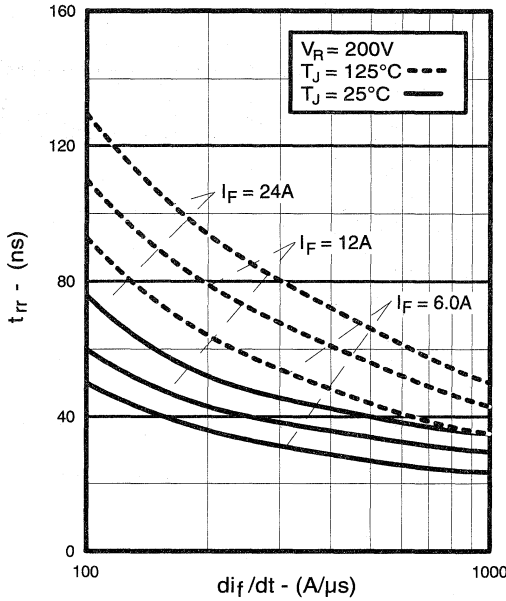


Fig. 14 - Typical Reverse Recovery vs. di_f/dt

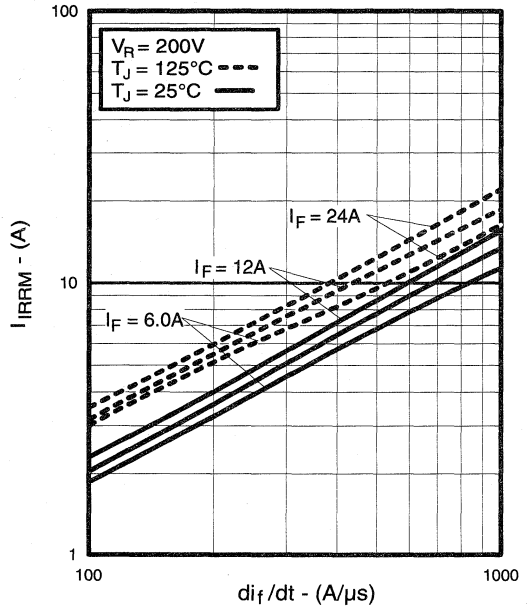


Fig. 15 - Typical Recovery Current vs. di_f/dt

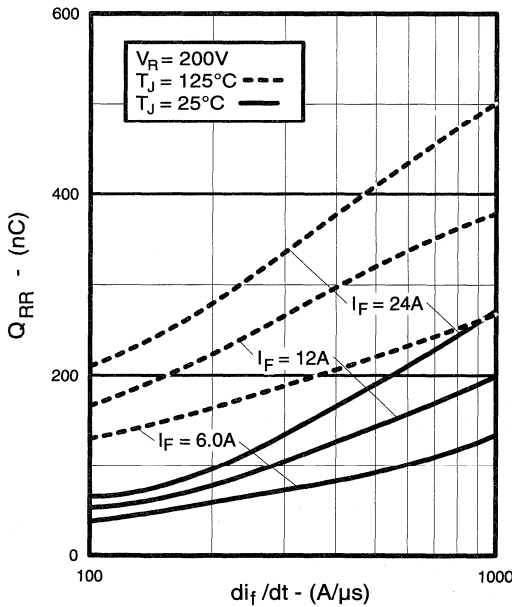


Fig. 16 - Typical Stored Charge vs. di_f/dt

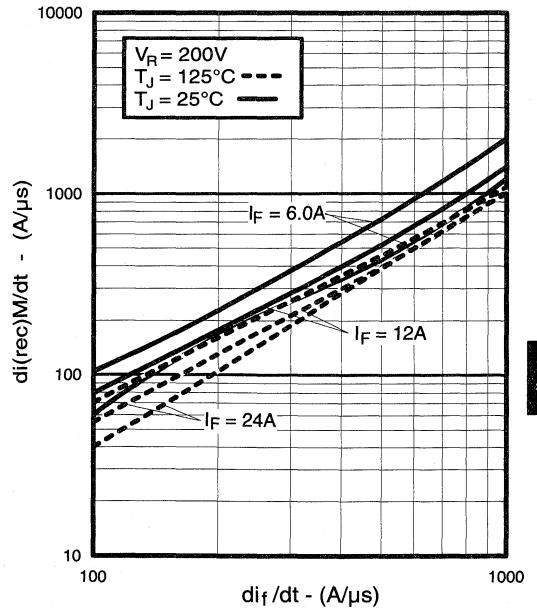


Fig. 17 - Typical $di_{(rec)M}/dt$ vs. di_f/dt

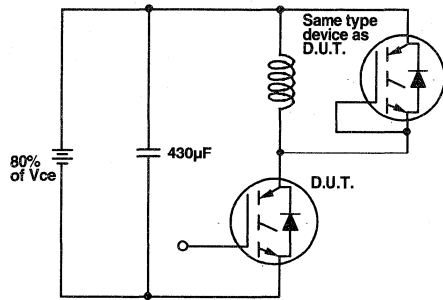


Fig. 18a - Test Circuit for Measurement of I_{LM} , E_{on} , $E_{off}(\text{diode})$, t_{rr} , Q_{rr} , I_{rr} , $t_{d(on)}$, t_r , $t_{d(off)}$, t_f

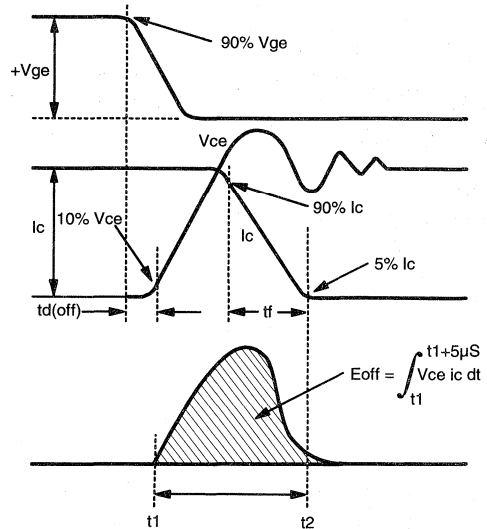


Fig. 18b - Test Waveforms for Circuit of Fig. 18a, Defining E_{off} , $t_{d(off)}$, t_f

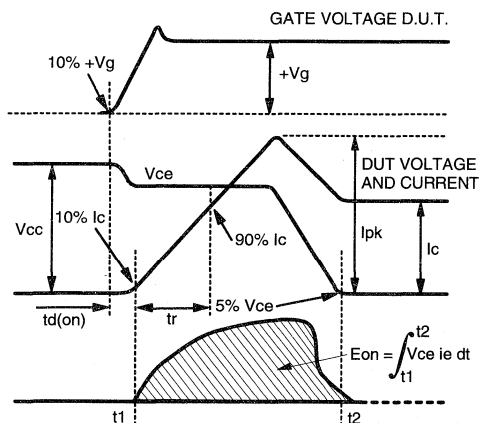


Fig. 18c - Test Waveforms for Circuit of Fig. 18a, Defining E_{on} , $t_{d(on)}$, t_r

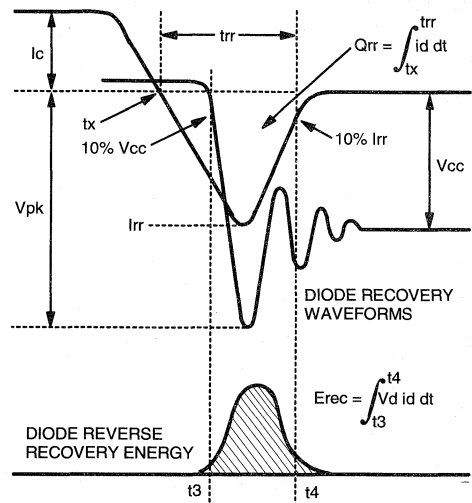


Fig. 18d - Test Waveforms for Circuit of Fig. 18a, Defining E_{rec} , t_{rr} , Q_{rr} , I_{rr}

Refer to Section D for the following:

Appendix D: Section D - page D-6

Fig. 18e - Macro Waveforms for Test Circuit of Fig. 18a

Fig. 19 - Clamped Inductive Load Test Circuit

Fig. 20 - Pulsed Collector Current Test Circuit

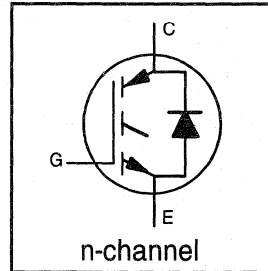
IRGBC20KD2-S

**INSULATED GATE BIPOLAR TRANSISTOR
WITH ULTRAFAST SOFT RECOVERY DIODE**

**Short Circuit Rated
UltraFast CoPack IGBT**

Features

- Short circuit rated -10µs @ 125°C, V_{GE} = 15V
- Switching-loss rating includes all "tail" losses
- HEXFRED™ soft ultrafast diodes
- Optimized for high operating frequency (over 5kHz)
See Fig. 1 for Current vs. Frequency curve

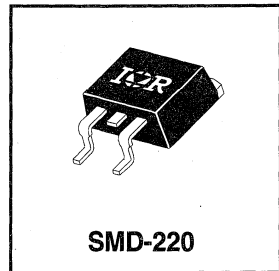


V _{CES} = 600V
V _{CE(sat)} ≤ 3.5V
@ V _{GE} = 15V, I _C = 6.0A

Description

Co-packaged IGBTs are a natural extension of International Rectifier's well known IGBT line. They provide the convenience of an IGBT and an ultrafast recovery diode in one package, resulting in substantial benefits to a host of high-voltage, high-current, applications.

These new short circuit rated devices are especially suited for motor control and other applications requiring short circuit withstand capability.



Absolute Maximum Ratings

	Parameter	Max.	Units
V _{CES}	Collector-to-Emitter Voltage	600	V
I _C @ T _C = 25°C	Continuous Collector Current	10	A
I _C @ T _C = 100°C	Continuous Collector Current	6.0	
I _{CM}	Pulsed Collector Current ①	20	
I _{LM}	Clamped Inductive Load Current ②	20	
I _F @ T _C = 100°C	Diode Continuous Forward Current	7.0	
I _{FM}	Diode Maximum Forward Current	20	
t _{sc}	Short Circuit Withstand Time	10	µs
V _{GE}	Gate-to-Emitter Voltage	± 20	V
P _D @ T _C = 25°C	Maximum Power Dissipation	60	W
P _D @ T _C = 100°C	Maximum Power Dissipation	24	
T _J	Operating Junction and	-55 to +150	°C
T _{STG}	Storage Temperature Range		
	Soldering Temperature, for 10 sec.	300 (0.063 in. (1.6mm) from case)	
	Mounting Torque, 6-32 or M3 Screw.	10 lbf•in (1.1 N•m)	

Thermal Resistance

	Parameter	Min.	Typ.	Max.	Units
R _{θJC}	Junction-to-Case - IGBT	—	—	2.1	°C/W
R _{θJC}	Junction-to-Case - Diode	—	—	3.5	
R _{θJA}	Junction-to-Ambient, (PCB Mount)**	—	—	40	
R _{θJA}	Junction-to-Ambient, typical socket mount	—	—	80	
Wt	Weight	—	2 (0.07)	—	g (oz)

** When mounted on 1" square PCB (FR-4 or G-10 Material)

For recommended footprint and soldering techniques refer to application note #AN-994.



Electrical Characteristics @ $T_J = 25^\circ\text{C}$ (unless otherwise specified)

	Parameter	Min.	Typ.	Max.	Units	Conditions
$V_{(BR)CES}$	Collector-to-Emitter Breakdown Voltage ^③	600	—	—	V	$V_{GE} = 0V, I_C = 250\mu A$
$\Delta V_{(BR)CES}/\Delta T_J$	Temp. Coeff. of Breakdown Voltage	—	0.37	—	V/°C	$V_{GE} = 0V, I_C = 1.0mA$
$V_{CE(on)}$	Collector-to-Emitter Saturation Voltage	—	2.4	3.5	V	$I_C = 6.0A, V_{GE} = 15V$
		—	3.6	—		$I_C = 10A$
		—	2.8	—		$I_C = 6.0A, T_J = 150^\circ\text{C}$
$V_{GE(th)}$	Gate Threshold Voltage	3.0	—	5.5		$V_{CE} = V_{GE}, I_C = 250\mu A$
$\Delta V_{GE(th)}/\Delta T_J$	Temperature Coeff. of Threshold Voltage	—	-11	—	mV/°C	$V_{CE} = V_{GE}, I_C = 250\mu A$
g_{fe}	Forward Transconductance ^④	1.9	3.3	—	S	$V_{CE} = 100V, I_C = 6.0A$
I_{CES}	Zero Gate Voltage Collector Current	—	—	250	μA	$V_{GE} = 0V, V_{CE} = 600V$
		—	—	1700		$V_{GE} = 0V, V_{CE} = 600V, T_J = 150^\circ\text{C}$
V_{FM}	Diode Forward Voltage Drop	—	1.4	1.7	V	$I_C = 8.0A$
		—	1.4	1.7		$I_C = 8.0A, T_J = 150^\circ\text{C}$
I_{GES}	Gate-to-Emitter Leakage Current	—	—	± 100	nA	$V_{GE} = \pm 20V$

Switching Characteristics @ $T_J = 25^\circ\text{C}$ (unless otherwise specified)

	Parameter	Min.	Typ.	Max.	Units	Conditions
Q_g	Total Gate Charge (turn-on)	—	17	26	nC	$I_C = 6.0A$
Q_{ge}	Gate - Emitter Charge (turn-on)	—	4.3	6.8		$V_{CC} = 480V$
Q_{gc}	Gate - Collector Charge (turn-on)	—	6.4	11		See Fig. 8
$t_{d(on)}$	Turn-On Delay Time	—	59	—	ns	$T_J = 25^\circ\text{C}$
t_r	Rise Time	—	38	—		$I_C = 6.0A, V_{CC} = 480V$
$t_{d(off)}$	Turn-Off Delay Time	—	110	210		$V_{GE} = 15V, R_G = 50\Omega$
t_f	Fall Time	—	80	120		Energy losses include "tail" and diode reverse recovery.
E_{on}	Turn-On Switching Loss	—	0.28	—		See Fig. 9, 10, 11, 18
E_{off}	Turn-Off Switching Loss	—	0.15	—	mJ	
E_{ts}	Total Switching Loss	—	0.43	0.90		
t_{sc}	Short Circuit Withstand Time	10	—	—	μs	$V_{CC} = 360V, T_J = 125^\circ\text{C}$ $V_{GE} = 15V, R_G = 50\Omega, V_{CPK} < 500V$
$t_{d(on)}$	Turn-On Delay Time	—	52	—	ns	$T_J = 150^\circ\text{C}$, See Fig. 9, 10, 11, 18
t_r	Rise Time	—	35	—		$I_C = 6.0A, V_{CC} = 480V$
$t_{d(off)}$	Turn-Off Delay Time	—	170	—		$V_{GE} = 15V, R_G = 50\Omega$
t_f	Fall Time	—	170	—		Energy losses include "tail" and diode reverse recovery.
E_{ts}	Total Switching Loss	—	0.7	—		mJ
L_E	Internal Emitter Inductance	—	7.5	—	nH	Measured 5mm from package
C_{ies}	Input Capacitance	—	350	—	pF	$V_{GE} = 0V$
C_{oes}	Output Capacitance	—	50	—		$V_{CC} = 30V$
C_{res}	Reverse Transfer Capacitance	—	4.7	—		$f = 1.0MHz$
t_{rr}	Diode Reverse Recovery Time	—	37	55	ns	$T_J = 25^\circ\text{C}$ See Fig. 14
		—	55	90		$T_J = 125^\circ\text{C}$
I_{rr}	Diode Peak Reverse Recovery Current	—	3.5	5.0	A	$T_J = 25^\circ\text{C}$ See Fig. 15
		—	4.5	8.0		$T_J = 125^\circ\text{C}$
Q_{rr}	Diode Reverse Recovery Charge	—	65	138	nC	$T_J = 25^\circ\text{C}$ See Fig. 16
		—	124	360		$T_J = 125^\circ\text{C}$
$di_{(rec)M}/dt$	Diode Peak Rate of Fall of Recovery During t_b	—	240	—	A/ μs	$T_J = 25^\circ\text{C}$ See Fig. 17
		—	210	—		$T_J = 125^\circ\text{C}$

Notes:

① Repetitive rating; $V_{GE}=20V$, pulse width limited by max. junction temperature. (See fig. 20)

② $V_{CC}=80\%(V_{CES}), V_{GE}=20V, L=10\mu H, R_G=50\Omega$, (See fig. 19)

③ Pulse width $\leq 80\mu s$; duty factor $\leq 0.1\%$.

④ Pulse width 5.0 μs , single shot.

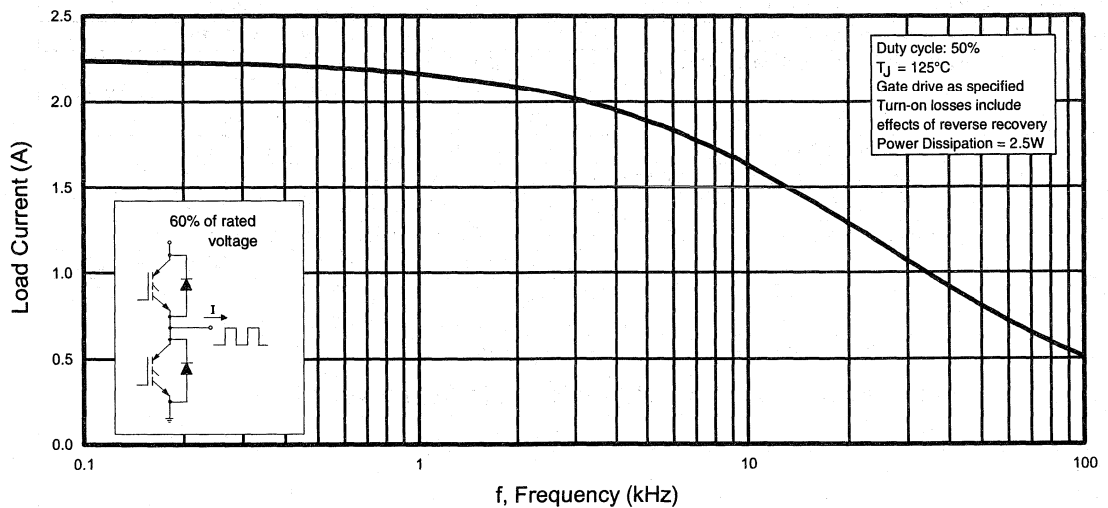


Fig. 1 - Typical Load Current vs. Frequency
(Load Current = I_{RMS} of fundamental)

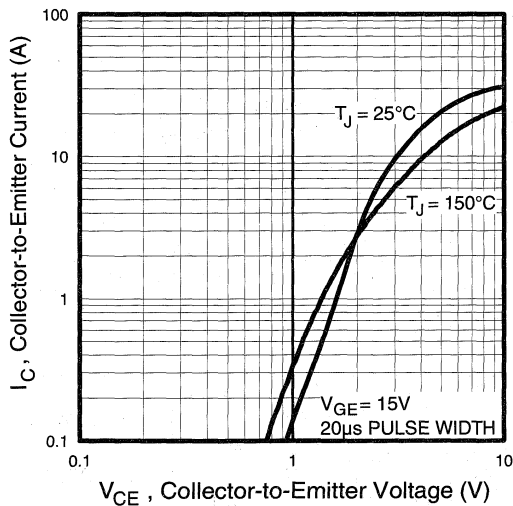


Fig. 2 - Typical Output Characteristics

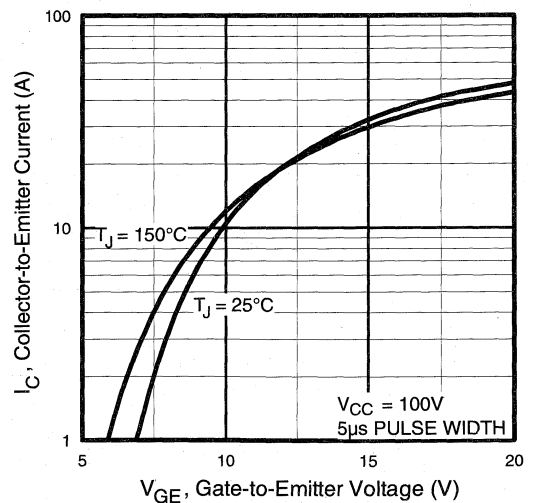


Fig. 3 - Typical Transfer Characteristics

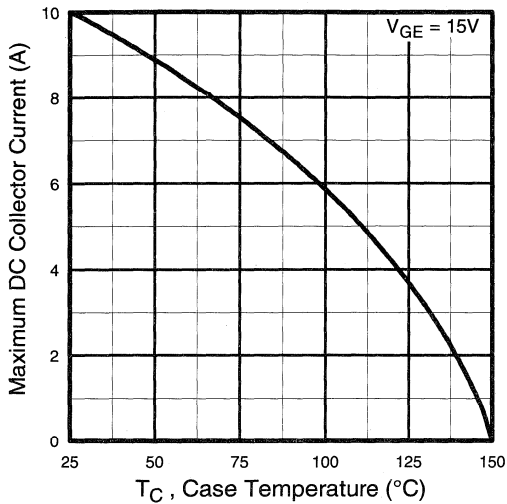


Fig. 4 - Maximum Collector Current vs. Case Temperature

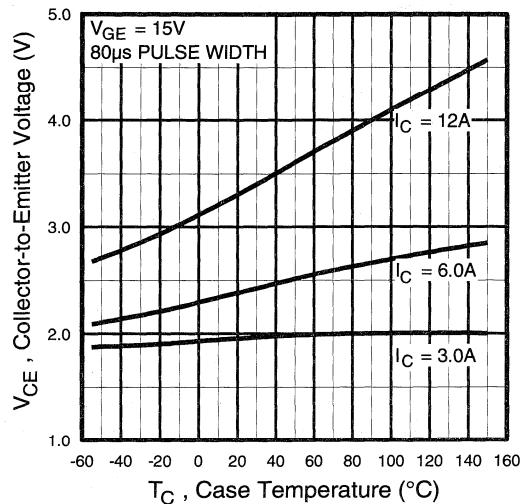


Fig. 5 - Collector-to-Emitter Voltage vs. Case Temperature

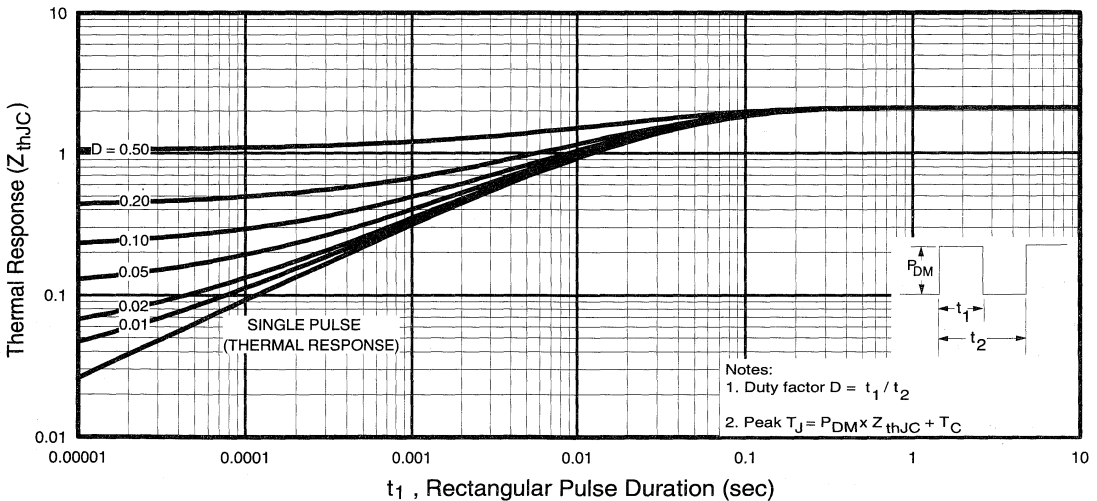


Fig. 6 - Maximum IGBT Effective Transient Thermal Impedance, Junction-to-Case

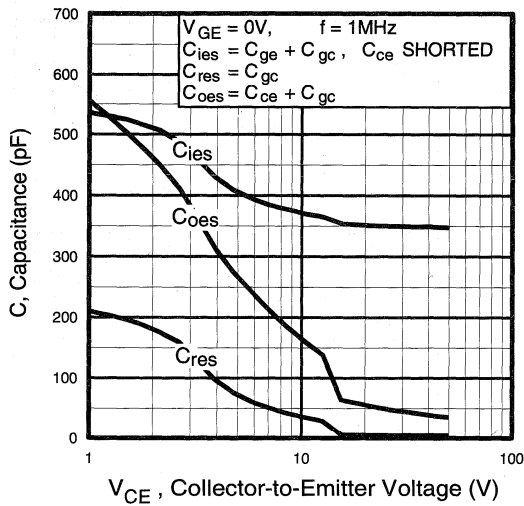


Fig. 7 - Typical Capacitance vs. Collector-to-Emitter Voltage

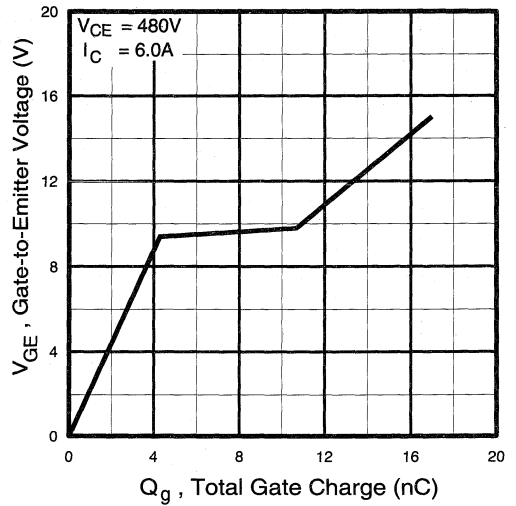


Fig. 8 - Typical Gate Charge vs. Gate-to-Emitter Voltage

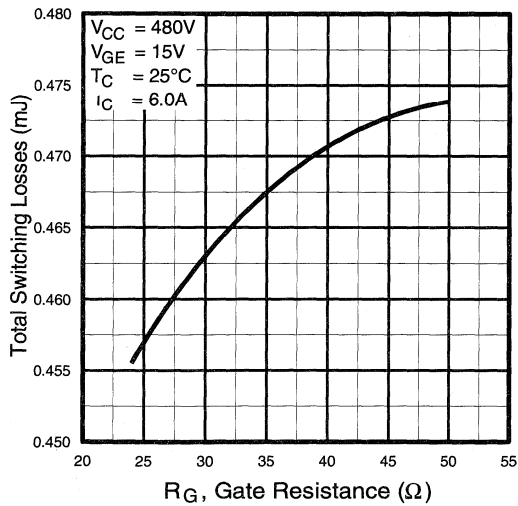


Fig. 9 - Typical Switching Losses vs. Gate Resistance

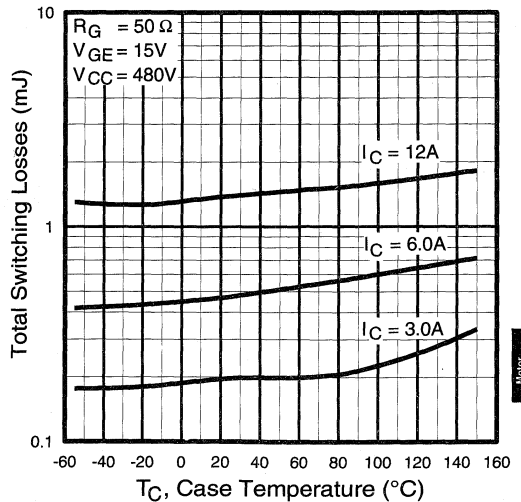


Fig. 10 - Typical Switching Losses vs. Case Temperature

Motor Control
Ultra-Fast
Co-Packs

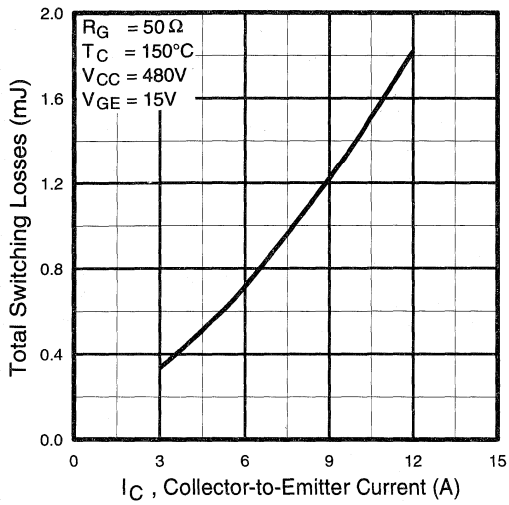


Fig. 11 - Typical Switching Losses vs. Collector-to-Emitter Current

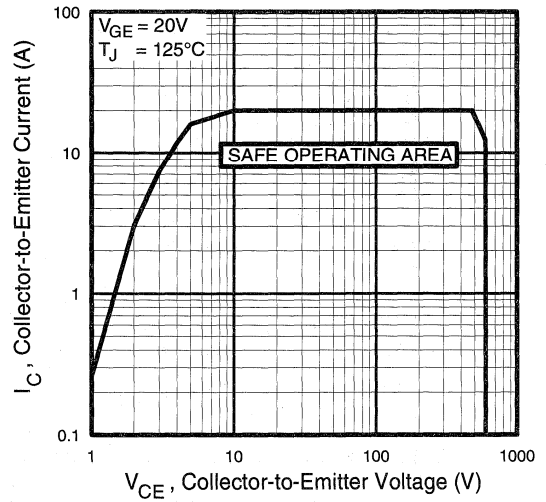


Fig. 12 - Turn-Off SOA

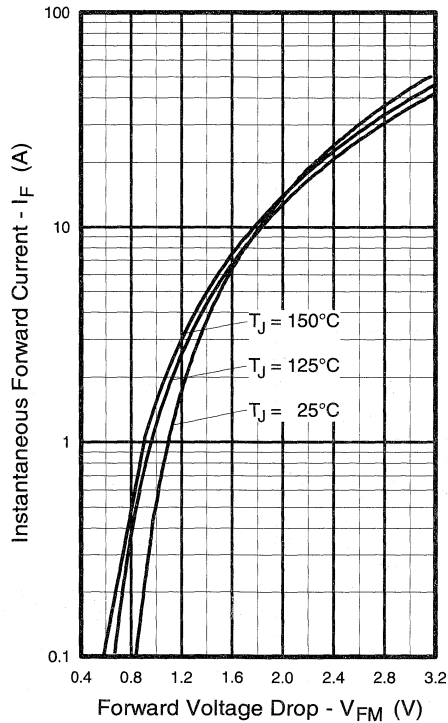


Fig. 13 - Maximum Forward Voltage Drop vs. Instantaneous Forward Current

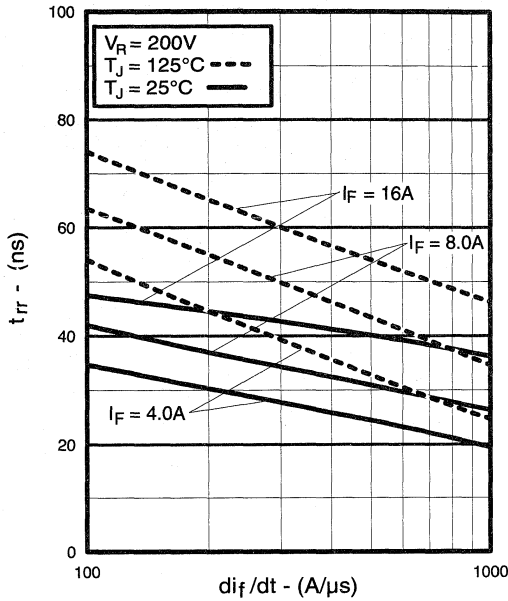


Fig. 14 - Typical Reverse Recovery vs. di_f/dt

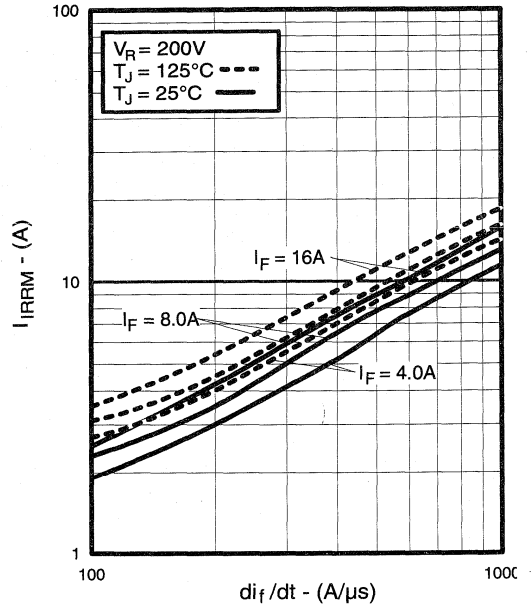


Fig. 15 - Typical Recovery Current vs. di_f/dt

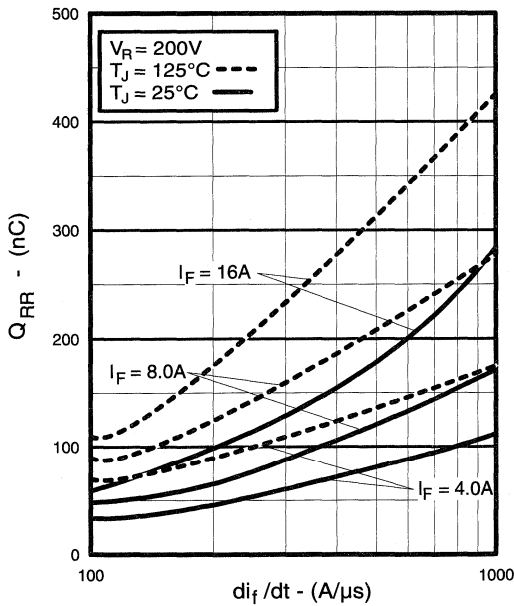


Fig. 16 - Typical Stored Charge vs. di_f/dt

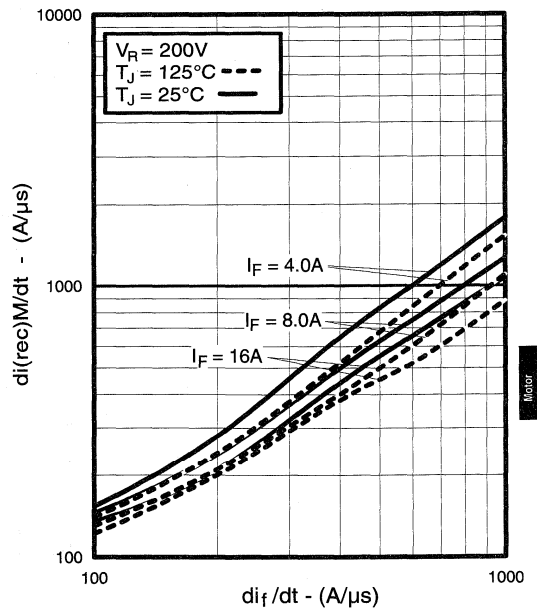


Fig. 17 - Typical $di_{(rec)M}/dt$ vs. di_f/dt

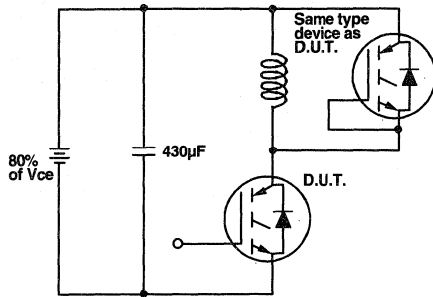


Fig. 18a - Test Circuit for Measurement of I_{LM} , E_{on} , $E_{off(diode)}$, t_{rr} , Q_{rr} , I_{rr} , $t_{d(on)}$, t_r , $t_{d(off)}$, t_f

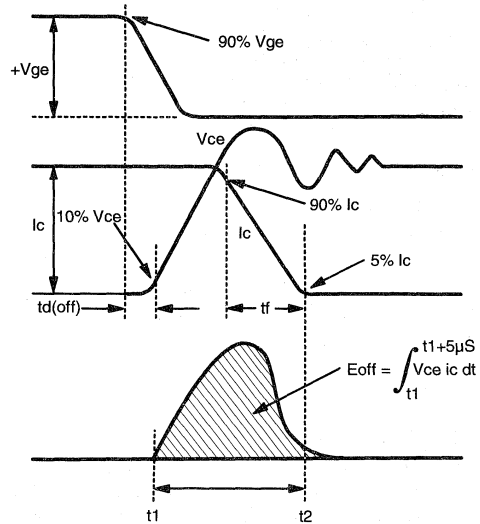


Fig. 18b - Test Waveforms for Circuit of Fig. 18a, Defining E_{off} , $t_{d(off)}$, t_f

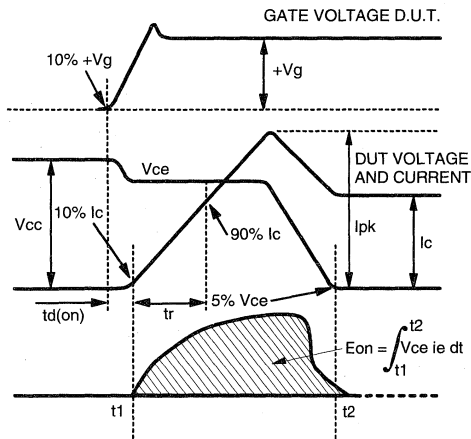


Fig. 18c - Test Waveforms for Circuit of Fig. 18a, Defining E_{on} , $t_{d(on)}$, t_r

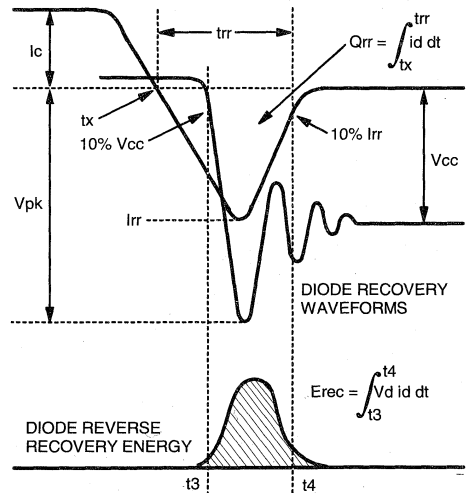


Fig. 18d - Test Waveforms for Circuit of Fig. 18a, Defining E_{rec} , t_{rr} , Q_{rr} , I_{rr}

Refer to Section D for the following:
Appendix D: Section D - page D-6

- Fig. 18e - Macro Waveforms for Test Circuit of Fig. 18a
- Fig. 19 - Clamped Inductive Load Test Circuit
- Fig. 20 - Pulsed Collector Current Test Circuit

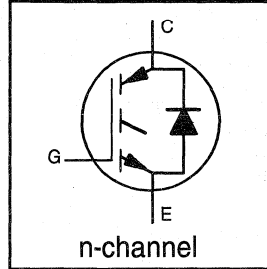
IRGBC30KD2-S

**INSULATED GATE BIPOLAR TRANSISTOR
WITH ULTRAFAST SOFT RECOVERY DIODE**

**Short Circuit Rated
UltraFast CoPack IGBT**

Features

- Short circuit rated -10µs @ 125°C, V_{GE} = 15V
- Switching-loss rating includes all "tail" losses
- HEXFRED™ soft ultrafast diodes
- Optimized for high operating frequency (over 5kHz)
See Fig. 1 for Current vs. Frequency curve

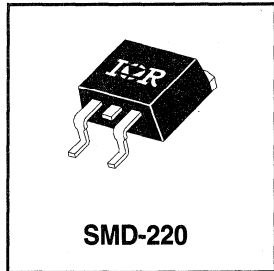


V _{CES} = 600V
V _{CE(sat)} ≤ 3.8V
@ V _{GE} = 15V, I _C = 14A

Description

Co-packaged IGBTs are a natural extension of International Rectifier's well known IGBT line. They provide the convenience of an IGBT and an ultrafast recovery diode in one package, resulting in substantial benefits to a host of high-voltage, high-current, applications.

These new short circuit rated devices are especially suited for motor control and other applications requiring short circuit withstand capability.



Absolute Maximum Ratings

	Parameter	Max.	Units
V _{CES}	Collector-to-Emitter Voltage	600	V
I _C @ T _C = 25°C	Continuous Collector Current	23	A
I _C @ T _C = 100°C	Continuous Collector Current	14	
I _{CM}	Pulsed Collector Current ①	46	
I _{LM}	Clamped Inductive Load Current ②	46	
I _F @ T _C = 100°C	Diode Continuous Forward Current	12	
I _{FM}	Diode Maximum Forward Current	46	
t _{sc}	Short Circuit Withstand Time	10	µs
V _{GE}	Gate-to-Emitter Voltage	± 20	V
P _D @ T _C = 25°C	Maximum Power Dissipation	100	W
P _D @ T _C = 100°C	Maximum Power Dissipation	42	
T _J	Operating Junction and	-55 to +150	°C
T _{STG}	Storage Temperature Range		
	Soldering Temperature, for 10 sec.	300 (0.063 in. (1.6mm) from case)	
	Mounting Torque, 6-32 or M3 Screw.	10 lbf•in (1.1 N•m)	

Thermal Resistance

	Parameter	Min.	Typ.	Max.	Units
R _{θJC}	Junction-to-Case - IGBT	—	—	1.2	°C/W
R _{θJC}	Junction-to-Case - Diode	—	—	2.5	
R _{θJA}	Junction-to-Ambient, (PCB Mount)**	—	—	40	
R _{θJA}	Junction-to-Ambient, typical socket mount	—	—	80	
Wt	Weight	—	2 (0.07)	—	g (oz)

** When mounted on 1" square PCB (FR-4 or G-10 Material)
For recommended footprint and soldering techniques refer to application note #AN-994.



Electrical Characteristics @ T_J = 25°C (unless otherwise specified)

	Parameter	Min.	Typ.	Max.	Units	Conditions
V _{(BR)CES}	Collector-to-Emitter Breakdown Voltage ^②	600	—	—	V	V _{GE} = 0V, I _C = 250μA
ΔV _{(BR)CES/ΔT_J}	Temp. Coeff. of Breakdown Voltage	—	0.30	—	V/°C	V _{GE} = 0V, I _C = 1.0mA
V _{CE(on)}	Collector-to-Emitter Saturation Voltage	—	2.5	3.8	V	I _C = 14A V _{GE} = 15V
		—	3.3	—		I _C = 23A See Fig. 2, 5
		—	2.5	—		I _C = 14A, T _J = 150°C
V _{GE(th)}	Gate Threshold Voltage	3.0	—	5.5		V _{CE} = V _{GE} , I _C = 250μA
ΔV _{GE(th)/ΔT_J}	Temperature Coeff. of Threshold Voltage	—	-13	—	mV/°C	V _{CE} = V _{GE} , I _C = 250μA
g _{fe}	Forward Transconductance ^④	3.3	6.5	—	S	V _{CE} = 100V, I _C = 14A
I _{CES}	Zero Gate Voltage Collector Current	—	—	250	μA	V _{GE} = 0V, V _{CE} = 600V
		—	—	2500		V _{GE} = 0V, V _{CE} = 600V, T _J = 150°C
V _{FM}	Diode Forward Voltage Drop	—	1.4	1.7	V	I _C = 12A See Fig. 13
		—	1.3	1.6		I _C = 12A, T _J = 150°C
I _{GES}	Gate-to-Emitter Leakage Current	—	—	±100	nA	V _{GE} = ±20V

Switching Characteristics @ T_J = 25°C (unless otherwise specified)

	Parameter	Min.	Typ.	Max.	Units	Conditions
Q _g	Total Gate Charge (turn-on)	—	39	58	nC	I _C = 14A
Q _{ge}	Gate - Emitter Charge (turn-on)	—	8.7	13		V _{CC} = 400V
Q _{gc}	Gate - Collector Charge (turn-on)	—	15	23		See Fig. 8
t _{d(on)}	Turn-On Delay Time	—	67	—	ns	T _J = 25°C
t _r	Rise Time	—	120	—		I _C = 14A, V _{CC} = 480V
t _{d(off)}	Turn-Off Delay Time	—	110	170		V _{GE} = 15V, R _G = 23Ω
t _f	Fall Time	—	94	140		Energy losses include "tail" and diode reverse recovery.
E _{on}	Turn-On Switching Loss	—	1.1	—		mJ
E _{off}	Turn-Off Switching Loss	—	0.5	—		
E _{ts}	Total Switching Loss	—	1.6	2.4		
t _{sc}	Short Circuit Withstand Time	10	—	—	μs	V _{CC} = 360V, T _J = 125°C V _{GE} = 15V, R _G = 23Ω, V _{CPK} < 500V
t _{d(on)}	Turn-On Delay Time	—	64	—	ns	T _J = 150°C, See Fig. 9, 10, 11, 18
t _r	Rise Time	—	100	—		I _C = 14A, V _{CC} = 480V
t _{d(off)}	Turn-Off Delay Time	—	190	—		V _{GE} = 15V, R _G = 23Ω
t _f	Fall Time	—	180	—		Energy losses include "tail" and diode reverse recovery.
E _{ts}	Total Switching Loss	—	2.2	—		mJ
L _E	Internal Emitter Inductance	—	7.5	—	nH	Measured 5mm from package
C _{ies}	Input Capacitance	—	740	—	pF	V _{GE} = 0V
C _{oes}	Output Capacitance	—	92	—		V _{CC} = 30V See Fig. 7
C _{res}	Reverse Transfer Capacitance	—	9.4	—		f = 1.0MHz
t _{rr}	Diode Reverse Recovery Time	—	42	60	ns	T _J = 25°C See Fig. 14
		—	80	120		T _J = 125°C
I _{rr}	Diode Peak Reverse Recovery Current	—	3.5	6.0	A	T _J = 25°C See Fig. 15
		—	5.6	10		T _J = 125°C
Q _{rr}	Diode Reverse Recovery Charge	—	80	180	nC	T _J = 25°C See Fig. 16
		—	220	600		T _J = 125°C
di _{(rec)M/dt}	Diode Peak Rate of Fall of Recovery During t _b	—	180	—	A/μs	T _J = 25°C See Fig. 17
		—	120	—		T _J = 125°C

Notes:

① Repetitive rating; V_{GE}=20V, pulse width limited by max. junction temperature. (See fig. 20)

② V_{CC}=80%(V_{CES}), V_{GE}=20V, L=10μH, R_G=23Ω, (See fig. 19)

④ Pulse width 5.0μs, single shot.

③ Pulse width ≤ 80μs; duty factor ≤ 0.1%.

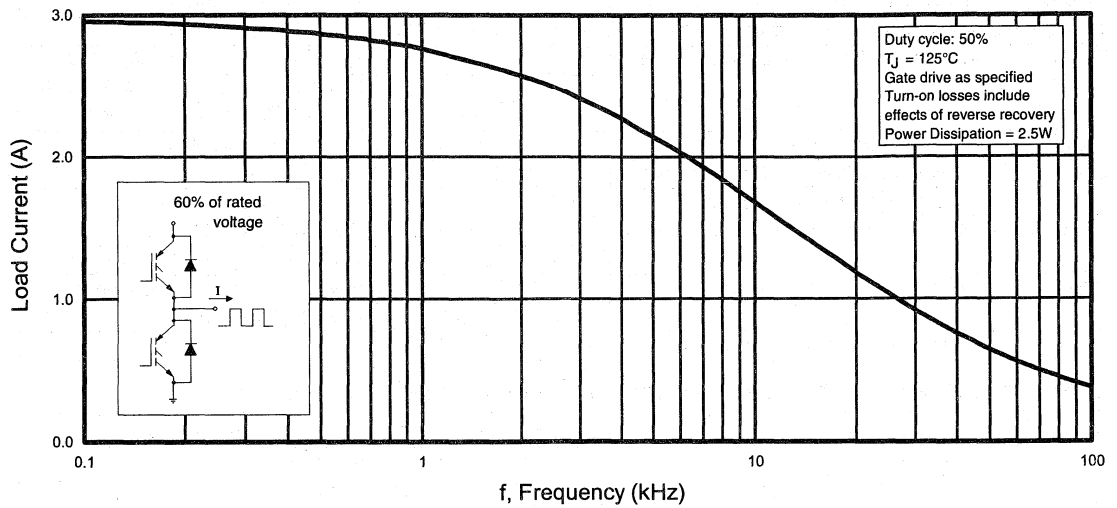


Fig. 1 - Typical Load Current vs. Frequency
 (Load Current = I_{RMS} of fundamental)

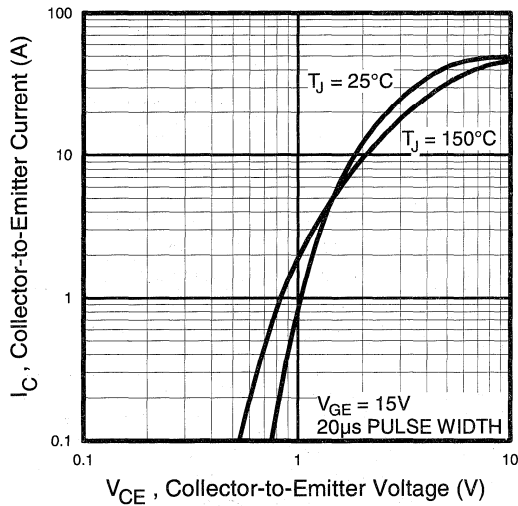


Fig. 2 - Typical Output Characteristics

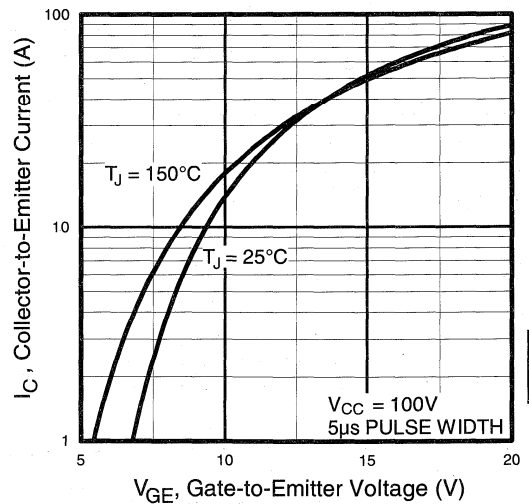


Fig. 3 - Typical Transfer Characteristics

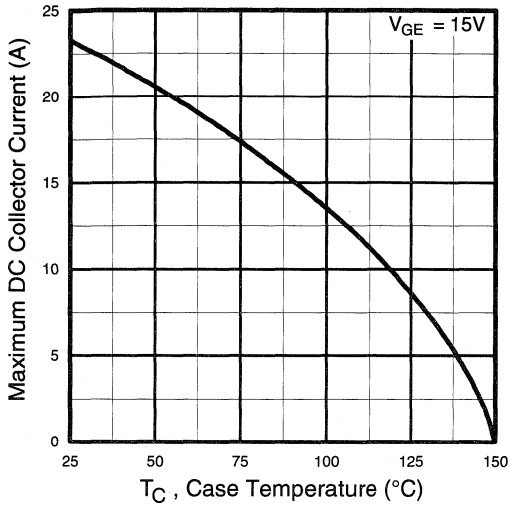


Fig. 4 - Maximum Collector Current vs. Case Temperature

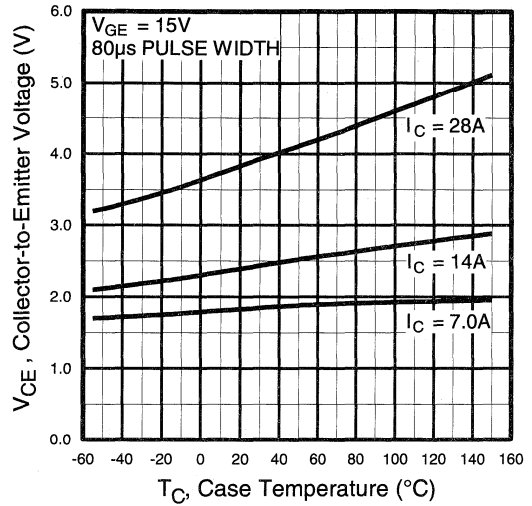


Fig. 5 - Collector-to-Emitter Voltage vs. Case Temperature

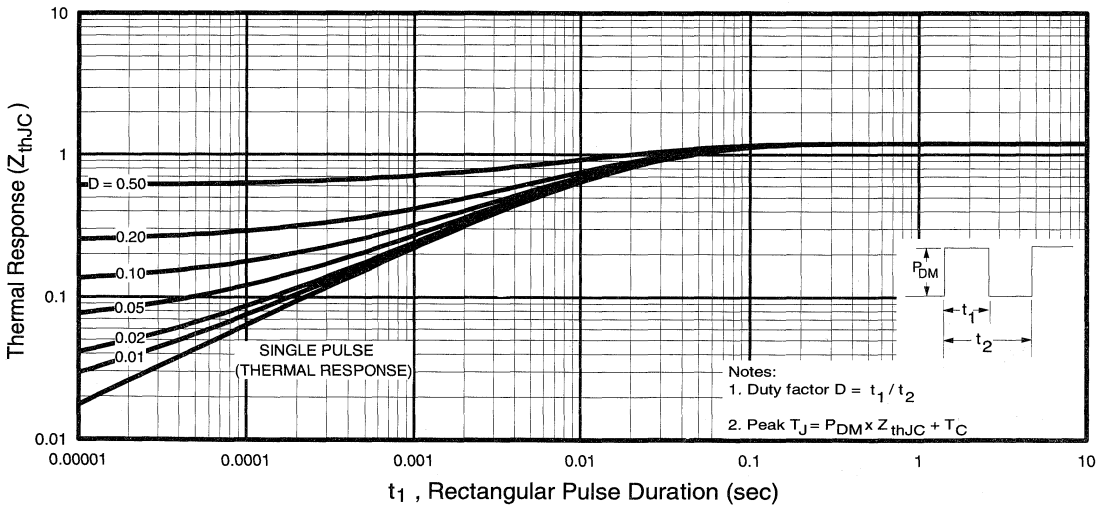


Fig. 6 - Maximum IGBT Effective Transient Thermal Impedance, Junction-to-Case

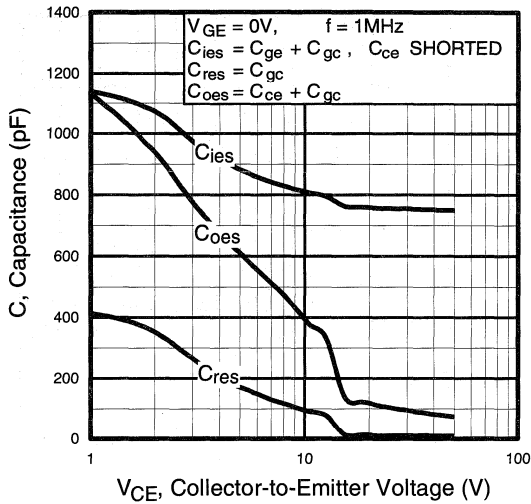


Fig. 7 - Typical Capacitance vs. Collector-to-Emitter Voltage

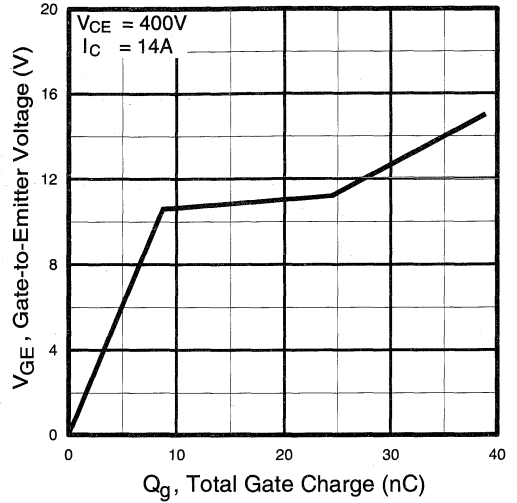


Fig. 8 - Typical Gate Charge vs. Gate-to-Emitter Voltage

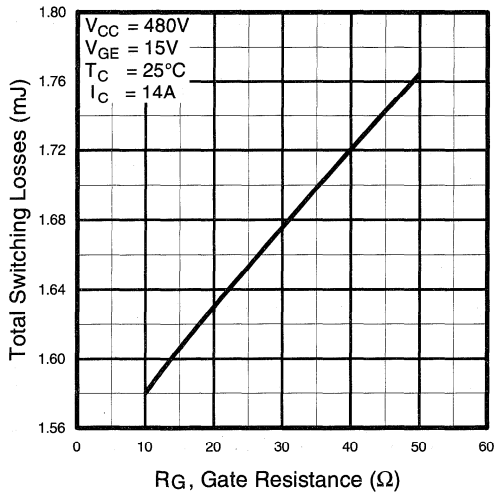


Fig. 9 - Typical Switching Losses vs. Gate Resistance

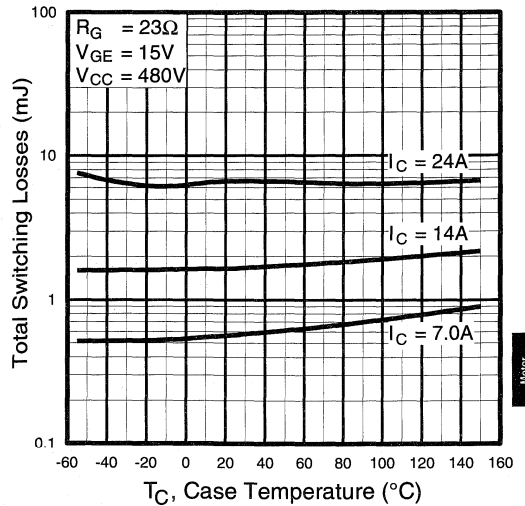


Fig. 10 - Typical Switching Losses vs. Case Temperature

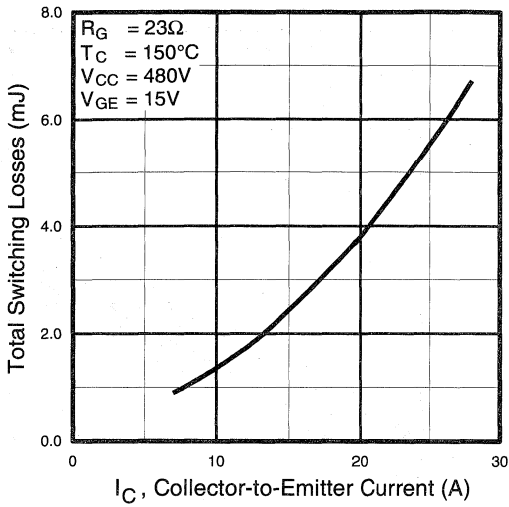


Fig. 11 - Typical Switching Losses vs. Collector-to-Emitter Current

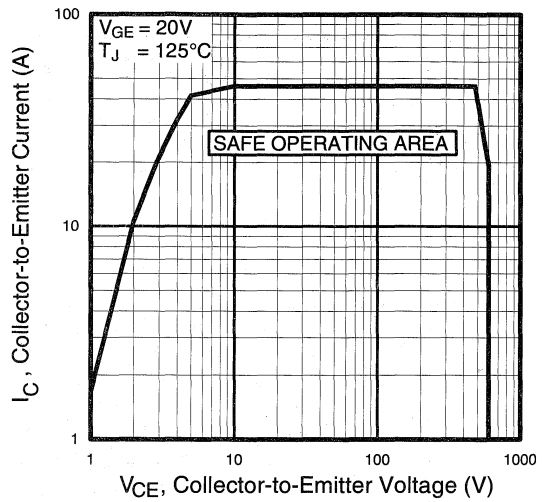


Fig. 12 - Turn-Off SOA

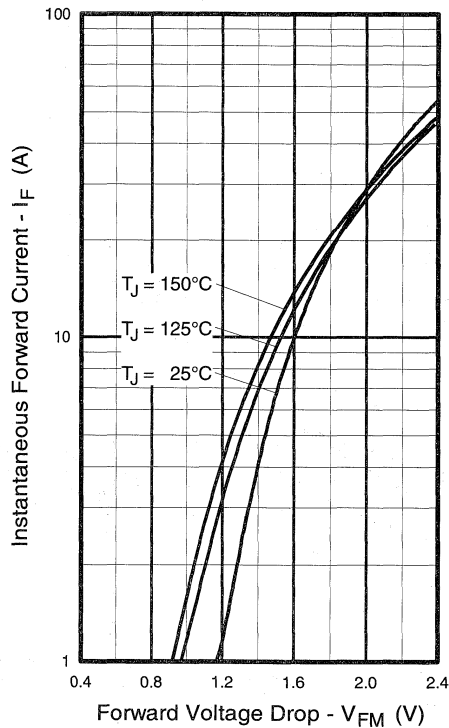


Fig. 13 - Maximum Forward Voltage Drop vs. Instantaneous Forward Current

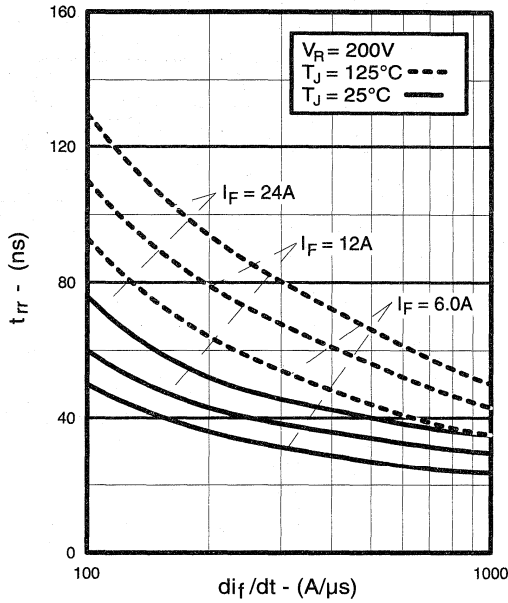


Fig. 14 - Typical Reverse Recovery vs. di_f/dt

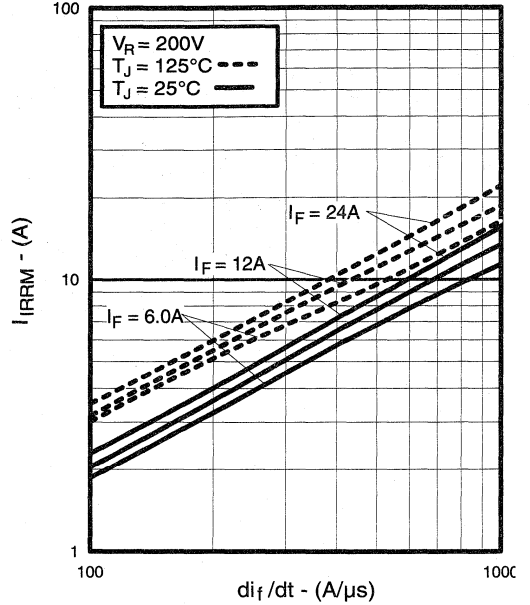


Fig. 15 - Typical Recovery Current vs. di_f/dt

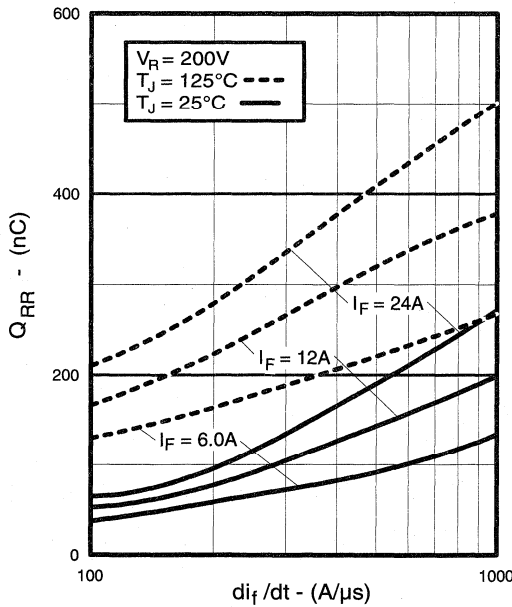


Fig. 16 - Typical Stored Charge vs. di_f/dt

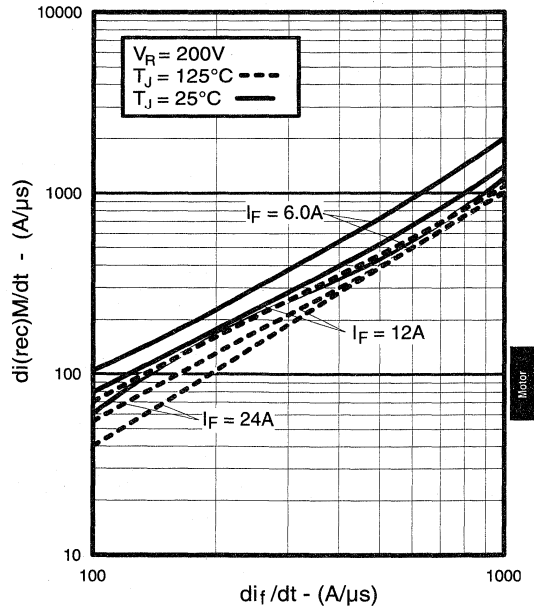


Fig. 17 - Typical $di_{(rec)M}/dt$ vs. di_f/dt

Motor
Control
Ultra-Fast
Cap-Packs

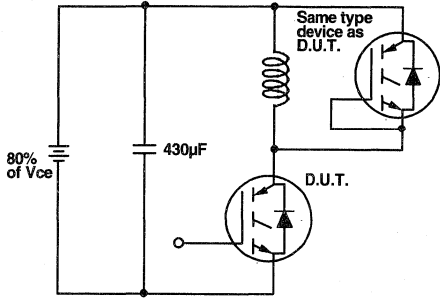


Fig. 18a - Test Circuit for Measurement of I_{LM} , E_{on} , $E_{off}(\text{diode})$, t_{rr} , Q_{rr} , I_{rr} , $t_{d(on)}$, t_r , $t_{d(off)}$, t_f

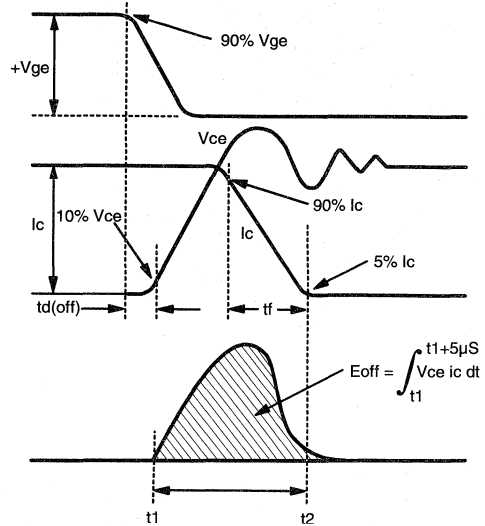


Fig. 18b - Test Waveforms for Circuit of Fig. 18a, Defining E_{off} , $t_{d(off)}$, t_f

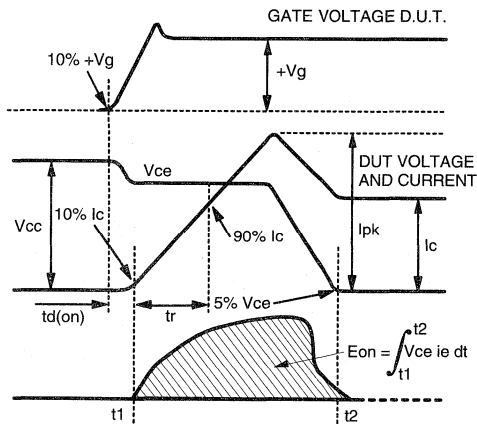


Fig. 18c - Test Waveforms for Circuit of Fig. 18a, Defining E_{on} , $t_{d(on)}$, t_r

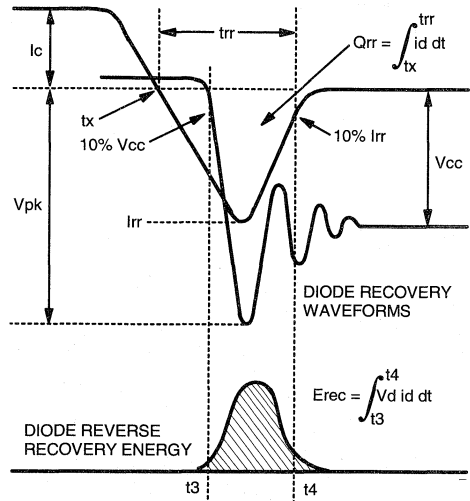


Fig. 18d - Test Waveforms for Circuit of Fig. 18a, Defining E_{rec} , t_{rr} , Q_{rr} , I_{rr}

Refer to Section D for the following:

Appendix D: Section D - page D-6

Fig. 18e - Macro Waveforms for Test Circuit of Fig. 18a

Fig. 19 - Clamped Inductive Load Test Circuit

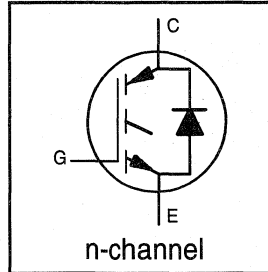
Fig. 20 - Pulsed Collector Current Test Circuit

INSULATED GATE BIPOLAR TRANSISTOR WITH ULTRAFAST SOFT RECOVERY DIODE

Short Circuit Rated
UltraFast CoPack IGBT

Features

- Short circuit rated -10 μ s @ 125°C, $V_{GE} = 15V$
- Switching-loss rating includes all "tail" losses
- HEXFRED™ soft ultrafast diodes
- Optimized for high operating frequency (over 5kHz)
See Fig. 1 for Current vs. Frequency curve



$$V_{CES} = 600V$$

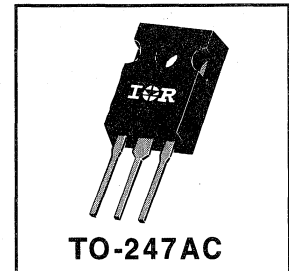
$$V_{CE(sat)} \leq 3.5V$$

$$@ V_{GE} = 15V, I_C = 6.0A$$

Description

Co-packaged IGBTs are a natural extension of International Rectifier's well known IGBT line. They provide the convenience of an IGBT and an ultrafast recovery diode in one package, resulting in substantial benefits to a host of high-voltage, high-current, applications.

These new short circuit rated devices are especially suited for motor control and other applications requiring short circuit withstand capability.



Absolute Maximum Ratings

	Parameter	Max.	Units
V_{CES}	Collector-to-Emitter Voltage	600	V
$I_C @ T_C = 25^\circ C$	Continuous Collector Current	10	A
$I_C @ T_C = 100^\circ C$	Continuous Collector Current	6.0	
I_{CM}	Pulsed Collector Current $\text{\textcircled{D}}$	20	
I_{LM}	Clamped Inductive Load Current $\text{\textcircled{D}}$	20	
$I_F @ T_C = 100^\circ C$	Diode Continuous Forward Current	7.0	
I_{FM}	Diode Maximum Forward Current	20	
t_{sc}	Short Circuit Withstand Time	10	μ s
V_{GE}	Gate-to-Emitter Voltage	± 20	V
$P_D @ T_C = 25^\circ C$	Maximum Power Dissipation	60	W
$P_D @ T_C = 100^\circ C$	Maximum Power Dissipation	24	
T_J	Operating Junction and	-55 to +150	$^\circ C$
T_{STG}	Storage Temperature Range		
	Soldering Temperature, for 10 sec.	300 (0.063 in. (1.6mm) from case)	
	Mounting Torque, 6-32 or M3 Screw.	10 lbf•in (1.1 N•m)	

Thermal Resistance

	Parameter	Min.	Typ.	Max.	Units
$R_{\theta JC}$	Junction-to-Case - IGBT	—	—	2.1	$^\circ C/W$
$R_{\theta JC}$	Junction-to-Case - Diode	—	—	3.5	
$R_{\theta CS}$	Case-to-Sink, flat, greased surface	—	0.24	—	
$R_{\theta JA}$	Junction-to-Ambient, typical socket mount	—	—	40	
Wt	Weight	—	6 (0.21)	—	g (oz)

Electrical Characteristics @ $T_J = 25^\circ\text{C}$ (unless otherwise specified)

	Parameter	Min.	Typ.	Max.	Units	Conditions
$V_{(BR)CES}$	Collector-to-Emitter Breakdown Voltage ^③	600	—	—	V	$V_{GE} = 0V, I_C = 250\mu A$
$\Delta V_{(BR)CES}/\Delta T_J$	Temp. Coeff. of Breakdown Voltage	—	0.37	—	V/ $^\circ\text{C}$	$V_{GE} = 0V, I_C = 1.0mA$
$V_{CE(on)}$	Collector-to-Emitter Saturation Voltage	—	2.4	3.5	V	$I_C = 6.0A, V_{GE} = 15V$
		—	3.6	—		$I_C = 10A$
		—	2.9	—		$I_C = 6.0A, T_J = 150^\circ\text{C}$
$V_{GE(th)}$	Gate Threshold Voltage	3.0	—	5.5		$V_{CE} = V_{GE}, I_C = 250\mu A$
$\Delta V_{GE(th)}/\Delta T_J$	Temperature Coeff. of Threshold Voltage	—	-11	—	mV/ $^\circ\text{C}$	$V_{CE} = V_{GE}, I_C = 250\mu A$
g_{fe}	Forward Transconductance ^④	1.9	3.3	—	S	$V_{CE} = 100V, I_C = 6.0A$
I_{CES}	Zero Gate Voltage Collector Current	—	—	250	μA	$V_{GE} = 0V, V_{CE} = 600V$
		—	—	1700		$V_{GE} = 0V, V_{CE} = 600V, T_J = 150^\circ\text{C}$
V_{FM}	Diode Forward Voltage Drop	—	1.4	1.7	V	$I_C = 8.0A$
		—	1.3	1.6		$I_C = 8.0A, T_J = 150^\circ\text{C}$
I_{GES}	Gate-to-Emitter Leakage Current	—	—	± 100	nA	$V_{GE} = \pm 20V$

Switching Characteristics @ $T_J = 25^\circ\text{C}$ (unless otherwise specified)

	Parameter	Min.	Typ.	Max.	Units	Conditions
Q_g	Total Gate Charge (turn-on)	—	17	26	nC	$I_C = 6.0A$
Q_{ge}	Gate - Emitter Charge (turn-on)	—	4.3	6.8		$V_{CC} = 400V$
Q_{gc}	Gate - Collector Charge (turn-on)	—	6.4	11		See Fig. 8
$t_{d(on)}$	Turn-On Delay Time	—	59	—	ns	$T_J = 25^\circ\text{C}$
t_r	Rise Time	—	38	—		$I_C = 6.0A, V_{CC} = 480V$
$t_{d(off)}$	Turn-Off Delay Time	—	110	210		$V_{GE} = 15V, R_G = 50\Omega$
t_f	Fall Time	—	80	120		Energy losses include "tail" and diode reverse recovery.
E_{on}	Turn-On Switching Loss	—	0.28	—	mJ	See Fig. 9, 10, 11, 18
E_{off}	Turn-Off Switching Loss	—	0.15	—		
E_{ts}	Total Switching Loss	—	0.43	0.90		
t_{sc}	Short Circuit Withstand Time	10	—	—	μs	$V_{CC} = 360V, T_J = 125^\circ\text{C}$ $V_{GE} = 15V, R_G = 50\Omega, V_{CPK} < 500V$
$t_{d(on)}$	Turn-On Delay Time	—	52	—	ns	$T_J = 150^\circ\text{C}$, See Fig. 9, 10, 11, 18
t_r	Rise Time	—	35	—		$I_C = 6.0A, V_{CC} = 480V$
$t_{d(off)}$	Turn-Off Delay Time	—	170	—		$V_{GE} = 15V, R_G = 50\Omega$
t_f	Fall Time	—	170	—		Energy losses include "tail" and diode reverse recovery.
E_{ts}	Total Switching Loss	—	0.65	—	mJ	diode reverse recovery.
L_E	Internal Emitter Inductance	—	13	—	nH	Measured 5mm from package
C_{ies}	Input Capacitance	—	350	—	pF	$V_{GE} = 0V$
C_{oes}	Output Capacitance	—	45	—		$V_{CC} = 30V$
C_{res}	Reverse Transfer Capacitance	—	4.7	—		$f = 1.0MHz$
t_{rr}	Diode Reverse Recovery Time	—	37	55	ns	$T_J = 25^\circ\text{C}$ See Fig.
		—	55	90		$T_J = 125^\circ\text{C}$ 14
I_{rr}	Diode Peak Reverse Recovery Current	—	3.5	5.0	A	$T_J = 25^\circ\text{C}$ See Fig.
		—	4.5	8.0		$T_J = 125^\circ\text{C}$ 15
Q_{rr}	Diode Reverse Recovery Charge	—	65	138	nC	$T_J = 25^\circ\text{C}$ See Fig.
		—	124	360		$T_J = 125^\circ\text{C}$ 16
$di_{(rec)M}/dt$	Diode Peak Rate of Fall of Recovery During t_b	—	240	—	A/ μs	$T_J = 25^\circ\text{C}$ See Fig.
		—	210	—		$T_J = 125^\circ\text{C}$ 17

Notes:

① Repetitive rating; $V_{GE}=20V$, pulse width limited by max. junction temperature. (See fig. 20)

② $V_{CC}=80\%(V_{CES}), V_{GE}=20V, L=10\mu H, R_G=50\Omega$, (See fig. 19)

③ Pulse width $\leq 80\mu s$; duty factor $\leq 0.1\%$.

④ Pulse width $5.0\mu s$, single shot.

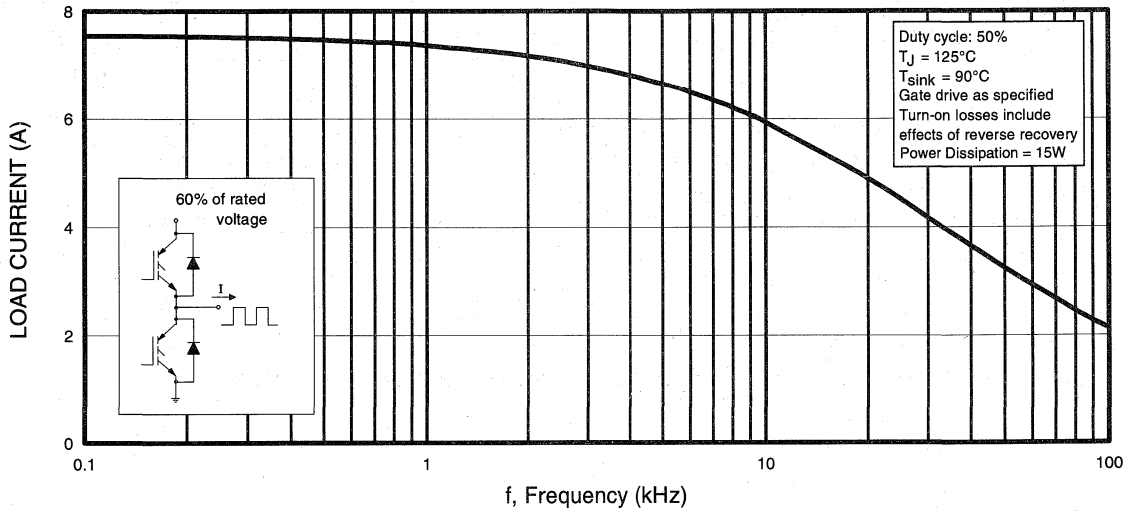


Fig. 1 - Typical Load Current vs. Frequency
(Load Current = I_{RMS} of fundamental)

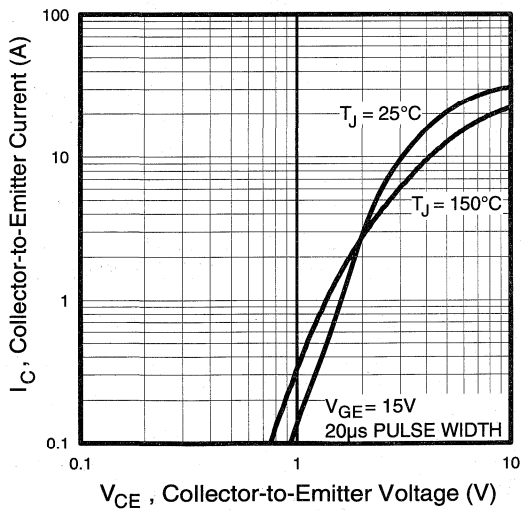


Fig. 2 - Typical Output Characteristics

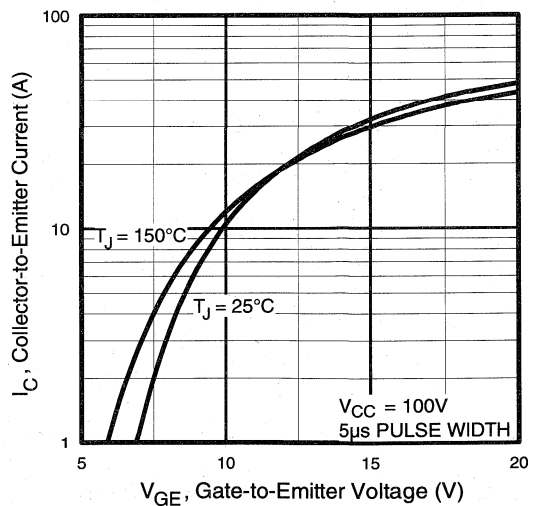


Fig. 3 - Typical Transfer Characteristics

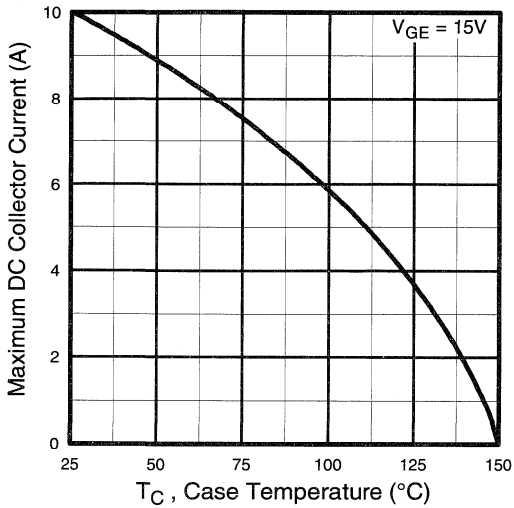


Fig. 4 - Maximum Collector Current vs. Case Temperature

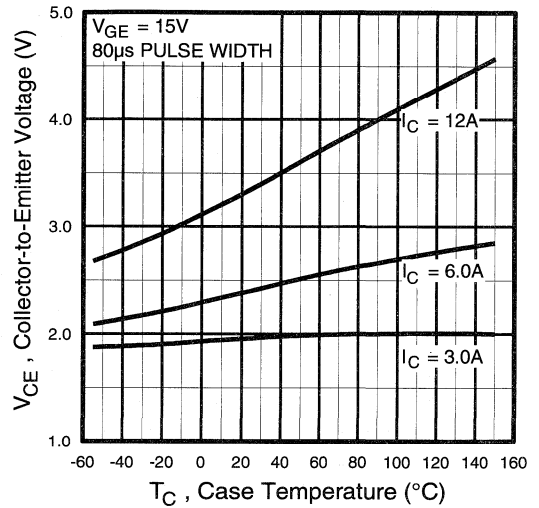


Fig. 5 - Collector-to-Emitter Voltage vs. Case Temperature

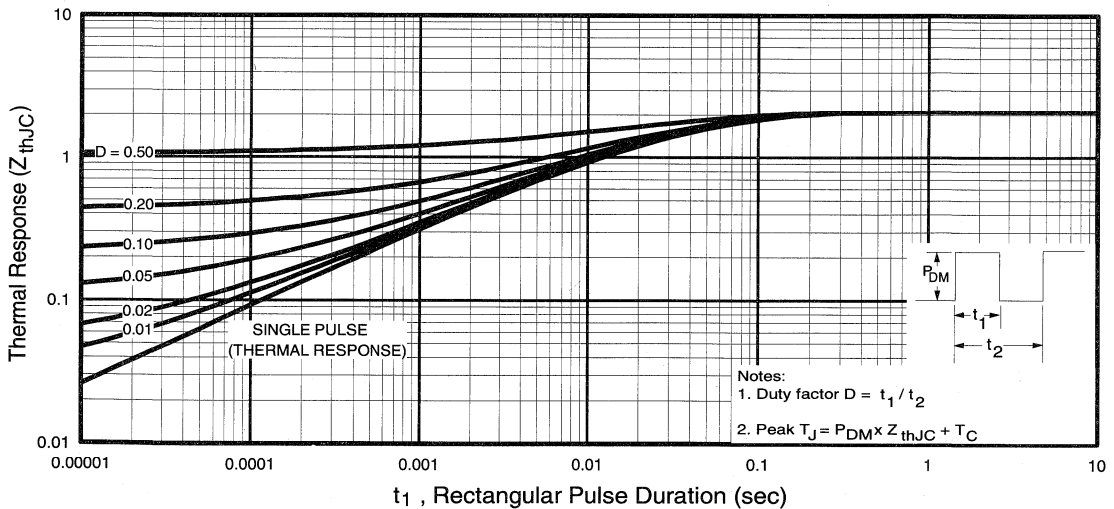


Fig. 6 - Maximum IGBT Effective Transient Thermal Impedance, Junction-to-Case

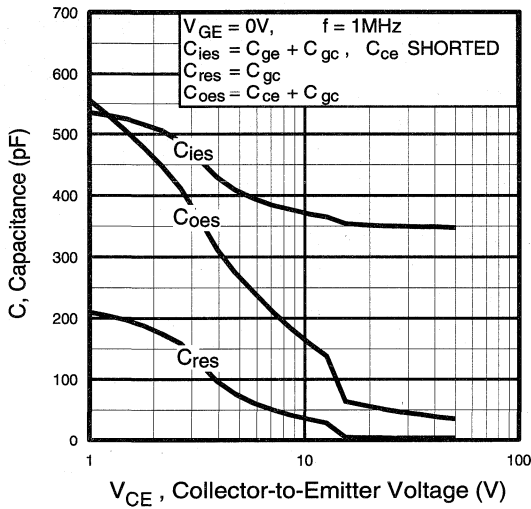


Fig. 7 - Typical Capacitance vs. Collector-to-Emitter Voltage

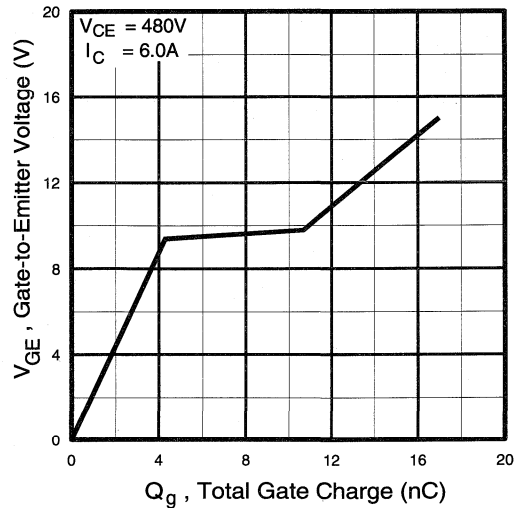


Fig. 8 - Typical Gate Charge vs. Gate-to-Emitter Voltage

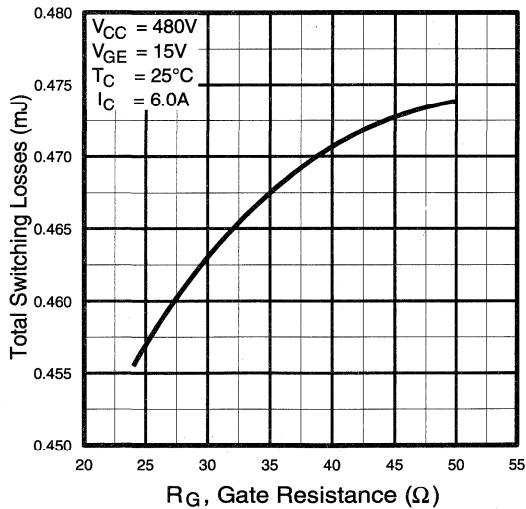


Fig. 9 - Typical Switching Losses vs. Gate Resistance

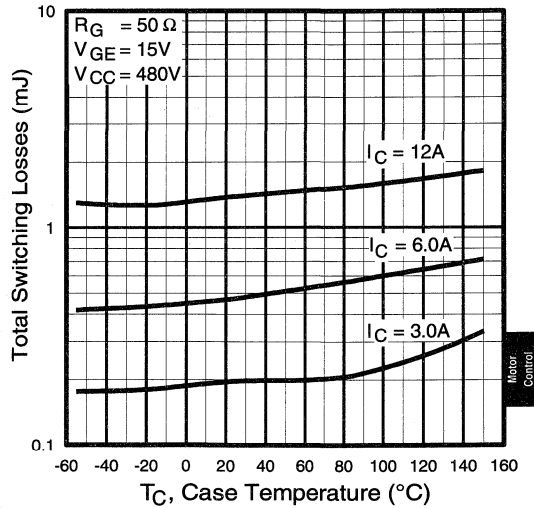


Fig. 10 - Typical Switching Losses vs. Case Temperature

Motor Control
 Ultra-Fast
 Co-Packs

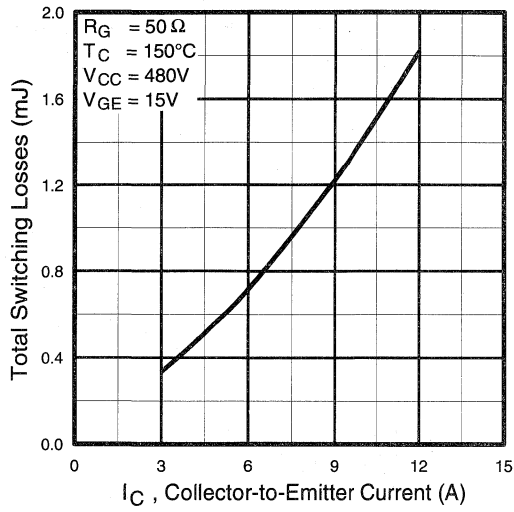


Fig. 11 - Typical Switching Losses vs. Collector-to-Emitter Current

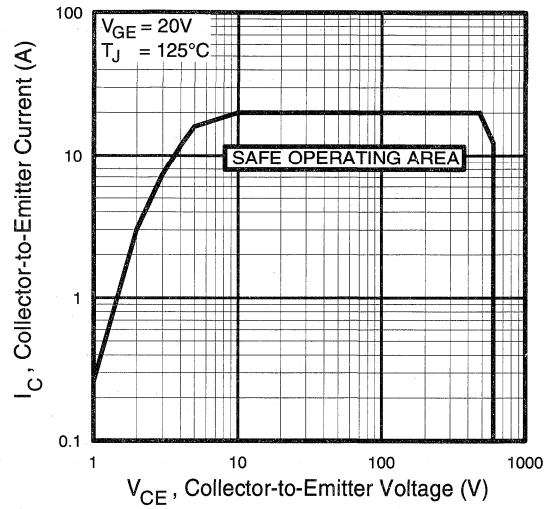


Fig. 12 - Turn-Off SOA

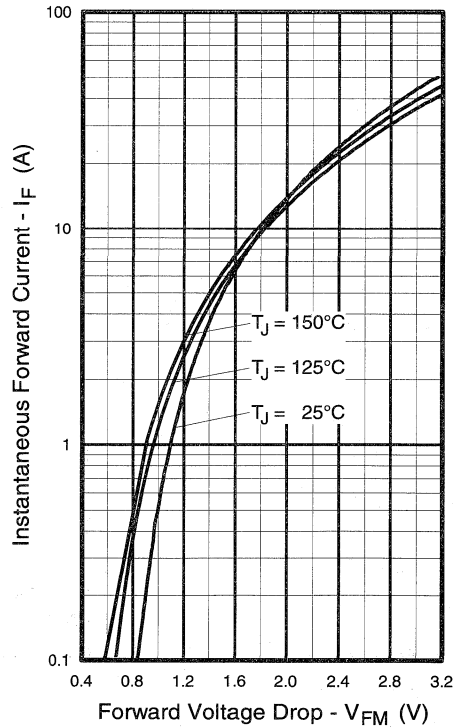


Fig. 13 - Maximum Forward Voltage Drop vs. Instantaneous Forward Current

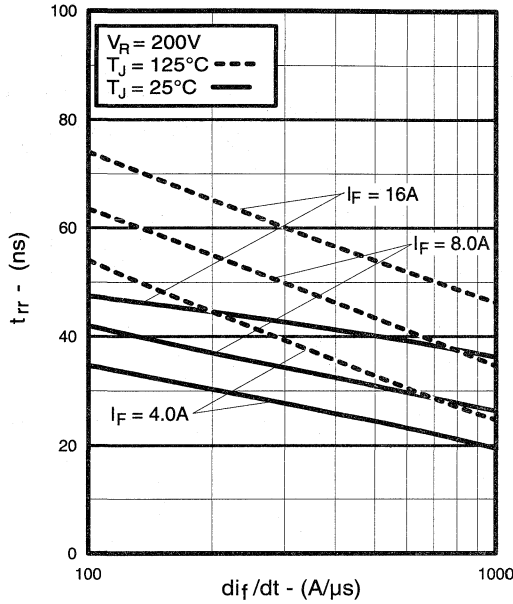


Fig. 14 - Typical Reverse Recovery vs. di_f/dt

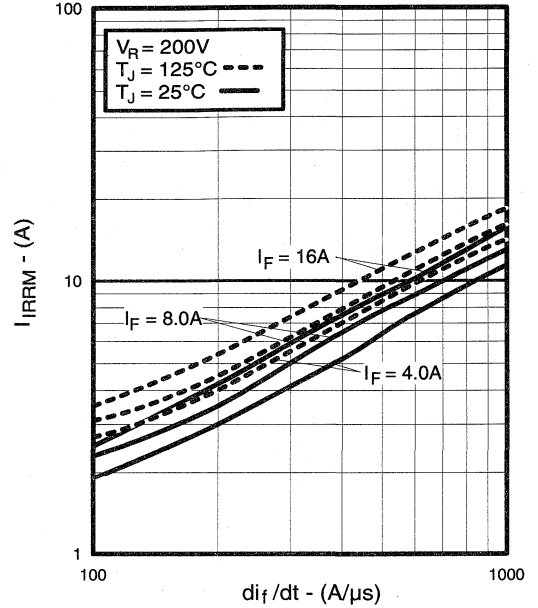


Fig. 15 - Typical Recovery Current vs. di_f/dt

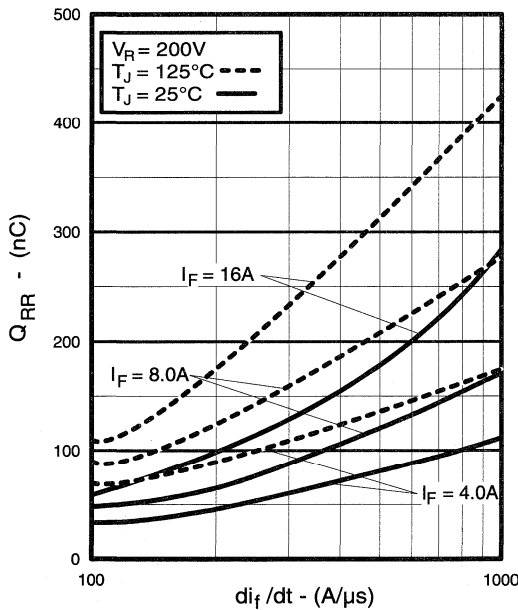


Fig. 16 - Typical Stored Charge vs. di_f/dt

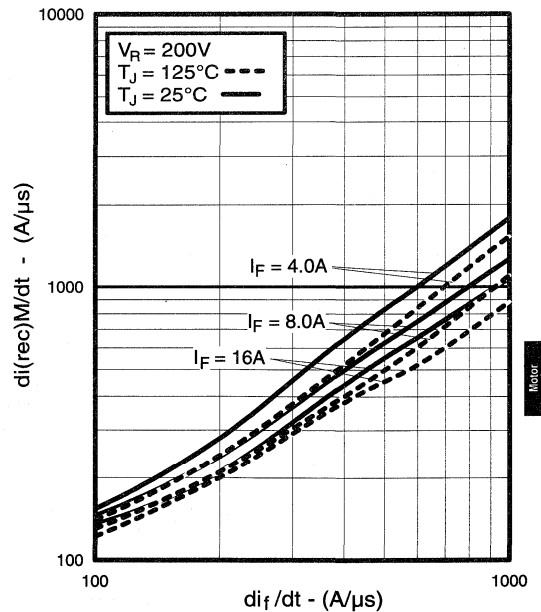


Fig. 17 - Typical $di_{(rec)}M/dt$ vs. di_f/dt

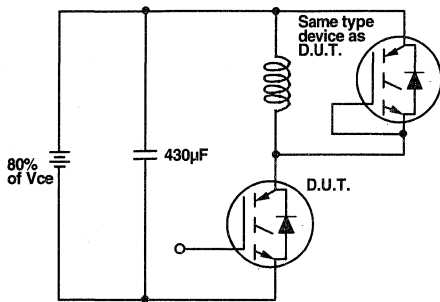


Fig. 18a - Test Circuit for Measurement of I_{LM} , E_{on} , $E_{off}(\text{diode})$, t_{rr} , Q_{rr} , I_{rr} , $t_{d(on)}$, t_r , $t_{d(off)}$, t_f

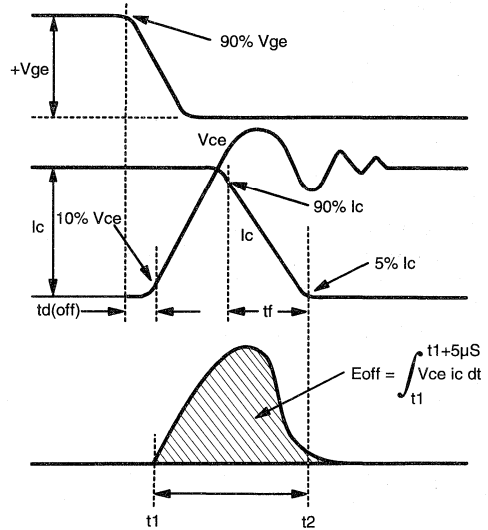


Fig. 18b - Test Waveforms for Circuit of Fig. 18a, Defining E_{off} , $t_{d(off)}$, t_f

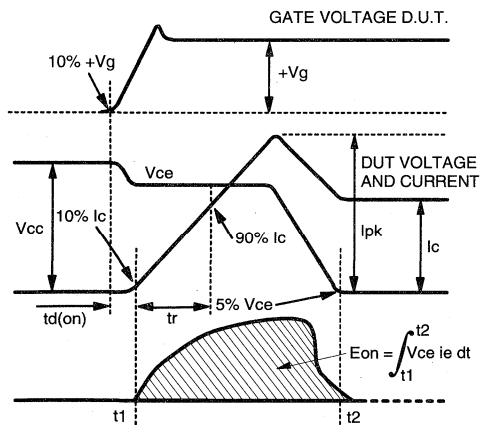


Fig. 18c - Test Waveforms for Circuit of Fig. 18a, Defining E_{on} , $t_{d(on)}$, t_r

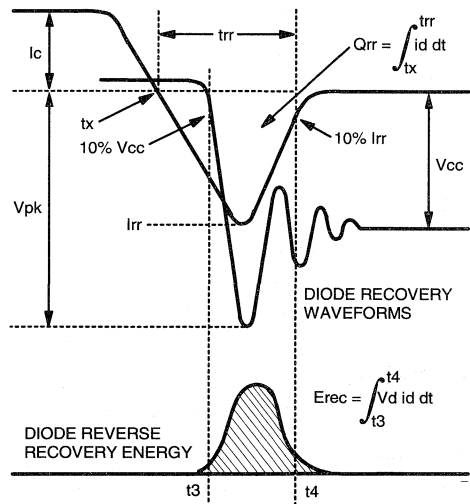


Fig. 18d - Test Waveforms for Circuit of Fig. 18a, Defining E_{rec} , t_{rr} , Q_{rr} , I_{rr}

**Refer to Section D for the following:
Appendix D: Section D - page D-6**

Fig. 18e - Macro Waveforms for Test Circuit of Fig. 18a

Fig. 19 - Clamped Inductive Load Test Circuit

Fig. 20 - Pulsed Collector Current Test Circuit

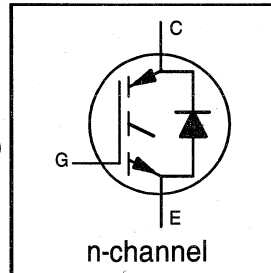
IRGPC30KD2

INSULATED GATE BIPOLAR TRANSISTOR
WITH ULTRAFAST SOFT RECOVERY DIODE

Short Circuit Rated
UltraFast CoPack IGBT

Features

- Short circuit rated -10 μ s @ 125°C, $V_{GE} = 15V$
- Switching-loss rating includes all "tail" losses
- HEXFRED™ soft ultrafast diodes
- Optimized for high operating frequency (over 5kHz)
See Fig. 1 for Current vs. Frequency curve

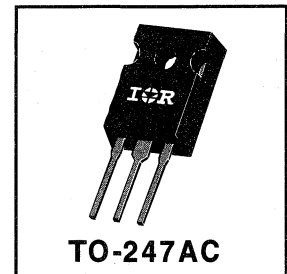


$V_{CES} = 600V$
 $V_{CE(sat)} \leq 3.8V$
@ $V_{GE} = 15V, I_C = 14A$

Description

Co-packaged IGBTs are a natural extension of International Rectifier's well known IGBT line. They provide the convenience of an IGBT and an ultrafast recovery diode in one package, resulting in substantial benefits to a host of high-voltage, high-current, applications.

These new short circuit rated devices are especially suited for motor control and other applications requiring short circuit withstand capability.



Absolute Maximum Ratings

	Parameter	Max.	Units
V_{CES}	Collector-to-Emitter Voltage	600	V
$I_C @ T_C = 25^\circ C$	Continuous Collector Current	23	A
$I_C @ T_C = 100^\circ C$	Continuous Collector Current	14	
I_{CM}	Pulsed Collector Current $\text{\textcircled{D}}$	46	
I_{LM}	Clamped Inductive Load Current $\text{\textcircled{2}}$	46	
$I_F @ T_C = 100^\circ C$	Diode Continuous Forward Current	12	
I_{FM}	Diode Maximum Forward Current	46	
t_{sc}	Short Circuit Withstand Time	10	
V_{GE}	Gate-to-Emitter Voltage	± 20	V
$P_D @ T_C = 25^\circ C$	Maximum Power Dissipation	100	W
$P_D @ T_C = 100^\circ C$	Maximum Power Dissipation	42	
T_J T_{STG}	Operating Junction and Storage Temperature Range	-55 to +150	$^\circ C$
	Soldering Temperature, for 10 sec.	300 (0.063 in. (1.6mm) from case)	
	Mounting Torque, 6-32 or M3 Screw.	10 lbf•in (1.1 Nm)	

Thermal Resistance

	Parameter	Min.	Typ.	Max.	Units
$R_{\theta JC}$	Junction-to-Case - IGBT	—	—	1.2	$^\circ C/W$
$R_{\theta JC}$	Junction-to-Case - Diode	—	—	2.5	
$R_{\theta CS}$	Case-to-Sink, flat, greased surface	—	0.24	—	
$R_{\theta JA}$	Junction-to-Ambient, typical socket mount	—	—	40	
Wt	Weight	—	6 (0.21)	—	g (oz)

Electrical Characteristics @ T_J = 25°C (unless otherwise specified)

	Parameter	Min.	Typ.	Max.	Units	Conditions
V _{(BR)CES}	Collector-to-Emitter Breakdown Voltage ^①	600	—	—	V	V _{GE} = 0V, I _C = 250μA
ΔV _{(BR)CES/ΔT_J}	Temp. Coeff. of Breakdown Voltage	—	0.30	—	V/°C	V _{GE} = 0V, I _C = 1.0mA
V _{CE(on)}	Collector-to-Emitter Saturation Voltage	—	2.5	3.8	V	I _C = 14A, V _{GE} = 15V I _C = 23A, T _J = 150°C See Fig. 2, 5
		—	3.3	—		
		—	2.5	—		
V _{GE(th)}	Gate Threshold Voltage	3.0	—	5.5		V _{CE} = V _{GE} , I _C = 250μA
ΔV _{GE(th)/ΔT_J}	Temperature Coeff. of Threshold Voltage	—	-13	—	mV/°C	V _{CE} = V _{GE} , I _C = 250μA
g _{fe}	Forward Transconductance ^②	3.3	6.5	—	S	V _{CE} = 100V, I _C = 14A
I _{CES}	Zero Gate Voltage Collector Current	—	—	250	μA	V _{GE} = 0V, V _{CE} = 600V V _{GE} = 0V, V _{CE} = 600V, T _J = 150°C
		—	—	2500		
V _{FM}	Diode Forward Voltage Drop	—	1.4	1.5	V	I _C = 12A, T _J = 150°C See Fig. 13
		—	1.3	1.4		
I _{GES}	Gate-to-Emitter Leakage Current	—	—	±100	nA	V _{GE} = ±20V

Switching Characteristics @ T_J = 25°C (unless otherwise specified)

	Parameter	Min.	Typ.	Max.	Units	Conditions
Q _g	Total Gate Charge (turn-on)	—	39	58	nC	I _C = 14A V _{CC} = 400V See Fig. 8
Q _{ge}	Gate - Emitter Charge (turn-on)	—	8.7	13		
Q _{gc}	Gate - Collector Charge (turn-on)	—	15	23		
t _{d(on)}	Turn-On Delay Time	—	67	—	ns	T _J = 25°C I _C = 14A, V _{CC} = 480V V _{GE} = 15V, R _G = 23Ω Energy losses include "tail" and diode reverse recovery.
t _r	Rise Time	—	120	—		
t _{d(off)}	Turn-Off Delay Time	—	110	170		
t _f	Fall Time	—	94	140		
E _{on}	Turn-On Switching Loss	—	1.1	—	mJ	See Fig. 9, 10, 11, 18
E _{off}	Turn-Off Switching Loss	—	0.5	—		
E _{ts}	Total Switching Loss	—	1.6	2.4		
t _{sc}	Short Circuit Withstand Time	10	—	—	μs	V _{CC} = 360V, T _J = 125°C V _{GE} = 15V, R _G = 23Ω, V _{C_{PK}} < 500V
t _{d(on)}	Turn-On Delay Time	—	64	—	ns	T _J = 150°C, See Fig. 9, 10, 11, 18 I _C = 14A, V _{CC} = 480V V _{GE} = 15V, R _G = 23Ω Energy losses include "tail" and diode reverse recovery.
t _r	Rise Time	—	100	—		
t _{d(off)}	Turn-Off Delay Time	—	190	—		
t _f	Fall Time	—	180	—		
E _{ts}	Total Switching Loss	—	2.2	—	mJ	
L _E	Internal Emitter Inductance	—	13	—	nH	Measured 5mm from package
C _{ies}	Input Capacitance	—	740	—	pF	V _{GE} = 0V V _{CC} = 30V, See Fig. 7 f = 1.0MHz
C _{oes}	Output Capacitance	—	92	—		
C _{res}	Reverse Transfer Capacitance	—	9.4	—		
t _{rr}	Diode Reverse Recovery Time	—	42	60	ns	T _J = 25°C See Fig. 14 T _J = 125°C
		—	80	120		
I _{rr}	Diode Peak Reverse Recovery Current	—	3.5	6.0	A	T _J = 25°C See Fig. 15 T _J = 125°C
		—	5.6	10		
Q _{rr}	Diode Reverse Recovery Charge	—	80	180	nC	T _J = 25°C See Fig. 16 T _J = 125°C
		—	220	600		
di _(rec) M/dt	Diode Peak Rate of Fall of Recovery During t _b	—	180	—	A/μs	T _J = 25°C See Fig. 17 T _J = 125°C
		—	120	—		

Notes:

① Repetitive rating; V_{GE}=20V, pulse width limited by max. junction temperature. (See fig. 2)

② V_{CC}=80%(V_{CES}), V_{GE}=20V, L=10μH, R_G= 23Ω, (See fig. 19)

④ Pulse width 5.0μs, single shot.

③ Pulse width ≤ 80μs; duty factor ≤ 0.1%.

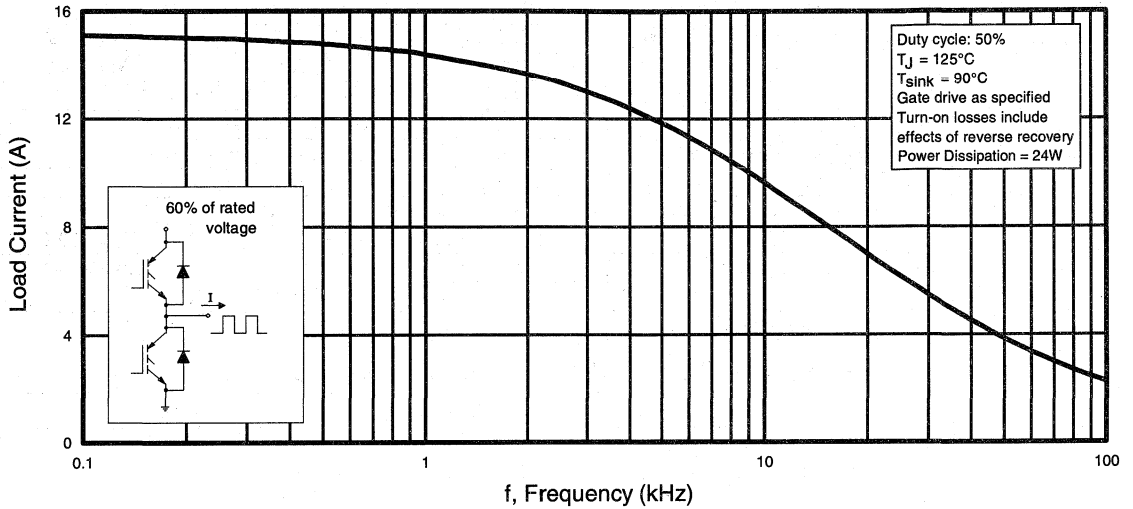


Fig. 1 - Typical Load Current vs. Frequency
(Load Current = I_{RMS} of fundamental)

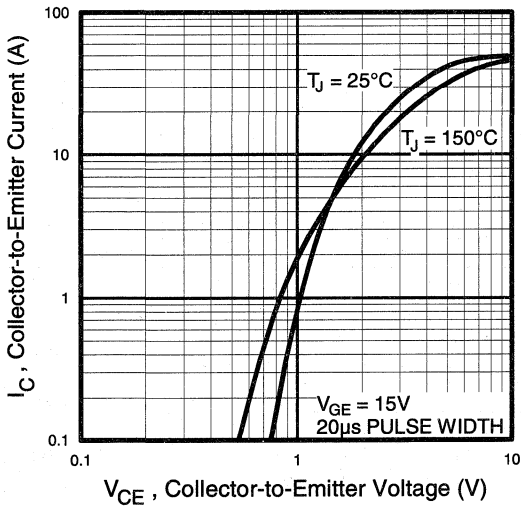


Fig. 2 - Typical Output Characteristics

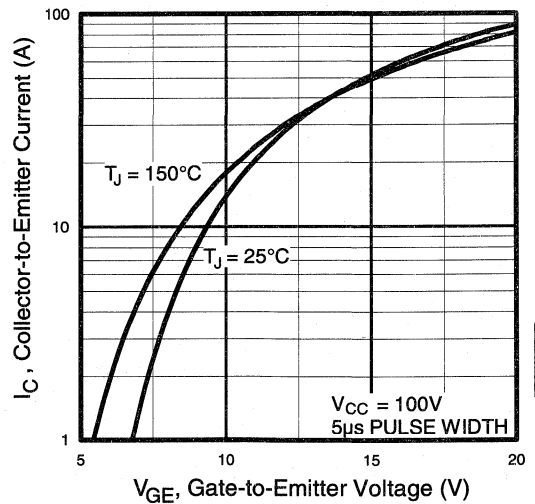


Fig. 3 - Typical Transfer Characteristics

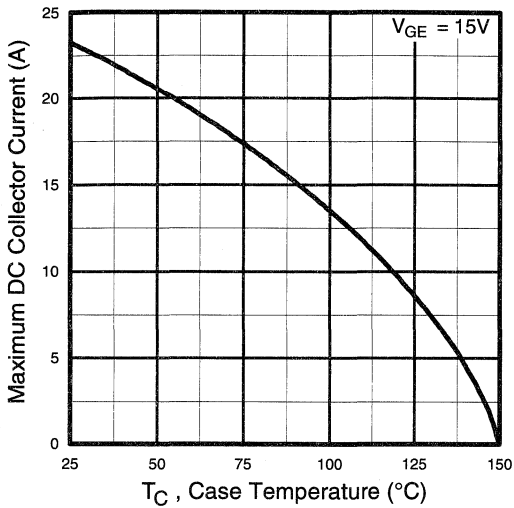


Fig. 4 - Maximum Collector Current vs. Case Temperature

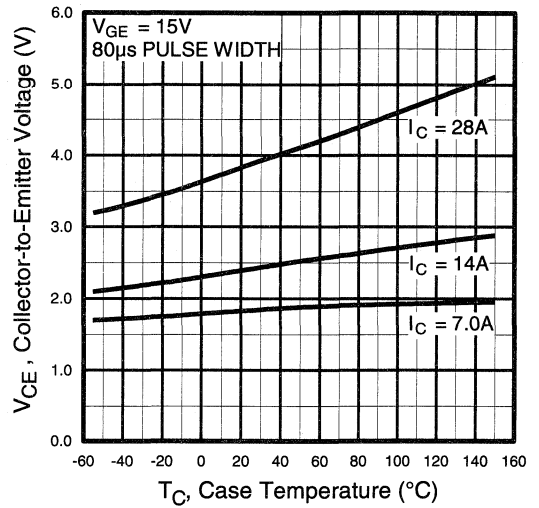


Fig. 5 - Collector-to-Emitter Voltage vs. Case Temperature

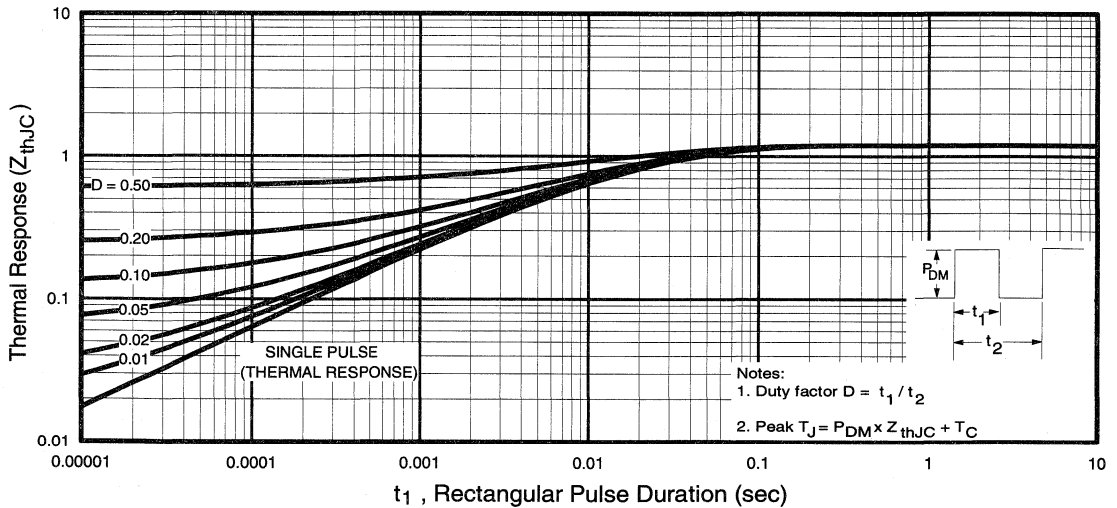


Fig. 6 - Maximum IGBT Effective Transient Thermal Impedance, Junction-to-Case

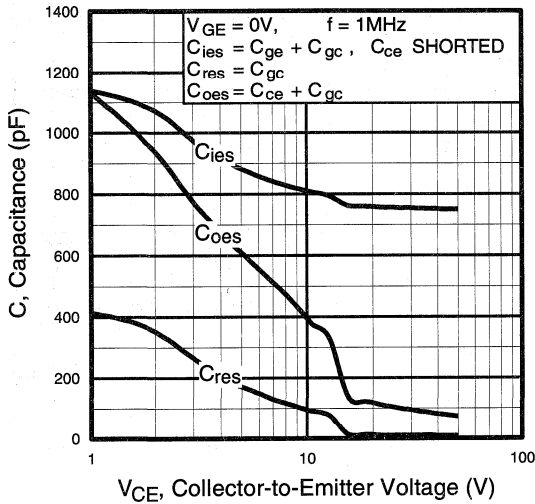


Fig. 7 - Typical Capacitance vs. Collector-to-Emitter Voltage

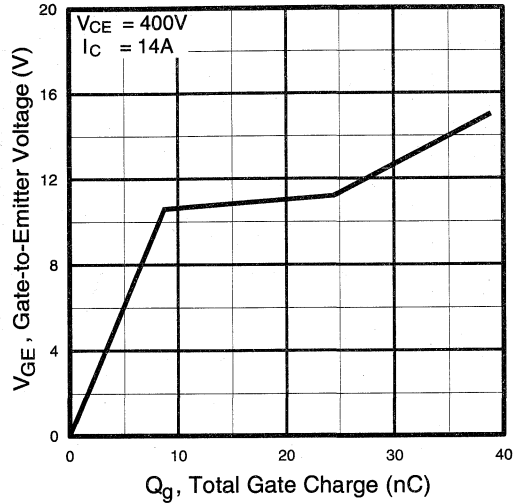


Fig. 8 - Typical Gate Charge vs. Gate-to-Emitter Voltage

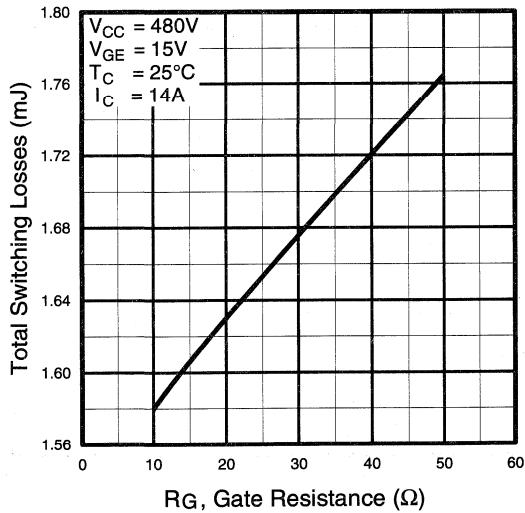


Fig. 9 - Typical Switching Losses vs. Gate Resistance

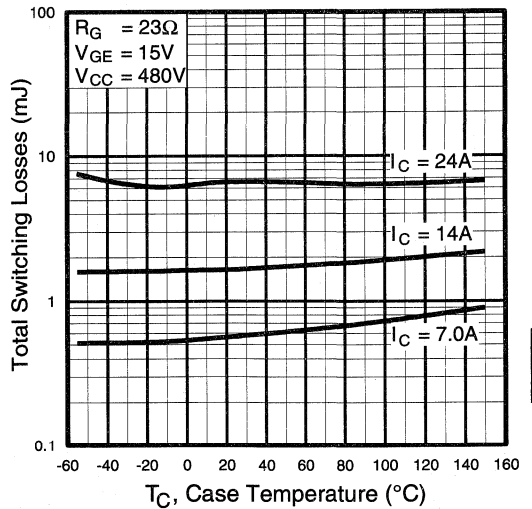


Fig. 10 - Typical Switching Losses vs. Case Temperature

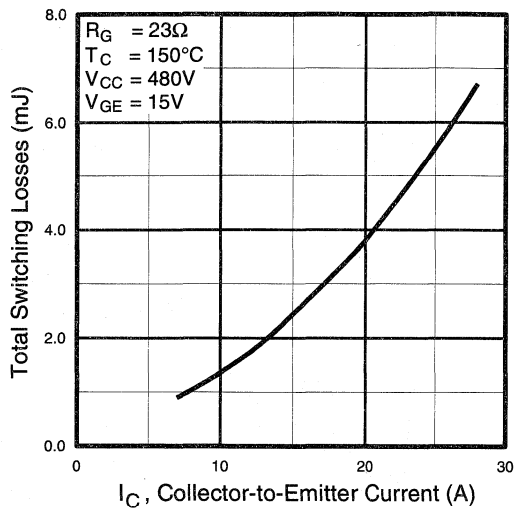


Fig. 11 - Typical Switching Losses vs. Collector-to-Emitter Current

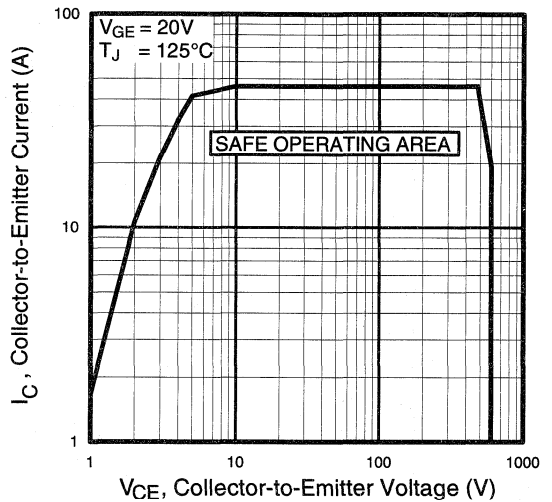


Fig. 12 - Turn-Off SOA

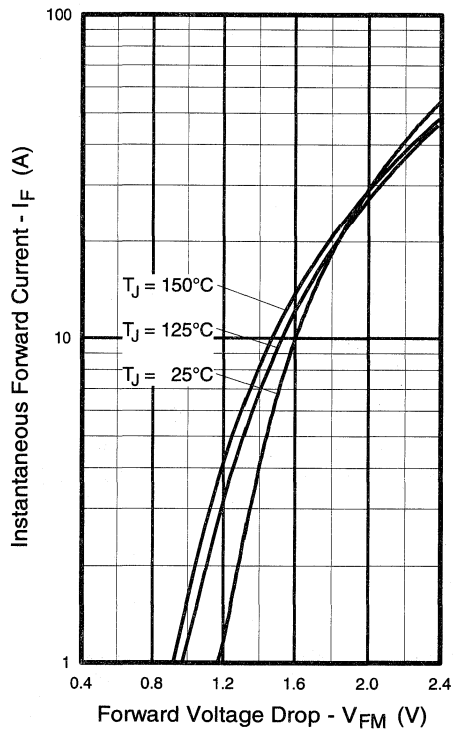


Fig. 13 - Maximum Forward Voltage Drop vs. Instantaneous Forward Current

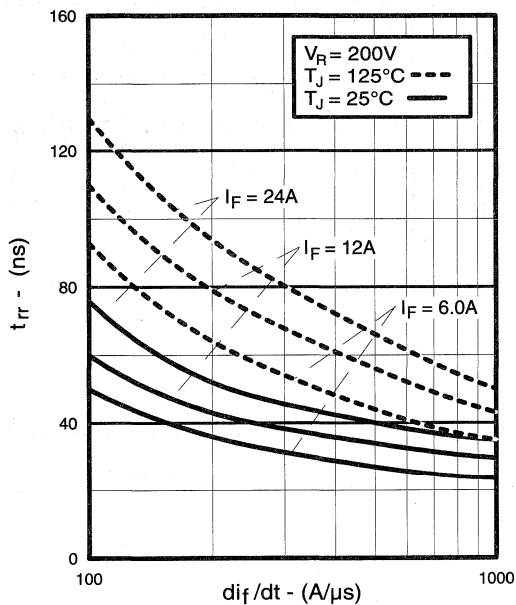


Fig. 14 - Typical Reverse Recovery vs. di_f/dt

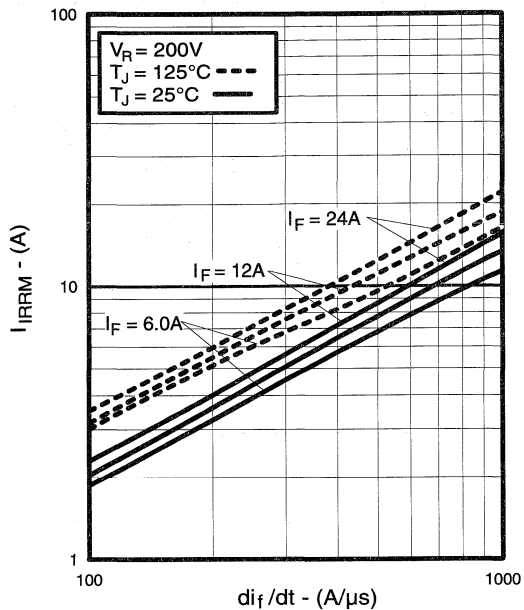


Fig. 15 - Typical Recovery Current vs. di_f/dt

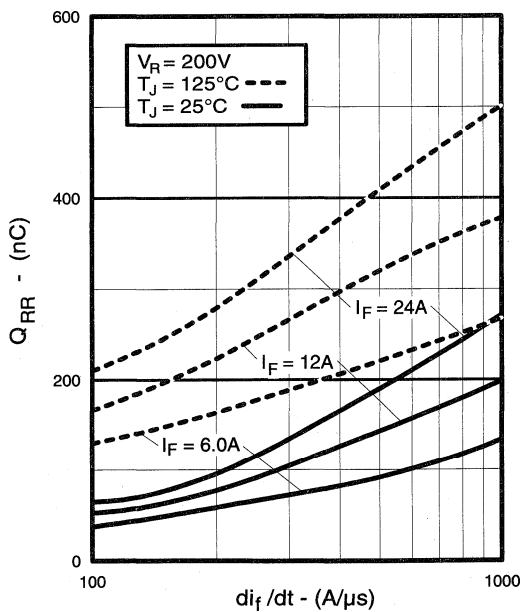


Fig. 16 - Typical Stored Charge vs. di_f/dt

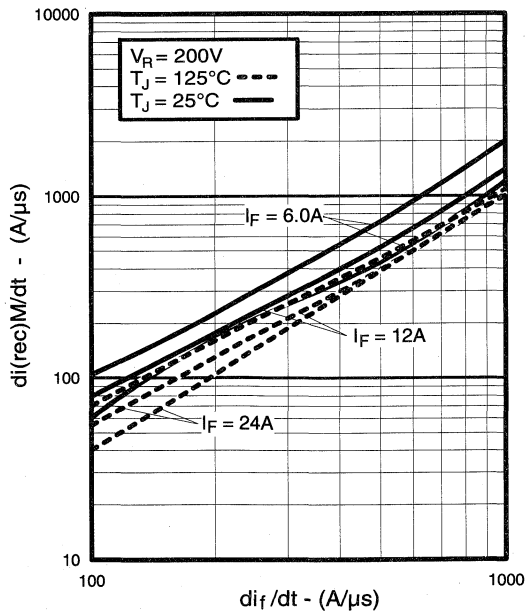


Fig. 17 - Typical $di_{(rec)M}/dt$ vs. di_f/dt

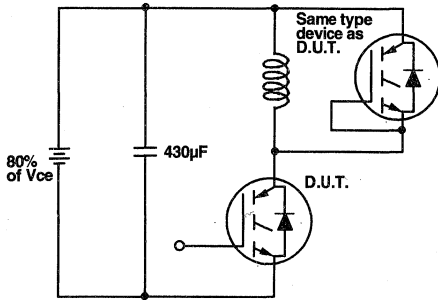


Fig. 18a - Test Circuit for Measurement of I_{LM} , E_{on} , $E_{off}(\text{diode})$, t_{rr} , Q_{rr} , I_{rr} , $t_{d(on)}$, t_r , $t_{d(off)}$, t_f

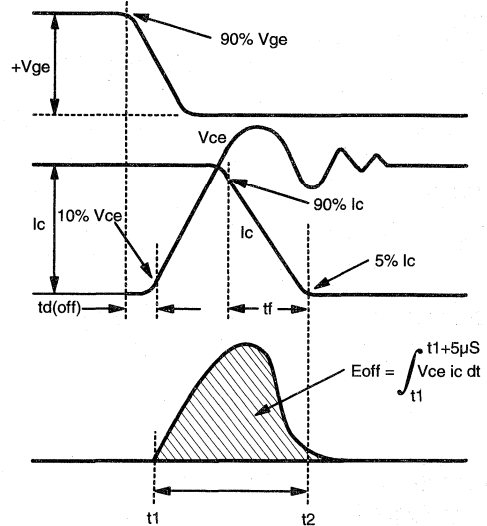


Fig. 18b - Test Waveforms for Circuit of Fig. 18a, Defining E_{off} , $t_{d(off)}$, t_f

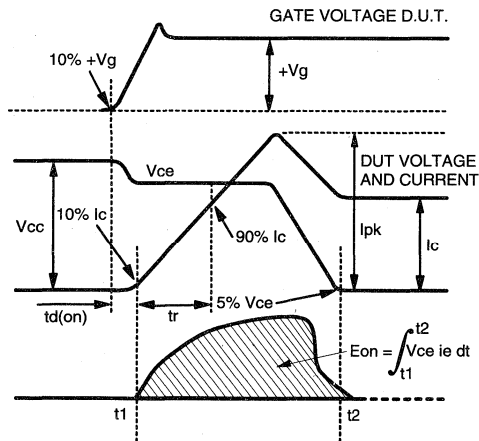


Fig. 18c - Test Waveforms for Circuit of Fig. 18a, Defining E_{on} , $t_{d(on)}$, t_r

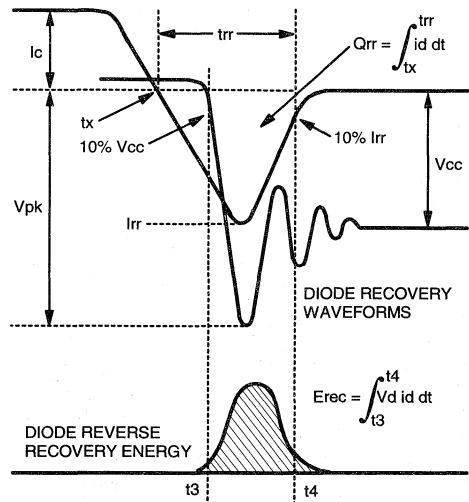


Fig. 18d - Test Waveforms for Circuit of Fig. 18a, Defining E_{rec} , t_{rr} , Q_{rr} , I_{rr}

Refer to Section D for the following:
Appendix D: Section D - page D-6

- Fig. 18e - Macro Waveforms for Test Circuit of Fig. 18a
- Fig. 19 - Clamped Inductive Load Test Circuit
- Fig. 20 - Pulsed Collector Current Test Circuit

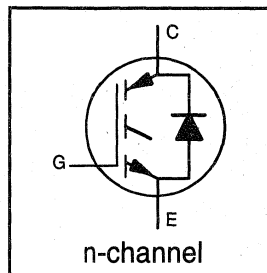
IRGPC40KD2

INSULATED GATE BIPOLAR TRANSISTOR
WITH ULTRAFAST SOFT RECOVERY DIODE

Short Circuit Rated
UltraFast CoPack IGBT

Features

- Short circuit rated -10 μ s @ 125°C, $V_{GE} = 15V$
- Switching-loss rating includes all "tail" losses
- HEXFRED™ soft ultrafast diodes
- Optimized for high operating frequency (over 5kHz)
See Fig. 1 for Current vs. Frequency curve



$$V_{CES} = 600V$$

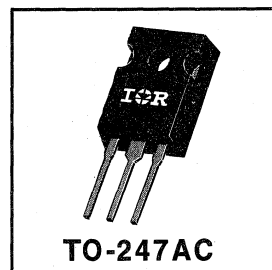
$$V_{CE(sat)} \leq 3.2V$$

$$@ V_{GE} = 15V, I_C = 25A$$

Description

Co-packaged IGBTs are a natural extension of International Rectifier's well known IGBT line. They provide the convenience of an IGBT and an ultrafast recovery diode in one package, resulting in substantial benefits to a host of high-voltage, high-current, applications.

These new short circuit rated devices are especially suited for motor control and other applications requiring short circuit withstand capability.



Absolute Maximum Ratings

	Parameter	Max.	Units
V_{CES}	Collector-to-Emitter Voltage	600	V
$I_C @ T_C = 25^\circ C$	Continuous Collector Current	42	A
$I_C @ T_C = 100^\circ C$	Continuous Collector Current	25	
I_{CM}	Pulsed Collector Current ①	84	
I_{LM}	Clamped Inductive Load Current ②	84	
$I_F @ T_C = 100^\circ C$	Diode Continuous Forward Current	15	
I_{FM}	Diode Maximum Forward Current	84	
t_{sc}	Short Circuit Withstand Time	10	μ s
V_{GE}	Gate-to-Emitter Voltage	± 20	V
$P_D @ T_C = 25^\circ C$	Maximum Power Dissipation	160	W
$P_D @ T_C = 100^\circ C$	Maximum Power Dissipation	65	
T_J	Operating Junction and	-55 to +150	$^\circ C$
T_{STG}	Storage Temperature Range		
	Soldering Temperature, for 10 sec.	300 (0.063 in. (1.6mm) from case)	
	Mounting Torque, 6-32 or M3 Screw.	10 lbf•in (1.1 N•m)	

Thermal Resistance

	Parameter	Min.	Typ.	Max.	Units
$R_{\theta JC}$	Junction-to-Case - IGBT	—	—	0.77	$^\circ C/W$
$R_{\theta JC}$	Junction-to-Case - Diode	—	—	1.7	
$R_{\theta CS}$	Case-to-Sink, flat, greased surface	—	0.24	—	
$R_{\theta JA}$	Junction-to-Ambient, typical socket mount	—	—	40	
Wt	Weight	—	6 (0.21)	—	g (oz)

Electrical Characteristics @ T_J = 25°C (unless otherwise specified)

	Parameter	Min.	Typ.	Max.	Units	Conditions
V _{(BR)CES}	Collector-to-Emitter Breakdown Voltage ^③	600	—	—	V	V _{GE} = 0V, I _C = 250μA
ΔV _{(BR)CES} /ΔT _J	Temp. Coeff. of Breakdown Voltage	—	0.46	—	V/°C	V _{GE} = 0V, I _C = 1.0mA
V _{CE(on)}	Collector-to-Emitter Saturation Voltage	—	2.1	3.2	V	I _C = 25A, V _{GE} = 15V
		—	2.8	—		I _C = 42A, V _{GE} = 15V
		—	2.5	—		I _C = 25A, T _J = 150°C
V _{GE(th)}	Gate Threshold Voltage	3.0	—	5.5		V _{CE} = V _{GE} , I _C = 250μA
ΔV _{GE(th)} /ΔT _J	Temperature Coeff. of Threshold Voltage	—	-13	—	mV/°C	V _{CE} = V _{GE} , I _C = 250μA
g _{fe}	Forward Transconductance ^④	7.0	14	—	S	V _{CE} = 100V, I _C = 25A
I _{CES}	Zero Gate Voltage Collector Current	—	—	250	μA	V _{GE} = 0V, V _{CE} = 600V
		—	—	3500		V _{GE} = 0V, V _{CE} = 600V, T _J = 150°C
V _{FM}	Diode Forward Voltage Drop	—	1.3	1.7	V	I _C = 15A, V _{GE} = 0V
		—	1.2	1.6		I _C = 15A, T _J = 150°C
I _{GES}	Gate-to-Emitter Leakage Current	—	—	±100	nA	V _{GE} = ±20V

Switching Characteristics @ T_J = 25°C (unless otherwise specified)

	Parameter	Min.	Typ.	Max.	Units	Conditions
Q _g	Total Gate Charge (turn-on)	—	61	92	nC	I _C = 25A
Q _{ge}	Gate - Emitter Charge (turn-on)	—	13	19		V _{CC} = 400V
Q _{gc}	Gate - Collector Charge (turn-on)	—	22	33		See Fig. 8
t _{d(on)}	Turn-On Delay Time	—	72	—	ns	T _J = 25°C
t _r	Rise Time	—	90	—		I _C = 25A, V _{CC} = 480V
t _{d(off)}	Turn-Off Delay Time	—	170	250		V _{GE} = 15V, R _G = 10Ω
t _f	Fall Time	—	140	220		Energy losses include "tail" and diode reverse recovery.
E _{on}	Turn-On Switching Loss	—	1.5	—		mJ
E _{off}	Turn-Off Switching Loss	—	1.5	—		
E _{ts}	Total Switching Loss	—	3.0	4.2		
t _{sc}	Short Circuit Withstand Time	10	—	—	μs	V _{CC} = 360V, T _J = 125°C V _{GE} = 15V, R _G = 10Ω, V _{CPK} < 500V
t _{d(on)}	Turn-On Delay Time	—	70	—	ns	T _J = 150°C, V _{CC} = 480V, V _{GE} = 15V, R _G = 10Ω
t _r	Rise Time	—	86	—		See Fig. 9, 10, 11, 18
t _{d(off)}	Turn-Off Delay Time	—	280	—		I _C = 25A, V _{CC} = 480V
t _f	Fall Time	—	270	—		V _{GE} = 15V, R _G = 10Ω
E _{ts}	Total Switching Loss	—	4.2	—		Energy losses include "tail" and diode reverse recovery.
L _E	Internal Emitter Inductance	—	13	—	nH	Measured 5mm from package
C _{ies}	Input Capacitance	—	1500	—	pF	V _{GE} = 0V
C _{oes}	Output Capacitance	—	190	—		V _{CC} = 30V
C _{res}	Reverse Transfer Capacitance	—	17	—		f = 1.0MHz
t _{rr}	Diode Reverse Recovery Time	—	42	60	ns	T _J = 25°C, I _F = 15A
		—	74	120		T _J = 125°C, I _F = 15A
I _{rr}	Diode Peak Reverse Recovery Current	—	4.0	6.0	A	T _J = 25°C, V _R = 200V
		—	6.5	10		T _J = 125°C, V _R = 200V
Q _{rr}	Diode Reverse Recovery Charge	—	80	180	nC	T _J = 25°C, di/dt = 200A/μs
		—	220	600		T _J = 125°C, di/dt = 200A/μs
di _{(rec)M} /dt	Diode Peak Rate of Fall of Recovery During t _b	—	188	—	A/μs	T _J = 25°C, di/dt = 200A/μs
		—	160	—		T _J = 125°C, di/dt = 200A/μs

Notes:

① Repetitive rating; V_{GE}=20V, pulse width limited by max. junction temperature. (See fig. 20)

② V_{CC}=80%(V_{CES}), V_{GE}=20V, L=10μH, R_G = 10Ω, (See fig. 19)

③ Pulse width ≤ 80μs; duty factor ≤ 0.1%.

④ Pulse width 5.0μs, single shot.

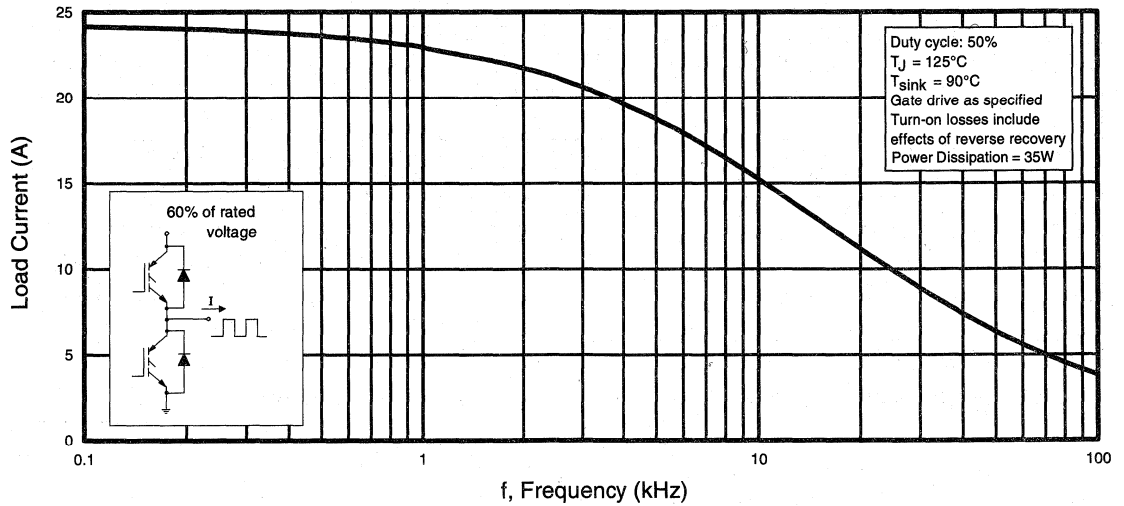


Fig. 1 - Typical Load Current vs. Frequency
 (Load Current = I_{RMS} of fundamental)

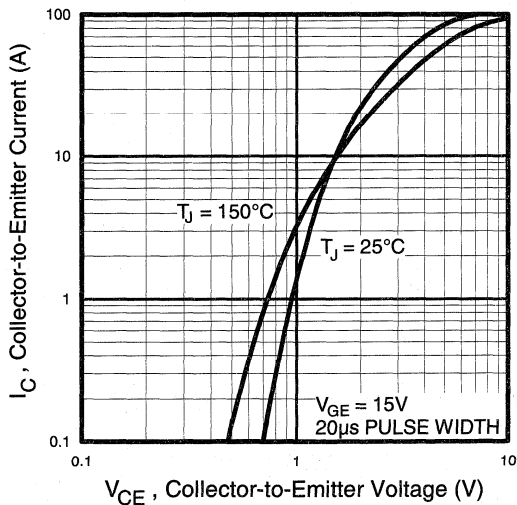


Fig. 2 - Typical Output Characteristics

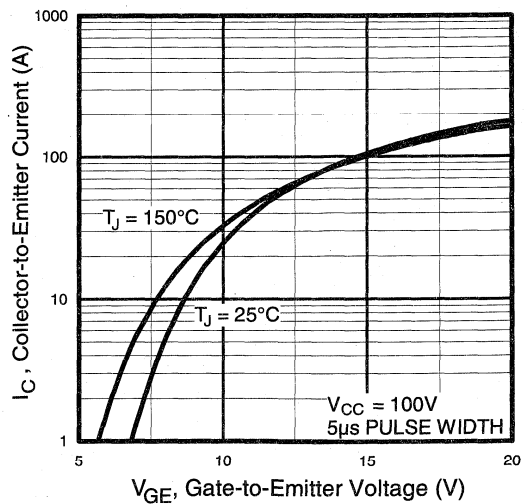


Fig. 3 - Typical Transfer Characteristics

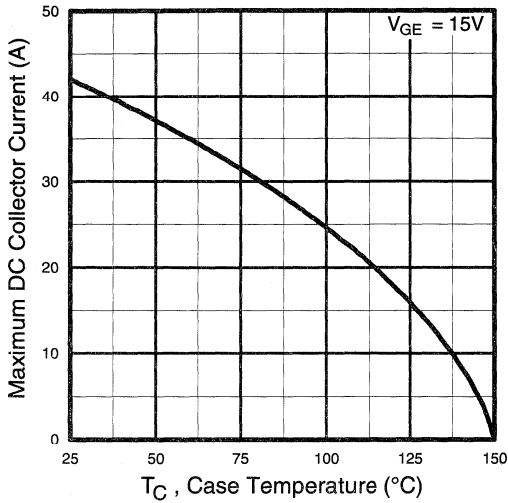


Fig. 4 - Maximum Collector Current vs. Case Temperature

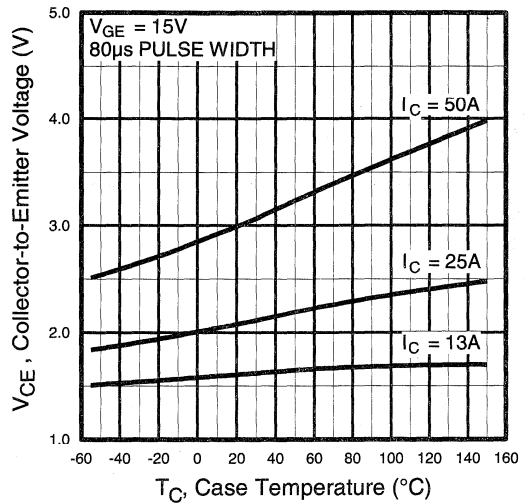


Fig. 5 - Collector-to-Emitter Voltage vs. Case Temperature

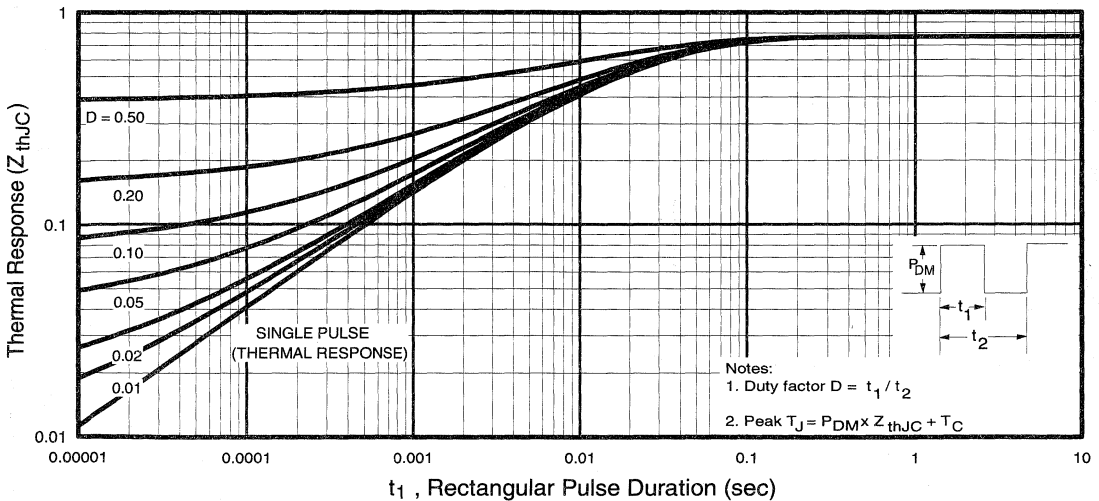


Fig. 6 - Maximum IGBT Effective Transient Thermal Impedance, Junction-to-Case

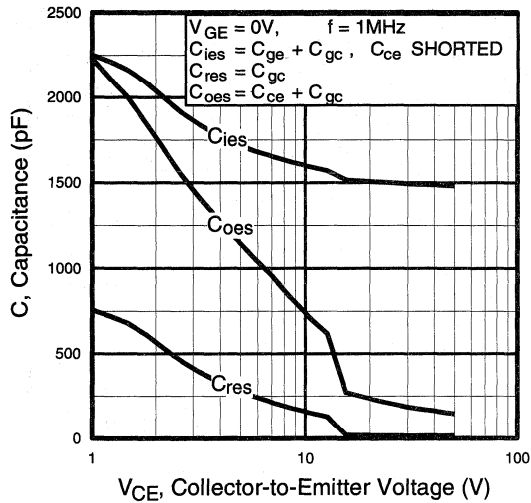


Fig. 7 - Typical Capacitance vs. Collector-to-Emitter Voltage

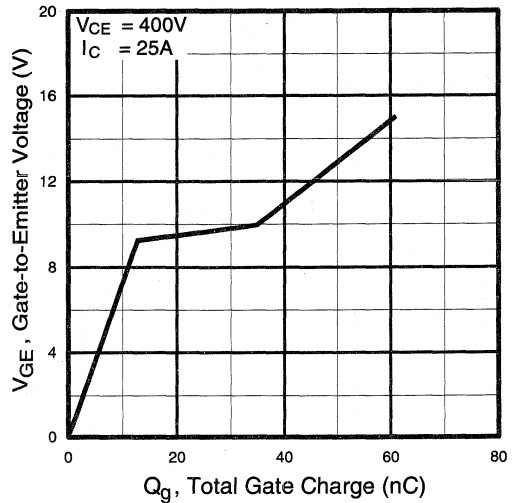


Fig. 8 - Typical Gate Charge vs. Gate-to-Emitter Voltage

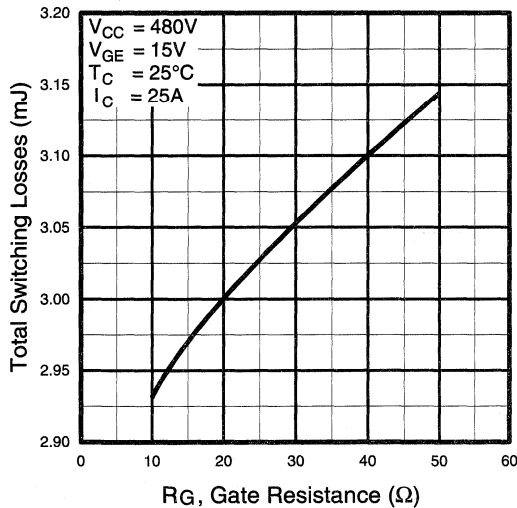


Fig. 9 - Typical Switching Losses vs. Gate Resistance

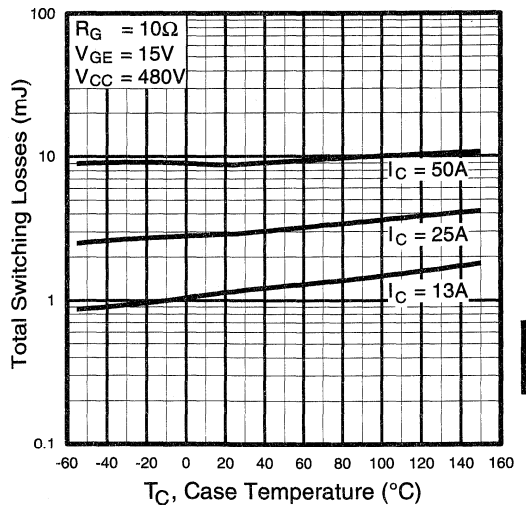


Fig. 10 - Typical Switching Losses vs. Case Temperature

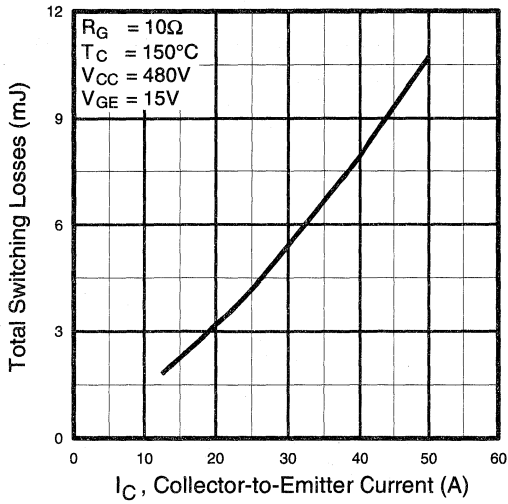


Fig. 11 - Typical Switching Losses vs. Collector-to-Emitter Current

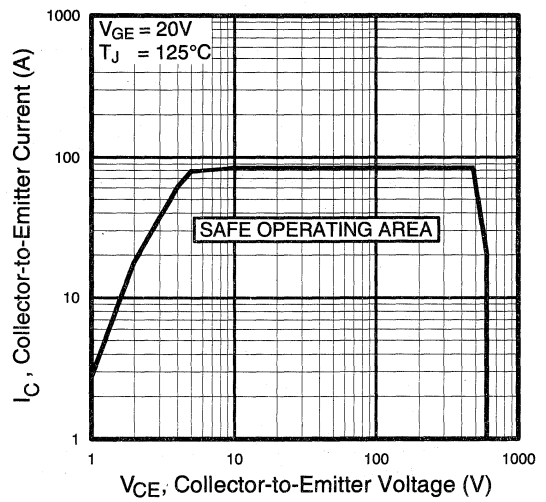


Fig. 12 - Turn-Off SOA

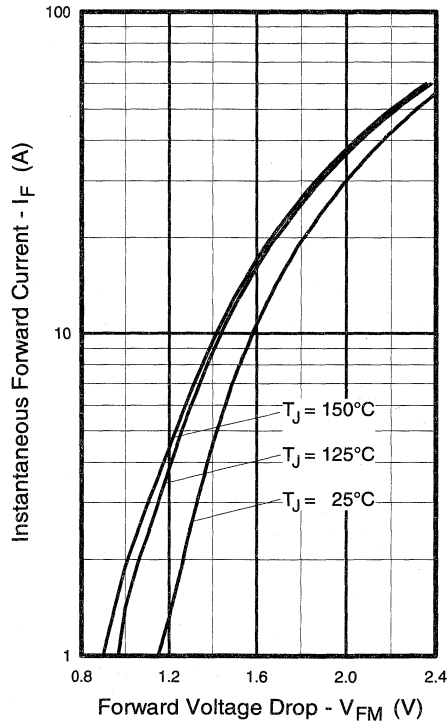


Fig. 13 - Maximum Forward Voltage Drop vs. Instantaneous Forward Current

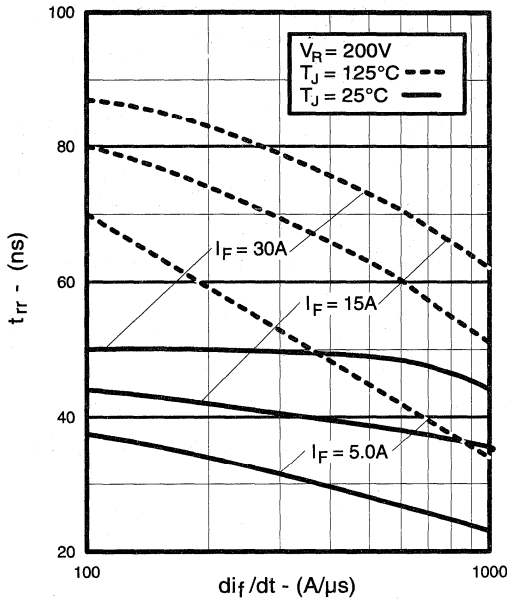


Fig. 14 - Typical Reverse Recovery vs. di_f/dt

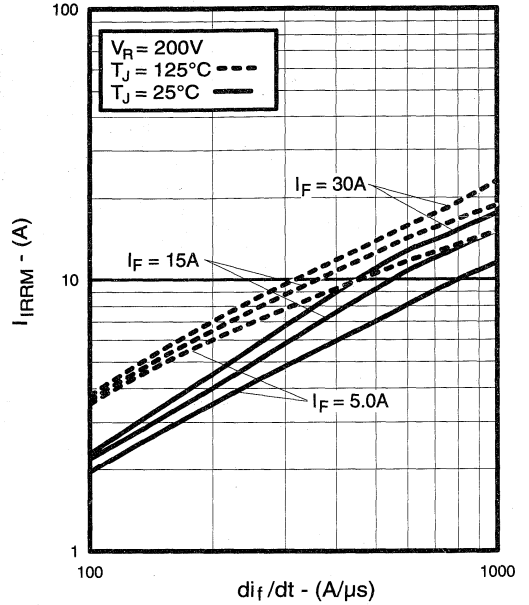


Fig. 15 - Typical Recovery Current vs. di_f/dt

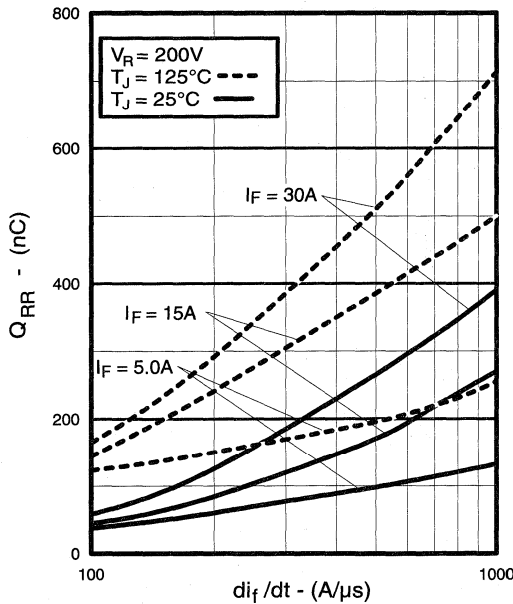


Fig. 16 - Typical Stored Charge vs. di_f/dt

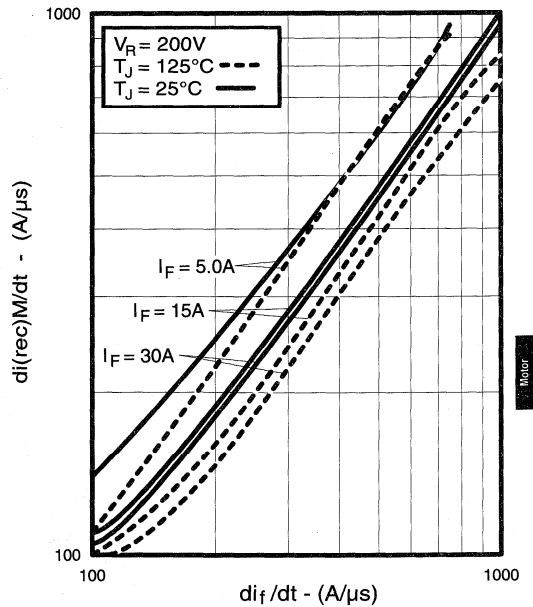


Fig. 17 - Typical $di_{(rec)M}/dt$ vs. di_f/dt

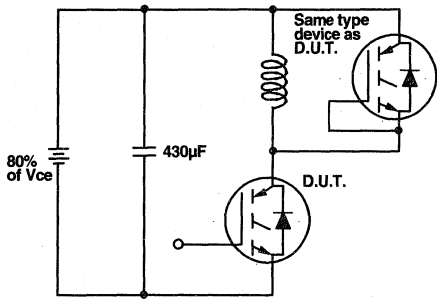


Fig. 18a - Test Circuit for Measurement of I_{LM} , E_{on} , $E_{off}(\text{diode})$, t_{rr} , Q_{rr} , I_{rr} , $t_{d(on)}$, t_r , $t_{d(off)}$, t_f

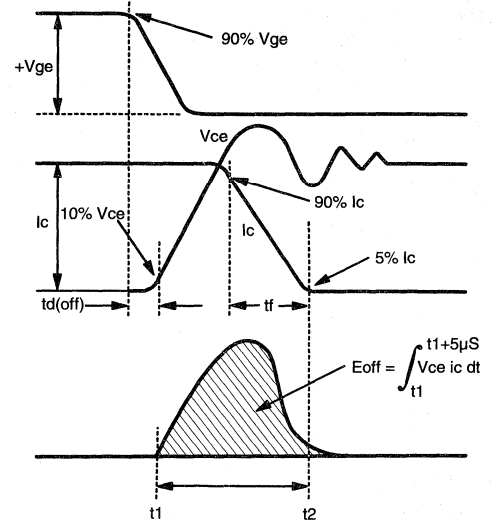


Fig. 18b - Test Waveforms for Circuit of Fig. 18a, Defining E_{off} , $t_{d(off)}$, t_f

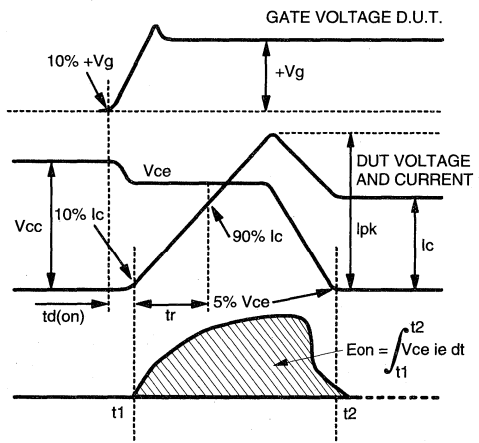


Fig. 18c - Test Waveforms for Circuit of Fig. 18a, Defining E_{on} , $t_{d(on)}$, t_r

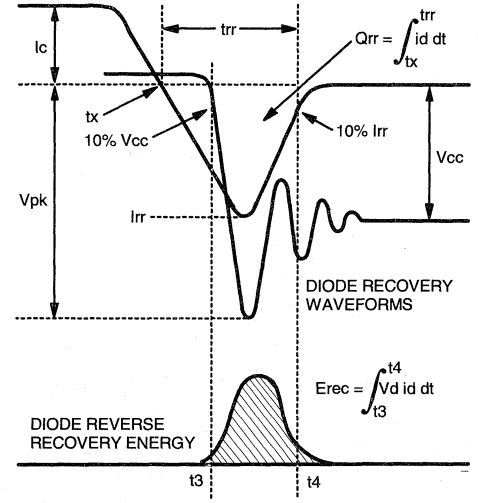


Fig. 18d - Test Waveforms for Circuit of Fig. 18a, Defining E_{rec} , t_{rr} , Q_{rr} , I_{rr}

Refer to Section D for the following:
Appendix D: Section D - page D-6

- Fig. 18e - Macro Waveforms for Test Circuit of Fig. 18a
- Fig. 19 - Clamped Inductive Load Test Circuit
- Fig. 20 - Pulsed Collector Current Test Circuit

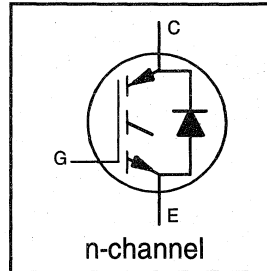
IRGPC50KD2

INSULATED GATE BIPOLAR TRANSISTOR
WITH ULTRAFAST SOFT RECOVERY DIODE

Short Circuit Rated
UltraFast CoPack IGBT

Features

- Short circuit rated $-10\mu\text{s}$ @ 125°C , $V_{GE} = 15\text{V}$
- Switching-loss rating includes all "tail" losses
- HEXFRED™ soft ultrafast diodes
- Optimized for high operating frequency (over 5kHz)

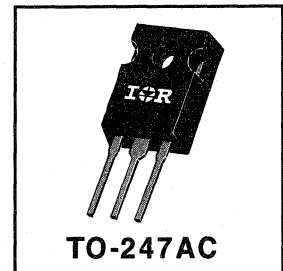


$V_{CES} = 600\text{V}$
 $V_{CE(sat)} \leq 2.7\text{V}$
@ $V_{GE} = 15\text{V}$, $I_C = 30\text{A}$

Description

Co-packaged IGBTs are a natural extension of International Rectifier's well known IGBT line. They provide the convenience of an IGBT and an ultrafast recovery diode in one package, resulting in substantial benefits to a host of high-voltage, high-current, applications.

These new short circuit rated devices are especially suited for motor control and other applications requiring short circuit withstand capability.



Absolute Maximum Ratings

	Parameter	Max.	Units
V_{CES}	Collector-to-Emitter Voltage	600	V
$I_C @ T_C = 25^\circ\text{C}$	Continuous Collector Current	52	A
$I_C @ T_C = 100^\circ\text{C}$	Continuous Collector Current	30	
I_{CM}	Pulsed Collector Current ①	100	
I_{LM}	Clamped Inductive Load Current ②	100	
$I_F @ T_C = 100^\circ\text{C}$	Diode Continuous Forward Current	25	
I_{FM}	Diode Maximum Forward Current	100	
t_{sc}	Short Circuit Withstand Time	10	μs
V_{GE}	Gate-to-Emitter Voltage	± 20	V
$P_D @ T_C = 25^\circ\text{C}$	Maximum Power Dissipation	200	W
$P_D @ T_C = 100^\circ\text{C}$	Maximum Power Dissipation	52	
T_J	Operating Junction and	-55 to +150	$^\circ\text{C}$
T_{STG}	Storage Temperature Range		
	Soldering Temperature, for 10 sec.	300 (0.063 in. (1.6mm) from case)	
	Mounting Torque, 6-32 or M3 Screw.	10 lbf•in (1.1 N•m)	

Thermal Resistance

	Parameter	Min.	Typ.	Max.	Units
$R_{\theta JC}$	Junction-to-Case - IGBT	—	—	0.64	$^\circ\text{C}/\text{W}$
$R_{\theta JC}$	Junction-to-Case - Diode	—	—	0.83	
$R_{\theta CS}$	Case-to-Sink, flat, greased surface	—	0.24	—	
$R_{\theta JA}$	Junction-to-Ambient, typical socket mount	—	—	40	
Wt	Weight	—	6 (0.21)	—	g (oz)

Electrical Characteristics @ $T_J = 25^\circ\text{C}$ (unless otherwise specified)

	Parameter	Min.	Typ.	Max.	Units	Conditions
$V_{(BR)CES}$	Collector-to-Emitter Breakdown Voltage ^③	600	—	—	V	$V_{GE} = 0V, I_C = 250\mu A$
$\Delta V_{(BR)CES}/\Delta T_J$	Temp. Coeff. of Breakdown Voltage	—	0.60	—	V/ $^\circ\text{C}$	$V_{GE} = 0V, I_C = 1.0mA$
$V_{CE(on)}$	Collector-to-Emitter Saturation Voltage	—	2.0	2.7	V	$V_{GE} = 15V$ $I_C = 30A$
		—	2.6	—		
		—	2.3	—		
$V_{GE(th)}$	Gate Threshold Voltage	3.0	—	5.5		$V_{CE} = V_{GE}, I_C = 250\mu A$
$\Delta V_{GE(th)}/\Delta T_J$	Temperature Coeff. of Threshold Voltage	—	-14	—	mV/ $^\circ\text{C}$	$V_{CE} = V_{GE}, I_C = 250\mu A$
g_{fe}	Forward Transconductance ^④	9.8	17	—	S	$V_{CE} = 100V, I_C = 30A$
I_{CES}	Zero Gate Voltage Collector Current	—	—	250	μA	$V_{GE} = 0V, V_{CE} = 600V$
		—	—	6500		$V_{GE} = 0V, V_{CE} = 600V, T_J = 150^\circ\text{C}$
V_{FM}	Diode Forward Voltage Drop	—	1.3	1.7	V	$I_C = 25A$
		—	1.2	1.5		$I_C = 25A, T_J = 150^\circ\text{C}$
I_{GES}	Gate-to-Emitter Leakage Current	—	—	± 100	nA	$V_{GE} = \pm 20V$

Switching Characteristics @ $T_J = 25^\circ\text{C}$ (unless otherwise specified)

	Parameter	Min.	Typ.	Max.	Units	Conditions	
Q_g	Total Gate Charge (turn-on)	—	120	200	nC	$I_C = 30A$ $V_{CC} = 400V$	
Q_{ge}	Gate - Emitter Charge (turn-on)	—	27	42			
Q_{gc}	Gate - Collector Charge (turn-on)	—	44	73			
$t_{d(on)}$	Turn-On Delay Time	—	74	—	ns	$T_J = 25^\circ\text{C}$ $I_C = 30A, V_{CC} = 480V$ $V_{GE} = 15V, R_G = 5.0\Omega$ Energy losses include "tail" and diode reverse recovery.	
t_r	Rise Time	—	100	—			
$t_{d(off)}$	Turn-Off Delay Time	—	260	460			
t_f	Fall Time	—	190	290			
E_{on}	Turn-On Switching Loss	—	2.1	—			
E_{off}	Turn-Off Switching Loss	—	0.9	—	mJ		
E_{ts}	Total Switching Loss	—	3.0	4.5			
t_{sc}	Short Circuit Withstand Time	10	—	—	μs	$V_{CC} = 360V, T_J = 125^\circ\text{C}$ $V_{GE} = 15V, R_G = 5.0\Omega, V_{CPK} < 500V$	
$t_{d(on)}$	Turn-On Delay Time	—	77	—	ns	$T_J = 150^\circ\text{C}$ $I_C = 30A, V_{CC} = 480V$ $V_{GE} = 15V, R_G = 5.0\Omega$ Energy losses include "tail" and diode reverse recovery.	
t_r	Rise Time	—	100	—			
$t_{d(off)}$	Turn-Off Delay Time	—	530	—			
t_f	Fall Time	—	360	—			
E_{ts}	Total Switching Loss	—	4.5	—			
L_E	Internal Emitter Inductance	—	13	—	nH	Measured 5mm from package	
C_{ies}	Input Capacitance	—	2900	—	pF	$V_{GE} = 0V$ $V_{CC} = 30V$ $f = 1.0MHz$	
C_{oes}	Output Capacitance	—	220	—			
C_{res}	Reverse Transfer Capacitance	—	30	—			
t_{rr}	Diode Reverse Recovery Time	—	50	75	ns	$T_J = 25^\circ\text{C}$	$I_F = 25A$ $V_R = 200V$ $di/dt = 200A/\mu s$
		—	105	160			
I_{rr}	Diode Peak Reverse Recovery Current	—	4.5	10	A	$T_J = 25^\circ\text{C}$	
		—	8.0	15		$T_J = 125^\circ\text{C}$	
Q_{rr}	Diode Reverse Recovery Charge	—	112	375	nC	$T_J = 25^\circ\text{C}$	
		—	420	1200		$T_J = 125^\circ\text{C}$	
$di_{(rec)}/dt$	Diode Peak Rate of Fall of Recovery During t_b	—	250	—	A/ μs	$T_J = 25^\circ\text{C}$	
		—	160	—		$T_J = 125^\circ\text{C}$	

Notes:

① Repetitive rating; $V_{GE} = 20V$, pulse width limited by max. junction temperature.

② $V_{CC} = 80\%(V_{CES}), V_{GE} = 20V, L = 10\mu H, R_G = 5.0\Omega$

④ Pulse width 5.0 μs , single shot.

③ Pulse width $\leq 80\mu s$; duty factor $\leq 0.1\%$.

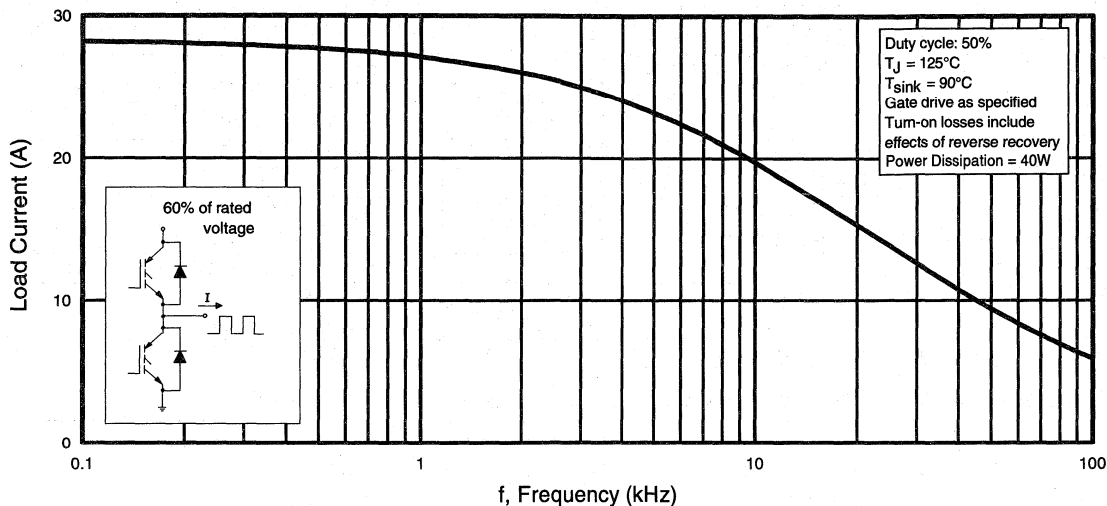


Fig. 1 - Typical Load Current vs. Frequency
(Load Current = I_{RMS} of fundamental)

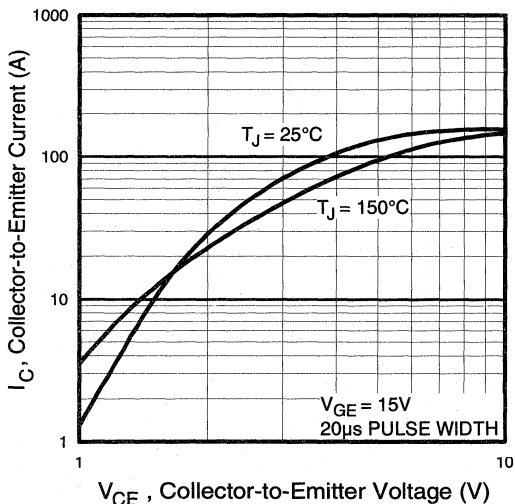


Fig. 2 - Typical Output Characteristics

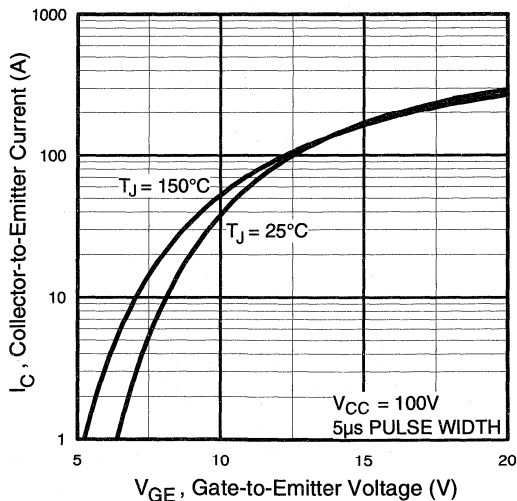


Fig. 3 - Typical Transfer Characteristics

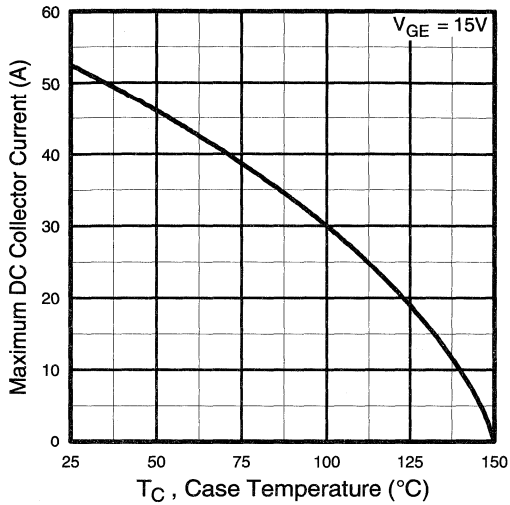


Fig. 4 - Maximum Collector Current vs. Case Temperature

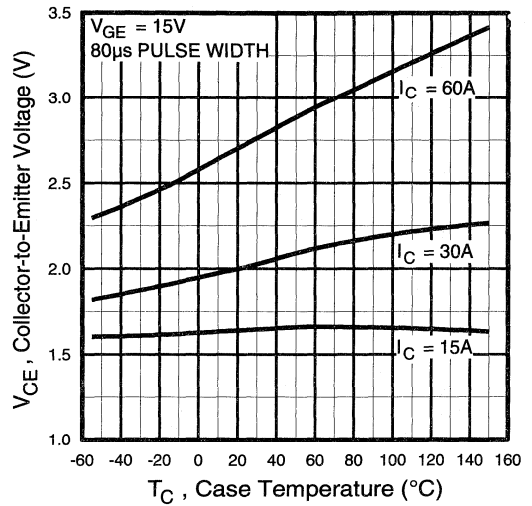


Fig. 5 - Collector-to-Emitter Voltage vs. Case Temperature

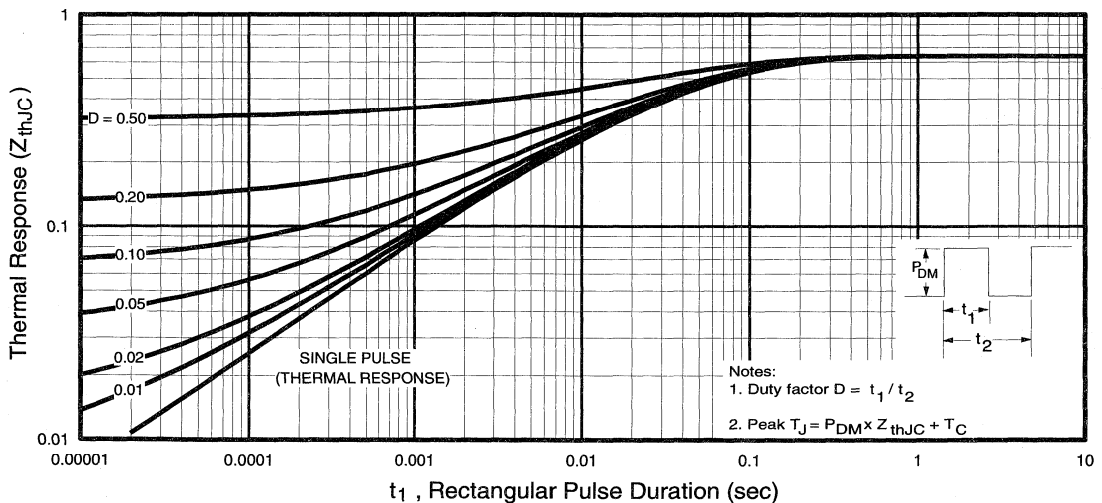


Fig. 6 - Maximum IGBT Effective Transient Thermal Impedance, Junction-to-Case

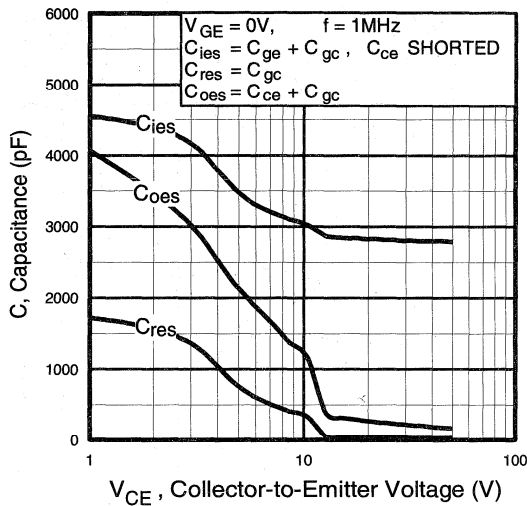


Fig. 7 - Typical Capacitance vs. Collector-to-Emitter Voltage

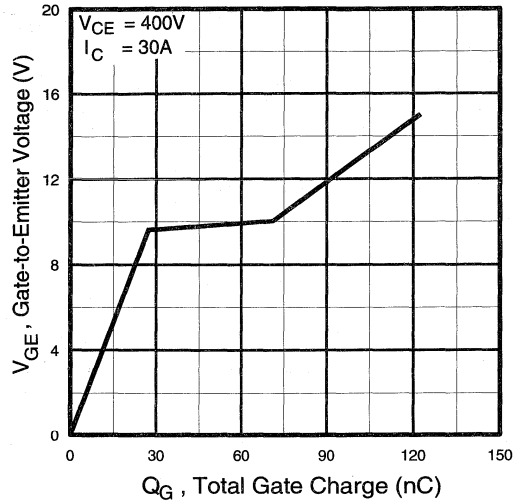


Fig. 8 - Typical Gate Charge vs. Gate-to-Emitter Voltage

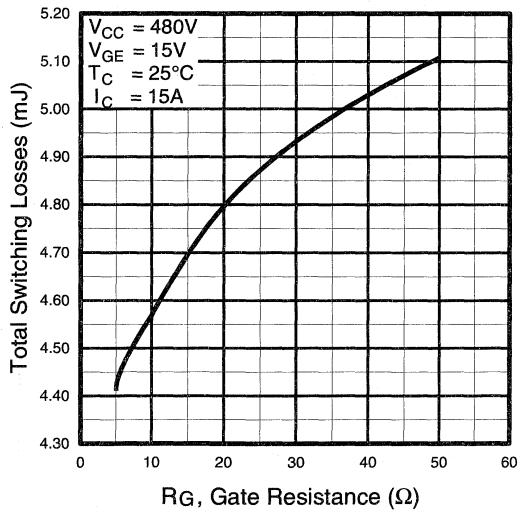


Fig. 9 - Typical Switching Losses vs. Gate Resistance

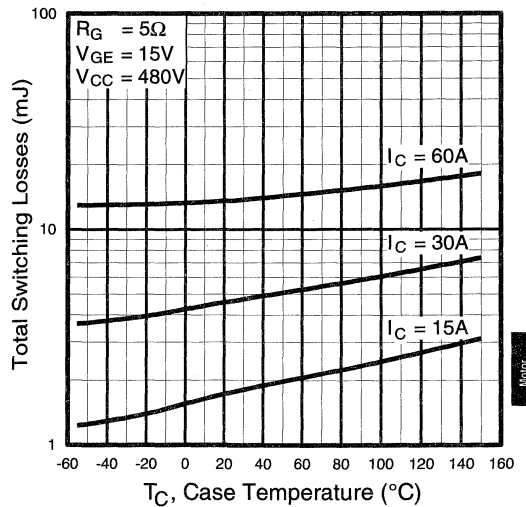


Fig. 10 - Typical Switching Losses vs. Case Temperature

Motor Control
 Ultra-Fast
 Co-Packs

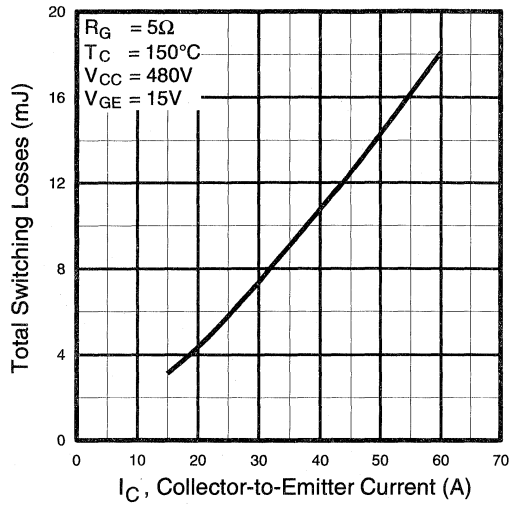


Fig. 11 - Typical Switching Losses vs. Collector-to-Emitter Current

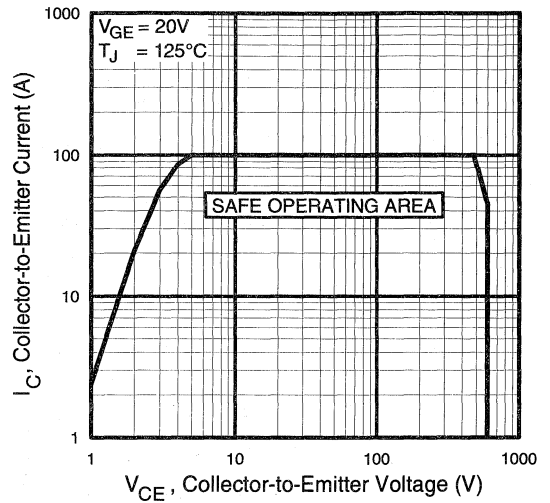


Fig. 12 - Turn-Off SOA

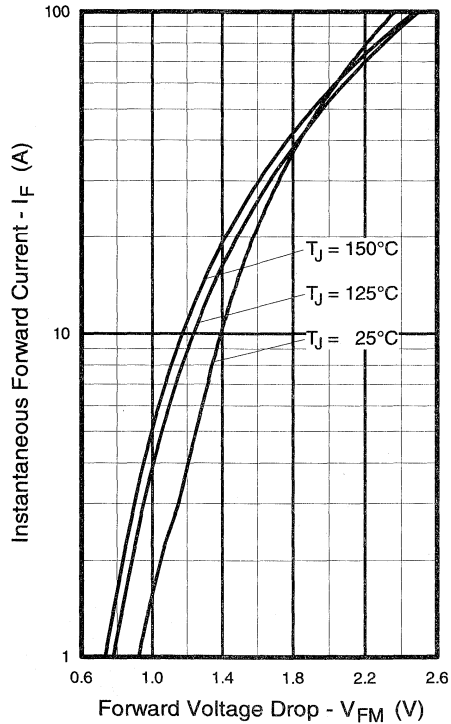


Fig. 13 - Maximum Forward Voltage Drop vs. Instantaneous Forward Current

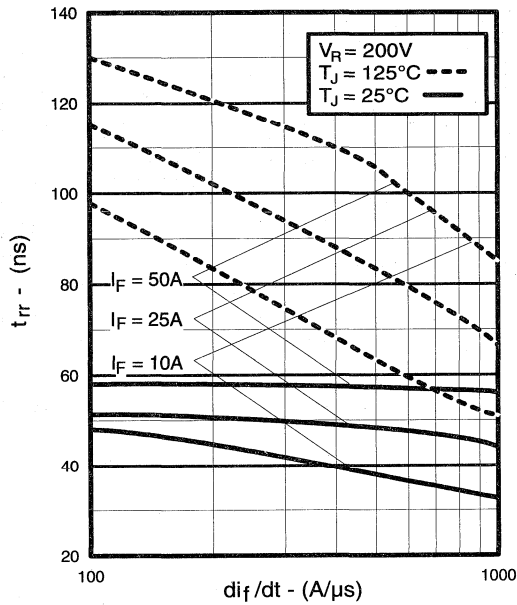


Fig. 14 - Typical Reverse Recovery vs. di_f/dt

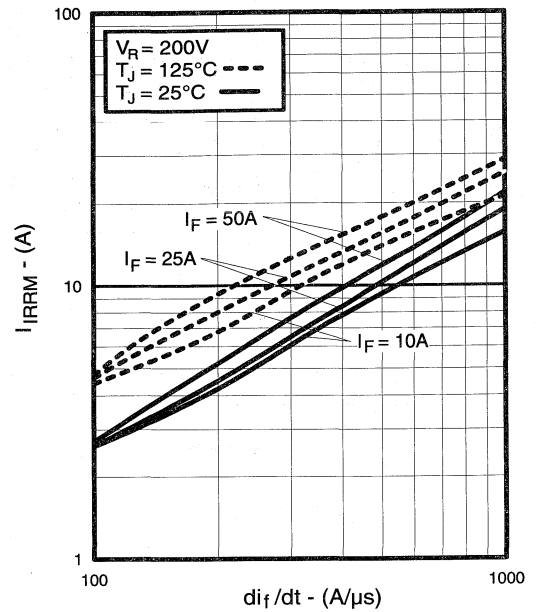


Fig. 15 - Typical Recovery Current vs. di_f/dt

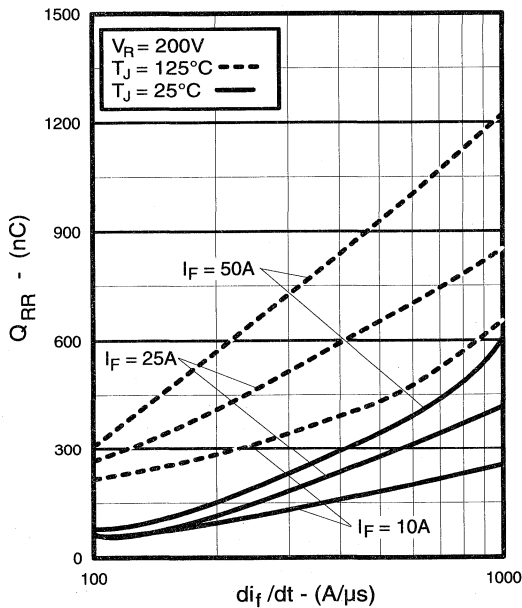


Fig. 16 - Typical Stored Charge vs. di_f/dt

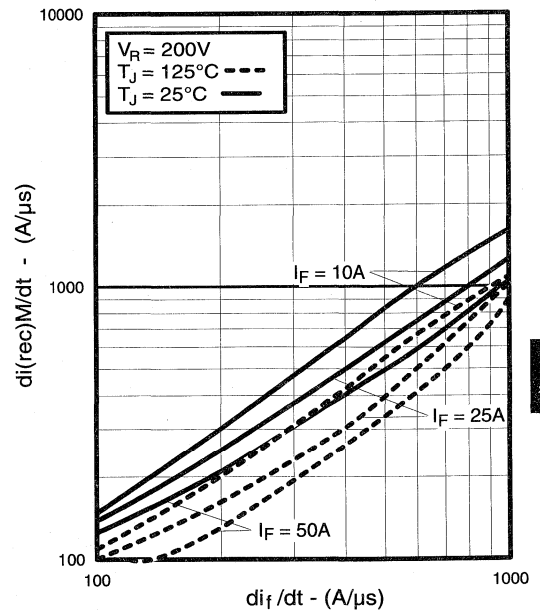


Fig. 17 - Typical $di_{(rec)M}/dt$ vs. di_f/dt

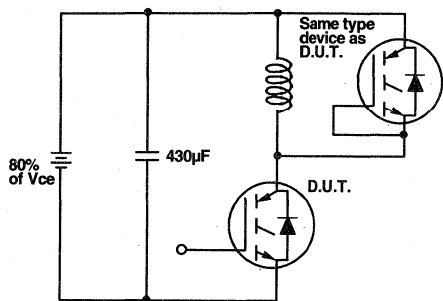


Fig. 18a - Test Circuit for Measurement of I_{LM} , E_{on} , $E_{off}(\text{diode})$, t_{rr} , Q_{rr} , I_{rr} , $t_{d(on)}$, t_r , $t_{d(off)}$, t_f

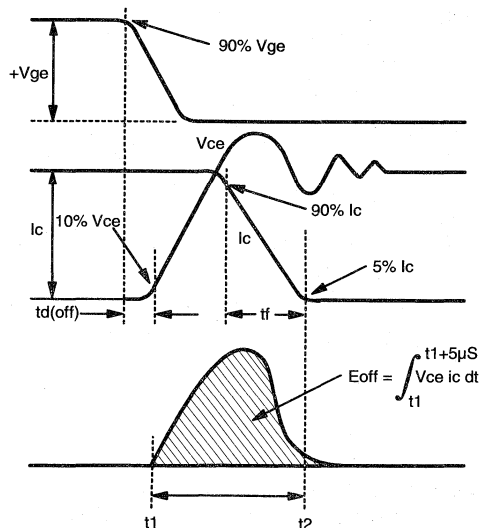


Fig. 18b - Test Waveforms for Circuit of Fig. 18a, Defining E_{off} , $t_{d(off)}$, t_f

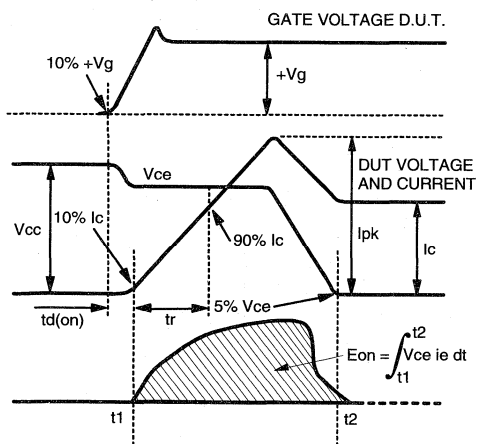


Fig. 18c - Test Waveforms for Circuit of Fig. 18a, Defining E_{on} , $t_{d(on)}$, t_r

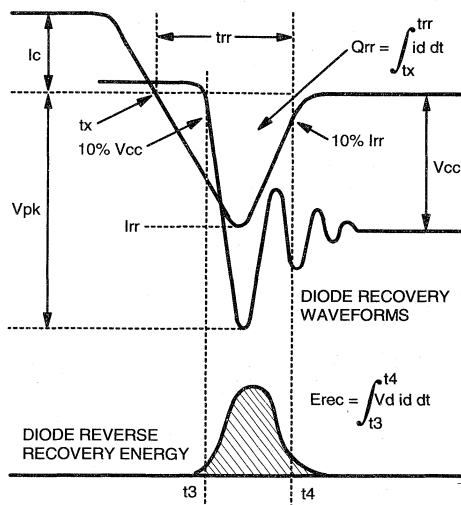


Fig. 18d - Test Waveforms for Circuit of Fig. 18a, Defining E_{rec} , t_{rr} , Q_{rr} , I_{rr}

Refer to Section D for the following:
Appendix D: Section D - page D-6

Fig. 18e - Macro Waveforms for Test Circuit of Fig. 18a

Fig. 19 - Clamped Inductive Load Test Circuit

Fig. 20 - Pulsed Collector Current Test Circuit

IGBT SIP MODULE

Short Circuit Rated UltraFast IGBT

Features

- Short Circuit Rated - $10\mu\text{s}$ @ 125°C , $V_{\text{GE}} = 15\text{V}$
- Fully isolated printed circuit board mount package
- Switching-loss rating includes all "tail" losses
- HEXFRED™ soft ultrafast diodes
- Optimized for high operating frequency (over 5kHz)

Product Summary

Output Current in a Typical 20 kHz Motor Drive

10 A_{RMS} with $T_{\text{C}} = 90^\circ\text{C}$, $T_{\text{J}} = 125^\circ\text{C}$, Supply Voltage 360Vdc, Power Factor 0.8, Modulation Depth 80%.

Description

The IGBT technology is the key to International Rectifier's advanced line of IMS (Insulated Metal Substrate) Power Modules. These modules are more efficient than comparable bipolar transistor modules, while at the same time having the simpler gate-drive requirements of the familiar power MOSFET. This superior technology has now been coupled to a state of the art materials system that maximizes power throughput with low thermal resistance. This package is highly suited to power applications and where space is at a premium.

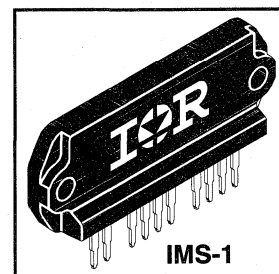
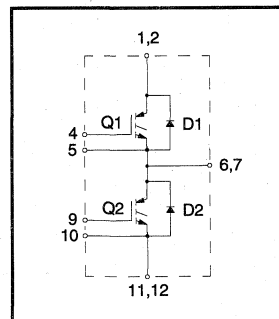
These new short circuit rated devices are especially suited for motor control and other totem-pole applications requiring short circuit withstand capability.

Absolute Maximum Ratings

	Parameter	Max.	Units
	V_{CES} Collector-to-Emitter Voltage	600	V
	I_{C} @ $T_{\text{C}} = 25^\circ\text{C}$ Continuous Collector Current, each IGBT	33	A
	I_{C} @ $T_{\text{C}} = 100^\circ\text{C}$ Continuous Collector Current, each IGBT	17	
	I_{CM} Pulsed Collector Current ①	100	
	I_{LM} Clamped Inductive Load Current ②	100	
	I_{F} @ $T_{\text{C}} = 100^\circ\text{C}$ Diode Continuous Forward Current	15	
	I_{FM} Diode Maximum Forward Current	100	
	t_{sc} Short Circuit Withstand Time	10	μs
	V_{GE} Gate-to-Emitter Voltage	± 20	V
	V_{ISOL} Isolation Voltage, any terminal to case, 1 min.	2500	V_{RMS}
	P_{D} @ $T_{\text{C}} = 25^\circ\text{C}$ Maximum Power Dissipation, each IGBT	83	W
	P_{D} @ $T_{\text{C}} = 100^\circ\text{C}$ Maximum Power Dissipation, each IGBT	33	
	T_{J} Operating Junction and	-40 to +150	$^\circ\text{C}$
	T_{STG} Storage Temperature Range		
	Soldering Temperature, for 10 sec.	300 (0.063 in. (1.6mm) from case)	
	Mounting torque, 6-32 or M3 screw.	5-7 lbf•in (0.55 - 0.8 N•m)	

Thermal Resistance

	Parameter	Typ.	Max.	Units
	$R_{\theta\text{JC}}$ (IGBT) Junction-to-Case, each IGBT, one IGBT in conduction	—	1.5	$^\circ\text{C/W}$
	$R_{\theta\text{JC}}$ (DIODE) Junction-to-Case, each diode, one diode in conduction	—	2.0	
	$R_{\theta\text{CS}}$ (MODULE) Case-to-Sink, flat, greased surface	0.1	—	
	W_{t} Weight of module	20 (0.7)	—	g (oz)



Motor Control UltraFast Modules

Electrical Characteristics @ $T_J = 25^\circ\text{C}$ (unless otherwise specified)

	Parameter	Min.	Typ.	Max.	Units	Conditions
$V_{(BR)CES}$	Collector-to-Emitter Breakdown Voltage ^③	600	—	—	V	$V_{GE} = 0V, I_C = 250\mu A$
$\Delta V_{(BR)CES}/\Delta T_J$	Temp. Coeff. of Breakdown Voltage	—	0.60	—	V/ $^\circ\text{C}$	$V_{GE} = 0V, I_C = 1.0mA$
$V_{CE(on)}$	Collector-to-Emitter Saturation Voltage	—	2.1	2.7	V	$I_C = 30A$ $V_{GE} = 15V$
		—	2.6	—		$I_C = 52A$
		—	2.3	—		$I_C = 30A, T_J = 150^\circ\text{C}$
$V_{GE(th)}$	Gate Threshold Voltage	3.0	—	5.5		$V_{CE} = V_{GE}, I_C = 250\mu A$
$\Delta V_{GE(th)}/\Delta T_J$	Temp. Coeff. of Threshold Voltage	—	-14	—	mV/ $^\circ\text{C}$	$V_{CE} = V_{GE}, I_C = 250\mu A$
g_{fe}	Forward Transconductance ^④	9.8	17	—	S	$V_{CE} = 100V, I_C = 30A$
I_{CES}	Zero Gate Voltage Collector Current	—	—	250	μA	$V_{GE} = 0V, V_{CE} = 600V$
		—	—	6500		$V_{GE} = 0V, V_{CE} = 600V, T_J = 150^\circ\text{C}$
V_{FM}	Diode Forward Voltage Drop	—	1.3	1.7	V	$I_C = 25A$
		—	1.2	1.5		$I_C = 25A, T_J = 150^\circ\text{C}$
I_{GES}	Gate-to-Emitter Leakage Current	—	—	± 500	nA	$V_{GE} = \pm 20V$

Switching Characteristics @ $T_J = 25^\circ\text{C}$ (unless otherwise specified)

	Parameter	Min.	Typ.	Max.	Units	Conditions	
Q_g	Total Gate Charge (turn-on)	—	120	200		$I_C = 30A$	
Q_{ge}	Gate - Emitter Charge (turn-on)	—	27	42	nC	$V_{CC} = 400V$	
Q_{gc}	Gate - Collector Charge (turn-on)	—	44	73			
$t_{d(on)}$	Turn-On Delay Time	—	74	—	ns	$T_J = 25^\circ\text{C}$ $I_C = 30A, V_{CC} = 480V$ $V_{GE} = 15V, R_G = 5.0\Omega$ Energy losses include "tail" and diode reverse recovery.	
t_r	Rise Time	—	100	—			
$t_{d(off)}$	Turn-Off Delay Time	—	260	460			
t_f	Fall Time	—	190	290			
E_{on}	Turn-On Switching Loss	—	1.9	—	mJ		
E_{off}	Turn-Off Switching Loss	—	2.6	—			
E_{ts}	Total Switching Loss	—	4.5	7.0			
t_{sc}	Short Circuit Withstand Time	10	—	—	μs	$V_{CC} = 360V, T_J = 125^\circ\text{C}$ $V_{GE} = 15V, R_G = 5.0\Omega, V_{CPK} < 500V$	
$t_{d(on)}$	Turn-On Delay Time	—	77	—	ns	$T_J = 150^\circ\text{C}$, $I_C = 30A, V_{CC} = 480V$ $V_{GE} = 15V, R_G = 5.0\Omega$ Energy losses include "tail" and diode reverse recovery.	
t_r	Rise Time	—	100	—			
$t_{d(off)}$	Turn-Off Delay Time	—	530	—			
t_f	Fall Time	—	360	—			
E_{ts}	Total Switching Loss	—	7.3	—	mJ		
C_{ies}	Input Capacitance	—	2900	—	pF	$V_{GE} = 0V$ $V_{CC} = 30V$ $f = 1.0MHz$	
C_{oes}	Output Capacitance	—	220	—			
C_{res}	Reverse Transfer Capacitance	—	30	—			
t_{rr}	Diode Reverse Recovery Time	—	50	75	ns	$T_J = 25^\circ\text{C}$ $T_J = 125^\circ\text{C}$	$I_F = 25A$
		—	105	160			
I_{rr}	Diode Peak Reverse Recovery Current	—	4.5	10	A	$T_J = 25^\circ\text{C}$ $T_J = 125^\circ\text{C}$	$V_R = 200V$
		—	8.0	15			
Q_{rr}	Diode Reverse Recovery Charge	—	112	375	nC	$T_J = 25^\circ\text{C}$ $T_J = 125^\circ\text{C}$	$di/dt = 200A/\mu s$
		—	420	1200			
$di_{(rec)M}/dt$	Diode Peak Rate of Fall of Recovery During t_b	—	250	—	A/ μs	$T_J = 25^\circ\text{C}$ $T_J = 125^\circ\text{C}$	
		—	160	—			

Notes: ① Repetitive rating; $V_{GE}=20V$, pulse width limited by max. junction temperature.

② $V_{CC}=80\%(V_{CES}), V_{GE}=20V, L=10\mu H, R_G = 5.0\Omega$.

④ Pulse width 5.0 μs , single shot.

③ Pulse width $\leq 80\mu s$; duty factor $\leq 0.1\%$.

Refer to Section D - page D-13 for Package Outline 4 - IMS-1 Package (10 pins)

IGBT SIP MODULE

Short Circuit Rated UltraFast IGBT

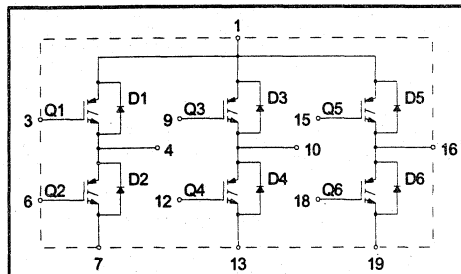
Features

- Short Circuit Rated - $10\mu\text{s}$ @ 125°C , $V_{GE} = 15\text{V}$
 - Fully isolated printed circuit board mount package
 - Switching-loss rating includes all "tail" losses
 - HEXFRED™ soft ultrafast diodes
 - Optimized for high operating frequency (over 5kHz)
- See Fig. 1 for Current vs. Frequency curve

Product Summary

Output Current in a Typical 20 kHz Motor Drive

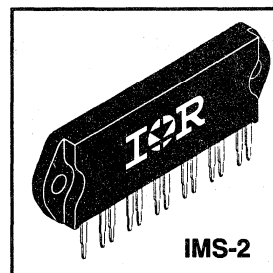
$3.5 A_{RMS}$ per phase (1.1 kW total) with $T_C = 90^\circ\text{C}$, $T_J = 125^\circ\text{C}$, Supply Voltage 360Vdc,
Power Factor 0.8, Modulation Depth 80% (See Figure 1)



Description

The IGBT technology is the key to International Rectifier's advanced line of IMS (Insulated Metal Substrate) Power Modules. These modules are more efficient than comparable bipolar transistor modules, while at the same time having the simpler gate-drive requirements of the familiar power MOSFET. This superior technology has now been coupled to a state of the art materials system that maximizes power throughput with low thermal resistance. This package is highly suited to power applications and where space is at a premium.

These new short circuit rated devices are especially suited for motor control and other totem-pole applications requiring short circuit withstand capability.



Absolute Maximum Ratings

	Parameter	Max.	Units
V_{CES}	Collector-to-Emitter Voltage	600	V
$I_C @ T_C = 25^\circ\text{C}$	Continuous Collector Current, each IGBT	5.7	A
$I_C @ T_C = 100^\circ\text{C}$	Continuous Collector Current, each IGBT	3.0	
I_{CM}	Pulsed Collector Current $\text{\textcircled{D}}$	11	
I_{LM}	Clamped Inductive Load Current $\text{\textcircled{Q}}$	11	
$I_F @ T_C = 100^\circ\text{C}$	Diode Continuous Forward Current	3.4	
I_{FM}	Diode Maximum Forward Current	11	
t_{sc}	Short Circuit Withstand Time	10	μs
V_{GE}	Gate-to-Emitter Voltage	± 20	V
V_{ISOL}	Isolation Voltage, any terminal to case, 1 min.	2500	V_{RMS}
$P_D @ T_C = 25^\circ\text{C}$	Maximum Power Dissipation, each IGBT	23	W
$P_D @ T_C = 100^\circ\text{C}$	Maximum Power Dissipation, each IGBT	9.1	
T_J	Operating Junction and	-40 to +150	$^\circ\text{C}$
T_{STG}	Storage Temperature Range		
	Soldering Temperature, for 10 sec.	300 (0.063 in. (1.6mm) from case)	
	Mounting torque, 6-32 or M3 screw.	5-7 lbf•in (0.55 - 0.8 N•m)	

Thermal Resistance

	Parameter	Typ.	Max.	Units
$R_{\theta JC}$ (IGBT)	Junction-to-Case, each IGBT, one IGBT in conduction	—	5.5	$^\circ\text{C/W}$
$R_{\theta JC}$ (DIODE)	Junction-to-Case, each diode, one diode in conduction	—	9.0	
$R_{\theta CS}$ (MODULE)	Case-to-Sink, flat, greased surface	0.1	—	
Wt	Weight of module	20 (0.7)	—	g (oz)

Electrical Characteristics @ $T_J = 25^\circ\text{C}$ (unless otherwise specified)

	Parameter	Min.	Typ.	Max.	Units	Conditions
$V_{(BR)CES}$	Collector-to-Emitter Breakdown Voltage ^③	600	—	—	V	$V_{GE} = 0V, I_C = 250\mu A$
$\Delta V_{(BR)CES}/\Delta T_J$	Temp. Coeff. of Breakdown Voltage	—	0.37	—	V/°C	$V_{GE} = 0V, I_C = 1.0mA$
$V_{CE(on)}$	Collector-to-Emitter Saturation Voltage	—	2.3	3.5	V	$I_C = 3.0A, V_{GE} = 15V$ See Fig. 2, 5
		—	2.7	—		
		—	2.2	—		
$V_{GE(th)}$	Gate Threshold Voltage	3.0	—	5.5		$V_{CE} = V_{GE}, I_C = 250\mu A$
$\Delta V_{GE(th)}/\Delta T_J$	Temperature Coeff. of Threshold Voltage	—	-11	—	mV/°C	$V_{CE} = V_{GE}, I_C = 250\mu A$
g_{fe}	Forward Transconductance ^④	1.9	3.3	—	S	$V_{CE} = 100V, I_C = 6.0A$
I_{CES}	Zero Gate Voltage Collector Current	—	—	250	μA	$V_{GE} = 0V, V_{CE} = 600V$ $V_{GE} = 0V, V_{CE} = 600V, T_J = 150^\circ\text{C}$
		—	—	1700		
V_{FM}	Diode Forward Voltage Drop	—	1.4	1.7	V	$I_C = 8.0A$ See Fig. 13 $I_C = 8.0A, T_J = 150^\circ\text{C}$
		—	1.3	1.6		
I_{GES}	Gate-to-Emitter Leakage Current	—	—	±500	nA	$V_{GE} = \pm 20V$

Switching Characteristics @ $T_J = 25^\circ\text{C}$ (unless otherwise specified)

	Parameter	Min.	Typ.	Max.	Units	Conditions
Q_g	Total Gate Charge (turn-on)	—	17	26	nC	$I_C = 6.0A$ $V_{CC} = 400V$ See Fig. 8
Q_{ge}	Gate - Emitter Charge (turn-on)	—	4.3	6.8		
Q_{gc}	Gate - Collector Charge (turn-on)	—	6.4	11		
$t_{d(on)}$	Turn-On Delay Time	—	60	—	ns	$T_J = 25^\circ\text{C}$ $I_C = 3.0A, V_{CC} = 480V$ $V_{GE} = 15V, R_G = 50\Omega$ Energy losses include "tail" and diode reverse recovery. See Fig. 9, 10, 11, 18
t_r	Rise Time	—	20	—		
$t_{d(off)}$	Turn-Off Delay Time	—	110	220		
t_f	Fall Time	—	50	110		
E_{on}	Turn-On Switching Loss	—	0.10	—		
E_{off}	Turn-Off Switching Loss	—	0.10	—	mJ	
E_{ts}	Total Switching Loss	—	0.20	0.27		
t_{sc}	Short Circuit Withstand Time	10	—	—	μs	$V_{CC} = 360V, T_J = 125^\circ\text{C}$ $V_{GE} = 15V, R_G = 50\Omega, V_{CPK} < 500V$
$t_{d(on)}$	Turn-On Delay Time	—	60	—	ns	$T_J = 150^\circ\text{C}$, See Fig. 9, 10, 11, 18 $I_C = 3.0A, V_{CC} = 480V$ $V_{GE} = 15V, R_G = 50\Omega$ Energy losses include "tail" and diode reverse recovery.
t_r	Rise Time	—	17	—		
$t_{d(off)}$	Turn-Off Delay Time	—	230	—		
t_f	Fall Time	—	130	—		
E_{ts}	Total Switching Loss	—	0.29	—		
C_{ies}	Input Capacitance	—	350	—	pF	$V_{GE} = 0V$ $V_{CC} = 30V$ See Fig. 7 $f = 1.0MHz$
C_{oes}	Output Capacitance	—	50	—		
C_{res}	Reverse Transfer Capacitance	—	4.7	—		
t_{rr}	Diode Reverse Recovery Time	—	37	55	ns	$T_J = 25^\circ\text{C}$ See Fig. 14 $T_J = 125^\circ\text{C}$ 14
		—	55	90		
I_{rr}	Diode Peak Reverse Recovery Current	—	3.5	5.0	A	$T_J = 25^\circ\text{C}$ See Fig. 15 $T_J = 125^\circ\text{C}$ 15
		—	4.5	8.0		
Q_{rr}	Diode Reverse Recovery Charge	—	65	138	nC	$T_J = 25^\circ\text{C}$ See Fig. 16 $T_J = 125^\circ\text{C}$ 16
		—	124	360		
$di_{(rec)M}/dt$	Diode Peak Rate of Fall of Recovery During t_b	—	240	—	A/ μs	$T_J = 25^\circ\text{C}$ See Fig. 17 $T_J = 125^\circ\text{C}$ 17
		—	210	—		

Notes:

- ① Repetitive rating; $V_{GE} = 20V$, pulse width limited by max. junction temperature. (See fig. 20)
- ② $V_{CC} = 80\%(V_{CES}), V_{GE} = 20V, L = 10\mu H, R_G = 50\Omega$, (See fig. 19)
- ③ Pulse width $\leq 80\mu s$; duty factor $\leq 0.1\%$.
- ④ Pulse width 5.0 μs , single shot.

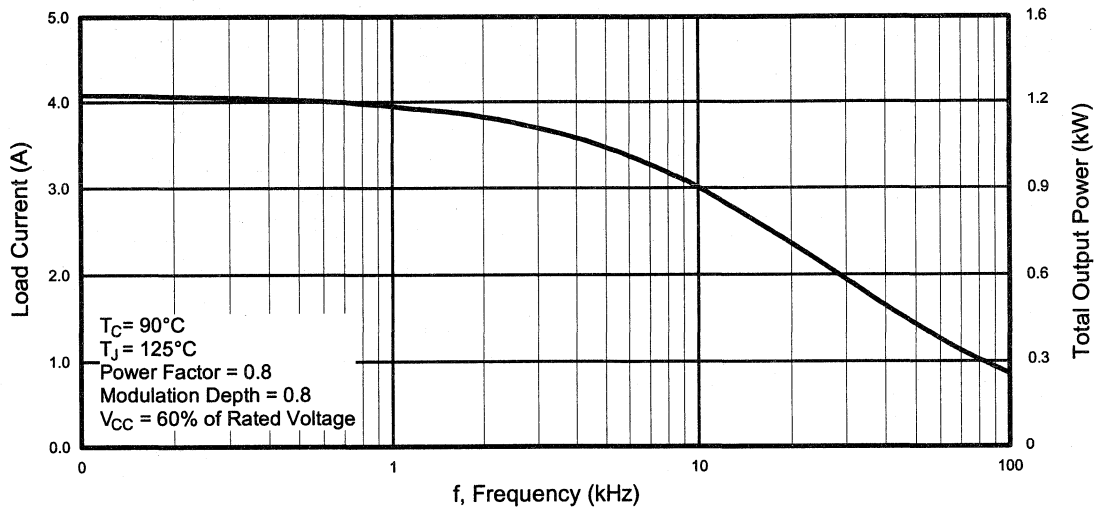


Fig. 1 - RMS Current and Output Power, Synthesized Sine Wave

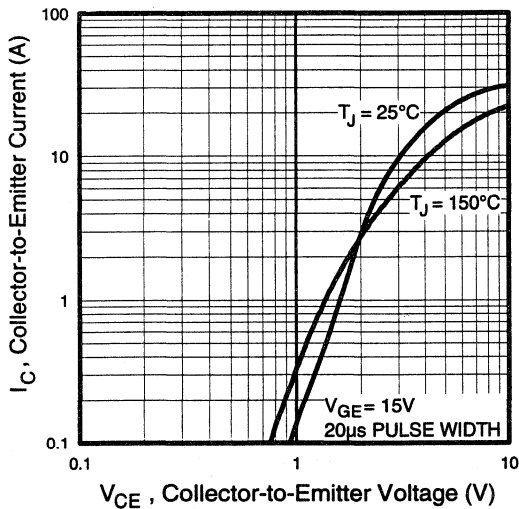


Fig. 2 - Typical Output Characteristics

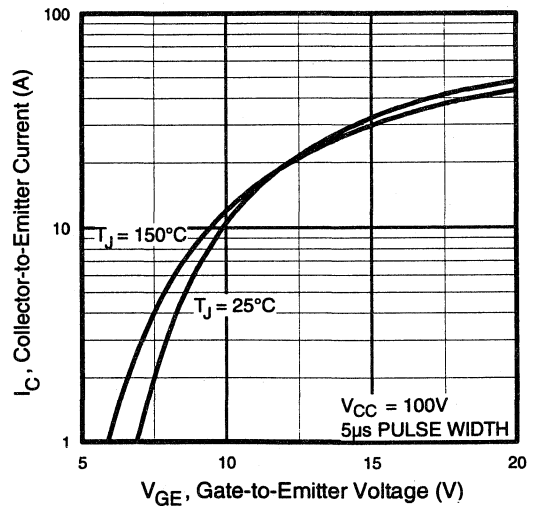


Fig. 3 - Typical Transfer Characteristics

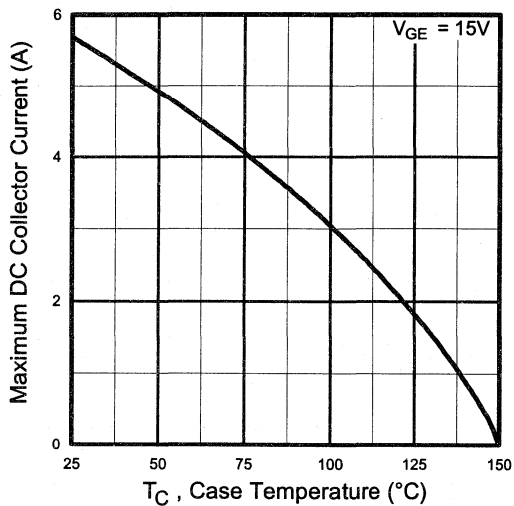


Fig. 4 - Maximum Collector Current vs. Case Temperature

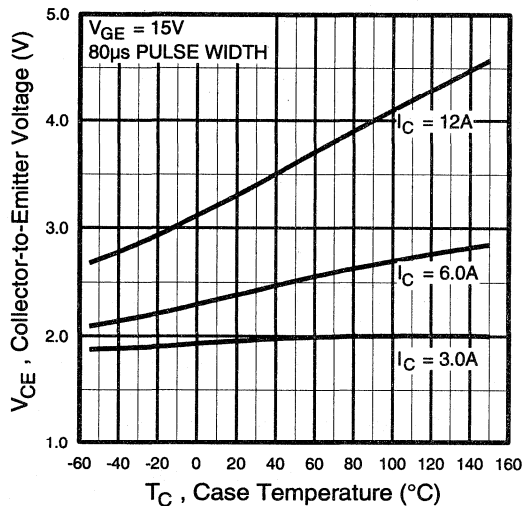


Fig. 5 - Collector-to-Emitter Voltage vs. Case Temperature

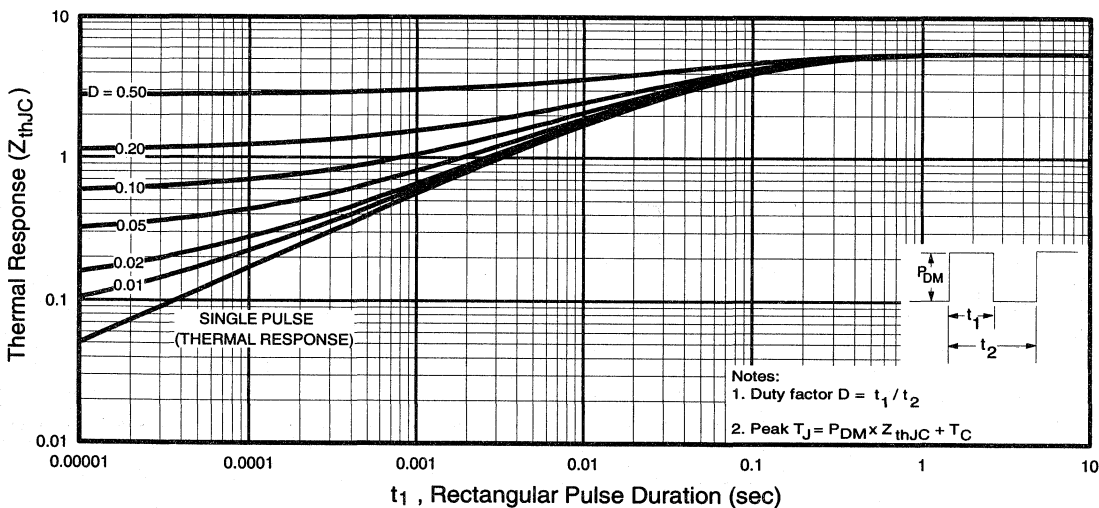


Fig. 6 - Maximum IGBT Effective Transient Thermal Impedance, Junction-to-Case

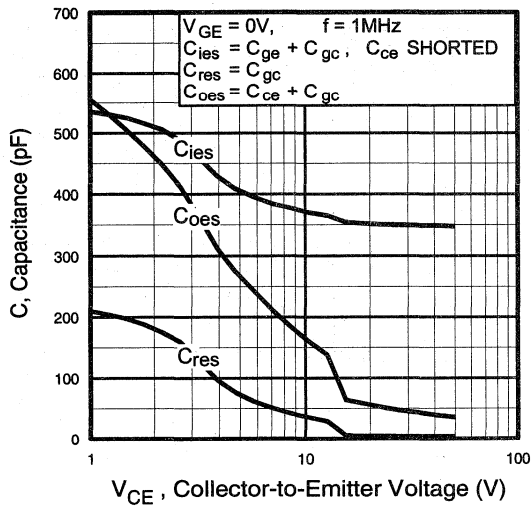


Fig. 7 - Typical Capacitance vs. Collector-to-Emitter Voltage

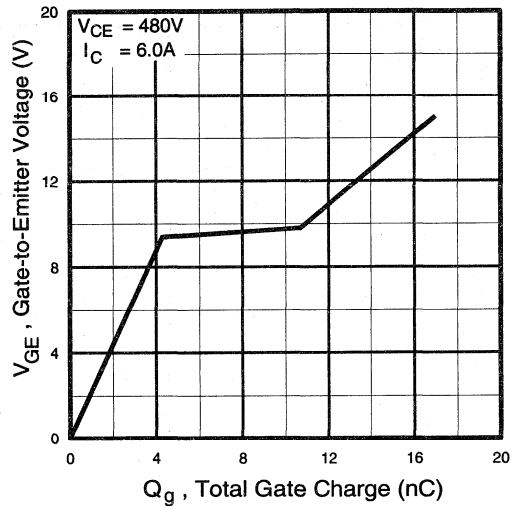


Fig. 8 - Typical Gate Charge vs. Gate-to-Emitter Voltage

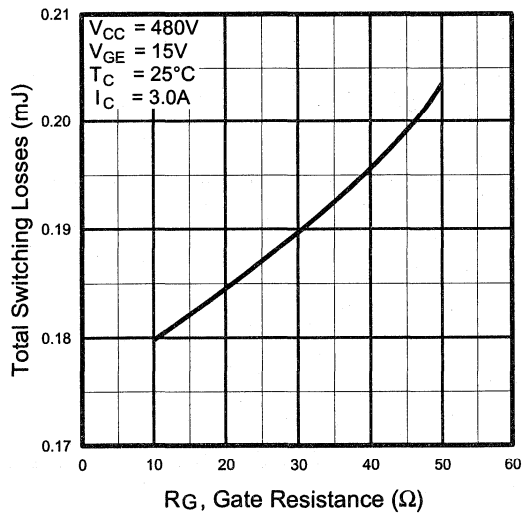


Fig. 9 - Typical Switching Losses vs. Gate Resistance

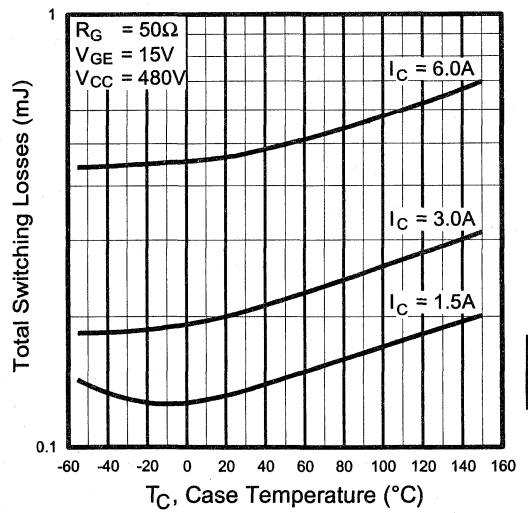


Fig. 10 - Typical Switching Losses vs. Case Temperature

Motor
Control
Ultra-Fast
Modules

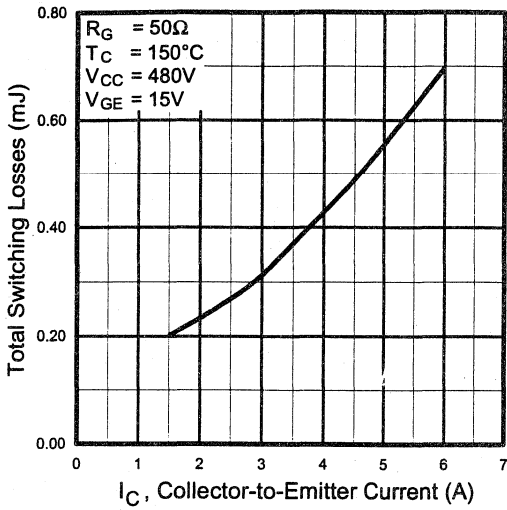


Fig. 11 - Typical Switching Losses vs. Collector-to-Emitter Current

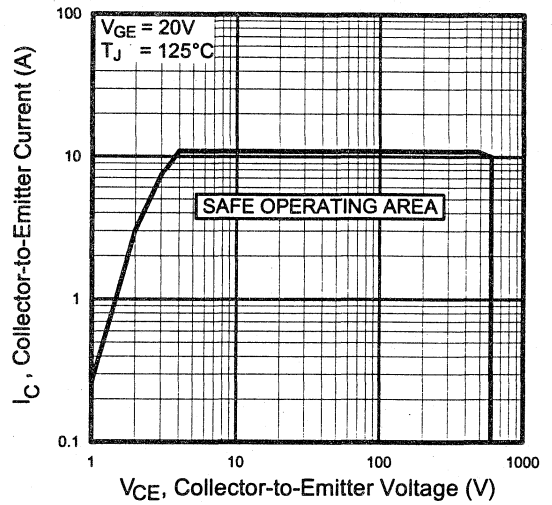


Fig. 12 - Turn-Off SOA

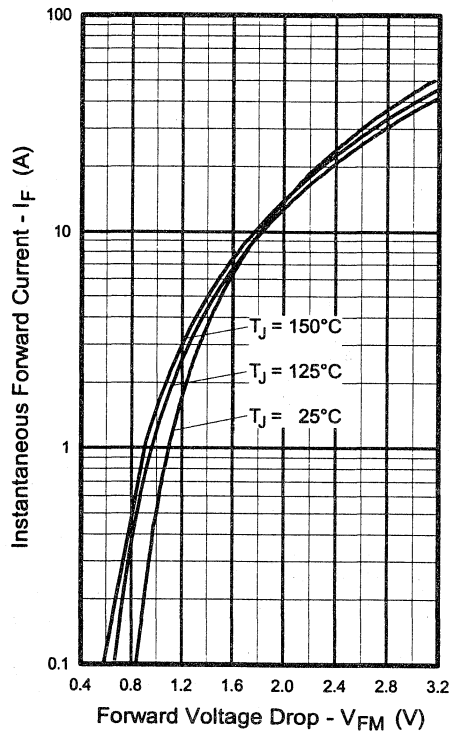


Fig. 13 - Maximum Forward Voltage Drop vs. Instantaneous Forward Current

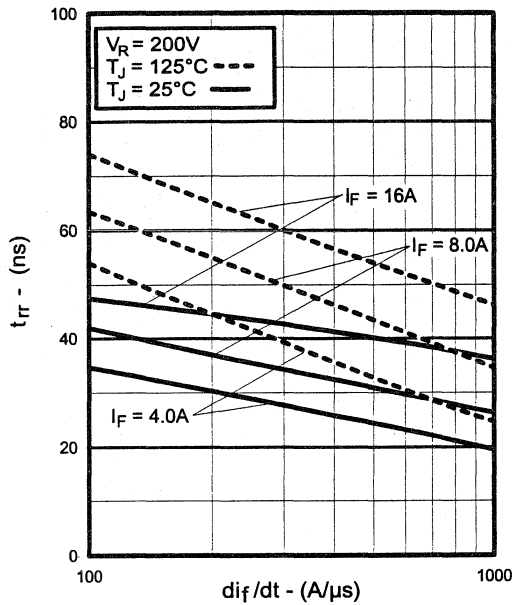


Fig. 14 - Typical Reverse Recovery vs. di_f/dt

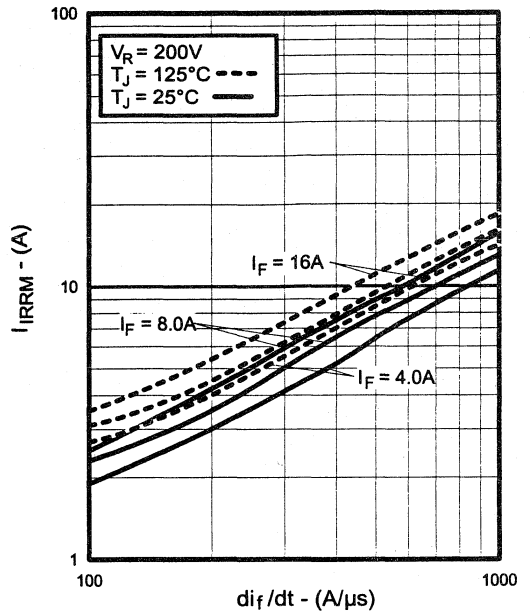


Fig. 15 - Typical Recovery Current vs. di_f/dt

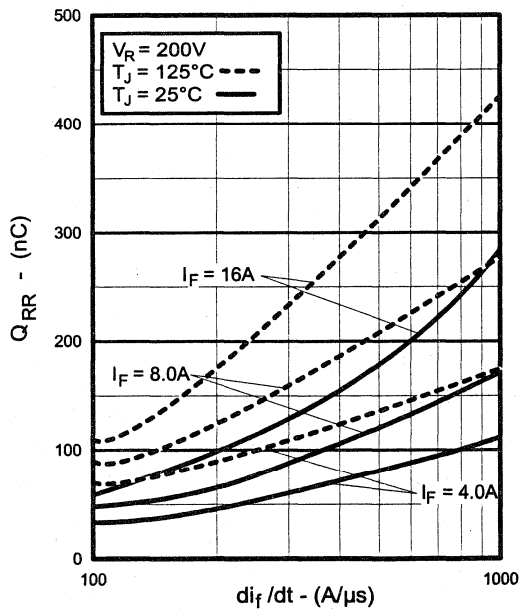


Fig. 16 - Typical Stored Charge vs. di_f/dt

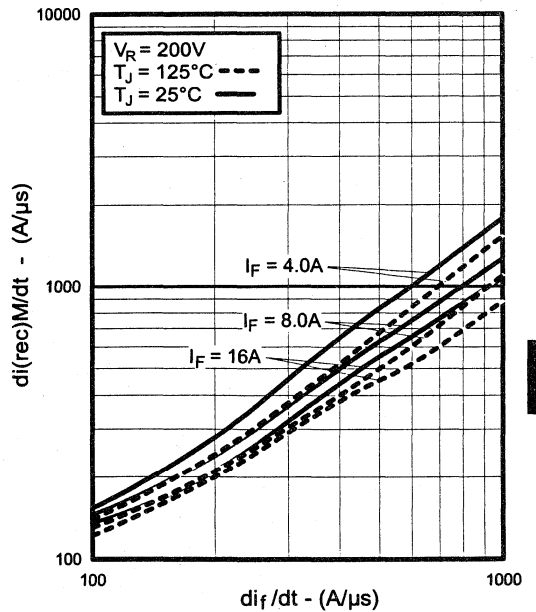


Fig. 17 - Typical $di_{(rec)M}/dt$ vs. di_f/dt

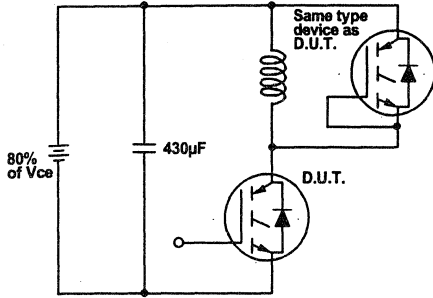


Fig. 18a - Test Circuit for Measurement of I_{LM} , E_{on} , $E_{off}(\text{diode})$, t_{rr} , Q_{rr} , I_{rr} , $t_{d(on)}$, t_r , $t_{d(off)}$, t_f

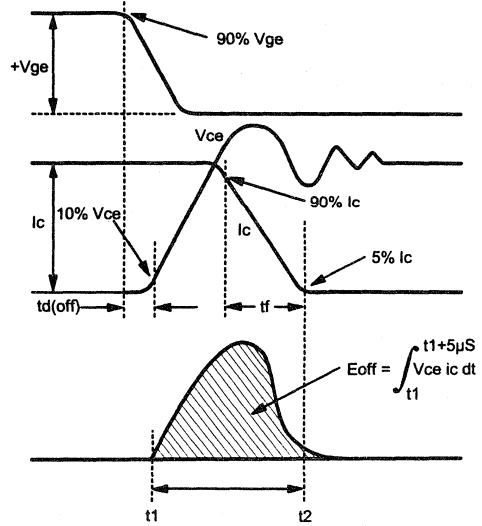


Fig. 18b - Test Waveforms for Circuit of Fig. 18a, Defining E_{off} , $t_{d(off)}$, t_f

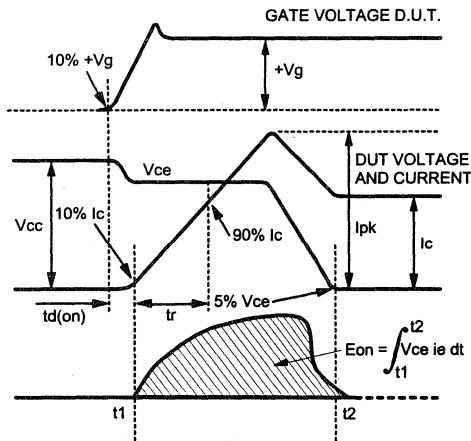


Fig. 18c - Test Waveforms for Circuit of Fig. 18a, Defining E_{on} , $t_{d(on)}$, t_r

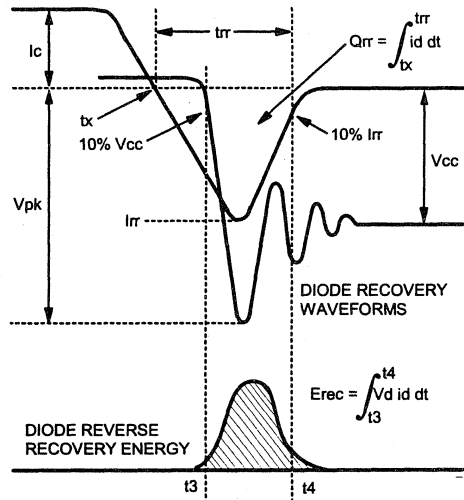


Fig. 18d - Test Waveforms for Circuit of Fig. 18a, Defining E_{rec} , t_{rr} , Q_{rr} , I_{rr}

Refer to **Section D** for the following:
Appendix D: Section D - page D-6

Fig. 18e - Macro Waveforms for Test Circuit of Fig. 18a

Fig. 19 - Clamped Inductive Load Test Circuit

Fig. 20 - Pulsed Collector Current Test Circuit

IGBT SIP MODULE

Short Circuit Rated UltraFast IGBT

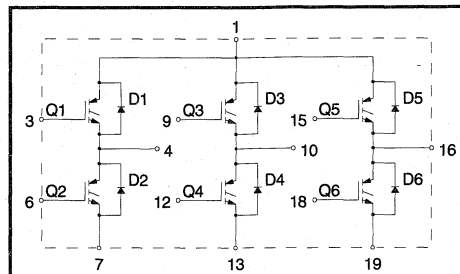
Features

- Short Circuit Rated - 10 μ s @ 125°C, V_{GE} = 15V
 - Fully isolated printed circuit board mount package
 - Switching-loss rating includes all "tail" losses
 - HEXFRED™ soft ultrafast diodes
 - Optimized for high operating frequency (over 5kHz)
- See Fig. 1 for Current vs. Frequency curve

Product Summary

Output Current in a Typical 20 kHz Motor Drive

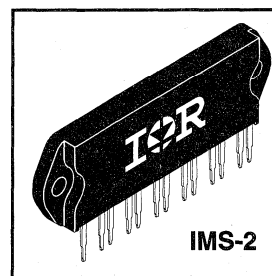
5.4 A_{RMS} per phase (1.7 kW total) with T_C = 90°C, T_J = 125°C, Supply Voltage 360Vdc, Power Factor 0.8, Modulation Depth 80% (See Figure 1)



Description

The IGBT technology is the key to International Rectifier's advanced line of IMS (Insulated Metal Substrate) Power Modules. These modules are more efficient than comparable bipolar transistor modules, while at the same time having the simpler gate-drive requirements of the familiar power MOSFET. This superior technology has now been coupled to a state of the art materials system that maximizes power throughput with low thermal resistance. This package is highly suited to power applications and where space is at a premium.

These new short circuit rated devices are especially suited for motor control and other totem-pole applications requiring short circuit withstand capability.



Absolute Maximum Ratings

	Parameter	Max.	Units
V _{CES}	Collector-to-Emitter Voltage	600	V
I _C @ T _C = 25°C	Continuous Collector Current, each IGBT	11	A
I _C @ T _C = 100°C	Continuous Collector Current, each IGBT	6.0	
I _{CM}	Pulsed Collector Current ①	22	
I _{LM}	Clamped Inductive Load Current ②	22	
I _F @ T _C = 100°C	Diode Continuous Forward Current	6.1	
I _{FM}	Diode Maximum Forward Current	22	
t _{sc}	Short Circuit Withstand Time	10	μ s
V _{GE}	Gate-to-Emitter Voltage	\pm 20	V
V _{ISOL}	Isolation Voltage, any terminal to case, 1 min.	2500	V _{RMS}
P _D @ T _C = 25°C	Maximum Power Dissipation, each IGBT	36	W
P _D @ T _C = 100°C	Maximum Power Dissipation, each IGBT	14	
T _J	Operating Junction and	-40 to +150	°C
T _{STG}	Storage Temperature Range		
	Soldering Temperature, for 10 sec.	300 (0.063 in. (1.6mm) from case)	
	Mounting torque, 6-32 or M3 screw.	5-7 lbf•in (0.55 - 0.8 N•m)	

Thermal Resistance

	Parameter	Typ.	Max.	Units
R _{θJC} (IGBT)	Junction-to-Case, each IGBT, one IGBT in conduction	—	3.5	°C/W
R _{θJC} (DIODE)	Junction-to-Case, each diode, one diode in conduction	—	5.5	
R _{θCS} (MODULE)	Case-to-Sink, flat, greased surface	0.1	—	
Wt	Weight of module	20 (0.7)	—	g (oz)

Electrical Characteristics @ $T_J = 25^\circ\text{C}$ (unless otherwise specified)

	Parameter	Min.	Typ.	Max.	Units	Conditions
$V_{(BR)CES}$	Collector-to-Emitter Breakdown Voltage ^③	600	—	—	V	$V_{GE} = 0V, I_C = 250\mu\text{A}$
$\Delta V_{(BR)CES}/\Delta T_J$	Temperature Coeff. of Breakdown Voltage	—	0.45	—	V/ $^\circ\text{C}$	$V_{GE} = 0V, I_C = 1.0\text{mA}$
$V_{CE(on)}$	Collector-to-Emitter Saturation Voltage	—	2.0	3.0	V	$I_C = 6.0\text{A}$ $V_{GE} = 15V$ See Fig. 2, 5
		—	2.5	—		
		—	2.1	—		
$V_{GE(th)}$	Gate Threshold Voltage	3.0	—	5.5		$V_{CE} = V_{GE}, I_C = 250\mu\text{A}$
$\Delta V_{GE(th)}/\Delta T_J$	Temperature Coeff. of Threshold Voltage	—	-13	—	mV/ $^\circ\text{C}$	$V_{CE} = V_{GE}, I_C = 250\mu\text{A}$
g_{fe}	Forward Transconductance ^④	3.0	6.0	—	S	$V_{CE} = 100V, I_C = 12A$
I_{CES}	Zero Gate Voltage Collector Current	—	—	250	μA	$V_{GE} = 0V, V_{CE} = 600V$
		—	—	2500		$V_{GE} = 0V, V_{CE} = 600V, T_J = 150^\circ\text{C}$
V_{FM}	Diode Forward Voltage Drop	—	1.4	1.7	V	$I_C = 12A$ See Fig. 13
		—	1.3	1.6		$I_C = 12A, T_J = 150^\circ\text{C}$
I_{GES}	Gate-to-Emitter Leakage Current	—	—	± 500	nA	$V_{GE} = \pm 20V$

Switching Characteristics @ $T_J = 25^\circ\text{C}$ (unless otherwise specified)

	Parameter	Min.	Typ.	Max.	Units	Conditions
Q_g	Total Gate Charge (turn-on)	—	34	52	nC	$I_C = 12A$ $V_{CC} = 400V$ See Fig. 8
Q_{ge}	Gate - Emitter Charge (turn-on)	—	7.8	12		
Q_{gc}	Gate - Collector Charge (turn-on)	—	13	21		
$t_{d(on)}$	Turn-On Delay Time	—	64	—	ns	$T_J = 25^\circ\text{C}$ $I_C = 6.0\text{A}, V_{CC} = 480V$ $V_{GE} = 15V, R_G = 23\Omega$ Energy losses include "tail" and diode reverse recovery.
t_r	Rise Time	—	24	—		
$t_{d(off)}$	Turn-Off Delay Time	—	130	200		
t_f	Fall Time	—	20	30		
E_{on}	Turn-On Switching Loss	—	0.23	—		
E_{off}	Turn-Off Switching Loss	—	0.17	—	mJ	See Fig. 9, 10, 11, 18
E_{ts}	Total Switching Loss	—	0.40	0.60		
t_{sc}	Short Circuit Withstand Time	10	—	—	μs	$V_{CC} = 360V, T_J = 125^\circ\text{C}$ $V_{GE} = 15V, R_G = 23\Omega, V_{CPK} < 500V$
$t_{d(on)}$	Turn-On Delay Time	—	58	—	ns	$T_J = 150^\circ\text{C}$, See Fig. 9, 10, 11, 18 $I_C = 6.0\text{A}, V_{CC} = 480V$ $V_{GE} = 15V, R_G = 23\Omega$ Energy losses include "tail" and diode reverse recovery.
t_r	Rise Time	—	24	—		
$t_{d(off)}$	Turn-Off Delay Time	—	240	—		
t_f	Fall Time	—	140	—		
E_{ts}	Total Switching Loss	—	0.61	—		
C_{ies}	Input Capacitance	—	740	—	pF	$V_{GE} = 0V$ $V_{CC} = 30V$ See Fig. 7 $f = 1.0\text{MHz}$
C_{oes}	Output Capacitance	—	100	—		
C_{res}	Reverse Transfer Capacitance	—	9.3	—		
t_{rr}	Diode Reverse Recovery Time	—	42	60	ns	$T_J = 25^\circ\text{C}$ See Fig. 14 $T_J = 125^\circ\text{C}$ 15
		—	80	120		
I_{rr}	Diode Peak Reverse Recovery Current	—	3.5	6.0	A	$T_J = 25^\circ\text{C}$ See Fig. 15 $T_J = 125^\circ\text{C}$ 15
		—	5.6	10		
Q_{rr}	Diode Reverse Recovery Charge	—	80	180	nC	$T_J = 25^\circ\text{C}$ See Fig. 16 $T_J = 125^\circ\text{C}$ 16
		—	220	600		
$di_{(rec)M}/dt$	Diode Peak Rate of Fall of Recovery During t_b	—	180	—	A/ μs	$T_J = 25^\circ\text{C}$ See Fig. 17 $T_J = 125^\circ\text{C}$ 17
		—	120	—		

Notes:

① Repetitive rating; $V_{GE} = 20V$, pulse width limited by max. junction temperature. (See fig. 20)

② $V_{CC} = 80\%(V_{CES}), V_{GE} = 20V, L = 10\mu\text{H}, R_G = 23\Omega$, (See fig. 19)

③ Pulse width $\leq 80\mu\text{s}$; duty factor $\leq 0.1\%$.

④ Pulse width $5.0\mu\text{s}$, single shot.

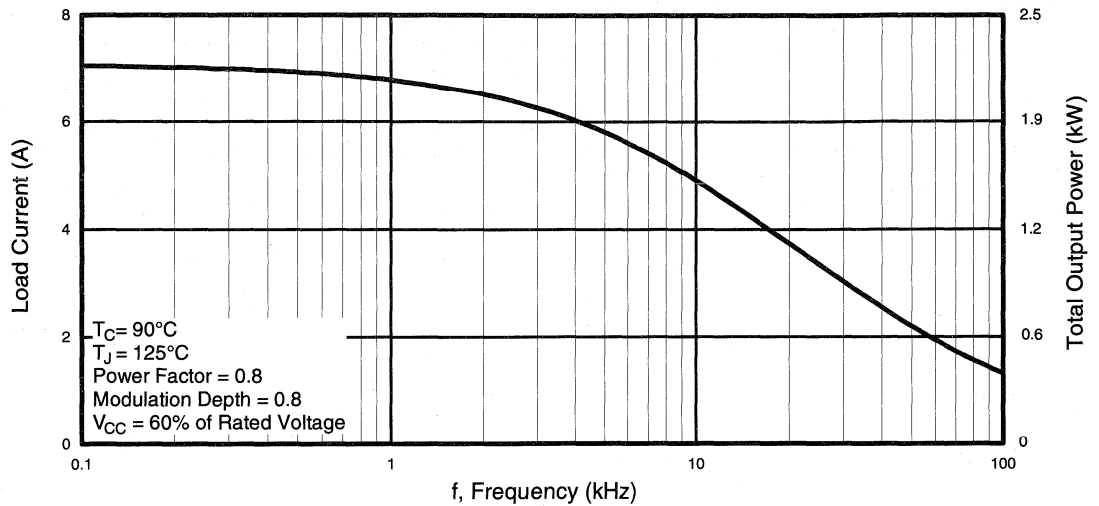


Fig. 1 - RMS Current and Output Power, Synthesized Sine Wave

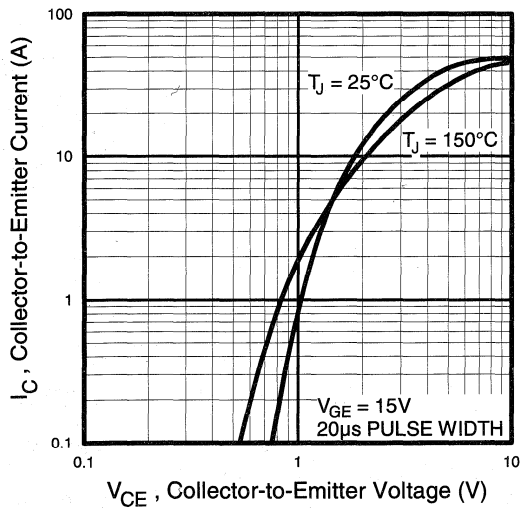


Fig. 2 - Typical Output Characteristics

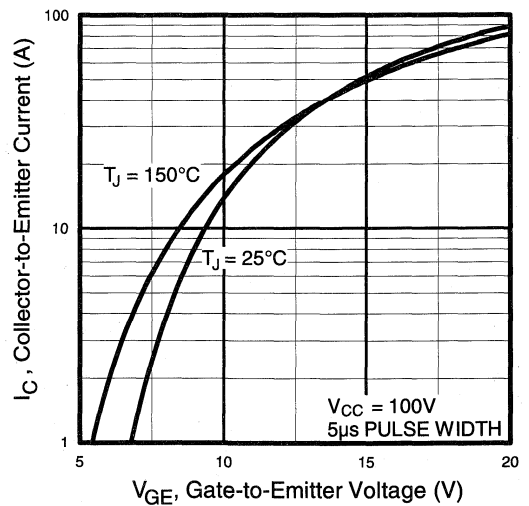


Fig. 3 - Typical Transfer Characteristics

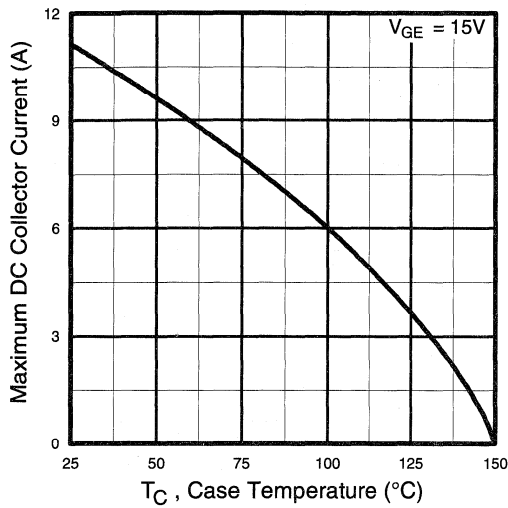


Fig. 4 - Maximum Collector Current vs. Case Temperature

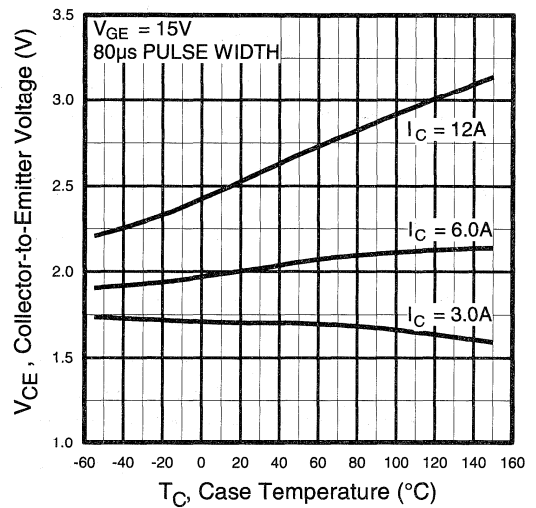


Fig. 5 - Collector-to-Emitter Voltage vs. Case Temperature

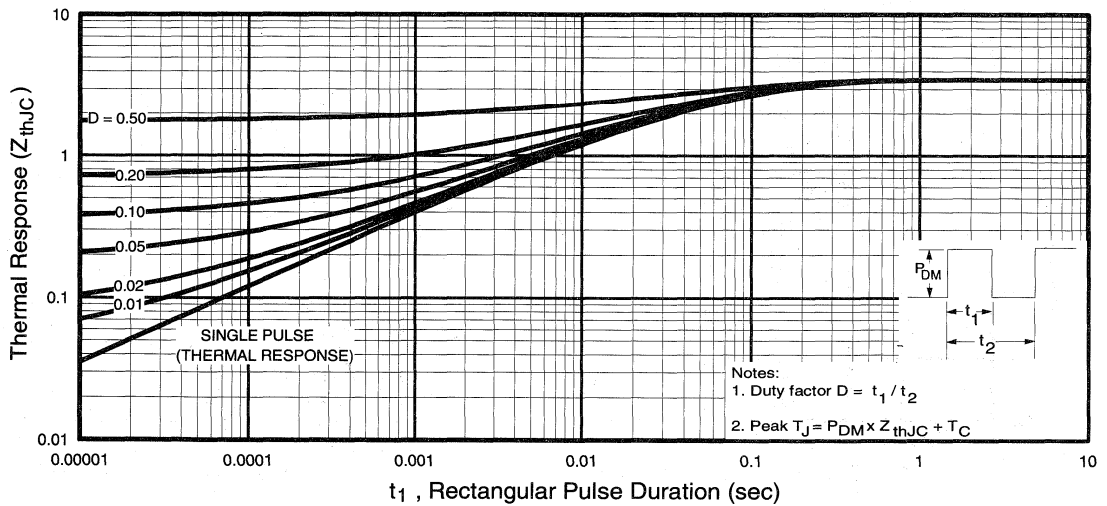


Fig. 6 - Maximum IGBT Effective Transient Thermal Impedance, Junction-to-Case

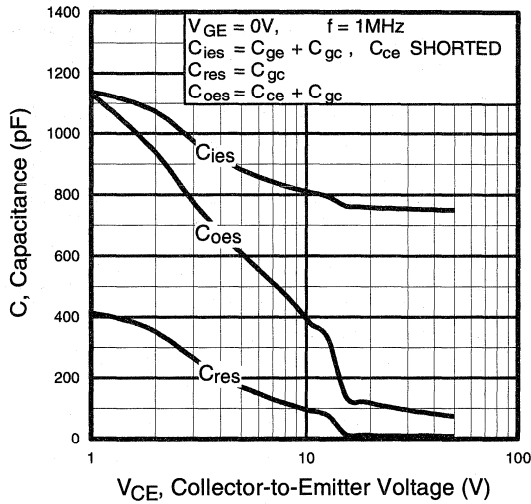


Fig. 7 - Typical Capacitance vs. Collector-to-Emitter Voltage

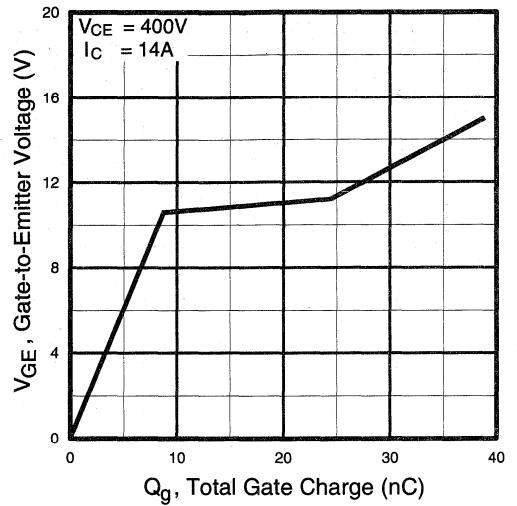


Fig. 8 - Typical Gate Charge vs. Gate-to-Emitter Voltage

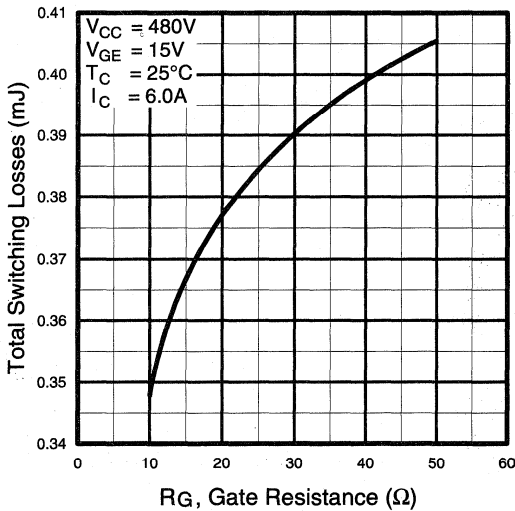


Fig. 9 - Typical Switching Losses vs. Gate Resistance

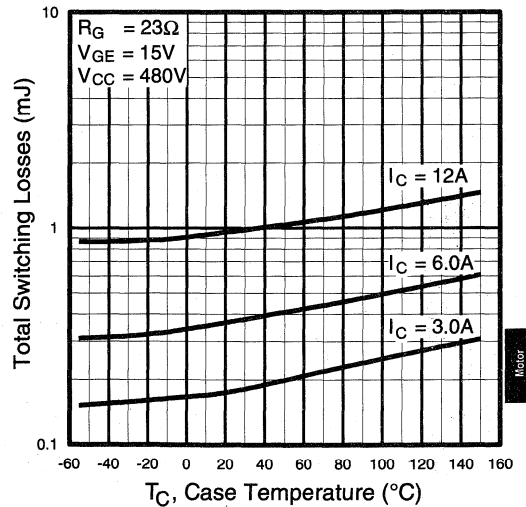


Fig. 10 - Typical Switching Losses vs. Case Temperature

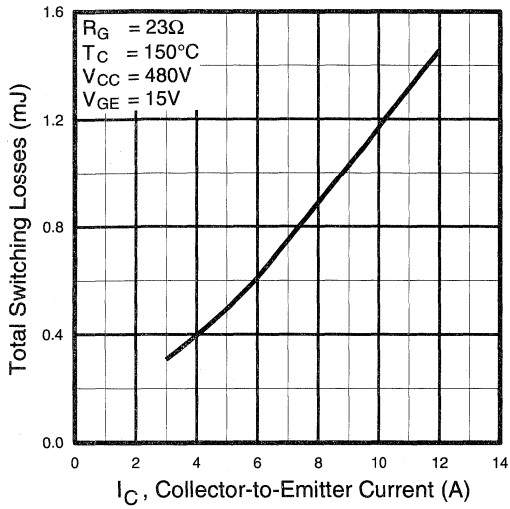


Fig. 11 - Typical Switching Losses vs. Collector-to-Emitter Current

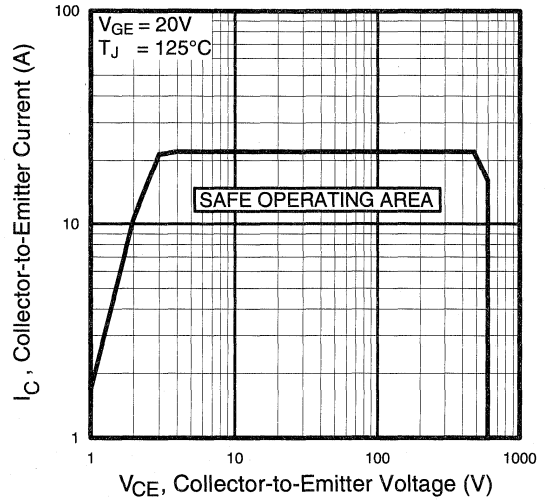


Fig. 12 - Turn-Off SOA

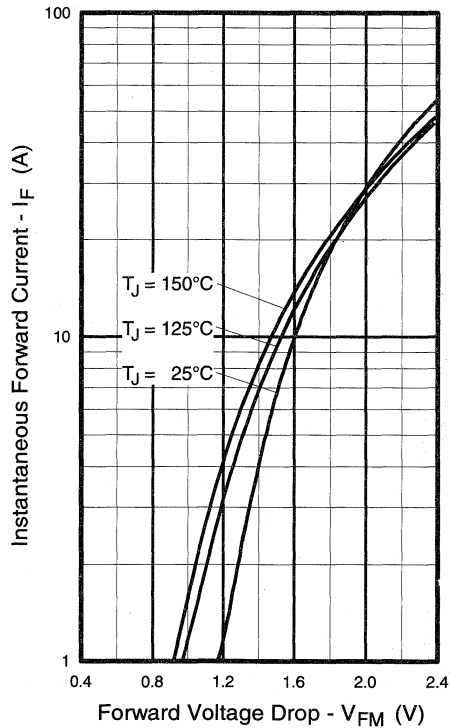


Fig. 13 - Maximum Forward Voltage Drop vs. Instantaneous Forward Current

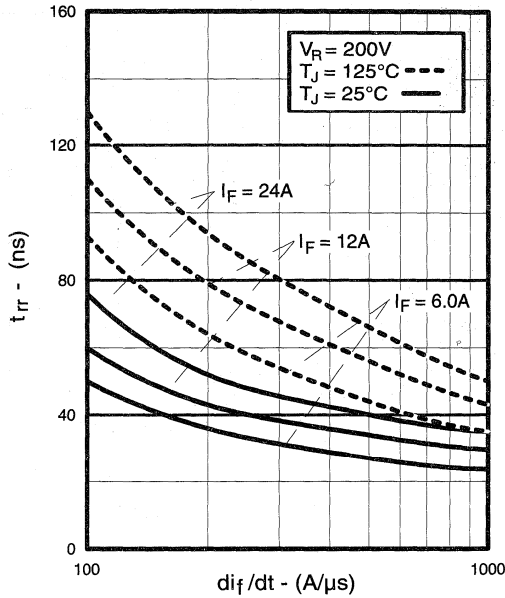


Fig. 14 - Typical Reverse Recovery vs. di_f/dt

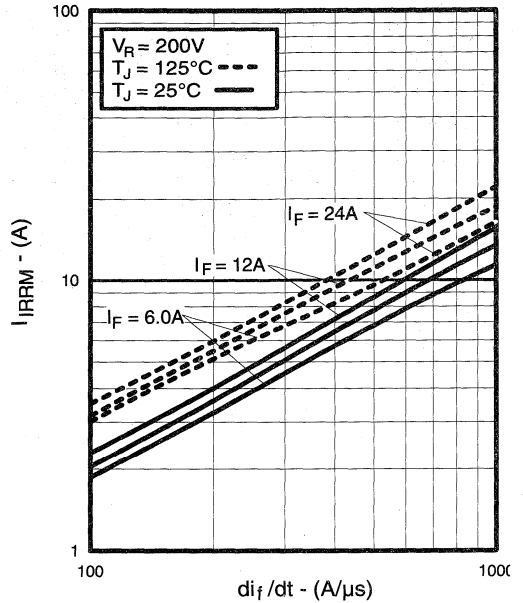


Fig. 15 - Typical Recovery Current vs. di_f/dt

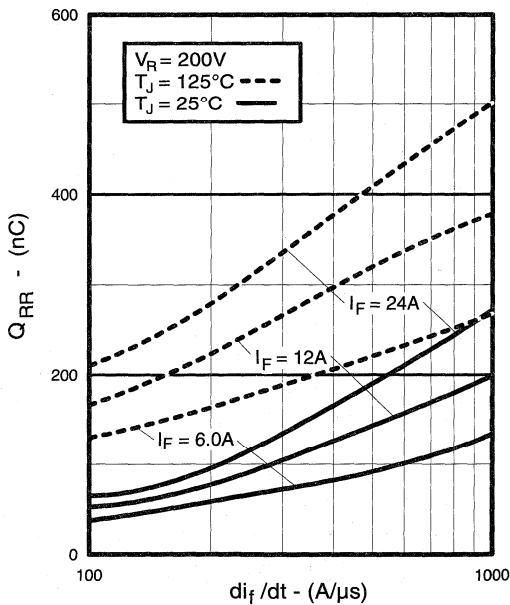


Fig. 16 - Typical Stored Charge vs. di_f/dt

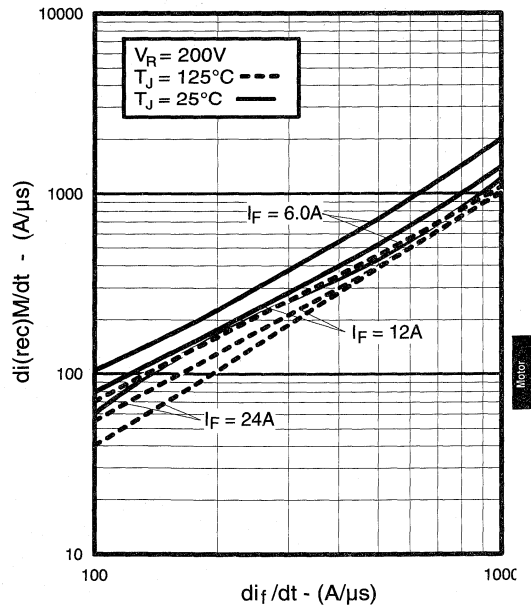


Fig. 17 - Typical $di_{(rec)M}/dt$ vs. di_f/dt

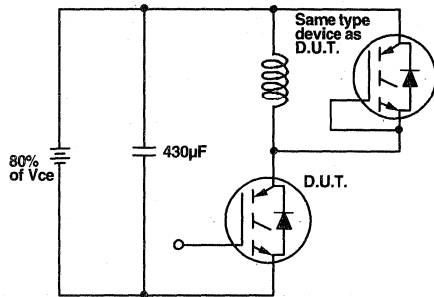


Fig. 18a - Test Circuit for Measurement of I_{LM} , E_{on} , $E_{off}(\text{diode})$, t_{rr} , Q_{rr} , I_{rr} , $t_{d(on)}$, t_r , $t_{d(off)}$, t_f

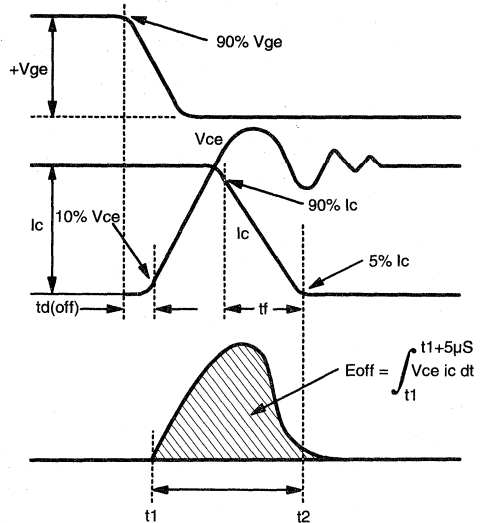


Fig. 18b - Test Waveforms for Circuit of Fig. 18a, Defining E_{off} , $t_{d(off)}$, t_f

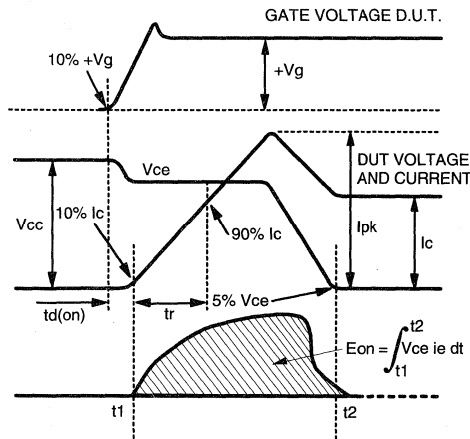


Fig. 18c - Test Waveforms for Circuit of Fig. 18a, Defining E_{on} , $t_{d(on)}$, t_r

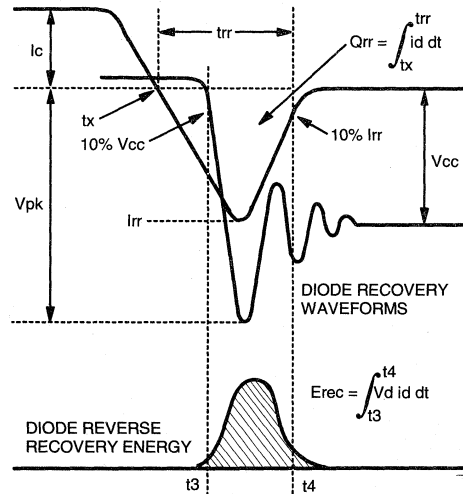


Fig. 18d - Test Waveforms for Circuit of Fig. 18a, Defining E_{rec} , t_{rr} , Q_{rr} , I_{rr}

Refer to Section D for the following:
Appendix D: Section D - page D-6

Fig. 18e - Macro Waveforms for Test Circuit of Fig. 18a

Fig. 19 - Clamped Inductive Load Test Circuit

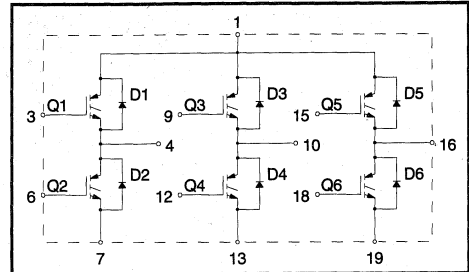
Fig. 20 - Pulsed Collector Current Test Circuit

IGBT SIP MODULE

Short Circuit Rated UltraFast IGBT

Features

- Short Circuit Rated - 10 μ s @ 125°C, V_{GE} = 15V
- Fully isolated printed circuit board mount package
- Switching-loss rating includes all "tail" losses
- HEXFRED™ soft ultrafast diodes
- Optimized for high operating frequency (over 5kHz)
- See Fig. 1 for Current vs. Frequency curve



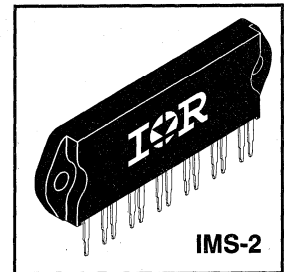
Product Summary

Output Current in a Typical 20 kHz Motor Drive

8.8 A_{RMS} per phase (2.7 kW total) with T_C = 90°C, T_J = 125°C, Supply Voltage 360Vdc, Power Factor 0.8, Modulation Depth 80% (See Figure 1)

Description

The IGBT technology is the key to International Rectifier's advanced line of IMS (Insulated Metal Substrate) Power Modules. These modules are more efficient than comparable bipolar transistor modules, while at the same time having the simpler gate-drive requirements of the familiar power MOSFET. This superior technology has now been coupled to a state of the art materials system that maximizes power throughput with low thermal resistance. This package is highly suited to power applications and where space is at a premium.



These new short circuit rated devices are especially suited for motor control and other totem-pole applications requiring short circuit withstand capability.

Absolute Maximum Ratings

	Parameter	Max.	Units
V _{CES}	Collector-to-Emitter Voltage	600	V
I _C @ T _C = 25°C	Continuous Collector Current, each IGBT	24	A
I _C @ T _C = 100°C	Continuous Collector Current, each IGBT	13	
I _{CM}	Pulsed Collector Current $\text{\textcircled{D}}$	48	
I _{LM}	Clamped Inductive Load Current $\text{\textcircled{Q}}$	48	
I _F @ T _C = 100°C	Diode Continuous Forward Current	9.3	
I _{FM}	Diode Maximum Forward Current	48	
t _{sc}	Short Circuit Withstand Time	10	μ s
V _{GE}	Gate-to-Emitter Voltage	± 20	V
V _{ISOL}	Isolation Voltage, any terminal to case, 1 min.	2500	V _{RMS}
P _D @ T _C = 25°C	Maximum Power Dissipation, each IGBT	63	W
P _D @ T _C = 100°C	Maximum Power Dissipation, each IGBT	25	
T _J	Operating Junction and	-40 to +150	°C
T _{STG}	Storage Temperature Range		
	Soldering Temperature, for 10 sec.	300 (0.063 in. (1.6mm) from case)	
	Mounting torque, 6-32 or M3 screw.	5-7 lbf•in (0.55 - 0.8 N•m)	

Thermal Resistance

	Parameter	Typ.	Max.	Units
R _{θJC} (IGBT)	Junction-to-Case, each IGBT, one IGBT in conduction	—	2.0	°C/W
R _{θJC} (DIODE)	Junction-to-Case, each diode, one diode in conduction	—	3.0	
R _{θCS} (MODULE)	Case-to-Sink, flat, greased surface	0.1	—	
Wt	Weight of module	20 (0.7)	—	g (oz)

Motor Control
 Ultra-Fast
 Modules

Electrical Characteristics @ $T_J = 25^\circ\text{C}$ (unless otherwise specified)

	Parameter	Min.	Typ.	Max.	Units	Conditions
$V_{(BR)CES}$	Collector-to-Emitter Breakdown Voltage ^②	600	—	—	V	$V_{GE} = 0\text{V}$, $I_C = 250\mu\text{A}$
$\Delta V_{(BR)CES}/\Delta T_J$	Temp. Coeff. of Breakdown Voltage	—	0.63	—	V/ $^\circ\text{C}$	$V_{GE} = 0\text{V}$, $I_C = 1.0\text{mA}$
$V_{CE(on)}$	Collector-to-Emitter Saturation Voltage	—	2.1	3.1	V	$I_C = 13\text{A}$ $V_{GE} = 15\text{V}$ See Fig. 2, 5
		—	2.6	—		
		—	2.2	—		
$V_{GE(th)}$	Gate Threshold Voltage	3.0	—	5.5		$V_{CE} = V_{GE}$, $I_C = 250\mu\text{A}$
$\Delta V_{GE(th)}/\Delta T_J$	Temp. Coeff. of Threshold Voltage	—	-13	—	mV/ $^\circ\text{C}$	$V_{CE} = V_{GE}$, $I_C = 250\mu\text{A}$
g_{fe}	Forward Transconductance ^③	11	18	—	S	$V_{CE} = 100\text{V}$, $I_C = 20\text{A}$
I_{CES}	Zero Gate Voltage Collector Current	—	—	250	μA	$V_{GE} = 0\text{V}$, $V_{CE} = 600\text{V}$ $V_{GE} = 0\text{V}$, $V_{CE} = 600\text{V}$, $T_J = 150^\circ\text{C}$
		—	—	3500		
V_{FM}	Diode Forward Voltage Drop	—	1.3	1.7	V	$I_C = 15\text{A}$ See Fig. 13 $I_C = 15\text{A}$, $T_J = 150^\circ\text{C}$
		—	1.2	1.6		
I_{GES}	Gate-to-Emitter Leakage Current	—	—	± 500	nA	$V_{GE} = \pm 20\text{V}$

Switching Characteristics @ $T_J = 25^\circ\text{C}$ (unless otherwise specified)

	Parameter	Min.	Typ.	Max.	Units	Conditions		
Q_g	Total Gate Charge (turn-on)	—	61	90	nC	$I_C = 20\text{A}$ $V_{CC} = 400\text{V}$ See Fig. 8		
Q_{ge}	Gate - Emitter Charge (turn-on)	—	13	20				
Q_{gc}	Gate - Collector Charge (turn-on)	—	22	35				
$t_{d(on)}$	Turn-On Delay Time	—	70	—	ns	$T_J = 25^\circ\text{C}$ $I_C = 13\text{A}$, $V_{CC} = 480\text{V}$ $V_{GE} = 15\text{V}$, $R_G = 10\Omega$ Energy losses include "tail" and diode reverse recovery. See Fig. 9, 10, 11, 18		
t_r	Rise Time	—	55	—				
$t_{d(off)}$	Turn-Off Delay Time	—	130	200				
t_f	Fall Time	—	47	71				
E_{on}	Turn-On Switching Loss	—	0.65	—				
E_{off}	Turn-Off Switching Loss	—	0.37	—				
E_{ts}	Total Switching Loss	—	1.0	1.5				
t_{sc}	Short Circuit Withstand Time	10	—	—			μs	$V_{CC} = 360\text{V}$, $T_J = 125^\circ\text{C}$ $V_{GE} = 15\text{V}$, $R_G = 10\Omega$, $V_{CPK} < 500\text{V}$
$t_{d(on)}$	Turn-On Delay Time	—	66	—			ns	$T_J = 150^\circ\text{C}$, See Fig. 9, 10, 11, 18 $I_C = 13\text{A}$, $V_{CC} = 480\text{V}$ $V_{GE} = 15\text{V}$, $R_G = 10\Omega$ Energy losses include "tail" and diode reverse recovery.
t_r	Rise Time	—	48	—				
$t_{d(off)}$	Turn-Off Delay Time	—	250	—				
t_f	Fall Time	—	140	—				
E_{ts}	Total Switching Loss	—	1.6	—				
C_{ies}	Input Capacitance	—	1500	—	pF	$V_{GE} = 0\text{V}$ $V_{CC} = 30\text{V}$ See Fig. 7 $f = 1.0\text{MHz}$		
C_{oes}	Output Capacitance	—	190	—				
C_{res}	Reverse Transfer Capacitance	—	17	—				
t_{rr}	Diode Reverse Recovery Time	—	42	60	ns	$T_J = 25^\circ\text{C}$ See Fig. 14 $T_J = 125^\circ\text{C}$ 14		
		—	74	120				
I_{rr}	Diode Peak Reverse Recovery Current	—	4.0	6.0	A	$T_J = 25^\circ\text{C}$ See Fig. 15 $T_J = 125^\circ\text{C}$ 15		
		—	6.5	10				
Q_{rr}	Diode Reverse Recovery Charge	—	80	180	nC	$T_J = 25^\circ\text{C}$ See Fig. 16 $T_J = 125^\circ\text{C}$ 16		
		—	220	600				
$di_{(rec)M}/dt$	Diode Peak Rate of Fall of Recovery During t_b	—	188	—	A/ μs	$T_J = 25^\circ\text{C}$ See Fig. 17 $T_J = 125^\circ\text{C}$ 17		
		—	160	—				

Notes:

① Repetitive rating; $V_{GE}=20\text{V}$, pulse width limited by max. junction temperature. (See fig. 20)

② $V_{CC}=80\%(V_{CES})$, $V_{GE}=20\text{V}$, $L=10\mu\text{H}$, $R_G=10\Omega$, (See fig. 19)

③ Pulse width $\leq 80\mu\text{s}$; duty factor $\leq 0.1\%$.

④ Pulse width $5.0\mu\text{s}$, single shot.

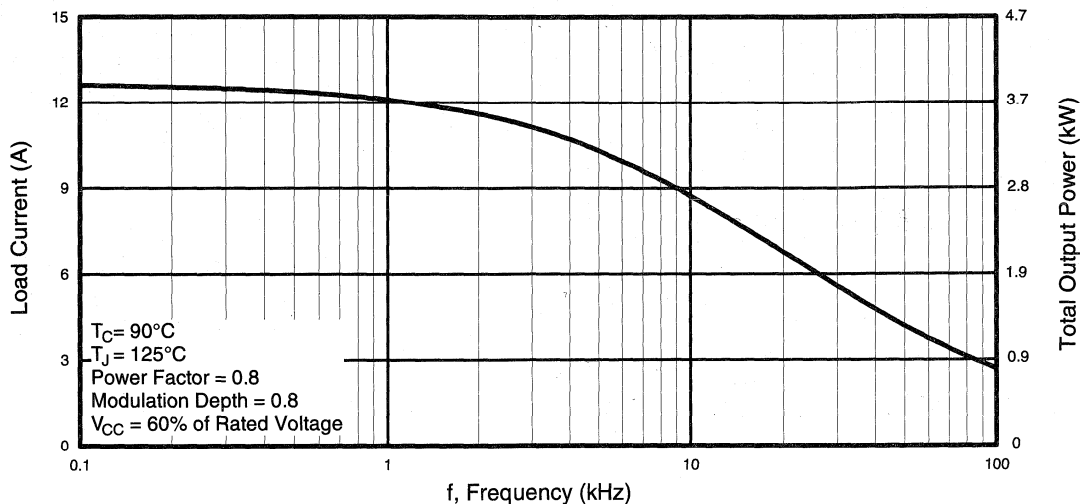


Fig. 1 - RMS Current and Output Power, Synthesized Sine Wave

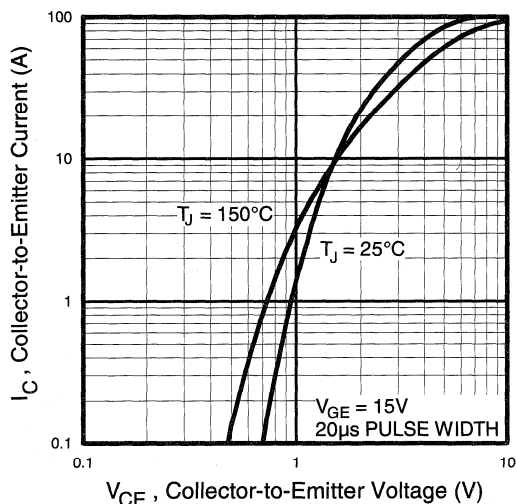


Fig. 2 - Typical Output Characteristics

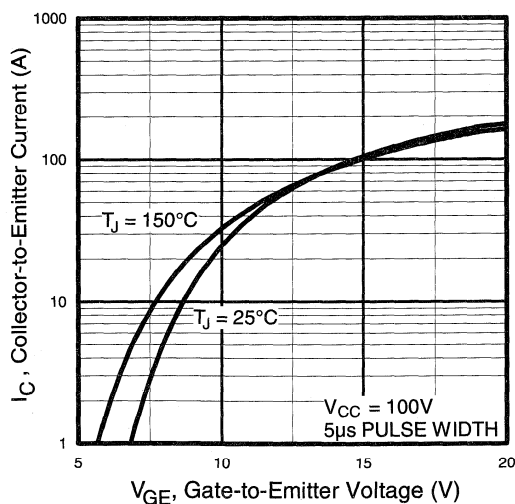


Fig. 3 - Typical Transfer Characteristics

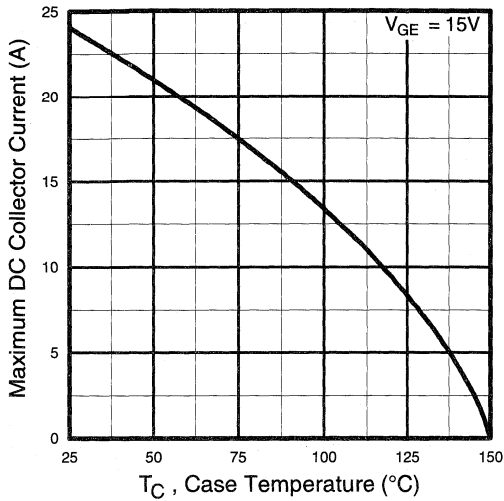


Fig. 4 - Maximum Collector Current vs. Case Temperature

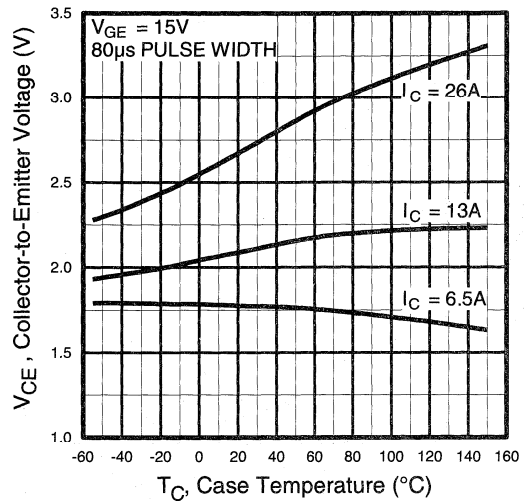


Fig. 5 - Collector-to-Emitter Voltage vs. Case Temperature

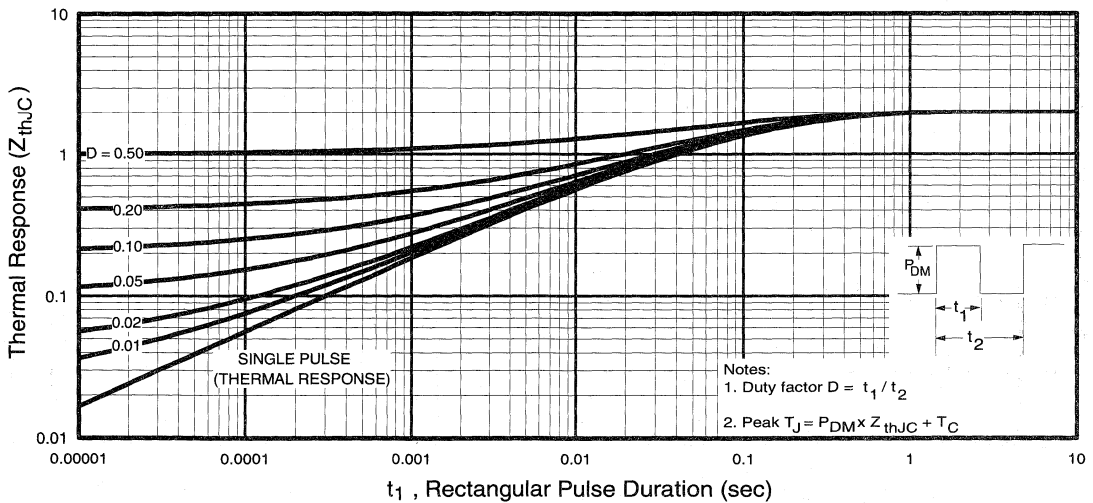


Fig. 6 - Maximum IGBT Effective Transient Thermal Impedance, Junction-to-Case

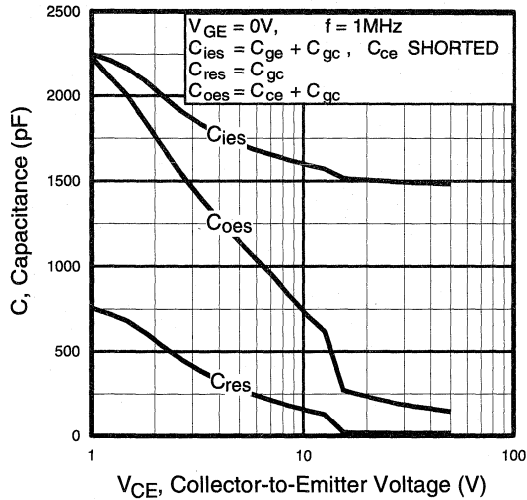


Fig. 7 - Typical Capacitance vs. Collector-to-Emitter Voltage

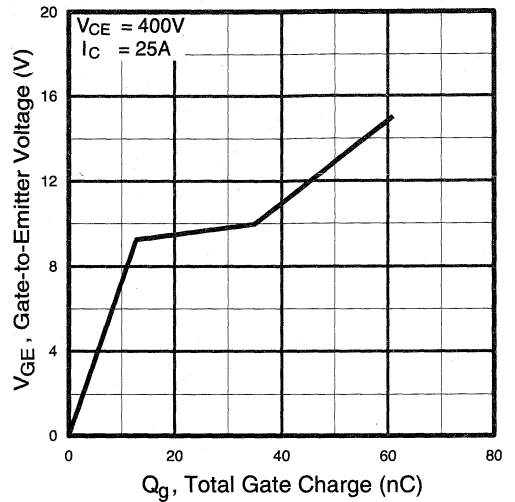


Fig. 8 - Typical Gate Charge vs. Gate-to-Emitter Voltage

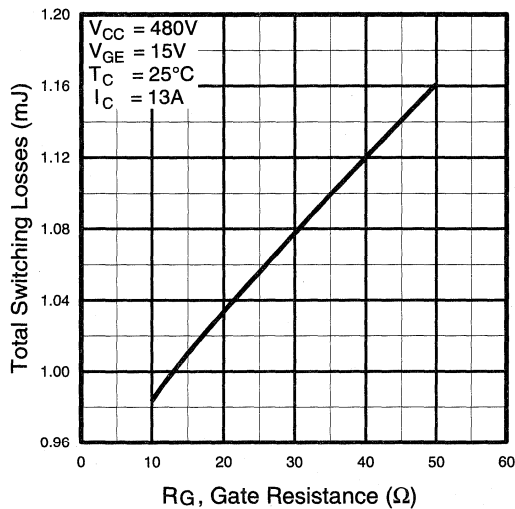


Fig. 9 - Typical Switching Losses vs. Gate Resistance

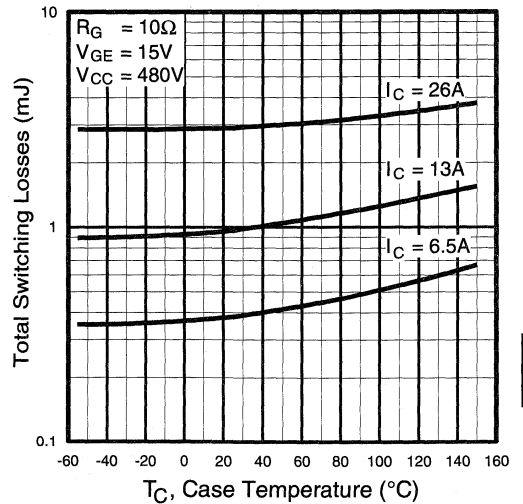


Fig. 10 - Typical Switching Losses vs. Case Temperature

Motor Control Ultra-Fast Modules

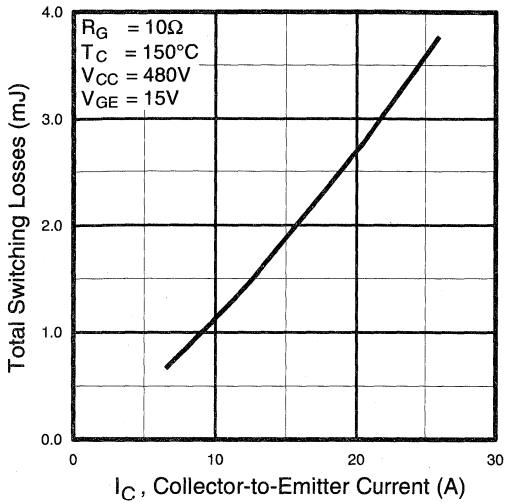


Fig. 11 - Typical Switching Losses vs. Collector-to-Emitter Current

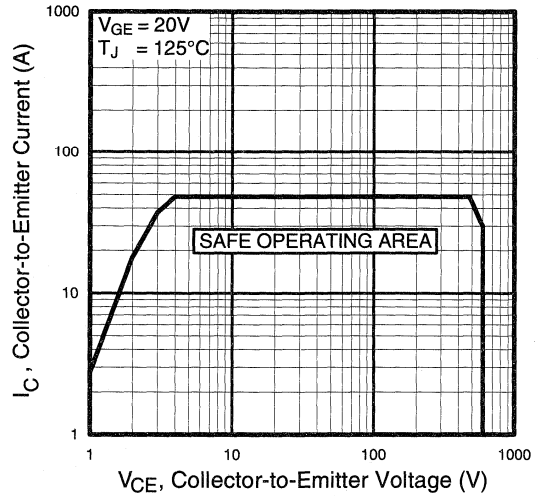


Fig. 12 - Turn-Off SOA

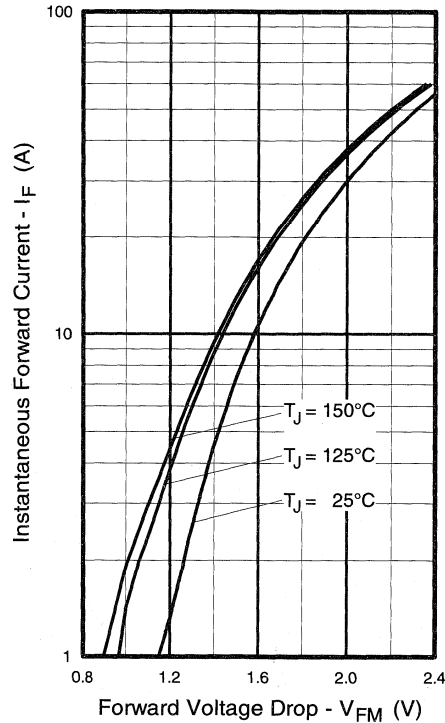


Fig. 13 - Maximum Forward Voltage Drop vs. Instantaneous Forward Current

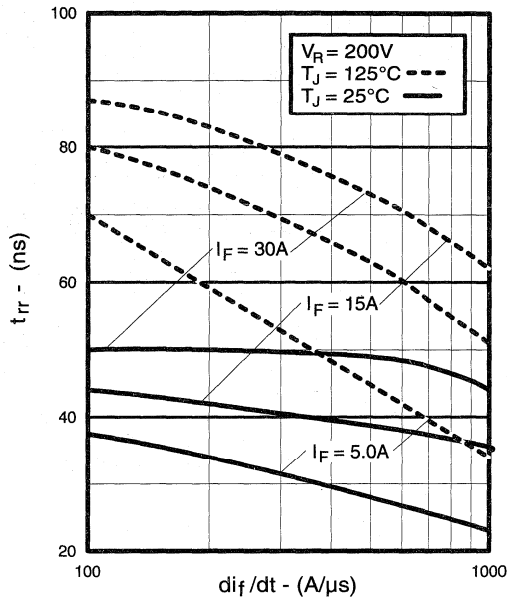


Fig. 14 - Typical Reverse Recovery vs. di_f/dt

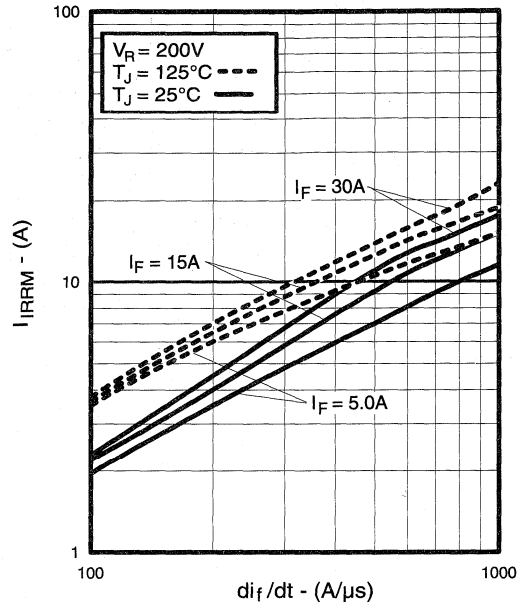


Fig. 15 - Typical Recovery Current vs. di_f/dt

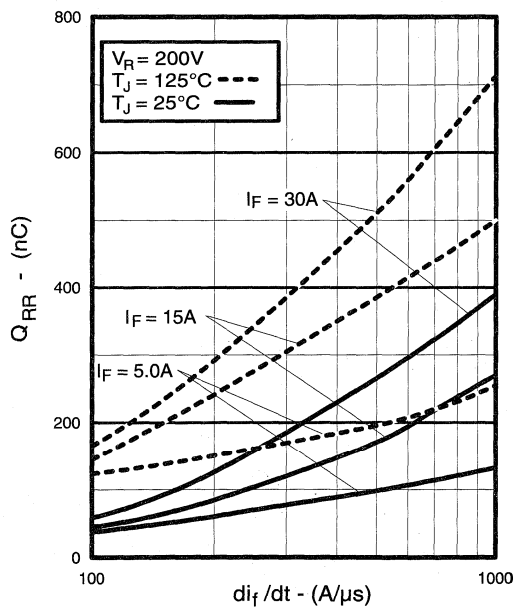


Fig. 16 - Typical Stored Charge vs. di_f/dt

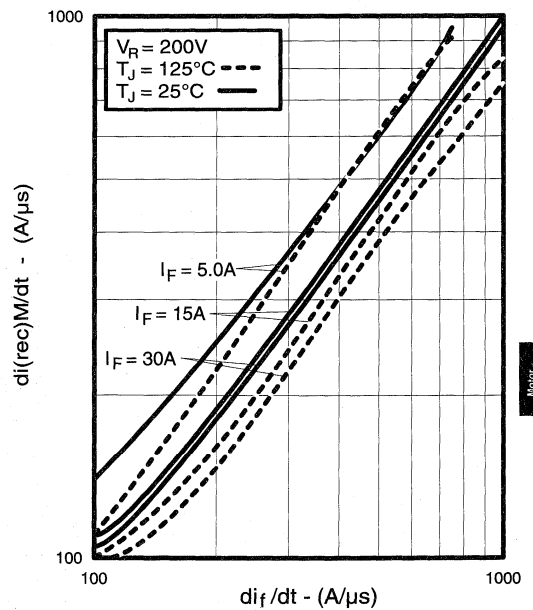


Fig. 17 - Typical $di_{(rec)M}/dt$ vs. di_f/dt

Motor
Control
Ultra-Fast
Modules

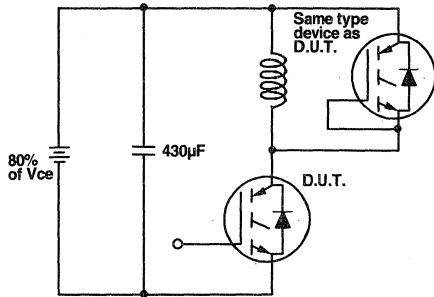


Fig. 18a - Test Circuit for Measurement of I_{LM} , E_{on} , $E_{off}(\text{diode})$, t_{rr} , Q_{rr} , I_{rr} , $t_{d(on)}$, t_r , $t_{d(off)}$, t_f

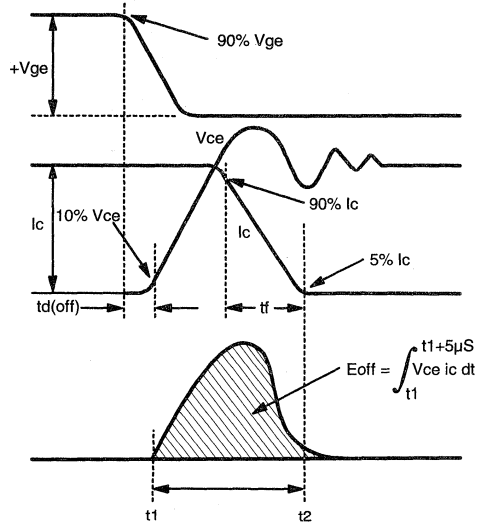


Fig. 18b - Test Waveforms for Circuit of Fig. 18a, Defining E_{off} , $t_{d(off)}$, t_f

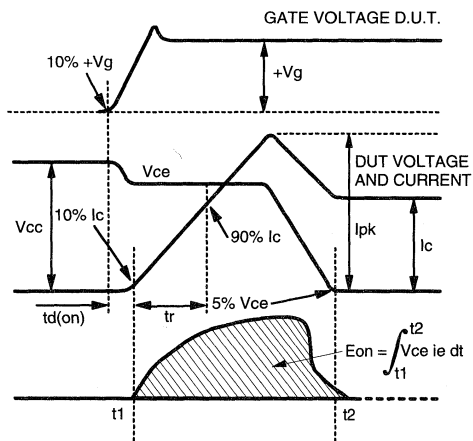


Fig. 18c - Test Waveforms for Circuit of Fig. 18a, Defining E_{on} , $t_{d(on)}$, t_r

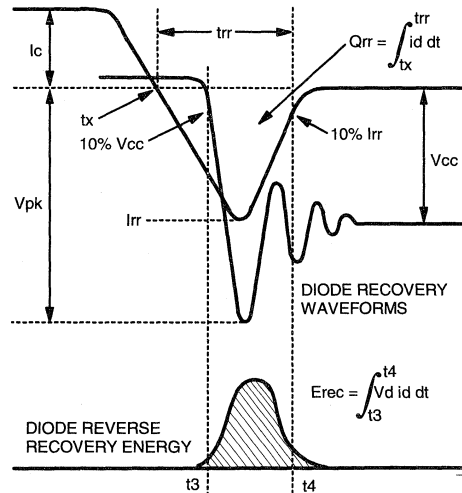


Fig. 18d - Test Waveforms for Circuit of Fig. 18a, Defining E_{rec} , t_{rr} , Q_{rr} , I_{rr}

Refer to Section D for the following:
Appendix D: Section D - page D-6

Fig. 18e - Macro Waveforms for Test Circuit of Fig. 18a

Fig. 19 - Clamped Inductive Load Test Circuit

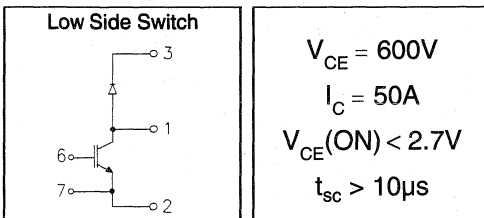
Fig. 20 - Pulsed Collector Current Test Circuit

IRGKIN050K06

"CHOPPER" IGBT INT-A-PAK

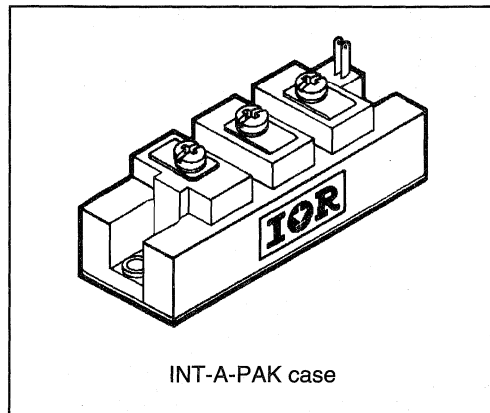
Low conduction loss IGBT

- Rugged Design
- Simple gate-drive
- Switching-Loss Rating includes all "tail" losses
- Short circuit rated



Description

IR's advanced IGBT technology is the key to this line of INT-A-PAK Power Modules. The efficient geometry and unique processing of the IGBT allow higher current densities than comparable bipolar power module transistors, while at the same time requiring the simpler gate-drive of the familiar power MOSFET. These modules are short circuit rated for applications such as motor control requiring this important feature.



Absolute Maximum Ratings

Parameter	Description	Value	Units
V_{CES}	Continuous collector to emitter voltage	600	V
$I_C @ T_C = 25^\circ C$	Continuous collector current	55	A
$I_C @ T_C = 85^\circ C$	Continuous collector current	30	
$I_C @ T_C = 100^\circ C$	Continuous collector current	20	
I_{LM}	Peak switching current	100	
I_{FM}	Peak diode forward current (1)	100	V
V_{GE}	Gate to emitter voltage	± 20	
V_{ISOL}	RMS isolation voltage, any terminal to case, $t = 1$ min	2500	W
$P_D @ T_C = 25^\circ C$	Power dissipation	240	
T_J	Operating junction temperature range	-40 to 150	$^\circ C$
T_{STG}	Storage temperature range	-40 to 125	

(1) Duration limited by max junction temperature.

Target Data



Electrical Characteristics - $T_J = 25^\circ\text{C}$, unless otherwise stated

Parameter	Description	Min	Typ	Max	Units	Test Conditions
BV_{CES}	Collector-to-emitter breakdown voltage	600	—	—	V	$V_{GE} = 0V, I_C = 500\mu A$
$V_{CE(ON)}$	Collector-to-emitter voltage	—	—	2.7		$V_{GE} = 15V, I_C = 50A$
		—	2.7	—		$V_{GE} = 15V, I_C = 50A, T_J = 125^\circ\text{C}$
V_{FM}	Diode forward voltage - maximum	—	1.8	2.0		$I_F = 50A, V_{GE} = 0V$
		—	1.75	—		$I_F = 50A, V_{GE} = 0V, T_J = 125^\circ\text{C}$
V_{Geth}	Gate threshold voltage	3.0	—	5.5	$I_C = 250\mu A$	
ΔV_{Geth}	Threshold voltage temperature coefficient	—	- 11	—	mV/°C	$V_{CE} = V_{GE}, I_C = 250\mu A$
g_{fe}	Forward transconductance	17	—	30	S(Ω)	$V_{CE} = 25V, I_C = 50A$
I_{CES}	Collector-to-emitter leakage current	—	—	500	μA	$V_{GE} = 0V, V_{CE} = 600V$
		—	—	5	mA	$V_{GE} = 0V, V_{CE} = 600V, T_J = 125^\circ\text{C}$
I_{GES}	Gate-to-emitter leakage current	—	—	± 500	nA	$V_{GE} = \pm 20V$

Dynamic Characteristics - $T_J = 125^\circ\text{C}$, unless otherwise stated

Parameter	Description	Min	Typ	Max	Units	Test Conditions
E_{on}	Turn-on switching energy	—	0.04	—	mJ/A	$R_G = 15\Omega, V_{CC} = 300V$
E_{off} (1)	Turn-off switching energy	—	0.06	—		$I_C = 50A, L_S = 100nH$
E_{ts} (1)	Total switching energy	—	—	0.12		$V_{GE} = \pm 15V$
$t_{d(on)}$	Turn-on delay time	—	200	—	ns	$R_G = 15\Omega, V_{CC} = 300V$
t_r	Rise time	—	500	—		$I_C = 50A$
$t_{d(off)}$	Turn-off delay time	—	250	—		$V_{GE} = \pm 15V$
t_f	Fall time	—	120	—		Resistive load, $T_J = 25^\circ\text{C}$
I_{rr}	Diode peak recovery current	—	20	—		$R_G = 15\Omega, V_{CC} = 300V$
t_{rr}	Diode recovery time	—	110	—	ns	$I_C = 50A$
Q_{rr}	Diode recovery charge	—	1.2	—	μC	$V_{GE} = \pm 15V$
Q_{ge}	Gate-to-emitter charge (turn-on)	13	—	21	nC	$V_{CC} = 480V$
Q_{gc}	Gate-to-collector charge (turn-on)	35	—	70		$I_C = 27A$
Q_g	Total gate charge (turn-on)	77	—	140		$V_{GE} = 15V$
C_{ies}	Input capacitance	—	2900	—	pF	$V_{GE} = 0V$
C_{oes}	Output capacitance	—	330	—		$V_{CC} = 30V$
C_{res}	Reverse transfer capacitance	—	40	—		$f = 1MHz$
t_{sc}	Short circuit withstand time	10	—	—	μs	$V_{CC} = 360V, V_{GE} = \pm 15V$ Min. $R_G = 15\Omega, V_{CEP} = 500V$

(1) Includes tail losses

Thermal and Mechanical Characteristics

Parameter	Description	Typ	Max	Units
R_{thJC} (IGBT)	Thermal resistance, junction to case, each IGBT	—	0.52	°C/W
R_{thJC} (Diode)	Thermal resistance, junction to case, each diode	—	0.90	
R_{thCS} (Module)	Thermal resistance, case to sink	0.041	0.100	
Wt	Weight of module	150	—	g

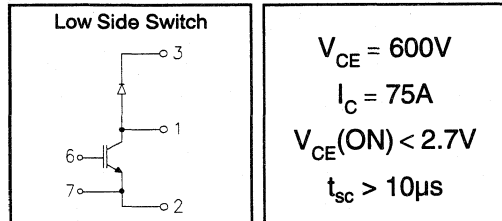
Refer to Section D - page D-15 for Package Outline 7 -INT-A-PAK, New - Low Side Switch

IRGKIN075K06

"CHOPPER" IGBT INT-A-PAK

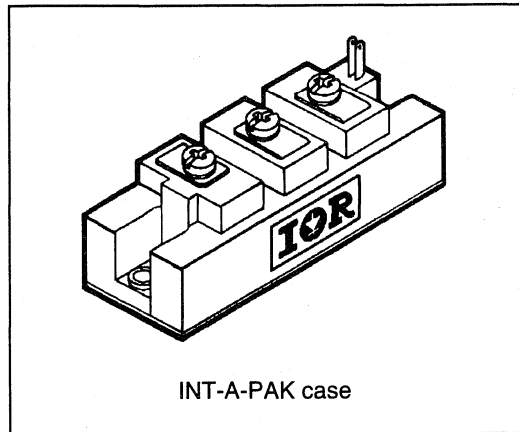
Low conduction loss IGBT

- Rugged Design
- Simple gate-drive
- Switching-Loss Rating includes all "tail" losses
- Short circuit rated



Description

IR's advanced IGBT technology is the key to this line of INT-A-PAK Power Modules. The efficient geometry and unique processing of the IGBT allow higher current densities than comparable bipolar power module transistors, while at the same time requiring the simpler gate-drive of the familiar power MOSFET. These modules are short circuit rated for applications such as motor control requiring this important feature.



Absolute Maximum Ratings

Parameter	Description	Value	Units
V_{CES}	Continuous collector to emitter voltage	600	V
$I_C @ T_C = 25^\circ C$	Continuous collector current	95	A
$I_C @ T_C = 85^\circ C$	Continuous collector current	55	
$I_C @ T_C = 100^\circ C$	Continuous collector current	40	
I_{LM}	Peak switching current	150	
I_{FM}	Peak diode forward current (1)	150	V
V_{GE}	Gate to emitter voltage	± 20	
V_{ISOL}	RMS isolation voltage, any terminal to case, $t = 1$ min	2500	W
$P_D @ T_C = 25^\circ C$	Power dissipation	391	
T_J	Operating junction temperature range	-40 to 150	$^\circ C$
T_{STG}	Storage temperature range	-40 to 125	

(1) Duration limited by max junction temperature.

Electrical Characteristics - $T_J = 25^\circ\text{C}$, unless otherwise stated

Parameter	Description	Min	Typ	Max	Units	Test Conditions
BV_{CES}	Collector-to-emitter breakdown voltage	600	—	—	V	$V_{GE} = 0\text{V}, I_C = 1\text{mA}$
$V_{CE(ON)}$	Collector-to-emitter voltage	—	—	2.7		$V_{GE} = 15\text{V}, I_C = 75\text{A}$
		—	2.7	—		$V_{GE} = 15\text{V}, I_C = 75\text{A}, T_J = 125^\circ\text{C}$
V_{FM}	Diode forward voltage - maximum	—	1.8	2.0		$I_F = 75\text{A}, V_{GE} = 0\text{V}$
		—	1.75	—		$I_F = 75\text{A}, V_{CE} = 0\text{V}, T_J = 125^\circ\text{C}$
V_{GEth}	Gate threshold voltage	3.0	—	5.5	$I_C = 500\mu\text{A}$	
ΔV_{GEth}	Threshold voltage temperature coefficient	—	-11	—	mV/ $^\circ\text{C}$	$V_{CE} = V_{GE}, I_C = 500\mu\text{A}$
g_{fe}	Forward transconductance	34	—	58	S(Ω)	$V_{CE} = 25\text{V}, I_C = 75\text{A}$
I_{CES}	Collector-to-emitter leakage current	—	—	1	mA	$V_{GE} = 0\text{V}, V_{CE} = 600\text{V}$
		—	—	10		$V_{GE} = 0\text{V}, V_{CE} = 600\text{V}, T_J = 125^\circ\text{C}$
I_{GES}	Gate-to-emitter leakage current	—	—	± 1	μA	$V_{GE} = \pm 20\text{V}$

Dynamic Characteristics - $T_J = 125^\circ\text{C}$, unless otherwise stated

Parameter	Description	Min	Typ	Max	Units	Test Conditions
E_{on}	Turn-on switching energy	—	0.04	—	mJ/A	$R_G = 15\Omega, V_{CC} = 300\text{V}$
E_{off} (1)	Turn-off switching energy	—	0.06	—		$I_C = 75\text{A}, L_S = 100\text{nH}$
E_{ts} (1)	Total switching energy	—	—	0.12		$V_{GE} = \pm 15\text{V}$
$t_{d(on)}$	Turn-on delay time	—	200	—	ns	$R_G = 15\Omega, V_{CC} = 300\text{V}$
t_r	Rise time	—	500	—		$I_C = 75\text{A}$
$t_{d(off)}$	Turn-off delay time	—	250	—		$V_{GE} = \pm 15\text{V}$
t_f	Fall time	—	120	—		Resistive load, $T_J = 25^\circ\text{C}$
I_{rr}	Diode peak recovery current	—	27	—		A
t_{rr}	Diode recovery time	—	110	—	ns	$I_C = 75\text{A}$
Q_{rr}	Diode recovery charge	—	1.7	—	μC	$V_{GE} = \pm 15\text{V}$
Q_{ge}	Gate-to-emitter charge (turn-on)	26	—	42	nC	$V_{CC} = 480\text{V}$
Q_{gc}	Gate-to-collector charge (turn-on)	70	—	140		$I_C = 54\text{A}$
Q_g	Total gate charge (turn-on)	150	—	280		$V_{GE} = 15\text{V}$
C_{ies}	Input capacitance	—	5800	—	pF	$V_{GE} = 0\text{V}$
C_{oes}	Output capacitance	—	660	—		$V_{CC} = 30\text{V}$
C_{res}	Reverse transfer capacitance	—	80	—		$f = 1\text{MHz}$
t_{sc}	Short circuit withstand time	10	—	—	μs	$V_{CC} = 360\text{V}, V_{GE} = \pm 15\text{V}$ Min. $R_G = 15\Omega, V_{CEP} = 500\text{V}$

(1) Includes tail losses

Thermal and Mechanical Characteristics

Parameter	Description	Typ	Max	Units
R_{thJC} (IGBT)	Thermal resistance, junction to case, each IGBT	—	0.32	$^\circ\text{C/W}$
R_{thJC} (Diode)	Thermal resistance, junction to case, each diode	—	0.48	
R_{thCS} (Module)	Thermal resistance, case to sink	0.041	0.100	
Wt	Weight of module	150	—	g

Refer to Section D - page D-15 for Package Outline 7 -INT-A-PAK, New - Low Side Switch

IRGKIN100K06

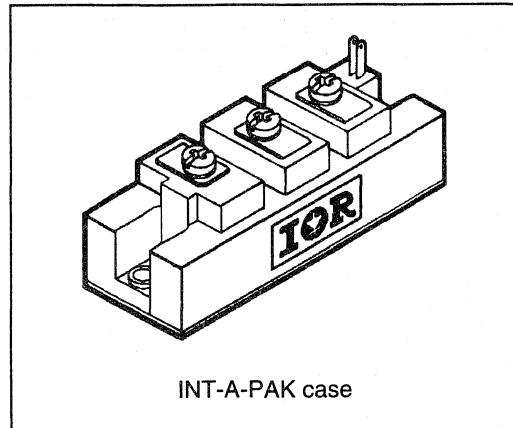
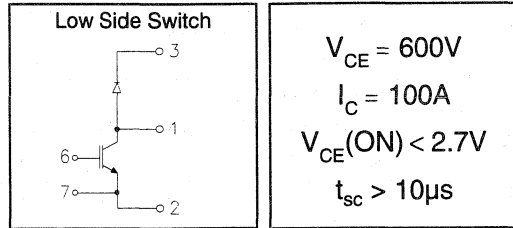
"CHOPPER" IGBT INT-A-PAK

Low conduction loss IGBT

- Rugged Design
- Simple gate-drive
- Switching-Loss Rating includes all "tail" losses
- Short circuit rated

Description

IR's advanced IGBT technology is the key to this line of INT-A-PAK Power Modules. The efficient geometry and unique processing of the IGBT allow higher current densities than comparable bipolar power module transistors, while at the same time requiring the simpler gate-drive of the familiar power MOSFET. These modules are short circuit rated for applications such as motor control requiring this important feature.



Absolute Maximum Ratings

Parameter	Description	Value	Units
V_{CES}	Continuous collector to emitter voltage	600	V
$I_C @ T_C = 25^\circ C$	Continuous collector current	130	A
$I_C @ T_C = 85^\circ C$	Continuous collector current	70	
$I_C @ T_C = 100^\circ C$	Continuous collector current	50	
I_{LM}	Peak switching current	200	
I_{FM}	Peak diode forward current (1)	200	V
V_{GE}	Gate to emitter voltage	± 20	
V_{ISOL}	RMS isolation voltage, any terminal to case, $t = 1 \text{ min}$	2500	
$P_D @ T_C = 25^\circ C$	Power dissipation	500	W
T_J	Operating junction temperature range	-40 to 150	$^\circ C$
T_{STG}	Storage temperature range	-40 to 125	

(1) Duration limited by max junction temperature.



Electrical Characteristics - $T_J = 25^\circ\text{C}$, unless otherwise stated

Parameter	Description	Min	Typ	Max	Units	Test Conditions
BVCES	Collector-to-emitter breakdown voltage	600	—	—	V	$V_{GE} = 0V, I_C = 1.5mA$
V _{CE(ON)}	Collector-to-emitter voltage	—	—	2.7		$V_{GE} = 15V, I_C = 100A$
		—	2.7	—		$V_{GE} = 15V, I_C = 100A, T_J = 125^\circ\text{C}$
V _{FM}	Diode forward voltage - maximum	—	1.8	2.0		$I_F = 100A, V_{GE} = 0V$
		—	1.75	—		$I_F = 100A, V_{GE} = 0V, T_J = 125^\circ\text{C}$
V _{GEth}	Gate threshold voltage	3.0	—	5.5	$I_C = 750\mu A$	
DV _{GEth}	Threshold voltage temperature coefficient	—	- 11	—	mV/°C	$V_{CE} = V_{GE}, I_C = 750\mu A$
g _{fe}	Forward transconductance	51	—	87	S(τ)	$V_{CE} = 25V, I_C = 100A$
I _{CES}	Collector-to-emitter leakage current	—	—	1.5	mA	$V_{GE} = 0V, V_{CE} = 600V$
		—	—	15		$V_{GE} = 0V, V_{CE} = 600V, T_J = 125^\circ\text{C}$
I _{GES}	Gate-to-emitter leakage current	—	—	± 1.5	μA	$V_{GE} = \pm 20V$

Dynamic Characteristics - $T_J = 125^\circ\text{C}$, unless otherwise stated

Parameter	Description	Min	Typ	Max	Units	Test Conditions
E _{on}	Turn-on switching energy	—	0.04	—	mJ/A	$R_G = 15W, V_{CC} = 300V$
E _{off} (1)	Turn-off switching energy	—	0.06	—		$I_C = 100A, L_S = 100nH$
E _{ts} (1)	Total switching energy	—	—	0.12		$V_{GE} = \pm 15V$
t _{d(on)}	Turn-on delay time	—	200	—	ns	$R_G = 15W, V_{CC} = 300V$
t _r	Rise time	—	500	—		$I_C = 100A$
t _{d(off)}	Turn-off delay time	—	250	—		$V_{GE} = \pm 15V$
t _f	Fall time	—	120	—		Resistive load, $T_J = 25^\circ\text{C}$
I _{rr}	Diode peak recovery current	—	40	—	A	$R_G = 15W, V_{CC} = 300V$
t _{rr}	Diode recovery time	—	110	—	ns	$I_C = 100A$
Q _{rr}	Diode recovery charge	—	2.2	—	μC	$V_{GE} = \pm 15V$
Q _{ge}	Gate-to-emitter charge (turn-on)	39	—	63	nC	$V_{CC} = 480V$
Q _{gc}	Gate-to-collector charge (turn-on)	105	—	210		$I_C = 81A$
Q _g	Total gate charge (turn-on)	225	—	420		$V_{GE} = 15V$
C _{ies}	Input capacitance	—	8700	—	pF	$V_{GE} = 0V$
C _{oes}	Output capacitance	—	990	—		$V_{CC} = 30V$
C _{res}	Reverse transfer capacitance	—	120	—		$f = 1MHz$
t _{sc}	Short circuit withstand time	10	—	—	μs	$V_{CC} = 360V, V_{GE} = \pm 15V$ Min. $R_G = 15\Omega, V_{CEP} = 500V$

(1) Includes tail losses

Thermal and Mechanical Characteristics

Parameter	Description	Typ	Max	Units
R _{thJC} (IGBT)	Thermal resistance, junction to case, each IGBT	—	0.25	°C/W
R _{thJC} (Diode)	Thermal resistance, junction to case, each diode	—	0.38	
R _{thCS} (Module)	Thermal resistance, case to sink	0.041	0.100	
Wt	Weight of module	150	—	g

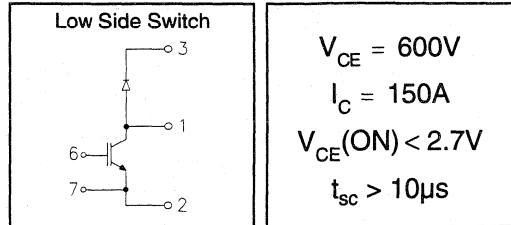
Refer to Section D - page D-15 for Package Outline 7 -INT-A-PAK, New - Low Side Switch

IRGKIN150K06

"CHOPPER" IGBT INT-A-PAK

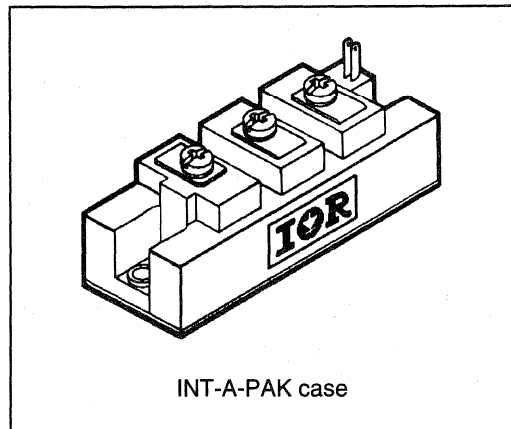
Low conduction loss IGBT

- Rugged Design
- Simple gate-drive
- Switching-Loss Rating includes all "tail" losses
- Short circuit rated



Description

IR's advanced IGBT technology is the key to this line of INT-A-PAK Power Modules. The efficient geometry and unique processing of the IGBT allow higher current densities than comparable bipolar power module transistors, while at the same time requiring the simpler gate-drive of the familiar power MOSFET. These modules are short circuit rated for applications such as motor control requiring this important feature.



Absolute Maximum Ratings

Parameter	Description	Value	Units
V_{CES}	Continuous collector to emitter voltage	600	V
$I_C @ T_C = 25^\circ C$	Continuous collector current	170	A
$I_C @ T_C = 85^\circ C$	Continuous collector current	95	
$I_C @ T_C = 100^\circ C$	Continuous collector current	70	
I_{LM}	Peak switching current	300	
I_{FM}	Peak diode forward current (1)	300	
V_{GE}	Gate to emitter voltage	± 20	V
V_{ISOL}	RMS isolation voltage, any terminal to case, $t = 1$ min	2500	
$P_D @ T_C = 25^\circ C$	Power dissipation	658	W
T_J	Operating junction temperature range	-40 to 150	$^\circ C$
T_{STG}	Storage temperature range	-40 to 125	

(1) Duration limited by max junction temperature.



Electrical Characteristics - $T_J = 25^\circ\text{C}$, unless otherwise stated

Parameter	Description	Min	Typ	Max	Units	Test Conditions
BV_{CES}	Collector-to-emitter breakdown voltage	600	—	—	V	$V_{GE} = 0V, I_C = 2mA$
$V_{CE(ON)}$	Collector-to-emitter voltage	—	—	2.7		$V_{GE} = 15V, I_C = 150A$
		—	2.7	—		$V_{GE}=15V, I_C=150A, T_J=125^\circ\text{C}$
V_{FM}	Diode forward voltage - maximum	—	1.8	2.0		$I_F = 150A, V_{GE} = 0V$
		—	1.75	—	$I_F=150A, V_{GE}=0V, T_J=125^\circ\text{C}$	
V_{Geth}	Gate threshold voltage	3.0	—	5.5	$I_C = 1mA$	
ΔV_{Geth}	Threshold voltage temperature coefficient	—	- 11	—	mV/ $^\circ\text{C}$	$V_{CE} = V_{GE}, I_C = 1mA$
g_{fe}	Forward transconductance	68	—	120	S(Ω)	$V_{CE} = 25V, I_C = 150A$
I_{CES}	Collector-to-emitter leakage current	—	—	2	mA	$V_{GE} = 0V, V_{CE} = 600V$
		—	—	20		$V_{GE}=0V, V_{CE}=600V, T_J=125^\circ\text{C}$
I_{GES}	Gate-to-emitter leakage current	—	—	± 2	μA	$V_{GE} = \pm 20V$

Dynamic Characteristics - $T_J = 125^\circ\text{C}$, unless otherwise stated

Parameter	Description	Min	Typ	Max	Units	Test Conditions
E_{on}	Turn-on switching energy	—	0.04	—	mJ/A	$R_G = 15\Omega, V_{CC} = 300V$
E_{off} (1)	Turn-off switching energy	—	0.06	—		$I_C = 150A, L_S = 100nH$
E_{ts} (1)	Total switching energy	—	—	0.12		$V_{GE} = \pm 15V$
$t_{d(on)}$	Turn-on delay time	—	200	—	ns	$R_G = 15\Omega, V_{CC} = 300V$
t_r	Rise time	—	500	—		$I_C = 150A$
$t_{d(off)}$	Turn-off delay time	—	250	—		$V_{GE} = \pm 15V$
t_f	Fall time	—	120	—		Resistive load, $T_J = 25^\circ\text{C}$
I_{rr}	Diode peak recovery current	—	50	—		A
t_{rr}	Diode recovery time	—	110	—	ns	$I_C = 150A$
Q_{rr}	Diode recovery charge	—	3	—	μC	$V_{GE} = \pm 15V$
Q_{ge}	Gate-to-emitter charge (turn-on)	52	—	84	nC	$V_{CC} = 480V$
Q_{gc}	Gate-to-collector charge (turn-on)	140	—	280		$I_C = 108A$
Q_g	Total gate charge (turn-on)	300	—	560		$V_{GE} = 15V$
C_{ies}	Input capacitance	—	11600	—	pF	$V_{GE} = 0V$
C_{oes}	Output capacitance	—	1320	—		$V_{CC} = 30V$
C_{res}	Reverse transfer capacitance	—	160	—		$f = 1MHz$
t_{sc}	Short circuit withstand time	10	—	—	μs	$V_{CC} = 360V, V_{GE} = \pm 15V$ Min. $R_G = 15\Omega, V_{CEP} = 500V$

(1) Includes tail losses

Thermal and Mechanical Characteristics

Parameter	Description	Typ	Max	Units
R_{thJC} (IGBT)	Thermal resistance, junction to case, each IGBT	---	0.19	$^\circ\text{C/W}$
R_{thJC} (Diode)	Thermal resistance, junction to case, each diode	---	0.28	
R_{thCS} (Module)	Thermal resistance, case to sink	0.041	0.100	
Wt	Weight of module	150	---	g

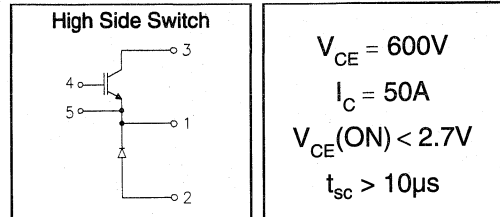
Refer to Section D - page D-15 for Package Outline 7 -INT-A-PAK, New - Low Side Switch

IRGNIN050K06

"CHOPPER" IGBT INT-A-PAK

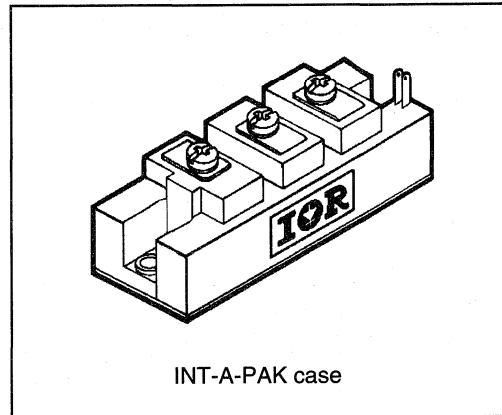
Low conduction loss IGBT

- Rugged Design
- Simple gate-drive
- Switching-Loss Rating includes all "tail" losses
- Short circuit rated



Description

IR's advanced IGBT technology is the key to this line of INT-A-PAK Power Modules. The efficient geometry and unique processing of the IGBT allow higher current densities than comparable bipolar power module transistors, while at the same time requiring the simpler gate-drive of the familiar power MOSFET. These modules are short circuit rated for applications such as motor control requiring this important feature.



Absolute Maximum Ratings

Parameter	Description	Value	Units
V_{CES}	Continuous collector to emitter voltage	600	V
$I_C @ T_C = 25^\circ C$	Continuous collector current	55	A
$I_C @ T_C = 85^\circ C$	Continuous collector current	30	
$I_C @ T_C = 100^\circ C$	Continuous collector current	20	
I_{LM}	Peak switching current	100	
I_{FM}	Peak diode forward current (1)	100	V
V_{GE}	Gate to emitter voltage	± 20	
V_{ISOL}	RMS isolation voltage, any terminal to case, $t = 1$ min	2500	W
$P_D @ T_C = 25^\circ C$	Power dissipation	240	
T_J	Operating junction temperature range	-40 to 150	
T_{STG}	Storage temperature range	-40 to 125	

(1) Duration limited by max junction temperature.

Target Data

IRGNIN050K06

Target Data



Electrical Characteristics - $T_J = 25^\circ\text{C}$, unless otherwise stated

Parameter	Description	Min	Typ	Max	Units	Test Conditions
BV_{CES}	Collector-to-emitter breakdown voltage	600	—	—	V	$V_{GE} = 0V, I_C = 500\mu A$
$V_{CE(ON)}$	Collector-to-emitter voltage	—	—	2.7		$V_{GE} = 15V, I_C = 50A$
		—	2.7	—		$V_{GE} = 15V, I_C = 50A, T_J = 125^\circ\text{C}$
V_{FM}	Diode forward voltage - maximum	—	1.8	2.0		$I_F = 50A, V_{GE} = 0V$
		—	1.75	—		$I_F = 50A, V_{GE} = 0V, T_J = 125^\circ\text{C}$
V_{GEth}	Gate threshold voltage	3.0	—	5.5		$I_C = 250\mu A$
ΔV_{GEth}	Threshold voltage temp. coefficient	—	-11	—	$\text{mV}/^\circ\text{C}$	$V_{CE} = V_{GE}, I_C = 250\mu A$
g_{fe}	Forward transconductance	17	—	30	$S(\tau)$	$V_{CE} = 25V, I_C = 50A$
I_{CES}	Collector-to-emitter leakage current	—	—	500	μA	$V_{GE} = 0V, V_{CE} = 600V$
		—	—	5	mA	$V_{GE} = 0V, V_{CE} = 600V, T_J = 125^\circ\text{C}$
I_{GES}	Gate-to-emitter leakage current	—	—	± 500	nA	$V_{GE} = \pm 20V$

Dynamic Characteristics - $T_J = 125^\circ\text{C}$, unless otherwise stated

Parameter	Description	Min	Typ	Max	Units	Test Conditions
E_{on}	Turn-on switching energy	—	0.04	—	mJ/A	$R_G = 15\Omega, V_{CC} = 300V$
$E_{off} (1)$	Turn-off switching energy	—	0.06	—		$I_C = 50A, L_S = 100\text{nH}$
$E_{ts} (1)$	Total switching energy	—	—	0.12		$V_{GE} = \pm 15V$
$t_{d(on)}$	Turn-on delay time	—	200	—	ns	$R_G = 15\Omega, V_{CC} = 300V$
t_r	Rise time	—	500	—		$I_C = 50A$
$t_{d(off)}$	Turn-off delay time	—	250	—		$V_{GE} = \pm 15V$
t_f	Fall time	—	120	—		Resistive load, $T_J = 25^\circ\text{C}$
I_{rr}	Diode peak recovery current	—	20	—		$R_G = 15\Omega, V_{CC} = 300V$
t_{rr}	Diode recovery time	—	110	—	ns	$I_C = 50A$
Q_{rr}	Diode recovery charge	—	1.2	—	μC	$V_{GE} = \pm 15V$
Q_{ge}	Gate-to-emitter charge (turn-on)	13	—	21	nC	$V_{CC} = 480V$
Q_{gc}	Gate-to-collector charge (turn-on)	35	—	70		$I_C = 27A$
Q_g	Total gate charge (turn-on)	77	—	140		$V_{GE} = 15V$
C_{ies}	Input capacitance	—	2900	—	pF	$V_{GE} = 0V$
C_{oes}	Output capacitance	—	330	—		$V_{CC} = 30V$
C_{res}	Reverse transfer capacitance	—	40	—		$f = 1\text{MHz}$
t_{sc}	Short circuit withstand time	10	—	—	μs	$V_{CC} = 360V, V_{GE} = \pm 15V$ Min. $R_G = 15\Omega, V_{CEP} = 500V$

(1) Includes tail losses

Thermal and Mechanical Characteristics

Parameter	Description	Typ	Max	Units
R_{thJC} (IGBT)	Thermal resistance, junction to case, each IGBT	—	0.52	$^\circ\text{C/W}$
R_{thJC} (Diode)	Thermal resistance, junction to case, each diode	—	0.90	
R_{thCS} (Module)	Thermal resistance, case to sink	0.041	0.100	
Wt	Weight of module	150	—	g

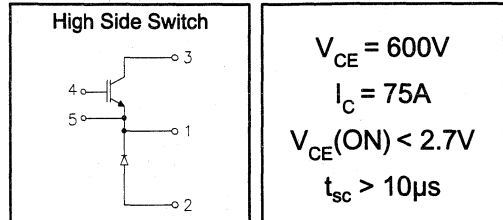
Refer to Section D - page D-16 for Package Outline 9 -INT-A-PAK, New - High Side Switch

IRGNIN075K06

"CHOPPER" IGBT INT-A-PAK

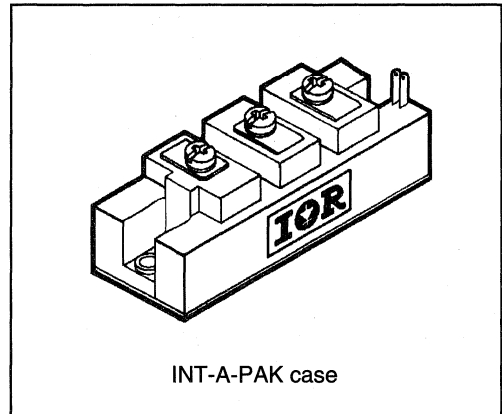
Low conduction loss IGBT

- Rugged Design
- Simple gate-drive
- Switching-Loss Rating includes all "tail" losses
- Short circuit rated



Description

IR's advanced IGBT technology is the key to this line of INT-A-PAK Power Modules. The efficient geometry and unique processing of the IGBT allow higher current densities than comparable bipolar power module transistors, while at the same time requiring the simpler gate-drive of the familiar power MOSFET. These modules are short circuit rated for applications such as motor control requiring this important feature.



Absolute Maximum Ratings

Parameter	Description	Value	Units
V_{CES}	Continuous collector to emitter voltage	600	V
$I_C @ T_C = 25^\circ C$	Continuous collector current	95	A
$I_C @ T_C = 85^\circ C$	Continuous collector current	55	
$I_C @ T_C = 100^\circ C$	Continuous collector current	40	
I_{LM}	Peak switching current	150	
I_{FM}	Peak diode forward current (1)	150	V
V_{GE}	Gate to emitter voltage	± 20	
V_{ISOL}	RMS isolation voltage, any terminal to case, $t = 1$ min	2500	
$P_D @ T_C = 25^\circ C$	Power dissipation	391	W
T_J	Operating junction temperature range	-40 to 150	$^\circ C$
T_{STG}	Storage temperature range	-40 to 125	

(1) Duration limited by max junction temperature.

Target Data

Electrical Characteristics - $T_J = 25^\circ\text{C}$, unless otherwise stated

Parameter	Description	Min	Typ	Max	Units	Test Conditions
BV_{CES}	Collector-to-emitter breakdown voltage	600	—	—	V	$V_{GE} = 0V, I_C = 1mA$
$V_{CE(ON)}$	Collector-to-emitter voltage	—	—	2.7		$V_{GE} = 15V, I_C = 75A$
V_{FM}	Diode forward voltage - maximum	—	1.8	2.0		$V_{GE} = 15V, I_C = 75A, T_J = 125^\circ\text{C}$
		—	1.75	—		$I_F = 75A, V_{GE} = 0V$
V_{Geth}	Gate threshold voltage	3.0	—	5.5		$I_C = 500\mu A$
DV_{Geth}	Threshold voltage temperature coefficient	—	-11	—	mV/ $^\circ\text{C}$	$V_{CE} = V_{GE}, I_C = 500\mu A$
g_{fe}	Forward transconductance	34	—	58	S(\bar{r})	$V_{CE} = 25V, I_C = 75A$
I_{CES}	Collector-to-emitter leakage current	—	—	1	mA	$V_{GE} = 0V, V_{CE} = 600V$
		—	—	10		$V_{GE} = 0V, V_{CE} = 600V, T_J = 125^\circ\text{C}$
I_{GES}	Gate-to-emitter leakage current	—	—	± 1	μA	$V_{GE} = \pm 20V$

Dynamic Characteristics - $T_J = 125^\circ\text{C}$, unless otherwise stated

Parameter	Description	Min	Typ	Max	Units	Test Conditions
E_{on}	Turn-on switching energy	—	0.04	—	mJ/A	$R_G = 15\Omega, V_{CC} = 300V$
E_{off} (1)	Turn-off switching energy	—	0.06	—		$I_C = 75A, L_S = 100nH$
E_{ts} (1)	Total switching energy	—	—	0.12		$V_{GE} = \pm 15V$
$t_{d(on)}$	Turn-on delay time	—	200	—	ns	$R_G = 15\Omega, V_{CC} = 300V$
t_r	Rise time	—	500	—		$I_C = 75A$
$t_{d(off)}$	Turn-off delay time	—	250	—		$V_{GE} = \pm 15V$
t_f	Fall time	—	120	—		Resistive load, $T_J = 25^\circ\text{C}$
I_{rr}	Diode peak recovery current	—	27	—	A	$R_G = 15\Omega, V_{CC} = 300V$
t_{rr}	Diode recovery time	—	110	—	ns	$I_C = 75A$
Q_{rr}	Diode recovery charge	—	1.7	—	μC	$V_{GE} = \pm 15V$
Q_{ge}	Gate-to-emitter charge (turn-on)	26	—	42	nC	$V_{CC} = 480V$
Q_{gc}	Gate-to-collector charge (turn-on)	70	—	140		$I_C = 54A$
Q_g	Total gate charge (turn-on)	150	—	280		$V_{GE} = 15V$
C_{ies}	Input capacitance	—	5800	—	pF	$V_{GE} = 0V$
C_{oes}	Output capacitance	—	660	—		$V_{CC} = 30V$
C_{res}	Reverse transfer capacitance	—	80	—		$f = 1MHz$
t_{sc}	Short circuit withstand time	10	—	—	μs	$V_{CC} = 360V, V_{GE} = \pm 15V$ Min. $R_G = 15\Omega, V_{CEP} = 500V$

(1) Includes tail losses

Thermal and Mechanical Characteristics

Parameter	Description	Typ	Max	Units
R_{thJC} (IGBT)	Thermal resistance, junction to case, each IGBT	—	0.32	$^\circ\text{C/W}$
R_{thJC} (Diode)	Thermal resistance, junction to case, each diode	—	0.48	
R_{thCS} (Module)	Thermal resistance, case to sink	0.041	0.100	
Wt	Weight of module	150	—	g

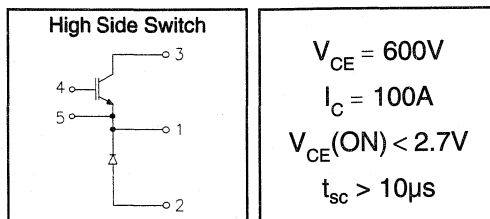
Refer to Section D -page D-16 for Package Outline 9 -INT-A-PAK, New - High Side Switch

IRGNIN100K06

"CHOPPER" IGBT INT-A-PAK

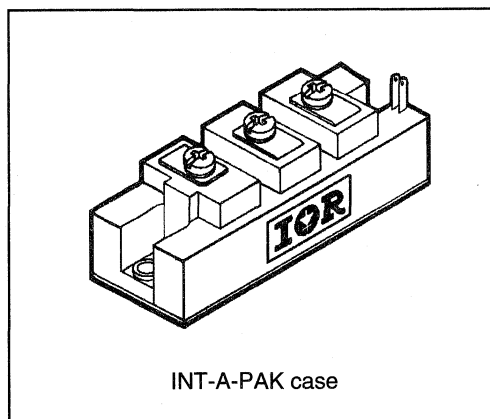
Low conduction loss IGBT

- Rugged Design
- Simple gate-drive
- Switching-Loss Rating includes all "tail" losses
- Short circuit rated



Description

IR's advanced IGBT technology is the key to this line of INT-A-PAK Power Modules. The efficient geometry and unique processing of the IGBT allow higher current densities than comparable bipolar power module transistors, while at the same time requiring the simpler gate-drive of the familiar power MOSFET. These modules are short circuit rated for applications such as motor control requiring this important feature.



Absolute Maximum Ratings

Parameter	Description	Value	Units
V_{CES}	Continuous collector to emitter voltage	600	V
$I_C @ T_C = 25^\circ C$	Continuous collector current	130	A
$I_C @ T_C = 85^\circ C$	Continuous collector current	70	
$I_C @ T_C = 100^\circ C$	Continuous collector current	50	
I_{LM}	Peak switching current	200	
I_{FM}	Peak diode forward current (1)	200	V
V_{GE}	Gate to emitter voltage	± 20	
V_{ISOL}	RMS isolation voltage, any terminal to case, $t = 1$ min	2500	W
$P_D @ T_C = 25^\circ C$	Power dissipation	500	
T_J	Operating junction temperature range	-40 to 150	
T_{STG}	Storage temperature range	-40 to 125	

(1) Duration limited by max junction temperature.

Target Data

Electrical Characteristics - $T_J = 25^\circ\text{C}$, unless otherwise stated

Parameter	Description	Min	Typ	Max	Units	Test Conditions
BV_{CES}	Collector-to-emitter breakdown voltage	600	—	—	V	$V_{GE} = 0V, I_C = 1.5mA$
$V_{CE(ON)}$	Collector-to-emitter voltage	—	—	2.7		$V_{GE} = 15V, I_C = 100A$
		—	2.7	—		$V_{GE} = 15V, I_C = 100A, T_J = 125^\circ\text{C}$
V_{FM}	Diode forward voltage - maximum	—	1.8	2.0		$I_F = 100A, V_{GE} = 0V$
		—	1.75	—		$I_F = 100A, V_{GE} = 0V, T_J = 125^\circ\text{C}$
V_{GEth}	Gate threshold voltage	3.0	—	5.5	$I_C = 750\mu A$	
ΔV_{GEth}	Threshold voltage temperature coefficient	—	-11	—	mV/ $^\circ\text{C}$	$V_{CE} = V_{GE}, I_C = 750\mu A$
g_{fe}	Forward transconductance	51	—	87	S(τ)	$V_{CE} = 25V, I_C = 100A$
I_{CES}	Collector-to-emitter leakage current	—	—	1.5	mA	$V_{GE} = 0V, V_{CE} = 600V$
		—	—	15		$V_{GE} = 0V, V_{CE} = 600V, T_J = 125^\circ\text{C}$
I_{GES}	Gate-to-emitter leakage current	—	—	± 1.5	μA	$V_{GE} = \pm 20V$

Dynamic Characteristics - $T_J = 125^\circ\text{C}$, unless otherwise stated

Parameter	Description	Min	Typ	Max	Units	Test Conditions
E_{on}	Turn-on switching energy	—	0.04	—	mJ/A	$R_G = 15\Omega, V_{CC} = 300V$
$E_{off} (1)$	Turn-off switching energy	—	0.06	—		$I_C = 100A, L_S = 100nH$
$E_{ts} (1)$	Total switching energy	—	—	0.12		$V_{GE} = \pm 15V$
$t_{d(on)}$	Turn-on delay time	—	200	—	ns	$R_G = 15\Omega, V_{CC} = 300V$
t_r	Rise time	—	500	—		$I_C = 100A$
$t_{d(off)}$	Turn-off delay time	—	250	—		$V_{GE} = \pm 15V$
t_f	Fall time	—	120	—		Resistive load, $T_J = 25^\circ\text{C}$
I_{rr}	Diode peak recovery current	—	40	—		$R_G = 15\Omega, V_{CC} = 300V$
t_{rr}	Diode recovery time	—	110	—	ns	$I_C = 100A$
Q_{rr}	Diode recovery charge	—	2.2	—	μC	$V_{GE} = \pm 15V$
Q_{ge}	Gate-to-emitter charge (turn-on)	39	—	63	nC	$V_{CC} = 480V$
Q_{gc}	Gate-to-collector charge (turn-on)	105	—	210		$I_C = 81A$
Q_g	Total gate charge (turn-on)	225	—	420		$V_{GE} = 15V$
C_{ies}	Input capacitance	—	8700	—	pF	$V_{GE} = 0V$
C_{oes}	Output capacitance	—	990	—		$V_{CC} = 30V$
C_{res}	Reverse transfer capacitance	—	120	—		$f = 1MHz$
t_{sc}	Short circuit withstand time	10	—	—	μs	$V_{CC} = 360V, V_{GE} = \pm 15V$ Min. $R_G = 15\Omega, V_{CEP} = 500V$

(1) Includes tail losses

Thermal and Mechanical Characteristics

Parameter	Description	Typ	Max	Units
R_{thJC} (IGBT)	Thermal resistance, junction to case, each IGBT	—	0.25	$^\circ\text{C/W}$
R_{thJC} (Diode)	Thermal resistance, junction to case, each diode	—	0.38	
R_{thCS} (Module)	Thermal resistance, case to sink	0.041	0.100	
Wt	Weight of module	150	—	g

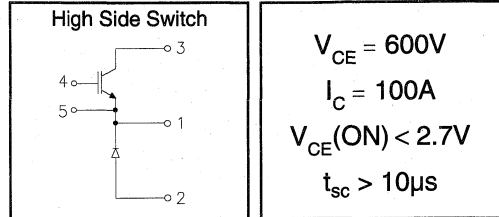
Refer to Section D - page D-16 for Package Outline 9 -INT-A-PAK, New - High Side Switch

IRGNIN150K06

"CHOPPER" IGBT INT-A-PAK

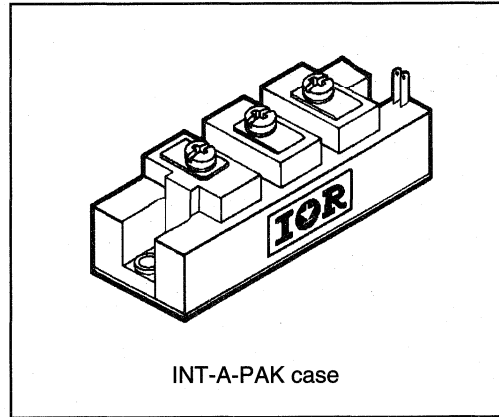
Low conduction loss IGBT

- Rugged Design
- Simple gate-drive
- Switching-Loss Rating includes all "tail" losses
- Short circuit rated



Description

IR's advanced IGBT technology is the key to this line of INT-A-PAK Power Modules. The efficient geometry and unique processing of the IGBT allow higher current densities than comparable bipolar power module transistors, while at the same time requiring the simpler gate-drive of the familiar power MOSFET. These modules are short circuit rated for applications such as motor control requiring this important feature.



Absolute Maximum Ratings

Parameter	Description	Value	Units
V_{CES}	Continuous collector to emitter voltage	600	V
$I_C @ T_C = 25^\circ C$	Continuous collector current	170	A
$I_C @ T_C = 85^\circ C$	Continuous collector current	95	
$I_C @ T_C = 100^\circ C$	Continuous collector current	70	
I_{LM}	Peak switching current	300	
I_{FM}	Peak diode forward current (1)	300	V
V_{GE}	Gate to emitter voltage	± 20	
V_{ISOL}	RMS isolation voltage, any terminal to case, $t = 1 \text{ min}$	2500	W
$P_D @ T_C = 25^\circ C$	Power dissipation	658	
T_J	Operating junction temperature range	-40 to 150	
T_{STG}	Storage temperature range	-40 to 125	

(1) Duration limited by max junction temperature.

Target Data

Electrical Characteristics - $T_J = 25^\circ\text{C}$, unless otherwise stated

Parameter	Description	Min	Typ	Max	Units	Test Conditions
BV_{CES}	Collector-to-emitter breakdown voltage	600	—	—	V	$V_{GE} = 0V, I_C = 1.5mA$
$V_{CE(ON)}$	Collector-to-emitter voltage	—	—	2.7		$V_{GE} = 15V, I_C = 100A$
		—	2.7	—		$V_{GE} = 15V, I_C = 100A, T_J = 125^\circ\text{C}$
V_{FM}	Diode forward voltage - maximum	—	1.8	2.0		$I_F = 100A, V_{GE} = 0V$
		—	1.75	—		$I_F = 100A, V_{GE} = 0V, T_J = 125^\circ\text{C}$
V_{GEth}	Gate threshold voltage	3.0	—	5.5		$I_C = 750\mu A$
ΔV_{GEth}	Threshold voltage temperature coefficient	—	-11	—	$mV/^\circ\text{C}$	$V_{CE} = V_{GE}, I_C = 750\mu A$
g_{fe}	Forward transconductance	68	—	120	$S(\Omega)$	$V_{CE} = 25V, I_C = 100A$
I_{CES}	Collector-to-emitter leakage current	—	—	2	mA	$V_{GE} = 0V, V_{CE} = 600V$
		—	—	20		$V_{GE} = 0V, V_{CE} = 600V, T_J = 125^\circ\text{C}$
I_{GES}	Gate-to-emitter leakage current	—	—	± 2	μA	$V_{GE} = \pm 20V$

Dynamic Characteristics - $T_J = 125^\circ\text{C}$, unless otherwise stated

Parameter	Description	Min	Typ	Max	Units	Test Conditions
E_{on}	Turn-on switching energy	—	0.04	—	mJ/A	$R_G = 15\Omega, V_{CC} = 300V$
E_{off} (1)	Turn-off switching energy	—	0.06	—		$I_C = 100A, L_S = 100nH$
E_{ts} (1)	Total switching energy	—	—	0.12		$V_{GE} = \pm 15V$
$t_{d(on)}$	Turn-on delay time	—	200	—	ns	$R_G = 15\Omega, V_{CC} = 300V$
t_r	Rise time	—	500	—		$I_C = 100A$
$t_{d(off)}$	Turn-off delay time	—	250	—		$V_{GE} = \pm 15V$
t_f	Fall time	—	120	—		Resistive load, $T_J = 25^\circ\text{C}$
I_{rr}	Diode peak recovery current	—	50	—		$R_G = 15\Omega, V_{CC} = 300V$
t_{rr}	Diode recovery time	—	110	—	ns	$I_C = 100A$
Q_{rr}	Diode recovery charge	—	3	—	μC	$V_{GE} = \pm 15V$
Q_{ge}	Gate-to-emitter charge (turn-on)	52	—	84	nC	$V_{CC} = 480V$
Q_{gc}	Gate-to-collector charge (turn-on)	140	—	280		$I_C = 81A$
Q_g	Total gate charge (turn-on)	300	—	560		$V_{GE} = 15V$
C_{ies}	Input capacitance	—	11600	—	pF	$V_{GE} = 0V$
C_{oes}	Output capacitance	—	1320	—		$V_{CC} = 30V$
C_{res}	Reverse transfer capacitance	—	160	—		$f = 1MHz$
t_{sc}	Short circuit withstand time	10	—	—	μs	$V_{CC} = 360V, V_{GE} = \pm 15V$ Min. $R_G = 15\Omega, V_{CEP} = 500V$

(1) Includes tail losses

Thermal and Mechanical Characteristics

Parameter	Description	Typ	Max	Units
R_{thJC} (IGBT)	Thermal resistance, junction to case, each IGBT	—	0.19	$^\circ\text{C/W}$
R_{thJC} (Diode)	Thermal resistance, junction to case, each diode	—	0.28	
R_{thCS} (Module)	Thermal resistance, case to sink	0.041	0.100	
Wt	Weight of module	150	—	g

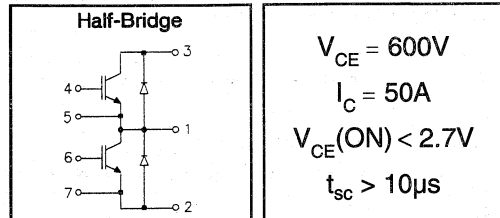
See Section D Package Outline 9 -INT-A-PAK, New - High Side Switch

IRGTIN050K06

"HALF-BRIDGE" IGBT INT-A-PAK

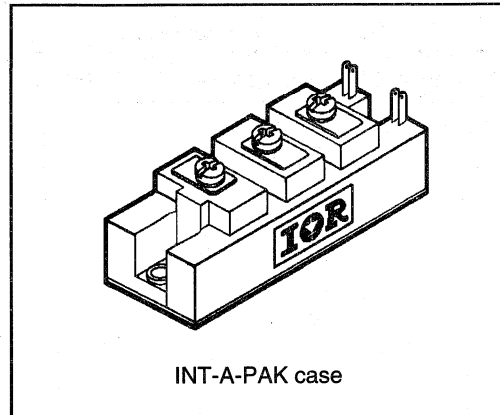
Low conduction loss IGBT

- Rugged Design
- Simple gate-drive
- Switching-Loss Rating includes all "tail" losses
- Short circuit rated



Description

IR's advanced IGBT technology is the key to this line of INT-A-PAK Power Modules. The efficient geometry and unique processing of the IGBT allow higher current densities than comparable bipolar power module transistors, while at the same time requiring the simpler gate-drive of the familiar power MOSFET. These modules are short circuit rated for applications such as motor control requiring this important feature.



Absolute Maximum Ratings

Parameter	Description	Value	Units
V_{CES}	Continuous collector to emitter voltage	600	V
$I_C @ T_C = 25^\circ C$	Continuous collector current	55	A
$I_C @ T_C = 85^\circ C$	Continuous collector current	30	
$I_C @ T_C = 100^\circ C$	Continuous collector current	20	
I_{LM}	Peak switching current	100	
I_{FM}	Peak diode forward current (1)	100	V
V_{GE}	Gate to emitter voltage	± 20	
V_{ISOL}	RMS isolation voltage, any terminal to case, $t = 1 \text{ min}$	2500	W
$P_D @ T_C = 25^\circ C$	Power dissipation	240	
T_J	Operating junction temperature range	-40 to 150	$^\circ C$
T_{STG}	Storage temperature range	-40 to 125	

(1) Duration limited by max junction temperature.

Target Data

Electrical Characteristics - $T_J = 25^\circ\text{C}$, unless otherwise stated

Parameter	Description	Min	Typ	Max	Units	Test Conditions
BV_{CES}	Collector-to-emitter breakdown voltage	600	—	—		$V_{GE} = 0V, I_C = 500\mu A$
$V_{CE(ON)}$	Collector-to-emitter voltage	—	—	2.7	V	$V_{GE} = 15V, I_C = 50A$
		—	2.7	—		$V_{GE} = 15V, I_C = 50A, T_J = 125^\circ\text{C}$
V_{FM}	Diode forward voltage - maximum	—	1.8	2.0		$I_F = 50A, V_{GE} = 0V$
		—	1.75	—		$I_F = 50A, V_{GE} = 0V, T_J = 125^\circ\text{C}$
V_{GEth}	Gate threshold voltage	3.0	—	5.5		$I_C = 250\mu A$
ΔV_{GEth}	Threshold voltage temp. coefficient	—	-11	—	mV/°C	$V_{CE} = V_{GE}, I_C = 250\mu A$
g_{fe}	Forward transconductance	17	—	30	S(τ)	$V_{CE} = 25V, I_C = 50A$
I_{CES}	Collector-to-emitter leakage current	—	—	500	μA	$V_{GE} = 0V, V_{CE} = 600V$
		—	—	5	mA	$V_{GE} = 0V, V_{CE} = 600V, T_J = 125^\circ\text{C}$
I_{GES}	Gate-to-emitter leakage current	—	—	± 500	nA	$V_{GE} = \pm 20V$

Dynamic Characteristics - $T_J = 125^\circ\text{C}$, unless otherwise stated

Parameter	Description	Min	Typ	Max	Units	Test Conditions
E_{on}	Turn-on switching energy	—	0.04	—	mJ/A	$R_G = 15\Omega, V_{CC} = 300V$
E_{off} (1)	Turn-off switching energy	—	0.06	—		$I_C = 50A, L_S = 100nH$
E_{ts} (1)	Total switching energy	—	—	0.12		$V_{GE} = \pm 15V$
$t_{d(on)}$	Turn-on delay time	—	200	—	ns	$R_G = 15\Omega, V_{CC} = 300V$
t_r	Rise time	—	500	—		$I_C = 50A$
$t_{d(off)}$	Turn-off delay time	—	250	—		$V_{GE} = \pm 15V$
t_f	Fall time	—	120	—		Resistive load, $T_J = 25^\circ\text{C}$
I_{rr}	Diode peak recovery current	—	20	—		$R_G = 15\Omega, V_{CC} = 300V$
t_{rr}	Diode recovery time	—	110	—	ns	$I_C = 50A$
Q_{rr}	Diode recovery charge	—	1.2	—	μC	$V_{GE} = \pm 15V$
Q_{ge}	Gate-to-emitter charge (turn-on)	13	—	21	nC	$V_{CC} = 480V$
Q_{gc}	Gate-to-collector charge (turn-on)	35	—	70		$I_C = 27A$
Q_g	Total gate charge (turn-on)	77	—	140		$V_{GE} = 15V$
C_{ies}	Input capacitance	—	2900	—	pF	$V_{GE} = 0V$
C_{oes}	Output capacitance	—	330	—		$V_{CC} = 30V$
C_{res}	Reverse transfer capacitance	—	40	—		$f = 1MHz$
t_{sc}	Short circuit withstand time	10	—	—	μs	$V_{CC} = 360V, V_{GE} = \pm 15V$ Min. $R_G = 15\Omega, V_{CEP} = 500V$

(1) Includes tail losses

Thermal and Mechanical Characteristics

Parameter	Description	Typ	Max	Units
R_{thJC} (IGBT)	Thermal resistance, junction to case, each IGBT	—	0.52	°C/W
R_{thJC} (Diode)	Thermal resistance, junction to case, each diode	—	0.90	
R_{thCS} (Module)	Thermal resistance, case to sink	0.041	0.100	
Wt	Weight of module	150	—	g

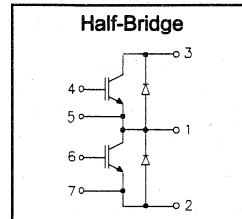
Refer to Section D - page D-17 for Package Outline11 -INT-A-PAK, New -Half Bridge

IRGTIN075K06

"HALF-BRIDGE" IGBT INT-A-PAK

Low conduction loss IGBT

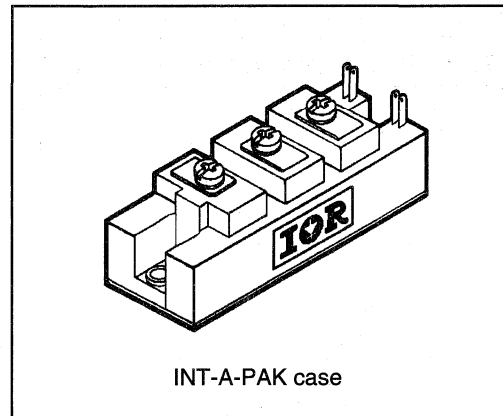
- Rugged Design
- Simple gate-drive
- Switching-Loss Rating includes all "tail" losses
- Short circuit rated



$V_{CE} = 600V$
$I_C = 75A$
$V_{CE(ON)} < 2.7V$
$t_{sc} > 10\mu s$

Description

IR's advanced IGBT technology is the key to this line of INT-A-PAK Power Modules. The efficient geometry and unique processing of the IGBT allow higher current densities than comparable bipolar power module transistors, while at the same time requiring the simpler gate-drive of the familiar power MOSFET. These modules are short circuit rated for applications such as motor control requiring this important feature.



Absolute Maximum Ratings

Parameter	Description	Value	Units
V_{CES}	Continuous collector to emitter voltage	600	V
$I_C @ T_C = 25^\circ C$	Continuous collector current	95	A
$I_C @ T_C = 85^\circ C$	Continuous collector current	55	
$I_C @ T_C = 100^\circ C$	Continuous collector current	40	
I_{LM}	Peak switching current	150	
I_{FM}	Peak diode forward current (1)	150	V
V_{GE}	Gate to emitter voltage	± 20	
V_{ISOL}	RMS isolation voltage, any terminal to case, $t = 1 \text{ min}$	2500	W
$P_D @ T_C = 25^\circ C$	Power dissipation	391	
T_J	Operating junction temperature range	-40 to 150	
T_{STG}	Storage temperature range	-40 to 125	

(1) Duration limited by max junction temperature.

Target Data

Electrical Characteristics - $T_J = 25^\circ\text{C}$, unless otherwise stated

Parameter	Description	Min	Typ	Max	Units	Test Conditions
BV_{CES}	Collector-to-emitter breakdown voltage	600	—	—	V	$V_{GE} = 0V, I_C = 1mA$
$V_{CE(ON)}$	Collector-to-emitter voltage	—	—	2.7		$V_{GE} = 15V, I_C = 75A$
		—	2.7	—		$V_{GE} = 15V, I_C = 75A, T_J = 125^\circ\text{C}$
V_{FM}	Diode forward voltage - maximum	—	1.8	2.0		$I_F = 75A, V_{GE} = 0V$
		—	1.75	—		$I_F = 75A, V_{GE} = 0V, T_J = 125^\circ\text{C}$
V_{GETh}	Gate threshold voltage	3.0	—	5.5	$I_C = 500\mu A$	
DV_{GETh}	Threshold voltage temperature coefficient	—	-11	—	mV/ $^\circ\text{C}$	$V_{CE} = V_{GE}, I_C = 500\mu A$
g_{fe}	Forward transconductance	34	—	58	S(Ω)	$V_{CE} = 25V, I_C = 75A$
I_{CES}	Collector-to-emitter leakage current	—	—	1	mA	$V_{GE} = 0V, V_{CE} = 600V$
		—	—	10		$V_{GE} = 0V, V_{CE} = 600V, T_J = 125^\circ\text{C}$
I_{GES}	Gate-to-emitter leakage current	—	—	± 1	μA	$V_{GE} = \pm 20V$

Dynamic Characteristics - $T_J = 125^\circ\text{C}$, unless otherwise stated

Parameter	Description	Min	Typ	Max	Units	Test Conditions
E_{on}	Turn-on switching energy	—	0.04	—	mJ/A	$R_G = 15\Omega, V_{CC} = 300V$
E_{off} (1)	Turn-off switching energy	—	0.06	—		$I_C = 75A, L_S = 100nH$
E_{ts} (1)	Total switching energy	—	—	0.12		$V_{GE} = \pm 15V$
$t_{d(on)}$	Turn-on delay time	—	200	—	ns	$R_G = 15\Omega, V_{CC} = 300V$
t_r	Rise time	—	500	—		$I_C = 75A$
$t_{d(off)}$	Turn-off delay time	—	250	—		$V_{GE} = \pm 15V$
t_f	Fall time	—	120	—		Resistive load, $T_J = 25^\circ\text{C}$
I_{rr}	Diode peak recovery current	—	27	—	A	$R_G = 15\Omega, V_{CC} = 300V$
t_{rr}	Diode recovery time	—	110	—	ns	$I_C = 75A$
Q_{rr}	Diode recovery charge	—	1.7	—	μC	$V_{GE} = \pm 15V$
Q_{ge}	Gate-to-emitter charge (turn-on)	26	—	42	nC	$V_{CC} = 480V$
Q_{gc}	Gate-to-collector charge (turn-on)	70	—	140	nC	$I_C = 54A$
Q_g	Total gate charge (turn-on)	150	—	280		$V_{GE} = \pm 15V$
C_{ies}	Input capacitance	—	5800	—	pF	$V_{GE} = 0V$
C_{oes}	Output capacitance	—	660	—		$V_{CC} = 30V$
C_{res}	Reverse transfer capacitance	—	80	—		$f = 1MHz$
t_{sc}	Short circuit withstand time	10	—	—	μs	$V_{CC} = 360V, V_{GE} = \pm 15V$ Min. $R_G = 15\Omega, V_{CEP} = 500V$

(1) Includes tail losses

Thermal and Mechanical Characteristics

Parameter	Description	Typ	Max	Units
R_{thJC} (IGBT)	Thermal resistance, junction to case, each IGBT	—	0.32	$^\circ\text{C/W}$
R_{thJC} (Diode)	Thermal resistance, junction to case, each diode	—	0.48	
R_{thCS} (Module)	Thermal resistance, case to sink	0.041	0.100	
Wt	Weight of module	150	—	g

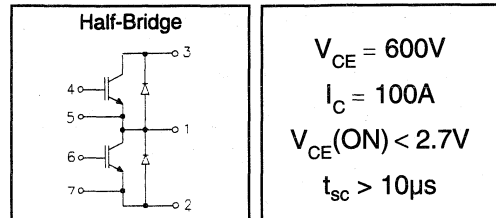
Refer to Section D - page D-17 for Package Outline11 -INT-A-PAK, New -Half Bridge

IRGTIN100K06

"HALF-BRIDGE" IGBT INT-A-PAK

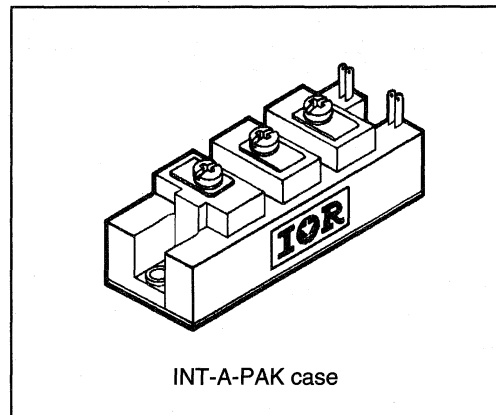
Low conduction loss IGBT

- Rugged Design
- Simple gate-drive
- Switching-Loss Rating includes all "tail" losses
- Short circuit rated



Description

IR's advanced IGBT technology is the key to this line of INT-A-PAK Power Modules. The efficient geometry and unique processing of the IGBT allow higher current densities than comparable bipolar power module transistors, while at the same time requiring the simpler gate-drive of the familiar power MOSFET. These modules are short circuit rated for applications such as motor control requiring this important feature.



Absolute Maximum Ratings

Parameter	Description	Value	Units
V_{CES}	Continuous collector to emitter voltage	600	V
$I_C @ T_C = 25^\circ C$	Continuous collector current	130	A
$I_C @ T_C = 85^\circ C$	Continuous collector current	70	
$I_C @ T_C = 100^\circ C$	Continuous collector current	50	
I_{LM}	Peak switching current	200	
I_{FM}	Peak diode forward current (1)	200	V
V_{GE}	Gate to emitter voltage	± 20	
V_{ISOL}	RMS isolation voltage, any terminal to case, $t = 1 \text{ min}$	2500	W
$P_D @ T_C = 25^\circ C$	Power dissipation	500	
T_J	Operating junction temperature range	-40 to 150	$^\circ C$
T_{STG}	Storage temperature range	-40 to 125	

(1) Duration limited by max junction temperature.

Target Data

Electrical Characteristics - $T_J = 25^\circ\text{C}$, unless otherwise stated

Parameter	Description	Min	Typ	Max	Units	Test Conditions
BV_{CES}	Collector-to-emitter breakdown voltage	600	—	—	V	$V_{GE} = 0V, I_C = 1.5mA$
$V_{CE(ON)}$	Collector-to-emitter voltage	—	—	2.7		$V_{GE} = 15V, I_C = 100A$
		—	2.7	—		$V_{GE} = 15V, I_C = 100A, T_J = 125^\circ\text{C}$
V_{FM}	Diode forward voltage - maximum	—	1.8	2.0		$I_F = 100A, V_{GE} = 0V$
		—	1.75	—		$I_F = 100A, V_{GE} = 0V, T_J = 125^\circ\text{C}$
V_{GETh}	Gate threshold voltage	3.0	—	5.5	$I_C = 750\mu A$	
ΔV_{GETh}	Threshold voltage temp. coefficient	—	-11	—	mV/ $^\circ\text{C}$	$V_{CE} = V_{GE}, I_C = 750\mu A$
g_{fe}	Forward transconductance	51	—	87	S(σ)	$V_{CE} = 25V, I_C = 100A$
I_{CES}	Collector-to-emitter leakage current	—	—	1.5	mA	$V_{GE} = 0V, V_{CE} = 600V$
		—	—	15		$V_{GE} = 0V, V_{CE} = 600V, T_J = 125^\circ\text{C}$
I_{GES}	Gate-to-emitter leakage current	—	—	± 1.5	μA	$V_{GE} = \pm 20V$

Dynamic Characteristics - $T_J = 125^\circ\text{C}$, unless otherwise stated

Parameter	Description	Min	Typ	Max	Units	Test Conditions
E_{on}	Turn-on switching energy	—	0.04	—	mJ/A	$R_G = 15\Omega, V_{CC} = 300V$
$E_{off(1)}$	Turn-off switching energy	—	0.06	—		$I_C = 100A, L_S = 100nH$
$E_{ts(1)}$	Total switching energy	—	—	0.12		$V_{GE} = \pm 15V$
$t_{d(on)}$	Turn-on delay time	—	200	—	ns	$R_G = 15\Omega, V_{CC} = 300V$
t_r	Rise time	—	500	—		$I_C = 100A$
$t_{d(off)}$	Turn-off delay time	—	250	—		$V_{GE} = \pm 15V$
t_f	Fall time	—	120	—		Resistive load, $T_J = 25^\circ\text{C}$
I_{rr}	Diode peak recovery current	—	40	—	A	$R_G = 15\Omega, V_{CC} = 300V$
t_{rr}	Diode recovery time	—	110	—	ns	$I_C = 100A$
Q_{rr}	Diode recovery charge	—	2.2	—	μC	$V_{GE} = \pm 15V$
Q_{ge}	Gate-to-emitter charge (turn-on)	39	—	63	nC	$V_{CC} = 480V$
Q_{gc}	Gate-to-collector charge (turn-on)	105	—	210		$I_C = 81A$
Q_g	Total gate charge (turn-on)	2250	—	420		$V_{GE} = 15V$
C_{ies}	Input capacitance	—	8700	—	pF	$V_{GE} = 0V$
C_{oes}	Output capacitance	—	9960	—		$V_{CC} = 30V$
C_{res}	Reverse transfer capacitance	—	120	—		$f = 1MHz$
t_{sc}	Short circuit withstand time	10	—	—	μs	$V_{CC} = 360V, V_{GE} = \pm 15V$ Min. $R_G = 15\Omega, V_{CEP} = 500V$

(1) Includes tail losses

Thermal and Mechanical Characteristics

Parameter	Description	Typ	Max	Units
R_{thJC} (IGBT)	Thermal resistance, junction to case, each IGBT	—	0.25	$^\circ\text{C/W}$
R_{thJC} (Diode)	Thermal resistance, junction to case, each diode	—	0.38	
R_{thCS} (Module)	Thermal resistance, case to sink	0.041	0.100	
Wt	Weight of module	150	—	g

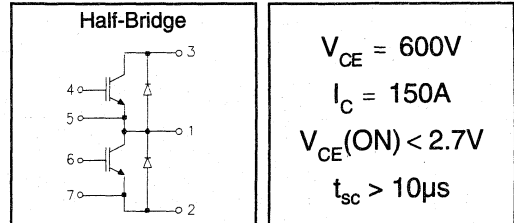
Refer to Section D -page D-17 for Package Outline11 -INT-A-PAK, New -Half Bridge

IRGTIN150K06

"HALF-BRIDGE" IGBT INT-A-PAK

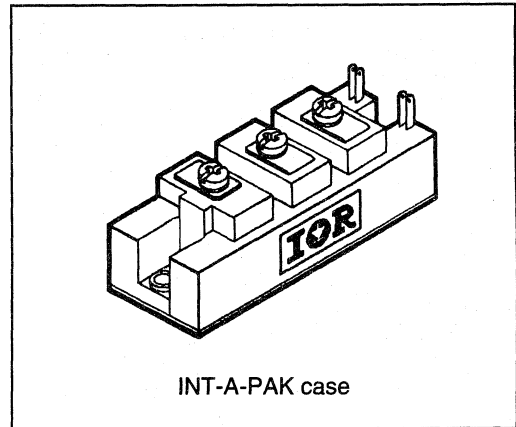
Low conduction loss IGBT

- Rugged Design
- Simple gate-drive
- Switching-Loss Rating includes all "tail" losses
- Short circuit rated



Description

IR's advanced IGBT technology is the key to this line of INT-A-PAK Power Modules. The efficient geometry and unique processing of the IGBT allow higher current densities than comparable bipolar power module transistors, while at the same time requiring the simpler gate-drive of the familiar power MOSFET. These modules are short circuit rated for applications such as motor control requiring this important feature.



Absolute Maximum Ratings

Parameter	Description	Value	Units
V_{CES}	Continuous collector to emitter voltage	600	V
$I_C @ T_C = 25^\circ C$	Continuous collector current	170	A
$I_C @ T_C = 85^\circ C$	Continuous collector current	95	
$I_C @ T_C = 100^\circ C$	Continuous collector current	70	
I_{LM}	Peak switching current	300	
I_{FM}	Peak diode forward current (1)	300	V
V_{GE}	Gate to emitter voltage	± 20	
V_{ISOL}	RMS isolation voltage, any terminal to case, $t = 1$ min	2500	
$P_D @ T_C = 25^\circ C$	Power dissipation	658	W
T_J	Operating junction temperature range	-40 to 150	$^\circ C$
T_{STG}	Storage temperature range	-40 to 125	

(1) Duration limited by max junction temperature.

Electrical Characteristics - $T_J = 25^\circ\text{C}$, unless otherwise stated

Parameter	Description	Min	Typ	Max	Units	Test Conditions
BV_{CES}	Collector-to-emitter breakdown voltage	600	—	—	V	$V_{GE} = 0V, I_C = 2mA$
$V_{CE(ON)}$	Collector-to-emitter voltage	—	—	2.7		$V_{GE} = 15V, I_C = 150A$
		—	2.7	—		$V_{GE} = 15V, I_C = 150A, T_J = 125^\circ\text{C}$
V_{FM}	Diode forward voltage - maximum	—	1.8	2.0		$I_F = 150A, V_{GE} = 0V$
		—	1.75	—		$I_F = 150A, V_{GE} = 0V, T_J = 125^\circ\text{C}$
V_{GEth}	Gate threshold voltage	3.0	—	5.5	$I_C = 1mA$	
DV_{GEth}	Threshold voltage temperature coefficient	—	- 11	—	$mV/^\circ\text{C}$	$V_{CE} = V_{GE}, I_C = 1mA$
g_{fe}	Forward transconductance	68	—	120	S(t)	$V_{CE} = 25V, I_C = 150A$
I_{CES}	Collector-to-emitter leakage current	—	—	2	mA	$V_{GE} = 0V, V_{CE} = 600V$
		—	—	20		$V_{GE} = 0V, V_{CE} = 600V, T_J = 125^\circ\text{C}$
I_{GES}	Gate-to-emitter leakage current	—	—	± 2	μA	$V_{GE} = \pm 20V$

Dynamic Characteristics - $T_J = 125^\circ\text{C}$, unless otherwise stated

Parameter	Description	Min	Typ	Max	Units	Test Conditions
E_{on}	Turn-on switching energy	—	0.04	—	mJ/A	$R_G = 15\Omega, V_{CC} = 300V$
E_{off} (1)	Turn-off switching energy	—	0.06	—		$I_C = 150A, L_S = 100nH$
E_{ts} (1)	Total switching energy	—	—	0.12		$V_{GE} = \pm 15V$
$t_{d(on)}$	Turn-on delay time	—	200	—	ns	$R_G = 15\Omega, V_{CC} = 300V$
t_r	Rise time	—	500	—		$I_C = 150A$
$t_{d(off)}$	Turn-off delay time	—	250	—		$V_{GE} = \pm 15V$
t_f	Fall time	—	120	—		Resistive load, $T_J = 25^\circ\text{C}$
I_{rr}	Diode peak recovery current	—	50	—	A	$R_G = 15\Omega, V_{CC} = 300V$
t_{rr}	Diode recovery time	—	110	—	ns	$I_C = 150A$
Q_{rr}	Diode recovery charge	—	3	—	μC	$V_{GE} = \pm 15V$
Q_{ge}	Gate-to-emitter charge (turn-on)	52	—	84	nC	$V_{CC} = 480V$
Q_{gc}	Gate-to-collector charge (turn-on)	140	—	280		$I_C = 108A$
Q_g	Total gate charge (turn-on)	300	—	560		$V_{GE} = 15V$
C_{ies}	Input capacitance	—	11600	—	pF	$V_{GE} = 0V$
C_{oes}	Output capacitance	—	1320	—		$V_{CC} = 30V$
C_{res}	Reverse transfer capacitance	—	160	—		$f = 1MHz$
t_{sc}	Short circuit withstand time	10	—	—	μs	$V_{CC} = 360V, V_{GE} = \pm 15V$ Min. $R_G = 15\Omega, V_{CEP} = 500V$

(1) Includes tail losses

Thermal and Mechanical Characteristics

Parameter	Description	Typ	Max	Units
R_{thJC} (IGBT)	Thermal resistance, junction to case, each IGBT	—	0.19	$^\circ\text{C/W}$
R_{thJC} (Diode)	Thermal resistance, junction to case, each diode	—	0.28	
R_{thCS} (Module)	Thermal resistance, case to sink	0.041	0.100	
Wt	Weight of module	150	—	g

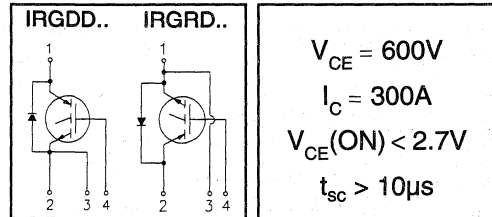
Refer to Section D - page D-17 for Package Outline11 -INT-A-PAK, New -Half Bridge

IRGDDN300K06 IRGRDN300K06

"SINGLE SWITCH" IGBT DOUBLE INT-A-PAK

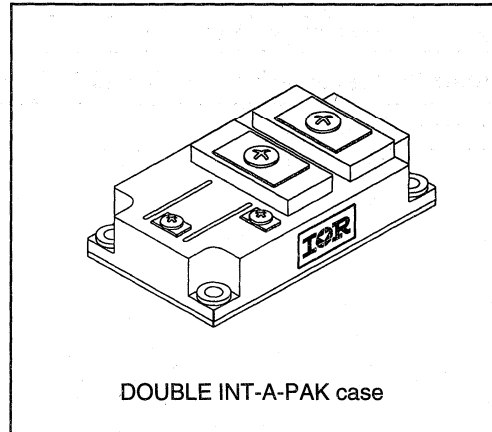
Low conduction loss IGBT

- Rugged Design
- Simple gate-drive
- Switching-Loss Rating includes all "tail" losses
- Short circuit rated



Description

IR's advanced IGBT technology is the key to this line of DOUBLE INT-A-PAK Power Modules. The efficient geometry and unique processing of the IGBT allow higher current densities than comparable bipolar power module transistors, while at the same time requiring the simpler gate-drive of the familiar power MOSFET. This superior technology has now been coupled to state of the art assembly techniques to produce a higher current module that is highly suited to power applications such as motor drives, uninterruptible power supplies, welding and power factor correction.



Absolute Maximum Ratings

Parameter	Description	Value	Units
V_{CES}	Continuous collector to emitter voltage	600	V
$I_C @ T_C = 25^\circ\text{C}$	Maximum Continuous collector current	340	A
$I_C @ T_C = 85^\circ\text{C}$	Maximum Continuous collector current	190	
$I_C @ T_C = 100^\circ\text{C}$	Maximum Continuous collector current	140	
I_{LM}	Peak switching current	600	
I_{FM}	Peak diode forward current (1)	600	V
V_{GE}	Gate to emitter voltage	± 20	
V_{ISOL}	RMS isolation voltage, any terminal to case, $t = 1 \text{ min}$	2500	
$P_D @ T_C = 25^\circ\text{C}$	Power dissipation	1563	$^\circ\text{C}$
T_J	Operating junction temperature range	-40 to 150	
T_{STG}	Storage temperature range	-40 to 125	

(1) Duration limited by max junction temperature.

Target Data

IRGDDN300K06

IRGRDN300K06

Target Data



Electrical Characteristics - $T_J = 25^\circ\text{C}$, unless otherwise stated

Parameter	Description	Min	Typ	Max	Units	Test Conditions
BV_{CES}	Collector-to-emitter breakdown voltage	600	—	—	V	$V_{GE} = 0V, I_C = 4mA$
$V_{CE(ON)}$	Collector-to-emitter voltage	—	—	2.7		$V_{GE} = 15V, I_C = 300A$
		—	2.7	—		$V_{GE} = 15V, I_C = 300A, T_J = 125^\circ\text{C}$
V_{FM}	Diode forward voltage - maximum	—	1.8	2.0		$I_F = 300A, V_{GE} = 0V$
		—	1.8	—		$I_F = 300A, V_{GE} = 0V, T_J = 125^\circ\text{C}$
V_{GEth}	Gate threshold voltage	3.0	—	5.5	$I_C = 2mA$	
ΔV_{GEth}	Threshold voltage temperature coefficient	—	-11	—	mV/°C	$V_{CE} = V_{GE}, I_C = 2mA$
g_{fe}	Forward transconductance	136	—	240	S(Ω)	$V_{CE} = 25V, I_C = 300A$
I_{CES}	Collector-to-emitter leakage current	—	—	4	mA	$V_{GE} = 0V, V_{CE} = 600V$
		—	—	40		$V_{GE} = 0V, V_{CE} = 600V, T_J = 125^\circ\text{C}$
I_{GES}	Gate-to-emitter leakage current	—	—	±4	μA	$V_{GE} = \pm 20V$

Dynamic Characteristics - $T_J = 125^\circ\text{C}$

Parameter	Description	Min	Typ	Max	Units	Test Conditions
E_{on}	Turn-on switching energy	—	0.04	—	mJ/A	$R_G = 15\Omega, V_{CC} = 300V$
E_{off} (1)	Turn-off switching energy	—	0.06	—		$I_C = 300A, L_S = 100nH$
E_{ts} (1)	Total switching energy	—	—	0.15		$V_{GE} = \pm 15V$
$t_{d(on)}$	Turn-on delay time	—	300	—	ns	$R_G = 15\Omega, V_{CC} = 300V$
t_r	Rise time	—	900	—		$I_C = 300A$
$t_{d(off)}$	Turn-off delay time	—	700	—		$V_{GE} = \pm 15V$
t_f	Fall time	—	120	—		Resistive Load, $T_J = 25^\circ\text{C}$
I_{rr}	Diode peak recovery current	—	110	—	A	$R_G = 15\Omega, V_{CC} = 300V$
t_{rr}	Diode recovery time	—	110	—		$I_C = 300A$
Q_{rr}	Diode recovery charge	—	6	—		$V_{GE} = \pm 15V$
Q_{ge}	Gate-to-emitter charge (turn-on)	104	—	168	nC	$V_{CC} = 480V$
Q_{gc}	Gate-to-collector charge (turn-on)	280	—	560		$I_C = 216A$
Q_g	Total gate charge (turn-on)	600	—	1120		$V_{GE} = 15V$
C_{ies}	Input capacitance	—	23200	—	pF	$V_{GE} = 0V$
C_{oes}	Output capacitance	—	2640	—		$V_{CC} = 30V$
C_{res}	Reverse transfer capacitance	—	320	—		$f = 1MHz$
t_{sc}	Short circuit withstand time	10	—	—	μs	$V_{CC} = 360V, V_{GE} = \pm 15V$ Min. $R_G = 15\Omega, V_{CEP} = 500V$

(1) Includes tail losses

Thermal and Mechanical Characteristics

Parameter	Description	Typ	Max	Units
R_{thJC} (IGBT)	Thermal resistance, junction to case, each IGBT	—	0.08	°C/W
R_{thJC} (Diode)	Thermal resistance, junction to case, each diode	—	0.12	
R_{thCS} (Module)	Thermal resistance, case to sink	0.023	0.050	
Wt	Weight of module	242	—	g

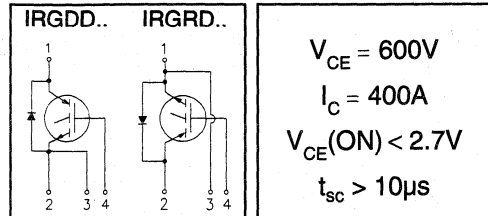
Refer to Section D - page D-18 for Package Outline 13 - Double INT-A-Pak Single Switch

IRGDDN400K06 IRGRDN400K06

"SINGLE SWITCH" IGBT DOUBLE INT-A-PAK

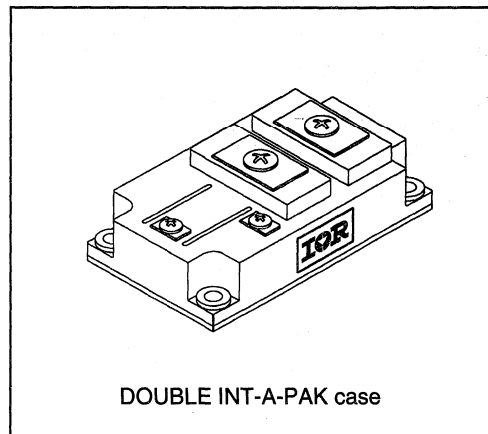
Low conduction loss IGBT

- Rugged Design
- Simple gate-drive
- Switching-Loss Rating includes all "tail" losses
- Short circuit rated



Description

IR's advanced IGBT technology is the key to this line of DOUBLE INT-A-PAK Power Modules. The efficient geometry and unique processing of the IGBT allow higher current densities than comparable bipolar power module transistors, while at the same time requiring the simpler gate-drive of the familiar power MOSFET. This superior technology has now been coupled to state of the art assembly techniques to produce a higher current module that is highly suited to power applications such as motor drives, uninterruptible power supplies, welding and power factor correction.



Absolute Maximum Ratings

Parameter	Description	Value	Units
V_{CES}	Continuous collector to emitter voltage	600	V
$I_C @ T_C = 25^\circ\text{C}$	Maximum Continuous collector current	520	A
$I_C @ T_C = 85^\circ\text{C}$	Maximum Continuous collector current	280	
$I_C @ T_C = 100^\circ\text{C}$	Maximum Continuous collector current	200	
I_{LM}	Peak switching current	800	
I_{FM}	Peak diode forward current (1)	800	V
V_{GE}	Gate to emitter voltage	± 20	
V_{ISOL}	RMS isolation voltage, any terminal to case, $t = 1 \text{ min}$	2500	
$P_D @ T_C = 25^\circ\text{C}$	Power dissipation	1984	$^\circ\text{C}$
T_J	Operating junction temperature range	-40 to 150	
T_{STG}	Storage temperature range	-40 to 125	

(1) Duration limited by max junction temperature.

Target Data

IRGDDN400K06 IRGRDN400K06

Target Data



Electrical Characteristics - $T_J = 25^\circ\text{C}$, unless otherwise stated

Parameter	Description	Min	Typ	Max	Units	Test Conditions
BV_{CES}	Collector-to-emitter breakdown voltage	600	—	—	V	$V_{GE} = 0V, I_C = 6mA$
$V_{CE(ON)}$	Collector-to-emitter voltage	—	—	2.7		$V_{GE} = 15V, I_C = 400A$
		—	2.7	—		$V_{GE} = 15V, I_C = 400A, T_J = 125^\circ\text{C}$
V_{FM}	Diode forward voltage - maximum	—	1.8	2.0		$I_F = 400A, V_{GE} = 0V$
		—	1.8	—		$I_F = 400A, V_{GE} = 0V, T_J = 125^\circ\text{C}$
V_{Geth}	Gate threshold voltage	3.0	—	5.5	$I_C = 3mA$	
DV_{Geth}	Threshold voltage temperature coefficient	—	-11	—	mV/°C	$V_{CE} = V_{GE}, I_C = 3mA$
g_{fe}	Forward transconductance	204	—	348	S(Ω)	$V_{CE} = 25V, I_C = 300A$
I_{CES}	Collector-to-emitter leakage current	—	—	6	mA	$V_{GE} = 0V, V_{CE} = 600V$
		—	—	60		$V_{GE} = 0V, V_{CE} = 600V, T_J = 125^\circ\text{C}$
I_{GES}	Gate-to-emitter leakage current	—	—	±6	μA	$V_{GE} = \pm 20V$

Dynamic Characteristics - $T_J = 125^\circ\text{C}$

Parameter	Description	Min	Typ	Max	Units	Test Conditions
E_{on}	Turn-on switching energy	—	0.04	—	mJ/A	$R_G = 15\Omega, V_{CC} = 300V$
E_{off} (1)	Turn-off switching energy	—	0.06	—		$I_C = 400A, L_S = 100nH$
E_{is} (1)	Total switching energy	—	—	0.15		$V_{GE} = \pm 15V$
$t_{d(on)}$	Turn-on delay time	—	300	—	ns	$R_G = 15\Omega, V_{CC} = 300V$
t_r	Rise time	—	900	—		$I_C = 400A$
$t_{d(off)}$	Turn-off delay time	—	700	—		$V_{GE} = \pm 15V$
t_f	Fall time	—	120	—		Resistive Load, $T_J = 25^\circ\text{C}$
I_{rr}	Diode peak recovery current	—	110	—		A
t_{rr}	Diode recovery time	—	110	—	ns	$I_C = 400A$
Q_{rr}	Diode recovery charge	—	6	—	μC	$V_{GE} = \pm 15V$
Q_{ge}	Gate-to-emitter charge (turn-on)	156	—	252	nC	$V_{CC} = 480V$
Q_{gc}	Gate-to-collector charge (turn-on)	420	—	840		$I_C = 324A$
Q_g	Total gate charge (turn-on)	900	—	1680		$V_{GE} = 15V$
C_{ies}	Input capacitance	—	34800	—	pF	$V_{GE} = 0V$
C_{oes}	Output capacitance	—	3960	—		$V_{CC} = 30V$
C_{res}	Reverse transfer capacitance	—	480	—		$f = 1MHz$
t_{sc}	Short circuit withstand time	10	—	—	μs	$V_{CC} = 360V, V_{GE} = \pm 15V$ Min. $R_G = 15\Omega, V_{CEP} = 500V$

(1) Includes tail losses

Thermal and Mechanical Characteristics

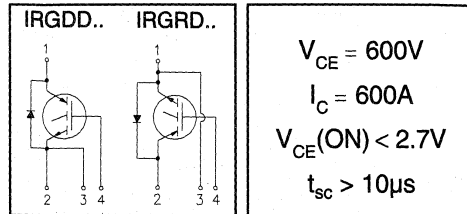
Parameter	Description	Typ	Max	Units
R_{thJC} (IGBT)	Thermal resistance, junction to case, each IGBT	—	0.063	°C/W
R_{thJC} (Diode)	Thermal resistance, junction to case, each diode	—	0.095	
R_{thCS} (Module)	Thermal resistance, case to sink	0.023	0.050	
Wt	Weight of module	242	—	g

Refer to Section D - page D-18 for Package Outline 13 - Double INT-A-Pak Single Switch

"SINGLE SWITCH" IGBT DOUBLE INT-A-PAK

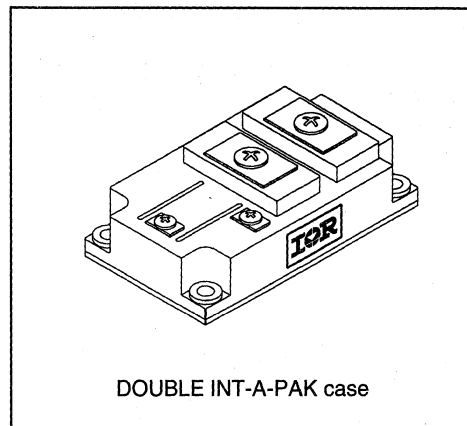
Low conduction loss IGBT

- Rugged Design
- Simple gate-drive
- Switching-Loss Rating includes all "tail" losses
- Short circuit rated



Description

IR's advanced IGBT technology is the key to this line of DOUBLE INT-A-PAK Power Modules. The efficient geometry and unique processing of the IGBT allow higher current densities than comparable bipolar power module transistors, while at the same time requiring the simpler gate-drive of the familiar power MOSFET. This superior technology has now been coupled to state of the art assembly techniques to produce a higher current module that is highly suited to power applications such as motor drives, uninterruptible power supplies, welding and power factor correction.



Absolute Maximum Ratings

Parameter	Description	Value	Units
V_{CES}	Continuous collector to emitter voltage	600	V
$I_C @ T_C = 25^\circ\text{C}$	Maximum Continuous collector current	680	A
$I_C @ T_C = 85^\circ\text{C}$	Maximum Continuous collector current	380	
$I_C @ T_C = 100^\circ\text{C}$	Maximum Continuous collector current	280	
I_{LM}	Peak switching current	1200	
I_{FM}	Peak diode forward current (1)	1200	
V_{GE}	Gate to emitter voltage	± 20	V
V_{ISOL}	RMS isolation voltage, any terminal to case, $t = 1 \text{ min}$	2500	
$P_D @ T_C = 25^\circ\text{C}$	Power dissipation	2604	
T_J	Operating junction temperature range	-40 to 150	$^\circ\text{C}$
T_{STG}	Storage temperature range	-40 to 125	

(1) Duration limited by max junction temperature.

Target Data

IRGDDN600K06 IRGRDN600K06

Target Data



Electrical Characteristics - $T_J = 25^\circ\text{C}$, unless otherwise stated

Parameter	Description	Min	Typ	Max	Units	Test Conditions
BV_{CES}	Collector-to-emitter breakdown voltage	600	—	—	V	$V_{GE} = 0V, I_C = 8mA$
$V_{CE(ON)}$	Collector-to-emitter voltage	—	—	2.7		$V_{GE} = 15V, I_C = 600A$
		—	2.7	—		$V_{GE} = 15V, I_C = 600A, T_J = 125^\circ\text{C}$
V_{FM}	Diode forward voltage - maximum	—	1.8	2.0		$I_F = 600A, V_{GE} = 0V$
		—	1.8	—		$I_F = 600A, V_{GE} = 0V, T_J = 125^\circ\text{C}$
V_{GEth}	Gate threshold voltage	3.0	—	5.5	$I_C = 4mA$	
DV_{GEth}	Threshold voltage temperature coefficient	—	-11	—	mV/ $^\circ\text{C}$	$V_{CE} = V_{GE}, I_C = 4mA$
g_{fe}	Forward transconductance	272	—	480	S(τ)	$V_{CE} = 25V, I_C = 600A$
I_{CES}	Collector-to-emitter leakage current	—	—	8	mA	$V_{GE} = 0V, V_{CE} = 600V$
		—	—	80		$V_{GE} = 0V, V_{CE} = 600V, T_J = 125^\circ\text{C}$
I_{GES}	Gate-to-emitter leakage current	—	—	± 8	μA	$V_{GE} = \pm 20V$

Dynamic Characteristics - $T_J = 125^\circ\text{C}$

Parameter	Description	Min	Typ	Max	Units	Test Conditions
E_{on}	Turn-on switching energy	—	0.04	—	mJ/A	$R_G = 15\Omega, V_{CC} = 300V$
E_{off} (1)	Turn-off switching energy	—	0.06	—		$I_C = 600A, L_S = 100nH$
E_{is} (1)	Total switching energy	—	—	0.15		$V_{GE} = \pm 15V$
$t_{d(on)}$	Turn-on delay time	—	300	—	ns	$R_G = 15\Omega, V_{CC} = 300V$
t_r	Rise time	—	900	—		$I_C = 600A$
$t_{d(off)}$	Turn-off delay time	—	700	—		$V_{GE} = \pm 15V$
t_f	Fall time	—	120	—		Resistive Load, $T_J = 25^\circ\text{C}$
I_{rr}	Diode peak recovery current	—	110	—		$R_G = 15\Omega, V_{CC} = 300V$
t_{rr}	Diode recovery time	—	110	—	ns	$I_C = 600A$
Q_{rr}	Diode recovery charge	—	6	—	μC	$V_{GE} = \pm 15V$
Q_{ge}	Gate-to-emitter charge (turn-on)	208	—	336	nC	$V_{CC} = 480V$
Q_{gc}	Gate-to-collector charge (turn-on)	560	—	1120		$I_C = 432A$
Q_g	Total gate charge (turn-on)	1200	—	2240		$V_{GE} = 15V$
C_{ies}	Input capacitance	—	46400	—	pF	$V_{GE} = 0V$
C_{oes}	Output capacitance	—	5280	—		$V_{CC} = 30V$
C_{res}	Reverse transfer capacitance	—	640	—		$f = 1MHz$
t_{sc}	Short circuit withstand time	10	—	—	μs	$V_{CC} = 360V, V_{GE} = \pm 15V$ Min. $R_G = 15\Omega, V_{CEP} = 500V$

(1) Includes tail losses

Thermal and Mechanical Characteristics

Parameter	Description	Typ	Max	Units
R_{thJC} (IGBT)	Thermal resistance, junction to case, each IGBT	—	0.048	$^\circ\text{C/W}$
R_{thJC} (Diode)	Thermal resistance, junction to case, each diode	—	0.070	
R_{thCS} (Module)	Thermal resistance, case to sink	0.023	0.050	
Wt	Weight of module	242	—	g

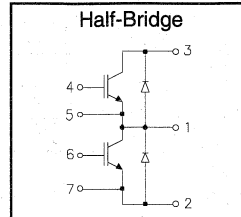
Refer to Section D - page D-18 for Package Outline 13 - Double INT-A-Pak Single Switch

IRGTDN150K06

"HALF-BRIDGE" IGBT DOUBLE INT-A-PAK

Low conduction loss IGBT

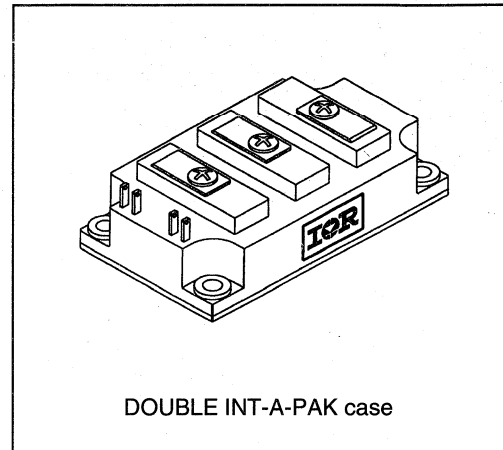
- Rugged Design
- Simple gate-drive
- Switching-Loss Rating includes all "tail" losses
- Short circuit rated



$V_{CE} = 600V$
$I_C = 150A$
$V_{CE(ON)} < 2.7V$
$t_{sc} > 10\mu s$

Description

IR's advanced IGBT technology is the key to this line of DOUBLE INT-A-PAK Power Modules. The efficient geometry and unique processing of the IGBT allow higher current densities than comparable bipolar power module transistors, while at the same time requiring the simpler gate-drive of the familiar power MOSFET. This superior technology has now been coupled to state of the art assembly techniques to produce a higher current module that is highly suited to power applications such as motor drives, uninterruptible power supplies, welding and power factor correction.



Absolute Maximum Ratings

parameter	Description	Value	Units
	Continuous collector to emitter voltage	600	V
25°C	Maximum Continuous collector current	170	A
5°C	Maximum Continuous collector current	95	
100°C	Maximum Continuous collector current	70	
	Peak IGBT switching current	300	
	Peak diode forward switching current (1)	300	
	Collector to emitter voltage	± 20	V
	Isolation voltage, any terminal to case, t = 1 min	2500	
	Power dissipation	781	W
	Storage temperature range	-40 to 150	°C
	Operating temperature range	-40 to 125	

1. Junction temperature.

Target Data

Electrical Characteristics - $T_J = 25^\circ\text{C}$, unless otherwise stated

Parameter	Description	Min	Typ	Max	Units	Test Conditions
BV_{CES}	Collector-to-emitter breakdown voltage	600	—	—	V	$V_{GE} = 0V, I_C = 2mA$
$V_{CE(ON)}$	Collector-to-emitter voltage	—	—	2.7		$V_{GE} = 15V, I_C = 150A$
		—	2.7	—		$V_{GE} = 15V, I_C = 150A, T_J = 125^\circ\text{C}$
		—	1.8	2.0		$I_F = 150A, V_{GE} = 0V$
V_{FM}	Diode forward voltage - maximum	—	1.75	—		$I_F = 150A, V_{GE} = 0V, T_J = 125^\circ\text{C}$
		3.0	—	5.5	$I_C = 1mA$	
V_{Geth}	Gate threshold voltage	3.0	—	5.5		
ΔV_{Geth}	Threshold voltage temp. coefficient	—	-11	—	mV/ $^\circ\text{C}$	$V_{CE} = V_{GE}, I_C = 1mA$
g_{fe}	Forward transconductance	68	—	120	S(t)	$V_{CE} = 25V, I_C = 150A$
I_{CES}	Collector-to-emitter leakage current	—	—	2	mA	$V_{GE} = 0V, V_{CE} = 600V$
		—	—	20		$V_{GE} = 0V, V_{CE} = 600V, T_J = 125^\circ\text{C}$
I_{GES}	Gate-to-emitter leakage current	—	—	± 2	μA	$V_{GE} = \pm 20V$

Dynamic Characteristics - $T_J = 125^\circ\text{C}$

Parameter	Description	Min	Typ	Max	Units	Test Conditions
E_{on}	Turn-on switching energy	—	0.04	—	mJ/A	$R_G = 15\Omega, V_{CC} = 300V$
E_{off} (1)	Turn-off switching energy	—	0.06	—		$I_C = 150A, L_S = 100nH$
E_{ts} (1)	Total switching energy	—	—	0.13		$V_{GE} = \pm 15V$
$t_{d(on)}$	Turn-on delay time	—	300	—	ns	$R_G = 15\Omega, V_{CC} = 300V$
t_r	Rise time	—	500	—		$I_C = 150A$
$t_{d(off)}$	Turn-off delay time	—	350	—		$V_{GE} = \pm 15V$
t_f	Fall time	—	120	—		Resistive Load, $T_J = 25^\circ\text{C}$
I_{rr}	Diode peak recovery current	—	60	—	A	$R_G = 15\Omega, V_{CC} = 300V$
t_{rr}	Diode recovery time	—	110	—	ns	$I_C = 150A$
Q_{rr}	Diode recovery charge	—	3	—	μC	$V_{GE} = \pm 15V$
Q_{ge}	Gate-to-emitter charge (turn-on)	52	—	84	nC	$V_{CC} = 480V$
Q_{gc}	Gate-to-collector charge (turn-on)	140	—	280		$I_C = 108A$
Q_g	Total gate charge (turn-on)	300	—	560		$V_{GE} = 15V$
C_{ies}	Input capacitance	—	11600	—	pF	$V_{GE} = 0V$
C_{oes}	Output capacitance	—	1320	—		$V_{CC} = 30V$
C_{res}	Reverse transfer capacitance	—	160	—		$f = 1MHz$
t_{sc}	Short circuit withstand time	10	—	—	μs	$V_{CC} = 360V, V_{GE} = \pm 15V$ Min. $R_G = 15\Omega, V_{CEP} = 500V$

(1) Includes tail losses

Thermal and Mechanical Characteristics

Parameter	Description	Typ	Max	Units
R_{thJC} (IGBT)	Thermal resistance, junction to case, each IGBT	—	0.16	$^\circ\text{C/W}$
R_{thJC} (Diode)	Thermal resistance, junction to case, each diode	—	0.24	
R_{thCS} (Module)	Thermal resistance, case to sink	0.032	0.075	
Wt	Weight of module	242	—	g

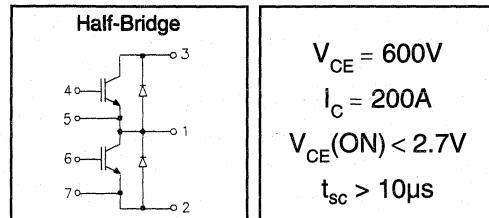
Refer to Section D -page D-17 for Package Outline 12 -Double INT-A-PAK Half Bridge

IRGTDN200K06

"HALF-BRIDGE" IGBT DOUBLE INT-A-PAK

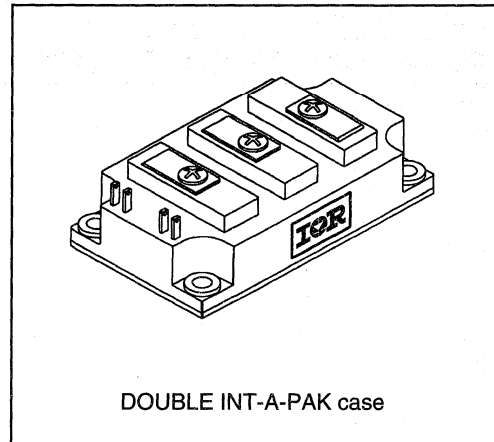
Low conduction loss IGBT

- Rugged Design
- Simple gate-drive
- Switching-Loss Rating includes all "tail" losses
- Short circuit rated



Description

IR's advanced IGBT technology is the key to this line of DOUBLE INT-A-PAK Power Modules. The efficient geometry and unique processing of the IGBT allow higher current densities than comparable bipolar power module transistors, while at the same time requiring the simpler gate-drive of the familiar power MOSFET. This superior technology has now been coupled to state of the art assembly techniques to produce a higher current module that is highly suited to power applications such as motor drives, uninterruptible power supplies, welding and power factor correction.



Absolute Maximum Ratings

Parameter	Description	Value	Units
V_{CES}	Continuous collector to emitter voltage	600	V
$I_C @ T_C = 25^\circ C$	Maximum Continuous collector current	260	A
$I_C @ T_C = 85^\circ C$	Maximum Continuous collector current	140	
$I_C @ T_C = 100^\circ C$	Maximum Continuous collector current	100	
I_{LM}	Peak IGBT switching current	400	
I_{FM}	Peak diode forward switching current (1)	400	V
V_{GE}	Gate to emitter voltage	± 20	
V_{ISOL}	RMS isolation voltage, any terminal to case, $t = 1 \text{ min}$	2500	°C
$P_D @ T_C = 25^\circ C$	Power dissipation	1000	
T_J	Operating junction temperature range	-40 to 150	
T_{STG}	Storage temperature range	-40 to 125	

(1) Duration limited by max junction temperature.

Target Data

Electrical Characteristics - $T_J = 25^\circ\text{C}$, unless otherwise stated

Parameter	Description	Min	Typ	Max	Units	Test Conditions
BV_{CES}	Collector-to-emitter breakdown voltage	600	—	—	V	$V_{GE} = 0V, I_C = 3mA$
$V_{CE(ON)}$	Collector-to-emitter voltage	—	—	2.7		$V_{GE} = 15V, I_C = 200A$
		—	2.7	—		$V_{GE} = 15V, I_C = 200A, T_J = 125^\circ\text{C}$
V_{FM}	Diode forward voltage - maximum	—	1.8	2.0		$I_F = 200A, V_{GE} = 0V$
		—	1.75	—		$I_F = 200A, V_{GE} = 0V, T_J = 125^\circ\text{C}$
V_{GEth}	Gate threshold voltage	3.0	—	5.5	$I_C = 1.5mA$	
ΔV_{GEth}	Threshold voltage temp. coefficient	—	-11	—	mV/ $^\circ\text{C}$	$V_{CE} = V_{GE}, I_C = 1.5mA$
g_{fe}	Forward transconductance	102	—	174	S(τ)	$V_{CE} = 25V, I_C = 200A$
I_{CES}	Collector-to-emitter leakage current	—	—	3	mA	$V_{GE} = 0V, V_{CE} = 600V$
		—	—	30		$V_{GE} = 0V, V_{CE} = 600V, T_J = 125^\circ\text{C}$
I_{GES}	Gate-to-emitter leakage current	—	—	± 3	μA	$V_{GE} = \pm 20V$

Dynamic Characteristics - $T_J = 125^\circ\text{C}$

Parameter	Description	Min	Typ	Max	Units	Test Conditions
E_{on}	Turn-on switching energy	—	0.04	—	mJ/A	$R_G = 15\Omega, V_{CC} = 300V$
$E_{off} (1)$	Turn-off switching energy	—	0.06	—		$I_C = 200A, L_S = 100nH$
$E_{ts} (1)$	Total switching energy	—	—	0.13		$V_{GE} = \pm 15V$
$t_{d(on)}$	Turn-on delay time	—	300	—	ns	$R_G = 15\Omega, V_{CC} = 300V$
t_r	Rise time	—	500	—		$I_C = 200A$
$t_{d(off)}$	Turn-off delay time	—	350	—		$V_{GE} = \pm 15V$
t_f	Fall time	—	120	—		Resistive Load, $T_J = 25^\circ\text{C}$
I_{rr}	Diode peak recovery current	—	90	—		$R_G = 15\Omega, V_{CC} = 300V$
t_{rr}	Diode recovery time	—	110	—	ns	$I_C = 200A$
Q_{rr}	Diode recovery charge	—	4.5	—	μC	$V_{GE} = \pm 15V$
Q_{ge}	Gate-to-emitter charge (turn-on)	78	—	126	nC	$V_{CC} = 480V$
Q_{gc}	Gate-to-collector charge (turn-on)	210	—	420		$I_C = 162A$
Q_g	Total gate charge (turn-on)	450	—	840		$V_{GE} = 15V$
C_{ies}	Input capacitance	—	17400	—	pF	$V_{GE} = 0V$
C_{oes}	Output capacitance	—	1980	—		$V_{CC} = 30V$
C_{res}	Reverse transfer capacitance	—	240	—		$f = 1MHz$
t_{sc}	Short circuit withstand time	10	---	---	μs	$V_{CC} = 360V, V_{GE} = \pm 15V$ Min. $R_G = 15\Omega, V_{CEP} = 500V$

(1) Includes tail losses

Thermal and Mechanical Characteristics

Parameter	Description	Typ	Max	Units
R_{thJC} (IGBT)	Thermal resistance, junction to case, each IGBT	—	0.125	$^\circ\text{C/W}$
R_{thJC} (Diode)	Thermal resistance, junction to case, each diode	—	0.190	
R_{thCS} (Module)	Thermal resistance, case to sink	0.032	0.075	
Wt	Weight of module	242	—	g

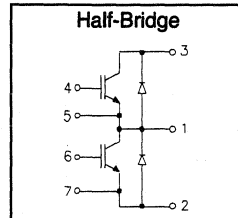
Refer to Section D - page D-17 for Package Outline 12 -Double INT-A-PAK Half Bridge

IRGTDN300K06

"HALF-BRIDGE" IGBT DOUBLE INT-A-PAK

Low conduction loss IGBT

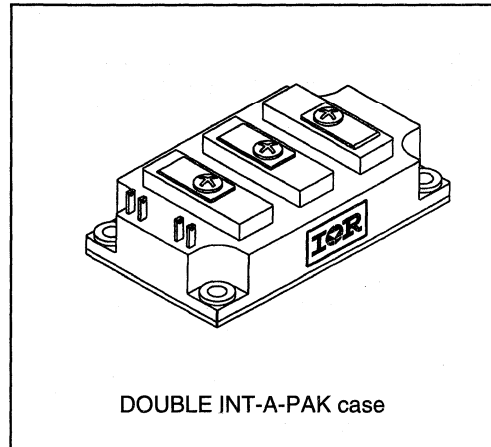
- Rugged Design
- Simple gate-drive
- Switching-Loss Rating includes all "tail" losses
- Short circuit rated



$V_{CE} = 600V$
$I_C = 300A$
$V_{CE(ON)} < 2.7V$
$t_{sc} > 10\mu s$

Description

IR's advanced IGBT technology is the key to this line of DOUBLE INT-A-PAK Power Modules. The efficient geometry and unique processing of the IGBT allow higher current densities than comparable bipolar power module transistors, while at the same time requiring the simpler gate-drive of the familiar power MOSFET. This superior technology has now been coupled to state of the art assembly techniques to produce a higher current module that is highly suited to power applications such as motor drives, uninterruptible power supplies, welding and power factor correction.



Absolute Maximum Ratings

Parameter	Description	Value	Units
V_{CES}	Continuous collector to emitter voltage	600	V
$I_C @ T_C = 25^\circ C$	Maximum Continuous collector current	340	A
$I_C @ T_C = 85^\circ C$	Maximum Continuous collector current	190	
$I_C @ T_C = 100^\circ C$	Maximum Continuous collector current	140	
ILM	Peak IGBT switching current	600	
IFM	Peak diode forward switching current (1)	600	
V_{GE}	Gate to emitter voltage	± 20	V
VISOL	RMS isolation voltage, any terminal to case, $t = 1 \text{ min}$	2500	
$P_D @ T_C = 25^\circ C$	Power dissipation	1316	W
T_J	Operating junction temperature range	-40 to 150	$^\circ C$
T_{STG}	Storage temperature range	-40 to 125	

(1) Duration limited by max junction temperature.

Target Data



Electrical Characteristics - $T_J = 25^\circ\text{C}$, unless otherwise stated

Parameter	Description	Min	Typ	Max	Units	Test Conditions
BV _{CE} S	Collector-to-emitter breakdown voltage	600	—	—	V	V _{GE} = 0V, I _C = 4mA
V _{CE(ON)}	Collector-to-emitter voltage	—	—	2.7		V _{GE} = 15V, I _C = 300A
		—	2.7	—		V _{GE} = 15V, I _C = 300A, T _J = 125°C
V _{FM}	Diode forward voltage - maximum	—	1.8	2.0		I _F = 300A, V _{GE} = 0V
		—	1.75	—		I _F = 300A, V _{GE} = 0V, T _J = 125°C
V _{GEth}	Gate threshold voltage	3.0	—	5.5	I _C = 2mA	
DV _{GEth}	Threshold voltage temperature coefficient	—	-11	—	mV/°C	V _{CE} = V _{GE} , I _C = 2mA
g _{fe}	Forward transconductance	136	—	240	S(Ω)	V _{CE} = 25V, I _C = 300A
I _{CE} S	Collector-to-emitter leakage current	—	—	4	mA	V _{GE} = 0V, V _{CE} = 600V
		—	—	40		V _{GE} = 0V, V _{CE} = 600V, T _J = 125°C
I _{GES}	Gate-to-emitter leakage current	—	—	±4	μA	V _{GE} = ±20V

Dynamic Characteristics - $T_J = 125^\circ\text{C}$

Parameter	Description	Min	Typ	Max	Units	Test Conditions
E _{on}	Turn-on switching energy	—	0.04	—	mJ/A	R _G = 15Ω, V _{CC} = 300V
E _{off} (1)	Turn-off switching energy	—	0.06	—		I _C = 300A, L _S = 100nH
E _{ts} (1)	Total switching energy	—	—	0.13		V _{GE} = ±15V
t _{d(on)}	Turn-on delay time	—	300	—	ns	R _G = 15Ω, V _{CC} = 300V
t _r	Rise time	—	500	—		I _C = 300A
t _{d(off)}	Turn-off delay time	—	350	—		V _{GE} = ±15V
t _f	Fall time	—	120	—		Resistive Load, T _J = 25°C
I _{rr}	Diode peak recovery current	—	110	—	A	R _G = 15Ω, V _{CC} = 300V
t _{rr}	Diode recovery time	—	110	—	ns	I _C = 300A
Q _{rr}	Diode recovery charge	—	6	—	μC	V _{GE} = ±15V
Q _{ge}	Gate-to-emitter charge (turn-on)	104	—	168	nC	V _{CC} = 480V
Q _{gc}	Gate-to-collector charge (turn-on)	280	—	560		I _C = 216A
Q _g	Total gate charge (turn-on)	600	—	1120		V _{GE} = 15V
C _{ies}	Input capacitance	—	23200	—	pF	V _{GE} = 0V
C _{oes}	Output capacitance	—	2640	—		V _{CC} = 30V
C _{res}	Reverse transfer capacitance	—	320	—		f = 1MHz
t _{sc}	Short circuit withstand time	10	—	—	μs	V _{CC} = 360V, V _{GE} = ±15V Min. R _G = 15Ω, V _{CEP} = 500V

(1) Includes tail losses

Thermal and Mechanical Characteristics

Parameter	Description	Typ	Max	Units
R _{thJC} (IGBT)	Thermal resistance, junction to case, each IGBT	—	0.095	°C/W
R _{thJC} (Diode)	Thermal resistance, junction to case, each diode	—	0.140	
R _{thCS} (Module)	Thermal resistance, case to sink	0.032	0.075	
Wt	Weight of module	242	—	g

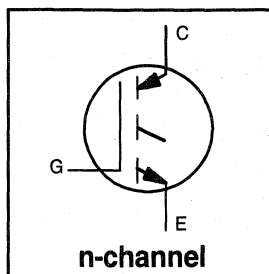
Refer to Section D - page D-17 for Package Outline 12 -Double INT-A-PAK Half Bridge

INSULATED GATE BIPOLAR TRANSISTOR

Short Circuit Rated
UltraFast IGBT

Features

- Short circuit rated - $10\mu\text{s}$ @ 125°C , $V_{\text{GE}} = 10\text{V}$
($5\mu\text{s}$ @ $V_{\text{GE}} = 15\text{V}$)
- Switching-loss rating includes all "tail" losses
- Optimized for high operating frequency (over 5kHz)
See Fig. 1 for Current vs. Frequency curve



$$V_{\text{CES}} = 1200\text{V}$$

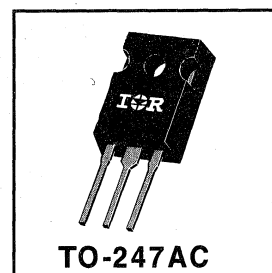
$$V_{\text{CE(sat)}} \leq 3.5\text{V}$$

$$\text{@ } V_{\text{GE}} = 15\text{V}, I_{\text{C}} = 20\text{A}$$

Description

Insulated Gate Bipolar Transistors (IGBTs) from International Rectifier have higher usable current densities than comparable bipolar transistors, while at the same time having simpler gate-drive requirements of the familiar power MOSFET. They provide substantial benefits to a host of high-voltage, high-current applications.

These new short circuit rated devices are especially suited for motor control and other applications requiring short circuit withstand capability.



Absolute Maximum Ratings

	Parameter	Max.	Units
V_{CES}	Collector-to-Emitter Voltage	1200	V
$I_{\text{C}} @ T_{\text{C}} = 25^\circ\text{C}$	Continuous Collector Current	36	A
$I_{\text{C}} @ T_{\text{C}} = 100^\circ\text{C}$	Continuous Collector Current	20	
I_{CM}	Pulsed Collector Current ①	72	
I_{LM}	Clamped Inductive Load Current ②	72	
t_{sc}	Short Circuit Withstand Time	10	μs
V_{GE}	Gate-to-Emitter Voltage	± 20	V
E_{ARV}	Reverse Voltage Avalanche Energy ③	20	mJ
$P_{\text{D}} @ T_{\text{C}} = 25^\circ\text{C}$	Maximum Power Dissipation	200	W
$P_{\text{D}} @ T_{\text{C}} = 100^\circ\text{C}$	Maximum Power Dissipation	78	
T_{J}	Operating Junction and	-55 to +150	°C
T_{STG}	Storage Temperature Range		
	Soldering Temperature, for 10 sec.	300 (0.063 in. (1.6mm) from case)	
	Mounting torque, 6-32 or M3 screw.	10 lbf•in (1.1N•m)	

Thermal Resistance

	Parameter	Min.	Typ.	Max.	Units
$R_{\theta\text{JC}}$	Junction-to-Case	—	—	0.64	°C/W
$R_{\theta\text{CS}}$	Case-to-Sink, flat, greased surface	—	0.24	—	
$R_{\theta\text{JA}}$	Junction-to-Ambient, typical socket mount	—	—	40	
Wt	Weight	—	6 (0.21)	—	g (oz)

Electrical Characteristics @ $T_J = 25^\circ\text{C}$ (unless otherwise specified)

	Parameter	Min.	Typ.	Max.	Units	Conditions
$V_{(BR)CES}$	Collector-to-Emitter Breakdown Voltage	1200	—	—	V	$V_{GE} = 0V, I_C = 250\mu A$
$V_{(BR)ECS}$	Emitter-to-Collector Breakdown Voltage ④	20	—	—	V	$V_{GE} = 0V, I_C = 1.0A$
$\Delta V_{(BR)CES}/\Delta T_J$	Temp. Coeff. of Breakdown Voltage	—	1.8	—	V/°C	$V_{GE} = 0V, I_C = 1.0mA$
$V_{CE(on)}$	Collector-to-Emitter Saturation Voltage	—	2.7	3.5	V	$I_C = 20A$ $I_C = 36A$ $I_C = 20A, T_J = 150^\circ\text{C}$ $V_{GE} = 15V$ See Fig. 2, 5
		—	3.4	—		
		—	2.6	—		
$V_{GE(th)}$	Gate Threshold Voltage	3.0	—	6.0		$V_{CE} = V_{GE}, I_C = 250\mu A$
$\Delta V_{GE(th)}/\Delta T_J$	Temperature Coeff. of Threshold Voltage	—	-15	—	mV/°C	$V_{CE} = V_{GE}, I_C = 250\mu A$
g_{fe}	Forward Transconductance ⑤	4.2	12	—	S	$V_{CE} = 100V, I_C = 20A$
I_{CES}	Zero Gate Voltage Collector Current	—	—	250	μA	$V_{GE} = 0V, V_{CE} = 1200V$ $V_{GE} = 0V, V_{CE} = 1200V, T_J = 150^\circ\text{C}$
		—	—	5000		
I_{GES}	Gate-to-Emitter Leakage Current	—	—	± 100	nA	$V_{GE} = \pm 20V$

Switching Characteristics @ $T_J = 25^\circ\text{C}$ (unless otherwise specified)

	Parameter	Min.	Typ.	Max.	Units	Conditions
Q_g	Total Gate Charge (turn-on)	—	94	140	nC	$I_C = 20A$ $V_{CC} = 400V$ $V_{GE} = 15V$ See Fig. 8
Q_{ge}	Gate - Emitter Charge (turn-on)	—	23	35		
Q_{gc}	Gate - Collector Charge (turn-on)	—	24	36		
$t_{d(on)}$	Turn-On Delay Time	—	36	—	ns	$T_J = 25^\circ\text{C}$ $I_C = 20A, V_{CC} = 960V$ $V_{GE} = 15V, R_G = 5.0\Omega$ Energy losses include "tail"
t_r	Rise Time	—	21	—		
$t_{d(off)}$	Turn-Off Delay Time	—	210	380		
t_f	Fall Time	—	180	290		
E_{on}	Turn-On Switching Loss	—	0.9	—	mJ	See Fig. 9, 10, 11, 14
E_{off}	Turn-Off Switching Loss	—	2.5	—		
E_{ts}	Total Switching Loss	—	3.4	5.1		
t_{sc}	Short Circuit Withstand Time	10	—	—	μs	$V_{GE} = 10V$ $V_{GE} = 15V$ $V_{CC} = 720V, T_J = 125^\circ\text{C}$ $R_G = 5.0\Omega, V_{CPK} < 1000V$
		5.0	—	—		
$t_{d(on)}$	Turn-On Delay Time	—	33	—	ns	$T_J = 150^\circ\text{C}$, $I_C = 20A, V_{CC} = 960V$ $V_{GE} = 15V, R_G = 5.0\Omega$ Energy losses include "tail"
t_r	Rise Time	—	22	—		
$t_{d(off)}$	Turn-Off Delay Time	—	420	—		
t_f	Fall Time	—	270	—		
E_{ts}	Total Switching Loss	—	6.7	—	mJ	See Fig. 10, 14
L_E	Internal Emitter Inductance	—	13	—	nH	Measured 5mm from package
C_{ies}	Input Capacitance	—	2600	—	pF	$V_{GE} = 0V$ $V_{CC} = 30V$ See Fig. 7 $f = 1.0MHz$
C_{oes}	Output Capacitance	—	140	—		
C_{res}	Reverse Transfer Capacitance	—	26	—		

Notes:

- ① Repetitive rating; $V_{GE}=20V$, pulse width limited by max. junction temperature. (See fig. 13b)
- ② $V_{CC}=80\%(V_{CES}), V_{GE}=20V, L=10\mu H, R_G=5.0\Omega$, (See fig. 13a)
- ③ Repetitive rating; pulse width limited by maximum junction temperature.
- ④ Pulse width $\leq 80\mu s$; duty factor $\leq 0.1\%$.
- ⑤ Pulse width $5.0\mu s$, single shot.

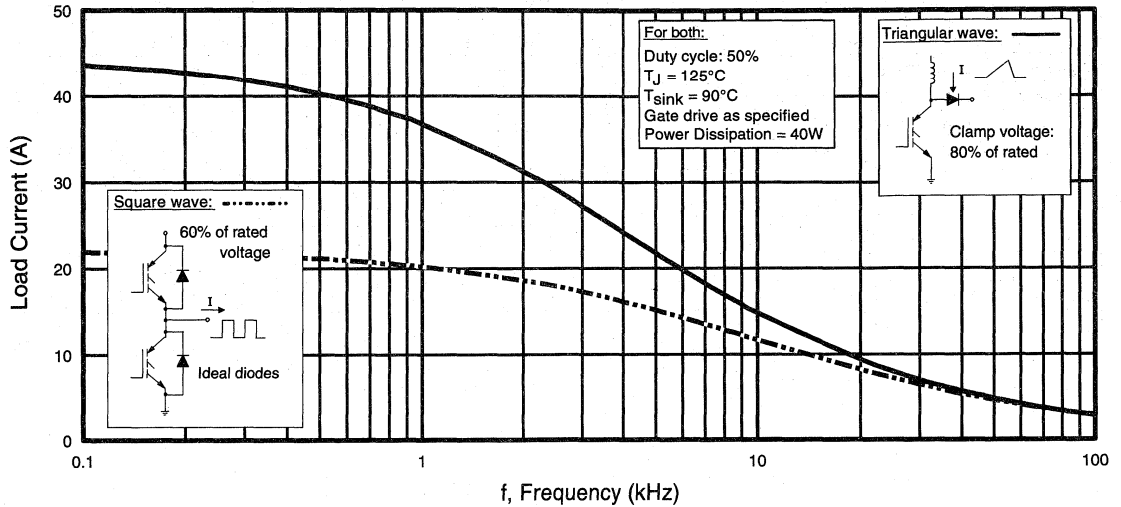


Fig. 1 - Typical Load Current vs. Frequency
 (For square wave, $I = I_{RMS}$ of fundamental; for triangular wave, $I = I_{PK}$)

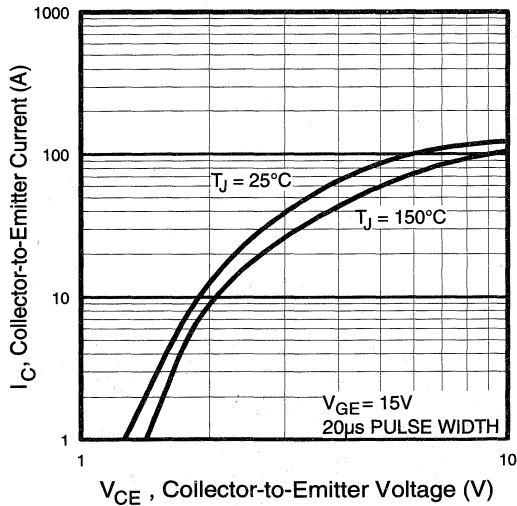


Fig. 2 - Typical Output Characteristics

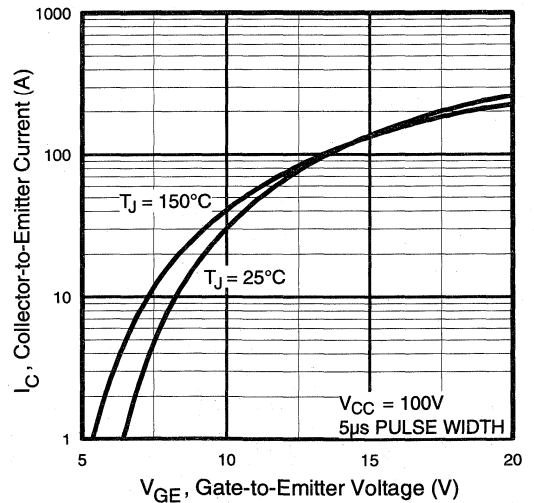


Fig. 3 - Typical Transfer Characteristics

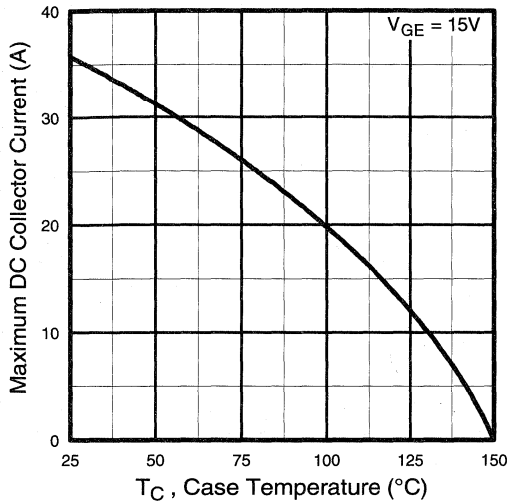


Fig. 4 - Maximum Collector Current vs. Case Temperature

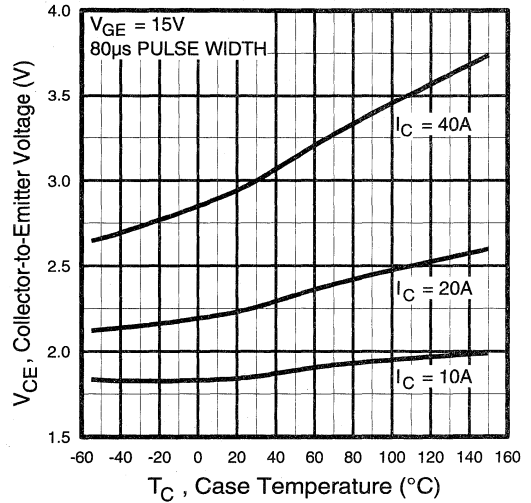


Fig. 5 - Collector-to-Emitter Voltage vs. Case Temperature

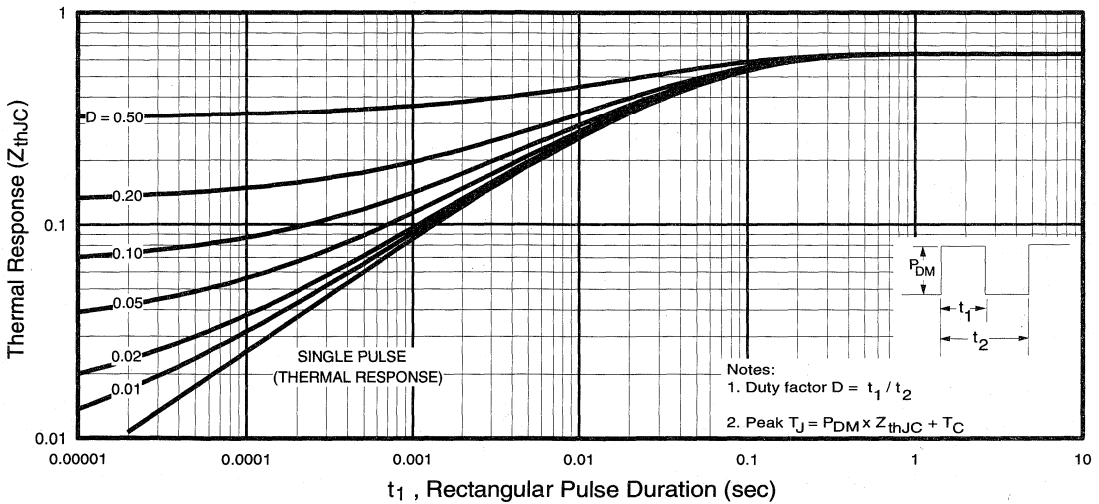


Fig. 6 - Maximum Effective Transient Thermal Impedance, Junction-to-Case

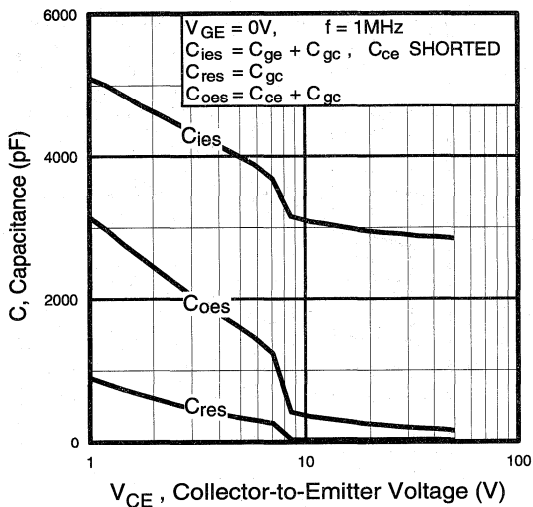


Fig. 7 - Typical Capacitance vs. Collector-to-Emitter Voltage

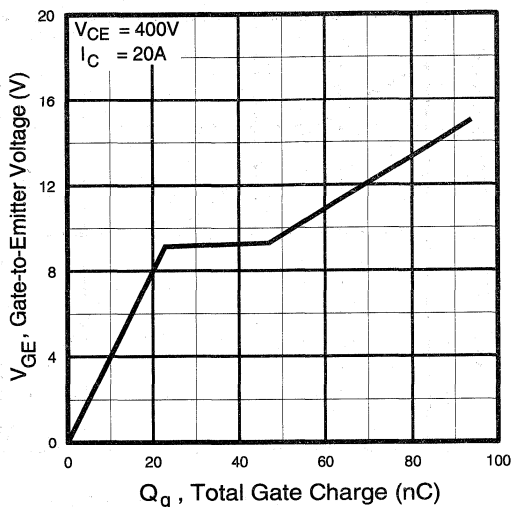


Fig. 8 - Typical Gate Charge vs. Gate-to-Emitter Voltage

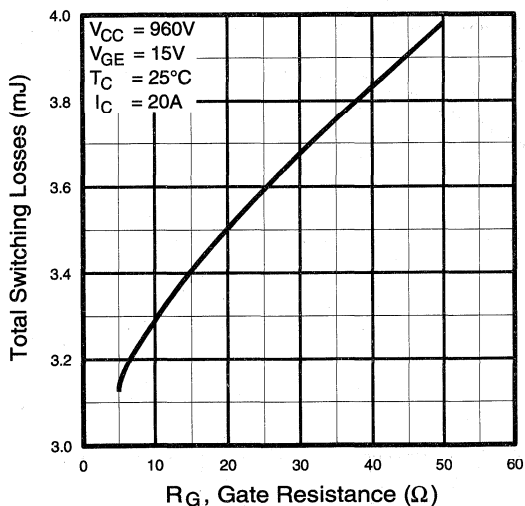


Fig. 9 - Typical Switching Losses vs. Gate Resistance

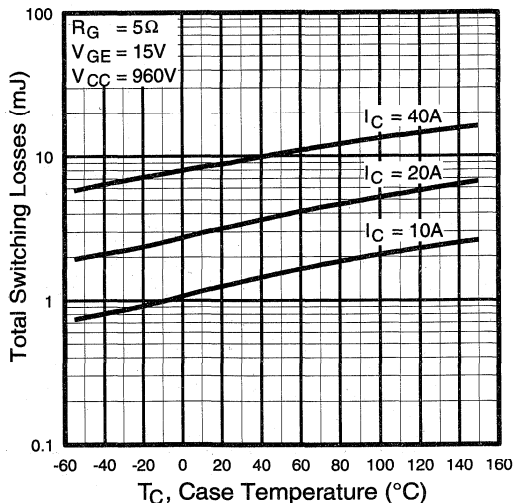


Fig. 10 - Typical Switching Losses vs. Case Temperature

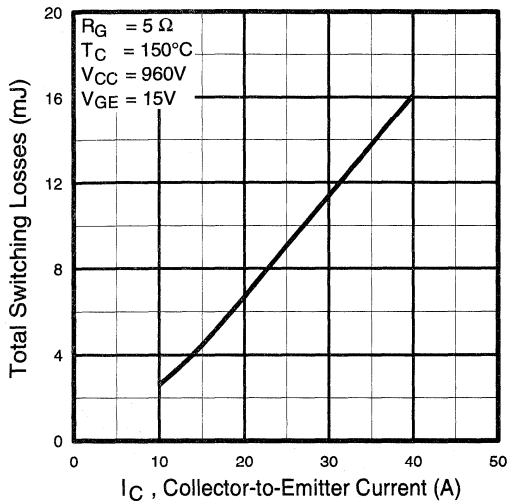


Fig. 11 - Typical Switching Losses vs. Collector-to-Emitter Current

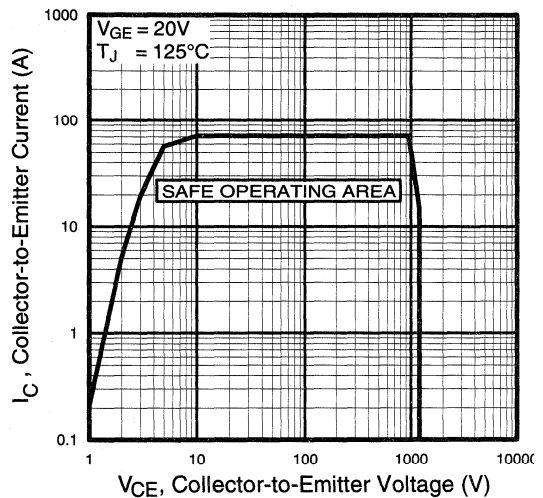


Fig. 12 - Turn-Off SOA

Refer to Section D for the following:

Appendix G: Section D- page D-9

- Fig. 13a - Clamped Inductive Load Test Circuit
- Fig. 13b - Pulsed Collector Current Test Circuit
- Fig. 14a - Switching Loss Test Circuit
- Fig. 14b - Switching Loss Waveform

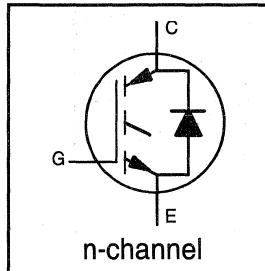
IRGPH50KD2

INSULATED GATE BIPOLAR TRANSISTOR
WITH ULTRAFAST SOFT RECOVERY DIODE

Short Circuit Rated
UltraFast CoPack IGBT

Features

- Short circuit rated -10 μ s @ 125°C, $V_{GE} = 10V$ (5 μ s @ $V_{GE} = 15V$)
- Switching-loss rating includes all "tail" losses
- HEXFRED™ soft ultrafast diodes
- Optimized for high operating frequency (over 5kHz)
See Fig. 1 for Current vs. Frequency curve



$$V_{CES} = 1200V$$

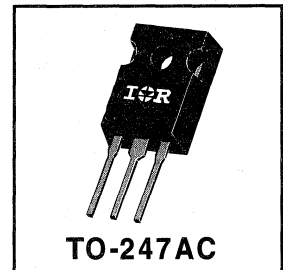
$$V_{CE(sat)} \leq 3.5V$$

$$@V_{GE} = 15V, I_C = 20A$$

Description

Co-packaged IGBTs are a natural extension of International Rectifier's well known IGBT line. They provide the convenience of an IGBT and an ultrafast recovery diode in one package, resulting in substantial benefits to a host of high-voltage, high-current, applications.

These new short circuit rated devices are especially suited for motor control and other applications requiring short circuit withstand capability.



Absolute Maximum Ratings

	Parameter	Max.	Units
V_{CES}	Collector-to-Emitter Voltage	1200	V
$I_C @ T_C = 25^\circ C$	Continuous Collector Current	36	A
$I_C @ T_C = 100^\circ C$	Continuous Collector Current	20	
I_{CM}	Pulsed Collector Current ①	72	
I_{LM}	Clamped Inductive Load Current ②	72	
$I_F @ T_C = 100^\circ C$	Diode Continuous Forward Current	16	
I_{FM}	Diode Maximum Forward Current	72	
t_{sc}	Short Circuit Withstand Time	10	μ s
V_{GE}	Gate-to-Emitter Voltage	± 20	V
$P_D @ T_C = 25^\circ C$	Maximum Power Dissipation	200	W
$P_D @ T_C = 100^\circ C$	Maximum Power Dissipation	78	
T_J	Operating Junction and Storage Temperature Range	-55 to +150	°C
T_{STG}	Soldering Temperature, for 10 sec.	300 (0.063 in. (1.6mm) from case)	
	Mounting Torque, 6-32 or M3 Screw.	10 lbf•in (1.1 N•m)	

Thermal Resistance

	Parameter	Min.	Typ.	Max.	Units
$R_{\theta JC}$	Junction-to-Case - IGBT	—	—	0.64	°C/W
$R_{\theta JC}$	Junction-to-Case - Diode	—	—	0.83	
$R_{\theta CS}$	Case-to-Sink, flat, greased surface	—	0.24	—	
$R_{\theta JA}$	Junction-to-Ambient, typical socket mount	—	—	40	
Wt	Weight	—	6 (0.21)	—	g (oz)

Electrical Characteristics @ $T_J = 25^\circ\text{C}$ (unless otherwise specified)

	Parameter	Min.	Typ.	Max.	Units	Conditions
$V_{(BR)CES}$	Collector-to-Emitter Breakdown Voltage ^②	1200	—	—	V	$V_{GE} = 0V, I_C = 250\mu\text{A}$
$\Delta V_{(BR)CES}/\Delta T_J$	Temperature Coeff. of Breakdown Voltage	—	1.8	—	V/ $^\circ\text{C}$	$V_{GE} = 0V, I_C = 1.0\text{mA}$
$V_{CE(on)}$	Collector-to-Emitter Saturation Voltage	—	2.7	3.5	V	$I_C = 20A, V_{GE} = 15V$ See Fig. 2, 5
		—	3.4	—		
		—	2.6	—		
$V_{GE(th)}$	Gate Threshold Voltage	3.0	—	6.0		$V_{CE} = V_{GE}, I_C = 250\mu\text{A}$
$\Delta V_{GE(th)}/\Delta T_J$	Temperature Coeff. of Threshold Voltage	—	-15	—	mV/ $^\circ\text{C}$	$V_{CE} = V_{GE}, I_C = 250\mu\text{A}$
g_{fe}	Forward Transconductance ^③	4.2	12	—	S	$V_{CE} = 100V, I_C = 20A$
I_{CES}	Zero Gate Voltage Collector Current	—	—	250	μA	$V_{GE} = 0V, V_{CE} = 1200V$
		—	—	6500		$V_{GE} = 0V, V_{CE} = 1200V, T_J = 150^\circ\text{C}$
V_{FM}	Diode Forward Voltage Drop	—	2.5	3.0	V	$I_C = 16A$ See Fig. 13
		—	2.1	2.5		$I_C = 16A, T_J = 150^\circ\text{C}$
I_{GES}	Gate-to-Emitter Leakage Current	—	—	± 100	nA	$V_{GE} = \pm 20V$

Switching Characteristics @ $T_J = 25^\circ\text{C}$ (unless otherwise specified)

	Parameter	Min.	Typ.	Max.	Units	Conditions
Q_g	Total Gate Charge (turn-on)	—	94	140	nC	$I_C = 20A$ $V_{CC} = 400V$ See Fig. 8
Q_{ge}	Gate - Emitter Charge (turn-on)	—	23	35		
Q_{gc}	Gate - Collector Charge (turn-on)	—	24	36		
$t_{d(on)}$	Turn-On Delay Time	—	70	—	ns	$T_J = 25^\circ\text{C}$ $I_C = 20A, V_{CC} = 800V$ $V_{GE} = 15V, R_G = 5.0\Omega$ Energy losses include "tail" and diode reverse recovery.
t_r	Rise Time	—	68	—		
$t_{d(off)}$	Turn-Off Delay Time	—	200	470		
t_f	Fall Time	—	190	320	mJ	See Fig. 9, 10, 11, 18
E_{on}	Turn-On Switching Loss	—	2.5	—		
E_{off}	Turn-Off Switching Loss	—	2.4	—		
E_{ts}	Total Switching Loss	—	4.9	8.7	μs	$V_{GE} = 10V, V_{CC} = 720V, T_J = 125^\circ\text{C}$ $V_{GE} = 15V, R_G = 5.0\Omega, V_{CPK} < 1000V$
t_{sc}	Short Circuit Withstand Time	10	—	—		
$t_{d(on)}$	Turn-On Delay Time	—	68	—	ns	$T_J = 150^\circ\text{C}$ See Fig. 9, 10, 11, 18 $I_C = 20A, V_{CC} = 800V$ $V_{GE} = 15V, R_G = 5.0\Omega$ Energy losses include "tail" and diode reverse recovery.
t_r	Rise Time	—	63	—		
$t_{d(off)}$	Turn-Off Delay Time	—	320	—		
t_f	Fall Time	—	310	—	mJ	diode reverse recovery.
E_{ts}	Total Switching Loss	—	7.5	—		
L_E	Internal Emitter Inductance	—	13	—	nH	Measured 5mm from package
C_{ies}	Input Capacitance	—	2600	—	pF	$V_{GE} = 0V$ $V_{CC} = 30V$ See Fig. 7 $f = 1.0\text{MHz}$
C_{oes}	Output Capacitance	—	140	—		
C_{res}	Reverse Transfer Capacitance	—	26	—		
t_{rr}	Diode Reverse Recovery Time	—	90	135	ns	$T_J = 25^\circ\text{C}$ See Fig. 14
		—	164	245		$T_J = 125^\circ\text{C}$
I_{rr}	Diode Peak Reverse Recovery Current	—	5.8	10	A	$T_J = 25^\circ\text{C}$ See Fig. 15
		—	8.3	15		$T_J = 125^\circ\text{C}$
Q_{rr}	Diode Reverse Recovery Charge	—	260	675	nC	$T_J = 25^\circ\text{C}$ See Fig. 16
		—	680	1838		$T_J = 125^\circ\text{C}$
$di_{(rec)M}/dt$	Diode Peak Rate of Fall of Recovery During t_b	—	120	—	A/ μs	$T_J = 25^\circ\text{C}$ See Fig. 17
		—	76	—		$T_J = 125^\circ\text{C}$

Notes:

- ① Repetitive rating; $V_{GE} = 20V$, pulse width limited by max. junction temperature. (See fig. 20)
- ② $V_{CC} = 80\%(V_{CES}), V_{GE} = 20V, L = 10\mu\text{H}, R_G = 5.0\Omega$, (See fig. 19)
- ③ Pulse width $\leq 80\mu\text{s}$; duty factor $\leq 0.1\%$.
- ④ Pulse width 5.0 μs , single shot.

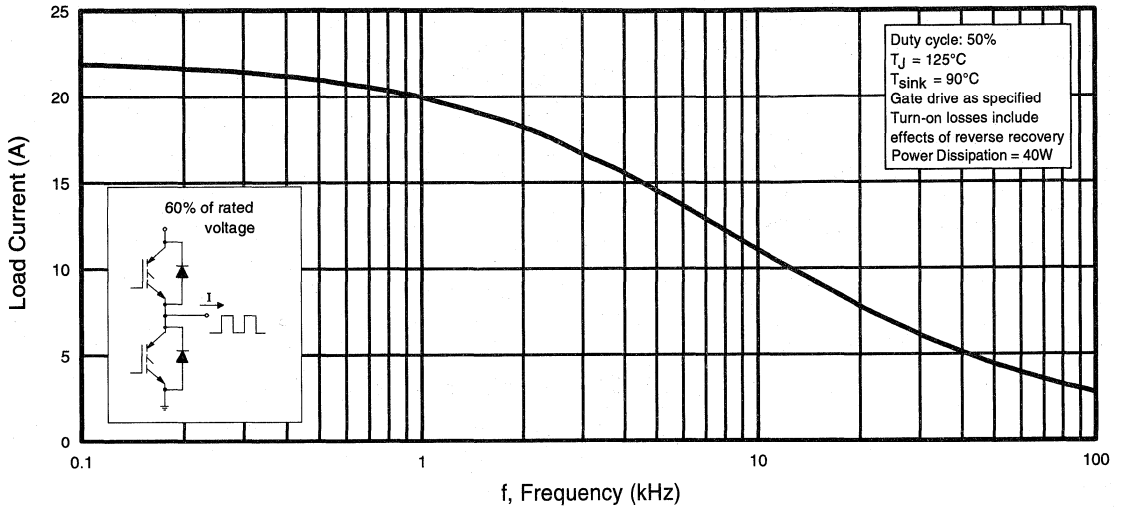


Fig. 1 - Typical Load Current vs. Frequency
(Load Current = I_{RMS} of fundamental)

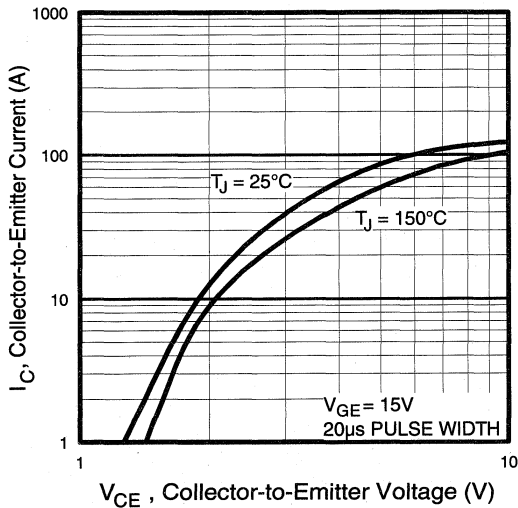


Fig. 2 - Typical Output Characteristics

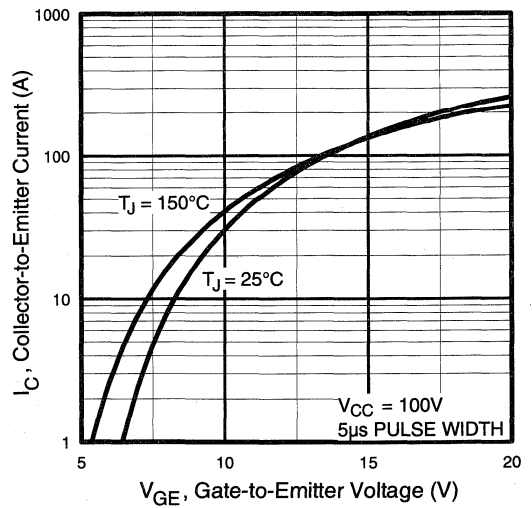


Fig. 3 - Typical Transfer Characteristics

Motor
Control
Ultra-Fast
Co-Packs

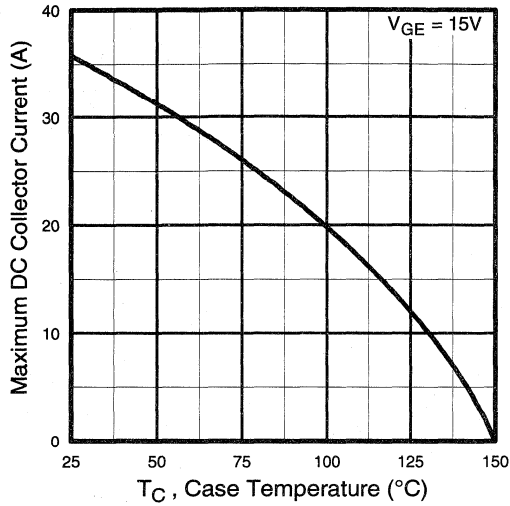


Fig. 4 - Maximum Collector Current vs. Case Temperature

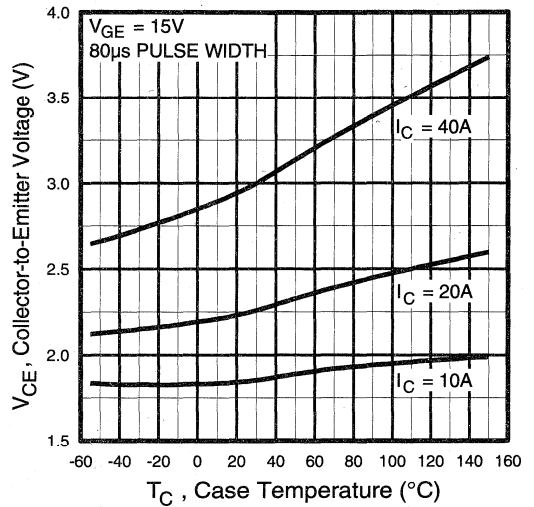


Fig. 5 - Collector-to-Emitter Voltage vs. Case Temperature

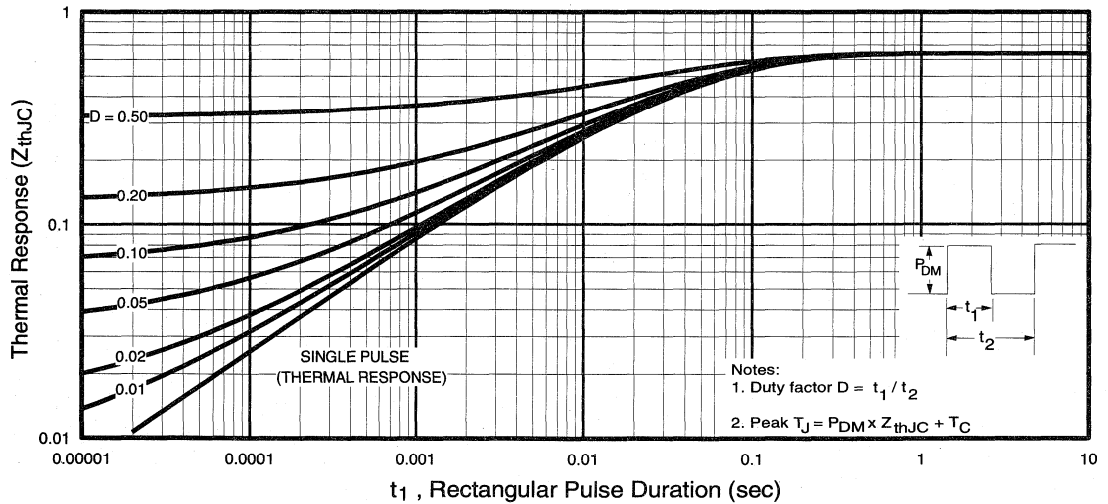


Fig. 6 - Maximum IGBT Effective Transient Thermal Impedance, Junction-to-Case

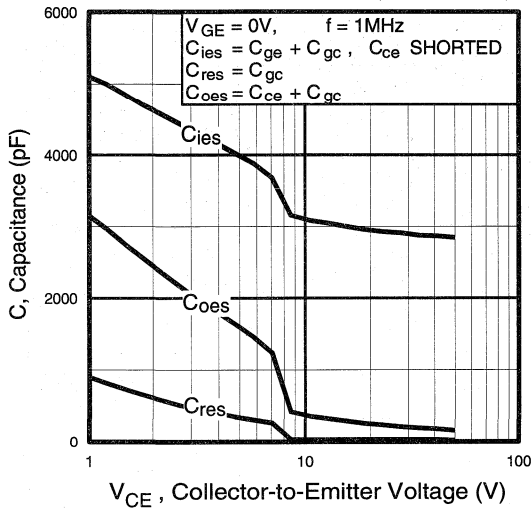


Fig. 7 - Typical Capacitance vs. Collector-to-Emitter Voltage

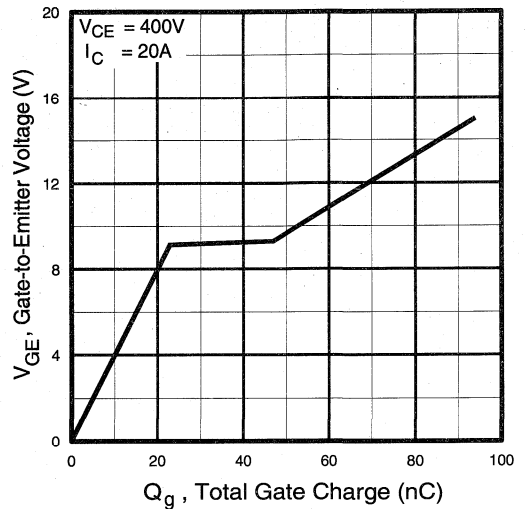


Fig. 8 - Typical Gate Charge vs. Gate-to-Emitter Voltage

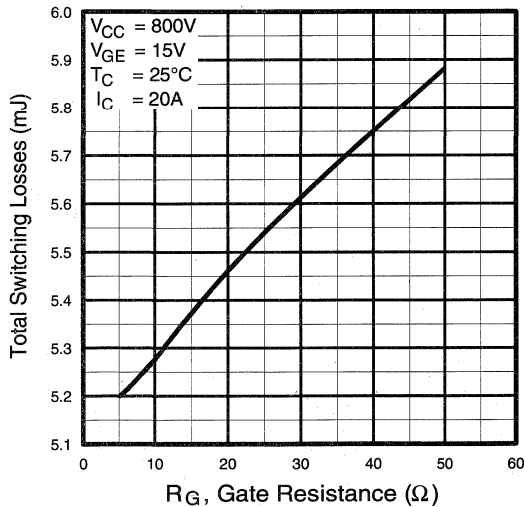


Fig. 9 - Typical Switching Losses vs. Gate Resistance

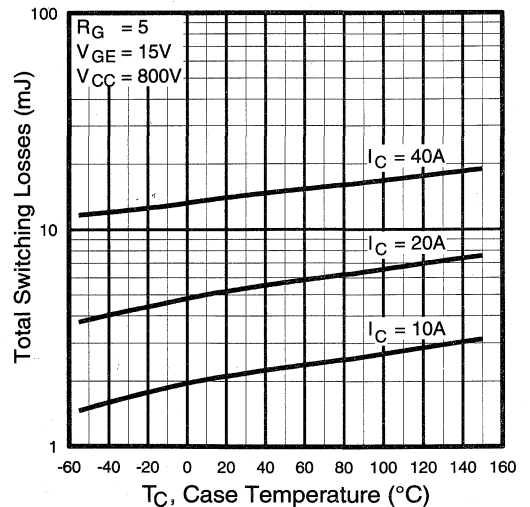


Fig. 10 - Typical Switching Losses vs. Case Temperature

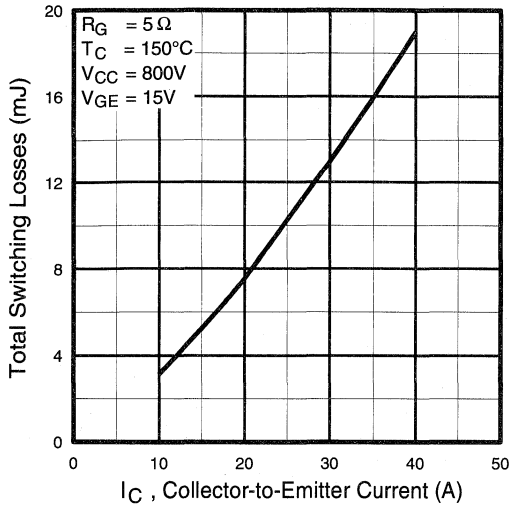


Fig. 11 - Typical Switching Losses vs. Collector-to-Emitter Current

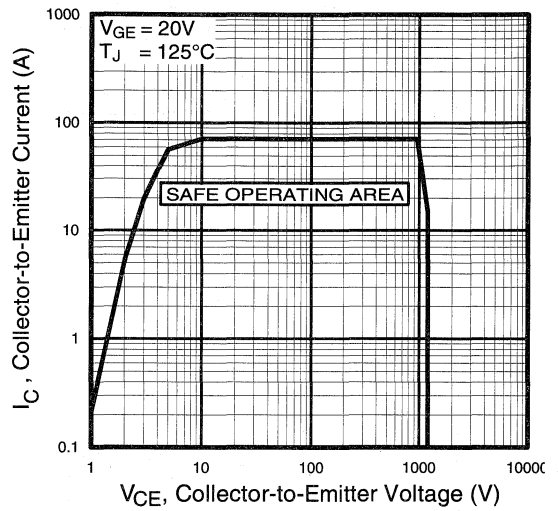


Fig. 12 - Turn-Off SOA

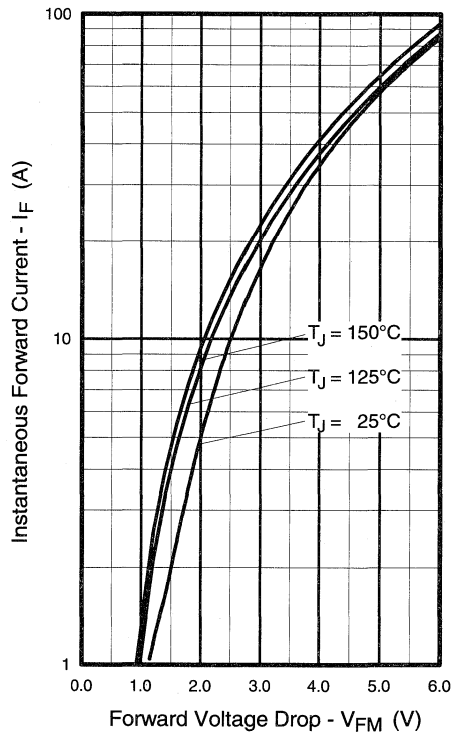


Fig. 13 - Maximum Forward Voltage Drop vs. Instantaneous Forward Current

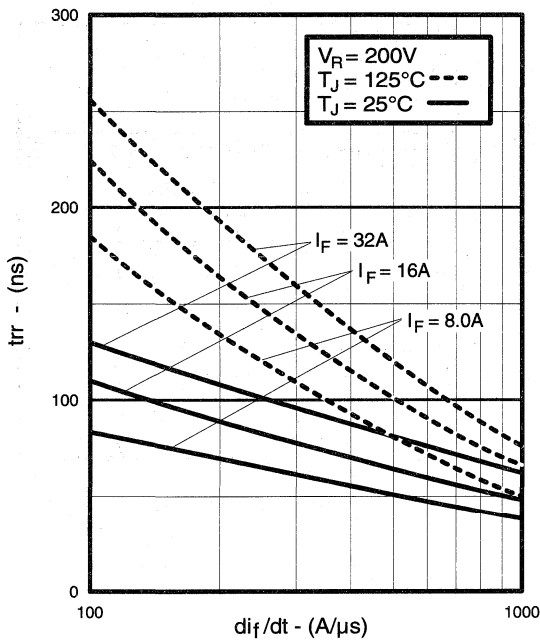


Fig. 14 - Typical Reverse Recovery vs. di_f/dt

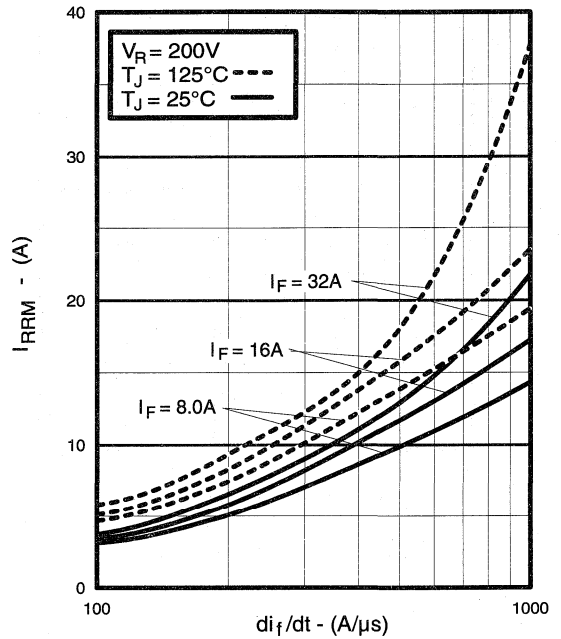


Fig. 15 - Typical Recovery Current vs. di_f/dt

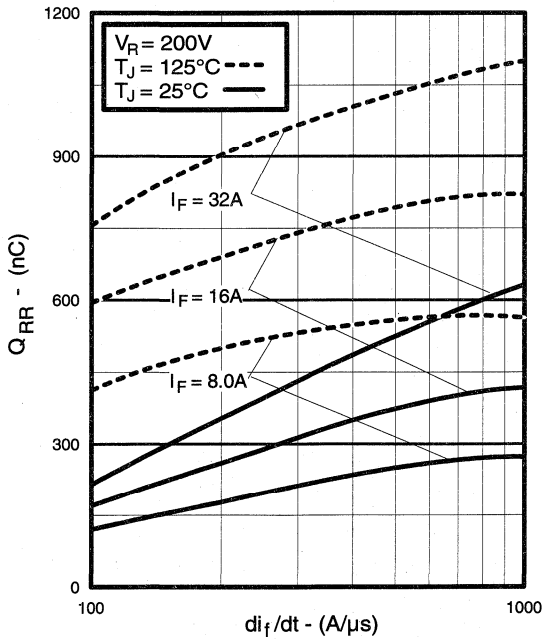


Fig. 16 - Typical Stored Charge vs. di_f/dt

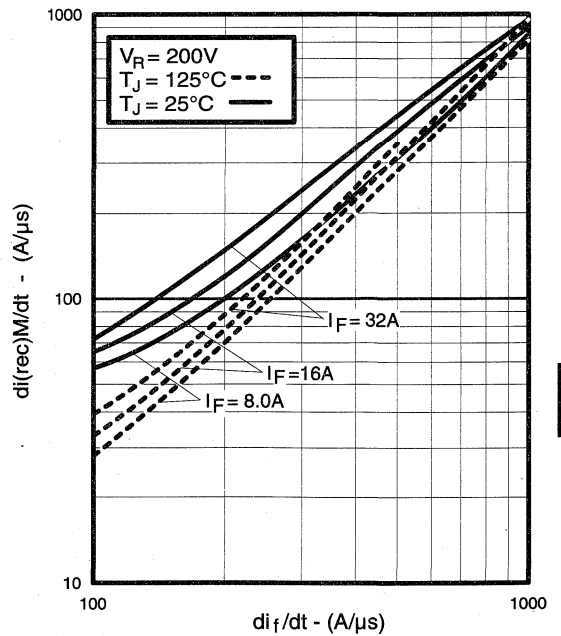


Fig. 17 - Typical $di_{(rec)M}/dt$ vs. di_f/dt

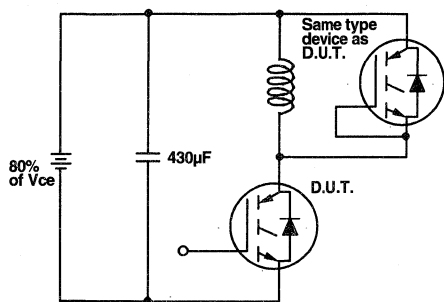


Fig. 18a - Test Circuit for Measurement of I_{LM} , E_{on} , $E_{off}(\text{diode})$, t_{rr} , Q_{rr} , I_{rr} , $t_{d(on)}$, t_r , $t_{d(off)}$, t_f

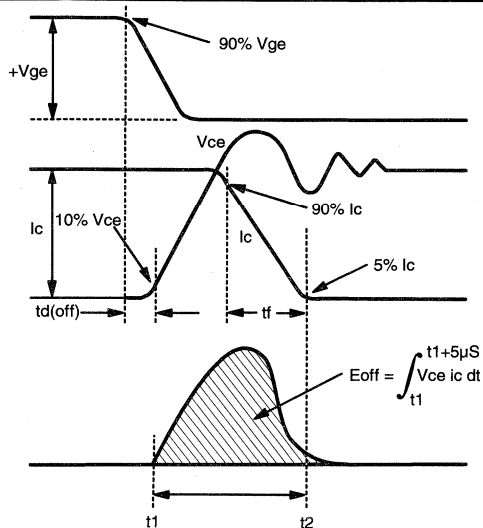


Fig. 18b - Test Waveforms for Circuit of Fig. 18a, Defining E_{off} , $t_{d(off)}$, t_f

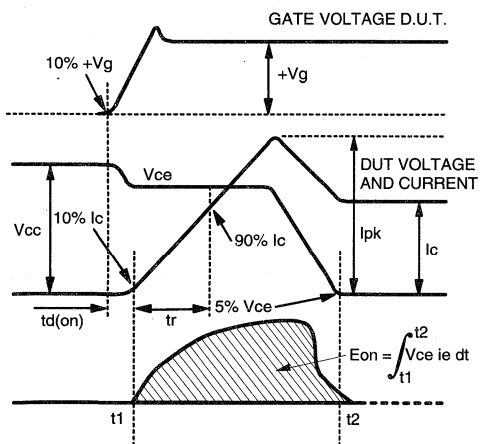


Fig. 18c - Test Waveforms for Circuit of Fig. 18a, Defining E_{on} , $t_{d(on)}$, t_r

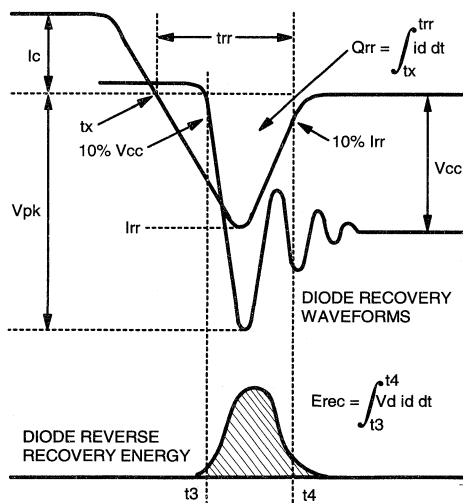


Fig. 18d - Test Waveforms for Circuit of Fig. 18a, Defining E_{rec} , t_{rr} , Q_{rr} , I_{rr}

Refer to Section D for the following:
Appendix H: Section D - page D-9

Fig. 18e - Macro Waveforms for Test Circuit of Fig. 18a

Fig. 19 - Clamped Inductive Load Test Circuit

Fig. 20 - Pulsed Collector Current Test Circuit

IGBT Designer's Manual

Other Information

Appendix

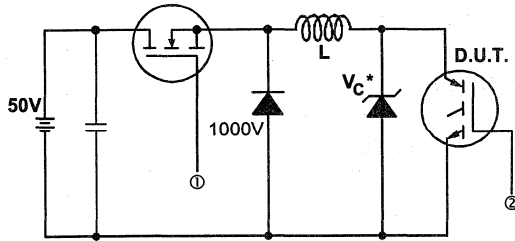
D

Appendix

Table of Contents

Appendices			
Appendix	Device Type	Voltage	Page No.
A	Discrete	500V	D-2
B	Co-Packs	500V	D-3
C	Discrete	600V	D-4
D	Co-Packs / IMS Modules	600V	D-5
E	Modules	600V	D-6
F	Discrete	900V	D-7
G	Discrete	1200V	D-8
H	Co-Packs	1200V	D-9
I	Modules	1200V	D-10

Case Outlines			
Case Outline Number	Case Style	Description	Page No.
1	TO-220AB		D-12
2	SMD-220		D-12
3	TO-247AC		D-13
4	IMS-1		D-13
5	IMS-2		D-14
6	INT-A-PAK	Old Low Side Switch	D-14
7	INT-A-PAK	New Low Side Switch	D-15
8	INT-A-PAK	Old High Side Switch	D-15
9	INT-A-PAK	New High Side Switch	D-16
10	INT-A-PAK	Old Half Bridge	D-16
11	INT-A-PAK	New Half Bridge	D-17
12	Double INT-A-PAK	New Half Bridge	D-17
13	Double INT-A-PAK	Single Switch Diode	
		Single Switch Complementary Diode	D-18
	SMD-220	Tape and Reel	D-18



* Driver same type as D.U.T.; $V_c = 80\%$ of $V_{ce(max)}$
 * Note: Due to the 50V power supply, pulse width and inductor will increase to obtain rated I_d .

Fig. 13a - Clamped Inductive Load Test Circuit

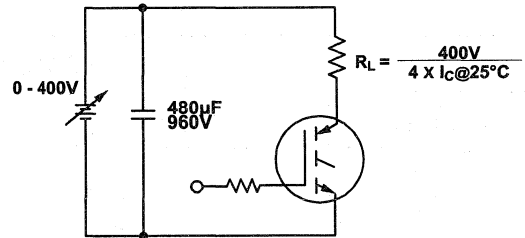


Fig. 13b - Pulsed Collector Current Test Circuit

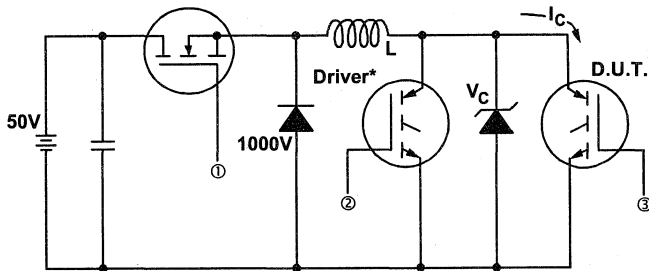


Fig. 14a - Switching Loss Test Circuit

* Driver same type as D.U.T., $V_c = 400V$

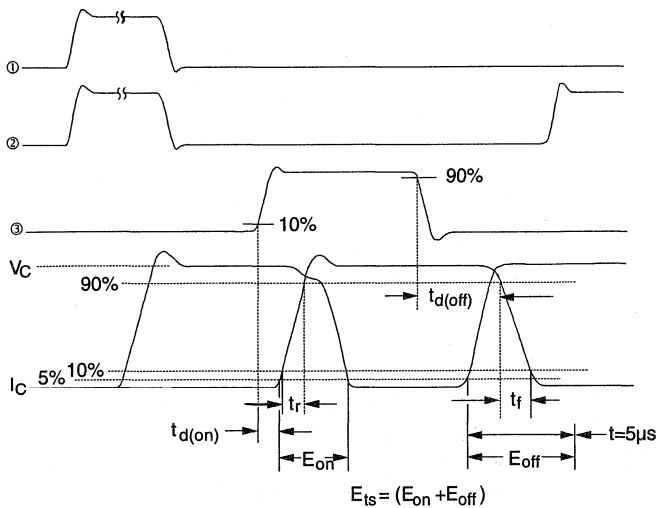


Fig. 14b - Switching Loss Waveforms

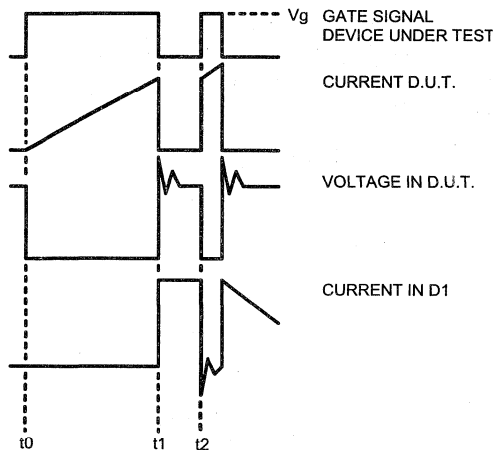


Fig. 18e - Macro Waveforms for Test Circuit of Fig. 18a

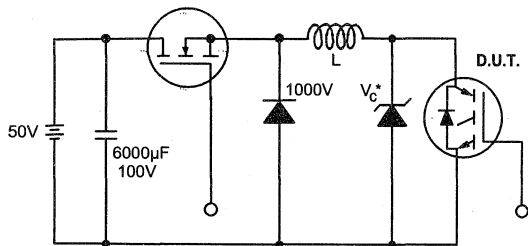


Fig. 19 - Clamped Inductive Load Test Circuit

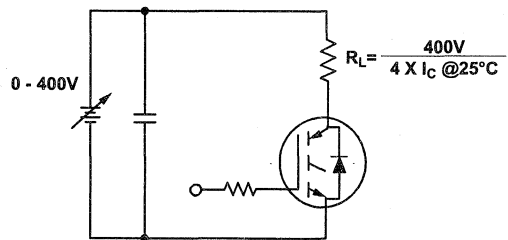
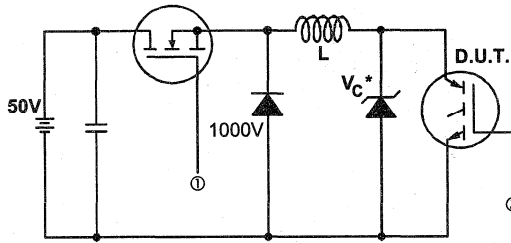


Fig. 20 - Pulsed Collector Current Test Circuit



* Driver same type as D.U.T.; $V_c = 80\%$ of $V_{ce(max)}$
 * Note: Due to the 50V power supply, pulse width and inductor will increase to obtain rated Id.

Fig. 13a - Clamped Inductive Load Test Circuit

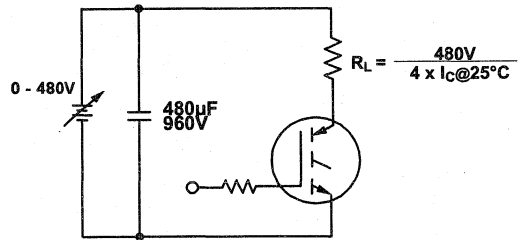


Fig. 13b - Pulsed Collector Current Test Circuit

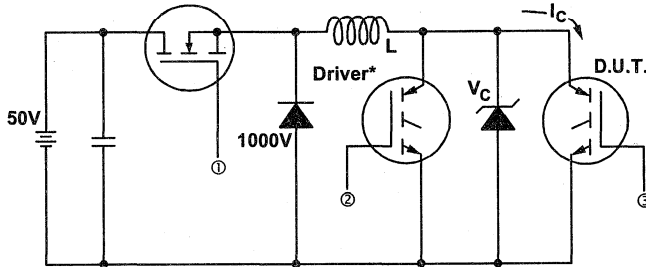


Fig. 14a - Switching Loss Test Circuit

* Driver same type as D.U.T., $V_c = 480V$

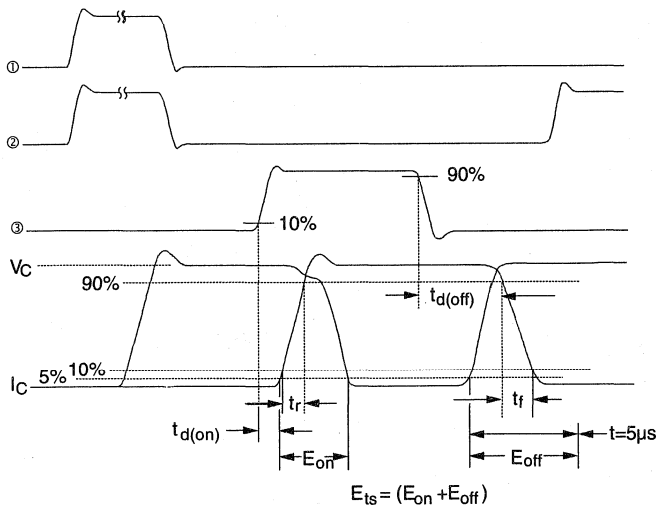


Fig. 14b - Switching Loss Waveforms

Appendix C - 600V Discretes

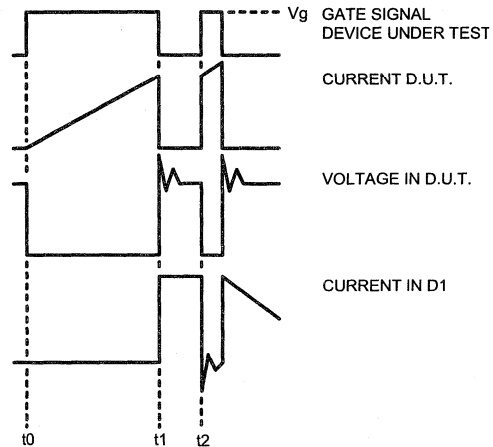


Fig. 18e - Macro Waveforms for Test Circuit of Fig. 18a

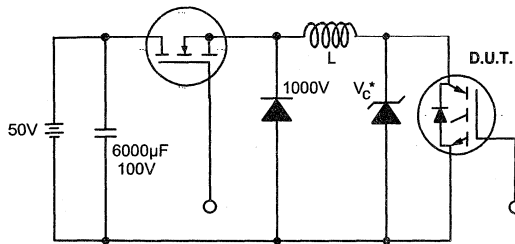


Fig. 19 - Clamped Inductive Load Test Circuit

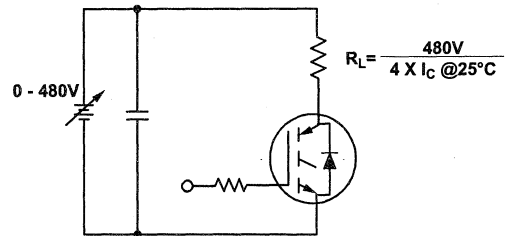


Fig. 20 - Pulsed Collector Current Test Circuit

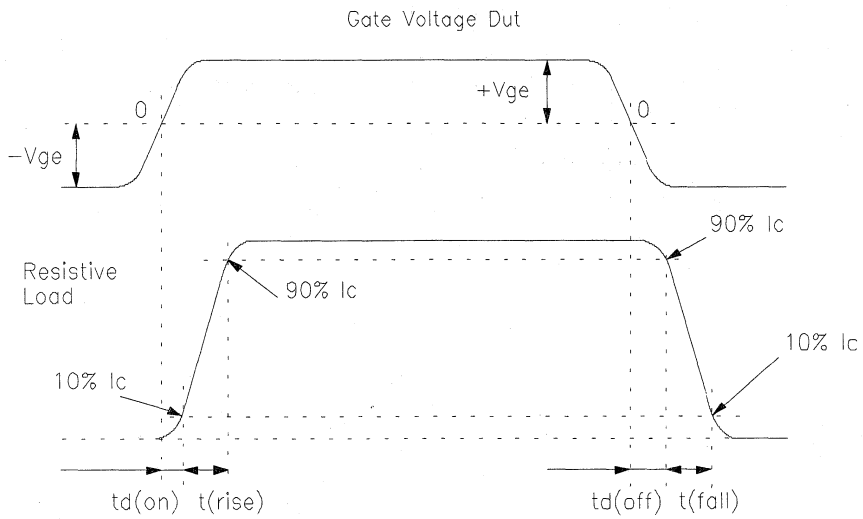


Fig. 19 - Waveforms for Switching Time

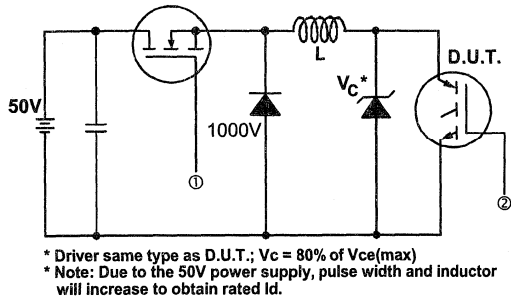


Fig. 13a - Clamped Inductive Load Test Circuit

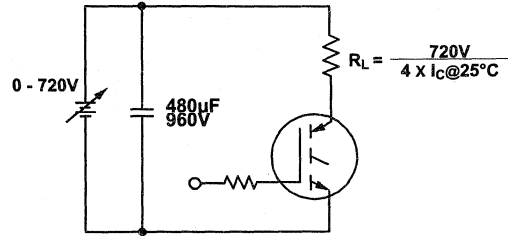


Fig. 13b - Pulsed Collector Current Test Circuit

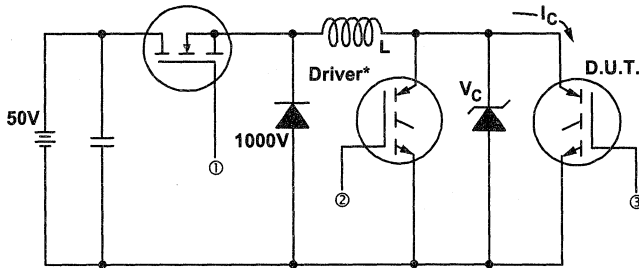


Fig. 14a - Switching Loss Test Circuit

* Driver same type as D.U.T., $V_c = 720V$

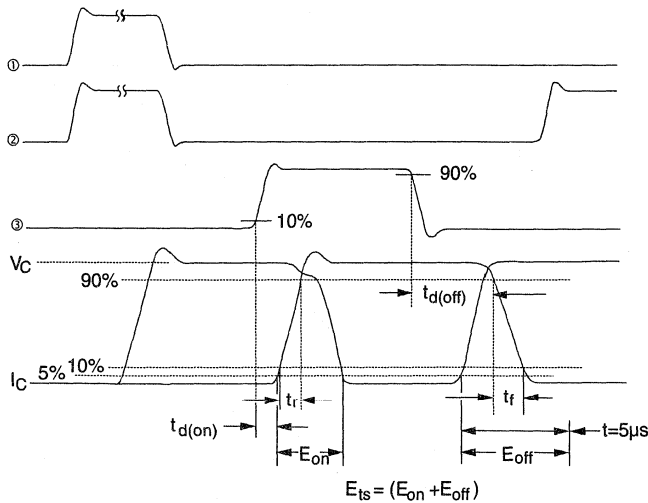
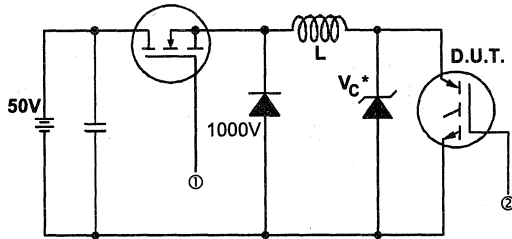


Fig. 14b - Switching Loss Waveforms



* Driver same type as D.U.T.; $V_c = 80\%$ of $V_{ce(max)}$
 * Note: Due to the 50V power supply, pulse width and inductor will increase to obtain rated I_d .

Fig. 13a - Clamped Inductive Load Test Circuit

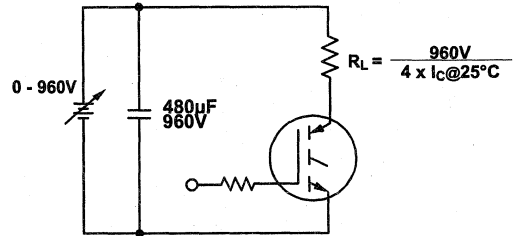


Fig. 13b - Pulsed Collector Current Test Circuit

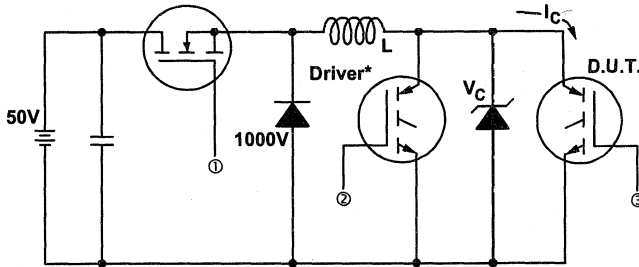


Fig. 14a - Switching Loss Test Circuit

* Driver same type as D.U.T., $V_C = 960V$

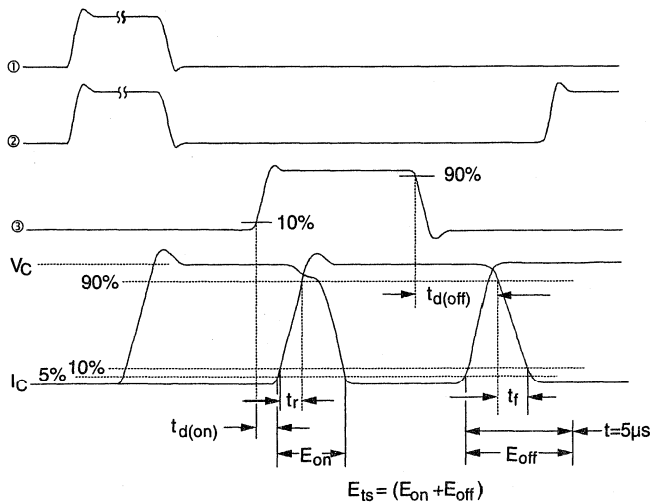


Fig. 14b - Switching Loss Waveforms

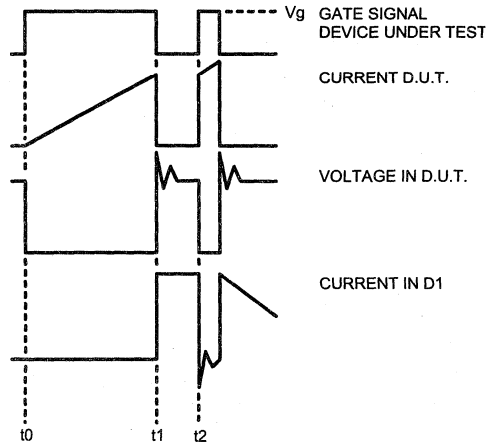


Fig. 18e - Macro Waveforms for Test Circuit of Fig. 18a

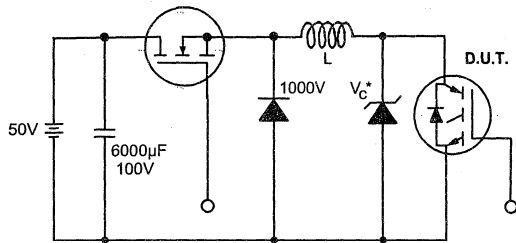


Fig. 19 - Clamped Inductive Load Test Circuit

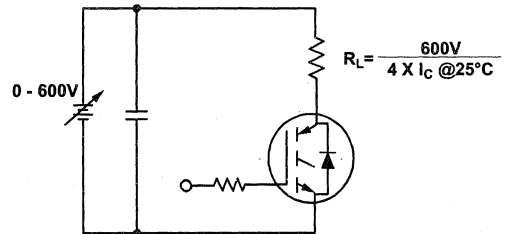


Fig. 20 - Pulsed Collector Current Test Circuit

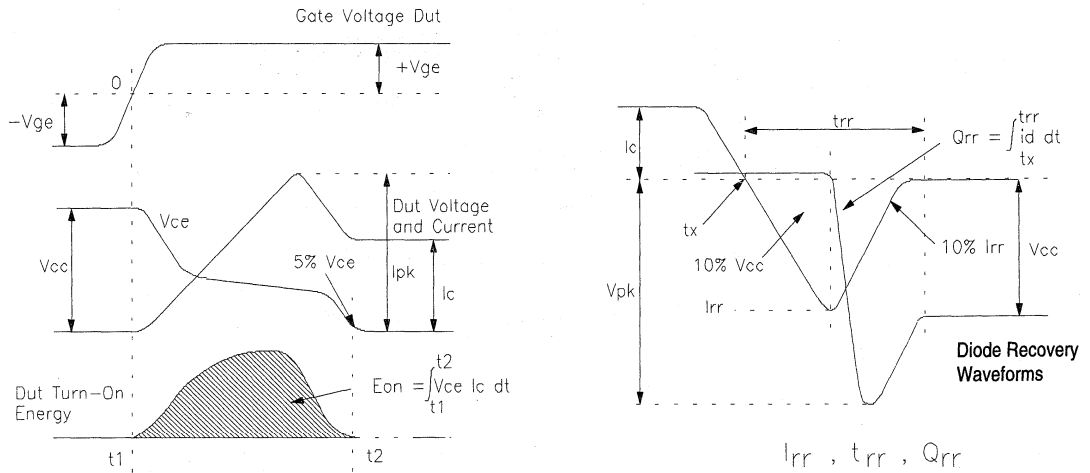


Fig. 19 - Test Waveforms for Circuit of Fig. 17, Defining E_{ON} , E_{REC} , Q_{RR}

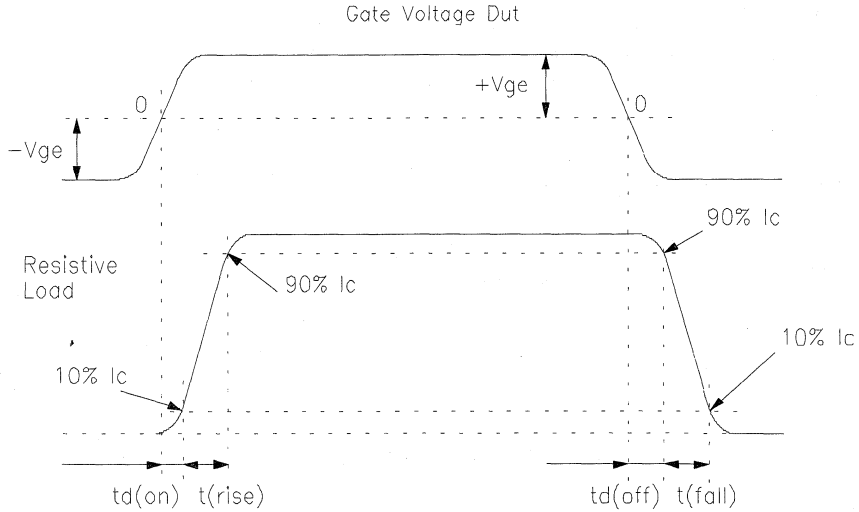
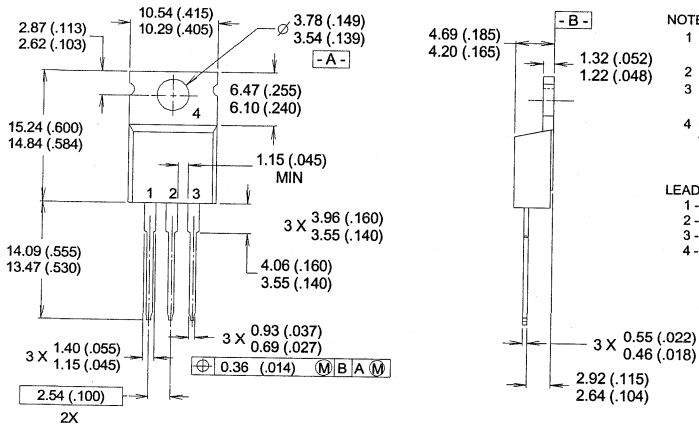


Fig. 20 - Waveforms for Switching Time

Case Outline 1 - TO-220AB

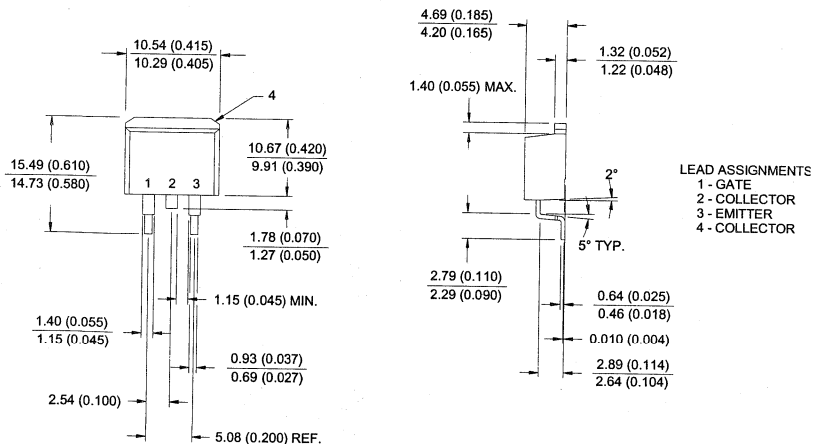


- NOTES:
- 1 DIMENSIONS & TOLERANCING PER ANSI Y14.5M, 1982.
 - 2 CONTROLLING DIMENSION : INCH.
 - 3 DIMENSIONS ARE SHOWN MILLIMETERS (INCHES).
 - 4 CONFORMS TO JEDEC OUTLINE TO-220AB.

- LEAD ASSIGNMENTS
- 1 - GATE
 - 2 - COLLECTOR
 - 3 - EMITTER
 - 4 - COLLECTOR

CONFORMS TO JEDEC OUTLINE TO-220AB
Dimensions in Millimeters and (Inches)

Case Outline 2 - SMD-220

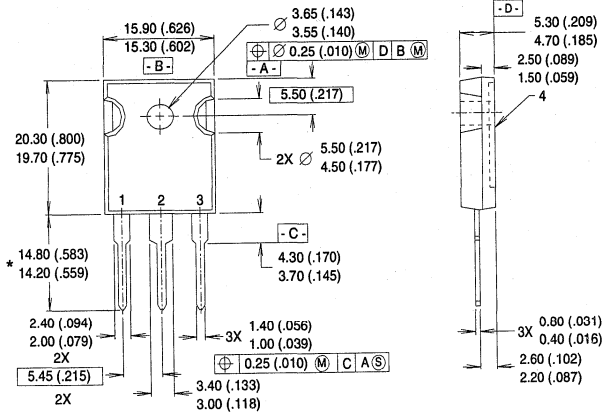


- LEAD ASSIGNMENTS
- 1 - GATE
 - 2 - COLLECTOR
 - 3 - EMITTER
 - 4 - COLLECTOR

OUTLINE SMD-220
Dimensions in Millimeters and (Inches)



Case Outline 3 - TO-247AC (TO-3P)



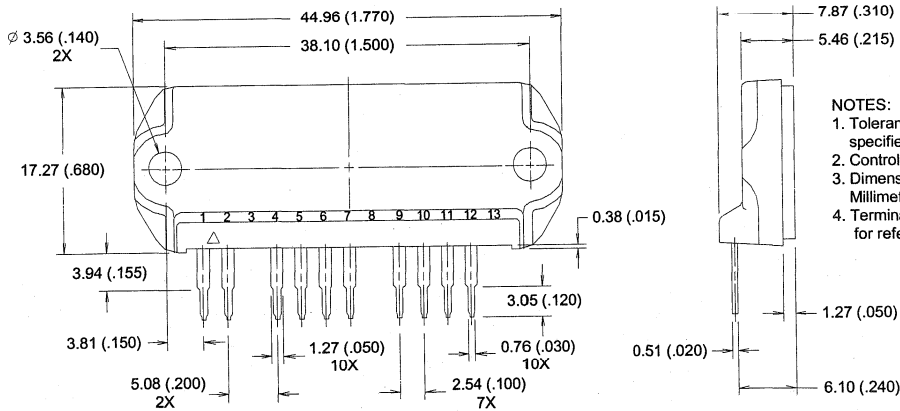
- NOTES:
- 1 DIMENSIONS & TOLERANCING PER ANSI Y14.5M, 1982.
 - 2 CONTROLLING DIMENSION - INCH.
 - 3 DIMENSIONS ARE SHOWN MILLIMETERS (INCHES).
 - 4 CONFORMS TO JEDEC OUTLINE TO-247AC.

- LEAD ASSIGNMENTS
- 1 - GATE
 - 2 - COLLECTOR
 - 3 - EMITTER
 - 4 - COLLECTOR

* LONGER LEADED (20mm) VERSION AVAILABLE (TO-247AD) TO ORDER ADD "E" SUFFIX TO PART NUMBER

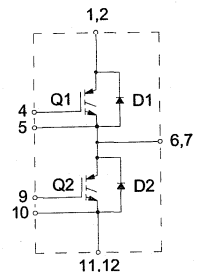
CONFORMS TO JEDEC OUTLINE TO-247AC (TO-3P)
Dimensions in Millimeters and (Inches)

Case Outline 4 - IMS-1

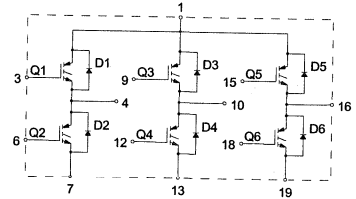
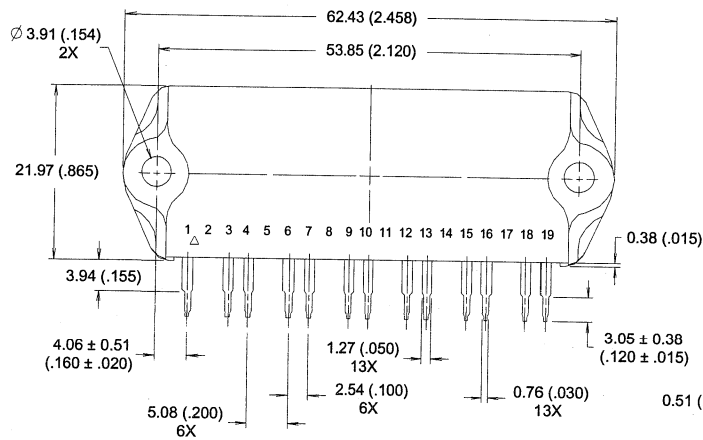


- NOTES:
1. Tolerance unless otherwise specified $\pm 0.254 (.010)$.
 2. Controlling Dimension: Inch.
 3. Dimensions are shown in Millimeter (Inches).
 4. Terminal numbers are shown for reference only.

IMS-1 Package Outline (10 Pins)
Dimensions in Millimeters and (Inches)



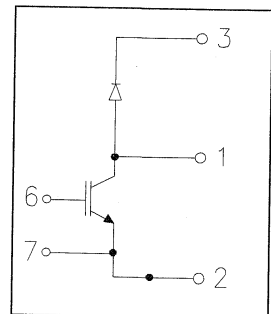
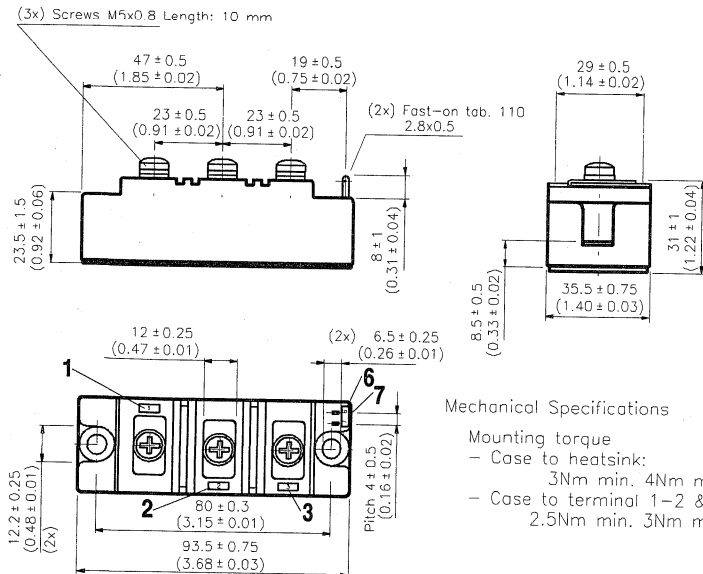
Case Outline 5 - IMS-2



- NOTES:
1. Tolerance unless otherwise specified $\pm 0.254 (.010)$.
 2. Controlling Dimension: Inch.
 3. Dimensions are shown in Millimeter (Inches).
 4. Terminal numbers are shown for reference only.

IMS-2 Package Outline (13 Pins)
 Dimensions in Millimeters and (Inches)

Case Outline 6 - INT-A-PAK Old Low SideSwitch



Mechanical Specifications

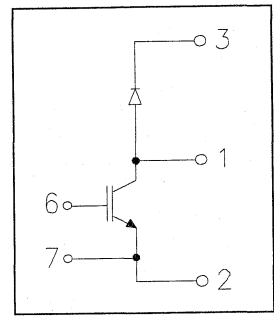
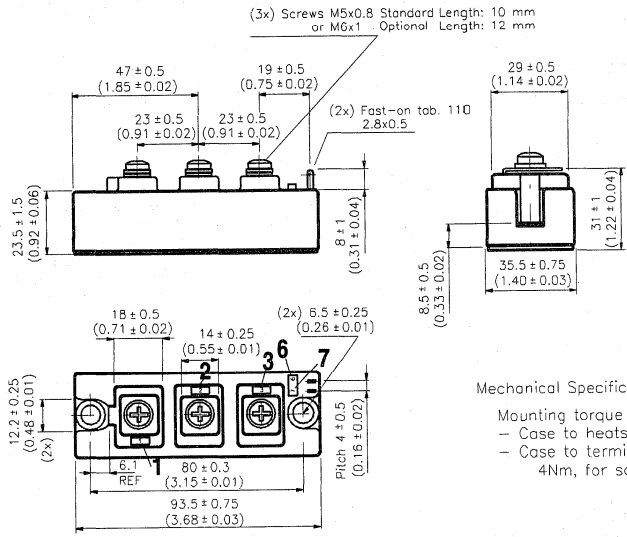
- Mounting torque
- Case to heatsink: 3Nm min. 4Nm max.
 - Case to terminal 1-2 & 3: 2.5Nm min. 3Nm max.

Numbers in bold indicate pin assignments

All dimensions in millimeters (inches)



Case Outline 7 - INT-A-PAK New Low Side Switch

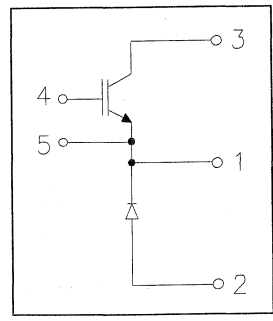
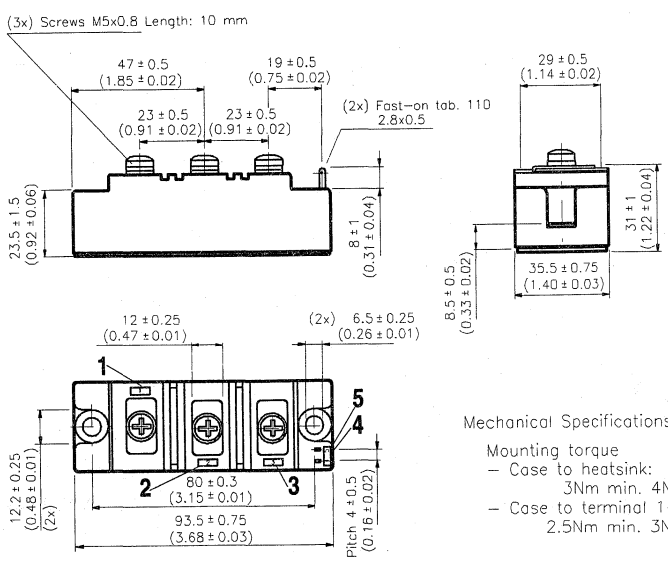


Numbers in bold indicate pin assignments

Mechanical Specifications
 Mounting torque
 - Case to heatsink: 5Nm
 - Case to terminal 1-2 & 3: 4Nm, for screws M5x0.8

All dimensions in millimeters (inches)

Case Outline 8 - INT-A-PAK Old High Side Switch



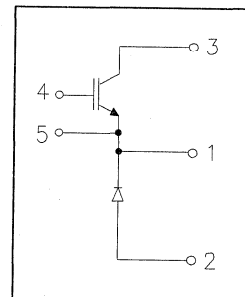
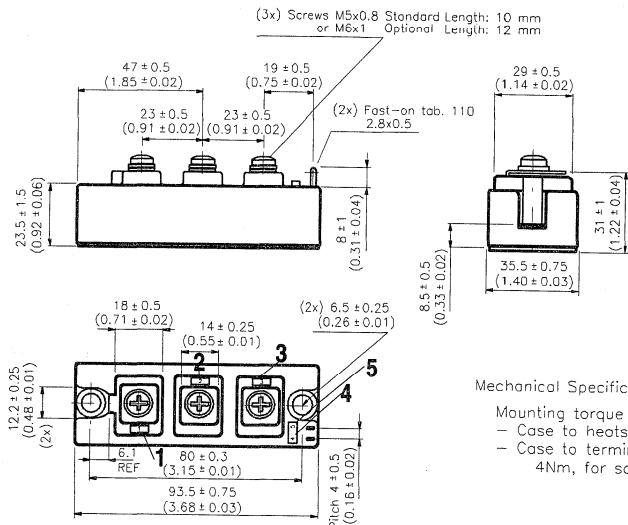
Numbers in bold indicate pin assignments

Mechanical Specifications
 Mounting torque
 - Case to heatsink: 3Nm min. 4Nm max.
 - Case to terminal 1-2 & 3: 2.5Nm min. 3Nm max.

All dimensions in millimeters (inches)



Case Outline 9 - INT-A-PAK New High Side Switch



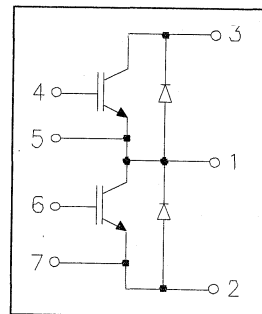
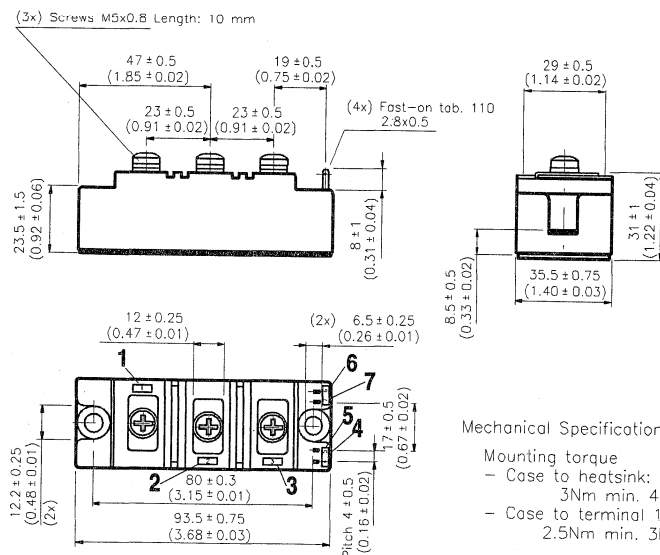
Numbers in bold indicate pin assignments

Mechanical Specifications

- Mounting torque
- Case to heatsink: 5Nm
 - Case to terminal 1-2 & 3: 4Nm, for screws M5x0.8

All dimensions in millimeters (inches)

Case Outline 10 - INT-A-PAK Old Half Bridge



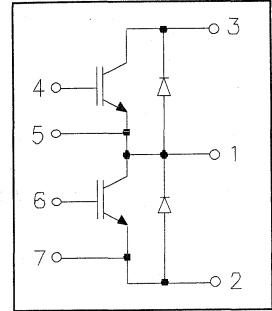
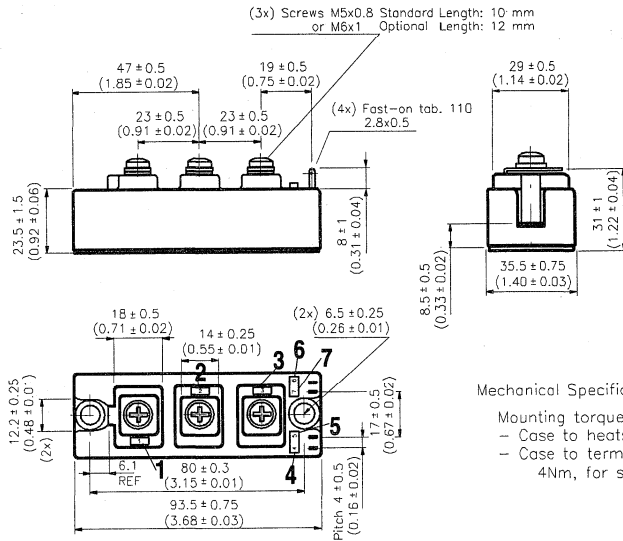
Numbers in bold indicate pin assignments

Mechanical Specifications

- Mounting torque
- Case to heatsink: 3Nm min. 4Nm max.
 - Case to terminal 1-2 & 3: 2.5Nm min. 3Nm max.

All dimensions in millimeters (inches)

Case Outline 11 - INT-A-PAK New Half Bridge



Numbers in bold indicate pin assignments

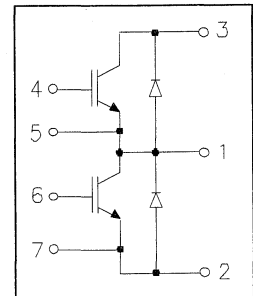
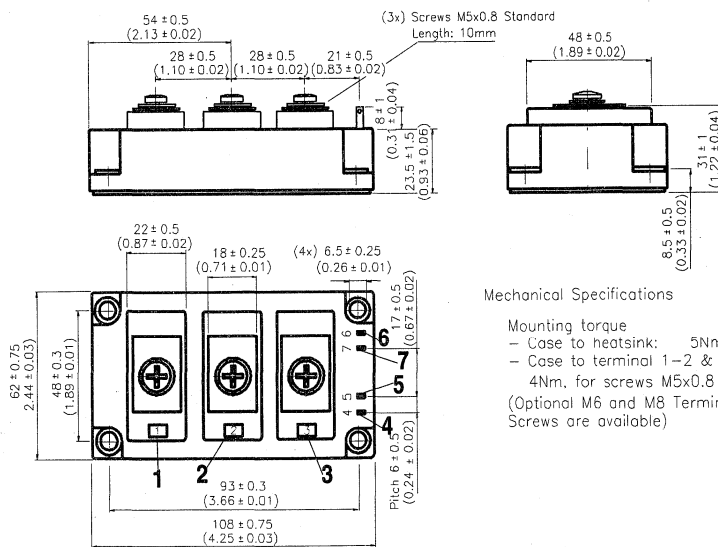
Mechanical Specifications

Mounting torque

- Case to heatsink: 5Nm
- Case to terminal 1-2 & 3: 4Nm, for screws M5x0.8

All dimensions in millimeters (inches)

Case Outline 12 -Double INT-A-PAK New Half Bridge



Numbers in bold indicate pin assignments

Mechanical Specifications

Mounting torque

- Case to heatsink: 5Nm
 - Case to terminal 1-2 & 3: 4Nm, for screws M5x0.8
- (Optional M6 and M8 Terminal Screws are available)

All dimensions in millimeters (inches)

IGBT Designer's Manual

Application Information

Other Information

Application
Information

E

Application
Information

IGBT Designer's Manual

IGBT Characteristics

(HEXFET is a trademark of International Rectifier)

by S. Clemente, A. Dubhashi, B. Pelly

Summary

This application note describes International Rectifier's Insulated Gate Bipolar Transistors (IGBTs).

Section I describes the characteristics of the device, its technology and the key trade-offs in its design, comparing it to MOSFETs and bipolar transistors.

Section II reviews the data sheet and explains the terms and test methods used to characterize the IGBT.

Section III contains an overview of the three families of IGBTs available from International Rectifier.

The major issues normally encountered in the design of an IGBT power conditioning circuit are covered in a companion application note AN-990, "Application Characterization of IGBTs."

Introduction

Switching speed, peak current capability, ease of drive, wide SOA, avalanche and dv/dt capability have made power MOSFETs the logical choice in new power electronic designs. These advantages, a natural consequence of being majority carrier devices, are partly mitigated by their conduction characteristics which are strongly dependent on temperature and voltage rating.

Furthermore, as the voltage rating goes up, the inherent reverse diode displays increasing Q_{RR} and T_{RR} which leads to increasing switching losses.

IGBTs on the other hand, being minority carrier devices, have superior conduction characteristics, while sharing many of the appealing features of power MOSFETs such as ease of drive, wide SOA, peak current capability and ruggedness. Generally speaking, the switching speed of an IGBT is inferior to that of power MOSFETs. However, as will be shown in Section III, a new line of IGBTs from International Rectifier has switching characteristics that are very close to those of power MOSFETs, without sacrificing the much superior conduction characteristics.

The absence of the integral reverse diode gives the user the flexibility of choosing an external fast recovery diode to match a specific requirement. This feature can be an advantage or a disadvantage, depending on the frequency of operation, cost of diodes, current requirement, etc.

The purpose of this application note is to provide the design engineer with a comprehensive understanding of this new class of devices, with special reference to those provided by International Rectifier.

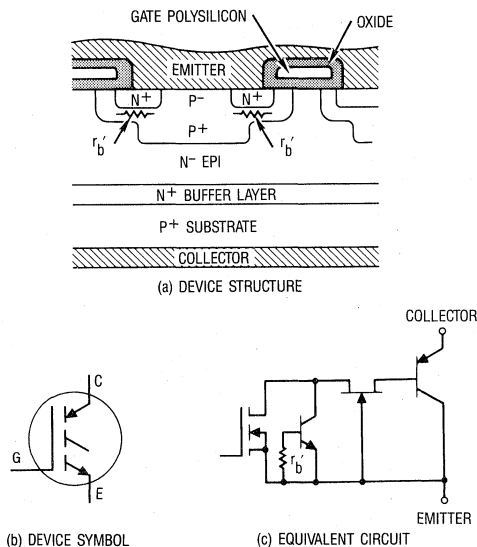


Figure 1. Silicon cross-section of an IGBT with its equivalent circuit and symbol (N-Channel, enhancement mode). The terminal called *collector* is, actually, the *emitter* of the PNP. In spite of its similarity to the cross-section of a power MOSFET, operation of the two transistors is fundamentally different, the IGBT being a minority carrier device.

Section I: The IGBT Technology and Characteristics

Except for the P+ substrate, the silicon cross-section of an IGBT (Figure 1) is virtually identical to that of a power MOSFET. Both devices share a similar polysilicon gate structure and P wells with N+ source contacts. In both devices the N-type material under the P wells is sized in thickness and resistivity to sustain the full voltage rating of the device.

However, in spite of the many similarities, the physical operation of the IGBT is closer to that of a bipolar transistor than to that of a power MOSFET. This is due to the P+ substrate which is responsible for the minority carrier injection into the N-region and the resulting conductivity modulation. In a power MOSFET, which does not benefit from conductivity modulation, a significant share of the conduction losses occur in the N-region, typically 70% in a 500V device.

As shown in the equivalent circuit of Figure 1, the IGBT consists of a PNP driven by an N-Channel MOSFET in a pseudo-Darlington configuration. The JFET supports most of the voltage and allows the MOSFET to be a low voltage type, and consequently have a low $R_{DS(on)}$.

The base region of the PNP is not brought out and the emitter-base PN junction, spanning the entire extension of the wafer cannot be terminated nor passivated. This influences the turn-off and reverse blocking behavior of the IGBT, as will be explained later. The breakdown voltage of this junction is about 20V and is shown in the IGBT symbol as an unconnected terminal (Figure 1).

A. Conduction Characteristics

As it is apparent from the equivalent circuit, the voltage drop across the IGBT is the sum of two components: a diode drop across the P-N junction and the voltage drop across the driving MOSFET. Thus, unlike the power MOSFET, the on-state voltage drop across an IGBT never goes below a diode threshold. The voltage drop across the driving MOSFET, on the other hand, has one characteristic that is typical of all low voltage MOSFETs: it is sensitive to gate drive voltage. This is apparent from Figures 12 and 13 where, for currents that are close to their rated value, an increase in gate voltage causes a reduction in collector-to-emitter voltage. This is due to the fact that, within its operating range, the gain of the PNP increases with current and an increase in gate voltage causes an increase in channel current, hence a reduction in voltage drop across the PNP. This is quite different from the behavior of a high voltage power MOSFET that is largely insensitive to gate voltage.

As the final stage of a pseudo-Darlington, the PNP is never in heavy saturation and its voltage drop is higher than what could be obtained from the same PNP in heavy saturation. It should be noted, however, that the emitter of an IGBT covers the entire area of the die, hence its injection efficiency and conduction drop are much superior to that of a bipolar transistor of the same size.

Two options are available to the device designer to decrease the conduction drop:

1. Reduce the on-resistance of the MOSFET. This can be done by increasing the die size and/or the packing density. Both have a negative impact on yield and cost.
2. Increase the gain of the PNP. As explained later, this option is limited by latch-up considerations.

International Rectifier has pursued the optimization of the MOSFET component of the IGBT to the point where its devices can be correctly referred to as a "conductivity modulated MOSFET" with its characteristic features of high speed, low voltage drop and efficient silicon utilization. Other semiconductor companies, on the other hand, have concentrated on the optimization of the bipolar part and the resulting product should be more correctly referred to as a "MOSFET-driven transistor" with a different set of characteristics.

The dramatic impact of conductivity modulation on voltage drop can be seen from Figure 2 which compares a HEXFET power MOSFET and an IGBT of the same die size. Temperature dependence, very significant in a power MOSFET, is minimal in an IGBT, just enough to ensure current sharing of paralleled devices at high current levels under steady state conditions, as shown in Figure 14 for the IRGBC20U. This same figure shows that the temperature dependence of the voltage drop is different

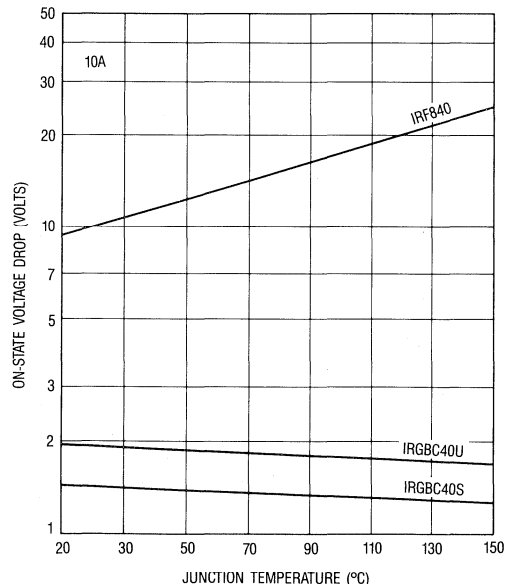


Figure 2. On-state voltage drop vs temperature of two IGBTs of different switching characteristics compared to those of a HEXFET of the same die size (IRGBC40S and IRGBC40U vs IRF840).

Conductivity modulation causes a dramatic improvement in the on-state voltage drop. To take the avalanche capability of the HEXFET into account, a 500V device is compared with 600V IGBTs.

at different current levels. This is because the diode component of this drop has a temperature coefficient that is initially negative becoming positive at higher current levels. The MOSFET component, on the other hand, is positive. The problem is made more complex by the fact that these two components are weighted differently at different current and temperatures.

In addition to reducing the voltage drop and its temperature coefficient, conductivity modulation virtually eliminates its dependence on the voltage rating. This is shown in Table I, where the conduction drops of four IGBTs of different voltage ratings are compared with those of HEXFETs at the same current density¹.

Table I: Dependence of Voltage Drop From Voltage Rating

Rated Voltage	IGBT	100	300	600	1200
	HEXFET	100	250	500	1000
Typical Voltage Drop @ 1.7A/mm ² , 100°C	IGBT	1.5	2.1	2.4	3.1
	HEXFET	2.0	11.2	26.7	100

The voltage rating of the HEXFET power MOSFETs used in this comparison are lower than the IGBTs to take into account their avalanche capability.

The voltage drop of a conductivity modulated device with minority lifetime killing may exhibit a peculiar behavior frequently referred to as ‘switchback’: the voltage drop at low current and low temperature is higher than expected, suddenly dropping to its expected value if current or temperature are increased. The term comes from the fact that, when using the step generator in a curve tracer, the trace suddenly ‘switches’ to the left of the screen as the gate voltage is increased.

This behavior is ascribed to lifetime killing which, in so far as it facilitates recombination, delays the onset of conductivity modulation. Hence, the voltage drop for current levels below conductivity modulation is higher than for a somewhat higher collector current, after conductivity modulation is established. This phenomenon is one of the causes of the ‘‘forward recovery’’ of fast (reverse recovery) diodes and of higher values of latching current in minority lifetime killed thyristors.

A trace of this phenomenon can be seen in the ‘‘bump’’ in the $V_{CE(sat)}$ portion of Figure 12. Notice that the bump disappears in Figure 13 because temperature increases the lifetime of the charges and speeds up the onset of conductivity modulation. Notice, also, that only the Ultrafast IGBTs exhibit this phenomenon, because of higher levels of lifetime killing.

B. Switching Characteristics

The biggest limitation to the turn-off speed of an IGBT is the lifetime of the minority carriers in the N- epi, i.e., the base of the PNP. Since this base is not accessible, external drive circuitry cannot be used to improve the

switching time. It should be remembered, though, that since the PNP is in a pseudo-Darlington connection, it has no storage time and its turn-off time is much better than the same PNP in heavy saturation. Even so, it may still be inadequate for many high frequency applications.

The charges stored in the base cause the characteristic ‘‘tail’’ in the current waveform of an IGBT at turn-off (Figure 3). As the MOSFET channel stops conducting, electron current ceases and the IGBT current drops rapidly to the level of the hole recombination current at the inception of the tail. This tail increases turn-off losses and requires an increase in the deadtime between the conduction of two devices in a half-bridge.

Traditional lifetime killing techniques and/or an N+ buffer layer to collect the minority charges at turn-off are commonly used to speed-up recombination time. Insofar as they reduce the gain of the PNP, these techniques increase the voltage drop. Pushed to the extreme, minority lifetime killing causes a quasi-saturation condition at turn-on, as shown in Figure 4, where the turn-on losses have become larger than the turn-off losses.

Thus, the gain of the PNP is constrained by conduction and turn-on losses on one hand, and by latching considerations on the other, as explained in the next section.

Like all minority carrier devices, the switching performance of an IGBT degrades with temperature. As can be seen in Figure 18, this phenomenon is less significant at high current levels.

IGBTs operated in zero current switching may exhibit quasi-saturation losses at turn-on that are somewhat higher than in switchmode circuits. The low di/dt that is characteristic of this mode of operation emphasizes the ‘‘switchback’’ phenomenon described in the previous section.

Similarly, with zero-voltage turn-off, the IGBT may experience a short burst of current if the complementary device is turned on soon after the current has ceased in the one that was conducting. This is due to the fact that the turn-on of the complementary device causes the supply voltage to appear across the first IGBT, thereby depleting its base region and causing a final sweep-out of the minority carriers that were still left there.

C. Latching

As shown in the cross-section of Figure 1, the IGBT is made of four alternate P-N-P-N layers. Given the necessary conditions ($\alpha_{NPN} + \alpha_{PNP} > 1$) the IGBT could latch-up like a thyristor.

The N+ buffer layer and the wide epi base reduce the gain of the PNP, while the gain of the NPN, which is the

¹Several papers make reference to a voltage dependence of the $R_{DS(on)}$ of a power MOSFET of the following type:

$$R = R_0 V^\alpha$$

with $\alpha = 2.5$, i.e., the on-resistance increases with the voltage rating at a higher

rate than a square law. In reality, assuming that a power law is a true representation of the underlying physical phenomena, the correct value would be ≈ 1.6 , as can be easily verified from the data sheets of any manufacturer. These data sheets will also contradict the common misconception that power MOSFETs have better silicon utilization at low voltage. In actual fact they achieve their highest power handling capability per unit area between 400V and 600V.

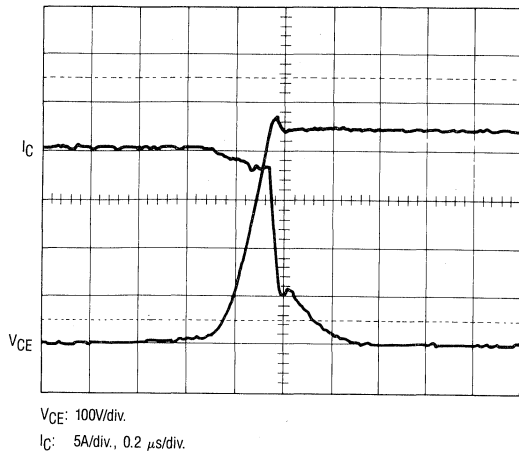


Figure 3. Turn-off waveform of a commercial IGBT at 25°C, rated current. Notice the clean break at the inception of the “tail”. Switching circuit as in Figure 16.

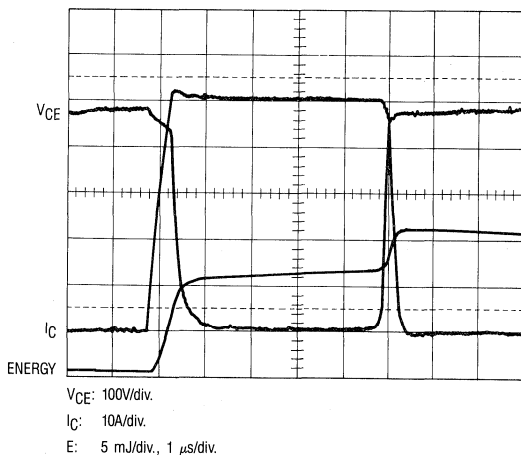


Figure 4. Switching waveforms of a commercially available IGBT with heavy lifetime killing. It takes approximately 0.5 μ s for the voltage to drop the last 50V. The energy plot shows that the losses at turn-on are twice as high as those at turn-off. Switching circuit as in Figure 16.

parasitic bipolar of the MOSFET, can be reduced with the same techniques [1] that are commonly employed to give HEXFETs their avalanche and dv/dt capability, mainly a drastic reduction of the r'_b . If this r'_b is not adequately reduced, “dynamic latching” could occur at turn-off when a high density of hole current flows in r'_b , taking the gain of the parasitic NPN to much higher values.

Latching should not occur under any of the operating conditions of current, temperature and dv/dt that the device may see within its rated limits of operation. IGBTs from International Rectifier are guaranteed not to latch at the maximum current that can be sustained with $V_{gs} = 20V$, $T_j = 150^\circ C$ and the highest dv/dt the device is capable of. At the same time, since a PNP with higher gain reduces conduction losses, International Rectifier has been careful not to reduce it beyond what is necessary for safe and reliable operation at the data sheet limits.

D. Safe Operating Area

The safe operating area (SOA) describes the capability of a transistor to withstand significant levels of voltage and current at the same time. The three main conditions that would subject an IGBT to this combined stress are the following:

1. Operation in short circuit. The current in the IGBT is limited by its gate voltage and transconductance and can reach values well in excess of 10 times its continuous rating. The level of hole current that flows underneath the N+ source contact can cause a drop across r'_b , large enough to turn on the NPN parasitic bipolar with possible latching. This is normally prevented by a reduction in r'_b , as mentioned in the previous section or by a reduction of the total device transconductance (essentially the gain of the PNP). This second technique increases conduction losses and reduces switching speed.

Lower power dissipation was deemed a more desirable feature than short circuit capability, particularly considering that simple protection circuitry can be added to the gate drive to protect the IGBT in those applications where a short circuit is a likely event.

2. Inductive turn-off, sometimes referred to as “clamped I_L .” In an inductive turn-off the voltage swings from a few volts to the supply voltage with constant current and with no channel current. These conditions are different from those described in the previous section in so far as the load current is totally made up of holes flowing through r'_b . For this reason some manufacturers suggest the use of gate drive resistors to slow down the turn-off dv/dt and maintain some level of electron current, thereby avoiding a potential “dynamic latching” condition. IGBTs from International Rectifier can be operated at their maximum switching speed without any problem. Reasons to limit the switching speed should be external to the device (e.g., overshoots due to stray inductance), rather than internal.

3. Operation as a linear amplifier. Linear operation exercises the SOA of the IGBT in a combination of the two modes described above, but in a less severe fashion. A device that is designed to withstand those stresses will be more than suited to operate as a linear amplifier. No second breakdown has been observed in IGBTs from International Rectifier in any mode of operation within the data sheet limit.

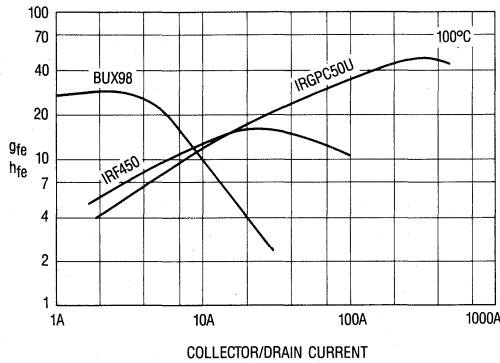


Figure 5. Current dependence of the transconductance of an IGBT compared to that of a HEXFET and to the gain of a bipolar of approximately the same die size. The IGBT, like the power MOSFET, is not "gain limited."

E. Transconductance

The current handling capability of a semiconductor can be limited by thermal constraints or by gain/transconductance constraints. While the "headline current rating" of power semiconductors is based solely on thermal considerations, it is entirely possible, as is frequently the case with bipolar transistors, that the device cannot operate at the current level it is thermally capable of, because its gain has fallen to very low values. As shown in Figure 5, the transconductance of an IGBT tops out at current levels that are well beyond its thermal capability, while the gain of a bipolar of similar die size is on a steep downslope within its current operating range.

The flattening out of transconductance occurs when the saturation effects in the MOSFET channel, that reduce the base current of the PNP, combine with the flattening of the gain of the PNP. Since temperature reduces the MOSFET channel current more than it increases the gain of the PNP, the saturation in transconductance occurs at lower current as the temperature increases.

Since lifetime killing reduces the gain of the PNP, the transconductance of fast IGBTs peaks at a lower level than those without lifetime killing. This, however, is a second order effect because the gain of the PNP is determined mainly by the N+ buffer layer.

The decrease in transconductance at very high current and its additional decrease with temperature helps protect the IGBT under short circuit conditions. With a gate voltage of 15V, the current density of a standard IGBT from International Rectifier reaches values of 10-20A/mm² in short circuit. This high transconductance is partly responsible for their superior switching and conduction characteristics.

Section II: The Data Sheet

International Rectifier prides itself on having one of the most comprehensive IGBT data sheets in the industry, with all the information required to operate the IGBT reliably. However, like all technical documents it requires a good understanding by the user of the different terms and conditions. These are briefly explained in the following sections.

A. The Headline Information

In addition to the mechanical layout, the front page gives the voltage and current ratings. The current rating is the industry standard dc current capability of the device with the case being maintained at 25°C.

The part number itself contains in coded form the key features of the IGBT. An explanation of the nomenclature is contained in Figure 6.

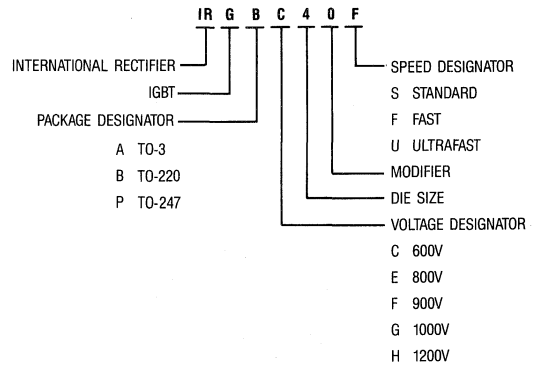


Figure 6. Simplified nomenclature code for commercial IGBTs from International Rectifier.

B. The Absolute Maximum Ratings

This table sets up a number of constraints on device operation that apply under any circumstance.

Continuous Collector Current @ $T_C = 25^\circ\text{C}$ and 100°C (I_C). This represents the dc current level that will take the junction to its rated temperature from the stipulated case temperature. It is calculated with the following formula:

$$I_C = \frac{\Delta T}{\theta_{j-c} \cdot V_{CE(on)} @ I_C}$$

where ΔT is the temperature rise from the stipulated case temperature to the maximum junction temperature $(150^\circ\text{C})^2$.

²Notice that $V_{CE(on)} @ I_C$ is not known because I_C is not known. It can be found with few iterations.

It is clear, from this formula, that a current rating has no meaning without a corresponding junction and case temperature. Since in normal applications the case temperature is much higher than 25°C, the associated rating is of no practical value and is only reported because transistors have been traditionally rated in this way. Figure 7 shows how this rating changes with case temperature, with a junction temperature of 150°C, for a specific device.

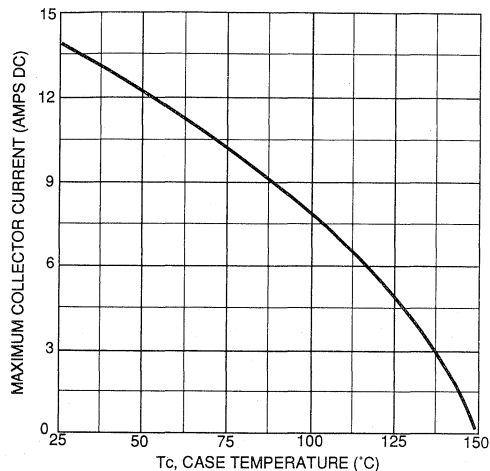


Figure 7. Maximum Collector Current vs. Case Temperature

Pulsed Collector Current (I_{CM}). Within its thermal limits, the IGBT can be used to a peak current well above the rated continuous DC current. The temperature rise during a high current transient can be calculated as indicated in Section IVC. The test circuit is shown in Figure 8.

Collector-to-Emitter Voltage (V_{CE}). Voltage across the IGBT should never exceed this rating, to prevent breakdown of the collector-emitter junction. The breakdown itself is guaranteed in the Table of Electrical Characteristics.

Maximum Gate-to-Emitter Voltage (V_{GE}). The gate voltage is limited by the thickness and characteristics of the gate oxide layer. Though the gate dielectric breakdown is typically around 80 volts, the user is limited to 20V to limit current under fault conditions and to ensure long term reliability.

Clamped Inductive Load Current (I_{LM}). This rating guarantees that the device is able to repetitively turn off the specified current with a clamped inductive load, as encountered in most applications. In fact, the test circuit (Figure 9) exposes the IGBT to the peak recovery current of the free-wheeling diode, which adds a significant component to the turn-on losses (Figure 10).

This rating guarantees a square switching SOA, i.e., that the device can sustain high voltage and high current simultaneously. The I_{LM} rating is specified at 150°C,

80% of the rated voltage and at four times the rated current at $T_C = 25^\circ\text{C}$. This is a simpler and more direct representation of the device capability than the traditional SOA curve that lends itself to many misunderstandings.

Reverse Avalanche Energy (E_{ARV}). This subject is covered in detail in the BV_{ECS} section of the electrical characteristics.

Maximum Power Dissipation @ 25°C and 100°C (P_D). It is calculated with the following formula:

$$P_D = \frac{\Delta T}{\theta_{j-c}}$$

The same comments that were made on the Continuous Collector Current apply to Power Dissipation.

Junction Temperature (T_j): the device can be operated in the industry standard range of -55°C to 150°C respectively.

C. Thermal Resistance

R_{thjc} , R_{thcs} , R_{thja} are needed for the thermal design, as explained in Section IV, C.

D. Electrical Characteristics

The purpose of this section is to provide a detailed characterization of the device so that the designer can predict with accuracy its behavior in a specific application.

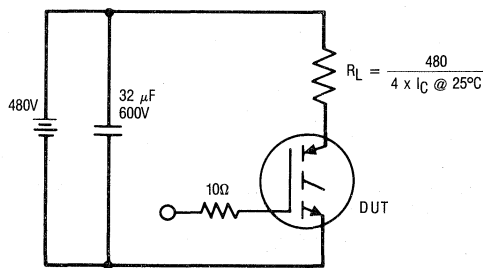


Figure 8. Pulsed Collector Current Test Circuit

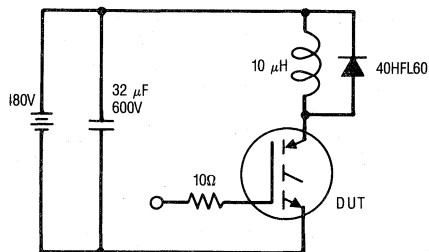
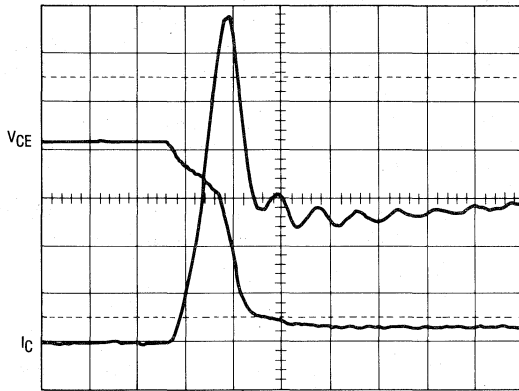


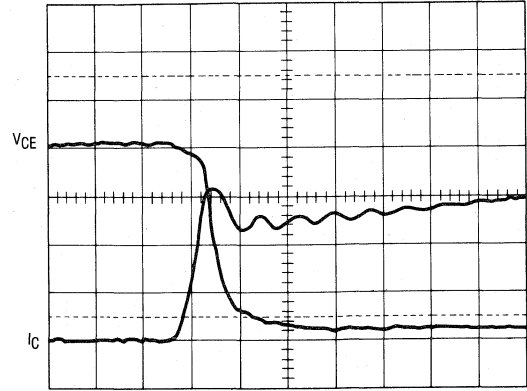
Figure 9. Clamped Inductive Load Test Circuit



V_{CE} : 100V/div.
 I_C : 5A/div., 0.1 μ s/div.

Figure 10a. Turn-on with a clamped inductive load and a fast recovery diode. Test circuit as in Figure 9.

The reverse recovery is a significant contributor to turn-on losses. To discriminate between the losses that are intrinsic to the IGBT and those due to the diode reverse recovery, the test circuit shown in Figure 16 has been used to generate the data sheet values.



V_{CE} : 100V/div.
 I_C : 5A/div., 0.1 μ s/div.

Figure 10b. Turn-on with an ideal diode (zener clamp). Test circuit as in Figure 16.

Collector-to-Emitter Breakdown Voltage (BV_{CES}). This parameter guarantees the lower limit of the distribution in breakdown voltage. Breakdown is defined in terms of a specific leakage current and has a positive temperature coefficient (listed in the table as $BV_{CES}/\Delta T$) of about 0.63V/°C. This implies that a device with 600V breakdown at 25°C would have a breakdown voltage of 550V at -55°C.

Emitter-to-Collector Breakdown Voltage (BV_{ECS}). This rating characterizes the reverse breakdown of the unterminated collector-base junction of the PNP. The relevance of this specification and its associated reverse avalanche energy can be better understood with reference to Figure 11. When an IGBT turns off and current is transferred to the diode across the complementary device, the turn-off di/dt in the stray inductance that is in series with the diode generates a reverse voltage spike across the IGBT (i.e., the collector voltage goes negative with respect to the emitter). This reverse voltage is typically less than 10V, though higher voltages can result from very high di/dt or poor layout. Since this reverse voltage can cause avalanche in the junction, International Rectifier IGBTs have an energy rating, given in the Absolute Maximum Ratings table, that is more useful to the designer than a traditional diode characterization. This rating is typically an order of magnitude more than what would be required by the user.

Collector-to-Emitter Saturation Voltage ($V_{CE(on)}$). Being the key rating to calculate conduction losses, this value is supported by three figures that provide a detailed characterization in temperature, current and gate voltage (Figures 12, 13, and 14 for the IRBGC20U). The Table of Switching Characteristics lists three values at two currents and two temperatures.

Gate Threshold Voltage ($V_{GE(th)}$). This is the range of voltage on the gate at which collector current starts to flow.

The variation in gate threshold with temperature is also specified ($V_{GE(th)}/\Delta T_j$). Typically the coefficient is -11 mV/°C, leading to a reduction of about 1.4V in the threshold voltage at high temperatures.

Forward Transconductance (g_{FE}). This parameter is measured by superimposing a small variation on a gate bias that takes the IGBT to its 100°C rated current in “linear” mode. As mentioned in Section 11, E, transconductance increases significantly with current so

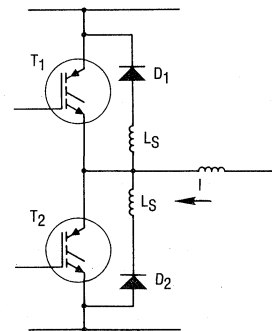


Figure 11. When T_2 goes off, load current flows into the diode in parallel with T_1 . The reverse turn-off di/dt of T_2 develops a voltage across the stray inductance in series with D_1 which reverse biases T_1 . IR's IGBTs have a specified reverse blocking capability (BV_{CES}) and an avalanche rating (ER_V).

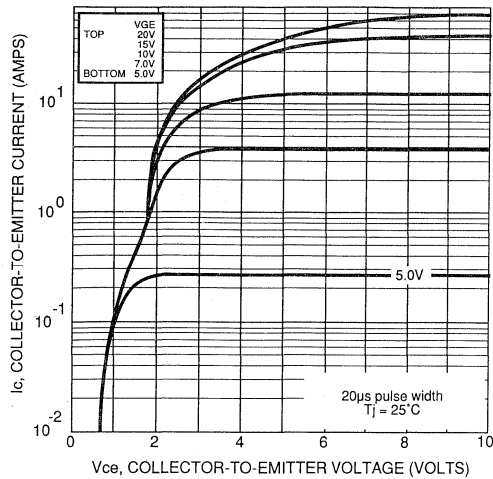


Figure 12. Typical Output Characteristics, $T_C = 25^\circ\text{C}$

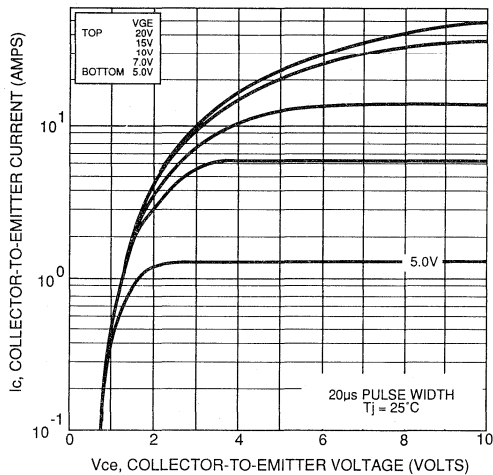


Figure 13. Typical Output Characteristics, $T_C = 150^\circ\text{C}$

that the “current throughput” of an IGBT is not limited by gain, as a bipolar, but by thermal considerations.

Zero-Gate-Voltage Collector Current (I_{CES}). This parameter guarantees the upper limit of the leakage distribution at the rated voltage and two temperatures. It complements the BV_{CES} rating seen above.

E. Switching Characteristics

Gate Charge Parameters (Q_g , Q_{ge} , Q_{gc}). Gate charge values of an IGBT are useful to size the gate drive circuit and estimating gate drive losses. Unfortunately they cannot be used to predict switching times, as for a power MOSFET, because of the minority carrier nature of this device. The test method and the characteristics described in the application note AN-944 [3] for power MOSFETs are also applicable to IGBTs. Figure 15 gives the typical

value of the total gate charge as a function of the voltage applied to the gate. The shape of the curve is explained in detail in AN-944.

Switching Times (t_d , t_r , t_f). The switching times are defined in a fairly conventional way (Figure 16):

- Turn-on delay time: 10% of gate voltage to 10% of collector current
- Rise time: 10 to 90% of collector current
- Turn-off delay time: 90% of gate voltage to 90% of collector voltage
- Fall time: 90 to 10% of collector current. The fall time definition is a problem with some IGBTs, because of the current tail, mentioned in Section IIB, a significant part of which may be below 10%. The voltage fall time, on the other hand, is not characterized in any way. Thus, two significant contributors to losses are not properly accounted for by the switching times and, for this reason, they should not be used to calculate switching losses. Switching losses are fully characterized as such in the data sheet, as explained in the next paragraph.

It should be remembered that IGBTs, like power MOSFETs, do not have a storage time. The turn-off delay is due to the Miller effect, as explained in Section IVA.

Switching times provide a useful guideline to establish the appropriate deadtime between the turn-off and subsequent turn-on of complementary devices in a half bridge configuration and the minimum and maximum pulse widths.

Switching Energy (E_{on} , E_{off} , E_{ts}). IGBTs from International Rectifier have a guaranteed switching energy providing a full characterization in terms of temperature, collector current and gate resistance (Figures 17, 18 and 19 for the IRBGC20U). This allows the designer to calculate the switching losses, without worrying about the actual current and voltage waveshapes, the tail and the quasi-saturation.

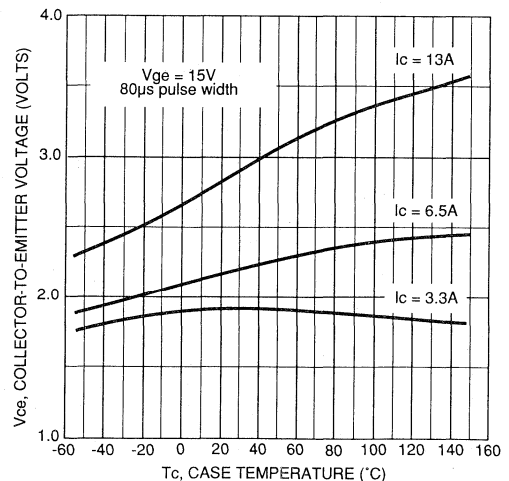


Figure 14. Collector-to-Emitter Saturation Voltage vs. Case Temperature

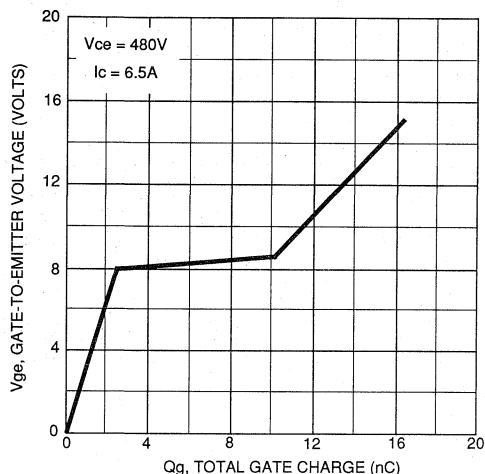


Figure 15. Typical Gate Charge vs. Gate-to-Emitter Voltage

Any test circuit for measuring switching losses has to satisfy two fundamental requirements:

1. It must simulate the switching conditions as they are encountered in a practical application, i.e., a clamped inductive load with continuous current flow.
2. It must reflect the losses that are attributable to the IGBT, and must be independent from those due to other circuit components, like the freewheeling diode.

The test circuit that meets these requirements is shown in Figure 16. Its operation is as follows:

The driver IGBT builds the test current in the inductor. When it is turned off, current flows in the zener. At this point the switching time and switching energy test begins, by turning on and off the device under test (DUT). The DUT will see the test current that was flowing into the inductor and the voltage across the zener, *without* any reverse recovery component from a free-wheeling diode. This test can exercise the IGBT to its full voltage and current without any spurious effect due to diode reverse recovery.

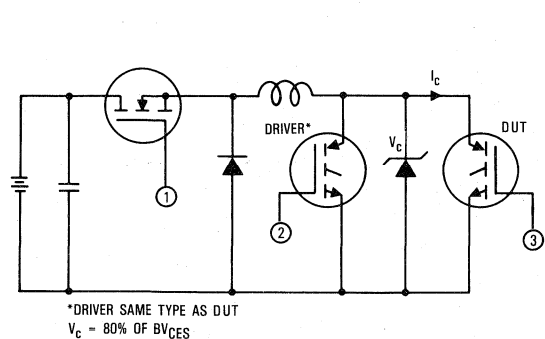


Figure 16. Switching Loss Test Circuit and Waveforms

The test method, on the other hand, must account for all losses that occur because of the switching operation, including the quasi-saturation at turn-on and the tail at turn-off. To fulfill this requirement, the energy figures reported in the data sheet are defined as follows:

E_{on}: From 5% of test current to 5% of test voltage. We feel that 5% is a reasonable compromise between the resolution of the instrumentation and the need to account for the quasi-saturation that could occur in some devices.

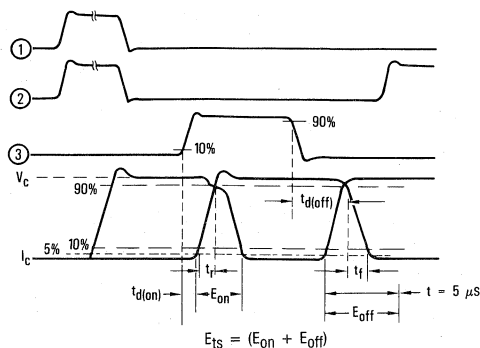
E_{off}: This energy is measured over a period of time that starts with 5% of test voltage and goes on for 5 μsec. While the current tail of most IGBTs would be finished well before that time, it was felt that the contribution of the leakage losses to the total energy is minimal.

E_{TS}: This is the sum of the turn-on and turn-off losses.

As shown in Figure 19, switching energy for International Rectifier IGBTs is closely proportional to current. This is not necessarily true for IGBTs from other manufacturers.

Internal Emitter Inductance (L_E). This is the package inductance between the bonding pad on the die and the electrical connection at the lead. This inductance slows down the turn-on of the IGBT by an amount that is proportional to the di/dt of the collector current, just like the Miller effect slows it down by an amount that is proportional to the collector dv/dt. With a di/dt of 1000 A/μsec, the voltage developed across this inductance is in excess of 7V.

Device Capacitances (C_{iee}, C_{oee}, C_{ree}). The test circuit and a brief explanation of the test method can be found in Figure 20. The output capacitance has the typical voltage dependence of a P-N junction. The reverse transfer (Miller) capacitance is also strongly dependent on voltage (inversely proportional), but in a more complex way than the output capacitance. The input capacitance, which is the sum of the gate-to-emitter and of the Miller capacitance, shows the same voltage dependence of the Miller capacitance but in a very attenuated form since the gate-to-emitter capacitance is much larger and voltage independent.



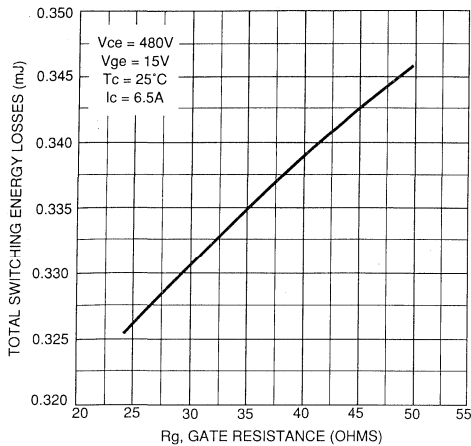


Figure 17. Typical Switching Losses vs. Gate Resistance

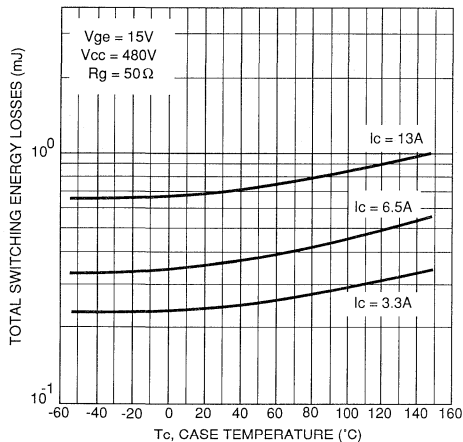


Figure 18. Typical Switching Losses vs. Case Temperature

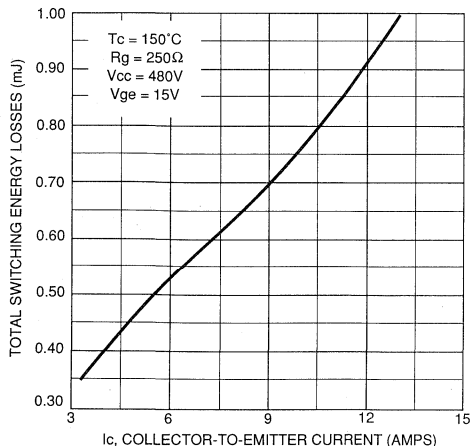


Figure 19. Typical Switching Losses vs. Collector Current

The Transfer Characteristic (Figure 21 for the IRGBC20U). This curve deviates from the traditional definition of transfer characteristic in one detail: the drain is not connected to the gate but to a fixed (100V) supply. When gate and drain are tied together, the curve is the boundary separating operation in full enhancement from operation in linear mode (sometimes referred to as "sat mode").

Figure 21 provides an indication of current when operated in short circuit. In the normal range of operation this curve shows a slight negative dependence on temperature and is largely independent from applied voltage.

Section III: The IGBT Families from IR

The discussion in Sections I and II can be summarized in a comparative table (Table II) that may be useful in placing different power transistors in the proper perspective. In general, the IGBT offers clear advantages in high voltage (>300V), high current (1-3 A/mm² of active area), and medium speed (to 10-20 kHz).

In a technological breakthrough, International Rectifier has developed a processing method that reduces the voltage drop per unit of current density to much lower

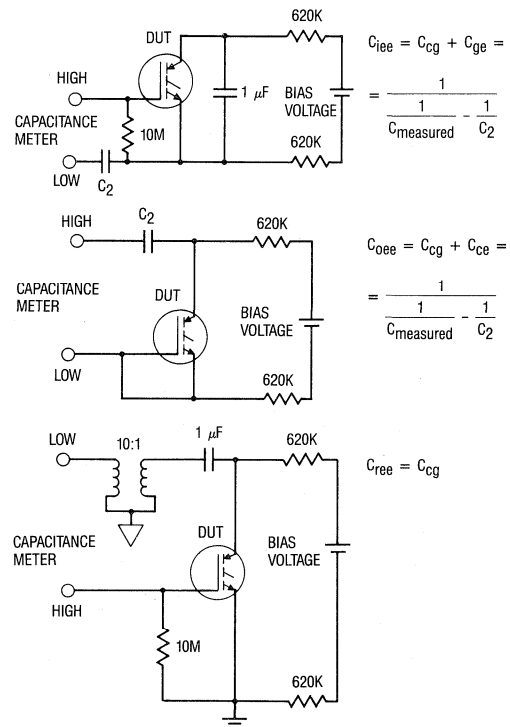


Figure 20. Capacitance test circuits. The IGBT is biased with 25V between collector and emitter. Two of its terminals are ac shorted with a large value capacitor. Capacitance is measured between these two terminals and the third.

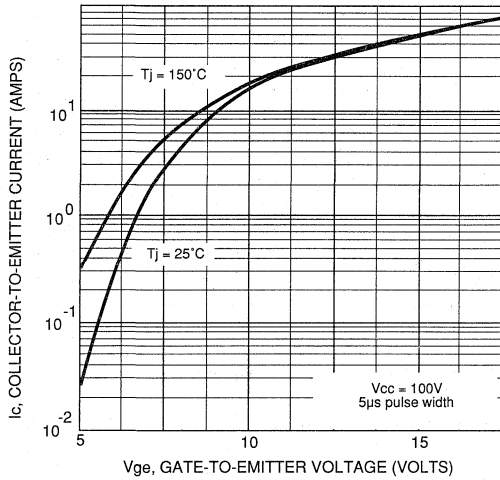
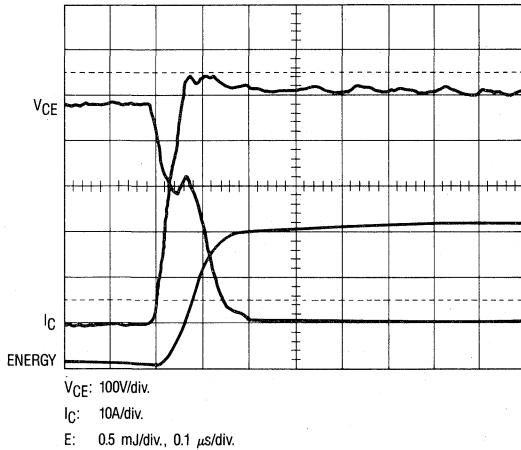


Figure 21. Typical Transfer Characteristics

values than are obtainable with state-of-the-art technology. This allows higher levels of minority lifetime killing and, consequently, much lower switching losses.

To maximize the value to the user of its technological breakthrough, International Rectifier has introduced three different families of devices with different crossover frequency: *Standard*, *Fast* and *UltraFast*.

IR's *Standard* IGBTs have been optimized for voltage drop and conduction losses and have the lowest voltage drop per unit of current density that is presently available in the market.

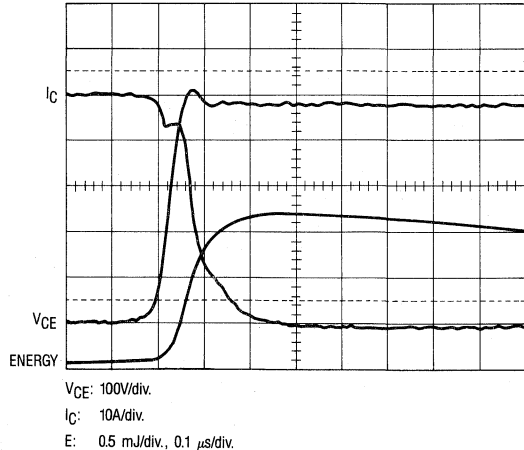


Turn-on. Current rise time is approximately 50 ns with a turn-on energy of 1.5 mJ.

Table II: Comparative Table of Power Transistor Characteristics

	Power MOSFETs	IGBTs	Bipolars	Darlingtons
Type of Drive	Voltage	Voltage	Current	Current
Drive Power	Minimal	Minimal	Large	Medium
Drive Complexity	Simple	Simple	High Large positive and negative currents are required	Medium
Current Density For Given Voltage Drop	High at low voltages	Very High Small trade-off with switching speed	Medium Severe trade-off with switching speed	Low
	Low at high voltages			
Switching Losses	Very Low	Low to Medium depending on trade-off with conduction losses	Medium to High depending on trade-off with conduction losses	High

IR's *UltraFast* IGBTs have been optimized for switching losses and have the lowest switching losses per unit of current density presently available in the market. As it is apparent from Figure 22, these devices have switching



Turn-off. Voltage rise time is approximately 50 ns with a current tail of 100 ns and a turn-off energy of 1.7 mJ. The tail contribution to these losses is 0.5 mJ. The drop in energy after the turn-off is due to the slowly resetting current transformer.

Figure 22. IRGPC50U switching 50A at 480V, 125°C. Test circuit is as shown in Figure 16.

speeds that are comparable to those of power MOSFETs in practical applications. They can operate comfortably at 50 kHz in PWM and significantly higher frequencies in resonant circuits.

IR's *Fast* devices offer a combination of low switching and low conduction losses that closely matches the switching characteristics of many popular bipolar transistors.

Table III shows the key features of the three families.

Table III: International Rectifier IGBT Families

Characteristic	Standard	Fast	Ultrafast
V _{CE}	1.3V	1.5V	1.9V
Switching Energy	0.54 mJ/A mm ²	0.16 mJ/A mm ²	0.055 mJ/A mm ²
Conduction Losses (50% dc)	0.625W	0.75W	0.95W

1A/mm², 100°C, Typical Values

REFERENCES

- [1] U.S. Patents No. 4,376,286 and 4,642,666
- [2] AN-937A: Gate Drive Characteristics and Requirements
- [3] AN-944: A New Gate Charge Factor
- [4] AN-978: High Voltage Floating MOS-Gate Driver IC
- [5] AN-967: PWM Motor Drive with HEXFET III

Application Characterization of IGBTs

(HEXFRED is a trademark of International Rectifier)

by Steve Clemente

Summary

This application note covers some of the major issues normally encountered in the design of an IGBT power conditioning circuit. It is the companion to AN-983A, "IGBT Characteristics," which covers the details of the device, rather than its application.

The main focus of this note is on the calculation of conduction and switching losses in a real application. Device optimization methods are suggested and tools are provided to perform it.

Finally, the problem of current sharing of paralleled devices is analysed, providing an insight into the mechanisms that bring about balanced operation.

I. Gate Drive Requirements

A. Impact of the impedance of the gate drive circuit on switching losses

The gate drive circuit controls directly the MOSFET channel of the IGBT and, through the drain current of the MOSFET, the base current of its bipolar portion. Since the turn-on characteristics of an IGBT are determined, to a large extent, by its MOSFET portion, the turn-on losses will be significantly affected by the gate drive impedance.

Turn-off characteristics, on the other hand, are chiefly determined by the minority carrier recombination mechanism, which is only indirectly affected by the MOSFET turn-off. An increase in gate drive impedance prolongs the Miller effect and causes a delay in the current fall time that is similar to a storage time. This delay is emphasized in Figure 1 with the addition of a 47 Ω gate resistor.

The impact of the gate drive impedance on total switching losses depends on the basic design of the IGBT and its

speed. The impact on *turn-on losses* is appreciable for all IGBTs from International Rectifier, regardless of speed. The impact on *turn-off losses* depends on the speed of the device: the faster the IGBT the greater its sensitivity to the gate drive impedance. In any event, *additional* gate drive impedance has a *marginal* impact, i.e. the same amount of additional drive impedance will have a lower effect if the gate drive impedance is already high.

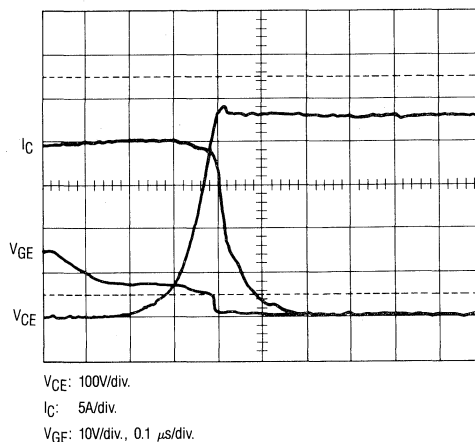


Figure 1. Turn-off waveform of an IRGBC40F with a 47 Ω gate resistor. Notice the turn-off delay of the current waveform during the Miller effect.

It follows that the *total switching losses* of standard devices will be marginally affected by the characteristics of the gate drive circuit, while the Ultrafast IGBTs are more sensitive to it and stand to benefit the most from a low impedance gate drive.

The specific dependence of the switching energy on gate drive resistance is shown in Figure 9 of the data sheet.

B. Impact of the gate drive impedance on noise sensitivity

As explained in Ref. [1], to reduce noise sensitivity and the risk of dv/dt -induced turn-on¹, the gate must be shorted to the emitter through a very low impedance.

Frequently a negative gate bias is used to improve noise immunity. An effective alternative is to design a layout that minimizes the inductance of the gate charge/discharge loops with parallel tracks or twisted wires for the gate drive. This can be as effective in taking care of this problem as the negative bias, eliminating the need for isolated negative supplies. In many cases the effects of a contained amount of dv/dt induced turn-on, i.e. a small increase in power dissipation, can be an appealing alternative to the added complexity of the negative gate bias.

C. Impact of gate drive impedance on “dynamic latching”

Some manufacturers suggest the use of significant amounts of gate resistance to reduce the possibility of “dynamic latch-up” (see Ref. [6], Section I.d), particularly when short circuit currents have to be switched off. This increases the switching energy and the sensitivity to dv/dt induced turn-on. Under these conditions a negative gate bias may be required.

Although IGBTs from International Rectifier will not latch even with no gate resistance, there may be practical reasons to add them, mainly to reduce the current spike at turn-on due to reverse recovery of the diode and reduce ringing. This resistance can be safely bypassed with an antiparallel diode to reduce the turn-off losses and the amount of dv/dt induced turn-on, as explained in Ref. [4], Section 3.b. For most applications, the circuit shown in Figure 2 provides a simple, low cost, high performance solution to the gate drive requirements of most applications.

D. Using gate voltage to improve short circuit capability

The gate terminal can be advantageously used to control the short-circuit withstand capability of the IGBT. A lower gate drive voltage reduces the collector current and the power dissipation during short circuit, at the expenses of a higher conduction drop. As an alternative, simple circuits can be implemented to reduce the gate voltage within 1-3 μs from the inception of the short circuit. Ref. [7] provides an example of how this function can be performed.

¹In a MOS-Gated transistor, any dv/dt that appears on the collector/drain is coupled to the gate through a capacitive divider consisting of the Miller capacitance and the gate-to-source/emitter capacitance. If the gate is not solidly clamped to the source/emitter, a large enough dv/dt will take the gate voltage beyond its threshold and the transistor will conduct. As it goes into conduction it clamps the dv/dt that is causing it to conduct so that the gate voltage never goes much beyond its threshold. The end result is a limited amount of “shoot-through” current, with an increase in power dissipation.

MOS-Gate Driver integrated circuits are available to perform the current limiting and short circuit protection function by means of the gate voltage. One such example is shown in Figure 3 and described in Ref. [10].

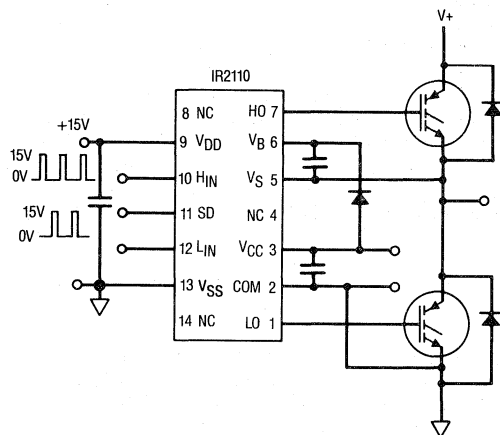


Figure 2. The IR2110 provides a simple, high performance, low cost solution to the problem of driving a Half-Bridge.

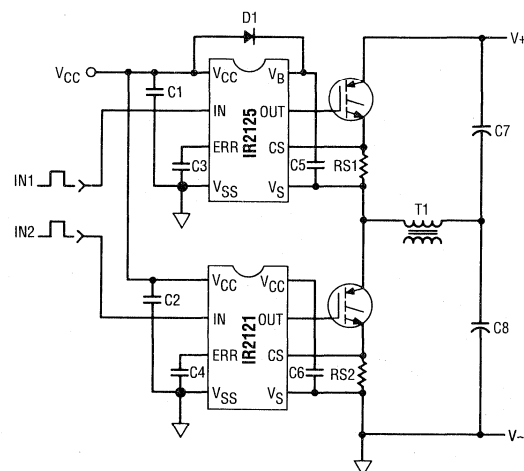


Figure 3. Short circuit protection performed with MOS gate driver ICs.

E. Contribution of "common emitter inductance" to the impedance of the gate drive circuit

The "common emitter inductance" is the inductance that is common to the collector circuit and the gate circuit (Figure 4a). This inductance establishes a feedback from the collector circuit to the gate circuit that is proportional to $L di_c/dt$. The voltage developed across this inductance subtracts from the applied gate voltage during the turn-on transient and adds to it during turn-off. In so doing, it slows down the switching.

This phenomenon is similar to the Miller effect, except that it is proportional to the di/dt of the collector current rather than the dv/dt of its voltage. In both cases the feedback is proportional to the transconductance of the IGBT, which is much larger than that of a MOSFET of the same die size. A di_c/dt of 0.5A/ns is quite common in IGBT circuits and voltages in the order of 10V could be expected in 20 nH of common emitter inductance, except that the feedback mechanism slows down the turn-on process and limits the di_c/dt .

No additional common emitter inductance should be added to what is already in the package. Separate wires to the emitter pin should be provided for the emitter and

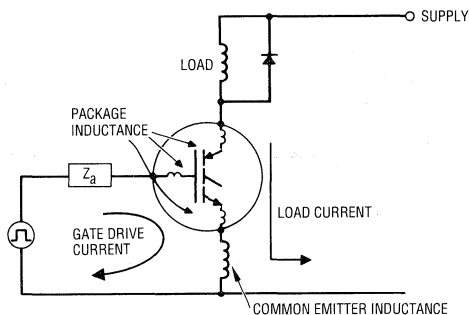


Figure 4a. "Common emitter inductance" is the inductance that is common to the collector current and the gate drive current

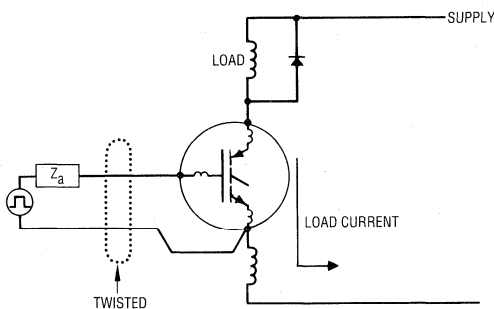


Figure 4b. "Common emitter inductance" can be eliminated by running separate wires to the emitter pin, one for the emitter, the other for the gate drive return.

the gate return, as shown in Figure 4b. The gate lead and the gate return lead should be twisted or run on parallel tracks to minimize inductance in the gate drive path. This improves immunity to dv/dt induced turn-on and reduces ringing in the gate.

F. Gate charge vs. input capacitance

The same general considerations can be made for the IGBTs as those made for power MOSFETs in [1] and [2]. Designers that are familiar with the limited usefulness of the input capacitance concept can safely skip this section.

Input capacitance is frequently used for two purposes:

- as a figure of merit of switching performance;
- as a reference point of design a gate drive circuit.

On both counts, the use of data sheet capacitance values gives results that are wrong or misleading.

As shown in Figure 5, IGBT capacitances change significantly with collector voltage to the point that no capacitance number is, in itself, meaningful unless a voltage is associated with it.

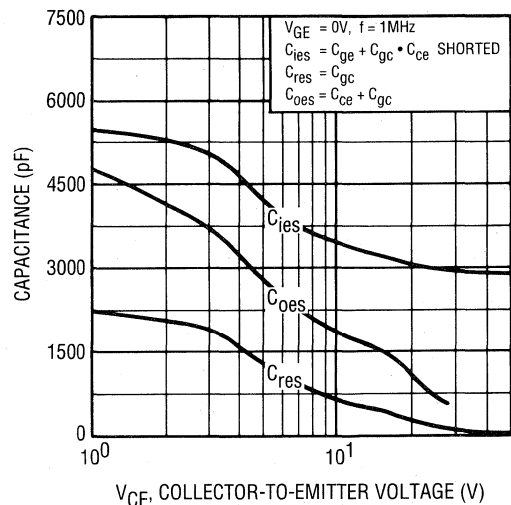


Figure 5. Typical capacitance vs V_{CE} , IRGPC50U. The variation of C_{res} and C_{ies} with collector voltage makes the concept of capacitance virtually useless.

Even disregarding the voltage dependence, input capacitance is not a good figure of merit of switching performance, neither for MOSFETs, nor for IGBTs. As far as MOSFETs go, a device with lower input capacitance can be slower than one with higher input capacitance, depending on threshold, transconductance and total gate charge (see Figure 6 of Ref. [2]). A conspicuous example of this is the fact that logic level devices are faster than their standard gate counterparts, in spite of a larger input capacitance [3].

Application Information

In the specific case of IGBTs, which are minority carrier devices, the switching behavior is dominated by injection and recombination phenomena and only the turn-on behavior is affected by gate drive conditions in a significant way.

As a guideline to design the gate drive circuit, the input capacitance underestimates the gate drive requirements. Normally, the charge required by the gate for one switching operation corresponds to an input capacitance that is two to three times larger than the data sheet value. As explained in Ref. [2], this is due to the Miller component of the input capacitance.

Thus, gate drive circuits designed on the basis of input capacitance are generally inadequate and result in poor switching operation, noise susceptibility and malfunction. The sizing of the gate drive circuit is more appropriately done using the gate charge specified in the data sheet, as explained in Ref. [2].

11. Switching Trajectories and Safe Operating Area Considerations

Minority carrier devices, when subjected to high levels of voltage and current, can experience uneven current distributions within the die that, taken beyond safe limits, can cause device failure. The current distribution takes different forms, depending on the sign of the di/dt associated with it. Hence, the Safe Operating Area curve, which was devised as a convenient representation of this limitation, is frequently differentiated into “Forward-Biased SOA” and “Reverse-Biased SOA”.

The Forward Biased SOA curve applies to operation in Class A or Class B or during short circuit, which can be considered an extreme case of Class B operation. Thermal limitations for pulsed operation are frequently included in this curve, even though the Transient Thermal Response curve provides this same information in a more comprehensive and accurate way. Operation in these conditions is guaranteed to the specified I_{CM} and $V_{(BR)CES}$, within the maximum junction temperature. Hence, the FBSOA curve, being “square”, has been omitted from the data sheet.

The Reverse Biased SOA applies when switching off a clamped inductive load, including the turn-off from a short circuit condition.

Figure 6 shows the importance of the Reverse Biased SOA. During the turn off of a clamped inductive load, the voltage across the transistor goes from the low value of $V_{CE(sat)}$ to the full supply voltage while the collector current stays constant. After the collector voltage exceeds the supply voltage by a diode drop, the diode starts to conduct, thereby taking over the inductor current from the transistor. Thus the trajectory of the operating point moves along a constant current line until it intercepts the supply voltage, at which point a voltage overshoot normally occurs, whose magnitude depends on the amount of stray inductance L_S and the turn-off speed. A more detailed explanation of the switching trajectories can be found in Ref. [15].

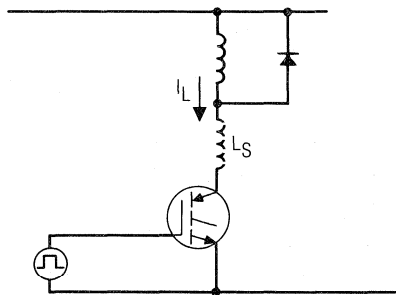


Figure 6a. Typical clamped inductive load

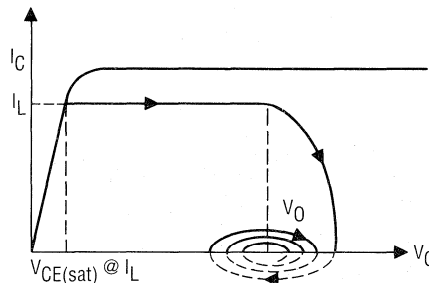


Figure 6b. During a turn-off transient, the trajectory of the operating point traverses the SOA curve. Second breakdown would place limits to the free evolution of the trajectory.

It will be appreciated that, for a safe commutation of the load current, the entire trajectory must lay within the turn-off SOA and that any limitation to the SOA will translate into a limitation of turn-off capability of inductive loads. Load-shaping snubbers have been used in conjunction with bipolar transistors to lower the trajectory below the second breakdown limit.

Due to the wide base and, hence, low gain of its bipolar portion, the second breakdown of International Rectifier's IGBTs occur at current and voltage levels that are significantly higher than what is normally encountered in a practical application, as shown in Figure 12 of the data sheets. Notice that the values therein contained apply at 125°C and that load-shaping snubbers are not necessary, as long as the switching trajectory is confined within the turn-off SOA.

During an inductive turn-off, a bipolar-mode device can undergo a partial loss of blocking capability, similar in many respects to second breakdown. This phenomenon is generally explained as being due to excessive concentration of minority carriers in the base region (13), rather than lateral thermal instability. For the IGBTs available from International Rectifier at the time of writing, this phenomenon occurs well beyond the SOA limits published in the data sheet.

In addition to load shaping, snubbers can be used to limit overshoots and/or reduce EMI. This function is not related to SOA and is covered in more detail in [11].

III. Conduction Losses

At any given time, the energy dissipated in the IGBT can be obtained with the following expression:

$$E = \int_0^t V_{CE}(i) i(t) dt$$

where t is the length of the pulse. Power is obtained by multiplying energy by frequency, if applicable. When the transistor is off $i(t) \approx 0$ and losses are negligible.

Unfortunately, no simple expression can be found for the voltage and current functions during a switching transient. Hence, for analytical expediency, we resort to a somewhat artificial distinction between conduction and switching losses.

We define conduction losses the losses that occur between the end of the turn-on interval and the beginning of the turn-off interval, as defined for the switching losses characterization. Since the turn-on energy is measured from 5% of the test current to 5% of the test voltage and the turn-off energy is measured starting from 5% of the test voltage, conduction losses occur when the voltage across the IGBT is less than 5% of the test, or supply, voltage (see Ref. 6, Section E).

The function $V_{CE}(i)$ in the formula above expresses the conduction behavior of the IGBT. International Rectifier characterizes the conduction losses in the following ways:

- with tabular information in the data sheet;
- with graphs in the data sheet;
- with the model parameters of Table I.

A. Calculating the voltage drop from data sheet parameters

The tabular information in the data sheet provides a few limit points that, with the help of the graphs, can be used to generate the information necessary to calculate the conduction losses.

To obtain the max voltage drop at any current and temperature, from the data sheet supplied values, a two step procedure can be followed.

First a typical value is obtained by interpolating a curve in Figure 5 of the data sheet at the desired current level. Then, to obtain a maximum value, the voltage drop read from this curve at the appropriate junction temperature is multiplied by the ratio between maximum and typical from the Table of Electrical Characteristics.

An additional correction may be required if the gate drive voltage is not 15V. Figures 2 and 3 of the data sheet can be used to make the necessary corrections.

If the current waveform is not constant during the conduction interval, it should be broken up into smaller

intervals, calculating the losses for each sub-interval and summing the results, rather than averaging or taking its RMS value.

An appealing alternative, for those cases where the current waveform has a simple mathematical expression, e.g. sinusoidal or triangular or trapezoidal, is to calculate the conduction losses with the integral above, with the help of the conduction model.

B. Conduction model

The solution of the integral requires a mathematical expression for the current waveform and one for the voltage drop. The expression shown below for the voltage drop as a function of current was found to be more than satisfactory for the general accuracy that is expected from these calculations.

$$V_{CE} = V_t + a I^b$$

Information on the accuracy of the model and how it was derived is contained in Appendix 1.

The specific parameters for the three families of IGBTs from International Rectifier can be found in Table I. The model parameters have been fitted with a simple linear regression over temperature.

Table I. Conduction Model Parameters for International Rectifier IGBTs

$$V_{CE} = (V_1 + V_2 T) + (a_1 + a_2 T) i(b_1 + b_2 T) \quad T \text{ in } ^\circ\text{C}$$

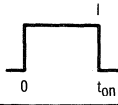

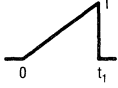
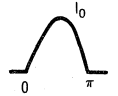
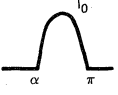
Part Number	V_1	V_2	a_1	a_2	b_1	b_2
IRGBC20F	0.905	-2.06E-03	0.241	7.08E-04	0.649	5.11E-04
IRGBC20S	0.810	-1.66E-03	0.173	2.90E-04	0.721	4.79E-04
IRGBC20U	1.071	-2.40E-03	0.669	-1.28E-03	0.353	2.29E-03
IRGBC30F	0.911	-1.98E-03	0.115	4.19E-04	0.721	2.95E-04
IRGBC30S	0.840	-1.64E-03	0.100	1.38E-04	0.760	5.10E-04
IRGBC30U	1.175	-2.75E-03	0.307	-3.13E-04	0.504	1.56E-03
IRGBC40F	0.901	-1.93E-03	0.072	2.17E-04	0.731	3.13E-04
IRGBC40S	0.824	-1.67E-03	0.052	6.52E-05	0.776	4.24E-04
IRGBC40U	1.171	-2.55E-03	0.320	-1.08E-03	0.419	2.24E-03
IRGPC40F	0.901	-1.93E-03	0.072	2.17E-04	0.731	3.13E-04
IRGPC40S	0.824	-1.67E-03	0.052	6.52E-05	0.776	4.24E-04
IRGPC40U	1.171	-2.55E-03	0.320	-1.08E-03	0.419	2.24E-03
IRGPC50F	0.871	-1.92E-03	0.045	1.19E-04	0.751	2.87E-04
IRGPC50S	0.820	-1.69E-03	0.033	3.42E-05	0.794	4.09E-04
IRGPC50U	1.099	-2.39E-03	0.202	-6.99E-04	0.466	1.92E-03

Table II shows the expressions to calculate conduction energy for five simple current waveforms, assuming that the conduction behavior is accurately expressed by the model shown in Table I.

As shown in Sections V and VI, this model, as well as the companion switching model that will be described in the next Section, is extremely useful in performing comparative evaluations for device optimization. Section VI shows how it can be used to simplify and automate the calculation of junction temperature for any operating condition.



Table II. Conduction Energy for Simple Waveforms

CURRENT WAVEFORM	MATHEMATICAL EXPRESSION	$E = \int V_{CE}(t) i(t) dt$, $V_{CE}(t) = V_t + ai^b$ $E = \int [V_t i(t) + ai(t)^{b+1}] dt$
	$i(t) = I$	$E = \int_0^{t_{on}} (I V_t + aI^{b+1}) dt = (IV_t + aI^{b+1}) t_{on}$
	$i(t) = I_1 + (I_2 - I_1) \frac{t}{t_1}$	$E = \int_0^{t_1} [V_t \left(I_1 + \frac{(I_2 - I_1)}{t_1} t \right) + a \left(I_1 + \frac{(I_2 - I_1)}{t_1} t \right)^{b+1}] dt = V_t \frac{(I_1 + I_2)}{2} t_1 + \frac{I_2^{b+2} - I_1^{b+2}}{(b+1)(I_2 - I_1)} \frac{at_1}{b+2}$
	$i(t) = I \frac{t}{t_1}$	$E = \int_0^{t_1} \left(V_t I \frac{t}{t_1} + a \left(I \frac{t}{t_1} \right)^{b+1} \right) dt = \frac{1}{2} IV_t t_1 + \frac{aI^{b+1}}{b+2} t_1$
	$i(t) = I_0 \sin \omega t$	$E = \int_0^T (V_t I_0 \sin \omega t + a I_0^{b+1} \sin^{b+1} \omega t) dt = \frac{2I_0}{\omega} \left[V_t + \frac{\sqrt{\pi}}{2} a I_0^b \frac{\Gamma\left(\frac{b+2}{2}\right)}{\Gamma\left(\frac{b+3}{2}\right)} \right]$ $T = 1/f = \text{Repetition rate of current pulse}$
	$i(t) = I_0 \sin \omega t$	for $\alpha = \frac{\pi}{2}$ $E = \frac{I_0}{\omega} \left[V_t + \frac{\sqrt{\pi}}{2} a I_0^b \frac{\Gamma\left(\frac{b+2}{2}\right)}{\Gamma\left(\frac{b+3}{2}\right)} \right]$ otherwise $E = \frac{I_0}{\omega} \left[V_t (1 + \cos \alpha) + a I_0^b \int_{\alpha}^{\pi} \sin^{b+1} \alpha d \alpha \right]$

IV. Losses in Hard Switching

Like conduction losses, “hard switching” operation is characterized in the following ways:

- with tabular information in the data sheet;
- with graphs in the data sheet;
- with the model parameters of Table III.

Table III. Switching Model Parameters for International Rectifier IGBTs

$$E_{on} = (h_1 + h_2T) I(k_1 + k_2T) \quad E_{off} = (m_1 + m_2T) I(n_1 + n_2T)$$

T in °C, E in mJ

Part Number	h_1	h_2	k_1	k_2	m_1	m_2	n_1	n_2
IRGBC20F	1.17E-02	2.21E-05	1.195	-1.53E-04	-9.18E-04	1.02E-03	1.358	-2.41E-03
IRGBC20S	1.67E-02	2.78E-06	1.178	3.41E-04	2.05E-01	2.51E-03	1.090	-5.96E-04
IRGBC20U	1.43E-02	9.73E-06	1.110	1.21E-04	-1.02E-02	3.58E-04	1.543	-3.75E-03
IRGBC30F	4.44E-03	2.65E-06	1.503	-1.59E-04	-1.29E-02	1.02E-03	1.498	-2.71E-03
IRGBC30S	6.21E-03	2.98E-06	1.467	1.22E-04	1.58E-01	2.75E-03	1.096	-6.94E-04
IRGBC30U	3.80E-03	1.18E-05	1.542	-6.01E-04	-2.05E-02	4.18E-04	1.880	-5.34E-03
IRGBC40F	3.34E-03	-1.10E-06	1.584	6.37E-04	-2.47E-02	1.04E-03	1.470	-2.85E-03
IRGBC40S	1.58E-03	2.08E-05	1.802	-1.25E-03	1.71E-01	3.23E-03	1.070	-6.23E-04
IRGBC40U	1.30E-03	1.08E-05	1.791	-8.66E-04	-1.38E-02	2.74E-04	1.829	-4.60E-03
IRGPC40F	3.34E-03	-1.10E-06	1.584	6.37E-04	-2.47E-02	1.04E-03	1.470	-2.65E-03
IRGPC40S	1.58E-03	2.08E-05	1.802	-1.25E-03	1.71E-01	3.23E-03	1.070	-6.23E-04
IRGPC40U	1.30E-03	1.08E-05	1.791	-8.66E-04	-1.38E-02	2.74E-04	1.829	-4.60E-03
IRGPC50F	5.40E-03	-1.40E-05	1.558	6.42E-04	-3.53E-02	1.12E-03	1.490	-2.81E-03
IRGPC50S	3.61E-03	2.61E-07	1.670	1.85E-04	1.44E-01	3.91E-03	1.079	-7.42E-04
IRGPC50U	4.52E-03	-6.10E-06	1.616	1.87E-04	-1.14E-02	2.13E-04	1.946	-4.82E-03

As explained in Ref. [6], Section E, the Switching Energy reported in the data sheet makes specific reference to a test circuit that simulates a clamped inductive load operated with an ideal diode. Hence, it does not include the losses in the IGBT when, in turning on, it carries the full load current, plus the reverse recovery current of the freewheeling diode.

It follows that, to obtain the total turn-on losses or the total switching losses, two components have to be calculated:

- turn-on or total losses with an ideal diode
- the additional turn-on losses in the IGBT due to the reverse recovery of the freewheeling diode.

The following sections show how to calculate these two components.

It should be kept in mind that active devices in flyback converters do not normally have turn-on losses, nor are they subject to recovery transients. The same is true for those bridge circuits where the output voltage and duty cycle is controlled by phase shifting the output of one leg with respect to the other, both being 50% duty cycle.

A. Calculation of switching losses with an ideal diode from data sheet information

Total switching losses with an ideal diode for any given current and temperature can be obtained from data sheet information following a three step procedure, similar to the one for obtaining the on-state voltage drop.

First a typical value is obtained, either by interpolating a curve in Figure 10 of the data sheet for the desired current, or by plotting another curve on Figure 10 for the appropriate temperature, from the values read from Figure 11 of the data sheet.

From this typical value a maximum value can be obtained by multiplying the typical by the ratio between maximum and typical that is in the Table of Switching Characteristics.

Finally, since the switching energy is proportional to voltage, the result is scaled by the ratio of the actual circuit voltage to the test voltage (normally 80% of device rated voltage).

An additional correction may be necessary to account for the gate resistor. This can be done with the help of Figure 9 of the data sheet.

B. Calculation of switching losses with an ideal diode from switching model

A simpler alternative to the method outlined below is to make use of the simple model shown in Table III, together with the specific parameters for the three families of IGBTs from International Rectifier. Losses calculated with these parameters assume the following:

- supply voltages equal to 80% of rated $V_{(BR)CES}$.
- a gate drive circuit similar to the one in the data sheet.
- ideal diode.

The results should be scaled linearly for the appropriate supply voltage and should be scaled according to Figure 9 of the data sheet to take into account a different gate drive impedance.

The accuracy of the model parameters obtained from the second linear regression (see Appendix 1) is good at temperatures over 70°C ($\pm 5\text{-}10\%$) but deteriorates at temperatures below 60°C ($-15\text{-}20\%$), occasionally negative numbers are obtained at 25°C). Fortunately, accuracy in this range is less important as it is far from the maximum operating temperature of a power device.

C. Contribution of the diode reverse recovery

In a typical clamped inductive load in continuous current mode, the turn-on of a switch causes a reverse recovery in the freewheeling diode and a large current spike in the device that is being turned on (Figure 7) [5]. This increases the turn-on losses in the IGBT with respect to the calculations of the previous sections and data sheet characterization. The *forward recovery* of the diode, on

the other hand, has a secondary impact on the turn-off losses and will not be analyzed here.

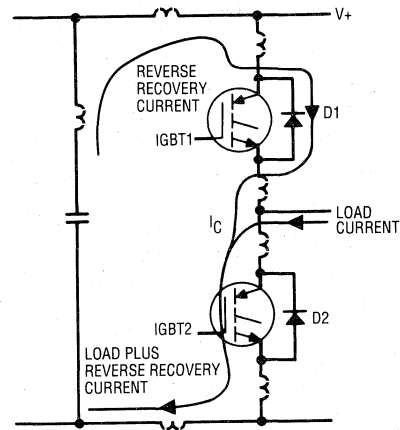


Figure 7a. Typical clamped inductive load showing stray circuit inductances. Load current was flowing in D1 previous to IGBT2 turning on. At turn-on IGBT2 takes over load current and reverse recovery current of D1.

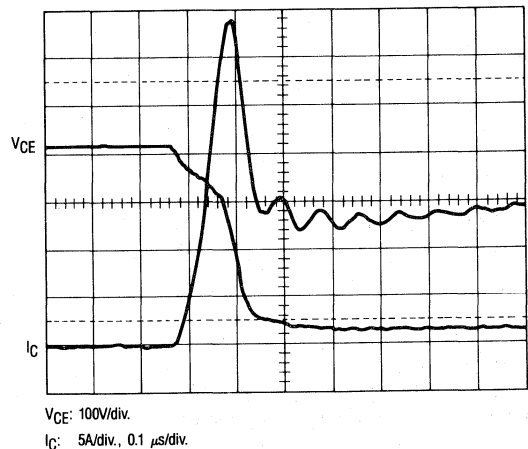


Figure 7b. Turn-on current in IGBT2.

No simple expression can be provided for these additional losses, as they depend on a number of factors: turn-on speed di/dt , stray inductance and diode characteristics. Several have been proposed, based on simplifying assumptions. The following assumes that the voltage across the diode stays close to 0V during the length of t_a , rising to the supply voltage during t_b .

$$E = V I_L \left[\left(1 + \frac{1}{2} \frac{I_{RR}}{I_L} \right) t_a + \frac{1}{4} \frac{I_{RR}}{I_L} t_b \right]$$

$$= V \left(I_L t_a + Q_a + \frac{1}{4} Q_b \right)$$

where V and I_L are supply voltage and load current, I_{rr} is the peak reverse recovery current, t_a and t_b are the two components of t_{rr} and Q_a and Q_b the charges associated with them. The first two terms represent the losses during t_a , one due to the load current, the other due to the reverse recovery current. The third term represents the losses during t_b , which are partly in the IGBT, partly in the diode.

The limitation of this approximation is that the voltage starts to rise across the diode (and fall across the IGBT) during t_a . In fact, it reaches the supply voltage at the point of $di/dt = 0$ of the reverse recovery current, which is the end of t_a . Hence, it yields values that are in excess of what would be reasonably encountered.

Assuming that the voltage starts to rise at $2/3 t_a$, the following expression could be used:

$$E = \frac{2}{3} V I_L \left(\frac{1}{3} \frac{I_{rr}}{I_L} + 1 \right) t_a$$

By increasing the gate drive resistance the peak reverse recovery current is reduced. The turn-on energy losses in the IGBT increase, though, because of the prolonged current rise time, as well as a prolonged t_a .

V. Trade-off Between Conduction And Switching Losses: Device Optimization

To compare different devices or technologies, silicon designers often resort to curves of voltage drop vs. current density like those shown in Figure 8. These curves ignore the dynamic behavior of the device and, since in a typical switchmode application a significant portion of the temperature rise is due to the switching losses, they are not useful in the device selection.

Furthermore, it is frequently inferred, from those curves, that a technology is superior if it is capable of operating at higher current densities. In a specific application, operation at higher current densities means smaller die sizes and, consequently, higher thermal resistances. If total losses stay the same, this implies higher operating junction temperature, with all its negative connotations.

It follows that, for a given thermal design, operation at higher current densities will be advantageous only if the higher thermal resistance is compensated by lower total losses.

To quantify these considerations a simple method has been developed comparing different power devices in a typical switchmode environment. This method takes all critical aspects into account: thermal constraints, conduction and switching losses.

The popular half-bridge operated with a clamped inductive load was chosen as the benchmark circuit to compare the performance of different IGBTs. Operating

conditions are listed in Figure 9. None of the operating conditions are critical and they can all be changed as

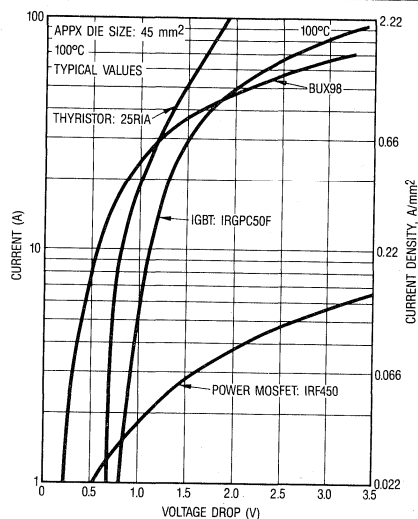


Figure 8. Conduction characteristics for devices of similar die size implemented in different technologies.

necessary. Flyback or resonant circuits could be used in place of the half-bridge to obtain results that are specifically tailored to a given application.

This figure shows in a clear and concise way to what extent higher switching frequencies impact the current output of the pair. It also provides a simple way of selecting the optimum device for the application, which is the one that gives the highest output current at the frequency of operation.

Once the thermal constraints are properly factored into the operating conditions, the graph carries important application information. In a motor control, the RMS component of the fundamental is directly related to torque. In a power supply, on the other hand, the total RMS content of the square wave contributes to power. The ratio between the two is 1.11.

Although the graph shown in Figure 9 can be generated with a relatively simple test circuit, we have made use of the model presented in the previous sections and of a spreadsheet like the one shown in Figure 10. Starting from the top, the IGBT model parameters are entered first, as appropriate for the junction temperature at which the performance is being evaluated².

Next the diode model is entered, which will be used to calculate the component of turn-on losses in the IGBT due to the reverse recovery of the diode. The conduction

²The model parameters in the spreadsheet of Figure 10 are obtained from measurements taken at the indicated temperature. They may differ from those listed in Tables I and III, which result from a linear regression over the temperature range (see Appendix 1).

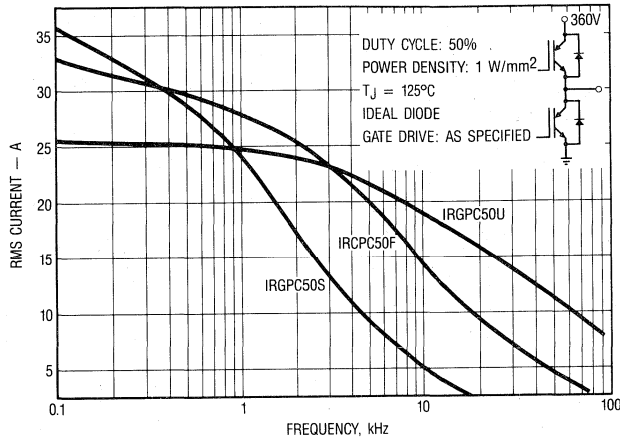


Figure 9. RMS current vs frequency for a Half Bridge with two IGBTs of same die size, same package, different speed, operated in the conditions indicated in the inset.

Part Number: IRGPC40U	
IGBT MODEL $T_j = 125$	
Conduction model:	$V_t = 0.86$ $a = 0.1834$ $b = 0.6999$
Turn-on model, ideal diode:	$h = 0.0028$ $k = 1.6741$
Turn-off model:	$m = 0.018$ $n = 1.2486$
DIODE MODEL $T_j = 125$	
Conduction model:	$V_t = 1.00$ $a = 0.040$ $b = 1.000$
Switching model:	Peak $I_{rr}/I_f = 1.00$ $t_a = 0.035$ $t_b = 0.030 \mu s$
Switching parameters at	480 V
Operating voltage:	360 V
Thermal resistance j-c	0.77 K/W
Thermal resistance c-s	0.24 K/W
Thermal resistance s-a	1.5 K/W
Allowable power dissipation	27.89 $^{\circ}Ta = 55$
Current for balanced losses	13.85 1E-05
Peak Current	A 13.85 8.00 10.00 15.00 17.50 19.50
CONDUCTION LOSSES	
Voltage drop	V 2.01 1.65 1.78 2.08 2.22 2.33
Losses (50% duty cycle)	W 13.94 6.58 8.89 15.60 19.42 22.68
SWITCHING LOSSES	
Turn-on, ideal diode	mJ 0.1685 0.0673 0.0977 0.1927 0.2494 0.2990
IGBT losses due to diode	mJ 0.2991 0.1728 0.2160 0.3240 0.3780 0.4212
Turn-off losses	mJ 0.3595 0.1812 0.2394 0.3972 0.4815 0.5512
Diode, switching losses	mJ 0.0374 0.0216 0.0270 0.0405 0.0473 0.0527
SUMMARY:	
Conduction losses	W 13.94 6.58 8.89 15.60 19.42 22.68
Sw. losses, ideal diode	mJ 0.53 0.25 0.34 0.59 0.73 0.85
Pole RMS Current (fund.)	A 12.46 7.20 9.00 13.50 15.75 17.55
Frequency, ideal diode	kHz 26.41 85.74 56.33 20.82 11.58 6.12
Sw. losses, real diode	mJ 0.83 0.42 0.55 0.91 1.11 1.27
Frequency, real diode	kHz 16.86 50.57 34.34 13.44 7.64 4.09

Figure 10. Spreadsheet to calculate Output current vs. Frequency curves.

model for the diode can also be entered for completeness and to calculate its conduction losses. This will not affect the losses in the IGBT but could provide useful information related to the total losses, efficiency, etc.

The reference voltage for the switching loss model (normally 80% of device rated voltage) is entered next, followed by the actual operating voltage that, for a rectified 220V line, would be approximately 360V.

Finally the thermal information is entered in the form of thermal resistance and ambient temperature, from which the allowable power dissipation is calculated.

The value "Current for balanced losses" is the current at which the conduction losses equal the switching losses for the specific thermal operating conditions. The corresponding frequency is shown at the bottom of the first column under "frequency, ideal diode". These values are calculated by means of a "solve for" function in the spreadsheet and are accurate to the number indicated on the right of the current value.

The rest of the spreadsheet performs the calculations of losses for different levels of current. Losses are broken down into two classes: conduction and switching. The formulas in the spreadsheet are described in the next section.

All the losses are summarized at the bottom. These values are used to generate the Current vs Frequency graph that is reported in each data sheet as Figure 1.

If the diode is co-packaged with the IGBT its losses cannot be dissociated from the losses in the main switching device. In this case the thermal information and allowable power dissipation should be for the combination of both devices. Losses should include conduction and switching losses of both devices and the formulas should be modified accordingly.



VI. The Analysis: Methods To Calculate Junction Temperature And Power Dissipation For A Given Operating Condition.

In the previous section we have developed an application related tool to compare the performance of different devices over temperature and frequency. In this section we present a different tool, aimed at analyzing the operating conditions of the power devices, particularly its junction temperature, *in a specific application environment*.

Since temperature affects conduction and switching losses which, in turn, affect temperature, a direct mathematical solution is not possible. However, the models introduced in Sections III and IV, applied iteratively and with the help of the "solve for" function available in most spreadsheets, permit the characterization of a given operating condition with relative ease.

Figure 11 shows an example of such a spreadsheet. It was designed to answer two different but related questions. The first is: What is the maximum current that can be obtained from a specific IGBT for a given junction temperature and a set of operating conditions. The alternative question is: What is the junction temperature, given a value of current. In other words, since current and temperature are interdependent, either one must be given so that the other can be calculated.

Thus, the spreadsheet is divided vertically in two parts: one for a known junction temperature, one for a known current. Horizontally, the spreadsheet is divided in three major parts: thermal operating conditions, device models and electrical operating conditions. As part of the analysis, conduction and switching losses are calculated, together with some output parameters related to the application. Individual entries are self-explanatory.

Notice that, for operation at fixed temperature, the model parameters are fixed. On the other hand, when the junction temperature is unknown, the model parameters are also unknown. Hence, starting from a reasonable junction temperature, at the top of the right hand section,

the model parameters are calculated and a new junction temperature is obtained, as shown at the bottom. The procedure is iterated by replacing the temperature at the top with the bottom one. Although only few iterations are necessary, the process can be automated with a simple macro.

The spreadsheet contains a correction factor to take into account the fact that the gate drive circuit may have a different resistance than the one that was used for data sheet (and model) characterization. Since many circuits have a "polarized gate resistors", i.e. a resistor with a parallel diode, two lines are provided for this purpose, one for turn-on and one for turn-off energy. The entries for these two lines can be obtained from Figure 9 of the data sheet. Although this figure does not distinguish between turn-on and turn-off losses, it offers a first-cut approximation to both. It should be remembered that the gate drive circuit used for device characterization is very

Part Number: IRGPC50U

THERMAL OPERATING CONDITIONS

Ambient temperature	°C	60.0
Thermal resistance j-to-c	°C/W	0.640
Thermal resistance c-to-s	°C/W	0.240
Thermal resistance s-to-a	°C/W	1.400

Allowable current at stated Tj Junction temperature for stated current

Power dissipation	W	28.5	*	29.16
Junction temperature	°C	125.0		126.50

IGBT MODEL

Vt, Vt1, Vt2	V	0.8000		0.7958	1.0994	-2.40E-03
a, a1, a2	Ohm	0.1120		0.1136	0.2021	-7.00E-04
b, b1, b2		0.7117		0.7085	0.4656	1.92E-03
h, h1, h2	mJ/A	0.0038		0.0037	0.0045	-6.10E-06
k, k1, k2		1.6376		1.6399	1.6162	1.87E-04
m, m1, m2	mJ/A	0.0128		0.0155	-0.0114	2.13E-04
n, n1, n2		1.3382		1.3360	1.9457	-4.82E-03
Reference voltage	V	480		480		

DIODE MODEL

Vt		0.8		0.8
a, b		0.04	1	0.04 1
Ratio Irr/Irf		1		1
ta, tb	µs	0.04	0.03	0.04

ELECTRICAL OPERATING CONDITIONS

RECT. WAVEFORM, CLAMPED IND. LOAD

Switching voltage	V	360		360
Operating Frequency	kHz	40		40
Duty cycle		0.45		0.45
Peak current	A	9.82		9.82 *
Voltage drop at peak current	V	1.37		1.37
Conduction losses	W	6.05		6.05
Turn-on losses	W	4.76		4.76
Correction factor for gate resistance		1.00		1.00
Corrected turn-on losses	W	4.76		4.76
Turn-off losses	W	8.14		9.87
Correction factor for gate resistance		1.00		1.00
Corrected turn-off losses	W	8.14		9.87
Turn-on losses due to diode recovery	W	9.55		8.48
Total losses	W	28.50		29.16
Junction Temperature	°C			126.49

RMS current, fundamental	A	8.84		8.84
RMS current, total	A	9.82		9.82
Output voltage, RMS fundamental	V	162.00		162.00
Output power, fundamental	kVA	1.59		1.59
Output power, total	kVA	1.77		1.77

*Data entered

Figure 11. Analysis of the operating conditions of an IGBT in a clamped inductive load.

stiff. If the application being analyzed has a weak gate drive, its internal impedance should be added to the actual value of gate resistor.

The current for a given junction temperature is obtained with a "solve for" function, changing the current until the total losses at the bottom equal the allowable power dissipation at the top.

The right-hand side of the spreadsheet can be used to do analyses of different type, like checking for thermal runaway. This can be easily done by increasing the ambient temperature at the top of the spreadsheet and

calculating the new junction temperature. In case of thermal runaway, successive iterations yield higher and higher junction temperatures.

This spreadsheet allows convenient analysis of the same circuit in different operating points, e.g. under stresses of transitory nature, like shorts in the output, where the junction temperature could be allowed to go to, say, 150°C. In this case the duty cycle would probably be lower and peak current higher.

In Appendix 1 we mentioned that the model parameters obtained from linear regression are less accurate than the model parameters derived from measurements at fixed temperatures. A trace of this can be found in Figure 11, where the left side of the spreadsheet uses fixed temperature parameters, while the right hand side calculates the parameters from the linear regression coefficients. As a result, in spite of the fact that the operating conditions are the same in both sides of the spreadsheet, there is a junction temperature discrepancy of 1.5°C.

The spreadsheet contains several formulas, most of them requiring no explanation. From the top:

- Power dissipation: the ratio between temperature rise and thermal resistance between junction and ambient.
- Model parameters are entered (left-hand column) or calculated as explained in Table I and in Appendix 1 (right-hand column).
- The peak current is the unknown in the left-hand column, calculated with the solve function, equalizing the total losses (at the bottom) with the allowable power dissipation (at the top). In the right-hand column it is a simple entry.
- The voltage drop is calculated from the model (Section III.B).
- Conduction losses depend on the specific application. Table II provides some common expressions.
- Turn-on and turn-off losses are calculated as explained in Table II and Appendix 1.
- The corrections for gate resistance are multiplication factors obtained from Figure 9 of the data sheet, for a known value of gate drive impedance.
- The turn-on losses due to diode recovery can be calculated as explained in Section IV.C.
- The total losses are the sum of conduction and switching losses, including losses due to diode recovery.
- The RMS value of the fundamental component of the output current depends on the output waveform. For a square wave is 0.9 times its peak value.
- The total RMS component of a square wave is 1.

— The RMS value of the fundamental component of output voltage is, for a square wave, 0.9 times half the DC-link voltage.

VII. Brief Notes On Thermal Design

Quite unlike bipolar transistors, whose fundamental limitation in a practical circuit is its limited gain, IGBTs, power MOSFETs and thyristors are thermally limited. Hence, a good thermal design is the key to its cost effective utilization.

When the objective of the thermal design is just the selection of the heatsink that keeps the junction at, or below, a given temperature, the following expression provides the answer.

$$R_{\theta S-A} = \frac{\Delta T}{P_D} - R_{\theta J-C} - R_{\theta C-S}$$

The power dissipation can be calculated with the help of the left-hand side of the spreadsheet of Figure 11.

In general, the objective of the thermal design is the selection of the best device-heatsink combination and may require an iterative use of the right-hand side of the spreadsheet of Figure 11.

In order to obtain a thermal resistance case-to-sink that is close to the data sheet value, the mounting torque should be close to the maximum specified in the data sheet. An excessive mounting torque causes the package to bow and may crack the die. An inadequate mounting torque, on the other hand, gives poor thermal performance.

The temperature rise due to pulses of short duration can be calculated with the transient thermal response curves (Data sheet Figure 6). The section "Peak Current Rating" in application note AN-949 [9], originally written for HEXFETs, describes the procedure in detail and is, in this respect, equally applicable to IGBTs.

For short pulses (50µs or less) the temperature rise calculated with the transient thermal response curve tends to be too conservative. A more accurate method to calculate temperature rise can be found in Ref. [8].

VIII. Guidelines On Paralleling

Whenever devices are operated in parallel, due consideration should be given to the sharing between devices to ensure that the individual units are operated within their limits.

The three most important parameters from this point of view are: voltage, current and junction temperature. Voltage unbalances will be briefly examined in a qualitative way in the next section with other general considerations. The effects of current and temperature unbalances will be analyzed in detail in the following sections.

A. General paralleling guidelines

Generally speaking, voltage equality is ensured by the fact that the devices are in parallel. However, under transient conditions, voltage differentials can appear across devices, due to di/dt effects in unequaled stray inductances.

The stray inductances of a typical power circuit, like the one shown in Figure 12, have different effects, depending on where they are situated. The effects of the emitter and collector inductances that are common to the paralleled pair have been analyzed in [11] and [14] and will be ignored here.

An unbalance of 10% in the stray inductances that are in series with each collector, combined with a di/dt unbalance of 10% translates in an unbalance of 20% in the overshoot seen at turn-off (81 vs. 121V). To minimize these differentials both di/dt 's and stray inductances have to be matched. However, if the overshoot does not violate the ratings of the IGBT, the differential in the turn-off losses is negligible.

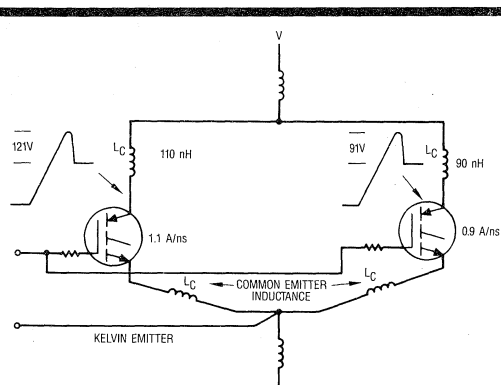


Figure 12. The effect of different di/dt and stray inductances on collector voltages.

The impact of the common emitter inductance on switching energy, on the other hand, is far from negligible, as explained in Section I.E. Furthermore, the IGBT with lower common source inductance turns off before the other, which is left to shoulder the entire load current during the turn-off transient [12]. It follows that switchmode operation of paralleled IGBTs should not be undertaken unless the common emitter inductances are matched in value.

Finally, like power MOSFETs, parasitic oscillation have been observed on paralleled IGBTs without individual gate resistors. It is assumed that the cause for this oscillation is the same as that reported in Ref. [12], Figure 17.

In summary, the following general guidelines should be followed when paralleling IGBTs:

- Use individual gate resistors to eliminate the risk of parasitic oscillation;
- Equalize common emitter inductance and reduce it to a value that does not greatly impact the total switching losses at the frequency of operation;
- Reduce stray inductance to values that give acceptable overshoots at the maximum operating current.

Stray components are minimized by a tight layout and equalized by symmetrical position of components and routing of connections.

These guidelines ensure that the voltage and switching unbalances due to the layout are negligible with respect to those due to the IGBTs themselves, analyzed in the next section.

B. Current and temperature unbalance

In this section we will examine the steady state conduction and temperature unbalance due to the IGBTs themselves and the effects of frequency and duty cycle.

The complexity of the algebraic equations does not allow a direct, closed form solution of general applicability. However, with the help of the models presented in Sections III and IV and a spreadsheet, we can establish the operating conditions of two paralleled IGBTs in a given application environment. The results, although specific to the application, provide a useful insight into the factors that come into play and their respective effects.

1. Selection Criteria For The IGBTs

As far as this analysis goes, two IGBTs (IRGPC50U) have been selected from a population of 15 devices from three different lots. The two IGBTs were at the two extremes of the distribution of voltage drop, one being the highest (IGBT 1), the other being the lowest (IGBT 2). Temperature and current were not a factor since both IGBTs remained, respectively, the highest and the lowest throughout the temperature and current range.

The conduction and switching parameters were generated for both IGBTs and are listed in the spreadsheets we will use to calculate the operating conditions, together with the average parameters for the entire population.

Notice that the analysis carried out in the following sections is based on two extreme but real IGBTs, chosen from a given population. As it should be expected, the IGBT with better conduction characteristics has worse switching characteristics.

From that same population we could have constructed the model for two *fictitious* IGBTs with extreme conduction *and* switching behavior. This, however, would have been at odds with the fundamental trade-off between conduction and switching characteristics, typical of the device itself.

2. The Thermal System

The heat generated by the two IGBTs is transmitted to a sink and, ultimately, to a common ambient. Two cases will be examined: common and separate heatsinks (Figure 13).

A common heatsink establishes a thermal coupling between the two dice that limits their temperature differential. As it will be seen later, if the thermal coupling is tight, as with dice mounted on the same spreader, the temperature differential is in the order of few degrees.

3. Steady State Operating Conditions

Being in parallel, the voltage drop across the IGBTs is the same. Hence, the IGBT with better conduction characteristics carries a larger share of the load current to make its voltage drop the same as the other. Its power dissipation and junction temperature are higher by an amount that depends on the thermal design, as we will now see.

For a given set of thermal conditions and a given common current, the individual currents and junction temperature can be calculated with a spreadsheet like the one shown in Figure 14. The spreadsheet is laid out to establish the operating point in the following way:

- Reasonable junction temperatures appear at the top of the Operating Conditions.
- The model parameters for that temperature are calculated.
- The current unbalance is calculated by means of the "solve" function. The equations that govern this relationship can be found in Appendix 2.
- Calculate conduction losses and temperature rise between junction and common sink for both IGBTs.
- Calculate temperature rise between common sink and ambient.
- Calculate both junction temperatures.
- Enter the junction temperatures thus calculated to the top of the box and repeat the process until the two temperatures become the same.

This process would, of course, be automated with a simple macro, as shown at the bottom of the figure.

The results of this analysis are shown in Figure 15. For low currents the conduction unbalance can be as high as 100%, i.e. one IGBT takes the entire current, operating, however, well within its limits. As the load current increases the current unbalance decreases and, long as the IGBTs are mounted on a common heatsink, the two temperatures stay within $\pm 10^\circ\text{C}$. The use of separate heatsinks causes large current unbalances and very significant temperature differentials.

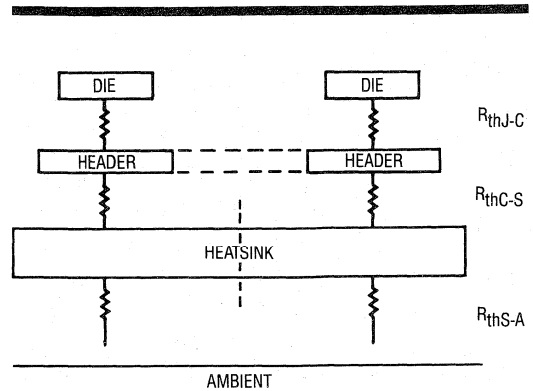


Figure 13. The characteristics of the thermal system of the paralleled IGBTs.

IGBT MODEL PARAMETERS

	IGBT 1 high drop	IGBT 2 low drop	nominal
Vt1	1.1784	1.0128	1.0994
Vt2	-0.0024	-0.0023	-0.0024
a1	0.3804	0.106	0.2021
a2	-0.0019	-7E-05	-0.0007
b1	0.3111	0.6148	0.4656
b2	0.0029	0.001	0.0019

APPLICATION ENVIRONMENT

Current	25
Ta	45
Rth s-a	1.20
Rth subs-sink	0.35
Rth j-subs	0.30 (single die)

OPERATING CONDITIONS

Tj	107.79	112.38	109.9
Vt	0.9197	0.7543	0.8356
a	0.1756	0.0984	0.1252
b	0.6194	0.7222	0.6766
Delta I	39.98%	5.00	-39.98%
I	7.50	17.50	12.50
Voltage drop	1.53	1.53	1.53
Cond. losses W	11.49	26.80	19.09
Delta T j-subs	3.45	8.04	5.73
Delta T subs-a		59.35	59.17
Tj	107.79	112.38	109.90
%	-1.91%	2.26%	0%

Alt-S {for b35, 1, 6, 1, b37}
7

Iterate {/ Math; Solve Go}
{/Block; Values} b29..d29 ~
b17 ~

Figure 14. Spreadsheet used to establish the operating conditions of two specific IGBTs in parallel. Model parameters are shown at the top. The parameters for the entire population are also listed for reference.

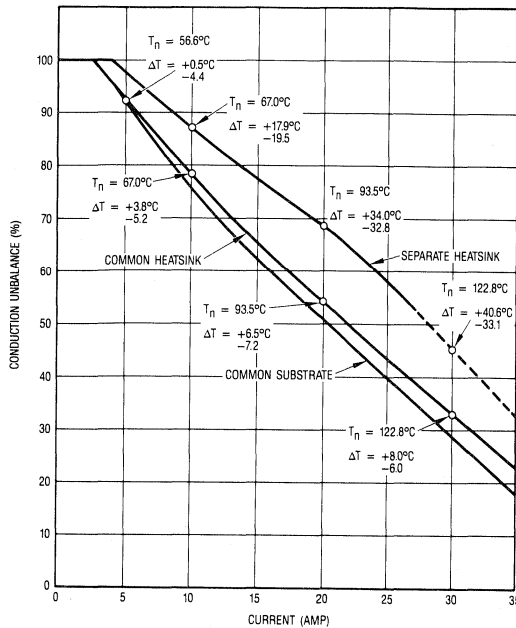


Figure 15. Conduction unbalance for two paralleled IGBTs as a function of current for three different thermal designs.

The first factor that keeps the unbalance in check is the thermal feedback between the two junctions. The one with higher power dissipation increases the sink temperature and, consequently, the junction temperature of the other, by an amount that is inversely proportional to the thermal resistance between the junctions. If the thermal coupling between dice is tight, the temperature differential cannot be significant.

The other factor that reduces the current unbalance is the temperature coefficient of the voltage drop. Although they are both negative, the IGBT with lower voltage drop has a lower temperature coefficient. As current and temperature increase, its voltage drop changes little, while the voltage drop of the IGBT that was carrying little current comes down significantly, thereby closing the gap in current, as well as temperature.

There is a third balancing mechanism: as collector current increases, the voltage drop of the two IGBTs converge toward the average of the distribution. This intrinsically reduces the unbalance at higher currents.

4. The Effect of Frequency and Duty Cycle

In a practical applications the two IGBTs would be operated at some frequency and the losses in both devices would have a switching component.

The IGBT that carries more current will also be switching a higher current. Hence, it has higher conduction, as well as higher switching losses. The unbalance in losses is further compounded by the fact that, as we have mentioned previously, this same IGBT exhibits a worse switching behavior, which further increases its switching losses.

IGBT MODEL PARAMETERS

	IGBT 1 high drop	IGBT 2 low drop	nominal
Vt1	1.1784	1.0128	1.0994
Vt2	-0.0024	-0.0023	-0.0024
a1	0.3804	0.106	0.2021
a2	-0.0019	-7E-05	-0.0007
B1	0.3111	0.6148	0.4656
b2	0.0029	0.001	0.0019
p1	-0.0033	-0.005	-0.0031
p2	0.0001	0.0002	0.0002
q1	1.8428	1.7941	1.7994
q2	-0.0027	-0.0029	-0.0026

APPLICATION ENVIRONMENT

Duty cycle	0.5		
Operating voltage	360		
Ipeak	44.43	Irms, pole, fund.	40.0
Ta	45		
Rth s-a	1.20		
Rth c-s	0.24		
Rth j-c	0.64		
Frequency (kHz)	0.4		

OPERATING CONDITIONS

Tj	115.64	123.13	118.43
Vt	0.9009	0.7296	0.8152
a	0.1607	0.0976	0.1192
b	0.6418	0.7325	0.693
p	0.0127	0.0186	0.0148
q	1.5306	1.4407	1.4915
i	16.15	-27.31%	28.28
Voltage drop	1.86	1.86	
Cond. losses W	15.01	26.29	20.41
Sw. losses W	0.27	0.69	0.45
Delta T j-sub	9.78	17.26	13.35
Delta T subs-a		60.85	60.07
Tj	115.62	123.11	118.42
%	-2.37%	3.96%	0%
Delta T	-2.8 °C	4.7 °C	0

Figure 16. Spreadsheet to calculate the operating conditions of two paralleled IGBTs operated in switchmode.

Thus, it would appear that a regenerative process is in place that will quickly take the junction temperature of the IGBT with lower conduction losses beyond its rated limits and that this regenerative process is accelerated by the operating frequency. In practice this does not happen and frequency helps bring about balanced operation, as we are about to see.

One additional unbalancing element, disregarded in the following calculations, is due the fact that, with a clamped inductive load, the IGBT that goes off last, ends up carrying the entire load current. This turn-off unbalance can be disregarded only to the extent that the turn-off times of the devices is short compared to the individual stray inductances, which tends to reduce this source of unbalance.

The operating conditions can be calculated with a spreadsheet similar to that shown in Figure 14, except that additional entries are required for the switching losses (Figure 16).

Curves of current and temperature unbalance have been generated for the popular "half-bridge" circuit, as shown in Figure 17a. From these curves we observe the following:

1. As the frequency increases the current unbalance decreases. The rate of decrease increases with frequency.
2. As the current increases the amount of unbalance decreases. This result is consistent with the observations made in the previous section.

3. As the frequency increases the temperature differential increases, then decreases rapidly.

The key balancing mechanism in this, as in the steady state mode of operation, is the different temperature coefficients of the voltage drop. As we have seen in the previous section, an increase in current causes an increase in temperature which, in turn, causes a reduction in voltage drop that is larger for the IGBT with a higher voltage drop. Hence, an increase in temperature results in a reduction in current unbalance.

Switching losses increase junction temperature of both IGBTs and contribute to reduce the current unbalance. However, the increase in temperature is higher for the IGBT which carries the higher current, on account of its higher conduction and switching losses. This delays the balancing mechanism and causes the increase in temperature differential noticeable in Figure 17 between 10 and 30 kHz ($I = 20A_{RMS}$).

The thermal coupling and the difference in temperature coefficients gradually cause a reduction in the current unbalance. This, in turn, reduces conduction and switching losses in the IGBT that was carrying more current, thereby bringing about a more balanced operating condition at an exponential rate.

For the specific IGBTs we have modelled the point of current balance occurs at a temperature that is somewhat higher than $150^{\circ}C$. At this point there will still be a temperature differential, on account of different switching losses. It is entirely possible that IGBTs with different characteristics may reach current balance at a lower temperature, beyond which the unbalance would reverse.

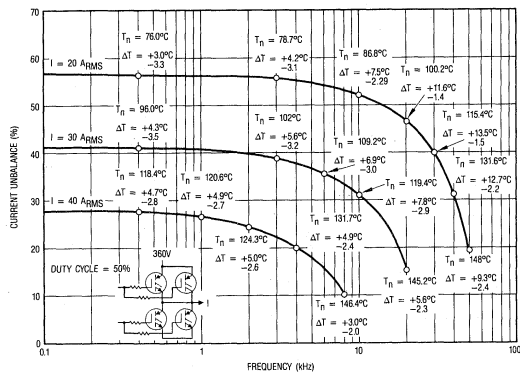
Operation at lower duty cycles is not significantly different from what we have just described (Figure 17b), except that the current unbalance for a given output current is lower.

This is due to the third balancing mechanism, whereby the voltage drops converge at higher currents. To generate the same output current with a lower duty cycle a higher peak current is necessary, with intrinsically better current sharing.

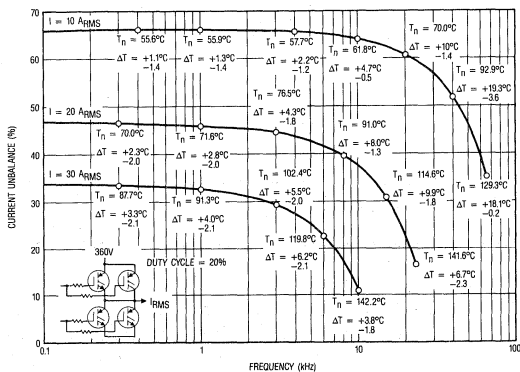
C. Conclusions

Although the analysis presented in the previous sections is limited to one specific type of IGBTs in a specific operating mode, the results have been found to be equally applicable to the other families of IGBTs available from International Rectifier at the time of writing. They can be summarized as follows:

1. Paralleled IGBTs will operate with a current unbalance that, in a practical application, can be as high as 50 to 70% at low currents. Temperature unbalance, on the other hand, is generally less than $10^{\circ}C$, provided they are on the same heatsink.



a. Duty cycle of 50%



b. Duty cycle of 20%

Figure 17. Current and temperature unbalance as a function of frequency of two IGBTs operated in parallel.

2. Three balancing mechanisms tend to reduce the current unbalance:
 - thermal feedback;
 - different temperature coefficients of the voltage drop;
 - converging voltage drop characteristics at higher currents.
3. The tighter the thermal coupling, the lower the unbalance. Operation of paralleled IGBTs on separate heatsinks should be avoided.
4. An increase in junction temperature reduces the unbalance, on account of the different temperature coefficients of the voltage drop. An increase in frequency has the same effect, for the same reason.
5. An increase in current reduces the unbalance, due to converging dynamic resistances. It would also cause an increase in temperature and, consequently, a further reduction in unbalance.
6. For a given output current, a decrease in duty cycle causes an increase in peak current, hence a reduction in unbalance. □

References

- | | |
|--|--|
| [1] AN-937A: Gate Drive Characteristics and Requirements | [9] AN-949: Current rating, SOA and High Frequency Switching Performance. |
| [2] AN-944: A New Gate Charge Factor | [10] International Rectifier data sheets PD-6.017 and PD-6.018 |
| [3] Switching Waveforms of the L ² FET, by C.F. Wheatley and H.R. Ronan IEEE Transactions on Power Electronics, April 1987 p. 81 | [11] AN-936: The Do's and Don'ts of Using Power HEXFETs |
| [4] AN-978: High Voltage Floating MOS-Gate Driver IC | [12] AN-941: A Chopper for Motor Speed Control |
| [5] AN-967: Using HEXFET III in PWM Inverters for Motor Drives and UPS Systems | [13] Nondestructive RBSOA characterization of IGBTs and MCTs by Dan Y. Chen, VPI Current, Fall 91 |
| [6] AN-983A: IGBT Characteristics | [14] AN-947: Understanding HEXFET switching performance. |
| [7] AN-984: Protecting IGBTs against Short Circuit | [15] Analysis and characterization of power MOSFET switching performance, by S.M. Clemente, A. Isidori, B.R. Pelly. Proceedings of Powercon 8, 1981, H2. |
| [8] Transient Thermal Response of Power Semiconductors to Short Power pulses, by S. Clemente, Proceedings of the European Power Conference, Florence 1991. | |

APPENDIX 1: Description of the curve fitting methods used to derive the model parameters.

The conduction model presented in Section III fulfills the basic requirements of accuracy and simplicity. As it shown in Table II, it lends itself to easy integration, thus providing a closed form expression for the conduction losses of common waveforms.

The parameters of the model are extracted from the averages and standard deviations taken at a given temperature on a population of IGBTs from three different lots, as shown in Table A.1.

Table A.1. Conduction Characteristics of a Population of IGBTs from three different Lots

VCE(ON) DEVICE LOT #'S:	TEMP 100°C					
	Ic (A) >	0.6	8	16	32	50
BC40F						
FS 4						
FQ 8						
FS 3						
1	0.694	1.127	1.418	1.925	2.460	
2	0.678	1.114	1.413	1.940	2.500	
3	0.677	1.097	1.382	1.885	2.400	
4	0.685	1.112	1.399	1.899	2.420	
5	0.711	1.178	1.485	2.010	2.570	
6	0.743	1.263	1.604	2.190	2.830	
7	0.732	1.223	1.541	2.090	2.670	
8	0.723	1.206	1.524	2.080	2.660	
9	0.746	1.264	1.602	2.190	2.810	
10	0.731	1.223	1.543	2.090	2.670	
11	0.694	1.157	1.470	2.010	2.600	
12	0.714	1.193	1.513	2.060	2.650	
13	0.714	1.189	1.506	2.050	2.650	
14	0.700	1.147	1.512	1.980	2.550	
15	0.706	1.151	1.470	1.990	2.560	
MINIMUM	0.677	1.097	1.382	1.885	2.400	
MAXIMUM	0.746	1.264	1.604	2.190	2.830	
AVERAGE	0.710	1.176	1.492	2.026	2.600	
STD	0.021	0.051	0.066	0.091	0.122	
AVG + 6STD	0.838	1.484	1.888	2.572	3.331	
AVG-6STD	0.581	0.868	1.097	1.480	1.869	

To calculate a and b the model is manipulated as follows:

$$V_{ce} = V_t + I^b$$

$$V_{ce} - V_t = a I^b$$

$$\ln(V_{ce} - V_t) = \ln a + b \ln I$$

This last expression is a straight line fit to the natural logarithms of I and $V_{ce} - V_t$. Using the least square method, the values of $\ln a$ and b can be obtained by the following formulas:

$$b = \frac{n \sum \left\{ (\ln I_i) \times [\ln(V_{ce} - V_t)]_i \right\} - \left[\sum (\ln I_i) \right] \times \left[\sum \ln(V_{ce} - V_t)_i \right]}{n \sum (\ln I_i)^2 - \left[\sum (\ln I_i) \right]^2}$$

$$\ln a = \frac{\sum \ln(V_{ce} - V_t)_i}{n} - b \frac{\sum (\ln I_i)}{n}$$

$$a = e^{\ln a}$$

The value of V_t has been defined as the voltage drop at a current density of approximately 0.035 a/mm², which, for the IGBT of Table A.1, corresponds to 0.6A. With this in mind, Table A.2 shows the calculations and the error.

The values entered in Table A.2 correspond to the averages of Table A.1. If the average-plus-three-sigma values had been entered, the model parameters would correspond to the data entered.

Table A.2. Calculation of the Voltage Drop Parameters

A	V	V cal	V-Vcal	Error	V-Vt	ln(V-Vt)	ln(I)	(XiYi)	
0.60	0.71	0.77	-0.0645	-9.08%					
800	1.18	1.17	0.0026	0.22%	0.4660	-0.7636	2.0794	-1.5878	
1600	1.49	1.50	-0.0035	-0.23%	0.7820	-0.2459	2.7726	-0.6818	
3200	2.03	2.04	-0.0155	-0.76%	1.3160	0.2746	3.4657	0.9517	
5000	2.60	2.58	0.0198	0.76%	1.8900	0.6366	3.9120	2.4903	
					n =	4	-0.0983	12.2298	1.1724
					b =	0.7614	Sum Yi	Sum Xi	Sum XiYi
					ln a =	-2.3524	Varian	0.4837	
					a =	0.0951			

This process can be repeated for different temperatures and a set of model parameters would be obtained. Each element of the set provides an accurate model of the specific IGBT at a specific temperature.



Unfortunately, in most design problems the junction temperature is the unknown (see Figure 11, 14 and 16) and fixed temperature parameters, like those shown in Table A.2 are not useful. Assuming that these parameters have a simple temperature dependence, a linear regression has been done, as shown in Table A.3. This provides the expression of the voltage drop as a function of current and temperature with which we have analyzed the operating conditions of Figure 11, 14 and 16. As shown in Table A.3 the accuracy of the parameter obtained with the linear regression is within few percent.

The switching model parameters are obtained in a very similar way, using the same type of expression, except for the threshold. The accuracy of the linear regression to calculate the temperature coefficients is acceptable for some IGBTs, particularly the Standard and the Fast, while an exponential regression is more accurate for the Ultra-fast. For the sake of simplicity, only the linear regression is listed in Tables I and III. □

Table A.3. Linear Regression for Temperature Coefficient of Voltage Drop Parameters

Temp	a	a (calc)	Error	b	b (calc)	Error	Vt	Vt Calc	Error
25		0.0778			0.7391			0.85	
50	0.0814	0.0832	-2.23%	0.7523	0.7469	0.72%	0.80	0.80	-0.40%
75	0.0899	0.0886	1.27%	0.7496	0.754-	-0.69%	0.76	0.76	0.28%
100	0.0951	0.0941	1.13%	0.7614	0.7626	-0.16%	0.71	0.71	0.34%
125	0.1009	0.0995	1.40%	0.7668	0.7704	-0.48%	0.66	0.66	0.26%
150	0.1030	0.1049	-1.86%	0.7829	0.7783	0.59%	0.61	0.61	-0.49%
500	0.4703			3.8129			3.5380	6.83E-02	
(XiYi) =	48.3873			(XiYi) =	383.2507		(XiYi) =	341.7250	
SxiΛ2 =	56250								
a	= a1 + a2*T			a1 = 0.0724			a2 = 2.17E-04		
b	= b1 + B2*T			b1 = 0.7313			b2 = 3.13E-04		
Vt	= Vt1 + Vt2*T			Vt1 = 0.9008			Vt2 = -1.9E-03		

APPENDIX 2: Equations to identify the operating point of paralleled IGBTs.

In the system described in sections IIX.B.1 and B.2 the parameters listed in the two top boxes of Figure 16 are known, whilst those listed in the third box have to be calculated. The two fundamental constraints that determine the current distribution between the IGBTs are the following:

- voltage drop across the two IGBTs is the same;
- the sum of the currents is the same and equal to the load current.

Imposing these two constraints to the voltage drop model we obtain the following:

$$V_{CE-1} = V_{CE-2}$$

$$V_{T1} + a_1 I_{L1}^{(b,1)} = V_{T2} + a_2 I_{L2}^{(b,2)}$$

$$\left(\frac{I_L}{2} + \Delta I \right) = \exp \left\{ \frac{1}{b_2} \ln \left[\frac{V_{T1} - V_{T2}}{a_2} + \frac{a_1}{q_2} \left(\frac{I_L}{2} - \Delta I \right)^{(b,1)} \right] \right\}$$

where the index after the dash identifies the IGBT, while the index before the dash identifies the model parameter, e.g. V_{T1-2} identifies the first threshold parameter (see Figure 14) of the second IGBT.

Since the key unknowns are ΔI , T_1 and T_2 , we need two additional expressions, which can be obtained from the thermal equations:

$$T_2 = T_A + I_L \left(V_{T2} - a_2 I_2^{(b,2)} \right) \theta_{SA} + \left(I_2 V_{T2} + a_2 I_2^{(b,2+1)} \right) \theta_{JS}$$

$$T_1 = T_A + I_L \left(V_{T2} + a_2 I_2^{(b,2)} \right) \theta_{SA} + \left[I \left(V_{T2} + a_2 I^{(b,2)} \right) - \left(I_2 V_{T2} + a_2 I_2^{(b,2+1)} \right) \right] \theta_{JS}$$

The first of these expression is calculated in the cell shown on the right of the Operating Conditions box with the “solve for” function, with the parameters shown in the box. Successive calculations of current and temperature yield the final result. For these calculations the following simplification was made in the first expression:

$$V_{T1} - V_{T2} \cong (V_{T2-1} - V_{T2-2}) (T_1 - T_2)$$

of minimal impact on overall accuracy. □

Introduction to the 600V ADD-A-pak™ and INT-A-pak™ IGBT Modules

by J. Catt, R. Chokhawala, B. Pelly

Summary

Insulated Gate Bipolar Transistor (IGBT) modules are the preferred switching components for currents above a few tens of amperes in applications such as inverters and choppers for motor control, uninterruptible power supplies, welders, induction heaters, active filters and power factor correctors. Compared with older bipolar transistor modules, IGBTs offer better efficiency, higher switching frequency, and simpler drive circuitry.

International Rectifier IGBT modules, in particular, have significantly superior characteristics over bipolar transistors, as well as over other types of IGBT modules. These superior characteristics are the result of a unique design that offers higher switching speed, better efficiency, and snubberless operation.

This application note introduces International Rectifier's initial 600V IGBT ADD-A-pak™ and INT-A-pak™ module offerings, explains their operating characteristics and data sheet ratings, and illustrates their superior performance capabilities.

Relationships Between Saturation Voltage and Switching Energy

The current that an IGBT can handle is determined by the amount of power dissipation that the current produces. The power dissipation is comprised of two major components. The first is the conduction loss due to the conduction voltage, $V_{CE(ON)}$. The second is the switching loss due to the energy dissipated each time the IGBT is switched on and off.

The switching energy depends upon the current and voltage at the instant of switching and the speed at which the IGBT switches from the "on" state to the "off" state, and vice versa.

The conduction loss is independent of frequency, whereas the switching loss is directly proportional to frequency.

A fundamental trade-off exists, in the design of an IGBT, between the conduction voltage and the switching energy. This is illustrated in Figure 1.

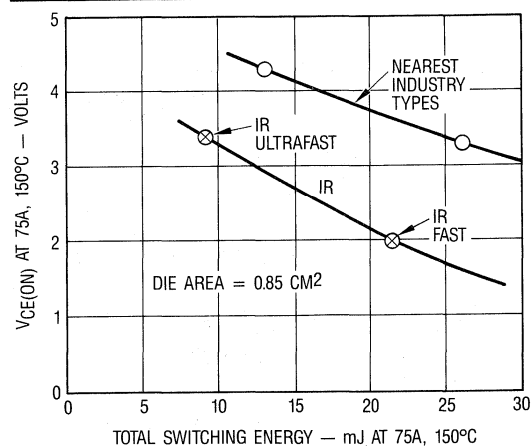


Figure 1. $V_{CE(ON)}$ versus switching energy relationships for the IR 600V IGBT modules and comparison with nearest industry types.

An IGBT designed for low conduction voltage will have relatively high switching energy; one designed for low switching energy will have relatively high conduction voltage. The former type will be more suited to lower frequency operation, where the average switching losses are low because the frequency is low; thus the total losses are minimized by optimizing the conduction losses. The latter type will be more suited to higher frequency operation, where the average switching losses are

significant and total losses are minimized by optimizing the characteristics of the IGBT for lower switching energy, but with correspondingly higher conduction voltage.

IR's IGBTs have a unique design structure which provides a fundamentally superior conduction voltage versus switching energy relationship. Figure 1 compares this relationship for IR's IGBT technology versus a corresponding relationship for a typical competitive IGBT technology.

IR's technology offers significantly lower switching energy for a given conduction voltage; conversely, it offers appreciably lower conduction voltage for a given switching energy.

The fundamentally superior characteristics of IR's IGBTs mean that they can be operated at higher current density than other industry types. This has the following important application advantages:

- The physical size of IR's module, for a given operating current, can generally be smaller than that of competitive types.
- Operating losses for a given current, voltage, and frequency are generally smaller. Efficiency is higher, and heatsink size can often be smaller, giving a more compact equipment design.
- For a given heatsink, operating current can often be significantly higher.

Fast And Ultrafast IGBT Families

Figure 1 illustrates a continuum of possible IGBT designs that could fit anywhere along the curve. International Rectifier has selected two points on this continuous design curve as the basis for two standard families of IGBTs called "Fast" and "Ultrafast."

The Fast IGBT family has relatively low conduction voltage, with correspondingly less than minimum possible switching energy; it is generally best suited to operation at frequencies below 10kHz.

The Ultrafast family has near-minimum switching energy, with correspondingly higher conduction voltage; it is best suited to frequencies above a few kHz, to well beyond 20kHz.

The above operating frequencies apply to circuits that employ "hard switching," i.e., to circuits in which the IGBTs must switch the full circuit current at the full circuit voltage.

Much higher operating frequencies are feasible in "soft switching" resonant circuits; in these circuits, even though the IGBT handles high current and high voltage, it is not required to *switch* high current at high voltage.

The Fast IGBT family can attain frequencies of about 80kHz in resonant circuits, while the Ultrafast IGBT family can achieve 200kHz or more in these circuits.

Package Outlines

IR's initial high current IGBT modules are offered in the company's ADD-A-pak and INTA-pak outlines. Pictures of these packages are shown in Figure 2. Outline drawings are shown in Figure 3.

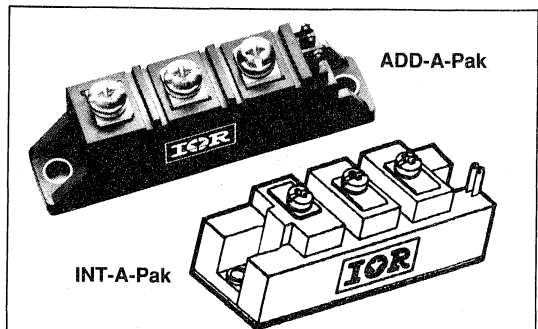


Figure 2. ADD-A-pak and INTA-pak modules.

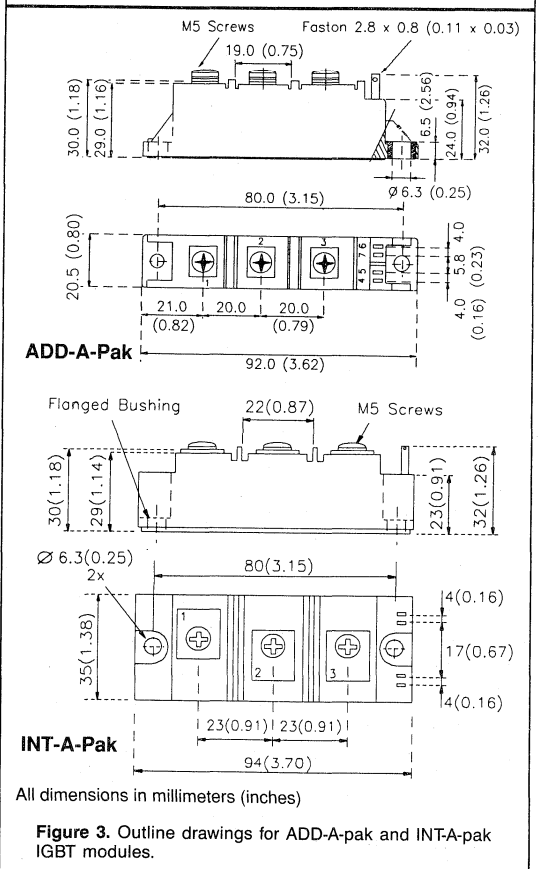


Figure 3. Outline drawings for ADD-A-pak and INTA-pak IGBT modules.

Both packages are industry-standards. The smaller Add-A-pak is a popular industry-standard for rectifiers, SCRs and MOSFETs. It has not previously been widely offered for IGBTs, but is well suited to IR's "silicon efficient"

IGBT technology. The INTA-pak is a well established industry-standard for rectifiers, SCRs, bipolar transistors and IGBTs.

Both packages have the same mounting hole dimensions and terminal heights as each other. The terminals of the ADD-A-pak are spaced on 20mm centers, versus 23mm centers for the INTA-pak.

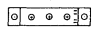
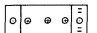

Due to IR's superior IGBT technology, the ADD-A-pak commonly will offer the same current capability, but with lower power dissipation than a competitive INTA-pak type IGBT module. It will often be possible, in a given application, to substitute IR's ADD-A-pak for a larger competitive INTA-pak type module, obtaining equivalent or better performance with otherwise minor design changes.

By the same token, IR's INTA-pak module offers the same current ratings as larger competitive "double" INTA-pak type modules and will often be able to replace these larger modules.

A comparison of the current ratings of IR's ADD-A-pak and INTA-pak modules, versus current ratings of competitive modules, is summarized in Table 1.

TABLE 1

Comparison of Continuous Current Ratings of 600V IR ADD-A-pak and INTA-pak Half-Bridge IGBT Modules Versus Other Industry Types

	Package Types			
	ADD-A-pak	INTA-pak	"Double INTA-pak"	
				
	International Rectifier		Other Industry Types	
Continuous Rated Current of 600V Half-Bridge Modules	35 - 90A	50 - 200A	15 - 100A	100 - 300A

Circuit Configurations

Standard circuit configurations for IR's present range of Add-A-pak and INTA-pak IGBT modules are the "half-bridge" and "chopper" configurations, illustrated in Figure 4.

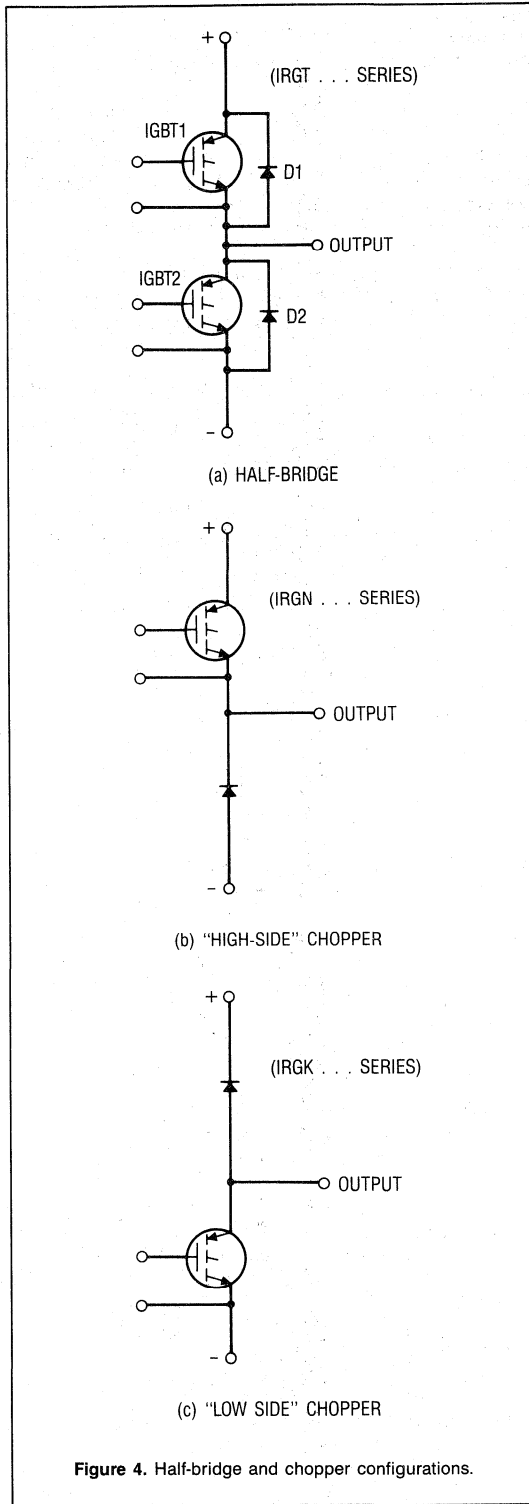


Figure 4. Half-bridge and chopper configurations.



The half-bridge is primarily intended for half-bridge, H-bridge, and 3-phase bridge circuits, as shown in Figure 5. The chopper is primarily intended for the buck, "double forward" and "boost" converter circuits, as shown in Figure 6.

It should be noted that the IGBT in the chopper module does not have an antiparallel diode connected across it.

The circuits in which the chopper module will typically be used usually do not fundamentally require an antiparallel diode, because the voltage across the IGBT does not normally reverse.

The reverse voltage capability of the IGBT is limited. If the practical circuit operation is such that a reverse voltage (even a transient) of greater than about 10V can occur, an external diode should be connected across the IGBT.

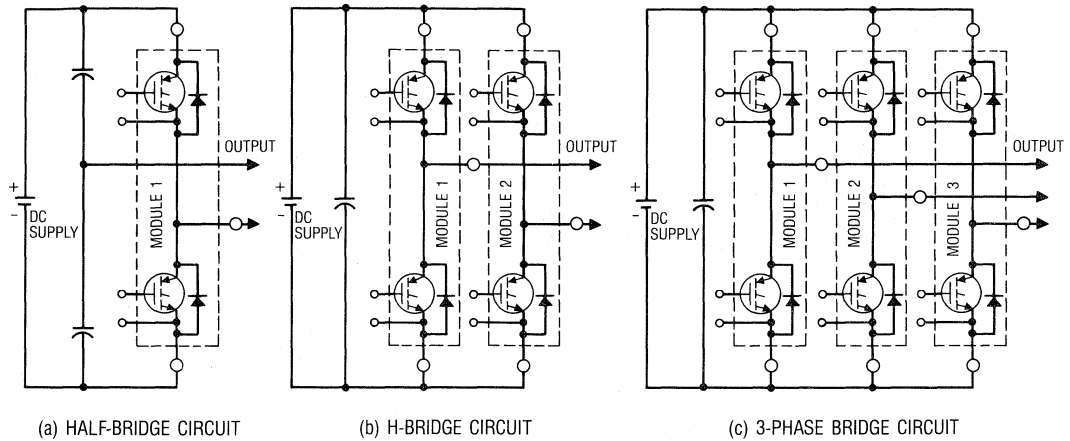


Figure 5. Typical circuits for half-bridge IGBT modules.

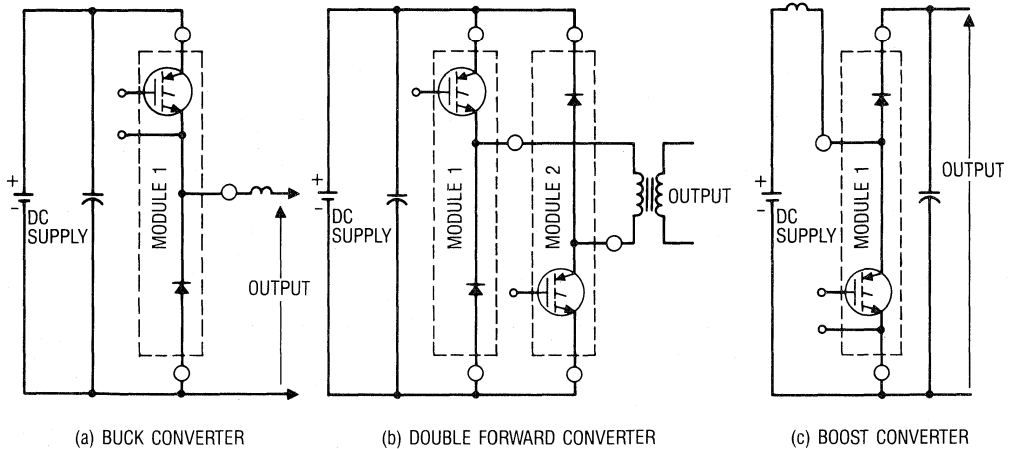


Figure 6. Typical circuits for chopper modules.

Current Ratings

Current ratings of the 600V "half-bridge" and "chopper" ADD-A-pak and INT-A-pak modules range from 35 to 200A. Table 2 gives a summary.

IGBT Conduction Characteristics

The conduction voltage, $V_{CE(ON)}$, of the IGBT is a

function of the collector current, the gate drive voltage, and the junction temperature.

Typical conduction characteristics are exemplified by those for International Rectifier's 90A Half-Bridge Fast ADD-A-pak IGBT module in Figure 7(a), and for the 65A Half-Bridge Ultrafast ADD-A-pak module in Figure 7(b).

Table 2

Ratings and Part-Numbers of IR's 600V ADD-A-pak and INT-A-pak Half-Bridge and Chopper IGBT Modules

ADD-A-pak						INT-A-pak					
FAST			ULTRAFAST			FAST			ULTRAFAST		
Continuous Current Amps	Part Number		Continuous Current Amps	Part Number		Continuous Current Amps	Part Number		Continuous Current Amps	Part Number	
	1/2 Bridge	Chopper		1/2 Bridge	Chopper		1/2 Bridge	Chopper		1/2 Bridge	Chopper
50	IRGTA050F06	IRGKA050F06 IRGNA050F06	35	IRGTA035U06	IRGKA035U06 IRGNA035U06	65	IRGTI065F06	IRGKI065F06 IRGNI065F06	50	IRGTI050U06	IRGKI050U06 IRGNI050U06
90	IRGTA090F06	IRGKA090F06 IRGNA090F06	65	IRGTA065U06	IRGKA065U06 IRGNA065U06	120	IRGTI120F06	IRGKI120F06 IRGNI120F06	90	IRGTI090U06	IRGKI090U06 IRGNI090U06
120		IRGKA120F06 IRGNA120F06	90		IRGKA090U06 IRGNA090U06	165	IRGTI165F06	IRGKI165F06 IRGNI165F06	115	IRGTI115U06	IRGKI115U06 IRGNI115U06
						200	IRGTI200F06	IRGKI200F06 IRGNI200F06	140	IRGTI140U06	IRGKI140U06 IRGNI140U06

NOTE "K" IN PART NUMBER FOR CHOPPER DENOTES "LOW SIDE" IGBT
"N" IN PART NUMBER FOR CHOPPER DENOTES "HIGH SIDE" IGBT

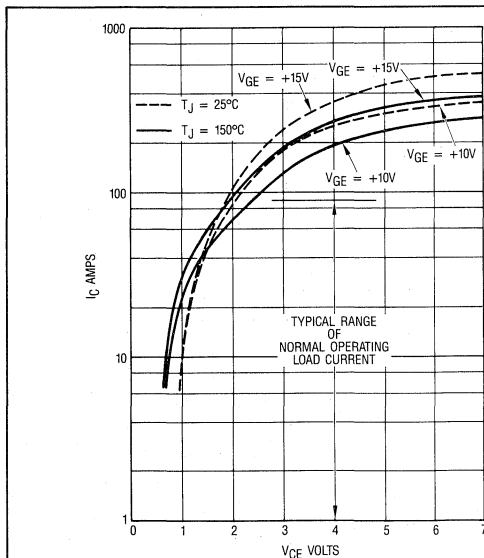


Figure 7a. Typical relationships between collector-emitter voltage V_{CE} , collector current I_C , gate-emitter drive voltage V_{GE} , and junction temperature T_J (IRGTA090F06 Fast module type).

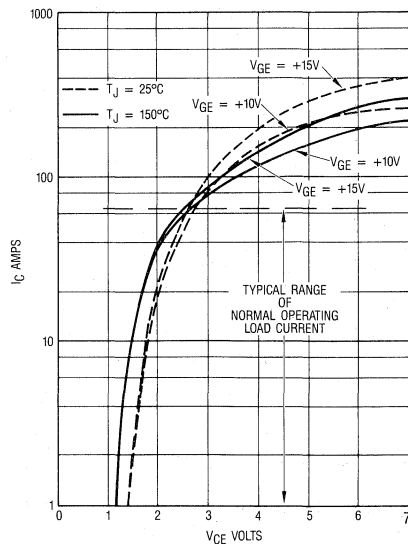


Figure 7b. Typical relationships between collector-emitter voltage V_{CE} , collector current I_C , gate-emitter drive voltage V_{GE} , and junction temperature T_J (IRGTA065U06 Ultrafast module type).

Within the range of typical application operating current, variation of the gate drive voltage between 10V and 15V has rather minor impact upon V_{CE} of the Ultrafast IGBT. For example, at 50A and $T_J = 150^\circ\text{C}$, $V_{CE(ON)}$ is typically 2.35V, with V_{GE} of 10V. Increasing V_{GE} to 15V decreases $V_{CE(ON)}$ by about 60mV – a relatively minor reduction.

Variation of the gate drive voltage has a more significant impact upon $V_{CE(ON)}$ of the Fast IGBT. For example, at 70A and $T_J = 150^\circ\text{C}$, $V_{CE(ON)}$ is typically 2.1V with $V_{GE} = 10\text{V}$, and 1.7V with $V_{GE} = 15\text{V}$.

Use of a lower, rather than higher, gate drive voltage has the advantage that it gives a lower “current ceiling,” at which the IGBT becomes “self current-limiting.” This may be beneficial in controlling the amplitude of and protecting against overload and fault current above the normal operating level.

Switching Characteristics

Effect of load inductance

The load connected to the output of a half-bridge or chopper module will almost invariably have an inductive component. This typically could be due to the inductance of a motor, the leakage inductance of a transformer, the inductance of an output filter, or simply the inductance of the wiring between the output terminal and the load.

Almost always, the load inductance will be at least a few micro Henries; this amount of inductance is sufficient to force the amplitude (and direction) of the current at the output terminal to stay practically unchanged during the short switching transition of the IGBT.

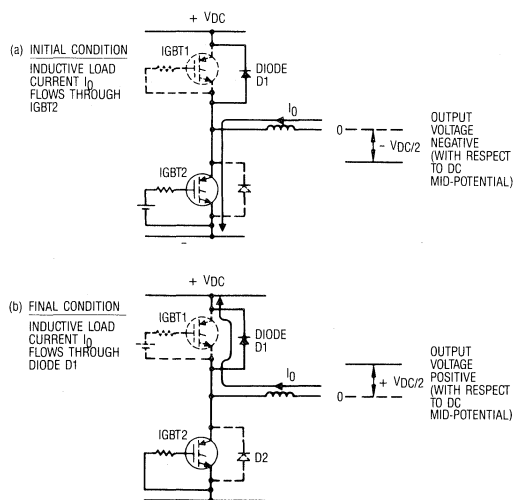


Figure 8. Initial and final conditions for commutation of inductive load current from the “lower” to the “upper” switch. IGBT 2 and diode D1 are active participants. IGBT 1 and diode D2 are “bystanders.”

Consider the situation, illustrated in Figure 8(a), in which current I_0 initially flows into the output terminal of the module via IGBT 2. When IGBT 2 is switched off, the output inductance prevents I_0 from instantaneously changing amplitude or direction. The output current is simply transferred to the antiparallel diode, D1, of the “opposite” IGBT, as illustrated in Figure 8(b).

Thus, the immediate effect of switching the IGBT off has been to reverse the polarity of the output voltage. The amplitude and direction of the output current instantaneously remain unaltered, because any significant change of the output current simply does not have time to occur during the “micro” period of the IGBT switching transition. This is by far the most common mode of switching an IGBT module; it is commonly referred to as “clamped inductive load” switching.

Following the switching transition itself, the amplitude and/or direction of the output current may change. This will be the intended result of the “macro” switching regime of the circuit.

For a given direction of output current, one IGBT and the antiparallel diode of the “opposite” IGBT of a half-bridge module are “active” current-carrying participants during the switching transition. The other IGBT and diode do not carry current and are essentially “bystanders.”

“Chopper” modules contain just one IGBT and one “freewheeling” diode, and inherently carry output current of just one polarity. The half-bridge’s “bystander” components, during the switching transition, are therefore physically absent from the chopper. Relatively minor effects of the capacitance of the half-bridge’s “bystander” components are therefore absent from the chopper; but otherwise the chopper’s switching operation is essentially the same as that of the half-bridge.

Effect of dc loop inductance

The basic circuit configuration of the half-bridge or chopper module ensures that a path is always provided via a diode for the flow of “inductive” output current, even if the IGBT is off. Thus – if there is no inductance in the “dc loop” – the voltage at the output of a half-bridge is rigidly clamped by the diodes; it cannot go above the upper dc bus voltage, nor below the lower dc bus voltage.

In practice, stray “dc loop” inductance exists, due to inductance of the dc bus capacitor, busbar or wiring inductance, and inductance of the internal connections of the module itself. This stray “dc-loop” inductance is represented by the “lumped” inductors L_{S1} and L_{S2} in Figure 9.

DC loop inductance “spoils” the rigid voltage clamping action; transient voltages are developed across this inductance during the switching intervals, due to rapidly changing current in the dc loop. The greater is this stray

inductance, the greater is its "spoiling" action and the greater is the amplitude of the overvoltage transient developed across the IGBTs and diodes during switching.

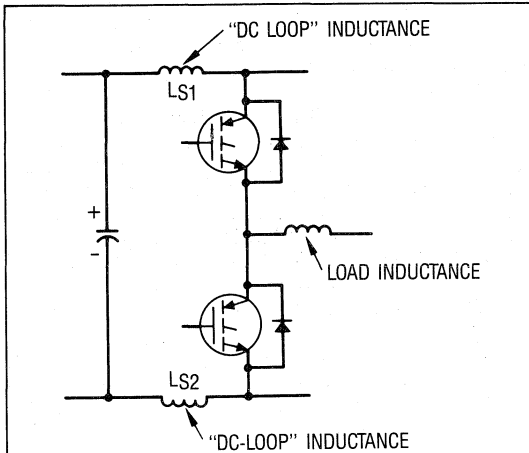


Figure 9. Equivalent circuit representing stray "dc loop" inductance.

Thus, while the value of the *load* inductance has essentially no impact upon the switching operation of the module, the value of the *dc loop* inductance has a major impact. The latter must be minimized to minimize the overvoltage switching transients across the IGBTs and diodes.

Turn-on and turn-off gate resistance

The switching performance of IR's IGBT modules will generally be optimized by using one value of "turn-on" gate resistance to charge the gate when turning on; and a second lower value of "turn-off" gate resistance to discharge the gate when turning off. This can be achieved with the circuit arrangement shown in Figure 10.

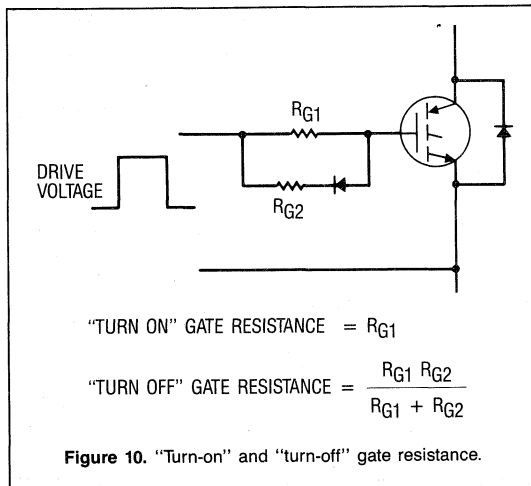


Figure 10. "Turn-on" and "turn-off" gate resistance.

Reference is made to "turn-on" and "turn-off" gate resistance in the following sections. The circuit arrangement in Figure 10 is tacitly assumed. Internal resistance of the drive voltage source itself (additional to R_{G1}/R_{G2}) is assumed to be comparatively small.

IGBT turn-on

Fundamentals of operation

During turn-on, the collector current of the IGBT is closely under the control of the applied gate-emitter voltage. This is similar to the turn-on operation of a power MOSFET.

The starting condition for "clamped inductive load" turn-on of the IGBT is with the output current, I_0 , flowing in the antiparallel diode of the opposite IGBT.

It helps to understand the operating waveforms to consider firstly the "theoretically ideal" case of no dc loop inductance and a "perfect" diode that has no reverse recovery charge. The modifying effects of reverse recovery and "dc loop" inductance will then be added.

Figure 11 shows idealized waveforms with no diode reverse recovery and no dc loop inductance. Gate voltage is applied at t_0 , via a series gate resistor. The gate-emitter voltage begins to rise, charging the gate-emitter capacitance of the IGBT. When the gate emitter voltage reaches the IGBT's threshold voltage, collector current starts to flow and the IGBT current rises in concert with the rising gate-emitter voltage. The diode current meanwhile decreases, the sum of the diode and IGBT currents remaining equal to the output current.

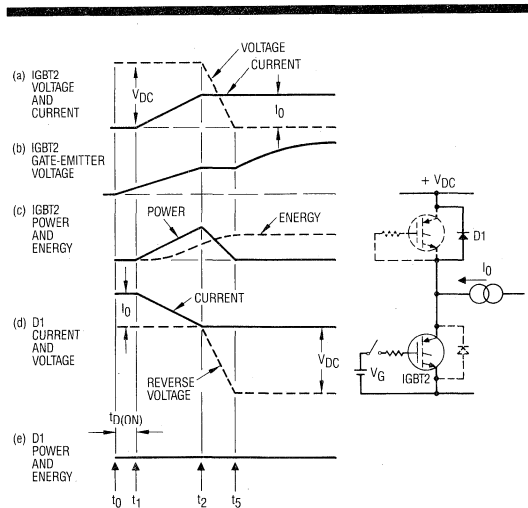


Figure 11. Idealized turn-on waveforms with no dc loop inductance and no diode reverse recovery.

Throughout the period t_1 to t_2 , the current in the diode is decreasing, but the diode is still in forward conduction. The voltage across the diode therefore remains at the diode's forward conduction level. This means that essentially the full dc bus voltage is "left" across the IGBT, which is simultaneously carrying an increasing share of the output current. The resulting instantaneous power loss in the IGBT, shown in Figure 11(c), is high.

The output current, I_0 , has transferred completely to the IGBT at time t_2 , while the diode current has simultaneously reached zero. The diode - assumed to have no reverse recovery - now starts to support reverse voltage. The diode voltage rises between t_2 and t_5 , while the voltage across the IGBT correspondingly falls. The IGBT voltage reaches it's "fully on" level at t_5 and the commutation process is complete.

The waveforms in Figure 12 illustrate the modifying effect of diode reverse recovery. Until time t_2 the waveforms are the same as in Figure 11. At t_2 , as before, the diode forward current has reached zero, but now the diode needs time to recover and cannot yet support reverse voltage. The diode starts to draw reverse recovery current from the dc supply and the IGBT current increases above the output current.

At time t_3 the IGBT current is equal to the sum of the output current and the peak reverse recovery current of the diode. The diode has begun to regain reverse blocking capability, and the reverse recovery current starts to decrease. At t_4 the diode's reverse recovery current reaches zero. At t_5 the IGBT voltage reaches it's "fully on" level and the commutation process is complete.

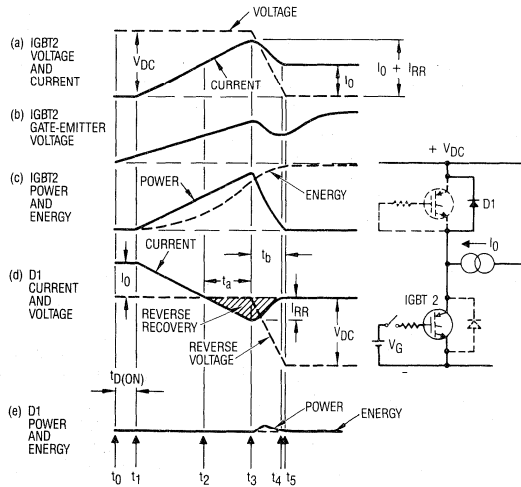


Figure 12. Idealized turn-on waveforms, with no dc loop inductance, illustrating the effect of diode reverse recovery.

Comparison of Figures 11(c) and (12c) shows that the reverse recovery of the diode accounts for significant additional turn-on energy dissipation in the IGBT, for two reasons. First, the peak IGBT current increases significantly above the output current. Second, the turn-on period is "stretched" by the recovery period of the diode. This elongation of the turn-on period, of itself, increases the turn-on energy, even without considering the extra recovery component of diode current.

A relatively small amount of switching energy is dissipated in the diode during the " t_b " recovery period as illustrated in Figure 12(e).

The effect of dc loop inductance is illustrated in Figure 13. As the IGBT current begins to rise at t_1 , the rate of change of current induces a voltage across the "dc loop" inductance, and the IGBT voltage starts to fall. The decreasing IGBT voltage causes current to flow through the gate-collector capacitance of the IGBT; this current is drawn from the gate circuit and diminishes the current available to charge the gate-emitter capacitance. This somewhat decreases the initial rate of rise of gate-emitter voltage and hence of the collector current.

During the period t_1 to t_2 , the collector voltage "floats" at an intermediate level that is less than the dc bus voltage, but much more than the conduction voltage of the IGBT. This "floating" collector voltage is sometimes misinterpreted as abnormal behaviour or "sluggishness" of the IGBT to turn on. Actually, it is simply the result of voltage "dropped" across the "dc loop" inductance, which would otherwise have been developed across the IGBT itself. This voltage drop in reality is beneficial during this time period because it *reduces* the voltage

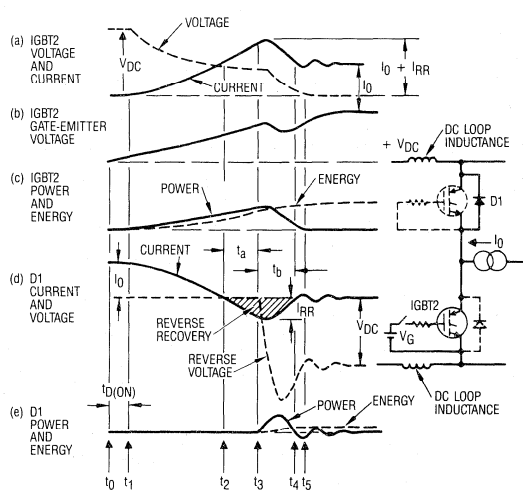


Figure 13. Idealized turn-on waveforms illustrating the effect of diode reverse recovery and dc loop inductance.

across the IGBT and hence also reduces the IGBT turn-on energy. (Turn-off energy, however, is increased.)

At time t_3 the diode begins to regain its reverse blocking capability; soon after, the diode reverse recovery current starts to decrease. At the peak of the reverse recovery current, the rate of change of current is zero and the voltage across the dc loop inductance is zero. At this instant, the sum of the IGBT and diode voltages is equal to the dc supply voltage.

As the recovery current starts to decrease, the di/dt and the voltage developed across the “dc loop” inductance change sign. The sum of the IGBT and diode voltages now *exceeds* the dc supply voltage and a transient overvoltage appears across the diode. This overvoltage is followed by a damped oscillation, caused by resonance of the loop inductance with the combined capacitance of the diode and that of the antiparallel “bystander” IGBT.

Comparison of Figures 12(c) and 13(c) shows that the dc loop inductance causes a significant *reduction* in the turn-on switching energy of the IGBT. This is actually beneficial at turn-on; but the benefit is short-lived because it is paid for by an approximately equal amount of *increased* switching energy during subsequent turn-off.

The dc loop inductance also increases the energy in the diode during the t_b recovery period, though this energy is comparatively small.

Effect of junction temperature on turn-on

The turn-on switching speed of IR’s IGBT is determined by majority carrier MOSFET-like action. Just as the switching speed of a MOSFET is independent of temperature, the switching speed of the IGBT at turn-on is also essentially independent of temperature. This is illustrated by the waveforms in Figure 14, which show that the rate of rise of current at turn-on is independent of temperature.

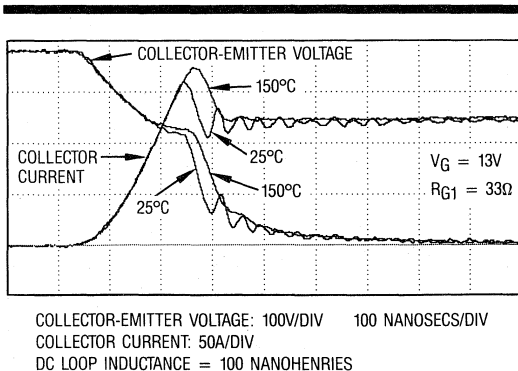


Figure 14. Oscilloscope waveforms of IGBT turn-on voltage and turn-on current at junction temperatures T_J of 25°C and 150°C (IRGTA065U06).

The minority carrier recovery characteristic of the diode, on the other hand, does depend on temperature. Peak reverse recovery current, reverse recovery charge and recovery time increase with increasing junction temperature. Thus, the peak IGBT turn-on current and the total turn-on energy in the IGBT increase with increasing temperature.

The waveforms in Figure 14 illustrate that the rate of change of diode current, during the “ t_b ” recovery period, is somewhat higher at lower temperature. Thus, the diode’s recovery is somewhat more “snappy” at lower temperature. The voltage overshoot caused by the diode recovery, therefore, tends to increase somewhat as junction temperature decreases.

Effect of gate voltage and gate resistance on turn-on

The rate of rise of the IGBT’s collector current at turn-on is controlled by the rate of rise of the gate-emitter voltage. The rise of gate-emitter voltage is determined by the charging current fed by the drive circuit to the gate-emitter capacitance, hence by the amplitude of the gate drive voltage and the value of gate resistance. Within certain limits, “high” gate drive voltage and “high” gate resistance will produce the same current rise time and turn-on energy dissipation as “low” gate drive voltage and “low” gate resistance.

Figure 15(a) through (c) illustrates typical turn-on waveforms for International Rectifier’s 90A Fast IGBT module, type IRGTA 090F06, with a gate resistance of 33 Ohms and gate drive voltages of 10, 13 and 15V, for an output current of 130A. The rate of rise of current increases and the turn-on energy decreases significantly as the gate drive voltage is increased.

During the final fall time of the collector voltage (i.e., after the peak of the diode recovery current), the drive current is drawn through the gate-emitter capacitance of the IGBT; the rate of discharge of this capacitance, hence also the final fall time of the collector voltage, therefore depend upon the amplitude of the drive current. Thus, the drive voltage and gate resistance control the final voltage fall time, as well as the current rise time.

Figure 15(d) illustrates the effect of reducing the gate drive voltage to 10V, and the gate resistance to 10 Ohms. The rise time of the current is about the same as with 15V and 33 Ohms; the final voltage fall time is slightly slower.

Generally, different combinations of gate drive voltage and gate resistance can be found that will result in approximately the same turn-on energy. This is the case so long as the amplitude of the gate drive voltage is more than sufficient to drive the IGBT into “full conduction,” which depends upon the amount of current being switched.

Generally, a minimum gate drive voltage of 10 to 11V ensures that IR’s IGBT modules are driven into full conduction, with “something to spare,” within their normal range of peak operating current.

Application Information

Comparison of turn-on characteristics of Fast and Ultrafast modules

Differences in switching performance between IR's Fast

and Ultrafast IGBTs reside in their turn-off, not turn-on, characteristics. For given IGBT die size, gate drive voltage and gate resistance, the turn-on operation of IR's Fast and Ultrafast modules is essentially the same.

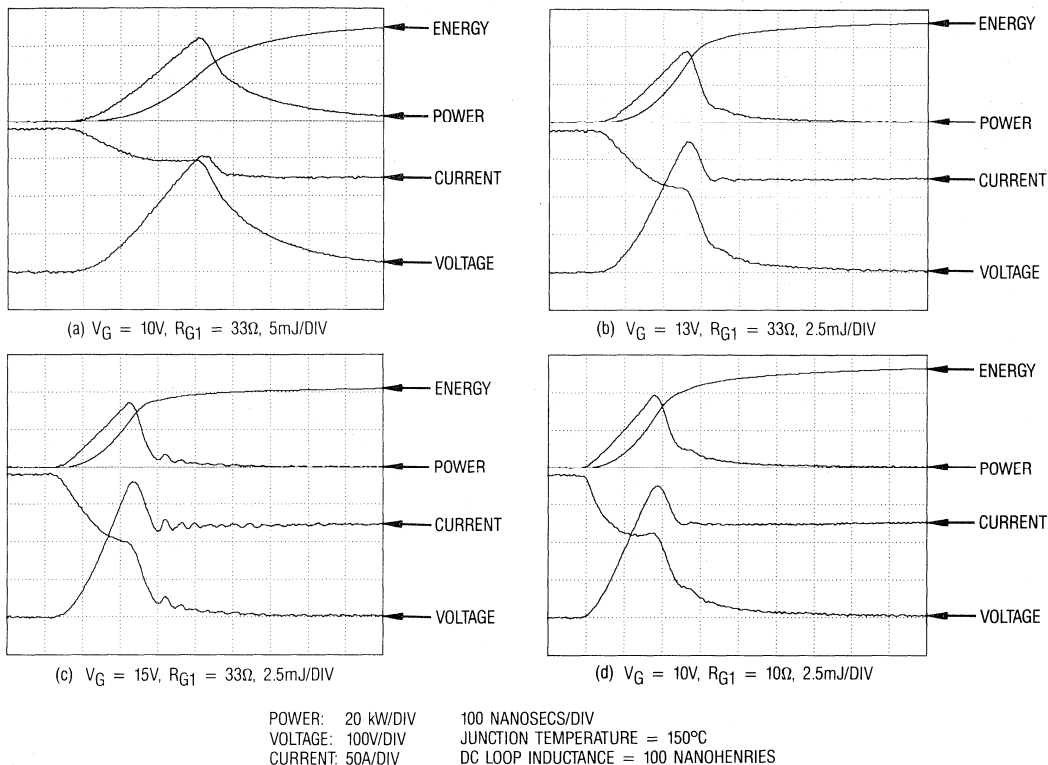


Figure 15. Oscilloscopes of IGBT turn-on current, voltage, power and energy for various combinations of applied gate-drive voltage V_G , and turn-on gate resistance R_{G1} (IRGTA090F06).

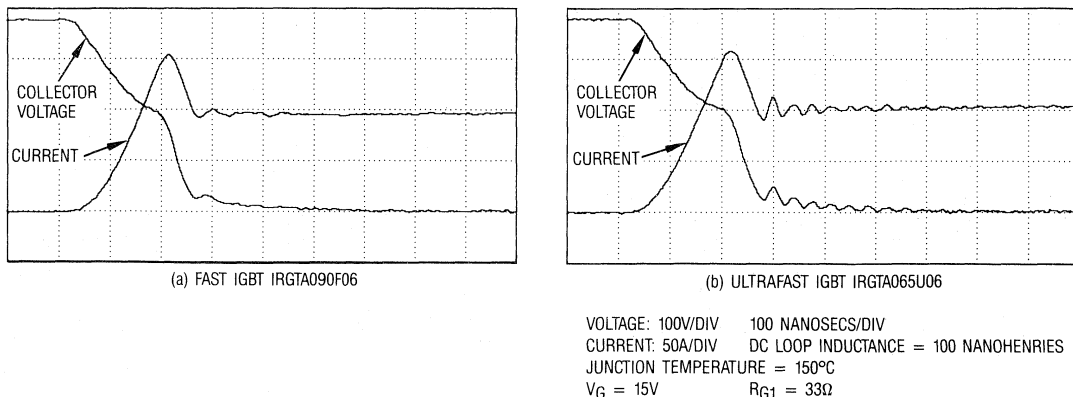


Figure 16. Oscilloscopes of IGBT turn-on voltage and current for Fast and Ultrafast modules.

Turn-on waveforms of IR's Fast and Ultrafast modules are compared in Figure 16. These waveforms confirm that both types dissipate essentially the same turn-on energy.

Relationships between turn-on energy and current

Typical relationships between turn-on energy and current, for International Rectifier's 90A Fast ADD-A-pak IGBT module and the 65A Ultrafast ADD-A-pak module, are shown in Figure 17.

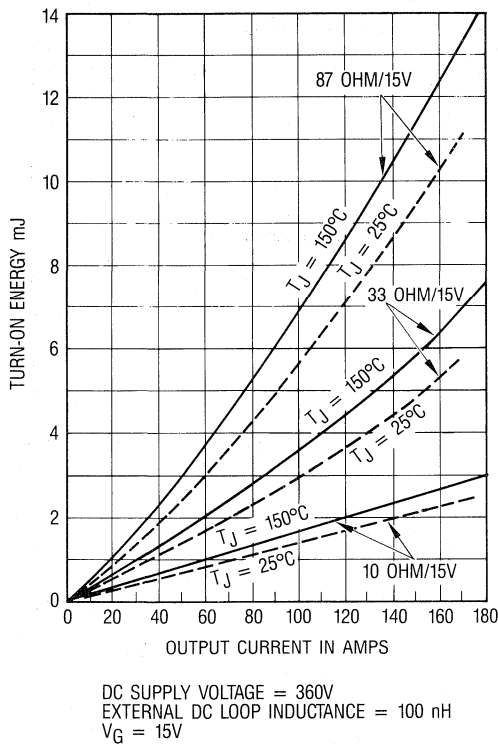


Figure 17. Typical relationships between turn-on energy and output current for the Fast (IRGTA090F06) and Ultrafast (IRGTA065U06) IGBT modules for different values of R_{G1} .

Note the quite linear relationship between collector current and turn-on energy. Because the relationship is "linear," it is convenient to express the switching energy in terms of millijoules per amp. The Fast and Ultrafast IGBT modules both have typical turn-on energy of 0.05mJ/A, with $R_G = 47$ Ohms, at $V_{CC} = 360V$.

dv/dt induced current and the influence of negative drive

When one IGBT of the half-bridge turns on, a quite high rate of change of voltage, typically about 10V/ns, is generated across the other one, as the outgoing diode

recovers. This dv/dt can cause the latter IGBT to conduct momentarily.

With reference to the equivalent circuit shown in Figure 18, when dv/dt is applied across the collector-emitter of the IGBT, potentially three components of current will flow. The first component is the charging current of the IGBT's output capacitance, I_{CO} ; this component is inevitable, because the output capacitance is physically always present.

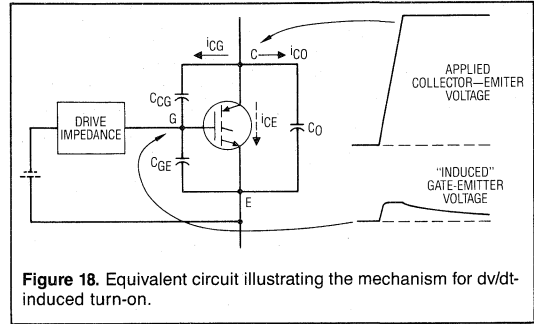


Figure 18. Equivalent circuit illustrating the mechanism for dv/dt-induced turn-on.

The second component, i_{CG} , is the charging current of the collector-gate capacitance. This charging current is also inevitable, but is quite small by comparison with the charging current of the output capacitance, because the collector-gate capacitance is small (about 10-15%) by comparison with the output capacitance.

The third component of current, i_{CE} , may or may not flow. It is caused by the "amplifying" effect of i_{CG} . The effect of i_{CG} flowing into the gate circuit impedance is to increase the gate-emitter voltage. If this voltage exceeds the gate threshold level, it will cause collector-emitter current to flow.

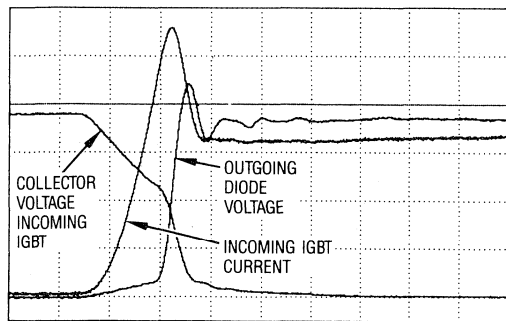
The flow of the dv/dt-induced, i_{CE} , component of current depends upon the magnitude of the dv/dt, which determines the magnitude of i_{CG} ; it also depends on the impedance of the gate drive circuit, which determines the amplitude of the gate voltage that results from i_{CG} . If the gate is tied to the emitter via a low impedance drive circuit, the induced gate voltage will be insufficient to turn on the IGBT.

It is quite common practice to apply a negative voltage to the gate of the IGBT when it is required to be off, to ensure that the gate voltage cannot rise to the threshold level and turn it on, when collector-emitter dv/dt is applied.

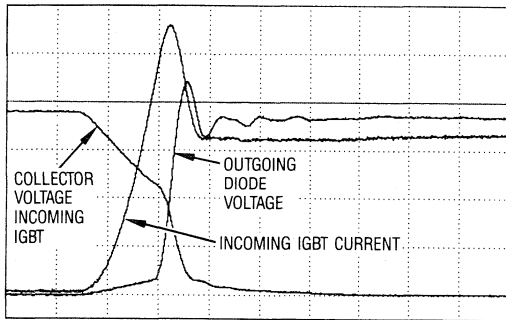
International Rectifier IGBTs do not require a negative gate drive for this purpose. It is recommended that a diode is connected across R_{G1} , to provide a low "turn-off" gate impedance, i.e., $R_{G2} = 0$ in Figure 10. It is, of course, necessary that any additional internal impedance of the drive circuit should be relatively low (not more than, say, 10 Ohms).

Figure 19 illustrates, for the IGTA090F06 module, that the turn-on waveforms actually remain essentially





(a) $V_{G2} = -18V$
 $R_{G2} = 0\Omega$ } FOR "OFF" IGBT



(b) $V_{G2} = 0V$
 $R_{G2} = 100\Omega$ } FOR "OFF" IGBT

VOLTAGE: 100V/DIV 100 NANOSECS/DIV
 CURRENT: 20A/DIV
 JUNCTION TEMPERATURE = 150°C
 $V_{G1} = 15V$
 $R_{G1} = 33\Omega$ } FOR INCOMING IGBT

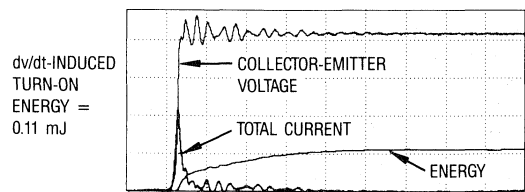
Figure 19. Typical turn-on oscillograms with "off" IGBT.

(a) "Heavily" biased, with $V_{G2} = -18V$, $R_{G2} = 0$.
 (b) "Loosely held off," with $V_{G2} = 0$ volts, $R_{G2} = 100$ Ohms. Illustrating minimal differences between two sets of conditions.

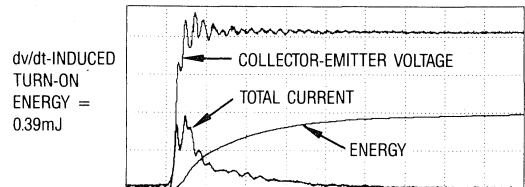
unchanged, between the quite extreme condition, of the gate of the non-conducting IGBT being firmly held off, with $V_G = -18V$ and $R_{G2} = 0$, to the much more "loose" condition, of $V_G = 0$ and $R_{G2} = 100$ Ohms. The waveforms are virtually the same in both cases, demonstrating the virtual absence of a dv/dt induced component of collector current.

The dv/dt across the IGBT due to the recovery of its antiparallel diode is typically about 10V/ns, as exemplified by the waveforms in Figure 19. It is possible to generate a much higher dv/dt , if the minimum value of turn-on gate resistance, R_{G1} , specified for snubberless switching, is disregarded and the IGBT is overdriven at turn-on, creating a high dv/dt across the other one.

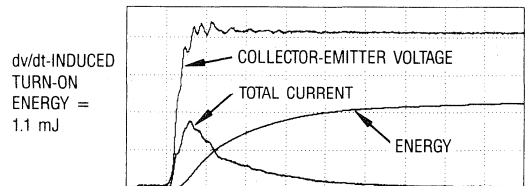
Figure 20(a) shows a rising collector voltage across the



(a) $V_{G2} = 0V$ $R_{G2} = 20\Omega$ 0.1mJ/DIV



(b) $V_{G2} = +1.4V$ $R_{G2} = 20\Omega$ 0.2mJ/DIV



(c) $V_{G2} = +2.3V$ $R_{G2} = 20\Omega$ 0.5mJ/DIV

VOLTAGE: 100V/DIV 100 NANOSECS/DIV
 CURRENT: 5A/DIV
 JUNCTION TEMPERATURE = 150°C

Figure 20. Oscillograms of collector-emitter voltage and dv/dt -induced turn-on current and energy when upper IGBT is overdriven "on" and positive gate bias is applied to lower IGBT (IRGTA050F06).

lower IGBT that has a maximum dv/dt of about 45V/ns, obtained by overdriving the upper IGBT. These waveforms were obtained with the 50A IRGTA050F06 module with essentially no output current, hence with no diode reverse recovery current, so that the dv/dt -induced IGBT current could be "isolated" for observation.

The waveforms in Figure 20(b) and (c) demonstrate the effect of positive gate bias applied to the lower IGBT, on its dv/dt -induced turn-on current. The threshold voltage of this device was about 4.1V at 25°C, which is typical. The purpose of applying positive gate bias was to determine how a "limit device," having a threshold voltage equal to the minimum specified value of 3.0V at 25°C, might behave with no negative gate bias.

It can be projected from these waveforms that a limiting

low-threshold device would dissipate about $280\mu\text{J}$ of dv/dt -induced turn-on energy, at the maximum rated junction temperature of 150°C (at which the threshold voltage is lowest and therefore the dv/dt -induced energy is highest), with a maximum applied dv/dt of $45\text{V}/\text{ns}$, with no negative gate bias. The corresponding average power dissipation at 20kHz would be 5.6W .

Considering that the maximum dv/dt needed to produce this quite “manageable” power dissipation is about 4X greater than a “real” typical operating value, it is clear that in practice the effect of dv/dt -induced turn-on will be minimal and that the use of negative gate bias, though permissible, is not necessary.

Snubberless Switching Safe Operating Area (SSSOA) for turn-on

International Rectifier IGBTs can reliably switch high current at high voltage. For most practical design purposes they do not require “snubber” components to “shape” the switching load-line.

Operation without snubbers is an important application advantage. It is therefore important to the circuit designer that the limits of the Snubberless Switching Safe Operating Area (SSSOA) are defined.

The critical factor that determines the limits of safe operation during turn-on is the transient overvoltage developed across the diode (and hence also across the antiparallel IGBT) as it recovers. The peak diode recovery voltage must be constrained within the rated voltage by setting appropriate limits on the operating conditions of the module.

The peak diode recovery voltage depends upon the dc supply voltage, the “dc loop” inductance and the peak diode reverse recovery current, in combination with the diode’s recovery “snap factor” (t_b/t_a).

The reverse recovery current and snap factor themselves depend upon the diode junction temperature, the initial amplitude of the diode forward current, i.e., the amplitude of the current being switched, and the rate of decrease of diode forward current, which is equal to the rate of increase of the IGBT current. As already discussed, the latter can be controlled by setting the value of the turn-on gate resistance, R_{G1} , in combination with the amplitude of the gate drive voltage.

The value of R_{G1} , for a given amplitude of gate drive voltage, is thus critical in determining the recovery voltage across the diode. For any level of dc supply voltage, dc loop inductance, switching current, gate drive voltage and junction temperature, the diode recovery voltage can be constrained within the rated value by appropriate choice of R_{G1} .

The SSSOA of the International Rectifier 600V IGBT modules is illustrated in Figure 49 (see page 29). It is specified for a maximum switching current, I_{LM} , of twice

TABLE 3

Turn-On Gate Resistance, R_{G1} , for Snubberless Switching Safe Operating Area. $V_G = 15\text{V}$.

IGBT Module Type	Turn-On Gate Resistance, R_{G1} Ohms
IRGTA050F06	82
IRGKA050F06	
IRGNA050F06	
IRGTA035U06	
IRGKA035U06	
IRGNA035U06	
IRGTI065F06	100
IRGKI065F06	
IRGNI065F06	
IRGTI050U06	82
IRGKI050U06	
IRGNI050U06	
IRGTA090F06	47
IRGKA090F06	
IRGNA090F06	
IRGTA065U06	
IRGKA065U06	
IRGNA065U06	
IRGTI120F06	56
IRGKI120F06	
IRGNI120F06	
IRGTI090U06	47
IRGKI090U06	
IRGNI090U06	
IRGKA120F06	42
IRGNA120F06	
IRGKA090U06	33
IRGNA090U06	
IRGTI165F06	
IRGKI165F06	42
IRGNI165F06	
IRGTI115U06	33
IRGKI115U06	
IRGNI115U06	
IRGTI200F06	27
IRGKI200F06	33
IRGNI200F06	
IRGTI140U06	27
IRGKI140U06	
IRGNI140U06	



the rated continuous current, at a dc supply voltage of 420V. These values of dc *supply* voltage exceed most normal maximum design levels of dc “bus” voltage for a 600V-rated IGBT.

A practically achievable maximum value of “external” dc loop inductance, of 100nH, is specified. This is the allowed dc loop inductance, external to the module, over and above the module’s internal inductance. (The user has no control over the latter.)

The IGBT and diode junction temperatures for the SSSOA are specified for a temperature range of 25°C to 150°C. The gate drive voltage is specified at 15V maximum.

The above conditions, which map the boundaries of the SSSOA, are complemented by a specified minimum value of turn-on gate resistance, R_{G1} . This minimum gate resistance ensures that the transient recovery voltage of the diode will not exceed the rated value, when switching under the specified maximum boundary conditions.

Table 3 gives a summary of the specified minimum values of R_{G1} , for the SSSOA of the 600V ADD-A-pak and INTA-pak modules.

The oscillograms in Figure 19, for the IRGTA090F06, illustrate the transient recovery voltage of the diode, with a value of R_{G1} of 33Ω, which is less (and therefore “worse-case”) than the minimum value of 47Ω specified for the SSSOA. The diode recovery voltage swings about 100V above the dc bus voltage.

Comparison of turn-on performance versus other industry types

As explained, the critical limiting factor during turn-on is the recovery voltage transient generated across the outgoing diode. It is necessary to restrain the turn-on speed of the IGBT by connecting a resistor in series with the gate to restrain the rate of rise of gate voltage, which in turn restrains the diode recovery voltage transient.

The “snappier” the diode’s reverse recovery, the more restraint must be placed on the rise time of the IGBT current. Thus, the recovery characteristic of the diode determines how much the turn-on speed of the IGBT must be “degraded,” hence, how much energy must be dissipated during turn-on.

The waveforms in Figure 21 show a comparison between the turn-on operation of the International Rectifier 65A Ultrafast IGBT module, and that of a competitive 600V, 75A module. The turn-on gate resistance for each module is 33 Ohms. The maximum di/dt of the diode recovery current during the “ t_b ” period is approximately the same for both types – about 1250A/μs for the IR module and 1000A/μs for the competitive module. This would produce an overvoltage transient in the order of 100 to 125V across a dc loop inductance of 100nH.

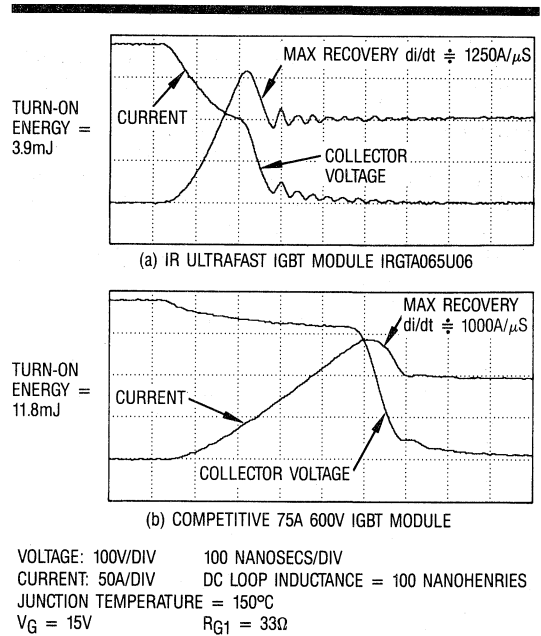


Figure 21. Comparison of oscillograms of IGBT turn-on voltage and current for IR and competitive modules. Current rise-time of competitive module is severely restrained by diode recovery characteristics.

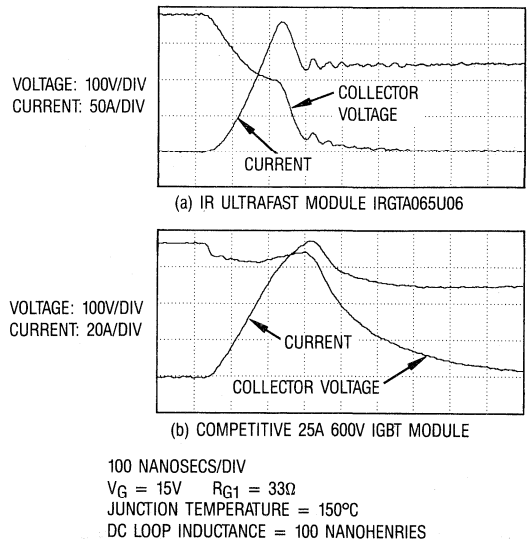


Figure 22. Comparison of oscillograms of IGBT turn-on voltage and current for IR and competitive modules. Both modules are switching at 2x continuous rated current. Turn-on voltage tail of competitive module is much more pronounced.

The rise time of IGBT current for the competitive module is about 450 nanoseconds, versus 170 nanoseconds for the IR module. The turn-on energy of the competitive module is more than 3X greater than that of the IR module.

Another phenomenon, evident in some industry types of IGBT modules, is low transconductance, which results in "tailing" of the collector voltage at turn-on at higher levels of current. The collector voltage of the IR IGBT falls within 100-200 nanoseconds after the recovery of the diode, to the final conduction level, even when turning on the full peak rated output current. This is illustrated in Figure 22(a), for the 600V, 65A Ultrafast module, switching on into an output current of 130A.

By contrast, Figure 22(b) shows the turn-on waveform for a 25A, 600V industry module, switching its peak rated current of 50A. This exhibits a significant voltage "tail" at turn-on, of almost 1 μ s duration.

IGBT Turn-off

Fundamentals of operation

IGBT turn-off is initiated by reducing to zero or reversing the gate drive voltage.

Whereas at turn-on the collector current is closely under the control of the gate-emitter voltage, the operation during turn-off is a somewhat "delayed reaction" to the removal of the gate drive voltage, because of the minority carrier lifetime of the IGBT.

Idealized waveforms that illustrate the operation during turn-off are shown in Figure 23. At t_0 , the applied gate drive voltage is reduced to zero. It is assumed here that

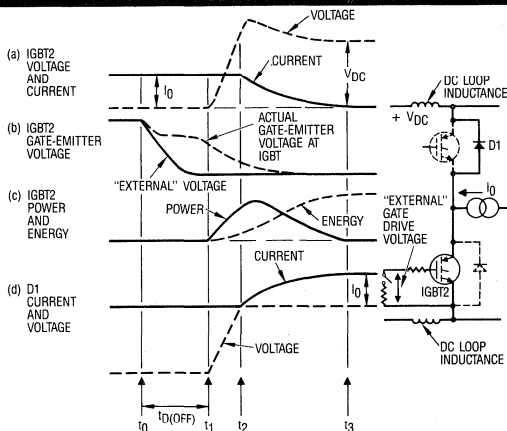
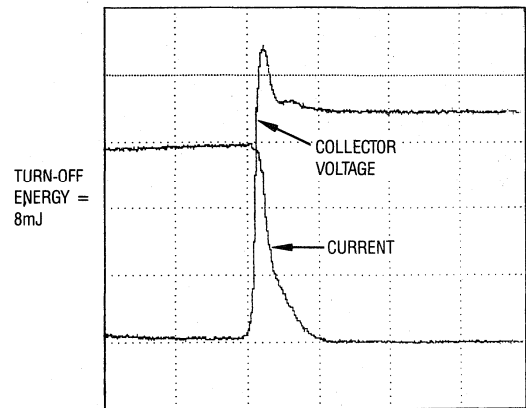


Figure 23. Idealized turn-off waveforms.

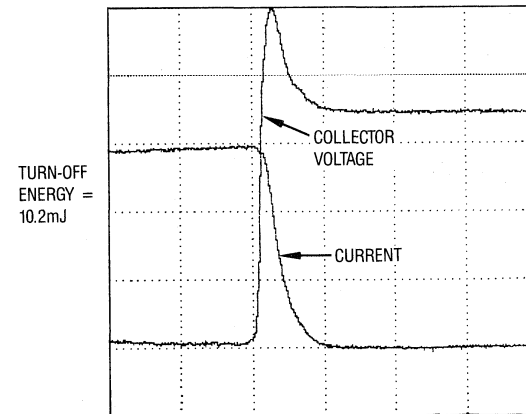
¹Footnote: The actual gate emitter voltage at the IGBT itself is somewhat different from the "external" gate emitter voltage, seen at the external gate-emitter terminals of the module, because of internal gate resistance built into the module. The internal gate resistance is generally "transparent" and need be of no concern to the user. It is mentioned here only to explain the observed external gate waveform at turn-off. All references to gate resistance in this application note are to external resistances.

the external (turn-off) gate drive resistance (R_{G2}) is low. The voltage seen at the external gate-emitter terminals¹ therefore decreases quite rapidly to zero, typically within about 200 nanoseconds. Within about the same period, the IGBT's collector voltage starts to rise. The full output current continues, for the time being, to flow in the IGBT; it does not start to transfer into the "opposite" diode until the IGBT's collector voltage reaches the dc supply voltage. Until this point is reached the diode is still reverse biased and inherently cannot conduct.

The IGBT's collector voltage reaches the dc supply voltage at time t_2 and current now starts to transfer to the diode. The decay of current is determined predominantly by the IGBT's "internal" characteristics, not by the gate voltage, which has already largely disappeared, nor, to any significant degree, by the dc loop inductance.



(a) DC-LOOP INDUCTANCE = 100nH



(b) DC LOOP INDUCTANCE = 200nH

VOLTAGE: 100V/DIV 500 NANOSECS/DIV
CURRENT: 50A/DIV
 $V_G = 15V$ $R_{G2} = 0$
JUNCTION TEMPERATURE = 125°C

Figure 24. Turn-off oscillograms demonstrating the effect of the dc loop inductance on the voltage overshoot and turn-off energy.

The “dc loop” inductance essentially has a di/dt “imposed” upon it. This inductance has little influence itself in determining the value of the di/dt .

The resulting induced voltage transient increases the IGBT’s voltage above the dc supply voltage. The voltage overshoot is essentially proportional to the value of the dc loop inductance, as illustrated by the waveforms in Figure 24.

Turn-off tail current

The idealized waveforms in Figures 23 and actual waveform of Figure 24 show a rather smooth “exponential” decay of the IGBT current during turn-off. This smooth turn-off current is typical for the International Rectifier IGBT at high junction temperature, where turn-off time and turn-off energy are highest.

At lower junction temperature, the turn-off current waveform subdivides into two distinct regions. In the first

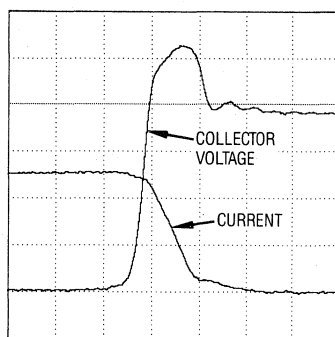
region, the current decreases rapidly; in the second region, a slower exponential “tail” occurs. This tail is due to recombination of minority carriers in the base region.

Turn-off current waveforms, at junction temperatures of 25°C and 150°C, are compared for the IR 65A, 600V Ultrafast module in Figure 25. The rapid initial rate of change of current, followed by the much slower “tail,” are evident at 25°C. At 150°C, the initial rate of change of current is slower and the initial amplitude of the tail current is higher. The two regions merge, and a clear “break” point is not distinguishable.

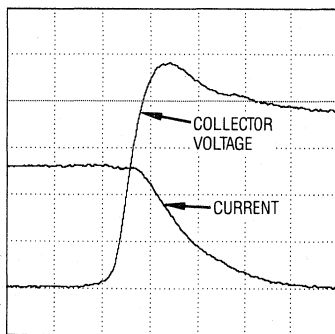
The total turn-off energy is highest at highest junction temperature. The voltage overshoot across the IGBT, however, is higher at lower junction temperature, at which the rate of decrease of current is higher.

Comparison of turn-off for Fast and Ultrafast modules

A comparison of the turn-off waveforms of the International Rectifier Fast and Ultrafast IGBT modules, at rated maximum junction temperature of 150°C, is illustrated in Figure 26.



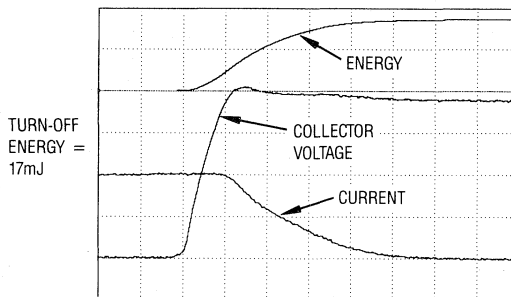
(a) JUNCTION TEMPERATURE = 25°C



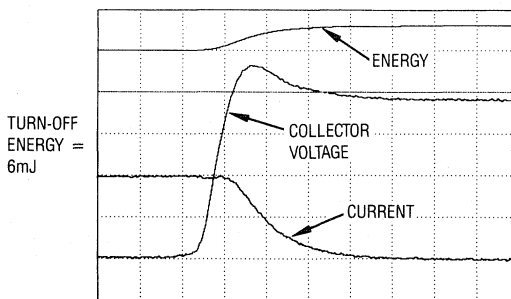
(b) JUNCTION TEMPERATURE = 150°C

VOLTAGE: 100V/DIV 100 NANOSECS/DIV
 CURRENT: 50A/DIV
 $V_G = 15V$ TURN-OFF $R_G = 33\Omega$
 DC LOOP INDUCTANCE = 100 NANOHENRIES

Figure 25. Comparison of IGBT turn-off voltage and current oscillograms at 25°C and 150°C (IRGTA065U06).



(a) FAST IGBT IRGTA090F06 200 NANOSECS/DIV



(b) ULTRAFAST IGBT IRGTA065U06 100 NANOSECS/DIV

VOLTAGE: 100V/DIV DC LOOP
 CURRENT: 50A/DIV
 ENERGY: 10mJ/DIV
 JUNCTION TEMPERATURE = 150°C
 $V_G = 15V$ TURN-OFF GATE RESISTANCE = 33Ω

Figure 26. Comparison of turn-off oscillograms for Fast and Ultrafast IGBT modules. Note change of time scale between (a) and (b).

The total “active” turn-off time (i.e., not including the initial turn-off delay time) of the Fast module is about 1 μ s; this is comprised of a voltage rise time of about 250ns and a current fall time of about 750ns.

The total “active” turn-off time of the Ultrafast module is about 400ns, comprised of a voltage rise time of about 100ns and a current fall time of about 300ns.

Total turn-off energy is about 0.17mJ/A at a V_{CC} of 360V for the Fast module and only 0.06mJ/A for the Ultrafast module.

Note the quite small overvoltage transient for the Fast IGBT, due to the slower current fall-time, versus the more significant overvoltage for the Ultrafast IGBT.

Effect of turn-off gate resistance

The turn-off gate resistance has a direct influence on the turn-off delay time, as illustrated by the waveforms in Figure 27. The higher the turn-off gate resistance, the longer the delay time taken for the gate-emitter voltage to decay to the point at which the collector voltage starts to rise significantly.

During the delay period, the internal gate-emitter voltage (Figure 23) stays practically constant, at a level corresponding to the amplitude of the collector current. This is caused by feedback from the collector voltage – which actually is rising slightly – via the collector-gate capacitance, which has a high value (and hence strong feedback effect) at low collector voltage.

The gate resistance also influences the rise time (t_1 to t_2) of the collector voltage. As the rise of the collector voltage gathers pace, the collector-gate capacitance decreases significantly and the collector-gate feedback becomes progressively weaker. Nonetheless, the higher the gate resistance, the more this “Miller” effect plays a part and the longer the voltage rise time. This is evident in the waveforms of Figure 27.

Gate turn-off resistance has only minor effect on the current fall time. The waveforms of collector current shown in Figure 27(a) through (c), for the 90A, 600V Fast module, with turn-off gate resistances of 0, 33, and 51 Ω , are virtually the same as one another.

The minor effect of the turn-off gate resistance on turn-off energy is exemplified in Figures 28 and 29.

Effect of negative gate bias

Reversing the gate drive voltage during turn-off reduces the turn-off delay time by discharging the gate emitter capacitance more quickly. It also somewhat decreases the voltage rise time. These effects are relatively minor, and would not normally, of themselves, be a sufficient reason for using negative gate drive.

Figures 28 and 29 illustrate that negative gate drive has only minor effect on turn-off energy.

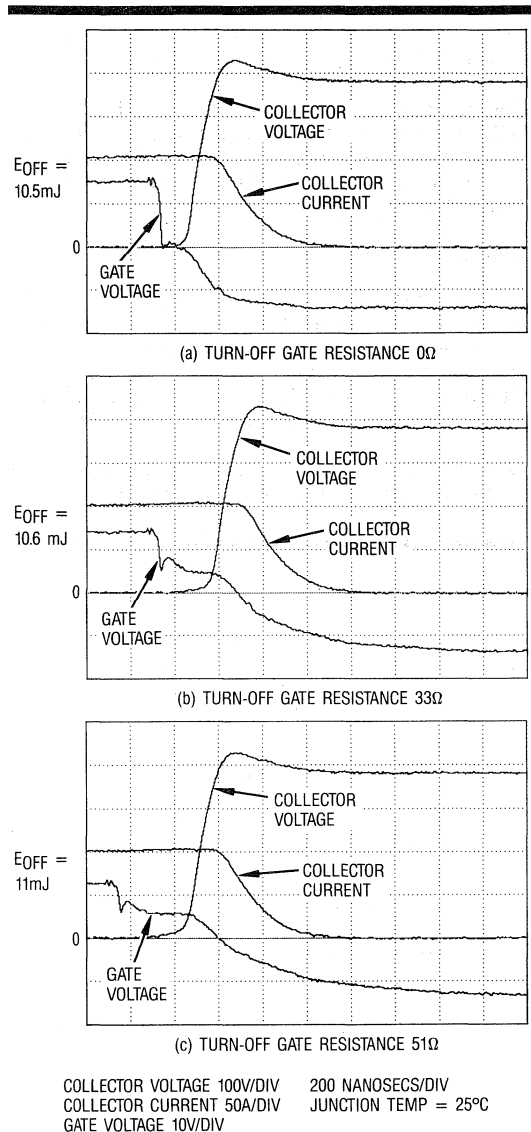
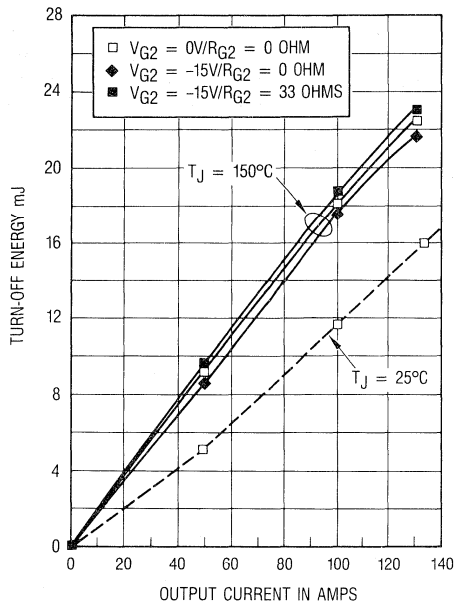


Figure 27. Oscilloscopes illustrating the effect of turn-off gate resistance on turn-off.

Relationships between turn-off energy and current

Relationships between turn-off energy and current for the IR 90A Fast ADD-A-pak IGBT module, and the 65A Ultrafast ADD-A-pak module, are shown in Figures 28 and 29 respectively.

The relationship between turn-off energy and turn-off current is quite linear. As explained above, the turn-off energy does not depend significantly on the value of the gate resistance, nor on whether negative drive voltage is applied.



DC LOOP INDUCTANCE = 100 nH
DC SUPPLY VOLTAGE = 360V

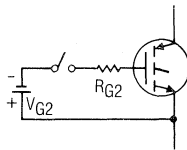
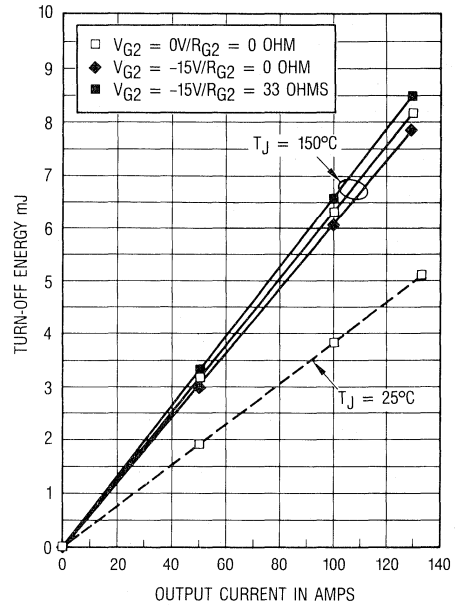


Figure 28. Typical turn-off energy vs. output current for Fast IGBT module type (IRGTA090F06).



DC LOOP INDUCTANCE = 100 nH
DC SUPPLY VOLTAGE = 360V

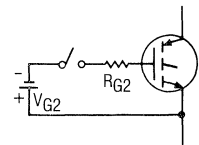


Figure 29. Typical turn-off energy vs. output current for Ultrafast IGBT module type (IRGTA065U06).

Because of the “linearity” of these relationships, it is convenient to express the turn-off energy of International Rectifier IGBTs in terms of millijoules per amp. The Fast IGBTs have typical turn-off energy, at $V_{CC} = 360V$, of about $0.17mJ/A$; the Ultrafast IGBTs have typical turn-off energy of about $0.05mJ/A$.

Snubberless Switching Safe Operating Area (SSSOA) for turn-off

The IR IGBT modules are latch-free and can reliably turn-off rated I_{LM} , equal to twice the continuous rated current, at maximum junction temperature, without a snubber.

The critical factor that determines the limits of the SSSOA for turn-off is the overvoltage transient developed across the IGBT, caused by the dc loop inductance.

The IGBT’s characteristic waveshape of turn-off current depends largely upon the IGBT itself and not much on

external circuit conditions. The maximum di/dt of the turn-off current tends to increase with decreasing junction temperature. Thus, the peak voltage developed across the IGBT at turn-off tends to increase with decreasing junction temperature.

The transient turn-off voltage must be constrained, by setting limits on the maximum dc supply voltage, in combination with the maximum permissible value of “external” dc loop inductance.

The SSSOA for the IR 600V ADD-A-pak and INT-A-pak modules is illustrated in Figure 49 (see page 29). This is guaranteed at rated I_{LM} , at a maximum dc supply voltage of 420V, with a maximum external dc loop inductance of 100nH, for junction temperatures ranging from 25°C to 150°C.

Snubberless operation at junction temperatures lower than 25°C may require some reduction of dc supply voltage and/or dc loop inductance, to keep the peak transient voltage during turn-off within the rated value.

Comparison of turn-off of IR's IGBTs versus other industry types

International Rectifier IGBTs are designed to optimize the relationship between turn-off switching energy and saturation voltage, while keeping the turn-off current waveform "soft," to minimize voltage overshoot.

Comparison of the turn-off waveforms of the 600V, 65A Ultrafast ADD-A-pak module, versus a comparable 600V, 75A industry type is illustrated in Figure 30.

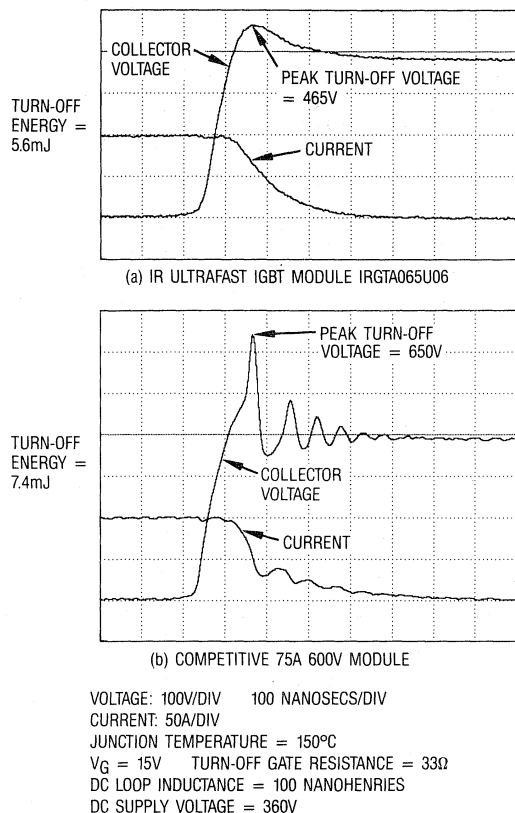


Figure 30. Comparison of turn-off oscillograms for the IR Ultrafast and competitive IGBT modules.

The turn-off current of the IR module is smooth, and overshoot of the collector voltage is well "damped." By contrast, the competitive module has a much more abrupt initial decay of current, a much greater voltage overshoot, (which goes well beyond the 600V rating), a significant turn-off voltage oscillation, a longer turn-off tail, and a higher turn-off energy.

These waveforms demonstrate that not all industry types of IGBT modules are well suited to snubberless switching.

Relationships between total switching energy and collector current

In most "hard" switching applications, the values of the current at turn-on and turn-off are essentially the same. For the purpose of calculating the total switching losses, the designer needs to know only the *total* switching energy, i.e., the sum of the turn-on and turn-off energies, at the maximum design current.

Figures 31 and 32 show typical relationships between the total switching energy and output current of the module, for the IR 600V Fast and Ultrafast modules respectively.

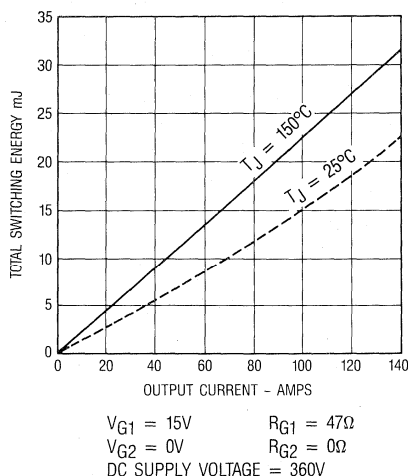


Figure 31. Typical total switching energy vs. output current for Fast IGBT module type (IRGTA090F06).

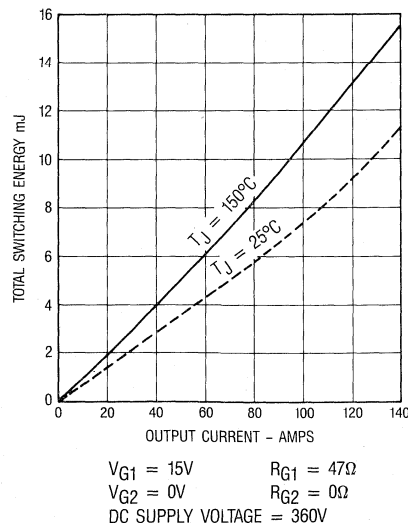


Figure 32. Typical total switching energy vs. output current for Ultrafast IGBT module type (IRGTA065U06).

The maximum value of total switching energy, (E_{TS}/A), at a nominal dc supply voltage of 360V and a junction temperature of 150°C, is 0.3mJ/A for IR's 600V Fast modules and 0.12mJ/A for the Ultrafast modules.

For any value of output current, I_0 , and dc supply voltage, V_{CC} , the total switching energy, E_{TS} , can be approximated as:

$$E_{TS} = I_0 \cdot \frac{V_{CC}}{360} \cdot (E_{TS}/A)$$

Average switching losses, P_{switch} , are simply the product of the total switching energy and the frequency, f :

$$P_{switch} = E_{TS} \times f.$$

Diode Characteristics

The diode is an essential element of all circuits in which the module is used. Moreover, as has been seen, the diode's recovery characteristic has a critical influence on the turn-on Snubberless Switching Safe Operating Area (SSSOA) and the turn-on switching energy of the IGBT.

The diode in the IR IGBT modules has a unique design structure that minimizes the recovery charge, while having the soft reverse recovery characteristic needed to minimize voltage overshoot and allow snubberless safe operation of the module.

Conduction characteristics

Typical relationships between the conduction voltage and current for the diode in the ADD-A-pak module, types IRGTA090F06 and IRGTA065U06, are shown in Figure 33.

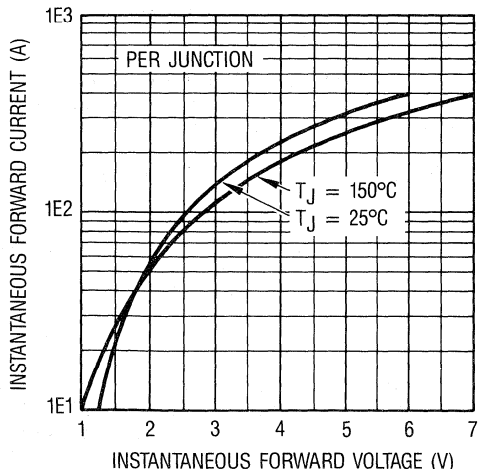


Figure 33. Typical conduction voltage characteristics of diode (IRGTA065U06 and IRGTA090F06).

Reverse recovery characteristic

Typical reverse recovery current waveforms for the diode are shown in Figure 34, for junction temperatures of 25°C and 150°C. Note the relative softness of the recovery current, characterized by a t_b/t_a ratio close to unity.

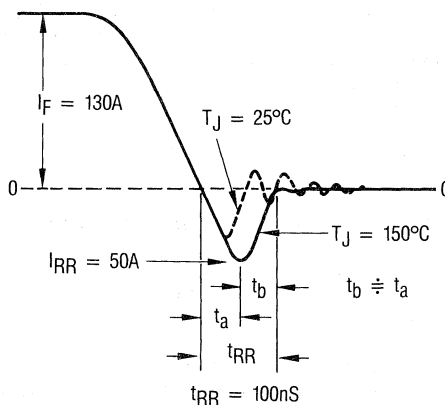


Figure 34. Typical reverse recovery waveforms for diode (IRGTA065U06 and IRGTA090F06).

Typical relationships between diode forward current, peak reverse current, reverse recovery time, and t_b/t_a , are shown in Figure 35.

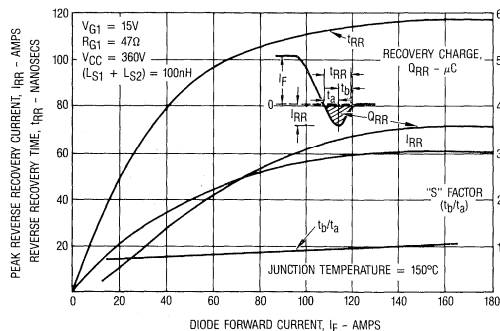


Figure 35. Typical reverse recovery characteristics of diode (IRGTA065U06 and IRGTA090F06).

Diode size

In most applications the diode is required to carry a significant average component of current under specific operating conditions. It is essential that the diode is sufficiently sized to meet the load demand upon it. It should not, however, be unnecessarily oversized; if it is, it will have "more than necessary" reverse recovery charge, which will unnecessarily increase the turn-on switching energy of the IGBT.

The size of the diode in the IR 600V IGBT modules is set to satisfy the loading to which the diode will be subjected in typical applications, such as uninterruptible power supplies, power factor correctors, switching power supplies and resonant converters.

In motor control applications, the diode will generally be sufficiently rated to handle all normal operating conditions, including full regenerative current flow. It may not, however, have sufficient capability to handle the more extreme operating condition of full rated current supplied continuously to a motor with a locked rotor, at zero fundamental output frequency. This design requirement, however, depends upon the torque specification of the drive and the type of motor and may not be needed.

General Summary of Switching Performance

The following major points relating to the switching performance of International Rectifier IGBT modules can be summarized:

- The IGBTs employ a unique design that offers a superior relationship between saturation voltage and switching energy, which minimizes the total losses.
- Differences in switching energy between Fast and Ultrafast IGBTs are due to differences in turn-off energy. Turn-on energy is essentially the same for both types.
- Turn-off energy of Fast IGBT modules is typically about 3 times the turn-on energy. Turn-off energy of Ultrafast IGBT modules is about equal to the turn-on energy.
- The 600V IGBTs have a rated maximum Snubberless Switching Safe Operating Area (SSSOA). They can safely achieve *snubberless* switching, at current up to twice the continuous rated load current, at dc bus voltage up to the maximum design levels usually encountered for 600V rated IGBTs, with a practically achievable value of stray dc loop inductance.
- The SSSOA is independent of the value of the load inductance.
- The critical factors that govern the SSSOA are the turn-on and turn-off voltage transients caused by stray dc loop inductance. The user should ensure that the stray inductance is within the value specified for the SSSOA, by careful attention to the circuit layout.
- The turn-on voltage transient is caused by the recovery current of the diode, interacting with stray dc loop inductance. The amplitude of this voltage transient stays about the same with varying junction temperature.
- The design of the diode in the IGBT modules minimizes the recovery charge, while maintaining the soft recovery characteristic needed to minimize turn-on voltage overshoot.
- The turn-on gate resistance governs the rate of rise of current at turn-on. This resistance is critical in controlling the diode recovery voltage transient and is a critical condition of the SSSOA.
- Turn-on energy is governed by the need to restrain the IGBT's turn-on speed, to keep the diode recovery voltage transient under control, not by the intrinsic turn-on speed of the IGBT.
- The turn-off voltage transient is caused by the falling current of the IGBT interacting with stray dc loop inductance. This voltage transient generally increases somewhat as junction temperature decreases, because the rate of change of IGBT turn-off current increases as junction temperature decreases.
- The turn-off voltage transient is not very significant for the Fast IGBT modules, but is more so for the Ultrafast modules because of their faster turn-off speed.
- The turn-off gate resistance has significant influence on the turn-off delay time, moderate influence on the turn-off voltage rise time and little influence on the current fall time.
- If stray dc loop inductance is greater than the maximum specified value of 100nH for the SSSOA, an appropriate reduction in the maximum dc bus voltage is necessary for snubberless switching.
- The relationships between switching energy and collector current are fairly linear, for both turn-on and turn-off. It is a reasonable approximation to express the switching energy in terms of a fixed value of "millijoules per amp."
- dv/dt induced IGBT turn-on is not significant with International Rectifier modules and negative gate bias is not needed to mitigate its effects.
- Negative gate bias generally has minor influence on switching operation and switching energy. It can be used, if desired, but is not mandatory.
- IR's IGBTs do not exhibit significant turn-on voltage tail.
- The turn-off current tail of IR's IGBTs is optimized to be "soft," while minimizing turn-off energy.

Understanding The Data Sheet

The International Rectifier data sheet contains all the critical information needed to design the IGBT module into a specific application. In general, IR's philosophy is to make the data sheet as user-friendly as possible, by specifying the ratings and characteristics so they are closely representative of actual circuit design conditions.

A step-by-step discussion follows of the major ratings and characteristics presented in the data sheet. The purpose



is to give insight into the data sheet specifications, to help the user apply International Rectifier modules correctly and take maximum advantage of their performance characteristics.

Absolute maximum ratings

I_C - Continuous collector current

Continuous collector current ratings are specified, for case temperatures of 25°C and 100°C.

These ratings are based on thermal limits. They define the maximum direct current that can be passed through the IGBT, with the “case” i.e., base temperature of the module held at the specified value, with an associated power dissipation that raises the junction temperature to the rated maximum value.

The rated continuous current of the IGBT at case temperature T_C is given by:

$$(I_C @ T_C) \times (V_{CE(ON)} @ I_C @ T_{Jmax}) \times R_{thJC} = (T_{Jmax} - T_C)$$

where

R_{thJC} = junction to case thermal resistance

T_{Jmax} = rated maximum junction temperature.

The I_C rating is based on an applied gate-emitter voltage, V_{GE} , (which determines the value of $V_{CE(ON)}$) of 15V.

In most applications, the IGBT would never be required to operate *continuously* at a *direct* current as high as the rated $I_C @ T_C = 25^\circ\text{C}$. This is because of the impracticality of keeping the case temperature at 25°C, while removing the associated heat.

The $I_C @ T_C = 25^\circ\text{C}$ “headline rating” is nonetheless a useful benchmark for comparison against other industry types, all of which have similarly based “headline” ratings.

The rated $I_C @ T_C = 100^\circ\text{C}$ is typically about 55% of the above “headline” rating; it is more representative of normal average operating current.

I_{OM} - Peak output current

I_{OM} is the absolute maximum peak repetitive *output* current of the module.

I_{LM} - Peak output switching current

I_{LM} is the peak *output* current that can be safely *switched repetitively*, under the stated conditions. It defines the “maximum current” boundary of the Snubberless Switching Safe Operating Area (SSSOA).

The peak IGBT *collector* current during turn-on is higher than I_{LM} because of additional diode reverse recovery

current. This higher turn-on current in the IGBT itself is permissible. It is allowed for in the I_{LM} *output* current rating. Therefore, so long as the design complies with the I_{LM} *output* current rating, the additional diode reverse recovery current need be of no concern in terms of complying with the rated switching current.

Distinction between I_{OM} and I_{LM}

The distinction should be drawn between the I_{OM} and I_{LM} ratings. I_{OM} is the maximum repetitive output current that can be permitted to *flow*, but repetitive *switching* should not be allowed at this current. I_{LM} is the maximum output current that can be repetitively *switched*. I_{OM} is normally 25% higher than I_{LM} .

The I_{OM} rating can be used to advantage, for example, in resonant circuits, where the peak *output* current is significantly higher than the peak *switching* current.

I_{FM} - peak diode forward current

I_{FM} is the maximum peak repetitive current that can be drawn through the diode. It has the same value as I_{OM} .

V_{CE} - Continuous collector-emitter voltage

V_{CE} is the maximum voltage that can be supported between collector and emitter terminals, with the gate connected to the emitter.

V_{GE} - Gate to emitter voltage

V_{GE} is the maximum voltage, of either polarity, that can be applied between the gate and emitter terminals.

The breakdown voltage of the gate oxide is typically several times the rated V_{GE} . Exceeding the rated V_{GE} will not necessarily cause breakdown. It should be avoided, however, because it can degrade long term reliability.

V_{ISOL} - Isolation voltage

V_{ISOL} is the maximum rms ac voltage (50 or 60Hz) that can be applied between any terminal and case.

P_{Dmax} - Power dissipation

P_{Dmax} is the maximum power that can be dissipated in each IGBT with the case temperature held at 25°C. It is based upon a junction-case temperature rise of ($T_{Jmax} - 25^\circ\text{C}$) and is therefore related to the junction to case thermal resistance by:

$$P_{Dmax} = \frac{(T_{Jmax} - 25^\circ\text{C})}{R_{thJC}} = \frac{125^\circ\text{C}}{R_{thJC}}$$

T_J – Operating junction temperature range

The upper and lower limits of the permissible range of operating junction temperature.

T_{STG} – Storage temperature range

The upper and lower limits of the permissible storage temperature range.

T – Mounting torque

The maximum and minimum limits of torque that should be applied to the screws.

Excessive torque applied to the terminal screws can cause internal damage; insufficient torque can result in a poor electrical connection. Insufficient torque applied to the base plate screws can cause poor thermal interface to the heatsink.

Static electrical characteristics

BV_{CES} – Collector to emitter breakdown voltage

BV_{CES} is the minimum voltage that will be developed across the collector-emitter junction at the specified collector current, with the gate shorted to the emitter.

BV_{CES}/T_J – Temperature coefficient of breakdown voltage

The collector-emitter breakdown voltage of an IGBT increases with junction temperature. For a 600V IGBT, the temperature coefficient of breakdown voltage is typically about 0.7V/°C.

Collector leakage current increases with increasing temperature; the collector leakage current at which the temperature coefficient is specified is therefore greater than the collector leakage current at 25°C.

The minimum breakdown voltage, BV_{CES} , is specified at 25°C. Since breakdown voltage decreases with temperature, BV_{CES} may be as low as 550V at $T_J = -40^\circ\text{C}$.

$V_{CE(ON)}$ – Collector to emitter conduction voltage

$V_{CE(ON)}$ is the collector-emitter conduction voltage, at the specified collector current, gate-emitter voltage, and junction temperature.

$V_{CE(ON)}$ is obviously a critically important characteristic, because it determines the conduction losses.

V_{FM} – Diode forward voltage

V_{FM} is the maximum diode forward voltage at the specified current and junction temperature.

V_{GEth} – Gate threshold voltage

As the gate-emitter voltage is increased from zero, significant collector current does not begin to flow, until the gate *threshold voltage* is attained. The IGBT is essentially “off” at gate emitter voltage less than the threshold value.

The gate threshold voltage is thus the gate-emitter voltage that brings the IGBT to the “threshold” of conduction; it is specified as the gate voltage that just initiates a small specified flow of collector current.

Maximum and minimum values of gate threshold voltage are specified.

V_{GEth}/T_J – Temperature coefficient of threshold voltage

Gate threshold voltage decreases as junction temperature increases. The V_{GEth}/T_J temperature coefficient defines the rate of decrease of threshold voltage with temperature.

V_{GEth}/T_J is typically 11mV/°C. An IGBT with minimum threshold voltage of 3.0V at 25°C would therefore have a threshold voltage of about 1.63V at 150°C.

g_{fe} – Forward transconductance

The “gain” of the IGBT is expressed in terms of its transconductance. The transconductance is the incremental change of collector current for an incremental change of gate voltage, at a defined operating point.

Maximum and minimum values of forward transconductance are specified.

I_{CES} – Collector to emitter leakage current

I_{CES} is the maximum collector-emitter leakage current, with the gate shorted to the emitter, at rated collector-emitter voltage. It is specified at junction temperatures of 25°C and 150°C.

I_{GES} – Gate to emitter leakage current

I_{GES} is the maximum gate to emitter leakage current at the rated gate-emitter voltage.

Dynamic characteristics

It is normal industry practice to specify the switching characteristics of the individual IGBT and diode elements of a module, as if each element was an independent “discrete” component.

These specified switching characteristics typically have rather remote relationship to actual operating conditions of the “integrated” module. For example, switching times of the IGBT are commonly specified with a resistive load, at a junction temperature of 25°C. In actual application, of course, the load is inductive, not resistive; the operating junction temperature is usually well in excess of 100°C, not 25°C.

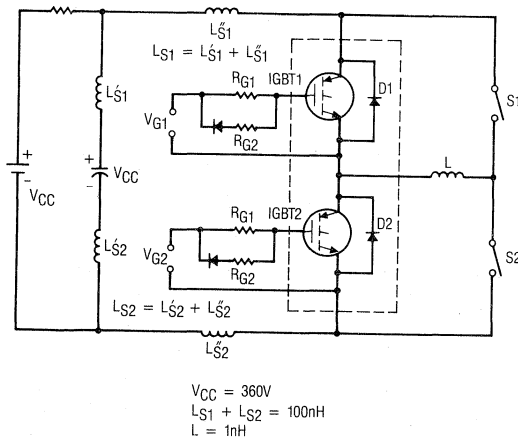
Switching performance of the diode is likewise specified rather arbitrarily, the reverse recovery characteristics being specified for conditions that often do not represent typical operation.

By contrast, the dynamic performance of International Rectifier IGBT modules is specified for operating conditions that are representative of actual application design conditions. Moreover, the dynamic switching performance is specified for the *integrated* module, so that the dynamic interaction between the diode and the IGBT is naturally included in the specifications.

The intent of the data sheet is to remove the “guesswork” so frequently necessary when designing with less application-informative data sheets. IR’s intent is to give the information needed so that simple design calculations, for actual operating conditions, can be made with confidence.

Dynamic test circuit

The test circuit that applies to the dynamic performance specification of International Rectifier half-bridge and chopper modules is essentially the *module itself*, as shown in Figure 36. “Macro” waveforms, that illustrate the dynamic sequencing of turn-on and turn-off for each IGBT, are shown in Figure 37.



SWITCH S1	POSITION S2	IGBT UNDER TEST	DIODE UNDER TEST	V_{G1}		V_{G2}	
				ON	OFF	ON	OFF
CLOSED	OPEN	IGBT2	D1	—	0 TO -15	+15	0 TO -15
OPEN	CLOSED	IGBT1	D2	+15	0 TO -15	—	0 TO -15

Figure 36. Dynamic test circuit for half-bridge and chopper modules.

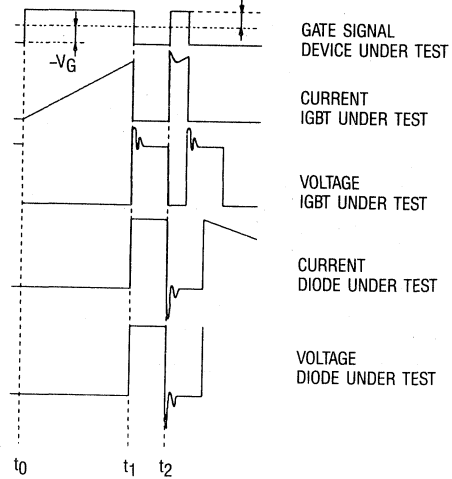


Figure 37. Macro waveforms for Figure 36 test circuit.

IGBT switching energy

The energy dissipated during switching is important to the circuit designer. He needs to know this to calculate the average switching losses. Most manufacturer’s data sheets do not specify the switching energy as such. The designer is left to estimate it, as best as possible, from the given switching times.

This is approximate at best; it is not possible to predict with any certainty the switching energy, under actual circuit operating conditions, from resistive load switching times at 25°C, particularly because these switching times typically do not include turn-on or turn-off “tailing.”

International Rectifier data sheets specify the actual switching energy, for actual application operating conditions, including the effects of “tailing.” Given these specifications, the switching times as such are not necessary for calculating switching losses. (The designer does, however, still need to know the switching times, for the purpose of setting switching “deadtimes” for the circuit.)

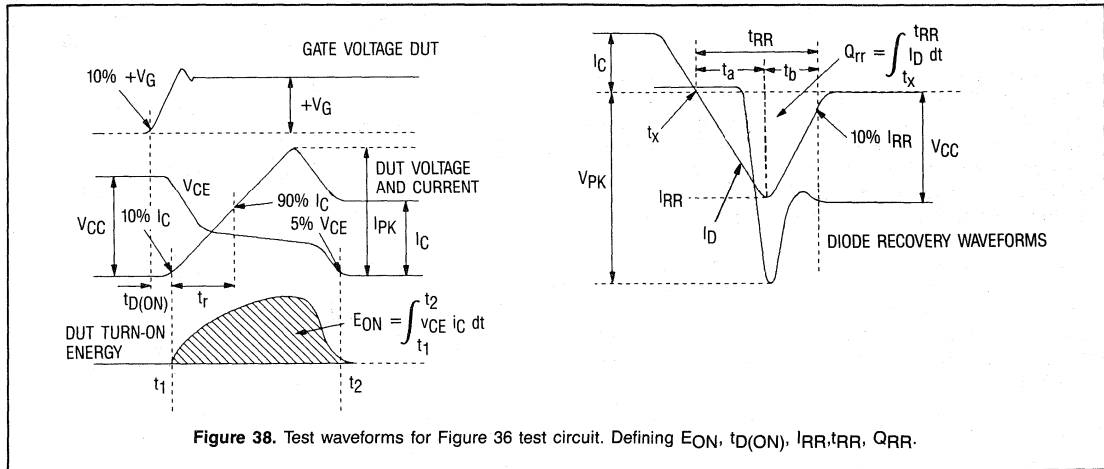
E_{ON} - Turn-on switching energy

E_{ON} is the total energy dissipated when the IGBT turns on, with pre-established “inductive” load current flowing in the diode of the opposite IGBT. The IGBT turn-on energy specified *includes* the component due to diode reverse recovery; as previously explained, this component is significant.

The turn-on energy is specified as a value of mJ/A for given values of dc supply voltage, dc loop inductance, gate drive voltage, and “turn-on” gate resistance. The specified

junction temperature is 150°C, representing a “worst-case” design situation.

The time-boundaries for measurement of E_{ON} are defined in Figure 38.



E_{OFF} – turn-off switching energy

E_{OFF} is the total energy dissipated when the IGBT turns off with “inductive” load current, including the energy due to the turn-off tail current.

The turn-off energy is specified as a value of mJ/A for given values of dc supply voltage, dc loop inductance, drive voltage, and “turn-off” gate resistance. Again, the specified junction temperature is 150°C.

The time-boundaries for measurement of E_{OFF} are defined in Figure 39. The termination point is arbitrarily set 5μs after the collector voltage begins to rise. The purpose is to ensure that all turn-off tail energy is included in E_{OFF} .

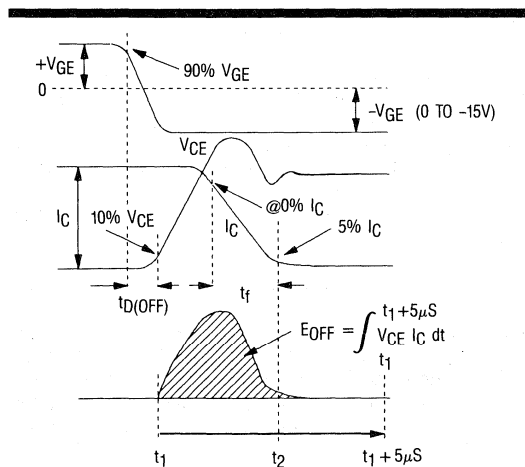
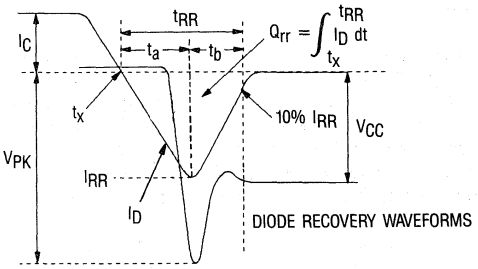


Figure 39. Test waveforms for Figure 36 circuit. Defining E_{OFF} , $t_{D(OFF)}$, t_f .



The turn-off tail time of the International Rectifier IGBT, in reality, is much less than 5μs. The 5μs measurement limit has been adopted as a standard, to allow meaningful comparisons of turn-off energy between different industry types, some of which have significantly longer tail times than the IR IGBTs.

E_{TS} – Total switching energy

E_{TS} is sum of the turn-on and turn-off switching energies.

E_{TS} is actually the only energy specification needed to calculate switching power losses, for applications in which IGBT turn-on and turn-off occur at essentially the same output current level.

A maximum limiting value of E_{TS} , in terms of mJ/A, is specified at given values of dc supply voltage, “dc loop” inductance, drive voltage, and gate resistance.

$t_{D(ON)}$ – Turn-on delay time

$t_{D(ON)}$ is the delay time between initiation of gate drive voltage and the start of IGBT collector current.

The time-boundaries for measurement of $t_{D(ON)}$ are defined in Figure 38.

t_r – Current rise time

t_r is the rise time of the current, with a clamped inductive load.

The time-boundaries for measurement of t_r are defined in Figure 38. The rise time terminates at the point when the IGBT current reaches 90% of the output current.

The actual IGBT current “overshoots” the output current, because of the diode recovery current. The rise time to the peak of the IGBT current is therefore significantly greater than to 90% of the output current.

t_{D(OFF)} – Turn-off delay time

t_{D(OFF)} is the delay time between the removal of gate drive voltage and the start of the voltage rise across the IGBT

The time-boundaries for measurement of t_{D(OFF)} are defined in Figure 39.

t_f – Current fall time

t_f is the fall time of the current, with a clamped inductive load, under the specified test conditions.

The time-boundaries for measurement of t_f are specified in Figure 39.

I_{RR}, t_{RR}, Q_{RR} – Diode reverse recovery characteristics

The diode reverse recovery characteristics, I_{RR}, t_{RR}, and Q_{RR}, are specified for given values of output current, dc supply voltage, dc loop inductance, gate drive voltage and turn-on gate resistance. The junction temperature is specified at 150°C, representing a worst-case design condition.

Definition of the diode reverse recovery characteristics is given in Figure 38.

The major effect of the diode reverse recovery is to increase the turn-on energy of the IGBT, as previously illustrated in Figure 13(c). This is taken into account in the E_{ON} specification for the IGBT.

Q_{GE}, Q_{GC}, Q_G – Gate charge

The gate charge characteristics apply to the IGBT *turning-on* into a clamped inductive load.

Q_{GE} is the charge that must be delivered by the drive circuit to bring the gate-emitter voltage to the point needed to sustain the specified collector current.

Q_{GC} is the charge that must be delivered by the drive circuit, to allow the voltage across the gate collector capacitance to fall from the specified initial value to the final conduction value.

Q_G, the total gate charge, is the sum of Q_{GE}, Q_{GC}, and an additional component, corresponding to the gate “overdrive” voltage. These three separate components of gate charge are defined in Figure 45 (see page 28).

The gate charge specification is useful for sizing the gate drive circuit and for determining the gate drive losses.

R_{thJC} (IGBT) and R_{thJC} (Diode)

R_{thJC} (IGBT) and R_{thJC} (diode) are the steady state junction to case thermal resistances of the IGBT and diode, respectively.

R_{thC-S} (module)

R_{thC-S} is the thermal resistance between the baseplate of the module and the heatsink on which the module is mounted. The external heatsink surface must be flat, smooth, and greased.

Graphical data

IR’s IGBT module data sheet contains a number of graphs, that supplement the tabulated ratings and characteristics.

These graphs will be exemplified, by reference to those in the data sheet for the ADD-A-pak module, type IRGTA090F06.

Output characteristics

Typical output characteristics, for junction temperatures of 25° and 150°C, are shown in Figures 40 and 41.

The output characteristics give the relationship between collector current and collector-emitter voltage, as a function of the applied gate-emitter voltage.

At collector currents at which the IGBT is “saturated,” increasing the amplitude of the gate drive voltage above a certain level does not have much impact on the collector-emitter “saturation” voltage.

As the collector current rises, a point is reached at which the collector-emitter voltage increases rapidly and operation moves into a “constant current” region. In this region, the current is a strong function of the gate voltage, but is fairly independent of the collector-emitter voltage.

Transfer characteristics

The transfer characteristic is the relationship between collector current and gate voltage, at a specified collector to emitter voltage. Typical transfer characteristics, for junction temperatures of 25°C and 150°C, are shown in Figure 42.

At relatively low gate voltage the collector current increases as the junction temperature increases. At higher gate voltage, the collector current decreases as the junction temperature increases.

Collector-emitter conduction voltage versus temperature

Typical relationships between V_{CE(ON)} and junction temperature, for varying levels of collector current, are shown in Figure 43.

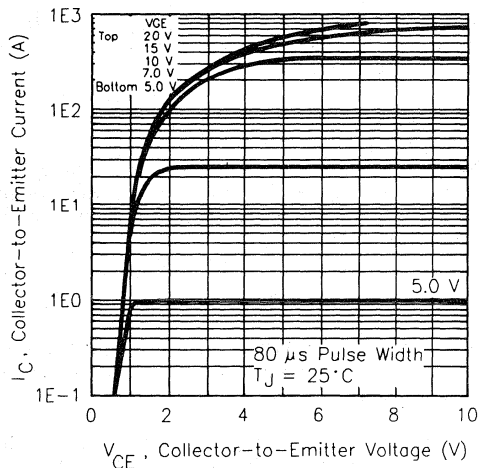


Figure 40. Typical output characteristics, $T_J = 25^\circ\text{C}$ (IRGTA090F06).

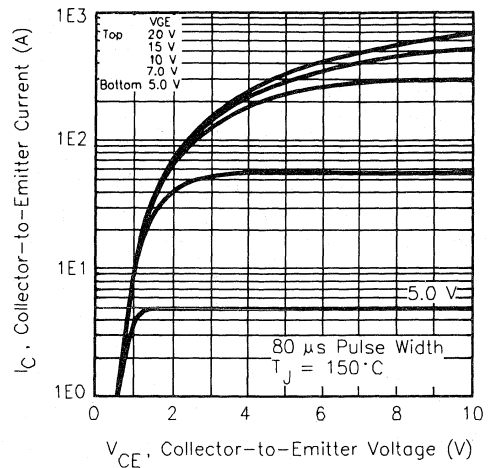


Figure 41. Typical output characteristics, $T_J = 150^\circ\text{C}$ (IRGTA090F06).

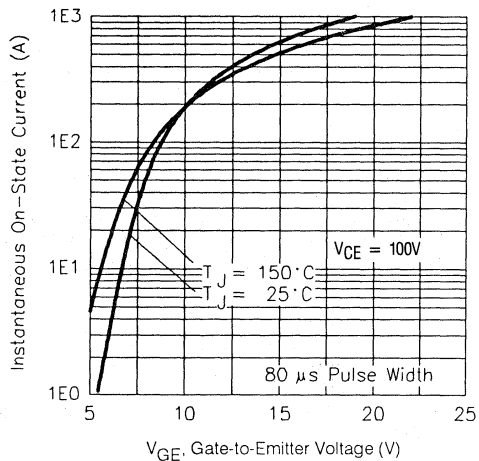


Figure 42. Typical transfer characteristics (IRGTA090F06).

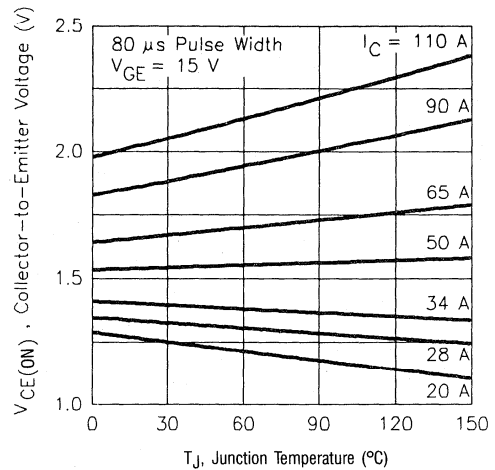


Figure 43. Typical $V_{CE(ON)}$ vs. junction temperature (IRGTA090F06).

At lower levels of collector current, $V_{CE(ON)}$ decreases with increasing temperature. At higher collector current, $V_{CE(ON)}$ increases with increasing temperature.

Capacitance versus collector-emitter voltage

Typical relationships between the IGBT's self-capacitive components and the collector-emitter voltage, are shown in Figure 44.

Self-capacitance increases as collector-emitter voltage decreases. It is essentially independent of temperature.

Note the very strong increase of C_{res} and C_{oes} as V_{GE} falls below about 20V.

Gate charge versus gate-emitter voltage

A typical relationship between gate charge and gate-emitter voltage is shown in Figure 45.

The Q_{GE} , Q_{GC} , and Q_G regions, discussed earlier, are indicated.

Reference can be made to IR's Application Note 944A, for further insights into the gate charge characteristic. That application note refers to power MOSFETs; but the principles are also applicable to the IGBT *turn-on* characteristics.

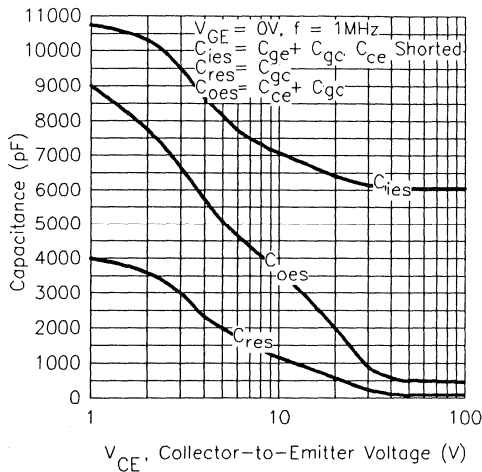


Figure 44. Typical capacitance vs. collector-to-emitter voltage (IRGTA090F06).

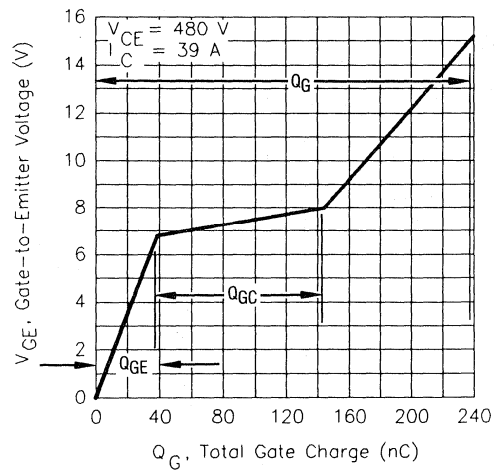


Figure 45. Typical gate charge vs. gate-to-emitter voltage (IRGTA090F06).

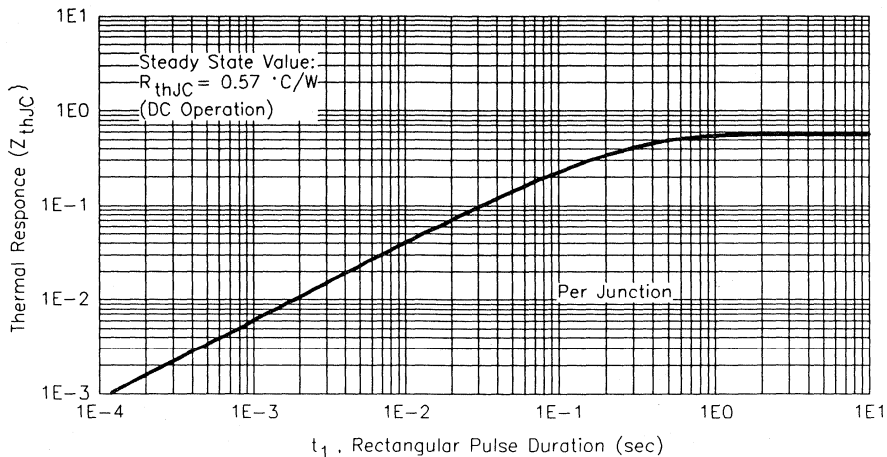


Figure 46. Maximum effective transient thermal impedance, junction-to-case (IRGTA090F06).

Transient junction to case thermal impedance

Maximum thermal impedance versus pulse duration is shown in Figure 46.

This curve defines the transient thermal impedance, in relation to the duration of the power pulse.

Transient thermal impedance is needed by the designer to calculate junction temperature under transient overload conditions and to calculate cycle-by-cycle fluctuations of junction temperature. The latter are generally not significant at operating frequencies higher than a few kHz.

Switching losses versus gate resistance

A typical relationship between total switching energy, E_{TS} , and gate resistance, R_{GI} , is shown in Figure 47.

The gate resistance has impact on the turn-on losses, but not much effect on the turn-off losses. The variation of total switching energy with gate resistance is therefore essentially due to the variation of the turn-on component of energy.

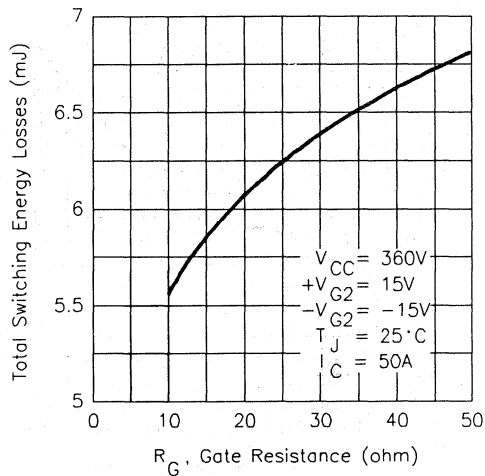


Figure 47. Typical switching losses vs. gate resistance (IRGTA090F06).

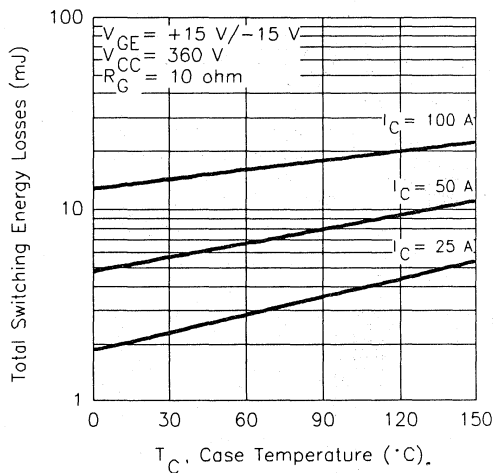


Figure 48. Typical switching losses vs. case temperature (IRGTA090F06).

Switching energy versus temperature

Switching energy increases as junction temperature increases.

Typical relationships between total switching energy and junction temperature are shown in Figure 48.

Snubberless Switching Safe Operating Area (SSSOA)

The SSSOA is shown in Figure 49.

It is important to appreciate that the SSSOA is defined

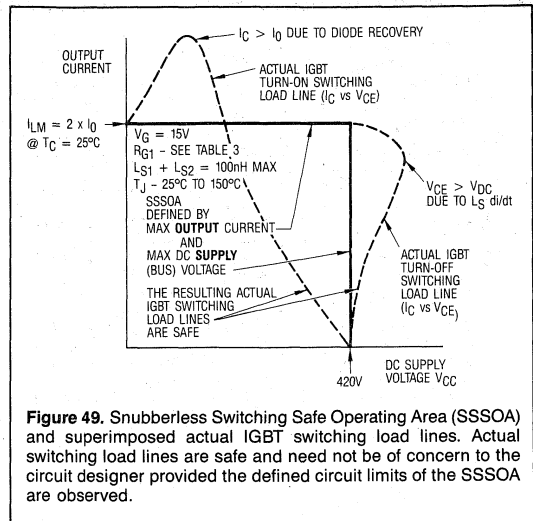


Figure 49. Snubberless Switching Safe Operating Area (SSSOA) and superimposed actual IGBT switching load lines. Actual switching load lines are safe and need not be of concern to the circuit designer provided the defined circuit limits of the SSSOA are observed.

in terms of the maximum dc supply voltage, V_{CC} and the maximum output current, I_0 . This is *not the same* as the normal industry method of defining the switching SOA, in terms of the IGBT's "own" collector-emitter voltage, V_{CE} and collector current, I_C .

During turn-off, the IGBT's "own" collector-emitter voltage, V_{CE} , exceeds the dc supply voltage, because of the overvoltage developed by the dc loop inductance. During turn-on, the IGBT's "own" current, I_C , exceeds the output current, because of the reverse recovery current of the diode.

The resulting "snubberless" dynamic switching load lines for the IGBT itself, shown in Figure 49, are *nonetheless safe* for IR's module. The "soft" switching characteristics of the IGBT and diode ensure that this is so.

A comparison of IR's SSSOA with the normal industry method for defining the switching safe operating area, often referred to as Reverse Bias Safe Operating Area, or RBSOA, is illustrated in Figure 50. The latter defines the IGBT's safe operating area during switching, in terms of the IGBT's "own" collector-emitter voltage and collector current.

Designing for snubberless switching, based on the RBSOA, is thwart with uncertainties. The designer must try to calculate the circuit operating limits that will ensure that the worst case dynamic switching load lines fit within the RBSOA. This calculation requires "worst-case" data on the diode's reverse recovery and IGBT turn-off characteristics - information that will not normally be found in the data sheet.

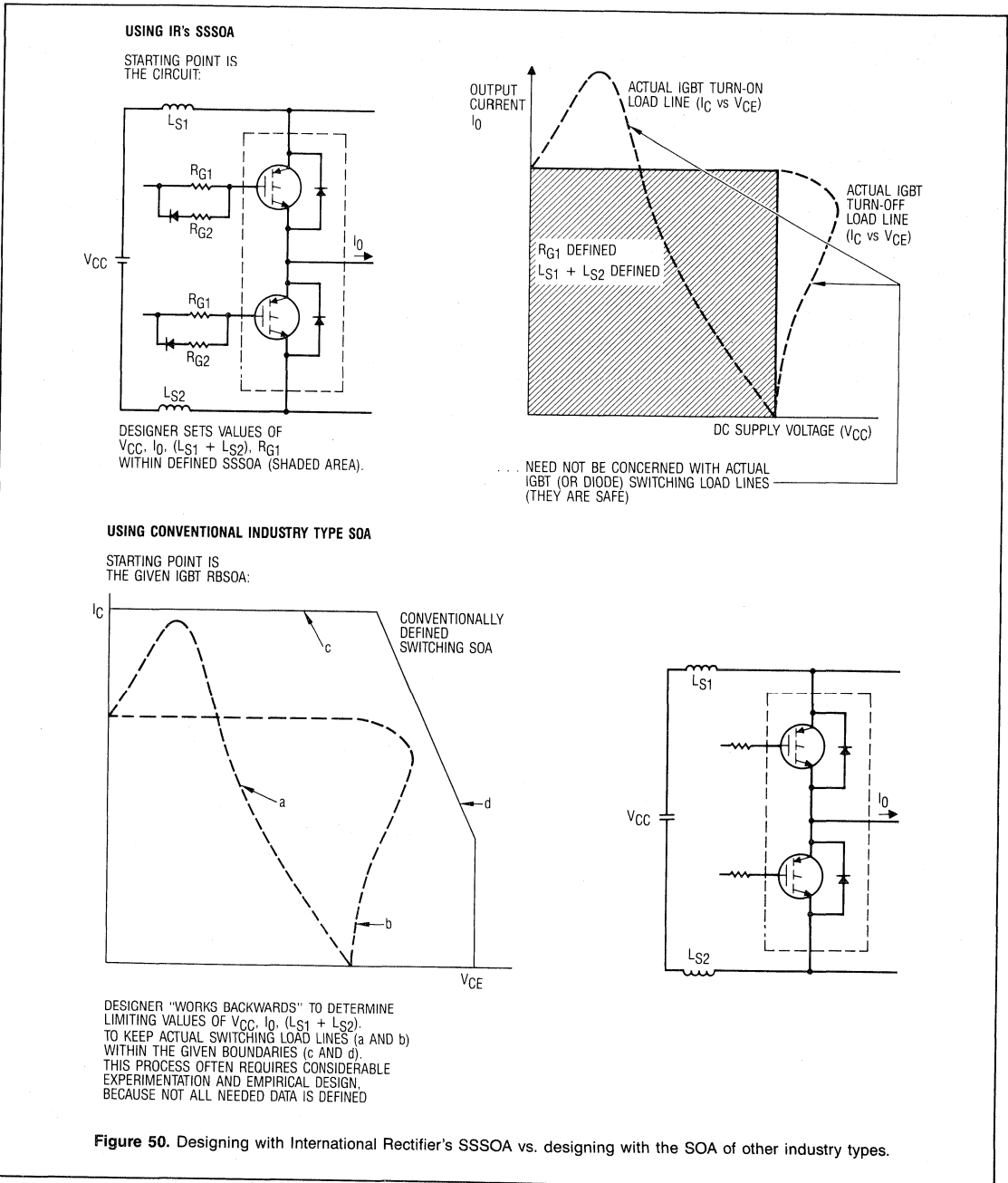
Usually, the designer must resort to an empirical approach to try to achieve "snubberless" compliance with the RBSOA. Faced with uncertain variability in the switching characteristics of the components, the designer will often fall back on the use of a snubber.

Designing with IR's SSSOA, by contrast, is simplicity itself. All that needs to be done is to set V_{CC} , I_0 , ($L_{S1} + L_{S2}$), R_{G1} , V_G and T_J within the specified limits. The design is then finished.

Derivation of the corresponding actual dynamic switching load lines for the IGBT itself is unnecessary. Compliance

with the SSSOA, of itself, ensures that the resulting switching load lines are safe.

In summary, snubberless operation with competitive types of IGBT modules is problematic and may not be feasible. Snubberless operation with International Rectifier modules is easy to design-for and guaranteed within the defined SSSOA.



Conclusions

The following conclusions relating to International Rectifier IGBT modules are summarized:

1. The IGBT modules generally have lower losses and can operate with a smaller heatsink and/or at higher frequency than other industry types.
2. The user has a choice of IGBT modules with "Fast" or "Ultrafast" switching characteristics.

Fast IGBT modules are generally best suited to operation at frequencies up to a few kHz in "hard" switching circuits. Frequencies to around 70kHz are practical in "resonant" circuits.

Ultrafast IGBT modules are generally best suited to operation in the 5-25kHz range in "hard" switching circuits. Frequencies in the 70-200kHz are practical in "resonant" circuits.

3. The size of the IR IGBT module is generally smaller than that of a competitive module of the same rating.

The ADD-A-pak IGBT module can often substitute

for a larger competitive INT-A-pak module, while having lower operating losses.

The INT-A-pak module can often substitute for a larger competitive "double INT-A-pak" module, while having lower operating losses.

6. IR's IGBTs and diodes have fast, "soft" switching characteristics. The "soft" switching characteristics allow snubberless operation.

An easy-to-use Snubberless Switching Safe Operating Area (SSSOA) is defined in the International Rectifier data sheet.

7. IR's IGBT modules do not require negative gate drive voltage.
8. International Rectifier data sheets for IGBT modules are "user friendly." They provide easily usable technical design information, that is directly related to actual circuit operating conditions. □

IGBT Designer's Manual

ACCURATE JUNCTION TEMPERATURE CALCULATION OPTIMIZES IGBT SELECTION FOR MAXIMUM PERFORMANCE AND RELIABILITY

S.M. Clemente and D.A. Dapkus II

Abstract - The power MOSFET, IGBT and thyristor are thermally-limited devices; that is, their power throughput is limited only by junction temperature. To get the most out of the device requires accurate calculation of the junction temperature under operating conditions. Unlike the power MOSFET, losses due to switching energy cannot be neglected in the calculations for the IGBT. Models based on both switching and conduction characteristics are developed. These models are used by a simple spreadsheet to allow the designer to quickly calculate the operating temperature of the IGBT. A procedure is presented which allows the designer to select the optimal IGBT for his particular application, based on thermal and reliability considerations. Thus, comparisons can be made between die sizes, switching speeds, saturation voltages, as well as heatsink sizes, and ultimately, final cost.

Introduction

One aspect in which the IGBT is similar to its cousin, the power MOSFET, is that it is a thermally-limited device. However, determining the power dissipation of an IGBT is more difficult, as switching losses cannot be neglected as in the MOSFET. For the IGBT, the total power dissipation is made up of three components: 1) turn-on, 2) conduction, and 3) turn-off.

Conduction losses are relatively simple to calculate if the current waveform is well behaved. However, the turn-on and turn-off losses are more difficult to calculate. We have developed a procedure to develop accurate models for all three regions. The models are accurate over a large range of currents and temperatures.

Using the models, it is possible to simulate the

junction temperature of an IGBT in a circuit. By adjusting the size of the IGBT and heatsink, it is possible to come to the best combination based on cost. As reliability is directly related to junction temperature, conservative thermal designs can be developed using the simulation tool presented here.

IGBTs are generally classified according to their switching speed. The faster the IGBT switches, the less

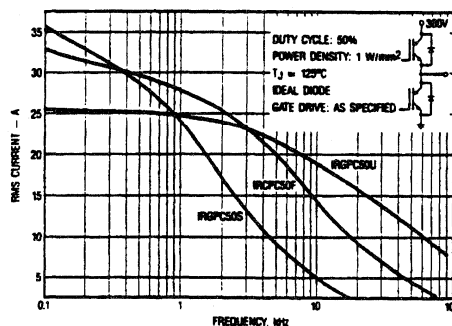


Figure 1 - RMS current vs. frequency for a Half-Bridge with two IGBTs of same die size, same package, different speed, operated in the conditions indicated in the inset

its switching losses. Of course there is a penalty for increased switching speed: conduction characteristics. Typically, IGBTs are divided into two groups: fast switching and low conduction loss. For a particular design, there is a frequency at which both devices have the same total loss. Above this frequency, it is desirable to use the fast switching IGBT, below, to use the low conduction IGBT.

For basic device comparisons, some manufacturers put current versus frequency graphs on their data sheets - that is, how much current one can expect to get out of a

certain circuit topology at a given frequency.

Figure 1 shows such a figure for the three families of 600V International Rectifier IGBTs. This figure was generated using the models developed in this paper. These figures are good for a basic figure of merit, however, unless the topology in question matches exactly the one used in the figure, the results will vary significantly. Thus, the model developed here is more general, and can be used to simulate any circuit topology under any conditions.

Background

Semiconductor companies spend considerable effort optimizing their silicon to obtain what they consider the best trade-off between conduction and switching characteristics. This is accomplished through a process called lifetime killing which increases switching speed at the expense of conduction losses. Conduction and short circuit withstand time characteristics are related to each other - the higher the conduction losses, the longer the short circuit withstand time, and vice versa. The amount of lifetime killing is chosen based on whether the device is to be a fast switching, or low conduction drop device. After the design is complete, the device undergoes testing to develop a data sheet. We have expanded on the testing typically done to develop three matrices: turn-on energy versus both current and temperature, turn-off energy versus both current and temperature, and finally, saturation voltage versus both current and temperature. Several lots are measured to ensure statistical deviations are taken into account (three in our case). The data is then averaged into a single set of three matrices. With the use of the three matrices, losses under any conditions (frequency, current, and temperature) are known. The matrices need to be pulled together to provide a method of automatically generating the losses under a particular set of conditions. This could be done using a lookup table and interpolating between points for values not in the matrices. As this is somewhat cumbersome to do, we settled on a method of approximating the data using curve fitting techniques. Using this method requires extra effort to reduce the data, but greatly simplifies matters when simulating device behavior under actual operating conditions. The error introduced by the curve fitting is within acceptable limits, and is detailed below.

The data required for these models has been acquired on the three families of International Rectifier's 600V IGBTs: Standard, Fast, and UltraFast™, which are classified according to their switching speed. Basic guidelines are: Standard speed IGBTs are typically used in applications where the switching frequency is under one kilohertz, while Fast speed IGBTs are used between three and eight kilohertz, and UltraFast™ IGBTs are used in applications above ten kilohertz. Of course, using the

models developed here, it is possible to optimize device selection based on the actual conditions at which the IGBT will be operated.

Development of Conduction Model

At any given time, the energy dissipated in the IGBT can be obtained with the following expression:

$$E = \int_0^t V_{CE}(i) \cdot i(\tau) d\tau$$

where t is the length of the pulse. Power is obtained by multiplying energy by frequency, if applicable. When the IGBT is off, $i(t) = I_{CES}$, the leakage current, and losses are negligible.

Unfortunately, no simple expression can be found for the voltage and current functions during a switching transient. Thus, for analytical expediency, we resort to a somewhat artificial distinction between conduction and switching losses.

We define conduction losses as the losses that occur between the end of the turn-on interval and the beginning of the turn-off interval, as defined for the switching losses characterization. Since the turn-on energy is measured from 5% of the test current to 5% of the test voltage, and turn-off energy is measured starting from 5% of the test voltage, conduction losses occur when the voltage across the IGBT is less than 5% of the test, or supply voltage (see Reference [1]).

To develop the conduction model, the matrix of conduction losses versus current and temperature was filled by taking laboratory measurements on three separate die lots, using five devices from each die lot. The temperature parameters were: 50, 75, 100, 125, and 150°C. Measurements were taken to identify "threshold," and four separate current densities. By "threshold," we mean the voltage collector to emitter that is developed when the IGBT carries appreciable current (approximately 0.035A/mm²).

Once the matrix was completed, it was fitted according to a power function of the form:

$$y = ax^b.$$

In terms of IGBT characteristics, this is:

$$V_{CE} = V_T + aI^b$$

where

$$\begin{aligned} V_{CE} &= \text{voltage drop across the IGBT} \\ V_T &= \text{drop across IGBT at "threshold,"} \\ I &= \text{current of interest.} \end{aligned}$$

The equation is then manipulated as follows:

$$V_{CE} - V_T = aI^b$$

$$\ln(V_{CE} - V_T) = \ln a + b \cdot \ln(I).$$

For a power function fit by the method of least squares, the values $\ln a$ and b are obtained by fitting a straight line to the set of ordered pairs $\{(\ln V_{CE} - V_T, \ln I)\}$ (see Reference [2]).

To determine the values of a and b , we use a straight line fit by the method of least squares:

$$b = \frac{n \sum_i \ln I_i \ln(V_{CE} - V_T)_i}{n \sum_i (\ln I_i)^2 - (\sum_i \ln I_i)^2}$$

$$= \frac{(\sum_i \ln I_i) [\sum_i \ln(V_{CE} - V_T)_i]}{n \sum_i (\ln I_i)^2 - (\sum_i \ln I_i)^2}$$

It can be shown that an alternate form of the denominator is:

$$n^2 \text{var}(\sum I_i)$$

Once the value of b has been calculated, the value of $\log a$ can be calculated as:

$$\log a = \frac{\sum_i (V_{CE} - V_T)_i - b \sum_i \ln I_i}{n}$$

Thus, for each of the temperatures, the values of a and b are calculated. Another linear regression is performed on these values to obtain an approximation according to the temperature of the form:

$$a = a_0 + a_1 \cdot T$$

$$b = b_0 + b_1 \cdot T$$

$$V_T = V_{T0} + V_{T1} \cdot T$$

where T designates the operating temperature in $^{\circ}\text{C}$.

It is then possible to calculate using just the results of the three linear regressions, the current, I (in A), and the operating temperature, T (in $^{\circ}\text{C}$) the V_{CE} across the IGBT:

$$V_{CE} = (V_{T0} + V_{T1} \cdot T) + (a_0 + a_1 \cdot T) I (b_0 + b_1 \cdot T)$$

The linear regression used to calculate the temperature coefficient has minimal effect on the accuracy of the models for the Standard and Fast IGBTs. An exponential

regression is more accurate for the UltraFast™. For the sake of simplicity, only the results of the linear regression are reported here.

The parameters for the three families of International Rectifier IGBTs can be found in the Appendix as Table I. Also found in the Appendix are graphs detailing the error introduced by the model. The error at low temperature is not particularly worrisome, as the device will usually be operated at higher temperatures. The graph depicts the error between measured and modeled values for size 5 International Rectifier IGBTs carrying a load current of 30A.

Table III of the Appendix lists the model parameters for the average data plus three sigma. These parameters may be used where a maximum simulation is required. The three sigma numbers are especially conservative as they describe a device that has both high conduction losses, and high switching losses. In reality, a device has one or the other, but not both. Thus, a device with higher than average conduction losses would have lower than average switching losses.

Development of Switching Model

As stated earlier, conduction losses are not the only losses of interest; the switching losses for IGBTs become more and more important as operating frequency increases. In order to see the whole picture, we need a method calculating the switching losses, both turn-on and turn-off.

The models for both turn-on and turn-off are developed exactly as the conduction model, with the exception that there is no "threshold" for the switching energies. As before, matrices of switching losses (either turn-on or turn-off) versus current and temperature are filled with laboratory-measured data. The same data reduction techniques are completed, resulting in the parameters in Table II of the Appendix. Also, Table IV lists the three sigma models for switching characteristics.

The expression to calculate the turn-on energy at a current I , and temperature T is:

$$E_{on} = (h_0 + h_1 \cdot T) I (k_0 + k_1 \cdot T)$$

Similarly, the expression to calculate the turn-off energy at a current I , and temperature T is:

$$E_{off} = (m_0 + m_1 \cdot T) I (n_0 + n_1 \cdot T)$$

Both these models assume the following operating conditions:

- Supply voltage is 80% of $V_{(BR)CES}$.
- Gate drive circuitry similar to the one in the data sheet, and
- Ideal diode.

The results should be scaled linearly for the appropriate supply voltage. The data sheet gate drive is what we consider to be a “stiff” gate drive: very low internal output impedance, and very low stray inductance in the path to the gate of the IGBT, and includes a separate emitter sense return path. If the gate drive in question is not terribly stiff, the results should be scaled according to Figure 9 of the data sheet which is “Typical Switching Losses versus Gate Resistance.” Use the sum of the external gate resistor and the internal resistance of the driver to obtain the resistance value to use when determining the scaling factor.

Changing the gate voltage does not significantly change the turn-off losses. However, decreasing the gate voltage does cause an increase in turn-on losses. This is most apparent in the UltraFast™ as the turn-on loss is a greater percentage of the total loss. Unfortunately, we have not been able to isolate how turn-on losses vary with gate voltage in a concise manner.

The model assumes an ideal diode, but with a typical clamped inductive load in continuous current mode, the turn-on of a switch causes a reverse recovery in the freewheeling diode and large current spike in the device that is being turned on. This increases the turn-on losses in the IGBT with respect to the model calculations and data sheet characterization. The forward recovery of the diode, on the other hand, has a second-order effect on the turn-off losses and will not be analyzed here.

No simple expressions can be provided for these additional turn-on losses, as they depend on a number of factors: turn-on speed di/dt , stray inductance, and diode characteristics. Several have been proposed, based on simplifying assumptions. The following assumes that the voltage across the diode is approximately zero volts during the length of t_a , rising to the supply voltage during t_b :

$$E = V \cdot I_L \left[(1 + \frac{1}{2} \cdot \frac{I_{rr}}{I_L} t_a + \frac{1}{4} \cdot \frac{I_{rr}}{I_L} t_b) \right]$$

$$= V(I_L t_a + Q_a + \frac{1}{2} Q_b)$$

where V and I_L are supply voltage and load current, I_{rr} is the peak reverse recovery current, t_a and t_b are the two

components of t_{rr} , and Q_a and Q_b are the charges associated with them (see Reference [3]). The first two terms represent the losses during t_a , one due to the load current, and the other due to the reverse recovery current. The third term represents the losses during t_b , which are partly in the IGBT, partly in the diode.

The limitation of this approximation is that the voltage starts to rise across the diode (and fall across the IGBT) during t_a . In reality, it reaches the supply voltage at the point of $di/dt=0$ of the reverse recovery current, which is the end of t_a . Hence, it yields values that are in excess of what would be reasonably encountered.

Assuming the voltage starts to rise at $2/3 t_a$, the following expression could be used:

$$E = \frac{2}{3} V \cdot I_L \left[\frac{1}{3} \frac{I_{rr}}{I_L} + 1 \right] t_a$$

By increasing the gate drive resistance which slows down turn-on, the peak reverse recovery current is reduced. However, turn-on energy losses in the IGBT increase because of the prolonged current rise time, as well as prolonged t_a .

If the diode is co-packaged with the IGBT, its losses cannot be dissociated from the losses in the main switching device. In this case, the thermal information and allowable power dissipation should be for the combination of both devices. Losses should include conduction and switching losses of both devices and the formulas should be modified accordingly.

Application Specific Simulation

Using the models developed in the previous sections, it is now possible to simulate the IGBT in an application. This simulation is more of a thermal simulation than an electrical one like SPICE would generate. Thermal analysis is critical as the final choice of the proper IGBT comes down to it.

Since temperature affects both conduction and switching losses, which, in turn, affect temperature, a direct mathematical solution is not possible. However, the models introduced in the previous sections can be applied iteratively, and with the help of the ‘solve for’ function available in most spreadsheets, permitting the characterization of a given operating condition with relative ease.

Figure 2 shows an example of such a spreadsheet. It was designed to answer two different, but related,

questions. The first: What is the maximum current that can be obtained from a specific IGBT for a given junction temperature and a set of operating conditions. The complementary question is: What is the junction temperature, given a value of current. In other words, since current and temperature are interdependent, one must be given so the other can be calculated.

Thus, the spreadsheet is divided vertically into two parts: one for a known junction temperature, and one for a known current. Horizontally, the spreadsheet is divided into three major parts: thermal operating conditions, device models, and electrical operating conditions. As part of the analysis, conduction and switching losses are calculated, together with some output parameters related to the application. Individual entries are self-explanatory.

Notice that, for operation at fixed temperature, the model parameters are fixed. On the other hand, when the junction temperature is unknown, the model parameters are also unknown. Hence, starting from a reasonable junction temperature, at the top of the right-hand section, the model parameters are calculated, and a new junction temperature is obtained, as shown at the bottom. The procedure is iterated by replacing the temperature at the top with the bottom one. Although only a few iterations are necessary, the process can be automated with a simple macro.

The spreadsheet contains a correction factor to take into account the fact that the gate drive circuit may have a different resistance than the one that was used for data sheet (and model) characterization. Since many circuits have a 'polarized gate resistor,' i.e., a resistor with a parallel diode, two lines are provided for this purpose, one for turn-on and one for turn-off energy. The entries for these two lines can be obtained from Figure 9 of the data sheet. Although this figure does not distinguish between turn-on and turn-off losses, it offers a first-cut approximation to both. It should be remembered that the gate drive circuit used for device characterization is very stiff. If the application being analyzed has a weak gate drive, its internal impedance should be added to the actual value of gate resistor.

The current for a given junction temperature is obtained with a 'solve for' function, changing the current until the total losses at the bottom equal the allowable power dissipation at the top.

The right-hand side of the spreadsheet can be used to do analyses of different types, like checking for thermal runaway. This can easily be done by increasing the ambient temperature at the top of the spreadsheet and calculating the new junction temperature. In the case of thermal runaway, successive iterations yield higher and higher junction temperatures.

This spreadsheet allows convenient analysis of the same circuit in different operating points, e.g., under stresses of transitory nature, like shorts in the output, where the junction temperature could be allowed to go to, say 150°C. In this case, the duty cycle would most likely be lower, and peak current higher.

As mentioned before, the model parameters obtained from linear regression are less accurate than the model parameters derived from measurements at fixed temperatures. A trace of this can be found in Figure 2, where the left side of the spreadsheet uses fixed temperature parameters, while the right side calculates the parameters from the linear regression coefficients. As a result, in spite of the fact that the operating conditions are the same in both sides of the spreadsheet, there is a junction temperature discrepancy of 3.93°C.

The spreadsheet contains several formulae, most of which require no explanation. From the top:

- Power dissipation: the ratio between temperature rise and thermal resistance between junction and ambient.
- Model parameters are entered (left-hand column) or calculated as explained in the previous sections (right-hand column).
- The peak current is the unknown in the left-hand column, calculated with the solve function, equalizing the total losses (at the bottom) with the allowable power dissipation (at the top). In the right-hand column, it is a simple entry.
- The voltage drop is calculated using the model.
- Conduction losses depend on the specific application. Figure 3 provides some common expressions.
- Turn-on and turn-off losses are calculated using the switching models.
- The corrections for gate resistance are multiplication factors obtained from Figure 9 of the data sheet, for a known value of gate drive impedance.
- The turn-on losses due to the diode recovery can be calculated as discussed previously.
- The total losses are the sum of conduction and switching losses, including losses due to diode recovery.

- The RMS value of the fundamental component of the output current depends on the output waveform. For a square wave, it is 0.9 times its peak value.
- The total RMS component of a square wave is 1.0.

Conclusion

Models for IGBT conduction and switching have been developed and fully characterized for use with International Rectifier's IGBTs. It is shown that the errors introduced by the models are within acceptable levels. Application of the models using a spreadsheet is detailed, which allows the designer to choose the optimal IGBT based on price/performance. By having an accurate knowledge of the operating temperature, reliability issues are addressed.

References

- [1] AN-983: "IGBT Characteristics," Section II.E
- [2] "Standard Mathematical Tables," The Chemical Rubber Co., 38th Ed.
- [3] AN-990 "Application Characterization of IGBTs"

PART NUMBER

IRGPC50U

THERMAL OPERATING CONDITIONS

Ambient temperature	° C	60
Thermal resistance j-to-c	° C/W	0.640
Thermal resistance c-to-s	° C/W	0.240
Thermal resistance s-to-a	° C/W	1.400

		Allowable current at stated T _J	Junction temperature for stated current
Power dissipation	W	28.5	30.23
	° C	125.0*	128.93

IGBT MODEL

V _t , V _{t1} , V _{t2}	V	0.8000		0.7900	1.0994	-2.40E-03
a, a1, a2	Ohm	0.1120		0.1119	0.2021	-7.00E-04
b, b1, b2		0.7117		0.7131	0.4656	1.92E-03
h, h1, h2	mJ/A	0.0038		0.0037	0.0045	-6.10E-06
k, k1, k2		1.6376		1.6403	1.6162	1.87E-04
m, m1, m2	mJ/A	0.0128		0.0161	-0.0114	2.13E-04
n, n1, n2		1.3382		1.3243	1.9457	-4.82E-03
Reference voltage	V	480		480		

DIODE MODEL

V _t		0.8		0.8	
a,b		0.04	1	0.04	1
ratio I _{rr} /I _f		1		1	
t _a , t _b	μ s	0.04	0.03	0.04	0.03

ELECTRICAL OPERATING CONDITIONS

RECT. WAVEFORM, CLAMPED IND. LOAD

Switching voltage	V	360	360
Operating Frequency	kHz	40	40
Duty cycle		0.45	0.45
Peak current	A	9.82	9.82*
Voltage drop at peak current	V	1.37	1.36
Conduction losses	W	6.05	6.01
Turn-on losses	W	4.76	4.75
Correction factor for gate resistance		1.00	1.00
Corrected turn-on losses	W	4.76	4.75
Turn-off losses	W	8.14	9.92
Correction factor for gate resistance	W	1.00	1.00
Corrected turn-off losses	W	8.14	9.92
Turn-on losses due to diode recovery	W	9.55	9.55
Total losses	W	28.50	30.23
Junction Temperature	° C		128.93

RMS current, fundamental	A	8.84	8.84
RMS current, total	A	9.82	9.82
Output voltage, RMS fundamental	V	162.00	162.00
Output power, fundamental	kVA	1.59	1.59
Output power, total	kVA	1.77	1.77

*: Data entered

Figure 2 - Sample spreadsheet showing application of models



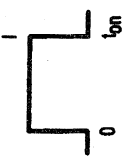
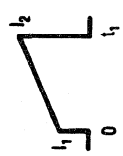
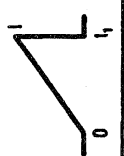
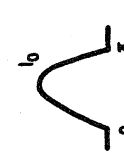
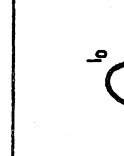
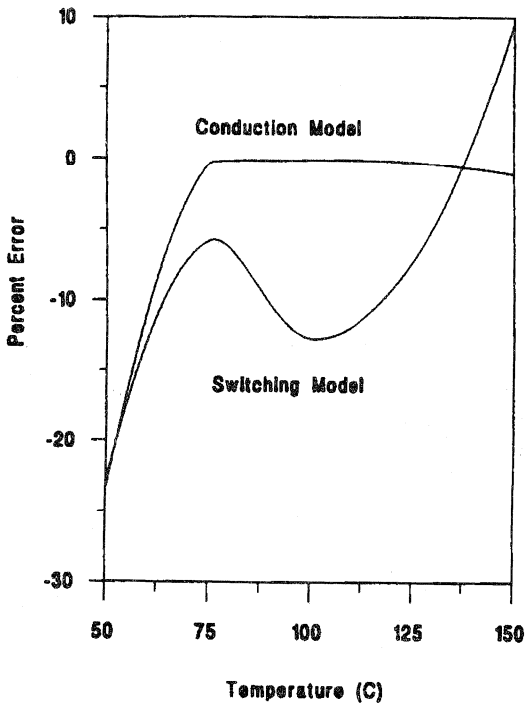
CURRENT WAVEFORM	MATHEMATICAL EXPRESSION	$E = \int v_{ce}(t) i(t) dt$, $v_{ce}(t) = V_t + a t^p$, $E = \int [V_t i(t) + a i(t)^{p+1}] dt$
	$i(t) = 1$	$E = \int_0^{t_{on}} (1 V_t + a t^{p+1}) dt = (V_t + a t^{p+1}) t_{on}$
	$i(t) = 1_1 + (1_2 - 1_1) \frac{t}{t_1}$	$E = \int_0^{t_1} \left[V_t \left(1_1 + \frac{(1_2 - 1_1)}{t_1} t \right) + a \left(1_1 + \frac{(1_2 - 1_1)}{t_1} t \right)^{p+1} \right] dt = V_t \frac{(1_1 + 1_2)}{2} t_1 + \frac{1_1^{p+2} - 1_2^{p+2}}{(1_2 - 1_1)} \frac{a t_1}{b + 2}$
	$i(t) = 1 \frac{t}{t_1}$	$E = \int_0^{t_1} \left(V_t \frac{t}{t_1} + a \left(\frac{t}{t_1} \right)^{p+1} \right) dt = \frac{1}{2} V_t t_1 + \frac{a t_1^{p+2}}{b + 2}$
	$i(t) = I_0 \sin \omega t$	$E = \int_0^{T/2} (V_t I_0 \sin \omega t + a I_0^p \sin^{p+1} \omega t) dt = \frac{2 I_0}{\omega} \left[V_t + \frac{\sqrt{\pi}}{2} a \frac{\Gamma\left(\frac{b+2}{2}\right)}{\Gamma\left(\frac{b+3}{2}\right)} \right]$
	$i(t) = I_0 \sin \omega t$	for $\alpha = \frac{\pi}{2}$ $E = \frac{I_0}{\omega} \left[V_t + \frac{\sqrt{\pi}}{2} a \frac{\Gamma\left(\frac{b+2}{2}\right)}{\Gamma\left(\frac{b+3}{2}\right)} \right]$ otherwise $E = \frac{I_0}{\omega} \left[V_t (1 + \cos \alpha) + a \int \sin^{p+1} \alpha d \alpha \right]$

Figure 3
Conduction Energy for Simple Waveforms

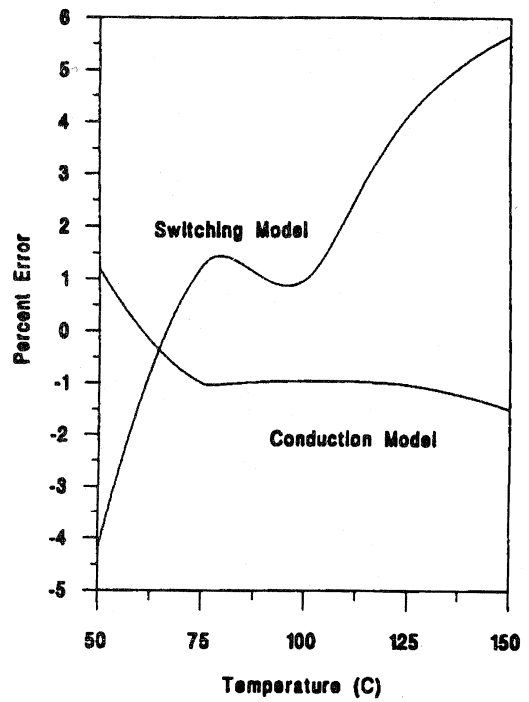
APPENDIX

- Graphs depicting model error
- Model parameters - These are updated as we develop new models

Model Error for IRGPC50F



Model Error for IRGPC50S



Model Error for IRGPC50U

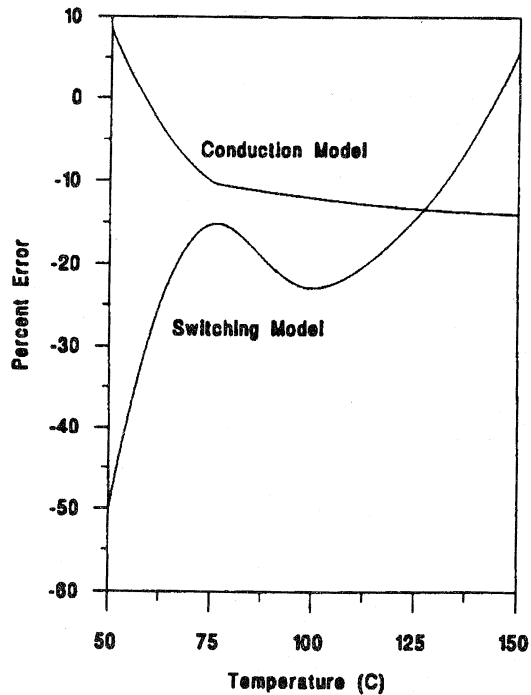


Table I - Conduction Model Parameters for International Rectifier IGBTs

Part Number	V_{T0}	V_{T1}	a_0	a_1	b_0	b_1
IRGBC20F	0.905	-2.06E-3	0.241	7.08E-4	0.649	5.11E-4
IRGBC20S	0.810	-1.66E-3	0.173	2.90E-4	0.721	4.79E-4
IRGBC20U	1.071	-2.40E-3	0.669	-1.28E-3	0.353	2.29E-3
IRGBC30F	0.911	-1.98E-3	0.115	4.19E-4	0.721	2.95E-4
IRGBC30S	0.840	-1.64E-3	0.100	1.38E-4	0.760	5.10E-4
IRGBC30U	1.175	-2.75E-3	0.307	-3.13E-4	0.504	1.56E-3
IRGBC40F	0.901	-1.93E-3	0.072	2.17E-4	0.731	3.13E-4
IRGBC40S	0.824	-1.67E-3	0.052	6.52E-5	0.776	4.24E-4
IRGBC40U	1.171	-2.55E-3	0.320	-1.08E-3	0.419	2.24E-3
IRGPC40F	0.901	-1.93E-3	0.072	2.17E-4	0.731	3.13E-4
IRGPC40S	0.824	-1.67E-3	0.052	6.52E-5	0.776	4.24E-4
IRGPC40U	1.171	-2.55E-3	0.320	-1.08E-3	0.419	2.24E-3
IRGPC50F	0.871	-1.92E-3	0.045	1.19E-4	0.751	2.87E-4
IRGPC50S	0.820	-1.69E-3	0.033	3.42E-5	0.794	4.09E-4
IRGPC50U	1.099	-2.39E-3	0.202	-6.99E-4	0.466	1.92E-3
IRGBF20F	1.162	-1.26E-3	1.214	-2.87E-3	0.205	3.23E-3
IRGBF30F	1.209	-1.84E-3	0.512	-1.12E-3	0.412	2.30E-3
IRGPF30F	1.209	-1.84E-3	0.512	-1.12E-3	0.412	2.30E-3
IRGPF40F	TBD	TBD	TBD	TBD	TBD	TBD
IRGPF50F	1.118	-1.95E-3	0.205	-5.10E-4	0.509	1.65E-3
IRGPH50F	1.324	-2.02E-3	0.179	1.02E-4	0.668	8.96E-4
IRGPH40F	1.286	-2.09E-3	0.103	6.04E-5	0.702	8.50E-4

Table II - Switching Model Parameters for International Rectifier IGBTs

Part Number	h_0	h_1	k_0	k_1	m_0	m_1	n_0	n_1
IRGBC20F	1.17E-2	2.21E-5	1.20	-1.53E-4	-9.18E-4	1.02E-3	1.36	-2.41E-3
IRGBC20S	1.67E-2	2.78E-6	1.18	3.41E-4	2.05E-1	2.51E-3	1.09	-5.96E-4
IRGBC20U	1.43E-2	9.73E-6	1.11	1.21E-4	-1.02E-2	3.58E-4	1.54	-3.75E-3
IRGBC30F	4.44E-2	2.65E-6	1.50	-1.59E-4	-1.29E-2	1.02E-3	1.50	-2.88E-3
IRGBC30S	6.21E-2	2.96E-6	1.47	1.22E-4	1.58E-1	2.75E-3	1.10	-6.94E-4
IRGBC30U	3.80E-3	1.18E-5	1.54	-6.01E-4	-2.05E-2	4.18E-4	1.88	-5.34E-3
IRGBC40F	3.34E-3	-1.10E-6	1.58	6.37E-4	-2.47E-2	1.04E-3	1.47	-2.65E-3
IRGBC40S	1.58E-3	2.08E-5	1.80	-1.25E-3	1.71E-1	3.23E-3	1.07	-6.23E-4
IRGBC40U	1.30E-3	1.08E-5	1.79	-8.66E-4	-1.38E-2	2.74E-4	1.83	-4.60E-3
IRGPC40F	3.34E-3	-1.10E-6	1.58	6.37E-4	-2.47E-2	1.04E-3	1.47	-2.65E-3
IRGPC40S	1.58E-3	2.08E-5	1.80	-8.66E-4	-1.38E-2	2.74E-4	1.83	-4.60E-3
IRGPC40U	1.30E-3	1.08E-5	1.79	-8.66E-4	-1.38E-2	2.74E-4	1.83	-4.60E-3
IRGPC50F	5.40E-3	-1.40E-5	1.56	6.42E-4	-3.53E-2	1.12E-3	1.49	-2.81E-3
IRGPC50S	3.61E-3	2.61E-7	1.67	1.85E-4	1.44E-1	3.91E-3	1.08	-7.42E-4
IRGPC50U	4.52E-3	-6.10E-6	1.62	1.87E-4	-1.14E-2	2.13E-4	1.95	-4.82E-3
IRGBF20F	5.21E-2	5.79E-5	0.86	2.71E-4	1.67E-2	4.83E-4	1.39	-7.64E-4
IRGBF30F	2.60E-2	2.64E-5	1.09	1.41E-4	1.42E-2	4.34E-4	1.33	-6.88E-4
IRGPF30F	2.60E-2	2.64E-5	1.09	1.41E-4	1.42E-2	4.34E-4	1.33	-6.88E-4
IRGPF40F	TBD	TBD	TBD	TBD	TBD	TBD	TBD	TBD
IRGPF50F	2.98E-2	6.60E-6	1.11	6.49E-6	-2.96E-3	4.60E-4	1.55	0.00
IRGPH50F	3.22E-2	-7.46E-6	1.23	5.44E-4	5.04E-3	1.23E-3	1.50	-1.84E-3
IRGPH40F	8.59E-4	1.09E-4	1.70	-1.66E-3	-7.19E-3	1.15E-3	1.54	-2.08E-3

Table III - Conduction Model Parameters for International Rectifier IGBTs
Average + 3 Sigma

Part Number	V_{T0}	V_{T1}	a_0	a_1	b_0	b_1
IRGBC20F	0.987	-2.20E-3	0.320	5.68E-4	0.595	8.79E-4
IRGBC20S	0.816	-1.59E-3	0.197	2.49E-4	0.785	4.70E-4
IRGBC20U	1.161	-2.45E-3	1.003	-3.03E-3	0.255	3.17E-3
IRGBC30F	0.958	-2.03E-3	0.134	3.64E-4	0.696	5.73E-3
IRGBC30S	0.862	-1.65E-3	0.118	1.39E-4	0.078	5.75E-4
IRGBC30U	1.409	-3.38E-3	0.589	-1.97E-3	0.313	2.79E-3
IRGBC40F	0.976	-2.04E-3	0.096	1.95E-4	0.689	5.79E-4
IRGBC40S	0.864	-1.72E-3	0.068	3.89E-5	0.785	5.86E-4
IRGBC40U	1.340	-2.63E-3	0.716	-3.05E-3	0.240	3.34E-3
IRGPC40F	0.976	-2.04E-3	0.096	1.95E-4	0.689	5.79E-4
IRGPC40S	0.864	-1.72E-3	0.068	3.89E-5	0.785	5.86E-4
IRGPC40U	1.340	-2.63E-3	0.716	-3.50E-3	0.240	3.34E-3
IRGPC50F	0.941	-2.04E-3	0.058	8.90E-5	0.719	5.10E-4
IRGPC50S	0.833	-1.65E-3	0.036	1.22E-5	0.796	6.12E-4
IRGPC50U	1.249	-2.54E-3	0.499	-2.71E-3	0.246	3.34E-3
IRGBF20F	1.162	-1.26E-3	2.234	-8.53E-3	-0.016	4.16E-3
IRGBF30F	1.209	-1.84E-3	1.148	-5.12E-3	0.160	3.89E-3
IRGPF30F	1.209	-1.84E-3	1.148	-5.12E-3	0.160	3.89E-3
IRGPF40F	TBD	TBD	TBD	TBD	TBD	TBD
IRGPF50F	1.118	-1.95E-3	0.413	-1.79E-4	0.368	2.47E-3
IRGPH50F	1.516	-2.27E-3	0.231	1.16E-4	0.632	1.08E-3
IRGPH40F	1.587	-2.64E-3	0.095	2.47E-4	0.832	6.17E-4

Table IV - Switching Model Parameters for International Rectifier IGBTs
Average + 3 Sigma

Part Number	h_0	h_1	k_0	k_1	m_0	m_1	n_0	n_1
IRGBC20F	9.79E-3	5.60E-5	1.29	-1.06E-3	2.05E-2	1.40E-3	1.31	-1.97E-3
IRGBC20S	1.74E-2	1.47E-6	1.29	2.52E-4	2.66E-1	3.08E-3	1.09	-6.21E-4
IRGBC20U	1.62E-2	-4.11E-6	1.11	5.11E-4	-1.14E-2	4.47E-4	1.53	-3.62E-3
IRGBC30F	4.61E-2	6.38E-6	1.56	-4.37E-4	-1.16E-2	1.27E-3	1.48	-2.71E-3
IRGBC30S	6.67E-2	7.74E-7	1.48	3.38E-4	2.16E-1	3.33E-3	1.07	-6.00E-4
IRGBC30U	4.53E-3	1.08E-5	1.59	-4.71E-4	-2.94E-2	6.04E-4	1.87	-5.41E-3
IRGBC40F	2.90E-3	1.25E-6	1.69	2.82E-4	-3.32E-2	1.42E-3	1.49	-2.81E-3
IRGBC40S	1.63E-3	2.55E-5	1.85	-1.71E-3	2.63E-1	4.62E-3	1.03	-6.22E-4
IRGBC40U	9.55E-4	1.59E-5	1.88	-1.63E-3	-1.92E-2	4.13E-4	1.73	-4.28E-3
IRGPC40F	2.90E-3	-1.25E-6	1.69	2.82E-4	-3.32E-2	1.42E-3	1.49	-2.81E-3
IRGPC40S	1.63E-3	2.55E-5	1.85	-1.71E-4	-2.63E-2	4.62E-3	1.03	-6.22E-3
IRGPC40U	9.55E-4	1.59E-5	1.88	-1.63E-3	-1.92E-2	4.13E-4	1.73	-4.28E-3
IRGPC50F	6.50E-3	-2.28E-5	1.55	9.86E-4	-4.34E-2	1.56E-3	1.47	-2.69E-3
IRGPC50S	4.06E-3	-2.27E-6	1.71	3.00E-4	1.98E-1	4.86E-3	1.09	-7.04E-4
IRGPC50U	3.22E-3	7.35E-6	1.75	6.81E-4	-1.88E-2	3.58E-4	1.90	-4.83E-3
IRGBF20F	5.47E-2	6.69E-5	0.944	2.70E-4	1.53E-2	7.75E-4	1.64	-2.29E-3
IRGBF30F	2.75E-2	2.32E-5	1.10	2.15E-4	2.26E-2	5.84E-4	1.37	-9.08E-4
IRGPF30F	2.75E-2	2.32E-5	1.10	2.15E-4	2.26E-2	5.84E-4	1.37	-9.08E-4
IRGPF40F	TBD	TBD	TBD	TBD	TBD	TBD	TBD	TBD
IRGPF50F	2.96E-2	-4.11E-6	1.15	1.55E-4	-3.40E-4	5.49E-4	1.57	-2.11E-3
IRGPH50F	3.38E-2	-5.04E-6	1.27	9.18E-4	1.71E-2	1.43E-3	1.49	-1.66E-3
IRGPH40F	4.79E-3	7.71E-5	1.70	-1.50E-3	-6.16E-3	1.41E-3	1.52	-2.15E-3

500V IGBTs REPLACE MOSFETS AT LOWER COST

by Laszlo Kiraly

Introduction:

International Rectifier's 500V IGBTs have switching characteristics that are very close to those of power MOSFETs, without sacrificing the superior conduction characteristics of IGBTs. They offer advantages over MOSFETs in high-voltage, hard-switching applications. These advantages include lower conduction losses and smaller die area for the same output power. The smaller die area results in lower input capacitance and cost.

Replacing MOSFETs with IGBTs:

Because the package style and pinouts of MOSFETs and IGBTs are identical, no mechanical or layout changes are required.

The gate drive requirement for IGBTs is similar to MOSFETs. A gate voltage between 12V and 15V is sufficient for turn-on, and no negative voltage is required at turn-off. The value of the series gate resistor may have to be increased to avoid ringing at the gate of the IGBT due to smaller die size.

1. Power Dissipation:

In high-voltage MOSFETs, power dissipation is mostly due to conduction losses; switching losses are negligible up to 50kHz. On the other hand, conduction losses in the IGBT are less than in the MOSFET, but switching losses become significant above 10kHz.

Design Example:

Switched DC Current	= 7.5A
Duty cycle	= 0.5
Bus voltage	= 310V
Junction temperature	= 125°C
MOSFET used	= IRFP450
$R_{DS(on)}$ (25°C)	= 0.4Ω
Operating frequency	= 50kHz
Current waveform	= square wave

On-resistance of the IRFP450 MOSFET at 125°C is (from the data sheet):

$$R_{DS(on)}(125^\circ\text{C}) = 0.816\Omega.$$

Conduction loss in the MOSFET at 125°C:

$$P_D = R_{DS(on)}(125^\circ\text{C}) * I^2 * D = 23\text{W}$$

Assuming 75ns switching times and 50kHz switching frequency, switching losses in the MOSFET at 7.5A are approximately:

$$P_{sw} = 6.5\text{W}$$

Total power loss in the MOSFET is:

$$P_{tot} = 29.5\text{W}$$

Replacing the MOSFET with an IRGP430U IGBT, conduction loss in the IGBT is:

$$P_C = V_{CE(125^\circ\text{C})} * I_c * D$$

On-state collector-emitter voltage at 125°C and 7.5 A is from Figure 5 on the data sheet:

$$V_{CE@125^{\circ}C} = 2.03V.$$

Conduction loss in the IGBT is:

$$P_c = 2.03V * 7.5A * 0.5 = 7.62W$$

Due to the IGBT's higher usable current density, the same power dissipation in the IGBT and MOSFET results in higher junction temperature for the IGBT because of higher junction-to-case thermal resistance.

To maintain junction temperature parity, the power dissipation in the IGBT needs to be reduced to:

$$P_{DIGBT} = P_D * (R_{\theta SA} + R_{\theta CSM} + R_{\theta JCM}) / (R_{\theta SA} + R_{\theta CSI} + R_{\theta JCI})$$

Where:

- $R_{\theta SA}$ Heatsink-to-ambient thermal resistance.
- $R_{\theta CSM}$ MOSFET case-to-sink thermal resistance
- $R_{\theta JCM}$ MOSFET junction-to-case thermal resistance.
- $R_{\theta CSI}$ IGBT case-to-sink thermal resistance.
- $R_{\theta JCI}$ IGBT junction-to-case thermal resistance.

Total power dissipation is composed of both conduction and switching losses. Conduction losses were calculated above. Applying the formula above results in $P_{DIGBT} = 23.2W$.

Maximum allowable power loss due to switching losses:

$$P_{SW} = P_{TOT} - P_{COND}$$

$$P_{SW} = 23.2W - 7.6W = 15.6W$$

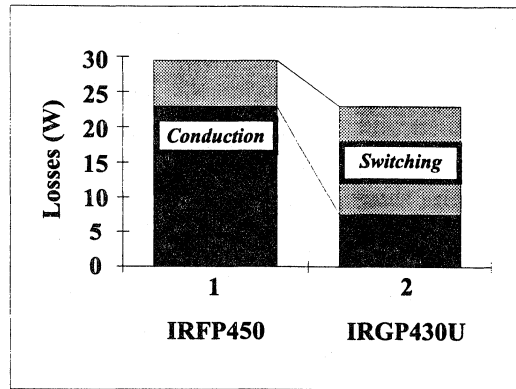


Figure 1 - Power losses in an IRGPC450 MOSFET and a IRGP430U IGBT at 7.5A current both switching at 50kHz.

Maximum switching frequency for same junction temperature in same thermal environment:

$$f_{max} = 10.3W / 0.226mJ = 56.4kHz$$

The switching energy number comes from data sheet information. It will be appreciated that, being operated with lower losses, the IGBT design is more efficient.

The sources of power dissipation in the IRFP450 MOSFET and IRGP430U IGBT are shown in Figure 1.

Selecting IGBT:

Figure 2 provides an easy method to select an IGBT which can replace IRFP460, IRFP450 or IRFP440 MOSFET in hard-switching applications. The first step is to find the proper curve in the chart, based on the MOSFET's part number. The part number of the recommended replacement IGBT is shown next to the curve. In general, a given MOSFET can be replaced with a two die size smaller 500V IGBT (e.g. IRFP450 → IRGP430U). The IGBT's die size is typically about 40% of the MOSFET's die size.

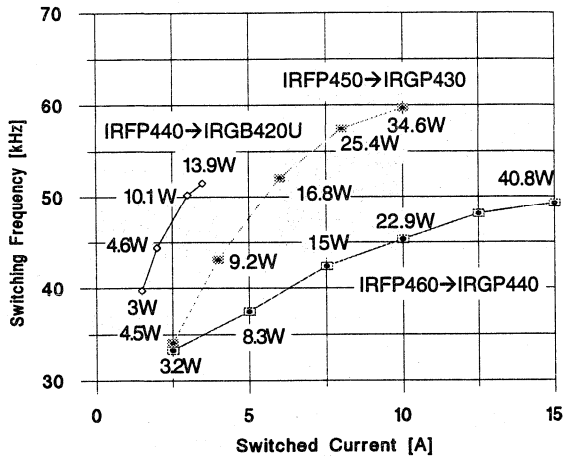


Figure 2 - Maximum operating frequency of IGBT vs. switched current. IGBT replaces 2-size larger MOSFET in hard-switching application. Operating IGBT at frequency indicated, junction temperature of IGBT equals junction temperature of MOSFET it replaces.
($T_{ambient} = 65^{\circ}C$, $T_j = 125^{\circ}C$, Duty cycle = 0.5)

The next step is to find the maximum operating frequency for the IGBT. By definition, at the maximum operating frequency the IGBT operates at the same junction temperature as the replaced MOSFET. To find the maximum operating frequency, select the operating current on the horizontal axis and read the maximum operating frequency on the vertical axis.

Using the power dissipation values for the IGBT in Figure 2, the heatsink can be sized for a given ambient temperature.

2. Gate Resistor and Snubber:

The smaller die size and input capacitance of the IGBT may result in faster switching speed than the MOSFET replaced. A larger-value gate resistor slows down turn-on speed, but has little effect on turn-off. Unlike the MOSFET, the turn-off speed of the IGBT cannot be controlled with a series gate

resistor.

High turn-off speed can generate excessive ringing and voltage spikes in the circuit. If a snubber is used, resizing the components helps reduce noise. Minimizing stray inductances in the wiring and transformer is the most effective way of reducing noise in new designs.

3. Emitter-Collector Diode:

In applications where the body diode of the MOSFET is used, IGBT-HEXFRED® diode Co-Paks improve performance and efficiency while reducing current spikes, due to better diode performance.

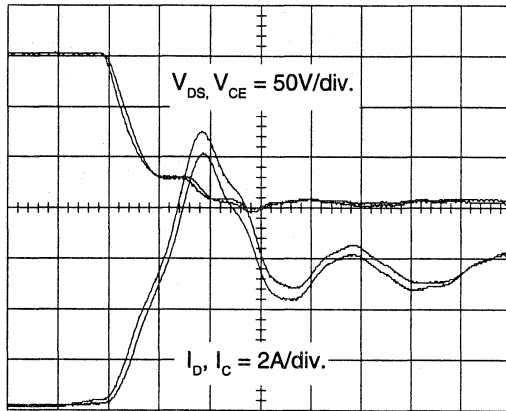
4. Test Results:

Figures 3 and 4 show the turn-on and turn-off waveforms for an IRFP450 MOSFET and an IRGP430U IGBT, both switching 5.5A at 160V. The switching waveforms were taken in a 400W, single-ended forward converter. Because of different die sizes, a 10 Ohm gate resistor was used for the MOSFET and 33 Ohm for the IGBT. The waveforms show same turn-on speed and faster turn-off for the IGBT.

5. Additional Information:

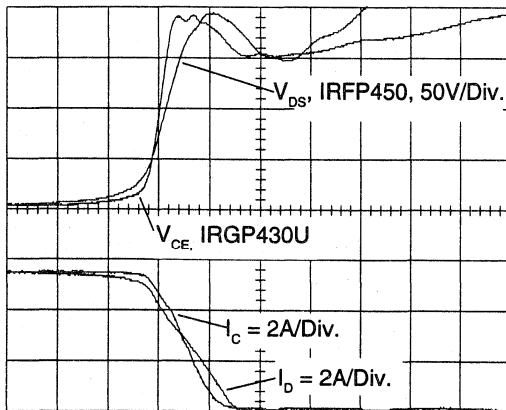
Application Note AN-990, *Application Characteristics of IGBTs*, provides details on how to calculate IGBT losses.

Application Note AN-983A, *IGBT Characteristics*, describes the fundamentals of IGBT operation.



Horiz.: 50ns/div.

Figure 3 - Turn-on waveforms. The IRFP450 and IRGP430 are switching 5.5A at 160V



Horiz.: 100ns/div

Figure 4 - Turn-Off Waveforms, 5.5A at 160V

MINIATURIZATION OF THE POWER ELECTRONICS FOR MOTOR DRIVES

By Gerry Limjuco & Dana Wilhelm

Introduction:

The power electronics for a fractional HP AC or BL-DC motor drive can be built in a volume not much larger than a pack of cigarettes. MOS Gate Drivers and co-packaged IGBTs in surface mounted TO-220 (IRGBC30UD2-S) are the key to achieve this level of power density (Figure 1).

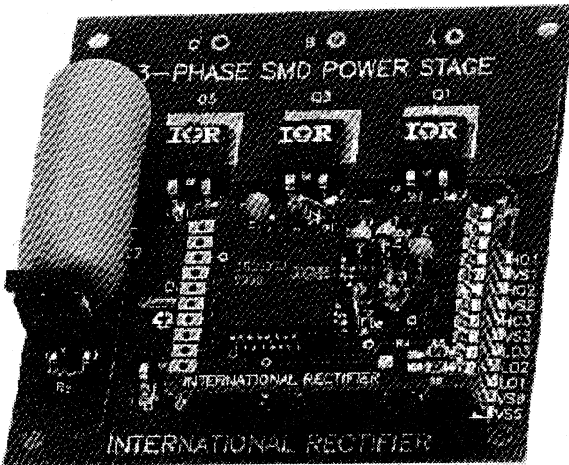


Figure 1: 3-Phase SMD Power Stage (Actual Size)

Figure 2 shows the schematic of the power stage. The input is the logic signal from the modulator (standard TTL/CMOS) and the outputs are the three phases to the motor.

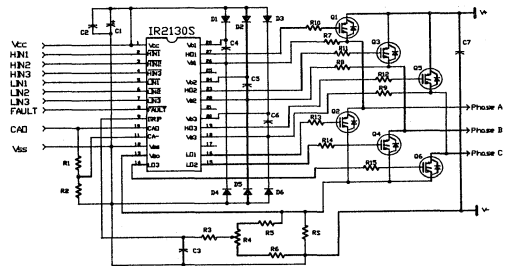


Figure 2: 3-Phase SMD Power Stage (Schematic Diagram - IR2130S)

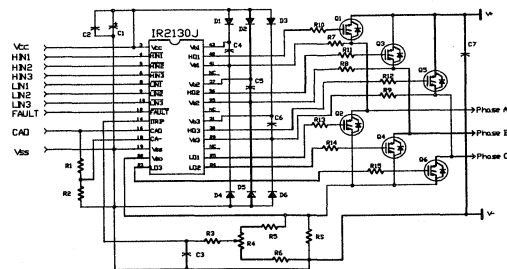


Figure 2A: 3-Phase SMD Power Stage (Schematic Diagram - IR2130J)

If isolation is required between the modulator and the power stage, it can be provided with inexpensive (low dv/dt) opto-isolators at the input of the IR2130 (Figure 3).

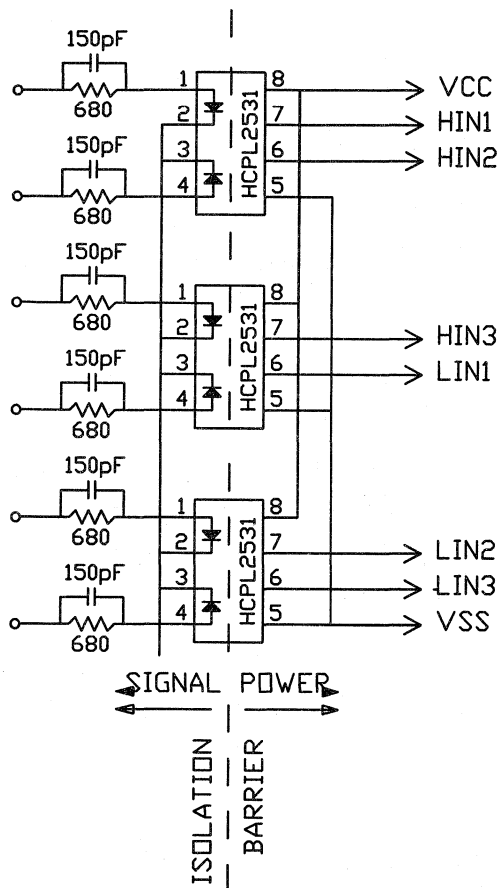


Figure 3: Input Isolation Stage

In addition to the logic inputs, the power stage requires a single 12-15V, 20mA supply. It can operate to bus voltages up to 600V.

The power stage is split into two boards, one with the power devices (Figures 4 & 4A), the other with the gate driver and overcurrent protection and shutdown.

Power Circuit

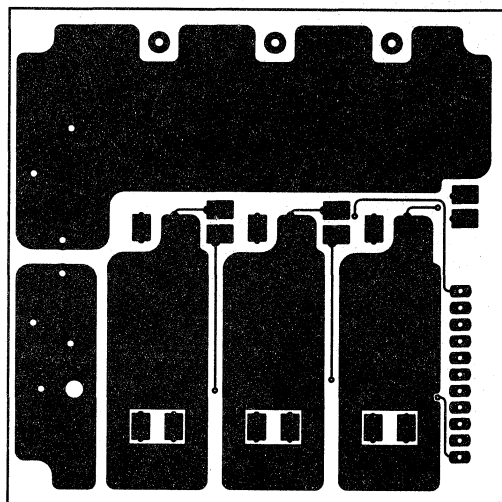


Figure 4: Power Circuit (top view)

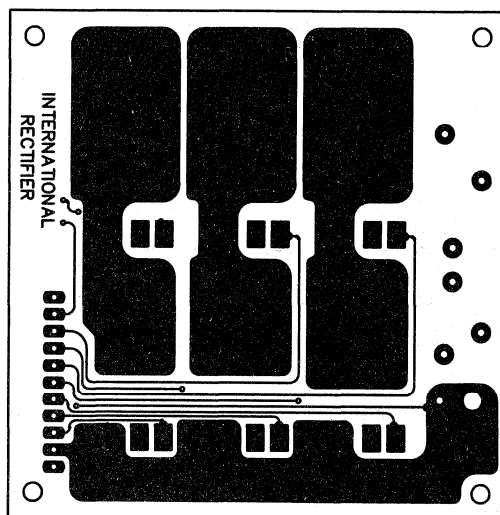


Figure 4A: Power Circuit (bottom view)

Figures 5 and 5A show the control board layout using IR2130S (SOIC), whereas Figures 6 and 6A show the control board layout using IR2130J (PLCC). Either of these control boards can be interconnected with the power board using standard .100" center headers into mating receptacles.

IR2130S Control Circuit

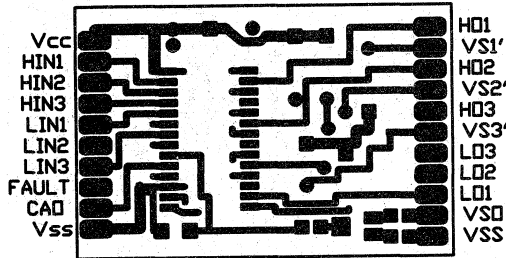


Figure 5: IR2130S Control Circuit (top view)

IR2130J Control Circuit

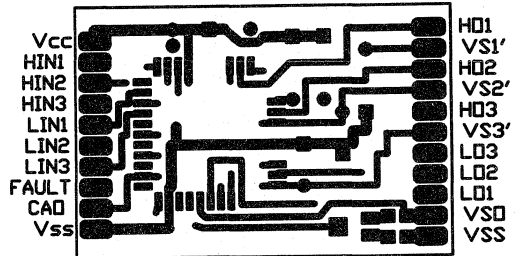


Figure 6: IR2130J Control Circuit (top view)

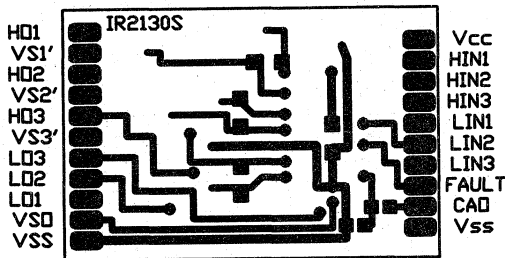


Figure 5A: IR2130S Control Circuit (bottom view)

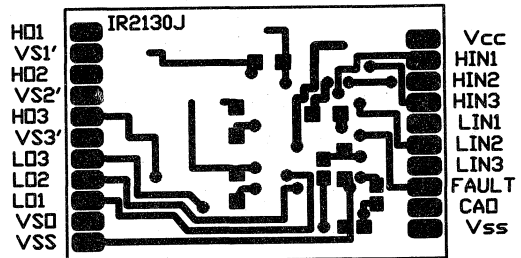


Figure 6A: IR2130J Control Circuit (bottom view)

Figure 7 shows how much current can be delivered to an AC motor operated with pulse-width modulation. Larger currents can be obtained from a board with better thermal characteristics than a standard FR4, 4 oz. copper. The thermal resistance between junction and air for this specific design was measured at 40°C/W per device. The attached sheet shows a breakdown of the different components of losses.

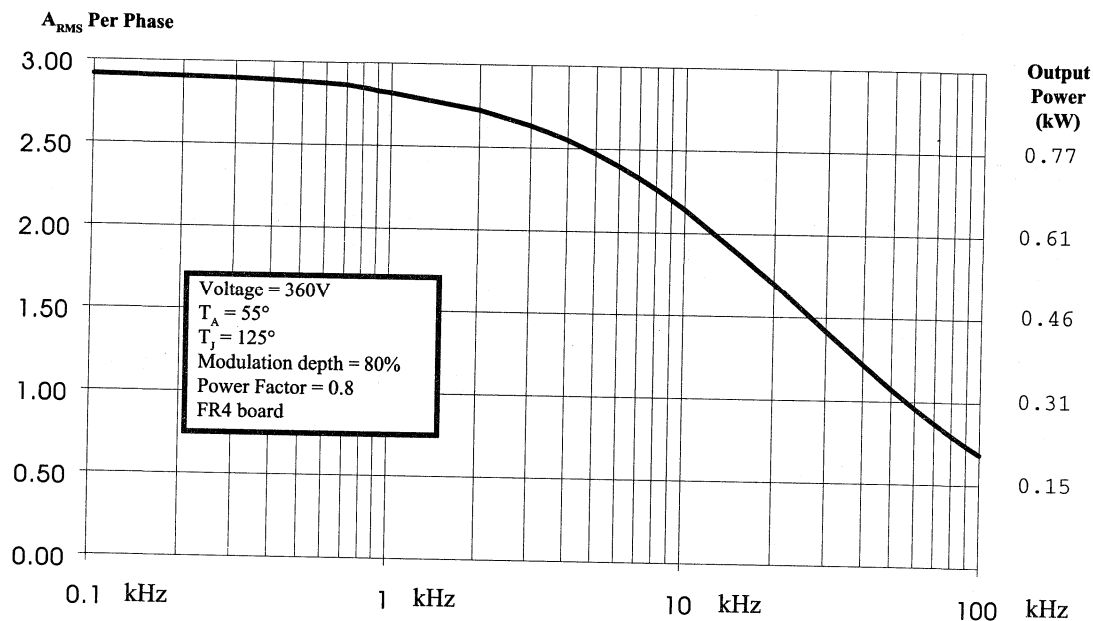
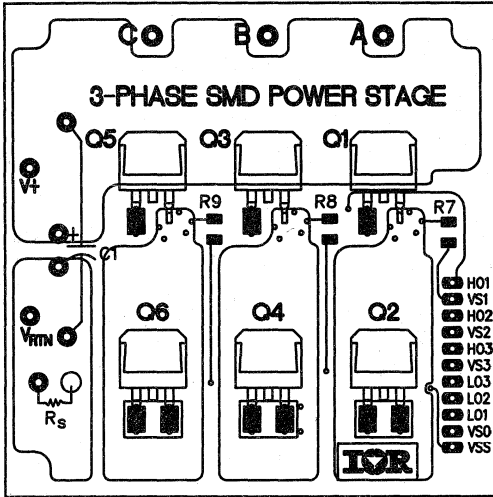


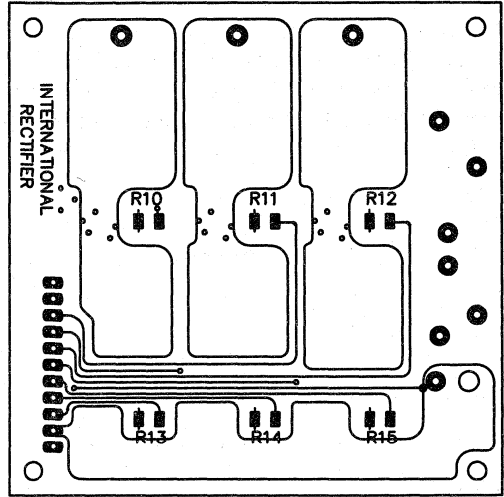
Figure 7: Typical Output vs. Frequency of a 3-Phase Bridge with IRGBC30UD2S

Components Placement Diagrams

Power Circuit



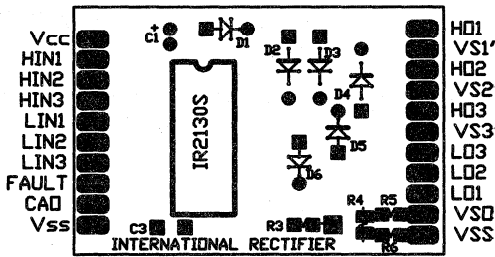
Top View



Bottom View

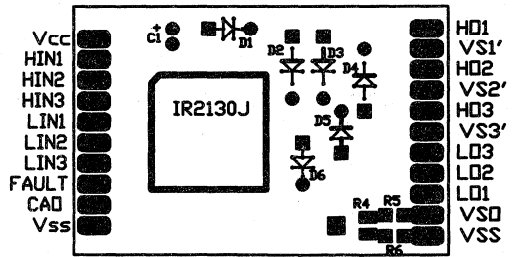
Control Circuit

IR2130S(SOIC)

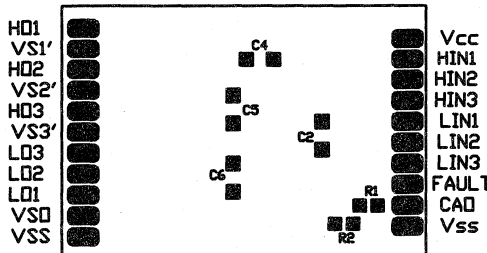


Top View

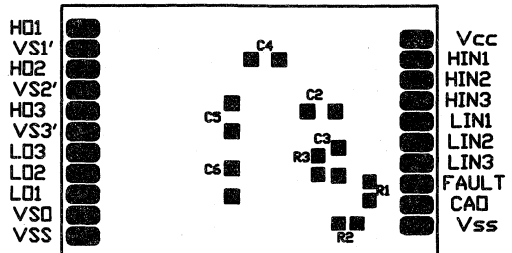
IR2130J(PLCC)



Top View



Bottom View



Bottom View

3-Phase SMD Power Stage Components List

IC	IR2130S or IR2130J MOS Gate Driver
Q1 - Q6	See Table I
R1	9.1k Ω , thick film resistor, type 0805
R2, R3	1.0k Ω , thick film resistor, type 0805
R4	50 Ω , Bourns trimmer type 3314G
R5, R6	10 Ω , thick film resistor, type 0805
R10, R11, R12, R13, R14, R15	100 Ω , thick film resistor, type 1206
R7, R8, R9	47 Ω , thick film resistor, type 1206
RS	.100 Ω , 16W, (Caddock type MP816)
D1-D6	10DF6 Ultra-fast recovery diode
C2	10 μ F, 25V tantalum capacitor
C3	1nF, 50V Ceramic capacitor, type 1206
C1, C4, C5, C6	0.1 μ F, 50V Ceramic capacitor, type 1206
C7	10 μ F, 450V Aluminum electrolytic capacitor
C8	(external - use appropriate value for intended application)
Header & Receptacle	0.100" center, square pins

Table I

Frequency	Short Circuit Rating Not Required	Short Circuit Rating Required
1 to 6 kHz	IRGBC30FD2-S or IRGBC20FD2-S	IRGBC30MD2-S or IRGBC20MD2-S
60 to 25kHz	IRGBC30UD2-S or IRGBC20UD2-S	IRGBC30KD2-S or IRGBC20KD2-S

For more information, please refer to:

- AN-983A IGBT Characteristics and Applications.
 - AN-985 The IR2130: A Six-Output, High Voltage MOS Gate Driver.
 - AN-978 High Speed, High Voltage IC Drive for HEXFET or IGBT Bridge Circuits.
 - AN-990 Application Characterization of IGBTs
- "An Algorithm for the Section of the Optimum Power Device" (Section 3) by Steve Clemente and Brian Pelly.
- "Accurate Junction Temperature Calculations" by Steve Clemente and Don Dapkus II.

APPLICATION PARAMETERS

Switching voltage	V	360		
Displacement angle	rad	0.64	Power factor	0.8
Modulation depth		0.8		

THERMAL OPERATING CONDITIONS

Ambient temperature	oC	55
Thermal resistance j-a	K/W	40.00

IGBT MODEL AND PARAMETERS: IRGBC30UD2-S (typical)

Temperature of ref. parameters	oC	125.00
Vt	V	0.83
a	Ohm	0.27
b		0.70
Gamma function, (b+2)/2	1.35	0.89
Gamma function, (b+3)/2	1.85	0.94
h	mJ/A	5.44E-3
k		1.45
Gamma function, (k+1)/2	1.23	0.91
Gamma function, (k+2)/2	1.73	0.91
m	mJ/A	2.63E-2
n		1.22
Gamma function, (n+1)/2	1.11	0.95
Gamma function, (n+2)/2	1.61	0.89
Reference voltage	V	480

DIODE MODEL

HFRD-2, 600 V

Tj = 125°C

Gamma

Conduction model:	Vt =	0.60	a =	0.12	b =	1.00	0.88623
Switching model:	Pk I _{rr} /I _f =	1.30	ta (us)=	0.30	tb (us)=	0.20	1



ELECTRICAL OPERATING CONDITIONS

Operating frequency	kHz	0.10	0.20	0.50	1.00	2.00	5.00	10.00	20.00	50.00
Peak current	A	4.12	4.11	4.08	4.02	3.91	3.61	3.20	2.50	1.52
RMS fund. voltage, line to neutra	V	129.60	129.60	129.60	129.60	129.60	129.60	129.60	129.60	129.60
RMS Current, fundamental	A	2.92	2.91	2.88	2.84	2.76	2.55	2.26	1.77	1.07
Output power, fundamental	kW	0.91	0.90	0.90	0.88	0.86	0.79	0.70	0.55	0.33
Voltage drop at peak current	V	1.56	1.56	1.55	1.55	1.53	1.49	1.44	1.34	1.19
Conduction losses	W	1.43	1.43	1.41	1.38	1.34	1.21	1.03	0.76	0.41
Turn-on losses, ideal diode	W	0.00	0.00	0.00	0.10	0.20	0.40	0.60	0.90	0.11
Correction factor for gate drive	23 Ohms	1.00	1.00	1.00	1.00	1.00	1.00	1.00	2.00	3.00
Corrected turn-on losses	W	0.00	0.00	0.00	0.10	0.20	0.40	0.60	0.17	0.32
Turn-on losses due to diode recov	W	0.00	0.00	0.10	0.20	0.40	0.10	0.17	0.26	0.40
Turn-off losses	W	0.00	0.10	0.20	0.30	0.60	0.14	0.24	0.36	0.49
Total IGBT losses	W	1.44	1.44	1.44	1.45	1.46	1.48	1.51	1.56	1.62
Diode conduction losses	W	0.31	0.31	0.31	0.30	0.29	0.26	0.22	0.16	0.90
Diode, switching losses	W	0.00	0.00	0.00	0.00	0.00	0.10	0.20	0.30	0.40
Total diode losses	W	0.31	0.31	0.31	0.30	0.29	0.27	0.24	0.19	0.13
Total losses in co-pak	W	1.75	1.75	1.75	1.75	1.75	1.75	1.75	1.75	1.75
Junction temperature	°C	125.00	125.00	125.00	125.00	125.00	125.00	125.00	125.00	125.00
Semiconductor Efficiency	%	98.84	98.84	98.83	98.81	98.78	98.68	98.51	98.09	96.85

CHOOSING BETWEEN MULTIPLE DISCRETES AND HIGH CURRENT MODULES

By Brian R. Pelly

Introduction

Many circuits using HEXFETs or IGBTs operate at current in the range of tens to hundreds of amps. IR's packages that cover this range are shown in Figure. 1.

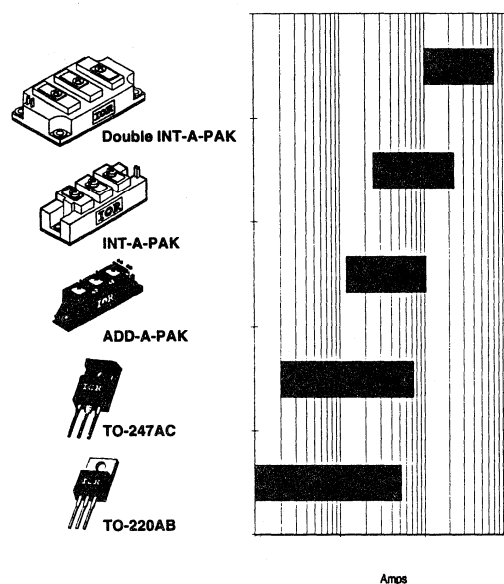


Figure 1. Current Ratings of Discrete TO-220AB, TO-247AC, and High Current Module Packages

The discrete TO-220 and TO-247 packages contain a single MOSFET, a single IGBT, or an IGBT with antiparallel HEXFRED fast recovery diode (Co-Pack). The TO-247 has a rated maximum current of 70A; full-load continuous operating design current of this package is typically in the range of 10 to 20A. Both the TO-220 and TO-247 discrete packages are manufactured in volume and offer low cost-per-ampere.

The isolated high current modules generally contain half-bridge, "chopper," or single switch configurations. Current ratings range from 25A, for a 1200V half-bridge Int-a-pak, to 600A, for a single-switch 600V Double Int-a-pak.

Attractive features of high current modules are that they are electrically isolated, easy to mount to heatsinks, and easy to interconnect with other modules to form the overall circuit. They also avoid the need for paralleling for currents up to several hundred amperes. Cost-per-ampere of high current modules is higher than for discretives, in terms of the basic semiconductor component cost — though not necessarily in terms of final system cost.

Figure 1 shows a range of overlap of current ratings covered by both discretes and high current modules. Within this range, the discrete often will offer the most cost-effective system design because of its lower cost-per-ampere.

TO-220 and TO-247 Co-Packs add to the attraction of the discrete packages for inverter circuits because they reduce the required number of components by 50%, compared to using discrete IGBTs with separate diodes.

The range of overlap where discretes can offer an alternative to high current modules can be extended by using multiple discretes in parallel.

Multiple discretes offer the potential for system cost savings versus high current modules because of the lower cost per ampere of the semiconductor *components*. Whether overall cost savings will be achieved will depend upon the design requirements for the specific application, and how these requirements will affect the total *system* cost.

This Design Tip presents a brief discussion and general guidelines that will assist the user in choosing between multiple discretes or high current modules for specific design situations.

Considerations for paralleling discretes are discussed sufficiently for a general qualitative understanding of the issues. The reader should refer to other, more specific, IR application literature for greater detail on paralleling.

Cost of Module as Function of Its Rated Current

As shown in Figure 1, a given module package covers a range of current ratings. A given module package, at its highest rating, contains the largest area of silicon die that it can accommodate; it is said to be "fully loaded." The same module with lower current ratings contains less than the full complement of silicon, and is "partially loaded."

Figure 2 illustrates that a fully loaded 200A, 600V Int-a-pak half-bridge has the same silicon die area as eight TO-247 Co-Packs. A partially loaded 50A, 600V Int-a-pak half-bridge, by contrast, contains the equivalent silicon of just two TO-247 packages.

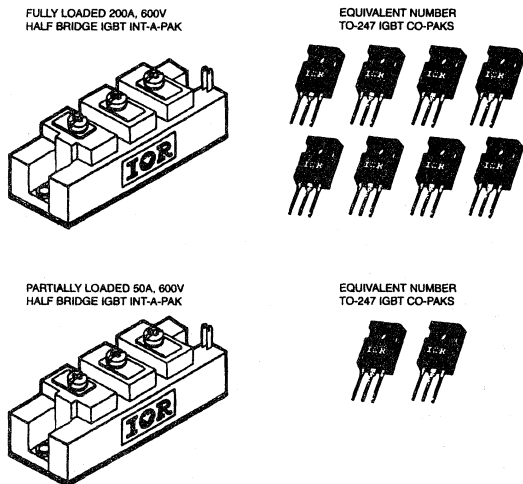


Figure 2. Equivalence Between IGBT INT-A-Paks of Different Current Ratings and TO-247 IGBT Co-Packs

Since module package cost is essentially fixed, independent of how much silicon goes inside it, a fully loaded module will inevitably have lower cost-per-amp than a partially loaded one.

Cost of Module versus Discretes

The simple construction of the discrete package, coupled to its high manufacturing volumes, ensures that the discrete's cost-per-ampere will always be less than that of a high current module. Cost-per-ampere of a fully loaded module may be 150% or more of the cost of the equivalent number of discrete components.

Against the *component* cost advantage of the discrete, the user must weigh additional assembly costs, derating needed for paralleling, and technical practicality of using multiple discretes. These factors depend upon the specific design requirements.

Electrical Connections

A basic difference between the discrete and the high current module is the method of making electrical connections to the package.

A discrete TO-220 or TO-247 is designed for soldering to a Printed Circuit Board (PCB). The maximum continuous operating current that can be handled by a PCB is typically less than 100A. This tends to set a natural limit on the number of discretes that can conveniently be connected in parallel.

High current modules, by contrast, have screw terminals; they are designed primarily for cable-lug or busbar connections, as illustrated in Figure 3(a). The high current module can also be connected directly via through-holes to a PCB, as illustrated in Figure 3(b). This

type of connection is best suited to operating currents below 100A.

(A) BUSBAR CONNECTION



(B) PCB CONNECTION

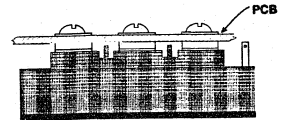


Figure 3. Methods of Making Connection to INT-A-Pak Module

Equalizing Junction Temperatures of Multiple Discretes

Paralleling of multiple discretes requires that power losses and — more importantly — junction temperatures of each device should be equalized as much as possible.

Some unbalance of losses is inevitable, because of differences in electrical characteristics between different devices. The variation of characteristics between individual devices will require a certain amount of current derating, typically around 20%. Even with this derating, good thermal coupling is necessary to force individual junction temperatures to "equalize."

The need for tight thermal coupling between the junctions of individual discretes weighs against an electrical isolation barrier, such as a "Silpad," being placed directly at the cooling surface of a TO-220 or TO-247. This places a thermal barrier between individual discretes and tends to decouple individual junction temperatures. For this reason, electrically isolated "Fullpak" TO-220 and TO-247 packages are not ideal for paralleling.

Parallel discretes should be mounted on a common heatsink. If electrical isolation is required, the discretes can be mounted on a common heatspreader to thermally couple the junctions. The heatspreader also serves the purpose of a mechanical carrier for the discretes during assembly. The isolation barrier is placed between the busbar and the main heatsink structure, as illustrated in Figure 4.

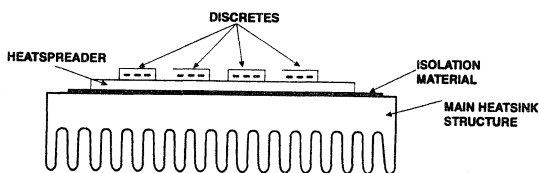


Figure 4. Use of Heatspreader to Provide Thermal Coupling Between Discretes

Unbalance due to Circuit Layout

External circuit unbalance due to non-symmetrical layout can cause significant differences in losses between parallel discretes. The most serious effects of non-symmetrical layout will be current unbalance during switching intervals and unbalanced switching losses. The most sensitive stray circuit elements to be balanced are the individual common emitter inductances. This is illustrated in Figure 5.

If switching losses are relatively small in relation to the conduction losses, a certain amount of circuit-induced unbalance of switching losses can be tolerated, and symmetrical layout will not be super-critical. This will depend on the design requirements of the application.

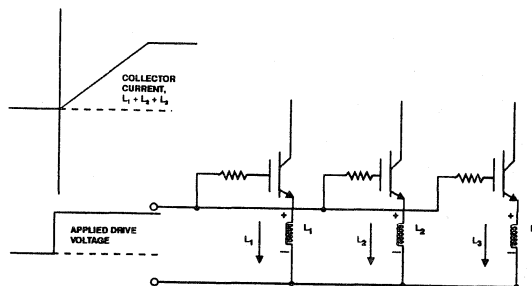


Figure 5. Common emitter circuit inductances L_1, L_2, L_3 develop $L di/dt$ voltages during switching, modifying the gate-emitter voltage applied to the IGBTs. Unbalanced inductances cause unbalanced drive voltages and unbalanced currents.

Switching losses will be low where switching frequency and/or switching voltage is relatively low. The simple in-line arrangement of discretes, shown in Figure 6(a), though not electrically symmetrical, can be satisfactory in these circumstances.

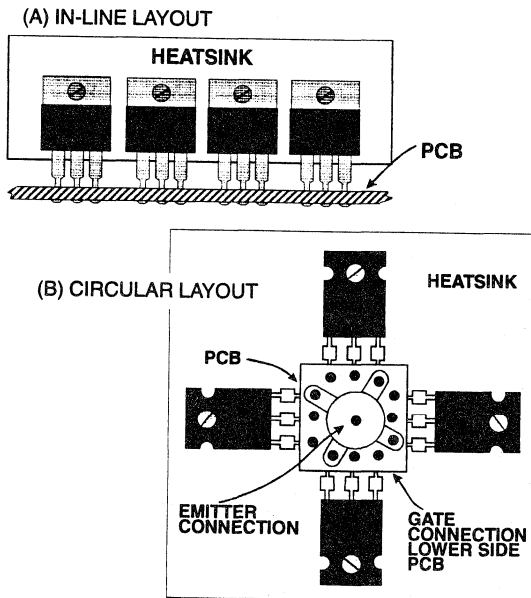


Figure 6. Different Layouts of Discretes

Where switching losses are significant, careful attention to layout is important. The symmetrical layout illustrated in Figure 6(b) is ideal, in terms of balancing individual common emitter inductances and equalizing switching losses.

Figures 7 and 8, for HEXFETs and IGBTs respectively, show typical boundaries of switching voltage and average device switching frequency that correspond to switching losses of 15% and 30% of the total device losses in hard switching applications¹. Layout will generally not be super-critical where switching losses are less than 15%; it becomes increasingly more so as switching losses increase above this level.

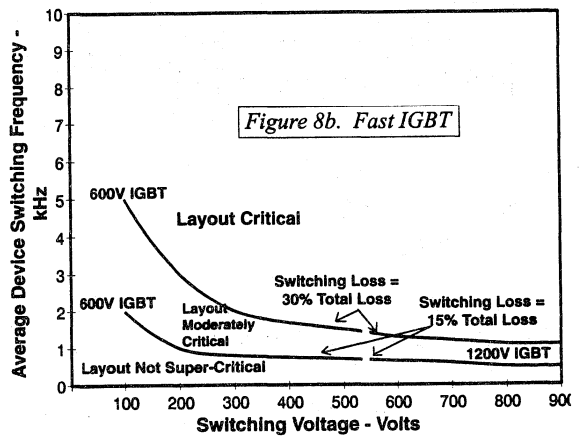
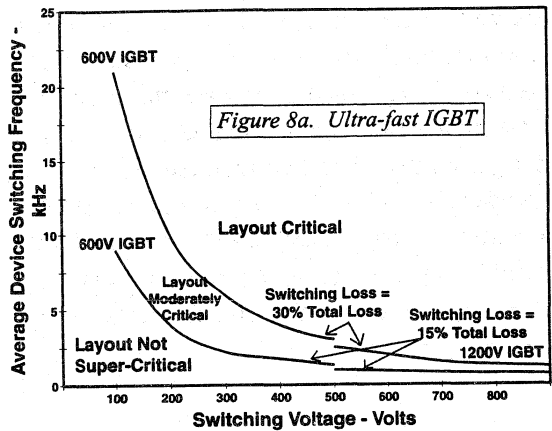
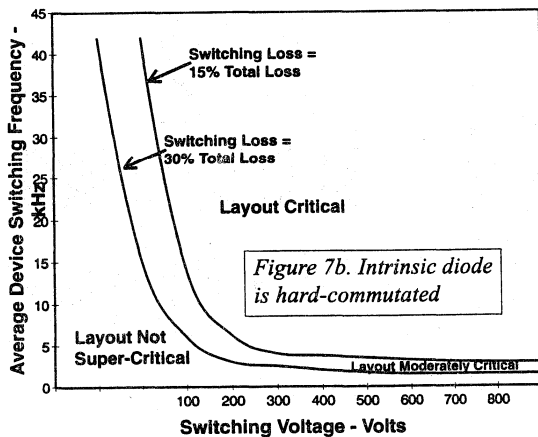
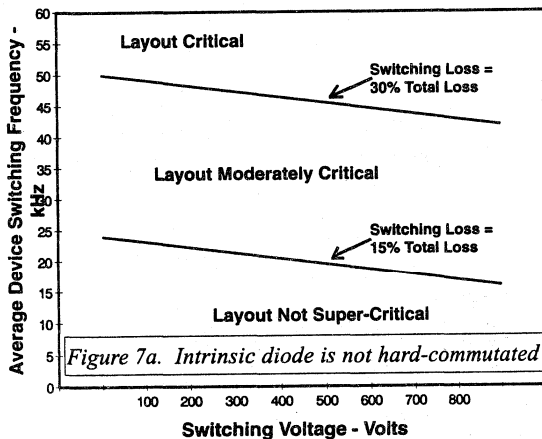


Figure 7(b) shows that if the HEXFET's internal diode is hard commutated — as is the case in sinusoidal PWM inverters — the area of operation for non-critical layout is generally restricted to low voltage operation because the switching losses caused by recovery of the HEXFET's intrinsic diode increase significantly as voltage increases.

¹ Note that the average device switching frequency in a sinusoidally modulated PWM inverter is *half* the output PWM frequency. Thus for this type of circuit, average device switching frequency should be multiplied by 2 to obtain the output PWM frequency.

Figures 7 and 8 are intended only as a general indication of the operating areas that are “easy” or “less easy” for parallel discretes, based on layout considerations.

Tables 1 and 2 relate this basic information to typical circuits.

Table 1 Design Situations for Multiple Discretes For Which Layout is not Super-critical	
Design Conditions	Typical Circuits
Operating frequency of HEXFET or IGBT is low	Line frequency inverter Line frequency ACswitch
Operating voltage of HEXFET or IGBT at switching instant is low	Inverters operating from battery voltage below 100 V Zero-voltage-switching resonant inverters
Operating current of HEXFET or IGBT at switching instant is low	Zero-current-switching resonant inverters
HEXFET internal diode is not hard-commutated	Forward, flyback, bridge inverters

Table 2 Design Situations for Multiple Discretes For Which Layout is Critical	
Design Conditions	Typical Circuits
Operating frequency and voltage of HEXFET are high, internal diode is hard-commutated	PWM inverter
Operating frequency and voltage of IGBT are high	PWM Inverter Buck Converter Boost Converter

Heatsink Mounting Area

The symmetrical layout of discretes shown in Figure 6(b), (two similar sections for a half-bridge) with the same silicon area as a fully loaded Int-a-pak, would require three to four times more heatsink mounting area.

The simpler, non-symmetrical, in-line arrangement of TO-247 Co-paks shown in Figure 6(a), on the other hand, with the same silicon area as a fully loaded Int-a-pak, would require slightly less heatsink area. The savings in heatsink area become more significant when in-line Co-Packs are compared against a partially loaded Int-a-pak.

Summary

Table 3 shows a summary of the factors that will influence the choice between multiple discretes and high current modules, and typical applications that are potentially suited to each design approach.

Table 3 Summary	
Factors that favor multiple discretes	Factors that favor high current module
A few discretes in parallel are needed	Beyond the capability of a few discretes in parallel
Current is below rating of fully loaded module	Fully loaded module is needed
High volume manufacturing geared to handling discretes	Low-to-medium volume manufacturing
Design time not critical	Important to minimize design time
Electrical isolation not required	Electrical isolation is required
Design will use printed circuit board	High-current cable-lug or busbar connections needed
HEXFET internal diode is not hard-commutated	Forward, flyback, bridge inverters
Typical Applications	
Line frequency inverters Low-voltage PWM inverters for UPS Line-frequency AC switches/breakers Electric vehicle controllers Resonant power supplies Resonant HF welders HEXFET switching power supplies	PWM AC motor drives Line voltage PWM inverters for UPS High current power factor correction

TRADE-OFF CONSIDERATIONS BETWEEN EFFICIENCY AND SHORT CIRCUIT CAPABILITY IN IGBTs

By Rahul Chokhawala

Switching devices are selected by system designers to reliably handle circuit currents under normal as well as estimated overload conditions. Under fault conditions however, a device is subjected to very high surge currents—with magnitude limited mainly by its own gain. Only timely control and removal of the fault current by some external means would save the switching device from failure. In applications where system fault is a possibility, external protection circuits are used to sense the fault and turn off the transistors by shutting down the base/gate drive in a time duration shorter than the short circuit withstand time — a measure of how long a device would survive under specified fault conditions.

There is a fundamental device trade-off between short circuit withstand time, t_{sc} , and transistor current-gain. The higher the gain of the transistor, the higher will be the fault current magnitude and the shorter will be the t_{sc} . The on-state voltage drop depends directly on the current-gain. High gain IGBTs have lower $V_{CE(sat)}$ but shorter t_{sc} . The lower-gain IGBTs, on the other hand, have a longer t_{sc} but only at the expense of the $V_{CE(sat)}$. The generalized plot in Figure 1 illustrates this trade-off.

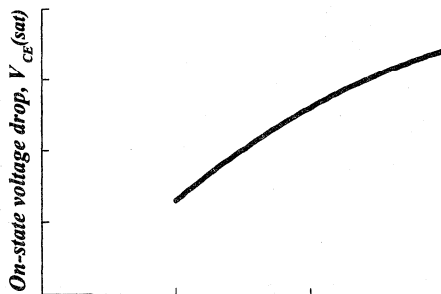


Figure 1 - Short Circuit time, t_{sc}

There also exists a device trade-off between current-gain and minority carrier life-time. The latter influences the amount of trapped charge in the IGBT—the shorter the carrier life-time, the faster the free-charge recombination process. The consequence is shorter turn-off current tail and, therefore, lower turn-off losses (E_{off}). The curves in Figure 2 show the generalized relationship between $V_{CE(sat)}$ and E_{off} for two different values of t_{sc} . As seen from this figure, the trade-off between $V_{CE(sat)}$ and E_{off} is improved as the short circuit withstand time requirement is relaxed.

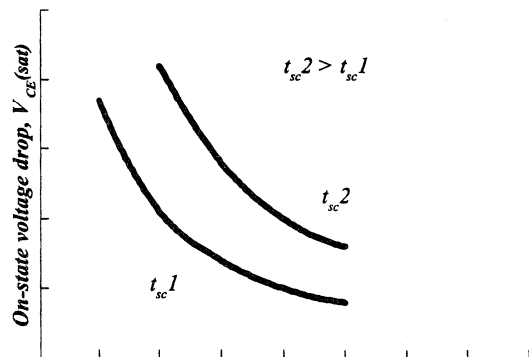


Figure 2 - Turn-Off Losses, E_{off} (a measure of stored charge)

The above trade-offs result in IGBTs with a more relaxed t_{sc} constraint being able to handle higher load currents.

Figure 3 shows generalized trends in allowable load current against switching frequency for IGBTs with "low" and "high" short circuit times. The shapes of the curves strictly depend on the $V_{CE(sat)}$ versus E_{off} trade-off.

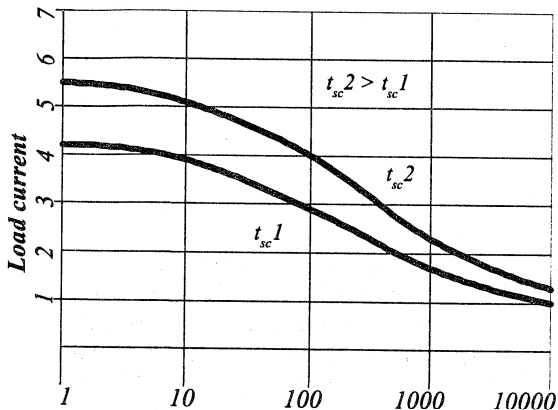


Figure 3 - Current vs. Frequency graph comparing standard IGBTs to short circuit rated IGBTs

In applications like uninterruptible power supplies, where the fault current is limited by the circuit components, the principal criterion for selection is the efficiency of the switching device. For such applications, devices not rated for long short circuit time, but designed to be more efficient, should be selected.

It should be noted that fast-reacting protection circuits are now available² to protect most efficient IGBTs, despite their reduced short circuit endurance times. Use of such circuits in association with high-efficiency IGBTs would enhance circuit efficiency without sacrificing system reliability.

¹ "A Discussion on IGBT Short Circuit Behavior and Fault Protection Schemes", presented at the APEC'93 conference.

² "IGBT Fault Current Limiting Current", presented at the IAS'93 Conference.

USING MOS-GATED POWER TRANSISTOR IN AC SWITCH APPLICATIONS

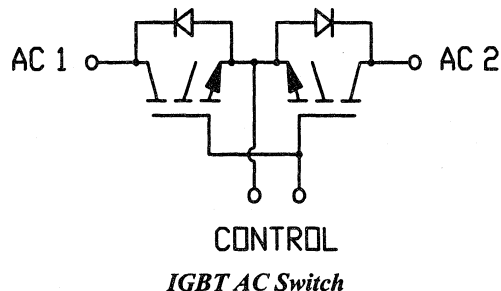
by Donald A. Dapkus II

Problem:

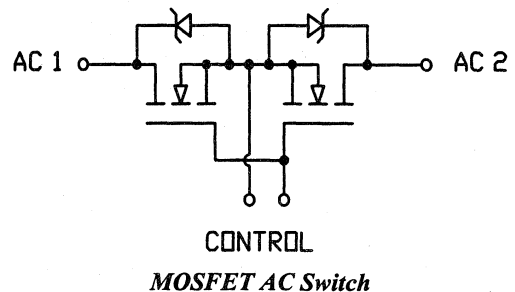
The IGBT and the power MOSFET are not suited to switching AC waveforms directly. The IGBT can only conduct current in one direction due to its use of conductivity modulation, while the power MOSFET has an anti-parallel diode that will conduct for every negative cycle. MOSFETs are the device of choice in applications below approximately 200V, while IGBTs will take over at higher voltages due to their relative voltage drops.

Solution:

By placing copackaged IGBTs (IGBT + HEXFRED® Ultrafast, ultra-soft recovery diode in the same package) in a series configuration (emitter to emitter), the problem of violating the conductivity modulation is solved. For each half of the AC waveform, one IGBT, and the opposite diode is in conduction. Of course, it is also possible to use discrete IGBTs with discrete diodes around each IGBT.



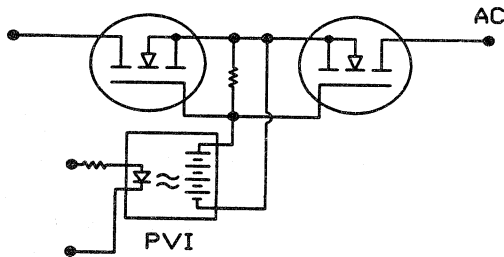
Similarly, by placing two power MOSFETs source-to-source, the intrinsic anti-parallel diodes will prevent each other from conducting. Also, the current flow will most likely be through both MOSFET channels, instead of opposite MOSFETs and diodes. The MOSFET channel is a bidirectional switch; i.e., it can conduct current in the reverse direction. If the voltage across the MOSFET channel is less than the VF of the intrinsic diode (which typically has a higher VF than discrete diodes), then the majority of the current will flow through the MOSFET channel instead of the intrinsic diode.



Driving the AC Switch:

No discussion of an AC switch would be complete without discussing the technique used to drive the devices. The gate drive for both the MOSFETs and IGBTs must be referenced to either the common sources or emitters of the devices. The problem is that this node will be swinging along the AC waveform. The two gates must be driven approximately 10V above this waveform. International Rectifier manufactures a photovoltaic isolator which generates an electrically isolated 10

VDC output upon receipt of a DC input signal. Depending on the devices being driven, switching times can be greater than 1 ms. For more information on this technique, please see Application Note GBAN-PVI-1 which appears in the Microelectronic Relay Designer's Manual (MPIC-5). This data book also contains the data sheet for the photovoltaic isolator, the PVI1050. A circuit is also provided in the AN to significantly speed up turn-off of the switch.



Driving the Switch

PARALLEL OPERATION OF IGBTs

by Donald A. Dapkus II

Power MOSFETs parallel extremely well due to their positive temperature coefficient. The IGBT, being a combination of a power MOSFET and BJT, cannot be simply described as having either a negative or positive temperature coefficient. The temperature coefficient is dependent on the technology used in the IGBT's design; even within the same technology, it changes depending on the current density. Following are a few simple guidelines that will ensure success in your parallel IGBT designs.

The objectives of this *Design Tip* are to:

1. Discuss general considerations for paralleling IGBTs.
2. Discuss the effect of thermal coupling on current and temperature unbalance.
3. Discuss one method of device selection to achieve better sharing and compare performance achieved.
4. Discuss multiple (> 2) parallel IGBT designs.

Background information on paralleling IGBTs is contained in Section VIII of Application Note AN-990.

1. General Considerations

Paralleling semiconductors is not a trivial matter. Items that must be considered to successfully parallel IGBTs are: gate circuitry, layout considerations, current unbalance, and temperature unbalance between devices. Paralleling to take advantage of lower price of smaller devices should not be attempted without due consideration of the technical risks. Experimental results should be obtained at the extremes of the manufacturing tolerances.

Gate Circuitry

The following is a list of suggestions to eliminate parasitic oscillation in *any* MOS-gated power transistor design:

1. Ensure the gate of the IGBT or MOSFET is looking into a stiff (voltage) source with as little impedance as practical. This advice applies equally well to both paralleled and single device designs.
2. Use at least 10Ω of gate isolation resistance on *each* device in parallel; locate the resistor physically close to the actual gate lead of the device.
3. Zener diodes in gate drive circuits may cause oscillations. Do not place them directly gate to emitter/source to control gate overvoltage, instead place them on the driver side of the gate isolation resistor(s), if required.
4. Capacitors in gate drive circuits may also cause

oscillations. Do not place them directly gate to emitter/source to control switching times, instead increase the gate isolation resistor. Capacitors slow down switching, thereby increasing the switching unbalance between devices.

Layout Considerations

The importance of the physical circuit layout increases with both current and frequency. Significant effort should be made to keep stray inductance to an absolute minimum. A poor layout can contribute the following problems: voltage overshoot, poor switching performance, and poor conduction performance. The layout should be as tight, compact, and symmetrical as practical, and as the operating frequency and/or current increases, so should the distribution of capacitance used to decouple the stray circuit inductance. Of particular importance is the stray inductance in the loop of the gate drive return. This will cause the gate of the IGBT to see a different voltage than expected. Reference [1] and Reference [2] page 40 cover some of the problems that can be caused by poor layout or inadequate gate drive.

Unbalance Current vs. Temperature

When paralleling power semiconductors, the first issue that comes to mind is how well they share the total current. But, semiconductors are more sensitive to temperature than to current, so the real issue is how closely they are matched in junction temperature and whether or not one of the devices approaches the rated junction temperature. As junction temperature directly correlates to reliability, it should be of primary concern to the designer.

Current Unbalance

Given two different IGBTs, each $V_{CE(on)}$ for any given current level will be slightly different. When these two IGBTs are operated in parallel, the $V_{CE(on)}$ across both devices is forced to be the same. Thus, for a given load current, one IGBT will carry more current than the other, resulting in a current unbalance. *As long as the current remains below the maximum specified on the data sheet,*

current unbalance is not critically important. At lower currents, it can be 75-100%.

Temperature Unbalance

Since the voltage drop is the same for both IGBTs, the device that carries more current has a higher junction temperature that may exceed the maximum rated junction temperature of 150°C. Combined with reliability issues, this factor should focus the designer's primary concern on temperature unbalance.

2. Thermal Coupling and Other Balancing Factors

Thermal coupling is the key to reducing temperature unbalance. If the thermal coupling between the two devices is tight, the temperature differential cannot be significant. The other factor that reduces current unbalance is the temperature coefficient of the voltage drop. The IGBT with the lower voltage drop has a lower temperature coefficient. As current and temperature increase, its voltage drop changes little, while the voltage drop of the IGBT that was carrying little current comes down significantly, thereby closing the gap in current as well as temperature.

The third balancing mechanism is due to one characteristic of the dynamic resistance of the devices. The IGBT with lower voltage drop has a higher dynamic resistance. This causes the two voltage drops to converge at higher currents.

Current unbalance may not be affected significantly by thermal coupling. This is shown in the figures in the following section depicting current unbalance for IGBTs mounted on both separate and common heat sinks. However, the more important criterion, temperature unbalance, *is* affected significantly. In fact, the figures in the following section show that the maximum current is limited by the hotter device exceeding the 150°C maximum junction temperature rating. See AN-990 Section VIII.B.3 for more information.

3. Device Selection

Device selection is an effective method to reduce derating that is intrinsically associated with paralleling and ensure that IGBTs are operated within data sheet limits. As a selection criterion, the voltage across each IGBT was measured at a certain current level. The configuration of this measurement is what we call “diode mode” (Figure 1), which means the gate is tied to the collector, and voltage is applied across that combined terminal and the emitter. The voltage is increased until the desired current is conducted through the IGBT. This measurement must be done in pulse mode to avoid device self-heating. The voltage required for this amount of current is recorded. This measurement not only takes into account variations in $V_{CE(on)}$, but also threshold, and g_{fs} . This “diode mode” voltage results in a convenient way to select IGBTs that will be paralleled. Matching only $V_{CE(on)}$ would be more appropriate for IGBTs not operated in switchmode. In the following two sections, simulations have been run on different pairs of IGBTs to compare temperature unbalance and current unbalance versus device variation measured using the “diode mode” voltage of the IGBT.

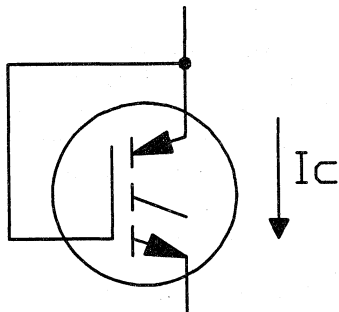


Figure 1 - Connection for Measuring “Diode Mode” Voltage, V_{diode}

Using this device selection strategy, we set out to devise a method of determining how well various pairs of IGBTs parallel in a typical half-bridge configuration. To this end, an empirical model was used for our IGBTs that models conduction and switching loss (see Reference [3]).

Five devices from each lot, using three lots, were examined and ranked in order of conduction voltage. Using this information, it is possible to obtain the operating point of IGBTs in parallel operation. To compare performance of various sets of IGBTs, graphs of percent current unbalance versus total current were developed. These graphs depict how much D.C. current unbalance can be expected for a given total current for a particular pair of IGBTs. Two cases are plotted - devices mounted on separate heat sinks and devices mounted on a common heat sink. Also generated were graphs of junction temperature of the higher of the two junctions versus total current. In these graphs, three curves are plotted: 1) perfectly matched devices with no unbalance, 2) devices unmatched by a value of DV_{diode} mounted on the same heat sink, and 3) devices unmatched by a value of ΔV_{diode} mounted on separate heat sinks.

Figure 2 depicts the percent current unbalance at different current levels for the two IRGPC50Fs at both ends of the spectrum: one has the lowest $V_{CE(on)}$, while the other has the highest $V_{CE(on)}$ of all the devices tested. The ΔV_{diode} for this pair of IGBTs was 0.69V. The operating conditions were: two devices mounted either on a common heat sink with an $R_{\theta SA}$ of $2^{\circ}\text{C}/\text{W}$, or else on separate heat sinks with $R_{\theta SA}$ s of $4^{\circ}\text{C}/\text{W}$ with an ambient temperature of 45°C .

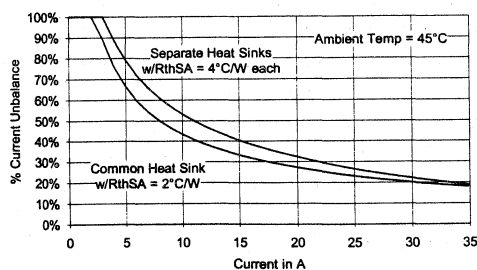


Figure 2 - Percent Current Unbalance versus Total Current, IRGPC50F with $\Delta V_{diode} = 0.69\text{V}$

As Figure 2 shows, at low currents one IGBT carries all the current. As the current increases, the unbalance improves due to the three balancing mechanisms we mentioned above for the lower curve (same heat sink, therefore tight thermal coupling) and just the two related to current for the upper curve (separate heat sink).

Figure 3 depicts the higher junction temperature of the two IGBTs in parallel for three different cases: 1) perfectly matched devices; 2) the above two devices mounted on the same heat sink; and 3) the above two devices mounted on different heat sinks. This figure provides the strongest argument for placing separate devices on the same heat sink: while conducting 20 A, the two worst case IGBTs' junction temperatures are within 2.5°C of the ideal case of perfectly matched IGBTs. However, the junction temperature of one of these same two devices mounted on separate heat sinks operates at an increased junction temperature of 16°C. Also note that the maximum allowable current is reduced from 35 A to 31 A. *All solely due to the devices' being mounted on separate heat sinks.*

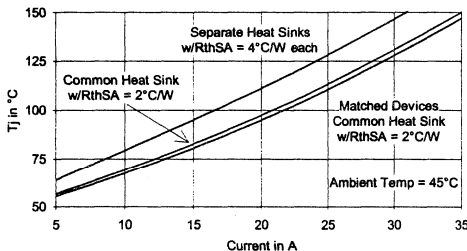


Figure 3 - Junction Temperature versus Total Current, IRGPC50F with $\Delta V_{diode} = 0.69V$

The two devices in Figures 2 and 3 exhibited the largest range in V_{diode} of all 15 devices tested. The difference in V_{diode} voltages was 0.69 V measured at 20 A. For two devices that had a difference of 0.33 V at 20A, the graphs are shown in Figures 4 and 5.

These devices, mounted on separate heat sinks, are limited to a maximum current of 33 A, while devices on a common heat sink can operate to 35 A. While conducting 20 A, the two IGBTs' junction temperatures are within 1.5°C of the ideal case of perfectly matched IGBTs when mounted on a common heat sink. The same two devices mounted on separate heat sinks operate at an increased junction temperature of 8.3°C.

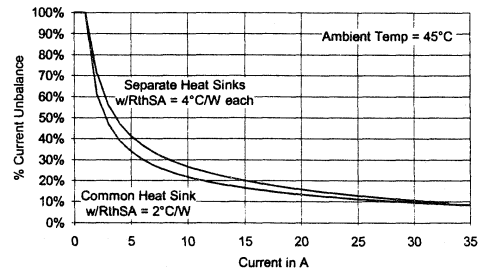


Figure 4- Percent Current Unbalance versus Total Current, IRGPC50F with $\Delta V_{diode} = 0.33V$

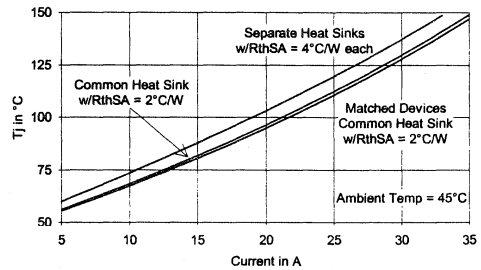


Figure 5 - Junction Temperature versus Total Current, IRGPC50F with $\Delta V_{diode} = 0.33V$

The following two graphs depict the correlation of current unbalance and junction temperature versus V_{diode} measurements. *From these two figures, it is possible to predict the operation of a parallel pair of IGBTs given the difference in their "diode mode" voltages.* Figure 7 reinforces the importance of mounting the devices on the same heat sink.

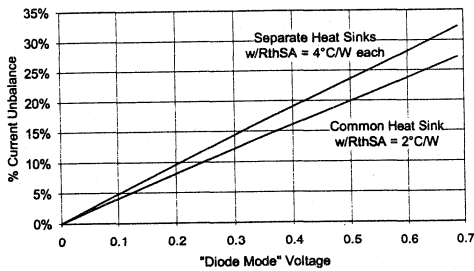


Figure 6 - Percent Current Unbalance versus ΔV_{diode} IRGPC50F

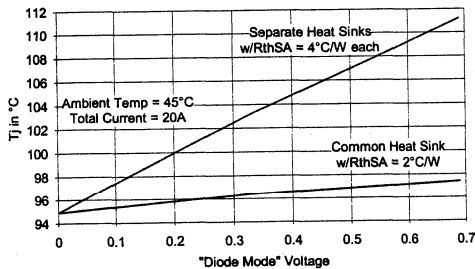


Figure 7 - Junction Temperature versus ΔV_{diode} IRGPC50F

Figure 8 depicts the reduction in output current in a half-bridge circuit due to junction temperature limitations between unmatched IGBTs. The circuit is operated under the same conditions as the previous ones, but instead of the current being fixed, the junction temperature is fixed at 125°C. Neither IGBT is allowed to exceed 125°C. The graph plots the maximum output current versus switching frequency. Notice that little or no derating is necessary under common applications or conditions.

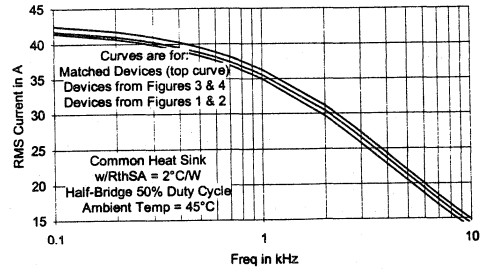


Figure 8 - Current versus Frequency Graph for Three Pairs of IRGPC50Fs with $\Delta V_{diode} = 0.00, 0.33, \& 0.69V$

The curves in Figure 8 were calculated assuming the two devices were mounted on a common heat sink. The case of separate heat sinks was not addressed due to concerns previously mentioned. The output current would be significantly reduced if the devices were on different heat sinks.

4. Multiple Paralleled Devices

The previous discussion has been limited to two paralleled devices, the only case that can be treated with simple analytical tools. This does not limit the generality of the conclusions, however, as in any group of paralleled devices, there will be two with extreme voltage drops. As explained in AN-990, these two are also likely to have extreme switching characteristics. The considerations of this Design Tip, specifically the selection criteria, would apply to these two extreme devices, with all others falling in between.

Conclusions

IGBTs can be paralleled if due precaution in layout, driving and heat sinking are taken. The critical parameter to be equalized is the junction temperature, as this directly correlates to the long term reliability of the devices. If the parallel IGBTs are mounted on the same heat sink, tight thermal feedback will be achieved. This feedback results in acceptable temperature unbalance in nearly all applications. A method of device selection targeted

for switchmode operation is presented, but it is generally not necessary unless the IGBTs are being used close to their maximum rating, i.e., with little or no derating.

References:

1. James B. Forsythe, *Paralleling of Power MOSFETs for Higher Power Output*, PowerCon '81
2. HEXFET Designer's Manual (HDM-1), 1992
3. Clemente, S., Dapkus, D., *Accurate Junction Temperature Calculation Optimizes IGBT Selection for Maximum Performance and Reliability*, PCIM'92 Conference Proceedings.

Gate Drive Considerations for IGBT Modules

Rahul Chokhawala

Jamie Catt

Brian Pelly

Abstract - The switching performance of an IGBT module depends upon the drive circuit characteristics and external dc loop inductance. This paper discusses the influence of these parameters on switching losses, diode recovery, switching voltage transients, short circuit operation and dv/dt induced current.

The paper is tutorial and identifies trends. It is intended as an aid to the circuit designer, to assist in applying the IGBT module to best advantage.

Introduction

The correlation between the gate charge transfer characteristics and the switching performance of MOSFETs is well established¹. A similar relationship exists for the 'turning on' of IGBTs, which is predominantly a majority carrier phenomenon. The MOSFET input stage of the IGBT drives the PNP transistor output stage and the turn-on event is greatly affected by the gate drive.

Turn-off for the IGBT, however, is more dependent on the bipolar characteristics. Minority carrier stored charges in the n-epi region re-combine at a rate determined by the carrier lifetime, with much less influence from the charge being removed from the gate.

The gate drive thus has only a minor influence on turn-off losses of the IGBT, while playing a major role in determining the switching losses at turn-on.

If switching losses were the only criteria in specifying a gate drive design, life would be simple. A high value for the gate drive voltage ($V_{G(on)}$) and

low value for the series gate resistance ($R_{G(on)}$) would ensure minimum turn-on losses. The switching loss, however, is only one parameter that needs to be considered when designing the gate drive.

Other technical concerns are:

- Diode recovery effect on switching loss.
- Diode recovery effect on voltage transients.
- Noise generated by the recovery of the diode.
- 'dc loop' inductance and voltage transients.
- Short circuit protection.
- Off state dv/dt protection.

This paper discusses the inter-relationships between these issues and the gate drive.

The IGBT Switching Process

The processes occurring in the IGBT when undergoing a transition between conduction and non-conduction states are known and quantified in texts dealing with modern power semiconductor device physics². The effect of circuit topology and external influences on these internal processes should be understood for an optimal design of the gate drive circuit.

The most common implementation of the IGBT module is in switching systems where the load inductance is sufficient to maintain a nearly constant current throughout the switching cycle. This is simulated by use of the 'Clamped Inductive Load' circuit, shown in Figure 1. This circuit is useful in examining the IGBT switching process as it introduces the external influences that exist in 'hard switched' inverter circuits³

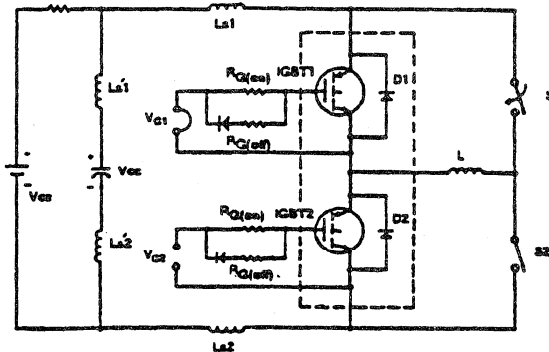


Figure 1. Switching test circuit
'dc loop' inductance $L_S = L_{S1} + L_{S1'} + L_{S2} + L_{S2'}$

With S1 closed and S2 open, the low side IGBT is made to conduct and a current is built up in the load inductor. When it is switched off, the load current continued to flow, freewheeling through the high side diode. The current remains essentially constant in the diode until the low side IGBT is turned on once more, when the current is re-directed from the diode back into the IGBT.

Complementary operation of the high-side IGBT and the low-side diode is achieved with S1 opened and S2 closed.

IGBT Turn-On:

During turn-on, the collector current of the IGBT is closely under the control of the applied gate-emitter voltage. This is similar to the turn on operation of a power MOSFET.

The starting condition for 'clamped inductive load' turn-on of the IGBT is with the output current, I_O , freewheeling through the anti-parallel diode of the opposite IGBT.

It helps to understand the operating waveforms to consider firstly the 'theoretically ideal' case of no 'dc loop' inductance and a 'perfect' diode that has no reverse recovery charge. The modifying effects of reverse recovery and 'dc loop' inductance will then be added.

Figure 2 shows idealized waveforms with no diode reverse recovery and no dc loop inductance. Gate voltage is applied at t_0 , via a series gate

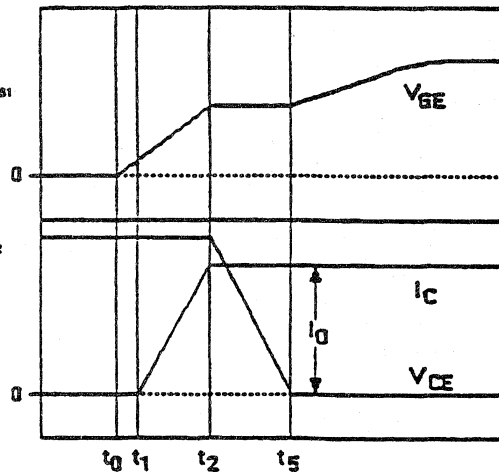


Figure 2. Idealized turn-on waveforms with no 'dc loop' inductance and no diode reverse recovery

resistor. The gate-emitter voltage (V_{GE}) begins to rise, charging the gate-emitter capacitance (C_{GE}) of the IGBT. When gate-emitter voltage reaches the IGBT's threshold voltage, collector current (i_C) starts to flow and the IGBT current rises in concert with the rising gate-emitter voltage. The diode current meanwhile decreases, the sum of the diode and IGBT currents remaining equal to the output current I_O .

Throughout the period t_1 to t_2 , the current in the diode is decreasing, but the diode is still in forward conduction. The voltage across the diode therefore remains at the diode's forward conduction level. This means that, essentially, the full dc bus voltage remains across the IGBT, which is simultaneously carrying an increasing share of the output current. The resulting instantaneous power loss in the IGBT is high during this interval.

The output current, I_O , has transferred completely to the IGBT at time t_2 , while the diode current has simultaneously reached zero. The diode — assumed to have no reverse recovery — now starts to support reverse voltage. The diode voltage rises between t_2 and t_3 , while the voltage across the IGBT (V_{CE}) correspondingly falls. The IGBT voltage reaches its 'fully on' level at t_3 and the commutation process is complete.

Figure 3 shows actual turn-on waveforms which include the effect of 'dc loop' inductance and diode reverse recovery.

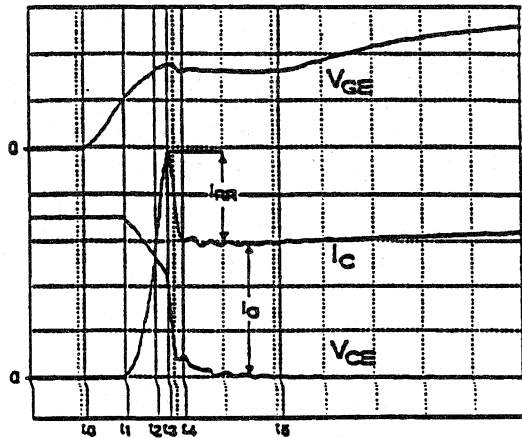


Figure 3. Actual turn-on waveforms with 'dc loop' inductance

IRGTA090F06 module. Tested at : 360V, 60A
 $L_S = 100\text{nH}$; $V_{CE} : 100\text{V/div}$, $I_C : 20\text{A/div}$
 $V_{GE} : 5\text{V/div}$, time : 200ns/div

As the IGBT current begins to rise at t_1 , the rate of change of current induces a voltage across the 'dc loop' inductance, and the IGBT voltage starts to fall. The decreasing V_{CE} causes current to flow through the gate-collector (Miller) capacitance (C_{GC} in Figure 13); this current is drawn from the gate circuit and diminishes the current available to charge the gate-emitter capacitance. This somewhat decreases the initial rate of rise of V_{GE} and, hence, of the i_C ¹.

At t_2 , as before, the diode forward current reaches zero, but now the diode needs time to recover and cannot yet support reverse voltage. The diode starts to draw reverse recovery current from the dc supply and the IGBT current increases above the output current.

At time t_3 , the IGBT current is equal to the sum of the output current I_O and the peak reverse recovery current, I_{RR} , of the diode. The diode has already begun to regain reverse blocking capability, and the reverse recovery current starts to decrease. The rise in voltage across the freewheel diode causes V_{CE} to fall rapidly. During this period, energy is dissipated in the IGBT as well as in the

diode. The negative dV_{CE}/dt couples a current from the gate to the collector through the C_{GC} , causing the gate-emitter voltage to drop momentarily.

At time t_4 some ringing develops due to the stray circuit inductances and capacitances.

During interval t_4 to t_5 , as the collector voltage settles to its 'steady state' level, the gate-emitter voltage is just sufficient to support the current. With constant gate drive output voltage on one side and constant V_{GE} on the other, the drive current through $R_{G(on)}$ is also constant. This current flows through the Miller capacitances C_{GC} . The rate of decay of the collector voltage dV_{CE}/dt , during the final phase of its fall, is equal to the ratio of i_{GC} over C_{GC} . dV_{CE}/dt reduces rapidly as V_{CE} approaches its full on-state value. This is due to the fact that at very low collector-emitter voltage, C_{GC} (as seen from the manufacturer's data sheet curves) increases by two to three orders⁴. Once V_{CE} settles to its 'steady state' value, dV_{CE}/dt is reduced to zero. The gate drive current at this time resumes charging the gate-emitter capacitance and the V_{GE} rises toward the gate drive voltage. The rise of gate voltage at t_5 is thus a good marker of the point at which the IGBT is in full conduction.

Reducing the gate drive current thus not only decreases the initial rise of the collector current, but also results in slower decay of the collector voltage. Both effects result in higher switching losses.

IGBT Turn-Off:

Figure 4 shows the gate voltage, current and voltage waveforms for the IGBT at turn-off.

At the initiation of turn-off, as the gate drive voltage is reduced, the gate-emitter capacitance begins to discharge. V_{CE} and i_C remain unchanged during this period t_0 to t_1 . At t_1 , the gate voltage is just sufficient to support the collector current.

The full output current continues, for the time being, to flow in the IGBT; it does not start to transfer into the 'freewheel' diode until the IGBT's collector voltage reaches the dc supply voltage. Until that point is reached, the diode is still reversed biased and inherently cannot conduct. Beyond t_1 ,

V_{CE} starts to slowly rise. The resultant dV_{CE}/dt couples a current into the gate-emitter capacitance through the C_{CG} . Due to this 'feedback' action, the V_{GE} stays nearly constant between t_1 and t_2 . The larger the gate resistance, the larger is this 'turn-off delay' time.

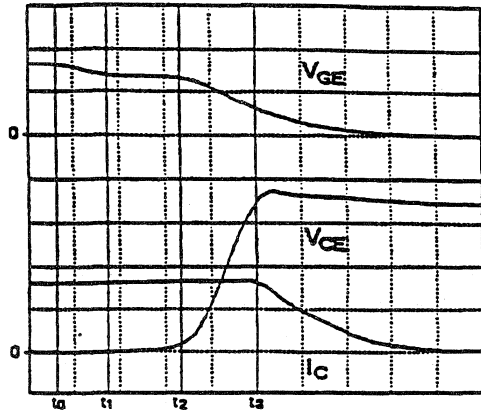


Figure 4. Turn-off waveforms IRGTA090F06 module. Tested at : 360V, 80A $L_S = 100nH$; $V_{CE} : 100V/div$, $I_C : 50A/div$ $V_{GE} : 5V/div$, time : 200ns/div

Beyond t_2 , as V_{CE} increases above 10V or so, the Miller capacitance, C_{CG} , reduces to a much smaller value, significantly reducing the magnitude of collector-to-gate feedback current. V_{GE} declines toward zero and V_{CE} increases rapidly toward the dc bus voltage; i_C , however, remains at the full output current I_O , as the diode is not yet forward biased.

The IGBT's collector voltage reaches the dc supply voltage at time t_3 and output current now starts to transfer to the diode. The decay of current is determined predominantly by the IGBT's internal characteristics, not as much by the gate voltage which has already largely disappeared, nor, to any significant degree, by the dc loop inductance.

The turn-off switching, converse to the turn-on, is predominantly a minority carrier event. Fall di/dt and turn-off tail current, upon which the turn-off losses depend, are determined mostly by the amount of stored charge and the minority carrier lifetime in the device. The current fall rate and tail time for 'high-speed' IGBTs are much faster than those for the 'low- $V_{CE(SAT)}$ ' types. Also, at elevated temperatures, due to greater stored charge, turn-off

times are longer. The shape of the turn-off current waveform also depends on the device/process design.

The gate drive parameters have only a marginal effect on the turn-off losses. This is demonstrated in the following section.

B. Switching Losses and Their Relationship to Gate Drive

Integrating the product of the current and voltage waveforms over the entire switching interval renders the amount of energy consumed by the switching process.

Switching energy is thus calculated according to the equation:

$$E(\text{switch}) = \int v(t)i(t) dt$$

As discussed, an increase in the gate drive voltage or decrease in the series gate resistance increases the rate at which the gate-emitter capacitance is charged. This results in a faster turn-on of the IGBT and a dramatic decrease in the turn-on switching losses. Table 1 shows turn-on losses for different combinations of series gate resistor $R_{G(on)}$ and gate drive voltage $V_{G(on)}$.

$V_{G(on)}$	$R_{G(on)}=10\Omega$	$R_{G(on)}=33\Omega$
10 Volts	6.5mJ	13.0mJ
13 Volts	3.0mJ	6.5mJ
15 Volts	2.5mJ	5.0mJ

Table 1. Turn On losses for differing gate voltage and series gate resistance.

IRGTA090F06: Low $V_{CE(on)}$ type IGBT module $V_{dc} = 380$ Volts, $I_O = 100$ Amps, $T_J = 150^\circ C$, $L_S = 100nH$.

In Figure 5, turn-on losses are plotted against gate drive voltage for two values of series gate resistances. It can be seen that, within certain limits, 'high' gate drive voltage and 'high' gate resistance will produce the same current rise time and turn-on energy dissipation as 'low' gate drive voltage and 'low' gate resistance. Thus, identical turn-on waveforms could be obtained with a $V_{G(on)} - R_{G(on)}$ combination of 15V - 50 Ω as with 10V - 10 Ω .

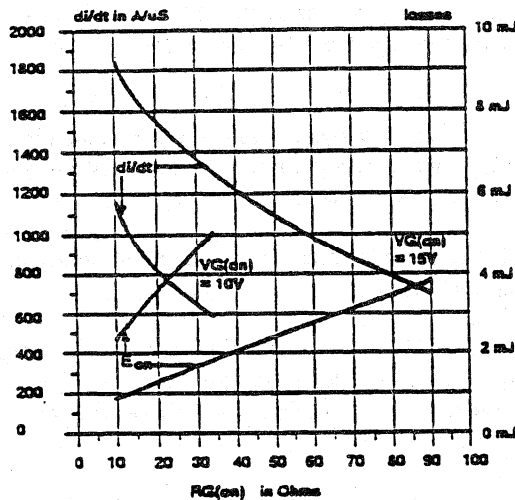
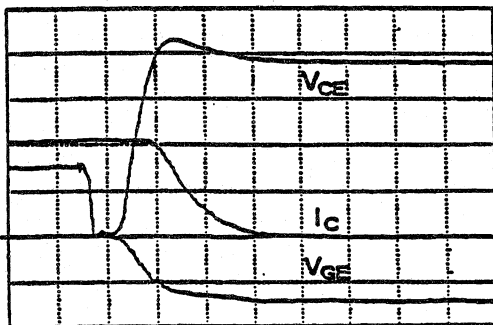
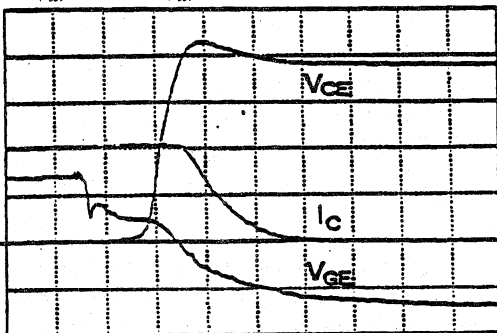


Figure 5. Turn-off di/dt and losses vs. $R_{G(on)}$ IRGTA090F06 module. Tested at : 360V, 50A 150°C, $L_S = 100nH$



6a. $V_{G(off)} = -15V, R_{G(off)} = 0\Omega$



6b. $V_{G(off)} = -15V, R_{G(off)} = 33\Omega$

Figure 6. Turn-off waveforms IRGTA090F06 module. Tested at : 360V, 100A 25°C, $L_S = 100nH, V_{CE} : 100V/div, I_C : 50A/div, V_{GE} : 10V/div, time : 200ns/div$

This is true, however, as long as gate drive voltage is high enough to support the peak turn-on current. The turn-off losses shown in Table 2 for the same device are found to vary very little with the gate drive. The bipolar stage of the IGBT exhibits tailing current at turn-off due to the stored minority carriers in the transistor base region, which must be allowed to re-combine and cannot be removed through the gate. The turn-off waveforms of Figures 6a and 6b also demonstrate this point.

$V_{G(off)}$	$R_{G(off)}$	$R_{G(off)}$	$R_{G(off)}$
0 Volts	0Ω	33Ω	51Ω
-15 Volts	10.1 mJ	10.6mJ	11.0mJ
	9.8mJ	10.2mJ	10.5mJ

Table 2 - Turn-off losses for differing gate voltage and series gate resistances.

The above results do not mean that the value of the turn-off gate resistance is unimportant. Other considerations are discussed later. In any case, manufacturers' recommendations should be followed.

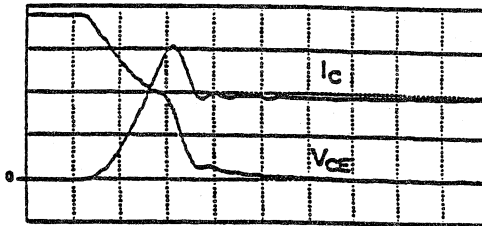
C: Freewheel Diode Recovery, EMI and Recovery Voltage Transients

The critical factor that determines the limits of safe operation during turn-on is the transient over-voltage developed across the diode (and, hence, also across the anti-parallel IGBT) as it recovers. The peak diode recovery voltage must be constrained within the rated voltage by setting appropriate limits on the operating conditions of the module. The peak diode recovery voltage depends upon the dc supply voltage, the 'dc loop' inductance and the peak diode reverse recovery current, in combination with the diode's recovery di/dt.

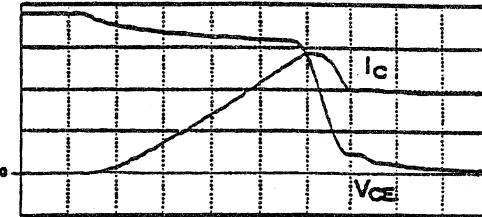
The peak reverse recovery current and recovery di/dt themselves depend upon the diode junction temperature, the initial amplitude of the diode forward current I_0 and the rate of decrease of the diode forward current, which is equal to the rate of increase of the IGBT current ($= di_{C(on)}/dt$). The diode recovery di/dt is approximately equal to $di_{C(on)}/dt$ over the diode 'snap factor' ($= t_b/t_s$). $di_{C(on)}/dt$, as already discussed, can be controlled by setting the value of the $R_{G(on)}$ in combination with the amplitude of $V_{G(on)}$.

Very low values of series gate resistor, besides producing high diode recovery voltage transients, could give rise to unacceptable ringing during recovery. The stray inductance and parasitic capacitance form a resonant circuit that will be set into damped oscillation. The electrical noise thus produced could interfere with control and protection circuits and would contribute to the total system EMI. This ringing is obviously not a good characteristic.

The reduction of the problem is simple; either reduce the gate drive voltage or increase the series gate resistor. This solution is, however, in direct conflict with reduction of the switching losses. A compromise needs to be made to satisfy the circuit performance criteria.



7a: 65A, 600V High-Speed Module with Soft Recovery, Low Q_{RR} Diode



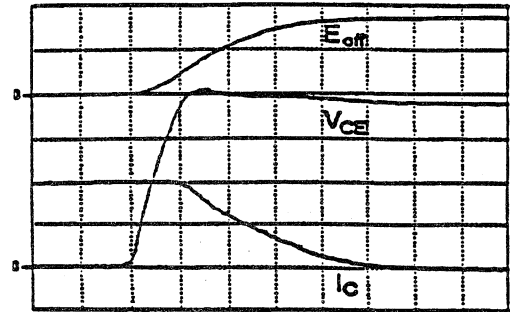
7b: 75A, 600V High-Speed Module with Higher Q_{RR} Diode

Figure 7. Turn-on waveforms
 Tested at : 380V, 100A, 150°C, $L_s = 100\text{nH}$
 $R_{G(\text{on})} = 33\Omega$, $V_{CE} : 100\text{V/div}$, $I_C : 50\text{A/div}$
 time : 100ns/div

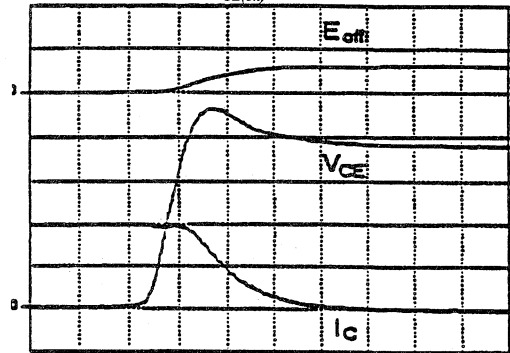
It should be noted that, while an IGBT by itself could be turned on extremely fast, thanks to its MOSFET-like turn-on, it is the recovery of the freewheel diode that forces the circuit designer to slow down the turn-on process using external means. Figures 7a and 7b compare turn-on waveforms of two IGBT modules; one with a softer recovery diode — higher value of t_b/t_a — than the other. The turn-on losses measured for the IGBT with softer companion diode were found to be only 33% (3.9mJ) of those for the IGBT with the snappier diode (11.9mJ).

D. 'DC Loop' Inductance and Voltage Transients

During turn-on, as mentioned in the previous section, diode recovery di/dt combined with the 'dc loop' inductance (shown as L_s in Figure 1) produces a recovery voltage transient. This recovery voltage transient needs to be limited to at least the rated breakdown voltage of the diode and the IGBT in parallel with it. A trade-off between this voltage overshoot and the turn-on losses is necessary. It is important that L_s is kept as low as possible.



8a: IRGTA090F06 Low $V_{CE(\text{on})}$ Module, 200ns/div

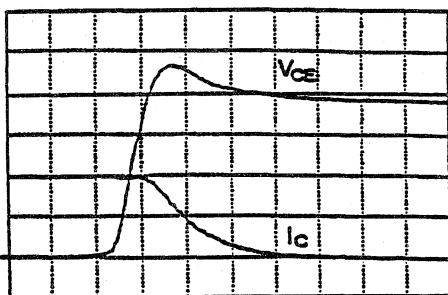


8b: IRGTA065U06 High-Speed Module, 100ns/div

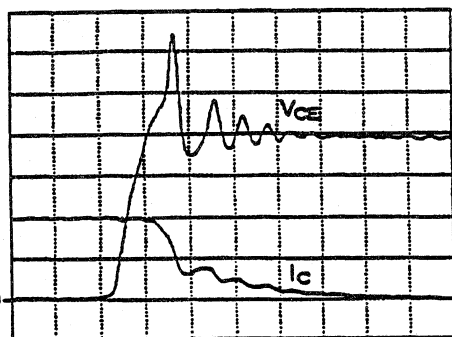
Figure 8. Turn-off waveforms
 Tested at : 380V, 100A, 150°C, $L_s = 100\text{nH}$
 $V/R_{G(\text{off})} = -1.5\text{V}/33\Omega$, $V_{CE} : 100\text{V/div}$, $I_C : 50\text{A/div}$
 energy : 10mJ/div

The turn-off transient voltage is also caused by di/dt induced voltage across the circuit stray inductance L_s as the current changes its path from the conducting IGBT to the freewheel diode. The magnitude of the induced voltage is proportional to the di/dt through the stray inductance.

The gate drive has only a minor influence on the current fall di/dt, while the minority carrier lifetime has a significant impact on the turn-off losses as well as on the fall rate of the current. Figures 8a and 8b illustrate turn-off of a low $V_{CE(on)}$ type IGBT module against that of a high-speed type module. The turn-off switching time and the turn-off energy are much lower with the high-speed device. The 'dc loop' inductance causes a higher voltage to be generated across the faster device. This over voltage may exceed the breakdown rating; for this reason the stray 'dc loop' inductances must be minimized to allow operation in the Snubberless Switching Safe Operating Area (SSSOA).



9a: Manufacturer 'A', 65A, 600V High-Speed Module



9b: Manufacturer 'B', 75A, 600V High-Speed Module

Figure 9. Turn-off waveforms
 Tested at : 380V, 100A, 150°C, $L_s = 100nH$
 $V/R_{G(off)} = -1.5V/33\Omega$, $V_{CE} : 100V/div$, $I_C : 50A/div$
 time : 100ns/div

A good data sheet will quote values for several variables in defining the SSSOA for an IGBT, including bus voltage, 'dc loop' inductance, gate drive voltage and series gate resistance³. Should any of these variables be exceeded, a snubber circuit may have to be used.

The waveforms of Figures 9a and 9b were obtained for high-speed devices of the same order of minority carrier lifetime from two different manufacturers. While the IGBT in Figure 9a compared to the one in Figure 9b is slightly faster, its current rate of fall is much less snappy. V_{CE} in Figure 9b rises to a much higher value and actually above the rating of 600V. In order to restrict the voltage overshoot, a much higher $R_{G(off)}$ is recommended for the snappier device than the softer one. This illustrates the fact that devices of near-identical lifetime, but different design (technology) could have vastly different turn-off waveforms.

E. Gate Drive and IGBT Short Circuit

It has been shown elsewhere that the ability of an IGBT to withstand fault currents can be improved by reducing the gate voltage applied to the device. The relationship between gate drive voltage and peak short-circuit current, as well as short-circuit withstand time, is illustrated in Figure 10. However, a reduction in gate drive voltage, as discussed earlier, should be accompanied by a reduction in the series gate resistor (see Figure 5) to avoid incurring increased turn-on switching energy.

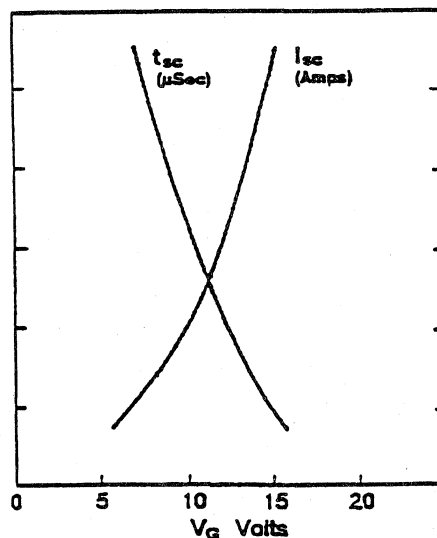


Figure 10. Generalized trends of short circuit current, I_{SC} and permissible short circuit time, t_{SC} with gate voltage, V_G

Two types of fault conditions may occur. The behavior of the device and the relationship to the gate drive circuitry should be understood for each case.

TYPE 1: Fault Under Load

A device may be subjected to short circuit while in normal conduction.

The waveforms in Figure 11 illustrates this type of fault. Initially, the IGBT is gated fully on ($V_{G(\text{on-state})} = 11.0\text{V}$) and is operating normally, carrying a steady load current within its ratings ($=80\text{A}$). The voltage across the device, V_{CE} , is low. A fault is imposed on the device at time t_0 . For this experiment, this was achieved by turning the complementary IGBT on, causing a shoot-through. The current increased rapidly, pulling the IGBT out of its full conduction state. The rise in the V_{CE} , as explained previously, causes a current i_{CG} to flow through the Miller capacitance, C_{CG} . Due to the presence of a high $R_{G(\text{off})}$ ($=100\Omega$), the gate-emitter voltage increases to a higher peak value ($=17\text{V}$). Consequently, the fault current for this high-gain/high-efficiency IGBT rises to over 1200A before

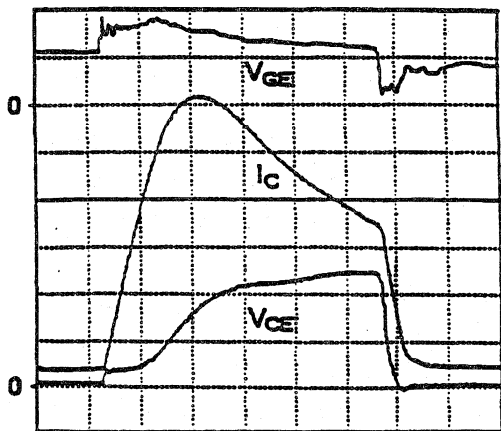


Figure 11. Fault under load test waveforms IRGT1090F06 - Tested at : 360V, $V_{G(\text{on-state})} = 11.0\text{V}$, $R_{G(\text{on})}$, $R_{G(\text{off})} = 100\Omega$, $V_{CE} : 100\text{V/div}$, $I_C : 200\text{A/div}$, $V_{GE} : 10\text{V/div}$, time : 500ns/div

declining, as V_{GE} dwindles back to its normal on-state value. The fault current in this experiment was removed by turning the complementary IGBT switch off.

Lowering the value of $R_{G(\text{off})}$ facilitates better clamping of the gate-emitter voltage, reducing the fault current magnitude significantly. As demon-

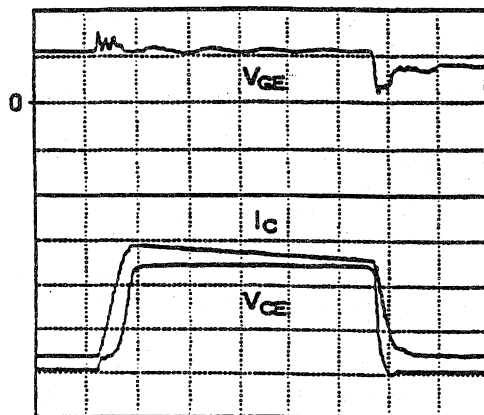


Figure 12. Fault under load test waveforms IRGT1090F06 - Tested at : 360V, $V_{G(\text{on-state})} = 11.0\text{V}$, $R_{G(\text{on})}$, $R_{G(\text{off})} = 10\Omega$, $V_{CE} : 100\text{V/div}$, $I_C : 200\text{A/div}$, $V_{GE} : 10\text{V/div}$, time : 500ns/div

strated in Figure 12, the fault current peak decreased to less than 600A when $R_{G(\text{off})}$ was reduced to 10Ω . The energy losses during the fault period declined from 462mJ to 338mJ.

Figure 13 shows the fault current test results for the same device, but with a higher $V_{G(\text{on-state})}$. As expected, the magnitude of the fault current increased accordingly. An increase in $V_{G(\text{on-state})}$ from 11V to 12.5V resulted in an increase in the fault current from 580A to 760A. The losses due to the fault increased from 338mJ to 410mJ.

Lower current and losses would obviously enable to device to better negotiate through the fault conditions. The short-circuit endurance time is increased, allowing the protection circuits longer time to react. IGBTs designed for higher operating efficiency due to inherently higher gain have less short-circuit endurance time than less-efficient devices.

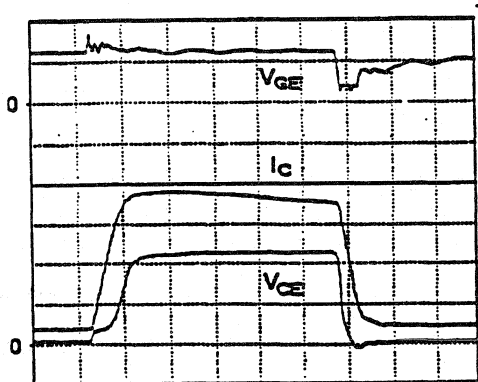


Figure 13. Fault under load test waveforms IRGTI090F06 - Tested at : 360V, $V_{G(on-state)} = 12.5V$, $R_{G(on)} = 100\Omega$, $R_{G(off)} = 10\Omega$, $V_{CE} : 100V/div$, $I_C : 200A/div$, $V_{GE} : 10V/div$, time : 500ns/div

TYPE 2: Hard Switch Fault

In this mode, the IGBT device is off and the system voltage is supported across the device. The IGBT is gated on into the fault. The rate at which the device begins to conduct current and the magnitude of the fault current are related to the charging rate of the input capacitance and the gate-drive voltage $V_{G(on)}$. This type of fault is described by the waveforms in Figure 14.

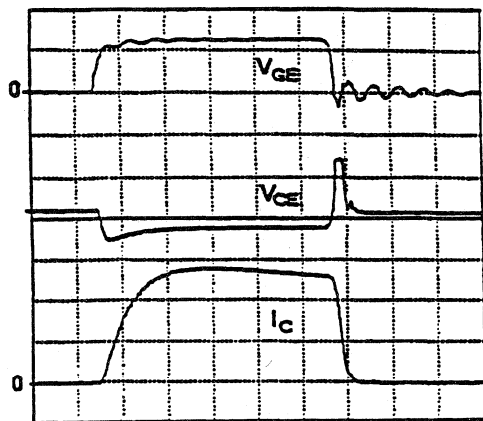


Figure 14. Hard switch fault test waveforms IRGTI090F06 - Tested at : 420V, $V_{G(on-state)} = 12.5V$, $R_{G(on)} = 33\Omega$, $R_{G(off)} = 0\Omega$, $V_{CE} : 100V/div$, $I_C : 200A/div$, $V_{GE} : 10V/div$, time : 1 μ s/div

During the pre-fault state, the full system voltage is supported by the device. Upon application of the gate signal, and following the gate-emitter voltage reaching gate-threshold voltage, i_C begins to rise. A notch is gouged out of V_{CE} due to the voltage drops occurring across the resistive and inductive elements of the circuit.

The fault current was ended by simply removing the gate drive. The rapid fall of the fault current, combined with the 'dc loop' inductance, causes V_{CE} to overshoot the supply voltage. In this case, the voltage overshoot the bus voltage by 130V. The rate of fall of fault current, and hence, the magnitude of V_{CE} can be controlled, to a certain degree, by increasing the value of $R_{G(off)}$. The device was re-tested with $R_{G(off)}$ increased to 33 Ω . As viewed from Figure 15, the resultant voltage overshoot declined to 100V.

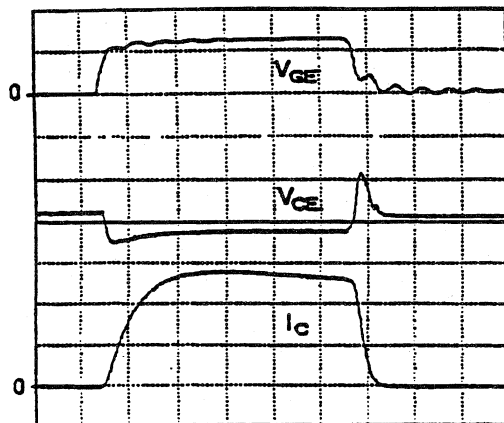


Figure 15. Hard switch fault test waveforms IRGTI090F06 - Tested at : 420V, $V_{G(on-state)} = 12.5V$, $R_{G(on)} = 33\Omega$, $R_{G(off)} = 33\Omega$, $V_{CE} : 100V/div$, $I_C : 200A/div$, $V_{GE} : 10V/div$, time : 1 μ s/div

Note that increasing $R_{G(off)}$ to reduce the over-voltage transient following short circuit is in conflict with other considerations discussed elsewhere. Again, a tradeoff will have to be made by the designer, based on the specific operating conditions.

It is obvious from Figures 14 and 15 that, for a hard switch fault, only a small positive dv/dt is generated across the IGBT. Thus, the Miller effect, a major consideration for the fault under load, is not as much of a nuisance for the hard switch fault,

particularly because the Miller capacitance is much lower at higher voltage. Thus, the hard switch fault can result in much lower fault current than the fault under load. This is probably why this case often used by the manufacturers to quote the short-circuit capabilities of their devices, as it is a less stressful test and will tend to give flattering results.

F: DV/DT EFFECT ON 'OFF' DEVICES

When one IGBT in a half bridge is turned on, a quite high dv/dt will be generated across the other one. This dv/dt can cause this second device to conduct momentarily, leading to additional losses 6. Potentially, there are components of current present, as seen from Figure 16⁴. The first component, i_{CO} , is the charging current of the IGBT's output capacitance, C_{CO} . This component is inevitable, as the output capacitance is always physically present.

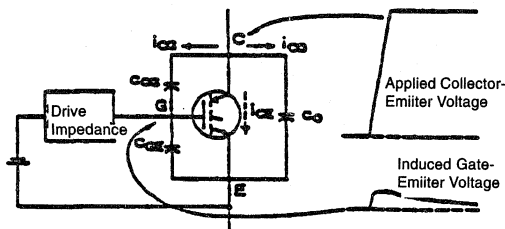
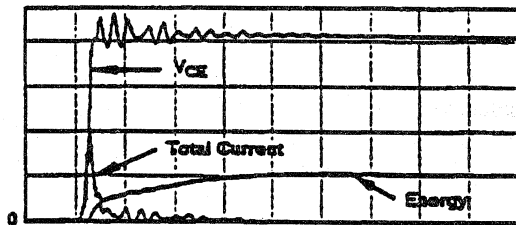


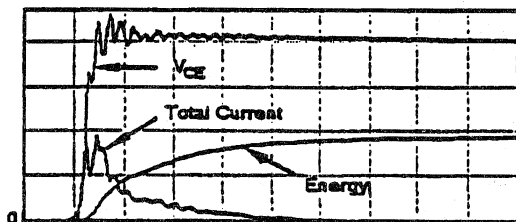
Figure 16. Equivalent circuit illustrating the mechanism for the dv/dt induced turn-on

The second component of current, i_{CG} , is due to the collector-gate capacitance, C_{CG} . This current is also inevitable, but is small in comparison to the charging current of the output capacitance. The collector-gate capacitance is generally about 10-15% of the value of the output capacitor.

The third component of current, i_{CE} , may or may not flow. This component is conducted through the IGBT due to the lifting of the gate voltage to a sufficient level by the collector-gate current. If the gate voltage exceeds the threshold level, it will allow the IGBT to conduct a current between the collector and emitter.



17a: 0V, $R_{G(off)} = 20\Omega$, 100mJ/div



17b: +1.4V, $R_{G(off)} = 20\Omega$, 200mJ/div

Figure 17. Oscillographs of collector-emitter voltage and dv/dt induced turn-on current and energy loss when the upper IGBT is over-driven 'on' and zero or positive bias is applied to the lower IGBT

IRGTA050F06 - Tested at : 45 μ s (max), 150°C
 V_{CE} : 100V/div, I_C : 5A/div, V_{GE} : 10V/div
 time : 100ns/div

The flow of the dv/dt induced current component depends upon the magnitude of the dv/dt , which determined the magnitude of collector gate current through the parasitic capacitance. It also depends upon the impedance of the gate drive circuit, which determines the amplitude of the induced gate voltage. If the gate is tied to the emitter via a low-impedance drive circuit, the gate voltage will be insufficient to turn on the IGBT.

It is quite common practice to apply a negative voltage to the gate of the IGBT when it is required to be off to ensure that the gate voltage cannot rise above the threshold level. Whether this is necessary will depend on the level of the gate threshold voltage, the C_{CG} characteristic of the particular IGBT and the maximum dv/dt the device will be expected to withstand. The dv/dt across the IGBT due to the recovery of its anti-parallel diode is typically about 10V/ns.

Figure 17a shows oscillograph results for a 600v/50A IGBT with gate threshold voltage of 4.1V

4.1V subjected to a voltage front with a maximum dv/dt of about 45V/ns. No negative bias was applied to the gate which was simply connected to the emitter through a 20Ω resistor. An initial output capacitance charging current of peak value 10A was measured. However, no conduction was recorded following the initial current spike, and losses were measured to be only 0.112mJ. Next, waveforms of Figure 17b were acquired with a positive bias of 1.4V applied to the gate, through a 20Ω resistor. The purpose of the positive gate bias was to demonstrate how a 'low' (2.7V in this case) gate threshold voltage device might behave with no negative gate bias. The device is forced into conduction following the output capacitance charge current. The losses increased to 0.39mJ.

Many gate drive circuits include a diode across the series gate resistor, polarizing it to a low resistance value in the reverse direction. This gives the advantage of controlled turn-on through the series gate resistor, and a low impedance path for the dv/dt induced current.

There is also a possibility that, confronted by very high dv/dt , an IGBT can 'latch up' ^{7,8}. Just as an SCR, the IGBT has four alternate P-N-P-N layers. Under normal operation, the sum of the gains of PNP and NPN is held to less than unity; a required condition to prevent 'latching' of the device. However, the flow of (dv/dt -related) capacitive current through the P base of NPN could elevate the transistor gain to initiate a regenerative 'latch-up.' Most IGBTs available on the market are designed to be 'latch free.' However, the recommendations of the specific manufacturer for avoiding latch-up should be adhered to.

Conclusions

The following tables summarize the effects of increasing either the gate drive voltage or the series gate resistor on the circuit operational parameters discussed in this paper.

Parameter	Increase in $R_{G(on)}$	Increase in $V_{G(on)}$
turn-on di/dt	decrease	increase
turn-on loss	increase	decrease
turn-on time	increase	decrease
I_{rec} diode	decrease	increase
V_{rec} diode	decrease	increase
EMI	decrease	increase
S/C time	negligible	decrease
S/C peak I	negligible	increase

Table 4. - Summary of Effects on Circuit Operation of Increase Series Gate Resistor or Gate Drive Voltage at Turn-On

Parameter	Increase in $R_{G(off)}$	Increase in $V_{G(off)}$
turn-off loss	marginal increase	marginal decrease
turn-off delay	increase	decrease
voltage rise time	increase	decrease
current fall time	marginal increase	marginal decrease
peak V_{off} IGBT	marginal decrease	marginal increase
S/C time	decrease	negligible
S/C peak I	increase	negligible
S/C peak V	decrease	increase
dv/dt sensitivity	increase	increase

Table 5. - Summary of Effects on Circuit Operation of Increased Series Gate Resistor or Gate Drive Voltage at Turn-Off

Each of the effects listed in Tables 4 and 5 must be weighed in the design of the gate drive circuit.

Acknowledgment

The authors wish to thank Dr. Richard Francis for his valuable suggestions and comments.

REFERENCES

1. Grant, J. Govar, Power MOSFET - Theory and Applications - New York; Wiley, 1989.
2. A. Hefner, "An Improved Understanding of the Transient Operation of the Power Insulated Gate Bipolar Transistor," IEEE trans. on Power Electronics, Oct. 1990.
3. J. Catt, R. Chokhawala, B. Pelly, "Introduction to the 600V Add-A-Pak and Int-A-Pak IGBT Modules," International Rectifier Corp., Applications note AN-988.
4. K. Gauen, "The Effect of MOSFET Output Capacitance in High Frequency Applications," IAS-IEEE Conf., Oct 1989.
5. G. Castino, A. Dubbashi, S. Clemente, B. Pelly, "Protecting IGBTs Against Short Circuit," The First Annual Motion Control Tech. Conf. West, Oct. 1990.
6. R. Letor, M. Melito, B. Ishaan, "Safe Behavior of IGBTs Submitted to a dv/dt ," Power Conversion Conf., June 1990.
7. S. Clemente, A. Dubbashi, B. Pelly, "IGBT Characteristics and Applications," International Rectifier Corp., Applications Note AN-983.
8. S. Biswas, B. Basak, K. Rajashelcara, "A Modular Gate Drive Circuit for Insulated Gate Bipolar Transistors," IAS-IEEE Conf., Oct. 1991.

A DISCUSSION ON IGBT SHORT CIRCUIT BEHAVIOR AND FAULT PROTECTION SCHEMES

Rahul Chokhawala

Jamie Catt

Laszlo Kiraly

Abstract - IGBTs are available with short circuit withstand times approaching those of bipolar transistors. These IGBTs can, therefore, be protected by the same relatively slow-acting circuitry.

The more efficient IGBTs, however, have lower short circuit withstand times. While protection of these types of IGBTs is not difficult, it does require a re-assessment of the traditional protection methods used for the bipolar.

An in-depth discussion on the behavior of IGBTs under different short circuit conditions is carried out and the effects of various parameters on permissible short circuit time are analyzed. The paper also re-examines the problem of providing short circuit protection in relation to the special characteristics of the most efficient IGBTs. The pros and cons of some of the existing protection circuits are discussed and, based on the recommendations, a protection scheme is implemented to demonstrate that reliable short circuit protection of these IGBTs can be achieved without difficulty in a PWM motor drive application.

Introduction

Power transistors used in motor-drive applications need to be protected from failure under external fault conditions. Such faults mostly result from the occurrence of a short circuit at the load end. Motor winding insulation failure, for example, may cause a fault in the system. Also, there is always a threat of wiring misconnections at the motor terminals, creating a possibility for the drive output terminals to be short-circuited. In the case

of dedicated motor drives — where the complete systems are assembled prior to shipping — such mistakes are not nearly as likely to occur. In applications such as uninterruptible power supplies, filter chokes used in the system would limit rate of rise of fault currents, allowing a slower over-current detection circuit to protect the system. In high-frequency welding power supplies, an application where IGBTs are becoming the favored devices, excessively high fault currents are prevented by the resonant nature of the power circuit and/or output transformer leakage inductance.

The switching devices are selected by system designers to reliably handle circuit currents under both normal and estimated overload conditions. Under fault conditions, however, a device could be subjected to very high surge currents — with magnitude limited mainly by its own gain. Only timely control and removal of the fault current by some external means would save the switching device from failure. In applications where a system fault is a possibility, external protection circuits are used to sense the faults and turn off the transistors by shutting down the base/gate drive. In all such applications, except where 'intelligent' modules are used, the protection circuit is connected externally to these devices.

Switching device manufacturers are expected to guarantee minimum short-circuit withstand time — a measure of how long a device would survive under specific test conditions. What complicates the picture is the fundamental device trade-off between short circuit withstand time and transistor current-gain. The higher the gain of the transistor,

the higher will be the fault current magnitude and the shorter will be the short circuit withstand time. [1], [2]. The generalized trade-off plot illustrated in Figure 1, is most important to the IGBT manufacturers due to the inherently higher gain of their devices. The low-gain IGBTs available today allow longer short circuit time at the expense of operating efficiency. The high-gain devices are more efficient, but require more 'alert' protection circuits.

IGBTs available in the initial phase of their evolution were of the low-gain type with short circuit time approaching that of BJTs. Designing-in of these devices has been, to a great part, responsible for the still-prevalent market demand for these less efficient but $>10\mu\text{s}$ short-circuit-time IGBTs. The present trend, however, is toward high-gain, low-loss IGBTs. The purpose of this paper is to show how various circuit parameters and fault conditions affect the short-circuit endurance time of these devices and how an effective protection scheme could be implemented. The intent is also to demonstrate, via a practical experiment, that such a scheme can provide full short circuit protection, even for more-efficient/high-gain IGBTs with modest intrinsic short circuit capability.

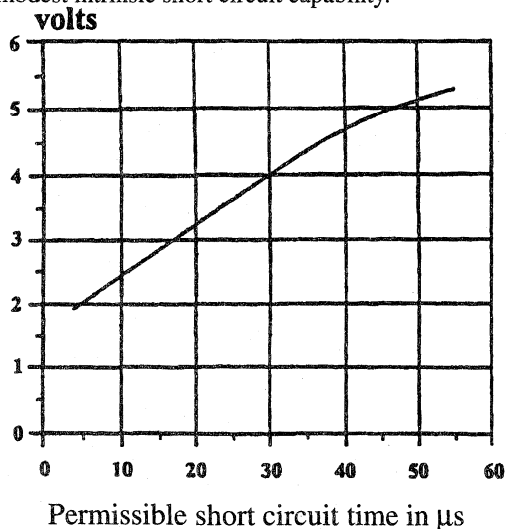


Figure 1. $V_{CE(on)}$ vs. t_{SC} . Generalized Trade-off Curve

The Failure Mechanisms

It can be seen from Figure 2 that an IGBT is a four-layer structure. The structure is similar to a MOSFET, except that a heavily-doped P-type layer is added. A PNP transistor is formed with its emitter at the substrate and its collector, the P body region, connected to the top layer metal. A parasitic NPN transistor is also formed with its collector in the N type epi region and its emitter also at the top layer metal. An equivalent circuit for the IGBT is also shown in Figure 2. The combination of the two transistors produces a structure similar to that of a thyristor [3].

The destruction of an IGBT under short circuit is always due to an excessive power dissipation generating high temperatures beyond the limits of the silicon. The high temperatures occur in concentrated locations due to nonuniformity of the dopant concentrations. The processes leading to the breakdown of the silicon may vary depending on the failure mode of the device. Some of these processes and their failure modes are discussed below.

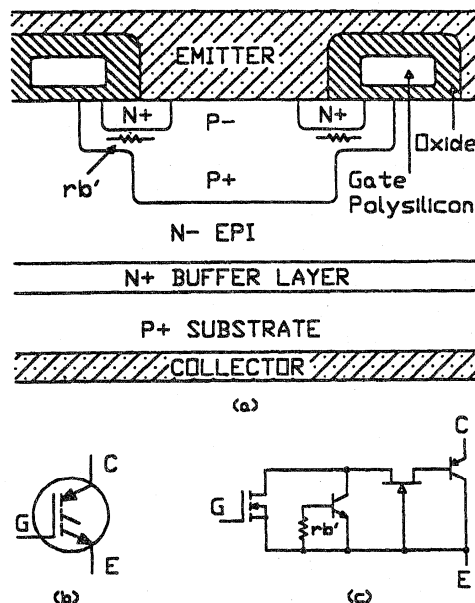


Figure 2. a) Silicon cross-section of an IGBT b) with its symbol, c) equivalent circuit

1) Exceeding Thermal Limit: If short circuit is sustained on a device, the power dissipation of the high current will cause a temperature rise to occur. This temperature rise in the die is extremely fast due to its fast thermal time constant. Exact calculations of the temperature rise are difficult due to the transient thermal impedance model not being accurate at the extremely high power dissipation occurring under short circuit conditions.

The silicon will not fail immediately even if the rated junction temperature for the device is exceeded. At approximately 250°C however, the doped silicon becomes intrinsic. Further rise in junction temperature would lead to exponential increase in the carrier concentration, resulting in thermal runaway [7]. The die becomes fatally damaged when the silicon begins to break down above 900°C. There also is possibility of silicon, near its surface, reaching metal-Silicon interface Eutectic temperature (577°C for Al-Si). If this takes place, contact-metal would migrate into the silicon and to the junctions, fatally harming blocking capability of the device in the process. These temperatures are reached in such a short time, after the die becomes intrinsic, that it is not possible to save the device by external means.

2) Latching: As described earlier, the four layer structure of the IGBT resembles that of a thyristor. The thyristor is prevented from operating by limiting the gain of the two transistors and reducing the value of the parasitic resistor r_b '.

Under fault conditions, excess current can flow through r_b ' as the MOSFET channel is reduced when attempting to turn off the IGBT. This excess current can cause a voltage across r_b ' that drives part of the IGBT structure into a latch condition. Once this occurs, control of the IGBT from the gate is not possible. An extremely low impedance is presented across the IGBT which was supporting the supply voltage. The high current, limited only by the supply impedance and high power dissipation, quickly destroys the device. Thus, an IGBT rated for long short circuit time may fail at turn-off simply due to 'dynamic latching.' Since the turn-off speed is, to some degree, dependent on the turn-off gate resistors, IGBT manufacturers must specify their values along with other test conditions.

3) Exceeding Voltage Rating: An IGBT may survive long short circuit time but fail when turned off. The fall rate of current induces a voltage equal to $L di/dt$ in the circuit stray inductances. This voltage overshoot, if too large, would cause the switching device to avalanche, resulting in failure due to excessive power surge or latching.

This mode of failure could be avoided by minimizing the circuit stray inductances on the DC side of the switching device, also called 'dc loop' inductance. See Figure 5. The objective could also be achieved by slowing the rate of fall of fault current which again, to some degree, is dependent on the turn-off series gate resistor, $R_{G(off)}$. The higher the value of $R_{G(off)}$, the slower the current rate of fall. The above is a subject of discussion in a later section.

Reliability

Short circuit is a fault condition that will drive the operation of the IGBT outside its safe operating area. A short circuit protection scheme, while saving a device from immediate failure, may not stop the long term reliability of the device from being affected. Care needs to be taken in specifying the short circuit capability of a device until the long term reliability effects are better known. For this reason, the designer should limit the short circuit stress to which the IGBT is subjected in an effort to reduce any detrimental effects on the reliability of the device. An effort should be made to immediately remove the IGBT fault current once the existence of fault condition is confirmed. It is thus advisable to protect a 10 μ s short circuit time IGBT in the range of 2 μ s.

IGBT Short Circuit Behavior

The ability of an IGBT to withstand fault currents can be improved by reducing the gate voltage applied to the device. A general trend in variation of short circuit current, I_{sc} , and time, t_{sc} , with gate drive voltage is illustrated in Figure 3. Reducing gate voltage to an IGBT reduces the magnitude of fault current through it and, as a result, extends the short circuit time.

In Figure 4, turn-on losses are plotted against gate drive voltage for two values of series gate resistors. It can be seen that within certain limits, 'high' gate drive voltage and 'high' gate resistance will produce the same current rise time and turn-on energy dissipation as 'low' gate drive voltage and 'low' gate resistance. Thus, for the device considered, identical turn-on waveforms could be obtained with a $V_{G(on)}$ - $R_{G(on)}$ combination of 15V - 50 Ω as with 10V - 10 Ω . This is only true, however, as long as the gate drive voltage is high enough to support the peak turn-on current [4].

Note that the turn-off switching losses are not an issue here, since they are largely unaffected by the gate drive.

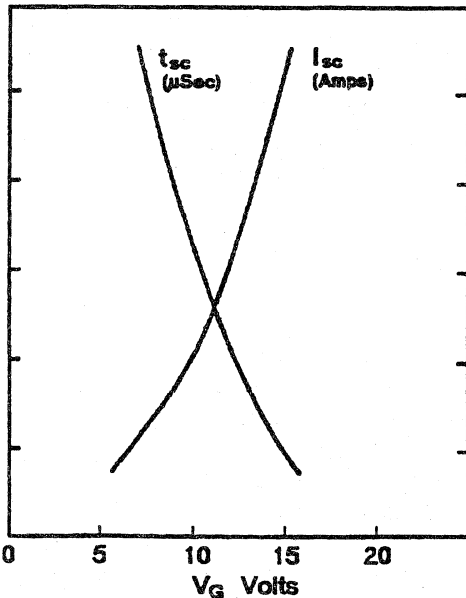


Figure 3. Generalized trends of short circuit current, I_{sc} and permissible short circuit time, t_{sc} with gate voltage V_G

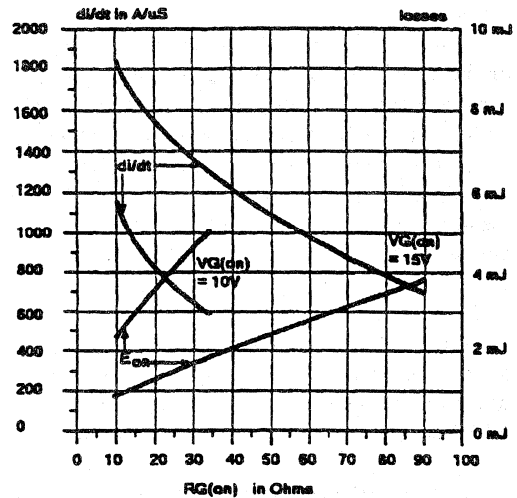


Figure 4. Turn-on di/dt and losses vs. $R_{G(on)}$
 IRGTA090F06 Tested at: 360V, 50A, 150°C.
 $L_S = 100nH$

Types of Faults:

Two types of fault conditions are possible. The behavior of IGBTs and the relationship to the gate drive circuitry should be understood for each case.

a) Fault Under Load: A device may be subjected to a short circuit while in normal conduction. The test circuit is shown in Figure 5. The waveforms in Figure 6 illustrate this type of fault. Initially, the IGBT is gated on and is operating normally, carrying a steady load current within its ratings

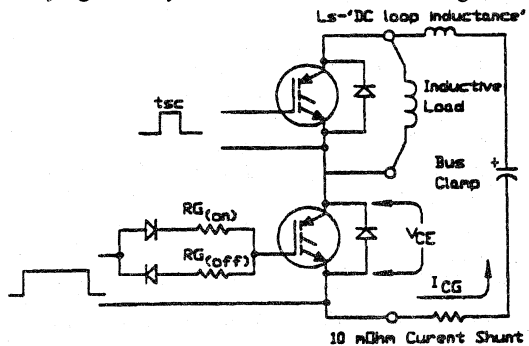


Figure 5. Short Circuit Test Circuit

(=80A). The voltage across the device, V_{CE} , is low. A fault is imposed on the device by turning on the complementary IGBT shown in Figure 5, causing a shoot-through. The current increased rapidly, pulling the IGBT out of its near saturation state. The rise in the V_{CE} caused a current I_{CG} to flow through the Miller capacitance, CC_G . Due to the presence of a high $R_{G(off)}$ (=100 Ω), the gate-emitter voltage jumps to a higher level (from 11V to 17V). Consequently, the fault current for this high-gain IGBT rises to over 1200A before declining as V_{GE} dwindles back to its normal on-state value. The fault current in this experiment was removed by turning off the complementary IGBT switch.

Lowering the value of $R_{G(off)}$ facilitates better clamping of the gate-emitter voltage, thereby significantly reducing the fault current magnitude. As demonstrated in Figure 7, the fault current peak decreases to less than 600A when $R_{G(off)}$ is reduced to 10 Ω .

An increase in V_G would result in an increase in the fault current magnitude. The IGBT has a better chance of survival with lower fault current

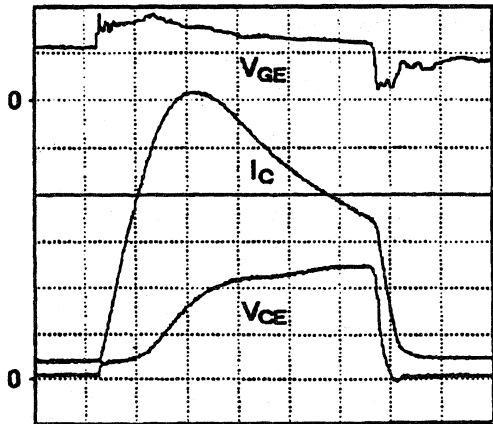


Figure 6. Fault Under Load test waveforms - IRGTA090F06 - Tested at: 360V, $V_{G(on-state)} = 11.0V$, $R_{G(on)} = 100\Omega$, $R_{G(off)} = 100\Omega$. V_{CE} : 100V/div, I_C : 200A/div, V_{GE} : 10V/div, Time: 500ns/div

level and, hence, lower resulting power dissipation. The short-circuit endurance time is increased, allowing the protection circuits longer time to react. IGBTs designed for higher operating efficiency, due to inherently higher gain, have less short-circuit endurance time than less efficient devices.

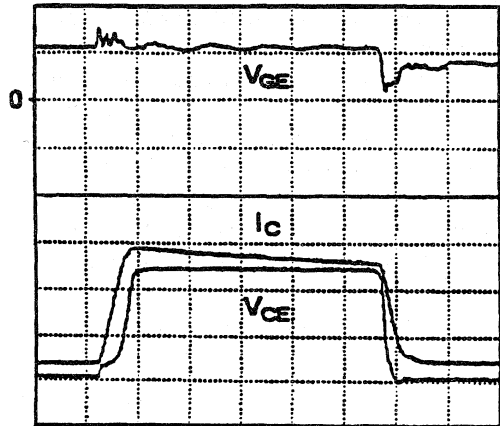


Figure 7. Fault Under Load test waveforms - IRGTA090F06 - Tested at: 360V, $V_{G(on-state)} = 11.0V$, $R_{G(on)} = 100\Omega$, $R_{G(off)} = 10\Omega$. V_{CE} : 100V/div, I_C : 200A/div, V_{GE} : 10V/div, Time: 500ns/div

b) Hard Switch Fault: The inductive load in Figure 5 is short circuited and the switching device is gated on directly into the fault. In this mode, the IGBT is off and the system voltage is supported across the device. The rate at which the device begins to conduct current and the magnitude of the fault current are related to the charging rate of the input capacitance and the gate-drive voltage V_G . This type of fault is described by the waveforms of Figure 8.

During the pre-fault stage the full system voltage is supported by the device. Upon application of the gate signal and following the gate-emitter voltage reaching gate-threshold voltage, I_C begins to rise. A notch is gouged out of V_{CE} due to the voltage drops occurring across the resistive and inductive elements of the circuit.

The fault current was ended by simply removing the gate drive. The rapid fall of the fault current

combined with the 'dc loop' inductance causes V_{CE} to overshoot the supply voltage. In this particular case, the voltage overshoots the bus voltage by 130V. The rate of fall of fault current and, hence, the magnitude of V_{CE} can be controlled, to a certain degree, by varying the value of $R_{G(off)}$. The device was retested with $R_{G(off)}$ increased to 33Ω . As shown in Figure 9, the resultant voltage overshoot decreases to 100V.

Note that increasing $R_{G(off)}$ to reduce the over-voltage transient following short circuit is in conflict with other considerations; the gate noise immunity and the dv/dt capability being the main ones, as discussed elsewhere [1]. A trade-off will have to be made by the designer, based on specific operating conditions.

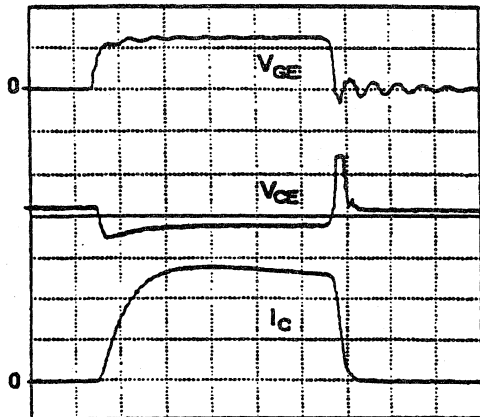


Figure 8. Hard Switch Fault test waveforms - IRGTA090F06

420V, $V_{G(on-state)} = 12.5V$, $R_{G(on)} = 33\Omega$, $R_{G(off)} = 0\Omega$. $V_{CE}: 100V/div$, $I_C: 200A/div$, $V_{GE}: 10V/div$, Time: $1\mu s/div$

It is obvious from Figures 8 and 9 that, for a hard switch fault, only a small positive dv/dt is generated across the IGBT. Thus, the Miller effect, a major consideration for the fault under load, has much less influence for the hard switch fault, particularly because the Miller capacitance is much lower at higher voltage. Thus, the hard switch fault can result in much lower fault current than the fault under load.

This is probably why the HSF test is used by most manufacturers to quote the short circuit

capabilities of their devices, as it is a less stressful test and will tend to give flattering results.

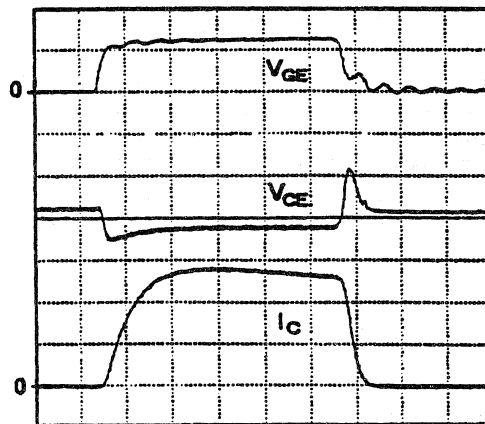


Figure 9. Hard Switch Fault test waveforms - IRGTA090F06

420V, $V_{G(on-state)} = 12.5V$, $R_{G(on)} = 33\Omega$, $R_{G(off)} = 33\Omega$. $V_{CE}: 100V/div$, $I_C: 200A/div$, $V_{GE}: 10V/div$, Time: $1\mu s/div$

Short Circuit Protection Schemes

Many schemes have been discussed over the last few years for protecting IGBTs under fault conditions [5]. All of these schemes have their advantages and disadvantages. The degree to which they perform the protection function for the cost of implementation is a decision to be made by the design engineer. The following attributes are considered desirable for a protection scheme to possess:

- (i) The scheme must implement a shutdown of the IGBT before device failure occurs. This should be true for all operating conditions the IGBT will be subjected to.
- (ii) The scheme should limit the peak fault current allowed to pass through the IGBT and therefore reduce the stress on the device and other parts of the system which are exposed to the high current.
- (iii) The scheme should be insensitive to noise and nuisance trips. Switching circuits generate noise due to high switching di/dt 's and stray circuit inductances. The fault detection method should ignore this noise as well as transient overcurrents due to such things as diode recovery.
- (iii) The scheme should be flexible enough to operate under 'Fault Under Load' and 'Hard Switch' type faults.

- (v) The scheme should not detrimentally affect the switching performance of the IGBT. This reflects on the operating efficiency of the system and the reliability of the part due to increased temperature.
- (vi) The scheme should not detrimentally affect the conduction performance of the IGBT. This reflects on the operating efficiency of the system and the reliability of the part due to increased temperature.
- (vii) The trip point of the scheme should be easy to set at some level that accurately defines the occurrence of a fault condition.
- (viii) The scheme should be inexpensive and simple to implement so as to not affect the economic viability of an application.

The above characteristics of a protection scheme are strongly linked to the detection method used to determine the existence of a fault condition. A review of some detection methods follows and their impact on the above points briefly summarized.

Resistor sensing: This method of fault detection is probably the most straight forward to understand. A shunt resistor is placed in the load current path and used to generate a voltage that is monitored by the protection circuit. The advantages of using sense resistors are:

- (1) Accurate current measurement suitable for both overcurrent and short circuit detection.
- (2) Signal may also be used for analog feedback.

The disadvantages of using sense resistors are:

- (1) Requires bulky, expensive low inductance sensing resistor.
- (2) Bad transient response due to the self inductance of the sense resistor and the wiring inductances. If the resistor is placed in the DC loop it will add unwanted inductance that may affect performance of the system.
- (3) The voltage from the sense resistor is not isolated from the main power circuit. This means that either the protection circuit may have to be isolated from the main logic circuitry of the fault detection signals passed through an isolation barrier which adds complexity to the system.

The use of current sensing IGBTs may involve a sensing resistor in the current sense path. This resistor can be a more convenient value than a

resistor in the main current path, however the cost trade-off of the more expensive IGBT, the limited availability and the consistency of the sense ratio from device to device will have to be evaluated.

Current transformer: This is another obvious method for fault current detection. A current transformer is placed around a conductor that is expected to carry any fault current and the output monitored. The advantages of using a current transformer are:

- (1) The transformer can be chosen to provide accurate AC sensing.
- (2) The transformer provides isolation between the power circuit and the protection circuit which can now be more conveniently referenced.
- (3) The protection circuit is current driven and can provide a high level signal output that offers more noise immunity.

The disadvantages of using a current transformer are:

- (1) The current transformer system cannot easily sense DC levels unless a more sophisticated (and expensive) DC transformer is used. The Hall Effect sensors provide one such example.
- (2) The design of an appropriate current transformer is not a trivial matter as it must be able to operate over a wide bandwidth. To respond to fast rising fault currents it must be able to operate up in the MHz region as well as down to the minimum switching frequency of the system.
- (3) The current transformer may be quite expensive.

VCE sensing: This scheme is also referred to as 'Desaturation Detection' [5], [6]. By definition, short circuit means that the only impedance seen by the supply is the switching device. The supply voltage will therefore appear across the device. For this to occur the IGBT is pulled out of its low on-state voltage mode and driven up the Output Characteristic Curve. This voltage across the device when it should be in the low on-state can be detected. The advantages of the VCE sensing method are:

- (1) No lossy current sense element is required in the circuit.
- (2) Circuit can be fast because of the low circuit inductances.
- (3) The circuit will be equally effective in AC and DC applications.

(4) The circuit is inexpensive and would be easy to integrate, as it uses simple passive components.

The disadvantages of the VCE sensing method are:

- (1) The circuit cannot be set to a known current level and gives a coarse fault/no-fault indication. The circuit will have to be set so that its detection level is above the maximum $V_{CE(on)}$ of the IGBT to determine when it is pulling out of saturation.
- (2) The circuit is not isolated from the power stage. This means that while an immediate action of removing the gate signal to the IGBT could be carried out locally, passing the error message to the logic circuitry (flagging) may require an isolation barrier, adding to the complexity of the system.
- (3) The circuit should provide blanking time to allow for the turn-on switching process.

A Practical Circuit

An inexpensive way to drive and fast-protect an IGBT is shown in Figure 10. The circuit uses the IR2125 MOS gate driver PIC [8]. The current sense feature of this device was modified to function as VCE-sense. During normal IGBT conduction, VCE is near saturation value and diode D1 is forward biased. The values of resistors R1, R2 and R3 are adjusted to keep the potential across R1 — also the PIC's CS pin — well below triggering value during normal operation. The IGBT gate drive remains unaffected.

When a fault occurs, perhaps due to accidental shorting of the load, rapid rise in VCE reverse biases the diode D1. The gate drive now starts to charge capacitor C6. The time constant $(R2+R3)C6$ is adjusted to provide a dead time which is long enough to allow for the turn-on switching to complete, or harmless capacitive loads transients. Note that IR2125 does have a built in dead time of 500ns. When the voltage at CS pin rises above the threshold level, the protection circuit inside the PIC is triggered. The gate drive is removed after reaction time, which is partly set by the capacitor C3 at the error pin. The reaction time of this protection circuit is as low as 1.5 μ s; which is fast enough to protect most efficient IGBTs. Detection of a fault is reported at the ERROR pin 3.

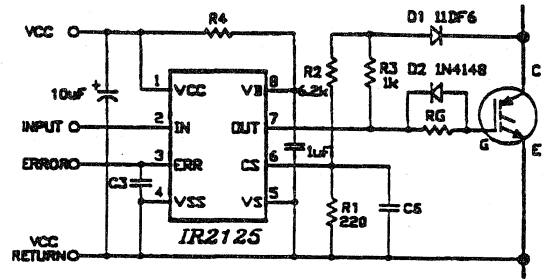


Figure 10. IGBT Gate Drive and Short Circuit Protection Scheme. VCE Sensing using IR2125 PIC

Note that the circuit in Figure 10 is configured to drive and protect a low side switch. IR2125 serves as both high side (to 500V) and low side driver. For high side operation, a boot-strap diode is required between VCC and VB pins. The purpose of resistor R4 is to de-couple the output stage from the input stage and help minimize IGBT switching noise feedback. Diode D2 provides low reverse impedance and reduces the Miller effects.

Short Circuit Protection of IGBTs in a 3-Phase PWM Motor Drive

The practical application of the protection circuit shown in Figure 10 was demonstrated using a 5HP AC motor drive. The system was set up as shown in Figure 11. To assure protection of the high-gain IGBTs used in this experiment, capacitor C6 was adjusted to react in 1.5 μ s and C3 was adjusted to achieve total reaction time of 3 μ s. The waveforms of Figure 12a illustrate operation of the above protection circuit. The figure shows PWM voltage and sinusoidal motor drive output current under blocked rotor condition. A short was forced across the motor drive output terminals at time t1. This activated the protection circuit, resulting in the IGBTs turning off. The IGBT fault current appears as a current spike in the inverter output current waveform. Figure 12b shows the IGBT current waveform during the fault condition, on an expanded time scale. The current shot up from 32A under blocked rotor conditions to 84A under fault conditions. For higher gate drive voltages, fault currents would have increased. The gate drive to the switching device was removed, saving it from

imminent failure. The flag output at the ERROR pin tripped a logic circuit which shut down further gating of all the IGBTs.

Note that by adjusting the value of capacitor at the ERROR pin the circuit reaction time could be further reduced.

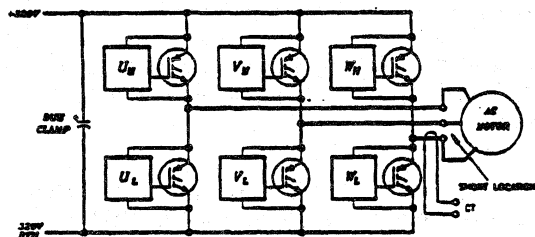


Figure 11. IGBT PWM 3-phase Motor Drive with VCE-Sensing Fault Protection Scheme

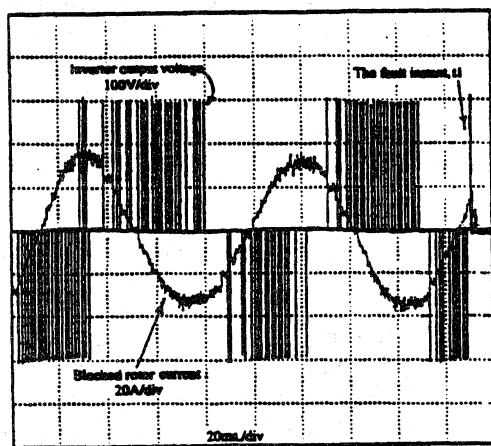


Figure 12. Short Circuit Test Under Blocked Rotor Condition. PWM inverter output voltage and motor current

The test was repeated with the motor running under no load conditions. The inverter output current waveform shown in Figure 13 reflects the small magnetizing motor current. The figure also shows the inverter PWM output voltage waveform. The output terminals of inverter were momentarily shorted out at instance t1. Just as in the earlier case, protection circuit action turned off the IGBTs in 5 μ s. The short was removed at t2. Thereafter, the motor current ceased to flow through the shorted

path and the sinusoidal back EMF voltage appeared at the motor terminal.

This illustration demonstrates the point that inexpensive circuits are available to (drive and) protect low-t_{sc}, but more efficient, IGBTs.

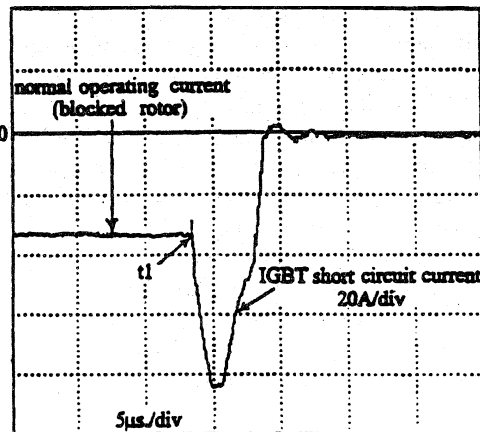


Figure 12b. IGBT current waveform

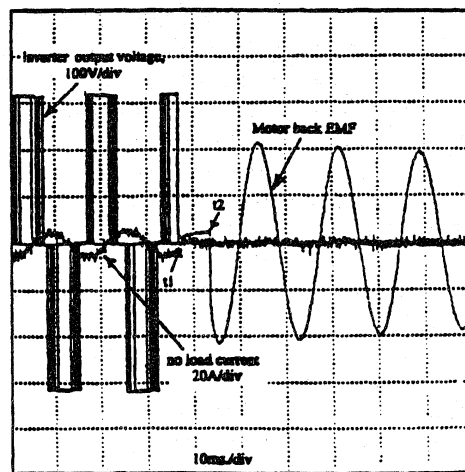


Figure 13. Short Circuit Test with the Motor in Free-Run. PWM inverter output voltage and motor current

Conclusions:

The issue of short circuit capability and protection of IGBTs is receiving a lot of discussion in certain applications. In particular, applications such as motor drives where there is potential for the end product user to incorrectly connect a system. The IGBT is a more efficient device than what is currently being used in these applications and, as such, has a lower short circuit capability and will require faster protection circuits than those for low-gain/less-efficient BJTs.

The failure modes and mechanisms of the IGBT have been discussed in an effort to determine the important criteria for a protection circuit. Methods of fault detection have also been discussed and their general advantages and disadvantages pointed out so that an appropriate detection method may be selected for a given application. The so-called 'VCE Detection' method appeared the most convenient and cost effective in our review.

Discussion and results of the protection circuit operation are presented. Usefulness of such a circuit in connection with a PWM motor drive was demonstrated. The results showed that even the most efficient IGBTs with the worst short circuit capability can be protected effectively without detrimentally affecting normal system operation.

References:

- [1] R. Chokhawala, J. Catt, B. Pelly, 'Gate Drive Considerations for IGBT Modules,' IAS-IEEE 1992.
- [2] C. Aniceto, R. Letor, 'How Short Circuit Capabilities Govern the Desired Characteristics of IGBTs,' Power Conversion - PCIM 1992.
- [3] S. Clemente, A. Dubhashi, B. Pelly, 'IGBT Characteristics and Applications,' International Rectifier Application Note AN-983A.
- [4] J. Catt, R. Chokhawala, B. Pelly, 'Introduction to the 600V ADD-A-Pak™ and INT-A-Pak™ IGBT Modules,' International Rectifier Application Note AN-988.
- [5] G. Castino, S. Clemente, A. Dubhashi, B. Pelly, 'Protecting IGBTs Against Short Circuit,' International Rectifier Application Note AN-984.
- [6] R. Locher, 'Short Circuit Proof IGBTs Simplify Overcurrent Protection,' IAS-IEEE 1991.
- [7] S. Gandhi, 'Semiconductor Power Devices,' A Wiley-Interscience Publication.
- [8] Arnold Alderman, Steve Clemente, 'MGDs: High Performance Integrated Drivers for Power MOSFETS and IGBTs,' Power Conversion - PCIM 1991.
- [9] J. Kassakian, M. Schlecht, G. Verghese, 'Principles of Power Electronics,' Addison Wesley 1991.

IGBT FAULT CURRENT LIMITING CIRCUIT

Rahul Chokhawala Giuseppe Castino

Abstract - There is a growing market demand for high efficiency yet long short-circuit withstand time IGBTs. The inherent device trade-off, however, does not allow device designers to achieve both goals simultaneously. The proposed circuits, by limiting the fault current magnitude, extends the short circuit withstand time of high efficiency (high-gain) IGBTs. Limiting of the fault current magnitude also results in reduced turn-off voltage transients; a desirable by-product, especially for higher current modules. Moreover, the adverse Miller effect is counterbalanced to a great degree. If the fault current is of short transient type, the circuit restores normal operation; a unique and desirable feature for noise-prone systems.

The circuit does not require an external DC supply to operate. This feature, combined with the simplicity of the circuit, renders itself feasible to be inserted in IGBT modules or be connected as an interface between the gate driver and module.

Introduction

Power transistors are used in electrical equipment to control and convert electrical power. The objective is achieved by switching these devices on and off at pre-determined instances. The devices are selected by system designers to reliably handle circuit currents both under normal conditions and under estimated overload conditions. However, under fault or short circuit conditions a power transistor may be subjected to very high surge currents — with the magnitude limited mainly by its own gain. Only timely control and removal of the fault current (by some external means) would save the device from impending failure.

In applications where system fault is a real possibility, motor-drive market being the prime example, external protection circuits are used to sense the fault and turn off the transistors by shutting down the base/gate drive. In all such applications, except where 'intelligent' modules are used, the protection circuit is connected externally to these devices.

Consequently, power semiconductor device manufacturers are expected to guarantee minimum short-circuit withstand time — a measure of how long a device would survive the fault current. A device trade-off exists between short circuit withstand time and current-gain of power transistors^{2,3}. That is, the higher the gain of the transistor, the higher will be the fault current magnitude and the shorter will be the short circuit withstand time. This trade-off is even more crucial for IGBT transistor manufacturers due to the inherently higher gain of these devices. The low-gain IGBTs available today allow longer short circuit time, but at the expense of operating efficiency. The high-gain devices, on the other hand, offer greater efficiency, but require quicker external protection circuits.

The market trend is to improve system efficiency. This, in turn, translates into demand for high-efficiency IGBTs. The requirement for longer short circuit time (10 μ s) IGBTs is still prevalent, especially for existing designs.

The proposed Fault Current Limiting Circuit, or FCLC, helps achieve both of the above objectives. The circuit operates by sensing the fault and

subsequently lowering the gate voltage. Lower gate voltage limits the magnitude of the fault current, and in doing so extends the short circuit withstand time^{4,5}. A time delay is introduced to allow for the duration of the switching transients or load circuit spikes; that resulting from motor cable charging current, for example. If the fault current is of transient type, lasting only for a few microseconds, the circuit restores the gate voltage and normal device operation is allowed to proceed unimpeded; a desirable feature for noise-prone systems. Note that many of the driver/protections ICs and 'smart' modules available on the market today do not have this diagnostic feature. A protection circuit should be designed in consideration of the following three principal causes of IGBT failures when subjected to short circuit conditions¹.

Exceeding Thermal Limit: If short circuit is sustained on a device, the power dissipation resulting from high current will cause a temperature rise to occur. This temperature rise in the die is extremely fast, due to its short thermal time constant. If the die temperature exceeds silicon intrinsic temperature (~250°C), the device loses blocking capability, making it impossible to save by gate control.

Reducing the fault current magnitude limits power dissipation in the IGBT die, thereby extending fault endurance time.

An IGBT may survive long short circuit time, but fail when being turned off due to the following scenarios:

Latching: As described elsewhere³, the four-layer structure of the IGBT resembles that of a thyristor. The thyristor is prevented from operating by limiting the gain of the two transistors and reducing the value of the base resistance of the NPN transistor, rb' .

When an IGBT is made to turn off under the fault conditions, a large portion of the device current is diverted to flow through the rb' as the MOSFET channel starts to turn off. The voltage drop developed across rb' could forward bias the base-emitter junction of the NPN transistor, turning

it on and initiating a regenerative latch-up of the IGBT.

Reducing the fault current at turn-off reduces the amount of current diverted into the rb' region, substantially decreasing the possibility of thyristor-like latch-up.

Exceeding Voltage Rating: The fall rate of large fault current induces a voltage, equal to Ldi/dt , in the external circuit stray inductances and internal package inductances. This voltage overshoot, if too large, would cause the switching device to avalanche, resulting in device failure if the energy stored in the stray inductances exceeds the avalanche capability of the transistor.

While the external circuit stray inductance could be greatly reduced by use of de-coupling capacitors, the internal package inductances remain out of the user's reach. Since the turn-off di/dt increases with current magnitude, it could easily reach a few thousand A/ μ s for high-current modules. The situation is worst at lower junction temperatures due to faster recombination of stored charges in the device. The resultant high di/dt could lead to large turn-off voltage overshoots across the IGBT die and cause failure.

This mode of failure can be avoided by slowing down the fault current turn-off di/dt . This is achieved by, 1) increasing the turn-off gate resistor, 2) ramping down the gate drive voltage, or 3) reducing the fault current magnitude before the turn-off.

Increasing the turn-off gate resistor is not an attractive solution, since it enhances the Miller effect¹. The other two solutions are free of such adverse effects.

It is clear from the above discussion that reducing the fault current magnitude can alleviate the three principal stresses primarily responsible for the failures of IGBTs under fault.

The proposed FCLC satisfies the following desirable attributes:

(i) The circuit should limit the peak fault current allowed to pass through the IGBT, and therefore

- reduce the stress on the device and other parts of the system which are exposed to the high current.
- (ii) The circuit should be insensitive to noise and nuisance trips. Switching circuits generate noise due to high switching di/dts and stray circuit inductances. The fault detection method should ignore this noise, as well as transient overcurrents due to such things as diode recovery.
 - (iii) The circuit should be flexible enough to operate under both 'fault during conduction' and 'switching into a fault' conditions.
 - (iv) The circuit should not detrimentally affect the switching and conduction behavior of the IGBT. This reflects on the operating efficiency of the system and the reliability of the part due to increased temperature.
 - (v) The trip point of the circuit should be easy to set at some level that accurately defines the occurrence of a fault condition.

II. OPERATION OF THE PROPOSED CIRCUIT

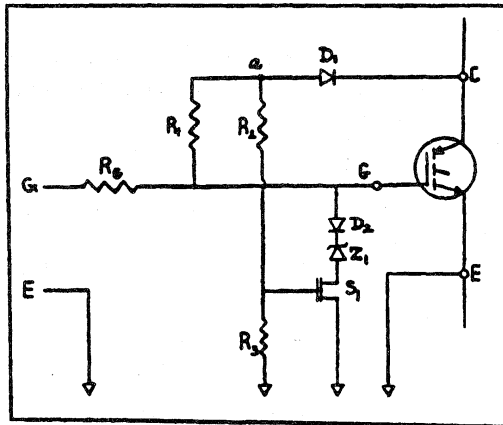


Figure 1. The proposed circuit

The proposed circuit shown in Figure 1 consists of the following elements:

- 1) Zener Z1 is selected to produce desired clamp voltage.
- 2) Diode D2 blocks negative off-state gate bias.
- 3) MOSFET S1 controls the state of operation of (activates/deactivates) the circuit.
- 4) Resistors R1, R2 and R3 form a voltage divider. Resistors Rg, R1, R2 and R3 are adjusted to

produce desired time constant $\tau_1 = [(RG+R1+R2) \times R3 / (RG+R1+R2+R3)] \times C_{iss}$. C_{iss} being the MOSFET input capacitance.

5) Fast diode D1 serves as a fault sensing element. Its voltage rating is the same as that of the protected IGBT.

The circuit uses V_{CE} sensing technique to detect the occurrence of a short circuit. By definition, short circuit means that the only impedance seen by the supply is the switching device. The supply voltage will, therefore, appear across the device. when this happens, the IGBT is pulled out of its low on-state voltage mode and driven up the output characteristic curve. The occurrence of high voltage across the device, when it should be in the low on-state, is detected by the proposed circuit.

Under normal operating conditions, gate drive voltage is applied across the gate and emitter terminals and the IGBT starts to conduct as the V_{GE} rises above the gate-threshold value. At the end of the turn-on transition, V_{CE} tails off toward its on-state level. The time duration for completion of this process varies between 100ns and 2 μ s, depending on the characteristics of the IGBT and the load current magnitude.

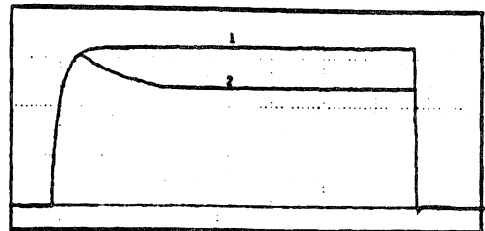


Figure 2. IGBT gate signals with FCLC connected.

Waveforms:

- #1 - Gate signal under normal operation
- #2 - Gate signal when the IGBT is turned on into an existing short circuit

Scales: V_{GE} : 5V/div, time: 1 μ s/div

Initially, with the gate drive voltage switched to the high-state and the IGBT still in the off-state, diode D1 is reverse biased. The gate drive begins to charge the gate of MOSFET S1 at a rate determined by the time constant τ_1 . This time constant is adjusted such that the MOSFET gate voltage

remains below its threshold value, at least prior to completion of the IGBT turn-on process. If the conduction proceeds normally, V_{CE} tails off toward its low on-state voltage level. As V_{CE} declines below the gate signal level (e.g. 15V), diode D1 is forward biased and the potential at point a starts to decrease with V_{CE} . As the turn-on process nears completion, voltage at node a is reduced to a few volts. Resistors R1 and R2 are adjusted to keep the MOSFET gate voltage below its threshold level under the above conditions. Consequently, the gate signal to the IGBT is left unaffected, as seen from waveform #1 of Figure 2.

If an IGBT is triggered into an existing short, V_{CE} remains at its off-state level as the supply voltage is forced across the collector and emitter terminals. Diode D1 now remains reverse biased and the potential at the MOSFET gate continues to rise toward a level that is determined by the gate voltage and relative values of resistors R1, R2 and R3. these resistors are selected to guarantee MOSFET turn-on under the above conditions. Once MOSFET S1 is on, the IGBT gate signal is clamped to a lower voltage, the value of which is determined mainly by the avalanche voltage of zener Z1. Consequently, the IGBT gate signal is brought down to a lower level, as seen from waveform #2 of Figure 2. For this illustration, the circuit components were adjusted to produce 1 μ s delay.

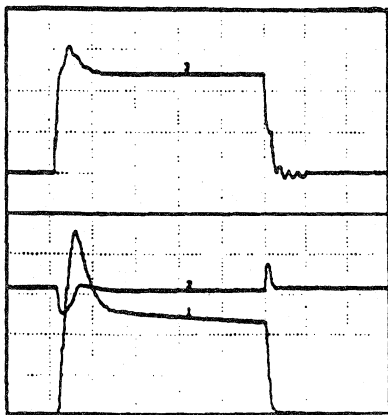


Figure 3. IGBT fault waveforms with FCLC connected

Waveform scales:

#1 - I_C : 100V/div, #2 - V_{CE} : 100A/div,
#3 - V_{GE} : 5V/div, time: 2 μ s/div

TPAP-4

By clamping the gate voltage to a lower level, the fault current magnitude is decreased, thereby reducing power dissipation in the IGBT die. The direct effect of reducing losses is the extension of device short circuit endurance time, as described earlier. Figures 3 through 5 compare short circuit waveforms with and without the FCLC circuit. Note the significant reduction in the fault current and corresponding energy dissipation. The fault current was brought down from 400A without the FCLC to 230A with the FCLC. The energy dissipation was reduced from 1.35J to 0.8J in 10 μ s.

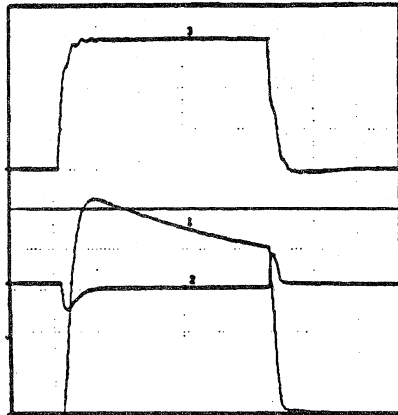


Figure 4. IGBT fault waveforms without FCLC connected

Waveform scales:

#1 - I_C : 100V/div, #2 - V_{CE} : 100A/div
#3 - V_{GE} : 5V/div, time: 2 μ s/div

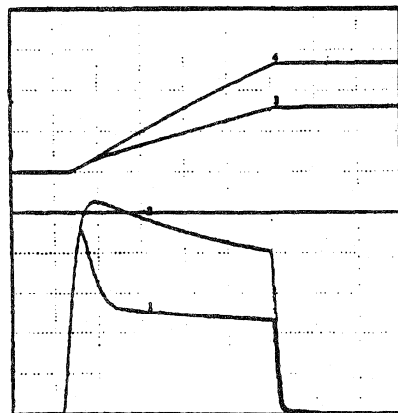


Figure 5. IGBT fault currents and energy losses with and without FCLC connected

Waveform scales:

#1 and #2 - I_C : 100V/div, #3 and 4 - E_{SC} :
0.5Joules/div, time: 2 μ s/div

The criteria in selection of clamp voltage, responsible for lowering these losses, are discussed below.

It is emphasized here again that the FCLC described in this paper serves only to extend IGBT short circuit withstand time. It is left for the slower-acting principal protection circuit to turn off the gate drive completely and disable further firing of the IGBTs.

In applications where narrow, but large, magnitude current spikes are common occurrences, such as motor cable capacitive currents, or noise-triggered shoot-through transients, it becomes necessary to restrict the level to which the gate voltage can be reduced. Such transients, if considered to be nondestructive, must not be allowed to cause nuisance tripping of the protective circuit that may lead to system shutdown. Therefore, the clamp voltage should be kept high enough to allow the circuit to 'unclamp' itself once the transient has passed. The proper value of the clamp voltage is determined by the knowledge of maximum estimated load current without pulling the device out of 'saturation.' The gate clamp voltage in Figure 3 (=12V) was selected to support twice the rated current of the test module. In actual applications, the maximum load current could be significantly less than the peak rated current, which would allow usage of much lower clamp voltage and thereby provide longer short circuit endurance time. The scenario discussed above is demonstrated in the following paragraphs.

Fault may occur while the IGBT is in conducting state. In Figure 6, the IGBT is conducting inductive load current prior to occurrence of the fault. As seen from this figure, V_{CE} rises rapidly from its low on-state level to the DC rail voltage. Diode D1 is now reverse biased and, just as in the previous case, the IGBT gate signal starts to charge the MOSFET input capacitance. This action is sped up by the recovery current of diode D1. Consequently, IGBT gate voltage is made to clamp in a shorter duration; a desirable effect, since under this type of fault, there is no need for a delay in circuit reaction. As a matter of fact, faster circuit reaction helps minimize the adverse Miller effect.

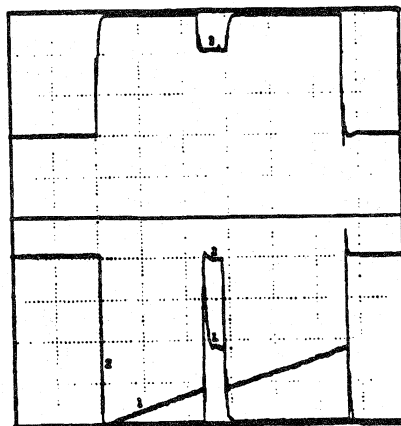


Figure 6. Fault under load with FCLC

Waveform scales:

#1 - I_C : 100V/div, #2 - V_{CE} : 200A/div,

#3 - V_{GE} : 5V/div, time: 10 μ s/div

The fault simulated in Figure 6 is of a transient type, with its duration set to 5 μ s. At the end of the fault, the IGBT current reverts back to the load current. V_{CE} returns to its on-state level, diode D1 switches back to its forward bias state, and the clamp circuit is turned off. As seen from the figure, the gate voltage is restored to its original value and the operation proceeds unimpeded. If the gate clamp voltage is reduced to a level that is too low, the IGBT will not support the load current, and the V_{CE} will remain high even after the transient fault has passed. The FCLC under such circumstances will remain latched on, thereby keeping the IGBT in 'pseudo-'fault state. This action will guarantee false tripping of the principal protection circuit and shutting down of the circuit operation. By properly selecting the clamp voltage, a nuisance tripping is thus avoided.

Note that with the reduced gate voltage, the short circuit withstand time of the IGBT is extended significantly. This allows usage of a slow-acting principal protection circuit.

III. ALTERNATE CIRCUITS

The circuit of Figure 1 requires selection of MOSFET S1 based on gate threshold voltage. If the IGBT selected has excessively high on-state voltage drop, it may not be possible to find suitable MOSFETs. The circuit shown in figure 7 elimi-

nates the problem of MOSFET selection. Zener Z2 is selected to offset the IGBT on-state voltage drop, no matter how high it may be. This way, when the IGBT is conducting worst case load current, it is assured the potential at the gate of MOSFET S1 is below its gate-threshold level, and the clamp circuit is made to stay in its off state.

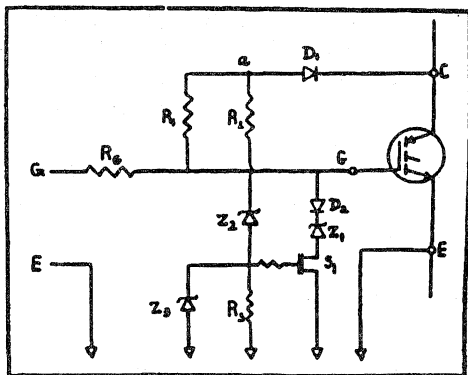


Figure 7. FCLC requiring no MOSFET selection

The circuit shown in Figure 8 is a two-stage corollary of the proposed FCLC. The short circuit protection is extended by lowering gate voltage in steps. After the first stage of operation, which also serves as the diagnostic period, the gate voltage level is reduced further. This is accomplished by the operation of MOSFET S2. The triggering mechanism is the same as in Case 1. The time constant $\tau 2$ governing the triggering of S2 is adjusted by properly selecting values of R4, R5 and C2. C2 is the sum of the MOSFET input capacitance and an external discrete capacitor. Waveforms #1 and #2 in Figure 9 show each of the two stages operating one at a time. Waveform #3 is a combination of the above two, and is the output (IGBT gate) signal of the two-stage FCLC under fault conditions. This could be compared with waveform #4 which is the gate signal without FCLC.

The purpose of this circuit is not only to extend the short circuit endurance time of the IGBTs, but also to greatly reduce the fault current level at turn-off. As described earlier, reducing the fault current magnitude at turn-off helps prevent the IGBT from latching up and lowers the turn-off voltage overshoot. Figures 10 and 11, respectively, compare

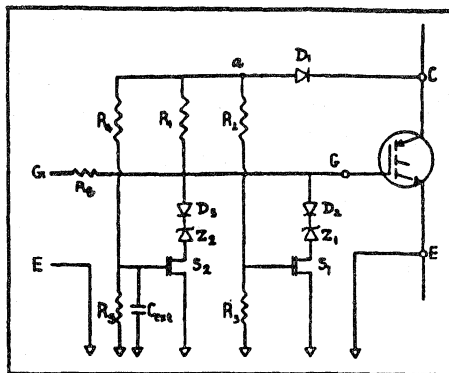


Figure 8. Two-stage FCLC

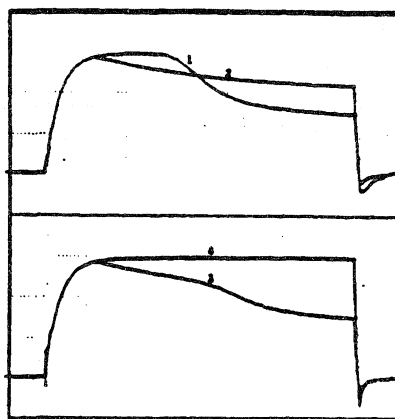


Figure 9. Gate signals under fault conditions - two-stage FCLC

Waveforms:

- #1 - Gate signal with only Z1 clamp connected
- #2 - Gate signal with only Z2 clamp connected
- #3 - Combined effects of Z1 and Z2
- #4 - Gate signal without FCLC connected

Scales: $V_{GE} : 5V/div$, time: $2\mu s/div$

the effect of single-stage and two-stage FCLC on the fault currents. Comparing these two figures with Figure 4 demonstrates the progressive decrease in the fault turn-off voltage overshoots. As demonstrated in Figure 12, IGBT fault current, which was 400A before connecting the FCLC, is reduced to 220A with the single-stage FCLC and down to 60A with the two-stage circuit. Figure 12 compares the gate voltages and corresponding fault currents from the above three cases. Figure 13 shows the resultant energy losses. Note the

significant lowering of dissipated energy with the two-stage FCLC. As a result, the short circuit withstand time of the IGBT protected is increased greatly. Figure 14 shows an IGBT enduring 30 μ s of short circuit time.

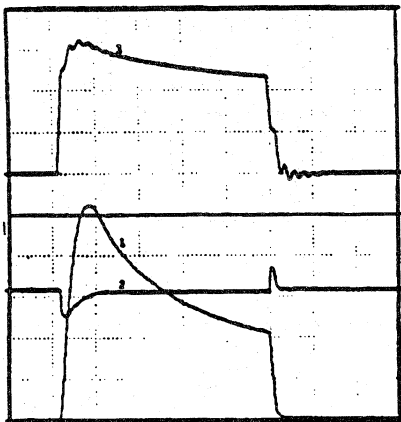


Figure 10. IGBT fault waveforms with single-stage FCLC

Waveforms:

#1 - I_C : 100V/div, #2 - V_{CE} : 100A/div,

#3 - V_{GE} : 5V/div, time: 2 μ s/div

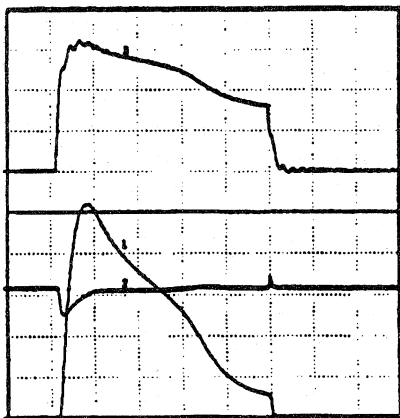


Figure 11. IGBT fault waveforms with two-stage FCLC

Waveforms:

#1 - I_C : 100V/div, #2 - V_{CE} : 100A/div,

#3 - V_{GE} : 5V/div, time: 2 μ s/div

In some applications, it may be desired to turn the IGBT completely off following the first diagnostic stage. This could be accomplished by lowering the clamp voltage to a level below the IGBT gate-threshold voltage.

V. SUMMARY

The IGBT fault current is controlled and the short circuit withstand time is prolonged by simply selecting the right gate clamp voltage. Lowered fault current, besides significantly reducing silicon losses, helps diminish the possibility of device latch-up, and lowers the magnitude of turn-off voltage overshoot. The normal operation of the IGBT is not interfered with. If the fault current is of short transient type, the circuit restores the gate signal and normal circuit operation continues unimpeded. The circuit consumes little power, which is derived from the gate signal itself. This feature, combined with the simplicity of the circuit, renders itself feasible to be inserted in the IGBT modules or be connected as an interface between the gate driver and IGBT.

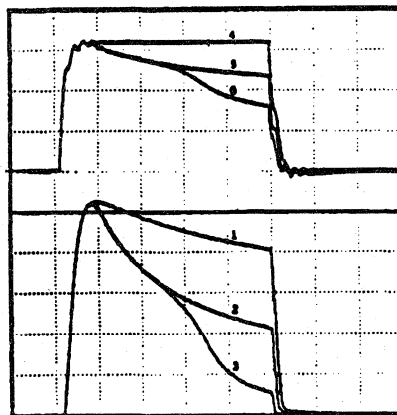


Figure 12. Comparison of test waveforms. IGBT gate voltages and corresponding fault current without and with single- and two-stage FCLC

Waveforms:

#1, #2, #3 - I_C : 100V/div

#4, #5, #6 - V_{CE} : 100A/div, time: 2 μ s/div

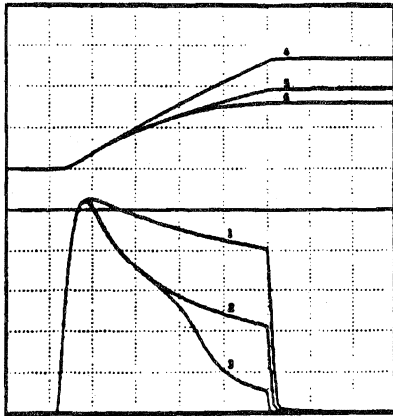


Figure 13. Comparison of test waveforms. IGBT fault currents and corresponding energy losses without and with single- and two-stage FCLC

Waveforms:

#1, #2, #3 - I_C : 100V/div

#4, #5, #6 - E_{SC} : 0.5Joules/div,

time: 2 μ s/div

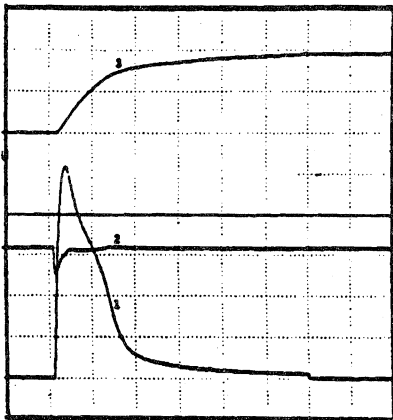


Figure 14. IGBT fault waveforms with two-stage FCLC

Waveforms:

#1 - I_C : 100V/div, #2 - V_{CE} : 100A/div,

#3 - V_{GE} : 5V/div, time: 2 μ s/div

References:

- 1) R. Chokhawala, J. Catt, L. Kiraly, "A Discussion on IGBT Short Circuit Behavior and Fault Protection Schemes," APEC-IEEE Conf., March 1992.
- 2) R. Chokhawala, J. Catt, B. Pelly, "Gate Drive Considerations for IGBT Modules," IAS-IEEE Conf., Oct. 1992.
- 3) C. Aniceto, R. Letor, B. Ishan, "How Short Circuit Capabilities Govern the Desired Characteristics of IGBTs," Power Conversion Conf., April 1992.
- 4) S. Clemente, A. Dubhashi, B. Pelly, "IGBT Characteristics and Applications," International Rectifier Applications Note AN-983-A.
- 5) G. Castino, A. Dubhashi, S. Clemente, B. Pelly, "Protecting IGBTs Against Short Circuit," International Rectifier Applications Note AN-984.

Snubber Considerations for IGBT Applications

Yi Zhang

Saed Sobhani

Rahul Chokhawala

Abstract - Snubber circuits can be used to protect fast-switching IGBTs from turn-on and turn-off voltage transients. Snubbers are available in various configurations and a clear understanding of their operation is necessary to make the appropriate selection. This paper will discuss pros and cons of these circuits. De-coupling capacitors, RCD voltage clamp circuit, RCD charge-discharge snubber are included in the discussion.

Introduction

When a power device is abruptly turned off, trapped energy in the circuit stray inductance is dissipated in the switching device, causing a voltage overshoot across the device. The magnitude of this transient voltage is proportional to the amount of stray inductance and rate of fall of turn-off current. The situation is at its worst for fast-switching IGBT modules. These devices switch high magnitudes of currents in a short duration of time, giving rise to potentially destructive voltage transients. The higher current modules normally consist of several IGBT chips in parallel. Each individual chip switches its share of the load current at a di/dt that is determined by the gate drive circuit. The total current and di/dt seen by the external power circuit is the sum of currents and di/dt s through each IGBT chip. The di/dt s produced could easily be few thousand A/ μ s. Proper attention needs to be paid to protect these devices from destruction.

Snubbers offer optimized protection against voltage transients during normal turn-on and turn-off switching. Using such protection circuits allows faster, yet safer, operation by containing the

operating loci within the boundaries of the rated Safe Operating Area. The paper discusses various snubber circuits, pros and cons of de-coupling capacitors, and RCD snubber-clamp circuits, RCD charge-discharge snubber are discussed. Circuit operations are analyzed and the test results are illustrated.

Note that the fault current shut-off transients are more effectively protected by considerably slowing the rate of fall of fault current. Fault current turn-off protection through electronic gate control is covered in detail elsewhere [1].

De-coupling capacitors

As mentioned earlier, the magnitude of transient voltage depends on the trapped energy in the circuit stray inductance, also called 'DC loop' inductance, L_s . As a preventive measure, steps should be taken to improve the circuit layout. Using laminated copper plates, minimizing the size of 'DC loop' and choosing source capacitance with inherently low self-inductance are ways to lower stray inductances [2]. De-coupling capacitors connected across the module's bus terminals, as shown in Figure 1a, are found to be useful for low-to-medium current applications. High-frequency polypropylene film capacitors are designed to fit IGBT terminal spacing for direct mounting. The resultant internal inductances are dramatically lower than conventional leaded capacitors. Figures 2a, 2b, 3a and 3b show turn-on and turn-off switching waveforms with and without a 1 μ F module-compatible de-coupling capacitor.



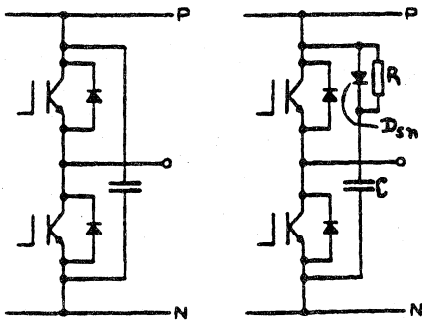


Figure 1a
de-coupling capacitor

Figure 1b
discharge restricted
de-coupling capacitor

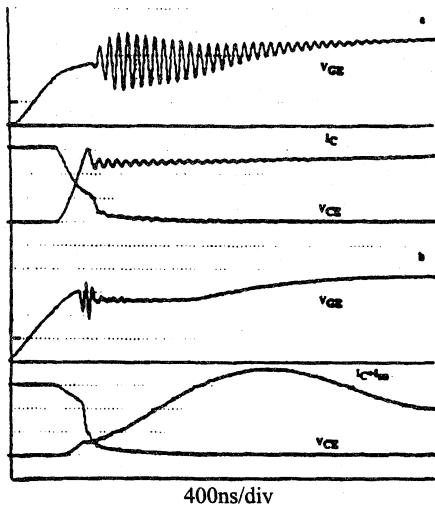


Figure 2a,b turn-on waveforms without and with de-coupling capacitor, respectively
Tested at 300V, 125A, 15V/39Ω, $C_{sn}=1\mu F$
 V_{CE} : 100V/div, I_C : 50A/div, V_{GE} : 5V/div

These figures show voltage across the IGBT (V_{CE}), the DC bus current (i.e. I_C in Figures 2a and 3a and I_C+I_{sn} in Figures 2b and 3b) and the gate voltage (V_{GE}). The actual current through the IGBT is not recorded in Figures 2b and 3b, since the de-coupling capacitor was directly screwed onto the module terminals and the path to the IGBT was not accessible for the current measurements. However, since the IGBT switching current is only marginally dependent on the effective external inductances, L_S (the principal difference between the two examples), it is assumed to be almost identical in both cases. It can also be shown that,

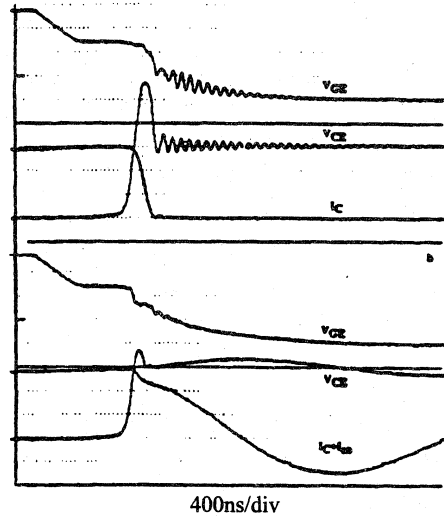


Figure 3a,b turn-off waveforms without and with de-coupling capacitor, respectively
Tested at 300V, 125A, 15V/39Ω, $C_{sn}=1\mu F$
 V_{CE} : 100V/div, I_C : 50A/div, V_{GE} : 5V/div

under a given set of conditions, the total switching losses are independent of the external stray inductances [3].

It is clear from the above figures that the use of de-coupling capacitors, by providing a 'non'-inductive path during the switching operation, eliminates severe voltage transients during switching and helps smooth the circuit waveforms. Note that, in Figure 3b, the voltage transient during turn-off is reduced to 370V from its dangerously high value of 570V in Figure 3a (rated voltage was 600V).

Due to the danger of destroying the device by over-voltage (caused by the recovering diode), the IGBT's turn-on switching speed is limited by using higher gate resistors. With the de-coupling capacitor in place, this constraint is removed. The gate resistor can now be reduced to a lower value, thereby allowing the IGBT to turn on faster and reducing overall switching losses.

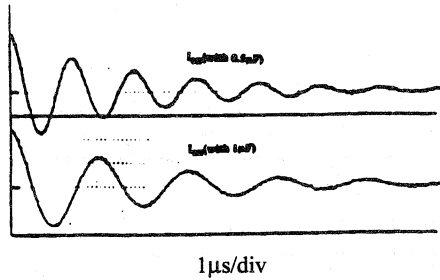


Figure 4 - snubber current waveforms at IGBT turn-off with 0.5µF and 1µF capacitors
Tested at 300V, 125A, 15V/39Ω, I_{SN} : 50A/div

The snubber capacitance value can be approximated from the following, based on the circuit stray inductance L_S , maximum switching current I_O , DC rail voltage V_{CC} and allowable peak voltage V_{pk} (Appendix II).

$$C_{sn} = L_S \cdot I_O^2 / (V_{pk} \cdot V_{CC})^2 \quad (1)$$

The overriding criterion in selecting the capacitor may be the RMS current limit of the de-coupling capacitor. IGBT switching sets off oscillations in the 'DC loop' between the de-coupling capacitor and the DC source. The oscillations are damped by the resistive stray elements in the loop. The resulting snubber currents are shown in Figure 4 and given by the following (Appendix I).

$$i_{sn} = I_O e^{-\alpha t} \cos(\beta t) \quad (2)$$

Where $\alpha = R/2L_S$ and $\beta = [4/L_S C_{sn} \cdot (R/2L_S)^2]^{1/2}$, R being the stray resistance in the loop that includes the capacitor's ESR. From Appendix II I_{RMS} in the capacitor is given by:

$$I_{RMS} = I_O (f_{sw} \cdot L_S / R_S)^{-1/2} \quad (3)$$

Since the capacitor's ESR is the dominant part of the total stray resistance, the worst-case losses in the capacitor can be approximated as follows:

$$ESR \cdot I_{RMS}^2 = 2 \cdot (\frac{1}{2} L_S I_O^2) \cdot f_{sw} \quad (4)$$

At higher frequencies and higher device currents, the oscillatory snubber currents may cause excessive heating in these high-frequency capacitors.

The capacitor should, therefore, be selected based on the limiting values give by (1) and (3). For load currents up to about 150A, and switching frequency of up to a few kHz, the de-coupling capacitors seem to provide optimal protection against normal switching transients. While this method provides low inductive path for the currents during switching, it is not a panacea for bad circuit layout, as higher L_S results in greater RMS currents in the capacitors (as seen from 3).

Discharge resistant circuit — Figure 1b

The circuit in Figure 1b operates on the same principal as the de-coupling capacitor, but only during turn-off switching. As the IGBT is turned off, the energy trapped in the stray 'DC loop' inductance is transferred to the capacitor. The diode D_{SN} , however, blocks any oscillations from occurring (see Figure 5). The excess charge on the capacitor is gradually discharged through the snubber resistor.

The disadvantage of this circuit is that the added element in the protection circuit, i.e. the blocking diode, increases the overall snubber inductance. Also, a direct-mounted, low-inductance snubber capacitor cannot be used in this case. This causes an increase in the VCE overshoot, as seen from Figure 5 compared to Figure 3b.

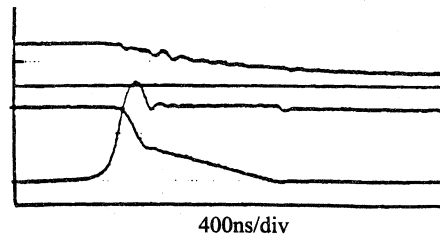


Figure 5 - turn-off waveforms with discharge restricted de-coupling capacitor
Tested at 300V, 125A, 15V/39Ω, $C_{sn}=1\mu F/20\Omega$
 V_{CE} : 100V/div, I_C : 50A/div, V_{GE} : 10V/div

The turn-on operation of this circuit is nearly identical to the one for the RCD clamp circuit to be discussed next. The snubber losses are given by (1) and (5), also in the next section.

RCD Snubber and clamp circuits

Figures 6a and 6b are two principal examples of RCD snubbers for high-current IGBT applications. While both circuits reduce transient voltages across switching devices, the charge-discharge snubber circuit in Figure 6b is also targeted for reducing IGBT turn-off losses. First, operation of the circuit in Figure 6a will be considered.

The ‘clamp’ circuit — Figure 6a

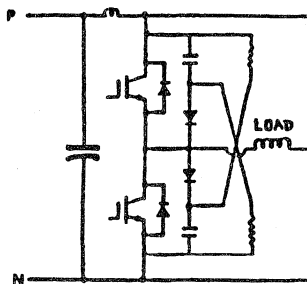


Figure 6a
RCD clamp-snubber

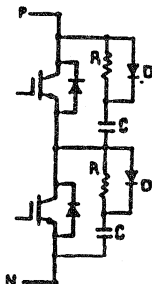


Figure 6b
RCD charge-discharge snubber

The operations of this RCD circuit during turn-on and turn-off switching are described below.

Turn-off — The function of this circuit is somewhat similar to a voltage clamp. During IGBT conduction time, the snubber capacitors are charged to the bus voltage. As the IGBT is turned off, the voltage across it, V_{CE} , rises rapidly. The circuit ‘DC loop’ stray inductance, L_s , may cause V_{CE} to rise above the bus voltage. As this occurs, the snubber diode is forward biased and the snubber is activated. The energy trapped in the stray inductance is now diverted to the snubber capacitor, which absorbs this incremental energy without a substantial rise in its voltage. The waveforms shown in Figure 7 illustrate turn-off behavior with and without the RCD clamp. The voltage overshoot has been substantially reduced from 210 volts to just 50 volts. Initially, a small stray inductance in the snubber circuit causes V_{CE} to peak slightly above V_{CC} .

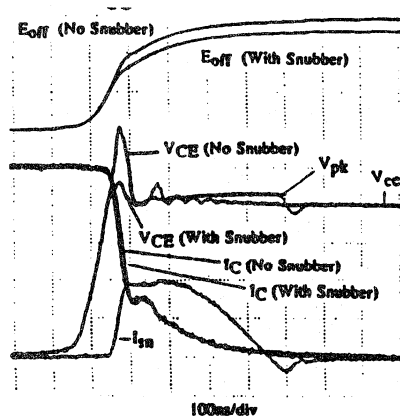


Figure 7 - turn-off waveforms with and without RCD snubber

Tested at 400V, 100A, 25°C, $L_s = 100\text{nH}$
 $V_G/R_G(\text{off}) = -8\text{V}/33\Omega$; $C_{sn} = 0.22\mu\text{F}$, $R_{sn} = 12\Omega$
 $V_{CE}: 100\text{V}/\text{div}$, $I_C/I_{sn}: 20\text{A}/\text{div}$, $E_{off}: 2\text{mJ}/\text{div}$

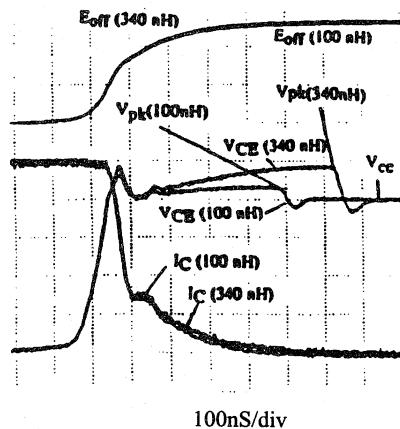


Figure 8 - turn-off waveforms with RCD snubber for two different L_s values (100nH, 340nH)

Tested at 400V, 100A, 25°C
 $V_G/R_G(\text{off}) = -8\text{V}/33\Omega$, $C_{sn} = 0.22\mu\text{F}$, $R_{sn} = 12\Omega$
 $V_{CE}: 100\text{V}/\text{div}$, $I_C: 20\text{A}/\text{div}$, $E_{off}: 2\text{mJ}/\text{div}$

Figure 8 displays the waveforms generated for two different stray inductances (100nH and 340nH). As illustrated in the Figure, the initial V_{CE} peak, which is dependent on the stray inductance within the snubber circuitry, is the same for both cases. The final voltage peak (V_{pk}) for the high inductance does, as expected, reach a higher value, since

there is more trapped energy ($\frac{1}{2} \cdot L_s \cdot I^2$) diverted to the same snubber capacitor. This value, however, is well within the voltage rating of the device and only marginally influences the losses in the IGBT, since it occurs when the current has reached a smaller value. The V_{pk} magnitude can be calculated from the formulae given in the following section.

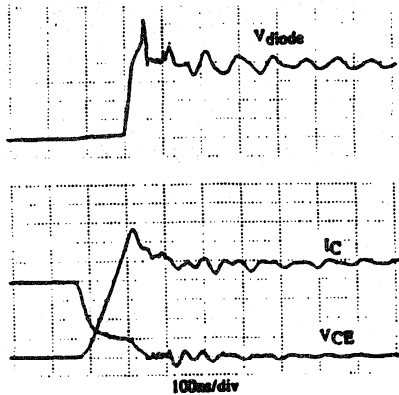


Figure 9 - turn-on waveforms with no RCD snubber protection

Tested at 400V, 100A, 25°C, $L_s=240nH$
 $V_G/R_G(on)=15V/5.1\Omega$
 $V_{CE}: 100V/div, I_C: 20A/div, V_{diode}: 100V/div$

Turn-on — Figure 9 displays the turn-on waveforms for an unprotected IGBT with a gate resistor (R_G) of 5.1Ω. The rapid rise in the IGBT current (1200 A/μs), combined with the circuit stray inductance (300 nH), caused the FWD to go through a severe reverse recovery process. As seen in the Figure, the FWD recovery voltage (=630V) actually exceeded the rated voltage of the module.

In order to bring this voltage down to a safe value, the turn-on di/dt was lowered by using a higher R_G . The results are shown in Figure 10. The increase in R_G , however, greatly increased the switching losses, as expected [3], [4].

The RCD clamp shown in Figure 6a is also effective in reducing turn-on voltage transients. As the IGBT current rises, the $L_s \cdot di/dt$ voltage loss causes the voltage across the positive and negative terminals of the module, V_{ab} , to drop by the same amount, (i.e. to $V_{CC} - L_s \cdot di/dt$). The snubber capacitors that were fully charged to V_{CC} now find

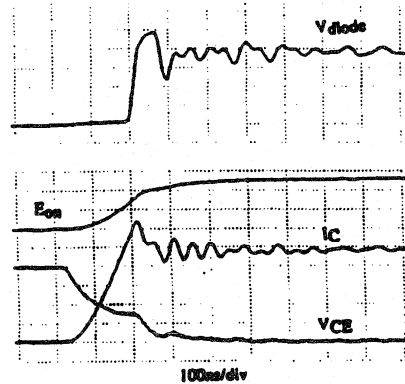


Figure 10 - turn-on waveforms with no RCD snubber protection

Tested at 400V, 100A, 25°C, $L_s=240nH$
 $V_G/R_G(on)=15V/33\Omega$
 $V_{CE}: 100V/div, I_C: 20A/div, V_{diode}: 100V/div, E_{on}: 1mJ/div$

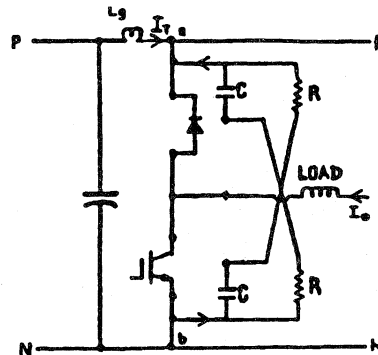


Figure 11 - equivalent circuit under turn-on conditions—low-side IGBT is switched on

a discharge path through the forward biased Free Wheel Diode (note that the FWD is on, freewheeling the load current), the IGBT and the snubber resistors. Figure 11 shows the equivalent circuit during turn-on. The snubber diodes are reverse biased and therefore not shown. The current paths are shown in the Figure. This snubber discharge current (I_{sn}) partially provides for the reverse recovery charge of the FWD. Thus, the total current seen by L_s is modified. This has a favorable effect on the magnitude of the reverse recovery voltage transient.

The waveforms shown in Figure 12 illustrate the snubber operation. Notice the complete elimination of the voltage transient, as well as reduction in the oscillations following turn-on. Another interesting fact is that this waveform was generated with R_G of 0.5Ω , which reduced the energy losses from 2.41 mJ in Figure 10 to 1.25 mJ, a savings of almost 50%. Therefore, this snubber not only clamps the turn-on voltage transient, it also enables the user to choose a value of R_G that produces minimal turn-on losses.

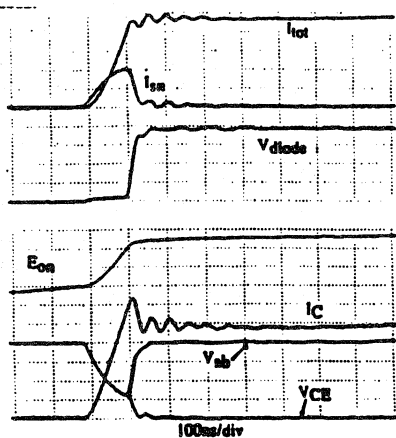


Figure 12 - turn-on waveforms with RCD snubber
 Tested at 400V, 100A, 25°C, $L_s=240nH$
 $V_G/R_G(on)=15V/0.5\Omega$, $C_{Sn}=0.22\mu F$, $R_{Sn}=12\Omega$
 V_{CE}/V_{diode} : 100V/div, $I_C/I_{sn}/I_{total}$: 20A/div, E_{on} : 0.5V/div,
 V_{ab} : 100V/div

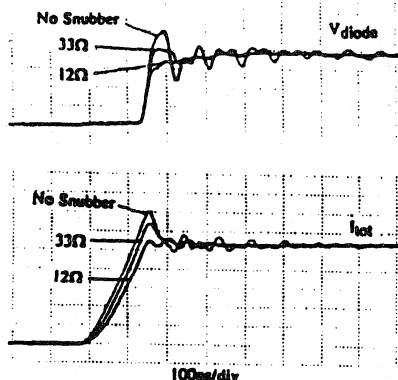


Figure 13 - effects of changing R_{Sn} values
 Tested at 400V, 100A, 25°C, $L_s=240nH$
 $V_G/R_G(on)=15V/33\Omega$, $C_{Sn}=0.22\mu F$, $R_{Sn}=12\Omega$, 33Ω
 V_{diode} : 100V/div, I_{total} : 20A/div

Figure 13 shows the effect of changing the snubber resistor (R_{Sn}) on turn-on waveforms. Lower R_{Sn} s provide for better snubbing action.

The value for the snubber components can be approximated from the expressions given below, based on circuit stray inductance (L_s), switching frequency (f_{sw}), maximum switching current (I_o), DC rail voltage (V_{CC}) and allowable peak voltage (V_{pk}). The derivations are show in Appendix II.

Snubber capacitor:

$$C_{Sn} = L_s \cdot I_o^2 / (V_{pk} - V_{CC})^2 \quad (1)$$

Snubber resistor:

$$R_{Sn} = 1 / (6 \cdot C_{Sn} \cdot f_{sw}) \quad (5)$$

Losses in snubber resistor:

$$PR = \frac{1}{2} \cdot C_{Sn} \cdot (V_{pk}^2 - V_{CC}^2) \cdot f_{sw} \quad (6)$$

The snubber diode should be of fast and soft recovery type to avoid severe oscillations following V_{pk} at turn-off. The resistor should be of non-inductive type to avoid oscillations at turn-on.

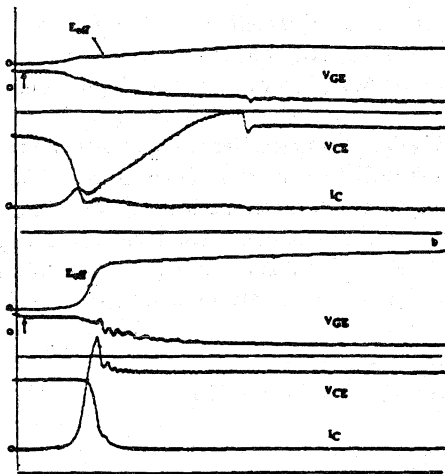
The charge-discharge circuit — Figure 6b

The charge-discharge snubber circuit in Figure 6b can be targeted for reducing turn-off dissipation in the IGBT. During IGBT turn-on, the snubber capacitor is fully discharged, and during turn-off it is fully charged. This circuit, unlike the one in Figure 6a, which essentially acts as a clamp, reduces the rate of rise of voltage across the IGBT at turn-off, imposing softer switching, and thereby reducing losses in the IGBT. The losses in the snubber are:

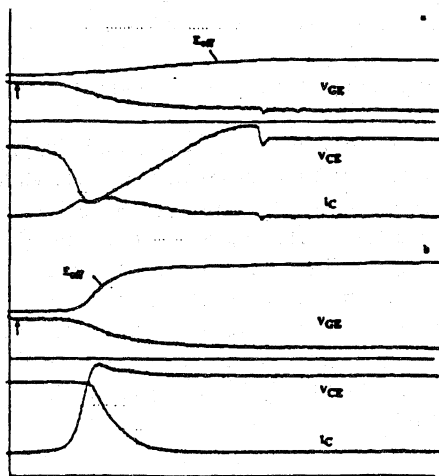
$$PR = \frac{1}{2} \cdot C_{Sn} \cdot V_{pk}^2 \cdot f_{sw} \quad (7)$$

As compared to (6), these losses are substantially higher.

Figures 14a and 14b show the results of testing a 150A 600V UltraFast™ IGBT module with and without a charge-discharge snubber. With a $0.5\mu F$ capacitor, the turn-off dv/dt was reduced from $3500V/\mu s$ to $300V/\mu s$, as shown in these Figures. As a result, turn-off losses were brought down from 11.2mJ to 3.4mJ (down 70%). The test was



Figures 14a, 14b -150A/600V UltraFast IGBT turn-off waveforms, with and without charge-discharge RCD snubber, respectively
 Tested at 340V, 150A, 125°C, 15V/39Ω,
 $C_{sn}/R_{sn}=0.5\mu F, 20\Omega$
 $V_{CE}: 100V/div, I_C: 50A/div, V_{GE}: 5V/div, E_{off}: 5mJ/div, Time scale: 400ns/div$



Figures 15a, 15b -150A/600V Fast IGBT turn-off waveforms, with and without charge-discharge RCD snubber, respectively
 Tested at 340V, 150A, 125°C, 15V/39Ω,
 $C_{sn}/R_{sn}=0.5\mu F, 20\Omega$
 $V_{CE}: 100V/div, I_C: 50A/div, V_{GE}: 5V/div, E_{off}: 5mJ/div, Time scale: 400ns/div$

repeated on a 150A, 600V low $V_{CE(sat)}$ -type module. The results are shown in Figures 15a and 15b. Again, savings were substantial as the turn-off losses decreased from 20mJ to 6.5mJ (down 68%),

due to slowing of the rate of rise of voltage. Low $V_{CE(sat)}$ -type IGBTs, due to their longer minority carrier lifetime, continue to incur higher turn-off losses under soft switching conditions, just as they do under hard switching conditions.

The reduction in turn-off losses directly depends on the load current, I_O . On the other hand, snubber losses depend predominantly on values of C_{sn} and V_{CC} , varying only marginally as the load current is increased (see equation 7). This is best demonstrated by the test results in Figure 16, which shows IGBT turn-off at much higher current (350A) with and without snubber. In terms of mJs per switching, the savings here were much more substantial (30mJ) than at 150A (13.5mJ). The snubber losses as given by (see equation 7) did not change much. Therefore, at higher currents, the savings in IGBT turn-off losses start to overshadow the losses in snubber circuit, making this circuit more applicable. Efficiency is greatly enhanced if an active feedback circuit is employed to return the trapped energy to the source.

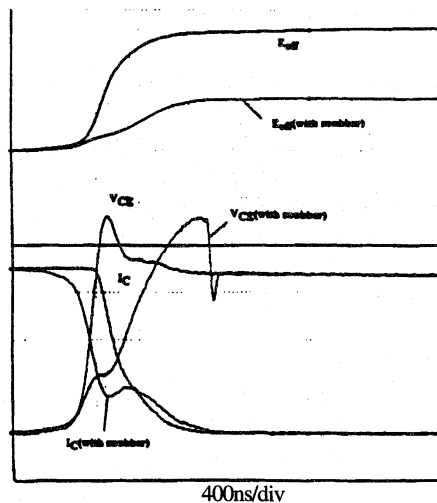


Figure 16 -150A/600V Fast IGBT turn-on waveforms, with and without charge-discharge RCD snubber
 Tested at 340V, 350A, 125°C, 15V/39Ω,
 $C_{sn}/R_{sn}=0.5\mu F, 33\Omega$
 $V_{CE}: 100V/div, I_C: 100A/div, E_{off}: 5mJ/div$

In bridge applications, the snubber capacitor across the opposite IGBT could produce extremely high shoot-through currents in the IGBT that is being turned on. The magnitude of this additional current could be as high as $V_{CC} \cdot [C_{sn}/L_s]^{1/2}$, with

the width of $\pi[C_{SN} \cdot L_s]^{1/2}$. Figure 17 shows turn-on waveforms with a 0.1 μ F snubber capacitor. The snubber-inflicted transients caused turn-on losses at 150A to increase from 9mJ to 16mJ. The impact of this additional current during turn-on becomes less severe as the load current is increased. In applications not involving bridge configurations (chopper circuits, for example), this charge-discharge snubber can be used with the consideration of turn-off stresses only. The freewheel diode can be effectively protected by a simpler RC snubber in such circuits [5].

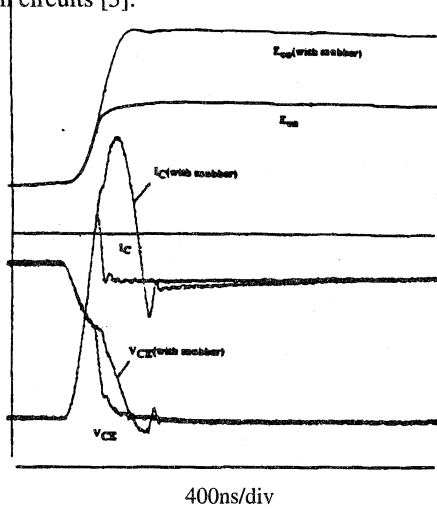


Figure 17 -150A/600V Fast IGBT turn-on waveforms, with and without charge-discharge RCD snubber
 Tested at 340V, 150A, 125°C, 15V/39Ω
 $C_{SN}/R_{sn}=0.1\mu F, 33\Omega$
 $V_{CE}: 100V/div, I_C: 50A/div, E_{off}: 5mJ/div$

Voltage transients during fault current turn-off

The short circuit current generated during fault conditions can be five to ten times the rated current. Shutting off such high currents too quickly can produce extremely high di/dts that are potentially detrimental to the IGBTs [6].

The snubber circuits discussed in the above section are not as practical when it comes to protecting transient voltage generated during short circuit conditions. As seen from equation (1), the required snubber capacitor value is proportional to the square of the device current. This means that the capacitor required will have to be 25 to 100 times larger than in normal switching operation. High-capacity, high-voltage snubber capacitors are large

and expensive, making the RCD scheme unattractive for high-current IGBT modules. Of equal importance, the snubber circuit connected at the terminals does not address the problem of the high-current module's internal L-di/dt voltage spike. More practical methods involve slowing the turn-off of the IGBTs under fault conditions, are discussed elsewhere [1].

Conclusions

The problem of switching voltage transients is an important subject that cannot be ignored, especially in applications using fast-switching IGBTs. This paper discussed principal protection circuits. Circuit operations were analyzed and the test results were illustrated. The following table summarizes the results.

Type	Advantages	Disadvantages
de-coupling capacitor	low snubber losses	
	directly and favorably affects turn-off and turn-on voltage stresses	
	newly available, module-compatible capacitors are more effective in limiting voltage transients	produces voltage and current oscillations in DC bus, forcing use of high RMS current limited snubber capacitors
more practical for lower current range		
discharge resistant de-coupling capacitor	low snubber losses	
	directly reduces turn-off voltage overshoots has a favorable effect on turn-on voltage transients	eliminates increased snubber inductance making protection less effective
	much quieter switching—snubber diode blocks oscillations	snappy diode could produce high recovery voltage spikes and dv/dts across IGBT/diode pair
more practical for medium current ranges		
RCD charge-discharge snubber circuit		very high snubber losses
	reduces turn-off voltage overshoots	requires more components
	could substantially reduce turn-off losses in transistor no oscillations in DC bus	increases turn-on losses in bridge configuration more complicated component selection
more practical for high-current, low bus voltage chopper applications		
RCD snubber-clamp circuit	Low snubber losses	
	directly reduces turn-off voltage overshoots favorable effect on turn-on voltage transients	
	no oscillations in DC bus	requires more components
most practical, especially for medium-high-current applications		

To recap, the module-compatible, high-frequency de-coupling capacitors were found to offer an optimal solution for low-current applications. The RCD snubber-clamp circuit was found to be the most effective and practical tool for medium- and high-current applications.

Appendix I

During short switching intervals, the inductive load current remains unchanged at I_o , as the main DC source and de-coupling capacitor supply it.

i.e., $is_n + is_p = I_o$ during switching (a)
where is_n is the de-coupling capacitor current and is_p is the current from the DC source.

Assuming ideal turn-on as the worst case for calculating snubber current, $is_w(0^-)=0$, $is_w(0^+)=I_o$, where is_w is the IGBT current.

Since is_p cannot change immediately, due to L_s , is_n supplies full load current initially. Under ensuing steady-state conditions, is_p supplies 100% of the load current.

That is:

$$\begin{aligned} is_n(0^+) &= I_o, is_p(0^+) = 0 & (b) \\ is_n(\text{inf.}) &= 0, is_p(\text{inf.}) = I_o & (c) \end{aligned}$$

The equations governing various circuit variables are:

$$\begin{aligned} V_{cc} &= L_s \cdot (di/dt) + V_{sn} + is_n \cdot ESR & (d) \\ di/dt + disp/dt &= 0 \text{ (from (a))} & (e) \\ is_n &= -C \cdot dV_{sn}/dt & (f) \end{aligned}$$

assuming that ESR of the high-frequency de-coupling capacitor constitutes most of the circuit stray resistance. Upon solving (d), (e) and (f) with the initial conduction (b) and (c), we get,

$$is_n = e^{-\alpha t} \cdot I_o \cos(\beta t) \quad (2)$$

At the point of turn-off we have:

$$\begin{aligned} is_n(0^+) &= -I_o, is_p(0^+) = I_o & (g) \\ is_n(\text{inf.}) &= 0, is_p(\text{inf.}) = 0 & (h) \end{aligned}$$

assuming ideal switching.

The equation remains the same as before, and we have

$$is_n = -e^{-\alpha t} \cdot I_o \cos(\beta t) \quad (\text{note the sign change})$$

i.e. $is_n(\text{off}) = -is_n(\text{on})$.

The total capacitor current is:

$$\begin{aligned} I_{rms} &= \sqrt{2T/T_{sw} \int (1/t) \cdot (is_n^2) dt} \\ &= \sqrt{2/T_{sw} \cdot \int [I_o \cdot e^{-\alpha t} \cos(\beta t)]^2 dt} \\ &= I_o \sqrt{1/T_{sw} \cdot \int [e^{-2\alpha t} (1 + \cos(2\beta t))] dt} \\ &= I_o \sqrt{1/(2\alpha T_{sw}) \cdot [1 + \alpha^2/(\alpha^2 + \beta^2)]} \end{aligned}$$

where $\alpha = ESR/2L_s$ and $\beta = \sqrt{[4/L_s C_{sn} - (ESR/2L_s)^2]}$
 $I_{rms} = I_o \sqrt{[f_{sw} \cdot (L_s/R + RC/4)]}$, $f_{sw} = 1/T$,
As $L_s/R \gg RC/4$

$$I_{rms} = I_o \sqrt{(f_{sw} \cdot L_s/R_s)} \quad (3)$$

The power loss in the ESR are:

$$\begin{aligned} Pr &= ESR \cdot I_{rms}^2 = f_{sw} \cdot L_s I_o^2 \\ &= 2 \cdot (1/2 \cdot L_s \cdot I_o^2) \cdot f_{sw} & (4) \end{aligned}$$

[$1/2 \cdot L_s \cdot I_o^2$ being the energy stored in L_s]

Appendix II

The expression (1), (5) and (6) are derived as follows:

At turn-off (see Figure 6a) as one of the two conducting IGBTs is gated off, collector-to-emitter voltage $v_{ce}(t)$, rises to the DC bus voltage V_{CC} . Beyond this point, load current freewheels through the diode across the other IGBT. The stray inductances (L_s), however, prolong the flow of current in the 'DC loop.' Two components of currents make up for the current $i(t)$ in L_s . They are IGBT turn-off current ($i_C(t)$) and the snubber current ($is_n(T)$), as marked in Figure 7.

For simplicity of calculations, it is assumed that the IGBT turns off instantly, i.e., $is_n(t) = i(t)$. This assumption is justified on the grounds that it only renders somewhat conservative the estimate of snubber capacitor value.

The equations governing various circuit variables are:

$$\begin{aligned} v_{ce}(t) &= V_{CC} + 1/C \int i(t) dt \\ \text{i.e., } V_{CC} - v_{ce}(t) &= -1/C \cdot \int i(t) dt & (a) \end{aligned}$$

$$v_{ce}(t) = V_{CC} - L \cdot di(t)/dt$$

$$\text{i.e., } di(t)/dt = [VCC - v_{ce}(t)]/L_s \quad (b)$$

From (a) and (b)

$$di(t)/dt = -1/L_s C \cdot i(t) dt \quad (c)$$

The following is the solution to the above equation:

$$i(t) = I_o \cdot \cos(t/\sqrt{L_s C}) \quad (d)$$

Where I_o is the load current at turn-off. The current is this a cosine function. In Figure 7 it can be observed that the combination of $i_C(t)$ and $I_{SN}(t)$ does follow cosine wave shape.

Differentiating (d),

$$di(t)/dt = -I_o/L_s C \cdot \sin(t/\sqrt{L_s C}) \quad (e)$$

From (b) and (e),

$$v_{ce}(t) = VCC + I_o \cdot \sqrt{L_s C} \cdot \sin(t/\sqrt{L_s C}) \quad (f)$$

v_{ce} is at maximum when $t/\sqrt{L_s C} = \pi/2$.

Therefore,

$$VCM = \text{maximum desired voltage across IGBT}$$

$$VCM = VCC + I_o \cdot \sqrt{L_s C} \quad (g)$$

From (g),

Snubber capacitor

$$C_{SN} = L_s \cdot I_o^2 / [VCM - VCC]^2 \quad (l)$$

The snubber capacitor is therefore charged to VCM at the end of turn-off. Before the next turn-off event, i.e. $1/f_{SW}$ later, C_{SN} should discharge back to its initial value of VCC. The snubber resistor (R_{SN}) selected according to the following expression fulfills the above requirement.

$$R_{SN} = 1/(6 \cdot C_{SN} \cdot f_{SW}) \quad (5)$$

The losses in R_{SN} at turn-off are therefore given by:

$$PR(\text{off}) = [1/2 \cdot C_{SN} \cdot (V_{pk}^2 - VCC^2)] \cdot f_{SW} \quad (f)$$

At turn-on (see Figures 11 and 12), as the IGBT is turned on, the switching $di(t)/dt$ causes voltage at module terminals $v_{ab}(t)$ to drop from its initial value of VCC to an amount equal to $L_s \cdot di/dt$. As explained in the article, this causes the snubber capacitors to discharge through R_{SN} s.

For simplicity, it is assumed that the turn-on di/dt is linear. It is further assumed that the peak turn-on current is 25% above the load current I_o at the switching instant. These assumptions will result in conservative estimates of snubber losses.

The snubber discharge current is:

$$i_{SN}(t) = [VCC - V_{ab}]/R_{SN} \quad (g)$$

where

$$V_{ab} = VCC - L_s \cdot di/dt \quad (h)$$

where

$$di/dt \text{ (a constant)} = di/dt = 0.9I_o/t_r \quad (i)$$

t_r is the rise time, specified under inductive load conditions. From (g), (h) and (i),

$$i_{SN}(t) = I_{SN} = [L_s \cdot 0.9I_o/t_r]/R_{SN}$$

$$I_{SN} = 0.9 \cdot L_s \cdot I_o / (t_r \cdot R_{SN}) \quad (j)$$

The losses in R_{SN} at turn-on are,

$$PR(\text{on}) = [0.9 \cdot L_s \cdot I_o / t_r \cdot R_{SN}]^2 \cdot R_{SN} \cdot T \cdot f_{SW} \quad (k)$$

where T, the snubber discharge time, is approximated to be interval between the beginning of the current rise and the point where current reaches its peak value ($=1.25I_o$).

$$T = 1.25I_o / [0.9I_o/t_r] = 1.39t_r \quad (l)$$

Combining (k) and (l),

$$PR(\text{on}) = [1.125 \cdot L_s^2 \cdot I_o^2 / (t_r \cdot R_{SN})] \cdot f_{SW} \quad (m)$$

From (f) and (m),

$$PR = [1/2 \cdot C_{SN} \cdot (V_{pk}^2 - VCC^2) + 1.125 \cdot L_s^2 \cdot I_o^2 / (t_r \cdot R_{SN})] \cdot f_{SW}$$

The second half of the above expression is an insignificant part of the total and can be neglected. The total losses in snubber resistor are, therefore,

$$PR = 1/2 \cdot C_{SN} \cdot (V_{pk}^2 - VCC^2) \cdot f_{SW} \quad (6)$$

References:

- [1] R. Chokhawala, S. Sobhani 'Switching Voltage Transient Protection Schemes for High Current IGBT Modules,' APEC-IEEE Conf., February 1994
- [2] Harald Vetter, 'High Performance Capacitors for Low-Inductance Circuits' Power Conversion, June 1991
- [3] International Rectifier Applications Note AN-983. 'IGBT Characteristics and Applications' by S. Clemente, A Dubhashi, B. Pelly
- [4] C. Aniceto, R. Letor, B. Ishan, 'How Short Circuit Capabilities Govern the Desired Characteristics of IGBTs,' Power Conversions Conf., April 1992
- [5] R. Chokhawala, E. Carroll, 'A Snubber Design Tool for P-N Junction Reverse Recovery Using a More Accurate Simulation of the Reverse Recovery Waveform,' IAS-IEEE Conf., October 1989
- [6] R. Chokhawala, J. Catt, L. Kiraly, 'A Discussion on IGBT Short Circuit Behavior and Fault Protection Schemes,' APEC-IEEE Conf., March 1992
- [7] Tore, Underland et al, 'A Snubber Configuration for both Power Transistors and GTO PWM Inverters', IEEE Conf. 1984

Switching Voltage Transient Protection Schemes for High Current IGBT Modules

Rahul Chokhawala

Saed Sobhani

Abstract - The emergence of high current and faster switching IGBT modules has made it imperative for designers to look at ways of protecting these devices against detrimental switching voltage transients that are a common side effect of these efficient transistors. This paper will discuss protection criteria for both normal switching operation and short circuit operation and will cover in detail some of the protection schemes that were designed to address these problems.

Introduction

When a power device is abruptly turned off, trapped energy in the circuit stray inductance is dissipated in the switching device, causing a voltage overshoot across the device. The magnitude of this transient voltage is proportional to the amount of stray inductance and the rate of fall of turn-off current. Large IGBT modules switch high magnitudes of currents in a short duration of time, giving rise to potentially destructive voltage transients. These higher current modules normally consist of several IGBT chips in parallel. Each individual chip switches its share of the load current at a di/dt that is determined by the gate drive circuit. The total current and di/dt seen by the external power circuit is the sum of currents and di/dts through each IGBT chip. The situation is at its worst when a short circuit current is rapidly turned off to protect the IGBT. The di/dts produced could easily be a few thousand A/ μ s. If proper attention is not paid to minimize resulting switching voltage transients, any attempt to save IGBTs by shutting them down under fault conditions may destroy the device.

This paper discusses various protection schemes. A transient voltage protection scheme optimized to protect IGBTs during normal switching operation may not protect the IGBTs under fault current shut-off processes. Separate schemes would normally be required to achieve both goals.

It is determined that snubbers and clamps offer optimized protection against voltage transients during normal switching operation. Operation of an RCD clamp circuit is described in detail. As illustrated in Figure 1, protection circuits allow faster, yet safer, operation by containing operating loci with the boundaries of the rated Safe Operating Area (SOA).

Fault current shut-off transients are more effectively protected by considerably slowing the rate of fall of fault current. Two novel protection schemes are introduced which protect IGBTs from potentially destructive voltage transients by slowing the rate of fall of fault current only under fault conditions. Circuit operations are analyzed and the test results are illustrated. Usefulness of an active clamp is also discussed in this section.

Voltage transients during normal switching operation

As mentioned earlier, the magnitude of transient voltage depends on the trapped energy in the circuit stray inductance, also called 'DC loop' inductance LS . As a preventive measure, steps should be taken to improve the circuit layout. Using copper plates separated by a thin sheet of insulating material, tightening the 'DC loop' and

choosing source capacitance with inherently low self-inductance are ways to lower stray inductances [1]. De-coupling capacitors connected across the module terminals can also be used to achieve this goal. High-frequency polypropylene capacitors designed for low internal lead inductance are found to be effective. Care should be taken in the selection of the de-coupling capacitor value to avoid oscillations in the DC loop which otherwise may result in excessive heating in the high-frequency capacitors. For modules rated up to 100A, de-coupling capacitors may provide optimal protection against voltage transients during normal switching.

One other way to prevent high-voltage transients from occurring is to slow the switching process by choosing a greater value of gate resistor. While this is an attractive method for fault current turn-off protection, it is not practical for protection against voltage transients during normal switching operation, as the efficiency of these devices is adversely affected. In the following discussion, more efficient ways of protecting devices will be presented.

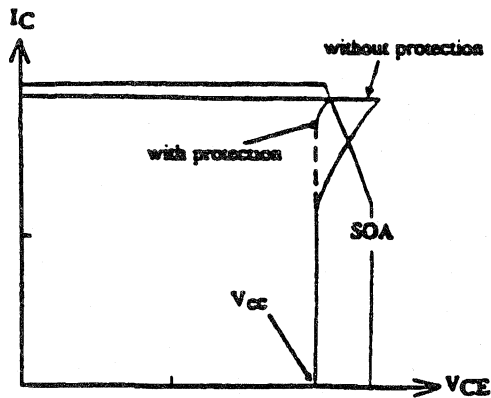


Figure 1 - Rated SOA curve and operating loci with and without switching voltage transient protection circuit

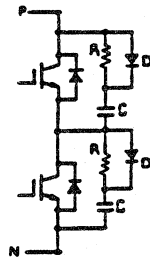


Figure 3. - RCD charge/discharge snubber

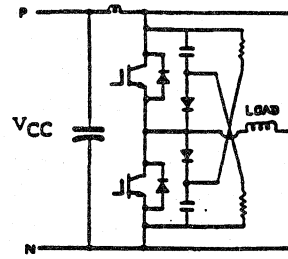


Figure 2. - RCD voltage clamp

RCD snubber and clamp circuits

Figures 2 and 3 are two examples of RCD snubbers for high-current IGBT applications. While both circuits are employed to reduce transient voltages across switching devices, the charge-discharge snubber circuit in Figure 3 is targeted also for reducing IGBT turn-off losses. During IGBT turn-on, the snubber capacitor is fully discharged, and during turn-off, it is charged. This circuit, unlike the circuit in Figure 2, which essentially acts as a clamp, reduces the rate of rise of voltage across the IGBT at turn-off, imposing softer switching and therefore reducing losses in the IGBT. The losses in the snubber, however, are substantially increased and are equal to $\frac{1}{2} \cdot C \cdot V_{pk}^2$, where V_{pk} is the voltage across the snubber capacitor at the end of the turn-off process and is equal to the DC bus plus an allowable overshoot voltage.

Due to the dual purpose that the circuit in Figure 3 serves, the trade-offs involved are complex. Since this paper concentrates only on switching voltage transient protection, discussion will be focused on the circuit in Figure 2. The effects of this snubber on turn-off and turn-on will be discussed separately in the following sections.

Turn-off

The RCD clamp of Figure 2 acts as a voltage clamp. During the IGBT conduction period, the snubber capacitors are charged to the bus voltage. As the IGBT is turned off, the voltage across it, V_{CE} , rises rapidly. The circuit 'DC loop' stray inductance, L_s , may cause V_{CE} to rise above the bus voltage. As this occurs, the snubber diode is forward biased and the snubber is activated. The

energy trapped in the stray inductance now is diverted to the snubber capacitor, which absorbs this incremental energy without substantial rise in its voltage. The waveforms shown in Figure 4 illustrate turn-off behavior with and without the RCD clamp. The voltage overshoot has been substantially reduced from 210 Volts to 50 Volts. Initially, a small stray inductance in the snubber circuit causes VCE to peak slightly above VCC.

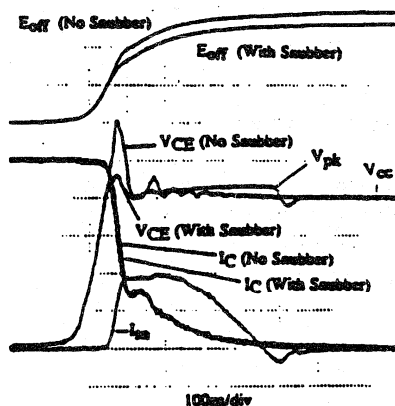


Figure 4 - Turn-off waveforms with and without RCD snubber. Tested at: 400V, 100A, 25°; $L_s = 100\text{nH}$, $V_G/R_{G(\text{off})} = -8\text{V}/33\Omega$; $C_{sn} = 0.22\text{nF}$, $R_{sn} = 12\Omega$; $V_{CE}: 100\text{V}/\text{div}$, $I_C/I_{sn}: 20\text{A}/\text{div}$, $E_{\text{off}}: 2\text{mJ}/\text{div}$

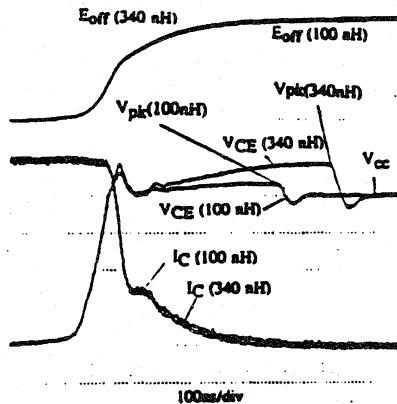


Figure 5 - Turn-off waveforms with RCD snubber for 2 different L_s values (100nH, 340nH). Tested at: 400V, 100A, 25°; $L_s = 100\text{nH}$, $V_G/R_{G(\text{off})} = -8\text{V}/33\Omega$; $C_{sn} = 0.22\text{nF}$, $R_{sn} = 12\Omega$; $V_{CE}: 100\text{V}/\text{div}$, $I_C/I_{sn}: 20\text{A}/\text{div}$, $E_{\text{off}}: 2\text{mJ}/\text{div}$

Figure 5 displays the waveforms generated for the two different stray inductances (100nH, 340nH). As illustrated in the Figure, the initial VCE peak — which is dependent on the stray inductance within the snubber circuitry — is the same for the two cases. The final voltage peak (V_{pk}) for the higher inductance does reach a higher value, as expected, since there is more trapped energy ($\frac{1}{2} \cdot L_s \cdot I^2$) diverted to the same snubber capacitor. This value, however, is well within the voltage rating of the device, and only marginally influences the losses in the IGBT, since it occurs when the current has reached a smaller value. The V_{pk} magnitude can be calculated from the formulae given in the following section.

Turn-on

Figure 6 displays the turn-on waveforms for an unprotected IGBT with a gate resistor (R_G) of 5.1Ω. The rapid rise in the IGBT current (1200 A/μs) combined with the circuit stray inductance (300nH), caused the FWD to go through a severe reverse recovery process. As seen in the Figure, the FWD recovery voltage (=630V) actually exceeded the rated voltage of the module.

In order to bring this voltage down to a safe value, the turn-on di/dt was reduced by using a higher R_G . The results are shown in Figure 7. The increase in R_G , however, greatly increased switching losses, as expected [2], [3].

The RCD clamp shown in Figure 2 is also effective in reducing turn-on voltage transients. As the IGBT current rises, the $L_s \cdot \text{di}/\text{dt}$ voltage loss causes the voltage across the positive and negative terminals of the module, V_{ab} , to drop by the same amount (i.e. to $V_{CC} - L_s \cdot \text{di}/\text{dt}$). The snubber capacitors that were fully charged to V_{CC} now find a discharge path through the forward biased freewheel diode (note that the FWD is on, free-wheeling the load current), the IGBT and the snubber resistors. Figure 8 shows the equivalent circuit during turn-on. The snubber diodes are reverse biased and, therefore, not shown. The current paths are shown in the Figure. This snubber

discharge current (I_{sn}) partially provides for the reverse recovery charge of the FWD, thus the total current seen by L_s is modified. This has a favorable effect on the magnitude of the reverse recovery voltage transient.

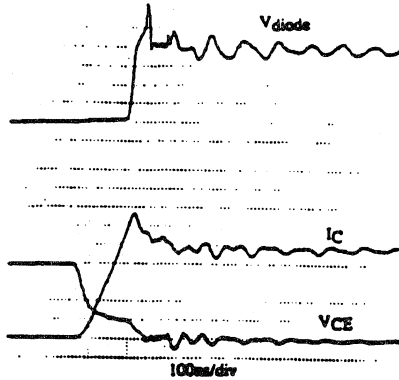


Figure 6 - Turn-on waveforms without RCD snubber. Tested at: 400V, 100A, 25°; $L_s = 240nH$, $V_G/R_{G(on)} = 15V/5.1\Omega$ $V_{CE}: 100V/div$, $I_C: 20A/div$, $V_{diode}: 100V/div$

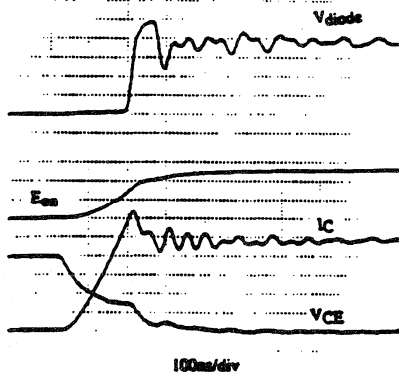


Figure 7 - Turn-on waveforms without RCD snubber. Tested at: 400V, 100A, 25°; $L_s = 240nH$, $V_G/R_{G(on)} = 15V/33\Omega$ $V_{CE}: 100V/div$, $I_C: 20A/div$, $V_{diode}: 100V/div$; $E_{on}: 1mJ/div$

The waveforms shown in Figure 9 illustrate the snubber operation. Note the complete elimination of the voltage transient and reduction in the oscillations following turn-on. Another interesting fact is that this waveform was generated with R_G of 0.5Ω , which reduced the energy losses from 2.41mJ in Figure 7 to 1.25mJ, a savings of almost 50%. Therefore, this snubber not only

clamps the turn-on voltage transient, but also enables the user to choose a value of R_G that produces minimal turn-on losses.

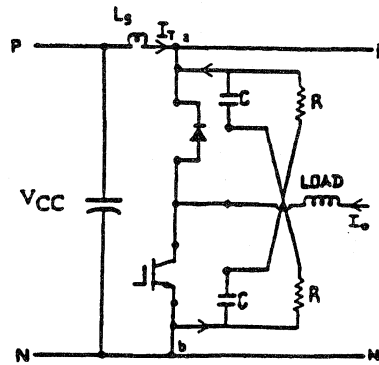


Figure 8 - Equivalent circuit under turn-on conditions. Low-side IGBT is switched on

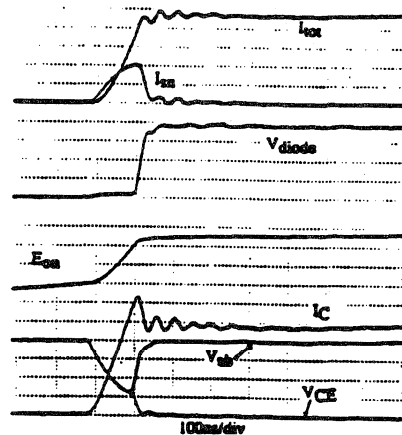


Figure 9 - Turn-on waveforms with RCD snubber. Tested at: 400V, 100A, 25°; $L_s = 240nH$, $V_G/R_{G(on)} = 15V/0.5\Omega$, $C_{sn} = 0.22\mu F$, $R_{sn} = 12\Omega$ $V_{CE}/V_{diode}: 100V/div$, $I_C/I_{sn}/I_{total}: 20A/div$, $E_{on}: 0.5mJ/div$; $V_{ab}: 100V/div$

Figure 10 shows the effect on turn-on waveforms of changing the snubber resistor (R_{sn}). Lower R_{sn} s provide for better snubbing action. The value for the snubber components can be approximated from the expressions give below, based on circuit stray inductance, L_s ; switching frequency, f_{sw} ; maximum switching current, I_O ; turn-on current rise time, t_r ; DC rail voltage, V_{CC} ; and allowable peak voltage, V_{pk} (Appendix I).

Snubber capacitor:

$$C_{sn} = L_s \cdot I_o^2 / (V_{pk} - V_{CC})^2 \quad (1)$$

Snubber resistor:

$$R_{sn} = 1 / (6 \cdot C_{sn} \cdot f_{sw}) \quad (2)$$

Losses in snubber resistor:

$$PR = [\frac{1}{2} \cdot C_{sn} (V_{pk}^2 - V_{CC}^2) + 1.125 \cdot L_s^2 \cdot I_o^2 / (t_r \cdot R_{sn})] \cdot f_{sw} \quad (3)$$

The snubber diode should be of fast and soft recovery type to avoid severe oscillations following V_{pk} at turn-off. The resistor should be of non-inductive type to avoid oscillations at turn-on.

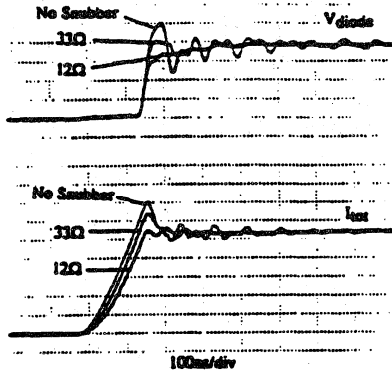


Figure 10 - Effects of changing R_{sn} values.

Tested at: 400V, 100A, 25°; $L_s = 240nH$,
 $V_G/R_{G(on)} = 15V/33\Omega$, $C_{sn} = 0.22\mu F$, $R_{sn} = 12\Omega, 33\Omega$
 $V_{diode} = 100V/div$, $I_{total} = 20A/div$

Voltage transients during fault current turn-off

The short circuit current generated during fault conditions can be five to ten times the rated current. Shutting off such high currents too quickly can produce extremely high di/dts that are potentially detrimental to the IGBTs [4].

The RCD clamp circuit discussed in the above section is not as practical when it comes to protecting transient voltages generated during short circuit conditions. As seen from the above expressions, the required snubber capacitor value is proportional to the square of the device current. This means that the capacitor required will have to be 25 to 100 times larger than in normal switching operation. High-capacity, high-voltage snubber capacitors are large and expensive, making the RCD scheme unattractive for high-current IGBT

modules. Also, voltage clamps connected external to the modules do not address the problem of internal inductive voltage spike. In the following sections, more practical methods are discussed, involving slowing the IGBTs' turn-off under fault conditions.

The IGBT fault current rate can be reduced by slowing the turn-off gate voltage signal. The simplest way of achieving this is to increase the gate resistor, but this is inefficient, since the trade-off is increased switching losses during normal conduction. In order to address this problem, two novel circuits are introduced that, through electronic gate control, effectively decrease the V_{GE} rate of fall only when a fault current is sensed, thereby avoiding any losses during normal switching operation. The first of these circuits uses a resistive method and the other uses a capacitive method. In the resistive method, a considerably higher-value gate resistor is switched in series with the IGBT gate. In the capacitive method, a considerably higher-value external capacitor is switched in parallel with the IGBT gate input capacitance.

Resistive method

The circuit in Figure 11 is composed of de-sat sense diode D1 and a P-channel MOSFET to switch-in higher value of resistor, R_{G2} , upon occurrence of a fault. Initially, when the IGBT is in the off state, the P-MOSFET is turned off. During normal turn-on, a step rise in voltage is applied to the IGBT gate through R_{G1} and the inherent body diode of the P-MOSFET. As V_{CE} , after a normal

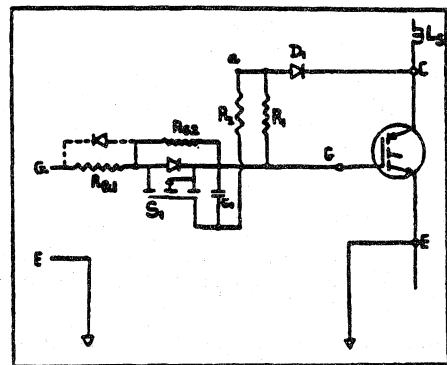


Figure 11 - Circuit for the resistive method

turn-on delay period, drops to its low on-state level, diode D1 is forward biased, and input capacitance of the P-MOSFET starts to charge. During normal conduction, therefore, the P-MOSFET remains gated on.

During normal turn-off operation, the gate drive output voltage is switched to its low state. The P-MOSFET gate capacitance begins to discharge. The values of C1, R1 and R2 are adjusted such that the MOSFET is kept on, at least until the IGBT turn-off is completed (for example, 1 μ s). Therefore, the IGBT turn-off losses are not affected.

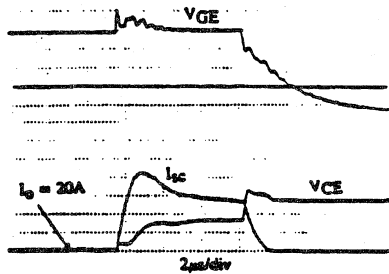


Figure 12 - Short circuit waveforms with resistive protection scheme for Fault Under Load conditions
 Tested at: 280V, 25°C; $L_s = 240\text{nH}$, $V_G/RG1 = -8\text{V}/33\Omega$
 $V_{CE} = 100\text{V}/\text{div}$, $V_{GE} = 5\text{V}/\text{div}$, $I_{sc} = 200\text{A}/\text{div}$

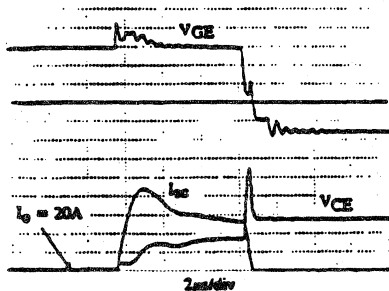


Figure 13 - Short circuit waveforms *without* resistive protection scheme for Fault Under Load conditions
 Tested at: 280V, 25°C; $L_s = 240\text{nH}$, $V_G/RG1 = -8\text{V}/33\Omega$
 $V_{CE} = 100\text{V}/\text{div}$, $V_{GE} = 5\text{V}/\text{div}$, $I_{sc} = 200\text{A}/\text{div}$

Fault under load

When a fault occurs during normal conduction, diode D1 goes into blocking mode, and the P-MOSFET input capacitance starts to discharge through resistors R1 and R2. The MOSFET is turned off as its gate voltage drops below the threshold value. Thereafter, the V_{GE} rate of fall is reduced significantly, as the discharge is now forced to take place through R_{G2} . The fault current fall rate is decreased accordingly. Note that if the IGBT is turned off while the MOSFET is still on, the circuit will not be effective, since R_{G2} is bypassed. This consideration placed an upper limit on the discharge time constant of the MOSFET (approx. 5 μ s).

Figures 12 and 13 display short circuit switching waveforms with and without the protection circuit. The initial current through the IGBT is 40A. When a fault occurs, the current initially shoots up to 800A, but settles down to 600A once the Miller effect on gate voltage is diminished (see gate waveforms). The MOSFET discharge time constant was adjusted to be $2.5\mu\text{s} [(r1+r2) \cdot (C_{iss}+C1)]$. Fault current was turned off after 6 μ s. The IGBT gate discharge rate was considerably slowed by the addition of R_{G2} (200 Ω), thereby reducing voltage overshoot from 270V to 60V.

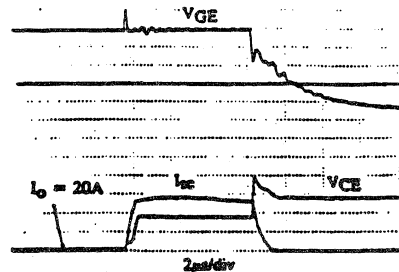


Figure 14- Short circuit waveforms with resistive protection scheme for Fault Under Load conditions with bypass diode across R_{G1}
 Tested at: 280V, 25°C; $L_s = 240\text{nH}$, $V_G/RG1 = -8\text{V}/0\Omega$
 $V_{CE} = 100\text{V}/\text{div}$, $V_{GE} = 5\text{V}/\text{div}$, $I_{sc} = 200\text{A}/\text{div}$

The Miller effect can be filtered out by bypassing R_{G1} with a diode. The IGBT gate voltage is now clamped to the gate drive output voltage. Figure 14 displays the resulting waveforms. Compare the results to Figure 12 (same protection circuit without the R_{G1} bypass diode).

The initial surge of current is eliminated. The slight increase in turn-off voltage overshoot (since RG1 is now bypassed during IGBT turn-off) can be compensated for by readjusting RG2 value.

Hard fault

This is the case where the device turns on directly into a fault and, therefore, the MOSFET is never turned on. Thus, the discharge path for VGE is through RG2. Figures 15 and 16 show the waveforms with and without the protection circuit. The voltage overshoot was reduced from 190V to only 10V. Note that this circuit increases the effective gate bias impedance during IGBT off time. This effect imposes an upper limit on RG2, the value of which is governed by the IGBT's characteristics and gate bias voltage.

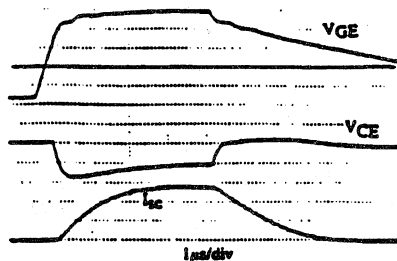


Figure 15- Short circuit waveforms with resistive protection scheme for Hard Fault condition
Tested at: 400V, 25°C; $L_s = 240\text{nH}$, $V_G/RG1 = -8\text{V}/33\Omega$
 $V_{CE}: 100\text{V}/\text{div}$, $V_{GE} = 5\text{V}/\text{div}$, $I_{sc}: 200\text{A}/\text{div}$

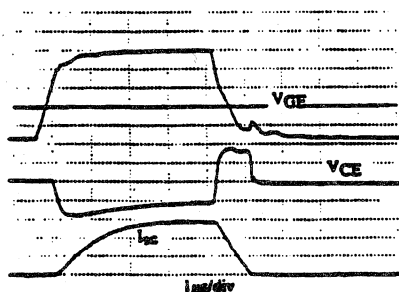


Figure 16- Short circuit waveforms without protection scheme for Hard Fault condition
Tested at: 400V, 25°C; $L_s = 240\text{nH}$, $V_G/RG1 = -8\text{V}/33\Omega$
 $V_{CE}: 100\text{V}/\text{div}$, $V_{GE} = 5\text{V}/\text{div}$, $I_{sc}: 200\text{A}/\text{div}$

Capacitive method

The circuit in Figure 17 is composed of desat diode D1, used to sense a fault condition, and an N-channel MOSFET to switch in a higher value of capacitor, C1, in parallel with the IGBT input capacitance upon occurrence of a fault.

During normal turn-on, after the normal turn-on delay, VCE drops to its low on-state level and diode D1 is forward biased. The MOSFET gate charge time constant $[(RG+R1+R2) \cdot R3 \cdot (C_{iss}+C3) / (RG+R1+R2+R3)]$ is adjusted such that it is not turned on prior to the IGBT turning on (e.g., 1ms). Therefore, during the conduction period, the MOSFET is in its off state. Zener diode Z2 is selected to offset large VCE(on) voltages. False triggering of the MOSFET is therefore prevented. When the gate drive is switched to its off state to turn the IGBT off, the MOSFET remains turned off. The normal switching operation is, therefore, not affected by the existence of this protection circuit.

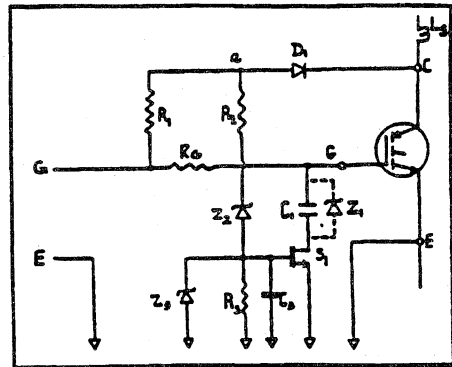


Figure 17 - circuit for the capacitive method

Fault under load

Once a fault occurs, the sense diode becomes reverse biased and the MOSFET gate input capacitance is charged by the gate drive power, through the voltage divider provided by RG, R1, R2 and R3. When the MOSFET turns on, capacitor C1 is switched in in parallel with the IGBT input capacitance. A drop is seen in the IGBT gate voltage since some charge is removed to charge the capacitor C1, which was initially

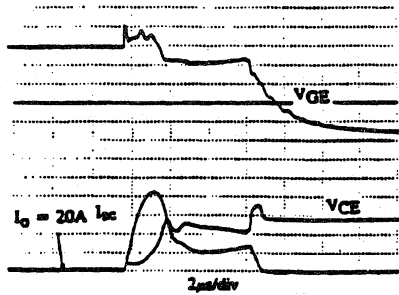


Figure 18- Short circuit waveforms *with* capacitive protection scheme for Fault Under Load condition
 Tested at: 280V, 25°C; $L_s = 240\text{nH}$, $V_G/R_{G(off)} = -8\text{V}/33\Omega$
 $V_{CE}: 100\text{V}/\text{div}$, $V_{GE} = 5\text{V}/\text{div}$, $I_{SC}: 200\text{A}/\text{div}$

charged to the off-bias voltage. This, in turn, lowers the value of the I_{SC} momentarily, reducing the energy losses during the short circuit period. The IGBT discharge time constant has increased, since it now includes capacitor C1 in parallel with the IGBT input capacitance. The fault current turn-off di/dt is therefore slowed, and the transient voltage is brought down substantially. Figure 18 shows the waveforms for the IGBT with the protection circuit. Compare this to the waveforms in Figure 13 without the protection circuit. Once again, turn-off voltage overshoot was reduced from 270V to 60V.

Hard fault

The operation of this protection circuit under hard fault is the same as described above.

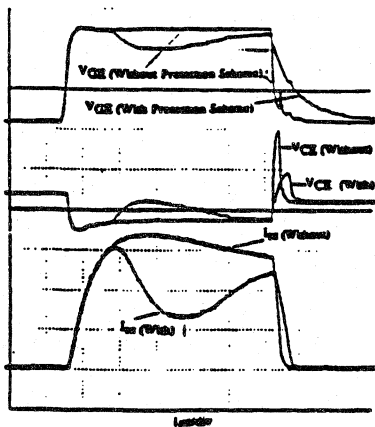


Figure 19- Short circuit waveforms *with and without* capacitive protection scheme for Hard Fault condition
 Tested at: 340V, 25°C; $L_s = 240\text{nH}$, $V_G/R_{G(off)} = -8\text{V}/33\Omega$
 $V_{CE}: 100\text{V}/\text{div}$, $V_{GE} = 10\text{V}/\text{div}$, $I_{SC}: 200\text{A}/\text{div}$

The upper limit of the MOSFET's gate charge time constant should be adjusted such that the MOSFET is fully turned on before the fault current is turned off (e.g. in less than 5 μs). Figure 19 displays the waveforms with and without the protection circuitry. As seen from the Figure, the voltage overshoot was brought down from 160V to 50V.

The functional usefulness of the circuit in Figure 17 can be increased by the simple addition of zener diode Z1 across capacitor C1 (indicated in the Figure). The circuit now serves the dual purpose of preventing turn-off voltage transient, as well as limiting fault current amplitude. The complete discussion on such a fault current limiting circuit is presented elsewhere [5].

Active voltage clamp

The circuit in Figure 20 contains avalanche diode Z1 in series with blocking diode D1, connected between the IGBT collector and gate. The avalanche diode is selected such that its voltage rating is less than the maximum allowable voltage at the IGBT module terminals. If this voltage limit is exceeded at turn-off, the avalanche current I_{Z1} in $R_{G(off)}$ would raise the gate-emitter voltage above its threshold level, therefore maintaining the IGBT in the conducting state. This feedback mechanism clamps V_{CE} to a safe value. The rate of decay of I_C is then equal to $(V_Z \cdot V_{CC})/L_s$, where V_Z is the clamp voltage and V_{CC} is the DC bus voltage. Figure 21 illustrates the operation of this clamp circuit. For comparison, results obtained without this protection circuit are shown in Figure 22. The peak turn-off voltage across 600V-rated IGBTs was reduced from 580V to a safer 460V.

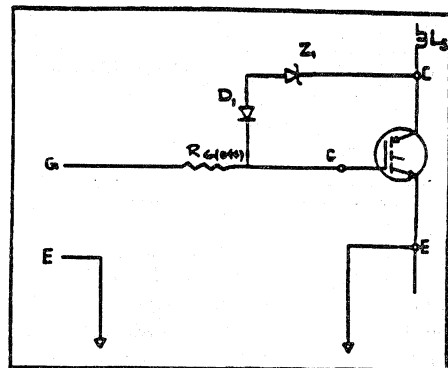


Figure 20 - circuit for zener clamp protection scheme

While the previously discussed (resistive and capacitive) circuits are activated immediately upon commencement of a fault, the circuit presently under consideration reacts only at turn-off. A slight delay in re-gating of the IGBT would result in potentially dangerous voltage spike. It was found that the combined junction capacitances of Z1 and D1, if high enough, speeds charging of the IGBT gate by providing a dV_{CC}/dt feedback. At the same time, these capacitances, if too high, would noticeably contribute to the adverse Miller effect under normal operating conditions. Proper selection of these components is, therefore, crucial to assure successful operation of this circuit. Also note that the value of $R_{G(off)}$, if too low, will make operation of this circuit less effective.

Except for unclamped inductive load applications, this circuit is not appropriate to protect against voltage transients during normal switching operation, as substantial losses are incurred in the IGBT due to operation of the voltage clamp. The losses per pulse are given by the following equation: $P_{SW} = \frac{1}{2} \cdot I_0^2 \cdot L_s \cdot [V_Z / (V_Z - V_{CC})] \cdot f_{sw}$

The value $\frac{1}{2} \cdot I_0^2 \cdot L_s$ is the energy trapped in the 'DC loop' stray inductance. For V_Z of 550V and V_{CC} of 400V, the additional losses per pulse in the IGBT are almost four times that value.

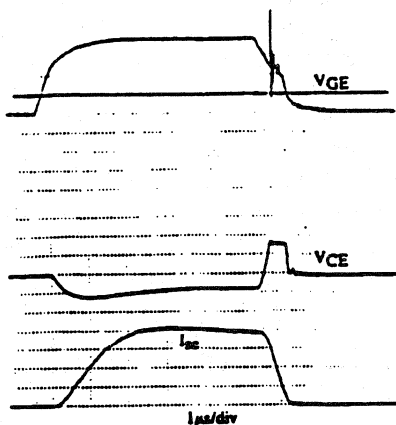


Figure 21- Short circuit waveforms with zener clamp protection scheme for Hard Fault condition
Tested at: 300V, 25°C; $L_s = 240nH$, $V_G/R_{G(off)} = -5V/33\Omega$
 $V_{CE}: 100V/div$, $V_{GE} = 5V/div$, $I_{sc}: 200A/div$

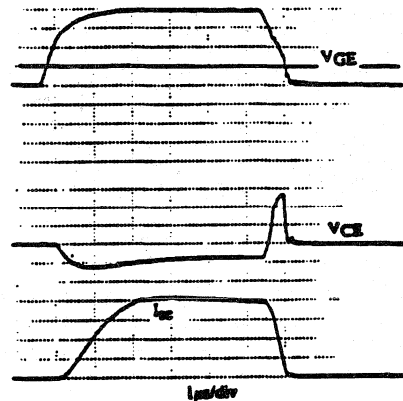


Figure 22 - short circuit waveforms without zener clamp protection scheme for hard fault condition
Tested at: 300V, 25°C; $L_s = 240nH$, $V_G/R_{G(off)} = -5V/33\Omega$
 $V_{CE}: 100V/div$, $V_{GE} = 5V/div$, $I_{sc}: 200A/div$

The additional losses inflicted by slower turn-off are not a major consideration during fault operation, as it is only a one-time operation. Usefulness of this circuit is, therefore, restricted to fault current protection.

Conclusions

The problem of switching voltage transients is an important subject that cannot be ignored, especially in applications where high-current IGBT modules are used. The paper discussed principal sources of voltage transients. Protection schemes that were designed and tested on high-current IGBT modules under normal switching operation and fault condition were described.

An RCD clamp circuit was the focus for the over voltage protection during normal switching operation. This low-loss circuit offers effective protection against voltage transients during normal turn-on and turn-off switching.

Voltage transients during fault current shut-off are more effectively protected by slowing the rate of fall of fault current. Two novel protection schemes, resistive and capacitive techniques, were introduced. These circuits, through electronic gate control, slow the rate of decay of gate voltage, thereby slowing the rate of fall of fault current. Operational characteristics of an active clamp circuit were also discussed in this section. Circuit operations were analyzed and the test results were illustrated.

Appendix I

Expressions 1-3 are derived as follows:

At turn-off (see Figure 2) as one of the two conducting IGBTs is gated off, collector-to-emitter voltage ($v_{ce}(t)$), rises to the DC bus voltage, V_{CC} . Beyond this point, load current freewheels through the diode across the other IGBT. The stray inductances (L_s), however, prolong flow of current in the 'DC loop.' Two components of currents make up for the current $i(t)$ in L_s . They are IGBT turn-off current ($i_c(t)$) and the snubber current ($i_{sn}(t)$), as marked in Figure 4.

For simplicity of calculation, it is assumed that the IGBT turns off instantly, i.e. $i_{sn}(t)$ is equal to $i(t)$. This assumption is justified on the grounds that it only renders somewhat conservative the estimate of snubber capacitor value.

The equations governing various circuit variables are:

$$\text{i.e., } \begin{aligned} v_{ce}(t) &= V_{CC} + 1/C \int i(t) dt \\ V_{CC} - v_{ce}(t) &= -1/C \cdot \int i(t) dt \end{aligned} \quad (a)$$

$$\text{i.e., } \begin{aligned} v_{ce}(t) &= V_{CC} - L \cdot di(t)/dt \\ di(t)/dt &= [V_{CC} - v_{ce}(t)]/L_s \end{aligned} \quad (b)$$

$$\text{From (a) and (b)} \quad di(t)/dt = -1/L_s C \cdot \int i(t) dt \quad (c)$$

$$\text{The following is the solution to the above equation:} \quad i(t) = I_o \cdot \cos(t/\sqrt{L_s C}) \quad (d)$$

Where I_o is the load current at turn-off. The current is thus a cosine function. In Figure 7 it can be observed that the combination of $i_c(t)$ and $I_{sn}(t)$ does follow cosine wave shape.

$$\text{Differentiating (d),} \quad di(t)/dt = -I_o/L_s C \cdot \sin(t/\sqrt{L_s C}) \quad (e)$$

$$\text{From (b) and (e),} \quad v_{ce}(t) = V_{CC} + I_o \cdot \sqrt{L_s/C} \cdot \sin(t/\sqrt{L_s C}) \quad (f)$$

v_{ce} is at maximum when $t/\sqrt{L_s C} = \pi/2$.

Therefore,

$$\begin{aligned} V_{CM} &= \text{maximum desired voltage across IGBT} \\ V_{CM} &= V_{CC} + I_o \cdot \sqrt{L_s/C} \end{aligned} \quad (g)$$

From (g),

Snubber capacitor

$$C_{sn} = L_s \cdot I_o^2 / [V_{CM} - V_{CC}]^2 \quad (l)$$

The snubber capacitor is therefore charged to V_{CM} at the end of turn-off. Before the next turn-off event, i.e. $1/f_{sw}$ later, C_{sn} should discharge back to its value of V_{CC} . The snubber resistor (R_{sn}) selected according to the following expression fulfills the above requirement.

$$R_{sn} = 1/(6 \cdot C_{sn} \cdot f_{sw}) \quad (5)$$

The losses in R_{sn} at turn-off are therefore given by:

$$PR(\text{off}) = [1/2 \cdot C_{sn} \cdot (V_{pk}^2 - V_{CC}^2)] \cdot f_{sw} \quad (f)$$

At turn-on (see Figures 8 and 9), as the IGBT is turned on, the switching $di(t)/dt$ causes voltage at module terminals $v_{ab}(t)$ to drop from its initial value of V_{CC} to an amount equal to $L_s \cdot di/dt$. As explained in the article, this causes the snubber capacitors to discharge through R_{sn} .

For simplicity, it is assumed that the turn-on di/dt is linear. It is further assumed that the peak turn-on current is 25% above the load current I_o at the switching instant. These assumptions will result in conservative estimates of snubber losses.

The snubber discharge current is:

$$i_{sn}(t) = [V_{CC} - V_{ab}]/R_{sn} \quad (g)$$

where

$$V_{ab} = V_{CC} - L_s \cdot di/dt \quad (h)$$

where

$$di/dt \text{ (a constant)} = di/dt = 0.9I_o/t_r \quad (i)$$

t_r is the rise time, specified under inductive load conditions. From (g), (h) and (i),

$$\begin{aligned} i_{sn}(t) &= I_{sn} = [L_s \cdot 0.9I_o/t_r]/R_{sn} \\ I_{sn} &= 0.9 \cdot L_s \cdot I_o / (t_r \cdot R_{sn}) \end{aligned} \quad (j)$$

The losses in R_{sn} at turn-on are,

$$PR(\text{on}) = [0.9 \cdot L_s \cdot I_o / (t_r \cdot R_{sn})]^2 \cdot R_{sn} \cdot T \cdot f_{sw} \quad (k)$$

where T , the snubber discharge time, is approximated to be interval between the beginning of the current rise and the point where current reaches its peak value ($=1.25I_o$).

$$T = 1.25I_o / [0.9I_o/t_r] = 1.39t_r \quad (l)$$

Combining (k) and (l),

$$PR(\text{on}) = [1.125 \cdot L_s^2 \cdot I_o^2 / (t_r \cdot R_{sn})] \cdot f_{sw} \quad (m)$$

From (f) and (m),

$$\begin{aligned} PR &= [1/2 \cdot C_{sn} \cdot (V_{pk}^2 - V_{CC}^2) \\ &\quad + 1.125 \cdot L_s^2 \cdot I_o^2 / (t_r \cdot R_{sn})] \cdot f_{sw} \end{aligned}$$

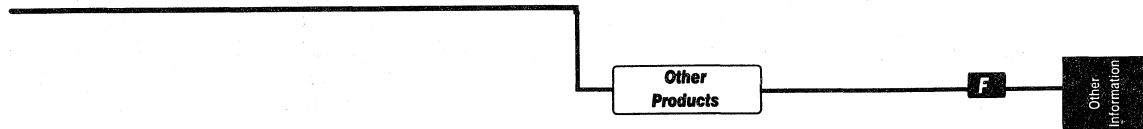
References:

- [1] Harald Vetter, 'High Performance Capacitors for Low-Inductance Circuits' Power Conversion, June 1991
- [2] C. Aniceto, R. Lator, B. Ishan, 'How Short Circuit Capabilities Govern the Desired Characteristics of IGBTs,' Power Conversions Conf., April 1992
- [3] International Rectifier Application Note AN-983A. 'IGBT Characteristics and Applications' by S. Clemente, A Dubhashi, B. Pelly
- [4] R. Chokhawala, J. Catt, L. Kiraly, 'A Discussion on IGBT Short Circuit Behavior and Fault Protection Schemes,' APEC-IEEE Conf., March 1992
- [5] R. Chokhawala, G. Castino, 'IGBT Fault Current Limiting Circuit,' IAS-IEEE Conf., October 1993
- [6] G. Castino, A. Dubhashi, S. Clemente, B. Pelly, 'Protecting IGBTs Against Short Circuit,' International Rectifier Application Note AN-984
- [7] Tore, Underland et al, 'A Snubber Configuration for both Power Transistors and GTO PWM Inverters', IEEE Conf. 1984

IGBT Designer's Manual

Other Information

Other Information



IGBT Designer's Manual

Table of Contents

Other Information	Section & Page No.
Available Literature from IR	F-3
Application Information	F-3
Microelectronic Relays	F-6
PIC Control Applications	F-9
HEXFET Power MOSFETs	F-15
PIC Power Switch	F-33
Power Interface Products	F-35
Diodes, Ultra-Fast Recovery	F-39
HEXFRED	F-41
Schottky Diode	F-45
Government & Space	F-57
PIC Application Materials	F-73
Bridges, Power Modules	F-74



Available Literature

DATABOOKS

GOVERNMENT AND SPACE PRODUCTS DESIGNER'S MANUAL	GSP-1
HEXFET DESIGNER'S MANUAL - APPLICATION NOTES & RELIABILITY DATA	HDM-1, VOL. 1
HEXFET DESIGNER'S MANUAL	HDM-1, VOL. 3
HEX-PAK DATABOOK	HPD-1
MICROELECTRONIC RELAY DESIGNERS MANUAL	MPIC-5
POWER MODULES DESIGNER'S MAUNAL	PMD-1
SCHOTTKY DIODE DESIGNER'S MANUAL	SDM-1
POWER SEMICONDUCTOR 1994 PRODUCT DIGEST	SFC-94
RECTIFIER POWER-STANDARD RECOVERY TYPES (SUPPLEMENT TO NRPM-2 & SHVR-2)	VDSR-2
RECTIFIER POWER - FAST RECOVERY TYPES (SUPPLEMENT TO FRPM-1)	VDFR-2
THYRISTOR POWER - INVERTER TYPES (SUPPLEMENT TO IPM-1)	VTI-2
THYRISTOR - PHASE CONTROL TYPES (SUPPLEMENT TO NTPM-2)	VTPC-2

SELECTION GUIDES

MICROELECTRONIC RELAYS	E1002F
HEXFET-POWER MOSFETS-IGBTs-INSULATED GATE BIPOLAR TRANSISTORS	E1003J
-POWER INTEGRATED CIRCUITS-POWER INTERFACE PRODUCTS	
SCHOTTKY BARRIER RECTIFIER DIODES	E1005G
ENCAPSULATED BRIDGE RECTIFIER	E1007E
INSULATED GATE BIPOLAR TRANSISTORS,HEXFET,HEXSENSE,LOGIC LEVEL,SCHOTTKY AND POWER SEMICONDUCTOR DIE	E1022C
SURFACE MOUNTED DEVICES	E1026A
HEXFRED-ULTRA FAST, SOFT RECOVERY DIODES	E1027
INSULATED GATE BIPOLAR TRANSISTORS-(IGBTs) AND IGBT/ULTRAFast DIODES (CO-PACK)	E1028
FULLPAK-FULLY ISOLATED POWER MOSFETS-HEXFETS	E1029

RELIABILITY REPORTS

POWER IC RELIABILITY REPORT, NUMBER 5, APRIL 1992	
MICROELECTRONIC POWER IC RELAY RELIABILITY REPORT, REPORT NUMBER 13, JULY 1990	
IR2110S RELIABILITY REPORT, POWER IC, REPORT NUMBER 3-AUGUST 1990	
SCHOTTKY RELIABILITY REPORT NUMBER 2, MARCH 31, 1992	
SCHOTTKY RELIABILITY REPORT, SEMI-ANNUAL, 2ND HALF, 1993	
HEXFET RELIABILITY REPORT, QUARTERLY REPORT	
CUSTOM PRODUCTS RELIABILITY REPORT NUMBER 9, JANUARY 1990	
PVI1050 PHOTOVOLTAIC ISOLATOR RELIABILITY REPORT NUMBER 14, DECEMBER 1990	
HEXFRED-ULTRA FAST, SOFT RECOVERY DIODE RELIABILITY REPORT JUNE, 1992	
IGBT MODULE RELIABILITY REPORT #1 - NOVEMBER, 1991	
IR2113 QUALIFICATION REPORT - AUGUST 1992	
SO-8 RELIABILITY REPORT, JULY 1993-SURFACE MOUNT TECHNOLOGY (REPORT NUMBER SMT-01)	

APPLICATION INFORMATION

POWER INTEGRATED CIRCUITS

USING THE IR8200 IN STEPPER MOTOR DRIVES	AN-982
USING THE PIH2001 STEPPER MOTOR DRIVER	AN-981
THE IR2130: A SIX-OUTPUT, HIGH VOLTAGE MOS GATE DRIVER	AN-985
ELECTRONIC BALLASTS USING THE COST-SAVING IR2155 DRIVER	AN-995
INTRODUCING THE IR8200 DMOS H-BRIDGE POWER IC	AN-979B
HV FLOATING MOS-GATE DRIVER IC	AN-978A
ESD TESTING OF MOS-GATED POWER TRANSISTORS	AN-986



Other Products from IR



APPLICATION INFORMATION, cont.

HEXFETs

HEXFET POWER MOSFET AVALANCHE RATINGS	AN-958
SPICE 2 COMPUTER MODELS FOR HEXFETS	AN-954A
APPLYING INTERNATIONAL RECTIFIER POWER MOSFETS	AN-930A
AN INTRODUCTION TO THE HEXSENSE CURRENT-SENSING DEVICE	AN-959B
USING HEXSENSE CURRENT-SENSE HEXFETS IN CURRENT-MODE CONTROL POWER SUPPLIES	AN-961B
MEASURING HEXFET CHARACTERISTICS	AN-957B
USING SURFACE MOUNTED DEVICES	AN-956A
PROTECTING POWER MOSFETS FROM ESD	AN-955
THERMAL AND MECHANICAL CONSIDERATIONS FOR FULLPAK APPLICATIONS	AN-972B
A 250 WATT CURRENT-CONTROLLED SMPS WITH SYNCHRONIOUS RECTIFICATION	AN-960A
SPICE COMPUTER MODELS FOR HEXFET POWER MOSFETS	AN-975B
THE HEX-PAK IR's HIGH POWER HEXFET MODULE	GBAN-HEX-1
A 500W 100 KHZ RESONANT CONVERTER USING HEXFETS	AN-965A
CHARACTERISTICS OF HEXFET III DICE	AN-964D
ECONOMIC, HIGH PERFORMANCE, HIGH FREQUENCY ELECTRONIC IGNITION WITH AVALANCHE RATED HEXFETS	AN-969
USING HEXFET III IN PWM INVERTERS FOR MOTOR DRIVES AND UPS SYSTEMS	AN-967A
HEXFET III: A NEW GENERATION OF POWER MOSFETS	AN-966A
HEXFETS IMPROVE EFFICIENCY, EXPAND LIFE OF ELECTRONIC LIGHTING BALLASTS	AN-973
A 70W BOOST-BUCK CONVERTER USING HEXSENSE CURRENT-MODE CONTROL	AN-962
A 230 WATT BUCK REGULATOR WITH HEXSENSE RECTIFIERS, STANDARD RECOVERY, FAST	AN-963
A MULTIPLE OUTPUT, OFF-LINE SWITCHING POWER USING HEXFETS	AN-952A
SWITCHING CHARACTERISTICS OF LOGIC LEVEL HEXFET POWER MOSFETS	AN-971
BIPOLAR POWER TRANSISTOR CHIPS FOR HYBRID ASSEMBLIES	AN-935
THE HEXFETS INTEGRAL BODY DIODE - ITS CHARACTERISTICS AND LIMITATIONS	AN-934B
A UNIVERSAL 100KHZ POWER SUPPLY USING A SINGLE HEXFET	AN-939A
GATE DRIVE CHARACTERISTICS AND REQUIREMENTS FOR POWER MOSFETS	AN-937B
THE DO'S AND DON'TS OF USING POWER HEXFETS	AN-936A
A CHOPPER FOR MOTOR SPEED CONTROL USING PARALLEL CONNECTED POWER HEXFETS	AN-941B
THERMAL AND MECHANICAL CONSIDERATIONS FOR FULLPAK APPLICATIONS	AN-994
HEXFET POWER MOSFETS IN LOW DROPOUT LINEAR POST-REGULATORS	AN-970
SWITCHING TRANSIENTS IN HIGH-FREQUENCY, HIGH-POWER CONVERTERS USING POWER MOSFETS	AN-933
RELIABILITY...THE KEY TO IR'S TO-220 DEVICES	AN-932
CUSTOM ASSEMBLY OF HEXFET DICE	AN-931D
AN INTRODUCTION TO INTERNATIONAL RECTIFIER P-CHANNEL HEXFETS	AN-940B
TRANSFORMER-ISOLATED HEXFET DRIVER PROVIDES VERY LARGE DUTY CYCLE RATIOS	AN-950B
SIMPLIFIED HEXFET POWER DISSIPATION AND JUNCTION TEMPERATURE CALCULATION SPEEDS HEATSINK DESIGN	AN-942
UNDERSTANDING AND USING POWER MOSFET RELIABILITY DATA	AN-
976A UNDERSTANDING HEXFET CURRENT RATINGS	AN-945
CURRENT RATINGS, SAFE OPERATING AREA AND HIGH FREQUENCY SWITCHING PERFORMANCE OF POWER MOSFETS	AN-949B
LINEAR POWER AMPLIFIER USING COMPLEMENTARY HEXFETS	AN-948A
UNDERSTANDING HEXFET SWITCHING PERFORMANCE	AN-947



Other Products from IR

MORE POWER FROM HEXDIPS AN-953

APPLICATION INFORMATION, cont.

HIGH VOLTAGE, HIGH FREQUENCY SWITCHING USING A CASCODE CONNECTION
 OF HEXFET AND BIPOLAR TRANSISTOR AN-946B

THE IMPACT OF HEXFETS ON PRODUCT PROFITABILITY: AN ECONOMIC DISCUSSION
 OF POWER MOSFETS AN-943

A NEW GATE CHARGE FACTOR LEADS TO EASY DRIVE FOR POWER MOSFET CIRCUITS AN-944A

AN INTRODUCTION TO HEXFET QUALITY AND RELIABILITY AN-977

THERMAL AND MECHANICAL CONSIDERATIONS FOR FULLPAK APPLICATIONS AN-994

HEXFREDS

THE HEXFRED ULTRAFAST DIODE IN PRW SWITCHING CIRCUITS AN-989

UTILIZING HEXFRED ULTRA-FAST RECOVERY DIODE DIE IN ASSEMBLY AN-993

IGBT VS HEXFET POWER MOSFETS FOR VARIABLE AN-980

MICROELECTRONIC RELAYS

THE PVI-A VERSATILE NEW CIRCUIT ELEMENT GBAN-PVI-1

SHORT CIRCUIT WITHSTAND CAPABILITY OF THE PHOTOVOLTAIC RELAY AN.107

THE SWITCHING LIFE OF BOSFET PHOTOVOLTAIC RELAYS AN.106

ADVANTAGES OF PHOTOVOLTAIC RELAYS IN MULTIPLEXERS AN.105

THE PHOTOVOLTAIC RELAY: A NEW SOLID STATE CONTROL DEVICE AN.104

THERMAL EVALUATION OF CHIPSWITCH IN PROGRAMMABLE CONTROLLERS AN.103

INDUCTIVE LOAD SWITCHING CHARACTERISTICS OF THE CHIPSWITCH AN.102

CHOOSING AN INPUT RESISTOR FOR A MICROELECTRONIC RELAY AN.101

AC LOAD SWITCHING WITH CHIPSWITCH MICROELECTRONIC RELAYS AN.100

MODULES

INTRODUCTION TO 600V ADD-A-PAK & INT-A-PAK IGBT MODULES AN-988

THE ADD A PAK POWER MODULE EXPLAINED GBAN-AP-1

THYRISTORS

CALCULATIONS OF CURRENT RATINGS AN-305

SCRs - THEIR PARAMETERS, SPECIFICATIONS, RATINGS AND CHARACTERISTICS AN-309

THERMAL AND HEAT TRANSFER DATA FOR HEAT EXCHANGERS AN-701

DESIGN TIPS

SOLVING NOISE PROBLEMS IN HIGH POWER, HIGH FREQUENCY PIC DRIVEN POWER STAGES DT 92-1

HIGH CURRENT BUFFER FOR MOS-GATE DRIVERS DT 92-2

USING STANDARD MOS GATE DRIVERS TO GENERATE NEGATIVE GATE BIAS FOR MOSFET's AND IGBT's ... DT 92-3

SIMPLE HIGH SIDE DRIVE PROVIDES FAST SWITCHING AND CONTINUOUS ON TIME DT 92-4

SPICE MODELS FOR MOS-GATED POWER DEVICES DT 92-5

CURRENT SENSING WITH THE IR2130 DT 92-6

TESTING HIGH-POWER SCRs AND DIODES DT 93-1

IR6000 DESIGN TIPS-DRIVING FILAMENTS, BRIDGE APPLICATIONS DT 93-2

CURRENT CAPABILITY OF TO-220 PACKAGE DT 93-4

MINIATURIZATION OF THE POWER ELECTRONICS FOR MOTOR DRIVES DT 93-6

KEEPING THE BOOTSTRAP CAPACITOR CHARGED IN BUCK CONVERTERS DT 94-1




SIMPLE ELECTRONIC BALLAST USING IR2155 MOS GATE DRIVER DT 94-3



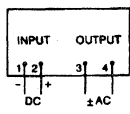
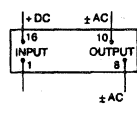
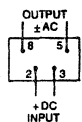
Microelectronic Relays

ChipSwitch® Solid State Relay

Other Products from IR




Part Number	Operating Voltage Range (V)RMS	Maximum Load Current @ 40°C A(RMS)	Trans. Overvolt V(Pk)	Turn-On Signal (DC)	Dielectric Strength Input/Output V(RMS)	Minimum Off-State dv/dt @ Rated V 25°C V/μs	Maximum Off State Leakage μA	Case Outline Number	Series
SP1210	20-140	1.0 Free Standing With Heat Sink	300	10mA				MR4	SP  1 Form A
SP2210	20-280		450	10mA	4000	600	10		
SP6210	20-280		600	10mA					
DP1210	20-140	1.0	300	10mA				MR2	DP  1 Form A
DP1610	20-140		300	3.5V					
DP2210	20-280		450	10mA	4000	600	10		
DP2610	20-280		450	3.5V					
DP6210	20-280		600	10mA					
DP6610	20-280		600	3.5V					
CS5005	20-280	0.3	500	5mA				MR1	CS  1 Form A
CS5010	20-280		500	10mA					
CS6005	20-280		600	5mA	4000	1200	10		
CS6010	20-280		600	10mA					


Wiring Diagram

			
Series	SP	DP	CS

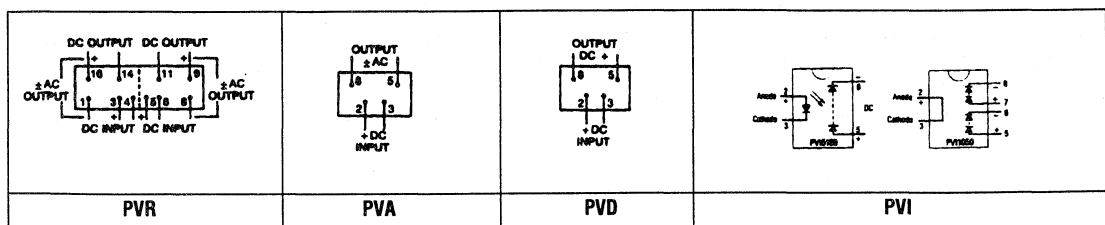
Other Products from IR

Microelectronic Relays PhotoVoltaic Relay

Part Number	Operating Voltage Range V(Pk)	Max. On-State Res. @ 25°C Ohms		Max Load Current @ 40°C (DC) mA	Nom. Control Current (DC) mA	Min. Off-State Res. Ohms	Dielectric Strength Input/Output V(RMS)	Max. Response Time On/Off μ sec	Maximum Thermal Offset Voltage @ 5mA Control μ V	Case Outline Number	Series
		AC/DC	DC								
PVR1300	± 100	5.0	1.5	700		10^8		300/50		MR3	PVR  2 Form A
PVR1301	± 100	5.0	1.5	700		10^{10}		300/50			
PVR2300	± 200	24	6.0	260	10	10^8	1500	100/50	0.2		
PVR3300	± 300	24	6.0	260		10^8		100/50			
PVR3301	± 300	24	6.0	260		10^{10}		100/50			
PVA1052	± 100	35		70	5.0	10^8		25/15		MR1	PVA  1 Form A
PVA1054	± 100	35		70	5.0	10^{10}		25/15			
PVA1352	± 100	5.0		315	5.0	10^8		300/50			
PVA1354	± 100	5.0		315	5.0	10^{10}		300/50			
PVA2352	± 200	24		130	5.0	10^8	2500	100/50	0.2		
PVA3054	± 300	160		40	5.0	10^{10}		25/15			
PVA3055	± 300	160		40	5.0	10^{11}		25/15			
PVA3324	± 300	24		130	2.0	10^{10}		100/50			
PVA3354	± 300	24		130	5.0	10^{10}		100/50			
PVAZ172	± 60	0.5		1200	10	10^8	1500	500/8000			
PVD1052	± 100		8.0	160	5.0	10^8		25/15		MR1	PVD  1 Form A
PVD1054	± 100		8.0	160	5.0	10^{10}		25/15			
PVD1354	+100		1.5	500	5.0	10^8	2500	300/50	0.2		
PVD2352	+200		6.0	220	5.0	10^{10}		100/50			
PVD3354	+300		6.0	220	5.0	10^{10}		100/50			
PVDZ172	+60		0.25	1400	10	10^8	1500				

Part Number	Number Outputs	Output Voltage V(DC)	Short Circuit Current μ A	Nom. Control Current (DC) mA	Dielectric Strength Input/Output V(RMS)	Case Outline Number	Series
PVI5050	1	5.0	5.0	10	2500	MR1	PVI 
PVI5100	1	5.0	10.0	10	2500		
PVI1050	2	5.0/10	10/5	10	2500		



Wiring Diagram



Microelectronic Relays

Safety Standards Qualifications

Other Products from IR

Part Number												
	Underwriter's Labs Recognition		Canadian Standards Certification									
	Standard	File	Standard	File								
SP1110 SP1210 SP2110 SP2210 SP6110 SP6210	UL508	E50015 E50015 E50015 E50015 E50015 E50015	C22.2	LR32053 LR32053 LR32053 LR32053 LR32053 LR32053								
DP1110 DP1210 DP1610 DP2110 DP2210 DP2610 DP6110 DP6210 DP6610		UL508		E50015 E50015 E50015 E50015 E50015 E50015 E50015 E50015 E50015	C22.2	LR32053 LR32053 LR32053 LR32053 LR32053 LR32053 LR32053 LR32053 LR32053						
CS5005 CS5010 CS6005 CS6101				UL508		E50015 E50015 E50015 E50015	C22.2	LR56615 LR56615 LR56615 LR56615				
PVA2352 PVA3324 PVA3354						UL508		E88583 E88583 E88583	—	—		
PVA3055 PVA3054 PVA1354 PVA1352 PVA1052 PVD3354 PVD2352 PVD1354 PVD1352 PVD1054 PVD1052 PVA2172 PVD2172								UL508		E88583 E88583 E88583 E88583 E88583 E88583 E88583 E88583 E88583 E88583 E88583 E88583 E88583	—	—

International Rectifier has expanded its power integrated circuit (PIC) product line to address additional applications which require both power and control.

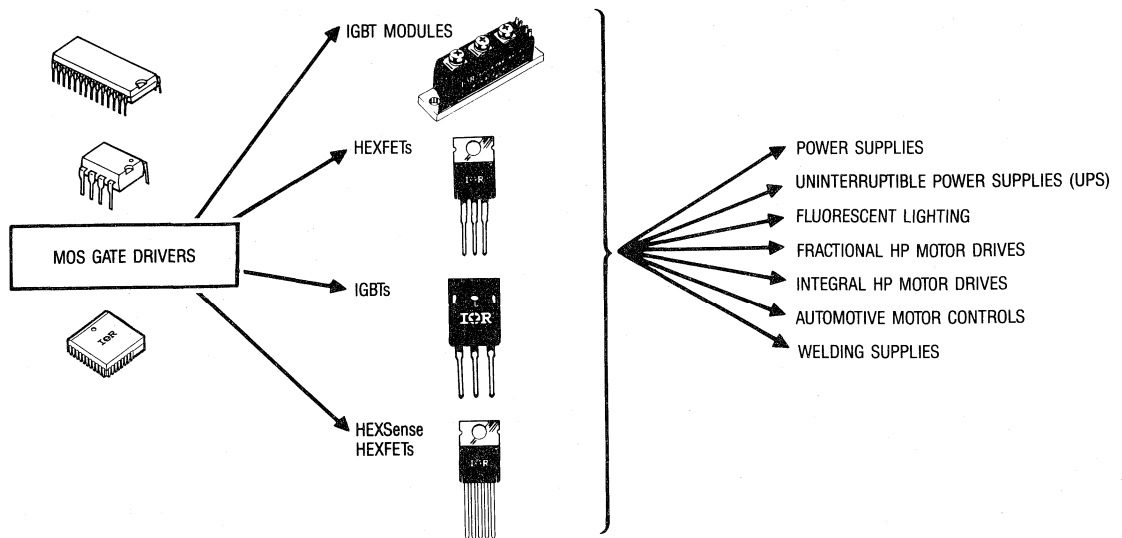
High Voltage Control IC (HV PIC)

With a voltage range to 600 volts, IR's unique high voltage junction isolated BCDMOS technology makes it possible to combine the power MOSFET with analog and digital control circuitry on a single silicon chip, producing a new family of off-line monolithic functions for power converters and motor control applications.

Features (HVPIC)

- Drivers for use with power MOSFETs and IGBTs
- Up to 600V rating
- Floating High Side Driver
- High Noise Immunity
- Low Power Consumption
- Undervoltage Shutdown

Use MOS gate drivers to drive power components for these applications.



Power Integrated Circuits

Application Selection Guide



Application	BALLAST				MOTOR DRIVE
	Half-Bridge		High Intensity Discharge	Full-Bridge	Six-Step Control
	Self-Oscillating Fluorescent	Synchronized Oscillating Fluorescent			
IR2110	Applicable	Applicable	Applicable	Applicable	Applicable
IR2111	Applicable	Applicable	Applicable	Preferred	Applicable
IR2112	Applicable	Applicable	Applicable	Applicable	Applicable
IR2113	Applicable	Applicable	Applicable	Applicable	Applicable
IR2121					
IR2125					
IR2130					Preferred
IR2132					Applicable
IR2155	Preferred	Preferred	Preferred	Preferred	

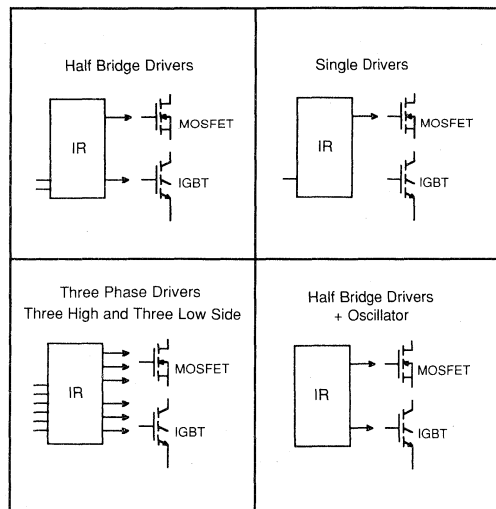
 Preferred

 Applicable

MOTOR DRIVE	POWER SUPPLY				Application
	High Side Switch	Half-Bridge	Full-Bridge		
PWM Control	Buck & Boost Converter	Resonant Mode Control	Square Wave Control	Phased Shifted PWM	
					IR2110
					IR2111
					IR2112
					IR2113
					IR2121
					IR2125
					IR2130
					IR2132
					IR2155

Preferred 
Applicable 

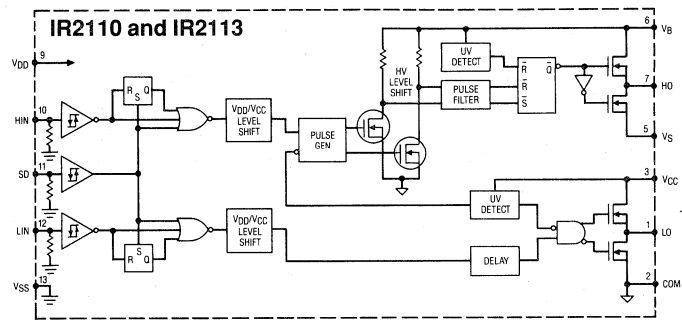
High Voltage Power MOSFET/IGBT Gate Drivers



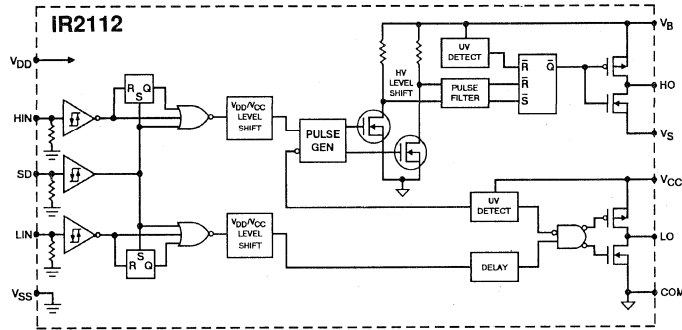
Features

- Drives single, pair, and six HEXFETs or IGBTs
- Floating High Side Driver
- Ground Referenced Low Side Driver
- Operates to either 500V or 600V
- High dv/dt and negative transient immunity
- CMOS Compatible Schmitt Trigger Inputs
- Low Quiescent Power Dissipation
- Undervoltage lockout with hysteresis – all channels
- Matched delay times for High and Low channels
- Latch immune CMOS

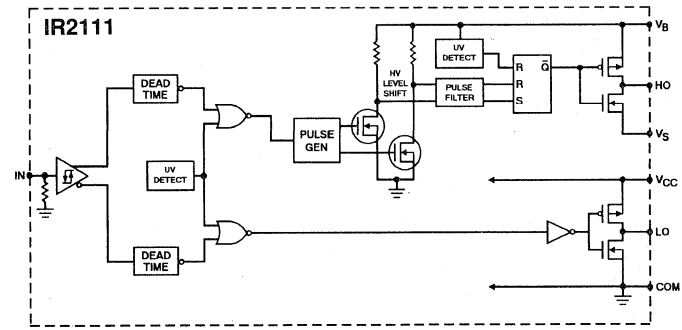
Part Number	Configuration	Maximum Floating Supply Offset Voltage	I _o Source, Sink	Schematic	(1) Case Outline	Notes	Case Style
IR2110	High Side	500V	2A / 2A	S1	P1		14 Pin DIP
IR2110-1	and				P2		14 Pin DIP w/o Pin 4
IR2110-2	Low Side				P3		16 Pin DIP w/o Pins 4 & 5
IR2110S					P4		16 Pin SOIC Wide Body
IR2111	Half Bridge	600V	200 / 420 mA	S3	P5		8 Pin DIP
IR2112	High Side	600V	200 / 420 mA	S2	P1		14 Pin DIP
IR2112-1	and				P2		14 Pin DIP w/o Pin 4
IR2112-2	Low Side				P3		16 Pin DIP w/o Pins 4 & 5
IR2112S					P4		16 Pin SOIC Wide Body
IR2113	High Side	600V	2A / 2A	S1	P1		14 Pin DIP
IR2113-1	and				P2		14 Pin DIP w/o Pin 4
IR2113-2	Low Side				P3		16 Pin DIP w/o Pins 4 & 5
IR2113S					P4		16 Pin SOIC Wide Body
IR2121	Low Side Current Limit	—	1A / 2A	S5	P5		8 Pin DIP
IR2125	High Side Current Limit	500V	1A / 2A	S6	P5		8 Pin DIP
IR2130	3 High Side	600V	200 / 420 mA	S7	P6	2.5 μs Dead-time	28 Pin DIP
IR2130J	and				P7		44 Pin PLCC w/o 12 leads
IR2130S	3 Low Side				P8		28 Pin SOIC Wide Body
IR2132	3 High Side	600V	200 / 420 mA	S7	P6	0.8 μs Dead-time	28 Pin DIP
IR2132J	and				P7		44 Pin PLCC w/o 12 leads
IR2132S	3 Low Side				P8		28 Pin SOIC Wide Body
IR2155	1/2 Bridge Self oscillating	600V	200 / 420 mA	S4	P5	555 Type timer	8 Pin DIP



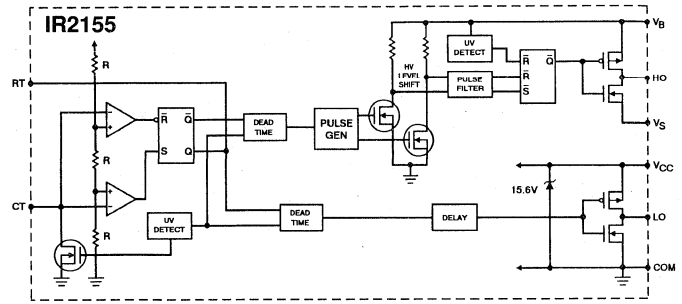
S1 – IR2110 and IR2113 Schematic



S2 – IR2112 Schematic



S3 – IR2111 Schematic



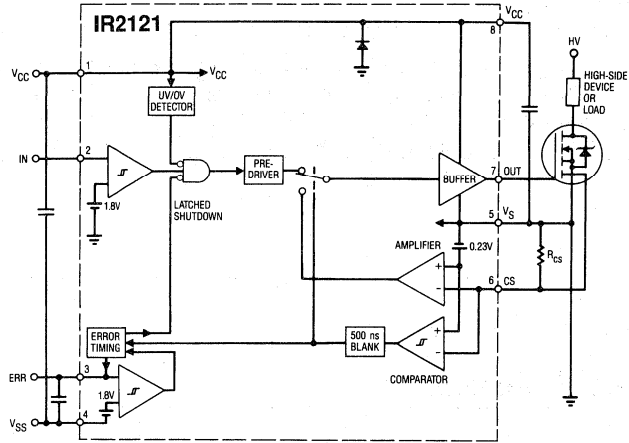
S4 – IR2155 Schematic



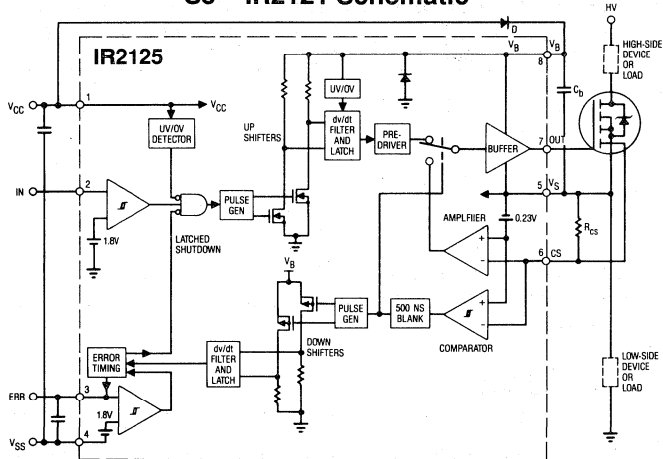
Power Integrated Circuits

Power MOSFET/IGBT

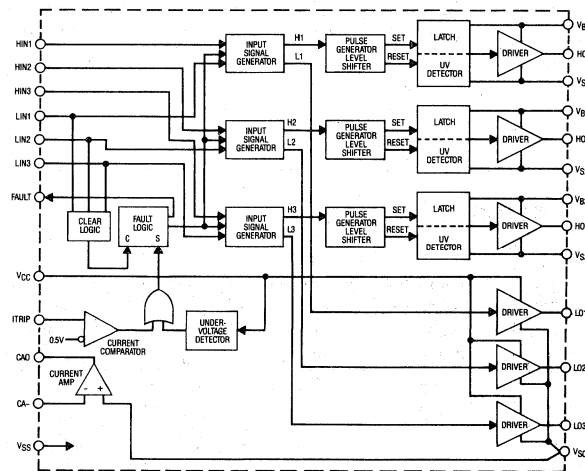
Gate Driver



S5 - IR2121 Schematic



S6 - IR2125 Schematic




S7 - IR2130 Schematic

Other Products from IR

SOT-89 N-Channel


HEXFET Power MOSFETs

Surface Mount

Part Number	V(BR) _{DSS} Drain-to-Source Breakdown Voltage (Volt)	R _{DS(on)} On-State Resistance (Ohms)	I _D Continuous Drain Current 25°C (Amps)	I _D Continuous Drain Current 100°C (Amps)	R _{thJA} Max Thermal Resistance (°C/W)	P _d @T _c = 25°C Max Power Dissipation (Watts)	Case Outline Number	Case Style
IRFS1Z0	100	2.4	0.82	0.52	35	3.6	H1	SOT-89 

Logic level HEXFETs are fully enhanced with 4 or 5V applied to the gate.


SOT-89 Logic Level N-Channel

Part Number	V(BR) _{DSS} Drain-to-Source Breakdown Voltage (Volt)	R _{DS(on)} On-State Resistance (Ohms)	I _D Continuous Drain Current 25°C (Amps)	I _D Continuous Drain Current 100°C (Amps)	R _{thJA} Max Thermal Resistance (°C/W)	P _d @T _c = 25°C Max Power Dissipation (Watts)	Case Outline Number	Case Style
IRLS0Z0	50	0.3	2.6	1.6	35	3.6	H1	SOT-89 


SO-8

The new SO-8 can accommodate a dual-die configuration allowing multiple devices to be used in an application with greatly reduced board space. Power dissipation of more than 1W is possible in a typical printed circuit board application. The SO-8 is designed for all soldering techniques.

SO-8 Logic Level N-Channel

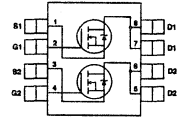
Part Number	V(BR) _{DSS} Drain-to-Source Breakdown Voltage (Volt)	R _{DS(on)} On-State Resistance (Ohms)	I _D Continuous Drain Current 25°C (Amps)	I _D Continuous Drain Current 100°C (Amps)	R _{thJA} Max Thermal Resistance (°C/W)	P _d @T _c = 25°C Max Power Dissipation (Watts)	Case Outline Number	Case Style
IRF7201	30	0.03	7.0	5.8	50	2.5	H2	SO-8 

SO-8 Logic Level P-Channel


Part Number	V(BR) _{DSS} Drain-to-Source Breakdown Voltage (Volt)	R _{DS(on)} On-State Resistance (Ohms)	I _D Continuous Drain Current 25°C (Amps)	I _D Continuous Drain Current 100°C (Amps)	R _{thJA} Max Thermal Resistance (°C/W)	P _d @T _c = 25°C Max Power Dissipation (Watts)	Case Outline Number	Case Style
IRF7202	-20	0.25	-2.5	-2.0	50	2.5	H2	SO-8 
IRF7203	-20	0.1	-4.3	-3.3	50	2.5		
IRF7204	-20	0.06	-5.3	-4.2	50	2.5		
IRF7205	-30	0.07	-5.3	-4.1	50	2.5		

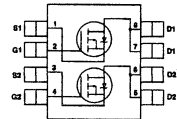
SO-8

The new SO-8 can accommodate a dual-die configuration, allowing multiple devices to be used in an application with greatly reduced board space. Power dissipation of more than 1W is possible in a typical printed circuit board application. The SO-8 is designed for all soldering techniques.




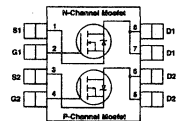
SO-8 Logic Level Dual N-Channel

Part Number	V(BR) _{DSS} Drain-to-Source Breakdown Voltage (Volt)	R _{DS(on)} On-State Resistance (Ohms)	I _D Continuous Drain Current 25°C (Amps)	I _D Continuous Drain Current 100°C (Amps)	R _{thJA} Max Thermal Resistance (°C/W)	P _d @T _c = 25°C Max Power Dissipation (Watts)	Case Outline Number	Case Style
IRF7101	20	0.1	3.5	2.8	62	2.0	H2	
IRF7102	50	0.3	2.0	1.6	62	2.0		
IRF7103	50	0.13	3.0	2.3	62	2.0		




SO-8 Logic Level Dual P-Channel

Part Number	V(BR) _{DSS} Drain-to-Source Breakdown Voltage (Volt)	R _{DS(on)} On-State Resistance (Ohms)	I _D Continuous Drain Current 25°C (Amps)	I _D Continuous Drain Current 100°C (Amps)	R _{thJA} Max Thermal Resistance (°C/W)	P _d @T _c = 25°C Max Power Dissipation (Watts)	Case Outline Number	Case Style
IRF7104	-20	0.25	-2.3	-1.8	62	2.0	H2	



SO-8 Logic Level Dual N/P-Channel

Part Number	V(BR) _{DSS} Drain-to-Source Breakdown Voltage (Volt)	R _{DS(on)} On-State Resistance (Ohms)	I _D Continuous Drain Current 25°C (Amps)	I _D Continuous Drain Current 100°C (Amps)	R _{thJA} Max Thermal Resistance (°C/W)	P _d @T _c = 25°C Max Power Dissipation (Watts)	Case Outline Number	Case Style
IRF7105	25 -25	0.1 0.25	3.5 -2.3	2.8 -1.9	62	2.0	H2	
IRF7106	20 -20	0.125 0.25	3.0 -2.5	2.5 -2.0	62	2.0		
IRF7107	20 -20	0.125 0.160	3.0 -2.8	2.5 -2.3	62	2.0		


Other Products from IR

HEXFET Power MOSFETs Surface Mount

SOT-223


The new SOT-223 is capable of dissipating more than 1W in a typical printed circuit board application. Its unique package design allows for maximum die size, optimum thermal performance and ease of surface-mount manufacturing; suitable for use with all soldering techniques.

SOT-223 N-Channel


Part Number	V(BR) _{DSS} Drain-to-Source Breakdown Voltage (Volt)	R _{DS(on)} On-State Resistance (Ohms)	I _D Continuous Drain Current 25°C (Amps)	I _D Continuous Drain Current 100°C (Amps)	R _{thJA} Max Thermal Resistance (°C/W)	P _d @T _c = 25°C Max Power Dissipation (Watts)	Case Outline Number	Case Style
IRFL014	60	0.20	2.7	1.7	40	3.1	H3	SOT-223 (TO-261AA) 
IRFL110	100	0.54	1.5	0.96	40	3.1		
IRFL210	200	1.5	0.96	0.60	40	3.1		
IRFL214	250	2.0	0.79	0.50	40	3.1		

Logic level HEXFETs are fully enhanced with 4 or 5V applied to the gate.

SOT-223 Logic Level N-Channel

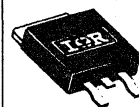
Part Number	V(BR) _{DSS} Drain-to-Source Breakdown Voltage (Volt)	R _{DS(on)} On-State Resistance (Ohms)	I _D Continuous Drain Current 25°C (Amps)	I _D Continuous Drain Current 100°C (Amps)	R _{thJA} Max Thermal Resistance (°C/W)	P _d @T _c = 25°C Max Power Dissipation (Watts)	Case Outline Number	Case Style
IRLL014	60	0.20	2.7	1.7	40	3.1	H3	SOT-223 (TO-261AA) 
IRLL110	100	0.54	1.5	0.93	40	3.1		

SOT-223 P-Channel

Part Number	V(BR) _{DSS} Drain-to-Source Breakdown Voltage (Volt)	R _{DS(on)} On-State Resistance (Ohms)	I _D Continuous Drain Current 25°C (Amps)	I _D Continuous Drain Current 100°C (Amps)	R _{thJA} Max Thermal Resistance (°C/W)	P _d @T _c = 25°C Max Power Dissipation (Watts)	Case Outline Number	Case Style
IRFL9014	-60	0.50	-1.8	-1.1	40	3.1	H3	SOT-223 (TO-261AA) 
IRFL9110	-100	1.2	-1.1	-0.69	40	3.1		

D-Pak (TO-252AA) N-Channel

Part Number	V(BR) _{DSS} Drain-to-Source Breakdown Voltage (Volt)	R _{DS(on)} On-State Resistance (Ohms)	I _D Continuous Drain Current 25°C (Amps)	I _D Continuous Drain Current 100°C (Amps)	R _{thJA} Max Thermal Resistance (°C/W)	P _d @T _c = 25°C Max Power Dissipation (Watts)	Case Outline Number	Case Style
IRFR014	60	0.20	7.7	4.9	5.0	25	H4	D-Pak (TO-252AA)
IRFR024	60	0.10	14	9.0	3.0	42		
IRFR110	100	0.54	4.3	2.7	5.0	25		
IRFR120	100	0.27	7.7	4.9	3.0	42		
IRFR210	200	1.5	2.6	1.7	5.0	25		
IRFR220	200	0.80	4.8	3.0	3.0	42		
IRFR214	250	2.0	2.2	1.4	5.0	25		
IRFR224	250	1.1	3.8	2.4	3.0	42		
IRFR310	400	3.6	1.7	1.1	5.0	25		
IRFR320	400	1.8	3.1	2.0	3.0	42		
IRFR420	500	3.0	2.4	1.5	3.0	42		
IRFRC20	600	4.4	2.0	1.3	3.0	42		



Logic level HEXFETs are fully enhanced with 4 or 5V applied to the gate.

D-Pak (TO-252AA) Logic Level N-Channel

Part Number	V(BR) _{DSS} Drain-to-Source Breakdown Voltage (Volt)	R _{DS(on)} On-State Resistance (Ohms)	I _D Continuous Drain Current 25°C (Amps)	I _D Continuous Drain Current 100°C (Amps)	R _{thJA} Max Thermal Resistance (°C/W)	P _d @T _c = 25°C Max Power Dissipation (Watts)	Case Outline Number	Case Style
IRLR014	60	0.20	7.7	4.9	5.0	24	H4	D-Pak (TO-252AA)
IRLR024	60	0.10	14	9.2	3.0	42		
IRLR110	100	1.54	4.3	2.7	5.0	25		
IRLR120	100	0.27	7.7	4.9	3.0	42		



D-Pak (TO-252AA) P-Channel

Part Number	V(BR) _{DSS} Drain-to-Source Breakdown Voltage (Volt)	R _{DS(on)} On-State Resistance (Ohms)	I _D Continuous Drain Current 25°C (Amps)	I _D Continuous Drain Current 100°C (Amps)	R _{thJA} Max Thermal Resistance (°C/W)	P _d @T _c = 25°C Max Power Dissipation (Watts)	Case Outline Number	Case Style
IRFR9014	-60	0.50	-5.1	-3.2	5.0	25	H4	D-Pak (TO-252AA)
IRFR9024	-60	0.28	-8.8	-5.6	3.0	42		
IRFR9110	-100	1.2	-3.1	-2.0	5.0	25		
IRFR9120	-100	0.60	-5.6	-3.6	3.0	42		
IRFR9210	-200	3.0	-1.9	-1.2	5.0	25		
IRFR9220	-200	1.5	-3.6	-2.3	3.0	42		



Other Products from IR

HEXFET Power MOSFETs Surface Mount

SMD-220

These devices provide the highest power capability and lowest possible on-resistance in a surface mount package. They can dissipate up to 2W in a typical surface mount application and are available in tape and reel.

SMD-220 N-Channel

Part Number	V(BR) _{DSS} Drain-to-Source Breakdown Voltage (Volt)	R _{DS(on)} On-State Resistance (Ohms)	I _D Continuous Drain Current 25°C (Amps)	I _D Continuous Drain Current 100°C (Amps)	R _{thJA} Max Thermal Resistance (°C/W)	P _d @T _c = 25°C Max Power Dissipation (Watts)	Case Outline Number	Case Style
IRFZ46S	50	0.024	50	38	1.0	150	H5	SMD-220
IRF1010S	55	0.014	75	53	1.0	150		
IRFZ14S	60	0.20	10	7.2	3.5	43		
IRFZ24S	60	0.10	17	12	2.5	60		
IRFZ34S	60	0.050	30	21	1.7	88		
IRFZ44S	60	0.028	50	36	1.0	150		
IRFZ48S	60	0.018	50	50	0.80	190		
IRF1310S	100	0.04	43	25	1.0	150		
IRF510S	100	0.54	5.6	4.0	3.5	43		
IRF520S	100	0.27	9.2	6.5	2.5	60		
IRF530S	100	0.16	14	10	1.7	88		
IRF540S	100	0.077	28	20	1.0	150		
IRF610S	200	1.5	3.3	2.1	3.5	36		
IRF620S	200	0.80	5.2	3.3	2.5	50		
IRF630S	200	0.40	9.0	5.7	1.7	74		
IRF640S	200	0.18	18	11	2.0	125		
IRF614S	250	2	2.7	1.7	3.5	36		
IRF624S	250	1.1	4.4	2.8	2.5	50		
IRF634S	250	0.45	8.1	5.1	1.7	74		
IRF644S	250	0.28	14	8.5	1.0	125		
IRF710S	400	3.6	2	1.2	3.5	36		
IRF720S	400	1.8	3.3	2.1	2.5	50		
IRF730S	400	1	5.5	3.3	1.7	74		
IRF740S	400	0.55	10	6.3	1.0	125		
IRF820S	500	3	2.5	1.6	2.5	50		
IRF830S	500	1.5	4.5	2.9	1.7	74		
IRF840S	500	0.85	8	5.1	1.0	125		




SMD-220


These devices provide the highest power capacity and lowest possible on-resistance in a surface mount package. They can dissipate up to 2W in a typical surface mount application and are available in tape and reel.

Logic level HEXFETs are fully enhanced with 4 or 5V applied to the gate.

SMD-220 Logic Level N-Channel

Part Number	V(BR) _{DSS} Drain-to-Source Breakdown Voltage (Volt)	R _{DS(on)} On-State Resistance (Ohms)	I _D Continuous Drain Current 25°C (Amps)	I _D Continuous Drain Current 100°C (Amps)	R _{thJA} Max Thermal Resistance (°C/W)	P _D @ T _C = 25°C Max Power Dissipation (Watts)	Case Outline Number	Case Style
IRL2203S	30	0.010	92	65	1.0	150	H5	SMD-220 
IRL3705S	50	0.012	80	57	1.0	150		
IRLZ14S	60	0.20	10	7.2	3.5	43		
IRLZ24S	60	0.10	17	12	2.5	60		
IRLZ34S	60	0.05	30	21	1.7	88		
IRLZ44S	60	0.28	50	36	1.0	150		
IRL520S	100	0.27	9.2	6.5	2.5	60		
IRL510S	100	0.54	5.6	4.0	3.5	43		
IRL530S	100	0.16	15	11	1.7	88		
IRL540S	100	0.077	28	20	1.0	150		
IRL620S	200	0.8	5.2	3.3	2.5	50		
IRL630S	200	0.4	9.0	5.7	1.7	74		
IRL640S	200	0.18	18	11	1.0	125		

SMD-220 P-Channel

Part Number	V(BR) _{DSS} Drain-to-Source Breakdown Voltage (Volt)	R _{DS(on)} On-State Resistance (Ohms)	I _D Continuous Drain Current 25°C (Amps)	I _D Continuous Drain Current 100°C (Amps)	R _{thJA} Max Thermal Resistance (°C/W)	P _D @ T _C = 25°C Max Power Dissipation (Watts)	Case Outline Number	Case Style
IRF9Z14S	-60	0.5	-6.7	-4.7	3.5	43	H5	SMD-220 
IRF9Z24S	-60	0.28	-11	-7.7	2.5	60		
IRF9Z34S	-60	0.14	-18	-13	1.7	88		
IRF9510S	-100	1.2	-4	-2.8	3.5	43		
IRF9520S	-100	0.6	-6.8	-4.8	2.5	60		
IRF9530S	-100	0.3	-12	-8.2	1.7	88		
IRF9540S	-100	0.2	-19	-13	1.0	150		
IRF9610S	-200	3.0	-1.8	-1.0	6.4	20		
IRF9620S	-200	1.5	-3.5	-2.0	3.1	40		
IRF9630S	-200	0.8	-6.5	-4.0	1.7	74		
IRF9640S	-200	0.5	-11	-6.8	1.0	125		

Other Products from IR


HEXFET Power MOSFETs Fully Isolated HEXFET

TO-220 FullPak


The FullPak outline is "overmolded" to provide a built-in isolation barrier from the external heatsink. The molding compound and package design provides a high isolation capability and low thermal impedance between the tab and external heatsink along with excellent creepage and clearance distances to meet safety requirements. Consequently, the FullPak requires no further external isolation barrier saving a significant amount of additional labor and reducing component count and cost.

Low charge Hexfets reduce gate charge by 40% or more and capacitances by up to 85% without any added device cost.

TO-220 FullPak N-Channel - "Low Charge"

Part Number	V(BR) _{DSS} Drain-to-Source Breakdown Voltage (Volt)	R _{DS(on)} On-State Resistance (Ohms)	I _D Continuous Drain Current 25°C (Amps)	I _D Continuous Drain Current 100°C (Amps)	R _{thJA} Max Thermal Resistance (°C/W)	P _d @ T _c = 25°C Max Power Dissipation (Watts)	Case Outline Number	Case Style
IRF1740GLC	400	0.55	6.0	39	3.1	40	H6	TO-220 FullPak 
IRF1840GLC	500	0.85	4.8	39	3.1	40		
IRF1840GLC	600	1.2	4.0	39	3.1	40		

TO-220 FullPak N-Channel

Part Number	V(BR) _{DSS} Drain-to-Source Breakdown Voltage (Volt)	R _{DS(on)} On-State Resistance (Ohms)	I _D Continuous Drain Current 25°C (Amps)	I _D Continuous Drain Current 100°C (Amps)	R _{thJA} Max Thermal Resistance (°C/W)	P _d @ T _c = 25°C Max Power Dissipation (Watts)	Case Outline Number	Case Style
IRF11010G	55	0.14	43	30	3.0	50	H6	TO-220 FullPak 
IRF1214G	60	0.20	8.0	5.7	5.5	27		
IRF1224G	60	0.10	14	10	4.1	37		
IRF1234G	60	0.050	20	14	3.6	38		
IRF1244G	60	0.028	30	21	3.1	48		
IRF1248G	60	0.018	37	26	3.0	50		
IRF1510G	100	0.54	4.5	3.2	5.5	27		
IRF1520G	100	0.27	7.2	5.1	4.1	37		
IRF1530G	100	0.16	9.7	6.9	3.6	39		
IRF1540G	100	0.077	17	12	3.1	48		
IRF11310G	100	0.040	21	15	3.0	50		
IRF1620G	200	0.80	4.1	2.6	4.1	30		
IRF1630G	200	0.40	5.9	3.7	3.6	32		
IRF1640G	200	0.18	9.8	6.2	3.1	40		
IRF1614G	250	2.0	2.1	1.3	5.5	23		
IRF1624G	250	1.1	3.4	2.2	4.1	30		
IRF1634G	250	0.45	5.6	3.5	3.6	32		
IRF1644G	250	0.28	7.9	5.0	3.1	40		
IRF1720G	400	1.8	2.6	1.7	4.1	30		
IRF1730G	400	1.0	3.7	2.3	3.6	32		
IRF1740G	400	0.55	5.4	3.4	3.1	40		
IRF1734G	450	1.2	3.4	2.1	3.6	35		
IRF1744G	450	0.63	4.9	3.1	3.1	40		
IRF1820G	500	3.0	2.1	1.3	4.1	30		
IRF1830G	500	1.5	3.1	2.0	3.6	32		
IRF1840G	500	0.85	4.6	2.9	3.1	40		
IRF18C20G	600	4.4	1.7	1.1	4.1	30		
IRF18C30G	600	2.2	2.5	1.6	3.6	35		
IRF18C40G	600	1.2	3.5	2.2	3.1	40		
IRF18E20G	800	6.5	1.4	0.86	4.1	30		
IRF18E30G	800	3.0	2.1	1.4	3.6	35		
IRF18F20G	900	8.0	1.2	0.79	4.1	30		
IRF18F30G	900	3.7	1.9	1.2	3.6	35		



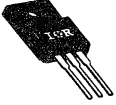
HEXFET Power MOSFETs

Fully Isolated HEXFET

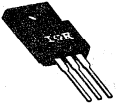
Other Products from IR

Logic-level HEXFETs are fully-enhanced with 4 or 5V applied to the gate.

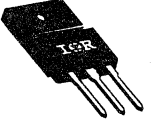
TO-220 FullPak Logic Level N-Channel

Part Number	V(BR) _{DSS} Drain-to-Source Breakdown Voltage (Volt)	R _{DS(on)} On-State Resistance (Ohms)	I _D Continuous Drain Current 25°C (Amps)	I _D Continuous Drain Current 100°C (Amps)	R _{thJA} Max Thermal Resistance (°C/W)	P _d @T _c = 25°C Max Power Dissipation (Watts)	Case Outline Number	Case Style
IRLI2203G	30	0.010	49	35	3.1	48	H6	TO-220 FullPak 
IRLI3705G	50	0.012	45	32	3.1	48		
IRLIZ14G	60	0.20	8.0	5.7	5.5	27		
IRLIZ24G	60	0.10	14	10	4.1	37		
IRLIZ34G	60	0.050	20	14	3.6	42		
IRLIZ44G	60	0.028	30	21	3.1	48		
IRLI520G	100	0.27	7.2	5.1	4.1	37		
IRLI530G	100	0.16	9.7	6.9	3.6	42		
IRLI540G	100	0.077	12	12	3.1	48		
IRLI620G	200	0.80	4.1	2.6	4.1	30		
IRLI630G	200	0.40	5.9	3.7	3.6	32		
IRLI640G	200	0.18	9.8	6.2	3.1	40		

TO-220 FullPak P-Channel

Part Number	V(BR) _{DSS} Drain-to-Source Breakdown Voltage (Volt)	R _{DS(on)} On-State Resistance (Ohms)	I _D Continuous Drain Current 25°C (Amps)	I _D Continuous Drain Current 100°C (Amps)	R _{thJA} Max Thermal Resistance (°C/W)	P _d @T _c = 25°C Max Power Dissipation (Watts)	Case Outline Number	Case Style
IRFI9214G	-60	0.50	-5.3	-3.8	5.5	27	H6	TO-220 FullPak 
IRFI9224G	-60	0.28	-8.5	-6.0	4.1	37		
IRFI9234G	-60	0.14	-12	8.5	3.6	38		
IRFI9520G	-100	0.60	-5.2	-3.6	4.1	37		
IRFI9530G	-100	0.30	-7.7	-5.4	3.6	38		
IRFI9540G	-100	0.20	-11	-7.6	3.1	48		
IRFI9620G	-200	1.5	-3.0	-1.9	4.1	30		
IRFI9630G	-200	0.80	-4.3	-2.7	3.6	40		
IRFI9640G	-200	0.50	-6.1	-3.9	3.1	40		

TO-3P FullPak Logic Level N-Channel

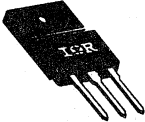
Part Number	V(BR) _{DSS} Drain-to-Source Breakdown Voltage (Volt)	R _{DS(on)} On-State Resistance (Ohms)	I _D Continuous Drain Current 25°C (Amps)	I _D Continuous Drain Current 100°C (Amps)	R _{thJA} Max Thermal Resistance (°C/W)	P _d @T _c = 25°C Max Power Dissipation (Watts)	Case Outline Number	Case Style
IRFIP044	60	0.028	43	30	1.5	100	H7	TO-247AC FullPak 
IRFIP054	60	0.014	64	45	1.3	120		
IRFIP140	100	0.077	23	16	1.5	100		
IRFIP150	100	0.055	31	22	1.3	120		
IRFIP240	200	0.18	14	8.9	1.5	83		
IRFIP250	200	0.085	22	14	1.3	96		
IRFIP244	250	0.28	11	6.9	1.5	44		
IRFIP254	250	0.14	17	11	1.3	96		
IRFIP340	400	0.55	8.0	5.1	1.5	83		
IRFIP350	400	0.30	11	7.0	1.3	96		
IRFIP440	500	0.85	6.4	4.0	1.5	83		
IRFIP448	500	0.60	7.4	4.7	1.4	89		
IRFIP450	500	0.40	10	6.5	1.3	96		

Other Products from IR

HEXFET Power MOSFETs Fully Isolated HEXFET

TO-3P FullPak P-Channel

Part Number	V(BR) _{DSS} Drain-to-Source Breakdown Voltage (Volt)	R _{DS(on)} On-State Resistance (Ohms)	I _D Continuous Drain Current 25°C (Amps)	I _D Continuous Drain Current 100°C (Amps)	R _{thJA} Max Thermal Resistance (°C/W)	P _d @T _c = 25°C Max Power Dissipation (Watts)	Case Outline Number	Case Style
IRFIP9140	-100	0.20	-15	-11	1.5	100	H7	TO-247AC FullPak
IRFIP9240	-200	0.50	-8.9	-5.6	1.5	83		


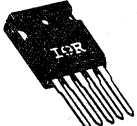


HEXSense

HEXSense Power MOSFETs provide the user with the ability to sense the current through the device by measuring a small proportion of the total drain current. The current-sensing is accomplished through the addition of the kelvin and current-sense connections providing for greater accuracy, wider bandwidths and cost-savings in current-mode applications.

HEXSENSE N-Channel

Part Number	V(BR) _{DSS} Drain-to-Source Breakdown Voltage (Volt)	R _{DS(on)} On-State Resistance (Ohms)	I _D Continuous Drain Current 25°C (Amps)	I _D Continuous Drain Current 100°C (Amps)	R _{thJA} Max Thermal Resistance (°C/W)	P _d @T _c = 25°C Max Power Dissipation (Watts)	Nominal Sense Number	Case Outline Number	Case Style
IRCZ24	60	0.10	17	12	2.5	60	820	H8	TO-220 Hexsense
IRCZ34	60	0.050	30	21	1.7	88			
IRCZ44	60	0.028	50	37	1.0	150			
IRC530	100	0.16	14	10	1.7	88			
IRC540	100	0.077	28	20	1.0	150			
IRC630	200	0.40	9.0	5.7	1.7	74			
IRC640	200	0.18	18	11	1.0	125			
IRC634	250	0.45	8.1	5.1	1.7	74			
IRC644	250	0.28	14	8.5	1.0	125			
IRC730	400	1.0	5.5	3.5	1.0	74			
IRC740	400	0.55	10	6.3	1.0	125			
IRC830	500	1.5	4.5	3.0	1.7	74			
IRC840	500	0.85	8.0	5.1	1.0	125			
IRCP054	60	0.014	70	64	0.65	230			


HEXFET Power MOSFETs

HEXDips


Other Products from IR

Low charge Hexfets reduce gate charge by 40% or more and capacitances by up to 85% without any added device cost.

HEXDIPS N-Channel "Low Charge"


Part Number	V(BR) _{DSS} Drain-to-Source Breakdown Voltage (Volt)	R _{DS(on)} On-State Resistance (Ohms)	I _D Continuous Drain Current 25°C (Amps)	I _D Continuous Drain Current 100°C (Amps)	R _{thJA} Max Thermal Resistance (°C/W)	P _d @T _c = 25°C Max Power Dissipation (Watts)	Case Outline Number	Case Style
IRFD010LC	600	10	0.25	12	120	1.3	H10	HEXDIPS (HD-1) 

HEXDIPS N-Channel


Part Number	V(BR) _{DSS} Drain-to-Source Breakdown Voltage (Volt)	R _{DS(on)} On-State Resistance (Ohms)	I _D Continuous Drain Current 25°C (Amps)	I _D Continuous Drain Current 100°C (Amps)	R _{thJA} Max Thermal Resistance (°C/W)	P _d @T _c = 25°C Max Power Dissipation (Watts)	Case Outline Number	Case Style
IRFD014	60	0.20	1.7	1.2	120	1.3	H10	HEXDIPS (HD-1) 
IRFD024	60	0.10	2.5	1.8	120	1.3		
IRFD120	100	2.4	0.50	0.36	120	1.3		
IRFD110	100	1.0	1.0	0.71	120	1.3		
IRFD120	100	0.27	1.3	0.94	120	1.3		
IRFD210	200	1.5	0.60	0.38	120	1.3		
IRFD220	200	0.80	0.80	0.50	120	1.3		
IRFD214	250	2.0	0.57	0.32	120	1.3		
IRFD224	250	1.1	0.76	0.43	120	1.3		
IRFD310	400	3.6	0.42	0.23	120	1.3		
IRFD320	400	1.8	0.60	0.33	120	1.3		
IRFD420	500	3.0	0.46	0.26	120	1.3		
IRFD620	600	4.4	0.32	0.21	120	1.3		

Logic-level HEXFETs are fully-enhanced with 4 or 5V applied to the gate.

HEXDIPS Logic Level N-Channel

Part Number	V(BR) _{DSS} Drain-to-Source Breakdown Voltage (Volt)	R _{DS(on)} On-State Resistance (Ohms)	I _D Continuous Drain Current 25°C (Amps)	I _D Continuous Drain Current 100°C (Amps)	R _{thJA} Max Thermal Resistance (°C/W)	P _d @T _c = 25°C Max Power Dissipation (Watts)	Case Outline Number	Case Style
IRLD014	60	0.20	1.7	1.2	120	1.3	H10	HEXDIPS (HD-1) 
IRLD024	60	0.10	2.5	1.8	120	1.3		
IRLD110	100	0.54	1.0	0.70	120	1.3		
IRLD120	100	0.27	1.3	0.94	120	1.3		

HEXDIPS P-Channel

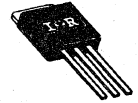
Part Number	V(BR) _{DSS} Drain-to-Source Breakdown Voltage (Volt)	R _{DS(on)} On-State Resistance (Ohms)	I _D Continuous Drain Current 25°C (Amps)	I _D Continuous Drain Current 100°C (Amps)	R _{thJA} Max Thermal Resistance (°C/W)	P _d @T _c = 25°C Max Power Dissipation (Watts)	Case Outline Number	Case Style
IRFD9014	-60	0.50	-1.1	-0.80	120	1.3	H10	HEXDIPS (HD-1) 
IRFD9024	-60	0.28	-1.6	-1.1	120	1.3		
IRFD9110	-100	1.2	-0.70	-0.49	120	1.3		
IRFD9120	-100	0.60	-1.0	-0.70	120	1.3		
IRFD9210	-200	3.0	-0.40	-0.25	120	1.3		
IRFD9220	-200	1.5	-0.56	-0.36	120	1.3		

Other Products from IR

HEXFET Power MOSFETs I-Pak

I-Pak (TO-251AA) N-Channel

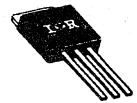
Part Number	V(BR) _{DSS} Drain-to-Source Breakdown Voltage (Volt)	R _{DS(on)} On-State Resistance (Ohms)	I _D Continuous Drain Current 25°C (Amps)	I _D Continuous Drain Current 100°C (Amps)	R _{thJA} Max Thermal Resistance (°C/W)	P _d @T _c = 25°C Max Power Dissipation (Watts)	Case Outline Number	Case Style
IRFU014	60	0.20	7.7	4.9	5.0	25	H11	I-Pak (TO-251AA)
IRFU024	60	0.10	14	9.0	3.0	42		
IRFU110	100	0.54	4.3	2.7	5.0	25		
IRFU120	100	0.27	7.7	4.9	3.0	42		
IRFU210	200	1.5	2.6	1.7	5.0	25		
IRFU220	200	0.80	4.8	3.0	3.0	42		
IRFU214	250	2.0	2.2	1.4	5.0	25		
IRFU224	250	1.1	3.8	2.4	3.0	42		
IRFU310	400	3.6	1.7	1.1	5.0	25		
IRFU320	400	1.8	3.1	2.0	3.0	42		
IRFU420	500	3.0	2.4	1.5	3.0	42		
IRFUC20	600	4.4	2.0	1.3	3.0	42		



Logic-level HEXFETs are fully-enhanced with 4 or 5V applied to the gate.

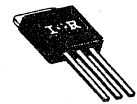
I-Pak (TO-251AA) Logic Level N-Channel

Part Number	V(BR) _{DSS} Drain-to-Source Breakdown Voltage (Volt)	R _{DS(on)} On-State Resistance (Ohms)	I _D Continuous Drain Current 25°C (Amps)	I _D Continuous Drain Current 100°C (Amps)	R _{thJA} Max Thermal Resistance (°C/W)	P _d @T _c = 25°C Max Power Dissipation (Watts)	Case Outline Number	Case Style
IRLU014	60	0.20	7.7	4.9	5.0	25	H11	I-Pak (TO-251AA)
IRLU024	60	0.10	14	9.2	3.0	42		
IRLU110	100	0.54	4.3	2.7	5.0	25		
IRLU120	100	0.27	7.7	4.9	3.0	42		



I-Pak (TO-251AA) P-Channel

Part Number	V(BR) _{DSS} Drain-to-Source Breakdown Voltage (Volt)	R _{DS(on)} On-State Resistance (Ohms)	I _D Continuous Drain Current 25°C (Amps)	I _D Continuous Drain Current 100°C (Amps)	R _{thJA} Max Thermal Resistance (°C/W)	P _d @T _c = 25°C Max Power Dissipation (Watts)	Case Outline Number	Case Style
IRFU9014	-60	0.50	-5.1	-3.2	5.0	25	H11	I-Pak (TO-251AA)
IRFU9024	-60	0.28	-8.8	-5.6	3.0	42		
IRFU9110	-100	1.2	-3.1	-2.0	5.0	25		
IRFU9120	-100	0.60	-5.6	-3.6	3.0	42		
IRFU9210	-200	3.0	-1.9	-1.2	5.0	25		
IRFU9220	-200	1.5	-3.6	-2.3	3.0	42		



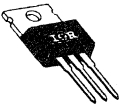
HEXFET Power MOSFETs

TO-220AB

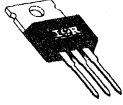
Other Products from IR

Logic-level HEXFETs are fully-enhanced with 4 or 5V applied to the gate.

TO-220AB Logic Level N-Channel

Part Number	V(BR) _{DSS} Drain-to-Source Breakdown Voltage (Volt)	R _{DS(on)} On-State Resistance (Ohms)	I _D Continuous Drain Current 25°C (Amps)	I _D Continuous Drain Current 100°C (Amps)	R _{thJA} Max Thermal Resistance (°C/W)	P _d @T _c = 25°C Max Power Dissipation (Watts)	Case Outline Number	Case Style
IRL2203	30	0.010	92	65	1.0	150	H12	TO-220AB 
IRL3705	50	0.012	80	57	1.0	150		
IRLZ14	60	0.20	10	7.2	3.5	43		
IRLZ24	60	0.10	17	12	2.5	60		
IRLZ34	60	0.050	30	21	1.7	88		
IRLZ44	60	0.028	50	36	1.01	150		
IRL510	100	0.54	5.6	4.0	3.5	43		
IRL520	100	0.27	9.2	6.5	2.5	60		
IRL530	100	0.16	15	11	1.7	88		
IRL540	100	0.077	28	20	1.0	150		

TO-220AB P-Channel

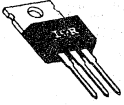
Part Number	V(BR) _{DSS} Drain-to-Source Breakdown Voltage (Volt)	R _{DS(on)} On-State Resistance (Ohms)	I _D Continuous Drain Current 25°C (Amps)	I _D Continuous Drain Current 100°C (Amps)	R _{thJA} Max Thermal Resistance (°C/W)	P _d @T _c = 25°C Max Power Dissipation (Watts)	Case Outline Number	Case Style
IRF9Z14	-60	0.50	-6.7	-4.7	3.5	43	H12	TO-220AB 
IRF9Z24	-60	0.28	-11	-7.7	2.5	60		
IRF9Z34	-60	0.14	-18	-13	1.7	88		
IRF9510	-100	1.2	-4.0	-2.8	3.5	43		
IRF9520	-100	0.60	-6.8	-4.8	2.5	60		
IRF9530	-100	0.30	-12	-8.2	1.7	88		
IRF9540	-100	0.20	-19	-13	1.0	150		
IRF9610	-200	3.0	-1.8	-1.0	6.4	20		
IRF9620	-200	1.5	-3.5	-2.0	3.1	40		
IRF9630	-200	0.80	-6.5	-4.0	1.7	74		
IRF9640	-200	0.50	-11	6.8	1.0	125		

Other Products from IR

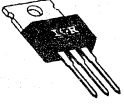
HEXFET Power MOSFETs TO-220AB

Low charge Hexfets reduce gate charge by 40% or more and capacitances by up to 85% without any added device cost.

TO-220AB N-Channel - "Low Charge"

Part Number	V(BR) _{DSS} Drain-to-Source Breakdown Voltage (Volt)	R _{DS(on)} On-State Resistance (Ohms)	I _D Continuous Drain Current 25°C (Amps)	I _D Continuous Drain Current 100°C (Amps)	R _{thJA} Max Thermal Resistance (°C/W)	P _d @ T _c = 25°C Max Power Dissipation (Watts)	Case Outline Number	Case Style
IRF740LC	400	0.55	10	39	1.0	125	H12	TO-220AB 
IRF840LC	500	0.85	8.0	39	1.0	125		
IRFBC40LC	600	1.2	6.2	39	1.0	125		
IRFBC10LC	600	10	1.2	12	3.5	36		

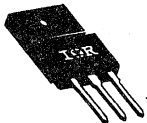
TO-220AB N-Channel

Part Number	V(BR) _{DSS} Drain-to-Source Breakdown Voltage (Volt)	R _{DS(on)} On-State Resistance (Ohms)	I _D Continuous Drain Current 25°C (Amps)	I _D Continuous Drain Current 100°C (Amps)	R _{thJA} Max Thermal Resistance (°C/W)	P _d @ T _c = 25°C Max Power Dissipation (Watts)	Case Outline Number	Case Style
IRFZ46	50	0.024	50	38	1.0	150	H12	TO-220AB 
IRF1010	55	0.014	75	53	1.0	150		
IRFZ14	60	0.20	10	7.2	3.5	43		
IRFZ24	60	0.10	17	12	2.5	60		
IRFZ34	60	0.050	30	21	1.7	88		
IRFZ44	60	0.028	50	36	1.0	150		
IRFZ48	60	0.018	50	50	0.80	190		
IRF510	100	0.54	5.6	4.0	3.5	43		
IRF520	100	0.27	9.2	6.5	2.5	60		
IRF530	100	0.16	14	10	1.7	88		
IRF540	100	0.077	28	20	1.0	150		
IRF1310	100	0.040	43	25	1.0	150		
IRF610	200	1.5	3.3	2.1	3.5	36		
IRF620	200	0.80	5.2	3.3	2.5	50		
IRF630	200	0.40	9.0	5.7	1.7	74		
IRF640	200	0.18	18	11	1.0	125		
IRF614	250	2.0	2.7	1.7	3.5	36		
IRF624	250	1.1	4.4	2.8	2.5	50		
IRF634	250	0.45	8.1	5.1	1.7	74		
IRF644	250	0.28	14	8.5	1.0	125		
IRF710	400	3.6	2.0	1.2	3.5	36		
IRF720	400	1.8	3.3	2.1	2.5	50		
IRF730	400	1.0	5.5	3.3	1.7	74		
IRF740	400	0.55	10	6.3	1.0	125		
IRF820	500	3.0	2.5	1.6	2.5	50		
IRF734	450	1.2	4.9	3.1	1.7	74		
IRF744	450	0.63	8.8	5.6	1.0	125		
IRF830	500	1.5	4.5	2.9	1.7	74		
IRF840	500	0.85	8.0	5.1	1.0	125		
IRFBC20	600	4.4	2.2	1.4	2.5	50		
IRFBC30	600	2.2	3.6	2.3	1.7	74		
IRFBC40	600	1.2	6.2	3.9	1.0	125		
IRFBE20	800	6.5	1.8	1.2	2.3	54		
IRFBE30	800	3.0	4.1	2.6	2.0	125		
IRFBF20	900	8.0	1.7	1.1	2.3	54		
IRFBF30	900	3.7	3.6	2.3	1.0	125		
IRFBG20	1000	11	1.4	0.86	2.3	54		
IRFBG30	1000	5.0	3.1	2.0	1.0	125		




Low charge Hexfets reduce gate charge by 40% or more and capacitances by up to 85% without any added device cost.

TO-247AC N-Channel - "Low Charge"

Part Number	V(BR) _{DSS} Drain-to-Source Breakdown Voltage (Volt)	R _{DS(on)} On-State Resistance (Ohms)	I _D Continuous Drain Current 25°C (Amps)	I _D Continuous Drain Current 100°C (Amps)	R _{thJA} Max Thermal Resistance (°C/W)	P _d @T _c = 25°C Max Power Dissipation (Watts)	Case Outline Number	Case Style
IRFP350LC	400	0.30	18	70	0.65	190	H13	TO-247AC 
IRFP360LC	400	0.20	23	98	0.45	280		
IRFP450LC	500	0.40	16	70	0.65	190		
IRFP460LC	500	0.27	20	98	0.45	280		
IRFPC50LC	600	0.60	13	70	0.65	190		
IRFPC60LC	600	0.40	16	98	0.45	280		

TO-247AC P-Channel

Part Number	V(BR) _{DSS} Drain-to-Source Breakdown Voltage (Volt)	R _{DS(on)} On-State Resistance (Ohms)	I _D Continuous Drain Current 25°C (Amps)	I _D Continuous Drain Current 100°C (Amps)	R _{thJA} Max Thermal Resistance (°C/W)	P _d @T _c = 25°C Max Power Dissipation (Watts)	Case Outline Number	Case Style
IRFP9140	-100	0.20	-21	-15	0.83	180	H13	TO-247AC 
IRFP9240	-200	0.50	-12	-7.5	0.83	150		

Other Products from IR

HEXFET Power MOSFETs TO-247AC

TO-247AC N-Channel

Part Number	V(BR) _{DSS} Drain-to-Source Breakdown Voltage (Volt)	R _{DS(on)} On-State Resistance (Ohms)	I _D Continuous Drain Current 25°C (Amps)	I _D Continuous Drain Current 100°C (Amps)	R _{thJA} Max Thermal Resistance (°C/W)	P _d @T _c = 25°C Max Power Dissipation (Watts)	Case Outline Number	Case Style
IRFP044	60	0.028	57	40	0.83	180	H13	TO-247AC
IRFP048	60	0.018	70	52	0.80	190		
IRFP054	60	0.014	70	64	0.65	230		
IRFP064	60	0.009	70	70	0.50	300		
IRFP140	100	0.077	31	22	0.83	180		
IRFP150	100	0.055	41	29	0.65	230		
IRFP240	200	0.18	20	12	0.83	150		
IRFP250	200	0.085	30	19	0.65	190		
IRFP260	200	0.055	46	29	0.45	280		
IRFP244	250	0.28	15	9.7	0.83	150		
IRFP254	250	0.14	23	15	0.65	190		
IRFP264	250	0.075	38	24	0.45	280		
IRFP340	400	0.55	11	6.9	0.83	150		
IRFP350	400	0.30	16	10	0.65	190		
IRFP360	400	0.20	23	14	0.45	280		
IRFP344	450	0.63	9.5	6.0	0.83	150		
IRFP354	450	0.35	14	9.1	0.65	190		
IRFP440	500	0.85	8.8	5.6	0.83	150		
IRFP448	500	0.60	11	6.6	0.70	180		
IRFP450	500	0.40	14	8.7	0.65	190		
IRFP460	500	0.27	20	13	0.45	280		
IRFPC30	600	2.2	4.3	2.7	1.2	100		
IRFPC40	600	1.2	6.8	4.3	0.83	150		
IRFPC50	600	0.60	11	7.0	0.65	180		
IRFPG60	600	0.40	16	10	0.45	280		
IRFPC48	600	0.82	8.9	5.6	0.73	170		
IRFPE30	800	3.0	4.1	2.6	1.0	125		
IRFPE40	800	2.0	5.4	3.4	0.83	150		
IRFPE50	800	1.2	7.8	4.9	0.65	190		
IRFPF30	900	3.7	3.6	2.3	1.0	125		
IRFPF40	900	2.5	4.7	2.9	0.83	150		
IRFPF50	900	1.6	6.7	4.2	0.65	190		
IRFPG30	1000	5.0	3.1	2.0	1.0	125		
IRFPG40	1000	3.5	4.3	2.7	0.83	150		
IRFPG50	1000	2.0	6.1	3.9	0.65	190		

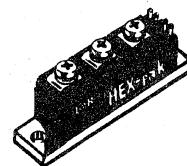
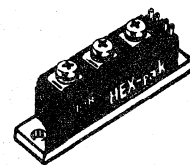


HEXFET Power MOSFETs HEX-Pak Modules

Other Products from IR

TO-240 N-Channel

Part Number	V_{DSS} Drain Source Voltage (Volt)	$R_{DS(on)}$ On-State Resistance (Ohms)	I_D Continuous Drain Current 25°C Case (Amps)	I_{DM} Pulse Drain Current (Amps)	P_D Max Power Dissipation (Watts)	Case Outline Number	Case Style			
IRFK2D054	60	0.010	120	480	500	H14	TO-240AA			
IRFK2D150	100	0.028	72	288						
IRFK2D250	200	0.043	54	216						
IRFK2D350	400	0.150	25	100						
IRFK2D450	500	0.200	22	88						
IRFK2DC50	600	0.350	18	72						
IRFK2DE50	800	0.600	12	48						
IRFK2F054	60	0.010	120	480						
IRFK2F150	100	0.028	72	288						
IRFK2F250	200	0.043	54	216						
IRFK2F350	400	0.150	25	100						
IRFK2F450	500	0.200	22	88						
IRFK2FC50	600	0.350	16	72						
IRFK2FE50	800	0.600	12	48						
IRFK3D150	100	0.020	125	435				625		
IRFK3D250	200	0.030	70	280						
IRFK3D350	400	0.100	37	148						
IRFK3D450	500	0.135	33	132						
IRFK3DC50	600	0.230	24	96						
IRFK3F150	100	0.020	125	435						
IRFK3F250	200	0.030	70	280						
IRFK3F350	400	0.100	37	148						
IRFK3F450	500	0.135	33	132						
IRFK3FC50	600	0.230	24	96						
IRFK4H054	60	0.005	150	960	500	H15	TO-240AA			
IRFK4H150	100	0.014	145	580						
IRFK4H250	200	0.021	108	432						
IRFK4H350	400	0.075	50	200						
IRFK4H450	500	0.100	44	176						
IRFK4HC50	600	0.175	35	140						
IRFK4HE50	800	0.300	26	104						
IRFK4J054	60	0.005	150	960						
IRFK4J150	100	0.014	145	580						
IRFK4J250	200	0.021	108	432						
IRFK4J350	400	0.075	50	200						
IRFK4J450	500	0.100	44	176						
IRFK4JC50	600	0.175	35	140						
IRFK4JE50	800	0.300	26	104						
IRFK6H054	60	0.003	350	1400				625		
IRFK6H150	100	0.010	150	720						
IRFK6H250	200	0.015	140	560						
IRFK6H350	400	0.050	75	300						
IRFK6H450	500	0.067	66	264						
IRFK6HC50	600	0.100	48	192						
IRFK6J054	60	0.003	350	1400						
IRFK6J150	100	0.010	150	720						
IRFK6J250	200	0.015	140	560						
IRFK6J350	400	0.050	75	300						
IRFK6J450	500	0.067	66	264						
IRFK6JC50	600	0.100	48	192						



Other Products from IR

HEXFET Power MOSFETs

Table I. HEXFET III Die

HEX Size	Part Number	V _{DS}	R _{DS(on)} Max	Die Outline Figure	Recomm. Source Bonding Wire		Equivalent Device Type
					mils	mm	
Z	IRFC1Z0	100	2.400	D1	3	0.08	IRFS1Z0
1	IRFC014	60	0.200	D2	5	0.13	IRFZ14
1	IRFC110	100	0.540	D3	5	0.13	IRF510
1	IRFC210	200	1.500	D4	5	0.13	IRF610
1	IRFC214	250	2.000	D4	5	0.13	IRF614
1	IRFC310	400	3.600	D5	5	0.13	IRF710
2	IRFC024	60	0.100	D6	10	0.25	IRFZ24
2	IRFC120	100	0.270	D7	8	0.20	IRF520
2	IRFC220	200	0.800	D8	8	0.20	IRF620
2	IRFC224	250	1.100	D8	8	0.20	IRF624
2	IRFC320	400	1.800	D9	8	0.20	IRF720
2	IRFC420	500	3.000	D9	8	0.20	IRF820
2	IRFCC20	600	4.400	D10	8	0.20	IRFBC20
2	IRFCE20	800	6.500	D11	5	0.13	IRFBE20
2	IRFCF20	900	8.000	D11	5	0.13	IRFBF20
2	IRFCG20	1000	11.500	D11	5	0.13	IRFBG20
3	IRFC034	60	0.050	D12	15	0.38	IRFZ34
3	IRFC130	100	0.160	D13	10	0.25	IRF530
3	IRFC230	200	0.400	D14	8	0.20	IRF630
3	IRFC234	250	0.450	D14	8	0.20	IRF634
3	IRFC330	400	1.000	D15	8	0.20	IRF730
3	IRFC430	500	1.500	D15	8	0.20	IRF830
3	IRFCC30	600	2.200	D16	8	0.20	IRFBC30
3	IRFCE30	800	3.200	D17	10	0.25	IRFBE30
3	IRFCF30	900	4.000	D17	10	0.25	IRFBF30
3	IRFCG30	1000	5.600	D17	10	0.25	IRFBG30
4	IRFC044	50/60	0.028	D19	20	0.15	IRFZ44
4.1	IRFC048	60	0.018	D24	20	0.15	IRFZ48
4	IRFC140	100	0.077	D20	15	0.38	IRF540
4	IRFC240	200	0.180	D21	15	0.38	IRF640
4	IRFC244	250	0.280	D21	15	0.38	IRF644
4	IRFC340	400	0.550	D22	12	0.30	IRF740
4	IRFC440	500	0.850	D22	12	0.30	IRF840
4.5	IRFC448	500/600	0.600	D25	12	0.30	IRFP448
4	IRFCC40	600	1.200	D22	12	0.30	IRFBC40
4	IRFCE40	800	2.000	D23	10	0.25	IRFBE40
4	IRFCF40	900	2.500	D23	10	0.25	IRFBF40
4	IRFCG40	1000	3.500	D23	10	0.25	IRFBG40
5	IRFC054	60	0.014	D26	25	0.64	IRFP054
5	IRFC150	100	0.055	D27	20	0.51	IRFP150
5	IRFC250	200	0.085	D27	20	0.51	IRFP250
5	IRFC254	250	0.140	D27	20	0.51	IRFP254
5	IRFC350	400	0.300	D27	20	0.51	IRFP350
5	IRFC450	500	0.400	D27	20	0.51	IRFP450
5	IRFCC50	600	0.600	D28	20	0.51	IRFPC50
5	IRFCE50	800	1.200	D29	10	0.25	IRFPE50
5	IRFCF50	900	1.600	D29	10	0.25	IRFPF50
5	IRFCG50	1000	2.000	D29	10	0.25	IRFPG50
6	IRFC060	60	-	D30	-	-	-
6	IRFC260	200	(.060)	D31	25	0.64	-
6	IRFC360	400	0.200	D32	25	0.64	IRFP360
6	IRFC460	600	0.270	D32	25	0.64	IRFP460



Table I. HEXFET III Die, cont.

HEX Size	Part Number	V _{DS}	R _{DS(on)} Max	Die Outline Figure	Recomm. Source Bonding Wire		Equivalent Device Type	
					mils	mm		
P-Channel HEXFETs								
1	IRFC9014	-60	0.500	D33	5	0.13	IRFR9014	
1	IRFC9110	-100	1.200	D34	5	0.13	IRF9510	
1	IRFC9210	-200	3.000	D35	5	0.13	IRF9610	
2	IRFC9024	-60	0.280	D36	10	0.25	IRF9Z24	
2	IRFC9120	-100	0.600	D37	8	0.20	IRF9520	
2	IRFC9220	-200	1.500	D38	8	0.20	IRF9620	
3	IRFC9034	-60	0.140	D39	12	0.30	IRF9Z34	
3	IRFC9130	-100	0.300	D40	10	0.25	IRF9530	
3	IRFC9230	-200	0.800	D41	8	0.20	IRF9630	
4	IRFC9044	-60	-	-	20	0.51	-	
4	IRFC9140	-100	0.200	D42	15	0.38	IRF9540	
4	IRFC9240	-200	0.500	D43	15	0.38	IRF9640	
Logic Level Die								
1	IRLC014	60	0.200	D2	5	0.13	IRLZ14	
1	IRLC110	100	0.540	D3	5	0.13	IRL510	
2	IRLC024	60	0.100	D6	10	0.25	IRLZ24	
2	IRLC120	100	0.270	D7	8	0.20	IRL520	
3	IRLC034	60	0.050	D12	15	0.38	IRLZ34	
3	IRLC130	100	0.160	D13	10	0.25	IRL530	
4	IRLC044	60	0.028	D18	20	0.51	IRLZ44	
4	IRLC140	100	0.077	D20	15	0.38	IRL540	
HEXSense Die								
HEX Size	Part Number	V _{DS}	R _{DS(on)} Max	Nominal Sense Ratio	Die Outline Figure	Recomm. Source Bonding Wire		Equivalent Device Type
						mils	mm	
2	IRCC024	60	0.100	780	D44	10	0.25	IRCZ24
3	IRCC034	60	0.050	1410	D45	15	0.38	IRCZ34
3	IRCC130	100	0.160	1430	D46	10	0.25	IRC530
3	IRCC230	200	0.400	1490	D46	8	0.20	IRC630
3	IRCC234	250	0.450	1490	D46	8	0.20	IRC634
3	IRCC330	400	1.000	1525	D46	8	0.20	IRC730
3	IRCC430	500	1.500	1520	D46	8	0.20	IRC830
4	IRCC044	60	0.028	2590	D47	20	0.51	IRCZ44
4	IRCC140	100	0.077	2680	D48	15	0.38	IRC540
4	IRCC240	200	0.180	2740	D48	15	0.38	IRC640
4	IRCC244	250	0.280	2770	D48	15	0.38	IRC644
4	IRCC340	400	0.550	2800	D48	12	0.30	IRC740
4	IRCC440	500	0.850	2780	D48	12	0.30	IRC840
5	IRCC054	60	0.014	2200	D49	25	0.64	IRCP054
5	IRCC150	100	0.055	(5440)	D50	20	0.51	-
5	IRCC250	200	0.085	(5680)	D50	20	0.51	-
5	IRCC254	250	0.140	(5440)	D50	20	0.51	-
5	IRCC350	400	0.300	(5440)	D50	20	0.51	-
5	IRCC450	500	0.400	(5440)	D50	20	0.51	-

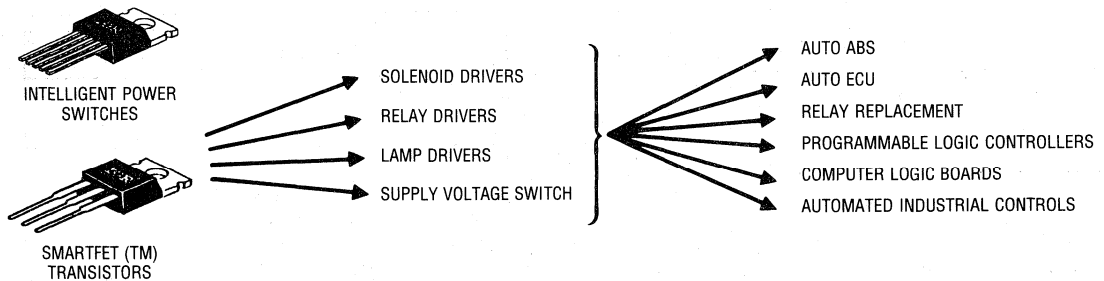
IPS & SmartFET™ (SIV-DCMOS)

For protected power MOSFET switches, International Rectifier employs a self isolated vertical DMOS/CMOS technology. This technology enables IR to provide low voltage (up to 60V) high side protected switches and up to 600V protected low side switches. These switches are used for high reliability systems in automotive, office equipment, industrial automation systems.

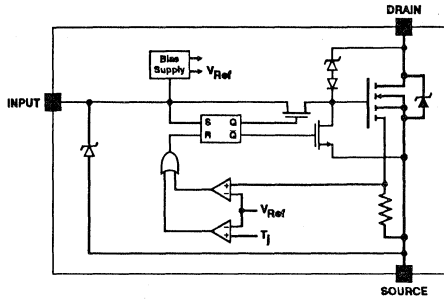
Features (SIVDCMOS)

- Power, control, and diagnostic on a Single Chip
- Overcurrent protection
- Overtemperature protection
- Overvoltage clamping
- Diagnostic
- High Avalanche/clamp energy rating

Use IPS and Smart FET transistors to drive power components for these applications



SmartFET™ Transistor

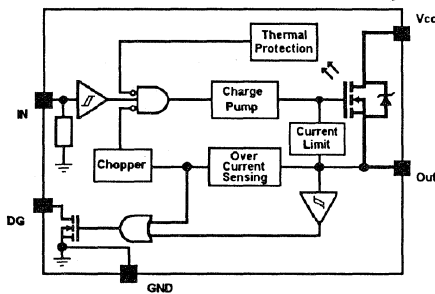


Features

- Extremely rugged for harsh operating environment
- Over-temperature protection
- Over-current protection
- Active drain to source clamp
- ESD protection
- Logic level input threshold
- Compatible with standard POWER MOSFET
- Monolithic construction

Part Number	Continuous Operating Voltage	Shutdown Current	Over Temperature Shutdown	Clamp Voltage (typ.)	On Resistance (max.)	Turn-On Time	Turn-Off Time	Case Outline P10*
	$V_{ds, max.}$ (V)	$I_{ds(isd), min.}$ (A)	$T_{j(isd), typ.}$ (°C)	$V_{ds, clamp}$ (V)	$R_{ds(on)}$ (Ω)	typ. (μs)	typ. (μs)	TO-220
IRSF3010	50	11	165	55	0.080	2.4	1.2	
IRSF3011	50	5	165	55	0.200	0.8	0.5	

High Side Protected DMOS Switch



Features

- High negative output clamp voltage
- Avalanche rated output power DMOS
- Over-temperature protection
- PWM current limit for short circuit protection
- ESD protection
- Open circuit detection in off-state
- Diagnostic feedback
- LSTTL/CMOS compatible logic input

Part Number	Continuous Operating Voltage	Current Limit	Over Temperature Shutdown	Clamp Voltage (typ.)	On Resistance (max.)	Turn-On Time	Turn-Off Time	Case Outline P9*
	$V_{ds, max.}$ (V)	$I_{LIM, min.}$ (A)	$T_{j(isd), typ.}$ (°C)	$V_{ds, clamp}$ (V)	$R_{ds(on)}$ (Ω)	typ. (μs)	typ. (μs)	TO-220 5 lead
IR6000	35	4	175	72	0.100	100	140	
IR6001	35	12	175	72	0.100	100	140	

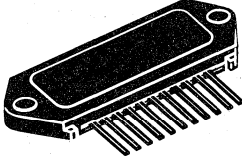
* Other packages available - consult factory.
For case outline drawings see page O-2.

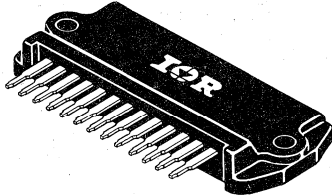
The Powerline and IMS Packages

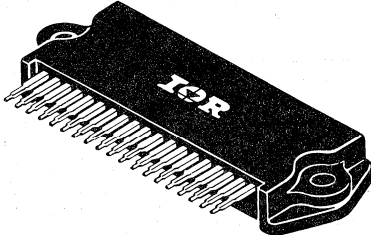
The Power Interface Products family are available in three different package outlines. All three are Single-In-Line Packages (SIP) printed circuit board compatible modules. The packages are the Powerline 1, IMS-1 and IMS-2 shown below. These packages are available with standard configurations as described on page and are also available for semi-custom design to meet your

specific circuit requirements. They may include HEXFET's, IGBT's, Logic Level HEXFET's, IC's, resistors, capacitors, Diodes, (Schottky, Zener or FRED's) chips as well as surface mount components. Customer specified lead forming and terminations are also available.

Powerline Packages for standard or semi-custom designs.

Max No. of Pins: 11 on 0.1" centers	<p style="text-align: center;">Powerline 1</p>  <p style="text-align: center;">1.5" x 0.5" x 0.13" power SIP</p>
Maximum Current: 10 Amps	
Power Range: 20 Watts to 100 Watts	
Circuit and Component Capability	
3 ϕ Bridge with HEX-2 Die and Diodes	
H Bridge with HEX-3 Die and Diodes	
1/2 Bridge with HEX-5 Die, Diodes, and Logic	
Typical Applications	
FHP Motors; Actuators; Power Amplifiers	

Max No. of Pins: 13	<p style="text-align: center;">IMS-1</p> 
Power Range: 20 Watts to 80 Watts	
Circuit and Component Capability	
3 ϕ Bridge with IGBT-2 Die and Diodes	
H-Bridge HEX-4 Die and Diodes	
Single Phase Leg with IGBT-5 Die and Diodes	
Typical Applications	
Power Supplies and Motor controls	

Max No. of Pins: 19	<p style="text-align: center;">IMS-2</p> 
Power Range: 30 Watts to 125 Watts	
Circuit and Component Capability	
3 ϕ Bridge with IGBT-4 Die and Diodes	
H-Bridge HEX-6 Die and Diodes	
Single Phase Leg with IR2110, IGBT-4 Die and Diodes	
Typical Applications	
Power Supplies and Motor controls	

For case outline drawing see page



Power Interface Products



HEXFET POWER MODULES

PART NUMBER	V _{DS} (V)	I _D MAX. (1) @ T _C = 45°C (AMPS)	MAX. R _{DS(ON)} PER SWITCH		V _{SD} (2) PER SWITCH		TYPICAL R _{THJC} (K/W)	CIRCUIT	CASE OUTLINE NUMBER (7)	NOTES	CASE STYLE
			LOW SIDE (OHMS)	HIGH SIDE (OHMS)	LOW SIDE (VOLTS)	HIGH SIDE (VOLTS)					

3 ϕ BRIDGES for brushless DC motors

IRFT002	60	6.1	0.10	0.28	1.25	-6.3	5.6	A	CP1	—	POWERLINE 1
CPY302F	60	6.1	0.10	0.28	1.25	1.5	5.6	B	CP1	(4)(6)	POWERLINE 1
IRFT001	100	3.6	0.30	0.60	2.5	-6.3	7.5	A	CP1	—	POWERLINE 1

FULL BRIDGES for stepper motors, brush DC motors, servo amplifiers, power supplies

CPY203E	60	10.1	0.05	0.14	1.6	1.5	5.6	C	CP1	(3)(4)(6)	POWERLINE 1
IRFT003	60	6.1	0.10	0.28	1.25	-6.3	3.8	G	CP1	—	POWERLINE 1

UNIPOLAR DRIVE for stepper motors, solenoid drives

CPY400H	100	7.8	0.18	—	2.5	1.5	5.3	F	CP1	(4)(6)	POWERLINE 1
---------	-----	-----	------	---	-----	-----	-----	---	-----	--------	-------------

IGBT POWER MODULES

PART NUMBER	V _{DS} (V)	P _D MAX. @ 25°C (W)	V _{CE} (V) @ (A)		CIRCUIT	CASE OUTLINE	NOTES	CASE STYLE
-------------	---------------------	--------------------------------	---------------------------	--	---------	--------------	-------	------------

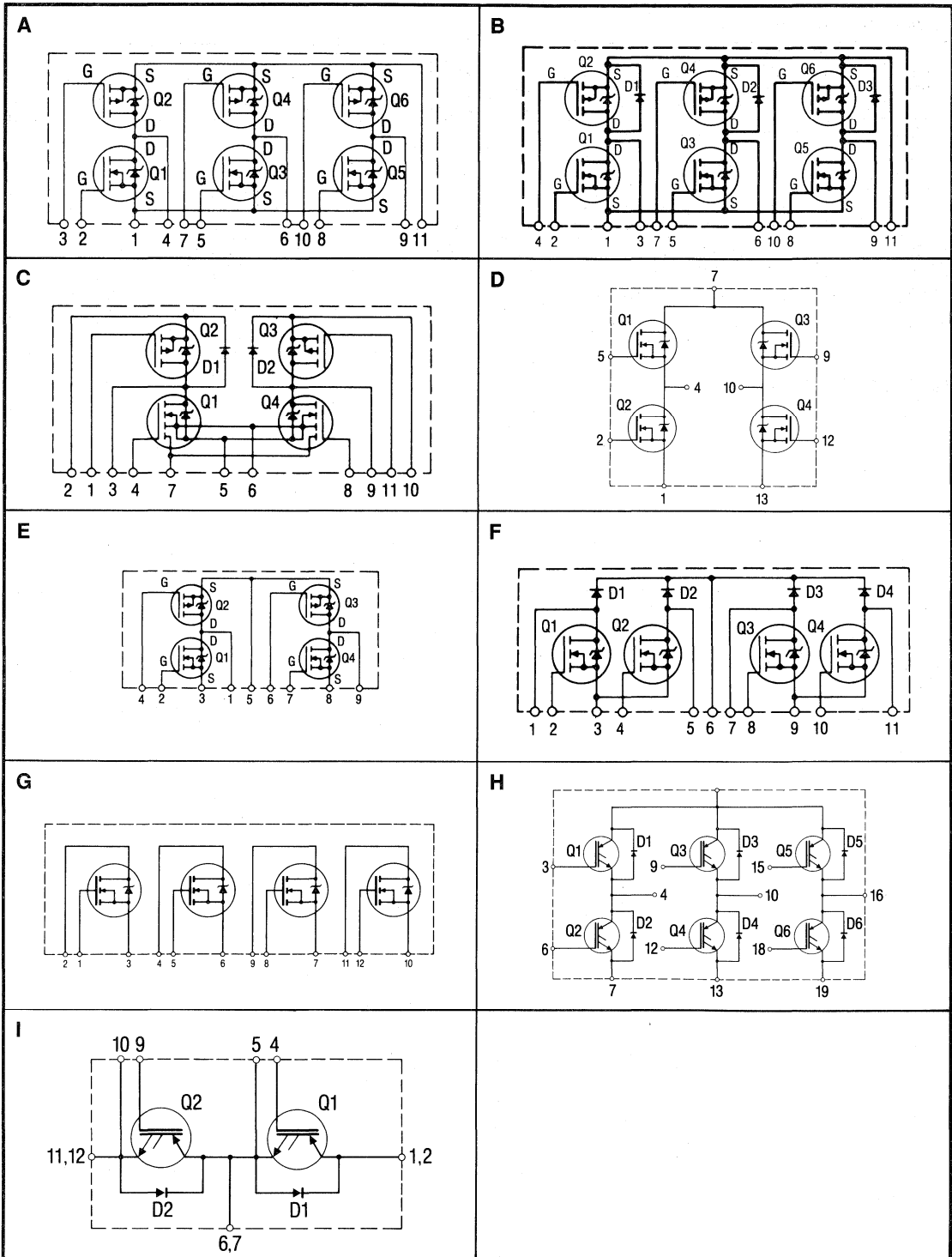
3 ϕ BRIDGES FOR AC MOTOR CONTROLS

CPU362MF	600	23	2.3	8.8	H	CP4	8	IMS-2
CPU362MU	600	23	2.5	7.2	H	CP4	9	IMS-2
CPV363MF	600	35.9	2.0	15.9	H	CP4	8	IMS-2
CPV363MU	600	35.9	2.8	13	H	CP4	9	IMS-2
CPV364MF	600	62.5	2.0	27	H	CP4	8	IMS-2
CPV364MU	600	62.5	3.1	28	H	CP4	9	IMS-2

HALF BRIDGES FOR AC MOTOR CONTROLS

CPU165MF	600	83	1.9	42	I	CP3	8	IMS-1
CPU165MU	600	83	2.7	83	I	CP3	9	IMS-1

- (1) Complementary pair; p-channel limited where applicable. (2) Typical; consult the data sheet for conditions. (3) Contains HEXSense® current-sensing die. (4) Includes freewheeling diodes across the p-channel die. (5) Employs gate-source zener diodes for ESD protection. (6) V_{SD} value given for reverse conduction through freewheeling diode. (7) For case outline drawing see page 0-2. (8) Using Fast IGBT. (9) Using UltraFast IGBT.



Custom solutions are readily available if the POWERLINE and IMS packages or standard circuit configurations do not meet your specific application needs. IR has years of experience designing and manufacturing custom products and can provide the flexibility and expertise necessary to meet your unique power packaging requirement.

Design Experience

The Power Interface Products Group is dedicated to meeting the design needs of the customer. Computer-aided design and thermal analysis capabilities are utilized to minimize the time and cost of achieving the most complex and demanding design requirements. The combined experience of our development team offers design support and customer responsiveness second to none.

Advanced Manufacturing

Our manufacturing facility houses a full compliment of automatic assembly and test equipment necessary to develop and manufacture power modules to meet virtually any application specific power packaging requirement. This facility offers flexibility to provide hybrid prototype quantities in a short cycle time and high volume capacity to meet your production requirements

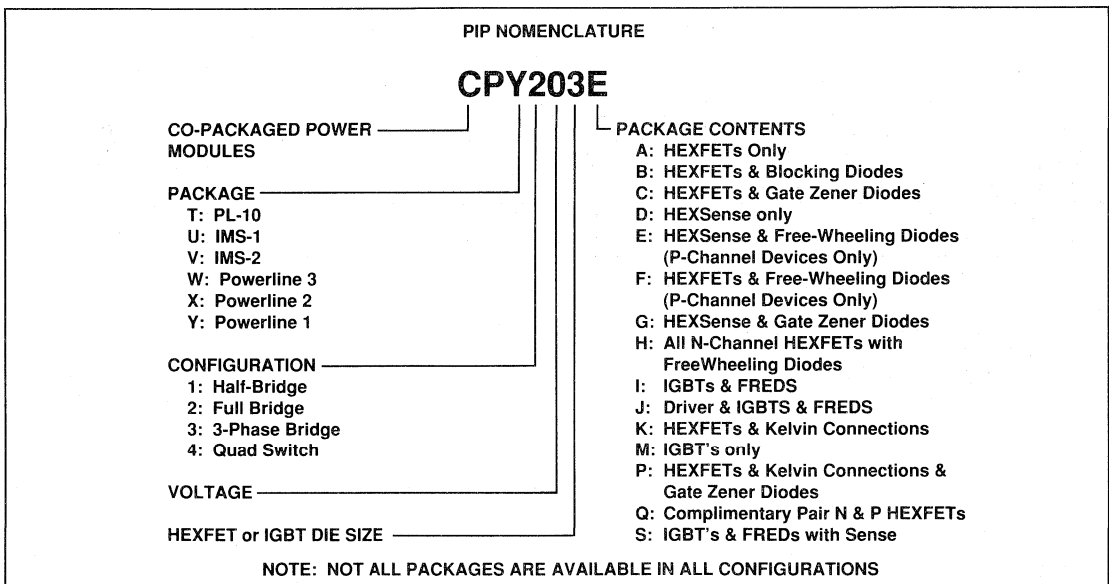
with delivery you can rely upon. Dedicated thick film or direct bond processing, design capability, automatic testing and lead forming capabilities provide the foundation for a total and immediate responsiveness to product quality, reliability, performance and delivery.

Technology Leadership

International Rectifier's established position as a technology leader in power semiconductors has allowed the Power Interface Products Group to establish itself as a leader in semiconductor power packaging. At the forefront of power hybrid technology, both screen printing thick film and direct bond lead-frame technologies are available. Ceramic Substrate or Insulated Metal Substrate technologies with integrated heat-sink systems are offered. Whatever your specific needs, the power packaging technologies are available to provide advanced integration for optimized performance in the minimal space required.

Contact Us Today

To find out more about the custom packaging capabilities at International Rectifier, contact your local sales office or the Power Interface Products Business Management Group.



Part Number	VRWM (V)	IF(AV) @ Tc		IFSM (1) @ 60 Hz (A)	VFM @ IF(AV) (V)	RthJC DC (°C/W)	Max. trr (ns)	Case Outline Number (6)	Notes	Case Style		
		(A)	(°C)									
10DF1	100	1	25	34	1.05	115	100	J5	(2)	DO-204AL DO-41		
10DF2	200	1	25	34	1.05	115	100					
10DF4	400	1	25	34	1.20	115	100					
10DF6	600	1	25	34	1.20	115	100					
10DF8	800	1	25	34	1.20	115	100					
11DF1	100	1	63	31.4	0.98	115	35					
11DF2	200	1	63	31.4	0.98	115	35					
11DF3	300	1	63	31.4	1.25	115	30					
11DF4	400	1	63	31.4	1.25	115	30					
30DF1	100	3	40	90	1.05	80	200	J6		D-201AD		
30DF2	200	3	40	90	1.05	80	200					
30DF4	400	3	40	90	1.25	80	200					
30DF6	600	3	40	90	1.25	80	200					
31DF1	100	3	57	62.8	0.98	80	35					
31DF2	200	3	57	62.8	0.98	80	35					
31DF3	300	3	57	62.8	1.25	80	30					
31DF4	400	3	57	62.8	1.25	80	30					
10MF2	200	1	122	28	0.98	160	50	J1	(3)	D-64		
10BF10	100	1	120	30	0.95	25	35				J2	SMB
10BF20	200	1	120	30	0.95	25	35					
10BF40	400	1	75	30	1.30	30	50					
10BF60	600	1	75	30	1.50	30	100					
10BF80	800	1	75	30	1.70	30	100					
10BF100	1000	1	75	30	1.70	30	100					
30BF10	100	3	120	60	0.95	12	35				J3	SMC
30BF20	200	3	120	60	0.95	12	35					
30BF40	400	3	75	60	1.40	15	50					
30BF60	600	3	75	60	1.50	15	100					
30BF80	800	3	75	60	1.70	15	100					
30BF100	1000	3	75	60	1.70	15	100					
30WF10F	100	3.3	104	31.4	1.35	8	30	J8	(3)	T0-252 D-PAK		
30WF20F	200	3.3	104	31.4	1.35	8	30					
30WF30F	300	3.3	104	31.4	1.35	8	30					
30WF40F	400	3.3	104	31.4	1.35	8	30					
50WF10F	100	5.5	104	47	1.1	6	40					
50WF20F	200	5.5	104	47	1.1	6	40					
50WF30F	300	5.5	104	47	1.1	6	40					
50WF40F	400	5.5	104	47	1.1	6	40					
6CWF10F	100	6.6	117	47	0.98	80	30					
6CWF20F	200	6.6	117	47	0.98	80	30					


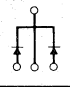
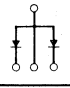
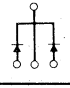
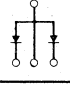

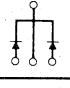
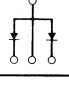













- (1) Following any rated load condition and with rated VRWM reapplied.
- (2) Available on tape and reel. See page 0-2.
- (3) For ordering information on tape and reel see page 0-2.
- (4) Reverse polarity – common anode devices.
- (5) For lead formed options see page 0-2.
- (6) For case outline drawing see page 0-2.

Diodes

Ultra-Fast Recovery

10–25 Amps




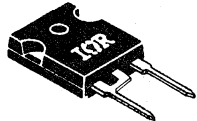
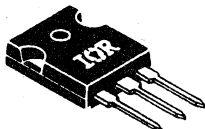


Part Number	V _{RWM} (V)	I _{F(AV)} @ T _C		I _{FSM} (1) @ 60 Hz (A)	V _{FM} @ I _{F(AV)} (V)	R _{thJC} DC (°C/W)	Max. t _{rr} (ns)	Case Outline Number (6)	Notes	Case Style		
		(A)	(°C)									
10CTF10	100	10	117	84	0.98	3	35	J9	(5)	TO-220AB 		
10CTF20	200	10	117	84	0.98	3	35					
10CTF30	300	10	112	84	1.25	3	45					
10CTF40	400	10	112	84	1.25	3	45					
10JTF10	100	10	117	84	0.98	3	35			J11	TO-247AA 	
10JTF20	200	10	117	84	0.98	3	35					
10JTF30	300	10	112	84	1.25	3	45					
10JTF40	400	10	112	84	1.25	3	45					
16CPF10	100	16	113	126	0.98	2	35	(4)	TO-247AA 			
16CPF20	200	16	113	126	0.98	2	35					
16CPF30	300	16	109	126	1.25	2	45					
16CPF40	400	16	109	126	1.25	2	45					
16JPF10	100	16	113	126	0.98	2	35	(4)		TO-247AA 		
16JPF20	200	16	113	126	0.98	2	35					
16JPF30	300	16	109	126	1.25	2	45					
16JPF40	400	16	109	126	1.25	2	45					
25CPF10	100	25	93	157	0.98	2	50		TO-247AA 			
25CPF20	200	25	93	157	0.98	2	50					
25CPF30	300	25	85	183	1.25	2	60					
25CPF40	400	25	85	183	1.25	2	60					
25JPF10	100	25	93	157	0.98	2	50	(4)		TO-247AA 		
25JPF20	200	25	93	157	0.98	2	50					
25JPF30	300	25	85	183	1.25	2	60					
25JPF40	400	25	85	183	1.25	2	60					

- (1) Following any rated load condition and with rated V_{RWM} reapplied.
- (2) Available on tape and reel. See page 0-2.
- (3) For ordering information on tape and reel see page 0-2.
- (4) Reverse polarity – common anode devices.
- (5) For lead formed options see page 0-2.
- (6) For case outline drawing see page 0-2.

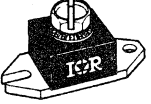
Other Products from IR

HEXFRED™
Discrete - 4-50 Amps

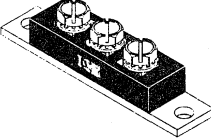
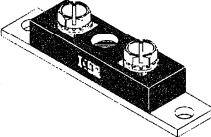
Part Number	V _{RWM} (V)	I _{F(AV)} @ T _C per Pkg.		V _{FM} @ I _{F(AV)} (V)	IR @ V _{RWM} (μA)	R _{thJC} per Pkg. °C/W	Max I _{RRM} (A)	Max t _{rr} (ns)	Case Outline Number	Case Style
		(A)	(°C)							
HFA04TB60S	600	4	106	1.8	3	5	5.2	42	J4	SMD-220 
HFA08TB60S		8	90	1.7	5	3.5	5	55		
HFA15TB60S		15	100	1.7	10	1.7	6	60		
HFA25TB60S		25	100	1.7	20	0.83	10	75		
HFA08TA60CS	600	8	100	1.8	3	2.5	5.2	42		
HFA16TA60CS		16	90	1.7	5	1.75	5	55		
HFA30TA60CS		30	100	1.7	10	0.85	6	60		
HFA04TB60	600	4	106	1.8	3	5	5.2	42	J10	TO-220AC 
HFA08TB60		8	90	1.7	5	3.5	5	55		
HFA15TB60		15	100	1.7	10	1.7	6	60		
HFA25TB60		25	100	1.7	20	0.83	10	75		
HFA08TA60C	600	8	100	1.8	3	2.5	5.2	42	J9	TO-220AB 
HFA16TA60C		16	90	1.7	5	1.75	5	55		
HFA30TA60C		30	100	1.7	10	0.85	6	60		
HFA08PB60	600	8	90	1.7	5	3.5	5	55	J12	TO-247AC (MOD) 
HFA15PB60		15	100	1.7	10	1.7	6	60		
HFA25PB60		25	100	1.7	20	0.83	10	75		
HFA16PA60C	600	16	90	1.7	5	1.75	5	55	J11	TO-247AC 
HFA30PA60C		30	100	1.7	10	0.85	6	60		
HFA50PA60C		50	100	1.7	20	0.42	10	75		

HEXFRED™ Modules - 90-320 Amps

Other Products from IR

Part Number	V _{RWM} (V)	I _{F(AV)} @ T _C per Pkg.		V _{FM} @ I _{F(AV)} (V)	IR @ V _{RWM} (μA)	R _{thJC} per Pkg. °C/W	Max I _{RRM} (A)	Max t _{rr} (ns)	Case Outline Number	Case Style
		(A)	(°C)							
HFA90NH40	400	90	89	1.60	20	0.40	5.5	32	J15	D-67 Half Pak 
HFA90NH40R	400	90	77	1.60	20	0.48	5.5	32		
HFA135NH40	400	135	89	1.60	30	0.27	6.0	36		
HFA135NH40R	400	135	75	1.60	30	0.33	6.0	36		
HFA180NH40	400	180	90	1.60	40	0.20	6.5	40		
HFA180NH40R	400	180	77	1.60	40	0.24	6.5	40		
HFA70NH60	600	70	100	1.43	40	0.40	5.6	32		
HFA70NH60R	600	70	90	1.43	40	0.48	5.6	32		
HFA105NH60	600	105	99	1.43	60	0.27	5.8	34		
HFA105NH60R	600	105	88	1.43	60	0.33	5.8	34		
HFA140NH60	600	140	99	1.43	80	0.20	6.0	36		
HFA140NH60R	600	140	90	1.43	80	0.24	6.0	36		

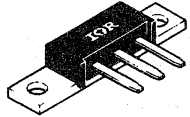
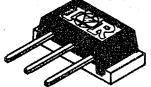

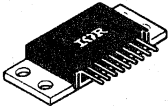
DOUBLER

Part Number	V _{RWM} (V)	I _{F(AV)} @ T _C per Pkg.		V _{FM} @ I _{F(AV)} (V)	IR @ V _{RWM} (μA)	R _{thJC} per Pkg. °C/W	Max I _{RRM} (A)	Max t _{rr} (ns)	Case Outline Number	Case Style
		(A)	(°C)							
HFA120MD40D	400	120	86	1.43	20	0.35	5.5	32	J17	TO-244AB Isolated 
HFA160MD40D	400	160	85	1.39	30	0.275	6.0	36		
HFA200MD40D	400	200	85	1.36	40	0.225	6.5	40		
HFA100MD60D	600	100	91	1.34	40	0.35	5.6	32		
HFA140MD60D	600	140	86	1.32	60	0.275	5.8	34		
HFA180MD60D	600	180	83	1.31	80	0.225	6.0	36		
HFA160NJ40D	400	160	98	1.55	20	0.20	5.5	32	J16	TO-244AB Non-Isolated 
HFA240NJ40D	400	240	97	1.55	30	0.135	6.0	36		
HFA320NJ40D	400	320	98	1.55	40	0.10	6.5	40		
HFA140NJ60D	600	140	100	1.43	40	0.20	5.6	32		
HFA210NJ60D	600	210	100	1.43	60	0.135	5.8	34		
HFA280NJ60D	600	280	100	1.43	80	0.10	6.0	36		


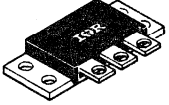
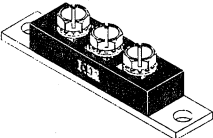
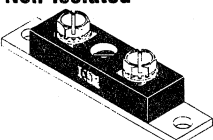
Other Products from IR

HEXFRED™
Modules - 60-320 Amps

CENTER TAP

Part Number	V _{RWM} (V)	I _{F(AV)} @ T _C per Pkg.		V _{FM} @ I _{F(AV)} (V)	IR @ V _{RWM} (μA)	R _{thJC} per Pkg. °C/W	Max I _{RRM} (A)	Max t _{rr} (ns)	Case Outline Number	Case Style
		(A)	(°C)							
HFA80NC40C HFA70NC60C	400 600	80 70	95 97	1.54 1.43	10 20	0.425 0.425	4.0 5.3	22 30	K10	D-61-8 
HFA80NC40CSM HFA70NC60CSM	400 600	80 70	92 94	1.54 1.43	10 20	0.45 0.45	4.0 5.3	22 30	K11	D-61-8SM 
HFA80NC40CSL HFA70NC60CSL	400 600	80 70	92 94	1.54 1.43	10 20	0.45 0.45	4.0 5.3	22 30	K12	D-61-8SL 
HFA75MB40C HFA60MB60C	400 600	75 60	90 98	1.49 1.38	10 20	0.50 0.50	4.0 5.3	22 30	K13	D-60 




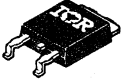

CENTER TAP

Part Number	V _{RWM} (V)	I _{F(AV)} @ T _C per Pkg.		V _{FM} @ I _{F(AV)} (V)	IR @ V _{RWM} (μA)	R _{thJC} per Pkg. °C/W	Max I _{RRM} (A)	Max t _{rr} (ns)	Case Outline Number	Case Style		
		(A)	(°C)									
HFA75MC40C HFA60MC60C	400 600	75 60	90 98	1.49 1.38	10 20	0.50 0.50	4.0 5.3	22 30	K16	TO-249AA Isolated 		
HFA80NK40C HFA70NK60C	400 600	80 70	98 100	1.54 1.43	10 20	0.40 0.40	4.0 5.3	22 30			K15	TO-249AA Non-Isolated 
HFA120MD40C HFA160MD40C HFA200MD40C HFA100MD60C HFA140MD60C HFA180MD60C	400 400 400 600 600 600	120 160 200 100 140 180	86 85 85 91 86 83	1.43 1.39 1.36 1.34 1.32 1.31	20 30 40 40 60 80	0.35 0.275 0.225 0.35 0.275 0.225	5.5 6.0 6.5 5.6 5.8 6.0	32 36 40 32 34 36	J23	TO-244AB - Isolated 		
HFA160NJ40C HFA240NJ40C HFA320NJ40C HFA140NJ60C HFA210NJ60C HFA280NJ60C	400 400 400 600 600 600	160 240 320 140 210 280	98 97 98 100 100 100	1.55 1.55 1.55 1.43 1.43 1.43	20 30 40 40 60 80	0.20 0.135 0.10 0.20 0.135 0.10	5.5 6.0 6.5 5.6 5.8 6.0	32 36 40 32 34 36			J22	TO-244AB Non-Isolated 

Other Products from IR

Schottky Diode


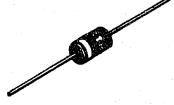
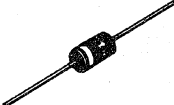

Surface Mount - Discrete
0.77 - 20 Amps

Part Number	VRRM (V)	I _{F(AV)} @ T _C		V _{FM} @ I _{FM} (V)	E _{AS} (mJ)	I _{AR} (A)	I _{RM} @ Rated V _{RWM} (mA)	Max. T _J (°C)	Case Outline Number	Case Style
		(A)	(°C)							
10MQ040	40	1.1	92	0.51			50	125	J1	D-64 
10MQ060	60	0.77	110	0.57	—	—	7.5			
10MQ090	90	0.77	110	0.65			5.0			
15MQ040	40	1.7		0.55	—	—	50			
10BQ015	15	1	78	0.34	5.0	0.2	12	100 150 150 175	J2	SMB 
10BQ040	40	1	112	0.53	18	0.2	4.0			
10BQ060	60	1	103	0.57	11	1.0	5.0			
10BQ100	100	1	152	0.78	9.7	1.0	1.0			
30BQ015	15	3	75	0.35	10	0.6	50	100 150 150 175	J3	SMC 
30BQ040	40	3	123	0.45	35	0.6	20			
30BQ060	60	3	122	0.52	35	3.4	20			
30BQ100	100	3	148	0.62	50	2.8	5			
30WQ03F	30	3.3	105	0.56	—	—	12	125	J8	T0-252AA (D-Pak) 
30WQ04F	40	3.3	105	0.56			12			
30WQ05F	50	3.3	104	0.60			20			
30WQ06F	60	3.3	104	0.60			20			
30WQ09F	90	3.3	103	0.74			2			
30WQ10F	100	3.3	103	0.74			2			
50WQ03F	30	5.5	92	0.60	—	—	20	125	J4	SMD-220 
50WQ04F	40	5.5	92	0.60			20			
50WQ05F	50	5.5	89	0.66			30			
50WQ06F	60	5.5	89	0.66			30			
50WQ09F	90	5.5	90	0.77			3			
50WQ10F	100	5.5	90	0.77			3			
6TQ035S	35	6	163	0.51	8	1.2	7	175	J4	SMD-220
6TQ045S	45									
8TQ080S	80	8	157	0.58	7.5	0.5	7	175		
8TQ100S	100									
10TQ035S	35	10	151	0.49	13	2	15	175		
10TQ045S	45									
12TQ035S	35	15	120	0.50	16	2.4	70	150		
12TQ045S	45									
18TQ035S	35	18	149	0.53	24	3.6	25	175		
18TQ045S	45									
19TQ015S	15	19	80	0.32	6.75	1.5	522	100		
20TQ035S	35	20	116	0.51	27	4	105	150		
20TQ045S	45									

Schottky Diode



Discrete
1.1 - 20 Amps

Other Products from IR

Part Number	VRRM (V)	I _F (AV) @ T _C		V _{FM} @ I _{FM} (V)	E _{AS} (mJ)	I _{AR} (A)	I _{RM} @ Rated V _{RWM} (mA)	Max. T _J (°C)	Case Outline Number	Case Style
		(A)	(°C)							
11DQ03 11DQ04 11DQ05 11DQ06 11DQ09 11DQ10	30 40 50 60 90 100	1.1 1.1 1.1 1.1 1.1 1.1	58 58 40 40 48 48	0.50 0.50 0.53 0.53 0.68 0.68	— —	— —	6 6 11 11 1 1	125	J5	D0-204AL (D0-41) 
31DQ03 31DQ04 31DQ05 31DQ06 31DQ09 31DQ10	30 40 50 60 90 100	3.3 3.3 3.3 3.3 3.3 3.3	35 35 19 19 25 25	0.51 0.51 0.53 0.53 0.69 0.69	— —	— —	25 25 30 30 4 4	125	J6	D0-201AD 
50SQ080 50SQ100	80 100	5	119	0.52	15	1	7	175	J7	D0-204AR 
80SQ035 80SQ040 80SQ045	35 40 45	8	119	0.44	10	1.6	15	175		
90SQ035 90SQ040 90SQ045	35 40 45	9	69	0.42	12	1.8	70	150		
95SQ015	15	9	55	0.25	4.5	1	348	100		
6TQ035 6TQ040 6TQ045	35 40 45	6	163	0.51	8	1.2	7	175		
MBR735 MBR745	35 45	7.5	120	0.57	—	1.0	15	150	J10	T0-220AC 
8TQ080 8TQ100	80 100	8	157	0.58	7.5	0.5	7	175		
MBR1035 MBR1045	35 45	10	120	0.57	—	1.0	15	150		
10TQ035 10TQ040 10TQ045	35 40 45	10	151	0.49	13	2	15	175		
12TQ035 12TQ040 12TQ045	35 40 45	15	120	0.50	16	2.4	70	150		
MBR1635 MBR1645	35 45	16	125	0.57	—	1.0	40	150		
18TQ035 18TQ040 18TQ045	35 40 45	18	149	0.53	24	3.6	25	175		
19TQ015	15	19	80	0.32	6.75	1.5	522	100		
20TQ035 20TQ040 20TQ045	35 40 45	20	116	0.51	27	4	105	150		

Other Products from IR

Schottky Diode Discrete 25 -90 Amps

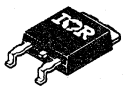

Part Number	VRRM (V)	$I_F(AV) @ T_C$		$V_{FM} @ I_{FM}$ (V)	E_{AS} (mJ)	I_{AR} (A)	$I_{RM} @ \text{Rated } V_{RWM}$ (mA)	Max. T_J (°C)	Case Outline Number	Case Style
		(A)	(°C)							
1N6391	45	25	115	0.78	40	6	40	175	J13	D0-203AA (D0-4) 
1N6095	30	25	105	0.86	40	6	250	125		
1N6096	40									
SD41	35	30	96	0.58	—	—	125	150		
20FQ035	35									
20F0040	40	30	111	0.47	40	6	150	150		
20F0045	45									
21FQ035	35									
21FQ040	40	30	107	0.51	40	6	150	150		
21FQ045	45									
30F0035	35									
30FQ040	40	30	144	0.54	40	6	35	175		
30FQ045	45									
1N6097	30	50	70	0.86	81	12	250	125	J14	D0-203AB (D0-5) 
1N6098	40									
SD51	35	60	90	0.66	—	—	200	150		
1N6392	45	60	115	0.68	101	15	60	175		
50HQ035	35									
50HQ040	40	60	101	0.53	81	12	200	150		
50HQ045	45									
51HQ035	35									
51HQ040	40	60	96	0.58	81	12	200	150		
51HQ045	45									
55HQ030	30	60	110	0.41	54	12	280	150		
60HQ080	80	60	118	0.70	15	1	20	175		
60HQ100	100									
75HQ035	35									
75HQ040	40	75	117	0.63	101	15	45	175		
75HQ045	45									
MBR7535	35	75	90	0.60	—	—	150	150		
MBR7545	45									
85HQ035	35									
85HQ040	40	85	112	0.62	114	17	45	175		
85HQ045	45									
95HQ015	15	95	44	0.39	9	2	1000	100		



Schottky Diode

Center Tap - Surface Mount
6.6 - 30 Amps

Other Products from IR

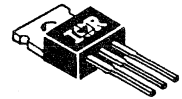
Part Number	VRRM (V)	I _{F(AV)} @ T _C		V _{FM} @ I _{FM} (V)	E _{AS} (mJ)	I _{AR} (A)	I _{RM} @ Rated V _{RWM} (mA)	Max. T _J (°C)	Case Outline Number	Case Style
		(A)	(°C)							
6CWQ03F	30	6.6	97	0.63			20	125	K1	TO-252AA (D-Pak) 
6CWQ04F	40	6.6	97	0.63			20			
6CWQ05F	50	6.6	92	0.67	—	—	30			
6CWQ06F	60	6.6	92	0.67			30			
6CWQ09F	90	6.6	94	0.79			3			
6CWQ10F	100	6.6	94	0.79			3			
10CTQ150S	150	10	145	0.86	6.75	0.30	7	175	K2	SMD-220 
12CTQ035S	35	12	157	0.63	8	1.2	7			
12CTQ045S	45									
15CTQ035S	35	15	123	0.65	10	1.5	32			
15CTQ045S	45									
MBRB1535CT	35	15	105	0.72	—	1.0	15			
MBRB1545CT	45									
16CTQ080S	80	16	145	0.69	7.5	0.5	7			
16CTQ100S	100									
20CTQ035S	35	20	145	0.68	13	2	15			
20CTQ045S	45									
MBRB2080CT	80									
MBRB2090CT	90	10	133	0.70	—	0.5	150			
MBRB20100CT	100									
25CTQ035S	35	30	102	0.64	20	3	70			
25CTQ045S	45									
30CTQ035S	35	30	127	0.70	20	3	15			
30CTQ045S	45									
30CTQ050S	50	30	97	0.71	13	1.5	45			
30CTQ060S	60									
32CTQ030S	30	30	109	0.53	13	3	97			

Other Products from IR

Schottky Diode

Center Tap - Discretes
10- 30 Amps

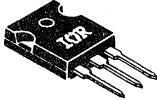


Part Number	VRRM (V)	I _{F(AV)} @ T _C		V _{FM} @ I _{FM} (V)	E _{AS} (mJ)	I _{AR} (A)	I _{RM} @ Rated V _{RWM} (mA)	Max. T _J (°C)	Case Outline Number	Case Style
		(A)	(°C)							
10CTQ150	150	10	145	0.86	6.75	0.30	7	175	K3	TO-220AB
12CTQ035 12CTQ040 12CTQ045	35 40 45	12	157	0.63	8	1.2	7	175		
15CTQ035 15CTQ040 15CTQ045	35 40 45	15	123	0.65	10	1.5	32	150		
MBR1535CT MBR1545CT	35 45	15	105	0.72	—	1.0	15	150		
16CTQ080 16CTQ100	80 100	16	145	0.69	7.5	0.57	175			
20CTQ035 20CTQ040 20CTQ045	35 40 45	20	145	0.68	13	2	15	175		
MBR2035CT MBR2045CT	35 45	20	135	0.72	—	1.0	15	150		
MBR2080CT MBR2090CT MBR20100CT	80 90 100	10	133	0.70	—	0.5	150	150		
MBR2535CT MBR2545CT	35 45	30 30	130	0.73	—	1.0	40	150		
25CTQ035 25CTQ040 25CTQ045	35 40 45	30	102	0.64	20	3	70	150		
30CTQ035 30CTQ040 30CTQ045	35 40 45	30	127	0.70	20	3	15	175		
30CTQ050 30CTQ060	50 60	30	97	0.71	13	1.5	45	150		
32CTQ030	30	30	109	0.53	13	3	97	150		



Schottky Diode

Center Tap - Discrete
30 - 60 Amps

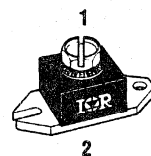
Other Products from IR

Part Number	VRRM (V)	I _{F(AV)} @ T _C		V _{FM} @ I _{FM} (V)	E _{AS} (mJ)	I _{AR} (A)	I _{RM} @ Rated V _{RWM} (mA)	Max. T _J (°C)	Case Outline Number	Case Style		
		(A)	(°C)									
30CPQ035 30CPQ040 30CPQ045	35 40 45	30	124	0.64	20	3	70	150	K4	T0-247AC (T0-3P) 		
30CPQ050 30CPQ060	50 60	30	112	0.70	13	1.5	45	150				
30CPQ080 30CPQ100	80 100	30	140	0.81	7.5	0.5	7	175				
30CPQ150	150	30	131	0.93	11.25	0.5	15	175				
MBR3035PT MBR3045PT	35 45	30	105	0.72	—	2.0	100	150				
40CPQ035 40CPQ040 40CPQ045	35 40 45	40	120	0.56	27	4	150	150				
40CPQ050 40CPQ060	50 60	40	120	0.64	18	2	96	150				
40CPQ080 40CPQ100	80 100	40	145	0.75	11.25	0.75	15	175				
MBR4045PT MBR4060PT MBR6045WT	45 60 45	40 40 60	103 101 100	0.72 0.77 0.69	20 13 —	3 1.5 2	70 45 150	150 150 150				
MBR3035CT MBR3045CT	35 45	30	105	0.72	—	2.0	60	150			K5	T0-204AA (T0-3) 
40CDQ035 40CDQ040 40CDQ045	35 40 45	40	135	0.71	27	4	25	175				
SD241	35	60	120	0.92	—	—	20	175				
60CDQ035 60CDQ040	35 40	60	112	0.80	40	6	25	175			K6	T0-204AE (T0-3 MOD) 

Other Products from IR

Schottky Diode Modules 120 - 180 Amps

Part Number	VRRM (V)	I _{F(AV)} @ T _C		V _{FM} @ I _{FM} (V)	E _{AS} (mJ)	I _{AR} (A)	I _{RM} @ Rated V _{RWM} (mA)	R _{thCS} /Leg (°C/W)	Max. T _J (°C)	Case Outline Number	Case Style
		(A)	(°C)								
120NQ035	35	120	99	0.52	81	12	400	0.40	150	J15	D-67 Half Pak
120NQ040	40										
120NQ045	45										
120NQ045R	45										
121NQ035	35	120	133	0.56	81	12	90	0.40	175		
121NQ040	40										
121NQ045	45										
121NQ045R	45										
122NQ030	30	120	110	0.41	54	12	560	0.40	150		
122NQ030R	30										
123NQ080	80	120	121	0.74	15	1	70	0.40	175		
123NQ100	100										
123NQ100R	100										
124NQ035	35	120	76	0.52	135	20	1200	0.40	125		
124NQ040	40										
124NQ045	45										
124NQ045R	45										
125NQ015	15	120	71	0.33	9	2	1780	0.40	100		
125NQ015R	15										
128NQ060	60	120	120	0.61	75	1.0	480	0.40	150		
128NQ060R	60										
129NQ150	150	120	139	0.74	290	1.0	45	0.40	175		
129NQ150R	150										
180NQ035	35	180	90	0.56	243	36	600	0.30	150		
180NQ040	40										
180NQ045	45										
180NQ045R	45										
181NQ035	35	180	125	0.56	243	36	135	0.30	175		
181NQ040	40										
181NQ045	45										
181NQ045R	45										
182NQ030	30	180	107	0.41	162	36	840	0.30	150		
182NQ030R	30										
183NQ080	80	180	116	0.74	15	1	105	0.30	175		
183NQ100	100										
183NQ100R	100										
185NQ015	15	180	66	0.34	9	2	2670	0.30	100		
185NQ015R	15										
188NQ060	60	180	120	0.61	75	1.0	720	0.30	150		
188NQ060R	60										
189NQ150	150	180	134	0.74	290	1.0	65	0.30	175		
189NQ150R	150										



Standard Configuration



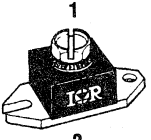
'R' Configuration
Reverse Polarity




Schottky Diode Modules 200 - 400 Amps

Other Products from IR


Part Number	VRRM (V)	$I_F(AV) @ T_C$		$V_{FM} @ I_{FM}$ (V)	E_{AS} (mJ)	I_{AR} (A)	$I_{RM} @$ Rated V_{RWM} (mA)	R_{thCS} /Leg (°C/W)	Max. T_J (°C)	Case Outline Number	Case Style
		(A)	(°C)								
240NQ035	35	240	96	0.55	324	48	800	0.20	150	J15	D-67 Half Pak
240NQ040	40										
240NQ045	45										
240NQ045R	45										
241NQ035	35	240	130	0.59	324	48	180	0.20	175		
241NQ040	40										
241NQ045	45										
241NQ045R	45										
242NQ030	30	240	111	0.42	216	48	1120	0.20	150		
242NQ030R	30										
243NQ080	80	240	120	0.74	15	1.0	140	0.20	175		
243NQ100	100										
243NQ100R	100										
244NQ035	35	240	75	0.52	270	40	2400	0.20	125		
244NQ040	40										
244NQ045	45										
244NQ045R	45										
245NQ015	15	240	70	0.34	9.0	2.0	3560	0.20	100		
245NQ015R	15										
248NQ060	60	240	120	0.61	75	1.0	960	0.20	150		
248NQ060R	60										
249NQ150	150	240	139	0.74	290	1.0	85	0.20	175		
249NQ150R	150										



1
2



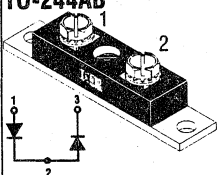
Standard Configuration



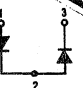
'R' Configuration
Reverse Polarity

DOUBLER

Part Number	VRRM (V)	$I_F(AV) @ T_C$		$V_{FM} @ I_{FM}$ (V)	E_{AS} (mJ)	I_{AR} (A)	$I_{RM} @$ Rated V_{RWM} (mA)	R_{thCS} /Leg (°C/W)	Max. T_J (°C)	Case Outline Number	Case Style
		(A)	(°C)								
203DNQ100	100	200	120	0.72	15	1.0	0.70	0.40	175	K17	TO-244AB
209DNQ150	150	200	100	0.80	32	1.0	50	0.40	175		
203DMQ100	100	200	100	0.72	15	1.0	0.70	0.70	175	K18	TO-244AB
209DMQ150	150	200	97	0.80	32	1.0	50	0.70	175		
400DMQ045	45	400	60	0.62	180	40	800	0.50	150		

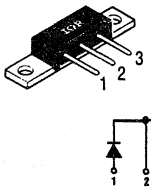
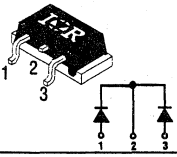
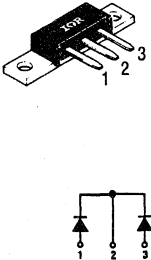


1
2
3



Other Products from IR

Schottky Diode Center Tap - Modules 60 - 80 Amps

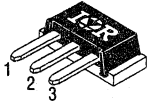
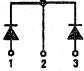
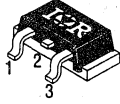
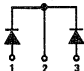

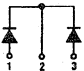

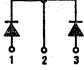
Part Number	VRRM (V)	I _{F(AV)} @ T _C		V _{FM} @ I _{FM} (V)	EAS (mJ)	I _{AR} (A)	I _{RM} @ Rated V _{RWM} (mA)	R _{thCS} /Leg (°C/W)	Max. T _J (°C)	Case Outline Number	Case Style
		(A)	(°C)								
60CNQ035	35	60	116	0.44	40	6.0	200	0.85	150	K7	D61-6 
60CNQ040	40										
60CNQ045	45										
61CNQ035	35	60	149	0.49	40	6.0	45	0.85	175		
61CNQ040	40										
61CNQ045	45										
62CNQ030	30	60	135	0.35	27	6.0	280	0.85	150		
63CNQ080	80	60	155	0.64	15	1.0	35	0.85	175		
63CNQ100	100										
60CNQ045SM	45	60	116	0.44	40	6.0	200	0.85	150		
61CNQ045SM	45	60	149	0.49	40	6.0	45	0.85	175		
62CNQ030SM	30	60	135	0.35	27	6.0	280	0.85	150		
63CNQ100SM	100	60	155	0.64	15	1.0	35	0.85	175		
60CNQ045SL	45	60	116	0.44	40	6.0	200	0.85	150	K9	SLD61-6 
61CNQ045SL	45	60	149	0.49	40	6.0	45	0.85	175		
62CNQ030SL	30	60	135	0.35	27	6.0	280	0.85	150		
63CNQ100SL	100	60	155	0.64	15	1.0	35	0.85	175		
80CNQ035	35	80	109	0.47	54	8.0	200	0.85	150	K10	D61-8 
80CNQ040	40										
80CNQ045	45										
81CNQ035	35	80	141	0.54	54	8.0	45	0.85	175		
81CNQ040	40										
81CNQ045	45										
81CNQ050	50										
82CNQ030	30	80	119	0.35	36	8.0	280	0.85	150		
83CNQ080	80	80	132	0.67	15	1.0	35	0.85	175		
83CNQ100	100										
84CNQ035	35	80	91	0.44	54	8.0	600	0.85	125		
84CNQ040	40										
84CNQ045	45										
85CNQ015	15	80	78	0.32	9.0	2.0	890	0.85	100		
88CNQ060	60	80	95	0.56	75	1.0	240	0.85	150		
89CNQ150	150	80	117	0.69	190	1.0	21	0.85	175		

Schottky Diode

Center Tap - Modules


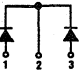
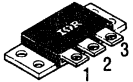
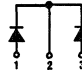
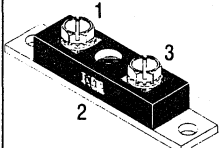
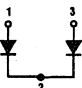
80 - 150 Amps

Other Products from IR

Part Number	VRRM (V)	I _{F(AV)} @ T _C		V _{FM} @ I _{FM} (V)	E _{AS} (mJ)	I _{AR} (A)	I _{RM} @ Rated V _{RWM} (mA)	R _{thCS} /Leg (°C/W)	Max. T _J (°C)	Case Outline Number	Case Style
		(A)	(°C)								
80CNQ045SM	45	80	109	0.47	54	8.0	200	0.85	150	K11	SMD61-8  
81CNQ045SM	45	80	141	0.54	54	8.0	45	0.85	175		
81CNQ050SM	50										
82CNQ030SM	30	80	119	0.35	36	8.0	280	0.85	150		
83CNQ100SM	100	80	132	0.67	15	1.0	35	0.85	175		
84CNQ045SM	45	80	91	0.44	54	8.0	600	0.85	125		
85CNQ015SM	15	80	78	0.32	9.0	2.0	890	0.85	100		
80CNQ045SL	45	80	109	0.47	54	8.0	200	0.85	150	K12	SLD61-8  
81CNQ045SL	45	80	141	0.54	54	8.0	45	0.85	175		
81CNQ050SL	50										
82CNQ030SL	30	80	119	0.35	36	8.0	280	0.85	150		
83CNQ100SL	100	80	132	0.67	15	1.0	35	0.85	175		
84CNQ045SL	45	80	91	0.44	54	8.0	600	0.85	125		
85CNQ015SL	15	80	78	0.32	9.0	2.0	890	0.85	100		
150CMQ035	35	150	71	0.60	101	15	200	1.00	150	K13	D-60  
150CMQ040	40										
150CMQ045	45										
151CMQ035	35	150	104	0.65	101	15	45	1.00	175		
151CMQ040	40										
151CMQ045	45										
152CMQ030	30	150	85	0.47	68	15	280	1.00	150		
153CMQ080	80	150	90	0.80	15	1.0	35	1.00	175		
153CMQ100	100										
150CNQ045	45	150	86	0.60	101	15	200	0.80	150	K14	D-60 Non-Isolated  
151CNQ045	45	150	118	0.65	101	15	45	0.80	175		
153CNQ100	100	150	107	0.80	15	1.0	35	0.80	175		

Other Products from IR

Schottky Diode Center Tap - Modules 130 - 220 Amps

Part Number	VRRM (V)	I _{F(AV)} @ T _C		V _{FM} @ I _{FM} (V)	E _{AS} (mJ)	I _{AR} (A)	I _{RM} @ Rated V _{RWM} (mA)	R _{thCS} /Leg (°C/W)	Max. T _J (°C)	Case Outline Number	Case Style		
		(A)	(°C)										
160CMQ035 160CMQ040 160CMQ045	35 40 45	160	69	0.60	108	16	200	1.00	150	K15	TO-249AA Isolated  		
161CMQ035 161CMQ040 161CMQ045	35 40 45	160	101	0.63	108	16	45	1.00	175				
162CMQ030 163CMQ080 163CMQ100	30 80 100	160	83 87	0.46 0.82	72 15	16 1.0	280 35	1.00 1.00	150 175				
168CMQ060	60	160	96	0.67	75	1.0	240	1.00	150				
160CNQ045 161CNQ045 162CNQ030 163CNQ100	45 45 30 100	160	100 120 107 112	0.60 0.63 0.46 0.82	108 108 72 15	16 16 16 1.0	200 45 280 35	0.80 0.80 0.80 0.80	150 175 150 175			K16	TO-249AA Non-Isolated  
200CNQ035 200CNQ040 200CNQ045	35 40 45	200	108	0.49	135	20	400	0.40	150				
201CNQ035 201CNQ040 201CNQ045 201CNQ050	35 40 45 50	200	138	0.58	135	20	90	0.40	175				
203CNQ080 203CNQ100	80 100	200	130	0.72	15	1.0	70	0.40	175				
208CNQ060 209CNQ150 220CNQ025 220CNQ030 224CNQ035 224CNQ040 224CNQ045	60 150 25 30 35 40 45	200 200 220 220 220	106 131 114 81	0.75 0.80 0.40 0.50	75 32 99 135	1.0 1.0 22 20	480 50 560 1200	0.40 0.40 0.40 0.40	150 175 150 125			K17	TO-244AB  

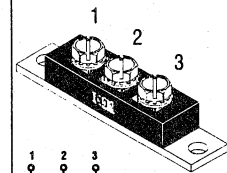
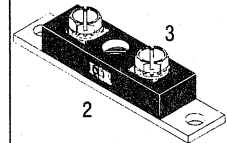
Schottky Diode

Center Tap - Modules

200 - 440 Amps

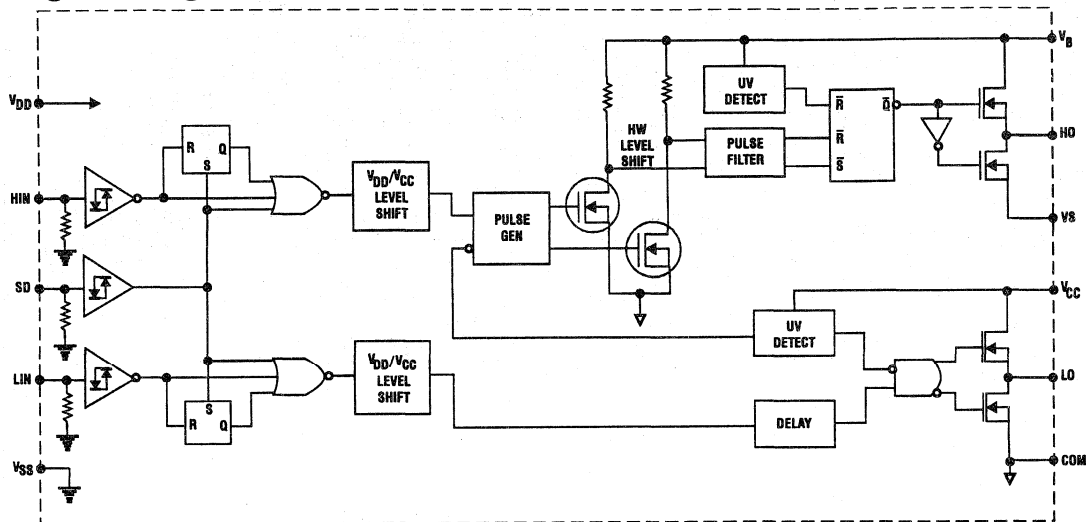
Other Products from IR

Part Number	VRRM (V)	I _{F(AV)} @ T _C		V _{FM} @ I _{FM} (V)	E _{AS} (mJ)	I _{AR} (A)	I _{RM} @ Rated V _{RWM} (mA)	R _{thCS} /Leg (°C/W)	Max. T _J (°C)	Case Outline Number	Case Style
		(A)	(°C)								
225CNQ015	15	220	74	0.32	9.0	2.0	2000	0.40	100	K17	TO-244AB Non-Isolated
300CNQ035	35	300	100	0.62	160	30	600	0.40	150		
300CNQ040	40	300	98	0.62	160	30	600	0.40	150		
300CNQ045	45	300	96	0.62	160	30	600	0.40	150		
301CNQ035	35										
301CNQ040	40	300	120	0.59	202	30	90	0.40	175		
301CNQ045	45										
301CNQ050	50										
303CNQ080	80	300	126	0.72	15	1.0	105	0.30	175		
303CNQ100	100										
309CNQ150	150	300	125	0.85	190	1.0	75	0.30	175		
400CNQ035	35										
400CNQ040	40	400	105	0.52	180	40	800	0.20	150		
400CNQ045	45										
401CNQ035	35										
401CNQ040	40	400	138	0.56	270	40	180	0.20	175		
401CNQ045	45										
403CNQ080	80	400	105	0.72	15	1.0	140	0.20	175		
403CNQ100	100										
408CNQ060	60	400	49	0.88	75	1.0	960	0.20	150		
409CNQ150	150	400	128	0.85	190	1.0	90	0.20	175		
440CNQ030	30	440	115	0.41	198	44	1120	0.20	150		
444CNQ035	35										
444CNQ040	40	440	81	0.51	270	40	2400	0.20	125		
444CNQ045	45										
445CNQ015	15	440	75	0.47	18	4.0	4000	0.20	100		
201CMQ045	45	200	110	0.58	135	20	90	0.70	175	K18	TO-244 AB Isolated
203CMQ100	100	200	100	0.72	15	1.0	70	0.70	175		
208CMQ060	60	200	95	0.75	75	1.0	480	0.50	150		
209CMQ150	150	200	97	0.80	32	1.0	50	0.70	175		
220CMQ030	30	220	95	0.40	99	22	560	0.70	150		
401CMQ045	45	400	120	0.56	270	40	180	0.50	175		
403CMQ100	100	400	85	0.72	15	1.0	140	0.50	175		
408CMQ060	60	400	109	0.88	75	1.0	960	0.50	150		
440CMQ030	30	440	63	0.41	198	44	1120	0.50	150		



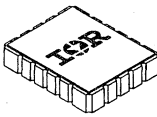
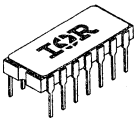
IR2110, IR2113

High Voltage MOS Gate Driver



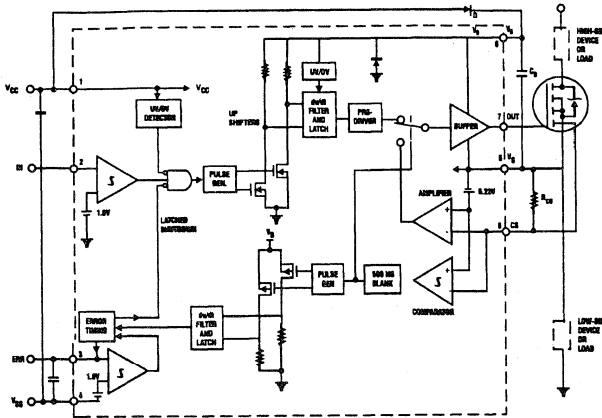
FEATURES

- Drives a pair of HEXFETs or IGBTs
- Two Independent Channel Drivers
 - One Floating High Side Driver
 - One Ground Referenced Low Side Driver
- Operates to 500V
- 2 Amperes Peak Current Drive Capability
- Operates to 500 KHz
- High dv/dt (>±50V/ns) Immunity
- CMOS and LSTTL Compatible Schmitt Trigger Inputs
- Low Quiescent Power Dissipation
- Undervoltage Lockout with Hysteresis (both channels)
- 25 ns Typical Switching Time (into 1000 pf load)
- Matched Delay Times for Both Channels (within 10 ns)
 - 120 ns Turn-on Delay
 - 94 ns Turn-off Delay
- Cycle by Cycle Edged Triggered Latched Shutdown
- Logic Supply Return Can Swing ±5v from Power Ground
- Floating Supply Offset -5V from Power Ground
- Latch Immune CMOS (withstands >2A reverse current at I/O pins)

Part Number	Vs Offset Supply Voltage (V)	Vb, Vc Output Voltage (V)	IOUT Sink, Source (A)	Case Outline Number	Case Style
IR2110E	10-500	10-20	2	P10	LCC 
IR2113E	10-600	10-20	2		
IR2110L	10-500	10-200	2	P12	MO-036AB 
IR2113L	10-600	10-20	2		

IR2125Z

Current Limiting MOS Gate Drivers

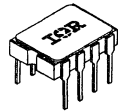


FEATURES

- Current detection and limiting loop to limit driven power transistor current
 - Trip point at 230mV with 30 mV hysteresis
 - Leading edge blanking time of 500 ns
- Error pin indicates fault conditions and programs shutdown time
 - Latched shutdown threshold at 1.8V
 - Source current of 100 μ A to charge timing capacitor
 - Filter time of 1 μ s for noise immunity
- Wide gate drive supply range from 10 to 20V
- Under and over-voltage lockout with hysteresis
- Output driver designed to drive MOS-gated power devices
 - $R_{(on)}$ of pull-up driver typically at 9 ohm
 - $R_{(on)}$ of pull-down driver typically at 3 ohm
 - Switching time of 43/27 ns typical t_r/t_f into 3300 pF load
- Propagation delay time of 140 ns typical

IR2125Z

- High voltage (500V) operation
- Floating supply designed for bootstrap operation
 - Operating offset range from -5 to +500V
 - dv/dt immunity rated at $\pm 50V/ns$
 - Quiescent power dissipation of 7.5 mW at 15V

Part Number	V _B Floating Supply	V _S Floating Supply Offset	V _{CC} Fixed Supply	V _O Output Voltage	Case Outline Number (1)	Case Style
IR2125Z	-0.5- (V _S + 20)	-5- 500V	-0.5- 20V	(V _S - 0.5) - (V _B + 0.5)	P11	MO-036AA 

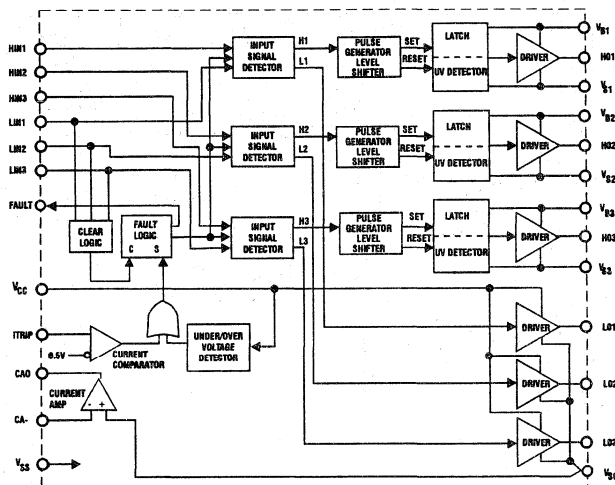
IR2130D

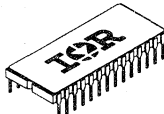
High Voltage Three Phase MOS Gate Driver

FEATURES

- High voltage (600V) operation
Output driver designed to drive MOS-gated power devices
—Output drive of 250mA/500mA typical source/sink
—Switching time of 75/35ns typical t_r/t_f into 1000pF load
- Independent half bridge drivers
—Three floating high voltage drivers
—Three ground referenced drivers
- Floating supply designed for bootstrap operation
—Operating offset range from -5 to +600V
—dv/dt immunity rated at +/-50V/ns
—Quiescent power dissipation of 30mW at 15V
- Over-current shut down turns off all six drive outputs
—Trip point at 485mV with 100mV hysteresis
—Leading edge blanking time with 100mV hysteresis
- Current amplifier provides linear voltage proportional to bridge current
- Input logic provides 2ms deadtime between high side and low side
—250ns min input filter for noise immunity
- Fault pin indicates over-current shut down and undervoltage lockout
- Propagation delay time of 630 ns/400ns typical t_{ON}/t_{OFF}
- Wide gate drive supply range from 10 to 20V
- Under-voltage lockout (8.65V typ) with hysteresis for all channels

FUNCTIONAL BLOCK DIAGRAM



Part Number	V_B	V_S Floating Supply Offset	V_{CC} Fixed Supply	Typical I_{Out} Source/Sink	(1) Case Outline Number	Case Style
IR2130D	$(V_{S1,2,3} + 10)$ $-(V_{S1,2,3} + 20)$	$(V_{SO}-5) -$ $(V_{SO} + 600)$	- 10 - 20V	250mA/ 500mA	P14	MO-038AB 

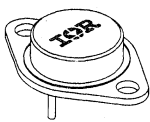
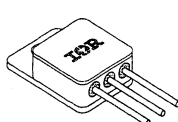
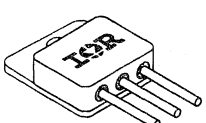
Government and Space

IGBT

Hermetic Packages

600 - 1200V

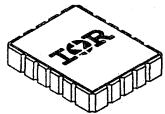

Other Products from IR

Part Number	V(BR)/CES (V)	V _{GE(th)} MIN (V)	V _{GE(th)} MAX (V)	I _C @ T _C = 25°C	I _C @ T _C = 100°C	E _{TS} TYP Loss @ T _J = 125		P _D Max. Power Dissipation	Case Outline Number	Case Style
						(mJ)	(A)			
IRGAC30F IRGAC30U IRGAC40F IRGAC40U IRGAC50F IRGAC50U	600	3.0	5.5	23	12	3.5	12	75	IG20	TO-204AE 
17				8	1.2	8	75			
38				20	9.0	20	125			
31				15	2.0	15	125			
45				30	10	30	150			
41				20	2.8	20	150			
IRGMC30F IRGMC30U IRGMC40F IRGMC40U IRGMC50F IRGMC50U	600	3.0	5.5	23	12	3.5	12	75	IG21	TO-254AA 
17				8	1.2	8	75			
35				20	9.0	20	125			
31				15	2.0	15	125			
35				30	10	30	150			
35				20	2.8	20	150			
IRGMVC50U IRGVH50F	600 1200	3.0 3.0	5.5 5.5	45 45	27 25	2.8 8.2	27 25	200 200	IG22	TO-258AA 
IRGMIC50U IRGIH50F	600 1200	3.0 3.0	5.5 5.5	45 45	27 25	2.8 8.2	27 25	200 200		

Other Products from IR

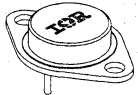
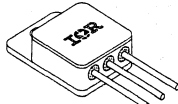
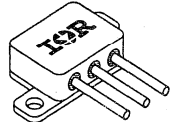

Government and Space

HEXFET Power MOSFETs
Radiation Hardened
N - and P-Channel

Part Number	V_{DSS} (V)	$R_{DS(on)}$ (Ohms)	$I_D@$ $T_C = 25^\circ C$ (A)	$I_D@$ $T_C = 100^\circ C$ (A)	R_{thJC} Max. (K/W)	$P_D@$ $T_C = 25^\circ C$ (W)	Case Outline Number	Case Style
IRHE7110	100	0.60	3.1	2.0	11	11	H20	LCC 
IRHE8110	100	0.60	3.1	2.0	11	11		
IRHE7130	100	0.18	8.0	5.0	5.8	22		
IRHE8130	100	0.18	8.0	5.0	5.8	22		
IRHE7230	200	0.40	4.5	2.5	5.8	22		
IRHE8230	200	0.40	4.5	2.5	5.8	22		
IRHE9130	-100	0.30	-6.0	-3.5	5.8	22		
IRHN7054	60	0.250	42	26	1.25	100	H21	SMD-1 
IRHN8054	60	0.250	42	26	1.25	100		
IRHN7130	100	0.18	10	6.0	3.125	40		
IRHN8130	100	0.18	10	6.0	3.125	40		
IRHN7150	100	0.055	29	18	1.25	100		
IRHN8150	100	0.055	29	18	1.25	100		
IRHN7230	200	0.40	6.0	4.0	3.125	40		
IRHN8230	200	0.40	6.0	4.0	3.125	40		
IRHN7250	200	0.10	21	13	1.25	100		
IRHN8250	200	0.10	21	13	1.25	100		
IRHN7450	500	0.45	9.0	5.0	1.25	100		
IRHN8450	500	0.45	9.0	5.0	1.25	100		
IRHN9130	-100	0.30	-8.0	-5.0	3.125	40		
IRHN9150	-100	0.120	-18	-11	1.25	100		
IRHF7110	100	0.60	3.5	2.2	8.3	15		
IRHF8110	100	0.60	3.5	2.2	8.3	15		
IRHF7130	100	0.18	8.0	5.0	5.0	25		
IRHF8130	100	0.18	8.0	5.0	5.0	25		
2N7261	100	0.18	8.0	5.0	5.0	25		
JANSH2N7261	100	0.18	8.0	5.0	5.0	25		
JANSR2N7261	100	0.18	8.0	5.0	5.0	25		
IRHF7230	200	0.40	5.5	3.5	5.0	25		
IRHF8230	200	0.40	5.5	3.5	5.0	25		
IRHF7234	250	0.48	4.8	3.0	5.0	25		
IRHF8234	250	0.48	4.8	3.0	5.0	25		
2N7262	200	0.40	5.5	3.5	5.0	25		
JANSH2N7262	200	0.40	5.5	3.5	5.0	25		
JANSR2N7262	200	0.40	5.5	3.5	5.0	25		
IRHF9130	-100	0.30	-6.5	-4.1	5.0	25		

Government and Space
HEXFET Power MOSFETs
Single Event Effect Hardened
N-Channel

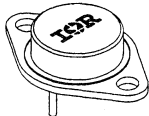

Other Products from IR

Part Number	BV _{DSS} (V)	R _{DS(on)} (Ohms)	I _D @ T _C = 25°C (A)	I _D @ T _C = 100°C (A)	R _{thJC} Max. (K/W)	P _D @ T _C = 25°C (W)	Case Outline Number	Case Style
IRH7250SE IRH7254SE IRH7450SE	200 250 500	0.10 0.120 0.45	26 23 11	17 15 7.0	0.83 0.83 0.83	150 150 150	H23	TO-204AA (TO-3) 
IRHM7250SE IRHM7254SE IRHM7360SE IRHM7450SE IRHM7460SE	200 250 400 500 500	0.100 0.120 0.22 0.45 0.315	26 23 22 11 19	16 15 14 7.0 12	0.83 0.83 0.5 0.83 0.5	150 150 250 150 250	H25	TO-254AA 
IRHI7460SE	500	0.315	21	13	0.42	300	H27	TO-259AA 
IRHN7250SE IRHN7254SE IRHN7450SE	200 250 500	0.10 0.120 0.45	21 20 9.0	13 11 5.0	1.25 1.25 1.25	100 100 100	H21	SMD-1 

Other Products from IR

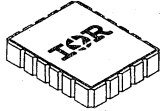

Government and Space

HEXFET Power MOSFETs
Radiation Hardened
N - and P-Channel

Part Number	V_{DSS} (V)	$R_{DS(on)}$ (Ohms)	$I_D@$ $T_C = 25^\circ C$ (A)	$I_D@$ $T_C = 100^\circ C$ (A)	R_{thJC} Max. (K/W)	$P_D@$ $T_C = 25^\circ C$ (W)	Case Outline Number	Case Style
IRH7054	60	0.025	45	32	0.83	150	H23 H24	TO-204AA/AE (TO-3) 
IRH8054	60	0.025	45	32	0.83	150		
IRH7130	100	0.18	14	9.0	1.67	75		
IRH8130	100	0.18	14	9.0	1.67	75		
IRH7150	100	0.055	38	24	0.83	150		
IRH8150	100	0.055	38	24	0.83	150		
IRH7230	200	0.40	9.0	6.0	1.67	75		
IRH8230	200	0.40	9.0	6.0	1.67	75		
IRH7250	200	0.10	26	17	0.83	150		
IRH8250	200	0.10	26	17	0.83	150		
IRH7450	500	0.45	11	7	0.83	150		
IRH8450	500	0.45	11	7	0.83	150		
IRH9130	-100	0.30	-11	-7.0	1.67	75		
IRH9150	-100	0.120	-21	-13	0.83	150		
IRHM7054	60	0.027	35	30	0.83	150	H29	MO-036AB 
IRHM8054	60	0.027	35	30	0.83	150		
IRHM7130	100	0.18	14	9.0	1.67	75		
IRHM8130	100	0.18	14	9.0	1.67	75		
IRHM7150	100	0.065	34	21	0.83	150		
IRHM8150	100	0.065	34	21	0.83	150		
2N7268	100	0.065	34	21	0.83	150		
JANSH2N7268	100	0.065	34	21	0.83	150		
JANSR2N7268	100	0.065	34	21	0.83	150		
IRHM7230	200	0.40	9.0	6.0	1.67	75		
IRHM8230	200	0.40	9.0	6.0	1.67	75		
IRHM7250	200	0.100	26	16	0.83	150		
IRHM8250	200	0.100	26	16	0.83	150		
IRHM7254	250	0.120	23	15	0.83	150		
IRHM8254	250	0.120	23	15	0.83	150		
2N7269	200	0.100	26	16	0.83	150		
JANSH2N7269	200	0.100	26	16	0.83	150		
JANSR2N7269	200	0.100	26	16	0.83	150		
IRHM7360	400	0.22	22	14	0.5	250		
IRHM8360	400	0.22	22	14	0.5	250		
IRHM7450	500	0.45	11	7.0	0.83	150		
IRHN8450	500	0.45	11	7.0	0.83	150		
2N7270	500	0.45	11	7.0	0.83	150		
JANSH2N7270	500	0.45	11	7.0	0.83	150		
JANSR2N7270	500	0.45	11	7.0	0.83	150		
IRHM9130	-100	0.30	-11	-7.0	1.67	75	H29	MO-036AB
IRHM9150	-100	0.120	-21	-13	0.83	150		
IRHG6110	100	0.70	1.0	0.6	17	1.4	H29	MO-036AB
	-100	1.4	-0.75	17	1.4	1.4		
IRHG7110	100	0.70	1.0	0.60	17	1.4		

Government and Space
HEXFET Power MOSFETs
Hermetic Packages
N - and P-Channel

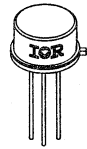
Other Products from IR

Part Number	V_{DSS} (V)	$R_{DS(on)}$ (Ohms)	$I_D@$ $T_C = 25^\circ C$ (A)	$I_D@$ $T_C = 100^\circ C$ (A)	R_{thJC} Max. (K/W)	$P_D@$ $T_C = 25^\circ C$ (W)	Case Outline Number	Case Style		
IRFE024	60	0.15	6.7	4.2	9.1	14	H20	LCC 		
IRFE110	100	0.60	3.1	2.0	11	11				
IRFE120	100	0.30	4.5	3.0	9.1	14				
IRFE130	100	0.18	7.4	4.7	5.8	22				
IRFE210	200	1.5	1.8	1.2	11	11				
IRFE220	200	0.80	2.8	1.8	9.1	14				
IRFE230	200	0.40	4.8	3.1	5.8	22				
IRFE310	400	3.6	1.2	0.74	11	11				
IRFE320	400	1.8	1.8	1.1	9.1	14				
IRFE330	400	1.0	3.0	1.9	5.8	22				
IRFE420	500	3.0	1.4	0.9	9.1	14				
IRFE430	500	1.5	2.5	1.6	5.8	22				
IRFE9024	-60	0.28	-5.4	-3.4	9.1	14				
IRFE9110	-100	1.2	-2.2	-1.4	11	11				
IRFE9120	-100	0.60	-3.5	-2.2	9.1	14				
IRFE9130	-100	0.30	-6.1	-3.8	5.8	22				
IRFE9210	-200	3.0	-1.3	-0.84	11	11				
IRFE9220	-200	1.5	-2.1	-1.5	9.1	14				
IRFE9230	-200	0.80	-3.6	-2.2	5.8	22				
IRFN044	60	0.040	34	21	1.67	75			H21	SMD-1 
IRFN054	60	0.027	45	28	1.25	100				
IRFN140	100	0.077	22	13.9	1.67	75				
IRFN150	100	0.070	27	19	1.25	100				
IRFN240	200	0.18	13.9	8.8	1.67	75				
IRFN250	200	0.100	22	14	1.25	100				
IRFN340	400	0.55	7.5	4.8	1.67	75				
IRFN350	400	0.315	11	7.0	1.25	100				
IRFN440	500	0.85	6.1	3.8	1.67	75				
IRFN450	500	0.415	10.4	6.6	1.25	100				
IRFNG40	1000	3.5	3.0	2.0	1.67	75				
IRFNG50	1000	2.0	4.5	2.8	1.25	100				
IRFN9140	-100	0.20	-14	-9.0	1.67	75				
IRFN9240	-200	0.51	-8.0	-5.0	1.67	75				

Other Products from IR

Government and Space HEXFET Power MOSFETs Hermetic Package N-Channel

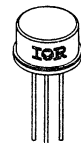
Part Number	V_{DSS} (V)	$R_{DS(on)}$ (Ohms)	$I_D@$ $T_C = 25^\circ C$ (A)	$I_D@$ $T_C = 100^\circ C$ (A)	R_{thJC} Max. (K/W)	$P_D@$ $T_C = 25^\circ C$ (W)	Case Outline Number	Case Style
IRFF024	60	0.15	8.0	5.7	6.25	20	H22	TO-205AF (TO-39)
IRFF110	100	0.60	3.5	2.25	8.3	15		
2N6782	100	0.60	3.5	2.25	8.3	15		
JANTX2N6782	100	0.60	3.5	2.25	8.3	15		
JANTXV2N6782	100	0.60	3.5	2.25	8.3	15		
IRFF120	100	0.30	6.0	3.5	6.25	20		
2N6788	100	0.30	6.0	3.5	6.25	20		
JANTX2N6788	100	0.30	6.0	3.5	6.25	20		
JANTXV2N6788	100	0.30	6.0	3.5	6.25	20		
IRFF130	100	0.18	8.0	5.0	5.0	25		
2N6796	100	0.18	8.0	5.0	5.0	25		
JANTX2N6796	100	0.18	8.0	5.0	5.0	25		
JANTXV2N6796	100	0.18	8.0	5.0	5.0	25		
IRFF210	200	1.5	2.25	1.50	8.3	15		
2N6784	200	1.5	2.25	1.50	8.3	15		
JANTX2N6784	200	1.5	2.25	1.50	8.3	15		
JANTXV2N6784	200	1.5	2.25	1.50	8.3	15		
IRFF220	200	0.80	3.5	2.25	6.25	20		
2N6790	200	0.80	3.5	2.25	6.25	20		
JANTX2N6790	200	0.80	3.5	2.25	6.25	20		
JANTXV2N6790	200	0.80	3.5	2.25	6.25	20		
IRFF230	200	0.40	5.5	3.5	5.0	25		
2N6798	200	0.40	5.5	3.5	5.0	25		
JANTX2N6798	200	0.40	5.5	3.5	5.0	25		
JANTXV2N6798	200	0.40	5.5	3.5	5.0	25		
IRFF310	400	3.6	1.25	0.80	8.3	15		
2N6786	400	3.6	1.25	0.80	8.3	15		
JANTX2N6786	400	3.6	1.25	0.80	8.3	15		
JANTXV2N6786	400	3.6	1.25	0.80	8.3	15		
IRFF320	400	1.8	2.0	1.25	6.25	20		
2N6792	400	1.8	2.0	1.25	6.25	20		
JANTX2N6792	400	1.8	2.0	1.25	6.25	20		
JANTXV2N6792	400	1.8	2.0	1.25	6.25	20		
IRFF330	400	1.0	3.0	2.0	5.0	25		
2N6800	400	1.0	3.0	2.0	5.0	25		
JANTX2N6800	400	1.0	3.0	2.0	5.0	25		
JANTXV2N6800	400	1.0	3.0	2.0	5.0	25		
IRFF420	500	3.0	1.5	1.0	6.25	20		
2N6794	500	3.0	1.5	1.0	6.25	20		
JANTX2N6794	500	3.0	1.5	1.0	6.25	20		
JANTXV2N6794	500	3.0	1.5	1.0	6.25	20		
IRFF430	500	1.5	2.5	1.5	5.0	25		
2N6802	500	1.5	2.5	1.5	5.0	25		
JANTX2N6802	500	1.5	2.5	1.5	5.0	25		
JANTXV2N6802	500	1.5	2.5	1.5	5.0	25		



Government and Space
HEXFET Power MOSFETs
Hermetic Package
P-Channel

Other Products from IR

Part Number	V_{DSS} (V)	$R_{DS(on)}$ (Ohms)	$I_D@$ $T_C = 25^\circ C$ (A)	$I_D@$ $T_C = 100^\circ C$ (A)	R_{thJC} Max. (K/W)	$P_D@$ $T_C = 25^\circ C$ (W)	Case Outline Number	Case Style
IRFF9024	-60	0.28	-6.4	-4.1	6.25	20	H22	TO-205AF (TO-39)
IRFF9110	-100	1.2	-2.5	-1.6	8.3	15		
IRFF9120	-100	0.60	-4.0	-2.6	6.25	20		
2N6845	-100	1.2	-2.5	-1.6	8.3	15		
JANTX2N6845	-100	1.2	-2.5	-1.6	8.3	15		
JANTXV2N6845	-100	1.2	-2.5	-1.6	8.3	15		
IRFF9130	-100	0.30	-6.5	-4.1	5.0	25		
2N6849	-100	0.30	-6.5	-4.1	5.0	25		
JANTX2N6849	-100	0.30	-6.5	-4.1	5.0	25		
JANTXV2N6849	-100	0.30	-6.5	-4.1	5.0	25		
IRFF9210	-200	3.0	-1.5	-0.97	8.3	15		
IRFF9220	-200	1.5	-2.5	-1.6	6.25	20		
2N6847	-200	1.5	-2.5	-1.6	6.25	20		
JANTX2N6847	-200	1.5	-2.5	-1.6	6.25	20		
JANTXV2N6847	-200	1.5	-2.5	-1.6	6.25	20		
IRFF9230	-200	0.80	-4.0	-2.4	5.0	25		
2N6851	-200	0.80	-4.0	-2.4	5.0	25		
JANTX2N6851	-200	0.80	-4.0	-2.4	5.0	25		
JANTXV2N6851	-200	0.80	-4.0	-2.4	5.0	25		

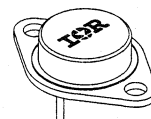


Other Products from IR

Government and Space

HEXFET Power MOSFETs
Hermetic Package
N-Channel

Part Number	V _{DSS} (V)	R _{DS(on)} (Ohms)	I _D @ T _C = 25°C (A)	I _D @ T _C = 100°C (A)	R _{thJC} Max. (K/W)	P _D @ T _C = 25°C (W)	Case Outline Number	Case Style
IRF034	60	0.500	25	16	1.67	75	H23 H24	TO-204AA/AE (TO-3)
IRF044	60	0.280	44	27	1.0	125		
IRF054	60	0.220	45	31	0.83	150		
IRF130	100	0.18	14	9.0	1.67	75		
2N6756	100	0.18	14	9.0	1.67	75		
JANTX2N6756	100	0.18	14	9.0	1.67	75		
JANTXV2N6756	100	0.18	14	9.0	1.67	75		
IRF140	100	0.077	28	20	1.0	125		
IRF150	100	0.055	38	24	0.83	150		
2N6764	100	0.055	38	24	0.83	150		
JANTX2N6764	100	0.055	38	24	0.83	150		
JANTXV2N6764	100	0.055	38	24	0.83	150		
IRF230	200	0.40	9.0	6.0	1.67	75		
2N6758	200	0.40	9.0	6.0	1.67	75		
JANTX2N6758	200	0.40	9.0	6.0	1.67	75		
JANTXV2N6758	200	0.40	9.0	6.0	1.67	75		
IRF240	200	0.18	18	11	1.0	125		
IRF250	200	0.085	30	19	0.83	150		
2N6766	200	0.085	30	19	0.83	150		
JANTX2N6766	200	0.085	30	19	0.83	150		
JANTXV2N6766	200	0.085	30	19	0.83	150		
IRF330	400	1.00	5.5	3.5	1.67	75		
2N6760	400	1.00	5.5	3.5	1.67	75		
JANTX2N6760	400	1.00	5.5	3.5	1.67	75		
JANTXV2N6760	400	1.00	5.5	3.5	1.67	75		
IRF340	400	0.55	10	6.0	1.0	125		
IRF350	400	0.300	14	9.0	0.83	150		
2N6768	400	0.300	14	9.0	0.83	150		
JANTX2N6768	400	0.300	14	9.0	0.83	150		
JANTXV2N6768	400	0.300	14	9.0	0.83	150		
IRF360	400	0.20	25	16	0.42	300		
IRF430	500	1.50	4.5	3.0	1.67	75		
2N6762	500	1.50	4.5	3.0	1.67	75		
JANTX2N6762	500	1.50	4.5	3.0	1.67	75		
JANTXV2N6762	500	1.50	4.5	3.0	1.67	75		
IRF440	500	0.85	8.0	5.0	1.0	125		
IRF450	500	0.400	12	7.75	0.83	150		
2N6770	500	0.400	12	7.75	0.83	150		
JANTX2N6770	500	0.400	12	7.75	0.83	150		
JANTXV2N6770	500	0.400	12	7.75	0.83	150		
IRF460	500	0.27	21	14	0.42	300		
IRFAC30	600	2.2	3.6	2.3	1.67	75		
IRFAC40	600	1.2	6.2	3.9	1.0	125		
IRFAE30	800	3.2	3.1	2.0	1.67	75		
IRFAE40	800	2.0	4.8	3.0	1.0	125		
IRFAE50	800	1.2	7.1	4.5	0.83	150		
IRFAF30	900	4.0	2.0	1.7	1.67	75		
IRFAF40	900	2.5	4.3	2.7	1.0	125		
IRFAF50	900	1.6	6.2	4.0	0.83	150		
IRFAG30	1000	5.6	2.3	1.5	1.67	75		
IRFAG40	1000	3.5	3.9	2.5	1.0	125		
IRFAG50	1000	2.0	5.6	3.5	0.83	150		



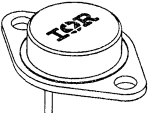
Government and Space

HEXFET Power MOSFETS

Hermetic Package

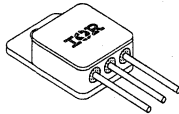
P-Channel

Other Products from IR

Part Number	BV_{DSS} (V)	$R_{DS(on)}$ (Ohms)	$I_D@$ $T_C = 25^\circ C$ (A)	$I_D@$ $T_C = 100^\circ C$ (A)	R_{thJC} Max. (K/W)	$P_D@$ $T_C = 25^\circ C$ (W)	Case Outline Number	Case Style
IRF9130	-100	0.3	-11	-7.0	1.67	75	H24 H25	TO-204AA/AE (TO-3) 
2N6804	-100	0.3	-11	-7.0	1.67	75		
JANTX2N6804	-100	0.3	-11	-7.0	1.67	75		
JANTXV2N6804	-100	0.3	-11	-7.0	1.67	75		
IRF9140	-100	0.2	-18	-11	1.0	125		
IRF9230	-200	0.80	-6.5	-4.0	1.67	75		
2N6806	-200	0.80	-6.5	-4.0	1.67	75		
JANTX2N6806	-200	0.80	-6.5	-4.0	1.67	75		
JANTXV2N6806	-200	0.80	-6.5	-4.0	1.67	75		
IRF9240	-200	0.5	-11	-7.0	1.0	125		

Other Products from IR

Government and Space HEXFET Power MOSFETs Hermetic Package N- and P-Channel

Part Number	V_{DSS} (V)	$R_{DS(on)}$ (Ohms)	$I_D@$ $T_C = 25^\circ C$ (A)	$I_D@$ $T_C = 100^\circ C$ (A)	R_{thJC} Max. (K/W)	$P_D@$ $T_C = 25^\circ C$ (W)	Case Outline Number	Case Style
IRFM044	60	0.04	35	28	1.0	125	H25	TO-254AA 
IRFM054	60	0.027	35	35	0.83	150		
IRFM064	60	0.017	35	35	0.5	250		
IRFM140	100	0.077	28	20	1.0	125		
2N7218	100	0.077	28	20	1.0	125		
JANTX2N7218	100	0.077	28	20	1.0	125		
JANTXV2N7218	100	0.077	28	20	1.0	125		
IRFM150	100	0.070	34	21	0.83	150		
2N7224	100	0.070	34	21	0.83	150		
JANTX2N7224	100	0.070	34	21	0.83	150		
JANTXV2N7224	100	0.070	34	21	0.83	150		
IRFM240	200	0.18	18	11	1.0	125		
2N7219	200	0.18	18	11	1.0	125		
JANTX2N7219	200	0.18	18	11	1.0	125		
JANTXV2N7219	200	0.18	18	11	1.0	125		
IRFM250	200	0.100	27.4	17	0.83	150		
2N7225	200	0.100	27.4	17	0.83	150		
JANTX2N7225	200	0.100	27.4	17	0.83	150		
JANTXV2N7225	200	0.100	27.4	17	0.83	150		
IRFM340	400	0.55	10	6.0	1.0	125		
2N7221	400	0.55	10	6.0	1.0	125		
JANTX2N7221	400	0.55	10	6.0	1.0	125		
JANTXV2N7221	400	0.55	10	6.0	1.0	125		
IRFM350	400	0.315	14	9.0	0.83	150		
2N7227	400	0.315	14	9.0	0.83	150		
JANTX2N7227	400	0.315	14	9.0	0.83	150		
JANTXV2N7227	400	0.315	14	9.0	0.83	150		
IRFM360	400	0.20	23	14	0.50	250		
IRFM440	500	0.85	8.0	5.0	1.0	125		
2N7222	500	0.85	8.0	5.0	1.0	125		
JANTX2N7222	500	0.85	8.0	5.0	1.0	125		
JANTXV2N7222	500	0.85	8.0	5.0	1.0	125		
IRFM450	500	0.415	12	8.0	0.83	150		
2N7228	500	0.415	12	8.0	0.83	150		
JANTX2N7228	500	0.415	12	8.0	0.83	150		
JANTXV2N7228	500	0.415	12	8.0	0.83	150		
IRFM460	500	0.27	19	12	0.5	250		
IRFMG40	1000	3.5	3.9	2.5	1.0	125		
IRFMG50	1000	2.0	5.6	3.5	0.83	150		
IRFM9140	-100	0.20	-18	-11	1.0	125		
2N7236	-100	0.20	-18	-11	1.0	125		
JANS2N7236	-100	0.20	-18	-11	1.0	125		
JANTX2N7236	-100	0.20	-18	-11	1.0	125		
JANTXV2N7236	-100	0.20	-18	-11	1.0	125		
IRFM9240	-200	0.51	-11	-7.0	1.0	125		
2N7237	-200	0.51	-11	-7.0	1.0	125		
JANS2N7237	-200	0.51	-11	-7.0	1.0	125		
JANTX2N7237	-200	0.51	-11	-7.0	1.0	125		
JANTXV2N7237	-200	0.51	-11	-7.0	1.0	125		

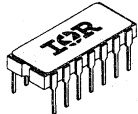
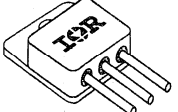
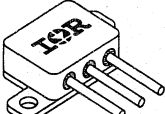
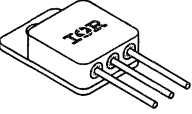


Government and Space

HEXFET Power MOSFETS

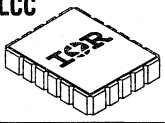




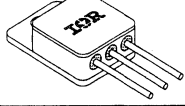
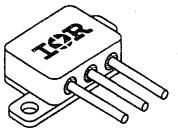
Other Products from IR

Hermetic Package
N- and P-Channel

Part Number	BV_{DSS} (V)	$R_{DS(on)}$ (Ohms)	$I_D@$ $T_C = 25^\circ C$ (A)	$I_D@$ $T_C = 100^\circ C$ (A)	R_{thJC} Max. (K/W)	$P_D@$ $T_C = 25^\circ C$ (W)	Case Outline Number	Case Style		
IRFG110	100	0.70	1.0	0.6	17	1.4	H29	MO-036AB 		
2N7334	100	0.70	1.0	0.6	17	1.4				
JANTX2N7334	100	0.70	1.0	0.6	17	1.4				
JANTXV2N7334	100	0.70	1.0	0.6	17	1.4				
IRFG5110	100 -100	0.70 0.70	1.0 -1.0	0.6 -0.6	17 17	1.4 1.4				
IRFG6110	100 -100	0.70 1.4	1.0 -0.75	0.6 -0.5	17 17	1.4 1.4				
2N7336	100 -100	0.7 1.4	1.0 -0.75	0.6 -0.5	17 17	1.4 1.4				
JANTX2N7336	100 -100	0.7 1.4	1.0 -0.75	0.6 -0.5	17 17	1.4 1.4				
JANTXV2N7336	100 -100	0.7 1.4	1.0 -0.75	0.6 -0.5	17 17	1.4 1.4				
IRFG9110	-100	1.4	-0.75	-0.5	17	1.4				
2N7335	-100	1.4	-0.75	-0.5	17	1.4				
JANTX2N7335	-100	1.4	-0.75	-0.5	17	1.4				
JANTXV2N7335	-100	1.4	-0.75	-0.5	17	1.4				
IRFV064	60	0.017	45	45	0.42	300			H26	TO-258AA 
IRFV360	400	0.20	25	16	0.42	300				
IRFV460	500	0.27	21	13	0.42	300				
IRFI064	60	0.017	45	45	0.42	300	H27	TO-259AA 		
IRFI360	400	0.20	25	16	0.42	300				
IRFI460	500	0.27	21	13	0.42	300				
IRFY044	60	0.035	20	20	2.1	60	H28	TO-257AB 		
IRFY120	100	0.31	7.3	4.6	4.1	30				
IRFY130	100	0.19	11	7.0	2.8	45				
IRFY140	100	0.092	18	12	2.1	60				
IRFY240	200	0.19	12	7.8	2.1	60				
IRFY340	400	0.55	6.9	4.4	2.1	60				
IRFY430	500	1.6	3.7	2.4	2.8	45				
IRFY440	500	0.85	5.5	3.5	2.1	60				
IRFY9120	-100	0.6	-5.3	-3.4	4.1	30				
IRFY9130	-100	0.31	-9.3	-5.8	2.8	45				
IRFY9140	-100	0.21	-13	-8.2	2.1	60				
IRFY9240	-200	0.50	-7.7	-4.9	2.1	60				

Other Products from IR

Government and Space Schottky Diode Hermetic Package 8 - 60 Amps

Part Number	V _{RRM} (V)	I _{F(AV)} @ T _C (A)	I _{F(AV)} @ T _C (C)	V _{FM} @ I _{FM} 25°C (V)	I _{RM} @V _{RRM} 25°C (mA)	Max. T _J	Case Outline Number	Case Style				
5EQ100 8EQ045	100 45	8 10	100 100	0.80 0.65	5 5	150 150	J30	LCC 				
15CLQ100 20CLQ045	100 45	15 20	100 100	0.90 0.69	5 5	150 150			K31	SMD-1 		
30FQ045 1N6391 JAN1N6391 JANTX1N6391 JANTXV1N6391	45 45 45 45 45	25 25 25 25 25	115 115 115 115 115	0.50 0.50 0.50 0.50 0.50	15 15 15 15 15	175 175 175 175 175	J13	DO-203AA (DO-4) 				
75HQ045 1N6392 JAN1N6392 JANTX1N6392 JANTXV1N6392 60HQ080 60HQ100	45 45 45 45 45 80 80	60 60 60 60 60 60 60	115 115 115 115 115 118 118	0.51 0.51 0.51 0.51 0.51 0.95 0.95	20 20 20 20 20 5 5	175 175 175 175 175 175 175			J14	DO-203AB (DO-5) 		
60CDQ035 60CDQ040 60CD0045	35 40 45	60 60 60	112 112 112	0.87 0.87 0.87	5 5 5	175 175 175			K6	TO-204AE 		
12CGQ150 15CGQ100 22CGQ045 22DGQ045 22GQ100 25GQ045	150 100 45 45 100 45	35 35 35 26 30 35	100 100 100 100 100 100	1.6 1.30 0.82 0.82 1.10 0.93	5 5 5 5 5 5	150 150 150 150 150 150					K32 J33 J34 J34	TO-254AA 
45CKQ100 60CKQ045	100 45	45 45	100 100	1.13 0.92	5 5	150 150						
45CIQ100 60CIQ045	100 45	45 45	100 100	1.13 0.92	5 5	150 150			K34	TO-259AA 		




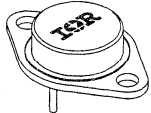
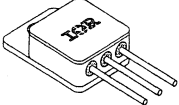
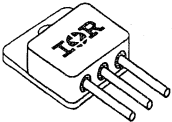
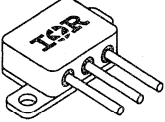
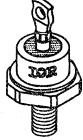
Government and Space

HEXFRED Diodes

Hermetic Packages

7 - 45 Amps

Other Products from IR

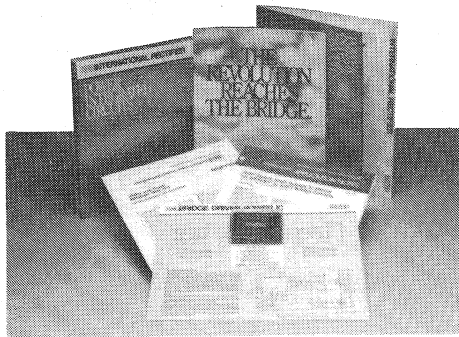
Part Number	V_{RWM}	$I_F(AV)@T_C$ (A)	$I_F(AV)@T_C$ (C)	$V_{FM}@I_{FM}$ 25°C (V)	$I_{RM}@V_{RWM}$ 25°C (mA)	R_{thJC} (°K/W)	Typ I_{RRM} (A)	Typ T_{rr} (nS)	Case Outline Number	Case Style
HFA40HF60 HFA40HF120	600 1200	12 7	100 100	1.7 3.0	10 20	2.50 2.50	10 10	75 135	J31	SMD-1 
HFA35HA60C HFA35HA120C	600 1200	30 15	100 100	2.0 4.3	10 20	2.00 2.00	6 8	60 95	K5	TO-204AA (TO-3) 
HFA35HB60 HFA35HB120 HFA35HB60C HFA35HB120C	600 1200 600 1200	22 11 30 15	100 100 100 100	1.7 3.0 2.0 4.3	10 20 10 10	1.50 1.50 2.00 2.00	10 10 6 8	75 135 60 95	J33 K32	TO-254AA 
HFA45HC60C HFA45HC120C	600 1200	45 28	100 100	2.0 3.9	10 20	1.20 1.20	10 10	75 135	K33	TO-258AA 
HFA45HI60G HFA45HI120C	600 1200	45 28	100 100	2.0 3.9	10 20	1.20 1.20	10 10	75 135	K34	TO-259AA 
HFA40HE60 HFA40HE120	600 1200	25 15	100 100	1.7 3.0	10 20	1.25 1.25	10 10	75 135	J14	DO-203AB (DO-5) 

Power Integrated Circuits

International
IR Rectifier

Application Materials:

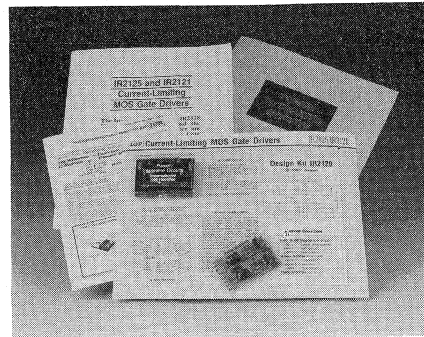
IR2119 DESIGN KIT FEATURING IR2110



KIT COMPONENTS

- 2 — IR2110 MOS Gate Drivers (500V, 2A)
- 2 — IR830 HEXFETs (500V, 4.5A) — Q1, Q2
- 1 — 10KF6 Diode (600V, 1A) — D1
- 1 — Capacitor (0.047 μ F, 50V) — C1
- 2 — Resistors (47 Ω , 1/4W, 5%) — R1, R2
- 1 — Resistor (10 Ω , 1/4W, 5%) — R3
- 1 — Kit PC Wiring Board (located under foam)

IR2129 DESIGN KIT FEATURING IR2125/IR2121



KIT COMPONENTS

- 1 — IR2125 MOS Gate Driver (500V)
- 1 — IR2121 MOS Gate Driver (20V)
- 2 — IRC830 HEXSense power FETs (500V) Q1, Q2
- 2 — Resistors (22 Ω , .25W, 5%) R1, R3
- 2 — Resistors (120 Ω , .25W, 5%) R2, R4
- 1 — 10KF6 Diode (600V) D1
- 2 — 1N4148 Diodes D2, D3
- 2 — Capacitors (1000pF, 100V, Ceramic) C1, C2
- 2 — Capacitors (10 μ F, 50V, Aluminum) C3, C4
- 2 — Capacitors (0.1 μ F, 100V, Ceramic) C5, C6
- 1 — Kit PC Wiring Board (located under foam)

ADDITIONAL POWER IC APPLICATION ARTICLES AVAILABLE FROM IR

NUMBER **Power IC Technology**

- ER91-1 "Trends in Integrated Power and Logic", by A. Alderman, D. Tam, P. Wood, P. Schugart presented at ELKOM March 7, 1991.
- ER92-1 "MGDs: High Performance Integrated Drivers for Power MOSFETs & IGBTs", by Arnold Alderman and Steve Clemente

IR2110

- ER90-1 "High Voltage Chipset for Offline System Designs", by David Tam and Dan Kinzer.
- ER90-3 "New High-Voltage Bridge Driver Simplifies PWM Inverter Design", by D. Grant and B. Pelly, presented at 1989 PCIM Conference.

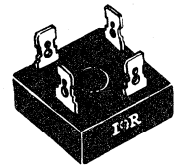
IR2125/IR2121

- ER91-2 "Power IC Driver Protects MOSFETs and IGBTs, operates to 500V", by P. Wood, PCIM March 1991 Reprint.

IR2130

- ER91-3 "A 600 Volt Interface IC for Three-Phase Bridge Circuits", by Chris Choi and Peter Wood

Part Number	U.S. Series	V _{RRM} (V)	I _O	T _C	V _{FM} @ I _F		I _{FSM} (3)	I _{FSM} (3)	R _{thJC} DC (1) (K/W)	Case Outline Number (4)	Notes	Case Style
			(A)	(°C)	(V)	(A)	50 Hz (A)	60 Hz (A)				
	100JB05L 100JB1L 100JB2L 100JB4L 100JB6L 100JB8L 100JB10L 100JB12L 100JB14L 100JB16L	50 100 200 400 600 800 1000 1200 1400 1600	10	65	1.3	16	125	130	3.5	B1	(2) (5)	D-34A
	26MB05A 26MB10A 26MB20A 26MB40A 26MB60A 26MB80A 26MB100A 26MB120A 26MB140A 26MB160A	250JB05L 250JB1L 250JB2L 250JB4L 250JB6L 250JB8L 250JB10L 250JB12L 250JB14L 250JB16L	25	65	1.1	40	335	350	1.7			
	36MB05A 36MB10A 36MB20A 36MB40A 36MB60A 36MB80A 36MB100A 36MB120A 36MB140A 36MB160A	35MB05A 35MB10A 35MB20A 35MB40A 35MB60A 35MB80A 35MB100A 35MB120A 35MB140A 35MB160A	35	60	1.2	55	400	420	1.2			



RU U.L.
RECOGNIZED
File no: E62320

(1) Value given for R_{thJC} is per module.
(2) RMS isolation voltage: 2700V-50 Hz.

(3) 100% V_{RRM} reapplied. T_j = T_j max. = 150°C.
(4) For case outline drawing see page 0-2.
(5) V_{FM} @ 25°C.

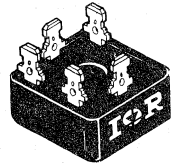
Bridges

Three Phase Diode

25-160 Amps

International
IOR Rectifier

Part Number	VRRM (V)	I _O T _C		VFM @ I _F		I _{FSM} (4)	I _{FSM} (4)	R _{thJC} DC (1) (K/W)	Case Outline Number (5)	Notes	Case Style
		(A)	(°C)	(V)	(A)	50 Hz (A)	60 Hz (A)				
26MT5 26MT10 26MT20 26MT40 26MT60 26MT80 26MT100 26MT120 26MT140 26MT160	50 100 200 400 600 800 1000 1200 1400 1600	25	70	1.26	40	300	314	1.42	B2	(3)	D-63
36MT5 36MT10 36MT20 36MT40 36MT60 36MT80 36MT100 36MT120 36MT140 36MT160	50 100 200 400 600 800 1000 1200 1400 1600	35	60	1.19	40	400	420	1.16			
60MT80K 60MT100K 60MT120K 60MT140K 60MT160K	800 1000 1200 1400 1600	60	85	1.75	100	350	370	0.370	B3	(2)	
70MT80K 70MT100K 70MT120K 70MT140K 70MT160K	800 1000 1200 1400 1600	70	85	1.55	100	400	420	0.292			
90MT80K 90MT100K 90MT120K 90MT140K 90MT160K	800 1000 1200 1400 1600	90	90	1.6	150	650	680	0.210			
110MT80K 110MT100K 110MT120K 110MT140K 110MT160K	800 1000 1200 1400 1600	110	90	1.4	150	800	840	0.178			
130MT80K 130MT100K 130MT120K 130MT140K 130MT160K	800 1000 1200 1400 1600	130	85	1.63	200	950	1000	0.155			
160MT80K 160MT100K 160MT120K 160MT140K 160MT160K	800 1000 1200 1400 1600	160	85	1.49	200	1200	1260	0.121			



UL U.L.
RECOGNIZED
File no: E62320



UL U.L.
RECOGNIZED
File no: E78996

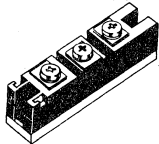
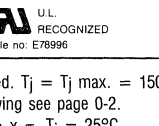
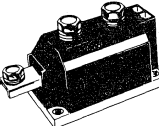
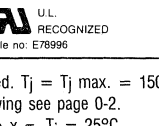
- (1) Value given for R_{thJC} is per module.
- (2) RMS isolation voltage: 4000V-50 Hz.
- (3) RMS isolation voltage: 2700V-50 Hz.

- (4) 100% VRRM reapplied. T_j = T_j max. = 150°C.
- (5) For case outline drawing see page 0-2.

Power Modules

Diode/Diode

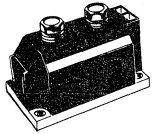

International
Rectifier

Part Number			V _{RRM} (V)	I _{F(AV)} @ T _C		I _{FSM} (7)		(9) V _{FM} (V)	R _{thJC} DC (1) (K/W)	Case Outline Number (8)	Notes	Case Style
(3)	(4)	(5)		(A)	(°C)	50 Hz (A)	60 Hz (A)					
IRKD166-04	IRKC166-04	IRKJ166-04	400							M5	(6) (10)	
IRKD166-06	IRKC166-06	IRKJ166-06	600									
IRKD166-08	IRKC166-08	IRKJ166-08	800									
IRKD166-10	IRKC166-10	IRKJ166-10	1000									
IRKD166-12	IRKC166-12	IRKJ166-12	1200	165	100	3350	3500	1.69	0.10			
IRKD166-14	IRKC166-14	IRKJ166-14	1400									
IRKD166-16	IRKC166-16	IRKJ166-16	1600									
IRKD166-18	IRKC166-18	IRKJ166-18	1800									
IRKD166-20	IRKC166-20	IRKJ166-20	2000									
IRKD196-04	IRKC196-04	IRKJ196-04	400									
IRKD196-06	IRKC196-06	IRKJ196-06	600									
IRKD196-08	IRKC196-08	IRKJ196-08	800									
IRKD196-10	IRKC196-10	IRKJ196-10	1000									
IRKD196-12	IRKC196-12	IRKJ196-12	1200									
IRKD196-14	IRKC196-14	IRKJ196-14	1400	195	100	4000	4200	1.38	0.10			
IRKD196-16	IRKC196-16	IRKJ196-16	1600									
IRKD196-18	IRKC196-18	IRKJ196-18	1800									
IRKD196-20	IRKC196-20	IRKJ196-20	2000									
IRKD196-22	IRKC196-22	IRKJ196-22	2200									
IRKD196-24	IRKC196-24	IRKJ196-24	2400									
IRKD236-04	IRKC236-04	IRKJ236-04	400							M6	(6) (10)	
IRKD236-06	IRKC236-06	IRKJ236-06	600									
IRKD236-08	IRKC236-08	IRKJ236-08	800									
IRKD236-10	IRKC236-10	IRKJ236-10	1000									
IRKD236-12	IRKC236-12	IRKJ236-12	1200	230	100	5500	5750	1.27	0.085			
IRKD236-14	IRKC236-14	IRKJ236-14	1400									
IRKD236-16	IRKC236-16	IRKJ236-16	1600									
IRKD236-18	IRKC236-18	IRKJ236-18	1800									
IRKD236-20	IRKC236-20	IRKJ236-20	2000									
IRKD250-04	IRKC250-04	IRKJ250-04	400									
IRKD250-06	IRKC250-06	IRKJ250-06	600									
IRKD250-08	IRKC250-08	IRKJ250-08	800									
IRKD250-10	IRKC250-10	IRKJ250-10	1000									
IRKD250-12	IRKC250-12	IRKJ250-12	1200	250	100	5900	6180	1.29	0.08			
IRKD250-14	IRKC250-14	IRKJ250-14	1400									
IRKD250-16	IRKC250-16	IRKJ250-16	1600									
IRKD250-18	IRKC250-18	IRKJ250-18	1800									
IRKD250-20	IRKC250-20	IRKJ250-20	2000									
IRKD270-04	IRKC270-04	IRKJ270-04	400							M6	(6) (10)	
IRKD270-06	IRKC270-06	IRKJ270-06	600									
IRKD270-08	IRKC270-08	IRKJ270-08	800									
IRKD270-10	IRKC270-10	IRKJ270-10	1000									
IRKD270-12	IRKC270-12	IRKJ270-12	1200									
IRKD270-14	IRKC270-14	IRKJ270-14	1400									
IRKD270-16	IRKC270-16	IRKJ270-16	1600	270	100	7500	7850	1.48	0.063			
IRKD270-18	IRKC270-18	IRKJ270-18	1800									
IRKD270-20	IRKC270-20	IRKJ270-20	2000									
IRKD270-22	IRKC270-22	IRKJ270-22	2200									
IRKD270-24	IRKC270-24	IRKJ270-24	2400									
IRKD270-26	IRKC270-26	IRKJ270-26	2600									
IRKD270-28	IRKC270-28	IRKJ270-28	2800									
IRKD270-30	IRKC270-30	IRKJ270-30	3000									
IRKD320-04	IRKC320-04	IRKJ320-04	400							M6	(6) (10)	
IRKD320-06	IRKC320-06	IRKJ320-06	600									
IRKD320-08	IRKC320-08	IRKJ320-08	800									
IRKD320-10	IRKC320-10	IRKJ320-10	1000									
IRKD320-12	IRKC320-12	IRKJ320-12	1200	320	100	8500	8900	1.28	0.063			
IRKD320-14	IRKC320-14	IRKJ320-14	1400									
IRKD320-16	IRKC320-16	IRKJ320-16	1600									
IRKD320-18	IRKC320-18	IRKJ320-18	1800									
IRKD320-20	IRKC320-20	IRKJ320-20	2000									

(1) Value given for R_{thJC} is per module.
(3) Doubler circuit.

(4) Center tap, circuit common cathode. Contact factory.
(5) Center tap, circuit common anode. Contact factory.
(6) RMS isolation voltage: 3000V-50 Hz.

(7) 100% V_{RRM} reapplied. T_J = T_J max. = 150°C.
(8) For case outline drawing see page 0-2.
(9) V_{FM} at I_{FM} = I_{F(AV)} × π, T_J = 25°C.
(10) All devices can be supplied with non toxic material. Add suffix N to part number.

Part Number	V _{RRM} (V)	I _{F(AV)} @ T _C		I _{FSM} (5)		(3) V _{FM} (V)	R _{thJC} DC (1) (K/W)	Case Outline Number (6)	Notes	Case Style
		(A)	(°C)	50 Hz (A)	60 Hz (A)					
IRKE270-04 IRKE270-06 IRKE270-08 IRKE270-10 IRKE270-12 IRKE270-14 IRKE270-16 IRKE270-18 IRKE270-20 IRKE270-22 IRKE270-24 IRKE270-26 IRKE270-28 IRKE270-30	400 600 800 1000 1200 1400 1600 1800 2000 2200 2400 2400 2600 3000	270	100	7500	7850	1.48	0.125	M6	(4) (7)	 
IRKE320-04 IRKE320-06 IRKE320-08 IRKE320-10 IRKE320-12 IRKE320-14 IRKE320-16 IRKE320-18 IRKE320-20	400 600 800 1000 1200 1400 1600 1800 2000	320	100	8500	8900	1.28	0.125			

(1) Value given for R_{thJC} is per module.

(3) V_{FM} at I_{FM} = I_{F(AV)} × π, T_J = 25°C.

(4) RMS isolation voltage: 3000V-50 Hz.

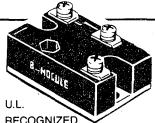
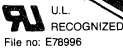
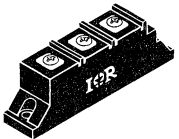

(5) 100% V_{RRM} reapplied. T_J = T_J max. = 150°C.

(6) For case outline drawing see page

(7) All devices can be supplied with non-toxic material.

Add suffix "N" to part number.

Diode/Diode

Part Number			V _{RRM} (V)	I _{F(AV)} @ T _C		I _{FSM} (7)		(9) V _{FM} (V)	R _{thJC} DC (1) (K/W)	Case Outline Number (8)	Notes	Case Style
(3)	(4)	(5)		(A)	(°C)	50 Hz (A)	60 Hz (A)					
B40D10 B40D20 B40D40 B40D60 B40D80 B40D100 B40D120	— — — — — — —	B40J10 B40J20 B40J40 B40J60 B40J80 B40J100 B40J120	100 200 400 600 800 1000 1200	40	85	550	575	1.31	0.60	M2	(2)	 
IRKD56/04 IRKD56/06 IRKD56/08 IRKD56/10 IRKD56/12	IRKC56/04 IRKC56/06 IRKC56/08 IRKC56/10 IRKC56/12	IRKJ56/04 IRKJ56/06 IRKJ56/08 IRKJ56/10 IRKJ56/12	400 600 800 1000 1200	55	100	1350	1420	1.35	0.325	M4	(2) (11)	 
IRKD61/14 IRKD61/16 IRKD61/18 IRKD61/20	IRKC61/14 IRKC61/16 IRKC61/18 IRKC61/20	IRKJ61/14 IRKJ61/16 IRKJ61/18 IRKJ61/20	1400 1600 1800 2000	60	90	1220	1270	1.35	0.325			
IRKD71/04 IRKD71/06 IRKD71/08 IRKD71/10 IRKD71/12	IRKC71/04 IRKC71/06 IRKC71/08 IRKC71/10 IRKC71/12	IRKJ71/04 IRKJ71/06 IRKJ71/08 IRKJ71/10 IRKJ71/12	400 600 800 1000 1200	70	100	1500	1570	1.30	0.285			
IRKD81/14 IRKD81/16 IRKD81/18 IRKD81/20	IRKC81/14 IRKC81/16 IRKC81/18 IRKC81/20	IRKJ81/14 IRKJ81/16 IRKJ81/18 IRKJ81/20	1400 1600 1800 2000	80	88	1350	1410	1.36	0.25			
IRKD91/04 IRKD91/06 IRKD91/08 IRKD91/10 IRKD91/12	IRKC91/04 IRKC91/06 IRKC91/08 IRKC91/10 IRKC91/12	IRKJ91/04 IRKJ91/06 IRKJ91/08 IRKJ91/10 IRKJ91/12	400 600 800 1000 1200	90	100	1700	1780	1.30	0.22			
IRKD101/14 IRKD101/16 IRKD101/18 IRKD101/20	IRKC101/14 IRKC101/16 IRKC101/18 IRKC101/20	IRKJ101/14 IRKJ101/16 IRKJ101/18 IRKJ101/20	1400 1600 1800 2000	100	87	1700	1780	1.34	0.22			

(1) Value given for R_{thJC} is per module.

(2) RMS isolation voltage: 3500V-50 Hz.

(3) Doubler circuit.

(4) Center tap, circuit common cathode. Contact factory.

(5) Center tap, circuit common anode. Contact factory.

(7) 100% V_{RRM} reapplied. T_J = T_J max. = 150°C.

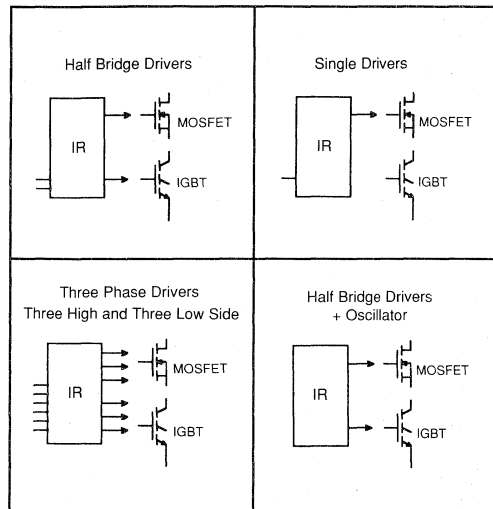
(8) For case outline drawing see page 0-2.

(9) V_{FM} at I_{FM} = I_{F(AV)} × π, T_J = 25°C.

(11) New generation of ADD-A-Pak modules are identified by a "/" (slash) in the part number instead of the "-" of the old part number. Consult factory for new type availability.



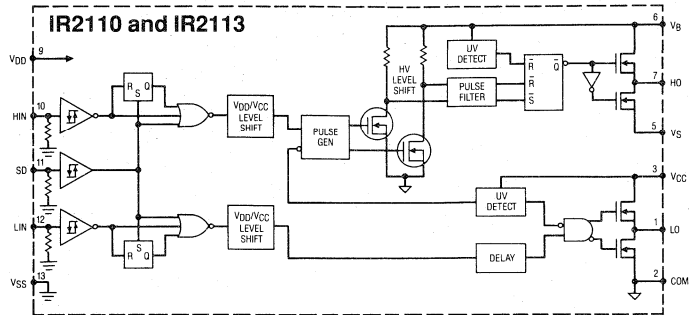
High Voltage Power MOSFET/IGBT Gate Drivers



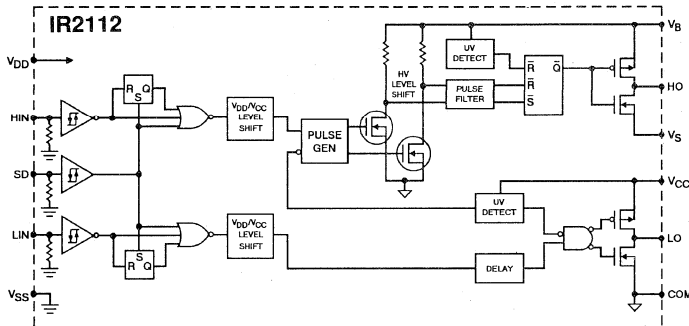
Features

- Drives single, pair, and six HEXFETs or IGBTs
- Floating High Side Driver
- Ground Referenced Low Side Driver
- Operates to either 500V or 600V
- High dv/dt and negative transient immunity
- CMOS Compatible Schmitt Trigger Inputs
- Low Quiescent Power Dissipation
- Undervoltage lockout with hysteresis – all channels
- Matched delay times for High and Low channels
- Latch immune CMOS

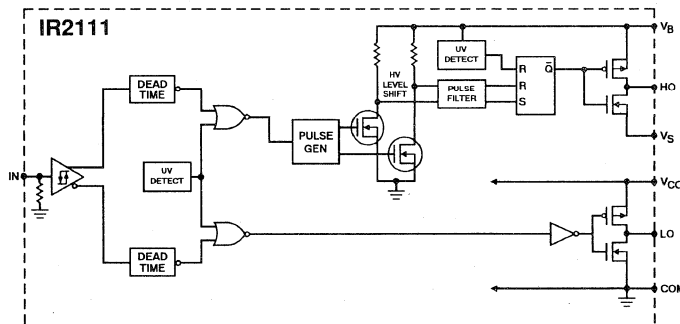
Part Number	Configuration	Maximum Floating Supply Offset Voltage	I _o Source, Sink	Schematic	(1) Case Outline	Notes	Case Style
IR2110	High Side	500V	2A / 2A	S1	P1		14 Pin DIP
IR2110-1	and				P2		14 Pin DIP w/o Pin 4
IR2110-2	Low Side				P3		16 Pin DIP w/o Pins 4 & 5
IR2110S					P4		16 Pin SOIC Wide Body
IR2111	Half Bridge	600V	200 / 420 mA	S3	P5		8 Pin DIP
IR2112	High Side	600V	200 / 420 mA	S2	P1		14 Pin DIP
IR2112-1	and				P2		14 Pin DIP w/o Pin 4
IR2112-2	Low Side				P3		16 Pin DIP w/o Pins 4 & 5
IR2112S					P4		16 Pin SOIC Wide Body
IR2113	High Side	600V	2A / 2A	S1	P1		14 Pin DIP
IR2113-1	and				P2		14 Pin DIP w/o Pin 4
IR2113-2	Low Side				P3		16 Pin DIP w/o Pins 4 & 5
IR2113S					P4		16 Pin SOIC Wide Body
IR2121	Low Side Current Limit	—	1A / 2A	S5	P5		8 Pin DIP
IR2125	High Side Current Limit	500V	1A / 2A	S6	P5		8 Pin DIP
IR2130	3 High Side	600V	200 / 420 mA	S7	P6	2.5 μs Dead-time	28 Pin DIP
IR2130J	and				P7		44 Pin PLCC w/o 12 leads
IR2130S	3 Low Side				P8		28 Pin SOIC Wide Body
IR2132	3 High Side	600V	200 / 420 mA	S7	P6	0.8 μs Dead-time	28 Pin DIP
IR2132J	and				P7		44 Pin PLCC w/o 12 leads
IR2132S	3 Low Side				P8		28 Pin SOIC Wide Body
IR2155	1/2 Bridge Self oscillating	600V	200 / 420 mA	S4	P5	555 Type timer	8 Pin DIP



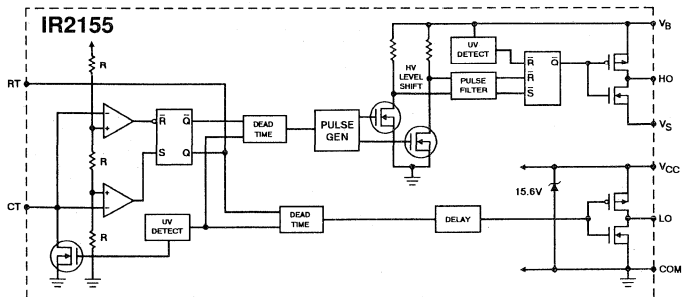
S1 – IR2110 and IR2113 Schematic



S2 – IR2112 Schematic



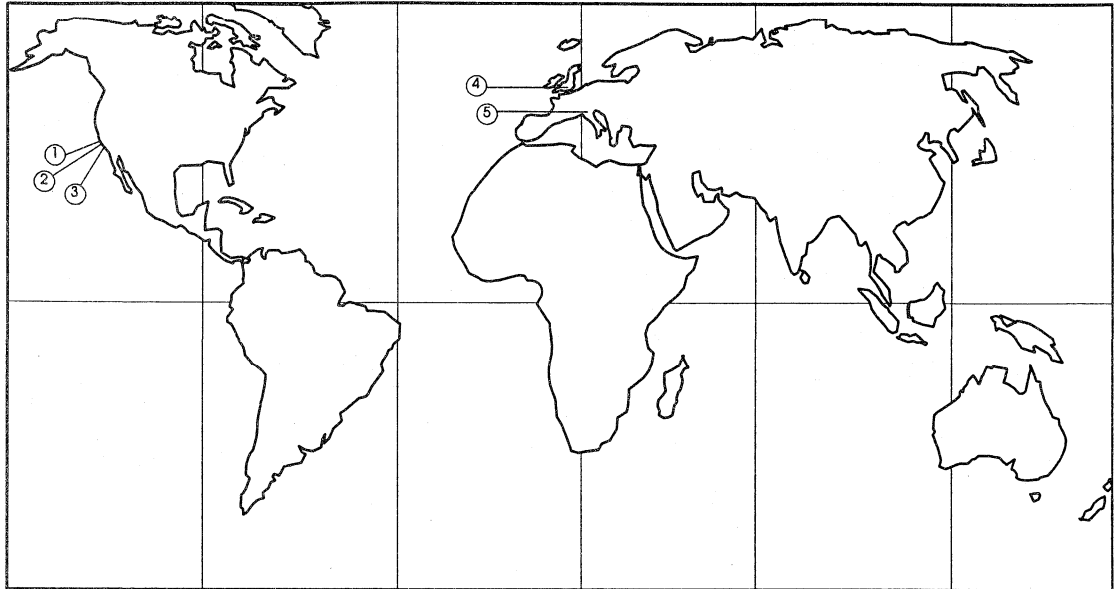
S3 – IR2111 Schematic



S4 – IR2155 Schematic

International Rectifier

...around-the-world manufacturing
to serve worldwide needs.



① **El Segundo, California**

- Power MOSFETs, custom hybrids, PICs, government/military hi-rel devices, microelectronic relays

② **HEXFET America
Rancho California, California**

- Dedicated to power MOSFETs, IGBTs

③ **Tijuana, Mexico**

- Schottkys, HEXFREDs, IGBTs, HEXFET, Alloyed Diodes

④ **Oxted, England**

- Power MOSFETs, IGBTs, Schottkys, Power ICs, HEXFREDs

⑤ **Turin, Italy**

- Diodes, thyristors, diode bridges, power modules

INTERNATIONAL RECTIFIER WORLDWIDE SALES AND SERVICE

WORLD HEADQUARTERS

233 KANSAS ST., EL SEGUNDO, CA 90245 USA · Tel: 310-322-3331 · FAX: 310-322-3332 · Telex: 66-4464

EUROPEAN HEADQUARTERS

HURST GREEN, OXTED, SURREY RH8 9BB, UK · Tel: (44) 0883 713 215 · FAX: (44) 08833 714 234 · Telex: 95219

NORTHAMERICA/U.S.A.

Eastern U.S.: 130 Commons Ct., Chadds Ford, PA · Tel: 610-358-5153 · FAX: 610-358-5172

Central U.S.: 1851 Hicks Rd., Suite C, Rolling Meadows, IL 60008 · Tel: 708-934-0020 · FAX: 708-934-0452

Southern U.S.: 4309 Neptune Rd., St. Cloud, FL 34769 · Tel: 407-957-4344 · FAX: 407-957-3933

Western U.S.: 222 Kansas St., El Segundo, CA 90245 · Tel: 310-607-8886 · FAX: 310-607-8116

Canada: 7231 Victoria Park Ave., Markham, Ontario L3R 2Z8 · Tel: 905-475-1897 · FAX: 905-475-8801 · Telex: 06 966 650

Mexico: Durazno 30, Centro Industrial Los Olivos, Tijuana, Baja California · Tel: 526-689-1200 · FAX: 526-689-3127

EASTERN EUROPE

Czechoslovakia: Macurova 1565/19, post. schranka c.30, 149 00 Praha 4 · Tel: 2 792 6831 · FAX: 2 792 6831

Hungary: Szent Istvan Park 15, H-1137 Budapest · Tel: 1 1298 822 · FAX: 1 1298 822

Poland: Ul. Gwiazdzista 13/100, 01-651 Warszawa · Tel: 022 39 8295 · FAX: 022 39 8295

WESTERN EUROPE

France: 123 Rue de Petit Vaux, 91360 Epinay sur Orge · Tel: 1 64 548 329 · FAX: 1 64 548 330

Germany: Saalburgstrasse 157, 61350 Bad Homburg · Tel: 6172 37066 · FAX: 6172 37065 · Telex: 410 404

Italy: Via Liguria 49, 10071 Borgaro, Torino · Tel: 011 451 0111 · FAX: 011 451 0220 · Telex: 221257

Switzerland: CH-8032 Zurich, Kirchenweg 5 · Tel: 01 386 8702 · FAX: 01 383 5108

SCANDINAVIA

Denmark: P.O. Box 88, Telefonvej 8, DK-2860 Soeborg · Tel: 45 39 57 71 50 · FAX: 45 39 57 71 52

Finland: Billskogsvagen 19, 02580 Sjundea St. · Tel: 0 262 8144 · FAX: 0 262 8150

Sweden: Box 86, S-162, 12 Vallingby 1, Stockholm · Tel: 08 870 035 · FAX: 08 874 242

ASIA

Hong Kong: Room 5, 20/F, Pacific Plaza, 418 Des Voeux Road West · Tel: 852 803 7380 · FAX: 852 540 5835

Japan: K&H Bldg., 2F, 3-30-4 Nishi-Ikebukuro 3-Chome, Toshima-Ku, Tokyo 171 · Tel: (03)3983-0641 · FAX: (03)3983-0642

Korea: Samku Bldg., 2020, 16-49 Hankang-ro 3ka, Youngsan-gu, Seoul 140-202 · Tel: 2 705 1280 · FAX: 2 705 1279

Singapore: 315 Outram Road, #10-02 Tan Boon Liat Building, 0316 · Tel: 65 221 8371 · FAX: 65 221 8372

Sales Offices, Agents and Distributors in Major Cities Throughout the World.



 International Rectifier

WORLD HEADQUARTERS: 233 KANSAS STREET • EL SEGUNDO, CA 90245 USA • 310-322-3331 • FAX 310-322-3332
EUROPEAN HEADQUARTERS: HURST GREEN, OXTED, SURREY RH8 9BB, ENGLAND • 0883-713215 • FAX 0883-714234